THE CHEMISTRY OF THE
ACTINIDE AND TRANSACTINIDE ELEMENTS

Joseph J. Katz

Glenn T. Seaborg

This work is dedicated to
Joseph J. Katz and Glenn T. Seaborg,
authors of the first and second editions of
The Chemistry of the Actinide Elements
and leaders in the field of actinide chemistry.

THE CHEMISTRY OF THE
ACTINIDE AND TRANSACTINIDE ELEMENTS

THIRD EDITION

Volume 1

EDITED BY

Lester R. Morss
Argonne National Laboratory,
Argonne, Illinois, USA

Norman M. Edelstein
Lawrence Berkeley National Laboratory,
Berkeley, California, USA

Jean Fuger
University of Liège,
Liège, Belgium

Honorary Editor
Joseph J. Katz
Argonne National Laboratory

Springer

Library of Congress Control Number: 2008922620

ISBN-10 1-4020-3555-1 (HB)
ISBN-10 1-4020-3598-5 (e-book)
ISBN-13 978-1-4020-3555-5 (HB)
ISBN-13 978-1-4020-3598-2 (e-book)

Published by Springer,
P.O. Box 17, 3300 AA Dordrecht, The Netherlands.

www.springer.com

Printed on acid-free paper

First published in 2006
Reprinted 2006
Reprinted with corrections in 2008

CONTENTS

Volume 1

Volume 2

Volume 3

Volume 4

Volume 5

CONTRIBUTORS

Irshad Ahmad
Argonne National Laboratory, USA

Thomas E. Albrecht-Schmitt
Auburn University, Alabama, USA

Mark R. Antonio
Argonne National Laboratory, USA

A. J. Arko
Los Alamos National Laboratory, USA (retired)

James V. Beitz
Argonne National Laboratory, USA (retired)

Jean Blaise
Laboratoire Aimé Cotton, Orsay, France

Jean-Philippe Blaudeau
High Performance Technologies, Inc., Wright-Patterson Air Force Base, Ohio, USA

Nicholas J. Bridges
The University of Alabama, USA

Edgar C. Buck
Pacific Northwest National Laboratory, Richland, Washington, USA

Carol J. Burns
Los Alamos National Laboratory, USA

Bruce E. Bursten
The University of Tennessee, USA

Gregory R. Choppin
Florida State University, USA

David L. Clark
Los Alamos National Laboratory, USA

Claude Degueldre
Paul Scherrer Institute, Switzerland

Peter K. Dorhout
Colorado State University, USA

Janusz Drożdżyński
University of Wroclaw, Poland

Patricia W. Durbin
Lawrence Berkeley National Laboratory, USA

Norman M. Edelstein
Lawrence Berkeley National Laboratory, USA

Moris S. Eisen
Technion -Israel Institute of Technology, Israel

P. Gary Eller
Los Alamos National Laboratory, USA (retired)

Mark Fred
Argonne National Laboratory, USA (deceased)

Blandine Fourest
Institut de Physique Nucléaire, Orsay, France

Jean Fuger
University of Liège, Belgium

Takeo Fujino
Tohoku University, Japan (retired)

Ingmar Grenthe
Royal Institute of Technology, Stockholm, Sweden

Keith E. Gutowski
The University of Alabama, USA

Richard G. Haire
Oak Ridge National Laboratory, USA

John M. Haschke
Actinide Science Consulting, Harwood, TX, USA

Ladia Havela
Charles University, Czech Republic

P. Jeffrey Hay
Los Alamos National Laboratory, USA

Siegfried S. Hecker
Los Alamos National Laboratory, USA

David E. Hobart
Los Alamos National Laboratory, USA

Darleane C. Hoffman
Lawrence Berkeley National Laboratory, USA

Gordon D. Jarvinen
Los Alamos National Laboratory, USA

Mark P. Jensen
Argonne National Laboratory, USA

Stephen G. Johnson
Idaho National Laboratory, USA

John J. Joyce
Los Alamos National Laboratory, USA

Nikolas Kaltsoyannis
University College London, UK

Joseph J. Katz
Argonne National Laboratory, USA (retired)

Takaumi Kimura
Japan Atomic Energy Agency, Japan

Harold W. Kirby *(deceased)*
Mound Laboratory, Miamisburg, Ohio, USA

Rudy J. M. Konings
European Commission, Joint Research Centre
Institute for Transuranium Elements, Karlsruhe, Germany

John R. Krsul
Argonne National Laboratory, USA (retired)

Jérôme Lacquement
CEA-Valrho, Marcoule, France

Gerard H. Lander
European Commission, Joint Research Centre
Institute for Transuranium Elements, Karlsruhe, Germany

Diana M. Lee
Lawrence Berkeley National Laboratory, USA

Jun Li
Pacific Northwest National Laboratory, Richland, Washington, USA

Guokui Liu
Argonne National Laboratory, USA

Gregg J. Lumetta
Pacific Northwest National Laboratory, Richland, Washington, USA

Charles Madic
CEA-Saclay, Gif-sur-Yvette, France

Jagdish N. Mathur
Bhabha Atomic Research Centre, Mumbai, India

Lester R. Morss
Argonne National Laboratory (retired) and
U.S. Department of Energy, Washington DC, USA

Boris F. Myasoedov
Russian Academy of Sciences, Moscow, Russia

Kenneth L. Nash
Washington State University, USA

Mary P. Neu
Los Alamos National Laboratory, USA

Robert A. Penneman
Los Alamos National Laboratory, USA (retired)

Valeria Pershina
Gesellschaft für Schwerionenforschung, Darmstadt, Germany

Joseph R. Peterson
The University of Tennessee, USA and
Oak Ridge National Laboratory, USA (retired)

Robin D. Rogers
The University of Alabama, USA

Wolfgang Runde
Los Alamos National Laboratory, USA

Wallace W. Schulz
Albuquerque, New Mexico, USA

Robert J. Silva
Lawrence Livermore National Laboratory, USA (retired)

Lynda Soderholm
Argonne National Laboratory, USA

Jerry L. Stakebake
Boulder, Colorado, USA

Ivan G. Tananaev
Russian Academy of Sciences, Moscow, Russia

Major C. Thompson
Savannah River National Laboratory, USA (retired)

Norbert Trautmann
Universität Mainz, Germany

Mathias S. Wickleder
Carl von Ossietzky Universität, Oldenburg, Germany

Stephen F. Wolf
Indiana State University, Terre Haute, Indiana, USA

Earl F. Worden, Jr.
Lawrence Livermore National Laboratory, USA (retired)

Jean-François Wyart
Laboratoire Aimé Cotton, Orsay, France

Zenko Yoshida
Japan Atomic Energy Agency, Japan

PREFACE

The first edition of this work (*The Chemistry of the Actinide Elements* by J. J. Katz and G. T. Seaborg) was published in 1957, nearly a half century ago. Although the chemical properties of thorium and uranium had been studied for over a century, and those of actinium and protactinium for over fifty years, all of the chemical properties of neptunium and heavier elements as well as a great deal of uranium chemistry had been discovered since 1940. In fact, the concept that these elements were members of an "actinide" series was first enunciated in 1944. In this book of 500 pages the chemical properties of the first transuranium elements (neptunium, plutonium, and americium) were described in great detail but the last two actinide elements (nobelium and lawrencium) remained to be discovered. It is not an exaggeration to say that *The Chemistry of the Actinide Elements* expounded a relatively new branch of chemistry.

The second edition was published in 1986, by which time all of the actinide elements had been synthesized and chemically characterized, at least to some extent. At this time the chemistry of the actinide elements had reached maturity. The second edition filled two volumes, with a chapter for each of the elements (the elements beyond einsteinium were combined in one chapter) and systematic treatment of various aspects of the chemical and electronic properties of the actinide elements, ions, and compounds due to the filling of the 5f subshell. Six transactinide elements had been synthesized by 1986 but their experimentally determined chemical properties occupied only 1.5 pages of text in the second edition.

This edition was initiated by the editors of the second edition (J. J. Katz, G. T. Seaborg, and L. R. Morss) in 1997. They realized that the study of the chemical properties of the actinide elements had advanced to produce distinct subdisciplines of actinide chemistry, for example actinide coordination chemistry, actinide X-ray absorption spectroscopy, itinerancy in actinide intermetallics, organoactinide chemistry, and actinide environmental chemistry. These fields had sufficiently matured so that scientists could make more substantial contributions to predicting and controlling the fate of actinides in the laboratory, in technology, and in the environment. We now understand and are able to predict with some degree of confidence the chemical bonding and reactivity of actinides in actinide materials, in actual environmental matrices and in proposed nuclear waste repositories. Most of the unique properties of the actinides are caused by their accessible and partly filled 5f orbitals. In addition to advances with the actinides, there have been research groups at nuclear research centers in several countries that have dedicated themselves to carry out significant and systematic experimental studies on the transactinide elements for several decades. For these reasons the editors initiated the writing of a third edition, with the enlarged title *The Chemistry of the Actinide and Transactinide Elements* that is both broader and deeper than the second edition.

The third edition follows the plan enunciated by the authors of the first edition: "This book is intended to provide a comprehensive and uniform treatment of the chemistry of the actinide [and transactinide] elements for both the nuclear technologist and the inorganic and physical chemist." To fulfill this plan consistent with the maturity of the field, the third edition is organized in three parts.

The first group of chapters follows the format of the first and second editions by beginning with chapters on individual elements or groups of elements that describe and interpret their chemical properties. A chapter on the chemical properties of the transactinide elements is included.

The second group, chapters 15-26, summarizes and correlates physical and chemical properties that are in general unique to the actinide elements, because most of these elements contain partially-filled shells of 5f electrons whether present as isolated atoms or ions, as metals, as compounds, or as ions in solution.

The third group of chapters (chapters 27-31) focuses on specialized topics that encompass contemporary fields related to actinide species in the environment, in the human body, and in storage or wastes. There are also two appendices that tabulate important nuclear properties of all actinide and transactinide isotopes.

Each chapter has been written to provide sufficient background for the substantial parts of the readership that are not specialists in actinide science, nuclear-science-related areas (nuclear physics, health physics, nuclear engineering), spectroscopy, or solid-state science (metallurgy, solid state physics). The editors hope that this work educates and informs those readers who are scientists and engineers that are unfamiliar with the field and wish to learn how to deal with actinides in their research or technology.

The editors are deeply indebted to the contributors of each chapter, all of whom agreed enthusiastically to write their chapters and all of whom did so as a labor of love as well as a long-term professional responsibility. We take special pleasure in thanking Dr. Emma Roberts, Senior Publishing Editor of Springer, who provided the resources to turn more than thirty manuscripts into this attractive and useful professional series of volumes. We also thank Roger Wayman and Aaliya Jetha of Springer and all the other professional staff at Springer and SPI Publisher Services who brought this work to completion.

The editors dedicate this work to Joseph J. Katz and Glenn T. Seaborg, the first authors of the first edition and second editions of *The Chemistry of the Actinide Elements.* They provided inspiration for the generations of scientists who followed them and they set high standards in their research. Dr. Katz guided and motivated the editors and authors of the third edition to produce a work that followed the model of the first and second editions and provided leadership as this edition was unfolding. Because of his insights and leadership as an inorganic, physical, and actinide chemist, we have asked Dr. Katz to be listed on the title page as honorary editor, and he has agreed to accept this role. The editors also dedicate this work to the memory of Professor Seaborg, the co-discover of plutonium and many other actinide and transactinide elements, and pioneer in actinide chemistry. We note with sadness that he participated in planning this edition but passed away before any of the chapters had been written. We believe that he would have been pleased to see how productive has been the research of the authors and many other actinide and transactinide scientists who follow his leadership.

All of us who have participated in the writing, editing, and publishing *The Chemistry of the Actinide and Transactinide Elements* express our hope that this new edition will make a substantive contribution to research in actinide and transactinide science, and that it will be an appropriate source of factual information on these elements for teachers, researchers, and students and for those who have the responsibility for utilizing the actinide elements to serve humankind and to control and mitigate their environmental hazards.

Lester R. Morss
Norman M. Edelstein
Jean Fuger

CHAPTER ONE

INTRODUCTION

Joseph J. Katz, Lester R. Morss, Norman M. Edelstein, and Jean Fuger

The actinide elements are the 15 chemical elements with atomic numbers 89 through 103, the first member of which is actinium and the last member is lawrencium (Fig. 1.1). The transactinide elements (those beyond the actinides) are the heaviest known chemical elements. Both the actinide and the transactinide elements have chemical properties that are governed by their outermost electronic subshells. Each of these groups of elements is a unique transition series (a group of elements in which d or f electronic subshells are being filled).

The actinides are the transition elements that fill the 5f subshell. The actinide series is unique in several respects:

- Most of the elements (those heavier than uranium) were first discovered by synthetic methods: bombardment of heavy atoms with neutrons in nuclear reactors, bombardment with other particles in accelerators, or as the result of nuclear detonations.
- All actinide isotopes are radioactive, with a wide range of nuclear properties, especially that of spontaneous and induced nuclear fission.
- They are all metals with very large radii, and exist in chemical compounds and in solution as cations with very large ionic radii.
- The metals exhibit an unusual range of physical properties. Plutonium, with six allotropes, is the most unusual of all metals.
- Many of the actinide elements have a large number of oxidation states. In this respect plutonium is unique, being able to exist in aqueous solution simultaneously in four oxidation states.
- In metallic materials and in some other compounds with elements lighter than plutonium, the 5f orbitals are sufficiently diffuse that the electrons in these orbitals are “itinerant” (delocalized, chemically bonding, often with unique magnetic moments and electrical conductivity). In metallic materials and in most compounds with elements heavier than plutonium the 5f electrons are “localized” (not contributing significantly to electrical conductivity or to chemical bonds). Materials with plutonium and adjacent

elements can exhibit both itinerant and localized behavior, depending on conditions such as temperature and applied pressure.

- Actinium (which has no 5f electrons in the metal, free atom, or in any of its ions) and the elements americium through lawrencium are similar in many respects to the lanthanide elements (the elements that fill the 4f electron subshell). The elements thorium through neptunium have some properties similar to those of the d transition elements.
- Relativistic contributions to electronic properties and spin–orbit effects are important in the chemical properties of actinides.

The transactinide elements are at the frontier of both the periodic table (Fig. 1.1) and the chart of the nuclides. Transactinide chemistry has been in existence since 1970. Although these elements have unique properties, they are very difficult to study because their synthesis and identification require unique nuclear reactions and rapid separations. The heaviest transactinide element for which chemical properties have been identified (at the time of writing of this work) is hassium (atomic number 108). Experimental evidence and theoretical studies to date indicate that the elements through 112 are part of a 6d transition series of elements.

1	2	3	4	5	6	7	8	9	10	11	12	13	14	15	16	17	18
1 H																	2 He
3 Li	4 Be											5 B	6 C	7 N	8 O	9 F	10 Ne
11 Na	12 Mg											13 Al	14 Si	15 P	16 S	17 Cl	18 Ar
19 K	20 Ca	21 Sc	22 Ti	23 V	24 Cr	25 Mn	26 Fe	27 Co	28 Ni	29 Cu	30 Zn	31 Ga	32 Ge	33 As	34 Se	35 Br	36 Kr
37 Rb	38 Sr	39 Y	40 Zr	41 Nb	42 Mo	43 Tc	44 Ru	45 Rh	46 Pd	47 Ag	48 Cd	49 In	50 Sn	51 Sb	52 Te	53 I	54 Xe
55 Cs	56 Ba	57 La	72 Hf	73 Ta	74 W	75 Re	76 Os	77 Ir	78 Pt	79 Au	80 Hg	81 Tl	82 Pb	83 Bi	84 Po	85 At	86 Rn
87 Fr	88 Ra	89 Ac	104 Rf	105 Db (Ha)	106 Sg	107 Bh	108 Hs	109 Mt	110 Ds	111 Rg	*112*	*113*	*114*	*115*	*116*	(117)	(118)
(119)	(120)	(121)	(154)														

LANTHANIDES	58 Ce	59 Pr	60 Nd	61 Pm	62 Sm	63 Eu	64 Gd	65 Tb	66 Dy	67 Ho	68 Er	69 Tm	70 Yb	71 Lu
ACTINIDES	90 Th	91 Pa	92 U	93 Np	94 Pu	95 Am	96 Cm	97 Bk	98 Cf	99 Es	100 Fm	101 Md	102 No	103 Lr
SUPERACTINIDES	(122)	(123)	(124)	(125)	(126)									(153)

Fig. 1.1 *The periodic table of the elements, showing placement of transactinides and superactinides through element* 154 (*see Chapter* 14). (*Italics indicate elements reported but not yet confirmed as of* 2005. *Undiscovered elements are shown in parentheses.*)

The transactinides are also unique in several respects:

- One-atom-at-a-time chemistry is required to compensate for low nuclear yields and short isotopic half-lives. Ingenious techniques have been developed to study their chemical properties in both gas phase and solution.
- Relativistic effects cause substantial contraction of the 7s (occupied), 7p (empty), and 6d (partially filled) orbitals. (Many electronic configurations have been calculated; see Chapter 14.) The contraction of the 7s orbitals stabilizes the $7s^2$ electron pair. The contraction of the 7p orbitals makes 7p terms accessible, e.g., the first excited multiplet of rutherfordium (element 104) outside the [Xe $5f^{14}$] core is calculated to be $6d7s^27p$.
- The first part of the transactinides constitutes a 6d transition series, with the calculated ionic radii intermediate between those of the 5d ions and actinide ions of the same charge. Relativistic effects decrease the polarizability of transactinide ions.
- Fundamental properties – electronic configurations, ionization energies of atoms and ions, oxidation–reduction potentials in solution – remain to be calculated theoretically and measured experimentally.

In the six decades that have elapsed since the "actinide concept" was enunciated by G. T. Seaborg, great advances have taken place in actinide and transactinide chemistry. As in many other important areas of science, new information and new concepts have accumulated to an extraordinary extent. This, in itself, would be ample justification for a comprehensive examination of the scientific aspects of the actinide elements. Of equal, or perhaps even greater, importance in the preparation of this third edition are the contributions that its many authors have made to provide the foundations for the solution of some of the most urgent technological and environmental problems that face humanity worldwide. We refer, of course, to the problems created by nuclear reactors used for electricity production; nuclear weapons production and dismantlement; the treatment and storage of nuclear wastes; and the cleanup of Cold War nuclear material sites. These are sources of acute global concern, in all of which the actinide elements are intimately involved.

In 1957, when the first edition of this work was published, the chemistry of the actinide elements was remarkably well developed, considering that the actinide concept itself had first been publicly described in 1945. (See Chapter 15, section 1.2, of this book) The elements thorium and uranium had already been studied by chemists for more than 100 years. Uranium enjoyed some small distinction as the heaviest element in nature, and as the terminus of the classical periodic table. In 1895 Becquerel had discovered that uranium undergoes radioactive decay, a discovery that permanently divested uranium of its obscurity, and that inaugurated the era of the Curies, Rutherford, Soddy, Hahn and Meitner, Fajans, and others who mapped the very complex radioactive transformations of the naturally occurring elements. The crucial importance of uranium, however, became fully apparent only after Fermi and his colleagues irradiated many of the elements, including uranium, with neutrons in the 1930s. They produced new radioactive species with chemical properties that were not identical with any of the known heavy elements. The Fermi group believed that they had created new elements heavier than uranium. In 1938 Hahn, Meitner, and Strassmann conducted definitive chemical experiments showing that the radioactive species produced by neutron irradiation of uranium were in fact fission fragments resulting from the cleavage of the uranium nucleus into smaller nuclei. Their experiments constituted the discovery of nuclear fission. The earlier formation of transuranium elements had been disproved, but the way to their synthesis was now open.

The first transuranium element, neptunium, was nevertheless the by-product of an investigation by McMillan and Abelson into the details of the fission process. While fission fragments recoil with enormous energy from a uranium nucleus undergoing fission, a radioactive species with a half-life of 2.3 days was observed to be formed with insufficient energy to escape from a thin film of irradiated uranium. Chemical investigation confirmed that a new element, neptunium, unknown in nature, with atomic number 93 and mass number 239, had been formed by neutron capture in ^{238}U.

$$^{238}_{92}\mathrm{U}+^{1}_{0}\mathrm{n} \rightarrow {}^{239}_{92}\mathrm{U} \xrightarrow[23.5\,\mathrm{min}]{\beta^-} {}^{239}_{93}\mathrm{Np} \quad (t_{1/2} = 2.36 \text{ days}) \tag{1.1}$$

The new prospects opened up by the discovery of the first transuranium element were rapidly explored, and soon the trickle became a flood. Table 1.1 lists the transuranium elements, the discoverers and the date of discovery, and the date of first isolation in weighable amount. The first of the transuranium elements to be synthesized on purpose, so to speak, was element 94 as the isotope of mass number 238. In 1940, Seaborg, McMillan, Kennedy, and Wahl at the University of California in Berkeley bombarded uranium oxide with 16 MeV deuterons produced in the 60 in. cyclotron and succeeded in isolating a long-lived alpha-particle emitter, chemically separable from both uranium and neptunium, which was identified as an isotope of element 94 and later given the name plutonium:

$$^{238}_{92}\mathrm{U} + {}^{2}_{1}\mathrm{H} \rightarrow {}^{238}_{93}\mathrm{Np} + 2^{1}_{0}\mathrm{n} \tag{1.2}$$

$$^{238}_{93}\mathrm{Np} \xrightarrow[2.1\mathrm{d}]{\beta^-} {}^{238}_{94}\mathrm{Pu} \quad (t_{1/2} = 87.7 \text{ years}) \tag{1.3}$$

Twenty isotopes of plutonium are now known. The plutonium isotope of major importance has always been the isotope of mass number 239. Research with ^{239}Pu has been strongly motivated by the fact that it was shown to be fissile by slow neutrons in the same way as ^{235}U, and would thus be able to sustain a neutron chain reaction. The isotope ^{239}Pu can thus be used for both military and nuclear energy purposes. To separate ^{235}U from ^{238}U requires an isotope separation of

Table 1.1 *The transuranium elements.*

Atomic number	*Element*	*Symbol*	*Discoverers and date of discovery*	*First isolation in weighable amount*
93	Neptunium	Np	E. M. McMillan and P. H. Abelson, 1940	L. B. Magnusson and T. J. LaChapelle, 1944
94	Plutonium	Pu	G. T. Seaborg, E. M. McMillan, J. W. Kennedy, and A. C. Wahl, 1940–41	
	Plutonium-239		J. W. Kennedy, G. T. Seaborg, E. Segrè, and A. C. Wahl, 1941	B. B. Cunningham and L. B. Werner, 1942
95	Americium	Am	G. T. Seaborg, R. A. James, L. O. Morgan, and A. Ghiorso, 1944–45	B. B. Cunningham, 1945
96	Curium	Cm	G. T. Seaborg, R. A. James, and A. Ghiorso, 1944	L. B. Werner and I. Perlman, 1947
97	Berkelium	Bk	S. G. Thompson, A. Ghiorso, and G. T. Seaborg, 1949	S. G. Thompson and B. B. Cunningham, 1958
98	Californium	Cf	S. G. Thompson, K. Street, Jr, A. Ghiorso, and G. T. Seaborg, 1950	B. B. Cunningham and S. G. Thompson, 1958
99	Einsteinium	Es	A. Ghiorso, S. G. Thompson, G. H. Higgins, G. T. Seaborg, M. H. Studier, P. R. Fields, S. M. Fried, H. Diamond, J. F. Mech, G. L. Pyle, J. R. Huizenga, A. Hirsch, W. M. Manning, C. I. Browne, H. L. Smith, and R. W. Spence, 1952	B. B. Cunningham, J. C. Wallmann, L. Phillips, and R. C. Gatti, 1961
100	Fermium	Fm	A. Ghiorso, S. G. Thompson, G. H. Higgins, G. T. Seaborg, M. H. Studier, P. R. Fields, S. M. Fried, H. Diamond, J. F. Mech, G. L. Pyle, J. R. Huizenga, A. Hirsch, W. M. Manning, C. I. Browne, H. L. Smith, and R. W. Spence, 1953	
101	Mendelevium	Md	A. Ghiorso, B. G. Harvey, G. R. Choppin, S. G. Thompson, and G. T. Seaborg, 1955	
102	Nobelium	No	A. Ghiorso, T. Sikkeland, J. R. Walton, and G. T. Seaborg, 1958	

Table 1.1 (*Contd.*)

Atomic number	*Element*	*Symbol*	*Discoverers and date of discovery*	*First isolation in weighable amount*
103	Lawrencium	Lr	A. Ghiorso, T. Sikkeland, A. E. Larsh, and R. M. Latimer, 1961	
104	Rutherfordium	Rf	A. Ghiorso, M. Nurmia, J. Harris, K. Eskola, and P. Eskola, 1969; Y. T. Oganessian, Y. V. Lobanov, S. P. Tretyakova, Y. A. Lasarev, I. V. Kolesov, K.A. Gavrilov, V. M. Plotko, and Y. V. Poluboyarinov, 1974	
105	Dubnium	Db	A. Ghiorso, M. Nurmia, K. Eskola, J. Harris, and P. Eskola, 1970; G. N. Flerov, Y.T. Oganessian, Y.V. Lobanov, Y. A. Lasarev, and S. P. Tretyakova, 1970	
106	Seaborgium	Sg	A. Ghiorso, J. M. Nitschke, J. R. Alonso, C. T. Alonso, M. Nurmia, G. T. Seaborg, E. K. Hulet, and R. W. Lougheed, 1974	
107	Bohrium	Bh	G. Münzenberg, S. Hofmann, F. P. Hessberger, W. Reisdorf, K. H. Schmidt, J. H. R. Schneider, P. Armbruster, C. C. Sahm, and B. Thuma, 1981	
108	Hassium	Hs	G. Münzenberg, P. Armbruster, H. Folger, F. P. Hessberger, S. Hofmann, J. Keller, K. Poppensieker, W. Reisdorf, K. H. Schmidt, H. J. Schott, M. E. Leino, and R. Hingmann, 1984	
109	Meitnerium	Mt	G. Münzenberg, P. Armbruster, F. P. Hessberger, S. Hofmann, K. Poppensieker, W. Reisdorf, J. R. H. Schneider, W. F. W. Schneider, K. H. Schmidt, C. C. Sahm, and D. Vermeulen, 1982	
110	Darmstadtium	Ds	S. Hofmann, V. Ninov, F. P. Hessberger, P. Armbruster, H. Folger, G. Münzenberg, H. J. Schött, A. G. Popeko, A. V. Yeremin, A. N. Andreyev, S. Saro, R. Janik, and M. Leino, 1995	

111	Roentgenium	Rg	S. Hofmann, V. Ninov, F. P. Hessberger, P. Armbruster, H. Folger, G. Münzenberg, H. J. Schött, A. G. Popeko, A. V. Yeremin, A. N. Andreyev, S. Saro, R. Janik, and M. Leino, 1995
112			S. Hofmann, F. P. Hessberger, D. Ackermann, G. Münzenberg, S. Antalic, P. Cagarda, B. Kindler, J. Kojouharova, M. Leino, B. Lonnel, R. Mann, A. G. Popeko, S. Reshitko, S. Saro, J. Uusitalo, and V. Yeremin, 2002[a]
113			Same as element 115[a]
114			Yu. Ts. Oganessian, V. K. Utyonkov, Yu. V. Lobanov, F. Sh. Abdullin, A. N. Polyakov, I. V. Shirokovsky, Yu. Ts. Tsyganov, G. G. Gulbekian, S. L. Bogomolov, B. N. Gikal, A. N. Metsentsev, S. Iliev, V. G. Subbotin, A. M. Sukhov, O. V. Ivanov, G. V. Buklanov, K. Subotic, M. G. Itkis, K. J. Moody, J. F. Wild, N. J. Stoyer, M. A. Stoyer, and R. W. Lougheed, 2000[a]
115			Yu. Ts. Oganessian, V. K. Utyonkov, Yu. V. Lobanov, F. Sh. Abdullin, A. N. Polyakov, I. V. Shirokovsky, Yu. Ts. Tsyganov, G. G. Gulbekian, S. L. Bogomolov, A. N. Metsentsev, S. Iliev, V. G. Subbotin, A. M. Sukhov, A. A. Voinov, G. V. Buklanov, K. Subotic, V. I. Zagrebaev, M. G. Itkis, J. J. Patin, K. J. Moody, J. F. Wild, M. A. Stoyer, N. J. Stoyer, D. A. Shaughnessy, J. M. Kenneally, and R. W. Lougheed, 2004[a]
116			Yu. Ts. Oganessian, V. K. Utyonkov, Yu. V. Lobanov, F. Sh. Abdullin, A. N. Polyakov, I. V. Shirokovsky, Yu. Ts. Tsyganov, G. G. Gulbekian, S. L. Bogomolov, B. N. Gikal, A. N. Metsentsev, S. Iliev, V. G. Subbotin, A. M. Sukhov, O. V. Ivanov, G. V. Buklanov, K. Subotic, M. G. Itkis, K. J. Moody, J. F. Wild, N. J. Stoyer, M. A. Stoyer, R. W. Lougheed, C. A. Laue, Ye. A. Karelin, and A. N. Tatarinov, 2000[a]

---

[a] Discovery claimed and published but not confirmed by IUPAC/IUPAP.

formidable proportions, but separating ^{239}Pu in pure form requires only a chemical separation from other elements, likewise an intimidating problem, but one that is in principle a considerably simpler undertaking.

In 1941, Kennedy, Seaborg, Segré, and Wahl successfully obtained ^{239}Pu by radioactive decay from ^{239}Np, which was first produced by irradiating natural ^{238}U with cyclotron-generated neutrons:

$$^{238}_{92}\mathrm{U} + ^{1}_{0}\mathrm{n} \rightarrow ^{239}_{92}\mathrm{U} + \gamma \tag{1.4}$$

$$^{239}_{92}\mathrm{U} \underset{23.5\ \mathrm{min}}{\xrightarrow{\beta^-}} ^{239}_{93}\mathrm{Np} \underset{2.36\ \mathrm{days}}{\xrightarrow{\beta^-}} ^{239}_{94}\mathrm{Pu} \quad (t_{1/2} = 24\ 110\ \text{years}) \tag{1.5}$$

The isotope plutonium-239 indeed turned out to be fissionable, with a slow neutron cross section 1.7 times that of uranium-235. Later work at the wartime Los Alamos Laboratory established conclusively that sufficient neutrons were emitted in the act of fission to sustain a nuclear chain reaction. The exigencies of World War II soon made available the massive resources necessary to convert the scientific possibilities of the transuranium elements into actuality, and the nuclear age was truly upon us. Seaborg (1982, 1992) has given a vivid eyewitness account of the discovery and early experiments with plutonium. This chronicle describes in unusual detail the problems that confronted the investigators in this strange and intimidating new field of research, and how they were solved.

Twelve transplutonium elements were added to the periodic table in the 30 years between 1944 and 1974. The syntheses of the elements with atomic number 95 through 106 required the development of new and ingenious experimental techniques as well as new conceptual frameworks, and these were elaborated with remarkable speed. Elements 95 and 96, named americium and curium, respectively, were first prepared in 1944 by bombardment of ^{239}Pu; curium was synthesized by irradiation of plutonium with helium ions (alpha particles), and soon thereafter americium was synthesized by multiple neutron capture in plutonium in a nuclear reactor. As was the case for neptunium and plutonium, chemical identification was essential; it was not until these elements were predicted to be part of an actinide (5f) transition series with +3 oxidation states that they were isolated and identified. By 1946 the chemical properties of americium and curium were already well defined, and by 1949 sufficient amounts of americium-241 and curium-242 had been accumulated to make it possible to undertake a search for the next members of the actinide series. Bombardment of elements 95 and 96 by helium ions accelerated in the 60 in. Berkeley cyclotron produced alpha-particle-emitting species that could be identified as isotopes of elements 97 and 98. These in turn were named berkelium and californium after their place of discovery. Again, prediction of their behavior as +3 ions in aqueous solution was essential. During this same period of time, magnetic and spectroscopic evidence confirmed that the transuranium elements were indeed members of a 5f series of elements; see the review by Gruen (1992).

The detonation of a thermonuclear device is capable of producing enormously high fluxes of neutrons. The first test thermonuclear explosion was set off at Eniwetok Atoll by the United States at the end of 1952. The huge numbers of neutrons produced by the explosion resulted in multineutron captures in the uranium-238 that was a part of the device. The capture of no fewer than 15 neutrons by a ^{238}U nucleus yielded an isotope of element 98:

$$^{238}_{92}\mathrm{U} + 15^{1}_{0}\mathrm{n} \rightarrow {}^{253}_{92}\mathrm{U} \xrightarrow{\text{multiple } \beta^- \text{ decays}} {}^{253}_{98}\mathrm{Cf} \tag{1.6}$$

Capture of the 15 neutrons must have been accomplished in a fraction of a microsecond, and the subsequent radioactive decay of uranium-253 via a series of beta-particle emissions to form californium-253 must have been completed in a short time. Californium-253 then undergoes decay by beta-particle emission (with a half-life of 17.8 days) to form einsteinium-253. Close examination of the debris from the nuclear explosion revealed another alpha-particle-emitting radioactive species that was identified as an isotope of element 100 with the mass number 255. The new elements were named einsteinium and fermium in honor of two of the most important progenitors of the nuclear age. The unexpected consequences of the vast numbers of neutrons released by the nuclear chain reaction thus led to the synthesis of two new elements and revealed the potential utility of high-flux nuclear reactors in the production of transplutonium elements. Following the earlier use of other reactors in the 1950s, the High-Flux Isotope Reactor (HFIR) and the transuranium processing facility, currently named Radiochemical Engineering Development Center (REDC) were built at Oak Ridge National Laboratory in the 1960s for the production of transcurium elements. The HFIR starting material is highly irradiated plutonium-239 already containing substantial amounts of heavier isotopes of plutonium. Prolonged exposure to the intense neutron flux of HFIR produces considerable amounts of plutonium-242, americium-243, and curium-244, which have been isolated and refabricated into new targets for irradiation in the HFIR. Work-up of these targets, a task of no mean proportions because of the intense radioactivity from fission products and the newly formed transcurium elements, yields heavy isotopes of curium, berkelium, and californium plus smaller quantities of einsteinium and fermium.

The discovery of elements 99 and 100 in a sense was a watershed in the search for elements of ever higher atomic number. The experimental methods developed to isolate and identify neptunium and plutonium, refined and elaborated, were adequate for the task of isolation and characterization of the transplutonium elements up to element 100. With the transfermium elements, matters became much more difficult. Among the isotopes of the elements uranium, neptunium, plutonium, and curium, there is at least one that has a half-life of 10^6 years or more. For americium and berkelium, the longest-lived isotopes, produced by neutron irradiation, have half-lives of the order of 10^4 years and 1 year, respectively. The most stable californium isotope has a half-life less than

1000 years, einsteinium a half-life less than a year, and fermium a half-life of about 3 months. The elements of atomic number greater than 100 have isotopes with lifetimes measured in days, hours, minutes, seconds, and fractions of a second. The short half-lives severely limit the amount of a heavier isotope that can be made. Whereas the elements up to atomic number 100 could be characterized with amazingly small amounts of material, these, nevertheless, still contained large numbers of atoms. All of the actinides with atomic numbers up to 99 have been studied with weighable amounts (Table 1.1) but there is no prospect for producing weighable amounts of heavier elements. The elements of higher atomic number had to be identified with as little as one atom of a new element. That this feat was achievable was a result of the rapid developments in nuclear systematics, which made it possible to predict the nuclear properties of new isotopes; the actinide concept, which predicted the chemical properties of transuranium elements; and the development of new experimental techniques, which made it possible to isolate a single atom of a new isotope almost simultaneously with its formation in a nuclear reaction, and to measure half-lives in the millisecond range.

On the complex subject of nuclear systematics, it will be sufficient here to mention that the great progress made in the theoretical understanding of the behavior of atomic nuclei allowed predictions about lifetimes and the nature of radioactive emissions and their energetics to be made with considerable confidence, and this played a major role in the search for new elements. The actinide concept similarly played a crucial part. When the first transuranium elements were studied in the laboratory, it soon became apparent that the new members of the periodic table did not have the chemical properties that might be expected of them if they were placed in traditional sequence after uranium. Neptunium did not behave like rhenium, and in no way did plutonium resemble osmium, which would have been positioned directly above plutonium had the first two transuranium elements merely been inserted in the next vacant positions in the periodic table directly after uranium. Because similarities in chemical behavior arise in the periodic table from similarities in electronic configuration of the ions of homologous elements, simple insertion of the transuranium elements into the periodic table would have precluded its use as a reliable guide to the chemistry of the new elements.

The actinide hypothesis advanced by Seaborg systematized the chemistry of the transuranium elements, and thus greatly facilitated the search for new elements. From the vantage point of the actinide concept, the transuranium elements are considered to constitute a second inner transition series of elements similar to the rare-earth elements. In the rare-earth series, successive electrons are added to the inner 4f shell beginning with cerium and ending with lutetium. In the actinide series, fourteen 5f electrons are added beginning, formally, with thorium (atomic number 90) and ending with lawrencium (atomic number 103). Although the regularities are not as pronounced in the actinide as in the lanthanide series, the concept of the actinide elements as members of a 5f transition series is now accepted and has served as a unifying principle in the evolution of the chemistry of the actinide elements. A more detailed discussion of the actinide hypothesis can be found in Chapter 15.

The first chemical studies on neptunium and plutonium were made using classical radiochemical techniques in the 1940s. Amounts far too small to be weighed were studied by tracer methods, where solutions are handled in ordinary-sized laboratory vessels. Concentrations of the order of 10^{-12} mol L^{-1} or less are not unusual in tracer work, and valuable information could be acquired on solutions containing only a few million atoms. The radioactive element is detected by its radioactivity, and the chemistry is inferred from its behavior relative to that of an element of known chemistry present in macro amounts. When weighable amounts were available, ultramicrochemical methods were used. These manipulations were and still are carried out with microgram or even lesser amounts of material in volumes of solution too small to be seen by the naked eye at concentrations normally encountered in the laboratory. Ultramicro methods make possible the isolation of small samples of pure chemical compounds, which can then be identified by X-ray crystallography or electron diffraction in a transmission electron microscope. All of the actinide elements are radioactive, and, except for thorium and uranium, special containment and shielded facilities are mandatory for safe handling of these substances. Gloved boxes are required (Fig. 1.2)

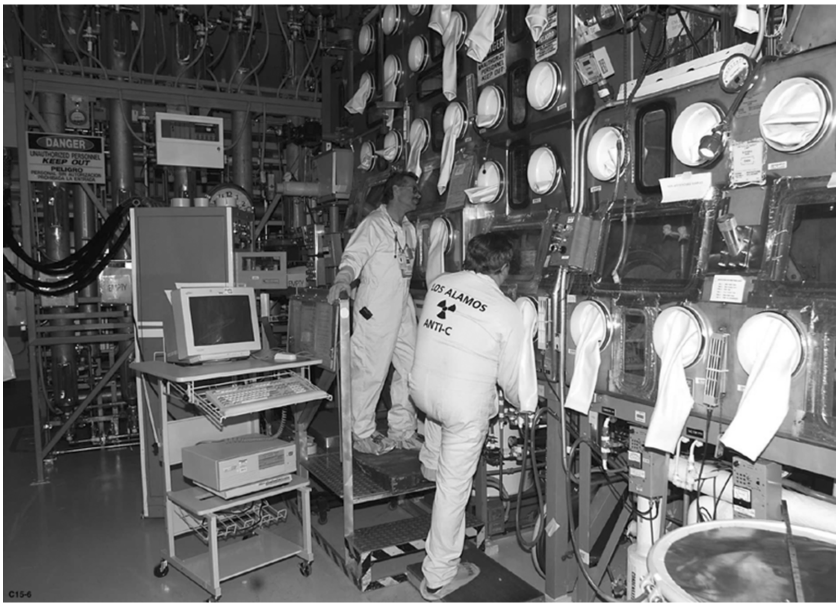

Fig. 1.2 *A modern laboratory with a bank of gloved boxes for carrying out experimental chemistry of transuranium elements.* (*Reproduced by permission of Los Alamos National Laboratory.*)

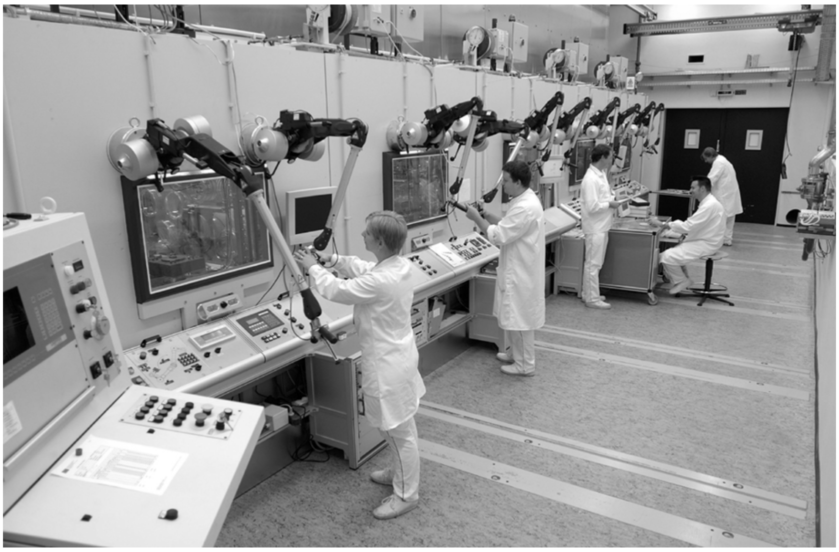

Fig. 1.3 *A hot-cell facility for remote synthesis and characterization of gram-scale transuranium materials.* (*Reproduced by permission of Institute for Transuranium Elements, Karlsruhe, part of the Joint Research Centre, European Commission.*)

and, where high levels of penetrating radiation (gamma rays or neutrons) are encountered, which is not infrequent, all manipulations may need to be performed by remote control (Figs. 1.3 and 1.4). Even when radiation can easily be shielded, as is the case with alpha-particle emitters, containment to prevent inhalation is still essential because of the toxicity of the transuranium elements. Inhaled transuranium isotopes may be deposited in the lungs and ingested isotopes may be translocated to the bone, where the intense alpha radioactivity over a period of time can give rise to neoplasms. The shorter the half-life, i.e., the higher the specific activity of the radioactive isotope, the more serious are the difficulties of experiments with macro amounts of material. Consequently, every effort has been made to produce long-lived isotopes. There are available isotopes of neptunium, plutonium, and curium with half-lives longer than 10^5 years, and isotopes of americium and californium that have half-lives of the order of 1000 years can be used in chemical studies. These long-lived isotopes greatly reduce the extent of radiolysis of water or other solvents for experiments in the liquid phase, they minimize radiation damage in the solid phase, and they also considerably reduce the health hazards in the experiment. Even with the longest-lived isotopes, most laboratory research with transuranium elements is carried out on the milligram or smaller scale.

The syntheses of the transfermium elements presented an even more challenging set of problems. Because of the short lifetimes of these isotopes, production by successive neutron capture in a high-flux reactor was not possible. Methods

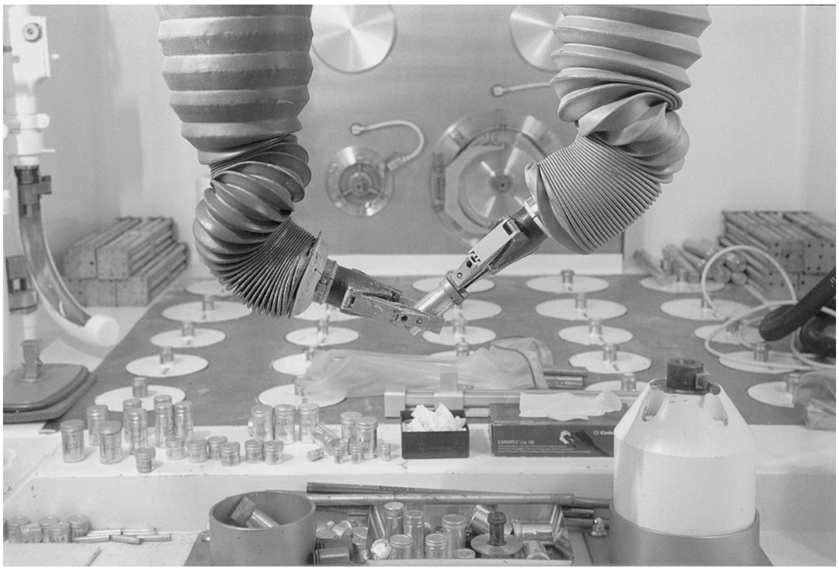

Fig. 1.4 *Example of an experimental setup within a hot-cell facility.* (*Reproduced by permission of Institute for Transuranium Elements, Karlsruhe, part of the Joint Research Centre, European Commission.*)

for the rapid collection of the newly formed isotopes had to be developed and very rapid separation procedures were required to isolate a pure product for identification. Ghiorso (1982) described in fascinating detail how these problems were surmounted. A newly formed nucleus contains sufficient energy to eject it from a target undergoing bombardment; the atom that recoils can be caught on a clean foil placed in close proximity to the target. The catcher foil can then be dissolved and the solution examined. For identification, ion-exchange chromatography proved to be ideal. Elution from an ion-exchange column can be carried out very rapidly. The order of elution is very specific and provides an unmistakable fingerprint for identification. In this way, it was possible to synthesize and identify element 101, subsequently named mendelevium, in experiments in which it was made one atom at a time. Even more highly refined collection procedures were evolved to complete the actinide series of elements by the discovery of nobelium (atomic number 102) and lawrencium (atomic number 103).

The transactinide elements 104 through 112 have been discovered at Berkeley and Darmstadt (see Table 1.1). Scientists at the Dubna Laboratory in Russia also made claims for the discovery of a number of these elements, but their evidence did not meet the accepted criteria for the discovery of new elements (Wilkinson *et al.*, 1991, 1993). No names have been suggested for elements heavier than 111, in conformity with the IUPAC rules for the naming of new elements (Koppenol, 2002). A surprising amount of information has accumulated about the oxidation states of the transfermium and transactinide ions in solution even though only a few atoms of any of these were available at any one time. Evidence for isotopes of elements heavier than 112 has been published by a consortium of scientists from Dubna and Livermore (Table 1.1). The chemistry of transactinide elements, and predicted chemical properties of these elements, is presented in Chapter 14.

One frontier is the synthesis of longer-lived isotopes and determination of chemical properties of additional transactinide elements (Chapter 14 of this work; Schädel, 2003). Numerous theoretical calculations have been made that indicate that there may be more than one "island" of relatively stable nuclei near the presently defined limits of the periodic table. In addition to the island of spherical stability originally predicted to be around atomic number $Z = 114$ and neutron number $N = 184$, other islands of spherical nuclei have been predicted at $Z = 120$ or 126 and $N = 184$ and at $Z = 120$ and $N = 172$. A predicted island of deformed nuclei at $Z = 108$ and $N = 162$ has already been confirmed experimentally. Because of the relatively long half-lives of isotopes conferred by closed nuclear shells, the goal of carrying out chemical studies with the elements at or near these islands is considered to be attainable by some scientists. The new techniques and theoretical understanding required to attain this goal will undoubtedly have profound consequences for nuclear and inorganic chemistry.

There are outstanding questions in actinide chemistry. One is the understanding of the bonding and electronic structure of the 5f electrons in condensed phases containing plutonium and adjacent elements. Another is the bonding and chemical behavior of actinides that may be released into the environment. To advance both of these frontiers, heavy-element chemists utilize modern instrumental techniques – X-ray absorption spectroscopy, laser fluorescence spectroscopy, electron microscopy, mass spectroscopy, neutron scattering, to name only a few – that make it possible to study the elements described in the subsequent chapters as pure materials, at extremely low concentrations, and under many unique conditions. Theoretical actinide and transactinide chemistry is advancing rapidly. Relativistic contributions to electronic properties that incorporate spin–orbit interactions are being calculated for bulk actinide solids, actinide metal surfaces, actinide complexes in solution, and transactinide atoms. Relativistic electronic structure theory utilizes time-dependent density functional theory and relativistic effective core potentials.

The actinide and transactinide elements in the last 65 years have played an important role in inorganic chemistry, in nuclear chemistry and physics, and in many other branches of science and technology. The actinide elements are also of crucial importance in energy resource development and, regrettably, in warfare. These elements are destined to continue to occupy the attention of scientists, engineers, environmentalists, and statesmen. We hope that these volumes will help provide the factual basis so necessary for the important research breakthroughs and technical decisions that will have to be made in future years.

REFERENCES

Ghiorso, A. (1982) *Actinides in Perspective* (ed. N. M. Edelstein), Pergamon Press, Oxford, pp. 23–56.

Gruen, D. M. (1992) *Transuranium Elements – A Half Century* (eds. L. R. Morss and J. Fuger), American Chemical Society, Washington, DC, pp. 63–77.

Koppenol, W. H. (2002) *Pure Appl. Chem.,* **74**, 787–791.

Schädel, M. (2003) *Chemistry of Superheavy Elements,* Kluwer Academic Publishers, Dordrecht.

Seaborg, G. T. (1982) *Actinides in Perspective* (ed. N. M. Edelstein), Pergamon Press, Oxford, pp. 1–22.

Seaborg, G. T. (1992) *Transuranium Elements – A Half Century* (eds. L. R. Morss and J. Fuger), American Chemical Society, Washington, DC, pp. 10–49.

Wilkinson, D. H., Wapstra, A. H., Uhelea, I., Barber, R. C., Greenwood, N. N., Hrynkiewicz, A., Jeannin, Y. P., Lefort, M., and Sakai, M. (1991) *Pure Appl. Chem.,* **63**, 879–886.

Wilkinson, D. H., Wapstra, A. H., Uhelea, I., Barber, R. C., Greenwood, N. N., Hrynkiewicz, A., Jeannin, Y. P., Lefort, M., and Sakai, M. (1993) *Pure Appl. Chem.,* **65**, 1764–1814.

ADDITIONAL SUGGESTED READINGS

Bagnall, K. W. (1972) *The Actinide Elements,* Elsevier, Amsterdam.

Bagnall, K. W. (ed.) (1972, 1975) *Lanthanides and Actinides* (MTP International Review of Science, Inorganic Chemistry, series 1, vol. 7, set. 2, vol. 7), Butterworths, London.

Blank, H. and Lindner, R. (eds.) (1976) *Plutonium 1975 and Other Actinides,* North Holland, Amsterdam.

Brown, D. (1968) *Halides of the Lanthanides and Actinides,* Wiley-Interscience, London.

Burney, G. A. and Harbour, R. M. (1974) *Radiochemistry of Neptunium*, Report NAS-NS 3060.

Carnall, W. T. and Choppin, G. R. (eds.) (1983) *Plutonium Chemistry* (ACS Symp. Ser. 216), American Chemical Society, Washington, DC.

Cleveland, J. M. (1979) *The Chemistry of Plutonium,* 2nd edn, American Nuclear Society, La Grange Park, IL.

Cordfunke, E. H. P. (1969) *The Chemistry of Uranium,* Elsevier, Amsterdam.

Edelstein, N. M. (ed.) (1980) *Lanthanide and Actinide Chemistry and Spectroscopy* (ACS Symp. Ser. 131), American Chemical Society, Washington, DC.

Edelstein, N. M. (ed.) (1982) *Actinides in Perspective,* Pergamon Press, Oxford and New York.

Edelstein, N. M., Navratil, J. D., and Schulz, W. W. (eds.) (1985) *Americium and Curium Chemistry and Technology,* Reidel, Dordrecht.

Erdös, P. and Robinson, J. M. (1983) *The Physics of Actinide Compounds,* Plenum, New York.

Fields, P. R. and Moeller, T. (eds.) (1967) *Lanthanide/Actinide Chemistry* (ACS Adv. Ser. 71), American Chemical Society, Washington, DC.

Freeman, A. J. and Darby, J. B. (eds.) (1974) *The Actinides: Electronic Structure and Related Properties,* Academic Press, New York.

Handbook on the Physics and Chemistry of Rare Earths, North-Holland, Amsterdam, New York; Elsevier Science, New York, NY, vols 17–19, 1993–1994.

Handbook on the Physics and Chemistry of the Actinides, North-Holland, Amsterdam, New York; Elsevier Science, New York, NY, 1984–1991, 6 volumes.

Hoffman, Darleane C. (2002) *Advances in Plutonium Chemistry, 1967–2000*, American Nuclear Society, La Grange Park, IL.

Kaltsoyannis, N. and Scott, P. (1999) *The f Elements,* Oxford University Press, Oxford.

Katz, J. J. and Rabinowitch, E. (1951) *The Chemistry of Uranium,* McGraw-Hill, New York. (Reprinted 1961 by Dover Publications, New York.)

Katz, J. J. and Rabinowitch, E. (eds.) (1958) *Chemistry of Uranium, 2 vols.* U.S. Atomic Energy Commission, Technical Information Service, Oak Ridge, TN, TID-5290.

Keller, C. (1971) *The Chemistry of the Transuranium Elements,* Verlag Chemie, Weinheim.

Los Alamos National Laboratory (2000) *Challenges in plutonium science*, *Los Alamos Science No. 26*, 2 vols, Los Alamos National Laboratory, Los Alamos, NM. http://www.fas.org/sgp/othergov/doe/lanl/pubs/number26.htm

Milyukova, M. S., Gusev, N. L., Sentyurin, I. G., and Sklyarenko, I. S. (1967) *Analytical Chemistry of Plutonium,* Israel Program for Scientific Translations, Jerusalem.

Myasoedov, B. F., Guseva, L. I., Lebedev, I. A., Milyukova, M. S., and Chmutova, M. S. (1974) *Analytical Chemistry of the Transplutonium Elements* (Engl. transl.), Wiley, New York.

Meyer, G. and Morss, L. R. (eds.) (1991) *Synthesis of Lanthanide and Actinide Compounds,* Kluwer Academic Publishers, Dordrecht.

Morss, L. R. and Fuger, J. (eds.) (1992) *Transuranium Elements – A Half Century,* American Chemical Society, Washington, DC.

Müller, W. and Blank, H. (eds.) (1976) *Heavy Element Properties,* North-Holland, Amsterdam.

Müller, W. and Lindner, R. (eds.) (1976) *Transplutonium 1975*, North-Holland, Amsterdam.

National Academy of Sciences (1959–86) *Series on Radiochemistry:* Stevenson, P. C. and Nervik, W. E. (1961) *Actinium,* NAS-NS-3020; Hyde, E. (1960) *Thorium,* NAS-NS-3004; Kirby, H. W. (1959) *Protactinium,* NAS-NS-3016; Gindler, J. (1961) *Uranium,* NAS-NS-3050; Burney, G. A. and Harbour, R. M. (1974) *Neptunium,* NAS-NS-3060; Coleman, G. H. and Hoff, R. W. (1965) *Plutonium,* NAS-NS-3058; Penneman, R. A. and Keenan, R. K. (1960) *Americium and Curium,* NAS-NS-3006; Higgins, G. H. (1960) *The Transcurium Elements,* NAS-NS-3031; Roberts, R. A., Choppin, G. R., and Wild, J. F. (1986). *Uranium, Neptunium and Plutonium, An Update,* NA-NS-3063. Volumes of this series can be found at http://lib-lanl.gov/radiochemistry/elements.htm.

Navratil, J. D. and Schulz, W. W. (eds.) (1980) *Actinide Separations* (ACS Symp. Ser. 117), American Chemical Society, Washington, DC.

Navratil, J. D. and Schulz, W. W. (eds.) (1981) *Transplutonium Elements – Production and Recovery* (ACS Symp. Ser. 161), American Chemical Society, Washington, DC.

Schädel, M. (2003) *Chemistry of Superheavy Elements,* Kluwer Academic Publishers, Dordrecht.

Schädel, M. (2006) *Angew. Chem. Int. Ed.*, **45**, 368–401.

Seaborg, G. T. (1958) *The Transuranium Elements,* Yale University Press, New Haven.

Seaborg, G. T. (1963) *Man-Made Transuranium Elements,* Prentice-Hall, Englewood Cliffs, NJ.

Seaborg, G. T. (1978) *Transuranium Elements, Products of Modern Alchemy,* Dowden, Hutchison and Ross, Stroudsburg, PA.

Seaborg, G. T. and Katz, J. J. (eds.) (1954) *The Actinide Elements* (Natl Nucl. Eng. Ser., Div. IV, 14A), McGraw-Hill, New York.

Seaborg, G. T., Katz, J. J., and Manning, W. M. (eds.) (1949) *The Transuranium Elements* (Natl Nucl. Eng. Ser., Div. IV, 14B), McGraw-Hill, New York.

Seaborg, G. T. and Loveland, W. D. (1990) *The Elements Beyond Uranium,* Wiley-Interscience, New York.

Schulz, W. W. (1976) *The Chemistry of Americium,* Report TID-26971, US Dept of Energy, Technical Information Center, Oak Ridge, TN.

Sterne, P. A., Gonis, A., and Borovoi, A. A. (1998) *Actinides and the Environment,* Kluwer Academic Publishers, Dordrecht.

Taube, M. (1974) *Plutonium – A General Survey,* Verlag Chemie, Weinheim.

Trotman-Dickenson, A. F. (exec. ed.) (1973) *Comprehensive Inorganic Chemistry,* vol. 5, The Actinides, Pergamon, Oxford.

Wick, O. J. (ed.) (1967) *Plutonium Handbook,* Gordon and Breach, New York, 2 vols.

CHAPTER TWO

ACTINIUM

H. W. Kirby and L. R. Morss

2.1 INTRODUCTION

The actinide series of elements encompasses all the 15 chemical elements that have properties attributable to the presence of low-lying 7p, 6d, and 5f orbitals such that their tripositive ions have electronic configurations $7p^06d^05f^n$, where $n = 0,1,2,\ldots,14$. According to this definition, actinium, element 89, is the first member of the actinide series of elements, although it has no 5f electrons in its metallic, gaseous, or ionic forms. As such, its position in group 3 (in current IUPAC terminology) or group 3B (commonly used in some American textbooks) of the periodic table is analogous to that of its homolog, lanthanum, in the lanthanide series. This definition, which includes actinium as the first of the actinides (Seaborg, 1994), parallels the accepted inclusion of lanthanum as the first member of the lanthanide series (Moeller, 1963).

The chemistry of actinium closely follows that of lanthanum. There are no qualitative differences between them; the only quantitative differences are those attributable to the difference in their ionic radii (1.12 Å for Ac^{3+} and 1.032 Å for La^{3+} in six-fold coordination) (Shannon, 1976 and Chapter 15, section 7.5, of this book). Because of this similarity, lanthanum is a nearly ideal surrogate for actinium in the development of preparative or analytical procedures. As a carrier for trace amounts of actinium, lanthanum suffers from only one disadvantage: Once mixed, the two elements behave like any pair of adjacent rare earths and can be separated only by ion-exchange chromatography, solvent extraction, or fractional crystallization.

The most important isotope of actinium is ^{227}Ac, a member of the naturally occurring uranium–actinium ($4n + 3$) family of radioelements. Its applications are derived from its unique radioactive properties. Although ^{227}Ac itself is essentially ($\geq$98%) a weak β^- emitter, with a moderately long half-life (21.773 years), its decay chain includes five short-lived α emitters. The net effect is one of high specific power and long service life, a combination that makes ^{227}Ac suitable as a heat source in thermoelectric generators on space missions to the outer planets and beyond. Recently ^{225}Ac and ^{228}Ac have found applications (see Section 2.9).

The early actinium literature (up to January 1940) was comprehensively reviewed by the staff of the Gmelin Institute, and an English translation is available (Gmelin, 1942). Later reviews and bibliographies have appeared with the waxing and waning of interest in possible applications of actinium (Clarke, 1954, 1958; Hagemann, 1954; Bagnall, 1957; Katz and Seaborg, 1957; Bouissières, 1960; Stevenson and Nervik, 1961; Salutsky, 1962; Sedlet, 1964; Kirby, 1967; Keller, 1977). The most recent monograph on actinium chemistry is the *Gmelin Handbook* supplement (Gmelin, 1981).

2.1.1 Historical

In 1899, André Debierne, in the laboratory of Pierre and Marie Curie, reported that he had found a new radioactive substance, whose chemistry closely followed that of titanium (Debierne, 1899). Six months later, he said that the titanium fraction was no longer very active, but that the radioactive material he was now recovering exhibited the same chemical behavior as thorium (Debierne, 1900). Debierne claimed the right of discovery and named the new substance actinium (*aktis*, ray). His claim was accepted uncritically at the time, but, in the light of what we now know of the chemical and nuclear properties of actinium, it is clear that his 1899 preparation contained no actinium at all and that his 1900 preparation was a mixture of several radioelements, possibly including actinium as a minor constituent (Kirby, 1971; Adloff, 2000).

In 1902, Friedrich Giesel reported a new 'emanation-producing' substance among the impurities he had separated with radium from pitchblende residues (Giesel, 1902). He correctly established many of its chemical properties, including the important fact that it followed the chemistry of the cerium group of rare earths. By 1903, he had concentrated and purified it to a point where lanthanum was the chief impurity and thorium was spectroscopically undetectable (Giesel, 1903). A year later, he proposed the name, emanium, for what was clearly a new radioelement (Giesel, 1904a).

Giesel's claim was vigorously attacked by Debierne (1904), who now had an emanation-producing substance of his own, which, he insisted, was the same as the substance he had originally named actinium, although the 1900 preparation had titanium- or thorium-like properties (Adloff, 2000). Debierne's claim prevailed, and has been propagated by historians (Ihde, 1964; Partington, 1964; Weeks and Leicester, 1968), largely because of the prestige of the Curies and the support of Rutherford (1904). The latter based his conclusion solely on the similarity in the decay characteristics of the "emanations" (i.e. ^{219}Rn) and the "active deposits" (^{211}Pb) given off by the samples supplied to him by the two claimants. Although some historical studies (Weeks and Leicester, 1968; Adloff, 2000) give both Debierne and Giesel credit for the discovery, Kirby (1971), Keller (1977), and the second author of this chapter believe that it is more appropriate to give credit for discovery of actinium to Giesel.

The actinium decay chain was sorted out rather quickly. In 1905, Godlewski (1904–5, 1905) and Giesel (1904b, 1905) independently reported the existence of actinium X (also referred to as "emanium X"), now known as ^{223}Ra, and showed it to be the direct source of the actinium emanation and its active deposit. The following year, Hahn (1906a,b) discovered radioactinium (^{227}Th), the immediate descendant of actinium and the parent of actinium X. ^{231}Pa, the parent of actinium, was discovered independently in 1918 by Soddy and Cranston (1918a,b) and by Hahn and Meitner (1918). The primordial origin of the actinium series ($4n + 3$ or uranium–actinium series, Fig. 2.1) was not finally resolved until 1935, when Dempster (1935) detected the uranium isotope of atomic weight 235 by mass spectroscopy.

2.2 NUCLEAR PROPERTIES

Of the 29 known isotopes of actinium (Table 2.1) only three are of particular significance to chemists. Two of these isotopes are the naturally occurring isotopes, ^{227}Ac (Fig. 2.1, $4n + 3$ or uranium–actinium series) and ^{228}Ac (mesothorium II, Fig. 2.2, $4n$ or thorium series). The third is ^{225}Ac, a descendant of reactor-produced ^{233}U (Fig. 2.3, $4n + 1$ or neptunium series).

2.2.1 Actinium–227

The isotope ^{227}Ac, a β^- emitter, is a member of the naturally occurring ^{235}U (AcU) decay series (Fig. 2.1). It is the daughter of ^{231}Pa and the parent of ^{227}Th (RdAc). It is also the parent, by a 1.38% α branch (Kirby, 1970; Monsecour *et al.*, 1974), of ^{223}Fr, which was discovered in 1939 by Perey (1939a,b). The half-life of ^{227}Ac is (21.772 ± 0.003) years (Jordan and Blanke, 1967; Browne, 2001), as determined by calorimetric measurements made over a period of 14 years. The thermal-neutron-capture cross section σ_t and the resonance integral are (762 ± 29) barn and (1017 ± 103) barn, respectively (1 barn = 10^{-28} m^2) (Monsecour and De Regge, 1975).

The β^- radiation of ^{227}Ac is so weak (0.045 MeV maximum) (Beckmann, 1955; Novikova *et al.*, 1960) that the nuclide was once thought to be 'rayless' (Marckwald, 1909; Rutherford, 1911). Even with modern nuclear spectrometers, neither the β^- nor the γ radiation is useful for analytical purposes because of interference from the rapidly growing decay products. On the other hand, ^{227}Ac is readily identified, even in the presence of its decay products,

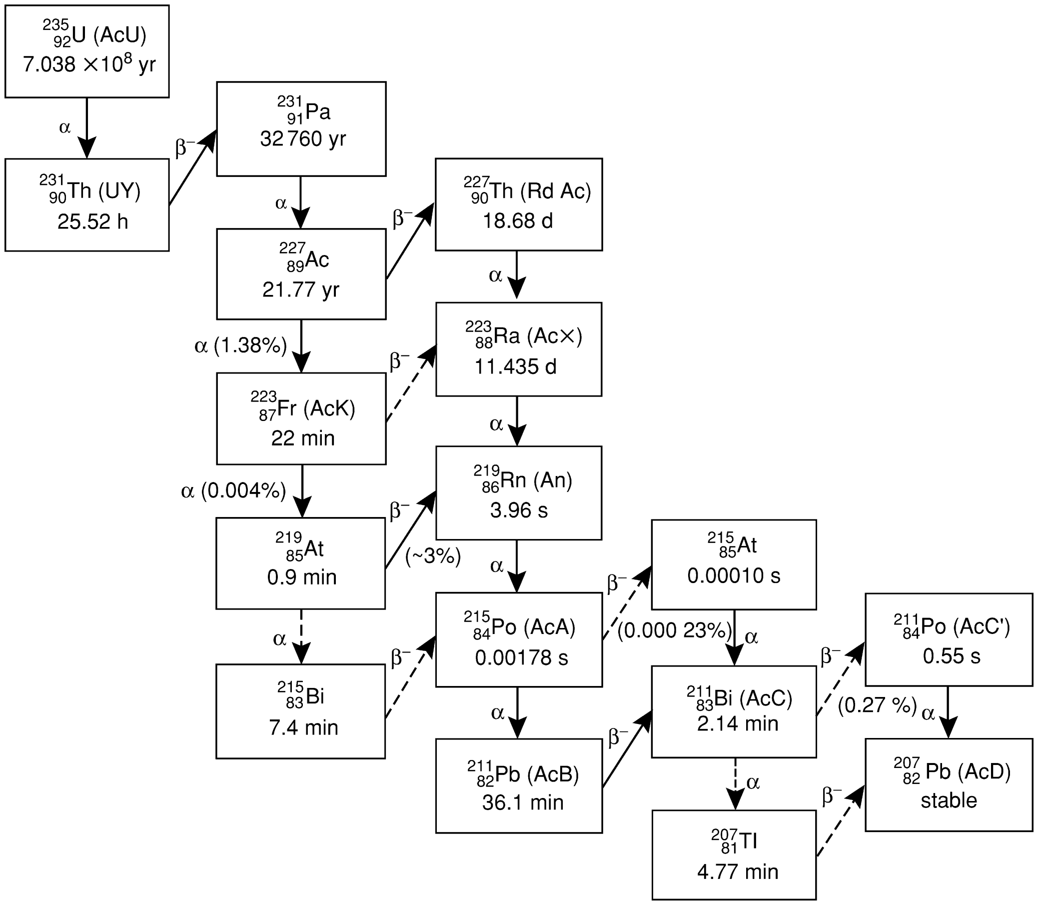

Fig. 2.1 *Uranium–actinium series* ($4n + 3$).

Table 2.1 *Nuclear properties of actinium isotopes.*[a]

Mass number	*Half-life*	*Mode of decay*	*Main radiations* (MeV)	*Method of production*
206	33 ms	α	α 7.750	^{175}Lu(^{40}Ar,9n)
	22 ms	α	α 7.790	
207	22 ms	α	α 7.712	^{175}Lu(^{40}Ar,8n)
208	95 ms	α	α 7.572	^{175}Lu(^{40}Ar,7n)
	25 ms	α	α 7.758	
209	0.10 s	α	α 7.59	^{197}Au(^{20}Ne,8n)
210	0.35 s	α	α 7.46	^{197}Au(^{20}Ne,7n) ^{203}Tl(^{16}O,9n)
211	0.25 s	α	α 7.48	^{197}Au(^{20}Ne,6n) ^{203}Tl(^{16}O,8n)
212	0.93 s	α	α 7.38	^{203}Tl(^{16}O,7n) ^{197}Au(^{20}Ne,5n)
213	0.80 s	α	α 7.36	^{197}Au(^{20}Ne,4n) ^{203}Tl(^{16}O,6n)
214	8.2 s	α ≥ 86% EC ≤ 14%	α 7.214 (52%) 7.082 (44%)	^{203}Tl(^{16}O,5n) ^{197}Au(^{20}Ne,3n)
215	0.17 s	α 99.91% EC 0.09%	α 7.604	^{203}Tl(^{16}O,4n) ^{209}Bi(^{12}C,6n)
216	~0.33 ms	α	α 9.072	^{209}Bi(^{12}C,5n)
216 m	0.33 ms	α	α 9.108 (46%) 9.030 (50%)	
217	69 ns	α	α 9.650	^{208}Pb(^{14}N,5n)
218	1.08 μs	α	α 9.20	^{222}Pa daughter
219	11.8 μs	α	α 8.66	^{223}Pa daughter
220	26.4 ms	α	α 7.85 (24%) 7.68 (21%) 7.61 (23%)	^{208}Pb(^{15}N,3n) ^{224}Pa daughter
221	52 ms	α	α 7.65 (70%) 7.44 (20%)	^{205}Tl(^{22}Ne,α2n) ^{208}Pb(^{18}O,p4n)
222	5.0 s	α	α 7.00	^{226}Ra(p,5n) ^{208}Pb(^{18}O,p3n)
222 m	63 s	α > 90% EC ~ 1% IT < 10%	α 7.00 (15%) 6.81 (27%)	^{208}Pb(^{18}O,p3n) ^{209}Bi(^{18}O,αn)
223	2.10 min	α 99% EC 1%	α 6.662 (32%) 6.647 (45%)	^{227}Pa daughter
224	2.78 h	EC ~ 90% α ~ 10%	α 6.211 (20%) 6.139 (26%)	^{228}Pa daughter
225	10.0 d	α	α 5.830 (51%) 5.794 (24%) γ 0.100 (1.7%)	^{225}Ra daughter
226	29.37 h	β^{-} 83% EC 17% α 6 × 10^{-3}%	α 5.399 β^{-} 1.10 γ 0.230 (27%)	^{226}Ra(d,2n)
227	21.772 yr	β^{-} 98.62% α 1.38%	α 4.950 (47%) 4.938 (40%) β^{-} 0.045 γ 0.086	Nature

Table 2.1 (*Contd.*)

Mass number	*Half-life*	*Mode of decay*	*Main radiations* (MeV)	*Method of production*
228	6.15 h	β^-	β^- 2.18 γ 0.991	Nature
229	62.7 min	β^-	β^- 1.09 γ 0.165	^{229}Ra daughter ^{232}Th(γ,p2n)
230	122 s	β^-	β^- 1.4 γ 0.455	^{232}Th(γ,pn)
231	7.5 min	β^-	β^- 2.1 γ 0.282	^{232}Th(γ,p) ^{232}Th(n,pn)
232	119 s	β^-		^{238}U + Ta
233	145 s	β^-		^{238}U + Ta
234	44 s	β^-		^{238}U + Ta

---

[a] Appendix II.

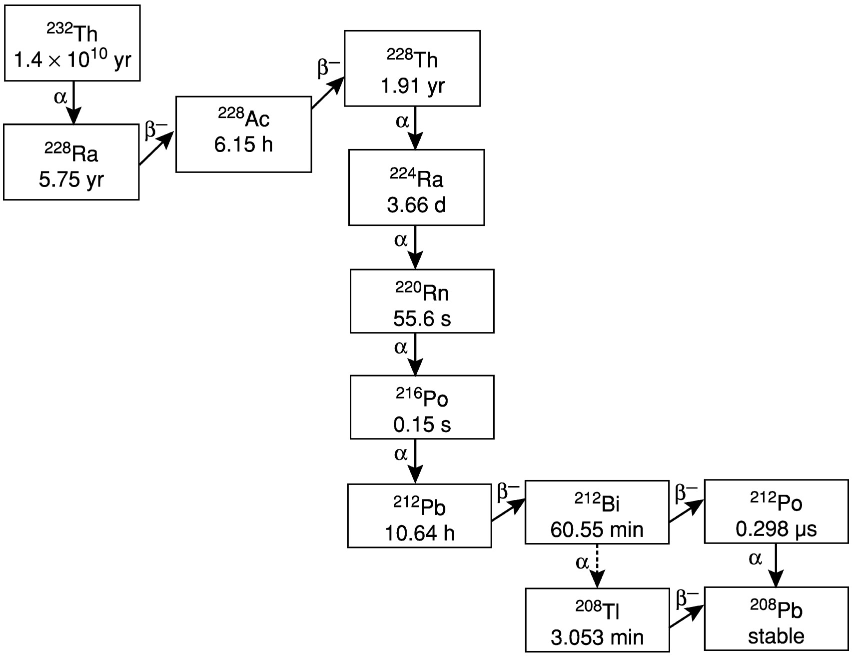

Fig. 2.2 *Thorium series* (4*n*).

by α spectrometry (Fig. 2.4), and a computational technique has been described for its quantitative determination by this method (Kirby, 1970).

The γ spectrum of ^{227}Ac in equilibrium with its decay products is shown in Fig. 2.5. The 235.9-keV γ-ray, which has an intensity of (12.3 ± 1.3)% of ^{227}Th

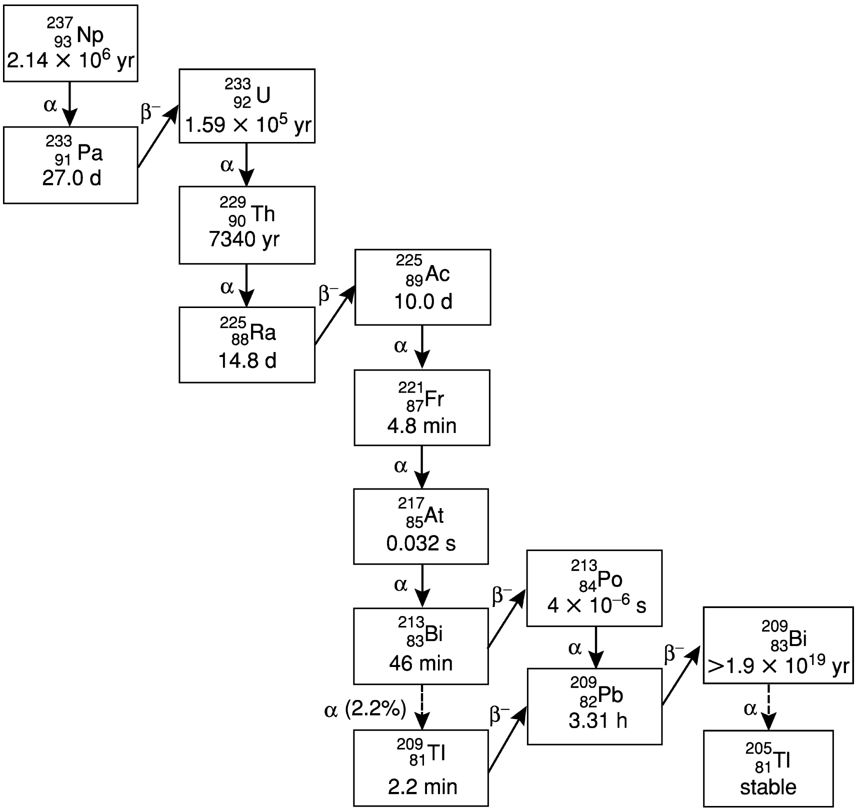

Fig. 2.3 *Neptunium series* ($4n + 1$).

α decay, can be used for quantitative analysis of ^{227}Ac. For a detailed level scheme, see the most recent critical compilation (Firestone and Shirley, 1996).

2.2.2 Actinium–228 (MsTh II or MsTh$_2$)

The isotope ^{228}Ac (mesothorium II or MsTh$_2$) is a member of the naturally occurring ^{232}Th decay chain. It is the daughter of 5.77-year ^{228}Ra (mesothorium I or MsTh$_1$) and the parent of 1.9116-year ^{228}Th (radiothorium).

All three nuclides were discovered by Otto Hahn (1905, 1907, 1908). The long-accepted half-life of ^{228}Ac (6.13 ± 0.03) h, reported in 1926 (Hahn and Erbacher, 1926), was redetermined to be (6.15 ± 0.02) h in 1985 (Skarnemark and Skalberg, 1985).

^{228}Ac has a complex β$^-$ spectrum (Bjornholm *et al.*, 1957; Arnoux and Giaon, 1969; Dalmasso *et al.*, 1974), but, unlike ^{227}Ac, more than 99% of the β$^-$ particles have maximum energies greater than 0.5 MeV so that its γ-ray spectrum (Novikova *et al.*, 1960) is a useful analytical tool. By contrast, the

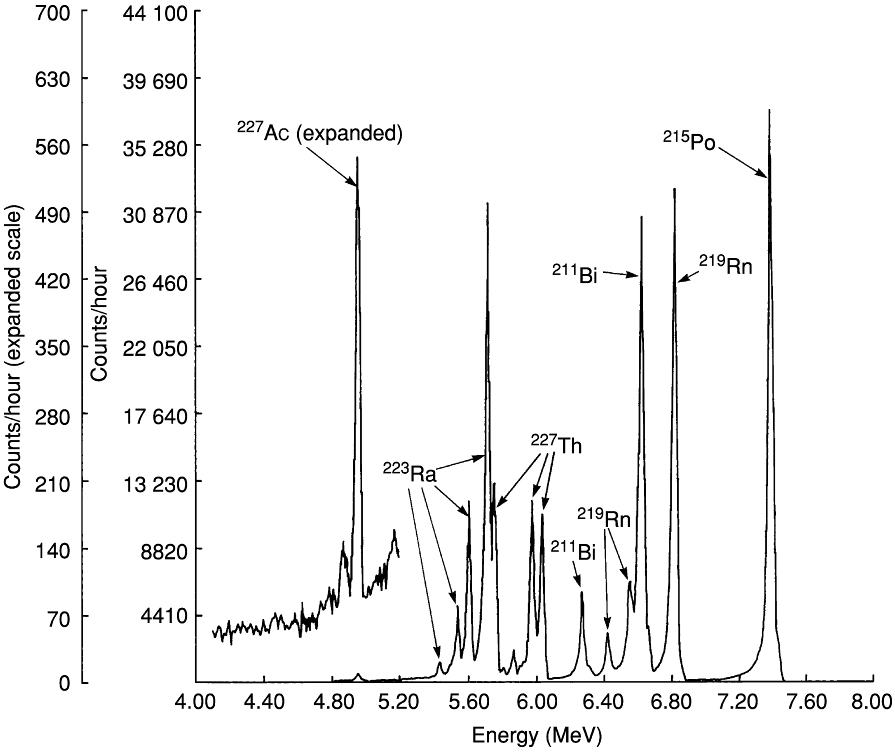

Fig. 2.4 *Alpha spectrum of* ^{227}*Ac in equilibrium with its decay products* (*Kirby,* 1970).

β^- and γ radiations from ^{228}Ra are too weak for routine detection; consequently, nearly all methods for the determination of ^{228}Ra are based on the isolation and counting of ^{228}Ac (Hahn and Erbacher, 1926). ^{228}Ac is frequently used as a tracer for other actinium isotopes (Bhatki and Adloff, 1964; Chayawattanangkur *et al.*, 1973).

A level scheme and a critical compilation of γ-ray energies for ^{228}Ac have been published (Horen, 1973).

2.2.3 Actinium-225

The isotope ^{225}Ac is an α emitter. It is a member of the $4n + 1$ decay series, of which ^{237}Np is the longest-lived member and progenitor (Fig. 2.3). In practice, however, ^{225}Ac is most easily obtained by milking a sample of ^{229}Th that was previously separated from aged ^{233}U (Valli, 1964). The latter isotope is itself produced by neutron bombardment of natural thorium (St. John and Toops, 1958; Hyde *et al.*, 1964):

$$^{232}\mathrm{Th}(\mathrm{n},\gamma)^{233}\mathrm{Th} \xrightarrow[22.3\ \mathrm{min}]{\beta^-} {}^{233}\mathrm{Pa} \xrightarrow[26.967\,\mathrm{d}]{\beta^-} {}^{233}\mathrm{U} \tag{2.1}$$

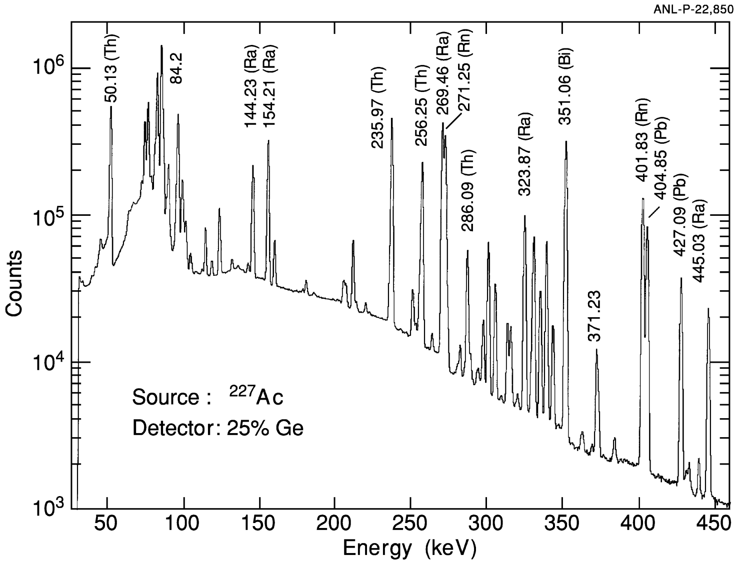

Fig. 2.5 *Gamma spectrum of ^{227}Ac in equilibrium with its decay products* (*I. Ahmad,* 2002).

Unfortunately, ^{229}Th is always more or less contaminated with ^{228}Th because of side reactions during the production of ^{233}U:

$$^{232}\text{Th}(\text{n},2\text{n})^{231}\text{Th} \xrightarrow[25.52\ \text{h}]{\beta^-} {}^{231}\text{Pa} \tag{2.2}$$

$$^{231}\text{Pa}(\text{n},\gamma)^{232}\text{Pa} \xrightarrow[1.31\ \text{d}]{\beta^-} {}^{232}\text{U} \xrightarrow[68.9\,\text{y}]{\alpha} {}^{228}\text{Th} \tag{2.3}$$

To obtain pure samples of ^{225}Ac, the presence of ^{228}Th in ^{229}Th is not a serious problem, because the ^{224}Ra daughter of ^{228}Th can be chemically separated from he ^{225}Ac, together with ^{225}Ra, after its milking from thorium. The ^{224}Ra must be removed to ensure the absence of its progeny ^{208}Tl, which emits a 2.6-MeV γ-ray.

The complex fine structure of the ^{225}Ac α spectrum was thoroughly investigated by Dzhelepov *et al.* (1967) and by Bastin-Scoffier (1967). A level scheme is given in a critical compilation (Maples, 1973).

2.3 OCCURRENCE IN NATURE

The natural occurrence of ^{227}Ac is proportional to that of its primordial ancestor, ^{235}U, which is widely distributed in the Earth's crust (Kirby, 1974). The average crustal abundance of uranium is 2.7 ppm (Taylor, 1964), of which

0.720 mass% is ^{235}U (Holden, 1977). Therefore, the natural abundance of ^{227}Ac (calculated from its half-life and that of ^{235}U) is 5.7×10^{-10} ppm. Based upon a crustal mass of 2.5×10^{25} g (to a depth of 36 km) (Heydemann, 1969), the global inventory of ^{227}Ac is estimated to be 1.4×10^{4} metric tons.

Although the $4n + 1$ family is not ordinarily considered to be 'naturally occurring' because its primordial ancestor has become extinct, both ^{237}Np and ^{225}Ac have been detected in uranium refinery wastes and ^{225}Ac has been found in ^{232}Th isolated from Brazilian monazite (Peppard *et al.*, 1952). These nuclides are believed to be formed continually in nature by the bombardment of natural thorium and uranium with neutrons arising from spontaneous fission of ^{238}U and from neutrons produced by (α,n) reactions on light elements:

$$^{238}\mathrm{U(n,2n)}\ ^{237}\mathrm{U} \xrightarrow[6.75\mathrm{d}]{\beta^-} {}^{237}\mathrm{Np} \tag{2.4}$$

$$^{232}\mathrm{Th}(\mathrm{n},\gamma)\ ^{233}\mathrm{Th} \xrightarrow[22.3\,\mathrm{min}]{\beta^-} {}^{233}\mathrm{U} \tag{2.5}$$

2.4 PREPARATION AND PURIFICATION

Uranium ores always contain large amounts of rare earths, and were thus generally unsatisfactory as sources of actinium before modern methods of rare earth separations were developed. The most concentrated actinium sample ever prepared from a natural raw material consisted of 0.5 mCi (~7 μg) of ^{227}Ac in less than 0.1 mg of La_2O_3 (Lecoin *et al.*, 1950).

In 1949, Peterson reported that ^{227}Ac could be synthesized by irradiating ^{226}Ra with thermal neutrons (Peterson, 1949):

$$^{226}\mathrm{Ra}(\mathrm{n},\gamma)\ ^{227}\mathrm{Ra} \xrightarrow[42.2\,\mathrm{min}]{\beta^-} {}^{227}\mathrm{Ac} \quad (\sigma_\mathrm{t} \cong 20\ \mathrm{barn}) \tag{2.6}$$

This reaction greatly simplified the chemical separations required to prepare macroscopic amounts of pure ^{227}Ac and, in 1950, Hagemann reported the isolation of 1.27 mg of ^{227}Ac from 1 g of neutron-irradiated ^{226}Ra (Hagemann, 1950).

Later work (Kirby *et al.*, 1956; Cabell, 1959; Monsecour and De Regge, 1975) showed that the neutron-capture cross section of ^{227}Ac is many times greater than that of ^{226}Ra (Fig. 2.6). A new problem is introduced, namely that of separating ^{227}Ac from the large amounts of 1.9-year ^{228}Th produced by the second-order reactions:

$$^{227}\mathrm{Ac}(\mathrm{n},\gamma)\ ^{228}\mathrm{Ac} \xrightarrow[6.15\ \mathrm{h}]{\beta^-} {}^{228}\mathrm{Th} \quad (\sigma_\mathrm{t} = 762\ \mathrm{barn}) \tag{2.7}$$

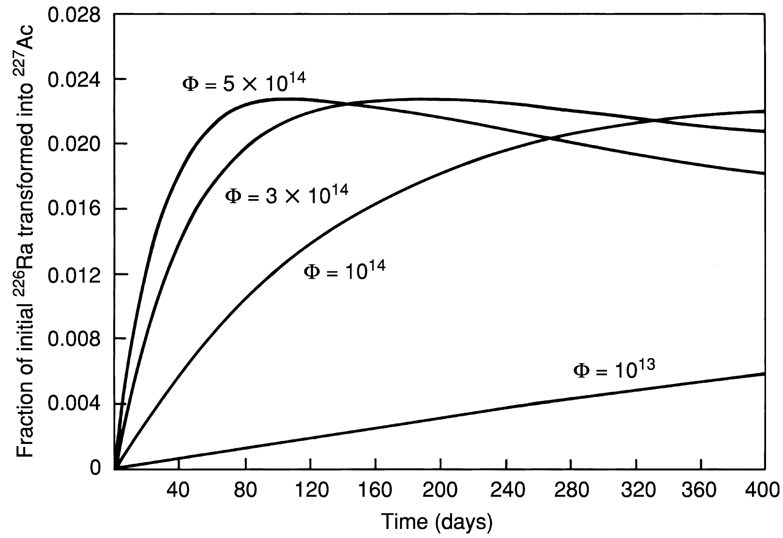

Fig. 2.6 *Growth of* ^{227}*Ac in neutron-irradiated* ^{226}*Ra at various thermal-neutron fluxes* Φ (*in* $\mathrm{cm^{-2}\ s^{-1}}$). *The calculations assume* $\sigma_t(^{226}Ra) = 20$ *barn and* $\sigma_t(^{227}Ac) = 795$ *barn* (*Gomm and Eakins,* 1968).

Nevertheless, neutron irradiation of ^{226}Ra remains the method of choice for the preparation of ^{227}Ac at either the tracer or the macroscopic level.

The isotope ^{225}Ac is best generated by separating it from the generator ^{229}Th (Geerlings *et al.*,1993; Tsoupko-Sitnikov *et al.*, 1996; Khalkin *et al.*, 1997). The ^{229}Th generator must be separated from ^{233}U. The isotope ^{233}U is synthesized by neutron irradiation of ^{232}Th, which contaminates the ^{229}Th with some ^{228}Th and its daughters.

The isotope ^{228}Ac can be generated by separating it from the generator ^{228}Ra, which can be isolated from natural ^{232}Th (Gmelin, 1981). Detailed procedures were given by Sekine *et al.* (1967). Sani (1970) and Mikheev *et al.* (1995) removed ^{228}Ra from aged ^{232}Th by cocrystallization with $Ba(NO_3)_2$. The ^{228}Ac that grew into ^{228}Ra was removed by extraction or by adding $GdCl_3$ to an aqueous solution of the ^{228}Ra in $Ba(NO_3)_2$ and coprecipitating Ac^{3+} with Gd $(OH)_3$ using $NH_3(g)$.

2.4.1 Purification by liquid–liquid extraction

Hagemann (1950, 1954) isolated the first milligram of ^{227}Ac from neutron-irradiated ^{226}Ra by liquid–liquid extraction with 2-thenoyltrifluoroacetone (TTA). Experience has shown (Engle, 1950; Stevenson and Nervik, 1961; Kirby, 1967), however, that TTA is not a suitable reagent for quantitative extraction of actinium because a relatively high pH (≥ 5.5, Fig. 2.7) is required

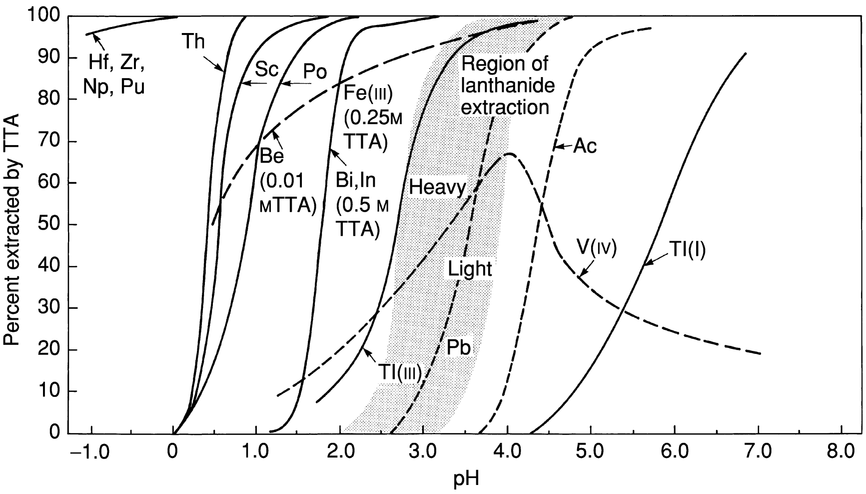

Fig. 2.7 *Extraction of various elements with thenoyltrifluoroacetone* (*TTA*). (*After Stevenson and Nervik,* 1961).

for efficient chelation but Ac^{3+} hydrolyzes above pH 7 and forms inextractable polymeric species when the pH is in the 'desirable' range, 6–7. The recovery of actinium requires tight pH control and speed of operation for satisfactory yields (Allison *et al.*, 1954; Tousset, 1961) that are usually not quantitative. The most effective application of TTA in the purification of ^{227}Ac is to remove ^{227}Th, which can be selectively and quantitatively extracted from moderately acid solutions. For this extraction, the pH_{50} (the pH at which 50% of the Th^{4+} is extracted or partitioned equally between the phases, i.e. $D = 1$) is 0.48 (Poskanzer and Foreman, 1961).

On the other hand, Sekine *et al.* (1967) found that, while the extraction of ^{228}Ac with TTA alone was not quantitative, a mixture of 0.1 M TTA and 0.1 M tri(*n*-butyl)phosphate (TBP) in CCl_4 gave reproducible distribution ratios and quantitative extraction of Ac^{3+} at pH ≥ 4.

Solvent extraction systems that have been applied to other actinide and lanthanide separations have also been applied to actinium separations from thorium and radium. Thus, Karalova *et al.* (1977a) studied the extraction of Ac(III) in aqueous nitrate solution by trioctylphosphine oxide dissolved in cyclohexane, *o*-xylene, carbon tetrachloride, octyl alcohol, or chloroform. Optimum extraction conditions were: $[NaNO_3] \geq 2$ M, pH 2, and cyclohexane as the partition solvent. Making the aqueous phase 8 M in lithium chloride appears to facilitate extraction with 0.1 M trioctylphosphine oxide (Karalova *et al.*, 1977b).

Trialkylphosphine oxide in aliphatic hydrocarbon solvents was used by Xu *et al.* (1983) for the solvent extraction separation of Ac(III) from La(III) in nitric acid solution. Amines and quaternary ammonium bases have also been used in solvent extraction systems for the separation of Ac(III) from rare earths and Am(III). Karalova *et al.* (1979a) examined the separation of Ac(III) from Eu(III) by extraction from aqueous solutions containing lithium nitrate at pH 2.5–3 with tri-*n*-octylamine in cyclohexane, and concluded that this partition system shows promise for the separation of Ac(III) from rare earths. A 0.5 M solution of the quaternary ammonium base Aliquat 336 (methyltrioctylammonium chloride) in xylene extracts Ac, Am, and Eu efficiently from aqueous alkaline ($pH > 11$) solutions containing ethylenediaminetetraacetic acid (EDTA) or 2-hydroxydiaminopropanetetraacetic acid; separation factors for Ac(III)/Am(III) and Ac(III)/Eu(III) greater than 100 were attained (Karalova *et al.*, 1978a, 1979b). A mixture of trialkylmethylammonium nitrate and TBP was reported by Mikhailichenko *et al.* (1982) to exert a weak synergistic effect on La(III) extraction and an antagonistic effect on Ac(III) extraction. Bis(2-ethylhexyl) phosphoric acid (HDEHP) has been successfully employed in the solvent extraction separation of ^{227}Ac(III), ^{227}Th(IV), ^{223}Ra(II), and ^{223}Fr(I) (Mitsugashira *et al.*, 1977). Karalova *et al.* (1978b) established that the actinium species extracted from 1 M perchloric acid is $AcX_3{\cdot}2HX$, and at higher perchloric acid concentrations is $HAc(ClO_4)_4{\cdot}2HX$.

The use of bis(2-ethylhexyl)phosphoric acid (HDEHP) as an extractant for Ac^{3+} has been little explored. Two studies have explored the fundamental mechanism of this extractant with Ac^{3+} (Szeglowski and Kubica, 1991) and the influence of colloidal rare earth particles on this extraction (Szeglowski and Kubica, 1990).

An unusual purification procedure is one in which actinium must be removed from rare earths on a commercial scale to minimize the level of radioactive contamination of the rare earth products (Kosynkin *et al.*, 1995). Uranium–rare earth phosphorites [fibrous apatites, generic formula $Ca_5(PO_4)_3(OH,F,Cl)$] have been processed commercially to remove both uranium and rare earths. After uranium was extracted from the dissolved phosphorite, cerium was removed by oxidation and precipitation from dilute acid. The trivalent rare earths and actinium remained in the aqueous phase and the actinium was removed from the rare earth fraction using mixer-settlers with mixtures of TBP and trialkyl amine (TAA) extractants in kerosene. Decontamination from a level of $\sim 10^{-8}$ Ci/(g rare earth oxides) to a level of $\sim 2 \times 10^{-11}$ Ci/(g rare earth oxides) has been achieved on an industrial scale.

2.4.2 Purification by ion-exchange chromatography

Cation-exchange chromatography is the simplest and most consistently effective method of separating sub-milligram amounts of ^{227}Ac from its principal decay products, 18.68-day ^{227}Th and 11.43-day ^{223}Ra (Gmelin, 1981). The resin most commonly employed is a strong cation-exchange resin such as Dowex 50 (Andrews and Hagemann, 1948; Cabell, 1959; Farr *et al.*, 1961; Eichelberger *et al.*, 1964; Nelson, 1964; De Troyer and Dejonghe, 1966; Baetslé *et al.*, 1967;

Baetslé and Droissart, 1973; Kraus, 1979; Boll *et al.*, 2005), but inorganic ion exchangers have also been used successfully (Huys and Baetslé, 1967; Monsecour and De Regge, 1975). The method is applicable to milking of ^{228}Ac tracer from its parent, 5.76 year ^{228}Ra (Bjornholm *et al.*, 1956, 1957; Duyckaerts and Lejeune, 1960; Bryukher, 1963; Bhatki and Adloff, 1964; Gomm and Eakins, 1966; Arnoux and Giaon, 1969; Monsecour *et al.*, 1973). A typical separation is illustrated in Fig. 2.8.

Anion-exchange chromatography is now used for bulk separation of ^{225}Ac and ^{223}Ra from ^{229}Th. The ^{225}Ac and ^{223}Ra are eluted in 2–4 bed volumes of 8 M HNO_3 and then ^{229}Th is stripped from the resin in 0.1 M HNO_3, after which the ^{229}Th can be recycled (Boll *et al.*, 2004).

Partition chromatography by reverse-phase and ion-exchange chromatography has been explored (Sinitsyna *et al.*, 1977, 1979). The radioisotopes of actinium were separated from other elements using trioctylamine, bis(2-ethylhexyl)phosphoric acid, and TBP as stationary phases on Teflon. Chromatography on a Teflon support was also investigated by Korotkin (1981). He used a mixture of TTA and TBP impregnated in Teflon to sorb the metal ions. Elution

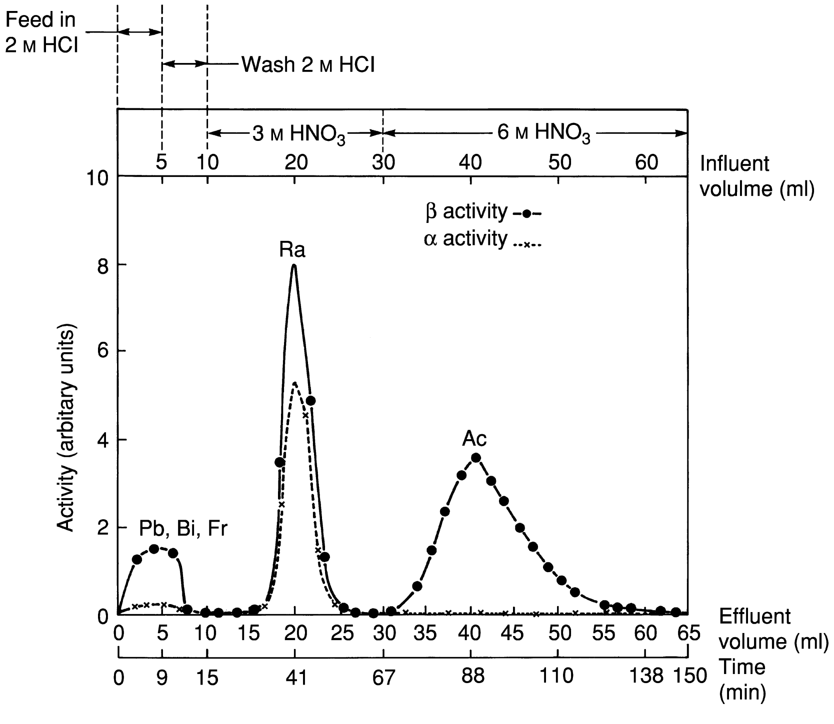

Fig. 2.8 *Separation of* ^{227}Ac *from its decay products by cation-exchange chromatography on Dowex* 50, *hydrogen form,* 200–400 *mesh,* 60°C (*Cabell,* 1959).

was by oxalate in a phthalate buffer. The procedure appears to have general utility for the rapid separation of actinides, lanthanides, and other metal ions. ^{227}Ac was separated from irradiated radium samples containing Pb, Tl, Bi, Po, and Th, and ^{225}Ac was separated from ^{233}U containing the same elements.

The inorganic cation exchanger, cryptomelane MnO_2 [a sorbent for large cations related to the mineral cryptomelane, $K(Mn^{4+},Mn^{2+})_8O_{16}$] is highly radiation-resistant and has distribution ratios (K_d values) for trivalent lanthanides and actinides that are orders of magnitude smaller than for Ra^{2+}. This ion exchanger has been used to separate $^{225}Ac^{3+}$ or $^{228}Ac^{3+}$ from $^{225}Ra^{2+}$ or $^{228}Ra^{2+}$ in radioisotope generators (Włodzimirska *et al.*, 2003).

2.4.3 Isolation of gram quantities of actinium

The history of large-scale actinium production is littered with the mutilated corpses of carefully designed processes, developed at the laboratory scale, which failed utterly, or required innumerable *ad hoc* modifications, when they were applied to the recovery of multi-Curie amounts of ^{227}Ac and ^{228}Th from multigram quantities of neutron-irradiated ^{226}Ra (Andrews and Hagemann, 1948; Engle, 1950; Kirby, 1951, 1952; Eichelberger *et al.*, 1964, 1965; De Troyer and Dejonghe, 1966; Foster, 1966; Baetslé *et al.*, 1967; Huys and Baetslé, 1967; Baetslé and Droissart, 1973).

Not the least of the problems is that posed by 3.824-day ^{222}Rn, a noble gas, which is evolved copiously and continuously by the decay of ^{226}Ra. The radioactive gaseous exhaust from the facility must be trapped and immobilized for several weeks while it decays to levels at which it can safely be released to the environment. (The maximum permissible concentration [inhalation derived air concentration (DAC)] of ^{222}Rn and its progeny in air in the workplace is very low, 3×10^{-8} μCi mL^{-1}) (U.S. Nuclear Regulatory Commission, 2005) Until now, this low level has been achieved by adsorbing the radon on activated charcoal at −75 to −180°C (Baetslé *et al.*, 1972), or by replacing the air at a sufficiently high rate, but chemical methods for removing radon and its daughters from the air by reaction with powerful fluorination reagents were also shown to bear promise for the removal of radon from air (Stein and Hohorst, 1982).

At the Belgian Nuclear Research Center (SCK-CEN, Mol), the irradiated $RaCO_3$ was dissolved in dilute nitric acid, and then precipitated as $Ra(NO_3)_2$ from 80% HNO_3, leaving nearly all the ^{227}Ac and ^{228}Th in solution. This step made the ^{226}Ra immediately available for recycling to the reactor; it also eliminated many of the severe radiolytic problems that develop when organic solvents or ion-exchange resins are in contact with large amounts of ^{226}Ra for extended periods of time.

The solution was then filtered, adjusted to 5 M HNO_3, and passed through a column of Dowex AG 1 × 8, an anion-exchange resin. ^{228}Th was quantitatively adsorbed (Danon, 1956, 1958), while the non-complexing cations (Fe, Ni, Cr) passed through the column unimpeded. ^{227}Ac, which appeared to be adsorbed to a slight extent by the resin, followed after a brief delay. The actinium was finally purified by oxalate precipitation (Salutsky and Kirby, 1956) and ignited to Ac_2O_3 at 700°C. The process gave excellent Ac/Th separations ($<0.01\%$ ^{228}Th) and 'reasonable' Ac purifications (Baetslé *et al.*, 1972; Baetslé, 1973).

The production capacity at Mol was about 20 g ^{227}Ac and 4 g ^{228}Th per year. As of the end of 1972, 2 g of Ac_2O_3 had been encapsulated as a prototype 30 W heat source and about 700 mg had been purified for the preparation of Ac–Be neutron sources. The ^{227}Ac production and separation facility at Mol was dismantled a few years later (Deworm *et al.*, 1979).

2.5 ATOMIC PROPERTIES

Meggers, Fred, and Tomkins (Meggers *et al.*, 1951, 1957; Meggers, 1957; Sugar, 1984) examined the emission spectra of actinium excited in a hollow cathode and in arcs and sparks between copper or silver electrodes. They reported some 500 lines characteristic of actinium in the spectral range 2062.00–7886.82 Å. Of these about 140 lines were assigned to the neutral atom, Ac I, more than 300 to singly ionized actinium, Ac II, and eight to doubly ionized actinium, Ac III. The lowest energy levels for identified configurations are given in Chapter 16 of this work (Table 16.1). The electron configuration of the Ac I (neutral Ac) ground state was found to be [Rn]($6d7s^2$) $^2D_{3/2}$; that of Ac II (Ac^+), ($7s^2$) $^1S_0$; and that of Ac III (Ac^{2+}), (7s) $^2S_{1/2}$. The first two ionization potentials were estimated to be 5.17 and 11.87 eV (Sugar, 1973, 1984). Similar values were calculated by Eliav *et al.* (1998), who also calculated the third ionization potential to be 17.518 or 17.512 eV by relativistic coupled-cluster methods. The first ionization potential was recently measured to be 5.3807(3) eV by resonant excitation of ^{227}Ac by laser spectroscopy in an external electric field (Backe *et al.*, 2002).

Analysis of interference spectrograms of the ^{227}Ac nucleus yielded the nuclear spin $I = 3/2$ (Tomkins *et al.*, 1951), and values of $\mu = (1.1 \pm 0.1)$ nuclear magnetons and $Q = +1.7$ barns for the magnetic and electric quadrupole moments, respectively (Fred *et al.*, 1955).

The foregoing comprises essentially all the experimentally determined data presently available on the properties of isolated actinium atoms and ions in the gas phase (see also Chapters 16 and 19). Theoretical calculations on such properties as energy levels (Brewer, 1971a,b; Nugent and Vander Sluis, 1971; Vander Sluis and Nugent, 1972, 1974; Nugent *et al.*, 1973b), ionization potentials (Carlson *et al.*, 1970; Sugar, 1973; Eliav *et al.*, 1998), and electron affinities (Eliav *et al.*, 1998) of actinium atoms and its free ions have also been made. There remain some discrepancies among some of these calculations or estimates that will only be resolved by better theoretical treatments and experimental measurements.

Consistent with the difference between the ionic radii of La^{3+} and Ac^{3+} (0.088 Å = 8.8 pm) (Shannon, 1976 and Section 15.7.5, Chapter 15), *ab initio* nonrelativistic and quasi-relativistic calculations of the bond lengths in monohydrides, monoxides, and monofluorides of all the lanthanide and actinide elements indicated a difference between La–X and Ac–X bond lengths of 10 pm (Küchle *et al.*, 1997). Another set of fully relativistic *ab initio* calculations of the bond lengths in monofluorides, monohydrides, and trihydrides revealed similar La–X and Ac–X bond-length differences; for LaH_3 and AcH_3 the bond-length difference calculated was also 10 pm (Laerdahl *et al.*, 1998).

2.6 THE METALLIC STATE

In 1953, Farr *et al.* (1953, 1961) prepared 10 μg of ^{227}Ac metal in an X-ray capillary by reduction of $AcCl_3$ with potassium vapor at 350°C. The diffraction pattern yielded two face-centered cubic (fcc) structures, which were attributed (by analogy to a parallel experiment with lanthanum) to actinium metal (a_0 = 5.311 ± 0.010 Å) and actinium hydride (a_0 = 5.670 ± 0.006 Å). The calculated densities were 10.07 and 8.35 g cm^{-1}, respectively. (The hydrogen in the 'actinium hydride' was of unknown origin.)

Milligram amounts of actinium metal were prepared by reduction of AcF_3 with lithium vapor in a molybdenum crucible (Stites *et al.*, 1955). The temperature range, 1100–1275°C, was critical for the reduction of AcF_3; at lower temperatures reduction was incomplete because the product metal did not melt, whereas at higher temperatures the yield was low because some of the AcF_3 was lost by volatilization.

The metal was reported to be silvery white in color, sometimes with a golden cast. It oxidizes rapidly in moist air to form a white coating of Ac_2O_3, which is somewhat effective in preventing further oxidation. Stites *et al.* (1955) estimated the melting point to be (1050 ± 50)°C. This melting point has been criticized as 'unreasonably low' (Matthias *et al.*, 1967) but is accepted in this work. A melting point of 1227°C has been estimated more recently (Arblaster, 1995). Based upon bonding contributions to the cohesive energy by 7s, 7p, and 6d electrons, Fournier (1976) estimated the melting point to be 1430°C and the enthalpy of sublimation ($\Delta_f H°$, Ac, g, 298 K) to be 396 kJ mol^{-1}. Other estimates of the enthalpy of sublimation are 406 kJ mol^{-1} (Wagman *et al.*, 1982) and 418 kJ mol^{-1} (David *et al.*, 1978; Ward *et al.*, 1986). The boiling point, estimated by extrapolation from vapor pressure measurements, is (3200 ± 300)°C (Foster and Fauble, 1960).

Subsequently, two metal preparations were made by the reduction of Ac_2O_3 with metallic thorium in high vacuum at 1750°C (Baybarz *et al.*, 1976), subliming the metal onto a tantalum condenser, and resubliming the metal to further purify it. X-ray data on these preparations of Ac metal suggest an fcc lattice with a_0 parameter of (5.317 ± 0.009) and (5.314 ± 0.001) Å in the two preparations (Baybarz *et al.*, 1976). Arblaster (1995) predicted that actinium metal should parallel metallic lanthanum and americium, with a double close-packed hexagonal allotrope at lower temperature and a body-centered cubic (bcc) allotrope at higher temperature.

Farr *et al.* (1953, 1961) reported that the metallic radius of actinium is 1.88 Å, but Zachariasen (1961, 1973) regarded this value as unreasonably similar to that of lanthanum (1.87 Å), because, in all isostructural compounds, the bond distances for actinium compounds are approximately 0.1 Å greater than those for the corresponding lanthanum compounds. By interpolation between the metallic radii of Ra and Th (2.293 and 1.798 Å, respectively), he predicted a value of 1.977 Å for Ac. On the other hand, Hill (1972) suggested that the lack of an appreciable increase in the metallic radius is a manifestation of a pronounced relativistic shrinkage in the 7s orbital of the neutral Ac atom, relative to such an effect on the 6s orbital of lanthanum. The fcc Ac prepared by Baybarz *et al.* (1976) corresponded to a metallic radius of 1.878 Å, supporting Hill's argument.

2.7 COMPOUNDS

With the sole exception of the questionable hydride mentioned in Section 2.6, almost all the compounds of actinium that have been positively identified by X-ray diffraction analysis are the result of a single study by Fried, Hagemann, and Zachariasen (Fried *et al.*, 1950). Each of the compounds was prepared from 10 μg of actinium or less, which was purified by TTA extraction (Hagemann, 1950) immediately before the start of the preparation. The small sample size was chosen to minimize the radiation health hazard and to reduce the fogging of the X-ray film by γ radiation from the rapidly growing actinium decay products. Even, so, it was necessary to prepare and photograph the compound within 24 h after purification. After purification of actinium from neutron-irradiated ^{226}Ra (Baetslé and Droissart, 1973) by ion exchange, Weigel and Hauske (1977) precipitated actinium oxalate on the 10 μg scale and identified it as the decahydrate from its X-ray powder pattern. It is isomorphous with similar compounds of the rare earths, plutonium, and americium.

Table 2.2 summarizes the preparative work and some of the properties of the ten known compounds of actinium. In addition, compounds thought to be the iodide, hydroxide, oxalate, oxyiodide, phosphate, and double salt with potassium sulfate were prepared but could not be identified (Fried *et al.*, 1950). Other unidentified compounds, suggested by chemical or thermogravimetric evidence, include the basic carbonate (Butterfield and Woollatt, 1968), the 8-hydroxyquinolate (Mosdzelewski, 1966; Keller and Mosdzelewski, 1967), and a double salt with ammonium nitrate (Kirby, 1969).

Table 2.2 *Preparation and properties of actinium compounds* (*Fried* et al., 1950; *Weigel and Hauske*, 1977; *Gmelin*, 1981).

	Preparation		*Crystal structure data*					
					Lattice parameters			
Compound	*Reaction*	*Temp.* (°C)	*Symmetry*	*Structure type*	a_0 (Å)	b_0 (Å)	c_0 (Å)	β (deg)
AcF_3	$Ac(OH_3)_3 + 3HF \rightarrow AcF_3 + 3H_2O$	700	trigonal	LaF_3	7.41 ± 0.01		7.53 ± 0.02	
	$Ac^{3+} + 3F^- \rightarrow AcF_3$	25						
$AcCl_3$	$2Ac(OH)_3 + 3CCl_4 \rightarrow 2AcC1_3 + 3CO_2 + 6HCl$	subl 960	hexagonal	UCl_3	7.62 ± 0.02		4.55 ± 0.02	
$AcBr_3$	$Ac_2O_3 + 2AlBr_3 \rightarrow 2AcBr_3 + A1_2O_3$	800	hexagonal	UCl_3	8.06 ± 0.04		4.68 ± 0.02	
AcOF	$AcF_3 + 2NH_3 + H_2O \rightarrow AcOF + 2NH_4F$	900–1000	cubic	CaF_2	5.931 ± 0.002			
AcOCl	$AcCl_3 + H_2O \rightarrow AcOCl + 2HCl$	1000	tetragonal	PbClF	4.24 + 0.02		7.07 ± 0.03	
AcOBr	$AcBr_3 + 2NH_3 + H_2O \rightarrow AcOBr + 2NH_4Br$	500	tetragonal	PbClF	4.27 ± 0.02		7.40 ± 0.03	
Ac_2O_3	$Ac_2(C_2O_4)_3 \rightarrow Ac_2O_3 + 3CO_2 + 3CO$	1100	hexagonal	La_2O_3	4.07 ± 0.01		6.29 ± 0.02	
Ac_2S_3	$Ac_2O_3 + 3H_2S \rightarrow Ac_2S_3 + 3H_2O$	1400	cubic	Ce_2S_3	8.97 ± 0.01			
$AcPO_4 \cdot 1/2H_2O$	$Ac^{3+} + PO_4^{3-} \rightarrow AcPO_4$	25	hexagonal	$LaPO_4 \cdot 1/2H_2O$	7.21 ± 0.02		6.64 ± 0.03	
$Ac_2(C_2O_4)_3 \cdot 10H_2O$[a]	$2Ac^{3+} + 3C_2O_4^{2-} \rightarrow Ac_2(C_2O_4)_3 \cdot 10H_2O$	25	monoclinic	$La_2(C_2O_4)_3 \cdot 10H_2O$	11.26	9.97	10.65	111.3

[a] From Weigel and Hauske (1977).

2.8 SOLUTION AND ANALYTICAL CHEMISTRY

All available evidence supports the conclusion (Moeller and Kremers, 1945), derived primarily from tracer and coprecipitation studies, that actinium is a homolog of lanthanum, fitting into the 7th period in the periodic table. The Ac^{3+}(aq) ion is more basic (less subject to hydrolysis) than the La^{3+}(aq) ion. As such, Ac^{3+} is the most basic tripositive ion known.

Aqueous solutions of actinium are colorless. In the only reported spectrophotometric study (Hagemann, 1954), no absorption was observed over the range 400–1000 nm. There was a slight amount of absorption between 300 and 400 nm, and a pronounced absorption maximum at 250 nm.

There has been limited work on the fundamental properties of Ac^{3+}(aq). Abramov *et al.* (1998) calculated the hydration Gibbs energy of Ac^{3+} to be -3034.7 kJ mol^{-1}.

2.8.1 Redox behavior

The only stable oxidation state of actinium in aqueous solution is 3+. A transitory Ac(ii) ion has been postulated by Bouissières, David, and coworkers (Bouissières *et al.*, 1961; Bouissières and Legoux, 1965; David and Bouissières, 1965, 1968; David, 1970a) to account for the amalgamation behavior of actinium, which resembled that of Eu(ii) and Sm(ii) more than that of La(iii). This hypothesis was reinforced by polarographic evidence: David (1970b,c) reported two waves in the polarogram of ^{228}Ac in $HClO_4$ at pH 1.9–3.1. He attributed the first wave to the reversible reaction:

$$Ac^{2+} + 2e^- + Hg \leftrightarrows Ac(Hg) \tag{2.8}$$

and the second to the irreversible reaction:

$$Ac^{3+} + 3e^- + Hg \rightarrow Ac(Hg) \tag{2.9}$$

From the half-wave potentials, he estimated the formal potential of the Ac(iii)/Ac(ii) couple to be -1.6 V and that of the Ac(iii)/Ac(0) couple to be -2.62 V. A later estimate was $E°(Ac^{3+}/Ac) = -2.13$ V (David *et al.*, 1978). However, Maly (1969) performed extractions of actinium and other elements from sodium amalgam in sodium acetate solutions as a function of pH and found that actinium extraction behavior was similar to that of the elements thorium to berkelium, i.e. that actinium reduction did not show evidence of the Ac(ii) ion.

Yamana *et al.* (1983) attempted to increase the stability of Ac^{2+}(aq) by complexing it with 18-crown-6. They noted a shift of the half-wave potential of about 0.15 V due to a complex, which they attributed to formation of an Ac^{2+}–crown complex and an Ac^{2+}(aq) ion with electronic configuration $[Rn]6d^1$ and ionic radius 1.25 Å. The $[Rn]6d^1$ configuration lies only 801 cm^{-1} above the [Rn]7s state in the free ion, so that the change of configuration is plausible.

However, Mikheev *et al.* (1995) noted that Nugent *et al.* (1973a) and Bratsch and Lagowski (1986) had calculated $E^\circ(\mathrm{Ac}^{3+}/\mathrm{Ac}^{2+})$ to be −4.9 and −3.3 V, respectively; the value $E^\circ(\mathrm{Ac}^{3+}/\mathrm{Ac}^{2+}) = -4.9$ V is adopted in Chapter 19 of this work. Either of these much more negative E° values would preclude the observation of Ac^{2+}(aq). Mikheev *et al.* (1994) found no evidence for Ac^{2+} in cocrystallization experiments with $\mathrm{Gd_2Cl_3}$ clusters or with Sm^{2+} in aqueous ethanol solution, a medium that should enhance the stability of Ac^{2+}. They recommended that the polarographic reduction of Ac^{3+}(aq) (David, 1970b,c) was actually reduction of water but they recommended further research on the $\mathrm{Ac}^{3+}/\mathrm{Ac}^{2+}$ couple.

The electrolysis of actinium at a mercury cathode has been used to separate tracer amounts of ^{228}Ac and 1.24 μg of ^{227}Ac from 3.10 mg of ^{231}Pa and an equilibrium amount of ^{227}Th. After 50 min of electrolysis in 0.17 M lithium citrate solution at a current density of 15 mA cm^{-2} the actinium was recovered by washing the amalgam with 0.1 M HCl. The overall yield was 85% and the decontamination factor was greater than 10^8 with respect to protactinium and thorium (David and Bouissières, 1966; Monsecour *et al.*, 1973).

2.8.2 Solubility

At the tracer level, actinium is carried quantitatively by any quantitative lanthanum precipitate, as well as by a wide variety of isomorphous and nonisomorphous carriers. The coprecipitation behavior of actinium was summarized in a useful table by Kahn (1951) and was exhaustively discussed in reviews (Bouissières, 1960; Sedlet, 1964; Kirby, 1967; Gmelin, 1981).

The relative amounts of actinium in partial precipitations of actinium tracer with lanthanum or other carriers are consistent with the relative solubilities of the compounds precipitated, where these are known or predictable. Unfortunately, however, with only two exceptions, quantitative solubility information is generally unavailable, because the dissolutions and precipitations that have been reported were usually incidental to some other objective, e.g. the preparation of compounds for crystallographic analysis (Table 2.2) (Weigel and Hauske, 1977).

Salutsky and Kirby (1956) precipitated tens of milligrams of ^{227}Ac from homogeneous solution with dimethyl oxalate and estimated the solubility of $\mathrm{Ac_2(C_2O_4)_3}$ in 0.25 M $\mathrm{H_2C_2O_4}$ (pH 1.2) to be 24 mg L^{-1}. That result is consistent with a more detailed study by Ziv and Shestakova (1965a), which shows, as expected, that the solubility of $\mathrm{Ac_2(C_2O_4)_3}$ varies with both the acidity and the oxalate concentration (Table 2.3). In a parallel study, the authors found that the solubility of $\mathrm{La_2(C_2O_4)_3}$ in 0.01 M $\mathrm{HNO_3}$ (pH 2.2) was 4.28×10^{-5} M, about half that of $\mathrm{Ac_2(C_2O_4)_3}$ under the same conditions. This unusual solubility of $\mathrm{Ac_2(C_2O_4)_3}$ may be due to radiolysis.

Ziv and Shestakova (1965b) also studied the solubility of $\mathrm{Ac(OH)_3}$ in $\mathrm{NH_4NO_3}$ solutions ($\mu = 0.001$ M). They observed a pronounced aging effect

Table 2.3 *Solubility of actinium oxalate in aqueous media at* 25°C (*Ziv and Shestakova,* 1965a).

Solvent	*pH*	*Solubility*		*Activity product*
		Ac^{3+} (mg L^{-1})	$Ac_2(C_2O_4)_3$ (M)	
0.01 M HNO_3	1.85	41.0	9.0×10^{-5}	7.5×10^{-27}
0.01 M HNO_3	2.00	40.0	8.8×10^{-5}	6.7×10^{-27}
0.01 M HNO_3	2.00	34.0	7.5×10^{-5}	2.1×10^{-27}
0.01 M HNO_3	2.00	30.0	6.5×10^{-5}	1.5×10^{-27}
H_2O	–	0.86	1.9×10^{-6}	2.7×10^{-27}
H_2O	–	1.5	3.3×10^{-6}	4.2×10^{-26}
H_2O	–	1.7	3.7×10^{-6}	8.0×10^{-26}
5×10^{-5} M $H_2C_2O_4$	3.4	2.5	5.5×10^{-6}	–
5×10^{-4} M $H_2C_2O_4$	3.0	1.2	2.6×10^{-6}	–
5×10^{-3} M $H_2C_2O_4$	2.3	0.96	2.1×10^{-6}	–
5×10^{-1} M $H_2C_2O_4$	0.9	7.85	1.73×10^{-5}	–

on both its solubility and the pH of its saturated solutions. For example, 1 h after precipitation the solubility was 3.6×10^{-8} g L^{-1} (1.59×10^{-8} M) and the pH was 10.4; 15 h later, the solubility had increased to 1.73×10^{-4} g L^{-1} and the pH had decreased to 9.1. After 27 days, the pH was 4.2. The authors attributed this decrease in pH to radiolysis of the solution by adsorbed ^{227}Th. Gamma radiation of aerated water also causes the pH to decrease: radiolysis by γ-rays produces nitric acid from dissolved O_2 and N_2 (Barkatt *et al.*, 1982). Another reason for the decrease of pH is that radiolysis of air by α particles at an air–water interface (Burns *et al.*, 1982) oxidizes nitrogen to acidic nitrogen oxides, which slowly acidifies the adjacent aqueous solution.

When ^{227}Ac was radiochemically purified before precipitation, the pH declined from 10.4 to only 8.3 in 166 days. From the activity product in various concentrations of NH_4NO_3, the solubility of aged $Ac(OH)_3$ was calculated to be 0.74 mg L^{-1}, which is higher than that for $La(OH)_3$. The corresponding equilibrium constants

$$M(OH)_3(s) + 3H^+(aq) \rightarrow M^{3+}(aq) + 3H_2O \ {}^*K_{s,0} \qquad (2.10)$$

(see Chapter 19, section 9, this book, for further discussion of $^*K_{s,0}$) at ionic strength 0.1 are $(1.26 \pm 0.04) \times 10^{24}$ for $Ac(OH)_3$ and 2.0×10^{20} for $La(OH)_3$. The higher solubility of $Ac(OH)_3$ can be attributed to the more basic character of the large Ac^{3+} ion, radiation damage of the crystallites, and/or to the tendency of radiolysis to produce more acidic conditions (Barkatt *et al.*, 1982; Burns *et al.*, 1982). A comparison of some solubility products for rare earth and actinide hydroxides is given in Chapter 19. The above evidence that $Ac(OH)_3$ is the most soluble of all f-element trihydroxides is consistent with Ac^{3+} being the most basic tripositive cation.

More recently, Kulikov *et al.* (1992) used electromigration to determine that ^{225}Ac is unhydrolyzed in aqueous solution of ionic strength 0.1 at 298 K until pH > 10. They determined the $*K_{s,0}$

$$\mathrm{Ac(OH)_3(s) + 3H^+(aq) \rightarrow Ac^{3+}(aq) + 3H_2O} \quad *K_{s,0} \tag{2.11}$$

to be 7.9×10^{31}. This value is much higher than that derived by Ziv and Shestakova or that expected by extrapolating from trivalent rare earths and actinide hydroxides.

2.8.3 Complexation

As in all its reactions, actinium closely resembles lanthanum in its behavior toward complexing agents. To the extent that they have been determined experimentally, the stability constants of actinium complexes (a selection is given in Table 2.4) are the same as, or slightly smaller than, those of the corresponding lanthanum complexes (Rao *et al.*, 1968, 1970; Shahani *et al.*, 1968; Sekine *et al.*, 1969; Sekine and Sakairi, 1969; Gmelin, 1981), in agreement with prediction from the similarity in their electronic configurations and their ionic radii (Kirby, 1967; Section 15.7.5). There is a linear dependence of log (formation constant) upon ionic radius, with Ac^{3+} always having the extreme position of largest ionic radius (Gmelin, 1981 and Section 15.7.5).

The hydrolysis of $Ac^{3+}(aq)$ is the smallest of all 3+ ions. Moutte and Guillaumont (1969) determined the equilibrium constant for the reaction

$$\mathrm{AcOH^{2+}(aq) + H_2O \rightarrow Ac(OH)_2^+(aq) + H^+(aq)} \tag{2.12}$$

to be 3.5×10^{-9} mol L^{-1}. Using the isotope ^{228}Ac, they determined that, at pH 8, 74% of the actinium in solution exists as $Ac(OH)^{2+}$ and 26% exists as $Ac(OH)_2^+$.

The Ac^{3+}–citrate complexes are sufficiently strong that citrate complexes almost all Ac^{3+} in 0.001 M citrate even at pH 8.1 (Moutte and Guillaumont, 1969). In addition to the complexes listed in Table 2.4, Ac^{3+} complexes have been studied with *trans*-1,2-diaminocyclohexanetetraacetic acid (DCTA), TTA and other diketones, arsenazo III, and other organic ligands (Gmelin, 1981).

Fukusawa *et al.* (1982) determined stability constants for chloro and bromo complexes of Ac(III), among many others, by a solvent extraction procedure. A much larger contribution from inner-sphere complex formation was observed in chloro than in bromo complexes for tripositive actinide ions. An empirical approach for predicting the stability of metal-ion complexes has been applied to actinium (Kumok, 1978).

On the basis of known and estimated ionic radii, Abramov *et al.* (1998) calculated the extraction constant K_{ex} of Ac^{3+} with bis(2-ethylhexyl)phosphoric acid (HDEHP) into toluene. The calculated K_{ex} value for Ac^{3+} is nearly an order of magnitude smaller than that for La^{3+}.

Table 2.4 *Cumulative stability constants of selected actinium complexes.*

Ligand	*Ionic strength* (μ)	$[H^+]$ (M)	*Stability constant*[a]	*Reference*
F^-	0.5	0.00025	$\beta_1 = 529 \pm 8$ $\beta_2 = (1.67 \pm 0.09) \times 10^5$ $\beta_3 = 8 \times 10^7$	Aziz and Lyle (1970)
F^-	0.1	0.016	$\beta_1 = 885$	Makarova *et al.* (1973)
Cl^-	1.0	1.0	$\beta_1 = 0.80 \pm 0.09$ $\beta_2 = 0.24 \pm 0.08$	Shahani *et al.* (1968)
Cl^-	4.0	0.01	$\beta_1 = 0.9$ $\beta_2 = 0.09$ $\beta_3 = 0.05$	Sekine and Sakairi (1969)
Br^-	1.0	1.0	$\beta_1 = 0.56 \pm 0.07$ $\beta_2 = 0.30 \pm 0.06$	Shahani *et al.* (1968)
NO_3^-	1.0	1.0	$\beta_1 = 1.31 \pm 0.12$ $\beta_2 = 1.02 \pm 0.12$	Shahani *et al.* (1968)
SO_4^{2-}	1.0–1.16	1.0	$\beta_1 = 15.9 \pm 1.3$ $\beta_2 = 71.4 \pm 7.3$	Shahani *et al.* (1968)
SO_4^2	1.0	pH 3–3.5	$\beta_1 = 22.9$ $\beta_2 = 479$	Sekine and Sakairi (1969)
SCN^-	1.0	pH 2	$\beta_1 = 1.11 \pm 0.07$ $\beta_2 = 0.82 \pm 0.08$	Rao *et al.* (1968)
SCN^-	5.0	pH 3–3.5	$\beta_1 = 0.18$ $\beta_2 = 0.35$	Sekine and Sakairi (1969)
$C_2O_4^{2-}$	1.0	pH 3–3.5	$\beta_1 = 3.63 \times 10^3$ $\beta_2 = 1.45 \times 10^6$	Sekine and Sakairi (1969)
$H_2PO_4^-$	0.5	pH 2–3	$\beta_1 = 38.8 \pm 5$	Rao *et al.* (1970)
Citrate	0.1	pH 2–3	$\beta_1 = 9.55 \times 10^6$	Makarova *et al.* (1974)
NTA^{-}[b]	0.1	pH $\approx$ 5	$\beta_3 = 4.3 \times 10^{14}$	Keller and Schreck (1969)
EDTA[c]	0.1	pH 2.8	$\beta_1 = 1.66 \times 10^{14}$	Makarova *et al.* (1972)

[a] $\beta_n = [MLn]/[M][L]^n$.

[b] HNTA, 2-naphthoyltrifluoroacetone.

[c] EDTA, ethylenediaminetetraacetic acid.

2.8.4 Radiocolloid formation

Kirby (1969) noted that when acidic aqueous solutions containing tracer amounts of Ac^{3+} and its progeny $^{227}Th^{4+}$ and $^{223}Ra^{2+}$ are dried on platinum disks, the actinium can be separated by redissolution in dilute NH_4NO_3(aq) and the radium by redissolution in dilute HF(aq), leaving the thorium on the disk. He described this separation as an application of ‘residue adsorption’; it may represent radiocolloid formation and selective redissolution at the metal surface.

Rao and Gupta (1961) studied the adsorption of ^{228}Ra and ^{228}Ac onto sintered glass and paper, and found that the adsorption of ^{228}Ac onto the glass increased with pH and time of aging. They studied the phenomenon by centrifugation; the ^{228}Ac fraction could be centrifuged at pH ≥ 5. Paper chromatography showed that the ^{228}Ac was immobile at a pH of 3 and higher, whereas Ba remained in solution. They concluded that the ^{228}Ac formed radiocolloids at pH ≥ 5.

2.8.5 Analytical chemistry of actinium

Sedlet (1964) published a complete set of procedures for analytical chemistry of actinium, primarily radiochemical procedures for ^{227}Ac. Kirby (1967) published a review that selected published and unpublished procedures that "will be of most value to the modern analytical chemist." Kirby also wrote the section on analytical chemistry in Gmelin (1981). Karalova (1979) reviewed the analytical chemistry of actinium. The analytical procedures that they described were based upon separation of actinium from other radioelements and then determination by measurement of the α, β, or γ radioactivity of a sample that has reached secular equilibrium with its daughters. The techniques suitable for tracer-level determination of ^{227}Ac are neutron activation analysis, by which ^{227}Ac can be determined at the level of 10^{-17} g, and total α, β, and γ radioactivity of a sample that has reached secular equilibrium with its daughters, by which ^{227}Ac can be determined at the level of 10^{-20} g. Recently a procedure for determination of ^{227}Ac in environmental samples by coprecipitation with lead sulfate, ion exchange, and α spectrometry after allowing the daughter isotopes ^{227}Th and ^{223}Ra to reach secular equilibrium (2–3 months) has been published (Martin *et al.*, 1995). The method requires the use of a short-lived actinium yield tracer, ^{225}Ac or ^{228}Ac. The lower limit of detection is $\sim$0.2 mBq per sample (7.5×10^{-16} g) at 95% confidence level.

The isotope ^{225}Ac, which is useful for tumor radiotherapy (see below), can be determined by α-spectrometric measurement of its α-emitting progeny ^{217}At (Martin *et al.*, 1995) or by γ spectrometry of the progeny ^{221}Fr and ^{213}Bi (McDevitt *et al.*, 2001).

2.9 APPLICATIONS OF ACTINIUM

2.9.1 Heat sources for radioisotope thermoelectric generators

The first practical use of actinium was to produce multi-Curie amounts of ^{227}Ac in order to take advantage of the energy released from the five α particles that are generated during its decay (Fig. 2.1) to produce electrical power for spacecraft and other devices that must operate for long periods of time in remote locations. An ambitious radioisotope thermoelectric generator (RTG) program was undertaken in Belgium to produce a 250 W_{th} thermoelectric generator fueled with 18 g of ^{227}Ac (Baetslé and Droissart, 1973). A prototype heat source that contained 2 g of ^{227}Ac was prepared but was not put into use (Baetslé and

Droissart, 1973). Kirby (Gmelin, 1981) listed the radioisotopes that can be used as thermoelectric heat sources. Of these, ^{238}Pu has been the most suitable; it has been used in almost all U.S. spacecrafts that utilized RTGs, beginning with 2.7-W SNAP–3B (Space Nuclear Auxiliary Power) generators for Transit 4A and 4B satellites in 1961 (Lange and Mastal, 1994; U.S. Department of Energy, 1987) and continuing to the three 276-W general purpose heat source (GPHS) RTGs in the Cassini probe, which was launched in 1997 and reached Saturn in 2004. (See also relevant sections in Chapter 7 and Chapter 15, section 11.2, this book.)

2.9.2 Neutron sources

Isotopes of elements with $Z \leq 20$ emit neutrons when they are bombarded by ~5 MeV α particles. Kirby (Gmelin, 1981) listed the properties of important (α,n) generators. The advantages of ^{227}Ac as a heat source are also those that make it attractive as an (α,n) generator. A few ^{227}Ac (α,n) generators have been constructed and used (Gmelin, 1981).

2.9.3 Alpha-particle generators for tumor radiotherapy

The 10-day α emitter ^{225}Ac has desirable properties for destroying rapidly growing cancer cells. After decay of ^{225}Ac to ^{221}Fr, four additional high-energy α decays and two β^- decays occur rapidly (Fig. 2.3), delivering ~40 MeV of high linear-energy-transfer radiation over a range of less than 100 μm. None of the decay events emits hard γ-rays, so that ^{225}Ac can deliver large doses to a tumor cell and negligible doses to surrounding healthy tissue (Tsoupko-Sitnikov *et al.*, 1996; Khalkin *et al.*, 1997; Boll *et al.*, 2005). To utilize this isotope for therapy, the principal challenges are to generate the isotope free of other radioisotopes, to deliver it to the cancer cell for a long enough period of time, to bind it firmly to the target call, and to retain the daughter radioisotopes (especially the ^{221}Fr$^+$ ion) at the target site. The *in vivo* stability of several macrocyclic complexes of ^{225}Ac have been evaluated. Deal *et al.* (1999) found the most promising complex to be that with 1,4,7,10,13,16-hexaazacyclohexadecane-*N*,*N*′,*N*″,*N*‴,*N*⁗-hexaacetic acid (HEHA); Ouadi *et al.* (2000) bifunctionalized an isothiocyanate derivative of HEHA for good covalent bonding to biomolecules. A procedure for delivering ^{225}Ac to tumors via bifunctional chelators related to the ligand 1,4,7,10-tetraazacyclododecane-1,4,7,10-tetraacetic acid (DOTA) has been described (McDevitt *et al.*, 2001). Kennel *et al.* (2000, 2002) evaluated radioimmunotherapy of mice with lung and other tumors using ^{225}Ac–HEHA conjugates with monoclonal antibodies; their studies concluded that the radiotoxicity of ^{225}Ac can only be controlled if conjugates that bind strongly with the daughters as well as with Ac$^+$ can be discovered.

As described in the earlier paragraph and in Section 2.2.3, ^{229}Th (α, $t_{1/2} = 7340$ years) is an appropriate generator from which ^{225}Ac can be removed periodically. At the time of writing, Oak Ridge National Laboratory is producing

50–60 mCi of ^{225}Ac from ^{229}Th every 8 weeks. Additional shipments of 5–20 mCi of ^{225}Ac are produced by ORNL every 2 weeks from the decay of the ^{225}Ra parent. The ^{225}Ac is shipped to hospitals and other research facilities (Boll *et al.*, 2005).

The isotope ^{225}Ac can also serve as a ^{213}Bi generator, which decays with a 45.6-min half-life (97.8% β, 2.2% α). The decay is accompanied by a 440-keV γ-ray, so that ^{213}Bi can be delivered to tumors with a bifunctional chelating agent for radioimmunotherapy as well as for imaging (Pippin *et al.*, 1995; Nikula *et al.*, 1999). Generators have been delivered to hospitals, where radioisotopically pure, chemically active ^{213}Bi can be eluted for radiotherapy, with minimum shielding every 5–6 h for at least 10 days. At the time of writing, the Institute for Transuranium Elements (Joint Research Centre of the European Commission, located at Karlsruhe, Germany) is producing and distributing ^{225}Ac/^{213}Bi generators.

2.9.4 Actinium-227 as a geochemical tracer

Nozaki (1984) demonstrated that the concentration of ^{227}Ac is higher than that of its progenitor ^{231}Pa in deep seawater; he proposed the use of natural ^{227}Ac as a tracer for circulation and mixing of seawater in deep ocean basins. Geibert *et al.* (2002) confirmed this phenomenon in several other oceanic locations and proposed that ^{227}Ac be used as a tracer for deep seawater circulation (diapycnal mixing, i.e. mixing across lines of equal density).

REFERENCES

Abramov, A. A., Eliseeva, O. V., and Iofa, B. Z. (1998) *Radiochemistry,* **40**, 302–5; *Radiokhimiya*, **40**, 292–5.

Adloff, J. P. (2000) *Radiochim. Acta,* **88**, 123–7.

Ahmad, I. (2002) Unpublished; personal communication to L. Morss.

Allison, M., Moore, R. W., Richardson, A. E., Peterson, D. T., and Voight, A. F. (1954) *Nucleonics,* **12**(5), 32–4.

Andrews, H. C. and Hagemann, F. (1948) in *Summary Report for April, May, and June 1948. Chemistry Division, Section C-I, ANL–4176* (eds. W. M. Manning and D. W. Osborne), pp. 13–6.

Arblaster, J. W. (1995) *Calphad,* **19**, 373.

Arnoux, M. and Giaon, A. (1969) *C. R. Acad. Sci. Paris,* **269B**, 317–20.

Aziz, A. and Lyle, S. J. (1970) *J. Inorg. Nucl. Chem.,* **32**, 1925–32.

Backe, H., Dretzke, A., Eberhardt, K., Fritsche, S., Grüning, C., Gwinner, G., Haire, R. G., Huber, G., Kratz, J. V., Kube, G., Kunz, P., Lassen, J., Lauth, W., Passler, G., Repnow, R., Schwalm, D., Schwamb, P., Sewtz, M., Thörle, P., Trautmann, N., and Waldek, A. (2002) *J. Nucl. Sci. Technol.*, (Suppl. 3), 86–9.

Baetslé, L. H., Dejonghe, P., Demildt, A. C., De Troyer, A., Droissart, A., and Dumont, G. (1967) *Ind. Chim. Belge,* **32** (2), 56–60.

Baetslé, L. H., Brabers, M. J., Dejonghe, P., Demildt, A. C., De Troyer, A., Droissart, A., and Poskin, M. (1972) *Proc. 4th UN Int. Conf. on Peaceful Uses of Atomic Energy*. A/CONF.49/P/287, United Nations, New York, pp. 191–203.

Baetslé, L. H. (1973) in *CEN-SCK Annual Scientific Report, 1972, Belgian Report BLG–481* (eds. R. Billiau, K. Bobin, W. Drent, and L. Hespeels), ch. 6.

Baetslé, L. H. and Droissart, A. (1973) Production and Applications of ^{227}Ac. Belgian Report BLG 483.

Bagnall, K. W. (1957) in *Chemistry of the Rare Radioelements: Polonium–Actinium,* Butterworths, London, pp. 15–45.

Barkatt, A., Barkatt, A., and Sousanpour, W. (1982) *Nucl. Technol.,* **60**, 218–27.

Bastin-Scoffier, G. (1967) *C. R. Acad. Sci. Paris,* **265B**, 863–5.

Baybarz, R. D., Bohet, J., Buijs, K., Colson, L., Müller, W., Reul, J., Spirlet, J. C., and Toussaint, J. C. (1976) *Transplutonium Elements. Proc. 4th Int. Transplutonium Elements Symp., 1975* (eds. W. Müller and R. Lindner), North Holland, Amsterdam, pp. 61–8.

Beckmann, W. (1955) *Z. Phys.,* **142**, 585–601.

Bhatki, K. S. and Adloff, J. P. (1964) *Radiochim. Acta,* **3**, 123–6.

Bjornholm, S., Nielsen, B., and Sheline, R. K. (1956) *Nature,* **178**, 1110–1.

Bjornholm, S., Nathan, O., Nielsen, O. B., and Sheline, R. K. (1957) *Nucl. Phys.,* **4**, 313–24.

Boll, R. A., Malkemus, D., and Mirzadeh, S. (2004) *Appl. Radiat. Isot.*, **62**, 667–9.

Bouissières, G. (1960) in *Nouveau Traité de Chimie Minérale* (ed. P. Pascal), Masson, Paris 7, pp. 1413–46.

Bouissières, G., Haïssinsky, M., and Legoux, Y. (1961) *Bull. Soc. Chim. Fr.*, 1028–30.

Bouissières, G. and Legoux, Y. (1965) *Bull. Soc. Chim. Fr.*, 386–8.

Bratsch, S. G. and Lagowski, J. J. (1986) *J. Phys. Chem.,* **90**, 307–12.

Brewer, L. (1971a) *J. Opt. Soc. Am.,* **61**, 1101–11.

Brewer, L. (1971b) *J. Opt. Soc. Am.,* **61**, 1666–82.

Browne, E. (2001) *Nucl. Data Sheets,* **93**, 763.

Bryukher, E. (1963) *Sov. Radiochem.,* **5**, 123–5; *Radiokhimiya*, **5**, 142–3.

Burns, W. G., Hughes, A. E., Marples, J. A. C., Nelson, R. S., and Stoneham, A. M. (1982) *J. Nucl. Mater.,* **107**, 245–70.

Butterfield, D. and Woollatt, R. (1968) *J. Inorg. Nucl. Chem.,* **30**, 801–5.

Cabell, M. J. (1959) *Can. J. Chem.,* **37**, 1094–1103.

Carlson, T. A., Nestor, C. W. J., Wasserman, N., and McDowell, J. F. (1970) Comprehensive Calculation of Ionization Potentials and Binding Energies for Multiply-Charged Ions, US Report ORNL-4562.

Chayawattanangkur, K., Herrmann, G., and Trautmann, N. (1973) *J. Inorg. Nucl. Chem.,* **35**, 3061–73.

Clarke, R. W. (1954) Actinium. A Bibliography of Unclassified and Declassified Atomic Energy Project Reports and References to the Published Literature (1906–1953), UK Report AERE Inf/Bib 95.

Clarke, R. W. (1958) Abstracts of Atomic Energy Project Unclassified Reports and Published Literature on the Actinide Elements (Papers dated 1957 noted up to February, 1958), Part I. Actinium, Protactinium, Neptunium, UK Report AERE C/R 2472.

Dalmasso, J., Herment, M., and Ythier, C. (1974) *C. R. Acad. Sci. Paris,* **278B**, 97–100.

Danon, J. (1956) *J. Am. Chem. Soc.,* **78**, 5953–4.

Danon, J. (1958) *J. Inorg. Nucl. Chem.,* **5**, 237–9.

David, F. (1970a) *Rev. Chim. Minér.,* **7**, 1–11.

David, F. (1970b) *C. R. Acad. Sci. Paris,* **271**, 440–2.

David, F. (1970c) *Radiochem. Radioanal. Lett.,* **5**, 279–85.

David, F. and Bouissières, G. (1965) *Bull. Soc. Chim. Fr.*, 1001–7.

David, F. and Bouissières, G. (1966) in *Physico-Chimie du Protactinium*, Colloques internationaux du CNRS, Paris, No. 154, pp. 301–6.

David, F. and Bouissières, G. (1968) *Inorg. Nucl. Chem. Lett.,* **4**, 153–9.

David, F., Samhoun, K., Guillaumont, R., and Edelstein, N. (1978) *J. Inorg. Nucl. Chem.,* **40**, 69–74.

Deal, K. A., Davis, I. A., Mirzadeh, S., Kennel, S. J., and Brechbiel, M. W. (1999) *J. Med. Chem.,* **42**, 2988–92.

Debierne, A. (1899) *C. R. Acad. Sci. Paris,* **129**, 593–5.

Debierne, A. (1900) *C. R. Acad. Sci. Paris,* **130**, 906–8.

Debierne, A. (1904) *C. R. Acad. Sci. Paris,* **139**, 538–40.

Dempster, A. J. (1935) *Nature,* **136**, 180.

De Troyer, A. and Dejonghe, P. (1966) in *Large Scale Production and Applications of Radioisotopes,* US Report DP–1066, edn 1, session III, pp. 63–9.

Deworm, J. P., Fieuw, G., and Marlein, J. (1979) *Ann. Belg. Ver. Stralingsbescherming,* **4**, 107–28; *Chem. Abstr.*, 93, 83093b.

Duyckaerts, G. and Lejeune, R. (1960) *J. Chromatogr.,* **3**, 58–62.

Dzhelepov, B. S., Ivanov, R. B., Mikhailova, M. A., Moskvin, L. N., Nazarenko, O. M., and Rodionov, V. F. (1967) *Bull. Acad. Sci. USSR, Phys. Ser.,* **31**, 563–74; *Dokl. Akad. Nauk USSR, Fiz. Ser.*, **31**, 568–80.

Eichelberger, J. F., Grove, G. R., and Jones, L. V. (1964) Mound Laboratory Progress Report for April, 1964. US Report MLM-1196, pp. 9–11.

Eichelberger, J. F., Grove, G. R., and Jones, L. V. (1965) Mound Laboratory Progress Report for November, 1964. US Report MLM-1227.

Eliav, E., Shmulyian, S., and Kaldor, U. (1998) *J. Chem. Phys.,* **109**, 3954–8.

Engle, P. M. (1950) Preliminary Report on the Actinium Separation Project. US Report MLM-454.

Farr, J. D., Giorgi, A. L., Money, R. K., and Bowman, M. G. (1953) The Crystal Structure of Actinium Metal and Actinium Hydride. US Report LA-1545, Los Alamos National Laboratory.

Farr, J. D., Giorgi, A. L., Bowman, M. G., and Money, R. K. (1961) *J. Inorg. Nucl. Chem.,* **18**, 42–7.

Firestone, R. B. and Shirley, V. S. (eds.) (1996) *Table of Isotopes,* Wiley, New York.

Foster, K. W. (1966) Radioisotopes for Heat Sources. II. Calculations for preparation of Ac-227 by Neutron Irradiation of Ra-226. US Report MLM-1297.

Foster, K. W. and Fauble, L. G. (1960) *J. Phys. Chem.,* **64**, 958–9.

Fournier, J. M. (1976) *J. Phys. Chem. Solids,* **37**, 235–44.

Fred, M., Tomkins, F. S., and Meggers, W. F. (1955) *Phys. Rev.,* **98**, 1514.

Fried, S., Hagemann, F., and Zachariasen, W. H. (1950) *J. Am. Chem. Soc.,* **72**, 771–5.

Fukusawa, T., Kawasuji, I., Mitsugashira, T., Sato, A., and Suzuki, S. (1982) *Bull. Chem. Soc. Jpn.,* **55**, 726–9.

Geerlings, M. W., Kaspersen, F. M., Apostolidis, C., and Van Der Hout, R. (1993) *Nucl. Med. Commun.,* **14**, 121–5.

Geibert, W., Rutgers van der Loeff, M. M., Hanfland, C., and Dauelsberg, H.-J. (2002) *Earth Planet. Sci. Lett.,* **198**, 147–65.

Giesel, F. (1902) *Ber. Dtsch. Chem. Ges.,* **35**, 3608–11.

Giesel, F. (1903) *Ber. Dtsch. Chem. Ges.,* **36**, 342–7.

Giesel, F. (1904a) *Ber. Dtsch. Chem. Ges.,* **37**, 1696–9.

Giesel, F. (1904b) *Ber. Dtsch. Chem. Ges.,* **37**, 3963–6.

Giesel, F. (1905) *Ber. Dtsch. Chem. Ges.,* **38**, 775–8.

Gmelin (1942) *Handbuch der Anorganischen Chemie, 8. Auflage, System-Nummer 40, Actinium und Isotope (MsTh2),* Verlag Chemie, Berlin, (English translation by G. A. Young (1954)). U.S. Report AEC-tr-l734.

Gmelin (1981) *Handbook of Inorganic Chemistry, Actinium*, 8th edn, System Number 40 Suppl. vol. 1, Springer-Verlag, Berlin.

Godlewski, T. (1904–5) *Nature,* **71**, 294–5.

Godlewski, T. (1905) *Phil. Mag.,* **10**, 35–45.

Gomm, P. J. and Eakins, I. D. (1966) The Determination of Actinium-227 in Urine. UK Report AERE-R 4972.

Gomm, P. J. and Eakins, J. D. (1968) *Analyst,* **93**, 228–34.

Hagemann, F. (1950) *J. Am. Chem. Soc.,* **72**, 768–71.

Hagemann, F. T. (1954) The Chemistry of Actinium, in *The Actinide Elements, Nat. Nucl. En. Ser. Div. IV, 14A* (eds. G. T. Seaborg and J. J. Katz), McGraw-Hill, New York, pp. 14–44.

Hahn, O. (1905) *Jahrb. Radioaktivitat Elektronik,* **2**, 233–66.

Hahn, O. (1906a) *Ber. Dtsch. Chem. Ges.,* **39**, 1605–7.

Hahn, O. (1906b) *Phys. Z.,* **7**, 855–64.

Hahn, O. (1907) *Ber. Dtsch. Chem. Ges.,* **40**, 1462–9.

Hahn, O. (1908) *Phys. Z.,* **9**, 146–8.

Hahn, O. and Meitner, L. (1918) *Phys. Z.,* **19**, 208–18.

Hahn, O. and Erbacher, O. (1926) *Phys. Z.,* **27**, 531–3.

Heath, R. L. (1974) Gamma-ray Spectrum Catalogue. Ge(Li) and Si(Li) Spectrometry. US Report ANCR-1000-2, 3rd edn, vol. 2.

Heydemann, A. (1969) in *Handbook of Geochemistry* (ed. K. H. Wedepohl), Springer-Verlag, New York, vol. 1, pp. 276–412.

Hill, H. H. (1972) *Chem. Phys. Lett.,* **16**, 114–8.

Holden, N. E. (1977) *Isotopic Composition of the Elements and Their Variation in Nature – A Preliminary Report, BNL-NCS–50605*; (1979) *Pure Appl. Chem.,* **52**, 2371.

Horen, D. J. (1973) *Nucl. Data Sheets,* **10**, 387–90.

Huys, D. and Baetslé, L. H. (1967) Separation of ^{226}Ra, ^{227}Ac and ^{228}Th by Ion Exchange. Belgian Report BLG 422.

Hyde, E. K., Perlman, I., and Seaborg, G. T. (1964) *The Nuclear Properties of the Heavy Elements*, vol. 2, Prentice-Hall, Englewood Cliffs, NJ, pp. 584–6.

Ihde, A. J. (1964) *The Development of Modern Chemistry,* Harper & Row, New York, p. 492.

Jordan, K. C. and Blanke, B. C. (1967) in *Standardization of Radionuclides, IAEA Proc. Series STI/PUB/139*. IAEA, Vienna, pp. 567–78.

Kahn, M. (1951) in *Radioactivity Applied to Chemistry* (eds. A. C. Wahl and N. A. Bonner) Wiley, New York, pp. 403–33.

Karalova, Z. K., Rodionova, L. M., Pyzhova, Z. I., and Myasoedov, B. F. (1977a) *Soviet Radiochem.,* **19**, 31–3; *Radiokhimiya*, **19**, 38–41.

Karalova, Z. K., Rodionova, L. M., Pyzhova, Z. I., and Myasoedov, B. F. (1977b) *Sov. Radiochem.,* **19**, 34–7; *Radiokhimiya,* **19**, 42–5.

Karalova, Z. K., Nekrasova, V. V., Pyzhova, Z. I., Rodionova, L. M., and Myasoedov, B. F. (1978a) *Radiokhimiya,* **20**, 845–50.

Karalova, Z. K., Rodionova, L. M., Pyzhova, Z. I., and Myasoedov, B. F. (1978b) *Sov. Radiochem.,* **20**, 30–3; *Radiokhimiya,* **20**, 42–6.

Karalova, Z. K. (1979) *Sov. Radiochem.,* **20**, 712–20; *Radiokhimiya,* **20**, 834–44.

Karalova, Z. K., Rodionova, L. M., Pyzhova, Z. I., and Myasoedov, B. F. (1979a) *Sov. Radiochem.,* **21**, 7–10; *Radiokhimiya*, **21**, 11–4.

Karalova, Z. K., Rodionova, L. M., Pyzhova, Z. I., and Myasoedov, B. F. (1979b) *Sov. Radiochem.,* **21**, 335–9; *Radiokhimiya*, **21**, 394–9.

Katz, J. J. and Seaborg, G. T. (1957) in *The Chemistry of the Actinide Elements*, Methuen, London, pp. 5–15.

Keller, C. and Mosdzelewski, K. (1967) *Radiochim. Acta,* **7**, 185–8.

Keller, C. and Schreck, H. (1969) *J. Inorg. Nucl. Chem.,* **31**, 1121–32.

Keller, C. (1977) *Chem.-Z.,* **101**, 500–7.

Kennel, S. J., Chappell, L. L., Dadachova, K., Brechbiel, M. W., Lankford, T. K., Davis, I. A., Stabin, M., and Mirzadeh, S. (2000) *Cancer Biotherapy Radiopharm.,* **15**, 235–44.

Kennel, S. J., Brechbiel, M. W., Milenic, D. E., Schlom, J., and Mirzadeh, S. (2002) *Cancer Biotherapy Radiopharm.,* **17**, 219–31.

Khalkin, V. A., Tsupko- Sitnikov, V. V., and Zaitseva, N. G. (1997) *Radiochemistry,* **39**, 481–90; *Radiokhimiya,* **39**, 483–92.

Kirby, H. W. (1951) Mound Laboratory Report for General Research. December 11, 1950 to April 2, 1951 (Actinium volume). US Report MLM-558, pp. 13–4.

Kirby, H. W. (1952) Tentative Procedure for the Analysis of Mixtures Containing Radium-226, Actinium-227 and Thorium-228. US Report MLM-773.

Kirby, H. W., Grove, G. R., and Timma, D. L. (1956) *Phys. Rev.,* **102**, 1140–1.

Kirby, H. W. (1967) *Prog. Nucl. Energy, Ser. IX,* **8(1)**, 89–139.

Kirby, H. W. (1969) *J. Inorg. Nucl. Chem.,* **31**, 3375–85.

Kirby, H. W. (1970) *J. Inorg. Nucl. Chem.,* **32**, 2823–37.

Kirby, H. W. (1971) *Isis,* **62**, 290–308.

Kirby, H. W. (1974) Geochemistry of the Naturally Occurring Radioactive Series. US Report MLM-2111.

Korotkin, Y. S. (1981) *Sov. Radiochem.,* **23**, 145–9; *Radiokhimiya,* **23**, 181–5.

Kosynkin, V. D., Moiseev, S. D., and Vdovichev, V. S. (1995) *J. Alloys Compds.,* **225**, 320–3.

Kraus, K. A. (1979) *J. Chromatogr.,* **178**, 163–8.

Küchle, W., Dolg, M., and Stoll, H. (1997) *J. Phys. Chem. A,* **101**, 7128–33.

Kulikov, E. V., Novgorodov, A. F., and Schumann, D. (1992) *J. Radioanal. Nucl. Chem., Lett.,* **164**, 103–8.

Kumok, V. N. (1978) *Sov. Radiochem.,* **20**, 590–4; *Radiokhimiya*, **20**, 691–4.

Laerdahl, J. K., Faegri, J., Visscher, L., and Saue, T. (1998) *J. Chem. Phys.,* **109**, 10806–17.

Lange, R. G. and Mastal, E. F. (1994) A tutorial review of radioisotope power systems in *A Critical Review of Space Nuclear Power and Propulsion, 1984–1993* (ed. M. S. El-Genk), American Institute of Physics, New York, pp. 1–20.

Lecoin, M., Perey, M., Riou, M., and Teillac, J. (1950) *J. Phys. Radium.,* **11**, 227–34.

Maly, J. (1969) *J. Inorg. Nucl. Chem.,* **31**, 1007–17.

Makarova, T. P., Sinitsyna, G. S., Stepanov, A. V., Shestakova, I. A., and Shestakov, B. I. (1972) *Sov. Radiochem.,* **14**, 555–8; *Radiokhimiya*, **14**, 538–41.

Makarova, T. P., Stepanov, A. V., and Shestakov, B. I. (1973) *Russ. J. Inorg. Chem.,* **18**, 783–785; *Zh. Neorg. Khim.,* **18**, 1845–9.

Makarova, T. P., Sinitsyna, G. S., Stepanov, A. V., Gritschenko, I. A., Shestakova, I. A., and Shestakov, B. I. (1974) *Chem. Abs.,* **82**, 176644.

Maples, C. (1973) *Nucl. Data Sheets,* **10**, 643–71.

Marckwald, W. (1909) *Am. Chem. J.,* **41**, 515–57.

Martin, P., Hancock, G. J., Paulka, S., and Akber, R. A. (1995) *Appl. Radiat. Isot.,* **46**, 1065–70.

Matthias, B. T., Zachariasen, W. H., Webb, G. W., and Engelhardt, J. J. (1967) *Phys. Rev. Lett.,* **18**, 781–4.

McDevitt, M. R., Ma, D., Lai, L. T., Simon, J., Borchardt, P., Frank, R. K., Wu, K., Pellegrini, V., Curcio, M. J., Miederer, M., Bander, N. H., and Scheinberg, D. A. (2001) *Science,* **294**, 1537–40.

Meggers, W. F., Fred, M., and Tomkins, F. S. (1951) *J. Opt. Soc. Am.,* **41**, 867–8.

Meggers, W. F. (1957) *Spectrochim. Acta,* **10**, 195–200.

Meggers, W. F., Fred, M., and Tomkins, F. S. (1957) *J. Res. NBS,* **58**, 297–315.

Mikhailichenko, A. I., Goryacheva, E. G., Aksenova, N. M., and Denisov, A. F. (1982) *Sov. Radiochem.,* **24**, 173–5; *Radiokhimiya,* **24**, 207–9.

Mikheev, N. B., Kamenskaya, A. N., Rumer, I. A., Kulyukhin, S. A., and Novichenko, V. L. (1994) *Radiokhimiya,* **36**, 160–2; *Radiochemistry,* **36**, 173–5.

Mikheev, N. B., Veleshko, I. E., Kamenskaya, A. N., and Rumer, I. A. (1995) *Radiokhimiya,* **37**, 322–5; *Radiochemistry,* **37**, 297–9.

Mitsugashira, T., Yamana, H., and Suzuki, S. (1977) *Bull. Chem. Soc. Jpn,* **50**, 2913–6.

Moeller, T. and Kremers, H. E. (1945) *Chem. Rev.,* **37**, 97–159.

Moeller, T. (1963) *The Chemistry of the Lanthanides*, Reinhold, New York.

Monsecour, M., De Regge, P., and Demildt, A. (1973) *Radiochem. Radioanal. Lett.,* **14**, 365–71.

Monsecour, M., De Regge, P., Demildt, A., and Baetslé, L. H. (1974) *J. Inorg. Nucl. Chem.,* **36**, 719–23.

Monsecour, M. and De Regge, P. (1975) *J. Inorg. Nucl. Chem.,* **37**, 1841–3.

Mosdzelewski, K. (1966) Die Extraktion der Elemente Radium, Actinium, Protactinium, Americium, und Curium mit 8-Hydroxychinolin, Thesis. German Report KFK–432.

Moutte, A. and Guillaumont, R. (1969) *Rev. Chim. Minér.,* **6**, 603–10.

Nelson, F. (1964) *J. Chromatogr.,* **16**, 538–40.

Nikula, T. K., McDevitt, M. R., Finn, R. D., Wu, C., Kozak, R. W., Garmestani, K., Brechbiel, M. W., Curcio, M. J., Pippin, C. G., Tiffany-Jones, L., Geerlings, M. W., Sr., Apostolidis, C., Molinet, R., Geerlings, M. W. Jr., Gansow, O. A., and Scheinberg, D. A. (1999) *J. Nucl. Med.,* **40**, 166–76.

Novikova, G. I., Volkova, E. A., Gol'din, L. L., Ziv, D. M., and Tret'yakov, E. F. (1960) *Sov. Phys. JETP,* **37**, 663–9; *Zh. Eks. Teor. Fiz.,* **37**, 928–37.

Nozaki, Y. (1984) *Nature,* **310**, 486–8.

Nugent, L. J., Baybarz, R. D., Burnett, J. L., and Ryan, J. L. (1973a) *J. Phys. Chem.,* **77**, 1528–39.

Nugent, L. J., Burnett, J. L., and Morss, L. R. (1973b) *J. Chem. Thermodyn.,* **5**, 665–78.

Nugent, L. J., and Vander Sluis, K. L. (1971) *J. Opt. Soc. Am.,* **61**, 1112–5.

Ouadi, A., Loussouarn, A., Remaud, P., Morandeau, L., Apostolidis, C., Musikas, C., Fauve-Chauvet, A., and Gestin, J.-F. (2000) *Tetrahedron Lett.,* **41**, 7207–9.

Partington, J. R. (1964) *A History of Chemistry*, Macmillan, London, vol. 4, p. 938.

Peppard, D. F., Mason, G. W., Gray, P. R., and Mech, J. F. (1952) *J. Am. Chem. Soc.,* **74**, 6081–4.

Perey, M. (1939a) *C. R. Acad. Sci. Paris,* **208**, 97–9.

Perey, M. (1939b) *J. Phys. Radium,* **10**, 435–8.

Peterson, S. (1949) *Natl. Nucl. En. Ser., Div. IV*, in *The Transuranium Elements* (eds. G. Seaborg, J. J. Katz, and W. M. Manning), McGraw-Hill, New York, vol. 14B, pp. 1393–4.

Pippin, C. G., Gansow, O. A., Brechbiel, M. W., Koch, L., Molinet, R., van Geel, J., Apostolidis, C., Geerlings, M. W., and Scheinberg, D. A. (1995) in *Chemist's Views of Imaging Centers* (ed. A. M. Emran), Plenum Press, New York, pp. 315–25.

Poskanzer, A. M. and Foreman, B. M. J. (1961) *J. Inorg. Nucl. Chem.,* **16**, 323–36.

Rao, C. L. and Gupta, A. R. (1961) *J. Chromatogr.,* **5**, 147–52.

Rao, C. L., Shahani, C. I., and Mathew, K. A. (1968) *Inorg. Nucl. Chem. Lett.,* **4**, 655–9.

Rao, V. K., Shahani, C. J., and Rao, C. L. (1970) *Radiochim. Acta,* **14**, 31–4.

Rutherford, E. (1904) *Phil. Trans. R. Soc. Lond.,* **204A**, 169–219.

Rutherford, E. (1911) in *Encyclopaedia Britannica*, 11th edn, vol. 22, pp. 795–802.

Salutsky, M. L. (1962) in *Comprehensive Analytical Chemistry* (eds. C. L. Wilson and D. W. Wilson), Elsevier, Amsterdam, 1C, pp. 492–6.

Salutsky, M. L. and Kirby, H. W. (1956) *Anal. Chem.,* **28**, 1780–2.

Sani, A. R. (1970) *J. Radioanal. Chem.,* **4**, 127–9.

Seaborg, G. T. (1994) Origin of the Actinide Concept, in *Handbook on the Chemistry and Physics of the Rare Earths* (eds. K. A. Gschneidner, L. Eyring, G. R. Choppin, and G. Lander), North-Holland, Amsterdam, 18, 1–27.

Sedlet, J. (1964) Actinium, Astatine, Francium, Polonium, and Protactinium, in *Treatise on Analytical Chemistry*, Part II, vol. 6 (eds. I. M. Kolthoff, P. J. Elving, and E. B. Sandell), Wiley, New York, pp. 435–610.

Sekine, T., Koike, Y., and Sakairi, M. (1967) *J. Nucl. Sci. Technol.,* **4**, 308–11.

Sekine, T., Koike, Y., and Hasegawa, Y. (1969) *Bull. Chem. Soc. Japan,* **42**, 432–6.

Sekine, T. and Sakairi, M. (1969) *Bull. Chem. Soc. Jpn.,* **42**, 2712–3.

Shahani, C. J., Mathew, K. A., Rao, C. L., and Ramaniah, M. V. (1968) *Radiochim. Acta,* **10**, 165–7.

Shannon, R. D. (1976) *Acta Crystallogr.,* **A32**, 751–67.

Sinitsyna, G. S., Shestakova, I. A., Shestakov, B. I., Plyushcheva, N. A., and Malyshev, N. A., Belyatskii, A. F. (1977) *Tezisy Dokl.-Konf. Anal. Khim. Radioakt.*, Nauka, Moscow.

Sinitsyna, G. S., Shestakova, I. A., Shestakov, B. I., Plyushcheva, N. A., Malyshev, N. A., Belyatskii, A. F., and Tsirlin, V. A. (1979) *Sov. Radiochem.,* **21**, 146–51; *Radiokhimiya,* **21**, 172–7.

Skarnemark, G. and Skalberg, M. (1985) *Int. J. Appl. Radiat. Isot.,* **36**, 439–41.

Soddy, F. and Cranston, J. A. (1918a) *Nature,* **100**, 498–9.

Soddy, F. and Cranston, J. A. (1918b) *Proc. R. Soc. Lond.,* **94A**, 384–404.

Stein, L. and Hohorst, F. A. (1982) *Envir. Sci. Technol.,* **16**, 419–22.

Stevenson, P. C. and Nervik, W. E. (1961) The Radiochemistry of the Rare Earths, Scandium, Yttrium and Actinium. US Report NAS-NS 3020. All the volumes of the series "The Radiochemistry of..." can be found on the site http://lib-www.lanl.gov/radiochemistry/elements.htm

Stites, J. G. Jr., Salutsky, M. L., and Stone, B. D. (1955) *J. Am. Chem. Soc.,* **77**, 237–40.

St. John, D. S. and Toops, E. C. (1958) Formation of U-232 During the Irradiation of Thorium. US Report DP-279.

Sugar, J. (1973) *J. Chem. Phys.,* **59**, 788–91.

Sugar, J. (1984) Personal communication to L. R. Morss.

Szeglowski, Z. and Kubica, B. (1990) *J. Radioanal. Nucl. Chem.,* **143**, 389–95.

Szeglowski, Z. and Kubica, B. (1991) *J. Radioanal. Nucl. Chem. Lett.,* **153**, 67–74.

Taylor, S. R. (1964) *Geochim. Cosmochim. Acta,* **28**, 1273–85.

Tomkins, F. S., Fred, M., and Meggers, W. F. (1951) *Phys. Rev.,* **84**, 168.

Tousset, J. (1961) Les Spectres Béta de Faible Energie de Que1ques Eléments Lourds, Thesis, Univ. Lyon (F.) French Report NP-13367.

Tsoupko-Sitnikov, V., Norseev, Y., and Khalkin, C. (1996) *J. Radioanal. Nucl. Chem.,* **205**, 75–83.

U.S. Department of Energy (1987) Atomic Power in Space: a History (excerpted in *Nuclear News*, May 2003, pp. 37–44).

U.S. Nuclear Regulatory Commission (2005) U.S. Code of Federal Regulations, 10 CFR 20.

Valli, K. (1964) *Ann. Acad. Sci. Fenn.*, *Ser. A*, VI, no. 165.

Vander Sluis, K. L. and Nugent, L. J. (1972) *Phys. Rev. A,* **6**, 86–94.

Vander Sluis, K. L. and Nugent, L. J. (1974) *J. Opt. Soc. Am.,* **64**, 687–95.

Wagman, D. D., Evans, W. E., Parker, V. B., Schumm, R. H., Halow, I., Bailey, S. M., Churney, K. L., and Nuttall, R. L. (1982) *J. Phys. Chem. Ref. Data*, **11**, Suppl. No. 2.

Ward, J. W., Kleinschmidt, P. D., and Peterson, D. E. (1986) in *Handbook on the Physics and Chemistry of the Actinides*, vol. 4 (eds. A. J. Freeman and C. Keller), ch. 7.

Weeks, M. E. and Leicester, H. M. (1968) *Discovery of the Elements*, Journal of Chemical Education, Easton, PA, p. 794.

Weigel, F. and Hauske, H. (1977) *J. Less-Common Met.,* **55**, 243–7.

Włodzimirska, B., Bartoś, B., and Bilewicz, A. (2003) *Radiochim. Acta,* **91**, 553–6.

Xu, J., He, P., and Zhu, Y. (1983) *He Huaxue Yu Fangshe Huaxue,* **5**, 202–10; *Chem. Abstr.*, **99**, 192397.

Yamana, H., Mitsugashira, T., and Shiokawa, Y. (1983) *J. Radioanal. Nucl. Chem.,* **76**, 19–26.

Zachariasen, W. H. (1961) in *The Metal Plutonium* (eds. W. N. Miner and A. S. Coffinberry), University of Chicago Press, Chicago, pp. 99–107.

Zachariasen, W. H. (1973) *J. Inorg. Nucl. Chem.,* **35**, 3487–97.

Ziv, D. M. and Shestakova, I. A. (1965a) *Sov. Radiochem.,* **7**, 168–75; *Radiokhimiya,* **7**, 166–75.

Ziv, D. M. and Shestakova, I. A. (1965b) *Sov. Radiochem.,* **7**, 176–86; *Radiokhimiya,* **7**, 175–87.

CHAPTER THREE

THORIUM

Mathias S. Wickleder, Blandine Fourest, and Peter K. Dorhout

3.1 HISTORICAL

In 1815 Berzelius analyzed a rare mineral from the Falun district. He assumed that the mineral contained a new element, which he named thorium after the ancient Scandinavian god of thunder and weather, Thor (Weeks and Leicester, 1968).

Unfortunately, 10 years later the mineral turned out to be simply xenotime, e.g. yttrium phosphate. However, in 1828, Berzelius was given a mineral by the Reverend Hans Morten Thrane Esmark. In that mineral Berzelius really discovered a new element and gave it the same name (Berzelius, 1829; Gmelin, 1955, 1986a; Weeks and Leicester, 1968). Consequently, he called the mineral from which he isolated the new element thorite. It is a silicate that contains significant amounts of uranium and should therefore be written as $(Th,U)SiO_4$. Although thorium was discovered in 1828, it virtually had no application until the invention of the incandescent gas mantle in 1885 by C. Auer von Welsbach. Thereafter the application of thorium developed into a wide array of products and processes (Gmelin, 1988b). Besides the above-mentioned incandescent gas mantles, the production of ceramics, carbon arc lamps, and strong alloys may serve as examples. To be mentioned is also its use as coating for tungsten welding rods, because it provides a hotter arc. Furthermore, when added to refractive glass, it allows for smaller and more accurate camera lenses. As minor important applications, the use of ThO_2 in producing more heat-resistant laboratory crucibles and its occasional use as a catalyst for the oxidation of ammonia to nitric acid and other industrial chemical reactions can be mentioned. Nevertheless, during the last decade the demand for thorium in non-nuclear applications has sharply decreased due to environmental concerns related to its radioactivity. The radioactivity of thorium is helpful for the dating of very old materials, e.g. seabeds or mountain ranges. Maybe the largest potential for thorium is its usage in nuclear energy. This is because ^{232}Th can be converted by thermal (slow) neutrons to the fissionable uranium isotope ^{233}U via the following reaction sequence:

$$^{232}\mathrm{Th(n,\gamma)} \rightarrow {}^{233}\mathrm{Th} \xrightarrow{\beta^-} {}^{233}\mathrm{Pa} \xrightarrow{\beta^-} {}^{233}\mathrm{U}$$

Fission of the ^{233}U can provide neutrons to start the cycle again. This cycle of reactions is known as the thorium cycle (Seaborg *et al.*, 1947; Katzin, 1952).

Conversion of ^{232}Th into ^{233}U provides the possibility to gain large amounts of slow-neutron-fissile material, several times the amount of uranium naturally present on Earth, and several hundred times the amount of the naturally occurring fissile uranium isotope ^{235}U (Seaborg and Katzin, 1951).

A number of advantages of thorium-based nuclear fuels exist in comparison with the presently utilized uranium–plutonium fuels (Rand *et al.*, 1975; Trauger, 1978). These include the inherent detectability of ^{233}U, its higher neutron yield, the fact that ^{233}U, unlike ^{239}Pu, can be mixed with ^{238}U so that it cannot directly be used in weapons manufacture, and the superior physical properties of thorium-based fuels that enhance reactor core safety and performance. The disadvantage of the use of thorium-based fuels is that thorium must be irradiated and reprocessed before the advantages of ^{232}Th can be realized. This reprocessing step, requiring more advanced technology than that needed for uranium fuels, and other factors have projected greater costs for thorium fuels. The nuclear technology has nevertheless matured with the development of high-temperature gas-cooled reactors.

3.2 NUCLEAR PROPERTIES

Thorium refined from ores free of uranium would be almost monoisotopic ^{232}Th, with less than one part in 10^{10} of ^{228}Th (radiothorium) produced by its own radioactivity decay chain (4*n* family). If the ore contains uranium, as is usually the case, practically undetectable concentrations of ^{231}Th (uranium Y) and ^{227}Th (radioactinium) are present, products of the $(4n + 3)$ decay chain that starts with ^{235}U. Also present are greater quantities of ^{230}Th (ionium), as well as lesser amounts of ^{234}Th (uranium X_1), which originate from the $(4n + 2)$ decay chain whose progenitor is ^{238}U. ^{229}Th is the first product in the $(4n + 1)$ decay series (English *et al.*, 1947; Hagemann *et al.*, 1947, 1950) derived from man-made ^{233}U formed as indicated in Section 3.1. The remaining thorium isotopes listed in Table 3.1 (see also Appendix II) are also synthetic, being formed directly by bombardment of lead or bismuth targets with energetic

Table 3.1 *Nuclear properties of thorium isotopes.*[a]

Mass number	*Half-life*	*Mode of decay*	*Main radiations* (MeV)	*Method of production*
209	3.8 ms	α	α 8.080	^{32}S + ^{182}W
210	9 ms	α	α 7.899	^{35}Cl + ^{181}Ta
211	37 ms	α	α 7.792	^{35}Cl + ^{181}Ta
212	30 ms	α	α 7.82	^{176}Hf(^{40}Ar,4n)
213	140 ms	α	α 7.691	^{206}Pb(^{16}O,9n)
214	100 ms	α	α 7.686	^{206}Pb(^{16}O,8n)
215	1.2 s	α	α 7.52 (40%) 7.39 (52%)	^{206}Pb(^{16}O,7n)
216	28 ms	α	α 7.92	^{206}Pb(^{16}O,6n)
217	0.237 ms	α	α 9.261	^{206}Pb(^{16}O,5n)
218	0.109 μs	α	α 9.665	^{206}Pb(^{16}O,4n) ^{209}Bi(^{14}N,5n)
219	1.05 μs	α	α 9.34	^{206}Pb(^{16}O,3n)
220	9.7 μs	α	α 8.79	^{208}Pb(^{16}O,4n)
221	1.68 ms	α	α 8.472 (32%) 8.146 (62%)	^{208}Pb(^{16}O,3n)
222	2.8 ms	α	α 7.98	^{208}Pb(^{16}O,2n)
223	0.60 s	α	α 7.32 (40%) 7.29 (60%)	^{208}Pb(^{18}O,3n)
224	1.05 s	α	α 7.17 (81%) 7.00 (19%) γ 0.177	^{228}U daughter ^{208}Pb(^{22}Ne,α2n)
225	8.0 min	α ≈ 90% EC ≈ 10%	α 6.478 (43%) 6.441 (15%) γ 0.321	^{229}U daughter ^{231}Pa(p,α3n)
226	30.57 min	α	α 6.335 (79%) 6.225 (19%) γ 0.1113	^{230}U daughter
227	18.68 d	α	α 6.038 (25%) 5.978 (23%) γ 0.236	nature
228	1.9116 yr	α	α 5.423 (72.7%) 5.341 (26.7%) γ 0.084	nature
229	7.340×10^{3} yr	α	α 4.901 (11%) 4.845 (56%) γ 0.194	^{233}U daughter
230	7.538×10^{4} yr	α	α 4.687 (76.3%) 4.621 (23.4%) γ 0.068	nature
231	25.52 h	β^{-}	β^{-} 0.302 γ 0.084	nature ^{230}Th(n,γ)
232	1.405×10^{10} yr $> 1 \times 10^{21}$ yr	α SF	α 4.016 (77%) 3.957 (23%)	nature

Table 3.1 (*Contd.*)

Mass number	*Half-life*	*Mode of decay*	*Main radiations* (MeV)	*Method of production*
233	22.3 min	β^-	β^- 1.23 γ 0.086	^{232}Th(n,γ)
234	24.10 d	β^-	β^- 0.198 γ 0.093	nature
235	7.1 min	β^-		^{238}U(n,α)
236	37.5 min	β^-	γ 0.111	^{238}U(γ,2p) ^{238}U(p,3p)
237	5.0 min	β^-		^{18}O + ^{238}U
238	9.4 min	β^-		^{18}O + ^{238}U

[a] Appendix II.

multi-nucleon projectiles, by decay of lightweight uranium isotopes, which are themselves synthetic and formed by nuclear bombardment, or by other miscellaneous nuclear reactions. Uranium ores that are relatively thorium-free can be processed to prepare multigram amounts of material with significant proportions of ionium, ^{230}Th. From one unselected ore residue, after removal of uranium, thorium was obtained (Hyde, 1952, 1960) that was 26.4% ionium and 73.6% ^{232}Th (Roll and Dempster, 1952).

3.3 OCCURRENCE OF THORIUM

Two volumes of the *Gmelin Handbook of Inorganic Chemistry* deal with the natural occurrence of thorium and give a comprehensive review of known thorium minerals (Gmelin, 1990a, 1991a). So only the most important features will be emphasized here. Thorium has a much wider distribution than is generally thought. In the Earth's crust it is three times as abundant as Sn, twice as abundant as As, and nearly as abundant as Pb and Mo. It occurs in the tetravalent state in nature and is frequently associated with U(IV), Zr(IV), Hf(IV), and Ce(IV) but also with the trivalent rare earth elements that are relatively close in ionic radii (Cuthbert, 1958; Frondel, 1958; Shannon, 1976).

Due to the isotypism of ThO_2 and UO_2 solid state solutions can be formed and depending on the uranium content the mixtures are named thorianite (75–100 mol% ThO_2), uranothorianite (25–75 mol% ThO_2), thorian uraninite (15–25 mol% ThO_2) and uraninite (0–15 mol% ThO_2). A second mineral with a high thorium content is thorite, $ThSiO_4$, from which the element has originally been discovered. Thorite has the tetragonal zircon-type of structure but also a monoclinic variant of $ThSiO_4$ is known, which is called huttonite (Taylor and

Table 3.2 *Thorium content of various minerals.*

Accessory mineral	*Th* (ppm)
monazite	25000 to 2×10^5
allanite	1000 to 20000
zircon	50 to 4000
titanite	100 to 600
epidote	50 to 500
apatite	20 to 150
magnetite	0.3 to 20
xenotime	Low

Ewing, 1978). In both modifications of $ThSiO_4$, substitution of PO_4^{3-} for SiO_4^{4-} is frequently observed with additional replacement of Th^{4+} by trivalent rare earth ions for charge compensation. SiO_4^{4-} ions may be also replaced by OH^- groups according to $Th(SiO_4)_{1-x}(OH)_{4x}$ leading to a new mineral, thorogummite.

However, in all the minerals given in Table 3.2, Th occurs as the minor constituent. From these minerals, monazite is of significant commercial interest because it is distributed throughout the world, and some of the deposits are very large. Monazite is a phosphate of high specific gravity that is found in the form of yellow to brown sand in nature (monazite sand). The chemical inertness of monazite makes it hard to process.

3.4 THORIUM ORE PROCESSING AND SEPARATION

Monazite can be only attacked by strong acid, which essentially transforms the phosphate ion to $H_2PO_4^-$ and H_3PO_4 and leaves the metal ions as water-soluble salts, or by strong alkali, which transforms the insoluble phosphates to insoluble metal hydroxides that can easily be dissolved in acid after removal from the supernatant solution of alkali phosphates.

Thorium in monazite follows the rare earths in either the acid or the alkali processes. Thorium can be separated from the rare earths in strong sulfuric acid solution (Fig. 3.1) by partial dilution and reduction of acidity (by ammonia addition) to about pH 1.0, at which point hydrated thorium phosphates, containing only small amounts of entrained rare earths, precipitate (Fig. 3.2). The acidity must be reduced to about pH 2.3 to ensure precipitation of the bulk of the rare earths. (Any uranium present in the process solution is separated from the rare earths at this step.) The crude precipitate of thorium phosphate is then treated with alkali to remove undesired sulfate and phosphate anions, and the thorium hydroxide residue may then be dissolved in nitric acid for subsequent

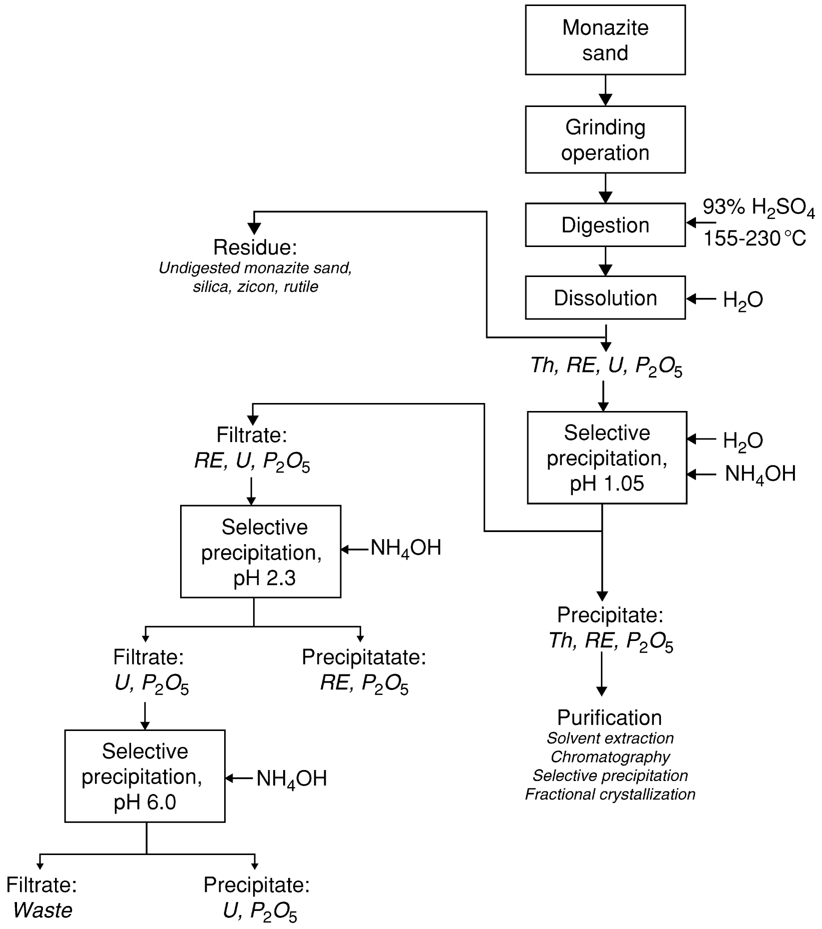

Fig. 3.1 *Simplified schematic diagram of sulfuric acid digestion of monazite sand and recovery of thorium, uranium, and the rare earths.*

purification. Purification is achieved efficiently by solvent extraction of the thorium with tri(*n*-butyl)phosphate (TBP) dissolved in kerosene, a procedure that separates thorium nitrate from rare earths and other non-extractable species. Numerous further extractants have been employed as pointed out in the *Gmelin Handbook* (Gmelin, 1985a).

The solid reaction product of the alkaline digestion of monazite (Fig. 3.3) may be dissolved in acid after separation from the supernatant solution. The solubility of the thorium-containing fraction, however, is a function of the conditions under which the alkaline digestion is performed. Too prolonged

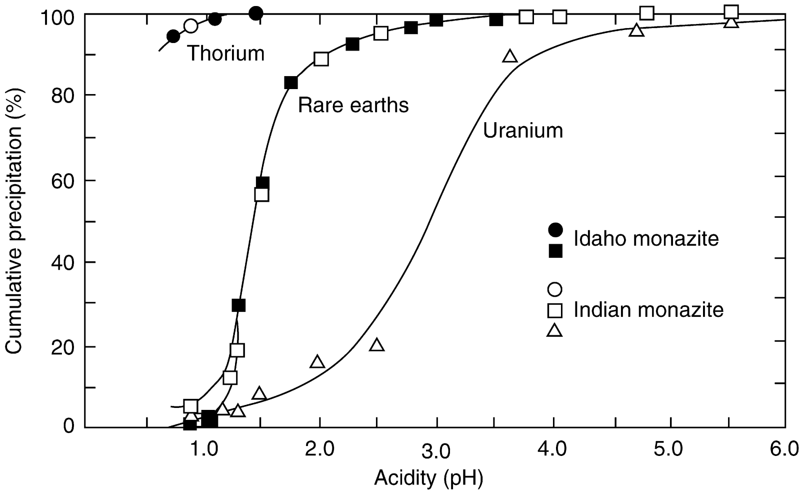

Fig. 3.2 *Effect of acidity on precipitation of thorium, rare earths, and uranium from a monazite–sulfuric acid solution of Idaho and Indian monazite sands: agitation time* 5 min; *dilution ratio,* 45 *to* 50 *parts water per one part monazite sand; digestion ratio of* 93% *sulfuric acid to digestion sands,* 1.77; *neutralizing agent,* 3.1% *ammonium hydroxide* (*Cuthbert,* 1958).

digestion at too high temperature may produce a product in which a large fraction of the thorium will not react readily with the acid used to dissolve the hydroxide cake. Presumably this is a consequence of the formation of ThO_2. Depending on whether hydrochloric, nitric, or sulfuric acid is used to dissolve the hydroxide cake, different procedures may be used in subsequent purification. Assuming the use of hydrochloric acid, which involves the fewest complications, a solution of thorium and rare earth chlorides is obtained. Differential precipitation of thorium from this solution again offers several choices: hydroxide (preferred), peroxide, or phosphate may be used to precipitate the thorium, or precipitation by carbonate may be used to separate the rare earths from thorium (and uranium), which form soluble anionic complexes. Final purification of thorium, again, is preferably made by solvent extraction (Marcus and Kertes, 1969; Gmelin, 1985a), but also chromatographic methods are applied (Kiriyama and Kuroda, 1978; Mayankutty *et al.*, 1982; Gmelin, 1990c, 1991b).

Thorium may also be recovered as a by-product from the treatment of uraninite or uranothorianite to obtain uranium. The thorium remaining in the solution of sulfuric acid after removal of the uranium is extracted into kerosene with the aid of long-chain amines. The thorium is part of a complex sulfate anion, which accompanies the protonated cationic amine into the organic phase. Neutralization of the quaternary ammonium cation precipitates the thorium from the organic phase or allows it to be back-extracted into an aqueous phase.

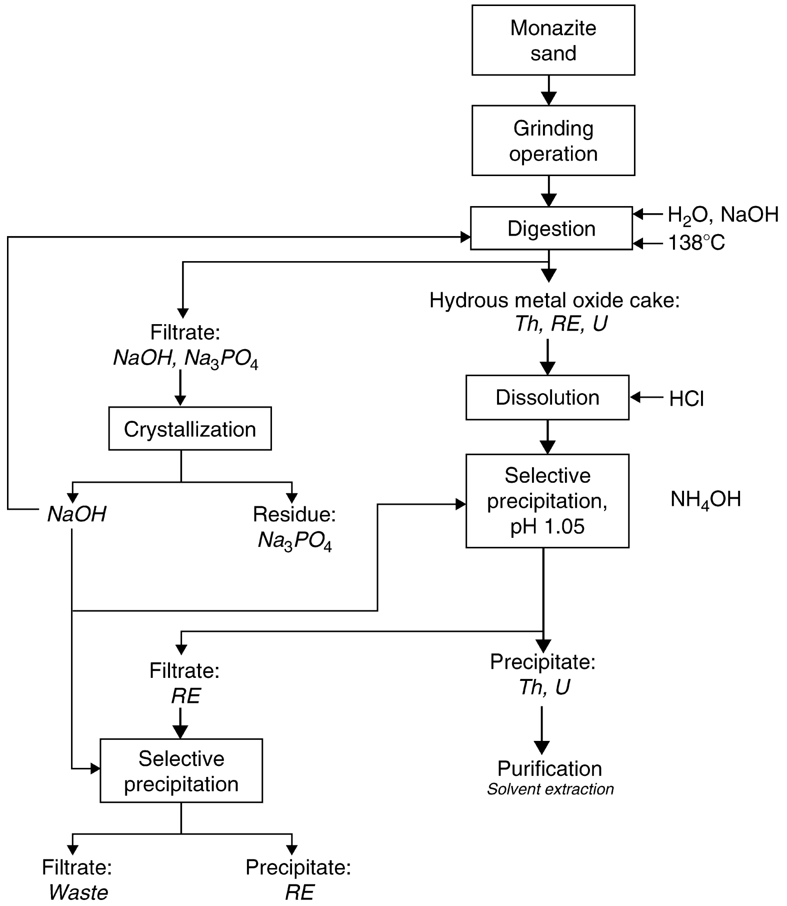

Fig. 3.3 *Simplified schematic diagram of caustic soda digestion of monazite sand and recovery of thorium, uranium, and the rare earths.*

3.5 ATOMIC SPECTROSCOPY OF THORIUM

The atomic spectroscopy of thorium provides not only information about the electronic states of thorium but also clues to the properties expected for elements of higher atomic number. The electronic structure of thorium and the related spectra will be discussed in more detail in Chapter 16 and are only summarized briefly here. Further details are also given in a volume of *Gmelin's Handbook* (Gmelin, 1989).

The four valence electrons of the neutral atom have available to them, in principle, the 5f, 6d, 7s, and 7p orbitals. The stable ground state configuration of the neutral thorium atom turns out to be $6d^27s^2$ ($^3F_2$) (Giacchetti *et al.*, 1974).

The $6d^37s$ ($^5F_1$) level is at higher energy by 5563.143 cm^{-1} and it is only at 7795.270 cm^{-1} that one encounters $5f6d7s^2$ ($^3H_4$). Still higher lie $6d7s^27p$ (10783.153 cm^{-1}), $6d^27s7p$ (14465.220 cm^{-1}), and $5f6d^27s$ (15618.98 cm^{-1}) (Zalubas, 1968).

The ionization potential of neutral Th was recently measured by resonance ionization mass spectrometry (RIMS) (Köhler *et al.*, 1997) as 6.3067(2) eV. The value obtained earlier (Sugar, 1974; Ackermann and Rauh, 1972) by extrapolation of spectroscopic data was 6.08 eV. The ground level of singly ionized Th is d^2s, followed by ds^2 (1859. 938 cm^{-1}), fs^2 (4490.256 cm^{-1}), fds (6168.351 cm^{-1}), d^3 (7001.425 cm^{-1}), and fd^2 (12485.688 cm^{-1}) (Zalubas and Corliss, 1974). It is a major step up in energy to configurations with either p contribution or to configurations that contain paired f-electrons: dsp is at 23372.582 cm^{-1}, followed by f^2s (24381.802 cm^{-1}), fsp (26488.644 cm^{-1}), d^2p (28243.812 cm^{-1}), fdp (30452.723 cm^{-1}), s^2p (31625.680 cm^{-1}), and f^2d (32620.859 cm^{-1}).

The ground state of doubly ionized thorium is 5f6d but the $6d^2$ configuration is only 63.267 cm^{-1} and the 5f7s is 2527.095 cm^{-1} higher (Racah, 1950). These are followed by 6d7s (5523.881 cm^{-1}), $7s^2$ (11961.133 cm^{-1}), $5f^2$ (15148.519 cm^{-1}), 5f7p (33562. 349 cm^{-1}), 6d7p (37280.229 cm^{-1}), and 7s7p (42259.714 cm^{-1}). These trends are continued in the triply ionized form (Klinkenberg and Lang, 1949), in which the ground level is 5f, and 6d is at 9193.245 cm^{-1}, 7s at 23130.75 cm^{-1}, and 7p at 60239.10 cm^{-1}.

Thus, with increasing ionic charge, configurations that include 5f electrons are stabilized with respect to others and the configurations containing 7p electrons become grossly destabilized. Effects in 7s and 6d systems are less but are still significant. The stabilization of the 5f electron in the triply charged ion is not sufficient however to make triply charged thorium a stable chemical species. The stable form is tetrapositive Th^{4+}, in which only the radon core of electrons is present.

Solid metallic thorium with the ground state configuration d^2s^2 has the 5f electrons in a reasonably broad energy band (Koelling and Freeman, 1971), about 5 eV above the Fermi level of 7.5–8.0 eV. This presumably is because the fds^2 level lies so low and interacts with the d^2s^2 level. Electron-binding energies for the various core levels of the atom have been determined (Nordling and Hagström, 1964), and the X-ray transitions have been determined with precision (Bearden, 1967; Bearden and Burr, 1967; Murthy and Redhead, 1974).

3.6 THORIUM METAL

A comprehensive treatment of the physical and chemical properties of thorium metal is given in the *Gmelin Handbook* (Gmelin, 1989, 1997). A brief summary on the most important properties shall be given here.

The preparation of thorium has been done by reducing halides or double halides by sodium, potassium, or calcium (Berzelius, 1829; Chydenius, 1863;

Nilson, 1876; Chauvenet, 1911). Furthermore, $ThCl_4$ can be reduced by sodium or electrolysis can be applied to a melt of thorium chloride or fluoride in sodium chloride or potassium chloride (Matignon and Delepine, 1901; Moissan and Hönigschmid, 1906; von Bolton, 1908; von Wartenberg, 1909; Chauvenet, 1911; Kaplan, 1956). Also, ThO_2 can be used as starting material and various reductants may be used (Ruff and Brintzinger, 1923; Marden and Rentschler, 1927). Care has to be taken when carbon or silicon is used because the formation of carbides and silicides may occur (Berzelius, 1829; Moissan and Étard, 1896, 1897; Hönigschmid, 1906a,b). In the so-called 'Sylvania process' calcium is used as the reducing agent (Dean, 1957; Smith *et al.*, 1975). Other reduction processes involve ThO_2 and aluminum or magnesium (Winkler, 1891; Leber, 1927). Both reactions are preferably carried out in the presence of zinc, making the reduction process thermodynamically favorable due to the formation of the intermetallic compound Th_2Zn_{17} (Spedding *et al.*, 1952). Zinc can easily be removed by vacuum distillation and leaves the metal mainly as a powder (Meyerson, 1956; Fuhrman *et al.*, 1957). Zinc is usually introduced as chloride or fluoride in the process (Briggs and Cavendish, 1971), but attempts have been made to use a zinc–magnesium alloy as reductant (Capocchi, 1971).

Unusual reductions include, for example, the reaction of $ThCl_4$ with $DyCl_2$ (Mikheev *et al.*, 1993). A method leading to high-purity thorium is the thermal decomposition of ThI_4 on a hot tungsten filament, known as the van Arkel–de Boer process (van Arkel and de Boer, 1925). This reaction is also used for the purification of thorium because the iodine formed in the reaction can be used to transport the crude metal from the low-temperature source to the hot wire. Another method to gain very pure thorium is the electrotransport that refines the high-grade thorium from the van Arkel–de Boer process further to a material containing less than 50 ppm impurities in total (Peterson and Schmidt, 1971).

Thorium appears as a bright silvery metal that has the highest melting point among the actinide elements while its density is the lowest one in the series except for Ac. Under ambient conditions, Th adopts the face-centered cubic (fcc) structure of copper that transforms to the body-centered cubic (bcc) structure of tungsten above 1360°C. Under high pressure, a third modification with a body-centered tetragonal lattice has been observed (Bridgman, 1935; Vohra, 1991, 1993; Vohra and Akella, 1991, 1992). Note that the transition conditions between the modifications depend remarkably on the amount of impurities in the metal (Smith *et al.*, 1975; Oetting *et al.*, 1976). The same is true for the properties like melting point, density (James and Straumanis, 1956), resistance, and others shown in Table 3.3, which summarizes selected properties of thorium as reported in two monographs (Smith *et al.*, 1975; Oetting *et al.*, 1976), and in the *Gmelin Handbook* (Gmelin, 1997).

Thorium metal is paramagnetic (ground state $6d^27s^2$) and shows a specific magnetic susceptibility of $0.412 \times 4\pi \times 10^{-9}$ m^3 kg^{-1} at room temperature (Greiner and Smith, 1971). The magnetic susceptibility is nearly

Table 3.3 *Some physical properties of thorium metal.*

melting point	2023 K
crystal structure	
face-centered cubic up to 1633 K	$a = 5.0842$ Å (298 K)
body-centered cubic from 1633–2023 K	$a = 4.11$ Å (1723 K)
body-centered tetragonal at high pressure	$a = 2.282$ Å, c = 4.411 Å (102 GPa)
atomic radius (from fcc structure)	1.798 Å
density	
from X-ray lattice parameters	11.724 g cm^{-3}
bomb reduced, as-cast	11.5–11.6 g cm^{-3}
arc melted, van Arkel metal	11.66 g cm^{-3}
enthalpy of sublimation (298 K)[a]	602 ± 6 kJ mol^{-1}
vapor pressure of the solid (1757–1956 K)	$\log p(\mathrm{atm}) = -28780\ (\mathrm{T/K})^{-1} + 5.991$
vapor pressure of the liquid (2020–2500 K)	$\log p(\mathrm{atm}) = -(29770 \pm 218)\ (\mathrm{T/K})^{-1} - (6.024 \pm 0.098)$
enthalpy of fusion	14 kJ mol^{-1}
elastic constants	
Young's modulus	7.2×10^{7} kPa
shear modulus	2.8×10^{7} kPa
Poisson's ratio	0.265
compressibility	17.3×10^{-8} cm^{2} N^{-1}
coefficient of thermal expansion (298–1273 K)	12.5×10^{-6} K^{-1}
electric resistivity	
electrorefined metal (298 K)	$15.7 \times 10^{-6}\ \Omega$ cm
temperature coefficient of resistance	3.6×10^{-3} K^{-1}
thermal conductivity (298 K)	0.6 W cm^{-1} K^{-1}
work function	3.49 eV
Hall coefficient (297 K)	-11.2×10^{-5} cm^{3} C^{-1}
emissivity (solid, 1600 K)	0.31

[a] Cox *et al.* (1989).

temperature-independent but it depends on the amount of impurities or dopants, respectively (Sereni *et al.*, 1987). Thorium is superconducting at low temperature (Meissner, 1929; de Haas and van Alphen, 1931). The transition temperature T_c is between 1.35 and 1.40 K, the critical magnetic field H_c has been found to be (159.22 ± 0.10) G for a high-purity sample (Decker and Finnemore, 1968). Thorium is an excellent example of a weakly coupled type-I superconductor that exhibits a complete Meissner effect and whose critical field curve $H_c(T)$ has a parabolic temperature dependence and is in good agreement with the predictions of the theory of Bardeen, Cooper, and Schrieffer (Bardeen *et al.*, 1957). The pressure dependence of H_c has been determined (Fertig *et al.*, 1972) and the specific heat discontinuity at T_c has been reported by several authors to be around 8.4 mJ mol^{-1} K^{-1} (Gordon *et al.*, 1966; Satoh and Kumagai, 1971, 1973; Luengo *et al.*, 1972a,b). Calculations on electron–phonon coupling have been also reported (Winter, 1978; Skriver and Mertig, 1985; Allen, 1987; Skriver *et al.*, 1988). The pressure dependence of the critical temperature has been followed up to 20 GPa (Palmy *et al.*, 1971; Rothwarf and Dubeck, 1973). Below 2.5 GPa T_c decreases linearly with pressure. The decrease flattens to a minimum around 7.4 GPa, increases slightly up to 10 GPa, before it smoothly decreases again. The pressure dependence of T_c has also been recently examined theoretically (Rosengren *et al.*, 1975; Mahalingham *et al.*, 1993). Furthermore, the dependence of T_c on impurities has been investigated (Guertin *et al.*, 1980).

The chemical reactivity of thorium is high. It is easily attacked by oxygen, hydrogen (Winkler, 1891; Matignon and Delepine, 1901; Sieverts and Roell, 1926; Nottorf *et al.*, 1952), nitrogen (Matignon, 1900; Kohlschütter, 1901; Matignon and Delepine, 1901), the halogens (Nilson, 1876; Moissan and Étard, 1896, 1897; von Wartenberg, 1909), and sulfur (Berzelius, 1829; Nilson, 1876; von Wartenberg, 1909) at elevated temperatures. Also carbon and phosphorus are known to form binary compounds with thorium (Strotzer *et al.*, 1938; Meisel, 1939; Wilhelm and Chiotti, 1950). Finely divided thorium is even pyrophoric (Raub and Engles, 1947). The reaction of bulky thorium with air under ambient conditions is low, but nevertheless corrosion is observed according to the investigations of several authors. Thorium reacts vigorously with hydrochloric acid. The reaction with hydrochloric acid always leaves a certain amount of a black residue (12 to 15%) behind, which was first thought to be ThO_2 that was originally present in the metal (Matignon and Delepine, 1901; Meyer, 1908; von Wartenberg, 1909). As discussed in Section 3.7.3, other studies have suggested that a lower-valent thorium oxide hydrate, $ThO{\cdot}H_2O$, is formed but it is much more likely that this compound is in fact an oxide hydride containing hydroxide and chloride ions according to ThO(X)H (X = combination of OH^- and Cl^-) (von Bolton, 1908; Karstens, 1909, Katzin, 1944, 1958; Karabash, 1958; Katzin *et al.*, 1962). This assumption is also supported by mass spectroscopic investigations that show Cl^- to be present in the residue (Ackermann and Rauh, 1973a). The reaction of thorium with other acids occurs slowly, with nitric acid even passivation is observed (Smithells, 1922; Schuler *et al.*, 1952). The latter can be overcome by adding small amounts of fluoride or fluorosilicate ions.

A great number of thorium alloys are known, including those with iron, cobalt, nickel, copper, gold, silver, platinum, molybdenum, tungsten, tantalum, zinc, bismuth, lead, mercury, sodium, beryllium, magnesium, and aluminum. Other systems, like Th/Cr and Th/U, are simply eutectics, and complete miscibility is found in the liquid and solid states with cerium. An overview of thorium alloys with main group metals can be found in the *Gmelin Handbook* (Gmelin, 1992a, 1997).

3.7 IMPORTANT COMPOUNDS

As Chapter 19 is devoted to the thermodynamic properties of the actinides and their compounds, data such as enthalpies of formation or entropies will not be given here, except when needed for the clarity of the discussion.

3.7.1 Hydrides

Reaction of thorium with hydrogen, and formation of two hydrides, ThH_2 and Th_4H_{15}, has been known for more than a century (Winkler, 1891). A substoichiometric dihydride with the fluorite-type of structure was observed by X-ray diffraction (XRD) along with the tetragonal ThH_{2-x} in a preparation of overall composition $ThH_{1.73}$ (Korst, 1962) as well as in dihydrides containing some ThO_2 (Peterson *et al.*, 1959). The well-known dihydride, which can be significantly substoichiometric, has a tetragonal structure (Nottorf *et al.*, 1952; Rundle *et al.*, 1952; Flotow and Osborne, 1978). The compound contains two metal atoms in the unit cell and is isotypic with ZrH_2 (Rundle *et al.*, 1948a; Nottorf *et al.*, 1952). The higher hydride (Matignon and Delepine, 1901; Sieverts and Roell, 1926; Rundle *et al.*, 1948a, 1952; Nottorf *et al.*, 1952; Zachariasen, 1953; Mueller *et al.*, 1977), Th_4H_{15} (= $ThH_{3.75}$), has a unique cubic structure, with the Th atom in 12-fold coordination of hydrogen atoms. The hydrogen atoms are coordinated by three and four thorium atoms as may be expressed by the formula $ThH_{9/3}H_{3/4}$ according to Niggli's formalism. The structure has also been determined for the deuterated analog Th_4D_{15} (Mueller *et al.*, 1977). Th_4H_{15} was the first metal hydride to be found to show superconductivity (Satterthwaite and Toepke, 1970; Satterthwaite and Peterson, 1972; Dietrich *et al.*, 1974). The transition temperature for superconductivity is 7.5–8 K, which is narrow, but not isothermal. Metallic conduction is exhibited at room temperature. Both the hydride and the deuteride are superconducting, with no apparent isotope effect. The existence of another crystalline form, with a 1% tetragonal distortion, that is non-superconducting has been suggested (Caton and Satterthwaite, 1977). The transition temperature is reversibly pressure-sensitive, with a slope of about 42 mK $kbar^{-1}$, up to a pressure of about 28 kbar. The heat capacities of ThH_2 and Th_4H_{15} have been measured from 5 to 350 K (Schmidt and Wolf, 1975; Miller *et al.*, 1976; Flotow and Osborne, 1978). As pointed out in more detail in Chapter 19, experimental values have been extrapolated to 800 K by Flotow *et al.* (1984).

The electronic structure of these binary thorium hydrides has been investigated by photoelectron spectroscopy (Weaver *et al.*, 1977) and nuclear magnetic resonance (NMR) spectroscopy (Schreiber, 1974; Lau *et al.*, 1977; Peretz *et al.*, 1978; Maxim *et al.*, 1979).

Powdered or sintered thorium metal reacts immediately and exothermically with hydrogen at room temperature, whereas massive metal may require heating to 300–400°C before reaction takes place. For the reaction with massive metal, an induction period that is a function of the impurity content of the metal was found (Nottorf *et al.*, 1952). In general, it is taken for granted that a consequence of the reaction of hydrogen on massive metal is a crumbling and powdering of the mass. However, it has been found (Satterwaithe and Peterson, 1972) that, at temperatures around 850°C, massive metal yields massive ThH_2, and then massive Th_4H_{15}, whereas even at 500°C the reaction fractures and cracks the massive metal. It is assumed that at high temperature, there is a sufficiently close match between the crystal structures of the metal and the hydride formed at that temperature that the incorporation of hydrogen can proceed without causing disruption of the solid.

At 900°C, in high vacuum, thorium hydride is completely decomposed to its elements. The decomposition product is grey to black, powdered, or in the form of an easily disintegrated mass. When it is desired to prepare thorium metal for some subsequent reaction, formation and decomposition of the hydride is generally used to accomplish this goal. The dissociation pressures of the two hydrides have been reported as (Nottorf *et al.*, 1952):

$$\log p(\mathrm{mmHg}) = -7700\ (T/K)^{-1} + 9.54 \quad (\mathrm{Th/ThH_2\ system})$$

$$\log p(\mathrm{mmHg}) = -4220\ (T/K)^{-1} + 9.50 \quad (\mathrm{ThH_2/Th_4H_{15}\ system})$$

Flotow *et al.* (1984) discuss in greater detail the hydrogen pressures associated with the Th–H_2 system as a function of the hydrogen composition of the solid phases and the temperatures.

Thorium hydride reacts readily with oxygen to form ThO_2. Many hydride preparations are in fact pyrophoric. ThO_2 can also be formed smoothly by reaction of thorium hydride with steam at 100°C. The reactions with oxygen and with steam are typical for the procedures commonly used for the synthesis of binary compounds of thorium. Pure thorium is necessary to prepare thorium hydride that is free of oxygen or moisture. Subsequent manipulation in the absence of air or moisture then assures the formation of pure binary compounds. Thus, in the range of 250–350°C, the hydride reacts smoothly with halogens as well as with hydrogen compounds of the halogens, sulfur, phosphorus, or nitrogen to give the corresponding binary compounds of thorium (Foster, 1945, 1950; Lipkind and Newton, 1952). Methane or carbon dioxide does not react with thorium hydride.

A number of ternary hydrides and deuterides has been reported (Table 3.4). The iron compounds $Th_2Fe_{17}D_x$ are structurally related to the respective alloy Th_2Fe_{17} and show interesting magnetic properties (Isnard *et al.*, 1993). The deuterides $ThZr_2D_x$ can be described as stuffed variant of the cubic Laves phases as it has been shown by neutron diffraction (van Houten and Bartram, 1971; Bartscher *et al.*, 1986). $ThZr_2H_{7+x}$ (and also the hexagonal $ThTi_2H_{6+x}$) combine an extremely large amount of hydrogen per unit volume with relatively low equilibrium vapor pressures of hydrogen at elevated temperatures. Both of

Table 3.4 *Crystallographic data of thorium hydrides and deuterides.*

		Lattice parameters			
Compound	*Space group*	*a* (Å)	*b* (Å)	*c* (Å)	*References*
ThH_2	I4/mmm	4.055		4.965	Flotow and Osborne, 1978[a]
Th_4H_{15}	$I\bar{4}3d$	9.11			Mueller *et al.* (1977)
Th_4D_{15}	$I\bar{4}3d$	9.11			Mueller *et al.* (1977)
$Th_2Fe_{17}D_{4.956}$	$R\bar{3}m$	8.7116		12.624	Isnard *et al.* (1993)
$Th_2Fe_{17}D_{4.668}$	$R\bar{3}m$	8.682		12.56	Isnard *et al.* (1993)
$Th_6Mn_{23}D_{16.2}$	$Fm\bar{3}m$	12.922			Hardman *et al.* (1980)
$Th_6Mn_{23}D_{16}$	$Fm\bar{3}m$	12.921			Hardman *et al.* (1980)
$Th_6Mn_{23}D_{16}$	P4/mmm	9.076		12.961	Hardman-Rhyne *et al.* (1984)
$Th_6Mn_{23}D_{28.5}$	$Fm\bar{3}m$	13.203			Hardman-Rhyne *et al.* (1984)
$ThZr_2D_6$	$Fd\bar{3}m$	9.151			Bartscher *et al.* (1986)
$ThZr_2D_{3.6}$	$Fd\bar{3}m$	9.042			Bartscher *et al.* (1986)
$ThZr_2D_{4.8}$	$Fd\bar{3}m$	9.112			Bartscher *et al.* (1986)
$ThZr_2D_{6.3}$	$Fd\bar{3}m$	9.154			Bartscher *et al.* (1986)
$ThNi_2D_2$	P6/mmm	3.87		3.951	Andresen *et al.* (1984)
$ThNi_2D_{2.6}$	P6/mmm	4.405		4.360	Andresen *et al.* (1984)
Th_2AlD_2	I4/mcm	7.702		6.23	Bergsma *et al.* (1961)
Th_2AlD_3	I4/mcm	7.676		6.383	Bergsma *et al.* (1961)
Th_2AlD_4	I4/mcm	7.629		6.517	Bergsma *et al.* (1961)
$Th_2AlD_{3.71}$	I4/mcm	7.6260		6.5150	Sorby *et al.* (2000)
$Th_2AlD_{2.75}$	$P\bar{4}2m$	7.6796		19.073	Sorby *et al.* (2000)
$Th_2AlD_{2.29}$	I4/mcm	7.7014		6.2816	Sorby *et al.* (2000)

[a] These authors use the F4/mmm setting with a = 5.734 Å. The F-centered cell has the diagonal of the ab-plane as axis, i.e. square root of twice the a axis of the I-centered cell.

these ternary hydrides are apparently stable in air. Unlike thorium hydride itself, the Th–Zr hydride is not superconducting (Satterthwaite and Peterson, 1972). Also the nickel phases $ThNi_2D_x$ are derived from the alloy $ThNi_2$ and show the deuterium atom in tetrahdral interstices of the metal atom network (Andresen *et al.*, 1984). The thorium manganese compounds $Th_6Mn_{23}D_x$ have been investigated frequently with respect to the D atom distribution in the lattice (Hardman *et al.*, 1980, 1982; Jacob, 1981; Carter, 1982; Hardman-Rhyne *et al.*, 1984). Furthermore, the ternary aluminum hydrides Th_2AlD_x have been reported in great detail (Bergsma *et al.*, 1961; Sorby *et al.*, 2000). Other hydrides, for example with cobalt and palladium are known, however not very well characterized in the most cases (Buschow *et al.*, 1975; Oesterreicher *et al.*, 1976).

3.7.2 Borides, carbides, and silicides

Three binary thorium borides are well characterized (du Jassonneix, 1905; Allard, 1932; Stackelberg and Neumann, 1932; Lafferty, 1951; Post *et al.*, 1956; Konrad *et al.*, 1996). ThB_6 contains a network of linked $[B_6]$ octahedra;

in ThB_4, $[B_2]$ dumbbells accompany the octahedra (Brewer *et al.*, 1951; Zalkin and Templeton, 1951; Blum and Bertaut, 1954). Investigations of the thorium–boron system at low boron concentrations showed that non-stoichiometric varieties of ThB_4 can be prepared (Rand *et al.*, 1975; Chiotti *et al.*, 1981). On the other hand, certain impurities (for example ThO_2) have been suggested to be accountable for the non-stoichiometry (Brewer *et al.*, 1951). The third boride, ThB_{12}, is isotypic with UB_{12} (Cannon and Hall, 1977; Cannon and Farnsworth, 1983). Furthermore, the borides ThB_{66} and ThB_{76} have been reported (Naslain *et al.*, 1971; Schwetz *et al.*, 1972), but it was not clear whether they are truly thorium–boron phases or if they are a metal-stabilized form of a boron allotrope.

Various ternary thorium borides have been prepared, especially those containing transition metals. The orthorhombic borides Th_2MB_{10} were obtained from the elements by arc melting and show a structure that is closely related to that of ThB_6 (Konrad and Jeitschko, 1995). Borides of the composition $ThMB_4$ have been recognized for $M = V$, Mo, W, Re, Cr, and Mo (Pitman and Das, 1960; Rogl and Nowotny, 1974; Konrad *et al.*, 1996). The crystal structures have been determined for $M = Cr$ and Mo, in which the boron atoms form infinite layers with the metal atoms in between similar to MgB_2. The chromium compound $ThCr_2B_6$ is isotypic with $CeCr_2B_6$ and shows metallic conduction and Pauli paramagnetism (Konrad and Jeitschko, 1995). The hexagonal borides $ThIr_3B_2$ and $ThRu_3B_2$ have been characterized magnetically and structurally. They contain discrete boride ions in prismatic coordination of the platin metal atoms (Hiebl *et al.*, 1980; Ku *et al.*, 1980). The magnetic properties have also been also determined for the rather complicated borides $R_{2-x}Th_xFe_{14}B$ ($R = Y$, Dy, Er) (Pedziwiatr *et al.*, 1986).

Further boron-containing thorium compounds are the borohydrides $Th(BH_4)_4$, $LiTh(BH_4)_5$, and $Li_2Th(BH_4)_6$ (Ehemann and Nöth, 1971). They contain the tetrahedral BH_4^- ion.

Carbides of thorium have been discussed in great detail in the *Gmelin Handbook* (Gmelin, 1992b). Thus only the most important items shall be given here briefly. Binary thorium carbides were obtained by the reaction of ThO_2 with carbon or the direct fusion of the elements (Troost, 1883; Moissan and Étard, 1896, 1897; Wilhelm and Chiotti, 1949, 1950). Three compositions, ThC_2, Th_2C_3, and ThC, are known (Fig. 3.4). ThC_2 occurs in three different modifications. At room temperature, a monoclinic unit cell is found (Jones *et al.*, 1987). Between 1430 and 1480°C, a rotation of the C_2 dumbbells starts, leading to a tetragonal structure that changes to cubic above 1480°C with complete rotational disorder of the C_2 units (Hunt and Rundle, 1951; Gantzel and Baldwin, 1964; Hill and Cavin, 1964; Langer *et al.*, 1964; Bowman *et al.*, 1968). The monocarbide, ThC, has the cubic NaCl structure. Both ThC_2 and ThC are refractory solids with high melting points (2655 ± 25 and 2625 ± 25, respectively). For ThC, the specific heat has been measured from 1.5 to 300 K (Danan, 1975). The third binary thorium carbide, Th_2C_3, has been observed at pressures

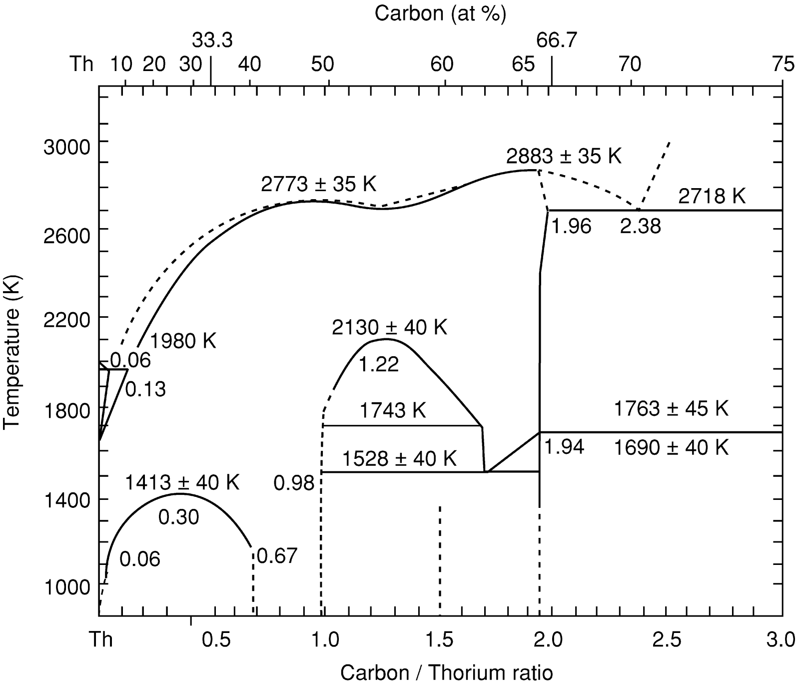

Fig. 3.4 *Phase diagram of the thorium–carbon system* (*Chiotti* et al., 1981).

above 33 kbar in the region of 1200°C (Krupka, 1970). It has the cubic structure of Pu_2C_3 and is a superconductor with T_c decreasing with increasing pressure (Giorgi *et al.*, 1976). Besides these three carbides, several non-stoichiometric phases have been found that can be seen as solid state solutions between α-Th and γ-ThC_2 (Chiotti *et al.*, 1967; Storms, 1967) that have cubic symmetry.

Upon heating ThC_2 to high temperature on a graphite filament, ThC_4^+ ions were observed (Asano *et al.*, 1974). ThC_2 burns in the air to form ThO_2 and reacts with sulfur or selenium vapor (Moissan and Étard, 1896, 1897). Halogens react with the carbide to give anhydrous halides. According to an early study (Lebeau and Damiens, 1913) the hydrolysis of the carbide produces a mixture of almost 60% hydrogen, 3.16% methane, 10.7% ethane, ~15% acetylene, ~3% ethylene, ~8% propylene and propane, and higher products. Other studies on the hydrolysis of ThC and ThC_2 report the formation of methane in the ThC case and the formation of ethane and hydrogen in the ThC_2 case (Kemper and Krikorian, 1962). It seems evident that not only the composition and purity of the carbide but also the actual hydrolysis conditions may be important factors.

A number of ternary carbides have been reported (Table 3.5). The boride carbides have the compositions ThBC, $Th_3B_2C_3$, and ThB_2C (Rogl, 1978, 1979;

Rogl and Fischer, 1989). ThBC and $Th_3B_2C_3$ contain CBBC units; in $Th_3B_2C_3$ additional C atoms are found (Fig. 3.5). For ThB_2C extended layers of connected B and C atoms are found with the thorium atoms located between the layers. In the nitride carbide ThCN (Benz, 1969; Benz and Troxel, 1971), dumbbell-shaped C_2 units and nitride ions are present (Benz *et al.*, 1972).

Several ternary carbide systems have been investigated, Th–M–C, with M being a transition metal element or a lanthanide, and a huge number of compounds are believed to exist (Gmelin, 1992b). However, only a few of them are structurally characterized. Specifically, for ruthenium and nickel, several structure determinations have been performed. In the former case, the compounds $Th_{11}Ru_{12}C_{18}$, $Th_2Ru_6C_5$, and $ThRu_3C$ were investigated (Aksel'rud *et al.*, 1990a,b; Wachtmann *et al.*, 1995). The carbon-rich species contain both C_2 units and single C atoms while $ThRu_3C$ can be regarded as a cubic closest packing of metal atoms with the carbon atoms in octahedral interstices. Two series of thorium iron carbides have been structutrally and magnetically investigated recently. They have the composition $ThFe_{11}C_{1+x}$ $(0 < x < 1)$ and $Th_2Fe_{17}C_x$ $(0 < x < 1)$, respectively (Isnard *et al.*, 1992a,b; Singh Mudher *et al.*, 1995). In the nickel system, three compounds were found: Th_2NiC_2, $Th_3Ni_5C_5$, and $Th_4Ni_3C_6$. According to the structure determination the latter two should be more correctly described as $Th_3Ni_{4.96}C_{4.79}$ and $Th_4Ni_{2.88}C_6$, respectively (Moss and Jeitschko, 1991a,b). Two carbides have been prepared in the system Th–Al–C, namely $Th_2Al_2C_3$ and $ThAl_4C_4$ (Gesing and Jeitschko, 1996). They are both methanides in the sense that they contain isolated carbon atoms. One lanthanide compound that has been structurally characterized is $CeThC_2$ (Stecher *et al.*, 1964).

According to the phase diagram Th–Si (Fig. 3.6) four binary thorium silicides exist (Stecher *et al.*, 1963; Chiotti *et al.*, 1981; Gmelin, 1993b): Th_3Si_5, Th_3Si_2, ThSi, and $ThSi_2$. The latter three are structurally known (Brauer and Mitius, 1942; Jacobson *et al.*, 1956; Brown, 1961). $ThSi_2$ is dimorphic and both the hexagonal (AlB_2 type) and the tetragonal modifications show the thorium atoms in 12-fold coordination of silicon atoms. In ThSi the silicon atoms are linked to zigzag chains (Si—Si distance: 2.49 Å) while Si_2 dumbbells (2.33 Å) are found in Th_3Si_2. Further silicides have been reported, for example Th_6Si_{11} (Brown and Norreys, 1961), but have not be confirmed up to now.

Various ternary silicides of thorium are known (Table 3.5). The largest group among them contains compounds of the composition ThM_2Si_2 with M being a transition metal element. For M = Cr, Mn, Fe, Co, Ni, Cu, and Tc, structure determinations have been performed (Ban and Sikirica, 1965; Leciejewicz *et al.*, 1988; Wastin *et al.*, 1993) and for part of the silicides, magnetic properties are known (Omejec and Ban, 1971; Ban *et al.*, 1975). The compounds are isotypic with each other and have tetragonal symmetry. The stucture consists of layers of edge connected $[ThSi_8]$ cubes that are separated by the transition metal atoms. Other silicides have the composition Th_2MSi_3 (M = M, Fe, Co, Ni, Cu, Ru, Rh, Pd, Os, Ir, Pt, Au) and are derived from the two modifications of $ThSi_2$ by substitution of transition metal atoms for silicon atoms (Ban *et al.*, 1975; Wang *et al.*, 1985; Albering *et al.*, 1994). In the same way, the silicides ThMSi (M = Au, Pd, Ni) are derived from the hexagonal form of $ThSi_2$ (Ban *et al.*, 1975; Wang *et al.*, 1985). Two new silicides of thorium have been reported recently with $ThCo_9Si_2$ and $ThRe_4Si_2$ (Albering and Jeitschko, 1995; Moze *et al.*, 1996).

In a few cases, quaternary compounds have also been investigated. For example the silicide–carbides $Th_2Re_{2.086}Si_xC$ ($x = 1.914$ and 1.904), $ThOs_{2.04}Si_{0.96}C$, and $ThOs_{2.284}Si_{0.716}C$ have been reported (Hüfken *et al.*, 1998, 1999), and the two lanthanide nitride carbides CeThNC and DyThNC are known (Ettmayer *et al.*, 1980).

3.7.3 Oxides, hydroxides, and peroxides

Thorium oxides have received considerable attention in the recent decades. They have been reviewed in the *Gmelin Handbook* (Gmelin, 1976, 1978), but the diverse chemistry of the simple binary oxide of thorium has yielded 435 patents since these days, out of which 53 are related to the catalytic behavior of ThO_2. An recent search of the Chemical Abstract Services database revealed over 540 journal articles and some 50 reports on catalysis. While ThO_2 has been studied as a complement to CeO_2 and HfO_2 in its chemistry, ThO has been postulated as a defect form of the fluorite or a ZnS structure (Katzin, 1958; Ackermann and Rauh, 1973b). Table 3.6 lists the binary oxides and the other chalcogenides (cf. Section 3.7.5) with their lattice constants. Thorium monoxide has been reported to form on the surface of thorium metal exposed to air (Rundle *et al.*, 1948b) but its preparation and isolation as a bulk black suspension was first reported in 1958 by Katzin as a result of the action of 2 to 12 N HCl solutions on thorium metal. The black powder reported appeared later to be a form of low-valent thorium oxide stabilized by HCl and H_2O. XRD studies revealed a cubic phase with a lattice constant of 5.302 Å and a pattern indicative of an fcc lattice – either a defect fluorite or ZnS-type (Ackermann and Rauh, 1973b). However, the 'monoxide' solid state compound appears to be a Th(IV) phase with the formula Th(H)(O)X, where X is a combination of OH^- and Cl^- (Katzin *et al.*, 1962). This seemed to explain the reaction of the black solid upon heating to yield HCl, H_2, H_2O, and ThO_2 under various conditions (Ackermann and Rauh, 1973b). This phase was also reported to be unstable to disproportionation under dynamic vacuum. Until now, however, there is no report on bulk-phase ThO available that is without question. On the other hand, ThO was reported in the vapor phase above a mixture of Th and ThO_2 at high temperatures (Darnell and McCollum, 1961; Ackermann and Rauh, 1973b; Hildenbrand and Murad, 1974a,b; Neubert and Zmbov, 1974).

Thorium dioxide (thoria) is somewhat hygroscopic. Reaction with nitric or hydrochloric acids followed by evaporation yields hydrates that have in the past been thought to resemble the so-called 'metaoxides' of tin and zirconium. The material may be dispersed as a positively charged colloid following evaporation

Table 3.5 *Crystallographic data of thorium borides, carbides, and silicides.*

		Lattice parameters				
Compound	*Space group*	*a* (Å)	*b* (Å)	*c* (Å)	*Angles* (°)	*References*
ThB_4	P4/mbm	7.256		4.113		Zalkin and Templeton (1950, 1953); Konrad *et al.* (1996)
ThB_6	Pm$\bar{3}$m	4.113				Konrad *et al.* (1996), Blum and Bertaut (1954)
ThBC	P$4_1$22	3.762		25.246		Rogl (1978)
ThB_2C	R$\bar{3}$m	6.676		11.376		Rogl and Fischer (1989)
$Th_3B_2C_3$	P2/m	3.703	3.773	9.146	$\beta = 100.06$	Rogl (1979)
$ThB_{66.8}O_{0.36}$	Fm$\bar{3}$c	23.53				Naslain *et al.* (1971)
$Na_{0.77}Th_{0.23}B_6$	Pm$\bar{3}$m	4.151				Blum and Bertaut (1954)
Th_2FeB_{10}	Pbam	5.627		4.183		Konrad and Jeitschko (1995)
Th_2CoB_{10}	Pbam	5.624		4.185		Konrad and Jeitschko (1995)
Th_2NiB_{10}	Pbam	5.646	11.204	4.173		Konrad and Jeitschko (1995)
$ThCrB_4$	Pbam	6.057	11.712	3.640		Konrad *et al.* (1996)
$ThCr_2B_6$	Immm	3.158	6.591	8.364		Konrad *et al.* (1996)
$ThMoB_4$	Cmmm	7.481	9.658	3.771		Rogl and Nowotny (1974)
$ThIr_3B_2$	P6/mmm	5.449		3.230		Ku *et al.* (1980)
$ThRu_3B_2$	P6/mmm	5.528		3.070		Hiebl *et al.* (1980)
ThC	Fm$\bar{3}$m	5.346				Kemper and Krikorian (1962)
ThC_2	C2/c	6.53	4.24	6.56	$\beta = 104.0$	Hunt and Rundle (1951)
ThC_2	C2/c	6.684	4.220	6.735	$\beta = 103.91$	Jones *et al.* (1987)
$ThC_{1.97}$	C2/c	6.692	4.223	6.744	$\beta = 103.1$	Bowman *et al.* (1968)
$ThC_{1.97}$	I4/mmm	4.221		5.394		Bowman *et al.* (1968)
$ThC_{1.97}$	Fm$\bar{3}$m	5.806				Bowman *et al.* (1968)
ThCN	C2/m	7.0249	3.9461	7.2763	$\beta = 95.67$	Benz *et al.* (1972)
$Th_2Al_2C_3$	Pnnm	5.406	11.556	3.5201		Gesing and Jeitschko (1996)
$ThAl_4C_4$	I4/m	8.231		3.3273		Gesing and Jeitschko (1996)
$ThFe_{11}C_{1+x}$	I4_1/amd	~10.20		~6.61		Isnard *et al.* (1992a)

Table 3.5 (*Contd.*)

		Lattice parameters				
Compound	*Space group*	*a* (Å)	*b* (Å)	*c* (Å)	*Angles* (°)	*References*
$Th_2Fe_{17}C_x$	R$\bar{3}$m	~8.6		~12.5		Isnard *et al.* (1992b)
Th_2NiC_2	I4/mmm	3.758		12.356		Moss and Jeitschko (1991b, 1989b)
$Th_3Ni_{4.96}C_{4.79}$	Cmca	13.961	7.174	7.07		Moss and Jeitschko (1991b, 1989b)
$Th_4Ni_{2.88}C_6$	C2/m	15.369	3.751	7.628	$\beta = 113.29$	Moss and Jeitschko (1991a, 1989a)
$ThRu_3C$	Pm$\bar{3}$m	4.227				Wachtmann *et al.* (1995)
$Th_2Ru_6C_5$	P4/mbm	9.113		4.186		Aksel'rud *et al.* (1990a)
$Th_{11}Ru_{12}C_{18}$	I4$\bar{3}$m	10.764				Aksel'rud *et al.* (1990b)
$Th_2Ru_6C_5$	P4/mbm	9.096		4.177		Wachtmann *et al.* (1995)
$Th_{11}Ru_{12}C_{18}$	I4$\bar{3}$m	10.754				Wachtmann *et al.* (1995)
$ThCeC_2$	Fm$\bar{3}$m	5.280				Stecher *et al.* (1964)
ThSi	Pbnm	5.89	7.88	4.15		Jacobson *et al.* (1956)
$ThSi_2$	P6/mmm	4.136		4.126		Brown (1961)
$ThSi_2$	$I4_1$/amd	4.126		14.346		Brauer and Mitius (1942)
$ThSi_2$	P6/mmm	3.985		4.220		Jacobson *et al.* (1956)
Th_3Si_2	P4/mbm	7.835		4.154		Jacobson *et al.* (1956)

$ThCr_2Si_2$	I4/mmm	4.043		10.577	Ban and Sikirica (1965)
$ThCr_2Si_2$	I4/mmm	4.0414		10.588	Leciejewicz *et al*. (1988)
$ThMn_2Si_2$	I4/mmm	4.021		10.493	Ban and Sikirica (1965)
$ThMn_2Si_2$	I4/mmm	4.0225		10.475	Leciejewicz *et al*. (1988)
$ThMn_2Si_2$	I4/mmm	4.019		10.483	Ban *et al*. (1975)
$ThFe_2Si_2$	I4/mmm	4.038		9.820	Ban and Sikirica (1965)
$ThFe_2Si_2$	I4/mmm	4.038		9.812	Leciejewicz *et al*. (1988)
$Th(Co_{0.5}Si_{1.5})$	P6/mmm	4.043		4.189	Wang *et al*. (1985)
$ThCo_9Si_2$	$I4_1/amd$	9.7914		6.3138	Moze *et al*. (1996)
$ThCo_2Si_2$	I4/mmm	4.015		9.760	Ban and Sikirica (1965)
$ThCo_2Si_2$	I4/mmm	4.0128		9.754	Leciejewicz *et al*. (1988)
$ThNi_2Si_2$	I4/mmm	4.076		9.551	Ban and Sikirica (1965)
$ThNi_2Si_2$	I4/mmm	4.0789		9.555	Leciejewicz *et al*. (1988)
$ThCu_2Si_2$	I4/mmm	4.104		9.864	Ban and Sikirica (1965)
$ThCu_2Si_2$	I4/mmm	4.1031		9.866	Leciejewicz *et al*. (1988)
$ThTc_2Si_2$	I4/mmm	4.184		10.063	Wastin *et al*. (1993)
$ThRe_4Si_2$	Pnnm	7.294	15.500	4.124	Albering and Jeitschko (1995)
ThAuSi	$P\bar{6}m2$	4.260		4.164	Albering *et al*. (1994)

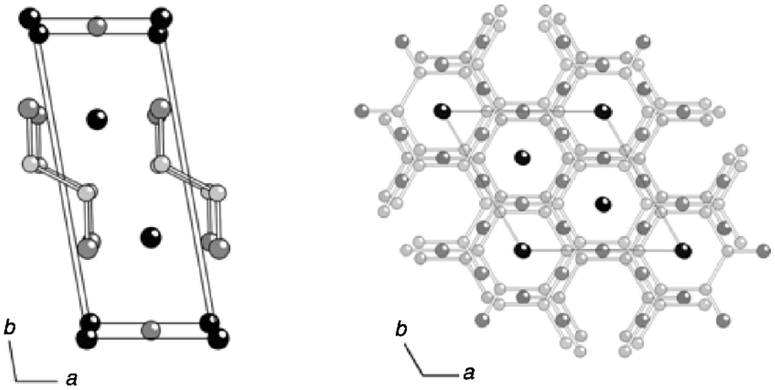

Fig. 3.5 *Crystal structures of $Th_3B_2C_3$ (left) and ThB_2C (right).*

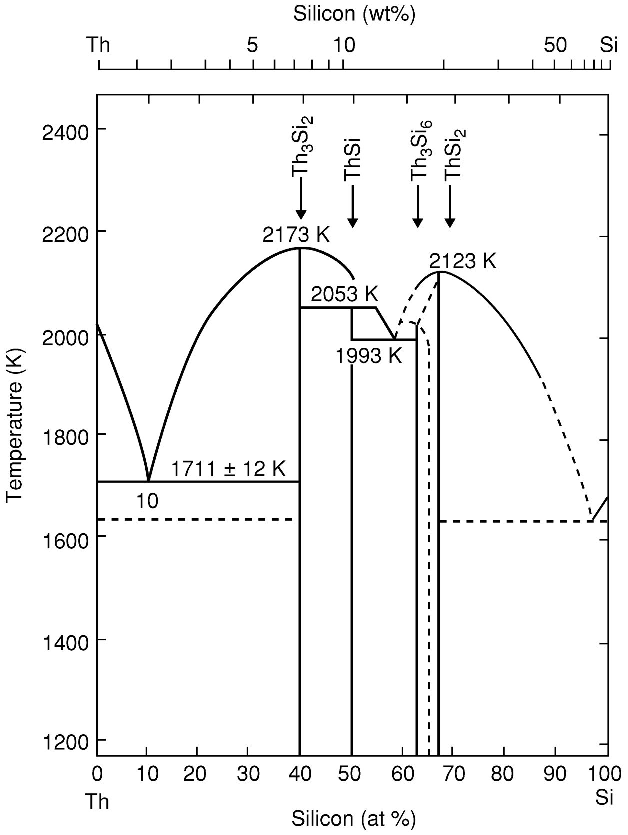

Fig. 3.6 *Phase diagram of the thorium–silicon system* (*Chiotti* et al., 1981).

Table 3.6 *Crystallographic data of thorium chalcogenides.*

		Lattice parameters				
Compound	*Space group*	*a* (Å)	*b* (Å)	*c* (Å)	*Angles* (°)	*References*
ThO	cubic	5.302				Katzin (1958); Ackermann and Rauh (1973b)
ThO_2	Fm$\bar{3}$m	5.592				Gmelin (1976, 1978)
ThOS	P4/nmm	3.963		6.747		Zachariasen (1949c)
ThS	Fm$\bar{3}$m	5.682				Zachariasen (1949c)
Th_2S_3	Pbnm	10.990	10.850	3.960		Zachariasen (1949c)
Th_7S_{12}	$P6_3/m$	11.063		3.991		Zachariasen (1949d)
ThS_2	Pmnb	4.267	7.264	8.617		Zachariasen (1949c)
Th_2S_5	Pcnb	7.623	7.677	10.141		Nöel and Potel (1982)
ThOSe	P4/nmm	4.038		7.019		D'Eye *et al.* (1952)
ThSe	Fm$\bar{3}$m	5.875				D'Eye *et al.* (1952)
Th_2Se_3	Pbnm	11.36	11.59	4.28		D'Eye *et al.* (1952)
Th_7Se_{12}	$P6_3/m$	11.570		4.230		D'Eye (1953)
$ThSe_2$	Pmnb	4.420	7.611	9.065		D'Eye (1953)
Th_2Se_5	Pcnb	7.922	7.937	10.715		Kohlmann and Beck (1999)
$ThSe_3$	$P2_1/m$	5.72	4.21	9.64	$\beta = 97.05$	Nöel (1980)
ThOTe	P4/nmm	4.120		9.563		D'Eye and Sellman (1954)
ThTe	Pm$\bar{3}$m	3.827				D'Eye and Sellman (1954)
Th_2Te_3	hexagonal	12.49		4.35		Graham and McTaggart (1960)
Th_7Te_{12}	P$\bar{6}$	12.300		4.566		Tougait *et al.* (1998)
$ThTe_2$	hexag. (?)	8.49		9.01		Graham and McTaggart (1960)
$ThTe_3$	monoclinic	6.14	10.44	4.31	$\beta = 98.4$	Graham and McTaggart (1960)

and the colloid can be 'salted out' by addition of electrolytes. The ignited oxide or the oxide sintered into larger particles is one of the most refractory substances known, showing limited reactivity with hot sulfuric acid or fusion with potassium hydrogen sulfate. Aqueous nitric acid with a few percentage of HF or sodium fluorosilicate provides a reasonable solution of the oxide (Smithells, 1922). Hot aqueous HF or gaseous HF at 250–750°C converts thoria to ThF_4 (Newton *et al.*, 1952b).

Amorphous thoria is said to crystallize from a suitable flux, for example sodium carbonate, potassium orthophosphate, or borax (Nordenskjöld and Chydenius, 1860; Nordenskjöld, 1861; Chydenius, 1863; Rammelsberg, 1873; Troost and Ouvrard, 1889; Duboin, 1909a,b). However, the use of borax as a flux is questionable, because ThO_2 is known to form ThB_2O_5 in the reaction with B_2O_3 (Baskin *et al.*, 1961).

Thorium dioxide has been studied as an active catalyst because of its reactivity with many gases, in addition to water. Dehydration of alcohols (Frampton, 1979; Siddham and Narayanan, 1979), dehydrogenation of alcohols (Thomke, 1977), and the hydration (Frampton, 1979) and hydrogenation of alkenes (Tanaka *et al.*, 1978) have been demonstrated. Other examples include copper–thorium oxide catalysts studied for the selective hydrogenation of isoprene (Bechara *et al.*, 1990a,b), decomposition of isopropanol (Aboukais *et al.*, 1993), and the oxidative coupling of methane (Zhang *et al.*, 2001). Indeed, the development of mixed-metal rare earth/thorium/copper oxides based on a perovskite parent structure have been shown to decompose NO_x (Gao and Au, 2000), to catalyze the reduction of NO by CO (Wu *et al.*, 2000), and to dehydroxylate phenol (Liu *et al.*, 1997). Lastly, thorium oxide, when heated, produces an intense blue light and mixed with ceria at 1%, produces a more intense white light. It is this property that was the basis for the thoriated gas mantle industry (Mason, 1964; Manske, 1965).

Thorium hydroxide is formed as a gelatinous precipitate when alkali or ammonium hydroxide is added to a solution of a thorium salt. This precipitate dissolves in dilute acids and, when fresh, in ammonium oxalate, alkali carbonates, sodium citrate, or sodium potassium tartrate solutions (Chydenius, 1863; Glaser, 1897; Jannasch and Schilling, 1905; Sollman and Brown, 1907). The hydroxide is also precipitated by the action of sodium nitrate (Baskerville, 1901) or potassium azide (Dennis and Kortright, 1894; Glaser, 1897; Wyrouboff and Verneuil, 1898a). Electrolysis of thorium nitrates is also said to yield a precipitate of hydroxide at the anode (Angelucci, 1907). Material dried at 100°C has been reported to correspond closely in composition to $Th(OH)_4$ (Clève, 1874), but other reports claim to find higher hydrates even at higher temperatures (Wyrouboff and Verneuil, 1905). Two forms of $ThO_2{\cdot}2H_2O$ ($=Th(OH)_4$), from precipitation in basic aqueous solution, have been distinguished, one of which is amorphous (Guymont, 1977). Further studies indicate that $Th(OH)_4$ is stable in the temperature range 260–450°C and is converted to the oxide at temperatures of 470°C and higher (Dupuis and Duval, 1949). Thermal analysis has shown that the decomposition of the hydroxide is a continuous process (Tiwari and Sinha, 1980). Thorium hydroxide absorbs atmospheric carbon dioxide very readily (Chydenius, 1863; Dennis and Kortright, 1894; Chauvenet, 1911). When boiled with thorium nitrate, $Th(OH)_4$ forms a positively charged colloid (Müller, 1906). The colloid formation is also observed if thorium hydroxide is treated with hydrous aluminum chloride, ferric chloride, uranyl nitrate, or hydrochloric acid (Szilard, 1907). The solubility product of $Th(OH)_4$ is discussed in Section 3.8.5.

Thorium peroxide had been reportedly known since 1885 as the product of the reaction between hydrogen peroxide and salts of thorium in solution (de Boisbaudran, 1885). The precipitate that forms can be a dense solid or a gelatinous paste. The solid has initially been described in the literature as hydrated thorium peroxide, 'Th_2O_7' (de Boisbaudran, 1885; Pissarsjewski, 1900; Schwarz and Giese, 1928). The existence of peroxide species was confirmed but it was pointed out that the respective anions of the initial thorium salt are part of the solid (Clève, 1885; Wyrouboff and Verneuil, 1898a; Hamaker and Koch, 1952a,b; Johnson *et al.*, 1965; Hasty and Boggs, 1971; Raman and Jere, 1973a,b; Jere and Santhamma, 1977). XRD studies revealed two phases if the precipitation occurs from thorium sulfate solution: $Th(OO)SO_4 \cdot 3H_2O$ precipitated from solutions of high H_2SO_4 concentration and a second phase is obtained from more weakly acidic solutions with a variable sulfate content and 3.0–3.8 peroxide oxygen atoms per thorium atom (Hamaker and Koch, 1952a). A Raman analysis of $Th(OO)SO_4 \cdot 3H_2O$ has been performed (Raman and Jere, 1973a,b) and suggests a formulation of the compound as 'tetraaquo-μ-peroxy-disulfatodithorium(IV)', with two bridging sulfato groups. Raman investigations have been also carried out for the peroxide obtained from a nitrate solution (Raman and Jere, 1973b). According to these measurements thorium peroxide nitrate showed a 'free' (D_{3h}) nitrate anion along with a bridging peroxide molecule between thorium atoms. However, also a nitrate-free peroxide has been obtained from the reaction of a refluxing aqueous solution of $Th(NO_3)_4 \cdot 4H_2O$, urea, and 30% hydrogen peroxide (Gantz and Lambert, 1957). The precipitate, described as a granular light blue-green powder, decomposes at 120°C to yield ThO_2 and water. Chemical analysis revealed a formula of $Th(OH)_3OOH$, equivalent to tin and zirconium analogs. The dried peroxide is insoluble in neutral solutions (aqueous) but is soluble in concentrated mineral acids. Thorium peroxide has also been reported by the action of hydrogen peroxide or sodium hypochlorite on thorium hydroxide, or by anodic oxidation of an alkaline thorium hydroxide suspension containing sodium chloride (Pissarsjewsky, 1902).

Like the double salts of the halides, thorium dioxide will form a similar 'double salt' of oxide with BaO and alkali metal oxides (K_2O, for example) in phases such as $BaThO_3$ and K_2ThO_3 (Brunn and Hoppe, 1977); however, neither the Sr form nor the Li form of these structures have been reported (Hoffmann, 1935; Naray-Szabo, 1951; Scholder *et al.*, 1968; Fava *et al.*, 1971; Nakamura, 1974). No reaction was seen with BeO (Ohta and Sata, 1974) and, although there is solid solution formation with the rare earth oxides, no reaction to form the 'double salt' phase Ln_2ThO_5 has been observed (Diness and Roy, 1969; Sibieude, 1970). Because of the reactivity of ThO_2–CuO mixtures, reactions that have included other transition metal oxides have yielded a number of unique phases including tetragonal perovskite phases such as $La_{1-x}Th_xCoO_3$ (Tabata and Kido, 1987), $La_{1-1.333x}Th_xNiO_3$ (Yu *et al.*, 1992), $Na_{.6667}Th_{.3333}TiO_3$ (Zhu and Hor, 1995), and the Ruddlesden–Popper manganites $Ca_{3-x}Th_xMn_2O_7$ (Lobanov *et al.*, 2003).

3.7.4 Halides

(a) Binary halides

The halides of thorium had been treated comprehensively in 1968 by Brown (1968), and the fluorides in particular have been reviewed by Penneman *et al.* (1973) and Taylor (1976). In addition, a later volume of the *Gmelin Handbook* has discussed thorium halides (Gmelin, 1993a).

The tetrahalides of thorium are known for the whole halogen series (Table 3.7). Thorium fluoride, ThF_4, can be obtained by various procedures (Moissan and Martinsen, 1905; Duboin, 1908a; Chauvenet, 1911; Lipkind and Newton, 1952). Precipitation from aqueous Th^{4+}-containing solutions leads to hydrates of ThF_4 that are, however, not easily dehydrated due to the formation of hydroxide or oxide fluorides (Briggs and Cavendish, 1971). Under careful conditions, for example under streaming HF or F_2 gas, dehydration to pure ThF_4 is possible (Pastor and Arita, 1974). Alternative routes avoiding aqueous media are the reaction of thorium metal or thorium carbide with fluorine (Moissan and Étard, 1896, 1897), or the action of hydrogen fluoride on other thorium halides, thorium oxide or hydroxide, and thorium oxalate or oxide carbonate (Newton *et al.*, 1952a). As mentioned in the Section 3.7.1, the reaction of thorium hydrides with fluorine provides a route to ThF_4 (Lipkind and Newton, 1952). An elegant way to obtain pure ThF_4 is the reaction of ThO_2

Table 3.7 *Crystallographic data of binary thorium halides.*

		Lattice parameters				
Compound	*Space group*	*a* (Å)	*b* (Å)	*c* (Å)	*Angles* (°)	*References*
ThF_4	C2/c	13.049	11.120	8.538	$\beta = 126.31$	Benner and Müller (1990)
β-$ThCl_4$	$I4_1$/amd	8.491		7.483		Brown *et al.* (1973)
α-$ThCl_4$	$I4_1$/a	6.408		12.924		Mason *et al.* (1974a)
β-$ThBr_4$	$I4_1$/amd	8.971		7.912		Madariaga *et al.* (1993)
α-$ThBr_4$	$I4_1$/a	6.737		13.601		Mason *et al.* (1974b)
ThI_4	$P2_1$/n	13.216	8.068	7.766	$\beta = 98.68$	Zalkin *et al.* (1964)
β-ThI_3	Cccm	8.735	20.297	14.661		Beck and Strobel (1982)
β-ThI_2	$P6_3$/mmc	3.97		31.75		Guggenberger and Jacobson (1968)

with NH_4HF_2. Ammonium hydrogen fluoride serves as the fluorinating agent and is much easier to handle than hydrogen fluoride itself. The reaction yields the ternary fluoride NH_4ThF_5 that decomposes above 300°C to the tetrafluoride (Asprey and Haire, 1973). The disadvantage of the method compared to the direct hydrofluorination is that an eight-fold excess of NH_4HF_2 is needed.

The monoclinic crystal structure of ThF_4 is isotypic with those of zirconium and hafnium fluoride and contains Th^{4+} ions in slightly distorted square antiprismatic coordination of fluoride ions (Zachariasen, 1949a; Asprey and Haire, 1973; Benner and Müller, 1990). Each of the fluorine atoms is attached to another thorium ion, leading to a three-dimensional structure according to ${}^{3}_{\infty}[ThF_{8/4}]$. Surprisingly, the thorium fluoride hydrate that can be precipitated from aqueous solution (Berzelius, 1829; Chydenius, 1863) has not been structurally characterized up to now. It is believed to be an octahydrate, which decomposes to a tetrahydrate on further drying and then finally to a dihydrate on heating (Chauvenet, 1911). The only hydrate of ThF_4 that is structurally known is $Th_6F_{24}\cdot H_2O$ ($=ThF_4\cdot 1/6H_2O$) (Cousson *et al.*, 1978). Similarly to the anhydrous fluoride it consists of three-dimensionally connected square antiprisms $[ThF_8]$. Six of these aniprisms are arranged in a way that empty voids are formed in which the water molecule resides having contact to two of the six Th^{4+} ions (Fig. 3.7). It is assumed that this compound can be obtained by

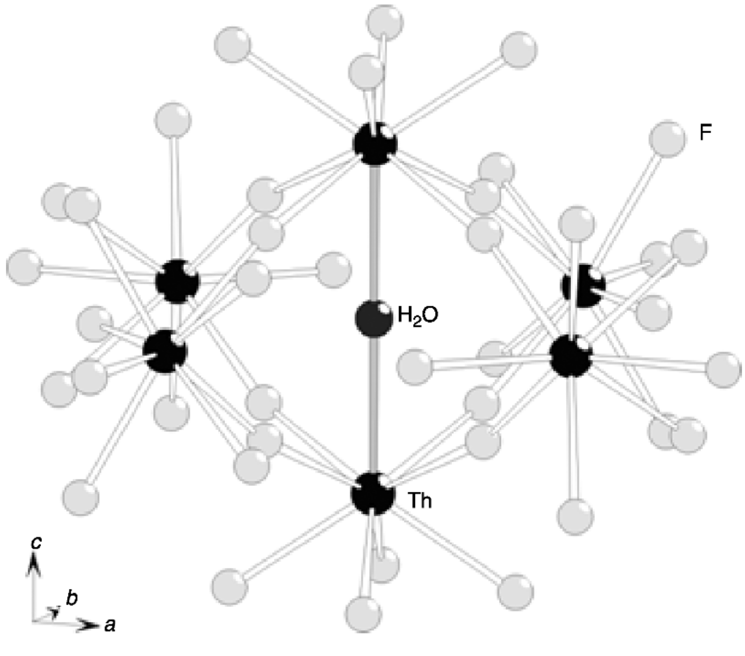

Fig. 3.7 *Detail of the crystal structure of $Th_6F_{24}\cdot H_2O$; the H_2O molecule resides in a void formed by six square antiprismatic $[ThF_8]$ polyhedra.*

careful dehydration of higher hydrates but usually hydrolysis is observed yielding $Th(OH)F_3 \cdot H_2O$ and then finally $ThOF_2$ (Marden and Rentschler, 1927; Zachariasen, 1949a; D'Eye, 1958). The structure of neither of the latter two compounds is known without some question. For $ThOF_2$, however, an orthorhombic unit cell has been determined, which has a close relationship to the hexagonal one of LaF_3. Probably the structure can be seen as an ordering variant of the LaF_3-type of structure. The treatment of $ThOF_2$ with steam at 900°C will yield thoria (Chydenius, 1863; Cline *et al.*, 1944).

Thorium tetrachloride, $ThCl_4$, can be crystallized from aqueous solution as an octahydrate, which is easily transformed to basic chlorides upon heating above 100°C (Chauvenet, 1911; Dergunov and Bergman, 1948; Knacke *et al.*, 1972a,b). Dehydration has also been done by refluxing the hydrates with thionyl chloride but the product was hard to get free of $SOCl_2$. Other routes have been employed to produce pure $ThCl_4$ (Chydenius, 1863) including the reaction of ThH_4 with HCl and the action of chlorine on thorium metal (Krüss and Nilson, 1887a; Lipkind and Newton, 1952), ThH_4, or thorium carbide (Nilson, 1876, 1882a,b, 1883; Moissan and Étard, 1896, 1897; von Wartenberg, 1909). Furthermore mixtures of chlorine and carbon or S_2Cl_2 were used for the chlorination of ThO_2 (Matignon and Bourion, 1904; Meyer and Gumperz, 1905; Bourion, 1909; von Wartenberg, 1909; Yen *et al.*, 1963), and also carbon tetrachloride (Matignon and Delepine, 1901; von Bolton, 1908; Knacke *et al.*, 1972a), phosgene (Baskerville, 1901; Karabasch, 1958), and phosphorus pentachloride (Smith and Harris, 1895; Matignon, 1908) were applied as chlorinating agents and mixtures of chlorine and CO or CO_2 for the chlorination of thorium oxalate and nitrate, respectively (Dean and Chandler, 1957). A facile synthesis of $ThCl_4$ is provided in the reaction of thorium metal with NH_4Cl in sealed tubes (Schleid *et al.*, 1987). Purification of $ThCl_4$ can be achieved by sublimation. $ThCl_4$ melts at 770°C (Moissan and Martinsen, 1905; Fischer *et al.*, 1939) and boils at 921°C. The results of vapor pressure measurements as a function of the temperature have been compiled (Fuger *et al.*, 1983).

$ThCl_4$ is dimorphic and exhibits a phase transition at 405°C (Mooney, 1949; Mucker *et al.*, 1969; Mason *et al.*, 1974a). The phase transition can only be observed under special conditions and in very pure samples. Usually the high-temperature phase β-$ThCl_4$ remains even at temperatures below 405°C as a metastable compound. Both the low-temperature phase α-$ThCl_4$ and the high-temperature phase β-$ThCl_4$ are tetragonal and show eight-fold coordinated Th^{4+} ions. The coordination polyhedra are slightly distorted dodecahedra that are connected via four edges to a three-dimensional structure. Thus, each of the chloride ligands are connected to two Th^{4+} ions. The difference in the two polymorphs results from small differences in the orientation of the $[ThCl_8]$ polyhedra with respect to each other (Fig. 3.8). The symmetry decreases from $I4_1/amd$ for β-$ThCl_4$ to $I4_1/a$ for α-$ThCl_4$. The two modifications of $ThCl_4$ are related in much the same way as are zicon ($ZrSiO_4$) and scheelite ($CaWO_4$).

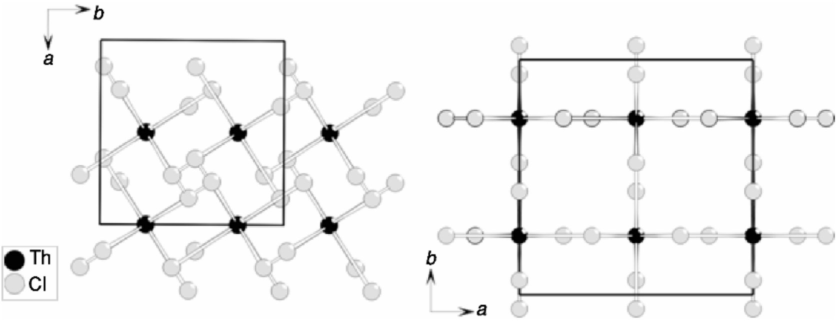

Fig. 3.8 *Projections of the crystal structures of* α*-ThCl*$_4$ (*right*) *and* β*-ThCl*$_4$ (*left*) *onto* (001).

In fact the structures of $ThCl_4$ result if the atoms in the tetrahedral centers (Si and W, respectively) are removed in the oxo-compounds. More recent investigations gave some evidence that there is a third modification of $ThCl_4$ below 70 K that has a complicated incommensurate structure related to that of α-$ThCl_4$ (Khan Malek *et al.*, 1982; Bernard *et al.*, 1983; Krupa *et al.*, 1987).

Structural data of $ThCl_4$ hydrates are not known up to now but the enthalpies of formation of the di-, tetra-, hepta- and octahydrates have been evaluated (Fuger *et al.*, 1983) from enthalpy of solution measurements (Chauvenet, 1911). Also the basic chlorides that are frequently observed as the products of the thermal treatment of the hydrates are poorly investigated (Bagnall *et al.*, 1968). It is only for the oxychloride $ThOCl_2$ that lattice parameters have been calculated from powder diffraction data based on the data given for $PaOCl_2$ (Bagnall *et al.*, 1968). The heat of formation of $ThOCl_2$ has been reported several times (Yen *et al.*, 1963; Korshunov and Drobot, 1971; Knacke *et al.*, 1972b; Fuger *et al.*, 1983) and will be discussed in proper context in Chapter 19. Chlorides of lower-valent thorium have been reported to form by electrochemical reduction of a $ThCl_4$/KCl melt (Chiotti and Dock, 1975) but these observations are still in need of confirmation.

Analogous to the tetrachloride, $ThBr_4$ can be obtained from aqueous solution, for example, by adding $Th(OH)_4$ to aqueous HBr. Depending on the drying conditions various hydrates may form. The main disadvantage of the wet route for preparing $ThBr_4$ is the contamination of the product with hydrolysis products like $ThOBr_2$. Dry routes to $ThBr_4$ include the action of bromine on thorium metal, ThH_4, ThC, or on mixtures of ThO_2 and C (Nilson, 1876; Troost and Ouvrard, 1889; Moissan and Étard, 1896, 1897; Matthews, 1898; Moissan and Martinsen, 1905; Fischer *et al.*, 1939; Young and Fletcher, 1939; Lipkind and Newton, 1952). Moreover, the reaction of gaseous HBr with ThH_4 (Lipkind and Newton, 1952) and of a mixture of S_2Cl_2 and gaseous HBr with ThO_2 have been employed (Bourion, 1907). Sublimation above 600°C in vacuum should be applied for purification. The temperature dependence of the vapor pressure has been investigated (Fischer *et al.*, 1939) and melting (679°C) and boiling (857°C) points have been reported (Fischer *et al.*, 1939; Mason *et al.*, 1974b).

As found for the tetrachloride, $ThBr_4$ is also dimorphic (D'Eye, 1950; Brown *et al.*, 1973; Fuger and Brown, 1973; Mason *et al.*, 1974b; Guillaumont, 1983). Both modifications, β-$ThBr_4$ and α-$ThBr_4$, are isotypic to the respective chlorides. The transition temperature is slightly higher compared to $ThCl_4$ and is determined to be 426°C. Again, the β-phase is found to remain metastable even below 426°C. The phase transition has been investigated in detail by means of nuclear quadrupolar resonance (NQR) on the ^{79}Br isotope (Kravchenko *et al.*, 1975). According to these experiments, the time to achieve complete conversion is strongly dependent on the previous treatment of the sample and is reduced after one conversion cycle has passed. Analogous to $ThCl_4$ another phase transition is found at lower temperature. According to NQR and electron paramagnetic resonance (EPR) measurements as well as neutron and X-ray diffractions, the transition is second order and occurs at 92 K (Kravchenko *et al.*, 1975). It is only observed in β-$ThBr_4$ and can be described as a continuous modulation of the bromide ions along the *c*-axis, leading to a complicated incommensurate structure (Madariaga *et al.*, 1993). The incommensurate low-temperature modifications of $ThBr_4$ and $ThCl_4$ have also been investigated spectroscopically on U^{4+}-doped samples (Krupa *et al.*, 1995).

There are two reports on the low-valent thorium bromides, $ThBr_3$ and $ThBr_2$ (Hayek and Rehner, 1949; Shchukarev *et al.*, 1956). They have been prepared from the elements in the desired molar ratio or, in the case of $ThBr_3$, by reduction of $ThBr_4$ with hydrogen. These bromides are highly reactive and show disproportionation at higher temperatures. Unfortunately no structural data are known. More recently the molecular species, $ThBr_3$, $ThBr_2$ and ThBr, have been identified by mass spectrometry in the bromination of thorium between 1500 and 2000 K (Hildenbrand and Lau, 1990).

None of the various hydrates of $ThBr_4$ that have been reported to contain 12, 10, 8, and 7 molecules of water, respectively (Lesinsky and Gundlich, 1897; Rosenheim and Schilling, 1900; Rosenheim *et al.*, 1903; Moissan and Martinsen, 1905; Chauvenet, 1911), are well characterized to date. The heat of solution has been determined in some cases and the thermal decomposition of the hydrates is known to lead to $Th(OH)Br_3$ and finally to $ThOBr_2$ (Chauvenet, 1911). The powder diffraction pattern of the oxybromide shows that this compound is not isotypic with $ThOCl_2$ but seems to have a lower symmetry (Bagnall *et al.*, 1968). $ThBr_4$ is also known to form solvates with amines (Rosenheim and Schilling, 1900; Rosenheim *et al.*, 1903), acetonitrile (Young, 1935), and trimethylphosphine (Al-Kazzaz and Louis, 1978).

Thorium tetraiodide (ThI_4) is most conveniently prepared by the reaction of the elements in sealed silica ampoules (Nilson, 1876; Moissan and Étard, 1896, 1897; Zalkin *et al.*, 1964). It is very important to exclude any traces of water or oxygen during the reaction to avoid contamination of the product with $ThOI_2$ or even ThO_2. Alternative procedures involve the reactions between ThH_4 and HI, and between thorium metal and a H_2/I_2 mixture (Lipkind and Newton, 1952). If only small amounts of ThI_4 are needed, the action of AlI_3 on ThO_2 might also be appropriate (Chaigneau, 1957). In the temperature range from 500 to 550°C, ThI_4 can be sublimed for purification under dynamic vacuum yielding yellow crystals. Knudsen cell effusion studies of ThI_4 have suggested dissociation through ThI_3, ThI_2, and ThI to thorium metal (Knacke *et al.*, 1978). On heating, ThI_4 reacts with ThO_2 to form the basic iodide $ThOI_2$ (Scaife *et al.*, 1965; Corbett *et al.*, 1969).

ThI_4 is not isotypic with the other tetrahalides. It has monoclinic symmetry and contains eight-fold coordinated Th^{4+} ions (Zalkin *et al.*, 1964). The coordination polyhedron can be seen as a distorted square antiprism. The polyhedra are linked in chains via two triangular faces leading to Th–Th distances of 4.48 Å. The chains are further connected via the two remaining iodine ligands into layers. The connectivity may be formulated as $^{2}_{\infty}[ThI^{f}_{6/2}I^{e}_{2/2}]$ (f = face; e = edge). These layers are held together only by van der Waals interactions (Fig. 3.9).

Two lower-valent thorium iodides, ThI_3 and ThI_2, are known. Both can be obtained by reduction reactions of ThI_4 with appropriate amounts of thorium metal in sealed tantalum tubes (Anderson and D'Eye, 1949; Hayek and Rehner, 1949; Hayek *et al.*, 1951; Clark and Corbett, 1963; Scaife and Wylie, 1964; Guggenberger and Jacobson, 1968). If hydrogen is used as the reducing reagent, the formation of iodide hydrides is observed (Struss and Corbett, 1978).

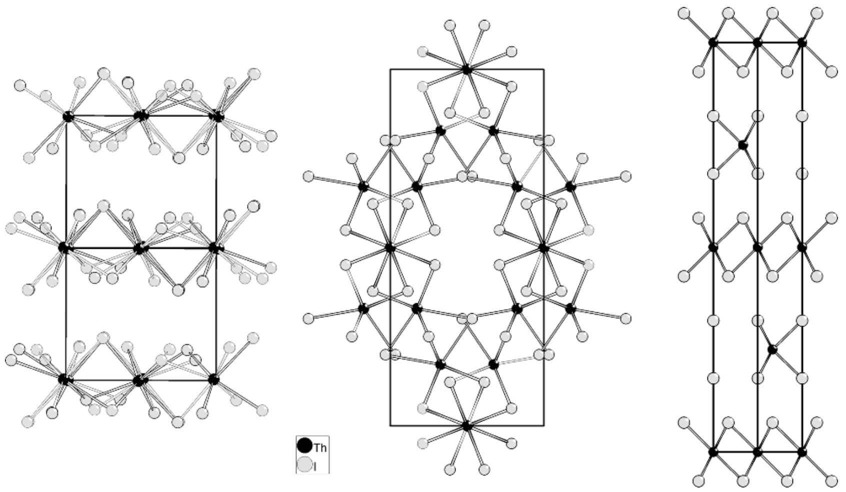

Fig. 3.9 *Crystal structures of the thorium iodides ThI_4 (left, as a projection onto the* (101) *plane),* β-*ThI_3 (middle, as a projection onto the* (001) *plane), and* β-*ThI_2 (right, as a projection onto the* (110) *plane).*

For the preparation of ThI_2, another route has been developed. The electrolysis of thorium metal in a solution of iodine and tetraethyl ammonium perchlorate in acetonitrile affords $ThI_2{\cdot}2CH_3CN$ that can be decomposed into ThI_2 *in vacuuo* (Kumar and Tuck, 1983).

Depending on the time, the reaction of ThI_4 and Th leads to two modifications of ThI_3 (Beck and Strobel, 1982). After a short period of 2–3 days, thin shiny rods of α-ThI_3 were obtained while long heating times led to compact crystals of β-ThI_3 that show a slight green to brass-colored luster. For α-ThI_3 only the lattice constants are known while a complete structure determination has been performed for β-ThI_3 (Beck and Strobel, 1982). It shows three crystallographically different thorium atoms in the unit cell, each of them in an eightfold coordination of iodide ions. Two of the $[ThI_8]$ polyhedra are square antiprismatic, the third one is a slightly elongated cube. The $[ThI_8]$ cubes are connected via four rectangular faces to $[ThI_8]$ square antiprisms (Fig. 3.9). One half of the square antiprisms is further connected to other cubes and, the second half to other square antiprisms, leading to a three-dimensional network. The Th–I bond distances suggest that thorium is in the tetravalent state in ThI_3 and has to be formulated according to $Th^{4+}(I^-)_3(e^-)$ with the electrons delocalized or involved in metal–metal bonds. The latter assumption is supported by the relatively short Th–Th distances of 3.46 to 3.80 Å.

ThI_2 is also found to adopt two different crystal structures (Clark and Corbett, 1963; Scaife and Wylie, 1964). Lustrous gold crystals of β-ThI_2 are obtained at 700 to 850°C while α-ThI_2 forms at 600°C. Both compounds are hexagonal but a structure determination has been performed only for β-ThI_2 (Guggenberger and Jacobson, 1968). The structure can be seen as a stacking variant of the CdI_2 structure (Fig. 3.9). It has a remarkable long *c*-axis (31 Å) and the stacking sequence of the iodide ions is ...ABCCBA... with the thorium atoms in octahedral and trigonal prismatic sites (Fig. 3.9). Judging from the Th–I bond distances, Th^{4+} is present in the structure and the free electrons, according to $Th^{4+}(I^-)_2(e^-)_2$, should be responsible for the electrical conductivity of the compound. The metal–metal distances, however, are remarkably longer than those found in ThI_3. Both subiodides, ThI_3 and ThI_2, exhibit peritectic decomposition above 850°C caused by disproportionations to ThI_4 and ThI_2 or ThI_4 and Th, respectively (Scaife and Wylie, 1964).

The formation of pseudo-halides of thorium (such as thiocyanate or selenocyanate) in organic solvents has been reported, but up to now, no binary compound is known (Golub and Kalibabchuk, 1967; Laubscher and Fouché, 1971; Golub *et al.*, 1974).

(b) Polynary halides

The systems AF/ThF_4, where A is an alkali or another monovalent metal ion, have been widely investigated (Brunton *et al.*, 1965). Phase diagrams of the

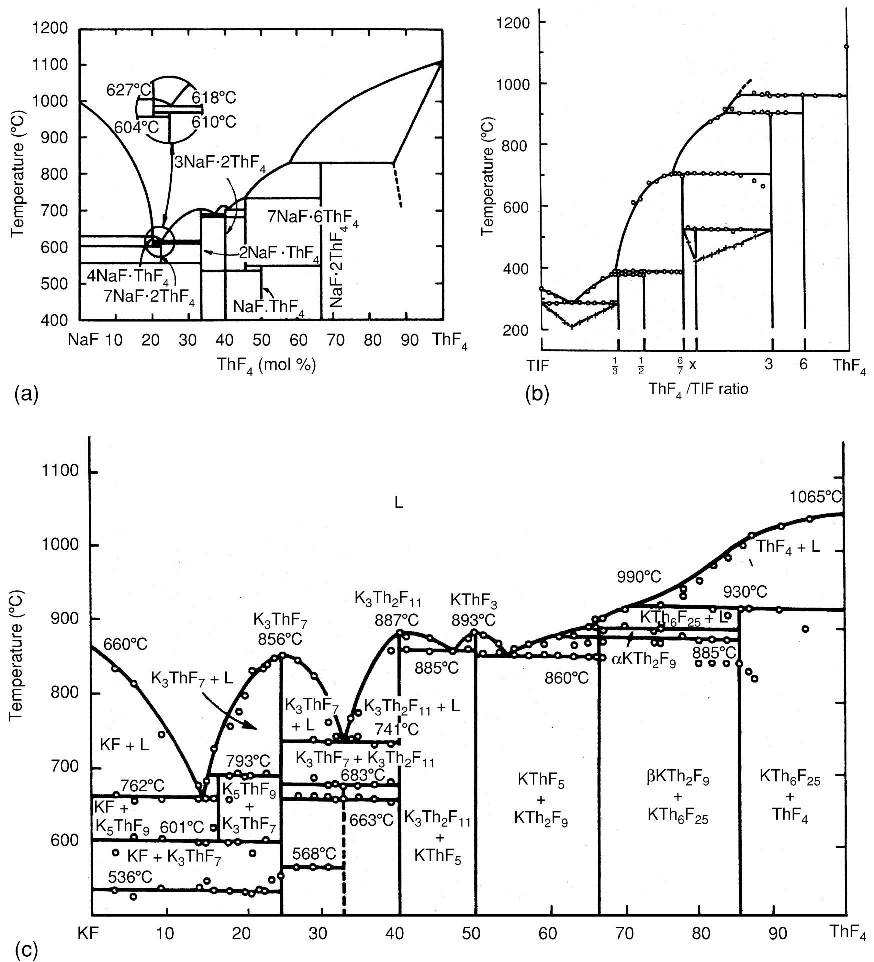

Fig. 3.10 *Phase diagrams of three AF/ThF$_4$ systems.* (*a*) *NaF/ThF$_4$* (*Thoma,* 1972). (*b*) *TlF/ThF$_4$* (*Avignant and Cousseins,* 1970). (*c*) *KF/ThF$_4$* (*Kaplan,* 1956).

systems NaF/ThF$_4$ (Thoma, 1972), KF/ThF$_4$ (Kaplan, 1956), and TlF/ThF$_4$ (Avignant and Cousseins, 1970) are given as examples in Fig. 3.10. Furthermore, the binary and also some ternary phase diagrams of ThF$_4$ with several other fluorides were determined. Table 3.8 surveys the phases that are reported to exist along with those found in the other halide systems. Unfortunately, only very few of these phases have been carefully characterized. In some cases lattice parameters of the compounds were determined by powder diffraction; moreover,

Table 3.8 *Detected phases in the systems with* ThX_4 ($X = F, Cl, Br$).

System	*Compounds*	*References*
$LiF–ThF_4$	Li_3ThF_7, $LiThF_5$, $LiTh_2F_9$, $LiTh_4F_{17}$	Thoma and Carlton (1961)
$NaF–ThF_4$	Na_4ThF_8, Na_3ThF_7, Na_2ThF_6, $Na_3Th_2F_{11}$, $Na_7Th_6F_{31}$, $NaThF_5$, $NaTh_2F_9$	Thoma and Carlton (1961); Thoma (1972); Brunton *et al.* (1965)
$KF–ThF_4$	K_5ThF_9, K_2ThF_6, $K_7Th_6F_{31}$, $KThF_5$, KTh_2F_9, KTh_6F_{25}	Thoma and Carlton (1961); Dergunov and Bergman (1948); Harris (1960)
$RbF–ThF_4$	Rb_3ThF_7, Rb_2ThF_6, $Rb_7Th_6F_{31}$ $RbTh_3F_{13}$, $RbTh_6F_{25}$	Thoma and Carlton (1961); Dergunov and Bergman (1948)
$CsF–ThF_4$	Cs_3ThF_7, Cs_2ThF_6, $CsThF_5$, $Cs_2Th_3F_{14}$, $CsTh_2F_9$, $CsTh_3F_{13}$, $CsTh_6F_{25}$	Thoma and Carlton (1961); Brunton *et al.* (1965)
$NH_4F–ThF_4$	$(NH_4)_4ThF_8$, $(NH_4)_3ThF_7$, $(NH_4)_2ThF_6$	Ryan *et al.* (1969); Penneman *et al.* (1971, 1976, 1968)
$N_2H_5F–ThF_4$	$(N_2H_5)_3ThF_7$, $(N_2H_5)ThF_5$	Glavic *et al.* (1973); Sahoo and Patnaik (1961)
$NH_3OH–ThF_4$	$(NH_3OH)ThF_4$	Satpathy and Sahoo (1968); Rai and Sahoo (1974)
$TlF–ThF_4$	Tl_3ThF_7, Tl_2ThF_6, $Tl_7Th_6F_{31}$, $TlThF_5$, $TlTh_3F_{13}$, $TlTh_6F_{25}$	Avignant and Cousseins (1970); Keller and Salzer (1967)
$LiCl–ThCl_4$	Li_4ThCl_8	Vdovenko *et al.* (1974)
$NaCl–ThCl_4$	$NaThCl_5$	Vdovenko *et al.* (1974)
$KCl–ThCl_4$	K_3ThCl_7, K_2ThCl_6, $KThCl_5$	Gershanovich and Suglobova (1980)
$RbCl–ThCl_4$	Rb_3ThCl_7, Rb_2ThCl_6, $RbThCl_5$, $RbTh_{1.6}Cl_{5.6}$	Gershanovich and Suglobova (1980)
$CsCl–ThCl_4$	Cs_3ThCl_7, Cs_2ThCl_6, $CsThCl_5$, $CsTh_3Cl_{13}$	Gershanovich and Suglobova (1980)
$BaCl_2–ThCl_4$	Ba_3ThCl_{10}, $Ba_3Th_2Cl_{14}$	Gorbunov *et al.* (1974)
$NaBr–ThBr_4$	$NaThBr_5$	Gershanovich and Suglobova (1981)
$KBr–ThBr_4$	K_2ThBr_6	Gershanovich and Suglobova (1981)
$RbBr–ThBr_4$	Rb_2ThBr_6	Gershanovich and Suglobova (1981)
$CsBr–ThBr_4$	Cs_2ThBr_6	Gershanovich and Suglobova (1981)

careful structure determinations remain scarce. Known crystallographic data are summarized in Table 3.9.

In the system LiF/ThF_4 four compounds are known to exist (Brown, 1968; Cousson *et al.*, 1977; Penneman *et al.*, 1973; Taylor, 1976), namely Li_3ThF_7, $LiThF_5$, $LiTh_2F_9$, and $LiTh_4F_{17}$. A complete structure analysis has been done for only one of these phases, namely Li_3ThF_7 (Cousson *et al.*, 1978;

Table 3.9 *Crystallographic data of polynary thorium halides* (*in italics: powder data*).

		Lattice parameters				
Compound	*Space group*	*a* (Å)	*b* (Å)	*c* (Å)	*Angles* (°)	*References*
$\mathrm{Li_3ThF_7}$	Ccca	8.788	8.768	12.958		Laligant *et al.* (1989)
$\mathrm{Li_3ThF_7}$	P4/ncc	6.206		12.940		Cousson *et al.* (1978); Laligant *et al.* (1992)
$LiThF_5$	$I4_1/a$	*15.10*		*6.60*		Keenan (1966)
$LiTh_2F_9$	*tetragonal*	*11.307*		*6.399*		Harris *et al.* (1959)
$\alpha\text{-}(\mathrm{Na_2ThF_6})_{1.333}$	$\mathrm{Fm\bar{3}m}$	5.687				Zachariasen (1949a)
$\beta_2\text{-}\mathrm{Na_2ThF_6}$	P321	5.989		3.835		Zachariasen (1948a)
$\delta\text{-}Na_2ThF_6$	*hexagonal*	*6.14*		*7.36*		Zachariasen (1948b)
$\mathrm{NaTh_2F_9}$	$\mathrm{I\bar{4}3m}$	8.722				Zachariasen (1948a, 1949b)
Na_4ThF_8	*cubic*	*12.706*				Zachariasen (1948b)
$Na_7Th_6F_{31}$	$R\bar{3}$	*14.96*		*9.912*		Keenan (1966)
$\mathrm{Na_3Li_4Th_6F_{31}}$	P3c1	9.906		13.282		Brunton and Sears (1969)
$\mathrm{Na_3BeTh_{10}F_{45}}$	$\mathrm{P4_2/ncm}$	11.803		23.420		Brunton (1973)
$\mathrm{Na_3ZnTh_6F_{29}}$	P321	10.166		13.255		Cousson *et al.* (1979b)
$\mathrm{Li_2CaThF_8}$	$\mathrm{I\bar{4}m2}$	5.109		11.013		Vedrine *et al.* (1973)
$\mathrm{KNaThF_6}$	$\mathrm{P\bar{3}}$	6.307		7.891		Brunton (1970)
$\alpha\text{-}(\mathrm{K_2ThF_6})_{1.333}$	$\mathrm{Fm\bar{3}m}$	5.994				Zachariasen (1948b, 1949a)
$\beta\text{-}\mathrm{K_2ThF_6}$	$\mathrm{P\bar{6}2m}$	6.578		3.822		Zachariasen (1948a)
$\mathrm{K_5ThF_9}$	$\mathrm{Cmc2_1}$	7.848	10.840	12.785		Ryan and Penneman (1971)
$\mathrm{K_7Th_6F_{31}}$	$\mathrm{R\bar{3}}$	15.293		10.449		Brunton (1971a)
$\mathrm{KTh_6F_{25}}$	$\mathrm{R\bar{3}m}$	8.313		25.262		Brunton (1972)
$\mathrm{RbTh_3F_{13}}$	$\mathrm{P2_1ma}$	8.649	8.176	7.445		Brunton (1971b)
Rb_3ThF_7	$Fm\bar{3}m$	*9.62*				Dergunov and Bergman (1948)
Rb_2ThF_6	$P\bar{6}2m$	*6.85*		*3.83*		Harris (1960)
$Rb_7Th_6F_{31}$	$R\bar{3}$	*9.58*			$\alpha = 106.9^{a}$	Brunton *et al.* (1965)
$RbTh_6F_{25}$	$R\bar{3}m$	*8.330*		*25.40*		Brunton *et al.* (1965)
Cs_3ThF_7	$Fm\bar{3}m$	*10.04*				Brunton *et al.* (1965)
$CsTh_6F_{25}$	$P6_3/mmc$	*8.31*		*16.91*		Brunton *et al.* (1965)

Table 3.9 (*Contd.*)

Compound	*Space group*	*Lattice parameters*				*References*
		a (Å)	*b* (Å)	*c* (Å)	*Angles* (°)	
$\mathrm{(NH_4)_4ThF_8}$	$\mathrm{P\bar{1}}$	8.477	8.364	7.308	$\alpha = 88.38$ $\beta = 96.08$ $\gamma = 106.33$	Ryan *et al.* (1969)
$\mathrm{(NH_4)_3ThF_7}$	Pnma	13.944	7.928	7.041		Penneman *et al.* (1971)
$\mathrm{(NH_4)_7Th_2F_{15}{\cdot}H_2O}$	$\mathrm{P2_13}$	12.573				Penneman *et al.* (1968)
$\mathrm{Tl_3ThF_7}$	$\mathrm{P2_1/m}$	9.793	8.464	10.712	$\beta = 117.20$	Gaumet *et al.* (1995)
$Tl_7Th_6F_{31}$	$R\bar{3}$	*15.60*		*10.84*		Avignant and Cousseins (1970)
$TlTh_6F_{25}$	$P6_3/mmc$	*8.31*		16.86		Avignant and Cousseins (1970)
$\mathrm{(SmTh_2F_{11})_{1.333}}$	Pnma	8.610	4.137	7.225		Abaouz *et al.* (1997)
$\mathrm{Zr_2ThF_{12}}$	I2/m	9.895	10.488	7.856		Taoudi *et al.* (1996)
$CaThF_6$		*6.994*		*7.171*		Keller and Salzer (1967); Salzer (1966)
$SrThF_6$		*7.150*		*7.313*		Keller and Salzer (1967); Salzer (1966)
$BaThF_6$		*7.419*		*7.516*		Keller and Salzer (1967); Salzer (1966)
$CdThF_6$		*6.963*		*7.109*		Keller and Salzer (1967); Salzer (1966)
$PbThF_6$		*7.245*		*7.355*		Keller and Salzer (1967); Salzer (1966)
$EuThF_6$		*7.124*		*7.360*		Keller and Salzer (1967); Salzer (1966)
$\mathrm{Cs_2ThCl_6}$	$\mathrm{P\bar{3}m1}$	7.614		6.038		Siegel (1956)
K_2ThCl_6	*Orthorh.*	*8.16*	*14.13*	*8.62*		Gershanovich and Suglobova (1981)
Rb_2ThCl_6	*Orthorh.*	*8.31*	*14.39*	*8.74*		Gershanovich and Suglobova (1981)
$\mathrm{In_2ThBr_6}$	C2/c	8.791	14.670	9.046	$\beta = 91.15$	Dronskowski (1995)
K_2ThBr_6	*trigonal*	*7.52*		*11.80*		Siegel (1956); Gershanovich *et al.* (1981);
	tetragonal	*11.478*		*7.94*		Brunton *et al.* (1965)
Rb_2ThBr_6	trigonal	*7.58*		*12.24*		Gershanovich and Suglobova (1981)

Cs_2ThBr_6	*tetragonal*	*11.37*		*10.69*	Siegel (1956); Gershanovich and Suglobava (1981)
	trigonal	*9.537*		*8.10*	Brunton *et al.* (1965)
$CaThBr_6$	Pmma	9.764	4.109	12.104	Beck and Kühn (1995)
$SrThBr_6$	Pmma	9.878	4.286	12.255	Beck and Kühn (1995)
$BaThBr_6$	Pmma	9.992	4.490	12.526	Beck and Kühn (1995)
$SnThBr_6$	*Pmma*	*9.143*	*4.209*	*12.716*	Beck *et al.* (1993)
$PbThBr_6$	*Pmma*	*9.191*	*4.228*	*12.68*	Beck *et al.* (1993)
$FeTh_6Br_{15}$	Im$\bar{3}$m	11.488			Böttcher *et al.* (1991a)
$CoTh_6Br_{15}$	Im$\bar{3}$m	11.507			Böttcher *et al.* (1991a)
$NaFeTh_6Br_{15}$	Im$\bar{3}$m	11.605			Böttcher *et al.* (1991a)
$Th_6Br_{15}H_7$	Im$\bar{3}$m	11.390			Böttcher *et al.* (1991a)
$Th_6Br_{15}D_7$	Im$\bar{3}$m	11.376			Böttcher *et al.* (1991a)
$Th_6H_7Br_{15}$	Im$\bar{3}$m	11.470			Böttcher *et al.* (1991b)
$Th_6D_7Br_{15}$	Im$\bar{3}$m	11.376			Böttcher *et al.* (1991b)
$Th_6Br_{14}C$	Cmca	15.764	14.160	13.123	Böttcher *et al.* (1991)
$K(Th_{12}N_6Br_{29})$	Pnnm	17.524	11.943	14.031	Braun *et al.* (1995)
ThNI	P4/nmm	4.107		9.242	Juza and Sievers (1968)
β-$PbThI_6$	P$\bar{3}$1c	7.748		13.789	Beck *et al.* (1993)
γ-$PbThI_6$	Cmcm	4.387	13.956	10.005	Beck *et al.* (1993)
β-$SnThI_6$	P$\bar{3}$1c	7.748		13.789	Beck *et al.* (1993)
β-$PbGeI_6$	*P$\bar{3}$1c*	*7.526*		*13.783*	Beck *et al.* (1993)
β-$CaThI_6$	*P$\bar{3}$1c*	*7.697*		*13.959*	Beck *et al.* (1993)
γ-$GeThI_6$	*Cmcm*	*4.248*	*13.92*	*9.991*	Beck *et al.* (1993)
γ-$SnThI_6$	*Cmcm*	*4.376*	*13.937*	*9.995*	Beck *et al.* (1993)
γ-$CaThI_6$	*Cmcm*	*4.278*	*14.02*	*10.10*	Beck *et al.* (1993)
γ-$SrThI_6$	*Cmcm*	*4.455*	*13.991*	*10.052*	Beck *et al.* (1993)
γ-$BaThI_6$	*Cmcm*	*4.685*	*13.76*	*10.015*	Beck *et al.* (1993)
γ-$EuThI_6$	*Cmcm*	*4.420*	*13.964*	*10.038*	Beck *et al.* (1993)

---

[a] rhombohedral setting.

Laligant *et al.*, 1989; Pulcinelli and de Almeida Santos, 1989). It is dimorphic but the linkage of the monocapped square antiprisms [ThF_9] is the same in the two modifications. They are connected via two common edges to layers according to the formulation ${}^{2}_{\infty}[\mathrm{ThF}^{e}_{4/2}\mathrm{F}^{t}_{5/1}]$ (e = edge, t = terminal). The layers are stacked along the *c*-axis. The different symmetry of the two modifications arises from the different positions of the Li^+ ions in the interlayer spacings, and their positions are temperature-dependent, making the compound a good ionic conductor (Laligant *et al.*, 1992). According to powder diffraction measurements, $LiThF_5$ is isotypic with $LiUF_5$ and contains a three-dimensional network of vertex-connected monocapped square antiprisms [ThF_9] that incorporate the Li^+ in a six-fold coordination (Keenan, 1966). The lattice parameter of the other two fluorides have been obtained by powder XRD (Harris *et al.*, 1959; Cousson *et al.*, 1978).

The system NaF/ThF_4 shows the formation of seven compounds (Table 3.8) (Rosenheim *et al.*, 1903; Dergunov and Bergman, 1948; Brunton *et al.*, 1965; Kaplan, 1956; Ryan and Penneman, 1971; Thoma, 1972). Na_2ThF_6 may either be cubic (α-Na_2ThF_6) or trigonal (β_2-Na_2ThF_6) (Table 3.9). The cubic modification is a variant of the CaF_2-type of structure with Na^+ and Th^{4+} occupying Ca^{2+} sites in a disordered fashion (Zachariasen, 1949b). The trigonal structure of Na_2ThF_6 is very similar to the structure of LaF_3 and contains both the Na^+ and the Th^{4+} ions in tricapped trigonal prismatic coordination of fluoride anions (Zachariasen, 1948b). The polyhedra are connected via triangular faces in the [001] direction and via common edges in the (001) plane. A third modification, δ-Na_2ThF_6, has been reported to be also trigonal but has not been proved yet (Zachariasen, 1948c; Penneman *et al.*, 1973). In $NaTh_2F_9$ the Th^{4+} are nine-fold coordinated by F^- ions. The polyhedra are connected via vertices according to ${}^{3}_{\infty}[\mathrm{ThF}_{9/2}]^{-0.5}$ to a three-dimensional network with the Na^+ ions incorporated for charge compensation (Zachariasen, 1948b, 1949a). In the complex structure of $Na_7Th_6F_{31}$ nine- and ten-fold coordinated Th^{4+} ions are present (Keenan, 1966; Penneman *et al.*, 1973).

An X-ray structure analysis is available for all of the six compounds that exist in the KF/ThF_4 system (Kaplan, 1956), except for $KThF_5$ (Table 3.9). α_1-K_2ThF_6 is isotypic with the respective sodium compound, while a slight difference is found between β_1-K_2ThF_6 and β_1-Na_2ThF_6 (Zachariasen, 1948c; Ryan and Penneman, 1971). The Th/F sublattice is the same in the two compounds, however, in the former the K^+ ions are located in tricapped trigonal prismatic voids, in the latter, Na^+ occupies octahedral sites. The complex fluoride $K_7Th_6F_{31}$ (Zachariasen, 1948c; Brunton, 1971a) shows isotypism to the sodium compound. K_5ThF_9, which has also been prepared from aqueous media (Wells and Willis, 1901), consists of monomeric distorted square antiprismatic $[ThF_8]^{4-}$ anions that are connected via K^+ ions (Ryan and Penneman, 1971). Furthermore there are isolated F^- ions in the structure that are not bonded to Th^{4+}. The structure of KTh_6F_{25} is a polymorph of the CsU_6F_{25}-type with the Th^{4+} ions in nine-fold coordination by fluoride ions (Brunton, 1972).

The tricapped trigonal prismatic polyhedra are linked via shared edges and vertices. The resulting three-dimensional network incorporates the K^+ ions in voids. Finally, a mixed sodium potassium fluoride is known: $NaKThF_6$ (Brunton, 1970).

Among the compounds found in the RbF/ThF_4 system (Dergunov and Bergman, 1948; Thoma and Carlton, 1961), Rb_2ThF_6, $Rb_7Th_6F_{31}$ and $RbTh_6F_{25}$ are isotypic to their respective potassium fluorides (Harris, 1960; Penneman *et al.*, 1973). Rb_3ThF_7 has the same cubic structure as K_3UF_7 and shows a highly disordered fluoride sublattice (Dergunov and Bergman, 1948).

The same is true for Cs_3ThF_7, which is one of the seven phases that are known to exist in the CsF/ThF_4 system (Thoma and Carlton, 1961; Penneman *et al.*, 1973). Unfortunately, lattice parameters are only available for one additional compound, $CsTh_6F_{25}$. It is isotypic to CsU_6F_{25} and can be seen as a polymorph of the KTh_6F_{25}-type wherein the Th^{4+} ions are in nine-fold and the Cs^+ ions in 12-fold coordination by fluoride ions (Brunton, 1971b; Penneman *et al.*, 1973).

Although the size of the ammonium ion is comparable to the radii of K^+ and Rb^+, the NH_4F/ThF_4 system contains only a few phases, namely $(NH_4)_2ThF_6$, $(NH_4)_3ThF_7$, and $(NH_4)_4ThF_8$ (Ryan *et al.*, 1969; Penneman *et al.*, 1971). The latter two have been structurally characterized. $(NH_4)_3ThF_7$ is not isotypic with the respective potassium or cesium compounds but crystallizes with orthorhombic symmetry (Penneman *et al.*, 1971). It contains chains of edge-sharing $[ThF_9]$ polyhedra with the formulation $^1_\infty[ThF_{4/2}F_{5/1}]$ that are separated by the NH_4^+ ions. Similar chains are found in the unique crystal structure of $(NH_4)_4ThF_8$. This latter compound contains, however, an additional fluoride ion that is not coordinated to any Th^{4+} so that it should be formulated as $(NH_4)_4[ThF_7]F$ (Ryan *et al.*, 1969).

As far as structural data are known, the compounds found in the TlF/ThF_4 system show a close relationship to the respective fluorides of the larger alkali metal ions (Avignant and Cousseins, 1970). Slight deviations may be observed as can be seen from the structure of Tl_3ThF_7 and are usually attributed to the stereochemical activity of the lone electron pair on Tl^+ (Gaumet *et al.*, 1995).

Several other systems with ThF_4 have been investigated with unusual components like N_2H_5F or even NH_3OH (Table 3.8) (Sahoo and Patnaik, 1961; Satpathy and Sahoo, 1968; Glavic *et al.*, 1973; Rai and Sahoo, 1974). Single crystal structures are not known in these cases. In addition, compounds with higher valent ions have been investigated. With divalent cations, a number of compounds are known that have essentially the LaF_3 structure type, wherein the La^{3+} positions are filled by Th^{4+} and the divalent cation, respectively (Zachariasen, 1949a; Keller and Salzer, 1967; Brunton, 1973). Anion-rich fluorides can be obtained when a small amount of Th^{4+} is doped in the CaF_2 lattice and complicated phases with severe disorder in the cation and anion lattice are described for lanthanide-containing compounds like $SmTh_2F_{11}$ (Abaouz *et al.*, 1997). Finally, the zirconium thorium fluoride $ThZr_2F_{12}$ is completely ordered and contains layers of vertex-shared $[ZrF_8]$ polyhedra that alternate with layers of Th^{4+} ions in nine-fold coordination by F^- ions (Taoudi *et al.*, 1996).

A few hydrates of ternary thorium fluorides are known. Probably the most remarkable hydrate has the composition $(NH_4)_7Th_2F_{15} \cdot H_2O$ (Penneman *et al.*, 1968, 1976) and contains the dimeric anion $[Th_2F_{15}(H_2O)]^{7-}$ in which the Th^{4+} ions are linked via three fluoride ions. Furthermore the lanthanide-containing phases $LaTh_4F_{19} \cdot H_2O$ and $ThEr_2F_{10} \cdot H_2O$ have been reported in which the lanthanide and the Th^{4+} ions occupy the same sites (Guery *et al.*, 1994; Le Berre *et al.*, 2000). Finally, the fluoride hydroxide $Li_3Th_5F_{22}OH$ should be mentioned, which incorporates the Li^+ ions in a three-dimensional network of $[ThF_9]$ and $[ThF_8OH]$ polyhedra (Cousson *et al.*, 1979a).

Polynary thorium fluorides with more than one additional cation have been rarely characterized (Table 3.9). Structural data are available for $Na_3Li_4Th_6F_{31}$ (Brunton and Sears, 1969), $KNaThF_6$ (Brunton, 1970), Li_2CaThF_8 (Vedrine *et al.*, 1973), $Na_3BeTh_{10}F_{45}$ (Brunton, 1973), and $Na_3ZnTh_6F_{29}$ (Cousson *et al.*, 1979b). $Na_3Li_4Th_6F_{31}$ has the same structure as $Na_7Th_6F_{31}$, with some of the Na^+ ions being substituted by Li^+. Similarly, the structure of $KNaThF_6$ is closely related to the structure of the potassium-only compound. Li_2CaThF_8 adopts the structure of $CaWO_4$, even if the symmetry is slightly different. The Li^+ ions occupy the tetrahedral positions of the tungsten atoms, while both Ca^{2+} and Th^{4+} are found on the calcium sites of $CaWO_4$. $Na_3BeTh_{10}F_{45}$ and $Na_3ZnTh_6F_{29}$ (Fig. 3.11) have crystal structures wherein the Th^{4+} ions are found mainly in an eight-fold coordination of fluoride ions (Brunton, 1973). The thorium polyhedra are linked in complicated three-dimensional networks

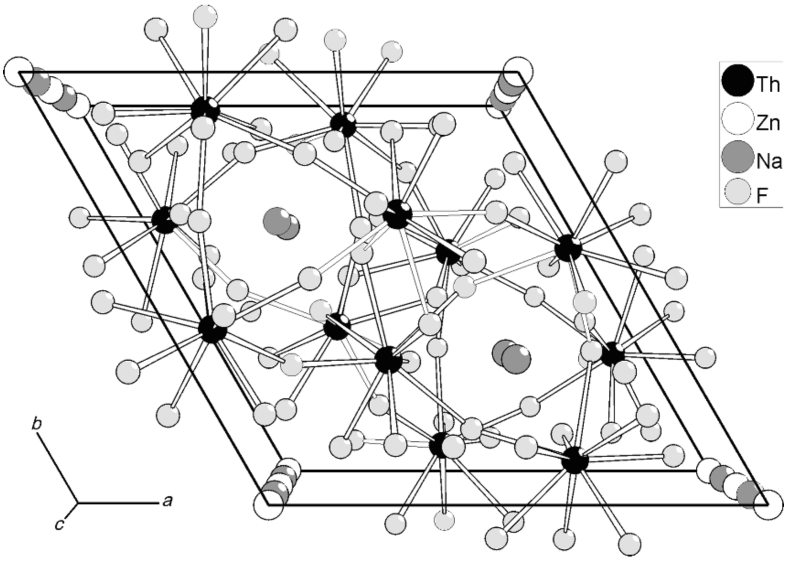

Fig. 3.11 *Crystal structure of the polynary $Na_3ZnTh_6F_{29}$.*

that incorporate the Na^+, Be^{2+}, and Zn^{2+} ions, respectively. The coordination number of the sodium ions range from six to eight. Be^{2+} is tetrahedrally coordinated, and Zn^{2+} is in the center of an octahedron.

Mixed chloride–fluorides, namely $LiThClF_4$, $CsTh_2ClF_8$, $SrThCl_2F_4$, and $BaThCl_2F_8$, have been reported but these compounds are in need of further characterization (Gudaitis *et al.*, 1972; Desyatnik *et al.*, 1974a,b).

Compared to the respective fluorides the number of well-characterized polynary thorium chlorides, bromides, or iodides is quite limited. According to phase diagram investigations containing $ThCl_4$, the compounds included in Table 3.8 are known to exist (Vdovenko *et al.*, 1974; Gershanovich and Suglobova, 1980). However, additional chlorides, which were not found in their respective phase diagrams, have been prepared by several authors (Rosenheim and Schilling, 1900; Rosenheim *et al.*, 1903; Chauvenet, 1911; Siegel, 1956; Ferraro, 1957; Adams *et al.*, 1963; Brown, 1966; Vokhmyakov *et al.*, 1973; Gorbunov *et al.*, 1974; Desyatnik and Emel'yanov, 1975). Unfortunately, the structure of only a few chlorides is known, all of them being exclusively hexachlorothorates containing the octahedral $[ThCl_6]^{2-}$ anion. Alkaline metal ions, Tl^+ and Cu^+, as well as divalent ions, for example Ba^{2+} or Pb^{2+}, may serve as counter-ions (Binnewies and Schäfer, 1973, 1974; Gorbunov *et al.*, 1974; Westland and Tarafder, 1983). Furthermore, alkyl ammonium ions can be used to crystallize the hexachlorothorate (Brown, 1966; Woodward and Ware, 1968). Occasionally, complex $[ThCl_5]^-$ and $[ThCl_7]^{3-}$ ions have been mentioned in the literature (Oyamada and Yoshida, 1975; Yoshida *et al.*, 1978). The enthalpies of formation of several thorium–alkali metal ternary chlorides have been reported. Experimental data on these chlorides, together with those on other actinide ternary halides are assembled and briefly discussed in Chapter 19.

Chloro compounds of thorium in which one or more chloride ions in $ThCl_4$ are replaced by other ligands have been prepared. These ligands can be trimethysilylamide, benzaldehyde, and methylsalicylate, for example (Bradley *et al.*, 1974).

The phase diagrams of $ThBr_4$ and the alkali metal bromides NaBr–CsBr show one compound to exist in each case (Ribas Bernat and Ramos Alonso, 1976; Ribas Bernat *et al.*, 1977; Gershanovich and Suglobova, 1981). For sodium, $NaThBr_5$ melts incongruently, and for the remaining alkali metals, the bromides A_2ThBr_6 ($A = K - Cs$) melt congruently. The structure of the equivalent sodium compound is not known, but for the compounds with heavier alkali metals, the lattice parameters have been derived from powder diffraction data. Although the data are not in entire agreement, it seems very likely that these compounds are (nearly) isotypic with the respective iodides and thus contain the octahedral $[ThBr_6]^{2-}$ anion. The same anion also occurs in the family of bromides, $AThBr_6$, with A being a divalent cation (cf. Table 3.9) (Beck and Kühn, 1995). An interesting exception is the unique crystal structure of In_2ThBr_6. It contains square antiprismatic $[ThBr_8]$ polyhedra that are linked in

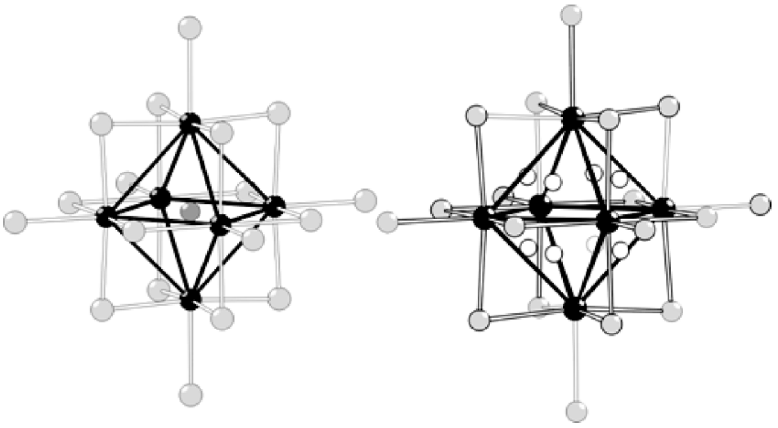

Fig. 3.12 *Octahedral* $[Th_6]$ *cluster in the crystal structures of* $Th_6Br_{15}Co$ *and* $Th_6Br_{14}H_7$*, respectively. The cobalt atom as well as the hydrogen atoms are stabilizing the cluster, which are surrounded by* 18 Br^- ions. *The hydrogen position are only occupied to* 7/8.

chains along [001] according to the formula $^1_\infty[ThBrF_{4/2}Br_{4/1}]$ via shared edges. The chains are held together by nine-fold coordinated In^+ ions (Dronskowski, 1995).

A series of reduced thorium bromides containing octahedral $[Th_6]$ clusters has been described recently. They have been prepared from $ThBr_4$ and thorium metal in the presence of either hydrogen, carbon, or a transition metal, leading to the compounds: MTh_6Br_{15} (M = Mn, Fe, Co, Ni), $Th_6Br_{14}C$, and $Th_6Br_{15}H_7$ (Böttcher *et al.*, 1991a,b). The transition metal and the carbon atom act as a stabilizing interstitial atom within the octahedron whereas the hydrogen atoms are located above the triangular faces of the empty octahedra. In each case, the $[Th_6]$ core is surrounded by 12 Br^- ions that are bridging the edges of the octahedron, and six additional anions attached to the vertices. The linkage of the $[(Th_6Br_{12})Br_6]$ units is different in $Th_6Br_{14}C$ compared to the metal-centered cubic phases, causing the slightly higher Th/Br ratio (Fig. 3.12). Another unique cluster compound is $KTh_{12}N_6Br_{29}$. It shows a core of six $[NTh_4]$ tetrahedra that are connected by sharing edges (Fig. 3.13) (Braun *et al.*, 1995).

Ternary iodides containing the octahedral $[ThI_6]^{2-}$ anion have been prepared with a number of different counter-cations, for example alkali metal ions, tetraalkyl ammonium ions, or $[As(C_6H_5)_4]^+$ (Bagnall *et al.*, 1965; Brown *et al.*, 1970a, 1976; Brendel *et al.*, 1985). The ThI_4/AI_2 systems with A being Ca, Sr, Sn, or Pb, have been investigated and for selected examples crystal structures have even been determined (Beck *et al.*, 1993). Ternary iodides have also been synthesized by the fusion of the binary iodides at elevated temperature with other divalent cations (Beck *et al.*, 1993). Finally, the mercury iodides $Hg_2ThI_8{\cdot}12H_2O$ and $Hg_5ThI_{14}{\cdot}18H_2O$ have been reported (Duboin, 1909a).

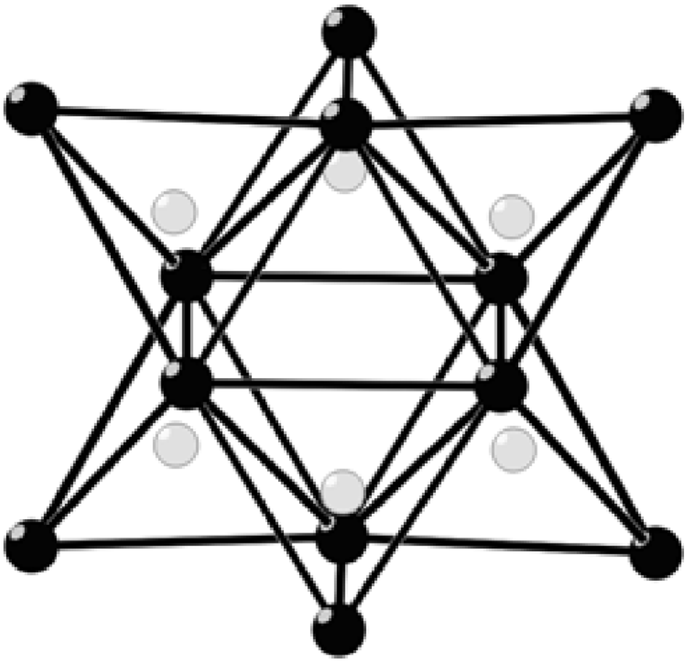

Fig. 3.13 [$Th_{12}N_6$] *core in the crystal structure of* $KTh_{12}N_6Br_{29}$. The unit consists of six linked [NTh_4] *tetrahedra. It might also be seen as an* [Th_6] *octahedron whith four of the six triangular faces capped by an additional thorium atom.*

3.7.5 Chalcogenides

The heavier analogs of oxides, the chalcogenides S, Se, and Te, all form compounds with thorium (Table 3.6). While some are based on simple crystal structures such as fluorite or NaCl, the richness of the electronic structures of sulfur, selenium, and tellurium lend themselves to forming more complex structures than the oxides. Binary thorium sulfur compounds can be prepared by the action of H_2S on the metal (Berzelius, 1829; Nilson, 1876; Moissan and Étard, 1896, 1897), the metal halide (Krüss and Volck, 1894; Duboin, 1908b), the metal hydride (Eastman *et al.*, 1950; Lipkind and Newton, 1952), or on thoria itself in the presence of carbon (Eastman *et al.*, 1950). Sulfur will react at elevated temperatures with the metal or thorium carbide and CS_2 with thoria will also form the binary sulfides. There are six generally recognized structurally characterized sulfides (including ThOS, which is not isostructural with ThS_2 or ThO_2) listed in Table 3.6 (Shalek, 1963). The sulfide with the lowest sulfur content (Khan and Peterson, 1976), ThS, stands out against ThO as not being like ZnS but rather forming the NaCl structure type (Zachariasen, 1949c). However, as mentioned earlier, the characterization of ThO remains a puzzle. ThS is metallic in appearance with a density of 9.56 g cm^{-3}. The compound sinters above 1950°C with no appreciable vapor pressure above its melting point (2200°C). The compound can be machined or polished and becomes superconducting near 0.5 K (Moodenbaugh *et al.*, 1978). The disulfide of thorium, ThS_2, is a purple-brown solid with the $PbCl_2$ structure and a density of 7.36 g cm^{-3}. It is reported to melt at 1905°C with considerable decomposition starting at 1500°C (Eastman *et al.*, 1950, 1951). Heating the disulfide in vacuum will yield a black phase, Th_7S_{12}, which melts around 1770°C (Zachariasen, 1949d; Eastman *et al.*, 1950, 1951). This compound has been mislabeled as Th_4S_7. The sesquisulfide is a brown-metallic phase, isotypic with stibnite, Sb_2S_3 (Zachariasen, 1949c). This phase also melts with no appreciable vapor pressure at high temperatures (2000°C), making it a useful high-temperature crucible material. An orange-brown material has been prepared via a lower-temperature reaction (400°C) between thorium metal and sulfur or between the hydride and excess H_2S. A 'polysulfide' phase was first identified as Th_3S_7 (Strotzer and Zumbusch, 1941) and later found (Graham and McTaggart, 1960) to evolve sulfur around 150°C to yield Th_2S_5, of tetragonal structure, although more recent studies found that it is correctly reported in the orthorhombic cell (Noël and Potel, 1982). ThOS, a yellow phase prepared from the action of thoria and CS_2 or thoria and sulfur (Krüss, 1894; Heindl and Loriers, 1974), forms in the PbFCl structure type, analogous with the rare earth series of compounds (Zachariasen, 1949c). ThOS hydrolyzes in acid solutions as do all the other binary sulfides of thorium (Dubrovskaya, 1971).

Selenium and tellurium form a series of compounds with thorium that are homologs of the sulfides. These compounds, listed in Table 3.6, are ThOSe, ThSe, Th_7Se_{12}, Th_2Se_3, $ThSe_2$, Th_2Se_5, and $ThSe_3$ (D'Eye *et al.*, 1952; D'Eye, 1953; Graham and McTaggart, 1960; Noël, 1980; Kohlmann and Beck, 1999). These phases have all been obtained by the reaction of selenium on thorium metal (D'Eye *et al.*, 1952) on the carbide, the halide, or the silicide of thorium (Moissan and Martinsen, 1905). Thorium selenides have also been produced by the reaction of hydrogen selenide gas on thorium bromide (Moissan and Martinsen, 1905). It has been reported that ThSe becomes superconducting at 1.6 K (Moodenbaugh, 1978), in contrast to earlier observations (Bucher and Staundenmann, 1968). A selenium analog to the polysulfide phase may be Th_7Se_{12} (D'Eye, 1953) or Th_2Se_5 (Graham and McTaggart, 1960). Another reported polyselenide is $ThSe_3$ (Noël and Potel, 1982), which is isotypic with USe_3 (Ben Salem *et al.*, 1984). Finally, the reaction of selenium with thoria yields ThOSe (D'Eye, 1953).

The tellurides of thorium exist in phases of similar stoichiometry but with slightly differing structures from those of the sulfides or selenides. For example, ThTe is found in the CsCl structure rather than the NaCl-type (D'Eye and Sellman, 1954). Several conflicting reports exist about the identity of a higher telluride, Th_3Te_8, although it has been confirmed to be $ThTe_3$, in a structure type analogous to the low-dimensional $ZrSe_3$-type (Graham and McTaggart, 1960). This same report also suggests that $ThTe_2$ is hexagonal rather than orthorhombic as in the $PbCl_2$-type found for $ThSe_2$. Recently, the missing link in the series, Th_7Te_{12}, was prepared and characterized as isostructural with the selenide (Tougait *et al.*, 1998). An early report on 'Th_3Te' has not been confirmed up to now and seems to be not very reliable (Montignie, 1947).

During the past decade, a series of interesting ternary and quaternary thorium chalcogenide phases have been prepared (Cody and Ibers, 1996; Wu *et al.*, 1997; Tougait *et al.*, 1998; Narducci and Ibers, 1998a,b, 2000; Choi *et al.*, 1998; Briggs-Piccoli *et al.*, 2000, 2001, 2002; Hess *et al.*, 2001). The series of layered tellurides and selenides of thorium, ATh_2Te_6, are based on the sesquiselenide or telluride structure type that has been, in effect, pried apart, reduced, and intercalated by an alkali metal (Cody and Ibers, 1996; Wu *et al.*, 1997; Tougait *et al.*, 1998). The review by Narducci and Ibers describes these reactions in detail (1998a). Indeed, a series of related transition metal compounds such as $KCuThSe_3$, $CuTh_2Te_6$, and $SrTh_2Se_5$ have been prepared from the action of tellurium or selenium, or their alkali metal salts, on thorium metal (Narducci and Ibers, 1998a, 2000).

Attempts were also made to prepare chalcophosphate analogs of the thorium phosphates discussed in Section 3.7.7e. The unique chemistry of thiophosphates and selenophosphates provided a rich set of compounds from homoleptic clusters of $[Th_2(PS_4)_6]^{10-}$ (Briggs-Piccoli *et al.*, 2002) to complex three-dimensional phases with a unique $(P_2Se_9)^{6-}$ anion building block in $Cs_4Th_4P_4Se_{26}$ (Briggs-Piccoli *et al.*, 2001).

3.7.6 Pnictides

The nitride of thorium, Th_3N_4, can be prepared by a variety of methods (Gmelin, 1987). One is the strong heating of the metal in the presence of N_2. At the turn of the last century, there was significant debate about the composition and color (chestnut, citron yellow, maroon, and black) of the thorium nitride that could be obtained by heating the metal in presence of N_2 (Matignon and Delepine, 1907; Düsing and Hüniger, 1931). The debate lingered into the 1960s and the variations in color have been attributed to vacancies in nitrogen and oxygen impurities. Indeed, the tan-colored Th_2N_3 is actually Th_2N_2O (Aronson and Auskern, 1966; Benz and Zachariasen, 1966). The golden yellow ThN (Chiotti, 1952; Olson and Mulford, 1965) may likely be seen as a thin layer on the surface of Th_3N_4 as it is the thermally stable product of all decomposition reactions of the other thorium nitrides (Aronson and Auskern, 1966). ThN displays metallic character when prepared as a thin film (Gouder *et al.*, 2002). The ThN phase is isotypic with all other actinide mononitrides and has the NaCl fcc structure (Auskern and Aronson, 1967; Benz *et al.*, 1967). ThN is a superconductor at low temperatures with an inverse dependence of pressure on the critical temperature (Dietrich, 1974).

The synthesis of the binary nitrides listed in Table 3.10 can be achieved most easily by the action of ammonia or nitrogen on heated thorium hydride

Table 3.10 *Crystallographic data of thorium pnictides.*

		Lattice parameters				
Compound	*Lattice symmetry*	*a* (Å)	*b* (Å)	*c* (Å)	*Angles* (°)	*References*
ThN	cubic	5.180				Evans and Raynor (1959)
Th_3N_4	rhombohedral	3.87		27.38		Bowman and Arnold (1971)
Th_2N_3	rhombohedral	3.883		6.187		Zachariasen (1949a)
ThP	cubic	5.840				Gingerich and Wilson (1965)
Th_3P_4	cubic	8.600				Meisel (1939); Zumbusch (1941)
Th_2P_{11}	monoclinic	17.384	10.104	19.193	$\beta = 117.62$	von Schnering *et al.* (1980)
ThP_7	orthorhombic	10.218	10.401	5.671		von Schnering and Vu (1986)
ThAs	cubic	5.978				Ferro (1955)
Th_3As_4	cubic	8.843				Ferro (1955)
$ThAs_2$	tetragonal	4.086		8.575		Ferro (1955); Pearson (1985)
ThSb	cubic	6.318				Ferro (1956)
Th_3Sb_4	cubic	9.371				Ferro (1956)
$ThSb_2$	tetragonal	4.352		9.172		Ferro (1956)
$ThBi_2$	tetragonal	4.492		9.298		Pearson (1985)

(Katzin, 1983). Metal powder heated in nitrogen will yield the nitrides; in the presence of ammonia, a hydride intermediate can be formed (Juza and Gerke, 1968). These hydrogen-containing species might be nitride-imides, nitride-amides, or pure amides of thorium, as investigations of the system Th–N–H have shown. Thoria treated with carbon and heated in a nitrogen atmosphere will also yield nitrides where a finely divided metal powder can be seen as an intermediate.

The reaction of binary nitrides with thorium halides leads to the halide nitrides ThNX (X = F, Cl, Br, I). They have been shown to adopt the BiOCl-type of structure (Juza and Sievers, 1968; Blunck and Juza, 1974). Complex metal nitrides such as Th_2NOP can be prepared by heating binary nitrides with thoria and thorium phosphides (Benz and Zachariasen, 1969; Barker and Alexander, 1974). Heating the nitrides in oxygen generally yields thoria as the product and the nitrides are moisture-sensitive. Several complex mixtures of double salts have been prepared recently, namely $Ca_xTh_{3-x}\,N_{4-2x}O_{2x}$, $Sr_xTh_{3-x}\,N_{4-2x}O_{2x}$, and $Sr_xTh_{1-x}N_xO_{1-x}$ (Brese and DiSalvo, 1995a). Ternary nitrides are the lithium compound Li_2ThN_2 (Palisaar and Juza, 1971) as well as the very unique nitride perovskite phase, $TaThN_3$ (Brese and DiSalvo, 1995b).

This latter cubic perovskite was prepared by the action of Ta_3N_5 and Th_3N_4 at 1400°C as well as by the reaction of $Ta_2Th_2O_9$ and Ca_3N_2 at 1500°C.

The heavier pnictide analogs all form similar binary phases to the nitride that have been characterized by single crystal XRD analysis except for ThBi that is conspicuously absent (Ferro, 1957). Analogously to ThN, ThP, ThAs, and ThSb adopt the fcc NaCl structure (Ferro, 1955, 1956; Gingerich and Wilson, 1965; Javorsky and Benz, 1967; Baskin, 1969). The same structure has been reported for all of the actinide and lanthanide mononitrides and pnictides, respectively. Interestingly, the lattice constant has been shown to decrease when going from Th to U, then to increase through Cm, and finally to decrease again (Lam *et al.*, 1974; Damien and de Novion, 1981) (Fig. 3.14).

Adachi and Imoto reported that the cubic ThP could be made as ThP_{1-x} where x varied from 0 to 0.6. This behavior dramatically affected the hardness of the phase as well as its conductivity (Adachi and Imoto, 1968). Indeed, at 1200°C, the phase ranges from $ThP_{0.4}$ to $ThP_{0.6}$. The non-stoichiometric phases show a weak paramagnetism and the room temperature resistivity of the metallic ThP decreased with an increasing P/Th ratio for the ThP_{1-x} phases. ThP forms a solid solution with UP and displays an antiferromagnetic phase transition at 23 K with up to 40% ThP (Adachi *et al.*, 1973). ThP undergoes a

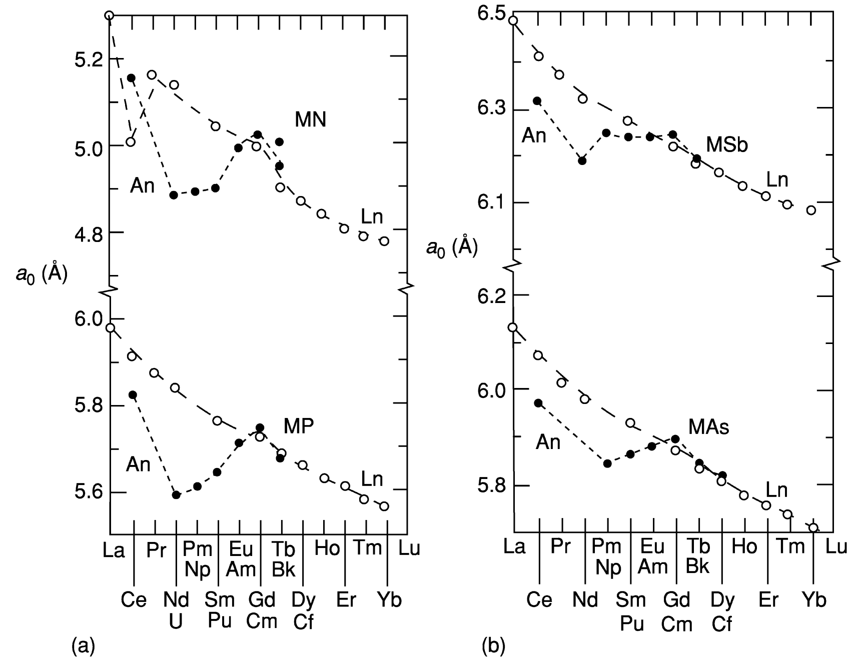

Fig. 3.14 *Lattice constants of actinide and lanthanide monopnicnitides: mononitrides and monophosphides (a); monoantimonides and monoarsenides (b) (Damien and de Novion, 1981).*

structural phase transition from the NaCl-type to the CsCl-type at 30 GPa (Staun Olsen *et al.*, 1988). The reaction between Th and Th_3P_4 at 1100°C will yield ThP (Gingerich and Wilson, 1965; Gingerich and Aronson, 1966; Javorsky and Benz, 1967). Th_3P_4 can be made by the direct combination of the elements (Gingerich and Wilson, 1965; Price and Warren, 1965), by heating $ThCl_4$ with phosphorus vapors (Moissan and Martinsen, 1905), and by the reaction of the hydride with phosphine gas (Lipkind and Newton, 1952). This phase of phosphide is a dark gray material, unlike the black ThP, and is unreactive in water. It releases phosphine upon action by acids and can be ignited to thorium phosphate by heating in air (Strotzer *et al.*, 1938; Meisel, 1939). Th_3P_4 is an n-type semiconductor with a band gap of 0.4 eV (Henkie *et al.*, 1976; Suzuki *et al.*, 1982). A very unique, phosphorus-rich Zintl phase was prepared by the action of phosphorus on thorium metal at 1040°C, yielding Th_2P_{11} (von Schnering *et al.*, 1980). This phase comprises chains of phosphorus atoms linked into two-dimensional nets comprising open and closed P_6 rings. This black, semiconducting phase (band gap of 0.3 eV) decomposes to Th_3P_4 upon heating to 1040°C in vacuum. Other complex ternary phosphides are known including $Th_5Fe_{19}P_{12}$, $ThFe_4P_2$, and $Th_2Mn_{12}P_7$ (Albering and Jeitschko, 1992; Jeitschko *et al.*, 1993). Finally, a dense, magnetoresistive skutterudite phase can be prepared from the elements to yield $ThFe_4P_{12}$ (Dordevic *et al.*, 1999).

In the thorium–arsenic system, ThAs and Th_3As_4 are black-gray compounds that are isomorphous with the associated phosphides and nitrides (Benz, 1968). Th_3As_4 is an n-type semiconductor with a band gap of 0.43 eV (Ferro, 1955; Warren and Price, 1964; Henkie and Markowski, 1978). In contrast to the Th–P system, a diarsenide, $ThAs_2$, is formed, which displays two modifications: a low-temperature phase (α), with the PbCl structure and a high-temperature phase (β) with the Fe_2As structure (Ferro, 1955; Hulliger, 1966). More complex mixtures of ThAs and ThS or ThSe have yielded compounds such as ThAsSe that display unique anomalous Kondo-like behavior (Henkie and Wawryk, 2002). Thorium antimony compounds form in the same structures as the arsenides, with ThSb, Th_3Sb_4, and $ThSb_2$ (Ferro, 1956; Hulliger, 1966, Chiotti *et al.*, 1981). Like the arsenide, ThSb undergoes a high-pressure phase transition from NaCl to the CsCl-type (Palanivel *et al.*, 1995). Kondo-like resistivity behavior was observed for solid solutions of USb and ThSb. The dilution of USb by ThSb lead to large modifications of the electrical transport properties, reflecting the change from antiferromagnetism to ferromagnetism with a concomitant decrease of the ordered magnetic moment per U atom (Frick *et al.*, 1982). In the thorium–bismuth system, three binary compounds with familiar structures are found: ThBi, $ThBi_2$, and Th_3Bi_4 (Ferro, 1957; Dahlke *et al.*, 1969). ThBi was reported as part of an alloy structure although a single crystal structure has not been determined (Borzone *et al.*, 1982). Another phase with the Mn_5Si_3-type was observed as well but was not confirmed by elemental analysis (Borzone *et al.*, 1982). Bismuth can be distilled from ThBi, yielding the thorium-rich Th_5Bi_3 hexagonal structure. During the U.S. breeder reactor program of the mid–1950s, breeder-blanket liquid Bi with a slurry of $ThBi_2$ suspended in the liquid bismuth showed promise but there was significant difficulty in suspending the inhomogeneous particles of $ThBi_2$ (Bryner and Brodsky, 1959).

3.7.7 Complex anions

Thorium compounds with complex anions play an important role in various fields, for example in separation techniques (cf. Section 3.4) and nuclear waste disposal, to name only two of them. Thus, this chemistry has been widely investigated, although often not in very detail, what is especially true with respect to structural characterizations. In the following the most important and more recent findings are summarized. For each complex anion an extra subdivision has been created and reliable crystallograhic data are presented in Table 3.11.

(a) Perchlorates

Thorium perchlorate is highly soluble in water and crystallizes, generally from acidic solution, in the form of the tetrahydrate $Th(ClO_4)_4{\cdot}4H_2O$ (Murthy and Patel, 1965). The structure of the tetrahydrate is not known, but the compound has been shown to decompose at 280°C to form $ThO(ClO_4)_2$ that finally forms ThO_2 at 335°C (Murthy and Patel, 1965). The oxide–perchlorate apparently will dissolve in water, and from XRD this is interpreted to be due to the formation of a tetrameric species (Bacon and Brown, 1969). An elegant (but somewhat dangerous) route to prepare anhydrous $Th(ClO_4)_4$ is the reaction of $ThCl_4$ with Cl_2O_6 (Koulkès-Pujo *et al.*, 1982). From X-ray powder diffraction, an orthorhombic lattice has been deduced with the space group probably being $P2_12_12$ (Ramamurthy and Patel, 1963). Due to the weak coordination tendency of the ClO_4^- ion, $Th(ClO_4)_4$ is frequently used to prepare coordination compounds of thorium in which the perchlorate anion in not included in the coordination sphere (Gmelin, 1985b, 1993a).

(b) Sulfates (VI, IV)

A detailed discussion of the older literature on thorium sulfates has been given by Mellor (1941). Thorium sulfates can be prepared by the reaction of various thorium salts, for example thorium nitrate, with concentrated sulfuric acid. Upon crystallization from aqueous solution, different hydrates can be obtained. At lower temperatures (0–45°C), $Th(SO_4)_2{\cdot}9H_2O$ has the lowest solubility (Clève, 1874; Roozeboom, 1890; Dawson and Williams, 1899). Nevertheless, the octahydrate is usually obtained even under these conditions (Clève, 1874; Krüss and Nilson, 1887b; Roozeboom, 1890; Koppel and Holtkamp, 1910). Furthermore, a hexahydrate has been mentioned and at higher temperature,

Table 3.11 *Crystallographic data of thorium compounds with oxo anions.*

		Lattice parameters				
Compound	*Space group*	*a* (Å)	*b* (Å)	*c* (Å)	*Angles* (°)	*References*
$Th(SO_4)_2 \cdot 8H_2O$	$P2_1/n$	8.51	11.86	13.46	$\beta = 92.65$	Habash and Smith (1983)
$Th(OH)_2SO_4$	Pnma	11.733	6.040	7.059		Lundgren (1950)
$K_4Th(SO_4)_4 \cdot 2H_2O$	$C\bar{1}$	10.096	16.75	9.762	$\alpha = 95.15$ $\beta = 95.22$ $\gamma = 91.00$	Arutyunyan *et al.* (1963)
$Na_2Th(SO_4)_3 \cdot 6H_2O$	$P2_1/c$	5.567	16.81	15.76	$\beta = 91.925$	Habash and Smith (1990)
$Cs_2Th(SO_4)_3 \cdot 2H_2O$	$P2_1/c$	6.415	15.95	13.078	$\beta = 90.88$	Habash and Smith (1992)
$Th(NO_3)_4 \cdot 5H_2O$	Fdd2	11.191	22.89	10.579		Taylor *et al.* (1966)
$Th(NO_3)_4 \cdot 4H_2O$	$P2_1/n$	7.438	17.530	9.183	$\beta = 99.72$	Charpin *et al.* (1987)
$ThOH(NO_3)_3 \cdot 4H_2O$	$P2_1/c$	6.772	11.693	13.769	$\beta = 102.63$	Johansson (1968a)
$(NH_4)_2Th(NO_3)_6$	$P2_1/n$	8.321	6.890	13.097	$\beta = 91.55$	Spirlet *et al.* (1992)
$MgTh(NO_3)_6 \cdot 8H_2O$	$P2_1/c$	9.080	8.750	13.610	$\beta = 97.03$	Scavnicar and Prodic (1965)
$(C(NH_2)_3)_6Th(CO_3)_5 \cdot 4H_2O$	B11b	16.15	16.70	13.23	$\gamma = 108.42$	Voliotis and Rimsky (1988)
$Na_6Th(CO_3)_5(H_2O)_{12}$	$P\bar{1}$	9.60	9.92	13.64	$\alpha = 90.47$ $\beta = 104.38$ $\gamma = 95.52$	Voliotis and Rimsky (1975)
$(C(NH_2)_3)_5(Th(CO_3)_3F_3)$	$P2_12_12_1$	9.53	29.79	9.11		Voliotis (1979)
$Na_6BaTh(CO_3)_6(H_2O)_6$	$R\bar{3}$	14.175		8.605		Yamnova *et al.* (1990)
$Th(P_2O_7)$	$Pa\bar{3}$	8.721				Burdese and Borlera (1963)
$KTh_2(PO_4)_3$	C2/c	17.57	6.863	8.138	$\beta = 101.77$	Matkovic *et al.* (1968)
$NaTh_2(PO_4)_3$	C2/c	17.37	6.81	8.13	$\beta = 101.13$	Matkovic *et al.* (1970)
$Pb_{0.5}Th_2(PO_4)_3$	C2/c	17.459	6.8451	8.1438	$\beta = 101.25$	El-Yacoubi *et al.* (1997)
$CuTh_2(PO_4)_3$	C2/c	22.029	6.7430	7.0191	$\beta = 108.58$	Louer *et al.* (1995)
$Na_2Th(PO_4)_2$	C2/c	7.01	21.50	9.12	$\beta = 111.02$	Galesic *et al.* (1984)

$KTh(P_3O_{10})$	$P2_12_12_1$	8.234	10.187	10.015		Ruzic Toros *et al.* (1974)
$Na_6(Th(PO_4)(P_2O_7))_2$	$P\bar{1}$	8.734	8.931	6.468	$\alpha = 93.33$ $\beta = 108.29$ $\gamma = 110.10$	Kojic-Prodic *et al.* (1982)
$Na_2Th(PO_4)_2$	$P2_1/c$	7.055	21.66	9.095	$\beta = 111.56$	Galesic *et al.* (1984)
$Th_4(PO_4)_4(P_2O_7)$	Pcam	12.865	10.437	7.0676		Bénard *et al.* (1996)
$KTh_2(VO_4)_3$	C2/c	18.564	7.157	8.077	$\beta = 101.05$	Quarton and Kahn (1979)
ThV_2O_7	Pnnm	7.216	6.964	22.80		Quarton *et al.* (1970)
$Pb_{0.5}Th_{0.5}(VO_4)$	$I4_1/a$	5.175		11.943		Andreetti *et al.* (1984)
$Pb_{0.5}Th_{0.5}(VO_4)$	$I4_1/amd$	7.428		6.590		Andreetti *et al.* (1984)
$Pb_{0.5}Th_{0.5}(VO_4)$	$P2_1/n$	7.046	7.3089	6.8066		Andreetti *et al.* (1984)
$Th(VO_3)_2O$	$Pn2_1a$	7.201	22.771	6.945		Launay *et al.* (1992)
$Th(MoO_4)_2$-I	Pbca	10.318	9.737	14.475		Cremers *et al.* (1983)
$Th(MoO_4)_2$-II	$P\bar{3}$	17.593		6.238		Larson *et al.* (1989)
$K_2Th(MoO_4)_3$	C2/c	17.649	12.143	5.3688	$\beta = 105.76$	Huyghe *et al.* (1991a)
$K_4Th(MoO_4)_4$	$I4_1/a$	11.586		13.069		Huyghe *et al.* (1991b)
$K_8Th(MoO_4)_6$	$P\bar{1}$	10.255	10.260	14.466	$\alpha = 75.87$ $\beta = 96.81$ $\gamma = 118.43$	Huyghe *et al.* (1993)
$Cu_2Th_4(MoO_4)_9$	$I\bar{4}3d$	14.477				Launay *et al.* (1998)
$CdTh(MoO_4)_3$	$P6_3/m$	9.803		6.350		Launay and Rimsky (1980)
$Th(OH)_2CrO_4 \cdot H_2O$	$P2_1/m$	7.67	6.11	6.94	$\beta = 113.91$	Lundgren and Sillen (1949)
$ThSiO_4$	$I4_1/amd$	7.133		6.319		Taylor and Ewing (1978)
$ThSiO_4$	$P2_1/n$	6.784	6.974	6.500	$\beta = 104.92$	Taylor and Ewing (1978)
$Ca_2ThSi_8O_{20}$	I422	7.483		14.893		Szymanski *et al.* (1982)
$Na_{12}Th_3(Si_8O_{19})_4 \cdot 18H_2O$	$R\bar{3}c$	29.124		17.260		Li *et al.* (2000)

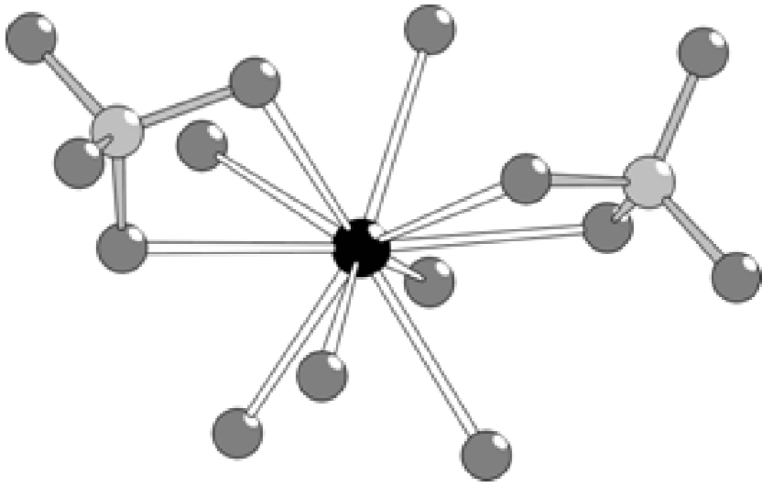

Fig. 3.15 *The* $[Th(SO_4)_2(H_2O)_6]$ *molecule in the crystal structure of* $Th(SO_4)_2{\cdot}8H_2O$.

a tetrahydrate is said to form (Roozeboom, 1890; Dawson and Williams, 1899; Wirth, 1912). A dihydrate was observed as an intermediate of the dehydration of higher hydrates (Rollefson, 1947) and $Th(SO_4)_2{\cdot}8H_2O$ has been structurally characterized (Fig. 3.15). It shows the Th^{4+} ions in a ten-fold coordination by oxygen atoms, which belong to six water molecules and two chelating sulfate ions. The coordination polyhedron is a distorted bicapped squared antiprism. The crystal structure is completed by two crystal water molecules (Habash and Smith, 1983).

The formation of basic thorium sulfates has also been frequently observed but these compounds are not well characterized (Krüss and Nilson, 1887b; Wyrouboff and Verneuil, 1898b, 1899; Meyer and Gumperz, 1905). $ThOSO_4$ has been reported to form upon dehydration of $ThOSO_4{\cdot}3H_2O$ but none of these compounds has been further investigated (Wyrouboff, 1901; Wöhler *et al.*, 1908; Hauser and Wirth, 1908; Barre, 1910, 1911; Halla, 1912). The structure is known only for $Th(OH)_2SO_4$, which has been thought to be $ThOSO_4{\cdot}H_2O$ (Lundgren, 1950). The thorium ions are connected as dimers by two OH^- ions. The coordination sphere of Th^{4+} is completed by four monodentate sulfate groups and the dimeric $[Th_2(OH)_2(SO_4)_8]$ units are linked into a three-dimensional network.

Various polynary sulfates containing alkali metals are thought to exist (Colani, 1909; Barre, 1912). The phase diagram of $Na_2SO_4/Th(SO_4)_2$ has been determined recently wherein the compound $Na_{12}Th(SO_4)_8$ is found (Fedorov and Fedorov, 2001). Solid state reactions of ThO_2 with $KHSO_4$, $K_2S_2O_8$, and $K_2S_2O_7$ afforded $K_4Th(SO_4)_4$ (Keskar *et al.*, 2000). Also the reactions of ThO_2 with $(NH_4)_2SO_4$, and mixtures of $(NH_4)_2SO_4$ with NH_4NO_3 or NH_4HF, have been studied (Singh Mudher *et al.*, 1995). Furthermore, the rubidium compound, $Rb_2Th(SO_4)_3$, has been synthesized. Despite these investigations no structural data of the anhydrous species have been reported until now. A little more information is available for the hydrated polynary sulfates (Cleve, 1874; Manuelli and Gasparinetti, 1902; Rosenheim *et al.*, 1903; Barre, 1910, 1911). According to very old data, they may contain alkali and thorium metal ions in a ratio of 1:1, 2:1, 3:1, and 4:1, but newer investigations determined the compositions as $A_2Th(SO_4)_3 \cdot xH_2O$ and $A_4Th(SO_4)_4 \cdot xH_2O$ (A = Na–Cs, NH_4) (Gmelin, 1986b), where the water content x varies from 2 to 6. Additionally, $M_6Th(SO_4)_5 \cdot 3H_2O$ (M = Cs, NH_4) and $(NH_4)_8Th(SO_4)_6 \cdot 2H_2O$ are known (Gmelin, 1986b). For several compounds, infrared spectroscopy (IR) data are available (Evstaf'eva *et al.*, 1966) and structure determinations have been done for $Na_2Th(SO_4)_3 \cdot 6H_2O$ (Habash and Smith, 1990), $Cs_2Th(SO_4)_3 \cdot 2H_2O$ (Habash and Smith, 1992), and $K_4Th(SO_4)_4 \cdot 2H_2O$ (Arutyunyan *et al.*, 1963). The sodium compound exhibits chains of ${}^{1}_{\infty}[Th(H_2O)_{3/1}(SO_4)_{6/2}]$ running along [100] in which the Th^{4+} ions are surrounded by six monodentate SO_4^{2-} ions and three H_2O molecules to form a tricapped trigonal prism. The chains are linked by the Na^+ ions and three non-coordinating water molecules are found in the unit cell. In $Cs_2Th(SO_4)_3 \cdot 2H_2O$ the $[Th(H_2O)_2(SO_4)_5]$ polyhedra are linked to layers according to ${}^{2}_{\infty}[Th(H_2O)_2(SO_4)_{4/2}(SO_4)_{1/1}]$ that are connected by the Cs^+ ions. For the Th^{4+} ions a coordination number of nine arises due to the chelating nature of two of the SO_4^{2-} groups. In $K_4Th(SO_4)_4 \cdot 2H_2O$ zigzag chains are found with the formula ${}^{1}_{\infty}[Th(H_2O)_{2/1}(SO_4)_{4/2}(SO_4)_{2/1}]$. One of the SO_4^{2-} ions acts as chelating ligand leading to a coordination number of 9 for Th^{4+}.

Thorium sulfates containing other counter-cations besides alkali metals are rarely described. They include the manganese compound $MnTh(SO_4)_3 \cdot 7H_2O$ that was obtained from an aqueous solution of the binary sulfates at 30°C, the tin compound, $Sn_2Th(SO_4)_4 \cdot 2H_2O$ (Weinland and Kühl, 1907), and the poorly characterized thallium sulfates (Fernandes, 1925). Finally, the organic guanidinium ion has been used for the precipitation of thorium sulfato complexes (Molodkin *et al.*, 1964).

With $Th(SO_3F)_4$, one fluorosulfate of thorium has been synthesized by the reaction of HSO_3F with thorium acetate. According to IR measurements the anions act as bidentate ligands. The thermal decomposition of the compound yields SO_2F_2 and $Th(SO_4)_2$ (Paul *et al.*, 1981).

Thorium sulfate (IV), $Th(SO_3)_2 \cdot xH_2O$, is said to form as a white precipitate when SO_2 is passed through a solution containing Th^{4+} ions or when an alkali metal sulfite is added (Clève, 1874; Chavastelon, 1900; Baskerville, 1901; Grossmann, 1905). Based on differential thermal analysis (DTA) investigations, the water content x is believed to be four (Golovnya *et al.*, 1967a,b). Hydrolysis of the thorium sulfites or their thermal decomposition leads to basic compounds with different compositions (Golovnya *et al.*, 1964, 1967a). Furthermore, various ternary sulfites containing alkali metal ions or the ammonium ion have been mentioned, but a more precise characterization is needed for these compounds

(Chavastelon, 1900; Golovnya *et al.*, 1967b,c). A number of organic solvates of thorium sulfites are reported, but again, further characterization is still needed (Golovnya *et al.*, 1967b).

(c) Nitrates

Nitrates of thorium may be prepared by dissolving $Th(OH)_4$ in nitric acid. Depending on the concentration of the acid, three different hydrates form upon evaporation. If the acid concentration is in the range between 1 and 54%, a pentahydrate crystallizes while a tetrahydrate is obtained at concentrations up to 75% (Ferraro *et al.*, 1954). Both hydrates have molecular structures. The tetrahydrate contains $[Th(NO_3)_4(H_2O)_4]$ molecules with all of the nitrate groups being attached in a chelating manner to the Th^{4+} ions, leading to a coordination number of 12 (Charpin *et al.*, 1987). In the non-centrosymmetric pentahydrate, $Th(NO_3)_4 \cdot 5H_2O$, there are also four chelating nitrate groups around Th^{4+} but only three additional H_2O molecules, yielding a coordination number of 11. The remaining water molecules are held via hydrogen bonds in the structure so that the compound has to be formulated according to $[Th(NO_3)_4(H_2O)_3] \cdot 2H_2O$ (Ueki *et al.*, 1966). The structure of the pentahydrate has also been determined by neutron diffraction so that exact hydrogen positions are known (Taylor *et al.*, 1966). Furthermore, thermodynamic data have been provided for the pentahydrate (Ferraro *et al.*, 1956; Cheda *et al.*, 1976; Morss and McCue, 1976).

From nearly neutral solutions, a hexahydrate was said to crystallize (Fuhse, 1897; Misciatelli, 1930a,b). Unfortunately it has not been structurally characterized and due to the well-known tendency of Th^{4+} compounds to hydrolyze, it might be possible that the hexahydrate is in fact a basic species. With $ThOH(NO_3)_3 \cdot 4H_2O$, another basic nitrate is known (Johansson, 1968a,b). As seen in Fig. 3.16, it contains the dimers $[Th_2(OH)_2(NO_3)_6(H_2O)_6]$, with the Th^{4+} ions in an 11-fold coordination by three H_2O molecules, two hydroxide ions, and three chelating nitrate groups. The dimers are arranged in the lattice with additional crystal water molecules. The thermal decomposition of thorium nitrate hydrates leads to ThO_2. According to DTA and thermogravimetry (TG) measurements, various intermediates can be observed (Tiwari and Sinha, 1980). Acidic thorium nitrates have been reported, for example $H_2Th(NO_3)_6{\cdot}3H_2O$, but unfortunately they have not been characterized (Moseley *et al.*, 1971). Also $Th(NO_3)_4{\cdot}2N_2O_5$, which is said to form in highly concentrated HNO_3, has not been investigated further (Kolb, 1913; Misciatelli, 1930a,b; Ferraro *et al.*, 1954, 1955).

Thorium nitrate is well soluble in water and various oxygen-containing organic solvents such as alcohols, ketones, ethers, and esters (Imre, 1927; Misciatelli, 1929; Templeton and Hall, 1947; Rothschild *et al.*, 1948; Yaffe, 1949; Bock and Bock, 1950). The solid solvate $Th(NO_3)_4 \cdot 3H_2O \cdot 3C_2H_5OCH_2CH_2OC_2H_5$ has been crystallized from a solution of thorium

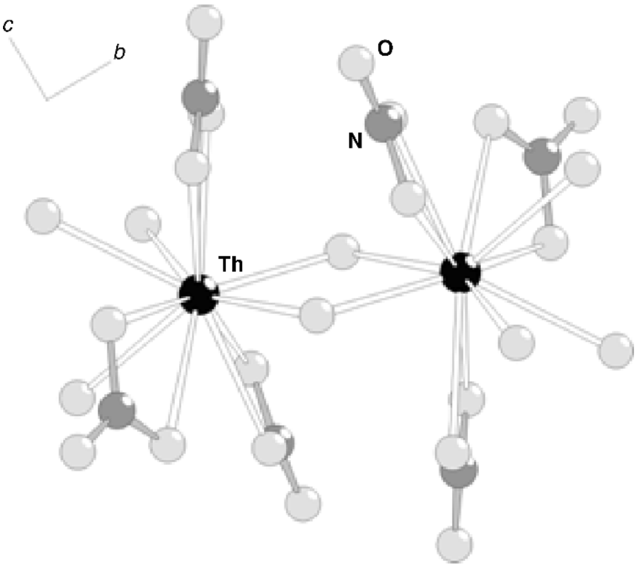

Fig. 3.16 *The dimeric unit* $[Th_2(OH)_2(NO_3)_6(H_2O)_6]$ *in the crystal structure of* $ThOH(NO_3)_3{\cdot}4H_2O$.

nitrate in the diethylether of ethyleneglycol (Katzin, 1948), and compounds with a variety of nitrogen bases in place of water are known (Kolb *et al.*, 1908; Kolb, 1913). It is possible to extract thorium nitrate from aqueous solution with an immiscible organic solvent if the aqueous phase is extremely concentrated, or if it contains high concentrations of ammonium nitrate (Templeton and Hall, 1947; Rothschild *et al.*, 1948; Hyde and Wolf, 1952; Newton *et al.*, 1952b). Since the rare earth metal ions do not extract well under the same conditions, being almost totally restricted to the aqueous phase, the procedure finds application in the preparation of pure thorium salts from ores containing rare earth elements.

A particularly useful liquid extractant is tri(*n*-butyl)phosphate (TBP) (Warf, 1949; Anderson, 1950), as well as other phosphate esters (Peppard, 1966, 1971; Shoun and McDowell, 1980). These compounds differ from ordinary nucleophilic solvents in that they interact specifically with the metal ion through the oxygen atom of the phosphoryl group to form a very strong solvation bond. In the case of thorium nitrate, this results in the formation of very stable complexes in the organic phase, with two and three molecules of phosphate per molecule of thorium nitrate (Katzin *et al.*, 1956). The TBP adduct is stable even against considerable dilution with 'inert' fluids such as benzene, CCl_4, or aliphatic hydrocarbons, which are themselves not solvents for thorium nitrate (Anderson, 1950; Katzin *et al.*, 1956). The coordination interaction of Th^{4+} in aqueous solution with phosphate esters is the basis of an important commercial process for the extraction and purification of thorium. Normally, addition of ammonia to the aqueous phase causes the formation of hydroxo complexes that reduce the efficiency of the thorium nitrate extraction. If this is coupled with addition of a neutral salting agent such as lithium nitrate, it is found that extraction is enhanced by formation of a hydroxynitrate of thorium. The polymeric complex has been formulated as $[Th_4(OH)_{10}(NO_3)_6(TBP)_4]$, thus contains one tri(*n*-butyl)phosphate molecule per thorium atom in contrast to the monomeric unhydrolyzed thorium nitrate complex (Klyuchnikov *et al.*, 1972). Thorium nitrate forms 1:1 or 1:2 complexes with crown ethers, depending on the size of the crown (Zhou *et al.*, 1981; Rozen *et al.*, 1982; Wang *et al.*, 1982). These can also be used as extractants (Wang *et al.*, 1983).

Organic donor molecules such as butylamine, dimethylamine, aromatic amine *N*-oxides, and others have been frequently used to prepare complexes with thorium nitrate (Rickard and Woolard, 1978). A compound with trimethylphosphine oxide, $Th(NO_3)_4 \cdot 3/8(Me_3PO)$, has been crystallographically characterized (Alcock *et al.*, 1978). It contains $[Th(NO_3)_3(Me_3PO)]^+$ cations and $[Th(NO_3)_6]^{2-}$ anions, a structural feature that is frequently displayed by transition metal–halide complexes (Katzin, 1966).

A number of ternary thorium nitrates with mono or divalent counter-cations are known (Jacoby, 1901; Meyer and Jacoby, 1901; Sachs, 1901). Those of the type $A_2Th(NO_3)_6$ contains the complex anion $[Th(NO_3)_6]^{2-}$ that shows the Th^{4+} ion in 12-fold coordination by oxygen atoms (Spirlet *et al.*, 1992). The latter contains six chelating nitrate groups, as it was shown from the structure determination of the ammonium compound. The same complex anion is found in the nitrates $BTh(NO_3)_6 \cdot 8H_2O$ with B = Mg, Mn, Co, Ni, Zn (Geipel, 1992). In this case, the counter-ions are octahedral $[B(H_2O)_6]^{2+}$ complexes according to the formulation $[B(H_2O)_6][Th(NO_3)_6] \cdot 2H_2O$ (Scavnicar and Prodic, 1965). Another series of ternary nitrates with monovalent cations includes members of the composition $ATh(NO_3)_5{\cdot}xH_2O$, with A = NH_4, Na, K. They have not been fully characterized, so the amount of crystal water is not known (Meyer and Jacoby, 1901; Molodkin *et al.*, 1971; Volkov *et al.*, 1974). Furthermore, the nitrates $K_3Th(NO_3)_7$ and $K_3H_3Th(NO_3)_{10}{\cdot}4H_2O$ have been reported, but again structural data are not known (Meyer and Jacoby, 1901; Molodkin *et al.*, 1971).

(d) Carbonates

Thorium hydroxide absorbs CO_2 readily (Berzelius, 1829; Chydenius, 1863; Clève, 1885; Chauvenet, 1911), where the end product is the hydrated $ThOCO_3$, and finally $Th(CO_3)_2{\cdot}0.5H_2O$ under high CO_2 pressures. The composition of this latter product has also been given as $Th(OH)_2CO_3{\cdot}2H_2O$ (Kharitonov *et al.*, 1969). Hydrates of the oxycarbonate are also produced by the action of sodium or ammonium carbonate on a solution of a thorium salt. The carbonate is somewhat soluble in excess alkali carbonate solution (Clève, 1885) because of the formation of complexes strong enough to prevent precipitation of thorium by ammonia, fluoride, or phosphate. Sodium hydroxide, however, will bring about precipitation (Sollman and Brown, 1907). The nature of the carbonato complexes (Dervin and Faucherre, 1973a,b; Shetty *et al.*, 1976) will be discussed in more detail in Section 3.8. Crystallization of these complexes is possible using various counter-cations, and compounds with Na^+, K^+, Tl^+, NH_4+, $(HGua)^+$ (guanidinium), Ca^{2+}, Ba^{2+}, and $[Co(NH_3)_6]^{3+}$ have been reported (Clève, 1874; Rosenheim *et al.*, 1903; Canneri, 1925; Rosenheim and Kelmy, 1932; Chernyaev *et al.*, 1958; Kharitonov *et al.*, 1969; Ueno and Hoshi, 1970; Dervin and Faucherre, 1973b; Dervin *et al.*, 1973; Voliotis and Rimsky, 1975, 1988). All of the salts are hydrated and the sodium compound, $Na_6Th(CO_3)_5 \cdot xH_2O$, has been reported to occur with a considerable range of hydration. In the crystal structures of $Na_6Th(CO_3)_5 \cdot 12H_2O$ and $[C(NH_2)_3]_6Th(CO_3)_5{\cdot}4H_2O$, the Th^{4+} ions are in ten-fold coordination by oxygen atoms (Voliotis *et al.*, 1977). In the mineral tuliokite, $Na_6BaTh(CO_3)_6 \cdot 6H_2O$, six chelating carbonate groups are attached to the Th^{4+} ion leading to a $[ThO_{12}]$ icosahedron (Yamnova *et al.*, 1990). Carbonates containing additional anions have been reported, for example $Na_5Th(CO_3)_4OH \cdot 9H_2O$, $Na_4Th(CO_3)_4 \cdot 7H_2O$, $(HGua)_4Th(CO_3)_4 \cdot 6H_2O$, $(HGua)_2Th(CO_3)_3 \cdot 5H_2O$, $K_3Th(CO_3)_3(OH) \cdot 5H_2O$, $(NH_4)_2Th(CO_3)_3 \cdot 6H_2O$, $Na_2Th(CO_3)_2(OH)_2 \cdot 10H_2O$, $K_2Th(CO_3)_2(OH)_2 \cdot 10H_2O$, and the fluoride carbonate $(HGua)_5Th(CO_3)_3F_3$ (Voliotis, 1979).

(e) Phosphates

Phosphates of thorium have been investigated for many years (Troost and Ouvrard, 1885; Johnson, 1889; Kauffmann, 1899; Hecht, 1928; King, 1945; Dupuis and Duval, 1949; Burdese and Borlera, 1963; Hubin, 1971; Laud, 1971). More recent studies were carried out in relation with the potential of phosphate matrices to be used as radioactive waste storage material, due to their resistance to radiation effects and their low solubilities (Baglan *et al.*, 1994; Merigou *et al.*, 1995; Genet *et al.*, 1996; Dacheux *et al.*, 1998; Volkov, 1999; Brandel *et al.*, 2001a,b). The system ThO_2/P_2O_5 has been studied in the 1960s and the phosphates $Th_3(PO_4)_4$, $(ThO_3)(PO_4)_2$, $(ThO)_2P_2O_7$, ThP_2O_7, and $ThO_2{\cdot}0.8P_2O_5$ have been reported. Recent investigations, however, show that $ThO_2{\cdot}0.8P_2O_5$ and the orthophosphate, $Th_3(PO_4)_4$, do not exist (Bénard *et al.*, 1996; Brandel *et al.*, 1998). Instead, the phosphate–diphosphate $Th_4(PO_4)_4P_2O_7$ has been obtained under similar conditions. Subsequently it has been shown that the compound can be synthesized applying dry or wet preparative routes and even single crystals have been grown. Besides ThP_2O_7 (Burdese and Borlera, 1963), the orthophosphate–disphosphate is the only structurally known binary thorium phosphate to date, although various other species, for example $ThOH(PO_4)$ and $Th_2(PO_4)_2HPO_4{\cdot}H_2O$, have been reported (d'Ans and Dawihl, 1929; Merkusheva, 1967; Molodkin *et al.*, 1968a; Brandel *et al.*, 2001a,b). In the crystal structure of the orthophosphate–diphosphate

(Bénard *et al.*, 1996), Th^{4+} is surrounded by four monodentate and one chelating PO_4^{3-} groups and one diphosphate ion. The latter suffers from a positional disorder. In ThP_2O_7, the Th^{4+} ions are octahedrally surrounded by six monodentate $P_2O_7^{4-}$ ions and the polyhedra are linked in a three-dimensional cubic network. The compound is thought to exhibit a second modification that has unfortunately not been structurally characterized.

Several ternary thorium phosphates are known, especially those with additional monovalent cations like alkali metals, silver, copper, and thallium (Wallroth, 1883; Palmer, 1895; Haber, 1897; Schmid and Mooney, 1964; Matkovic and Sljukic, 1965; Matkovic *et al.*, 1966, 1968, 1970; Molodkin *et al.*, 1970; Topic *et al.*, 1970; Popovic, 1971; Laügt, 1973; Ruzic Toros *et al.*, 1974; Kojic-Prodic *et al.*, 1982; Galesic *et al.*, 1984; Arsalane and Ziyad, 1996). Phosphates with the composition $MTh_2(PO_4)_3$ (M = Na, K) show ferroelectric properties and are thus of special interest. In the crystal structure, the Th^{4+} ions are nine-fold coordinated by oxygen atoms that belong to seven PO_4^{3-} ions. Two of the latter are chelating ligands. The linkage of the polyhedra leads to parallel layers (100) that are further linked into a three-dimensional network in [100] direction. The Na^+ or K^+ ions in $MTh_2(PO_4)_3$ can be replaced by Pb^{2+} ions, leading to the composition $Pb_{0.5}Th_2(PO_4)_3$ without structural changes (El-Yacoubi *et al.*, 1997). The structure of $CuTh_2(PO_4)_3$ is very similar, although the coordination number of Th^{4+} is lowered to eight. Another characteristic feature of the structure is the linear two-fold coordination of the Cu^+ ions (Louer *et al.*, 1995).

(f) Vanadates

The vanadates of thorium have been investigated to a much lesser extent than the respective phosphates. They seem to parallel the structural chemistry of the phosphates (Le Flem and Hagenmuller, 1964; Le Flem *et al.*, 1965; Quarton *et al.*, 1970; Baran *et al.*, 1974; Elfakir *et al.*, 1987), but high-quality structure determinations are rare. For example, such determinations have been performed for $MTh_2(VO_4)_3$ (M = K, Rb) and 'ThV_2O_7' (Quarton and Kahn, 1979; Elfakir *et al.*, 1987, 1989; Nabar and Mangaonkar, 1991; Launay *et al.*, 1992; Pai *et al.*, 2002). The latter compound is not a divanadate but a mixed *ortho*-vanadate–*catena*-vanadate with the formula $Th(VO_4)(VO_3)$ (Fig. 3.17). Other structurally characterized vanadates include $BaMTh(VO_4)_3$ (M = La, Pr) that adopt the monazite structure type (Nabar and Mhatre, 2001) and the silver compound, $AgTh_2(VO_4)_3$, in the zircon-type (Elfakir *et al.*, 1990). Monazite-, scheelite-, and zircon-type structures have also been frequently observed for other ternary or quaternary thorium *ortho*-vanadates, namely $Pb_{0.5}Th_{0.5}(VO_4)$ (Botto and Baran, 1981; Andreetti *et al.*, 1984; Calestani and Andreetti, 1984), $MLaTh(VO_4)_3$ (M = Sr, Pb) (Nabar and Mhatre, 1982), and $CdMTh(VO_4)_3$ (M = La, Yb) (Nabar *et al.*, 1981). Furthermore, a hydrogenvanadate, Th $(HVO_4)_2{\cdot}5H_2O$, is said to precipitate, when VO_4^{3-} is added to solution of a thorium salt (Clève, 1874; Volck, 1894; Neish, 1904).

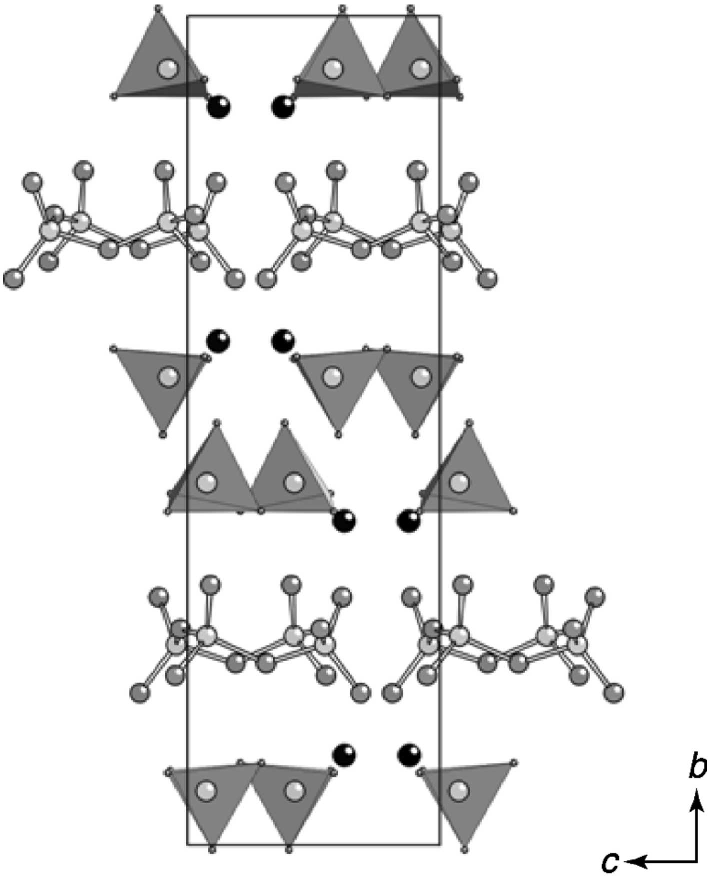

Fig. 3.17 *Crystal structure of Th(VO_4)(VO_3) (or ThV_2O_7). The structure contains isolated* ortho-*vanadate ions (drawn as tetrahedra) and* catena-*vanadate strands.*

(g) Molybdates

One compound, Th(MoO_4)$_2$, is found in the system ThO_2/MoO_3 (Zambonini, 1923; Thoret *et al.*, 1970; Pagès and Freundlich, 1971; Thoret, 1971, 1974). It can be obtained by fusion of the binary oxides or as a hydrate by adding ammonium or alkali metal molybdate to Th^{4+} solutions (Metzger and Zons, 1912; Banks and Diehl, 1947; Trunov and Kovba, 1963; Trunov *et al.*, 1966; Thoret *et al.*, 1968). Th(MoO_4)$_2$ is dimorphic. The orthorhombic low-temperature form shows the Th^{4+} ion in an eight-fold coordination by eight monodentate MoO_4^{2-} groups (Thoret *et al.*, 1970; Thoret, 1974). The molybdate tetrahedra are coordinated to four Th^{4+} ions, leading to a three-dimensional network. In the high-temperature trigonal modification, one set of thorium ions are coordinated by six oxygen atoms while the other set has tricapped trigonal-prismatic coordination polyhedra (Cremers *et al.*, 1983; Larson *et al.*, 1989).

With alkali metal molybdates, M_2MoO_4, $Th(MoO_4)_2$ forms a great variety of compounds (Barbieri, 1913; Thoret, 1971, 1974; Bushuev and Trunov, 1974). The compositions $M_2Th_4(MoO_4)_9$, $M_2Th_2(MoO_4)_5$, $M_2Th(MoO_4)_3$, $M_4Th(MoO_4)_4$, $M_6Th(MoO_4)_5$, and $M_8Th(MoO_4)_6$ have been reported, but only very few of them are properly characterized. In $K_2Th(MoO_4)_3$ the Th^{4+} ions are coordinated by eight oxygen atoms that belong to one chelating and six monodentate MoO_4^{2-} ions (Huyghe *et al.*, 1991a). The $[Th(MoO_4)_7]$ polyhedra are linked to chains along [001] that are held together by K^+ ions. $K_4Th(MoO_4)_4$ consists of a three-dimensional network with the formula $^3_\infty[Th(MoO_4)_{8/2}]$, where the potassium ions are found in holes in the structure (Huyghe *et al.*, 1991b). All of the MoO_4^{2-} groups are monodentate, leading to a coordination number of eight for Th^{4+}. The potassium-rich molybdate $K_8Th(MoO_4)_6$ contains isolated $[Th(MoO_4)_6]^{8-}$ ions in which Th^{4+} attains a coordination number of eight due to the chelating nature of two of the six molybdate groups (Huyghe *et al.*, 1993). The cadmium compound $CdTh(MoO_4)_3$ shows the Th^{4+} ions in tricapped trigonal-prismatic coordination of nine monodentate MoO_4^{2-} groups (Launay and Rimsky, 1980). The prisms are connected to columns along the *c*-axis that are stacked in a hexagonal fashion. In this way channels are formed in which the Cd^{2+} ions reside in an octahedral coordination. $Cu_2Th_4(MoO_4)_9$ has a complicated three-dimensional structure with nine-fold coordinated thorium ions (Launay *et al.*, 1998).

(h) Chromates

Upon addition of dichromate to a solution containing Th^{4+}, the thorium chromate $Th(CrO_4)_2 \cdot 3H_2O$ precipitates at room temperature (Palmer, 1895; Haber, 1897; Britton, 1923). At higher temperatures, a monohydrate precipitates (Palmer, 1895). Both hydrates have been investigated by optical microscopy and seem to be hexagonal or rhombic (Vasilega *et al.*, 1980). According to thermal investigations $Th(CrO_4)_2 \cdot 3H_2O$ dehydrates by a three-step mechanism (Vasilega *et al.*, 1980). Above 280°C, the anhydrous chromate is obtained that remains stable up to 620°C where it decomposes to ThO_2 and Cr_2O_3. Under acidic conditions, for example in concentrated chromic acid, $Th(CrO_4)_2 \cdot CrO_3 \cdot 3H_2O$ is found as the equilibrium solid in the system $ThO_2/CrO_3/H_2O$ (Palmer, 1895; Britton, 1923). None of these compounds is structurally characterized, but the basic chromate, $Th(OH)_2CrO_4 \cdot H_2O$ (Palmer, 1895; Britton, 1923), has been investigated by means of XRD (Lundgren and Sillen, 1949). Its crystal structure contains zigzag-chains of hydroxo-bridged Th^{4+} ions along [010]. Further linkage of the thorium ions is achieved through bonding to CrO_4^{2-} ions.

(i) Miscellaneous oxometallates

A limited number of thorium compounds with oxo-anions other than those discussed above have been mentioned in the literature. The arsenates of thorium are obviously related to the phosphates (Le Flem, 1967; Hubin, 1971; Chernorukov *et al.*, 1974a,b), while the tungstates resemble the molybdates (de Maayer *et al.*, 1972; Thoret, 1974). Thorium *ortho*-germanate, $ThGeO_4$, has been shown to be dimorphic (Bertaut and Durif, 1954; Perezy Jorba *et al.*, 1961; Harris and Finch, 1972) and adopts either the zircon or the scheelite structure type (Ennaciri *et al.*, 1986). This compound has been used as a host lattice for trivalent lanthanides (Gutowska *et al.*, 1981). Besides the most important silicate minerals thorite, huttonite, and thorogummite already mentioned in Section 3.3, a number of complex silicate minerals is known, which are, however, often not characterized completely. Structural data are, for example, available for ekanite, $Ca_2ThSi_8O_{20}$ (Szymanski *et al.*, 1982), and $Ca_6Th_4(SiO_4)_6O_2$, which has the apatite type of structure (Engel, 1978). Furthermore the structure of the mineral thornasite, $Na_{12}Th_3(Si_8O_{19})_4 \cdot 18H_2O$, has been reported recently (Li *et al.*, 2000). One borate, $Th(B_2O_5)$, has been structurally investigated. It contains $B_2O_5^{4-}$ ions and eight-fold coordinated Th^{4+} ions (Baskin *et al.*, 1961; Cousson and Gasperin, 1991).

Additional thorium compounds with transition metal oxo-anions such as the perrhenates should be mentioned. $Th(ReO_4)_4 \cdot 4H_2O$ was obtained from $Th(OH)_4$ and $HReO_4$ (Silvestre *et al.*, 1971; Zaitseva *et al.*, 1984). Its structure is not known but is has been shown to dehydrate in four steps yielding $Th(ReO_4)_4$, which finally decomposes to $Th_2O(ReO_4)_6$ (Zaitseva *et al.*, 1984). $Th(ReO_4)_4$ forms ternary compounds with alkali perrhenates and mixed anionic species with WO_4^{2-} and MoO_4^{2-} (Silvestre, 1978).

Other oxo-metallates reported are the titanate $ThTi_2O_6$ (brannerite structure) (Perezy Jorba *et al.*, 1961; Radzewitz, 1966; Ruh and Wadsley, 1966; Loye *et al.*, 1968; Kahn-Harari, 1971; Zunic *et al.*, 1984; Mitchell and Chakhmouradian, 1999), the niobate $ThNb_4O_{12}$ (Keller, 1965; Trunov and Kovba, 1966; Alario-Franco *et al.*, 1982), and the tantalates $ThTa_2O_7$, $Th_2Ta_2O_9$ (Keller, 1965; Schmidt and Gruehn, 1989, 1990), $Th_2Ta_6O_{19}$ (Busch *et al.*, 1996), and $Th_4Ta_{18}O_{53}$ (Busch and Gruehn, 1996) have been reported. Structurally, however, they are preferably described as double oxides rather than oxo-metallates. Values for the enthalpies of formation of thorite, huttonite (Mazeina *et al.*, 2005) and thorium brannerite (Helean *et al.*, 2003) are given in Chapter 19.

(j) Carboxylates and related organic salts

Carboxylate complexes of thorium have been frequently investigated with respect to the role they may play in solvent extraction processes. Carboxylates and related salts have also been employed in gravimetric analyses for thorium, either by direct weighing if the compound is stoichiometric, or after ignition to thorium dioxide. Thus, there are a large number of papers describing these compounds. Most of them have been mentioned in the *Gmelin Handbook* (Gmelin, 1988a), so only selected examples will be presented here.

The most investigated groups among the carboxylates are formates and acetates. Formates and formato complexes can be obtained by the reaction of formic acid with $ThCl_4$ or other salts of Th^{4+}. In acid solution, $Th(OOCH)_4$, is formed, which has been shown to be polymorphic (Mentzen, 1969, 1971a,b; Greis *et al.*, 1977) and may contain different amounts of crystal water (Claudel and Mentzen, 1966; Thakur *et al.*, 1980). If the pH of the solution increases above 6, basic formates start to form. They may have different compositions like $ThOH(OOCH)_3$, $Th(OH)_2(OOCH)_2$, and $Th(OH)_3(OOCH)$ (Gmelin, 1988a) but they have not been structurally characterized. Various metal ions have been used to crystallize formato complexes, such as $MTh(OOCH)_5$ (M = K, Rb, Cs, NH_4) and $MTh(OOCH)_6$ (M = Sr, Ba). All these complexes have been characterized by thermal analysis and vibrational spectroscopy (Molodkin *et al.*, 1968b; Gmelin, 1988a).

The structural knowlegde of thorium acetates and acetato complexes is also quite limited, although quite a number of compounds have been described. The tetraacetate, $Th(CH_3COO)_4$, is said to be isotypic with the respective uranium acetate (Eliseev *et al.*, 1967; Bressat *et al.*, 1968; Gmelin, 1988a), and similar to the formates, various hydrates and basic salts are known. Derivatives of acetic acid such as CF_3COOH, CCl_3COOH, $CHCl_2COOH$, $CH_2ClCOOH$, $C_6H_5CH_2COOH$, $C_6H_5CH(OH)COOH$, naphtyl acetic acid, and others, have been used to prepare the respective salts (Katzin and Gulyas, 1960; Gmelin, 1988a). Even bromo- and iodoacetates are known. Among the chloroacetates, one compound has been investigated crystallographically. It has the composition $[Th_6(CHCl_2\ COO)_{12}(OH)_{12}(H_2O)_2]$ and shows an octahedral $[Th_6]$ core surrounded by the ligands.

With increasing complexity of the carboxylic acids, less is known structurally about their thorium compounds. The compounds prepared include glycolates, propionates, butyrates, and their derivatives. Furthermore, compounds with unsaturated mono carboxylic acids have been reported, for example crotonates and cinnamates.

The largest group of thorium salts of dicarboxylic acids are the oxalates and oxalato complexes, for which some crystallographic data are available (Gmelin, 1988a). More complex dicarboxylic acids have been employed, and even the thorium salts of long-chain acids like sebacic acid, $HOOC(CH_2)_8COOH$, are known. The latter has been used, along with *m*-nitrobenzoic acid (Neish, 1904), picrolonic acid (Hecht and Ehrmann, 1935; Dupuis and Duval, 1949), or 'ferron' (7-iodo-8-hydroxyquinoline-5-sulfonic acid), for analytical purposes (Dupuis and Duval, 1949).

3.7.8 Coordination compounds

Coordination compounds of thorium are of special interest because the knowledge of their behavior and their properties is fundamental for the understanding of separation processes (for example, the thorium extraction [THOREX] process that involves tri(*n*-butyl)phosphate complexes) (Peppard and Mason, 1963), see Chapter 24, the development of decontamination methods, and the treatment of radioactive waste. Thus, the number of compounds reported in literature is very large. The *Gmelin Handbook* provides a comprehensive overview of the compounds investigated until 1983 (literature closing date) (Gmelin, 1985b). A more recent review (Agarwal *et al.*, 2000) covers thorium compounds with neutral oxygen donor ligands. These ligands can be divided with respect to the atom to which the oxygen donor is bonded: ligands containing a C–O group may, for example, be alcohols, phenols, ketones, esters, ethers, formamide, acetamide, those containing a N–O group are typically pyridine and quinoline *N*-oxides or even nitrosyl chloride and P=O, As=O, and S=O groups are known for the respective phosphine, arsine, and sulfoxides. The group of neutral oxygen donor ligands is probably the most investigated, but also a great number of complexes with neutral nitrogen donor ligands are known (Vigato *et al.*, 1977). Besides NH_3 (Matthews, 1898; von Bolton, 1908; Clark, 1924), the ligands are higher amines, hydrazine and its derivatives, and pyridine and its derivatives (Matthews, 1898;Adi and Murty, 1978; Al-Daher and Bagnall, 1984). Coordination compounds with charged ligands besides the above-mentioned carboxylates have been also frequently investigated. Among these ligands are the diketonates and related ligands, tropolone and its derivatives, and a great number of Schiff base ligands (Biradar and Kulkarni, 1972).

One of the most important thorium coordination compounds is thorium tetrakis(acetylacetonate), $Th(acac)_4$, which can be sublimed at temperatures below its melting point of 171°C (Urbain, 1896). This is also true for most of the substituted acetylacetonates, for example the trifluoromethylacetylacetonate, whose structure has been determined and that shows the thorium atoms in square antiprismatic coordination of oxygen atoms (Wessels *et al.*, 1972). These compounds are generally efficiently extracted into water-immiscible solvents, a property that has been used, for example, with thenoyltrifluoroacetone, to measure complexation of thorium with various anions (Calvin, 1944; Day and Stoughton, 1950). Another ligand that has been studied in more detail is 8-hydroxyquinoline ('oxine') and its derivatives (Frazer and Rimmer, 1968; Abraham and Corsini, 1970; Corsini and Abraham, 1970; Singer *et al.*, 1970; White and Ohnesorge, 1970). Also heteroleptic species involving oxine and another ligand, for example dimethylsulfoxide, are known (Singer *et al.*, 1970; Andruchow and Karraker, 1973). As a thorium complex with eight-fold thorium coordination with sulfur atoms, thorium(IV) tetrakis(*N*,*N*-diethyldithiocarbamate) should be mentioned (Brown *et al.*, 1970b). A path to related compounds is through intermediates such as $Th(NEt_2)_4$ (Bradley and Gitlitz, 1969; Watt and Gadd, 1973), which, when treated with CXY (X,Y = O, S, Se etc.), gives carbamates, thiocarbamates, mixed compounds like $Th[OSCN(CH_3)_2]_4$, and even $Th(Se_2CNEt_2)_4$ (Bagnall and Yanir, 1974). It is very surprising that despite the large number of complexes that have been prepared, the number of structure determinations is very limited.

3.7.9 Organothorium compounds

As Chapters 25 and 26 are devoted to the synthesis, the characterization and the properties of the organoactinide compounds, only selected examples shall be mentioned briefly here.

Thorocene, $Th(COT)_2$ (COT = cyclo-octatetraene), has been prepared by treating $ThCl_4$ in tetrahydrofuran (THF) with $K_2(COT)$ at dry-ice temperature (Streitwieser and Yoshida, 1969). The yellow crystals of $Th(COT)_2$ sublime at 0.01 mmHg pressure and 160°C. Thorocene, isomorphous with $U(COT)_2$ (uranocene) (Avdeef *et al.*, 1972), is unstable in air, decomposes in water, and undergoes thermal decomposition without melting above 190°C. Gas-phase photoelectron spectra have been used to elucidate the bonding in thoracene (Fragala *et al.*, 1976; Clark and Green, 1977). This compound has also been prepared by treating ThF_4 with Mg(COT) (Starks *et al.*, 1974). In addition, a number of half-sandwich Th(IV) complexes with COT have been reported (LeVanda *et al.*, 1980; Zalkin *et al.*, 1980).

Numerous complexes with the cyclopentadienyl (Cp^-) anion have been reported. $Th(Cp)_4$ was first prepared by the reaction of $ThCl_4$ with KCp (Fischer and Treiber, 1962). This compound sublimes between 250 and 290°C at 10^{-3} to 10^{-4} mmHg. Tris(cyclopentadienyl) halides and alkoxides of thorium have been synthesized (Ter Haar and Dubeck, 1964; Marks *et al.*, 1976), and, in general, these air-sensitive compounds sublime below 200°C and 10^{-3} to 10^{-4} mmHg pressure. Related tris(indenyl)thorium halides and alkoxides have been prepared (Laubereau *et al.*, 1971; Goffart *et al.*, 1975, 1977). The only bis (cyclopentadienyl)thorium dihalide reported is $ThI_2(Cp)_2$, prepared from ThI_4 and $Mg(Cp)_2$ (Reid and Wailes, 1966), whereas it is believed that the chloride analog would be unstable, similar to the uranium compound (Ernst *et al.*, 1979). In contrast, the permethylated Cp derivative $C_5(CH_3)_5^-$ (=Cp*) has been used to prepare stable dichlorides, $(Cp^*)_2ThCl_2$ (Manriquez *et al.*, 1978; Blake *et al.*, 1998). The CpTh trihalides have been described to exist as adducts with ethers, $CpThX_3 \cdot 2L$ (L = tetrahydrofurane or 1/2 dimethoxyethane [DME]) (Bagnall *et al.*, 1978). Analogous indenyl (Goffart *et al.*, 1980) and Cp* compounds have also been reported (Mintz *et al.*, 1982).

Tetrabenzylthorium, $Th(CH_2C_6H_5)_4$, is the best-characterized thorium homoalkyl compound reported to date (Köhler *et al.*, 1974). The light-yellow, air-sensitive, crystalline compound decomposes slowly at room temperature. A second tetrahydrocarbyl thorium complex has been reported, $Th(CH_3)_4(dmpe)_2$ (dmpe = bis(dimethylphosphino)ethane), prepared by the reaction of $ThCl_4(dmpe)_2$ with CH_3Li (Edwards *et al.*, 1981). It is stable up to –20°C in the absence of air and moisture. These two thorium phosphine complexes, along with $Th(OC_6H_5)_4(dmpe)_2$ and $Th(CH_2C_6H_5)_4(dmpe)_2$, were the first isolated and characterized species of their kind (Edwards *et al.*, 1984). Tetraallylthorium, $Th(C_3H_5)_4$, has been reported and decomposes slowly above 0°C (Wilke *et al.*, 1966).

The reaction of the Cp– (Marks and Wachter, 1976), indenyl– (Goffart *et al.*, 1977), and Cp*–thorium chlorides (Fagan *et al.*, 1981; Fendrick, 1984) with alkylating or arylating reagents has yielded the corresponding π-ligand thorium hydrocarbyls. In a thermodynamic study on the series $(Cp^*)_2ThR_2$, it was observed that the bond disruption enthalpies of the thorium–ligand σ-bonds were about 250–335 kJ mol^{-1}, significantly greater than similar transition metal bond enthalpies (Bruno *et al.*, 1983).

More recent investigations on organothorium chemistry were intended to introduce new ligands in that field and to synthesize low-valent thorium compounds. For example, the bicyclic pentalene dianion $C_8H_6^{2-}$ has been used to prepare a new type of thorium sandwich complex. The crystal structure, as well as the photoelectron spectra, of $[Th\{C_6H_4(Si^iPr_3\text{–}1{,}5)_2\}_2]$ was reported (Cloke and Hitchcock, 1997; Cloke *et al.*, 1999). Another very interesting ligand, the dicarbollide anion $C_2B_9H_{11}^{2-}$, should be mentioned: it is found in the complexes $[Li(THF)_4]_2[Th(\eta^5\text{-}C_2B_9H_{11})_2X_2]$ (X = Cl, Br, I) (Rabinovich *et al.*, 1997).

The number of potentially low-valent organothorium complexes is still very limited. Two forms of $Th(C_5H_5)_3$ have been reported. Purple $Th(C_5H_5)_3$ was prepared by sodium naphtalide reduction of $Th(C_5H_5)_3Cl$ in THF. The latter was removed under vacuum (Kanellakopulos *et al.*, 1974). According to X-ray powder diffraction measurements, the compound is isotypic with the analogs of heavier 5f elements and has an effective magnetic moment of $0.331\mu_B$. The green form of $Th(C_5H_5)_3$ was formed via photolysis of $Th(C_5H_5)_3[(CH(CH_3)_2]$ in benzene solution and has a magnetic moment of $0.404\mu_B$ (Kalina *et al.*, 1977). A recent example is $[Th\{COT(TBS)_2\}_2][K(DME)_2]$ – with $COT(TBS)_2$ = $\eta\text{-}C_8H_6(t\mathrm{Bu}Me_2Si)_2\text{–}1{,}4$ – that has been prepared by the reaction of a suspension of $[Th\{COT(TBS)_2\}_2]$ in DME with elemental potassium (Parry *et al.*, 1999). Furthermore, the first organometallic compounds of divalent thorium have been reported recently. They contain the complex Et_8-calix[4]tetrapyrrole ligand and are potentially divalent synthons (Korobkov *et al.*, 2003).

3.8 SOLUTION CHEMISTRY

3.8.1 Redox properties

Thorium is known to have only one stable oxidation state in aqueous solution, the tetravalent state, $Th^{4+}(aq)$ (Gmelin, 1988c).

Th(III) has been recently claimed by Klapötke and Schulz (1997) to be formed by reaction of $ThCl_4$ with HN_3 in slightly acidic solution and to be stable for at least 1 h. Reportedly, the reaction involved:

$$Th^{4+} + HN_3 \rightarrow Th^{3+} + 1.5N_2 + H^+$$

Yet, the reaction has been shown to be thermodynamically impossible by Ionova *et al.* (1998). First, the stabilization of d-electrons by the crystal field effect is not sufficient to assign, as suggested by Bratsch and Lagowski (1986), a value of –3.0 V to the redox potential of the couple M^{4+}/M^{3+}. Besides, a value between –3.35 and –3.82 V, in the same range as the previously published one, –3.7 V (Nugent *et al.*, 1973), is much more probable. Secondly, the reducing ability of HN_3 has been overestimated and the authors concluded that the spectra published by Klapötke and Schulz (1997), as a proof of the existence of Th^{3+}(aq) (broad absorption signal centered around 460 nm and intense peaks at 392, 190 and below 185 nm), correspond, in fact, to azido–chloro complexes of Th(IV).

3.8.2 Structure of the aqueous Th^{4+} ion

The LIII-edge extended X-ray fine structure (EXAFS) experiments on 0.03–0.05 M Th(IV) in 1.5 M $HClO_4$ solutions have clearly defined the structure of the Th(IV) aqua ion (Moll *et al.*, 1999). A least-squares refinement of the data leads to a Th–O distance of (2.45 ± 0.01) Å and a coordination number of (10.8 ± 0.5) which is larger than the older values estimated by Johansson *et al.* (1991) from low-angle X-ray scattering (LAXS) results (8.0 ± 0.5 water molecules at 2.485 Å) or by Fratiello *et al.* (1970) from ^1H NMR data at low temperatures and higher concentrations (nine water molecules in the first hydration sphere).

The results of Moll *et al.* are consistent with the structural parameters obtained in the same study for U^{4+}(aq) (CN = 10 ± 1; $R = 2.42 \pm 0.01$ Å) and previously by Allen *et al.* (1997) for Np^{4+}(aq) (CN = 11.2 ± 0.4; $R = 2.40 \pm 0.01$ Å). A correlation between the hydration number (higher than 6) of highly charged metal ions and the bond distance shows also that a M–O distance of 2.45 Å is in favor of a hydration number closer to 10 (Sandström *et al.*, 2001). More precise systematics and correlation between the space around the cation and its charge have been proposed by David and Vokhmin (2003). They give consistent coordination numbers of Th^{4+}, U^{4+}, Np^{4+}, and Pu^{4+}: 11.0, 10.65, 10.2, and 10.0, respectively. The same authors have evaluated the corresponding ionic radii, 1.178 Å for Th^{4+}, and a size of the coordinated water molecule of 1.335 Å, by assuming a pure electrostatic bond. It would result in a larger cation–oxygen distance of 2.51 Å. The observed difference with experimental data (0.06 Å) has been interpreted by a covalent effect and the effective charge of the Th^{4+} aquo ion has been evaluated to be 3.82 (David and Vokhmin, 2003). Finally, the same authors have determined the number of water molecules in a second hydration sphere as 13.4.

3.8.3 Thermodynamics of the Th^{4+}(aq) ion

The data on the standard enthalpy of formation, entropy, and corresponding Gibbs energy, adopted in this review and shown in Table 3.12, are those given in the compilation of Martinot and Fuger (1985), except for a small difference in the standard Gibbs energy of formation, due to the use of a more recent value for the entropy of Th(cr) (see Chapter 19).

Table 3.12 *Main thermodynamic properties of the thorium aqueous ion at* 25°C (*see text for references*).

$E°(Th^{4+}/Th)$	$\Delta_f H°$(kJ mol^{-1})	$\Delta_f G°$(kJ mol^{-1})	$S°$ (J K^{-1} mol^{-1})
−(1.828 ± 0.015) V/NHE	−(769.0 ± 2.5)	−(705.5 ± 5.6)	−(422.6 ± 16.7)

Thermodynamic models have been proposed recently by David and Vokhmin (2001) to evaluate the Gibbs hydration energy and the entropy of the aquo ions. Corresponding values are $\Delta_{hyd}G°(Th^{4+}) = -6100$ kJ mol^{-1} and $S°(Th^{4+},aq) = -438$ J mol^{-1} K^{-1} (David and Vokhmin, 2003). The entropy value is consistent with the experimental value, –(422.6 ± 16.7) J K^{-1} mol^{-1} (Martinot and Fuger, 1985).

The standard state partial molar heat capacities and volumes of Th^{4+}(aq) have been recently determined from 10 to 55°C under conditions minimizing complications due to hydrolysis and ion-pairing equilibria or ion–ligand complexation (measurements on aqueous solutions containing $Th(ClO_4)_4$ in dilute $HClO_4$ (Hovey, 1997)). The values obtained at 25°C, $C_p°(Th^{4+},aq) = -(224 \pm 3)$ J $K^{-1}mol^{-1}$ and $V°(Th^{4+},aq) = -(60.6 \pm 0.5)$ cm^3 mol^{-1}, appear as more negative than those of any monoatomic aqueous ion. These results are also quite different from the previous estimations: $C_p°(Th^{4+},aq) = -(1 \pm 11)$ J K^{-1} mol^{-1} (Morss and McCue, 1976) recalculated as −(60 ± 11) J K^{-1} mol^{-1} using a newer $C_p°(NO_3^-$,aq) value, –72 J K^{-1} mol^{-1} (Hovey, 1997) and $V°(Th^{4+},aq)$ = –53.5 and –54.6 cm^3 mol^{-1} from the values given in the International Critical Tables (1928) for the standard state partial molar volumes of $ThCl_4$(aq) and $Th(NO_3)_4$(aq), respectively.

3.8.4 Hydrolysis behavior

Being the largest actinide tetravalent ion, Th^{4+}(aq) is also the least hydrolyzable of them (Onosov, 1971). Because of its size, it is less hydrolyzable than many other multi-charged ions such as iron(III); tetravalent thorium may therefore be studied over a larger range of concentrations, at pH values up to 4. However, its tendency to undergo polynucleation reactions and colloid formation, as well as the low solubility of its hydroxide or hydrous oxide, limit the possibilities of investigation. For these reasons, the oxide/hydroxide solubility products and hydrolysis constants published in the literature show great discrepancies.

Very recently, Neck and Kim (2001) have proposed a critical review and a comprehensive set of thermodynamic constants at zero ionic strength and 25°C. In the first part of their work, they compared the frequently accepted constants of Baes *et al.* (1965), Baes and Mesmer (1976), Brown *et al.* (1983), Grenthe and Lagerman (1991), and Ekberg and Albisson (2000). All these data, which are reported in Table 3.13, are based on potentiometric titrations at 15, 25, or 35°C with relatively low thorium concentrations (2×10^{-4} to 10^{-5} M).

Ekberg and Albinsson have performed, in addition, solvent extraction experiments with a total concentration of Th(IV) in the range 10^{-5} to 10^{-7} M. It should be outlined that, under the conditions usually applied in potentiometric and solvent extraction studies ($[\mathrm{Th}]_{\mathrm{tot}} = 2 \times 10^{-4}$ to 2×10^{-2} M; pH = 2.5–4; Kraus and Holmberg, 1954; Hietanen and Sillen, 1964; Baes *et al.*, 1965; Nakashima and Zimmer, 1984), polynuclear species are of major importance and laser-induced breakdown detection (LIBD) has shown that a considerable amount of colloids were present at $\log[\mathrm{H}^+] \leq -(1.90 \pm 0.02)$ for $\log[\mathrm{Th}]_{\mathrm{tot}} = -(2.04 \pm 0.02)$ and at $\log\,[\mathrm{H}^+] \leq -(2.40 \pm 0.03)$ for $\log[\mathrm{Th}]_{\mathrm{tot}} = -(4.05 \pm 0.02)$ (Bundschuh *et al.*, 2000). We can also cite the work of Moulin *et al.* (2001) who recently applied electrospray ionization–mass spectrometry to determine the hydrolysis of Th(IV) in dilute solution, but the equilibrium constants so-determined $\log K^\circ_{11} = -(2.0 \pm 0.2), \log K^\circ_{12} = -(4.5 \pm 0.5), \text{and} \log K^\circ_{13} = -(7.5 \pm 1.0)$ are so large, compared to those obtained from the above-cited well-established methods, that it is difficult to consider them as reliable.

As we can see from Table 3.13, the first mononuclear hydrolysis constants found by Brown *et al.* (1983) and Ekberg and Albinsson (2000) are about one order of magnitude higher than the constants derived by Baes and Mesmer (1976) and Grenthe and Lagerman (1991). Moreover, the hydrolysis constants reported for $\mathrm{Th(OH)}_2^{2+}$, $\mathrm{Th(OH)}_3^{+}$, and $\mathrm{Th(OH)_4(aq)}$ differ between authors by several orders of magnitude. In order to select the best available data, Neck and Kim (2000) estimated the 'unknown' formation constants of $\mathrm{Th(OH)}_n^{(4-n)+}$ by two methods.The first one, method A, is based on the empirical intercorrelation between hydrolysis constants of actinide ions at different oxidation states. The second method, B, developed by the authors consists of applying a semiempirical approach, in which the decrease of the stepwise complexation constants for a given metal–ligand system is related to the increasing electrostatic repulsion between the ligands. From their results collected in Table 3.13, Neck and Kim concluded that the higher $\log \beta^\circ_{11}$ values, in the range 11.7–11.9, and the lower $\log \beta^\circ_{13}$ and $\log \beta^\circ_{14}$ values (Ekberg and Albinsson, 2000) should be preferred. Consequently, their selected values are $\log \beta^\circ_{1n} = (11.8 \pm 0.2), (22.0 \pm 0.6), (31.0 \pm 1.0)$, and (39.0 ± 0.5) for $n = 1, 2, 3$, and 4, respectively (Neck and Kim, 2000). These data have been used to plot the speciation diagrams given in Fig. 3.18.

Following a similar approach, Moriyama *et al.* (1999) analyzed the mononuclear hydrolysis constants of actinide ions by using a simple hard sphere model. Systematic trends were thus obtained, from which the values given in Table 3.13 have been deduced ($\log \beta^\circ_{1n} = 12.56$, 23.84, 32.76, and 40.40 for $n = 1, 2, 3$, and 4, respectively). These values are intermediate between the two series calculated by Neck and Kim (2000) and are in rather good agreement with the averages of literature data ($\log \beta^\circ_{1n} = 11.27$, 22.43, 33.41, and 40.94 for $n = 1, 2, 3$, and 4, respectively) given by Moriyama *et al.* (1999).

Table 3.13 *Experimental and estimated hydrolysis constants proposed for Th(IV) at 25°C and defined as follows ([i] and γ_i denoting the concentration and the activity coefficient of the species i):*

$$K_{1-n} = [Th(OH)_n^{(4-n)+}][H^+]^n/[Th^{4+}]$$

$$\beta^\circ_{1-n} = [Th(OH)_n^{(4-n)+}](\gamma_{Th(OH)n})/[Th^{4+}](\gamma_{Th})[OH^-]^n(\gamma_{OH})^n$$

The values at $I = 0$ (log β°_{1n}) have been calculated by Neck and Kim (2001) by applying the specific interaction theory (SIT) following the NEA Thermochemical Data Base project (Grenthe et al., 1992).

References	*Method*	*Medium*	log β^o_{1-1} (*log* K_{1-1})	log β^o_{1-2} (*log* K_{1-2})	log β^o_{1-3} (*log* K_{1-3})	log β^o_{1-4} (*log* K_{1-4})
Hietanen and Sillen (1964)	potentiometry and coulometry	3 M NaCl	(–2.65/ <–2.33)			
Baes *et al.* (1965); Baes and Mesmer (1976)	potentiometry	1 M $NaClO_4$	11.0 ± 0.2 (–4.12 ± 0.03)^{a}	22.2 ± 0.2 (–7.81 ± 0.03)^{a}	<30.3^{b}	40.1 ± 0.3^{b}
Brown *et al.* (1983)	potentiometry	0.1 M KNO_3	11.7 ± 0.1 (–2.98 ± 0.07)			
Nakashima and Zimmer (1984)	solvent extraction	0.5 M KNO_3	11.8 ± 0.2 (–3.28)			
Bruno *et al.* (1987)	potentiometry	3 M $NaClO_4$	(–4.13 ± 0.06)			(–15.07 ± 0.2)
Moon (1989)	ThO_2 solubility	0.1 M $NaClO_4$	12.42 ± 0.02^{c}	22.46 ± 0.15^{c}	34.36 ± 0.07^{c}	42.58 ± 0.08^{c}
	$Th(OH)_4$ solubility	0.5 M $NaClO_4$	12.58 ± 0.02^{c}	22.35 ± 0.15^{c}	34.42 ± 0.07^{c}	42.76 ± 0.08^{c}
Grenthe and Lagerman (1991)	potentiometry	3 M $NaClO_4$	10.9 ± 0.3 (–4.35 ± 0.09)		32.7 ± 0.4 (–12.3 ± 0.2)	42.4 ± 0.4 (–16.65 ± 0.04)
Ekberg and Albinsson (2000)	potentiometry and solvent extraction	1 M $NaClO_4$	11.9 ± 0.2 (–3.3 ± 0.1)	21.4 ± 0.2 (–8.6 ± 0.1)	30.6^{d} (–13.8)^{d}	39.0 ± 0.5 (–19.4 ± 0.5)
Moriyama *et al.* (1999)	hard sphere model		12.56	23.84	32.76	40.40
Neck and Kim (2001)	estimation A		13.4	26.5	36.7	43.9
	estimation B		11.9	22.9	31.4	37.0
	selection		11.8 ± 0.2	22.0 ± 0.6	31.0 ± 1.0	38.5 ± 1.0

[a] Values based on the data of Kraus and Holmberg (1954).
[b] Values based on the data of Nabivanets and Kudritskaya (1964).
[c] Not extrapolated to zero ionic strength.
[d] Interpolated values (15–35°C).

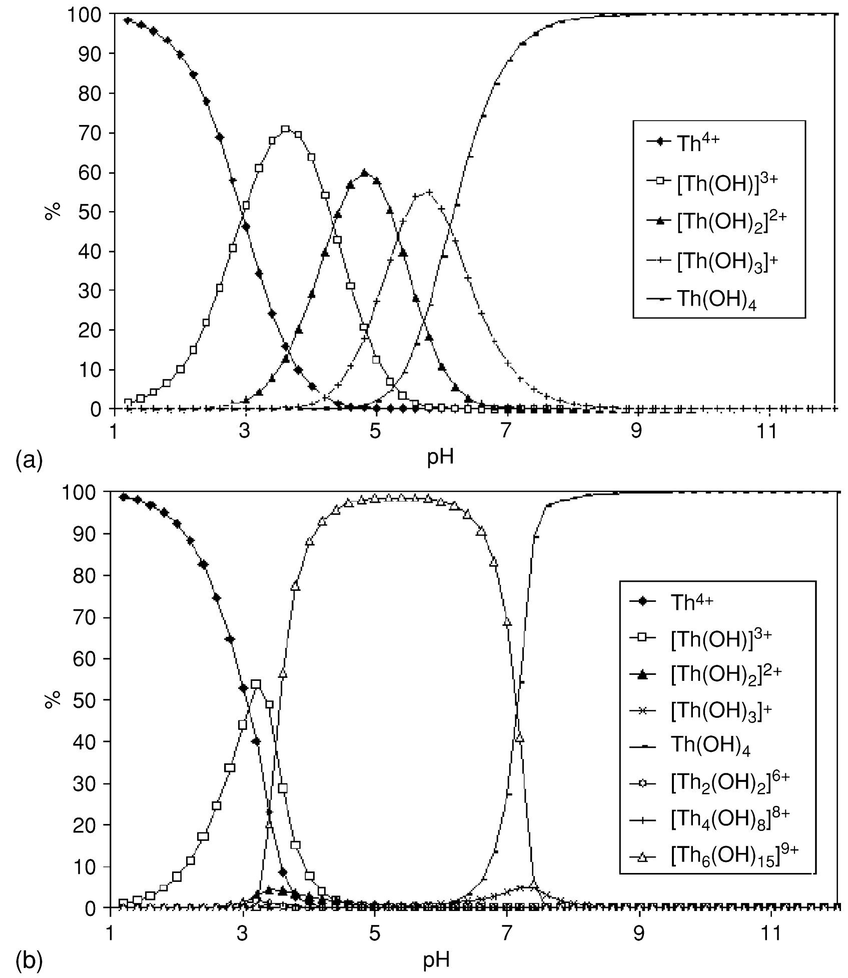

Fig. 3.18 *Thorium speciation diagrams in non-complexing aqueous solution* (*calculated for* 0.1 M *NaCl by using the hydrolysis constants given in Tables* 3.13 *and* 3.14 (*Neck and Kim,* 2001; *Ekberg and Albinsson,* 2000) *and the PHREEQUE program, version* 2.2). (*a*) *Species distribution for low concentrations of Th*(*IV*) (= 10^{-8}M *in the present case*). (*b*) *Species distribution for* $[Th]_{tot} = 0.1$ M, *considering the possible formation of only three polynuclear species:* $Th_2(OH)_2^{6+}$, $Th_4(OH)_8^{8+}$, *and* $Th_6(OH)_{15}^{9+}$.

3.8.5 Solubility

(a) In non-complexing media

In perchlorate media, an average hydroxyl number, *n* (OH^- groups bound per thorium), of about 2.5 can be reached without delayed precipitation. All hydrolyzed solutions contain polymeric species and the weight-average degree of polymerization increases with the degree of hydrolysis (Danesi *et al.*, 1968; Hietanen and Sillen, 1964). The presence of the $Th_2(OH)_2^{6+}$ polymer is well recognized in most of the studies (Hietanen and Sillen, 1964; Baes *et al.*, 1965; Milic, 1971, 1981; Milic and Suranji, 1982; Moon, 1989), but other polymers such as $Th_2(OH)_3^{5+}$ (Milic, 1981, Moon, 1989), $Th_2(OH)_4^{5+}$ (Moon, 1989), $Th_4(OH)_8^{8+}$ (Baes *et al.*, 1965; Ekberg and Albinsson, 2000), $Th_4(OH)_{12}^{4+}$ (Brown *et al.*, 1983), $Th_5(OH)_{12}^{8+}$ (Lefèbvre, 1957), $Th_6(OH)_{14}^{10+}$ (Milic, 1981), $Th_6(OH)_{15}^{9+}$ (Baes *et al.*, 1965; Brown *et al.*, 1983; Ekberg and Albinsson, 2000) have been found as well. The corresponding conditional constants collected in Table 3.14 show a rather reasonable agreement between the different studies for the species commonly detected. The experimental conditions, especially the total thorium concentration involved in the measurements, may explain why different sets of polynuclear species are discussed in the different studies (some species can have a too low concentration to be detected and/or can precipitate). However, it is interesting to note that $Th_6(OH)_{15}^{9+}$ is the only polynuclear species expected to predominate in the simple Th(IV)/H_2O system, when the total Th(IV) concentration exceeds $\sim 10^{-3}$ M (and up to at least 1 M) and for a pH range centered around 4.5–5 (see Fig. 3.18(b)).

The structure of highly hydrolyzed thorium salt solutions has been studied by electronic microscopy (Dobry *et al.*, 1953; Dzimitrowickz *et al.*, 1985) and light or X-ray scattering techniques (Dobry *et al.*, 1953; Hentz and Johnson, 1966; Magini *et al.*, 1976). The details of this structure are dependent on sample history. At room temperature, the hydrolysis complexes contain a small number of Th(IV) atoms probably situated at the corners of slightly distorted face-sharing tetrahedral. At higher temperatures, small crystallites (~40 Å) are formed, which have the ThO_2 structure. These crystallites tend to join to other crystallites, in random orientation, to form particles of up to 170 Å in diameter (Magini *et al.*, 1976). Finally, the small fragments of fluorite can be connected (e.g. cross-linking by oxide bridges) in a random manner into larger, porous agglomerates irregular in shape and size up to 800–15000 Å (Dzimitrowickz *et al.*, 1985). In dilute colloidal solutions ($[Th]_{tot} < 10^{-2}$ mol L^{-1}), filamentous particles with a statistic average length of 700 Å are observed; they are wound into compact balls in more concentrated solutions (Dobry *et al.*, 1953).

The solubility products reported for the thorium oxide and hydroxide species show considerable discrepancies (Table 3.15). The reasons can be found in: (1) the characteristics of the solid phase (degree of crystallization, morphology, etc.), which depend on the history of its preparation (hydrolysis reaction, pretreatment, aging); (2) the composition of the solution (pH range, ionic strength); (3) the method of evaluating the total concentration of thorium in solution (cutting size for the phase separation); (4) the generally too simplified chemical model used to derive the solubility product; and (5) the set of hydrolysis constants used in the data treatment.

Concerning the first point, it is important to distinguish between the amorphous fresh hydroxide precipitate, just washed prior to experiments,

Table 3.14 *Conditional hydrolysis constants proposed for the polynuclear species of Th(IV) and defined as follows ([i] denoting the concentration of the species i):*

$$K_{x-y} = [Th_x(OH)_y^{(4x-y)+}]\,[H^+]^y/[Th^{4+}]^x.$$

Medium (*reference*)	$-logK_{2\text{–}2}$	$-logK_{2\text{–}3}$	$-logK_{2\text{–}4}$	$-logK_{4\text{–}8}$	$-logK_{4\text{–}12}$	$-logK_{6\text{–}14}$	$-logK_{6\text{–}15}$
3 M $NaClO_4$ (Hietanen and Sillen, 1964)	4.70 ± 0.05	8.83 ± 0.21				36.53 ± 0.19	40.37 ± 0.23
1 M $NaClO_4$ (Baes *et al.*, 1965)	4.61 ± 0.02			19.01 ± 0.02			36.76 ± 0.02
3 M $NaClO_4$ (Brown *et al.*, 1983)					30.55 ± 0.03		34.4 ± 0.03
3 M $NaClO_4$ (Bruno *et al.*, 1987)	4.74 ± 0.04			19.15 ± 0.04		33.83 ± 0.03	
0.5 M $NaClO_4$	−2.05 ± 0.04	9.79 ± 0.11	−3.07 ± 0.04				
0.1 M $NaClO_4$ (Moon, 1989)	5.89 ± 0.10						
3 M $NaClO_4$ (Grenthe and Lagerman, 1991)	5.10 ± 0.17	7.87 ± 0.05		19.6 ± 0.2	34.86 ± 0.05	33.67 ± 0.05	
1 M $NaClO_4$ (Ekberg and Albinsson, 2000)				19.1[a]			39.5[a]

[a] Values used, after correction for the ionic strength, in the PHREEQUE program in order to calculate the speciation curves plotted in Fig. 3.18.

Table 3.15 *Conditional solubility product, K_{sp}, and estimated value at infinite dilution, K°_{sp}, proposed for Th oxide and hydroxide species at 17–25°C and defined as follows ([i] and γ_i denoting the concentration and the activity coefficient of the species i):*

$$K_{sp} = [Th^{4+}][OH^-]^4$$

$$K^{\circ}_{sp} = K_{sp}(\gamma_{Th})(\gamma_{OH})^4 (for Th(OH)_4, am)$$

$$K^{\circ}_{sp} = K_{sp}(\gamma_{Th})(\gamma_{OH})^4 (a_w)^{(x=2)} (for ThO_2.xH_2O, s).$$

References	*Solid*	*Solution*	*$log[Th]_{tot}$ at pH > 5*	K_{sp}	K°_{sp}
Nabivanets and Kudritskaya (1964)	Th(IV) hydroxide or hydrous oxide	0.1 M $NaClO_4$ (17°C)	−6.3	−44.7	−46.8
Ryan and Rai (1987)	$ThO_2. \cdot xH_2O$(am) (hydrous oxide)	0.1 M $NaClO_4$	−8.8 ± 0.2	−45.2	−45.5
Felmy *et al.* (1991)		0.6 M NaCl and KCl (room temp.)	−8.5 ± 0.6		-47.3^b
Moon (1989)	$Th(OH)_4$(am)	0.5 M $NaClO_4$ (18°C)	−8.2 ± 0.3	−50.52 ± 0.08	−46.6
				-43.5^a	−52.9
	ThO_2(cr) (700°C)	0.1 M $NaClO_4$(25°C)	−8.2 ± 0.3	−50.76 ± 0.08	-53.6^b
Östhols *et al.* (1994)	microcrystalline	0.5 M $NaClO_4$ (25°C)		−45.1	−48.7
	$ThO_2 \cdot 2.5H_2O$				-48.2^b
Bundschuh *et al.* (2000)	colloidal ThO_2(cr)	0.5 M NaCl (25°C)		−49.54 ± 0.22	−52.8 ± 0.3
Neck and Kim (2001)	$Th(OH)_4$(am)		−8.5 ± 0.6		−47.0 ± 0.8
	ThO_2(cr)		−8.5 ± 0.6		−53.5 ± 0.7

[a] Value calculated by Neck and Kim (2001) with the use of an other set of hydrolysis constants.

[b] Values calculated by Neck and Kim (2001) by applying the specific interaction theory (SIT) following the NEA Thermochemical Data Base project (Grenthe *et al.*, 1992).

the hydrous oxide or microcrystalline $ThO_2 \cdot nH_2O$ showing very broad X-ray powder diffraction peaks, and the well-crystallized thorine, obtained after appropriate heating steps. The four other points have to be taken into account to select and interpret the various solubility curves published in the literature. This task has been recently accomplished by Neck and Kim (2001). First, they analyzed the solubility data obtained for amorphous Th(IV) precipitates (not treated at higher temperature but only washed with water) at $I \leq 1$ M by using a chemical model that includes all mononuclear species $Th(OH)_n^{(4-n)+}$ up to $n = 4$ and two polynuclear species, $Th_4(OH)_{12}^{4+}$ and $Th_6(OH)_{15}^{9+}$. For this purpose, they chose the hydrolysis constants, $\log K_{4-12}$ and $\log K_{6-15}$, given in Table 3.14 and derived by Brown *et al.* (1983) from potentiometric titrations at pH = 3–4, in combination with their selected data for the mononuclear hydrolysis species (see Table 3.13).

By monitoring the initial colloid generation (with size of 16–23 nm) as a function of pH and Th(IV) concentration with the use of LIBD, Bundschuh *et al.* (2000) determined a value of $\log K^{\circ}_{sp}$ equal to $-(52.8 \pm 0.3)$ (also calculated with the specific interaction theory (SIT) coefficients of Nuclear Energy Agency Thermochemical Database Project [NEA-TDB] data), which corresponds both to the solubility products of crystalline ThO_2 (values of Moon (1989) revisited by Neck and Kim (2001) [see Table 3.15]) and to the value calculated from thermochemical data for ThO_2, $\log K^{\circ}_{sp} = -(54.2 \pm 1.3)$ (Rai *et al.*, 1987). The difference is ascribed to a particle size effect and it is concluded that the colloids formed in the coulometric pH titration experiments consist of crystalline thorium dioxide. This conclusion is also supported by the work of Dzimitrowickz *et al.* (1985).

Moreover, it is evident from Fig. 3.19 that the degree of crystallization of ThO_2 influences its solubility behavior essentially in acidic media. At pH < 2.5, the experimental solubility curve of ThO_2(cr) seems to indicate an equilibrium between the solid phase and Th^{4+}(aq) (slope of −4 for the microcrystalline precipitates only). However, such an equilibrium has never been observed when the dissolution process is studied from under-saturation (Hubert *et al.*, 2001; Neck, 2002). With increasing pH, the solubility data deviate more and more from the expected curve. The hydrolysis of the Th^{4+} ions leads to increased Th(IV) concentrations, which are not in equilibrium with ThO_2(cr), but with an amorphous surface layer of $Th(OH)_4$ covering the crystalline solid, as judiciously explained by Neck and Kim (2001). In fact, kinetic effects play an important role in the overall process, as outlined by Hubert *et al.* (2001).

(b) In complexing media

The precipitation of thorium by various inorganic and organic ligands and the characterization of the resulting solids were treated at some length in Section 3.7.7. Therefore the discussion here will be limited to the role of the carbonate

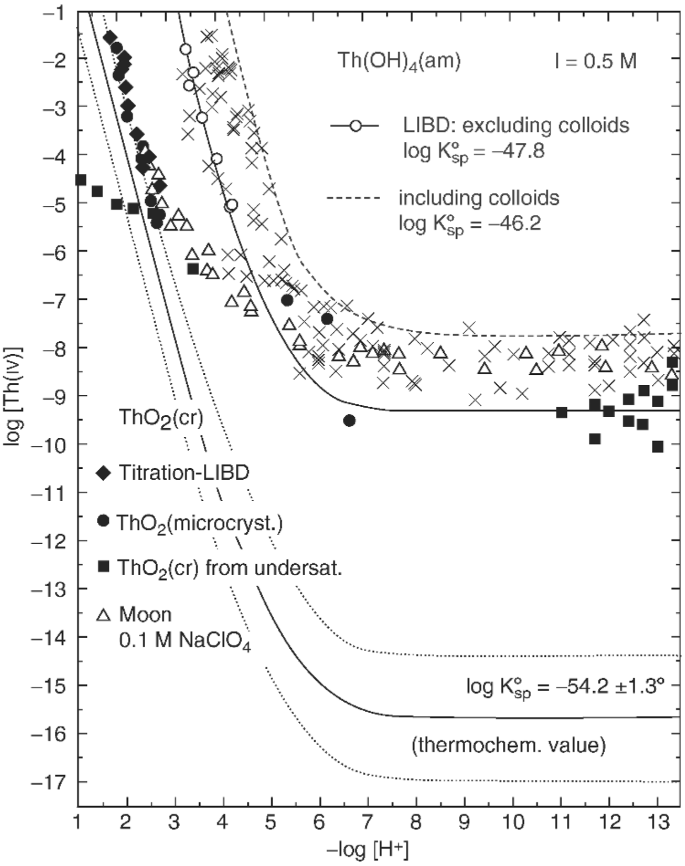

Fig. 3.19 *Experimental and calculated solubility of ThO_2(cr) in comparison with that of Th(IV) hydroxide or hydrous oxide at* $I = 0.5$ M *and* 25°C (*Neck,* 2002). *The experimental data for ThO_2(cr) are those determined by Neck* (2002) *by titration–LIBD and from under- and oversaturation* (*filled symbols*) *and by Moon* (1989) *in* 0.1 M $NaClO_4$ *at* 18°C (*open triangles*). *The solubility data for amorphous precipitates* (*crosses*) *are taken from Moon* (1989), *Felmy et al.* (1997), *Östhols et al.* (1994), *Rai et al.* (1997), *Neck and Kim* (2000), *all data being at* $I = 0.5$–0.6 M *and* 18–25°C. *The curves calculated for the two kinds of solids and for* $I = 0.5$ M *are based on the hydrolysis constants selected by Neck and Kim* (2001) *and on the solubility products* $\log K^{\circ}_{sp}(ThO_2, cr) = -(54.2 \pm 1.3)$ (*Rai et al.,* 1987) *and* $\log K^{\circ}_{sp}(Th(OH)_4, am) = -(47.0 \pm 0.8)$ (*Neck and Kim,* 2001).

and the phosphate ions on the solubility of thorium and, consequently, on its behavior in natural waters.

The presence of carbonates in solution greatly increases the solubility of thorium dioxide. An increase by one order of magnitude of the carbonate concentration (in the range 0.1–2.0 M Na_2CO_3) leads to an increase by about five orders of magnitude of the solubility of hydrous ThO_2(am) (Rai *et al.*, 1995). Moreover, for a fixed carbonate concentration [1 M Na_2CO_3 (Rai *et al.*, 1995) or $pCO_2 = 0.1$ atm (Östhols *et al.*, 1994)], a large pH dependency is observed. The fitting of their solubility data has lead Östhols *et al.* (1994) to propose the following equilibrium constants:

$$ThO_2 + H^+ + H_2O + CO_3^{2-} \leftrightarrow Th(OH)_3CO_3^-;\ \log K_{131} = 6.11 \pm 0.19,\ \log K^\circ_{131} = 6.78 \pm 0.30$$

$$ThO_2 + 4H^+ + 5CO_3^{2-} \leftrightarrow Th(CO_3)_5^{6-};\ \log K_{105} = 42.12 \pm 0.32,\ \log K^\circ_{105} = 39.64 \pm 0.40$$

that were calculated by using the hydrolysis constants determined in 3 M $NaClO_4$ by Grenthe and Lagerman (1991) and were corrected to 0.5 M $NaClO_4$ (Grenthe *et al.*, 1992) .

The ion interaction model of Pitzer has been developed, extending to high concentration, and applied satisfactorily by Felmy *et al.* (1997) to describe, on the basis of the above equilibria, the solubility data obtained by both Rai *et al.* (1995) and Östhols *et al.* (1994) in the aqueous Na^+–HCO_3^- – CO_3^{2-}–OH^-–ClO_4^- –H_2O system. They have estimated $\log K^\circ_{105}$ to be 37.6 and log K°_{131} to be 6.78; these values are identical or close to those previously determined by Östhols *et al.* (1994). However, a considerable uncertainty in the determination of the value for $\log K^\circ_{105}$, due to the introduction of large mixing terms with the bulk anionic species, has been outlined by the authors.

The effect of phosphate on the solubility of microcrystalline ThO_2 has been observed to be very limited (Östhols, 1995). The only data for which there is a significant deviation from the solubility of ThO_2(am) as predicted in the absence of phosphates, are those obtained in 0.1 M phosphate solutions in the pH range 10.5–13. Here, a small increase in solubility has been found. However, an analysis of the solid phase has shown a small but significant phosphate content. This suggests the formation of a sparingly soluble thorium phosphate in the experiments, meaning that there will eventually be a decrease of the thorium solubility in the presence of excess amounts of phosphate.

It has been concluded from other solubility measurements (Fourest *et al.*, 1999) carried out on a synthesized thorium phosphate–diphosphate, $Th_4(PO_4)_4P_2O_7$ (incorrectly named 'Th orthophosphate' in a previous study (Baglan *et al.*, 1994)) that the total concentration of Th(IV) in solution ($-3 < \log [Th] < -7$ for $0 < pH < 5$) is mainly controlled by the precipitation of two compounds: $Th(HPO_4)_2$ in acidic media ($pH < 4.5$) and $Th(OH)_4$ in basic and near-neutral media. However, more recently, Thomas *et al.* (2000) and Brandel *et al.* (2001b) have characterized by electron probe microanalysis (EPMA), XRD, IR, TGA, and DTA, the crystallized phase formed during the dissolution of $Th_4(PO_4)_4P_2O_7$, when the saturation of the leachate is reached. They have shown that the thorium concentration in phosphate-containing solutions is controlled by the precipitation of the thorium phosphate–hydrogenphosphate hydrate, $Th_2(PO_4)_2(HPO_4) \cdot H_2O$, which has a very low solubility product: $\log K^\circ_{sp} = -(66.6 \pm 1.2)$ (Thomas *et al.*, 2001).

3.8.6 Complexation

(a) Inorganic ligands

To our knowledge, the formation of Th(IV) complexes with most of the common inorganic ligands, such as F^-, Cl^-, SO_4^{2-}, andNO_3^{2-}, has not been re-investigated recently (Hogfeld, 1982). The stability constants of the corresponding equilibria, collected in Table 3.16, are those previously reported by Langmuir and Herman (1980) in their review paper. From these values, it can be concluded that weak 1:1 complexes are formed with chloride and nitrate anions and that higher order complexes, even if they have been pointed out in the literature (Langmuir and Herman, 1980; Fuger *et al.*, 1992), are unimportant. Colin-Blumenfeld (1987) has thus shown, through thermodynamic calculations, that $Th(NO_3)_2^2+$ can only exist in acidic solutions (pH < 3.2) containing high concentrations of nitrates (>0.1 M). Similarly, $Th(Cl)_2^{2+}$ is expected to be found only at pH < 4 and for $[Cl^-]_{tot} > 0.5$ M (Colin-Blumenfeld, 1987).

On the contrary, strong complexes of Th(IV) are formed with F^- and SO_4^{2-} and particularly with carbonate and phosphate ligands which are known to appreciably affect the speciation of Th(IV) in natural waters. A very strong complexation of Th(IV) by the HPO_4^{2-} species is indicated by the stability constants published by Moskvin *et al.* (1967) (see Table 3.16). These data are found in many databases used for geochemical modeling, but they were derived from solubility of an ill-defined solid thorium phosphate in acidic phosphate media (hydrogen concentration of 0.35 M). They cannot explain the ThO_2 solubility results obtained by Östhols (1995). Moreover, extraction experiments by acetylacetone in the two-phase system 1 M $Na(H)ClO_4$/toluene carried out by Engkvist and Albinsson (1994) at pH 8 and 9 (HPO_4^{2-} being thus the dominant species) give cumulative stability constants of Th^{4+}/HPO_4^{2-} much lower than the values published earlier; these new β values suffer, however, from large uncertainties.

The stability constants known for $Th^{4+}/H_2PO_4^-$ and Th^{4+}/H_3PO_4, and reported in Table 3.16, are those collected by Langmuir and Herman (1980). They have not been checked by subsequent studies, but their role is of minimal importance in the speciation of thorium in neutral and basic media. No data have been published on the complexation of Th^{4+} by the PO_4^{3-} ions, except the following equilibrium proposed by Östhols (1995):

$$Th^{4+} + 4H_2O + PO_4^{3-} \leftrightarrow Th(OH)_4PO_4^{3-} + 4H^+ \quad \log K = -(14.90 \pm 0.36)(0.35\ \text{M})$$

Finally, mention can be made of the study of Fourest *et al.* (1994). The solubility curves obtained by equilibrating solid thorium phosphate-diphosphate and highly concentrated phosphate solutions have led to the determination of $ThO(HPO_4)_3(H_2PO_4)^{5-}$ and $ThO(HPO_4)_3(H_2PO_4)_2^{6-}$ as the presumed complex forms of Th(IV) at pH 6–7 and for $0.3 < [PO_4]_{tot} < 0.8$ and $0.8 < [PO_4]_{tot} < 1.5$ M, respectively.

Table 3.16 *Cumulative formation constants of the Th(IV) complexes formed with the main inorganic ligands at* 25°C.

Complex	*log* β_{1xn}	*I* (M)	*References*
ThF^{3+}	8.03	0	Langmuir and Herman (1980)
ThF_2^{2+}	14.25	0	Langmuir and Herman (1980)
ThF_3^{+}	18.93	0	Langmuir and Herman (1980)
ThF_4	22.31	0	Langmuir and Herman (1980)
$ThCl^{3+}$	1.09	0	Langmuir and Herman (1980)
$ThCl_2^{2+}$	0.80	0	Langmuir and Herman (1980)
$ThCl_3{}^{+}$	1.65	0	Langmuir and Herman (1980)
$ThCl_4$	1.26	0	Langmuir and Herman (1980)
$ThSO_4^{2+}$	5.45	0	Langmuir and Herman (1980)
$Th(SO_4)_2$	9.73	0	Langmuir and Herman (1980)
$Th(SO_4)_3^{2-}$	10.50	0	Langmuir and Herman (1980)
$Th(SO_4)^{4-}$	8.48	0	Langmuir and Herman (1980)
$ThNO_3^{3+}$	0.94	0	Langmuir and Herman (1980)
$Th(NO_3)_2^{2+}$	1.97	0	Langmuir and Herman (1980)
$Th(OH)_4PO_4^{3-}$	–14.9 ± 0.36	0.35	Östhols (1995)
$Th(HPO_4)^{2+}$	10.8	0.35	Langmuir and Herman (1980)
	(8.7 – 9.7)	1	Engkvist and Albinsson (1994)
$Th(HPO_4)_2$	22.8	0.35	Langmuir and Herman (1980)
	(15 – 17.3)	1	Engkvist and Albinsson (1994)
$Th(HPO_4)_3^{2-}$	31.3	0.35	Langmuir and Herman (1980)
	(21–23)	1	Engkvist and Albinsson (1994)
$ThH_2PO_4^{3+}$	4.52	0	Langmuir and Herman (1980)
$Th(H_2PO_4)_2^{2+}$	8.88	0	Langmuir and Herman (1980)
$ThH_3PO_4^{4+}$	1.9	2	Langmuir and Herman (1980)
$Th(OH)_3CO_3^{-}$	41.5	0	Östhols *et al.* (1994)
$Th(CO_3)_5^{6-}$	21.6[a]	0.05	Joao *et al.* (1995)
	32.3	0	Östhols *et al.* (1994)
	27.1[b]	0	Felmy *et al.* (1997)

[a] Recalculated by Östhols *et al.* (1994) (see text) to be 33.2 in 1 M carbonate media.
[b] Derived by using the K°_{sp} value of Ryan and Rai (1987) given in Table 3.15.

Despite the studies mentioned above, the thermodynamic database for tetravalent actinides remains rather poor for the complexation with inorganic anions, such as carbonate, phosphate, sulfate, fluoride, and chloride, which are dominant in natural aquatic systems. Consequently, a new semiempirical approach (based on an energy term describing the interligand electrostatic repulsion) has been developed by Neck and Kim (2000) with a first application for the mononuclear complexes with a high number of carbonate ligands. For such a ligand, this model predicts a slight decrease from $\log\beta_4^{\circ}$ to $\log\beta_5^{\circ}$ and a strong decrease from $\log\beta_5^{\circ}$ to $\log\beta_6^{\circ}$. Hence the pentacarbonate complex is expected to be the limiting Th(IV)–carbonate complex at high carbonate concentration. Moreover, the existence of $Th(CO_3)_5^{6-}$ has been confirmed by several experiments using various methods: cryoscopy, conductometry, and ionic exchange (Dervin and Faucherre, 1973a), solvent extraction followed by neutron activation (Joao *et al.*, 1987, 1995), solubility of amorphous or microcrystalline ThO_2 (Rai *et al.*, 1995; Felmy *et al.*, 1997; Östhols *et al.*, 1994) and X-ray absorption (Felmy *et al.*, 1997). The pentacarbonate complex structure is also well established in solid phase investigations (Voliotis and Rimsky, 1975). The stability constant values published in the frame of these works for the corresponding reaction:

$$Th^{4+} + 5CO_3^{2-} \leftrightarrow Th(CO_3)_5^{6-}$$

are collected in Table 3.16. The value obtained by Joao *et al.* (1987) recalculated by taking into account the complex really formed between Th(IV) and ethylenediaminetetraacetic acid (EDTA) at high pH (Th(OH)Y and not ThY) (Östhols *et al.*, 1994) is in general agreement with the value estimated by these authors. The estimation of Faucherre and Dervin (1962) from measurements of freezing point depressions is open to criticism, because only the dominant reaction is postulated and Th(IV) hydrolysis is neglected in the data treatment. The remaining values (Östhols *et al.*, 1994; Rai *et al.*, 1995; Felmy *et al.*, 1997) depend on the hydrolysis constants applied for their evaluation.

X-ray absorption spectroscopy (XAS) data (Felmy *et al.*, 1997) have clearly shown a change in speciation at low bicarbonate concentrations (0.01 M solution), but the total thorium concentration was too low to allow a definitive identification of the species. Solubility data of amorphous or microcrystalline ThO_2 have been most satisfactorily explained by the introduction of a mixed $Th(OH)_3CO_3$ (Östhols *et al.*, 1994; Felmy *et al.*, 1997) with $\log K^\circ_{131} = 41.5$ (see Table 3.16).

(b) Organic ligands

The organic species, such as oxalate ($C_2O_4^{2-}$), citrate ($C_6H_5O_7^{3-}$), and EDTA ($C_{10}H_{12}O_8N_2^{4-}$), form strong complexes with thorium and ‘organic’ complexation can predominate in natural waters over ‘inorganic’ by orders of magnitude, even when the concentrations of organic ligands are low as compared with inorganic ones (Langmuir and Herman, 1980).

The interaction of Th(IV) with citrate has been investigated both by potentiometry in 0.1 M chloride solution (Raymond *et al.*, 1987) and solvent extraction (thenoyltrifluoro-acetone [TTA] or dibenzoylmethane [DBM] in toluene) in perchlorate (0.1–14 M $NaClO_4$; pH: 1.8–4.0) and chloride (0.1–5.0 M NaCl; pH: 3) solutions (Choppin *et al.*, 1996). The former study covers a wider pH range (pH: 1–6) and a larger set of stability constants has been derived from the results than in the latter one. However, attention should be paid to the choice of hydrolysis constants used to fit the results. Moreover, the contribution of mixed hydroxy species, not yet identified, can be expected to be more important in basic media. Nevertheless, a relatively good agreement is observed for the two $Th(Cit)^+$ formation constants (see Table 3.17).

Table 3.17 *Cumulative formation constants of the Th(IV) complexes with some organic ligands at* 25°C.

Complex	$\log \beta^{o}_{1n}$	*References*
$Th(Cit)^{+}$	16.17	Nebel and Urban (1966)
	14.13	Raymond *et al.* (1987)
	13.7 ± 0.1	Choppin *et al.* (1996)
$Th(Cit)_2^{2-}$	24.94	Nebel and Urban (1966)
	24.29	Raymond *et al.* (1987)
$ThH(Cit)_2^{-}$	16.6 ± 0.1	Choppin *et al.* (1996)
$ThH_2(Cit)_2$	31.9 ± 0.1	Choppin *et al.* (1996)
$Th(Cit)_2(OH)_2^{4-}$	14.67	Raymond *et al.* (1987)
$Th(Cit)_3^{5-}$	28.0	Raymond *et al.* (1987)
$ThH(Cit)_3^{4-}$	33.31	Raymond *et al.* (1987)
$ThC_2O_4^{2+}$	10.6	Moskvin and Essen (1967)
	9.30	Langmuir and Herman (1980)
	9.8	Erten *et al.* (1994)
$Th(C_2O_4)_2$	20.2	Moskvin and Essen (1967)
	18.54	Langmuir and Herman (1980)
	17.5	Erten *et al.* (1994)
$Th(C_2O_4)_3^{2-}$	26.4	Moskvin and Essen (1967)
	25.73	Langmuir and Herman (1980)
$Th(C_2O_4)_4^{4-}$	29.6	Moskvin and Essen (1967)
$Th(HC_2O_4)^{3+}$	11.0	Erten *et al.* (1994)
$Th(HC_2O_4)_2^{2+}$	18.13	Erten *et al.* (1994)
ThEDTA	25.30	Langmuir and Herman (1980)
$ThHEDTA^{+}$	17.02	Langmuir and Herman (1980)

The Th(IV)/oxalate constants determined by using solvent extraction techniques (TTA and bis(2-ethylhexyl)phosphoric acid [HDEHP] in toluene; pH: 1.3–4.0; $I = 1, 3, 5, 7$, and 9 M) (Erten *et al.*, 1994) appear somewhat different from the values previously obtained from solubility measurements, but the approach of Moskvin and Essen (1967) has already been subjected to some criticism in the case of the phosphate ligands (Östhols, 1995).

Other anions of organic acids, such as formate, acetate, chloroacetate, tartrate, malate, salicylate, sulfosalicylate, and so on, form complexes with Th(IV). They are too numerous to be listed in Table 3.16, but the corresponding stability constants can be found in various compilations: Sillen and Martell (1964, 1971), Perrin (1982), or the most recent database issued by the National Institute of Standards and Technology (NIST, 2002).

Humic and fulvic acids have been identified as efficient complexing agents for ions such as Th^{4+}. Their influence on thorium mobilization in natural waters have been discussed in several publications (Choppin and Allard, 1985; Cacheris and Choppin, 1987; Miekeley and Küchler, 1987). The Th(IV)–humate complex has been recently analyzed by X-ray photoelectron spectroscopy (XPS)

(Schild and Marquardt, 2000). The XPS study corroborates EXAFS results (Denecke *et al.*, 1999) according to which Th(IV) is predominantly bound to carboxylic groups of humic acids.

3.8.7 Analytical chemistry

As Chapter 30 is devoted to trace analysis of actinides in geological, environmental, and biological matrices, only summarized considerations will be given here, centered on the determination of thorium in natural waters. Extensive information on the techniques used in analytical chemistry of thorium, including the 'classical' gravimetric, titrimetric, and photometric methods, is also given in the *Gmelin Handbook* (1990b).

Because of its low solubility and its ability to be sorbed as hydroxo complexes, the concentration of thorium in natural waters is, in general, below 0.1 μg L^{-1} and its quantitative determination is difficult. The most important analytical methods for the determination of Th(IV) in the range of low concentrations have been compiled and discussed by Hill and Lieser (1992). In most cases, a preconcentration step – coprecipitation, solvent extraction, and/or ion exchange separation – is performed prior to the measurement.

Inductively coupled plasma mass spectrometry (ICP-MS) is the most sensitive method with usual limits of detection around 0.01 μg kg^{-1} (Gray, 1985) and a reported limit value as low as 0.2 ng kg^{-1} (Chiappini *et al.*, 1996), but this method needs costly pieces of equipment. Two other methods exhibit low detection limits (0.1 μg kg^{-1}) and are well suited for routine analysis (Hill and Lieser, 1992):

- Spectrophotometry, with the procedure described by Keil (1981) coupling preliminary extraction and Th(IV) complexation with arsenazo;
- Voltammetry, with the procedure reported by Wang and Zadeii (1986) using a chelating reagent (with a concentration to be optimized).

However, in practical applications, drawbacks are encountered with both methods due to the presence of uranium and aluminium, respectively. To avoid these drawbacks, a selective preconcentration of Th(IV) is thus necessary (Hill and Lieser, 1992).

Gamma- and alpha-spectrometries, with sensitivity around 1 μg kg^{-1} (Singh *et al.*, 1979; Kovalchuk *et al.*, 1982; Jiang and Kuroda, 1987), are essentially used for isotopic determinations. However, these standard radiochemical techniques require preconcentration and long counting times. ^{228}Th can be determined from two successive gamma-measurements of the ^{224}Ra daughters, but a delay of 20 days is necessary to obtain reliable results for ^{228}Th (Surbeck, 1995). The chemical separation techniques for the classical alpha-spectrometry have been reviewed by De Regge and Boden (1984). These techniques often need optimization because around 50% of the initial activity can be lost at the chemical separation stage (Vera Tomé *et al.*, 1994). Liquid scintillation spectrometers, which allow discrimination between alpha and beta decays, and are commercially available, offer, in combination with selective extractive scintillators, a more advantageous solution to the problem of the isotopic determination of ^{232}Th, ^{230}Th, and ^{228}Th, in spite of a low-energy resolution compared to alpha-spectrometry (Dacheux and Aupiais, 1997). With the PERALS (name registered to Ordela, Inc.) system, a limit of detection as low as 0.2 μg kg^{-1} can be reached for ^{232}Th [value obtained for 250 mL and 3 days of counting (Dacheux and Aupiais, 1997)]. Moreover, PERALS spectrometry can be associated to six short liquid–liquid extraction steps to isolate Th from other actinides (U, Pu, Am, and Cm) prior to its detection at very low levels (the use of spikes during the chemical procedure is necessary for complex matrices).

REFERENCES

Abaouz, A., Taoudi, A., and Laval, J. P. (1997) *J. Solid State Chem.*, **130**, 277–83.

Aboukais, A., Bechara, R., Aissi, C. F., Bonnelle, J. P., Ouqour, A., Loukah, M., Coudurier, G., and Vedrine, J. C. (1993) *J. Chem. Soc., Faraday Trans.*, **89**, 2545–9.

Abraham, J. and Corsini, A. (1970) *Anal. Chem.*, **42**, 1528–31.

Ackermann, R. J. and Rauh, E. G. (1972) *J. Chem. Thermodyn.*, **4**, 521–32.

Ackermann, R. J. and Rauh, E. G. (1973a) *High Temp. Sci.*, **5**, 463–73.

Ackermann, R. J. and Rauh, E. G. (1973b) *J. Inorg. Nucl. Chem.*, **35**, 3787–94.

Adachi, H. and Imoto, S. (1968) *Technol. Rep. Osaka Univ.*, **18**, 377.

Adachi, H., Imoto, S., and Kuki, T. (1973) *Phys. Lett. A*, **44**, 491–2.

Adams, D. M., Chatt, J., Davidson, J. M., and Gerratt, J. (1963) *J. Chem. Soc.*, 2189–94.

Adi, M. B. and Murty, A. S. R. (1978) *Curr. Sci.*, **47**, 539–41.

Agarwal, R. K., Agarwal, H., and Arora, K. (2000) *Rev. Inorg. Chem.*, **20**, 1–61.

Aksel'rud, L. G., Bodak, O. I., Aslan, A. N., Marusin, E. P., and Mazus, M. D. (1990a) *Kristallografiya*, **35**, 199–201; (1990a) *Sov. Phys., Crystallogr.*, **35**, 120–1.

Aksel'rud, L. G., Bodak, O. I., Marusin, E. P., and Aslan, A. M. (1990b) *Kristallografiya*, **35**, 487–90.

Alario-Franco, M. A., Grey, I. E., Joubert, J. C., Vincent, H., and Labeau, M. (1982) *Acta Crystallogr.*, **A38**, 177–86.

Albering, J. H. and Jeitschko, W. (1992) *Z. Naturforsch.*, **47b**, 1521–5.

Albering, J. H. and Jeitschko, W. (1995) *Z. Kristallogr.*, **210**, 686.

Albering, J. H., Poettgen, R., Jeitschko, W., Hoffmann, R.-D., Chevalier, B., and Etourneau, J. (1994) *J. Alloys*, **206**, 133–9.

Alcock, N. W., Esperas, S., Bagnall, K. W., and Wang, H.-Y. (1978) *J. Chem. Soc. Dalton Trans.* 638–46.

Al-Daher, A. G. M. and Bagnall, K. W. (1984) *J. Less Common Metals*, **97**, 343–8.

Al-Kazzaz, Z. M. S. and Louis, R. A. (1978) *Z. Anorg. Allg. Chem.*, **440**, 286–8.

Allard, G. (1932) *Bull. Soc. Chim.*, **51**, 1213–5.

Allen, P. B. (1987) *Phys. Rev.*, **B36**, 2920–3.

Allen, P. G., Bucher, J. J., Shuh, D. K., Edelstein, N. M., and Reich, T. (1997) *Inorg. Chem.*, **36**, 4676–83.

Anderson, J. S. and D'Eye, R. W. M. (1949) *J. Chem. Soc.*, (Suppl. Issue 2), S244–8.

Anderson, M. R. (1950) USAEC Document ISC-116.

Andreetti, G. D., Calestani, G., and Montenero, A. (1984) *Z. Kristallogr.*, **168**, 41–51.

Andresen, A. F., Fjellvag, H., and Maeland, A. J. (1984) *J. Less Common Metals*, **103**, 27–31.

Andruchow, W. J. and Karraker, D. G. (1973) *Inorg. Chem.*, **12**, 2194–6.

Angelucci, O. (1907) *Atti Acad. Nazl. Lincei*, **16**, 196–8.

Aronson, S. and Auskern, A. B. (1966) *J. Phys. Chem.*, **70**, 3937–41.

Arsalane, S. and Ziyad, M. (1996) *Mater. Res. Bull.*, **31**, 156–71.

Arutyunyan, E. G., Porai-Koshits, M. A., and Molodkin, A. K. (1963) *Zh. Strukt. Khim.*, **4**, 276–7.

Asano, M., Kubo, K., and Sasaki, N. (1974) *Kyoto Daigaku Genshii Energi Kenkyosho Iho*, **46**, 33.

Asprey, L. B. and Haire, R. G. (1973) *Inorg. Nucl. Chem. Lett.*, **9**, 1121–8.

Auskern, A. B. and Aronson, S. (1967) *J. Phys. Chem. Solids*, **28**, 1069–71.

Avdeef, A., Raymond, K. N., Hodgson, K. O., and Zalkin, A. (1972) *Inorg. Chem.*, **11**, 1083–8.

Avignant, D. and Cousseins, J. C. (1970) *C. R. Acad. Sci. Paris C*, **271**, 1446–8.

Bacon, W. E. and Brown, G. H. (1969) *J. Phys. Chem.*, **73**, 4163–6.

Baes, C. F. Jr, Meyer, N. J., and Roberts, C. E. (1965) *Inorg. Chem.*, **4**, 518–27.

Baes, C. F. and Mesmer, R. E. (1976) *The Hydrolysis of Cations*, Reprint edn, Krieger Publishing company, Malabar, FL, Copyright 1976 by John Wiley, p. 158.

Baglan, N., Fourest, B., Guillaumont, R., Blain, G., Le Du, J. F., and Genet, M. (1994) *New J. Chem.*, **18**, 809–16.

Bagnall, K. W., Brown, D., Jones, P. J., and du Preez, J. G. H. (1965) *J. Chem. Soc.*, 350–3.

Bagnall, K. W., Brown, D., and Easey, J. F. (1968) *J. Chem. Soc. A*, 288–91.

Bagnall, K. W. and Yanir, E. (1974) *J. Inorg. Nucl. Chem.*, **36**, 777–9.

Bagnall, K. W., Behesti, A., and Heatley, F. (1978) *J. Less Common Metals*, **61**, 63–9.

Ban, Z. and Sikirica, M. (1965) *Acta Crystallogr.*, **18**, 594–9.

Ban, Z., Omejec, L., Szytula, A., and Tomkowicz, Z. (1975) *Physica Status Solidi A*, **27**, 333–8.

Banks, C. V. and Diehl, H. (1947) *Anal. Chem.*, **19**, 222–4.

Baran, E. J., Gentil, L. A., Pedregosa, J. C., and Aymonino, P. J. (1974) *Z. Anorg. Allg. Chem.*, **410**, 301–12.

Barbieri, G. A. (1913) *Atti Acad. Nazl. Lincei*, **22**, 781–6.

Bardeen, J., Cooper, L. N., and Schrieffer, J. R. (1957) *Phys. Rev.*, **108**, 1175–204.

Barker, M. G. and Alexander, I. C. (1974) *J. Chem. Soc., Dalton Trans.*, 2166–70.

Barre, M. (1910) *C. R. Acad. Sci. Paris*, **150**, 1599–602.

Barre, M. (1911) *Ann. Chim. Phys.*, **8** (24), 145–256.

Barre, M. (1912) *Bull. Soc. Chim.*, **11**, 646–8.

Bartscher, W., Rebizant, J., Boeuf, A., Caciuffo, R., Rustichelli, F., Fournier, J. M., and Kuhs, W. F. (1986) *J. Less Common Metals*, **121**, 455–6.

Baskerville, C. (1901) *J. Am. Chem. Soc.*, **23**, 761–4.

Baskin, Y., Harada, Y., and Handwerk, J. H. (1961) *J. Am. Ceram. Soc.*, **44**, 456–9.

Baskin, Y. (1969) *J. Am. Ceram. Soc.*, **52**, 54–5.

Bearden, J. A. (1967) *Rev. Mod. Phys.*, **39**, 78–124.

Bearden, J. A. and Burr, A. F. (1967) *Rev. Mod. Phys.*, **39**, 125–42.

Bechara, R., D'Huysser, A., Aissi, C. F., Guelton, M., Bonnelle, J. P., and Abou-Kais, A. (1990a) *Chem. Mater.*, **2**, 522–6.

Bechara, R., Wrobel, G., Aissi, C. F., Guelton, M., Bonnelle, J. P., and Abou-Kais, A. (1990b) *Chem. Mater.*, **2**, 518–22.

Beck, H. P. and Strobel, C. (1982) *Angew. Chem.*, **94**, 558–9.

Beck, H. P., Thiel, W., and Schuster, M. (1993) *Z. Anorg. Allg. Chem.*, **619**, 221–7.

Beck, H. P. and Kühn, F. (1995) *Z. Anorg. Allg. Chem.*, **621**, 1649–54.

Ben Salem, A., Meerschaut, A., and Rouxel, J. (1984) *C. R. Acad. Sci. Paris*, **299**, 617–9.

Bénard, P., Brandel, V., Dacheux, N., Jaulmes, S., Launay, S., Lindecker, C., Genet, M., Louer, D., and Quarton, M. (1996) *Chem. Mater.*, **8**, 181–8.

Benner, G. and Müller, B. G. (1990) *Z. Anorg. Allg. Chem.*, **588**, 33–42.

Benz, R. and Zachariasen, W. H. (1966) *Acta Crystallogr.*, **21**, 838–40.

Benz, R., Hoffmann, C. G., and Rupert, G. N. (1967) *J. Am. Chem. Soc.*, **89**, 191–7.

Benz, R. (1968) *J. Nucl. Mater.*, **25**, 233–5.

Benz, R. (1969) *J. Nucl. Mater.*, **31**, 93–8.

Benz, R. and Zachariasen, W. H. (1969) *Acta Crystallogr. B*, **25**, 294–6.

Benz, R. and Troxel, J. E. (1971) *High Temp. Sci.*, **3**, 422–32.

Benz, R., Arnold, G. P., and Zachariasen, W. H. (1972) *Acta Crystallogr. B*, **28**, 1724–7.

Bergsma, J., Goedkoop, J. A., and van Vucht, J. H. N. (1961) *Acta Crystallogr.*, **14**, 223–8.

Bernard, L., Currat, R., Delamoye, P., Zeyen, C. M. E., and Hubert, S. (1983) *J. Phys. Chem.*, **16**, 433–56.

Bertaut, F. and Durif, A. (1954) *C. R. Acad. Sci. Paris*, **238**, 2173–5.

Berzelius, J. J. (1829) *K. Sven. Vetenskapsakad. Handl.*, **9**, 1–30; (1829) *Pogg. Ann.*, **16**, 385–415.

Binnewies, M. and Schäfer, H. (1973) *Z. Anorg. Allg. Chem.*, **395**, 77–81; (1974) *Z. Anorg. Allg. Chem.*, **407**, 327–44.

Binnewies, M. and Schäfer, H. (1974) *Z. Anorg. Allg. Chem.*, **410**, 149–55.

Biradar, N. S. and Kulkarni, V. H. (1972) *Z. Anorg. Allg. Chem.*, **387**, 275–9.

Blake, P. C., Edelman, M. A., Hitchcock, P. B., Hu, J., Lappert, M. F., Tian, S., Müller, G., Atwood, J. L., and Zhang, H. (1998) *J. Organomet. Chem.*, **551** (1–2), 261–70.

Blum, P. and Bertaut, F. (1954) *Acta Crystallogr.*, **7**, 81–6.

Blunck, H. and Juza, R. (1974) *Z. Anorg. Allg. Chem.*, **410**, 9–10.

Bock, R. and Bock, E. (1950) *Z. Anorg. Chem.*, **263**, 146–8.

Borzone, G., Borsese, A., and Ferro, R. (1982) *J. Less Common Metals*, **84**, 165–72.

Böttcher, F., Simon, A., Kremer, R. K., Buchkremer-Hermanns, H., and Cockcroft, J. K. (1991a) *Z. Anorg. Allg. Chem.*, **598**, 25–44.

Böttcher, F., Simon, A., Kremer, R. K., Buchkremer-Hermanns, H., and Cockcroft, J. K. (1991b) *Angew. Chem.*, **103**, 79–80.

Botto, I. L. and Baran, E. J. (1981) *Acta Sud. Am. Quim.*, **1**, 143–50.

Bourion, F. (1907) *C. R. Acad. Sci. Paris*, **145**, 243–6.

Bourion, F. (1909) *C. R. Acad. Sci. Paris* **148**, 170–1; (1910).

Bowman, A. L., Krikorian, N. H., Arnold, G. P., Wallace, T. C., and Nereson, N. G. (1968) *Acta Crystallogr. B*, **24**, 1121–3.

Bowman, A. L. and Arnold, G. P. (1971) *Acta Crystallogr. B*, **27**, 243–4.

Bradley, D. C. and Gitlitz, M. H. (1969) *J. Chem. Soc. A*, 980–4.

Bradley, D. G., Ghotra, J. S., and Hart, F. A. (1974) *Inorg. Nucl. Chem. Lett.*, **10**, 209–11.

Brandel, V., Dacheux, N., Pichot, E., and Genet, M. (1998) *Chem. Mater.*, **10**, 345–50.

Brandel, V., Dacheux, N., and Genet, M. (2001a) *Radiochemistry* **43**, 16–21. (Moscow, Russian Federation) (Translation of Radiokhimiya)

Brandel, V., Dacheux, N., Genet, M., and Podor, R. (2001b) *J. Solid State Chem.*, **159**, 139–48.

Bratsch, S. G. and Lagowski, J. J. (1986) *J. Phys.Chem.*, **90**, 307–12.

Brauer, G. and Mitius, A. (1942) *Z. Anorg. Allg. Chem.*, **249**, 325–39.

Braun, T. P., Simon, A., Böttcher, F., and Ueno, F. (1995) *Angew. Chem.*, **107**, 647–8.

Brendel, W., Samartzis, T., Brendel, C., and Krebs, B. (1985) *Thermochim. Acta*, **83**, 167–72.

Brese, N. E. and Di Salvo, F. J. (1995a) *J. Solid State Chem.*, **120**, 372–5.

Brese, N. E. and Di Salvo, F. J. (1995b) *J. Solid State Chem.*, **120**, 378–80.

Bressat, R., Claudel, B., Giorgio, G., and Mentzen, B. (1968) *J. Chim. Phys.*, **65**, 1615–7.

Brewer, L., Sawyer, D. L., Templeton, D. H., and Dauben, C. H. (1951) *J. Am. Ceram. Soc.*, **34**, 173–9.

Bridgman, P. W. (1935) *Phys. Rev.*, **48**, 825–47.

Briggs, G. G. and Cavendish, J. H. (1971) AEC Report NLCO-1080.

Briggs-Piccoli, P. M., Abney, K. D., Schoonover, J. R., and Dorhout, P. K. (2000) *Inorg. Chem.*, **39**, 2970–6.

Briggs-Piccoli, P. M., Abney, K. D., Schoonover, J. R., and Dorhout, P. K. (2001) *Inorg. Chem.*, **40**, 4871–5.

Briggs-Piccoli, P. M., Abney, K. D., and Dorhout, P. K. (2002) *J. Nucl. Sci. Tech.*, **3**, 611–5.

Britton, H. T. S. (1923) *J. Chem. Soc.*, 1429–35.

Brown, A. (1961) *Acta Crystallogr.*, **14**, 860–5.

Brown, A. and Norreys, J. J. (1961) *J. Inst. Methods*, **89**, 238–40.

Brown, D. (1966) *J. Chem. Soc.*, 766–9.

Brown, D. (1968) *Halides of the Lanthanides and Actinides,* John Wiley, London.

Brown, D., Fowles, G. W. A., and Walton, R. A. (1970a) *Inorg. Synth.*, **12**, 225–32.

Brown, D., Holah, D. G., and Rickard, C. E. F. (1970b) *J. Chem. Soc. A*, 423–5.

Brown, D., Hall, T. L., and Moseley, P. T. (1973) *J. Chem. Soc., Dalton Trans.*, 686–91.

Brown, D., Lidster, P., Whittaker, B., and Edelstein, N. (1976) *Inorg. Chem.*, **15**, 511–4.

Brown, P. L., Ellis, J., and Sylva, R. N. (1983) *J. Chem. Soc., Dalton Trans.*, 31–4.

Brunn, H. and Hoppe, R. (1977) *Z. Anorg. Allg. Chem.*, **430**, 144–54.

Bruno, J. W., Marks, T. J., and Morss, L. R. (1983) *J. Am. Chem. Soc.*, **105**, 6824–32.

Bruno, J., Casas, I., Lagerman, B., and Munoz, M. (1987) in *Scientific Basis for Nuclear Waste Management X (Pittsburg, PA)* (eds. J. K. Bates and W. B. Seefelt), *M R S Symposium Proceedings* ANL-IL (USA): pp. 153–60.

Brunton, G. D., Insley, H., McVay, T. N., and Thoma, R. E. (1965) ORNL-3761.

Brunton, G. and Sears, D. R. (1969) *Acta Crystallogr. B*, **25**, 2519–27.

Brunton, G. (1970) *Acta Crystallogr. B*, **26**, 1185–7.

Brunton, G. (1971a) *Acta Crystallogr. B*, **27**, 2290–2.

Brunton, G. (1971b) *Acta Crystallogr. B*, **27**, 1823–6.

Brunton, G. (1972) *Acta Crystallogr. B*, **28**, 144–7.

Brunton, G. (1973) *Acta Crystallogr. B*, **29**, 2976–8.

Bryner, J. S. and Brodsky, M. B. (1959) *Proc. Second UN Int. Conf. on the Peaceful Uses of Atomic. Energy*, 2nd, Geneva, 1958, **7**, 207–15.

Bucher, E. and Staundenmann, J. L., private communication cited by Hulliger, F. (1968) *Struct. Bonding*, **4**, 83–229.

Bundschuh, T., Knopp, R., Kim, J. I., and Fanghänel, Th (2000) *Radiochim. Acta*, **88**, 625–9.

Burdese, A. and Borlera, M. L. (1963) *Ann. Chim.*, **53**, 344–55.

Busch, J. and Gruehn, R. (1996) *Z. Anorg. Allg.*, **622**, 640–8.

Busch, J., Hofmann, R., and Gruehn, R. (1996) *Z. Anorg. Allg.*, **622**, 67–75.

Buschow, K. H. J., Van Mal, H. H., and Miedema, A. R. (1975) *J. Less Common Metals*, **42**, 163–78.

Bushuev, N. N. and Trunov, V. K. (1974) *Dokl. Akad. Nauk SSSR*, **217**, 827–9; *Dokl. Chem.*, **217**, 533–5.

Cacheris, W. P. and Choppin, G. R. (1987) *Radiochim. Acta*, **42**, 185–90.

Calestani, G. and Andreetti, G. D. (1984) *Z. Kristallogr.*, **168**, 41–51.

Calvin, M. (1944) Report CN-2486.

Canneri, G. (1925) *Gazz. Chim. Ital.*, **55**, 39–44.

Cannon, J. F. and Hall, H. T. (1977) in *The Rare Earths in Modern Science and Technology* (eds. G. J. McCarthy and J. J. Rhyne), Plenum, New York, pp. 219–24.

Cannon, J. F. and Farnsworth, P. B. (1983) *J. Less Common Metals*, **92**, 359–68.

Capocchi, J. D. T. (1971) *Met. Ass. Brasil Metais.*, **27**, 881–90.

Carter, F. L. (1982) *Rare Earth Mod. Sci. Technol*, **3**, 479–80.

Caton, R. and Satterthwaite, C. B. (1977) *J. Less Common Metals*, **52**, 307–21.

Chaigneau, M. (1957) *Bull. Soc. Chim. Fr.*, 886–8.

Charpin, P., Chevrier, G., Lance, M., Nierlich, M., and Vigner, D. (1987) *Acta Crystallogr. C*, **43**, 1239–41.

Chauvenet, E. (1911) *Ann. Chim. Phys.*, **8** (23), 425–90.

Chavastelon, R. (1900) *C. R. Acad. Sci. Paris*, **130**, 781–2.

Cheda, J. A. R., Westrum, E. F. Jr, and Morss, L. R. (1976) *J. Chem. Thermodyn.*, **8**, 25–9.

Chernorukov, N. G., Moskvichev, E. P., and Zhuk, M. I. (1974a) *Kristallographiya*, **19**, 1084–5.

Chernorukov, N. G., Sibrina, G. F., and Moskvichev, E. P. (1974b) *Radiokhimiya*, **16**, 412–3.

Chernyaev, I. I., Golovina, V. A., and Molodkin, A. K. (1958) *Proc. Second UN Int. Conf. on the Peaceful Uses of Atomic Energy*, **28**, 203–9.

Chiappini, R., Taillade, J. M., and Brébion, S. (1996) *J. Anal. At. Spectrom.*, **11**, 497–503.

Chiotti, P. (1952) *J. Am.Ceram. Soc.*, **35**, 123–30.

Chiotti, P., Korbitz, F. W., and Dooley, G. J. (1967) *J. Nucl. Mater.*, **23**, 55–67.

Chiotti, P. and Dock, C. H. (1975) *J. Less Common Metals*, **41**, 225–39.

Chiotti, P., Akhachinskij, V. V., Ansara, I., and Rand, M. H. (1981) in *The Chemical Thermodynamics of Actinide Elements and Compounds,* part 5, *The Actinide Binary Alloys* (eds. F. L. Oetting, V. A. Medvedev, M. H. Rand, and E. F. Westrum Jr), STI/PUB/424/5, IAEA, Vienna.

Choi, K.-S., Patschke, R., Billinge, S. J. L., Waner, M. J., Dantus, M., and Kanatzidis, M. G. (1998) *J. Am. Chem. Soc.*, **120**, 10706.

Choppin, G. R. and Allard, B. I. (1985) in *Handbook on the Physics and Chemistry of Actinides,* vol. 3, ch. 11 (eds. A. J. Freeman and C. Keller), Elsevier, Amsterdam, 407–29.

Choppin, G. R., Erten, H. N., and Xia, Y.-X. (1996) *Radiochim. Acta*, **74**, 123–7.

Chydenius, J. J. (1863) *Pogg. Ann.*, **119**, 43.

Clark, G. L. (1924) *Am. J. Sci.*, **7**, 1–23.

Clark, R. J. and Corbett, J. D. (1963) *Inorg. Chem.*, **2**, 460–3.

Clark, J. P. and Green, J. C. (1977) *J. Chem. Soc., Dalton Trans.*, 505–8.

Claudel, B. and Mentzen, B. (1966) *Bull. Soc. Chim. France*, 1547–52.

Clève, P. T. (1874) *Bull. Soc. Chim. Paris*, **21**, 115–23.

Clève, P. T. (1885) *Bull. Soc. Chim. Paris*, **43**, 53–8.

Cline, D., Tevebaugh, R., and Warf, J. (1944) Report CC-1981.

Cloke, F. G. N. and Hitchcock, P. B. (1997) *J. Am. Chem. Soc.*, **119**, 7899–900.

Cloke, F. G. N., Grenn, J. C., and Jardine, C. N. (1999) *Organometalics*, **18**, 1080–6.

Cody, J. A. and Ibers, J. A. (1996) *Inorg. Chem.*, **35**, 3836.

Colani, A. (1909) *C. R. Acad. Sci. Paris*, **149**, 207–10.

Colin-Blumenfeld, M. (1987) Thesis, University of Nancy I (France), 182–4.

Corbett, J. D., Guidotti, R. A., and Adolphson, D. G. (1969) *Inorg. Chem.*, **8**, 163–5.

Corsini, A. and Abraham, J. (1970) *Talanta*, **17**, 439–42.

Cousson, A., Pagès, M., Cousseins, J. C., and Vedrine, A. (1977) *J. Cryst. Growth*, **40**, 157–60.

Cousson, A., Pagès, M., and Chevalier, R. (1978) *Acta Crystallogr. B*, **34**, 1776–8.

Cousson, A., Pagès, M., and Chevalier, R. (1979a) *Acta Crystallogr. B*, **35**, 1564–6.

Cousson, A., Tabuteau, A., Pagès, M., and Gasperin, M. (1979b) *Acta Crystallogr. B*, **35**, 2674–6.

Cousson, A. and Gasperin, M. (1991) *Acta Crystallogr. C*, **47**, 10–2.

Cox, J. D., Wagman, D. D., and Medvedev, V. A. (1989) *CODATA Key Values for Thermodynamics,* Hemisphere Publishers, New York.

Cremers, T. L., Eller, P. G., and Penneman, R. A. (1983) *Acta Crystallogr. C*, **39**, 1165–7.

Cuthbert, F. L. (1958) *Thorium Production Technology,* Addison-Wesley, Reading, MA.

d'Ans, J. and Dawihl, W. (1929) *Z. Anorg. Allg. Chem.*, **178**, 252–6.

Dacheux, N. and Aupiais, J. (1997) *Anal. Chem.*, **69**, 2275–82.

Dacheux, N., Podor, R., Chassigneux, B., Brandel, V., and Genet, M. (1998) *J. Alloys Compds*, **271–273**, 236–9.

Dahlke, O., Gans, W., Knacke, O., and Müller, F. (1969) *Z. Metallk.*, **60**, 465–8.

Damien, D. and de Novion, C. H. (1981) *J. Nucl. Mater.*, **100**, 167–77.

Danan, J. (1975) *J. Nucl. Mater.*, **57**, 280–2.

Danesi, P. R., Magini, M., Margherita, S., and D'Alessandro, G. (1968) *Energy. Nucl.*, **15**, 333–9.

Darnell, A. J. and McCollum, W. A. (1961) USAEC Report NAA-SR-6498.

Dawson, H. M. and Williams, P. (1899) *Proc. Chem. Soc.*, **15**, 210–1.

David, F. and Vokhmin, V. (2001) *J. Phys. Chem.*, **105**, 9704–9.

David, F. and Vokhmin, V. (2003) *New J. Chem.*, **27**, 1627–32.

Day, R. A. Jr and Stoughton, R. W. (1950) *J. Am. Chem. Soc.*, **72**, 5662–6.

de Boisbaudran, L. (1885) *C. R. Acad. Sci. Paris*, **100**, 605–7.

de Haas, W. J. and van Alphen, P. V. (1931) *Proc. Acad. Sci. Amsterdam*, **34**, 70–4.

de Maayer, P., de Bruyne, R., and Brabers, M. J. (1972) *J. Am. Ceram. Soc.*, **55**, 113.

de Regge, P. and Boden, R. (1984) *Nucl. Instrum. Methods Phys. Res.*, **223**, 181–7.

Dean, O. C. (1957) *Adv. Nucl. Eng., Proc. Second Nucl. Eng. Sci. Conf.*, **1**, 66–73. Philadelphia.

Dean, O. C. and Chandler, J. M. (1957) *Nucl. Sci. Eng.*, **2**, 57–72.

Decker, W. R. and Finnemore, D. K. (1968) *Phys. Rev.*, **172**, 430–6.

Denecke, M. A., Bublitz, D., Kim, J. I., Moll, H., and Farkes, I. (1999) *J. Synchrotron Radiat.*, **6**, 394–6.

Dennis, L. M. and Kortright, F. L. (1894) *Am. Chem. J.*, **16**, 79–83.

Dergunov, E. P. and Bergman, A. G. (1948) *Dokl. Akad. Nauk SSSR*, **60**, 391–4.

Dervin, J. and Faucherre, J. (1973a) *Bull. Soc. Chim. Fr.*, 2926–9.

Dervin, J. and Faucherre, J. (1973b) *Bull. Soc. Chim. Fr.*, 2929–33.

Dervin, J., Faucherre, J., Herpin, P., and Voliotis, S. (1973) *Bull. Soc. Chim. Fr.*, 2634–7.

Desyatnik, V. N., Kurbatov, N. N., Raspopin, S. P., and Trifonov, I. I. (1974a) *Zh. Fiz. Khim.*, **48**, 237; *Russ. J. Phys. Chem.,* **48**, 145.

Desyatnik, V. N., Raspopin, S. P., and Trifonov, I. I. (1974b) *Zh. Neorg. Khim.*, **19**, 842–3; *Russ. J. Inorg. Chem.,* **19**, 459–60.

Desyatnik, V. N. and Emel'yanov, N. M. (1975) *Zh. Prikl. Khim.*, **48**, 1382–4.

D'Eye, R. W. M. (1950) *J. Chem. Soc.*, 2764–6.

D'Eye, R. W. M., Sellman, P. G., and Murray, J. R. (1952) *J. Chem. Soc.*, 255–62.

D'Eye, R. W. M. (1953) *J. Chem. Soc.*, 1670–2.

D'Eye, R. W. M. and Sellman, P. G. (1954) *J. Chem. Soc.*, 3760–6.

D'Eye, R. W. M. (1958) *J. Chem. Soc.*, 196–9.

Dietrich, M. (1974) Report KFK-2098.

Dietrich, M., Gey, W., Rietschel, A., and Satterthwaite, C. B. (1974) *Solid State Commun.*, **15**, 941–3.

Diness, A. M. and Roy, R. (1969) *J. Mater. Sci.*, **4**, 613–24.

Dobry, A., Guinand, S., and Mathieu-Sicaud, A. (1953) *J. Chim. Phys. et Phys. Chim. Biol.*, **50**, 501–11.

Dordevic, S. V., Dilley, N. R., Bauer, E. D., Basov, D. N., Maple, M. B., and Degiorgi, L. (1999) *Phys. Rev. B: Conden. Matter Mater. Phys.*, **60**, 11321.

Dronskowski, R. (1995) *Inorg. Chem.*, **34**, 4991–5.

du Jassonneix, B. (1905) *C. R. Acad. Sci. Paris*, **141**, 191–3; (1906) *Bull. Soc. Chim.*, **3** (35), 278–80.

Duboin, A. (1908a) *C. R. Acad. Sci. Paris*, **146**, 489–91.

Duboin, A. (1908b) *C. R. Acad. Sci. Paris*, **146**, 815–7.

Duboin, A. (1909a) *Ann. Chim. Phys.*, **8** (16), 256–88.

Duboin, A. (1909b) *Ann. Chim. Phys.*, **8** (17), 354–64.

Dubrovskaya, G. N. (1971) *Zh. Neorg. Khim.*, **16**, 12–5; *Russ. J. Inorg. Chem.*, **16**, 6–8.

Dupuis, T. and Duval, C. (1949) *C. R. Acad. Sci. Paris*, **228**, 401–2.

Düsing, W. and Hüniger, M. (1931) *Techn. Wiss. Abhandl. Osram-Konzern*, **2**, 357–65.

Dzimitrowickz, D. J., Wiseman, P. J., and Cherns, D. (1985) *J. Colloid Interface Sci.*, **103**(1), 170–7.

Eastman, E. D., Brewer, L., Bromley, L. A., Gilles, P. W., and Lofgren, N. L. (1950) *J. Am Chem. Soc.*, **72**, 4019–23.

Eastman, E. D., Brewer, L., Bromley, L. A., Gilles, P. W., and Lofgren, N. L. (1951) *J. Am. Ceram. Soc.*, **34**, 128–34.

Edwards, P. G., Andersen, R. A., and Zalkin, A. (1981) *J. Am. Chem. Soc.*, **103**, 7792–4.

Edwards, P. G., Andersen, R. A., and Zalkin, A. (1984) *Organometallics*, **3**, 293–8.

Ehemann, M. and Nöth, H. (1971) *Z. Anorg. Allg. Chem.*, **386**, 87–101.

Ekberg, C. and Albinsson, Y. (2000) *J. Solution Chem.*, **29**(1), 63–86.

Elfakir, A., Mahe, P., and Quarton, M. (1987) *Z. Kristallogr.*, **181**, 235–9.

Elfakir, A., Souron, J. P., and Quarton, M. (1989) *Powder Diffraction*, **4**, 165–7.

Elfakir, A., Souron, J. P., and Quarton, M. (1990) *Powder Diffraction*, **5**, 219–20.

Eliseev, A. A., Molodkin, A. K., and Ivanova, O. M. (1967) *Russ. J. Inorg. Chem.*, **12**, 1507–8.

El-Yacoubi, A., Brochu, R., Serghini, A., Louer, M., Alami Talbi, M., and Louer, D. (1997) *Powder Diffraction*, **12**, 76–80.

Engel, G. (1978) *Mater. Res. Bull.*, **13**, 43–8.

Engkvist, I. and Albinsson, Y. (1994) *Radiochim. Acta*, **58/59**, 139–42.

English, A. C., Cranshaw, T. E., Demers, P., Harvey, J. A., Hincks, E. P., Jelly, J. V., and May, A. N. (1947) *Phys. Rev.*, **72**, 253–4.

Ennaciri, A., Kahn, A., and Michel, D. (1986) *J. Less Common Metals.*, **124**, 105–9.

Ernst, R. D., Kennelly, W. J., Day, V. W., and Marks, T. J. (1979) *J. Am. Chem. Soc.*, **101**, 2656–64.

Erten, H. N., Mohammed, A. K., and Choppin, G. R. (1994) *Radiochim. Acta*, **66/67**, 123–8.

Ettmayer, P., Waldhart, J., Vendl, A., and Banik, G. (1980) *Monatsh. Chem.*, **111**, 1185–8.

Evans, D. S. and Raynor, G. V. (1959) *J. Nucl. Mater.*, **1**, 281–8.

Evstaf'eva, O. N., Molodkin, A. K., Dvoryantseva, G. G., Ivanova, O. M., and Struchkova, M. I. (1966) *Russ. J. Inorg. Chem.*, **11**, 697–702.

Fagan, P. J., Manriquez, J. M., Maatta, E. A., Seyam, A. M., and Marks, T. J. (1981) *J. Am. Chem. Soc.*, **103**, 6650–7.

Faucherre, J. and Dervin, J. (1962) *C. R. Acad. Sci.*, **255**, 2264–6.

Fava, J., Le Flem, G., Devalette, M., Rabardel, L., Coutures, J.-P., Foëx, M., and Hagenmuller, P. (1971) *Rev. Int. Hautes Temp. Refract.*, **8**, 305–10.

Fedorov, P. I. and Fedorov, P. P. (2001) *Zh. Neorg. Khim.*, **46**, 1571–2; *Russ. J. Inorg. Chem.*, **46**, 1422–4.

Felmy, A. R., Rai, D., and Mason, M. J. (1991) *Radiochim. Acta*, **55**, 177–85.

Felmy, A. R., Rai, D., Sterner, S. M., Mason, M. J., Hess, N. J., and Conradson, S. D. (1997) *J. Solution. Chem.*, **26**, 233–48.

Fendrick, C. M., Mintz, E. A., Schertz, L. D., Marks, T. J., and Day, V. W. (1984) *Organometallics*, **3**, 819–21.

Fernandes, L. (1925) *Gazz. Chim. Ital.*, **55**, 3–6.

Ferraro, J. R., Katzin, L. I., and Gibson, G. (1954) *J. Am. Chem. Soc.*, **76**, 909–11.

Ferraro, J. R., Katzin, L. I., and Gibson, G. (1955) *J. Am. Chem. Soc.*, **77**, 327–9.

Ferraro, J. R., Katzin, L. I., and Gibson, G. (1956) *J. Inorg. Nucl. Chem.*, **2**, 118–24.

Ferraro, J. R. (1957) *J. Inorg. Nucl. Chem.*, **4**, 283–6.

Ferro, R. (1955) *Acta Crystallogr.*, **8**, 360

Ferro, R. (1956) *Acta Crystallogr.*, **9**, 817–8.

Ferro, R. (1957) *Acta Crystallogr.*, **10**, 476–7.

Fertig, W. A., Moodenbaugh, A. R., and Maple, M. B. (1972) *Phys. Lett.*, **38A**, 517–8.

Fischer, E. O. and Treiber, A. (1962) *Z. Naturforsch. B*, **17**, 276–7.

Fischer, W., Gewehr, R., and Wingchen, H. (1939) *Z. Anorg. Allg. Chem.*, **242**, 161–92.

Flotow, H. E. and Osborne, D. W. (1978) *J. Chem. Thermodyn.*, **10**, 537–51.

Flotow, H. E., Haschke, F. M., Yamauchi, S. (1984) in *The Chemical Thermodynamics of Actinide Elements and Compounds* (eds. V. A. Medredev, M. H. Raud, E. F. Westrum Jr., part 9, The Actinide Hydrides), STI/PuB/424/9, IAEA, Vienna.

Foster, L. S. (1945) Report CT-3370.

Foster, L. S. (1950) Report AECD-2942.

Fourest, B., Baglan, N., Guillaumont, R., Blain, G., and Legoux, Y. (1994) *J. Alloys Compds*, **213/214**, 219–25.

Fourest, B., Lagarde, G., Perrone, J., Brandel, V., Dacheux, N., and Genet, M. (1999) *New J. Chem.*, **23**, 645–9.

Fragala, I., Condorelli, G., Zanella, P., and Tondello, E. (1976) *J. Organomet. Chem.*, **122**, 357–63.

Frampton, O. D. (1979) *Res. Discl.*, **183**, 364.

Fratiello, A., Lee, R. E., and Schuster, R. E. (1970) *Inorg. Chem.*, **9**, 391–2.

Frazer, M. J. and Rimmer, B. (1968) *J. Chem. Soc. A*, 2273–5.

Frick, B., Schoenes, J., Vogt, O., and Allen, J. W. (1982) *Solid State Commun.*, **42**, 331.

Frondel, C. (1958) *Systematic Mineralogy of Uranium and Thorium*, Geological Survey Bulletin no. 1064, U.S. Govt.

Fuger, J. and Brown, D. (1973) *J. Chem. Soc., Dalton Trans.*, 428–34.

Fuger, J., Parker, V. B., Hubbard, W. N., and Oetting, F. L. (1983) in *The Chemical Thermodynamics of Actinide Elements and Compounds,* part 8, *The Actinide Halides* (eds. F. L. Oetting, V. A. Medvedev, M. H. Rand, and E. F. Westrum Jr), STI/PUB/424/8, IAEA, Vienna.

Fuger, J., Khodakovsky, I. L., Sergeyeva, E. I., Medvedev, V. A., and Navratil, J. D. (1992) in *The Chemical Thermodynamics of Actinide Elements and Compounds,* part 12, *The Actinide Aqueous Inorganic Complexes* (eds. F. L. Oetting, V. A. Medvedev, M. H. Rand, and E. F. Westrum Jr), STI/PUB/424/12, IAEA, Vienna.

Fuhrman, N., Holden, R. B., and Whitman, C. I. (1957) USAEC Report SCNC-185.

Fuhse, O. (1897) *Z. Angew. Chem.*, **10**, 115–6.

Galesic, N., Matkovic, B., Topic, M., Coffou, E., and Sljukic, M. (1984) *Croat. Chem. Acta*, **57**, 597–608.

Gantz, D. E. and Lambert, J. L. (1957) *J. Phys. Chem.*, **61**, 112–4.

Gantzel, P. K. and Baldwin, N. L. (1964) *Acta Crystallogr.*, **17**, 772–3.

Gao, L. Z. and Au, C. T. (2000) *Catalysis Lett.*, **65**, 91–8.

Gaumet, V., El-Ghozzi, M., and Avignant, D. (1995) *Eur. J. Solid State Inorg. Chem.*, **32**, 893–905.

Geipel, G. (1992) *Z. Kristallogr.*, **35**, 608–28.

Genet, M., Brandel, V., Dacheux, N., and Lindecker, C. (1996) in *PCT Int. Appl.* (Centre National De La Recherche Scientifique, Fr.). WO 9630300, 35 pp.

Gershanovich, A. Y. and Suglobova, I. G. (1980) *Sov. Radiochem.*, **22**, 201–5.

Gershanovich, A. Y. and Suglobova, I. G. (1981) *Sov. Radiochem.*, **23**, 170–3.

Gesing, T. M. and Jeitschko, W. (1996) *J. Alloys Compds*, **240**, 9–15.

Giacchetti, A., Blaise, J., Corliss, C. H., and Zalubas, R. (1974) *J. Res. NBS*, **78A**, 247–81.

Gingerich, K. A. and Wilson, D. W. (1965) *Inorg. Chem.*, **4**, 987–93.

Gingerich, K. A. and Aronson, S. (1966) *J. Phys. Chem.*, **70**, 2517–23.

Giorgi, A. L., Hill, H. H., Szklarz, E. G., and White, R. W. (1976) Report LA-UR-76-1535.

Glaser, C. (1897) *Chem. News*, **75**, 145–7, 157–8.

Glavic, P., Slivnik, J., and Bole, A. (1973) *J. Inorg. Nucl. Chem.*, **35**, 427–32.

Gmelin Handbook of Inorganic Chemistry, 8th edn, Thorium, System No. 44, Springer Verlag, Berlin.

(1955) Main volume (reprint 1978).

(1976) vol. C2, Ternary and Polynary Oxides.

(1978) vol. C1, Compounds with Noble Gases, Hydrogen, Oxygen.

(1985a) vol. C2, Solvent Extraction.

(1985b) vol. E, Coordination Compounds.

(1986a) vol. A2, History, Isotopes, Recovery.

(1986b) vol. C5, Compounds with S, Se, Te, B.

(1987) vol. C3, Compounds with Nitrogen.

(1988a) vol. C7, Compounds with Carbon: Carbonates, Thiocyanates, Alkoxides, Carboxylates.

(1988b) vol. A3, Technology, Uses, Irradiated Fuel, Reprocessing.

(1988c) vol. D1, Properties of Ions in Solutions.

(1989) vol. A4, General Properties. Spectra. Recoil Reactions.

(1990a) vol. A1a, Natural Occurrence. Minerals(Excluding Silicates).

(1990b) vol. C5, Analysis, Biological Behavior.

(1990c) vol. D3, Ion Exchange.

(1991a) vol. A1b, Minerals (Silicates). Deposits.Mineral Index.

(1991b) vol. D4, Chromatography. Chemistry in Nonaqueous Solutions.

(1992a) vol. B2, Alloys with Metals of Group I to IV.

(1992b) vol. C6, Carbides.

(1993a) vol. C4, Compounds with F, Cl, Br, I.

(1993b) vol. C8, Compopunds with Si, P, As,Sb, Bi, and Ge.

(1997) vol. B1, Thorium Metal.

Goffart, J., Fuger, J., Gilbert, B., Hocks, L., and Duyckaerts, G. (1975) *Inorg. Nucl. Chem. Lett.*, **11**, 569–83.

Goffart, J., Gilbert, B., and Duyckaerts, G. (1977) *Inorg. Nucl. Chem. Lett.*, **13**, 189–96.

Goffart, J., Piret-Meunier, J., and Duyckaerts, G. (1980) *Inorg. Nucl. Chem. Lett.*, **16**, 233–4.

Golovnya, V. A., Molodkin, A. K., and Tverdokhlebov, V. N. (1964) *Zh. Neorg. Khim.*, **9**, 2032–34; *Russ. J. Inorg. Chem.*, **9**, 1097–8.

Golovnya, V. A., Molodkin, A. K., and Tverdokhlebov, V. N. (1967a) *Zh. Neorg. Khim.*, **12**, 2377–87; *Russ. J. Inorg. Chem.*, **12**, 1254–9.

Golovnya, V. A., Molodkin, A. K., and Tverdokhlebov, V. N. (1967b) *Zh. Neorg. Khim.*, **12**, 2729–39; *Russ. J. Inorg. Chem.*, **12**, 1439–44.

Golovnya, V. A., Molodkin, A. K., and Tverdokhlebov, V. N. (1967c) *Zh. Neorg. Khim.*, **12**, 2075–85; *Russ. J. Inorg. Chem.*, **12**, 1092–8.

Golub, A. M. and Kalibabchuk, V. A. (1967) *Zh. Neorg. Khim.*, **12**, 2370–6; *Russ. J. Inorg. Chem.*, **12**, 1249–53.

Golub, A. M., Dabeka, R. V., and Koval, V. T. (1974) *Komplexobrazovanie Ekstr. Aktinoidov Lantanoidov*, 97–101.

Gorbunov, L. V., Desyatnik, V. N., Raspopin, S. P., and Trifonov, I. I. (1974) *Zh. Neorg. Khim.*, **19**, 3093–5; *Russ. J. Inorg. Chem.*, **19**, 1692–3.

Gordon, J. E., Montgomery, H., Noer, R. J., Pickett, G. R., and Tobóu, R. (1966) *Phys. Rev.*, **152**, 432–7.

Gouder, T., Havela, L., Black, L., Wastin, F., Rebizant, J., Boulet, P., Bouexiere, D., Heathman, S., and Idiri, M. (2002) *J. Alloys Compds*, **336**, 73–6.

Graham, J. and McTaggart, F. K. (1960) *Aust. J. Chem.*, **13**, 67–73.

Gray, A. L. (1985) *Spectrochim. Acta*, **40B**, 1525–37.

Greiner, J. D. and Smith, J. F. (1971) *Phys. Rev. B.*, **4**, 3275–7.

Greis, O., Bohres, E. W., and Schwochau, K. (1977) *Z. Anorg. Allg. Chem.*, **433**, 111–8.

Grenthe, I. and Lagerman, B. (1991) *Acta Chem. Scand.*, **45**, 231–8.

Grenthe, I., Fuger, J., Konings, R. J. M., Lemire, R. J., Muller, A. B., Nguyen-Trung, C., and Wanner, H. (1992) OECD, NEA-TDB: Chemical Thermodynamics, vol. 1, *The Chemical Thermodynamics of Uranium,* Elsevier, North-Holland, Amsterdam, pp. 683–98.

Grossmann, H. (1905) *Z. Anorg. Chem.*, **44**, 229–36.

Gudaitis, M. N., Desyatnik, V. N., Raspopin, S. P., and Trifonov, I. I. (1972) *Zh. Neorg. Khim.*, **17**, 2841–2; *Russ. J. Inorg. Chem.*, **17**, 1489.

Guertin, R. P., Bulman, J. B., Huber, J. G., and Parks, R. D. (1980) *Physica B/C*, **102**, 151–4.

Guery, J., Gao, Y., Guery, C., and Jacoboni, C. (1994) *Eur. J. Solid State Inorg. Chem.*, **31**, 187–96.

Guggenberger, L. J. and Jacobson, R. A. (1968) *Inorg. Chem.*, **7**, 2257–60.

Guillaumont, R. (1983) *Radiochim. Acta*, **32**, 129–37.

Gutowska, M., Wanklyn, B. M., and Porcher, P. (1981) *Physica B*, **111**, 257.

Guymont, M. (1977) *C. R. Acad. Sci. Paris C*, **285**, 345–8.

Habash, J. and Smith, A. J. (1983) *Acta Crystallogr. C*, **39**, 413–5.

Habash, J. and Smith, A. J. (1990) *Acta Crystallogr. C*, **46**, 957–60.

Habash, J. and Smith, A. J. (1992) *J. Crystallogr. Spectr. Res.*, **22**, 21–4.

Haber, L. (1897) *Monatsh. Chem.*, **18**, 687–99.

Hagemann, F., Katzin, L. I., Studier, M. H., Ghiorso, A., and Seaborg, G. T. (1947) *Phys. Rev.*, **72**, 252.

Hagemann, F., Katzin, L. I., Studier, M. H., Seaborg, G. T., and Ghiorso, A. (1950) *Phys. Rev.*, **79**, 435–43.

Halla, F. (1912) *Z. Anorg. Chem.*, **79**, 260–2.

Hamaker, J. W. and Koch, C. W. (1952a) in Katzin (1952), paper 7.2, p. 318.

Hamaker, J. W. and Koch, C. W. (1952b) in Katzin (1952), paper 7.3, p. 339.

Hardman, K., Rhyne, J. J., Smith, K., and Wallace, W. E. (1980) *J. Less Common Metals*, **74**, 97–102.

Hardman, K., Rhyne, J. J., Prince, E., Smith, H. K., Malik, S. K., and Wallace, W. E. (1982) *Rare Earth Mod. Sci. Technol.*, **3**, 477–8.

Hardman-Rhyne, K., Smith, H. K., and Wallace, W. E. (1984) *J. Less Common Metals*, **96**, 201–11.

Harris, L. A., White, G. D., and Thoma, R. E. (1959) *J. Phys. Chem.*, **63**, 1974–5.

Harris, L. A. (1960) *Acta Crystallogr.*, **13**, 502.

Harris, L. A. and Finch, C. B. (1972) *Am. Mineral.*, **57**, 1894–8.

Hasty, R. A. and Boggs, J. E. (1971) *J. Inorg. Nucl. Chem.*, **33**, 874–6.

Hauser, O. and Wirth, F. (1908) *Z. Anorg. Chem.*, **60**, 242–6.

Hayek, E. and Rehner, T. (1949) *Experientia*, **5**, 114.

Hayek, E., Rehner, T., and Frank, A. (1951) *Monatsh. Chem.*, **82**, 575–87.

Hecht, F. (1928) *Z. Anal. Chem.*, **75**, 28–39.

Hecht, F. and Ehrmann, W. (1935) *Z. Anal. Chem.*, **100**, 87–98.

Heindl, F. and Loriers, J. (1974) *Bull. Soc. Chim. Fr.*, 377–8.

Helean, K. B., Navrotsky A., Lumpkin, G. R., Colella, M., Lian, J., Ewing, R. C., Ebbinghaus B., and Catalano, J. G. (2003) *J. Nucl. Mater.*, **320**, 231–44.

Henkie, Z., Markowski, P. J., and Zdanowicz, E. (1976) *Proc. Second Int. Conf. on Electronic Structure of Actinides,* Wroclaw (Poland), pp. 425–9.

Henkie, Z. and Markowski, P. J. (1978) *J. Phys. Chem. Solids*, **39**, 39–43.

Henkie, Z. and Wawryk, R. (2002) *Solid State Commun.*, **122**, 1–6.

Hentz, F. C. and Johnson, J. S. (1966) *Inorg. Chem.*, **5**, 1337–44.

Hess, R. F., Abney, K. D., Burris, J. L., Hochheimer, H. D., and Dorhout, P. K. (2001) *Inorg. Chem.*, **40**, 2851–9.

Hiebl, K., Rogl, P., Uhl, E., and Sienko, R. J. (1980) *Inorg. Chem.*, **19**, 3316–20.

Hietanen, S. and Sillen, L. G. (1964) *Acta Chem. Scand.*, **18**, 1018–9.

Hildenbrand, D. L. and Murad, E. (1974a) *J. Chem. Phys.*, **61**, 5466–7.

Hildenbrand, D. L. and Murad, E. (1974b) *J. Chem. Phys.*, **61**, 1232–7.

Hildenbrand, D. L. and Lau, K. H. (1990) *J. Chem. Phys.*, **93**, 5983–9.

Hill, N. A. and Cavin, O. B. (1964) *J. Am. Ceram. Soc.*, **47**, 360–1.

Hill, R. and Lieser, K. H. (1992) *Fresenius J. Anal. Chem.*, **342**, 337–40.

Hoffmann, A. (1935) *Z. Phys. Chem. B*, **28**, 65–77.

Hogfeldt, E. (1982) *Stability Constants of Metal-ion Complexes.* part A, *Inorganic Ligands, IUPAC Chemical Data Series*, no. 21, Pergamon Press, Oxford, p. 122.

Hönigschmid, O. (1906a) *Monatsh. Chem.*, **27**, 205–12.

Hönigschmid, O. (1906b) *C. R. Acad. Sci. Paris*, **142**, 157–9.

Hovey, J. K. (1997) *J. Phys. Chem.*, **101**, 4321–34.

Hubert, S., Barthelet, K., Fourest, B., Lagarde, G., Dacheux, N., and Baglan, N. (2001) *J. Nucl. Mater.*, **297**, 206–13.

Hubin, R. (1971) *Spectrochim. Acta*, **27A**, 311–9.

Hüfken, T., Witte, A. M., and Jeitschko, W. (1998) *J. Alloys Compds*, **266**, 158–63.

Hüfken, T., Witte, A. M., and Jeitschko, W. (1999) *J. Solid State Chem.*, **142**, 279–87.

Hulliger, F. (1966) *Nature*, **209**, 499–500; (1968) *J. Less Common Metals*, **16**, 113–7.

Hunt, E. B. and Rundle, R. E. (1951) *J. Am. Chem. Soc.*, **73**, 4777–81.

Huyghe, M., Lee, M.-R., Quarton, M., and Robert, F. (1991a) *Acta Crystallogr.*, **C47**, 244–6.

Huyghe, M., Lee, M.-R., Quarton, M., and Robert, F. (1991b) *Acta Crystallogr.*, **C47**, 1797–9.

Huyghe, M., Lee, M.-R., Jaulmes, S., and Quarton, M. (1993) *Acta Crystallogr.*, **C49**, 950–4.

Hyde, E. K. (1952) in Katzin (1952), paper 9.7, p. 554.

Hyde, E. K. and Wolf, M. J. (1952) in Katzin (1952), paper 3.12, p. 197.

Hyde, E. K. (1960) *The Radiochemistry of Thorium,* NAS-NS–3004, National Research Council, Springfield, VA.

Imre, L. (1927) *Z. Anorg. Allg. Chem.*, **164**, 214–8; **166**, 1–15.

International Critical Tables (1928) vol. 3, McGraw-Hill, New York, pp. 51–95.

Ionova, G., Madic, C., and Guillaumont, R. (1998) *Polyhedron*, **17**, 1991–5.

Isnard, O., Soubeyroux, J. L., Fruchart, D., Jacobs, T. H., and Buschow, K. H. J. (1992a) *J. Phys.: Conden. Matter*, **4**, 6367–74.

Isnard, O., Soubeyroux, J. L., Fruchart, D., Jacobs, T. H., and Buschow, K. H. J. (1992b) *J. Alloys Compds*, **186**, 135–45.

Isnard, O., Miraglia, S., Soubeyroux, J. L., Fruchart, D., Deportes, J., and Buschow, K. H. J. (1993) *J. Phys.: Cond. Matter*, **5**, 5481–90.

Jacob, I. (1981) *Solid State Commun.*, **40**, 1015.

Jacobson, E. L., Freeman, R. D., Tharp, A. G., and Searcy, A. W. (1956) *J. Am. Chem. Soc.*, **78**, 4850–2.

Jacoby, R. (1901) *Die Doppelnitrate des vierwertigen Ceriums und des Thoriums, Berlin,* as cited in Mellor, J. W. (1941) *A Comprehensive Treatise on Inorganic and Theoretical Chemistry*, vol. VII, Longmans, Green & Co., London, p. 251.

James, W. J. and Straumanis, M. E. (1956) *Acta Crystallogr.*, **9**, 376–9.

Jannasch, P. and Schilling, J. (1905) *J. Prakt. Chem.* **72**, 26–34.

Javorsky, C. A. and Benz, R. (1967) *J. Nucl. Mater.*, **23**, 192–8.

Jeitschko, W., Pollmeier, P. G., and Meisen, U. (1993) *J. Alloys Compds*, **196**, 105–9.

Jere, G. V. and Santhamma, M. T. (1977) *J. Less Common Metals*, **55**, 281–4.

Jiang, F. S. and Kuroda, P. K. (1987) *Radiochim. Acta*, **42**, 23–28.

Joao, A., Bigot, S., and Fromage, F. (1987) *Bull. Soc. Chim.*, **1**, 42–4.

Joao, A., Burrows, H. D., Zikovsky, L., and Lipponen, M. (1995) *Radiochim. Acta*, **68**, 177–83.

Johansson, G. (1968a) *Acta Chem. Scand.*, **22**, 389–98.

Johansson, G. (1968b) *Acta Chem. Scand.*, **22**, 399–409.

Johansson, G., Magini, M., and Ohtaki, H. (1991) *J. Solution Chem.*, **20**(8), 775–92.

Johnson, G. L., Kelly, M. I., and Cuneo, D. R. (1965) *J. Inorg. Nucl. Chem.*, **27**, 1787–91.

Johnson, K. R. (1889) *Berl. Dtsch. Chem. Ges.*, **22**, 976–80.

Jones, D. W., McColm, I. J., Steadman, R., and Yerkess, J. (1987) *J. Solid State Chem.*, **68**, 219–26.

Juza, R. and Gerke, H. (1968) *Z. Anorg. Allg. Chem.*, **363**, 245–57.

Juza, R. and Sievers, R. (1968) *Z. Anorg. Allg. Chem.*, **363**, 258–72.

Kahn-Harari, A. (1971) *Rev. Int. Hautes Temp. Refract.*, **8**, 71–84.

Kalina, D. G., Marks, T. J., and Wachter, W. A. (1977) *J. Am. Chem. Soc.*, **99**, 3877–9.

Kanellakopulos, B., Dornberger, E., and Baumgärtner, F. (1974) *Inorg. Nucl. Chem. Lett.*, **10**, 155–60.

Kaplan, G. E. (1956) *Proc. Int. Conf. on the Peaceful Uses of Atomic Energy*, Geneva, 1955, vol. 8, pp. 184–7.

Karabasch, A. G. (1958) *Zh. Neorg. Khim.*, **3**, 986–95.

Karstens, H. (1909) *Z. Elektrochem.*, **15**, 33–4.

Katz, J. J. and Seaborg, G. T. (1957) *The Chemistry of the Actinide Elements,* Methuen, London, 58.

Katzin, L. I. (1944) Memorandum to G. T. Seaborg on October 14.

Katzin, L. I. (1948) Report AECD-2213.

Katzin, L. I. (1952) *Production and Separation of* U^{233}*: Collected Papers*, Natl. Nucl. En. Ser., Div. IV, 17B, Report TID–5223, USAEC, Oak Ridge, Tenn.

Katzin, L. I., Ferraro, J. R., Wendlandt, W. W., and McBeth, R. L. (1956) *J. Am. Chem. Soc.*, **78**, 5139–44.

Katzin, L. I. (1958) *J. Am. Chem. Soc.*, **30**, 5908–10.

Katzin, L. I. and Gulyas, E. (1960) *J. Phys. Chem.*, **64**, 1347–50.

Katzin, L. I., Kaplan, L., and Seitz, T. (1962) *Inorg. Chem.*, **1**, 963–4.

Katzin, L. I. (1966) in *Transition Metal Chemistry, A Series of Advances,* vol. 3 (ed. R. L. Carlin), Marcel Dekker, New York, pp. 56–88.

Katzin, L. I. (1983) *Kirk-Othmer Encyclopoedia of Chemical Technology,* 3rd edn, **22**, 989–1002.

Kauffmann, O. (1899) PhD Thesis, University of Rostok, Germany.

Keenan, T. K. (1966) *Inorg. Nucl. Chem. Lett.*, **2**, 153–6; 211–4.

Keil, R. (1981) *Fresenius Z. Anal. Chem.*, **305**, 374–8.

Keller, C. (1965) *J. Inorg. Nucl. Chem.*, **27**, 1233–46.

Keller, C. and Salzer, M. (1967) *J. Inorg. Nucl. Chem.*, **29**, 2925–34.

Kemper, C. P. and Krikorian, N. H. (1962) *J. Less Common Metals*, **4**, 244–51.

Keskar, M., Kasar, U. M., and Singh Mudher, K. D. (2000) *J. Nucl. Mater.*, **282**, 146–51.

Khan Malek, C., Péneau, A., and Guibé, L. (1982) *J. Mol. Struct.*, **83**, 201–12.

Khan, A. S. and Peterson, D. T. (1976) *J. Less Common Metals*, **50**, 103–6.

Kharitonov, Yu. Ya., Molodkin, A. K., and Balakaeva, T. A. (1969) *Zh. Neorg. Khim.*, **14**, 2761–7; *Russ. J. Inorg.Chem.*, **14**, 1453–6.

King, E. L. (1945) Ph.D. Thesis, University of California.

Kiriyama, T. and Kuroda, R. (1978) *Anal. Chim. Acta*, **101**, 207–10.

Klapötke, T. M. and Schulz, A. (1997) *Polyhedron*, **16**(6), 989–91.

Klinkenberg, P. F. A. and Lang, R. J. (1949) *Physica*, **15**, 774–88.

Klyuchnikov, V. M., Zaitsev, L. M., and Apraksin, I. A. (1972) *Zh. Neorg. Khim.*, **17**, 2269–73.

Knacke, O., Müller, F., and van Rensen, E. (1972a) *Phys. Chem.*, **80**, 82–90.

Knacke, O., Müller, F., and van Rensen, E. (1972b) *Z. Phys. Chem.*, **80**, 91–100.

Knacke, O., Münstermann, E., and Probst, H. (1978) *Ber. Bunsen Ges.*, **82**, 154–9.

Koelling, D. D. and Freeman, A. J. (1971) *Solid State Commun.*, **9**, 1369–72.

Köhler, E., Brüser, W., and Thiele, K.-H. (1974) *J. Organomet. Chem.*, **76**, 235–40.

Köhler, S., Deißenberger, R., Eberhardt, K., Erdmann, N., Herrmann, G., Huber, G., Kratz, J. V., Nunnemann, M., Passler, G., Rao, P. M., Riegel, J., Trautmann, N., and Wendt, K (1997) *Spectrochim. Acta B*, **52**, 717–26.

Kohlmann, H. and Beck, H. P. (1999) *Z. Kristallogr.*, **214**, 341–5.

Kohlschütter, V. (1901) *Liebig's Ann.*, **317**, 158–89.

Kojic-Prodic, B., Slukic, M., and Ruzic Toros, Z. (1982) *Acta Crystallogr.*, **B38**, 67–71.

Kolb, A., Melzer, G., Merckle, A., and Teufel, C. (1908) *Z. Anorg. Chem.*, **60**, 123–33.

Kolb, A. (1913) *Z. Anorg. Chem.*, **83**, 143–8.

Konrad, T. and Jeitschko, W. (1995) *Z. Naturforsch.*, **50b**, 1195–9.

Konrad, T., Jeitschko, W., Danebrock, M. E., and Evers, C. B. H. (1996) *J. Alloys Compds*, **234**, 56–61.

Koppel, I. and Holtkamp, H. (1910) *Z. Anorg. Chem.*, **67**, 266–92.

Korobkov, I., Gambarotta, S., and Yap, G. P. A. (2003) *Angew. Chem.*, **115**, 838–42.

Korshunov, B. G. and Drobot, D. V. (1971) *Zh. Neorg. Khim.*, **16**, 556–7.

Korst, W. L. (1962) *Acta Crystallogr.*, **15**, 287–8.

Koulkès-Pujo, A. M., Martin-Rovet, D., Folcher, G., Plissionier, M., and Pascal, J. L. (1982) *Nouv. J. Chim.*, **6**, 571–2.

Kovalchuk, E. L., Smolnikov, A. A., and Temmoev, A. H. (1982) *Phys. Appl.*, **8**, 297–303.

Kraus, K. A. and Holmberg, R. W. (1954) *J. Phys. Chem.*, **58**, 325–30.

Kravchenko, E. A., Ivanova, O. M., and Ilin, E. G. (1975) *Zh. Neorg. Khim.*, **20**, 2556–7.

Krupa, J. C., Khan Malek, C., Delamoye, P., Moine, B., and Pedrini, C. (1987) *Phys. Status Solidi B*, **140**, 289–300.

Krupa, J. C., Delamoye, P., and Milicic-Tang, A. (1995) *Zh. Prikl. Spek.*, **62**, 167–78.

Krupka, M. C. (1970) *J. Less Common Metals*, **20**, 135–40.

Krüss, G. and Volck, C. (1894) *Z. Anorg. Chem.*, **5**, 75–9.

Krüss, G. and Nilson, L. F. (1887a) *Z. Phys. Chem.*, **1**, 301–6.

Krüss, G. and Nilson, L. F. (1887b) *Ber. Dtsch. Chem. Ges.*, **20**, 1665–76.

Krüss, G. (1894) *Z. Anorg. Chem.*, **6**, 49–56.

Ku, H. C., Meisner, G. P., Acker, F., and Johnston, D. C. (1980) *Solid State Commun.*, **35**, 91–6.

Kumar, N. and Tuck, D. G. (1983) *Inorg. Chem.*, **22**, 1951–2.

Lafferty, J. M. (1951) *J. Appl. Phys.*, **22**, 299–309.

Laligant, Y., Le Bail, A., Avignant, D., Cousseins, J. C., and Ferey, G. (1989) *J. Solid State Chem.*, **80**, 206–12.

Laligant, Y., Ferey, G., El Ghozzi, M., and Avignant, D. (1992) *Eur. J. Solid State Inorg. Chem.*, **29**, 497–504.

Lam, D. J., Darby, J. B. Jr, and Nevitt, M. V. (1974) in *The Actinides: Electronic Structure and Related Properties,* ch. 4 (eds. A. J. Freeman and J. B. Darby), Academic Press, New York.

Langer, S., Baldwin, N., Gantzel, P., Kester, F., and Hancock, C. (1964) in *Nuclear Metallurgy,* vol. 10 (eds. J. T. Waber, P. Chiotti, and W. N. Miner), Edward Bros., Ann Arbor, p. 359.

Langmuir, D. and Herman, J. S. (1980) *Geochim. Cosmochim. Acta*, **44**, 1753–66.

Larson, E. M., Eller, P. G., Cremers, T. L., Penneman, R. A., and Herrick, C. C. (1989) *Acta Crystallogr.*, **C45**, 1669–72.

Lau, K. F., Vaughan, R. W., and Satterthwaite, C. B. (1977) *Phys. Rev. B*, **15**, 2449–57.

Laubereau, P. G., Ganguly, J., Burns, J. H., Benjamin, B. M., Atwood, J. L., and Selbin, J. (1971) *Inorg. Chem.*, **10**, 2274–80.

Laubscher, A. E. and Fouché, K. F. (1971) *J. Inorg. Nucl. Chem.*, **33**, 3521–35.

Laud, K. R. (1971) *J. Am. Ceram. Soc.*, **54**, 296–8.

Laügt (1973) *J. Appl. Crystallogr.*, **6**, 299–301.

Launay, S. and Rimsky, A. (1980) *Acta Crystallogr.*, **B36**, 910–2.

Launay, S., Mahe, P., Quarton, M., and Robert, F., J. (1992) *J. Solid State Chem.*, **97**, 305–13.

Launay, S., Jaulmes, S., Lucas, F., and Quarton, M. (1998) *J. Solid State Chem.*, **136**, 199–205.

Le Berre, F., Boucher, E., Allain, M., and Courbion, G. (2000) *J. Mater. Chem.*, **10**, 2578–86.

Le Flem, G. (1967) Thése de Doctorat, Bordeaux.

Lebeau, P. and Damiens, A. (1913) *C. R. Acad. Sci. Paris*, **156**, 1987–9.

Leber, A. (1927) *Z. Anorg. Allg. Chem.*, **166**, 16–26.

Leciejewicz, J., Siek, S., and Szytula, A. (1988) *J. Less Common Metals*, **144**, 9–13.

Lefèbvre, J. (1957) *Bull. Soc. Chim.*, **14**, 227–33.

Le Flem, G. and Hagenmuller, P. (1964) *Rev. Hautes Temp. Refract.*, **1**, 149–52.

Le Flem, G., Hardy, A., and Hagenmuller, P. (1965) *C. R. Acad. Sci. Paris C*, **260**, 1663–5.

Lesinsky, J. and Gundlich, C. (1897) *Z. Anorg. Chem.*, **15**, 81–3.

Le Vanda, C., Solar, J. R., and Streitwieser, A. Jr (1980) *J. Am. Chem. Soc.*, **102**, 2128–9.

Lipkind, H. and Newton, A. S. (1952) in Katzin (1952), paper 7.8, p. 398.

Li, Y.-P., Krivovichev, S. V., and Burns, P. C. (2000) *Am. Miner.*, **85** 1521–5.

Liu, C., Zhao, Z., Yang, X., Ye, X., and Wu, Y. (1997) *Sci. China, Ser. A: Math., Phys., Astron.*, **40**, 1210.

Lobanov, M. V., Li, S., and Greenblatt, M. (2003) *Chem. Mater.*, **15**, 1302–8.

Louer, M., Brochu, R., Louer, D., Arsalane, S., and Ziyad, M. (1995) *Acta Crystallogr.*, **B51**, 908–13.

Loye, O., Laurelle, P., and Harari, A. (1968) *C. R. Acad. Sci. Paris C*, **266**, 454–6.

Luengo, C. A., Cotiguola, J. M., Sereni, J. G., Sweedler, A. R., and Maple, M. B. (1972a) *Proc. 13th Int. Conf. Low Temp. Phys.,* Boulder, Colorado, 585–9.

Luengo, C. A., Cotiguola, J. M., Sereni, J. G., Sweedler, A. R., Maple, M. B., and Huber, J. G. (1972b) *Solid State Commun.*, **10**, 459–63.

Lundgren, G. (1950) *Ark. Kem.*, **2**, 535–49.

Lundgren, G. and Sillen, L. G. (1949) *Naturwiss.*, **36**, 345–6.

Madariaga, G., Perez-Mato, J. M., and Aramburu, I. (1993) *Acta Crystallogr.*, **B49**, 244–54.

Magini, M., Cabrini, A., Scibona, G., Johansson, G., and Sandström, M. (1976) *Acta Chem. Scand. A*, **30**, 437–47.

Mahalingham, A., Kalpana, G., Kansalaya, B., Palanivel, B., and Rajagopalan, M. (1993) *Phys. Status Solidi B*, **178**, 185–97.

Manriquez, J. M., Fagan, P. J., and Marks, T. J. (1978) *J. Am. Chem. Soc.*, **100**, 3939–41.

Manske, W. J. (1965) *Luminescent Gas Mantles and Their Mountings*, Minnesota Mining and Manufacturing Company, 32 pp.

Manuelli, C. and Gasparinetti, B. (1902) *Gazz. Chim. Ital.*, **32**, 523–31.

Marcus, Y. and Kertes, A. S. (1969) *Ion Exchange and Solvent Extraction of Metal Complexes,* Wiley-Interscience, London.

Marden, J. W. and Rentschler, H. C. (1927) *Ind. Eng. Chem.*, **19**, 97–103.

Marks, T. J. and Wacher, W. A. (1976) *J. Am. Chem. Soc.*, **98**, 703–10.

Marks, T. J., Seyam, A. M., and Wachter, W. A. (1976) *Inorg. Synth.*, **16**, 147–51.

Mason, D. M. (1964) Technical Report – Institute of Gas Technology (Chicago), No. 9, 19 pp.

Mason, J. T., Jha, M. C., and Chiotti, P. (1974a) *J. Less Common Metals*, **34**, 143–51.

Mason, J. T., Jha, M. C., Bailey, D. M., and Chiotti, P. (1974b) *J. Less Common Metals*, **35**, 331–8.

Martinot, L. and Fuger, J. (1985) in *Standard Potentials in Aqueous Solution* (eds. A. J. Bard, R. Parsons, and J. Jordan), IUPAC, Marcel Dekker, New York, ch. 21, p. 640.

Matignon, C. (1900) *C. R. Acad. Sci. Paris*, **131**, 837–9.

Matignon, C. and Delepine, M. (1901) *C. R. Acad. Sci. Paris.*, **132**, 36–8.

Matignon, C. A. and Bourion, R. (1904) *C. R. Acad. Sci. Paris*, **138**, 631–3.

Matignon, C. and Delepine, M. (1907) *Ann. chim. phys.*, **10**, 130–44.

Matignon, C. A. (1908) *C. R. Acad. Sci. Paris*, **147**, 1292–3.

Matkovic, B. and Sljukic, M. (1965) *Croat. Chem. Acta*, **37**, 115–6.

Matkovic, B., Sljukic, M., and Prodic, B. (1966) *Croat. Chem. Acta*, **38**, 69–70.

Matkovic, B., Prodic, B., and Sljukic, M. (1968) *Bull. Soc. Chim. Fr.*, 1777–9.

Matkovic, B., Kojic-Prodic, B., Sljukic, M., Topic, M., Willett, R. D., and Pullen, F. (1970) *Inorg. Chim. Acta*, **4**, 571–6.

Matthews, J. M. (1898) *J. Am. Chem. Soc.*, **20**, 815–39; 839–43.

Maxim, P., Müller, R., and Schnabel, B. (1979) *Physica*, **24**, 53–6.

Mayankutty, P. C., Jangida, B. L., and Sundaresan, M. (1982) *Separat. Sci. Technol.*, **17**, 1327–37.

Mazeina, L., Ushakov, S. V., Navrotsky, A., and Boatner, L. A. (2005) *Geochim. Cosmochim. Acta* **69**, 4675–783.

Meisel, K. (1939) *Z. Anorg. Allg. Chem.*, **240**, 300–2.

Meissner, W. (1929) *Naturwissenschaften*, **17**, 390–1; (1930) *Z. Phys.*, **61**, 191–8.

Mellor, J. W. (1941) *A Comprehensive Treatise on Inorganic and Theoretical Chemistry,* vol. VII, Longmans, Green & Co., London, p. 241.

Mentzen, B. F. (1969) *Rev. Chim. Miner.*, **6**, 713–25.

Mentzen, B. F. (1971a) *J. Solid State Chem.*, **3**, 12–9.

Mentzen, B. F. (1971b) *J. Solid State Chem.*, **3**, 20–5.

Merigou, C., Le Du, J. F., Genet, M., Ouillon, N., and Chopin, T. (1995) *New J. Chem.*, **19**, 1037–45.

Merkusheva, S. A., Skorik, N. A., Kumok, V. N., and Serebrennikov, V. V. (1967) *Radiokhimiya*, **9**, 723–5; *Sov. Radiochem.*, **9**, 683–5.

Metzger, F. J. and Zons, F. W. (1912) *Ind. Eng. Chem.*, **4**, 493–5.

Meyer, R. J. and Jacoby, R. (1901) *Z. Anorg Chem.*, **27**, 359–89.

Meyer, R. J. and Gumperz, A. (1905) *Berl. Dtsch. Chem. Ges.*, **38**, 817–25.

Meyer, R. J. (1908) *Z. Elektrochem.*, **14**, 809–10; (1909) *Z. Elektrochem.*, **15**, 105–6.

Meyerson, G. A. (1956) *Proc. Int. Conf. on the Peaceful Uses of Atomic Energy*, Geneva, 1955, vol. 8, pp. 188–93.

Miekeley, N. and Küchler (1987) *Inorg. Chim. Acta*, **140**, 315–9.

Mikheev, N. B., Kulyhukin, S. A., and Kamenskaya, A. N. (1993) *Radiokhimiya*, **35**, 1; *Sov. Radiochem.*, **35**, 249.

Milic, N. A. (1971) *Acta Chem. Scand.*, **25**, 2487–98.

Milic, N. B. (1981) *J. Chem. Soc. Dalton*, 1445–9.

Milic, N. A. and Suranji, T. M. (1982) *Can. J. Chem.*, **60**, 1298–303.

Miller, J. F., Caton, R. H., and Satterthwaite, C. B. (1976) *Phys. Rev. B*, **14**, 2795–800.

Mintz, E. A., Moloy, K. G., Marks, T. J., and Day, V. W. (1982) *J. Am Chem. Soc.*, **104**, 4692–5.

Misciatelli, P. (1929) *Phil. Mag.*, **7**, 670–4.

Misciatelli, P. (1930a) *Gazz. Chim. Ital.*, **60**, 833–8.

Misciatelli, P. (1930b) *Gazz. Chim. Ital.*, **60**, 882–5.

Mitchell, R. H. and Chakhmouradian, A. R. (1999) *Phys. Chem. Miner.*, **26**, 396–405.

Moissan, H. and Étard, A. (1896) *C. R. Acad. Sci. Paris*, **122**, 573

Moissan, H. and Étard, A. (1897) *Ann. Chim. Phys.*, **7** (12), 427–32.

Moissan, H. and Martinsen, M. (1905) *C. R. Acad. Sci. Paris*, **140**, 1510–5.

Moissan, H. and Hönigschmid, O. (1906) *Ann. Chim. Phys.*, **8** (8), 182–92.

Moll, H., Denecke, M. A., Jalilehvand, F., Sandström, M., and Grenthe, I. (1999) *Inorg. Chem.*, **38**, 1795–9.

Molodkin, A. K., Skotnikova, E. G., and Arutyunyan, E. (1964) *Zh. Neorg. Khim.*, **9**, 2705–9; *Russ. J. Inorg. Chem.*, **9**, 1458–61.

Molodkin, A. K., Petrov, K. I., Balakayeba, T. A., and Kuchumova, A. N. (1968a) *Zh. Neorg. Khim.*, **13**, 3209–15; *Russ. J. Inorg. Chem.*, **13**, 1654–7.

Molodkin, A. K., Ivanova, O. M., Kozina, L. E., and Petrov, K. I. (1968b) *Russ. J. Inorg. Chem.*, **13**, 694–9.

Molodkin, A. K., Balakayeva, T. A., and Kuchumova, A. N. (1970) *Zh. Neorg. Khim.*, **15**, 1152–3; *Russ. J. Inorg. Chem.*, **15**, 589–90.

Molodkin, A. K., Belyakova, Z. V., and Ivanova, O. M. (1971) *Zh. Neorg. Khim.*, **16**, 1582–9; *Russ. J. Inorg. Chem.*, **16**, 835–9.

Montignie, E. (1947) *Bull. Soc. Chim. Fr.*, 748–9.

Moodenbaugh, A. R., Johnston, D. C., Viswanathan, R., Shelton, R. N., Delong, L. E., and Fertig, W. A. (1978) *J. Low Temp. Phys.*, **33**, 175–203.

Moon, H. C. (1989) *Bull. Korean Chem. Soc.*, **10**(3), 270–2.

Mooney, R. C. L. (1949) *Acta Crystallogr.*, **2**, 189–91.

Morss, L. R. and McCue, M. C. (1976) *J. Chem. Eng. Data*, **21**, 337–41.

Moriyama, H., Kitamura, A., Fujiwara, K., and Yamana, H. (1999) *Radiochim. Acta*, **87**, 97–104.

Morss, L. R. and McCue, M. C. (1976) *J. Chem. Eng. Data*, **21**, 337–41.

Moseley, P. T., Sanderson, S. W., and Wheeler, V. J. (1971) *J. Inorg. Nucl. Chem.*, **33**, 3975–6.

Moss, M. A. and Jeitschko, W. (1989a) *Z. Kristallogr.*, **186**, 204–5.

Moss, M. A. and Jeitschko, W. (1989b) *Z. Kristallogr.*, **186**, 204.

Moss, M. A. and Jeitschko, W. (1991a) *Z. Anorg. Allg. Chem.*, **603**, 57–67.

Moss, M. A. and Jeitschko, W. (1991b) *Z. Metallkunde*, **82**, 669–74.

Moskvin, A. I. and Essen, L. N. (1967) *Russ. J. Inorg. Chem.*, **12**, 359–62.

Moskvin, A. I., Essen, L. N., and Bukhtiyarova, T. N. (1967) *Russ. J. Inorg. Chem.*, **12**, 1794–5.

Moulin, C., Amekraz, B., Hubert, S., and Moulin, V. (2001) *Anal. Chim. Acta*, **441**, 269–79.

Moze, O., Brueck, E., de Boer, F. R., and Buschow, K. H. J. (1996) *J. Magn. Magn. Mater.*, **152**, 341–4.

Mucker, K., Smith, G. S., Johnson, Q., and Elson, R. E. (1969) *Acta Crystallogr. B*, **25**, 2362–5.

Mueller, M. H., Beyerlein, R. A., Jorgensen, J. D., Brun, T. O., Satterthwaite, C. B., and Caton, R. (1977) *J. Appl. Crystallogr.*, **10**, 79–83.

Müller, A. (1906) *Berl. Dtsch. Chem. Ges.*, **39**, 2857–9; (1908) *Z. Anorg. Chem.*, **57**, 311–22.

Murthy, M. S. and Redhead, P. A. (1974) *J. Vac. Sci. Technol.*, **11**, 837–42.

Murthy, P. R. and Patel, C. C. (1965) *Indian Chem.*, **3**, 134–5.

Nabar, M. A., Mhatre, B. G., and Vasaikar, A. P. (1981) *J. Appl. Crystallogr.*, **14**, 469–70.

Nabar, M. A. and Mhatre, B. G. (1982) *J. Solid State Chem.*, **45**, 135–9.

Nabar, M. A. and Mangaonkar, S. S. (1991) *Eur. J. Solid State Inorg. Chem.*, **28**, 549–52.

Nabar, M. A. and Mhatre, B. G. (2001) *J. Alloys Compds*, **323–4**, 83–5.

Nabivanets, B. I. and Kudritskaya, L. N. (1964) *Ukr. Khim. Zh.*, **30**, 891–5.

Nakamura, T. (1974) *Chem. Lett.*, 429–34.

Nakashima, T. and Zimmer, E. (1984) *Radiochim. Acta*, **37**, 165–7.

Naray-Szabo, L. (1951) in *Crystal Structures,* vol. 1 (ed. R. W. Wyckoff), Interscience Publishers, New York, no. 1, 30.

Narducci, A. A. and Ibers, J. A. (1998a) *Chem. Mater.*, **10**, 2811–23.

Narducci, A. A. and Ibers, J. A. (1998b) *Inorg. Chem.*, **37**, 3798–801.

Narducci, A. A. and Ibers, J. A. (2000) *Inorg. Chem.*, **39**, 688–91.

Naslain, R., Etourneau, J., and Kasper, J. S. (1971) *J. Solid State Chem.*, **3**, 101–11.

Nebel, D. and Urban, G. (1966) *Z. Phys. Chem. (Leipzig)*, **233**, 73–84.

Neck, V. and Kim, J. I. (2000) *Radiochim. Acta*, **88**, 815–22.

Neck, V. and Kim, J. I. (2001) *Radiochim. Acta*, **89**, 1–16.

Neck, V (2002) *ANDRA project: Solution Chemistry of Actinides and Radium; Lot 2: Cement water Environment, 3rd Annual and Final Report to Phase 3* "*Experimental Programme*", FZK-INE 002/02 Report.

Neck, V., Müller, R., Bouby, M., Altmaier, M., Rothe, J., Denecke, M. A., and Kim, J. I. (2002) *Radiochim. Acta*, **90**, 485–94.

Neish, A. C. (1904) *J. Am. Chem. Soc.*, **26**, 780–3.

Neubert, A. and Zmbov, K. F. (1974) *High Temp. Sci.*, **6**, 303–8.

Newton, A. S., Lipkind, H., Keller, W. H., and Iliff, J. E. (1952a) in Katzin (1952), paper 8.3, p. 419.

Newton, A. S., Johnson, O., Tucker, W., Fisher, R. W., and Lipkind, H. (1952b) in Katzin (1952), paper 8.6, p. 462.

Nilson, L. F. (1876) *Berl. Dtsch. Chem. Ges.*, **9**, 1142.

Nilson, L. F. (1882a) *Berl. Dtsch. Chem. Ges.*, **15**, 2537.

Nilson, L. F. (1882b) *C. R. Acad. Sci. Paris*, **95**, 727.

Nilson, L. F. (1883) *Berl. Dtsch. Chem. Ges.*, **16**, 153.

NIST (2002) NIST Critically Selected Stability Constants of Metal Complexes:version 7.0.NIST Standard Reference Database 46, National Institute of Standards and Technology, Gaithersburg, MD.

Noël, H. (1980) *J. Inorg. Nucl. Chem.*, **42**, 1715–7.

Noël, H. and Potel, M. (1982) *Acta Crystallogr. B*, **38**, 2444–5.

Nordenskjöld, A. E. and Chydenius, J. J. (1860) *Pogg. Ann.*, **110**, 642.

Nordenskjöld, A. E. (1861) *Pogg. Ann.*, **114**, 612.

Nordling, C. and Hagström, S. (1964) *Z. Phys.*, **178**, 418–32.

Nottorf, R. W., Wilson, A. S., Rundle, R. E., Newton, A. S., and Powell, J. E. (1952) in Katzin (1952), paper 7.6, p. 350.

Nugent, L. J., Baybarz, R. D., Burnett, J. L., and Ryan, J. L. (1973) *J. Phys. Chem.*, **77**, 1528–39.

Oesterreicher, H., Clinton, J., and Bittner, H. (1976) *J. Solid State Chem.*, **16**, 209–10.

Oetting, F. L., Rand, M. H., and Ackermann, R. J. (1976) in *The Chemical Thermodynamics of Actinide Elements and Compounds*, part 1, *The Actinide Elements* (eds. F. L. Oetting, V. A. Medvedev, M. H. Rand, and E. F. Westrum Jr), STI/PUB/424/1, IAEA, Vienna.

Östhols, E., Bruno, J., and Grenthe, I. (1994) *Geochim. Cosmochim. Acta*, **58**, 613–23.

Östhols, E. (1995) *Radiochim. Acta*, **68**, 185–90.

Ohta, T. and Sata, T. (1974) *Yogyo Kyoka Shi*, **82**, 387–401.

Olson., W. M. and Mulford, R. N. R. (1965) *J. Phys. Chem.*, **69**, 1223–6.

Omejec, L. and Ban, Z. (1971) *Z. Anorg Allg. Chem.*, **380**, 111–7.

Onosov, V. N. (1971) *Tr. Ural. Politekh. Inst.*, **193**, 21–7.

Oyamada, R. and Yoshida, S. (1975) *J. Phys. Soc. Japan*, **38**, 1786.

Pagès, M. and Freundlich, W. (1971) *C. R. Acad. Sci. Paris C*, **272**, 1861–2.

Pai, M. R., Wani, B. N., and Gupta, N. M. (2002) *J. Mater. Sci. Lett.*, **21**, 1187–90.

Palanivel, B., Kalpana, G., and Rajagopalan, M. (1995) *Mater. Res. Soc. Symp. Proc.*, **364**, 1095.

Palisaar, A.-P. and Juza, R. (1971) *Z. Anorg. Allg. Chem.*, **384**, 1–11.

Palmer, C. (1895) *Am. Chem. J.*, **17**, 374–9.

Palmy, C., Flach, R., and De Trey, P. (1971) *Physica*, **55**, 663–8.

Parry, J. S., Cloke, F. G. N., Coles, S. J., and Hursthouse, M. B. (1999) *J. Am. Chem. Soc.*, **121**, 6867–71.

Pastor, R. C. and Arita, K. (1974) *Mater. Res. Bull.*, **9**, 579–83.

Paul, R. C., Singh, S., and Verma, R. D. (1981) *J. Indian Chem. Soc.*, **58**, 24–5.

Pearson, W. B. (1985) *Z. Kristallogr.*, **171**, 23–39.

Pedziwiatr, A. T., Wallace, W. E., and Burzo, E. (1986) *J. Magn. Magn. Mater.*, **61**, 177–82.

Penneman, R. A., Ryan, R. R., and Rosenzweig, A. (1968) *J. Chem. Soc. Chem. Commun.*, 990–1.

Penneman, R. A., Ryan, R. R., and Kressin, I. K. (1971) *Acta Crystallogr. B*, **27**, 2279–83.

Penneman, R. A., Ryan, R. R., and Rosenzweig, A. (1973) *Struct. Bonding*, **13**, 1–52.

Penneman, R. A., Ryan, R. R., and Larson, A. C. (1976) *Proc. Moscow Symp. on Chem. Transuranium Elements, 1972,* Pergamon Press, Oxford, , pp. 265–9.

Peppard, D. F. and Mason, G. W. (1963) *Nucl. Sci. Eng.*, **16**, 382–8.

Peppard, D. F. (1966) *Adv. Inorg. Chem. Radiochem.*, **9**, 1–80.

Peppard, D. F. (1971) *Annu. Rev. Nucl. Sci.*, **21**, 365–96.

Peretz, M., Zamir, D., and Hadari, Z. (1978) *Phys. Rev. B*, **18**, 2059–65.

Perezy Jorba, M., Mondange, H., and Collongues, R. (1961) *Bull. Soc. Chim. Fr.*, 79–81.

Perrin, D. D. (1982) *Stability Constants of Metal-ion Complexes, Part B-Organic Ligands,* IUPAC Chemical Data Series, n°21, Pergamon Press, Oxford.

Peterson, D. T. and Schmidt, F. A. (1971) *J. Less Common Metals*, **24**, 223–8.

Peterson, D. T., Westlake, D. G., and Rexer, J. (1959) *J. Am. Chem. Soc.*, **81**, 4443–5.

Pissarsjewski, L. (1900) *J. Russ. Phys.-Chem. Ges.*, **32**, 609–27.

Pissarsjewsky, L. (1902) *Z. Anorg. Chem.*, **31**, 359–67.

Pitman, D. T. and Das, D. K. (1960) *J. Electrochem. Soc.*, **107**, 763–6.

Popovic, S. (1971) *J. Appl. Cryst.*, **4**, 240–1.

Post, B., Moskowitz, D., and Glaser, F. S. (1956) *J. Am. Chem. Soc.*, **78**, 1800–2.

Price, C. E. and Warren, I. H. (1965) *J. Electrochem. Soc.*, **112**, 510–3.

Pulcinelli, S. H. and de Almeida Santos, R. H. (1989) *J. Fluorine Chem.*, **42**, 41–50.

Quarton, M., Rimsky, H., and Freundlich, W. (1970) *C. R. Acad. Sci. Paris C*, **271**, 1439–41.

Quarton, M. and Kahn, A. (1979) *Acta Crystallogr.*, **C35**, 2529–32.

Rabinovich, D., Chamberlin, R. M., Scott, B. L., Nielsen, J. B., and Abney, K. D. (1997) *Inorg. Chem.*, **36**, 4216–7.

Racah, G. (1950) *Physica*, **16**, 651–66.

Radzewitz, H. (1966) Report KFK-433.

Rai, H. C. and Sahoo, B. (1974) *Indian J. Chem.*, **12**, 1302–3.

Rai, D., Swanson, J. L., and Ryan, J. L. (1987) *Radiochim. Acta*, **42**, 35–41.

Rai, D., Felmy, A. R., Moore, D. A., and Mason, M. J. (1995) *Mater. Res. Soc. Symp. Proc.*, **353**, 1143–50.

Rai, D., Felmy, A. R., Sterner, S. M., Moore, D. A., Mason, M. J. M., and Novak, C. F. (1997) *Radiochim. Acta*, **79**, 239–47.

Ramamurthy, P. and Patel, C. C. (1963) *J. Inorg. Nucl. Chem.*, **25**, 310–2.

Raman, V. and Jere, G. V. (1973a) *Indian J. Chem.*, **11**, 1318–9.

Raman, V. and Jere, G. V. (1973b) *Indian J. Chem.*, **11**, 31–4.

Rammelsberg, C. (1873) *Pogg. Ann.*, **150**, 198.

Rand, M. H., von Goldbeck, O., Ferro, R., Girgis, K., and Dragoo, A. L. (1975) in *Thorium: Physico-Chemical Properties of its Compounds and Alloys* (ed. O. Kubaschewski), IAEA, Vienna.

Raub, E. and Engles, M. (1947) *Metallforsch.*, **2**, 115–9.

Raymond, D. P., Duffield, J. R., and Williams, D. R. (1987) *Inorg. Chim. Acta.*, **140**, 309–13.

Reid, A. F. and Wailes, P. C. (1966) *Inorg. Chem.*, **5**, 1213–6.

Ribas Bernat, J. G. and Ramos Alonso, V. (1976) *Ion (Madrid)*, **36**, 11–3.

Ribas Bernat, J. G., Ramos Alonso, V., and Balcazar Pinal, J. L. (1977) *Ann. Quim.*, **73**, 1425–7.

Rickard, C. E. F. and Woolard, D. C. (1978) *Inorg. Nucl. Chem. Lett.*, **14**, 207–10.

Rogl, P. and Nowotny, H. (1974) *Monatsh. Chem.*, **105**, 1082–98.

Rogl, P. (1978) *J. Nucl. Mater.*, **73**, 198–203.

Rogl, P. (1979) *J. Nucl. Mater.*, **79**, 154–8.

Rogl, P. and Fischer, P. (1989) *J. Solid State Chem.*, **78**, 294–300.

Roll, W. and Dempster, A. J. (1952) in Katzin (1952), paper 9.22, p. 639.

Rollefson, G. K. (1947) unpublished work cited in Report CB-3717.

Roozeboom, H. W. B. (1890) *Z. Phys. Chem.*, **5**, 198–216.

Rosengren, A., Ebbsjö, I., and Johansson, B. (1975) *Phys. Rev. B*, **12**, 1337–42.

Rosenheim, A. and Schilling, J. (1900) *Berl. Dtsch. Chem. Ges.*, **33**, 977–80.

Rosenheim, A., Samter, V., and Davidsohn, J. (1903) *Z. Anorg. Chem.*, **35**, 424–53.

Rosenheim, A. and Kelmy, M. (1932) *Z. Anorg. Allg. Chem.*, **206**, 31–43.

Rothschild, B. F., Templeton, C. C., and Hall, N. F. (1948) *J. Phys. Col. Chem.*, **52**, 1006–20.

Rothwarf, F. and Dubeck, L. W. (1973) *Solid State Commun.*, **13**, 1645–9.

Rozen, A. M., Nikolotova, Z. A., Kartasheva, N. A., Luk'yanenko, N. G., and Bogatskii, A. V. (1982) *Dokl. Akad. Nauk SSSR*, **263**, 1165–9.

Ruff, O. and Brintzinger, H. (1923) *Z. Anorg. Allg. Chem.*, **129**, 267–75.

Ruh, R. and Wadsley, A. D. (1966) *Acta Crystallogr.*, **21**, 974–8.

Rundle, R. E., Wilson, A. S., Nottorf, R., and Rauchle, R. F. (1948a) Report AECD-2120.

Rundle, R. E., Baenziger, N. C., Wilson, A., McDonald, R. A., Chiotti, P., and Rundle, R. E. (1948b) *Acta Crystallogr.*, **1**, 180–7.unpublished data cited in

Rundle, R. E., Schull, C. G., and Wollan, E. O. (1952) *Acta Crystallogr.*, **5**, 22–6.

Ruzic Toros, Z., Kojic-Prodic, B., Liminga, R., and Popovic, S. (1974) *Inorg. Chim. Acta*, **8**, 273–8.

Ryan, R. R., Penneman, R. A., and Rosenzweig, A. (1969) *Acta Crystallogr. B*, **25**, 1958–62.

Ryan, R. R. and Penneman, R. A. (1971) *Acta Crystallogr. B*, **27**, 829–33.

Ryan, J. L. and Rai, D. (1987) *Inorg. Chem.*, **26**, 4140–2.

Sachs, A. (1901) *Z. Kristallogr.*, **34**, 162–70.

Sahoo, B. and Patnaik, D. (1961) *Curr. Sci.*, **30**, 293–4.

Salzer, M. (1966) Report KFK-385.

Sandström, M., Persson, I., Jalilehvand, F., Lindquist- Reis, P., Spangberg, D., and Hermansson, K. (2001) *J. Synchrotron Radiat.*, **8**, 657–9.

Satoh, T. and Kumagai, K. (1971) *Proc. 12th Int. Conf. Low Temp. Phys.*, Tokyo, 347–9.

Satoh, T. and Kumagai, K. (1973) *J. Phys. Soc. Jpn.*, **34**, 391–5.

Satpathy, K. C. and Sahoo, B. (1968) *Curr. Sci.*, **37**, 435–6.

Satterthwaite, C. B. and Toepke, I. L. (1970) *Phys. Rev. Lett.*, **25**, 741–3.

Satterthwaite, C. B. and Peterson, D. T. (1972) *J. Less Common Metals*, **26**, 361–8.

Scaife, D. E. and Wylie, A. W. (1964) *J. Chem. Soc.*, 5450–8.

Scaife, D. E., Turnbull, A. G., and Wylie, A. W. (1965) *J. Chem. Soc.*, 1432–7.

Scavnicar, S. and Prodic, B. (1965) *Acta Crystallogr.*, **18**, 698–702.

Schleid, ThMeyer, and G., Morss, R. L. (1987) *J. Less Common Metals*, **132**, 69–77.

Schmid, W. F. and Mooney, R. W. (1964) *J. Electrochem. Soc.*, **111**, 668–73.

Schmidt, H. G. and Wolf, G. (1975) *Solid State Commun.*, **16**, 1085–7.

Schmidt, H. G. and Gruehn, R. (1989) *J. Less Common Metals*, **156**, 75–86.

Schmidt, H.G. and Gruehn, R. (1990) *J. Less Common Metals*, **158**, 275–85.

Scholder, R., Räde, D., and Schwarz, H. (1968) *Z. Anorg. Allg. Chem.*, **362**, 149–68.

Schild, D. and Marquardt, C. M. (2000) *Radiochim. Acta*, **88**, 587–91.

Schreiber, D. S. (1974) *Solid State Commun.*, **14**, 177–9.

Schuler, F. W., Steahly, F. L., and Stoughton, R. W. (1952) in Katzin (1952), paper 7.1, p. 307.

Schwarz, R. and Giese, H. (1928) *Z. Anorg. Allg. Chem.*, **176**, 209–32.

Schwetz, K., Ettmayer, P., Kieffer, R., and Lipp, A. (1972) *J. Less Common Metals*, **26**, 99–104.

Seaborg, G. T., Gofman, J. W., and Stoughton, R. W. (1947) *Phys. Rev.*, **71**, 378.

Seaborg, G. T. and Katzin, L. I. (1951) *Production and Separation of* U^{233}*: Survey*, Natl. Nucl. En. Ser., Div. IV, 17A, Report TID–5222, USAEC, Oak Ridge, Tenn.

Sereni, J. G., Nieva, G., Huber, J. G., Braun, E., Oster, F., Brück, E., Roden, B., and Wohlleben, D. (1987) *J. Magn. Magn. Mater.*, **63/64**, 597–9.

Shalek, P. D. (1963) *J. Am. Ceram. Soc.*, **46**, 155–61.

Shannon, R. D. (1976) *Acta Crystallogr. A,* **32**, 751–67.

Shchukarev, S. A., Novikov, G. I., and Suvorov, A. V. (1956) *Russ. J. Inorg. Chem.*, **9**, 13–8.

Shetty, S. Y., Sathe, R. M., and Shanker Das, M. (1976) *Indian J. Chem.*, **14A**, 719–20.

Shoun, R. R. and McDowell, W. J. (1980) in Actinide Separations (ACS Symp. Ser. no. 117), American Chemical Society, Washington, DC, pp. 71–87.

Sibieude, F. (1970) *C. R. Acad. Sci. Paris C*, **271**, 130–3.

Siddham, S. and Narayanan, K. (1979) *J. Catal.*, **59**, 405–22; Karuppannasamy, S., Narayanan, K., and Pilai, C. N. (1980) *J. Catal.*, **63**, 433–7.

Siegel, S. (1956) *Acta Crystallogr.*, **9**, 827.

Sieverts, A. and Roell, E. (1926) *Z. Anorg. Allg. Chem.*, **153**, 289–308.

Sillen, L. G. and Martell, A. (1964) *Stability Constants of Metal-ion Complexes*, Special Publication n°17, The Chemical Society, Burlington House, London, p. 534.

Sillen, L. G. and Martell, A. (1971) Stability Constants of Metal-ion Complexes, Supplement n°1, Special Publication n°25, The Chemical Society, Burlington House, London, p. 203.

Silvestre, J. P. (1978) *Rev. Chim. Miner.*, **15**, 412–22.

Silvestre, J. P., Pagès, M., and Freundlich, W. (1971) *C. R. Acad. Sci. Paris C*, **272**, 1808–10.

Singer, N., Studd, B. F., and Swallow, A. G. (1970) *J. Chem. Soc. Chem. Commun.*, 342–8.

Singh, N. P., Ibrahim, S. A., Cohen, N., and Wrenn, M. E. (1979) *Anal. Chem.*, **51**, 207–10; 1978–81.

Singh Mudher, K. D., Keskar, M., and Venugopal, V. (1995) *Proceedings of Nuclear and Radiochemistry Symposium* (eds. S. G. Kulkarni, S. B. Manohar, D. D. Sood), Kalpakkam, India, pp. 234–5.

Skriver, H. L. and Mertig, I. (1985) *Phys. Rev.*, **B32**, 4431–41.

Skriver, H. L., Eriksson, O., Mertig, I., and Mrosan, E. (1988) *Phys. Rev.*, **B37**, 1706–10.

Smith, E. F. and Harris, H. B. (1895) *J. Am. Chem. Soc.*, **17**, 654–6.

Smith, J. F., Carlson, O. N., Peterson, D. T., and Scott, T. E. (1975) *Thorium: Preparation and Properties,* Iowa State University Press, Ames, Iowa.

Smithells, C. J. (1922) *J. Chem. Soc.*, 2236–8.

Sollman, T. and Brown, E. D. (1907) *Am. J. Physiol.*, **18**, 426–56.

Sorby, M. H., Fjellvag, H., Hauback, B. C., Maeland, A. J., and Yartys, V. A. (2000) *J. Alloys Compds*, **309**, 154–64.

Spedding, F. H., Wilhelm, H. A., Keller, W. H., Iliff, J. E., and Neher, C. (1952) in Katzin (1952), paper 8.4, p. 428.

Spirlet, M. R., Rebizant, J., Apostolidis, C., Kanellakopoulos, B., and Dornberger, E. (1992) *Acta Crystallogr.*, **C48**, 1161–4.

Stackelberg, M. V. and Neumann, F. (1932) *Z. Phys. Chem. B*, **19**, 314–20.

Starks, D. V., Parsons, T. C., Streitwieser, A. Jr, and Edelstein, N. (1974) *Inorg. Chem.*, **13**, 1307–8.

Staun Olsen, J., Gerward, L., Benedict, U., Luo, H., and Vogt, O. (1988) Report KU-HCOE-FL-R-88-8(Fys. Lab., Univ. Copenhagen, Copenhagen, Den.) 15 pp.; (1989) *J. Appl.Crystallogr.*, 22, 61–3.

Stecher, P., Benesovsky, F., and Nowotny, H. (1963) *Monatsh. Chem.*, **94**, 549–64.

Stecher, P., Neckel, A., Benesovsky, F., and Nowotny, H. (1964) *Planseeber. Pulvermetall.*, **12**, 181–95.

Storms, E. K. (1967) *Refractory Carbides,* Academic Press, New York and London, p. 160.

Streitwieser, A. Jr and Yoshida, N. (1969) *J. Am. Chem. Soc.*, **91**, 7528.

Strotzer, E. F., Biltz, W., and Meisel, K. (1938) *Z. Anorg. Allg. Chem.*, **238**, 69–80.

Strotzer, E. F. and Zumbusch, M. (1941) *Z. Anorg. Allg. Chem.*, **247**, 415–28.

Struss, A. W. and Corbett, J. D. (1978) *Inorg. Chem.*, **17**, 965–9.

Sugar, J. (1974) *J. Chem. Phys.*, **60**, 4103.

Surbeck, H. (1995) *Sci. Total Environ.*, **173–174**, 91–9.

Suzuki, T., Takagi, S., Niitsuma, N., Takegahara, K., Kasuya, T., Yanase, A., Sakakibara, T., Date, M., Markowski, P. J., and Henkie, Z. (1982) *High Field Magnetism, Proc. Int. Symp.*, pp. 183–7.

Szilard, B. (1907) *J. Chem. Phys.*, **5**, 488–94.

Szymanski, J. T., Owens, D. R., Roberts, A. C., Ansell, H. G., and Chao, G. Y. (1982) *Can. Mineral.*, **20**, 65–75.

Tabata, K. and Kido, H. (1987) *Phys. Status Solidi A*, **99**, K121.

Tanaka, Y., Hattori, H., and Tanabe, K. (1978) *Bull. Chem. Soc. Jpn*, **51**, 3641–2; Tanaka, K. and Okuhara, T. (1980) *J. Catal.*, **65**, 1–8.

Taoudi, A., Mikou, A., and Laval, J. P. (1996) *Eur. J. Solid State Inorg. Chem.*, **33**, 1051–62.

Taylor, J. C., Mueller, M. H., and Hitterman, R. L. (1966) *Acta Crystallogr.*, **20**, 842–51.

Taylor, J. C. (1976) *Coord. Chem. Rev.*, **20**, 197–273.

Taylor, M. and Ewing, R. C. (1978) *Acta Crystallogr.*, **B34**, 1074–5.

Templeton, C. C. and Hall, N. F. (1947) *J. Phys. Coll. Chem.*, **51**, 1441–9.

Ter Haar, G. L. and Dubeck, M. (1964) *Inorg. Chem.*, **3**, 1648–50.

Thakur, L., Thakur, A. K., and Ahmad, M. F. (1980) *Indian J. Chem.*, **A19**, 792–5.

Thoma, R. E. and Carlton, T. S. (1961) *J. Inorg. Nucl. Chem.*, **17**, 88–97.

Thoma, R. E. (1972) *J. Inorg. Nucl. Chem.*, **34**, 2747–60.

Thomas, A. C., Dacheux, N., Le Coustumer, P., Brandel, V., and Genet, M. (2000) *J.Nucl. Mater.*, **281**, 91–105.

Thomas, A. C., Dacheux, N., Le Coustumer, P., Brandel, V., and Genet, M. (2001) *J.Nucl. Mater.*, **295**, 249–64.

Thomke, K. (1977) *Z. Phys. Chem.*, **107**, 99–108.

Thoret, J., Rimsky, A., and Freundlich, W. (1968) *C. R. Acad. Sci. Paris C*, **267**, 1682–4.

Thoret, J., Rimsky, A., and Freundlich, W. (1970) *C. R. Acad. Sci. Paris C*, **270**, 2045–7.

Thoret, J. (1971) *C. R. Acad. Sci. Paris C*, **273**, 1431–4.

Thoret, J. (1974) *Rev. Chim. Minér.*, **11**, 237–61.

Tiwari, R. N. and Sinha, D. N. (1980) *Indian Chem. J.*, **14**, 25–8.

Topic, M., Prodic, B., and Popovic, S. (1970) *Czech J. Phys.*, **20**, 1003–6.

Tougait, O., Potel, M., and Noël, H. (1998) *Inorg. Chem.*, **37**, 5088–91.

Trauger, D. B. (1978) *Ann. Nucl. Energy*, **5**, 375–403.

Troost, L. (1883) *C. R. Acad. Sci. Paris*, **116**, 1229

Troost, L. and Ouvrard, L. (1885) *C. R. Acad. Sci. Paris*, **101**, 210–2; (1886) *C. R. Acad. Sci. Paris*, **102**, 1422–7; (1887) *C. R. Acad. Sci. Paris*, **105**, 30–4.

Troost, L. and Ouvrard, L. (1889) *Ann. Chim. Phys.*, **6** (17), 227–45.

Trunov, V. K. and Kovba, L. M. (1963) *Vestn. Mosk. Univer., Ser. II, Khim.*, **18**, 60–3.

Trunov, V. K. and Kovba, L. M. (1966) *Zh. Strukt. Khim.*, **7**, 896–7.

Trunov, V. K., Efremova, A., and Kovba, L. M. (1966) *Radiokhimiya*, **8**, 717–18; *Sov. Radiochem.*, **8**, 658–9.

Ueki, T., Zalkin, A., and Templeton, D. H. (1966) *Acta Crystallogr.*, **20** 836–41.

Ueno, K. and Hoshi, M. (1970) *J. Inorg. Nucl. Chem.*, **32**, 3817–22.

Urbain, G. (1896) *Bull. Soc. Chim.*, **3** (15), 347–9.

van Arkel, A. E. and de Boer, J. H. (1925) *Z. Anorg. Allg. Chem.*, **148**, 345–50.

Van Houten, R. and Bartram, S. (1971) *Metall. Trans.*, **2**, 527–30.

Vasilega, N. D., Tishchenko, A. F., Lugovskaya, E. S., Badaev, Yu. V., and Pavlikov, V. N. (1980) *Dopov. Akad. Nauk Ukr. RSR*, **B11**, 34–8.

Vdovenko, V. M., Gershanovich, A. Y., and Suglobova, I. G. (1974) *Sov. Radiochem.*, **16**, 863–5.

Vedrine, A., Barackic, L., and Cousseins, J. C. (1973) *Mater. Res. Bull.*, **8**, 581–8.

Vera Tomé, F., Jurado Vargas, M., and Martin Sanchez, A. (1994) *Appl. Radiat. Isot.*, **45**, 449–52.

Vigato, P. A., Casellato, U., and Vidali, M. (1977) *Gazz. Chim. Ital.*, **107**, 61–6.

Vohra, Y. K. (1991) *Scr. Met. Mater.*, **25**, 2787–9.

Vohra, Y. K. and Akella, J. (1991) *Phys. Rev. Lett.*, **67**, 3563–6.

Vohra, Y. K. and Akella, J. (1992) *High Pressure Res.*, **10**, 681–5.

Vohra, Y. K. (1993) *Physica B*, **190**, 1–4.

Vokhmyakov, A. N., Desyatnik, V. N., and Kurbatov, N. N. (1973) *At. Energy (USSR)*, **35**, 424.

Volck, C. (1894) *Z. Anorg. Chem.*, **6**, 161–7.

Voliotis, S. and Rimsky, A. (1975) *Acta Crystallogr.*, **B31**, 2615–20.

Voliotis, S. (1979) *Acta Crystallogr. B*, **35**, 2899–904.

Voliotis, S., and Rimsky, A. (1988) *Acta Crystallogr.*, **B44**, 77–88.

Volkov, Yu. F., Kapshukov, I. I., and Vasil'ev, V. Ya. (1974) *1st Vses. Konf. Khim. Urana*, p. 26.

Volkov, Yu. F. (1999) *Radiochemistry (Moscow) (Translation of Radiokhimiya)*, **41**, 168–74.

Voliotis, S., Fromage, F., Faucherre, J., and Dervin, J. (1977) *Rev. Chim. Minér.*, **14**, 441–6.

von Bolton, W. (1908) *Z. Elektrochem.*, **14**, 768–70.

von Schnering, H. G., Wittmann, M., and Nesper, R. (1980) *J. Less Common Metals*, **76**, 213–26.

von Schnering, H. G. and Vu, D. (1986) *J. Less Common Metals*, **116**, 259–70.

von Wartenberg, H. (1909) *Z. Elektrochem.*, **15**, 866–72.

Wachtmann, K. H., Moss, M. A., Hoffmann, R.-D., and Jeitschko, W. J. (1995) *J.Alloys Compds*, **219**, 279–84.

Wallroth, K. A. (1883) *Bull. Soc. Chim.*, **2** (39), 316–22.

Wang, W., Chen, B., Wang, A., Yu, M., and Liu, X. (1982) *He Huaxue Yu Fangshe Huaxue*, **4**, 139–46.

Wang, W., Chen, B., Jin, Z., and Wang, A. (1983) *J. Radioanal. Chem.*, **76**, 49–62.

Wang, X. Z., Ng, W. L., Chevalier, B., Etourneau, J., and Hagenmuller, P. (1985) *Mater. Res. Bull.*, **20**, 1229–38.

Wang, J. and Zadeii, J. M. (1986) *Anal. Chim. Acta*, **188**, 187–94.

Warf, J. C. (1949) *J. Am. Chem. Soc.*, **71**, 3257–8.

Warren, I. H. and Price, C. E. (1964) *Adv. Energy Conversion*, **4**, 169.

Wastin, F., Rebizant, J., Spirlet, J. C., Sari, C., Walker, C. T., and Fuger, J. (1993) *J.Alloys Compds*, **196**, 87–92.

Watt, G. W. and Gadd, K. F. (1973) *Inorg. Nucl. Chem. Lett.*, **9**, 203–5.

Weaver, J. H., Knapp, J. A., Eastman, D. E., Peterson, D. T., and Satterthwaite, C. B. (1977) *Phys. Rev. Lett.*, **39**, 639–42.

Weeks, M. E. and Leicester, H. M. (1968) *Discovery of the Elements*, 7th edn, Easton, PA.

Weinland, R. F. and Kühl, H. (1907) *Z. Anorg. Chem.*, **54**, 244–52.

Wells, H. L. and Willis, J. M. (1901) *Am. J. Sci.*, **12**, 191–2.

Wessels, G. F. S., Leipoldt, J. G., and Bok, L. D. C. (1972) *Z. Anorg. Allg. Chem.*, **393**, 284–94.

Westland, A. D. and Tarafder, M. T. H. (1983) *Can. J. Chem.*, **61**, 1573–7.

White, G. M. and Ohnesorge, W. E. (1970) *Anal. Chem.*, **42**, 504–8.

Wilhelm, H. A. and Chiotti, P. (1949) Report AECD-2718.

Wilhelm, H. A. and Chiotti, P. (1950) *Trans. Am. Soc. Met.*, **42**, 1295–310.

Wilke, G., Bogdanivic, B., Hardt, P., Heimbach, P., Keim, W., Kröner, M., Oberkirch, W., Tanaka, K., Steinrücke, E., Walter, D., and Zimmermann, H. (1966) *Angew. Chem.* (*Int. Edn. Engl.*), **5**, 151–64.

Winkler, C. (1891) *Berl. Dtsch. Chem. Ges.*, **24**, 873–99.

Winter, H. (1978) *Conf. Ser. Inst. Phys.*, **39**, 713–5.

Wirth, F. (1912) *Z. Anorg. Chem.*, **76**, 174–200.

Wöhler, L., Plüddemann, W., and Wöhler, P. (1908) *Ber. Dtsch. Chem. Ges.*, **41**, 703–17.

Woodward, L. A. and Ware, M. J. (1968) *Spectrochim. Acta*, **24A**, 921–5.

Wu, E. J., Pell, M. A., and Ibers, J. A. (1997) *J. Alloys Compds.*, **255**, 106

Wu, Y., Zhao, Z., Liu, Y., and Yang, X. (2000) *J. Mol. Catal. A. Chem.*, **155**, 89–100.

Wyrouboff, G. and Verneuil, A. (1898a) *Bull. Soc. Chim.*, **3** (19), 219–27.

Wyrouboff, G. and Verneuil, A. (1898b) *C. R. Acad. Sci. Paris*, **128**, 1573–5.

Wyrouboff, G. and Verneuil, A. (1899) *Bull. Soc. Chim.*, **3** (21), 118–43.

Wyrouboff, G. (1901) *Bull. Soc. Miner.*, **24**, 105–16.

Wyrouboff, G. and Verneuil, A. (1905) *Ann. Chim. Phys.*, **6**, 441–507.

Yaffe, L. (1949) *Can. J. Res. B*, **27**, 638–45.

Yamnova, N. A., Pushcharovskii, D. Y., and Voloshin, A. V. (1990) *Dokl. Akad. Nauk SSSR*, **310**, 99–102.

Yen, K.-F., Li, S.-C., and Novikov, G. I. (1963) *Zh. Neorg. Khim.*, **8**, 89–93; *Russ. J. Inorg. Chem.*, **8**, 44–7.

Yoshida, S., Oyamada, R., and Kawamura, K. (1978) *Bull. Chem. Soc. Japan*, **51**, 25–7.

Young, R. C. (1935) *J. Am. Chem. Soc.*, **57**, 997–9.

Young, R. C. and Fletcher, H. G. (1939) in *Inorganic Synthesis,* vol. I (ed. H. S. Booth), McGraw-Hill, New York, pp. 51–4.

Yu, Z., Gao, L., Yuan, S., and Wu, Y. (1992) *J. Chem. Soc., Faraday Trans.*, **88**, 3245–9.

Zachariasen, W. H. (1948a) Report AECD-2163.

Zachariasen, W. H. (1948b) *Acta Crystallogr.*, **1**, 265–8.

Zachariasen, W. H. (1948c) *J. Am. Chem. Soc.*, **70**, 2147–51.

Zachariasen, W. H. (1949a) *Acta Crystallogr.*, **2**, 388–90.

Zachariasen, W. H. (1949b) *Acta Crystallogr.*, **2**, 390–3.

Zachariasen, W. H. (1949c) *Acta Crystallogr.*, **2**, 291–6.

Zachariasen, W. H.(1949d) *Acta Crystallogr.*, **2**, 288–91.

Zachariasen, W. H. (1953) *Acta Crystallogr.*, **6**, 393–5.

Zaitseva, L. L. Vakhrushin, YuA., and Shepel'kov, S. V. (1984) *Zh. Neorg. Khim.*, **29**, 768–72; *Russ. J. Inorg. Chem.*, **29**, 443–5.

Zalkin, A. and Templeton, D. H. (1950) *J. Chem. Phys.*, **18**, 391.

Zalkin, A. and Templeton, D. H. (1953) *Acta Crystallogr.*, **6**, 269–72.

Zalkin, A., Forrester, J. D., and Templeton, D. H. (1964) *Inorg. Chem.*, **3**, 639–44.

Zalkin, A., Templeton, D. H., Le Vanda, C., and Streitwieser, A. Jr (1980) *Inorg. Chem.*, **19**, 2560–3.

Zalubas, R. (1968) *J. Opt. Soc. Am.*, **58**, 1195–9.

Zalubas, and R. Corliss, C. H.(1974) *J. Res. NBS*, **78A**, 163–246.

Zambonini, F. (1923) *C. R. Acad. Sci. Paris*, **176**, 1473–5.

Zhang, H. B., Lin, G. D., Wan, H. L., Liu, Y. D., Weng, W. Z., Cai, J. X., Shen, Y. F., and Tsai, K. R. (2001) *Catal. Lett.*, **73**, 141–7.

Zhou, M. L., Jin, J. N., Xu, S. C., Liu, M. Z., Xu, D. Q., Peng, Q. X., Qi, and Sh., J. (1981) *Huaxue Yu Fangshe Huaxue*, **3**, 136–40.

Zhu, W. J. and Hor, P. H. (1995) *J. Solid State Chem.*, **120**, 208–9.

Zumbusch, M. (1941) *Z. Anorg. Allg. Chem.*, **245**, 402–8.

Zunic, T. B., Scavnicar, S., and Grobenski, Z. (1984) *Croat. Chem. Acta*, **57**, 645–51.

CHAPTER FOUR

PROTACTINIUM

Boris F. Myasoedov, H. W. Kirby, and Ivan G. Tananaev

4.1 INTRODUCTION

Protactinium, element 91, is one of the most rare of the naturally occurring elements and may well be the most difficult of all to extract from natural sources. Protactinium is, formally, the third element of the actinide series and the first having a 5f electron. The superconducting properties of protactinium metal provide clear evidence that Pa is a true actinide element (Smith *et al.*, 1979). Its chemical behavior in aqueous solution, however, would seem to place it in group VB of the Mendeleev's table, below Ta and Nb.

The predominant oxidation state is 5+. Pa(v) forms no simple cations in aqueous solution and, like Ta, it exhibits an extraordinarily high tendency to undergo hydrolysis, to form polymers, and to be adsorbed on almost any available surface. These tendencies undoubtedly account for the many reports of erratic and irreproducible behavior of protactinium as well as for its frustrating habit of disappearing in the hands of inexperienced or unwary investigators. A useful review of the chemical properties of Pa important in an analytical context has been made by Pal'shin *et al.* (1970) and Myasoedov *et al.* (1978).

The most important natural isotope is ^{231}Pa, but the industrial importance of Pa stems chiefly from the role of its artificial isotope, ^{233}Pa, as an intermediate in the production of fissile ^{233}U in thorium breeder reactors. It was, in fact, the need for a relatively stable isotope that could be used for macroscopic chemical studies, which was responsible for the revival of interest in the recovery of ^{231}Pa from natural sources (Katzin, 1952). The result has been a rapid growth in our understanding of Pa chemistry, as summarized in numerous critical review articles (Gmelin, 1942, 1977; Elson, 1954; Katz and Seaborg, 1957; Haïssinsky and Bouissières, 1958; Kirby, 1959; Salutsky, 1962; Brown and Maddock, 1963; Sedlet, 1964; Guillaumont and deMiranda, 1966; Keller, 1966a; Brown and Maddock, 1967; Guillaumont *et al.*, 1968; Brown, 1969; Muxart *et al.*, 1969; Muxart and Guillaumont, 1974; Morgan and Beetham, 1990), books (Cotton *et al.*, 1999) and presentations (Weigel 1978; Jung *et al.*, 1993; Greenwood and Earnshaw 1997; Sime, 1997).

4.1.1 Discovery of protactinium

During the preparation of the periodic table Mendeleev (1872) placed in the vacant space in group V between Th(IV) and U(VI) an unknown hypothetical element No. 91 named 'eka-tantalum' with atomic mass of about 235, and chemical properties similar to Nb and Ta. Forty years later, Russell (1913), Fajans (1913a,b), and Soddy (1913a,b) independently proposed the radioactive displacement principles, i.e. two simple rules for reconciling the chemical and radioactive properties of the 33 radioelements known at that time: (1) if a radioelement emits an α particle, its position in the Mendeleev's table is shifted two places to the left, or (2) if it emits a β^--particle, its position is shifted one place to the right. When the rules were applied systematically, there was one obvious discrepancy: the only known link between ^{238}U and ^{234}U, both in group VI, was element UX, a β^--emitter whose chemistry was identical with that of thorium, in group IV. It was necessary to postulate the existence of an unknown β^--emitter, in the space in the periodic table reserved by Mendeleev (1872).

Before the end of 1913, Fajans and his student, Göhring, had shown that element UX was actually a mixture of two distinct radioelements: UX_1 (^{234}Th) and UX_2 (^{234m}Pa), which gave off hard β^--rays, had a half-life of 1.15 min, and was chemically similar to Ta (Göhring, 1914a,b). They named the new element, '*brevium*' (Bv) (*brĕvis* (Latin): short, brief), because of its short half-life (Göhring, 1914b).

An analogous problem existed with respect to the origin of actinium (Göhring, 1914a). It was clear that Ac could not be a 'primary' radioelement, because its half-life was only about 30 years (Curie, 1911). On the other hand, although there was a constant ratio of Ac to U in nature (Boltwood, 1906, 1908), Ac could not be part of the main U–Ra series, because the ratio was far too low. According to the displacement laws, Ac, in group III, could only be the product either of a β^--emitter in group II or of an α-emitter in group V. The first possibility was eliminated when Soddy (1913b) proved that Ra, the only group II element in the U–Ra series, was not the parent of Ac. The only remaining alternative was an α-emitting isotope of UX_2.

In 1913, Soddy had reported the growth of Ac in two lots of UX, separated from 50 kg of uranium 4 years earlier (Soddy, 1913a). This suggested that Ac was being produced from UX 'through an intermediate substance'. Five years later Soddy and Cranston (1918) [see also Sackett (1960)] had confirmed the growth beyond doubt and had separated the parent of Ac by sublimation from pitchblende in a current of air containing CCl_4 at incipient red heat. This method was later applied by Malm and Fried (1950, 1959) to the separation of ^{233}Pa from neutron-irradiated ^{232}Th.

Almost simultaneously, Hahn and Meitner (1918) reported their independent discovery of the parent of Ac in the siliceous residue resulting from the treatment of pulverized pitchblende with hot concentrated HNO_3. They proposed the name, *protactinium*. Preliminary estimates indicated that the half-life of the new isotope was between 1200 and 180 000 years. Since the name, *brevium*, was obviously inappropriate for such a long-lived radioelement, Fajans and Morris (1913) proposed that the name of element-91 be changed to *protactinium* (linguistic purists at first insisted on calling it *protoactinium*, because '*proto* is better Greek' (Grosse, 1975), but the name *protactinium* (Pa) was restored officially in 1949 (Anonymous, 1949)).

There was still no direct evidence as to the origin of protactinium. In 1911, Antonoff (1911) had separated uranium Y – UY (^{231}Th) from a purified U solution. UY was chemically similar to Th and Antonoff (1913) suggested that this might be the point at which the Ac series branched off from the U series. In 1917, Piccard (1917) suggested that, in addition to the two known isotopes of uranium, uranium I and II (UI and UII), there might also exist a third long-lived isotope, actinouranium (AcU). AcU would decay by α-emission to yield UY, which, in turn, would decay by β^--emission to give an isotope of *brevium*. Piccard's hypothesis was confirmed experimentally in 1935, when Dempster (1935) discovered AcU (^{235}U) by mass spectrography.

4.1.2 Isolation of protactinium

The new element was isolated for the first time in 1927, when Grosse (1927, 1928) reported that he had prepared about 2 mg of essentially pure Pa_2O_5. By the end of 1934, Grosse with Agruss had developed a process for the large-scale recovery and purification of Pa (Grosse, 1934a; Grosse and Agruss, 1934, 1935a). They had isolated more than 0.15 g of Pa_2O_5, reduced it to the metal, and determined its atomic weight to be 230.6 ± 0.5 (Grosse, 1934b). In the same year, Graue and Kading (1934a,b) recovered 0.5 g of pure Pa (as K_2PaF_7) from 5.5 tons of pitchblende residues, an achievement that would not be equaled, let alone surpassed, for the next quarter of a century.

The development of atomic energy led to the processing of most of the world's known reserves of high-grade uranium ores and to the accumulation of vast stockpiles of process wastes. Among these, at the Springfields refinery of the United Kingdom Atomic Energy Authority (UKAEA) was the '*ethereal sludge*', a siliceous precipitate that had separated during the ether extraction of U from dilute HNO_3 solution. This material, amounting to some 60 tons, contained about 4 ppm of Pa, or more than ten times its equilibrium concentration in unprocessed pitchblende. Since the sludge also contained about 12 tons of U, it was economically attractive to recover both elements, with most of the development and production cost being borne by the U recovery. The process that was finally adopted yielded 127 g of 99.9% pure ^{231}Pa (Goble *et al.*, 1958; Nairn *et al.*, 1958; Jackson *et al.*, 1960a,b; Collins *et al.*, 1962; Hillary and Morgan, 1964) at a cost of about US$500 000 (CRC Handbook, 1997).

The UKAEA has generously made its stockpile of Pa available to the rest of the world at nominal cost, thereby touching off intensive investigation of Pa chemistry at many laboratories. Thanks to this concentrated effort, the new era in Pa research that started in the mid-1950s has now reached maturity. Three international conferences were convened, devoted entirely to the chemical, physical, and nuclear properties of Pa (Oak Ridge National Laboratory, 1964; Bouissières and Muxart, 1966; Born, 1971).

4.2 NUCLEAR PROPERTIES

At present, there are 29 known isotopes of Pa (Table 4.1), but only three are of particular significance to chemists. They are the naturally occurring isotopes, ^{231}Pa and ^{234}Pa, and reactor-produced ^{233}Pa. The characteristics of α-decay of Pa isotopes with mass numbers (A) till 224 were presented by Andreev *et al.* (1996b). Hyde (1961, undated) and Hyde *et al.* (1964) had exhaustively reviewed the nuclear properties of all the isotopes with A ranging from 225 to 237.

A new nuclide ^{239}Pa produced recently by multi-nucleon transfer reactions ^{238}U(p,2n)^{239}Pa (Yuan *et al.*, 1996). Protactinium was chemically separated from the uranium target and other produced elements. From the ^{239}Pa β^--decay a half-life of (106 ± 30) min was observed.

For details concerning the more recently discovered isotopes, the reader should consult the original references (Meitner *et al.*, 1938; Ghiorso *et al.*, 1948; Gofman and Seaborg, 1949; Hyde *et al.*, 1949; Meinke *et al.*, 1949, 1951, 1952, 1956; Harvey and Parsons, 1950; Barendregt and Tom, 1951; Keys, 1951; Browne *et al.*, 1954; Crane and Iddings, 1954; Zijp *et al.*, 1954; Wright *et al.*, 1957; Hill, 1958; Arbman *et al.*, 1960; Takahashi and Morinaga, 1960; Albridge *et al.*, 1961; Baranov *et al.*, 1962; Bjørnholm and Nielsen, 1962, 1963; Subrahmanyam, 1963; Wolzak and Morinaga, 1963; McCoy, 1964; Bastin *et al.*, 1966; Bjørnholm *et al.*, 1968; Hahn *et al.*, 1968; Trautmann *et al.*, 1968; Briand *et al.*, 1969; Borggreen *et al.*, 1970; dePinke *et al.*, 1970; Laurens *et al.*, 1970; Varnell, 1970; Holden and Walker, 1972; Sung-Ching-Yang *et al.*, 1972; Lederer and Shirley, 1978; Folger *et al.*, 1995; Yuan *et al.*, 1995, 1996; Andreev *et al.*, 1996a; Nishinaka *et al.*, 1997).

4.2.1 Protactinium-231

^{231}Pa, an α-emitter with fixed atomic weight 231.03588 ± 0.0002 (Delaeter and Heumann, 1991), is a member of the naturally occurring ^{235}U decay ($4n + 3$) chain. It is the daughter of ^{231}Th and the parent of ^{227}Ac, from which it derives

Table 4.1 *Nuclear properties of protactinium isotopes.*

Mass number	*Half-life*	*Mode of decay*	*Main radiations* (MeV)	*Method of production*
212	5.1 ms	α	α 8.270	^{182}W(^{35}Cl,5n)
213	5.3 ms	α	α 8.236	^{170}Er(^{51}V,8n)
214	17 ms	α	α 8.116	^{170}Er(^{51}V,7n)
215	14 ms	α	α 8.170	^{181}Ta(^{40}Ar,6n)
216	0.2 s	α	α 7.865	^{197}Au(^{24}Mg,5n)
217	4.9 ms	α	α 8.340	^{181}Ta(^{40}Ar,4n)
	1.6 ms	α	α 10.160	
218	0.12 ms	α	α 9.614 (65%)	^{206}Pb(^{16}O,4n)
219	53 ns	α	α 9.900	^{204}Pb(^{19}F,4n)
220	0.78 μs	α	α 9.15	^{204}Pb(^{19}F,3n)
221	5.9 μs	α	α 9.080	^{209}Bi(^{16}O,4n)
222	5.7 ms	α	α 8.54 (∼30%)	^{209}Bi(^{16}O,3n)
			∼8.18 (50%)	^{206}Pb(^{19}F,3n)
223	6 ms	α	α 8.20 (45%)	^{208}Pb(^{19}F,4n)
			8.01 (55%)	^{205}Tl(^{22}Ne,4n)
224	0.9 s	α	α 7.49	^{208}Pb(^{19}F,3n)
225	1.8 s	α	α 7.25 (70%)	^{232}Th(p,8n)
			7.20 (30%)	^{209}Bi(^{22}Ne,α2n)
226	1.8 min	α 74%	α 6.86 (52%)	^{232}Th(p,7n)
		EC 26%	6.82 (46%)	
227	38.3 min	α ∼85%	α 6.466 (51%)	^{232}Th(p,6n)
		EC ∼15%	6.416 (15%)	
			γ 0.065	
228	22 h	EC ∼98%	α 6.105 (12%)	^{232}Th(p,5n)
		α ∼2%	6.078 (21%)	^{230}Th(p,3n)
			γ 0.410	
229	1.5 d	EC 99.5%	α 5.669 (19%)	^{230}Th(d,3n)
		α 0.48%	5.579 (37%)	^{229}Th(d,2n)
230	17.7 d	EC 90%	α 5.345	^{230}Th(d,2n)
		β^- 10%	β^- 0.51	^{232}Th(p,3n)
		α 3.2×10^{-3}%	γ 0.952	
231	3.28×10^4 yr	α	α 5.012 (25%)	nature
			4.951 (23%)	
			γ 0.300	
232	1.31 d	β^-	β^- 1.29	^{231}Pa(n,γ)
			γ 0.969	^{232}Th(d,2n)
233	27.0 d	β^-	β^- 0.568	^{233}Th daughter
			γ 0.312	^{237}Np daughter
234	6.75 h	β^-	β^- 1.2	nature
			γ 0.570	
234 m	1.175 min	β^- 99.87%	β^- 2.29	nature
		IT 0.13%	γ 1.001	
235	24.2 min	β^-	β^- 1.41	^{235}Th daughter
				^{235}U(n,p)
236	9.1 min	β^-	β^- 3.1	^{236}U(n,p)
			γ 0.642	^{238}U(d,α)
237	8.7 min	β^-	β^- 2.3	^{238}U(γ,p)
			γ 0.854	^{238}U(n,pn)
238	2.3 min	β^-	β^- 2.9	^{238}U(n,p)
			γ 1.014	
239	106 min	β^-		^{18}O + ^{238}U

its name (Fig. 4.1). Reported half-lives have ranged from 32 000 years ± 10% (Grosse, 1932) to (34 300 ± 300) years (Van Winkle *et al.*, 1949); three recent determinations (Kirby, 1961; Brown *et al.*, 1968a; Robert *et al.*, 1969) yield a weighted average of (32 530 ± 250) years (at the 95% confidence level). Therefore ^{231}Pa is the only isotope easy to access in multi-gram quantities. The thermal-neutron cross section is (211 ± 2) barn (Simpson *et al.*, 1962; Gryntakis and Kim, 1974). The spontaneous fission half-life is 1.1×10^{16} years (Segrè, 1952), which gives the correlation of 0.3 of a fission per 1 g Pa per min.

The complex fine structure of the ^{231}Pa alpha-spectrum can be resolved with a passivated implanted planar silicon detector (Fig. 4.2). Baranov *et al.* (1962, 1968), using a double-focusing magnetic spectrometer, found at least 19 α-groups with energies ranging from 4.51 to 5.06 MeV and additional low-abundance groups have been detected by α–γ coincidence measurements (Lange and Hagee, 1968). Predictably, the γ-ray spectrum, as recorded with a high-resolution Ge detector, is even more complex (Fig. 4.3): 92 γ-rays have been reported, with energies up to 609 keV (dePinke *et al.*, 1970; Leang, 1970). A detailed level scheme is given in the critical compilation by Artna-Cohen (1971). The prominent γ photopeak at 27.35 keV is easily detectable even with a NaI(Tl) crystal; it uniquely identifies ^{231}Pa in the presence of other naturally occurring γ-emitters (Fig. 4.4).

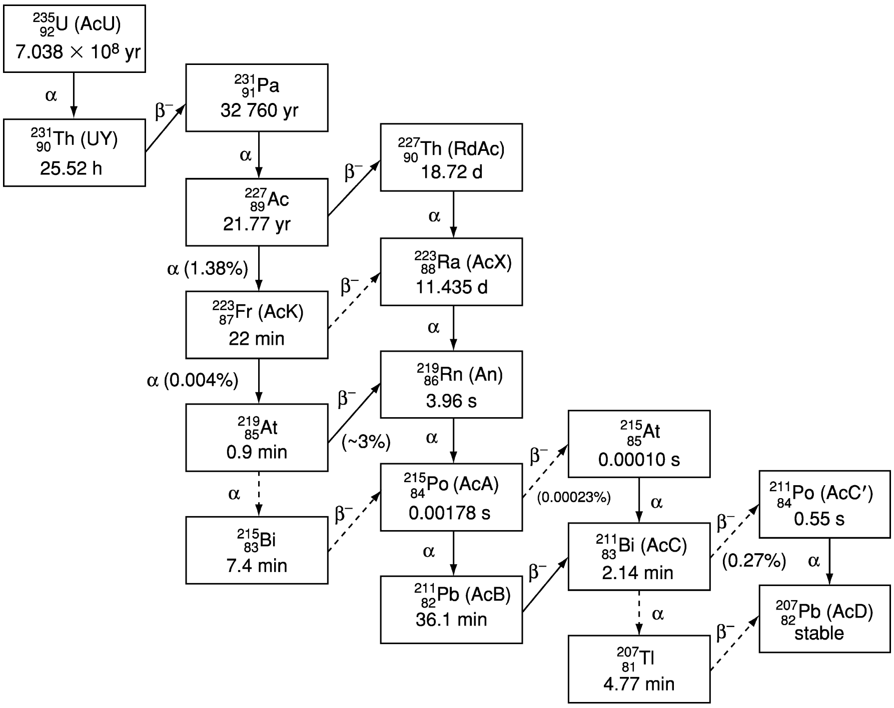

Fig. 4.1 *Uranium–actinium series* (4*n* + 3).

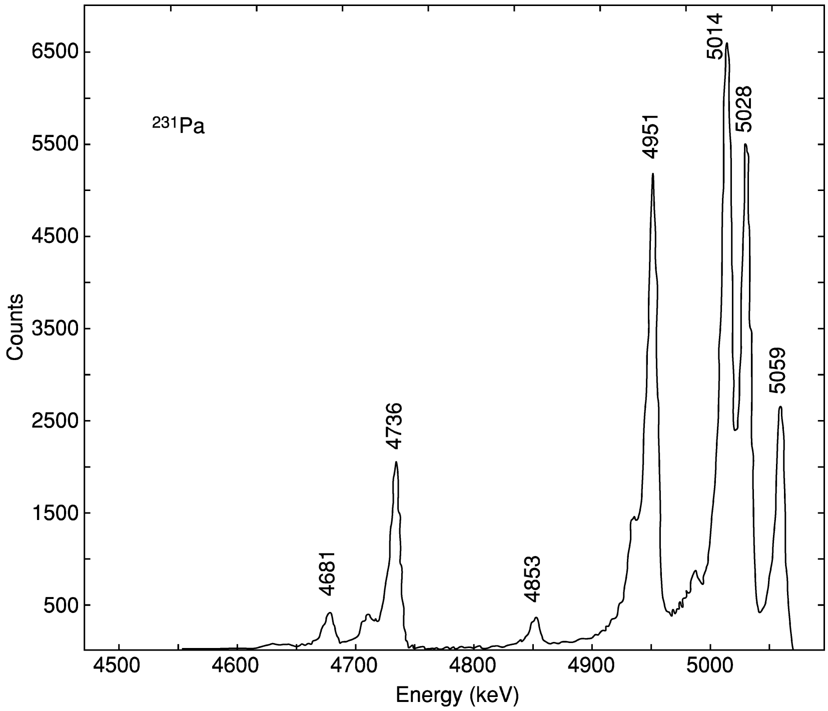

Fig. 4.2 *Alpha-spectrum of* ^{231}*Pa measured with a passivated implanted planar silicon detector* (*Ahmad,* 2004).

^{231}Pa can be separated from reprocessed U ores, or alternatively, produced by either of the two nuclear reactions: ^{232}Th(n,2n)^{231}Th (Nishina *et al.*, 1938) or ^{230}Th(n,γ)^{231}Th (Hyde, 1948). In principle, this would eliminate many of the problems attendant on the isolation of ^{231}Pa. However, neutron irradiation of ^{232}Th yields large amounts of ^{233}Pa and other undesirable contaminants, but relatively little ^{231}Pa (Table 4.2) (Schuman and Tromp, 1959; Codding *et al.*, 1964). The ^{230}Th route is only superficially more attractive, since the richest sources of ^{330}Th found thus far in U refinery waste streams and residues have always been associated with at least eight times as much ^{232}Th (Figgins and Kirby, 1966). Protactinium was not formed in the amalgam and could be also separated from thorium (David and Bouissières, 1966).

4.2.2 Protactinium-233

^{233}Pa is the only artificial isotope of Pa thus far produced in weighable amounts; the first gram was isolated in 1964 by a group at the National Reactor Testing Station in Idaho (Codding *et al.*, 1964). ^{233}Pa derives its importance from the

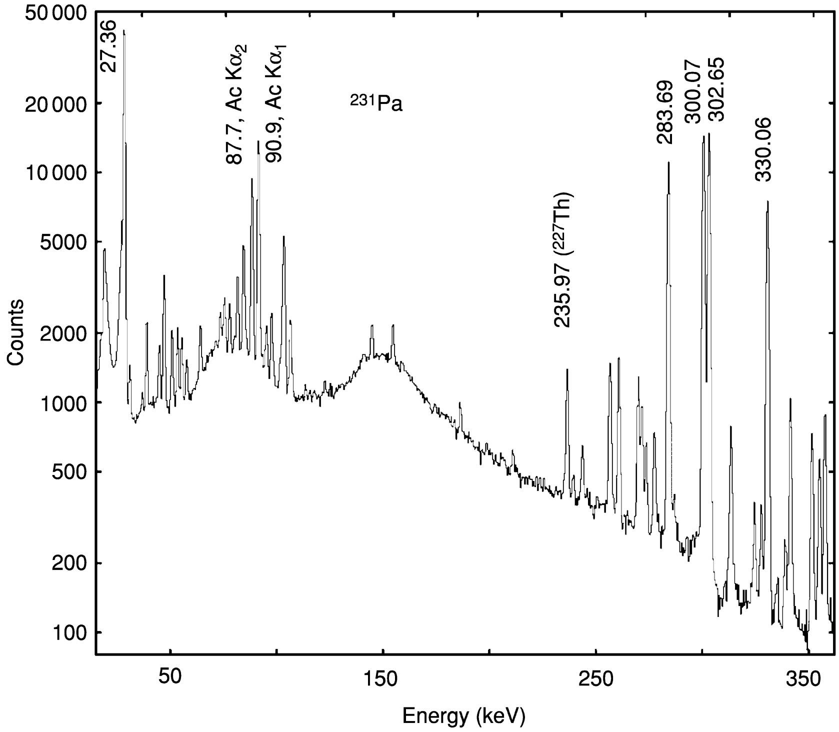

Fig. 4.3 *γ-Ray spectrum of ^{231}Pa measured with a 25% efficiency germanium detector* (*Ahmad*, 2004).

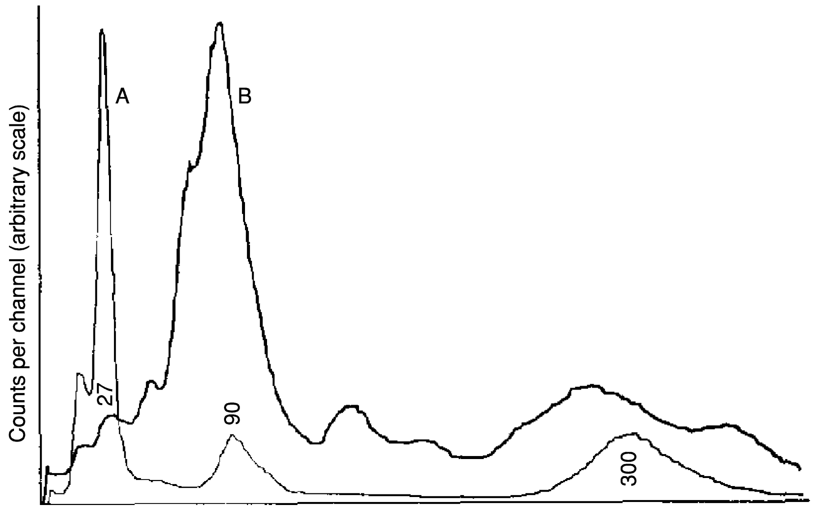

Fig. 4.4 *γ-Ray spectrum of ^{231}Pa observed with a NaI(Tl) crystal: curve A, freshly purified ^{231}Pa; curve B, raw material (~0.3 ppm ^{231}Pa).*

Table 4.2 *Calculated composition of* 100 g *of* ^{232}*Th after thermal-neutron irradiation* (*Codding* et al., 1964) (*thermal flux* = 5 × 10^{14} n $cm^{-2}s^{-1}$; *resonance flux* = (*thermal flux*)/12; *nvt* = 1.2 × 10^{21} n cm^{-2}).

Nuclide	*Amount*
^{231}Pa	98.6 g
^{232}Th	~1 mg
^{233}Pa	950 mg
^{233}U	320 mg
^{235}U	65 mg
^{235}U	5 mg
fission products	60 mg

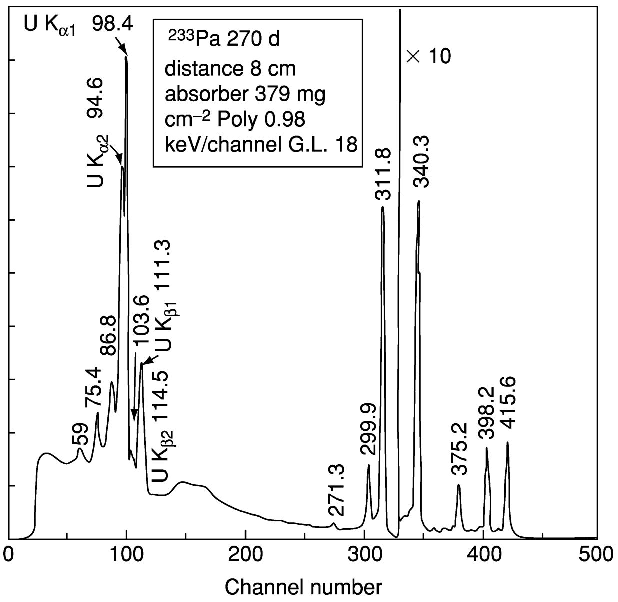

Fig. 4.5 *γ-Ray spectrum of* ^{233}*Pa observed with a Ge*(*Li*) *detector. Reproduced from Crouthamel* et al. (1970) *with permission from Pergamon Press.*

fact that it is an intermediate in the production of fissile ^{233}U. The reaction, discovered in 1938 by Meitner *et al.* (1938) (Sime, 1997) is:

$$^{232}\text{Th}\,(\text{n},\gamma)\,^{233}\text{Th}\,(\beta^-;22\ \text{min}) \rightarrow {}^{233}\text{Pa}(\beta^-;\ 27\,\text{days}) \rightarrow {}^{233}\text{U}$$

^{233}Pa has largely replaced ^{234}Pa as a tracer because of its favorable half-life (26.95 ± 0.06) days (Wright *et al.*, 1957), its relative ease of preparation (cf. Table 4.2), and its readily detectable gamma spectrum (Fig. 4.5). Using this isotope a large volume of important data on protactinium chemistry had been provided.

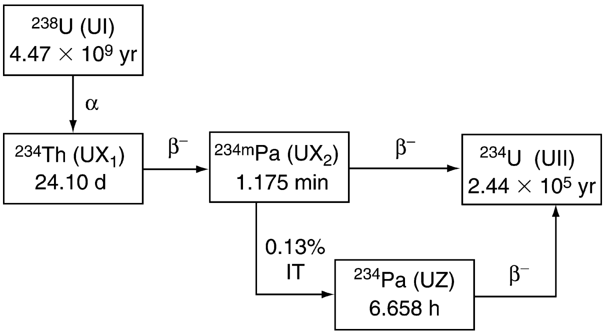

Fig. 4.6 *Genetic relationships of the* UX_1*–*UX_2*–UZ complex.*

4.2.3 Protactinium-234

The nuclide ^{234}Pa occurs naturally in two isomeric forms: ^{234m}Pa, discovered by Fajans and Göhring (1913a,b), and ^{234}Pa, discovered afterward by Hahn (1921). Their genetic relationships are indicated in Fig. 4.6. Both are β^--emitters, decaying to ^{234}U, but ^{234m}Pa is metastable and, in 0.13% of its disintegrations, it decays to its ground state by isomeric transition, yielding ^{234}Pa (Bjørnholm and Nielsen, 1963). The extraordinarily complex decay scheme of ^{234}Pa (Ellis, 1970; Ardisson and Ardisson, 1975) is difficult to study, because the intense sources needed for high-resolution spectrometry are not readily available. However, 0.8 Ci of ^{234}Th was extracted from several tons of ^{238}U, making possible the definitive study by Bjørnholm *et al.* (1967, 1968). The gamma-spectrum of ^{234}Pa (in equilibrium with ^{238}U and ^{234}Th) is shown in Fig. 4.7 (Crouthamel *et al.*, 1970).

4.3 OCCURRENCE IN NATURE

Since the half-life of ^{231}Pa is short in geological terms, its natural occurrence is closely tied to that of ^{235}U, its primordial ancestor. Uranium isotopes are widely distributed in the Earth's crust (Kirby, 1974). The average crustal abundance of U is 2.7 ppm (Taylor, 1964), of which 0.711 wt% is ^{235}U (Grundy and Hamer, 1961); therefore, the natural abundance of ^{231}Pa (calculated from its half-life and that of ^{235}U) is 0.87×10^{-6} ppm – only slightly less than that of ^{226}Ra. Assuming that the crustal mass (to a depth of 36 km) is 2.5×10^{25} g (Heydemann, 1969), the global inventory of ^{231}Pa is 2.2×10^7 metric tons.

The pronounced hydrolytic tendency of Pa is the basis of a method for dating marine sediments less than 10^6 years old (Sackett, 1960; Roshalt *et al.*, 1961, 1962; Sakanoue *et al.*, 1967; Thomson and Walton, 1971, 1972; Kirby, 1974). In an undisturbed geological formation, thematic Pa:U = 3.2×10^{-7}, but this ratio

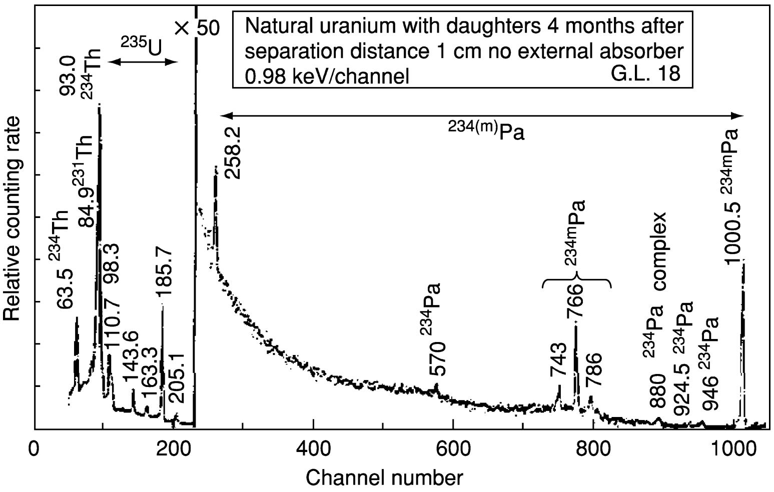

Fig. 4.7 *γ-Ray spectrum of* UX_1*–*UX_2*–UZ in equilibrium with* ^{238}U*. Reproduced from Crouthamel* et al. (1970) *with permission from Pergamon Press.*

is altered when the deposit is leached with groundwater and the U is carried to sea. At the pH of seawater, both Pa and Th hydrolyze and deposit together on the ocean floor, leaving the U in solution as UO_2^{2+}. Because ^{231}Pa and ^{230}Th decay moved at different rates, their ratio at various depths can be used to determine the rate of sedimentation.

^{231}Pa/^{235}U ages were also determined for 17 carnotites from two areas in Israel (Kaufman *et al.*, 1995). For the determination of ^{231}Pa in solids, a new method, more than ten times more precise than those determined by decay counting, based on thermal ionization mass spectroscopy (TIMS) of protactinium in carbonates was created. Carbonates between 10 and 250 000 years old can now be dated with this ^{231}Pa method. Barbados corals that have identical ^{231}Pa and ^{230}Th ages indicate that the timing of sea level change over parts of the last glacial cycle is consistent with the predictions of the Astronomical Theory (Edwards *et al.*, 1997).

^{233}Pa has not itself been detected in nature, but traces of both ^{237}Np, its parent, and ^{225}Ac, its descendant, have been identified in a U refinery waste stream (Peppard *et al.*, 1952). It may, therefore, be inferred that ^{233}Pa is being continually formed in nature by the reaction:

$$^{238}\mathrm{U}\,(\mathrm{n},2\mathrm{n})\,^{237}\mathrm{U}\,(\beta^-;\ 6.75\,\mathrm{days}) \rightarrow {}^{237}\mathrm{Np}\,(\alpha;\ 2.14\times10^6\,\mathrm{years}) \rightarrow {}^{233}\mathrm{Pa}.$$

The natural neutron output in pitchblende is about 0.05 ng^{-1} s^{-1}, attributable about equally to spontaneous fission of ^{238}U and (α,n) reactions of light elements (McKay, 1971).

4.4 PREPARATION AND PURIFICATION

No large-scale separation of ^{231}Pa has ever been made from virgin ores because the element has little commercial value. Weighable amounts of Pa have always been obtained from U refinery residues. Indeed, the economic realities are such that it is rarely possible even to optimize the segregation of Pa in a single waste stream or residue. More typically, the Pa is fractionated at every stage in the beneficiation and extraction of U from its ores.

Before the development of atomic energy, pitchblende ores were processed primarily for their Ra content. The pulverized ore, after being roasted with Na_2CO_3, was leached with aqueous solutions of H_2SO_4 or HNO_3 (or both) and the acid-insoluble material was digested with NaOH or Na_2CO_3 solutions. The residue was then leached with hydrochloric acid to recover the Ra (Curie, 1913). The final residue retained a greater or lesser fraction of the original Pa according to the relative proportions of the acids used in the digestion; a higher H_2SO_4 concentration and higher total acidity favored the dissolution of Pa (Reymond, 1931). This *Rückrückstände,* or 'residue of residues', was the raw material used by Hahn and Meitner (1918) for their discovery of ^{231}Pa, by Grosse (1927, 1928) in the isolation of the first milligram amounts, and by Graue and Kading (1934a) in the recovery of 0.5 g of the element. The analysis of one such residue is given in Table 4.3.

During and after World War II, an ether extraction process was used for the purification of U. The acid solution resulting from the ore digestion was treated with Na_2CO_3 to precipitate some of the less basic metals, while leaving the U in solution as a carbonate complex. Katzin *et al.* (1950) found that the carbonate precipitate contained 0.30–0.35 ppm of Pa and subsequent processing of this material yielded about 25 mg of pure Pa (Kraus and Van Winkle, 1952; Larson *et al.*, 1952; Thompson *et al.*, 1952). When the process was modified to eliminate the carbonate precipitation, the Pa passed through the ether extraction step into the aqueous raffinate, from which Elson *et al.* (1951) recovered 35 mg of pure material.

A later modification produced a precipitate in the aqueous waste stream, which, according to Salutsky *et al.* (1956), carried down nearly all the Pa. This material was periodically filtered off and eventually yielded a total of about 2 g of Pa (Kirby, 1959; Hertz *et al.*, 1974; Figgins *et al.*, 1975).

The aqueous raffinate from the ether extraction was treated with lime and the filtered precipitate was stored for future recovery of U and other commercially valuable metals. The accumulated material was later treated by a process of which the relevant steps were: digestion with sulfuric acid, followed by extraction with bis(2-ethylhexyl)phosphoric acid (HDEHP), and finally back-extraction with sodium carbonate solution. The waste solutions and residues were discharged to a tailings pond, where, for all practical purposes, much of the Pa and ^{230}Th were irretrievably lost. In 1972, the process was modified by

Table 4.3 *Analyses of some ^{231}Pa raw materials.*

Riickriickstände (*Grosse and Agruss*, 1935*a*)		*Ethereal sludge* (*Nairn* et al., 1958)		*Cotter concentrate* (*Ishida*, 1975)	
Constituent	*Amount (%)*	*Constituent*	*Amount (%)*	*Constituent*	*Amount (%)*
SiO_2	60	U	28.3	U_3O_8	13.8
Fe_2O_3	22	Fe	7.7	Fe	~30
PbO	8	Si	6.4	Si	~4
Al_2O_3	5	Ba	~3	Na	~60
MnO	1	Zr	2.7	Mo	≤ 2
CaO	0.6	Mo	2.7	V	≤ 1
MgO	0.5	F^-	1.8	Al	≥ 0.3
Ti	0.3	NH_4^+	1.7	Th	0.15
Zr	0.1	Ca	1.5	Ti	0.1
HF and others	–	V	0.9	Ca	0.07
Graphite	0.1	Ti	0.44	Cu	0.05
Pa_2O_5	3×10^{-3}	Pb	0.4	Zr	0.04
		Al	0.27	Mg	0.04
		P	0.15	Ni	0.03
		Sr	0.09	Mn	0.01
		Nb, Ta	<0.1	Cr	0.01
		Mg, Ni, Cr, Co, Mn, & Sn	<0.01	B	0.002
				Be	7×10^{-4}
		Pa	$3.7 \times I0^{-4}$	Pa	4×10^{-5}

adding enough sodium hydroxide to the Na_2CO_3 strip solution to cause total precipitation of the U, thus minimizing any further loss of Pa and ^{230}Th (Haubach, 1967; Figgins and Hertz, 1972a,b, 1973). The filtered precipitate ('*Cotter concentrate*') consists of some 2000 tons (dry weight) of mixed oxides and carbonates (Table 4.3) and contains an estimated 30 tons of U_3O_8, 14 kg of ^{230}Th, and 75 g of Pa. This material has been processed at Mound Laboratory.

At the Windscale refinery of the UKAEA, after removal of a sulfate precipitate containing the Ra, the solution was buffered to pH ~2 and the U was precipitated by the addition of hydrogen peroxide. The peroxide precipitate carried down more than 80% of the Pa and, when it was redissolved in nitric acid, the low acidity encouraged the formation of a siliceous Pa-containing sludge, which deposited on the walls of the ether extraction plant and its ancillary vessels. This '*ethereal sludge*' was collected and drummed, pending future recovery of U. It proved to be the richest source of Pa ever found, ultimately yielding 127 g of the pure element (Goble *et al.*, 1958; Nairn *et al.*, 1958; Jackson *et al.*, 1960a; Collins *et al.*, 1962). The gross chemical composition of '*ethereal sludge*' is shown in Table 4.3.

4.4.1 Industrial-scale enrichment of siliceous residues

At ultra-micro concentrations with respect to other metals ions, Pa scarcely exhibits a chemistry of its own. Consequently, the procedure adopted to recover Pa from ‘natural’ sources is usually dictated less by the chemistry of Pa than by the gross chemical and physical characteristics of the source and, sometimes, by the sheer quantity of material to be processed.

The problems are magnified by the extreme complexity and variability of the sources from which ^{231}Pa is obtained, but one problem common to nearly all natural sources has been the ubiquitous presence of silica, and nearly all authors have resorted, at one stage or another, to alkaline fusion or digestion for its removal. Grosse (1934a) and Grosse and Agruss (1934, 1935a) recovered more than 100 g of pure Pa_2O_5 from 1.2 tons of *Rückrückstände,* a material composed largely of SiO_2 and Fe_2O_3 (Table 4.3). The principal steps in the enrichment process were: (1) leaching with hydrochloric acid to eliminate Fe and the more basic oxides; (2) fusing the residue with NaOH and leaching the cooled melt with water to remove soluble silicates and Pb; (3) dissolving the residue in hydrochloric acid and heating to coagulate the remaining SiO_2; (4) washing the precipitate with 20% NaOH solution and dissolving the residue in hydrochloric acid; (5) precipitating Zr (and Pa) by the addition of phosphoric acid; and (6) fusing the ZrP_2O_7 with KOH to eliminate PO_4^{3-} and the last of the SiO_2. The plant product contained more than 85% of the original Pa in a concentration of 1:5000 – an enrichment factor of about 600. Graue and Kading (1934a,b) recovered 700 mg of Pa from 5.5 tons of *Rückrückstände* by essentially the same process, except that the raw material was first fused with NaOH and then leached with hydrochloric acid. The large quantity of SiO_2 that remained in the residue was eliminated by fuming with hydrofluoric acid.

4.4.2 Enrichment of carbonate precipitates

Pa in trace amounts may fractionate unpredictably during dissolution or precipitation of a multi-component mixture. To inhibit such fractionation, many authors have introduced carriers such as Ta (Hahn and Meitner, 1918), Zr (Graue and Kading, 1934a; Grosse and Agruss, 1935a), or Ti (Zavizziano, 1935; Emmanuel-Zavizziano, 1936; Kirby, 1959), which carry Pa quantitatively when they are precipitated as phosphates or hydrated oxides.

Larson *et al.* (1952) leached a carbonate precipitate with nitric acid and digested the resultant SiO_2 gel with 10% NaOH solution to which La carrier was added to minimize losses of Pa in the alkaline solution. However, Thompson and co-workers (1952), by first digesting the carbonates with 40% NaOH, were able to remove enough SiO_2 to prevent gel formation when the metathesized residue was dissolved in 1 M HNO_3. There was no loss of Pa to the alkaline solution, probably because the residue already contained appreciable amounts of both Zr and Ti. The Pa was concentrated from the 1 M HNO_3

solution by adsorption on a MnO_2 precipitate formed *in situ* (Grosse and Agruss, 1935b; Katzin and Stoughton, 1956). Two additional cycles of MnO_2 precipitation and redissolution in HNO_3 were followed by a hydrolytic precipitation of Ti and Zr from 5 M HNO_3. The precipitate that carried down the Pa was taken up in hydrofluoric acid and evaporated to dryness in the presence of perchloric acid to eliminate SiO_2, giving a 1000-fold enrichment of the Pa with a 65% yield.

Carrying by MnO_2 is a key step in the recovery of Pa from *Cotter concentrate* (Hertz *et al.*, 1974). The solids are digested in HNO_3 solution and filtered to yield a solution that is 2–3 M in HNO_3. Essentially all the U and ^{230}Th and 50–85% of the Pa are dissolved; the undissolved residue is reserved for further digestion. The U is extracted with di-*S*-butylphenyl phosphonate (DSBPP) and the Pa and ^{230}Th are quantitatively extracted with tri-*n*-octylphosphine oxide (TOPO). ^{230}Th is stripped from the TOPO with 0.3 M H_2SO_4 and the Pa with 0.5 M $H_2C_2O_4$. Addition of potassium permanganate to the oxalic acid solution yields a precipitate of 5 g of MnO_2 containing 1–6 mg of Pa, for an enrichment factor of 500–2500.

4.4.3 Enrichment of aqueous raffinates

After the sodium carbonate precipitation step was omitted from the Mallinckrodt process, the aqueous raffinate from the diethyl ether extraction of U contained about 0.2 mg L^{-1} of Pa and 1–10 g L^{-1} for other elements (chiefly Ca, Fe, and rare earths). Elson *et al.* (1951) extracted this weakly acid solution of nitrates with 5% of its volume of tri(*n*-butyl)phosphate (TBP) and stripped the TBP with one-fourth of its volume of 0.5 M HF solution. Rare earths and Th isotopes precipitated, but the Pa remained in solution. Al^{3+} was added to complex the F^- and the solution was contacted with di-isopropylcarbinol (DIPC), which extracted 70–90% of the Pa. Back-extraction into 10% H_2O_2 gave another 20-fold volume reduction and yielded a product that contained about 4% Pa by weight, with Ca and U as the principal impurities. The overall yield was only 5–35%, however, primarily because of the poor extractability of Pa into TBP at low acidity. Peppard *et al.* (1957) later found that Pa is efficiently extracted by TBP from 5 M HCl.

In a Russian process (Shevchenko *et al.*, 1958b), the U ore is digested with nitric acid and extracted as slurry with a 10% solution of TBP in kerosene. About 75–85% of the ^{230}Th and 50–55% of the Pa pass into solution, but neither is appreciably extracted by the TBP. After phase separation and filtration, the aqueous solution is made 2 M in HNO_3 and contacted with a 15% solution of mixed mono- and di-isoamylphosphoric acids (DIAPA) in isoamylacetate. A single-stage extraction with an organic:aqueous volume ratio of 1:20 recovers 75–85% of the ^{230}Th and 82–89% of the Pa. After back-extraction with saturated aqueous $(NH_4)_2CO_3$, Fe and other heavy metals are precipitated as sulfides and the carbonate is decomposed by heating and acidification.

The ^{230}Th and Pa are precipitated with NH_4OH and calcined to yield a concentrate containing up to 1% ^{230}Th and about 0.01% Pa in a matrix of U, P, Ti, Zr, Sc, and other impurities. The Pa is separated from ^{230}Th and Sc by fluoride precipitation, which leaves Pa in the solution, from which it is coprecipitated with Zr as a phosphate in the presence of H_2O_2. The Pa:Zr ratio in the concentrate is usually 1:400 or higher.

The adsorption behavior of protactinium on zirconium phosphate cation exchanger from ammonium chloride, hydrochloric acid, and hydrochloric acid–alcohol media has been investigated (Souka *et al.*, 1975c). The distribution coefficients in solvent mixtures of hydrochloric acid and various alcohols depend on both alcohol content and acid concentration. Similar investigations have been carried out for nitric acid systems (Souka *et al.*, 1976a). Sorption of protactinium on silica gel has also attracted attention. Adsorption of ^{233}Pa on silica gel has been investigated as a possible procedure for obtaining isotopically pure uranium-233 (Chang and Ting, 1975a). Protactinium-233 sorption from oxalic acid system has been studied; a 1:1 complex of Pa and oxalate is formed in these systems and the observed adsorption is well correlated to the concentration of the oxalate complexes (Bykhovskii *et al.*, 1977). Hydrophobic silica gel has been prepared by silylation; uptake of protactinium from mixtures of hydrochloric acid and lower aliphatic alcohols increases with increasing molecular weight of the aliphatic alcohol (Caletka and Spěváčkova, 1975).

4.4.4 Enrichment of ethereal sludge

Aqueous hydrofluoric acid is the most consistently effective solvent for Pa(v), with which it forms strong anionic complexes (Guillaumont and deMiranda, 1966; Guillaumont *et al.*, 1968). It has the added advantage of dissolving the oxides of most of the elements with which Pa is normally associated in nature (Si, Fe, Ta, Zr, Ti, etc.). If Al^{3+} is added to such a solution in sufficient quantity to mask all the F^-, a precipitate forms, which carries the Pa quantitatively.

In an enrichment method reported by Goble *et al.* (1958), ethereal sludge was leached with 0.5 M HNO_3, which dissolved about 90% of the U. The residue, which retained more than 95% of the Pa, was leached with 0.5 M HF and Al sheets were suspended in the solution. After 5 days or more, the Pa separated quantitatively as a black deposit on the aluminum, from which it was loosened by treatment with 0.2 M NaOH. The precipitate was washed with dilute NaOH solution and dissolved in 8 M HCl, from which it was extracted with di-isobutylketone (DIBK). The DIBK was stripped with 8 M HCl containing a little HF. Addition of $AlCl_3$ permitted a second cycle of DIBK extraction and stripping. The crude HCl–HF product from 100 kg of sludge was 200 mg of Pa (77% yield) in 0.5 L of solution containing about 10 g of solids.

Unfortunately, this ingenious and inexpensive process failed when attempts were made to apply it on a tonnage scale, apparently because fluorides (from CaF_2 slag) had been dispersed throughout the sludge during a re-drumming operation. This resulted in unacceptable losses of Pa during the initial leaching with dilute HNO_3 solution. Furthermore, the deposition of Pa on Al plates proved too slow and cumbersome for operation on a tonnage scale.

The process that was finally adopted is outlined in Fig. 4.8 (Nairn *et al.*, 1958; Collins *et al.*, 1962). The U and Pa were dissolved by leaching the sludge with a mixture of HNO_3 and HF. After extraction of the U with TBP, Al^{3+} as chloride was added to the raffinate. A precipitate is formed, which carried down 80–95% of the Pa, with an enrichment factor of approximately 10. The precipitate was

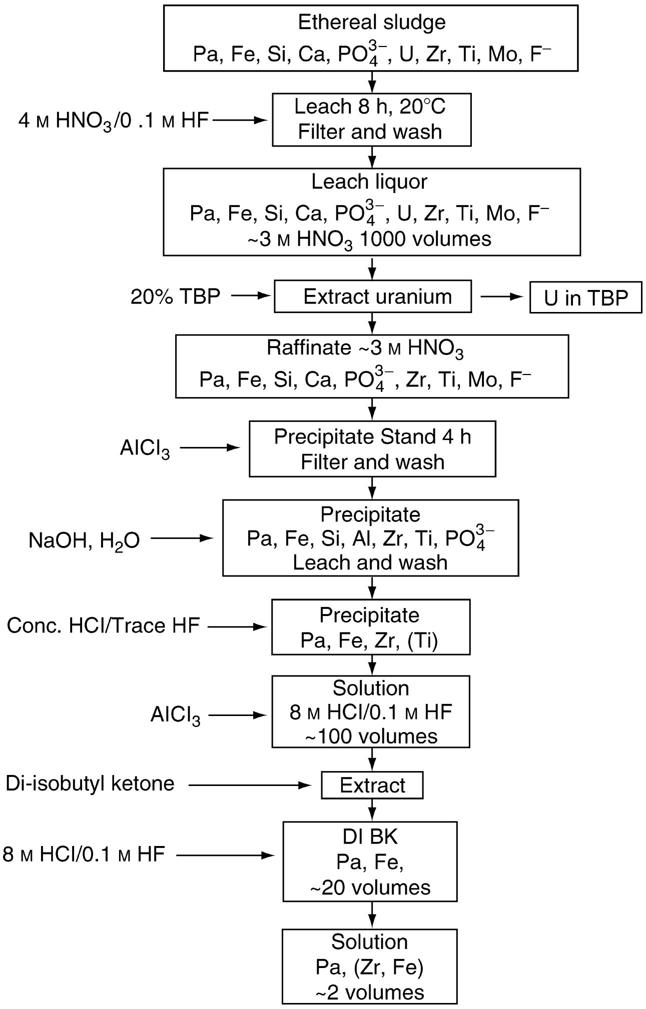

Fig. 4.8 *Recovery of protactinium and uranium from ethereal sludge* (*Nairn* et al., 1958).

digested with 10–35% NaOH to remove Si, Al, and, especially, PO_4^{3-}. The residue was dissolved in 8 M HCl and 0.1 M HF and aluminum chloride was added in a molar ratio of Al:F > 5. The solution was extracted with DIBK and stripped with 8 M HCl and 0.1 M HF. A second cycle of DIBK extraction and stripping yielded 52.4 L of an aqueous solution containing 126.75 g of Pa, 3.25 g of Zr, and 1.42 g of Fe (it was later learned that the product also contained 0.1–4% Nb) (Walter, 1963; Brown *et al.*, 1966a; Jenkins *et al.*, 1975).

Salutsky *et al.* (1956) recovered 0.5 mg of Pa from 5 kg of a material similar to ethereal sludge but only one-tenth as rich. The principal features of the method were: (1) dissolution in 1 M HCl, (2) saturation of the solution with sodium chloride, and (3) boiling to coagulate a small precipitate (chiefly Ca and Si), which quantitatively carried down the Pa. The precipitate was digested with NaOH solution to solubilize silicates and the residue was dissolved in 9 M HCl; this became the feed solution for purification of the Pa by anion exchange. However, attempts to apply this simple process to other batches of the same material failed because of the inhomogeneity of the raw material. Batchwise development and processing ultimately recovered approximately 2 g of Pa from 20 tons of residue, but only after substantial modification of the process, including (Kirby, 1959): addition of Ti as a carrier; dissolution of HCl-insoluble residues in sulfuric acid; extraction with isopropyl ether to reduce the Fe concentration to manageable proportions; and concentration of the Pa by several cycles of extraction into di-isobutylcarbinol (DIBC) and stripping with H_2O_2.

4.4.5 Purification of macroscopic amounts of ^{231}Pa

Preliminary enrichment processes such as those described above afford a high degree of decontamination from Si, Fe, U, Th, Ti, and most bivalent and trivalent elements, including the ^{231}Pa decay products (Fig. 4.1). However, Zr, Ta, and Nb are usually enriched along with the Pa and most recent work has been directed primarily at the separation of those elements, of which Nb is the most troublesome.

Methods reported for the purification of Pa after its enrichment from natural sources are so numerous that only a selected few can be mentioned here. For details of other methods, readers should consult the following reviews (Gmelin, 1942, 1977; Haïssinsky and Bouissières, 1958; Brown and Maddock, 1963, 1967; Pal'shin *et al.*, 1970) and the original publications cited therein.

(a) Precipitation and crystallization

The addition of KF to a solution of Pa(v) in hydrofluoric acid quantitatively precipitates K_2PaF_7 and separates Pa from Zr, Nb, Ti, and Ta (Grosse, 1928; Graue and Kading, 1934b; Bouissières and Haïssinsky, 1951; Cunningham, 1966).

On the other hand, during the fractional crystallization of the double ammonium fluorides, Pa crystallizes before Zr, but after Ti and Ta (Bachelet and Bouissières, 1947). Haïssinsky (Haïssinsky and Bouissières, 1951; Bouissières and Haïssinsky, 1951) separated Pa from Ta, Zr, and Ti by reducing Pa(v) to Pa(iv) with Zn amalgam in 2 M HF. The PaF_4 precipitate was redissolved in aqueous HF or H_2SO_4 in the presence of H_2O_2 or a current of air, which reoxidized the Pa.

Precipitation by H_2O_2 has been widely used to separate Pa from Nb, Ta, and Ti (Grosse, 1930; Bachelet and Bouissières, 1944, 1947; Goble *et al.*, 1958). Walter (1963) decontaminated 500 mg of Pa of about 4% Nb by adding H_2O_2 to a 40% H_2SO_4 solution of the Pa and neutralizing with ammonium hydroxide. Pal'shin *et al.* (1968a) mixed 4.1 mg of Pa with 8 mg each of Nb, Ta, and Zr in 0.25–0.5 M $H_2C_2O_4$, then precipitated the Pa by adding H_2O_2 (to 7.5%) and HCl (to 1.2 M). The precipitate, which formed during an 8–12 h period at room temperature, contained less than 1% total impurities.

The hydrolytic behavior of Pa was used by Kirby (1966) and by Kirby and Figgins (1966) to separate it from up to 13 times as much Nb. When hydrochloric acid was added to a 1 M $H_2C_2O_4$ solution containing equal amounts of the two elements, the precipitate, which developed on heating, contained 94.4% of the Pa and 2.0% of the Nb. Final purification was achieved by dissolution of the precipitate in 7 m H_2SO_4 and evaporation to fumes of SO_3, yielding Pa crystals of undetermined composition, in which the Nb content was reduced from 0.3 to 0.05% in a single stage. According to Brown and Jones (1964) and Bagnall *et al.* (1965), Pa crystallizes quantitatively as $H_3PaO(SO_4)_3$ when Pa_2O_5 is dissolved in a mixture of HF and H_2SO_4 and the solution is evaporated until all F^- has been eliminated. Two recrystallizations of a 10 g batch of Pa reduced the Nb contamination from 4 to 0.18%.

Myasoedov *et al.* (1968c) reported that Pa is quantitatively precipitated by phenylarsonic acid (PAA) from 1 to 7 N HCl, HNO_3, or H_2SO_4. In the absence of $H_2C_2O_4$, Sn(iv), Zr, Nb, Ta, and Ti are also precipitated; however, Pa is separated from Nb and Zr (but not from Ta) when PAA is added to a 2.5 M H_2SO_4 solution containing 0.1 M $H_2C_2O_4$. Both trace and major amounts of Pa have been separated from Nb, Zr, and Fe by this method.

Protactinium was isolated from liquid radioactive waste by sodium silicate, potassium silicate, and an alumina sol mixed in ratios by volume of 1:0.1 to 1. As an example, 0.94 mL of water glass containing 200 g L^{-1} of sodium silicate, and 100 mL of liquid waste containing 20 ppm of uranium was stirred, then 0.94 mL of the same water glass was added and stirred into the mixture along with 1.88 mL of an alumina sol for 10 min. Negatively charged silica particles and positively charged alumina particles absorb U and β^--decay nuclides (Pa) (Mitsubishi, 1995).

The protactinium distribution in a fluoride melt in the presence of solid oxide phases has been calculated (Alekseev *et al.*, 1988, 1989).

(b) Ion exchange

Numerous studies have demonstrated that Pa(v) at trace levels can be separated from the usual contaminants by sorption on anion-exchange resins from hydrochloric acid solutions (Kraus and Moore, 1950, 1951, 1955; Kahn and Hawkinson, 1956; Kraus *et al.*, 1956; Maddock and Pugh, 1956; Hill, 1958; Bunney *et al.*, 1959; Lebedev *et al.*, 1961; D'yachkova *et al.*, 1962; El-Dessouky, 1966; Hicks *et al.*, 1978; Kluge and Lieser, 1980; Alhassanieh *et al.*, 1999; Raje *et al.*, 2001). Typically, the feed solution is 9–10 M HCl, from which Pa(v) is strongly sorbed in anion-exchange resins such as Dowex-1, along with Fe(iii), Ta(v), Nb(v), Zr(iv), U(iv), and U(vi); Th(iv) is only weakly sorbed and appears in the feed effluent. The eluent is a mixture of HCl and HF acids, the concentration of each depending upon the separation required. For example, Zr and Pa are both eluted with 9 M HCl and 0.004 M HF, but Zr may be eluted with 6–7 M HCl, without significant desorption of Pa (Fig. 4.9).

However, attempts to apply this procedure to the purification of weighable amounts of Pa have usually been unsatisfactory, primarily because of the low capacity of the resin (5–50 μg of Pa per gram of resin) and the strong tendency of Pa to hydrolyze in HCl solutions in the absence of complexing anions (Nairn *et al.*, 1958; Kirby, 1959; Collins *et al.*, 1962). Nevertheless, several authors (Jackson *et al.*, 1960a; Stein, 1966; Suzuki and Inoue, 1966) have reported the successful purification of gram quantities of Pa by anion-exchange procedures in which a stable feed solution was prepared by first dissolving the Pa in 9 M HCl

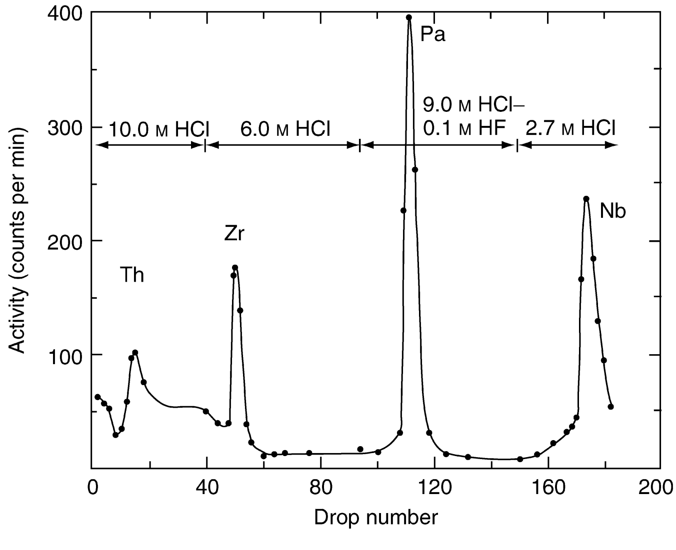

Fig. 4.9 *Separation of Th, Zr, Pa, and Nb on Dowex-*1 *anion-exchange column* (*Hill,* 1958).

containing some HF and then eliminating the F^- by complexing it with Al^{3+} or by evaporation. Sorption properties of Zr, HF, Nb, Ta, and Pa at trace levels towards a macroporous anion exchanger in HF and HCl media were investigated with two ion-exchange methods: static and dynamic. Variations of the distribution coefficients as a function of HCl and HF concentration in the range 0.02–0.8 M for both acids were presented in the form of contour plots and some of the most promising separation possibilities were pointed out (Trubert *et al.*, 1998).

Keller (1963) found that Pa(V), Nb(V), and Ta(V) are all strongly sorbed by an anion exchanger (Dowex-1) from pure hydrofluoric acid solution. However, an increase in $[H^+]$ suppresses the dissociation of HF and sharply reduces the distribution coefficient (K_d) of Pa. Chetham-Strode and Keller (1966) observed that, in >10 M HF, the K_d of Pa was more than an order of magnitude lower than that of Nb and they applied these observations to the separation of Nb and various alkali- and alkaline-earth metal ions from 1 g of Pa_2O_5. The impure Pa was loaded on Dowex-1-Ax10 in 2.5 M HF and eluted with 17 M HF; the product was contaminated only by ^{227}Th, a decay product of ^{231}Pa. Jenkins *et al.* (1975) have reported the purification of approximately 35 g of Pa by this method, with high decontamination factors for Si, Mg, Fe, Al, Cu, and Nb.

The separation of Zr, Ha, Nb, Ta, and Pa was performed on a macroporous anion-exchange resin BIO-RAD AG MP1® in HF media (Monroy-Guzman *et al.*, 1996) and a mixture of 0.01–4.0 M NH_4SCN and 0.05–3.0 M HF media to determine its analytical potential for the quantitative separation of these elements. It was found that the SCN^- concentration in mixtures NH_4SCN–HF had a strong influence on the adsorption of these ions. The K_d of these elements could be explained in terms of the formation of species: $[MF_x]^{(n-x)-}$, $[M(SCN)_y]^{(n-y)-}$, or $[MOF_x]^{(n-x-y)-}$ and $[MO(SCN)_y]^{(n-(2+y)-}$, and mixed fluorothiocyanates of the type $[M(F)_x(SCN)_y]^{(n-x-y)-}$ anionic complexes (Monroy-Guzman *et al.*, 1997).

El-Sweify *et al.* (1985) calculated the distribution of Pa, other actinides, and fission products between the chelating ion exchanger Chelex–100 and certain carboxylic acid solutions.

(c) Solvent extraction and extraction chromatography

Pal'shin *et al.* (1970) have exhaustively reviewed the analytical applications of solvent extraction and Guillaumont and deMiranda (1971) have reviewed the published data as they relate to the ionic species of Pa and the mechanism of its extraction. At tracer levels ($<10^{-4}$ M), Pa(V) is efficiently extracted from aqueous solutions by a wide variety of organic solvents (Hyde and Wolf, 1952; Elson, 1954; Sedlet, 1964); however, only a few have been found useful at macroscopic levels. Dimethyl sulfoxide (DMSO) and the related compounds, diphenyl sulfoxide, and dibenzyl sulfoxide, have received some scrutiny, but it is not clear whether these complexing agents have particular utility for protactinium separation (Reddy and Reddy, 1977; Reddy *et al.*, 1977; Chakravortty and Mohanly, 1979; Chakravortty *et al.*, 1986). As with ion exchange, the chief problems encountered in scaling up tracer-level procedures have been the low capacities of most solvents and the hydrolysis of Pa(v) in the aqueous phase, leading to the formation of 'inextractable polymers'. The most successful extractions of Pa at concentrations up to about 10 g L^{-1} have been with certain ketones, such as di-isopropylketone (DIPK) and DIBK (Goble and Maddock, 1958; Brown *et al.*, 1966a; Myasoedov *et al.*, 1966b) and long-chain alcohols, notably DIBC (Moore, 1955; Kirby, 1959; Brown and Jones, 1964; Scherff and Hermann, 1964; Brown *et al.*, 1966a; Sotobayashi *et al.*, 1977; Pathak *et al.*, 1999a,b).

DIBK was used in some studies for isolation of protactinium from raw materials (Katzin *et al.*, 1950; Katzin, 1952; Kraus and VanWinkle, 1952; Larson *et al.*, 1952; Thompson *et al.*, 1952) and from neutron-irradiated thorium (Meinke, 1946; Hyde and Wolf, 1952; Hill, 1958; Van Winkle and Kraus, 1959; Hyde *et al.*, 1951). Brown *et al.* (1966a) dealt with the problem of hydrolysis by precipitating Pa(v) from aqueous acid solutions with NH_4OH, redissolving the hydrated oxide in either 9 M H_2SO_4 and 0.5 M HF or 9 M HCI and 0.5 M HF, and then complexing the F^- with H_3BO_3. The use of sulfuric acid systems is preferred because of the greater stability of the Pa(v) complexes in that medium. In HCl and HF solutions, hydrolysis proceeds rapidly after the F^- is masked by reaction with $A1^{3+}$ or BO_3^{3-}. After adjustment of the aqueous phase to 4.5 M H_2SO_4 and 6 M HCl, the Pa(v) is extracted with DIBK, stripped with 9 M H_2SO_4 containing some H_2O_2, and re-extracted with DIBC (Fig. 4.10).

The method is said to give good decontamination from nearly all the usual impurities, including Si, Al, Fe, Nb, Zr, Ta, and ^{231}Pa decay products.

DIBC was also used for extraction studies of Pa, Nb, and element 105 – dubnium (Db) from aqueous HBr and HCl. It was shown that the extraction behavior of Db is closer to that of Nb than to Pa. The decreasing extractability from HBr (Pa $>$ Nb $>$ Db) is likely to be due to an increasing tendency of these elements to form a non-extractable polynegative complex species in concentrated HBr in the sequence Pa $<$ Nb $<$ Db (Gober *et al.*, 1992).

Milligram amounts of Pa(v) were extracted from H_2SO_4, HCl or HNO_3 acid solutions by isoamyl alcohol containing 1% PAA or 4% benzeneseleninic acid; good separation from many impurities was reported (Myasoedov *et al.*, 1966a, 1968a). Tetraphenylarsonium chloride has also been studied as a possible extractant for protactinium from hydrochloric or oxalic acid solutions (Abdel Gawad *et al.*, 1976; Souka *et al.*, 1976b). Other extraction agents have also been explored. Thus, l-phenyl-2-methyl-3-hydroxy-4-pyridone dissolved in chloroform (Tamhina *et al.*, 1976, 1978; Herak *et al.*, 1979) quantitatively extracted Pa from hydrochloric acid solution, and Pa can be separated from uranium and/or thorium by appropriate adjustment of the acidity. The antibiotic, tetracycline, was used in radiochemical analytical separations of protactinium from other actinide elements (Saiki *et al.*, 1981) and 5,7-dichloro-8-hydroxyquinoline

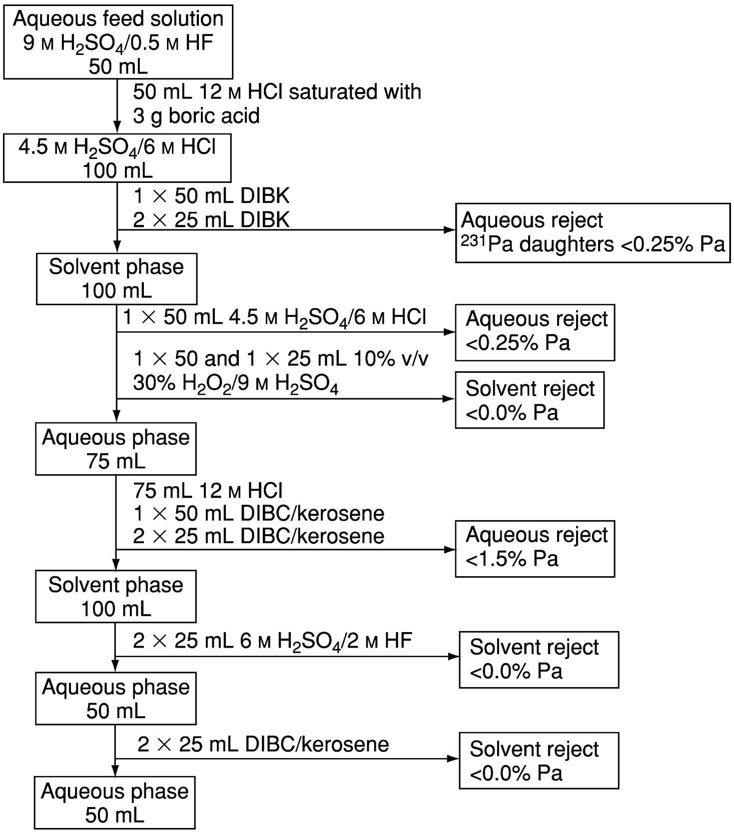

Fig. 4.10 *Purification scheme for* 555 mg *of Pa.* (*According to Brown* et al., 1966*a*.) *Reproduced with permission from Pergamon Press.*

was investigated for the separation of protactinium from niobium, tantalum, and zirconium by solvent extraction (Vaezi-Nasr *et al.*, 1979).

Myasoedov and Pal'shin (1963) and Davidov *et al.* (1966c) proposed an effective method for isolation of Pa from uranium ores and products of their reprocessing by liquid–liquid extraction with the chelating complexing reagent 3,6-bis-[(2-arsenophenyl)azo]-4,5-dihydroxy-2,7-naphthalene disulfo acid (Arsenazo-III) in isoamyl alcohol. It was shown that an effective extraction of Pa from strong acid media, even in the presence of a great amount of Al, Fe(III), Mn(II), rare earth metals, and other elements, took place. The growth of U, Zr, Th, and particularly Nb concentrations in the solutions led to a diminution of Pa isolation. This method was used for analytical control of the separation of gram amounts of Pa(V) under plant conditions.

Thenoyltrifluoroacetone (TTA) had been used for separation and purification of Pa from several elements (Meinke and Seaborg, 1950; Meinke, 1952; Bouissières *et al.*, 1953; Moore, 1955, 1956; Brown *et al.*, 1959; Moore *et al.*, 1959; Poskanzer and Foreman, 1961a,b; Myasoedov and Muxart, 1962a). TTA extraction has been applied to the extraction of Pa from 10 M HCI in which $PaOCl_6^{3-}$ appears to be a principal species (Duplessis and Guillaumont, 1979). Triphenylphosphine oxide (TPPO), triphenylarsine oxide (Maghrawy *et al.*, 1989), and mixtures of TTA and either TBP, TOPO, or TPPO have been investigated (Kandil *et al.*, 1980); a combination of TTA and TOPO has found use in the separation of protactinium and thorium by solvent extraction (Kandil and Ramadan, 1978). TBP (Peppard *et al.*, 1957; Souka *et al.*, 1975b; Svantesson *et al.*, 1979), HDEHP (Shevchenko *et al.*, 1958a; Brown and Maddock, 1963; Myasoedov and Molochnikova, 1968; Myasoedov *et al.*, 1968b; Maghrawy *et al.*, 1988), and di-2-ethyl-hexyl isobutylamide (D2EHIBA) (Pathak *et al.*, 1999a,b) have high capacities for Pa(v), but are relatively unselective.

The extraction by *N*-benzoylphenylhydroxylamine (BPHA) from HCl, and H_2SO_4 solutions was used for the separation of Pa(v) from other elements by Pal'shin *et al.* (1963) and Myasoedov *et al.* (1964). It was found that protactinium complexes with BPHA were extracted by benzene or other solvents from aqueous solutions with a wide range of acid concentrations. D'yachkova and Spitsyn (1964) studied the protactinium, zirconium, and niobium behavior by extraction with BPHA from sulfuric acid solutions. The isolation of the above elements was carried out with 0.2–0.5% solution BPHA in chloroform. The largest difference in extraction ability for these elements was observed with H_2SO_4 concentrations in the aqueous phase greater than 7 N. Rudenko *et al.* (1965) and Lapitskii *et al.* (1966) carried out the separation of protactinium from uranium and thorium by extraction with 0.1 M BPHA solution in chloroform from 4 M HCl.

The Pa(v) extraction by cupferron (CP) had been studied by Maddock and Miles (1949). It was found that Pa was easily extracted by CP in both oxygen-containing and inert solvents from inorganic acid media. Spitsyn and Golutvina (1960) used the extraction with CP for the separation of ^{233}Pa from large amounts of manganese. Rudenko *et al.* (1965) and Lapitskii *et al.* (1965) reported that the neocupferron (NCP), an analog of CP, can be also used for the separation of protactinium from uranium, thorium, and other elements. Uranium and thorium are not extracted by NCP from 2 M HCl solutions, whereas protactinium isolation by a 0.01 M solution of this reagent in chloroform is about 90%. These authors used NCP for isolation of ^{233}Pa from irradiated thorium.

The extraction of Pa by 1-phenyl-3-methyl-4-benzoylpyrazolone (PMBP) in benzene solution from H_2SO_4 media effectively isolated this element from large amounts of Fe(III), La, Nb(v), Th(IV), and U(VI) (Pal'shin *et al.*, 1970). Hence, Pa extraction and isolation by 0.1 M solution of PMBP in benzene from 5 N H_2SO_4 is greater than 98%. For the complete separation of Pa from Zr by this method, a 12% solution of H_2O_2 had been used.

The quantitative extraction of protactinium salicylate with acetone at pH 4 from saturated calcium chloride solutions was reported by Nikolaev *et al.* (1959). Under these conditions zirconium, thorium, uranium, and plutonium are extracted with protactinium. The extraction with salicylate can be used for the separation of protactinium from rare earth and other di- and tervalent elements. The quantitative extraction of protactinium oxychinolate with chloroform from solutions with pH 3–9 was described (Keller, 1966a).

Extraction by tertiary amines in early work was explored only at levels of 10^{-4} M or less, but this procedure shows promise because it permits the extraction of Pa(v) from HF-containing solutions (Moore, 1960; Muxart and Arapaki-Strapelias, 1963; Guillot, 1966; Muxart *et al.*, 1966b; Pal'shin *et al.*, 1971; Moore and Thern, 1974).

The extraction behavior of protactinium in mixtures of uranium, thorium, and neptunium with trilaurylamine from sulfonic acid solutions (Souka *et al.*, 1975c) indicates low distribution coefficients at high acid concentrations; the addition of hydrochloric acid appreciably enhances extraction. The extraction of protactinium (v) with trioctylamine (TOA) dissolved in xylene from thiocyanate solutions containing uranium and thorium have been successfully accomplished (Nekrasova *et al.*, 1975a); tracer amounts of Pa can exist in monomeric form in thiocyanate media for several months, but at Pa(v) concentrations greater than 10^{-6} M, polymers form and the efficacy of TOA as an extractant is seriously impaired (Nekrasova *et al.*, 1975b). Columns impregnated with TOA in a liquid chromatographic system were also used for the separation of ^{262,263}Db in HCl–HF media from Pa and Nb. The data obtained confirm the non-tantalum-like behavior of dubnium in 0.5 M HCl and 0.01 M HF media, and corroborate previously suggested structural differences between the halide complexes of dubnium, niobium, and protactinium, on the one hand, and those of tantalum on the other hand (Zimmerman *et al.*, 1993). Dubnium was shown to be adsorbed on the column from 12 M HCl and 0.02 M HF solutions together with its lighter homologs Nb, Ta, and the pseudohomolog Pa. In elutions with 10 M HCl and 0.025 M HF, 4 M HCl and 0.02 M HF, and 0.5 M HCl and 0.01 M HF, the extraction sequence Ta > Nb > Db > Pa was observed (Paulus *et al.*, 1998, 1999).

The formation of polymers of Pa(v) in the extractions by quaternary ammonium base Aliquat 336 from strongly alkaline solutions can be minimized by the addition of a hydroxycarboxylic acid or aminopolycarboxylic acid (Myasoedov *et al.*, 1980). While the extractability of Pa(v) can be enhanced, the separations are poor. For the systematic study of halide complexation of the group V elements, new batch extraction experiments for Nb, Ta, and Pa were performed with the Aliquat 336 in pure HF, HCl, and HBr solutions. Based on these results, new chromatographic column separations were designed to study separately the fluoride and chloride complexation of Db with Automated Rapid Chemistry Apparatus II (ARCA II). In the system Aliquat 336-HF, after feeding the activity onto the column in 0.5 M HF, dubnium did not elute in 4 M HF (Pa fraction) but showed a higher distribution coefficient close to that of

Nb (and Ta). In the system Aliquat 336-HCl, after feeding onto the column in 10 M HCl, dubnium showed a distribution coefficient in 6 M HCl close to that of Nb establishing an extraction sequence Pa $>$ Nb greater than or equal to Db $>$ Ta, which was theoretically predicted by considering the competition between hydrolysis and complex formation (Paulus *et al.*, 1998, 1999). Separation of ^{231}Pa from U and other impurities has been provided by an extraction-chromatographic method using quaternary ammonium-Kel-F materials (Zhang Xianlu *et al.*, 1993).

Extraction of protactinium(V) chloro complexes by tricaprylamine and its separation from Th(IV), U(VI), and rare earths has been described (El-Yamani and Shabana, 1985).

(d) Large-scale recovery of protactinium-231

Brown and Whittaker (1978) have described a new, ‘relatively simple’ method for the recovery and purification of protactinium-231. It has been applied with signal success to the recovery of Pa from various residues containing 1.73 g of protactinium in a state of high chemical and radiochemical purity. Efficient separation of ^{231}Pa was readily effected by dissolving the ^{231}Pa-containing residues in 5 M hydrofluoric acid. Excess ammonia is added to precipitate the hydrous oxides, which after several washes with water are redissolved in 2 M nitric acid. This precipitate is considerably enriched in ^{231}Pa. Washing the precipitated hydrous oxides with 0.5–4.0 M HNO_3 and/or 0.5 M HNO_3 and 0.3 M H_2O_2, in which protactinium(V) hydrous oxide, is essentially insoluble, removes much of the impurities carried in the initial hydrous oxide precipitation. Repetition of this cycle twice more yields Pa_2O_5 of high purity. The final traces of silicon are then removed by dissolving the hydrous oxides in 20 M HF and evaporating the solution to dryness. Recovery yields range from 92 to 96% from initial samples containing 30–75 wt% ^{231}Pa. The purity of the product is generally greater than 99%; it is also radiochemically pure.

4.4.6 Preparation of pure ^{234}Pa and ^{234m}Pa

Because of its short half-life, 1.17 min ^{234m}Pa is frequently used for classroom demonstrations of radioactive decay and growth (Booth, 1951; Carsell and Lawrence, 1959; Overman and Clark, 1960). Pure ^{234m}Pa (and its ground-state isomer, 6.7 h ^{234}Pa) can be coprecipitated directly from a 6 M HCl solution of $(NH_4)_2U_2O_7$ with BPHA (Cristallini and Flegenheimer, 1963). The procedure is rapid and gives a high degree of decontamination from both U and Th.

However, most authors prefer to make a preliminary separation of 24.1 day ^{234}Th, from which the ^{234m}Pa (and ^{234}Pa) can be repeatedly ‘milked’. The classical procedure of Crookes (1900) is still one of the most widely used for this purpose (Harvey and Parsons, 1950; Barendregt and Tom, 1951;

Bouissières *et al.*, 1953; Forrest *et al.*, 1960; Bjørnholm and Nielsen, 1963): 10–200 g of $UO_2(NO_3)_2 \cdot 6H_2O$ are dissolved in diethyl ether. The aqueous phase formed by the water of crystallization retains the ^{234}Th and some U. Repeated extraction with fresh ether removes the remaining U. Alternatively, the ^{234}Th is purified and concentrated by coprecipitation with $Fe(OH)_3$ in the presence of $(NH_4)_2CO_3$ (Hahn, 1921; Harvey and Parsons, 1950), by cation exchange from HCl solution (Zijp *et al.*, 1954; Suner *et al.*, 1974), by anion exchange from HNO_3 solution (Bunney *et al.*, 1959), or by extraction with tertiary amines (Moore and Thern, 1974; Carswell and Lawrence, 1959).

Once the ^{234}Th has been purified, the ^{234m}Pa and ^{234}Pa quickly regain equilibrium and can be isolated by any of the methods described above for the purification of ^{231}Pa, except, of course, carrier-free precipitation. Solvent extraction is the most suitable, because of its speed and selectivity, at tracer levels, Pa(v) is rapidly and quantitatively separated from Th(iv) by extraction from 6 M HCl solution with any number of organic solvents, notably DIPK, DIBK, DIPC, and DIBC (Moore, 1955; Myasoedov *et al.*, 1966a). The ^{234}Th remains in the aqueous phase. To prepare ^{234m}Pa free of ^{234}Pa, the first two or three organic extracts are discarded and, after 10–15 min, the re-grown ^{234m}Pa is extracted with fresh solvent (Bjørnholm and Nielson, 1963).

Fajans and Göhring (1913b) first separated *brevium* by selective adsorption on lead plates and by coprecipitation with Ta_2O_5. The addition of ^{232}Th keeps the mixture of ^{234}Th and ^{234m}Pa more quantitatively in solution (Guy and Russell, 1923; Jacobi, 1945). Hahn (1921) coprecipitated the mixture of ^{234}Th and ^{234m}Pa with LaF_3, leaving ^{234}Pa in the filtrate. Zijp *et al.* (1954) concentrated ^{234}Pa by MnO_2 precipitations (Maddock and Miles, 1949), alternating with extraction by TTA (Meinke, 1952).

Bjørnholm *et al.* (1967) milked 0.5–1 mCi of ^{234}Pa from 0.8 mCi of ^{234}Th by extraction into hexone (methyl isobutyl ketone, MIK) from 6 M HC1 solution. It is noteworthy, however, that many of the same problems were encountered in the initial concentration of ^{234}Th from 2 tons of U metal as in scaling up laboratory procedures for the concentration of macroscopic amounts of ^{231}Pa from natural sources.

4.4.7 Preparation of pure ^{233}Pa

Irradiation of 1 g ^{232}Th (as metal, oxide, chloride, nitrate, or basic carbonate) for 1 day in a thermal-neutron flux of 2×10^{14} n cm^{-2} s^{-1} will produce approximately 5 Ci of ^{233}Pa (Schuman and Tromp, 1959). Detailed procedures for the isolation of ^{233}Pa from Th targets are given in several review articles (Hyde and Wolf, 1952; Hyde, 1954, 1956; Haïssinsky and Bouissières, 1958; Kirby, 1959; Pal'shin *et al.*, 1970). In general, the target is dissolved in concentrated HCl or HNO_3 (usually containing 0.01–0.1 M HF as a catalyst) and the ^{233}Pa is separated from Th and other impurities by one, or a combination, of the anion-exchange and solvent extraction methods described above. Alternatively, 3 g of Th metal irradiated in a reactor with an irradiation time of 1 day in a thermal flux of 3×10^{13} n cm^{-2} s^{-1} are dissolved in nitric acid. The ^{233}Pa is adsorbed on an anion-exchange column, eluted, then is extracted by TOPO (Kuppers and Erdtmann, 1992).

A preliminary concentration by coprecipitation (Katzin and Stoughton, 1956; Fudge and Woodhead, 1957; Katzin, 1958) is often used, and was, in fact, the method adopted by Codding *et al.* (1964) to isolate 1 gram of ^{233}Pa after solvent extraction with MIK or DIPK gave unaccountably poor yields. Leaching the MnO_2 with a mixture of HNO_3 and H_2O_2 removed the Mn without loss of ^{233}Pa, which was subsequently dissolved in 6 M H_2SO_4 and re-precipitated with HNO_3. On the other hand, Schulz (1972) reported good extraction of ^{233}Pa by DIBC from 7.4 M HNO_3 solutions containing 1.4 M Th $(NO_3)_4$ and 480 Ci L^{-1} of ^{233}Pa. Macroscopic amounts of ^{233}Pa have also been recovered from HNO_3 solutions of irradiated ThO_2 by adsorption on powdered unfired Vycor glass and silica gel (Moore and Rainey, 1964; Goode and Moore, 1967); at tracer levels, ^{233}Pa has been separated from Th targets by adsorption on silica gel (Davydov *et al.*, 1965; Spitsyn *et al.*, 1969; Chang *et al.*, 1974; Chang and Ting, 1975b), on quartz sand (Sakanoue and Abe, 1967), and on activated charcoal saturated with PAA (Pal'shin *et al.*, 1966). Separations with cation and chelating resins (Kurodo and Ishida, 1965; Myasoedov *et al.*, 1969), by paper chromatography and paper electrophoresis (Vernois, 1958, 1959; Myasoedov *et al.*, 1969), and by reversed-phase partition chromatography (Fidelis *et al.*, 1963) have also been reported.

4.4.8 Toxic properties

^{231}Pa is dangerous to organisms, similar to other α-emitters with comparatively short half-lives. Once in organisms it accumulates in kidneys and bones. The maximum amount of protactinium considered not harmful after absorption by an organism is 0.03 μCi. It corresponds to 0.5 μg ^{231}Pa. Protactinium-231, contained in the air as an aerosol, is 2.5×10^{8}-fold more toxic than hydrocyanic acid at the same concentrations (Bagnall, 1966a). Therefore all operations with weighable amounts of ^{231}Pa are carried out in special isolated boxes.

4.4.9 Applications of protactinium

Pa was used for the preparation of a scintillator for detecting X-rays, comprising complex oxides of Gd, Pa, Cs, rare earth metals and other elements. This scintillator, which can significantly increase relative light emission outputs without increasing background, is used in for detecting X-rays, particularly in an X-ray computed tomography apparatus (Hitachi Metals, 1999). The coating material for a color cathode ray tube with bright green fluorescence was created by doping wih Pa (Toshiba, 1995).

Mixed oxides of Nb, Mg, Ga and Mn, doped with 0.005–0.52% Pa_2O_5, were used as high temperature dielectrics (up to 1300°C) for ceramic capacitors (Fujikawa *et al.*, 1996).

One of the important applications of Pa can be in the determination of ancient subjects using a $^{231}Pa/^{235}U$ dating method. This method was used for the dating of one of the Qafzeh human skulls, Qafzen 6, excavated in 1934 by Neuville and Stekelis and conserved at the Institut de Paléontologie Humaine in Paris, by non-destructive gamma-ray spectroscopy. A long-term measurement resulted in an age of (94 ± 10) Ka and confirmed the great antiquity of the Proto-Cro-Magnons of the Near East, contributing to the establishment of modern man's chronology (Yokoyama *et al.*, 1997). The Neanderthal hominid Tabun C1, found in Israel by Garod and Bate, was attributed to either layer B or C of their stratigraphic sequence. Gamma-ray spectroscopy of the $^{231}Pa/^{235}U$ ratios of two bones from this skeleton was used to determine their age. Calculations gave the age of the Tabun C1 mandible as 345 Ka. This suggests that Neanderthals did not necessarily coexist with the earliest modern humans in the region. The early age determined for the Tabun skeleton would suggest that Neanderthals survived as late in the Levant as they did in Europe (Schwarcz *et al.*, 1998). Uranium-series dating of bones and teeth from the Chinese Paleolithic sites has also been used (Chen and Yuan, 1988).

As a result of the development of the nuclear industry (e.g. nuclear power engineering and nuclear powered fleets), a considerable amount of radioactive wastes and spent nuclear fuel is accumulating in the world. Geological disposal of solid and solidified nuclear waste is considered as being economical, technically and ecologically the most feasible approach to completion of the nuclear fuel cycle. Thus determination of chemical behavior of actinides elements, Pa included, is an important problem of environmental science.

The sorption behavior of Pa, which is a decay product of uranium, was studied on the principal rock types from the potential areas selected for construction of a repository. The sorption distribution coefficients (K_d) of Pa were determined under ambient conditions in oxic and anoxic (N_2) atmospheres using natural fresh and brackish groundwater; and the values obtained were 0.07–2.3 and 1.7–12 $m^3\ kg^{-1}$, respectively (Kulmala *et al.*, 1998). Pickett and Murrell (1997) presented the first survey of $^{231}Pa/^{235}U$ ratios in volcanic rocks; such measurements were made possible by new mass spectrometric techniques. It was shown that the high $^{231}Pa/^{235}U$ ratios in basalts reflect a large degree of discrimination between two incompatible elements, posing challenges for modeling of melt generation and migration. Fundamental differences in $^{231}Pa/^{235}U$ ratios among different basaltic environment are likely related to differences in melting zone conditions (e.g. melting rate). Strong disequilibria in continental basalts demonstrate that Pa–U fractionation is possible in both garnet and spinel mantle stability fields.

4.5 ATOMIC PROPERTIES

Experimental measurements (Marrus *et al.*, 1961; Giaechetti, 1966; Richards *et al.*, 1968) and theoretical calculations (Judd, 1962; Wilson, 1967, 1968) agree that the ground state configuration of the neutral Pa atom is almost certainly [Rn] $5f^2 6d^1 7s^2$. However, some unpublished calculations by Maly (cited by Cauchois (1971)) indicated that the total relativistic energy of that structure was 0.9 eV higher than that of a $5f^1 6d^2 7s^2$ configuration, implying that the latter may be the more stable of the two. Giaechetti (1967) found that the ground state configuration of the first ion of Pa (Pa^{1+}) was $5f^2 7s^2$ and this was confirmed by theoretical calculations, which also yielded $5f^2 6d^1$, $5f^2$ and $5f^1$ as the ground state configurations of Pa^{2+}, Pa^{3+} and Pa^{4+}, respectively. Crystal structure stabilities and the electronic structure of Pa have been discussed by Wills and Ericsson (1992).

The emission spectrum of Pa was first recorded by Schüler and Gollnow (1934), who reported a large number of lines in the visible region, many of which showed hyperfine splitting patterns, indicating a nuclear spin of 3/2 for ^{231}Pa. Tomkins and Fred (1949) listed 263 lines in the ultraviolet region sensitive to copper spark excitation. The emission spectrum excited by a microwave discharge tube was measured by Richards and co-workers (1963, 1968), who recorded some 14 000 lines between 3 μm and 400 nm, about half of which were fitted into a level scheme of about 200 even and 300 odd levels.

Table 4.4 lists recommended X-ray atomic energy levels, based on the X-ray wavelengths re-evaluated by Bearden (1967) and by Bearden and Burr (1967).

The Mössbauer effect has been studied by Croft *et al.* (1968) with the 84.2 keV γ-ray of ^{231}Pa, following β$^-$-decay of ^{231}Th; resonance absorption was detected

Table 4.4 *Recommended values of the atomic energy levels* (eV) *of Pa* (*measured values of the X-ray absorption energies are shown in parentheses*) (*Bearden and Burr*, 1967).

Level	*Energy* (eV)	*Level*	*Energy* (eV)
K	1 12 601.4 ± 2.4	$\mathrm{N_{I}}$	1387.1 ± 1.9
$\mathrm{L_{I}}$	21 104.6 ± 1.8	$\mathrm{N_{II}}$	1224.3 ± 1.6
	(21 128)		
$\mathrm{L_{II}}$	20 313.7 ± 1.5	$\mathrm{N_{III}}$	1006.7 ± 1.7
	(20 319)		
$\mathrm{L_{III}}$	16 733.1 ± 1.4	$\mathrm{N_{IV}}$	743.4 ± 2.1
	(16 733)		
$\mathrm{M_{I}}$	5366.9 ± 1.6	$\mathrm{N_{V}}$	708.2 ± 1.8
$\mathrm{M_{II}}$	5000.9 ± 2.3	$\mathrm{N_{VI}}$	371.2 ± 1.6
$\mathrm{M_{III}}$	4173.8 ± 1.8	$\mathrm{N_{VII}}$	359.5 ± 1.6
$\mathrm{M_{IV}}$	3611.2 ± 1.4	$\mathrm{O_{I}}$	309.6 ± 4.3
	(3608)	$\mathrm{O_{II}}$	
$\mathrm{M_{V}}$	3441.8 ± 1.4	$\mathrm{O_{III}}$	222.9 ± 3.9
	(3436)	$\mathrm{O_{IV}}$	94.1 ± 2.8
		$\mathrm{O_{V}}$	

with absorbers of both Pa_2O_5 and PaO_2. No isomer shift between the valence states was observed.

4.6 THE METALLIC STATE

Grosse (1934a) prepared metallic Pa by two methods: (1) Pa_2O_5 was bombarded for several hours with 35 kV electrons at a current strength of 5–10 mA and (2) the pentahalide (Cl, Br, I) was heated on a tungsten filament at a pressure of 10^{-6} to 10^{-5} torr. Later authors have prepared the metal by reduction of PaF_4 with the vapors of Ba (Sellers *et al.*, 1954; Bansal, 1966; Cunningham, 1966, 1971; Dod, 1972), Li (Fowler *et al.*, 1965; Cunningham, 1971), or Ca (Marples, 1966). A Zn–Mg reductant is said to yield an impure Pa product (Lee and Marples, 1973).

In the method used by Cunningham and his co-workers at Berkeley (Cunningham, 1971; Dod, 1972), PaF_4 is mixed with barium in a crucible fabricated from a single crystal of BaF_2 (or LiF) and supported in a tantalum foil cylinder. The assembly is evacuated to below 10^{-6} torr and heated inductively to 1250–1275°C for 4–5 min. The BaF_2 crucible is then melted by raising the temperature to 1600°C for 1.5 min and then molten Pa metal agglomerates as a small sphere at the bottom of the Ta support ring. Individual preparations are limited to about 15 mg.

Subsequently, individual preparations of Pa metal of up to 0.5 g have been successfully executed by a modified Van Arkel technique (Baybarz *et al.*, 1976; Brown *et al.*, 1977; Bohet and Muller, 1978; Brown, 1982; Spirlet, 1982). The starting material is protactinium carbide obtained by reduction of Pa_2O_5 with carbon. Heating the protactinium carbide with I_2 generates volatile PaI_5, which is then decomposed on a heated tungsten filament or, better, a sphere (Spirlet, 1979) using induction heating. Protactinium can be precipitated from diluted HF, H_2SO_4 solutions as a fine film on several metal plates (Zn, Al, Mn, and other) (Camarcat *et al.*, 1949; Haïssinsky and Bouissières, 1958; Stronski and Zelinski, 1964). The electrolytic reduction of Pa from NH_4F solutions in the presence of triethylamine at pH 5.8 and 10–20 mA cm^{-2} also has been realized (Emmanuel-Zavizziano and Haïssinsky, 1938). Preparation of a protactinium measurement source by the electroplating method also has been reported by Li Zongwei *et al.* (1998).

The availability of pure, single-crystal Pa metal has made possible the measurement of important physical parameters that cast light on the electronic structure of Pa and for the calculation of its optical properties (Gasche *et al.*, 1996). A theoretical calculation by Soderling and Eriksson (1997) predicted that protactinium metal will undergo a phase transition to the α-U orthorhombic structure below 1 Mbar (1 Mbar $\sim$100 GPa) pressure. At higher pressures, the β-phase re-enters into the phase diagram and at the highest pressures an ideal *hcp* structure becomes stable. Hence, Soderling and Eriksson expect Pa to undergo a sequence of transitions, with the first transition taking place at 0.25 Mbar and the subsequent ones above 1 Mbar. The β→α-U transition is triggered by the pressure-induced promotion of the spd-valence electrons to 5f states. In this regard Pa approaches uranium, which at ambient conditions has one more 5f electron than Pa at similar conditions. At higher compression of Pa, the 5f band broadens and electrostatic interactions in combination with Born–Mayer repulsion become increasingly important and drive Pa gradually to more close-packed structures. At ultra-high pressures, the balance between electrostatic energy, Born–Mayer repulsion, and one-electron band energy stabilizes the *hcp* (ideal packing) structure.

Recent experimental results (Haire *et al.*, 2003) confirm that the stable room temperature and pressure phase of Pa metal is the body-centered tetragonal (*bct*) phase. Under high pressure this phase is stable until 77(5) GPa (77 GPa ~0.77 Mbar) where it is converted to orthorhombic, the α-uranium phase, with a small (0.8%) volume collapse. The relative volume of the *bct* phase decreased smoothly from 1 atm down to a volume ratio of ~0.7 before the high-pressure phase transformation. Experiments continued to a pressure of 130 GPa with no further phase change but with a smooth decrease in the volume of the orthorhombic phase of ~0.62. Haire *et al.* (2003) attribute the structural phase change to an increase in 5f bonding at the higher pressures.

The superconducting properties of Pa metal have been described by Smith *et al.* (1979), who determined the superconducting transition temperature and upper critical magnetic field. Since the superconducting properties of Pa are markedly affected by its 5f electronic structure, it is now evident that Pa is a true actinide element. The heat capacity of a single Pa crystal in the temperature range 4.9–18 K has been reported (Stewart *et al.*, 1980). The unit cell volume of Pa metal first decreases and then increases on cooling from 300 to 50 K (Benedict *et al.*, 1979). The importance of the expansion coefficient in the explanation of specific-heat parameters has been discussed by Mortimer (1979). A Mössbauer resonance of ^{231}Pa at 84.2 keV in Pa metal has been reported; the electric field gradient in Pa metal is $|eq_Z| = (2.05 \pm 0.15) \times 10^{18}$ V cm^{-2} (Friedt *et al.*, 1978; Rebizant *et al.*, 1979). The vapor pressure of liquid Pa metal in the temperature range 2500–2900 K has been measured by a combination of mass spectrometry and Knudsen effusion techniques; the vapor pressure (in Pascals) is given (Bradbury, 1981) by:

$$\log[P(\mathrm{Pa(liq)})] = -[(31\,328 \pm 375)/T] + (10.83 \pm 0.13).$$

Pa metal is malleable and ductile (Zachariasen, 1952; Sellers *et al.*, 1954). Other physical properties are summarized in Table 4.5. The enthalpy of sublimation of Pa(s) at 298 K has been calculated to be 660 (Bradbury, 1981) or 570 kJ mol^{-1} (Kleinschmidt *et al.*, 1983).

Metallic Pa is attacked by 8 M HCl, 12 M HF, or 2.5 M H_2SO_4, but the initial reaction ceases quickly, possibly because of the accumulation of a protective layer resulting from the hydrolysis of Pa(V) or Pa(IV) at the metal surface.

Table 4.5 *Some physical properties of protactinium metal.*

Property	*Observed or calculated value*(*s*)	*References*
crystal structure	body-centered tetragonal (14/*mmm*)	Zachariasen (1952); Asprey *et al.* (1971)
	high temp. form is fcc or bcc	
lattice parameters (Å)	$a = 3.925 \pm 0.005$, $c = 3.238 \pm 0.007$ (RT)	Zachariasen (1952); Sellers *et al.* (1954)
	$a = 3.924 \pm 0.001$, $c = 3.239 \pm 0.0005$ (18°C)	Marples (1966)
	(*a*/*c* approaches 1 with increased temperature)	
	$a = 3.929 \pm 0.001$, $c = 3.241 \pm 0.002$ (RT)	Cunningham (1966)
	$a = 3.921 \pm 0.001$, $c = 3.235 \pm 0.001$ (RT)	Bohet (1977)
	$a = 5.02$ (high temperature form fcc)	Asprey *et al.* (1971)
	$a = 5.018$ (high temperature form fcc)	Bohet (1977)
	$a = 3.81$ (high temperature form bcc)	Marples (1965)
X-ray density (g cm^{-3})	15.37 ± 0.08	Zachariasen (1952)
metallic radius (Å)	1.63 for coordination number 12	Zachariasen (1952)
melting point (°C)	1575 ± 20	Marples (1966)
	1560 ± 20	Cunningham (1966)
	1565 ± 20	Cunningham (1971)
	1562 ± 15	Dod (1972)
vapor pressure (atm)	1×10^{-8} at ~2400 K	Cunningham (1971)
	5.1×10^{-5} at 2200 K	Murbach (1957)
magnetic susceptibility (emu mol^{-1}; 20–298 K)	$(250 \pm 50) \times 10^{-6}$ (temperature-independent)	Cunningham (1966)
	$(268 \pm 14) \times 10^{-6}$ (temperature-independent)	Bansal (1966)
	$(189 \pm 6.5) \times 10^{-6}$ (temperature-independent)	Dod (1972)
superconducting transition temperature (K)	1.4	Fowler *et al.* (1965, 1974)
	?	Smith *et al.* (1979)
	2	Francis and Theng-Da Tchang (1935)
	2	Launay and Dolechek (1947)

Table 4.6 *Preparation and structure of protactinium–noble-metal alloy phases* (*Erdmann*, 1971; *Erdmann and Keller*, 1971, 1973).

Compound	*Reduction temperature* (°C)	*Structure type*	*Lattice parameters* (Å)	
			a	*c*
Pt_3Pa	1250 ± 50	Cd_3Mg (hex)	5.704	4.957
Pt_5Pa	1200 ± 50	Ni_5U	7.413	
Ir_3Pa	1550 ± 50	Cu_3Au	4.047	
Rh_3Pa	1550 ± 50	Cu_3Au	4.037	
$Be_{13}Pa$	1300 ± 50	$NaZn_{13}$	10.26	

The metal does not react with 8 M HNO_3 even in the presence of 0.01 M HF. The most effective solvent found thus far is a mixture of 8 M HCl and 1 M HF (Cunningham, 1971).

According to Dod (1972), metal samples exposed to air at room temperature show little or no tarnishing over a period of several months. A slight loss of metallic luster was observed when a sample of Pa metal was heated in air for 1 h at 100°C. Heating for 1 h at 300°C caused the sample to turn grayish white and begin to disintegrate. Pa metal exposed to O_2, H_2O, or CO_2 at 300 and 500°C yielded Pa_2O_5; reaction with NH_3 and H_2 produced PaN_2 and PaH_3, respectively. The metal reacts quantitatively with excess I_2 above 400°C to yield a sublimate of crystalline, black PaI_5 (Sellers *et al.*, 1954; Brown *et al.*, 1967b).

4.6.1 Alloys

Erdmann and Keller (Erdmann, 1971; Erdmann and Keller, 1971, 1973) have prepared Pa–noble-metal alloy phases by reduction of Pa_2O_5 with highly purified H_2 in the presence of Pt, Ir, and Rh. Preparation conditions and some properties of these intermetallic compounds are listed in Table 4.6. Reaction of Pa_2O_5 with beryllium metal has been reported by Benedict *et al.* (1975) to form $Be_{13}Pa$.

4.7 SIMPLE AND COMPLEX COMPOUNDS

4.7.1 Protactinium hydride

Perlman and Weisman (1951) and Sellers *et al.* (1954) reacted H_2 with Pa metal at about 250°C and a pressure of about 600 torr, and obtained a black flaky substance, isostructural with β-UH_3. The compound was cubic, with a unit cell constant $a = (6.648 \pm 0.005)$ Å. However, Dod (1972) reported the formation at 100, 200, and 300°C of a gray, powdered substance that is isostructural with α-UH_3. The unit cell constant of α-PaH_3 is (4.150 ± 0.002) Å for the product obtained at 100 and 200°C and (4.154 ± 0.002) Å at 300°C. Subsequently, Brown (1982) prepared α- and β-PaH_3 at 250 and 400°C, respectively.

4.7.2 Protactinium carbides

Lorenz *et al.* (1969) prepared PaC by reduction of Pa_2O_5 with graphite at reduced pressure and temperatures above 1200°C. The product obtained at 1950°C was face-centered cubic (*fcc*) (NaCl type) with $a = (5.0608 \pm 0.0002)$ Å. At 2200°C, some additional weak lines, attributable to PaC_2, were observed; this structure was body-centered tetragonal with $a = (3.61 \pm 0.01)$ Å and $c = (6.11 \pm 0.01)$ Å. According to Sellers *et al.* (1954), PaC was 'probably' prepared by the reduction of PaF_4 with Ba in a carbon crucible. The magnetic susceptibility of PaC between 4 K and room temperature was measured by Hery *et al.* (1977). The magnetic susceptibility of PaC is weak (about -50×10^6 (emu cg)·mol^{-1}) and essentially independent of temperature, which may be taken to indicate the absence of 5f electrons and the presence of Pa(v) in the compound. Theoretical calculations by Maillet (1982) suggest that in ThC 5f electron participation in the bonding is minimal, but that in PaC the 5f electron bonding contribution is important.

4.7.3 Protactinium oxides

The known binary oxides of Pa are listed in Table 4.7. White Pa_2O_5 is obtained when the hydrated oxide, $Pa_2O_5 \cdot nH_2O$, and a wide variety of protactinium compounds as well are heated in oxygen or air above 500°C (Kirby, 1961) or 650°C (Sellers *et al.*, 1954; Keller, 1977). Thermochemical studies (Kleinschmidt and Ward, 1986) and differential thermal analysis shows three endothermic peaks, with maxima at 80, 390, and 630°C, and an exothermic peak, whose maximum occurs at 610°C (Stchouzkoy *et al.*, 1968). Several crystal modifications can be prepared, depending on the temperature to which the Pa_2O_5 is heated (Stchouzkoy *et al.*, 1964, 1966b; Roberts and Walter, 1966).

Black PaO_2 is prepared by the reduction of Pa_2O_5 with H_2 at 1550°C (Sellers *et al.*, 1954). Pa dioxide did not dissolve in H_2SO_4, HNO_3, or HCl solutions but reacted with HF because of the Pa(iv) oxidation to the pentavalent state by O_2 (Pal'shin *et al.*, 1970). Four intermediate phases have been identified by reduction of the pentoxide and oxidation of the dioxide (Roberts and Walter, 1966). A monoxide has been claimed to exist as a coating on metal preparations (Sellers *et al.*, 1954).

The heat of formation of Pa_2O_5 is about 106 kJ mol^{-1} as calculated by Augoustinik (1947). Pa_2O_5 did not dissolve in concentrated HNO_3 (Jones, 1966), but dissolved in HF and in a HF + H_2SO_4 mixture (Codding *et al.*, 1964) and reacted at high temperatures with solid oxides of metals of groups I and II of the periodic table (Pal'shin *et al.*, 1970).

Ternary oxides and oxide phases of different compositions and structures have been prepared by reaction of PaO_2 and Pa_2O_5 with the oxides of other elements (Table 4.8) (Keller, 1964a,b, 1965a–c, 1966a,b, 1971; Keller and Walter, 1965; Keller *et al.*, 1965; Iyer and Smith, 1966).

Table 4.7 *Binary oxides of protactinium.*

Composition	*Symmetry*	*Lattice constants*				*Temp, range of existence* (°C)	*References*
		a (Å)	*b* (Å)	*c* (Å)	α (deg.)		
PaO	cubic (NaCl)	4.961					Sellers *et al.* (1954)
PaO_2	fcc (CaF_2)	5.509					Roberts and Walter (1966)
PaO_2	fcc	5.505					Sellers *et al.* (1954)
$PaO_{2.18}$–$PaO_{2.21}$	fcc	5.473					Roberts and Walter (1966)
$PaO_{2.33}$	tetragonal	5.425		5.568			Roberts and Walter (1966)
$PaO_{2.40}$–$PaO_{2.42}$	tetragonal	5.480		5.416			Roberts and Walter (1966)
$PaO_{2.42}$–$PaO_{2.44}$	rhombohedral	5.449			89.65		Roberts and Walter (1966)
Pa_2O_5	fcc	5.446				650–700	Sellers *et al.* (1954)
Pa_2O_5	tetragonal	5.429		5.503		700–1000	Roberts and Walter (1966)
Pa_2O_5	tetragonal	10.891		10.992		700–1050	Stchouzkoy *et al.* (1968)
Pa_2O_5	hexagonal	3.820		13.225		1050–1500	Stchouzkoy *et al.* (1968)
Pa_2O_5	hexagonal	3.817		13.220		1000–1500	Roberts and Walter (1966)
Pa_2O_5	orthorhombic	6.92	4.02	4.18		?	Sellers *et al.* (1954)
Pa_2O_5	rhombohedral	5.424			89.76	1240–1400	Roberts and Walter (1966)

Table 4.8 *Polynary oxides of protactinium* (*Keller*, 1966*a*, 1971; *Palshin* et al., 1970).

Compound	*Structure type*	*Lattice constants*			
		a (Å)	*b* (Å)	*c* (Å)	*β* (deg.)
$LiPaO_3$	unknown				
Li_3PaO_4	tetragonal (Li_3UO_4)	4.52		8.48	
Li_7PaO_6	hexagonal (Li_7BiO_6)	5.55		15.84	
$(2–4)Li_2O \cdot Pa_2O_5$	cubic (fluorite phase)				
$(2–4)Na_2O \cdot Pa_2O_5$					
$NaPaO_3$	orthorhombic ($GdFeO_3$)	5.82	5.97	8.36	
Na_3PaO_4	tetragonal (Li_3SbO_4)	6.68			
$KPaO_3$	cubic ($CaTiO_3$)	4.341			
$RbPaO_3$	cubic ($CaTiO_3$)	4.368			
$CsPaO_3$	unknown				
$BaPaO_3$[a]	cubic ($CaTiO_3$)	4.45			
$SrPaO_3$[a]	unknown				
$Ba(Ba_{0.5}Pa_{0.5})O_{2.75}$	cubic (Ba_3WO_6)	8.932			
$GaPaO_4$	unknown				
$(La_{0.5}Pa_{0.5})O_2$	cubic (CaF_2)	5.525			
$Ba(LaO_{0.5}Pa_{0.5})O_3$	cubic (Ba_3WO_6)	8.885			
α-$PaGeO_4$	tetragonal ($CaWO_4$)	5.106		11.38	
β-$PaGeO_4$[a]	tetragonal ($ZrSiO_4$)	7.157		6.509	
α-$PaSiO_4$[a]	tetragonal ($ZrSiO_4$)	7.068		6.288	
β-$PaSiO_4$[a]	monoclinic ($CePO_4$)	6.76	6.92	6.54	104.83
Pa_2O_5/ThO_2	cubic (fluorite phase)				
$PaO_2 \cdot 2Nb_2O_5$[a]	tetragonal ($Th_{0.25}NbO_3$)	7.76		7.81	
$PaO_2 \cdot 2Ta_2O_5$[a]	tetragonal ($Th_{0.25}NbO_3$)	7.77		7.79	
$Pa_2O_5 \cdot 3Nb_2O_5$	hexagonal ($UTa_3O_{0.67}$)	7.48		15.81	
$Pa_2O_5 \cdot 3Ta_2O_5$	hexagonal ($UTa_3O_{10.67}$)	7.425		15.76	

[a] Could not be prepared in the pure state; always contained varying amounts of Pa(v).

The pale yellow product, which precipitates upon addition of H_2O_2 to a solution of Pa(v) in 0.25 M H_2SO_4, has been assigned the formula $Pa_2O_9 \cdot 3H_2O$ (Stchouzkoy *et al.*, 1966b). It is considered to be an unstable peroxide with a composition that varies with time over the range $Pa_2O_x \cdot 3H_2O$ with $5 < x < 9$.

4.7.4 Protactinium halides

Methods for preparing all the binary halides and many of the oxyhalides of Pa(iv) and Pa(v) are summarized schematically in Figs. 4.11, 4.12, and 4.13; those compounds which have been fully characterized are listed in Table 4.9. The preparative methods shown in Figs. 4.11 and 4.12 use an aqueous acid solution of Pa(v) as the starting material for the synthesis of binary protactinium halides. PaF_5 can be prepared by fluorination of PaC at 570 K or $PaCl_5$ at 295 K. The reaction products are isostructural with β-UF_5 (Brown *et al.*, 1982a). $PaF_5 \cdot 2H_2O$ is prepared by the evaporation of Pa solution in 30% HF

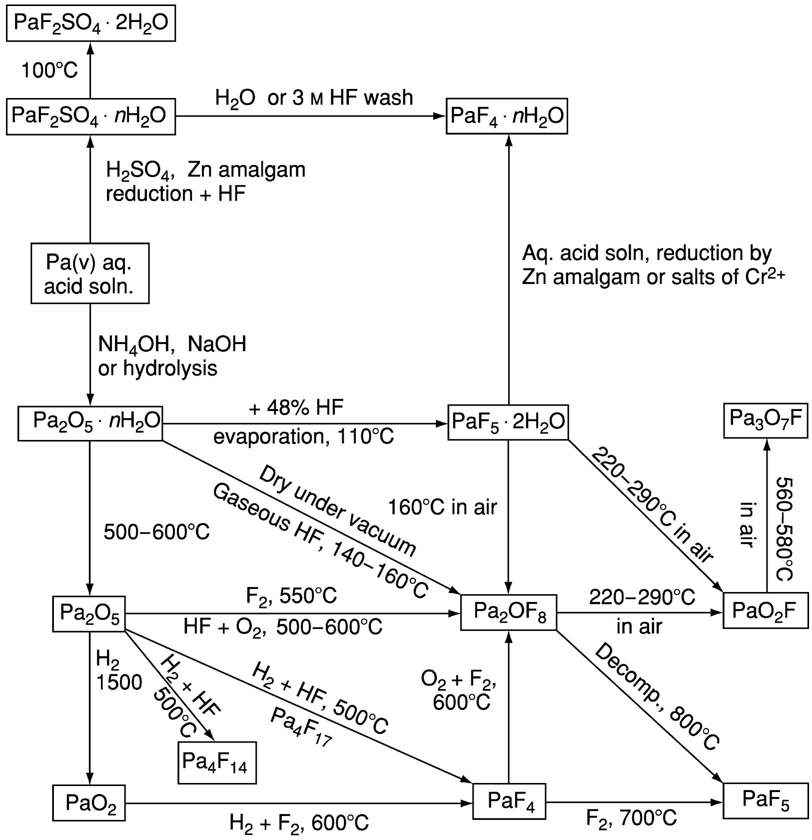

Fig. 4.11 *Preparation of some fluoride derivatives of Pa*(*IV*) *and Pa*(*V*) (*Muxart and Guillaumont*, 1974; *Pal'shin* et al., 1968a).

(Grosse, 1934c). Protactinium carbide is also useful in the preparation of other binary penta- and tetrahalides. Brown *et al.* (1976a) treated PaC with I_2 at 400°C, Br_2 at 350°C, and $SOCl_2$ at 200°C to obtain PaI_5, $PaBr_5$, and $PaCl_5$, respectively. PaI_4 was obtained by reaction of PaC with PaI_5 at 600°C or by the treatment with HgI_2 at 500°C. These compounds were also prepared by reactions of Pa_2O_5 with $Cl_2 + CCl_4$ at 300°C ($\rightarrow PaCl_5$) (Pissot *et al.*, 1966); CCl_4 at 400°C ($\rightarrow PaCl_4$) (Sellers *et al.*, 1954); $AlBr_3$ at 317°C ($\rightarrow PaBr_5$); and AlI_3 at $\leq$300°C ($\rightarrow PaI_5$) (D'Ege *et al.*, 1963) and so on.

Protactinium pentafluoride is reduced to PaF_4 by PF_3 but no reaction occurs with AsF_3. $PaCl_5$ and $PaCl_4$ are formed from PaF_5 and PaF_4 by reaction with PCl_3 and $SiCl_4$, respectively. PaF_5 reacts with CCl_4 to give $PaCl_xF_{5-x}$ (x probably 1), but no reaction is observed with PaF_4 (O'Donnell *et al.*, 1977). Whereas UF_5 is very soluble in acetonitrile, PaF_5 forms a sparingly soluble complex. An adduct $PaF_5 \cdot 2Ph_3PO$ forms on addition of TPPO to PaF_5 in acetonitrile

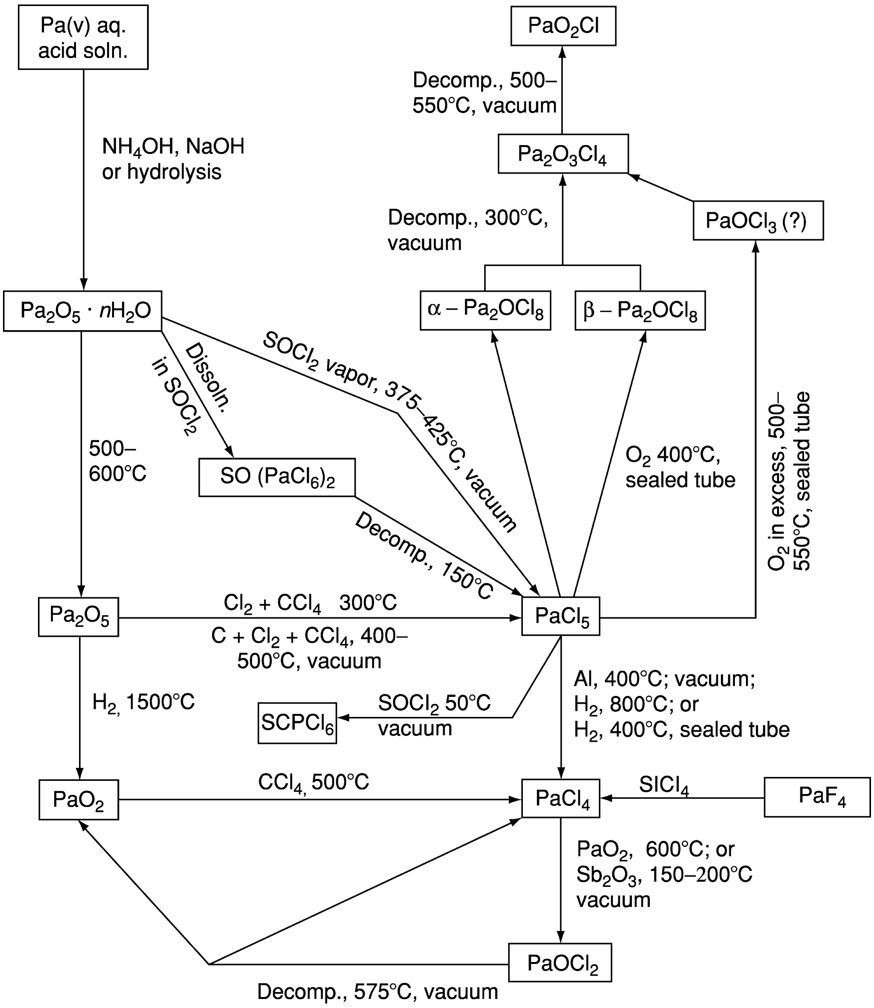

Fig. 4.12 *Preparation of some chlorides and oxychlorides of Pa*(IV) *and Pa*(V) (*Muxart and Guillaumont*, 1974; *Pal'shin* et al., 1968*a*).

(Brown *et al.*, 1982b). Brown (1979) found still another $PaBr_5$ crystal structure, designated γ, isostructural with β-UCl_5.

Of the possible halides of Pa(III), only PaI_3 has been reported so far (Scherer *et al.*, 1967). It is a dark brown compound (not black as originally reported) (Wilson, 1967), prepared by heating PaI_5, for several days at 10^{-6} torr and 360–380°C. Its tentative identification is based primarily on the similarity of its X-ray powder pattern to that of CeI_3.

All the binary halides are volatile at moderate temperatures, a property that has been used for the separation of ^{233}Pa from irradiated ThO_2 as well as for the

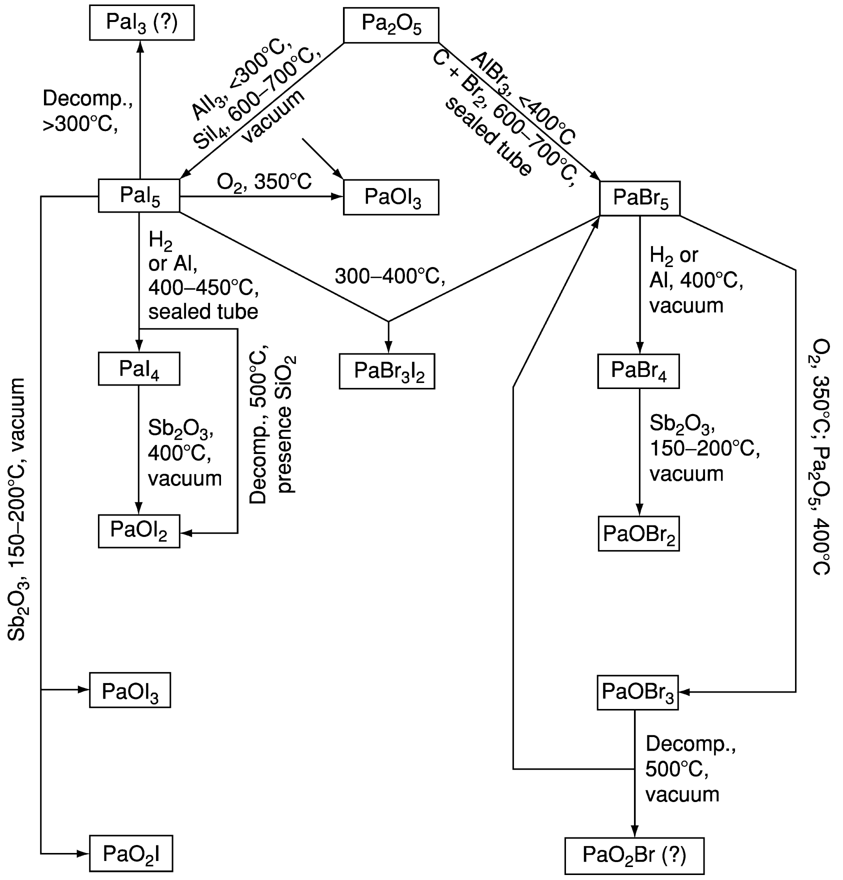

Fig. 4.13 *Preparation of some bromide and iodide derivatives of Pa(IV) and Pa(V) (Muxart and Guillaumont*, 1974; *Pal'shin* et al., 1968*a*).

preparation of radiochemically pure ^{231}Pa and ^{234}Pa (Malm and Fried, 1950; Merinis *et al.*, 1966; Brown, 1971). The vapor pressures of $PaCl_5$ and $PaBr_5$ have been measured by Weigel *et al.* (1969, 1974) in the temperature range 490–635 K; the boiling points, extrapolated to 760 torr, were 420 and 428°C, respectively. The thermal stability studies of Brown and co-workers (1976b) show that PaI_4 is stable up to a temperature of 330°C, and that PaI_5 is stable to 200–300°C.

Numerous alkali fluoro complexes of Pa(v) have been identified (Table 4.10). The first, K_2PaF_7, was prepared by Grosse (1934a) for use in determining the atomic weight of ^{231}Pa. Complexes of the form $MPaF_6$ (M = Li, Na, K, Rb, Cs, Ag, NH_4) can be prepared by crystallization from aqueous HF solutions containing equimolar amounts of Pa(v) and the alkali fluorides, but $LiPaF_6$ and $NaPaF_6$ are best prepared by evaporating the equimolar mixture to dryness and

Table 4.9 *Halides and oxyhalides of protactinium.*

Compound	*Symmetry*	*Structure type or space group*	*Lattice constants*				*References*
			a (Å)	*b* (Å)	*c* (Å)	*Angle* (deg.)	
PaF_4	monoclinic	UF_4	12.86	10.88	8.54	$\beta = 126.34$	Soddy and Cranston (1918); Sellers *et al.* (1954); Asprey *et al.* (1967)
Pa_2F_9 (or Pa_4F_{17})	bcc cubic	U_2F_9	8.507				Brown (1966); Stein (1966)
PaF_5	tetragonal	β-UF_5	11.525		5.218		Brown (1971)
			11.53		5.19		Stein (1964)
Pa_2OF_8	bcc	U_2F_9	8.406				Stein (1964)
							Brown and Easey (1970)
PaO_2F	orthorhombic	–	6.894	12.043	4.143		Brown and Easey (1970)
Pa_3O_7F	orthorhombic	$Cmm2(C_{20}^{11})$	6.947	12.030	4.203		Brown and Easey (1970)
$PaCl_4$	tetragonal	UCl_4	8.377		7.479		Brown and Jones (1967c)
					7.482		Sellers *et al.* (1954)
$PaCl_5$	monoclinic	C2/*c*	10.35	12.31	8.82	$\beta = 111.8$	Brown and Maddock (1963)
$PaOCl_2$	orthorhombic	*Pbam*	15.332	17.903	4.012		Dodge *et al.* (1968); Bagnall *et al.* (1968a)
$PaBr_4$	tetragonal	UCl_4	8.824		7.957		Brown and Jones (1967c)
α-$PaBr_5$	monoclinic	$P2_1/c$	12.69	12.82	9.92	$\beta = 108$	Brown and Petcher (1969)
β-$PaBr_5$	monoclinic	$P2_1/n$	8.385	11.205	8.950	$\beta = 91.1$	Brown *et al.* (1968b); Brown and Petcher (1969)
γ-$PaBr_5$	triclinic	P1	7.52(1)	10.21(1)	6.74(1)	$\alpha = 89.27(5)$; $\beta = 117.55(6)$; $\gamma = 109.01(5)$	Merinis *et al.* (1966)
			9.25	12.12	9.13		D'Ege *et al.* (1963)
$PaOBr_3$	monoclinic	C2	16.911	3.871	9.334	$\beta = 113.67$	Brown *et al.* (1968b)
PaI_3(?)	orthorhombic	CeI_3	4.33	14.00	10.02		Scherer *et al.* (1967)
PaI_4							Brown *et al.* (1976b)
PaI_5	orthorhombic	–	7.22	21.20	6.85		Maddock (1960)
PaO_2I	hexagonal	–	12.64		4.07		Brown *et al.* (1967b)

Table 4.10 *Some fluoro complexes of Pa(IV) and Pa(V).*

Compound	*Symmetry*	*Structure type or space group*	*Lattice constant*				*References*
			a (Å)	*b* (Å)	*c* (Å)	*Angle* (deg.)	
$LiPaF_5$	tetragonal	$LiUF_5$	14.96		6.58		Asprey *et al.* (1967)
$Na_7Pa_6F_{31}$	rhombohedral	$Na_7Zr_6F_3$,	9.16			$\alpha = 107.09$	Asprey *et al.* (1967)
$K_7Pa_6F_{31}$	rhombohedral	$Na_7Zr_6F_3$,	9.44			$\alpha = 107.15$	Asprey *et al.* (1967)
$Rb_7Pa_6F_{31}$	rhombohedral	$Na_7Zr_6F_{31}$	9.64			$\alpha = 107.00$	Asprey *et al.* (1967)
$(NH_4)_4PaF_8$	monoclinic	–	13.18	6.71	13.22	$\beta = 17.17$	Asprey *et al.* (1967)
$NaPaF_6$	tetragonal	–	5.35		3.98		Asprey *et al.* (1966)
NH_4PaF_6	orthorhombic	$RbPaF_6$	5.84	11.90	8.03		Asprey *et al.* (1966); Brown (1973)
$KPaF_6$	orthorhombic	$RbPaF_6$	5.64	11.54	7.98		Asprey *et al.* (1966); Brown (1973)
$RbPaF_6$	orthorhombic	*Cmca*	5.86	11.97	8.04		Asprey *et al.* (1966); Brown (1973)
$CsPaF_6$	orthorhombic	$RbPaF_6$	6.14	12.56	8.06		Asprey *et al.* (1966); Brown (1973)
K_2PaF_7	monoclinic	*C2/c*	13.760	6.742	8.145	$\beta = 125.17$	Brown and Easey (1966)
Cs_2PaF_7	monoclinic	K_2PaF_7	14.937	7.270	8.266	$\beta = 125.32$	Brown *et al.* (1967a)
Li_3PaF_8	tetragonal	$P4_22_12(D^6)$	10.386		10.89		Brown and Easey (1965, 1966)
Na_3PaF_8	tetragonal	14 *mmm*	5.487		10.89		Brown and Easey (1965, 1966)
K_3PaF_8	fcc	F*m3m*	9.235				Brown and Easey (1966)
Cs_3PaF_8	fcc	F*m3m*	9.937				Brown and Easey (1966)
Rb_3PaF_8	fcc	F*m3m*	9.6				Asprey *et al.* (1966); Brown (1973)

fluorinating the dried residue (Asprey *et al.*, 1966). The heptafluoroprotactinates, M_2PaF_7 (M = K, NH_4, Rb, Cs), are precipitated by the addition of acetone to a 17 M HF solution containing Pa(v) and an excess of the appropriate alkali fluoride. NaF in a 3:1 molar ratio to Pa(v) yields Na_3PaF_8, but the other octafluoroprotactinates (v) are most easily prepared by the reaction:

$$M_2PaF_7 + MF \rightarrow M_3PaF_8$$

at 450°C in an atmosphere of dry argon or by fluorination of the product obtained by evaporation of an HF solution containing 3:1 MF and Pa(v) (Brown and Easey, 1966).

The fluoro complexes of Pa(IV) are prepared either by H_2 reduction of a Pa(v) complex at 450°C or by heating stoichiometric amounts of the alkali fluoride with PaF_4 in a dry argon atmosphere (Asprey *et al.*, 1967).

$Pa_2O_5 \cdot nH_2O$ reacts vigorously with $SOCl_2$ at room temperature to yield stable solutions containing up to 0.5 M Pa(v). The product is probably $SO(PaCl_6)_2$ which decomposes at 150°C under vacuum. Hexa- and octachloroprotactinates (v) are precipitated when CS_2 is added to $SOCl_2$ solutions containing equal amounts of $PaCl_5$ and MCl (M = $N(CH_3)_4$, $N(C_2H_5)_4$, $NH_2(CH_3)_2$, and $(C_6H_5)_4As$). Hexachloro complexes with Cs^+ and NH_4^+ precipitate when the component halides are reacted in $SOCl_2$/ICl mixtures (Bagnall and Brown, 1964). Hexabromoprotactinate (v) complexes, $MPaBr_6$ (M = $N(CH_3)_4$, $N(C_2H_5)_4$), have been prepared by vacuum evaporation of stoichiometric quantities of $PaBr_5$ and the tetraalkylammonium bromide dissolved in anhydrous CH_3CN (Brown and Jones, 1967b).

Axe and co-workers (Axe, 1960, Axe *et al.*, 1960, Axe *et al.*, 1961) observed the paramagnetic resonance spectrum of Pa^{4+} in single crystal of Cs_2ZrCl_6, crystallized from a melt containing approximately 500 μg of $^{231}PaCl_4$. The $5f^1$ structure was confirmed, as was the nuclear spin of 3/2. The resonance spectrum was found to be isotropic, with a spectroscopic splitting factor $g = -1.14$. Hendricks *et al.* (1971) measured the magnetic susceptibility of $PaCl_4$ from 3.2 to 296 K and found a ferromagnetic transition at about 182 K.

$PaCl_4$ is virtually insoluble in $SOCl_2$, but hexachloro- and hexabromoprotactinates (IV), M_2PaX_6 (X = Cl, Br; M = $N(CH_3)_4$ and $N(C_2H_5)_4$), have been prepared by reaction of PaX_4 with the tetraalkylammonium halide in CH_3CN. Cs_2PaCl_6 is precipitated on the addition of CsCl to a solution of $PaCl_4$ in concentrated HCl. The hexaiodo complex, $[(C_6H_5)_3CH_3As]_2PaI_6$, was also prepared from the component iodides dissolved in CH_3CN (Brown and Jones, 1967a). The electronic structures and optical transition energies of PaX_6^{2-} (X = F, Cl, Br, I) were calculated by quasi-relativistic density functional methods (Kaltsoyannis and Bursten 1995; Kaltsoyannis 1998). Analysis of the $5f^1 \rightarrow 6d^1$ transitions in PaX_6^{2-} (X = Cl, Br) and $ThBr_4:Pa^{4+}$ was reported by Edelstein *et al.* (1988), and the EPR spectra of $ThBr_4:Pa^{4+}$ in the incommensurate phase was detected (Zwanenburg *et al.*, 1988). The fluorescence and absorption spectra between the ground $5f^1$ and the excited $6d^1$ configurations of

Pa^{4+} diluted into a single crystal of Cs_2ZrCl_6 were analyzed (Piehler *et al.*, 1991; Edelstein *et al.*, 1992).

Numerous halide complexes of Pa(IV) and Pa(V) are formed with oxygen donor ligands, such as substituted phosphine oxides (Brown *et al.*, 1966b, 1970a,b), hexamethylphosphoramide (Brown and Jones, 1966a), DMSO (Bagnall *et al.*, 1968b), tropolone (Brown and Rickard, 1970), *N*,*N*-dimethylacetamide (Bagnall *et al.*, 1969), acetylacetone (Brown and Rickard, 1971b), and *N*,*N*-diethyldithiocarbamate (Heckley *et al.*, 1971). In addition, complexes with sulfur and selenium donors have been reported (Brown *et al.*, 1971).

The ground state electronic structures of PaX_6^{2-} (X = F, Cl, Br, I), UX_6^- (X = F, Cl, Br), and NpF_6 have been calculated using both non-relativistic and relativistic implementations of the discrete-variational X alpha (DV-X alpha) method. A significant amount of metal–ligand covalent bonding is found, involving both 6d and 5f metal orbitals. The 5f contribution to the bonding levels increases significantly from PaX_6^{2-} to UX_6^- to NpX_6 but remains approximately constant as the halogen is altered in PaX_6^{2-} and UX_6^-. In contrast, the 6d atomic orbital character of the halogen-based levels increases from UF_6^- to UBr_6^- and a similar, though less marked, trend is observed in PaX_6^{2-}. The electronic transition energies have been calculated using the transition-state method. The relativistic calculations are far superior to the non-relativistic ones in both qualitatively and quantitatively describing the electronic spectra. The stabilization of the metal 5f atomic orbitals with respect to the halogen *n*p levels from Pa to Np results in the more energetic $f \rightarrow f$ transitions in NpF_6 being masked by the onset of a ligand-to-metal charge transfer band. In the remaining molecules, the $f \rightarrow f$ transitions occur well removed from charge transfer bands (Kaltsoyannis, 1998).

Several chloro complexes and one bromo complex for which crystallographic data are available are listed in Table 4.11.

4.7.5 Protactinium pnictides

Protactinium pnictide compounds have been prepared and constitute a new category of Pa compounds that have several features of more than usual interest. The protactinium phosphide, PaP_2, was prepared by reaction of elemental phosphorus with protactinium hydride; thermal dissociation of PaP_2 forms Pa_3P_4 (Table 4.12) (Wojakowski *et al.*, 1982). The diarsenide, $PaAs_2$, can be obtained by heating together PaH_3 and elemental arsenic at 400°C; heating $PaAs_2$ to 840°C results in decomposition of $PaAs_2$ to form Pa_3As_4 (Hery *et al.*, 1978). $PaAs_2$ has a tetragonal structure of the anti-Fe_2As type, and Pa_3As_4 crystallizes in a body-centered structure of the Th_3P_4-type (Table 4.12). Single crystals of $PaAs_2$, Pa_3As_4, PaAs, and Pa_3Sb_4 were prepared from the elements by a Van Arkel procedure using vapor transport; iodine was the transporting agent and deposition occurred on an induction-heated tungsten support (Calestani *et al.*, 1979a,b). Hery and co-workers (1979) have obtained Pa_3Sb_4 and $PaSb_2$ by heating PaH_3 with antimony.

Table 4.11 *Some chloro and bromo complexes of Pa(IV) and Pa(V).*

		Lattice constants				
Compound	*Symmetry*	*a* (Å)	*b* (Å)	*c* (Å)	*Angle* (deg.)	*References*
Cs_2PaCl_6	trigonal	7.546		6.056		Brown and Jones (1967a)
$(NMe_4)_2PaCl_6$	fcc	13.08				Brown and Jones (1967a)
$(NEt_4)_2PaCl_6$	orthorhombic	14.22	14.75	13.35		Brown and Jones (1966a,b)
$(NMe_4)_2PaBr_6$	fcc	13.40				Brown and Jones (1967a,b)
$Pa(Trop)_4Cl$,DMSO	triclinic	9.87	12.60	15.96	$\alpha = 119.8$; $\beta = 103.6$; $\gamma = 103.0$	Brown and Rickard (1970)
$(NEt_4)_2PaOCl_5$	monoclinic	14.131	14.218	13.235	$\beta = 91.04$	Brown and Rickard (1971a); Brown *et al.* (1972)
$Pa(Acac)_2Cl_3$	monoclinic	8.01	23.42	18.63	$\beta = 98.9$	Bagnall *et al.* (1969)

Me, methyl; Et, ethyl; Trop, tropolonate; DMSO, dimethyl sulfoxide; Acac, acetylacetonate.

Table 4.12 *Crystallographic data for some miscellaneous compounds of protactinium.*

		Lattice parameters				
Compound	*Symmetry*	*a* (Å)	*b* (Å)	*c* (Å)	γ (deg.)	*References*
$H_3PaO(SO_4)_3$	hexagonal	9.439		5.506		Bagnall *et al.* (1965)
$H_3PaO(SeO_4)_3$	hexagonal	9.743		5.679		Bagnall *et al.* (1965)
PaOS	tetragonal	3.832		6.704		Sellers *et al.* (1954)
$[N(C_2H_5)_4]_4Pa(NCS)_8$	tetragonal	11.65		23.05		Al-Kazzaz *et al.* (1972)
$[N(C_2H_5)_4]_4Pa(NCSe)_8$	tetragonal	11.82		23.49		Al-Kazzaz *et al.* (1972)
$Pa(HCOO)_4$	tetragonal	7.915		6.517		Bohres (1974); Greis *et al.* (1977)
$HPaOP_2O_7$	fcc	5.92				LeCloarec (1974)
$(PaO)_4(P_2O_7)_3$	monoclinic	12.23	13.44	8.96	113.88	LeCloarec (1974); Lux *et al.* (1980)
$Pa_2O_5{\cdot}Pa_2O_5$	orthorhombic	5.683	12.06	14.34		LeCloarec (1974); Lux *et al.* (1980)
PaP_2	tetragonal	3.898		7.845		Bhandari and Kulkarni (1979)
[a]$Pa(Trop)_5$	tetragonal	9.759		9.46		Bhandari and Kulkarni (1979)

[a] Trop, tropolone.

The magnetic susceptibility of $PaAs_2$ and $PaSb_2$ has been measured from 4 K to room temperature. PaAs, $PaAs_2$, and $PaSb_2$ exhibit temperature-independent paramagnetism (Hery *et al.*, 1978). Self-consistent band structure calculations show that PaN and PaAs have about one f-electron, and hence they are expected to be paramagnetic; these results have been confirmed by experiment (Hery, 1979; Brooks *et al.*, 1980).

4.7.6 Miscellaneous compounds

Pa_2O_5 is insoluble in nitric acid but the freshly prepared hydroxide, the pentachloride, the pentabromide, and the complex $SO(PaCl_6)_2$ all dissolve in fuming HNO_3 to form stable solutions of at least 0.5 M Pa(V). Vacuum evaporation of such solutions yields $PaO(NO_3)_3 \cdot xH_2O$ $(1 < x < 4)$. The reaction of Pa(V) halides with N_2O_5 in anhydrous CH_3CN yields $Pa_2O(NO_3)_4 \cdot 2CH_3CN$. Complexes of the type $MPa(NO_3)_6$ (M = Cs, $N(CH_3)_4$, $N(C_2H_5)_4$) have been prepared by reaction of the hexachloroprotactinates (V) with liquid N_2O_5 at room temperature (Brown and Jones, 1966b; Jones, 1966).

When a solution of Pa(V) in a mixture of HF and H_2SO_4 is evaporated until all F^- ion has been eliminated, $H_3PaO(SO_4)_3$ crystallizes almost quantitatively. The analogous selenato complex, more stable in acid (6 M HCl) or basic (NH_4OH) media, is obtained from HF/H_2SeO_4 mixtures. The sulfato-complex decomposes to $HPaO(SO_4)$ at 375°C (Bagnall *et al.*, 1965; Bagnall, 1966b) and to Pa_2O_5 at 750°C (Pal'shin *et al.*, 1968b). The binary chalcogenides, β-PaS_2 and γ-$PaSe_2$, have been prepared by Hery (1979). PaOS was obtained by the reaction of $PaCl_5$ with a mixture of H_2S and CS_2 at 900°C (Sellers *et al.*, 1954). $PaF_2SO_4 \cdot 2H_2O$ is precipitated when a solution of Pa(IV) in 4.5 M H_2SO_4 is added to 3 M HF (Stein, 1966). Crystallographic data for some S and Se compounds are given in Table 4.12.

The addition of hydrochloric acid to a solution of Pa(V) oxalate causes the precipitation of $PaO(C_2O_4)(OH) \cdot xH_2O$ $(x \sim 2)$ (Muxart *et al.*, 1966a). On the other hand, the addition of acetone instead of acid yields $Pa(OH)(C_2O_4)_2 \cdot 6H_2O$ (Davydov and Pal'shin, 1967).

Phenylarsonic acid forms a white flocculent precipitate with Pa(V) in neutral or acid solutions. The compound is believed to have the composition $H_3PaO_2(C_6H_6AsO_3)_2$ (Myasoedov *et al.*, 1968c).

Complexes of the type $[N(C_2H_5)_4]_4PaR_8$ (R = NCS or NCSe) have been prepared by reaction of $PaCl_4$ with stoichiometric amounts of KCNS or KCNSe in anhydrous CH_3CN (Table 4.12) (Al-Kazzaz *et al.*, 1972). The bis(phthalocyaninato)complexes of Pa(IV), $(C_{32}H_{16}N_8)_2Pa$, have been prepared by neutron irradiation of the corresponding thorium $^{233}ThPc_2$ complex by the reactions (Lux *et al.*, 1970, 1971):

$$^{232}ThPc_2(n,\gamma)\,^{233}ThPc_2 \rightarrow {}^{233}PaPc_2 + \beta^-$$

Spectroscopically pure bis(phthalocyaninato)protactinium(IV) ($PaPc_2$) was prepared by reaction between $PaI_4 \cdot 4CH_3CN$ and *o*-phthalic dinitrile in

1-chloronaphthalene followed by purification by sublimation. $PaPc_2$ is isostructural with $ThPc_2$ and UPc_2 (Lux *et al.*, 1980). Tetrakis(cyclopentadienyl)Pa(IV), $(C_5H_5)_4Pa$, was prepared by treating Pa_2O_5 with a mixture of $Cl_2 + CCl_4$ in an argon stream at 600°C, then fusing the reaction product with $Be(C_2H_5)_2$ at 65°C (Keller, 1964b; Baumgartner *et al.*, 1969). Protactinium(IV) tropolone, $Pa(Trop)_4$, has been prepared by reaction of $PaCl_4$ or $PaBr_4$ with lithium tropolonate, Li(Trop) in methylene chloride; in the presence of excess Li (Trop) in dimethyl formamide, $LiPa(Trop)_5$ is formed (Brown and Richard, 1970). However, when protactinium pentethoxide, which is obtained by reaction of $PaCl_5$ with sodium ethoxide in anhydrous alcohol (Maddock and Pires deMatos, 1972; Bagnall *et al.*, 1975), is treated with tropolone, the complex Pa $(Trop)_5$ is obtained. $Pa(Trop)_5$ has been crystallized and its crystal structure parameters are determined (Table 4.12) (Bhandari and Kulkarni, 1979). Complexes of the actinide elements with cyclooctatetrene have been obtained by reaction of an actinide halide with cyclooctatetrene anion. The bis(η^8-tetramethylcyclooctatetradiene) complex of Pa has been prepared by reaction of Pa borohydride, $Pa(BH_4)_4$, with tetramethylcyclooctatetrene dianion (Solar *et al.*, 1980). The preparation of the anhydrous tetraformate, $Pa(HCOO)_4$, has been reported by the reaction of $PaCl_4$ with O_2-free HCOOH at 60°C in an argon atmosphere for 4 h (Table 4.12) (Bohres, 1974; Bohres *et al.*, 1974).

Freshly precipitated Pa(V) hydroxide or peroxide dissolves readily in 14 M H_3PO_4. However, upon aging, the hydrated orthophosphate, $PaO(H_2PO_4)_3 \cdot 2H_2O$, crystallizes out. Calcination of this product yields, successively: the anhydrous orthophosphate, $PaO(H_2PO_4)_3$ between room temperature and 300°C; the trimetaphosphate, $PaO(PO_3)_3$, stable to 900°C; the pyrophosphate, $(PaO)_4(P_2O_7)_3$, at 1000°C; and an unidentified phase with the gross composition $Pa_2O_5 \cdot P_2O_5$ at 1200°C (LeCloarec *et al.*, 1970, 1976; LeCloarec and Muxart, 1971; LeCloarec, 1974). Crystallographic data for several phosphates are given in Table 4.12. Protactinium(V) perrhenate, $PaO(ReO_4)_3 \cdot xH_2O$, has been prepared by reaction of Pa_2O_5 and Re_2O_7 (Silvestre *et al.*, 1977).

Protactinium(IV) borohydride, $Pa(BH_4)_4$, has been prepared by treating PaF_4 with aluminum borohydride, $Al(BH_4)_3$. It is a relatively unstable solid at 20°C, but exhibits high volatility as do other actinide borohydrides. $Pa(BH_4)_4$ is isostructural with $U(BH_4)_4$ (Banks *et al.*, 1978; Banks, 1979; Banks and Edelstein, 1980). The molecular compound, $Pa(BH_3CH_3)_4$, has been synthesized from the reaction of $PaCl_5$ or $PaCl_4$ with $Li(BH_3CH_3)$. Its optical and NMR spectra have been obtained. Because of the T_d symmetry at the Pa^{4+} site, the dipolar shift is zero and the temperature-dependent proton and ^{11}B shifts are attributed to spin delocalization mechanisms. The ^1H NMR peaks of both the bridging and terminal protons shift to lower field as the temperature is decreased. These observations are inconsistent with a spin-polarization mechanism, which assumes that the temperature-dependent shifts are proportional to the average value of the electron spin in the 5f orbitals. In addition, new synthetic routes to $Pa(BH_4)_4$ and $Pa(MeCp)_4$ (MeCp = methylcyclopentadienyl) are described. They are simpler and more convenient than the earlier published methods and take advantage of the unexpected solubility of $PaCl_5$ in aromatic hydrocarbons (Kot and Edelstein, 1995). The 5f–6d absorption spectrum of $Pa^{4+}/CsZrCl_6$ (Edelstein *et al.*, 1992) and magnetic data of tetravalent protactinium(IV) (Edelstein and Kot, 1993) also were reported.

4.8 SOLUTION CHEMISTRY

Two oxidation states, Pa(IV) and Pa(V), have been definitely established in aqueous solution (Haïssinsky and Bouissières, 1948, 1951; Bouissières and Haïssinsky, 1949), but all attempts to demonstrate the existence of Pa(III) in solution have led to negative or inconclusive results (Elson, 1954; deMiranda and Maddock, 1962; Musikas, 1966). Both Pa(IV) and Pa(V) show strong tendencies to hydrolyze in the absence of complexing agents and most studies of the ionic species of Pa in aqueous solution have therefore been carried out at the tracer level. Furthermore, the instability of Pa(IV) toward reoxidation has made it difficult to obtain reproducible data on this oxidation state, so that, until quite recently, little quantitative information has been available about the aqueous chemistry of Pa(IV).

The behavior of protactinium in aqueous solution has been very thoroughly reviewed by Guillaumont, Bouissières, and Muxart (Guillaumont *et al.*, 1968; Bouissières, 1971; Muxart and Guillaumont, 1974) and by Pal'shin *et al.* (1970); those reviews should be consulted for more detail than can be given here. For a general discussion of the techniques used in the determination of stability constants, see Rossotti and Rossotti (1961), Fronaeus (1963), or Ahrland *et al.* (1973).

4.8.1 Hydrolysis of Pa (V) in non-complexing media

The hydrolytic behavior of Pa(V) has been studied by a large number of investigators (Jakovac and Lederer, 1959; Guillaumont, 1966a, 1971; Liljenzin and Rydberg, 1966; Scherff and Hermann, 1966; Suzuki and Inoue, 1966, 1969; Kolarich *et al.*, 1967; Mitsuji and Suzuki, 1967; D'yachkova *et al.*, 1968a; Mitsuji, 1968; Liljenzin, 1970; Cazaussus *et al.*, 1971) whose conclusions are summarized schematically in Figs. 4.14 and 4.15 (Bouissières, 1971).

The hydrolysis of Pa(V) is usually studied in perchloric acid solutions, because ClO_4^- is considered to be a non-complexing anion. However, the presence of small amounts of weakly complexing anions does not affect the results. Thus, <0.5 M HNO_3, <1 M HCl, <0.01 M H_2SO_4, or <0.01 M $H_2C_2O_4$, are all equivalent to $HClO_4$ of the same acidity.

In solutions of constant ionic strength ($\mu = 3$; 10^{-5} M$<$ $[H^+] < 3$ M), the least hydrolyzed cation is $PaOOH^{2+}$. At $[H^+] < 1$ M, $PaO(OH)_2^+$ begins to form and becomes predominant at pH ~3. At higher pH values, the neutral species, $Pa(OH)_5$, is formed. At tracer levels these species are in equilibrium (Fig. 4.14), but, at concentrations of Pa(V) close to saturation, polymers are

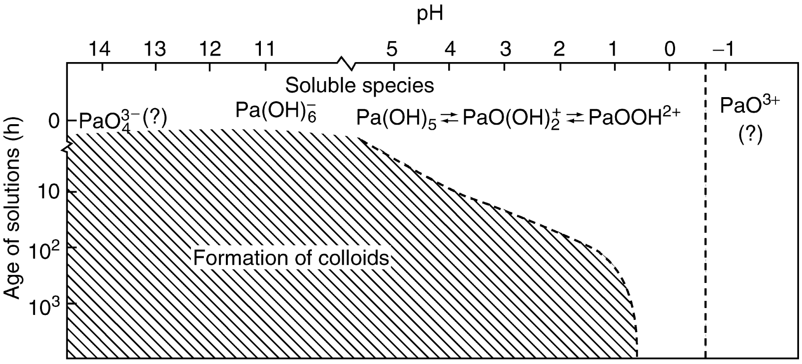

Fig. 4.14 *Hydrolysis of tracer-level Pa(v) in $HClO_4$ solution (Bouissières,* 1971).

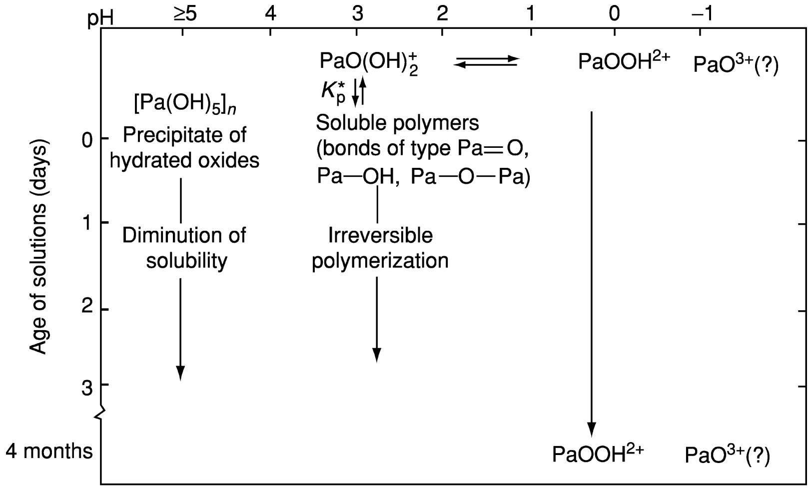

$K_p^* = [Pa_p]/[Pa_{p-1}][PaO(OH_2^+] \approx 3 \times 10^7$, with $Pa_p \equiv$ polymers of p atoms

Fig. 4.15 *Hydrolysis of Pa(v) in $HClO_4$ solution at* $[Pa(v)] = 10^{-5}$ M *(Bouissières,* 1971).

formed, a process that rapidly becomes irreversible (Fig. 4.15). At pH 5–6, the hydrated oxide is precipitated. In alkaline solution ($\mu = 0.1$) minute concentrations of $Pa(OH)_6^-$ are formed, and at $[H^+] \geq 3$ M the existence of PaO^{3+} has been suggested.

The hydrolysis reactions of Pa(v) may be written as:

$$PaO^{3+} + H_2O \leftrightarrow PaO(OH)^{2+} + H^+ \qquad (4.1)$$

$$PaO(OH)^{2+} + H_2O \leftrightarrow PaO(OH)_2^+ + H^+ \qquad (4.2)$$

$$PaO(OH)_2^+ + 2H_2O \leftrightarrow Pa(OH)_5 + H^+ \qquad (4.3)$$

with the corresponding equilibrium reaction constants K_1, K_2, and K_3. Since the species PaO^{3+} has only been suggested but never proven, only the latter two hydrolysis reactions and corresponding hydrolysis constants can be measured. Early studies on Pa(v) hydrolysis were reported by Guillaumont (1966a) and Bouissières (1971).

Recently Trubert *et al.* (Le Naour *et al.*, 2003; Trubert *et al.*, 1998, 2002, 2003) have obtained the hydrolysis constants for Pa(v) at the tracer level ($\sim 10^{-12}$ M using ^{233}Pa) from the variations of the partition coefficient of Pa(v) in the system: TTA/toluene/Pa(v)/H_2O/H^+/Na^+/ClO_4^- . These experiments were performed as a function of the concentrations of TTA and H^+ at ionic strengths of $0.1 \le \mu \le 3$ M and temperatures of 10°C $\le T \le$ 60°C. From the hydrolysis constants obtained under these conditions extrapolations to zero ionic strength were performed using the specific ion interaction theory (SIT) (Grenthe and Puigdomenech, 1997). The equilibrium constants obtained are given in Table 4.13. Thermodynamic data related to the hydrolysis equilibria were derived from the temperature dependence of the hydrolysis constants at infinite dilution and are given in Table 4.14.

Table 4.13 *Equilibrium constants for the hydrolysis of Pa*(*v*) *at zero ionic strength* (*from Trubert* et al., 2003).

T	log K_2^0	log K_3^0
(°C)	$PaO(OH)^{2+} + H_2O \leftrightarrow PaO(OH)_2^+ + H^+$	$PaO(OH)_2^+ + 2H_2O \leftrightarrow Pa(OH)_5 + H^+$
10	–1.32 ± 0.15	–6.7 ± 0.4
25	–1.24 ± 0.02	–7.03 ± 0.15
40	–1.22 ± 0.1	–5.3 ± 1.0
60	–1.19 ± 0.12	–5.4 ± 0.9

Table 4.14 *Standard thermodynamic data at* 25°C *derived from the experimental hydrolysis equilibria of Pa*(*v*). *The thermodynamic values for the hydrolysis reaction forming Pa*(*OH*)$_5$ *are considered to be estimates* (*from Trubert* et al., 2003).

$PaO(OH)^{2+} + H_2O \leftrightarrow PaO(OH)_2^+ + H^+$	$PaO(OH)_2^+ + 2H_2O \leftrightarrow Pa(OH)_5 + H^+$
$\Delta_r H^\circ = (5.7 \pm 1.3)$ kJ mol^{-1}	$\Delta_r H^\circ = (61 \pm 31)$ kJ·mol^{-1}
$\Delta_r C_p^\circ = (-200 \pm 89)$ J K^{-1} mol^{-1}	
$\Delta_r G^\circ = (7.1 \pm 0.1)$ kJ mol^{-1}	$\Delta_r G^\circ = (36.3 \pm 4)$ kJ mol^{-1}
$\Delta_r S^\circ = (-4.5 \pm 4.7)$ J K^{-1} mol^{-1}	$\Delta_r S^\circ = (81 \pm 118)$ J K^{-1} mol^{-1}

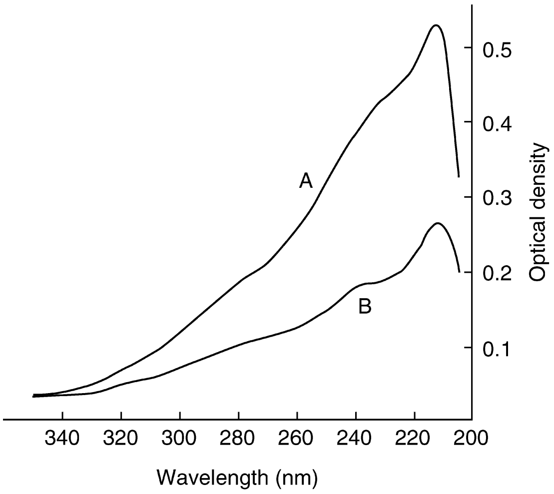

Fig. 4.16 *Absorption spectra of Pa(*v*) in* 11.5 M *$HClO_4$. The solution was prepared by dissolution of the hydroxide. Curve A, fresh solution; curve B, solution aged for* 1 *day or longer.* [*Pa(*v*)*] ~ 10^{-5} M (*Guillaumont*, 1966*c*).

The absorption spectrum of Pa(v) in 11.5 M $HClO_4$ is shown in Fig. 4.16 (Guillaumont, 1966c); similar spectra are obtained at lower acidities. The absorption maximum at about 200–210 nm is attributed to the Pa═O bond in $PaO(OH)_2^+$ and $PaOOH^{2+}$; this bond persists even in sulfuric acid media up to 4 M concentration.

4.8.2 Complexes of Pa(v) in mineral acid solutions

In the absence of strong complexing agents, such as F^- and certain organic reagents, the aqueous complexes of Pa(v) are all oxo- or hydroxo complexes. Consequently, Pa(v) in aqueous solution is rarely present as a single species but rather exists as a mixture of several complexes or hydrolyzed species. These may be characterized by solvent extraction or ion-exchange methods, which, because of differences in the experimental conditions, such as ionic strength, acidity, concentration of the ligand, age of the solution, etc., may yield ambiguous or mutually contradicting interpretations.

The relative complexing tendencies of inorganic anions with respect to Pa(v) are:

$$F^- > OH^- > SO_4^{2-} > Cl^- > Br^- > I^- > NO_3^- \geq ClO_4^-$$

(a) Ionic species of Pa(v) in nitric acid solution

In general, NO_3^- is a poor complexing anion for Pa(v) but freshly prepared solutions, in which [Pa(v)] $\leq 10^{-5}$ M and [HNO_3] ≥ 1 M, are fairly stable. Such systems contain monomeric nitratohydroxo complexes of the form $[\mathrm{Pa(OH)}_n(\mathrm{NO_3})_m]^{5-n-m}$, where $n \geq 2$ and $m \leq 4$ (Hardy *et al.*, 1958). The transition from cationic to anionic forms occurs at $[\mathrm{HNO_3}] \approx$ 4–5 M. Stability constants for several suggested species in this medium are listed in Table 4.15.

(b) Ionic species of Pa(v) in hydrochloric acid solution

Solutions of Pa(v) in hydrochloric acid are generally unstable with respect to hydrolytic condensation when [Pa] $\geq 10^{-3}$ M, although complete precipitation may take as long as several weeks (Kirby, 1966). If the freshly precipitated hydroxide is dissolved in 12 M HCl and then diluted to [Pa] $\leq 10^{-4}$ M and 1 M < [HCl] < 3 M, the solution is reasonably stable and will then contain a mixture of monomeric chloro complexes in thermodynamic equilibrium. It is generally agreed that, for [HCl] < 1 M and [Pa] < 10^{-5} M, the species present are the same as those described above for perchloric acid media, while, for [HCl] $\approx$ 3 M, the predominant species is $\mathrm{PaOOHCl^+}$. The complexes that have been proposed to explain the solvent extraction and ion-exchange behavior of Pa(v) at higher acidities are summarized in Table 4.16. The study of complex formation of Pa in aqueous HCl solutions of medium and high concentrations and the electronic structures of anionic complexes of $[\mathrm{PaCl_6}]^-$, $[\mathrm{PaOCl_4}]^-$, $[\mathrm{Pa(OH)_2Cl_4}]^-$, and $[\mathrm{PaOCl_5}]^{2-}$ have been calculated using the relativistic Dirac–Slater discrete-variational method. The charge density distribution analysis has shown that protactinium has a slight preference for the $[\mathrm{PaOCl_5}]^{2-}$ form or for the pure halide complexes with coordination number higher than six under these conditions. On the other hand, Ta occupies a specific position in the group and has the highest tendency to form the pure halide complex $[\mathrm{TaCl_6}]^-$; niobium has equal tendencies to form the $\mathrm{NbCl_6}$ and $[\mathrm{NbOCl_5}]^{2-}$ species (Pershina *et al.*, 1994).

There are no data on the species of protactinium in HBr and HI solutions. Goble and co-workers (1956, 1958) suggested on the basis of ^{231}Pa extraction from HBr and HI aqueous solutions that bromide and iodide complexes of protactinium are less stable than the chloride complexes.

(c) Fluoro complexes of Pa(v)

The solubility of Pa(v) is relatively high at all concentrations of hydrofluoric acid; thus, 0.05 M HF dissolves 3.9 g $\mathrm{L^{-1}}$ of ^{231}Pa and 20 M HF dissolves at least 200 g $\mathrm{L^{-1}}$ of the pentoxide (Bagnall *et al.*, 1965). The solubility of Pa(v) is estimated to be 11.2 g $\mathrm{L^{-1}}$ in 8 M HCl and 0.6 M HF and at least 125 g $\mathrm{L^{-1}}$ in 8 M HCl and 5 M HF (Chilton, 1964). Solutions of Pa(v) in aqueous HF are very stable with respect to hydrolysis and are probably the only systems that contain no polymeric species.

A great many complexes have been proposed to explain the behavior of Pa(v) in aqueous HF (deMiranda and Muxart, 1965; Bukhsh *et al.*, 1966a,b;

Table 4.15 *Stability constants for some suggested nitrate complexes of Pa(*v*).*

μ	$[H^+]$ (M)	$[NO_3^-]$ (M)	*Suggested species*	*Stability constants*	*References*
1	1	≤1	$[PaO_x(OH)_{4-2x}NO_3]^\circ$	$K_1 = 0.68$	Nowikow and Pfrepper (1963)[a]
			$[PaO_x(OH)_{4-2x}(NO_3)_2]^-$	$K_2 = 3.0$	
			$[PaO_x(OH)_{2-2x}(NO_3)_3]^-$	$K_4 = 11.93$	
2	2	≤1		$K_1 = 0.79$	
				$K_2 = 0.74$	
4	4	≤1		$K_1 = 0.63$	
				$K_2 = 0.21$	
1	1	≤1	$(PaNO_3)^{4+}$	$K_1 = 1.43$	Kolarich *et al.* (1967)
			$[Pa(NO_3)_2]^{3+}$	$K_2 = 0.07$	
6	6	1–3	$[Pa(NO_3)_5]^0$		Stanik and Ilmenkova (1963)
6	6	3–6	$[Pa(NO_3)_6]^-$	$K_6 = 0.141$	
			$[Pa(NO_3)_7]^{2-}$	$K_7 = 1.09$	
5–6	5	0.4–5	$[Pa(OH)_2(NO_3)]^{2+}$	$K_1 = 17$	Spitsyn *et al.* (1964); Khlebnikov *et al.* (1966)
			$[Pa(OH)_2(NO_3)_2]^+$	$K_2 = 127$	
			$[Pa(OH)_2(NO_3)_3]^0$	$K_3 = 540$	
			$[Pa(OH)_2(NO_3)_4]^-$	$K_4 = 1380$	

[a] Only the ratio $[Pa]:[NO_3^-]$ was determined.

Table 4.16 *Suggested chloro complexes of Pa*(*v*) *as a function of HCl concentration* (*after Guillaumont* et al., 1968).

[*HCl*] (M)	$Pa(OH)_nCl_m^{5-n-m}$			
1	$PaOOH^{2+}$	$PaOOH^{2+}$		
2	$PaOOHCl^{+}$	$PaOOHCl^{+}$		$Pa(OH)Cl_3^{+}$
3	$PaO_2Cl_2^{-}$	$PaOOHCl_2$ $PaOCl_3$	$Pa(OH)Cl_3^{+}$ $Pa(OH)_2Cl_3$	$Pa(OH)_3Cl^{+}$ $Pa(OH)_2Cl_2^{+}$
4	PaO_3^{+}	$POOHCl_3^{-}$	$Pa(OH)Cl_4$	$Pa(OH)_2Cl_3$ $Pa(OH)Cl_4$
5	$PaOCl_4^{-}$	$PaOCl_4^{-}$	$Pa(OH)_2Cl_4^{-}$	$Pa(OH)_2Cl_4^{-}$
6	$PaOHCl_6^{2-}$	$PaOCl_5^{2-}$	$Pa(OH)Cl_5^{-}$	$Pa(OH)Cl_5^{-}$
7	$PaCl_6^{-}$		$PaCl_6^{-}$	$PaCl_6^{-}$
8	$PaCl_7^{2-}$		$PaCl_7^{2-}$	
>8	$PaCl_8^{3-}$ or $POHCl_7^{3-}$	$PaOCl_6^{3-}$		
References	Scherff and Herrman (1966)	Guillaumont (1966c); Muxart *et al.* (1966a,b)	Casey and Maddock (1959a,b)	Shankar *et al.* (1963)

deMiranda, 1966; Guillaumont, 1966a,c; Guillaumont and deMiranda, 1966; Guillot, 1966; Kolarich *et al.*, 1967; Bonnet and Guillaumont, 1969; Plaisance and Guillaumont, 1969); their regions of existence are summarized in Fig. 4.17. Those for which stability constants have been determined are listed in Table 4.17. Only two species exist in a pure state: PaF_7^{2-}, which is present over the range 10^{-3} M < [HF] < 4–8 M, and PaF_8^{3-}, which can exist only when $[F^-] > 0.5$ M and 10^{-7} M $< [H^+] < 10^{-2}$ M. In more acid media, 1 M $< [H^+] <$ 3 M and $[F^-] \approx 10^{-4}$ M, the dominant heptafluoro complex is $HPaF_7^-$; this species would also exist in 10–12 M HF, because the $[F^-]$ is limited to about 10^{-2} M by the equilibrium constants: $K_1 = ([HF]/([H^+] \cdot [F^-])) = 935$ M^{-1} and $K_2 = ([HF_2]/([HF] \cdot [F^-])) = 3.12$ M^{-1} (Plaisance and Guillaumont, 1969). At [HF] $< 10^{-3}$ M, PaF_7^{2-} is replaced by complexes of successively lower F:Pa ratios, then by oxo and hydroxyfluoro complexes and, finally, by uncomplexed species.

(d) Behavior of Pa(v) in sulfuric acid solution

Freshly precipitated Pa(v) hydroxide is readily soluble in moderately concentrated H_2SO_4 and permanently stable solutions, containing up to 90 g L^{-1} of ^{231}Pa in approximately 2.5 M H_2SO_4, have been reported (Thompson, 1952; Kirby, 1959, 1966; Brown *et al.*, 1961; Campbell, 1964; Bagnall *et al.*, 1965; Takagi and Shimojima, 1965; Kirby and Figgins, 1966). The solubility falls off sharply at both ends of the acid concentration range, yielding amorphous hydrated oxides or colloids in <1 M H_2SO_4 and crystalline $H_3PaO(SO_4)_3$ in

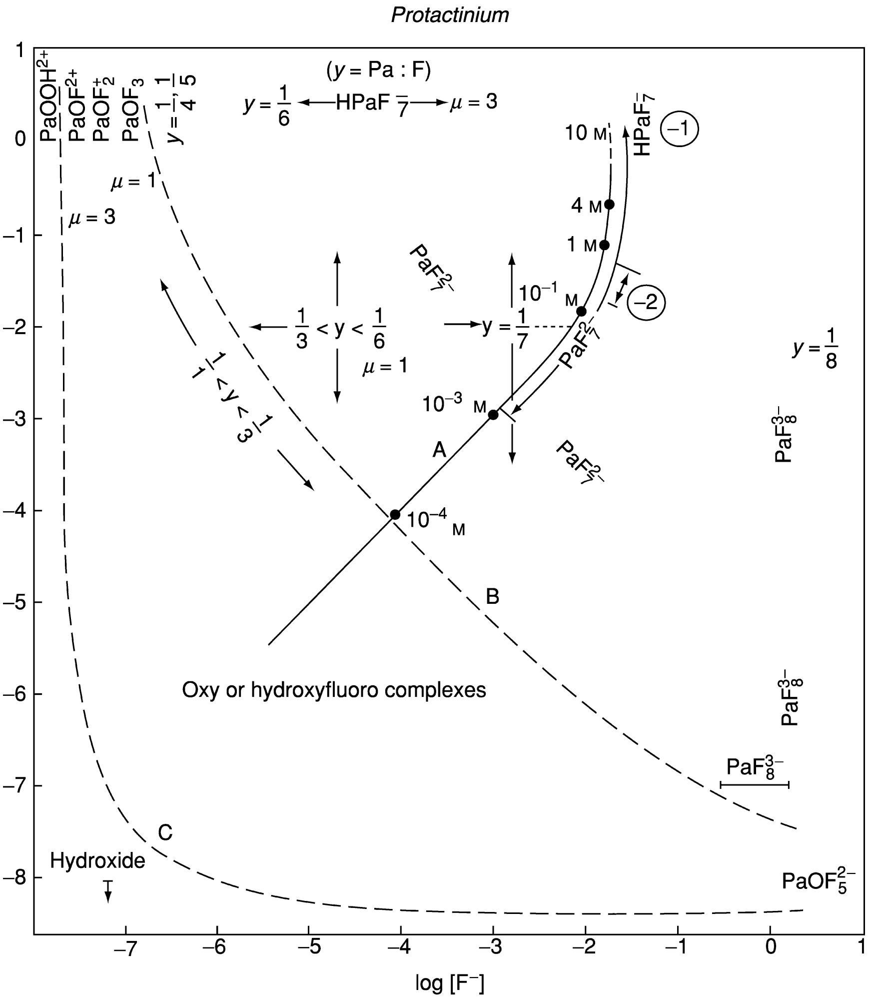

Fig. 4.17 *Fluoro complexes of Pa(*v*) as a function of* [*HF*], [*H*$^+$], *and* [*F*$^-$] (*Guillaumont* et al., 1968).

concentrated H_2SO_4 (Bagnall *et al.*, 1965; Takagi and Shimojima, 1965; Stchouzkoy *et al.*, 1966b, 1968).

The sulfate complexes of Pa(v) that have been deduced from tracer-level studies ([Pa] $\leq 10^{-4}$ M) are listed in Table 4.18. The absorption spectra of Pa(v) in H_2SO_4 are shown in Fig. 4.18 (Guillaumont *et al.*, 1960; Guillaumont, 1966c).

Table 4.17 *Stability constants for some suggested fluoride complexes of Pa*(*V*).

μ	[H^+] (M)	[F^-] (M)	*Suggested species*	*Stability constants*	*References*
1	≤ 0.1	≤ 0.1	PaF_3^{2+}	$\log K_3 = 4.9$	Bukhsh *et al.* (1966a)
			PaF_4^+	$\log K_4 = 4.8$	
			PaF_5	$\log K_5 = 4.5$	
			PaF_6^-	$\log K_6 = 4.4$	
			PaF_7^{2-}	$\log K_7 = 3.7$	
			PaF_8^{3-}	$\log K_8 = 1.7$	
3	1–3	$\leq 10^{-6}$	$Pa(OH)_2F^{2+}$	$K_1 = 3.6 \times 10^3$	Guillaumont (1966a,c)
			$Pa(OH)_2F_2^+$	$K_2 = 4.45 \times 10^7$	
			$Pa(OH)_2F_3$	$K_3 = 8.2 \times 10^{10}$	
1	1	$\leq 10^{-6}$	PaF^{4+}	$K_1 = 9 \times 10^3$	Kolarich *et al.* (1967)
			PaF_2^{3+}	$K_2 = 3 \times 10^3$	
			PaF_3^{2+}	$K_3 = 1.1 \times 10^3$	

Table 4.18 *Stability constants for some suggested sulfate complexes of Pa*(*V*).

μ	[H^+] (M)	[SO_4^{2-}] (M)	*Suggested species*	*Stability constants*	*References*
1	1	≤ 1	$[PaO_x(OH)_{4-2x}SO_4]^-$	$K_1 = 0.94$	Nowikow and
				$K_2 = 7.39$	Pfrepper (1963)[a]
2	2	≤ 1	$[PaO_x(OH)_{2-2x}(SO_4)_2]^-$	$K_1 = 1.14$	
				$K_2 = 14.70$	
3	1–3	≤ 3	$PaOSO_4^+$	$K_1 = 19.3$	Guillaumont (1966c)
			$PaO(SO_4)_2^-$	$K_2 = 320$	
1	1	≤ 1	$PaSO_4^{3+}$	$K_1 = 120$	Kolarich *et al.* (1967)[a]
			$Pa(SO_4)_2^+$	$K_2 = 1.7$	
1.38	0.3	≤ 0.4	$Pa(OH)_2SO_4^+$	$K_1 = 6.4$	Mitsuji and Suzuki (1967c)
1	0.1–1	≤ 0.2	$PaOOH(HSO_4)^+$	$K_1 = 31$	LeCloarec *et al.* (1973)
		≤ 0.2	$PaO(HSO_4)_2^+$	$K_2 = 250$	

[a] Only the ratio [Pa]:[SO_4^{2-}] was determined.

(e) Miscellaneous complexes of Pa(v) with inorganic ligands

The absorption spectra and the formation constants of complexes formed by tracer-level Pa(v) in phosphoric acid solution have been reported by LeCloarec and Muxart (1973), LeCloarec *et al.* (1973), and LeCloarec (1974). The species identified were $PaO(OH)\ ^-(H_2PO_4)^+$, $HPaO(H_2PO_4)_2^{2+}$, $PaO(H_2PO_4)_2^+$, and $PaO(H_2PO_4)_3$.

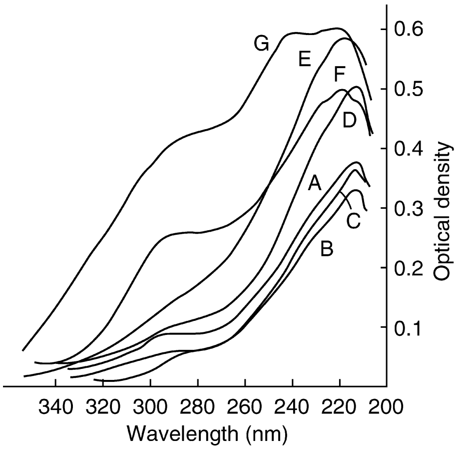

Curve	$[H_2SO_4]$ (M)	[*Pa(v)*] (M)
A	0.7	0.35×10^{-4}
B	1.32	0.40×10^{-4}
C	2.2	0.45×10^{-4}
D	4.1	0.42×10^{-4}
E	6.5	0.49×10^{-4}
F	9	0.18×10^{-4}
G	18	0.19×10^{-4}

Fig. 4.18 *Absorption spectra of Pa*(*v*) *in* H_2SO_4 *solution* (*Guillaumont*, 1966*c*).

The addition of ≤ 1 M H_2O_2 to a solution of ^{233}Pa in aqueous $HClO_4$ (1 M $\leq$ $[H^+]$ ≤ 3 M) leads to the formation of the following peroxy complexes: $PaO(OH)(HO_2)^+$, $PaO(OH)(HO_2)_2$, $PaO(HO_2)^{2+}$, and $PaO(HO_2)_2^+$, according to Stchouzkoy *et al.* (1969). Association constants for the 1:1 and 1:2 complexes of Pa(v) with IO_3^- have been reported by Kolarich *et al.* (1967).

Pa(v) forms mixed complexes in solutions containing more than one type of ligand. For example, a species identified as $PaO(H_2PO_4)_3(HSO_4)^-$ is found in a mixture of 0.35 M H_3PO_4 and 0.22 M H_2SO_4 (LeCloarec *et al.*, 1973). Mixed complexes are also formed in hydrochloric or nitric acid solutions containing $\leq 10^{-2}$ M HF (Hardy *et al.*, 1958; Casey and Maddock, 1959b; Shankar *et al.*, 1963; Plaisance and Guillaumont, 1969). Formation constants have been determined for the unidentified mixed complexes formed by Pa(v) in 3–6 M HNO_3 to which HCl, $(NH_4)_2SO_4$, $(NH_4)_2HPO_4$, or H_3AsO_4 was added (Davydov *et al.*, 1966b).

Finally, the existence of a perprotactinate ion with a charge of 3– is suggested by the fact that Pa(v) ($\sim 3 \times 10^{-4}$ M) is soluble in alkaline media in the presence of H_2O_2 (Stchouzkoy *et al.*, 1966a).

4.8.3 Organic complexes of Pa(v) in aqueous solution

Only a few systematic studies have been done of the aqueous complexes of Pa(v) with organic reagents. Galateanu and co-workers (1962a,b, 1966), Moskvin *et al.* (1963) used the ion-exchange method to determine the stability constants of the complexes formed with a number of organic acids (Table 4.19). Stability constants have also been reported for complexation by acetylacetone (Liljenzin and Rydberg, 1966; D'yachkova *et al.*, 1968b; Liljenzin, 1970),

Table 4.19 *Stability constants of complexes formed by Pa(*v*) with various organic acids* ($\mu = 0.25$) (*Galateanu and Lapitskii,* 1962*a,b*; *Moskvin* et al., 1963; *Galateanu*, 1966; *Lapitskii and Galateanu*, 1963).

		Stability constant for Pa:ligand ratio		
Acid	*pH*	1:1	1:2	1:3
lactic ($\leq$0.1 M)	1.5–2.7	1.75×10^2		
α-hydroxyisobutyric ($\leq$0.5 M)	0.98–1.2		3.0×10^3	1.0×10^7
mandelic ($\leq$0.5 M)	1.0–1.1	9.1×10^2		
malic ($\leq$0.65 M)	0.8–0.87	8.3×10^2	6.3×10^4	
tartaric ($\leq$0.65 M)	0.75–0.8	1.7×10^2	2.1×10^4	
trihydroxyglutaric ($\leq$0.7 M)	0.95–1.2	9.1×10^2	7.7×10^7	
oxalic ($\leq$0.7 M)[a]	0.7–0.8	3.6×10^2	8.0×10^5	1.1×10^6
citric ($\leq$0.7 M)[b]	0.7–0.95	4.5×10^3	2.3×10^5	6.3×10^8
aconitic ($\leq$0.7 M)	0.75–0.8	1.5×10^2		
ethylenediaminetetraacetic acid ($\leq$0.02 M)[c]	2.4–2.7	1.5×10^8	9.1×10^{11}	
amygdalic ($\leq$0.5 M)	1.1	8.5×10^2		

[a] cf. Carrere (undated); Davydov *et al.* (1966a,b); Guillaumont (1966a,c).
[b] cf. Guillaumont (1968).
[c] cf. Shiokawa *et al.* (1969).

DIAPA (Mikhailov, 1960), and TTA (Guillaumont, 1965a; D'yachkova *et al.*, 1968a).

Oxalic acid has been singled out for special attention because of its importance in the analytical and process chemistry of ^{231}Pa. Davydov and Pal'shin (1967) found that the solubility of Pa(v) at 25°C remained low in <0.05 M $H_2C_2O_4$, but increased sharply from 0.33 to 4 g L^{-1} or more between 0.05 and 0.5 M $H_2C_2O_4$. The low solubility was attributed to the formation of hydroxy complexes with a Pa:C_2O_4 ratio of 1:1, while the higher solubility was explained by the formation of complexes with a 1:2 ratio. Casey and Maddock (1959b) suggested the existence of complexes of the form $Pa(C_2O_4)_3^-$, and $Pa(C_2O_4)_4^{3-}$, but Guillaumont (1966a,c) suggested that these were preceded by the formation of $PaOC_2O_4^+$ and $PaO(C_2O_4)_2^+$.

It was shown that protactinium(v) forms a colored compound with Arsenazo-III in highly acidic solutions with a 1:1 ratio (Pal'shin *et al.*, 1962). Complex compounds formed with a large number of other organic reagents, such as 8-oxyquinoline (Maddock and Miles, 1949; Vernois *et al.*, 1963), BPHA (Cristallini and Flegenheimer, 1963; D'yachkova and Spitsyn, 1964), tannin (Elson *et al.*, 1951; Casey and Maddock, 1959a), 1-phenyl-3-methyl-4-benzoyl-pyrazolone-5 (Myasoedov and Molochnikova, 1968), pyrogallol, catechol, and gallic acid (Casey and Maddock, 1959a), and are used in the analytical chemistry of protactinium. However, literature data on the composition and stability of these compounds are absent.

4.8.4 Redox behavior in aqueous solution

The standard electrode potential of the Pa(v)/Pa(iv) couple has been estimated to be –0.1 V (vs. normal hydrogen electrode [NHE]) by Fried and Hindman (1954) and –0.25 V by Haïssinsky and Pluchet (1962), the latter value being based on a measured electrochemical potential of –0.29 ± 0.03 V in 6 M HCl.

Pa(iv) was prepared by Haïssinsky (Haïssinsky and Bouissières, 1948, 1951; Bouissières and Haïssinsky, 1949), who reduced 0.1–2 mg of ^{231}Pa(v) with solid Zn amalgam or $CrCl_2$ in 1–3 N HCl or H_2SO_4. Brown *et al.* (1959) found that Zn amalgam gave complete reduction in 5–6 h only if the initial solution was ≥ 6 M in HCl; lower acidities led to the formation of colloidal Pa(v), which was difficult to reduce. Mitsuji (1967a,b) used liquid Zn amalgam to obtain complete reduction in a few minutes of 4×10^{-4} M ^{231}Pa(v) in 1–11 M HCl or 0.05–9 M H_2SO_4. Tracer-level Pa(v) could not be completely reduced unless Cr(iii) was added to the system. ^{233}Pa(iv) has also been obtained by dissolution of neutron-irradiated ^{232}Th metal in 1 M HCl by Manier and co-workers (1969, 1970) or of neutron-irradiated $^{232}ThX_4$ (X = Cl, Br, I) in 0.02 M $ThCl_4$ (Carlier, 1971; Carlier and Genet, 1972a,b). In the first case, the yield of Pa(iv) was about 20%; in the second, it varied with the nature of the irradiated halogen and the pH of dissolution, ranging from less than 20% at pH ≤ 3 to approximately 80% for $ThCl_4$ at pH 5.5.

Musikas (1966) has described the electrolytic reduction of 10^{-3} M ^{231}Pa(v) in 8 M HCl, 0.5 M H_2SO_4, and 5 M NH_4F (pH 7.2). Electrolysis at 50 mA for 5 h completely reduced Pa(v) in 8 M HCl to Pa(iv). The reduction of 10^{-13} M Pa(v) on a Pt–H_2 electrode in aqueous solutions of acetylacetone at pH > 7 has also been reported (Liljenzin and Rydberg, 1966).

The polarography of Pa has been studied in various aqueous media (Elson, 1954; deMiranda and Maddock, 1962; Musikas, 1966; Schwochau and Astheimer, 1970; Astheimer and Schwochau, 1973). All solutions gave at least one wave, corresponding to the one-electron change, Pa(v)→Pa(iv), and in some cases a second wave, which might represent either the reduction, Pa(iv)→Pa(iii), or, more probably, the catalytic reduction of H^+. For example, with $[NH_4F] = 3.84$ M, pH 7.2, $[^{231}\text{Pa(v)}] = (2.3–9.5) \times 10^{-4}$ M, the wave height at $E_{1/2} = -1.29$ V (vs. standard calomel electrode [SCE]) was proportional to [Pa], but that of the second wave ($E_{1/2} = -1.57$ V) was not (deMiranda and Maddock, 1962). In DMSO, the reduction of $PaCl_4$ led directly to Pa(0) in a single step ($E_{1/2} = -1.49$ V), with the 3+ oxidation state omitted (Astheimer and Schwochau, 1973).

The behavior of protactinium in the TmI_2–TmI_3–THF system (THF, tetrahydrofuran) was studied by the cocrystallization method. In the presence of Tm^{2+}, microamounts of Pa cocrystallize with the solid phase of TmI_3 solvate, the cocrystallization coefficient (K_c) being nearly 1. A similar K_c for this system was obtained with Ce. Thus, in THF in the presence of Tm^{2+}, protactinium is probably reduced to the oxidation state 3+ (Kulyukhin *et al.*, 1996, 1997). Attempts to reduce Pa(v) to the trivalent state by Sm(ii) or Tm(ii) in chloride melts at high temperatures were reported by Mikheev *et al.* (1992). Using a cocrystallization method of Pa with the Sm(II) and Tm(II) system, the authors proposed that under these conditions the stabilization of the Pa(III) species was obtained. In the system with PrOCl, the Pa(III) reduction to Pa(II) has been detected. The standard redox potential of Pa(III)/Pa(II) couple has been calculated as –2.59 ± 0.1 V (vs. NHE) (Mikheev *et al.*, 1993a,b). Pa(II) also was produced by interaction of ^{233}Pa(V) with the cluster PrI_2 (Kazakevich *et al.*, 1993). It was shown that An = Pa, U, Np, Pu with the electronic configuration ($5f^{n-1}6d$) in the divalent state, were stabilized in clusters of the type $(Pr,An)I_2$ in the $LiI–PrI_2–PrI_3$ system (Kulyukhin and Mikheev, 1998). The influence of the electronic configurations of Pa^{2+} (f^3 and f^2d) and Pa^{3+} (f^2 and fd) upon the stability of divalent and trivalent protactinium and their redox potentials was examined by Guillaumont *et al.* (1996). An analysis of the stabilization of the configuration $5f^26d$ (Pa^{2+}) led to predictions of the relative scale for the $E^{\circ}_{\mathrm{Pa(III)/Pa(II)}}$ potentials which depend on the medium and on ligands. For this purpose the relation between the energy ($f^3 \rightarrow f^2d$) for Pa(II) in water ($Pa^{2+}\cdot aq$) and in solid ($Pa^{2+}:CaF_2$) was established. The values of the redox potentials were discussed on the basis of the 6d electron stabilization of Pa^{2+} and destabilization of Pa^{3+} ions. The standard redox potential $E^{\circ}_{\mathrm{Pa(III)/Pa(II)}}$ was estimated to be around −4.0 V, and for the couple Pa(IV)/Pa(III) about –2.1 V (vs. NHE). This result was confirmed by a measurement of E_{fd} in Pa^{4+}(aq) and by correlation of E_{fd} for Pa^{2+}(aq), Pa^{3+}(aq), and Pa^{4+}(aq) with the corresponding redox potentials (Guillaumont *et al.* 1996). Standard reduction potentials are given in Chapter 19, Fig. 19.9.

Pa(IV) in aqueous solution is rapidly oxidized by air, but the rate of oxidation is decreased by the exclusion of O_2 and by the presence of complexing anions (Brown *et al.*, 1959; Brown and Wilkins, 1961; Guillaumont, 1966b; Bagnall and Brown, 1967; Mitsuji, 1967a). Guillaumont *et al.* (1960) found that the stability of ^{231}Pa(IV) increased with increase in $[H_2SO_4]$ or [HCl], but Myasoedov *et al.* (1966b) reported the opposite effect. The oxidation rate was increased by ultraviolet light or heat. In the absence of air, Pa(IV) in a neutral solution of 2.2 M $N(CH_3)_4F$ was oxidized at the rate of about 1% per day (deMiranda and Muxart, 1964). Mitsuji (1967a) has proposed the reaction:

$$2Pa^{4+} + 2H^+ \leftrightarrow 2Pa^{5+} + H_2$$

The half-life for the oxidation of ^{233}Pa(IV) in the absence of redox buffers decreases exponentially with increase in $[H^+]$, but the formation of complexes tends to stabilize the 4+ oxidation state. The stability of Pa(IV) is greatly enhanced by a decrease in the dielectric constant; thus, in 0.6 M $HClO_4$ (10% H_2O/90% C_2H_5OH), the half-life for oxidation was 40 h, as compared with $\tau_{1/2}$ ~1 h in a pure aqueous solution (Manier *et al.*, 1969; Manier, 1970; Manier and Genet, 1970). The oxidation of Pa(IV) by molecular halogens is first-order with respect to both [^{233}Pa(IV)] and [Cl_2, or Br_2, or I_2] (Carlier, 1971; Carlier and Genet, 1972a).

4.8.5 Aqueous chemistry of Pa(iv)

The most characteristic property of Pa(iv) in aqueous solution is that, unlike Pa(v), it is precipitated by hydrofluoric acid (Haïssinsky and Bouissières, 1948; Bouissières and Haïssinsky, 1949). It is also precipitated by $\mathrm{IO_3^-}$, $\mathrm{PO_4^{3-}}$, $\mathrm{P_2O_6^{4-}}$, phenylarsonate, and saturated $\mathrm{K_2SO_4}$, but forms soluble carbonate, citrate, and tartrate complexes (Haïssinsky and Bouissières, 1951). $\mathrm{PaF_4}$ is soluble in 15 M $\mathrm{NH_4F}$ (Haïssinsky *et al.*, 1961).

The spectrophotometry of Pa(iv) has been investigated in perchloric (Brown and Wilkins, 1961), hydrochloric (Fried and Hindman, 1954; Brown *et al.*, 1959; Guillaumont *et al.*, 1960; Brown and Wilkins, 1961; Bagnall and Brown, 1967; Mitsuji, 1967a), hydrobromic (Brown and Wilkins, 1961), and sulfuric (Guillaumont *et al.*, 1960; Brown and Wilkins, 1961; Myasoedov *et al.*, 1966b; Mitsuji, 1967a) acid solutions and in neutral fluoride media (Haïssinsky *et al.*, 1961; deMiranda and Muxart, 1964; Asprey *et al.*, 1967). The reduction of Pa(v) in acid solutions is accompanied by the disappearance of the prominent absorption band at 210–215 nm (Figs. 4.16 and 4.18) and the appearance of bands at 225–230, 255–265, and 275–290 nm. Beer's law is not followed in hydrochloric acid solutions, but, for (0.65–1.5) × 10^{-4} M Pa(iv) in 0.5–6 M $\mathrm{H_2SO_4}$, the molar extinction coefficient (ε) is about 1500 L $\mathrm{M^{-1}\,cm^{-1}}$ at 290 nm (Myasoedov *et al.*, 1966b). In neutral fluoride media, the spectrum is different according to the nature of the medium: in $\mathrm{NH_4F}$, bands are observed at 355 and 250 nm (Haïssinsky *et al.*, 1961); but in $\mathrm{N(CH_3)_4F}$, the absorption maxima are at 344 and 323 nm, with $\varepsilon = 0.08$ and 0.037 $\mathrm{M^{-1}\,cm^{-1}}$, respectively (deMiranda and Muxart, 1964).

Pa(iv) hydrolyzes less readily than Pa(v). In 3 M $\mathrm{HClO_4}$, the dominant species are $\mathrm{Pa^{4+}}$ and $\mathrm{PaOOH^{2+}}$ (cf. Fig. 4.14). As the acidity is decreased at constant ionic strength ($\mu = 3$), $\mathrm{Pa(OH)^{3+}}$, $\mathrm{PaO^{2+}}$ or $\mathrm{Pa(OH)_2^{2+}}$, and $\mathrm{PaO(OH)^+}$ or $\mathrm{Pa(OH)_3^-}$ appear successively; their hydrolysis constants, as determined by Guillaumont (1965b, 1966b), are 0.725, 0.302, and 0.017, respectively. Estimates of the relative amounts of these species as a function of $[\mathrm{H^+}]$ are indicated in Fig. 4.19.

Mitsuji (1968), however, finds that $\mathrm{Pa(OH)_2^2}$+ is the most probable ionic species at pH 0.4–1.1 ($\mu = 0.5$). Lundqvist (1974c,d, 1975) believes that $\mathrm{PaO^{2+}}$ is more probable, because of the high stability of that ion toward both ethylenediaminetetraacetic acid (EDTA) and acetylacetone. He finds no evidence for species either more or less hydrolyzed than $\mathrm{Pa(OH)_2^{2+}}$ at pH 0–10.

There is, as yet, little information about the complexes formed by Pa(iv). Guillaumont (1966a,c) has calculated the formation constants of the following complexes at $\mu = 3$, $[\mathrm{H^+}] = 3$ M, and $[\mathrm{Cr^{2+}}] = 10^{-2}$ M: $\mathrm{PaCl^{3+}}$ ($K_1 < 1$). $\mathrm{PaCl_2^{2+}}$ ($K_2 = 1$), $\mathrm{PaSO_4^{2+}}$ ($K_1 = 42$), $\mathrm{Pa(SO_4)_2}$ ($K_2 = 153$), $\mathrm{PaF^{3+}}$ ($K_1 = 5.34 \times 10^4$), and $\mathrm{PaF_2^{2+}}$ ($K_2 = 1.8 \times 10^3$). Muxart *et al.* (1966b) found no anionic chloro complexes except at high acidity, e.g. $\mathrm{PaCl_6^{2-}}$ in ~8 M HCl. Mitsuji (1968) finds that $\mathrm{Pa(SO_4)(OH)^+}$ ($K = 320$) is the most probable ionic species formed by $\mathrm{HSO_4^-}$ at

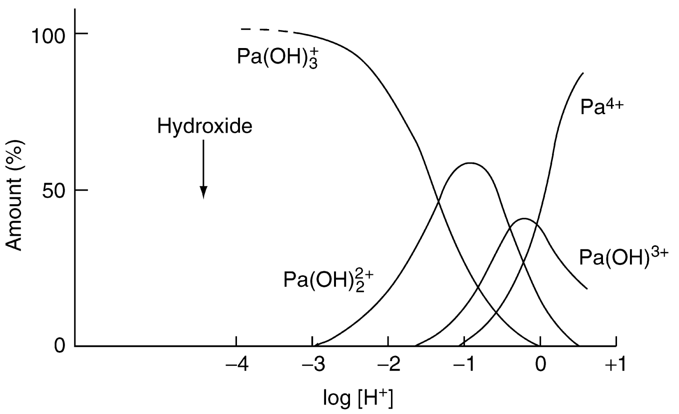

Fig. 4.19 *Distribution of the ionic species of* ^{233}*Pa(IV) as a function of* [H^+] *in non-complexing media of ionic strength* $\mu = 3$ (*Guillaumont*, 1966*a*).

pH 0.4–1.1, $\mu = 0.5$, 10°C. A comparable value is reported by Lundqvist (1974c), who has also determined stability constants for the complexes formed by ^{233}Pa(IV) with acetylacetone (Lundqvist, 1974a; Lundqvist and Rydberg, 1974), TOPO (Lundqvist, 1974b), EDTA (Lundqvist and Andersson, 1974), and benzoylacetone (Lundqvist, 1975).

Recently, the $6d^1 \rightarrow 5f^1$emission spectrum of Pa^{4+} in aqueous acidic solution was reported. The peak maximum was at 460 nm with a half-width of (61.6 ± 1.4) nm and a lifetime of (16 ± 2) ns (Marquardt *et al.*, 2004).

4.9 ANALYTICAL CHEMISTRY

Protactinium determination in natural materials is very complicated because of the extremely small content of Pa in the samples, as well as its tendency to hydrolyze. The presence of other elements, with chemical properties similar to protactinium, highly influences the behavior of protactinium in solutions.

Spectral, spectrophotometric, gravimetric, and other methods are used for the determination of macroquantities of protactinium. However, they are often invalid for the analysis of natural objects that contain very small amounts of protactinium. In these cases radiometric methods are preferable but they need careful purification of protactinium from macroelements and other radioactive materials.

4.9.1 Radiometric methods

The basis of the simplest methods for the determination of the long-lived protactinium isotope, ^{231}Pa, in natural objects (the ores, rocks, waste products), various solutions, and other samples is the measurements of α-activity and

γ-rays. The determination of the artificial protactinium isotope, ^{233}Pa, also is usually carried out by measurements of its γ-rays or β-particles.

(a) The determination of ^{231}Pa by α-counting

The large specific activity of ^{231}Pa isotope, equal to 10^6 alpha decays min^{-1} mg^{-1} of element (Bagnall, 1966a) allows the use of this method for the determination of submicrogram amounts of protactinium after its isolation in the radiochemically pure state.

α-Counters, such as ionization chambers, scintillation or proportional counters, are utilized for the measurements of α-activity of protactinium samples. Absolute quantities of protactinium are determined by comparison of the α-activity of the protactinium sample without other α-emitting isotopes with the activity of standard samples of ^{231}Pa, ^{239}Pu, RaD (^{210}Pb) + RaE (^{210}Bi) + RaF (^{210}Po), ^{210}Po, measured under the same conditions.

Usually protactinium samples for α-counting are prepared by evaporation of a known aliquot of the solution under investigation, after placing it on a platinum, stainless steel, or glass plate.

Thin layers are formed by placing the organic phase directly on a plate for counting, for instance, after extraction of protactinium with DIBK (Scherff and Hermann, 1964; Rona *et al.*, 1966).

Multichannel alpha-spectrometers are used for control of radiochemical purity of isolated samples (Salutsky *et al.*, 1957; Spitsyn and D'yachkova, 1960; Myasoedov and Pal'shin, 1963; Suzuki and Inoue, 1966). ^{231}Pa also can be characterized with enough reliability by its γ-rays spectrum (Salutsky *et al.*, 1956, 1957; Barnett, 1957; Suzuki and Inoue, 1966). Samples for alpha-spectrometers can be prepared by the electrolytic technique (Ko, 1956, 1957; Shimojima and Takagi, 1964; Smith and Barnett, 1965).

The application of alpha-spectrometers with high resolution ($\sim$0.5%) in some cases allows the determination of protactinium without separation from other α-emitters (Glover *et al.*, 1959; Jackson *et al.*, 1960b; Brown and Maddock, 1967). The alpha-spectrum of ^{231}Pa has the following main groups of α-particles: 5.046 (10%), 5.017 (23%), 5.001(24%), 4.938 (22%), and 4.722–4.666 MeV (13%) (Hyde, 1961). So 79% of ^{231}Pa α-particles emitted have energies within the interval 4.85–5.15 MeV. Measurements in this energy range with the alpha-spectrometer, previously calibrated with a pure ^{231}Pa sample, allow the determination of protactinium in the presence of other radioactive elements. Only ^{227}Ac (α-particles energy is 4.947 MeV) slightly influences measurements in this case. The effect of ^{227}Ac may be excluded completely if the protactinium α-particle energies in the interval 5.001–5.041 MeV are measured with a spectrometer that has a silicon detector with resolution of about 0.1%. The alpha-spectrometric method, developed by Glover *et al.* (1959), allows the determination of up to 10^{-4}% of protactinium in various natural objects with a relative precision of ±5%.

(b) The determination of ^{231}Pa by the γ-rays

The measurement of ^{231}Pa γ-rays is widely used for the quick determination of the protactinium concentration in the absence of other radioactive admixtures in solutions, in salts, and compounds of protactinium after their dissolution, and also for control of the protactinium behavior during its separation from waste solutions and solid residue (Barnett, 1957, 1958; Guillaumont *et al.*, 1960; Haïssinsky *et al.*, 1961; Stchouzkoy and Muxart, 1962; Miranda and Muxart, 1964a,b; Guillaumont, 1966a,c; Pissot *et al.*, 1966; Stchouzkoy *et al.*, 1966a,b).

In the γ-ray spectrum of ^{231}Pa there are three maxima, corresponding to the energies of γ-rays 27, 95, and 300 keV. The quantitative determination of protactinium is carried out with γ-spectrometers by comparison of γ-ray intensities from the sample under investigation in the region 300 keV with the intensity of the standard, containing a known amount of radiochemically pure protactinium. The sensitivity of this method is approximately 1×10^{-6} g Pa. So, for instance, it can determine 1.4×10^{-6} g Pa in a 5 g sample. The precision of this method is ±5% (Salutsky *et al.*, 1957). ^{227}Ac (0.095 and 280 keV) and ^{226}Ra (0.080 and 320 keV) prevent the determination.

(c) The determination of ^{234}Pa

The immediate short-lived daughters of U-238 are Th-234 and Pa-234. These nuclides are β^--emitters having energy bands that overlap the uranium bands in a liquid scintillation spectrum. ^{234}Pa is a high-energy β^--emitter that can be further identified and quantified from its Cerenkov radiation. Energy spectra were collected on the Packard 2500AB liquid scintillator analyzer for uranium solutions in diisopropylnaphthalene and pseudocumene-based scintillator cocktails. Calibration curves were prepared for nitric, hydrochloric, and sulfuric acid media (Huntley *et al.*, 1986; Grudpan *et al.*, 1990; Bower *et al.*, 1994).

(d) The determination of ^{233}Pa

Quantitative determination of ^{233}Pa is carried out by β^--particles (Fudge and Woodhead, 1956; McIsaak and Freinling, 1956; McCormac *et al.*, 1960; Sakanoue *et al.*, 1964) as well as γ-rays (Fudge and Woodhead, 1956; Moore and Reynolds, 1957; Arden *et al.*, 1962; Stricos, 1966) by comparison of the intensity of the sample under investigation with the intensity of a standard containing a known amount of ^{233}Pa.

The absolute amount of ^{233}Pa in a standard is determined by the β^--activity measurement on 4π-counters (Fudge and Woodhead, 1956; McCormac *et al.*, 1960).

A method, developed for the determination of absolute amounts ^{233}Pa in irradiated metallic thorium, consists of the measurement of ^{233}Pa β-particles after its chemical separation (McCormac *et al.*, 1960). This method is quick and simple and provides 70–80% protactinium yield and high degree of purification of protactinium from fission elements (10^6 times). For the separation of ^{233}Pa in a radiochemically pure state for its determination in neutron-irradiated thorium, Moore and Reynolds (1957) used the extraction with DIBC from 6 M HCl in the presence of oxalic acid, with almost all admixtures remaining in aqueous phase.

Fudge and Woodhead (1956) carried out the radiochemical purification of protactinium by ^{233}Pa precipitation with niobium tannate in the presence of EDTA. The separation of niobium and protactinium was carried out by paper chromatography or by protactinium precipitation with barium fluorozirconate.

4.9.2 Radioactivation methods

A quite large value of the thermal-neutron cross-section (^{231}Pa, 211 barns) (Smith *et al.*, 1956; Holtzman, 1962) allows the use of the nuclear reaction $^{231}\mathrm{Pa}(n,\gamma)^{232}\mathrm{Pa}$ for protactinium determination. In some cases it is better to measure ^{232}U, the daughter of the ^{232}Pa decay product, after the separation of uranium in a radiochemically pure state. This method allows the determination of 10^{-8} to 10^{-10} g of ^{231}Pa (Sakanoue *et al.*, 1965).

4.9.3 Spectral and X-ray methods

Spectral methods are not practical for the direct determination of protactinium in natural samples and other materials because of the low sensitivity and experimental complications. Usually emission spectral analysis is applied only for the detection of admixtures (Nb, Fe, Mg, Al, Sn, Cu, Si, and others) in pure samples of protactinium (Sackett, 1960; Spitsyn and D'yachkova, 1960; Walter, 1963; Birks *et al.*, 1965; Cunningham, 1966; Kirby and Figgins, 1966; Roberts and Walter, 1966).

The emission spectrum of protactinium has been investigated (Schüller and Gollnow, 1934; Thompson, 1951; Richards and Atherton, 1961, 1963; Richards *et al.*, 1961; Giaechetti, 1966). There are a few thousand lines in the range 2650–25 000 Å, and many of them have hyperfine structure. Tomkins and Fred (1949) observed 263 lines in the range 2640.3–4371.4 Å; the most sensitive and definite lines are at 3957.8, 3054.6, and 3053 Å. The sensitivity of protactinium determination is 0.2 μg Pa by use of these lines with the copper spark method. According to the data of Spitsyn and D'yachkova (1960), lines at 2732.2, 2743.9, and 2755.9 Å are also characteristic for protactinium. The X-ray spectrum of Pa_2O_5 has been investigated by Russell (1913) and Grosse and co-workers (Beuthe and Grosse, 1930; Pierce and Grosse, 1935; Grosse, 1939). Twenty-one lines of the L-series were found in the range 1088.5×10^{-11} to 586.6×10^{-11} cm and 14 lines of M-series in the range 518.2×10^{-11} to 252.2×10^{-11} cm. The information about other lines in these series has been reported in the literature (Dolejsek and

Kunzl, 1936; Cauchois and Hulubel, 1947; Cauchois and Bonnelle, 1966). A more recent compilation is given in Browne *et al.* (1954).

A comparative study of the photoacoustic spectra of lanthanide and actinide oxides (protactinium included) has been given by Heinrich *et al.* (1986).

4.9.4 Electrochemical methods

(a) Polarographic

The application of the polarographic method for the determination of protactinium is limited by the irreversibility of the Pa reduction process on the mercury drop electrode in many media.

(b) Potentiometric and amperometric

An oxidimetric method for Pa(IV) determination in chloride and sulfate solutions by titration with 6.7×10^{-2} M $FeCl_3$ solution was described by Musikas (1966). The final point was determined by a potentiometric method at a given current of 5 μA and an amperometric method at a given potential of 0.2 V. The platinum electrode was used as the indicator electrode, and a saturated calomel electrode was used as reference electrode. The titration was carried out in a special cell with a magnetic stirrer under nitrogen atmosphere.

The relative error for 3.65×10^{-2} to 4.08×10^{-2} M Pa in 6–8 N HCl or 1.0–1.8 N H_2SO_4 was nearly ±3%. The method is used for determination of the extent of Pa(V) reduction by an electrolytic method with the application of an amalgamated silver electrode.

4.9.5 Spectrophotometric methods

(a) Methods based on the Pa light absorption in mineral acids solutions

The absorption spectra of penta- and tetravalent protactinium in aqueous solutions of hydrochloric acid (Fried and Hindman, 1954; Nairn *et al.*, 1958; Brown *et al.*, 1959; Casey and Maddock, 1959a; Guillaumont *et al.*, 1959, 1960; Guillaumont, 1966c), sulfuric (Guillaumont *et al.*, 1960; Brown *et al.*, 1961; Brown and Wilkins, 1961; Guillaumont, 1966c; Myasoedov *et al.*, 1966b), perchloric (Guillaumont *et al.*, 1960; Brown and Wilkins, 1961; Guillaumont, 1966a,c) acids, and in neutral fluoride solutions (Miranda and Muxart, 1964a,b) have been studied rather completely. Protactinium complexes with inorganic ligands highly absorb in the ultraviolet part of spectrum at wavelength <250 nm. Protactinium determination by light absorption in solutions of inorganic acids is used very rarely because of the low sensitivity and selectivity of these methods, and also because of complications connected with work in ultraviolet part of the spectrum. Nevertheless the existence of characteristic bands in the absorption spectra of protactinium allow their use for the determination of protactinium concentration and for identification of protactinium valence state in some cases.

(b) Methods based on reactions with organic reagents

Effective spectrophotometric methods for the determination of microgram amounts of protactinium with application of organic reagents have been described. The advantage of such methods is their high sensitivity and the possibility of protactinium determination without previous separation from other radioactive elements that usually prevent radiometric determination of protactinium. Spectrophotometric methods for the determination in very acidic solutions are especially worthwhile. In this case complications connected with the hydrolysis of protactinium ions are excluded, and the selectivity of determination, reproducibility, and reliability of the methods increase considerably.

Pentavalent protactinium forms a stable complex with Arsenazo-III, hence this reaction is accompanied by the change of the red color of the reagent to green after mixing. The formation of the colored compound takes place in a wide interval of acidity: from slightly acidic media to 10 N H_2SO_4 or HCl and even in more concentrated solutions. Absorbance of the solution of protactinium complex compound reaches a maximum immediately after the reagent addition and does not change for at least 24 h. The reaction of Pa with the reagent is rather sensitive; the molar extinction coefficient at 660 nm is equal to 2.2×10^4 L· M^{-1} cm^{-1}. The error of the protactinium determination at the concentration 0.3–3.1 mg L^{-1} in the absence of interfering elements is ±3.5% (Pal'shin *et al.*, 1962).

According to the data of Pal'shin *et al.* (1962) the complex compound of protactinium with Arsenazo-III is quantitatively extracted by an equal volume of isoamyl alcohol from solutions with sulfuric acid concentration >2 M. The extraction of the protactinium compound from very acidic solutions of sulfuric acid gave high selectivity. In addition there is no necessity for the previous separation of contaminants. The error of the protactinium determination at a concentration 3 mg L^{-1} is less than 3% in the presence of a 10^4-fold amounts of Fe(III), Al, Ni; 10^3-fold amounts of Cr(III), La, Mn(II); 200-fold amounts of Bi(III), Sn(IV), Zr, Nb, Mo(VI), U(VI); and 100-fold amounts of Th and Ti(IV).

Pa(V) forms with TTA a colored complex compound, slightly soluble in aqueous solutions, but very soluble in many organic solvents (Myasoedov and Muxart, 1962a,b; Pal'shin and Myasoedov, 1963). The extraction-photometric method of protactinium determination with TTA is rather sensitive (~1 mg L^{-1} Pa) and highly selective. The molar extinction coefficient of protactinium complex with TTA is equal to 1.4×10^4 and 0.9×10^4 L· M^{-1} cm^{-1} at 430 and 440 nm, respectively. Beer's law is followed for concentrations of Pa in the solution over the range from 1.3 to 8.7 mg L^{-1}.

4.9.6 Gravimetric methods

Gravimetric methods of protactinium determination are used relatively rarely because of their low sensitivity. Nowadays this method is applied mainly for the determination of milligram amounts of Pa in solutions and in compounds. Protactinium is isolated from solutions in the form of insoluble compounds with inorganic or organic reagents. The choice of reagent for precipitation depends on the presence of other elements in solution.

The weighing of Pa_2O_5 is the final operation in most gravimetric determinations of protactinium after its precipitation in the form of hydroxide, peroxide, iodate, phenylarsonate, cupferronate, and following calcinations at 600–1000°C under air for 1–2 h. Pa_2O_5 is suitable and stable weight form for the determination, but it has a large conversion coefficient to protactinium, equal to 0.852. This limits the application of the determination to relatively large amounts of protactinium. The use of phenylarsonate of protactinium is more preferable as the weight form (Myasoedov *et al.*, 1968a). In this case the conversion coefficient is equal to 0.346. The calcinations of the protactinium compounds usually are carried out in platinum crucibles in order to regenerate the element. Concentrated HF or a mixture of HF + H_2SO_4 is used for dissolution of Pa_2O_5.

(a) Protactinium hydroxide

For weight determination protactinium hydroxide is obtained usually by precipitation of protactinium ions from solutions of mineral acids or their mixtures with ammonium hydroxide. The composition of the formed precipitate depends on precipitation conditions and can be represented as $Pa_2O_5 \cdot xH_2O$. Under precipitation by NaOH or KOH solutions it is necessary to wash thoroughly the precipitate to remove the adsorbed alkali metal ions. The precipitation of protactinium hydroxide is often used for analysis of some protactinium compounds (Grosse, 1934c; Sellers *et al.*, 1954; Bagnall and Brown, 1964; Bagnall *et al.*, 1965; Bukhsh *et al.*, 1966a,b; Stchouzkoy *et al.*, 1966a; Davydov and Pal'shin, 1967).

(b) Protactinium phenylarsonate

Phenylarsonic acid precipitates Pa(v) practically quantitatively from neutral solutions and from solutions of HCl, HNO_3, H_2SO_4, and $HClO_4$ at acids concentration <5 N. The precipitate composition, dried at 120–180°C, corresponds to the formula $H_3PaO_2(C_6H_5AsO_3)_2$. The precipitate is stable and is not changed in weight during heating for few hours at the above-mentioned temperature. As described above, protactinium phenylarsonate can be used for gravimetric determination. This compound may also be converted to Pa_2O_5 by calcination at 1000°C.

The precipitation of protactinium as phenylarsonate from acid solutions can be carried out in the presence of Ni, Co, Cr, La, Fe(III), Mn, Cu, Ti, Th, U, and other elements. Zr, Nb, Ta, fluoro-, and phosphate ions prevent the determination (Myasoedov *et al.*, 1968a).

(c) Protactinium peroxide

Hydrogen peroxide precipitates protactinium from solutions of mineral acids (HNO_3, HCl, H_2SO_4, and $HClO_4$) in the form of amorphous white protactinium peroxide, $Pa_2O_5 \cdot 3H_2O$ (Stchouzkoy and Muxart, 1962; Marples, 1965; Stchouzkoy *et al.*, 1966b). This compound is not stable in air, therefore, the protactinium determination is performed with the calcination of the precipitate to Pa_2O_5. The precipitation of protactinium peroxide from acid solutions can be carried out in the presence of Ni, Co, Cr, Mg, Mn, and other elements, and small quantities of iron. La, Th, U, Zr, and F^- ions prevent the determination. Stchouzkoy and Muxart (1962) recommend carrying out the $Pa_2O_5 \cdot 3H_2O$ precipitation from 0.25 M H_2SO_4 solution, obtained by dissolution of freshly precipitated protactinium hydroxide in sulfuric acid or by some other method.

Pal'shin *et al.* (1968a) applied oxalic acid to increase the selectivity of precipitation with hydrogen peroxide. It was shown that the extent of precipitation of protactinium peroxide from oxalic acid solutions increases with increasing HCl concentration. When the molar relation $H_2C_2O_4$:HCl is equal to 1:5 the extent of precipitation reaches a steady value, and at sufficient excess of hydrogen peroxide the precipitation is quantitative. The method allows determining protactinium in complex solutions and also in the presence of large amounts of zirconium, niobium, and tantalum.

(d) Protactinium iodate

Iodic acid and its salts precipitate Pa(V) from acid solutions in the form of a white volumetric precipitate. Upon standing, especially after heating on a water bath, the precipitate is compressed and is transformed into crystalline form. The composition of protactinium iodate precipitate is not established. According to the data of Kirby (1959) the quantitative precipitation of protactinium (~99.5%) occurs from previously heated solution of protactinium in 0.7 M H_2SO_4 under the addition of a drop at a time of excess 15% HNO_3. The weight determination is performed by calcination of the precipitate to Pa_2O_5 at 800°C (Codding *et al.*, 1964; 1966).

(e) Protactinium cupferronate

There is an indication that CP quantitatively precipitates protactinium from tartaric acid solutions (SalesGrande, 1950) and from solutions of mineral acids (Maddock and Miles, 1949). However, conditions of protactinium precipitation and composition of the formed precipitate have not been investigated in detail. The calcination of protactinium cupferronate at 1000°C leads to the formation of Pa_2O_5 that can be used for weight determination of protactinium.

4.9.7 Determination of protactinium in the environment

High-sensitivity mass spectrometric measurements of the naturally occurring radionuclides ^{231}Pa and ^{230}Th in the deep Canada Basin and on the adjacent shelf indicate high particle fluxes and scavenging rates in this region. The data obtained suggest that offshore advection of particulate material from the shelves contributes to scavenging of reactive materials in areas of permanent ice cover (Edmonds *et al.*, 1998). The scavenging of ^{231}Pa and ^{230}Th was investigated also in the Atlantic Sector of the Pacific Ocean (Yang *et al.*, 1986), and Southern Ocean by combining results from sediment trap and *in situ* filtration studies (Walter *et al.*, 2001). The U–Th–Pa model was realized for environment samples aging (Cheng *et al.*, 1998).

A new technique for the determination of ^{231}Pa in silicate rocks by isotope dilution mass spectroscopy was described (Bourdon *et al.*, 1999). This technique permits the determination down to a 100 fg of ^{231}Pa with a 1–2% uncertainty at the 2 sigma level. The first high-precision ^{231}Pa measurements in a manganese crust applying TIMS using the double filament techniques were described (Pickett *et al.*, 1994). The detection limit using TIMS is at least one order of magnitude lower, and the statistical uncertainty – six to eight times better than for alpha-spectroscopy. Thus, the older section of manganese crust from the Northern Equatorial Pacific could be measured precisely for their Pa-231 activity. The data described by Fietzky *et al.* (1999) reveal significant variations in ^{231}Pa activity for the last 150 ka, which corroborate existing alpha-spectroscopy results. If the growth rate was constant between 0 and 450 ka, the protactinium flux from the water column into manganese encrustations must have been variable. Thus, ^{231}Pa is not suitable for dating marine Mn/Fe deposits.

The determination of ^{231}Pa in environmental and soil materials (Harbottle and Evans, 1997) and in uranium ore samples is provided by gamma-ray spectrometer with high-purity germanium (Zhang Qingwen *et al.*, 1991).

LIST OF ABBREVIATIONS

Arsenazo-III	3,6-bis-[(2-arsonophenyl)azo]-4,5-dihydroxy-2,7-naphthalene disulfo acid
BPHA	*N*-benzoylphenylhydroxylamine
CP	Cupferron
HDEHP	bis(2-ethylhexyl)phosphoric acid
DIAPA	di-isoamylphosphoric acids
DIBC	di-isobutylcarbinol

DIBK	di-isobutylketone
DIPC	di-isopropylcarbinol
DIPK	di-isopropylketone
DMSO	dimethyl sulfoxide
DSBPP	di-*S*-butylphenyl phosphonate
EDTA	ethylenediaminetetraacetic acid
fg	femtogram
Hexone (or MIK)	methyl isobutyl ketone
Ka	thousand years ago
ng	nanogram
NCP	neocupferron
NHE	normal hydrogen electrode
PAA	phenylarsonic acid
Pc	phthalocyaninato
PMBP	1-phenyl-3-methyl-4-benzoylpyrazolone
SCE	standard calomel electrode
TBP	tri(*n*-butyl)phosphate
THF	tetrahydrofuran
TIMS	thermal ionization mass spectroscopy
TOA	trioctylamine
TOPO	tri-*n*-octylphosphine oxide
TPPO	triphenylphosphine oxide
TTA	thenoyltrifluoroacetone
UKAEA	United Kingdom Atomic Energy Authority

REFERENCES

Abdel Gawad, A. S., Souka, N., and Girgis, C. (1976) *J. Radioanal.*, **31**, 377–82.

Ahmad, I. (2004) Argonne National Laboratory, unpublished work.

Ahrland, S., Liljenzin, J. O., and Rydberg, J. (1973) in Comprehensive Inorganic Chemistry, vol. 5 (eds. J. C. Bailor, Jr., H. J. Emeleus, R. Nyholm, and A. F. Trotman-Dickenson), Pergamon, Oxford, pp. 465–635.

Albridge, R. G., Hollander, J. M., Gallagher, C. J., and Hamilton, J. H. (1961) *Nucl. Phys.*, **27**, 529–53.

Alekseev, V. A., Morozova, Z. E., and Ziv, V. S. (1988) *Radiokhimiya*, **29**, 344–9.

Alekseev, V. A., Morozova, Z. E., and Ziv, V. S. (1989) *Radiokhimiya*, **30**, 322–6.

Alhassanieh, O., Abdul-Hadi, A., Ghafar, M., and Aba, A. (1999) *Appl. Rad. Isotopes*, **51**, 493–8.

Al-Kazzaz, A. M. S., Bagnall, K. W., Brown, D., and Whittaker, B. (1972) *J. Chem. Soc. Dalton Trans.*, 2273–7.

Andreev, A. M., Bogranov, D. D., Yeremin, A. V., Kabachenko, A. P., Malyshev, O. N., Ter Akopian, T. A., and Chepigin, V. I. (1996a) *Izvestiya Akademii Nauk. Ser. Fiz.*, **60**, 186–8.

Andreev, A. M., Popeko, A. G., Yeremin, A. V., Hofman, S., Hessberger, F. P., Folder, H., Ninov, V., and Saro, S. (1996b) *Izvestiya Akademii Nauk. Ser. Fiz.*, **60**, 148–53.

Anonymous (1949) *Chem. Eng. News*, **27**, 2996–9.
Antonoff, G. N. (1911) *Phil. Mag.*, **22**, 419–32.
Antonoff, G. N. (1913) *Phil. Mag.*, **26**, 1058.
Arbman, E., Bjornholm, S., and Nielsen, O. B. (1960) *Nucl. Phys.*, **21**, 406–37.
Arden, I. W., Booth, E., and Perkins, M. (1962) U.K. Atomic Energy Authority Research Group. Report No AERE-AM90.
Ardisson, G. and Ardisson, C. (1975) *Radiochem. Radioanal. Lett.*, **21**, 357–64.
Artna-Cohen, A. (1971) *Nucl. Data B*, **6**, 225–55.
Asprey, L. B., Kruse, F. H., Rosenzweig, A., and Penneman, R. A. (1966) *Inorg. Chem.*, **6**, 659–61.
Asprey, L. B., Kruse, F. H., and Penneman, R. A. (1967) *Inorg. Chem.*, **6**, 544–8.
Asprey, L. B., Fowler, R. D., Lindsay, J. D., White, R. W., and Cunningham, B. B. (1971) *Inorg. Nucl. Chem. Lett.*, **7**, 977–80.
Astheimer, L. and Schwochau, K. (1973) *J. Inorg. Nucl. Chem.*, **35**, 223–30.
Augoustinik, A. I. (1947) *Zh. Prikl. Khim.*, **20**, 327.
Axe, J. D. (1960) U.S. Report UCRL-9293.
Axe, J. D., Kyi, R.-T., and Stapleton, H. J. (1960) *J. Chem. Phys.*, **32**, 1261.
Axe, J. D., Stapleton, H. J., and Jeffries, C. D. (1961) *Phys. Rev.*, **121**, 1630–7.
Bachelet, M. and Bouissières, G. (1944) *Bull. Soc. Chim.*, **11**, 169–71.
Bachelet, M. and Bouissières, G. (1947) *Bull. Soc. Chim.*, **14**, 281–3.
Bagnall, K. W. and Brown, D. (1964) *J. Chem. Soc.*, 3021–5.
Bagnall, K. W., Brown, D., and Jones, P. J. (1965) *J. Chem. Soc.*, 176–81.
Bagnall, K. W. (1966a) *Radiochim. Acta*, **5**, 1.
Bagnall, K. W. (1966b) in *Physico-Chimie du Protactinium* (eds. G. Bouissières and R. Muxart), Centre National de la Recherche Scientifique, Orsay, Paris, pp. 88–92.
Bagnall, K. W. and Brown, D. (1967) *J. Chem. Soc. A*, 275–8.
Bagnall, K. W., Brown, D., and Easey, J. F. (1968a) *J. Chem. Soc. A*, 288–91.
Bagnall, K. W., Brown, D., Holah, D. H., and Lux, F. (1968b) *J. Chem. Soc. A*, 465–70.
Bagnall, K. W., Brown, D., Lux, F., and Wirth, G. (1969) *Z. Naturforsch.*, **B24**, 214–21.
Bagnall, K. W. (1972) *The Actinide Elements,* Elsevier, Amsterdam.
Bagnall, K. W., Bhandari, A. M., Brown, D., Lidster, P. E., and Whittaker, B. (1975) *J. Chem. Soc. Dalton Trans.*, 1249–52.
Banks, R. H., Edelstein, N. M., Rietz, R. R., Templelon, D. H., and Zalkin, A. (1978) *J. Am. Chem. Soc.*, **100**, 1857–8.
Banks, R. H. (1979) Lawrence Berkeley Laboratory Report LBL-10292.
Banks, R. H. and Edelstein, N. M. (1980) *Am. Chem. Soc. Symp. Ser.*, **131**, 331–48.
Bansal, B. M. (1966) U.S. Report UCRL-16787.
Baranov, A. A., Kulakov, V. M., Samilov, P. S., Zelenkov, A. G., Rodinov Yu, F., and Pirozhkov, S. V. (1962) *Sov. Phys. JETP*, **14**, 1052–9.
Baranov, A. A., Kulakov, V. M., and Shatinskii, V. M. (1968) *Sov. J. Nucl. Phys.*, **7**, 442–5.
Barendregt, F. and Tom, S. (1951) *Physica*, **17**, 817–20.
Barnett, M. K. (1957) *J. Inorg. Nucl. Chem.*, **4**, 358.
Barnett, M. K. (1958) *Khimiya & Khim. Tekhnologiya*, **3**, 150.
Bastin, G., Leang, C. F., and Walen, R. J. (1966) *Compt. Rend. Acad. Sci. Paris B*, **262**, 89–92.

Baumgartner, F., Fischer, E. O., Kanellakopulos, B., and Laubeneau, P. (1969) *Angew. Chem.*, **8**, 202.

Baybarz, R. D., Bohet, J., Buijs, K., Colson, L., Muller, W., Reul, J., and Spirlet, J. C. (1976) in *Proc. 4th Int. Transptutonium Element Symp.*, Baden, pp. 61–8.

Bearden, J. A. (1967) *Rev. Mod. Phys.*, **39**, 78–124.

Bearden, J. A. and Burr, A. F. (1967) *Rev. Mod. Phys.*, **39**, 125–42.

Benedict, V., Buijs, K., Dufour, C., and Toussaint, J. C. (1975) *J. Less Common Metals*, **42**, 345–54.

Benedict, U., Dufour, C., and Mayne, K. (1979) *J. Phys. Colloq.*, **4**, 103–5.

Beuthe, H. and Grosse, A. (1930) *A. Phys. Z*, **61**, 170.

Bhandari, A. M. and Kulkarni, D. K. (1979) *Curr. Sci.*, **48**, 577–8.

Birks, F. T., Tomas, A. M., and Milner, G. W. C. (1965) UK Atomic Energy Authority Research Group. Report NAER-E-R-4615, p. 17.

Bjørnholm, S. and Nielsen, O. B. (1962) *Nucl. Phys.*, **30**, 488–512.

Bjørnholm, S. and Nielsen, O. B. (1963) *Nucl. Phys.*, **42**, 642–59.

Bjørnholm, S., Westgaard, L., Mason, T., and Nielsen, H. S. (1967) *Radiochim. Acta*, **8**, 204–6.

Bjørnholm, S., Borggreen, J., Davies, D., Hansen, N. J. S., Pedersen, J., and Nielsen, H. S. (1968) *Nucl. Phys. A*, **118**, 261–301.

Bohet, J. (1977) *Comm. Eur. Communities (Rep.) EUR 5882.*

Bohet, J. and Muller, W. (1978) *J. Less Common Metals*, **57**, 185–9.

Bohres, E. W. (1974) German Report JUL-1080-NC.

Bohres, E. W., Hauck, J., Schenk, H. J., and Schwochau, K. (1974) in *Proc. 16th Int. Conf. Coord. Chem.*, **2**, 166.

Boltwood, B. B. (1906) *Am. J. Sci.*, **22**, 537–8.

Boltwood, B. B. (1908) *Am. J. Sci.*, **25**, 269–98.

Bonnet, M. and Guillaumont, R. (1969) *Radiochim. Acta*, **12**, 98–107.

Booth, A. H. (1951) *J. Chem. Educ.*, **28**, 144–5.

Borggreen, J., Valli, K., and Hyde, E. K. (1970) *Phys. Rev. C*, **2**, 1841–62.

Born, H.-J. (ed.) (1971) *Tagungsber. 3 Int. Pa-Konf.*, Schloss-Elmau. 15–18 April 1969, German Report BMBW-FBK 71–17.

Bouissières, G. and Haïssinsky, M. (1949) *J. Chem. Soc. Suppl.*, **2**, 256–8.

Bouissières, G. and Haïssinsky, M. (1951) *Bull. Soc. Chem.*, **18**, 557–60.

Bouissières, G., Marty, N., and Teillac, J. (1953) *Compt. Rend. Acad. Sci. Paris*, 324–6.

Bouissières, G. and Muxart, R. (eds) (1966) *Physico-Chimie du Protactinium*, Centre National de la Recherche Scientifique, Orsay, Paris , 2–8 July 1965.

Bouissières, G. (1971) in *Tagungsber. 3 Int. Pa-Konf.* (ed. H.-J. Born), Schloss-Elmau, 15–18 April 1969, German Report BMBW-FBK 71–17, Paper No. 26.

Bourdon, B., Joron, J. L., and Allegre, C. J. (1999) *Chem. Geol.*, **157**, 147–51.

Bower, K., Angel, A., Gibson, R., Robinson, T., Knobeloch, D., and Smith, B. (1994) *J. Radioanal. Nucl. Chem. Articles*, **181**, 97–107.

Bradbury, M. H. (1981) *J. Less Common Metals*, **78**, 207–18.

Briand, J.-P., Chevallier, P., Borg, J., and Teillas, J. (1969) *Compt. Rend. Acad. Sci. Paris B*, **269**, 582–5.

Brooks, M. S. S., Calestani, G. J., Spirlet, C., Rebizant, J., Mueller, W., Fournier, J. M., and Blaise, A. (1980) *Physica B&C*, **102**, 84–7.

Brown, D., Smith, A. J., and Wilkins, R. G. (1959) *J. Chem. Soc.*, 1463–6.

Brown, D. and Wilkins, R. G. (1961) *J. Chem. Soc.*, 3804–7.

Brown, D., Sato, T., Smith, A. J., and Wilkins, R. G. (1961) *J. Inorg. Nucl. Chem.*, **23**, 91–101.

Brown, D. and Maddock, A. G. (1963) *Quart. Rev.*, **17**, 289–341.

Brown, D. and Jones, P. J. (1964) *J. Inorg. Nucl. Chem.*, **26**, 2296–7.

Brown, D. and Easey, J. F. (1965) *Nature*, **205**, 589.

Brown, D. (1966) in *Physico-Chimie du Protactinium* (eds. G. Bouissières and R. Muxart), Centre National de la Recherche Scientifique, Orsay, Paris, 2–8 July 1965, pp. 147–53.

Brown, D. and Easey, J. F. (1966) *J. Chem. Soc. A*, 254–8.

Brown, D. and Jones, P. J. (1966a) *Chem. Commun.*, 280.

Brown, D. and Jones, P. J. (1966b) *J. Chem. Soc. A*, 733–7.

Brown, D. and Jones, P. J. (1966c) *J. Chem. Soc. A*, 874–8.

Brown, D., Dixon, S. N., and Jones, P. J. (1966a) *J. Inorg. Nucl. Chem.*, **28**, 2529–33.

Brown, D., Easey, J. F., and DuPreez, J. G. H. (1966b) *J. Chem. Soc. A*, 258–61.

Brown, D. and Jones, P. J. (1967a) *J. Chem. Soc. A*, 243–7.

Brown, D. and Jones, P. J. (1967b) *J. Chem. Soc. A*, 247–51.

Brown, D. and Jones, P. J. (1967c) *J. Chem. Soc. A*, 719–23.

Brown, D. and Maddock, A. G. (1967) in *Prog. Nucl. Energy Ser.*, IX, pp. 3–47.

Brown, D., Easey, J. F., and Holah, D. G. (1967a) *J. Chem. Soc. A*, 1979–80.

Brown, D., Easey, J. F., and Jones, P. J. (1967b) *J. Chem. Soc. A*, 1698–702.

Brown, D., Kettle, S. F. A., and Smith, A. J. (1967c) *J. Chem. Soc. A*, 1429–34.

Brown, D., Dixon, S. N., Glover, K. M., and Rogers, F. J. G. (1968a) *J. Inorg. Nucl. Chem.*, **30**, 19–22.

Brown, D., Petcher, T. J., and Smith, A. J. (1968b) *Nature*, **271**, 737–8.

Brown, D. (1969) *Adv. Inorg. Chem. Radiochem.*, **12**, 1–51.

Brown, D. and Petcher, T. J. (1969) *Acta Crystallogr. B*, **25**, 178–82.

Brown, D. and Easey, J. F. (1970) *J. Chem. Soc. A*, 3378–81.

Brown, D. and Rickard, C. E. F. (1970) *J. Chem. Soc. A*, 3373–7.

Brown, D., Hill, J., and Rickard, C. E. F. (1970a) *J. Chem. Soc. A*, 476–80.

Brown, D., Hill, J., and Rickard, C. E. F. (1970b) *J. Chem. Soc. A*, 497–501.

Brown, D. (1971) in *Tagungsber. 3 Int. Pa-Konf.* (ed. H.-J. Born), Schloss-Elmau, 15–18 April 1969, German Report BMBW-FBK 71-17, Paper No. 32.

Brown, D. and Rickard, C. E. F. (1971a) *J. Chem. Soc. A*, 81–7.

Brown, D. and Rickard, C. E. F. (1971b) in *Tagungsber. 3 Int. Pa-Konf.* (ed. H.-J. Born), Schloss-Elmau, 15–18 April 1969, German Report BMBW-FBK 71-17, Paper No. 21.

Brown, D., Hill, J., and Rickard, C. E. F. (1971) in *Tagungsber. 3 Int. Pa-Konf.* (ed. H.-J. Born), Schloss-Elmau, 15–18 April 1969, German Report BMBW-FBK 71-17, Paper No. 22.

Brown, D., Reynolds, C. T., and Mosely, P. T. (1972) *J. Chem. Soc. Dalton Trans.*, 857–9.

Brown, D. (1973) in *Comprehensive Inorganic Chemistry*, vol. 5 (eds. J. C. Bailar, Jr, H. J., Emeleus, R. Nyholm, and A. F. Trotman-Dickenson), Pergamon, Oxford, pp. 151–217.

Brown, D., De Paoli, G., and Whittaker, B. (1976a) *J. Chem. Soc. Dalton Trans.*, 1336–8.

Brown, D., Whittaker, B., and Di Paoli, G. (1976b) UK Report, Atomic Energy Research Establishment AERE-R8367.

Brown, D., Tso, T. C., and Whittaker, B. (1977) *J. Chem. Soc. Dalton Trans.*, 2291–6.

Brown, D. and Whittaker, B. (1978) *J. Less Common Metals*, **61**, 161–70.

Brown, D. (1979) *Inorg. Nucl. Chem. Lett.*, **15**, 219–23.

Brown, D. (1982) in *Actinides in Perspective* (ed. N. Edelstein), Pergamon Press, Oxford, pp. 343–59.

Brown, D., Barry, J. A., and Holloway, J. H. (1982a) UK Report, Atomic Energy Research Eslablishment, AERE-R10415.

Brown, D., Whittaker, B., Benny, J. A., and Holloway, J. H. (1982b) *J. Less Common Metals*, **86**, 75–84.

Browne, C. I., Hoffman, D. C., Smith, H. L., Bunker, M. E., Mize, J. P., Stanner, J. W., Moore, R. L., and Bologna, J. P. (1954) *Phys. Rev.*, **95**, 827.

Bukhsh, M. N., Flegenheimer, J., Hall, F. M., Maddock, A. G., and deMiranda, C. F. (1966a) *J. Inorg. Nucl. Chem.*, **28**, 421–31.

Bukhsh, M. N., Flegenheimer, J., Hall, F. M., Maddock, A. G., and deMiranda, C. F. (1966b) in *Physico-Chimie du Protactinium* (eds. G. Bouissières and R. Muxart), Centre National de la Recherche Scientifique, Orsay, Paris, pp. 195–207.

Bunney, L. R., Ballou, N. E., Pascual, J., and Foti, S. (1959) *Anal. Chem.*, **31**, 324–6.

Bykhovskii, D. N., Kuzmina, M. A., and Lazkhina, G. S. (1977) *Radiokhimiya*, **19**, 178–84.

Calestani, G., Spirlet, J. C., and Mueller, W. (1979a) *J. Phys. Colloq.*, **4**, 106–7.

Calestani, G., Spirlet, J. C., Rebizant, J., and Mueller, W. (1979b) *J. Less Common Metals*, **68**, 207–12.

Caletka, R. and Spěváčkova, V. (1975) *Radiochem. Radioanal. Lett.*, **23**, 37–42.

Camarcat, M., Bouissières, G., and Haïssinsky, M. (1949) *J. Chem. Phys.*, **46**, 153.

Campbell, D. O. (1964) in *Proc. Protactinium Chem. Symp.,* 25–26 April 1963, U.S. Report TID-7675, Gatlinburg, Tennessee, pp. 87–103.

Carlier, R. (1971) French Report FRNC-TH-91.

Carlier, R. and Genet, M. (1972a) *Radiochem. Radioanal. Lett.*, **10**, 91–7.

Carlier, R. and Genet, M. (1972b) *Radiochim. Acta*, **18**, 11–16.

Carrere, J. P. (undated) unpublished results cited by Muxart and Guillaumont (1974) in *Complements au Noueveau Traite de Chimie Minerale* (eds. A. Pacault and G. Pannetier), Masson, Paris, p. 2.

Carsell, O. J. and Lawrence, J. J. (1959) *J. Chem. Educ.*, **36**, 499–501.

Carswell, D. J. and Lawrence, J. J. (1959) *J. Inorg. Nucl. Chem.*, **11**, 69–74.

Casey, A. T. and Maddock, A. G. (1959a) *J. Inorg. Nucl. Chem.*, **10**, 58.

Casey, A. T. and Maddock, A. G. (1959b) *J. Inorg. Nucl. Chem.*, **10**, 289–305.

Cauchois, Y. and Hulubel, H. (1947) Constantes selectionees Longueurs D'onde des Emmissions X et des Discont. D'Adsorption X. Hermann, Paris.

Cauchois, Y. and Bonnelle, C. (1966) in *Physico-Chimie du Protactinium* (eds. G. Bouissières and R. Muxart), Centre National de la Recherche Scientifique, Orsay, Paris, 2–8 July 1965, p. 21.

Cauchois, Y. (1971) in *Tagungsher. Int. Pa-Konf.* (ed. H.-J. Born), Schloss-Elmau, 15–18 April 1969, German Report BMBW-FBK 71–17.

Cazaussus, A., Arapaki-Strapelius, H., and Muxart, R. (1971) *Radiochem. Radioanal. Lett.*, **6**, 297–306.

Chakravortty, V. and Mohanly, S. R. (1979) *Radiochem. Radioanal. Lett.*, **41**, 275–8.

Chakravortty, V., Mohanly, S. R., and Dash, K. C. (1986) *Radiochim. Acta*, **40**, 89–94.

Chang, H.-P., Ho, C.-K., Ting, G., and Wu, S.-C. (1974) *Nucl. Sci. J.*, **11**, 73–81.

Chang, H.-P. and Ting, G. (1975a) *Ho Tzu K'oHsueh.*, **12**, 119–32.

Chang, H.-P. and Ting, G. (1975b) Taiwan Report INER-64-D–0167.

Chen, T. and Yuan, S. (1988) *Archaeometry*, **30**, 59–76.

Cheng, H., Edwards, R. L., Murrell, M. T., and Benjamin, T. M. (1998) *Geochimica et Cosmochimica Acta*, **62**, 3437–52.

Chetham-Strode, A., Jr. and Keller, O. L., Jr. (1966) in *Physico-Chimie du Protactinium* (eds. G. Bouissières and R. Muxart), Centre National de la Recherche Scientifique, Orsay, Paris, 2–8 July 1965, pp. 189–93.

Chilton, J. M. (1964) in *Proc. Protactinium Chem. Symp.*, 25–26 April 1963, U.S. Report TID-7675, Gatlinburg, Tennessee, pp. 157–9.

Codding, J. W., Berreth, J. R., Schuman, R. P., Burgus, W. H., and Deal, R. A. (1964) U.S. Report IDO-17007.

Codding, J. W., Berreth, J. R., Schuman, R. P., Burgus, W. H., Deal, R. A., and Simpson, F. B. (1966) in *Physico-Chimie du Protactinium* (eds. G. Bouissières and R. Muxart), Centre National de la Recherche Scientifique, Orsay, Paris, 2–8 July 1965, p. 325.

Collins, D. A., Hillary, J. J., Nairn, J. S., and Phillips, G. M. (1962) *J. Inorg. Nucl. Chem.*, **24**, 441–59.

Cotton, F. A., Wilkinson, G., Murillo, C. A., and Bochmann, M. (1999) in *Advanced Inorganic Chemistry*, 6th edition. John Wiley & Sons. Inc. Technical and Medical Division 605 Third Avenue; NY 10158–0012 ISBN 0-471-19957-5; Chapter 20 The Actinide Elements, P. 1130.

Crane, W. W. T. and Iddings, G. M. (1954) *Phys. Rev.*, **95**, 1702–3.

CRC Handbook of Chemistry and Physics and the American Chemical Society, Last Updated 12/19/1997, CST Information Service Team.

Cristallini, O. and Flegenheimer, J. (1963) *Radiochim. Acta*, **1**, 157–61.

Croft, W. L., Stone, J. A., and Pillinger, W. L. (1968) *J. Inorg. Nucl. Chem.*, **30**, 3203–8.

Crookes, W. (1900) *Proc. R. Soc.*, **66**, 409–22.

Crouthamel, C. E., Adams, F., and Dams, R. (1970) *Applied Gamma-Ray Spectrometrv,* Pergamon, Oxford.

Cunningham, B. B. (1966) in *Physico-Chimie du Protactinium* (eds. G. Bouissières and R. Muxart), Centre National de la Recherche Scientifique, Orsay, Paris, 2–8 July 1965, pp. 45–8.

Cunningham, B. B. (1971) in *Tagungsber. 3 Int. Pa-Konf.* (ed. H.-J. Born), Schloss-Elmau, 15–18 April 1969, German Report BMBW-FB-K, Paper No. 14.

Curie, P. (1911) *Le Radium*, **8**, 353–4.

Curie, M. (1913) *Ann. Chim. Phys.*, **30**, 125–6.

David, F. and Bouissières, G. (1966) in *Physico-Chimie du Protactinium* (eds. G. Bouissières and R. Muxart), Centre National de la Recherche Scientifique, Orsay, Paris, 2–8 July 1965, p. 301.

Davydov, A. V., Myasoedov, B. F., Novikov, Yu. P., Palei, P. N., and Pal'shin, E. S. (1965) *Nucl. Sci. Abst.*, **20**, 27–62.

Davydov, A. V., Marov, I. N., and Palei, P. N. (1966a) *Sov. J. Inorg. Chem.*, **11**, 1316.

Davydov, A. V., Marov, I. N., and Palei, P. N. (1966b) in *Physico-Chimie du Protactinium* (eds. G. Bouissières and R. Muxart), Centre National de la Recherche Scientifique, Orsay, Paris, 2–8 July 1965, pp. 181–8.

Davydov, A. V., Myasoedov, B. F., Novikov, Yu. P., Palei, P. N., and Pal'shin, E. S. (1966c) *Tr. Kom. Anal. Khim. Akad. Nauk SSSR*, **15**, 64–79.

Davydov, A. V. and Pal'shin, E. S. (1967) *Atomnaya Energiya*, **32**, 487–90.

D' Ege, R., Maddock, A. G., and Toms, D. I (1963). Unpublished observations cited by Brown.

Delaeter, J. R. and Heumann, K. G. (1991) *J. Phys. Chem. Refer. Data*, **20**, 1313–35.

deMiranda, C. F. and Maddock, A. G. (1962) *J. Inorg. Nucl. Chem.*, **24**, 1623–33.

deMiranda, C. F. and Muxart, R. (1964) *Bull. Soc. Chim. Fr.*, 2174–6.

deMiranda, C. F. and Muxart, R. (1965) *Bull. Soc. Chim. Fr.*, 387–9.

deMiranda, C. F. (1966) in *Physico-Chimie du Protactinium* (eds. G. Bouissières and R. Muxart), Centre National de la Recherche Scientifique, Orsay, Paris, 2–8 July 1965, pp. 127–34.

Dempster, A. J. (1935) *Nature*, **136**, 180.

dePinke, A. G., deSilviera, E. F., and Costa, N. L. (1970) *Phys. Rev. C*, **2**, 572–86.

Dod, R. L. (1972) U.S. Report LBL-659.

Dodge, R. P., Smith, G. S., Johnson, Q., and Elson, R. E. (1968) *Acta Crystallogr. B*, **24**, 304–12.

Dolejsek, V. and Kunzl, V. (1936) *Nature*, **138**, 590.

Duplessis, J. and Guillaumont, R. (1979) *Radiochem. Radioanal. Lett.*, **37**, 159–63.

D'yachkova, R. A., Spitsyn, V. I., and Nazarov, P. P. (1962) *Radiokhimiya*, **4**, 77–81.

D'yachkova, R. A. and Spitsyn, V. I. (1964) *Radiokhimiya*, **6**, 102.

D'yachkova, R. A., Khlebnikov, V. P., and Spitsyn, V. I. (1968a) *Sov. J. Inorg Chem.*, **13**, 439–42.

D'yachkova, R. A., Khlebnikov, V.P., and Spitsyn, V. I. (1968b) *Radiokhimiya*, **10**, 17–21.

Edelstein, N. M., Brown, D., Whittaker, B., Rajnak, K., Naik, R. C., and Krupa, J. C. (1988) *Inorg. Chem.*, **27**, 3186–9.

Edelstein, N. M., Krupa, J. C., and Kot, W. K. (1992) *J. Chem. Phys.*, **96**, 1–4.

Edelstein, N. M. and Kot, W. K. (1993) *J. Alloys & Comp.*, **193**, 82–7.

Edmonds, H. N., Moren, S. B., Hoff, J. A., Smith, J. N., and Edwards, R. L. (1998) *Science*, **280**, 405–7.

Edwards, R. L., Cheng, H., Murrell, M. T., and Goldstein, S. J. (1997) *Science*, **276**, 782–6.

El- Dessouky, M. M. (1966) *Microchim. Acta*, **2**, 461–6.

Ellis, Y. A. (1970) *Nucl. Data B*, **4**, 581–621.

Elson, R. E., Mason, G. W., Peppard, D. F., Sellers, P. O., and Studier, M. H. (1951) *J. Am. Chem. Soc.*, **73**, 4974–5.

Elson, R. E. (1954) *The Actinide Elements* (eds. G. T. Seaborg and J. J. Katz), McGraw-Hill, New York, pp. 103–29.

El-Sweify, F. H., Aly, H. F., Abdel-Rahman, A., and Shabana, R. (1985) *Radiochim. Acta*, **38**, 211–4.

El-Yamani, I. S. and Shabana, E. I. (1985) *J. Radioanal. Nucl. Chem. Lett.*, **88**, 209–16.

Emmanuel-Zavizziano, H. and Mme (1936) *Compt. Rend. Acad. Sci. Paris*, **202**, 1052–4.

Emmanuel-Zavizziano, H. and Haïssinsky, M. (1938) *Compt. Rend. Acad. Sci. Paris*, **206**, 1102.

Erdmann, B. (1971) German Report KFK-1444.

Erdmann, B. and Keller, C. (1971) *Inorg. Nucl. Chem. Lett.*, **7**, 675–83.

Erdmann, B. and Keller, C. (1973) *J. Solid State Chem.*, **7**, 40–8.

Fajans, K. (1913a) *Phys. Z*, **14**, 131–6.

Fajans, K. (1913b) *Phys. Z*, **14**, 136–42.

Fajans, K. and Göhring, O. (1913a) *Naturwissenschaften*, **I**, 339.

Fajans, K. and Göhring, O. (1913b) *Phys. Z*, **14**, 877–84.

Fajans, K. and Morris, D. F. C. (1913) *Nature*, **244**, 137–8.

Fidelis, J., Gwozdz, R., and Siekierski, S. (1963) *Nukleonika*, **8**, 224–7.

Fietzke, J., Bollhofer, A., Frank, N., and Mangini, A. (1999) *Nuclear Instr. Meth. Phys. Res. Sec. B*, **149**, 353–60.

Figgins, P. E. and Kirby, H. W. (1966) U.S. Report MLM-1349.

Figgins, P. E. and Hertz, M. R. (1972a) U.S. Report MLM-1903, pp. 6–17.

Figgins, P. E. and Hertz, M. R. (1972b) U.S. Report MLM-1955, pp. 7–13.

Figgins, P. E. and Hertz, M. R. (1973) U.S. Report MLM-2013, pp. 48–55.

Figgins, P. E., Hertz, M. R., and Stringham, W. S. (1975) U.S. Report MLM-2198, pp. 33–8.

Folger, H., Hartmann, W., Hessberger, F. P., Hoffman, S., Klemm, J., Munzenberg, G., Nilov, V., Thalheimer, W., and Armbruster, P. (1995) *Nucl. Instrum. Meth. Phys. Res. A*, **362**, 64–9.

Forrest, J. H., Lyle, S. J., Martin, G. R., and Maulden, J. J. (1960) *J. Inorg. Nucl. Chem.*, **15**, 210–4.

Fowler, R. D., Matthias, B. T., Asprey, L. B., Hill, H. H., Lindsay, J. D. G., Olsen, C. E., and White, R. W. (1965) *Phys. Rev. Lett.*, **15**, 860–7.

Fowler, R. D., Asprey, L. B., Lindsayand, J. D. G., and White, R. W. (1974) in *Low-Temperature Physics, LT13*, vol. 3 (ed. K. D. Timmerhaus), Plenum, New York, pp. 377–81.

Francis, M. and Theng-Da Tchang. (1935) *Phil. Mag.*, **20**, 626.

Fried, S. and Hindman, J. C. (1954) *J. Am. Chem. Soc.*, **76**, 4863–4.

Friedt, J. M., Kalvius, G. M., Poinsot, R., Rebizant, J., and Spirlet, J. C. (1978) *Phys. Lett. A*, **69**, 225–7.

Fronaeus, S. (1963) *Technique of Inorganic Chemistry*, vol. 1 (eds. H. B. Jonassen and A. Weissberger), Interscience, New York, pp. 1–36.

Fudge, A. J. and Woodhead, J. L. (1956) *Analyst*, **81**, 417.

Fudge, A. J. and Woodhead, J. L. (1957) *Chem. Ind.*, **17**, 1122.

Fujikawa, N., Fujioka, Y., Ojima, H., Osawa, S., and Yamakuchi, Y. (1996) Japan Patent 08151260-A, U.S. Patent 5650367-A, C04B-035/46, H01B-003/12.

Galateanu, I. and Lapitskii, A. V. (1962a) *Dokl. Akad. Nauk. SSSR (Angl. Transl.)*, **147**, 983–7.

Galateanu, I. and Lapitskii, A. V. (1962b) *Radiokhimiya*, **4**, 371–5.

Galateanu, I. (1966) *Can. J. Chem.*, **44**, 647–55.

Gasche, T., Johansson, B., and Brooks, M. S. (1996) *Phys. Rev. B. (Cond. Matt.)*, **54**, 2446–52.

Ghiorso, A., Meinke, W. W., and Seaborg, G. T. (1948) *Phys. Rev.*, **74**, 695–6.

Giaechetti, A. (1966) *J. Opt. Soc. Am.*, **56**, 653–7.

Giaechetti, A. (1967) *J. Opt. Soc. Am.*, **57**, 728–33.

Glover, K. M., Golden, A. J., Maddock, A. G., and Toms, D. J. (1959) Atomic Energy Research Establ. (GB), Report AERE-R-2971.

Gmelin (1942) *Gmelin Handbuch der Anorganischen Chemie – Protactinium und Isotope. System-Nummer 51 Verlag Chemie (1942) Verlag Chemie*. Springer Verlag, Berlin.

Gmelin (1977) *Gmelin Handbuch der Anorganischen Chemie – Protactinium und Isotope. System-Nummer 51Verlag Chemie (1977). Weinheim: Suppl.*, Vols. 1 and 2, Springer-Verlag, Berlin.

Gober, M. K., Kratz, J. V., Zimmermann, H. P., Schädel, M., Bruchle, W., Schimpf, E., Gregorich, K., Turler, E. A., Hannink, N. J., Czerwinski, K. R., Kadkhodayan, B., Lee, D. M., Nurmia, M. J., Hoffman, D. C., Gaggeler, H., Jost, D., Kovacs, J., Cherer, U. W., and Weber, A. (1992) *Radiochim. Acta*, **57**, 77–84.

Goble, A. G., Golden, J., and Maddock, A. G. (1956) *Can. J. Chem.*, **34**, 284.

Goble, A. G. and Maddock, A. G. (1958) *J. Inorg. Nucl. Chem.*, **7**, 94.

Goble, A. G., Golden, J., Maddock, A. G., and Toms, D. J. (1958) in *Prog. Nuct. Energy Ser. III*, 2: pp. 86–98.

Gofman, J. W. and Seaborg, G. T. (1949) *The Transuranium Elements. Div. IV, Natl. Nucl. En. Ser., 14B* (eds. G. T. Seaborg, J. J. Katz, and W. M. Manning), McGraw-Hill, New York, pp. 1427–30.

Göhring, O. (1914a) *Phys. Z*, **15**, 642–5.

Göhring, O. (1914b) Dissertation, p. 21. T. H., Karlsruhe.

Goode, J. H. and Moore, J. G. (1967) U.S. Report ORNL-3950.

Graue, G. and Kading, H. (1934a) *Naturwissenschaften*, **22**, 386–8.

Graue, G. and Kading, H. (1934b) *Angew. Chem.*, **47**, 650–3.

Greenwood, N. N. and Earnshaw, A. (1997) in *Chemistry of the Elements*, 2nd edn, Elsevier, Butterworth-Hainman, London, UK, Chapters 30–31.

Greis, O., Bohres, E. W., and Schwochau, K. (1977) *Z. Anorg. Allg. Chem.*, **433**, 111–8.

Grenthe, I. and Puigdomenech, I. (eds) (1997) *Modeling in Aquatic Chemistry*, OECD/NEA, Paris.

Grosse, A. V. (1927) *Naturwissenschaften*, **15**, 766–7.

Grosse, A. V. (1928) *Ber. Dtsch. Chem. Ges.*, **61B**, 233–45.

Grosse, A. V. (1930) *J. Am. Chem. Soc.*, **52**, 1742–7.

Grosse, A. V. (1932) *Naturwissenschaften*, **20**, 505.

Grosse, A. V. (1934a) *J. Am. Chem. Soc.*, **56**, 2200–1.

Grosse, A. V. (1934b) *J. Am. Chem. Soc.*, **56**, 2501.

Grosse, A. V. (1934c) *Science*, **80**, 512.

Grosse, A. V. and Agruss, M. S. (1934) *J. Am. Chem. Soc.*, **56**, 2200.

Grosse, A. V. and Agruss, M. S. (1935a) *Ind. Eng. Chem.*, **27**, 422–6.

Grosse, A. V. and Agruss, M. S. (1935b) *J. Am. Chem. Soc.*, **57**, 438–9.

Grosse, A. V. (1939) *Phys. Rev.*, **55**, 584.

A. V. Grosse, (1975) Personal communication.

Grudpan, K., Punyodom, W., and Singjanusong, P. (1990) in *Nuclear Science and Techn. Conf.,* 23–25 April 1990, Bangkok, Thailand.

Grundy, B. R. and Hamer, A. N. (1961) *J. Inorg. Nucl. Chem.*, **23**, 148–50.

Gryntakis, E. M. and Kim, J. I. (1974) *J. Inorg. Nucl. Chem.*, **36**, 1447–52.

Guillaumont, R., Muxart, R., Bouissières, G., and Haïssinsky, M. (1959) *Compt. Rend. Acad. Sci. Paris*, **248**, 3298.

Guillaumont, R., Muxart, R., Bouissières, G., and Haïssinsky, M. (1960) *J. Chim. Phys.*, **57**, 1019–28.

Guillaumont, R. (1965a) *Bull. Soc. Chim. Fr.*, 135–9.

Guillaumont, R. (1965b) *Compt. Rend. Acad. Sci. Paris*, **260**, 1416–8.

Guillaumont, R. (1966a) *Rev. Chim. Miner.*, **3**, 339–73.

Guillaumont, R. (1966b) in *Physico-Chimie du Protactinium* (eds. G. Bouissières and R. Muxart), Centre National de la Recherche Scientifique, Orsay, Paris, 2–8 July 1965, pp. 165–79.

Guillaumont, R. (1966c) Theses. La faculte des sciences de l'universite de Paris.

Guillaumont, R. and deMiranda, C. F. (1966) *Rev. Chim. Miner.*, **3**, 861–72.

Guillaumont, R. (1968) *Bull. Soc. Chim. Fr.*, 1956–61.

Guillaumont, R., Bouissières, G., and Muxart, R. (1968) *Actinides Rev.*, **1**, 135–63.

Guillaumont, R. (1971) in *Tagungsber. 3 Int. Pa-Konf.* (ed. H.-J. Bom). Schloss-Elmau, 15–18 April 1969, German Report BMBW-FBK 71–17, Paper No. 31.

Guillaumont, R. and deMiranda, C. F. (1971) *Solvent Extr. Rev.*, **1**, 105–49.

Guillaumont, R., Ionova, G. V., Krupa, J. C., and David, F. (1996) *Radiochim. Acta*, **75**, 97–103.

Guillot, P. (1966) in *Physico-Chimie du Protactinium* (eds. G. Bouissières and R. Muxart), Centre National de la Recherche Scientifique, Orsay, Paris, 2–8 July 1965, pp. 239–48.

Guy, W. G. and Russell, A. S. (1923) *J. Chem. Soc.*, **123**, 2618–31.

Hahn, O. and Meitner, L. (1918) *Phys. Z*, **19**, 208–18.

Hahn, O. (1921) *Ber. Dtsch Chem. Ges. B*, **54**, 1131–42.

Hahn, R. L., Roche, M. F., and Toth, K. S. (1968) *Nucl. Phys. A*, **113**, 206–14.

Haire, R. G., Heathman, S., Idiri, M., Le Bihan, T., Lindbaum, A., and Rebizant, J. (2003) *Phys. Rev. B*, **67**, 134101-1-10.

Haïssinsky, M. and Bouissières, G. (1948) *Compt. Rend. Acad. Sci. Paris*, **226**, 573–94.

Haïssinsky, M. and Bouissières, G. (1951) *Bull. Soc. Chim.*, 146–8.

Haïssinsky, M. and Bouissières, G. (1958) *Noweau Traits de Chimie Minérale* (ed. P. Pascal), Masson, Paris, pp. 617–80.

Haïssinsky, M., Muxart, R., and Arapaki, H. (1961) *Bull. Soc. Chim. Fr.*, 2248.

Haïssinsky, M. and Pluchet, E. (1962) *J. Chim. Phys.*, 608–10.

Harbottle, G. and Evans, C. V. (1997) *Radioact. Radiochem.*, **8**, 38–46.

Hardy, C. J., Scargill, D., and Fletcher, J. M. (1958) *J. Inorg. Nucl. Chem.*, **7**, 257–75.

Harvey, B. G. and Parsons, B. I. (1950) *Phys. Rev.*, **80**, 1098–9.

Haubach, W. J. (1967) Unpublished memorandum, 15 August.

Heckley, P. R., Holah, D. G., and Brown, D. (1971) *Can. J. Chem.*, **49**, 1151–60.

Heinrich, G., Ache, H. J., and Guesten, H. (1986) *Appl. Spectrosc.*, **40**, 363–8.

Hendricks, M. E., Jones, E. R. Jr, Stone, J. A., and Karraker, D. G. (1971) *J. Chem. Phys.*, **55**, 2993–7.

Herak, M. J., Prpic, I., and Tamhina, B. (1979) in *CIM Spec. Vol., Proc. Int. Solvent Extr. Conf.* 1977, pp. 462–6.

Hertz, M. R., Figgins, P. E., and Watrous, R. M. (1974) U.S. Report MLM–2168, pp. 31–5.

Hery, Y., Wojakowski, A., Baidron, M., and De Novion, C. H. (1977) in *Proc. 2nd Int. Conf. Electron. Structure Actinides, Zakl. Norimienia Ossolinskich, Wydawn. Polish Akad. Nauk*, Wroclaw, Poland, pp. 343–7.

Hery, Y., Damien, D., Haessler, M., and De Novion, E. H. (1978) *Radiochem. Radioanal. Lett.*, **32**, 283–92.

Hery, Y. (1979) Report CEA-R-4971.

Hery, Y., Damien, D., and Charvillat, J. P. (1979) *Radiochem. Radioanal. Lett.*, **37**, 17–26.

Heydemann, A. (1969) *Handbook of Geochemistry*, vol. 1 (ed. K. H. Wedepohl), Springer-Verlag, New York, pp. 376–412.

Hicks, H. G., Stevenson, P. C., and Schweiger, J. S. (1978) *J. Chromatogr*, 527–33.

Hill, M. W. (1958) U.S. Report UCRL-8423.

Hillary, J. J. and Morgan, A. R. (1964) *Ind. Chemist*, **40**, 131–6.

Hitachi Metals Ltd (1999) Japan Patent JP11166177-A, C09K–011/00.

Holden, N. E. and Walker, F. W. (1972) *Chart of the Nuclides,* 11th edn, General Electric Co., Schenectady, New York.

Holtzman, R. B. (1962) Atomic Energy Commission, Report ANL-6474. p. 42.

Huntley, D. J., Calvert, S. E., Thomson, J., and Nissen, M. K. (1986) *Can. J. Earth Sci.*, **23**, 959–66.

Hyde, E. K. (1948) U.S. Report ANL-4183.

Hyde, E. K., Studier, M. H., Hopkins, H. H. Jr, and Ghiorso, A. (1949) *The Transuranium Elements, Div. IV. 14B* (eds. G. T. Seaborg, J. J. Katz, and W. M. Manning), Natl. Nucl. Energy Ser., McGraw-Hill, New York, pp. 1439–41.

Hyde, E. K., Katzin, L. I., and Wolf, M. J. (1951) U.S. Patent 2978294.

Hyde, E. K. and Wolf, M. J. (1952) U.S. Report T1D-5223 (ed. L. I. Katzin), pp. 197–222.

Hyde, E. K. (1954) *The Actinide Elements, Div. IV, 14A* (eds. G. T. Seaborg and J. J. Katz), Natl. Nucl. Energy Ser., McGraw-Hill, New York, pp. 542–95.

Hyde, E. K. (1956) in *Proc. Int. Conf. on Peaceful Uses of Atomic Energy,* vol. 7, 8–20 August 1955 (Geneva). United Nations, New York, pp. 281–303.

Hyde, E. K. (1961) U.S. Report UCRL-9458.

Hyde, E. K., Perlman, J., and Seaborg, G. T. (1964) *The Nuclear Properties of the Heavy Elements,* vol. 2. Prentice-Hall, Englewood Cliffs, New York.

Hyde, E. K. (undated) U.S. Report UCRL-10612.

Ishida, Y. E. (1975) Unpublished results.

Iyer, P. N. and Smith, A. J. (1966) in *Physico-Chimie du Protactinium* (eds. G. Bouissières and R. Muxart), Centre National de la Recherche Scientifique, Orsay, Paris, 2–8 July 1965, pp. 81–5.

Jackson, N., Rogers, F. J. G., and Short, J. F. (1960a) UK Report AERE-R 3311.

Jackson, N., Rogers, F. J. G., and Short, J. F. (1960b) UK Report AERE-R 3377.

Jacobi, E. (1945) *Helv. Chim. Acta*, **28**, 757–8.

Jakovac, Z. and Lederer, M. (1959) *J. Chromatogr.,* **2**, 411–7.

Jenkins, I. L., Scargell, D., and Wain, A. G. (1975) *J. Inorg. Nucl. Chem.*, **37**, 257–9.

Jones, P. J. (1966) in *Physico-Chimie du Protactinium* (eds. G. Bouissières and R. Muxart), Centre National de la Recherch Scientifique, Orsay, Paris, 2–8 July 1965, pp. 93–8.

Judd, B. R. (1962) *Phys. Rev.*, **125**, 613–25.

Jung, B., Seaborg, G. T., and Edelstein, N. M. (1993) in *205th American Chemical Society National Meeting*, 28 March–2 April, 1993, Denver, CO.

Kahn, S. and Hawkinson, D. E. (1956) *J. Inorg. Nucl. Chem.*, **3**, 155–6.

Kaltsoyannis, N. and Bursten, B. E. (1995) *Inorg. Chem.*, **34**, 2735–44.

Kaltsoyannis, N. (1998) *J. Alloys Comp.*, **271–273**, 859–62.

Kandil, A. T. and Ramadan, A. (1978) *Radiochim. Acta*, **25**, 107–9.

Kandil, A. T., Abdel Gawad, A. S., and Ramadan, A. (1980) *Radiochim. Acta*, **27**, 39–42.

Katz, J. J. and Seaborg, G. T. (1957) *The Chemistry of the Actinide Elements*, Methuen, London, pp. 67–93.

Katzin, L. I., Van Winkle, Q., and Sedlet, J. (1950) *J. Am. Chem. Soc.*, **72**, 4815–7.

Katzin, L. I. (ed.) (1952) *Production and Separation of* ^{233}U, U.S. Report TID-5223.

Katzin, L. I. and Stoughton, R. W. (1956) *J. Inorg. Nucl. Chem.*, **3**, 229–32.

Katzin, L. I. (1958) USA Patent 2847273, August 12, 1958. *Cit Nucl. Sci. Abstr. 13*. 1007, 1959.

Kaufman, A., Ku, T. L., and Luo, S. D. (1995) *Chem. Geol.*, **120**, 175–81.

Kazakevich, M. Z., Mikheev, N. B., Kulyukhin, S.A., and Rumer, I.A. (1993) *Radiokhimiya*, **5**, 28–30.

Keller, C. (1963) *Radiochim. Acta*, **1**, 147–56.

Keller, C. (1964a) *J. Inorg. Nucl. Chem.*, **26**, 2069–74.

Keller, C. (1964b) German Report KFK 225.

Keller, C. (1965a) *J. Inorg. Nucl. Chem.*, **27**, 321–7.

Keller, C. (1965b) *J. Inorg. Nucl. Chem.*, **27**, 797–800.

Keller, C. (1965c) *J. Inorg. Nucl. Chem.*, **27**, 1233–46.

Keller, C. and Walter, K. H. (1965) *J. Inorg. Nucl. Chem.*, **27**, 1253–60.

Keller, C., Koch, L., and Walter, K. H. (1965) *J. Inorg. Nucl. Chem.,* **27**, 1225–32.

Keller, C. (1966a) *Angew. Chem.*, **5**, 23–35.

Keller, C. (1966b) in *Physico-Chimie du Protactinium* (eds. G. Bouissières and R. Muxart), Centre National de la Recherche Scientifique, Orsay, Paris, 2–8 July 1965, pp. 71–9.

Keller, C. (1971) in *Tagungsber 3 Int. Pa-Konf.* (ed. H.-J. Born). Schloss-Elmau, 15–18 April 1969, German Report BMBW-FBK 71–17, Paper No. 8.

Keller, C. (1977) in *Gmelin Handbuch der Anorganischen Chemie – Protactinium, Suppl.,* vol. 2, Springer-Berlag, Berlin, pp. 6–34.

Keys, J. D. (1951) Thesis. McGill University.

Khiebnikov, V. P., D'yachkova, R. A., and Spitsyn, V. I. (1966) *Radiokhimiya*, **8**, 119–24.

Kirby, H. W. (1959) *The Radiochemistry of Protactinium*, U.S. Report NAS-NS-3016, p. 440.

Kirby, H. W. (1961) *J. Inorg. Nucl. Chem.*, **18**, 8–12.

Kirby, H. W. (1966) *Physico-Chimie du Protactinium* (eds. G. Bouissières and R. Muxart), Centre National de la Recherche Scientifique, Orsay, Paris, 2–8 July 1965, pp. 283–91.

Kirby, H. W. and Figgins, P. E. (1966) in *Physico-Chimie du Protactinium* (eds. G. Bouissières and R. Muxart), Centre National de la Recherche Scientifique, Orsay, Paris, 2–8 July 1965, pp. 275–81.

Kirby, H. W. (1974) U.S. Report MLM-2111.

Kleinschmidt, P. D., Ward, J. W., and Haire, R. G. (1983) in *Proc. Symp. High Temp. Materials Chem. II* (eds. D. Cubiciotti and Z. A. Munir), Electrochemical Society, Pennington, NJ, pp. 23–31.

Kleinschmidt, P. D. and Ward, J. W. (1986) *J. Less Common Metals*, **121**, 121.

Kluge, E. and Lieser, K. H. (1980) *Radiochim. Acta*, **27**, 161–70.

Ko, R. (1956) *Nucleonics*, **14**, 74.

Ko, R. (1957) *Nucleonics*, **15**, 72.

Kolarich, R. T., Ryan, V. A., and Schuman, R. P. (1967) *J. Inorg. Nucl. Chem.*, **29**, 783–97.

Kot, W. K. and Edelstein, N. M. (1995) *New J. Chem.*, **19**, 641–54.

Kraus, K. A. and Moore, G. E. (1950) *J. Am. Chem. Soc.*, **72**, 4293–4.

Kraus, K. A. and Moore, G. E. (1951) *J. Am. Chem. Soc.*, **73**, 2900–2.

Kraus, K. A. and Van Winkle, Q. (1952) U.S. Report TID-5223, pp. 259–71.

Kraus, K. A. and Moore, G. E. (1955) *J. Am. Chem. Soc.*, **77**, 1383.

Kraus, K. A., Moore, G. E., and Nelson, F. (1956) *J. Am. Chem. Soc.*, **78**, 2692–5.

Kulmala, S., Hakanen, M., and Lindgerg, A. (1998) *Radiokhimiya*, **40**, 519–21.

Kulyukhin, S. A., Kamenskaya, A. N., Mikheev, N. B., and Rumer, I. A. (1996) in *Fourth Conf.: Nucl. & Radiochem. C-P21*, 8–13 September, St. Malo, France.

Kulyukhin, S. A., Kamenskaya, A. N., Mikheev, N. B., Rumer, I. A., Novichenko, V. L., and Kazakevich, M. Z. (1997) *Radiokhimiya*, **39**, 501–3.

Kulyukhin, S. A. and Mikheev, N. B. (1998) *Radiokhimiya*, **40**, 296–8.

Kuppers, G. and Erdtmann, G. L. (1992) *J. Radioanal. Nucl. Chem. Articles*, **160**, 425–34.

Kurodo, R. and Ishida, V. (1965) *J. Chromatogr.*, **18**, 438–40.

Lange, R. C. and Hagee, G. R. (1968) *Nucl. Phys. A*, **124**, 412–28.

Lapitskii, A. V. and Galateanu, I. (1963) *Radiokhimiya*, **5**, 298–302.

Lapitskii, A. V., Rudenko, N. P., and Saed A. Gavad (1965) *Radiokhimiya*, **7**, 139.

Lapitskii, A. V., Rudenko, N. P., and Saed, A. Gavad (1966) in *Physico-Chimie du Protactinium* (eds. G. Bouissières and R. Muxart), Centre National de la Recherche Scientifique, Orsay, Paris, 2–8 July 1965, p. 249.

Larson, R. G., Katzin, L. I., and Hausman, E. (1952) U.S. Report TID-5223, pp. 272–5.

Launay, J. and Dolechek, R.L. (1947) *Phys. Rev.*, **72**, 141.

Laurens, W., Ten Brink, B. O., and Wapstra, A. H. (1970) *Nucl. Phys. A*, **152**, 463–80.

Leang, C. F. (1970) *J. Phys.*, **31**, 269–76.

Lebedev, I. A., Pirozhkov, S. V., Semochkin, V. M., and Yakovlev, G. N. (1961) *Radiokhimiya*, **3**, 258–60.

Le Cloarec, M.-F., Kovacevic, S., and Muxart, R. (1970) *Rev. Chim. Miner.*, **7**, 735–45.

Le Cloarec, M.-F. and Muxart, R. (1971) in *Tagungsber. 3 Int. Pa-Konf.* (ed. H.-J. Born), Schloss-Elmau, German Report BMBW-FBK 71–17, 15–18 April 1969, Paper No. 11.

Le Cloarec, M. F. and Muxart, R. (1973) *Radiochim. Acta*, **20**, 7–10.

Le Cloarec, M. F., Guillaumont, R., deMiranda, C. F., and Franck, J. C. (1973) *Radiochim. Acta*, **20**, 1–6.

Le Cloarec, M.-F. (1974) Thesis, University of Paris.

Le Cloarec, M.-F., Dartyge, J. M., Kovacevic, S., and Muxart, R. (1976) *J. Inorg. Nucl. Chem.*, **38**, 737–9.

Lederer, C. M. and Shirley, V. S. (eds) (1978) *Table of Isotopes*, 7th edn, Wiley, New York.

Lee, J. A. and Marples, J. A. C. (1973) in *Comprehensive Inorganic Chemistry*, vol. 5 (eds. J. C. Bailar Jr, H. J. Emeleus, R. Nyholm, and A. F. Trotman-Dickenson), Pergamon, Oxford, pp. 5–73.

Le Naour, C., Trubert, D., and Jaussaud, C. (2003) *J. Solution Chem.*, **32**, 489–504.

Liljenzin, J. O. and Rydberg, J. (1966) in *Physico-Chimie du Protactinium* (eds. G. Bouissières and R. Muxart). Centre National de la Recherche Scientifique. Orsay, Paris, 2–8 July 1965, pp. 255–72.

Liljenzin, J. O. (1970) *Acta Chem. Scand.*, **24**, 1655–61.

Li, Z., Pan, Q., Guo, J., Yuan, S., Fang, K., and Yang, W. (1998) *Nucl. Technol.*, **21**, 7–10.

Lorenz, R., Scherff, H. L., and Toussaint, N. (1969) *J. Inorg. Nucl. Chem.*, **31**, 2381–90.

Lundqvist, R. (1974a) *Acta Chem. Scand. A*, **28**, 243–7.

Lundqvist, R. (1974b) *Acta Chem. Scand. A*, **28**, 358–61.

Lundqvist, R. (1974c) in *Int. Solvent Extr. Conf.*, Lyon, 8–14 September, Paper No. 143.

Lundqvist, R. (1974d) Thesis. Chalmers University of Technology and University of Gothenburg, Sweden.

Lundqvist, R. and Andersson, J. E. (1974) *Acta Chem. Scand. A*, **28**, 700–2.

Lundqvist, R. and Rydberg, J. (1974) *Acta Chem. Scand. A*, **28**, 399–406.

Lundqvist, R. (1975) *Acta Chem. Scand. A*, **29**, 231–5.

Lux, F., Ammentorp-Schmidt, F., Dempf, D., Graw, D., and Hagenberg, W. (1970) *Radiochim. Acta*, **14**, 57–61.

Lux, F., Brown, D., Dempf, D., Fischer, R. D., and Hagenberg, W. (1971) in *Tagungsber. 3 Int. Pa-Konf.* (ed. H.-J. Born), Schloss-Elmau, 15–18 April 1969, German Report BMBW-FBK 71–17, Paper No. 23.

Lux, F., Beck, O. F., Kraus, H., Brown, D., and Tso, C. (1980) *Z. Naturforsch. B. Anorg. Chem. Org. Chem. B*, **35**, 564–7.

Maddock, A. G. and Miles, G. L. (1949) *J. Chem. Soc. Suppl.*, **2**, 253–6.

Maddock, A. G. and Pugh, W. (1956) *J. Inorg. Nucl. Chem.*, **2**, 114–17.

Maddock, A. G. (1960) Unpublished observations cited by Brown (1969).

Maddock, A. G. and Pires de Matos, A. (1972) *Radiochim. Acta*, **18**, 71–4.

Maghrawy, H. B., Marie, S. A., and Ayoub, E. J. (1988) *J. Radioanal. Nucl. Chem. Lett.*, **121**, 429–40.

Maghrawy, H. B., Aly, H. F., and El-Reefy, S. A. (1989) *Radiochim. Acta*, **46**, 127–30.

Maillet, C. P. (1982) *J. Phys. Chem. C*, **15**, 6371–8.

Malm, J. G. and Fried, S. (1950) U.S. Report ANL-4490, pp. 53–5.

Malm, J. G. and Fried, S. (1959) U.S. Patent 2 893 825.

Manier, M., Carlier, R., and Genet, M. (1969) *Radiochem. Radioanal. Lett.*, **2**, 133–8.

Manier, M. (1970) French Report NP-18348.

Manier, M. and Genet, M. (1970) *Rev. Chim. Miner.*, **7**, 1087–100.

Marples, J. A. C. (1965) *Acta Crystallogr.*, **18**, 815.

Marples, J. A. C. (1966) in *Physico-Chimie du Protactinium* (eds. G. Bouissières and R. Muxart), Centre National de la Recherche Scientifique, Orsay, Paris, 2–8 July 1965, pp. 39–43.

Marquardt, C. M., Panak, P. J., Apostolidis, C., Morgenstern, A., Walther, C., Klenze, R., and Fanghänel, Th. (2004) *Radiochim. Acta*, **92**, 445–447.

Marrus, R., Nierenberg, W. A., and Winocur, J. (1961) *Nucl. Phys.*, **23**, 90–106.

McCormac, J. J., Cripps, F. H., and Wiblin, W. A. (1960) *Anal. Chim. Acta*, **22**, 408.

McCoy, J. D. (1964) *Soc. Sci. Fenn. Commentat. Phys. Math.*, **30**, 1–37.

McIsaac, L. D. and Freinling, E. C. (1956) *Nucleonics*, **14**, 10–65.

McKay, H. A. C. (1971) *Principles of Radiochemistry*, CRC Press, Cleveland, Ohio, p. 232.

Meinke, W. W. (1946) U.S. Report AECD-2738.

Meinke, W. W., Ghiorso, A., and Seaborg, G. T. (1949) *Phys. Rev.*, **75**, 314–5.

Meinke, W. W. and Seaborg, G. T. (1950) *Phys. Rev.*, **78**, 475.

Meinke, W. W., Ghiorso, A., and Seaborg, G. T. (1951) *Phys. Rev.*, **81**, 782–98.

Meinke, W. W. (1952) *J. Chem. Phys.*, **20**, 754.

Meinke, W. W., Ghiorso, A., and Seaborg, G. T. (1952) *Phys. Rev.*, **85**, 429–31.

Meinke, W. W., Wick, G. C., and Seaborg, G. T. (1956) *J. Inorg. Nucl. Chem.*, **3**, 69–92.

Meitner, L., Strassmann, F., and Hahn, O. (1938) *Z. Phys.*, **109**, 538–52.

Mendeleev, D. I. (1872) *Ann. Chem. Pharm. Suppl.*, **8**, 133–229.

Merinis, J., Legoux, Y., and Bouissières, G. (1966) in *Physico-Chimie du Protactinium* (eds. G. Bouissières and R. Muxart), Centre National de la Recherche Scientifique, Orsay, Paris, 2–8 July 1965, pp. 307–14.

Mikhailov, V. A. (1960) *Radiokhimiya*, **1**, 188–94.

Mikheev, N. B., Kulyukhin, S. A., and Konovalova, N. A. (1992) *Radiokhimiya*, **3**, 23–6.

Mikheev, N. B., Kamenskaya, A. N., Kulyukhin, S. A., and Rumer, I. A. (1993a) *Mendeleev Comm.*, 198.

Mikheev, N. B., Kamenskaya, A. N., Rumer, I. A., Kulyukhin, S. A., and Auerman, L. N. (1993b) *Radiokhimiya*, **5**, 24–6.

Miranda, C. F. and Muxart, R. (1964a) *Bull. Soc. Chim. France*, 387.

Miranda, C. F. and Muxart, R. (1964b) *Bull. Soc. Chim. France*, 2174.

Mitsubishi Materials, Corporation (1995) Japan Patent. B01J-020/10, G21F-009/10.

Mitsuji, T. (1967a) *Bull. Chem. Soc. Japan*, **40**, 2091–5.

Mitsuji, T. (1967b) *Bull. Chem. Soc. Japan*, **40**, 2822–5.

Mitsuji, T. and Suzuki, S. (1967) *Bull. Chem. Soc. Japan*, **40**, 821–6.

Mitsuji, T. (1968) *Bull. Chem. Soc. Japan*, **41**, 115–19.

Monroy-Guzman, F., Constantinescu, O., Hussonnois, M., Kim, J. B., Brillard, L., and Trubert, D. (1996) *J. Radioanal. Nucl. Chem. Lett.*, **208**, 461–6.

Monroy-Guzman, F., Trubert, D., Brillard, L., Hussonnois, M., and Le Naour, C. (1997) *Quimica Anal.*, **16**, 43–7.

Moore, F. L. (1955) *Anal. Chem.*, **27**, 70–2.

Moore, F. L. (1956) *Anal. Chem.*, **28**, 997.

Moore, F. L. and Reynolds, S. A. (1957) *Anal. Chem.*, **29**, 1596.

Moore, F. L., Fairman, W. D., Ganchoff, J. G., and Surac, J. G. (1959) *Anal. Chem.*, **31**, 1148.

Moore, F. S. (1960) U.S. Report NAS-NS 3101.

Moore, J. G. and Rainey, R. H. (1964) in *Proc. Protactinium Chem. Symp.*, Gatlinburg, Tenn., 25–26 April 1963, U.S. Report TID-7675, pp. 16–34.

Moore, F. L. and Thern, G. G. (1974) *Radiochem. Radioanal. Lett.*, **19**, 117–25.

Morgan, J. and Beetham, C. (1990) Report No.: NSS/R-220, ANS-2358-R4.

Mortimer, M. J. (1979) *J. Phys. Colloq.*, **4**, 124–9.

Moskvin, A. I., Galateanu, I., and Lapitskii, A. V. (1963) *Dokl. Akad. Nauk. SSSR*, **149**, 264–6.

Murbach, E. W. (1957) U.S. Report NAA-SR-1988.

Musikas, C. (1966) French Report CEA-R-3023.

Muxart, R. and Arapaki-Strapelias, H. (1963) *Bull. Soc. Chim.*, 888–91.

Muxart, R., Guillaumont, R., and Vernois, J. (1966a) *Compt. Rend. Acad. Sci. Paris C*, **262**, 888–9.

Muxart, R., Guillaumont, R., and Arapaki-Strapelias, H. (1966b) *Physico-Chimie du Protactinium* (eds. G. Bouissières and R. Muxart), Centre National de la Recherche Scientifique, Orsay, Paris, 2–8 July 1965, pp. 225–38.

Muxart, R., Guillaumont, R., and Bouissières, G. (1969) *Actinides Rev.*, **1**, 223–74.

Muxart, R. and Guillaumont, R. (1974) *Complements au Noueveau Traite de Chimie Minerale* (eds. A. Pacault and G. Pannetier), Masson, Paris, p. 2.

Myasoedov, B. F. and Muxart, R. (1962a) *J. Anal. Chem. (USSR)*, **17**, 340–2.

Myasoedov, B. F. and Muxart, R. (1962b) *Bull. Soc. Chim. France*, 237–9.

Myasoedov, B. F. and Pal'shin, E. S. (1963) *Zhurn. Anal. Khim.*, **18**, 596–602.

Myasoedov, B. F., Pal'shin, E. S., and Paley, P. N. (1964) *Zhurn. Anal. Khim.*, **19**, 105–10.

Myasoedov, B. F., Pal'shin, E. S., and Molochnikova, N. P. (1966a) *Zhurn. Anal. Khim.*, **21**, 599–606.

Myasoedov, B. F., deMiranda, C. F., and Muxart, R. (1966b) *Zhurn. Anal. Khim.*, **21**, 946–50.

Myasoedov, B. F. and Molochnikova, N. P. (1968) *Zhurn. Anal. Khim.*, **23**, 681.

Myasoedov, B. F., Pal'shin, E. S., and Molochnikova, N. P. (1968a) *Zhurn. Anal. Khim.*, **23**, 66–71.

Myasoedov, B. F., Pal'shin, E. S., and Molochnikova, N. P. (1968b) *Zhurn. Anal. Khim.*, **23**, 786–7.

Myasoedov, B. F., Pal'shin, E. S., and Molochnikova, N. P. (1968c) *Zhurn. Anal. Khim.*, **23**, 1312–17.

Myasoedov, B. F., Eliseeva, O. P., and Sawwin, S. B. (1969) *J. Radioanal. Chem.*, **2**, 369–76.

Myasoedov, B. F., Davydov, A. V., and Nekrasova, V. V. (1978) *Radiokhimiya*, **6**, 851–8.

Myasoedov, B. F., Karalova, Z. K., Nekrasova, V. V., and Rodionova, I. M. (1980) *J. Inorg. Nucl. Chem.*, **42**, 1495–9.

Nairn, J. S., Collins, D. A., McKay, H. A. C., and Maddock, A. G. (1958) in *Proc. 2nd UN Int. Conf. on Peaceful Uses of Atomic Energy*, 1–13 September 1958, Geneva, vol. 17, pp. 216–35.

Nekrasova, V. V., Pal'shin, E. S., and Myasoedov, B. F. (1975a) *Zh. Anal. Khim.*, **30**, 1122–6.

Nekrasova, V. V., Pal'shin, E. S., and Myasoedov, B. F. (1975b) *Zh. Anal. Khim.*, **30**, 2267–9.

Nikolaev, A. V., Kurnakova, A. G., and Rumyantseva, Z. G. (1959) *Zhurn. Neorg. Khim.*, **4**, 1682.

Nishina, Y., Yasaki, T., Kimura, K., and Ikawa, M. (1938) *Nature*, **142**, 874.

Nishinaka, I., Nagame, Y., Tsukada, K., Ikezoe, H., Sueki, K., Nakahara, H., Tanikawa, M., and Ohtsuki, T. (1997) *Phys. Rev. C*, **56**, 891–9.

Nowikow, J. and Pfrepper, G. (1963) *Z. Naturforsch. B*, **18**, 993–1001.

Oak Ridge National Laboratory (1964) in *Proc. Protactinium. Chem. Symp.*, Gatlinburg, Tenn., 25–26 April 1963. U.S. Report T1D 7675.

O'Donnell, T. A., Waugh, A. B., and Randall, C. H. (1977) *J. Inorg. Nucl. Chem.*, **39**, 1597–600.

Overman, R. T. and Clark, H. M. (1960) *Radioisotope Techniques*, McGraw-Hill, New York, pp. 326–9.

Pal'shin, E. S., Myasoedov, B. F., and Palei, P.N. (1962) *Zhurn. Anal. Khim.*, **17**, 471.

Pal'shin, E. S. and Myasoedov, B. F. (1963) *Zhurn. Anal. Khim.*, **18**, 750

Pal'shin, E. S., Myasoedov, B. F., and Novikov, Yu. P. (1963) *Zhurn. Anal. Chim.*, **18**, 657.

Pal'shin, E. S., Myasoedov, B. F., and Novikov, Yu. P. (1966) *Zhurn. Anal. Khim.*, **21**, 851–6.

Pal'shin, E. S., Myasoedov, B. F., and Ivanova, L. A. (1968a) *Zhurn. Anal. Khim.*, **23**, 758–61.

Pal'shin, E. S., Myasoedov, B. F., and Davydov, A. V. (1968b) *Analytical Chemistry of Protactinium* (ed. A. P. Vinogradov), Nauka, Moscow, pp. 16–19 (in Russian).

Pal'shin, E. S., Myasoedov, B. F., and Davydov, A. V. (1970) *Analytical Chemistry of Protactinium*, Ann Arbor-Humphrey, Ann Arbor.

Pal'shin, E. S., Davydov, A. V., Palei, P. N., and Ivanova, L. A. (1971) in *Tagungsher. 3 Int. Pa-Konf.* (ed. H.-J. Born), Schloss-Elmau, 15–18 April 1969, German Report BMBW-FBK 71–17.

Pathak, P. N., Manchnda, V. K., Ruikar, P. B., and Veeraraghavan, R. (1999a) *Radiochim. Acta*, **86**, 129–34.

Pathak, P. N., Manchnda, V. K., Purushotham, D. S. C., Rama Rao, G. A., Manohar, S. B., and Reddy, A. V. R. (1999b) in *Conference: NUCAR 99: Nuclear and Radiochemistry Symposium*, Mumbai, India.

Paulus, W., Kratz, J. V., Strub, E., Zauner, S., Bruchle, W., Pershina, V., Schädel, M., Schausten, B., Adams, J. L., Gregorich, K. E., Hoffman, D. C., Lane, M. R., Laue, C., Lee, D. M., McGrath, C. A., Shaughnessy, D. K., Strellis, D.A., and Sylwester, E. R. (1998) *J. Alloys Comp.*, **271**, 292–5.

Paulus, W., Kratz, J. V., Strub, E., Zauner, S., Bruchle, W., Pershina, V., Schädel, M., Schausten, B., Adams, J. L., Gregorich, K. E., Hoffman, D. C., Lane, M. R., Laue, C., Lee, D. M., McGrath, C. A., Shaughnessy, D. K., Strellis, D. A., and Sylwester, E. R. (1999) *Radiochim. Acta*, **84**, 69–77.

Peppard, D. F., Mason, G. W., Grayand, P. R., and Mech, J. F. (1952) *J. Am. Chem. Soc.*, **74**, 6081–4.

Peppard, D. F., Mason, G. W., and Gergel, M. V. (1957) *J. Inorg. Nucl. Chem.*, **3**, 370–8.

Perlman, M. N. and Weisman, S. J. (1951) USA Patent 2558377, June 26, 1951.

Pershina, V., Fricke, B., Kratz, J. V., and Ionova, G. V. (1994) *Radiochim. Acta*, **64**, 37–48.

Piccard, A. (1917) *Arch. Sci. Phys. Naturelles*, **44**, 161–4.

Pickett, D. A., Williams, R. W., and Murrell, M. T. (1994) *Anal. Chem.*, **66**, 1044–9.

Pickett, D. A. and Murrell, M. T. (1997) *Earth Planet. Sci. Lett.*, **148**, 259–71.

Piehler, D., Kot, W. K., and Edelstein, N. (1991) *J. Chem. Phys.*, **94**, 942–8.

Pierce, W. E. and Grosse, A. (1935) *Phys. Rev.*, **47**, 532.

Pissot, A. M., Muxart, R., and Miranda, C. F. (1966) *Bull. Soc. Chim. France*, 1757.

Plaisance, M. L. and Guillaumont, R. (1969) *Radiochim. Acta*, **12**, 32–7.

Poskanzer, A. M. and Foreman, B. M. (1961a) *Atomnaya Tekhnika za Rubezhom*, **8**, 33.

Poskanzer, A. M. and Foreman, B. M. (1961b) *J. Inorg. Nucl. Chem.*, **16**, 323.

Rajaram, M. and Scott, C. E. (2000) U.S. Patent C03C-013/04. 2000-6136736-A.

Raje, N., Swain, K. K., Kumar, S. R., Parthasarathy, R., and Mathur, P. K. (2001) *J. Radioanal. Nucl. Chem. Lett.*, **247**, 115–20.

Rebizant, J., Spirlet, J. C., Friedt, J. M., Poinsot, R., and Kalvius, G. M. (1979) *J. Phys. Colloq.*, **4**, 133.

Reddy, A. S. and Reddy, S. K. (1977) *Sep. Sci.*, **12**, 661–4.

Reddy, A. S., Ramakrishna, V. V., and Patel, S. K. (1977) *Radiochem. Radioanal. Lett.*, **28**, 445–52.

Reymond, F. (1931) *J. Chim. Phys.*, **28**, 409–10.

Richards, E. W. T. and Atherton, N. J. (1961) Atomic Energy Research Establishment (Great Britain). Report AERE-R-3851.

Richards, E. W. T., Ridgeliy, A., Atherton, N. J., and Wise, H. S. (1961) *Nature*, **192**, 4444.

Richards, E. W. T. and Atherton, N. J. (1963) *Spectrochim. Acta*, **19**, 971–87.

Richards, E. W. T., Stephen, J., and Wise, H. S. (1968) *Spectrochim. Acta B*, **23**, 635–42.

Robert, J., deMiranda, C. F., and Muxart, R. (1969) *Radiochim. Acta*, **11**, 104–7.

Roberts, L. E. J. and Walter, A. J. (1966) in *Physico-Chimie du Protactinium* (eds. G. Bouissières and R. Muxart), Centre National de la Recherche Scientifique, Orsay, Paris, 2–8 July 1965, pp. 51–9.

Rona, E., Muse, L., and Brandau, B. L. (1966) in *Physico-Chimie du Protactinium* (eds. G. Bouissières and R. Muxart), Centre National de la Recherche Scientifique, Orsay, Paris, 2–8 July 1965, p. 333.

Roshalt, J. N., Emiliani, C., Geise, J., Koczy, F. F., and Wangersky, P. J. (1961) *J. Geol.*, **69**, 162–85.

Roshalt, J. N., Emiliani, C., Geiss, J., Koczy, F. F., and Wangersky, P. J. (1962) *J. Geophys. Res.*, **67**, 2907–11.

Rossotti, F. J. C. and Rossotti, H. (1961) *The Determination of Stability Constants and Other Equilibrium Constants in Solution*, McGraw-Hill, New York.

Rudenko, N. P., Saed A. Gavad, and Lapitskii, A. V. (1965) *Radiokhimiya*, **7**, 32.

Russell, A. S. (1913) *Chem. News*, **107**, 49–52.

Sackett, W. M. (1960) *Science*, **132**, 1761–2.

Saiki, M., Nestasi, M. J. C., and Lima, F. W. (1981) *J. Radioanal. Chem.*, **64**, 83–116.

Sakanoue, M., Oosawa, M., Sakai, T., and Ishida, K. J. (1964) *J. At. Energy Soc. Japan*, **6**, 503.

Sakanoue, M., Takagi, E., Abe, M., and Oosawa, M. (1965) *J. At. Energy Soc. Japan*, **7**, 404.

Sakanoue, M. and Abe, M. (1967) *Radioisotopes*, **16**, 645–51.

Sakanoue, M., Konishi, K., and Komura, K. (1967) Paper SM–87/28, in *Symp. on Radioactive Dating and Methods of Low-Level Counting. Monaco*, 2–10 March 1967, IAEA Report STI/PUB/152, Vienna.

Sales Grande, M. R. (1950) *Rev. Quim. Appl.*, **1**, 184.

Salutsky, M. L., Shaver, K., Elmlinger, A., and Curtis, M. L. (1956) *J. Inorg. Nucl. Chem.*, **3**, 995–8.

Salutsky, M. L., Curtis, M. L., Shaver, K., Elmlinger, A., and Miller, R. A. (1957) *Anal. Chem.*, **29**, 373.

Salutsky, M. L. (1962) *Comprehensive Analytical Chemistry* (eds. C. L. Wilson and D. W. Wilson), EIsevier, Amsterdam, pp. 570–80.

Scherer, V., Weigel, F., and Van Ghemen, M. (1967) *Inorg. Nucl. Chem. Lett.*, **3**, 589–95.

Scherff, H.-L. and Hermann, G. (1964) *Radiochim. Acta*, **2**, 141–6.

Scherff, H.-L. and Hermann, G. (1966) *Radiochim. Acta*, **6**, 53–61.

Schüler, H. and Gollnow, H. (1934) *Naturwissenschaften*, **22**, 511.

Schulz, W. W. (1972) U.S. Report ARH-2420.

Schuman, R. P. and Tromp, R. L. (1959) U.S. Report IDO-16571.

Schwarcz, H. P., Simpson, J. J., and Stringer, C. B. (1998) *J. Human Evol.*, **35**, 635–45.

Schwochau, V. and Astheimer, L. (1970) *J. Inorg. Nucl. Chem.*, **32**, 119–26.

Sedlet, J. (1964) *Treatise on Analytical Chemistry*, part II, vol. 6 (eds. I. M. Kolthof, T. P. J. Elving, and E. B. Sandell), Wiley, New York, pp. 435–610.

Seelmann-Eggebert, M., Keller, C., and Zundel, G. (1961) Kernforschungszentrum Karlsruhe, Report KFK-41.

Segrè, E. (1952) *Phys. Rev.*, **86**, 21–8.

Sellers, P. A., Fried, S., Elson, R. F., and Zachariasen, W. H. (1954) *J. Am. Chem. Soc.*, **76**, 5935–8.

Shankar, J., Venkateswarlu, K. S., and Gopinathan, C. (1963) *J. Inorg. Nucl. Chem.*, **25**, 57–66.

Shevchenko, V. B., Mikhailov, V. A., and Zavalsky, Yu. P. (1958a) *Sov. J. Inorg. Chem.*, **3**, 1955.

Shevchenko, V. B., Zolotulcha, S. I., Kascheyev, N. F., Tsaryov, S. A., Mikhailov, V. A., and Toropchenova, G. A. (1958b) in *Proc. 2nd UN Int. Conf. on Peaceful Uses of Atomic Energy*, vol. 4, 1–13 September 1958, Geneva, pp. 40–3.

Shimojima, H. and Takagi, J. (1964) *J. Inorg. Nucl. Chem.*, **26**, 253.

Shiokawa, T., Kikuchi, M., and Omori, T. (1969) *Inorg. Nucl. Chem. Lett.*, **5**, 105–9.

Silvestre, J. P., Le Cloarec, M.-F., and Cazaussus, A. (1977) *Radiochem. Radioanal. Lett.*, **31**, 367–71.

Sime, R. L. (1997) Abstracts of Papers of the American Chemical Society **213**, 15.

Simpson, F. B., Burgus, W. H., Evans, J. E., and Kirby, H. W. (1962) *Nucl. Sci. Eng.*, **12**, 243–9.

Smith, G. and Barnett, G. A. (1965) *J. Inorg. Nucl. Chem.*, **27**, 975.

Smith, J. L., Spirlet, J. C., and Mueller, W. (1979) *Science*, **151**, 188–90.

Smith, R. R., Alloy, H. P., Lewis, R. H., and Does, A. V. (1956) *Phys. Rev.*, **101**, 1053.

Soddy, F. (1913a) *Chem. News*, **107**, 97–9.

Soddy, F. (1913b) *Nature*, **91**, 634–5.

Soddy, F. and Cranston, J. A. (1918) *Proc. R. Soc. A*, **94**, 384–404.

Soderling, P. and Eriksson, O. (1997) *Phys. Rev. B*, **56**, 10719–21.

Solar, J. P., Burghard, H. P. G., Banks, R. H., Streitwieser, A., and Brown, D. (1980) *Inorg. Chem.*, **19**, 2186–8.

Sotobayashi, T., Suzuki, T., and Kudo, H. (1977) *J. Radioanal. Chem.*, **36**, 145–52.

Souka, N., Shabana, R., and Hafey, F. (1975a) *Radiochim, Acta*, **22**, 45–8.

Souka, N., Shabana, R., and Hafey, F. (1975b) *J. Radioanal. Chem.*, **27**, 401–10.

Souka, N., Abdel- Gawad, A. S., Shabana, R., and Farah, K. (1975c) *Radiochim, Acta*, **22**, 180–2.

Souka, N., Shabana, R., and Farah, K. (1976a) *J. Radioanal. Chem.*, **33**, 215–22.

Souka, N., Shabana, R., and Girgis, C. (1976b) *Isotopenpraxis*, **12**, 164–6.

Spirlet, J. C. (1979) *J. Phys. Colloq.*, **40**, 87–94.

Spirlet, J. C. (1982) *Actinides in Perspective* (ed. N. Edelstein), Pergamon Press, Oxford, pp. 361–80.

Spitsyn, V. I. and D'yachkova, R. A. (1960) *Dokl. Akad. Nauk. SSSR*, **134**, 1111.

Spitsyn, V. I. and Golutvina, M. M. (1960) *Atomnaya Energiya*, **8**, 117.

Spitsyn, V. I., D'yachkova, R. A., and Khlebnikov, V. P. (1964) *Dokl. Akad. Nauk. SSSR*, **157**, 677–80.

Spitsyn, V. I., D'yachkova, R. A., and Kamenskaya, A. N. (1969) *Dokl. Akad. Nauk. SSSR*, **184**, 35–7.

Stanik, I. E. and Il'menkova, L. I. (1963) *Radiokhimiya*, **5**, 209–15.

Stchouzkoy, T. and Muxart, R. (1962) *Bull. Soc. Chim. France*, 2176.

Stchouzkoy, T., Pezeral, H., Bouissières, G., and Muxart, R. (1964) *Compt. Rend. Acad. Sci. Paris*, **259**, 3016–18.

Stchouzkoy, T., Muxart, R., and Bouissières, G. (1966a) *Compt. Rend. Acad. Sci. Paris C*, **262**, 1845–7.

Stchouzkoy, T., Pezerat, H., and Muxart, R. (1966b) in *Physico-Chimie du Protactinium* (eds. G. Bouissières and R. Muxart), Centre National de la Recherche Scientifique, Orsay, Paris, 2–8 July 1965, pp. 61–77.

Stchouzkoy, T., Muxart, R., Pezerat, H., and Dhers, J. (1968) *Rev. Chim. Miner.*, **5**, 1085–101.

Stchouzkoy, T., Muxart, R., and Guillaumont, R. (1969) *Rev. Chim. Miner.*, **6**, 411–25.

Stein, L. (1964) *Inorg. Chem.*, **3**, 995–8.

Stein, L. (1966) in *Physico-Chimie du Protactinium* (eds. G. Bouissières and R. Muxart), Centre National de la Recherche Scienlifique, Orsay, Paris, 2–8 July 1965, pp. 101–6.

Stewart, G. R., Smith, J. L., Spirlet, J. C., and Mueller, W. (1980) in *Superconductivity in d- and f-band Metals (Proc. Conf.) 1979* (eds. H. Subl and M. B. Maple), Academic Press, New York, pp. 65–70.

Stricos, D. P. (1966) Kholes At. Power Lab. KAPL-M-6554. Contract W-31–109-eng. 52.

Stronski, I. and Zelinski, A. (1964) *Nucleonica*, **9**, 801.

Subrahmanyam, V. B. (1963) U.S. Report UCRL-11082.

Suner, A., La Gamma de Bastioni, A. M., and Botbol, J. (1974) in Preparasion de Microcuries de ^{234}Th, Argentine Report CNEA 380.

Sung-Ching-Yang, G. Y., Druin, V. A., and Trofimov, A. S. (1972) *Sov. J. Nucl Phys.*, **14**, 725–6.

Suzuki, S. and Inoue, Y. (1966) *Bull. Chem. Soc. Japan*, **39**, 1705–15.

Suzuki, S. and Inoue, Y. (1969) *Bull. Chem. Soc. Japan*, **42**, 1916–21.

Svantesson, J., Hagstrom, I., Persson, G., and Liljenzin, G. (1979) *J. Inorg. Nucl. Chem.*, **41**, 383–9.

Takagi, J. and Shimojima, H. (1965) *J. Inorg. Nucl. Chem.*, **27**, 405–9.

Takahashi, K. and Morinaga, H. (1960) *Nucl. Phys.*, **15**, 664–77.

Tamhina, B., Gojnierac, A., and Herak, M. J. (1976) *Microchim. Acta*, **2**, 569–78.

Tamhina, B., Gojnierac, A., and Herak, M. J. (1978) *J. Inorg. Nucl. Chem.*, **40**, 335–8.

Taylor, S. R. (1964) *Geochim. Cosmochim. Acta*, **28**, 1273–85.

Thompson, R. C. (1951) U.S. Atomic Energy Commission, Report TID-5222.

Thompson, R. C. (1952) *Production and Separation of U*^{233} (ed. L. I. Katzin), U.S. Report T1D-5223, pp. 291–5.

Thompson, R. C., Van Winkle, Q., and Malm, J. G. (1952) U.S. Report TID-5223, pp. 276–86.

Thomson, J. and Walton A. (1971–72) *Proc. R. Soc. Edinburgh (B)*, **72/73**, 167–82.

Tomkins, F. S. and Fred, M. (1949) *J. Opt. Soc. Am.*, **39**, 357–63.

Toshiba Denshi Eng KK (1995) Japan Patent 07188653-A; C09K-011/56; C09K-011/84.

Trautmann, N., Denig, R., Kaffnell, N., and Herrmann, G. (1968) *Z. Naturforsch. A*, **23**, 2127–30.

Trubert, D., Guzman, F. M., Le Nauor, C., Brillard, L., Hussonnois, M., and Constantinescu, O. (1998) *Analytica Chim. Acta*, **374**, 149–58.

Trubert, D., Le Naour, C., and Jaussaud, C. (2002) *J. Solution Chem.*, **31**, 261–9.

Trubert, D., Le Naour, C., Jaussaud, C., and Mrad, O. (2003) *J. Solution Chem.*, **32**, 505–17.

Vaezi- Nasr, F., Duplessis, J., and Guillaumont, R. (1979) *Radiochem. Radioanal. Lett.*, **37**, 153–7.

Van Winkle, Q., Larson, R. G., and Katzin, L. I. (1949) *Am. Chem. Soc.*, **7**, 2585–96.

Van Winkle, Q. and Kraus, K. A. (1959) U.S. Patent 2910345.

Varnell, L. (1970) *Nucl. Phys. A*, **144**, 429–40.

Vernois, J. (1958) *J. Chromatogr.*, **1**, 52–61.

Vernois, J. (1959) *J. Chromatogr.*, **2**, 155–61.

Vernois, J., Conte, P., and Muxart, R. (1963) *Bull. Soc. Chim. France*, 403.

Walter, A. J. (1963) *J. Inorg. Nucl. Chem.*, **25**, 1301.

Walter, H. J., Geigert, W., van der Loeff, M. M. R., Fischer, G., and Bathmann, U. (2001) *Deep-Sea Res. Part I*, **48**, 471–93.

Weigel, F., Hoffman, G., and Ter Meer, N. (1969) *Radiochim. Acta*, **11**, 210–14.

Weigel, F., Hoffman, G., Wishnevsky, V., and Brown, D. (1974) *J. Chem. Soc. Dalton Trans.*, 1473–6.

Weigel, F. (1978) in *Handbuch der Präparativen Anorganischen Chemie, Aktiniden*, vol. 2 (ed. G. Brauer), Ferdinand Enke, Stuttgart, pp. 1117–322.

Wills, J. M. and Ericsson, O. (1992) *Phys. Rev. B. (Cond. Mat.)*, **45**, 13879–90.

Wilson, M. (1967) *J. Opt. Soc. Am.*, **57**, 429–30.

Wilson, M. (1968) *J. Opt. Soc. Am.*, **58**, 855–6.

Wojakowski, A., Damien, D., and Hery, Y. (1982) *J. Less Comm. Metals*, **83**, 169–74.

Wolzak, G. and Morinaga, H. (1963) *Radiochim. Acta*, **1**, 225–6.

Wright, H. W., Wyatt, E. I., Reynolds, S. A., Lyon, W. S., and Handley, T. H. (1957) *Nucl. Sci. Eng.*, **2**, 427–30.

Yang, H. S., Masuda, A., Sokai, H., and Nozaki, Y. (1986) *Geocimica Cosmochim. Acta*, **50**, 81–9.

Yokoyama, Y., Falgueres, C., and deLumley, M. A. (1997) *Compt. Rend. Acad. Sci. Paris. Séries II. Fasc. Sciences de la terre et des planètes*, **324**, 773–9.

Yuan, S., Yang, W., Mou, W., Zhang, X., Li, Z., Yu, X., Gu, J., Guo, Y., Gan, Z., Liu, H., and Guo, J. (1995) *Zeit. für Phys. A*, **352**, 235–6.

Yuan, S., Yang, W., Mou, W., Zhang, X., and Li, Z. (1996) *Chinese Physics Lett.*, **13**, 896–98.

Zachariasen, W. H. (1952) *Acta Crystallog.*, **5**, 19–21.

Zavizziano, H. (1935) *Compt. Rend. Acad. Sci. Paris*, **200**, 1843–5.

Zhang Qingwen, Tan Fuwen, Lin Chao, and Chen Yingqiang (1991) *Uranium Geology. China*, **7**, 251–3.

Zhang Xianlu, Xia Kailan, and Liu Husheng (1993) *Uranium Mining Metallurgy*, **12**, 189–93.

Zijp, W. L., Tom, S., and Sizoo, G. J. (1954) *Physica*, **20**, 727–35.

Zimmerman, H. P., Gober, M. K., Kratz, J. V., Schädel, M., Bruchle, W., Schimpf, E., Gregorich, K. E., Turler, A., Czerwinski, K. R., Hannink, N. J., Kadkhodan, B. D. M., Lee Nurmia, M. J., Hoffman, D. C., Gaggeler, H., Jost, D., Kovacs, J., Scherer, U. W., and Weber, A. (1993) *Radiochim. Acta*, **60**, 11–6.

Zwanenburg, G. J., Krupa, C., de Boer, E., and Keijzers, C. P. (1988) *J. Molec. Struct.*, **173**, 397–404.

CHAPTER FIVE

URANIUM*

Ingmar Grenthe, Janusz Drożdżyński, Takeo Fujino,
Edgar C. Buck, Thomas E. Albrecht-Schmitt, and
Stephen F. Wolf

5.1 HISTORICAL

Uranium compounds have been used as colorants since Roman times (Caley, 1948). Uranium was discovered as a chemical element in a pitchblende specimen by Martin Heinrich Klaproth, who published the results of his work in 1789. Pitchblende is an *impure* uranium oxide, consisting partly of the most reduced oxide uraninite (UO_2) and partly of U_3O_8. Earlier mineralogists had considered this mineral to be a complex oxide of iron and tungsten or of iron and zinc, but Klaproth showed by dissolving it partially in strong acid that the solutions yielded precipitates that were different from those of known elements. Therefore he concluded that it contained a new element (Mellor, 1932); he named it after the planet Uranus, which had been discovered in 1781 by William Herschel, who named it after the ancient Greek deity of the Heavens.

---

* Part of this chapter is based on Chapter 5 in the previous edition authored by the late Fritz Weigel.

The name 'Uranus' was first proposed by Johann Elert Bode in conformity with the other planetary names from classical mythology, but this name for the planet did not come into common use until 1850. However, uranium was accepted as the name for the chemical element.

The pure oxide UO_2 isolated by Klaproth by reduction was believed to be the elemental form until 1841, when Eugène-Melchior Péligot (1841a,b) showed that Klaproth's 'partially metallic' substance was in reality the oxide UO_2. Péligot (1841b, 1842, 1844) succeeded in preparing metallic uranium by reducing the tetrachloride with potassium. Péligot may thus properly be considered the founder of modern uranium chemistry; he was the first to use the word 'uranyl' to designate the yellow salts of uranium.

In the elaboration of the periodic table, Mendeleev assigned in 1872 an atomic weight of 240 and a highest valence of six to uranium, rather than the value of 120 that was then commonly used based on the assumption that uranium was trivalent. Mendeleev's reason was that he could not place an element with atomic weight 120 in group III of the periodic table; thus he conferred upon uranium the distinction of having the highest atomic weight in the periodic table. An atomic weight of nearly 240 was firmly established by Zimmerman (1882) by determining the mass ratios of several oxides and sodium uranyl acetate. The valence and atomic weight were confirmed by determination of the vapor density of UCl_4 and later of UF_6 and the atomic number 92 was established (Hahn, 1925) from nuclear decay systematics.

The principal use of uranium during the first century after its discovery (and for the previous two millenia) was as a colorant for ceramics and glasses. The obscurity surrounding the element was permanently dissipated by the discovery of Henri Becquerel (1896) that uranium emits penetrating rays. In connection with investigations of the fluorescence and phosphorescence of uranium salts that had been undertaken by generations of Becquerels (Zhang and Pitzer, 1999), H. Becquerel placed photographic plates that were covered with black paper near any salt or other material containing uranium. Whether the material was phosphorescent or not, he found that the emulsion was blackened by emanations that passed through the paper. He compared this phenomenon to that of X-rays, which had been announced only a few weeks earlier by Roentgen. Later Becquerel showed that the penetrating rays could discharge an electroscope. Shortly thereafter, Marie Curie developed quantitative techniques for measuring the radioactivity of uranium. She and others also found thorium to be radioactive and discovered by chemical separations that there were other elements present at trace levels in the uranium ore. Working with her husband Pierre, she discovered and named polonium and radium and described this property of these heavy elements as 'radioactivity'.

Because the Curies recognized that ores of uranium and thorium are much more radioactive than purified compounds of these elements, they and other radiochemists (e.g. Rutherford, Fajans, and Soddy) separated other radioelements and identified their chemical and nuclear transformations. The luminescent and medical properties of radium created a market for uranium ores and the processed radium that far exceeded the use of uranium as a colorant for glasses.

By 1911, the atomic weight of uranium had been refined to 238.5 (Gmelin, vol. A2, 1980a). The natural isotope ^{235}U was discovered in 1935 by mass spectrometry. The artificial isotope ^{239}U, which is the precursor of ^{239}Np and ^{239}Pu, was postulated and identified by Hahn and coworkers (Hahn *et al.*, 1937; Meitner *et al.*, 1937) as a 23 min half-life intermediate to transuranium elements that were not identified until the famous studies of Seaborg and coworkers 3 years later.

Despite these important discoveries, the crucial importance of uranium was not established until Hahn and Strassman (1939) discovered nuclear fission in late 1938. Since then, the chemistry, materials science, and nuclear properties of uranium have occupied a central position in the field of nuclear energy. Most schemes so far proposed for the release of nuclear energy involve the naturally occurring fissionable ^{235}U, fertile ^{238}U, or the artificial fissionable ^{233}U in one way or another, so that the chemistry and technology of uranium have become of great scientific and technical importance. For these reasons many reviews dealing with uranium chemistry, technology, and metallurgy have been published. The main volume on uranium of the *Gmelin Handbook of Inorganic Chemistry* (Gmelin, 1936) and a chapter by Mellor (1932) are the earliest comprehensive reviews of uranium chemistry prior to the discovery of fission. The Manhattan Project work was summarized in a number of volumes of the National Nuclear Energy Series (Katz and Rabinowitch, 1951, 1958; Seaborg and Katzin, 1951; Vance and Warner, 1951; Katzin, 1952; Warner, 1953; Wilkinson, 1962). These volumes deal with the chemistry of uranium and its compounds, ^{233}U, metallurgy, and technology of uranium, respectively. The most recent monograph on the chemistry of uranium is that by Cordfunke (1969). The most comprehensive treatment of all phases of uranium chemistry is the multi-volume uranium supplement to the *Gmelin Handbook of Inorganic Chemistry* (1975–1996).

5.2 NUCLEAR PROPERTIES

Uranium, as it occurs in nature, consists of a mixture of the three isotopes ^{238}U, ^{235}U, and ^{234}U. The relative abundances of ^{238}U, ^{235}U, and ^{234}U have been measured by various investigators, and 'best values' for the ^{238}U, ^{235}U, and ^{234}U relative abundances have been chosen through a review of the literature by Holden (1977). We have accepted these values and they are listed in Table 5.1. One has to keep in mind, however, that the isotopic ratio of the uranium isotopes in nature may vary as much as 0.1%. By utilizing mass spectrometric and nuclear disintegration data, the (chemical) atomic weight of natural uranium is calculated to be (238.0289 ± 0.0001). The isotope ^{238}U is the parent of the

Table 5.1 *Natural abundance of the uranium isotopes* (*Holden*, 1977).

Abundance (*at%*)		
Mass number	*Range*	*'Best' value*
234	0.0059–0.0050	0.005 ± 0.001
235	0.7202–0.7198	0.720 ± 0.001
238	99.2752–99.2739	99.275 ± 0.002

natural $4n + 2$ radioactive series, and the isotope ^{235}U is the parent of the natural $4n + 3$ radioactive series. ^{234}U arises from ^{238}U by radioactive decay and these two isotopes are thus linked to each other, but ^{235}U appears to be of independent origin.

The isotope ^{235}U, which exists in nature to the extent of 0.72%, and was identified by Dempster (1935) using mass spectrometry. This isotope is of special importance since it undergoes fission with slow neutrons.

Complete fission of ^{235}U gives rise to an energy equivalent of about 2×10^7 kWh kg^{-1} (corresponding to about 200 MeV per fission). Advantage can be taken of the fissionability of ^{235}U not only to generate large amounts of power but also to synthesize other important actinide elements. Uranium with its natural isotopic composition can be used in nuclear reactors to generate neutrons. The chain reaction is sustained by the excess neutrons produced by the fission of ^{235}U, while neutrons in excess of those required to propagate the chain reaction can be captured by the other natural isotope to produce plutonium:

$$^{235}\mathrm{U} + \mathrm{n} \rightarrow \text{fission products} + \text{energy} + 2.5\,\text{neutrons}$$

$$^{238}\mathrm{U} + \mathrm{n} \rightarrow {}^{239}\mathrm{U}$$

$$^{239}\mathrm{U} \xrightarrow{\beta^-} {}^{239}\mathrm{Np} \xrightarrow{\beta^-} {}^{239}\mathrm{Pu}$$

The abundant isotope ^{238}U can in this way be converted to plutonium-239, which, like ^{235}U, is also fissionable with slow neutrons.

A large number of synthetic isotopes of uranium have been prepared. The isotope ^{233}U, which was discovered by Seaborg, Gofman, and Stoughton (Katzin, 1952, paper 1.1), is particularly noteworthy, because it also undergoes fission with slow neutrons. Separation of this isotope from neutron-irradiated ^{232}Th is discussed (Thorex Process) in Chapter 24. Some of the other synthetic isotopes have particular utility as tracers for uranium. This is the case for beta-emitting ^{237}U and alpha-emitting ^{232}U, both of which have found extensive use in chemical and physical studies. The isotope ^{232}U is formed by alpha bombardment on ^{232}Th, or in the decay of the short-lived ^{232}Pa, which in turn may be obtained by neutron irradiation of ^{231}Pa. Procedures for the isolation of ^{232}U from this source have been described (Leuze *et al.*, 1962, 1963; Chilton, 1963).

The naturally occurring ^{234}U appears also in the α decay of ^{238}Pu (87.7 years). Separation of this ^{234}U from its parent furnishes a simple way to obtain isotopically pure ^{234}U (Figgins and Bernardinelli, 1966).

The various isotopes of uranium are listed in Table 5.2.

5.3 OCCURRENCE IN NATURE

The most important oxidation states of uranium in natural environments are 4+ and 6+. Compounds containing tetravalent uranium are insoluble in mildly acidic to alkaline conditions, whereas, those containing the linear uranyl moiety $(O{=}U{=}O)^{2+}$ are highly soluble and mobile. In solution, UO_2^{2+} forms soluble complexes with carbonate, oxalate, and hydroxide; UO_2^{2+} is also highly susceptible to adsorption either by organic matter, Fe oxyhydroxides, or by precipitation with various anions, such as hydroxide, silicate, vanadate, arsenate, and phosphate. In groundwater systems U(VI) is reduced to U(IV) if an effective reductant is present, such as H_2S. Other reducing agents may be fossil plants, methane, and transported humic material. Uranium minerals display an extraordinary wide structural and chemical variability, resulting from the different chemical conditions under which U minerals are formed.

Elucidation of the mechanisms of uranium sorption by mineral surfaces, refinements of complex U-mineral structures, and chemical bonding are needed to improve current models from uranium cycling in the aquo- and geospheres in order to describe the behavior of uranium in the environment. In past years, uranium mineralogy was more concerned with the economic quality of U-deposits; however, today we are equally concerned with the hazard presented by former uranium mines and nuclear waste sites to the local environment and population. This has placed greater emphasis on understanding the role of uranium sorption and for developing accurate thermodynamic and kinetic models for uranium attenuation. There are ~200 minerals that contain uranium as an essential component (Burns, 1999a; Finch and Murakami, 1999). Of these, the U(VI) minerals constitute the largest portion. Burns and coworkers have developed a novel approach for describing and classifying the uranyl phases, based on polymerization of coordination polyhedra of higher bond valence, which permits easy visualization of these extremely complex structures (Burns *et al.*, 1996; Burns, 1999a). Mineral descriptions are divided according to the major anionic component and structural similarities. In Table 5.3 a list of uranium minerals with the current information on composition, space group, and lattice parameters has been provided. Hill (1999) provided a similar list of uranium minerals and related synthetic phases; recent studies have identified new phases and errors in the previous entries.

Improved understanding of uranium mineralogy gives insight into the evolution of uranium deposits, possible mechanisms for uranium and radionuclide retardation following the weathering of nuclear waste materials, and the fate of

Table 5.2 *Nuclear properties of uranium isotopes.*[a]

Mass number	*Half-life*	*Mode of decay*	*Main radiations* (MeV)	*Method of production*
217	16 ms	α	α 8.005	^{182}W(^{46}Ar,5n)
218	1.5 ms	α	α 8.625	^{197}Au(^{27}Al,6n)
219	42 μs	α	α 8.680	^{197}Au(^{27}Al,x)
222	1.0 μs	α	α 9.500	W(^{40}Ar,xn)
223	18 μs	α	α 8.780	^{208}Pb(^{20}Ne,5n)
224	0.9 ms	α	α 8.470	^{208}Pb(^{20}Ne,4n)
225	59 ms	α	α 7.879	^{208}Pb(^{22}Ne,5n)
226	0.35 s	α	α 7.430	^{232}Th(α,10n)
227	1.1 min	α	α 6.87	^{232}Th(α,9n) ^{208}Pb(^{22}Ne,3n)
228	9.1 min	$\alpha \geq 95\%$ $\mathrm{EC} \leq 5\%$	α 6.68 (70%) 6.60 (29%) γ 0.152	^{232}Th(α,8n)
229	58 min	$\mathrm{EC} \sim 80\%$ $\alpha \sim 20\%$	α 6.360 (64%) 6.332 (20%) γ 0.123	^{230}Th(^{3}He,4n) ^{232}Th(α,7n)
230	20.8 d	α	α 5.888 (67.5%) 5.818 (31.9%) γ 0.072	^{230}Pa daughter ^{231}Pa(d,3n)
231	4.2 d	$\mathrm{EC} > 99\%$ $\alpha\ 5.5 \times 10^{-3}\%$	α 5.46 γ 0.084	^{230}Th(α,3n) ^{231}Pa(d,2n)
232	68.9 yr $\approx 8 \times 10^{13}$ yr	α SF	α 5.320 (68.6%) 5.264 (31.2%) γ 0.058	^{232}Th(α,4n)
233	1.592×10^{5} yr 1.2×10^{17} yr	α SF	α 4.824 (82.7%) 4.783 (14.9%) γ 0.097	^{233}Pa daughter
234	2.455×10^{5} yr 2×10^{16} yr	α SF	α 4.777 (72%) 4.723 (28%)	nature
235	7.038×10^{8} yr 3.5×10^{17} yr	α SF	α 4.397 (57%) 4.367 (18%) γ 0.186	nature
235 m	25 min	IT		^{239}Pu daughter
236	2.3415×10^{7} yr 2.43×10^{16} yr	α SF	α 4.494 (74%) 4.445 (26%)	^{235}U(n,γ)
237	6.75 d	β^-	β^- 0.519 γ 0.60	^{236}U(n,γ) ^{241}Pu daughter
238	4.468×10^{9} yr 8.30×10^{15} yr	α SF	α 4.196(77%) 4.149 (23%)	nature
239	23.45 min	β^-	β^- 1.29 γ 0.075	^{238}U(n,γ)
240	14.1 h	β^-	β^- 0.36 γ 0.044	^{244}Pu daughter
242	16.8 min	β^-	β^- 1.2 γ 0.068	^{244}Pu(n,2pn)

---

[a] Appendix II.

Table 5.3 *List of natural minerals with uranium as an essential component.*

Mineral	*Formula*	*Space group*	*a* (Å)	*b* (Å)	*c* (Å)	*Angle* (°)	*References*
uranium oxide	UO_2	*Fm*3*m*	5.4682				Roberts *et al.* (1990)
natural uraninite	$[U^{4+}_{1-x-y-z-u}U^{6+}_x(Th^{4+})_u REE^{3+}_y M^{2+}_z]O_{2+x-(0.5y)-z}$	*Fm*3*m*	5.470–5.443				Janeczek and Ewing (1992)
uranyl oxide hydrates							
dehydrated schoepite	$(UO_2)_4O(OH)_6 \cdot H_2O$		6.86	4.26	10.20		Finch *et al.* (1998)
ianthinite	$[U^{4+}_2(UO_2)_4O_6(OH)_4(H_2O)_4](H_2O)_5$	$P2_1cn$	7.178	11.473	30.39		Burns *et al.* (1997a)
meta-schoepite	$(UO_2)_4O(OH)_6 \cdot 5H_2O$	*Pbcn*	14.6861	13.9799	16.7063		Weller *et al.* (2000)
schoepite	$[(UO_2)_8O_2(OH)_{12}](H_2O)_{12}$	$P2_1ca$	14.337	16.813	14.731		Finch *et al.* (1996a)
wyartite	$Ca[U^{5+}(UO_2)_2(CO_3)O_4(OH)](H_2O)_7$	$P2_12_12_1$	11.2706	7.1055	20.807		Burns and Finch (1999)
peroxides							
meta-studtite	$(UO_2)O_2(H_2O)_2$		6.50	8.78	4.21		Deliens and Piret (1983a)
studtite	$[(UO_2)(O_2)(H_2O)_2](H_2O)_2$	C2/c	14.068	6.721	8.428	$\beta = 123.356$	Burns and Hughes (2003)
metal uranyl oxyhydroxides							
agrinierite	$K_2(Ca_{0.65}Sr_{0.35})[(UO_2)_3O_3(OH)_2]_2 \cdot 5H_2O$	*F*2*mm*	14.094	14.127	24.106		Cahill and Burns (2000)
bauranoite	$BaU_2O_7 \cdot 4.5H_2O$	No unit cell data					Rogova *et al.* (1973)
becquerelite	$Ca[(UO_2)_3O_2(OH)_3]_2(H_2O)_8$	$Pn2_1a$	13.8378	12.3781	14.9238		Burns and Li (2002)
billietite	$Ba[(UO_2)_3O_2(OH)_3]_2(H_2O)_4$	$Pbn2_1$	12.0720	30.167	7.1455		Pagoaga *et al.* (1987)
compreignacite	$K_2[(UO_2)_3O_2(OH)_3]_2(H_2O)_7$	*Pnmn*	14.8591	7.1747	12.1871		Burns (1998c)
protasite	$Ba[(UO_2)_3O_3(OH)_2](H_2O)_3$	*Pn*	12.2949	7.2206	6.9558	$\beta = 90.401$	Pagoaga *et al.* (1987)
rameauite	$K_2CaU_6O_{20} \cdot 9H_2O$	*C*2/*c*	13.97	14.26	14.22	$\beta = 121.02$	Gaines *et al.* (1997)
uranosphaerite	$Bi(UO_2)O_2OH$	$P2_1/n$	7.559	7.811	7.693	$\beta = 92.88$	Hughes *et al.* (2003)
vandenbrandeite	$(UO_2)Cu(OH)_4$	$P\bar{1}$	7.855	5.449	6.089	$\alpha = 91.44$ $\beta = 101.90$ $\gamma = 89.2$	Rosenzweig and Ryan (1977)

Table 5.3 (*Contd.*)

Mineral	*Formula*	*Space group*	*a* (Å)	*b* (Å)	*c* (Å)	*Angle* (°)	*References*
Pb–uranyl oxyhydroxides							
calciouranoite	$(Ca,Ba,Pb)U_2O_7 \cdot 5H_2O$	No data					
clarkeite	$(NaCa_{0.5}Pb_{0.5})[(UO_2)O(OH)](H_2O)_{0-1}$	*R*-3*m*	3.954		17.73		Finch and Ewing (1997)
curite	$Pb_{3+x}(H_2O)_2[((UO_2)_4O_{4+x}(OH)_{3-x}]_2$	*Pnam*	12.551 (12.53–12.58)	13.003 (13.01–13.03)	8.390 (8.39–8.40)		Taylor *et al.* (1981)
fourmarierite	$Pb_{1-x}[(UO_2)_4O_{3-2x}(OH)_{4+2x}](H_2O)_4$	*Bb*2$_1$*m*	13.986 (14.00–14.03)	16.400 (16.40–16.48)	14.293 (14.32–14.38)		Piret (1985)
masuyite	$Pb[(UO_2)_3O_3(OH)_2](H_2O)_3$	*Pn*	12.241	7.008	6.983	$\beta = 90.40$	Burns and Hanchar (1999)
meta-calciouranoite	$(Ca,Ba,Pb,K,Na)O \cdot UO_3 \cdot 5H_2O$	No data					
meta-vandendriesscheite	$PbU_7O_{22} \cdot nH_2O \quad n < 12$	*Pmma*	14.07	41.31	43.33		Roberts *et al.* (1990)
richetite	$M_xPb_{8.57}[(UO_2)_{18}(OH)_{12}]_2(H_2O)_{41}$	*P*1	20.9391	12.1000	16.3450	$\alpha = 103.87$ $\beta = 115.37$ $\gamma = 90.27$	Burns (1998b)
sayite	$Pb_2[(UO_2)_5O_6(OH)_2](H_2O)_4$	$P2_1/c$	10.704	6.960	14.533	$\beta = 116.81$	Piret *et al.* (1983)
spriggite	$Pb_3[(UO_2)_6O_8(OH)_2](H_2O)_3$	*C*2/*c*	28.355	11.990	13.998	$\beta = 104.248$	Brugger *et al.* (2004)
vandendriesscheite	$Pb_{1.57}[(UO_2)_{10}O_6(OH)_{11}](H_2O)_{11}$	*Pbca*	14.1165	41.478	14.5347		Burns (1997)
wölsendorfite	$Pb_{6.2}Ba_{0.4}[(UO_2)_{14}O_{19}(OH)_4](H_2O)_{12}$	*Cmcm*	14.131	13.885	55.969		Burns (1999b)
uranyl silicates							
haiweeite group (*U:Si* = *1:3*)							
coutinhoite	$Th_xBa_{(1-2x)}(H_2O)_y(UO_2)_2Si_5O_{13} \cdot H_2O$ With $0 \leq x \leq 0.5$ and $0 \leq y \leq (2+x)$	*Cmmb*	14.1676	14.1935	35.754		Atencio *et al.* (2004)
haiweeite	$Ca[(UO_2)_2Si_5O_{12}(OH)_2](H_2O)_3$	*Cmcm*	7.125	17.937	18.342		Burns (2001b)
weeksite	$K_{1.26}Ba_{0.25}Ca_{0.12}[(UO_2)_2(Si_5O_{13})]H_2O$	*Cmmb*	14.209	14.248	35.869		Jackson and Burns (2001)

uranophane group (*U:Si* = *1:1*)							
boltwoodite	$K_{0.56}Na_{0.42}[(UO_2)(SiO_3OH)](H_2O)_{1.5}$	$P2_1/m$	7.0772	7.0597	6.6479	$\beta = 104.982$	Burns (1998d)
cuprosklodowskite	$Cu(UO_2)_2(SiO_3OH)_2 \cdot 6H_2O$	$P\bar{1}$	7.052	9.267	6.655	$\alpha = 109.23$ $\beta = 89.84$ $\gamma = 110.01$	Rosenzweig and Ryan (1975)
kasolite	$Pb[(UO_2)(SiO_4)](H_2O)$	$P2_1/c$	6.704	6.932	13.252	$\beta = 104.22$	Ryan and Rosenzweig (1977)
oursinite	$(Co_{0.86}Mg_{0.10}Ni_{0.04}) \cdot O_2 \cdot UO_2 \cdot 2SiO_2 \cdot 6H_2O$	*Aba*2 *or Abam*	12.74	17.55	7.050		Deliens and Piret (1983b)
sklodowskite	$Mg(H_3O)_2[(UO_2)(SiO_4)]_2 \cdot 4H_2O$	$C2/m$	17.382	7.047	6.610	$\beta = 105.9$	Ryan and Rosenzweig (1977)
sodium boltwoodite	$(Na,K)(H_3O)[(UO_2)(SiO_4)] \cdot H_2O$	$P2_12_12_1$	27.2	7.02	6.65		Stohl and Smith (1981)
swamboite	$(UO_2)_{0.33}[(UO_2)(SiO_4)]_2 \cdot 6H_2O$	$P2_1/a$	17.64	21.00	20.12	$\gamma = 103.4$	Deliens and Piret (1981)
α-uranophane	$Ca(UO_2)_2(SiO_3OH)_2(H_2O)_5$	$P2_1$	15.909	7.002	6.665	$\beta = 97.27$	Ginderow (1988)
β-uranophane	$Ca(UO_2)_2(SiO_3OH)_2(H_2O)_5$	$P2_1/a$	13.966	15.443	6.632	$\gamma = 91.38$	Viswanathan and Harnett (1986)
other U silicates							
arapovite	$U(Ca,Na)_2(K_{1-x}\square_x)(Si_8O_{20})$, $x \sim 0.5$	$P4/mcc$	7.5505		14.7104		Uvarova *et al.* (2004)
ciprianiite	$Ca_4[(Th,U)(REE)]Al_2(Si_4B_4O_{22})(OH, F)_2]$	$P2/a$	19.032	4.746	10.248	$\gamma = 110.97$	della Ventura *et al.* (2002)
lepersonnite-Gd	$CaO(Gd,Dy)_2O_3 \cdot 24UO_3 \cdot 8CO_2 \cdot 4SiO_2 \cdot 60H_2O$	*Pnnm or Pnn*2	16.23	38.74	11.73		Deliens and Piret (1982)
soddyite	$(UO_2)_2[SiO_4](H_2O)_2$	*Fddd*	8.334	11.212	18.688		Demartin *et al.* (1992)
uranosilite	$(Mg,Ca)_4(UO_2)_4(Si_2O_5)_{5.5}(OH)_5 \cdot 13H_2O$	*Pmmb or Pmcb*	11.60	14.68	12.83		Walenta (1983)
orthosilicates							
coffinite	$U(SiO_4)_{1-x}(OH)_{4x}$	$I4_1/amd$	6.979		6.252		Fuchs and Gebert (1958)
uranyl carbonates							
albrechtschraufite	$Ca_4Mg(UO_2)_2(CO_3)_6F_2 \cdot 17H_2O$	$P\bar{1}$	13.562	13.406	11.636	$\alpha = 115.72$ $\beta = 107.66$ $\gamma = 92.86$	Mereiter (1984)

Table 5.3 (*Contd.*)

Mineral	*Formula*	*Space group*	*a* (Å)	*b* (Å)	*c* (Å)	*Angle* (°)	*References*
andersonite	$Na_2Ca[(UO_2)(CO_3)_3](H_2O)_5$	$R\text{-}3m$	17.904		23.753		Mereiter (1986)
astrocyanite-Ce	$Cu_2(Ce,Nd,La)_2UO_2(CO_3)_5(OH)_2 \cdot 1.5H_2O$	$P6/mmm$	14.96		26.86		Deliens and Piret (1990b)
bayleyite	$Mg_2[(UO_2)(CO_3)_3](H_2O)_{18}$	$P2_1/a$	26.560	15.256	6.505	$\gamma = 92.90$	Mayer and Mereiter (1986)
bijvoetite-Y	$[M_8^{3+}(H_2O)_{25}(UO_2)_6O_8(OH)_8(CO_3)_{16}](H_2O)_{14}$	$B12_11$	21.234	12.958	44.911	$\beta = 90.00$	Li et *al.* (2000)
blatonite	$UO_2CO_3 \cdot H_2O$		15.79		23.93		Vochten and Deliens (1998)
čejkaite	$Na_4(UO_2)(CO_3)_3$	$P1$ *or* $P\bar{1}$	9.291	9.292	12.895	$\alpha = 90.73$ $\beta = 90.82$ $\gamma = 120$	Ondruš *et al.* (2003)
fontanite	$Ca[(UO_2)_3(CO_3)_2O_2](H_2O)_6$	$P2_1/n$	6.968	17.276	15.377	$\beta = 90.064$	Hughes and Burns (2003)
grimselite	$K_3Na[(UO_2)(CO_3)_3](H_2O)$	$P\text{-}62c$	9.302		8.260		Li and Burns (2001b)
joliotite	$UO_2CO_3 \cdot nH_2O \quad n = 1.5\text{–}2.0$	$P222$	8.16	10.35	6.32		Walenta (1976)
kamotoite-Y	$Y_2O_4(UO_2)_4(CO_3)_3 \cdot 14H_2O$	$P2_1/a$	21.22	12.93	12.39	$\gamma = 115.3$	Gaines *et al.* (1997)
liebigite	$Ca_2UO_2(CO_3)_3 \cdot 11H_2O$	$Bba2$	16.699	17.557	13.697		Mereiter (1982a)
mckelveyite-Y	$Ba_3Na(Ca,U)Y(CO_3)_6 \cdot 3H_2O$	$P\bar{1}$	9.142	9.141	7	$\alpha = 102.51$ $\beta = 115.67$ $\gamma = 59.99$	Roberts *et al.* (1990)
meta-zellerite	$CaUO_2(CO_3)_2 \cdot 3H_2O$	$Pbnm$	9.718	18.226	4.965		Roberts *et al.* (1990)
oswaldpeetersite	$(UO_2)_2CO_3(OH)_2 \cdot 4H_2O$	$P2_1/c$	4.1425	14.098	18.374	$\beta = 103.62$	Vochten *et al.* (2001)
rabbittite	$Ca_3Mg_3(UO_2)_2(CO_3)_6(OH)_4 \cdot 18H_2O$		32.6	23.8	9.45	$\beta = 90$	Gaines *et al.* (1997)
roubaultite	$Cu_2[(UO_2)_3(CO_3)_2O_2(OH)_2](H_2O)_4$	$P\bar{1}$	7.767	6.924	7.850	$\alpha = 92.16$ $\beta = 90.89$ $\gamma = 93.48$	Ginderow and Cesbron (1985)
rutherfordine	UO_2CO_3	$Pmmn$	4.845	9.205	4.296		Finch *et al.* (1999b)
schröckingerite	(*listed under uranyl sulfates*)						
shabaite-Nd	$Ca(Nd,Sm,Y)_2UO_2(CO_3)_4(OH)_2 \cdot 6H_2O$	$P2$, Pm, *or* $P2_1/m$	9.208	32.09	8.335	$\beta = 90.3$	Deliens and Piret (1990a)
sharpite	$Ca(UO_2)_6(CO_3)_5(OH)_4 \cdot 6H_2O$		21.99	15.63	4.48		Gaines *et al.* (1997)
swartzite	$CaMgUO_2(CO_3)_3 \cdot 12H_2O$	$P2_1/m$	11.080	14.634	6.439	$\beta = 99.43$	Mereiter (1986)

urancalcarite	$Ca(UO_2)_3CO_3(OH)_6 \cdot 3H_2O$	*Pmcm* *or* $P2_1cn$	15.42	6.97	16.08		Deliens and Piret (1984a)
voglite	$Ca_2CuUO_2(CO_3)_4 \cdot 6H_2O$	$P2_1$	25.97	24.5	10.7	$\beta = 104$	Gaines *et al.* (1997)
widenmannite	$Pb_2UO_2(CO_3)_3$		8.99	9.36	4.95		Walenta (1976)
zellerite	$Ca(UO_2)(CO_3)_2(H_2O)_5$	*Pbnm*	11.22	19.25	4.93		Roberts *et al.* (1990)
znucalite	$CaZn_{11}(UO_2)(CO_3)_3(OH)_{20}(H_2O)_4$	$P\bar{1}$	12.692	25.096	11.85	$\alpha = 89.08$ $\beta = 91.79$ $\gamma = 90.37$	Ondruš *et al.* (1990)
uranyl phosphates							
althupite	$ThAl(UO_2)[(UO_2)_3(PO_4)_2O(OH)]_2(OH)_3(H_2O)_{15}$	$P\bar{1}$	10.953	18.567	13.504	$\alpha = 72.64$ $\beta = 68.20$ $\gamma = 84.21$	Piret and Deliens (1987)
ankoleite	$K_2(UO_2)_2(PO_4)_2 \cdot 6H_2O$	*P4/nmm*	6.993		8.891		Gaines *et al.* (1997)
asselbornite	$(Pb,Ba)(UO_2)_6(BiO)_4[(As,P)O_4]_2(OH)_{12} \cdot 3H_2O$	*Im3m*	15.66				Gaines *et al.* (1997)
autunite	$Ca[(UO_2)(PO_4)]_2 \cdot 11H_2O$	14/*mmm*	7.00		20.67		Locock and Burns (2003a)
bassetite	$Fe^{2+}(UO_2)_2(PO_4)_2 \cdot 8H_2O$	$P2_1/m$	6.98	17.07	7.01	$\beta = 90.32$	Roberts *et al.* (1990)
bergenite	$Ca_2Ba_4[(UO_2)_3O_2(PO_4)_2]_3(H_2O)_{16}$	$P2_1/c$	10.092	17.245	17.355	$\beta = 113.678$	Locock and Burns (2003c)
chernikovite	$(H_3O)_2(UO_2)(PO_4)_2 \cdot 6H_2O$	*P4/nmm*	7.02		9.043		Gaines *et al.* (1997)
coconinoite	$Fe_2Al_2(UO_2)_2(PO_4)_4SO_4(OH)_2 \cdot 20H_2O$	*C2/c*	12.5	12.97	23	$\beta = 106.6$	Young *et al.* (1966)
dewindtite	$Pb(UO_2)_3(PO_4)_2(OH)_2 \cdot 3H_2O$	*Bmmb*	16.031	17.264	13.605		Piret *et al.* (1990)
dumontite	$Pb_2[(UO_2)_3(PO_4)_2(OH)_4](H_2O)_5$	$P2_1/m$	8.118	16.819	6.983	$\beta = 109.03$	Locock and Burns (2003b)
françoisite-Nd	$Nd[(UO_2)_3(PO_4)_2O(OH)](H_2O)_6$	$P2_1/c$	9.298	15.605	13.668	$\beta = 112.77$	Piret *et al.* (1988)
furongite	$Al_2UO_2(PO_4)_2 \cdot 8H_2O$	$P\bar{1}$	17.87	14.18	12.18	$\alpha = 67.8$ $\beta = 77.5$ $\gamma = 79.9$	Shen and Peny (1981)
kamitugaite	$PbAl(UO_2)_5[(P,As)O_4]2(OH)_9 \cdot 5H_2O$	$P\bar{1}$	10.98	15.96	9.068	$\alpha = 95.1$ $\beta = 96.1$ $\gamma = 80$	Deliens and Piret (1984b)
lehnerite	$Mn(UO_2)_2(PO_4)_2 \cdot 8H_2O$	$P2_1/n$					Gaines *et al.* (1997)
lermontovite	$U^{4+}PO_4 \cdot OH \cdot H_2O$		9.74	19	10.01		Gaines *et al.* (1997)
meta-autunite	$Ca[(UO_2)(PO_4)]_2 \cdot 6H_2O$	*P4/nmm*	6.96		8.40		Gaines *et al.* (1997)

Table 5.3 (*Contd.*)

Mineral	*Formula*	*Space group*	*a* (Å)	*b* (Å)	*c* (Å)	*Angle* (°)	*References*
meta-torbenite	$Cu[(UO_2)(PO_4)]_2(H_2O)_8$	*P*4/*n*	6.9756		17.349		Locock and Burns (2003d)
meta-uranocircite-I	$Ba[(UO_2)(PO_4)]_2(H_2O)_7$	$P2_1$	6.943	17.634	6.952	$\beta = 89.95$	Locock *et al.* (2005b)
meta-vanmeersscheite	$U(UO_2)_3(PO_4)_2(OH)_6 \cdot 2H_2O$		34.18	33.88	14.07		Piret and Deliens (1982)
mundite	$Al(UO_2)_3(PO_4)_2(OH)_3 \cdot 5.5H_2O$		17.08	30.98	13.76		Gaines *et al.* (1997)
ningyoite	$(U^{4+},Ca,Ce)_2[PO_4]_2 \cdot 1\text{–}2H_2O$		6.8040	12.0117	6.3504		Gaines *et al.* (1997)
parsonsite	$Pb_2[(UO_2)(PO_4)_2](H_2O)n$, where $0 \leq n \leq 0.5$	$P\bar{1}$	6.842	10.383	6.670	$\alpha = 101.5$ $\beta = 110.84$ $\gamma = 88.09$	Sejkora *et al.* (2002)
phosphatian walpurgite	$(UO_2)Bi_4O_4[(As,P)O_4]_2 \cdot 2H_2O$	$P\bar{1}$	7.124	10.392	5.492	$\alpha = 101.22$ $\beta = 109.93$ $\gamma = 87.93$	Sejkora *et al.* (2004)
phosphuranylite	$KCa(H_3O)_3(UO_2)[(UO_2)_3(PO_4)_2O_2]_2(H_2O)_8$	*Cmcm*	15.899	13.740	17.300		Demartin *et al.* (1991)
phuralumite	$Al_2(UO_2)_3(PO_4)_3(OH)_2 \cdot 13H_2O$	$P2_1/a$	13.836	20.918	9.428		Piret *et al.* (1979)
phurcalite	$Ca_2(UO_2)_3O_2(PO_4)_2 \cdot 7H_2O$	*Pbca*	17.415	16.035	13.598		Atencio *et al.* (1991)
przhevalskite	$Pb_2(UO_2)_3(PO_4)_2(OH)_4 \cdot 3H_2O$	*Cmmm*	8.57	11.01	6.93		Gmelin (1981d)
ranunculite	$HAlUO_2PO_4(OH)_3 \cdot 4H_2O$		11.1	17.7	18.0	$\beta = 90$	Gaines *et al.* (1997)
renardite	(not a mineral species possible mixture of dewindtite and phosphuranylite (Čejka, 1999)						
sabugalite	$HAl(UO_2)_4(PO_4)_4 \cdot 16H_2O$		6.96		19.3		Frondel (1951a)
saléeite	$Mg[(UO_2)(PO_4)]_2 \cdot 10H_2O$	$P2_1/c$	6.951	19.947	9.896	$\beta = 135.17$	Miller and Taylor (1986)
threadgoldite	$Al(UO_2)_2(PO_4)_2OH \cdot 8H_2O$	*C*2/*c*	20.168	9.847	19.719		Khosrawan-Sazedj (1982b)
torbernite	$Cu[(UO_2)(PO_4)]_2(H_2O)_{12}$	*P*4/*nnc*	7.0267		20.807		Locock and Burns (2003d)
triangulite	$Al_3(UO_2)_4(PO_4)_4(OH)_5 \cdot 5H_2O$		10.39	10.56	10.6	$\alpha = 116.4$ $\beta = 107.8$ $\gamma = 113.4$	Gaines *et al.* (1997)

tristramite	*listed under uranyl sulfates*						
ulrichite	$Cu[Ca(H_2O)_2(UO_2)(PO_4)_2](H_2O)_2$	$P2_1/c$	12.84	6.996	13.007	$\beta = 91.92$	Kolitsch and Giester (2001)
upalite	$Al(UO_2)_3(PO_4)_2O(OH) \cdot 7H_2O$	$P2_1/a$	13.704	16.82	9.332	$\gamma = 111.5$	Piret and Declercq (1983)
uramphite	$NH_4UO_2PO_4 \cdot 3H_2O$		7.01		9.05		Gmelin (1981d)
uranocircite	$Ba[(UO_2)(PO_4)]_2(H_2O)_{10}$	$P2/c$	7.01	6.99	21.2	$\beta = 103.7$	Locock *et al.* (2005b)
uranospathite	$Al_{1-x}\square_x[(UO_2)(PO_4)]_2(H_2O)_{20+3x}F_{1-3x}$, $0 < x < 0.33$	$Pnn2$	30.020	7.0084	7.0492		Locock *et al.* (2005c)
vochtenite	$(Fe,Mg)Fe[(UO_2)(PO_4)]_2 \cdot 8H_2O$		12.606	19.99	9.99	$\beta = 102.52$	Gaines *et al.* (1997)
vanmeersscheite	$U(OH)_4[(UO_2)_3(PO_4)_2(OH)_2](H_2O)_4$	$P2_1mn$	17.06	16.76	7.023		Piret and Deliens (1982)
vyacheslavite	$UPO_4(OH) \cdot nH_2O$		6.96	9.1	12.38		Gaines *et al.* (1997)
xiangjiangite	$(Fe,Al)(UO_2)_4(PO_4)_2(SO_4)_2OH \cdot 22H_2O$	$C2/c$	12.54	12.98	23.8	$\beta = 108.6$	Zhang *et al.* (1992)
yingjiangite	$(K_{1-x}Ca_x)(UO_2)_3(PO_4)_2(OH)_{1+x} \cdot 4H_2O$ $x = 0.35$	$Bmmb$	15.707	17.424	13.692		Zhangru *et al.* (1986)
uranyl arsenates							
arsenuranospathite	$HAl(UO_2)_4(AsO_4)_4 \cdot 40H_2O$	$P4_2/n$	7.16		30.37		Gaines *et al.* (1997)
arsenuranylite	$Ca(UO_2)_4(AsO_4)_2(OH)_4 \cdot 6H_2O$		15.4	17.4	13.77		Gaines *et al.* (19970
asselbornite	$(Pb,Ba)(UO_2)_6(BiO)_4(AsO_4)_2(OH)_{12} \cdot 3(H_2O)$	$Im3m$	15.66				Sarp *et al.* (1983)
abernathyite	$K[(UO_2)(AsO_4)]_2(H_2O)_3$	$P4/ncc$	7.176		18.126		Ross and Evans (1964)
chadwickite	$(UO_2)H(AsO_3)$		11		15.96		Walenta (1998)
hallimondite	$Pb_2[(UO_2)(AsO_4)_2](H_2O)_n$, where $0 \leq n \leq 0.5$	$P\bar{1}$	7.123	10.469	6.844	$\alpha = 100.57$ $\beta = 94.80$ $\gamma = 91.27$	Walenta (1965)
heinrichite	$Ba[(UO_2)_2(AsO_4)]_2(H_2O)_{10}$	$P2/c$	7.1548	7.1340	21.290	$\beta = 104.171$	Locock *et al.* (2005b)
hügelite	$Pb_2[(UO_2)_3O_2(AsO_4)_2](H_2O)_5$	$P2_1/m$	31.066	17.303	7.043	$\beta = 96.492$	Locock and Burns (2003b)
kahlerite	$Fe(UO_2)_2(AsO_4)_2 \cdot 12H_2O$	$P4_2/n$	14.3		21.97		Gaines *et al.* (1997)
meta-heinrichite	$Ba[(UO_2)(AsO_4)]_2(H_2O)_7$	$P2_1$	7.08	17.7	7.09	$\beta = 90.02$	Locock *et al.* (2005b)
meta-kahlerite	$Fe(UO_2)_2(AsO_4)_2 \cdot 8H_2O$	$P4/mmm$	7.16		8.62		Gaines *et al.* (1997)
meta-kirchheimerite	$Co(UO_2)_2(AsO_4)_2 \cdot 8H_2O$	$P4/mmm$	7.16		8.60		Gaines *et al.* (1997)
meta-lodevite	$Zn(UO_2)_2(AsO_4)_2 \cdot 10H_2O$	$P4_2/m$	7.16		17.20		
meta-novácekite	$Mg(UO_2)_2(AsO_4)_2 \cdot 4\text{–}8H_2O$	$P4/n$	7.16		8.58		Roberts *et al.* (1990)

Table 5.3 (*Contd.*)

Mineral	*Formula*	*Space group*	*a* (Å)	*b* (Å)	*c* (Å)	*Angle* (°)	*References*
meta-zeunerite	$Cu[(UO_2)(AsO_4)]_2(H_2O)_8$	*P4/n*	7.1094		17.416		Locock and Burns (2003d)
novacekite	$Mg(UO_2)_2(AsO_4)_2 \cdot 12H_2O$	*P4₁/n*	7.16		20.19		Frondel (1951b)_
orthowalpurgite	$(UO_2)Bi_4O_4(AsO_4)_2 \cdot 2H_2O$	*Pbcm*	5.492	13.324	20.685		Krause *et al.* (1995)
séelite	$Mg(UO_2)(AsO_3)_{0.7}(AsO_4)_{0.3} \cdot 7\beta\beta H_2O$	*C2/m*	18.207	7.062	6.661	$\beta = 99.65$	Frondel (1951b)
trögerite	$(UO_2)_3(AsO_4)_2 \cdot 12H_2O$	*P4/mmm*	7.16		8.8		Gaines *et al.* (1997)
uranospinite	$Ca[(UO_2)(AsO_4)]_2(H_2O)_{11}$	*Pnma*	14.35	20.66	7.17		Lockock *et al.* (2005b)
walpurgite	$(UO_2)Bi_4O_4(AsO_4)_2 \cdot 2H_2O$	$P\bar{1}$	7.135	10.426	5.494	$\alpha = 101.47$ $\beta = 110.82$ $\gamma = 88.20$	Mereiter (1982b)
zeunerite	$Cu[(UO_2)(AsO_4)]_2(H_2O)_{12}$	*P4/nnc*	7.1797		20.857		Locock and Burns (2003d)
uranyl molybdates							
calcurmolite	$Ca(UO_2)_3(MoO_4)_3(OH)_2(H_2O)_{11}$						Gaines *et al.* (1997)
deloryite	$Cu_4(UO_2)(MoO_4)_2(OH)_6$	*C2/m*	19.94	6.116	5.52	$\beta = 104.2$	Pushcharovsky *et al.* (1996)
iriginite	$[(UO_2)Mo_2O_7(H_2O)_2](H_2O)$	*Pbcm*	6.705	12.731	11.524		Krivovichev and Burns (2000)
moluranite	$U^{4+}(UO_2)_2Mo_5O_{19} \cdot 12H_2O$	*amorphous*					Roberts *et al.* (1990)
mourite	$U^{4+}Mo_5O_{12}(OH)_{10}$	*P2/c*	24.443	7.182	9.901	$\beta = 102.22$	Gaines *et al.* (1997)
tengchongite	$CaO_6UO_3 \cdot 2MoO_3 \cdot 12H_2O$		15.616	13.043	17.716		Chen *et al.* (1986)
sedovite	$U(MoO_4)_2$		3.36	11.08	6.42		Roberts *et al.* (1990)
umohoite	$[(UO_2)MoO_4(H_2O)](H_2O)$	*P2₁/c*	6.3748	7.5287	14.628	$\alpha = 82.64$ $\beta = 85.95$ $\gamma = 89.91$	Krivovichev and Burns (2000b)
uranyl vanadates							
carnotite	$[K_2(UO_2)_2(VO_4)_2 \cdot 1\text{–}3H_2O]$	*P21/a*	10.51	8.45	7.32	$\gamma = 106.08$	Appleman and Evans (1965)
curienite	$Pb[(UO_2)_2(V_2O_8)](H_2O)_5$	*Pcan*	10.40	8.45	16.34		Borène and Cesbron (1971)

francevillite	$Ba_{0.96}Pb_{0.04}[(UO_2)_2(V_2O_8)](H_2O)_5$	*Pcan*	10.419	8.510	16.763		Mereiter (1986)
fritzscheite	$Mn(UO_2)_2(PO_4,VO_4)_2 \cdot 10H_2O$	*Pnam*	10.59	8.25	15.54		Roberts *et al.* (1990)
margaritasite	$(Cs,K,H_3O)_2(UO_2)_2(VO_4)_2 \cdot H_2O$	$P2_1/a$	10.514	8.425	7.25	$\gamma = 106.01$	Roberts *et al.* (1990)
meta-tyuyamunite	$Ca(UO_2)_2(VO_4)_2 \cdot 3–5H_2O$	*Pnam*	10.54	8.49	17.34		Roberts *et al.* (1990)
meta-vanuralite	$Al(UO_2)_2(VO_4)_2OH \cdot 8H_2O$	*P*1	10.46	8.44	10.43	$\alpha = 75.88$ $\beta = 102.83$ $\gamma = 90$	Roberts *et al.* (1990)
rauvite	$Ca(UO_2)_2V_{10}O_{28} \cdot 16H_2O$	(*no unit cell data*)					
sengierite	$Cu_2[(UO_2)_2(V_2O_8)](OH)_2(H_2O)_6$	$P2_1/a$	10.599	8.093	10.085	$\gamma = 103.42$	Piret *et al.* (1980)
strelkinite	$NaUO_2VO_4 \cdot 3H_2O$	*Pnmm*	10.64	8.36	32.72		Gaines *et al.* (1997)
tyuyamunite	$Ca(UO_2)_2(VO_4)_2 \cdot 5–8H_2O$	*Pnan*	10.36	8.36	20.4		Roberts *et al.* (1990)
uvanite	$U_2V_6O_{21} \cdot 15H_2O$	(*no unit cell data*)					
vanuralite	$Al(UO_2)_2(V^{5+}O_4)_2(OH) \cdot 11H_2O$		10.55	8.44	24.52	$\beta = 103$	Roberts *et al.* (1990)
vanuranylite	$(H_3O,Ba,Ca,K)_{1.6}(UO_2)_2(VO_4)_2 \cdot 4H_2O$	*C*2/*c*	10.49	8.37	20.2	$\beta = 90$	Roberts *et al.* (1990)
uranyl tungstates							
uranotungstite	$(Fe^{2+},Ba,Pb)(UO_2)_2WO_4(OH)_4(H_2O)_{12}$		9.22	13.81	7.17		Walenta (1985)
uranyl sulfates							
deliensite	$Fe(UO_2)_2(SO_4)_2(OH)_2 \cdot 3H_2O$	*Pnnm or Pnn*2	15.908	16.274	6.903		Vochten *et al.* (1997)
Co-zippeite	$Co(H_2O)_{3.5}[(UO_2)_2(SO_4)O_2]$	*C*2/*m*	8.650	14.252	17.742	$\beta = 104.092$	Burns *et al.* (2003)
coconinoite	$Fe_2Al_2(UO_2)_2(PO_4)_4SO_4(OH)_2 \cdot 20H_2O$		12.5	12.97	23	$\beta = 106.6$	Young *et al.* (1966)
jáchymovite	$(UO_2)_8(SO_4)(OH)_{14} \cdot 13H_2O$	(*no unit cell data*)					Brugger *et al.* (2003)
johannite	$Cu(UO_2)_2(SO_4)_2(OH)_2 \cdot 8H_2O$	$P\bar{1}$	8.903	9.499	6.812	$\alpha = 109.87$ $\beta = 112.01$ $\gamma = 100.40$	Mereiter (1982c)
marecottite	$Mg_3(H_2O)_{18}[(UO_2)_4O_3(OH)(SO_4)_2]_2(H_2O)_{10}$	$P\bar{1}$	10.815	11.249	13.851	$\alpha = 66.224$ $\beta = 72.412$ $\gamma = 69.95$	Brugger *et al.* (2003)
Mg-zippeite	$Mg_2(H_2O)_{11}[(UO_2)_2(SO_4)O_2]_2$	$P2_1/c$	8.6457	17.2004	18.4642	$\beta = 102.119$	Burns *et al.* (2003)
meta-uranopilite	$(UO_2)_6SO_4(OH)_{10} \cdot 5H_2O$	no unit cell data					Roberts *et al.* (1990)
Ni-zippeite	$Ni_2(UO_2)_6(SO_4)_3(OH)_{10} \cdot 16H_2O$	no unit cell data					Roberts *et al.* (1990)

Table 5.3 (*Contd.*)

Mineral	*Formula*	*Space group*	*a* (Å)	*b* (Å)	*c* (Å)	*Angle* (°)	*References*
rabejacite	$Ca(UO_2)_4(SO_5)_2(OH)_6 \cdot 6H_2O$		8.73	17.09	15.72		Deliens and Piret (1993)
schröckingerite	$NaCa_3(UO_2)(CO_3)_3(SO_4)F \cdot 10H_2O$		9.341		12.824		Li *et al.* (2001a)
Na-zippeite	$Na_5(H_2O)_{12}[(UO_2)_8(SO_4)_4O]_5(OH)_3$	$P2_1/n$	17.6425	14.6272	17.6922	$\beta = 104.461$	Burns *et al.* (2003)
tristramite	$(Ca,U^{4+},Fe^{3+})(PO_4,SO_4) \cdot 2H_2O$	$P6_222$	6.919		6.422		Gaines *et al.* (1997)
uranopilite	$(UO_2)_6[(SO_4)O_2(OH)_6(H_2O)]_6(H_2O)_8$	$P\bar{1}$	8.896	14.029	14.33	$\alpha = 96.610$ $\beta = 98.472$ $\gamma = 99.802$	Burns (2001a)
Zn-zippeite	$Zn(H_2O)_{3.5}[(UO_2)_2(SO_4)O_2]$	$C2/m$	8.6437	14.1664	17.701	$\beta = 104.041$	Burns *et al.* (2003)
zippeite	$K_3(H_2O)_3[(UO_2)_4(SO_4)_2O_3(OH)]$	$C2$	8.7524	13.9197	17.6972	$\beta = 104.178$	Burns *et al.* (2003)
uranyl selenites and tellurites							
cliffordite	$UO_2(Te_3O_7)$	$Pa\bar{3}$	11.335				Branstätter (1981)
derriksite	$Cu_4[(UO_2)(SeO_3)_2](OH)_6$	$Pn2_1m$	5.570	19.088	5.965		Ginderow and Cesbron (1983a)
demesmaekerite	$Cu_5Pb_2(UO_2)_2(SeO_3)_6(OH)_6(H_2O)_2$	$P\bar{1}$	11.955	10.039	5.639	$\alpha = 89.78$ $\beta = 100.36$ $\gamma = 91.34$	Ginderow and Cesbron (1983b)
guilleminite	$Ba[UO_2)_3(SeO_3)_2O_2](H_2O)_3$	$P2_1nm$	7.084	7.293	16.881		Cooper and Hawthorne (1995)
haynesite	$(UO_2)_3(OH)_2(SeO_3)_2 \cdot 5H_2O$	$Pncm$	8.025	17.43	6.953		Gaines *et al.* (1997)
larisaite	$Na(H_3O)(UO_2)_3(SeO_3)_2O_2 \cdot 4H_2O$	$P11m$	6.9806	7.646	17.249	$\beta = 90.039$	Chukanov *et al.* (2004)
marthozite	$Cu^{2+}[(UO_2)_3(SeO_3)_2O_2](H_2O)_8$	$Pbn2_1$	6.9879	16.4537	17.2229		Cooper and Hawthorne (2001)
moctezumite	$PbUO_2(TeO_3)_2$	$P2_1/c$	7.813	7.061	13.775	$\beta = 93.71$	Swihart *et al.* (1993)
piretite	$Ca(UO_2)_3(SeO_3)_2(OH)_4 \cdot 4(H_2O)$	$Pmnm$	7.01	17.135	17.606		Vochten *et al.* (1996)
schmitterite	UO_2TeO_3	$Pca2_1$	10.161	5.363	7.862		Meunier and Galy (1973)

euxenite–pyrochlore (mineral structures obtained by heating)							
betafite	$(Ca,Na,U)_2(Ti,Nb,Ta)_2O_6(OH)$	$Fd3m$	10.31				Gaines *et al.* (1997)
calciobetafite	$(Ca,RE,Th,U)_2(Nb,Ta,Ti)_2O_7$	$Fd3m$	10.2978				Mazzi and Munno (1983)
calciosamarskite	$(Ca,Fe^{3+},U,Y)NbO_4$	Metamict					Hanson *et al.* (1999)
euxenite-y	$(Y,Ca,Ce,U,Th)(Nb,Ta,Ti)_2O_6$	$Pcan$	5.52	14.57	5.166		Gaines *et al.* (1997)
ishikawaite	$(U,Fe,Y,Ce)(Nb,Ta)O_4$	Metamict					Hanson *et al.* (1999)
kobeite-y	$(Y,U)(Ti,Nb)_2(O,OH)_6$		5.021				Gaines *et al.* (1997)
liandratite	$U^{6+}(Nb,Ta)_2O_8$	$P\bar{3}1m$	6.36		4.01		Mucke and Strunz (1978)
petscheckite	$U^{4+}Fe^{2+}(Nb,Ta)_2O_8$	$P\bar{3}1m$	6.42		4.02		Mucke and Strunz (1978)
samarskite	$(Fe,Y,Ce,U)(Nb,Ta,Ti)O_4$	$Pbcn$	5.498	14.34	5.12		Warner and Ewing (1993)
uranopyrochlore	$(U,Ca,Ce)_2(Nb,Ta)_2O_6(OH,F)$	$Fd3m$	10.44				Gaines *et al.* (1997)
uranmicrolite	$(U,Ca,Ce)_2(Ta,Nb)_2O_6(OH,F)$	$Fd3m$	10.4				Gaines *et al.* (1997)
uranopolycrase	$(U,Y)(Ti,Nb)_2O_6$	$Pbcn$	14.51	5.558	5.173		Gaines *et al.* (1997)
brannerites							
brannerite	$(U,Ca,Y,Ce)(Ti,Fe)_2O_6$	$C2/m$	9.79	3.72	6.87	$\beta = 118.25$	Pabst (1954)
thorutite	$(Th,U,Ca)Ti_2(O,OH)_6$	$C2/m$	9.822	3.824	7.036	$\beta = 118.83$	Roberts *et al.* (1990)
Fe–Ti oxides							
davidite-la	$(La,Ce)(Y,U,Fe)(Ti,Fe)_{20}(O,OH)_{38}$	$R\bar{3}$	10.375		20.909		Gatehouse *et al.* (1979)
dessauite	$(Sr,Pb)(Y,U)(Ti,Fe^{3+})_{20}O_{38}$	$R\bar{3}$	9.197			$\alpha = 68.75$	Orlandi *et al.* (1997)

other anthropogenic sources of uranium of environmental concern. The long-term behavior of nuclear waste materials such as high-level waste (HLW) glass, spent UO_2 nuclear fuel (SNF), and U-bearing waste forms, can be predicted, in part, by understanding the geochemical behavior of uranium. Other forms of uranium contamination of immediate concern are located at uranium production facilities, mines, and, more recently, battlefields where depleted uranium weapons have been used. Concerns about the fate of uranium in the environment have been addressed by employing several micro-analytical techniques to identify and characterize the nature of the contaminants (Bertsch *et al.*, 1994; Buck *et al.*, 1996; Morris *et al.*, 1996; Duff *et al.*, 1997, 2002).

Burns *et al.* (1997a) have theorized that many of the alteration phases that form during waste form corrosion may be capable of incorporating key radionuclides, including Np, Tc, and Pu. The potential for uranium secondary phases to incorporate radionuclides and thus curtail their migration is of significant scientific interest (Buck *et al.*, 1997; Chen *et al.*, 1999, 2000; Li and Burns, 2001a; Burns *et al.*, 2004a). A key to predicting the thermodynamic properties of these complex U(VI) minerals is to understand the nature of the connectivity between uranium polyhedra. Finch and Murakami (1999) have reported measured and estimated thermodynamic data for 14 uranyl silicate and carbonate minerals. Additional data is published elsewhere on uranium phases (Grenthe *et al.*, 1995), studtite (Hughes-Kubatko *et al.*, 2003), and new experimental thermodynamic measurements have now been obtained from the uranyl carbonates, uranophane, and uranyl phosphates (Hughes-Kubatko *et al.*, 2005). In addition to the natural U-minerals, a wealth of complex synthetic U(VI) phases have now been explored as potential, mesoporous materials, catalysts, and waste forms.

5.3.1 Mineralogy and classification of uranium deposits

Extensive reviews of uranium mineralogy and the origin of uranium deposits have been made by Finch and Murakami (1999) and Plant *et al.* (1999), respectively. Uranium deposits can be classified into 14 groups. These are: unconformity related, sandstone, quartz–pebble conglomerate, veins, breccia complex, intrusive, phosphorite, collapse breccia, volcanic, surficial, metasomatite, metamorphic, lignite, and black shale. Uranium is precipitated in reducing environments, sandstones rich in organic matter or iron sulfides, phosphate-rich sediments, shales where uranium is concentrated in organic matter, and lignite and coals. Enrichment of uranium in lignite or coal can create environmental problems when these sources are burned. Uranium undergoes a series of complex fractionation events, resulting in highly variable levels in different rock types. Owing to its relatively large size (the ionic radius of U^{4+} is 0.940 Å) in eight-fold coordination with oxygen (Farges *et al.*, 1992), tetravalent uranium is incompatible in silicate melts, depending on alkali content and the presence of nonbonding oxygens. Uranium is preferentially partitioned into small volume, low-temperature melts, and becomes progressively more concentrated, so that certain types of highly evolved granite, rhyolite,[1] and alkaline complexes contain significant quantities of uranium (Plant *et al.*, 1999). Uranium is usually present in accessory minerals such as zircon ($ZrSiO_4$), monazite {(Ce, La, Nd, Th)PO_4}, and pyrochlore (general formula AB_2O_7), many of which are also observed in synthetic ceramic HLW forms (Ewing, 1999). Although the levels of Th and U in terrestrial igneous rocks are variable, the Th/U ratio is relatively constant at about 3.8 (Taylor and McLennan, 1985). Although the most important uranium oxidation states of environmental and geological significance are considered to be U(IV) and U(VI), there is increasing evidence for the role of U(V) in uranium minerals (Burns and Finch, 1999; Colella *et al.*, 2005).

There are numerous U-deposits worldwide and some of these have been studied in great detail, some owing to their relevance to HLW disposal and the environmental fate of uranium, as well as being sources for unique uranium minerals. Understanding the geochemical behavior of uranium at these sites provides the basis for predictive modeling of uranium in the environment and also helps build confidence in the feasibility of geological waste isolation. Uranium deposits at Oklo, Peña Blanca, Shinkolobwe, and Koongarra will be described briefly below.

(a) Oklo, Gabon (Sandstone deposit)

The geochemical behavior of the natural fission reactors at Oklélobondo and Bangombé (Oklo), located in a Precambrian[2] sedimentary basin in Gabon (Africa) have been discussed by Brookins (1990), Hidaka and Holliger (1998), and Janeczek (1999). The Bamgombé site in the Oklo region is of particular interest as it is located at shallow depths. Furthermore, as full-scale mining was never commenced, the ore deposit has been left almost intact. Electron microprobe analysis (EMPA) of uraninite in contact with U(VI) phases indicates that the alteration resulted in increased concentrations of Si, P, S, Zr, Ce, and Nd. The dissolution of accessory apatite {$Ca_5(PO_4)_3(OH,Cl,F)$}, monazite and sulfides resulted in the retardation of uranium through the formation of secondary minerals, including phosphatian coffinites and iron–uranyl phosphate hydroxide hydrates (i.e. bassetite {$Fe^{2+}(UO_2)_2(PO_4)_2 \cdot 8H_2O$}). Jensen *et al.* (2002) investigated the mineralogy of the uranium deposits at Bamgombé and compared their experimental observations with thermodynamic predictions based on groundwater conditions. The primary U-minerals at Bamgombé are uraninite and minor coffinite [$U(SiO_4)_{4-x}(OH)_{4x}$]. The uranyl minerals include fourmarierite {$Pb_{1-x}[(UO_2)_4O_{3-2x}(OH)_{4+2x}] \cdot 4H_2O$}, bassetite possibly associated with {$U(HPO_4)_2 \cdot 2H_2O$} or chernikovite {$(H_3O)_2[(UO_2)(PO_4)]_2 \cdot 6H_2O$},

---

[1] Derived from the rapid cooling of a very viscous granitic magma.

[2] Between 2.5 and 1.8 billion years ago.

torbernite $\{Cu[(UO_2)(PO_4)]_2 \cdot 8\text{–}12H_2O\}$, Ce-rich françoisite $\{(Nd,Y,Sm,Ce)(UO_2)_3(PO_4)_2O(OH)(H_2O)_6\}$, and uranopilite $\{(UO_2)_6(SO_4)O_2(OH)_6(H_2O)_6 \cdot 8H_2O\}$. Autunite $\{Ca[(UO_2)(PO_4)]_2 \cdot 11H_2O\}$ has also been reported. Eh–pH diagrams predict that coffinite, $U(HPO_4)_2 \cdot H_2O$, and $UOF_2 \cdot H_2O$ are the only stable U(IV) phases and that uranopilite, torbernite, and bassetite will become stable during oxidative alteration.

(b) Peña Blanca, Chichuhua District, Mexico (Breccia Pipe)

The Sierra de Peña Blanca District, Chihuahua, Mexico consists of a gently dipping Tertiary[3] volcanic pile that covers a calcareous basement of Cretaceous age[4] (Cesbron *et al.*, 1993; Pearcy *et al.*, 1994). Peña Blanca is part of a much more extensive range of volcanic uranium deposits that extend from the McDermitt caldera at the Oregon–Nevada border through the Marysvale district of Utah and Date Creek Basin in Arizona and south into the Peña Blanca (Finch, 1996). In the Nopal I deposit, the ignimbritic tuffs[5] have been hydrothermally altered and U-mineralization is located within a breccia pipe structure at the intersection of several faults. The uraninite deposition under reducing conditions (8 ± 5) Ma ago has precluded the accumulation of significant amounts of lead. Later tectonic forces elevated the deposit above the local water table, exposing it to oxidizing conditions. The site is a convincing geochemical analog of the proposed HLW repository at Yucca Mountain, Nevada. The initial corrosion products from the oxidative dissolution of uraninite are uranyl oxide hydrates, including ianthinite $\{[U_2^{4+}(UO_2)_4O_6(OH)_4(H_2O)_4](H_2O)_5\}$ (Burns *et al.*, 1997b), schoepite $\{[(UO_2)_8O_2(OH)_{12}](H_2O)_{12}\}$, and dehydrated schoepite $\{(UO_2)_4O(OH)_6 \cdot H_2O\}$ (Leslie *et al.*, 1993). Ianthinite is unusual in that it contains both U^{6+} and U^{4+}. The phase has a narrow stability range and will easily degrade. It will form in oxygen-deficient environments, such as under localized reducing environments at Shinkolobwe (Finch and Ewing, 1992).

Uranyl silicates, uranophane $\{Ca(UO_2)_2(SiO_3OH)_2(H_2O)_5\}$, are the predominant U-phases at Nopal I, comprising more than 95% of all U-bearing minerals. They either replace earlier formed U-phases or form euhedral[6] crystals within open voids and fractures. The uranophanes at Nopal I have been dated at 3.2 Ma, suggesting that alteration of the initial uraninite took millions of years under the oxidizing environment. The paragenesis[7] of U-phases was similar to that observed in laboratory tests by Wronkiewicz *et al.* (1992) on synthetic UO_2 apart from the occurrence of the mixed uranium valence phase,

---

[3] ~5–45 million years ago.

[4] ~65–130 million years ago.

[5] Deposits of hot incandescently glowing ash (tuff) from volcanic activity.

[6] Well-formed crystal with regular shape.

[7] Refers to the order of mineral formation.

ianthinite that has not been observed in corrosion tests with UO_2 (Wronkiewicz *et al.*, 1996) or SNF (Finch *et al.*, 1999a; Wronkiewicz and Buck, 1999).

(c) Shinkolobwe (Sandstone U-deposit)

Uranium minerals from the 1.8-Ga-old Shinkolobwe deposit, located in the Katanga District of the Democratic Republic of the Congo, have been extensively described and discussed by Finch and Ewing (1992) and in references therein. The deposit has been exposed since Tertiary times and extensive weathering has significantly altered or replaced uraninite. Uranium mineralization occurs along fracture zones where meteoric[8] waters have penetrated. The uranyl silicates, uranophane and cuprosklodowskite $\{Cu(UO_2)_2(SiO_3OH)_2 \cdot 6H_2O\}$, are ubiquitous and replace becquerelite, compreignacite $\{K_2[(UO_2)_3O_2(OH)_3]_2(H_2O)_7\}$, vandendriesscheite $\{Pb_{1.57}[(UO_2)_{10}O_6(OH)_{11}](H_2O)_{11}\}$, fourmarierite, billietite $\{Ba[(UO_2)_3O_2(OH)_3]_2(H_2O)_4\}$ and schoepite by reaction with the silica-rich groundwater. As the groundwater interacts with the host rocks, it becomes increasingly more enriched in silica, resulting in the precipitation of uranophane. Finch *et al.* (1995) argued that the cyclical weather pattern explained the simultaneous occurrence of both becquerelite and uranophane. Becquerelite has been estimated to be 10^5 to 10^6 years old based on the $^{230}Th/^{234}U$ ratios being close to 1.0 in these minerals (Finch *et al.*, 1996b).

(d) Koongarra

Koongarra is located in a tropical monsoon climate with long dry seasons (Edghill, 1991). The host rock is quartz-rich schist[9] and the primary uranium mineral, uraninite, has been subjected to weathering for more than 1 million years. The alteration of chlorite produces Fe^{3+} minerals that become associated with some uranium. In the primary ore deposit uraninite has been altered to curite $\{Pb_3[(UO_2)_8O_8(OH)_6] \cdot 3H_2O\}$, and sklodowskite $\{Mg(H_3O)_2[(UO_2)(SiO_4)]_2 \cdot 4H_2O\}$. However, Murakami *et al.* (1997) have shown that upstream from the deposit, saléeite $\{Mg[(UO_2)(PO_4)]_2 \cdot 10H_2O\}$, has replaced sklodowskite and granular apatite and is the predominant mechanism for fixing uranium. In a transmission electron microscopy (TEM) study by Lumpkin *et al.* (1999) on Koongarra mineral substrates, uranium was observed to preferentially sorb to the iron oxide minerals (goethite, α-FeOOH, and possibly ferrihydrite) rather than the clay minerals.

---

[8] Groundwater of atmospheric origin (i.e. rain, snow, etc.).

[9] A thinly layered crystalline rock.

5.3.2 Reduced uranium phases

Uraninite is a common accessory mineral in pegmatites and peraluminous granites and is the most important source of dissolved uranium in groundwaters emanating from weathered granite terrains. Uraninite possesses the fluorite structure, nominally UO_{2+x}. U(IV) is coordinated by eight O atoms in a cubic arrangement, and each O atom bonds to four U^{4+} ions. Stoichiometric UO_2 is unknown in nature and is always partially oxidized in addition to containing radiogenic lead and commonly thorium, calcium, and lanthanides. Stoichiometric UO_2 (a = 5.47 Å) forms a complete solid solution with ThO_2 (a = 5.6 Å) following Végard's Law. Janeczek and Ewing (1992) proposed the formula $\{(U^{4+}_{1-x-y-z}U^{6+}_{x}Ln^{3+}_{y}M^{2+}_{z}\square_{v})O_{2-x-0.5y-z-2v}\}$ (where $\square$ denotes a vacancy).

It is possibly inappropriate to term uraninite (as well as coffinite and brannerite), as a primary uranium mineral as it can precipitate from aqueous solutions under reducing conditions or through microbial processes (e.g. sulfur-reducing bacteria (Spirakis, 1996; Fredrickson *et al.*, 2002)). Primary reduced uranium minerals are usually coarse grained and present in granites and pegmatites. They have high Th and consequently larger unit cells. Hydrothermal vein[10] uraninites typically have minor lanthanides, Y, Ca, and Th absent. Low-temperature sedimentary uraninites are devoid of lanthanides and Th, but may contain Ca, Si, and P. Grandstaff (1976) observed a correlation between dissolution rate and the mole fraction of impurity cations (Pb and Th). The decrease was attributed to the buildup of low-solubility impurities in the surface as U was preferentially leached. Similar processes have been observed in corroded SNF (Buck *et al.*, 2004).

The most common U-ore is fine grained uraninite, sometimes termed pitchblende, similar to the term used for fine-grained quartz (chalcedony); pitchblende is not a mineral name but a textural term. The name 'pitch' does not come from its black, resinous appearance, and botyroidal habit[11] but from the german word 'pech' meaning bad luck (Piekarski and Morfeld, 1997). Radiogenic lead can reach levels of 15–20 wt.% in ancient uraninites. Janeczek and Ewing (1991) observed lead contents of 14 wt.% in an 1800-Ma-old uraninite specimen from the Eldorado mine in Canada. The presence of lead in uraninite results in auto-oxidation and can lead to high U(VI)/U(IV) ratios in uraninite. Auto-oxidation at the uraninite deposit at Cigar Lake has led to U (VI)/U(IV) ratios from 0.02 to as high as ~0.75 according to X-ray photoelectron spectroscopy (XPS) studies by Sunder *et al.* (1996), despite the highly anoxic conditions prevalent in the deposit. Sunder and coworkers also examined uraninites from Oklo and found a similar range of ratios for uraninites.

---

[10] A vein formed by the crystallization of minerals from predominantly hot water solutions of igneous origin.

[11] A globular growth of minerals.

Oxidation of uraninite results in a decrease of the unit cell parameter, whereas α-decay damage has the opposite effect through the formation of defects and voids. Uraninites typically experience more than 10 displacements per atom over periods of millions of years; yet, the high rate of self-annealing prevents metamictization[12] of the uraninite. Cationic substitutions (radiogenic Pb, Th, Ca, and Ln) increase the unit cell parameter (Janeczek and Ewing, 1991). The large ionic radius of Pb^{2+} results in a substantial increase in the unit cell with increasing age of the uraninite. The presence of silicium and phosphorus in partly altered uraninite is due most likely due to the precipitation of phosphatian coffinite.

(a) U(IV) phosphates and molybdates

The UO_2–P_2O_5 system includes uranium meta-phosphate $U(PO_3)_4$, uranium diphosphate UP_2O_7, uranium oxide phosphate $(UO)_3(PO_4)_2$, and uranium oxide diphosphate $(UO)_2P_2O_7$. Douglass (1962) first characterized both orthorhombic $U(PO_3)_4$ and its isostructural plutonium analog. Brandel *et al.* (1996) synthesized two additional phosphates, uranium uranyl phosphate $U(UO_2)(PO_4)_2$, that formed in air at 1000–1200°C, which may be the only mixed valence uranium phosphate known, and diuranium oxide phosphate $U_2O(PO_4)_2$ that was formed at 1350°C in an inert atmosphere. Attempts by Brandel *et al.* (1996) to produce uranium orthophosphate, $U_3(PO_4)_4$, were unsuccessful confirming earlier data, indicating that this phase does not exist (Gmelin, 1981d).

A number of hydrous U(IV) phosphates exist in nature and some of these have been observed in secondary alteration phases formed during laboratory corrosion tests on HLW glass (Bates *et al.*, 1992). These phases have been described as brockite- and rhabdophane-related phases and contain U, Th, Ln, and Pu (Buck and Bates, 1999). Ningyoite, $\{(U^{4+},Ca,Ce)_2[PO_4]_2 \cdot 1\text{–}2H_2O\}$, is a member of the rhabdophane group of phosphates (Gaines *et al.*, 1997). Ningyoite is a translucent brown to greenish mineral observed at the Ningyo-Toge mine, Japan. The phase may form a solid solution with U-bearing brockite, $\{Ca_{z-y}(U^{4+}_{1-x}Th^{4+}_{x})_{y/2}(PO_4)_2 \cdot nH_2O\}$; in addition CO_3 and SO_4 may substitute for PO_4.

Lermontovite $\{U^{4+}(PO_4)OH\}$ and vyacheslavite $\{U^{4+}(PO_4)(OH) \cdot 2.5H_2O\}$ form under reduced conditions in hydrothermal deposits associated with sulfides.

(b) Uranium orthosilicate

Coffinite and the thorium orthosilicate, thorite, $(Th,U)SiO_4$, are widespread in igneous and metamorphic rocks and are important ore minerals in some uranium and thorium deposits (Speer, 1982). These silicates are tetragonal and

---

[12] Process of alteration of crystalline to non-crystalline structure through radioactive decay.

isostructural with zircon (Fuchs and Gebert, 1958). Because they can be primary in origin, they have been used in geochronological studies. Coffinite occurs as a primary uranium ore mineral in unoxidized, uranium–vanadium ores of the Colorado Plateau, USA; however, it is also found in hydrothermal, vein deposits with pitchblende, with variable composition where $(OH)^-$ substitutes for $(SiO_4)^{4-}$. Some studies have suggested that the ubiquitous occurrence of organic matter with secondary coffinite indicates a possible biogenic origin (Spirakis, 1996).

(c) Uranium in silicate melts and glasses

The partitioning of uranium into silicate melts depends on the oxygen fugacity, melt composition, and redox conditions. Under mildly reducing conditions, U(v) is present as an octahedrally coordinated species. Under very reducing conditions, such as that prevailing in silicate magmatic melts, U(iv) is the dominant uranium species. Data obtained by Farges *et al.* (1992) with extended X-ray absorption fine structure analysis (EXAFS) indicated that U(iv) is present in six coordinated sites in silicate glasses with a mean U–O distance of ≈ 2.26–2.29 Å. Uranium(iv) is expected to occupy similar sites in the melt. The solubility of uranium in silicate liquids is enhanced by high alkali content and the presence of nonbonding oxygens (NBO)[13] and non-framework oxygens (NFO).[14] There is a strong correlation between uranium solubility and the NBO/T ratio (where T is the number of tetrahedral cations). Up to 18 wt% U(iv) can be dissolved in sodium trisilicate glass; whereas less than 1 wt% of U(iv) will dissolve in a glass with albite (Na alumino-silicate) composition. The formation of bonds between NBO and NFO is favored because these oxygens have lower bond strength. The solubility of actinides in alkali silicate glasses decreases in the order Th > U > Np > Pu owing to decreasing ionic size and increasing actinide–oxygen bond strength. The solubilities of U(v) and U(iv) are also affected by alkali content due to variation in bond strength. Uranium(iv) and U(v) are generally incompatible with magmatic systems and tend to partition strongly into late stage formed minerals, such as zircon, titanite, or apatite. Farges *et al.* (1992) suggest that if melts have a heterogeneous distribution of bonding oxygens (BO) and NBO, uranium will become enriched in the NBO-enriched regions. With increasing magmatic differentiation,[15] the BO content of the melt increases, as a consequence U(iv) will partition to late crystallizing minerals, such as pyrochlore or zircon.

Farges *et al.* (1992) determined the U–O bond lengths in U(vi)-containing silicate glasses as $U–O_{ax} \approx 1.77$–1.85 Å and $U–O_{eq} \approx 2.18$–2.25 Å, characteristic

---

[13] Oxygen bonded to one Si^{4+} and an indeterminate number of other cations (Ellison *et al.*, 1994).
[14] Oxygen bonded exclusively to cations other than Si^{4+}.
[15] The process of chemical and mechanical evolution of a magma in the course of its crystallization such that different rock types are formed from the same original magma.

of the uranyl species. U(VI) is the dominant oxidation state observed in radioactive borosilicate waste glasses. XPS measurements performed on SON68-type borosilicate waste glass by Ollier *et al.* (2003) revealed two oxidation states in the glass: about 20% U(IV) and 80% U(VI) present in two different environments, uranate- and uranyl-sites, respectively. As a consequence of bond strength considerations, U(VI) also bonds primarily to NBO and NFO in both crystalline and amorphous silicates. U(V) is six-coordinated with a mean U–O bond distance of 2.19–2.24 Å (Farges *et al.*, 1992).

Karabulut *et al.* (2000) have investigated the local structure of uranium in a series of iron phosphate glasses with EXAFS and determined that the all uranium was present as U(IV).

(d) Uranium niobates, tantalates, and titanates

There are a number of complex tantalum, niobium, and titanium oxides that may contain uranium as an essential element. These phases are mainly observed in granitic rocks and granite pegmatites[16] and have been difficult to characterize as they commonly occur in the aperiodic metamict state owing to their age and radionuclide content. A common feature of these minerals is that niobium, tantalum, and titanium atoms occupy octahedral sites, and a structural framework that is formed by octahedral corner or edge sharing (Finch and Murakami, 1999).

The structures of the ixiolite, samarskite, and columbite groups, ideally $A^{3+}B^{5+}O_4$, are all derivatives of the α-PbO_2 structure. Ishikawaite $\{(U^{4+},Fe,Y,Ce)(Nb,Ta)O_4\}$ is the U-rich variety of samarskite and calciosamarskite is the Ca-rich variety. Because these minerals are chemically complex, metamict, and pervasively altered, their crystal chemistry and structure are poorly understood (Hanson *et al.*, 1999). Many of these phases are of interest because of their occurrence in designer crystalline ceramic waste forms for immobilization of actinides (Gieré *et al.*, 1998; Ewing, 1999). In particular, zirconolites, pyrochlores, and brannerites have been proposed for immobilizing transuranics. These phases will be discussed in more detail.

(*i*) *Zirconolite*

Zirconolite is an accessory mineral crystallizing under different geological conditions and in a wide range of generally SiO_2-poor rock types (Gieré *et al.*, 1998). Zirconolite has been found in mesostasis areas of ultrabasic cumulates, in granitic pegmatites, in carbonatites,[17] in nepheline syenites, and in other igneous formations. Zirconolite has been observed commonly in lunar late-stage

---

[16] Late stage crystallization from an igneous intrusion.

[17] Rock consisting of >50% carbonate minerals.

mesostasis areas of lunar basalts.[18] It is also a common constituent of designer titanate ceramic waste forms (Gieré *et al.*, 1998; Ewing, 1999). Natural zirconolite is a reddish-brown mineral with an appearance similar to that of ilmenite; however, the grains are typically anhedral and <0.1 mm in diameter, and easily overlooked.

Zirconolite, $CaZrTi_2O_7$, belongs to a group of anion-deficient superstructures of the fluorite-type, which have been found to be the most versatile phases for the incorporation of HLW elements. Zirconolite is termed the aristotype of the group (i.e. the structurally simplest member of the series). All have the general formula $[A_2B_2X_7]$ (A = Ca, Na, Ln, U, Th, Zr, Ti; B = Ti, Nb, Ta, Al, Fe; X = O, F) (Mazzi and Munno, 1983; Bayliss *et al.*, 1989). Zirconolite does not appear to incorporate uranium and lanthanides by isomorphic substitution; rather, distinct phases form depending on the particular elements present in the mineral. Elements may not be distributed uniformly throughout the zirconolite but concentrated in extended defects, which can lead to the formation of zirconolite polytypes (White, 1984). These are constructed by stacking modular units in a variety of orientations with respect to the arrangement of the interlayer cations. Each module consists of two hexagonal tungsten bronze layers and interposed cations. The zirconolite-type phases have been described in the literature as zirconolite, zirkelite, pyrochlore, and polymignyte. The three natural zirconolites are orthorhombic zirconolite, known as zirconolite-3O, trigonal zirconolite, known as as zirconolite-3T, and the more common monoclinic zirconolite called zirconolite-2M. The cubic form is termed zirkelite and for metamict minerals, the name polymignyte is used.

Geochemical studies by Lumpkin and coworkers (Lumpkin *et al.*, 1988, 1995; Lumpkin and Ewing, 1995) have shown that zirconolite is highly durable in the presence of hydrothermal fluids and low-temperature groundwaters. Uranium in zirconolite is mobilized only under conditions of high temperature and pressure in hydrothermal fluids. At lower temperatures alteration takes place because previous radiation induced damage; this may result in the release of radiogenic lead. However, uranium remains relatively unaffected by the alteration process.

(*ii*) *Pyrochlore*

Minerals of the pyrochlore group have the general formula $A_{1-2}B_2O_6X_{0-1}$ (Greegor *et al.*, 1989). Three subgroups are defined on the basis of the major B-site cations. The B-site is occupied by Ti, Nb, or Ta; however, Al, Fe^{3+}, Zr, Sn, and W may also be possible. Microlite and natural pyrochlore both contain more niobium and tantalum than titanium (see Fig. 5.1a). The H_2O content in

---

[18] Zirconolite was reported in rocks collected on Apollo 10 (mare basalt) and Apollo 14 (recrystallized breccia) moon missions.

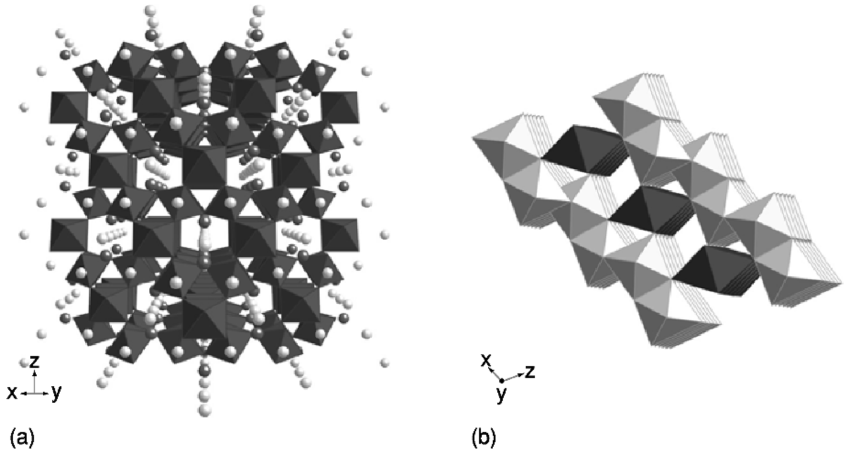

Fig. 5.1 *Structure of* (*a*) *pyrochlore* (*diagram displays grey circles = A site, dark circles = B site, and* TiO_6 *octahedra*) *and* (*b*) *brannerite* (*diagram shows uranium as dark-colored polyhedra and* TiO_6 *octahedra as gray*) (*courtesy of Prof. R. Gieré, University of Freiberg, Germany*).

the natural minerals ranges from 10 to 15 wt%, but will increase if the mineral has undergone alteration. These groups can be further subdivided based on the A-site occupation which can be Na, Ca, Mn, Fe^{2+}, Sr, Sb, Cs, Ba, rare earths, Pb, Bi, Th, and U. Natural pyrochlore minerals occur predominantly in three host rock categories: carbonatites, nepheline syenites, and granitic pegmatites.

(*iii*) *Evidence for U*(*V*) *in pyrochlores and zirconolite*

Fortner *et al.* (2002) used X-ray absorption spectroscopy near-edge structure (XANES) analysis to suggest that U(v) is present in a synthetic pyrochlore ceramic produced under reducing (Ar/H_2) conditions. The authors argue that uranium substitutes for titanium on the B-site in pyrochlore and suggest that this will also occur in natural pyrochlore-type minerals. This result is partially supported by findings by Vance *et al.* (2001) who determined that zirconolite, ($CaU_xZr_{1-x}Ti_2O_7$) oxidized at 1400°C in air, formed U(v) at the expense of U(IV) and that zirconolites with available charge-compensating lanthanides, also resulted in U(IV) to U(v) oxidation, even when sintered in an argon gas environment. The oxidation of U(IV) to U(v) is accompanied by a significant decrease in ionic size, suggesting that uranium is unlikely to enter the calcium site, but rather prefers the zirconium site. Although the presence of significant amounts of U(v) in these titanate phases has not been established by quantitative EMPA data on synthetic (Gieré *et al.*, 2002) and natural zirconolites and pyrochlores (Gieré *et al.*, 1998), the strong observed correlation between Ca and U in natural zirconolites, indicates substitution on the A-site rather than the B-site.

(*iv*) *Brannerite*

After uraninite and coffinite, brannerite is the most important uranium ore mineral. At the large uranium deposit of the El'kon District of the Aldan Shield, Siberia, brannerite is the dominant uranium phase (Miguta, 1997). Ifill *et al.* (1996) report that brannerite at the Elliot lake U-deposit in Canada formed mainly by replacement of uranium in TiO_2-rich relicts of magnetite–ilmenite intergrowths. The uranium was derived from diagenetic dissolution of uraninite. Brannerite, ideally $\{(U,Th)_{1-x}Ti_{2+x}O_6\}$, is a monoclinic accessory phase that is completely metamict (amorphous) as a result of the α-decay damage from the constituents uranium and thorium. As with many of these metamict U-minerals, the structure can be recrystallized on heating. Many cation substitutions have been identified for both uranium (Pb, Ca, Th, Y and Ce) and titanium (Si, Al, Fe) in natural brannerites (Vance *et al.*, 2001) (see Fig. 5.1b).

Brannerite is also formed in the titanate-based nuclear waste-form crystalline ceramics under reducing conditions. Finnie *et al.* (2003) and Colella *et al.* (2005) examined synthetic U(v) phases and natural brannerites with XPS and electron energy-loss spectroscopy. The average valence state in the natural brannerites was close to 5.0.

5.3.3 Uranium(VI) phases

Carbonate dominates the speciation of uranium in alkaline environments, while sulfate complexation is of importance in slightly acidic oxidizing media. The U(VI) phases represent an extremely diverse and complex series of minerals. In this section, the U(VI) minerals will be discussed by first introducing the various uranium mineral structures and then their occurrence on the basis of the major complexing anion, and finally a mention of uranium sorption on soil minerals.

Uranyl oxyhydroxides that form in U-rich aqueous solutions can be represented by the general formula $\{M_n[(UO_2)_xO_y(OH)_z](H_2O)_m\}$, where M represents divalent cations, including Ca^{2+}, Pb^{2+}, Ba^{2+}, and Sr^{2+}. However, uranyl oxyhydroxides are only stable in groundwaters devoid of carbonate, sulfate, and/or vanadate ligands.

(a) Bonding in uranyl polyhedra

Burns *et al.* (1996) developed a hierarchical structural classification for U(VI) minerals and other inorganic phases, based on the polymerization of coordination polyhedra. The linear uranyl (Ur) ion is coordinated by four, five, or six anions (ϕ: O^{2-}, OH^-, H_2O), with the oxygen atoms of the uranyl ion forming the apices of square ($Ur\phi_4$), pentagonal ($Ur\phi_5$), and hexagonal ($Ur\phi_6$) bipyramids. The equatorial U–O bond lengths for $Ur\phi_4$, $Ur\phi_5$, and $Ur\phi_6$, are 2.26(8), 2.34(10), and 2.46(12) Å, respectively. The polyhedra possess very asymmetrical charge distributions, $O_{Ur} \sim -1.7$and $U–O_{eq} \sim -0.5$ as discussed in more detail in

Section 5.8. Uranyl minerals with uranium as the only high-valence cation invariably contain sheets [the exception being studtite (Burns and Hughes, 2003)], as do the naturally occurring uranyl vanadates, uranyl molybdates, and most uranyl sulfates. A majority of the uranyl silicates contain sheets except for soddyite $\{(UO_2)_2[SiO_4](H_2O)_2\}$ and weeksite $\{K_{1.26}Ba_{0.25}Ca_{0.12}[(UO_2)_2(Si_5O_{13})]H_2O\}$ (Jackson and Burns, 2001), which involve frameworks of U(VI) polyhedra. Uranyl carbonates are exceptional because they often contain isolated uranyl tricarbonate clusters, although rutherfordine, UO_2CO_3 (cf. Fig. 5.54), and roubaultite $\{Cu_2(UO_2)_3(CO_3)_2O_2(OH)_2](H_2O)_4\}$, contain uranyl carbonate sheets. The uranyl selenites demesmaekerite $\{Cu_5Pb_2(UO_2)_2(SeO_3)_6(OH)_6(H_2O)_2\}$, and derriksite, $\{Cu_4[(UO_2)(SeO_3)_2](OH)_6]\}$, contain chains of polyhedra, whereas guillemenite, $\{Ba[UO_2)_3(SeO_3)_2O_2](H_2O)_3\}$, and haynesite, $\{(UO_2)_3(OH)_2(SeO_3)_2 \cdot 5H_2O\}$, both contain uranyl selenite sheets. Uranyl arsenates either contain autunite-type sheets or chains, as in the structures of walpurgite, $\{(UO_2)Bi_4O_4(AsO_4)_2 \cdot 2H_2O\}$, and orthowalpurgite, $\{(UO_2)Bi_4O_4(AsO_4)_2 \cdot 2H_2O\}$.[19] Relatively few uranium minerals are based upon chains, although recent structural refinements indicate that these types of U^{6+} minerals are more common that previously thought. Examples include: the only know peroxide mineral, studtite (Burns and Hughes, 2003); the uranyl tellurides, moctezumite $\{PbUO_2(TeO_3)_2\}$, derriksite, and demesmaekerite; the uranyl sulfate uranopilite; the uranyl arsenates, walpurgite, orthowalpurgite, and their phosphate analog, phosphowalpurgite $\{(UO_2)Bi_4O_4(PO_4)_2 \cdot 2H_2O\}$ (Sejkora *et al.* 2004); and parsonsite $\{Pb_2[(UO_2)(PO_4)_2]\}$. Locock *et al.* (2005a) have also shown that the synthetic arsenic-bearing analog of parsonsite, hallimondite $\{Pb_2[(UO_2)(AsO_4)_2]\}$, is also a chain structure.

(b) Geometries of uranyl polyhedra

The crystal chemistry of U(VI) is rich in diversity, yet it is relatively rare for uranyl solids to form frameworks. The distribution of bond strengths within uranyl bipyramidal polyhedra generally permits polymerization only through the equatorial ligands, resulting in chains or sheets. Linkages in the third dimension may be facilitated by additional polyhedra such as silicate, molybdate, vanadate, or phosphate.

The U(VI) minerals that are based on infinite polyhedra sheets with edge- and corner-sharing polyhedra can be better described by the topological arrangement of anions that occur within the sheets (Miller *et al.*, 1996; Burns and Hill, 2000a). Similar to a method described by Aléonard *et al.* (1983) for U_3O_8 structures, the procedure is as follows: Each anion that is not bonded to at least two cations within the sheet, and not an equatorial anion of a bipyramid or

---

[19] The compositions of orthowalpurgite and walpurgite as written are identical; however, the structures are not (Mereiter, 1982b; Krause *et al.*, 1995).

pyramid within the sheet, is removed from further consideration. Cations are removed along with all cation–anion bonds, leaving an array of unconnected anions. Anions are joined by lines, with only those anions that may be considered as part of the same coordination polyhedra being connected. Anions are removed from further consideration, leaving a series of lines that represent the anion topology. The anion topology does not contain any information about the cation population of the sheet from which the topology was derived (see Fig. 5.2). The P chain is composed of edge-sharing pentagons, the R chain contains rhombs, and the H chain contains edge-sharing hexagons. The arrowhead chains (U and D), which have a directional aspect, contain both pentagons and triangles, arranged such that each triangle shares an edge with a pentagon and the opposite corner with another pentagon in the chain. Generation of anion topologies using chain-stacking sequences is an elegant method for describing the relationships among the complex U(VI) sheet recently found in several minerals. The following describes a number of the possible anion topologies in the U(VI) minerals (see Burns, 1999a for a more complete list).

(*i*) *Protasite* (α-U_3O_8) *anion topology*

The protasite anion topology is the basis of sheets that occur in protasite $\{Ba[(UO_2)_3O_3(OH)_2](H_2O)_3\}$, becquerelite (Burns and Li, 2002), billietite (Pagoaga *et al.*, 1987), richetite $\{M_xPb_{8.57}[(UO_2)_{18}(OH)_{12}]_2(H_2O)_{41}\}$ (Burns, 1998b), compreignacite (Burns, 1998c), agrinierite $\{K_2(Ca_{0.65}Sr_{0.35})[(UO_2)_3O_3(OH)_2]_2\cdot 5H_2O\}$ (Cahill and Burns, 2000), and masuyite $\{Pb[(UO_2)_3O_3(OH)_2](H_2O)_3\}$ (Burns and Hanchar, 1999), as well as a synthetic cesium uranyl oxide hydrate (Hill and Burns, 1999). As such, it is apparent that sheets based on this topology are compatible with a range of interlayer configurations involving Ba, Ca, Pb, K, and Cs. This simple anion topology contains only triangles and pentagons (see Fig. 5.2a).

Only P and D chains are required to develop the protasite anion topology, with the repeat sequence PDPD... The protasite anion topology does not distinguish between O^{2-} and OH^- anions and the distribution of anions is not identical between different minerals possessing the protasite structure type. Becquerelite, billietite, and compreignacite have identical anion distributions, $[(UO_2)O_3(OH_3)]^-$ but masuyite and protasite do not.

(*ii*) *Fourmarierite anion topology*

Sheets based upon the fourmarierite anion topology (see Fig. 5.2b) occur in fourmarierite (Piret, 1985) and schoepite (Finch *et al.*, 1996a). In schoepite, the sheets are neutral, with H_2O groups being the only constituents of the interlayer. In fourmarierite, the sheets have a different distribution of O and OH^-, resulting in a charged sheet that is balanced by Pb^{2+} in the interlayer. The anion topology can be obtained with a chain-stacking sequence involving P, D, and U chains, with the sequence PDUPUD.... Li and Burns (2000a) have refined the structures of several fourmarierite specimens from various localities. All the crystals are orthorhombic.

(*iii*) *Vandendriesscheite anion topology*

Vandendriesscheite is the most common Pb-bearing uranyl oxyhydroxide, occurring at numerous weathered uraninite deposits, often in association with schoepite. The anion topology of vandendriesscheite (see Fig. 5.2c) is exceptionally complex, with a primitive repeat of 41.4 Å (Burns, 1997). Only vandendriesscheite contains a sheet based upon this topology, which can be constructed using P, U and D chains in the sequence PDUPUPUPU DPDPDPDUPUPUP.... It contains sections that are identical to the PDPD... (or PUPU...) repeats of the protasite anion topology, with the junction between such sections involving the DU sequence of the fourmarierite anion topology. Thus, the vandendriesscheite anion topology is a structural intermediate between these two simpler anion topologies.

(*iv*) *Sayrite anion topology*

Sayrite $\{Pb_2[(UO_2)_5O_6(OH)_2](H_2O)_4\}$ (Piret *et al.*, 1983), is the only mineral that contains sheets based upon the sayrite anion topology, which involves U, D, P and R chains. The chains are arranged in such a way that each P chain is flanked by two arrowhead chains with the same sense (direction), giving UPU or DPD sequences. These two sequences alternate in the anion topology, and are separated by R chains, giving the sequence RUPURDPDRUPU...

(*v*) *Curite anion topology*

The structure of curite (Taylor *et al.*, 1981; Li and Burns, 2000b) contains sheets based upon the curite anion topology, which cannot be described as a simple chain-stacking sequence using only the U, D, P and R chains. A chain with pentagons, triangles, and squares is required. It has a directional sense owing to the presence of an arrowhead (a pentagon and a triangle sharing an edge), and is designated U_m and D_m, for up and down (modified) pointing chains, respectively. The curite anion topology can be characterized by the chain-stacking sequence U_mDU_mD...

(*vi*) *β-U_3O_8 anion topology*

The β-U_3O_8 sheet anion topology (see Fig. 5.2d) is the basis of the sheets in ianthinite (Burns *et al.*, 1997b), as well as the sheets in β-U_3O_8. This topology can conveniently be described using a chain-stacking sequence involving U, D, and R chains with the repeat sequence DRUDRU...

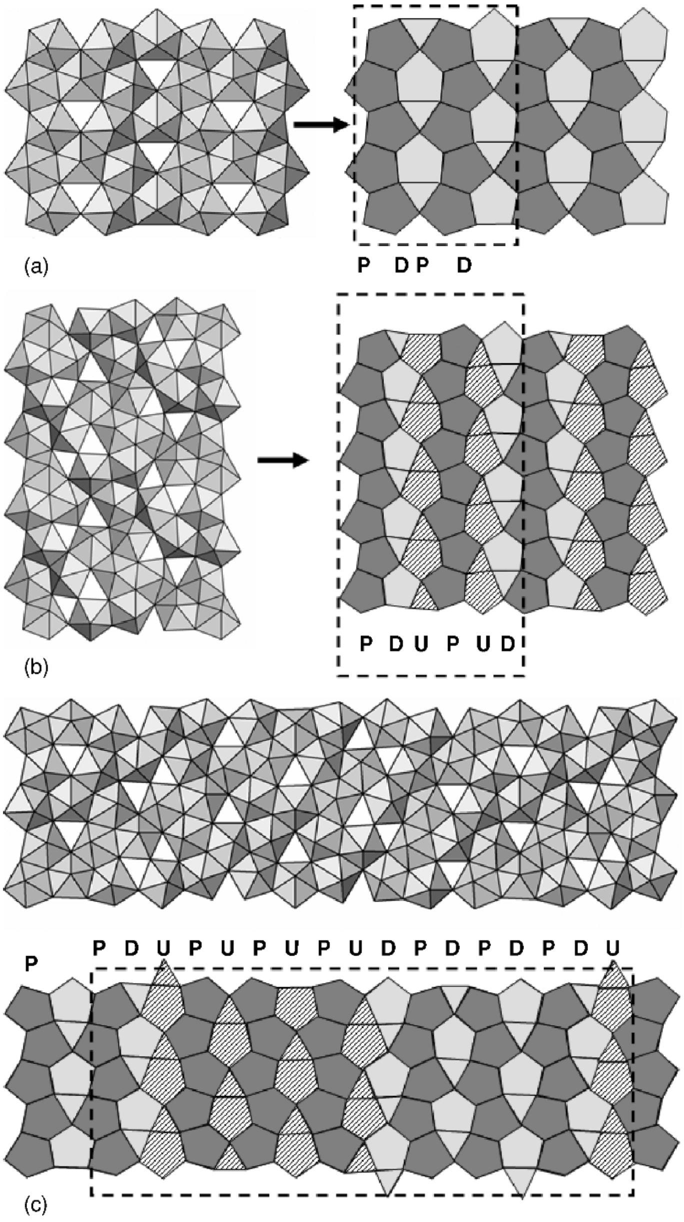
(a)
P D P D
(b)
P D U P U D
P
P D U P U P U P U D P D P D P D U
(c)

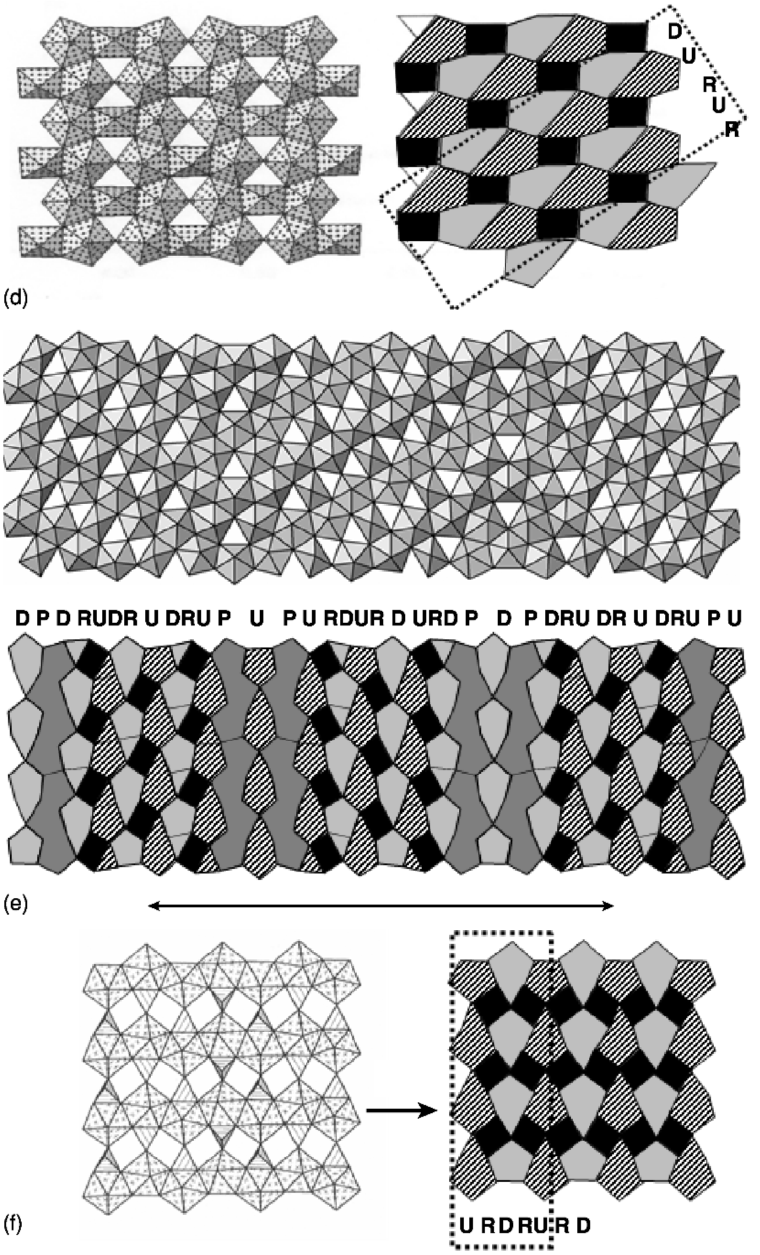

Fig. 5.2 (*a*) *Protasite* (α-U_3O_8) *structure and anion topology with anion repeat* (*adapted from Burns,* 1999). (*b*) *Fourmarierite structure and anion topology, showing the structural repeat.* (*c*) *Vandendriesscheite structure and anion topology.* (*d*) β-U_3O_8 *structure and anion topology* (*adapted from Brugger* et al., 2004). (*e*) *Wölsendorfite anion topology and the complex anion topology.* (*f*) *Uranophane anion topology showing anion repeat* (*adapted from Burns*, 1999).

(*vii*) *Wölsendorfite anion topology*

The versatility of this method for visualizing complex structures is beautifully demonstrated in the description of the structure of wölsendorfite (Burns, 1999b). The structure contains unique $Ur\phi_4$ square bipyramids and six unique $Ur\phi_5$ pentagonal bipyramids that link by sharing equatorial corners and edges to form infinite sheets that are parallel to (100). The interlayer between the uranyl sheets contains Pb^{2+} and Ba^{2+} cations, as well as H_2O groups that are either bonded to the interlayer cations or are held in the structure by H-bonding only. This complex anion topology possesses a primitive repeat of 56 Å (see Fig. 5.2e). It may be constructed using R, D, P, and U chains, with the repeat sequence DRUDRUDRUPDPDRUDRUDRUPDP... The repeat sequence involves the strings DRUDRUDRU and PDP, which are slabs of the β-U_3O_8 and protasite anion topologies, respectively. Thus, the wölsendorfite anion topology is structurally intermediate between the β-U_3O_8 and protasite anion topologies.

(*viii*) *Uranophane anion topology*

All minerals based on the uranophane topology contain pentagons of the anion topology (see Fig. 5.2f).

The uranophane sheet consists of chains of $Ur\phi_5$ bipyramids linked by bridging, isolated SiO_4 tetrahedra, and is common to uranophane, boltwoodite $\{K_{0.56}Na_{0.42}[(UO_2)(SiO_3OH)](H_2O)_{1.5}\}$, cuprosklodowskite, kasolite $\{Pb[(UO_2)(SiO_4)](H_2O)\}$, and sklodowskite. The difference between α-uranophane and β-uranophane depends on the orientation of the silicate tetrahedron. In kasolite, the apical O atoms of the SiO_4 tetrahedra bond to two Pb^{2+} cations in the interlayer (Catalano and Brown, 2004).

(c) Prediction of crystal morphology of U(VI) sheet minerals

The bond valence approach is commonly used to evaluate the analysis of a crystal structure. It provides a means to check bond lengths, the valence state of ions with the structure, as well as providing a method to describe hydrogen bonding (Burns, 1999a). The bond valence approach can be used to identify the valence state of the U cation in well-refined crystal structures. Schindler *et al.* (2004) and Schindler and Hawthorne (2004) have developed a method for predicting the stability of sheet uranyl minerals using the bond-valence deficiency of the sheet edges. Schindler *et al.* (2004) have shown that the surface structure of an edge is characterized by the bond-valence deficiency of anion terminations along chains of polyhedra parallel to the edge, and by the shift and orientation of adjacent layers. The stability of the edges also depends on the arrangement of the interstitial cations between the layers. The edges of the sheet-like uranyl minerals are more reactive than the basal surfaces because the equatorial O-atoms on the edges bond to fewer U^{6+} atoms than oxygen in the sheet, and hence must satisfy their individual bond-valence requirements through a higher degree of protonation (Schindler *et al.*, 2004). The interaction of the uranyl mineral edge surface with aqueous species controls crystal growth, dissolution, and sorption of other species, including other actinides. These interactions depend on the surface structure of an edge, the pH, and saturation index with respect to the mineral.

(d) Uranyl oxyhydroxides

The uranyl oxyhydrates are not only of importance in the geochemistry of uranium, but they are also one of the primary phases generated during the oxidative dissolution of SNF. Uranyl oxyhydroxides form in U-rich aqueous solutions and develop early during the oxidative dissolution of uraninite ores deposits; hence, they are expected to be the older U(VI) minerals in an oxidized deposit. The complexity of these structures combined with their propensity to dehydrate made their structure characterization difficult; Finch *et al.* (1996a) reported the full structure determination of schoepite and Weller *et al.* (2000) refined the structure of meta-schoepite $\{(UO_2)_4O(OH)_6 \cdot 5H_2O\}$. The uranyl oxyhydroxides are based on electrostatically neutral polyhedral sheets of the form $[(UO_2)_xO_y(OH)_z]$ and no interlayer cations. Water molecules occupy the interlayer sites, linking adjacent sheets through H-bonds. Meta-schoepite possesses one less water molecule than schoepite, leading to 2.8% reduction in the *c*-axis and 0.6 and 0.9% in the *a*- and *b*-directions, respectively. Hughes-Kubatko *et al.* (2005) have shown that meta-schoepite is thermodynamically unstable relative to dehydrated schoepite and have suggested that sodium may be an essential element in natural meta-schoepite. The $U–O_{ax}$ and $U–O_{eq}$ bond lengths in schoepite vary with pH. Allen *et al.* (1996a) determined that $U–O_{ax}$ distances are 1.80, 1.84, and 1.86 Å and $U–O_{eq}$ distances are 2.38, 2.36 and 2.32 Å, at pH 7, 9, and 11, respectively. At pH 11, the uranyl group becomes elongated and the $U–O_{eq}$ bond contracts, such that the structure resembles a clarkeite-like alkali metal uranate. Clarkeite-like sodium uranates have been observed during dissolution of soddyite (Giammar and Hering, 2002) and in the highly caustic environment of the Hanford tank wastes in Washington, USA (Deutsch *et al.*, 2004). Pseudomorphic replacement of pegamatic uraninite by clarkeite $\{(NaCa_{0.5}Pb_{0.5})[(UO_2)O(OH)](H_2O)_{0-1}\}$ may occur during metasomatic alteration by oxidizing hydrothermal fluids (Finch and Ewing, 1997).

The alkali uranyl oxyhydroxides may play an important role in attenuating radionuclides in the environment, including neptunium (Li and Burns, 2001a; Burns *et al.*, 2004a), strontium (Burns and Li, 2002), and cesium (Hoskins and Burns, 2003).

(e) Pb–uranyl oxyhydroxides

As uranium decays to lead, the lead enters cation vacancies in the interlayer, leaving a uranium vacancy in the structural sheet. Although Pb–uranyl oxyhydroxides will form directly from uraninite alteration, many Pb–uranyl minerals are formed though the accumulation of radiogenic lead in nominally Pb-free uranium phases. Accumulation of lead will also destabilize the structure of some U(VI) minerals. For example, Finch and Ewing (1997) have demonstrated that clarkeite will eventually transform to wölsendorfite or curite. Lead is not incorporated into rutherfordine, soddyite, or uranophane, minerals that may replace early-formed lead uranyl oxyhydroxides. However, several uranyl phosphates and arsenates will incorporate lead. Indeed, Finch and Ewing (1992) suggested that curite, one of the last minerals remaining after complete oxidative dissolution of uraninite, may act as substrate for nucleation of certain phosphates. Burns and Hill (2000b) have synthesized a strontium analog of curite that may be relevant to HLW disposal.

Spriggite, $\{Pb_3[UO_2)_6O_8(OH)_2](H_2O)_3\}$, has been identified by Brugger *et al.* (2004). The structure is based on $[(UO_2)_6O_8(OH)_2]^{6+}$ sheets of uranyl polyhedra of the β-U_3O_8 anion topology with Pb^{2+} and H_2O in the interlayer. Spriggite has the highest Pb:U ratio (1:2.00) of all known lead uranyl oxide hydrates. Finch and Murakami (1999) have suggested a reaction pathway for increasing alteration of hydrated lead uranyl oxyhydroxides where the molar proportion of PbO can be correlated with the molar proportion of H_2O. With increasing PbO content, charge compensation in the sheet structure results in OH^- substitution for O^{2-}. The U–O_{eq} bonds in the $Ur\phi_5$ pentagonal bipyramids are considerably longer and of lower bond valence than the U^{6+}–O bonds in the $Ur\phi_4$ square bipyramids. The change in uranyl ion coordination from pentagonal to square helps satisfy bond-valence requirements of OH^- in the anion site. Hence, the spriggite adopts $Ur\phi_4$ square bipyramids, whereas the structure of vandendriesscheite (Pb:U = 1:6.36) consists entirely of $Ur\phi_5$ pentagonal bipyramids. Vandendriesscheite, one of the most common Pb-bearing uranyl oxyhydroxides, contains two symmetrically distinct Pb^{2+} cations in the interlayer; both bonded to H_2O groups. The two Pb^{2+} cations (Pb(1) and Pb(2)) are bonded to five and six O_{ur} atoms of adjacent sheets of uranyl polyhedra, respectively. Richetite possesses an extraordinarily complex structure (Burns, 1998b). The phase has been reported at the Shinkolobwe and Jáchymov U-deposits.

(f) Uranyl peroxides

The U-bearing phases, studtite and meta-studtite $\{(UO_2)O_2(H_2O)_2\}$, are the only known peroxide minerals that form during the buildup of α-generated H_2O_2 on the surface of natural uraninite (Walenta, 1974; Deliens and Piret, 1983a; Finch and Ewing, 1992). Burns and Hughes (2003) determined that the structure of studtite is monoclinic, contains one symmetrically distinct U^{6+} cation and four O atoms, two of which occur as H_2O groups. The U^{6+} cation occurs as part of a linear uranyl ion, and each U^{6+} cation is bonded to six additional O atoms, two of which are H_2O groups, and four that are O atoms of the peroxide groups. Unlike all other uranyl oxide hydrate minerals, studtite is not based upon sheet of uranyl polyhedra, but contains polymerized uranyl polyhedra in only one dimension. The occurrence of chains rather sheets in U(VI) minerals is usually due to distortions in the polyhedra, normally the result of lone pairs (e.g. in Se- and Bi-bearing uranium minerals); however, in studtite, the presence of peroxide at the equatorial positions of the uranyl polyhedra results in distorted hexagonal bipyramids, with the peroxide O–O edge length of 1.46 Å. Typical O–O edge length in uranyl hexagonal bipyramid is 2.4 Å with nitrate or carbonate ligands. This distortion may prevent the formation of two-dimensional layer structures (see Fig. 5.56a).

Radiolysis of water at spent nuclear fuel may create an additional complexity for predicting UO_2 paragenesis in a geological repository (Satonnay *et al.*, 2001; Amme, 2002). Studtite and meta-studtite have been identified by McNamara *et al.* (2003) on the surface of corroding commercial spent fuel replacing the meta-schoepite that precipitated earlier. As the H_2O_2 concentration increased with time, studtite and meta-studtite became the dominant alteration phases. H_2O_2 is consumed in the presence of carbonate (Sunder *et al.*, 2004), forming peroxo complexes with H_2O_2 and U(VI) (Amme, 2002).

(g) Uranyl carbonates and calcite

Uranyl carbonates tend to form in evaporative environments or under high p_{CO_2} conditions. They are structurally diverse and only relatively few of the uranyl carbonates (rutherfordine (Finch *et al.*, 1999b), roubaultite, bijvoetite $\{[M_8^{3+}(H_2O)_{25}(UO_2)_{16}O_8(OH)_8(CO_3)_{16}](H_2O)_{14}\}$, where M is Y or Ln (Li *et al.*, 2000), and wyartite (Burns and Finch, 1999) consist of sheets of polyhedra that contain a cation of high valence. Other uranium carbonates contain isolated clusters similar to those observed in solution (Allen *et al.*, 1995). The optical signature of the UO_2^{2+} bands in liebigite $\{Ca_2UO_2(CO_3)_3 \cdot 11H_2O\}$, andersonite $\{Na_2Ca[(UO_2)(CO_3)_3](H_2O)_5\}$, and schröckingerite $\{NaCa_3(UO_2)(CO_3)_3(SO_4)F \cdot 10H_2O\}$, that all contain uranyl tricarbonate clusters, are almost identical (Čejka, 1999).

The uranyl monocarbonates (rutherfordine, joliotite $[UO_2CO_3 \cdot nH_2O]$, blatonite $[UO_2CO_3 \cdot H_2O]$, and urancalcarite $\{Ca(UO_2)_3CO_3(OH)_6 \cdot 3H_2O)\}$) are thermodynamically stable, having solubilities comparable to some uranyl oxide hydrates. The uranyl carbonate mineral grimselite, $\{K_3Na[(UO_2)(CO_3)_3](H_2O)\}$ (Li and Burns, 2001b), contains uranyl tricarbonate complexes of composition $[(UO_2)(CO_3)_3]^{4-}$, which occur as an isolated polyhedra in each of the structures, cf. Fig. 5.53. Schröckingerite contains $Na\phi_6$ octahedron, an SO_4 tetrahedron, and three symmetrically distinct $Ca\phi_8$ polyhedra (Hayden and Burns, 2002). The structure contains isolated units of uranyl tricarbonate and sulfate tetrahedra that are coordinated to low-valence cations. Bayleyite, $\{Mg_2[(UO_2)(CO_3)_3](H_2O)_{18}\}$, contains three symmetrically distinct $Mg(H_2O)_6$ octahedra, as well as a $(UO_2)(CO_3)_3$ cluster, and six symmetrically distinct H_2O groups. Swartzite, $\{CaMgUO_2(CO_3)_3 \cdot 12H_2O\}$, contains $Ca\phi_8$ polyhedra and a $Mg(H_2O)_6$ octahedron.

At a partial pressure of $CO_2 > 10^{-2.2}$ atm, rutherfordine becomes the stable uranium phase with respect to dehydrated schoepite; however, the schoepite–rutherfordine equilibrium indicates that p_{CO_2} must be $>10^{-1.9}$ atm before schoepite becomes unstable with respect to rutherfordine. Schoepite is thus expected to be the U-solubility-controlling phase in waters exposed to atmospheric conditions. Rutherfordine would be expected to replace schoepite in environments where the p_{CO_2} pressure is higher, possibly in a repository environment or in saturated soils. Replacement of schoepite by rutherfordine has been observed at the Shinkolobwe U-deposit (Finch and Ewing, 1992). The structure of rutherfordine was elucidated by Finch *et al.* (1999b) and can be represented by an anion topology that consists of edge-sharing hexagons that share corners, creating pairs of edge-sharing triangles. The rutherfordine sheet is obtained by populating all the hexagons in the anion topology with uranyl ions and one half of the triangles are populated with CO_3 groups. The sheets are held together via van der Waals forces. An identical sheet structure occurs in synthetic $(UO_2)(SeO_3)$.

Burns and Finch (1999) reported the structure of a mixed uranium valence mineral, wyartite that contains U(v) and U(vi). The structure of wyartite contains three symmetrically distinct U positions. The U1 and U2 cations are each strongly bonded to two O atoms with U–O bond lengths of ~1.8 Å, consistent with a linear uranyl ion, whereas the U3 site has seven anions at the corners of a pentagonal bipyramid, with U–O bond lengths of 2.07 and 2.09 Å. A bond valence analysis showed that the U3 site is coordinated by six O atoms and one H_2O group. Two of the O atoms of the bipyramid are shared with a CO_3 group and the sum of bond valences incident at the U3 site is 5.07, in agreement with the assignment of U(v) in this site. Urancalcarite is structurally similar to wyartite and commonly associated with wyartite in nature. Finch and Murakami (1999) suggest that wyartite may oxidize to uranocalcarite. Schindler and coworkers (Schindler and Hawthorne, 2004; Schindler *et al.*, 2004) proposed the formation of the mixed U(v)–U(vi) mineral, wyartite II, on surface of calcite during interaction of acidic and basic uranyl-bearing solutions with calcite.

The structure of fontanite, $\{Ca[(UO_2)_3(CO_3)_2O_2](H_2O)_6$, has been refined by Hughes and Burns (2003) as a monoclinic phase that consists of two symmetrically distinct $Ur\phi_5$ units, one $Ur\phi_6$ unit, and two CO_3 triangles. It is observed in the weathered zone of the Rabejac uranium deposit in Lodève, Hérault, France, where it is associated with billietite and uranophane. Both fontanite and roubaultite possess anion topologies similar to phosphuranylite $\{KCa(H_3O)_3(UO_2)[(UO_2)_3(PO_4)_2O_2]_2(H_2O)_8\}$.

Several uranyl carbonates that contain lanthanides have been described. Bijvoetite is found in association with uraninite, sklodowskite, and uranophane in the oxidized zone at the Shinkolobwe mine (Li *et al.*, 2000). The structure of bijvoetite is extremely complex and contains 16 unique carbonate groups, 39 symmetrically distinct H_2O groups, and 8 unique M^{3+} sites that are occupied by variable amounts of yttrium, dysprosium, and other lanthanides. Astrocyanite $\{Cu_2(Ce,Nd,La)_2UO_2(CO_3)_5(OH)_2 \cdot 1.5H_2O\}$, is another rare earth-bearing uranyl carbonate that is observed as an oxidation product of uraninite. These complex rare earth uranyl carbonates may play an important role in the long-term behavior of released transuranic elements following corrosion of nuclear materials in a geologic repository.

The occurrence of trace amounts of uranyl ions in natural calcite has posed a long-standing problem in crystal chemistry because of speculation that the size and shape of the uranyl ion may preclude its incorporation in a stable lattice position in calcite. The incorporation of uranium in calcite and aragonite provides the basis for U-series age-dating which are commonly adopted for marine and terrestrial carbonates. Uranium is enriched in aragonite relative to calcite owing to the nature of the coordination environment in U-bearing aragonite. Reeder *et al.* (2000) have demonstrated using EXAFS that the dominant aqueous species $UO_2(CO_3)_3^{4-}$ is retained by the uranyl in aragonite, essentially intact. In contrast, a different equatorial coordination occurs in calcite, characterized by fewer nearest oxygens at a closer distance, reflecting that the CO_3 groups are monodentate. The uranyl ion has a more stable and well-defined local environment when co-precipitated with aragonite; however, Reeder *et al.* (2000) argue that as aragonite is metastable with respect to calcite, retention of U(VI) by calcite is likely to be temporary. In contrast, Kelly *et al.* (2003) examined a 13 700-year-old U-rich calcite from a speleothem in northernmost Italy. X-ray absorption spectroscopy data indicated substitution of U(VI) for a Ca^{2+} and two adjacent CO_3^{2-} ions in calcite. This data implied that uranyl has a stable lattice position in natural calcite and suggested that uranium may become incorporated in calcite over long time scales.

Sturchio *et al.* (1998) reported the occurrence of U^{4+} in calcite based on XANES core spectroscopic analysis and concluded that this explained the anomalously high concentrations of uranium observed in calcite in reducing environments. Substitution of Ca^{2+} by Na^{+} was suggested as a possible mechanism to charge balance the structure. The calculated U–O distances reported by Sturchio *et al.* (1998) were (2.21 ± 0.02) Å and (2.78 ± 0.03) Å for U^{4+} in calcite, whereas Reeder *et al.* (2001) estimated $U–O_{eq}$ to be 2.33 Å and $U–O_{ax}$ as 1.80 Å. Interestingly, Sturchio *et al.* (1998) showed a good match of their measured U–O bond lengths with a natural brannerite, where U–O bond lengths were reported as 2.28 and 2.82 Å. However, natural brannerite minerals have recently been shown to be U(V) phases (Finnie *et al.*, 2003; Colella *et al.*, 2005).

(h) Uranyl sulfates

Uranyl sulfates are important in systems where sulfides (e.g. pyrite) are being oxidized. Initial oxidation causes an increase in acidity of the system; however, the acidity may be buffered by the dissolution of carbonate in the surrounding rock, leading to the formation of gypsum. Uranyl sulfates usually occur where uranyl carbonates are absent (and vice versa), owing to the different pH conditions where these minerals will dominate. Uranyl sulfate minerals typically occur as microcrystalline crusts, finely intergrown with other uranyl sulfates and/or monocarbonates. They are common at uranium mines where they form during evaporation of acid sulfate-rich mine drainage waters.

Burns (2001a) and Burns *et al.* (2003) have performed structural refinements on a number of monoclinic zippeite-group U(VI) phases, including zippeite

$\{K_3(H_2O)_3[(UO_2)_4(SO_4)_2O_3(OH)]\}$, sodium-zippeite $\{Na_5(H_2O)_{12}[(UO_2)_8(SO_4)_4O_5(OH)_3]\}$, Mg-zippeite $\{Mg(H_2O)_{3.5}[(UO_2)_2(SO_4)O_2]\}$, Zn-zippeite $\{Zn(H_2O)_{3.5}[(UO_2)_2(SO_4)O_2]\}$, and Co-zippeite $\{Co(H_2O)_{3.5}[(UO_2)_2(SO_4)O_2]$. Each structure contains the zippeite-type layers that consist of chains of edge-sharing $Ur\phi_5$ units that are cross-linked by vertex sharing with sulfate tetrahedra. Marecottite, $\{Mg_3(H_2O)_{18}[(UO_2)_4O_3(OH)(SO_4)_2]_2(H_2O)_{10}\}$, is based on uranyl layers composed of chains of edge-sharing $Ur\phi_5$ biyramids that are linked by vertex-sharing sulfate tetrahedra, identical to zippeite (Brugger *et al.*, 2003). Marecottite and zippeite can co-exist as has been observed in samples from the Jáchymov mine in the Czech Republic. Uranopilite is the only known uranyl sulfate mineral to form chains. The structure consists of clusters of six distinct $Ur\phi_5$ bipyramids that are linked together into a chain by sulfate tetrahedra bonded to two oxygens from each cluster. Adjacent chains are only hydrogen-bonded (Burns, 2001a).

(i) Uranyl silicates

Because of the ubiquity of dissolved silica in most groundwaters, uranyl silicates are the most abundant U(VI) minerals. The uranyl silicates are divided into three groups based on their U:Si ratios (Stohl and Smith, 1981). Accordingly, the structural trends in the uranyl silicates are also dependent on the U:Si ratio (Stohl and Smith, 1981; Finch and Murakami, 1999; Burns, 2001b). In phases with the U:Si ratio of 2:1 and 1:1, no polymerization of the SiO_4 tetrahedra occurs, whereas phases with 1:3 ratios contain chains of vertex-sharing silica tetrahedra. As the U:Si ratio approaches 1:4, the structures contain sheets of SiO_4 tetrahedra. In soddyite, with a ratio of 2:1, each silica tetrahedron shares two of its edges with other uranyl polyhedra, but in structures with the ratio 1:1, only one edge of each silica tetrahedron is shared with a second uranyl polyhedron and each silica tetrahedron is linked to other uranyl polyhedra by vertex sharing.

Uranophane is one of the most common uranyl minerals, and its ubiquity suggests that the uranyl silicates are important phases controlling uranium concentrations in groundwater (Finch and Ewing, 1992). α-Uranophane and β-uranophane have distinctly different crystallographic data and stabilities. Differences in stability were amply illustrated in the study by Cesbron *et al.* (1993) where they failed to synthesize β-uranophane whereas α-uranophane was produced. Both calcium uranyl silicates are common in most oxidized uranium deposits.

The 1:3 silicates (weeksite and haiweeite) are only known from Si-rich environments such as tuffaceous rocks but are commonly observed during the laboratory weathering of borosilicate waste glasses (Ebert *et al.*, 1991; Feng *et al.*, 1994). The structure of weeksite, originally described by Outebridge *et al.* (1960), has been refined by Jackson and Burns (2001). Haiweeite, named for the Haiwee reservoir, California, USA, has been identified at the Nopal I deposit in Peña Blanca, Mexico, where it is associated with uranophane. The structure of weeksite consists of chains of edge-sharing $Ur\phi_5$ pentagonal bipyramids that share edges with SiO_4 tetrahedra. The chains are linked through disordered SiO_4 tetrahedra to form complex sheets, which in turn form a framework through linkage with SiO_4 tetrahedra (Burns, 1999b).

The only known thorium uranyl silicate mineral, coutinhoite, has been described by Atencio *et al.* (2004) as being isostructural with weeksite. The open channels created by the silicate framework structure are thought to permit the incorporation of Th^{4+}. Oursinite, $\{(Co_{0.86}Mg_{0.10}Ni_{0.04})\cdot O_2\cdot UO_2\cdot 2SiO_2\cdot 6H_2O\}$, was first reported by Deliens and Piret (1983b) from Shinklolobwe. The phase formed from the oxidation of Co- and Ni-bearing sulfides and demonstrates the ability for U(VI) phases to incorporate a range of elements. Lepersonnite, $\{CaO(Gd,Dy)_2O_3\cdot 24UO_3\cdot 8CO_2\cdot 4SiO_2\cdot 60H_2O\}$, is a pale yellow uranyl silicate from the Shinkolobwe mine that was first described by Deliens and Piret (1982). The reported compositions of oursinite, lepersonnite, and coutinhoite have immediate implications for radioactive waste disposal for the possible retention of radionuclides, including plutonium, in the environment.

Soddyite is the only known mineral with a U:Si ratio of 2:1; it is also the most common of the uranyl minerals that have structures based on frameworks of polyhedra of higher valence. The structure of soddyite consists of $Ur\phi_5$ units that share equatorial edges to form chains. The chains are cross-linked by sharing edges with SiO_4 tetrahedra in such a way that each tetrahedron shares two of its edges with adjacent chains (Burns, 1999b). Based on observations at the Nopal I site, Pearcy *et al.* (1994) suggested that the precipitation of soddyite may be kinetically more favorable than the formation of other U^{6+} silicates. Soddyite may form from uranophane exposed to dilute metoric waters that are low in carbonate and with a pH below 7. Uranosilite, $\{(Mg,Ca)_4(UO_2)_4(Si_2O_5)_{5.5}(OH)_5\cdot 13H_2O\}$, has only been reported in nature at a site in Menzenschwand, Germany (Walenta, 1983). Burns *et al.* (2000) reported the occurrence of a new U(VI) silicate from the corrosion of a borosilicate glass with formula $\{KNa_3(UO_2)_2(Si_4O_{10})_2(H_2O)_4\}$, with a U:Si ratio of 1:4. This phase was demonstrated to be structurally distinct from the phase synthesized by Plesko *et al.* (1992). Burns and co-authors suggested that this novel U(VI) silicate may incorporate Np(V).

(j) Uranyl phosphates and arsenates

Uranyl phosphates and arsenates constitute about one-third of the ~200 described uranium minerals (see Table 5.3); yet only a fraction of these have well-defined structures. In groundwaters where $\log\{[PO_4^{3-}]_T/[CO_3^{2-}]_T\} > -3.5$, uranyl phosphate complexes dominate over uranyl carbonate complexes (Sandino and Bruno, 1992). Finch and Ewing (1992) suggested that the occurrence of uranyl phosphates in the most weathered zones of the Koongarra U-deposit indicated that higher oxidation potentials may be necessary for uranyl phosphate precipitation, as uranyl silicates were observed at depth. However, saléeite ($Mg(UO_2)_2(PO_4)_2\cdot 10H_2O$) was observed on the surface of apatite where the groundwater was undersaturated with respect to saléeite, indicating that the mineralization occurred by local saturation (Murakami *et al.*, 1997).

Laboratory studies have demonstrated that surface mineralization of saléeite on fluoro-apatite where localized release of Ca and P facilitates autunite formation and U^{6+} uptake (Ohnuki *et al.*, 2004).

Uranyl arsenates are often structurally analogous to the corresponding uranyl phosphates; e.g. the isostructural mineral species abernathyite, $\{K[(UO_2)(AsO_4)](H_2O)_3\}$, and meta-ankoleite, $\{K[(UO_2)(PO_4)](H_2O)_3\}$. Many of the natural uranyl phosphates and arsenates may exhibit complete solid solution formation between end-members. However, in hügelite, $\{Pb_2[(UO_2)_3O_2(AsO_4)_2](H_2O)_5\}$, the presence of arsenic makes the unit cell four times larger than that reported for dumontite, $\{Pb_2[(UO_2)_3(PO_4)_2(OH)_4](H_2O)_5\}$ (Locock and Burns, 2003b). Both structures possess the phospuranylite anion topology. In hügelite, the interlayer contains four symmetrically distinct Pb^{2+} cations. Unlike the lead uranyl oxyhydroxides, hügelite contains only $Ur\phi_5$ and $Ur\phi_6$ polyhedra; yet, it possesses a high U:Pb ratio.

Uranyl arsenates and phosphates may be divided into groups depending on the U:P or U:As ratio. However, a structural classification is more encompassing. The uranium phosphates and arsenates can be separated into four groups: (i) autunite structure; (ii) 3:2 phosphuranylite structure; (iii) uranophane structure; and (iv) chain structures.

(*i*) *Autunite structures*

The most important uranyl phosphates in terms of natural abundance are the autunites and meta-autunite groups. The autunite group of minerals is tetragonal uranyl arsenates and phosphates. The group possesses the general formula $M(UO_2)_2(XO_4)_2 \cdot 8\text{–}12H_2O$ where M may be Ba, Ca, Cu, Fe^{2+}, Mg, Mn^{2+} or $\frac{1}{2}(HAl)$ and X is As or P. Takano (1961) obtained unit cell parameters for an autunite specimen from Ningyo Pass, Japan ($a = 6.989$ Å and $c = 20.63$ Å). These were virtually identical to those obtained by Locock and Burns (2003a) on a synthetic autunite. The Pb uranyl oxide hydrate, curite is commonly associated with uranium phosphates such as autunite, torbernite, and parsonsite (Vochten and Deliens, 1980). Finch and Ewing (1992) suggested that the (010) face of curite consists of $\equiv (UO_2) - OH_2^+$ surface species that may provide a reactive pathway for attachment of $(HPO_4)^{2-}$ groups, forming $\equiv (UO_2)\text{-}OPO_3\text{-}H_3O^0$. This species, once deprotonated, would have the equivalent stoichiometry of chernikovite. Heinrichite $\{Ba[(UO_2)(AsO_4)]_2(H_2O)_{10}\}$ was originally assumed by Gross *et al.* (1958) to be tetragonal, despite the observation of biaxial optical properties. Locock *et al.* (2005b) have refined the structures of several of the barium-bearing phases that possess the autunite sheet structure, including heinrichite and meta-uranocircite $\{Ba[(UO_2)(PO_4)]_2(H_2O)_7\}$ type I and II. There is only the loss of one H_2O group and a slight decrease in the interlayer spacing, from $d_{020} = 8.82$ Å to $d_{020} = 8.43$ Å from going from meat-uranocircite I to II; however, there is a significant re-arrangement in the Ba atomic positions. Table 5.3 lists new refinements from Locock *et al.* (2005b) for these autunite structures; however, because of the difficulties in obtaining suitable natural specimens, some are based synthetic phases and predictions. These have been listed owing to the apparent inconsistencies in earlier published data. Locock *et al.* (2005c) have published a refinement of uranospathite $\{Al_{1-x}\square_x[(UO_2)(PO_4)]_2(H_2O)_{20+3x}\, F_{1-3x}\}$ with $0 < x < 0.33$ and confirmed the presence of fluorine, the absence of H_3O^+, and a higher Al content in the structure; the empty square in the formula indicates a vacancy. Locock *et al.* (2005c) have described uranospathite as the "Dogwood sandwich" of the autunite group with an interlayer spacing, d_{200} of 15.01Å, possessing 21 H_2O groups per formula unit (*pfu*). The discovery that uranospathite and other aluminum uranyl phosphates possess a number of different hydration states has called into question the traditional division of these minerals into autunite and meta-autunite sub-groups based on the 10-12 H_2O *pfu* and 6-8 H_2O *pfu*, respectively.

(*ii*) *Phosphuranylite structures*

The phosphuranylite group consists of mainly orthorhombic phases with structure sheets of the composition $[(UO_2)_3(O,OH)_2(PO_4)_2]$. Phosphuranylite is remarkable because it contains all three types of Ur polyhedra. The $Ur\phi_5$ and $Ur\phi_6$ occur in the uranyl sheet and the $Ur\phi_4$ occur in the interlayer (Burns, 1999a). It is one of the few minerals with uranium in an interlayer position. Torbernite and meta-torbernite are hydrous copper uranium phosphates, the only difference between the two being the number of water molecules present; the length of the *c*-axis depends on the water content. The structure of monoclinic bergenite, the barium phosphuranylite phase $\{Ca_2Ba_4[(UO_2)_3O_2(PO_4)_2]_3(H_2O)_{16}\}$, has been refined by Locock and Burns (2003c).

(*iii*) *Uranophane structures*

The uranophane structure type occurs in only a few uranium phosphates and arsenates. Ulrichtite, $Cu[Ca(H_2O)_2(UO_2)(PO_4)_2](H_2O)_2$, and the mixed valence arsenite–arsenate uranyl mineral, Séelite, $\{Mg(UO_2)(AsO_3)_{0.7}(AsO_4)_{0.3}\cdot 7H_2O\}$. The name ulrichite was once used as a term for pitchblende; however, the structure of this $Ca–Cu^{2+}$ mineral has now been refined by Kolitsch and Giester (2001).[20] The structure consists of elongated CuO_6 octahedra that are corner linked by two PO_4 octahedra, edge- and corner-sharing $Ur\phi_5$, CaO_8, and PO_4 polyhedra. These form heteropolyhedral sheets parallel to (001) that are linked by the elongated CuO_6 octahedra.

(*iv*) *Chain structures*

Chain structures occur in walpurgite, orthowalpurgite, phosphowalpurgite, hallimondite, and parsonsite. Burns (2000) solved the structure of parsonsite

---

[20] Problems with the ulrichite structure as described by Birch *et al.* (1988) were recognized by Burns (1999a).

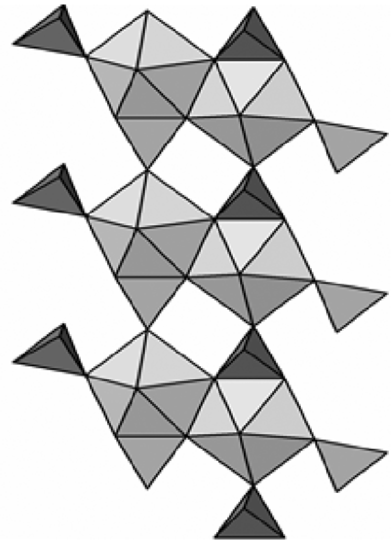

Fig. 5.3 *Parsonsite, the chain uranyl phosphate phase* (*adapted from Locock and Burns*, 2003).

and found that it was composed of uranyl phosphate chains rather than sheets as observed in the autunite and phosphuranylite minerals. The structure consists of Urϕ_5 polyhedra edge-sharing dimers that are cross-linked with two distinct phosphate tetrahedra by edge- and vertex- sharing. Two symmetrically distinct Pb^{2+} cations link the uranyl phosphate chains (see Fig. 5.3).

One of the Pb positions, Pb(1) is coordinated by 9 oxygen atoms, with Pb–O bond lengths ranging from 2.35 to 3.16 Å. Pb(2) is coordinated by 6 oxygens with a distinctly one-sided polyhedral geometry owing to the presence of a lone pair of electrons on the Pb cation. The Pb(2)–O bond lengths range from 2.28 to 3.15 Å. Common to other uranium phases, the lone pair distortion may be responsible for the formation of chains rather than sheets.

Based on structural refinements and infrared spectroscopy, Locock *et al.* (2005a) have shown that parsonsite does not contain any structural water. In most uranyl phosphates and arsenates, water occurs as a hydrate H_2O, either coordinating interlayer cations, or occurring as interstitial H_2O groups. Although Locock *et al.* (2005a) detected water in hallimondite, this was determined not to be critical to structural integrity.

(*v*) *Synthetic uranyl phosphates and arsenates*

Synthetic varieties have also revealed structural differences between phosphate and arsenate uranyl phases that contain the large alkali cations cesium and rubidium. These phosphate and arsenate phases are not isostructural. For example, cesium uranyl arsenates are not isostructural with cesium uranyl phosphates, but show a homeotypic framework with identical coordination geometries and polyhedral connectivity. The presence of arsenic expands the framework relative to phosphorus and so the cesium uranyl arsenate has a unit-cell volume ~7% greater than the corresponding phosphate.

(*vi*) *Uranium*(*VI*) *phosphates in the environment*

Because of their low solubilities, phosphate and arsenate minerals are of considerable environmental importance for understanding the mobility of uranium in natural systems and they may control the concentration of uranium in many groundwaters. In alkaline environments, dewindite {$Pb(UO_2)_3(PO_4)_2(OH)_2 \cdot 3H_2O$} is stable at low lead concentrations; whereas dumontite is the stable phase in Pb-rich environments. In acid environments, parsonsite is prevalent at high lead levels and przhevalskite {$Pb_2(UO_2)_3(PO_4)_2(OH)_4 \cdot 3H_2O$} occurs under low lead concentrations (Nriagu, 1984). Jerden and Sinha (2003) examined the long-term sequestration of uranium by U(VI) phosphate mineral precipitation at the Coles Hill uranium deposit in Virginia, USA where uranium is released by the oxidation and chemical weathering of an apatite-rich, coffinite–uraninite orebody. Meta-autunite was observed by Buck *et al.* (1996) and Morris *et al.* (1996) in contaminated soils from a former uranium processing plant at Fernald, Ohio, USA.

Significant uraniferous phosphorite deposits occur in Tertiary sediments in Florida, Georgia, and North and South Carolina and in the Hahotoé-Kpogamé U-deposits in Togo, West Africa (Gnandi and Tobschall, 2003). The Florida Phosphorite Uranium Province has yielded large quantities of uranium as a by-product of the production of phosphoric acid fertilizer (Finch, 1996). The discovery that bacteria can reduce U(VI), which appears to precipitate as uraninite, has led to the concept of *in situ* bioremediation of U-contaminated groundwater; however, another possible microbial process for uranium immobilization is the precipitation of U-phosphates. Macaskie *et al.* (2000) have demonstrated that *Citrobacter* sp. will bioprecipitate uranyl phosphate with exocellularly produced phosphatase enzyme. In a similar study by Basnakova *et al.* (1998) a nickel uranyl phosphate was observed in experiments with *Citrobacter* sp.

(k) Uranyl vanadates

Uranyl vanadates comprise some of the most insoluble uranyl minerals, forming whenever dissolved uranium comes in contact with dissolved vanadate anions. The K-bearing uranyl vanadate, carnotite, is possibly the most important source of secondary (U^{6+}) uranium ore minerals, providing ~90% of the uranium production from secondary deposits. It is a lemon-yellow mineral with an earthy luster, a yellow streak, and a specific gravity of about 4. It occurs most commonly in soft, powdery aggregates of finely crystalline material or in thin films or stains on rocks or other minerals. The most noted occurrences of carnotite are in the Colorado Plateau (Zhao and Ewing, 2000), on the western edge of the Black Hills, South Dakota, USA, and in the Ferghana basin in Kyrgyzstan. It occurs in sandstones in flat-lying, irregular, partially bedded ore bodies. If present in sufficient quantity, carnotite will color the rock bright yellow; but in poorer deposits, particularly below 0.20 percent U_3O_8, it may be difficult to distinguish the uranium mineral from the sandstone itself.

Using solid state reactions, Dion *et al.* (2000) synthesized two new alkali uranyl vanadates, $M_6(UO_2)_5(VO_4)_2O_5$ with M = Na, K, by and determined their structures from single-crystal XRD. Both structures consisted of $[(UO_2)_5(VO_4)_2O_5]^{6-}$ corrugated layers parallel to the (100) plane. The layers contained VO_4 tetrahedra, $Ur\phi_5$ pentagonal bipyramids, and distorted $Ur\phi_4$ octahedra. The $Ur\phi_5$ units were linked by sharing opposite equatorial edges to form zigzag infinite chains parallel to the *c*-axis. These chains were linked together on one side by VO_4 tetrahedra and on other side by $Ur\phi_4$ and $Ur\phi_5$ corner-sharing units.

(l) Uranyl selenites and tellurites

In nature, uranyl selenite minerals form where Se-bearing sulfides are undergoing oxidative dissolution. Selenium occurs as Se(IV), in the selenite anion, SeO_3^{2-}, however, Finch and Murakami (1999) suggested that Se(VI) minerals may be expected under sufficiently oxidizing conditions. Natural uranyl selenites and tellurites include the minerals derriksite, demesmaekerite, guilleminite, larisaite $\{Na(H_3O)(UO_2)_3(SeO_3)_2O_2\cdot 4H_2O\}$ (Chukanov *et al.*, 2004), and marthozite, $\{Cu[(UO_2)_3(SeO_3)_2O_2](H_2O)_8\}$. The three known uranyl tellurites are cliffordite $\{UO_2(Te_3O_7)\}$, moctezumite $\{PbUO_2(TeO_3)_2\}$, and schmitterite $\{UO_2(TeO_3)\}$. The selenites and tellurites are based upon infinite chains of polymerized polyhedra of higher valence. The chain structures observed with moctezumite and derriksite contains $Ur\phi_5$ and $Ur\phi_4$ bipyramids as well as $Te^{4+}O_3$ and $Se^{4+}O_3$ triangles. They are strongly distorted owing to the presence of a lone pair of electrons on the cation. The crystal structure of marthozite has been refined by Cooper and Hawthorne (2001). There are two unique selenium sites, each occupied by Se^{4+} and coordinated by three O atoms, forming a triangular pyramid with Se at the apex, indicative of the presence of a stereoactive lone pair. The Se–O bond length is $\sim$1.70 Å. The structure possesses one Cu site coordinated by 4 H_2O groups and two O atoms. The structural unit is a sheet of composition $[(UO_2)_3(SeO_3)_2O_2]$, which is topologically identical to the structural unit in guilleminite $\{Ba[(UO_2)_3(SeO_3)_2O_2](H_2O)_3\}$. Adjacent sheets are linked through interstitial Cu^{2+} cations *via* Cu^{2+}-O bonds and *via* H-bonds that involve both (H_2O) groups bonded to Cu^{2+} and interstitial (H_2O) groups.

A number of uranyl selenites containing alkaline metals (Almond *et al.*, 2002), as well as Ag and Pb (Almond and Albrecht-Schmitt, 2002) have been prepared. The structures consist of $[(UO_2)(SeO_3)_2]^{2-}$ sheets constructed from $Ur\phi_5$ units that are linked by SeO_3^{2-} anions, similar to the natural minerals. Synthetic $Sr[(UO_2)_3(SeO_3)_2O_2]\cdot 4H_2O$ prepared in supercritical water was found to possess the same anion topology as is found in guilleminite and marthozite; however, this phase could not be prepared under ambient or hydrothermal conditions (Almond and Albrecht-Schmitt, 2004).

(m) Uranyl molybdates

Uranyl molybdates are common minerals formed by weathering of uraninite and Mo-bearing minerals (Finch and Murakami, 1999). Umohoite $\{[(UO_2)(MoO_2)](H_2O)_4\}$, is commonly partially replaced by iriginite $\{[(UO_2)(MoO_3OH)_2(H_2O)](H_2O)\}$, which also consists of polyhedra sheets. Iriginite, however, has a distinctive anion-topology arrangement of chains of pentagons and squares that share edges, and zigzag chains of edge sharing squares and triangles (Krivovichev and Burns, 2000a). In the structure of iriginite, each pentagon of the anion topology is populated by an $Ur\phi_5$ polyhedron, two-thirds of the squares are populated with $Mo^{6+}O_6$ octahedra that occur as edge-sharing dimers; the triangles, as well as one-third of the squares, are empty. There have been reports of substantial variability of the *c* dimension of umohoite possibly due to variation of the H_2O content or polytypism that may account for the observed variation in unit-cell parameters (Krivovichev and Burns, 2000b).

The sheets of uranyl and molybdate polyhedra in iriginite and umohoite have features in common. The umohoite to iriginite transformation during alteration of U–Mo deposits, corresponding to a change of the U:Mo ratio from 1:1 to 1:2, involves a change of anion topology to one with a smaller number of edges shared between coordination polyhedra. The uranophane anion-topology is the basis of the umohoite sheet. Construction of the anion topology requires the U and D arrowhead chains as well as the R chain, with the chain-stacking sequence URDRURDR... The iriginite anion-topology contains the same chains as the umohoite (uranophane) anion-topology, but the chain-stacking sequence is DRRRURRRDRRRURRR... The ratio of arrowhead (U and D) chains to R chains in the umohoite and iriginite anion topologies is 1:1 and 1:3, respectively. In the umohoite sheet, all rhombs of the R chains are populated with Mo^{6+} cations, whereas in the iriginite sheet, only two-thirds of the rhombs contain Mo^{6+}, with the remaining third empty. The result is U:Mo ratios of 1:1 and 1:2 in the umohoite and iriginite sheets, respectively. The iriginite anion-topology may be derived from that of umohoite by expansion of the umohoite anion-topology along a vector within the sheet that is perpendicular to the arrowhead chain, together with the insertion of two additional **R** chains between adjacent arrowhead chains. This transformation mechanism requires addition of Mo^{6+} to populate the rhombs of the **R** chains. Another mechanism for obtaining the iriginite anion-topology from that of umohoite is the replacement of every second URD sequence in the umohoite anion-topology with an **R** chain. This mechanism requires the removal of the U^{6+} that populated the **D** and **U** arrowhead chains. Krivovichev and Burns (2000a,b) have suggested that this may appear to be the most likely mechanism of the umohoite-to-iriginite transformation (see Fig. 5.4).

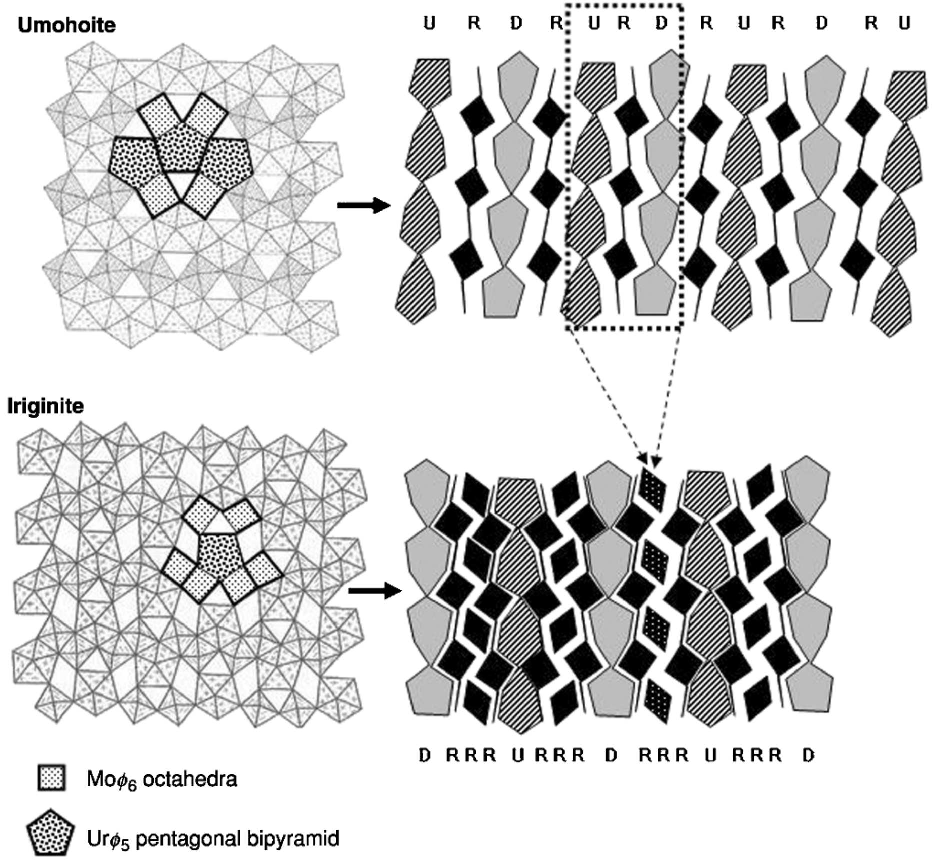

Fig. 5.4 *Diagram showing a possible mechanism for the umohoite to iriginite transformation* (*adapted from Krivovichev and Burns*, 2000a,b). *The iriginite structure can be obtained from umohoite through the replacement of every second URD sequence in the unmohoite anion topology with an R chain. This mechanism requires removal of the* U^{6+} *that occupied the D and U arrowhead chains.*

Mourite {$U^{4+}Mo^{6+}{}_5O_{12}(OH)_{10}$}, is a rare U^{4+} mineral containing molybdenum that is observed in oxidized zones in association with umohoite occurring as dark violet crusts and scaly aggregates in the Kyzylsai uranium deposit in Kazakhstan associated with umohoite. Krivovichev and Burns (2002a–c, 2003a) have described several synthetic uranyl molybdates, including Rb, Cs, Ag, and Tl species, respectively.

(n) Uranyl tungstates

Only one natural uranium tungstate is known, uranotungstite {$(Fe^{2+},Ba,Pb)(UO_2)_2WO_4(OH)_4(H_2O)_{12}$}; however, there are a wealth of synthetic U(IV) and U(VI) tungstates that have been reported in the literature. The phase UO_2WO_4 is isostructural with UO_2MoO_4, suggesting that the W^{6+} cations are tetrahedrally coordinated by O atoms. Given the structural similarities of Mo(VI) and W(VI), it might be expected that a variety of U(VI)–W(VI) phases should form. The phases $UO_2W_3O_{10}$ and $Na_2UO_2W_2O_8$, has been described but their structures are unknown. U(IV) tungsten bronzes have received considerable attention. The structures consist of ReO_3-type slabs of corner-sharing $W^{6+}O_6$ octahedra. A number of lithium uranyl tungstates ion conductors, such as $Li_2(UO_2)(WO_4)_2$ and $Li_2(UO_2)_4(WO_4)_4O$, have been prepared by high-temperature solid state reactions (Obbade *et al.*, 2004).

(o) Uranium association with clay minerals and zeolites

Chisholm-Brause *et al.* (2001) have identified four distinct uranyl complexes on montmorillonite that co-exist under certain conditions. Inner sphere and exchange-site complexes persist over a range of solution conditions. The uranyl ion sorbs onto montmorillonite at low pH *via* ion exchange, leaving the inner-sphere uranyl aquo-ion structure intact (Dent *et al.*, 1992; Sylwester *et al.*, 2000). At near neutral pH and in the presence of a competing cation, inner-sphere complexation with the surface predominates. Adsorption of the uranyl onto silica and γ-alumina surfaces appears to occur *via* an inner-sphere, bidentate complexation with the surface, with the formation of polynuclear surface complexes occurring at near-neutral pH (Sylwester *et al.*, 2000). Pabalan *et al.* (1993) have performed laboratory tests on the sorptive properties of zeolitic materials for uranium; the sorption is strongly dependent on pH. At near neutral pH U(VI) was strongly sorbed but under conditions where carbonate- and ternary hydroxyl-carbonate-complexes are present the sorption decreased substantially. Della Ventura *et al.* (2002) have discovered a new lanthanide borosilicate minerals of the hellandite group where uranium appears to be incorporated into a borosilicate cage structure. The phase, called ciprianiite {$Ca_4[(Th,U)(REE)]Al_2(Si_4B_4O_{22})(OH,F)_2]$}, formed with a syenitic ejectum[21] collected close at

---

[21] Literally, the violent volcanic explosion of mainly alkali feldspar (syenite) intrusive rock.

Tre Croci within a pyroclastic formation belonging to the Vico volcanic complex (Latium, Italy). Uvarova *et al.* (2004) reported another U^{4+} bearing silicate, arapovite $\{U(Ca,Na)_2(K_{1-x}\square_x)Si_8O_{20}\}$ from the Dara-i-Pioz moraine, Tien-Shan Mountains, Tajikistan.

The thorium and uranium uptake from their aqueous solutions by pristine and NaCl-pretreated zeolite-bearing volcanoclastic rock samples from Metaxades (Thrace, Greece) has been studied using a batch-type method (Misaelides *et al.*, 1995). The concentration of the solutions varied between 50 mg L^{-1} and 20 g L^{-1}. The NaCl pretreatment of the materials improved the thorium, but not the uranium, uptake. The absolute thorium uptake by the pretreated material, determined using neutron activation and X-ray fluorescence techniques, reached 12.41 mg g^{-1}, whereas the uranium uptake by the raw material was 8.70 mg g^{-1}. The distribution coefficients (K_d) indicated that the relative thorium and uranium uptake is higher for initial concentrations below 250 mg L^{-1}. The zeolitic materials were very stable despite the initial low pH of the solutions used; however, the pH increased significantly with time due to the simultaneous hydrogen-ion uptake. The thorium and uranium uptake is a complex function of the aqueous chemistry of the elements, the nature of the constituent minerals, and the properties of the zeolitic rock specimens. The various metal species are bound through different sorption processes such as ion-exchange, adsorption, and surface precipitation. Microporous minerals (zeolites, phyllosilicates) are mainly responsible for the large sorption capacity of the rock samples studied.

5.4 ORE PROCESSING AND SEPARATION

Because of the complexity of many uranium ores and the usual low concentrations of uranium present, the economic recovery of uranium often poses a difficult problem for the chemist. Physical concentration methods (flotation, gravitational, electromagnetic, etc.) have met with only limited success for uranium. The chemical methods used for the recovery of uranium from ores thus have to be designed to treat large ore volumes economically. Because of this and because uranium is a very electropositive metal, most direct pyrochemical methods are not applicable and processes usually involve modern aqueous extractive metallurgy. In this section the more important aspects of the extractive metallurgy of uranium will be described with emphasis on the chemical principles involved.

Uranium ores vary in chemical complexity from the relatively simple pitchblendes, which are accompanied by perhaps 10 other minerals, to exceedingly complex and refractory uranium-bearing titanites, niobates, and tantalates containing rare earths and many other metals. Included are uranium minerals accompanied by major admixtures of ill-defined organic compounds. Some pitchblende ores may have as many as 40 elements present from which uranium must be separated. Many uranium deposits are variable in composition, resulting in an almost daily variation in the composition of the starting materials. Such variations are minimized by stockpiling methods. Nevertheless there have been many *ad hoc* procedures elaborated to meet special chemical situations. Most such highly specialized methods will have little interest for this discussion. The general features common to most procedures will, however, be pertinent. All methods that have been commonly used comprise the following steps: (1) pre-concentration of the ore; (2) a leaching operation to extract the uranium into an aqueous phase – this step frequently being preceded by roasting or calcination to improve the extraction; and (3) recovery of the uranium from the pregnant leach liquors by ion exchange, solvent extraction, or direct precipitation, and in the case of ion-exchange or solvent extraction products by a final precipitation. Special methods may be used for recovery of by-product uranium. The product of these operations is a high-grade concentrate, which is usually further purified at a site other than the uranium mill.

The extractive metallurgy of uranium has been discussed in detail in various books (Vance and Warner, 1951; Clegg and Foley, 1958; Harrington and Ruehle, 1959; Chervet, 1960; Bellamy and Hill, 1963; Gittus, 1963; Galkin and Sudarikov, 1966; Merritt, 1971) and in collections of papers (United Nations, 1955, 1958, 1964; IAEA, 1966, 1970). There is also a bibliography on feed materials (Young, 1955). The most comprehensive collection of data is the multi-volume supplement to the *Gmelin Handbook of Inorganic Chemistry* (Gmelin, 1975–1996), more particularly its volume (A3) on Technology and Uses (Gmelin, 1981a). Many other references can be found in these sources.

5.4.1 Pre-concentration

Most uranium ores contain only small amounts of uranium, and because leaching is a relatively expensive operation, much effort has been expended to reduce the magnitude of the leaching operation by pre-concentration of the ore. Physical concentration methods (gravitational, electrostatic, flotation) and various sorting methods have been either used or proposed for upgrading of uranium ores. Unfortunately such beneficiation methods have not achieved great success, only a few of the uranium ores processed being amenable to physical beneficiation processes. Only in a few cases can appreciable concentration of uranium be achieved without excessive loss to tailings.

Uranium minerals as well as other minerals, with which they are closely associated, are denser than many gangue materials and successful gravity separation methods are sometimes possible. Such gravity separations are complicated by the fact that uranium minerals tend to concentrate in the fines upon crushing or grinding of some ores. This property has been used to some advantage in that a certain degree of mechanical concentration can be achieved by a gentle grinding followed by screening. Electrostatic methods generally give low recoveries or low concentration factors. Magnetic separation methods have generally been used to remove gangue materials such as magnetite, ilmenite, garnet, etc. Flotation methods have received considerable laboratory attention although they do not appear to have been widely applied. Flotation of undesirable gangue materials such as sulfides has met with some success, but no flotation agents have been developed for uranium minerals that give concentration factors approaching those obtained in the processing of sulfide minerals. Flotation has met with some success in splitting carbonate-containing ores into a carbonate and a non-carbonate fraction so that the former fraction can be leached by the carbonate method and the other with sulfuric acid. Both manual and mechanical sorting methods have been applied to the upgrading of uranium ores. In this procedure individual lumps of ore are sorted either by hand or by mechanical devices usually on the basis of radiation readings for the individual lumps. Merritt (1971) reviewed various mechanical upgrading techniques in some detail.

5.4.2 Roasting or calcination

It is frequently desirable to subject ores to high-temperature calcination prior to leaching. Several functions can be performed by such roasting operations. An oxidizing roast can remove carbonaceous material and put the uranium in soluble form. It can oxidize sulfur compounds to avoid subsequent polythionate and sulfur poisoning of ion-exchange resins. It removes other reductants, which might consume oxidant during the leaching step. Reducing roasts can convert uranium to the reduced state and prevent dissolution of uranium during by-product recovery.

Roasting also improves the characteristics of many ores. Many of them contain clays (particularly of the montmorillonite class), which cause thixotropic slurries and create problems in leaching, settling, and filtering. Dehydration of these clays alters their physical properties and decreases these problems.

Roasting with sodium chloride is commonly used with vanadium-containing ores to convert the vanadium to a soluble form. Sodium vanadate is formed, which is believed to form soluble uranyl vanadates (Merritt, 1971). Salt roasting has also been used to convert silver to silver chloride for easier separation from soluble components.

5.4.3 Leaching or extraction from ores

The object of this procedure is to extract the uranium present in the ore into solution, usually aqueous, from which the recovery and purification of the uranium from accompanying metals can be carried out. The leaching operation is usually the first of the chemical manipulations to which the ore is subjected, and all present chemical processing methods for any type of ore involve digestion of the ore with either acid or alkaline reagents. The acid reagent may be generated *in situ* by bacterial or high-pressure oxidation of sulfur, sulfides and Fe(II) in the ore to sulfuric acid and ferric [Fe(III)] species. The choice of a reagent for a particular case will be determined primarily by the chemical nature of the uranium compounds present in the ore and the gangue materials that accompany them.

The extraction of uranium from the majority of the ores is generally more complete by acid leaching than with alternative leaching procedures and is therefore used in most mills. While other acids can be used, sulfuric acid is employed because of its lower price, except when hydrochloric acid is available as a by-product of salt roasting. As a general principle only uranium (VI) minerals are readily dissolved in sulfuric acid. For uranium minerals, such as uraninite, pitchblende, and others, containing uranium in lower oxidation states, oxidizing conditions must be provided to ensure complete extraction. Oxidizing conditions are provided by agents such as manganese dioxide, chlorate ion, ferric ion, chlorine, or molecular oxygen. Manganese dioxide and chlorate ion are most commonly used and iron must be present in solution as a catalyst in order for either of them to be effective.

Manganese dioxide to the extent of perhaps 5 kg per ton (but typically about one-half of this in U.S. practice) or up to 1.5 kg $NaClO_3$ per ton of ore are usually adequate for all but the very refractory ores. Free ferric-ion concentrations larger than 0.5 g L^{-1} generally give adequate dissolution rates. Sufficient iron is normally provided by the ores themselves and by the ore-grinding process. Typical dissolution reactions are

$$UO_2 + 2Fe^{3+} \rightarrow UO_2^{2+} + 2Fe^{2+}$$

$$2Fe^{2+} + MnO_2 + 4H^+ \rightarrow 2Fe^{3+} + Mn^{2+} + 2H_2O$$

$$6Fe^{2+} + ClO_3^- + 6H^+ \rightarrow 6Fe^{3+} + Cl^- + 3H_2O$$

To avoid excessive consumption of oxidant this is in general not added to the acidified ore until the reaction with free iron and sulfides is practically complete. Manganese can be recovered at later stages as manganese(II) hydroxide followed by ignition in air at 300°C to the dioxide. When only a small fraction of the uranium is in reduced form, agitation with air is often sufficient to maintain oxidation by ferric ion. Various other oxidants are effective, including chlorine, permanganate, bromine, etc., but cost or difficulty of handling (corrosiveness, etc.), have relegated their use to very special situations. Proper addition of oxidizing agent can be controlled by an empiric potentiometric measurement of the redox potential. If the potential between a platinum and a calomel electrode inserted into the digesting ore mixture is adequately controlled, the iron will be present principally as Fe^{3+} and suitable oxidizing conditions will have been imposed (Woody and George, 1955).

The most common form in which acid leaching is applied is in the form of aqueous leaching with agitation. The sulfuric acid concentration is adjusted so that it close to pH 1.5 at the end of the leaching period; the period of extraction is generally 4–48 h, in U.S. practice typically 4–24 h. Elevated temperatures and higher acid concentrations increase the rate of extraction but are often uneconomic and result in higher reagent consumption, increased corrosion, and increased dissolution of non-uranium minerals. Counter-current leaching in several stages is sometimes used but is less common than single stage processes. Recycle circuits have also been devised to use the acid leachant more efficiently. A less common procedure is acid pugging, in which a small amount of dry, ground ore is mixed with a more concentrated acid to form a plastic mass, which is allowed to cure and then leached with water. Percolation leaching, in which solution percolates slowly through an ore bed, is well-suited to ores in which the uranium minerals occur as coatings on sand grains, particularly when the ore is of low grade. A variation of percolation leaching that has important application to low-grade ores is heap leaching, in which 5–10 m deep piles of ore of about 100 m length are leached by slow percolation of an acid solution that is collected in the pile drainage. *In situ* leaching is another method that has been applied to certain ore bodies with low permeability of the rock underlying the deposit and adequate porosity of the ore body itself. In this procedure, wells are drilled into the ore body and leachant is pumped into some of these while the enriched solutions are pumped from other wells.

Two acid leaching methods require no reagent addition in some ores containing sulfides or sulfur. These methods are pressure leaching, in which air is the oxidant at elevated temperatures ($\sim$150°C) and pressures, and bacterial leaching, where air is also the oxidant but at temperatures near ambient. In both cases uranium dissolution is brought about by the oxidation of iron and sulfur compounds to Fe^{3+} and sulfuric acid. Typical reactions in pressure leaching are

$$\begin{aligned}&4FeS_2 + 15O_2 + 2H_2O \rightarrow 2Fe_2(SO_4)_3 + 2H_2SO_4\\&UO_2 + Fe_2(SO_4)_3 \rightarrow UO_2SO_4 + 2FeSO_4\\&4FeSO_4 + 2H_2SO_4 + O_2 \rightarrow 2Fe_2(SO_4)_3 + 2H_2O\end{aligned}$$

Similar overall reactions occur in bacterial leaching through the action of bacteria, such as *Thiobacillus ferrooxidans* and others, on ferrous ion, sulfur, and sulfides. Although there are several reported advantages of high-pressure leaching, such as improved extraction and shorter extraction times, particularly with refractory ores, there is also larger corrosion and higher maintenance costs and the method has received little actual use. Bacterial leaching appears to be particularly attractive as a low-cost recovery method for very low-grade ores when used with heap or *in situ* leaching.

While acid leaching is excellent for many ores, and is essential for primary refractory ores such as euxenite, davidite, and brannerite, it is subject to certain limitations. Most uranium minerals are soluble in dilute sulfuric acid with an oxidant present, but many ores contain other minerals such as calcite, dolomite, and magnesite, which consume sufficient amounts of acid to make acid leaching uneconomic. In such cases, carbonate solutions are used to extract uranium.

Carbonate leaching is usually carried out with sodium carbonate. The utility of carbonate solutions arises from the high stability of the uranyl(VI) tricarbonate ion, $UO_2(CO_3)_3^{4-}$, in aqueous solution at low hydroxide-ion concentration. Uranium(VI) is thus soluble in carbonate solution, unlike the vast majority of other metal ions, which form insoluble carbonates or hydroxides in these solutions. The sodium carbonate leaching is thus inherently more selective than the sulfuric acid procedure. In general, compounds of uranium(VI) are readily soluble in carbonate leach solutions although silicates dissolve, albeit with some difficulty. Minerals containing uranium in its lower oxidation states are insoluble in carbonate solutions, and oxidants are required. Under oxidizing conditions, simple uranium oxides and some other uranium(IV) minerals such as coffinite can be leached, particularly at elevated temperature.

In addition to the advantage of low reagent consumption in carbonate-containing ores, carbonate leaching is relatively (but not completely) specific for uranium and carbonate solutions, which are moderately non-corrosive. Disadvantages include lower uranium extraction than by acid leaching and that the method is not suitable for ores having high gypsum or sulfide content. Important refractory minerals such as euxenite, brannerite, and davidite are not attacked significantly without a prior fusion step. Since few ore components other than uranium minerals are attacked to any appreciable extent by carbonate solutions, any uranium imbedded in gangue will escape leaching. A carbonate leach thus requires sufficiently fine grinding to liberate the uranium. Economics dictate that the reagents must be recovered and recycled in the carbonate leach process.

Oxygen (often under pressure) is the commonly used oxidant in carbonate leaching and the dissolution of simple uranium oxide follows the reactions (Merritt, 1971).

$$2UO_2 + O_2 \rightarrow 2UO_3$$

$$UO_3 + H_2O + 3CO_3^{2-} \rightarrow UO_2(CO_3)_3^{4-} + 2OH^-$$

$$OH^- + HCO_3^- \rightarrow CO_3^{2-} + H_2O$$

As shown in the equations above, bicarbonate is used to prevent increase in the hydroxide concentration, which would result in precipitation of uranates or polyuranates by the reaction

$$2UO_2(CO_3)_3^{4-} + 6OH^- + 2Na^+ \rightarrow Na_2U_2O_7 + 6CO_3^{2-} + 3H_2O$$

The detailed dissolution mechanisms are more complex than represented here and several possible alternatives have been proposed (Clegg and Foley, 1958; Wilkinson, 1962; Merritt, 1971). Although air is the most commonly used oxidant in carbonate leaching, other oxidants have been used. Potassium permanganate was commonly used in the past but was expensive and replaced by pressurized leaching at 95–120°C in air. This was followed by the use of cupric–ammonia complexes, a catalyst for air oxidation, but current practice is toward simply using air at atmospheric pressure and longer dissolution times at about 75–80°C in Pachuca-type (air-agitated) tanks (Merritt, 1971). Pure oxygen has been used (Woody and George, 1955) in place of air with some advantages. Other oxidants that have been considered are NaOCl, H_2O_2, and $K_2S_2O_8$. Various catalysts such as $MgCl_2$, Ag_2SO_4, $K_3Fe(CN)_6$, copper–cyanide complexes, and copper–, nickel–, and cobalt–ammonia complexes have also been studied.

Although sodium carbonate is the only reagent used commercially in alkaline leaching, ammonium carbonate has been extensively tested in the laboratory and pilot plant (Merritt, 1971). Since the concentrations of sodium carbonate and bicarbonate used are typically 0.5–1.0 M, the recovery of reagents is necessary. The specificity of carbonate leaching for uranium is such that the uranium can usually be recovered from the leach solution by precipitation as sodium polyuranates ('diuranate') with sodium hydroxide. The filtrate is then treated with carbon dioxide to regenerate the desired carbonate/bicarbonate ratio.

While the amounts of carbonate, bicarbonate, and oxygen consumed during leaching are usually very small, side reactions may occur with other constituents of the ores, which consume substantial amounts of carbonate. Particularly important parasitic reactions are due to sulfide minerals and gypsum and, at higher temperatures and pressures, silica and alumina:

$$2FeS_2 + 15/2O_2 + 8CO_3^{2-} + 7H_2O \rightarrow 2Fe(OH)_3 + 4SO_4^{2-} + 8HCO_3^-$$

$$CaSO_4 + CO_3^{2-} \rightarrow CaCO_3 + SO_4^{2-}$$

$$SiO_2 + H_2O + 2CO_3^{2-} \rightarrow SiO_3^{2-} + 2HCO_3^-$$

$$Al_2O_3 \cdot 3H_2O + 2CO_3^{2-} \rightarrow 2AlO_2^- + 2HCO_3^- + 2H_2O$$

Flotation may be used to reduce the initial sulfide content to tolerable limits.

Organic materials in some ores cause difficulties in the carbonate leach process and various schemes for handling this problem are reviewed by Merritt (1971). A simplified flow sheet for carbonate leaching is shown in Fig. 5.5.

Clarification is the separation of ore slimes from the aqueous uranium extract and constitutes the final step in ore extraction of uranium. It is a necessary step except when the resin-in-pulp ion-exchange process is used, in which case only partial clarification is necessary, and when *in situ*, heap, or percolation leaching has been used, since the ore itself acts as an effective filter medium in these leaching techniques and clear solutions are obtained. Solution clarification has in the past been one of the most difficult problems in uranium recovery, but flocculants have been developed (Clegg and Foley, 1958) to improve settling of clays and other slimy ore constituents. These have greatly improved liquid–solid separation technology and most ores can now be handled satisfactorily in liquid–solid separation equipment with the proper choice and use of flocculants.

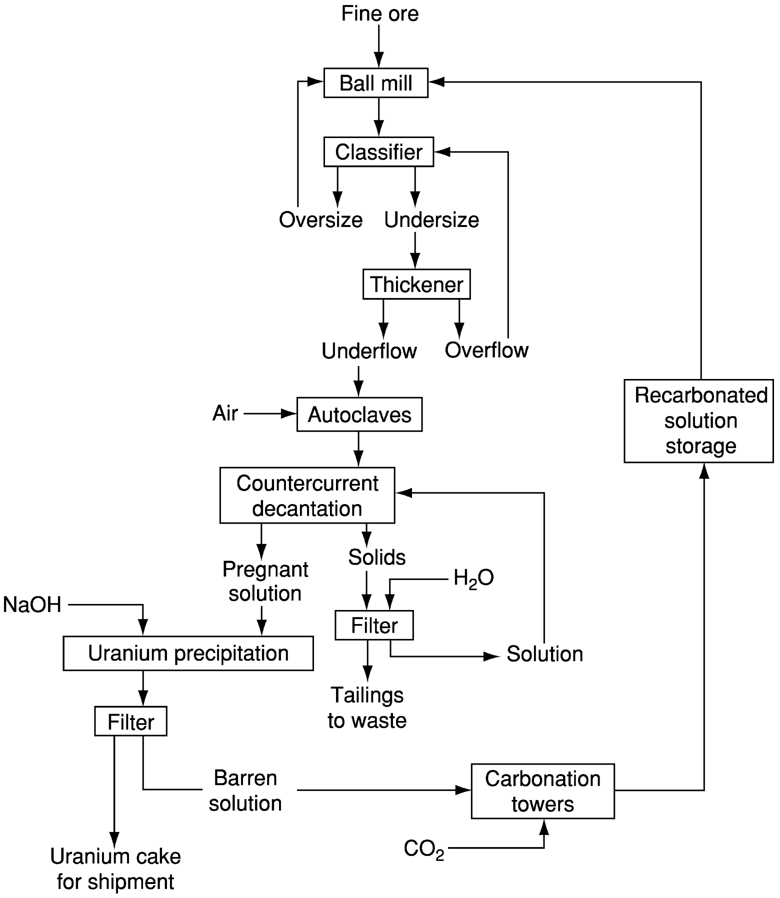

Fig. 5.5 *Flow sheet of raw ore leach for unoxidized or primary uranium of Eldorado Mining and Refining Ltd, Beaverlodge, Saskatchewan* (*Stephens and McDonald*, 1956).

Flocculants used include polyacrylamides, guar gums, and animal glues. For the resin-in-pulp process, only the coarser ore particles (325 mesh) are removed and slime contents of 5% to as high as 20% solids can be handled depending on exact process design. Clegg and Foley (1958) and Merritt (1971) review clarification in detail.

5.4.4 Recovery of uranium from leach solutions

The recovery of uranium from leach solutions can be achieved by a variety of methods including ion exchange, solvent extraction, and chemical precipitation. Each of the various procedures listed above can be applied to acid or alkaline leach liquors, although in general they will not be equally applicable. Although various precipitation methods were extensively used in the past, they were generally cumbersome and complex if significant uranium purification was to be achieved. Currently operating uranium mills, with the exception of some that employ carbonate leaching, all use ion exchange or solvent extraction, or both, to purify and concentrate the uranium before a final product precipitation. Because of the selectivity of carbonate leaching, precipitation from carbonate leach solutions produces a fairly pure uranium concentrate, but for acid leach solutions, ion exchange or solvent extraction is always employed.

(a) Ion exchange

The recovery of uranium by ion exchange is of great importance. Uranium(VI) is selectively absorbed from both sulfate and carbonate leach solutions as anionic complexes using anion-exchange resins. The loaded resin is rinsed, and the uranium eluted with a sodium chloride or an acid solution. The uranium is then precipitated from the eluate and recovered as a very pure uranium concentrate. This process can be carried out with either stationary columns of ion-exchange resin through which clarified leach liquors are passed; alternatively the resin may be moved through the leach liquor in agitated baskets. This resin-in-pulp process does not require complete clarification of the leach liquor.

The degree of purification of the uranium by these ion-exchange processes is related to the selectivity of the anion-exchange resins for the anionic uranyl sulfate or carbonate complexes relative to that of impurity species. Cationic impurities are not absorbed and many anionic species are absorbed less strongly than are the uranyl complexes and are displaced by them. The impurities can be left in the ion exchangers during uranium elution, but often they are so strongly absorbed as to act as exchanger poisons that require elaborate removal steps.

The uranyl species absorbed by the exchangers from carbonate solution appears to be exclusively the $UO_2(CO_3)_3^{4-}$ complex, but from sulfate solutions more than one species is absorbed (Ryan, 1962). Although it has been reported (OECD-NEA, 1982) that below pH 2 the only uranyl sulfate complex in the resin is $UO_2(SO_4)_3^{4-}$, spectral studies of the resin phase (Ryan, 1962) indicate that, although $UO_2(SO_4)_3^{4-}$ is present over at least the pH range 0.5–4.5, it is not the only uranyl species. The ratio of uranyl species in the resin phase changes with pH but is almost unaffected by change in total aqueous phase sulfate concentration at any given pH. Even if the affinity of anion-exchange resins for complex anions may be very high, high distribution coefficients do not necessarily mean that an appreciable fraction of the uranium is present as anionic species in the aqueous phase. Both weak-base or strong-base resins can be used with the sulfate system, but only the strong-base resins in the basic carbonate solutions. In practice, the resin choice is governed by several factors, including absorption and elution kinetics, resin particle size, the physical and chemical stability of the resin, the selectivity and ease of removal of resin poisons, hydraulic characteristics, and exchange capacity. Typically, resins of moderately low cross-linking and moderately large particle size are used and several resins have been marketed specifically for uranium processing.

Elution of the uranium from anion-exchange resins in either the sulfate or the carbonate processes is normally made with approximately 1 M sodium or ammonium chloride or nitrate solutions. In the sulfate process the eluent is acidified, and in the carbonate process some carbonate or bicarbonate is added to prevent hydrolysis. Special elution techniques are used for vanadium recovery when it is co-absorbed in the carbonate process (Merritt, 1971).

Although uranyl sulfate and carbonate complexes have a higher affinity for the resin than most impurity ions, they are not extremely strongly sorbed and some impurity ions are more strongly absorbed. In the acid system such ions include pentavalent vanadates, molybdenum sulfate complexes, polythionates, and in South African ores treated for gold recovery, cobalt cyanide complexes and thiocyanate. Vanadates are more strongly absorbed than uranium in the carbonate process except at high pH values. In addition, some other weakly sorbed ions may be present in sufficiently high concentration to compete for resin sites, resulting in decreased uranium loading; some of these may also alter absorption kinetics. Some of the strongly held ions and others such as silicate, titanium, thorium, hafnium, niobium, antimony, and arsenate and phosphate complexes, which polymerize or hydrolyze in the resin phase, are not readily removed during the normal elution process. They gradually build up in the resins where they act as poisons and require special removal procedures (Merritt, 1971).

Merritt (1971) and Clegg and Foley (1958) have reviewed the uranium ion-exchange processes in detail along with the various specialized problems encountered and their treatment. They have discussed specific flow sheets, processing rates, back-cycle methods for reagent conservation, and processing equipment for fixed-bed, moving-bed, basket resin-in-pulp, and continuous resin-in-pulp ion-exchange processes.

(b) Solvent extraction

Solvent extraction has a distinct advantage over ion exchange for uranium purification from leach liquors because of the ease with which it can be operated in a continuous counter-current flow process. It has a disadvantage, however, in the incomplete phase separation, due to emulsion formation, third-phase formation, etc. In addition solvent losses constitute both a monetary loss and a potential pollution problem in the disposal of spent leach liquor. Because solvent losses are related to overall solution volume, solvent extraction usually has an advantage for leach solutions with concentrations above about 1 g U per liter, and ion exchange has an advantage for low-grade solutions with concentrations appreciably less than 1 g U per liter (Merritt, 1971). Solvent extraction processes are not economically advantageous for carbonate leach solutions. Two types of alkyl phosphoric acids and secondary and tertiary alkylamines, have been used industrially for uranium extraction from sulfate leach liquors. These extraction reagents are normally used as relatively dilute solutions in an inert diluent such as kerosene. Modifiers such as long-chain alcohols and neutral phosphate esters are typically added to prevent third-phase formation to increase amine salt solubility in the diluent, and to improve phase separation.

Amine extraction from sulfate leaching is analogous to anion exchange in that anionic uranyl sulfate complexes are extracted by the alkylammonium cations. The species extracted, at least by tertiary amines, is predominantly the $UO_2(SO_4)_3^{4-}$ complex in the pH range ($1 < pH < 2$) normally used in commercial processing. The concentration of other uranyl species increases with decreasing pH (Ryan, 1962). There is considerable variation in affinity and selectivity for uranium with the structure of the amine. Typical commercially used tertiary amines give extraction coefficients of 100–140, whereas *N*-benzylheptadecylamine gives extraction coefficients as high as 8000 (Merritt, 1971). Such specialized amines, if made available at a reasonable cost, will be capable of recovering uranium from very dilute leach solutions but might require more complex stripping procedures. Amines extract other anions to varying degree and thereby decrease uranium extraction efficiency. Nitrate interference is severe and chloride interference is more severe for secondary than for tertiary amines. These factors are important for the choice of stripping agent and the recycling of solutions. Molybdenum is extracted more strongly than uranium. It builds up as a poison in the amine, finally causing serious problems by precipitating at the organic–aqueous interface, and special molybdenum stripping procedures are used to counteract this problem (Merritt, 1971). Vanadium is also extracted to some extent. Various ions are effective in stripping uranium from the solvent. Nitrate has such high affinity for the amine that it must be removed in the carbonate or hydroxide regeneration step before the next extraction cycle; however this is not necessary in solutions containing chloride, except with secondary amines having high chloride affinity. Another procedure uses ammonium sulfate with pH carefully controlled in the range 4.0–4.3, since poor stripping or poor phase separation occurs outside this range. Direct precipitation of uranium from the organic phase has been proposed (Brown *et al.*, 1958).

The alkylphosphoric acid extractants have the advantage over amines of fewer phase separation problems due to suspended solids and of having good extraction efficiency in the presence of dilute nitrate, chloride, and sulfate. On the other hand, they suffer from lower selectivity for uranium since the alkyl phosphates extract cations and many of the impurities including iron in the leach solutions. Special methods for removing or rendering these impurities non-extractable have been devised. Alkylphosphoric acid extraction has been referred to as 'liquid cation exchange'. The dialkyl phosphates appear to be dimers and four dialkyl phosphates are required to extract one uranyl ion (Baes *et al.*, 1958; Blake *et al.*, 1958). Addition of neutral phosphate esters increases the uranium extraction coefficient of alkylphosphoric acids (synergistic effect). Stripping of bis(2-ethylhexyl)phosphoric acid is normally carried out with carbonate solution, but monodecylphosphoric acid requires 10 M HCl for stripping.

In addition to the solvent extraction procedures discussed above, mixed amine–alkylphosphoric acids have also been used. Other processes include both ion-exchange and solvent-extraction steps as well as special methods for removing and in some cases recovering interfering ions such as molybdenum. Solvent extraction methods have also been studied in cases where the leach solution is not clarified, solvent-in-pulp, but solvent losses are then very high. Merritt (1971) has reviewed the commercial practice in detail and gives many further references.

(c) Chemical precipitation

Before the use of ion-exchange and solvent extraction methods for the removal and purification of uranium from leach liquors, precipitation techniques were used on clarified leach liquors. Much effort was spent during the late 1940s to develop selective precipitation processes; most of these techniques are obsolete and will not be discussed here but they are reviewed by Wilkinson (1962) and by Merritt (1971).

The product from typical acid process anion-exchange or solvent extraction processes is an acid solution of mixed nitrate or chloride and sulfate. The two principal methods of precipitation of uranium from these are neutralization with sodium hydroxide, magnesia, or ammonia, or the precipitation of the peroxide $UO_4 \cdot xH_2O$ in the pH range 2.5–4.0 with hydrogen peroxide. In the neutralization procedure a preliminary pH adjustment to 3.5–4.2 is made to precipitate and remove iron if it exceeds specifications. Phosphate, if present, is also removed in this step as iron phosphate. Uranium precipitation is then accomplished at a pH of 6.5–8.0. Since the cations used (Na^+, M^{2+}, or $NH_4{}^+$) contaminate the product by formation of insoluble polyuranates, the choice of precipitant will depend on cost, physical nature of the precipitate formed, product specifications, etc. Most U.S. plants now use ammonia, which can be removed by heating of the product, but there is also some use of magnesia. The peroxide precipitation process is more specific although the cost is somewhat higher, a higher-purity product is obtained. Ferric ions must be removed to a concentration less than 0.5 g L^{-1} in order to prevent catalytic decomposition of hydrogen peroxide in a preliminary precipitation step; alternatively the decomposition is prevented by precipitation from very cold solutions or by complexing the iron. The precipitates (‘yellow cake’) are dried, and in the case of the ammonia, precipitated material of composition approximately $(NH_4)_2U_2O_7$ (ammonium diuranate) may be heated to form U_3O_8 or UO_3, depending on temperature. The magnesium and sodium polyuranates are stable to low-temperature calcination.

Precipitation from alkaline solution is carried out with either clarified carbonate leach solution or with alkaline eluting or stripping solutions from ion exchange or solvent extraction. The three methods include addition of strong base, acidification followed by CO_2 removal and neutralization, and reduction to U(IV). The latter method is the only one capable of direct recovery of any vanadium present; the other ones do not result in complete recovery or complete separation. Sodium hydroxide does not completely precipitate uranium from carbonate solution; despite this, the filtrate is recarbonated and recycled. The product consists of sodium polyuranates. Acidification, carbon dioxide removal by boiling, and neutralization (usually with ammonia or magnesia) is preferred for the high-uranium-concentration carbonate strip solutions from solvent extraction since the volume is low and recycling of reagents is not so important. Reduction of uranyl(VI) carbonate solutions results in precipitation of hydrated U(IV) oxide. Reduction methods include hydrogen reduction under pressure in the range 100–200°C with appropriate catalyst, electrolytic reduction, and sodium amalgam reduction. Vanadium is reduced and co-precipitated with uranium. Merritt (1971) has reviewed precipitation conditions, flow sheets, and plant practice in detail.

(d) By-product uranium

In South Africa, uranium is recovered as a by-product of gold recovery by conventional methods after the recovery of gold by cyanide leaching. Uranium has also been recovered as a by-product from crude phosphoric acid by both ion exchange and solvent extraction methods. In anion exchange, U(VI) is absorbed and concentrated by absorption of uranyl phosphate complexes, but resin capacities are uneconomically low. Solvent extraction has normally involved use of alkyl pyrophosphate extraction of U(IV) (Greek *et al.*, 1957), but other schemes utilize extraction of U(VI) and synergistic combinations of phosphates. References to previous work in this field are given in a paper on this subject (Deleon and Lazarević, 1971).

(e) Refining to a high-purity product

The normal product of uranium milling operations, ‘yellow cake’ or calcined ‘yellow cake’, is not sufficiently pure to be of nuclear grade and is normally further refined to produce nuclear-grade material (IAEA, 1980). There has been some emphasis on further upgrading in the mill to produce a high-grade product by using multiple stages of solvent extraction and/or ion exchange, special stripping methods, more selective precipitation methods, or combinations of these (see Merritt, 1971 for further detail). The usual refining operation has normally been carried out either by tri(*n*-butyl)phosphate (TBP) extraction from nitric acid solutions or by distillation of uranium hexafluoride, since this is the feed for isotope enrichment plants.

Solvent extraction and fluoride volatility processes are currently used for uranium refining. A schematic flow diagram of a typical TBP/kerosene extraction process is shown in Fig. 5.6; a fluoride volatility process flow sheet is shown in Fig. 5.7. The TBP extraction from nitric acid solution makes use of the very selective tendency of actinides to form nitrate- or mixed nitrate–solvent complexes, as discussed further in Chapters 23 and 24. This process replaces the earlier and more hazardous diethyl ether extraction from nitrate solution. The extraction reaction is

$$\mathrm{UO_2(NO_3)_x^{2-x} + (2-\mathit{x})NO_3^- + 2TBP \rightarrow UO_2(NO_3)_2(TBP)_2}$$

where $x = 0\text{–}2$. Thorium is the only normally encountered impurity element having an appreciable distribution coefficient into a kerosene-TBP phase from nitric acid solution, but its distribution is sufficiently low that it can be transferred to the aqueous phase by high uranium loading of the organic phase.

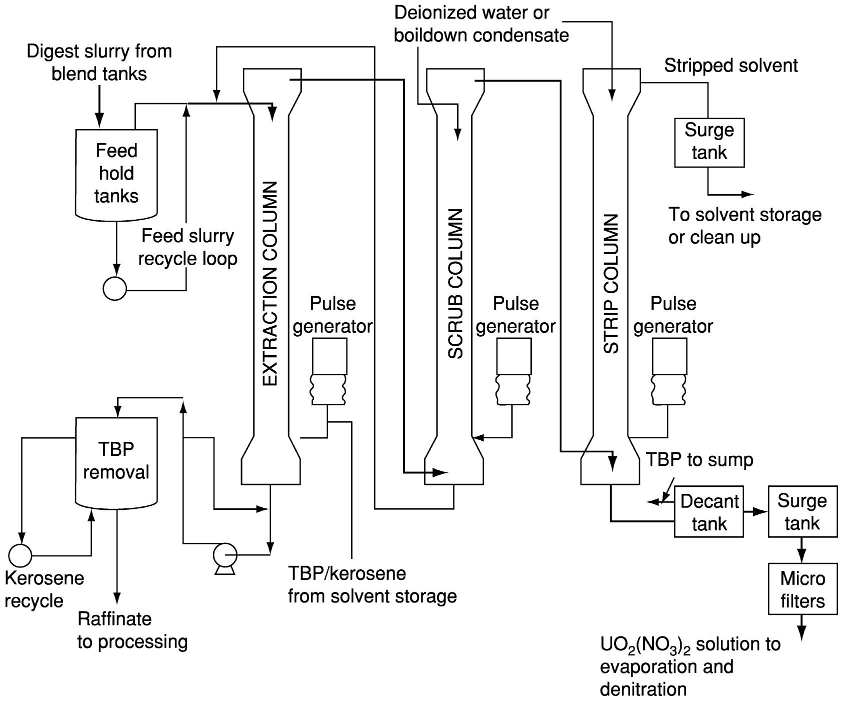

Fig. 5.6 *Schematic flow diagram: TBP/kerosene extraction system at the Fernald refinery* (*Harrington and Ruehle*, 1959).

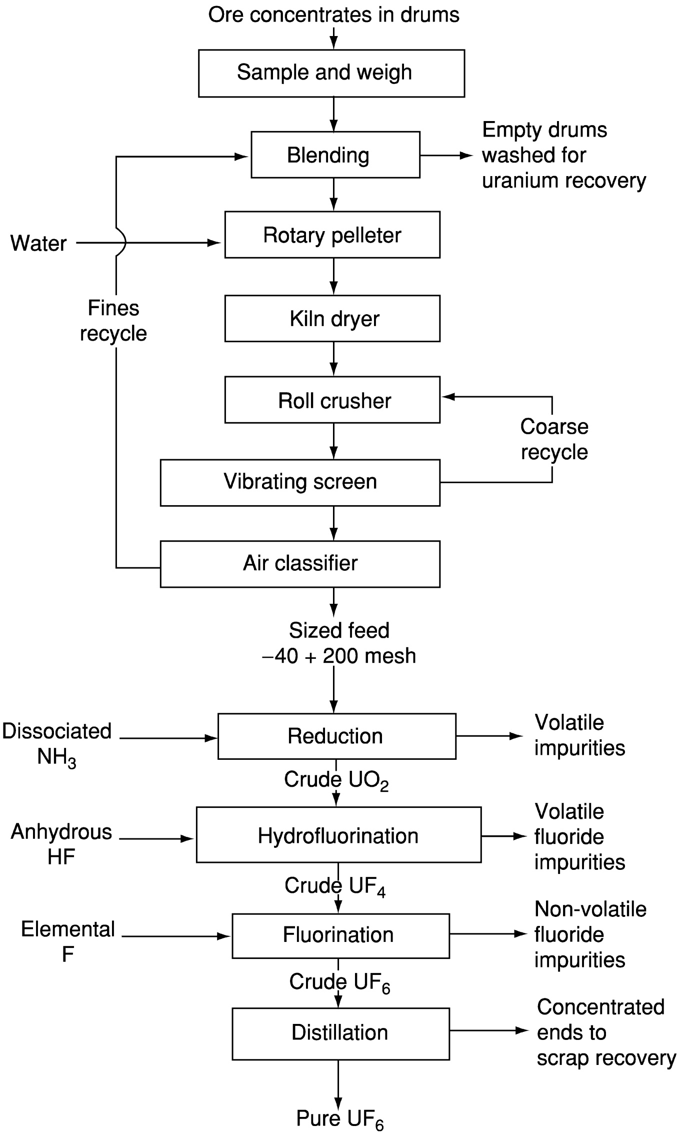

Fig. 5.7 *Overall process flow diagram for fluoride volatility process for the refining of ore concentrates* (*Ruch* et al., 1959).

The purified uranium is stripped from the organic phase with water, converted to UO_3, reduced with hydrogen to UO_2, and converted to UF_4 with hydrogen fluoride at elevated temperatures. The UF_4 can either be reduced to uranium metal for natural uranium reactors or be fluorinated to UF_6 for isotopic enrichment for production of other types of reactor fuel. The fluoride volatility process makes use of reduction to UO_2 followed by direct fluorination, using the cheaper hydrogen fluoride to make UF_4 followed by F_2 to prepare UF_6. The UF_6 is fractionally distilled to produce a high-purity UF_6 for isotopic enrichment. The chemistry and operating conditions of the TBP refining process, the conversion to UO_3, UO_2, and finally to UF_4 are reviewed in detail in the book edited by Harrington and Ruehle (1959). Ruch *et al.* (1959) have described the refining of ore concentrates by uranium hexafluoride distillation.

Hyman *et al.* (1955) have converted uranium ore concentrates to UF_6 by means of liquid-phase fluorination using bromine trifluoride, BrF_3 (b.p. 126°C). While not applicable to raw ore, the procedure may be readily applied to concentrates. Results of experiments along these lines are summarized in Table 5.4. Since fluorine in the form of BrF_3 is rather expensive, it is worthwhile to introduce as much fluorine as possible via the inexpensive reagent hydrogen fluoride (which cannot, of course, be used to convert lower uranium fluorides to uranium hexafluoride), and then to complete the fluorination process with bromine trifluoride. This reduction of fluorine consumption may be readily accomplished by a preliminary hydrofluorination at 600°C. This treatment fluorinates silica and other gangue materials present in the ore concentrate and converts uranium(IV) to UF_4. Thus, two-thirds of the fluorine in the final UF_6 product is introduced by the relatively inexpensive hydrogen fluoride rather than by bromine trifluoride. Since uranium hexafluoride is used for the isotope separation of uranium, chlorination procedures have not received nearly as extensive investigation, because of the serious corrosion problems created by the use of chlorine at elevated temperatures.

Table 5.4 *Fluorination of various ore concentrates with BrF_3 (Hyman* et al., 1955).

Ore concentrate			
Source	*U content* (%)	*Uranium retained by residue*[a,b] (%)	*F_2 consumption*[a,c] (cm^3 *F_2(STP) per* g U)
rand concentrate	68.1	0.16, 0.07	383, 419
rand concentrate	68.1	0.73, 0.10[d]	133, 138[d]
intermediate plant concentrate	23.3	1.45, 0.81	805, 767
intermediate plant concentrate	32.6	0.55, 1.00	552, 735

[a] Duplicate runs are given for each sample and treatment.

[b] (Grams U in residue/grams U in initial concentrate) × 100.

[c] To form UF_6 from 1 g U as metal requires 282.5 cm^3 F_2; to form UF_6 from 1 g U as UF_4 requires 94.2 cm^3 F_2.

[d] After hydrofluorination.

5.5 PROPERTIES OF FREE ATOMS AND IONS

Uranium, being one of the elements with the largest atomic number, has a very complex electronic structure. This is manifested in its spectral properties as they appear in the X-ray, UV/visible and fluorescence spectra. Details of the electronic energy levels deduced experimentally and from quantum chemical calculations are discussed in detail in Chapter 16 and in the following sections where the properties of compounds and complexes are described. The focus in Section 5.9 is on the interpretation of solid state spectra using the crystal field model and in Section 5.10 on solution spectra, including fluorescence spectroscopy of uranyl(VI) species.

5.6 URANIUM METAL

Uranium metal was used in earlier reactor systems but is now largely replaced in commercial reactors by ceramic uranium dioxide. Large-scale production of uranium metal requires elevated temperature where the high reactivity of uranium with most common refractory materials and metals makes the selection of reaction vessels a difficult problem. Finely divided uranium reacts even at room temperature with all the components of the atmosphere except the noble gases. However, contrary to the situation with titanium and zirconium, the introduction of small amounts of oxygen or nitrogen does not have an adverse effect on the mechanical properties of the metal. There are three different phases of metallic uranium below the melting point, α-, β-, and γ-uranium, each with its specific structure and physical properties. A detailed discussion of the physical properties is given in Chapter 21 on actinide metals and a short description on uranium metal and alloys in the following section.

5.6.1 Preparation of uranium metal

The element uranium is strongly electropositive, resembling aluminum and magnesium in this respect; consequently uranium metal cannot be prepared by reduction with hydrogen. Uranium metal has been prepared in a number of ways: reduction of uranium oxide with strongly electropositive elements, such as calcium, electro-deposition from molten-salt baths, thermal decomposition, decomposition of uranium halides (van Arkel de Boer ‘hot wire’ method), and reduction of uranium halides (UCl_3, UCl_4, UF_4) with electropositive metals (Li, Na, Mg, Ca, Ba). Only the last method is of current importance. For details, the reader is referred to two comprehensive surveys (Katz and Rabinowitch, 1951; Warner, 1953) and of older work to a review by Wilkinson (1962) and to the *Gmelin Handbook of Inorganic Chemistry* (1981a).

Both uranium tetrafluoride and tetrachloride are reducible with calcium and magnesium, while uranium dioxide can be reduced with calcium and probably magnesium. Finely divided uranium is pyrophoric and a massive metal product is therefore desired; this can be achieved by ensuring that the entire reaction mixture is fluid for a sufficiently long time for uranium metal to collect; this requires a slag with a moderately low melting point. Calcium oxide and magnesium oxide slags have melting points well above 2500°C, and are therefore less useful than calcium fluoride and magnesium fluoride, with melting points 1423°C and 1261°C, respectively. Uranium tetrachloride is very hygroscopic, and subject to oxidation in air and therefore the much more stable uranium tetrafluoride is preferred. Magnesium is the reagent of choice for reduction, since it is available in large quantities with a high degree of purity and can also be handled in air without special precautions. Details of a process based on these considerations are described by Wilhelm (1956) and in the books by Warner (1953) and by Harrington and Ruehle (1959).

For small-scale production of ^{233}U or ^{235}U in metallic state the batch size is limited by their critical mass of these isotopes and calcium is the preferred reductant. Bertino and Kirchner (1945), have described the special procedures for ^{233}U, and Patton *et al.* (1963) and Baker *et al.* (1946) those for ^{235}U.

Uranium ore concentrates are first purified by solvent extraction with TBP in kerosene as the immiscible solvent in the manner described in Section 5.4.4e. The purified uranyl nitrate is then decomposed thermally to UO_3. The trioxide is reduced with hydrogen to the dioxide, which in turn is converted to uranium tetrafluoride, 'green salt', by high-temperature hydrofluorination. The tetrafluoride is then reduced to metallic uranium with magnesium. A flow sheet of the production of uranium from ore concentrates is given in Fig. 5.8.

The temperature reached during the reduction reaction exceeds 1300°C where magnesium metal has a very high vapor pressure; hence, the reaction must be carried out in a sealed container (bomb). Such bombs are made in various sizes from standard seamless pipes. Their lengths range from 91.4 to 114.3 cm (36 to 45 in.), their diameters up to 33 cm (13 in.).

Uranium prepared by the metallothermic processes described above is of sufficient purity for most purposes. However, it may be further purified by molten-salt electrolysis (Slain, 1950; Noland and Marzano, 1953; Niedrach and Glamm, 1954; Blumenthal and Noland, 1956) using alkali or alkaline-earth chloride as electrolytes. UF_4, UCl_4, or UCl_3 are dissolved in these electrolytes. The material to be purified is used as the anode, molybdenum, or tantalum as the cathode; a diaphragm, usually of a sintered, porous ceramic material, separates the anode and the cathode.

Other methods that have been employed in uranium purification include zone melting (Whitman *et al.*, 1955; Antill, *et al.*, 1961) and hot-wire deposition (Fine *et al.*, 1945; Prescott *et al.*, 1946). Because of the low melting point of uranium, the latter method is only of limited value.

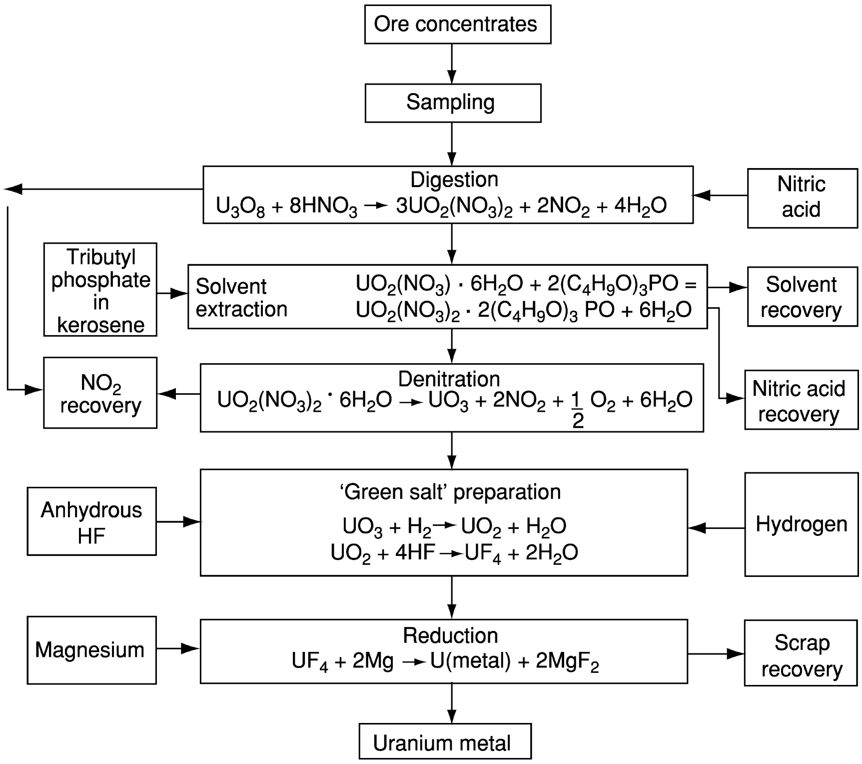

Fig. 5.8 *Flow sheet for the production of uranium metal by reduction of* UF_4 *with magnesium* (*Kelley,* 1955).

(a) Physical properties of uranium metal

(*i*) Crystal structure

Uranium metal has three crystalline phases below the melting point at (1134.8 ± 2.0)°C. The α-phase is the room-temperature modification of uranium; it is orthorhombic with space group No. 63, *Cmcm* and unit cell parameters $a = 2.854$ Å, $b = 5.87$ Å, and $c = 4.955$ Å (Barrett *et al.*, 1963; Lander and Müller, 1970) and one uranium at the site 4c in the space group.

The structure consists of corrugated sheets of atoms, parallel to the *ac*-plane and perpendicular to the *b*-axis. Within the sheets the atoms are tightly bonded, whereas the forces between atoms in adjacent sheets are relatively much weaker (Fig. 5.9). This arrangement is highly anisotropic and resembles the layer structures of arsenic, antimony, and bismuth. In the α-uranium structure, the U–U distances in the layer are (2.80 ± 0.05) Å and between adjacent layers

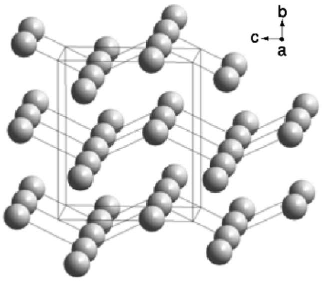

Fig. 5.9 *The structure of α-uranium from Lander and Müller* (1970). *It is a layer structure with puckered ac-layers perpendicular to the b-axis; the uranium–uranium distances in the layer are* (2.80 ± 0.05) Å *and between the layers* 3.26 Å.

3.26 Å. The physical properties of the α-phase are a reflection of its structure, e.g. the strongly anisotropic coefficient of thermal expansion. The average value of the thermal expansion coefficient over the temperature range 25–325°C is 26.5, –2.4, and 23.9 × 10^{-6} °C^{-1}, respectively, along *a*, *b*, and *c*. A chemical consequence of the unique orthorhombic structure of α-uranium is that the formation of solid solutions with metals of the common structure types is severely restricted.

The β-phase of uranium exists between 668 and 775°C; it has a complex structure with six crystallographically independent atoms in the tetragonal unit cell (Donohue and Einspahr, 1971). The space group is $P4_2/mnm$, $P4_2nm$, or $P4n2$, with unit cell parameters $a = 5.656$ Å and $b = c = 10.759$ Å. The lattice parameters were determined in an alloy with 1.4% chromium at 720°C, and in uranium powder in the temperature range where the phase is stable. The tetragonal lattice is a stacked layer structure with layers parallel to the *ab* plane of the unit cell at *c*/4, *c*/2, and 3*c*/4. Additional high-precision measurements are required to solve the structure completely (Donohue and Einspahr, 1971).

The γ-phase of uranium is formed at temperatures above 775°C; it has a body-centered cubic (bcc) structure with the cell parameter $a = 3.524$ Å; the phase stabilized at room temperature by the addition of molybdenum that forms an extensive series of solid solutions with γ-uranium.

(b) General properties

Foote (1956), Holden (1958), and Wilkinson and Murphy (1958) have described the physical metallurgy of uranium and Oetting *et al.* (1976) and Rand and Kubaschewski (1963) the thermodynamic properties of uranium metal.

A number of physical and thermal properties of elemental uranium are collected in Table 5.5. Uranium is not a refractory metal like chromium, molybdenum, or tungsten; it is among the densest of all metals, being exceeded in this respect only by some of the platinum metals and by α-Np and α-Pu.

Table 5.5 *Physical and thermal properties of uranium* (*Oetting* et al., 1976).

melting point	(1408 ± 2) K
vapor pressure	
1720–2340 K (Pattoret *et al.*, 1964)	$\log p(\text{atm}) = -(26210 \pm 270)\ T^{-1}$ $+ (5.920 \pm 0.135)$
1480–2420 K (Ackerman and Rauh, 1969)	$\log p(\text{atm}) = -(25230 \pm 370)\ T^{1}$ $+ (5.71 \pm 0.17)$
X-ray density (α-uranium) (Lander and Müller, 1970)	$19.04\ \text{g cm}^{-3}$
enthalpy of sublimation	
$\Delta_f H°(\text{U, g, 298.15 K})$	$(533 \pm 8)\ \text{kJ mol}^{-1}$[a]
enthalpy	
$H°(298.15\ \text{K}) - H°(0\ \text{K})$	$6364\ \text{J mol}^{-1}$
entropy	
$S°(298.15\ \text{K})$	$(50.20 \pm 0.20)\ \text{J K}^{-1}\ \text{mol}^{-1}$[a]
heat capacity	
$C_p^{\circ}(298.15\ \text{K})$	$(27.669 \pm 0.050)\ \text{J K}^{-1}\ \text{mol}^{-1}$
transformation points	
α to β	(942 ± 2) K
β to γ	(1049 ± 2) K
enthalpies of transformation	
$\Delta_{trs}H$ (α to β)	$2791\ \text{J mol}^{-1}$
$\Delta_{trs}H$ (β to γ)	$4757\ \text{J mol}^{-1}$
$\Delta_{fus}H$ (γ to liq)	$9142\ \text{J mol}^{-1}$
enthalpy and specific heat functions	
α-uranium (298–942 K)	$H_T - H_{298} = 26.920T - 1.251 \times 10^{-3}T^2 + 8.852 \times 10^{-6}T^3 + 0.7699 \times 10^5T^{-1}$ $8407.828\ (\text{J mol}^{-1})$ $C_p = 26.920 - 2.502 \times 10^{-3}T + 26.556 \times 10^{-6}T^2 - 0.7699 \times 10^5T^{-2}\ (\text{J K}^{-1}\ \text{mol}^{-1})$
β-uranium (942–1049 K)	$H_T - H_{298} = 42.920T - 14326.020\ (\text{J mol}^{-1})$ $C_p = 42.92(\text{J K}^{-1}\ \text{mol}^{-1})$
γ-uranium (1049–1408 K)	$H_T - H_{298} = 38.280T - 4698.690\ (\text{J mol}^{-1})$ $C_p = 38.28\ (\text{J K}^{-1}\ \text{mol}^{-1})$
uranium (liquid)	$H_T - H_{298} = 48.650T - 10137.120\ (\text{J mol}^{-1})$ $C_p = 48.65\ (\text{J K}^{-1}\ \text{mol}^{-1})$
thermal conductivity at 298.15 K (Ho *et al.*, 1972)	$27.5\ \text{J m}^{-1}\ \text{s}^{-1}\ \text{K}^{-1}$
electrical resistivity (300 K) (Arajs and Colvin, 1964)	$28 \times 10^{-8}\ \Omega\ \text{m}$

[a] CODATA key value (Cox *et al.*, 1989).

The electrical resistivity of uranium is about 16 times higher than that of copper, 1.3 times that of lead and approximates that of hafnium (Gale and Totemeier, 2003).

An important mechanical property (Table 5.6) of uranium is its plastic character, allowing easy extrusion. The mechanical properties are very sensitive

Table 5.6 *Average mechanical properties of uranium* (*Grossman and Priceman,* 1954; *Wilkinson and Murphy,* 1958).

modulus of elasticity	1758×10^6 kPa
Poisson ratio at zero stress	0.20
shear modulus	73.1×10^6 kPa
bulk modulus	97.9×10^6 kPa
proportional limit	2.068×10^4 kPa
yield strength	
0.1% offset	1.8617×10^5 kPa
0.2% offset	2.2754×10^5 kPa
compressibility	
β_{100}	0.758 ± 7%
β_{010}	0.296 ± 16%
β_{001}	0.141 ± 16%
β_{v}	1.195 ± 6%

to the pre-history of the sample, and are strongly dependent on crystal orientation, fabrication, and heat treatment. Despite its plastic nature, uranium has a definite yield point with a well-defined, but very low, proportional limit. The ultimate tensile strength of uranium varies between 3.44×10^5 and 13.79×10^5 kPa, depending on the cold working and previous thermal history of the sample. Uranium rapidly loses strength at elevated temperatures, the tensile strength falling from 1.862×10^5 kPa at 150°C to 0.827×10^5 kPa at 600°C.

The Brinell hardness of rolled polycrystalline α-uranium varies between 2350 and 2750 MN m^{-2} at 23°C (Samsonov, 1968). The hardness is strongly affected by impurities. Cold working increases the hardness with up to 50%. Above 200°C, the hardness falls off rapidly. γ-Uranium is so soft as to make fabrication difficult, while the β-phase is harder and considerably more brittle than the α-phase.

(c) Magnetic susceptibility and related properties

The solid-state properties of uranium have been the subject of a relatively recent exhaustive review (Lander *et al.*, 1994). Some pertinent physical properties taken from this review are given here. Although many measurements have been performed on uranium metal, the description and full understanding of its properties is still not complete. Uranium metal is weakly paramagnetic and exhibits almost temperature-independent paramagnetism with a room temperature value of 390×10^{-9} emu mol^{-1}. (Fournier and Troć, 1985). α-Uranium exhibits an anomaly at 43 K apparent in the magnetic susceptibility data and in other measurements. This anomaly and further phase transformations observed at 37 and 23 K have been attributed to charge density waves. α-Uranium exhibits a superconducting transition at low temperatures that can be described by the Bardeen–Cooper–Schreiffer (BCS) theory. The maximal T_c value for

Table 5.7 *Components of uranium resistivity tensor at* 273 K.

References	$\rho[100]$ (μΩ cm)	$\rho[110]$ (μΩ cm)	$\rho[110]$ (μΩ cm)
Brodsky *et al.* (1969)	36.1 ± 0.2	20.6 ± 0.2	26.0 ± 0.2
Berlincourt (1959)	39.4	25.5	26.2
Pascal *et al.* (1964)	39.1	23.6	30.2
Raetsky (1967)	34.7	23.6	20.3

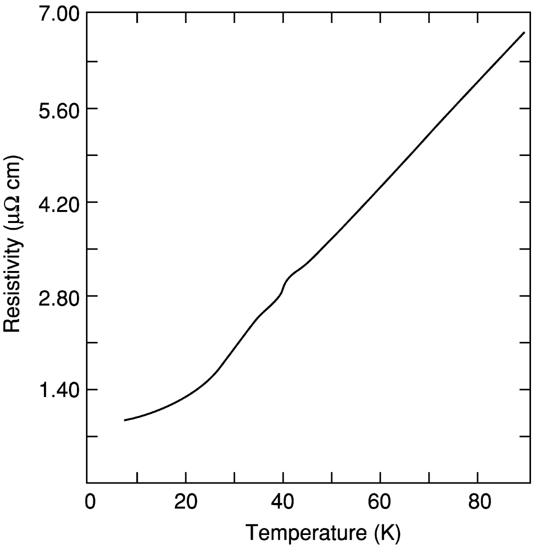

Fig. 5.10 *Resistivity–temperature curve for α-uranium along the* [010] *axis* (*Brodsky* et al., 1969).

α-uranium is ~2–2.3 K at a pressure of ~1.0–1.1 GPa. The 0.1013 MPa (1 atm) value of T_c is taken as ≤0.1 K.

(d) Electrical and related properties

The temperature dependence of the resistivity of uranium single crystals has been measured by a number of authors and the components of the resistivity tensor are given in Table 5.7. The resistivity–temperature curve for α-uranium along the [010] direction is shown in Fig. 5.10. Many other physical properties of elemental uranium have been determined, such as elastic moduli, heat capacity, de Haas-van Alphen measurements, transport properties and others. The reader is referred to Lander *et al.* (1994) and to Chapter 21 for further discussion.

Table 5.8 *Reactions of uranium with various metals* (*Saller and Rough,* 1955*; Rough and Bauer,* 1958*; Chiotti* et al., 1981). *IS and SS denote intensely studied and slightly studied, respectively.*

Class	*Behavior*		*Metals*
I	form intermetallic compounds	IS	Al, As, Au, B, Be, Bi, Cd, Co, Cu, Fe, Ga, Ge, Hg, Ir, Mn, Ni, Os, Pb, Pd, Pt, Rh, Ru, Sb, Sn
II	form solid solutions but no intermetallic compounds	SS	In, Re, Tc, Tl, Mo, Nb, Pu, Ti, Zr
III	form neither solid solutions	IS	Ag, Cr, Mg, Ta, Th, V, W
	nor intermetallic compounds	SS	lanthanides, Li, Na, K, Ca, Sr, Ba

5.6.3 Uranium intermetallic compounds and alloys

The most noticeable features of the behavior of uranium with other metals are the formation of intermetallic compounds with a wide variety of alloying metals and the extensive ranges of solid solutions in α- and β-uranium. Table 5.8 summarizes the alloying behavior with the metallic elements. Saller and Rough (1955), Pfeil (1956), Rough and Bauer (1958), Hansen and Anderko (1958), Elliott (1965), Shunk (1969), and Wilkinson (1962) have given comprehensive and informative descriptions of the general behavior of the alloying elements, including numerous phase diagrams. The thermodynamics of uranium alloy systems was reviewed by Chiotti *et al.* (1981).

A large number of intermetallic compounds have been characterized by X-ray crystallographic methods and by conventional metallographic techniques. The *Gmelin Handbook of Inorganic Chemistry* gives a comprehensive review of the properties of the uranium alloys with alkali metals, alkaline earths, and elements of main groups III and IV (Gmelin, 1989, vol. B2), with transition metals of groups IB to IVB (Gmelin, 1994, vol. B3), and with transition metals of groups VB to VIIB (Gmelin, 1995a, vol. B4), including the effects of irradiation, which are also discussed in the volume on technology and uses of uranium (Gmelin, 1981a, vol. A3).

Among uranium intermetallic phases of interest may be mentioned the transition-metal compounds U_6Mn, U_6Fe, U_6Co, and U_6Ni, which are distinguished by their hard and brittle nature. Uranium forms intermetallic phases with noble metals and the phase diagrams for U–Ru, U–Rh, U–Pd, U–Os, U–Ir, and U–Pt systems have been assessed by Chiotti *et al.* (1981), a compilation that also provides information on a number other intermetallic phases. The compounds of uranium with the light platinum metals, Ru, Rh, and Pd, are of interest in the pyrometallurgical reprocessing of metallic fuels, because the

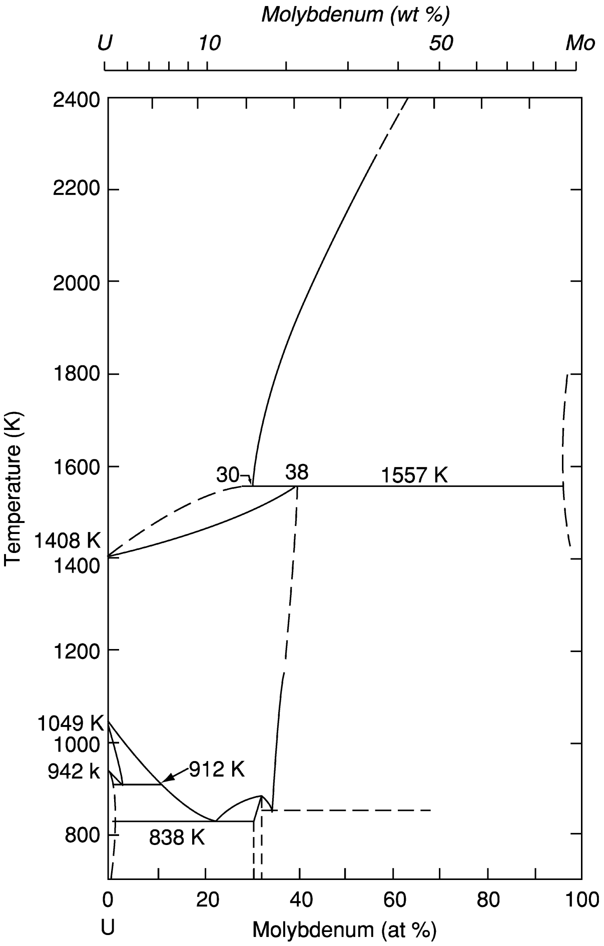

Fig. 5.11 *Phase diagram of the uranium–molybdenum system* (*Chiotti* et al., 1981).

noble metals form alloys that remain with the uranium when the fuel is processed for fission-product removal by oxidative slagging.

Elements of class III in many cases form simple eutectic systems. Molybdenum, titanium, zirconium, niobium, and plutonium form extensive solid solutions with uranium at elevated temperatures. No intermediate phases are detected for the U–Nb system, whereas the U–Mo, U–Pu, U–Ti, and U–Zr systems all show metastable phases. The uranium–molybdenum system is shown in Fig. 5.11 and illustrates the general features of the small but important class of true alloying elements. The uranium alloys have unusual physical properties that are discussed in Chapter 21.

Table 5.9 *Chemical reactions of uranium metal.*

Reactant	*Reaction temperature*[a] (°C)	*Products*
H_2	250	α- and β-UH_3
C	1800–2400	UC; U_2C_3; UC_2
N_2	700	UN, UN_2
P	1000[b]	U_3P_4
O_2	150–350	UO_2, U_3O_8
S	500	US_2
F_2	250	UF_6
Cl_2	500	UCl_4, UCl_5, UCl_6
Br_2	650	UBr_4
I_2	350	UI_3, UI_4
H_2O	100	UO_2
HF(g)	350[b]	UF_4
HCl(g)	300[b]	UCl_3
NH_3	700	$UN_{1.75}$
H_2S	500[b]	US, U_2S_3, US_2
NO	400	U_3O_8
N_2H_4	25	$UO_2(NO_3)_2 \cdot 2NO_2$
CH_4	635–900[b]	UC
CO	750	$UO_2 + UC$
CO_2	750	$UO_2 + UC$

[a] Reaction temperature with massive metal.
[b] Reaction temperature with powdered uranium (from decomposition of UH_3).

5.6.4 Chemical properties of uranium and its alloys

Uranium metal is a highly reactive substance that can react with practically all of the elements in the periodic table with the exception of the noble gases. Some of the more important chemical reactions of uranium are listed in Table 5.9.

Wilkinson (1962) has discussed in detail the corrosion of massive uranium by various gaseous agents, such as dry oxygen, dry air, water vapor, carbon monoxide, carbon dioxide, and others, as well as the pyrophoricity of this element. Totemeier (1995) has written a more recent review of the corrosion and pyrophoricity behavior of uranium (and plutonium) with oxygen, water vapor, and aqueous solutions in terms of reaction rates, products, and reaction mechanisms.

From a practical point of view, the reactions of uranium with oxygen, nitrogen, and water are probably the most significant. Uranium metal exposed to oxygen, water, or air undergoes reaction even at room temperature. The kinetics of corrosion of uranium by various reagents such as dry and moist oxygen, dry and moist air, water vapor and hydrogen, and the pyrophoricity of uranium, as well as that of plutonium, are discussed in detail in Chapter 29 devoted to handling, storage, and disposal of these elements and their relevant compounds.

Uranium dissolves very rapidly in aqueous hydrochloric acid. The reaction frequently yields considerable amounts of a black solid, presumably a hydrated uranium oxide but very likely containing some hydrogen. The addition of a small amount of fluorosilicate ion prevents the appearance of the black solid during dissolution in hydrochloric acid. Non-oxidizing acids, such as sulfuric, phosphoric, and hydrofluoric, react only very slowly with uranium, whereas nitric acid dissolves massive uranium at a moderate rate. With finely divided uranium, the dissolution in nitric acid may approach explosive violence. Uranium metal is inert to alkalis. Addition of oxidizing agents such as peroxide to sodium hydroxide solution leads to the dissolution of uranium and to the formation of ill-defined water-soluble peroxyuranates.

5.7 COMPOUNDS OF URANIUM

Ever since the discovery of uranium in 1789, its compounds have been synthesized and studied, so that a wealth of information has accumulated over the years. Much of this information may be found in the books by Katz and Rabinowitch (1951, 1958) and in the various volumes of the Supplement Series of the *Gmelin Handbook of Inorganic Chemistry* (1975–1996), which constitute probably the most comprehensive collection of information on uranium compounds.

For obvious reasons, such as lack of space, it is impossible to give a complete account of every uranium compound known to date. Rather, representative examples will be discussed with emphasis on preparation, structure, and chemical properties; information and discussion of thermodynamic properties of uranium and other actinide compounds are found in Chapter 19. In its compounds, uranium exhibits the oxidation states 3+, 4+, 5+, and 6+, with 4+ and 6+ as the predominant ones. Also, mixed valence and non-stoichiometric compounds are known.

While general features of the structures of uranium compounds, both from coordination and chemical points of view, will be discussed in Section 5.9, structures pertaining to each family of compounds will be described in the following subsections.

5.7.1 The uranium–hydrogen system

The uranium–hydrogen system has been reviewed by Katz and Rabinowitch (1951), Mallett *et al.* (1955), Libowitz (1968), Flotow *et al.* (1984), and Ward (1985). An extensive review has been given in the *Gmelin Handbook* (Gmelin, 1977, vol. C1). The kinetics of the reaction of hydrogen on uranium is discussed in detail in Chapter 29, describing the handling, storage, and disposition of plutonium and uranium. This topic will therefore not be developed here.

(a) Preparative methods

β-UH_3 forms rapidly as fine black or dark gray powder when uranium turnings or powder, as well as large massive lumps, are heated to 250°C in a vacuum followed by the introduction of H_2 gas into the reaction system (Spedding *et al.*, 1949; Libowitz and Gibb. Jr, 1957). Crystalline β-UH_3 may be prepared as gray, fibrous crystals at 30 atm H_2 and 600–700°C in an autoclave using a uranium nitride crucible as the primary container inside the pressure vessel.

α-UH_3 can only be prepared by slow reaction at temperatures below about −80°C. The α-phase is unstable, and the products are usually a mixture with more than 50% β-UH_3 (Mulford *et al.*, 1954; Abraham and Flotow, 1955). Purer α-UH_3 has been obtained by the diffusion method: Fine reactive uranium metal powder, formed by thermal decomposition of β-UH_3, was kept below −78°C in an Ar (or He) filled cryostat at a pressure of 0.25–0.40 atm, to which H_2 was introduced with an adequately low rate (reaction period: 20 days). More than 80% of the product was α-UH_3 (Wicke and Otto, 1962).

(b) Crystal structures

α-UH_3 is cubic with space group *Pm*3*n*. Two uranium atoms occupy (0,0,0) and (1/2,1/2,1/2), and six hydrogen atoms ±(1/4,0,1/2), ±(1/2,1/4,0), and ±(0,1/2,1/4) positions. The crystallographic data are listed in Table 5.10.

β-UH_3 also has a cubic structure with space group *Pm*3*n*, the same as in α-UH_3, but with different atom positions, $2U_I$ in (0,0,0) and (1/2,1/2,1/2), and

Table 5.10 *Crystallographic data of uranium hydrides.*

Compound	*Symmetry*	*Space group*	*a* (Å)	*z*	*X-ray density* (g cm^{-3})	*References*
α-UH_3	cubic	*Pm*3*n*	4.160(1)	2	11.12	Mulford *et al.* (1954); Wicke and Otto (1962);
			4.153(2)			Caillat *et al.* (1953)
α-UD_3	cubic	*Pm*3*n*	4.150	2	11.34	Wicke and Otto (1962); Grunzweig-Genossar *et al.* (1970);
			4.147(3)		11.36	Johnson *et al.* (1976)
α-UT_3	cubic	*Pm*3*n*	4.142(2)	2	11.55	Johnson *et al.* (1976)
β-UH_3	cubic	*Pm*3*n*	6.6444(8)	8	10.92	Rundle (1947, 1951)
β-UD_3	cubic	*Pm*3*n*	6.633(3)	8	11.11	Rundle (1947, 1951)
β-UT_3	cubic	*Pm*3*n*	6.625(3)	8	11.29	Johnson *et al.* (1976)

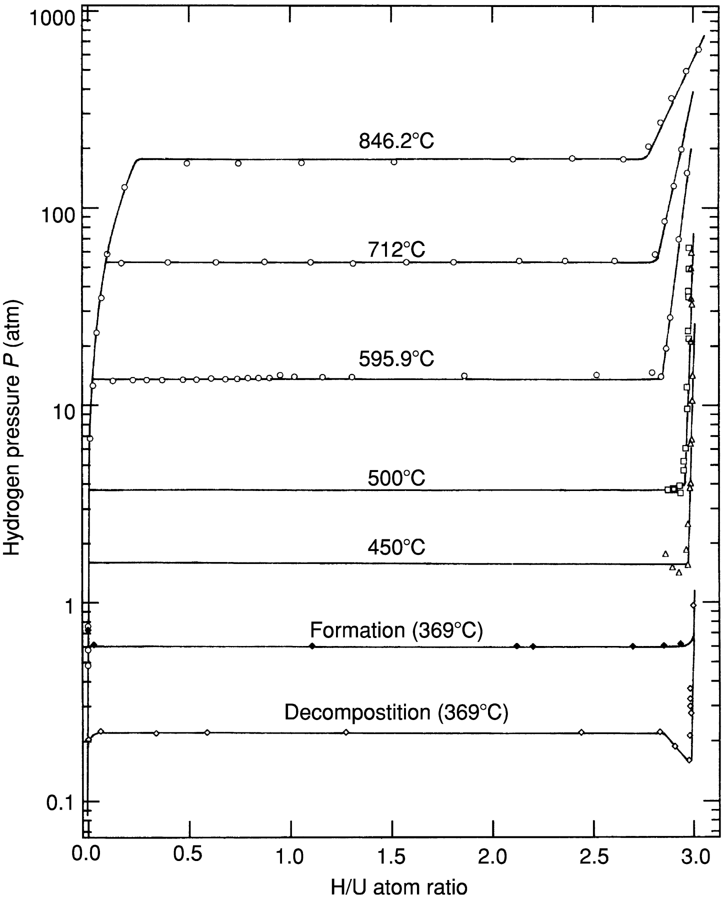

Fig. 5.12 *Hydrogen pressure versus composition isotherms for the system* $U–UH_3–H_2$. *Formation and decomposition curves at* 369°C: *Wicke and Otto* (1962); 450 *and* 500°C *curves: Libowitz and Gibb, Jr.* (1957); 595.9, 712, *and* 846.2°C *curves: Northrup, Jr.* (1975).

$6U_{II}$ in ±(1/4,0,1/2) and their equivalent positions. The hydrogen position was determined by neutron diffraction of β-UD_3 (Rundle, 1951). The hydrogen atoms are located in the 24(*k*) position, where each hydrogen atom is equidistant from four uranium neighbors within the experimental error, i.e., $12H_I$ in ±(5/16,0,±5/32) and $12H_{II}$ in ±(11/32,±1/2,3/16).

(c) Phase relations and dissociation pressures

A pressure–composition (isotherm) diagram of the $U–UH_3–H_2$ system is shown in Fig. 5.12; the region of the existence of α-hydride phase is not given because this phase is unstable and transforms irreversibly to β-UH_3 at higher

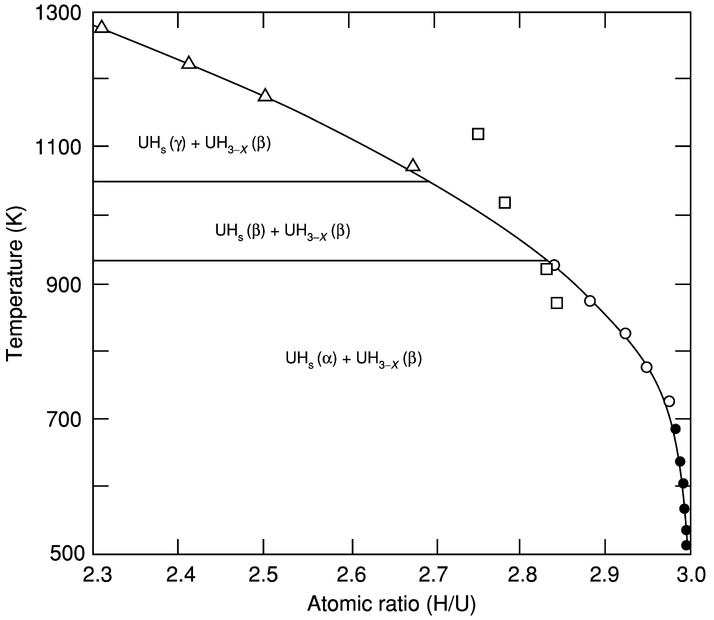

Fig. 5.13 *Phase diagram of the uranium–hydrogen system in the range H/U* = 2.3–3.0 (*from Flotow* et al., 1984). *UH_s (α, β, and γ) represent uranium metal phases (α, β, and γ), respectively, with dissolved hydrogen.* •: *Besson and Chevallier* (1964); ○: *Libowitz and Gibb, Jr.* (1957); □: *Northrup, Jr.* (1975); △: *Lakner* (1978). *Reproduced by the permission of the Atomic Energy Agency, Vienna.*

temperatures. The equilibrium H_2 pressure over α-UH_3 is much higher than that over β-UH_3, but no quantitative data are available. The rate of the α → β transformation is relatively low; α-UH_3 changes to β-UH_3 in a few hours at 250°C (Wicke and Otto, 1962).

The β-hydride phase, β-UH_{3-x}, has a relatively wide range of hydrogen hypostoichiometry at higher temperatures. The slight hyperstoichiometry at 846.2°C shown in Fig. 5.12 is an experimental artefact caused by hydrogen permeation from the sample vessel (Northrup, Jr., 1975).

Fig. 5.13 shows the hypostoichiometric range for uranium trihydride up to 1300 K (Flotow *et al.*, 1984). At 1280 K, the lower limit of the β-hydride phase attains to $UH_{2.3}$.

The solubility of hydrogen in uranium metal increases with increasing temperature (Fig. 5.12). The data determined by Mallett and Trzeciak (1958) obey Sieverts law.

$$\alpha\text{-U: } \log S(\mathrm{H/U}) = 1/2 \log p_{\mathrm{H_2}}(\mathrm{atm}) - 2.874 - 388\,T^{-1}\ (T < 942\,\mathrm{K}),$$
$$\beta\text{-U: } \log S(\mathrm{H/U}) = 1/2 \log p_{\mathrm{H_2}}(\mathrm{atm}) - 1.778 - 892\,T^{-1}(942 < T < 1049\,\mathrm{K}),$$
$$\gamma\text{-U: } \log S(\mathrm{H/U}) = 1/2 \log p_{\mathrm{H_2}}(\mathrm{atm}) - 2.238 - 227\,T^{-1}\ (1049 < T < 1408\,\mathrm{K}),$$
$$\text{Liquid U: } \log S(\mathrm{H/U}) = 1/2 \log p_{\mathrm{H_2}}(\mathrm{atm}) - 1.760 - 587\,T^{-1}\ (T > 1408\,\mathrm{K}),$$

where S is the solubility measured as the atom ratio. It may be noteworthy that finely divided uranium chemisorbs much larger amounts of hydrogen than those given by the previous equations (e.g. about 100 times larger at 295°C and 0.15 mmHg H_2).

Below 400°C the hydrogen pressure for formation of hydrides is not the same as that for the decomposition in the region of two solid phases (plateau region). Spedding *et al.* (1949) reported that the decomposition and formation pressures at 357°C were 0.176 and 0.188 atm, respectively. Wicke and Otto (1962) indicated that this difference is 170% at 369°C as shown in Fig. 5.12. Various explanations of the hysteresis and the dip in the decomposition process have been proposed (Libowitz, 1968; Condon and Larson, 1973); there is a possibility that traces of oxygen play a role. Using very pure uranium samples, no evidence of hysteresis was found and the time to attain equilibrium was quite short (Meusemann and von Erichsen, 1973; Condon, 1980).

The plateau hydrogen pressures are given by the equation

$$\ln p(\text{atm}) = A - BT^{-1}$$

where $A = 14.55$ and $B = 10233$ for UH_3 in the temperature range 298–942 K (Chiotti, 1980). For uranium trideuteride, UD_3, Flotow *et al.* (1984) assessed the measured data by Spedding *et al.* (1949), Wicke and Otto (1962), Destriau and Sériot (1962), and Carlson (1975), and recommended the values $A = 15.046$ and $B = 10362$ (500–800 K), which were obtained by averaging the results of Spedding *et al.* (1949) and Wicke and Otto (1962). The data for uranium tritritide, UT_3, are meager. The recommended A and B values (Flotow *et al.*, 1984) are those obtained by averaging the results of Flotow and Abraham (1951) and of Carlson (1975); they are $A = 14.57$ and $B = 9797$ in the temperature range 600–800 K. The above equilibrium pressures are considerably lower than the pressures derived from calorimetric data for UH_3, UD_3, and UT_3 (Flotow *et al.*, 1984).

(d) Thermodynamic properties

The heat capacity, entropy, and enthalpy of formation of UH_3, UD_3, and UT_3 (β forms) at 298 K are listed in Table 5.11.

Table 5.11 *Heat capacity, entropy, and enthalpy of formation of* β-UH_3, β-UD_3, *and* β-UT_3 *at* 298.15 K (*Flotow* et al., 1984).

Compound	C_p°(298.15 K) (J K^{-1}mol^{-1})	S°(298.15 K) (J K^{-1}mol^{-1})	$\Delta_f H^\circ$ (298.15K) (kJ mol^{-1})
β-UH_3	49.29 ± 0.08	63.68 ± 0.13	– 126.98 ± 0.13
β-UD_3	64.98 ± 0.08	71.76 ± 0.13	– 129.79 ± 0.13
β-UT_3	74.43 ± 0.75	79.08 ± 0.79	–130.29 ± 0.21

Flotow and Osborne (1967) and Flotow *et al.* (1959) have measured the low-temperature heat capacity of $UH_3(\beta)$ from 1.4 to 23 K and from 5 to 350 K, respectively. Abraham *et al.* (1960) have reported the low-temperature heat capacity of UD_3 from 5 to 350 K and Ward *et al.* (1979) that from 4 to 17 K.

Although no experimental heat capacity data have been published for $UT_3(\beta)$, Flotow *et al.* (1984) obtained the estimated C_p values using semiempirical equations to estimate the optical mode contributions of the hydrogen lattice vibrations. Abraham *et al.* (1960) found that the sum of the lattice heat capacity associated with the acoustic modes, the electronic heat capacity, and the magnetic heat capacity, agreed within 0.08 $JK^{-1}mol^{-1}$ for $UH_3(\beta)$ and $UD_3(\beta)$, which means that this part of heat capacity is virtually the same for UH_3, UD_3, and UT_3. Moreover, they showed that this could be represented by a linear function of temperature. On this basis, Flotow *et al.* (1984) calculated the optical mode contributions of UT_3 by using the Einstein heat capacity function to estimate the heat capacity of UT_3.

The heat capacity of UH_3 and UD_3 up to 800 K was also obtained by this method as shown in Fig. 5.14. The sharp anomaly in the vicinity of 170 K is due to the ferromagnetic–paramagnetic transition of the β-hydride phases.

(e) Electrical resistivity

The electrical resistivity, ρ, of β-hydride increases with increasing temperature as in metals. Ward *et al.* (1979) measured the electrical resistivity of β-UD_3 from 2.4 to 300 K. The ρ vs T curve has an anomaly due to a magnetic transition at 166 K. These resistivities are in good agreement with the unpublished data of Flotow for β-UH_3 communicated to Grunzweig-Genossar *et al.* (1970). The resistivity of β-hydride is about ten times higher than that of uranium metal.

(f) Magnetic properties and the nature of bonding

The history of magnetic studies of uranium hydrides is described in the review of Troć and Suski (1995). In the earlier work, α-UH_3 was considered to be ferromagnetic at low temperatures with T_C the same as, or close to that of β-UH_3. However, the neutron diffraction study on α-UD_3 (Lawson *et al.*, 1991) revealed the α-hydride phase to be non-magnetic at least above 15 K, i.e. the apparent ferromagnetism was due to β-hydride impurities in the α-hydride samples.

β-Hydride is ferromagnetic at low temperatures. The magnetic data for β-UH_3 and β-UD_3 are shown in Table 5.12. At the Curie temperature, the λ-type heat capacity anomaly has also been observed at 170.5 and 167.6 K for β-UH_3 and β-UD_3, respectively (Fig. 5.14). The lower Curie temperature in the deuteride is associated with the somewhat shorter U–U distance, resulting in a change of the exchange integrals for the Weiss field (Ward, 1985). The electrical

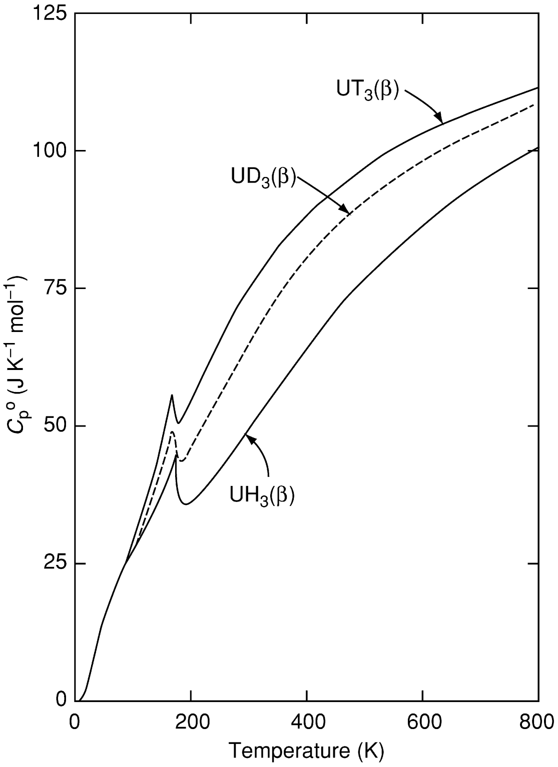

Fig. 5.14 *Heat capacities of $UH_3(\beta)$, $UD_3(\beta)$, and $UT_3(\beta)$* (*Flotow* et al., 1984).

resistivity for β-UD_3 changed at the Curie temperature (166 K) (Ward *et al.*, 1979). Andreev *et al.* (1998) report that the Curie temperature of β-UH_3 decreases with increasing external pressure from 175 K (0 kbar) to 169 K (8 kbar). In Table 5.12, the saturation uranium magnetic moments obtained by neutron diffraction are far larger than those obtained by magnetization measurements, possibly a result of a large magnetic anisotropy in β-UH_3 (Bartscher *et al.*, 1985). The neutron diffraction studies of β-UH_3 carried out at the ferromagnetic temperatures revealed that the two U_I and six U_{II} atoms, which occupy different crystallographic positions in space group *Pm*3*n*, are magnetically equivalent giving the same magnetic moment; no (110) reflection peak was observed in the diffraction patterns (Wilkinson *et al.*, 1955; Bartscher *et al.*, 1985; Lawson *et al.*, 1990). Increased external pressure lowers the saturation magnetic moment of uranium from $1\mu_B$(0 kbar) to $0.985\mu_B$(10 kbar) at 4.2 K (Andreev *et al.*, 1998). The effective uranium moments in Table 5.12 are those obtained from the slope of the Curie–Weiss curves in the paramagnetic range of temperatures.

Table 5.12 *Magnetic data for β-UH_3 and β-UD_3.*

Hydride	*Ferromagnetic Curie temperature* T_C(K)	*Paramagnetic Curie temperature* θ_p(K)	*Saturation uranium moment* $\mu_S(\mu_B)$	*Effective paramagnetic uranium moment* $\mu_{eff}(\mu_B)$	*References*
β-UH_3	174	174	0.65 (80 K)	2.44	Trzebiatowski *et al.* (1954)
	173		0.9 (78 K)	2.79	Gruen (1955)
	181	173	0.9 (2.1 T, 4.2 K)		Lin and Kaufmann (1956)
	168	180	1.18 (6 T, 1.3 K)		Henry (1958)
	181	176	0.7	2.24	Karchevskii and Buryak (1962)
	175		1.0 (40 T, 4.2 K)		Andreev *et al.* (1998)
	175		1.39 (ND)		Shull and Wilkinson (1955)
			1.45 (NMR)		Barash *et al.* (1984)
			1.54 (ND)		Lawson *et al.* (1990)
β-UD_3	172	172		2.44	Trzebiatowski *et al.* (1954)
			0.98 (6 T, 1.3 K)		Henry (1958)
	177.5	175.2		2.24	Karchevskii and Buryak (1962)
		166	0.87 (5.34 T)	2.26	Ward *et al.* (1979)
			1.39 (ND)		Wilkinson *et al.* (1955)
	178		1.45 (ND, 10 K)		Bartscher *et al.* (1985)

ND: neutron diffraction.

Grunzweig-Genossar *et al.* (1970) assume that uranium is composed of uranium ions and protons (deuterons) in a high-density interacting electron gas. The magnetic moments arise from 5f electrons. The uranium ions are magnetically coupled through the polarized conduction electrons by the RKKY interaction, which can explain the ferromagnetic ordering below ~180 K and the large Knight shift obtained by their nuclear magnetic resonance (NMR) measurement, i.e. $K = 0.40\chi_{\mathrm{M}}$, where χ_{M} is the molar magnetic susceptibility. The second moment and line-shape data suggest that the 5f electrons ($Z \sim 2.5$ conduction electrons per uranium atom) are localized and do not form a band as in metallic uranium.

Cinader *et al.* (1973) measured the NMR spin-lattice relaxation time in the paramagnetic state at 189–700 K. In addition to the time-dependent dipolar interaction through hydrogen diffusion, the relaxation time was dependent on (1) the direct interaction between the conduction electrons and the protons (deuterons) causing Korringa relaxation, and (2) the indirect RKKY (Ruderman-Kittel-Kasuya-Yosida) interaction. The density of states of the s-type conduction electrons at the Fermi level was 1.65 states per eV. A model with a spherical Fermi surface and free electron behavior in the RKKY interaction, results in U^{3+} and H^{-} as the ionic species.

(g) Chemical properties

Uranium hydride is very reactive and, in most respects its reactions resemble those of the finely divided uranium metal; in fact, reactions that occur at temperatures where the hydrogen decomposition pressures are high may be those of the metal. Uranium hydride ignites spontaneously in air, but gradual oxidation at low oxygen pressures at room temperature results in the formation of a protective film of oxide on the surface of hydride particles, which prevents the hydride from ignition. Adsorption of a variety of electron-pair-donor compounds can reduce the pyrophoric properties.

Uranium hydride is used as a starting material in many reactions, including the preparation of finely divided uranium metal. Hydrogen, deuterium, and tritium may be stored as UH_3, UD_3, and UT_3, respectively. These gases are released when the compounds are heated to the decomposition temperatures. Gram quantities of UH_3 reacts slowly with water, but larger samples react violently and produce high temperatures (Newton *et al.*, 1949). UH_3 reacts slowly with solution of non-oxidizing acids such as HCl and weak acids such as CH_3COOH, but vigorously with HNO_3. UH_3 reacts with H_2SO_4 to form S, SO_2, and H_2S, and with H_3PO_4 to form UPO_4. UH_3 is unstable in strong bases and reduces aqueous solutions of $AgNO_3$ and $HgCl_2$. At elevated temperatures, UH_3 reacts with O_2, hydrogen halides, H_2S, HCN, NH_3, N_2, CO_2, CH_4, and C_2H_2 (acetylene), but not with liquid hydrocarbons and chlorinated solvents, although an explosive reaction occurs with CCl_4. The reactions of UH_3 with most compounds are thermodynamically favored, and many cases where the

Table 5.13 *Reactions of uranium hydride.*

Reagent	*Reaction temperature* (°C)	*Product*
O_2	ignites at room temperature	U_3O_8
H_2O	350	UO_2
H_2S	400–500	US_2
N_2	250	U_2N_3
NH_3	250	U_2N_3
PH_3	400	UP
Cl_2	250	UCl_4
CCl_4	250 possibility of explosion at 25°C	UCl_4
HCl	250–300	UCl_3
HF	200–400	UF_4
Br_2	300–350	UBr_4
HBr	300	UBr_3
CO_2	300	UO_2

reactions do not proceed are a result of kinetic inhibition (Haschke, 1991). Typical reactions of uranium hydride are given in Table 5.13.

(h) Other uranium hydride compounds

(*i*) *Uranium*(IV) *borohydride,* $U(BH_4)_4$

The volatile $U(BH_4)_4$ is obtained as dark green crystals by the reaction

$$UF_4 + 2Al(BH_4)_3 \rightarrow U(BH_4)_4 + 2Al(BH_4)F_2.$$

Purification is made by vacuum sublimation (Schlesinger and Brown, 1953).

$U(BH_4)_4$ is tetragonal with space group $P4_32_12$ having four formula units in the unit cell. The lattice parameters are $a = (7.49 \pm 0.01)$ Å and $c = (13.24 \pm 0.01)$ Å. The positions of U, B, and H have been determined by X-ray and neutron diffraction analyses (Bernstein *et al.*, 1972a,b).

In vacuo and in an inert-gas atmosphere, $U(BH_4)_4$ is fairly stable, but it is immediately decomposed by oxygen or moisture. Bernstein and Keiderling (1973) determined the molecular structure from optical and nuclear magnetic resonance spectra.

The vapor pressure of $U(BH_4)_4$ is given by the equation

$$\log p(\text{mmHg}) = 13.354 - 4265T^{-1}.$$

$U(BH_4)_3$ is a red solid, which has been observed as a by-product in the synthesis of $U(BH_4)_4$. Because of its pyrophoric properties, it has not been well characterized (Schlesinger and Brown, 1953).

(*ii*) *UNiAlH*$_y$ *and related compounds*

The intermetallic compounds UXAl (X = Ni, Co, Mn) absorb hydrogen on heating in the temperature range 20–250°C at high H_2 pressures. The maximum hydrogen content attained at 20°C corresponds to $UNiAlH_{2.74}$ ($p_{H_2} = 55$ atm), $UCoAlH_{1.2}$ (40 atm), and $UMnAlH_{0.15}$ (40 atm) (Drulis *et al.*, 1982). UNiAl absorbs the largest amount of hydrogen in these compounds, though lower maximum hydrogen absorption values have been reported, at room temperature and 70 atm viz. $UNiAlH_{2.5}$ (Jacob *et al.*, 1984), and $UNiAlD_{2.2}$ at 30°C and 50 atm D_2 (Yamamoto *et al.*, 1998). The lower limit of the hydride phase is $y = 0.7$–0.8 (Yamamoto *et al.*, 1994, 1998; Yamanaka *et al.*, 1999). The hydrogen solubility in the UNiAl metal appears to obey Sieverts law in the hydrogen concentration region below 0.02 H per formula unit UNiAl (Yamanaka *et al.*, 1999).

The symmetry and space group of $UNiAlH_y$ are the same as those for UNiAl. The structure consists of alternate planes containing three Al (in 3f) and two Ni (2c) atoms at $z = 0$ and three U (3g) and one Ni (1b) atoms at $z = 1/2$. The hydrogen atoms are located in the center of one of the adjacent U_3Ni tetrahedra, in the bipyramid U_3Al_2, and in the bipyramid Al_3Ni_2 (Kolomiets *et al.*, 2000). The lattice parameter a increases whereas b decreases slightly with increasing value of y (Drulis *et al.*, 1982; Jacob *et al.*, 1984; Yamamoto *et al.*, 1994; Yamanaka *et al.*, 1999; Kolomiets *et al.*, 2000). This variation, expressed in Å, is approximately represented by the equations $a = 6.736 + 0.187y$ and $c = 4.037 - 0.028y$ in the range $0.8 \leq y \leq 2.7$. The hydrogenation of UNiAl is accompanied by a volume change. The quotient $\Delta V/V$ attains a value of 0.124 for both hydride ($y = 2.3$) and deuteride ($y = 2.1$). In addition, the X-ray diffraction peak intensities indicate a positional shift of the U atoms from (0.572, 0, 1/2) in UNiAl to (2/3, 0, 1/2) in $UNiAlH_{2.3}$. These changes are supposed to favor the accommodation of a larger amount of hydrogen (Kolomiets *et al.*, 2000).

The desorption isotherms of $UNiAlH_y$ have two sloping plateaus, which suggests the existence of two hydride phases (Jacob *et al.*, 1984). The partial molar enthalpy and entropy of hydrogen for the non-stoichiometric $UNiAlH_y$ varies with the y value. $\Delta\bar{H}(H_2)$ and $\Delta\bar{S}(H_2)$ were –53 kJ (mol H_2)$^{-1}$ and –88 J K^{-1} (mol H_2)$^{-1}$, respectively, for $UNiAlH_{1.35}$, and –41 kJ (mol H_2)$^{-1}$ and –95 J K^{-1} (mol H_2)$^{-1}$ for $UNiAlH_{2.30}$ (Drulis *et al.*, 1982). The values measured by Jacob *et al.* (1984) are comparable with the above values: $\Delta\bar{H}(H_2)$ and $\Delta\bar{S}(H_2)$ were −64 kJ (mol H_2)$^{-1}$ and –90 J K^{-1} (mol H_2)$^{-1}$, respectively, for $UNiAlH^{1.2}$, and −47 kJ (mol H_2)$^{-1}$ and –94 J K^{-1} (mol H_2)$^{-1}$, respectively, for $UNiAlH_{2.0}$.

The incorporation of hydrogen into UNiAl leads to a large increase in the antiferromagnetic ordering temperature from 19 K to 90–100 K. The transition temperatures for $UNiAlH_{2.3}$ and $UNiAlD_{2.1}$ are 99 and 94 K, respectively (Kolomiets *et al.*, 2000). According to Zogal *et al.* (1984), $UNiAlH_{1.9}$ has magnetic transitions at 122 and 34 K, where the second transition possibly refers to the hydride at the lower phase limit. The magnetic susceptibility in the paramagnetic region is represented by the modified Curie–Weiss equation. The effective moment, μ_{eff}, the paramagnetic Curie temperature, θ_{p}, and the temperature-independent susceptibility, χ_{o}, are 2.42 μ_{B}/f.u., –42 K and 7×10^{-9} $\mathrm{m^3\,mol^{-1}}$, respectively, for $\mathrm{UNiAlH_{2.3}}$. The values are 2.43 μ_{B}/f.u., –50 K and 8×10^{-9} $\mathrm{m^3\,mol^{-1}}$, respectively, for $\mathrm{UNiAlD_{2.1}}$ (Kolomiets *et al.*, 2000).

$\mathrm{U(Fe_{1-x}Ni_x)Al}$ with $x \geq 0.7$ absorbs hydrogen forming $\mathrm{U(Fe_{1-x}Ni_x)AlH_y}$ hydrides. Raj *et al.* (2000) studied the magnetic properties of $\mathrm{U(Fe_{0.3}Ni_{0.7})AlH_y}$, and found that no other hydride phase was formed above or below $y = 0.8$. $\mathrm{U(Fe_{0.3}Ni_{0.7})AlH_y}$ is ferromagnetic with $T_{\mathrm{C}} = 15$ K ($y = 0$) and 90 K ($y = 0.8$). Magnetization of $\mathrm{U(Fe_{0.3}Ni_{0.7})Al}$ at 5.5 T gave a saturation moment of $\cong 0.3\mu_{\mathrm{B}}$/f.u. The value for the hydride ($y = 0.8$) was much higher, $\cong 0.9\mu_{\mathrm{B}}$/f.u., indicating considerable increase in the ferromagnetic correlations. Other intermetallic hydrides, e.g. $\mathrm{U_5Ni_4PdH_{1.0}}$ (Drulis *et al.*, 1982), $\mathrm{UCoH_{2.7}}$ (Andreev *et al.*, 1986; Yamamoto *et al.*, 1991), and $\mathrm{UTi_2D_y}$ (Yamamoto *et al.*, 1995) have also been studied.

5.7.2 The uranium–oxygen system

(a) Binary uranium oxides

(*i*) *Preparative methods*

Comprehensive information on the preparation of actinide oxides including uranium oxides is given in a monograph by Morss (1991).

UO(s)

Although UO gas is one of the main species over $\mathrm{U(l)+UO_{2-x}}$ at high temperatures, solid UO ($Fm\bar{3}m$, $a = 4.92$ Å) with NaCl-type structure is very unstable and its formation has not been definitely established. When $\mathrm{UO_2}$ was heated with uranium metal at high temperatures, a fcc phase was produced only in cases of considerable carbon contamination (Rundle *et al.*, 1948). Carbon is thought to promote the reaction. It is possible that UC or UN must be present for the formation of the UO phase (Rundle *et al.*, 1948; Cordfunke, 1969).

UO_2(s)

$\mathrm{UO_2}$ is prepared by hydrogen reduction of $\mathrm{UO_3}$ or $\mathrm{U_3O_8}$ between 800 and 1100°C (Katz and Rabinowitch, 1951; Belle, 1961; Wedermeyer, 1984). The $\mathrm{H_2}$ gas used for this purpose should not contain impurity of $\mathrm{O_2}$ in order to avoid oxidation to hyperstoichiometric $\mathrm{UO_{2+x}}$, which occurs on cooling at temperatures below 300°C. The $\mathrm{UO_2}$ pellets for reactor fuel are reduced at much higher temperatures around 1700°C in order to approach the theoretical density. For laboratory use, other reductants such as CO, C, $\mathrm{CH_4}$, and $\mathrm{C_2H_5OH}$ may be used, but they offer no advantages over H_2 (Katz and Rabinowitch, 1951; Wedermeyer, 1984; Roberts and Walter, 1966). NH_3 is not suitable (Belle, 1961). Commercial methods of UO_2 synthesis start from the peroxide $UO_4 \cdot 2H_2O$, ammonium diuranate with the approximate composition $(NH_4)_2U_2O_7$ or ammonium uranyl carbonate $(NH_4)_4UO_2(CO_3)_3$ followed by air calcination at 400–500°C. Subsequent H_2 reduction at 650–800°C yields UO_2 with high surface area. The nuclear fuel pellets are produced by cold pressing of these powders, followed by sintering.

$U_4O_9(s)$

U_4O_9 can be prepared from the stoichiometric amounts of UO_2 and U_3O_8 according to the reaction $5UO_2 + U_3O_8 = 2U_4O_9$. The reactants are ground in an agate mortar and the mixture is sealed in an evacuated quartz ampoule, and then heated at 1000°C for about 2 weeks until the sample is completely homogenized. The sample is slowly cooled to room temperature over a period of 2 weeks (Gotoo and Naito, 1965; Westrum, Jr. *et al.*, 1965). U_4O_9 has three phases: α-U_4O_9 that transforms into β-U_4O_9 on heating to ~350 K, and β-U_4O_9 that transforms into γ-U_4O_9 at ~850 K (Labroche *et al.*, 2003b). These transformations are reversible.

$U_3O_7(s)$

Three polymorphs of α, β, and γ are known for U_3O_7; all of them are tetragonal. α-U_3O_7 with *c/a* ratios 0.986–0.991 is prepared by oxidizing UO_2 at temperatures below 160°C (Hoekstra *et al.*, 1961; Westrum, Jr. and Grønvold, 1962). To prepare a single phase with $O/U \approx 2.33$, the use of reactive UO_2, which is obtained by low-temperature reduction of UO_3 by H_2, is recommended (Hoekstra *et al.*, 1961). Oxidation of UO_2 in air at 200°C yields β-U_3O_7 with *c/a* ratios between 1.027 and 1.032 (Garrido *et al.*, 2003). The oxidation of standard uranium dioxide ceases at $UO_{2.33}$ at temperatures below 200°C and no formation of U_3O_8 takes place (Hoekstra *et al.*, 1961). Allen and Tyler (1986) report that well-crystallized single-phase β-U_3O_7 was obtained by oxidation at 230°C for 16 h. The γ-U_3O_7 ($U_{16}O_{37}$) phase, which has *c/a* ratios of 1.015–1.017 and smaller O/U ratios of 2.30–2.31 (Hoekstra *et al.*, 1961; Westrum, Jr. and Grønvold, 1962; Hoekstra *et al.*, 1970; Nowicki *et al.*, 2000), is formed when U_4O_9 is oxidized at 160°C (Hoekstra *et al.*, 1961). This compound has also been prepared as a mixture with monoclinic U_8O_{19} on heating a pellet of mixed UO_2 and UO_3 at $\geq$400°C under high pressures (15–60 kbar) (Hoekstra *et al.*, 1970).

$U_2O_5(s)$

High-pressure syntheses by Hoekstra *et al.* (1970) identified three U_2O_5 phases (α-U_2O_5, β-U_2O_5 and γ-U_2O_5). α-U_2O_5 was prepared by heating a mixture of UO_2 and U_3O_8 at 400°C and 30 kbar for 8 h. At 500°C, a pressure of 15 kbar was enough to prepare α-U_2O_5. Hexagonal β-U_2O_5 is formed at 40–50 kbar pressure at temperatures higher than 800°C. Monoclinic γ-U_2O_5 was sometimes

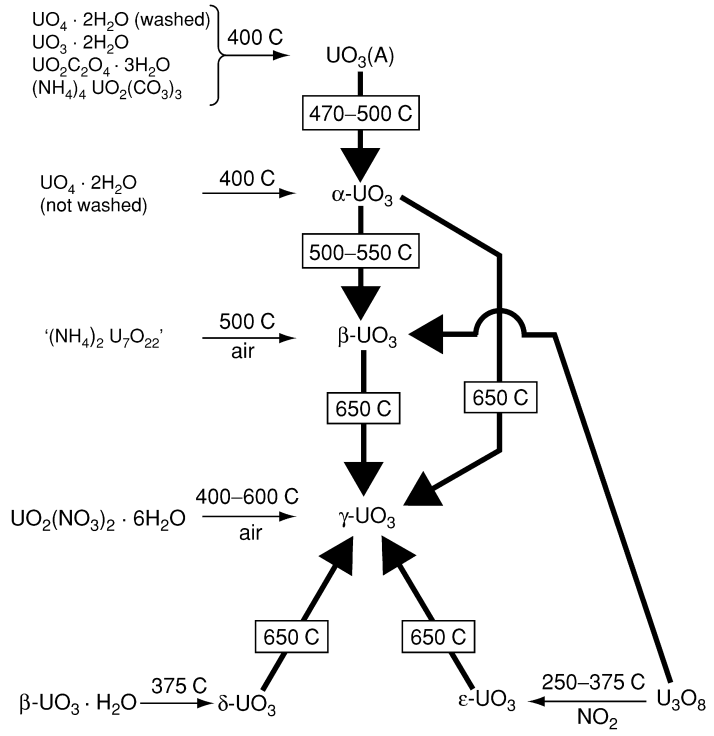

Fig. 5.15 *Flow sheet for the preparation of various UO_3 modifications: Bold lines refer to high O_2 pressure* (*Hoekstra and Siegel*, 1961; *Cordfunke*, 1969).

obtained when the UO_2 and U_3O_8 mixture was heated above 800°C at a pressure of 60 kbar.

$U_3O_8(s)$

α-U_3O_8 is prepared by oxidation of UO_2 in air at 800°C followed by slow cooling (Loopstra, 1970a). β-U_3O_8 is prepared by heating α-U_3O_8 to 1350°C in air or oxygen, followed by slow cooling (cooling rate: 100 K per day) to room temperature (Loopstra, 1970b).

$UO_3(s)$

Seven modifications are known for UO_3: A, α, β, γ, δ, ε, and ζ-UO_3. The methods of their syntheses are outlined in the flow sheet of Fig. 5.15 (Hoekstra and Siegel, 1961; Cordfunke, 1969).

Amorphous UO_3 (A-UO_3) forms when any of the compounds $UO_4 \cdot 2H_2O$ (washed with H_2O), $UO_3 \cdot 2H_2O$, $UO_2C_2O_4 \cdot 3H_2O$ and $(NH_4)_4UO_2(CO_3)_3$ is heated in air at 400°C. Because of the difficulty to remove residual traces of nitrogen and carbon, it is preferable to use either of the first two of the above compounds (Hoekstra and Siegel, 1961). α-UO_3 is prepared by crystallization of A-UO_3 at 485°C for 4 days. The heating time can be shortened at 500°C but a pressure of 40 atm oxygen is then needed (Hoekstra and Siegel, 1961). β-UO_3 is prepared by heating 'ammonium diuranate' or uranyl nitrate rapidly in air at 450–500°C. The crystallinity of β-UO_3 is improved by keeping the sample at 500°C (not higher) for 4–6 weeks (Debets, 1966). This compound is also obtained by heating at 500–550°C under 30–40 atm O_2. γ-UO_3 is formed slowly at 500–550°C in 6–10 atm O_2. At 650°C and 40 atm O_2, all α, β, δ, and ε-UO_3 compounds convert to the γ-phase. γ-UO_3 can be prepared directly in air by heating uranyl nitrate hexahydrate to 400–600°C (Hoekstra and Siegel, 1958; Engmann and de Wolff, 1963). Stoichiometric δ-UO_3 is obtained by heating β-$UO_2(OH)_2$ (= β-$UO_3 \cdot H_2O$) at 375–400°C for more than 24 h (Hoekstra and Siegel, 1961). At 415°C, the oxygen-deficient δ-phase forms (Wait, 1955). ε-UO_3 is prepared by oxidizing U_3O_8 at 350°C in $NO_2(g)$. The reaction goes to completion in a few seconds (Gruen *et al.*, 1951). At a temperature of 400°C, the reaction rate levels off as the stability limit of ε-UO_3 is approached (Hoekstra and Siegel, 1961). The high-pressure modification ζ-UO_3 forms at 30 kbar and 1100°C (Hoekstra *et al.*, 1970).

UO_3 hydrates

The existence of six compounds, i.e. $UO_3 \cdot 2H_2O$, α-$UO_3 \cdot 0.8H_2O$, α-$UO_2(OH)_2$, β-$UO_2(OH)_2$, γ-$UO_2(OH)_2$, and $U_3O_8(OH)_2$, has been confirmed in the UO_3–water system. $UO_3 \cdot 2H_2O$ is prepared by exposure of anhydrous UO_3 to water at 25–75°C. An alternative method is to add 0.65 g $La(OH)_3$ to 50 mL 0.2 M $UO_2(NO_3)_2$ solution. The hydroxide dissolves slowly, accompanied by an increase in solution pH from 2.2 to 4.0. Digestion of the clear solution at 55°C causes a gradual precipitation of a portion of the uranium as bright yellow crystals of $UO_3 \cdot 2H_2O$ (Hoekstra and Siegel, 1973). Water-deficient α-phase monohydrate, α-$UO_3 \cdot 0.8H_2O$, was prepared by heating $UO_3 \cdot 2H_2O$ in air at 100°C or by heating either $UO_3 \cdot 2H_2O$ or UO_3 in water at 80–200°C (Dell and Wheeler, 1963). Stoichiometric α-$UO_2(OH)_2$ (= α-$UO_3 \cdot H_2O$) was prepared in hydrothermal experiments at temperatures approaching 300°C (Harris and Taylor, 1962; Taylor, 1971).

Stoichiometric β-$UO_2(OH)_2$ (or β-$UO_3 \cdot H_2O$) is prepared by the action of water on $UO_3 \cdot 2H_2O$ or UO_3 at 200–290°C in a sealed reactor (Dawson *et al.*, 1956). It is also formed by the hydrolysis of uranyl salt solutions (cf. γ-$UO_2(OH)_2$). γ-$UO_2(OH)_2$ (or γ-$UO_3 \cdot H_2O$) is obtained when 0.65 g $La(OH)_3$ is added to 50 mL of 0.2 M $UO_2(NO_3)_2$ and subsequent heating of the solution to 80–90°C; digestion of the solution leads to slow precipitation of γ-$UO_2(OH)_2$ (Hoekstra and Siegel, 1973). There may be no region of true thermodynamic stability for the γ-phase. Continued digestion for several weeks eventually gives β-$UO_2(OH)_2$ as the sole product. $U_3O_8(OH)_2$ (= $UO_3 \cdot 1/3H_2O$ or $H_2U_3O_{10}$, i.e. hydrogen triuranate) is prepared by hydrothermal reaction of $UO_3 \cdot 2H_2O$ or UO_3 at temperatures between 300 and 400°C. Although no solid solution range has been observed for this compound, appreciable variations in water content from 0.33 to 0.50 have been reported (Siegel *et al.*, 1972).

Uranium peroxide tetrahydrate, $UO_4 \cdot 4H_2O$, is obtained when the precipitate, grown from the uranyl nitrate solution of $pH = 2$ on addition of hydrogen peroxide solution, is dried at room temperature (Silverman and Sallach, 1961); the dihydrate, $UO_4 \cdot 2H_2O$, is prepared by heating $UO_4 \cdot 4H_2O$ at 90°C.

(*ii*) *Preparation of single crystals*

The basic method to prepare single crystals of UO_2 is to melt UO_2 powders. Arc melting (Brit and Anderson, 1962) and solar furnace heating (Sakurai *et al.*, 1968) techniques have been adopted for this purpose. The vapor deposition method has also been used, where an electric current was passed through a hollow cylinder of UO_2. UO_2 sublimed from the hot central part of the inner surface of the cylinder and deposited at the cooler end, forms large hemispherical single crystals of 4–12 mm (van Lierde *et al.*, 1962). Recrystallization also yields single crystals in the central part of UO_2 rod when the current is directly passed through the specimen (Nasu, 1964).

Single crystals of the length 5 cm have been prepared by means of the floating zone technique. In this case, the preheated UO_2 rods were heated by induction eddy-currents (Chapman and Clark, 1965). Robins (1961) obtained single crystals of 3 mm length by electrolysis of uranyl chloride in fused alkali chloride melts.

Formation of single crystals by chemical transport reactions has been studied by a number of researchers. Naito *et al.* (1971) examined the transport of UO_2, U_4O_9, and U_3O_8 from 1000 to 850°C in sealed quartz tubes using the transporting agents HCl, Cl_2, I_2, Br_2, and Br_2+S_2. Although the transport rate was very low in I_2 ($0.002\ \text{mg h}^{-1}$), it was high enough in Cl_2 of 4 mmHg pressure ($23\ \text{mg h}^{-1}$) and in Br_2+S_2 with partial pressures (2.5 ± 0.2) mmHg ($12.5\ \text{mg h}^{-1}$) to obtain single crystals. Single crystals of UO_2 were deposited on UO_2 substrates with (100) and (111) orientations by the chemical transport method using Cl_2 as the transporting agent (Singh and Coble, 1974). At Cl_2 pressures below 10 mmHg and high substrate temperatures (>950°C), good single crystals free from cracking caused by epitaxial growth were obtained.

Faile (1978) reported the formation of large single crystals of UO_2 by the use of $TeCl_4$ as transport agent. UO_2 was transported in a sealed fused quartz tube from the source end at 1050°C over a temperature gradient to the deposition end at 950°C. The maximum weight of the obtained single crystals was 1 g. $TeCl_4$ has also been used successfully for the preparation of single crystals of other actinide dioxides (Spirlet *et al.*, 1979).

(*iii*) *Crystal structures*

The crystal structures of uranium oxides in the composition range $2.00 \leq O/U \leq 2.375$, which includes UO_2 and polymorphs of U_4O_9 and U_3O_7, are closely related to the fluorite structure. On the other hand, the crystal structures of

U_3O_8 and many of the UO_3 polymorphs are based on the layer structures, which are characterized by the existence of UO_2^{2+} uranyl groups arranged normal to the plane of the layers. The lattice parameters of the uranium oxides are shown in Table 5.14.

UO_2, UO_{2+x}

Stoichiometric uranium dioxide crystallizes in a fcc structure (space group $Fm\bar{3}m$), where the uranium atoms occupy the positions 0,0,0; 1/2,1/2,0; 1/2, 0, 1/2 and 0, 1/2, 1/2 and the oxygen atoms occupy the 1/4, 1/4, 1/4 and its equivalent positions. As the temperature is raised, the anisotropic thermal vibration causes the oxygen atoms to move to the $1/4 + \delta$, $1/4 + \delta$, $1/4 + \delta$ positions, where $\delta = (0.016 \pm 0.001)$ at 1000°C (Willis, 1964a).

In the hyperstoichiometric uranium dioxide, UO_{2+x}, the interstitial oxygen atoms occupy two different sites of the UO_2 lattice, which are displaced by about 1 Å along the <110> and <111> directions from the cubic coordinated interstitial position. These oxygen atoms are denoted as O' and O'', respectively. Together with these interstitial atoms, it was observed that vacancies were formed at the normal oxygen sites, although the uranium sublattice remained undisturbed (Willis, 1964b). Willis (1978) later analyzed the neutron diffraction data for $UO_{2.12}$ at 800°C by taking into account the anharmonic contribution to the Debye–Waller factor. The occupancy numbers of O' and O'' and the vacant lattice oxygens were calculated to be equal within one standard deviation, indicating that the defect complex has a 2:2:2 configuration of oxygen defects. The two O'' oxygen atoms displace two normal oxygen atoms forming two O' atoms and two oxygen vacancies.

A model that assumes a chain-like coordination of the 2:2:2 clusters along <110> directions has been proposed (Allen *et al.*, 1982). However, it failed to give a satisfactory agreement between the observed and calculated neutron intensities (Willis, 1987). There may be a similarity between the clusters present in UO_{2+x} and $Fe_{1-x}O$. In the non-stoichiometric $Fe_{1-x}O$, the Roth clusters (Roth, 1960) or Koch–Cohen clusters (Koch and Cohen, 1969) are thought to be statistically distributed. These clusters have different structures but their compositions are close to that of Fe_3O_4 (Anderson, 1970), which is formed as an ordered phase when the concentration of clusters exceeds a certain value. In the case of UO_{2+x}, the possibility of disordered arrangement of cuboctahedral clusters exists, as U_4O_9 might be composed of ordered cuboctahedral clusters.

U_4O_9

The low-temperature phase α-U_4O_9 transforms to β-U_4O_9 at 340–350 K, which is accompanied by an anomaly in the specific heat at 348 K (Westrum, Jr. *et al.*, 1965) or 330 K (Gotoo and Naito, 1965) and of a dilatation at 293–359 K (Grønvold, 1955). The lattice parameter decreases with increasing temperature in this range (Ferguson and Street, 1963), but no anomaly was observed in the

Table 5.14 *Physical properties of the stoichiometric uranium oxides.*

					Lattice parameters					*Density* (g cm^{-3})		
Formula	*Color*	*m.p.*(K)	*Space group*	*Symmetry*	*a* (Å)	*b* (Å)	*c* (Å)	*Angle* (deg)	*Z*	*Exp.*	*X-ray or ND*	*References*
UO_2	brown to black	3138	$Fm\bar{3}m$	fcc	5.4704				4	10.95	10.964	IAEA (1965); Winslow (1971)
U_4O_9	black		$I\bar{4}3d$	bcc	5.441 × 4				64		10.299	IAEA (1965); Ishii *et al.* (1970a); Bevan *et al.* (1986)
$U_{16}O_{37}$(*)	black			tetragonal	5.407		5.497				11.366	Hoekstra *et al.* (1970)
U_8O_{19}(*)	black			monoclinic	5.378	5.559	5.378	$\beta =$ 90.27		11.34	11.402	Hoekstra *et al.* (1968)
α-U_3O_7	black			tetragonal	5.447		5.400			10.62		Hoekstra *et al.* (1961); Westrum, Jr. and Grønvold (1962)
β-U_3O_7	black			tetragonal	5.383		5.547			10.60		Hoekstra *et al.* (1961); Garrido *et al.* (2003)
γ-U_3O_7 ($U_{16}O_{37}$)	black			tetragonal	5.407		5.497					Hoekstra *et al.* (1970)
α-U_2O_5	black			monoclinic	12.40	5.074	5.675	$\beta =$ 99.2	4	10.5	10.47	Hoekstra *et al.* (1970); Spitsyn *et al.* (1972)
β-U_2O_5	black			hexagonal	3.813		13.18		2	10.76 to 11.38	11.15	Hoekstra *et al.* (1970)
γ-U_2O_5	black			monoclinic	5.410	5.481	5.410	$\beta =$ 90.49	2	10.36	11.51	Hoekstra *et al.* (1970)
$U_{13}O_{34}$	black		*Cmcm* (or *Cmc* or *Ama*)	orthorhombic	6.740	3.964×13	4.143×2		4		8.40	Spitsyn *et al.* (1972)

U_8O_{21}			*Pmma*	orthorhombic	6.796	3.958×8	4.145×2		4		8.341	Spitsyn *et al.* (1972)
$U_{11}O_{29}$			*Pnma* (or *Pna*$_2$)	orthorhombic	6.765	3.956×11	4.140×2		4		8.40	Spitsyn *et al.* (1972)
α-U_3O_8	green black		*C*2*mm*	orthorhombic	6.716	11.960	4.147		2		8.395	Loopstra (1970b)
β-U_3O_8	green black		*Cmcm*	orthorhombic	7.069	11.445	8.303		4		8.326	Loopstra (1970b)
$U_{12}O_{35}$(*)	olive green			orthorhombic	6.91	3.92	4.16		2	7.72	8.39	Hoekstra *et al.* (1970)
A-UO_3	orange	723(d)		amorphous						6.80		Hoekstra and Siegel (1961)
α-UO_3	beige	723(d)	(*C*222 derived)	orthorhombic	6.84	43.45	4.157		19	7.30	7.44	Siegel and Hoekstra (1971a); Greaves and Fender (1972)
β-UO_3	orange	803(d)	*P*2$_1$	monoclinic	10.34	14.33	3.910	$\beta =$ 99.03	10	8.25	8.30	Hoekstra and Siegel (1961); Debets (1966)
γ-UO_3	yellow	923(d)	*Fddd*	orthorhombic	9.813	19.93	9.711		32	7.80	8.00	Hoekstra and Siegel (1961); Siegel and Hoekstra (1971b)
δ-UO_3	deep red	673(d)	*Pm*3*m*	cubic	4.16				1	6.69	6.60	Wait (1955); Hoekstra and Siegel (1961)
ε-UO_3	brick red	673(d)		triclinic	4.002	3.841	4.165	$\alpha =$ 98.10 $\beta =$ 90.20 $\gamma =$ 120.17	1	8.54	8.67	Hoekstra and Siegel (1961); Kovba *et al.* (1963)
ζ-UO_3	brown		*P*2$_1$2$_1$2$_1$	orthorhombic	7.511	5.466	5.224		4	8.62	8.86	Siegel *et al.* (1966); Hoekstra *et al.* (1970)

(d): decomposes.
(*): Parameters for these phases refer to a pseudo-cell.

magnetic susceptibility (Gotoo and Naito, 1965). The transition was claimed to be due to disordering of oxygen with U^{4+}–U^{5+} rearrangement (Naito *et al.*, 1967; Fournier and Troć, 1985). Belbeoch *et al.* (1967) reported that α-U_4O_9 has a rhombohedral structure, slightly distorted from a cubic structure with the lattice parameters $a = 5.4438n$ (n: an integer) and $\alpha = 90.078°$ at 20°C. The transition is possibly of order–disorder type coupled with a small change in crystal structure.

Another transition from β-U_4O_9 to γ-U_4O_9 occurs at higher temperatures around 850 K. An X-ray diffraction analysis showed the transition temperature to be 823–973 K (Blank and Ronchi, 1968), while the heat capacity measurement gave 900–950 K (Grønvold *et al.*, 1970). A transition between 813–893 K was observed for the specimens of $2.228 \leq O/U \leq 2.25$ (Naito *et al.*, 1973) using X-ray diffraction and electrical conductivity measurements. This β/γ transition is assumed to be based on the order–disorder mechanism (Blank and Ronchi, 1968; Naito *et al.*, 1973). According to Seta *et al.* (1982), there was no clear anomaly or variation in the heat capacity curves in the above temperature range. Instead they observed two small peaks for hypostoichiometric U_4O_{9-y} ($UO_{2.22}$ and $UO_{2.235}$) at 1000 and 1100 K.

The crystal structure of α-U_4O_9 has not yet been solved, but it is supposed to be closely related to that of strictly cubic β-U_4O_9, with the space group $I\bar{4}3d$. Electron diffraction measurements on α-U_4O_9 showed that the superlattice reflections all obeyed the special extinction rules for the $\bar{4}$ sites of the space group $I\bar{4}3d$ (Blank and Ronchi, 1968). Bevan *et al.* (1986) suggest that α-U_4O_9 consists of cuboctahedral clusters centered on 12(a) or 12(b) sites similar to the crystal structure of β-U_4O_9, although the anion sublattice may be perturbed.

Bevan *et al.* (1986) collected single-crystal neutron diffraction data for β-U_4O_9 at 230 and 500°C. A partial Patterson synthesis obtained using only the superlattice reflections supported the cuboctahedral cluster model. Fig. 5.16 shows a sketch of the cuboctahedral oxygen cluster formed by 12 anions located at the vertices of a cuboctahedron and with a 13th oxygen atom situated in its center. The cube surrounding the cluster has an edge length close to the lattice parameter of the fcc cell of the uranium sublattice (the individual cations are not shown in the figure). In β-U_4O_9, the discrete U_6O_{37} cuboctahedral clusters are arranged on $\bar{4}$ axes with positions 12(b) of $I\bar{4}3d$.The displacement of oxygen in the cluster gives rise to the O′ interstitial atoms of Willis. The cuboctahedral cluster contains the Willis 2:2:2 clusters as a component. The structure contains twelve U_6O_{37} clusters per unit cell. There are 60 extra anions per unit cell, and the composition is then $U_{256}O_{572}$, i.e. the β-U_4O_9 phase has the composition U_4O_{9-y} with $y = 0.062$.

U_3O_7

The U_3O_7 polymorphs all crystallize in the tetragonal system but none of their space groups have been specified. The axial ratio *c/a* is here an important parameter to classify the different polymorphs. α-U_3O_7, which is prepared by

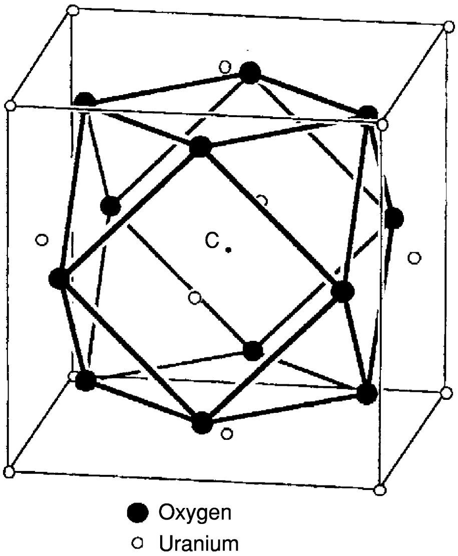

Fig. 5.16 *A schematic diagram of the cuboctahedral cluster. Eight oxygen anions inside the cationic cube are replaced by* 12 *anions located along the* <110> *directions from the center C.* (*from Garrido* et al. (2003), *reproduced by the permission of Elsevier*).

oxidation of UO_2 in air at temperatures of 120–175°C, has *c/a* ratios less than 1 (0.986–0.991) (Pério, 1953b; Westrum, Jr. and Grønvold, 1962). The *c/a* ratios for β-U_3O_7, prepared by oxidizing UO_2 in air at temperatures 160–250°C, are 1.027–1.032 (Hoekstra *et al.*, 1961; Simpson and Wood, 1983; McEachern and Taylor, 1998). In the range of O/U ratios between 2.26 and 2.33, the *c/a* ratio of α-U_3O_7 did not vary in a systematic way between 0.986 and 0.989, while that of β-U_3O_7 seemed to increase very slightly with increasing O/U ratio (Hoekstra *et al.*, 1961). The γ-U_3O_7 ($U_{16}O_{37}$) phase with *c/a* ratios of 1.015–1.016 appears in a range where the O/U ratios are 2.30–2.31 (Westrum, Jr. and Grønvold, 1962; Hoekstra *et al.*, 1970; Tempest *et al.*, 1988), which are significantly smaller than those of α-U_3O_7 and β-U_3O_7.

In the recent studies on β-U_3O_7, it was found that all the uranium atoms and 70% of the oxygen atoms were hardly affected by the oxidation of UO_2 to U_3O_7; however, the remaining 30% of the oxygen atoms changed their location to new sites which are shifted 0.31 Å along $\langle 110 \rangle$ vectors from the holes in the fluorite framework of UO_2. This result, based on a neutron diffraction analysis, is consistent with the assumption that the excess oxygen atoms in β-U_3O_7 are accommodated in the cuboctahedral oxygen clusters (Garrido *et al.*, 2003) as in the case of β-U_4O_9.

According to a theoretical study by Nowicki *et al.* (2000), the crystal structures of U_3O_7 differ from that of UO_2 by the presence of the cuboctahedral

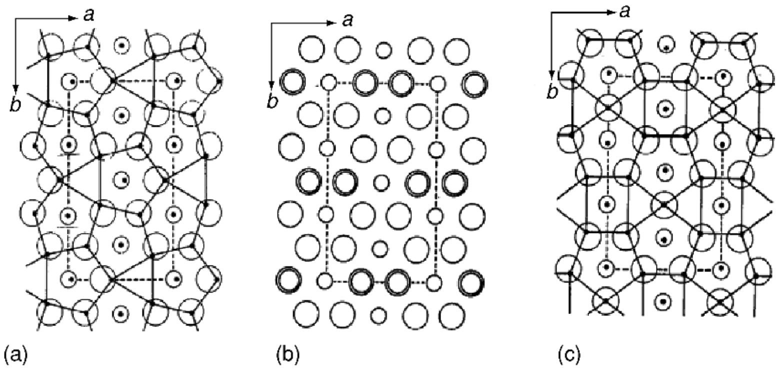

Fig. 5.17 *Atom arrangements on the sections perpendicular to the c-axis (Loopstra, 1970b). (a) α-U_3U_8; (b) hypothetical 'ideal' UO_3; (c) β-U_3O_8. The dots in the figure represent the actual positions. Isolated dots: uranium atoms; dots connected by full-drawn lines denote oxygen atoms. In (a), the section is at $z = 0$, and in (c), the origin is shifted b/3 at $z = 1/4$. Reproduced by permission of the International Union of Crystallography.*

clusters centered at specified ordered positions, and the arrangement of the clusters can be expressed as a stacking of identical polyatomic modules. A single module contains clusters arranged in a square pattern. The square sides have a length approximately equal to $R_1 = \sqrt{2.5}a_{\mathrm{UO_2}} \approx 0.86$ Å. The thickness of the modules is close to $1.5a_{\mathrm{UO_2}} \approx 0.82$ Å. The various polytypes found in U_3O_7 can be rationalized with different stacking order of these modules; the small change in the energy of formation of the crystal reflects the interaction between the clusters.

U_3O_8

α-U_3O_8 is orthorhombic (*C2mm*; $a = 6.716$ Å, $b = 11.96$ Å, $c = 4.1469$ Å; $z = 2$) (Loopstra, 1962). β-U_3O_8 is also orthorhombic (*Cmcm*; $a = 7.069$ Å, $b = 11.445$ Å, $c = 8.303$ Å; $z = 4$) (Loopstra, 1970b), and the crystal structures of these two modifications are very similar. Fig. 5.17 depicts the relation of α- and β-U_3O_8 with the hypothetical 'ideal' UO_3 structure. The idealized α-U_3O_8 structure (Fig. 5.17a) is derived from a layer of the hypothetical 'ideal' UO_3 (Fig. 5.17b) by removing one oxygen atom from every third row. The idealized β-U_3O_8 structure is obtained by replacing two oxygen atoms by a single one, located halfway between them (Fig. 5.17c). Fig. 5.17a and c show that the actual structures are only slightly distorted from the hypothetical ideal positions, which are represented in Fig. 5.17 by small circles (uranium atoms) and large circles (oxygen atoms). In α-U_3O_8, all uranium atoms are coordinated with oxygen atoms forming pentagonal bipyramids. In β-U_3O_8 the layers are stacked along the *c*-axis so that a set of chains of uranium atoms is formed at $x = 0$, $y = 0$ and $x = 1/2$, $y = 1/2$. The other uranium atoms form chains in the *c* direction, in which the oxygen coordination is alternately pentagonal bipyramidal and distorted octahedral.

α-U_3O_8 shows a λ-type anomaly in the specific heat at 208.5°C (Girdhar and Westrum, Jr., 1968). At this first-order phase transformation temperature, the orthorhombic pseudo-hexagonal α-U_3O_8 changes to a hexagonal structure ($P\bar{6}2m$; a = 6.812 Å, c = 4.142 Å; z = 1) (Loopstra, 1970a). Although the high- and low-temperature phases are closely related, there is an essential difference in the atom arrangement. In the high-temperature phase the uranium atoms occupy a single three-fold position, whereas at room temperature (in the low-temperature phase) they are located at two-fold and four-fold positions making it possible for the uranium atoms to have different localized charges.

Allen and Holmes (1995) pointed out the resemblance in the crystal structures of UO_2 and α-U_3O_8. The UO_2 fluorite structure can be transformed to the layer structure of α-U_3O_8 by displacing the (111) planes in UO_2. A displacement of 2.23 Å along the ⟨112⟩ direction in the (111) plane brings the outermost uranium layer directly above the second layer of the structure of α-U_3O_8.

UO_3

The crystal structure of α-UO_3 was first reported as trigonal ($P\bar{3}m1$; a = 3.971 Å, c = 4.170 Å) (Zachariasen, 1948a). However, the later neutron powder diffraction data could not be adequately described in this way. Loopstra and Cordfunke (1966) published a structure assignment using an orthorhombic unit cell ($C2mm$; a = 3.961 Å, b = 6.860 Å, c = 4.166 Å). This structure is close to the former one, since in both cases there are linear chains of O–U–O–U–O with the uranium surrounded by six additional oxygen atoms lying approximately in a plane normal to the chains. The reassignment to the orthorhombic cell reduced the R-value from 0.35 to 0.19, but this is still high. Neither of the structures proposed could explain the abnormally low experimental density and the infrared absorption spectrum; the experimental densities were 7.25 g cm^{-3} (Loopstra and Cordfunke, 1966) or 7.30 g cm^{-3} (Siegel and Hoekstra, 1971a), which are much lower than the X-ray density of 8.39 g cm^{-3}. Strong infrared absorption was observed around 930 cm^{-1} (Hoekstra and Siegel, 1961; Carnall *et al.*, 1966). This is typical of the antisymmetric stretching vibration of the linear uranyl group with the U–O bond distance of about 1.7 Å (Jones, 1959), but isolated uranyl groups do not exist in either of the above crystal structures.

A characteristic feature of a large number of solid uranium(VI) oxides is that they contain uranyl groups (UO_2^{2+}) with collinear atom arrangement (O–U–O) (Zachariasen, 1954b). The U–O bond (primary bond) of the uranyl group is a strong covalent bond (cf. Section 5.8.3c), giving short bond distances of 1.7–1.9 Å. The antisymmetric vibration of O_I–U–O_I, where O_I denotes the oxygen atoms in the uranyl group, gives rise to a strong infrared absorption in the frequency range of 600–950 cm^{-1}. The oxygen atoms (O_{II}), bound to uranium in a plane perpendicular to the linear uranyl group, form secondary bonds which are weaker than the U–O_I bonds. The U–O_{II} bond distances are longer, usually between 2.1 and 2.5 Å. The uranyl groups are often seen in the uranium oxides having layer structures. The collinear axis of the uranyl group is along the c-axis of such crystals with the four to six U–O_{II} bonds formed in the a–b plane.

Greaves and Fender (1972) carried out a structure refinement based on the assumption that α-UO_3 is formed by introducing statistically distributed vacancies into the uranium sublattice of α-U_3O_8 so as to re-establish an O/U ratio of three. For each missing uranium atom there were two displaced oxygen atoms in the z-direction. Refinement of diffraction data using this model for the α-U_3O_8 structure (space group *C*222) of Andresen (1958) decreased the R-value to 0.031 and the theoretical density to 7.44 g cm^{-3}; the U–O distance in the uranyl groups was 1.64 Å. The same refinement based on the *C*2*mm* space group of Loopstra (1962) yielded fairly reasonable values of the uranium occupation number, 0.82, and the U–O distance, 1.58 Å, but the R-value (0.13) and the uranium and oxygen temperature factors were somewhat higher. The superlattice reflections observed in both the neutron and electron diffraction patterns could be indexed on an orthorhombic unit cell with dimensions a = 6.84 Å, b = 43.45 Å, and c = 4.157 Å.

The crystal structure of high-pressure phase, ζ-UO_3, is orthorhombic ($P2_12_12_1$; a = 7.511 Å, b = 5.466 Å, c = 5.224 Å) (Siegel *et al.*, 1966). There are no uranium vacancies in this UO_3 modification as shown by the agreement of the measured density (8.62 g cm^{-3}) with the X-ray density (8.85 g cm^{-3}). In this structure each uranium atom is bonded to seven oxygen atoms, leading to shared [UO_7] configurations with bridging oxygen atoms in the plane perpendicular to the UO_2-axis, identified by two short collinear bonds of 1.80 and 1.85 Å. The other five coordinated oxygen atoms form a puckered pentagonal coordination geometry around the uranyl groups.

(*iv*) *Phase relations*

There have been numerous reports on the phase relations and thermodynamic properties of the uranium–oxygen system. Rand *et al.* (1978) made an assessment of thermodynamic data and presented a phase diagram of this system. Recently, Chevalier *et al.* (2002) and Guéneau *et al.* (2002) published critical reviews. In two recent papers Labroche *et al.* (2003a,b) critically assessed the composition range and oxygen potential of uranium oxides in the UO_2–U_3O_8 region taking into account the uncertainties of the published data.

Uranium–uranium dioxide region

Hypostoichiometric UO_{2-x} exists as a single phase or as a mixture with liquid. Since the formation energy of an oxygen vacancy in UO_2 is much higher than that of interstitial oxygen, the lower phase boundary of single phase UO_{2-x} is very close to O/U = 2.0 up to ~1500 K. In the phase diagram of Rand *et al.* (1978), this phase boundary has been obtained up to 2500 K by using the relation $\ln x = (3.877 \pm 0.094) - (13130 \pm 210)T^{-1}$ proposed by Winslow (1973) based on examination of the relevant experimental data. In the recent critical review on the thermodynamic properties in the uranium–oxygen system, Chevalier *et al.* (2002) presented the phase diagram of the U–UO_2 region by careful selection of the experimental data from Blum *et al.* (1963),

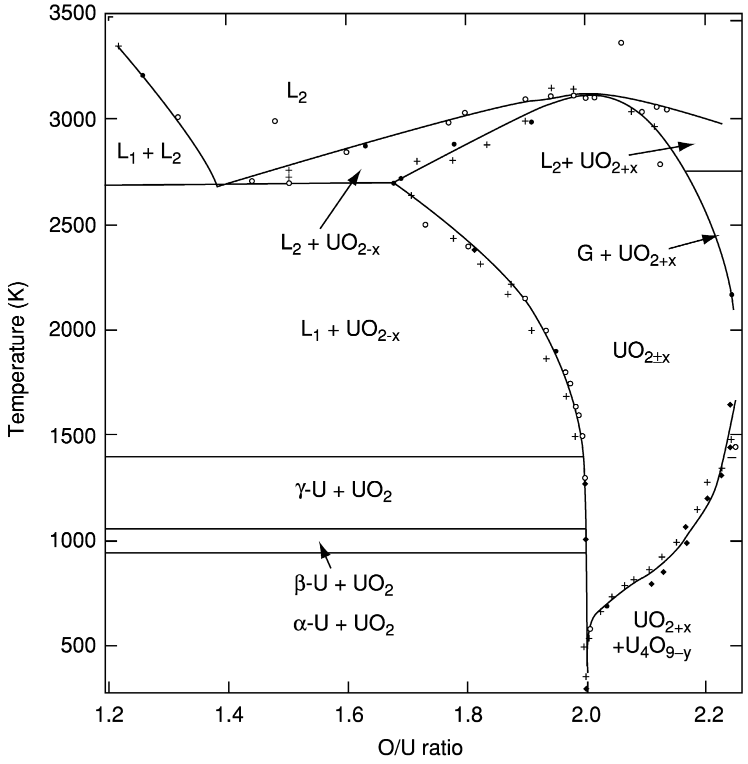

Fig. 5.18 *Partial phase diagram of the U–UO_2 system assembled from values in Rand* et al. (1978), *Chevalier* et al. (2002), *and Guéneau* et al. (2002).

Bates (1964, 1966), Martin and Edwards (1965), Edwards and Martin (1966), Guinet *et al.* (1966), Bannister (1967), Tetenbaum and Hund (1968, 1970), Ackermann *et al.* (1969), Latta and Fryxell (1970), Ackermann and Rauh (1972), Garg and Ackermann (1977, 1980), and Guéneau *et al.* (1998). Guéneau *et al.* (2002) presented the phase diagram of this region using the data from Cleaves *et al.* (1945), Martin and Edwards (1965), Edwards and Martin (1966), Bannister (1967), Hein *et al.* (1968), Ackermann *et al.* (1969), Kjaerheim and Rolstad (1969), Latta and Fryxell (1970), Tachibana *et al.* (1985), and Guéneau *et al.* (1998). Fig. 5.18 shows a phase diagram of the U–UO_2 region ($1.2 \leq$ O/U ≤ 2.0) and the UO_{2+x} region with $x \leq 0.25$ drawn by using the selected values from Rand *et al.* (1978), Chevalier *et al.* (2002), and Guéneau *et al.* (2002).

The monotectic temperatures for the reaction $L_2 = UO_{2-x} + L_1$ are (2773 ± 30) K (Edwards and Martin, 1966), (2743 ± 30) K (Guinet *et al.*, 1966) and (2693 ± 70) K (Bannister, 1967). The reported compositions of the liquid L_2 phase at the monotectic temperature are O/U = (1.3 ± 0.1) (Edwards and Martin, 1966), 1.18 (Guinet *et al.*, 1966), (1.53 ± 0.05) (Bannister, 1967) and

1.46 (Latta and Fryxell, 1970). The measured composition of the liquid L_1 phase at this temperature was O/U = 0.05 (Edwards and Martin, 1966; Latta and Fryxell, 1970). The O/U ratios of solid UO_{2-x} are in reasonable agreement: 1.67 (Latta and Fryxell, 1970; Rand *et al.*, 1978), 1.64 (Edwards and Martin, 1966), 1.60 (Guinet *et al.*, 1966), and (1.62 ± 0.06) (Bannister, 1967). The ratio O/U is decreased to ≈1.67 at the lower phase boundary of single phase UO_{2-x} at the monotectic temperature. Above the monotectic temperature the O/U ratio at the lower phase boundary increases to $UO_{2.00}$, until the maximum melting temperature is reached. At the monotectic temperature, three condensed phases, i.e. oxygen-saturated liquid uranium metal L_1 ($UO_{0.05}$), liquid L_2 of a composition $UO_{1.39}$, and solid UO_{2-x} ($UO_{1.67}$) coexist in equilibrium.

$UO_{2.00}$–$UO_{2.25}$ region

Stoichiometric uranium dioxide, UO_2, shows a first-order transition at 30.8 K. This is a magnetic transition, and below that temperature UO_2 is antiferromagnetic, with a structure of type I (Fournier and Troć, 1985), accompanied by an internal distortion in the oxygen sublattice (Faber, Jr. and Lander, 1976). At the transition temperature, a discontinuity in the lattice parameter vs temperature curve (Marples, 1976) and a sharp anomaly in the heat capacity with an entropy increment of 3.6 $J\,K^{-1}\,mol^{-1}$ (Westrum, Jr. and Grønvold, 1962; Huntzicker and Westrum, Jr., 1971) were observed.

Uranium dioxide is stoichiometric at low temperatures, but exhibits a hyperstoichiometric (UO_{2+x}) homogeneity range above 500 K; this range increases with increasing temperature. The upper phase boundary of single phase UO_{2+x} has been extensively studied at temperatures between 500 and 1950 K. The boundary increases with increasing temperature up to (1398 ± 8) K (Blackburn, 1958; Roberts and Walter, 1961; Anthony *et al.*, 1963; Belbeoch *et al.*, 1967; Blank and Ronchi, 1968; van Lierde *et al.*, 1970; Dodé and Touzelin, 1972; MacLeod, 1972; Matsui and Naito, 1975; Labroche *et al.*, 2003b), at which the U_4O_9 phase decomposes to UO_{2+x} and U_3O_{8-z} ($UO_{2.61}$) peritectoidally. The upper phase boundary of UO_{2+x} above that temperature increases only slightly with increasing temperature up to 1950 K.

The phase diagram in the region $2.0 \leq O/U \leq 3.0$ is shown in Fig. 5.19, where the upper phase boundary of UO_{2+x} was obtained by referring to the literature (Blackburn, 1958; Schaner, 1960; Aronson *et al.*, 1961; Roberts and Walter, 1961; Kiukkola, 1962; Markin and Bones, 1962a; Hagemark and Broli, 1966; Kotlar *et al.*, 1967a; Bannister and Buykx, 1974; Saito, 1974; Picard and Gerdanian, 1981; Labroche *et al.*, 2003b). The U_4O_9 phase has a narrow homogeneity range; the reported lower phase boundary is located between the O/U ratios of 2.228 and 2.235 (Blackburn, 1958; Schaner, 1960; Roberts and Walter, 1961; Kotlar *et al.*, 1968; van Lierde *et al.*, 1970; Inaba and Naito, 1973; Picard and Gerdanian, 1981; Labroche *et al.*, 2003b). This boundary is almost unchanged with temperature from room temperature to the peritectic temperature. The reported upper phase boundaries have the O/U values mostly between

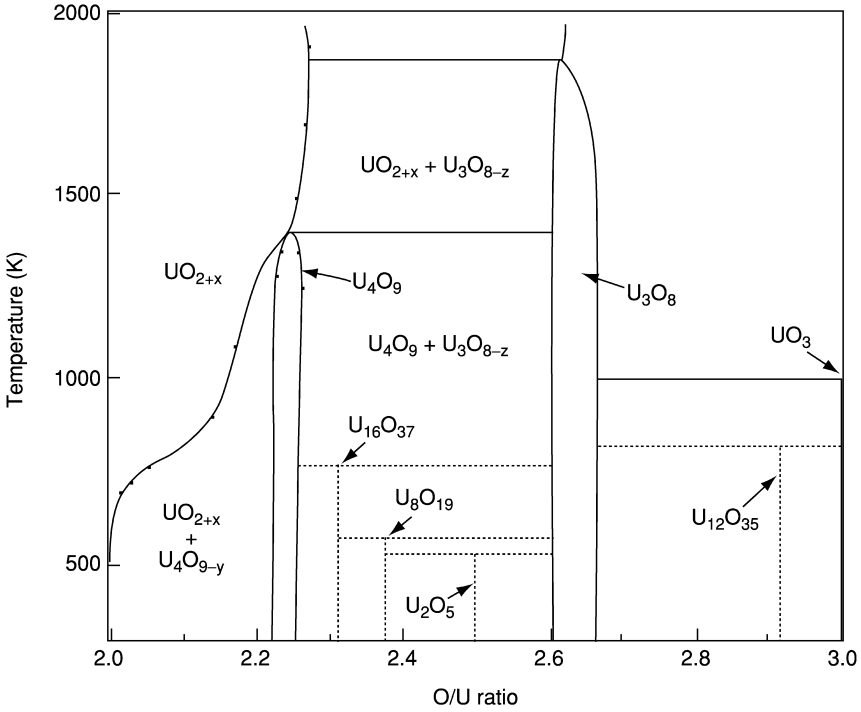

Fig. 5.19 *Phase diagram of the U–O system in the region* 2.0 ≤ *O/U* ≤ 3.0.

2.24 and 2.25 (Blackburn, 1958; Schaner, 1960; Roberts and Walter, 1961; Kotlar *et al.*, 1968; van Lierde *et al.*, 1970; Inaba and Naito, 1973; Picard and Gerdanian, 1981; Labroche *et al.*, 2003b), and many of the papers indicate the uppermost composition to have O/U = 2.242. It is generally assumed that also the upper phase boundary does not change substantially with temperature.

U_4O_9 shows no low-temperature anomaly in the heat capacity due to a magnetic transition observed for UO_2. This is interesting if one considers the close resemblance in the crystal structures between U_4O_9 and UO_2. Instead, the low-temperature modification α-U_4O_9 undergoes a non-magnetic second-order transition to β-U_4O_9 at 340–350 K giving rise to a λ-type specific heat anomaly. The enthalpy and entropy increments of this transition for $U_4O_{9\text{-}y}$ with O/U = 2.246–2.254 are 630–710 J mol^{-1} and 1.9–2.2 J K^{-1} mol^{-1}, respectively (Gotoo and Naito, 1965; Westrum, Jr., *et al.*, 1965; Grønvold *et al.*, 1970; Inaba and Naito, 1973). β-U_4O_9 transforms into γ-U_4O_9 at around 850 K. According to Bevan *et al.* (1986), the maximum O/U atom ratio of the β-U_4O_9 phase should be 2.2345 (cf. section on U_4O_9), which supports the hypostoichiometries at the upper phase boundary observed for U_4O_9. The phase transitions α/β and β/γ are reversible, as described in the crystal structure section.

$UO_{2.25}$–$UO_{2.667}$ region
Most compounds in the composition range of $2.25 \leq O/U \leq 2.5$, i.e. α- and β-U_3O_7, γ-U_3O_7 ($U_{16}O_{37}$), U_8O_{19}, and β- and γ-U_2O_5 have fluorite-type structures. α-, β-, and γ-U_3O_7 have been prepared under ambient atmosphere, but U_8O_{19} and α-, β-, and γ-U_2O_5 were formed only at high pressures (15–60 kbar). On this basis, U_8O_{19} and U_2O_5 are regarded as metastable phases, which are thermodynamically unstable at atmospheric pressure (Hoekstra *et al.*, 1970). The phases for which the stability has not been established are indicated in Fig. 5.19 by broken lines. U_3O_7 decomposes at 700°C in air to U_4O_9 and U_3O_8 (Pério, 1953a; Grønvold, 1955). Although β-U_3O_7 shows no low-temperature transitions, α-U_3O_7 exhibits a small λ-type anomaly at 30.5 K with enthalpy and entropy increments of 11 J mol^{-1} and 0.4 J K^{-1} mol^{-1}, respectively. This transition is assumed to be of magnetic origin (Westrum, Jr. and Grønvold, 1962). The other oxides $U_{13}O_{34}$ ($UO_{2.615}$) and $U_{11}O_{29}$ ($UO_{2.636}$) have been described (Kovba *et al.*, 1972; Spitsyn *et al.*, 1972), but no information is given for their stability at low temperatures and pressures.

Two modifications of U_3O_8, i.e. α- and β-U_3O_8, crystallize both in orthorhombic system and their crystal structures are very similar. These compounds are not based on the fluorite structure but are composed of the layer structures related to the hypostoichiometric ‘ideal’ UO_3 structure (Section 5.7.2a(iii)), which has uranyl bonds perpendicular to the layer planes. The difficulty to rearrange the oxygen atoms in these infinite layer structures is probably the reason for the slow equilibration between U_3O_8 and the gas phase at different temperatures and the oxygen partial pressures. The O/U ratio of the U_3O_8 phase varies with the experimental methods (Gerdanian and Dodé, 1965; Fujino *et al.*, 1981; Srirama Murti *et al.*, 1989). Labroche *et al.* (2003a) suggested that the reason for the scattered data is dissolution of atmospheric nitrogen in the oxides. Although the measured data at the lower phase boundary of U_3O_8 phase are not in good agreement above 1000 K (Labroche *et al.*, 2003b), the ratios O/U are in general between 2.595 and 2.62 (Blackburn, 1958; Hagemark and Broli, 1966; Kotlar *et al.*, 1967b; Ackermann and Chang, 1973; Caneiro and Abriata, 1984). This phase boundary does not change with temperature up to ~1600 K. Above 1000 K, the upper phase boundary was observed to have O/U = 2.667 (stoichiometric U_3O_8) up to ~1400 K (Ackermann and Chang, 1973; Caneiro and Abriata, 1984). At an ambient pressure of 0.21 atm O_2, however, the compound becomes hypostoichiometric above 873 K (Cordfunke and Aling, 1965; Rodriguez de Sastre *et al.*, 1967; Ackermann and Chang, 1973). On the other hand, at lower temperatures of 773–873 K, freshly prepared U_3O_8 samples often show hyperstoichiometry with O/U = 2.670. Moreover, a hysteresis is seen in the O/U ratio in heating and cooling cycles. Repetition of the heating and cooling cycle results in formation of compounds of lower O/U ratios (Dharwadkar *et al.*, 1975; Fujino *et al.*, 1981). Similar hysteresis phenomena for U_3O_{8-z} have also been observed in oxygen partial pressure vs O/U ratio isotherms (Caneiro and Abriata, 1984) and the electrical conductivity (Ishii *et al.*, 1970b;

Dharwadkar *et al.*, 1978). Slow formation of another phase in α-U_3O_8 may take place at temperatures of 1273–1573 K; according to Hoekstra *et al.* (1955); this is possibly the U_8O_{21} phase with a homogeneity range extending between the compositions $UO_{2.60}$ and $UO_{2.65}$. A slightly different composition range, $UO_{2.617}$–$UO_{2.655}$, has also been reported (Caneiro and Abriata, 1984). It is possible that the proper stoichiometry of β-U_3O_8 is U_8O_{21}, since β-U_3O_8 has been prepared by heating α-U_3O_8 to 1623 K followed by slow cooling to room temperature (Loopstra, 1970b). However in the majority of reports, the phase in this region of compositions is considered to be hypostoichiometric U_3O_8 (i.e. U_3O_{8-z}) (Kotlar *et al.*, 1967a; Ackermann and Chang, 1973; Labroche *et al.*, 2003a,b).

α-U_3O_8 shows a λ-type transition in the heat capacity at 25.3 K with associated enthalpy and entropy increments of 50 J mol^{-1} and 2.3 J K^{-1} mol^{-1}, respectively (Westrum, Jr. and Grønvold, 1959, 1962). This is due to a para-antiferromagnetic transition (Leask *et al.*, 1963). α-U_3O_8 shows three other transitions at higher temperatures: 490, 570, and 850 K. The reported temperature for the 490 K transition varies between 480 and 490 K (Girdhar and Westrum, Jr., 1968; Maglic and Herak, 1970; Inaba *et al.*, 1977; Naito *et al.*, 1982). For the 570 K transition, the reported temperatures are between 562 and 576 K (Inaba *et al.*, 1977; Naito *et al.*, 1982, 1983). The 850 K transition has been observed in one study using adiabatic calorimetry (Inaba *et al.*, 1977). Naito *et al.* (1983) proposed an electronic ordering on uranium atoms with displacement of oxygen atoms as the origin of the above transitions.

$UO_{2.667}$–UO_3 region

Hoekstra and Siegel (1961) regard the $UO_{2.9}$ phase ($U_{12}O_{35}$), which is formed by partial decomposition of amorphous UO_3, as a distinct compound because on heating amorphous UO_3 the O/U ratio remains virtually constant over a 100 K temperature interval from 450 to 550°C. The pycnometric density measured for $UO_{2.9}$ is considerably lower than the theoretical density. This is similar to the case of α-UO_3 assigned to a *C2mm* orthorhombic cell with $a = 3.961$ Å, $b = 6.860$ Å, and $c = 4.166$ Å (Loopstra and Cordfunke, 1966). Thus the crystal structure of $UO_{2.9}$ may also have vacant uranium sites as in the α-UO_3 structure.

For UO_3, one amorphous and six crystalline modifications are known. When α-UO_3 is heated in air with a constant heating rate, it decomposes to U_3O_8 passing through a non-stoichiometric range with the O/U ratios between 3.0 and ca. 2.95 (Hoekstra and Siegel, 1961). The δ- and ε-UO_3 compounds convert to U_3O_8 at about 450°C in air with no evidence of a non-stoichiometric oxide range. However, if the heating rate is low, they do not decompose directly, instead re-oxidation of the partially reduced oxides to γ-UO_3 takes place. Also in the γ-UO_3 there is no measurable oxygen non-stoichiometry. The γ-phase is more stable and decomposes to U_3O_8 at higher temperatures of 620–700°C. ζ-UO_3 is formed by heating U_3O_8 at 500°C under high pressures of 15–60 kbar interval produced by a pyrophyllite tetrahedral assembly. This compound is unstable at the ambient pressure (Hoekstra *et al.*, 1970). No magnetic transition has been observed for UO_3 (Jones *et al.*, 1952).

In the uranium trioxide–water system, six compounds have been well established (Dawson *et al.*, 1956; Harris and Taylor, 1962; Debets and Loopstra, 1963; Dell and Wheeler, 1963; Cordfunke and Debets, 1964; Bannister and Taylor, 1970; Taylor, 1971; Siegel *et al.*, 1972; Hoekstra and Siegel, 1973; Vita *et al.*, 1973; Tasker *et al.*, 1988). The physical properties for these compounds are listed in Table 5.15 together with those for uranium peroxide hydrates.

(*v*) *The heat capacity of UO_2*

The low-temperature heat capacity of UO_2 shows a very sharp λ-type anomaly of magnetic origin (Fournier and Troć, 1985) at 30.44 K (Huntzicker and Westrum, Jr., 1971) or 28.7 K (Jones *et al.*, 1952). The entropy increment is 3.6 J K^{-1} mol^{-1} (Westrum, Jr, and Grønvold, 1962). Faber, Jr. and Lander (1976) carried out a neutron diffraction and scattering study on this transition. They showed that the anomaly took place at 30.8 K and that it could be explained as a first-order transition from the low-temperature antiferromagnetic state of type I, associated with an internal distortion of the oxygen sublattice, to the paramagnetic state. The low-temperature (5–346 K) heat capacity data of Huntzicker and Westrum, Jr. (1971) are in good agreement with those of Grønvold *et al.* (1970) (304–1006 K) in the range of overlapping temperatures.

The high-temperature heat capacity of UO_2 has been studied extensively because of the importance of this compound as nuclear fuel; several critical reviews have also been published (Browning, 1981; Browning *et al.*, 1983; Naito, 1989; Ronchi and Hyland, 1994; Fink, 2001; Carbajo *et al.*, 2001). The selected data of heat capacities are shown in Fig. 5.20 together with the correlations calculated by the MATPRO equation (Hagrman, 1995) and by the Fink equations with functional and polynomial forms. In the figure two sets of data of Ronchi *et al.* (1999) are shown for high temperatures, and the data of Huntzicker and Westrum, Jr. (1971) and Grønvold *et al.* (1970) are shown for low and intermediate temperatures. Since the heat capacities of the functional and polynomial equations differ by at most 1%, the latter equation is recommended because of its simplicity (Fink, 2001). This equation, which is based on a combined analysis of the reported data (Moore and Kelley, 1947; Hein and Flagella, 1968; Hein *et al.*, 1968; Ogard and Leary, 1968; Leibowitz *et al.*, 1969; Fredrickson and Chasanov, 1970; Grønvold *et al.*, 1970; Huntzicker and Westrum, Jr., 1971; Ronchi *et al.*, 1999), for $298.15 \leq T \leq 3120$ K is:

$$\begin{aligned} C_\mathrm{p}(T)(\mathrm{J\ K^{-1}\ mol^{-1}}) = {} & 52.1743 + 87.951\,\tau - 84.2411\,\tau^2 + 31.542\,\tau^3 \\ & - 2.6334\,\tau^4 - 0.71391\,\tau^{-2}, \end{aligned}$$

where, $\tau = T(\mathrm{K})/1000$. The MATPRO equation (Hagrman, 1995) gives somewhat lower C_p values at higher temperatures.

The λ-type transition found by Bredig (1972) at 2670 K has been confirmed by other researchers (Hutchings *et al.*, 1984; Ralph and Hyland, 1985; Hiernaut *et al.*, 1993). Hiernaut *et al.* (1993) modeled the transition in $UO_{2.00}$ as

Table 5.15 *Physical properties of the uranium trioxide hydrates and of the uranium peroxide hydrates.*

				Lattice parameters					*Density* ($g\ cm^{-3}$)		
Formula	*Color*	*Space group*	*Symmetry*	*a* (Å)	*b* (Å)	*c* (Å)	*Angle* (deg)	*Z*	*Exp.*	*X-ray or ND*	*References*
α-$UO_3 \cdot 0.8H_2O$			orthorhombic	4.27–4.30	10.19–10.24	6.86–6.96		4	6.63		Dawson *et al.* (1956)
α-$UO_2(OH)_2$ (=α-$UO_3 \cdot H_2O$)	greenish yellow	*Cmca*	orthorhombic	4.242	10.302	6.868		4	6.73		Taylor (1971); Hoekstra and Siegel (1973)
β-$UO_2(OH)_2$ (=β-$UO_3 \cdot H_2O$)	yellow-green	*Pbca*	orthorhombic	5.6438	6.2867	9.9372		4	5.73		Bannister and Taylor (1970); Hoekstra and Siegel (1973)
γ-$UO_2(OH)_2$ (=γ-$UO_3 \cdot H_2O$)	gray-chamois	$P2_1/c$	monoclinic	6.419	5.518	5.561	$\beta = 112.77$	2	5.56		Cordfunke and Debets (1964); Hoekstra and Siegel (1973)
$UO_2(OH)_2 \cdot H_2O$ (=$UO_3 \cdot 2H_2O$) (schoepite)	bright yellow	*Pbna*	orthorhombic	13.977	16.696	14.672		32	5.00		Debets and Loopstra (1963); Tasker *et al.* (1988); Hoekstra and Siegel (1973)
$U_3O_8(OH)_2$	violet		triclinic	6.802	7.417	5.556	$\alpha = 108.5$ $\beta = 125.5$ $\gamma = 88.2$	1		6.85	Siegel *et al.* (1972)
$UO_4 \cdot 4H_2O$	pale yellow	*C*2, *Cm* or *C*2/*m*	monoclinic	11.85	6.78	4.245	$\beta = 93.47$	2	5.15		Debets (1966)
$UO_4 \cdot 2H_2O$	pale yellow	*Immm*	orthorhombic	6.502	4.216	8.778		2			Debets (1966)

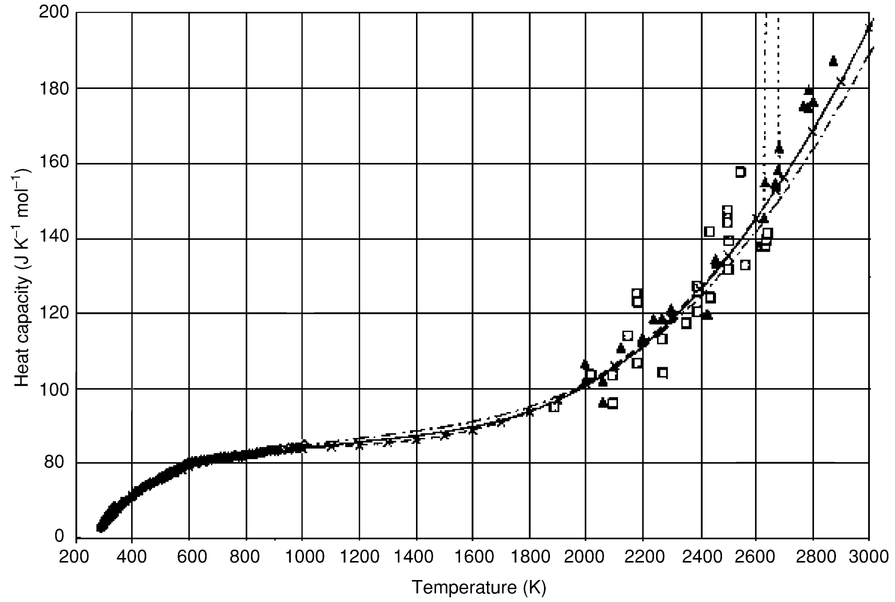

Fig. 5.20 *Recommended equations and data for the heat capacity of* UO_2 (*Fink*, 2001). ▲: *Table data of Ronchi* et al. (1999); □: *Graph data of Ronchi* et al. (1999); ◇ *Grønvold* et al. (1970); ○: *Huntzicker and Westrum, Jr.* (1971); ——: *Functional form equation* (*Fink*, 2001); –×–×–: *Polynomial form equation* (*Fink*, 2001); ------: *Phase transition*; —·—·—: *MATPRO equation* (*Hagrman*, 1995).

a second-order transition involving oxygen Frenkel disorder. The transition temperature of hypostoichiometric uranium dioxide (UO_{2-x}) increases with increasing x. Their model explains the shift as due to the change from a λ-transition to a first-order phase transition in UO_{2-x}.

The discussion on the heat capacity of UO_2 can be divided into the following four regions (Ronchi and Hyland, 1994):

(1) *Room temperature – 1000* K *region*. The increase in the heat capacity is caused by the harmonic lattice vibrations with a smaller contribution from thermal excitation of localized electrons of U^{4+} in the crystal field.

(2) *1000–1500* K *region*. The heat capacity increases with increasing anharmonicity of the lattice vibrations as shown by thermal expansion.

(3) *1500–2670* K *region*. The heat capacity increase in this region is mainly ascribed to the formation of lattice and electronic defects. The C_p peak at 2670 K is due to the oxygen Frenkel defects as determined by neutron scattering measurements.

(4) *Region above 2670* K. The peak of the heat capacity drops sharply by rapid saturation of the defects. At temperatures from 2700 K to the melting point, the concentration of Schottky defects increases.

(*vi*) *Oxygen potential and other thermodynamic properties*

A large number of reports have been published on the partial molar thermodynamic quantities $\Delta\bar{G}(O_2)$, $\Delta\bar{H}(O_2)$, and $\Delta\bar{S}(O_2)$ for non-stoichiometric uranium oxides. These studies have been carried out mainly by means of thermogravimetric method (Gerdanian, 1964; Gerdanian and Dodé, 1965; Hagemark and Broli, 1966; Kotlar *et al.*, 1967b; Ugajin, 1983; Matsui and Naito, 1985a) and emf method (Aronson and Belle, 1958; Kiukkola, 1962; Markin and Bones, 1962a,b; Marchidan and Matei, 1972; Saito, 1974; Nakamura and Fujino, 1987); however, tensimetric (Roberts and Walter, 1961), quenching (Anthony *et al.*, 1963), and Knudsen effusion (Blackburn, 1958) techniques have also been used.

In the two-phase regions of solid oxides, the equilibrium oxygen pressure over uranium oxides, p_{O_2}(atm), which is related with the oxygen potential of the oxides $\Delta\bar{G}(O_2)$ by the equation $\Delta\bar{G}(O_2) = RT \ln p_{O_2}$, is a function of only temperature. For the UO_{2+x}–U_4O_{9-y} two-phase region, Saito (1974) showed that $\log p_{O_2}$ is:

$$\log p_{O_2}(\text{atm}) = -105.7 - 5136\,T^{-1} + 33.46 \log T \tag{5.1}$$

The previous equation describes the measured data from the literature (Aronson and Belle, 1958; Blackburn, 1958; Roberts and Walter, 1961; Kiukkola, 1962; Markin and Bones, 1962b; Kotlar *et al.*, 1967b; Marchidan and Matei, 1972; Saito, 1974; Nakamura and Fujino, 1987), although it gives gradually too low values at temperatures above 1323 K (Roberts and Walter, 1961; Nakamura and Fujino, 1987).

For the U_4O_9–U_3O_{8-z} two-phase region, $\log p_{O_2}$ is represented by (Saito, 1974)

$$\log p_{O_2}(\text{atm}) = 7.996 - 16\,330\,T^{-1} \tag{5.2}$$

or (Roberts and Walter, 1961)

$$\log p_{O_2}(\text{atm}) = 8.27 - 16\,760\,T^{-1}. \tag{5.3}$$

The difference in $\log p_{O_2}$ of equations (5.2) and (5.3) is 0.20 at $T = 900$ K, which decreases to 0.033 at $T = 1400$ K.

The oxygen potential of UO_{2+x} in the single-phase region is a function of the composition x and temperature. A number of experimental $\Delta\bar{G}(O_2)$ isotherms plotted against O/U ratio of UO_{2+x} for various temperatures in the range 1173–1773 K have been reported (Aukrust *et al.*, 1962; Markin and Bones, 1962a,b; Hagemark and Broli, 1966; Ugajin, 1983; Matsui and Naito, 1985a). The scatter in the experimental $\Delta\bar{G}(O_2)$ data seems to increase as the O/U ratio decreases in the composition range below 2.01, where $\Delta\bar{G}(O_2)$ rapidly decreases with decreasing O/U ratio.

Fig. 5.21 shows $\Delta\bar{G}(O_2)$ for UO_{2+x} as a function of the O/U ratio expressed by an equation which consists of component equations giving experimental values in polynomial forms (Nakamura and Fujino, 1987) with small modifications for

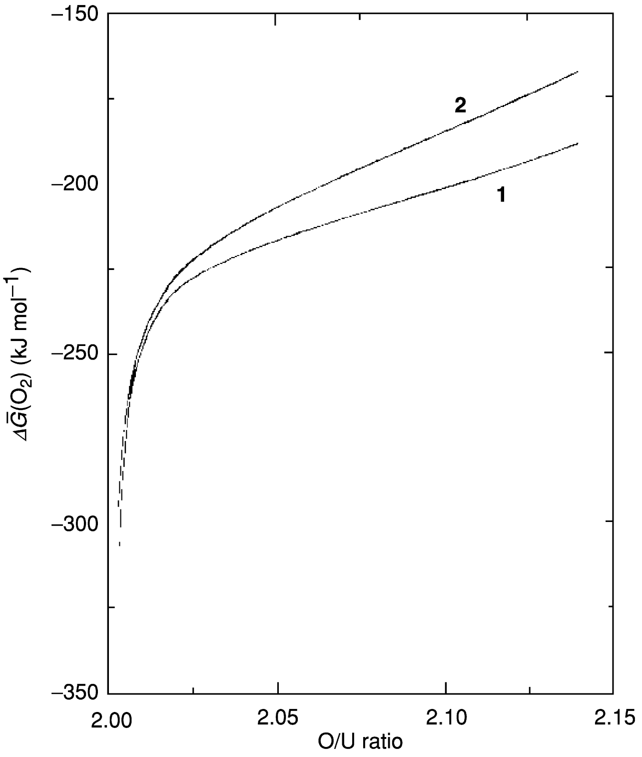

Fig. 5.21 *Oxygen potential as a function of O/U ratio. Curve* 1, 1173 K; *curve* 2, 1373 K.

$\Delta\bar{G}(O_2)$ below O/U = 2.02. The lowest O/U ratio shown in the figure is 2.003, below which the $\Delta\bar{G}(O_2)$ values approach those at $x = 0$, i.e. –633.3 and –588.4 kJ mol^{-1} for 1173 and 1373 K, respectively. These values are obtained from the equation $\Delta\bar{G}(O_2) = -897\,000 + 224.8\ T$ J mol^{-1} at $x = 0$ assessed by Lindemer and Besmann (1985) for temperatures between 873 and 1673 K.

The partial molar entropy of oxygen, $\Delta\bar{S}(O_2) = -\mathrm{d}\Delta\bar{G}(O_2)/\mathrm{d}T$, was in most papers regarded as temperature independent and on this basis differentiation of $\Delta\bar{G}(O_2)$ was made without specifying temperature. There have been rather wide scattering in the reported values of the partial molar enthalpy of oxygen, $\Delta\bar{H}(O_2)$, and the entropy, $\Delta\bar{S}(O_2)$. This is significantly reduced when $\Delta\bar{S}(O_2)$ is treated as a temperature-dependent quantity: $\mathrm{d}\Delta\bar{S}(O_2) = \bar{C}_p(O_2)\mathrm{d}T/T$ where $\bar{C}_p(O_2)$ is the partial molar heat capacity of oxygen expressed as a polynomial of $\log x$ (Nakamura and Fujino, 1987). In this case, $\Delta\bar{H}(O_2)$ also becomes temperature-dependent because of the relation $\Delta\bar{H}(O_2) = \Delta\bar{G}(O_2) + T\Delta\bar{S}(O_2)$.

Fig. 5.22a compares the calculated $\Delta\bar{H}(O_2)$ vs x curves obtained by using the above $\bar{C}_p(O_2)$ values with the literature data. Fig. 5.22b compares the $\Delta\bar{S}(O_2)$ vs x curves. The derived $\Delta\bar{H}(O_2)$ curve at 1323 K is in good agreement

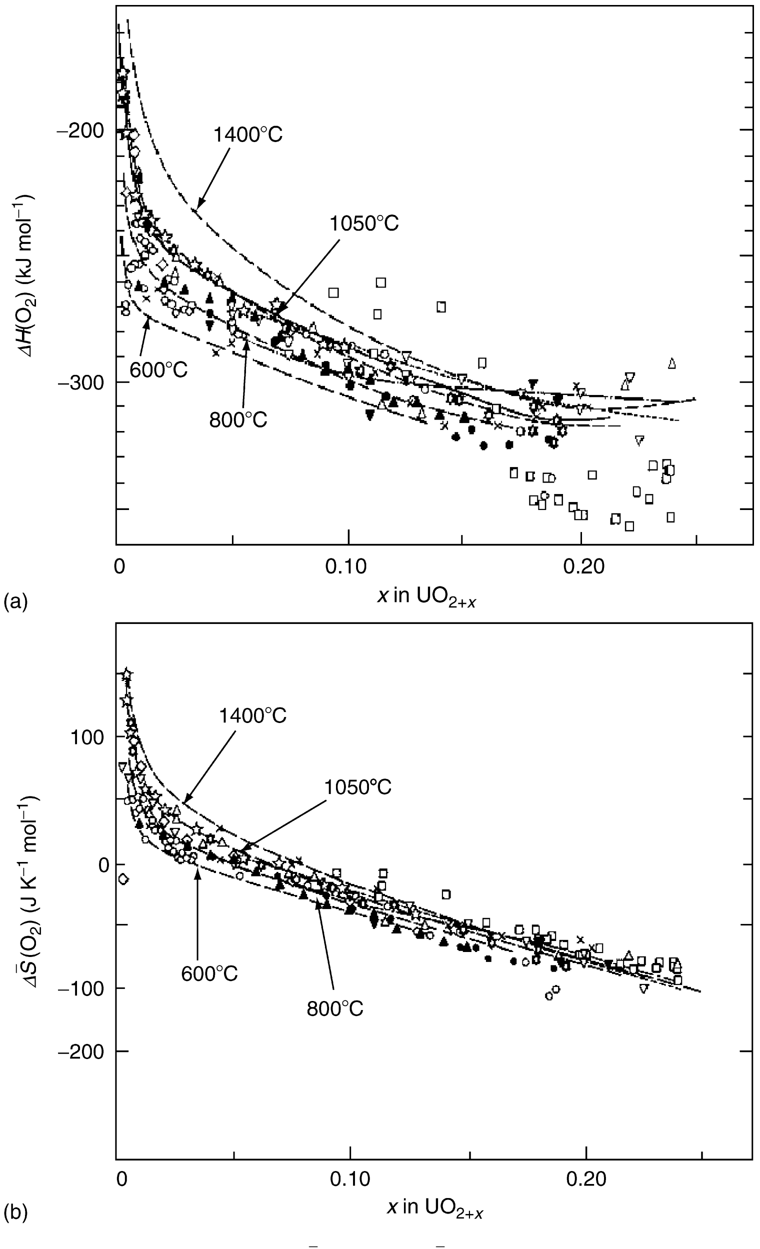

Fig. 5.22 (*a*) and (*b*): *Variation of* $\Delta\bar{H}(O_2)$ *and* $\Delta\bar{S}(O_2)$, *respectively*, *with composition x at* 873, 1073, 1323, *and* 1673 K *in the region* $0 \leq x \leq 0.25$ (*Nakamura and Fujino,* 1987). ★: *sample a* (*Nakamura and_Fujino,* 1987); ☆: *sample b* (*Nakamura and Fujino,* 1987); — — —: *least squared* $\Delta\bar{H}(O_2)$ *and* $\Delta\bar{S}(O_2)$ *curves* (*Nakamura and Fujino* 1987); ——: *Picard and Gerdanian* (1981) *at* 1323 K; ○: *Markin and Bones* (1962*a,b*); △: *Kiukkola* (1962); •: *Saito* (1974); ▲: *Gerdanian and Dodé* (1965); ▽: *Hagemark* et al. (1962, 1966); ▾: *Marchidan and Matei* (*1972*); ×: *Aronson and Belle* (1958); ◇: *Ugajin* (1983); □: *Roberts and Walter* (1961); -----: *Rand and Kubaschewski* (1963) *at* 1273 K; —·—·—: *Rand* et al. (1978). *Reproduced by the permission of Elsevier*.

with the measured curve of Picard and Gerdanian (1981). Most reported values of the temperature-independent $\Delta\bar{H}(O_2)$ and $\Delta\bar{S}(O_2)$ are within the curves derived using temperature-dependent $\Delta\bar{H}(O_2)$ and $\Delta\bar{S}(O_2)$ in the range 1073–1323 K.

Labroche *et al.* (2003a) made a critical assessment of the thermodynamic data for UO_{2+x} taking into account the uncertainties in the measurements. The result showed that $\log p_{O_2}$ could be represented by equations of the form $\log p_{O_2} = A - BT^{-1}$ with A and B varying with the O/U ratio in the range 2.01–2.23. On the other hand, this treatment revealed that the x dependence of $\log p_{O_2}$ could not be given with adequate accuracy by the above simple formulas if the temperature range is larger.

Gerdanian and Dodé (1968) determined $\Delta\bar{H}(O_2)$ by measuring the evolved heat when a small amount of oxygen was passed over UO_{2+x} in a Calvet-type microcalorimeter. This technique made it possible to measure $\Delta\bar{H}(O_2)$ close to the stoichiometric composition as shown in Fig. 5.23.

In this figure, $\Delta\bar{H}(O_2)$ increased very sharply with increasing O/U ratio from <–800 kJ mol^{-1} at $UO_{2.0003}$, and then attained a maximum of about

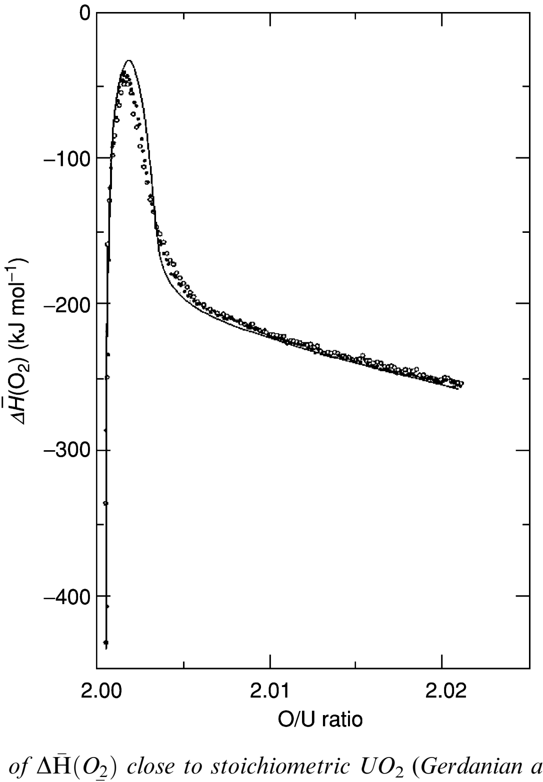

Fig. 5.23 *Change of* $\Delta\bar{H}(O_2)$ *close to stoichiometric* UO_2 (*Gerdanian and Dodé*, 1968). •: run 1; ○: *run* 2;———: $\Delta\bar{H}(O_2)$ *corrected for systematic experimental errors.*

–29 kJ mol^{-1} at $UO_{2.0018}$. The curve afterwards decreased and became progressively linear above O/U = 2.01.

No significant anomaly has been observed for $\Delta\bar{G}(O_2)$ in the above composition range (Markin and Bones, 1962a), though precise determination could not be made at small O/U ratios near stoichiometric UO_2 due to rapid change of $\Delta\bar{G}(O_2)$. When there is no anomaly in $\Delta\bar{G}(O_2)$, $\Delta\bar{S}(O_2)$ should have the sharp peak at the same composition as $\Delta\bar{H}(O_2)$. Gerdanian (1974) showed that the $\Delta\bar{H}(O_2)$ anomaly could be well described by assuming that the formation of the Willis (2:2:2) cluster is the predominant reaction. At the same time he commented that the choice of cluster structures and ionic charges was not crucial and it could be changed if another appropriate and consistent set of $\Delta\bar{H}(O_2)$ and $\Delta\bar{S}(O_2)$ was selected. Actually, the $\Delta\bar{H}(O_2)$ anomaly can also be interpreted by the oxygen Frenkel disorder and Willis (2:1:2) cluster formation reactions coupled with the intrinsic hole–electron formation reaction (Nakamura and Fujino, 1986).

(*vii*) *Vaporization of* UO_2

The vaporization of uranium oxides has been studied mainly on stoichiometric and hypostoichiometric uranium dioxides. The vaporization data concerning U_3O_8 and U_4O_9 phases (Ackermann *et al.*, 1960; Ackermann and Chang, 1973) have attracted only little attention (Naito and Kamegashira, 1976). The vaporization behavior of uranium dioxide may be discussed for the temperature regions below and above the melting point. In the region below the melting point, vaporization has been studied using a variety of techniques such as Knudsen mass effusion, Langmuir surface evaporation, mass spectrometry, and transpiration. The important gaseous species are U(g), UO(g), UO_2(g), UO_3(g), O(g), and O_2(g). The transpiration method can only give total pressures. The partial pressures of each of the uranium-bearing species are measured by means of the Knudsen cell - mass spectrometer technique. In the temperature range 1890–2420 K, the partial pressure of UO_2(g) measured by the latter method (Pattoret *et al.*, 1968) was $\log p_{UO_2}(\text{atm}) = 8.60 - 30850\,T^{-1}$.

In order to obtain the total pressure, it is necessary to measure the pressures of the other gaseous species. However, since the partial pressure p_{UO_2} over uranium dioxide near the stoichiometric composition is (94 ± 3)% of the total pressure at 2150 K (Pattoret *et al.*, 1968; Ackermann *et al.*, 1979), the total pressure is very close to p_{UO_2}. Ackermann *et al.* (1979) compared, at 2150 K, the reported values of the total pressure (10^{-6} atm), the apparent heat of sublimation (kJ mol^{-1}) obtained from a plot of log p_{total} versus $1/T$, and the apparent entropy of sublimation for UO_2(s) (J K^{-1} mol^{-1}). The values are 1.21, 596.2, and 164 (Ackermann *et al.*, 1956); 1.91, 627.6, and 182 (Ivanov *et al.*, 1962); 0.577, 587.9, and 154 (Voronov *et al.*, 1962); 1.32, 635.1, and 183 (Ohse, 1966); 0.914, 589.5, and 159 (Alexander *et al.*, 1967); 1.97, 617.1, and 178 (Gorban, *et al.*, 1967); 1.81, 590.8, and 165 (Pattoret *et al.*, 1968) and 1.16, 598.7, and 165 (Tetenbaum and Hunt, 1970), respectively. The ΔH_V values spread in a range from 585 to 635 kJ mol^{-1}. The Langmuir method (Voronov *et al.*, 1962) yields low total pressures. The pressure data obtained by the transpiration method (Alexander *et al.*, 1967; Tetenbaum and Hunt, 1970) also tend to be low, which is supposed to be caused by more rapid loss of material giving rise to composition gradient in uranium dioxide during transpiration evaporation. The transpiration total pressures in the form of $\log p_{\text{total}} = A - BT^{-1}$, measured at temperatures between 2500 and 2900 K for $UO_{1.88}$(s) (Szwarc and Latta, 1968), were in good agreement with those of Tetenbaum and Hunt (1970) measured over the temperature range 2080–2705 K, but the total pressures for $UO_{1.92}$ (s) and $UO_{1.94}$ (s) were low; approximately two-third to half of the values of Tetenbaum and Hunt (1970).

For hypostoichiometric uranium dioxide, the pressure of UO(g) becomes comparable to p_{UO_2}or, depending on the composition of the solid, higher than p_{UO_2}. Storms (1985) measured p_{UO} as a function of composition between U(l) + UO_{2-x}(s), and $UO_{2.0}$(s) in the temperature range 1667–2175 K using a mass spectrometer equipped with a tungsten Knudsen cell. The gas-phase reaction $2UO_2(g) = UO(g) + U(g)$ was assumed to be in equilibrium in the cell and its equilibrium constant should be independent of the solid composition. Thus, the uranium activity, a_U, and the partial enthalpy of vaporization of U(g), $\Delta\bar{H}_U$, were obtained by adopting the two-phase mixture U(l) + UO_{2-x}(s) as the reference in which a_U was measured to be unity below 2100 K. The partial pressures of U(g), UO(g), and UO_2(g) were expressed as a function of temperature and a_U. From the gas-phase equilibrium $UO_3(g) + UO(g) = 2UO_2(g)$, p_{UO_3} was also given as a (T, a_U) function using the $\Delta_f G^o(UO_3, g)$ data. The pressures p_U and p_{UO_2} were then obtained in terms of temperature, a_U, and $\Delta_f G^o(UO_2, s)$. The partial pressures and the total pressures over various compositions of UO_{2-x}(s) at 2000 K are shown in Fig. 5.24.

The sum of the partial pressures of U(g), UO(g), and UO_2(g) over U(l) + UO_2(s) at 2300 K was in good agreement with that of Ackermann *et al.* (1969), but it was about one-third that of Pattoret *et al.* (1968). The partial pressures of O_2 over U(l) + UO_{2-x} measured recently by Baïchi *et al.* (2002) using the twin-cell method are, for example, $\sim 1 \times 10^{-19}$, $\sim 1 \times 10^{-18}$, and $\sim 1 \times 10^{-17}$ atm for 2000, 2100, and 2200 K, respectively. The above O_2 pressure at 2000 K is in accord with that of Fig. 5.24.

The congruently vaporizing composition (CVC) changes with temperature as reported in the literature (Ackermann *et al.*, 1960, 1969; Pattoret *et al.*, 1968; Edwards *et al.*, 1969). The calculated relation between temperature and the O/U ratio for CVC by Storms (1985) is in reasonable accord with these data: Up to 2100–2200 K, CVC is O/U = 2.00. As the temperature rises above these temperatures, CVC decreases nearly linearly with increasing temperature to O/U = 1.95–1.96 at 2700 K.

The total vapor pressures over uranium dioxide above its melting point measured by the transpiration technique (Reedy and Chasanov, 1972), pulsed

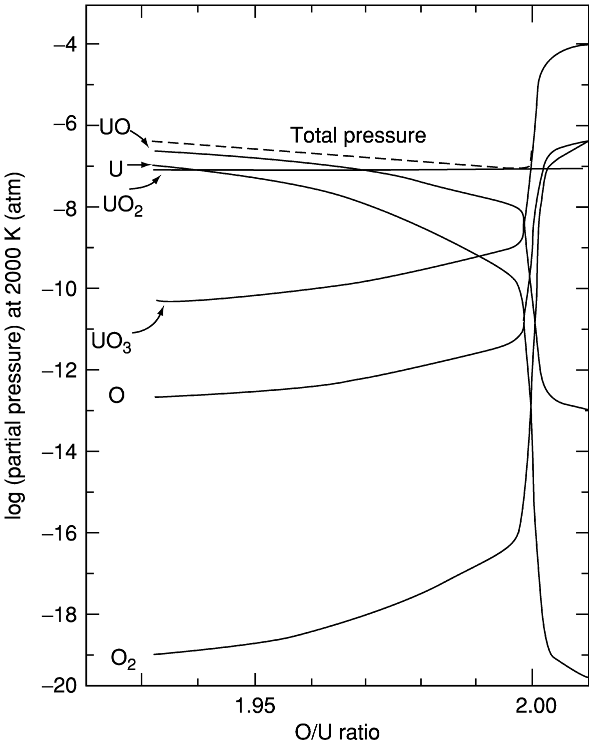

Fig. 5.24 *Partial pressures and total pressure over UO_{2-x} of various compositions at* 2000 K (*from Storms*, 1985, *reproduced by the permission of Elsevier*).

laser surface heating (Asami *et al.*, 1975; Bober *et al.*, 1975; Tsai *et al.*, 1975; Babelot *et al.*, 1977), and electron beam heating (Benson, 1977) have been compared by Ohse *et al.* (1979). In the latter monograph, a discussion was made of the methods to measure the equilibrium pressure from the evaporation rate of the gaseous species generated by dynamic, non-equilibrium pulse heating techniques. The upper temperature limit of the transpiration measurements was 3400 K for hypostoichiometric uranium dioxide of O/U = 1.94 (Reedy and Chasanov, 1972). The total pressure data above 4200 K showed a small curvature toward high pressures due to the composition change of liquid uranium dioxide to hypostoichiometry (Babelot *et al.*, 1977). In the case where the correction was made for this deviation by normalizing to O/U = 2.00 in forced congruency evaporation mode, a straight line was obtained in the $\log p_{\text{total}}$ vs. $1/T$ plot. The scattering of the corrected data (Asami *et al.*, 1975; Bober *et al.*, 1975; Tsai *et al.*, 1975; Babelot *et al.*, 1977; Benson, 1977) around the straight line is reasonable in the temperature range 3120–5000 K.

The suggested total pressure up to 5000 K by the IAEA Specialists' Meeting (1978) is

$$\log p_{\text{total}}(\text{MPa}) = 28.65 - 34\,930\,T^{-1} - 5.64 \log T.$$

The data of the equation of state for UO_2 were obtained using the principle of corresponding states (Browning *et al.*, 1978), the method of rectilinear diameters (Partington, 1949; Ohse *et al.*, 1979), and significant structure theory (Vilcu and Misdolea, 1967; Lu *et al.*, 1968). The values of critical temperature, T_c(K), critical pressure, p_c(atm), and critical density, ρ_c(g cm^{-3}) calculated by means of the principle of corresponding states are: 7300, 1915, and 3.16 (Meyer and Wolfe, 1964); 7300, 1900, and 3.16 (Menzies, 1966). The values obtained by the method of rectilinear diameters are 9110, 1230, and 1.59 (Miller, 1965). Gillan (1975) obtained the critical values on the basis of the significant structure theory. The values changed greatly when using the vapor pressures measured over UO_2(s) at lower temperatures from 6960, 1070, and 1.64 (Ohse, 1966) to 9330, 1450, and 1.63 (Tetenbaum and Hunt, 1970), respectively. Fischer *et al.* (1976), obtained the values 7560, 1210, and 1.66 using the experimental data of Ohse (1966).

(*viii*) *Diffusion*

Oxygen self-diffusion in hypostoichiometric uranium dioxide takes place by the vacancy mechanism. The self-diffusion coefficient, D^*, is expressed as

$$D^* \cong D_V^O = A_V \theta_V (1 - \theta_V) \exp(-\Delta H_V^O / RT),$$

where D_V^O, A_V, θ_V and ΔH_V^O are the oxygen self-diffusion coefficient of vacancy, pre-exponential factor, oxygen vacancy concentration (site fraction), and migration enthalpy of vacancy motion, respectively. Most of the observed values for ΔH_V^O are between 48 and 58 kJ mol^{-1} (Matzke, 1981, 1987; Bayovlu and Lorenzelli, 1984). Kim and Olander (1981) report 48.9 kJ mol^{-1}. The theoretically calculated enthalpy is 52 kJ mol^{-1} (Jackson *et al.*, 1986).

For stoichiometric UO_2, the oxygen diffusion mechanism changes with temperature: At low temperatures, thermal oxygen vacancies are the primary species contributing to oxygen mobility, whereas thermal interstitial oxygens predominate at high temperatures. In the range of 800–1800°C, both defects have significant mobility. Calculation suggests $D_i \approx D_V$ at 1400°C (Kim and Olander, 1981). The activation enthalpy of oxygen migration for stoichiometric UO_2, Q, has been determined to be 247 kJ mol^{-1} (Marin and Contamin, 1969), which is related to the enthalpy of oxygen Frenkel defect formation, H_F, by $Q = \Delta H_V^O + H_F/2$. This equation gives $H_F = 396$ kJ mol^{-1} for $\Delta H_V^O = 50$ kJ mol^{-1} (Murch and Catlow, 1987).

For hyperstoichiometric uranium dioxide, UO_{2+x}, the oxygen self-diffusion is considered to occur via the structural interstitial oxygen ions. By plotting D^* against $1/T$, the migration enthalpy of interstitial oxygens, ΔH_i^O, has been measured to be ca. 96 kJ mol^{-1} (Belle, 1969; Contamin *et al.*, 1972; Murch and Catlow, 1987) or 99.6 kJ mol^{-1} (Breitung, 1978) for x values between 0.01 and 0.1. The calculated $\Delta H_{\mathrm{i}}^{\mathrm{O}}$ value is 62 kJ mol^{-1} (Jackson *et al.*, 1986).

The chemical diffusion coefficient of oxygen, $\tilde{D}^{\mathrm{O}}$, describes the movement of oxygen ions under the oxygen concentration gradient of hyperstoichiometric UO_{2+x}; it is expressed as (Lay, 1970; Breitung, 1978):

$$\tilde{D}^{\mathrm{O}} = D^{*}\,\frac{(2+x)}{2RT}\,\frac{\mathrm{d}[\Delta\overline{G}(\mathrm{O}_2)]}{\mathrm{d}x}$$

The $\tilde{D}^{\mathrm{O}}$ values are higher than the oxygen self-diffusion coefficient, D^{*}, by several orders of magnitude. The $\tilde{D}^{\mathrm{O}}$ values calculated by the above equation are comparable with the experimental values for the x values up to 2.14 (Marin, 1968; Bittel *et al.*, 1969; Carter and Lay, 1970; Lay, 1970).

Uranium self-diffusion in uranium dioxide also depends on oxygen non-stoichiometry. For $x \geq 0$, the uranium vacancies are mainly responsible for uranium diffusion, while in the range of significant hypostoichiometry the interstitial uranium atoms become predominant. The activation enthalpies of uranium migration, Q_{U}, were measured to be 540 and 250 kJ mol^{-1} for UO_2 and UO_{2+x}, respectively (Matzke, 1987).

The calculated Q_{U} values are 1200 and 750 kJ mol^{-1} for UO_2 and UO_{2+x}, respectively (Jackson *et al.*, 1986). The uranium self-diffusion coefficient, D_{U}^{*}, is smaller than oxygen diffusion coefficient, D^{*}, by a factor of 10^5 at 1400°C. Another feature is the pronounced dependence of D_{U}^{*} on non-stoichiometry. D_{U}^{*} increases approximately proportionally with increasing x^2 from UO_2 to $\mathrm{UO}_{2.20}$ at 1400–1600°C by about five orders of magnitude (Marin and Contamin, 1969).

(*ix*) *Electrical conductivity*

UO_2, UO_{2+x}

The electrical conductivity of hyperstoichiometric uranium dioxide is caused by positive holes (Tagawa *et al.*, 1975). Although the measured values of mobility of the holes are scattered over a rather wide range, viz. from 0.0015 cm^2 V^{-1} s^{-1} at room temperature (Nagels *et al.*, 1964) to 0.021 cm^2 V^{-1} s^{-1} at 600°C or 0.055 cm^2 V^{-1} s^{-1} at 1100°C (Aronson *et al.*, 1961), these mobilities are much lower than those for usual band-type semiconductors for which the mobility is larger than 1 cm^2 V^{-1} s^{-1} (Tuller, 1981).

To explain the above conduction behavior of uranium dioxide, the small polaron model is used, where the holes are assumed to move in the oxide structure dragging the local distortion of the lattice caused by the electrical interaction. de Coninck and Devreese (1969) measured the electrical conductivity and thermoelectric power of UO_{2+x} having $x = 0.001$ and reported that the small polaron model could be applied with a nearly linear dependence of $\ln(\sigma T^{3/2})$ against $1/T$, where σ is the electrical conductivity. The holes and electrons are localized on individual atoms, giving the species of U^{5+} and U^{3+}, respectively; the electrical conduction occurs as a result of their hopping in the crystal (Catlow and Pyper, 1979). For wider range of x values of UO_{2+x}, the electrical conductivity follows (Aronson *et al.*, 1961; Winter, 1989)

$$\sigma T = 3.8 \times 10^6 (n+p)(1-n-p)e^{-0.3/kT},$$

where n and p are the electron and hole concentrations, respectively. The activation energy of conduction was measured to be 0.3 eV.

Based on Seebeck data, Winter (1989) claims the same mobility for electrons and holes in UO_{2+x}. The ratio σ_p/σ_n is larger than 1 for $x > 0$, and smaller than 1 for $x < 0$. Since one of the electronic defects always has a concentration higher than that of the ionic defects and the electronic mobilities are much higher, the ionic conductivity is insignificant. The conductivities for nominally stoichiometric UO_2 with $x \sim 10^{-3}$ can be represented by the above equation (Bates *et al.*, 1967; Winter, 1989). At $x = 0$, the intrinsic conductivity by the U^{5+} and U^{3+} charge carriers produced by a disproportionation reaction $2U^{4+} = U^{5+} + U^{3+}$ becomes important. The above reaction parameters were given by a band gap of 2 eV and a vibrational entropy of $2k$ (Winter, 1989).

For UO_{2+x} at 500–1400°C, the electrical conductivities plotted against x decrease nearly linearly with decreasing x below $x = 0.1$ in the direction $\sigma \rightarrow 0$. The conductivity changes in the different measurements, but there is a fairly good consistency in the σ values of the samples having larger x values: For $x = 0.1$ at 1000°C, for example, $\sigma \approx 30\ \Omega^{-1}\ \mathrm{cm}^{-1}$ (Aronson *et al.*, 1961), which is close to the conductivity obtained by Dudney *et al.* (1981). The other reported values are $\approx 10\ \Omega^{-1}\ \mathrm{cm}^{-1}$ (Matsui and Naito, 1985b) and $\approx 1.5\ \Omega^{-1}\ \mathrm{cm}^{-1}$ (Ishii *et al.*, 1970c), while the measured values of Lee (1974) are much lower.

U_3O_{8-z}

There are no large differences in the electrical conductivity between U_3O_{8-z} and UO_{2+x}. The conductivities for U_3O_{8-z} are $\sigma \approx 10^{-1}$ and $10^{-3}\ \Omega^{-1}\mathrm{cm}^{-1}$ at 730 and 230°C, respectively, when the oxygen partial pressure is 150 mmHg. Contrary to the conduction behavior of UO_{2+x}, however, σ for U_3O_{8-z} increases with decreasing p_{O_2} (in the range 10^2 to 10^{-2} mmHg O_2), suggesting that the main carriers are electrons (George and Karkhanavala, 1963). A change of slope in the $\log \sigma$ vs $1/T$ plots, resulting from a phase transition, was observed at 723 K. The activation energies of conduction were 0.64 and 1.10 eV below and above the transition, respectively. The transition temperature varies with non-stoichiometry from 658 K ($UO_{2.667}$, i.e. stoichiometric U_3O_8) to 923 K ($UO_{2.558}$ to $UO_{2.650}$) (Ishii *et al.*, 1970b). At higher temperatures of 1111–1190 K, another σ anomaly has been measured, presumably due to the formation of U_8O_{21+x} (Dharwadkar *et al.*, 1978).

(x) *Chemical properties*

UO_2 is oxidized to U_3O_8 on heating in air at temperatures of 600–1300°C. When UO_3 is heated in air above 600°C, the compound is reduced to U_3O_8. U_3O_8 has been used as a standard material for chemical analysis of uranium oxides

Table 5.16 *Reactions of uranium oxides.*

		Products of the following oxides		
Reagent	*Temperature* (°C)	*UO_2*	*U_3O_8*	*UO_3*
H_2(g)	>750	—	UO_2	UO_2
CO(g)	>750	—	UO_2	UO_2
HF(g)	550	UF_4	$UO_2F_2 + UF_4$	UO_2F_2
F_2(g)	400	UF_6 (>500°C)	UF_6	UF_6
CCl_4(g)	400	UCl_4	$UCl_4 + UCl_5$	$UCl_4 + UCl_5$
$SOCl_2$(g)	450	UCl_4	UCl_4	UCl_4
H_2S(g)	1000	UOS	UOS	UOS
C(s)	1500–1700	UC (UC_2)	UC (UC_2)	UC (UC_2)
C(s) + Cl_2(g)	1000	UCl_4	UCl_4	UCl_4
C(s) + CS_2(g)	1000	US_2	US_2	US_2
C(s) + N_2(g)	1700–1900	UN	UN	UN

because of its high stability in air. However, U_3O_8 is now recognized as a compound that is rather difficult to obtain in strictly stoichiometric composition; the O/U ratio deviates significantly from 8/3 depending on the heating temperature, time, and thermal history.

Stoichiometric UO_2 can be obtained by heating uranium oxides in H_2 or CO gas streams at temperatures 750–1700°C (Table 5.16). However, if the H_2 gas contains an O_2 impurity, the formed UO_2 is oxidized to non-stoichiometric UO_{2+x} during the cooling process at temperatures below 300°C. The reaction of UO_2 with air at room temperature deserves special attention, as the reaction is dependent on particle size and reactivity. Very fine UO_2 powder formed by the hydrogen reduction at lower temperatures below 800°C may be pyrophoric. Even though large particles are usually not pyrophoric, the O/U ratio increases steadily with time of exposure to air. UO_2 can take up appreciable quantities of oxygen for particle diameters of about 0.05–0.08 μm. When the particle size is 0.2–0.3 μm or larger, UO_2 is fairly stable to oxidation (Belle, 1961). UO_2 pellets sintered at around 1700°C are not oxidized for years due to protection by slightly oxidized thin surface films.

Some reactions of uranium oxides with chemical reagents are shown in Table 5.16. For the reaction with C(graphite), the product is UC if the mixing mole ratio of carbon and UO_2 is $C/UO_2 = 3$, and UC_2 if $C/UO_2 = 4$.

An interesting reaction between uranium oxides and liquid N_2O_4 has been observed (Gibson and Katz, 1951). Anhydrous uranium oxides react with liquid N_2O_4 to yield $UO_2(NO_3)_2 \cdot N_2O_4$. A similar reaction with N_2O_5 (Gibson *et al.*, 1960) may be used to prepare anhydrous $UO_2(NO_3)_2$. It was found that the reaction between metal and liquid N_2O_4 also gives $UO_2(NO_3)_2 \cdot N_2O_4$ (Addison and Hodge, 1961).

Uranium oxides dissolve in mineral acids such as HNO_3, $HClO_4$, HCl, and H_2SO_4. In HCl, H_2SO_4, and strong phosphoric acid, the mean valence of uranium does not change from that in the solid state before dissolution. Sintered UO_2 pellets dissolve in HNO_3 with a slow rate, but the dissolution can be accelerated if a small amount of NH_4F is added, due to the formation of fluoro-complexes of uranium. The addition of a small amount of H_2O_2 to HNO_3 is also effective to enhance the dissolution rate of UO_2 in laboratory experiments; in this way no contamination of the solution takes place.

The mechanism of dissolution of UO_2 in H_2O_2 aqueous solution has been studied by a number of researchers. It is regarded as a second-order reaction with a rate constant 8×10^{-7} m min^{-1} (based on the surface-to-solution volume ratio) (Ekeroth and Jonsson, 2003). The plausible mechanism is a slow electron transfer step producing $UO^{+}_{2(\mathrm{surface})} + OH^{\bullet}$ followed by a rapid reduction of the radical $OH^{\bullet}$ to OH^{-}. The $UO^{+}_{2(\mathrm{surface})}$ ions are oxidized to $UO^{2+}_{2(\mathrm{surface})}$ by $OH^{\bullet}$ or by disproportionation (Shoesmith and Sunder, 1994; Ekeroth and Jonsson, 2003). Carbonate ions increase the solubility of $UO^{2+}_{2(\mathrm{surface})}$ (Grenthe *et al.*, 1984). The above mechanism is consistent with the results by other oxidants, viz. $IrCl_6^{2-}$, MnO_4^{-}, $Fe(EDTA)^{-}$, $CO_3^{\bullet -}$, $HO_2^{\bullet}$, and O_2 (Bard and Parsons, 1985; Wardman, 1989; Huie *et al.*, 1991).

(b) Alkali metal uranates and alkaline-earth metal uranates

In Table 5.17, some physico-chemical properties and crystal structures are shown for ternary alkali metal uranates and alkaline-earth metal uranates.

(*i*) *Uranates*(*VI*)

The most frequently encountered uranates(VI) are a series of compounds of types $M_2^{+}U_nO_{3n+1}$ (M^{+}: alkali metals) and $M^{2+}U_nO_{3n+1}$ (M^{2+}: alkaline-earth metals), but other compounds such as $M_4^{+}UO_5$, $M_2^{2+}UO_5$, $M_3^{2+}UO_6$, and $M_2^{2+}U_3O_{11}$ are also well known.

Preparation

Carbonates, nitrates, or chlorides of alkali or alkaline-earth elements are mixed with the calculated amounts of U_3O_8 or UO_3. Uranates(VI) are obtained by heating the mixtures in air or oxygen at temperatures 500–1000°C. Because of higher volatility of rubidium and cesium oxides, the uranates of these elements are prepared by heating at lower temperatures of 600–700°C (Hoekstra, 1965). The alkaline-earth oxides are also used as starting materials. Reaction temperatures above 1000°C can be used for the preparation of alkaline-earth uranates on account of very low vapor pressures of alkaline-earth oxides.

A number of stoichiometric sodium uranates (α- and β-Na_2UO_4, $Na_2U_2O_7$, α-Na_4UO_5, etc.) have been prepared following a procedure described by Jayadevan *et al.* (1974) by calcining well-characterized thermally labile double sodium uranium salts such as carbonates, oxalates, and acetates. This technique avoids high-temperature treatment and decreases losses by vaporization. This is

Table 5.17 *Some physico-chemical properties and crystal structures for alkali and alkaline earth metal uranates.*

Formula	*Physico-chemical properties*	*Space group*	*Symmetry*	*Lattice parameters*				*Z*	*Density* (g cm^{-3})		*References*
				a (Å)	*b* (Å)	*c* (Å)	*Angle* (deg)		*Exp*	*X-ray or ND*	
U(VI) compounds											
Li_2UO_4	not hygroscopic. α→β transformation 1573 K. excitation and infrared spectra	α-phase: (*Fmmm*)	orthorhombic	(6.04	5.11	10.52)			6.13		Zachariasen (1946); Kovba *et al.* (1958); Efremova *et al.* (1959, 1961c); Neuhaus and Recker (1959); Spitsyn *et al.* (1961a); Bereznikova *et al.* (1961); Prigent and Lucas (1965); Hoekstra (1965); Ohwada (1970a); Kovba (1971a); O'Hare and Hoekstra (1974b); Hauck (1974); Krol (1981); Volkovich *et al.* (1998)
		Pnma		10.547	6.065	5.134					
		β-phase:	hexagonal	3.912		16.52					
Na_2UO_4	yellow. hygroscopic. infrared spectra	α-phase: *Cmmm*	orthorhombic	9.76	5.73	3.50			5.71		Wisnyi and Pijunowski (1957); Spitsyn *et al.* (1961a,b); Kovba *et al.* (1961a); Scholder and Glser (1964); Hoekstra (1965); Ohwada (1970a); Kovba (1971a); Cordfunke and Loopstra (1971); O'Hare and Hoekstra (1973); Osborne *et al.* (1974); Gebert *et al.* (1978); Volkovich *et al.* (1998)
		β-phase: (*Fmmm*)	orthorhombic	5.98	5.807	11.70			5.51		
		Pnma		11.708	5.804	5.970					
K_2UO_4	yellow. hygroscopic. infrared spectra	α-phase: *I4/mmm*	tetragonal	4.344		13.13			4.66		Hoekstra and Siegel (1956); Wisnyi and Pijunowski (1957); Spitsyn *et al.* (1961a,b); Hoekstra (1965); Ohwada (1970b); Kovba (1971a); O'Hare and Hoekstra (1974b); Volkovich *et al.* (1998)
				4.335		13.13					
			orthorhombic	7.98	6.91	19.78					
		β-phase:	pseudo-cubic	4.32							
Rb_2UO_4	yellow. hygroscopic. infrared spectra	*I4/mmm*	tetragonal	4.354		13.86			4.52	6.02	Spitsyn *et al.* (1961a,b); Hoekstra (1965); Ohwada (1970b); Kovba and Trunova (1971); O'Hare and Hoekstra (1974b)
				4.353		13.869					
Cs_2UO_4	orange. very hygroscopic. infrared spectra	*I4/mmm*	tetragonal	4.39		14.82					Spitsyn *et al.* (1961a,b); Hoekstra (1965); Ohwada (1970b); O'Hare and Hoekstra (1974a); van Egmond (1976b)
				4.3917		14.803					
$MgUO_4$	yellow. not hygroscopic, infrared spectra	*Imma*	orthorhombic	6.520	6.595	6.924				7.28	Zachariasen (1954a); Lambertson and Mueller (1954); Rüdorff and Pfitzer (1954); Klíma *et al.* (1966); Jakeš and Schauer (1967); Ohwada (1972); Jakeš and Křivý (1974); O'Hare *et al.* (1977)
				6.499	6.592	6.921					

$CaUO_4$	yellow, not hygroscopic, infrared and far infrared spectra	$R\bar{3}m$	rhombohedral	6.266			$\alpha = 36.03$	1			Zachariasen (1948b); Wisnyi and Pijunowski (1957); Leonidov (1960); Kovba *et al.* (1961b); Anderson and Barraclough (1963); Carnall *et al.* (1965); Jakeš *et al.* (1966); Loopstra and Rietveld (1969); Voronov *et al.* (1972)
				6.2683			$\alpha = 36.04$				
			hexagonal-indexing	3.87		17.54					
				3.876		17.558					
$SrUO_4$	α-phase: orange red. β-phase: yellow, infrared and Raman spectra	α-phase: $R\bar{3}m$ (isostructural with $CaUO_4$)	rhombohedral	6.54			$\alpha = 35.53$				Zachariasen (1948b); Rüdorff and Pfitzer (1954); Ippolitova *et al.* (1959, 1961b); Keller (1962a); Klíma *et al.* (1966); Reshetov and Kovba (1966); Cordfunke and Loopstra (1967); Loopstra and Rietveld (1969); Ohwada (1970a); Brisi (1971); Sawyer (1972); Voronov *et al.* (1972); Fujino *et al.* (1977); Tagawa and Fujino (1977); Tagawa *et al.* (1977)
				6.551			$\alpha = 34.82°$		7.84		
			hexagonal-indexing	3.991		18.361					
		β-phase: *Pbcm* (isostructural with $BaUO_4$)	orthorhombic	5.4896	7.9770	8.1297				7.26	
$BaUO_4$	orange yellow. infrared spectra	*Pbcm*	orthorhombic	5.751	8.135	8.236		4			Samson and Sillén (1947); Rüdorff and Pfitzer (1954); Wisnyi and Pijunowski (1957); Ippolitova *et al.* (1961c); Allpress (1964); Klíma *et al.* (1966); Reis, Jr. *et al.* (1976)
				5.7553	8.1411	8.2335					
				5.744	8.136	8.237					
$LiU_{0.83}O_3$	α, β, and γ-phases ($Li_2O \cdot 1.60UO_3 = Li_{22}U_{18}O_{65}$)		orthorhombic	20.382	11.511	11.417		2	6.6	6.66	Kovba (1971b); Hauck (1974); Prins and Cordfunke (1983); Griffiths and Volkovich (1999)
$Li_2U_2O_7$	yellow. existence confirmed. electronic and infrared spectra		rhombohedral								Efremova *et al.* (1961c); Kovba *et al.* (1961b); Spitsyn *et al.* (1961c); Hoekstra (1965); Kovba (1971b); Toussaint and Avogadro (1974); Hauck (1974); Prins and Cordfunke (1983); Volkovich *et al.* (1998); Griffiths and Volkovich (1999)
			orthorhombic	20.4	11.6	11.1					
$Na_2U_2O_7$	orange colored. infrared and far-infrared spectra		hexagonal	3.94		17.80					Sutton (1955); Neuhaus (1958); Kovba *et al.* (1961b); Spitsyn *et al.* (1961c); Hoekstra (1965); Carnall *et al.* (1965, 1966); Kovba (1970, 1972a); Cordfunke and Loopstra (1971); Battles *et al.* (1972); Volkovich *et al.* (1998)
			orthorhombic	3.725	6.660	11.88					
		C2/m	monoclinic	12.796	7.822	6.896	$\beta = 111.42$				
$K_2U_2O_7$	infrared and far-infrared spectra. possibility of two phases	α-phase: $R\bar{3}m$	hexagonal	3.99		19.71					Kovba *et al.* (1958, 1961b); Ippolitova and Kovba (1961); Spitsyn *et al.* (1961c); Hoekstra (1965); Carnall *et al.* (1965); Allpress *et al.* (1968); Anderson (1969); Kovba (1972a); Volkovich *et al.* (1998)
				3.985		19.643					
				3.998		19.77					

Table 5.17 (*Contd.*)

Formula	*Physico-chemical properties*	*Space group*	*Symmetry*	*Lattice parameters* *a* (Å)	*b* (Å)	*c* (Å)	*Angle* (deg)	*Z*	*Density* (g cm^{-3}) *Exp*	*X-ray or ND*	*References*
$Rb_2U_2O_7$	decomposes at 1473 K. infrared spectra	$R\bar{3}m$	hexagonal	4.01		20.81					Kovba *et al.* (1961b); Spitsyn *et al.* (1961c); Hoekstra (1965); Allpress *et al.* (1968); Anderson (1969); Kovba and Trunova (1971)
				4.00		20.57					
				4.004		20.83			6.33	6.50	
$Cs_2U_2O_7$	orange yellow. infrared spectra	α-phase: *C*2/*m*	monoclinic	14.528	4.2638	7.605	$\beta = 112.93$				Hoekstra (1965); Kovba and Trunova (1971); Kovba *et al.* (1974); Cordfunke *et al.* (1975); van Egmond (1976c)
		β-phase: *C*2/*m*	monoclinic	14.516	4.3199	7.46	$\beta = 113.78$				
		γ-phase: *P*6/*mmc*	hexagonal	4.106		14.58			6.62		
CaU_2O_7	yellow or orange green. infrared spectra	two orthogonal axes with 14.06 and 4.00 Å exist									Hoekstra and Katz (1952); Bereznikova *et al.* (1961); Jakeš *et al.* (1966); Cordfunke and Loopstra (1967); Brochu and Lucas (1967)
SrU_2O_7	magnetic susceptibility. infrared spectra										Hoekstra and Katz (1952); Klíma *et al.* (1966); Cordfunke and Loopstra (1967); Brochu and Lucas (1967)
BaU_2O_7	yellow. infrared spectra	*I*4$_1$/*amd*	tetragonal	7.127		11.95					Hoekstra and Katz (1952); Allpress (1964, 1965)
$Li_2U_3O_{10}$	infrared spectra		tetragonal	5.63		12.28		2		7.62	Efremova *et al.* (1961c); Spitsyn *et al.* (1961c); Hoekstra (1965); Kovba (1970, 1972c); Prins and Cordfunke (1983); Volkovich *et al.* (1998)
		α-phase: *P*2$_1$/*c*	monoclinic	6.821	18.91	7.300	$\beta = 121.56$		6.85	7.35	
		β-phase: *P*2	monoclinic	6.805	19.067	7.250	$\beta = 121.12$			7.32	
$K_2U_3O_{10}$	infrared spectra										Prigent and Lucas (1965); Anderson (1969)
$Cs_2U_3O_{10}$	no existence claimed										Efremova *et al.* (1961b); Cordfunke *et al.* (1975)
MgU_3O_{10}	yellow or orange yellow. infrared spectra		hexagonal	3.79		4.080					Rüdorff and Pfitzer (1954); Polunina *et al.* (1961); Klíma *et al.* (1966)
				7.57		16.32					
$K_2U_4O_{13}$	existence not confirmed	*P*6$_3$	hexagonal	14.29		14.014			6.7	6.6	Efremova *et al.* (1959); Allpress *et al.* (1968); Anderson (1969); Kovba (1970)
$Rb_2U_4O_{13}$	yellow. decomposes at 1473 K	*Pb*$_3$/*m* (or *Pb*$_3$)	hexagonal	14.307		14.298		8	6.85	7.0	Ippolitova *et al.* (1961a); Spitsyn *et al.* (1961c); Kovba and Trunova (1971)
$Cs_2U_4O_{13}$	forms by Cs_2CO_3+ $4UO_3$ at 873 K	*Cmcm*	orthorhombic	13.494	15.476	39.56			6.8	6.88	Efremova *et al.* (1959); Spitsyn *et al.* (1961c); Cordfunke (1975); Cordfunke *et al.* (1975); van Egmond (1976a)
CaU_4O_{13}	tan colored. decomposes to CaU_2O_7 at 1333 K in air		orthorhombic	6.656	4.161	4.030					Cordfunke and Loopstra (1967)

SrU_4O_{13}	dark purple. decomposes to $Sr_2U_3O_{11}$ at 1403 K		monoclinic (pseudo-orthorhombic)	6.734	4.193	4.065	$\beta = 90.16$				Cordfunke and Loopstra (1967)
$Cs_2U_5O_{16}$	solid solution with $Cs_2U_4O_{13}$		monoclinic	13.465	15.561	15.928	$\beta = 92.78$			6.82	Cordfunke *et al.* (1975); van Egmond (1976a)
$Li_2U_6O_{19}$	decomposes to $Li_2U_{2.7}O_9$ at 1263 K		othorhombic	6.701	4.01	4.148					Kovba (1970); Hauck (1974); Fujino *et al.* (1983)
$K_2U_6O_{19}$	existence doubtful		orthorhombic	6.95	3.90	7.19					Efremova *et al.* (1959); Kovba (1961); Spitsyn *et al.* (1961c); Allpress *et al.* (1968); Anderson (1969)
$K_2U_7O_{22}$	forms by the reaction of K_2CO_3 and $UO_4 \cdot nH_2O$	*Pbam*	orthorhombic	6.945	19.533	7.215		2	7.1	7.11	Kovba (1961, 1970)
$Rb_2U_7O_{22}$	decomposes at 1273 K	*Pbam*	orthorhombic	6.958	19.590	7.279				7.32	Efremova *et al.* (1959); Spitsyn *et al.* (1961c); Kovba and Trunova (1971)
$Cs_2U_7O_{22}$	decomposes at 1273 K	*Pbam*	orthorhombic	6.949	19.711	7.3955				7.485	Efremova *et al.* (1959); Spitsyn *et al.* (1961c); Cordfunke *et al.* (1975); van Egmond (1976b)
Li_4UO_5	gold colored. hygroscopic. excitation and infrared spectra	*I4/m*	tetragonal	6.736 6.720		4.45 4.451			5.28	5.41	Scholder (1958); Efremova *et al.* (1959, 1961c); Kovba (1962); Hoekstra and Siegel (1964); Reshetov and Kovba (1966); Ohwada (1971); Hauck (1974); Krol (1981)
Na_4UO_5	red to salmon pink. very hygroscopic. infrared spectra	*I4/m*	tetragonal	7.576 7.536		4.641 4.630			4.95	5.11	Findley *et al.* (1955); Efremova *et al.* (1959); Kovba (1962); Hoekstra and Siegel (1964); Cordfunke and Loopstra (1971); Ohwada (1971); Battles *et al.* (1972)
K_4UO_5	possibility of no existence remains		othorhombic	3.50	8.58	12.95				4.19	Efremova *et al.* (1959, 1961a); Hoekstra and Siegel (1964)
Rb_4UO_5	preparation $Rb_2CO_3 + UO_3$ at 1273 K		tetragonal	8.18		13.73				6.00	Efremova *et al.* (1959); Ippolitova *et al.* (1961a)
Ca_2UO_5	yellow. infrared spectra	$P2_1/c$	monoclinic	7.9137	5.4409	11.4482	$\beta = 108.803$		5.55	5.67	Bereznikova *et al.* (1961); Sawyer (1963); Jakeš *et al.* (1966); Cordfunke and Loopstra (1967); Loopstra and Rietveld (1969)
Sr_2UO_5	yellow. infrared and Raman spectra	$P2_1/c$	monoclinic	8.1043	5.6614	11.9185	$\beta = 108.985$		6.08	6.34	Sawyer (1963); Keller (1964); Cordfunke and Loopstra (1967); Loopstra and Rietveld (1969); Allen and Griffiths (1977)
Li_6UO_6	yellow. infrared spectra	α-phase:	hexagonal	8.338		7.352					Scholder and Glser (1964); Hauck (1973); Prins and Cordfunke (1983)
Ca_3UO_6	pale yellow. decomposes at 1773 K. infrared spectra	$P2_1$ (cryolite structure)	monoclinic	5.7275	5.9564	8.2982	$\beta = 90.568$		5.1	5.34	Rüdorff and Pfitzer (1954); Ippolitova *et al.* (1959); Bereznikova *et al.* (1961); Jakeš *et al.* (1966); Rietveld (1966); Brisi (1969); Loopstra and Rietveld (1969); Voronov *et al.* (1972); Kemmler-Sack and Seemann (1975)

Table 5.17 (*Contd.*)

Formula	*Physico-chemical properties*	*Space group*	*Symmetry*	*Lattice parameters*				*Z*	*Density* (g cm^{-3})		*References*
				a (Å)	*b* (Å)	*c* (Å)	*Angle* (deg)		*Exp*	*X-ray or ND*	
Sr_3UO_6	pale yellow. infrared and Raman spectra	*P*2$_1$	monoclinic	5.9588	6.1795	8.5535	$\beta = 90.192$	2		6.17	Rüdorff and Pfitzer (1954); Scholder and Brixner (1955); Ippolitova *et al.* (1959); Sleight and Ward (1962); Rietveld (1966); Cordfunke and Loopstra (1967); Loopstra and Rietveld (1969); Kemmler-Sack and Seemann (1975); Allen and Griffiths (1977)
Ba_3UO_6	pale yellow. stable up to high temperatures. infrared and charge transfer spectra	$Fm\bar{3}m$ $(NH_4)_3FeF_6$ type structure	cubic	8.922 8.90							Rüdorff and Pfitzer (1954); Scholder and Brixner (1955); Ippolitova *et al.* (1959, 1961c); Rietveld (1966);
			tetragonal	6.825		8.943					
			orthorhombic	44.63	44.31	8.973			6.75	6.98	Kemmler-Sack and Seemann (1975)
$Ca_2U_3O_{11}$	ocher. decomposes to CaU_2O_7 and $CaUO_4$ at 1173 K		triclinic	6.186	6.212	6.186	$\alpha = \gamma = 37.12$ $\beta = 37.56$				Cordfunke and Loopstra (1967)
$Sr_2U_3O_{11}$	cognac colored. stable to 1573 K. infrared and Raman spectra		triclinic	6.484	6.523	6.484	$\alpha = \gamma = 35.44$ $\beta = 36.10$				Cordfunke and Loopstra (1967); Allen and Griffiths (1977)
$Ba_2U_3O_{11}$	orange. stable to 1773 K. infrared spectra										Allpress (1964)
U(v) and U(iv) compounds											
$LiUO_3$	black purple. magnetic properties. electronic spectra	*R*3*c* $LiNbO_3$ type	rhombohedral	5.901			$\alpha = 54.60$	1	7.46	7.67	Rüdorff and Leutner (1957); Rüdorff and Menzer (1957); Kovba (1960); Rüdorff *et al.* (1962); Kemmler (1965); Kemmler-Sack *et al.* (1967); Kemmler-Sack (1968b); Keller (1972); Selbin *et al.* (1972a)
$NaUO_3$	red brown. magnetic susceptibility. electronic spectra. no existence of uranyl group	*Pbnm* $GdFeO_3$ type	orthorhombic	5.775 5.776	5.905 5.910	8.25 8.283				7.33	Rüdorff and Leutner (1957); Rüdorff and Menzer (1957); Ippolitova *et al.* (1961d); Rüdorff *et al.* (1962); Prigent and Lucas (1965); Kemmler-Sack *et al.* (1967); Kemmler-Sack and Rüdorff (1967); Kemmler-Sack (1968b); Bartram and Fryxell (1970); Cordfunke and Loopstra (1971); King (1971); Battles *et al.* (1972); Keller (1972); Selbin *et al.* (1972a); Lyon *et al.* (1977)

Na_xUO_3	green. $0 < x \leq 0.14$		orthorhombic ($Na_{0.025}UO_{3-x}$)	6.718	11.90	4.142		8.0	8.29	Greaves *et al.* (1973)
			hexagonal ($Na_{0.10}UO_3$)	3.955		4.163		7.2	7.69	
KUO_3	brown. magnetic susceptibility. electronic spectra	*Pm3m* $CaTiO_3$ type	cubic	4.290 4.299				6.85	6.84	Ippolitova *et al.* (1961d); Rüdorff *et al.* (1962); Kemmler-Sack *et al.* (1967); Kemmler-Sack and Rüdorff (1967); Kemmler-Sack (1968b); Selbin *et al.* (1972a)
$RbUO_3$	pale brown. Rb_xUO_3 ($0.8 \leq x \leq 1$). magnetic susceptibility. electronic spectra	*Pm3m*	cubic	4.323				7.5	7.63	Ippolitova and Kovba (1961); Rüdorff *et al.* (1962); Kemmler-Sack *et al.* (1967); Kemmler-Sack and Rüdorff (1967); Kemmler-Sack (1968b); Selbin *et al.* (1972a)
$CaUO_3$	black. no existence claimed	*Iam* Mn_2O_3 type	cubic (high pressure form: *fcc*, $a = 5.38$ Å)	10.727						Alberman *et al.* (1951); Young and Schwartz (1963); Brochu and Lucas (1967)
$SrUO_3$	dark brown	(deformed $CaTiO_3$ type)	orthorhombic	6.101 6.03	8.60 6.18	6.17 8.62				Scholder and Brixner (1955); Lang *et al.* (1956); Furman (1957); Brisi (1960); Keller (1964)
$BaUO_3$	brown. magnetic susceptibility	*Pm3m* $CaTiO_3$ type	cubic	4.40 4.387 (pseudo-cubic) 4.411				7.98		Rüdorff and Pfitzer (1954); Scholder and Brixner (1955); Lang *et al.* (1956); Furman (1957); Trzebiatowski and Jabłoński (1960); Fujino and Naito (1969); Braun *et al.* (1975)
$Ca_{2.5}U_{1.33}O_{5.83}$	electronic spectra	deformed $CaTiO_3$ type	monoclinic	5.767	5.974	8.349	$\beta = 89.8$		6.10	Kemmler-Sack and Seemann (1974)
$Sr_{2.5}U_{1.33}O_{5.83}$	same crystal structure as $Ca_{2.5}U_{1.33}O_{5.83}$.		monoclinic	6.178	6.023	8.629	$\beta = 89.8$	6.33	6.51	Kemmler-Sack and Seemann (1974)
$Ba_{2.67}U_{1.33}O_6$	brown. magnetic susceptibility. electronic spectra		cubic	8.901				7.10	7.34	Kemmler-Sack and Wall (1971)
Ca_2UO_4	forms by the reaction of $CaO+UO_2$ below 2023 K									Alberman *et al.* (1951)
Sr_2UO_4	forms by heating Sr_2UO_5 in H_2.									Scholder and Brixner (1955)
Ba_2UO_4	forms by the same method as Sr_2UO_4. possibility of no existence									Scholder and Brixner (1955); Trzebiatowski and Jabłoński (1960)
Ba_3UO_5	no existence reported	α-phase: β-phase: $Fm\bar{3}m$	tetragonal cubic	6.291 8.915		8.982				Trzebiatowski and Jabłoński (1960); Keller (1964); Charvillat *et al.* (1970); Braun *et al.* (1975)
Li_3UO_4	ocher colored. magnetic susceptibility. electronic spectra		tetragonal	4.49		8.5				Scholder (1960); Scholder and Glser (1964); Blasse (1964); Kemmler-Sack *et al.* (1967); Kemmler-Sack (1968b)

Table 5.17 (*Contd.*)

				Lattice parameters					*Density* (g cm^{-3})		
Formula	*Physico-chemical properties*	*Space group*	*Symmetry*	*a* (Å)	*b* (Å)	*c* (Å)	*Angle* (deg)	*Z*	*Exp*	*X-ray or ND*	*References*
Na_3UO_4	pale brown.	$Fm\bar{3}m$	cubic	4.77					6.5		Scholder (1960); Pepper (1964); Scholder and Glser (1964); Addison (1969); Bartram and Fryxell (1970); Marcon (1972); O'Hare *et al.* (1972); Osborne and Flotow (1972); Fredrickson and Chasanov (1972)
	low temperature C_p.	NaCl type		4.79–4.80							
	high temperature			4.74							
	C_p (298–1200 K).	$P4_232$	cubic	9.543 (to explain superstructure lines)							
	formula claimed to be $Na_{11}U_5O_{16}$	$Fd3m$	cubic	9.574							
Li_7UO_6	pale green. magnetic		rhombohedral	6.61			$\alpha = 53.27$				Scholder and Glser (1964); Keller *et al.* (1965); Kemmler-Sack *et al.* (1967); Kemmler-Sack (1968b); Hauck (1969); Selbin *et al.* (1965)
	susceptibility.		(hexagonal indexing)	5.52		15.80					
	electronic spectra			5.55		15.76					
$Cs_2U_4O_{12}$	$\alpha \rightarrow \beta$ at 898 K, and	α-phase: $R\bar{3}m$	rhombohedral	10.9623			$\alpha = 89.402$				Cordfunke *et al.* (1975); Cordfunke (1975); van Egmond (1975); Cordfunke and Westrum, Jr. (1979)
	$\beta \rightarrow \gamma$ at 968 K. stable	β-phase: $P2_1$	monoclinic	7.886	8.002	10.793	$\beta = 92.62$				
	in air up to 1523 K	γ-phase: $Fd3m$	cubic	11.2295							
MgU_2O_6	black. magnetic	$Fm\bar{3}m$	cubic	5.284							Hoekstra and Katz (1952); Keller (1964); Kemmler-Sack *et al.* (1967); Kemmler-Sack and Rüdorff (1967); Kemmler-Sack (1968b); Fujino and Naito (1970); Selbin *et al.* (1972a); Fujino (1972)
	susceptibility.	CaF_2 type		5.275							
	electronic spectra.			5.281							
	Mg and U atoms statistically distributed.										
CaU_2O_6	black. magnetic susceptibility	$Fm\bar{3}m$ CaF_2 type	cubic	5.379						8.71	Hoekstra and Katz (1952); Hoekstra and Siegel (1956); Brochu and Lucas (1967)
SrU_2O_6	black. magnetic susceptibility	$Fm\bar{3}m$ CaF_2 type	cubic	5.452						9.07	Hoekstra and Katz (1952); Hoekstra and Siegel (1956); Brochu and Lucas (1967); Tagawa *et al.* (1977)
BaU_2O_6	black. magnetic susceptibility (85–300 K)	$Fm\bar{3}m$ CaF_2 type	cubic	5.63							Hoekstra and Katz (1952); Scholder and Brixner (1955); Hoekstra and Siegel (1956); Keller (1964); Brochu and Lucas (1967)
CaU_3O_9	non-stoichiometric region in CaU_3O_{9-x}		cubic	super-structure line							Young and Schwartz (1962, 1963)
$Ba_2U_2O_7$	magnetic susceptibility. electronic spectra		monoclinic (pseudo tetragonal)	11.56	11.31	11.56	$\beta \approx 90$		7.46	7.58	Kemmler-Sack and Rüdorff (1967); Kemmler-Sack (1968a,b)

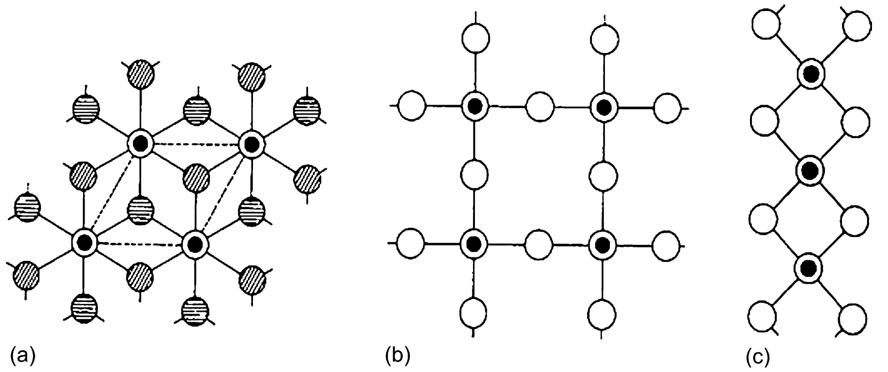

Fig. 5.25 *Schematic atom arrangement around a uranyl group (Zachariasen, 1954b); the notation is as follows: ◉: the inner filled circles show U in the plane of the page; the outer empty circles denote O_I, one above and the other below the plane of the page; ○: denotes O_{II} in the plane of the page; ◍: denotes O_{II} slightly above the plane of the page and ⊜: denotes O_{II} slightly below the plane. (a) Hexagonal coordination by six O_{II} atoms (β-Li_2UO_4, $CaUO_4$, α-$SrUO_4$). Each uranium atom is coordinated with six oxygen atoms in an approximately planar arrangement. The axis of the collinear U_I–U–O_I group is normal to the plane of the page. (b) Tetragonal coordination by four O_{II} atoms forming an infinite plane ($BaUO_4$). Uranium is octahedrally coordinated by four O_{II} atoms and two O_I atoms. Each octahedron shares four corners with adjacent octahedra forming a layer structure extended in the bc plane. The Ba atoms are located between the layers and link them by electrostatic force. (c) Tetragonal coordination by four O_{II} atoms forming an infinite chain ($MgUO_4$). The octahedra share two opposite edges, resulting in formation of chains along the a-axis. Reproduced by the permission of the International Union of Crystallography.*

discussed in Tso *et al.* (1985). Note that the technique is also discussed by Keller (1972) for BaU_2O_7 and $Ba_2U_3O_{11}$.

Crystal structures

An important feature of $M_2^+U_nO_{3n+1}$ and $M^{2+}U_nO_{3n+1}$ type uranates(VI) is their layer structure and the existence of the uranyl groups, UO_2^{2+}, in the crystals.

The structure of monouranates ($n = 1$) is characterized by the layer planes; the oxygen atoms on this plane are coordinated to uranium atoms forming secondary bonds. The primary bonds between the uranium and oxygen atoms of the uranyl group, O_I–U–O_I, are collinear and perpendicular to the layer plane. The atom arrangements around the uranyl groups are schematically drawn in Fig. 5.25 (Zachariasen, 1954b).

For β-Li_2UO_4 (Zachariasen, 1945), $CaUO_4$ and α-$SrUO_4$ (Zachariasen, 1948b), each uranium atom is coordinated to six oxygen atoms (cf. Fig. 5.25a, viewed from the *c*-axis). The axis of the UO_2^{2+} group in the figure is normal to the page, while three of six O_{II} atoms are located about 0.5 Å above and remaining three O_{II} atoms about 0.5 Å below the plane through uranium and perpendicular to the UO_2^{2+} axis. The oxygen atoms coordinated to uranium in

$BaUO_4$ and $MgUO_4$ form a deformed octahedron, where each O_{II} oxygen atom acts as a bridge between two adjacent uranium atoms. In $BaUO_4$ the octahedra share corners (Fig. 5.25b), but in $MgUO_4$ they share edges (Fig. 5.25c). As a consequence, infinite layers are formed in $BaUO_4$ and infinite chains in $MgUO_4$. The alkali or alkaline-earth metals occupy the positions between the layers and bind them together by electrostatic force (Zachariasen, 1954b).

There are no uranyl groups in Li_4UO_5 and Na_4UO_5, and the structure instead contains four orthogonal planar U–O_I bonds (with the distance 1.99 Å in both Li_4UO_5 and Na_4UO_5), yielding UO_4^{2-}; in addition, there are also two collinear U–O_{II} bonds (Li_4UO_5: 2.23 Å; Na_4UO_5: 2.32 Å) (Hoekstra and Siegel, 1964). The octahedra produced in this way are linked to bridges through the diagonally located O_{II} atoms, resulting in formation of a structure containing octahedral chains running along the *c*-axis. $M_3^{2+}UO_6$-type compounds (M = Ca, Sr, Ba) crystallize into distorted perovskite structures ($2[M_{1/4}U_{1/4}][M_{5/4}U_{1/4}]O_3$), where the alkaline-earth atoms and uranium atoms corresponding to $[M_{1/4}U_{1/4}]$ occupy the octahedral sites in an ordered manner (Keller, 1964; Morss, 1982; Williams *et al.*, 1984).

Physicochemical properties

Alkali metal monouranates(VI) are hygroscopic except for Li_2UO_4, and mostly yellow colored; some diuranates are orange or red-orange. The uranates(VI) of the heavy alkali metals are volatile on heating in air. The antisymmetric stretching vibration of UO_2^{2+} in uranates(VI) gives a strong absorption in the IR range of 600–900 cm^{-1}. The frequency changes depending on the bonding strength of the coordinated oxygen atoms. Since the U–O_I bonds of the uranyl group are much stronger, this vibration can be treated approximately as an isolated linear three-atom system of CO_2-type (Jones, 1958). The U–O_I distances calculated from the infrared frequencies using the empirical Badger equation are mostly in good agreement with those obtained by diffraction experiments (Hoekstra and Siegel, 1964; Allpress, 1965; Hoekstra, 1965; Carnall *et al.*, 1966).

A phase transformation coupled with oxygen non-stoichiometry has been observed for $SrUO_4$ and $CdUO_4$ (Tagawa and Fujino, 1978, 1980). α-$SrUO_4$ can be reduced to non-stoichiometric $SrUO_{4-x}$ with the maximum x value of 0.2–0.3. On heating α-$SrUO_4$ at different oxygen partial pressures from 10 to 600 mmHg and heating rates of 1–5 K min^{-1}, the compound is rapidly reduced to $SrUO_{3.8-3.9}$ at about 800°C. The solid is then immediately re-oxidized to stoichiometric composition by absorbing oxygen from the gaseous phase. At the same time, it transforms into β-$SrUO_4$. The atom rearrangement in the phase transformation may be accelerated by the formation of vacancies in the oxygen sublattice of α-$SrUO_4$.

Magnetic susceptibilities have been measured for $MgUO_4$, $SrUO_4$, $BaUO_4$, CaU_2O_7, SrU_2O_7, and BaU_2O_7 (Brochu and Lucas, 1967). In these compounds U(VI) is expected to be diamagnetic, but a weak paramagnetism was observed; this is ascribed to covalency in the uranyl group (Bell, 1969).

(*ii*) *Uranates* (*v*) *and* (*iv*)

Uranates(v) of $M^{+}UO_3$ (M = Li, Na, K, Rb), $M_3^{+}UO_4$ (M = Li, Na), and $M^{2+}U_2O_6$ (M = Mg, Ca, Sr, Ba) types are the most well known, as are the uranates(iv) of $M^{2+}UO_3$ (M = Ca, Sr, Ba) type.

Preparation

To prepare uranates(v), a symproportionation reaction is widely used, where the uranates(iv) and (vi) are first mixed in 1:1 uranium atom ratio, after which the mixture is heated in an evacuated sealed quartz ampoule. An example is the reaction $Li_2UO_4 + UO_2 = 2LiUO_3$, which takes place at 650–750°C. Another method is to reduce uranates(vi) by H_2 at elevated temperatures; the reaction condition should be carefully defined in order to form uranates(v). Since the uranates of alkaline-earth metals are not volatile, the high-temperature reduction method by H_2 can be used to prepare the corresponding uranates(iv).

For some uranates(vi) having high equilibrium oxygen pressures, uranates(v) can be prepared by heating the uranate(vi) in a vacuum at high temperature. The $M^{2+}U_2O_6$ compounds are prepared by the reaction

$$M^{2+}U_2O_7 = M^{2+}U_2O_6 + 1/2O_2$$

at 1100°C (M = Mg, Ca, Sr, Ba). It is, however, rather difficult to obtain stoichiometric uranates(v) by this method.

Crystal structures

Uranates(v) and (iv) do not contain uranyl groups and as a result, their crystal structures are in general not of the layer type and in many cases simpler. The compounds of $M^{+}UO_3$ and $M^{2+}UO_3$, with the exception of $CaUO_3$ (cubic Mn_2O_3-type structure), have perovskite or deformed perovskite-type structures. $LiUO_3$ crystallizes into a rhombohedrally distorted $LiNbO_3$ structure, as a result of the small ionic radius of Li^{+}. $NaUO_3$ has an orthorhombic $GdFeO_3$ structure with small distortions from cubic perovskite structure. KUO_3 and $RbUO_3$ have cubic perovskite structures, and $BaUO_3$ a cubic or pseudo-cubic perovskite structure.

In the uranates(v) of $M_3^{+}UO_4$-type, Li_3UO_4 crystallizes in a tetragonally distorted NaCl-type structure, in which the lithium and uranium atoms are located in the cation sites in an ordered manner with an atom ratio of 3:1. All $M^{2+}U_2O_6$ compounds have cubic fluorite-type structures, where the alkaline-earth metal atoms and uranium atoms are statistically distributed with an atom ratio of 1:2 over the cation sites.

Physico-chemical properties

Most uranates(v) and (iv) are brown to black. An exception is the pale green Li_7UO_6. Uranates(v) and (iv) dissolve in dilute mineral acids. The dissolution rate in HNO_3 is higher than those in HCl and H_2SO_4 (Trzebiatowski and

Jabłoński, 1960; Scholder and Gläser, 1964; Brochu and Lucas, 1967). Li_3UO_4 is oxidized to Li_2UO_4 in air even at room temperature. Na_3UO_4 absorbs significant amounts of oxygen, water, and CO_2 at room temperature. On heating the uranates(V) or uranates(IV) in air, they are readily oxidized to uranates(VI).

Electronic spectra have been measured for $LiUO_3$, $NaUO_3$, KUO_3, $RbUO_3$, MgU_2O_6, CdU_2O_6, Li_3UO_4, Li_7UO_6, $Ba_2U_2O_7$, etc. in the range 4000–40000 cm^{-1} (Kemmler-Sack *et al.*, 1967). The crystal field parameters were determined for $LiUO_3$ and Li_3UO_4 from the optical absorption electronic spectra (Lewis *et al.*, 1973; Kanellakopulos *et al.*, 1980; Hinatsu *et al.*, 1992a,b). For KUO_3 and $RbUO_3$, the octahedral crystal field around a U^{5+} atom was consistently calculated with a spin–orbit coupling constant of 1770 cm^{-1} (Kemmler-Sack *et al.*, 1967; Selbin *et al.*, 1972a).

Magnetic susceptibilities have been measured for $LiUO_3$, $NaUO_3$, KUO_3, $RbUO_3$, Li_3UO_4, Li_7UO_6, MgU_2O_6, CdU_2O_6, and $Ba_2U_2O_7$ at temperatures 85–473 K (Rüdorff and Menzer, 1957; Kemmler-Sack, 1968a). In the paramagnetic temperature range, the Curie constant changed with the coordination number. The magnetic susceptibilities for M^+UO_3 (M = Li, Na, K, Rb) were measured in a wider temperature range from 4.2 K to room temperature (Keller, 1972; Miyake *et al.*, 1979, 1982; Kanellakopulos *et al.*, 1980). The electron paramagnetic resonance (EPR) spectra for U^{5+} ions doped in $LiNbO_3$, which has the same crystal structure as $LiUO_3$, gave a signal at $g = 0.727$ (Lewis *et al.*, 1973). The EPR signals were also observed for pure M^+UO_3 but they were very broad (Miyake *et al.*, 1979, 1982). $LiUO_3$ showed a ferromagnetic transition at 16–17 K (Miyake *et al.*, 1979, 1982; Hinatsu *et al.*, 1992b).

Li_3UO_4 has a distorted NaCl-type structure and its magnetic properties have been studied by measuring the EPR spectra and magnetic susceptibility in an extended temperature range down to 4.2 K (Keller, 1972; Lewis *et al.*, 1973; Kanellakopulos *et al.*, 1980; Miyake *et al.*, 1982; Hinatsu *et al.*, 1992a). The experimental magnetic susceptibility can be well described by assuming the $5f^1$ electron of U^{5+} in an octahedral crystal field with a small tetragonal distortion with the crystal field parameters obtained from the electronic spectra (Hinatsu *et al.*, 1992a). $NaUO_3$ gives a magnetic transition at 32 K (Miyake *et al.*, 1977) or 35 K (Keller, 1972), for which a λ-type anomaly has also been observed in the heat capacity (Lyon *et al.*, 1977). The EPR and magnetic susceptibility studies for $M^{2+}U_2O_6$ (M = Mg, Ca, Cd, Sr) have been carried out (Brochu and Lucas, 1967; Miyake *et al.*, 1993; Miyake and Fujino, 1998). The anomalies of magnetic origin have been observed at 4–7 K.

(*iii*) *Non-stoichiometry*

The non-stoichiometry in uranates can be classified into three types. The first type occurs when part of the alkali metal in the uranate is lost as an oxide by vaporization on heating, viz. $Na_{2-2x}U_2O_{7-x}$ is formed from $Na_2U_2O_7$ by the loss of $x Na_2O$ ($0 \leq x \leq 0.07$) (Carnall *et al.*, 1966; Anderson, 1969). The second type is caused by non-stoichiometric dissolution of alkali metal in a uranium oxide. An example is Na_xUO_3 ($0 \leq x \leq 0.14$) (Greaves *et al.*, 1973). The third type is the most common non-stoichiometry, i.e. the oxygen non-stoichiometry. Examples of such uranates are $Na_2U_2O_{7-x}$ ($0 \leq x \leq 0.5$) (Anderson, 1969), $K_2U_2O_{7-x}$ (Spitsyn *et al.*, 1961b), $Cs_2U_4O_{13-x}$ (Cordfunke *et al.*, 1975), $CaUO_{4-x}$ ($0 \leq x \leq 0.5$) (Anderson and Barraclough, 1963), α-$SrUO_{4-x}$ ($0 \leq x \leq 0.5$) (Tagawa and Fujino, 1977), CaU_2O_{7-x} ($0 \leq x \leq 0.13$) and SrU_2O_{7-x} ($0 \leq x \leq 0.4$) (Hoekstra and Katz, 1952), SrU_4O_{13-x} (Cordfunke and Loopstra, 1967; Tagawa *et al.*, 1977). Rhombohedral $CaUO_4$ and α-$SrUO_4$, which crystallographically are very similar to ionic UO_2, show a wide range of non-stoichiometries, while β-$SrUO_4$ and $BaUO_4$ with increased covalency have virtually no non-stoichiometry. Examples of the third type of non-stoichiometric compounds derived from uranate(v) are MgU_2O_{6+x} ($-0.16 \leq x \leq 0.03$), CaU_2O_{6+x} ($-0.05 \leq x \leq 0.05$), SrU_2O_{6+x} ($-0.05 \leq x \leq 0.4\sim0.6$), and BaU_2O_{6+x} ($x \leq 0.86$) (Hoekstra and Katz, 1952).

The non-stoichiometric uranates are produced by heating in reducing atmospheres, but generally the U(VI) state is more stable in ternary uranates than in binary uranium oxides. This trend is more pronounced for the uranates with higher M/U ratios (M = alkali metals or alkaline-earth metals). The experimental fact that alkali and alkaline-earth metal uranates(VI) strictly without U(V) and U(IV) are formed under certain conditions when heated in air was utilized for the determination of oxygen in uranium oxides (Fujino *et al.*, 1978b).

(c) Transition metal uranates

Table 5.18 shows the crystallographic properties of ternary transition metal uranates. In this section the uranates of some non-transition metals such as Sb, Tl, Pb, and Bi are included because of the resemblance of their properties. Here we present an overview of preparation methods and crystal structures. For more detailed information, the reader is referred to the following review articles (Hoekstra and Marshall, 1967; Keller, 1972, 1975).

(*i*) *Preparative methods*

The most general 'dry' method for preparation is to heat thoroughly ground mixtures of transition metal oxides and UO_3 (or U_3O_8) in air. $CrUO_4$, $MnUO_4$, and $CoUO_4$ can be synthesized by heating the mixed oxides for 1 day at 1000–1100°C (Hoekstra and Marshall, 1967). $CuUO_4$ is obtained by heating below 875°C. Triuranates, MU_3O_{10} (M = Mn, Co, Ni, Cu, Zn), are prepared by heating the mixtures of M/U = 1/3 at 875°C. Although Ni, Cu, and Zn triuranates are readily obtained as stoichiometric compounds, Mn and Co triuranates tend to remain oxygen-deficient.

Nitrates, viz. $M(NO_3)_2 + UO_2(NO_3)_2$ (Weigel and Neufeldt, 1961), can also be used as starting materials for preparing MUO_4 (M = Cu, Zn, Cd, Hg),

Table 5.18 *Crystallographic properties of transition metal uranates.*

				Lattice parameters					*Density* (g cm^{-3})		
Formula	*Color*	*Space group*	*Symmetry*	*a* (Å)	*b* (Å)	*c* (Å)	*Angle* (deg)	*Z*	*Exp.*	*X-ray or ND*	*References*
$EuUO_3$			orthorhombic	6.020	6.165	8.606					Berndt *et al.* (1976)
$U_{0.25}NbO_3$	brown		tetragonal	7.727		7.792			5.72		Keller (1975)
$U_{0.25}TaO_3$	brown		tetragonal	7.739		7.773			8.23		Keller (1975)
U_xWO_3 ($x<0.16$–0.2)			cubic	3.78–3.81							Keller (1975)
$CrUO_4$	dark brown	*Pbcn*	orthorhombic	4.871	11.787	5.053			7.72	8.12	Rüdorff *et al.* (1967); Hoekstra and Marshall (1967); Keller (1975)
$MnUO_4$		*Imma*	orthorhombic	6.645	6.983	6.749					Hoekstra and Marshall (1967); Keller (1972)
$FeUO_4$	black	*Pbcn*	orthorhombic	4.888	11.937	5.110					Rüdorff *et al.* (1967); Hoekstra and Marshall (1967); Keller (1972, 1975)
$CoUO_4$	dark brown	*Imma*	orthorhombic	6.497	6.952	6.497				8.17	Hoekstra and Marshall (1967); Keller (1972, 1975)
α-$NiUO_4$		*Pbcn*	orthorhombic	4.820	11.627	5.188					Hoekstra and Marshall (1967); Keller (1972, 1975)
β-$NiUO_4$		*Imma*	orthorhombic	6.472	6.870	6.472					Hoekstra and Marshall (1967); Keller (1972, 1975)
$CuUO_4$	coffee brown	*P*2$_1$/*n*	monoclinic	5.475	4.957	6.569	$\beta = 118.87$	2			Hoekstra and Marshall (1967); Siegel and Hoekstra (1968); Keller (1972)
$ZnUO_4$	bright red	*Imma*	orthorhombic	6.492	6.994	6.574					Hoekstra and Marshall (1967); Keller (1972)
α-$CdUO_4$	brownish yellow		orthorhombic	7.01	6.836	3.519					Ippolitova *et al.* (1961e); Keller (1972)

β-$CdUO_4$	brownish yellow	$R\bar{3}m$	rhombohedral	3.587		17.41		2			Ippolitova *et al.* (1961e); Keller (1972)
$HgUO_4$	orange		orthorhombic	11.12	6.87	6.48					Keller (1972)
$PbUO_4$	red	*Pbcm*	orthorhombic	5.528	7.952	8.180					Keller (1972)
$BiUO_4$	gray black	$Fm\bar{3}m$	cubic	5.481				4	10.3	10.31	Rüdorff *et al.* (1967)
α-Ag_2UO_4	deep brown		tetragonal	11.70		5.87			7.57	7.41	Keller (1972)
β-Ag_2UO_4	deep brown		tetragonal	4.66		6.38			6.46	6.20	Keller (1972)
Tl_2UO_4	yellow orange		tetragonal	4.468		13.10					Keller (1972)
Cd_2UO_5	orange yellow	$P2_1/c$	monoclinic	8.074	5.312	11.52	$\beta = 100.52$	4		7.74	Keller (1972)
$UTiO_5$			orthorhombic	6.31	7.35	15.56					Dickens *et al.* (1993)
UVO_5	black	*Pbma*	orthorhombic	12.31	7.19	4.115					Keller (1975)
$UNbO_{5(+x)}$			orthorhombic	6.459	3.785	4.036					Keller (1975)
$UTaO_{5.17}$	dark gray		orthorhombic	6.463	3.780	3.980					Keller (1975)
$UMoO_5$		*Pbcm*	orthorhombic	4.115	12.761	7.338					Keller (1975)
$UTeO_5$		$Pca2_1$	orthorhombic	10.161	5.363	7.862					Meunier and Galy (1973)
CoU_2O_6	dark brown		hexagonal	9.095		4.990			8.55	8.79	Kemmler-Sack and Rüdorff (1967); Keller (1975)
NiU_2O_6	red brown	*P*321	hexagonal	9.015		5.103			8.64	8.75	Kemmler-Sack and Rüdorff (1967); Keller (1975)
CdU_2O_6			cubic	5.357					9.66	9.858	Kemmler-Sack and Rüdorff (1967)
Cr_2UO_6	black	$P\bar{3}1m$	hexagonal	4.988		4.620			7.01	7.31	Keller (1975)
Cd_3UO_6	light orange		monoclinic	8.262	5.733	5.623	$\beta = 89.53$				Keller (1972)
Pb_3UO_6	dark red	*Pnam*	orthorhombic	13.71	12.36	8.21					Keller (1972)
UV_2O_6		$P\bar{3}1m$	hexagonal	4.988		4.768			7.09	7.06	Keller (1975)

Table 5.18 (*Contd.*)

				Lattice parameters					*Density* (g cm^{-3})		
Formula	*Color*	*Space group*	*Symmetry*	*a* (Å)	*b* (Å)	*c* (Å)	*Angle* (deg)	Z	*Exp.*	*X-ray or ND*	*References*
CdU_2O_7	yellow										Keller (1972)
$Cd_2U_2O_7$			rhombohedral	10.72			$\alpha = 91.30$				Kemmler-Sack and Rüdorff (1967)
$Tl_2U_2O_7$			orthorhombic	6.902	7.971	19.643					Keller (1972)
$U_{2/3}Nb_2O_7$		$Fd3$	cubic	10.38					5.2	5.4	Keller (1975)
$Co_3U_2O_8$		$Pnnm$	orthorhombic	5.11	10.30	6.15		2			Bacmann (1973); Keller (1975)
UV_2O_8	yellow green	$Pnma$	orthorhombic	5.70	11.78	10.42			4.50	4.45	Keller (1975)
UTa_2O_8	yellow	$P\bar{3}1m$	hexagonal	6.41		3.95			8.3		Keller (1975)
UMo_2O_8		$Pban$	orthorhombic	20.08	7.32	4.11			6.13		Keller (1975)
U_2MoO_8		$P2_12_12$	orthorhombic	6.734	23.24	4.115					Keller (1975)
U_2WO_8		$P2_12_12$	orthorhombic	6.711	23.28	4.091					Keller (1975)
MnU_3O_{10}	light brown		hexagonal	3.80		4.14					Hoekstra and Marshall (1967); Keller (1972)
FeU_3O_{10}			orthorhombic	6.51	7.53	16.14					Keller (1972, 1975)
CoU_3O_{10}	deep brown		hexagonal	3.79		4.08					Hoekstra and Marshall (1967); Keller (1972, 1975)
NiU_3O_{10}	yellow brown		monoclinic	7.525	6.545	16.126	$\beta = 91$				Hoekstra and Marshall (1967); Keller (1972, 1975)
CuU_3O_{10}	deep red		monoclinic	7.575	6.473	16.679	$\beta = 91$				Hoekstra and Marshall (1967); Keller (1972)

ZnU_3O_{10}	red brown		hexagonal	7.56			16.418			Hoekstra and Marshall (1967); Keller (1972)
UV_3O_{10}	black	*Fddd*	orthorhombic	12.00	6.926	16.17				Keller (1975)
$UNb_3O_{10(+x)}$		*Fddd*	orthorhombic	7.38	12.78	15.96		5.95	5.98	Keller (1975)
$UTa_3O_{10(+x)}$			hexagonal	7.416		15.770		8.41		Keller (1975)
$U(WO_4)_2$			orthorhombic	9.545	10.245	14.26				Keller (1975)
$U_2V_2O_{11}$	green	$P2_1/m$	monoclinic	9.29	13.24	7.27	$\beta \approx 100$			Keller (1975)
Y_6UO_{12}	pale yellow-green	$R\bar{3}$	hexagonal	9.934	9.364			5.91	6.00	Aitken *et al.* (1964); Bartram (1966)
La_6UO_{12}	reddish-orange	$R\bar{3}$	hexagonal	10.473		9.984			9.63	Aitken *et al.* (1964); Hinatsu *et al.* (1988)
Pr_6UO_{12}		$R\bar{3}$	hexagonal	10.301		9.800				Aitken *et al.* (1964)
Nd_6UO_{12}		$R\bar{3}$	hexagonal	10.254		9.748				Aitken *et al.* (1964)
Sm_6UO_{12}		$R\bar{3}$	hexagonal	10.148		9.630				Aitken *et al.* (1964)
Gd_6UO_{12}		$R\bar{3}$	hexagonal	10.076		9.529				Aitken *et al.* (1964)
Tb_6UO_{12}		$R\bar{3}$	hexagonal	10.013		9.465				Aitken *et al.* (1964)
Ho_6UO_{12}		$R\bar{3}$	hexagonal	9.935		9.368				Aitken *et al.* (1964)
Tm_6UO_{12}		$R\bar{3}$	hexagonal	9.826		9.248				Aitken *et al.* (1964)
Yb_6UO_{12}		$R\bar{3}$	hexagonal	9.826		9.248				Aitken *et al.* (1964)
Lu_6UO_{12}		$R\bar{3}$	hexagonal	9.797		9.204				Aitken *et al.* (1964); Bartram (1966)
$Y_5U_2O_{12}$		$R\bar{3}$	hexagonal	10.01		9.36		6.88	6.83	Bartram (1966)
$U_2V_6O_{21}$	brown	*Fddd*	orthorhombic	11.995	6.94	16.17				Keller (1975)
$UMo_{10}O_{32}$		*Cccm*	orthorhombic	16.18	14.48	19.18				Keller (1975)
$UMo_{11}O_{35}$			orthorhombic	19.66	14.41	16.11		5.01		Keller (1975)
α-$U_3Mo_{20}O_{64}$		*Cccm*	orthorhombic	8.246	28.76	19.78				Keller (1975)
γ-$U_3Mo_{20}O_{64}$		*Pbmn*	orthorhombic	4.134	14.33	9.873		5.08	5.18	Keller (1975)
$U_5W_{19}O_{67}$		*Pcmm*	orthorhombic	7.814	7.271	38.67				Keller (1975)

because of their high reactivity. In this case, reaction temperatures not higher than 600°C are recommended for M = Cu, Zn, and Cd to avoid the formation of U_3O_8. $HgUO_4$ forms at 400°C. Ag_2UO_4 has been synthesized by heating a mixture of $AgNO_3$ and UO_2 to 500°C and maintaining this temperature for a period of 15 min. Above 500°C, Ag_2UO_4 begins to decompose with precipitation of metallic silver.

For preparing $FeUO_4$ and FeU_3O_{10}, the symproportionation reaction method in a sealed tube gives a good result. $FeUO_4$ is synthesized by heating either a mixture of $FeO + UO_3$ or $2Fe_2O_3 + U_3O_8 + UO_2$ at 1050°C in evacuated sealed quartz tubes. When a mixture of $Fe_2O_3 + U_3O_8 + 3UO_3$ is heated at 880°C, FeU_3O_{10} forms (Hoekstra and Marshall, 1967). $BiUO_4$ is prepared by heating a mixture of $2Bi_2O_3 + U_3O_8 + UO_2$ at 900–1000°C (Rüdorff *et al.*, 1967). The compounds MU_2O_6 (M = Co, Ni, Cd) have been prepared by heating the mixtures of $MUO_4 + UO_2$ at 800°C (Kemmler-Sack and Rüdorff, 1967). Single crystals of CuU_3O_8 and NiU_3O_{10} were grown by the reaction of UO_3 with the molten anhydrous transition metal chlorides in evacuated sealed silica tubes at 600–650°C for several weeks (Hoekstra and Marshall, 1967).

MU_3O_{10} with M = Mn, Co, and Zn were prepared by hydrothermal reactions using a platinum-lined Morey bomb in which the transition metal oxides and γ-UO_3 were heated in 0.06 M H_2SO_4 solution for 5 days at 350°C (Hoekstra and Marshall, 1967).

MUO_4 (M = Ni, Zn, Co, Mn) was successfully synthesized in experiments where a mixture of oxides was heated for 30 min at 1000°C under high pressures of 30–40 kbar using a tetrahedral anvil. However, the triuranates of these transition metals and $FeUO_4$ did not form by this method (Hoekstra and Marshall, 1967).

(*ii*) *Crystal structures*

$MnUO_4$ and $CoUO_4$ have the infinite chains of edge-sharing oxygen octahedra in the direction normal to the *c*-axis, characteristic of the $MgUO_4$ structure; these compounds crystallize in the same space group. The space group of $CrUO_4$, $FeUO_4$, and α-$NiUO_4$ is different from that of the above two compounds, and the lengths of the uranium–oxygen bonds that are expected to belong to uranyl groups are longer (2.05–2.06 Å) than those in $MnUO_4$ and $CoUO_4$. In these three compounds, the distorted UO_6 octahedra form infinite chains along the *c*-axis and less deformed MO_6 (M = Cr, Fe, Ni) octahedra are running parallel in the direction of the *c*-axis. Similar chain structures are also observed in the crystals of $USbO_5$, $UTiO_5$, and $UMoO_5$ (Dickens *et al.*, 1993). These structures are built from parallel layers of edge-sharing UO_m and MO_n polygons, linked together by metal–oxygen–metal chains or pillars running perpendicularly to the layers. In Pb_3UO_6, the infinite chains are formed by sharing the corners of distorted UO_6 octahedra in the direction of the *c*-axis.

The crystal structure of Pb_3UO_6 is wholly different from those of Ca_3UO_6 and Sr_3UO_6 (Sterns, 1967).

In the system PbO–U_2O_5, cubic $Pb_{1.5}U_2O_{6.5}$ (a = 11.16 Å) accommodates PbO until the $Pb_{2.5}U_2O_{7.5}$ composition is attained, resulting in a slight distortion to a rhombohedral structure (a = 11.23 Å, $\alpha = 90.25°$). This homogeneity range is regarded as derived from pyrochlore-type $Pb_2U_2O_7$ by addition or subtraction of PbO (Kemmler-Sack and Rüdorff, 1966).

$CuUO_4$ comprises a third group of crystal structures among the transition metal monouranates (Siegel and Hoekstra, 1968). The compound is monoclinic with space group $P2_1/n$. The coordination geometry is distorted octahedral with short collinear uranyl bonds, each of length 1.90 Å. The uranyl groups are in the direction nearly normal to a planar and almost square array of secondary uranium–oxygen bonds of lengths 2.15 and 2.24 Å.

Rare-earth oxides form solid solutions with UO_2 in an extended composition range. At the high atom ratio of RE/U = 6 (RE = rare-earth metals), however, the compounds of the composition RE_6UO_{12} crystallize in rhombohedral systems. In RE_6UO_{12} the uranium atom is surrounded by six oxygen atoms that form a distorted octahedron. All the U–O bond distances in the octahedron are 2.34 Å (La_6UO_{12}), and no uranyl groups exist in the crystal (Hinatsu *et al.*, 1988). $Y_5U_2O_{12}$ is produced along with Y_6UO_{12} giving a very similar crystal structure with similar lattice parameters. In $Y_5U_2O_{12}$, half the uranium atoms occupy the Y position (18f) in a disordered manner (Bartram, 1966).

(d) Solid solutions with UO_2

Uranium dioxide forms solid solutions with the oxides of alkaline-earth elements, rare-earth elements, some transition elements (Mn, Zr, Nb, Cd), and actinide elements (Th, Np, Pu, Am, Cm, etc.). The solid solution with PuO_2 (MOX) is important as nuclear fuel. Description on mixed oxide fuel, MOX, is given in Chapter 7.

The solid solutions are prepared by heating intimate mixtures of metal (M) oxides and uranium oxides usually in reducing atmosphere at temperatures between 1000 and 2000°C. The oxide powders are in most cases mechanically mixed, but other techniques such as coprecipitation (Keller *et al.*, 1972; Miyake *et al.*, 1986) and evaporation from aqueous solutions (Markin *et al.*, 1970; Lindemer and Sutton, Jr., 1988) have also been adopted. In the solid solutions, the dissolved foreign metal atoms and host uranium atoms are statistically distributed on the metal sites of the fluorite-type cubic crystals of UO_2 (Rüdorff *et al.*, 1967; Keller *et al.*, 1969; Hutchings *et al.*, 1985; Martin *et al.*, 2003). The solid solution can be written as $M_yU_{1-y}O_{2+x}$, where x is defined (in this section) to take on both positive and negative values. A considerable number of publications on the magnetic properties are available since the magnetic properties of uranium and metals, M, of varying oxidation state can be studied in the same fluorite-type fcc crystal field in these solid solutions; detailed description is given in Chapter 20. Recent progress on this subject is written in a review (Fujino and Miyake, 1991).

(*i*) *Lattice parameter change with composition*

The lattice parameter of cubic solid solution changes nearly linearly with the increase of y and x in $M_yU_{1-y}O_{2+x}$. The differential coefficient, $\partial a/\partial y$, where a is the lattice parameter in Å, can have both negative and positive values depending on the metal ion M^{n+}. Table 5.19 shows the observed $\partial a/\partial y$ and $\partial a/\partial x$ for various solid solutions (Fujino and Miyake, 1991). The underlined values in the table are those obtained from the lattice parameters of the stoichiometric solid solutions at the upper limit of the y-values, i.e. $M^{3+}_{0.5}U_{0.5}O_{2.00}$ and $M^{2+}_{0.33}U_{0.67}O_{2.00}$.

As seen in the table, the coefficient $\partial a/\partial y$ is large for the metals with large ionic radii, although correction for valence state of the metals is required for a more detailed discussion. Investigations to determine the functional relation between these quantities have been performed (Ohmichi *et al.*, 1981; Fujino and Miyake, 1991). The differential coefficient of the oxygen non-stoichiometry, $\partial a/\partial x$, in Table 5.19 have in general the values $-0.3 \leq \partial a/\partial x \leq -0.24$ for $x < 0$ and $-0.13 \leq \partial a/\partial x \leq -0.11$ for $x > 0$ regardless of the M metal.

(*ii*) *The solid solution regions*

$M^{4+}_yU_{1-y}O_{2+x}$

Zr SOLID SOLUTIONS The solubility data on this system are diverse. The Zr solid solution with $y = 0.15$ was obtained by heating at 1500°C (Une and Oguma, 1983a); at 1750°C, solid solutions with y values up to 0.3 were obtained (Aronson and Clayton, 1961). The solid solution with the highest y value, 0.35, has been obtained by heating the mixture of $UO_2(NO_3)_2 \cdot 6H_2O$ and $ZrOCl_2 \cdot 8H_2O$ in H_2 at 1650°C (Hinatsu and Fujino, 1985). The Zr solid solution is regarded as metastable at lower temperatures.

Th SOLID SOLUTIONS Th solid solutions are formed continuously from $y = 0$ to 1 for $x = 0$. However, for $x > 0$, there is an upper limit in the solubility. According to Paul and Keller (1971), the single-phase solid solutions under 1 atm O_2 exist below $y = 0.45$, 0.40, and 0.36 at 1100, 1400, and 1550°C, respectively. The lower limits at $p_{O_2} = 0.2$ atm are $y = 0.383$, 0.359, 0.253, and 0.068 for 700, 1200, 1400, and 1500°C, respectively (Gilpatrick *et al.*, 1964), which is in agreement with the value of $y = 0.22$ below 1400°C reported by Anderson *et al.* (1954). The maximum x value is 0.25 at temperatures between 1250 and 1550°C for $y \leq 0.5$. At lower temperatures of 600–1100°C, the upper limit of x decreases to 0.12–0.14 for y values below 0.4 (Cohen and Berman, 1966; Paul and Keller, 1971).

Table 5.19 *Lattice parameter change with composition of solid solutions* $M_yU_{1-y}O_{2+x}$ (*Fujino and Miyake,* 1991).

Element	$\partial a/\partial y$	$\partial a/\partial x$	*References*
Zr	–0.302		Cohen and Schaner (1963);
	–0.301		Hinatsu and Fujino (1985)
Th	0.163 ($y \leq 0.05$)	–0.14 ($x > 0$)	Cohen and Berman (1966)
	0.127 ($0.1 \leq y \leq 0.5$)		
Np	–0.146		Tabuteau *et al.* (1984)
Pu	–0.0747 ($x = 0$)	–0.345 ($x < 0$)	Schmitz *et al.* (1971);
	–0.0727 ($x < 0$)		
		–0.313 ($x < 0$)	Martin and Shinn (1971);
		–0.274 ($x < 0$)	Mignanelli and Potter (1986)
Sc	–0.438		Hinatsu and Fujino (1986);
	–0.521		Keller *et al.* (1972)
Y	–0.233		Fukushima *et al.* (1981);
	–0.254		Weitzel and Keller (1975);
	–0.266		Ohmichi *et al.* (1981)
La	0.094 ($x > 0$)	–0.131 ($x > 0$)	Hinatsu and Fujino (1987);
	0.06 ($x < 0$)	–0.2 ($x < 0$)	
	0.073 ($x = 0$)		Weitzel and Keller (1975);
		–0.285 ($x < 0$)	Hill *et al.* (1963)
Ce	–0.067		Mignanelli and Potter (1983);
	–0.06		Lorenzelli and Touzelin (1980);
	–0.057 ($x = 0$)		Hinatsu and Fujino (1988a);
		–0.321 ($x < 0$)	Markin *et al.* (1970);
		–0.288 ($y = 0.282$, $-0.015 \leq x < 0$)	Norris and Kay (1983)
Pr	–0.007	–0.127 ($x > 0$)	Yamashita *et al.* (1985);
		–0.397 ($x < 0$)	
	–0.015		Hinatsu and Fujino (1988c)
Nd	–0.047	–0.112 ($x > 0$)	Hinatsu and Fujino (1988b);
	–0.057		Fukushima *et al.* (1983);
	–0.058		Weitzel and Keller (1975);
	–0.075		Ohmichi *et al.* (1981);
		–0.30 ($x < 0$)	Wadier (1973)
Sm	–0.118		Fukushima *et al.* (1983);
	–0.121		Rüdorff *et al.* (1967)
Eu	–0.138		Fukushima *et al.* (1983);
	–0.144		Ohmichi *et al.* (1981);
	–0.151	–0.30 ($x < 0$)	Fujino *et al.* (1990)
Gd	–0.164		Fukushima *et al.* (1982);
	–0.171		Rüdorff *et al.* (1967);
	–0.173	–0.24 ($x < 0$)	Ohmichi *et al.* (1981)
Ho	–0.267		Weitzel and Keller (1975)
Yb	–0.315		Rüdorff *et al.* (1967)
Lu	–0.356		Weitzel and Keller (1975)
Mg	–0.568	–0.117 ($x > 0$)	Fujino and Naito (1970);
	–0.546		Kemmler-Sack and Rüdorff (1967);
	–0.559		Keller (1964)

Table 5.19 (*Contd.*)

Element	$\partial a/\partial y$	$\partial a/\partial x$	*References*
Ca	–0.310	–0.102 ($x > 0$) –0.190 ($x < 0$)	Yamashita and Fujino (1985);
	–0.213	–0.10 ($x > 0$)	Hinatsu and Fujino (1988d);
	–0.289		Loopstra and Rietveld (1969)
Sr	–0.098	–0.109 ($x > 0$) –0.244 ($x < 0$)	Fujino *et al.* (1988);
	–0.055		Hoekstra and Katz (1952)
Mn	–0.499		Kemmler-Sack and Rüdorff (1967)
Cd	–0.340		Keller (1962b); Kemmler-Sack and Rüdorff (1967)
Bi	0.149		Rüdorff *et al.* (1967)

$M_y^{4+\sim3+}U_{1-y}O_{2+x}$

Ce SOLID SOLUTIONS Ce solid solutions are formed continuously from $y = 0$ to 1 for $x = 0$. For $x < 0$, the region of the single-phase solid solution is restricted to $y \leq 0.35$ (Markin *et al.*, 1970) or $y \leq 0.2$ (Lorenzelli and Touzelin, 1980). Above this value up to $y = 0.7$, the products are two phases $(Ce,U)O_{2.00}$ and $(Ce,U)O_{2-x}$ at room temperature. Further reduction results in formation of single-phase solid solutions. The x values for the single-phase solid solutions are $x < -0.04$, –0.12, –0.19, and –0.24 for $y = 0.1$, 0.3, 0.5, and 0.7, respectively (Lorenzelli and Touzelin, 1980).

In the hyperstoichiometric range of $0 \leq x \leq 0.18$, the solid solutions with $y < 0.5$ are a single phase at room temperature. Air-oxidized hyperstoichiometric solid solutions crystallize in a fluorite-type single phase in the region of high Ce concentrations (Hoch and Furman, 1966). Single-phase regions exist in $y = 0.56$–1.0 (1100°C), 0.43–1.0 (1250 °C), and 0.26–1.0 (1550°C) (Paul, 1970). Single phases with $y = 0.6$–1.0 at 1100°C have also been reported (Tagawa *et al.*, 1981a).

$M_y^{n+}U_{1-y}O_{2+x}$ ($n = 3$ and 2)

SOLID SOLUTIONS IN REDUCING ATMOSPHERE The solid solutions obtained by heating in reducing atmospheres are generally hypostoichiometric. The x values are highly negative when strong reductants such as H_2 or CO are used. The single-phase regions of fcc solid solutions with M metals (M = rare-earth elements, alkaline-earth metals, and Cd) are shown in Table 5.20. In reducing atmosphere, the single-phase solid solution forms essentially in a range starting from $y = 0$. For M^{2+} metals, the maximum y values are around 1/3. If the monoxides of Mg and Ba are heated with UO_2 in a vacuum, the solubility is very low even at high temperatures due to shortage of oxygen (cf. Table 5.20).

Table 5.20 *Single phase regions of fcc solid solutions* $M_yU_{1-y}O_{2+x}$ *with M elements (rare-earth elements, alkaline-earth elements and Cd) prepared in reducing atmospheres. Concentrations of the M elements are shown in* mol%.

	Temperature (°C)					
Element	1100	1250	1400	1550	1700	*References*
Sc	0–1.6	0–1.8	0–2.1	0–2.9 (H_2)		Keller *et al*. (1972)
Y					0–50 (H_2)	Bartram *et al*. (1964);
					0–65 (2000°C, vacuum)	Ferguson and Fogg (1957)
La		0–82				Diehl and Keller (1971);
				0–54 (1750°C, vacuum)		Wilson *et al*. (1961);
				0–75 (1750°C, H_2 or vac.)		Hill *et al*. (1963)
Pr		0–70 (1350°C, vacuum)				Yamashita *et al*. (1985)
Eu		0–42 (Ar)				Berndt *et al*. (1976);
				0–53 (1600°C, vacuum)		Grossman *et al*. (1967);
				0–50~60 (vacuum)		Fujino *et al*. (1990)
Gd					0–80 (H_2) 0–50 (Ar)	Beals and Handwerk (1965)
Mg	0–33 ($MgUO_4$+MgU_3O_{10}+UO_2, 1100–1300°C, He)					Fujino and Naito (1970);
				0–5 (MgO+UO_2, 2350°C, vac.)		Anderson and Johnson (1953)
Ca	0–33 ($CaUO_4$+U_3O_8+UO_2, 1100–1300°C, vacuum)				0–40 (2000°C)	Brisi *et al*. (1972);
						Voronov and Sofronova (1972);
		3–33 (1200–1400°C, He)		0–20(CaO+UO_2, 1650°C, vac.)		Yamashita and Fujino (1985);
						Alberman *et al*. (1951)
Sr	0–30 ($SrUO_4$+U_3O_8+UO_2, 1200–1400°C, ~1 Pa O_2)					Fujino *et al*. (1988);
	33 (SrU_2O_7, vacuum)					Hoekstra and Siegel (1956);
						Ippolitova *et al*. (1961b);
		0–20 (1300°C)				Brisi *et al*. (1972)
Ba	33 (BaU_2O_7, 1200°C, vacuum)					Hoekstra and Siegel (1956);
	33 (BaU_2O_7, 600°C, NH_3)					Brochu and Lucas (1967);
				0–3 (BaO+UO_2, vac.)		Kleykamp (1985)
Cd	0–33 ($CdUO_4$+UO_2, vacuum sealed tube)					Kemmler-Sack and Rüdorff (1967)

SOLID SOLUTIONS IN OXIDIZING ATMOSPHERE The single-phase regions of fcc solid solutions prepared in oxidizing atmospheres are shown in Table 5.21. UO_2 is oxidized to U_3O_8 when heated in oxidizing atmospheres unless mixed with the M elements. Hence, the lower limit of the fcc single phase is not $y = 0$ but at higher values. The x value changes with y value in a rather simple way for rare-earth solid solutions: For Nd solid solutions heated under $p_{O_2} = 1$ atm at 1100°C for example, the mean uranium valence remains constant (+5) when the y value is in a region between ~0.3 and 0.5, i.e. x changes as $x=1/2-y$. The uranium valence then increases linearly from +5 to +6 when y increases from 0.5 to 0.67, during which $x = 0$. For the solid solutions in a higher y range, 0.67–0.75, the uranium valence is U(VI). Here, the x value decreases linearly from 0 to –0.125 ($x=1-3y/2$) with increasing y value in order to satisfy the charge neutrality condition (Keller and Boroujerdi, 1972).

(*iii*) *Oxygen potentials*

$M^{4+}_{y}U_{1-y}O_{2+x}$

Zr SOLID SOLUTIONS The oxygen potential of $Zr_yU_{1-y}O_{2+x}$ solid solution is lower than that of UO_{2+x}. At 1250 K, the $\Delta\bar{G}(O_2)$ value for Zr solid solution with $y = 0.3$ is –270 kJ mol^{-1} at $x = 0.05$ (Aronson and Clayton, 1961), while that for UO_{2+x} at $x = 0.05$ is ca. –210 kJ mol^{-1}. The low $\Delta\bar{H}(O_2)$ of $Zr_yU_{1-y}O_{2+x}$ has been suggested to explain the low $\Delta\bar{G}(O_2)$ of this solid solution. The $\Delta\bar{H}(O_2)$ values vary between –480 and –355 kJ mol^{-1} for $Zr_yU_{1-y}O_{2+x}$, which are significantly lower than those between –355 and –270 kJ mol^{-1} for $Th_yU_{1-y}O_{2+x}$ (Aronson and Clayton, 1960, 1961; Une and Oguma, 1983a).

Th SOLID SOLUTIONS Dissolution of Th causes an increase in $\Delta\bar{G}(O_2)$ with increasing value of y. The difference in $\Delta\bar{G}(O_2)$ between Th solid solution and UO_{2+x} is small if the concentration of Th is low (viz., $y = 0.1$). However, at high Th concentration with $y = 0.71$ ($x = 0.05$), $\Delta\bar{G}(O_2)$ of the solid solution at 1250 K is as high as –150 kJ mol^{-1} (Aronson and Clayton, 1960). This value is 60 kJ mol^{-1} higher than $\Delta\bar{G}(O_2)$ of $UO_{2.05}$ at the same temperature. There have been other thermodynamic studies on this solid solution (Tanaka *et al.*, 1972; Ugajin, 1982; Ugajin *et al.*, 1983; Matsui and Naito, 1985a).

$M^{4+\sim 3+}_{y}U_{1-y}O_{2+x}$

Ce SOLID SOLUTIONS Because two oxidation states, Ce^{3+} and Ce^{4+}, are possible for Ce in oxides, the oxygen potential of Ce solid solution changes over a wide range of x-values from negative to positive values, giving rise to a rapid ('vertical') change of $\Delta\bar{G}(O_2)$ at $x = 0$. The shape of the $\Delta\bar{G}(O_2)$ curve is very similar to that of $Pu_yU_{1-y}O_{2+x}$, but the $\Delta\bar{G}(O_2)$ values of $Ce_yU_{1-y}O_{2+x}$ are markedly higher. Namely, $\Delta\bar{G}(O_2)$ for $Ce_{0.25}U_{0.75}O_{1.95}$ is as high as –460 kJ mol^{-1} at 1200°C, compared to the value of –570 kJ mol^{-1} for $Pu_{0.25}U_{0.75}O_{1.95}$.

Table 5.21 *Single-phase regions of fcc solid solutions* $M_yU_{1-y}O_{2+x}$ *with M elements (rare-earth elements and Mg) prepared in oxidizing atmospheres. Atmosphere is* O_2 (1 atm) *unless otherwise described. Concentrations of the M elements are shown in* mol%.

Element	*Temperature* (°C)					*References*
	1100	1200	1300	1400	1500	
Sc	49.5–63.8	48.5–64.0 (1250°C)		45.5–64.9	42.1–65.5 (1510°C) ~0–65.7 (1550°C)	Keller *et al.* (1972)
Y	33–60 (1000°C, air)					Bartram *et al.* (1964);
		30–65 (air)				Hund *et al.* (1965)
La	31.5–51.5 68.5	28.5–55 63.5–69.5	26.5–75	25–82	24–82 (1550°C)	Diehl and Keller (1971);
	79.5–82	79–82	77–82		30–80 (1650°C)	Hill *et al.* (1963);
	30–45, 70–90 (1000°C, air)					Tagawa *et al.* (1983)
Pr	38.6–71.9	39.9–71.2	41.4–70.2	43.2–69.0	45.3–67.1	de Alleluia *et al.* (1981);
		30–60 (1250°C)				Jocher (1978);
			32–71 (1350°C, air)			Yamashita *et al.* (1985)
Nd	35.0–74.5	33–81 (1250°C)		25–81	13–81 (1550°C)	Boroujerdi (1971); Keller and Boroujerdi (1972)
Sm	50–60 (1000°C, air)					Tagawa *et al.* (1981b)
Eu	39–72	36–72 (1250°C)		30–72	25–72	Tanamas (1974);
	38–64 (air)					Haug and Weigel (1963)
Gd					30–60 (1700°C, air)	Beals and Handwerk (1965)
Dy	48.4–74.9	44.1–72.8 (1250°C)		35.0–72.8	14.2–72.2 (1550°C)	de Alleluia *et al.* (1981)
Ho	47.0–64.0	43.0–64.0 (1250°C)		33.0–64.0	19.0–64.0 (1550°C)	Keller *et al.* (1969)
Er	49.0–62.5	45.0–62.5 (1250°C)		41.0–62.5	21.5–62.5 (1550°C)	Keller *et al.* (1969)
Tm	48.5–64.0	45.0–64.0 (1250°C)		34.0–64.0	15.0–64.0 (1550°C)	Keller *et al.* (1969)
Yb	48.5–64.5	45.0–64.5 (1250°C)		38.5–64.5	16.5–64.5 (1550°C)	Keller *et al.* (1969)
Lu	48.0–65.5	45.0–65.5 (1250°C)		43.0–65.5	41.0–65.5 (1550°C)	Keller *et al.* (1969)
Mg			36–39 (1300°C, air)	12–39 (1500°C, air)	~0–39 (1600°C, air) max. 37 (1600–1700°C, air)	Sugisaki *et al.* (1973); Budnikov *et al.* (1958)

This difference has been attributed to the higher $\Delta\bar{G}(O_2)$ value of CeO_{2-x} (Panlener *et al.*, 1975) compared with that of PuO_{2-x} (Woodley, 1981). The $\Delta\bar{G}(O_2)$ measurements of the Ce solid solutions have been carried out by a number of researchers (Hoch and Furman, 1966; Markin and Crough, 1970; Ducroux and Baptiste, 1981; Norris and Kay, 1983; Nagarajan *et al.*, 1985).

Pr AND Am SOLID SOLUTIONS The Pr solid solutions have lower values of $\Delta\bar{G}(O_2)$ than the solid solutions with solely M^{3+} rare-earth ions, because of the two possible oxidation states, Pr^{3+} and Pr^{4+} (Jocher, 1978; Fujino and Miyake, 1991). The situation is the same for Am solid solutions, although their $\Delta\bar{G}(O_2)$ values are markedly higher than those of Pu and Ce solid solutions (Bartscher and Sari, 1983).

$M^{3+}_{y}U_{1-y}O_{2+x}$

A large number of oxygen potential measurements for the M^{3+} solid solutions have been carried out. These comprise solid solutions of Y (Aitken and Joseph, 1966; Hagemark and Broli, 1967; Nakajima *et al.*, 2002), La (Hagemark and Broli, 1967; Stadlbauer *et al.*, 1974; Matsui and Naito, 1986), Pr (Jocher, 1978; Fujino and Miyake, 1991), Nd (Wadier, 1973; Une and Oguma, 1983c), Eu (Tanamas, 1974; Lindemer and Brynestad, 1986; Fujino *et al.*, 1990, 1999), and Gd (Une and Oguma, 1982, 1983b; Lindemer and Sutton, Jr. 1988).

$\Delta\bar{G}(O_2)$ for $M^{3+}_{y}U_{1-y}O_{2+x}$ can be defined from $x = -y/2$ to positive x values; the measured oxygen potential increases with increasing x value, passing through an inflection point at $x = 0$, where $\Delta\bar{G}(O_2)$ increases very rapidly. The dissolution of M^{3+} metals enhances $\Delta\bar{G}(O_2)$ more than do the M^{4+} metals. The $\Delta\bar{G}(O_2)$ value increases with increasing y, but the $\Delta\bar{G}(O_2)$ curve gradually levels off at high M^{3+} concentrations. In a series of rare-earth solid solutions, the La solid solution shows the highest $\Delta\bar{G}(O_2)$ values, which is assumed to be associated with the fact that La^{3+} has the largest ionic radius of these M^{3+} ions. With increasing atomic number of the lanthanides, $\Delta\bar{G}(O_2)$ is lowered, although the $\Delta\bar{G}(O_2)$ difference between the Nd and Gd solid solutions is small. Fig. 5.26 shows the oxygen potential of $Gd_yU_{1-y}O_{2+x}$ as a function of O/(Gd+U) ratio ($=2 + x$).

The Eu solid solutions show a much higher value of $\Delta\bar{G}(O_2)$ than the other M^{3+} solid solutions (Lindemer and Brynestad, 1986). This is possibly due to the coexistence of Eu^{2+} and Eu^{3+} in the solid solutions (Fujino *et al.*, 1990). It is noteworthy that the inflection point of $\Delta\bar{G}(O_2)$ for Eu solid solutions is shifted to a range of $x < 0$ values. This is also observed for $M^{2+}_{y}U_{1-y}O_{2+x}$, supporting the presence of Eu^{2+} in the Eu solid solutions.

$M^{2+}_{y}U_{1-y}O_{2+x}$

The oxygen potential of $Mg_yU_{1-y}O_{2+x}$ (Fujino and Naito, 1970; Fujino *et al.*, 1978a; Tateno *et al.*, 1979) is significantly higher than those of $M^{3+}_{y}U_{1-y}O_{2+x}$. Moreover, the x values at which the 'vertical' change of $\Delta\bar{G}(O_2)$ takes place,

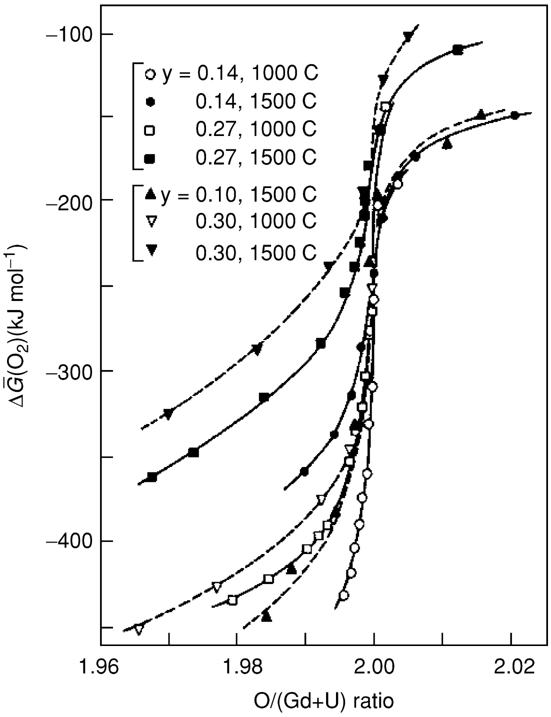

Fig. 5.26 *Oxygen potential of* $Gd_yU_{1-y}O_{2+x}$ *as a function of O/(Gd+U) ratio (Fujino and Miyake,* 1991*). Solid lines: Une and Oguma* (1983*b*)*; Broken lines: Lindemer and Sutton, Jr.* (1988)*. Reproduced by the permission of Elsevier.*

which are also the inflection points, are negative in contrast to the M^{4+} and M^{3+} solid solutions, where the value of x at the inflection is zero. This negative shift for $Mg_yU_{1-y}O_{2+x}$ becomes more pronounced at higher values of y, viz., $x = -0.07$ at $y = 0.3$ (1200–1500°C) (Sugisaki and Sueyoshi, 1978).

The high $\Delta\bar{G}(O_2)$ values are supposed to be rationalized by a configurational entropy change. Dissolution of M^{2+} metals in UO_2 results in formation of a larger number of U^{5+} ions in the solid solution crystals, which increases the number of ways, W, of arranging the cations on the cation sites. The entropy, $\Delta\bar{S}(O_2)$, described by the relation $\Delta\bar{S}(O_2) = 2R\,\partial \ln W/\partial(xN)$, where N is the Avogadro's number (Aronson and Clayton, 1960; Hagemark and Broli, 1967; Fujino and Miyake, 1991), shows therefore a significant decrease. For the Mg solid solutions Fujino *et al.* (1992, 1995, 1997b) claim that the $\Delta\bar{G}(O_2)$ shift is explained if the charge complexes of the form, ($M^{2+}2U^{5+}$), in which the corresponding cations have their normal sites, are formed together with ($M^{2+}U^{5+}$) complexes. In the oxygen potential curves for (Mg,Gd,U)O_{2+x} (Fujino *et al.*, 2001a) and (Mg,Ce,U)O_{2+x} (Fujino *et al.*, 2001b), the shift to negative x values is even larger than in the Mg solid solution.

When the oxygen partial pressure is very low, high concentrations of Mg cannot dissolve in UO_2. The solubility of Mg is in a range $0.1 < y < 0.15$ for $p_{O_2} = 10^{-15}$–10^{-19} atm at 1200°C (Fujino *et al.*, 1997a).

5.7.3 Uranium borides, carbides, silicides, and related compounds

Non-oxide p-block compounds of uranium represent a large family that share certain similarities with oxides in that non-stoichiometric compounds exist; these are especially well noted for the heavy p-block elements of a semi-metallic nature (e.g. Sb and Te). Oxidation state assignment for uranium in some of these compounds can be very tedious, owing to the presence of homoatomic bonding between main group elements where the $E\cdots E$ ($E =$ main group element) contacts between main group elements is intermediate in length between a full single bond and a van der Waals contact. This phenomenon is particularly common in antimonides and tellurides. Full descriptions of all known binaries and especially of ternary and quaternary phases are not possible in the present context. Further historical details can be found in Waber *et al.* (1964), Eding and Carr (1961), Freeman and Darby (1974), and in a series of IAEA bibliographies (Maximov, 1963, 1965, 1967).

(a) Uranium–boron system

The only known binary uranium borides are UB_2, UB_4, and UB_{12}. The crystal structure data for these compounds are given in Table 5.22. The former compounds have been prepared by direct reaction of the elements at high temperatures (Wedekind and Jochem, 1913). Mixtures of UB_{12} and UB_4 have also been deposited by fused-salt electrolysis (Andrieux, 1948; Andrieux and Blum, 1949). It has recently been demonstrated that UB_4 can be prepared by the solid-state metathesis reaction of UCl_4 with MgB_2 at 850°C (Lupinetti *et al.*, 2002).

$$UCl_4 + 2MgB_2 \rightarrow UB_4 + 2MgCl_2$$

A view of the structure of UB_4 is shown in Fig. 5.27.

The phase diagram of the U–B system is shown in Fig. 5.28 (Howlett, 1959, 1960; Elliott, 1965; Chiotti *et al.*, 1981).

In addition, there is mass spectroscopic evidence that supports the existence of UB and UB_2 in the gas phase (Gingerich, 1970). The dissociation energies D_0° were reported as (318 ± 33) kJ mol^{-1} for UB and (949 ± 42) kJ mol^{-1} for UB_2.

Uranium borides are remarkably inert, and borides have been proposed as a potential form for storing transuranium waste generated from the nuclear fuel cycle (Lupinetti *et al.*, 2002). There are some differences in reactivity of the uranium borides with respect to one another. UB_4 is generally more reactive

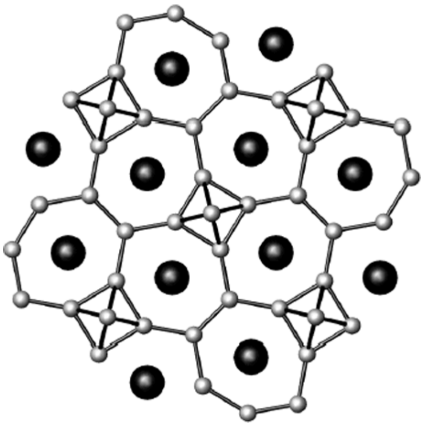

Fig. 5.27 *A view down the c-axis of the structure of UB_4. U–B bonds have been omitted for clarity.*

than UB_{12}. For example, boiling HF, HCl, and H_2SO_4 attack UB_{12} very slowly, but react more rapidly with UB_4, allowing for the separation of the two compounds. Both UB_4 and UB_{12} can be dissolved in HNO_3–H_2O_2 mixtures.

Ternary uranium borides have been extensively investigated for their rich variation in bonding and their complex physical properties. Compounds in this class include $U_5Mo_{10}B_{24}$, which contains three different kinds of B polyanions: two-dimensional puckered sheets formed from six- and eight-membered rings, planar ribbons composed of six-membered B rings, and chains of condensed eight-membered rings (Konrad and Jeitschko, 1996). UNi_4B has been extensively investigated and is a geometrically frustrated antiferromagnetic compound that partially orders below $T_N = 20$ K (Mentink *et al.*, 1998).

(b) Uranium–carbon system

The uranium–carbon system has been studied by a number of teams including Rundle *et al.* (1948), Esch and Schneider (1948), Litz *et al.* (1948), Wilhelm *et al.* (1949), and Mallett *et al.* (1952). The uranium–carbon system bear some similarities with that of uranium with other first-row p-block elements in that in addition to discrete, stoichiometric compounds, there are three known phases, UC, UC_2, and U_2C_3 that can be of variable composition. The complex phase diagram of the uranium–carbon system is shown in Fig. 5.29.

Among other things this diagram demonstrates that UC and UC_2 are completely miscible with one another at elevated temperatures and under these conditions the entire range UC–UC_2 is homogeneous. At lower temperatures, miscibility is much more limited and the exact extent of variability in composition for each of the carbides is still to be determined.

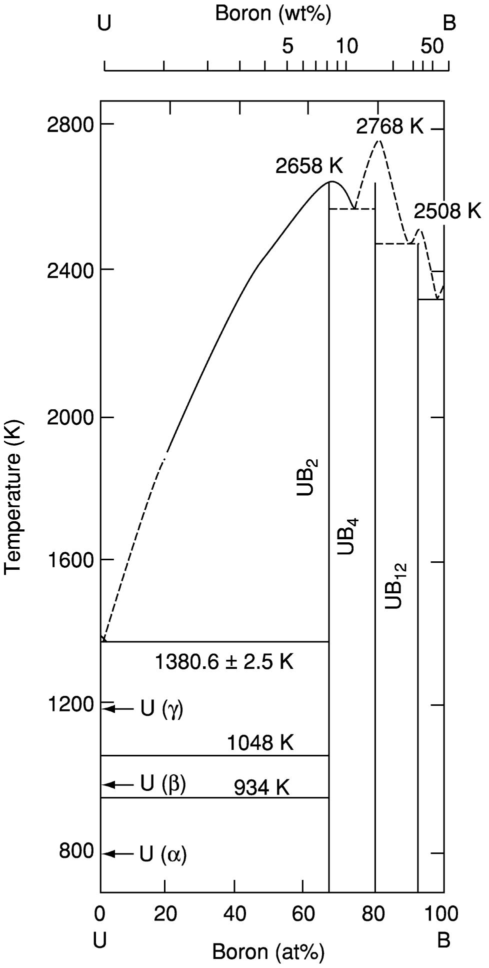

Fig. 5.28 *Phase diagram of the uranium–boron system* (*Chiotti* et al., 1981).

Litz *et al.* (1948) were the first to study the preparation of UC and UC_2. U_2C_3 is an unusual compound in that it has not been prepared by the direct reaction of the elements at high temperatures; this reaction invariably yields UC and UC_2 (Mallet *et al.*, 1952). However, U_2C_3 is obtained when a mixture of UC and UC_2 is heated in the range 1250–1800°C *in vacuo*. It is essential that the fused mixture be given a certain amount of stressing and cold working to initiate the nucleation necessary for the formation of the U_2C_3 phase; once formed it is stable at room temperature. Table 5.22 lists some of the crystallographic data for the uranium carbides. An illustration of the structure of UC_2 is shown in Fig. 5.30.

Table 5.22 *Crystallographic data for the stoichiometric binary uranium compounds with boron and group* IV *elements* (*Chiotti* et al., 1981).[a]

				Lattice parameters				*Density* (g cm^{-3})	
Formula	*Color*	*Space group*	*Symmetry*	*a* (Å)	*b* (Å)	*c* (Å)	*Z*	*Meas.*	*X-ray*
UB_2	metallic	*P*6/*mmm*	hexagonal	3.1293[b] 3.1314[c]		3.9893[b] 3.9857[c]	1	12.8	12.82
UB_4	metallic	*P*4/*mbm*	tetragonal	7.075		3.979	4	9.32	9.38
UB_{12}	metallic	*Fm*3*m*	fcc	4.4773			4	5.65	5.825
$UC(\delta_1)$	gray-black	*Fm*3*m*	fcc	4.961			4		13.63
U_2C_3	black	$I\bar{4}3d$	cubic	8.088			8		12.88
$UC_2(\zeta)$	light gray	*I*4/*mmm*	tetragonal	3.5266		6.0023	2		11.68
$UC_2(\delta_2)$	light gray		cubic	5.488			4		
$USi_3(l)$		*Pm*3*m*	cubic	4.060			1		8.15
$USi_{1.88}(\eta)$[d]	silvery	*I*4$_1$/*amd*	tetr. bc	3.948 3.930		13.67 14.06	4	7.27	8.98
$U_3Si_5(\tau)$[e]	silvery	*P*6/*mmm*	hexagonal	3.843		4.069	1	7.27	9.25
$USi(\zeta)$[f]	black	*Pbnm*	orthorhombic	5.66	7.67	3.91	4	9.30	10.40
$U_3Si_2(\varepsilon)$		*P*4/*mbm*	tetragonal	7.3299		3.9004	2	11.31	12.20
$U_3Si(\delta)$		*I*4/*mcm*	tetr. bc	6.029		9.696	4		15.58
UGe_3	metallic	*Pm*3*m*	cubic	4.2062			1		10.37
UGe_2[g]	metallic	*Cmmm*	orthorhombic	4.036	14.928	4.116	4		10.26
UGe[j]	metallic	*Pbcm*	orthorhombic	9.827	8.932	5.841	12		12.07
U_5Ge_4[k]	metallic	*P*6$_3$/*mcm*	hexagonal	8.744		5.863	2		12.67
U_3Ge_3	metallic								
U_5Ge_3[l,m]		*P*6$_3$/*mcm*	hexagonal	8.58		5.79	2		12.66
U_7Ge[h,m]									

Table 5.22 (*Contd.*)

				Lattice parameters				*Density* (g cm^{-3})	
Formula	*Color*	*Space group*	*Symmetry*	*a* (Å)	*b* (Å)	*c* (Å)	*Z*	*Meas.*	*X-ray*
USn_3	metallic	*Pm*3*m*	cubic	4.626			1		10.0
U_3Sn_5	metallic								
U_5Sn_4									
UPb_3[g]	metallic	*Fm*3*m*	cubic	4.7915					12.93
UPb[g,i]	metallic		tetr. bc	11.04		10.60			
			tetr. fc	4.579		5.259			13.27

[a] Unless otherwise mentioned, the data are taken from Chiotti *et al.* (1981).

[b] Boron-rich phase.

[c] Boron-poor phase.

[d] $USi_{1.88}$ is also referred to as α-USi_2.

[e] U_3Si_5 is also referred to as β-USi_2.

[f] According to Laugier *et al.* (1971), USi is tetragonal. The orthorhombic structure is due to oxygen.

[g] Boulet *et al.*, (1997a).

[h] Existence of these compounds deduced from vapor pressure data taken by Alcock and Grieveson (1962, 1963).

[i] The different lattice constants are due to different interpretations of powder patterns.

[j] Boulet *et al.* (1997b).

[k] Boulet *et al.* (1997c).

[l] Marakov and Bykov (1959). May be the same phase as U_5Ge_4.

[m] The existence of U_5Ge_3 and U_7Ge has been called into question (Boulet *et al.*, 1997c), and they are likely mixture of U_5Ge_4 and U metal dissolving 3% of germanium.

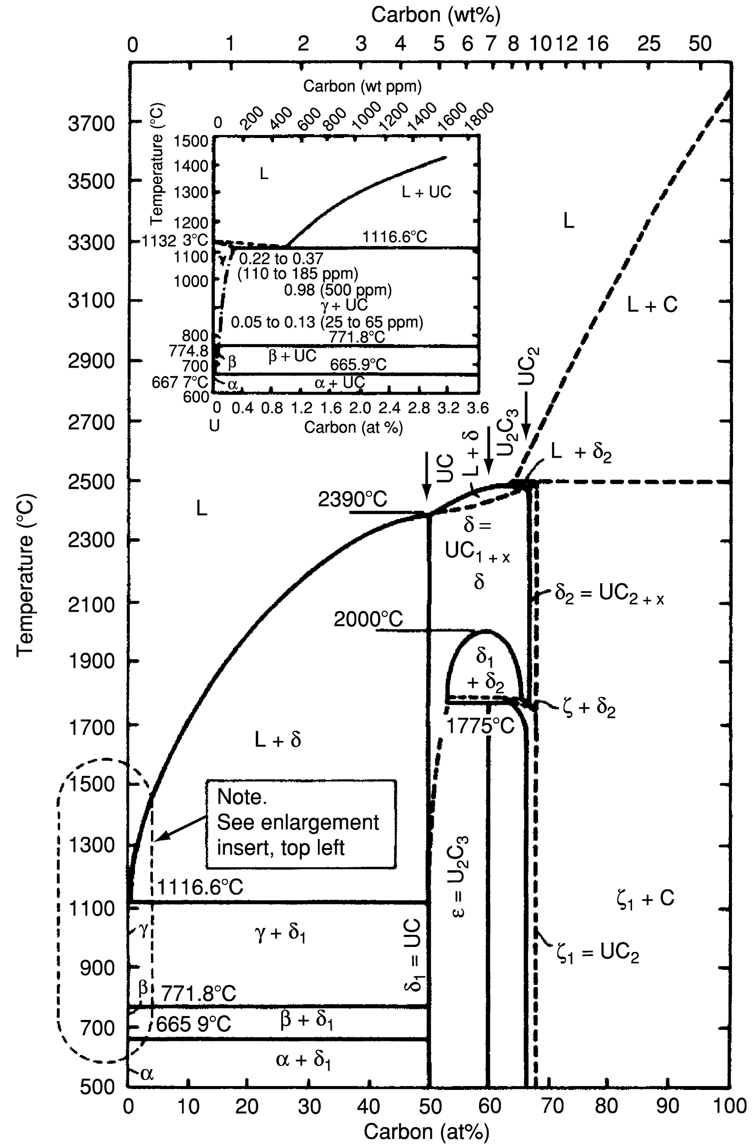

Fig. 5.29 *Phase diagram of the uranium–carbon system* (*Wilkinson,* 1962).

The uranium carbides can undergo a number of hydrolysis reactions; finely divided UC_2 is pyrophoric. The carbides react with water to yield a variety of products. Lebeau and Damien (1913) found that upon hydrolysis of UC_2, in addition to hydrogen, methane, and ethane, significant amounts of liquid and

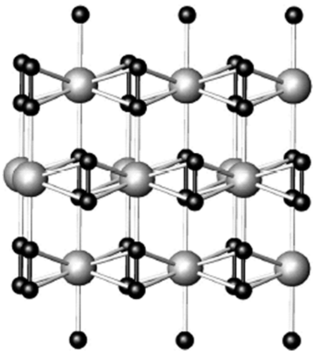

Fig. 5.30 *A view down the a-axis of the structure of UC_2.*

solid hydrocarbons are produced. Litz (1948) made an exhaustive study of the hydrolysis of UC and UC_2, the value of which is limited by the fact that he worked only at temperatures above 83°C and did not measure the quantity of gas evolved or analyze the solid residue for carbon compounds. Bradley and Ferris (1962, 1964) made a very careful study of the hydrolysis of arc-melted UC (1962) and of UC_2, U–UC mixtures, and UC–UC_2 mixtures (1964) at temperatures between 25 and 99°C. In the case of UC, the hydrolysis yielded a gelatinous, hydrous uranium(IV) oxide and a gaseous mixture (93 mL (STP) per gram UC), which consisted of 86 vol% methane, 11 vol% hydrogen, 1.8 vol% ethane, and small quantities of saturated C_3–C_6 hydrocarbons. The gaseous products contained all the carbon originally present in the carbide.

The total amount of carbon originally present in the carbide was also recovered in the hydrocarbon hydrolysis products of UC_2, U–UC, and UC–UC_2 mixtures. In the case of arc-melted $UC_{(1.85 \pm 0.03)}$, 36 different hydrocarbons were identified. The reaction product contained 15 vol% methane, 28 vol% ethane, 7 vol% C_3–C_6 alkanes, 8 vol% alkenes, 0.6 vol% alkynes, 1 vol% unidentified un-saturates, and 40 vol% hydrogen. Approximately 25% of the total carbon was found as a water-insoluble wax. In the hydrolysis of UC–UC_2 mixtures, a linear decrease of the volume percentage of CH_4 and linear increases of the percentages of hydrogen and the C_2–C_8 hydrocarbons were observed as the combined C/U atom ratio increased from 1.0 to 1.85. For UC–UC_2 mixtures, less methane than expected was evolved. This indicates that some polymerization of C units had occurred.

Bunnell *et al.* (1975) studied the hydrolysis of bare and defect-coated UC_2 fuel bead cores by water vapor at $p_{H_2O} = 24$–76 mmHg. They studied the reaction products by optical and scanning electron microscopies, identified hydrogen, methane, and ethane as the major reaction products, and measured the activation energy to be (25.4 ± 2.9) kJ mol^{-1}.

In air, UC_2 decomposes completely in a week, presumably as a result of hydrolysis. According to Mallet *et al.* (1952), U_2C_3 does not react appreciably with water even at 75°C. UC_2 appears to be stable in air at 300°C, but is completely converted to oxide in air within 4 h at 400–500°C. UC_2 reacts at 1100°C with nitrogen to form uranium nitride. Since the reactions of the carbides are greatly affected by the particle size of the solid and the previous thermal history of the sample, no far-reaching conclusions should be drawn regarding the relative reactivity of the uranium carbides.

The uranium carbides have found an important application as nuclear fuels in fast reactors. This type of application and related properties has been discussed in a number of uranium carbide conferences (see Proceedings, 1960a,b, 1961, 1963). One of the problems with reprocessing the spent fuels from these reactors is that oxalic acid is also produced in the dissolution of mixed uranium and plutonium carbides in HNO_3. Complexation of UO_2^{2+} by oxalate can account for the problems of incomplete uranium and plutonium extraction in the PUREX process for fuel reprocessing (Choppin *et al.*, 1983).

Ternary carbides, such as $U_2Al_3C_4$, can be prepared by melting the elements in a carbon crucible in a high-frequency radiofrequency (RF) furnace (Gesing and Jeitschko, 1995). The structure of $U_2Al_3C_4$ is closely related to that of Al_4C_3. Much like binary uranium carbides, $U_2Al_3C_4$ undergoes hydrolysis reactions in dilute HCl resulting in the formation of 74 (wt.)% methane, 8% ethane and ethylene, and 18% saturated and unsaturated higher hydrocarbons.

Laser-ablated U atoms react with CO in a noble gas matrix to form CUO (Li *et al.*, 2002). This molecule exhibits different stretching frequencies in a solid Ar matrix from those in a solid Ne matrix. Further experiments suggest that Ar atoms interact directly with CUO molecules to form an actinide–noble gas compound. The combination of experimental and theoretical methods suggests that multiple Ar atoms interact with a single CUO molecule.

(c) Uranium–silicon system

The uranium–silicon system is remarkably rich and a large number of uranium silicides including U_3Si, U_3Si_2, USi, U_3Si_5, $USi_{1.88}$, and USi_3 have been prepared and crystallographically characterized (Zachariasen, 1949a; Kaufman *et al.*, 1957). The phase diagram, shown in Fig. 5.31, is based on earlier work reported in the compilations by Hansen and Anderko (1958), Elliott (1965), and Shunk (1969), and in the paper by Vaugoyeau *et al.* (1971), which has been assessed and discussed by Chiotti *et al.* (1981).

Further details on the composition ranges of the two phases U_3Si_5 and $USi_{1.88}$ are given by Vaugoyeau *et al.* (1971). U_3Si_5 melts congruently at 2043 K (1770°C) and has a composition range $USi_{1.71}$ to $USi_{1.78}$ (63–64 at % Si) in the temperature range 1000–1300°C. The phase $USi_{1.88}$, in the same temperature range, has a composition span $USi_{1.79}$ to $USi_{1.84}$ (64–64.8 at % Si).

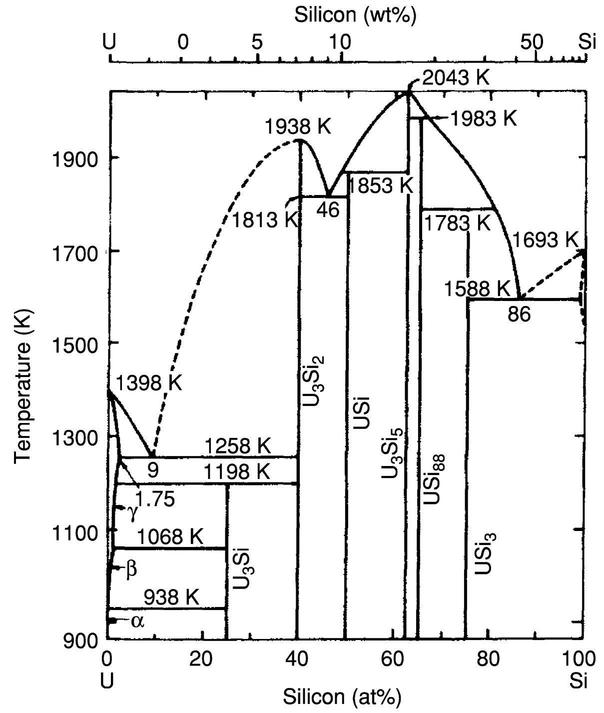

Fig. 5.31 *Phase diagram of the U–Si system* (*Chiotti* et al., 1981).

The two-phase region between the two compounds is very narrow. The compound USi was shown to decompose peritectically at 1580°C and has a narrow homogeneity range. The eutectic between U_3Si_2 and USi occurs at 1540°C and 46 at % Si.

As can be inferred from this information and from the data in Table 5.22, the U–Si phase diagram is very complicated. However, the uranium silicides are of technical importance. For instance, compounds such as $U(Al,Si)_3$ are formed in the layer between the uranium metal and the aluminum can in natural uranium fuel elements (Cunningham and Adams, 1957). Because of the chemical inertness of some of the uranium silicides, these compounds promise more applications. Crystal structures of the U–Si compounds are also summarized in Table 5.22.

Ternary uranium silicides are well established from compounds such as UCu_2Si_2 (Fisk *et al.*, 2003), $U_2Nb_3Si_4$ (Le Bihan *et al.*, 2000), and URu_2Si_2 (Sugiyama and Onuki, 2003). Single crystals of UCu_2Si_2 prepared from a Cu flux undergo a 50 K antiferromagnetic transition below the 100 K ferromagnetic transition (Fisk *et al.*, 2003).

$U_2Nb_3Si_4$ is weakly ferromagnetic below 35 K (Le Bihan *et al.*, 2000). Finally, URu_2Si_2 is one of the most studied heavy fermion materials (Sugiyama and Onuki, 2003).

(d) Uranium–germanium, uranium–tin, and uranium–lead systems

The uranium–germanium system is as complex as that of uranium silicides. U_7Ge (*vide infra*), U_5Ge_3 (*vide infra*), U_5Ge_4, UGe_2, and UGe have all been characterized and subjected to extensive physical property measurements (Onuki *et al.*, 1992). The compound originally formulated as U_3Ge_4 has been shown to be a mixture of UGe and U_3Ge_5. Detailed studies including magnetic structure determination via neutron diffraction have been performed on UGe_2, which is an unusual example of a ferromagnetic superconductor (Saxena, 2000; Sheikin *et al.*, 2000; Nishioka *et al.*, 2002).

This compound was originally reported to crystallize in the $ZrSi_2$ (*Cmcm*) structure type, but in fact crystallizes in the $ZrGa_2$ (*Cmmm*) type (Oikawa *et al.*, 1996; Boulet *et al.*, 1997a). U_5Ge_3 and U_7Ge both undergo a transition to a superconducting phase below 2 K (Onuki *et al.*, 1990). However, the existence of both of these compounds has been called into question (Boulet *et al.*, 1997c), and they are likely mixture of U_5Ge_4 and U metal dissolving 3% of germanium.

The uranium–tin phase diagram has been described by Palenzona and Manfrinetti (1995). U_5Sn_4 (Ti_5Ga_4-type), USn (ThIn-type), USn_2 ($ZrGa_2$-type), U_3Sn_7 (Ce_3Sn_7-type), and USn_3 ($AuCu_3$-type) were identified from this work. Dhar *et al.* (1998) have assessed the magnetic properties of these compounds. U_5Sn_4 and USn are ferromagnetically ordered below 62 and 49 K, respectively; USn_2 and U_3Sn_7 attain an antiferromagnetic state near 80 K. Shunk (1969) and Chiotti *et al.* (1981) have reported the phase diagram for the uranium–lead system.

5.7.4 Uranium pnictides

The systems U–N, U–P, U–As, U–Sb, and U–Bi have been studied in great detail. In particular, the monopnictides UN, UP, and UAs have found major interest because of their solid-state properties, which are relatively easy to study because of their cubic (NaCl) structure. Physical and crystallographic data of the pnictides are summarized in Table 5.23.

The thermodynamic properties of uranium and other actinide nitrides are briefly summarized in Chapter 19. Additional information on uranium nitrides and heavier pnictides is available in Gmelin (1981b, vol. C7; 1981d, vol. C14).

(a) Uranium–nitrogen system

Rundle *et al.* (1948) established the existence of the following uranium nitride phases: UN, U_2N_3, and $UN_{1.75}$, while the phase UN_2 could not be confirmed. Berthold *et al.* (1957) and Berthold and Delliehausen (1966) succeeded, however, in preparing a phase $UN_{1.90}$ by reacting uranium hydride with ammonia at

Table 5.23 *Crystallographic data of uranium pnictides* (*Rough and Bauer,* 1958; *Hansen and Anderko,* 1958; *Waber* et al., *1964; Elliot,* 1965; *Shunk,* 1969).[a]

					Lattice parameters			Density	
Formula	*Color*	*m.p.* (°C)	*Space group*	*Symmetry*	*a* (Å)	*c* (Å)	Z	*X-ray*	*Exp.*
UN	metallic	2850	$Fm3m$	fcc	4.889		4	14.32	
UN[b]			$R\bar{3}m$	rhombohedral	3.170	8.635	3	16.7	
α-U_2N_3			$Ia3$	cubic	10.678		16	11.24	
β-U_2N_3[c]			$P\bar{3}m1$	hexagonal	3.700	5.825		12.45	
$UN_{1.45}$	black				10.700				
UN_x[d]									
$UN_{1.76}$	black			bcc	10.628				
$UN_{1.90}$	black								
UP	metallic	2610	$Fm3m$	fcc	5.5889		4	10.23	
UP[b]			$R\bar{3}m$	rhombohedral	7.583	9.433	12	11.41	
U_3P_4	metallic		$I\bar{4}3d$	bcc	8.207		4		
UP_2	grey		$P4/nmm$	tetragonal	3.808	7.780	2		
UAs	metallic	2705[e]	$Fm3m$	fcc	5.7788		4	10.77	
U_3As_4	metallic		$I\bar{4}3d$	bcc	8.507		4		

UAs_2	metallic		$P4/nmm$	tetragonal	3.954	8.116	2	9.8	
$U_5Sb_4^g$	metallic		$P6_3/mcm$	hexagonal	9.237	6.211	2	12.14	
USb	metallic	1850	$Fm\bar{3}m$	fcc	6.203		4		
U_3Sb_4	metallic	1695^f	$I\bar{4}3d$	bcc	9.113		4	10.84	10.7
USb_2	metallic	1335^f	$P4/mmm$	tetragonal	4.272	8.759	2	10.04	10.5
α-UBi(δ_1)	metallic		$Fm\bar{3}m$	cubic	6.364		4	11.52	
β-UBi(δ_2)	metallic	$1400–1450^e$	$P4/nmm$	tetr.bc	11.12	10.55	24	13.6	
U_3Bi_4 (ε)	metallic	1150^f	$I\bar{4}3d$	bcc	9.350		4	12.57	12.8
UBi_2	metallic	1010^f	$P4/nmm$	tetragonal	4.445	8.908	2	12.38	12.36

---

[a] Unless otherwise mentioned, the data are taken from Rough and Bauer (1958), Hansen and Anderko (1958), Waber *et al.* (1964), Elliot (1965), Shunk (1969).

[b] High-pressure phase (Olsen *et al.*, 1985, 1988).

[c] Masaki and Tagawa (1975).

[d] Solid solutions ranging from $UN_{1.45}$ through $UN_{1.76}$, lattice constant decreasing from 10.700 to 10.628 Å.

[e] With decomposition.

[f] With peritectic decomposition.

[g] Paixão *et al.* (1994). This phase was originally formulated as U_4Sb_3.

elevated temperatures. Bugl and Bauer (1964) have studied the U–N system in detail.

The nitrides can be prepared by reaction of very pure uranium metal (or uranium hydride prepared from such metal) with nitriding agents. The surface of the uranium metal has to be pickled with nearly concentrated HNO_3, and then washed with organic solvents to remove even traces of oxide and oil films, which might lead to the formation of oxide or carbide contaminants. The nitriding agents also have to be of high purity. Uranium mononitride can be prepared (i) by reaction of uranium metal (or uranium hydride) with nitrogen or ammonia, (ii) by the thermal decomposition of higher nitrides at or above 1300°C, or (iii) by the reduction of higher nitrides with uranium metal. U_2N_3 can be prepared by reacting UC with NH_3 or a N_2/H_2 gas mixture (Nakagawa *et al.*, 1997). The reaction with ammonia is advantageous because NH_3 acts as both a nitriding agent and as a carbon-clearing agent. Fitzmaurice and Parkin (1994) report that various uranium nitrides could be prepared from the self-propagating reaction of UCl_4 with Li_3N.

Mallett and Gerds (1955) made a kinetic study of the reaction of uranium metal with nitrogen in the temperature range 550–900°C and at atmospheric pressure. Surface reaction products were identified by X-ray diffraction methods. At 775–900°C it was found that all three nitride phases were present. The intermediate nitride U_2N_3 is prepared by similar methods or by reduction of $UN_{1.75}$ with hydrogen. Since U_2N_3 loses nitrogen above 700°C *in vacuo*, the preparative procedure must take this into account. The nitride $UN_{1.75}$ cannot be prepared at all by reaction of the metal with nitrogen, unless a high pressure of nitrogen is used. There appears to be a two-phase region between UN and U_2N_3, but the region between U_2N_3 and $UN_{1.75}$ appears to be homogeneous. A tentative phase diagram of the system is shown in Fig. 5.32.

All of the higher uranium nitrides are thermally unstable relative to UN. UN is easily oxidized by air and is decomposed by water vapor; it is not attacked by either hot or cold hydrochloric or sulfuric acids, but is attacked by molten alkali. U_2N_3 can be used for the catalytic cracking of ammonia (Rizzo da Rocha *et al.*, 1995). Schmitz-Dumont *et al.* (1954) described the interesting uranium compound uranyl amide, $UO_2(NH_2)_2$. This compound can be prepared by the reaction of potassium uranyl nitrate, $KUO_2(NO_3)_3$, with potassium amide in liquid ammonia. Uranyl amide is a brown, amorphous substance that is unaffected by dry oxygen at room temperature. Moisture, however, converts the amide to ammonium diuranate. The uranium amido chlorides, UNH_2Cl_2 and $U(NH_2)_2Cl$, can be obtained by reacting UCl_3 with ammonia at 450 to 500°C. Increased heating of these compounds results in their conversion to U(NH)Cl and then $UN_{1.73-1.75}$ (Berthold and Knecht, 1965a).

The reaction of Li_3N with UH_3 at 900°C results in the formation of $LiUN_2$ (Jacobs *et al.*, 2003). The structure is related to the anatase type with the octahedral sites occupied by Li. Ca_3UN_4 can be prepared by reacting Ca $(NH_2)_2$ and UH_3 between 600 and 1000°C (Heckers *et al.*, 2003). X-ray and

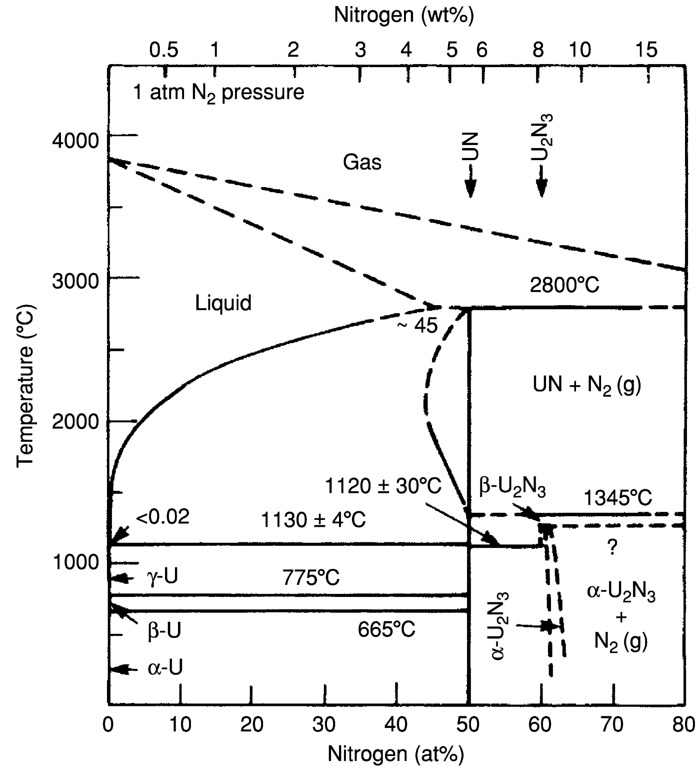

Fig. 5.32 *Phase diagram of the U–N system* (*Shunk*, 1969).

neutron diffraction studies on this phase show that it crystallizes in the NaCl structure type with statistical occupation of the cation site by three Ca atoms and one U atom.

(b) Uranium–phosphorus, uranium–arsenic, and uranium–antimony, and uranium–bismuth systems

In the systems U–P, U–As, U–Sb, and U–Bi, the compounds UX, U_3X_4, and UX_2 (where X = P, As, Sb, or Bi) have been reported. Compounds UX have the cubic NaCl structure for all X, with the exception of β-UBi, which is tetragonal body-centered. U_3X_4 is body-centered cubic and UX_2 tetragonal for all X.

At least four methods have been applied for preparation of the pnictides: direct synthesis from the elements in an autoclave (Albutt *et al.*, 1964) or in a sealed tube, for instance (Iandelli, 1952).

$$2U + P_4 \rightarrow 2UP_2$$

the reaction of uranium hydride with phosphine or arsine, for instance

$$UH_3 + PH_3 \rightarrow UP + 3H_2$$

and finally by circulating gaseous phosphine or arsine over slightly heated hydride (Baskin and Shalek, 1964; Baskin, 1969). For the preparation of the phosphides, a PH_3-loaded stream of argon is passed over the hydride, which is heated at 400–500°C. For the preparation of the arsenides, AsH_3 is reacted with UH_3 at 300°C. The reaction products are annealed at 1200–1400°C. Single crystals of UAs_2 have been grown by reacting uranium metal with a Cs_3As_7 flux (Albrecht-Schmitt *et al.*, 2000). Finally, uranium phosphides, arsenides, and antimonides can be prepared from the reaction of UCl_4 with sodium pnictides (Fitzmaurice and Parkin, 1994).

Buhrer (1969), Spirlet (1979), and Vogt (1982) succeeded in growing single crystals of most uranium pnictides by gas-phase transport, using $TeCl_4$, I_2, and other transporting agents. The crystals grown in this manner allow the determination of physical properties such as magnetic susceptibilities, magnetic phase diagrams (Busch *et al.*, 1979a), or the measurement of the de Haas–van Alphen effect (Henkie *et al.*, 1981); the uranium pnictides are particularly well suited for such measurements. Normally, they should exhibit isotropic behavior because of their structure, but the presence of anisotropy in the cubic crystals suggests the formation of magnetic domains. U_3P_4 and U_3As_4 are both metallic ferromagnets with itinerant 5f electrons (Inada *et al.*, 2001).

The binary compounds of the systems U–Sb and U–Bi may be prepared directly from the elements, or by reacting uranium with alkali metal antimonide and bismuthide fluxes. The binary phase diagram of U–Sb was originally investigated by Beaudry and Daane (1959). Among the binary compounds discovered in this system was a uranium-rich phase (δ) that forms a eutectic with USb at 1770°C. This compound was originally formulated as U_4Sb_3. Magnetic susceptibility measurements on a compound with this nominal composition show ferromagnetic behavior below 86 K (Troć, 1992). However, later microprobe analysis, neutron scattering, and single crystal X-ray diffraction data were utilized to establish that the actual composition of this phase is U_5Sb_4 (Paixão *et al.*, 1994); this compound crystallizes in the Ti_5Ga_4 structure type. Paixão *et al.* (1994) have demonstrated that U_5Sb_4 shows highly anisotropic ferromagnetic behavior below 86 K.

5.7.5 Uranium chalcogenides

The binary, ternary, and quaternary uranium sulfides, selenides, and tellurides have been the subject of intense investigation for more than 160 years. U–Po compounds are currently unknown owing to the high radioactivity and rarity of polonium. A significant number of the chalcogenide phases deduced before 1980 were reinvestigated over the past two decades, primarily by single-crystal X-ray diffraction, as a number of previously known compounds were assigned incorrect space groups, unit cells, and compositions.

(a) Uranium–sulfur system

Uranium sulfide in the form of US_2 was first prepared in the mid-1800s (Péligot, 1842; Herrmann, 1861). This compound was followed by the preparation of US and U_2S_3, which were identified by Alibegoff (1886); these studies pre-date the discovery of X-rays. Systematic X-ray powder diffraction investigations did not take place until 1943 (Strotzer *et al.* 1943), when seven distinct phases were identified from their powder patterns, but these were not indexed. The phase diagram of the uranium–sulfur system is shown in Fig. 5.33.

Based on later systematic studies of the uranium–sulfur system by Eastman *et al.* (1950), Zachariasen (1949b) was able to elucidate the crystal structures of many of the previously synthesized phases. Mills (1974) has compiled thermodynamic data for these phases. Crystal structure data for the uranium chalcogenides and oxychalcogenides are given in Table 5.24.

The uranium sulfides can be prepared by heating uranium or uranium hydride with H_2S, or by heating the elements together in a sealed tube. Lower sulfides may be obtained by thermal decomposition of the higher sulfides *in vacuo* at high temperatures. γ-US_2 can be prepared from what is thought to be a topotactic reaction of U_3S_5 with sulfur (Kohlmann and Beck, 1997).

α-UX_2 compounds (X = S, Se) were previously reported to crystallize in *I*4/*mcm*, but based on single crystal X-ray data they are now known to crystallize in *P*4/*ncc* (Noël and Le Marouille, 1984). U_3S_5 has been the subject of a large number of studies that have concluded that the compound is mixed-valent, containing both U^{3+} and U^{4+}; it can be formulated as $(U^{3+})_2(U^{4+})(S^{2-})_5$ (Noël and Prigent, 1980; Kohlmann and Beck, 2000). A view of the structure of U_3S_5 is shown in Fig. 5.34.

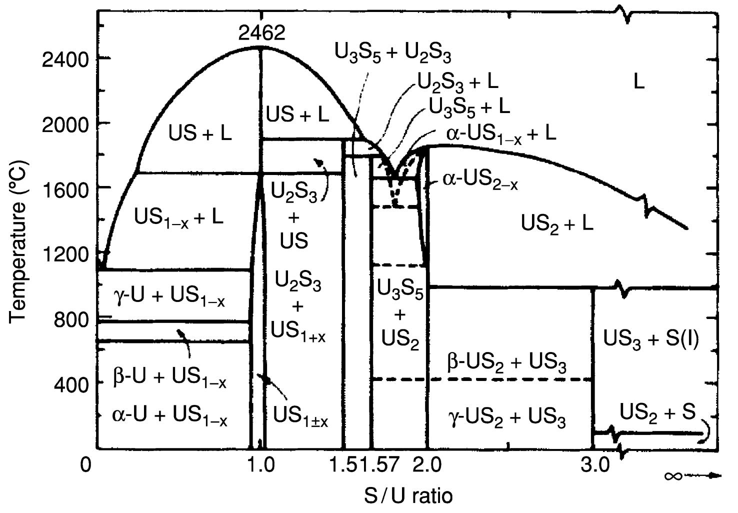

Fig. 5.33 *Tentative phase diagram of the U–S system* (*Cordfunke,* 1969).

Table 5.24 *Crystallographic data for uranium chalcogenides and oxychalcogenides.*[a]

					Lattice parameters					Density (g/cm^3)		
Formula	*Color*	*m.p.* (°C)	*Space group*	*Symmetry*	*a*	*b*	*c*	β	*Z*	*Obs.*	*Calc.*	*References*
UOS	Black		$P4/nmm$	tetrag.	3.483		6.697		2		9.64	Picon and Flahaut (1968)
US	silvery black	2462	$Fm\bar{3}m$	cubic	5.484				4		10.87	Zachariasen (1949b)
U_2S_3	Blue-black	1850	$Pbnm$	orthor.	10.34	10.58	3.885		4	8.94	8.96	Picon and Flahaut (1968)
U_3S_5	Blue-black			orthor.	7.42	8.11	11.74		4	8.16	8.26	Potol *et al.* (1972)
α-US_2^b	Steel gray	1850	$P4/ncc$	tetrag.	10.293		6.374		10		8.01	Noël and Le Marouille (1984)
β-US_2	Steel gray		$Pbab$	orthor.	4.4803	7.439	4.1209		4	8.07	8.09	Suski *et al.* (1972)
γ-US_2	Steel gray		$P\bar{6}2m$	hexag.	7.236		4.062		3	8.12	8.17	Picon and Flahaut (1968); Daoudi *et al.* (1996); Kohlmann and Beck (1997)
US_3	Black, shiny		$P2_1/m$	monoc.	5.40	3.90	18.26	80.5	4	5.9	5.86	Picon and Flahaut (1968); Marcon (1969)
UOSe	black[c]		$P4/nmm$	tetrag.	3.9035		6.9823		2	10.40	10.38	Murasik *et al.* (1968)
USe	Black		$Fm\bar{3}m$	fcc	5.7399				4		11.13	Kruger and Moser (1967)
U_3Se_4	Black, shiny	1680[d]	$I\bar{4}3d$	cubic	8.820				4	10.07	9.97	Khodadad (1960); Khodadad (1961); Noël (1985a)

U_2Se_3	Black	1610	$Pnma$	orthor.	10.94	11.33	4.06	4	9.42	9.40	Khodadad (1959, 1961)
U_3Se_5	Black	1560^d	$Pnma$	orthor.	12.292	8.459	7.799	4	9.04	9.14	Breeze and Brett (1972)
U_7Se_{12}	Black		$P6_3/m$	hexag.	11.385		4.099	1			Breeze and Brett (1972)
α-USe_2^e	Black	1460	$I4/mcm$	tetrag.	10.765		6.660	10		9.03	Noël and Le Marouille (1984)
β-USe_2	$black^f$		$Pnma$	orthor.	7.455	4.2320	8.964	4	9.08	9.3	Breeze and Brett (1972); Noël *et al.* (1996)
γ-USe_2	Black		$P\bar{6}2m$	hexag.	7.6376		4.1924	3	9.07	9.31	Breeze and Brett (1972); Kohlmann and Beck (1997)
USe_3	Black, shiny	1160^d	$P2_1/m$	monoc.	5.652	4.056	10.469	2	7.25	7.25	Breeze and Brett (1972); Ben Salem *et al.* (1984)
UOTe	Gray-black		$P4/nmm$	tetrag.	4.004		7.491	2	10.55		Klein-Haneveld and Jellinek (1964); Breeze *et al.* (1971)
U_2O_2Te	Gray-black		$I4/m$	tetrag.	3.9640		12.564	2			Breeze *et al.* (1971)
UTe	Gray-black	1740	$Fm\bar{3}m$	fcc	6.150			4	10.37	10.55	Kruger and Moser (1967); Klein-Haneveld and Jellinek (1964)
U_3Te_4	Black	1540^d	$I\bar{4}3d$	cubic	9.3980			4	9.80	9.81	Matson *et al.* (1963)
α-U_2Te_3	Black, shiny		$I\bar{4}3d$	cubic	9.3960			4	9.02	9.81	Matson *et al.* (1963)

Table 5.24 (*Contd.*)

					Lattice parameters					Density (g/cm^3)		
Formula	*Color*	*m.p.* (°C)	*Space group*	*Symmetry*	*a*	*b*	*c*	β	*Z*	*Obs.*	*Calc.*	*References*
β-U_2Te_3	Black	1500^d	*Pnma*	orthor.	12.175	4.370	11.828		4		9.06	Suski *et al.* (1976); Tougait *et al.* (1998b)
α-U_3Te_5	Black			hexag.	12.25		4.23					Ellert *et al.* (1975)
β-U_3Te_5	Black	1300^d		orthor.	7.99	8.73	12.88					Slovyanskikh *et al.* (1977)
γ-U_3Te_5	Black		*Pnma*	orthor.	16.098	4.210	14.060		4		9.42	Tougait *et al.* (1998a)
U_7Te_{12}	Black		$P\bar{6}$	hexag.	12.312		4.260		1		9.49	Breeze *et al.* (1971); Breeze and Brett (1971); Tougait *et al.* (1998c)
$UTe_{1.77}$	Black		*P4/nmm*	tetrag.	4.243		8.946		2		9.8	Klein-Haneveld and Jellinek (1969); Klein-Haneveld and Jellinek (1970)
$UTe_{1.78}$	Black			orthor.	4.162	6.134	13.973		4			Breeze *et al.* (1971)

α-UTe_2	Dark gray	1180[d]	*Immm*	orthor.	4.1619	6.1277	13.961		4	9.20	Klein-Haneveld and Jellinek (1970); Boehme *et al.* (1992)
β-UTe_2	Black		*Pnnn*	orthor.	4.24	6.16	14.52		4	8.68	Ellert *et al.* (1971)
U_3Te_7	Black	950[d]									Montignie (1947)
α-UTe_3	Black	935[d]	*P*2_1/*m*	monoc.	6.0987	4.2229	10.325	98.2	2	7.83	Breeze *et al.* (1971); Boehme *et al.* (1992); Stoewe (1996a)
β-UTe_3	Black		*Cmcm*	orthor.	4.338	24.743	4.338		4	8.85	Noël and Levet (1989)
U_2Te_5	Black		*C*2/*m*	monoc.	34.42	4.181	6.074	95.4	4	8.5	Stoewe (1996b); Tougait *et al.* (1997)
$U_{0.9}Te_3$[g]	Black		*Cmcm*	monoc.	4.3537	24.792	4.3541		4	8.4	Stoewe (1997a)
UTe_5		490[d]	*Pnma*	orthor.	17.915	10.407	4.220		4		Slovyanskikh *et al.* (1967); Noël (1985b)

---

[a] Compiled from Gmelin (1981, vol. C11, 1984, vol. C10) and from original literature.

[b] Old sources listing α-US_2 refer to $US_{1.80}$-$US_{1.93}$. The single crystal structure of α-US_2 is known.

[c] Most of the selenides and tellurides, if prepared in sealed tubes, are obtained as free-running black powders. In some cases, single crystals have been prepared by gas-phase transport.

[d] Peritectic decomposition temperature of the solid-state phase.

[e] α-USe_2 can refer to the phase $USe_{1.88}$ and has variable lattice parameters.

[f] Obtained as black crystals with metallic luster.

[g] This compound has been previously reported in the literature as $UTe_{3.38}$. Powder diffraction data suggests that the uranium content may equal $U_{0.724}Te_3$ (Boehme *et al.*, 1992).

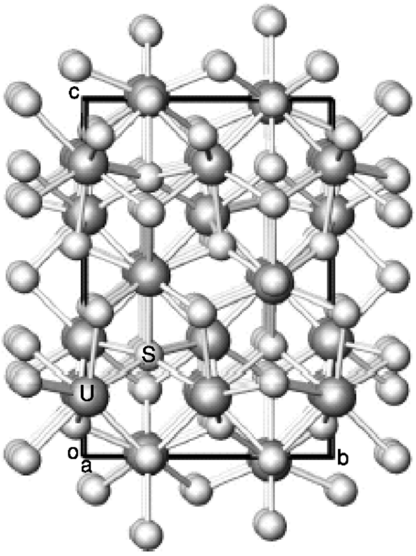

Fig. 5.34 *A view down the a-axis of the structure of U_3S_5. This is a mixed valence compound and should be formulated as $(U^{3+})_2(U^{4+})(S^{2-})_5$.*

(b) Uranium–selenium and uranium-tellurium systems

The selenides and tellurides of uranium have also been studied extensively. A large number of individual phases have been identified and characterized by their X-ray patterns. The crystallographic data of the individual phases have also been summarized in Table 5.24. The phase diagrams of the systems U–Se and U–Te are shown in Figs. 5.35 and 5.36, respectively.

The β modification of UTe_3, which was originally thought to adopt the $NdTe_3$ structure type, has been shown to be non-stoichiometric with uranium defects, giving rise to a formulation of $U_{0.9}Te_3$ (Stoewe, 1997a). This compound is identical to the previously known binary uranium telluride, formulated as $UTe_{3.38}$, and shows variable composition with U content ranging from 0.87 to 0.93. X-ray powder diffraction data suggest even a larger defect concentration consistent with a formula of $U_{0.724}Te_3$ (Boehme *et al.*, 1992). Te–Te bonding exists in a number of uranium telluride phases, making oxidation state assignment difficult. For example, one-dimensional tellurium chains exist in UTe_2. Therefore the compound is not $(U^{4+})(Te^{2-})_2$ but rather $(U^{3+})(Te^{2-})(Te^{1-})$ (Stoewe, 1997b). A view of the structure of UTe_2 is shown in Fig. 5.37.

The selenides and tellurides can be prepared by similar methods as the sulfides, i.e. reaction of uranium powder prepared from the hydride with H_2Se or H_2Te, synthesis from the elements at controlled temperatures in sealed tubes, or thermal decomposition of the higher selenides or tellurides. For a more detailed description of the solid-state properties of USe and UTe,

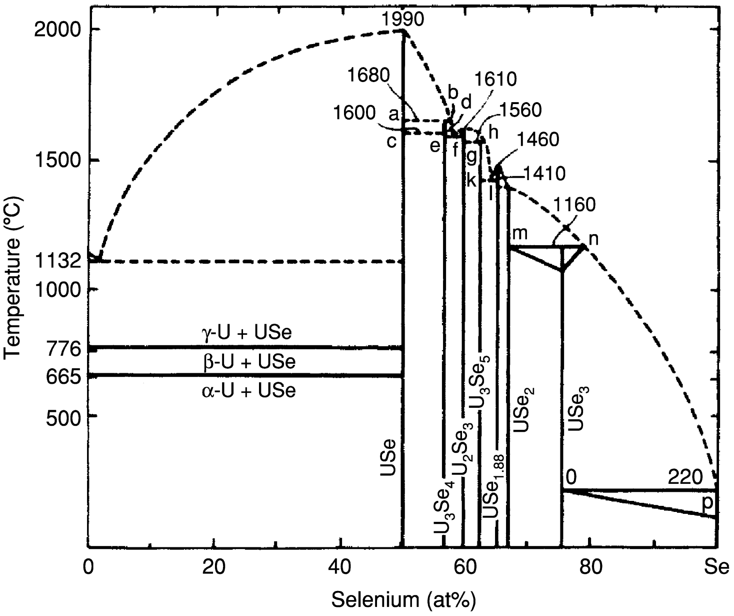

Fig. 5.35 *Phase diagram of the U–Se system* (*Klein-Haneveld and Jellinek*, 1964).

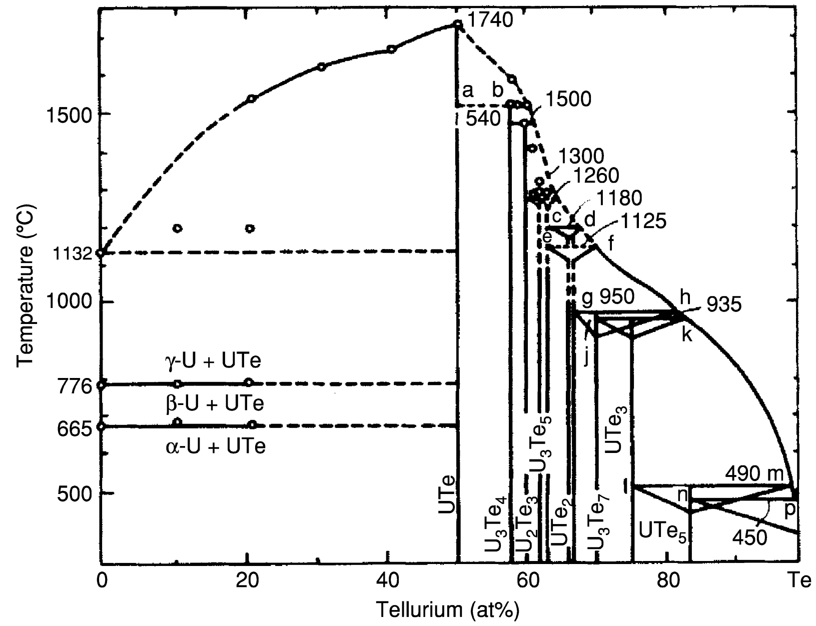

Fig. 5.36 *Phase diagram of the U–Te system* (*Slovyanskikh* et al., 1977).

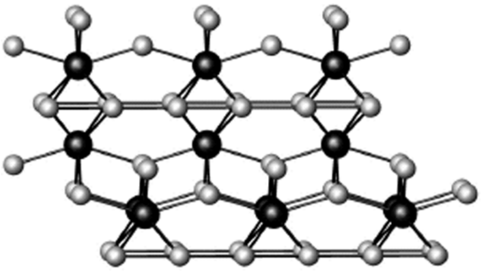

Fig. 5.37 *A view down the a-axis of the structure UTe_2. There are one-dimensional chains formed from Te–Te bonding, leading to the composition* $(U^{3+})(Te^{-})(Te^{2-})$.

see *Gmelin* (1981c, vol. C11) and the Proceedings of the International Conference on the Physics of Actinides and Related 4f Materials (Wachter, 1980). U_2Te_5 has been prepared from the direct reaction of the elements, and single crystals grown by using $TeBr_4$ as a chemical transport reagent (Stoewe, 1996b). Uranium chalcogenides can also be prepared by reacting UCl_4 with Li_2X (X = S, Se, Te) (Fitzmaurice and Parkin, 1994). Narducci and Ibers (1998) have reviewed the ternary and quaternary uranium chalcogenides. These compounds range from simple perovskite-type compounds with ABX_3 (X = S, Se, Te) formula to complex, tellurium-deficient compounds such as one-dimensional $Cs_8Hf_5UTe_{30.6}$ (Cody *et al.*, 1995; Cody and Ibers, 1995). The oxidation state of uranium in these compounds is often called into question due to the presence of Te ··· Te contacts on the order of 3 Å, which are considerably shorter than the van der Waals distance (4.10 Å), but longer than a full Te–Te single bond (2.76 Å). This results in a formal oxidation state for the tellurium with a non-integral value; hence, the oxidation state of uranium is ambiguous.

5.7.6 Uranium halides and related compounds

The halides and complex halides are one of the most thoroughly studied classes of uranium compounds. They have found use in many industrial applications, uranium hexafluoride, tetrachloride, and trichloride in large-scale isotope separation of ^{235}U and uranium tetrafluoride as a component of molten-salt reactor fuels as well as for the preparation of uranium metal. The most stable halides are formed with uranium in the 6+ and 4+ oxidation states. Experimental investigations gave evidence for increasing U 5f participation in the chemical bonds in the more covalent compounds. Ionicity is largest for halides with uranium in higher oxidation states and with the more electronegative halogens. An exception to this rule is UF_3, which is reported to be more covalent than UCl_3 (Thibaut *et al.*, 1982). Uranium in oxidation states 5+ and 6+ forms linear uranyl groups UO_2^+ and UO_2^{2+}. These possess covalent, substitution inert bonds and act like single species with respect to the halogen atoms. Lau and Hildenbrand (1982, 1984) have presented thermochemical data for gaseous

U–F_n and U–Cl_n species (where $n = 1, 2, 3, 4,$ or 5), obtained from mass spectrometric investigations of high-temperature reaction equilibria.

The chemistry of uranium halides has been reviewed in numerous papers and books, e.g. Katz and Sheft (1960), Hodge (1960), Pascal (1962–1970), Bagnall (1967, 1987), Caillat (1961), Chatalet (1967), Brown (1968, 1972, 1973, 1979), Johnson *et al.* (1974), Manes (1985), and Eick (1994). Several reviews were devoted to particular aspects of the halides: the crystallographic data of actinide halides have been reported by Taylor (1976a) and of their binary compounds with non-metallic elements by Benedict (1987); the results of spectroscopic investigations were presented by Carnall (1982), Carnall and Crosswhite (1985), Baer (1984), and Wilmarth and Peterson (1981); the magnetism of actinide compounds by Santini *et al.* (1999); EPR by Kanellakopulos (1983); the thermodynamic data by Kubaschewski and Alcock (1979), Fuger *et al.* (1983), Grenthe *et al.* (1992), and Guillaumont *et al.*, (2003); the industrial production of uranium hexafluoride by Hellberg and Schneider (1981), and the properties of uranium in molten salts and metals by Martinot (1984, 1991). A number of review papers have been also devoted to a particular oxidation state or group of uranium halides, e.g. *Structural systematics in actinide fluoride complexes* (Penneman *et al.*, 1973), *Verbindungen mit Fluor* (Bacher and Jacob, 1980), *Actinide fluorides* (Freestone and Holloway, 1991), *Uranium hexafluoride. Its chemistry related to its major application* (Bacher and Jacob, 1986), *Compounds of uranium with chlorine, bromine, iodine* (Brown, 1979), *Heptavalent actinides* (Keller, 1985), *Complex compounds of uranium* (Bagnall, 1979), *Comprehensive coordination chemistry II – The Actinides* (Burns *et al.*, 2004), *Magnetochemistry of uranium*(V) *complexes and compounds* (Miyake, 1991), *Chemistry of tervalent uranium* (Drożdżyński, 1991). In order to keep the reference number at a reasonable limit these review articles will be frequently cited as the source of chemical and physical properties of the compounds. In each of the following subsections the uranium halides and related compounds are discussed in order of increasing valence state and some of their physical properties summarized in subsequent tables. Although references to original literature data have been kept in these tables, the citation of thermodynamic data have been limited to the most important binary compounds as Chapter 19 of this work is devoted to thermodynamic properties of the actinides.

(a) Tervalent halides and complex halides

The first tervalent uranium compound, UCl_3, was prepared by Péligot (1842), and until the end of the 1960s the binary trihalides have been almost the only ones investigated. The crucial reason was the large sensitivity to oxidation and very poor solubility in aprotic organic solvents of all at that time known uranium(III) compounds. During the last 30 years the development of new experimental methods made it possible to prepare almost 150 uranium(III) compounds (Drożdżyński, 1991). However, the uranium trihalides and complex halides still remain the only relatively well-investigated group.

The stability of the trihalides decreases with increase in the atomic number of the halide. Apart from UF_3, all the halides are more or less hygroscopic and easily oxidized in air. In aqueous solutions they are rapidly oxidized but in pure, thoroughly deoxygenated solvents the U^{3+} ions are fairly stable. Concentrated hydrochloric acid gives intensely deep-red solutions, characteristic of the $[UCl_n]^{3-n}$ complex anions. With the exception of UF_3, UCl_3 and uranium(III) fluoro complexes, the halides are also readily soluble in some more polar solvents. The compounds exhibit a variety of colors (see Table 5.25). The preparation of somewhat more stable hydrated uranium(III) complexes have also been reported. Since all of them are readily soluble in water they are efflorescent in a humid atmosphere. For binary halides the following anion polyhedra have been identified: five capped trigonal prism (UF_3), tricapped trigonal prism (UCl_3, UBr_3), and bicapped trigonal prism (UI_3).

The synthesis of uranium(III) halides and complex halides requires a rather complex equipment and strictly oxygen-free conditions. At temperatures higher than 600°C the syntheses ought to be carried out in tantalum or molybdenum tubes in order to avoid side reactions with silica; Drożdżyński (1991) has reported a survey of the preparation methods.

Trivalent uranium has a [Rn] $5f^3$ electronic configuration with the $^4I_{9/2}$ ground state. A number of crystal-field analyses of high-resolution low-temperature absorption spectra have been reported for U^{3+}-doped single crystals of $LiYF_4$ (S_4) (Simoni *et al.*, 1995), $LaCl_3$ (C_{3h}) (Crosswhite *et al.*, 1980; Carnall, 1989; Karbowiak *et al.*, 2002a), $LaBr_3$ (C_{3h}) (Sobczyk *et al.*, 2005), RbY_2Cl_7 (C_{2v}) (Karbowiak *et al.*, 1997), K_2UX_5 (C_s) ($X = Cl$, Br or I) (Karbowiak *et al.* 1998a), Cs_2NaYCl_6 (O_h) and Cs_2LiYCl_6 (O_h) (Karbowiak *et al.*, 1998b), Ba_2YCl_7 (C_1) Karbowiak *et al.*, 2002b, Cs_2NaYBr_6 (Karbowiak *et al.*, 2003a), $CsCdBr_3$ (Karbowiak *et al.*, 2003b), $Cs_3Lu_2Cl_9$(C_{3v}) and $Cs_3Y_2I_9$ (C_{3v}) (Karbowiak *et al.* 2005a). Such analyses have been also performed for polycrystalline samples of UCl_3 and UBr_3 (C_{3h}) (Sobczyk *et al.*, 2003), $UCl_3 \cdot 7H_2O$ (C_i) (Karbowiak *et al.*, 2001), $CsUCl_4 \cdot 3H_2O$ (C_s), $NH_4UCl_4 \cdot 4H_2O$ (C_2) (Karbowiak *et al.*, 2000), and $ZnCl_2$-based glass (Dereń *et al.*, 1998). However, only the U^{3+}-doped single crystals of $LaCl_3$ and $LiYF_4$ exhibit suitable site symmetry for precise energy-level investigations, using selection rules for electric and magnetic dipole transitions. The energy levels of the U^{3+} ion in the different site symmetries were assigned and fitted to a semiempirical Hamiltonian representing the combined atomic and crystal-field interactions. *Ab initio* calculations made it possible to use a simplified parametrization and the determination of the starting values in the angular overlap model in cases where the U^{3+} ion had the lowest site symmetry (Karbowiak *et al.*, 2000). The free ion and crystal-field parameters obtained from an analysis of low-temperature absorption spectra of thin films of UF_3, UCl_3, and UBr_3 are presented in Table 5.25. In addition, an analysis of low-temperature absorption, luminescence, and excitation

Table 5.25 *Properties of selected uranium(III) halides and complex halides.*[a]

Formula	*Selected properties and physical data*[b]	*Lattice symmetry, lattice constants (Å), conformation and density (g cm^{-3})*[c]	*Remarks regarding information available and references*
UF_3	grey to black powder or purplish black crystals. density: 8.9 g cm^{-3}; disproportionates above 1000°C UF_3(cr): $\Delta_f G^o_m = -1432.5\ (4.7)^\dagger$, $\Delta_f H^o_m = -1501.4(4.7)^\dagger$, $S^o_m = 123.4\ (0.4)^\dagger$; $C^o_{p,m} = 95.1(0.4)^\dagger$. UF_3(g): $\Delta_f G^o_m = -1062.9\ (20.2)^\dagger$, $\Delta_f H^o_m = -1065.0\ (20)^\dagger$, $S^o_m = 347.5(10)^\dagger$; $C^o_{p,m} = 76.2(5.0)^\dagger$. $\log p(\text{mm Hg}) = 4187T^{-1} + 3.945$ $\mu_{\text{eff.}} = 3.67$ B.M. (125–300K)[d]; $\theta = -110$ K. $\mu_{\text{eff.}} = 3.66$ B.M. (293–723K)[d]; $\theta = -98$ K, Atomic and crystal-field parameters: $E_{\text{avg}} = 20\,006\ (30)$, $F^2 = 38068\ (108)$, $F^4 = 32256\ (177)$, $F^6 = 16372\ (198)$, $\zeta_{5f} = 1613\ (11)$; $\alpha = 26.1\ (6)$, $\beta = -793\ (40)$, $\gamma = 2085\ (104)$; $T^2 = [298.0]$, $T^3 = [48.0]$, $T^4 = [255.0]$, $T^6 = [-285.0]$, $T^7 = [332.0]$, $T^8 = [305.0]$; $M^0 = [0.67]$, $M^2 = [0.37]$, $M^4 = [0.26]$; $P^2 = [1276]$, $P^4 = [608]$, $P^6 = [122]$;$B^2_0 = 216(60)$, $B^2_2 = -319(49)$, $B^4_0 = 1479\ (78)$, $B^4_2 = 679(62)$, $B^4_4 = 1615(62)$, $B^6_0 = 2373\ (79)$, $B^6_2 = -2201\ (62)$, $B^6_4 = -1631(630)$, $B^6_6 = -1106\ (63)$; $n = 75$; $rms = 33.6$.	hexagonal; C^3_{6v}, $P6_3cm$, No. 185; $Z = 6$; or trigonal: $P\bar{3}c1$, D^4_{3d}, No. 165; Z = 6, CN = 11, $a = 7.173$, $c = 7.341$; d(calc.) = 8.95 to 8.99; d(exp.) = 9.18. LaF_3 structure type; The bond lengths to the corresponding prism atoms in $P\bar{3}cl$ are 3.01 (2×), 2.48 (2×) and 2.63 (2×) and in $P6_3cm$ these are 2.53 (2×), 2.81 (2×), 2.45 and 3.09, respectively. The cap atoms in both structures have fit firmly (bond lengths 2.42–2.48.)	*X-ray single-crystal and neutron diffraction data* (Zalkin *et al.*, 1967; Taylor 1976a; Zachariasen, 1975); *Synthesis* (Runnals, 1953; Warf, 1958; Friedman *et al.*, 1970; Berndt, 1973); *absorption spectra* (Schmieder *et al.*, 1970); *photoelectron spectra* (Thibaut *et al.*, 1982); *crystal-field analysis* (Drożdżyński *et al.*, 2002); *mechanical and thermal properties* (Bacher and Jacobs, 1980); *EPR, NMR and magnetic susceptibility data* (Berger and Sienko, 1967; Dao, Nguyen Nghi *et al.*, 1964; Kanellakopulos, 1983); *fused-salt systems* (Martinot, 1984); *thermodynamic properties* (Brown, 1973, 1979; Grenthe *et al.*, 1992; Guillaumont *et al.*, 2003)

Table 5.25 (*Contd.*)

Formula	*Selected properties and physical data*[b]	*Lattice symmetry, lattice constants* (Å)*, conformation and density* (g cm^{-3})[c]	*Remarks regarding information available and references*
$NaUF_4$	peritectic decomposition point of α-$NaUF_4$: 775°C; α–β transformation temp. 595°C	hexagonal, C_{3h}^1, $P\bar{6}$, No. 174; $a =$ 6.167, $c =$ 3.770; d(calc.) = 5.92; tricapped trigonal prism sharing ends to form chain	*X-ray powder diffraction data; fused salt systems* (Brunton *et al*., 1965; Bacher and Jacob, 1980)
Na_2UF_5		cubic, space centered, $Z = 4$; $a =$ 7.541(6); d(calc.) = 5.87	*X-ray powder diffraction data; fused salt systems* (D'Eye and Martin, 1957; Bacher and Jacob, 1980)
KUF_4	dark-blue		(Bacher and Jacob, 1980)
K_2UF_5	peritectic point: 848°C	cubic; CaF_2 structure type ; $a =$ 6.62 (1); $Z =$ 1.6; d(calc.) = 3.74	*X-ray powder diffraction data; fused salt systems* (Volkov *et al*., 1979)
K_3UF_6	purple-brown, extremely moisture sensitive	cubic, face centered; $a =$ 9.20	*X-ray powder diffraction data; fused salt systems* (Thoma and Penneman, 1965; Thoma *et al*., 1966)
$K_3U_2F_9$	peritectic point: 750°C	cubic; CaF_2structure type ; $a =$ 6.00 (1); $Z =$ 0.8; d(calc.) = 4.67	*X-ray powder diffraction data; fused salt systems* (Volkov *et al*., 1979)
$RbUF_4$		hexagonal; KYF_4 structure type ; $a =$ 8.54(1), $c =$ 10.72(2); $Z =$ 6, d(calc.) = 5.84	*X-ray powder diffraction data; fused salt systems* (Boraopkova *et al*., 1971)
Rb_3UF_6	purple-brown, extremely moisture sensitive	cubic, face centered; $a =$ 9.5074	*X-ray powder diffraction data; fused salt systems* (Thoma and Penneman, 1965; Thoma *et al*., 1966; Chirkst, 1981)
Cs_3UF_6	purple-brown, extremely moisture sensitive	cubic, face centered; $a =$ 10.6	*X-ray powder diffraction data; fused salt systems* (Thoma and Penneman, 1965; Thoma *et al*., 1966; Chirkst, 1981)

$UZrF_7$	reddish-brown, slowly oxidizes in air at room temperature; $\mu_{\text{eff.}} = 3.80$ B.M. (100–300 K)^{d}; $\theta = -85$ K	monoclinic, isotypic with $SmZrF_7$, $a = 6.1000(6)$, $b = 5.833(8)$ $c = 8.436(10)$; $\beta = 102.69(7)$; $Z = 2$; $V = 292.81$; d(calc) = 5.25; d(exp.) = 5.40.	*X-ray powder diffraction data; magnetic susceptibility data* (Fonteneau and Lucas, 1974)
UZr_2F_{11}	slowly oxidizes in air at room temperature. $\mu_{\text{eff.}} = 3.90$ B.M. (100–300 K)^{d}; $\theta = -101$ K	monoclinic; $a = 5.308(6)$, $b = 6.319(8)$, $c = 8.250(8)$, $\beta = 105.41(5)°$, $Z = 2$; $V = 266.81$; d(calc.) = 5.22	*X-ray powder diffraction data; magnetic susceptibility data* (Fonteneau and Lucas, 1974). *general properties* (Bacher and Jacob, 1980)
UCl_3	dark red needles or fine crystalline olive-green powder; hygroscopic; soluble in acetic acid.m.p. = 835°C; b.p. = 1657 °C; density: 5.51 g cm^{-3}; Oxidizes in air at room temperatures; UCl_3(cr): $\Delta_f G^o_m = -796.1\ (2.0)^{\dagger}$, $\Delta_f H^o_m = -863.7\ (2.0)^{\dagger}$, $S^o_m = 158.1\ (0.5)^{\dagger}$; $C^o_{p,m} = 95.10\ (0.5)^{\dagger}$. UCl_3(g): $\Delta_f G^o_m = -521.7\ (20.2)^{\dagger}$, $\Delta_f H^o_m = -523.0(20\ )^{\dagger}$, $S^o_m = 380.3\ (10.0)^{\dagger}$; $C^o_{p,m} = 82.4\ (5.0)^{\dagger}$. $\log p(\text{mmHg}) = -11149\ T^{-1} + 8.90$ (590–790 K) $\log p(\text{mmHg}) = -11552T^{-1} + 8.97$ (>790 K); Atomic and crystal-field parameters: $\mu_{\text{eff.}} = 3.76$ B.M. (70–300 K)^{d}; $\theta = -75$ K; $T_N = 20$ K; $\mu_{\text{eff.}} = 3.03$ B.M. (350–509 K)^{d}; $\theta = -29$ K; $E_{\text{avg}} = 19\,331(42)$, $F^2 = 37719(154)$, $F^4 = 30370(202)$, $F^6 = 19477(218)$, $\zeta_{5f} = 1606(13)$; $\alpha = 31(5)$, $\beta = -939(40)$, $\gamma = 2087(115)$; $T^2 = 460(81)$; $T^3 = 59(25)$, $T^4 = 159(39)$, $T^6 = -144(46)$, $T^7 = 356(42)$, $T^8 = [300]$; $M^0 = [0.663]$; $P^2 = 1639(65)$; $B^2_0 = 370(42)$, $B^4_0 = -359(76)$, $B^6_0 = -1704(74)$; $B^6_6 = 935(60)$; $n = 58$; $rms = 35.8$	hexagonal; C^2_{6h}, $P6_3/m$, No. 176; the coordination polyhedron is a symmetrically tricapped trigonal prism arranged in columns in the c-direction; $a = 7.452(6)$, $c = 4\ .328(4)$; d(U–Cl) = 2.928(3), (6×); d(U–Cl) = 2.934(5), (3×); d(U–Cl) = 4.816(4) (to neighbor chain); d(Cl–Cl) = 3.342(5); d(Cl–Cl) = 3.410(3); (face atom-cape atom); d(calc.) = 5.51	*X-ray single crystal data* (Schleid *et al.*, 1987; Murasik *et al.*, 1985; Taylor and Wilson, 1974f); *synthesis* (Brown, 1968, 1979; Drożdżyński, 1991, 1988a); *thermodynamic properties* (Rand and Kubaschewski, 1963; Brown, 1973, 1979; Grenthe *et al.*, 1992; Guillaumont *et al.*, 2003). *magnetic susceptibility data*, (Handler and Hutchison, 1956; Jones *et al.*, 1974; Dawson, 1951); *NIR, visible and UV low temperature absorption spectra and crystal-field analysis of UCl_3 and U^{3+}:$LaCl_3$*, (Carnall, 1989; Karbowiak *et al.*, 2002; Sobczyk *et al.*, 2003); *photoelectron spectra* (Thibaut *et al.*, 1982)

Table 5.25 (*Contd.*)

Formula	*Selected properties and physical data*[b]	*Lattice symmetry, lattice constants* (Å)*, conformation and density* (g cm^{-3})[c]	*Remarks regarding information available and references*
$UCl_3 \cdot 7H_2O$	grayish-ink-blue needles, readily soluble in numerous organic solvents; relatively resistant to oxidation by air at temperatures lower than 15°C; loses some of its crystallization water at higher temperatures or at high vacuum; may be completely dehydrated at 260°C. $\mu_{\text{eff.}} = 2.95$ B.M. (10–300 K)[d]; $\theta = -32.7$ K; Atomic and crystal-field parameters: $E_{\text{avg}} = 19827(17)$, $F^2 = 40488(58)$, $F^4 = 32544(81)$, $F^6 = 22866(75)$, $\zeta_{5f} = 1622(10)$; $\alpha = 28(5)$, $\beta = -622(35)$, $\gamma = 1148$; $T^2 = 306$, $T^3 = 42$, $T^4 = 188$, $T^6 = -242$, $T^7 = 447$, $T^8 = 300$; $M^0 = 0.672$, $M^2 = 0.372$, $M^4 = 0.258$; $P^2 = 1216$, $P^4 = 608$, $P^6 = 122$; $B^2_0 = -126(76)$, $B^2_1 = [-109]$, $\text{Im}B^2_1 = -423(47)$, $B^2_2 = -209(53)$, $\text{Im}B^2_2 = -350(55)$, $B^4_0 = 188(106)$, $B^4_1 = [-99]$, $\text{Im}B^4_1[-81]$, $B^4_2 = [-66]$, $\text{Im}B^4_2 = [-238]$, $B^4_3 = [136]$, $\text{Im}B^4_3 = -529(83)$, $B^4_4 = [374]$, $\text{Im}B^4_4 = [-491]$, $B^6_0 = [-130]$, $B^6_1 = 428(90)$, $\text{Im}B^6_1 = [-77]$, $B^6_2 = [171]$, $\text{Im}B^6_2 = 133\ [100]$, $B^6_3 = [-251]$, $\text{Im}B^6_3 = [-14]$, $B^6_4 = -489(110)$, $\text{Im}B^6_4 = -1832(81)$, $B^6_5 = [160]$, $\text{Im}B^6_5 = 1197(96)$, $B^6_6 = -498(98)$, $\text{Im}B^6_6 = -241(91)$; $rms = 36$; $n = 94$	triclinic; $P\bar{1}$, C^1_i, No.2; $a = 7.902(1)$; $b = 8.210(2)$, $c = 9.188(2)$; $\alpha = 70.53(3)$; $\beta = 73.14(3)$; $\gamma = 81.66(3)$; $V = 537.0(2)$; $Z = 2$; d(calc.) = 2.910. The crystals are built up from separate $[U_2Cl_2(H_2O)_{14}]^{4+}$ units and Cl^- ions. The characteristic features of this structure are dimers, formed by two uranium ions connected through the (Cl1) bridging chlorine atoms. d(U–Cl) = 2.915(1) and 2.894(1); d(U–O) = from 2.515(3) to 2.573(3)	*X-ray single crystal data* (Mech *et al.*, 2005); *magnetic susceptibility data; NIR and visible absorption spectrum, decomposition* (Drożdżyński, 1985); *crystal-field analysis, low temperature absorption spectrum* (Karbowiak *et al.*, 2001)

$UCl_3 \cdot 6H_2O$	purple plates	monoclinic; $P12/n1$; $a = 9.732(2)$, $b = 6.593(1)$, $c = 8.066(2)$, $\alpha = 90$, $\beta = 93.56(3)$; $\gamma = 90$; $V = 516.51$; $Z = 2$; d(calc.) = 2.909; The basic units of the crystal structure are Cl^- anions and $[UCl_2(H_2O)_6]^+$ cations. The U as well as O(1), O(2) and O(3) atoms are each eight-coordinated, whereas the Cl(2) and Cl(1) chloride atoms are seven and six coordinated, respectively. The characteristic feature of this structure is the existence of hydrogen bonds, which link the uranium eight–coordinated polyhedra, forming a three–dimensional network	*X-ray single crystal data* (Mech *et al.*, 2005)
$UCl_3 \cdot CH_3CN \cdot 5H_2O$	deep-red; soluble in polar organic solvents; IR (cm^{-1}): 2260m, 2270sh (ν_2, symm. $C \equiv N$ stretching); 1367 (ν_3, symm. CH_3 deform.); 926m (ν_4, symm. C–C stretching); 2298 ($\nu_3 + \nu_4$, combination band); 1035 (ν_7, degenerate CH_3 rocking); $\mu_{eff.} = 3.39$ B.M .(65–300 K)^d, $C = 1.430$ emu·K·mol^{-1}, $\theta = -65.7$ K, $T_N = 12$ K	monoclinic; $a = 12.96(2)$, $b = 12.98(3)$, $c = 6.62(1)$; $\beta = 101.7(2)$; $Z = 4$, $V = 1007.2$; d(calc.) = 3.14	*X-ray powder diffraction data; magnetic susceptibility data; IR, NIR and visible absorption spectra; decomposition*, (Zych and Drożdżyński, 1986)
$UCl_3 \cdot 2H_2O \cdot 2CH_3CN$	deep dark reddish needles	$P\bar{1}$, C_i^1, No.2; $a = 7.153(1)$, $b = 8.639(2)$, $c = 10.541(2)$; $\alpha = 108.85(3)$, $\beta = 105.05(3)$, $\gamma = 93.57(3)$; $V = 587.6(3)$; $Z = 2$; d(calc.) = 2.61; d(U–Cl) = 2.775; d(U–Cl) to the bridging anions = 2.860–2.901; d(U–O) = 2.468–2.485; d(U–U) = 4.605.	*X-ray single crystal data* (Mech *et al.*, 2005)

Table 5.25 (*Contd.*)

Formula	*Selected properties and physical data*[b]	*Lattice symmetry, lattice constants (Å), conformation and density (g cm^{-3})*[c]	*Remarks regarding information available and references*
		The U^{3+} ion is eight coordinated by five chloride ions, two water molecules and one methyl cyanide, which are forming a distorted bicapped trigonal prism The characteristic feature of this structure is the link of the uranium atoms through the two common edges of the Cl1 and Cl3 chlorine atoms into an infinitive zigzag chain in the [010] direction	
$CsUCl_4$	deep ink-blue; soluble in polar organic solvents; $\mu_{eff.} = 3.16$ B.M. (60–300 K)[d]; $\theta = -36$ K; $C = 1.2146$ emu·K·mol^{-1}	could not be unambiguously indexed	*X-ray powder diffraction data; magnetic susceptibility data; NIR, Vis, and UV absorption spectra* (Karbowiak and Drożdżyński, 1998a)
K_2UCl_5	purple; soluble in polar organic solvents, m.p. = 608°C – congruently; $\mu_{eff.} = 3.77$ B.M. (130–300K)[d)]; $\theta = -33.5$ K; $T_N = 13.2$ K; IR(cm^{-1}): ν(U–Cl, stretching) = 140–220	orthorhombic; D_{2h}^{16}, *Pnm*, No. 62; Z = 4; Monocapped trigonal prisms [UCl_7] are connected via two opposite common edges to chains; $a = 12.7224(7)$, $b = 8.8064(6)$, $c = 7.9951(5)$; $V = 1348.8(1)$; d(calc.) = 3.68	*single crystal and X-ray powder diffraction data; IR, NIR, and Vis absorption spectra; magnetic susceptibilities* (Drożdżyński and Miernik, 1978; Krämer *et al*., 1994); *luminescence and low temperature spectra of U^{3+}:K_2LaCl_5* (Andres *et al*., 1996); *magnetic phase transitions* (Keller *et al*., 1995); *crystal-field analysis* (Karbowiak *et al*., 2000); *fused salt systems* (Suglobova and Chirkst, 1981)

Rb_2UCl_5	violet-red; soluble in polar organic solvents; m.p. = 575°C–incongruently; $\mu_{\mathrm{eff.}} = 3.44$ B.M. (150–300 K)^d; $\theta = -32.0$ K; $T_N = 8.6$ K; IR (cm^{-1}): ν(U–Cl, stretching) = 100–260	orthorhombic; D_{2h}^{16}, *Pnma,* No. 62; $Z = 4$; Monocapped trigonal prisms [UCl_7] are connected via two opposite common edges to chains; $a = 13.1175(8)$, $b = 8.9782(6)$, $c = 8.1871(7)$; $V = 1451.19(2)$; d(calc.) = 4.04; d(U–Cl) = 2.774 to 2.846; d(U–U) = 4.651 (interchain); d(U–U) = 7.88 (intrachain)	*X-ray powder diffraction data; IR, NIR and visible absorption spectrum; magnetic susceptibilities* (Drożdżyński and Miernik, (1978); Krämer *et al.*, 1994); *fused salt systems* (Suglobova and Chirkst, 1981)
Cs_2UCl_5	m.p. = 370°C – decomposition in solid state	rhombic; $a = 12.03$, $b = 9.76$, $c = 9.37$; $Z = 4$, d(calc.) = 4.08	*X-ray powder diffraction data; fused salt systems* (Suglobova and Chirkst, 1981)
$(NH_4)_2UCl_5$	violet; $\mu_{\mathrm{eff.}} = 3.54$ B.M. (17–220 K)^d; $\theta = -26.0$ K; $\mu_{\mathrm{eff.}} = 3.47$ B.M. (220–300 K)^c; $\theta = -37.5$ K; $T_N = 7.8$ K; IR(cm^{-1}): ν(U–Cl, stretching) = 140–260		*IR, NIR,and Vis absorption spectra; magnetic susceptibilities* (Drożdżyński and Miernik, 1978)
$SrUCl_5$	deep olive-green; $\mu_{\mathrm{eff.}} = 3.65$ B.M. (90–300 K)^d $C = 1.653$ emu·K·mole^{-1}, $\theta = -127$ K	could not be indexed	*X-ray powder diffraction data; magnetic susceptibility data; NIR and Vis absorption spectra*, (Karbowiak and Drożdżyński, 1998b)
$[(CH_3)_3N]_3 \cdot UCl_6$	dark violet-blue; IR (cm^{-1}): 110m [δ(UCl_6) A_u]; 123m,b [δ(UCl_6) E_u] 203s [lattice or cation vib.]; 236s [ν_s(UCl_6) A_u]; 259s [ν_{as}(UCl_6) E_u]. Raman (cm^{-1}): 79sh [lattice]; 89w [δ(UCl_6) E_g]; 104w [δ(UCl_6) B_g]; 131m [lattice or cation vib.]; 226vs [ν_{as}(UCl_6) A_g]; 237sh [ν'(UCl_6) A_g]; 268w [ν_s(UCl_6) B_g]; $\mu_{\mathrm{eff.}} = 3.36$ B.M. (200–300K)^d; $\theta = 17$; $T_N = 4.8$ K; $C = 1.5058$ emu·K·mole^{-1}	tetragonal; $a = 13.020$, $c = 7.825$; $Z = 2$; $V = 1326.48$; d(calc.) = 1.68	*X-ray powder diffraction data; IR, Raman, NIR and Vis absorption spectra; magnetic susceptibility data* (Karbowiak *et al.*, 1996a)

Table 5.25 (*Contd.*)

Formula	*Selected properties and physical data*[b]	*Lattice symmetry, lattice constants* (Å)*, conformation and density* (g cm^{-3})[c]	*Remarks regarding information available and references*
RbU_2Cl_7	pale-brown; soluble in polar organic solvents; IR (cm^{-1}):281s, 271s, 210s, 202vs, 195sh, 190vs, 181vs, 169vs, 150sh [ν(U–Cl)]; 130m, 125m, 114m, 90m [δ(Cl–U–Cl)]; 83sh, 70m, 55w [T'(Rb/U)]; RS (in cm^{-1}): 262w, 227 s,b, 189s,165s [ν(U–Cl)]; 142m, 120m, 95w [δ(Cl–U–Cl)]; 85m, 62m T'(Rb/U); $\mu_{\mathrm{eff.}} = 3.76$ B.M., $C = 1.750$ emu·K·mole^{-1}, $\theta = -80$ K	rhombic; $a = 12.86(5)$, $b = 6.89(1)$, $c = 12.55(2)$; $Z = 4$, d(calc) = 4.80(3), $RbDy_2Cl_7$ structure type	*X-ray powder diffraction data* (Suglobova and Chirkst, 1981); Volkov *et al.*, 1987); *NIR and Vis low temperature absorption spectrum; magnetic susceptibility data; IR transmission and Raman spectra* (Karbowiak *et al.*, 1996b); *luminescence and excitation spectra* (Karbowiak *et al.*, 1996d); *low temperature absorption spectrum and crystal-field analysis of* U^{3+}*:*RbY_2Cl_7 (Karbowiak *et al.*, 1997)
Ba_2UCl_7	deep black-brown; soluble in polar organic solvents; $\mu_{\mathrm{eff.}} = 3.25$ B.M., (105–300 K)[d], $C = 1.310$ emu·K·mole^{-1}, $\theta = -95$ K	monoclinic; C_{2h}^5, $P2_1/c$, No. 14; $a = 7.20$, $b = 15.61$, $c = 10.66$; $\beta = 91.1°$, $V = 1197$; d(calc.) = 4.22	*X-ray powder diffraction data* (Volkov *et al.*, 1987); Suglobova and Chirkst, 1981); *magnetic susceptibility data; IR, NIR and Vis absorption spectra* (Karbowiak and Drożdżyński, (1998b)
Cs_2LiUCl_6	deep ink-blue; $\mu_{\mathrm{eff.}} = 3.56$ B.M. (85–300)[d]; $C = 1.571$ emu·K·mole^{-1}, $\theta = -103$ K	regular; O_h^5, $Fm3m$, No. 225; $a = 10.671$; $Z = 4$; $V = 1218.03$; d(calc.) = 3.9444	*X-ray powder diffraction data, NIR, Vis and UV absorption spectra, magnetic susceptibilities* (Karbowiak and Drożdżyński, 1998a); *absorption, vibronic and emission spectra; crystal-field analysis* (Karbowiak *et al.*, 1996e; Karbowiak *et al.*, 1998b)

K_2NaUCI_6		hexagonal; C_{3v}^1, $P3m1$, No.156; isostructural with α-K_2LiAlF_6; a = 7.28(1), c = 17.79(2); Z = 3; V = 816.53; d(calc.) = 3.35(1)	*X-ray powder diffraction data* (Volkov *et al.*, 1987; Aurov *et al.*, 1983); *thermodynamic data* (Aurov and Chirkst, 1983)
Rb_2NaUCI_6		trigonal; a = 7.27(2), c = 35.51(10); Z = 6; d(calc.) = 3.93(3), d(exp.) = 3.98(2); Rb_2LiAlF_6 and Cs_2NaCrF_6 structure type	*X-ray powder diffraction data* (Volkov *et al.*, 1987; Aurov *et al.*, 1983); *thermodynamic data* (Aurov and Chirkst, 1983)
Cs_2NaUCl_6	ink-blue; soluble in polar organic solvents; $\mu_{eff.} = 2.49$ B.M. $(4–20)^d$; $\theta = 0.53$ K. $\mu_{eff.} = 2.92$ B.M. $(25–50)^d$; $\theta = 9.6$ K	cubic; O_h^5, $Fm3m$, No.225; a = 10.937 (1); V = 1308.3(5); Z = 4, d(U–Cl) = 2.723(9), d(U–U) = 7.734; d(calc.) = 3.754	*single crystal data* (Spirlet *et al.*, 1988); *magnetic properties* (Hendricks *et al.*, 1974); *thermodynamic properties* (Aurov and Chirkst, 1983; Schoebrechts *et al.*, 1989); *NIR, Vis and UV low temperature absorption and luminescence spectra; crystal-field analysis* (Karbowiak *et al.*, 1998b); *IR spectra* (Mazurak *et al.*, 1988).
NaU_2Cl_6 or $(Na^+)(U^{3+})_2(e^-)(Cl^-)_6$		hexagonal; C_{6h}^2, $P6_3/m$., No 176; a = 7.5609(3), c = 4.3143(3); Z = 1; d(U–Cl) = 2.945(6×) and 2.977(3×), d(Na–Cl) = 2.878(6×)].	*single crystal data* (Schleid and Meyer, 1989)
$KUCl_4 \cdot 4H_2O$	violet-red; soluble in polar organic solvents; IR (cm^{-1}): 650, 610 (U–OH_2 rocking); 470s (U–OH_2 wagging); 300w ν(U–OH_2 stretching); 222sh, 214s, 198s ν(U–Cl, stretching); 166s ν(U–Cl–U, stretching or lattice); 130s δ(Cl–U–Cl, stretching or lattice); 107s, 88sh (lattice modes); $\mu_{eff.} = 3.72$ B.M. $(100–300\ K)^d$; $C = 1.716$ emu·K·mole^{-1}; $\theta = -69.3$ K	orthorhombic; a = 6.971, b = 6.638, c = 11.317; Z = 2; V = 523.6; d(calc.) = 3.11	*X-ray powder diffraction data; magnetic susceptibility data; IR, NIR and Vis spectra* (Drożdżyński, 1988b)

Table 5.25 (*Contd.*)

Formula	*Selected properties and physical data*[b]	*Lattice symmetry, lattice constants* (Å)*, conformation and density* (g cm^{-3})[c]	*Remarks regarding information available and references*
$RbUCl_4 \cdot 4H_2O$	violet-red; soluble in polar organic solvents; IR (cm^{-1}): 660 (U–OH$_2$, rocking); 486s (U–OH$_2$, wagging); 300sh, 290ms [ν(U–OH$_2$), stretching]; 228s, 216sh, 197s [ν(U–Cl) stretching]; 165ms [ν(U–Cl–U), stretching or lattice]; 130s [δ(Cl–U–Cl), bending]; 99 ms (lattice modes); $\mu_{\text{eff.}} = 3.74$ B.M. (100–300 K)[d]; $C = 1.734$ emu·K·mole^{-1}, $\theta = -66.2$ K	orthorhombic; $a = 6.999$, $b = 6.673$, $c = 11.375$; $Z = 2$; $V = 531.3$; d(calc.) = 3.36	*X-ray powder diffraction data; magnetic susceptibility data; IR, NIR and Vis absorption spectra* (Drożdżyński, 1988b)
$NH_4UCl_4 \cdot 4H_2O$	dark red-violet; soluble in polar organic solvents; IR (cm^{-1}): 650, 610 (U–OH$_2$, rocking); 494s (U–OH$_2$, wagging); 299ms [ν(U–OH$_2$) stretching]; 222s, 202s ν(U–Cl, stretching); 175ms [ν(U–Cl–U), stretching or lattice]; 130s [δ(Cl–U–Cl), bending]; 114ms, 84sh (lattice modes); $\mu_{\text{eff.}} = 3.53$ B.M. (100–240 K)[d]; $C = 1.560$ emu·K·mole^{-1}, $\theta = -72.5$ K. Atomic and crystal-field parameters: $F^2 = 39911(85)$, $F^4 = 33087(149)$, $F^6 = 22048(160)$, $\zeta_{5f} = 1627.3(8.8)$; $\alpha = 33.0(3.7)$, $\beta = -973.1(\ 29.3)$, $\gamma = 1316.9(85.4)$; $T^2 = 306$, $T^3 = 42$, $T^4 = 188$, $T^6 = -242$, $T^7 = 447$, $T^8 = 300$;	orthorhombic; D_2^3, $P2_12_12$, No. 18; $a = 7.002(2)$, $b = 11.354(3)$, $c = 6.603(2)$; $Z = 2$; $V = 524.94(14)$. The U^{3+} cation is coordinated by four Cl$^-$, ions and four H$_2$O molecules. The crystal is build up from eight-coordinated U^{3+} polyhedrons, which are connected together by O-H··Cl hydrogen bonds. d(U–Cl) (2×) = 2.845(4); d(U–Cl)) (2×) = 2.847(4); d(U–O) (2×) = 2.510(11); d(U–O) (2×) = 2.568(10); d(calc.) = 2.973, d(exp.) = 2.97	*single crystal diffraction data; magnetic susceptibility data; IR, NIR and Vis low temperature absorption spectra* (Drożdżyński, 1988b); *low temperature absorption spectra and crystal-field analysis* (Karbowiak *et al.*, 2000)

	$M^0 = 0.672$, $M^2 = 0.372$, $M^4 = 0.258$; $P^2 = 1216$, $P^4 = 608$, $P^6 = 122$; $B_0^2 =$ 721(47) / [698], $B_2^2 = 428$ (39) / [403], Im$B_2^2 = -460$ (39) / [–515], $B_0^4 =$ [–814], $B_2^4 =$ [–858], Im$B_2^4 =$ [118], B_4^4 = [–670], Im$B_4^4 =$ [–22], $B_0^6 =$ [–403], $B_2^6 =$ [–612], Im$B_2^6 =$ [838], $B_4^6 =$ [–549], Im$B_4^6 =$ [–197], $B_6^6 =$ [–1063], Im$B_6^6 =$ [–96], *rms* = 30, *n* = 83		
$KUCl_4{\cdot}3H_2O$	green; hygroscopic and air sensitive; IR(cm^{-1}): ν(U–OH$_2$, rocking) = 635s, 575s; ν(U–OH$_2$, wagging) = 480; ν(U–OH), stretching = 425, 280sh; ν(U–Cl), stretching = 260s, 238, 202; ν(U–Cl–U), stretching or lattice = 169, 125; δ(Cl–U–Cl), bending = 144, 125; ν(stretching and bending modes of coordinated water) = 1600; (3170, 3215, 3360, 3420); $\mu_{\text{eff.}}$ = 3.70 B.M. (150–300 K)^d; $C =$ 1.7033 emu·K·mole^{-1}, $\theta = -80$ K	monoclinic; $a = 6.9373$, $b = 7.2658$, $c = 9.5209$; $\beta = 96.71$; $Z = 2$; $V = 476.62$; d(calc.) = 3.30	*X-ray powder diffraction data; IR, NIR and Vis absorption spectra; magnetic susceptibility data* (Karbowiak and Drożdżyński, 1993)
$RbUCl_4{\cdot}$ $3H_2O$	greenish-brown to brown; hygroscopic and air sensitive; IR (cm^{-1}): ν(U–OH$_2$, rocking) = 650, 615, 600; ν(U–OH$_2$, wagging) = 485; ν(U–OH), stretching = 380, 285sh; ν(U–Cl), stretching = 255s, 220, 190; ν(U–Cl–U), stretching or lattice = 151, 157; δ(Cl–U–Cl), bending = 132, 127, 121, 118; ν(stretching and bending modes of coordinated water) = 1565, 1580, 1605, 3470; (93180, 3210, 3350, 3420, 3470); $\mu_{\text{eff.}}$ = 3.57 B.M. (100–300 K)^d, $C =$ 1.5766 emu·K·mole^{-1}, $\theta = -64$ K	monoclinic; $a = 8.8986$, $b = 6.9738$; $c = 8{,}0517$; $\beta = 100$; $Z = 2$; $V = 490.75$; d(calc.) = 3.51	*X-ray powder diffraction data; IR, NIR and Vis absorption spectra; magnetic susceptibility data* (Karbowiak and Drożdżyński, 1993)

Table 5.25 (*Contd.*)

Formula	*Selected properties and physical data*[b]	*Lattice symmetry, lattice constants* (Å)*, conformation and density* (g cm^{-3})[c]	*Remarks regarding information available and references*
$CsUCl_4 \cdot 3H_2O$	brown-green; soluble in polar organic solvents; $CsUCl_4 \cdot 3H_2O$; $\mu_{\mathrm{eff.}} = 3.39$ B.M., $C = 1.430$ emu·K·mole^{-1}, $\theta = -67.7$ K. Free ion and crystal-field parameters: $F^2 = 39876(58)$, $F^4 = 33279(77)$, $F^6 = 23598(68)$, $\zeta_{5f} = 1648.3(10.3)$; $\alpha = 26.2(4.3)$, $\beta = -889(38)$, $\gamma = 1131(94)$; $T^2 = 306$, $T^3 = 42$, $T^4 = 188$, $T^6 = -242$, $T^7 = 447$, $T^8 = 300$; $M^0 = 0.672$, $M^2 = 0.372$, $M^4 = 0.258$; $P^2 = 1216$, $P^4 = 608$, $P^6 = 122$; $B^2_0 = -411(46)$ / [–390], $B^2_2 = 614(45)$ / [573], Im$B^2_2 = 610(46)$ / [614], $B^4_0 =$ [–699], $B^4_2 =$ [–398], Im$B^4_2 =$ [–525], $B^4_4 =$ [–1039], Im$B^4_4 =$ [–49], $B^6_0 =$ [–1046], $B^6_2 =$ [–58], Im$B^6_2 =$ [794], $B^6_4 =$ [–119], Im$B^6_4 =$ [–173], $B^6_6 =$ [–27], Im$B^6_6 =$ [–691], *rms* = 34; $n = 77$	monoclinic; C^2_{2h}, $P2_1/m$., No. 11; $a = 7.116(1)$, $b = 8.672(2)$, $c = 8.071(2)$; $\beta = 99.28(3)$; $Z = 4$; $V = 956.96$; d(U–Cl) = 2.957(3×), d(U–O) = 2.552 (3×) (mean values); tricapped trigonal prism consisting of six Cl and three O atoms (representing the water molecules)	*single crystal diffraction data* (Krämer *et al.*, 1991); *synthesis, magnetic susceptibility data; IR, NIR and Vis low temperature absorption spectra; crystal-field analysis* (Karbowiak *et al.*, 1993, 2000)
$NH_4UCl_4 \cdot 3H_2O$	greenish-brown to brown; hygroscopic and air sensitive; IR (cm^{-1}): ν(U–OH$_2$, rocking) = 615sh, 590s; ν(U–OH$_2$, wagging) = 470s; ν(U–OH), stretching = 385, 290sh; ν(U–Cl), stretching = 266s, 232; ν(U–Cl–U), stretching or lattice = 172; δ(Cl–U–Cl), bending = 147, 128; ν(stretching and bending modes	monoclinic; $a = 13.7693$, $b = 8.8990$, $c = 7.8643$; $\beta = 95.65$; $Z = 4$; $V = 956.95$; d(calc.) = 3.12	*X-ray powder diffraction data; IR, NIR and Vis absorption spectra; magnetic susceptibility data* (Karbowiak and Drożdżyński, 1993)

	of coordinated water) = 1585, 1600; $\nu_4(NH_4)$ = 1404 vs; $\nu_2(NH_4)$ = 1670, $\nu_4+\nu_6(NH_4)$ = 1770, $2\nu_4-\nu_5(NH_4)$ = 2710, $\nu_1(NH_4)$ = 3040, $\nu_3(NH_4)$ = 3110vs. $\mu_{eff.}$ = 3.71 B.M. (75–300 K)^d; C = 1.7073 emu·K·mole^{-1}, $\theta = -54$ K		
UOCl	red; UOCl (cr): $\Delta_f G^o_m = -785.7$ (4.9)†, $\Delta_f H^o_m = -833.9(4.2)^\dagger$, S^o_m = 102.5 (8.4)†; $C^o_{p,m}$ = 71.0 (5.0)†. $\mu_{eff.}$ = 3.40 B.M. (240–300 K)^d; $\theta = -145$ K	tetragonal; D^7_{4h}, $P4/nmm$, No. 129; (PbFCl type of unit cell); a = 4.043, c = 6.882; Z = 2; CN = 9; d(U–Cl) = 2.373(2×), d(U–Cl) = 3.074(1×), d(U–Cl) = 3.150(4×)	*single crystal diffraction data* (Schleid and Meyer; 1988; Brown and Edwards, 1972); *IR and magnetic susceptibility data* (Levet and Noël, 1981); *photo-electron spectra* (Thibaut *et al*., 1982); *themodynamic data* (Grenthe *et al*., 1992; Guillaumont *et al*., 2003)
U(NH)Cl		tetragonal; D^7_{4h}, $P4/nmm$, No.129; a = 3.972(5), b = 3.972(5), c = 6.81 (1); Z = 2; V = 107.44; d(calc.) = 8.91	*crystallographic data* (Berthold, and Knecht, 1966)
$Cs_2U[Cl_9O_3(TaCl)_6]$		trigonal/rhombohedral; D^2_{3d}, $P\bar{3}1c$, No.163; a = 9.1824(5), c = 17.146(2); Z = 2; V = 1252.01; d(calc.) = 5.75	*structural and theoretical studies of bondings in the cluster* (Ogliaro *et al*., 1998)
UBr_3	reddish-brown; air sensitive; soluble in acetic acid, dimethylacetamid; density: 6.53 g cm^{-3}; m.p. = 835°C, b.p. = 1537°C UBr_3(cr): $\Delta_f G^o_m = -673.2$ (4.2)†, $\Delta_f H^o_m = -698.7$ (4.2)†, S^o_m = 192.98 (0.50)†; $C^o_{p,m}$ = 105.83 (0.50)†. UBr_3(g): $\Delta_f G^o_m = -408.1$ (20.5)†, $\Delta_f H^o_m = -371$ (20)†, S^o_m = 403.0 (15.0)†; $C^o_{p,m}$ = 85.2 (5.0)†. $\log p$(mmHg) = $-16420T^{-1} + 22.95 - 3.02 \log T$ (298–1000 K). $\log p$(mmHg) = $-15000T^{-1} + 27.54 - 5.03 \log T$ (1000–1810 K)	hexagonal, (UCl_3 type of structure), C^2_{6h}, $P6_3m$, No.176; a = 7.942(2), c = 4.441(2), (a = 7.9519, c = 4.448; Z = 2, CN = 9; d(calc.) = 6.54; d(U–Br) = 3.145 (3.150) to the three capping Br atoms, d(U–Br) = 3.062(3.069∼) to the six Br atoms at the prism vertices, d(Br–Br) = 3.652(3.663) at the trigonal prism face edge and d(U–U) = 4.441Å (4.448) along the c-direction. The face Br–U–Br angle is 73.21(73.3). Values in parentheses were taken from Krämer and Meyer (1989)	*X-ray single crystal data* (Levy *et al*., 1975; Krämer and Meyer, 1989); *magnetic susceptibility data*: (Jones *et al*., 1974); *thermodynamic properties* (Rand and Kubaschewski, 1963; Grenthe *et al*., 1992; Guillaumont *et al*., 2003); *NIR, Vis and UV absorption spectra; fused salt systems* (Sobczyk *et al*., 2003; Karbowiak *et al*., 2003a; Brown, 1979); *photoelectron spectra* (Thibaut *et al*., 1982)

Table 5.25 (*Contd.*)

Formula	*Selected properties and physical data*[b]	*Lattice symmetry, lattice constants* (Å)*, conformation and density* (g cm^{-3})[c]	*Remarks regarding information available and references*
	$\mu_{\text{eff.}} = 3.57$ B.M. (25–76K)[d]; $\theta = -54$ K, $T_N = 15$ K; $\mu_{\text{eff.}} = 3.29$ B.M. (350–483K)[d]; $\theta = 25$K, $T_N = 15$ K; Atomic and crystal-field parameters: $E_{\text{avg}} = 19213(74)$, $F^2 = 37796(265)$, $F^4 = 30940(313)$, $F^6 = 20985(315)$, $\zeta_{5f} = 1604(19)$; $\alpha = 27(8)$, $\beta = -823(54)$, $\gamma = 1647(168)$; $T^2 = 374(125)$, $T^3 = 29(34)$, $T^4 = 262(58)$, $T^6 = -258(77)$, $T^7 = 264(60)$, $T^8 = [300]$; $M^0 = [0.6630]$; $P^2 = 1707(89)$; $B_0^2 = 410(50)$, $B_0^4 = -452(86)$, $B_0^6 = -1637(77)$, $B_6^6 = 722(63)$; $n = 47$; $rms = 36.5$		
$UBr_3{\cdot}6H_2O$	red	monoclinic; $P2/n$; $a = 10.061$, $b = 6.833$, $c = 8.288$; $\beta = 92.99$; $V = 285.00$	*X-ray powder diffraction and thermal decomposition data* (Brown *et al.*, 1968)
K_2UBr_5	dark violet; Polar organic solvents; m.p. = 625°C – congruently; ν(U–Br) stretching vibrations (cm^{-1}): 110m, 124m, and 145s,br	orthorhombic; D_{2h}^{16}, *Pnma,* No. 62; $a = 13.328(1)$, $b = 9.2140(7)$, $c = 8.4337(5)$, $Z = 4$, $V = 1559.5(2)$; CN = 6; d(calc.) = 4.53	*X-ray powder diffraction data; magnetic data; NIR, Vis an UV absorption spectra* (Krämer *et al.*, 1993, 1994); *magnetic phase transitions* (Keller *et al.*, 1995); *IR and thermodynamic data* (Suglobova and Chirkst, 1978a; Fuger *et al.*, 1983); melting point diagrams (Vdovenko *et al.*, 1974a)
Rb_2UBr_5	violet; polar organic solvents; m.p. = 600°C – congruently; ν(U–Br) stretching vibrations (cm^{-1}): 111m, 124m, and 144s,br	orthorhombic; D_{2h}^{16}, *Pnma,* No. 62; $a = 13.670(1)$, $b = 9.3900(8)$, $c = 8.6046(4)$; $Z = 4$; $V = 1663.1(2)$. CN = 6	*X-ray powder diffraction data; magnetic data; NIR, Vis an UV absorption spectra* (Krämer *et al.*, 1994); *IR and thermodynamic data*:

			(Suglobova and Chirkst, 1978a; Fuger *et al*., 1983); melting point diagrams (Vdovenko *et al*., 1974a)
Cs_2UBr_5	violet; m.p. = 420°C, congruently; ν (U–Br) stretching vibrations(cm^{-1}): 110m, 124m, and 149s,br	rhombic; isostructural with Cs_2DyCl_5; $a = 15.79(4)$, $b = 9.85(5)$, $c = 7.90(1)$; $Z = 4$, CN = 6, d(calc.) = 4.85(4)	*X-ray powder diffraction data* (Volkov *et al*., (1987); *IR and thermodynamic data* (Suglobova and Chirkst, 1978a,b; Fuger *et al*., 1983); melting point diagrams (Vdovenko *et al*., 1974a)
Rb_3UBr_6	dark-violet; m.p. = 695°C, congruently	cubic; face centered; $a = 11.03(2)$, d(calc.) = 4.79	*X-ray powder diffraction data* (Vodovenko *et al*., 1974a).
Cs_3UBr_6	dark-violet; m.p. = 758°C, congruently;	cubic; face centered; $a = 11.51(2)$; d(calc) = 4.83	*X-ray powder diffraction data; thermodynamic properties* (Aurov and Chirkst, 1983)
K_2NaUBr_6	–	tetragonal; D^3_{4h}, $P4/nbm$, No. 125; $a = 10.81(1)$, $c = 11.30(1)$; $Z = 4$, d(calc.) = 4.09, d(exp.) = 4.04	*X-ray powder diffraction and thermodynamic data* (Aurov *et al*., 1983); *thermodynamic properties* (Aurov and Chirkst, 1983)
Cs_2NaUBr_6	–	P-cubic; T^6_h, $Pa3$, No. 205; $Z = 4$, $a = 11.439(2)$, d(calc.) = 4.44	*X-ray powder diffraction and thermodynamic data* (Aurov *et al*., 1983); *thermodynamic properties* (Aurov and Chirkst, 1983)
UOBr	$\mu_{eff.} = 3.67$ B.M. (250–300K)^d; $\theta = -140$ K	tetragonal; (PbFCl type of unit cell), D^7_{4h}, $P4/nmm$, No.129; $a = 4.063(1)$, $c = 7.447(2)$; CN = 9	*X-ray powder diffraction data; IR and magnetic susceptibility data* (Levet and Noël, 1981; *photoelectron spectra* (Thibaut *et al*., 1982)
$K_2UBr_5\cdot 2CH_3CN\cdot 6H_2O$	brown-red		*magnetic susceptibility data; decomposition; IR, NIR and Vis and UV absorption spectra* (Zych and Drożdżyński, 1991)
$Rb_2UBr_5\cdot CH_3CN\cdot 6H_2O$	blue-violet		*magnetic susceptibility data; decomposition; IR, NIR and Vis absorption spectra* (Zych and Drożdżyński, 1991)

Table 5.25 (*Contd.*)

Formula	*Selected properties and physical data*[b]	*Lattice symmetry, lattice constants (Å), conformation and density* (g cm^{-3})[c]	*Remarks regarding information available and references*
$(NH_4)[UBr_2\cdot(CH_3CN)_2\cdot(H_2O)_5]Br_2$	grayish-green to brown crystalline solid; air sensitive; soluble in organic solvents like methanol, ethanol, formic acid, dimethyl-formamide, tributhylphosphate etc. IR (cm^{-1}): $\nu(H_2O)$ with hydrogen bond character = 3325s,b; (3114s,b; 2952w); $\nu(CH_3)$ = 2921w; (2851w); combination band = 2307w; $\nu_s(C{\equiv}N)$ = 2273w; $\delta(HOH)$ = 1606m; $\delta_{as}(CH_3)$ = 1399s; (1378s); $\delta_s(CH_3)$ = 1189w, 1144w; $\delta(U{-}OH_2)$ = 1078w; $\rho(CH_3)$ = 1044w; $\nu(C{-}C)$ = 971w, 938w, 922w; $\rho(U{-}OH_2)$ = 887w, 770w,721w; $\omega(U{-}OH_2)$ = 663vs,b, 670vs,b, 400–590s,vb; $\nu(U{-}OH_2)$ = 387m, 306m; $\nu(UN_2)$ = 202m; $\nu(UBr_2)$ = 157m,b, 115sh; $\delta(UBr_2)$ = 82w; (62w, 59w,47w, 37w) Raman; $\nu_s(C{\equiv}N)$ = 2280m; $\delta(HOH)$ = 1631m;$\delta_{as}(CH_3)$ = 1415w; (1356m); $\delta_s(CH_3)$ = 1261w, 1186w; $\delta(U{-}OH_2)$ = 1123m; $\rho(CH_3)$ = 1063m; $\nu(C{-}C)$ = 952w, 826w;	orthorhombic; D_{2h}^{16}, *Pnma* No. 62; $a = 8.98(2)$, $b = 9.99(2)$, $c = 20.24(4)$; $Z = 4$; $V = 1816(7)$ Å^3; d(U–Br1) = 3.074(4) (2×), d(U–O1) = 2.538(12) (2×), d(U–O2) = 2.549(14) (2×), d(U–N1) = 2.517(30) (1×), d(U–N2) = 2.688(26) (1×), d(U–O3) = 2.652(20) (1×), d(calc.) = 2.74	*single crystal diffraction data; magnetic susceptibility data; IR, Raman, NIR, Vis and UV spectra; factor group analysis* (Zych *et al.*, 1993; Zych and Drożdżyński, 1990b)

	ρ(U–OH$_2$) = 729w; ω(U–OH$_2$) = 651w, 611w, 536w; ν(U–OH$_2$) = 536w, 455m,b, 326w; ν(UN$_2$) = 282w; ν(UBr$_2$) = 195sh, 149		
UI$_3$	black; extremely moisture sensitive, soluble: methanol, ethanol, ethyl acetate, dimethyl-acetamide, acetic acid; m.p. = 766°C; UI$_3$(cr): $\Delta_f G^o_m = -466.1\ (4.9)^\dagger$, $\Delta_f H^o_m = -466.9\ (4.2)^\dagger$, $S^o_m = 221.8\ (8.4)^\dagger$; $C^o_{p,m} = 112.1\ (6.0)^\dagger$; UI$_3$(g): $\Delta_f G^o_m = -198.7\ (25.2)^\dagger$, $\Delta_f H^o_m = -137\ (25)^\dagger$, $S^o_m = 431.2\ (10.0)^\dagger$; $C^o_{p,m} = 86.0\ (5.0)^\dagger$. $\mu_{\text{eff.}} = 3.65$ B.M. (25–200 K)^d; $\theta = -34$ K, $T_N = 3.4$K; $\mu_{\text{eff.}} = 3.31$ B.M. (350–394 K)^d; $\theta = 5$ K	orthorhombic; (TbCl$_3$ and PuBr$_3$ structure type); D^{17}_{2h}, *Cmcm*, No. 63; $a = 4.334(6)$, $b = 14.024(18)$, $c = 10.013(13)$; $Z = 4$. The coordination polyhedron is a bicapped trigonal prism the third capping Br$^-$ anion being withdrawn by bonding with another U atom; d(U–I1) = 3.165(12) (2×) and d(U–I2) = 3.244(8) (4×) (to the prism iodine atoms), d(U–I2) (2×) = 3.456(11) (to the cap iodine atoms), d(I2–I2) = 3.679(18) Å and d(U–U) = 4.328(5) Å. d(calc.) = 6.78	*X-ray single crystal and neutron diffraction data* (Zachariasen, 1948a; Levy *et al*., 1975; Murasik *et al*., 1981); *thermodynamic data* (Brown, 1979; Guillaumont *et al*., 2003); *e diffuse reflectance spectra* (Barnard *et al*., 1973); *magnetic data* (Dawson, 1951; Jones *et al*., 1974; Murasik *et al*., 1981; 1985)
UI$_3$·4CH$_3$CN	dark-brown	monoclinic; $a = 9.6168$, $b = 8.7423$, $c = 7.1858$; $\beta = 92.99$; $Z = 2$; $V = 603.31$; d(calc.) = 4.08; d(U–Il) = 3.165(12) (2×) and d(U–I2) (4×) = 3.244(8) (to prism iodines), d(U–I2) (2×) = 3.456(11) (to cap iodine atoms), d(I2–I2) = 3.679(18) and d(U–U) = 4.328(5) Å	*X-ray powder diffraction data; magnetic susceptibility data; IR, NIR, Vis and UV absorption spectra* (Drożdżyński and du Preez, 1994)
UI$_3$(THF)$_4$	dark-purple	monoclinic; C^5_{2h}, $P2_1/c$; No. 14; $a = 8.750(3)$, $b = 16.706(16)$, $c = 17.697\ (16)$; $\beta = 93.64(3)$; $Z = 4$; $V = 2582$	*synthesis and reactivity; single crystal X-ray diffraction data; thermal gravimetric analysis; vibrational spectrum; ^{1}H NMR spectrum; electronic absorption spectrum* (Avens *et al*., 1994)

Table 5.25 (*Contd.*)

Formula	*Selected properties and physical data*[b]	*Lattice symmetry, lattice constants* (Å)*, conformation and density* (g cm^{-3})[c]	*Remarks regarding information available and references*
K_2UI_5	deep-blue	orthorhombic; D_{2h}^{16}, *Pnma*, No. 62; monocapped trigonal prisms [UCl_7] are connected via two opposite common edges to chains; CN = 6; $a = 14.293(1)$, $b = 9.8430(5)$, $c = 9.1067(5)$; $Z = 4$; $V = 1929.1(2)$; d(U–I) = 3.182 to 3.275; d(U–U) = 5.143 (interchain); d(U–U) = 7.778 (intrachain)	*X-ray powder diffraction data, magnetic data, NIR, Vis an UV absorption spectra, magnetic phase transitions* (Krämer *et al.*, 1994; Keller *et al.*, 1995); *low temperature absorption spectrum of* U^{3}*:*K_2LaI_5 (Andres *et al.*, 1996); *crystal-field analysis* (Karbowiak *et al.*, 1998a); *IR and thermodynamic data* (Suglobova and Chirkst, 1978)
Rb_2UI_5	blue-violet	orthorhombic; D_{2h}^{16}, *Pnma*, No.62; $a = 14.546(2)$, $b = 9.249(1)$, $c = 10.026(2)$; $Z = 4$; $V = 2031.1(5)$Å, CN = 6	*X-ray powder diffraction data; magnetic data; NIR, Vis and UV absorption spectra* (Krämer *et al.*, 1994); *IR and thermodynamic data* (Suglobova and Chirkst, 1978)
UOI	deep blue; $\mu_{\text{eff.}} = 3.56$ B.M. (220–300K)$^{d)}$; $\theta = -150$ K	tetragonal; (PbFCl type of unit cell), D_{4h}^{7}, *P*4/*nmm*; No. = 129; $a = 4.062(1)$, $c = 9.208(2)$; CN = 9	*X-ray powder diffraction data;IR and magnetic susceptibility data* (Levet and Noel, 1981)
$UBrCl_2$	black with a greenish tinge; m.p. = 800°C; $UBrCl_2$(cr): $\Delta_f G_m^o = -760.3(9.8)^{\dagger}$, $\Delta_f H_m^o = -812.1(8.4)^{\dagger}$, $S_m^o = 175.7(16.7)$		*thermodynamic data* (MacWood, 1958; Brown, 1979; Grenthe *et al.*, 1992; Guillaumont *et al.*, 2003)

UBr_2Cl	black with a greenish tinge; m.p. = 775°C; $UBr_2Cl(cr)$ $\Delta_f G^o_m = -714.4$ (9.8)[†], $\Delta_f H^o_m = -750.6$ (8.4)[†], $S^o_m =$ 192.5 (16.7)[†]	*thermodynamic data* (MacWood, 1958; Brown,1979; Grenthe *et al.*, 1992; Guillaumont *et al.*, 2003)
other mixed halides: (i) UCl_2I; (ii) $UClI_2$; (iii) UBr_2I; (iv) $UBrI_2$.	extremely moisture sensitive; (i) black, m.p. ~750; (ii) black, m.p. ~725; (iii) black, m.p. ~700; (iv) black, m.p. ~690	

---

[*] Estimated values.

[†] Values recommended by the Nuclear Energy Agency (Guillaumont *et al.*, 2003).

[a] Values have been selected in part from review articles (Brown, 1979; Bacher and Jacob, 1980; Freestone and Holloway, 1991; Grenthe *et al.*,1992; Guillaumont *et al.*, 2003).

[b] m.p. = melting point (°C); b.p.. = boiling point (°C); (cr) = crystalline; (g) = gaseous; thermodynamic values in kJ mol^{-1}, or J K^{-1} mol^{-1} at 298.15 K, unless otherwise mentioned; $\Delta_f G^o_m$, standard molar Gibbs energy of formation; $\Delta_f H^o_m$, standard molar enthalpy of formation; S^o_m, standard molar entropy; $C^o_{p,m}$(J K^{-1} mol^{-1}), standard molar heat capacity; log p (mmHg) = $-AT^{-1} + B - C \log T$: vapor pressure equation for indicated temperature range; IR = infrared active; lat. = lattice vibrations; val. = valence vibrations; def. = deformation vibrations; all values in cm^{-1}; vs: very strong; s: strong; m: medium; ms: medium strong; w: weak; sh: shoulder; b: broad; C, Θ, paramagnetic constants from the Curie Weiss law $C = \chi'_M(T\text{-}\Theta)$; $\mu_{eff} = 2.84\sqrt{C}$ - effective magnetic moment; T_N, ordering temperature; atomic and crystal-field parameters; F^k and ζ_{5f} = electrostatic and spin–orbit interaction; α, β, γ; = two-body correction terms; $T^i t_i$ (i = 2,3,4,6,7,8) = three-particle configuration interaction; M^j (j = 0, 2 and 4) = spin–spin and spin–other–orbit relativistic corrections; P^k (k = 2, 4 and 6) = electrostatically correlated spin-orbit perturbation; B^k_q, crystal-field parameters; values in brackets indicate parameter errors; parameters in square brackets were kept constant during the final fitting procedure; standard deviation: $rms = \sum_i \left[(\Delta_i)^2/(n-p)\right]^{1/2}$ [cm^{-1}], where Δ_i is the difference between the observed and calculated energies, n is the number of levels fitted and p is the number of parameters freely varied.

[c] All values are in Å and angles are in degrees; d, density [g cm^{-3}]; CN, coordination number, V = molar volume [cm^3 mol^{-1}].

[d] Temperature range with linear relationship of χ_M^{-1} against T.

spectra of co-doped (U^{4+},U^{3+}):Ba_2YCl_7 single crystals has been also reported (Karbowiak *et al.*, 2003c) Efficient luminescence was observed at 7 K from both the $^4G_{7/2}$ and $^4F_{9/2}$ levels of the U^{3+} ions and from the $^1D_2$ and $^1I_6$ levels of U^{4+}. For the U^{4+}ions a very strong anti-Stokes emission was noticed due to energy transfer processes. Contrary to U^{4+} for which emission was observed even at room temperature the emission of U^{3+} ions is strongly quenched by temperature. Owing to the presence of U^{3+} and U^{4+} ions in the host crystal, an energy transfer between these ions has been proved. Analyses of the nephelauxetic effect and crystal field splittings of the K_2UX_5 (X = Cl, Br or I) series of compounds have also been reported (Karbowiak *et al.*, 1998a).

The absorption spectra of $NH_4UCl_4 \cdot 4H_2O$ and $CsUCl_4 \cdot 3H_2O$ recorded at 298 and 4.2 K, presented in Fig. 5.38 (Karbowiak *et al.*, 2000) are typical for most uranium(III) compounds. In the 4000–15800 cm^{-1} region the spectra consist of relatively intense, sharp, and well-separated absorption lines.

A comparison of the spectra shows significant differences in the visible range connected with the appearance of strong and broad f–d bands, allowed by the Laporte rule. For $CsUCl_4 \cdot 3H_2O$ the first f–d bands are located at about 23000 cm^{-1}, while in $NH_4UCl_4 \cdot 4H_2O$ they are shifted about 5000 cm^{-1} toward the infrared region. For the isostructural series of complex halides of the composition U^{3+}:K_2LaX_5 (X = Cl, Br, I), the substitution of the Cl^- by I^- results in a significantly smaller shift of about 1000 cm^{-1} (Karbowiak *et al.*, 1998a). Drożdżyński (1985, 1991) and Karbowiak *et al.* (1996c) report a close relationship between the increase of covalence/decrease of the uranium–halogenide distances, and the red shift of the first intense f–d bands. The crystal-field symmetry is another factor, which can influence the position of the f–d bands. However, this seems to be a minor factor, since there is no simple dependence of the energy of the first f–d transition on the site symmetry of the U^{3+} ion. For example in K_2UCl_5 (C_s) and Cs_2NaUCl_6 (O_h) (Karbowiak *et al.*, 1998a,b) the first f–d transitions occur at similar energies of 14300 and 15000 cm^{-1}, respectively, while for UCl_3 (D_{3h}) they appear at 23000 cm^{-1} (Karbowiak *et al.*, 2002a). An extensive analysis of the $5f^3 \rightarrow 5f^2 6d^1$ transitions in low temperature absorption spectra of U^{3+} ions incorporated in various single crystals were reported by Seijo and Barandiran (2001), Karbowiak and Drożdżyński (2004) and Karbowiak (2005a,b). Temperature-induced line broadening and line shift measurements have been chosen as method for the determination of the electron–phonon coupling parameters for U^{3+} doped in K_2LaCl_5 (Ellens *et al.*, 1998), $LaCl_3$ and $LaBr_3$ single crystals (Karbowiak *et al.*, 2003d). The value of the electron–phonon coupling parameter, $\bar{\alpha}$, was found to be considerably lower in $LaCl_3$ than in K_2LaCl_5 but larger than that of Nd^{3+} in $LaCl_3$. The electron–phonon coupling is also stronger for U^{3+} in the tribromide as compared with the trichloride host; this has been attributed to a larger covalency of the first compound.

Intensity calculations of $5f^3 \rightarrow 5f^3$ transitions in tervalent uranium, based on the Judd–Ofelt theory were performed both for solution (Drożdżyński, 1978, 1984) and solid-state spectra (Drożdżyński and Conway, 1972, Karbowiak and

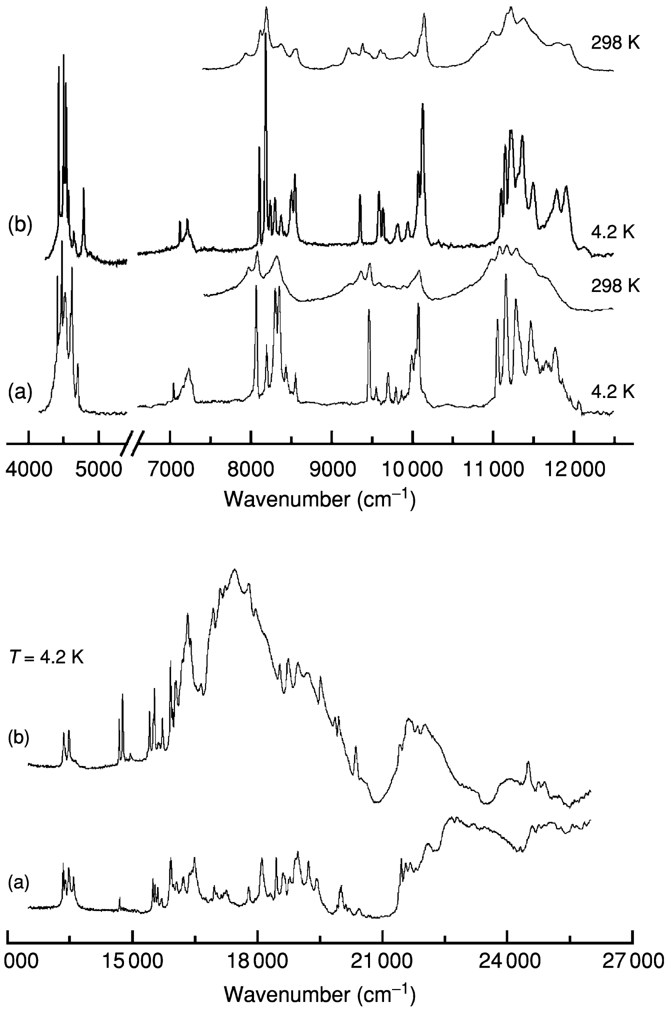

Fig. 5.38 *Absorption spectra of thin films of* $CsUCl_4 \cdot 3H_2O$ (*a*) *and* $NH_4UCl_4 \cdot 4H_2O$ *recorded at* 4.2 *and* 298 K (*from Karbowiak* et al., 2000 *reproduced by the permission of Elsevier*).

Drożdżyński, 2003). The analyses have shown a rather poor agreement between the observed and calculated oscillator strengths. So far, a relatively small r.m.s. deviation, of the order 10^{-6} to 10^{-7}, has been obtained only for the absorption spectra of UCl_3 in hexamethylphosphortriamide (Drożdżyński and Kamenskaya, 1978) and of UCl_3-doped $ZnCl_2$-based glass (Dereń *et al.*, 1998).

For almost all the halides and complex halides, magnetic susceptibility measurements were carried out over wide temperature ranges. The paramagnetic constants from the Curie–Weiss law $\chi'_{\mathrm{m}}. = C/(T - \theta)$ and the effective magnetic moments $\mu_{\mathrm{eff}} = 2.84\mu_{\mathrm{B}}$ were determined for a large number of compounds (see Table 5.25). The trihalides show remarkable cooperative effects, which were studied both experimentally (Murasik *et al.*, 1980, 1985, 1986) and theoretically (Łyżwa and Erdös, 1987; Plumer and Caillé, 1989). UCl_3 and UBr_3 undergo an unusual magnetic phase transition for actinide compounds. A one-dimensional, short-range magnetic order along the z-axis of the hexagonal lattice develops at about 15 K for UBr_3 and 22 K for UCl_3, which results from strong antiferromagnetic interactions between the nearest neighbors. A three-dimensional ordering appears in UBr_3 and UCl_3 when the uranium magnetic moments order to a '0+–' configuration in each plane perpendicular to the z-axis at $T_{\mathrm{N}} = 6.5$ and 5.3 K, respectively. At temperatures below $T_{\mathrm{t}} = 2.7$ K for UBr_3 and $T_{\mathrm{t}} = 2.5$ K for UCl_3 the magnetic moments exhibit smaller values and become oriented parallel to the equivalent x- or y-axis. The observed reorientation of the moments is reported to be rare in the actinide ions due to a usually strong anisotropy, which determines the direction of the moment (Santini *et al.*, 1999).

An extensive physical analysis of the magnetic interactions and magnetic ordering phenomena, as well as the crystal-field splitting in the K_2UX_5 (X = Cl, Br or I) series of compounds, were performed on the basis of the Ising model (Keller *et al.*, 1995). The application of elastic and inelastic neutron scattering experiments along with specific heat measurements made it possible to obtain a consistent picture of the magnetic phases. An analysis of the IR and Raman spectra of this series of compounds and of RbU_2Cl_7 is also available (Karbowiak *et al.*, 1996a; Hanuza *et al.*, 1999). Drożdżynski (1991) has summarized paramagnetic resonance measurements for U^{3+} ions substituted in CaF_2, SrF_2, and $LaCl_3$ single crystals. Some physical properties of tervalent uranium halides and related compounds are collected in Table 5.25.

(*i*) *Uranium trifluoride and uranium*(*III*) *fluoro complexes*

Uranium trifluoride

Uranium trifluoride is most conveniently prepared by reduction of UF_4 with metallic aluminum or finely powdered uranium. In the former case the reagents are placed in a graphite crucible and heated up to 900°C where the reaction proceeds smoothly and the excess of aluminum and by-products sublime from the reaction zone (Runnals, 1953). In the latter one, stoichiometric quantities of cleaned uranium turnings and UF_4 are placed in a nickel tube and heated to about 250°C in a stream of pure hydrogen (Warf, 1958). The finely divided UH_3 was decomposed at 400°C, after which the tube should be shaken in order to obtain an intimate mixture that was then heated to 700–900°C to give the pure trifluoride (Friedman *et al.*, 1970). The reduction with other metals such as Be, Mg, Ti, or Zr, as well as UN or U_2N_3, at 900–950°C has also been found suitable for the synthesis. The use of the nitrates has some technical advantages since they prevent the formation of corrosive by-products. Reduction with Li, Na, Cs, Mg, Ca, Sr, and Ba yields metallic uranium. The preparation of ultrapure UF_3 by reduction of UF_4 with hydrogen at 1020 to 1050 (± 20)°C has been reported by Berndt and Erdman (1973).

Uranium trifluoride is a gray to black solid. Separate crystals show a deep-violet color under the microscope. As compared to other uranium(III) compounds the trifluoride is remarkably stable on air at room temperature. At higher temperatures UF_3 oxidizes and at 900°C it is quantitatively converted into U_3O_8. The compound is thermally unstable even in an inert atmosphere and disproportionates to UF_4 and U at about 1000°C and to a smaller extent (0.1% per hour) also at 800°C. UF_3 is insoluble in water and cold aqueous acids but slowly undergoes oxidation. This proceeds with the formation of uranium(IV) and uranyl compounds at 100°C. UF_3 dissolves rapidly in nitric acid–boric acid mixtures. Chlorine, bromine, and iodine react to give UF_3X ($X = Cl$, Br or I).

UF_3 has the LaF_3-type structure but the symmetry is reported to be either trigonal (space group $P\bar{3}c1$, D_{3d}^4, No. 185) or hexagonal (space group $P6_3cm$, C_{6v}^3, No. 165). Two coordination numbers 9 and 11 are also taken into consideration (Taylor, 1976a). Both structures may be considered as distorted ideal polyhedra with a bimolecular hexagonal cell (space group $P6_3/mmc$) (Schlyter, 1953). The polyhedra are fully capped trigonal prisms in which fluorine atoms ($CN = 11$) are located on all corners and outside the two triangular and the three square boundary planes. The main difference between the different structures is a slight displacement of the atoms forming the prism and the atoms outside the triangular surfaces normal to *c*-axis (Taylor, 1976a). Other crystallographic data are listed in Table 5.25.

A good quality absorption spectrum of UF_3 was obtained by means of the teflon disk technique (Schmieder *et al.*, 1970) and in chlorinated naphthalene at 4.2 K (Drożdżyński and Karbowiak, 2005). For the latter data a crystal-field analysis has also been performed. There is a large shift of the L′S′J′ multiplets towards higher wave numbers, as compared with other U^{III} low-temperature spectra. Some absorption spectra were also recorded in fused-salt systems: LiF–Be_2, LiF–BeF_2–ZrF_4, and LiF–NaF–KF (Martinot, 1984).

The magnetic susceptibility of UF_3 has been measured between 2 and 300 K (Berger and Sienko, 1967) and between 293 and 723 K (Nguyen-Nghi *et al.*, 1964). For both temperature ranges a linear relationship of $1/\chi'_M$ vs T was reported. The effective magnetic moment of 3.67 BM is close to the free ion value.

Uranium trifluoride monohydrate and uranium(III) fluoro complexes

$UF_3 \cdot H_2O$ was prepared from an uranium(III) solution in 1 M HCl or in anhydrous methanol by precipitation with ammonium fluoride (Barnard *et al.*, 1973). The green gelatinous precipitate appears in the latter case to be brown after drying due to some U(IV) impurities. The hydrate is reported to be far more reactive than the anhydrous fluoride and is immediately oxidized in air, giving a pale green uranium(IV) substance. The compound was characterized by magnetic susceptibility measurements, but the results may not be reliable.

The formation of a number alkali fluorouranates(III) and complexes of UF_3 with ZrF_4 has been known for a long time (Bacher and Jacob, 1980). KUF_4, K_2UF_5, K_3UF_6, Rb_3UF_6, and Cs_3UF_6 were prepared by heating UF_4 and metallic uranium with the appropriate alkali fluoride at 1000°C (Thoma *et al.*, 1966). $NaUF_4$ and Na_2UF_5 were identified during investigations of the binary fused-salt system NaF–UF_3. Some of the complex fluorides were characterized by X-ray powder diffraction (Table 5.25) but more detailed information is still not available.

$UZrF_7$ was prepared by reduction of a mixture of UF_4 and ZrF_4, either with metallic zirconium or with metallic uranium at about 800°C; UZr_2F_{11} was identified in a systematic study of the $UZrF_7$–ZrF_4 binary system (Fonteneau and Lucas, 1974). The fluorides are not stable and slowly oxidize even at room temperature. The compounds were characterized by magnetic susceptibility measurements in the 100–300 K range and by X-ray powder diffraction analyses (Table 5.25).

(*ii*) *Uranium trichloride and uranium*(III) *complex chlorides*

Uranium trichloride

Uranium trichloride may be prepared by a number of methods (Brown, 1979; Drożdżyński, 1991). One of the most convenient is the action of gaseous hydrogen chloride on uranium hydride. Attractive alternative methods involve the reduction of uranium tetrachloride with zinc, metallic uranium, or uranium hydride.

$$UH_3 + 3HCl \xrightarrow{350^\circ C} UCl_3 + 3H_2$$

$$3UCl_4 + Al \xrightarrow{400^\circ C} 3UCl_3 + AlCl_3$$

Small amounts of pure UCl_3 may also be prepared by thermal vacuum decomposition of $NH_4UCl_4 \cdot 4H_2O$ (Drożdżyński, 1988a, 1991). The compound obtained by the latter method is reactive and tractable for synthetic purposes, in contrast to that obtained by reduction with metals.

Uranium trichloride is obtained either in the form of a fine olive-green powder or as dark-red crystals. It is not soluble in anhydrous organic solvents but it dissolves somewhat in glacial acetic acid, showing a characteristic transient red color. UCl_3 dissolves in polar organic solvents, provided the compound or the solvents have absorbed some gaseous hydrogen chloride before. In aqueous solutions it is more or less rapidly oxidized. UCl_3 reacts with chlorine to form a mixture of higher valence chlorides, and with bromine and iodine to yield $UBrCl_3$ and UCl_3I, respectively. The reaction with ammonia, acetonitrile, tetrahydrofuran (THF), and phenazine yields a number of unstable adducts.

UCl_3 is hygroscopic, but in contrast to other uranium halides no absorption of water is reported at p_{H_2O} less than 320 Pa (2.4 mmHg). It is a strong reducing agent both in solution and in solid state. Several metals such as calcium or lithium reduce UCl_3 to metallic uranium but the reaction has not been widely applied. UCl_3 melts at 837°C and disproportionates to U and UCl_4 at 840°C. A number of fused-salt systems containing UCl_3 have been investigated and the formation of some chloro complexes has also been reported (Bacher and Jacob, 1980).

Uranium trichloride has hexagonal symmetry (Zachariasen, 1948a,c; Murasik *et al.*, 1985; Schleid *et al.*, 1987) with the space group $P6_3/m - C_{6h}^2$. The coordination polyhedron is a symmetric tricapped trigonal prism arranged in columns in the *c*-direction. Each column is surrounded trigonally by three others at 1/2*c* in such a manner that the prism atoms of one chain become the cap atoms of the neighboring one. The packing view of UCl_3 along the [001] direction is shown on Fig. 5.39. The trichlorides Ac–Am and La–Nd have the same type of structure; some of the crystal data are listed in Table 5.25.

High-resolution polarized absorption spectra of $LaCl_3{:}U^{3+}$ single crystals (Karbowiak *et al.*, 2002) and unpolarized spectra of a polycrystalline UCl_3 sample in chlorinated naphathalene have been recorded at 4.2 K in the 4000–30000 cm^{-1} range (Sobczyk *et al.*, 2003). The experimental energy levels of the U^{3+} ion in the compounds were fitted to a semi-empirical Hamiltonian employing free-ion operators, one-electron crystal-field operators, and two-particle correlation crystal-field (CCF) operators, resulting in the determination of crystal-field parameters and the assignment/reassignment of the recorded $5f^3 \rightarrow 5f^3$ transitions. The effects of selected CCF operators on the splitting of

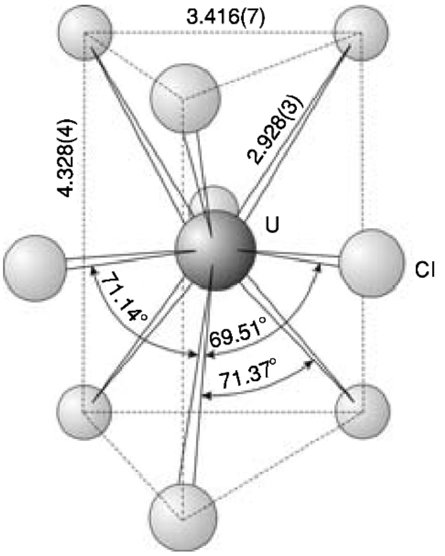

Fig. 5.39 *The tricapped trigonal prism configuration of halogen atoms in UCl_3 and UBr_3 (distances in Å are for UCl_3; after Murasik* et al., 1985).

some specific U^{3+} multiplets have also been investigated. The so far most accurate analysis of the band intensity, based on the Judd–Ofelt theory (Karbowiak and Drożdżyński, 2003), has been based on the obtained electronic wave functions and a room temperature absorption spectrum of UCl_3. A good agreement between the observed and calculated oscillator strengths has been obtained by combining the recorded band areas of some multiplets. In order to check the correctness of the calculations, the obtained intensity parameters, Ω_λ, have been used for the determination of transition probabilities and these in turn for the calculations of radiative lifetimes. A good-quality UCl_3 absorption spectrum has been obtained also by means of teflon disk technique (Schmieder *et al.*, 1970).

The magnetic properties of uranium trichloride have been the subject of extensive investigations (Santini *et al.*, 1999; Drożdżyński, 1991). The inverse magnetic susceptibility as a function of the temperature follows the Curie-Weiss law in two different temperature ranges and exhibits an antiferromagnetic transition at 22 K. Neutron diffraction studies revealed the existence of three-dimensional long-range anti-ferromagnetic ordering below the Néel temperature $T_N = 6.5K$ (Murasik *et al.*, 1981, 1985).

Uranium trichloride hydrates and hydrated uranium(III) chloro complexes

Two hydrates of UCl_3 are known, the heptahydrate, $UCl_3 \cdot 7H_2O$ and the hexahydrate, $UCl_3 \cdot 6H_2O$. The heptahydrate was obtained by reduction of an UCl_4 solution consisting of acetonitrile, propionic acid, and water (Drożdżyński, 1985) with liquid zinc amalgam in an inert atmosphere whereas the reduction is most conveniently accomplished in an all glass apparatus with provisions for precipitation, filtration, and drying in an inert gas atmosphere (Drożdżyński, 1979). It is interesting to note that a few years earlier Habenschuss and Spedding (1980) predicted the possible formation of this compound on the basis of ionic size considerations. $UCl_3 \cdot 7H_2O$ is a crystalline ink-blue solid, readily soluble in numerous organic solvents. The compound is relatively resistant to oxidation by air at temperatures lower than 15°C. At higher temperatures it loses some of its crystallization water and in high vacuum it may be completely dehydrated at 200°C (Drożdżyński, 1985).

X-ray single crystal analyses of the heptahydrate and of the less hydrated $UCl_3 \cdot 6H_2O$ compound have been reported (Mech *et al.*, 2005) (see Table 5.25). In the heptahydrate the crystals are built from separate $[U_2Cl_2(H_2O)_{14}]^{4+}$ units and Cl^- ions. The characteristic features of this structure are dimers, formed by two uranium ions connected through the (Cl1) bridging chlorine atoms. Whereas the basic units of the crystal structure of $UCl_3 \cdot 6H_2O$ are Cl^- anions and $[UCl_2(H_2O)_6]^+$ cations. The basic units of the crystal structure of $UCl_3 \cdot 6H_2O$ are Cl^- anions and $[UCl_2(H_2O)_6]^+$ cations. The U atom is eight-coordinated through six water molecules and two chlorine atoms. In this structure the characteristic feature is the existence of hydrogen bonds, which link the uranium eight-coordinated polyhedra, forming a three-dimensional network.

The presence of water molecules in the inner coordination sphere was also confirmed by the solid-state absorption spectrum of $UCl_3 \cdot 7H_2O$, which is very similar with that of the U^{3+} aquo ion (Drożdżyński, 1978) and exhibits significant differences in comparison to those of the less hydrated uranium(III) complex chlorides (Zych and Drożdżyński, 1986; Drożdżyński, 1988b). A detailed crystal-field level analysis, based on a very good quality low-temperature spectrum, is also available (Karbowiak *et al.*, 2001). The heptahydrate exhibits Curie–Weiss dependence in the temperature range 10 to 300 K. The derived magnetic moment $\mu_{\text{eff.}} = 2.95$ B.M. is much lower than the 'free ion' value of ca. 3.7 B.M., presumably due to the crystal field of the water molecules.

The synthesis and characterization of a number of hydrated complex chlorides of the formulas $MUCl_4 \cdot 5H_2O$ (Barnard *et al.*, 1972b), $MUCl_4 \cdot 4H_2O$ (M = K, Rb or NH_4) (Drożdżyński, 1988b; Karbowiak and Drożdżyński, 1993), $MUCl_4 \cdot 3H_2O$ (M = Cs, K, Rb, or NH_4) (Karbowiak and Drożdżyński, 1993, 1999), and $UCl_3 \cdot CH_3CN \cdot 5H_2O$ (Zych and Drożdżyński, 1986) have been reported.

The pentahydrates were prepared by shaking a U(III) solution in 11 M HCl with the appropriate halide MCl (M = K, Rb, or NH_4) at 0°C. The U^{III} solution was prepared either by dissolving $U_2(SO_4)_3 \cdot 8H_2O$ or by dissolving a uranium (III) double sulphate in 11 M HCl (Barnard *et al.*, 1972a). The preparation of the tetrahydrates can be achieved using a general route reported by Drożdżyński (1979). In this method the reduction of a solution of UCl_4, methyl cyanide, propionic acid, and water with zinc amalgam in anaerobic conditions generates an immediate precipitation of the tetrachlorouranate(III) tetrahydrate (Drożdżyński, 1988b). The formation of the pentahydrates has not been confirmed by X-ray investigations. Apart from some expected similarities between the compounds of the series, one can also note differences, e.g. that the tetrahydrates are reported to be readily soluble in dry methanol or ethanol, in contrast to the pentahydrates. The tetrahydrates are also much more resistant to oxidation and hydrolysis in dry air and temperatures below 15°C, and can be easily transformed into the anhydrous salts by thermal dehydration at high vacuum. One may note also a red shift of the $5f^3 \rightarrow 5f^3$ transitions and relatively large differences in the plots of the reciprocal susceptibilities as well as in the derived effective magnetic moments.

Structure investigations revealed that $(NH_4)UCl_4 \cdot 4H_2O$ belongs to the orthorhombic system, space group $P2_12_12$. The crystal is built up from separate $[U(H_2O)_4Cl_4]^-$ and NH_4^+ ions. The eight-coordinated U^{3+} polyhedra are connected by $O{-}H \cdots Cl$ hydrogen bonds forming a three-dimensional network (Karbowiak *et al.*, 1996c). X-ray powder diffraction patterns show that the other members of the series could also be indexed on the basis of the orthorhombic cell (Karbowiak *et al.*, 1996c). $(NH_4)UCl_4 \cdot 4H_2O$ is an excellent starting material for the preparation of numerous other uranium(III) compounds.

The $MUCl_4 \cdot 3H_2O$ series of compounds was also obtained by reduction of appropriate acetonitrile solutions of UCl_4 and MCl (where M = K, Rb, Cs, or NH_4) with liquid zinc amalgam, but using somewhat different conditions than those used to prepare the tetrahydrates (Karbowiak and Drożdżyński, 1993). In contrast to the deep purple-red colors of the penta- and tetrahydrates the latter ones show green to brown colors. In this series the first broad and strong $5f^3 \rightarrow 5f^2 6d^1$ bands were observed in the absorption spectra at wavenumbers higher than 21 000 cm^{-1}.

Single-crystal X-ray analysis is available for $CsUCl_4 \cdot 4H_2O$ (Krämer *et al.*, 1991). The compound crystallizes in the monoclinic system, space group: $P2_1/m$ (Table 5.25). Uranium has a coordination number of nine (tricapped trigonal prism) consisting of six chlorine atoms and three oxygen atoms (representing water) with mean distances of 2.957 and 2.552 Å, respectively. Cesium is surrounded by eight chlorine atoms in the shape of a distorted cube, which is capped by two non-bonded water ligands at a mean distance of 3.602 Å. One can view the structure as a linking of the polyhedra $[U(Cl1)_4(Cl2)_2(H_2O)_3]$ through two common edges of chloride (Cl1) ligands at two triangular faces of the trigonal prism of chloride ions to an infinite zigzag chain in the [010] direction. X-ray powder diffraction analyses show that the remaining three members of the series could be indexed on the basis of the same monoclinic cell, and that they presumably are isostructural.

For the tri- and tetrahydrates the first broad and strong $5f^3 \rightarrow 5f^2 6d^1$ bands are observed in the absorption spectra at about 21 500 and 16 000 cm^{-1}, respectively. The red shift of these bands has been attributed to the formation of inner sphere complexes with some of the uranium–ligand bond lengths of a markedly more covalent character than that of the U^{3+} aqua-ion, e.g. in $UCl_3 \cdot 7H_2O$ (Drożdżyński, 1991; Karbowiak *et al.*, 1996c). The magnetic susceptibility constants from the Curie–Weiss law are listed in Table 5.25.

Anhydrous uranium(III) chloro complexes

The largest group of well-characterized uranium(III) compounds is formed by chloro complexes such as $CsUCl_4$ (Karbowiak and Drożdżyński, 1998c), M_2UCl_5 (M = K, Rb, Cs. or NH_4) (Drożdżyński and Miernik, 1978; Meyer *et al.*, 1983), $SrUCl_5$ (Karbowiak and Drożdżyński, 1998b), $[(CH_3)_3N]_3UCl_6$ (Karbowiak *et al.*, 1996a); MU_2Cl_7 (M = K, Rb, Ph_4As or Ph_4P) (Drożdżyński, 1991; Karbowiak *et al.*, 1996b); Ba_2UCl_7 (Karbowiak *et al.* 1998d); M_2NaUCl_6 (M = K, Rb or Cs) (Aurov *et al.*, 1983; Volkov *et al.*, 1987), and Cs_2LiUCl_6 (Karbowiak and Drożdżyński, 1998a).

Most of the complex chlorides can be conveniently prepared by heating stoichiometric amounts of the component halides in graphite-coated quartz tubes. The $(NH_4)_2UCl_5$, $Ph_4AsU_2Cl_7$, and $Ph_4PU_2Cl_7$ compounds were obtained by reduction of appropriate uranium tetrachloride solutions in acetonitrile with liquid zinc amalgam (Drożdżyński, 1991; Drożdżyński and Miernik, 1978). Also the complexes with the general formulas M_2UCl_5 and MU_2Cl_7 can be prepared in this way (Drożdżyński, 1979). All the syntheses were carried out in an inert atmosphere or high vacuum of ca. 10^{-4} Pa. Spectroscopic studies and crystal-field analysis of U^{3+}:RbY_2Cl_7 and U^{3+}:Li_2NaYCl_6 single crystals were reported by Karbowiak *et al.* (1996b, 1977) and Karbowiak *et al.* (1996e, 1998b), respectively.

The formation of number of uranium(III) chloro complexes has also been observed during investigations of binary and ternary phase systems (Brown, 1979). The complexes display a variety of colors (Table 5.25). All of them are hygroscopic but are somewhat resistant to oxidation in dry air. Unlike UCl_3 the complex chlorides are readily soluble in numerous polar organic solvents.

K_2UCl_5 and Rb_2UCl_5 crystallize in the orthorhombic system and are isotypical with the K_2PrCl_5/Y_2HfS_5 structures, their space group is *Pnma*, $Z = 4$ (Krämer *et al.*, 1994). The coordination polyhedron is a monocapped trigonal prism [UCl_7], connected via two opposite common edges to chains, $[UCl1_{1/1}Cl2_{1/1}Cl3_{1/1}Cl4_{4/2}]^{-2}$, that run in the [010] direction of the unit cell. The relatively short U^{3+}–U^{3+} distance through the common edge, equal to 4.556 Å, is assumed to be responsible for antiferromagnetic transitions at 8.6 to 13.2 K. The temperature dependence of the inverse molar susceptibilities in the 20–300 K range follows the Curie–Weiss law in two temperature ranges, separated by a slight but apparent break at 130, 150, and 220 K, respectively, for K_2UCI_5, Rb_2UCl_5, and $(NH_4)_2UCl_5$. The effective magnetic moments range from 3.47 B.M. for $(NH_4)_2UCl_5$ to 3.99 B.M. for K_2UCI_5 (Drożdżyński and Miernik, 1978). Some other magnetic susceptibility constants determined from the Curie–Weiss law are listed in Table 5.25.

Solid-state electronic spectra of thin mulls of the compounds show all characteristic features of the uranium(III) complex anions with strong $5f^3 \rightarrow 5f^2 6d^1$ bands starting at ca. 18000 cm^{-1}. The complexes exhibit very similar far-IR spectra with one broad and not well-resolved band in the region 100–240 cm^{-1} assigned to U-Cl stretching modes. An analysis of magnetic phase transitions and crystal-field splittings in the K_2UX_5 (X = Cl, Br, or I) series of complex halides is reported by Keller *et al.*(1995).

Single-crystal X-ray data show that Cs_2NaUCl_6 (Spirlet *et al.*, 1988) crystallizes with the ideal cryolite arrangement. Each of the uranium or sodium ions is octahedrally surrounded by six chloride ions at the distance of 2.723(9) and 2.746(9) Å, respectively. The cesium ions (site symmetry T_d) are surrounded by 12 equidistant chloride ions with d(Cs–Cl) = 3.867(8) Å (for other data see Table 5.25). The enthalpies of formation of the hexachloro complexes are also available (Aurov and Chirkst, 1983; Schoebrechts *et al.*, 1989).

It is interesting to note the preparation of a reduced metallic uranium chloride which has been formulated as NaU_2Cl_6 or $(Na^+)(U^{3+})_2(e^-)(Cl^-)_6$ (Schleid and

Meyer, 1989). The extra electrons provided by the incorporation of the sodium atom are reported to occupy the 6d band of uranium. The compound is isostructural with $NaPr_2Cl_6$ and may be described as a stuffed derivative of UCl_3 (hexagonal symmetry, space group $P6_3/m$). Other available information about the compounds is compiled in Table 5.25.

Complexes of UCl_3 with neutral donor ligands

Ammonia adducts of the composition $UCl_3 \cdot 7NH_3$ and $UBr_3 \cdot 6NH_3$ were obtained by treatment of the halides with gaseous ammonia at room temperature and a pressure of 1013 hPa (Eastman and Fontana, 1958; Berthold and Knecht, 1965b, 1968). Since heating in a stream of nitrogen up to 45°C formed a relatively stable $UCl_3 \cdot 3NH_3$ complex, indicating that the compounds contain some loosely bound ammonia. At higher temperatures this adduct decomposes into $UCl_3 \cdot NH_3$, which is stable up to 300°C.

According to MacCordick and Brun (1970) the heating of UCl_3 with an excess of acetonitrile in sealed tube at 80°C results in the separation of a brown, hygroscopic solid of the formula $UCl_3 \cdot CH_3CN$. However, an attempt to repeat the preparation was unsuccessful (Barnard *et al.*, 1973).

A purple adduct of the composition $UCl_3(THF)_x$ has been prepared by reduction of a UCl_4 solution in THF with stoichiometric amounts of NaH or an excess of Na_2C_2. The obtained purple solution of $UCl_3(THF)_x$ is reported to be a useful starting material for numerous syntheses (Moody and Odom, 1979; Andersen, 1979; Moody *et al.*, 1982).

Hart and Tajik (1983) have reported the preparation of numerous air sensitive uranium(III) complexes with cyclic polyethers and aromatic diamines by reduction with liquid zinc amalgam in acetonitrile or acetonitrile/propionic acid solutions of UCl_4 and the appropriate ligand, e.g. $(UCl_3)_3$(benzo-15-crown-5)$_2 \cdot 1.5CH_3CN$ (yellow-orange), $(UCl_3)_3$(benzo-15-crown-5)$_2$ (deep red), UCl_3 (cyclohexyl-15-crown-5) (red-purple), $(UCl_3)_3$(18-crown-6)$_2$ (red-brown), $(UCl_3)_5$(dibenzo-18-crown-6)$_3$ (deep-red), $(UCl_3)_5$(*cis-syn-cis*-dicyclohexyl-18-crown-6)$_3$ (red), UCl_3(1,10 phenantroline)$_2$ (violet-purple) and UCl_3(2,2′-bipyridile)$_2$. The complexes are insoluble or react with common organic solvents. The preparation of several trivalent uranium complexes with crown ethers, oxygen donor or amine ligands has also been reported by other authors e.g. UCl_3(15-crown-5)(red), UCl_3(18-crown-6), UCl_3(benzo-15-crown-5) (red) by Moody *et al.* (1979, 1982), as well as $(UCl_3)_3$(18-crown-6)$_2$ (red-brown), $(UCl_3)_2$(2,2′-bipyridine)$_3$ (bright-green) and $(UCl_3)_2$(dimethoxyethane)$_3$ (brown) by Rossetto *et al.* (1982). All complexes are hygroscopic and more or less rapidly oxidized by atmospheric air. They exhibit some characteristic features of U(III) absorption spectra with very intense f–d transitions in the visible and/or ultraviolet region. Infrared data are indicative to decide if the coordination takes place through the ligand nitrogen or oxygen atoms. Some of the complexes have also been characterized by magnetic susceptibility measurements at 298 K (Hart and Tajik, 1983).

(*iii*) *Uranium tribromide and uranium*(*III*) *bromo complexes*

Uranium tribromide

Uranium tribromide can most conveniently be prepared by the reaction of uranium hydride with gaseous hydrogen bromide at 300°C. The method is also suitable for a large-scale preparation (Brown, 1979). Alternative methods include the reduction of UBr_4 by metallic zinc or finely divided uranium at about 600°C. Since UBr_3 reacts with quartz at that temperature, the reaction ought to be performed in a sealed tantalum or molybdenum vessel. In small quantities it may be readily prepared by thermal vacuum decomposition of $NH_4UBr_4 \cdot 5CH_3CN \cdot 6H_2O$ (Zych and Drożdżynski, 1990a). Other preparation procedures such as a direct combination of the elements or the reaction between uranium oxalate and gaseous hydrogen bromide seem to be less convenient (Brown, 1979).

UBr_3 is a dark-brown substance, much more hygroscopic and sensitive to oxidation in air than UCl_3. Rapid oxidation occurs on dissolution in water and in numerous organic solvents. It gives, however, somewhat more stable solutions in formamide, methyl acetate, dimethylacetamide, and acetic acid. Reactions with chlorine and bromine yield UCl_4 and UBr_4, respectively. UBr_3 is reduced by calcium to metallic uranium at high temperatures.

Uranium tribromide is isostructural with UCl_3. The unit cell data are given in Table 5.25. The interatomic distances of the tricapped trigonal prismatic coordination polyhedron obtained from neutron diffraction studies (Levy *et al.*, 1975) and by Krämer and Meyer (1989) (values in parentheses) are: d(U–Br) = 3.145 Å (3.150 Å) to the three capping Br atoms, d(U–Br) = 3.062 Å (~3.069 Å) to the six Br atoms at the prism vertices, d(Br–Br) = 3.652 Å (3.663 Å) at the trigonal prism face edge and d(U–U) = 4.441 Å (4.448 Å) along the c-direction.

Using low-temperature, high-resolution absorption and fluorescence spectra of UBr_3 doped into single crystals of $LaBr_3$ (Paszek, 1978) and K_2LaBr_5 (Karbowiak *et al.*, 1998a) a complete crystal-field analysis in the 4000–22000 cm^{-1} absorption range has been performed. Magnetic susceptibility measurements in the 4.5–483 K range show an antiferromagnetic transition at $T_N = (15 \pm 0.5)$ K. The effective magnetic moments equal to 3.92 and 3.57 B.M. have been determined from the temperature ranges where a plot of $1/\chi_M$ against T is linear.

Uranium tribromide hexahydrate

Uranium tribromide may be converted to the hexahydrate by controlled exposure to oxygen-free water vapor (Brown *et al.*, 1968). On prolonged pumping the obtained red-colored hexahydrate slowly loses most of the coordinated water until the composition approximates $UBr_3 \cdot H_2O$. Complete dehydration occurs with a slow and gradual increase of temperature to about 100°C. X-ray powder diffraction pattern shows that $UBr_3 \cdot 6H_2O$ is isostructural with the monoclinic lanthanide trihalide hexahydrates (Table 5.25). Further information is not available.

Uranium(III) bromo complexes

Bromouranates(III) of the composition M_2UBr_5 and M_3UBr_6 ($M = K$, Rb or Cs) have been identified during investigations of the binary fused-salt systems (Vdovenko *et al.*, 1974a; Volkov *et al.*, 1987). The pentabromouranates(III) may also be prepared by fusion of the appropriate components. Complexes of the M_3UBr_6 type are high-temperature phases and decompose on cooling into the alkali bromide and the corresponding pentabromouranate(III). The melting points and regions of existence of the hexabromouranates(III) increase with an increase in the atomic number of the alkali metal. An opposite tendency is observed in the series of pentabromouranates(III) (Vdovenko *et al.*, 1974a). Suglobova and Chirkst (1978a) have reported the thermodynamic properties of some of the bromo complexes.

X-ray powder diffraction analyses reveal that the hexabromouranates(III) have a face-centered cubic symmetry whereas the pentabromouranates(III) are isostructural with the rhombic Tl_2AlF_6. On this basis, it has been assumed (Suglobova and Chirkst, 1978b) that the structure of the pentabromouranates (III) contains distorted UBr_6 octahedra, which combine into parallel chains through common vertices. Aurov *et al.* (1983) and Aurov and Chirkst (1983) have reported X-ray powder diffraction and thermodynamic data for K_2NaUBr_6 and Cs_2NaUBr_6 by (Table 5.25).

A royal-blue $UBr_3(THF)_4$ adduct has been obtained by a gentle dissolution of uranium metal turnings in THF at a reaction temperature near 0°C (Avens *et al.*, 1994). The compounds $K_2UBr_5 \cdot 2CH_3CN \cdot 6H_2O$, $Rb_2UBr_5 \cdot CH_3CN \cdot 6H_2O$ and $(NH_4)[UBr_2(CH_3CN)_2(H_2O)_5]Br_2$ were obtained from acetonitrile solutions of UBr_4 and the appropriate ammonium or alkali metal bromide, by reduction with liquid zinc amalgam (Zych and Drożdżyński, 1990b, 1991; Zych *et al.*, 1993). All compounds are well characterized by various physical methods (Table 5.25). Single crystal X-ray data are available for $(NH_4)[UBr_2(CH_3CN)_2(H_2O)_5]Br_2$, (Zych *et al.*, 1993).

(*iv*) *Uranium(III) iodide and uranium(III) iodo complexes*

Uranium triiodide

A convenient and widely used method for the preparation of uranium triiodide involves the action of iodine vapors on finely divided uranium metal, either in sealed or flow systems at 570 and 525°C, respectively. Large quantities of high purity UI_3, in the form of black crystals, are collected in the 375–450°C condensing zone of a flow system apparatus first reported by Gregory (1958). Alternative procedures employ the reduction of uranium tetraiodide with zinc metal or finely divided uranium metal, reaction between uranium hydride and methyl iodide, and vacuum thermal decomposition of UI_4 at 225–235°C (Brown, 1979).

UI_3 is a jet-black, highly hygroscopic crystalline solid, sensitive to oxidation in air. Even at elevated temperatures the triiodide is corrosive and attacks glass, which at 800°C is reduced to silicon. The compound reacts with iodine, methylchloride, and uranium tetrachloride to yield UI_4, UCl_4, and $UClI_3$, respectively. UI_3 dissolves in aqueous solutions, methanol, ethanol, ethyl acetate, dimethylacetamide, and acetic acid forming unstable U(III) solutions. Spontaneous oxidation within 1 min was observed in organic solvents like dioxan, pyridine, acetonitrile, dimethylformamide, or acetone (Barnard *et al.*, 1973).

UI_3 possesses the orthorhombic $PuBr_3$-type structure (Zachariasen, 1948a). The structure (space group $Ccmm$ - D_{2h}^{17}) was studied in detail also by neutron diffraction profile analysis (Levy *et al.*, 1975; Murasik *et al.*, 1981). The coordination polyhedron is a distorted bicapped trigonal prism layered in planes perpendicular to the *a*-axis.

Diffuse reflectance spectra have been reported in the 4000–30000 cm^{-1} range at room temperature and 90 K (Barnard *et al.*, 1973). In the series of uranium (III) halides one may observe a pronounced red shift of the first $5f^3 \rightarrow 5f^2 6d^1$ bands from about 23000 cm^{-1} in the spectrum UF_3 to about 13400 cm^{-1} forUI_3.

Magnetic susceptibility measurements have shown an antiferromagnetic transition at $T_N = (3.4 \pm 0.2)$ K as well as a second susceptibility maximum at 1.5 K. UI_3 exhibits a first-order magnetic phase transition. The compound orders antiferromagnetically at $T_N = 2.6$ K, resulting in the appearance of a magnetic sublattice (Parks and Moulton, 1968). Neutron scattering investigations reveal hysteresis of the integretated neutron intensity of the magnetic reflections versus temperature, which confirms that the phase transition is of the first order (Murasik *et al.*, 1986).

Complexes with neutral donor ligands

The reaction of elemental iodine with an excess of oxide-free uranium metal turnings in appropriate coordinating solvents at 0°C yields dark purple $UI_3(THF)_4$, purple $UI_3(dme)_4$, black $UI_3(py)_4$ (Avens *et al.*, 1994), and a dark brown $UI_3(CH_3CN)_4$ (Drożdżyński and du Preez, 1994) (THF, tetrahydrofuran; dme, 1,2-dimethoxyethane; py, pyridine). These organic-solvent soluble Lewis base adducts are reported to be key starting materials for the preparation of variety of inorganic and organometallic uranium complexes. Single-crystal X-ray diffraction data show that $UI_3(THF)_4$ is mononuclear with a pentagonal bipyramidal coordination geometry about the uranium ion. Two iodide atoms, with an average U–I lengths of 3.111(2) Å are axially coordinated. The third iodide atom and the four THF ligands lie in the equatorial plane with the U–I distance of 3.167(2) Å and average U–O distances of 2.52(1) Å (Avens *et al.*, 1994). Other available information is listed in Table 5.25.

(*v*) *Uranium*(*III*) *oxide halides and mixed halides*

The uranium(III) oxide halides UOCI, UOBr, and UOI were prepared by heating stoichiometric mixtures of UO_2X_2, UO_2, and U or UX_4, U_3O_8 and U (X = Cl, Br or I), for 24 h at 700°C (Levet and Noël, 1981). The chemical properties of UOCI, UOBr, and UOI have not been reported.

The X-ray powder diffraction patterns are consistent with the tetragonal PbFCl-type of structure (*P*4/*nmm*). In a recent investigation, the structure was refined by single-crystal X-ray analysis and the atomic positions were determined (Schleid and Meyer, 1988). A plot of the inverse paramagnetic susceptibility against temperature follows the Curie–Weiss law from about 220 to 300 K with μ_{eff} of 3.40, 3.67, and 3.56 B.M. for UOCl, UOBr, and UOI, respectively. All of the oxide halides are weak ferromagnets with nearly the same transition temperatures ranging from 190 to 183 K. Some IR data are also available (Levet and Noël, 1981).

The preparation of a number of uranium(III) mixed halides with the general formulas UXY_2 and UX_2Y, where X = Cl or Br and Y = Cl or I were reported (Gregory, 1958), but very little information about their properties is available. $UClBr_2$ was obtained by reduction of UCl_3Br with hydrogen at 400°C. The UBr_3 by-product is removed from the substance by treatment with iodine. One of the most convenient methods for the preparation of UCl_2Br is reported to be the fusion of a 2:1 molar ratio of UCl_3 and UBr_3 at 850°C. The solid-state reaction between UCl_3 and UI_3 has been also applied successfully for the preparation of $UClI_2$. The remaining mixed halides, i.e. UCl_2I, UBr_2I, and $UBrI_2$ have usually been obtained by thermal decomposition of UCl_2I_2 and UBr_2I_2 at 400°C, and of $UBrI_3$ at 375°C (see also Table 5.25).

(b) Tetravalent halides and complex halides

Uranium tetrahalides and complex halides have so far been the most extensively investigated group of uranium compounds besides those in the 6+ oxidation state. The tetrahalides are not stable on exposure to air however with some exceptions, e.g. that of UF_4. They are more or less hygroscopic and after a time the compounds get oxidized in air. The large chemical stability of UF_4 is mainly due to its high lattice energy. Apart from the fluorides most of the compounds are readily soluble in polar solvents. Aqueous solutions are slowly oxidized to U(VI) species, but in pure and thoroughly deoxygenated solvents U^{4+} is fairly stable. The typical colors vary from pale olive green to deep bluish-green. In few cases black, brown, and blue colors have also been noticed (Table 5.26). The synthesis of binary uranium(IV) halides usually requires strictly oxygen-free conditions. The coordination polyhedra in the binary tetrahalides are more or less distorted forms of a square antiprism (UF_4), a dodecahedron (UCl_4), or a pentagonal bipyramid (UBr_4). The tetrahalides form stable solid complexes with a large variety of ligands, e.g. of the UX_4L_2-type (X = Cl. Br, or I)

Table 5.26 *Properties of selected uranium*(IV) *halides and complex halides.*[a]

Formula	*Selected properties and physical constants*[b]	*Lattice symmetry, lattice constants* (Å), *conformation and density* (g cm^{-3})[c]	*Remarks regarding information available and references*
UF_4	emerald green; non-volatile; almost insoluble in water and organic solvents; soluble in oxidizing solutions; m.p. = 1036°C; density: 6.70 g cm^{-3}; $\mu_{\mathrm{eff.}}$ = 3.28 B.M.; θ = –116 K (77–500 K)[d]; $\mu_{\mathrm{eff.}}$ = 2.83 B.M.; θ = –146 K (75–295K)[d]; $\mu_{\mathrm{eff.}}$ = 2.79 B.M; (1–300 K)[d] UF_4(cr): $\Delta_f G^o_m = -1823.5\ (4.2)^\dagger$, $\Delta_f H^o_m = -1914.2\ (4.2)^\dagger$, $S^o_m = 151.7\ (0.2)^\dagger$; $C^o_{p,m} = 116.0\ (0.1)^\dagger$. UF_4(g): $\Delta_f G^o_m = -1576.9\ (6.7)^\dagger$, $\Delta_f H^o_m = -1605.2\ (6.5)^\dagger$, $S^o_m = 360.7\ (5.0)^\dagger$; $C^o_{p,m} = 95.1\ (3.0)^\dagger$. $\log p$(mmHg) = $22.60 - 16400T^{-1} - 3.02 \log T$ (298–1309 K). $\log p$(mmHg) = $28.05 - 15300 \cdot T^{-1} - 5.03 \log T$ (1309–1755 K); IR (cm^{-1}): 404(s)[ν(U–F)]; 194 (s) [ν(F–U–F), bending]; Energy levels parameters (cm^{-1}): $F^2 = 44\,784$, $F^4 = 43\,107$, and $F^6 = 25654$; $\zeta_{5f} = 1761.0(3.4)$, $\alpha = 34.74$, $\beta = -767.3$, and $\gamma = 913.9$; $P^2 = 2715\ (94)$; $B^2_0 = 1183(28)$, $B^2_2 = 29(27)$, $B^4_0 = -2714(99)$, $B^4_2 = 3024(71)$, $B^4_4 = -3791(53)$, $B^6_0 = -1433\ (148)$,$B^6_2 = 1267(101)$, $B^6_4 = -1391\ (93)$ and $B^6_6 = 1755(82)$; *rms* = 31; $n = 69$	monoclinic; C^6_{2h}, *C*2/2, No. 15; a = 12.73 [12.7941], b = 10.753 [10.7901]; c = 8.404 [8.3687 90]; β = 126.33 [126.25]; [V = 931.68]; Z = 12; *d*(calc.) = 6.71], *d*(exp.) = 6.71; *d*(U–F) distances: 2.23–2.354. Antiprism linked in 3-dimensions by sharing all corners. Each uranium atom has eight fluorine neighbours arranged in a slightly distorted square antiprism. In square brackets are given the data of Kern *et al.*, (1994)	*synthesis* (Halstead *et al.*, 1982; Bacher and Jacob, 1980, Freestone and Holloway, 1990); *crystallographic data and temperature variation of structural parameters*, (Larson *et al.*, 1964; Keenan and Asprey, 1969; Kern *et al.*, 1994); *thermodynamic data* (Grenthe *et al.*, 1992; Guillaumont *et al.*, 2003); *magnetic data, IR, NIR; Raman spectra; Photo-acoustic spectra, ESCA spectra; redox reactions; applications for nuclear fuel* (Conway, 1959; Bacher and Jacob, 1980; *crystal-field spectra* (Carnall *et al.*, 1991); *Vis and UV spectra* (Conway, 1959; Bacher and Jacob, 1980); *photo-electron spectra* (Thibaut *et al.*, 1982)

Table 5.26 (*Contd.*)

Formula	*Selected properties and physical constants*[b]	*Lattice symmetry, lattice constants* (Å), *conformation and density* (g cm^{-3})[c]	*Remarks regarding information available and references*
$UF_4 \cdot 4/3H_2O$	grass-green	monoclinic; $d = 5.79$. The water molecules are bonded through O–H–F bridges	*crystallographic data* (Gagarinskii *et al.*, 1965; Khanaev *et al.*, 1967)
$UF_4 \cdot 2H_2O$	IR (cm^{-1}): 2950, 3365, and 3840	cubic; O_h^5, $Fm\bar{3}m$, No.225; $a = 5.701(0.012)$; d(calc.) = 6.32; $Z = 2$; d(U–U) = 2.465, d(F–F) = 2.846	*crystallographic data* (Dawson *et al.*, 1954; Bakakin, 1965), *NMR data* (Gabuda *et al.*, 1969)
$UF_4 \cdot 2.5H_2O$	slightly soluble in water (0.1g L^{-1}), soluble in dimethylammonium acetate; stable up to 100°C; $UF_4 \cdot 2.5H_2O$ (cr): $\Delta_f G_m^o = -2440.3$ (6.2)†, $\Delta_f H_m^o = -2671.5(4.3)^\dagger$, $S_m^o = 263.5(15.0)^\dagger$; $C_{p,m}^o = 263.7$ (15.0)†	orthorhombic; D_{2h}^{16}, *Pnam,* No.62; $a = 12{,}75$, $b = 11.12$, $c = 7.05$; d(calc.) = 4.74; $Z = 8$; d(U1–F) (5×) = 2.29; d(U1–O) (4×) = 2.63–2.84; d(U2—F) (9×) = 2.39	*crystallographic data* (Dawson *et al.*, 1954; Borisov and Zaniedporovski, 1971; Zadneporovskii and Borisov, 1971);*^{1}H-NMR, ^{19}F-NMR, IR data*, *thermodynamic data* (Bacher and Jacob, 1980; Grenthe *et al.*, 1992; Guillaumont *et al.*, 2003).
$UF_4 \cdot 7H_2O$		cubic; O_h^5, $Fm\bar{3}m$, No.225; $a = 5.65$ (1); $V = 180.36$; $Z = 2$; d(calc.) = 6.01	*crystallographic data* (Dawson *et al.*, 1954)
$LiUF_5$	dark-green; m.p. 605°C*	tetragonal; C_{4h}^6, $I4_1/a$; No.88; $a = 14.8592(96)$, $c = 6.5433(9)$; $Z = 16$; $V = 90.3$; d(calc.) = 6.23; the U atom is surrounded by nine F ions in a tricapped trigonal prismatic array. Adjacent prisms share edges and corners to form network	*crystallographic data* (Brunton, 1966; Keenan, 1966; Penneman *et al.*, 1973)

Li_3UF_7		tetragonal; D_{4h}^7, *P*4*nmn*, No.129; *a* = 6.132, *c* = 6.391	*crystallographic data* (Thoma and Penneman, 1965)
Li_4UF_8	m.p. = 496°C (incongr.)	orthorhombic; D_{2h}^{16}, *Pnma*; No.62; *a* = 9.960, *b* = 9.883, *c* = 5.986; *Z* = 4; *d*(calc.) = 4.71; *V* = 589.23; the coordination polyhedron is a triangular prism with pyramids on two of the prism faces; each U atom has 8 F^- neighbours at 2.29 (0.02) and a ninth at 3.30(0.03); CN. = 8	*crystallographic data; IR spectra* (Barton *et al.*, 1958; Brunton, 1967)
LiU_4F_{17}	yellowish-green or green square prism; 775°C*	*a* = 8.990, *c* = 11.387	*crystallographic data* (Jove and Cousson, 1977; Cousson *et al.*, 1977)
Li_2CaUF_8		tetragonal; D_{2d}^9, $I\bar{4}m2$, No. 119; *a* = 5.2290(12), *c* = 11.0130(18); *Z* = 2; *V* = 301.12; *d*(exp.) = 4.85, *d*(calc.) = 4.9.	*crystallographic data* (Védrine *et al.*, 1973; 1979)
Li_2CdUF_8		tetragonal; D_{2d}^9, $I\bar{4}$ (or $I\bar{4}m2$), No.119; *a* = 5.222(0.002), *c* = 10.952(0.005); *Z* = 2; *d*(exp.) = 4.85, *d*(calc.) = 4.86.	*crystallographic data* (Védrine *et al.*, 1973)
α-Na_2UF_6	blue; m.p. = 673°C; IR(cm^{-1}): *ν*(U–F) = 375(s); ν(F–U–F), bending = 192(s); 258(m), *ν*(Na–F) = 258(m); other: 146w	cubic; O_h^5, $Fm\bar{3}m$, No 225; *a* = 5.565(4); *Z* = 4; *V* = 172.34; *d*(calc.) = 5.11	*crystallographic data* (Zachariasen, 1948d; Mighell and Ondik, 1977)
$β_2$-Na_2UF_6		trigonal/rhombohedral; D_3^2, *P*321, No 150; *a* = 5.95(1), *c* = 3.7(1); *Z* = 1; *V* = 114.97; *d*(calc.) = 5.75; tricapped trigonal prism sharing ends to form chain	*crystallographic data* (Zachariasen, 1948d)

Table 5.26 (*Contd.*)

Formula	*Selected properties and physical constants*[b]	*Lattice symmetry, lattice constants* (Å), *conformation and density* (g cm^{-3})[c]	*Remarks regarding information available and references*
γ-Na_2UF_6	$\mu_{eff.} = 3.13$ to 3.23 B.M.; $\theta = -84$ to -89 K (14–300 K)[d]	orthorhombic; D_{2h}^{25}, *Immm*, No 71; $a = 5.56$, $b = 4.01$, $c = 11.64$; the coordination geometry in UF_9 chains is a tricapped trigonal prism (structure type of β_1-K_2UF_6)	*crystallographic data* (Zachariasen, 1948d; Mighell and Ondik, 1977); *magnetic data* (Bacher and Jacob, 1980)
δ-Na_2UF_6	m.p. = 648°C	hexagonal; C_3^1, *P*3, No.143; $a = 6.112(2)$, $c = 7.240(2)$; $Z = 2$; $V = 234.23$; d(calc.) = 5.64; in the asymmetric unit cell are two U ions; each has nine nearest F^- ions at the corners of capped trigonal prisms; d(U–F) ranges from 2.23 to 2.42(1)	*crystallographic data* (Brunton *et al.*, 1965; Cousson *et al.*, 1979)
Na_3UF_7	geenish-blue; m.p. = 629°C; $\mu_{eff.} = 3.40$ B.M.; $\theta = 290$ K (74–300 K)[d] or $\mu_{eff.} = 3.30$ B.M.; $\theta = 81$ K $\mu_{eff.} = 3.38$ B.M.; $\theta = 290$ K; (for 195–473 K range). IR (cm^{-1}): ν(U–F) = 380(s); ν(F–U–F), bending = 217(s); ν(Na–F) = 240 (m); other, 146w	tetragonal; D_{4h}^{17}, *I*4/*mmm,* No.139; $a = 5.488$, $c = 10.896$	*crystallographic data* (Zachariasen, 1948a; Mighell and Ondik, 1977); *magnetic data* (Bacher and Jacob, 1980)
NaU_2F_9	yellowish-green; m.p. = 660°C (dec.); IR (cm^{-1}): ν(U–F) = 360(s); ν(F–U–F), bending = 194(s); ν(Na-F) = 260(m); other, 145w		*IR data* (Ohwada *et al.*, 1972)

$Na_7U_2F_{15}$	green	orthorhombic; D_{2h}^{23}, *Fmmm*, No.69; $a = 17{,}7$, $b = 29.8$, $c = 12.7$	*crystallographic data* (Thoma *et al.*, 1963; Mighell and Ondik, 1977)
$Na_5U_3F_{17}$		cubic; $a = 5.589$	*crystallographic data* (Thoma *et al.*, 1963).
$Na_7U_6F_{31}$	green; m.p. = 718°C; IR(cm^{-1}): ν(U–F) = 383(s); ν(F–U–F), bending = 193(s); ν(Na–F) = 241(m)	rhombohedral; C_{3i}^{2}, $R\bar{3}$, No.148; $a = 14.72$, $c = 9.84$; $Z = 3$; $V = 615.5$ Å^3; CN = 8; isostructural with $Na_7Zr_6F_{31}$ in which the basic coordination geometry about central ion is approx. square antiprismatic, and six antiprisms share corners to form an octahedral cavity which encloses the additional F atom.	*crystallographic data* (Thoma *et al.*, 1963; Mighell and Ondik, 1977)
$NaKUF_6$		hexagonal; C_3^1, *P*3, No.143; $a = 6.24$, $c = 7.80$; $Z = 2$; *d*(calc.) = 5.23	*crystallographic data* (Brunton *et al.*, 1965)
$NaRbUF_6$	pale green, purple interference	hexagonal; C_3^1, *P*3, No. 143; $a = 6.29$, $c = 8.13$; $Z = 2$; *d*(calc.) = 5.49	*crystallographic data* (Brunton *et al.*, 1965); *optical data* (Bacher and Jacob, 1980)
α-K_2UF_6	green; $\mu_{eff.} = 3.45$ B.M.; $\theta = -108$K (74–300 K)^d; IR(cm^{-1}): ν(U–F)val. = 360s, 292s; ν(F–U–F)def. = 217sv; 161m, ν(F–U–F)def. or ν(K–F)lat. = 147m; ν(K–F)lat. = 84w	cubic with disordered cations; O_h^5, $Fm\bar{3}m$, No 225; $a = 5.946(1)$; $Z = 4$; $V = 210.22$; *d*(calc.) = 4.53	*crystallographic data* (Zachariasen, 1948d); *magnetic data* (Bacher and Jacob, 1980)
β_1-K_2UF_6	drab olive; m.p. = 755°C*; stable between 608 –and 755°C; below 608°C decomposes to K_3UF_7 + $K_7U_6F_{31}$	hexagonal; D_{3h}^3, $P\bar{6}2m$, No.189; $a = 6.5528(2)$, $c = 3.749(1)$; $Z = 1$; $V = 139.41$; *d*(calc.) = 5.1235; tricapped trigonal prisms share the triangular faces perpendicular to the three fold axis of the ideal polyhedron to form infinite chains	*crystallographic data* (Zachariasen, 1948a; Brunton, 1969a, Penneman *et al.*, 1973; Bacher and Jacob, 1980; *IR spectra* (Soga *et al.*, 1972)

Table 5.26 (*Contd.*)

Formula	*Selected properties and physical constants*[b]	*Lattice symmetry, lattice constants* (Å), *conformation and density* (g cm^{-3})[c]	*Remarks regarding information available and references*
β$_2$-K_2UF_6	green	hexagonal; D_3^2, $P321$, No.150; a = 6.54(2); c = 4.04; Z = 1; V = 150.02; d(calc.) = 4.76. tricapped trigonal prism sharing ends to form chain	*crystallographic data* (Zachariasen, 1948d); *IR spectra* (Soga *et al.*, 1972)
α-K_3UF_7	deep-green; m.p. = 957°C; IR (cm^{-1}): ν(U–F)val. = 362s; ν(F–U–F)def. = 206s; ν(F–U–F)def. or ν(K–F)lat. = 120m; ν(K–F)lat. = 80w	cubic; O_h^5, $Fm\bar{3}m$, No.225; a = 9.22 (2); Z = 4; V = 783.78, d(calc.) = 4.14; the seven F atoms are statistically distributed over fluorite lattice sites	*crystallographic data, IR spectra* (Zachariasen, 1954c; Burns and Duchamp, 1962; Bacher and Jacob, 1980); *IR spectra* (Soga *et al.*, 1972)
β-K_3UF_7		orthorhombic; D_{2h}^{13}, $Pmmn$, No.59 or $Pmn2_1$, C_{2v}^7, No. 31; a = 6.58, b = 8.31, c = 7.22	*crystallographic data* (Burns and Duchamp, 1962)
$K_7U_6F_{31}$	green; m.p. = 789°C (congr.); IR: ν(U–F)val. = 380s, 319m; 244sh, 200m; ν(F–U–F) def. = 244sh, 200m; ν(F–U–F) def. or ν(K–F) lat. = 153m, 114m; ν(K–F) lat. = 80w	rhombohedral; C_{3i}^2, $R\bar{3}$, No. 148; a = 9.376, α = 107.20; Z = 1; CN = 8; d(calc.) = 5.58; isostructural with $Na_7Zr_6F_{31}$; square antiprisms sharing corners, with one fluorine atom in a cavity	*crystallographic data, IR spectra* (Brunton *et al.*, 1965); *IR spectra* (Soga *et al.*, 1972)
KU_2F_9	green; m.p. = 765°C (incongr.) with formation of UF_6; IR (cm^{-1}): ν(U–F)val. = 360s, 331s, 290sh; ν(F–U–F) def. = 235m, 204m; ν(F–U–F)def. or ν(K–F)lat. = 160m, 148m, 118w; ν(K–F)lat. = 85w	orthorhombic; D_{2h}^{16}, $Pnma$, No 62; a = 8.7021, b = 11.4769, c = 7.0350; Z = 4; V = 702.61; CN = 9; d(calc.) = 6.4851; tricapped trigonal prism, sharing ends and edges; d(U–F) = 2.29–2.39	*X-ray powder diffraction and single crystal data, IR spectra* (Brunton *et al.*, 1965; Brunton, 1969b); *IR spectra* (Soga *et al.*, 1972)

KU_6F_{25}	metastable	hexagonal; D_{6h}^4, *P*6_3*/mmc,* No.194; $a = 8.18$, $c = 16.42$; *d*(calc.) = 6.73; $Z = 2$; tricapped trigonal prism, sharing edges and corners to form double rings of six polyhedra each	*crystallographic data* (Burton *et al*., 1965; Zachariasen, 1948d); *IR spectra* (Soga *et al*., 1972)
RbU_6F_{25}	deep-green; m.p. = 832°C (incongr. with formation of UF_4)	hexagonal; D_{6h}^4, *P*6_3*/mmc*, No.194; $a = 8.195$, $c = 16.37$; $Z = 2$; *d*(calc.) = 6.908; tricapped trigonal prism, sharing edges and corners to form double rings of six polyhedra each	*crystallographic data* (Mighell and Ondik, 1977; Brunton *et al*., 1965); *IR spectra* (Soga *et al*., 1973)
Rb_2UF_6	green; m.p. = 818°C (incongr)	orthorhombic; D_{2h}^{17}, *Cmcm*, No.63; $a = 6.958(2)$, $b = 12.042(5)$, $c = 7.605(5)$; $Z = 4$; $V = 637.21$; *d*(calc.) = 5.45; the structure is of the K_2ZrF_6 type and consists of infinitive chains of UF_8 polyhedra in the form of dodecahedra with triangular faces (ideal symmetry D_{2d})	*X-ray powder and single crystal diffraction data* (Kruse, 1971; Kruse and Asprey, 1962); *IR spectra* (Soga *et al*., 1973)
Rb_3UF_7	pale green; m.p. = 995°C (congr.)	cubic; O_h^5, $Fm\bar{3}m$, No.225; $a = 9.5667$; the seven F atoms are statistically distributed over fluorite lattice sites	*crystallographic data* (Bacher and Jacob, 1980); *IR spectra* (Soga *et al*., 1973)
$Rb_7U_6F_{31}$	green; m.p. = 675°C (incongr.)	rhombohedral; C_{3i}^2, $R\bar{3}$, No. 148; $a = 9.595$; $\alpha = 107.67$, $Z = 1$; CN = 8; *d*(calc.) = 6.02; structure type of $Na_7Zr_6F_{31;}$ square antiprisms sharing corners, with one fluorine atom in a cavity	*crystallographic data* (Burton *et al*., 1965; Thoma *et al*., 1958); *IR spectra* (Soga *et al*., 1973)

Table 5.26 (*Contd.*)

Formula	*Selected properties and physical constants*[b]	*Lattice symmetry, lattice constants* (Å), *conformation and density* (g cm^{-3})[c]	*Remarks regarding information available and references*
other complex fluorides with rubidium: $RbUF_5$ (green blue, m.p. = 735°C; IR(cm^{-1}):ν_{UF} = 370, 330, 302 cm^{-1}, RbU_3F_{13}, $Rb_2U_3F_{14}$ (m.p. = 722°C*)			*general properties* (Bacher and Jacob, 1980)
$CsUF_5$	greenish-blue (or sky blue); m.p. = 735°C.		
CsU_2F_9	deep-green crystals	monoclinic; C^6_{2h}, $C2/c$, No.15; a = 15.649(3), b = 7.087(1), c = 8.689 (2); β = 118·11(2); Z = 4, V = 849.98; CN = 8 1/2 (effective); d(exp.). = 6.4; d(calc.) = 6.09; tricapped trigonal prism, one prism corner statistically only half-occupied. Contains 8-coordinate U in edge-sharing polyhedra forming U_4F_{16} sheets	*crystallographic data* (Rosenzweig *et al.*, 1973)
CsU_6F_{25}	deep-green; m.p. = 867°C (incongr.) with formation of UF_4	hexagonal; D^4_{6h}, $P6_3/mmc$, No.194; a = 8.2424(4), c = 16.4120(20); Z = 2; V = 965.61; d(calc.) = 7; tricapped trigonal prism, sharing edges and corners to form double rings of six polyhedra each	*crystallographic data* (Brunton *et al.*, 1965, 1971)

Cs_2UF_6	greenish- blue to light blue; m.p. = 800°C*		*general properties* (Bacher and Jacob, 1980)
$Cs_2U_3F_{14}$	bluish-green; m.p. = 737°C (incongr.) with formation of $Cs_2U_3F_{14}$	monoclinic; C_{2h}^2, $P2_1/m$, No.11 or $P2_1$, C_2^2, No.4; $a = 8.39$, $b = 8.46$, $c = 20.88$; $\beta = 119.89°$	*crystallographic data* (Brunton *et al.*, 1965); *magnetic susceptibilities* (Bacher and Jacob, 1980)
Cs_3UF_7	pale blue; m.p. = 970°C	cubic; O_h^5, $Fm\bar{3}m$, No.225; $a = 9.90$; CN = 7; structure type of K_3UF_7; d(calc.) = 7.92.	*crystallographic data* (Penneman *et al.*, 1973; Brunton *et al.*, 1965)
α-NH_4UF_5	over 190°C decomposes partly to β-NH_4UF_5	rhombohedral; C_{3i}^2, $R\bar{3}$, No.148; $a = 9.55$; $\alpha = 107.4$	*crystallographic data* (Benz *et al.*, 1963; Penneman *et al.*, 1974); *magnetic susceptibilities* (Bacher and Jacob, 1980)
β-NH_4UF_5	polymeric	monoclinic; C_{2h}^5, $P2_1/c$, No.14; $a = 7.799(5)$, $b = 7.158(5)$, $c = 8.762 (7)$; $\beta = 116.45$; $Z = 4$; $V = 437.94$; d(calc.) = 5.32; CN = 9	*crystallographic data* (Penneman and Ryan, 1974) *magnetic susceptibilities* (Bacher and Jacob, 1980)
γ-$(NH_4)_2UF_6$	decomposes under He over 220°C to NH_4F+$(NH_4)_7U_6F_{31}$	orthorhombic; C_{2v}^2, $Pmc2_1$, No.26 or D_{2h}^5, $Pmcm$, No.51; $a = 4.05$, $b = 7.03$, $c = 11.76$; $Z = 2$; d(calc.) = 3.9	*crystallographic data* (Penneman *et al.*, 1964a); *magnetic and optical data* (Bacher and Jacob, 1980)
$(NH_4)_4UF_8$	deep green; over 130°C decomposes in air to NH_4F + $(NH_4)_2UF_6$	monoclinic; C_{2h}^6, $C2/c$, No.15; $a = 13.126$, $b = 6.692$, $c = 13.717$; $\beta = 121.32$; $Z = 4$; CN = 8; d(exp.) = 2.96; d(calc.) = 2.982; d(U–F) = 2.25–2.33; discrete distorted tetragonal antiprismatic array	*X-ray powder and single crystal data*; (Rosenzweig and Cromer, 1970); *thermodynamic data, magnetic and optical data* (Bacher and Jacob, 1980)
$NH_4U_3F_{13}$	decomposes in vacuum at 300–400°C to UF_4	orthorhombic; C_{2v}^2, $Pmc2_1$, No. = 26; $a = 8.045(2)$, $b = 8.468(2)$, $c = 7.375(2)$; $V = 502.42$; $Z = 2$; d(calc.) = 6.47	*crystallographic data* (Abazli *et al.*, 1980)

Table 5.26 (*Contd.*)

Formula	*Selected properties and physical constants*[b]	*Lattice symmetry, lattice constants* (Å), *conformation and density* (g cm^{-3})[c]	*Remarks regarding information available and references*
$(NH_4)_7U_6F_{31}$	m.p. > 150°C (dec.); under He gas to UF_4; exists in α, β, γ and δ forms	rhombohedral; C_{3i}^2, $R\bar{3}$, No.148; $a = 9.55$; $\alpha = 107.4$; CN = 8; square antiprisms sharing corners, with one fluorine atom in a cavity; structure type of $Na_7Zr_6F_{31}$.	*crystallographic data* (Benz *et al.*, 1963; Penneman *et al.*, 1964a); *thermodynamic data, magnetic and optical properties* (Bacher and Jacob, 1980)
$(NH_3OH)UF_5$		orthorhombic; D_2^1, $P222$, No.16; C_{2v}^1, $Pmm2$, No.25 or D_{2h}^1, $Pmmm$, No.47; $a = 10.963$, $b = 14.9024$, $c = 10.4391$	*crystallographic data* (Ratho *et al.*, 1969)
$N_2H_5UF_5$		orthorhombic; D_2^1, $P222$, or C_{2v}^1, $Pmm2$; $a = 7.941$, $b = 6.372$, $c = 7.478$; $Z = 4$	*crystallographic data* (Ratho and Patel, 1968); *thermodynamic data; magnetic susceptibilities; IR spectra, decomposition data.* (Bacher and Jacob, 1980)
$[N(C_2H_5)_4]_2UF_6$	white cryst.; air and moisture sensitive; IR (cm^{-1}):ν(U–F) = 405; $F^2 = 49699$, $\varsigma_{5f} = 1970$; $B_0^4 = 10\,067(113)$, $B_0^6 = 22(72)$; $rms = 67$		*general properties* (Ryan *et al.*, 1974); *electronic spectra, crystal-field parameters* (Wagner *et al.*, 1977)
other complex fluorides with hydrazinium: $(N_2H_5)_2UF_6$, $(N_2H_5)_3UF_7$			*general properties* (Bacher and Jacob, 1980)
$UN_{0.95}\,F_{1.2}$	uranium oxidation number = +4.05	tetragonal; D_{2h}^5, $P4/n$, No.85; $a = 3.951$ $c = 5.724$; $Z = 2$; $V = 89.35$; d(calc.) = 10.19	*crystallographic data* (Jung and Juza, 1973)

$Ca_{0.925}\,U_{0.075}\,F_{2.15}$		cubic; O_h^5; $Fm\bar{3}m$; No.225; $a = 5.507(3)$, $Z = 4$; $V = 167.01$; d(calc.) = 3.81	*neutron diffraction data* (Laval *et al.*, 1987)
$CaUF_6$	green; $\mu_{\text{eff.}} = 3.25$ B.M.; $\theta = -101$ (74–300 K)^d	hexagonal (LaF_3 type); D_{3d}^4, $P\bar{3}c1$, No.165; $a = 6.928$, $c = 7.127$; d(calc.) = 6.59	*crystallographic data* (Keller and Salzer, 1967) *magnetic data* (Bacher and Jacob, 1980)
$SrUF_6$		hexagonal (LaF_3 type); D_{3d}^4, $P\bar{3}c1$, No.165; $a = 7.122$, $c = 7.293$; d(calc.) = 6.83	*crystallographic data* (Keller and Salzer, 1967)
$BaUF_6$		hexagonal (LaF_3 type); D_{3d}^4, $P\bar{3}c1$, No.165; $a = 7.403$, $c = 7.482$; d(calc.). = 6.86	*crystallographic data* (Keller and Salzer, 1967)
$PbUF_6$	green	hexagonal (LaF_3 type); D_{3d}^4, $P\bar{3}c1$, No.165; $a = 7.245$, $c = 7.355$; d(calc.) = 8.33	*crystallographic data* (Keller and Salzer, 1967)
other complex fluorides with lead: $Pb_3U_2F_{14}$, Pb_6UF_{16}.			*general properties* Bacher and Jacob (1980)
$TlUF_5$	m.p. = 640°C	monoclinic; C_{2h}^5, $P2_1/c$; No.14; $a = 8.222(2)$, $b = 13.821(4)$, $c = 8.317(5)$; $\beta = 102.53(3)$; $Z = 8$; $V = 922.6$; d(calc.) = 7.74; tricapped trigonal prismatic at U	*infrared spectra* (Soga *et al.*, 1973); *crystallographic data* (Avignant *et al.*, 1980, 1982)
Tl_2UF_6	m.p. = 598°C (eutec.)	orthorhombic; $a = 4.07$, $b = 6.97$, $c = 11.56$; $Z = 2$; d(calc.) = 7.54	*crystallographic data* (Avignant and Cousseins, 1971)
Tl_3UF_7	m.p. = 542°C (incongr.)	cubic; $a = 9437$; $Z = 2$; $d = 7.92$	*crystallographic data* (Avignant and Cousseins, 1971)
Tl_4UF_8	m.p. = 317°C*		
$Tl_7U_6F_{31}$		hexagonal; $a = 15.39$, $c = 10.80$; $Z = 3$; d(calc.) = 7.74	*crystallographic data* (Avignant and Cousseins, 1977; Avignant *et al.*, 1977)
TlU_3F_{13}	m.p. = 674°C (incongr)	orthorhombic; $a = 8.49$, $b = 8.04$, $c = 7.38$.; Z = 2; d(calc.) = 7.68	*crystallographic data* (Avignant *et al.*, 1977)

Table 5.26 (*Contd.*)

Formula	*Selected properties and physical constants*[b]	*Lattice symmetry, lattice constants* (Å), *conformation and density* (g cm^{-3})[c]	*Remarks regarding information available and references*
TlU_6F_{25}		hexagonal; $a = 8.18$, $c = 16.46$; $d = 7.19$	*crystallographic data* (Avignant *et al.*, 1977)
$TlUO_3F_{11}$		monoclinic; C_s^3, *Cm*, No. 8; $a = 14.051(3)$, $b = 8.106(3)$, $c = 8.389(2)$, $\beta = 90.00(3)$; $Z = 4$; $V = 955.49$; d(calc.) = 7.95	*crystallographic data* (Hsini *et al.*, 1986)
YUF_7		monoclinic; $a = 8.19$, $b = 8.27$, $c = 11.17$; $\beta = 92.66$	*crystallographic data; magnetic properties* (Denes *et al.*, 1973)
$TmUF_7$		monoclinic; $a = 8.19$, $b = 8.27$, $c = 11.19$; $\beta = 92.73$	*crystallographic data; magnetic properties* (Denes *et al.*, 1973)
$YbUF_7$		monoclinic; $a = 8.18$, $b = 8.25$, $c = 11.20$; $\beta = 92.70$; d(calc.) = 6.93	*crystallographic data; magnetic properties* (Denes *et al.*, 1973)
$LuUF_7$		monoclinic; $a = 8.17$, $b = 8.24$, $c = 11.18$; $\beta = 92.48$	*crystallographic data; magnetic properties* (Denes *et al.*, 1973)
$CuU_2F_{10}\cdot 8H_2O$		orthorhombic; $a = 8.73$, $b = 7.16$, $c = 20.78$, $Z = 4$, d(calc.) = 4.48.	*crystallographic data* (Charpin *et al.*, 1968)
$ZnUF_6\cdot 5H_2O$		orthorhombic; $a = 14.34$, $b = 15.72$, $c = 8.05$; $Z = 8$; d(calc.) = 3.71	*crystallographic data* (Charpin *et al.*, 1969)
$MnUF_6\cdot 8H_2O$		monoclinic; $a = 12.37$, $b = 6.98$, $c = 8.06$; $\beta = 93.33$; $Z = 4$; d(calc.) = 4.41	*crystallographic data* (Charpin *et al.*, 1969)
$CoU_2F_{10}\cdot 5H_2O$		monoclinic; $a = 11.07$, $b = 7.10$, $c = 8.81$; $\beta = 94.17$; $Z = 2$; d(calc.) = 4.16	*crystallographic data* (Charpin *et al.*, 1968)
InU_2F_{11}		monoclinic; $a = 5.430$, $b = 6.407$, c = 8.402, $\beta = 104.62(4)$	*crystallographic data* (Champarnaud-Mesjard and Gaudreau, 1976)

$NiU_2F_{10}\cdot 8H_2O$		monoclinic; $a = 11.05$, $b = 7.08$, $c = 8.86$; $\beta = 93.33$; $Z = 2$; d(calc.) = 4.17	*crystallographic data* (Charpin *et al.*, 1968)
UOF_2	UOF_2(cr): $\Delta_f G^o_m = -1434.1\ (6.4)^\dagger$, $\Delta_f H^o_m = -1504.6\ (6.3)^\dagger$, $S^o_m = 119.2\ (4.2)^{\dagger.}$		*thermodynamic data* (Grenthe *et al.*, 1992; Guillaumont *et al.*, 2003)
$UO_2F_{0\cdot25}$	dark grey to black; mixed valence compound (U^{IV} and U^{V}); oxidation state 4.25	octahedral; fluorite type of structure; $a = 5.49$; $Z = 4$; d(exp.) = 11.0. One anion per unit cell is occupying inter-net places	(Kemmler-Sack, 1967, 1969)
$UOF_2\cdot H_2O$	$UOF_2\cdot H_2O$(cr): $\Delta_f G^o_m = -1674.5\ (4.1)^\dagger$, $\Delta_f H^o_m = -1802.0(3.3)^\dagger$, $S^o_m = 161.1(8.4)^\dagger$		*IR spectra* (Jacob and Bacher, 1980); *thermodynamic properties*, (Grenthe *et al.*, 1992; Guillaumont *et al.*, 2003)
UCl_4	light green needles or dark-green octahedra; m.p. = 590°C; b.p. = 789°C; density: 4.725 g cm^{-3}; $\mu_{eff.} = 3.29$ B.M.; $\theta = -65$ K (90 – 551 K)^d hygroscopic; soluble in polar organic solvents; insoluble in ethyl acetate, chloroform and benzene. UCl_4(cr): $\Delta_f G^o_m = -929.6\ (2.5)^\dagger$, $\Delta_f H^o_m = -1018.8\ (2.5)^\dagger$, $S^o_m = 197.200(0.8)^\dagger$; $C^o_{p,m} = 121.8\ (0.4)^\dagger$. UCl_4(g): $\Delta_f G^o_m = -789.4\ (4.9)^\dagger$, $\Delta_f H^o_m = -815.4\ (4.7)^\dagger$, $S^o_m = 409.3\ (5.0)^\dagger$; $C^o_{p,m} = 103.5\ (3.\ 0)^\dagger$ $\log p$ (mmHg) $= -11350T^{-1} + 23.21 - 3.02 \log T$ (298–863 K) $\log p$(mmHg) $= -9950\ T^{-1} + 28.96 - 5.53 \log T$ (863–1062 K); IR and Raman vibrations(cm^{-1}): 311 (R), 270 (R, IR), 240 (R, IR),	tetragonal; D^{19}_{4h}, $I4_1/amd$, No.141; $a = 8.3018(4)$, $c = 7.4813(6)$, $Z = 4$; d(calc.) = 4.87; each uranium atom is bonded to eight chlorine atoms; the coordination polyhedron is a dodecahedron ($\bar{4}2m$); d(U–Cl) = 2.889(1) and 2.644(2) (4 times each); Cl–U–Cl angles: 3.141(8) and 3.540(1). The Cl–Cl approaches are 3.141(8), 3.097(8) and 3.540(1); structure refined data: $a = 8.3018(4)$, $b = 8.3018(4)$, $c = 7.4813(6)$; $V = 515.61$; d(calc.) = 4.89	*crystallograhic data* (Brown, 1979; Taylor and Wilson, 1973a); *structural transitions anticipating melting* (Bros *et al.*, 1987); *structure refinement* (Schleid *et al.*, 1987) *temperature absorption spectra, crystal-field energy level structure* (Malek *et al.*, 1986a,b); Brown, 1979; Hecht and Gruber, 1974; Clifton *et al.*, 1969; McLaughlin, 1962; Żołnierek *et al.*, 1984; *thermodynamic data* (Rand and Kubaschewski, 1963 ; Grenthe *et al.*, 1992; Brown, 1979; Guillaumont *et al.*, 2003); *magnetic properties* (Hendricks *et al.*, 1971; Dawson, 1951; Gamp *et al.*, 1983); *electrical and optical properties* (Brown, 1979); *IR and*

Table 5.26 (*Contd.*)

Formula	*Selected properties and physical constants*[b]	*Lattice symmetry, lattice constants* (Å), *conformation and density* (g cm^{-3})[c]	*Remarks regarding information available and references*
	172 (R), 153 (R, IR), and 102(R, IR); $\mu_{eff.} = 3.29$; $\theta = -62$ K Energy level parameters: $F^2 = 42561(235)$, $F^4 = 39440(634)$, and $F^6 = 24174(185)$; $\zeta_{5f} = 1805(8)$, $\alpha = 30.9(1)$, $\beta = -576(168)$; $B_0^2 = -903(151)$, $B_0^4 = 766(220)$, $B_4^4 = -3091(185)$, $B_0^6 = -1619(482)$ and $B_4^6 = -308(280)$. $F_2 = 172.6$, $F_4 = 38.79$, $F_6 = 2.565$; $M^0 = [0.99]$, $M^2 = [0.55]$ and $M^4 = [0.38]$; $P^2 = P^4 = P^6 = [500]$		*Raman spectra* (Bohres *et al.*, 1974); *photoelectron spectra* (Thibaut *et al.*, 1982)
$UCl_4(CH_3CN)_4$	grey-green cryst; soluble in CH_3CN; loses CH_3CN *in vacuo* >40°C; IR (cm^{-1}): ν(CN) = 2278; $\mu_{eff.} = 2.89$ B.M.; $\theta = -158$ K	monoclinic; C_{2h}^6, $C2/c$, No.15; $a = 14.677(4)$; $b = 8.452(2)$; $c = 13.9559(3)$; $\beta = 91.77(2)$; $Z = 4$; d(calc.) = 2.087; d(U–Cl) = 2.624(2) and 2.614(2); d(U–N) = 2.599(6) and 2.567(6). The U atom is eight-coordinated with a dodecahedral arrangement. The C atoms occupy the dodecahedral B sites and the N atoms the A site	*crystallographic data* (Cotton *et al.*, 1984; Van den Bossche *et al.*, 1986); *infrared data* (Kumar and Tuck, 1984)
Li_2UCl_6	m.p. = 448.8 °C ; IR (cm^{-1}): ν(U–Cl) = 232w, 258, 287w	hexagonal; D_{6h}^4, $P6_3/mmc$, No. 194; $a = 11.191(5)$, $b = 11.191(5)$, $c = 6.0365(1)$; $Z = 3$; $V = 654.72$; d(calc.) = 3.53	*crystal structure from multiphase powder neutron profile refinement* (Bendall *et al.*, 1983); *magnetic properties* (Trzebiatowski and Mulak, 1970); *thermodynamic data* Vdovenko *et al.*, 1974b; Fuger *et al.*, 1983)

Na_2UCl_6	m.p. = 445.6 °C; IR (cm^{-1}): ν(U–Cl) = 240w, 260, 286w	trigonal/rhombohedral; D_{3d}^3, $P\bar{3}m1$, No.164; $a = 11.8062(9)$, $b = 11.8062(9)$, $c = 6.3243(2)$; $Z = 3$; $V = 763.42$; d(calc.) = 3.24	*crystal structure from multiphase powder neutron profile refinement* (Bendall *et al.*, 1983); *magnetic properties* (Trzebiatowski and Mulak, 1970); *thermodynamic data* Vdovenko *et al.*, 1974b; Fuger *et al.*, 1983)
Rb_2UCl_6	IR (cm^{-1}):ν(U–Cl) = 267; 285w	trigonal; D_{3d}^5, $R\bar{3}m$, No.166; $a = 7.34$, $c = 5.89$; d(calc.) = 3.68; each U atom is surrounded by six Cl atoms at the vertices of an octahedron	*crystallographic data* (Vdovenko *et al.*, 1972a); *magnetic properties* (Trzebiatowski and Mulak, 1970); *thermodynamic data* (Vdovenko *et al.*, 1974b; Fuger *et al.*, 1983)
α-Cs_2UCl_6	green crystals; m.p. = 670°C; IR and Raman data (cm^{-1}): $v_1 = 307$, $v_3 = 262$, $v_4 = 115$, $v_5 = 125$, $v_6 = 88$; Energy level parameters (T_d): $F_2 = 189.358$, $F_4 = 33.469$, $F_6 = 3.927$, $F^2 = 42605$, $F^4 = 36447$, $F^6 = 28909$; $\varsigma_{5f} = 1800.104$; $A_4^o\langle r^4\rangle = 901.381$ $A_6^o\langle r^6\rangle = 85.426$; $B_0^4 = 7211.0$, $B_4^4 = (4309)$ $B_0^6 = 1366.8$ $B_4^6 = (-2554)$; $rms = 163$; $n = 21$	trigonal; D_{3d}^5, $R\bar{3}m$, No 166; $a = 7.478$, $c = 6.026$; each U atom is surrounded by six Cl atoms at the vertices of an octahedron	*crystallographic data* (Siegel, 1956); *IR and Raman data* (Brown *et al.*, 1975; Brown, 1979); *crystal-field spectra* (Johnston *et al.*, 1966); *magnetic properties* (Trzebiatowski and Mulak, 1970); *thermodynamic data* Vdovenko *et al.*, 1974b; Fuger *et al.*, 1983)
β-Cs_2UCl_6	appears in a polymorphic transition at 510°C; IR and Raman data: $v_1 = 308$, $v_2 = 230$, $v_3 = 267$, $v_4 = 116$, $v_5 = 126$, $v_6 = 89$	trigonal; $a = 7.50$, $c = 12.00$; d(calc.) = 4.04; (for a rapidly quenched sample); for the refined structure: trigonal/rhombohedral; D_{3d}^3,$P\bar{3}m1$; No.164; $a = 7.5037(3)$, $b = 7.5037(3)$, $c = 6.0540(4)$; $Z = 1$; $V = 295.21$; 95.21	*crystallographic data* (Vdovenko *et al.*, 1972b); *structure refinement* (Schleid *et al.*, 1987) *IR and Raman data* (Shamir and Silberstein, 1975; Shamir *et al.*, 1975)
$Cs_2U[O_3Cl_9(Nb\ Cl)_6]$		trigonal/rhombohedral; D_{3d}^2, $P\bar{3}1c$, No.163; $a = 9.2080(7)$, $c = 17.0950(30)$; $Z = 2$; $V = 1255.25$; d(calc.) = 4.34	*crystal structure* (Cordier *et al.*, 1997)

Table 5.26 (*Contd.*)

Formula	*Selected properties and physical constants*[b]	*Lattice symmetry, lattice constants* (Å), *conformation and density* (g cm^{-3})[c]	*Remarks regarding information available and references*
$[N(CH_3)_4]_2UCl_6$	green cryst.; soluble in CH_3CN, H_2O; IR and Raman data (cm^{-1}): $\nu_1 = 284$, $\nu_2 = 230$, $\nu_5 = 123$, $\nu_6 = 87$	cubic face centered; $a = 13.06$; d(calc.) = 1.788, d(exp.) = 1.791	*crystallographic data* (Staritzky and Singer, 1952); *IR and Raman data* (Silberstein, 1972; Brown, 1979)
$[N(C_2H_5)_4]_2UCl_6$	green cryst.; soluble in CH_3CN, H_2O; crystals undergo reversible phase change at 94°C; IR and Raman data (cm^{-1}): $\nu_1 = 293$, $\nu_3 = 254$, $\nu_4 = 110$, $\nu_5 = 110$, $\nu_6 = 78$; $F^2 = 43170(2181)$, $\varsigma_{5f} = 1774(35)$; $B_0^4 = 7463(432)$, $B_0^6 = 992(258)$; *rms* = 168	orthorhombic; D_{2h}^{23}, *Fmmm*, No.69; $a = 14.23$, $b = 14.73$, $c = 13.33$; d(calc.) = 1.693	*crystallographic data* (Staritzky and Singer, 1952); *IR and Raman data* (Brown *et al.*, 1975; Brown, 1979); *electronic spectra, crystal-field parameters* (Wagner *et al.*, 1977)
$[P(C_6H_5)_3C_2H_5]_2UCl_6$		triclinic; C_1^1, $P\bar{1}$, No.2; $a = 10.53(1)$, $b = 10.95(1)$, $c = 10.31(1)$; $\alpha = 113.22(5)^\circ$, $\beta = 105.20(5)$, $\gamma = 80.40(5)$; $Z = 1$; d(calc.) = 1.631, d(exp.) = 1.64; d(U-Cl): = 2.621(2), 2.627(1) and 2.623(1)	*crystallographic data* (Caira *et al.*, 1978)
$UCl(H_2PO_2)_3(H_2O)_2$		orthorhombic; D_{2h}^{11}, *Pbcm*, No.57; $a = 7.559(2)$, $b = 10.111(2)$, $c = 14.680(2)$; $Z = 4$; $V = 1121.98$, d(calc.) = 2.99	*synthesis, structure, vibrational spectra* (Tanner *et al.*, 1992)
$UCl(PO_4)2H_2O$		tetragonal; C_{4h}^5, *I*4/*m*, No.87; $a = 14.631(2)$, $b = 14.631(2)$, $c = 6.662(1)$; $Z = 8$; $V = 1426.11$; d(calc.) = 3.77	*crystallographic data* (Benard-Rocherulle *et al.*, 1997)

other uranium(IV) chloro complexes: (i) $KUCl_5$; (ii) $RbUCl_5$; (iii) $CsUCl_5$, (iv) K_2UCl_6; (v) Cs_2UCl_6 (vi) Ag_2UCl_6; (vii) $KNaUCl_6$; (viii) $SrUCl_6$; (ix) $BaUCl_6$; (x) Rb_4UCl_8; (xi) KU_3Cl_{13}; (xii) $KNaUCl_6$; (xiii) CsU_2Cl_9; (xiv) $Cs_3U_2Cl_{11}$	(i) m.p. = 345°C* (ii) m.p. = 360°C* (iii) (iv) IR (cm^{-1}):ν(U–Cl) = 250w, 263, 286w (v) green cryst.; m.p. 670°C (vi) m.p. = 407°C; $\varDelta H^o_{fus}$ = 35.4 (2.1) (vii) (viii) m.p. = 560°C (ix) m.p. = 382°C* (x) m.p. = 406.3°C (xi) (xii) (xiii)		*thermodynamic and IR data* (Brown, 1979; Suglobova and Chirkst, 1978a, Vdovenko *et al.*, 1974b; Fuger *et al.*, 1983); *magnetic properties* (Brown, 1979)
$UOCl_2$	green; moisture sensitive; insoluble in organic solvents; soluble in H_2O; b.p.>400°C; $UOCl_2$(cr): $\varDelta_f G^o_m$ = –998.5 (2.7)†, $\varDelta_f H^o_m$ = –1069.3 (2.7)†, S^o_m = 138.32 (0.21)†; $C^o_{p,m}$ = 95.06 (0.42)†; paramagnetic $\mu_{eff.}$ = 3.13 B.M. (above 40 K); exhibits magnetic ordering below 31 K	orthorhombic; D^9_{2h}, *Pbam*, No.55; a = 15.255, b = 17.828, c = 3.992; d(U(1)–O) = 2.20–2.40; d(U(1)–Cl) = 2.66–3.15; d(U(2)–O) = 2.17–2.33; d(U(2)–Cl) = 2.88–3.01; d(U(3)–O) = 2.22–2.35; d(U(3)–Cl) = 2.70–3.51; the arrangement around U(1) is dodecahedral (CN = 8; 3O, 5Cl); that around U(2) is trigonal (CN = 7; 3O, 4Cl) and that around U (3) is approx. dodecahedral-1 (C.N. = 7; 3O, 4Cl)	*crystallographic data, neutron diffraction data* (Bagnall *et al.*, 1968; Taylor and Wilson, 1974a); *infrared spectra* (Bagnall *et al.*, 1968) *thermodynamic data* (Brown, 1979; Grenthe *et al.*, 1992;Guillaumont *et al.*, 2003); *magnetic properties, ir spectra* (Levet.and Noël, 1979); *photoelectron spectra* (Thibaut *et al.*, 1982)
UNCl		tetragonal; D^7_{4h}, *P*4/*nmm*, No.129; a = 3.979, c = 6.811; Z = 2; V = 107.83; d(calc.) = 8.85; d(exp) = 8.78. The compound is isostructural with PbFCl;	*crystallographic data* (Juza and Sievers, 1965; Juza and Meyer, 1969; Yoshihara *et al.*, 1971)

Table 5.26 (*Contd.*)

Formula	*Selected properties and physical constants*[b]	*Lattice symmetry, lattice constants* (Å), *conformation and density* (g cm^{-3})[c]	*Remarks regarding information available and references*
		d(U–Cl$_1$) = 3.17 (4×); d(U–N) = 2.30; d(Cl$_1$–Cl$_1$) = 3.98; d(Cl$_1$–Cl$_2$) = 3.23; d(N–Cl) = 3.29; d(N–N) = 2.81	
UClF$_3$	emerald green cryst.; m.p. = 444°C*; b.p. = 550–650°C (in vacuo subl.) UClF$_3$(cr): $\Delta_f G^o_m$ = –1606 (5.)†, $\Delta_f H^o_m$ = –1690 (5)†, S^o_m = 185.4 (4.2)†; $C^o_{p,m}$ = 120.9 (4.2)†	orthorhombic; *Abam* or C^{17}_{2v}, *Aba*2, No.41; a = 8.673(2), b = 8.69(1), c = 8.663(5); Z = 8; d(calc.) = 6.72	*crystallographic data* (Savage, 1956; Staritzky and Douglass, 1956); *thermodynamic data; fused salt system* (Brown, 1979; Grenthe *et al.*, 1992; Guillaumont *et al.*, 2003)
other chloride fluorides: (i) UCl$_2$F$_2$, (ii) UCl$_3$F.	(i) green; m.p. = 460°C*. UCl$_2$F$_2$(cr): $\Delta_f G^o_m$ = –1376(6)†, $\Delta_f H^o_m$ = –1466 (5)†, S^o_m = 174.1 (8.4)†; $C^o_{p,m}$ = 119.7 (4.2)†. (ii) m.p. = 530°C*; UCl$_3$F(cr): $\Delta_f G^o_m$ = –1147(5)†, $\Delta_f H^o_m$ = –1243 (5)†, S^o_m = 162.8 (4.2)†; $C^o_{p,m}$ = 118.8(4.2)†		*thermodynamic data; fused salt system* (Brown, 1979; Grenthe *et al.*, 1992; Guillaumont *et al.*, 2003)
UBr$_4$	brown to black-brown cryst; moisture sensitive; soluble in Me$_2$CO, EtOH; m.p. = 519°C; b.p. = 777°C; sublimes in a Br$_2$-N$_2$ stream. $\mu_{\text{eff.}}$ = 3.12 B.M; θ = –35 K; (77–569 K)[d] . UBr$_4$(cr): $\Delta_f G^o_m$ = –767.4 (3.5)†, $\Delta_f H^o_m$ = –802.1 (2.5)†, S^o_m = 238.5 (8.4)†; $C^o_{p,m}$ = 128.0 (4.2)†. UBr$_4$(g): $\Delta_f G^o_m$ = –634.6 (5.0)†, $\Delta_f H^o_m$ =	monoclinic; C^3_{2h}, *C*2/*m*, No.12; a = 10.92(2), b = 8.69(3), c = 7.05(1); β = 93.9(1); Z = 4; d(calc.) = 5.55, d(exp.) = 5.35. The Br anions form a pentagonal bipyramid around the U atom. The bipyramids are linked into two-dimensional sheets by double bromide bridging of the U cations. d(U–Br) = 2.85(2) to 2.95(2)	*synthesis* (Brauer, 1981) *crystallographic data* (Douglass and Staritzky, 1957; Taylor and Wilson, 1974d,e; Levy *et al.*, 1975; Korba, 1983); *thermodynamic data;* (Grenthe *et al.*, 1992; Guillaumont *et al.*, 2003); *magnetic data* (Dawson, 1951; Hendricks, 1971); *photoelectron spectra* (Thibaut *et al.*, 1982)

	–605.6 (4.7)†, S^o_m = 451.9 (5.0)†; $C^o_{p,m}$ = 106.9 (3.0)†. log*p* (mmHg) = –10800 T^{-1} +23.15–3.02 log*T* (298–792 K) log *p* (mmHg) = –8770 T^{-1} + 27.93 – 5.53 log*T* (792–1050 K); Energy level parameters: F_2 = 191, F_4 = 34, F_6 = 4, ζ_{5f} = 1976, $A(r^4)$ = –490 and $A(r^6)$ = –15 (in cm^{-1}); ν_{U-Br} = 233 cm^{-1} (vapor)	(in the pentagonal ring) and 2.78 (3) and 2.61(4) (to the apical bromides); the axial Br–U–Br angle = 177(1)°	
$[UBr(H_2O)_8]Br_3(H_2O)$		triclinic; C_i^1, $P\bar{1}$, No.2; *a* = 8.234 (4), *b* = 12.781(7), *c* = 7.168(2), α = 97.76(3), *β* = 98.36(2)° *γ* = 85.38(4); *Z* = 2; *V* = 738.07; *d*(calc.) = 3.24	*crystallographic data* (Rabinovich *et al.*, 1998)
Li_2UBr_6		trigonal/rhombohedral; D^2_{3d}, $P\bar{3}1c$; No = 163; *a* = 6.8896(4), *c* = 12.6465(9); *γ* = 120; *Z* = 2; *V* = 519.86	*crystallographic data; phase transitions by neutron diffraction* (Maletka *et al.*, 1998)
Na_2UBr_6	m.p. = 533°C; ν(U–Br)as. = 164w, 180, 202w	trigonal/rhombohedral; D^3_{3d}, $P\bar{3}m1$; No. = 164; *a* = 12.4368(1), *c* = 6.6653(2); *V* = 892.83; *Z* = 3	*crystallographic data* (Vdovenko *et al.*, 1973b; Bogacz *et al.*, 1980); *thermodynamic data* (Vdovenko *et al.*, 1973a, 1974c; Fuger *et al.*, 1983); *Visible and, IR data* (Brown, 1979; Suglobova and Chirkst, 1978)
K_2UBr_6	m.p. = 672°C; ν(U–Br)as. = 185, 208w	trigonal; *a* = 10.94, *c* = 10.67; *d*(calc.) = 4.11, *d*(exp.) = 4.12	*crystallographic data* (Vdovenko *et al.*, 1973b); *thermodynamic data* (Vdovenko *et al.*, 1973a, 1974c; Fuger *et al.*, 1983); *Visible and IR data* (Suglobova and Chirkst, 1978a; Brown, 1979)

Table 5.26 (*Contd.*)

Formula	*Selected properties and physical constants*[b]	*Lattice symmetry, lattice constants* (Å), *conformation and density* (g cm^{-3})[c]	*Remarks regarding information available and references*
Rb_2UBr_6	m.p. = 722°C*; ν(U–Br)as. = 192	cubic face centered; O_h^5, $Fm\bar{3}m$, No.225; $a = 10.94$; $V = 1309.34$. The U atoms are surrounded by an octahedral array of Br atoms at distances of 2.74; d(calc.) = 4.48, d(exp.) = 4.048	*crystallographic data* (Vdovenko *et al.*, 1973a; Maletka *et al.*, 1996b); *thermodynamic data* (Vdovenko *et al.*, 1973a, 1974c; Fuger *et al.*, 1983); *visible-near IR data* (Suglobova and Chirkst, 1978a; Brown, 1979)
Cs_2UBr_6	m.p. = 756°C; vibrational modes (cm^{-1}): ν_1(R) = 197, ν_2(R) = (155), ν_3(IR) = 195, ν_4 = (IR) = 84, ν_5(R) = 87, $L = 5$; $F_2 = 84.112$, $F_4 = 35.542$, $F_6 = 3.818$, $\zeta_{5f} = 1792.306$, $B_0^4 = 6593$, $B_0^6 = 1195$	cubic face centered; O_h^5, $Fm\bar{3}m$, No.225; $a = 11.07$; $V = 1356.57$. The U atoms are surrounded by an octahedral array of Br atoms at distances of 2.767; d(Br–Br) = 3.914; d(calc.) = 4.78, d(exp.) = 4.74	*crystallographic data*, (Vdovenko *et al.*, 1973a); *thermodynamic data* (Vdovenko *et al.*, 1973a, 1974c; Fuger *et al.*, 1983); *visible and IR spectral data* (Johnston *et al.*, 1966; Chodos, 1972; Suglobova and Chirkst, 1978a; Brown, 1979); *crystal-field analysis* (Johnston *et al.*, 1966)
UNBr		tetragonal; D_{4h}^7, $P4/nmm$, No.129; $a = 3.944$, $c = 7.950$; $Z = 2$; d(calc.) = 8.913; d(exp.) = 8.64; The compound is isostructural with BiOCl; d(U–Br) = 3.234; d(U–N) = 2.280	*crystallographic data*; (Juza and Meyer, 1969)
$[N(CH_3)_4]_2UBr_6$	vibrational modes (cm^{-1}): ν_3(IR) = 181; ν(U–Br) = 190–195	cubic face centered; O_h^5, $Fm\bar{3}m$, No.225; $a = 13.37$; d(calc.) = 2.405	*crystallographic data* (Brown, 1966)
$[N(C_2H_5)_4]_2UBr_6$	IR (cm^{-1}): ν(U–Br) = 178; energy level parameters: $F_2 = 181.63(12)$ (or $F^2 = 40867$), $\zeta_{5f} = 1756(41)$, $B_0^4 = 6946(609)$, $B_0^6 = 999(252)$; $rms = 176$		*IR and energy level analyses* (Brown, 1966; Wagner *et al.*, 1977)

$[P(C_6H_5)_3C_2H_5]_2UBr_6$		monoclinic; C^2_{2h}, $P2_1/m$, No.11; $a = 10.45(1)$, $b = 13.51(1)$, $c = 15.46(1)$; $\beta = 96.67(5)$; $Z = 2$; d(calc.) = 1.990, d(exp). = 1.96; d(U–Br): = 2.757(2), 2.776 (2) and 2.777(2)	*crystallographic data* (Caira *et al.*, 1978)
$[P(C_6H_5)_4]_2[UBr_6]\cdot 4CH_3CN$	green crystals; extremely sensitive towards oxygen and moisture	monoclinic; C^5_{2h}, $P2_1/c$, No.14; $a = 9.818(3)$, $b = 20.101(4)$, $c = 15.493(3)$, $\beta = 98.79(2)$; $Z = 2$; $V = 3022$; d(calc.) = 1.72; d(U–Br1) = 2.754 (1); d(U–Br2) = 2.778(1); d(U–Br3) or O = 2.768(1); Br(1)–U–Br(2) = 89.2(1); Br(1)–U–Br(3) (or O) = 90.4(1); Br(2)–U–Br(3) (or O) = 89.6(1).	*synthesis and crystallographic data* (Bohrer *et al.*, 1988)
$UBr(PO_2H_2)_3\cdot 2H_2O$		orthorhombic; D^{11}_{2h}, $Pbcm$, No. 57; $a = 7.488(5)$, $b = 10.192(2)$, $c = 15.203(5)$; $Z = 2$; $V = 1160.26$.	*X-ray crystallographic and spectroscopic structural studies* (Tanner *et al.*, 1993)
$UBr(PO_4)(H_2O)_2$		tetragonal; C^5_{4h}, $I4/m$, No.87; $a = 14.7480(7)$, $c = 6.6810(4)$; $V = 1453.14$; $Z = 8$; d(calc.) = 4.1.	*crystallographic data* (Benard-Rocherulle *et al.*, 1997)
$UBrCl_3$	greenish brown; hygroscopic; m.p. = 521°C; b.p. = 784°C; $UBrCl_3$(cr): $\Delta_f G^o_m = -893.5\ (9.2)^\dagger$, $\Delta_f H^o_m = -967.3\ (8.4)^\dagger$, $S^o_m = 213.4\ (12.6)^\dagger$	tetragonal; $a = 8.434$, $c = 7.690$	*thermodynamic data* (MacWood, 1958; Brown, 1979; Grenthe *et al.*, 1992; Guillaumont *et al.*, 2003)
UBr_2Cl_2	dark green; hygroscopic; m.p. = 510°C; b.p. = 1053 °C; UBr_2Cl_2 (cr): $\Delta_f G^o_m = -850.9\ (9.8)^\dagger$, $\Delta_f H^o_m = -907.9\ (8.4)^\dagger$, $S^o_m = 234.3\ (16.7)^\dagger$		*thermodynamic data* (MacWood, 1958; Brown, 1979; Grenthe *et al.*, 1992; Guillaumont *et al.*, 2003)
UBr_3Cl	greenish brown; hygroscopic; m.p. = 502°C; b.p. = 774°C UBr_3Cl(cr): $\Delta_f G^o_m = -807.1\ (9.8)^\dagger$, $\Delta_f H^o_m = -852.3\ (8.4)^\dagger$, $S^o_m = 238.5\ (16.7)^\dagger$		*thermodynamic data* (MacWood, 1958; Brown, 1979; Grenthe *et al.*, 1992; Guillaumont *et al.*, 2003)

Table 5.26 (*Contd.*)

Formula	*Selected properties and physical constants*[b]	*Lattice symmetry, lattice constants* (Å), *conformation and density* (g cm^{-3})[c]	*Remarks regarding information available and references*
$UOBr_2$	greenish yellow: $UOBr_2$(cr): $\Delta_f G^o_m = -929.6\ (8.4)^\dagger$, $\Delta_f H^o_m = -973.6\ (8.4)^\dagger$, $S^o_m = 157.57\ (0.29)^\dagger$; $C^o_{p,m} = 98.0\ (0.4)^\dagger$		*thermodynamic data* (Greenberg and Westrum, 1956; Rand and Kubaschewski, 1963; Brown, 1979; Grenthe *et al.*, 1992; Guillaumont *et al.*, 2003); *photoelectron spectra* (Thibaut *et al.*, 1982)
UI_4	black lustrous crystals; moisture sensitive; m.p. = 506°C; density: 5.6 g cm^{-3}; m.p. = 506°C; b.p. = 757°C; $\mu_{eff.} = 2.98$ B.M; (1–300 K)[d] . UI_4(cr): $\Delta_f G^o_m = -512.7\ (3.8)^\dagger$, $\Delta_f H^o_m = -518.3\ (2.8)^\dagger$, $S^o_m = 263.6\ (8.4)^\dagger$; $C^o_{p,m} = 126.4\ (4.2)^\dagger$. UI_4(g): $\Delta_f G^o_m = -369.6\ (6.2)^\dagger$, $\Delta_f H^o_m = -305.0\ (5.7)^\dagger$, $S^o_m = 499.1\ (8.0)^\dagger$; $C^o_{p,m} = 108.8\ (4.0)^\dagger$. $\log p\ (\text{mmHg}) = -12330\ T^{-1} + 26.62 - 3.52 \log T$ (298–779 K), $\log p\ (\text{mmHg}) = -9310\ T^{-1} + 28.57 - 5.53 \log T$ (779–1030 K): IR data (cm^{-1}): 178m, 165s, 132,s, 122m, 104vw, 92m, 55m	monoclinic; C^6_{2h}, $C2/c$, No. 15; $a = 13.967(6)$, $b = 8.472(4)$, $c = 7.510(3)$; $\beta = 90.54(5)$; $Z = 4$; $V = 888.7$; d(calc.) = 5.57. Close-packed hexagonal iodine atoms form zigzag chains of edge-sharing octahedra ($UI_2I_{4/2}$). d(U–I(1) bridging) = 3.08(2) and 3.11(2); d(U-I(2) terminal) = 2.92(2)(2×); d(U—U) = 4.55	*crystallographic and neutron diffraction data* (Levy *et al.*, 1980, Taylor, 1987); *thermodynamic data*; (Fuger and Brown, 1973; Brown, 1979; Guillaumont *et al.*, 2003)
Li_2UI_6		trigonal/rhombohedral; D^2_{3d}, $P\bar{3}1c$, No. = 163; $a = 7.3927(8)$, $c = 13.826(2)$; $V = 654.39$; $Z = 2$; d(U–I) = 3.013	*neutron diffraction and electrical conductivity data* (Maletka *et al.*, 1996a)

Na_2UI_6		trigonal/rhombohedral; C_{3i}^2, $R\bar{3}$, No.148; $a = 7.7001(6)$, $c = 20.526$; $Z = 3$; $V = 1053.97$; d(U–I) $= 2.992$	*crystallographic data* (Maletka *et al.*, 1992, 1995)
$EuUI_6$		monoclinic; C_s^4, Cc, No.9; $a = 8.006(4)$, $b = 12.998(5)$, $c = 15.194(5)$; $\beta = 106.2(1)$; $V = 1518.34$; $Z = 4$; d(U–I) $= 3.035$ to 3.218	*X-ray powder diffraction data* (Beck and Kuehn, 1995)
$BaUI_6$		monoclinic; C_s^4, Cc, No.9; $a = 8.845(5)$, $b = 13.834(7)$, $c = 15.753(8)$; $\beta = 107.5(1)$; $V = 1838.35$; $Z = 4$; d(U–I) $= 3.164$ to 3.241	*X-ray powder diffraction data* (Beck and Kuehn, 1995)
M_2UI_6 (M = $N(C_2H_5)_4$, $N(C_4H_9)_4$, $N(C_6H_5)(CH_3)_3$, $As(C_6H_5)_4$).	red; extremely moisture sensitive; soluble in anhydrous methyl cyanide and acetone; vibrational mode in (cm^{-1})UI_6^{2-}: $\nu_1 = 143$ to 156; $\nu_2 = 119$, $\nu_3 = 135$ to 143; $\nu_4 = 60$ to 65, $\nu_5 = 62$ to 66; $\nu_6 = 44$ to 47; energy level parameters for $[N(C_2H_5)_4]_2UI_6$: $F^2 = 38188\ (2422)$, $\zeta_{5f} = 1724(39)$, $B_0^4 = 6338(676)$, and $B_0^6 = 941\ (289)$		*electronic and IR spectra; crystal-field analysis; magnetic susceptibility data* (Wagner *et al.*, 1977; Brown, 1979)
UOI_2	rose-brown cryst; decomposes slowly at room temp; hygroscopic; soluble in H_2O; U–O vibrations (cm^{-1}): 520(w), 475(m), 420 (m), 280(w), and 250(sh); paramagnetic; $\mu_{\mathrm{eff.}} = 3.34$ B.M	orthorhombic; D_{2h}^9, $Pbam$, No.55; isostructural with $UOCl_2$ ($PaOCl_2$ struct. type); $a = 17.853(5)$, $b = 20.05(2)$, $c = 4.480(5)$	*crystallographic data; magnetic susceptibility data, infrared spectra* (Levet and Noël, 1979)
UNI		tetragonal; D_{4h}^7, $P4/nmm$, No.129; $a = 3.990$, $c = 9.206$; $Z = 2$;	*crystallographic data*; (Juza and Meyer, 1969)

Table 5.26 (*Contd.*)

Formula	*Selected properties and physical constants*[b]	*Lattice symmetry, lattice constants* (Å), *conformation and density* (g cm^{-3})[c]	*Remarks regarding information available and references*
		$V = 146.56$; *d*(calc.) = 8.58; *d*(exp) = 8.50; isostructural with BiOCl	
(i) UF_3I; (ii) $UClI_3$; (iii) UCl_2I_2; (iv) UCl_3I; (v) $UBrI_3$; (vi) UBr_2I_2; (vii) UBr_3I; (viii) UCl_2BrI; (ix) $UClBr_2I$.	(i) brownish black; (ii) black, m.p.<500°C; $UClI_3$ (cr): $\Delta_f G^o_m = -615.8\ (11.4)^†$, $\Delta_f H^o_m = -643.8\ (10.0)^†$, $S^o_m = 242\ (18)^†$; (iii) black, m.p.<500°C; UCl_2I_2 (cr): $\Delta_f G^o_m = -723.4\ (11.3)^†$, $\Delta_f H^o_m = -768.8\ (10.0)^†$, $S^o_m = 237\ (18)^†$; (iv) black, m.p.<490°C, UCl_3I(cr): $\Delta_f G^o_m = -829.9\ (8.8)^†$, $\Delta_f H^o_m = -898.3\ (8.4)^†$, $S^o_m = 213.4\ (8.4)^†$; (v) black, m.p.<500°C $UBrI_3$(cr): $\Delta_f H^o_m = -589.6\ (10.0)^†$;		*thermodynamic data*, (MacWood, 1958; Brown, 1979; Grenthe *et al.*, 1992; Guillaumont *et al.*, 2003)

(vi) dark, brown; m.p.<500°C
UBr_2I_2 (cr): $\Delta_f H_m^o = -660.4$
(10.0)[†];
(vii) dark brown, m.p. 478°C,
UBr_3I $\Delta_f H_m^o = -727.6$ (8.4)[†],
sublimes without decomposition;
(viii) black, m.p. < 500°C;
(ix) black, m.p. < 500°C.

---

[*] Peritectic decomposition point.

[†] Values recommended by the Nuclear Energy Agency (Guillaumont *et al.*, 2003) .

[a] Values have been selected in part from review articles (Brown, 1979, Bacher and Jacob, 1980; Freeman,1991; Grenthe *et al.*,1992; Guillaumont *et al.*, 2003);

[b] m.p. = melting point (°C); b.p(°C). = boiling point; (cr) = crystalline; (g) = gaseous; thermodynamic values in kJ mol^{-1}, or J $K^{-1}mol^{-1}$ at 298.15 K, unless otherwise mentioned; $\Delta_f G_m^o$, standard molar Gibbs energy of formation; $\Delta_f H_m^o$– standard molar enthalpy of formation; S_m^ostandard molar entropy; $C_{p,m}^o$, standard molar heat capacity; log p (mm Hg) = $-AT^{-1} + B - C \log T$: vapour pressure equation for indicated temperature range; IR = infrared active; L = lattice vibrations; val. = valence vibrations; def. = deformation vibrations; all values in cm^{-1}; s:strong; m: medium; w: weak; sh: shoulder; Energy levels parameters: F_k, F^k, ζ_{5f} = electrostatic and spin–orbit interaction parameters; α, β, γ; = two-body correction; M^j ($j = 0$, 2 and 4) = spin-spin and spin-other-orbit relativistic corrections; P^k = the electrostatically correlated spin-orbit perturbation parameters; B_q^k = crystal-field parameters; values in brackets indicate parameter errors; standard deviation: $rms = \sum_i \left[(\Delta_i)^2/(n-p)\right]^{1/2}$[$cm^{-1}$], where Δ_i is the difference between the observed and calculated energies, n is the number of levels fitted and p is the number of parameters freely varied.

[c] All values are in Å and angles are in degrees; CN, coordination number; d represents density in g cm^{-3}, V = molar volume [cm^3 mol^{-1}].

[d] Temperature range with linear relationship of χ_M^{-1} against T.

with arsine oxides or phosphine oxides (du Preez *et al.*, 1977b; du Preez and Zeelie, 1987).

Tetravalent uranium has a [Rn]$5f^2$ electronic configuration. The ground state is nominally $^3H_4$. The earlier studies of absorption spectra of tetravalent halides in the solid state, aqueous solutions, organic solvents, and in doped host crystals have been compiled in a review article by Carnall (1982). Krupa (1987) analyzed the spectroscopic properties of the ions in solids with their characteristic $5f^2 \rightarrow 5f^2$ transitions. In contrast to the uranium(III) spectra, the spin–orbit interactions in different compounds are of the same order of magnitude and the f–d transitions have been observed at higher energies beginning near 40000–45000 cm^{-1}. For a number of halides and complex halides, low-temperature absorption spectra have been recorded and the energy levels of the U^{4+} ion in different site symmetries were assigned and fitted to a semiempirical Hamiltonian representing the combined atomic and crystal-field interactions. An analysis of octahedral UX_6^{2-} spectra for a series of $(NEt_4)_2UX_6$ salts (X = F, Cl, Br or I) was reported by Wagner *et al.* (1977). The authors have noticed that the Slater parameter F^2 diminishes by ~20% for the series and the crystal-field parameters are different from those of the comparable octahedral PaX_6^{2-} and UX_6^{2-} halides. Analyses of the energy-level structure of U^{4+} ion doped in an isomorphic series of tetragonal ($I4_1/amd$) host crystals such as $ThSiO_4$, $ThCl_4$, and $ThBr_4$ (Delamoye *et al.*, 1983; Simoni *et al.*, 1988; Malek *et al.*, 1986a,b; Malek and Krupa, 1994) led to consistent sets of free ion and crystal-field parameters with a least square deviation (r.m.s.) between 36 and 71 cm^{-1}. In these host crystals, U^{4+} experiences a rather weak crystal field, which justifies the same theoretical approach as for the Ln^{3+} ions; this is in contrast to that in higher symmetry sites as found in $U(BD_4)_4/Hf(BD_4)_4$ (site symmetry T_d; Rajnak *et al.*, 1998), Cs_2UX_6 (X = Cl or Br) (site symmetry O_h; Johnston *et al.*, 1966; Satten *et al.*, 1983) or U^{4+}: $CsCdBr_3$ (disturbed O_h site symetry; Karbowiak *et al.*, 2005b) where the crystal field splitting is approximately twice as large with the r.m.s. deviation of 100 to 150 cm^{-1}. As a result, mixing of crystal field components of different multiplets in close proximity may occur. In an analysis of the absorption spectrum of Cs_2UBr_6 single crystals, Faucher *et al.* (1996) have shown that the inclusion of configuration interactions with the higher lying $5f^17p^1$ electronic configuration in the fitting procedure may considerably improve the r.m.s. deviation.

An analysis of (U^{4+}, U^{3+}):BaY_2Cl_7 single crystals (Karbowiak *et al.*, 2003b) enabled the assignment of 60 observed $5f^2 \rightarrow 5f^2$ transitions from absorption, excitation, and luminescence spectra, which encompasses all but the $^1S_0$ multiplet. A comparison of the scalar crystal field parameters,

$$N_v = \left[\sum_{k,2} (B_2^k)^2 \frac{4\pi}{(2k+1)} \right]^{1/2}$$

(Auzel and Malta, 1983), indicates that the main factor determining the crystal-field strength is not the nature of the ligand but the site symmetry of the central ion; this is in contrast to that for Ln^{3+} and U^{3+} ions. Energy transfer has been demonstrated between uranium ions in the 3+ and 4+ oxidations states. A very strong anti-Stokes emission was observed for the U^{4+} ions.

In all cases in which the uranium ions are occupying sites of inversion symmetry, as in UCl_6^{2-}, the observed band structure consists almost exclusively of vibronic side bands and their progressions could be used to deduce the electronic transitions. The analysis of absorption spectra of UF_4 in a KBr pellet at 4 K as well as of U^{4+}(aq.) at 298 K have been reported by Cohen and Carnall (1960) and Carnall *et al.* (1991). The authors have also compared the crystal-field interactions of UF_4, NpF_4, and PuF_4. The absorption spectrum of thin films of a mixture of UF_4 with chlorinated naphthalene (refraction index 1.635) at 7 K is shown in Fig. 5.40 (Drożdżyński and Karbowiak, 2005) and is typical for most uranium(IV) compounds. In this region the spectra consist of relatively intense and sharp absorption lines. The intra-configurational $5f^3 \rightarrow 5f^3$ transitions result in 91 non-degenerated crystal field levels.

Magnetic susceptibility measurements have been carried out over wide temperature ranges for almost all halides and complex halides. The paramagnetic constants from the Curie–Weiss law $\chi'_m = C/(T - \theta)$ and the effective magnetic moments ($\mu_{eff} = 2.84\sqrt{c}\mu_{B+}$) for some of the compounds are collected in Table 5.26. Hexachloro uranates(IV) show temperature-independent paramagnetism between 4 and 300 K with $\chi_M = 2000 \times 10^{-6}$ emu.

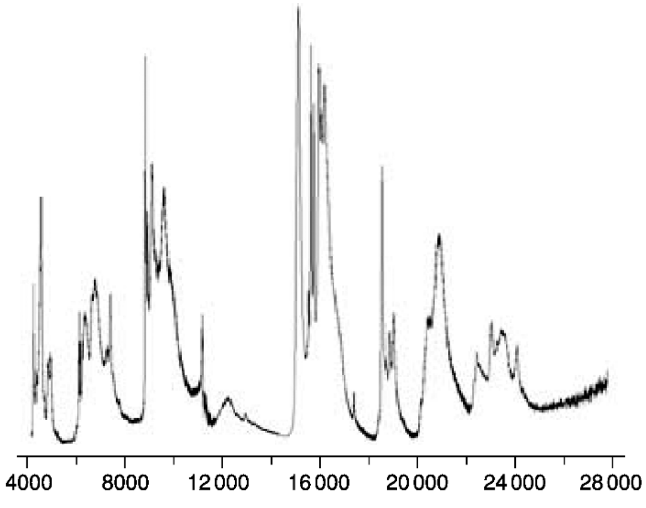

Fig. 5.40 *Absorption spectrum of thin films of a mixture of UF_4 with chlorinated naphthalene at* 7 K (*Drożdżyński and Karbowiak*, 2005).

(*i*) *Uranium tetrafluoride and complex uranium(IV) fluoro compounds*

Uranium tetrafluoride

Uranium tetrafluoride has important industrial applications in the conversion of uranium ore to UF_6 and in the production of UO_2. The former is a key compound in the uranium enrichment process and UO_2 is a nuclear fuel. The usefulness of UF_4 in these two processes depends on its large chemical stability and an almost complete insolubility in aqueous solutions. Fluoride melts containing UF_4 have also proved to be suitable in 'homogeneous reactors'. The preparation of UF_4 has been extensively investigated (Brown, 1968, 1979; Bacher and Jacob, 1980; Freestone and Holloway, 1991). Most of the procedures are based either on precipitation from aqueous solutions or on high-temperature reactions in anhydrous conditions. In the first method, aqueous uranyl solutions are reduced to U(IV) by $SnCl_2$, $Na_2S_2O_4$, $FeSO_4$, CuCl, $CrCl_3$, $TiCl_3$, and SO_2 (combined with Cu^{2+}ions), or electrochemically; after reduction, two hydrates, $UF_4 \cdot 2.5H_2O$ and $UF_4 \cdot nH_2O$, with $0.5 < n < 2$, are obtained by precipitation with F^- (Allen *et al.*, 1950; Anderson *et al.*, 1950; Dawson *et al.*, 1954). The preparation from aqueous solutions based on electrolytic reductions of uranyl solutions has found industrial application in the Excer Process (ion exchange conversion, electrolytic reduction (Higgins and Roberts, 1956; Marinsky, 1956; Bacher and Jacob, 1980).

Since it is difficult to remove water without hydrolytic reactions, UF_4 produced by aqueous processes is not suitable for reduction to metal or for conversion to UF_6. Consequently, it has been customary to prepare UF_4 by high-temperature reactions. One of the most convenient methods to produce UF_4 on a large scale employs heating of UO_2 in an excess of anhydrous HF at 400–600°C.

$$UO_2 + 4HF \xrightarrow{550^\circ C} UF_4 + 2H_2O$$

This and similar methods result in the formation of a highly reactive form of the dioxide. If the starting material is a non-stoichiometric oxide, it is essential to insert H_2 in order to avoid reactions such as:

$$U_3O_8 + 8HF \rightarrow 2UO_2F_2 + UF_4 + 4H_2O$$

Ruehle (1959) describe the synthesis of UF_4 using a stirred fluidized-bed hydrofluorination reactor. The chemistry of the reaction has been discussed by Dawson *et al.* (1954).

On a large scale the compound may be prepared by thermal decomposition of $UO_4 \cdot 2H_2O$ to UO_3 at 250°C followed by reduction with hydrogen to UO_2 at 600°C and fluorination to UF_4 with NH_4HF_2 at 150°C (Van Impe, 1954). Alternatively, UF_4 may be obtained in a similar route using uranium(IV) acetate or by reaction of UO_2 with SF_4 at 500°C.

Other satisfactory methods involve the direct reduction of UO_3 to UF_4 by ammonia–hydrogen fluoride mixtures at 500–750°C and by NH_4F, NH_4HF_2, or a mixture of NH_4HF_2 and hydrazine fluoride. Also various freons, in particular, CF_2Cl_2, are useful fluorinating agents for UO_2, UO_3, and $(NH_4)_3U_4O_{16}F_3$ (Evers and Reynolds, 1954; Van Impe, 1954).

Attractive alternatives for the preparation of smaller amounts include the heating of metallic uranium with anhydrous hydrogen fluoride in a sealed tube at 225–250°C and treating UH_3 or uranium with hydrogen fluoride vapours at 250–350°C or with a mixture of $H_2 + HF$ at 250°C (Brown, 1979).

Since UF_6 is the starting material for ^{235}U enrichment, it is also a convenient preparatory material for enriched metallic uranium via uranium tetrafluoride. The preparation of UF_4 from UF_6 may be performed by:

(i) reduction with H_2 in the gaseous phase (Smiley and Brater, 1958, 1960; Bacher and Jacob, 1980)

$$UF_6 + H_2 \overset{630^\circ C}{\rightarrow} UF_4 + 2HF$$

(ii) reduction with chlorinated hydrocarbons C_2HCl_3, C_2Cl_4, and CCl_4 (Bacher and Jacob, 1980, 1986)

$$UF_6 + 2CCl_4 \xrightarrow{200^\circ C,\, p=29\, bar} UF_4 + 2CCl_3F + Cl_2$$

(iii) the reaction with Me_3SiX (Brown *et al.*, 1983)

$$UF_6 + 2Me_3SiX \rightarrow 2Me_3SiF + X_2 + UF_4 (X = Cl\ or\ Br)$$

On technical scale the reaction (i) may be performed either in a 'hot-wall reactor', by heating the outside wall of the reactor up to 650°C, or in a 'cold-wall reactor' in which the energy is supplied by the reaction

$$F_2 + H_2 \rightarrow 2HF$$

The temperature of the reactor wall is kept between 150 and 200°C. In order to achieve a complete conversion in the reactions (ii) and (iii), a substantial excess of CCl_4 and a molar ratio 1:2 of UF_6 to Me_3SiX is essential (Bacher and Jacob, 1980; Hellberg and Schneider, 1981).

Uranium tetrafluoride is an emerald-green high melting polymeric solid, entirely insoluble in water. However it may be dissolved in the presence of reagents that can form fluoride complexes, such as Fe^{3+}, Al^{3+}, or boric acid, for example. It is a good starting material for the synthesis of UF_6 and production of uranium metal by reduction with calcium or magnesium. The reduction may also be performed with Li, La, or Al whereas Zr, Be, Ti, or hydrogen leads to uranium trifluoride. The compound is stable in air at room temperature, which makes it useful as an intermediate product in the conversion of uranium ore to UF_6. For sublimation *in vacuo*, a stainless steel tube with a molybdenum liner has been used (Dawson *et al.*, 1954). Uranium tetrafluoride reacts with strong oxidizing reagents such as Ce^{4+}, concentrated perchloric acid, nitric acid and, nitric acid–boric acid or sulphuric acid–ammonium persulphate mixtures with the formation of the appropriate uranyl salt solutions.

UF_4 is monoclinic, with the same structures as those of zirconium and hafnium tetrafluorides. The structure at different temperatures has been examined in detail by Kern *et al.* (1994), using neutron diffraction on polycrystalline samples. The unit cell of UF_4 contains 12 formula units with four (U1) and eight (U2) sites having C_2 symmetry. Each uranium atom has eight fluorine neighbors arranged in a slightly distorted square antiprism. A basic repeating unit of five uranium atoms is arranged in a slightly distorted pyramid. Four of them are forming a rhomb-shaped base, and the fifth comprises the apex of the pyramid. For other details see Table 5.26.

The thermodynamic properties of UF_4 have been analyzed in detail by Rand and Kubaschewski (1963), Kubaschewski and Alcock (1979), and Fuger *et al.* (1983). The heat capacity from 1.3 to 20 K has been measured by Burns *et al.* (1960) and between 5 and 300 K by Osborne *et al.* (1955).

Carnall *et al.* (1991) have reported an analysis of the low-temperature crystal-field absorption spectrum of UF_4. The authors found a good agreement between the experimentally observed and calculated band structure using an effective Hamiltonian with orthogonalized free-ion operators. The initial crystal-field parameter values were calculated on the basis of a superposition model for An^{4+} sites with C_2 symmetry. The values obtained are listed in Table 5.26. The parameters have been obtained in a fit of 69 observed crystal-field levels of UF_4; the r.m.s. error is 31 cm^{-1}. The spin–spin and spin–orbit parameters, $M^0 = 0.775$, $M^2 = 0.434$, and $M^4 = 0.294$, were assigned on the basis of *ab initio* calculations and were not varied in the fitting. The electrostatically correlated spin–orbit perturbation parameters P^4 and P^6 were constrained by keeping the ratios P^4/P^2 and P^6/P^2 constant, equal to 0.5 and 0.1, respectively. The magnitude of the total crystal-field strength expressed by the scalar parameter N_v (Auzel and Malta, 1983), is equal to 2700 (assuming the C_{2v} approximation).

Uranium tetrafluoride hydrates

The reaction of U(IV) solutions with 4–20% aqueous fluoride solutions results in the precipitation of $UF_4 \cdot 2.5H_2O$. A number of hydrates with smaller water content, $UF_4 \cdot nH_2O$ (where $0.5 < n < 2$), was obtained by controlled thermal decomposition. $UF_4 \cdot 2.5H_2O$ is the most stable one: in vacuum up to 25°C and in air up to 100°C. The compound may be converted to $UF_4 \cdot 0.5H_2O$ at 100–120°C with the maintenance of its structure. A complete dehydration occurs at 500–550°C in a stream of N_2 or HF. However, it still retains some of the structure of $UF_4 \cdot 2.5H_2O$ and, contrary to UF_4, it may be readily rehydrated to $UF_4 \cdot 2.5H_2O$. All UF_4 hydrates with lower water content may also be gradually converted back to this stable form. The solubility of $UF_4 \cdot 2.5H_2O$ in water is 0.1 $g \cdot L^{-1}$ (Bacher and Jacob, 1980).

$UF_4 \cdot 2.5H_2O$, $UF_4 \cdot 2H_2O$, and $UF_4 \cdot 4/3H_2O$ have orthorhombic *Pnma*, cubic $Fm\bar{3}m$, and a monoclinic structure, respectively, as revealed by X-ray diffraction and NMR data. Crystallographic data are given in Table 5.26.

The three-dimensional network contains channels in which coordinated and free water molecules are located (Zadneporovskii and Borisov, 1971).

Complex uranium(IV) fluorides

Metal fluoride–uranium tetrafluoride fused salt systems have been extensively studied because of their usefulness as fertile fuel materials, coolants, and heat transfer media in the Molten-Salt Reactor Experiment (MSRE), Molten-Salt Breeder Reactor, and the Aircraft Nuclear Propulsion (ANP) projects. Numerous ternary and polynary uranium(IV) fluorides have been characterized by determination of their crystallographic parameters (see Table 5.26) but there are fewer studies of their chemical and thermodynamic properties. The application of the compounds in molten-salt reactor technology has been reviewed in a number of articles (Thoma and Grimes, 1957; Thoma, 1959, 1971, 1972; Grimes and Cuneo, 1960; Rosenthal *et al.*, 1972; Grimes, 1978). Caillat (1961), Brown (1968), Bacher and Jacob (1980), Martinot (1984), Bagnall (1987), Freestone and Holloway (1991) and others have reviewed their general properties. Various complex compounds are listed in Table 5.27 with an indication of their melting behavior when available.

A number of ternary and quaternary fused salt systems such as LiF–BeF_2–UF_4 (Thoma, 1959; Jones *et al.*, 1959) and NaF–BeF_2–UF_4 (Thoma, 1959) were important for the MSRE and ANP projects. The $MgUF_6$ and $CaUF_6$ fluorides are of importance for the production of uranium by high-temperature reduction of UF_4 with calcium or magnesium. Systems with ammonium or hydrazinium cations have found application in the preparation of high-purity UF_4 by decomposition of the corresponding complex fluorides. A typical phase diagram of some importance for the molten-salt reactor projects is presented in Fig. 5.41.

The general methods for the preparation of the compounds (Bacher and Jacob, 1980; Freestone and Holloway, 1991) include: (i) solid state reaction between the component fluorides in an inert atmosphere; (ii) reactions between UF_4 or UO_2 and the alkali metal fluoride or carbonate in HF or HF–O_2 mixtures; (iii) reductions of UF_6 with appropriate alkali metal fluorides; (iv) controlled thermal decomposition of tetravalent uranium fluoro complexes of higher stoichiometry (e.g. $(NH_4)_4U^{IV}F_8$) or the treatment of other fluoro complexes with fluorine, (v) precipitation from aqueous solutions, followed by heating in air, *in vacuo* or fluorine, and (vi) hydrogen reduction of higher valence state fluoro complexes and precipitation from aqueous solutions.

The structures for the majority of the fluoro complexes are well established; typical examples are those with the UF_7^{3-}, UF_8^{4-} anions, but octahedral UF_6^{2-} complexes are also known. The cubic K_3UF_7 structure contains UF_7^{3-} pentagonal bipyramids, while the uranium coordination in Li_4UF_8 is described as a bicapped triangular prism (Brunton, 1967; Freestone and Holloway, 1991). Compounds of the $M^{II}UF_6$ (M^{II} = Ca, Sr, Ba, or Pb) adopt the LaF_3 structure (Keller and Salzer, 1967). U(IV) in $LiUF_5$, KU_2F_9, and $M^IU_3F_{13}$ (M^I = Rb or

Table 5.27 *Melting behavior of uranium*(IV) *complex fluorides and chlorides.*

System	*Complex fluorides*[a]
LiF-UF_4	LiU_3F_{13}, Li_2UF_6, Li_4UF_8 (P), Li_3UF_7, $LiUF_5$ (P), LiU_4F_{17} (P)
NaF-UF_4	$NaUF_5$, $Na_7U_2F_{15}$, Na_3UF_7 (C), Na_2UF_6 (P), $Na_5U_3F_{17}$ (P), $Na_7U_6F_{31}$ (C), NaU_2F_9 (D)
KF-U_4	KUF_5, K_3UF_7 (C), K_2UF_6 (P), KU_3F_{14}, $K_7U_6F_{31}$ (P), KU_2F_9 (P), KU_6F_{25}
RbF-UF_4	RbU_2F_9, Rb_3UF_7 (C), Rb_2UF_6 (P), $Rb_7U_6F_{31}$ (P), $RbUF_5$ (C), $Rb_2U_3F_{14}$ (P), RbU_3F_{13} (P), RbU_6F_{25} (P)
CsF-UF_4	Cs_3UF_7 (C), Cs_2UF_6 (P), $CsUF_5$ (C), $Cs_2U_3F_{14}$, CsU_2F_9, CsU_6F_{25}
NH_4F-UF_4	$(NH_4)_4UF_8$, $(NH_4)_2UF_6$, $(NH_4)_7U_6F_{31}$, NH_4UF_5, $NH_4U_3F_{13}$
N_2H_5F-UF_4	$(N_2H_5)_3UF_7$, $(N_2H_5)_2UF_6$, $N_2H_5UF_5$
NH_3OHF-UF_4	$(NH_3OH)UF_5$
LiF-CaF_2-UF_4	Li_2CaUF_8
LiF-CdF_2-UF_4	Li_2CdUF_8
MgF_2-UF_4	$MgUF_6$
CaF_2-UF_4	$CaUF_6$ (P)
BaF_2-UF_4	$BaUF_6$
SrF_2-UF_4	$SrUF_6$
TlF-UF_4	Tl_4UF_8, Tl_2UF_6, $Tl_7U_6F_{31}$, $TlUF_5$, TlU_3F_{13}, TlU_6F_{25}
SnF_2-UF_4	Sn_2UF_8 (P), $SnUF_6$ (P)
PbF_2-UF_4	$PbUF_6$, Pb_6UF_{16} (C), $Pb_3U_2F_{14}$ (C)
	complex chlorides[a]
LiCl-UCl_4	Li_2UCl_6 (C)
NaCl-UCl_4	Na_2UCl_6 (C)
KCl-Ucl_4	K_2UCl_6 (C), $KUCl_5$ (P), KU_3Cl_{13} (P), K_2UCl_6 (C)
RbCl-UCl_4	Rb_2UCl_6 (C), $Rb_3U_2Cl_{11}$ (P), $RbUCl_5$ (C), RbU_3Cl_{13} (P)
CsCl-UCl_4	Cs_2UCl_6 (C), CsU_2Cl_9 (P), $Cs_3U_2Cl_{11}$ (P), $CsUCl_5$ (P)

[a] C: congruent melting, E: eutectic, P: incongruent melting, D: decomposition.

NH_4) has tricapped trigonal prism coordination geometry. A structure with linear chains of polyhedra with a distorted cubic arrangement has been proposed for γ-Na_2UF_6 (Zachariasen, 1948a). Infinite chains are also present in the β_1-K_2UF_6 structure, where they are formed by tricapped trigonal prisms that share the triangular faces perpendicular to the three-fold axis of the ideal polyhedron (Zachariasen, 1948a). The structure of Rb_2UF_6 (Kruse, 1971) consists of infinite chains of $[UF_8]$ units with triangular faced dodecahedral geometry (of the K_2ZrF_6-type) whereas in $(NH_4)_2UF_6$ the chains of antiprism are linked by s edges on opposite square faces (Penneman *et al.*, 1974). Compounds of the $M^I_7U_6F_{31}$ type (M^I = Na, K, Rb, or NH_4) are isostructural with $Na_7Zr_6F_{31}$ (Burns *et al.*, 1968) and have a coordination geometry that is approximately square antiprismatic. The six antiprisms share corners to form an octahedral cavity, which encloses one F atom. Additional information on the structures and crystallographic data of uranium(IV) fluoro complexes are given in Table 5.26.

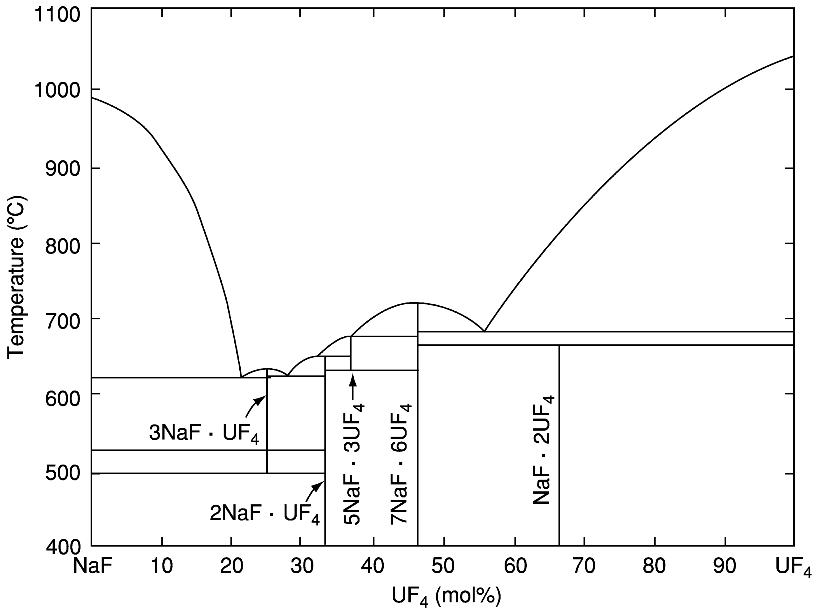

Fig. 5.41 *Phase diagram of the NaF–UF_4 system* (*Thoma,* 1959).

Numerous UF_4 complexes with quaternary ammonium compounds such as amines, pyridine, quinoline, and guanidine have been chemically and structurally characterized (Bacher and Jacob, 1980).

(*ii*) *Uranium*(IV) *oxide fluorides and nitride fluorides*

The melting of stoichiometric amounts of UO_2 and UF_4 yields UOF_2. From aqueous U(IV) solutions, the green hydrates $UOF_2 \cdot 2H_2O$ and $UOF_2 \cdot H_2O$ precipitates. Numerous non-stoichiometric uranium oxide fluorides, rich in oxygen, have been obtained by interactions of UF_4 with uranium oxides in the absence of oxygen at 400–550°C (Bacher and Jacob, 1980). The uranium atoms have an oxidation number that is either 5+, or a mixture of 5+ and 6+. In $UO_2F_{0.25}$, the oxidation number is 4+ and 5+. The compounds are non-volatile or difficult to volatilize; they have structures related to that of uranium oxide. The crystallographic data of $UO_2F_{0.25}$ are given in Table 5.26.

Heating of uranium nitride ($UN_{1.33}$) and uranium tetrafluoride leads to the formation of nitride fluorides of composition between UNF and $UN_{0.98}F_{1.20}$. The formal oxidation number of uranium in these compounds varies between 4 and 4.14. A tetragonal high-temperature and an orthorhombic low-temperature phase have been claimed to exist in this composition range. X-ray investigations of the tetragonal phase revealed a close structural relationship with lanthanum oxide fluoride (Jung and Juza, 1973). The interaction of uranium nitride with an excess of UF_4 at 950°C leads to UF_3 and with an excess of UN to UNF (Tagawa, 1975).

(*iii*) *Uranium tetrachloride and uranium*(*IV*) *complex chlorides*

Uranium tetrachloride

Uranium tetrachloride is a suitable starting material for the synthesis of a large range of uranium compounds due to its ease of preparation and solubility in numerous polar organic solvents. It has also found application as charge material for calutron ion sources in the electromagnetic separation of uranium isotopes (Akin *et al.*, 1950). Since it has been the subject of an extensive research, numerous methods for the synthesis have been developed (Brown, 1979). Most of them are based on chlorination of uranium oxides with an extensive range of powerful chlorinating agents such as CCl_4, $COCl_2$, $SOCl_2$, S_2Cl_2, Cl_2, $Cl_2C{=}CClCCl_3$ as well as of S_2Cl_2/Cl_2 and Cl_2/He mixtures that can be used both in gaseous and liquid phases. The direct combination of uranium and chlorine leads to a complex mixture of uranium chlorides and does not yield pure UCl_4. This may most conveniently be obtained either by liquid-phase chlorination of UO_3, $UO_4 \cdot 2H_2O$, U_3O_8, UO_2Cl_2 (but not UO_2) with hexachloro propene, $Cl_2C{=}CCl{-}CCl_3$ (Hermann and Suttle, 1957) or by converting UO_2 to the tetrachloride by carbon tetrachloride at 450°C (Brown, 1979):

$$UO_2 + CCl_4 \overset{450^\circ C}{\rightarrow} UCl_4 + CO_2$$

Since the particle size of uranium dioxide is important for the synthesis, a reactive form of UO_2 should be used, formed by decomposition of uranyl oxalate in presence of hydrogen at 300°C. On laboratory scale, the simplest method involves the refluxing of UO_3 with a five-fold excess of hexachloro propene (b.p. 210°C) at atmospheric pressure. Uranium tetrachloride is insoluble in the reaction mixture and precipitates quantitatively as the reaction progresses. Due to extensive hydrolysis, the anhydrous chloride cannot be recovered from aqueous solutions.

In syntheses involving chlorine or the higher uranium oxides, usually small amounts of UCl_5 are formed. This is, however, thermally unstable and loses chlorine by heating in a stream of carbon dioxide or nitrogen. Uranium tetrachloride may be easily purified by sublimation *in vacuo*, or in a stream of a dry inert gas. A recommended route is also vapor-phase transport by the $UCl_4 \cdot AlCl_3$ complex, which proceeds rapidly already at 350°C (Gruen and McBeth, 1968). The chorination of UO_3 using liquid CCl_4 was used on a large scale to obtain UCl_4, which was used as charge material for the calutron ion sources used in the electromagnetic separation of uranium isotopes. Under a pressure of 20 atm, the chlorination yielded UCl_5, which was thermally decomposed to UCl_4 in an inert gas. Details of these processes can be found in Akin *et al.* (1950).

Uranium tetrachloride forms dark-green hygroscopic crystals, which must be handled in a dry atmosphere. At 600°C, in air it converts into U_3O_8. The compound is insoluble in non-polar organic solvents such as chloroform or carbon tetrachloride but dissolves readily in numerous polar solvents, usually with complex formation, which enables the recovery of the anhydrous compound by evaporation. In water, it undergoes hydrolysis, which is complete at 100°C. The reaction of UCl_4 with hydrogen, zinc, or UN results in the formation of uranium trichloride. Reaction with HBr or HI yields UBr_3 and UI_3, respectively. Reduction to uranium metal takes place when the tetrachloride is heated with Li, Na, K, Mg, Ca, and Al.

Metallic uranium is also obtained by electrolytic reduction of molten UCl_4 or its solutions in fused salts media such as NaCl–KCl. Reduction with magnesium also leads to metallic uranium, whereas insoluble U(III) species are formed on reduction with Zn, Pb, and Bi. Uranium trichloride is formed in a LiCl–KCl melt by reduction with uranium or aluminum. The interaction of UCl_4 with chlorine at 115–125°C yields mixtures of UCl_5 and UCl_6, whereas in fused salt media at 400–700°C it leads to the formation of UCl_6. The reaction with fluorine gas, HBr, or HI converts UCl_4 to UF_6, UBr_4, and mixed chloride iodides, respectively.

Uranium tetrachloride crystallizes in the space group $I4_1/amd$, with tetragonal symmetry; it is isostructural with other actinide tetrachlorides. Each uranium atom is bonded to eight chlorine atoms in a dodecahedral arrangement. The crystallographic data are listed in Table 5.26. High-quality absorption spectra of UCl_4 were obtained (Brown, 1979) both for powdered samples, single crystals, in the vapor phase, and in a nitrogen matrix at 4 K (Clifton *et al.*, 1969). Numerous spectra were also recorded in different non-aqueous solvents. Successful investigations of U^{4+} spectra in the solid state started with a parametric analysis of U^{4+}-doped $ThBr_4$ single crystals by Delamoye *et al.* (1983). On this basis, consistent sets of atomic and crystal field parameters have been obtained also for isomorphic $ThCl_4$:U^{4+} and UCl_4 of D_{2d} symmetry (Malek *et al.*, 1986a,b). The data for UCl_4 are listed in Table 5.26. The parameters have been obtained by fitting 60 observed crystal-field levels of UCl_4 with a r.m.s. error of 60 cm^{-1}. The configuration interaction parameter $\gamma = 1200$, the spin–spin and spin–other orbit parameters, $M^0 = 0.99$, $M^2 = 0.55$ and $M^4 = 0.38$, and the electrostatically correlated spin–orbit perturbation parameters $P^2 = P^4 = P^6 = 500$ (all in cm^{-1}) have been used as constants in the fitting (Malek *et al.*, 1986b). The magnitude of the total crystal-field strength expressed by the scalar parameter (Auzel and Malta, 1983) N_v is equal to 1224.

The magnetic susceptibility of UCl_4 has been measured in wide temperature ranges: 100–350 K, $\mu_{eff} = 3.18$ B.M.; 350–500 K, $\mu_{eff} = 3.18$ B.M., $\theta = -31$ K (Bommer, 1941); 77–500 K, $\mu_{eff} = 3.29$ B.M., $\theta = -62$ K (Dawson, 1951); 77–450–775; 825–1200 K, $\mu_{eff} = 3.33$, 3.50, and 3.60 B.M., respectively (Trzebiatowski and Mulak, 1970). A deviation from the Curie–Weiss law was found at very low temperatures. The best fit between the experimental and the calculated curves was achieved using the values obtained by Hecht and Gruber (1974) with $A_6^4\langle r^6\rangle$ increased to 1561.8 cm^{-1}. The crystal-field parameters deduced by Mulak and Żołnierek (1977) are different from those obtained from spectroscopic data.

It has been shown (Gamp *et al.*, 1983) that the previous susceptibility measurements made on powdered UCl_4 samples are not reproducible because of a re-orientation effect caused by the high anisotropy of the susceptibility of this material. For single crystals, the anisotropic magnetic susceptibility $\chi_{\|}$ (along the tetragonal axis), measured between 1.6 and 350 K, is found to be almost temperature-independent and about 30 times smaller than $\chi_{\perp}$ at low temperatures (Gamp *et al.*, 1983). Chlorine-35 nuclear quadrupole resonance has been observed in solid UCl_4 at 77 K and a frequency of (6.24 ±0.03) MHz (Carlson, 1969). Some other physical data are summarized in Table 5.26.

Complex uranium(*IV*) *chlorides*

A large number of hexachloro uranium(IV) compounds of the formulas $M^I_2UCl_6$ and $M^{II}UCl_6$ have been prepared by reactions in non-aqueous and aqueous media and by solid state reactions of the component halides (where M^I = Li, Na, K, Rb, Cs, Ag, $N(CH_3)_4$, $N(C_2H_5)_4$, $As(C_6H_5)_4$, C_5H_5NH, $N(CH_3)_2(C_6H_5CH_2)_2$, $P(C_2H_5)_3H$, $P(C_4H_9)_3H$, $P(C_6H_5)_2H_2$, $P(C_2H_5)_4$ etc. and M^{II} = Be, Ca, Ba, Sr, etc.). The chlorination of a mixture of U_3O_8 and NaCl at high temperatures yields Na_2UCl_6. The formation of numerous complex tetravalent chloro compounds (see Table 5.27) has also been observed during investigations of binary and ternary fused salt systems containing UCl_4.

The results of investigations on phase equilibria, spectroscopic and electrochemical properties of uranium tetrachloride in molten salt systems have been reviewed by Brown (1979) and Martinot (1984). Investigations of Gruen and McBeth (1968, 1969) and Schäfer (1975) and Binnewies and Schäfer (1974) have given evidence for the existence of uranium(IV) vapor phase complexes such as $UCl_4 \cdot AlCl_3$, $TlUCl_5$, $CuUCl_5$, Tl_2UCl_6, TlU_2Cl_9, $BeUCl_8$, In_2UCl_{10}, $ThUCl_8$, and Cu_2UCl_5. In the UCl_4–HCl–H_2O system, five hydrates have been identified among which $UCl_4 \cdot 9H_2O$ and $UCl_4 \cdot 5H_2O$ are stable at 0 and 40°C, respectively (Brown, 1979).

The action of oxygen and nitrogen donor ligands on UCl_4 solutions in non-aqueous solvents results in the formation of stable adducts of different UCl_4 to ligand stoichiometries (Brown, 1979; du Preez and Zeelie, 1989):

- (1:1): methylene bis-diphenylphosphine, ethylene bis-diphenylphosphine, α-α-dimethylmalonamide;
- (1:2): pyridine, triphenylphosphine oxide, 1,2–dimethoxyethane, 1,2-bis-methylthioethane, 1,10-phenanthroline, 1,8-diaminonaphthalene, 1,2-diaminobenzene, dimethyl sulfoxide, di-*tert*-butylsulfoxide;
- (1:2, 1:6): trimethylphosphine oxide;
- (1:2, 1:4): ammonia;
- (1:3): dioxan, tetrahydrofuran, trimethylphosphine, pyrrolidine;
- (1:4): phosphorous oxide trichloride, ROH (R = CH_3, C_2H_5, C_3H_9, i-C_3H_9), ethylenediamine, piperidine, methyl cyanide;
- (1:6): acetamide, hydrazine;

- (1:7, 1:5, 1:3): dimethylsulphoxide;
- (2:3): malonamide, glutaramide, dimethylglutaramide;
- (2:5):dimethylformamide, pyrazine, 1,2-diaminobenzene, pyrazine-2-carboxamide; dimethylacetamide.

In alternative syntheses, the reaction between uranium tetraacetate and acetates of M^I cations (M^I = K, Rb, Cs, NH_4, or $N(CH_3)_4$) in an acetyl chloride–acetic acid mixture has been used. The use of $CsUCl_6$ as a convenient starting material for the preparation of the complexes has also been reported.

The chlorine atoms may by replaced by a variety of anions in metathetic reactions involving uranium tetrachloride in non-aqueous media such as formic acid, acetic acid, sodium diethyldithiocarbamate (Nadtc), tertaethylammonium diethyldiselenocarbamate ($N(C_2H_5)_4$dsc), sodium acetylacetonate (Na-acac), tropolone (Htrop), $LiNR_2$ (R = C_2H_5, C_3H_7, C_6H_5, KC_5H_5), $NaNH_2$ (in NH_3), $NaBH_4$, and many other compounds. Electrochemical oxidation of anodic uranium into acetonitrile solutions of Cl_2 results in the formation of $UCl_4 \cdot 4CH_3CN$ in good yield. The compound may be converted into other UCl_4 adducts, e.g. with dimethylsulfoxide (1:3), 2,2′-bipyridine (1:2), Ph_3PO (1:2) etc. (Kumar and Tuck, 1984).

The chloro complexes are to some extent soluble in organic solvents such as ethanol, methyl cyanide, thionyl chloride, nitromethane, etc. with the exception of the compounds containing alkali metal cations. In aqueous hydrochloric acid solutions, the solubility of the complexes decreases markedly with the increase of the acid concentration. Liquid zinc amalgam reduction of solutions of M_2UCl_6 (where M = NH_4, K, or Rb) with an excess of NH_4Cl, KCl, or RbCl in anhydrous methyl cyanide results in the formation of the trivalent complexes, M_2UCl_5 (Drożdżyński and Miernik, 1978).

The crystallographic data of the hexachloro uranium(IV) compounds are listed in Table 5.26. The compounds with Cs^+, Rb^+, $N(CH_3)_4^+$, $As(C_2H_5)_4^+$, $P(C_6H_5)H^+$, and other cations exhibit a non-magnetic ground state A_1 with no thermal population of the excited states of the ground multiplet $^3H_4$, resulting in a temperature-independent paramagnetism between 4 and 350 K with $\chi_{mole} \cong 2000 \times 10^6$ cm^3 mol^{-1}. The magnetic susceptibility of Rb_2UCl_6 and Cs_2UCl_6 has been measured at higher temperatures and show an approximate Curie–Weiss dependence above 400 K. The magnetic susceptibilities of other chloro compounds (with M = Li, Na, or K) have a somewhat more complex temperature dependence with limited ranges of temperature-independent paramagnetism, e.g. $KUCl_5$ exhibits Curie–Weiss dependence in the 77 to 600 K and 600–1200 K ranges with $\mu_{eff} = 3.52$ and 3.64 B.M., respectively. Solid state reactions of stoichiometric mixtures of Cs_2UCl_6 and Sb_2O_3 at 300°C *in vacuo* yields a dark olive brown uranium(IV) oxochloro compound of the formula Cs_2UOCl_4, for which Watt *et al.* (1974) reported infrared and powder diffraction data.

(*iv*) *Uranium*(*IV*) *oxychloride and oxochloro complexes*

$UOCl_2$ can be prepared by heating uranium dioxide in an excess of molten uranium tetrachloride followed by vacuum sublimation of the excess of tetrachloride at about 450°C (Brown, 1979), or by the following reaction:

$$3UCl_4 + Sb_2O_3 \rightarrow 3UOCl_2 + 2\,SbCl_3$$

This latter synthesis ought to be carried out *in vacuo* around 400°C where by-products sublimate from the reaction zone (Bagnall *et al.*, 1968).

Uranium(IV) oxide dichloride is a green, moisture-sensitive, and thermally unstable solid. It readily dissolves in water and aqueous nitric acid, but is insoluble in organic solvents. At 170°C, CCl_4 may convert the compound to the tetrachloride; anhydrous liquid hydrogen fluoride may convert it to the tetrafluoride.

$UOCl_2$ is isostructural with some $MOCl_2$ oxychlorides (where M = Pa, Th, or Np). The oxychlorides crystallize in the orthorhombic system (see Table 5.26) and the structure contains $U_3O_3Cl_3$ chains running parallel to the *c*-axis that are linked by chlorine bridges. There are three types of polyhedra around the non-equivalent uranium atoms in the chains: around U(1), dodecahedra (CN = 8; from 3O and 5 Cl); around U(2), tricapped trigonal prism (CN = 9; 4O, 5Cl) and around U(3) monocapped trigonal prisms (CN = 7; 3O, 4Cl) (Taylor and Wilson, 1974a); all coordination polyhedra are distorted from the ideal shape. A dark olive-brown to blue-brown oxochloro complex of the formula Cs_2UOCl_4 was prepared by heating together Cs_2UCl_6 with Sb_2O_3 at 300°C *in vacuo* (Watt *et al.*, 1974).

(*v*) *Uranium*(*IV*) *perchlorates*

Uranium(IV) perchlorate, $U(ClO_4)_4$, is unknown, but a few uranium(IV) perchlorato compounds have been isolated. Bagnall *et al.* (1962) and Bagnall and Wakerley (1974) have described the preparation and reactions in non-aqueous media of oxygen donor complexes of the formula $U(ClO_4)_4 \cdot 4L$ (L = octamethyl phosphoramide) and $U(ClO_4)_4 \cdot 4L'$ (L′ = dimethylacetamide, trimethylphosphine oxide, or hexamethylphosphoramide). Interaction of solid U $(HPO_4)_2 \cdot xH_2O$ with 10 M $HClO_4$ results in the formation of hydrated phosphate perchlorates of the formula $U(H_2PO_4)_2(ClO_4)_2 \cdot xH_2O$ ($x = 4$ and 6).

(*vi*) *Uranium tetrabromide and uranium*(*IV*) *complex bromides*

Uranium tetrabromide

A wide variety of methods for the preparation of uranium tetrabromide have been reported (Brown, 1979); the product may then be purified by sublimation *in vacuo* or in a stream of an inert gas. Since the compound is extremely moisture-sensitive, the carrier gases must be carefully dried. The most convenient and widely used preparation methods involve (i) the conversion of UO_2 or

U_3O_8 to the tetrabromide by heating, with a mixture of carbon, in a stream of bromine at 700–900°C, (ii) reactions between UO_2, UO_3, or $UOBr_3$ with carbon tetrabromide at about 170°C, (iii) reactions between UO_2 and a sulfur–bromine mixture under reflux at about 170°C, and (iv) direct bromination of uranium metal, either in a flow system, for example, a helium–bromine mixture at about 650°C, or in sealed evacuated vessels at 500–700°C.

Uranium tetrabromide is a deep brown, very hygroscopic solid, insoluble in non-polar organic solvents but soluble or reacting with numerous polar solvents. HBr is evolved on dissolution in methanol, ethanol, phenol, acetic acid, aniline, or on exposure to moist air. In non-aqueous solvents, the tetrabromide forms complex compounds with numerous organic ligands such as nitriles, amides, sulfoxides, phosphine oxides, or arsine oxides, e.g. $UBr_4 \cdot 4CH_3CN$, $UBr_4 \cdot 4CH_3CON(CH_3)_2 \cdot CH_3COCH_3$, $UBr_4 \cdot nCH_3CON(CH_3)_2$ ($n = 2.5$ or 5), $UBr_4 \cdot 8CO(NH_2)_2$, $UBr_4 \cdot 6(CH_3)_2SO$, $UBr_4 \cdot 2L$ (L = $(C_6H_5)_3PO$, $[(CH_3)_2N]_3PO$, $(C_2H_5)_3PO$, $(CH_3)_3AsO$, $(C_6H_5)_3AsO$, $(C_2H_5)_3AsO$, $(CH_3)_3AsO$, $UBr_4 \cdot 6(CH_3)_3PO$, $UBr_4 \cdot 6L'$ (L′ = $(CH_3)_3AsO$ and $(C_2H_5)_3AsO$). Reduction with alkali or alkaline earth metals at high temperatures and hydrogen at 450–700°C yields uranium metal and uranium tribromide, respectively. Uranium tetrabromide may be converted to the tetrachloride by chlorine and to UO_2Br_2 by dry oxygen at 150–160°C. The preparation and crystal structure of octaaquabromo uranium(IV) tribromide monohydrate, $[UBr(H_2O)_8]Br_3(H_2O)$ (Table 5.26) have been reported by Rabinovich *et al.* (1998).

Uranium tetrabromide crystallizes in the monoclinic space group *C*2/*m* (see Table 5.26), with pentagonal bipyramid coordination at the uranium atom; the polyhedra are linked into infinite two-dimensional sheets by double bromine bridges between the uranium atoms (Taylor and Wilson, 1974d,e).

Good-quality low-temperature absorption spectra as well as solution, reflectance, and transmission spectra of UBr_4 are available. The energy level parameters obtained from least-squares fitting of the observed and calculated energy levels are listed in Table 5.26. Absorption bands observed in the range 41 400–32 160 cm^{-1} were assigned to $5f^2 \rightarrow 5f^1 6d^1$ transitions; a charge transfer band was identified at 30 165 cm^{-1}. Magnetic susceptibility measurements reveal a Curie–Weiss behavior in the temperature range 77–569 K, with $\theta = -35$ K and $\mu_{eff} = 3.12$ B.M (Brown, 1979; Dawson, 1951).

Uranium(IV) *ternary and polynary bromides and bromo compounds*

Cooling curves obtained from melting point diagrams show that only complexes of the M_2UBr_6-type are formed in the UBr_4–MBr system (M = Na, K, Rb, or Cs). They may conveniently be prepared by heating the component bromides in evacuated silica ampoules (Vdovenko *et al.*, 1973a,b). In addition to synthetic methods, phase transitions and crystallographic data for Li_2UBr_6 have been reported (Maletka *et al.*, 1998). Hexabromo compounds containing large organic cations are formed in anhydrous methyl cyanide solutions as a result of reactions at 0°C between UBr_4 and a number of alkylammonium or phosphonium bromides, e.g. $[N(CH_3)_4]_2UBr_6$, $[N(C_2H_5)_4]_2UBr_6$, (Brown, 1979). Hexabromouranates(IV) may also be prepared by reactions of UBr_4 with aniline, ethylenediamine, and 8-hydroxyquinoline (Sara, 1970).

$UBr_4 \cdot 2CH_3CN$ in good yield is formed by electrochemical oxidation of uranium in CH_3CN/Br_2 solution under an inert atmosphere. Using a two-fold excess of different neutral ligands in a solution of this compound in acetone gives rise to UBr_4 adducts, e.g. $UBr_4 \cdot 2Ph_3O$ and $UBr_4 \cdot 6$dmso (dmso = dimethylsulfoxide) (Kumar and Tuck, 1984). The preparation of UBr_4 adducts has also been reported by du Preez and Zeelie (1989), e.g. $UBr_4 \cdot (tbso)_2$ (tbso = di-*tert*-butyl phosphoxide), $UBr_4(dmso)_2$ (dimethylsulfoxide) and $UBr_4 \cdot 4CH_3CN$. Evaporation of UBr_5 solutions containing 1 or more than 3 mol equivalents of methyl cyanide in dichloromethane yields $UBr_4 \cdot CH_3CN$ and $UBr_4 \cdot 3CH_3CN$, respectively. The synthesis, crystal structure, and IR data of $P(C_6H_5)_4UBr_6$, $P(C_6H_5)_4[UBr_6] \cdot 2CCl_4$, $[P(C_6H_5)_4]_2[UBr_6] \cdot 4CH_3CN$, and $[P(C_6H_5)_4]_2[UO_2\ Br_4] \cdot 2CH_2Cl_2$ were reported by Bohrer *et al.* (1988) (see Table 5.26).

The hexabromo complexes containing large organic cations have green-blue color; they dissolve readily in water, aqueous hydrobromic acid, and a number of polar non-aqueous organic solvents. They may be purified by crystallization, e.g. from methylcyanide or nitromethane. The compounds react with aqueous ammonia and liquid ammonia forming hydrous oxides and the insoluble $[N(C_2H_5)_4]_2UBr_6$ complex, respectively.

Rb_2UBr_6, Cs_2UBr_6, and $[N(CH_3)_4]_2UBr_6$ crystallize with face-centered cubic symmetry. The crystallographic data of these and some other hexabromouranates(IV) are listed in Table 5.26. Spectroscopic and magnetic susceptibility investigations performed for a number of octahedral uranium(IV) chloro- and bromo-complex compounds by Day and Venanzi (1966) show a temperature-independent paramagnetism, which results from interactions between the A_1 ($^3H_4$) ground state and the first excited state T_1 ($^3H_4$). Using the relative field strengths obtained from magnetic data, the authors have obtained the following values of the energy parameters: $\Delta = 1177\ cm^{-1}$ and $\theta = 2096\ cm^{-1}$ [where $\Delta = 8/33\ (B_0^4 + 35/13 B_0^6)$ and $\theta = 2/33\ (5B_0^4 - 210/13 B_0^6)$; $B_0^4 = 6481.5\ cm^{-1}$, $B_0^6 = 804\ cm^{-1}$]. The observed interactions are in an octahedral field best described by the orbital energy differences $\Delta(a_{2u} \rightarrow t_{2u})$ and $\theta(t_{2u} \rightarrow t_{1u})$.

Spectroscopic investigations reveal a coordination geometry with octahedral geometry both in the solid and in non-aqueous solutions; vibronic side bands are prominent in the spectra of the complexes and permit the assignment of a number of electronic transitions and the determination of the electrostatic, spin–orbit, and crystal-field parameters, e.g. for Cs_2UBr_6: (Johnston *et al.*, 1966) and for $[N(C_2H_5)_4]_2UBr_6$: (Wagner *et al.*, 1977) (see Table 5.26). From the spectral data the following ligand field parameters have been obtained: $\theta = 2378$, $\Delta = 828\ cm^{-1}$, $\zeta_{5f} = 1792\ cm^{-1}$ (or $B_0^4 = 6592.5\ cm^{-1}$, $B_0^6 = 1194.8\ cm^{-1}$) and $\theta = 2336$, $\Delta = 1127\ cm^{-1}$, $\zeta_{5f} = 998.95\ cm^{-1}$ (or $B_0^4 = 6946.5\ cm^{-1}$, $B_0^6 = 998.95\ cm^{-1}$) for Cs_2UBr_6 and $[N(C_2H_5)_4]_2UBr_6$, respectively. As one would expect the $5f^2 \rightarrow 5f^1 6d^1$ transitions, recorded for $[N(C_2H_5)_4]_2UBr_6$, lie between those observed for the hexachloro and hexaiodo uranates(IV), i.e. at 27400(sh), 29400, 30400, 31500(sh), 33100, 37000, and 39000 cm^{-1} (Ryan, 1972). Spectral investigations of the compound in non-aqueous solvents reveal hydrogen bonding to primary, secondary, and tertiary alkylammonium ions that partially distorts the octahedral field in the UBr_6^{2-} complex, making the $5f^2 \rightarrow 5f^2$ electronic transitions allowed. The analysis of the visible and near IR spectra demonstrates vibronic frequencies within the ranges: 180–184 cm^{-1} (ν_3), 72–74 cm^{-1} (ν_4), and at 58 cm^{-1} (ν_6).

(*vii*) *Uranium*(*IV*) *oxide dibromide and nitride bromides*

Useful preparative methods for $UOBr_2$ (Brown, 1979) involve heating of UO_2 in a stream of CS_2 at 900°C to form $U_3O_2S_4$ followed by bromination at 600°C:

$$U_3O_2S_4 + 6Br_2 \rightarrow 2UOBr_2 + UBr_4 + 2S_2Br_2$$

or by heating of stoichiometric amounts of Sb_2O_3 and UBr_4 at about 150°C *in vacuo* (Bagnall *et al.*, 1968):

$$Sb_2O_3 + 3UBr_4 \rightarrow 3\,UOBr_2 + 2SbBr_3$$

Uranium(IV) oxide dibromide is a non-volatile, pale yellow, air-sensitive solid, readily soluble in water with the formation of a green solution from which a black solid slowly deposits. It decomposes above 600°C *in vacuo* to form UO_2 and UBr_4. The reported thermodynamic data (Greenberg and Westrum, Jr., 1956; Rand and Kubaschewski, 1963; Grenthe *et al.*, 1992; Guillaumont *et al.*, 2003) are listed in Table 5.26.

As in the corresponding chloride systems, the ammonolysis of UBr_4 at elevated temperatures leads to the formation of uranium nitride via amido, imido, and nitride bromides (Burk, 1967; Burk and Naumann, 1969). Since the composition of the decomposition products varies with temperature, the pure phases cannot easily be obtained (Brown, 1959). Juza and Meyer (1966, 1969) have obtained a dark-brown $UN_{1.03}Br_{1.03}$ phase on heating UBr_4-ammoniates at 400°C in gaseous ammonia. The compound can also be prepared by solid-state reactions of UN with UBr_4 at 600–900°C. It is insoluble in water and has the BiOCl-type structure with the space group *P*4/*nmm*. The crystallographic data are listed in Table 5.26.

(*viii*) *Uranium tetraiodide and uranium*(*IV*) *complex iodides*

Uranium tetraiodide

The most convenient and widely used method for the preparation of UI_4 involves the direct combination of the elements at about 500°C, either in a gas-flow system or in sealed vessels (see Brown, 1979); it is a black, moisture-sensitive solid. It rapidly decomposes on exposure to air and is also thermally

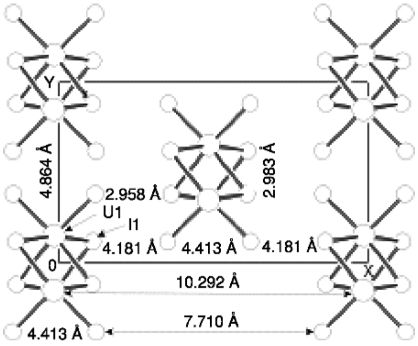

Fig. 5.42 *View along zigzag chains in UI_4 (distances are taken from Levy* et al., 1980).

unstable, liberating iodine with the formation of UI_3. The tetraiodide may also readily be reduced to UI_3 by hydrogen at moderate temperatures. The interaction of UI_4 with chlorine yields UCl_4, and with uranium tetrahalides it forms the mixed halides: UCl_2I_2, $UClI_3$, UBr_2I_2, and $UBrI_3$. Like other uranium halides the tetraiodide also forms complexes with organic ligands, e.g. $UI_4 \cdot 4$dma (dma = dimethylacedamide), $UI_4 \cdot 2$tbso (tbso = di-*tert*-butyl sulfoxide), $UI_4 \cdot 8$dmso (dmso = dimethyl sulfoxide), $UI_4 \cdot 6$dibso (dibso = di-isobutylsulfoxide), $UI_4 \cdot xNH_3$ (x = 4, 5, or 10) and $UI_4 \cdot 8$L (L = ε-caprolactam, α-$UI_4 \cdot$ tpao$_2$, β-$UI_4 \cdot$ tpao$_2$, $UI_4 \cdot$ tpao$_4$, and $UI_4 \cdot$ tpao$_6$ (tpao = triphenylarsine oxide) (Brown, 1979; du Preez and Zeelie, 1987, 1989).

The crystal structure of UI_4 has been solved using X-ray and powder neutron diffractions (Levy *et al.*, 1980; Taylor, 1987). The monoclinic structure (Table 5.26) contains uranium atoms with an approximately octahedral coordination, where the uranium atoms are linked by double iodide bridges, forming zigzag chains (Fig. 5.42). Two terminal iodide ions in the *cis* position are completing the coordination sphere of the uranium atom.

Uranium(iv) iodo complexes

Hexaiodo uranium(iv) compounds of the M_2UI_6-type (where M = $N(C_2H_5)_4$, $N(C_4H_9)_4$, $N(C_6H_5)(CH_3)_3$, and $As(C_6H_5)_4$) have been obtained from reactions of the component halides in anhydrous methyl cyanide followed by crystallization in an ice bath or by vacuum evaporation of the solvent. Alternatively, the treatment of uranium(iv) hexachloro or hexabromo complexes with anhydrous liquid hydrogen iodide may be used (Bagnall *et al.*, 1965; Brown *et al.*, 1976). The hexaiodo uranium(iv) compounds are stable, but extremely moisture-sensitive, red colored solids. Exposure to the atmosphere, addition of dilute aqueous acids, or ammonia results in immediate decomposition. The compounds are soluble in anhydrous methyl cyanide and acetone and liberate iodine on heating above 200°C.

From an analysis of the spectral data for $[N(C_2H_5)_4]_2UI_6$ the following electrostatic, spin–orbit, and crystal-field parameters were obtained (in cm^{-1}): $F^2 = 38188(2422)$, $\zeta_{5f} = 1724(39)$, $B_0^4 = 6338(676)$, and $B_0^6 = 992(252)$ (Wagner *et al.*, 1977). Magnetic susceptibility measurements of $[As(C_6H_5)_4]_2UI_6$ have shown that the compound exhibits a temperature-independent paramagnetism in the 84–300 K range with $\chi_{\text{mole}} = 2146(30) \times 10^{-6}$ cm^3 mol^{-1} (Bagnall *et al.*, 1965), analogous to that in the hexachloro and hexabromo uranium(IV) compounds.

(*ix*) *Uranium*(*IV*) *oxide di-iodide and nitride iodide*

UOI_2 can be prepared by heating U_3O_8, U, and I_2 at 450°C in a sealed Pyrex tube. The compound is iso-structural with $UOCl_2$ (orthorhombic symmetry in space group *Pbam*, see Table 5.26) and has $\mu_{\text{eff}} = 3.34$ B.M, as determined from magnetic susceptibility measurements (Levet and Noël, 1979).

The reaction of uranium tetraiodide with gaseous ammonia at temperatures above ~350°C yields uranium nitride iodide, UNI. It may be also obtained by heating uranium nitride with uranium tetraiodide. The compound has tetragonal symmetry (space group *P*4/*nmm*) and is iso-structural with the chloride and bromide analogues (see Table 5.26).

(*x*) *Uranium*(*IV*) *mixed halides and mixed halogeno compounds*

Phases of the composition of $UClF_3$, UCl_2F_2, and UCl_3F occur in the UCl_4–UF_4 system. All are melting incongruently and are thermally unstable, the order being $UClF_3 > UCl_2F_2 > UCl_3F$. The last compound may be prepared by (i) chlorination of UO_2F_2 in refluxing hexachloropropene, (ii) chlorination of UF_3 with chlorine at 350–380°C and by heating of UF_4 in a CCl_4 vapor at 420°C. UCl_3F, obtained in this way, is somewhat contaminated with unreacted starting materials and by-products (UCl_4 or $UOCl_2$). The X-ray powder data obtained for UCl_3F are listed in Table 5.26. A number of ternary chloride fluorides were identified in the $M^{I}Cl$–UF_4 and $M^{II}Cl_2$–UF_4 phase diagrams (where M^{I} = Li, Na, K, Rb, or Cs and M^{II} = Mg or Ca) (Brown, 1979).

The preparation and thermodynamic data of uranium(IV) mixed halides containing bromine have been reported by MacWood (1958). Solid-state reactions of stoichiometric quantities of UCl_4 and UBr_4 yield $UBrCl_3$ at 750°C and UBr_2Cl_2 and $UBrCl_3$ at 590°C. The former may also be prepared by bromination of UCl_3 at 500°C. Some thermodynamic data of these compounds are listed in Table 5.26.

The following mixed tetravalent halides containing iodide anions: (i) UCl_3I, (ii) UCl_2I_2, (iii) $UClI_3$, (iv) UBr_3I, (v) UBr_2I_2, and (vi) $UBrI_3$ (Brown, 1979) have be obtained in pure form. Satisfactory preparation methods involve: (i) iodination of UCl_3 at 500°C in a atmosphere of iodine, (ii) fusion of equimolar amounts of UI_4 and UCl_4 in the presence of small amount of iodine, (iii) fusion of UCl_4 and either UI_3 (at 600°C) or UI_4, (iv) iodination of UBr_3 at 500°C, (v) iodination of UBr_2I at 500°C, or fusion of UBr_4 and UI_4 at 520°C followed by sublimation in a stream of iodine, and (vi) fusion of a 1:3 mole ratio of UBr_4 and UI_4, followed by sublimation at a low pressure of iodine. The compounds are dark-brown or black and undergo rapid hydrolysis in a humid atmosphere. Their melting points range from 478 and 490°C for UBr_3I and UCl_3I, respectively, to somewhat less than 500°C for the remaining mixed halides. All compounds readily lose iodine on heating *in vacuo*, except of $UBrI_3$, which can be sublimed without decomposition. A number of thermodynamic data are available for these compounds (see Table 5.26). The stability of the chloride iodides increases with increasing iodide content. A reverse stability trend is reported for the bromide iodides.

The preparation of uranium(IV) mixed halgeno-compounds by fusion methods and mixed halgeno compounds with donor ligand have been also reported, e.g. $M^I_2UX_2Y_2$ (where M^I = Na, K or Cs, X = Cl, and Y = Br), $K_2UCl_4I_2$, $K_2UBr_4I_2$, $UCl_3I \cdot 8CO(NH_2)_2$, $UI_2Cl_2 \cdot 5DMA$ (DMA = *N*,*N*-dimethylacetamide), and $UClI_3 \cdot 5DMA$ (Gregory, 1958; Brown, 1968).

(*xi*) *Nitrogen-containing uranium halides*

Uranium nitride chlorides, bromides, and iodides

High-temperature ammonolysis of UCl_4, UBr_4, or UI_4 leads to the corresponding uranium nitride chloride, bromide, and iodide. The formation of UNCl and UNBr proceeds via a number of intermediates such as $U(NH_2)Cl_3$, $U(NH)_2Cl_2$, or UNCl. Other routes to UNCl involve high-temperature interaction of UCl_4 and $UN_{1.33}$ as well as solid-state reactions between UCl_4 and aluminium or silicium at about 800°C in a nitrogen atmosphere. Crystallographic data for UNCl (Juza and Sievers, 1965; Juza and Meyer, 1969) are listed in Table 5.26.

A dark brown compound of the formula $UN_{1.03}Br_{1.03}$ was obtained on heating uranium tetrabromide ammoniates in gaseous ammonia for 48–60 h. The compound may also be prepared by heating uranium nitride and the tetrabromide at 600–900°C (Juza and Meyer, 1969). It is insoluble in water but dissolves slowly in 2 M H_2SO_4 with the formation of a green solution. UNBr is converted to uranium nitride in gaseous ammonia at temperatures over 750°C. The compound crystallizes in the BiOCl-type of structure, space group $P4/nmm$, D^7_{4h}, the same as the corresponding UNCl and UNI compounds (see Table 5.26).

The preparation of UNI can be achieved by ammonolysis of uranium tetraiodide at about 350°C or by heating uranium nitride with UI_4. The compound has the BiOCl-type structure and is isostructural with the chloride and bromide analogs (Juza and Meyer, 1969; see Table 5.26).

(c) Pentavalent halides and complex halides

Uranium halides in the pentavalent oxidation state exhibit a tendency to hydrolysis and disproportionation into U(IV) and U(VI) species. However, in the absence of substances that cause hydrolysis, diproportionation does not occur spontaneously (Bacher and Jacob, 1980). Stable solutions of uranium(V) have been obtained, for example, by heating a mixture of UO_3 with thionyl chloride under prolonged refluxing, or by dissolving UF_5 in methyl cyanide, dimethylformamide or Me_2SO as well as of UCl_5 and UBr_5 in some organic solvents (Selbin and Ortego, 1969; Brown, 1979; Halstead *et al.*, 1979). Uranium hexachloride decomposes easily in solvents like carbon tetrachloride, methylene dichloride, or 1,2-dichlorethane and is therefore a suitable starting material for the preparation of uranium(V) compounds on a laboratory scale. The synthesis and properties of various uranium(V) compounds and complexes have been reviewed by Selbin and Ortego (1969). The preparation of UX_6^- (X = F, Cl, Br or I) complexes and the oxohalide complexes $[UOF_5]^{2-}$, $[UOCl_5]^{2-}$, and $[UOBr_5]^{2-}$ has been reported by Ryan (1971). The chemical properties of the compounds, their stability against disproportionation in various non-aqueous halide solutions as well as some aspects of their absorption spectra are also discussed. The halides and complex halides have a variety of colors – from pale blue and red brown to yellow (Table 5.28). The coordination geometry of uranium(V) halides are: octahedral (α-UF_5), pentagonal bipyramidal (β-UF_5), and edge-sharing octahedral (U_2Cl_{10} units).

Uranium(V) has a [Rn]$5f^1$ electronic configuration with the $^4F_{5/2}$ (Γ_7) ground state. A number of spectra in solutions, solids, and gas phase are available (Ryan, 1971; Edelstein *et al.*, 1974; Leung and Poon, 1977; Bacher and Jacob, 1980; Eichberger and Lux, 1980; Carnall and Crosswhite, 1985). The analysis of the spectra has been based on a strong ligand-field model. The site symmetry of the U^{5+} ion is frequently found to be octahedral or distorted octahedral (Carnall and Crosswhite, 1985). The combined ligand field and spin–orbit interaction split the parent ^2F state into the Γ_7, Γ_8, Γ_7', Γ_8', and Γ_6 components. The spectra of U^{5+} in the approximate octahedral sites of the different compounds have very similar f–f band energy and relative intensities, e.g. the spectra of $[N(C_2H_5)_4]_2UOCl_5$ (Selbin *et al.*, 1972a), UCl_5 single crystals (Leung and Poon, 1977), UCl_5 in $SOCl_2$ (Karraker, 1964), and $(UCl_5)_2$ or $UCl_5 \cdot AlCl_3$ in the vapor phase (Gruen and McBeth, 1969). Spectroscopic studies and semi-empirical theoretical calculations of energy levels of UOX_5^{2-} species (X = F, Cl, or Br) in the corresponding tetraethylammonium oxopentahalide complexes reveal that each of the six electronic transitions is shifted to higher energy in the expected order: $Br^- < Cl^- < F^-$. The spin–orbit coupling constants obtained in the best fits also increase in this same order: 1750, 1770, and 1850 cm^{-1}. For a number of uranium(V) halides and complex halides, magnetic susceptibility measurements were carried out over wide temperature ranges. The paramagnetic constants from the Curie–Weiss law $\chi'_M = C/(T-\theta)$ and the effective

Table 5.28 *Properties of selected uranium(*V*) halides, mixed valence halides and complex halides.*[a]

Formula	*Selected properties and physical constants*[b]	*Lattice symmetry, lattice constants* (Å), *polyhedron type and density* (g cm^{-3})[c]	*Remarks regarding information available and references*
α-UF_5	grayish-white or bluish-white crystals; moisture sensitive; soluble in CH_3CN, C_2H_5CN, DMF and Me_2SO; disproportionate over 150°C to $U_2F_9 + UF_6$; m.p. = 348 (+13, –16)°C in a UF_6 atmosphere of 1.6–4.6 bar; density = 5.81g cm^{-3}; α-UF_5: $\Delta_f G^o_m = –1968.7\ (7.0)^\dagger$, $\Delta_f H^o_m = –2075.3\ (5.9)^\dagger$, $S^o_m = 199.6\ (12.6)^\dagger$, $C^o_{p,m} = 132.2\ (4.2)^\dagger$. UF_5(g): $\Delta_f G^o_m = –1862.1\ (15.3)^\dagger$, $\Delta_f H^o_m = –1913\ (15)^\dagger$, $S^o_m = 386.4\ (10.0)^\dagger$; $C^o_{p,m} = 110.6\ (5.0)$. IR: 580s,br, 398s; $\log p_{\text{solid}}$(mmHg) = – (8001 ± 664)/T^{-1} + (13.994 ± 1.119) $\log p_{\text{liquid}}$ (mmHg) = –(5388 ± 803) T^{-1} + (9.819 ± 1.236).Raman (cm^{-1}): 627.5s, 503m, 223m; $\lvert g \rvert = 0.892$;	tetragonal; C^5_{4h}, $I4/m$, No. 87; a = 6.5259(3), c = 4.4717(2), Z = 2; V = 190.44; CN = 6; d(calc.) = 5.81; UF_6 octahedra are bridged by *trans*-fluorides with d(U–F1) = 2.235(1) to give an infinite linear chain parallel to the c-axis. The remaining four F atoms in the octahedron are bound to one U atom with d(U–F2) = 1.995(7)	*crystallographic and neutron powder data; UV, Vis, IR and Raman spectra; heat capacity* (Zachariasen, 1949c; Osborne *et al.*, 1955; Burns *et al.*, 1960; Paine *et al.*, 1976; Eller *et al.*, 1979; Howard *et al.*, 1982); *thermodynamic data* (Rand and Kubaschewski, 1963; Kubaschewski and Alcock, 1979; Fuger *et al.*, 1983; Grenthe *et al.*, 1992; Guillaumont *et al.*, 2003); *magnetic susceptibility data, chemical properties* (Eller *et al.*, 1979; Brown, 1968, 1973); *optical spectra and crystal-field analysis* (Hecht *et al.*, 1986b); *photoelectron spectra* (Thibaut *et al.*, 1982)
β-UF_5	pale yellow; moisture sensitive; soluble in CH_3CN, C_2H_5CN, DMF and Me_2SO; β-UF_5: $\Delta_f G^o_m = –1970.6(5.6)^\dagger$, $\Delta_f H^o_m = –2083.2\ (4.2)^\dagger$, $S^o_m = 179.5\ (12.6)^\dagger$; $C^o_{p,m} = 132.2\ (12.0)^\dagger$. IR (cm^{-1}): 623s,sh, 567s, 508s, 405s; Raman: 623s, 610s, 280m.	tetragonal; D^{12}_{2d}, $I\bar{4}2d$, No. 122; a = 11.469(5), c = 5.215(2); Z = 8; CN = 7; V = 685.97; d(calc.) = 6.45	*crystallographic and neutron diffraction data, IR and Raman spectra, thermodynamic data, chemical properties* (Brown, 1968; Paine *et al.*, 1976; Ryan *et al.*, 1976; Bacher and Jacob, 1980; Taylor and Waugh, 1980; Grenthe *et al.*, 1992; Guillaumont *et al.*,

	$\mu_{\text{eff.}} = 2.24$ B.M.; $\theta = -75.4$ K (125–420 K)		2003); *magnetic susceptibility data* (Nguyen-Nghi *et al.*, 1964b) *optical spectra and crystal-field analysis* (Hecht *et al.*, 1986b); *solution spectra* (Halstead *et al.*, 1979)
U_2F_9 (mixed valence)	black; uranium oxidation number = +4.5; disproportionates into UF_4 and UF_6; U_2F_9(cr): $\Delta_f G^o_m = -3812\ (17)^{\dagger}$, $\Delta_f H^o_m = -4016\ (18)^{\dagger}$, $S^o_m = 329\ (20)^{\dagger}$; $C^o_{p,m} = 251.0\ (16.7)^{\dagger}$	cubic; body centered; T^3_d, $I\bar{4}3m$, No. 217; $a = 8.462(2)$; [$a = 8.4716$: (Howard *et al.* 1982)]; $Z = 4$; $V = 607.99$; CN = 9; d(calc.) = 7.091; the structure consists of a three-dimensionally bridged network composed of tricapped trigonal prismatic UF_9 units; $d(U–F_1) = 2.37(2), 2.21(2)$; $d(U–F_2) = 2.266(3)$; F1–U–F1 = 119.5(1), 71.2(3); F1–U–F2 = 67.0(5), 128.4(9)	*crystallographic and neutron diffraction data; reflectance spectrum* (Zachariasen,1949d; Eller *et al.*, 1979; Laveissière, 1967; Taylor, 1976a,b; Howard *et al.*, 1982); *thermodynamic data* (Bacher and Jacob, 1980; Grenthe *et al.*, 1992; Guillaumont *et al.*, 2003)
U_4F_{17} (mixed valence)	black; uranium oxidation number = +4.25; disproportionates into UF_4 and UF_6; U_4F_{17}(cr) $\Delta_f G^o_m = -7464\ (30)^{\dagger}$, $\Delta_f H^o_m = -7850\ (32)^{\dagger}$, $S^o_m = 631\ (40)^{\dagger}$, $C^o_{p,m} = 485.3\ (33.0)^{\dagger}$	monoclinic; deformed UF_4 lattice; C^6_{2h}, $C2/c$, No. 15; $a = 12.09(0.08)$, $b = 10.81(2)$, $c = 8.29(4)$; $\beta = 128.0(8)$; $Z = 12$; CN = 8 (UF_4); d(calc.) = 7.07	*crystallographic data* (Chatelet, 1967); *thermodynamic data* (Bacher and Jacob, 1980; Grenthe *et al.*, 1992; Guillaumont *et al.*, 2003)
$(H_3O)UF_6$	blue-green; above 68(1) °C decomposes to $UF_4 + UO_2F_2$; $(H_3O)UF_6$(cr):$\Delta_f H^o_m = -2641.4\ (3.2)^{\dagger}$	cubic; $a = 5.2229(5)$	*X-ray powder diffraction data; VIS, NIR and IR spectra, EPR data* (Masson *et al.*, 1976); *thermodynamic data* (Grenthe *et al.*, 1992; Guillaumont *et al.*, 2003)
Other hydrated fluorides: $HUF_4{\cdot}2.5H_2O$; $HUF_4{\cdot}1.25H_2O$;	blue or light blue		*general properties* (Bacher and Jacob, 1980)

Table 5.28 (*Contd.*)

Formula	*Selected properties and physical constants*[b]	*Lattice symmetry, lattice constants* (Å), *polyhedron type and density* (g cm^{-3})[c]	*Remarks regarding information available and references*
$LiUF_6$	pale blue; EPR: $g_o = -0.768$; $\|\Delta g\| = 0.022$; $\Delta H = 109$ Oe; angle of distortion 0.13°; $\|g\| = 0.768$; $g_{\|\|} = -0{,}801$, $g\perp = -0.753$; $\varsigma = 1969$; IR and Raman(cm^{-1}): $\nu_1 = 622$, $\nu_2 = 439$, $\nu_3 = 515$, $\nu_4 = 152$, $\nu_5 = 222, 232$, $\nu_6 = 107^e$	rhombohedral; C_{3i}^2, $R\bar{3}$, No. 148; structure type of $LiSbF_6$; $a = 5.262$, $c = 14.295$	*crystallographic data* (Brown, 1968, 1973; Penneman *et al.*, 1973); *absorption spectra, IR data, ESR data* (Hecht *et al.*, 1986a; Rigny and Plurien, 1967; Allen *et al.*, 1978; Halstead *et al.*, 1979; Bacher and Jacob, 1980)
α-$NaUF_6$	pale blue; air sensitive; EPR: $g_o = -0.745$; angle of distortion 0.65° $g_{\|\|} = -0.8175$, $g\perp = -0.708$; $\varsigma = 1965$; IR and Raman (cm^{-1}): $\nu_1 = 621$, $\nu_2 = 449$, $\nu_3 = 520$, $\nu_4 = 122^e$, 132^e, $\nu_5 = 206, 209$, $\nu_6 = 72^e$	rhombohedral; C_{3i}^2, $R\bar{3}$, No.148; structure type of $LiSbF_6$; $a = 5.596$, $c = 15.526$	*crystallographic data* (Brown, 1968, 1973; Penneman *et al.*, 1973); *absorption spectra* (Bacher and Jacob, 1980; Hecht *et al.*, 1986a); *thermodynamic data* (Kudriashov *et al.*, 1978; Fuger *et al.*, 1983); *ESR data* (Rigny and Plurien, 1967; Halstead *et al.*, 1979)
β-$NaUF_6$	pale blue; air sensitive; EPR: $\|g\| = 0.748$; $\|\Delta g\| = 0.107$; $\Delta H = 57$ Oe; angle of distortion = 0.65°	cubic fcc; O_h^5, $Fm3m$, No. 225; $NaTaF_6$ structure type; $a = 8.608$	*crystallographic data* (Brown, 1968, 1973; Penneman *et al.*, 1973) *thermodynamic data* (Kudriashov *et al.*, 1978; Fuger *et al.*, 1983); *spectroscopic data* (Moskvin and Zaitseva, 1962)
KUF_6	yellow-green; air sensitive	orthorhombic; D_{2h}^{18}, $Cmca$, No. 64; CN = 6; $RbPaF_6$ structure type; $a = 5.61$, $b = 11.46$, $c = 7.96$; dodecahedron sharing edges to form chains	*crystallographic data* (Brown, 1968, 1973; Penneman *et al.*, 1973); *absorption sp*ectra (Bacher and Jacob, 1980) *thermodynamic data* (Kudriashov *et al.*, 1978; Fuger *et al.*, 1983)
$RbUF_6$	yellow-green;		*crystallographic data* (Penneman *et al.*, 1973 ; Brown, 1968, 1973);

		orthorhombic; D_{2h}^{18}, *Cmca*, No. 64; $RbPaF_6$ structure type; $a = 5.82$, $b = 11.89$, $c = 8.03$	*absorption spectra* (Bacher and Jacob, 1980); *thermodynamic data* (Kudriashov *et al.*, 1978; Fuger *et al.*, 1983); *crystal-field calculations* (Amberger *et al.*, 1983)
$CsUF_6$	pale blue to green blue; (ν(U–F) = 503s; EPR: $\lvert g\rvert = 0.709$; $\lvert g\rvert = 0.709$; $\lvert\Delta g\rvert = 0.210$; angle of distortion = 1.25°; $g_{\parallel} = -0{,}928$, $g\perp = -0.681$; $\varsigma = 1985\ \mathrm{cm}^{-1}$; IR and Raman ($\mathrm{cm}^{-1}$): $\nu_1 = 608$, $\nu_2 = 452$, $\nu_3 = 505$, $\nu_4 = 126\text{–}130^{e}$, $\nu_5 = 190, 213$, $\nu_6 = 60^{e}$	rhombohedral; C_{3i}^{2}, $R\bar{3}$, No. 148; $KCsF_6$ structure type, $a = 8.04$, $c = 8.39$; dodecahedron sharing edges to form chains	*crystallographic data* (Brown, 1968, 1973; Penneman *et al.*, 1973); *absorption spectra, NMR-spectra; IR and Raman spectra* (Bacher and Jacob, 1980, Carnall and Crosswhite, 1985; Hecht *et al.*, 1986a; Geichman *et al.*, 1962); *magnetic susceptibilities* (Mulak and Żołnierek, 1972); *ESR spectra* (Rigny and Plurien, 1967); *thermodynamic data* (Kudriashov *et al.*, 1978; Fuger *et al.*, 1983)
NH_4UF_6	yellow-green; $\mu_{\mathrm{eff}} = 1.74$ B.M. (93–200 K); $\mu_{\mathrm{eff}} = 2.25$ B.M. (200–390 K)^{d}	orthorhombic; D_{2h}^{18}, *Cmca*, No.64; $RbPaF_6$ structure type; $a = 5.83$, $b = 11.89$, $c = 8.03$; dodecahedron sharing edges to form chains	*crystallographic data* (Brown, 1968, 1973; Penneman *et al.*, 1973; *absorption spectra; magnetic susceptibility* (Nguyen-Nghi *et al.*, 1965; Bacher and Jacob, 1980)
$AgUF_6$	decomposes at 230°C to F_2, UF_4 and AgF	tetragonal; $a = 5.42$, $c = 7.95$	*crystallographic data* (Brown, 1968, 1973; Penneman *et al.*, 1973)
$TlUF_6$		orthorhombic; D_{2h}^{18}, *Cmca,* No.64; $a = 5.96$, $b = 11.55$, $c = 8.00$.	*crystallographic data* (Charpin, 1965)
$UF_5(SbF_5)_2$		monoclinic; C_{2h}^{5}, $P2_1/c$, No. = 14; $a = 8.110(4)$, $b = 14.129(6)$, $c = 10.032(6)$; $\beta = 96.97(5)°$; $Z = 4$; $V = 1141.03$; d(calc.) = 4.46	*crystallographic data* (Sawodny *et al.*, 1980)

Table 5.28 (*Contd.*)

Formula	*Selected properties and physical constants*[b]	*Lattice symmetry, lattice constants* (Å), *polyhedron type and density* (g cm^{-3})[c]	*Remarks regarding information available and references*
$NOUF_6$	greenish-white; IR (cm^{-1}): ν(U–F) = 2333, 550s, 509sh; Raman: 616, 495, 441, 225, 206; $\lvert g \rvert = 0.748$	cubic; T_h^7, $Ia3$, No. 206; a = 10.464; d(exp.) = 4.30(5)	*crystallographic data* (Brown, 1973; Penneman *et al.*, 1973; *chemical reactivity, absorption spectra; IR and Raman spectra* (Geichman *et al.*, 1962; Bacher and Jacob, 1980); *ESR spectra* (Rigny *et al.*, 1971)
$C_{36}H_{30}P_2NUF_6$ bis (triphenylphosphine) iminium hexafluorouranate(V)	exhibits an unusual g-tensor with $\lvert g_1 \rvert = 0.79$, $\lvert g_2 \rvert = 0.69$, $\lvert g_3 \rvert = 0.65$ which is attributed to low site symmetry and/or very small distortions of the UF_6^- octahedron	triclinic; C_i^1, $P\bar{1}$, No. 2; a = 14.553 (9), b = 12.110(7), c = 12.384(8); $\alpha = 73.08(4)°$, $\beta = 95.40(5)°$, γ = 64.64(4)°; Z = 2; d(exp.) = 1.62, d(calc.) = 1.62; the U atom lies in a general position in the cell; d(U–F) = distances range between 2.00(1) and 2.061.	*crystal structure, EPR spectra* (Eastman *et al.*, 1981)
$Co(UF_6)_2{\cdot}4H_2O$		triclinic; a = 11.52, b = 10.11, c = 5.22; $\alpha = 91.30°$, $\beta = 91.30°$, $\gamma = 90.0°$; d(exp.) = 4.52	*crystallographic data* (Montoloy and Plurien, 1968)
other hexa- and heptafluoro complexes: (i) K_2UF_7; Rb_2UF_7; (ii) Cs_2UF_7; (iii), (iv) $(NH_4)_2UF_7$; (v) $N_2H_6UF_7$; (vi) $N_2H_6(UF_6)_2$; (vii) NO_2UF_6; (viii) $(NH_3OH)UF_6$; (ix) $As(C_6H_5)_4UF_6$; (x) $Cu(UF_6)_2{\cdot}4H_2O$.			*general properties* (i–iv) Penneman *et al.*, 1964b; (v) Frlec *et al.* (1966), (vi) Frlec and Hyman (1967) (vii) Gleichman *et al.*,1961 (i–x) Bacher and Jacob, 1980

Na_3UF_8	pale blue; $\mu_{\text{eff.}} = 2.29$ B.M.	tetragonal; D_{4h}^{17}, $I4/mmm$, No.139; Na_3PaF_8 structure type; $a = 5.470$, $c = 10.940$	*crystallographic data* (Brown, 1973; Penneman *et al.*, 1973; Freestone and Holloway, 1991); *magnetic susceptibility,* ^{19}*F-NMR spectra* (Bacher and Jacob, 1980)
K_3UF_8	pale blue	fcc cubic; O_h^5, $Fm\bar{3}m$, No. 225, $a = 9.20$	*crystallographic data* (Brown, 1973; Penneman *et al.*, 1973; Freestone and Holloway, 1991); *IR spectra* (Bacher and Jacob, 1980)
Rb_3UF_8		fcc cubic; O_h^5, $Fm\bar{3}m$, No. 225, $a = 9.60$	*crystallographic data* (Brown, 1968; Bacher and Jacob, 1980; Freestone and Holloway, 1991); *absorption spectra and spectral data* (Bacher and Jacob, 1980; Penneman *et al.*, 1964b)
Cs_3UF_8		fcc *cubic;* O_h^5, $Fm\bar{3}m$, No.225	*X-ray powder diffraction data, absorption spectra, magnetic susceptibilities* (Bacher and Jacob, 1980)
Ag_3UF_8		cubic; $a = 4.36$; d(exp.) $= 6.49$	*crystallographic data* (Brown, 1973; Penneman *et al.*, 1973; Freestone and Holloway, 1991); *IR spectra* (Bacher and Jacob, 1980)
Tl_3UF_8		cubic; $a = 4.75$	*crystallographic data* (Bougon and Plurien, 1965; Freestone and Holloway, 1991). (Bacher and Jacob, 1980)

Table 5.28 (*Contd.*)

Formula	*Selected properties and physical constants*[b]	*Lattice symmetry, lattice constants* (Å), *polyhedron type and density* (g cm^{-3})[c]	*Remarks regarding information available and references*
other octafluoro complexes:			
$(NH_4)_3UF_8$.			
$N_2H_6(UF_6)_2$	bluish-green; $\mu_{eff} = 1.61$ B.M. (80–293 K)		*magnetic susceptibility, IR and Raman data* (Frlec *et al.*, 1966; Frlec and Hyman, 1967)
$N_2H_6UF_7$	yellow; $\mu_{eff} = 1.66$ B.M. at 273 K (160–280 K); $\theta = 111$ K		*magnetic susceptibility, IR and Raman data* (Frlec *et al.*, 1966; Frlec and Hyman, 1967)
$(NH_3OH)UF_6$	blue; $\mu_{eff} = 152$ B.M. at 300 K; (the Curie–Weiss law is not obeyed)		*magnetic susceptibility, IR and Raman data* (Frlec and Hyman, 1967)
$[N(C_2H_5)_4]_2UOF_5$	pink; air sensitive; IR data (cm^{-1}): ν(U–O) = 852, 760 cm^{-1}; $\|g\| = 0.58$		*IR data* (Ryan, 1971); *EPR and crystal-field spectra* (Selbin and Sherrill, 1974)
$[N(C_2H_5)_4]_2$ $UOF_5 \cdot 2H_2O$	pink; air sensitive; IR data: ν(U–O) = 872, 780 cm^{-1}		*IR data* (Ryan, 1971)
UO_2F		monoclinic; $a = 8.22$, $b = 6.81$, $c = 32.08$; $\beta = 90.5$	*X-ray powder diffraction, optical and magnetic data* (Kemmler-Sack, 1967, 1969)
$UO_2F_{0.25}$	deep-gray to black	cubic; fluorite type of structure; $a = 5.49$; $Z = 4$; d(calc.) = 11.4; d(exp.) = 11.0	*X-ray powder diffraction, optical and magnetic data* (Kemmler-Sack, 1967, 1969)
(i) $NaSrU_2O_6F$ (ii) $KSrU_2O_6F$ (iii) $RbSrU_2O_6F$ (iv) $TlSrU_2O_6F$ (v) $NaBaU_2O_6F$		cubic; O_h^7, $Fd3m$, No. 227; (i) $a = 11.16$ (ii) $a = 11.27$ (iii) $a = 11.34$ (iv) $a = 11.27$	*crystallographic data* (Kemmler-Sack, 1968c)

(vi) $KBaU_2O_6F$ (vii) $RbBaU_2O_6F$ (viii) $TlBaU_2O_6F$ (ix) $KPbU_2O_6F$ (x) $RbPbU_2O_6F$ (xi) $TlPbU_2O_6F$		(v) $a = 11.31$ (vi) $a = 11.39$ (vii) $a = 11.45$ (viii) $a = 11.40$ (ix) $a = 11.33$ (x) $a = 11.36$ (xi) $a = 11.36$	
$UZr_6O_{14}F$		orthorhombic; C_{2v}^9, $Pna2_1$, No.33; $a = 5.328(1)$, $b = 36.64(1)$, $c = 5.065(1)$; $Z = 4$; $V = 988.78$; d(calc.) = 6.91	*crystallographic data* (Papiernik *et al.*, 1980, 1983)
α-UCl_5	red-brown; very moisture sensitive; in water disproportionates to U(IV) and U(VI); soluble in CS_2, CCl_4 and $SOCl_2$. m.p. = dec; density = 3.81 g cm^{-3}. UCl_5(cr): $\Delta_f G_m^o = -930.1$ (3.9)†, $\Delta_f H_m^o = -1039.0$ (3.0)†, $S_m^o = 242.7$ (8.4)†; $C_{p,m}^o = 150.6$ (8.4)†. UCl_5(g): $\Delta_f G_m^o = -849.6$ (15.1)†, $\Delta_f H_m^o = -900$ (15)†, $S_m^o = 438.7$ (10.0)†; $C_{p,m}^o = 123.6$ (5.0)†. $\log p$ (mmHg) = $-3307\ T^{-1}$ +3.361 $\mu_{\text{eff.}} = 2.00$ B.M, $\theta = -99$ K, (14–300 K); ESR: $\lvert g \rvert = 1.188$; IR (cm^{-1}): 360, 340, 320, 308sh, 263, 227, 177, 169, 150, 127, 116, 102, 64; Raman (cm^{-1}): 367, 324, 130;crystal-field data (cm^{-1}): $B_0^4 = 134.79$ (1125), $B_0^6 = 158.6(745)$, $\varsigma_{5f} = 1559(115)$	monoclinic; C_{2h}^2, $P2_1/n$, No.11; structure based on cubic close packing of Cl atoms in which U atoms occupy one-fifth of the octahedral holes; two such octahedra share one edge forming a U_2Cl_{10} unit; d[U–Cl(1)] = 2.70, d[U–Cl(1')] = 2.67, d[U–Cl(2)] and d[U–Cl(4)] = 2.43, d[U–Cl(3)] and d[U–Cl(5)] = 2.44; $a = 7.99$, $b = 10.69$, $c = 8.48$; $\beta = 91.5$; $Z = 4$; d(calc.) = 3.81	*synthesis:* (Rediess and Sawodny, 1982); *crystallographic data* (Smith *et al.*, 1967; Brown, 1973); *thermodynamic data* (Grenthe *et al.*, 1992; Guillaumont *et al.*, 2003); *electrical properties, optical data and crystal-field analysis* (Leung and Poon, 1977; Brown, 1979; Carnall and Crosswhite, 1985); *photoelectron spectra* (Thibaut *et al.*, 1982); *IR and Raman spectra*; (Brown, 1979); *magnetic properties and electron spin resonance data* (Handler and Hutchison, 1956; Fuji *et al.*, 1979; Miyake, 1991)
β-UCl_5	red-brown	triclinic; C_i^1, $P\bar{1}$, No.2; $a = 7.07$, $b = 9.65$, $c = 6.35$; $\alpha = 89.1$,	*crystallographic data* (Müller and Kolitsch, 1974)

Table 5.28 (*Contd.*)

Formula	*Selected properties and physical constants*[b]	*Lattice symmetry, lattice constants* (Å), *polyhedron type and density* (g cm^{-3})[c]	*Remarks regarding information available and references*
		$\beta = 117.36$, $\gamma = 108.54$; structure based on hexagonal close packing of Cl atoms. In the U_2Cl_{10} units the U–Cl distances of the bridging atoms are 2.70 and those involving the terminal Cl atoms are ranging from 2.43 to 2.45	
$Cl_4UCl_2UCl_4$		triclinic; C_i^1, $P\bar{1}$, No.2; $a = 7.07$, $b = 9.65$, $c = 35.89$; $\alpha = 89.1$, $\beta = 117.36$, $\gamma = 108.54$; $Z = 1$; $V = 360.4$; d(calc.) = 3.83	*crystallographic data* (Müller and Kolitsch, 1974); *spectral data* (Gruen and McBeth, 1969)
$(SCl_3)(UCl_6)$		orthorhombic; D_2^4, $P2_12_12_1$, No. 19; $a = 10.668(10)$, $b = 10.712(4)$, $c = 11.333(6)$; $Z = 4$; $V = 1295.09$; d(calc.) = 3.02	*crystallographic data* (Sawodny *et al.*, 1983)
UCl_5 adducts: $UCl_5 \cdot Cl_2C = CClCOCl$; $UCl_5 \cdot Ph_3PO$; $UCl_5 \cdot SOCl_2$; $UCl_5 \cdot AlCl_3(g)$.			*general properties* (Sillén and Martell, 1964; Bagnall *et al.*, 1964; Gruen and McBeth, 1969)
$LiUCl_6$	IR data (cm^{-1}): $\nu_1 = 343$; $\nu_2 = 293$; $\nu_5 = 160$		*infrared and Raman data* (Stumpp and Piltz, 1974)
α-$NaUCl_6$	yellow; IR data (cm^{-1}): $\nu_1 = 343$; $\nu_2 = 273$; $\nu_5 = 136$	cubic; O_h^5, $Fm\bar{3}m$, No. 225, $a = 9.86(2)$; $Z = 4$; d(U-Cl) = 4.93; d(calc.) = 3.26	*X-ray powder diffraction data*; *thermodynamic data* (Kudryashov *et al.*, 1978; Fuger *et al.*, 1983); *infrared and Raman data* (Stumpp and Piltz, 1974)
β-$NaUCl_6$	yellow	trigonal; C_{3i}^2, $R\bar{3}$, No.148; $a = 6.56$ (1), $c = 18.68(3)$; $Z = 3$; d(U-Cl) =	*X-ray powder diffraction data; thermodynamic data* (Kudryashov

		4.90; *d*(calc.) = 3.37, *d*(exp.) = 3.15	*et al*., 1978; Fuger *et al*., 1983); *infrared and Raman data* (Stumpp and Piltz, 1974)
$KUCl_6$	yellow; IR data (cm^{-1}): $v_1 = 343$; $v_2 = 286$; $v_5 = 141$	orthorhombic; D_{2h}^{18}, *Cmca*, No.64; $a = 6.97(1)$, $b = 14.14(3)$, $c = 9.66(2)$; $Z = 4$; d(U-Cl) = 6.23; d(calc.) = 3.40	*X-ray powder diffraction data; thermodynamic data* (Kudryashov *et al*., 1978; Fuger *et al*., 1983); *infrared and Raman data* (Stumpp and Piltz, 1974)
$RbUCl_6$	deep yellow; moisture and oxygen sensitive; m.p. >280 °C;; IR data (cm^{-1}): $v_1 = 341$; $v_2 = 273$; $v_5 = 136$	orthorhombic; D_{2h}^{18}, *Cmca,* No. 64; $a = 6.92(1)$, $b = 14.14(3)$, $c = 9.66(2)$; $Z = 4$; d(U-Cl) = 6.23; d(calc.) = 3.74	*X-ray powder diffraction data*; *thermodynamic data* (Kudryashov *et al*., 1978; Fuger *et al*., 1983); *infrared and Raman data* (Stumpp and Piltz, 1974)
$CsUCl_6$	yellow; moisture sensitive; soluble in $SOCl_2$; m.p. = 360°C; μ_{eff} = 1.71 B.M., $\theta = -161$ K, (83–308 K); IR data (cm^{-1}): $v_1 = 342$; $v_2 = 280$; $v_5 = 139$	cubic; O_h^5, $Fm\overline{3}m$, No. 225; $a = 10.22(1)$; $Z = 4$; d(calc.) = 3.61, d(U–Cl) = 5.11	*X-ray powder diffraction data; thermodynamic data* (Kudryashov *et al*., 1978; Fuger *et al*., 1983); *infrared and Raman data* (Stumpp and Piltz, 1974)
$TlUCl_6$	orange yellow; IR data (cm^{-1}): $\nu_1 = 348$; $v_2 = 283$; $v_5 = 147$		*infrared and Raman data* (Stumpp and Piltz, 1974)
$UCl_5 \cdot PCl_5$ (= $[PCl_4]^+[UCl_6^-]$)	orange-red; air sensitive; IR data (cm^{-1}): $v_1 = 343$; $v_2 = 271$; $v_5 = 130$	triclinic; C_i^1, $P\bar{1}$, No.2; $a = 7.038(4)$, $b = 7.373(4)$; $c = 13.706(8)$; $\alpha = 89.38(3)$, $\beta = 88.80(3)°$, $\gamma = 105.20(3)°$; $Z = 2$; $V = 686.09$, d(calc.) = 3.02; d(U–Cl) = 2.474(13) to 2.517(14); Cl–U–Cl = 88.6(5) to 92.1(6); the compound is isomorphous with $PCl_5 \cdot NbCl_5$ and $PCl_5 \cdot TaCl_5$, consisting of an assemblage of octahedral $U(1)Cl_6^-$, $U(2)Cl_6^-$ and tetrahedral PCl_4^+ groups. The array of the chlorine atoms are hexagonal	*crystal and molecular structure* (Taylor and Waugh, 1983); *infrared and Raman data* (Stumpp and Piltz, 1974)

Table 5.28 (*Contd.*)

Formula	*Selected properties and physical constants*[b]	*Lattice symmetry, lattice constants* (Å), *polyhedron type and density* (g cm^{-3})[c]	*Remarks regarding information available and references*
		close packed, while the polyhedra are regular within experimental errors	
$[P(C_6H_5)_3CH_2(C_6H_5)]UCl_6$	orange crystals; discolors on exposure to air	monoclinic; C^5_{2h}, $P2_1/c$, No.14; $a = 11.72(1)$, $b = 18.78(1)$, $c = 13.61(1)$; $\beta = 105.71(2)$; $Z = 4$; d(calc.) = 1.851, d(exp.) = 1.85(1). Each uranium atom is surrounded by a slightly distorted octahedron of six crystallographically independent Cl atoms at U–Cl distances ranging from 2.469(7) to 2.513(7)	*crystallographic data* (de Wet *et al.*, 1978)
$[C(N_3)_3]UCl_6$	IR data (cm^{-1}): $\nu_1 = 347$; $\nu_3 = 314$; $\nu_4 = 127$; $\nu_5 = 129$	hexagonal; D^1_{3d}, $P\bar{3}1m$, No.162; $a = 8.19(2)$, $c = 6.43(5)$; d(U–Cl) = 2.56	*crystallographic data; infrared and Raman data* (Kolitsch and Müller, 1974)
$[N(CH_3)_4]UCl_6$	yellow; air sensitive; soluble in $MeNO_2$, MeCN, Me_2CO, Et_2O; $\mu_{eff.} = 1.62$ B.M.; $\theta = -161$K; IR data (cm^{-1}): $\nu_1 = 345$; $\nu_2 = 278$; $\nu_5 = 134$; $\nu_6 = 95$; ν(U–Cl)as = 310		*Infrared and Raman data* (Shamir and Silberstein, 1975, Shamir *et al.*, 1975)
$[N(C_2H_5)_4]UCl_6$	deep yellow cryst.; soluble in $MeNO_2$, MeCN, Me_2CO, Et_2O; IR data (cm^{-1}): $\nu_3 = 310$; $\nu_4 = 122$; ν(U–Cl)as. = 303–310; $\|g\| = 1.12$		*absorption spectra and crystal-field analysis* (Ryan, 1971; Edelstein *et al.*, 1974); *infrared and Raman data* (Ryan, 1971); *ESR data* (Edelstein *et al.*, 1974)

$[N(C_3H_7)_4]UCl_6$	yellow; air sensitive; soluble in $SOCl_2$, $MeNO_2$, MeCN, Me_2CO, Et_2O; IR data (cm^{-1}): $\nu_1 = 340$; $\nu_2 = 278$; $\nu_3 = 310$; $\nu_4 = 121$; $\nu_5 = 129$; $\nu_6 = 91$	*infrared and Raman data* (Shamir and Silberstein, 1975, Shamir *et al*., 1975)
$[As(C_6H_5)_4]UCl_6$	yellow cryst.; soluble in $MeNO_2$, MeCN, Me_2CO, Et_2O; $\mu_{\text{eff.}} = 2.14$ B.M.; $\theta = -280$ K; IR data (cm^{-1}): $\nu_1 = 340$; $\nu_2 = 276$; $\nu_3 = 319$; $\nu_4 = 124$; $\nu_5 = 124$	*infrared and Raman data* (Kolitsch and Müller, 1975)
other hexachloro complexes: $AgUCl_6$; $Ba(UCl_6)_2$; $[NH_2(CH_3)_2]UCl_6$; $[N(CH_3)_4]_3UCl_8$;		*general properties* (Brown, 1979)
$[(N(C_2H_5)_4]_2UOCl_5$	blue; assignment of electronic bands in D_4 symmetry: $\Gamma_7 \rightarrow \Gamma_6 = 1555$, $\Gamma_7 \rightarrow \Gamma_7 = 5050$, $\Gamma_7 \rightarrow \Gamma_7 = 6161$, $\Gamma_7 \rightarrow \Gamma_6 = 8584$, $\Gamma_7 \rightarrow \Gamma_7 = 10616$, $\Gamma_7 \rightarrow \Gamma_6 = 16835$; IR data ($cm^{-1}$): ν(U–O) = 913, 813; other observed bands: 296, 253, 197, and 120	*infrared* (Ryan, 1971) *and electronic spectral data* (Selbin *et al*., 1972a)
$UOCl_3$	brown; moisture sensitive, dissolves in alcohols and $MeNO_2$; sl. soluble in acetone and CCl_4; soluble. in water with decomposition; $UOCl_3$(cr): $\Delta_f G^o_m = -1045.6\ (8.3)^\dagger$, $\Delta_f H^o_m = -1140.0\ (8.0)^\dagger$, $S^o_m = 170.7\ (8.4)^\dagger$; $C^o_{p,m} = 117.2\ (4.2)^\dagger$. IR ($cm^{-1}$): 450, 615, 750, 845, 965	*synhthesis* (Brauer, 1981); *thermodynamic and infrared data* (Brown, 1979; Grenthe *et al*., 1992; Guillaumont *et al*., 2003)

Table 5.28 (*Contd.*)

Formula	*Selected properties and physical constants*[b]	*Lattice symmetry, lattice constants* (Å), *polyhedron type and density* (g cm^{-3})[c]	*Remarks regarding information available and references*
UO_2Cl	violet brown or reddish grey; air sensitive; decomposes >600°C and in aqueous media; not soluble in organic solvents; UO_2Cl(cr): $\Delta_f G^o_m = -1095.2\ (8.4)^\dagger$, $\Delta_f H^o_m = -1171.1\ (8.0)^\dagger$, $S^o_m = 112.5\ (8.4)^\dagger$; $C^o_{p,m} = 88\ (5)^\dagger$. $\mu_{eff} = 1.86$ B.M., $\Theta = -95$ K		*thermal and magnetic properties data* (Brown, 1979; Grenthe *et al.*, 1992; Guillaumont *et al.*, 2003); *magnetic properties* (Levet, 1969); *photoelectron spectra* (Thibaut *et al.*, 1982)
$(UO_2)_2Cl_3$ (mixed valence)	black-brown; contains hexa- and pentavalent uranium; hygroscopic, forms $(UO_2)_2Cl_3{\cdot}7H_2O$ on exposure to air; dissolves slowly in H_2O and dilute mineral acids $\Delta_f G^o_m = -2234.8\ (2.9)^\dagger$, $\Delta_f H^o_m = -2404.5\ (1.7)^\dagger$, $S^o_m = 276\ (8)^\dagger$; $C^o_{p,m} = 203.6(5.0)^\dagger$	orthorhombic; $a = 5.833(2)$, $b = 20.978(2)$, $c = 11.9266(5)$; $Z = 8$, d(calc.) = 5.88, d(exp.) = 6.02	*crystallographic data* (Cordfunke *et al.*, 1977); *thermodynamic data* (Cordfunke *et al.*, 1977; Grenthe *et al.*, 1992; Guillaumont *et al.*, 2003)
$U_2O_2Cl_5$	$\Delta_f G^o_m = -2037.3\ (4.9)^\dagger$, $\Delta_f H^o_m = -2197.4\ (4.2)^\dagger$, $S^o_m = 326.3\ (8.4)^\dagger$; $C^o_{p,m} = 219.4(5.0)^\dagger$	orthorhombic; D^{19}_{2h}, *Cmmm*, No.65; $a = 8.431(3)$, $b = 13.663(3)$, $c = 4.106(2)$; $Z = 2$; $V = 472.98$; d(calc.) = 4.81	*crystallographic data* (Levet *et al.*, 1980); *thermodynamic data* (Cordfunke *et al.*, 1983; Grenthe *et al.*, 1992; Guillaumont *et al.*, 2003)
$U_5O_{12}Cl$	$\Delta_f G^o_m = -5518.0\ (12.4)^\dagger$, $\Delta_f H^o_m = -5854.4\ (8.6)^\dagger$, $S^o_m = 465\ (30)^\dagger$	orthorhombic; D^5_{2h}, *Pmma*, No.51; $a = 7.111(9)$, $b = 19.625(12)$, $c = 4.130(2)$; $Z = 2$; $V = 576.36$; d(calc.) = 8.17	*crystallographic data* (Cordfunke *et al.*, 1985); *thermodynamic data* (Cordfunke *et al.*, 1985; Grenthe *et al.*, 1992; Guillaumont *et al.*, 2003)

UBr_5	deep-brown, dec.. UBr_5(cr): $\Delta_f G_m^o = -769.3$ (9.2)†, $\Delta_f H_m^o = -810.4$ (8.4)†, $S_m^o = 292.9$ (12.6)†; $C_{p,m}^o = 160.7$ (8.0)†. UBr_5(g): $\Delta_f G_m^o = -668.2$ (15.3)†, $\Delta_f H_m^o = -648$ (15)†, $S_m^o = 498.7$ (10.0)†; $C_{p,m}^o = 129.0$ (5.0) $\mu_{eff.} = 1.42$ B.M. ($\chi_g = 1.316 \times 10^{-6}$ at 291 K), (11–291 K)	triclinic; C_1^1; $P\bar{1}$, No. 2; $a = 7.449$ (7), $b = 10.127(14)$, $c = 6.686(4)$; $\alpha = 89.25(12°)$, $\beta = 117.56(4)°$, $\gamma = 108.87(9)°$; $Z = 2$; $V = 417.46$; d(calc.) = 5.07; d(U–Br) = 2.81(7) and 2.94(7) for bridging atoms and 2.58(7) to 2.58(7) for terminal atoms	*crystallographic data* (Levy *et al.*, 1978); *magnetic susceptibility data* (Eichberger,, 1979); *photoelectron spectra* (Thibaut *et al.*, 1982); *thermodynamic data* (Grenthe *et al.*, 1992; Guillaumont *et al.*, 2003)
$P(C_6H_5)_4[UBr_6]$	brown crystals; extremely oxygen- and moisture-sensitive; soluble in CH_2Cl_2	monoclinic; C_{2h}^6, $C2/c$, No.15; $a = 23.155(4)$, $b = 6{,}950(3)$, $c = 18.052$ (3); $\beta = 96.38(2)°$; $Z = 4$; $V = 2887$; d(calc.) = 3.07 d(U–Br1 and U–Br2) = 2.669(3); d(U–Br3 or U–O) = 2.654(4); Br–U–Br = 89.9(11) and O–U–O = 88.8(1) or 89.9(1)	*synthesis and crystallographic data* (Bohrer *et al.*, 1988) *absorption spectra; ESR data* (Eichberger and Lux, 1980; Edelstein *et al.*, 1974); *infrared spectra* (Brown, 1979)
$P(C_6H_5)_4[UBr_6]\cdot 2CCl_4$	almost black crystals; IR (cm^{-1}): ν(U–Br) = 215	monoclinic; C_{2h}^5, $P2_1/c$; No.14; $a = 11.115(3)$, $b = 21.142(5)$, $c = 17.187(5)$, $\beta = 95.42(3)°$; $Z = 4$; $V = 4021$; d(calc.) = 2.25; d(U–Br) = 2.603(4) to 2.679(3); d(U–O) = 2.674(4); Br1–U–Br2 = 89.3(1) Br1–U–Br3 (or O) = 89.5(1) Br2–U–Br3 (or O) = 91.1(1)	*synthesis and crystallographic data* (Bohrer *et al.*, 1988)
$MUBr_6$ [M = (i) Na, K, Rb, (ii) Cs, NH_4, (iii) $N(C_2H_5)_4$, $N(C_4H_9)_4$, $As(C_6H_5)_4$,	brown to black; IR data (cm^{-1}) for $N(C_2H_5)_4UBr_6$: $\nu_3 = 215$; $\nu_4 = 87$; ν(lattice) = 62→68; ν_6 (IR and R inactive) = 61; (i) $\lvert g \rvert = 1.245$; (ii) $\lvert g \rvert = 1.21$; (iii) $\lvert g \rvert = 1.21$		*absorption spectra; ESR data* (Eichberger and Lux, 1980; Edelstein *et al.*, 1974); *infrared spectra* (Brown, 1979); *crystal-field analysis for $[N(C_2H_5)_4]UBr_6$* (Ryan, 1971, Eichberger and Lux, 1980)

Table 5.28 (*Contd.*)

Formula	*Selected properties and physical constants*[b]	*Lattice symmetry, lattice constants* (Å), *polyhedron type and density* (g cm^{-3})[c]	*Remarks regarding information available and references*
M_2UOB_5 (i) M = N $(C_2H_5)_4$ and (ii) As $(C_6H_5)_4$.	IR: 919, 817 (U–O, stetch.), 250, 190 and 80 cm^{-1}; for (i): green solid; $\varsigma_{5f} = 1750$ cm^{-1}, $\Gamma_6 = 16194$, $\Gamma_7 = 10460$, $\Gamma_6 = 8163$, $\Gamma_7 = 6080$, $\Gamma_7 = 4865$, $\Gamma_7 = 1490$, $\Gamma_7 = 0$; $\|g\| = 1.24$; (ii) green solid		*absorption spectra; ESR data; infrared spec tra* (Selbin and Sherrill, 1974; Brown, 1979)
$[N(C_2H_5)_4]_2UBr_6\cdot 2.5$ $N(C_2H_5)_4Br$	green; IR data (cm^{-1}): ν(M–O) = 919, 817; ν(M–Br) = 190s, 80m.		*infrared data* (Ryan, 1971)
$UOBr_3$	brown; $UOBr_3$ (cr): $\Delta_f G_m^o$ = –901.5 (21.3)†, $\Delta_f H_m^o$ = –954(0)†, S_m^o = 205.0 (12.6)†; $C_{p,m}^o$ = 120.9 (4.2)†	monoclinic; C_2^3, *C*2, No.5; *a* = 16.24, *b* = 3.7, *c* = 9.0; β = 110.5	*crystallographic data* (Brown, 1973); *thermodynamic data* (Rand and Kubaschewski, 1963; Grenthe *et al*., 1992; Guillaumont *et al*., 2003)
UO_2Br	brown-black; μ_{eff} = 1.76 B.M., Θ = –200 K	orthorhombic; D_{2h}^{17}, *Cmcm*, No. 63; *a* = 4.106(1), *b* = 20.200 (5), *c* = 3.980(1); *d*(calc.) = 6.97. The coordination polyhedron is a pentagonal bipyramid with two Br and three U atoms; *d*(U–Br) = 2.939(3) in the base of the pentagon; *d*(U–O1) = 2.17(1)×2	*crystallographic data* (Levet *et al*., 1977); *magnetic susceptibility data* (Levet, 1969); *thermodynamic data* (Shchukarev *et al*., 1959); *photoelectron spectra* (Thibaut *et al*., 1982)

		and d(U–O'1) = 2.30(3) = 2.30(3) in the base of the pentagon; d(U–O2) = 2.054(1))×2 at the apices; d(Br–Br) = 3.870(6). The angles are: O(2)–U–(O2) = 176.8 (2); O(2)–U–O'(1) = 90.6(4); Br–U–Br = 85.2(2); Br–U–O(1) = 70.7(2)	
$[N(C_2H_5)_4]_2UOBr_5$; $[As(C_6H_5)_4]_2UOBr_5$; $[N(C_2H_5)_4]_2UOBr_5 \cdot 2.5N(C_2H_5)_4Br$	IR vibrations for $UOBr_5^{2-}$ species (cm^{-1}): 919, 817, 250, 190, and 80; ν(U–O, stretch.) = 919, 817		*absorption spectra; crystal-field analysis* (Selbin and Sherrill, 1974); *infrared spectra* (Ryan, 1971)

---

* Peritectic decomposition point.

† Values recommended by the Nuclear Energy Agency (Grenthe *et al*., 1992; Guillaumont *et al*., 2003).

* *R*, *rhombohedral* (*hexagonal parameters given*).

[a] Values have been selected in part from review articles (Brown, 1979; Bacher and Jacob, 1980; Freeman,1991; Grenthe *et al*., 1992; Guillaumont *et al*., 2003).

[b] m.p. = melting point (°C); b.p. = boiling point (°C); (cr) = crystalline; (g) = gaseous; thermodynamic values in kJ mol^{-1}, or J K^{-1} mol^{-1} at 298.15 K, unless otherwise mentioned; $\Delta_f G_m^o$ (kJ mol^{-1}), standard molar Gibbs energy of formation; $\Delta_f H_m^o$(kJ mol^{-1}), standard molar enthalpy of formation; S_m^o, standard olar entropy; $C_{p,m}^o$(J K^{-1} mol^{-1}), standard molar heat capacity; log p (mmHg) = $-AT^{-1} + B - C \log T$, vapor pressure equation for indicated temperature range; IR = infrared active; val. = valence vibrations; def. = deformation vibrations; stretch. = stretching; all values in cm^{-1}; s: strong; m: medium; w: weak; sh: shoulder; ς_{5f} = spin-orbit interaction parameter; B_2^k-crystal-field parameters; $\mu_{eff.}$ = effective magnetic moment; B.M. = Bohr magneton.

[c] All values are in Å and angles are in degrees; CN, coordination number; d = density [g cm^{-3}], V = molar volume [cm^3 mol^{-1}].

[d] Temperature range with linear relationship of χ_M^{-1} against T.

[e] Deduced from measurements in excited states spectra.

magnetic moments $\mu_{\text{eff}} = 2.84\sqrt{c}\mu_B$ along with some other physical constants are summarized in Table 5.28.

(*i*) *Uranium pentafluoride and uranium*(*V*) *complex fluorides*

Uranium pentafluoride

The pentafluoride exists in two crystalline modifications: a high-temperature α-UF_5 (over 150°C) and a low-temperature β-UF_5 form (below 125°C). The general preparation procedures involve either the oxidation of UF_4 or reduction of UF_6 (Bacher and Jacob, 1980). Halogen fluorides, some noble gas fluorides, and CoF_3, VF_3, and OF_2 may be used as oxidation reagents. The formation of α-UF_5 can be achieved by fluorine oxidation of UF_4 at 150°C, or the conversion of UCl_5 by gaseous HF at 300°C; the low-temperature form may be prepared by the reaction with anhydrous liquid HF (AHF) and UCl_6 or UCl_5. The β-form may be also obtained by reduction of UF_6 by silicium powder, NH_3, or $SOCl_2$. This compound is also formed in AHF in the presence of gold plates, by pyrolysis of NH_4UF_7, photolysis of UF_6 by UV light, and by reaction of $NOUF_6$ in a solution of AHF and BF_3. The reduction of UF_6 to UF_5 has also been achieved in hydrogen bromide and CF_3COOH. Some of the preparation methods are of little practical importance because of small yields, an impure product, or inconvenient starting materials. On laboratory scale the most convenient procedures involve photoreduction of UF_6 in the presence of H_2, CO, or SO_2. The reaction between UF_4 and UF_6 results in the formation of β-UF_5 below 125°C and α-UF_5 at 230–250°C. β-UF_5 is formed also in the following reaction at molar ratios 1.1 to 1 between UF_6 and $(CH_3)_3SiX$ (Brown *et al.*, 1983):

$$UF_6 + (CH_3)_3SiX \rightarrow (CH_3)_3SiF + 1/2X_2 + UF_5 \quad (X = \text{Cl or Br})$$

The pentafluoride is a hygroscopic crystalline solid, which disproportionates even in a humid atmosphere, according to reaction

$$2UF_5 + 3H_2O \rightarrow UF_4 + UO_2F_2 \cdot H_2O + 4HF$$

In aqueous solutions this reaction results in the precipitation of the hydrated tetrafluoride and the formation of a solution of uranyl fluoride. Above 150°C, UF_5 disproportionates slowly to U_2F_9(s) and UF_6(g). The disproportionation reaction can be limited by the presence of UF_6(g); the temperature dependence of the vapor pressure follows the equations (Wolf *et al.*, 1965):

$$\log p_{\text{solid}}(\text{mmHg}) = -8001\,T^{-1} + 13.99$$
$$\log p_{\text{liquid}}(\text{mmHg}) = -5388\,T^{-1} + 9.82$$

UF_5 can be reduced to UF_4 by H_2 or Ni (at 600°C) and by some covalent fluorides such as PF_3, AsF_3, or $AsCl_3$. Halide exchange reactions were observed with BCl_3, $TiCl_4$, and PCl_3, the products being respectively, BF_3, TiF_4, and PF_3, in addition to UF_4 and UCl_6.

Uranium pentafluoride dissolves without hydrolytic decomposition in 48–50% hydrofluoric acid, forming relatively stable blue solutions from which $(H_3O)UF_6 \cdot 1.5H_2O$ crystallizes; by addition of RbF or CsF, the blue MUF_6 salts (M = Rb or Cs) are formed. Uranium pentafluoride dissolves in acetonitrile and reacts with alkali fluorides and sodium ethoxide, NaOEt, to form $M[UF_4]$ and $U_2(OEt)_{10}$, respectively.

The structure of α-UF_5 consists of infinite chains of UF_6 octahedra, bridged by *trans*-fluorides to give a linear chain parallel to the *c*-axis. The remaining four fluorine atoms are single bonded to uranium. The low-temperature β-form is isostructural with PaF_5 and NpF_5 and consists of an eight-coordinate arrangement with a geometry intermediate between dodecahedral and square antiprismatic (Ryan *et al.*, 1976; Eller *et al.*, 1979). The crystal packing of β-UF_5 is shown on Fig. 5.43. Other crystallographic data are listed in Table 5.28.

Theoretical model calculations performed using the vibrational spectrum of monomeric UF_5 molecules isolated in an Ar-matrix indicate a square-pyramidal structure in which the U atoms are located above the equatorial plane formed by the fluorine atoms (Paine *et al.*, 1976).

In non-aqueous solvents such as nitriles, dimethyl sulfoxide, and dimethylformamide, uranium pentafluoride forms stable solutions containing UF_6^- anions and solvated UF_4^+ cations. From these solutions several adducts and complex

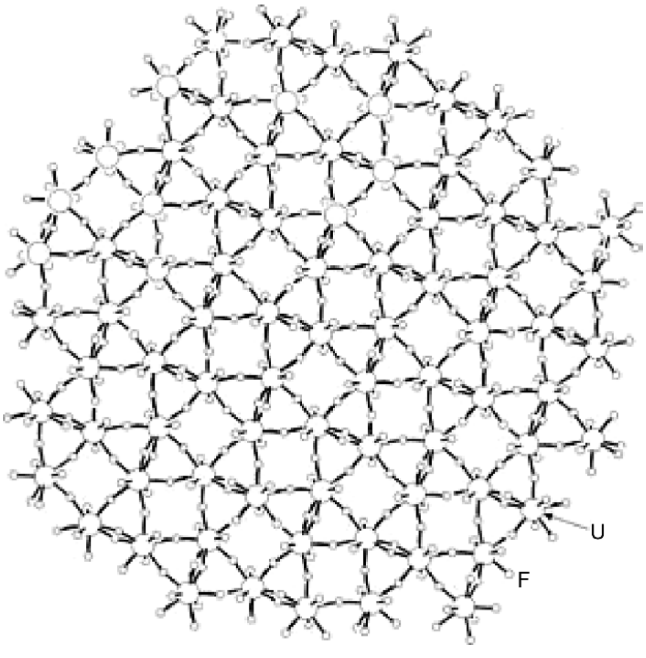

Fig. 5.43 *Crystal packing view of β-UF_5 (from Ryan* et al., 1976).

fluorides have been isolated, for example, $UF_5 \cdot CH_3CN$, $[UF_4(Me_2SO)_3][UF_6]$, $[UF_4(DMF)_3][UF_6]$, $[(C_6H_5N(CH_3)_3][UF_6]$, $[(C_6H_5)_3PNP(C_6H_5)_3][UF_6]$, Na $[UF_6]$, and $K[UF_6]$ (Berry *et al.*, 1977; Halstead *et al.*, 1979). The compounds and their solutions have been characterized by electronic, infrared, Raman, and EPR spectra.

*Complex uranium(*v*) fluoro compounds*

A number of fluorouranates(v) have been characterized by determination of their crystallographic data and their chemical and thermodynamic properties (see Table 5.28). Additional information in the reviews of Chatalet (1967), Penneman *et al.* (1967), Ryan (1971), Brown (1972), Bacher and Jacob (1980), and Freestone and Holloway (1991). Complex compounds identified in a number of selected fused salt systems are listed in Table 5.29.

The compounds may be prepared by a variety of methods (Bacher and Jacob, 1980; Freestone and Holloway, 1991): (i) solid state reactions between UF_5 and the appropriate alkali fluorides in an inert atmosphere at 300°C constitute a general route to most of the fluoro complexes; (ii) melting of mixtures of hexa- and octafluoro complexes leads to the formation of the heptafluoro complex compounds; (iii) solid state reactions or reduction of UF_6 with NH_3 yield ammonium fluorouranates; (iv) treatment of equimolar mixtures of UF_5 and the appropriate alkali fluoride with anhydrous HF yields the hexafluorouranates(v); (v) oxidation of UF_4–alkli fluoride mixtures with fluorine also leads to the hexafluoruranates; and (vi) $RbUF_6$ may be also obtained by crystallization from solutions of RbF and UF_5 in concentrated HF.

The pentafluoro uranates may disproportionate into U(iv) and U(vi). However, they are relatively stable in the absence of substances that cause hydrolysis. Ohwada (1976) and Soulié (1978) suggest that the U–F bonds in the fluorouranates(v) are partly covalent (68 to 77% as compared to 46.3 and 35%, respectively, in UF_4 and β-K_2UF_5). The bonds in UF_5 are assumed to have

Table 5.29 *Uranium(*v*) complex fluorides identified in molten salt systems.*

System	*Complex fluorides*
LiF-UF_5	$LiUF_6$
NaF-UF_5	$NaUF_6$, Na_3UF_8
KF-UF_5	KUF_6, K_2UF_7, K_3UF_8
RbF-UF_5	$RbUF_6$, Rb_2UF_7, Rb_3UF_8
CsF-UF_5	$CsUF_6$, Cs_2UF_7, Cs_3UF_8
NH_4F-UF_5	NH_4UF_6, $(NH_4)_2UF_7$, $(NH_4)_3UF_8$
$N_2H_6F_2$-UF_5	$N_2H_6UF_7$, $N_2H_6(UF_6)_2$
$(NH_3OH)F$-UF_5	$(NH_3OH)UF_6$

a nearly 100% covalent character. The pentafluoro uranates of the M_2UF_7 type (M = K, Rb, Cs, or NH_4) have the same type of powder patterns ($P2_1/c$, C^5_{2h}, No. 14) as that of K_2NbF_7 where the coordination polyhedon is a monocapped trigonal prism (Brown and Walker, 1966). The analysis of the spectral data for $CsUF_6$ (Carnall and Crosswhite, 1985) made it possible to assign the electronic transitions from the Γ_7 ground state to the excited levels Γ_8, $\Gamma_{7'}$, $\Gamma_{8'}$ and Γ_6 of the $5f^1$ electronic configuration. The spin–orbit coupling parameter ς_{5f} and the B^2_0, B^4_0, and B^6_0 crystal-field parameters determined for the D_{3d} site symmetry are equal to 1910.2(13), 534.2(139), –14866(66) and 3305(78) cm^{-1}, respectively.

Pentavalent oxide fluorides and oxide fluoride complexes

White U_2OF_8 oxide fluoride has been obtained by heating of UF_4 in an intermittent oxygen flow at 850°C (Kirslis *et al.*, 1950; Freestone and Holloway, 1991). The compound disproportionates in vacuo at 300°C to form a mixture of uranyl fluoride and uranium hexa and tetrafluoride. The existence of this compound has not been confirmed by other authors (Ekstrom *et al.*, 1974). A series of uranium oxide fluoride phases, UO_xF_y, containing uranium in the oxidation state 5+ ($UO_{2.33}F_{0.33}$ to $UO_{2.00}F_{1.00}$), a mixture of 5+ and 6+ ($UO_{2.58}F_{0.17}$ to $UO_{2.17}F_{0.83}$) and a mixture of 4+ and 5+ ($UO_{2.00}F_{0.25}$) have been obtained by heating UF_4 with UO_3 or U_3O_8 at 400–500°C *in vacuo* (Kemmler-Sack, 1967, 1969). The possible structures of these phases have been discussed on the basis of X-ray powder, magnetic, and spectral data.

A number of complexes of the $M^IM^{II}U_2O_6F$-type (where M^I = Na, K, Rb, or Tl and M^{II} = Ba, Sr, or Pb) were obtained by heating appropriate mixtures of the component fluorides and oxide fluorides at 500–900°C *in vacuo*, e.g. (i) M^IF with $M^{II}UO_4$, and UO_2; (ii) $M^{II}F_2$ with $M_2{}^IUO_4$, $M^{II}UO_4$, and UO_2, and (iii) M^IUO_2 with $M^{II}O$, UO_3, UO_2, and UF_4 (Kemmler-Sack, 1968a). All complexes have cubic symmetry (Kemmler-Sack, 1968b,c) with similar lattice parameters (Table 5.28). Reflectance spectra of the compound have been analyzed on the basis of the $5f^1$ configuration of the U(v) ion in an octahedral field.

Two additional complex oxide fluoride compounds, $[N(C_2H_5)_4]_2UOF_5$ and $[N(C_2H_5)_4]_2UOF_5 \cdot 2H_2O$, have also been isolated. The hydrated compound is formed by hydrolysis of the corresponding UCl_6 salt in a saturated solution of $[N(C_2H_5)_4]F \cdot nH_2O$ in an ethanol–acetone mixture. The complex is easily dehydrated in vacuum (Ryan, 1971). Both compounds are pink colored and oxygen-sensitive. UOF_5^{2-} solutions may be stabilized by an excess of $[N(C_2H_5)_4]F$. Addition of water results in a rapid disproportionation of UOF_6^{2-} to U^{IV} and U^{VI} species. An analysis of the absorption spectra of $[N(C_2H_5)_4]_2UOF_5$ in solid state and in an acetonitrile solution made it possible to make an assignment of the six electronic transitions based on a D_4 ligand field model (Selbin and Sherrill, 1974).

(*ii*) *Uranium pentachloride and uranium*(*v*) *complex chlorides*

Uranium pentachloride

Uranium pentachloride may be prepared by a number of methods, but only a few of them result in high yields and high purity due to the instability of the compound towards thermal decomposition and disproportionation; these reactions take place below 100°C at pressures between 10^5 Pa (1 atm) and 133×10^{-4} Pa, respectively:

$$UCl_5 \xrightarrow{10^5 Pa} UCl_4 + 1/2Cl_2 \text{ and}$$

$$2UCl_5 \xrightarrow{133 \times 10^{-4} Pa} UCl_4 + UCl_6$$

At normal pressure, the disproportionation is complete in the range 100 to 175°C.

One of the most satisfactory preparative methods is to use liquid phase chlorination of UO_3 or U_3O_8 with carbon tetrachloride at 80–250°C under pressure and UCl_5 as catalyst (Brown, 1979). The most convenient laboratory method involves decomposition of UCl_6 at room temperatures in carbon tetrachloride, methylene dichloride, or 1,2-dichloroethane. Another relatively simple method is the reduction of UO_3 by silicon tetrachloride at 400°C followed by vacuum removal of the excess of reagent from the resulting solution of UCl_5 in $SiCl_4$ (Selbin *et al.*, 1968).

Uranium pentachloride is obtained as dark brown crystals, which exist in two crystal modifications. The more often encountered α-UCl_5 is obtained by recrystallization from CCl_4 and the β-UCl_5 is formed by crystallization of UCl_6 from carbon tetrachloride or methylene dichloride (Kolitsch and Müller, 1974). UCl_5 is very hygroscopic and immediately disproportionates into U(IV) and U(VI) in aqueous solutions. It reacts instantly with a number of organic solvents such as alcohols, acetone, dimethyl ether, diethyl ether, ethyl acetate, formamide, or dioxane. In some anhydrous organic solvents such as carbon tetrachloride, carbon disulfide, and thionyl chloride, it forms relatively stable solutions; it is insoluble in benzene, xylene, or isopropyl ether. Impure samples may be recrystallized from carbon tetrachloride and separated from UCl_4 by dissolution and recrystallization from liquid chlorine. Hydrogen reduces UCl_5 to UCl_4 at 250–300°C. Anhydrous gaseous or liquid hydrogen fluoride converts it to UF_5 and fluorine oxidizes it to UF_6. The reactions of UCl_5 with some univalent chlorides yield $N(CH_3)_4UCl_6$, $As(C_6H_5)_4UCl_6$, or $N(CH_3)_2H_2UCl_6$ (Bagnall *et al.*, 1964).

The structures of the monoclinic α-UCl_5 (space group $P2_1/n$) and triclinic β-UCl_5 (space group $P\bar{1}$) are based on a cubic or hexagonal close packing of the chlorine atoms. In the first one, the uranium atoms occupy one-fifth of the octahedral holes and two octahedra are forming a dimeric U_2Cl_{10} unit by sharing a common edge. The structure of the β phase contains the same

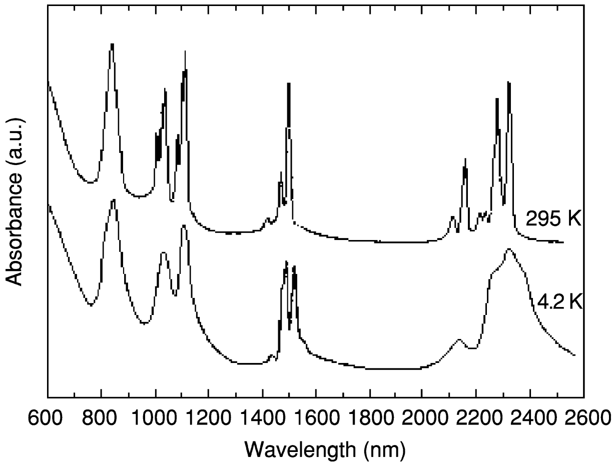

Fig. 5.44 *Absorption spectrum of* UCl_5 *single crystals at* 4.2 *and* 295 K (*partially adapted from Leung and Poon*, 1977). *Reproduced with the permission of Copyright Clearance on Government of Canada Works.*

U_2Cl_{10} units (Table 5.28). The following ligand-field parameters have been reported from an analysis of the UCl_5 spectrum: $\varsigma_{5f} = 1559(115)$, $B_0^4 = 13479$ (1125) and $B_0^6 = -158.6(745)$ (Leung and Poon, 1977). The electronic absorption spectra of the two UCl_5 crystal modifications (see Fig. 5.44) are identical and similar to those of the hexachlorouranates(v).

The magnetic susceptibility follows the Curie–Weiss law in the 14–300 K temperature range. Different effective magnetic moments were reported: according to Rüdorff and Menzer (1957), they range from 1.05 B.M. at 77 K to 1.42 B.M. at 398 K, while Handler and Hutchison (1956) report $\mu_{eff} = 2.00$ B. M. at 300 K with $\Theta = -99$ K.

Complex uranium(v) *chloride compounds*

The isolation of numerous pentavalent uranium complexes with ligands containing N, P, As, S, Se, and Te donor atoms has been reported (Selbin and Ortego, 1969; Brown,1972, 1979). Thus, complexes of UCl_5L-type are formed with triphenylphosphine oxide, thionyl chloride, phenazine, 2,2′-bipyridyl, ethylene bis(diphenylphosphine), triphenylphosphine, trioctylphosphine, diarsine, anthrone, benzanthrone, methyleneanthrone, triphenylbismuthine, diphenyldisulphide, Ph_2Se_2, and Ph_2Te_2; those of the $UCl_5{\cdot}2L$-type – with pyrazine, phthalazine, methyl cyanide, pyridine, 1,10-phenanthroline, 2-mercaptopyridine, ethylene bis-salicylaldiamine, 8-hydroxyquinoline, anthrone, benzil, benzanthrone, and triphenylphosphine oxide, while $UCl_5{\cdot}3L$ complexes are formed with dioxane and tetramethyl amine.

The preparation of $[N(CH_3)_4]_3UCl_8$ and a number of $MUCl_6$ complexes (where M = $N(CH_3)_4$, $N(CH_3)_2H_2$, $N(C_2H_5)_4$, $N(C_3H_7)_4$, $N(C_3H_9)_4$,

$N(C_4H_9)_4$, $P(C_6H_5)_4$, $As(C_6H_5)_4$, NH_4, K, Rb, etc.) has been achieved by addition of carbon disulfide to thionyl chloride solutions of U(v) using the appropriate MCl compound (Bagnall *et al.*, 1964; Brown, 1979). A convenient alternative method to prepare $MUCl_6$ complexes (where M = $N(C_2H_5)_4$, As $(C_6H_5)_4$, or $N(CH_3)_4$) employs chlorine oxidation in nitromethane solutions (Ryan, 1974). UCl_5tcac (tcac is the acronym for $Cl_2C{=}CClCOCl$) has been reported (Fuji *et al.*, 1979) to be a useful starting material for the preparation of $RbUCl_5$, $(n\text{-}C_3H_7)_4NUCl_5$, and a number of UCl_5 adducts with different donor ligands. Other convenient routes to the U(v) complexes involve the addition of MCl (where M = NH_4, $As(C_6H_5)_4$, or $N(CH_3)_4$) to uranium hexachloride in methylene dichloride (Brown, 1979). The reactions between UO_3, $SOCl_2$, and MCl (M = Na, K, Rb, Cs, NH_4, Ag, Ba, or Tl) in sealed vessels at 180–200°C also lead to uranium(v) hexachloro complexes (Stumpp, 1969); the reaction between UO_3 and PCl_5 results in the formation of $UCl_5 \cdot PCl_5$. The last compound should be formulated as $[PCl_4]^+[UCl_6]^-$ (Brown, 1969). Gruen and McBeth (1969) have reported the formation of a uranium(v) chloro complexes in the vapor phase according to the reaction

$$UCl_4 + \frac{1}{2}Cl_2 + AlCl_3 \rightarrow UCl_5 \cdot AlCl_3$$

The analysis of the high-temperature electronic spectrum indicates that the compound should be formulated as $[AlCl_4]^+[UCl_6]^-$.

The hexachlorouranates(v) are very hygroscopic. On exposure to air they are hydrolyzed with disproportionation to U(iv) and U(vi). With the exception of those containing alkali metal cations, they are soluble in numerous organic solvents such as methyl cyanide, diethyl ether, acetone, nitromethane, or phosphorous oxytrichloride. $CsUCl_6$ is reported to react in inert solvents with oxygen donor ligands forming $UCl_5 \cdot L$ adducts. Structure data and references to heats of formation determinations of several uranium(v) chloro-complexes are listed in Table 5.28. Spin–orbit and crystal field parameters, $\varsigma_{5f} = (1913)$, $B^4_0 = 12209(710)$, and $B^6_0 = -39(776)$, were determined for $N(C_2H_5)_4UCl_6$ by Edelstein *et al.* (1974). The magnetic susceptibility of $CsUCl_4$, $[(CH_3)_2H_2]UCl_6$, $[N(CH_3)_4]UCl_6$, and $[As(C_2H_5)_4]UCl_6$ exhibits a Curie–Weiss dependence in two temperture ranges: 140–205 K and 210–310 K. The effective magnetic moments and Weiss constants (in brackets) range between 1.71 (161 K) and 2.14 B.M. (280 K) (Bagnall *et al.*, 1964; Brown, 1979). In the 250–310 K range $[N(CH_3)_4]_3UCl_8$ has a temperature-independent paramagnetism ($\chi_{mole} = 1100 \times 10^{-6}\ cm^3\ mol^{-1}$).

(*iii*) *Uranium*(*v*) *and mixed valence oxide chlorides*

The most convenient methods for the preparation of $UOCl_3$ involve heating of stoichiometric amounts of (i) UO_3 and $MoCl_5$ at 200–220°C *in vacuo*, (ii) UCl_4 and UO_2Cl_2 at about 370°C, or (iii) UO_2Cl_2 with WCl_5, $ReCl_5$, or $MoOCl_3$ at about 200°C (Brown, 1979). The mechanism of the first reaction is:

$$UO_3 + MoCl_5 \rightarrow UO_2Cl_2 + MoOCl_3$$
$$UO_2Cl_2 + MoOCl_3 \rightarrow UOCl_3 + \uparrow MoO_2Cl_2$$

The brown, moisture-sensitive solid is insoluble in non-polar organic solvents like carbon tetrachloride and benzene, but dissolves without decomposition in anhydrous ethanol. In the latter, it reacts with $C_6H_5N \cdot HCl$ to give $[C_6H_5NH]_2UOCl_5$. In other alcohols, acetone, and water, the compound dissolves with decomposition. Hydrolysis of $UOCl_3$ results in the formation of polymeric –U–O–U–O– chains. The reduction with $MoOCl_3$, $MoCl_5$, or $ReCl_5$ *in vacuo* around 200°C leads to UCl_4.

The preparation of UO_2Cl can be achieved by heating equimolar quantities of UO_2Cl_2 and UO_2 at 590°C *in vacuo* (Levet, 1969) or by reduction of UO_3 with $MoCl_3$ (Eliseev *et al.*, 1972). Uranium(v) dioxide monochloride is a brown-violet, air-sensitive solid. It is insoluble in organic solvents and decomposes to UO_2 and Cl_2 at 600°C in an inert atmosphere. UO_2Cl is reduced to UCl_4 by $MoCl_5$ at about 200°C and to $UOCl_2$ when heated with $MoOCl_3$. It exhibits Curie–Weiss dependence between 86 and 295 K with $\mu_{eff} = 1.86$ B.M. and $\Theta = -95$ K (Levet, 1969).

There is also a mixed valence state oxide chloride, $(UO_2)_2Cl_3$, which may be obtained by thermal decomposition of UO_2Cl_2 in high vacuum at 400–500°C, or by heating UO_2 and $UOCl_2$ in the molar ratio of 1:3 at 500°C; at higher temperature (500–650°C), UO_2Cl is formed. The black-brown solid has orthorhombic symmetry (Table 5.28) and dissolves slowly in water and in dilute mineral acids (Cordfunke *et al.*, 1977, Brown, 1979). On exposure to the atmosphere, the compound converts into the heptahydrate $(UO_2)_2Cl_3 \cdot 7H_2O$.

(*iv*) *Complex uranium*(*v*) *oxochlorides*

Brown (1979) has described methods for the preparation and characterization of a number of uranium(v) oxochloro-compounds, such as M_2UOCl_5 (where M = $N(C_2H_5)_4$, $N(C_2H_5)_3H$, $As(C_6H_5)_4$, or C_5H_5NH), $[N(C_2H_5)_4]UOCl_5{\cdot}L$ (where L = phtalazine or 1,10-phenantroline), $[LH]_2UOCl_5{\cdot}L$ (where L = pyridine, quinoline, isoquinoline, α- and β-picoline), and $[C_5H_5NH]_2UOCl_5 \cdot 2.5C_5H_5NHCl$. The complex $[C_5H_5NH]_2UOCl_5$ may be obtained by the addition of pyridine to an ethanolic solution of $UCl_5 \cdot SOCl_2$ saturated with hydrogen chloride; $[N(C_2H_5)_3H]_2UOCl_5$ by photolysis of $UO_2Cl_2 \cdot 2C_5H_5N$ in dry ethanol; and $[N(C_2H_5)_4]_2UOCl_5$ or $[As(C_2H_5)_4]_2UOCl_5$ by controlled hydrolysis in nitromethane of the corresponding hexachloro complexes. They are slightly soluble in nitromethane where they may react with other species to yield different uranium(IV), (V), or (VI) complexes. The oxopentachloro compounds are moisture-sensitive and undergo rapid disproportionation in water-containing solvents with the exception of $[N(C_2H_5)_4]_2UOCl_5$ and $[As(C_2H_5)_4]_2UOCl_5$ that are moderately stable on exposure to air. Reactions between $[N(C_2H_5)_4]_2UOCl_5$ and nitrogen heterocyclic compounds in nitromethane or nitrobenzene yield complexes of uranyl(VI) or U(IV) (Selbin *et al.*, 1972b, 1973; Brown, 1979).

The electronic absorption spectra of $[UOCl_5]^{2-}$ in solid state and non-aqueous solvents are essentially identical (Ryan, 1971). A good agreement between observed and calculated energy levels of $[N(C_2H_5)_4]_2UOCl_5$ is obtained assuming D_4 symmetry and using the following crystal field parameters: $\tau = 700\ \text{cm}^{-1}$ and $\varsigma_{5f} = 1770\ \text{cm}^{-1}$, where τ is a parameter which depends on the radial function and ς_{5f} is the spin–orbit coupling parameter (Selbin *et al.*, 1972a).

(*v*) *Uranium pentabromide and uranium*(*V*) *complex bromides*

Uranium pentabromide

The most convenient method for the preparation of UBr_5 is bromination of either uranium metal or uranium tetrabromide at 55°C, or at room temperatures in the presence of catalytic amounts of methyl cyanide (Brown, 1979). The compound is a dark brown solid and is extremely sensitive to moisture. It disproportionates rapidly on dissolution in water and in various organic solvents like ethanol, acetone, dioxane, and ethylacetate. In chloroform and bromoform, the rate of disproportionation is much slower. Stable solutions may be obtained on dissolution in anhydrous, oxygen-free methyl cyanide and methylene dichloride. A number of stable $UBr_5 \cdot L$ complexes with oxygen donors like $L = (C_6H_5)_3PO$ or $[(CH_3)_2N]_3PO$ have been prepared by bromine oxidation of UBr_4 in the presence of the ligand. Interactions with univalent bromides in thionyl bromide result in the formation of hexabromourantes(V), $MUBr_6$. Uranium pentabromide crystallizes with triclinic symmetry, space group $P\bar{1}$ and is isostructural with β-UCl_5 (see Table 5.28).

Ternary and polynary bromides and bromo compounds of uranium(*V*)

Hexabromouranates(V) of the formula $MUBr_6$ (where M = Na, K, Rb, Cs, NH_4, $N(CH_3)_4$, $N(C_2H_5)_4$, $N(C_4H_9)_4$, $As(C_6H_5)_4$, $P(C_6H_5)_4$, etc.) have been prepared by a variety of methods (Brown, 1979): (i) bromine oxidation of the appropriate tetravalent M_2UBr_6 compounds in non-aqueous solutions, e.g. nitromethane; (ii) halogen exchange reactions between the chloro complexes and an excess of liquid boron tribromide; (iii) reactions between thionyl bromide solutions of pentavalent uranium (prepared by dissolution of UO_3 in the solvent under refluxing) and the appropriate MBr; and (iv) reaction of UBr_6^{2-} and $UO_2Br_4^{2-}$ in nitromethane or methyl cyanide in the presence of anhydrous HBr according to the reaction

$$UBr_6^{2-} + UO_2Br_4^{2-} + 10HBr \rightarrow 2UBr_6^- + 2H_3O^+ + 4HBr_2^-$$

The hexabromouranates have a brown-black color and are rapidly decomposed on dissolution in water or in the presence of moisture. $[As(C_6H_5)_4]UBr_6$ and $[N(C_2H_5)_4]UBr_6$ form stable solutions in anhydrous methylene dichloride and nitromethane. In the last solvent, the presence of bromine is required to avoid reduction to uranium(IV). The complexes with M = $N(CH_3)_4$, $N(C_2H_5)_4$, and $N(C_4H_9)_4$ dissolve also in methylene dibromide and dibromoethane.

Vibronic side-bands dominate in the solid state and solution spectra of the bromo complexes, which indicates an octahedral or close to octahedral stereochemistry. An assignment of the electronic transitions in $[N(C_2H_5)_4]UBr_6$ from the Γ_7 ground level to the Γ_6, Γ_7, and Γ_8 excited levels of the $5f^1$ electronic configuration has been made (Edelstein *et al.*, 1974). The spin–orbit coupling parameter ς_{5f} and the B_0^4 and B_0^6 crystal-field parameters determined from the fitting procedure are 1761(31), 10953(350) and –1058(274) cm^{-1}, respectively (Ryan, 1971; Eichberger and Lux, 1980). There are IR vibronic frequencies at 215 (ν_3) and 87 (ν_4) and at 61 cm^{-1} (ν_6); the identification of the infrared (IR) and Raman inactive (ν_6) vibration has been made by Brown *et al.* (1970). The first electron transfer band in a solution of anhydrous nitromethane has been registered at 17400 cm^{-1}, from which a value of 2.22 for the uncorrected optical electronegativity was deduced (Ryan, 1971).

(*vi*) *Uranium*(V) *oxide bromides*

Uranium(V) *oxide tribromide*

Uranium(V) oxide tribromide, $UOBr_3$, may be conveniently prepared by heating UO_3 in a stream of nitrogen and carbon tetrabromide vapour at 110°C. $UOBr_3$ is a moisture-sensitive and thermally unstable compound, slowly evolving bromine even at room temperatures. It is converted to UO_2Br_2 or UBr_4 by heating in oxygen at 148°C and with CBr_4 at 165°C, respectively. When heated at 200–300°C in a nitrogen atmosphere $UOBr_3$ converts to $UOBr_2$. In water and ethanol, acetone, ethyl acetate, and dioxan, it disproportionates to U(IV) and U(VI) species. The compound is insoluble in non-polar organic solvents like CCl_4 or CS_2.

Uranium(V) *dioxide monobromide*

The preparation of UO_2Br can be achieved by thermal decomposition of UO_2Br_2 in a sealed evacuated glass tube (Levet *et al.*, 1977) or by heating the latter compound in a nitrogen–bromine mixture around 320°C (Gueguin, 1964). It may also be prepared by heating UO_3 at 250°C in a mixture of H_2 and HBr, or by treating UO_2Cl_2 with HBr (Levet, 1965). UO_2Br is a moisture-sensitive black-brown solid. When heated in an inert atmosphere (400–500°C), it decomposes to UO_2 and Br_2. It reacts with chorine (400°C) and oxygen (300°C) to yield UO_2Cl_2 and UO_3, respectively.

The compound has an orthorhombic symmetry in the space group *Cmcm* (No. 63). The coordination polyhedron is a pentagonal bipyramid with two bromine and three oxygen atoms in the equatorial plane and two oxygen atoms at the apices. The uranium atoms are linked in double chains by the sharing of three coordinated oxygen atoms. The structural arrangement is similar to those in $PaOBr_3$, U_3O_8 and $PaCl_5$ and the compound is isostructural with PaO_2Br, NbO_2Br, TaO_2Br, NbO_2I and TaO_2I (Levet *et al.*, 1977). Crystallographic data are listed in Table 5.28. Magnetic susceptibility data are reported by Levet (1969) and the effective magnetic moment is 1.76 B.M. with $\Theta = -200$ K.

(*vii*) *Ternary and polynary uranium*(*v*) *oxide bromides and oxobromo compounds*

Green oxybromo complexes of the formulas $[As(C_6H_5)_4]_2UOBr_5$, $[N(C_2H_5)_4]_2UOBr_6 \cdot 2.5N(C_2H_5)_4Br$, etc. have been obtained by controlled hydrolysis of hexabromouranates(v) in acetone or acetone–nitromethane mixtures at –75°C (Ryan, 1971; Brown, 1979). The complexes are significantly less stable than their fluoro and chloro analogs. They are moisture-sensitive and rapidly disproportionate in numerous anhydrous solvents, such as nitromethane.

Selbin *et al.* (1972a) and Selbin and Sherrill (1974) have presented an interpretation of the electronic spectra of UBr_6^- and $UOBr_5^{2-}$ and have shown the effect of perturbing the $5f^1$ orbital energy levels successively by a tetragonal distortion of the octahedral field and spin–orbit coupling. Semi-empirical theoretical calculations of energy levels of UBr_6^- and $UOBr_5^{2-}$ have been performed in order to locate and assign all electronic transitions in these $5f^1$ species. The first electron transfer transition was observed at 26 700 cm^{-1}. As compared with UBr_6^- species it is shifted by 9300 cm^{-1} to higher frequencies, equivalent to 0.3 eV. This change is reported to result from the pronounced anisotropic nature of the $UOBr_5^{2-}$ complex (Ryan, 1971).

(*viii*) *Intermediate uranium halides*

The reaction of solid UF_4 with gaseous UF_6 results in a gradual formation of intermediate fluorides with a composition between UF_4 and $UF_{4.5}$, depending on the temperature used and the partial pressure of uranium hexafluoride: U_2F_9 (= $UF_{4.5}$), U_4F_{17} (= $UF_{4.25}$), and U_5F_{22} (= $UF_{4.2}$) (Eller *et al.*, 1979; Bacher and Jacob, 1980).

$$3UF_4 + UF_6 \rightleftharpoons 2U_2F_9 \quad (200\,^\circ C)$$

$$7UF_4 + UF_6 \rightleftharpoons 2U_4F_{17} \quad (300\,^\circ C)$$

Agron (1958) has studied the chemical equilibria in these systems; the forward reactions take place at temperatures between 225–300 and 270–350°C, respectively. Agron (1958) has also reported the conditions of formation, equilibrium, dissociation, and the thermodynamics of the disproportionation reactions.

Intermediate uranium fluorides may also be prepared by reduction of UF_6 with HBr by a careful control of the reactant stoichiometry in reactions between

UF_3 and iodine, SiH_4 or PF_3. There are only two oxidation states, U(IV) and U(V), in U_2F_9 as shown by spectroscopic analyses. U_4F_{17} and U_2F_9 are slowly hydrolyzed, in water with the formation of $UF_4 \cdot nH_2O$, UO_2^{2+}, and F^-, and in moist air with the formation of $UO_2F_2 \cdot xHF \cdot yH_2O$. Organic solvents such as C_6H_6, $CHCl_3$, or CCl_4 react with U_2F_9 with reduction to UF_4.

U_4F_{17} has a monoclinic structure that is a distorted version of that of UF_4 (Chatalet, 1967). In U_2F_9 the uranium atoms are nine-coordinated with a tricapped trigonal prismatic arrangement (Zachariasen, 1949d; Taylor, 1976a,b).

Investigation of the UCl_3–UF_4 phase diagram identified mixed valence phases $2UCl_3 \cdot UF_4$ and $UCl_3 \cdot 7UF_4$ that melt incongruently at 625 and 760°C, respectively.

The preparation and characterization of a mixed-valence oxide chloride of the composition $(UO_2)_2Cl_3$ has been reported by Cordfunke *et al.* (1977). The compound is formed by thermal decomposition of anhydrous UO_2Cl_2 at 400–500°C in high vacuum, or by the reaction of UO_2 and UO_2Cl_2 in evacuated quartz tubes at temperatures between 400 and 800°C. On the basis of comparable uranium compounds, such as U_3O_8, the authors have assumed that uranium is present in both oxidation states 6+ and 5+. Structure data of the intermediate halides are given in Table 5.28.

(d) Hexavalent halides and complex halides

Uranium hexahalides and complex halides have been the most extensively investigated uranium compounds due to their commercial applications. The stability of the halides decreases with increasing atomic number of the halide anion, e.g. UCl_6 is much more prone to thermal decomposition than UF_6, and no simple halides are formed with iodine or bromine in this oxidation state. The hexahalides react violently with water at room temperatures to form soluble uranyl halides; they are also readily soluble in polar organic solvents, in many cases with formation of complexes. The uranyl ion (UO_2^{2+}) forms weak complexes with halide ions, with the exception of fluoride cf. Table 5.34, p.349. Hexavalent halides and complex halides are typically yellow and in a few cases colorless (e.g. UF_6) or green (e.g. UCl_6) (see Table 5.30).

Hexavalent uranium has the $[Rn]5f^0$ electronic configuration. The ground state is formally $^1S_0$. There are numerous reports on absorption and fluorescence spectra of hexavalent halides and uranyl halogeno complexes in the solid state, aqueous solutions, and organic solvents that are discussed in a review article by Carnall (1982). The spectra of UO_2^{2+} compounds exhibit a characteristic vibrational fine structure in the visible–ultraviolet region due to coupling with the stretch modes in the linear UO_2 unit. The absorption spectrum of UF_6 displays a similar complex vibronic structure, which is observed to be superimposed on broad and intense charge transfer bands centered near 26670 and 38460 cm^{-1}. An analysis of the spectrum (Lewis *et al.*, 1976) has

Table 5.30 *Properties of selected uranium(VI) halides and complex halides.*[a]

Formula	*Selected properties and physical data*[b,c]	*Lattice symmetry, lattice constant* (Å), conformation and density (g cm^{-3})	*Remarks regarding information available and references*
UF_6	colorless; extremely hygroscopic; m.p. = 64.02 (1136 torr); reacts vigorously with water; soluble: liq. Cl_2, Br_2, CCl_4, CH_3Cl; gives dark red fuming solution with nitrobenzene. bond energies (kJ mol^{-1}): average bond: 523.4 first bond: 286; second bond: 422.9. ionization potential: 14.0 eV $\Delta_f H^o_m$(cr) = –2197.7(1.8)† $\Delta_f H^o_m$(g) = –2148.6(1.9)† S^o_m(g) = 376.3(1.0)† $C^o_{p,m}$(cr) = 166.8(0.2)† $C^o_{p,m}$(g) = 129.4(0.5† sublimation: $\Delta_{sub}H_m$(298.15K) = 49.1(5)† fusion: $\Delta_{fus}H_m$ (329.69K) = 18.8 vaporization: $\Delta_{vap}H_f$(337.202K) = 28.8 triple point : 337.20 K at p = 1522 mbar vapor pressure: solid (273.15–337.17K): log p (mmHg)‡ = 6.38363 + 0.0075377t – [942.76/t+ 183.416)]; liquid (337.17–383.15K):	solid: orthorhombic; D^{16}_{2h}; *Pnma*, No.62; a = 9.900, b = 8.962, c = 5.207; [from neutron diffraction data a = 9.654(3), b = 8.776(4) c = 5.084(3); V = 430.73; d(calc.) = 5.43]; Z = 4; V = 462; d(calc.) = from 4.93 to 5.43, d(exp.) = 4.87; the molecule appears to have an undistorted octahedral structure; distances in the UF_6 octahedron: d(U–F1) = 1.981(4), d(U–F2) = 1.989(4), d(U–F3) (2×) = 1.979 (3), d(U–F4) (2×) = 1.978(3), d(F···F) = from 2.784 to 2.806; F–U–F = 89.78 to 90.20; F2–U–F1 = 179.9°; F4–U–F3 (2×) = 179.6; liquid: octahedral, space group O_h, a = 1.996; gaseous: octahedral, space group O_h, a = 1.996	*X-ray single crystal data* (Hoard and Stroupe, 1959; Levy *et al.*, 1976; Rigny, 1965); *neutron diffraction data* (Taylor and Wilson 1975b; Levy *et al.*, 1983)*; structure in liquid and gaseous states; NMR, IR, Raman, vis, UV, photoelectron and fluorescence spectra; physical constants* (Stoller and Richards, 1961 Lewis *et al.*, 1976; Downs, 1986); *IR and Raman data* (McDowell *et al.*, 1974); *mechanical and thermal properties, phase diagram, phase transformation, thermal conductivity, stability, diffusion coefficients, magnetic susceptibility; paramagnetic resonance; sorption on solids, thermal conductivity, dielectric polarization, transport phenomena, electrical properties, chemical properties; handling, reactions with UF_6, industrial applications* (Bacher and Jacob, 1980, 1986)

log p(mmHg)‡ = 6.99646 –
[1126.288/(t+ 221.963)];
above 383.15K : log p(mmHg)‡ =
7.69069 – [1683.165/(t +
302.148)]
sublimation point: 56.54°C at
760 mmHg
vapor density(326–405K): may be
considered ideal at 298K;
$P(1+1.2328 \times 10^{6}\ T^{-3}\ P)\cdot V = RT$.
critical constants:
  temperature: 503.35(20)K
  pressure: 45.5(5) atm
  density: 1.39 g cm^{-3}
thermal conductivity:
  liquid (345.15K):
  $k = 16.02\times10^{-4}$ J cm^{-1}s^{-1}K^{-1}
  gas‡ $k = (6.104 + 0.002568t)$
  $\times10^{-5}$ J cm^{-1} s^{-1} K^{-1}
density (g cm^{-3}):
  solid: 5.060 (at 298.15K); 4.87
  (at 335.65K);
  liquid‡ : $\rho = 3.630–5.805\times10^{-3}$
  $(t–64.0)$ –1.36 $(t–64.0)^{2}$
  (at 333.15 to 436.15K)
viscosity, η (cP):
  liquid: 0.731 at 340.35K; 0.663
  at 348.15K.
  gas‡ : (1.67–0.0044t) ×10^{-}
^{2} surface tension, γ (N cm^{-1}):
  16.8(3) × 10^{-5} at 343.15K;
  13.1(3) 10^{-5}at 373.15K

Table 5.30 (*Contd.*)

Formula	*Selected properties and physical data*[b,c]	*Lattice symmetry, lattice constant* (Å), conformation and density (g cm^{-3})	*Remarks regarding information available and references*
	refractive index: liquid (Na D line): $n_D = 1.3580$ (4) at 343.15K gas (5100 Å): $n-1 = 5.2 \times 10^{-4}$ pK^{-1} (p in mmHg) fundamental frequencies (IR and Raman, cm^{-1}): v_1 (R) = 667.1 ; v_2 (R) = 534.1; v_3 (IR) = 625.5; v_4 (IR) = 186.2; v_5 (R) = 200.3; v_6 (inact.) = 143 dielectric constants: liquid: $\varepsilon^{-1} = 2.18 \cdot 10^{-6}$ at 65°C and $p =$ 2745.9 kPa gaseous $\varepsilon^{-1} = 3815.4 \times 10^{-6}$ at 28.2°C $\varepsilon^{-1} = 3221.9 \times 10^{-6}$ at 83.1°C magnetic susceptibility: UF_6 exhibits temperature independent paramagnetism molar susceptibility: $\chi_M = (42.7 \pm 2.6) \times 10^{-6}$ cm^{3}mol^{-1} molar polarization: $P_M = 31.453$ (25) cm^3 mol^{-1} (average value for 326–426 K) dipole moment: $\mu \approx 0$ ($\ll 10^{-18}$ Debye)		

$NaUF_7$	white to pale green; very hygroscopic; decomposes over 20°C to $Na_2UF_8 + UF_6$; Raman (solid): 636, 554, 540, 516, 463, 441, 430, 312, 305sh, 243, 218; (L): 111, 91, 57, 35; $\log p$ (mmHg) = $(11.06 \pm 0.02) - 3.48 \times 10^3 T^{-1}$ (T in K)	dimorphic; the high-temperature form is cubic, face centered, $a = 8.511$; $Z = 4$. The low-temperature form is monoclinic. The UF_7^- anion is octahedral with predominant covalent character	*crystallographic data* (Bougon *et al.*, 1976a); *IR, Raman, vis and UV spectra; physical constants, thermodynamic data, thermal decomposition; paramagnetic resonance; NMR* (Brown, 1968; Bacher and Jacob, 1980)
Na_2UF_8	yellow; very hygroscopic; decomposes to $UF_6 + NaF$; Raman (cm^{-1}): 607(10), 440(0.2), 410(0.6), 372(0.5), 343(.7) 303 (1.1), 284(1.1), 170(0.7), 141(0.3); $\log p$ (mmHg) = $(9.25 \pm 0.02) - 4.18 \times 10^3 T^{-1}$	tetragonal; space centered; D_{4h}^{17}; *I*4/*mmm*, No. 139; $a = 5.27$; $c = 11.20$; each U atom is surrounded by eight equidistant F atoms with d(U–F) = 2.29; d(F–F) = 2.63 and 2.97. Each Na atom is also surrounded by 8 F atoms with d(Na–F) = 2.37 and d(F–F) = 2.63 and 2.97	*crystallographic data* (Malm *et al.*, 1966); *IR, Raman, vis and UV spectra; physical constants, thermodynamic data, thermal decomposition* (Bougon *et al.*, 1976a; Katz, 1964); *magnetic susceptibility; paramagnetic resonance; NMR* (Brown, 1968; Bacher and Jacob, 1980).
KUF_7	extremely hygroscopic; decomposes at 100°C to $K_2UF_8 + UF_6$; IR(cm^{-1}): 626w,580sh, 540,s, 497s, 457w, 438w, 314w, 296sh, 256w, 234s, 202s, 140m, 100(L); Raman (solid): 623, 544, 517, 502, 455, 440, 311, 253, 232, 212, 201, 100L, 31L	dimorphic; the high-temperature form is cubic, $a = 5.22$	*crystallographic data* (Bougon *et al.*, 1976a); *IR and Raman spectra; thermal decomposition* (Brown, 1968; Bacher and Jacob, 1980)
K_2UF_8	extremely hygroscopic; decomposes at 300°C to $UF_6 + F_2 + K_2UF_7 + K_3UF_8$; IR: 598m, 510s,br, 460sh, 390sh, 294vw, 260s, 232s,br	orthorhombic; $a = 6.038$, $b = 12.899$, $c = 8.728$	*crystallographic data* (Bougon *et al.*, 1976a); *IR and Raman spectra; thermal decomposition* (Brown, 1968; Bacher and Jacob, 1980)
K_3UF_9		orthorhombic; $a = 6.974$, $b = 7.534$, $c = 9.768$	*crystallographic data* (Iwasaki *et al.*, 1981)

Table 5.30 (*Contd.*)

Formula	*Selected properties and physical data*[b,c]	*Lattice symmetry, lattice constant* (Å), conformation and density (g cm^{-3})	*Remarks regarding information available and references*
$RbUF_7$	extremely hygroscopic: $4RbUF_7 + H_2O \rightarrow Rb_4UO_2F_6 + 3UO_2F_2 + 16HF$; decomposes in vacuum at 210°C to UF_6 + Cs_2UF_8; IR(cm^{-1}): 625w, 550, br, 482w, 457m, 442w, 230m, 210m; (L.): 100, 53, 35. at –170°C; Raman: 625(10), 520(0.1), 443 (0,9), 310(0.5), 248(0.5), 215(0.4)	dimorphic; the high temperature form is cubic; $a = 5.385(5)$	*crystallographic data* (Bougon *et al*., 1976a); *IR and Raman spectra; thermal decomposition* (Brown, 1968; Bacher and Jacob, 1980)
Rb_2UF_8	very hygroscopic; decomposes over 350°C to $UF_6 + F_2$ + Rb_2UF_7 or Rb_3UF_8	orthorhombic; $a = 6.265(16)$, $b = 13.479(37)$, $c = 8.776(21)$	*crystallographic data* (Bougon *et al*., 1976a); *IR and Raman spectra; thermal decomposition*; (Brown, 1968; Bacher and Jacob, 1980)
Rb_3UF_9		orthorhombic; $a = 8.121$, $b = 7.612$, $c = 9.614$	*crystallographic data* (Iwasaki *et al*., 1981).
$CsUF_7$	yellow; hygroscopic; decomposes to $Cs_3UF_8 + UF_6$ at 210°C in vacuum; IR(cm^{-1}): 618vw, 605m, 540sh, 507s, 450sh, 200br, 170; Raman: 622, 462sh, 444, 312, 249, 211	the high-temperature form is cubic with $a = 5.517(5)$. At 15(1)°C it transforms to a tetragonal structure with $a = 5.30$ and $c = 5.37$	*crystallographic* data (Bougon *et al*., 1976a); *IR and Raman spectra; thermal decomposition* (Bacher and Jacob, 1980)
Cs_2UF_8	very hygroscopic; decomposes to $Cs_3UF_8 + UF_6 + F_2$ over 400°C	orthorhombic; $a = 6.480(10)$, $b = 14.036(22)$, $c = 9.272(12)$	*crystallographic data* (Bougon *et al*., 1976a); *IR and Raman spectra* (Brown, 1968; Bacher and Jacob, 1980)

NH_4UF_7	decomposes at 100–170°C to $UF_5 + NH_4F + HF + N_2$; IR(cm^{-1}): 625(10), 447(1.25), 314(0.55), 250 (0.76), 215(1.74), 195(1.53)	cubic; $a = 5.393(5)$	*crystallographic data* (Bougon *et al.*, 1976a); *IR and Raman spectra; thermal decomposition* (Bacher and Jacob, 1980)
$(NH_4)_2UF_8$	Raman (cm^{-1}): 592(10), 470(0.3), 420(0.3), 321(1.4), 286(1.5), 112 (L), 38(L)	orthorhombic; $a = 6.305(13)$; $b = 13.431(23)$, $c = 9.018(16)$	*crystallographic data* (Bougon *et al.*, 1976a); *IR, Raman spectra* (Bacher and Jacob, 1980).
$N_2H_5UF_7$	yellow		*synthesis* Bacher and Jacob (1980).
$NOUF_7$	hygroscopic; decomposes to $NOF + UF_6$ with reversible formation of $NOUF_7$. IR(cm^{-1}): 624vw, 604m, 540sh, 508s, 450sh, 420vw, 208vw, 188vw, 120(L); Raman (solid): 627, 446sh, 434, 310, 240, 210	cubic (high-temperature form); $a = 5.334(70)$; $Z = 1$; CN = 7; d(exp.) = 4.5. At room temperatures the lattice is composed of NO^+ cations and UF_7^- anions. Below –16°C exists β-$NOUF_7$ of lower symmetry.	*crystallographic data* (Geichman *et al.*, 1963; Bougon *et al.*, 1976a); *NMR, IR and Raman spectra* (Brown, 1968; Bacher and Jacob, 1980)
NO_2UF_7	hygroscopic; decomposes to $NO_2F + UF_6$ with reverse formation of NO_2UF_7	tetragonal; $a = 5.74$, $c = 2$	*crystallographic data* (Geichman *et al.*, 1963); *IR spectra and thermodynamic data* (Brown, 1968; Bacher and Jacob, 1980)
$(NO_2)_2UF_8$	IR (cm^{-1}): 590sh, 534sh, 510s, 498sh, 208w, 160m	orthorhombic; D_{2h}^{15}, *Pbca*, No.61; $a = 8.795(1)$, $b = 13.247(2)$, $c = 11.942(2)$; $Z = 8$; $V = 1391.33$; CN = 8. d(calc.) = 4.3 The lattice is composed of NO^+ cations and UF_8^{2-} anions. The coordination polyhedron around the uranium atom is a slightly distorted cube with an almost O_h symmetry	*crystallographic data* (Bougon *et al.*, 1976b; Seppelt and Hwang, 2000), *NMR, IR and Raman spectra* (Brown, 1968; Bacher and Jacob, 1980)
other fluorouranate (VI): $Na_3U_2F_{15}$, $K_3U_2F_{15}$, Rb_3UF_9, Cs_3UF_9,	$Na_3U_2F_{15}$ and $K_3U_2F_{15}$ are extremely hygroscopic		Bacher and Jacob (1980)

Table 5.30 (*Contd.*)

Formula	*Selected properties and physical data*^{b,c}	*Lattice symmetry, lattice constant* (Å), conformation and density (g cm^{-3})	*Remarks regarding information available and references*
$NH_4(UO_2)F(SeO_4) \cdot H_2O$		orthorhombic; D_{2h}^{16}, *Pnma*, No.62; $a = 8.450(4)$, $b = 13.483(5)$, $c = 13.569(5)$; $V = 1545.93$; $Z = 8$; d(calc.) = 4.02	*crystallographic data* (Blatov *et al.*, 1989)
α-UOF_4	orange; hygroscopic; decomposes at 200 to 250°C into $UO_2F_2 + UF_4$; reacts with $H_2O \rightarrow UO_2F_2$. UOF_4(cr): $\Delta_f G_m^o = -1816.3\ (4.3)^\dagger$, $\Delta_f H_m^o = -1924.6\ (4.0)^\dagger$, $S_m^o = 195\ (5)^\dagger$. UOF_4(g): $\Delta_f G_m^o = -1704.814\ (20.142)^\dagger$, $\Delta_f H_m^o = -1763\ (20)^\dagger$, $S_m^o = 363.2\ (8.0)^\dagger$, $C_{p,m}^o = 108.1\ (5.0)$ IR ($U^{16}OF_4$) (cm^{-1}): ν(U–O, valence, terminal) = 893; ν(U–F$_{trans.}$, terminal) = 667s, ν(U–F$_{cis.}$, valence, terminal) = 558; 478m (L); 375s,br (L); Raman: ν(U–O stretch, terminal) = 890s; ν(U–F$_{trans.}$, stretch, terminal) = 660s, ν(U–F$_{cis.}$, stretch, terminal) = 552m	trigonal/rhombohedral; C_{3v}^5, *R3m*, No.160; $a = 13.095(6)$, $c = 5.658\ (2)$; $V = 840.24$; $Z = 9$, d(calc.) = 5.87; The idealized coordination sphere of the U atom consists of a pentagonal bipyramid formed by the light atoms; one O and one F atom occupy indistinguishable axial positions with d(U–O) = 1.870(16) and d(U–F1) = 1.884 (17), d(U–F2(a)) = 2.273, d(U–F2 (b)) = 2.270(11), d(U–F3) = 2.050 (5); O–U–F(1) = 179.2, U–F(2)–U = 153.2(7) (received from neutron diffraction analysis)	*crystallographic data* (Paine *et al.*, 1975); *neutron powder diffraction data* (Levy *et al.*, 1977), *electronic, IR and Raman spectra* (Jacob and Polligkeit, 1973; Paine *et al.*, 1975; Bacher and Jacob, 1980). *thermodynamic data* (Grenthe *et al.*, 1992; Guillaumont *et al.*, 2003)
$UOF_4(SbF_5)_2$		monoclinic; C_{2h}^5, $P2_1/c$, No.14; $a = 7.864(16)$, $b = 14.704(8)$, $c = 9.980\ (8)$; $\beta = 99.8(1)$; $Z = 4$; $V = 1137.17$; d(calc.) = 4.46	*crystallographic data; NMR-investigations* (Bougon, *et al.*, 1979)

$KUOF_5$	hygroscopic	orthorhombic; *a* = 8.02(1), *b* = 11.28(2), *c* = 5.55(1). Each uranium atom is surrounded by eight light atoms forming a dodecahedron. The dodecahedra are linked together by fluorine atoms	*crystallographic data, IR and Raman spectra* (Joubert *et al*., 1978a)
$RbUOF_5$	hygroscopic	orthorhombic; *a* = 8.07(1), *b* = 11.73(2), *c* = 5.77(1). Each uranium atom is surrounded by eight light atoms forming a dodecahedron. The dodecahedra are linked together by fluorine atoms to form infinite chains	*crystallographic data, IR and Raman spectra* (Joubert *et al*., 1978a)
$CsUOF_5$		rhombohedral; C_{3i}^2, $R\overline{3}$, No.148; *a* = 5.41(1); α = 95.57(8)°; *V* = 155.9; *d*(calc.) = 5.13, *d*(exp.) = 5.1(5). The unit cell is very close to that of $CsUF_6$	*neutron powder diffraction and, NMR data* (Joubert *et al*., 1978b; Bougon *et al*., 1978)
NH_4UOF_5	hygroscopic	orthorhombic; *a* = 8.08(1), *b* = 11.59(2), *c* = 5.77(2). Each uranium atom is surrounded by eight light atoms forming a dodecahedron. The dodecahedra are linked together by fluorine atoms to form infinite chains.	*crystallographic data, IR and Raman spectra* (Joubert *et al*., 1978a)
$AgUOF_5$		tetragonal; *a* = 5.370, *c* = 8.043	*crystallographic data* (Malm, 1980)
UO_2F_2	light yellow-green; decomposes in a He stream at 700–900°C to $UF_6 + U_3O_8 + O_2$; sublimes in the presence of HF over 550°C; may be transported with partial	rhombohedral; D_{3d}^5, $R\overline{3}m$, No = 166; *a* = 5.755(1); α = 42,72(5)°; *Z* = 1; CN = 8; *d*(calc.) = 6.37, *d*(exp.) = 5.8; *d*(U–O) = 1.91 (2×); *d*(U–F) = 2.50 (6×)	*synthesis* (Brauer, 1981); *X-ray and neutron powder diffraction data* (Atoji and McDermott, 1970); Zachariasen, 1948e); Bacher and Jacob, 1980) *IR and*

Table 5.30 (*Contd.*)

Formula	*Selected properties and physical data*^{b,c}	*Lattice symmetry, lattice constant* (Å), conformation and density (g cm^{-3})	*Remarks regarding information available and references*
	decomposition in a He stream at 825°C. UO_2F_2(cr): $\Delta_f G_m^o =$ –1557.3 (1.3)†, $\Delta_f H_m^o =$ –1653.5 (1.3)†, $S_m^o = 135.56$ (0.42)†; $C_{p,m}^o =$ 103.22 (0.42)†. UO_2F_2(g): $\Delta_f G_m^o =$ –1318.1 (10.2)†, $\Delta_f H_m^o =$ –1352.5 (10.1)†, $S_m^o = 342.7$ (6.0)†; $C_{p,m}^o =$ 86.4 (3.0)†. IR ($U^{16}O_2F_2$)(cm^{-1}): v_3 ($v_{asym.}UO_2$) = 1020vs; v_4(L.) = inactive; ν_7 ($L[UF_{6/3}]$) = 260; v_8($\delta_{asym.}UO_2$) = 238s. Raman (cm^{-1}): v_1 ($\nu_{sym.}UO_2$) = 918vs; v_2(L) = inactive (?); v_5($L[UF_{6/3}]$) = 444vw; ν_6 ($\delta_{sym.}$ UO_2) = 183m; v_7	neutron powder diffraction data: $a = 4.192$; $c/3 = 5.520$; d(U–O) = 1.74(0.02) (2×); d(U–F) = 2.429 (0.002) (6×). The structure consists of layers of U atoms, which are 5.22 Å apart from each other. The axes of the UO_2 groups are perpendicular to the there planes. The fluorine atoms are 0.61 Å above and below the uranium planes, and weak O···O and O···F bonds holds the layer together	*Raman spectra, chemical properties, conversion of UO_2F_2 to UF_6*. (Bacher and Jacob, 1980); *photoelectron spectroscopy* (Thibaut *et al.*, 1982) *thermodynamic data* (Grenthe *et al.*, 1992; Guillaumont *et al.*, 2003)
$UO_2F_2{\cdot}nH_2O$ ($n =$ 1,2,3,4) $UO_2FOH{\cdot}H_2O$; $UO_2FOH{\cdot}2H_2O$	monohydrate (yellow solid, soluble in H_2O, $v_{U=O} = 990$ cm^{-1}); dihydrate (yellow solid, soluble in H_2O, $\nu_{U=O} = 966$ cm^{-1}); formed when anhydrous compound is exposed to moist air. $UO_2F_2{\cdot}3H_2O$ (cr): $\Delta_f G_m^o =$ –2269.7 (6.9)†, $\Delta_f H_m^o =$ –2534.4 (4.4)†, $S_m^o = 270$ (18)†; $UO_2FOH{\cdot}H_2O$ (cr): $\Delta_f G_m^o =$ –1721.7 (7.5)†, $\Delta_f H_m^o =$ –1894.5 (8.4)†, $S_m^o = 178$ (38UO_2F $OH{\cdot}2H_2O$ (cr): $\Delta_f G_m^o =$ – 1961.0 (8.4)†, $\Delta_f H_m^o =$ –2190.0 (9.4)†, S_m^o = 223 (38)†		*general properties* (Bacher and Jacob, 1980); *thermodynamic data* (Grenthe *et al.*, 1992; Guillaumont *et al.*, 2003)

$UO_2F_2(SbF_5)_3$		monoclinic; C_{2h}^5, $P2_1/c$, No.14; a = 11.040(7); b = 12.438(12); c = 12.147(8); γ = 111.16(20); Z = 4; V = 1555.51; d(calc.) = 4.09	*crystallographic data and characterization* (Fawcett *et al.*, 1982)
$[UO_2F_2\{CO(NH_2)_2\}_2]_2$		monoclinic; $P2_1/b$; a = 10.240(1), b = 10.983(1), c = 8.254(1); β = 98.65(1); Z = 4; d(U–F) = 2.23(2)–2.39(2); d(U–O) = 2.36(2) 2× and 1.72(2) 2×	*crystallographic data* (Mikhailov *et al.*, 1976a)
$Rb_2UO_2F_4 \cdot H_2O$		orthorhombic; C_{2h}^{15}, $Pbca$, No. = 61; a = 8.881(3), b = 14.547(6), c = 11.975(4); Z = 8; d(calc.) = 4.59; V = 1547.07	*crystallographic data* (Brusset *et al.*, 1972)
$Cs_2UO_2F_4 \cdot H_2O$		monoclinic; C_{2h}^5, $P2_1/c$, No.14; a = 8.06(1), b = 12.18(1), c = 9.29(1); β = 109.12(4); Z = 4; V = 861.7, d(calc.) = 4.85	*crystallographic data* (Nguyen Quy Dao, 1972)
$K_3UO_2F_5$	yellow; $v_1(UO_2^{2+}) = 803\,cm^{-1}$, $v_3(UO_2^{2+}) = 863\,cm^{-1}$	tetragonal; C_{4h}^6, $I4_1/a$, No.88; a = 9.159(4), c = 18.170(8); Z = 8; V = 1524.23; d(calc.) = 4.2; pentagonal $UO_2F_5^{2-}$ units are held together by potassium ions	*crystallographic data* (Zachariasen, 1954d; Vodovatov *et al.*, 1984; Lychev *et al.*, 1986); *thermodynamic data* (Fuger *et al.*, 1983)
$Cs_3UO_2F_5$	yellow	cubic; T_h^3, $Fm3$, No.202; a = 9.833 (5); Z = 4; V = 950.73; d(calc.) = 5.33	*crystallographic data* (Rebenko *et al.*, 1968; Brusset and Nguyen Quy Dao, 1971); *thermodynamic data* (Fuger *et al.*, 1983).
$(NH_4)_3UO_2F_5$	yellow	monoclinic; C_s^3, Cm, No.8; a = 29.22, b = 9.48, c = 13.51; β = 136.11°; V = 2594.15; d(calc.) = 3.22. Distorted pentagonal bipyramid	*crystallographic data* (Brusset *et al.*, 1969)

Table 5.30 (*Contd.*)

Formula	*Selected properties and physical data*[b,c]	*Lattice symmetry, lattice constant* (Å), conformation and density (g cm^{-3})	*Remarks regarding information available and references*
$K_2[UO_2F_2(C_2O_4)]$	yellow, stable in air, soluble in water; insoluble in common organic solvents. IR (cm^{-1}): $\nu_{as}(C{=}O) = 1650$vs,b; $\nu_s(C–O) + \nu(C–C) + \delta(O–C{=}O) = 1355$s, 1316s, 1480w, 1455m, 1415w, 1360m, 1315vs.; $\nu_{as}(UO_2) = 905$. Other bands; 3610s, 3500s, 2920w, 845m, 800vs, 782w, 740w, 490s, 450s	triclinic; C_i^1, $P\bar{1}$, No. 2; $a = 10.981$, $b = 11.038$, $c = 12.629$; $\alpha = 108.00°$, $\beta = 86.79°$, $\gamma = 123.99°$; $Z = 2$; d(calc.) = 1.31, d(exp.) = 1.36	*crystallographic data and IR spectral bands* (Chakravorti *et al.*, 1978)
$K_4[UO_2F_2(C_2O_4)_2]$	yellow, stable in air, soluble in water; insoluble in common organic solvents; $\nu_{as}(C{=}O) = 1720$vs, 1655vs; $\nu_s(C–O)+\nu(C–C)+\delta(O–C{=}O) = 1410$vs, 1295vs; $\nu_{as}(UO_2) = 890$vs; Other bands: 3500s, 2910w, 830w, 790vs, 485s, 400s, in cm^{-1}	triclinic; C_i^1, $P\bar{1}$, No. 2; $a = 8.768$, $b = 8.777$, $c = 14.857$; $\alpha = 101.58°$, $\beta = 114.27°$, $\gamma = 85.27$; $Z = 4$; d(calc.) = 4.16, d(exp.) = 4.08	*crystallographic data and IR spectral bands* (Chakravorti *et al.*, 1978)
$K_2[(UO_2)_2F_4(C_2O_4)]$	yellow, stable in air, soluble in water; insoluble in common organic solvents; $\nu_{as}(C{=}O) = 1640$, 1610vs; $\nu_s(C–O)+\nu(C–C)+\delta(O–C{=}O) = 1365$m, 1318vs; $\nu_{as}(UO_2) = 920$vs; Other bands: 3630s, 3460s, 3220w, 2920w, 855s, 795vs, in cm^{-1}	monoclinic; $a = 10.792$, $b = 12.028$, $c = 10.615$; $\beta = 136.88$; $Z = 2$; d(calc.) = 2.92, d(exp.) = 2.83	*crystallographic data and IR spectral bands* (Chakravorti *et al.*, 1978)

$Na_2(UO_2)_2\,(SiO_4)F_2$	The compound is structurally related to soddyite, and is formed during uranyl silicate synthesis in teflon-lined bombs	tetragonal; D_{4h}^{19}, $I4_1/amd$, No.141; $a = 6.975(8)$, $c = 18.31(2)$; $Z = 4$; $V = 890.79$	*crystallographic data* (Blaton *et al.*, 1999)
$Cs_2[(UO_2)_2F_6(H_2O)_2]$		monoclinic; C_{2h}^{5}, $P2_1/c$, No.14; $a = 6.027(2)$, $b = 11.505(2)$, $c = 9.389(2)$; $\beta = 95.72(2)°$; $Z = 2$; $V = 647.8$; d(calc.) = 4.9	*crystallographic data* (Mikhailov *et al.*, 1979)
$[Na_3(UO_2)_2F_7](H_2O)_6$	yellow, transparent crystals: dehydration of the compound gives: $[Na_3(UO_2)_2F_7](H_2O)_2$ at 25–91°C : $[Na_3(UO_2)_2F_7]$ at 150–200°C; at higher temperatures (235–300°C) it decomposes to a mixture of $Na_3UO_2F_5$, UO_2F_2, $NaUO_2F_3$, and $Na(UO_2)_2F_5$	triclinic; C_i^1, $P\bar{1}$, No.2; $a = 6.997(1)$, $b = 7.176(1)$, $c = 8.630(1)$; $\alpha = 77.84(1)^o$, $\beta = 113.30(1)^o$, $\gamma = 104.95(1)^o$; $Z = 1$; $V = 381.62$; d(calc.) = 3.7; d(U–U)single bridge = 4.632(1) and 4.003(1) double bridge; d(U–O1) = 1.79(1), d(U–O2) = 1.77(1); d(U–F) = from 2.21 to 2.39; the structure consists of $[(UO_2)_2F_6{\cdot}F_{2/2}]^{3-}$ chains of complex ions formed by double and single F bridges alternatively	*crystallographic, thermogravimetric and IR data* (Nguyen Quy Dao *et al.*, 1981)
$[K_3(UO_2)_2F_7](H_2O)_2$		triclinic; C_i^1, $P\bar{1}$, No.2; the structure consists of $(UO_2)_2F_7^{3-}$ chains of complex ions formed by double and single F bridges alternatively	*crystallographic data and physicochemical properties* (Mikhailov *et al.*, 1972a; Nguyen Quy Dao and Chourou, 1974)
$K_5(UO_2)_2F_9$		monoclinic; C_{2h}^{6}, $C2/c$, No. = 15; $a = 19.860(1)$, $b = 6.110(1)$, $c = 11.706(4)$; $\beta = 102.58(4)°$; $V = 1386.36$; $Z = 4$; d(calc.) = 4.34	*crystallographic data* (Brusset *et al.*, 1974; *Nguyen Quy Dao and Chourou,S.(1972)* Mikhailov *et al.*, 1972b); *thermodynamic data* (Fuger *et al.*, 1983)
$Cs_2(NH_4)[(UO_2)_2F_7]$		orthorhombic; D_{2h}^{25}, $Immm$, No.71; $a = 6.526(2)$, $b = 8.553(3)$, $c = 12.434(2)$; $Z = 2$; $V = 694.03$; d(calc.) = 4.58	*crystallographic data* (Ivanov *et al.*, 1980)

Table 5.30 (*Contd.*)

Formula	*Selected properties and physical data*^{b,c}	*Lattice symmetry, lattice constant* (Å), conformation and density (g cm^{-3})	*Remarks regarding information available and references*
$Rb_2[(UO_2)_3F_8(H_2O)]\cdot 3H_2O$		orthorhombic; C_{2v}^{16}, *Ama*2, No. = 40; $a = 8.4624(8)$, $b = 14.343(1)$, $c = 13.916(1)$; $V = 1689.07$; $Z = 4$; d(calc.) = 4.74	*crystallographic data* (Mikhailov *et al.*, 1976b)
$K_2\,[(UO_2)_3\,F_8(H_2O)]\cdot 3H_2O$		orthorhombic; C_{2v}^{16}, *Ama*2, No.40; $a = 8.39(5)$, $b = 14.12(8)$, $c = 13.66(8)$; $V = 1618.26$; $Z = 4$; d(calc.) = 4.56	*crystallographic data* (Nguyen Quy Dao., 1979)
$K_2(UO_2F_2)(SO_4)\cdot H_2O$		monoclinic; C_{2h}^5, $P2_1/c$, No. = 14; $a = 9.2634(18)$, $b = 8.6722(18)$, $c = 11.0195(15)$; $\beta = 101.60(1)°$; d(calc.) = 3.83; $V = 867.16$; $Z = 4$	*crystallographic data* (Alcock *et al.*, 1980)
$Ni_2[(UO_2)F_4]_2\cdot 14H_2O$		monoclinic; C_{2h}^5, $P2_1/c$, No.14; $a = 10.141(1)$, $b = 11.901(1)$, $c = 9.510(1)$; $\beta = 96.80(1)$; $V = 1139.67$; $Z = 4$; d(calc.) = 3.09	*crystallographic data* (Ivanov *et al.*, 1982)
$Ni_3[(UO_2)_2F_7]_2\cdot 18H_2O$		monoclinic; C_{2h}^2, $P2_1/m$, No.11; $a = 9.132$, $b = 16.925$, $c = 12.500$; $\gamma = 114.62°$	*crystallographic data* (Ivanov *et al.*, 1981)
$Cs_3UO_3F_5$		cubic; $a = 9.869$	*crystallographic data* (Rebenko *et al.*, 1968)
$U(OTeF_5)_6$		monoclinic; C_{2h}^3, $C/2m$, No. 12; d(calc) = 3.56; $a = 10.30(1)$, $b = 16.61(2)$, $c = 9.98(1)$; $\beta = 114.14(6)°$; $Z = 2$; $V = 1558.09$; d(calc.) = 3.56	*crystallographic data* (Templeton *et al.*, 1976)

UCl_6	black to dark green crystalline material; extremely moisture sensitive; slightly soluble in some organic solvents: CCl_4, $CHCl_3$; hydrolyzes in moist air; reacts vigorously with water to form UCl_2O_2. m.p. = 177.5°C. UCl_6(cr): $\Delta_f G_m^o = -937.1\ (3.0)^{\dagger}$, $\Delta_f H_m^o = -1066.5\ (3.0)^{\dagger}$, $S_m^o = 285.5\ (1.7)^{\dagger}$; $C_{p,m}^o = 175.7\ (4.2)^{\dagger}$. UCl_6(g): $\Delta_f G_m^o = -901.6\ (5.2)^{\dagger}$, $\Delta_f H_m^o = -985.5\ (5.0)^{\dagger}$, $S_m^o = 438.0\ (5.0)^{\dagger}$; $C_{p,m}^o = 147.2\ (3.0)^{\dagger}$. vapour pressure: $\log p$ (mmHg) = $-4000T^{-1} + 10.20$ (298–450 K). IR and Raman (cm^{-1}): v_1 (R) = 367, v_2 (R) = 321, v_3 (IR) = 343, v_4 (IR) = 101, and v_5 (R) = 133	hexagonal; D_{3d}^3, $P\bar{3}m1$, No. 164; $a = 10.95$, $c = 6.016(6)$; $Z = 3$; d(calc.) = 3.594, d(exp.) = 3.17–3.36. Chlorine atoms form an almost regular octahedron around U(1) with d(U–Cl) = 2.47 and Cl–U–Cl angles of 86.6 and 93.4°; the array around U(2) is slightly distorted; d(U–Cl) lie between 2.41(4) and 2.51(4); the Cl–U–Cl angles are of 79.7, 98.0 and 90.4	*synthesis* (Rediess and Sawodny, 1982), *crystallographic and neutron diffraction data* (Zachariasen, 1948c, Taylor and Wilson, 1974b); *thermodynamic data* (Brown, 1973, 1979; Grenthe *et al.*, 1992; Guillaumont *et al.*, 2003), *UV, vis, infrared and Raman spectra; magnetic susceptibility data* (Brown, 1979 and references therein)
$[P(C_6H_5)_4]UOCl_5$	deep orange-red moisture sensitive crystals. IR (cm^{-1}): ν(U–O) = 834, δ(U–O) = 231; Raman: ν(U–O) = 836, δ(U–O) = 229; . ν(U–Cl) = 345, 341(sh), 302, 298, 291 (IR); and 347, 341, 293 (R)	tetragonal; C_{4h}^3, $P4/n$, No. 85; $a = 13.264(5)$; $c = 7.621(5)$; $Z = 2$; d(calc.) = 1.924, d(exp.) = 1.916; d(U–O) = 1.76(1). The structure is composed of octahedral anions and cations with the $\bar{4}$ (S_4) symmetry. Both ions are forming linear stacks parallel to c. d(U–Cl) = 2.636(2) in the equatorial plane and 2.433(4) in the axial bond	*crystallographic dat*a (de Wet and du Preez, 1978); *infrared data* (Bagnall *et al.*, 1975)
UO_2Cl_2	golden-yellow; very hygroscopic; m.p. = 570–578°C very volatile >775°C; soluble H_2O, acetone, alcohol, and common polar organic	orthorhombic; D_{2h}^{16}, $Pnma$, No. 62; $a = 5.725$, $b = 8.409$, $c = 8.720$; $Z = 4$; d(calc.) = 5.349; d(exp.) = 5.28; The U coordination polyhedron is a pentagonal	*crystallographic data* (Debets, 1968; Taylor and Wilson, 1973b); *thermodynamic data* (Cordfunke *et al.*, 1976; Grenthe *et al.*, 1992; Guillaumont *et al.*, 2003)

Table 5.30 (*Contd.*)

Formula	*Selected properties and physical data*^{b,c}	*Lattice symmetry, lattice constant* (Å), conformation and density (g cm^{-3})	*Remarks regarding information available and references*
	solvents. UO_2Cl_2 (cr): $\Delta_f G^o_m$ = –1145.9 (1.3)†, $\Delta_f H^o_m$ = –1243.6 (1.3)†, S^o_m = 150.54 (0.21)†; $C^o_{p,m}$ = 107.86 (0.17)†. UO_2Cl_2 (g): $\Delta_f G^o_m$ = –939.0 (15.1)†, $\Delta_f H^o_m$ = –970.3 (15.0)†, S^o_m = 373.4 (6.0)†; $C^o_{p,m}$ = 92.6 (3.0)†. IR (cm^{-1}): ($\nu_{as}(B_{1u}+B_{3u})$ = 958vs, 946vs; $\nu_s(B_{1u})$ = 832s; $\nu_s(B_{3u})$ = 781s; ν(U···O) = 320w; δ(O–U–O)(B_{1u}, $B_{2u,}$ B_{3u}) = 727w, 258m, 200s; ν(U–Cl) = 97s, 80.5s; Raman: $\nu_{as}(A_g)$ = 940m; $\nu_s(B_{2g})$ = 848m; $\nu_s(A_g)$ = 767vs; ν(overtone or combination) = 750w; ν(U···O) = 340w; δ(O–U–O)(B_{1g}, B_{2g}, B_{3g}) = 270w; 255vw, 240w; δ(O–U–O) (A_g) = 197m; ν(U–Cl) = 178s, 105s	bipyramid with uranyl oxygen atoms at the apices: *d*(U–O, uranyl) = 1.78(2) and 1.73(1). Three Cl and one O atoms form the equatorial pentagon: *d*(U–Cl) = 2.73 and 2.75; *d*(U–O, pentagon) = 2.52(2); pentagonal angles in ring: ≈72; uranyl angle O–U–O = 178.8(8); angles in the bipyramid: ≈90°	*electronic absorption, luminescence and fluorescence spectra* (Brown, 1979); *IR and Raman data* (Bullock, 1969; Perrin and Caillet, 1976); *photoelectron spectroscopy* (Thibaut *et al.*, 1982)
$UO_2Cl_2{\cdot}H_2O$	yellow powder; hygroscopic; soluble in H_2O, EtOH, Me_2CO; dec. > 300°C. $UO_2Cl_2{\cdot}H_2O$(cr): $\Delta_f G^o_m$ = –1405.0 (3.3)†, $\Delta_f H^o_m$ = –1559.8 (2.1)†, S^o_m = 192.5 (8.4)†. IR (cm^{-1}): 150w, 182m, 208m, 240mw, 280m, 962vs, br, 1602vs, 3450ms. Raman: 52mw (sharp), 58w (sharp), 136w, 176m, 203m, br, 245ms, 869vs (sharp)	monoclinic system; C^2_{2h}, $P2_1/m$, No.11; *a* = 5.847(9), *b* = 8.596 (13), *c* = 5.543(9); β = 97.51(8); CN = 7; *d*(calc.) = 4.34; *d*(U–Cl) = 2.75(1) and 2.80(1); *d*(U–O) = 1.70 and 1.74(3); *d*(U–O)(water) = 2.46	*crystallographic and neutron diffraction data* (Taylor and Wilson, 1974c); *infrared and Raman data* (Gerding *et al.*, 1975); *thermodynamic data* (Grenthe *et al.*, 1992; Guillaumont *et al.*, 2003)

$UO_2Cl_2 \cdot 3H_2O$	yellow-green, fluorescent; deliquescent in air; extremely soluble in water, alcohol and ether $UO_2Cl_2 \cdot 3H_2O$(cr): $\Delta_f G^o_m$ = –1894.6 (3.0)†, $\Delta_f H^o_m$ = –2164.8 (1.7)†, S^o_m = 272.0 (8.4)†. IR (cm^{-1}): (B_{1u}, B_{2u}, B_{3u}): 93w,150m, 220sh, $v_2(UO_2^{2+})$ = 255s, v(free H_2O) = 435br, 590br, $v_1(UO_2^{2+})$ = 879 (sharp), $v_3(UO_2^{2+})$ = 950s, 955s, $\nu_2(H_2O)$ = 1570sh, 1595m, 1610sh, $(v_1+v_3)(UO_2^{2+})$ = 1830w, 1835sh, v(combination) = 2230w, $v_1+v_3(H_2O)$ = 3250vs,br	orthorhombic; C^9_{2v}, $Pn2_1a$, No.11; $a = 12.738(5)$, $b = 10.495(5)$, c = 5·47(2)	*crystallographic data* (Debets, 1968; Caville and Poulet, 1974; Brown, 1979); *infrared and Raman data* (Caville and Poulet, 1974); *thermodynamic data* (Brown, 1979; Grenthe *et al.*, 1992; Guillaumont *et al.*, 2003)
$[(UO_2)_4Cl_2O_2(OH)_2(H_2O)_6] \cdot (H_2O)_4$		monoclinic; C^5_{2h}, $P2_1/c$; No.14; a = 11.645(1), b = 10.101(1), c = 10.206(1); β = 105.77(1), Z = 2; V = 1155.31	*crystal structure* (Aberg, 1971, 1976)
$Li_2UO_2Cl_4$		monoclinic; C^3_{2h}, $C2/m$, No.12; a = 11.63, b = 7.56, c = 5.58; β = 95.7°	*crystallographic data* (Vorobei *et al.*, 1971); *infrared and thermodynamic data* (Brown, 1979)
$Na_2UO_2Cl_4$		monoclinic; C^3_{2h}, $C2/m$, No.12; a = 11.53, b = 7.56, c = 5.60; β = 94.41	*crystallographic data* (Vorobei *et al.*, 1971); *infrared and thermodynamic data* (Brown, 1979)
$Rb_2UO_2Cl_4$		monoclinic; C^3_{2h}, $C2/m$, No.12; a = 11.65, b = 7.42, c = 5.58; β = 98.6	*crystallographic data* (Vorobei *et al.*, 1971); *infrared and thermodynamic data* (Brown, 1979)
$Rb_2UO_2Cl_4 \cdot 2H_2O$		triclinic; C^1_i, $P\bar{1}$, No.2; a = 6.795 (5); b = 6.929(5), c = 7.457(4),	*crystallographic data* (Anson *et al.*, 1996)

Table 5.30 (*Contd.*)

Formula	*Selected properties and physical data*[b,c]	*Lattice symmetry, lattice constant* (Å), conformation and density (g cm^{-3})	*Remarks regarding information available and references*
		$\alpha = 91.96(5)$, $\beta = 102.13(5)$, $\gamma = 118.82(6)$; $Z = 1$; $V = 296.95$; d(calc.) = 3.46	
$Cs_2UO_2Cl_4$	IR and Raman (symmetry in D_{4h}) (cm^{-1}): A_{1g}(R) ν(O–U–O) sym. str. = 831; A_{2u}(IR) ν(O–U–O) asym. str. = 916; E_u(IR) ν(O–U–O) bend. = 252; A_{1g}(R) ν(U–Cl) sym.str. = 264; B_{2g}(R) ν(U–Cl) str. = 230; E_u(IR) ν(O–Cl) = 238; B_{1g}(R) ν(U–Cl) in plane bend. = 131; E_u(IR) ν(U–Cl) in plane bend. = 112; A_{2u}(IR) ν(U–Cl) out of plane bend. = 112; B_{1u} ν(U–Cl) out of plane bend. = 91****; E_g(R) ν(O–U–O) rock = 205–200; Lattice modes: 93(R), 73(R), 69(R), 56 (IR), 53(R), 48(R)	monoclinic; C_{2h}^3, *C2/m*, No.12; $a = 11.92(2)$, $b = 7.71(2)$, $c = 5.83(1)$; $\beta = 99.66(3)$; d(calc.) = 4.26; d(U–O) = 1.81; d(U–Cl) = 2.62; O–U–O = 180; data from the neutron refinement: monoclinic; C_s^3, *Cm*, No.8; $a = 12.005(8)$, $b = 7.697(3)$, $c = 5.850(3)$; $\beta = 100.00(4)$; $Z = 2$; $V = 532.34$; d(calc.) = 4.23	*crystallographic data* (Hall 1966; Vorobei *et al.*, 1971); *infrared and Raman data* (Denning *et al.*, 1976; Brown, 1979); *neutron diffraction refinement* (Tutov *et al.*, 1991) *thermodynamic data* (Brown, 1979; Fuger *et al.*, 1983)
$Cs(UO_2)_2Cl_5$		orthorhombic; $a = 11.17(5)$, $b = 12.80(5)$, $c = 838(5)$; d(calc.) = 4.715	*crystallographic data* (Bevz *et al.*, 1970)
$[N(CH_3)_4]_2UO_2Cl_4$		tetragonal; D_{4h}^{14}, *P4$_2$/mmm*, No. 136; $a = 9.175(5)$, $c = 11.745(6)$; d(U–O) = 1.724(7); d(U–Cl) = 2.646(4) and 2.660(3); O–U–O = 180°	*crystallographic data* (Di Sipio *et al.*, 1974a); *infrared and Raman data*, *thermodynamic data* (Brown, 1979)

$[N(C_2H_5)_4]_2UO_2Cl_4$	triclinic; C_i^1, $P\bar{1}$, No. 2; $a = 9.997(5)$, $b = 10.064(5)$, $c = 12.914(5)$; $\alpha = 90.00(5)$, $\beta = 90.69(5)$, $\gamma = 90.00(5)$; d(U–O) = 1.76(2) and 1.77(3); d(U–Cl) = 2.65(1), 2.67(1) and 2.68(1)(2×); O–U–O = 180.0(1)	*crystallographic data* (Bois *et al.*, 1976a); *infrared and Raman data*, *thermodynamic data* (Brown, 1979)
$[N(C_2H_5)_3H]_2UO_2Cl_4$	tetragonal; C_{4h}^6, $I4_1/a$, No. 88; $a = 13.465(5)$, $c = 24.18(1)$; d(calc.) = 1.84; d(U–O) = 1.75(1); d(U–Cl) = 2.663(5) and 2.672(5); O–U–O = 179(1)	*crystallographic data* (Bois *et al.*, 1976b); *infrared and Raman, thermodynamic data* (Brown, 1979)
$[N(C_3H_7)_4N]_2UO_2Cl_4$	triclinic; C_i^1, $P\bar{1}$, No.2; $a = 10.890(5)$, $b = 17.257(7)$, $c = 11.076(5)$; $\alpha = 95.4(1)$, $\beta = 106.1(1)$, $\gamma = 114.9(13)$; $Z = 4$. The structure consists of tetrahedral $[CH_3CH_2CH_2]^+$ cations and bipyramidal $[UO_2Cl_4]^{2-}$ anions held together by Van der Waals forces. The U–O(2) bond distances [1.58(2)] are significantly shorter than the usual distances reported for uranyl U–O bonds (1.68–1.77) in hexacoordinated U (VI) compounds	*crystallographic data* (Di Sipio *et al.*, 1974b)
$[N(C_4H_9)_4]_2UO_2Cl_4$	monoclinic; C_{2h}^5, $P2_1/c$, No. 14; $a = 15.533(6)$, $b = 15.466(6)$, $c = 20.438(8)$; $\beta = 118.2(2)$; d(U–O) = 1.68(1) and 1.69(1); d(U–Cl) = 2.646(6), 2.648(5), 2.656(6) and 2.671(5); O–U–O = 178.1(5)°. The structure is built up of flattened $[UO_2Cl_4]^{2-}$ bipyramids and tetrahedral $[Bu_4N]^+$ ions held together by Van der Waals forces	*crystallographic data* (Di Sipio *et al.*, 1974c); *Infrared and Raman, thermodynamic data* (Brown, 1979)

Table 5.30 (*Contd.*)

Formula	*Selected properties and physical data*[b,c]	*Lattice symmetry, lattice constant* (Å), conformation and density (g cm^{-3})	*Remarks regarding information available and references*
$[LH]_2UO_2Cl_4$[f]		monoclinic; C^3_{2h}, $C2/m$, No.12; ($P2_1/n$; No.14; non standard setting of P_21/c); $a = 11.199$, $b = 6.968$, $c = 23.675$; $\beta = 97.50$; d(U–O) = 1.78(1); d(U–Cl) = 2.66 (1) and 2.69(1); O–U–O = 180.0.	*crystallographic data* (Marzotto *et al.*, 1973; Clemente *et al.*, 1974)
$[L'H]_2UO_2Cl_4$ CH_3CN[g]		triclinic; C^1_i, $P\bar{1}$, No. 2; $a = 12.77$ (1), $b = 23.12(2)$, $c = 8.11(1)$; $\alpha = 94.33(3)$, $\beta = 89.43(3)$, $\gamma = 98.22$ (3); d(exp.) = 1.60; d(U–O) = 1.784(2) and 1.789(12); d(U–Cl) = 2.705(6), 2.706(4), 2.697(6) and 2.699(6); O–U–O = 179(1)	*crystallographic data* (Graziani *et al.*, 1975)
$UO_2(ClO_4)_2$	forms complexes with various donors ligands, e.g. DMSO and urea; soluble in H_2O; IR (cm^{-1}) (C_s): $\nu_8 = 1270, 1234$, $\nu_6 = 1116, 1114$; $\nu_1 = 1048$, $\nu_2 = 974$, $\nu_7 = 640$, $\nu_9 = 627$, $\nu_3 = 600$, $\nu_5 = 481$, $\nu_4 = 455$, $\nu_3(UO^{2+}_{2(as)}) = 996$, $\nu_3(UO^{2+}_{2(sym)}) = 900$		*infrared data* (Vdovenko *et al.*, 1964)
(i) $UO_2(ClO_4)_2 \cdot H_2O$ (ii) $UO_2(ClO_4)_2 \cdot 3H_2O$ (iii) $UO_2(ClO_4)_2 \cdot 5H_2O$	(i) IR (cm^{-1})(C_s): $\nu_8 = 1250, 1231$, $\nu_6 = 1136, 1114$; $\nu_1 = 1075$, $\nu_2 = 996$, $\nu_7 = 646$, $\nu_9 = 633$, $\nu_3 = 613$, $\nu_5 = 470$, $\nu_4 = 450$, $\nu_3(UO^{2+}_{2(as)}) = 974$, $\nu_3(UO^{2+}_{2(sym)}) = 896$		*infrared data* (Vdovenko *et al.*, 1964)

	(ii) IR (cm$^{-1)}$ (C_{3v}): $v_4 = 1192$, 1162, $v_1 = 1035$, 1017; $v_2 =$ 874, $v_5 = 645$, $v_3 = 619$, $v_6 =$ 460, $v_3(UO^{2+}_{2(as)}) = 967$, $v_3(UO^{2+}_{2(sym)}) = 892$. (iii) IR (cm^{-1}) ($T_d$): $v_3 = 1030$ to 1160, $v_1 = 930$; $v_4 = 624$, $v_3(UO^{2+}_{2(as)}) = 958$, $v_3(UO^{2+}_{2(sym)}) = 898$		
$UO_2(ClO_4)_2{\cdot}7H_2O$	soluble in: H_2O, EtOH, CH_3Cl, pyridine, DMSO etc.: loses H_2O at 270°C, dec. at 375°C; IR (cm^{-1}) (T_d): $v_3 = 1110$, $v_1 = 932$; $v_4 = 624$, $v_3(UO^{2+}_{2(as)}) = 958$, $v_3(UO^{2+}_{2(sym)}) =$ 888	orthorhombic; C^5_{2v}, $Pca2_1$, No. 29; $a = 9.302(4)$, $b = 14.692(6)$, $c =$ 10.842(5); $Z = 4$; $d_{cal.} = 2.75$. The structure contains $[UO_2(OH_2)_5]^{2+}$ and ClO_4^- ions and two H_2O molecules per U atom. The coordination polyhedron is a distorted bipyramid with d(U–O) = 1.62(7) and 1.80(3) in the uranyl group and 2.35 to 2.55 for the coordinated water molecules.	*crystallographic data* (Alcock and Esperäs, 1977); *Infrared data* (Vdovenko *et al.*, 1964); *absorption ,fluorescence and luminescence spectra* (Carnall, 1982)
$UO_2(HMPTA)_4$ $(ClO_4)_2$; HMPTA = hexamethyl-phosphor-triamide = $[(CH_3)_2N]_3PO$.	$v_3(ClO_4^-) = 1095$, $v_4(ClO_4^-) = 624$, $v_{as}(UO_2^{2+}) = 917$	orthorhombic; D^{15}_{2h}, $Pbca$, No. 61; $a = 45, 818(5)$, $b = 14.273(5)$, $c = 15.381(5)$; $V = 10056$	*crystallographic data* (Nassimbeni and Rodgers, 1976); *infrared spectra* (Gusev *et al.*, 1985)
(i) $K_xUO_3Cl_x (x \approx 0.8)$. (ii) $Rb_xUO_3Cl_x$ $(x \approx 0.8)$. (iii) $Cs_xUO_3Cl_x$ $(x \approx 0.9)$.		monoclinic; C^2_{2h}, $P2_1/m$, No.11. (i) $a = 8.55$, $b = 4.10$, $c = 7.00$; $\beta = 104.22$. (ii) $a = 8.734(2)$, $b = 4.118(2)$, $c = 7.718(2)$; $\beta = 105.34$. (iii) $a = 8.56$, $b = 4.11$, $c = 7.35$; $\beta = 104.56$; d(exp.) = 5.43. d(U–O) = 1.82(6); 1,85(9); 2.30(7); 2.17(7); d(U–Cl) = 2.98(2); O–U–O = 180.	*crystallographic data* (Allpress *et al.*, 1968)

Table 5.30 (*Contd.*)

Formula	*Selected properties and physical data*[b,c]	*Lattice symmetry, lattice constant* (Å), conformation and density (g cm^{-3})	*Remarks regarding information available and references*
(i) $Rb_2U_2O_5Cl_4 \cdot 2H_2O$[d] (ii) $Cs_2U_2O_5Cl_4 \cdot 2H_2O$		monoclinic; C_{2h}^5, $P2_1/c$, No. 14; (i) $a = 8.540(11)$, $b = 8.096(8)$, $c = 21.735(32)$; $\beta = 111.74(11)°$; d(U–O) = 1.78(2×), 2.203*, 2.268*, 2.289* and 2.509; d(U–Cl) = 2.743, 2.781, 2.800*, 2.804*, 2.825*, and 2.845*, O–U–O = 180.0 (ii) $a = 8.82(2)$, $b = 8.27(1)$, $c = 22.17(4)$; $\beta = 112.03(10)$; d(calc.) = 4.30	*crystallographic data* (Perrin, 1977a)
(i) $K_4U_5O_{16}Cl_2$ (ii) $Rb_4U_5O_{16}Cl_2$		monoclinic; C_{2h}^5, $P2_1/c$, No. 14; (i) $a = 9.96$, $b = 6.99$, $c = 19.60$; $\beta = 134.97°$ (ii) $a = 10.21$, $b = 7.01$, $c = 19.64$; $\beta = 134.22$; d(calc.) = 6.13	*crystallographic data* (Allpress *et al.*, 1968)
(i) $La_3(UO_6Cl_3)$ (ii) $Pr_3(UO_6Cl_3$ (iii) $Nd_3(UO_6Cl_3)$		hexagonal; C_{6h}^2, $P6_3/m$, No.176; (i) $a = 9.5155(16)$, $c = 5.6132(16)$; $Z = 2$; $V = 440.15$ (ii) $a = 9.3957(6)$, $c = 5.5470(5)$; $Z = 2$; $V = 424.08$ (iii) $a = 9.3668(5)$, $c = 5.5300(7)$; $Z = 2$; $V = 420.18$	*crystallographic data* (Henche *et al.*, 1993)
$(NH_4)_2[(UO_2)_4O_2(OH)_2Cl_4(H_2O)_4] \cdot 2H_2O$		triclinic; $a = 12.12(1)$, $b = 12.31(1)$, $c = 7.99(1)$; $\alpha = 111.2(1)$, $\beta = 95.1(1)$, $\gamma = 138.1(1)$	*crystallographic data* (Perrin, 1977b)

$K_2[(UO_2)_4O_2(OH)_2Cl_4(H_2O)_4] \cdot 2H_2O^e$		triclinic; $a = 12.15(2)$, $b = 12.33(1)$, $c = 8.026(9)$; $\alpha = 110.5(1)$, $\beta = 96.3(1)$, $\gamma = 138.7(1)$; d[U(1)–O] = 1.767(6), 1.774(7), 2.205(2)*, 2.39(2)*, and 2.45(2)**; d[U(2)–O] = 1.795(6), 1.786(6), 2.246(19)*, 2.256(14)*, 2.39(2)*, and 2.41(1)**; d(U-Cl) = 2.873(9)*; O–U–O = 175.6(7)	*crystallographic data* (Perrin, 1977b; Perrin and Le Marouille, 1977)
$Rb_2[(UO_2)_4O_2(OH)_2Cl_4(H_2O)_4] \cdot 2H_2O$		triclinic; $a = 12.25(2)$, $b = 12.32(2)$, $c = 7.95(1)$; $\alpha = 110.4(1)$, $\beta = 95.6(1)$, $\gamma = 138.4(1)$	*crystallographic data* (Perrin, 1977b)
$Rb_4[(UO_2)_4O_2Cl_8(H_2O)_2]\cdot 2H_2O$		monoclinic; C_{2h}^5, $P2_1/c$, No.14; $a = 8.540(11)$, $b = 8.096(8)$, $c = 21.735(32)$; $\beta = 111.74(11)$; $Z = 2$; $V = 1395.87$; d(calc.) = 4.3	*crystallographic data* (Perrin, 1977a)
$Cs_3[(UO_2)_3O_2(OH)_3]_2Cl\cdot(H_2O)_3$		monoclinic; C_2^3, $C2$, No.5; $a = 19.6150(50)$, $b = 7.239(2)$, $c = 12.064(3)$; $\beta = 127.929(4)$; $Z = 2$; $V = 1351.17$; d(calc.) = 5.59	*synthesis and structural characterization* (Li *et al.*, 2001)
$[N(C_6H_5CH_2)(CH_3)_3]_4\cdot[UO_2Cl_3O]_2^h$		monoclinic; C_{2h}^5, $P2_1/c$, No. 14; $a = 8.869(5)$, $b = 11.013(5)$, $c = 25.60(1)$; $\beta = 103.66(10)$; $Z = 4$; d(calc.) = 1.89; mean d(U–O, peroxy) = 2.30; the mean d(U–O, uranyl) = 1.78; mean d(U–Cl, uranyl) = 2.71; 1. O–U–O = 179.3 (1.0)	*crystallographyic data* (Boeyens and Haegele, 1976; Haegele and Boeyens, 1977)
UO_2Br_2	bright red; hygroscopic, thermally unstable; soluble in Me_2CO, Et_2O, EtOH, MeCN, H_2O; slowly loses Br_2 at room temp. UO_2Br_2 (cr): $\Delta_f G_m^o = -1066.4\ (1.8)^\dagger$, $\Delta_f H_m^o = -1137.4\ (1.3)^\dagger$, $S_m^o = 169.5\ (4.2)^\dagger$; $C_{p,m}^o = 116\ (8)^\dagger$. IR (cm^{-1}): 905s (stretching), 945, 930, and 825		*thermodynamic data* (Prins *et al.*, 1978; Grenthe *et al.*, 1992; Guillaumont *et al.*, 2003); *IR spectra* (Prigent, 1958); *photoelectron spectroscopy* (Thibaut *et al.*, 1982)

Table 5.30 (*Contd.*)

Formula	*Selected properties and physical data*^{b,c}	*Lattice symmetry, lattice constant* (Å), conformation and density (g cm^{-3})	*Remarks regarding information available and references*
$UO_2Br_2{\cdot}H_2O$; $UO_2Br_2{\cdot}3H_2O$.	$UO_2Br_2{\cdot}H_2O$(cr): $\Delta_f G^o_m = -1328.6$ (2.5)†, $\Delta_f H^o_m = -1455.9$ (1.4)†, $S^o_m = 214$ (7)†. $UO_2Br_2{\cdot}3H_2O$(cr): $\Delta_f G^o_m = -1818.5$ (5.6)†, $\Delta_f H^o_m = -2058.0$ (1.5)†, $S^o_m = 304$ (18)†.		*thermodynamic data* (Grenthe *et al.*, 1992; Guillaumont *et al.*, 2003)
$(UO_2)_2(OH)_2$ $Br_2(H_2O)_4]$	$UO_2OHBr(H_2O)_2$(cr): $\Delta_f G^o_m = -1744.2$ (4.4)†, $\Delta_f H^o_m = -1958.2$ (1.3)†, $S^o_m = 248$ (14)†	isostructural with the chloride analogue (monoclinic; C^5_{2h}, $P2_1/c$, No.14)	*X-ray powder diffraction data* (Peterson, 1961); *IR spectra* (Perrin, 1970); *thermodynamic data* (Prins *et al.*, 1978; Grenthe *et al.*, 1992; Guillaumont *et al.*, 2003)
$[UO_2Br_2]{\cdot}3C_4H_8O$	light brown cryst.; soluble in THF	monoclinic; C^5_{2h}, $P2_1/c$, No.14; $a = 6.931(3)$, $b = 17.032(4)$, $c = 16.257(4)$; $\beta = 94.25(5)$; $V = 1914$ (2); $Z = 4$; d(calc.) = 2.242; the coordination polyhedron is a bipyramid with a non-planar pentagonal base made up of two Br^- anions three O atoms from the THF molecules. The two uranyl O atoms are in the apical positions; d(U–O) = 1.75(1), 1.77(1), 2.45(2), 2.47(1), 2.46(2); d(U–Br) = 2.845 (3), 2.856(3)	*crystallographic data* (Rebizant *et al.*, 1987)
$Cs_2UO_2Br_4$	yellow; IR (cm^{-1}): ν(U–O, asym. stretch.) = 895–934; ν(O–U–O deformation) = 243–263; ν(U–Br	monoclinic; C^5_{2h}, $P2_1/a$, No.14; $a = 9.959(3)$, $b = 9.806(5)$, $c = 6.415$ (5); $\beta = 104.8(2)$; d(calc.) = 4.51;	*crystallographic data* (Mikhailov and Kuznetzov, 1971); *infrared and Raman data* (Brown, 1979);

	stretch.) = 160–180; Raman: ν(U–O sym. stretch.) = 826–835, ν(U–O–Br bend.) = 190–198, ν(U–Br stretch.) = 167–172, 81–83 ν(U–Br bending mode) = 81–83	d(U–O) = 1,70(5); d(U–Br) = 2.83 (1)(2×) and 2.80(1)(2×)	*thermodynamic data* (Fuger *et al.* (1983)
$(NH_4)_2UO_2Br_4(H_2O)_2$		triclinic; C_i^1, $P\bar{1}$, No.2; $a = 6.8850$ (9), $b = 6.887(1)$, $c = 7.7370(7)$; $\alpha = 94.44(1)°$, $\beta = 98.78(1)$, $\gamma = 116.79(1)$; d(U-O) = 1.766(6); d(U–Br) = 2.813 (average); $Z = 1$; $V = 319.17$; d(calc.) = 3.44. The structure consists of $[UO_2Br_4]^{2-}$ and $[NH_4]^+$ ions. The U ions are octahedrally coordinated and the symmetry of $[UO_2Br_4]^{2-}$ is approx. D_{4h}	*crystallographic dat*a (Van den Bossche *et al.*, 1987)
$[N(CH_3)_4]_2UO_2Br_4$	yellow; IR (cm^{-1}): ν(U–O, asym. stretch.) = 895–934; ν(O–U–O, deformation) = 243–263; ν(U–Br, stetch.) = 160–180; Raman: ν(U–O, sym. stretch.) = 826–835, ν(U–O–Br, bend.) = 190–198, ν(U–Br, stretch.) = 167–172, 81–83; ν(U–Br, bending mode) = 81–83	tetragonal; D_{4h}^{14}, $P4_2/mmm$, No. 136; $a = 9.350(5)$, $c = 11.695(6)$; d(calc.) = 2.40; d(U–O) = 1,76(2); d(U–Br) = 2.783(6)(2×) and 2.828 (4) 2×	*crystallographic data* (Di Sipio *et al.* 1974a); *infrared and Raman data* (Brown, 1979)
$[N(C_3H_7)_4]_2UO_2Br_4$	yellow; IR (cm^{-1}): ν(U–O, asym. stretch.) = 895–934; ν(O–U–O, deformation) = 243–263; ν(U–Br, stetch.) = 160–180; Raman: ν(U–O, sym. stretch.) = 826–835, ν(U–O–Br, bend.) = 190–198, ν(U–Br, stretch.) = 167–172, 81–83 cm^{-1} ν(U–Br, bending mode) = 81–83.	monoclinic; $P2_1/n$; $a = 13.706(6)$, $b = 12.270(6)$, $c = 10.758(5)$; $\beta = 89.9(2)$; d(U–O) = 1,698(7); d(U–Br) = 2.837(2)(2×) and 2.829(6) 2×	*crystallographic dat*a (Di Sipio *et al.*, 1974d); *Infrared and Raman data* (Brown, 1979)

Table 5.30 (*Contd.*)

Formula	*Selected properties and physical data*[b,c]	*Lattice symmetry, lattice constant* (Å), conformation and density (g cm^{-3})	*Remarks regarding information available and references*
$[N(C_4H_9)_4]_2UO_2Br_4$		triclinic; C_i^1, $P\bar{1}$, No.2; $a = 18.62$ (2), $b = 11.52(1)$, $c = 11.50(1)$; $\alpha = 100.75(8)$, $\beta = 93.70(8)$, $\gamma = 115.96$ (8); $Z = 2$. The structure is built up of $[Bu_4N]^+$ and $[UO_2Br_4]^{2-}$ ions. The four Br anions are arranged around the linear UO_2 group to form a distorted to square bipyramidal octahedral coordination polyhedron. The U–Br moiety is strictly planar. The cations are tetrahedral. Alternating layers of anions and cations are linked by Van der Waals forces	*crystallographic dat*a (Di Sipio *et al.*, 1977)
$[P(C_6H_5)_4]_2$ $[UO_2\ Br_4]$ $\cdot 2CH_2Cl_2$	yellow	monoclinic; C_{2h}^6, $C2/c$, No.15; $a = 20.063(8)$, $b = 13.206(4)$, $c = 20.425(9)$; $\beta = 98.78(4)$; $V = 5348$; Z = 4; *d*(calc.) = 3.07 *d*(U–Br1) = 2.83.6(3); *d*(U–Br2) = 2.814(3); *d*(U–Br3 or U–O) = 1.72(2); Br–U–Br and O–U–O = 92.4(1) and 88.3(5)	*synthesis and crystallographic data* (Bohrer *et al.*, 1988)
$[C_7H_{16}NO_2]_2$ $UO_2Br_4{}^i$	yellow; IR (cm^{-1}): *ν*(U–O, asym. stretch.) = 895–934; *ν*(O–U–O deformation) = 243–263; *ν*(U–Br	orthorhombic; D_{2h}^{16}, *Pnma*, No. 62; $a = 13.60(2)$, $b = 20.943)$, $c = 9.22$ (2); *d*(calc.) = 2.23; *d*(U–O) = 1,80	*crystallographic data* (Marzotto *et al.*, 1974); *Infrared and Raman data* (Brown, 1979)

	stetch.) = 160–180; Raman: v(U–O sym. stretch.) = 826–835, v(U–O–Br bend.) = 190–198, v(U–Br stretch.) = 167–172 cm^{-1}, 81–83, v(U–Br bending mode) = 81–83 cm^{-1}	(3); d(U–Br) = 2.804(4), 2.792 (4) and 2.859(2) 2×	
(i) $K_2[(UO_2)_4 O_2(OH)_2 Br_4(H_2O)_4] \cdot 2H_2O$ (ii) $Rb_2[(UO_2)_4O_2 (OH)_2Br_4(H_2O)_4] \cdot 2H_2O$		triclinic; C_i^1, $P\bar{1}$, No. 2. (i) $a = 12.42(2)$, $b = 12.46(1)$, $c = 8.08(1)$; $\alpha = 109.4(1)^o$, $\beta = 97.2(1)$, $\gamma = 139.0(1)$. (ii) $a = 12.47(2)$, $b = 12.34(2)$, $c = 8.07(3)$; $\alpha = 109.0(1)$, $\beta = 97.2(1)$, $\gamma = 138.6(1)$	*crystallographic data* (Perrin, 1977b)
$K_xUO_3Br_x$ ($x = 0.9$)		monoclinic; C_{2h}^2, $P2_1/m$, No.11; $a = 9.57$, $b = 4.14$, $c = 6.89$; $\beta = 11.77$	*crystallographic data* (Allpress *et al.*, 1968)
$UO_2(HMPTA)_4 (BrO_4)_2$ HMPTA = hexamethyl-phosphortriamide = $[(CH_3)_2N]_3PO$.	IR (cm^{-1}):$\nu_3(BrO_4^-) = 871$, $\nu_{as}UO_{2(as)}^{2+} = 917$	orthorhombic; D_{2h}^{15}, $Pbca$, No. 61; $a = 46.18(10)$, $b = 14.40(4)$, $c = 15.56(4)$; $V = 10347$	*crystallographic data and infrared spectra* (Gusev *et al.*, 1985)
$K_2[(UO_2)_3 (IO_3)_4 O_2)]$		triclinic; C_i^1, $P\bar{1}$, No.2; $a = 7.0372(5)$, $b = 7.7727(5)$, $c = 8.9851(6)$; $\alpha = 93.386(1)$, $\beta = 105.668(1)$, $\gamma = 91.339(1)$; $Z = 1$; $V = 471.98$	*crystallographic data* (Bean *et al.*, 2001b)
$Ba[(UO_2)_2(IO_3)_2 O_2)] H_2O$		monoclinic; C_{2h}^5, $P2_1/c$, No. 14; $a = 8.062(4)$, $b = 6.940(3)$,$c = 21.665(10)$; $\beta = 98.049(10)$; $Z = 4$; $V = 1200.22$	*crystallographic data* (Bean *et al.*, 2001b)
$Ag_4(UO_2)_4 (IO_3)_2 (IO_4)_2 O_2$		monoclinic; C_{2h}^5, $P2_1/c$, No.14; $a = 15.040(7)$, $b = 8.051(4)$, $c = 18.3320(80)$; $\beta = 100.738(7)$; $V = 2180.9$; $Z = 4$	*crystallographic data* (Bean *et al.*, 2001a)

Table 5.30 (*Contd.*)

Formula	*Selected properties and physical data*^{b,c}	*Lattice symmetry, lattice constant* (Å), conformation and density (g cm^{-3})	*Remarks regarding information available and references*
(i) $UO_2(IO_3)_2$;. (ii)$UO_2(HMPTA)_4(IO_4)_2$ HMPTA = hexamethyl-phosphortriamide = $[(CH_3)_2N]_3PO$	(i) $UO_2(IO_3)_2$(cr): $\Delta_f G^o_m = -1250.2$ (2.4)†, $\Delta_f H^o_m = -1461.3$ (3.6)†, $S^o_m = 279$ (9)† (ii) IR (cm^{-1}):$\nu_3(IO_4^-) = 843$, $\nu_{as}(UO_2^{2+}) = 917$	orthorhombic; D^{15}_{2h}; *Pbca*, No. 61; $a = 46.52(10)$, $b = 14.50(4)$, $c = 15.66(4)$; $V = 10563$	*crystallographic data and infrared spectra* (Gusev *et al.*, 1985)

---

[*] Bridging oxygen or chlorine distances.

[**] U–O distances to the water molecule.

[***] Estimated values.

[****] Value obtained from a force constant calculation (IR inactive).

[†] Values recommended by the Nuclear Energy Agency (Grenthe *et al.*,1992; Guillaumont *et al.*, 2003).

[‡] equation expressed in°C.

[a] Values have been selected in part from review articles (Brown, 1979; Bacher and Jacob 1980; Freeman,1991; Grenthe *et al.*, 1992; Guillaumont *et al.*, 2003.).

[b] m.p. = melting point; b.p(°C). = boiling point; (cr) = crystalline; (g) = gaseous; thermodynamic values in kJ mol^{-1}, or J K^{-1} mol^{-1} at 298.15 K, unless otherwise mentioned; $\Delta_f G^o_m$, - standard molar Gibbs energy of formation; $\Delta_f H^o_m$, standard molar enthalpy of formation; S^o_m (J K^{-1} mol^{-1}), standard molar entropy; $C^o_{p,m}$, standard molar heat capacity; log *p* (mmHg) = $-AT^{-1} + B - C \log T$: vapor pressure equation for indicated temperature range; R = Raman active; IR = infrared active; vs: very strong; s: strong; m: medium; ms: medium strong; w: weak; sh: shoulder; b: broad; L: lattice; all values are in cm^{-1}.

[c] All values are in Å and angles are in degrees; CN, coordination number; *d*, density [g cm^{-3}], *V* = molar volume [cm^3 mol^{-1}].

[d] The anion is $[(UO_2)_4O_2Cl_8(H_2O)_2]^4$.

[e] The anion is $[(UO_2)_4O_2(OH)_2Cl_4(H_2O)_4]^{2-}$.

[f] L = thiamine ($C_{12}H_{16}ClN_4OS$).

[g] L′ = 2,6-diacetylpyridine-bisphenyl hydrazone.

[h] The anion is $[(UO_2)_2Cl_6(\mu\text{-}O_2)]^{4-}$.

[i] Acetylcholine cation.

shown the existence of several progressions in the symmetric stretching frequency (ν_1) coupled with other modes. Two non-phonon transitions, originating at 24564 and 25265 cm^{-1}, are associated with the first band and four other with origins at 30331, 31032 (observed directly), 32120, and 32821 cm^{-1} with the second one; they could be located in the low-temperature spectra of the compound. The observed fine structure has been explained in terms of electric–dipole forbidden transitions from the t_{1u} $(\pi+\sigma)$ orbitals of the fluorine atoms to the empty 5f orbitals of the uranium atoms. A strong absorption band without vibronic structure, observed at about 46730 cm^{-1}, has been assigned as a charge transfer transition.

Since the ground state of UO_2^{2+} does not contain unpaired electrons the uranyl compounds are either diamagnetic or weakly paramagnetic. The octahedral hexahalides exhibit a weak, almost temperature-independent, paramagnetism.

(*i*) *Uranium hexafluoride and uranium*(VI) *complex fluorides*

Uranium hexafluoride

Uranium hexafluoride is the only uranium compound that is readily volatilized and is therefore used for uranium isotope separation by gas diffusion, gas centrifugation, liquid thermal diffusion, or in mixtures with a light auxiliary gas like H_2 or He (separation nozzle). The uranium enrichment technologies have been surveyed by Becker (1979) and Ehrfeld and Ehrfeld (1980), for example. Due to the importance of UF_6, the physical and chemical properties of UF_6, including commercial syntheses, have been extensively studied. The literature is covered in a number of reviews (Caillat, 1961; Brown, 1968; Bacher and Jacob, 1980, 1982, 1986; Hellberg and Schneider, 1981; Freestone and Holloway, 1991). A scheme of reactions leading to UF_6 is shown in Fig. 5.45.

Some important preparative procedures are based on the following reagents (Bacher and Jacob, 1980; Freestone and Holloway, 1991):

(1) reaction of elemental fluorine with U, UF_4 (at 340°C), U_4F_{17}, U_2F_9 (at 300°C), UF_5 (at 270°C), $NaUF_5$ (at 340°C), UO_2 (at 500°C), UO_3 (at 400°C), U_3O_8 (at 360°C), UO_2F_2 (at 340°C), $Na_2U_2O_7$, CaU_2O_7, UCl_5 (at –20 to 30°C), UO_2HPO_4 (at 370°C), UC_2 (at 350°C); e.g.

$$U_3O_8 + 17F_2 \xrightarrow{360^\circ C} 3UF_6 + 8F_2O$$
$$CaU_2O_7 + 7F_2 \rightarrow 2UF_6 + CaF_2 + 7/2O_2$$

(2) reaction of bromine trifluoride with U (at 50–125°C), U_2F_9 (at 170°C, leading to UF_4), UO_2, UO_3, U_3O_8, UO_2F_2; e.g.

$$U_3O_8 + 6BrF_3 \rightarrow 3UF_6 + 3Br_2 + 4O_2$$

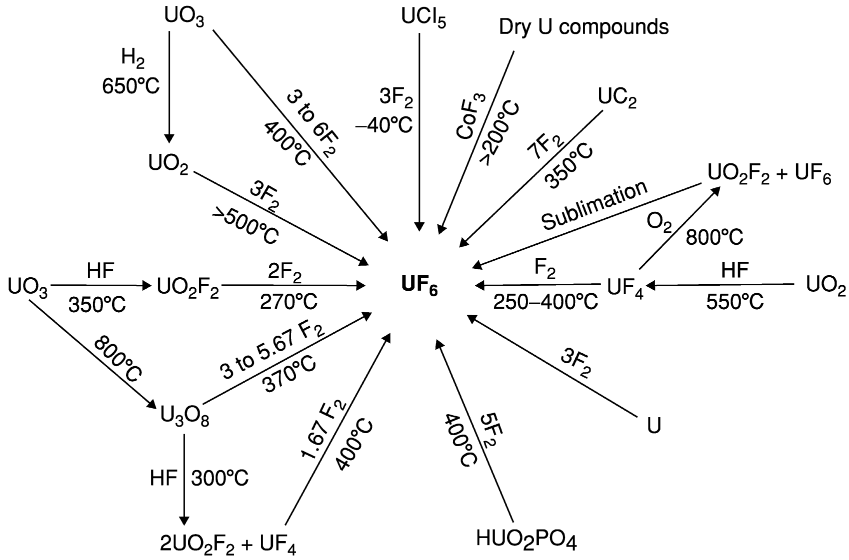

Fig. 5.45 *Reactions leading to UF_6 (adapted from Katz and Rabinowitch,* 1951).

(3) reaction of hydrogen fluoride with UO_2 (at 550°C), $Na_2U_2O_7$, UCl_5; e.g.

$$UCl_5 + 5HF \rightarrow UF_5 + 5HCl$$

followed by reactions (6b) and (6c) below;

(4) reaction with low temperature fluorinating agents: O_2F_2 with U_3O_8; KrF_2 with UF_4, and UO_2 and U_3O_8 in the gaseous phase or at room temperatures in HF solutions;

(5) reaction with other reagents:

(a) $O_2 + 2UF_4$ (at 660–800°C) $\rightarrow UF_6 + UO_2F_2$
(b) $3BrF_5 + U$ (at 50–125°C) $\rightarrow UF_6 + 3BrF_3$
(c) $3ClF_3 + U$ (at 25–75°C) $\rightarrow UF_6 + 3ClF$
(d) $2CoF_3 + UF_4$ (at 250°C) $\rightarrow UF_6 + 2CoF_2$

(6) decomposition reactions with disproportionation:

(a) $2U_4F_{17}$ (at 270–350°C) $\rightarrow 7UF_4 + UF_6$
(b) $3UF_5$ (at 170°C) $\rightarrow U_2F_9 + UF_6$
(c) $2U_2F_9$ (at >500°C) $\rightarrow 3UF_4 + UF_6$
(d) $9UO_2F_2$ (at >700°C) $\rightarrow 3UF_6 + 2U_3O_8 + O_2$.

As indicated above, the fluoride obtained by means of the reaction given in (3) can be converted to UF_6, using double decomposition with subsequent disproportionation (reactions 6b and 6c). The separation from UF_4 and an excess of HF can be achieved by heating, followed by fractional distillation. The method based on reaction (5a) is also a convenient route, not involving the use of gaseous fluorine; UO_2F_2 is formed as a by-product, but can be converted to UF_4 by reduction and to UF_6 by hydrofluorination. An attractive method on laboratory scale uses reactions (5d) (Weigel, 1958). The by-product CoF_2 can easily be separated from UF_6 and regenerated with fluorine. The general route for purification of UF_6 employs trap-to-trap distillation followed by condensing the hexafluoride at about –80°C.

The production of UF_6 on an industrial scale is achieved mainly by oxidative fluorination of uranium oxides or lower fluorides by fluorine at elevated temperatures. A uranium ore concentrate is first purified by solvent extraction or by ion exchange methods. From this concentrate, $(NH_4)_2U_2O_7$ (ammonium diuranate, ADU, yellow cake) or $UO_2(NO_3)_2 \cdot 6H_2O$ (UNH) is then precipitated. ADU is converted to UO_2 by calcination in the presence of H_2 whereas UNH is first pyrolyzed to UO_3 and then reduced by H_2 to UO_2.

A detailed description of the commonly applied direct fluorination technology of UF_4

$$UF_4(s) + F_2(g) \rightarrow UF_6(g)$$

has been published by Smiley and Brater (1956) and Brater and Smiley (1958). In the conversion flow sheet shown in Fig. 5.46, the fluorination reactor used is either a flame reactor or a fluidized-bed reactor (Harrington and Ruehle, 1959). In the first one UF_4 is fed to the top of the reactor having a length of 3.60 m, diameter of 20 cm, and a capacity of 380 kg per hour. The highly exothermic fluorination reaction takes place over a length of $\sim$1 m at the top of the reactor where a flame with temperatures up to 1100°C is formed. In order to suppress corrosion, the temperature of the reactor walls is maintained below 540°C. For a maximum yield of UF_6 a temperature limit of 450°C, which eliminates the formation of intermediate fluorides, is required. The off-gases contain $\sim$75% UF_6 and have their outlet at the lower part of the reactor. All unreacted solids are collected, powdered, mixed with fresh UF_4 and transmitted again to the feed.

In the second method, UF_4 is fluorinated with F_2 at 500°C in a Monel fluidized-bed reactor with an annual production capacity of 4400 to 7400 tons of UF_6. The UF_4 feed material and fluorine gas are mixed continuously by means of a conveyor screw and a gas distributor (6–20 $cm^3\ s^{-1}$), respectively. For stabilization of the fluidized bed CaF_2 is added to the feed. It serves also to prevent sintering of UF_4 and as a heat transfer material. The product obtained in both types of reactors is passed through Monel filters in order to remove UF_4 dust and is then condensed, first at +4 to –15°C and finally at –40°C. The condensers are then heated to 80°C and UF_6, which liquefies at that temperature under its own pressure, is drained into transport cylinders, which have a volume of up to about 4 m^3, weigh around 2.36 tons, and have a capacity

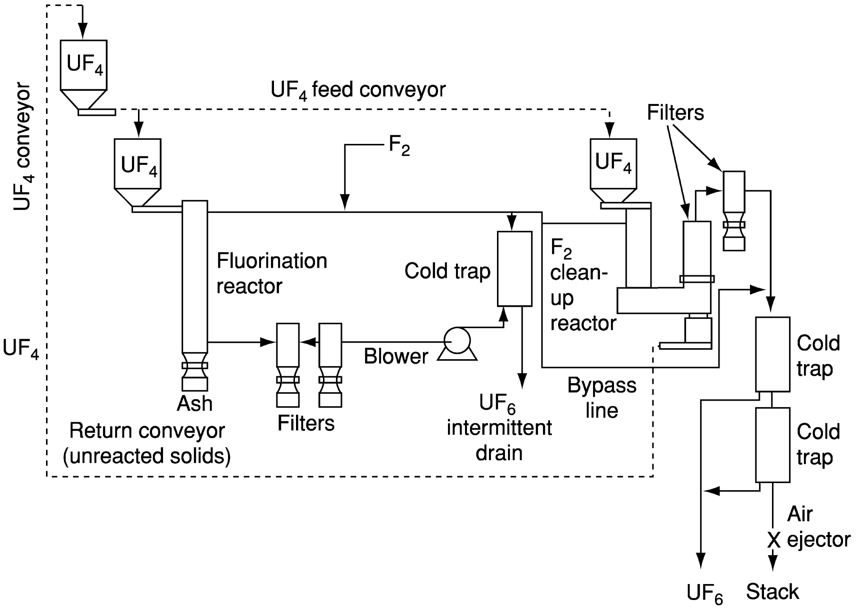

Fig. 5.46. *Schematic flow diagram for uranium hexafluoride production* (*Harrington and Ruehle*, 1959).

of 12.5–14 tons (Keller, 1956). The crude product usually contains numerous volatile impurities such as SiF_6, CF_4, SF_4, MoF_6, CrO_2F_2, or VF_5 as well as some less volatile compounds like MoF_4, VOF_3, and other transition metal fluorides. Since stringent purity specifications are required of commercial UF_6 for isotope separations, the impurities are removed by fractionation at temperatures and pressures above the triple point and by absorption–desorption techniques. At room temperature, UF_6 has a pressure of ca. 120 mmHg; it is thus possible to handle it as a gas in the separation of ^{235}U from natural uranium. For large-scale applications, solid UF_6 is delivered to isotope separation plants in containers, which are then placed into a steam-heated autoclave in which UF_6 builds up a high enough pressure to flow as a gas into the attached diffusion cascade for the separation process (Arendt *et al.*, 1957).

Uranium hexafluoride forms low-melting orthorhombic (space group *Pnma*) colorless crystals which sublime at 56.5°C at atmospheric pressure. The compound has a triple point at 64.02°C and a pressure of 1137 mmHg (Hoard and Stroupe, 1959; Rigny, 1965, 1966; Levy *et al.*, 1976). The structure of solid UF_6 was first determined by Hoard and Stroupe (1959) and later in a number of X-ray and neutron diffraction studies (Levy *et al.*, 1976; Jacob and Bacher, 1980). It consists of hexagonal close-packed fluorine ions with uranium atoms in octahedral holes. The crystallographic data of UF_6 are listed in Table 5.30 together with selected physical data.

The structure of UF_6 in the liquid and gaseous states is perfectly octahedral (point group O_h) with U–F bond lengths in solid UF_6 equal to 1.996 Å. The compound has a temperature-independent paramagnetism with a molar susceptibility of $\chi_{\text{mole}} = 43 \times 10^{-6}\ \text{cm}^3\ \text{mol}^{-1}$, after correction for a diamagnetic contribution of $\chi_{\text{mole}} = 106 \times 10^{-6}\ \text{cm}^3\ \text{mol}^{-1}$. Carnall (1982) has published extensive analyses of the absorption and fluorescence spectra of UF_6. The absorption spectrum of UF_6 in visible to the near-UV range is similar to that of the UO_2^{2+} ion; in the range 200–420 nm there is only one broad band at 375 nm.

The compound is highly reactive and extremely moisture-sensitive. It reacts with most elements but is relatively stable towards oxygen, chlorine, bromine, carbon dioxide, and noble gases even at elevated temperatures. UF_6 has a significant solubility in liquid chlorine and bromine. Thermodynamic calculations have shown that UF_6 is thermally stable below 1000 K; dissociation starts between 1100 and 1450 K. Since UF_6 is rapidly hydrolyzed by water with the formation of HF it is recommended to store the compound in teflon, Kel-F, nickel, or Monel containers.

$$\mathrm{UF_6 + 2\,H_2O \rightarrow UO_2F_2 + 4HF}$$

It can be also stored in quartz or Pyrex tubes by using NaF and KF as HF 'getters'.

Uranium hexafluoride is a powerful fluorinating agent with a vapor pressure of 115 mm at 25°C. Bacher and Jacob (1982) have classified, as discussed below, a number of reactions of UF_6.

Oxidative fluorination results in a simultaneous formation of lower uranium fluorides. UF_6 oxidizes elements or their fluorides in low oxidation states to yields fluorides in higher oxidation state, e.g. with alkali, alkaline earth metals, B, Al, Ga, In, C, Si, Ge, Sn, Pb, As, Sb, S, Se, and Te binary fluorides are formed; lower fluorides such as PF_3, SF_4, MoF_5, or WF_4 are oxidized to higher fluorides:

$$n\mathrm{UF_6 + M(s) \rightarrow} n\mathrm{UF_5(s) + MF}_n$$

Lower oxides are converted to oxyfluorides whereas chlorides and bromides yield fluorides in presence of an excess of UF_6 with formation of Cl_2 and Br_2, respectively:

$$n\mathrm{UF_6 + 2MX}_n \rightarrow n\mathrm{UF_4 + 2MF}_n + n\mathrm{X_2} \quad (\mathrm{X = Cl\,or\,Br})$$

The high fluorination efficiency of UF_6 is also demonstrated by interactions with SO_3 that leads to the formation of the peroxide $S_2O_6F_2$ (Wilson *et al.*, 1977; Masson *et al.*, 1978). The effective first bond dissociation energy of UF_6, according to the the reaction scheme

$$\mathrm{UF_6 \rightarrow (UF_5)_{solid} + F}$$

is equal to (134.0 ± 29.3) kJ mol^{-1}, and is of the same order of magnitude as the bond energy of elemental F_2 (153.2 kJ mol^{-1}, Jacob and Bacher, 1986).

Reaction of UF_6 with other highly electronegative groups may lead to a total or partial substitution of the fluorine atoms with retained oxidation state of uranium as in the vapor phase hydrolysis:

$$UF_6 + 3H_2O \rightarrow UO_2F_2 \cdot H_2O + 4HF$$

and the hydrolysis in liquid HF:

$$UF_6 + nH_2O \rightarrow UO_nF_{(6-2n)} + 2nHF \quad (\text{where } n = 1 \text{ or } 2)$$

or in exchange reactions where fluorine is replaced by groups such as Cl, OCH_3, and $OTeF_5$:

$UF_6 + 6BCl_3 \rightarrow UCl_6 + 6BCl_2F$ (with excess of BCl_3) (O'Donnell *et al.*, 1966)
$UF_6 + 6Si(OCH_3)_4 \rightarrow U(OCH_3)_6 + 6SiF(OCH_3)_3$ (with excess of $Si(OCH_3)_4$) (Jacob, 1982).

UF_6 is a strong Lewis acid that can bind fluoride from Lewis bases such as MF (where M = Na, K, Cs, Rb, NH_4, N_2H_5, NO, and NO_2) under the formation of the corresponding heptafluorouranates(VI), MUF_7 and octafluorouranates(VI), M_2UF_8. UF_6 can oxidize various metals, as well as NO, NO_2, and I_2 in other less common reactions. These reactions are due to the high electron affinity of UF_6 (5.2 eV) and to a favorable lattice energy when fluorouranates(V) are formed, e.g.:

$$NO \rightarrow NO^+ + e \quad +9.2\text{ eV}$$

$$UF_6 + e \rightarrow UF_6^- \quad -5.2\text{ eV}$$

$$NO^+ + UF_6^- \rightarrow NOUF_6 \quad -\text{lattice energy}$$

The hexafluoride is reduced to the tetravalent state by a number of reagents, e.g. HCl (250°C), PF_3, HBr (80°C), CCl_4, CS_2, H_2S, amorphous carbon as well as $SiCl_4$, $AsCl_3$, $SbCl_3$, PBr_5, and BBr_3, with the formation of the appropriate free halogen. Reduction with H_2 is slow and may be carried out at 650°C, or in pressurized systems at 300°C. Exposure of UF_6 to UV light or photocatalytic reduction with HBr, SO_2, or CO yield β-UF_5:

$$2UF_6 \xrightarrow{h\nu} (UF_5)_{\text{solid}} + 1/2F_2$$

$$2UF_6 + X \xrightarrow{h\nu} 2\beta\text{-}(UF_5)_{\text{solid}} + XF_2 \quad (X = H_2, CO, \text{ or } SO_2).$$

Alpha radiation from hexafluoride enriched with ^{235}U or ^{234}U results in significant reduction to lower fluorides.

A number of binary phase diagrams of uranium hexafluoride with fluorine and elements of the 7th main group have been reported (Bacher and Jacob, 1980). Simple eutectic types were observed in the UF_6–BrF_3, UF_6–BrF_5, and UF_6–BrF_2 systems. Some deviation from ideality was found for the UF_6–BrF_3, UF_6–BrF_5, UF_6–ClF_3, and UF_6–BrF_3 systems. In all of these systems, the solid phases are pure stoichiometric compounds. The UF_6–HF phase diagram investigated by Rutledge *et al.* (1953) has practical importance due to the common presence of HF in UF_6. In the phase diagram shown in Fig. 5.47 there is a complete miscibility above 100°C and above a pressure of 10 atm.

The system possesses an eutectic point at –85°C with less than 0.5 mol% of UF_6. The separation of HF from UF_6–HF solutions by distillation is limited due to the appearance of azeotropes.

Complex uranium(vi) *fluorides*

Bacher and Jacob (1980) and Freestone and Holloway (1991) have compiled data on the synthesis and characterisation of numerous fluorouranate(vi) compounds listed below in Table 5.31; some of their physical data are presented in Table 5.30.

NaF has found practical application in nuclear processing. It absorbs UF_6 quickly and has the largest absorption capacity of all alkali metal fluorides. The sodium fluorouranates(vi) formed in the process can easily be thermally dissociated to UF_6 (Bacher and Jacob, 1986).

Several methods have been applied for the preparation of the fluoro complexes (Bacher and Jacob, 1980; Freestone and Holloway, 1991), e.g.: (i) most of

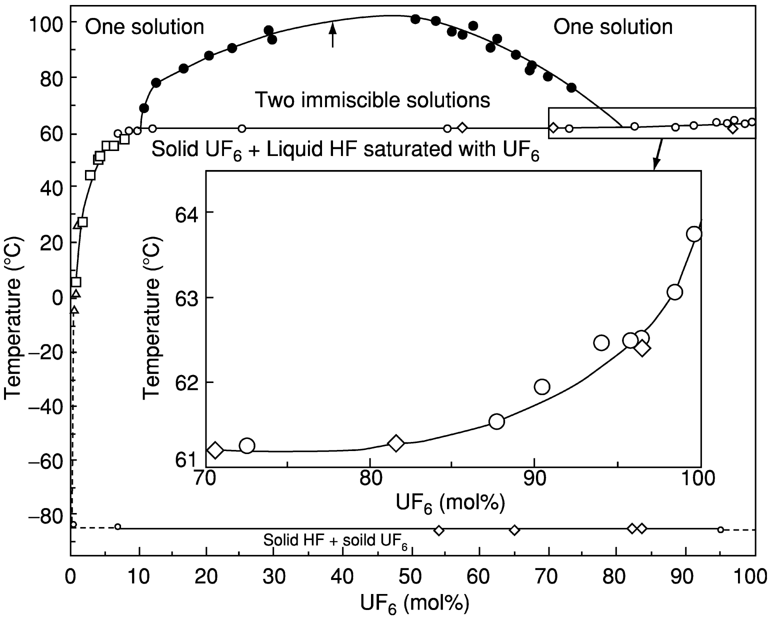

Fig. 5.47 *Phase diagram of the binary system UF_6-HF* (*Rutledge* et al., 1953). •, *Visual observation of disappearance of two liquid layers;* □, *visual observation of precipitation of solid UF_6;* Δ, *filter cell;* ○, *freezing point cell–K2 potentiometer;* ◇, *freezing point cell–white potentiometer. The thin arrow indicates rupture of polyethylene tube.*

Table 5.31 *Identified uranium*(VI) *complex fluorides.*

System	*Complex fluorides*
$NaF–UF_6$	$NaUF_7$, Na_2UF_8, Na_3UF_9, $Na_3U_2F_{15}$
$KF–UF_6$	KUF_7, K_2UF_8, K_3UF_9, $K_3U_2F_{15}$
$RbF–UF_6$	$RbUF_7$, Rb_2UF_8, Rb_3UF_9
$CsF–UF_6$	$CsUF_7$, Cs_2UF_8, Cs_3UF_9
$NH_4F–UF_6$	NH_4UF_7, $(NH_4)_2UF_8$
$N_2H_5F–UF_6$	$N_2H_5UF_7$, $N_2H_6(UF_6)_2$
$NO_xF–UF_6$	$NOUF_7$, NO_2UF_7, $(NO)_2UF_8$

the compounds can be obtained by the reaction of gaseous UF_6 with solid MF (where M = Na, K, Rb, Cs, or NH_4). In some cases, the reactions are carried out at higher temperatures and pressures. The products may be however contaminated by unreacted solid fluorides; (ii) the interaction of a large excess of liquid UF_6 with solid MF yields MUF_7 (M = K, Rb, or Cs); (iii) complex fluorides of the formula MUF_7 or M_2UF_8 are formed by interaction of UF_6 with NaF, KF, RbF, CsF, AgF, or TlF_3 by using appropriate solutions or suspensions in perfluoroheptane, C_7F_{16}, C_8F_{16}, ClF_3, or anhydrous HF; (iv) fluorination of a M_2UF_6 (M = Rb or Cs) or a NaF–UF_4 mixture with F_2 results in the formation of M_2UF_8 and $NaUF_7$, respectively; (v) the M_2UF_8 octafluoro uranate(VI) may also be prepared by thermal decomposition of the corresponding sodium (at 60–145°C), potassium (at 130°C), rubidium (at 150°C), and cesium (180–200°C) heptafluoro uranates; (vi) the reaction between UF_6 and liquid or gaseous ammonia yields NH_4UF_5 and NH_4UF_6, respectively. In the latter case also, a mixture of NH_4UF_5 and UF_5 may be obtained; (vii) the condensing of UF_6 in a suspension of NH_4F in tetrachloroethane yields NH_4UF_7; (viii) the corresponding hydrazinium $N_2H_5UF_7$, nitrosonium $NOUF_7$, and nitronium NO_2UF_7 salts are prepared by direct reaction of the component fluorides, the former in anhydrous hydrofluoric acid.

The fluoro uranates(VI) are extremely moisture-sensitive solids, very susceptible to hydrolysis. With some exception (e.g. NH_4UF_7, which decomposes to UF_5 or UF_4, depending of the applied temperature) they decompose to UF_6 when heated. The UF_6–bromine fluorides and the UF_6–HF systems (HF removal) have also found application in the fluorination reactions in nuclear reprocessing.

(*ii*) *Uranium*(VI) *oxide fluorides and complex oxide fluorides*

Uranium(VI) *oxide tetrafluoride, UOF_4*

UOF_4 can most conveniently be prepared either by the interaction of an excess of UF_6 with quartz wool in liquid HF

$$3UF_6 + SiO_2 \overset{\text{HF (liquid)}}{\rightarrow} 3UOF_4 + SiF_4$$

or by reaction with an excess of B_2O_3

$$3UF_6 + B_2O_3 \rightarrow 3UOF_4 + 2BF_3$$

Uranium oxide tetrafluoride is an orange solid with a shade of red. It is nonvolatile and decomposes at 200–250°C without melting. At 250°C in vacuum UOF_4 decomposes spontaneously in an exothermic reaction to UF_6 and UO_2F_2. The reaction proceeds quantitatively and may be used for purity checking. UOF_4-hydrate is formed after some time in moist air, but liquid water results in a rapid hydrolysis. UOF_4 reacts with KF and NH_4F in liquid HF to form $MUOF_5$ type of salts. Fluorination of UOF_4 by ClF_5, ClF_3, or $ClOF_3$ at room temperature yields UF_6:

$$ClF_5 + 2UOF_4 \rightarrow ClO_2F + 2UF_6$$

UOF_4(cr) has trigonal symmetry in the space group $R3m$ and a pentagonal bipyramidal coordination geometry formed by the O and F atoms. Some physical data are given in Table 5.30.

Uranium(VI) oxide difluoride (uranyl fluoride), UO_2F_2

One of the simplest methods to prepare UO_2F_2 is by heating of UO_3 in gaseous HF at 300–500°C. Other satisfactory routes employ fluorination of uranium oxides at 350°C and oxidation of UF_4 with O_2 at 600–800°C. The compound is a pale yellow solid with a green hue, slightly soluble in water, methanol, and ethanol. Recrystallization from water results in the formation of $UO_2F_2 \cdot 2H_2O$. Controlled action of H_2O in a closed vessel yields hydrates $UO_2F_2 \cdot nH_2O$ ($n = 1$ to 4). The reaction of an excess of UF_6 with water vapour at 60°C leads to the formation of $UO_2F_2 \cdot 1.53H_2O$. Adducts of the $UO_2F_2 \cdot L(H_2O)$ and $UO_2F_2 \cdot nL$ ($n = 1$ to 4) type are formed by interactions with oxygen or nitrogen donor ligands (L) such as NH_3, pyridine (py), tributylphosphine oxide (tbpo), dimethylsulfoxide (dmso), antipyrine (antypy), 2,2′-dipyridyl (dipy), dimethylformamide (dmf), acetamide (aa), dimethylacetamide (dma), urea (ur), dimethylurea (dmur), and tetramethylurea (tmur) (Shchelokov *et al.*, 1977; Bagnall, 1979, 1987; Mass, 1979). IR and Raman data are available for most of the compounds. The nature of the uranium–oxygen bonds in UO_2^{2+} depends on the electron donor properties of the ligands, which result in variations of the UO_2^{2+} ν_1 and ν_2 frequencies that provide valuable structural information. The k_{UO} force constants, determined from both of these frequencies, decrease in the series (Shchelokov *et al.*, 1977) $H_2O >$ aa $>$ dma $>$ dmur $>$ dmso $>$ dmf $>$ tmur$\sim$antipy $>$ ur.

The total energy, molar entropy, heat capacity, and vibration frequencies of the compound in the gas phase have been calculated by *ab initio* methods to obtain thermodynamic data for reactions. They agree well with experimental values and previous results (Privalov *et al.*, 2002).

UOF_2 is converted to UF_6 by gaseous fluorides such as XeF_6 (25°C), BrF_3 (25°C), ClF_3 (50–160°C), ClF (64–150°C), ClO_2F (100–150°C), ClF_5 (>120°C)

F_2 (>300°C), BrF_5 (250°C), SF_4 (>300°C), and VF_5 (100°C). The reactions proceed with much greater difficulty than oxidative fluorination of UF_4 or UF_5 (Bacher and Jacob, 1980). The compound crystallizes with a rhombohedric structure in the space group $R\overline{3}m$. Selected crystallographic data are given in Table 5.30. Besides, Otey and LeDoux (1967) have identified an oxide fluoride of the composition $U_3O_5F_8$ and suggested the existence of an intermediate, $U_2O_3F_6$ compound.

Hexavalent oxide fluoride complexes

There is a large variability in the stoichiometry of the very large number of reported hexavalent oxide fluorides: M^IUOF_5, $M^I(UO_2)_2F_5$, $M^IUO_2F_3$, $M^I_2UO_2F_4$, $M^I_3UO_2F_5$, $M^I_3(UO_2)F_3$, $M^I_3(UO_2)_2F_7$, $M^I_4(UO_2)_2F_8$, $M^I_5(UO_2)F_9$ (where M^I is usually an alkali metal ion), $M^{II}(UO_2)F_4$ (where M^{II} = Ca, Pb, Cu, Zn, or Cd) and $M^{II}(UO_2)_2F_6$ (where M^{II} = Sr, Ba, or Mg) (Freestone and Holloway, 1991). Many of the compounds were identified from phase diagram investigations. The complexes of the M^IUOF_5-type (M = K, Rb, Cs, NH_4) have been prepared by interaction of UOF_4 with the appropriate MF fluoride in liquid sulfur dioxide or anhydrous HF (Joubert and Bougon, 1975; Joubert *et al.*, 1978a,b). Hydrated complexes of the $M^{II}(UO_2)F_4 \cdot 4H_2O$ (M^{II} = Zn, Cd, Cu, Mn, Co, or Ni) were obtained by crystallization from aqueous solutions. A number of fluoro-oxalato compounds of the $[UO_2F(C_2O_4)_2(H_2O)]^{3-}$ and $[UO_2F_3(C_2O_4)(H_2O)]^{3-}$ types with alkali metals, ammonium, and guanidinium have been reported by Chernyayev (1966) and Shchelokov and Belomestnykh (1968a,b). Fluoro-oxalato compounds of the types $M_2[UO_2F_2(C_2O_4)]$, $M_4[UO_2F_2(C_2O_4)_2]$, and $M_2[(UO_2)_2F_4(C_2O_4)]$ (where M = Rb or K) are obtained by mixing of saturated solutions of $H[UO_2F_3] \cdot H_2O$ with alkali metal oxalates in different mole ratios (Chakravorti *et al.*, 1978). Some crystallographic data and IR spectral bands are collected in Table 5.30.

Numerous hydrated and anhydrous uranyl fluoro compounds have been obtained from aqueous solutions by varying the preparation conditions with a given alkali metal or organic base cation (Brown, 1968; Bacher and Jacob, 1980), e.g. $CsUO_2F_3$, $CsUO_2F_3 \cdot H_2O$, $NaUO_2F_3 \cdot xH_2O$ (x = 2 and 4), $CsUO_2F_4 \cdot H_2O$, $M_3UO_2F_5$ (M = Na, K, Rb, Cs, NH_4), $M_4(UO)_2F_5 \cdot 2H_2O$ (M = K, R, Cs), $M^I(UO_2)_2F_5 \cdot xH_2O$, $M^IUO_2F_3 \cdot xH_2O$ and $M^I(UO_2)_3F_7 \cdot xH_2O$ (where M^I is an organic base and x varies from 0 to 6). The MF/UO_2F_2 ratio in aqueous solutions has a significant influence on the stoichiometry of the complexes obtained. With a large excess of MF one usually obtains the $M_3UO_2F_5$ type of complexes. When the ratio is less than 3 one obtains di- or polynuclear complexes. The compounds obtained using the preparative methods described above can be rationalized from information on the equilibrium constants of the complexes present (cf. Section 5.9).

In $CsUOF_5$, the fluorine and oxygen atoms form a pseudo-octahedral surrounding of the uranium atom. In the other $MUOF_5$ (M = NH_4, K or Rb) oxide fluorides, uranium is eight coordinated with dodecahedral coordination geometry. The structure consists of chains formed by surface sharing of individual dodecahedra through bridging fluoride ligands. (Joubert *et al.*, 1978a,b). Some structural details are also available for other hexavalent oxide fluoride complexes (see Table 5.30).

(*iii*) *Uranium hexachloride*

Uranium hexachloride may be obtained by thermal decomposition of UCl_5 at 120–150°C *in vacuo*. The green UCl_6 crystals are collected on a cold finger and purified from contaminating UCl_5 by sublimation in vacuum at 75–100°C or distillation in a stream of an inert gas at a low pressure. On laboratory scale it is best prepared by condensing an excess of BCl_3 onto UF_6 at –196°C and allowing the vessel with the compounds to warm up slowly. It is not necessary to purify the product by sublimation since the by-products are volatile at room temperatures (Brown, 1979).

UCl_6 is an extremely moisture-sensitive, black to dark green crystalline solid. The compound is reported to melt at (177.5 ± 2.5)°C, but it readily liberates chlorine at temperatures higher than $\approx$120°C. It reacts violently with water to form uranyl(VI) solutions. Hydrogen reduces UCl_6 to UCl_4 at 250°C. Reaction of UCl_6 with anhydrous liquid hydrogen fluoride or UF_6 converts it to UF_4 and UF_5, respectively. The hexachloride is slightly soluble in carbon tetrachloride, liquid chlorine, methyl chloride, isobutyl bromide, and thionyl chloride. On prolonged storage in carbon tetrachloride, it decomposes forming crystalline red-brown, volatile U_2Cl_{10}. The decomposition reaction proceeds much faster in 1,2-dichloroethane and methylene dichloride. The reduction in the last solvent appears to be photochemically mediated. Interaction with chlorides such as NH_4Cl, $(C_6H_5)_4AsCl$, and $(CH_3)_4NCl$ yields the appropriate $MUCl_6$ hexachloorouranate(V) compounds.

UCl_6 has hexagonal symmetry, space group D^3_{3d}; $P\bar{3}m1$ (Zachariasen, 1948f). The structure has been refined with neutron and X-ray powder diffraction data by Taylor and Wilson (1974b) and can be described as a hexagonal close packing of chlorine atoms with uranium atoms in one-sixth of the octahedral holes. The chlorine atoms form an almost regular octahedron around the U(1) located at 0,0,0 while the geometry around U(2) at 1/3, 2/3, 0.518 is slightly distorted (Fig. 5.48).

The absorption spectra for UCl_6 in the solid state, vapor phase, and solutions in perfluoroheptane in the UV–Vis range have been reported and analyzed (Brown, 1979). Charge transfer bands were observed at 17000 and 20800 cm^{-1} for solid UCl_6 and at 21000 and 20800 cm^{-1} in the vapor phase. Some X-ray and physical data of the compound are summarized in Table 5.30.

(*iv*) *Uranium*(*VI*) *dioxide dichloride, UO_2Cl_2, and related compounds*

Uranium(*VI*) *dioxide dichloride* (*uranyl chloride*)

Since the literature on uranium(VI) dioxide dichloride is very extensive (Brown, 1979), the results of investigations presented in this section must necessarily be incomplete. The most attractive methods for the preparation of UO_2Cl_2 involve

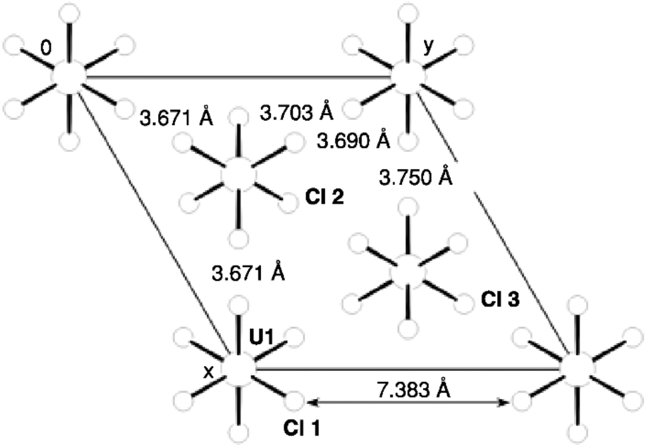

Fig. 5.48 *View of the crystal packing of* UCl_6 (*distances are taken from Taylor and Wilson*, 1974*b*).

the oxidation of UCl_4 at temperatures between 300 to about 350°C or the dehydration of $UO_2Cl_2 \cdot H_2O$. The last method may readily be performed by heating in a stream of gaseous HCl or HCl + Cl_2 mixtures at 400–450°C. UO_2Cl_2 may be also obtained by electrochemical oxidation of uranium in an acetonitrile solution of Cl_2 in the presence of oxygen. This solution of UO_2Cl_2 may be used for the preparation of numerous adducts, e.g. $(Et_4N)_2UO_2Cl_4$ (Kumar and Tuck, 1984).

The anhydrous compound is a yellow, hygroscopic solid, readily soluble in a number of organic solvents, in many cases with complex formation. It is not soluble in non-polar organic solvents. Thermal decomposition in air leads to formation of a mixture of α-UO_3 and $UO_{2.9}$ at 460°C and to U_3O_8 at higher temperature. The compound decomposes to UO_2 and Cl_2 on heating in a nitrogen atmosphere. Vacuum thermal decomposition results first in the formation of an intermediate state $(UO_2)_2Cl_3$ and next, at 450°C, of a mixture of UO_3 and U_3O_8. UO_2Cl_2 may be converted to $UOCl_3$ by reaction with UCl_4 *in vacuo* at 370°C.

The reaction of UO_2Cl_2 solutions with a variety of ligands in both aqueous and non-aqueous media results in the formation of a large number of stable compounds of different UO_2Cl_2:ligand stoichiometry, e.g.:

- (1:1): with methyl cyanide, methylmalonamide, benzophenone; acetyl chloride, 1,10-phenantroline and *N*,*N*,*N*′,*N*′- teramethyl-α,α-dimethylmalonamide;
- (1:1,5): with *N*,*N*,*N*′,*N*′-tetramethylmalonamide, *N*,*N*,*N*′,*N*′-tetramethylglutaramide;
- (1:2): aniline, pyridine, ethanol, acetic anhydride, diethyl ether, acet-*p*-phenetidine, 1,10-phenantroline, dimethylurea, tetramethylurea,

trialkyl-phosphine, triaryl-phosphine, 2,2′-bipyridine, and 4-methoxoy-pyridine-*N*-oxide;
- (1:3): with 4-methylpyridine-*N*-oxide, *N*,*N*-dimethylformamide, ethylurea, diethylurea;
- (1:4): hydrazine, urea, 1,3-dimethylurea and 4-chloropyridine-*N*-oxide etc.

A number of uranyl chloro-complexes have been identified during investigations of the MCl–UO_2Cl_2, $CuCl_2$–UO_2Cl_2, and NaCl–KCl–UO_2Cl_2 phase diagrams (where M = Li, Na, K, Rb, or Cs) (Brown, 1979).

UO_2Cl_2 has orthorhombic symmetry, space group *Pnma* (see Table 5.30). Uranium has pentagonal bipyramidal coordination geometry with two uranyl oxygen atoms at the apices; there are four chlorine atoms and one oxygen atom in the equatorial plane, the latter an "yl" oxygen atom from neighbouring uranium. The pentagons form chains parallel to the *b* axis by sharing Cl–Cl edges (Taylor and Wilson, 1973b). Electronic absorption spectra in the solid state and solutions in non-aqueous media and luminescence spectra have been discussed in numerous papers (Brown, 1979; Wells, 1990). Some physical data are listed in Table 5.30.

Uranyl(VI) chloride hydrates and hydroxide chlorides

The following compounds have been identified $UO_2Cl_2 \cdot 3H_2O$, $UO_2Cl_2 \cdot H_2O$, $[(UO_2)_2(OH)_2Cl_2(H_2O)_4]$, $[(UO_2)_4O_2(OH)_2Cl_2(H_2O)_6]$, and $4UO_3 \cdot HCl \cdot 8H_2O$ (Brown, 1979). The tri- and monohydrate are most conveniently prepared by slow evaporation from concentrated uranyl(VI) hydrochloric acid solutions over KOH and P_2O_5, or from an aqueous solution in dry air at room temperature; they form yellow hygroscopic powders. The hydrates are readily soluble in water and in various organic solvents such as ether, acetone, ethyl acetate, and a number of alcohols. The trihydrate may be dehydrated to $UO_2Cl_2 \cdot H_2O$ and then readily converted to the anhydrous salt by heating in a stream of dry hydrogen chloride or a HCl + Cl_2 mixture. When heated in an inert atmosphere, it is converted at about 220°C to impure UO_2Cl_2 and at temperatures above 400°C to U_3O_8 (Brown, 1979). $UO_2Cl_2 \cdot H_2O$ reacts with $P(C_6H_5)_4Cl$ by refluxing in a thionyl chloride solution to give $[P(C_6H_5)_4]UOCl_5$ on cooling. With smaller cations reductive chlorination to hexachlorouranates(V) occurs.

$UO_2Cl_2 \cdot H_2O$ and $UO_2Cl_2 \cdot 3H_2O$ have monoclinic ($P2_1/m$) and orthorhombic ($Pn2_1a$) symmetry, respectively. Neutron diffraction studies of $UO_2Cl_2 \cdot H_2O$ (Taylor and Wilson, 1974c) show that uranium has the common pentagonal bipyramidal coordination geometry with four chlorine and one water oxygen atoms in the equatorial plane. Infinite chains similar to those in UO_2Cl_2 are formed by sharing two Cl–Cl edges (Table 5.30).

Three basic hydroxide chlorides are observed in the UO_3–HCl–H_2O phase diagram at 25°C, but only one, $[(UO_2)_2(OH)_2Cl_2(H_2O)_4]$, is reported to be congruently soluble (Prins and Cordfunke, 1975). The compound may be easily obtained as hydrolysis product of a UO_2Cl_2 solution prepared by dissolution of

UO_3 in concentrated HCl (Åberg, 1969). Thermal decomposition of the compound in air leads first to the hemi-hydrate $UO_2(OH)Cl \cdot 0.5H_2O$ at 80–120°C, from which the nearly anhydrous salt, $UO_2(OH)Cl$ is formed at about 250°C. The compound crystallizes with monoclinic symmetry (see Table 5.30) and has a structure in which two linear uranyl units are linked through a double OH bridge, the remaining coordination sites are occupied by one Cl atom and four O atoms from two H_2O molecules, resulting in an irregular planar pentagon (Åberg, 1969).

(*v*) *Uranium*(*VI*) *oxochloro complexes*

The typical representatives of this group have the composition: M^IUOCl_5 (e.g. $M = P(C_6H_5)_4$, $M^I_2UO_2Cl_4$ (e.g. M = Li, Na, K, Rb Cs, NH_4, $P(C_6H_5)_4$, $N(C_2H_5)_4$, and others), $M^I_2UO_2Cl_4 \cdot 2H_2O$ (M = Li, Na, K, Rb, or NH_4), $M^{II}UO_2Cl_4 \cdot 2H_2O$ (M = Mg, Ca, Sr, Ba, Zn, Zn, Cd, and others), $M^IUO_2Cl_3$ (e.g. $M = P(C_6H_5)_4$, $N(C_{10}H_{21})_4$, and others), $M^I(UO_2)_2Cl_5$ (e.g. M = Na, K, Rb, Cs, or NH_4), $M^I_2U_2O_5Cl_4$ (M = Na, K, Rb, or Cs), $M^I_2U_2O_5Cl_4 \cdot xH_2O$ (M = Na, K, Rb or Cs), $KNa_2(UO_2)_2Cl_7$, KUO_3Cl, $K_2U_3O_8Cl_4$, and $K_2(UO_2)_xCl_{2x+2}$ ($x = 2$, 3, or 4). The compounds have been prepared by variety of methods (Brown, 1979), most commonly by crystallization from organic solvents (methyl cyanide or ethanol solutions) or aqueous hydrochloric acid solutions of the corresponding chlorides, as well as by solid-state reactions. Some of them are air-sensitive (e.g. $[P(C_6H_5)_4]UOCl_6$) or are hydrated on exposure to moist air ($M^I_2UO_2Cl_4$ where M = Li to Rb and NH_4); they are soluble in some organic solvents.

Structure data (Brown, 1979) are available for a number of the compounds (see Table 5.30). In $M^I_2UO_2Cl_4$ there are discrete $UO_2Cl_4^{2-}$ units with linear O–U–O groups. The structure of $M_2U_2O_5Cl_4 \cdot 2H_2O$ (M = Rb or Cs) consists of discrete planar tetranuclear anions, $[(UO_2)_4O_2Cl_8(H_2O)_2]^{4-}$, in which the uranyl groups in the equatorial plane are linked by oxygen and chloride bridges. In the structure of $[N(C_6H_5CH_2)(CH_3)_3]_4[UO_2Cl_3O]_2$ there are puckered sheets of binuclear $[Cl_3O_2U\text{-}(\mu\text{-}O_2)\text{-}UO_2Cl_3]^{4-}$ anions parallel to (001), which are interleaved by the cations. The anion is built of two identical, distorted pentagonal bipyramides sharing the peroxo-group as a common edge. Oxochlorouranates of the formula $Ln_3UO_6Cl_3$ (Ln = La, Pr, or Nd) were prepared by heating stoichiometric amounts of $LnOCl/Ln_2O_3/U_3O_8$ (Ln = La or Nd) or $PrOCl/Pr_6O_{11}/U_3O_8$ in silica ampoules at 800–1000°C in an excess of chlorine (Henche *et al.*, 1993). The crystals were investigated by X-ray diffraction methods (see Table 5.30) and high-resolution electron microscopy.

(*vi*) *Uranium*(*VI*) *perchlorates and related compounds*

The synthesis and characterization of uranyl(VI) perchlorate, $UO_2(ClO_4)_2$ and its hydrates $UO_2(ClO_4)_2 \cdot xH_2O$ ($x = 0$, 1, 3, 5, or 7) have been investigated by a number of authors (Brown, 1979). The heptahydrate has been obtained by crystallization from aqueous solution at room temperatures. Vacuum drying of the compound at that temperature leads to the pentahydrate, and vacuum dehydration over sulfuric acid to the trihydrate. Further vacuum drying converts the latter to the monohydrate; in the temperature range 100–140°C anhydrous perchlorate $UO_2(ClO_4)_2$ is formed (Vdovenko *et al.*, 1963). All of the compounds are readily soluble in water and polar organic solvents, in many cases with the formation of stable uranyl(VI) perchlorate complexes. The interaction with oxygen and nitrogen donor ligands leads to the formation of the following types of complexes:

$UO_2(ClO_4)_2 5L$: where L = pyridine, pyridine-*N*-oxide, antipyrene, dimethylsulfoxide, dimethylselenoxide, dimethylformamide, diphenylsulfoxide, thioxane oxide, urea, 1,3-dimethylurea, 1,3-diethylurea, hexamethylphosphoramide.

$UO_2(ClO_4)_2 4L$: where L = trimethylphosphine oxide, triphenylphosphine oxide, tripropylphosphine oxide.

$UO_2(ClO_4)_2 3L$: where L = octamethylphosphoramide, camphor, methyl cyanide, nonamethylimido-diphosphoramide.

$UO_2(ClO_4)_2 2L$: where L = tributylphosphate, tributylphosphine oxide, nitromethane, dibutyl ether.

$UO_2(ClO_4)_4 \cdot 7H_2O$ crystallizes in the orthorhombic space group $Pca2_1$ The structure consists of $[UO_2(OH_2)_5]^{2+}$ and ClO_4^- ions, with two additional water of solvation. The crystal structure is held together by an extensive network of hydrogen bonds.The coordination polyhedron is a distorted pentagonal bipyramid (Alcock and Esperas, 1977). Some crystallographic and infrared data are are listed in Table 5.30.

(*vii*) *Uranium*(*VI*) *oxide bromides and complex oxobromo compounds*

Uranyl(*VI*) *bromide and related complexes*

One of the most convenient methods for the preparation of UO_2Br_2 is the reaction of anhydrous UBr_4 with oxygen at a carefully controlled temperature in the range 150–160°C; at higher temperature, U_3O_8 is formed (Brown, 1979). An alternative method involves the electrochemical anodic oxidation of uranium in CH_3CN/Br_2 solution in the presence of dry oxygen. The resulting solution of UO_2Br_2 may also be used for the preparation of adducts by adding a two-fold excess of the appropriate ligand (Kumar and Tuck, 1984).

The compound is a bright red, hygroscopic solid which turns yellow on exposure to moisture. It is thermally unstable and appears to lose bromine slowly even at room temperature. The decomposition is complete within 48 h in an inert atmosphere at 350°C. UO_2Br_2 is extremely soluble in water and polar organic solvents. Numerous complex compounds have been prepared by reactions with a variety of ligands in anhydrous solvents, for example, of the following types: UO_2Br_2L (L = methyl cyanide), $UO_2Br_2 2L$ (L = acetic anhydride, ether, *N*,*N*–dimethylacetamide, antipyrine, *N*-methylacetanilide,

$(CH_3)_3PO$, $(C_2H_5)_3PO$, $(C_6H_5)_3PO$, etc), UO_2Br_23L (L = dimethylformamide), UO_2Br_24L (L = dimethylsulfoxide) $UO_2Br_2 \cdot xNH_3$ ($x = 2$, 3, and 4), $UO_2Br_4 \cdot (LH)_2$ (L = 2,2′-dipyridine,1,10-phenanthroline) and $(Et_4N)_2UO_2Br_4$. In addition, a number of oxo-tetrabromo complexes of the $M_2UO_2Br_4$ (M = Cs, $P(C_6H_5)_3CH_3$, $P(C_6H_5)_3H$, $P(CH_3)_3H$, $P(C_6H_5)_3C_6H_5CH_2$, etc.) and $M_2UO_2Br_4 \cdot 2H_2O$ (M = NH_4, K, or Rb) types have been obtained by reaction of UO_2Br_2 with the appropriate ligands in HBr or in anhydrous organic solvents (Brown, 1979, Kumar and Tuck, 1984).

Uranyl(VI) hydroxide bromide and bromide hydrates

A stable hydrate of the formula $UO_2Br_2 \cdot 3H_2O$ is obtained in the form of dark yellow needles by crystallization from an aqueous solution of HBr and UO_2Br_2, followed by vacuum drying (Peterson, 1961). The dehydration of the trihydrate over phosphoric acid leads to the formation of the monohydrate $UO_2Br_2 \cdot H_2O$. The hydrates may be also obtained by other methods (Brown, 1979). Crystallization of UO_2Br_2 from acid-deficient solutions leads to the formation of $UO_2(OH)Br \cdot 2H_2O$ (alternative formulations are: $[U_2O_5(H_2O)]Br_2 \cdot 4H_2O$ or $[UO_2(OH)_2UO_2]Br_2 \cdot 4H_2O$). The compound is isostructural with its chloride analog $[UO_2(OH)_2UO_2]Cl_2 \cdot 4H_2O$; it is converted to $UO_2(OH)Br$ when heated at 200°C.

The hydrates are readily soluble in water and numerous organic solvents like ethanol, ether, amyl alcohol, etc. $M_2UO_3Br_2$ (M = NH_3 or K) is formed by reacting the monohydrate with ammonia gas or a stiochiometric quantity of KOH (Brown, 1979). According to Peterson (1961) the trihydrate is stable in dry air and may lose one molecule of water at 60°C without decomposition.

Uranium(VI) oxobromo complexes

The synthesis and characterization of a large number of complex oxobromo compounds containing uranium(VI) have been summarized by Brown (1979). Oxo-tetrabromo complexes of the $M_2UO_2Br_4 \cdot 2H_2O$ type (M = NH_4, Na, K, or Rb) were prepared from aqueous or alcoholic HBr solutions of uranyl bromide by precipitation with appropriate MBr. The anhydrous analogs were obtained by heating at 120°C in an inert atmosphere. With large cations, for example Cs^+ or pyridinium, only anhydrous complexes of the $M_2UO_2Br_4$-type are formed.

Other anhydrous complexes of this type were prepared by reactions of uranyl bromide solutions in ethanol or methyl cyanide with various phosphonium bromides (e.g. $P(C_6H_5)_3C_4H_9Br$, $P(C_6H_5)_3HBr$, $P(C_6H_5)_3C_6H_5CH_2)Br$, $P(C_2H_5)_3HBr$, and $P(C_3H_7)_3HBr$) as well as with $N(C_2H_5)_4Br$ (in ethanol), $N(CH_3)_4Br$ (in a C_2H_5OH–HBr mixture), choline bromide, $(C_5H_{14}NO)Br$ (in methanol), and acetylcholine bromide, $(C_7H_{16}NO_2)Br$ (in methanol). The reaction of UO_2Br_2 with tetradecylammonium bromide in anhydrous benzene results in the formation of a viscous liquid of the $[N(C_{10}H_{21})_4]UO_2Br_3$. In the presence of traces of water in benzene compound converts into the oxo-tetrabromo complex.

The oxobromo complexes are yellow and readily soluble in aqueous solutions; those with organic cations also in anhydrous solvents such as acetone, benzene, methyl cyanide, and nitromethane. Structure investigations reveal a distorted octahedral geometry in complexes with M = Cs, $N(CH_3)_4$, $N(C_3H_7)_4$, and $C_7H_{16}NO_2$, where the U–O and U–Br bond distances range from 1.70 to 1.90 and 2.78 to 2.86 Å, respectively. For structural data, see Table 5.30. Extensive information on the infrared and Raman spectra is also available (Brown, 1979). On the basis of these data the observed frequencies for various oxotetrabromo complexes can be assigned as follows:

IR (cm^{-1}): ν(U–O, asym. stretch.) = 895–934; ν(O–U–O deformation) = 243–263; ν(U–Br stetch.) = 160–180; Raman (cm^{-1}): ν(U–O sym. stretch.) = 826–835, ν(U–O–Br bend.) = 190–198, ν(U–Br stretch.) = 167–172 ν(U–Br bending mode) = 81–83. The fluorescence spectrum of $Cs_2UO_2Br_4$ measured at 14.3 K reveals the existence of two sites of different symmetry, which has been supported by the observed differences in the fluorescence relaxation time. The solution spectra of $[N(C_{10}H_{21})_4]UO_2Br_3$ and $[N(C_{10}H_{21})_4]UO_2Br_4$ in anhydrous benzene have absorption bands at 508, 491, 483, 447, and 431 nm and at 497, 480, 464, and 449 nm, respectively. For $[P(C_6H_5)_3H]_2 \cdot UO_2Br_3$ in methyl cyanide solution these bands appear at 19800, 20080, 20790, 21550, 20220, and 22880 cm^{-1}. As one should expect, the absorption bands of the solid state reflectance spectra of $[C_5H_{14}NO]_2UO_2Br_4$ and $[C_7H_{16}NO_2]UO_2Br_4$ are somewhat shifted towards longer wavelengths as compared to their chloro analogs.

The reactions of uranyl bromide with various metal bromides in aqueous HBr lead to the formation of the following hydrated bromo compounds:

$MUO_2Br_4 \cdot xH_2O$ (M = Sr, $x = 3$; M = Zn, Mg, $x = 4$; M = Ca, $x = 8$);
$MUO_2Br_5 \cdot xH_2O$ (M = La, $x = 3$; M = Y, $x = 5$);
$MUO_2Br_6 \cdot 4H_2O$ (M = Ce or Th);
$MU_3O_8Br_5 \cdot xH_2O$ (M = Co, $x = 12$; M = Sc, $x = 8$), and
$Be_2UO_2Br_6 \cdot 8H_2O$, $Mn_3UO_2Br_8 \cdot 11H_2O$, and $HgU_3O_8Br_4 \cdot 4H_2O$

The complexes may be dehydrated in an oxygen atmosphere at about 200°C. $LaUO_2Br_5$, YUO_2Br_5, and $CeUO_2Br_5$ are converted to $LaUO_2(O_2)Br$, $YUO_2(O_2)Br$, and $LaUO_2(O_2)Br$, respectively, at 290–305°C. Decomposition at high temperature results in the formation of appropriate uranates, $CaUO_4$, Mn_3UO_6, $Co_2U_6O_{21}$, and HgU_3O_{10}, etc. The heating of $K_2UO_2Br_4$ at 250°C and $(NH_4)_2K_2UO_2Br_4$ at 250–350°C in an oxygen atmosphere results in the formation of $K_2UO_3Br_2$ and $(NH_4)_2UO_3Br_2$, respectively. $K_2UO_3Br_2$ may be also prepared by interaction of uranyl bromide monohydrate with KOH, or by heating K_2UO_4 with gaseous hydrogen bromide, whereas $(NH_4)_2UO_3Br_2$ is obtained by action of gaseous NH_3 on $UO_2Br_2 \cdot H_2O$. Compounds of the composition $K_2U_2O_6Br_2$ and $K_2U_3O_9Br_2$ have been prepared by heating K_2UO_4 or $K_2U_3O_{10}$ with gaseous HBr, respectively. A phase of the composition $K_xUO_3Br_x$ ($x = 0.9$) is obtained when UO_3 and KBr are heated at 300–550°C *in vacuo*. The compound is isostructural with $K_xUO_3Cl_x$ (see Table 5.30).

The interaction of $M_2UO_2Br_4 \cdot 2H_2O$ (M = K or Rb) with $UO_2(OH)_2$ results in the formation of compounds containing the tetranuclear unit $M_2[(UO_2)_4O_2(OH)_2Br_4(H_2O)_4] \cdot 2H_2O$. The complexes lose four H_2O molecules in an inert atmosphere at 60°C and form $M_2U_4O_{11}Br_4$ at ≈200°C. The compounds are triclinic ($P\bar{1}$) and isostructural with the chloro analogs (see Table 5.30).

(*viii*) *Uranium*(*VI*) *compounds with iodine*

$UI_4 \cdot 4$dmf is obtained by electrochemical oxidation of uranium anodes in *N*,*N*-dimethylformamide (dmf) (Kumar and Tuck, 1984). The preparation of an extremely unstable UO_2I_2 has been reported in a number of papers (Brown, 1979; du Preez and Zeelie, 1989). The compound has not been obtained in a pure form but relatively stable compounds, such as $UO_2I_2 \cdot 4$dmf (yellow, m.p. = 156°C; dmf = dimethylformamide), $UO_2I_2 \cdot 2$tppo (orange red, m.p. = 268°C; tppo = triphenylphosphine oxide), $UO_2I_2 \cdot 2$tmu (orange, tmu = *N*,*N*,*N*′,*N*′-tetramethylurea), $UO_2I_2 \cdot 5CO(NH_2)_2 \cdot H_2O$ (orange-red), $UO_2I_2 \cdot 2$hmpa (orange, hmpa = hexamethylphosphoric triamide), $UO_2I_2 \cdot xNH_3$ ($x = 2$ or 3), $UO_2I_2 \cdot 2$tbso (yellow-green, tbso = di-*tert*-butyl sulfoxide), $UO_2I_2 \cdot 2$dmeu (dmeu = *N*,*N*′-dimethylethylene urea), $(PPh_4)_2UO_2I_4$ (black), $UO_2I_2 \cdot 2Et_2O$ (decomposes at room temperature by evolving iodine), may be separated from solutions in water and various organic solvents (for example, ether, methanol, ethanol, amyl alcohol, methyl acetate, ethyl acetate, pyridine) (Brown, 1989; du Preez and Zeelie, 1989). A red uranyl(VI) iodo compound, $[P(C_6H_5)_3C_4H_9]_2UO_2I_4$, has been obtained by interaction of uranyl(VI) iodide with phosphonium iodide in a methyl cyanide solution (Day and Venanzi, 1966).

The addition of soluble iodides to uranyl nitrate solutions at room temperatures results in the formation of the uranyl(VI) iodide dihydrate, $UO_2(IO_3)_2 \cdot 2H_2O$. The compound is converted to α-$UO_2(IO_3)_2 \cdot H_2O$ when UO_2NO_3 and iodic acid are mixed in boiling nitric acid. β-$UO_2(IO_3)_2 \cdot H_2O$ is formed by recrystallization from water in the absence of acid. The compound $(UO_2)_2I_2O_9$ has been obtained by addition of potassium periodate to a cold solution of $UO_2(NO)_2$. The preparation of a number of uranium(VI) iodato and periodato complexes has also been reported: $KUO_2(IO_3)_3 \cdot 3H_2O$, $(KIO_4)_2(UO_2)_2O_2 \cdot 5H_2O$, $[Co(NH_3)_6][(UO_2)_2(IO_3)_7] \cdot 10H_2O$, $K_2I_2O_5(UO_2)_2$, $H(UO_2)_2IO_6 \cdot 8H_2O$, $NaH_2UO_2IO_6 \cdot 7H_2O$, $Ba(H_2UO_2IO_6)_2 \cdot xH_2O$ (Brown, 1979).

(*ix*) *Mixed halogeno-complexes*

Mixed uranyl(VI) halogeno-compounds $M^I_2UO_2Cl_2Br_2$ (M^I = NH_4, Na, K, or Cs), $Cs_2UO_2X_3Y$ (X and Y = Cl or Br), $[N(C_{10}H_{21})_4]_2[UO_2X_3I]$ (where X = Cl or Br), and $[P(C_6H_5)_3C_4H_9]_2[UO_2Cl_2Br_2]$, $[P(C_6H_5)_3C_4H_9]_2[UO_2Br_2I_2]$ have been obtained by interaction of uranyl halides with appropriate univalent bromides or iodides in aqueous HBr solutions, or in anhydrous organic solvents such as benzene and methyl cyanide. Alternative routes to these and similar mixed halogeno complexes have been also reported (Brown, 1968, 1979). $Cs_2UO_2BrCl_3$ and $Cs_2UO_2Br_3Cl$ (Ellert *et al.*, 1965) have been obtained by varying the HBr concentration in the interaction between CsBr and $UO_2Cl_2 \cdot H_2O$ The preparation of the dihydrate $K_2UO_2Br_2Cl_2 \cdot 2H_2O$ has been achieved by crystallization from 20% HCl containing KBr and UO_2Cl. Dehydration of the compound in an inert atmosphere at 110°C leads to $K_2UO_2Br_2Cl_2$ (Lucas, 1964). Dihydrates of the composition $M_2UO_2Br_{4-x}Cl_x$ ($M = NH_4$ or Rb; $x = 1$, 2, or 3) have also been isolated (Kharitonov *et al.*, 1967).

Complexes containing alkali metal cations are soluble in water and aqueous acetic acid solution; those containing phosphonium or tetralkylammonium cations are soluble in numerous non-aqueous solvents like methyl cyanide, benzene, and ethanol. In water, hydrolysis takes place. Dehydration of the compound in an inert atmosphere at $\approx$110°C leads to the anhydrous complexes (Lucas, 1964).

X-ray powder diffraction data are available for $Cs_2UO_2Cl_2Br_2$, $Cs_2UO_2BrCl_3$, $Cs_2UO_2Br_3Cl$ (Ellert *et al.*, 1965), $K_2UO_2Cl_2Br_2$, $K_2UO_2Br_2Cl_2 \cdot 2H_2O$, and $K_2U_2O_5Cl_2Br_2$ (Lucas, 1964). The ν(U–O) asymmetric stretching vibrations occur at 905–910 cm^{-1} for $M_2UO_2Br_{4-x}Cl_x \cdot 2H_2O$ ($M = NH_4$, K or Rb) and at 907–922 cm^{-1} for various anhydrous complexes. In the IR spectrum of $[P(C_6H_5)_4]UOBr_4Cl$, they appear at 838 cm^{-1}.

The metal–halogen stretching frequencies have been reported for: $[P(C_6H_5)_3C_4H_9]_2UO_2Br_2Cl_2$, $\nu(U\text{–}Cl) = 260\ cm^{-1}$; $[N(C_{10}H_{21})_4]_2UO_2BrCl_3$, $\nu(U\text{–}Cl) = 255\ cm^{-1}$, $\nu(U\text{–}Br) = 165\ cm^{-1}$; $[N(C_{10}H_{21})_4]_2UO_2Cl_3I$, $\nu(U\text{–}Cl) = 236\ cm^{-1}$, and $\nu(U\text{–}I) = 135\ cm^{-1}$, with the uranyl deformation mode at 261 cm^{-1} (Brown, 1979). The first high-intensity bands in the visible spectra of $[N(C_{10}H_{21})_4]_2UO_2Cl_3I$, and $[N(C_{10}H_{21})_4]_2UO_2BrCl_2I$ in benzene solutions, were recorded at about 20000 cm^{-1} (Vdovenko *et al.*, 1969).

5.8 CHEMICAL BONDING IN URANIUM COMPOUNDS

5.8.1 U(III) and U(IV) compounds

In general, the discussion of chemical bonding in U(III) and U(IV) compounds is related to metal–organic complexes as discussed in Chapters 25 and 26. A recent review of the organometallic chemistry of lanthanides and actinides has been given by Hyeon *et al.* (2005). An early example is given in a study by Bursten and Strittmatter (1987) that discussed the bonding in $[Cp_3UCO]$ and $[Cp_3UCO]^+$, where Cp is cyclopentadiene, $\eta^5\text{-}C_5H_5$. They suggested an extensive U(III) 5f–CO π-back-bonding, an effect that decreases significantly on oxidation to U(IV). The coordination of dinitrogen in $[\{U(NN'_3)\}_2(\mu_2\text{–}\eta^2:\eta^2\text{–}N_2)]$, where NN'_3 is $N(CH_2CH_2NSiBu^tMe_2)_3$, was studied by Roussel and Scott (1998). The end-on coordination is consistent with U → N back-bonding, but the authors suggest that the effect is minor. The role of the 5f orbitals in back-bonding has also been studied by comparison with the bonding in lanthanide compounds in oxidation states 3+ and 4+. A typical example is given in a study by Berthet *et al.* (2002) of the selective complexation of U(III) over Ce(III) and Nd(III) in 2,2′:6,2″-terpyridine complexes. This ligand forms much stronger complexes with uranium than cerium in solution. The authors probed the possible reasons behind this by determination of the X-ray crystal structure of the complexes $[MI_2(terpy)_2]I$, M = Ce, Nd, $[CeI_2(terpy)_2(H_2O)]I$, and $[UI_2(terpy)_2(pyridine)]I$. They suggest that the shortening of the average M–N distance by 0.05 Å in the uranium complex as compared to that of cerium might be a result of a stronger π back-bonding interaction between uranium and the terpyridyl ligand. The evidence for back-bonding is indirect and more direct information is necessary to draw definite conclusions, e.g. Di Bella *et al.* (1996) point out, based on electronic structure calculations and photoelectron spectroscopic data, that the bonding in isoleptic 4f and 5f M(III) bis-(cyclopentadienyl) is very similar. Experimental data and quantum chemical calculations on different model systems indicate 5f orbital participation in chemical bonding, but the extent of this and its chemical effects are far from clear. A detailed discussion of the quantum chemistry of uranium and other actinides is given in Chapter 17.

Roos and Gagliardi have used quantum chemical methods to explore the stability and possible existence of compounds with U–U bonds, similar to those found for some d-transition elements, e.g. Cr, Mo, W, Tc and Re. They predicted stable diatomic U_2 with a quintuple U–U bond and a bond distance of 2.43 Å (Gagliardi and Roos, 2005a). Gagliardi *et al.*, (2005) found that also U_2^{2+} is a stable ion with several low-lying electronic states, all with U–U bond distances around 2.30 Å.

Compounds containing U–U bonds have been identified by matrix isolation techniques; $H_2U–UH_2$ by Souter *et al.* (1997) and O-U–U-O by Gorokhov *et al.* (1974). In their most recent paper Gagliardi and Roos (2005b) have studied the stability and chemical bonding in U_2Cl_6, $U_2Cl_6^{2-}$, $U_2(OCHO)_4$, $U_2(OCHO)_6^{2-}$, and $U_2(OCHO)_4Cl_2^{2-}$. It seems unlikely that compounds where the formal oxidation state of uranium is +2 can be prepared, but those with the oxidation state of +3 seem more probable. $U_2Cl_6^{2-}$, has a similar structure and bonding as $Re_2Cl_6^{2-}$, with the eclipsed conformation as the most stable one. The weakest bond is found in $U_2(OCHO)_4Cl_2^{2-}$, where the U–U distance is 2.80 Å.

5.8.2 UF_5 and UF_6 compounds

The bonding in these compounds has been discussed by Rosén and Fricke (1979), Wadt and Hay, (1979), and Onoe *et al.* (1993, 1997); these compounds can presumably be used as models for the bonding also in other uranium(V) and uranium(VI) halides. The authors point out that there is extensive involvement of 5f, 6p, and 6d orbitals in the U–F bonds, the orbital population in the 7s and 7p orbitals is smaller, and relativistic effects are of great importance for the chemical bonding. The participation of the 5f orbitals in the bonding explains the fluxional geometry of UF_5 between C_{4v} and D_{3h} (Onoe *et al.*, 1997).

5.8.3 Uranyl(v) and uranyl(vi) compounds

The linear "yl"-ions in aqueous systems are unique for the actinide elements; in other "yl"-ions, such as VO_2^+, MoO_2^{2+}, and WO_2^{2+}, the oxygen atoms are mutually *cis*, thereby maximizing $(p_\pi) \rightarrow M(d_\pi)$ bonding. A linear MO_2^{2+} group is known in compounds of technetium, rhenium, ruthenium, and osmium, but the corresponding aqua-ions are unknown (a recent discussion of the electronic structure of these *trans*-dioxometal complexes is found in Hummel *et al.*, 2006). The short U(vi)–O_{yl} bond distance, approximately 1.75 Å, indicates a strong multiple uranium–oxygen bonding, one of σ and two of π character. The uranium–"yl" distance in UO_2^+ is somewhat longer due to the smaller effective charge of uranium (Vallet *et al.*, 2004a). The orbitals involved in the uranium–"yl"-oxygen bonds have been extensively discussed (see Denning, 1992; Kaltsyoannis, 2000; Matsika *et al.*, 2001 for a review); the MO diagram in Fig. 5.49 illustrates the bonding.

The bonding molecular orbitals are $\sigma_g^2\ \sigma_u^2\ \pi_g^4\ \pi_g^4$ with 5fδ and 5fφ as the lowest unoccupied orbitals. The bonding orbitals have mainly O 2p character and the uranyl(vi) ion can therefore be described as $O^{2-}{\equiv}U^{6+}{\equiv}O^{2-}$.

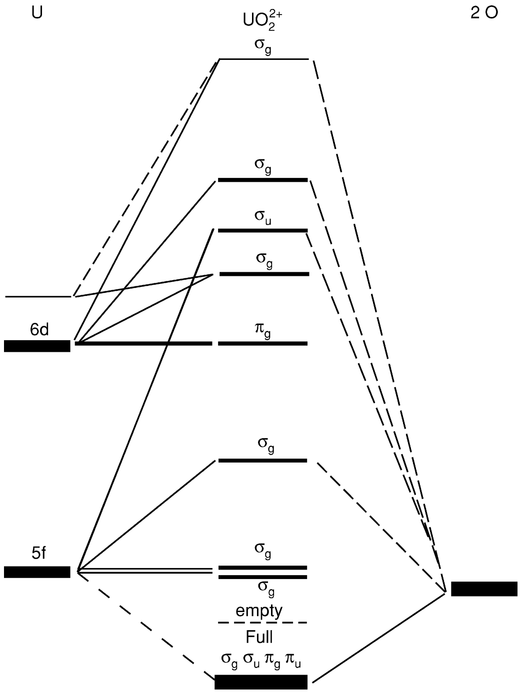

Fig. 5.49 *Schematic molecular orbital diagram for the uranyl(*vi*) ion.*

The nonbonding and antibonding orbitals have 5f and 6d character. The ordering of the bonding orbitals and the HOMO in UO_2^{2+} is not straightforward (de Jong *et al.*, 1999); Denning (1992) and later Kaltsyoannis (2000) suggested the order $\pi_g < \pi_u < \sigma_g << \sigma_u$, where σ_u is the highest occupied orbital. The significant energy gap between the σ_g and σ_u orbitals is traced to the filled–filled interactions between the semi-core 6p orbitals and the σ_u valence level, the 'pushing from below' mechanism. Triatomic UN_2 and UON^+ are isoelectronic with UO_2^{2+} and Pyykkö *et al.* (1994) suggested that these and other triatomic groups could have a significant stability. This was confirmed in experimental studies by Brown and Denning (1996) who prepared a number of stable compounds containing the linear –N≡U=N– and O=U=N– groups and discussed their chemical bonding. Kaltsyoannis (2000) made a more detailed study using density functional methods and concluded that the U–N bond is significantly more covalent than the U–O bond in UON^+ and UO_2^{2+} and that the uranium f-orbitals play a more important role than the d-orbitals in the metal to ligand bonding. He also pointed out that the U–N bond in iminato complexes is best described as a triple bond.

The previous correlation diagram can also be used to describe the bonding in UO_2^+, where the single 5f electron is located in one of the nonbonding 5fδ or 5fφ orbitals.

Tatsumi and Hoffmann (1980) and Wadt (1981) have discussed the electronic reasons for the change from the linear geometry in UO_2^{2+} to the *cis*-geometry in MoO_2^{2+}. Dyall (1999) and Straka *et al.* (2001) have discussed the bonding in actinyl ions and showed that the 5f character in the M–O bond increases steadily through the actinide series, while the 6d population remains nearly constant. The nonlinear O–M–O bonds are a result of an increased 6d population. As a result of the strong covalent U–O_{yl} bonding, the formal charge of uranium is much lower than +6, +2.43 for $UO_2(H_2O)_5^{2+}$ in gas phase (Vallet *et al.*, 2004a); the charge of the 'yl' oxygen atoms is –0.43. Because of their negative charge, the 'yl' oxygen atoms in UO_2^{2+} and UO_2^+ are Lewis bases, resulting in the formation of 'cation–cation' complexes of type O=U=O- - - M (Section 5.10.2f). The negative charge on the 'yl'-oxygen atoms varies with the nature of the ligands in the equatorial plane and by proper ligand choice, the Lewis basicity of the 'yl'-oxygen atoms can be significantly increased, resulting in coordination of strong Lewis acids such as $B(C_6F_5)_3$ (Sarsfield and Helliwell, 2003). The charges on U and oxygen in $UO_2(H_2O)_5^+$ are 2.19 and –0.66, respectively (Vallet *et al.*, 2004a), making the uranyl(v) oxygen atoms even stronger Lewis bases than in uranyl(vi). A more detailed discussion of the electronic structure and energy levels of the other oxidation states of uranium is given in Chapter 16. The slight variations in the effective charge of uranium in different compounds result in small differences in the U–O_{yl} bond distance and the effect is also noticeable as small changes in the vibrational stretch frequencies of the UO_2 group in infrared and Raman spectra. In the same way the 'yl'-stretch frequency is lower in UO_2^+ than in UO_2^{2+}, indicating a weaker bond in the former ion.

5.9 STRUCTURE AND COORDINATION CHEMISTRY OF URANIUM COMPLEXES IN SOLUTION AND THE SOLID STATE

The structure of complexes in solution is characterized by their coordination geometry, coordination number, and bond distances. The coordination geometry in solid-state structures is also influenced by additional factors, such as the efficiency of packing, the charge distribution in the structure, and the formation of hydrogen bond networks. The solid-state structures are often good models for bond distances and coordination geometry in solution. The structure in solution refers to discrete ions and molecules, more or less solvated, depending on the nature of the solvent and the charge of the complex. In some cases solid-state structures may contain discrete ions and molecules, but in general, the solid is better regarded as a 'polymer'. For example, $UO_2CO_3(s)$ is a layer structure that does not contain isolated UO_2CO_3 units (see Fig. 5.54), while $Na_4UO_2(CO_3)_3(s)$ contains discrete complexes of $UO_2(CO_3)_3^{4-}$ (Fig. 5.53).

The three-dimensional structures can be described using polyhedra and nets, and for simple structures, using packing of spheres (Chapters 3 and 4 in Wells, 1990). Polynuclear complexes are more common in the solid state than in solution, presumably as a result of the stronger electrostatic interactions in the solid phase. The water solvent with its high dielectric constant and strong hydrogen bond donor/acceptor properties reduces the stability of polynuclear complexes, except those involving hydroxide and oxide donors. Polynuclear fluoride complexes are very common in the solid state (Allen *et al.*, 2000), but are not formed in significant amounts in aqueous solution. This is presumably a result of the strong hydrogen bond acceptor properties of fluoride that makes hydrogen bonding to the water more favored than fluoride bridge formation between uranium atoms.

The stoichiometry, coordination number, and the number of available donor atoms per uranium atom indicate whether a certain compound contains isolated complexes, or if chains, layer structures, or three-dimensional networks are formed. Networks are common in oxide, uranate, phosphate, arsenate, and silicate compounds where they are a result of the sharing of oxygen donor atoms between two or more metal ions. These compounds are sparingly soluble and have a variable stoichiometry, (*cf.* Section 5.7.2).

The structure principles are demonstrated in the structure models of uranium compounds in oxidation states 3+, 4+, and 6+ described in the following sections. The largest number of structures are found for uranium(VI) compounds, many of which can be prepared from aqueous solution. In these compounds, the linear UO_2 unit is inert and the additional ligands in the coordination sphere are located in, or close to the plane through uranium and perpendicular to the UO_2 axis; the number of coordinated ligands in the plane varies between four and six; in solution, these ligands are labile, i.e. they can rapidly exchange with free ligand or in ligand substitution reactions as discussed in Section 5.10.3.

5.9.1 Uranyl(VI) compounds

The coordination chemistry of U(VI) differs from that of the d-transition and main-group elements. The common coordination geometry in UO_2^{2+} complexes with small ligands is a pentagonal bipyramid, with all labile ligands in the plane perpendicular to the linear UO_2 unit. Other coordination geometries are possible; a number of oxides and uranates have distorted octahedral or pentagonal bipyramidal structure, (Section 5.7.2.2, Fig. 5.25). Isolated ions of $UO_2(OH)_4^{2-}$ are found in the compound $[Co(NH_3)_6]_2[UO_2(OH)_4]_3 \cdot xH_2O$, the X-ray structure of which was determined by Clark *et al.* (1999) (Fig. 5.50), $UO_2(OH)_4^{2-}$ has a square bipyramidal geometry also in solution (Clark *et al.*, 1999; Wahlgren *et al.*, 1999; Moll *et al.*, 2000a); this geometry may also occur in complexes where there is a strong steric interference between coordinated organic ligands. The tetra-hydroxide complex has also been studied using quantum chemical methods (Schreckenbach *et al.*, 1998; Wahlgren *et al.*, 1999; Vallet *et al.*, 2001).

The structure of $K_2UO_2(SO_4)_2 \cdot 2H_2O$ is an example of pentagonal bipyramidal coordination consisting of uranium(VI) bipyramids linked in three dimensions by bridging sulfate groups (Niinistö *et al.*, 1979). Each sulfate acts as a bridge between two uranium atoms, leaving two non-coordinated sulfate oxygen atoms. The remaining coordination site on uranium is occupied by one of the two water molecules (Fig. 5.51).

A different structure (Burns and Hayden, 2002) still with pentagonal bipyramidal coordination is found in $Na_{10}[UO_2(SO_4)_4](SO_4)_2 \cdot 3H_2O$, shown in Fig. 5.52. This structure contains discrete complexes where the five-coordination in the equatorial plane is achieved by one chelating and three monodentate sulfate ions.

A hexagonal bipyramidal geometry with six ligands in the equatorial plane is in general obtained with ligands that can form chelates that have a small distance between their donor atoms. Examples are nitrates, $M[UO_2(NO_3)_3]$, where M = NH_4, K, Rb, Cs, and Tl (Zalkin *et al.*, 1989), carbonates such as $K_4UO_2(CO_3)_3$ (Anderson *et al.*, 1980), and acetates (Navaza *et al.*, 1991); these

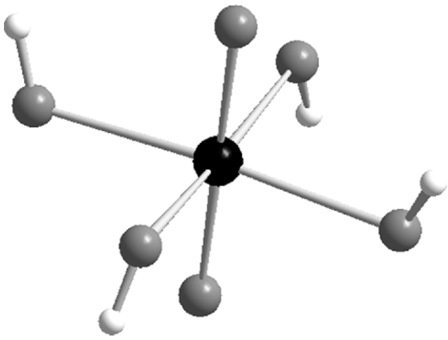

Fig. 5.50 *The structure of* $UO_2(OH)_4^{2-}$ (*from Clark* et al., 1999).

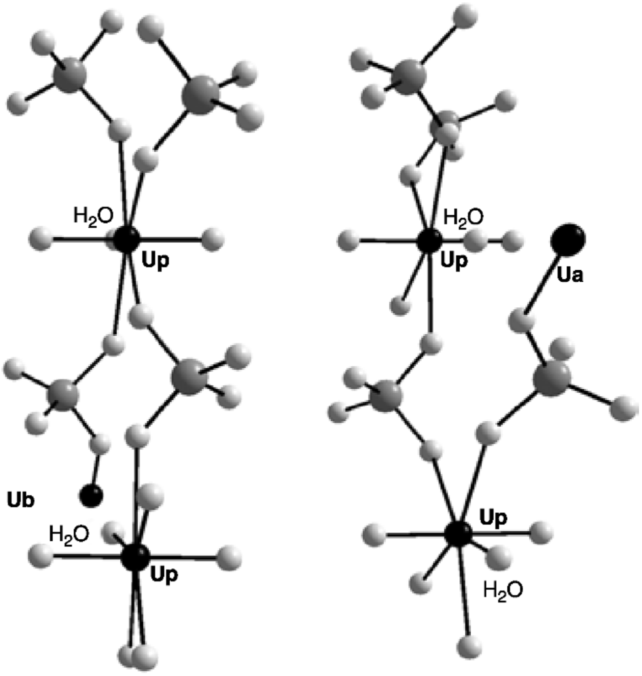

Fig. 5.51 *Coordination geometry and the three-dimensional linking in* $K_2UO_2(SO_4)_2 \cdot 2H_2O$ *(from Niinistö* et al., 1979). *The uranium atoms denoted* U_p *are located in the same plane and those denoted* U_a *and* U_b *in planes above and below this. The potassium atoms and one of the water molecules (not shown in the figure) provide additional links between the coordination polyhedra through coordination to the back end of the sulfate ions and through hydrogen bonding.*

compounds contain nine oxygen donors per uranium and from the geometry of the ligand, it is obvious that at most two per ligand can be coordinated to the same uranium atom. The donor atoms form hexagonal bipyramidal coordination together with the 'yl'-oxygen atoms. This results in structures that are composed of discrete complexes (Fig. 5.53). However, it is also feasible to have isomers; isolated pentagonal bipyramidal geometry is obtained if one of the ligands is coordinated through a single oxygen atom as in $UO_2(\text{oxalate})_3^{4-}$, discussed by Vallet *et al.* (2003). The only way to distinguish between these alternatives is through a structure determination or by using quantum chemical methods.

In UO_2CO_3(s), there are three oxygen donors per uranium and therefore the structure cannot contain isolated complexes; it turns out to be a layer structure where each oxygen donor is shared between two adjacent uranium atoms giving rise to hexagonal bipyramidal coordination (Fig. 5.54). This coordination geometry is very similar to that in the tris-carbonato complex (Fig. 5.53), but the three-dimensional structure of the latter is very different.

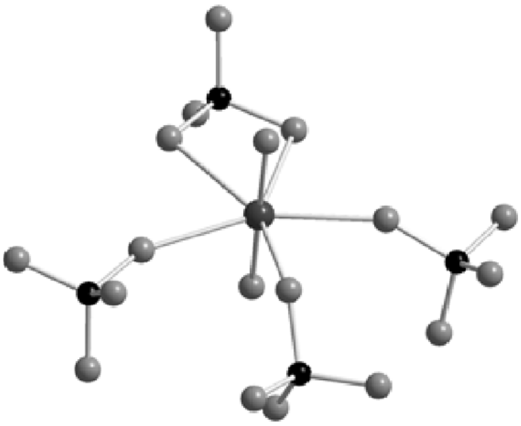

Fig. 5.52 *The coordination geometry of the* $UO_2(SO_4)_4^{6-}$ *ion in* $Na_{10}[UO_2(SO_4)_4](SO_4)_2 \cdot 3H_2O$ (*Burns and Hayden,* 2002). *One sulfate ion forms a chelate while the other three sulfate ions are monodentate.*

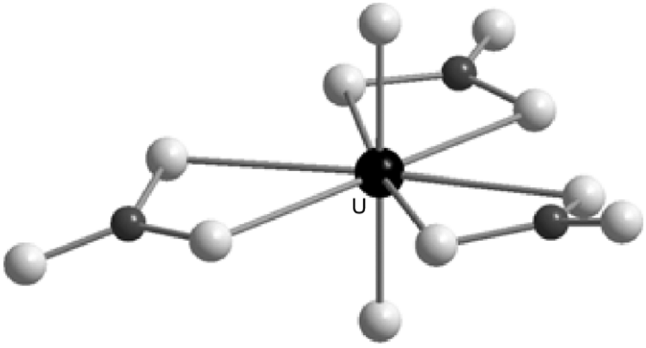

Fig. 5.53 *The coordination geometry, a hexagonal bipyramid, in* $K_4UO_2(CO_3)_3$ (*from the X-ray structure of Anderson* et al., 1980). *The ion* $[UO_2(CO_3)_3]^{4-}$ *occurs as discrete units in the structure; these units are linked through coordination to the counter ion* K^+.

Rare examples of six-coordination are also known in compounds containing organic ligands, e.g. $[UO_2(OTf)_2(bipy)_2]$ and $[UO_2(phen)_3][OTf]_2$, where bpy and phen denote bipyridine and phenantroline, respectively, and OTf^- the weakly coordinating triflate ion. Berthet *et al.* (2003) have determined the structure (Fig. 5.55) of these compounds, where the six nitrogen donors in the ligands are separated into two parallel and staggered equilateral triangles, (N2, N4, N6) and (N1, N3, N5) with the UO_2-axis perpendicular to the triangles. The uranium atom is equidistant, about 0.6 Å from these planes. The distortion is a result of geometric constraints in the chelating ligands.

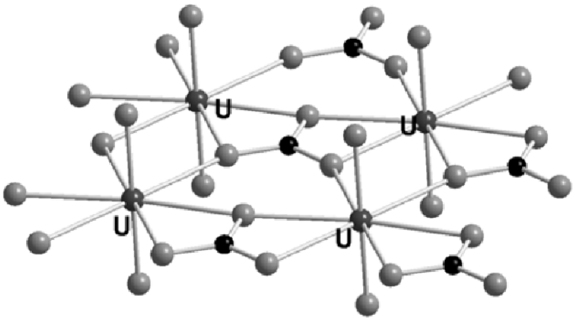

Fig. 5.54 *Part of the layer structure in $UO_2CO_3(s)$ showing the hexagonal bipyramidal coordination geometry of U(VI). By sharing each of the carbonate oxygens between two adjacent uranium atoms, six coordination in the plane perpendicular to the linear UO_2^{2+} ion is achieved. The structure is based on the X-ray study of Christ* et al. (1955).

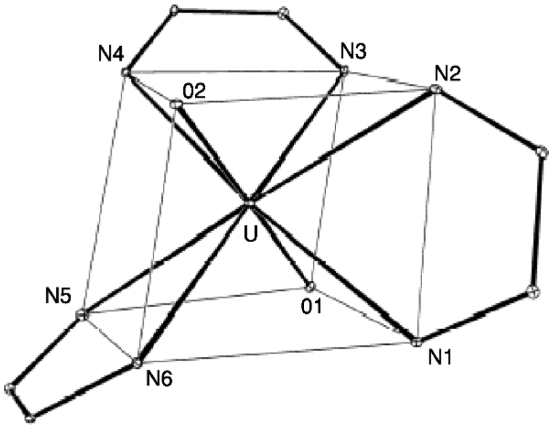

Fig. 5.55 *The coordination geometry for the six-coordinated U(VI) in $[UO_2(OTf)_2(bipy)_2]$ and $[UO_2(phen)_3][OTf]_2$; bpy denotes bipyridine, phen denotes phenantroline, and OTf the weakly coordinating triflate ion (from Berthet* et al., 2003, *reproduced by the permission of Royal Society of Chemistry).*

Uranium(VI) forms a number of peroxide complexes both in solution and in the solid state where the peroxide ligand is bonded 'side-on' to uranium as shown in Fig. 5.56a and b. The first one is the very rare mineral studtite, $UO_2(O_2)(H_2O)_2$ (Burns *et al.*, 2003); this compound has also been identified as a corrosion product on $UO_2(s)$ formed as a result of α-radiolysis (Sattonnay *et al.*, 2001); the second one is the structure of $Na_4[UO_2(O_3)_2](H_2O)_9$ from Alcock (1968). A number of other peroxide compounds and complexes in solution have been prepared by adding hydrogen peroxide to uranyl(VI) solutions; the sulfate and malonate systems were studied by Gurevich *et al.* (1971a,b);

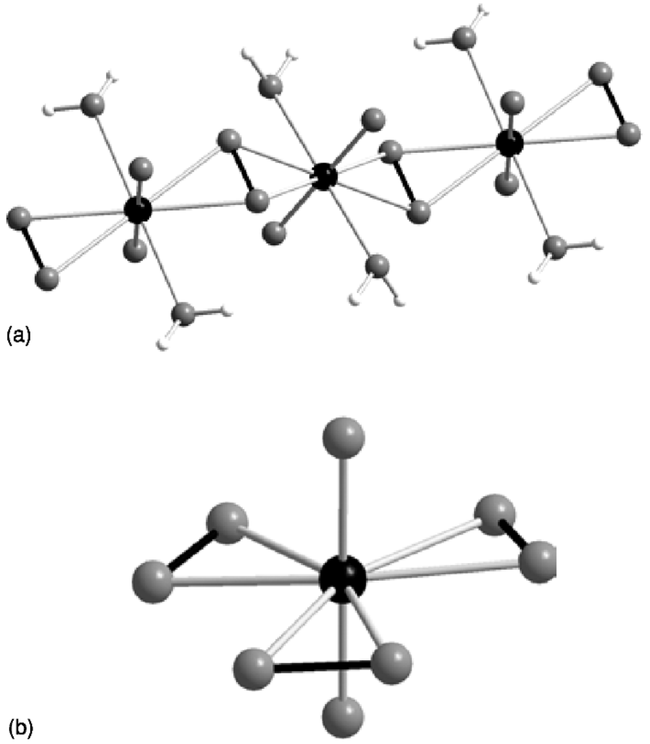

Fig. 5.56 (*a*) *The structure of studtite* (*from Burns* et al., 2003). *The peroxide group* (*black bond*) *is bridging two uranyl*(*vi*) *ions and forms a hexagonal bipyramidal coordination geometry around uranium together with two coordinated water molecules.* (*b*) *The structure of* $Na_4[UO_2(O_2)_3](H_2O)_9$ (*from Alcock,* 1968). *The structure contains discrete complexes with hexagonal bipyramidal coordination geometry.*

the oxalate system by Moskvin (1968); the uranyl(vi)-monoperoxo species was characterized by Djogic and Branica (1992). Self-assembled uranyl peroxide nanosphere clusters of 24, 28, and 32 polyhedra (some containing neptunyl) that crystallize from alkaline solution have been characterized (Burns *et al.*, 2005).

5.9.2 Uranium(iii) compounds

The structures of U(iii) complexes are expected to be very similar to those of the other trivalent actinides; the coordination chemistry of which has been extensively studied as they are chemically more stable than the corresponding U(iii) compounds. A point of interest is if there are differences in bonding between trivalent lanthanides and their actinide homologs. A comparison of equilibrium constants indicates that the actinide complexes are somewhat more stable, but the difference is not large. In the same way there are no large differences in bond distances and coordination geometry; the differences that do exist may be due to the larger ionic radius of the actinide homologs as compared to the corresponding lanthanides. Uranium(III) compounds are characterized by high coordination numbers, eight and nine coordination are predominating as in the corresponding lanthanide(III) compounds. There are no structure determinations of uranium(III) complexes of simple inorganic ligands in solution, but it is reasonable to assume that their coordination geometry is similar to those of the trivalent lanthanides and transuranium elements (Allen *et al.*, 2000). Examples of solid uranium(III) compounds are given by Chernyayev (1966) and Mehdoui *et al.* (2004), the latter also provides comparisons between U(III) and lanthanide(III) compounds.

Fig. 5.57 shows the structure of $K_3U(SO_4)_3 \cdot 3H_2O$ from Barnard *et al.* (1972a); it contains nine-coordinated U(III) through two chelating and two mono-dentate sulfate ions and three coordinated water molecules that form a strongly distorted trigonal prism around uranium.

5.9.3 Uranium(IV) compounds

Uranium(IV) forms both normal and basic salts with most inorganic ligands. The formation of basic salts is the result of the strong hydrolysis of U(IV) and these compounds contain coordinated hydroxide and/or oxide in addition to donor atoms from the other ligand. The relatively large ionic radius, 0.93 Å (eight coordination), and the high charge of U^{4+} results in high and often variable coordination numbers in different compounds, eight, nine and ten are

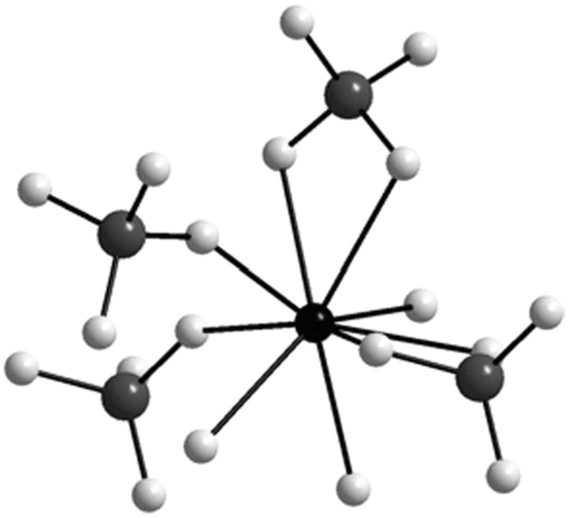

Fig. 5.57 *The coordination geometry of U(III) in $K_3U(SO_4)_3 \cdot 3H_2O$ (Barnard* et al.*, 1972a); uranium is nine-coordinated through two chelating and two monodentate sulfate ligands and three coordinated water molecules. The coordination polyhedron is strongly distorted from all the ideal geometries.*

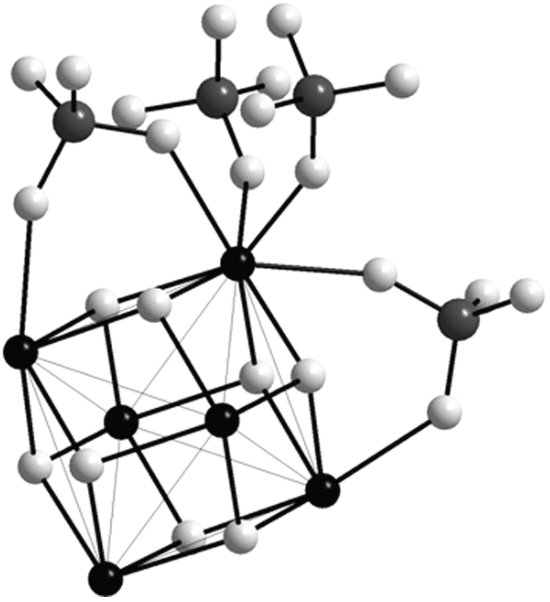

Fig. 5.58 *Structure of* $U_6(SO_4)_6O_4(OH)_4(s)$. *The characteristic structure element is an octahedron of six uranium(IV) ions (black) shown in the lower part of the figure. The oxide and hydroxide ions (light gray) are placed outside the eight triangular faces of this octahedron. The sulfate ions (sulfur is dark gray) are coordinated outside the octahedron and act as bridges between the U(IV) ions within the octahedron and between adjacent octahedra (not shown in the figure). Uranium(IV) is eight-coordinated in this compound. The structure is based on the X-ray study of Lundgren* (1952).

the most common ones. Uranium(IV) is in this respect similar to the elements in the lanthanide group, notably Ce(IV). Two examples of the coordination geometry of uranium(IV) in solid compounds are given in Figs. 5.58 and 5.59.

Fig. 5.59, based on an X-ray study of Fuchs and Gebert (1958), shows the structure of the mineral coffinite, $USiO_4$. A coordination number of eight can only be achieved by sharing all oxygen atoms in the silicate between two U(IV) atoms. The coordination geometry is best described as a triangular dodecahedron (Kepert, 1982, p. 153), the two 'arms' of which are indicated by the black full drawn lines.

The coordination number of the U(IV) and Th(IV) aqua ions in solution has been discussed based on data from Large-Angle X-ray Scattering (LAXS) and Extended X-ray Absorption Fine structure Spectroscopy (EXAFS). These methods provide accurate bond distances, while the determination of the coordination number is more uncertain, (9 ± 1). The high coordination number is retained in $UF^{3+}(aq)$, as indicated by EXAFS data (Moll *et al.*, 1999); these data demonstrate a pronounced difference in bond distance between coordinated fluoride and water; the U–F distance is 2.15 Å and the $U–H_2O$ distance 2.45 Å. The large variability of the coordination geometry in complexes of tetravalent actinides is demonstrated also by the structure of

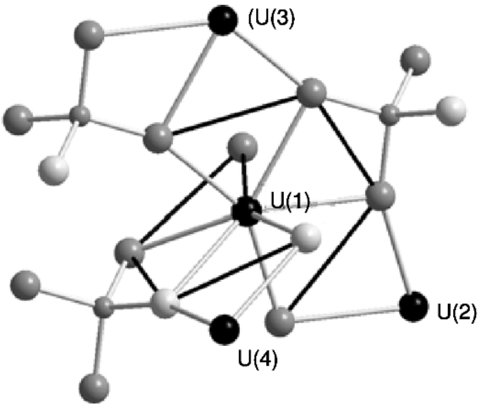

Fig. 5.59 *The structure of* $USiO_4$ *from Fuchs and Gebert* (1958). *The silicate group forms both a chelate and acts as a bridge between adjacent uranium atoms U*(2–4). *The chelate bonding is shown in the figure; the two remaining oxygen atoms in the silicate group are coordinated to adjacent uranium*(IV) *atoms not shown in the figure. The black full-drawn lines connect the atoms in the 'arms' of the dodecahedral coordination polyhedron. Each arm is approximately planar and the two planes are perpendicular.*

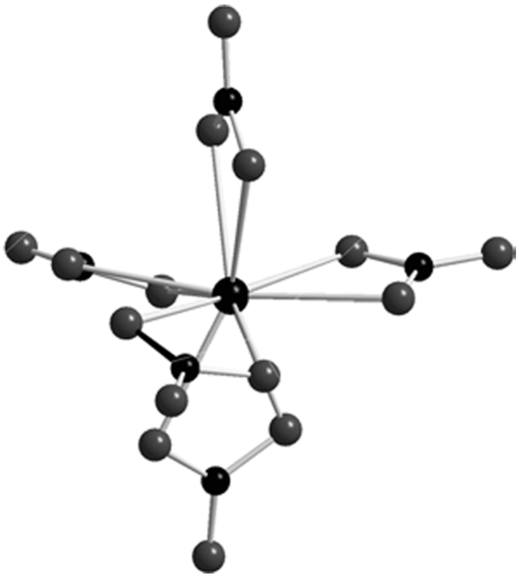

Fig. 5.60 *The structure of* $Th(CO_3)_5^{6-}$ *and the isostructural* $U(CO_3)_5^{6-}$ *from Voliotis and Rimsky* (1975).

$Na_6[Th(CO_3)_5] \cdot 12H_2O$ from Voliotis and Rimsky (1975), shown in Fig. 5.60; the corresponding uranium compound is isostructural. The carbonate ligands are arranged in an approximately trigonal bipyramidal arrangement around the central actinide ion; this geometry is very different from the common ones for ten-coordination, as discussed by Kepert (1982, p. 188). We may describe each carbonate ligand with one 'effective' charge because of its small ligand bite, resulting in a trigonal bipyramidal charge distribution in a geometry that minimizes the electrostatic repulsion between the ligands.

Another example of the variable coordination geometry is given by the structure of tetra(glycolato)uranium(IV) dihydrate, $[U(HOCH_2COO)_4] \cdot 2H_2O$ where uranium is ten-coordinated as indicated by Fig. 5.61, based on the structure data of Alcock *et al.* (1980). A recent example of the variable coordination geometry of U(IV) is the structure of the azide complex $U(N_3)_7^{3-}$, with an approximately pentagonal bipyramidal coordination geometry (Crawford *et al.*, 2005). The azide ion is linear, but the angle U–N–N–N is highly variable (from 120° to 180°).

5.9.4 Uranyl(V) compounds

There are few experimental data on the structure and bonding of uranyl(V) complexes, the only example is the structure of the uranyl(V) triscarbonate complex studied in solution using EXAFS (Docrat *et al.*, 1999). The complex has

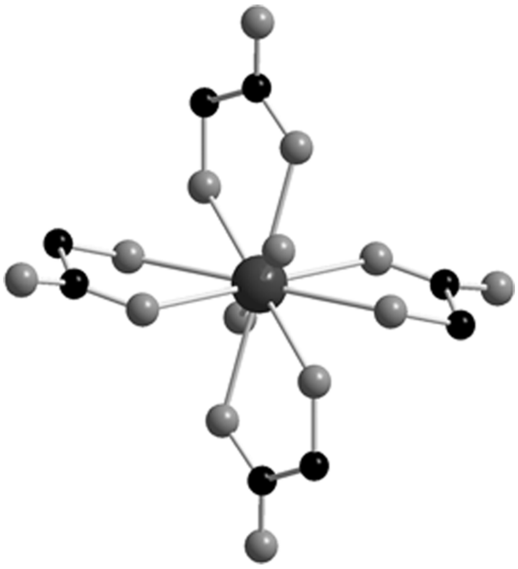

Fig. 5.61 *The coordination geometry in tetra(glycolato)uranium(IV) dihydrate from Alcock* et al. (1980). *The structure contains discrete ten-coordinated complexes* $[U(HOCH_2COO)_4(OH_2)_2]$ *with zero charge.*

hexagonal bipyramidal geometry similar to that of the uranyl(VI) triscarbonate complex, *cf*. Fig. 5.53. The corresponding information on neptunyl(V) complexes should provide good models also for the corresponding U(V) species. The geometry of the uranyl(V) and -(VI) carbonate complexes are supported by quantum chemical calculations by Gagliardi *et al.* (2001). The predominant coordination geometry is presumably a pentagonal or hexagonal bipyramid, with the labile ligands in the plane perpendicular to the linear UO_2 unit. The lower charge of the central atom results in the formation of weaker complexes and somewhat longer U–L distances than for the corresponding U(VI) complexes.

5.9.5 Uranium compounds of organic ligands

There is an abundance of organic ligands that form solid uranium complexes and we will restrict the examples to simple carboxylates, α-hydroxy and amino carboxylates.

The same structural principles as observed with the inorganic ligands are found also among the organic ones; the main difference between the two groups is that the geometry of the organic ligands puts additional constraints on the availability of the various donor atoms for bonding to uranium. In addition, the larger versatility of many organic ligands also opens up the possibility to form structural and bonding isomers.

Stoichiometric information on the constitution of complexes in solution can be obtained by an array of experimental methods (Rossotti and Rossotti, 1961), but this rarely gives information on structure and bonding. As is the case of inorganic ligands, the important methods to obtain structural information from solution are LAXS or EXAFS methods. However, both of them provide only limited structural information in the form of radial distribution functions, i.e. the distance from the central uranium atom to the atoms in the first and second coordination spheres and the number of such distances. In the case of LAXS one can also obtain information on the distances between the coordinated donor atoms. Allen *et al.* (1996b) give examples of the use of EXAFS for the deduction of structure models of uranyl(VI) tartrate, citrate, and malate complexes. Jiang *et al.* (2002) have investigated the structure and bonding of uranyl(VI) imino- and oxy-diacetate compounds and identified different modes of coordination of the ligands, an example that the stoichiometry of a complex does not provide sufficient information to identify the mode of coordination. In order to obtain more precise structure data it is often necessary to obtain additional structural information, such as provided by NMR spectroscopy (Szabó *et al.*, 1997, 2000; Moll *et al.*, 2000a,b) or by quantum chemical methods (Schreckenbach *et al.*, 1998; Tsushima *et al.*, 2001; Vallet *et al.*, 2001, 2004b; Yang *et al.*, 2003). The uranyl(VI) oxalate system provides a good example of different modes of bonding of the oxalate ligand in solid compounds and the structure of $UO_2(\text{oxalate})_3^{4-}$ complex in solution (Vallet *et al.*, 2003). The ground state structure predicted by the quantum chemical methods is the one that is found experimentally (Fig. 5.62a–c).

The stoichiometry and the value of the stability constants of the complexes given in Tables 5.33–5.37 give some indications of the mode of bonding of the ligands, in particular whether a certain ligand forms a chelate or not. A comparison between acetate and glycolate is instructive: acetate can only coordinate through the carboxylate group, either using one oxygen donor or both. In the latter case a four-membered chelate ring is formed. Glycolate can bind in the same way if only the carboxylate group is involved and one then expects a stability constant of the same magnitude for both ligands. However, glycolate can also form a chelate by using one donor atom from each of the carboxylate and the α-OH groups, in which case a five-membered chelate ring is formed. Chelate formation results in a large increase in the stability constant, *cf.* the $\log\beta_n$ values for the acetate and glycolate complexes of U(IV) in Table 5.36. The stability constants, with the exception of $\log\beta_1$, are slightly larger for the U(VI) acetate than those for the glycolate complexes, which strongly indicates the same mode of bonding of acetate and glycolate in the U(VI) complexes (Beck and Nagypál, 1990; Grenthe *et al.*, 1997). The stepwise equilibrium constants for the formation of $UO_2(ox)$ ($\log\beta_1 = 5.99$), $UO_2(ox)_2^{2-}$ ($\log K_2 = 4.65$ for the reaction $UO_2(ox) + ox^{2-} \rightleftharpoons UO_2(ox)_2^{2-}$) are large compared to the value for the formation of $UO_2(ox)_3^{4-}$ ($\log K_3 = 0.36$ for the reaction $UO_2(ox)_2^{2-} + ox^{2-} \rightleftharpoons UO_2(ox)_3^{4-}$), indicating that the third oxalate does not form a chelate. This assumption has been verified both by experimental EXAFS data from solution and by quantum chemical calculations (Vallet *et al.*, 2003) as shown in Fig. 5.62a–c. These data also illustrate the possible occurrence of isomers.

5.10 URANIUM CHEMISTRY IN SOLUTION

5.10.1 The uranium aqua ions

The most stable oxidation state of uranium in aqueous solution is 6+, with the linear uranyl(VI) ion, UO_2^{2+}, as the stable entity. The only known uranium ion in the 5+ oxidation state in aqueous solution is the linear dioxouranium(V) ion, UO_2^+. Aqueous solutions containing U^{4+} are stable in the absence of oxidation agents like dissolved oxygen. Aqueous solutions containing U^{3+} are rapidly oxidized under evolution of hydrogen. The relative stability of the various oxidation states is strongly depending on the pH of the solution and on the presence of complexing ligands as indicated in Fig. 5.63. The rate of the redox transformations between the different oxidation states of uranium is rapid when there is no change in chemical composition between the oxidized and reduced forms, otherwise it is very slow. This means that the reactions $UO_2^{2+} + e^- \rightleftharpoons UO_2^+$ and $U^{4+} + e^- \rightleftharpoons U^{3+}$ are fast, while $UO_2^{2+} + 4H^+ + 2e^- \rightleftharpoons U^{4+} + 2H_2O$ is slow.

The kinetics of the redox transformations in aqueous actinide systems has been described in a report by Newton (1975) (Section 5.10.3i). The structures and chemical properties of actinide aqua ions are discussed and compared in

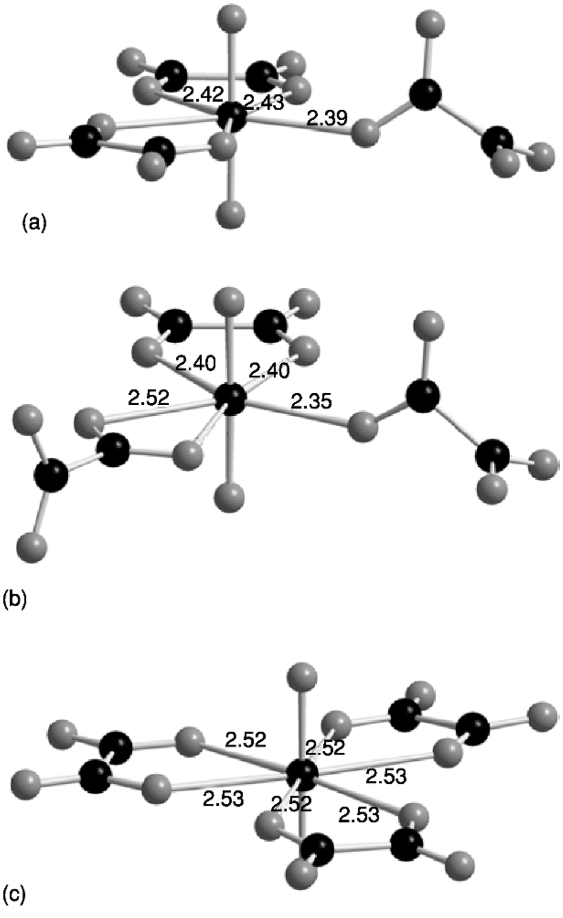

Fig. 5.62 (*a–c*) *Perspective views of three* $[UO_2(oxalate)_3]^{4-}$ *isomers, where* (*a*) *is the most stable one from Vallet* et al. (2003). *By using quantum chemical methods one can estimate the relative stability of the different isomers. The uranium atom and the carbon atoms are black and the oxygen atoms gray; distances are in ångströms. The bond distances for the ground state isomer a obtained from quantum chemical calculations agree with those obtained from EXAFS data in solution within* 0.03 Å. *The same mode of bonding has also been found in solid-state structures, but here there are no discrete complexes as the oxalate ligands act as bridges between adjacent uranium atoms.*

Chapter 23, section 2; a comparison of the complex formation properties of actinides is given in Chapter 23, sections 3–8. The kinetics of actinide reactions are compared and discussed in Chapter 23, sections 10 and 11.

Aqueous solutions of UO_2^+ are prone to disproportionation and the range of stability of U(v) is therefore small, a fact that makes it difficult to study its solution chemistry.

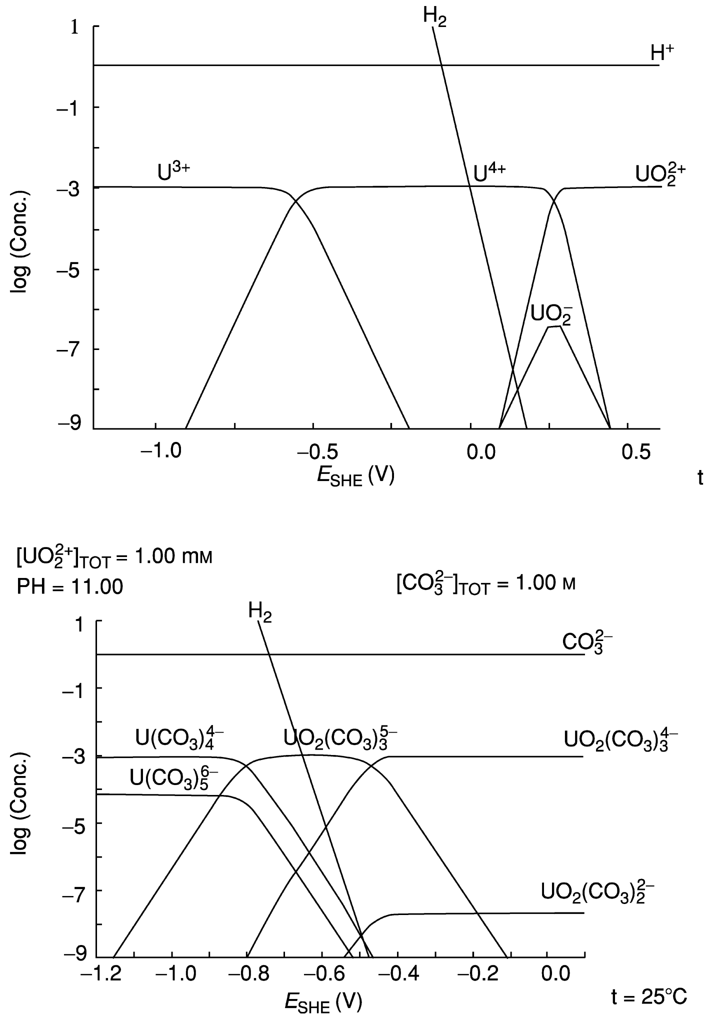

Fig. 5.63 *Logarithmic diagrams showing the distribution of U^{3+}, U^{4+}, UO_2^+ and UO_2^{2+} as a function of the redox potential in* 1 M *perchloric acid* (*the first diagram*), *and in* 1 M *Na_2CO_3* (*the second diagram*). *U*(*V*) *is predominant between* –0.7 *and* –0.4 V *in the second diagram.*

The oxygen atoms in UO_2^{2+} and UO_2^+ are kinetically inert and their rate of exchange with oxygen from water is slow, with a half-life of approximately 5×10^4 h in 1 M perchloric acid for the former (Gordon and Taube, 1961a), but much faster for the latter as indicated by the fact that UO_2^+ catalyzes the oxygen exchange between UO_2^{2+} and water (Gordon and Taube, 1961b).

However no exchange rate has been determined for UO_2^+ alone. The rate of exchange of the 'yl' oxygen atoms with the water solvent is strongly catalyzed by light in the near UV/visible region and varies with the chemical composition of the complexes present in solution as discussed in Section 5.10.3, where also some spectroscopic characteristics of the various species are described.

Solutions of U^{3+}, U^{4+}, and UO_2^{2+} can be used to prepare complexes in solution and various solid compounds using standard techniques. A treatise by Chernyayev (1966) gives an excellent account of the compounds prepared from aqueous media.

(a) Tripositive uranium, U^{3+}

Aqueous solutions of U^{3+} can be prepared by dissolving uranium trichloride in water. Alternatively, solutions of U(IV) or U(VI) can be reduced by electrolysis at a mercury cathode (Barnard *et al.*, 1967, 1972b; Weigel, 1958). The course of the reduction can conveniently be observed by the colour of the solutions in *incandescent* light: Solutions of U(VI) are yellow, while those of U(IV) and U(III) are green and wine red, respectively. These colors cannot be observed in fluorescent light. There are only few studies of the chemical properties of U^{3+} and its complexes in solution (Section 5.8.6); however the properties can often be estimated from those of the trivalent lanthanides. The standard redox potential of the U^{4+}/U^{3+} redox couple and the Gibbs energy and enthalpy of formation, entropy and heat capacity of U^{3+}(aq) have been reviewed by Grenthe *et al.* (1992) and Guillaumont *et al.* (2003). These data are reported in Table 5.32.

There is no structural information available on the U^{3+}(aq) ion, however the structure of Pu^{3+}(aq) has been determined (Matonic *et al.*, 2001) by a single-crystal X-ray diffraction study of $[Pu(H_2O)_9][CF_3SO_3]_3$. In addition, the structures of trivalent lanthanides and Am(III) and Cm(III) have been determined in solution using EXAFS (Allen *et al.*, 2000). The solid Pu(III) compound contains discrete nine-coordinated complexes that are very similar to those found among the trivalent lanthanides, in the same way the bond distances and coordination number determined from the EXAFS data are close to those in lanthanide(III) and actinide(III) complexes, indicating an aqua-ion of the composition $U(H_2O)_9^{3+}$ for trivalent uranium.

(b) Tetrapositive uranium, U^{4+}

U(IV) in the form of U^{4+}(aq) is a very strong acid and accordingly hydrolyzed except in solutions with a hydrogen ion concentration larger than 0.5 M. The hydrolysis will be discussed in Section 5.10.2b. Uranium(IV) species can be prepared by electrolysis of corresponding uranium(VI) solutions at low pH using a two-compartment cell and a mercury cathode, U(III) is formed simultaneously, but is rapidly oxidized by blowing air through the cathode

Table 5.32 *The redox potentials, Gibbs energy and enthalpy of formation, molar entropy, and heat capacity for the different uranium aqua ions under standard state conditions* (298.15 K, 0.1 MPa) *in pure water solvent at zero ionic strength* (*Grenthe* et al., 1992; *Guillaumont* et al., 2003).

Species and redox reaction	$E°$ (V)	$\Delta_f G^\circ_m$ (kJ mol^{-1})	$\Delta_f H^\circ_m$(kJ mol^{-1})	S°_m (J K^{-1} mol^{-1})	$C^\circ_{p,m}$ (J K^{-1} mol^{-1})
U^{3+}(aq)		–(476.5 ± 1.8)	–(489.1 ± 3.7)	–(188 ± 14)	–(150 ± 50)
$U^{4+} + e^- \rightleftharpoons U^{3+}$	–(0.553 ± 0.004)				
U^{4+}(aq)		–(529.9 ± 1.8)	–(591.2 ± 3.3)	–(417 ± 13)	–(220 ± 50)
UO_2^+(aq)		–(961.0 ± 1.8)	–(1025.1 ± 3.0)	–(25 ± 8)	–
$UO_2^{2+} + e^- \rightleftharpoons UO_2^+$	(0.0878 ± 0.0013)				
UO_2^{2+}(aq)		–(952.6 ± 1.7)	–(1019.0 ± 1.5)	–(98.2 ± 3.0)	(42.4 ± 3.0)
$UO_2^{2+} + 4H^+ + 2e^- \rightleftharpoons U^{4+} + 2H_2O$	(0.2673 ± 0.0012)				

compartment. Acid solutions of U(IV) are only slowly oxidized by oxygen but the situation is very different in the presence of strong complexing agents where the oxidation is very rapid and great experimental care has to be taken in order to keep the 4+ oxidation state. Uranium(IV) in acid solution can also be obtained by reduction of U(VI) with hydrogen using platinum black as a catalyst. The coordination number of the U^{4+}(aq) in solution has been studied by LAXS (Johansson, 1992) and by EXAFS (Moll *et al.*, 1999); the U–O distance is (2.42 ± 0.01) Å and the coordination number (9 ± 1). The coordination number is not well defined and the energy difference between isomers with different geometries is probably small (Kepert, 1982), an assumption supported by quantum chemical data on Th^{4+}(aq) by Yang *et al.* (2001, 2003). The rate constant for the exchange between coordinated and bulk water has been determined using ^{17}O NMR spectroscopy as discussed in section 5.10.3 (b). Experimental data for the redox potential and other thermodynamic quantities for U^{4+}(aq) have been reviewed (Grenthe *et al.*, 1992; Guillaumont *et al.*, 2003) and selected values are given in Table 5.32.

(c) Dioxouranium(V), UO_2^+

The 5+ oxidation state of uranium has a very narrow range of existence in aqueous solution, (Fig. 5.63). Millimolar solutions of UO_2^+ can be prepared by reduction of UO_2^{2+} with zinc amalgam or hydrogen, or by dissolving UCl_5 in water. A more convenient method is to irradiate a 0.5 M 2-propanol–0.2 M $LiClO_4$ solution of uranium(VI) at a pH between 1.7 and 2.7, with UV radiation from a Hg lamp (Howes *et al.*, 1988). The uranium(V) solution formed is not thermodynamically stable, but the rate of oxidation is so slow that there is little decomposition during 1 h.

There is no experimental information on the structure of UO_2^+(aq) and the number of coordinated water molecules. However, as judged by the chemical similarity between U(V) and Np(V) complexes, it is reasonable to assume that they also have a similar coordination geometry, as exemplified by the coordination geometry of different Np(V) carbonate complexes in solution is given by Clark *et al.* (1996); these structures are also very similar to those of the corresponding U(VI) system (Docrat *et al.*, 1999; Gagliardi *et al.*, 2001). Vallet *et al.* (2004a) have used quantum chemical models to predict that the most probable constitution of UO_2^+(aq) is $UO_2(H_2O)_5^+$, with pentagonal bipyramidal geometry. The thermodynamics of UO_2^+(aq) has been reviewed (Grenthe *et al.*, 1992; Guillaumont *et al.*, 2003) and the redox potential for the reaction: $UO_2^{2+}(aq) + e^- \rightleftharpoons UO_2^+(aq)$, and other thermodynamic data for UO_2^+(aq) from these reviews are given in Table 5.32. U(V) is an intermediate in the photochemical reduction of uranium(VI) (Heidt and Moon, 1953).

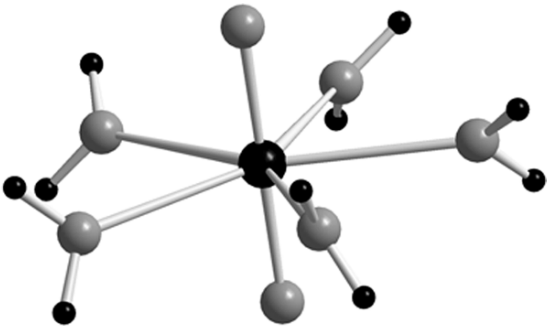

Fig. 5.64 *The coordination geometry of* $UO_2(H_2O)_5^{2+}$ *and* $UO_2(H_2O)_5^{+}$, *deduced from quantum chemical calculations using a solvent model as discussed by Vallet* et al. (2001, 2004). *Only the bond distances differ between the two structures; the U–O water distances are* 2.47 Å *in the uranyl*(VI) *aqua ion and* 2.63 Å *in the corresponding uranyl*(V) *species. The U–*O_{yl} *distance is* 0.1 Å *longer in the uranyl*(V) *compound than in the corresponding uranyl* (VI) *compound.*

(d) Dioxouranium(VI), UO_2^{2+}

The 6+ state is the most stable of the oxidation states of uranium and has accordingly been extensively studied. A large number of different compounds have been prepared from aqueous solution both by simple crystallization, by using hydrothermal techniques and other methods; numerous examples are given in other parts of this chapter. Under certain circumstances, the oxo ligands can undergo ligand exchange, scrambling, and substitution reactions; the ligand exchange reactions are in general slow but are strongly photo-catalyzed and these reactions are discussed in Section 5.10.3. The structure of the aqua ion $UO_2(H_2O)_5^{2+}$ in solution has been determined using LAXS (Åberg *et al.*, 1983) and EXAFS techniques (Wahlgren *et al.*, 1999; Sémon *et al.*, 2001; Neuefeind *et al.*, 2004b); more detailed studies have been made using quantum chemical methods (Spencer *et al.*, 1999; Wahlgren *et al.*, 1999; Hay *et al.*, 2000; Vallet *et al.*, 2001). Guilbaud and Wipff (1993), Hagberg *et al.* (2005) have determined the structure by using molecular dynamics simulations, a method that also gives some information on the structure of the second hydration sphere. The structure of the aqua ion is shown in Fig. 5.64. The redox potentials for reactions involving UO_2^{2+}(aq), and the standard Gibbs energy and enthalpy of formation, the molar entropy, and heat capacity of UO_2^{2+}(aq) from the reviews by Grenthe *et al.* (1992) and Guillaumont *et al.* (2003) are given in Table 5.32. The rate of exchange between coordinated water and the pure water solvent has been studied using ^{17}O NMR (Farkas *et al.*, 2000a), and these data are discussed in section 5.10.3(b).

5.10.2 Aqueous uranium complexes

Uranium is a very strong Lewis acid and a hard electron acceptor in all its different oxidation states. This means that the donor–acceptor interactions follow the sequences:

$$F^- \gg Cl^- > Br^- \approx I^-; O \gg S > Se; N \gg P \approx As$$

where the donors are either simple ions like fluoride, or part of a larger ion/molecule like carbonate. These sequences are expected if the donor–acceptor interactions are dominated by electrostatic forces. There is extensive information in the literature on the chemical thermodynamics of uranium complexes. Most of these data are compiled in *Stability Constants, Special Publications* No. 6 (Bjerrum *et al.*, 1957), No. 7 (Bjerrum *et al.*, 1958), No. 17 (Sillén and Martell, 1964), No. 25 (Sillén and Martell, 1971), and in the International Union of Physical and Applied Chemistry (IUPAC) Chemical Data Series, *Stability Constants of Metal-Ion Complexes, Part A* (Högfeldt, 1982) and *Part B* (Perrin, 1979). There are several critical evaluations of the compiled data; the series *Critical Stability Constants*, Vols 1–6, by Martell and Smith, is now available in a computer database that also includes the necessary software, *NIST Standard Reference Database* 46 (NIST, 2004). Grenthe *et al.* (1992) and Guillaumont *et al.* (2003) have given a more detailed critical evaluation of thermodynamic data for uranium, including a discussion of many of the experimental investigations on which the selected data are based.

The high Lewis acidity results in extensive hydrolysis of uranium that decreases in the order U(IV) > U(VI) >> U(III) > U(V). Another effect of the high Lewis acidity is that coordinated uranium exerts a very strong inductive effect on coordinated ligands, e.g. the dissociation constant of the proton in the α-hydroxy group of coordinated α-hydroxy carboxylic acids can increase by more than 13 orders of magnitude (Szabó and Grenthe, 2000) on coordination to uranium(VI); a similar effect is also found in some Th(IV) complexes (Toraishi *et al.*, 2002) and therefore most likely also in U(IV) complexes:

$$HOCH_2COO^- \rightleftharpoons {}^-OCH_2COO^- + H^+; pK \approx 17$$
$$UO_2(HOCH_2COO^-) \rightleftharpoons UO_2({}^-OCH_2COO^-) + H^+; pK = 3.6.$$

A similar example is found in the structure of the complex $[UO_2L(MeO)(MeOH)]_2$ where L is a thiosemicarbazone (Santos and Abram, 2004); this complex contains one coordinated (MeOH) and one deprotonated (MeO^-) methanol ligand. The ‘inductive effect’ is an electron redistribution in the coordinated ligand; if this is an organic species it will result in a changed ligand reactivity, a fact that has been used in preparative chemistry (van Axeel Castelli *et al.*, 2000).

(a) Uranium(III) and uranyl(V) complexes

Uranium(III) is a very strong reducing agent that is oxidized by water, hence no stable complexes can be maintained in aqueous solution. However, the chemical properties of uranium(III) are expected to be very similar to those of trivalent lanthanides, actinium(III) and the transuranium elements in oxidation state 3+. Guidance on the magnitude of equilibrium constants for U(III) species can therefore be obtained from databases for lanthanide(III) and actinide(III) elements: examples are given in Tables 5.34 and 5.36. The differences in chemical properties between U(III) and other An(III) ions and the corresponding Ln(III) species can be exploited by proper choice of ligand. This is a useful strategy for the design of An(III)/Ln(III) separation processes (Karmazin *et al.*, 2002). The narrow range of existence of uranium(V) in aqueous solution results in very little quantitative information on equilibrium constants. In view of the large chemical similarity between actinides in the same oxidation state, one may use the equilibrium constants for Np(V) complexes as estimates for the corresponding U(V) complexes (Chapter 6, section 9).

(b) Hydrolysis of uranium

A summary of the stoichiometry and equilibrium constants of the various hydroxide complexes are given in Table 5.33: they refer to reactions of the type

$$p\mathrm{M} + q\mathrm{H_2O} \rightleftharpoons \mathrm{M}_p(\mathrm{OH})_q + q\mathrm{H}^+$$

where all charges except for H^+ have been omitted for simplicity, and where M denotes, UO_2^{2+} UO_2^+, U^{4+}, or U^{3+}; the equilibrium constants are taken from Grenthe *et al.* (1992), Guillaumont *et al.* (2003) and Baes and Mesmer (1976).

In most of the experimental determinations of hydrolytic equilibria it is not possible to decide if the species formed contain coordinated hydroxide and/or oxide; the reason being that $2OH^- \equiv O^{2-}$ in experiments where the equilibrium constants and the stoichiometry are deduced from measurements of the free hydrogen ion concentration; this is an example of the so-called 'proton ambiguity' (Rossotti and Rossotti, 1961). The following example illustrates the point:

$$3\mathrm{UO_2^{2+}} + 5\mathrm{H_2O} \rightleftharpoons (\mathrm{UO_2})_3(\mathrm{OH})_5^+ + 5\mathrm{H}^+$$
$$3\mathrm{UO_2^{2+}} + 5\mathrm{H_2O} \rightleftharpoons (\mathrm{UO_2})_3(\mathrm{O})(\mathrm{OH})_3^+ + 5\mathrm{H}^+ + \mathrm{H_2O}$$

Both reactions result in the formation of five H^+ and can therefore not be distinguished. As the activity of water is a constant, the stability constant is the same for both stoichiometric formulations. This tri-nuclear complex was originally formulated as $(UO_2)_3(OH)_5^+$, but when structural data became available the actual composition turned out to be $(UO_2)_3(O)(OH)_3^+$, with the structure given in Fig. 5.65 (Åberg, 1978).

Table 5.33 *Stoichiometry and stability constants for the hydrolysis complexes of uranium. The stability constants refer to zero ionic strength and a temperature of* 25°C*; data from Grenthe* et al. (1992), *Guillaumont* et al. (2003), *and Baes and Mesmer* (1976).

Uranium(VI) Chemical reaction	$log^*\beta_{p,q}$	*Uranium(IV) Chemical reaction*	$log^*\beta_{p,q}$
$UO_2^{2+} + H_2O \rightleftharpoons UO_2OH^+ + H^+$	–5.25	$U^{4+} + H_2O \rightleftharpoons UOH^{3+} + H^+$	–0.54
$UO_2^{2+} + 2H_2O \rightleftharpoons UO_2(OH)_2(aq) + 2H^+$	–12.15	$U^{4+} + 2H_2O \rightleftharpoons U(OH)_2^{2+} + 2H^+$	–2.6[a]
$UO_2^{2+} + 3H_2O \rightleftharpoons UO_2(OH)_3^- + 3H^+$	–20.25	$U^{4+} 3H_2O \rightleftharpoons U(OH)_3^+ + 3H^+$	–5.8[a]
$UO_2^{2+} + 4H_2O \rightleftharpoons UO2(OH)_4^{2-} + 4H^+$	–32.40	$U^{4+} + 4H_2O \rightleftharpoons U(OH)_4(aq) + 4H^+$	–10.3[a]
$2UO_2^{2+} + H_2O \rightleftharpoons (UO_2)_2OH^{3+} + H^+$	–2.7	$6U^{4+} + 15H_2O \rightleftharpoons U_6(OH)_{15}^{9} + 15H^+$	–16.9
$2UO_2^{2+} + 2H_2O \rightleftharpoons (UO_2)_2(OH)^{2+} + 2H^+$	–5.62	Uranium(v): Estimates from Np(v) data	
$3UO_2^{2+} + 5H_2O \rightleftharpoons (UO_2)_3(OH)_5^+ + 5H^+$	–15.55	$UO_2^+ + H_2O \rightleftharpoons UO_2OH(aq) + H^+$	≈–11.3
$3UO_2^{2+} + 7H_2O \rightleftharpoons (UO_2)_3(OH)_7^+ + 7H^+$	–32.7	$UO_2^+ + 2H_2O \rightleftharpoons UO_2(OH)_2^- + 2H^+$	≈–23.6
$4UO_2^{2+} + 7H_2O \rightleftharpoons (UO_2)_4(OH)_7^+ + 7H$	–21.9	Uranium(III): Estimates from Cm(III) data	
		$U^{3+} + H_2O \rightleftharpoons UOH^{2+}$	–7.6
		$U^{3+} + 2H_2O \rightleftharpoons U(OH)_2^{2+}$	–15.7

---

[a] Estimates from Baes and Mesmer (1976).

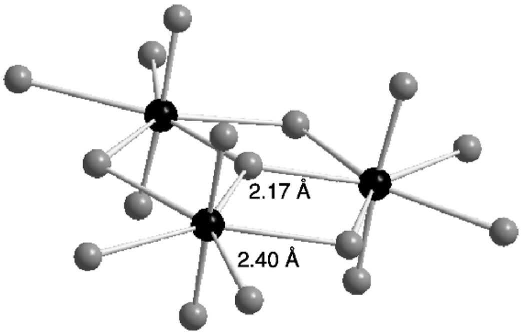

Fig. 5.65 *The structure of* $(UO_2)_3(O)(OH)_3^+$ *(from Åberg,* 1978). *The bond distance between uranium and the bridging oxide and hydroxide groups are* 2.17 Å *and* 2.40 Å, *respectively.*

Except at very low total concentrations of uranium, the polynuclear hydroxide complexes are predominant for all oxidation states, with the possible exception of U(v). There are no experimental data for U(iii), but its behavior can be estimated from the chemically analogous Cm(iii) ion, for which precise data are available.

The coordination chemistry of $U(OH)_4$(aq) and UF_4(aq) (Section 5.10.2c) deserves a comment. Because of the strong inductive effect of uranium on the dissociation of H^+ from coordinated water one would have expected the formation of anionic hydroxide complexes according to

$$U(OH)_4(H_2O)_n \rightleftharpoons U(OH)_5(H_2O)_{n-1}^- + H^+$$

if water is present in the first coordination sphere. However, there is no experimental indication of the formation of negatively charged hydroxide complexes even in 1 M hydroxide solutions. A coordination number of four is unlikely in view of the large ionic radius of U^{4+}. A possible resolution of this dilemma might be that the complex formulated as $U(OH)_4$(aq) is a polymer, e.g. a tetramer $U_4(OH)_{16}$ with one of the A_4X_{16}-type structures (Wells, 1990, p. 201), where the coordination number of A, in this case uranium(iv), is six. Hydroxide and fluoride ions have similar size and often replace one another in solid-state structures. One might therefore expect that their coordination geometry is similar also in aqueous solution. However, UF_4(aq) is not the limiting stoichiometry in aqueous solution where two negatively charged fluoride complexes UF_5^- and UF_6^{2-} have been identified (Table 5.34). This indicates a coordination number of at least six in the U(iv)–fluoride system, the same as the coordination number for $U(OH)_4$(aq) if this has an $U_4(OH)_{16}$ structure. Polynuclear complexes, e.g. U_4F_{16}(aq) do not form because of the poor bridging ability of fluoride in aqueous solution.

Table 5.34 *Stoichiometry and stability constants of uranium complexes of some common inorganic ligands at zero ionic strength and a temperature of* 25°C. *Data from Grenthe* et al. (1992) *and Guillaumont* et al. (2003). *The stability constants for U*(*III*) *have been estimated from the corresponding constants for Cm*(*III*). *Charges of the complexes have been deleted, to simplify notations.*

	$log \beta_n$			
Chemical reaction	$M \equiv UO_2^{2+}$	$M \equiv UO_2^{+}$	$M \equiv U^{4+}$	$M \equiv U^{3+}$
$M + F^- \rightleftharpoons MF$	5.1		9.3	~3.4
$M + 2F^- \rightleftharpoons MF_2$	8.6		16.2	
$M + 3F^- \rightleftharpoons MF_3$	10.9		21.6	
$M + 4F^- \rightleftharpoons MF_4$	11.7		25.6	
$M + 5F^- \rightleftharpoons MF_5$	11.5		27.0	
$M + 6F^- \rightleftharpoons MF_6$	–		29.1	
$M + Cl^- \rightleftharpoons MCl$	0.17		1.7	~0.24
$M + 2Cl^- \rightleftharpoons MCl_2$	–1.1			~–0.74
$M + NO_3^- \rightleftharpoons MNO_3$	0.3		1.5	
$M + SO_4^{2-} \rightleftharpoons MSO_4$	3.15		6.6	~3.3
$M + 2SO_4^{2-} \rightleftharpoons M(SO_4)_2$	4.14		10.5	~3.7
$M + PO_4^{3-} \rightleftharpoons MPO_4$	13.2			
$M + HPO_4^{2-} \rightleftharpoons MHPO_4$	7.2			
$M + H_2PO_4^- \rightleftharpoons MH_2PO_4$	1.12			
$M + CO_3^{2-} \rightleftharpoons MCO_3$	9.68			
$M + 2CO_3^{2-} \rightleftharpoons M(CO_3)_2$	16.9			
$M + 3CO_3^{2-} \rightleftharpoons M(CO_3)_3$	21.6	12.7		
$M + 4CO_3^{2-} \rightleftharpoons M(CO_3)_4$			35.1	
$M + 5CO_3^{2-} \rightleftharpoons M(CO_3)_5^{6-}$			34.0	

(c) Complexes between uranium and other inorganic ligands

Uranium(IV) and uranium(VI) form very strong fluoride complexes, while those formed with Cl^-, Br^-, and I^- are weak. There are no experimental data for halide complexes of U(V) and U(III); however, data from the chemically analogous Np(V) and Cm(III) indicate that they are all weak, the strongest being the fluoride complexes. The strength of complexes containing ligands with oxygen donors, such as sulfate, sulfite, phosphate, carbonate, silicate, and nitrate increases strongly with the charge and base strength of the ligand. However, complexes of the strongest bases such as $HSiO_4^{3-}$ and SiO_4^{4-} are difficult to study in aqueous solution because of competition from OH^- (and the formation of sparingly soluble hydrous oxides) at the high pH where these ions are present in significant amounts.

Strong complexes are also formed between UO_2^{2+} and the peroxide ion and the mode of coordination of the ligand is known from solid state structures (Fig. 5.56a and b). Examples of uranyl(VI) peroxide complex formation in solution have been given by Djogic and Branica (1992), Gurevich *et al.* (1971a,b), and

Moskvin (1968). However, most of the stability constants are uncertain (Sillén and Martell, 1971; NIST, 2004).

Ternary complexes of the type MA_qH_r may be formed when the ligand is the anion of a polyprotic acid.

The stoichiometry and equilibrium constants of uranium complexes of inorganic ligands are given in Table 5.34 where the data are taken from Grenthe *et al.* (1992) and Guillaumont *et al.* (2003). The structure of the complexes may be inferred from the known coordination geometry of the central uranium atom and from the structure of the ligand. However, quantitative information requires other methods, either X-ray or neutron diffraction data from solid compounds containing the ligands, or from EXAFS spectroscopy of solutions. It is interesting to note that the tetrahedral sulfate (Moll *et al.*, 2000b) and phosphate ions (Dusausoy *et al.*, 1996) rarely form chelates in solid compounds. In most cases the ligands are bonded either through a single oxygen donor, or act as a bridge between different uranium atoms (Figs. 5.51, 5.52, 5.57, and 5.58). In solution, however, EXAFS data indicate that the sulfate ion forms a bidentate chelate in $UO_2(SO_4)_2^{2-}$ and in ternary hydroxide–sulfate complexes (Moll *et al.*, 2000b) but not in $UO_2SO_4(aq)$ (Neuefeind *et al.*, 2004a). On the other hand, carbonate invariably forms complexes where the ligand is chelate-bonded to uranium via two oxygen atoms (Fig. 5.66).

The data in Table 5.34 provide the experimental basis for describing uranium as a strong Lewis acid, or as a hard acceptor. Uranium also forms complexes of moderate stability with inorganic nitrogen donors like azide, N_3^-, and thiocyanate, SCN^- (Table 5.35). Uranium does not form ammine complexes in aqueous solution; ammines are strong bases and under the conditions where complexes might form the pH is so high that the stronger uranium hydroxide complexes predominate. However, N-donor complexes are found in organic ligands of various types, some examples are given in Table 5.36.

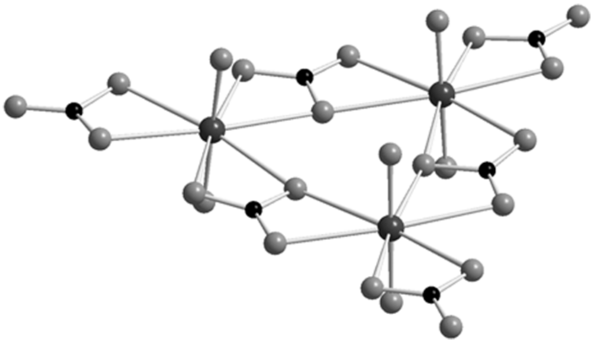

Fig. 5.66 *The structure of* $(UO_2)_3(CO_3)_6^{6-}$ *from Allen* et al. (1995). *Three terminal carbonate ligands form bidentate chelates and the remaining three act as bridges between the uranium atoms. The structure is closely related to that of* $UO_2(CO_3)_3^{4-}$ *containing three bidentate carbonate ligands.*

Table 5.35 *Equilibrium constants for uranium azide and thiocyanate complexes at zero ionic strength and a temperature of* 25°C. *Data from Grenthe* et al. (1992) *and Guillaumont* et al. (2003).

			$\log \beta_n$	
Chemical reaction	*$\log \beta_n$ U(VI)*	*Chemical reaction*	*$M^{n+} \equiv U^{4+}$*	*$M^{n+} \equiv UO_2^{2+}$*
$UO_2^{2+} + N_3^- \rightleftharpoons UO_2N_3^+$	2.58	$M^{n+} + SCN^- \rightleftharpoons MSCN^{(n-1)+}$	1.4	2.97
$UO_2^{2+} + 2N_3^- \rightleftharpoons UO_2(N_3)_2$	4.3	$M^{n+} + 2SCN^- \rightleftharpoons M(SCN)_2^{(n-2)+}$	1.2	4.3
$UO_2^{2+} + 3N_3^- \rightleftharpoons UO_2(N_3)_3^-$	5.7	$M^{n+} + 3SCN^- \rightleftharpoons M(SCN)_3^{(n-3)+}$	2.1	–
$UO_2^{2+} + 4N_3^- \rightleftharpoons UO_2(N_3)_4^{2-}$	4.9			

(d) Complexes between uranium and some important organic ligands

Two groups of ligands will be discussed, those containing carboxylate functional groups alone and those containing in addition one or more hydroxy or amino/imino groups; the first group is exemplified by acetate and oxalate, and the second by glycolate, glycine, iminodiacetate, and ethylenediaminetetraacetate ($EDTA^{4-}$). The stoichiometry and stability constants for the corresponding UO_2^{2+} and U^{4+} complexes are listed in Table 5.36. There is no experimental information available for U(III) and the equilibrium constants have been estimated from corresponding data for trivalent lanthanides and other trivalent actinides. The first chemical issue to be discussed is the mode of bonding of the ligand; the stoichiometry and the magnitude of the stability constants provide some insight, but more precise information requires direct structure information, either from X-ray or neutron diffraction, EXAFS spectroscopy, or from quantum chemistry. The relative magnitude of the stepwise stability constants often gives indication of changes in the mode of bonding of the ligand and structural changes of the complexes. An example is the stepwise stability constants of oxalate complexes of U(VI) (Table 5.36). It is also tempting to relate the very small equilibrium constant for the reaction $U(CO_3)_4^{4-} + CO_3^{2-} \rightleftharpoons U(CO_3)_5^{6-}$ (Table 5.34) to a structural rearrangement from a trigonal bipyramid arrangement of the carbonate ligands in $U(CO_3)_5^{6-}$ with CN = 10, (Fig. 5.60), to a tetrahedral arrangement with CN = 8 in $U(CO_3)_4^{4-}$ (the carbonate ligand is modelled with a single point change). The small stability constant for $UO_2(Hgly)^{2+}$, where Hgly is the "zwitter-ion" form of glycine, $^+H_3NCH_2COO^-$ indicates that the ligand is bonded only at the carboxylate end.

The equilibrium constants for the glycine complexes also deserve a comment. The predominant form of glycine at pH < 8 is the zwitter-ion; this means that one has to take the possible formation of complex with the formally uncharged zwitter-ion into account, which has not always been done in the

Table 5.36 *Stability constants for complexes between U(VI), U(IV), and U(III), and some organic ligands; acetate (ac^-); glycolate/α-hydroxyactate (α-ac^-), oxalate (ox^{2-}), glycinate ($glyc^-$), iminodiacetate ($IMDA^{2-}$), ethylenediamine-tetraacetate ($EDTA^{4-}$). The equilibrium constants are taken from Smith and Martell* (1989). *For some of the reactions, we have tabulated the equilibrium constant for the corresponding Th(IV) and Ce(III) complexes that should be good models for U(IV) and U(III).*

Chemical reaction	*log* β_n *U(VI)*	*Chemical reaction*	*log* β_n $M^{n+} \equiv U^{4+}$	*log* β_n $M^{n+} \equiv U^{3+}$
$UO_2^{2+} + ac^- \rightleftharpoons UO_2(ac)^+$	2.44	$M^{n+} + ac^- \rightleftharpoons M(ac)^{n-1}$	3.9	1.9
$UO_2^{2+} + 2ac^- \rightleftharpoons UO_2(ac)_{22}$	4.42	$M^{n+} + 2ac^- \rightleftharpoons M(ac)_2^{n-2}$	6.9	3.1
$UO_2^{2+} + 3ac^- \rightleftharpoons UO_2(ac)_3^-$	6.43	$M^{n+} + 3ac^- \rightleftharpoons M(ac)_3^{n-3}$	9.0	3.7
$UO_2^{2+} + \alpha{-}ac^- \rightleftharpoons UO_2(\alpha{-}ac)^+$	2.72	$M^{n+} + 4ac^- \rightleftharpoons M(ac)_4^{n-4}$	10.3	
$UO_2^{2+} + 2\alpha{-}ac^- \rightleftharpoons UO_2(\alpha{-}ac)_2$	4.45	$M^{n+} + 5ac^- \rightleftharpoons M(ac)_5^{n-5}$	11.0	
$UO_2^{2+} + 3\alpha{-}ac^- \rightleftharpoons UO_2(\alpha{-}ac)_3^-$	5.70	$M^{n+} + \alpha - ac^- \rightleftharpoons M(\alpha - ac)^{n-1}$	4.4	2.7
$UO_2^{2+} + ox^{2-} \rightleftharpoons UO_2(ox)$	5.99	$M^{n+} + 2\alpha - ac^- \rightleftharpoons M(\alpha - ac)_2^{n-2}$	8.3	4.5
$UO_2^{2+} + 2ox^{2-} \rightleftharpoons UO_2(ox)_2^{2-}$	10.64	$M^{n+} + 3\alpha - ac^- \rightleftharpoons M(\alpha - ac)_3^{n-3}$	11.8	5.3
$UO_2^{2+} + 3ox^{2-} \rightleftharpoons UO_2(ox)_3^{4-}$	11.0	$M^{n+} + ox^{2-} \rightleftharpoons M(ox)^{n-2}$	8.8	4.9
$UO_2^{2+} + Hgly \rightleftharpoons UO_2(Hgly)^{2+}$	1.16	$M^{n+} + 2ox^{2-} \rightleftharpoons M(ox)_2^{n-4}$	16.8	8.3
$UO_2^{2+} + 2gly^- \rightleftharpoons UO_2(gly)_2^{a}$	13.0			
$UO_2^{2+} + IMDA^{2-} \rightleftharpoons UO_2(IMDA)$	8.75	$M^{n+} + 3ox^{2-} \rightleftharpoons M(ox)_3^{n-6}$	22.8	10.2
$UO_2^{2+} + HIMDA^- \rightleftharpoons UO_2(HIMDA)$	2.41	$M^{n+} + 4ox^{2-} \rightleftharpoons M(ox)^{n-8}$	27.2	11.7
$UO_2^{2+} + HEDTA^{3-} \rightleftharpoons UO_2(HEDTA)^-$	6.35	$M^{n+} + IMDA^{2-} \rightleftharpoons M(IMDA)^{n-2}$	9.7	6.2
		$M^{n+} + EDTA^{4-} \rightleftharpoons M(EDTA)^{n-4}$	25.7	15.9

[a] From Szabó and Grenthe (2000).

published studies. The corresponding complexes with gly$^-$ are strong as indicated by log $k = 13.0$ for the reaction $UO_2^{2+} + 2gly^- \rightleftharpoons UO_2(gly)_2(aq)$ (Szabó and Grenthe, 2000). Aliphatic nitrogen donors are strong bases and the competition between H^+ prevents coordination to uranium unless the pH is above 6. The interpretation of experimental results is then complicated by the possible formation of binary and ternary complexes containing hydroxide. Sessler *et al.* (2001) have reviewed complex formation between uranium and macrocyclic ligands; these complexes together with organometallic complexes of uranium are discussed in Chapter 25.

(e) Ternary uranium complexes

Most experimental studies of uranium complexes in aqueous solution have been made in two-component systems (metal ion and ligand). Accordingly, most of the published equilibrium constant data refer to binary M_pL_q complexes. However, in experimental studies performed in water one must also take the possibility of the formation of ternary $M_pL_q(OH)_r$ complexes into account. When the ligand is a polyprotic acid also species of the type $M_pL_qH_r$ may form (the phosphate complexes in Table 5.34). The 'proton ambiguity' referred to in the case of hydroxide complexes, cf. $(UO_2)_3(OH)_5^+$ vs. $(UO_2)_3(O)(OH)_3^+$), is also found in other cases, notably for polyprotic ligands. An example is the UO_2^{2+}–glycolate system where there is a large difference in the dissociation constants of the carboxylate and α-hydroxy group. When studying the complex formation with this ligand using potentiometric methods, it is not possible to distinguish between the following two reactions:

$$UO_2^{2+}(aq) + HOCH_2COO^- \rightleftharpoons UO_2(OCH_2COO) + H^+$$

and

$$UO_2^{2+}(aq) + HOCH_2COO^- + H_2O \rightleftharpoons UO_2(HOCH_2COO)(OH) + H^+$$

To decide on the stoichiometry of the complex formed, it is necessary to use other methods, e.g. NMR spectroscopy as discussed by Szabó *et al.* (2000) and Toraishi *et al.* (2003).

It is possible to use coordination chemical data to decide on the conditions where ternary complexes containing different ligands (except OH^- and protonated ligands) may form; Beck and Nagypál (1990) and Grenthe *et al.* (1997) have discussed this issue and point out that the strength of a ternary complex MA_qB_r depends strongly on the strength of the binary complexes MA_q and MB_r and the steric constraints imposed by metal ion and ligands. Hence, ternary complexes are not common even in multicomponent systems; most of them contain fluoride or hydroxide, both strong donors that do not impose large steric constraints on the second ligand. Table 5.37 gives examples of some ternary uranium(VI) complexes. Note that the presence of the strongly binding oxalate and carbonate ligands has only a moderate influence on the strength of

Table 5.37 *Stoichiometry and stepwise equilibrium constants for reactions of the type* $UO_2AF_r + F^- \rightleftharpoons UO_2AF_{r+1}$. *Charges have been omitted for simplicity. The data are from Aas* et al. (1998) *and refer to a* 1 M $NaClO_4$ *ionic medium at* 25°C. *For comparison* $\log K_q$ *for the stepwise formation of the binary complexes* $UO_2F_q^{2-q}$ *are* 4.54, 3.44, *and* 2.43, *respectively.*

	log K		
A	$UO_2A + F^- \rightleftharpoons UO_2AF$	$UO_2AF + F^- \rightleftharpoons UO_2AF_2$	$UO_2AF_2 + F^- \rightleftharpoons UO_2AF_3$
Oxalate	3.93	2.55	1.72
Carbonate	4.08	2.30	1.91

bonding of fluoride as compared to that in the binary fluoride system. Ternary uranium(IV) complexes containing hydroxide/oxide ligands are abundant both in solid state structures and in solution. An example of the latter is U(EDTA) $(OH)^-$, where the equilibrium constant for the reaction $U(EDTA)(aq) + H_2O \rightleftharpoons U(EDTA)(OH)^- + H^+$ is equal to $\log^*K = -9.3$ (Smith and Martell, 1989), indicating a very large decrease in the acid strength of coordinated water from that in U^{4+}(aq), where $\log^*K$ is equal to –0.54 (see Table 5.33).

(f) Complex formation between UO_2^+ and other cations

The lower effective nuclear charge on uranium (V) as compared to uranium(VI) in uranyl ions results in a correspondingly larger negative charge of the 'yl' oxygen atoms (Vallet *et al.* (2004a). Electrostatic interactions between the 'yl' oxygen in MO_2^+ and the high positive effective charge of M(VI) in MO_2^{2+} is probably the reason for the formation of weak cation–cation complexes between the two. Newton and Baker (1965) were first to identify these species for UO_2^+ and UO_2^{2+} and Sullivan *et al.* (1961) for NpO_2^+ and UO_2^{2+}; Frolov and Rykov (1979) have reviewed the field.

5.10.3 Reaction mechanisms of ligand substitution reactions

The analysis of the rate and mechanism of chemical reactions requires information on the experimental rate equation and the thermodynamics of the reaction studied; in addition the structure and coordination geometry of reactants, intermediates, and products provide important clues on the microscopic details of the reaction. The rate equation describes how the rate of reaction depends on the concentration of different chemical species in the reacting system, some of them may appear as reactants/products in the total (stoichiometric) reaction, but this is not always the case. The rate equation may be simple or complex depending on the mechanism; details on the analysis of rate equations are given in standard texts on chemical kinetics, e.g. Katakis and Gordon (1987), Wilkins (1991) and Espenson (1995). 'Mechanism' is defined as the sequence of elementary reactions that transform the reactant(s) to product(s); these different steps can rarely be studied in isolation, but have to be inferred from the experimental rate equation and the activation parameters $\Delta H^{\neq}$, $\Delta S^{\neq}$, and $\Delta V^{\neq}$ of the reaction. The rate equation rarely provides a unique mechanistic model for a certain reaction: one reason is that it contains only stoichiometric information on the rate determining step and the fast equilibria preceding this, but no information on the fast reactions following the rate-determining step. The mechanism deduced from the rate equation is usually referred to as the *stoichiometric mechanism* of the reaction; the *intimate mechanism* describes the molecular details of a certain reaction, e.g. the timing of bond breaking and bond formation.

The information on rates and mechanisms of ligand substitution reactions in uranium complexes is limited and in general only includes information on rate equations, while the mechanistic discussions are much more speculative. Most experimental data refer to uranyl(VI) complexes where three reviews provide some details. Lincoln (1979) and Tomiyasu and Fukutomi (1982) have reviewed reactions that mostly take place in non-aqueous solvents, while Nash and Sullivan (1998) have reviewed the kinetics and mechanism of actinide redox and complexation reactions in aqueous solution. Vallet *et al.* (2004b) have discussed the combination of experimental and quantum chemical methods for the elucidation of the intimate mechanism of solvent exchange and ligand substitution in uranyl(VI) complexes.

Substitution reactions of simple unidentate ligands in uranium complexes are in general very fast and require special experimental methods (stopped-flow, temperature jump and other relaxation methods; NMR spectroscopy). Only the uranyl(VI) fluoride system has been studied in detail (Szabó *et al.*, 1996).

Most of the experimental studies of ligand substitution have been made using multidentate ligands. These reactions involve several elementary reactions, chelate ring opening/ring closure, and ligand dissociation/association steps. In addition, the ligands are often protolytes and the rate equation therefore depends on the hydrogen ion concentration. All these factors result in complicated rate equations from which it is difficult to deduce the reaction mechanism. The activation parameters, $\Delta H^{\neq}$, $\Delta S^{\neq}$, and $\Delta V^{\neq}$ (of which only the first two are known for reactions involving uranium) provide additional mechanistic information that in some cases can be corroborated by quantum chemical methods as will be described later. The ligand substitution reactions with multidentate ligands are conveniently followed using conventional stopped-flow spectrophotometric methods. Experiments of this type start from a system that is not in equilibrium and its evolution is then followed until equilibrium has been attained. In many cases the reaction has to be followed by using a color indicator and this introduces additional complications when deducing the reaction mechanism (Friese *et al.*, 2001).

A more direct method to obtain mechanistic information on ligand exchange reactions is to use NMR equilibrium dynamics with ^{1}H, ^{13}C, ^{17}O, and ^{19}F as the NMR-active nuclei. The use of ^{17}O-enriched UO_2^{2+} and ternary complexes containing fluoride have been particularly useful as the high sensitivity and wide chemical shift scales of these nuclei makes it possible to study a very large range of exchange rates. A typical example is the exchange reaction

$$UO_2(H_2O)_5^{2+} + H_2O^* \rightleftharpoons UO_2(H_2O^*)_5^{2+} + H_2O$$

that was studied using proton-NMR in mixed water–acetone media by Ikeda *et al.* (1979a) and Bardin *et al.* (1998) and by ^{17}O-NMR in water by Farkas *et al.* (2000a). An analogous example is the exchange between dimethyl sulfoxide (DMSO) and $UO_2(DMSO)_5^{2+}$ in DMSO solvent that was studied by Ikeda *et al.* (1979b). It should be noted that the NMR methods give information on all reactions that contribute to the dynamics at the reaction center. Hence one can use one NMR-active ligand as a probe to provide information on the dynamics of other ligands that are not easily studied using NMR, an example is the use of ^{19}F-NMR to estimate of the rate of water exchange in $UO_2(oxalate)F(H_2O)_2^-$ and $UO_2(oxalate)F_2(H_2O)^{2-}$ (Szabó *et al.*, 1997).

The range of rates that can be studied using NMR depends on the magnitude of the chemical shift between the NMR-active nuclei located in different exchanging sites, the larger the chemical shift the faster processes can be studied. The NMR method can be used in different ways: (a) as an analytical tool where the concentration is measured as a function of time. This method can only be used if the rate of exchange is slow in comparison with the time for measurement; (b) using magnetization transfer, which is a method appropriate for reactions with half-lives of a few seconds; (c) by measurement of the line-broadening which is the method for study of the fastest reactions. The NMR-active nuclei may be located in different chemical surroundings in the same complex allowing studies of intramolecular exchange, or located in different species, e.g. a complex and free ligand, making studies of intermolecular exchange possible. In order to provide accurate data the different sites must have similar concentrations.

It is often difficult, or impossible to use the NMR method to study the rate and mechanism of the formation of the first complex in systems where strong complexes are formed (Szabó *et al.*, 1996) because the free ligand concentration is here very small. In these cases stopped-flow technique is a useful alternative; on the other hand, NMR spectroscopy is superior when studying the rate and mechanism of limiting complexes (Ikeda *et al.*, 1984; Szabó *et al.*, 1997). A summary of experimental kinetic data is given in Tables 5.38 and 5.39, and a general discussion of the mechanistic conclusions in the following section.

(a) Reaction mechanisms

The Eigen–Wilkins mechanism describes the stoichiometric mechanism for many ligand substitution reactions; it includes the following two steps where N denotes the coordination number:

$$[(H_2O)_N M]^{n+} + [(H_2O)L^-] \rightleftharpoons [(H_2O)_N M \ldots L]^{(n-1)} + H_2O \qquad (1)$$

$$[(H_2O)_N M \ldots L]^{(n-1)+} \rightarrow [M(H_2O)_{N-1}L]^{(n-1)+} + H_2O \qquad (2)$$

Table 5.38 *Rate constants at* 25°C *and activation enthalpies for water exchange in* $U^{3+}(aq)$, $U^{4+}(aq)$, *and* $UO_2^{2+}\,(aq)$. *The rate constant for U*(III) *has been estimated from data on the trivalent lanthanides* (*Helm and Merbach,* 1999). *There is no experimental information on ligand exchange mechanisms in any actinide*(V) *species.*

Exchange reaction	k_{ex} (s^{-1})	*Activation enthalpy,* $(\Delta H^{\neq})$ (kJ mol^{-1})	*Activation entropy,* $(\Delta S^{\neq})$ (J K^{-1} mol^{-1})	*References*
$U(H_2O)_9^{3+} + H_2O^* \rightleftharpoons U(H_2O^*)_9^{3+} + H_2O$	$\approx 10^8$	–	–	Helm and Merbach (1999)
$U(H_2O)_9^{4+} + H_2O^* \rightleftharpoons U(H_2O^*)_9^{4+} + H_2O$	5.4×10^6	34	–16	Farkas *et al.* (2000b)
$UO_2(H_2O)_5^{2+} + H_2O^* \rightleftharpoons UO_2(H_2O^*)_5^{2+} + H_2O$; in water at 25°C	1.3×10^6	26	–40	Farkas *et al.* (2000a)
in water–acetone 1/4.38 at –70°C and at 25°C	3.6×10^2 9×10^5	42	12	Ikeda *et al.* (1979a)
In water–acetone 1/1.86 at –70°C and at 25°C	8×10^2 4.6×10^5	32	–30	Bardin *et al.* (1998)

Reaction (1) describes the formation of an outer-sphere ion pair; this is a fast diffusion controlled equilibrium reaction with equilibrium constants K_{os}. The second reaction is rate-determining with the rate constant k_2 (unit s^{-1}); it involves the substitution of water in the first coordination sphere of the metal ion with a ligand from the second coordination sphere. This situation may arise when L is a unidentate ligand, but also for polydentate ligands, when the rate of chelate ring-closure is fast. The rate equation deduced from the two elementary reactions is often approximated by the expression

$$\frac{-\mathrm{d}[M(H_2O)]}{\mathrm{d}t} = \frac{k_2 K_{os}[M(H_2O)][L]}{1 + K_{os}[L]} \cong k_2 K_{os}[M(H_2O)][L]$$

K_{os} is usually estimated using the Fuoss equation (Fuoss, 1958).

For reactions where the experimental rate equation has the form

$$\frac{-\mathrm{d}[M(H_2O)]}{\mathrm{d}t} = k_{obs}[M(H_2O)][L]$$

we have $k_{obs} = k_2 K_{os}$. The analysis of experimental rate data using the Eigen–Wilkins mechanism is described by Katakis and Gordon (1987) and Wilkins (1991). The intimate mechanism of the water–ligand exchange can be associative, A, dissociative, D, or of interchange type, I. The assignment is based on the identification of intermediates (A and D); if no intermediates are identified the reaction is classified as interchange (I) (Langford and Gray, 1965). The A intermediate has a higher and the D intermediate a lower coordination number than that of the reactant; in both cases there are two transition states along the reaction pathway. As no intermediate is formed in the interchange mechanism there is only one transition state. A rate constant k_{obs}, that is largely independent on the chemical nature of the entering ligand, indicates that the reaction mechanism is of dissociative type; the rate constant that depends strongly on the entering ligand is a characteristic of an associative mechanism. Szabó *et al.* (1996) have discussed fluoride exchange reactions in $UO_2F_n^{2-n}$ complexes using the Eigen–Wilkins mechanism.

The accessible coordination number at the metal center is often an important indicator when selecting the reaction mechanism. The characteristic coordination number for U(VI) and U(V) is five, but complexes with coordination numbers four and six are not uncommon; also U(IV) and U(III) have variable coordination numbers (9 ± 1). Hence, the coordination number is of little value as a mechanistic indicator in these cases, as neither associative nor dissociative mechanisms can be excluded. The size and charge of the metal ion and the ligand are also important for the mechanism; large ligands cannot enter the first coordination sphere until room is available through the dissociation of water. If water dissociation is rate determining, the intimate mechanism of the ligand exchange is dissociative; if the entry of the ligand from the second coordination sphere is rate determining the mechanism is associative.The simplest and most fundamental of the exchange reactions takes place between the aqua ions and the water solvent and this rate is often an important indicator for the mechanism of ligand substitution reactions of the Eigen–Wilkins type.

(b) Rates and mechanism of water exchange

The rate of water exchange has been studied both by proton NMR line-broadening at low temperature in mixed water–acetone solvents and in water containing 1 M $NaClO_4$. A complicating factor in experiments of this type is that it is not possible to vary the concentration of water in a pure water solvent; this is possible in the mixed water–acetone solvent. In the latter case, however, the concentration changes are often so large that the interpretation of the experimental data is ambiguous. Rate constants and activation parameters for the water exchange reactions are given in Table 5.38.

Because of the fast rate of exchange it is not possible to identify intermediates in these reactions and the rate equation alone is not sufficient to make a mechanistic assignment. This can be obtained by comparing the experimental activation energy with those for the D, A, and I mechanisms (Scheme 5.1), obtained using quantum chemical methods to identify the pathway of lowest activation energy; this value can then can be compared with the experimental data (Vallet *et al.*, 2001, 2004b). The theoretical activation energy of the pathways D, A, and I are 74, 19, and 21 kJ mol^{-1}, respectively; the dissociative pathway can be ruled out because of its high activation energy, while both the A and I mechanisms are consistent with the experimental value,

Table 5.39 *Experimental rate constants and activation parameters for some ligand substitution and ligand exchange reactions in aqueous uranyl(*VI*) systems studied by NMR and stopped-flow methods. The NMR experiments have been made in equilibrium systems where the rates of the forward reaction and the reverse reaction are equal. The stopped-flow experiments have been made under non-equilibrium conditions. The reactions in the table are in some cases elementary reactions; in other cases the mechanism is more complex and involves consecutive and/or parallel reactions. The ligand notation is: acetate ≡ ac; oxalate ≡ ox; picolinate ≡ pic; i-pentyl- picolinate ≡ i-pent-pic; 5-nitro-picolinate ≡ NO*$_2$*-pic; dipicolinate ≡ dipic; oxydiacetate ≡ oda. The following notation is used for the different fluoride ligands:* [a] *central fluoride,* [b,c] *edge fluorides. The rate constant in the forward and reverse directions is denoted +1 and –1, respectively;* k_{ex} *denotes an exchange reaction without net chemical change.*

Reaction	k_{obs} (s^{-1})	$\Delta H^{\neq}$ (kJ mol^{-1})	$\Delta S^{\neq}$ (J K^{-1} mol^{-1})	*References*
	NMR data at –5°C			
$UO_2(ac)F_3^{2-} + ac^{-*} \rightleftharpoons$ $UO_2(ac^*)F_3^{2-} + ac^-$	$k_1 = 2 \times 10^3$ s^{-1} $k_{-1} = 2.5 \times 10^4$ $M^{-1}s^{-1}$	–	–	Aas *et al.* (1999)
$UO_2(ac)_3^- \rightleftharpoons UO_2(ac)_2 + ac^-$	$k_1 = 2.7 \times 10^3$ s^{-1} $k_{-1} = 3.8 \times 10^5$ M^{-1} s^{-1}	22 ± 3	–61 ± 9	Aas *et al.* (1999)
$UO_2CO_3F_3^{3-} + F^{-*} \rightleftharpoons$ $UO_2CO_3F_3^{*3-} + F^-$	$k_{\mathrm{ex}} = 14.2 \pm 2.1^{a,b,c}$ s^{-1}	53.7 ± 1.6	–15.7 ± 0.8	Szabó and Grenthe (1998)
$UO_2CO_3F_3^{3-} + C^*O_3^{2-} \rightleftharpoons$ $UOC^*O_3F_3^{3-} + CO_3^{2-}$	$k_{\mathrm{ex}} = 8$ s^{-1} at pH 8.5	–	–	
$UO_2(pic)F_3^{3-} + F^{-*} \rightleftharpoons$ $UO_2(pic)F^*{}_3^{3-} + F^-$	$k_{\mathrm{ex}} = 24.4 \pm 0.6^a$ s^{-1}; $k_{\mathrm{ex}} = 12.8 \pm 0.3^{b,c}$ s^{-1}	61.4 ± 1.6	14.6 ± 0.5	Szabó and Grenthe (1998)
$UO_2(i\text{-pent-pic})F_3^{3-} + F^{-*} \rightleftharpoons$ $UO_2(i\text{-pent-pic})F^*{}_3^{3-} + F^{-*} \rightleftharpoons$	$k_{\mathrm{ex}} = 18.2 \pm 1.8^a$ s^{-1} ; $k_{\mathrm{ex}} = 13.9 \pm 1.1^{b,c}$ s^{-1}	59.7 ± 1.2	10.4 ± 0.8	
$UO_2(NO_2\text{-pic})F_3^{3-} + F^{-*} \rightleftharpoons$ $UO_2(NO_2\text{-pic})F^*{}_3^{3-} + F^-$	$k_{\mathrm{ex}} = 16.0 \pm 1.2^{a,b,c}$ s^{-1}	60.3 ± 2.6	14.6 ± 0.6	
$UO_2(pic)F_3^{3-} + pic^{-*} \rightleftharpoons$ $UO_2(pic*)F_3^{3-} + pic^-$	$k_{\mathrm{ex}} = 4.7 \pm 0.2$ s^{-1}	56.2 ± 4.2	–16.3 ± 1.2	
$UO_2(NO_2\text{-pic})F_3^{3-} + NO_2\text{-}pic^{-*} \rightleftharpoons UO_2(NO_2\text{-pic}^*)F_3^{3-} + NO_2\text{-pic}^-$	$k_{\mathrm{ex}} = 55$ s^{-1}	59.4	11.3 ± 0.4	

		picolinate ring rotation		
pic	k_{ex}=300 s^{-1}	40.1 ± 2.4	–46.7 ± 2.8	Szabó and Grenthe (1998)
i-pent- pic	$k_{ex} = 90$ s^{-1}	46.8 ± 1.5	–32.8 ± 1.0	
NO_2-pic	$k_{ex} = 2060$ s^{-1}	49.6 ± 3.4	3.3 ± 1.2	
$UO_2(ox)F_3^{4-} + F^{-*} \rightleftharpoons$ $UO_2(ox)F_3^{*4-} + F^-$	$k_{ex} = 21.6 \pm 2.4^{a,b,c}$ s^{-1}	58.9 ± 3.4	12.4 ± 1.0	Szabó and Grenthe (1998)
(In D_2O)	$k_{ex} = 14.1 \pm 0.8^{a,b,c}$ s^{-1}	60.4 ± 2.0	18.9 ± 0.6	
$UO_2(ox)F_3^{4-} + ox^{2-*} \rightleftharpoons$ $UO_2(ox^*)F_3^{4-} + ox^{2-}$	$k_{ex} = 6.2 \pm 0.2$ s^{-1}	70.2 ± 5.6	23.1 ± 1.8	
$UO_2(ox)F(H_2O)_2^- + H_2O^* \rightleftharpoons$ $UO_2(ox)F(H_2O^*)_2^- + H_2O$	$k_{ex} = 1.6 \times 10^4$ s^{-1}	45.4 ± 3.8	–11.3 ± 0.5	Szabó *et al.* (1997) Farkas *et al.* (2000)
$UO_2(ox)F_2(H_2O)_2^- + H_2O^* \rightleftharpoons$ $UO_2(ox)F_2(H_2O^*)^{2-} + H_2O$	$k_{ex} = 1.6 \times 10^3$ s^{-1}			Szabó *et al.* (1997)
$UO_2(ox)_2F_3^- + F^{-*} \rightleftharpoons$	$k_{ex} = 12.3 \pm 1.0$ s^{-1}	40.8 ± 2.0	–74.8 ± 3.6	Szabó and Grenthe (1998)
$UO_2(ox)_2F^{*3-} + F^-$		47.1 ± 2.6	–56.3 ± 3.2	
(In D_2O)	8.7 ± 1.5 s^{-1}	42.0 ± 3.4	–73.3 ± 5.8	
$UO_2(ox)_2F^{3-} + ox^{2-*} \rightleftharpoons$ $UO_2(ox^*)_2F^{3-} + ox^{2-}$				
$UO_2(ox)_2(H_2O)^{2-} + ox^{2-*} \rightleftharpoons$ $UO_2(ox^*)_2(H_2O)^{2-} + ox^{2-*}$	$k_{ex} = 1.6 \times 10^3$ s^{-1}	31 ± 2	–56 ± 5	Aas *et al.* (1999)
$UO_2^{2+} + SO_4^{2-} \rightleftharpoons UO_2SO_4$	$k_1 = 3.4 \times 10^3$ M^{-1} s^{-1} $k_{-1} = 80$ s^{-1}			Moll *et al.* (2000b)
$UO_2F_4(H_2O)^{2-} + F^- \rightleftharpoons UO_2F_5^{3-}$	$k_1 \approx 4 \times 10^3$ M^{-1} s^{-1} $k_{-1} = 6.5 \times 10^3$ s^{-1}			Vallet *et al.* (2002)
		stopped-flow data at 25°C $\mu = 0.10$ M		
$UO_2^{2+} + dipic^{2-} \rightleftharpoons UO_2(dipic)$;		47.3 ± 2.6	–39 ± 9	Friese *et al.* (2001)
pH = 1.0	$k_1 = 0.94 \times 10^3$ M^{-1} s^{-1} $k_{-1} = 0.74$ s^{-1}	62.4 ± 1.6	–41 ± 6	
pH = 3.0	$k_1 = 3.21 \times 10^3$ M^{-1} s^{-1}	55.3 ± 1.3	6 ± 4	
	$k_{-1} = 0.38$ s^{-1}	57.1 ± 9.1	–61 ± 31	
$UO_2^{2+} + oda^{2-} \rightleftharpoons UO_2(oda)$;	$k_1 = 3.4$ M^{-1} s^{-1}	62.1 ± 2.8	–27 ± 9	Friese *et al.* (1998)
pH = 3.0	$k_{-1} = 0.43$ s^{-1}	58.0 ± 1.2	–57 ± 4	

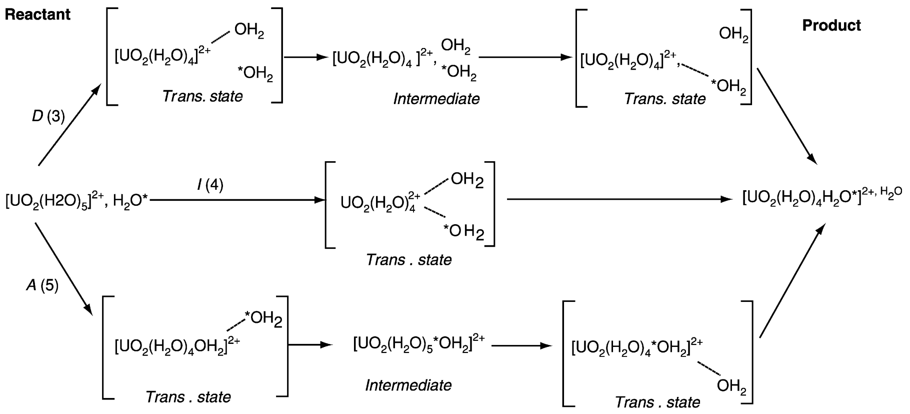

Scheme 5.1 *The scheme shows the dissociative (D), associative (A) and interchange (I) pathways for the water exchange between* $UO_2(OH_2)_5^{2+}$ *and water solvent from Vallet* et al. (2001) (*by permission of the American Chemical Society*).

$\Delta H^{\neq} = 26$ kJ mol^{-1}. The small difference in activation energy between these two pathways is understandable from the very similar structures of their transition states (Fig. 5.67a and b).

There are no experimental water exchange data for

$$UO_2(H_2O)_5^+ + H_2O^* \rightleftharpoons UO_2(H_2O^*)_5^+ + H_2O$$

However, the reaction has been studied using quantum chemical methods (Vallet *et al.* 2004a). In this system no stable intermediate $UO_2(H_2O)_6^+$ was found, hence the reaction cannot be associative. It was only possible to identify the reaction pathway for the dissociative mechanism with the electronic activation energy $\Delta E^{\neq} = 36.4$ kJ mol^{-1}. As judged by the activation energy one would expect the rate of water exchange to be slower in the uranyl(v) aquo-ion than that for the A/I mechanisms of the uranyl(vi) ion. However, the rate of reaction is determined by the Gibbs energy of activation, $\Delta G^{\neq} = \Delta H^{\neq}(\approx \Delta E^{\neq}) - T\,\Delta S^{\neq}$, where the activation entropy is larger for the D than for the A/I reactions (Wilkins, 1991, p. 202). Hence it is a reasonable assumption that the rate of water exchange in $UO_2(H_2O)_5^+$ is not too different from that in $UO_2(H_2O)_5^{2+}$.

The rate of water exchange and the activation energy for the reaction

$$U(H_2O)_n^{4+} + H_2O^* \rightleftharpoons U(H_2O^*)_n^{4+} + H_2O$$

has been determined experimentally (Farkas *et al.*, 2000b). The coordination number *n* is probably (9 ± 1), the rate constant 5.4×10^6 s^{-1} at 298 K and the activation enthalpy 34 kJ mol^{-1}. From the experimental data alone, it is not possible to determine the reaction mechanism. However, a quantum chemical study by Yang *et al.* (2003) of the water exchange in the corresponding thorium system indicates that the water exchange between $Th(H_2O)_9^{4+}$ and the water

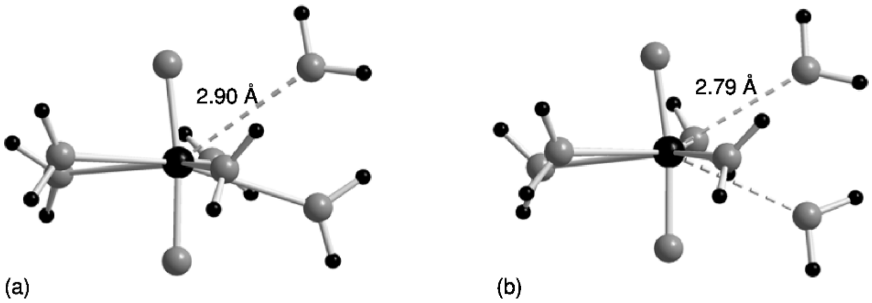

Fig. 5.67 (*a*) *Transition state in the A mechanism for the water exchange in the uranyl*(vi) *aqua ion. The geometry of the intermediate is very close to that of the I transition state*; *the bond distance in the entering and leaving water molecules are both* 2.65 Å. (*b*) *Transition state in the I mechanism. The U–H_2O distance for the two ligands above and below the equatorial plane in the I transition state is* 2.79 Å.

solvent takes place through an associative mechanism; from this we suggest that the mechanism is the same also for $U(H_2O)_9^{4+}$.

There are no experimental data for ligand exchange reactions in U(iii) complexes, but Helm and Mehrbach (1999) have made extensive studies of the water exchange reactions of the trivalent lanthanides that are chemically very similar to the trivalent actinides. Based on these data, one expects the substitution mechanisms on U(iii) to be similar to the nine-coordinated early lanthanides and to follow a dissociative mechanism.

(c) Water exchange in uranyl(vi) and uranium(iv) complexes

It is often assumed that the rate of water exchange at metal complexes is larger than that of the corresponding aqua ions. This does not seem to be the case for uranyl(vi) complexes as shown by the rate constant of water exchange in $UO_2(oxalate)F(H_2O)_2^-$ and $UO_2(oxalate)F_2(H_2O)^{2-}$, that are approximately 2×10^3 s^{-1} (Table 5.39); this is much smaller than that of $UO_2(H_2O)_5^{2+}$ ($k_{ex} = 1.3 \times 10^6$ s^{-1}; Szabó *et al.*, 1997). The rate constant of water exchange in $UF(H_2O)_8^{3+}$ is not significantly different from that in $U(H_2O)_9^{4+}$ (Farkas *et al.*, 2000b).

(d) Rates and mechanisms of complex formation reactions with inorganic and organic ligands

The rates and mechanisms of complex formation reactions have been studied both in equilibrium systems using NMR methods and in non-equilibrium systems using mainly stopped-flow and relaxation methods. In the former case the reactions are typically

$$ML_n + L^* \rightleftharpoons ML_n^* + L;$$

The rate constants in the forward and reverse directions are denoted k_1 and k_{-1}, respectively; as the system is in equilibrium the *rates* in the forward and reverse directions are the same. This is not the case in the non-equilibrium reactions where one often can arrange the experimental conditions so that the reverse reaction can be neglected; that is the reactions studied are of the type

$$\mathrm{ML}_n + \mathrm{L} \rightarrow \mathrm{ML}_{n+1}$$

Some examples of experimental data, rate constants, and activation parameters are given in Table 5.39. The rate equations and reaction mechanisms have been deduced by investigating how the reaction rate depends on the concentration of reactants, products, and catalysts like H^+. The mechanistic deductions are complicated for multidentate ligands that in general are moderately strong bases; the rate of reaction is therefore often strongly dependent on the pH. Hines *et al.* (1993), Ekstrom and Johnson (1974), and Pippin and Sullivan (1989) give examples of such systems using the ligands diphosphonic acids and 4-(2-pyridylazo) resorcinol. However, the mechanisms of these reactions are far from clear. The rates of exchange for the ligands in Table 5.39 have been studied in more detail and some general comments about rate constants and mechanisms can therefore be made.

The rate of dissociation of coordinatively saturated complexes varies strongly with the strength of the complexes, e.g. from $2.7 \times 10^3\ \mathrm{s}^{-1}$ for the acetate exchange in $UO_2(\text{acetate})_3^-$ to $0.38\ \mathrm{s}^{-1}$ for the rate of dissociation of UO_2(dipicolinate); the latter ligand forms a very strong three-dentate chelate complex. The rate of formation and dissociation of UO_2(dipicolinate) and $UO_2(CO_3)F_3^{3-}$ are proton-catalyzed; the same is certainly the case for UO_2(oxydiacetate), but here there is only experimental data at one pH.

For multidentate ligands the mode of coordination is not always known and it is also unlikely that the formation or dissociation of such complexes takes place in one step. Hence, the experimental rate equation does not provide information on the rate-determining step. Some information may be obtained using the Eigen–Wilkins mechanism as exemplified by the rate constant for the formation of UO_2(dipicolinate) and UO_2SO_4. Both rate constants have nearly the same value (Table 5.39) indicating that the reaction is not strongly dependent on the entering ligand; this is a typical feature of dissociative reactions where the rate of water dissociation from the first coordination sphere is rate-determining. However, in the Eigen–Wilkins mechanism the experimental rate constant is a product of the rate of water exchange and the equilibrium constant for the formation of an outer-sphere complex with the entering ligand. A crude estimate of K_{os} for sulfate and dipicolinate is 5–50 M^{-1}, which would correspond to a rate constant for the water dissociation equal to $(0.7–0.07) \times 10^3\ \mathrm{s}^{-1}$. This is very different from the experimental value for the water exchange, indicating that the mechanism is more complex, suggesting that the rate of chelate ring closure/ring opening might have a significant effect on the rate of formation/dissociation of the complexes. Hurwitz and Kustin (1967) have studied the rate and mechanism of reactions between UO_2^{2+} and SO_4^{2-}, SCN^-, CH_3COO^-, and $ClCH_2COO^-$ using the temperature jump method. The rate of complex formation with sulphate is 180 $\mathrm{M}^{-1}\ \mathrm{s}^{-1}$ at 20°C, very different from the value obtained by Moll *et al.* (2000b) using NMR. This is not an ionic strength effect that would result in a larger rate constant at lower ionic strength (Wilkins, 1991, p. 110). The bimolecular rate constants for the formation of the 1:1 complex between UO_2^{2+} and actate and monochloracetate are 1050 and 110 $\mathrm{M}^{-1}\ \mathrm{s}^{-1}$. Hurwitz and Kustin (1967) note that the most significant feature of their observations is the relative slowness of the substitution reactions and their strong ligand dependence. This indicates that the substitution reactions are associative.

Jung *et al.* (1988) have determined the rate and mechanism of the formation and decomposition of the binuclear hydroxide complex $[(UO_2)_2(OH)_2]^{2+}$. The rate is sufficiently slow so that NMR line broadening of $U^{17}O_2^{2+}$ can be used. The rate equation is

$$\mathrm{Rate} = k_2[UO_2^{2+}][UO_2OH^+] - k_{-2}K_a[H^+][(UO_2)_2(OH)_2^{2+}]/2$$

where K_a is the equilibrium constant for the reaction $(UO_2)_2(OH)_2^{2+} + H^+ \rightleftharpoons (UO_2)_2(OH)^{3+} + H_2O$. The suggested mechanism consists of two steps:

$$UO_2^{2+}UO_2OH^+ \rightleftharpoons (UO_2^{2+} \ldots UO_2(OH^+)) \rightarrow [UO_2 - (OH) - UO_2]^{3+}$$

that are followed by the fast reaction

$$(UO_2)_2(OH)^{3+} + H_2O \rightleftharpoons (UO_2)_2(OH)_2^{2+} + H^+.$$

The first step is the formation of an outer-sphere ion pair and the second is rate determining. The estimated rate constant for this step is $7.6 \times 10^5\ \mathrm{s}^{-1}$, close to the rate of water exchange in the aqua ion. Frei and Wendt (1970) have studied the rate of dissociation of the binuclear complex using the stopped-flow method and also they suggested a mechanism where a single OH-bridged intermediate is formed.

Ligand exchange between a limiting complex (the complex with the largest number of coordinated ligands) and free ligand is most conveniently studied by using NMR methods. A typical example is the rate of ligand exchange for the reaction

$$UO_2F_5^{3-} + {}^*F^- \rightleftharpoons UO_2{}^*F_5^{3-} + F^-$$

As one reactant is a coordinatively saturated complex it is unlikely that the ligand exchange takes place according to an associative mechanism. It also turns out that the rate of ligand exchange for the above and many other reactions involving limiting complexes is independent on the concentration of free ligand, confirming that the exchange mechanism is dissociative (Vallet *et al.*, 2002). This result is supported by quantum chemical calculations, which demonstrate that there is no stable intermediate $UO_2F_6^{4-}$ (Ikeda *et al.*, 1984; Szabó *et al.*, 1997; Vallet *et al.*, 2002).

(e) Mechanisms of intramolecular reactions

Important examples within this group are chelate ring opening/ring closure reactions, exemplified by the complex UO_2(picolinate)F_3^{2-}, (Fig. 5.68) (Szabó *et al.*, 1997; Vallet *et al.*, 2004b) and the experimental data in Table 5.39. In this complex there are three non-equivalent fluoride ligands, F_A, F_B and F_C, as shown in the ^{19}F NMR spectrum. The central peak, F_C, is narrow, indicating a slow exchange on the NMR time-scale while the other two peaks are broad, corresponding to a rate constant of 300 s^{-1} for the exchange between the F_A and F_B sites. This exchange is a result of an intramolecular process as the intermolecular exchange between coordinated and free fluoride is much slower, k_{obs} = 13 s^{-1} for F_A and F_B and 24 s^{-1} for F_C. The intramolecular exchange between F_A and F_B is the result of a a chelate ring opening/closure reaction that results in a rotation of the picolinate ligand and an exchange of the F_A and F_B sites The rate of exchange for the intermolecular exchange of picolinate is much slower, 4.7 s^{-1}.

The exchange between the different isomers of UO_2(picolinate)$_2F^-$ (Fig. 5.69) probably also takes place through a ring opening/ring closure reaction; a similar reaction mechanism has also been proposed for the kinetics of intra- and

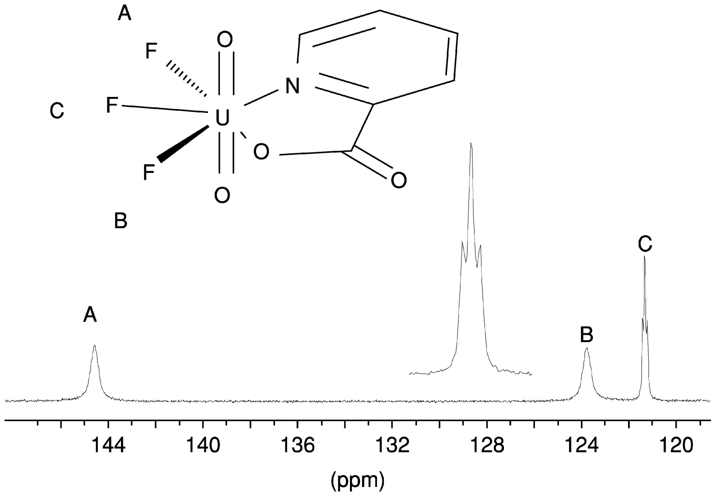

Fig. 5.68 *The ^{19}F NMR spectrum of UO_2(picolinate)F_3^{2-}at –5°C showing peaks for the three different fluorides (from Szabó* et al. *(1997), reproduced by the permission of American Chemical Society). There is no visible spin–spin coupling in the exchanged broadened peaks for fluorides A and B. Spin–spin coupling, a collapsed doublet of doublets, is evident in the narrow peak C, cf. the insert.*

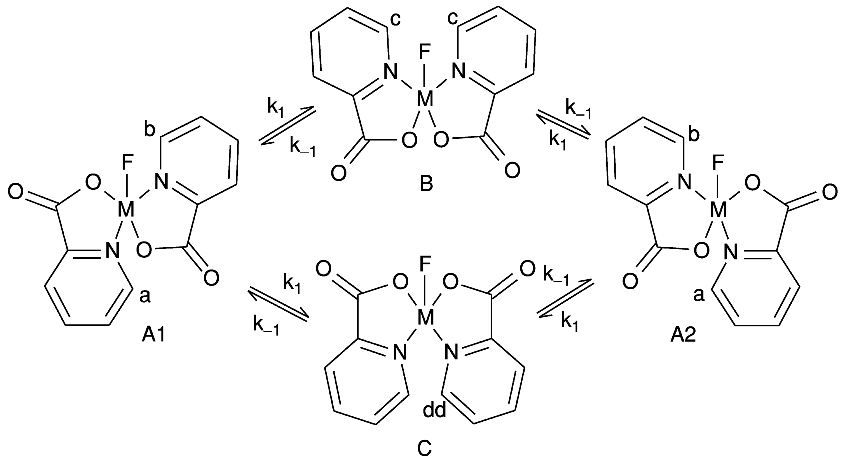

Fig. 5.69 *Different isomers of the complex $UO_2(picolinate)_2^{F-}$ and the possible exchange pathways between them* (*from Szabó* et al. (1997), *reproduced by the permission of American Chemical Society*). *The exchange presumably takes place through chelate ring opening/ring closure reactions.*

intermolecular exchange reactions of nonamethyl-imidodiphosphoramide (NIPA) in $UO_2(NIPA)_3^{2+}$ (Bokolo *et al.*, 1981).

Intramolecular reactions of the type encountered in $UO_2(picolinate)_2F^-$ do not necessarily proceed through chelate ring opening/ring closure as exemplified by $UO_2(acac)_2L$, in Fig. 5.70, where acac is a β-diketonate like acetylacetonate or dibenzoylmethanate and L an uncharged ligand such as dimethylsulfoxide (DMSO) (Ikeda *et al.*, 1984). The two methyl groups in the acetylacetone ^{13}C NMR spectrum are equivalent at room temperature due to fast exchange, but not at low temperature. The rate of intermolecular exchange between coordinated and free acac is slow and the fast exchange between the two methyl groups is therefore not the result of chelate ring opening/ring closure but of the fast dissociation/reentry of the ligand L that also results in exchange between the methyl groups (Fig. 5.70); the chelate ring opening is a very slow reaction.

Kramer and Maas (1981) have studied the fluxionality in U(VI) complexes of trifluoroacetylacetonate and various uncharged bases and suggest that the fluxionality of the complexes is a result of an intramolecular base migration; however, it is difficult to envisage that such a reaction is geometrically feasible.

(f) Rate and mechanism of ligand exchange in non-aqueous systems

The proposed mechanisms and activation parameters for ligand exchange in uranyl(VI) complexes between a number of uncharged ligands in non-aqueous systems are given in Table 5.40. The experimental rate constant k_{obs} for many of the reactions is given by

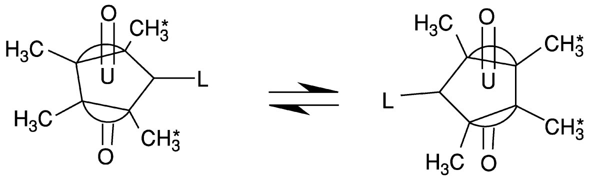

Fig. 5.70 *Ligand exchange in acetylacetonato complex $UO_2(acac)_2L$. The methyl groups in the coordinated acetylacetonate are non-equivalent as a result of their different chemical surroundings. The two sites are in fast exchange at room temperature as a result of the fast dissociation/re-entry of the ligand L.*

$$k_{\mathrm{obs}} = k_1 + k_2[\mathrm{L}],$$

where [L] is the free ligand concentration. In most systems k_2 is equal to zero, indicating a dissociative mechanism as seen in Table 5.40. When $k_2 \neq 0$ the rate of exchange depends on the ligand concentration, indicating an associative pathway. The difference in exchange mechanism for water (associative or associative interchange mechanism) and the dissociative pathway for the ligands in Table 5.40 is probably due to the larger steric constraints for the latter ligands. The occurrence of two parallel pathways, e.g. for DMSO indicates that the energy difference between complexes with four-, five-, and six-coordinated DMSO ligands is small. It is worth noting that there is no connection between the suggested mechanisms and the activation entropy for these reactions that all involve an uncharged ligand.

(g) Rate and mechanism of 'yl'-oxygen exchange in uranyl(VI) and uranyl(V) complexes: isotope exchange reactions

The rate of exchange between the 'yl'-oxygen atoms in UO_2^{2+}(aq) and the water solvent is very slow, the half-life is 5000 to 10000 h as demonstrated by Gordon and Taube (1961a) using ^{18}O-enriched uranyl(VI). They noticed that the rate of exchange depends on the hydrogen ion concentration and that the reaction was photo-catalyzed. The fact that the exchange is very fast in the photo-excited state of the uranyl(VI) aqua ion (Bell and Buxton, 1974) has been used to prepare uranyl(VI) complexes where the 'yl'-oxygens are isotope-enriched in ^{17}O or ^{18}O (Howes *et al.*, 1988). The rate of exchange of the 'yl'-oxygens and the water solvent is strongly catalyzed by UO_2^+(aq) (Gordon and Taube, 1961b). These two observations indicate that the exchange is related to the weakening of the U–O$_{\mathrm{yl}}$ bond. In the photo-excited state, this is the result of transfer of a bonding electron to an empty f-orbital, and in UO_2^+(aq) from the f-electron that is localized in a nonbonding f-orbital (Vallet *et al.*, 2004a). There are few precise and reproducible experimental observations and the mechanism for the exchange reaction has therefore not yet been clarified. Gordon and Taube (1961b) suggested that the rate law for the UO_2^+-catalyzed exchange

Table 5.40 *Mechanisms and activation parameters for the exchange of monodentate uncharged ligands, L, in the uranyl(*VI*) complexes $UO_2L_5^{2+}$ and $UO_2L_4^{2+}$. The solvent is deuterated acetone or dichloromethane. The ligands are: dimethylsulfoxide (DMSO),* N,N,*-dimethylacetamide (DMA), trimethylphosphate (TMP), triethylphosphate (TEP),* N-*methylacetamide (NMA), diethylphosphate (DEP), tetramethylurea (TMU), and hexamethylphosphoramide (HMPA).*

Complex	*Solvent*	*Mechanism*	$\Delta H^{\neq}$ (kJ mol^{-1})	$\Delta S^{\neq}$ (J K^{-1} mol^{-1})	*References*
$UO_2(DMSO)_5^{2+}$	CD_3COCD_3	D	39	–48	Honan *et al.* (1978); Ikeda *et al.* (1979b)
		D	54	6	
		A	39	–28	
$UO_2(DMA)_5^{2+}$	CD_2Cl_2	D	43	–44	Bowen *et al.* (1976)
$UO_2(TMP)_5^{2+}$	"	D or I_d	25	–110	Crea *et al.* (1977)
$UO_2(TEP)_5^{2+}$	"	D or I_d	44	–48	Crea *et al.* (1977)
$UO_2(NMA)_5^{2+}$	"	D	67	45	Honan *et al.* (1979)
$UO_2(DEP)_5^{2+}$	"	D	32	–54	Bowen *et al.* (1979)
$UO_2(TMU)_5^{2+}$	"	D	80	85	Ikeda *et al.* (1979b)
$UO_2(HMPA)_5^{2+}$	"	D	14	–172	Honan *et al.* (1978)
		A	22	–120	

$U^*O_2^{2+} + H_2O \rightleftharpoons UO_2^{2+} + H_2{}^*O$ is first order in $[UO_2^+]$ and suggest the mechanism

$$UO_2^+ + H_2{}^*O \rightleftharpoons U^*O_2^+ + H_2O$$

$$U^*O_2^+ + UO_2^{2+} \rightleftharpoons U^*O_2^{2+} + UO_2^+$$

where the first reaction is assumed to be fast, but the details of the oxygen exchange are not known and quantum chemical studies, similar to those of Schreckenbach *et al.* (1998) and Clark *et al.* (1999) on UO_2^{2+}, have not been made to our knowledge. Howes *et al.* (1988) have studied the second reaction and use the experimental data, in combination with the Marcus' cross-relations, to estimate the rate constant for the outer-sphere self-exchange to be in the range 1–15 M^{-1} s^{-1}, a value that is in good agreement with quantum chemical estimates by Privalov *et al.* (2004).

There are a number of other experimental studies of exchange between uranyl (VI) complexes and water, using ^{17}O-enriched uranyl(VI). This exchange is pH-dependent and much faster than in the $UO_2^{2+}(aq)$. The half-life is less than 1 h in the pH range where polynuclear complexes containing hydroxide/oxide bridges are present (Moll *et al.*, 2000b); the rate of exchange is much slower in $UO_2(OH)_4^{2-}$ and $UO_2(OH)_5^{3-}$ and very slow in limiting complexes that do not contain water or hydroxide in the first coordination sphere. Schreckenbach *et al.* (1998) and Clark *et al.* (1999) have discussed the mechanism, however the estimated activation energy seems large (160 kJ mol^{-1}).

(h) Isotopic exchange reactions involving uranium

Isotopic exchange using ^{233}U as a probe has been used to study the rate and mechanism of exchange reactions between UO_2^{2+}, UO_2^{+}, and U^{4+}. These studies have been made in acid solutions where the degree of hydrolysis is known. The exchange can take place either through bond breaking/bond formation or through electron transfer. The following exchange reaction is a typical example (Rona, 1950; Masters and Schwartz, 1961):

$$U^{4+}(aq) + {}^{*}UO_2^{2+}(aq) + 2H_2O \underset{k_r}{\overset{k_f}{\rightleftharpoons}} 2{}^{*}UO_2^{+}(aq) + 4H^{+}$$

where *U denotes uranium enriched in ^{233}U. The reaction follows two parallel pathways where the rate of exchange for the forward reaction at [U(IV)] < 0.01 M is equal to

$$\text{Rate} = k_f[U^{4+}][UO_2^{2+}][H^+]^{-3} \quad \text{with } k_f = 2.1 \times 10^{-7}\ \text{M}^{-1}\ \text{s}^{-1} \text{ at } 25°\text{C}$$

Imai (1957) studied the rate for the reverse reaction and found

$$\text{Rate} = k_r[UO_2^{+}]^2[H^+] \quad \text{with } k_r = 436\ \text{M}^{-2}\ \text{s}^{-1} \text{ at } 25°\text{C}$$

The ratio $k_r/k_f = 2 \times 10^9$ M^4 is in good agreement with the experimental equilibrium constant 1×10^9 M^4, indicating that both reactions have the same transition state. A slightly lower value of $k_r \approx 130$, was determined by Kern and Orleman (1949). The rate of exchange of the forward reaction is slow because it goes thermodynamically 'uphill', a result of the extensive bond breaking/bond formation during the exchange. The reverse reaction is fast because the reaction is now thermodynamically favored.

The intimate mechanism for most isotope exchange reactions is not known; for the U(IV)–U(V)–U(VI) reaction there is only information on the stoichiometry of the activated complex, $[HOUOUO_2^{3+}]^{\neq}$ and the activation energy 157 kJ mol^{-1}. At U(IV) concentrations higher than 0.01 M, there is a significant contribution from a second reaction pathway and the rate of exchange is now

$$\text{Rate} = k[U^{4+}]^2[UO_2^{2+}][H^+]^{-2}$$

but the mechanistic implications are not clear.

It is often difficult to decide if isotope exchange takes place through bond breaking/bond formation, or as a result of electron transfer; the isotope exchange between uranyl(VI) and uranyl(V) and other actinyl ions are typical examples. Kato *et al.* (1970) studied the exchange between UO_2^{2+} and U^{4+} by measuring the transfer of ^{18}O-enriched 'yl' oxygen to water. The rate constant was 6.5×10^{-4} M^{-1} s^{-1}, is very different from that of Masters and Schwartz (1961) that used different experimental conditions. Kato *et al.* suggested that the activated complex has the composition $[U(IV)U(VI)]^{\neq}$ and that the rate of oxygen exchange and electron exchange are of the same order of magnitude.

A number of the redox reactions to be discussed in the following section have been investigated experimentally using isotope exchange technique.

(i) Rate and mechanism of redox reactions

These reactions are in general studied using isotope exchange as exemplified by

$$U^*O_2^{2+}(aq) + UO_2^+(aq) \rightleftharpoons UO_2^{2+}(aq) + U^*O_2^+(aq)$$

The rate of exchange has been studied using ^{18}O-enriched UO_2^{2+} by following the isotope distribution using mass spectroscopy after separation of U(VI) and U(V) (Gordon and Taube, 1961b; Masters and Schwartz, 1961). The experimental rate of exchange is equal to

$$\text{Rate} = k_{obs}[UO_2^{2+}][UO_2^+]$$

with $k_{obs} \approx 50$ M^{-1} s^{-1} (Gordon and Taube, 1961b), close to the more accurate determination of the corresponding exchange reaction between Np(VI) and Np(V), $k_{obs} \approx 110$ M^{-1} s^{-1}, determined by Cohen *et al.* (1954). Howes *et al.* (1988) report rate constants in the range 1–15 M^{-1} s^{-1}. Privalov *et al.* (2004) have discussed the mechanism for the U(V)–U(VI) electron exchange between the aqua-ions, the fluoride, and the carbonate complexes using quantum chemical methods. Both outer-sphere and inner-sphere mechanisms were studied; the former for the aqua ions using the Marcus model and the latter using an inner-sphere model for binuclear complexes containing hydroxide, fluoride, and carbonate bridges. The calculated rate constant for the homogeneous electron exchange (outer-sphere) between $UO_2^{2+}(aq)$ and $UO_2^+(aq)$ is 26 M^{-1} s^{-1} in fair agreement with experimental data. The rate of electron transfer for the inner-sphere reactions is much faster, but here there are no experimental data that can be used for comparison. This study provides a model for the intimate reaction mechanisms as exemplified by the following structure of the precursor and transition state structures (Fig. 5.71).

The kinetics of redox reactions is also discussed in Chapter 23.

Rate constants and reaction mechanisms for a number of redox reactions involving uranium have been reported by Newton (1975) and in the second edition of this book (Katz *et al.*, 1986). It is not possible to discuss all this

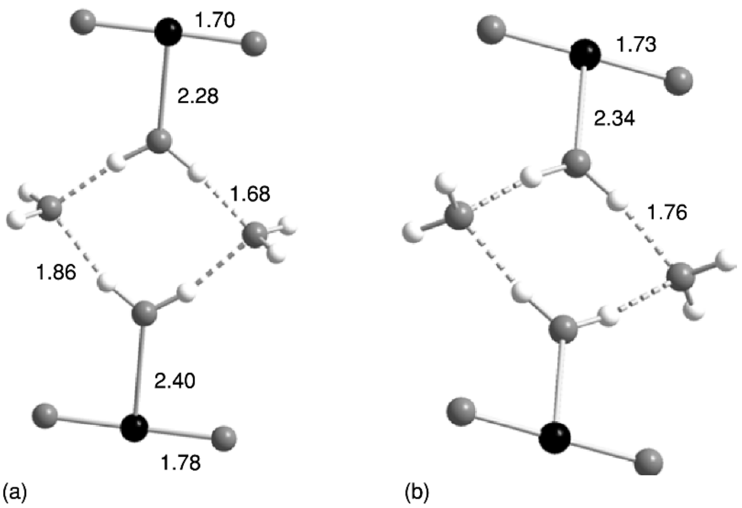

Fig. 5.71 *Quantum chemical model of the precursor* $[UO_2^{2+} \ldots UO_2^{+}]$ *in the outer-sphere electron transfer reaction* $U^*O_2^{2+}(aq) + UO_2^{+}(aq) \rightleftharpoons UO_2^{2+}(aq) + U^*O_2^{+}(aq)$ *from Privalov* et al. (2004). *The model is focused on the bridge between the two uranyl ions and their complete coordination spheres are therefore modeled using a continuum model.* (*a*) *shows the precursor with uranyl(*V*) and uranyl(*VI*) ions and* (*b*) *the transition state where the two uranyl ions are equivalent.*

information and we have accordingly selected a few examples that illustrate the interpretation of the experimental rate laws. A prerequisite for the mechanistic discussion is information on the equilibrium system, i.e. the complexes present in the test solutions under different experimental conditions. When determining the experimental rate law, care must be taken to identify possible parallel reaction pathways and possible catalysts. We will discuss the oxidation of U(IV) with Pu(VI) as this reaction is not only of scientific interest, but also important in nuclear reprocessing (Newton, 1958). In acid solutions of moderate concentration of the reactants, there is a complete reduction of Pu(VI) to Pu(III). When the reactant concentrations are about 10^{-4} M 96% of the U(IV) reacts according to

$$2\mathrm{Pu(VI)} + \mathrm{U(IV)} \rightleftharpoons 2\mathrm{Pu(V)} + \mathrm{U(VI)}$$

and the remaining 4% react according to

$$2/3\mathrm{Pu(VI)} + \mathrm{U(IV)} \rightleftharpoons 2/3\mathrm{Pu(III)} + \mathrm{U(VI)}$$

The latter two equations only represent the change in oxidation states of the actinides but do not account for the overall stoichiometry. At constant hydrogen ion concentration, the experimental rate law is

$$-\frac{\mathrm{d}[\mathrm{Pu}(\textsc{vi})]}{\mathrm{d}t} = 2k''[\mathrm{Pu}(\textsc{vi})][\mathrm{U}(\textsc{iv})]$$

This rate equation requires that the activated complex has the composition $[\mathrm{Pu(VI)}\cdots\mathrm{U(IV)}]^{\neq}$; as the hydrogen ion concentration is constant, there is no information of the hydrogen ion concentration dependence of the reaction rate. Based on this limited information, a possible reaction mechanism that involves the following two elementary reactions has been suggested (charges have been omitted):

$$\mathrm{Pu}(\textsc{vi}) + \mathrm{U}(\textsc{iv}) \rightleftharpoons \mathrm{Pu}(\textsc{v}) + \mathrm{U}(\textsc{v})$$

$$\mathrm{Pu}(\textsc{vi}) + \mathrm{U}(\textsc{v}) \rightleftharpoons \mathrm{Pu}(\textsc{v}) + \mathrm{U}(\textsc{vi})$$

The first reaction is rate-determining as it involves a major rearrangement between the coordination spheres of reactants and products, while the second is fast because these rearrangements are minor.

Additional mechanistic information is obtained by investigating how the rate of reaction depends in the hydrogen ion concentration. One finds that the rate is

$$-\frac{\mathrm{d}[\mathrm{Pu}(\textsc{vi})]}{\mathrm{d}t} = 2k''\left(1 + \frac{K}{[\mathrm{H}^+]}\right)[\mathrm{PuO}_2^{2+}]\,[\mathrm{U}^{4+}]$$

This rate law suggests that there are two parallel pathways according to the following elementary reactions:

$\mathrm{U}^{4+} + \mathrm{H_2O} = \mathrm{UOH}^{3+} + \mathrm{H}^+$ (a fast equilibrium prior to the rate-determining step);

$\mathrm{UOH}^{3+} + \mathrm{PuO}_2^{2+} \rightleftharpoons \mathrm{HOUOPuO}^{5+}$ (rate-determining step in a reversible reaction);

$\mathrm{HOUOPuO}^{5+} = \mathrm{OUOPuO}^{4+} + \mathrm{H}^+$ (a fast equilibrium reaction);

$\mathrm{OUOPuO}^{4+} + \mathrm{H_2O} \rightleftharpoons \mathrm{UO}_2^+ + \mathrm{PuO}_2^+ + 2\mathrm{H}^+$ (a slow equilibrium reaction).

The elementary reactions above provide information on the stoichiometric mechanism, but not the details at the microscopic level, as that exemplified in Fig. 5.71 for the electron transfer reaction

$$\mathrm{U^*O}_2^{2+}(\mathrm{aq}) + \mathrm{UO}_2^{+}(\mathrm{aq}) \rightleftharpoons \mathrm{UO}_2^{2+}(\mathrm{aq}) + \mathrm{U^*O}_2^{+}(\mathrm{aq}).$$

5.10.4 Fluorescence properties and photochemistry of uranyl(VI) complexes

Only light that is absorbed by a substance is effective in producing a photochemical change; Grotthuss and Draper stated this principle of photochemical activation in 1818, long before the quantum theory. According to quantum theory, the primary step of a photochemical reaction is the activation of *one* molecule by *one* absorbed quantum of radiation. The absorption of a photon leads to a transition from a singlet ground state to a singlet excited state; this is followed by a number of very fast processes with lifetimes in the picosecond

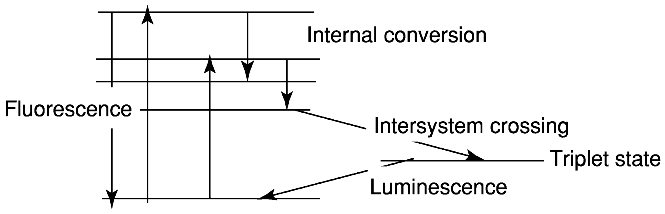

Fig. 5.72 *Molecular energy levels where the arrows denote the corresponding process for energy loss of the excited states. The ground state is a singlet, the excitation takes place without change of spin. The excited states can lose energy by fluorescence back to the ground state, via internal conversion from higher to lower excited states and by intersystem crossing to the triplet state. The typical fluorescence lifetime in the excited state is* 10^{-8} *to* 10^{-9} s *and for internal conversion* 10^{-12} s. *The energy loss from the triplet state to the ground state takes place either by luminescence/phosphorescence or thermally. In addition energy dissipation can take place through non-radiative decay and collisional quenching.*

range that take place before any photochemical reaction can occur. *Fluorescence* takes place from an excited singlet to the ground state, *internal conversion* between the excited singlet states, and *intersystem crossing* from the lowest excited singlet state to the triplet state (Fig. 5.72). The lifetime of the triplet state is long (micro to milliseconds) in comparison with that of the singlet states; the radiative emission from triplet to singlet is called phosphorescence. The long lifetime of the triplet also makes thermal energy dissipation possible.

There are other energy dissipation pathways than fluorescence from the excited states such as non-radiative transfer of the excitation energy to vibrational excitation in the coordinated ligands and the solvent and in collisional pathways, so called dynamic quenching; a more detailed discussion is given by Szabó *et al.* (2006). The intensity of fluorescence or phosphorescence depends on the competition between these physical and chemical processes. The quantum yield, Q_Y, is defined as the ratio between the number of photons emitted and absorbed and this quantity is accordingly strongly dependent on the different quenching mechanisms

$$Q_Y = \frac{1/\tau_n}{1/\tau_n + k_{nr}} = \frac{\tau}{\tau_n}$$

where τ_n is the lifetime in the absence of non-radiative processes and k_{nr} the rate constant for non-radiative decay; τ is the lifetime in the presence of non-radiative processes. In systems with dynamic quenching it is $1/\tau = 1/(1/\tau_n + k_{nr} + k_q)$, where k_q is the rate constant for collision quenching.

In addition to these quenching processes, the fluorescence intensity may also depend on static quenching that is the result of the formation of a non-fluorescent complex with a ligand, L, in the ground state. In order to understand and use information of fluorescence intensity and fluorescence lifetimes, it is essential to be able to distinguish and quantify all these mechanisms. Static and dynamic quenching can be distinguished by lifetime analysis (Toraishi *et al.*, 2004).

In steady-state excitation the concentration of excited molecules and therefore the fluorescence intensity is constant. Hence, we have the following relations in the absence and presence of quenching:

$$\frac{dI^*}{dt} = f - (1/\tau_0)[I^*] = 0;$$

and

$$\frac{dI^*}{dt} = f - \left(1/\tau_0 + k_q[L][I^*]\right) = 0$$

where f is the light flux, I^* is the concentration of the fluorescent species with a lifetime τ_0 in the absence of the quencher L. k_q is the rate constant for fluorescence decay in the presence of L. Hence

$$\left(\frac{I}{I_0}\right)^{-1} = \frac{1/\tau_0 + k_q[\mathrm{L}]}{1/\tau_0} = 1 + k_q\tau_0[\mathrm{L}]$$

where I and I_0 represent the measured fluorescence intensity in the presence and absence of L; this is the Stern–Volmer equation. The fraction of excited fluorophores relative to the total is equal to

$$\left(\frac{I}{I_0}\right) = \left(\frac{\tau}{\tau_0}\right)$$

which for the case of only static quenching in the ground state reduces to $(I/I_0) = 1$ because then $\tau = \tau_0$.

In uranyl(VI) systems where the ligand is a strong quencher, the rate constant k_q is very large; it is then not possible to detect the fluorescence spectrum for the complexes (e.g. Moll *et al.*, 2003).

The photochemistry of uranium compounds is a ‘classical’ field of research that dates back to the Becquerels more than 100 years ago. The experimental quantities are the excitation and emission spectra and the lifetime(s) of the excited state(s) as a function of chemical parameters. The chemistry of photo-excited UO_2^{2+} has been extensively studied, both as a tool for synthesis, as a method to determine equilibrium constants in ground and excited states, and for elucidation of luminescence quenching mechanisms. Recent reviews by Baird and Kemp (1997), Fazekas *et al.* (1998), and Yusov and Shilov (2000) provide an introduction to the literature.

The photo-oxidation of oxalic acid was used in the first chemical actinometers to measure photon flux based on the reactions

$$\begin{aligned}&UO_2^{2+} + h\nu \rightarrow (UO_2^{2+})^*;\\&(UO_2^{2+})^* + (COOH)_2 \rightarrow UO_2^{2+} + CO_2 + CO + H_2O\end{aligned}$$

The actinometer must be calibrated to determine the quantum efficiency at the wavelength used.

The excited states responsible for luminescence emission have a charge-transfer character as a result of excitations from the σ_u or σ_g bonding U–O orbitals to an empty f-orbital via internal conversion and intersystem crossing as outlined in Fig. 5.72. The resulting triplet state is $^3\Delta_g$, or to be more precise the $\Omega = 1_g$ component of the relativistic $^3\Delta_g$ state (Zhang and Pitzer, 1999; Matsika *et al.*, 2001) and the transition to the ground state is accordingly spin forbidden, which accounts for the long lifetime. The very long lifetime in comparison with those from electronically excited states of organic molecules is the basis for the photo-reactivity of $(UO_2^{2+})^*$. The photo-excited state is a very strong oxidant with an estimated oxidation potential of 2.6 V. The probable deactivation pathways are (Fazekas *et al.*, 1998):

- intra-molecular radiationless deactivation via O-H stretch modes of coordinated water;
- intra-molecular energy transfer to vibrational modes of the water solvent as in rare-earth metal ions;
- electron transfer and radical formation

  $$(UO_2^{2+})^* + H_2O \rightarrow UO_2^+ + (H_2O^+)^*;$$

  or hydrogen abstraction

  $$(UO_2^{2+})^* + H_2O \rightarrow UO_2H^+ + OH^*$$

The experimental basis for photochemical studies is provided by fluorescence spectroscopy and measurements of the decay of the fluorescence as a function of chemical parameters. The terminology is often misleading, the majority of the experimental 'fluorescence' spectra of uranyl(VI) systems refer to phosphorescence, often denoted luminescence. In the following we will use the luminescence terminology. Despite all experimental efforts there is no consensus about the primary deactivation processes. The luminescence properties of the uranyl(VI) ion in water solution can be used as an example. When the pH is increased in the UO_2^{2+}–water system, the peaks of the emission spectrum are displaced towards longer wavelength. At the same time, the luminescence lifetime is no longer mono-exponential; this is presumably a result of the formation of hydroxide complexes (Fazekas *et al.*, 1998). Moriyasu *et al.* (1977) made similar observations on other uranyl(VI) systems where complexes with fluoride and phosphate were formed, in particular they observed a strong enhancement of both the luminescence intensity and its lifetime that is the basis for an analytical method to determine uranium in low concentration. The increase of the lifetime of the triplet state is assumed to be a result of shielding of the uranyl ion from water that is an efficient quencher. Some authors explain the non-exponential luminescence decay by exciplex formation (Deschaux and Marcantanatos, 1979), other by a reversible crossing between two different excited uranyl states (Formosinho and Da Graca Miguel, 1984; Formosinho *et al.*, 1984). Billard and Lützenkirchen (2003) have discussed the problems encountered when analyzing experimental luminescence data in terms of elementary reactions as discussed below.

Laser-induced fluorescence spectroscopy is extensively used as a tool for the analytical determination of trace amounts of uranium as described in Chapter 30. The technique is also used to determine equilibrium constants and the speciation of uranium(VI) in aqueous solution both in laboratory and environmental systems. This raises the question if the measured equilibrium constant, K_{app}, refers to the ground or the excited state, a problem that has been discussed by Billard and Lützenkirchen (2003). Their starting point is the following mechanistic scheme (Scheme 5.2): where K is the equilibrium constant in the ground state, k_1 and k_{-1} the rate constants for the formation and dissociation of ML*, and λ_1 and λ_2 the rate constants for decay of M* and ML*.

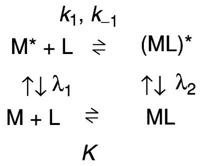

Scheme 5.2 *Mechanistic scheme for the complex formation between M and L in ground and excited state. The notation is explained in the text.*

In the experimental studies, time-resolved spectra are measured at different total concentrations of M and L, where the former is the fluorescence probe and the latter is assumed to be non-absorbing at the excitation wavelength. Scheme 5.2 has been used to deduce rate constants k_1 and k_{-1} and information on ground state and excited state chemistry from the amplitude of the emission spectra and ground state concentrations. In the case where there is no interaction between M* and L, or when the rate constants k_1 and $k_{-1} \ll \lambda_1$ and λ_2, Scheme 5.2 is reduced to Scheme 5.3 as follows:

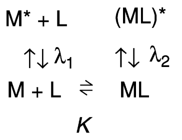

Scheme 5.3 *Mechanistic scheme for reactions where the complex formation in the excited state can be neglected.*

where the measured lifetimes now represent M* and ML*. Billard and Lützenkirchen (2003) discuss the conditions under which K_{app} is a satisfactory approximation for the equilibrium constant K in the ground state. In their Model A, k_1 and $k_{-1} \ll \lambda_1$ and λ_2 and $K_{\mathrm{app}} = K$ is then a good approximation. When k_1 and $k_{-1} \gg \lambda_1$, the chemistry in the excited state is dominating and the apparent equilibrium constant, K_{app} is then equal to

$$K_{\mathrm{app}} = K^* \frac{\alpha\tau_1}{\beta\tau_2}$$

where α and β are the molar absorption coefficients and τ_1 and τ_2 the lifetimes of M* and ML* (Model C). In systems where k_1 and $k_{-1} \approx \lambda_1$ and λ_2, one has to use numerical simulations to deduce the rate constants from the experimental data (Model B). K^* is the equilibrium constant for the formation of ML*.

Billard and Lützenkirchen (2003) discuss a number of time-resolved laser fluorescence studies of uranyl complexes using the model outlined above. For example, in the uranyl–hydroxide system can be described by either Model A or B. Lopez and Birch (1997) observed two decay times that were independent of pH in the range 2.5–4.5, indicating that $K_{\mathrm{app}} = K$.

(a) Quenching mechanisms of the uranyl ion

Quenching is in general described by the Stern–Volmer mechanism as described previously; it can proceed through a number of different reactions as outlined by Baird and Kemp (1997). Quenching by halide ions most likely takes place by electron transfer as indicated by the fact that the quenching efficiency depends on the oxidation potential, and decreases in the order $I^- > Br^- > Cl^- > F^-$; metal ions in low oxidation states like Ag^+, Fe^{2+}, and Mn^{2+} are also efficient quenchers that also act through an electron transfer mechanism.

Many organic compounds are very efficient quenchers and the mechanism involves either a process where the quencher forms a short-lived exciplex with the excited uranyl, or an electron transfer. In the latter case, the relative quenching rate depends on the ionization potential of the quencher (as for the halide ions). Burrows and Kemp (1974) have reviewed quenching reactions with different alcohols where hydrogen abstraction may be an important quenching mechanism as indicated by large primary hydrogen isotope effects.

The lifetime of the excited uranyl ion, $(UO_2^{2+})^*$ depends strongly on the total concentration of uranium (self-quenching), an observation that has been described by Deschaux and Marcantonatos (1979) and others as due to the formation of the binuclear exciplex

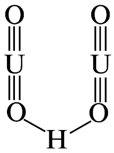

(b) Photochemistry of the uranyl(VI) ion

Rabinowitch and Belford (1964), Balzani and Carassiti (1970), and Güsten (1983) have reviewed the photochemistry of uranyl(VI) with organic substrates. The reactions involve oxidation of the substrate and reduction to uranyl(V); in the absence of oxygen, a subsequent fast reaction leads to formation of uranyl (VI) and uranium(IV). In the presence of oxygen, uranyl(V) is rapidly oxidized to uranyl(VI) and accordingly the uranyl(VI) ion acts as a photo-catalyst, e.g. for the oxidation of alkanes, alkenes, alcohols, and aldehydes. The uranyl ion has also been used as a photo-catalyst for DNA footprinting as described in Section 5.11. All these reactions seem to take place by hydrogen abstraction from a C–H bond, followed by uranium-mediated product formation (Wang *et al.*, 1995). The mechanism can schematically be described by the following reactions, where SH_2 is the organic substrate, and S_{ox} the final oxidation product, an aldehyde or carboxylic acid.

$$SH_2 + (UO_2^{2+})^* \rightarrow SH^+ + UO_2^+ + H^+;$$
$$2SH^+ \rightarrow SH_2 + S_{ox};$$
$$2UO_2^+ \rightarrow UO_2^{2+} + U(\text{IV}).$$

5.11 ORGANOMETALLIC AND BIOCHEMISTRY OF URANIUM

There is an extensive organometallic chemistry for uranium(III) and uranium (IV); in fact, most of the organometallic chemistry as described in Chapters 25 and 26 deals with uranium and a detailed description of the synthesis and properties of organometallic uranium compounds can be found there. For historical reasons, we will here mention a few examples; the field was started by Wilkinson with the preparation of $(\eta^5\text{-cyclopentadienyl})_3UCl$ (Reynolds and Wilkinson, 1956), followed by reports from Fischer and Hristidu (1962) of additional cyclopentadienyl compounds, e.g. tetrakis(η^5-cyclopentadienyl)uranium(IV) (Fischer and Hristidu, 1962). The 'sandwich' compound uranocene, bis(π-cyclooctatetraene) uranium(IV), $U(C_5H_5)_2$ was prepared by Streitweiser and Müller-Westerhoff (1968). These compounds are π-complexes where uranium is coordinated by the cyclic ligands through their delocalized π-orbitals. Other complexes with the cyclopentadienyl ion $C_5H_5^-$ are $U(\eta^5\text{-}C_5H_5)_3$, $U(\eta^5\text{-}C_5H_5)_4X$, where X is an alkyl group, an alkoxy group, or BH_4. For description of these and other metal organic compounds the reader is referred to Chapter 25.

The biochemistry of uranium is totally dominated by investigations of the coordination of the uranyl(VI) ion to proteins, DNA/RNA and polysaccharide coatings in cell walls. In the proteins, the bonding takes place at the carboxylate and amino groups, in DNA/RNA at the phosphate groups, and in the polysaccharides at deprotonated OH groups. The strong binding of uranium has been used to make heavy-atom derivatives in protein crystallography (Tame, 2000) and as staining reagent in electron microscopy (Gray, 1994, 2001).

Photochemical oxidation of polydeoxynucleotides by UO_2^{2+} has been used for footprinting of DNA (Nielsen *et al.*, 1988). This is a technique used to identify the DNA region where a particular protein is bonded. It involves labeling of one end of a DNA chain with ^{32}P; addition of UO_2^{2+} that binds to the phosphate groups and then irradiation with near-UV light to obtain photo-excited uranyl(VI) that abstracts a hydrogen from a nearby C–H group, resulting in cleavage of the DNA backbone diester chain both in single- and double-stranded DNA. The cleavage is random and not sensitive to the base sequence; it results in ^{32}P fragments of different lengths that can be identified through gel electrophoresis. When a protein is bonded to certain base sequences of DNA, these regions are not accessible to UO_2^{2+} and are therefore protected from cleavage; this results in a different fragmentation pattern and the base sequence where protein bonding takes place can therefore be identified. For details, see Stryer (1988). An important advantage of this method, as compared to the use of DNA-se enzymes as 'scissor', is the small size of the uranyl(VI) ion compared to the enzymes.

The uranyl ion has been used as a very efficient regioselective and stereoselective catalyst for the synthesis of oligonucleotides in solution (Sawai *et al.*, 1989, 1990, 1992, 1996; Shimazu *et al.*, 1993).

Uranium in the form of uranyl(VI) compounds is taken up by living organisms. In mammals the uranium is bonded to proteins, e.g. transferrin, with a residence time of several hours during which it is gradually transported and incorporated into bone tissue. The residence time is long and removal requires an extensive treatment with different sequestering agents (Scapolan, 1998). A detailed discussion of the behavior of uranium and other actinides is given in Chapter 31.

5.12 ANALYTICAL CHEMISTRY

There is wide array of options available for the determination of uranium including both classical wet chemical and instrument-based spectrometric techniques. The purpose of this section is to provide an overview of the analytical techniques and methods applicable to the determination of uranium in a variety of matrices with an emphasis on those techniques and methods useful for samples with uranium concentrations larger than 1 μg per gram of sample. An extensive review of the techniques and methods that are used for the determination of uranium at trace and ultra-trace (less than 1 μg per gram of sample) concentrations in geological, environmental, and biological matrices is given in Chapter 30.

5.12.1 Chemical techniques

(a) Sample preparation

Most bulk analytical techniques require that a stable, aqueous solution be prepared prior to analysis and element determination. The dissolution of uranium containing compounds and materials is typically performed either by fluxed fusion decomposition or acid dissolution. Fluxed fusion decomposition is the first step in many standard classical wet chemical procedures used for the determination of uranium at major and minor concentrations in uranium containing ores. Ingamells and Pitard (1986) describe a chemical method for the determination of uranium in silicate minerals. In this method a several-gram quantity of silicate material is decomposed via fusion with Na_2O_2 in a platinum crucible. The fusion mass is dissolved in dilute HNO_3 and uranium is precipitated with a mixture of Na_2CO_3 and K_2CO_3 (Sandell, 1959). This precipitate is evaporated and redissolved in dilute HNO_3 before further purification or direct determination of uranium. Other fluxes that can be used for the fusion of uranium containing materials include hydroxides, carbonates, bisulfates, hydrosulfates, pyrosulfates, tetraborates, and metaborates (Dean, 1995).

Nearly all uranium compounds and uranium containing alloys can be dissolved in HNO_3. As briefly discussed in Section 5.6.4, uranium metal dissolves very rapidly in HCl, but a voluminous black residue is left unless a small amount of fluosilicate ion is present. uranium containing minerals, such as autunite, carnallite, gummite, phosphuranylite, torbernite, tyuyammite, uraninite, and uranophane will dissolve via open vessel digestion with HNO_3, HCl, and H_2SO_4 (Meites, 1963). Acid leaching with HNO_3, HCl, or H_2SO_4 has been used for industrial scale recovery of uranium from its ores. The various leaching processes for uranium ores are discussed in more detail in Section 5.4.3. A mixture of HF and HNO_3 can be employed when dissolution of silicates is required. When this mixture is used, complete recovery of uranium requires conversion of UF_4 to a soluble form by fuming with $HClO_4$ or H_2SO_4 or by complexation of F^- with H_3BO_3.

Separation and preconcentration of uranium can be achieved by most of the common chemical and physical separation methods: precipitation, coprecipitation, volatilization, electrolysis, liquid–liquid extraction, and ion-exchange chromatography. The simplest methods for the separation of uranium from solution are by precipitation or coprecipitation. Precipitation of uranium can be accomplished using inorganic and organic precipitants (Gindler, 1962). The formation of many precipitates in uranium containing solutions that also contain other anions and cations typically yields a group separation of uranium along with other elements. Uranium will coprecipitate from a carbonate-free solution with Fe(III) and Al(III) hydroxides. Carbonate is removed by heating the solution. Coprecipitation is accomplished by adding a macroscopic amount of Fe(III) or Al(III) to an acidified solution and adjusting the solution pH to basic with the addition of NH_4OH. Separation of uranium can also be accomplished by coprecipitation with $Ca(OH)_2$, $(NH_4)_2CO_3$, and $(NH_4)_2S$ (Rodden and Warf, 1950). Precipitation of uranium from acidic solutions can be performed fairly selectively as a peroxide or oxalate.

Electrochemical separation of uranium can be accomplished via Hg-cathode electrolysis and electrolytic deposition on a variety of solid metal electrodes (Casto, 1950) as well as electrodialysis and pyrometallurgical processes (Gindler, 1962). Electrodeposition from an electrolyte matrix adjusted to pH 3.5 onto a metal planchet is the most common method for the preparation of a thin sample for high-resolution alpha-spectrometric determination (Kressin, 1977 and references therein). Further discussion on sample preparation by electrodeposition for alpha spectrometry is given in Chapter 30, section 3.1.

Liquid–liquid extraction of uranium can be accomplished using organic acids, ketones, ethers, esters, alcohols, and phosphoric acid derivatives (Lally, 1992). In many cases, extraction of uranium can be greatly enhanced with the addition of nitrate salts to the solution (Gindler, 1962). Uranium(IV) can be extracted with ethyl acetate after treatment of an acidified solution with $Al(NO_3)_3 \cdot 9H_2O$ (Guest and Zimmerman, 1955). Uranium(VI) can be extracted with 25% TBP in toluene (Mair and Savage, 1986). Methyl isobutyl ketone has been used in large-scale uranium-separation processes. Recently, several uranium-specific exchange resins have been developed for the separation of uranium from acidic matrices. While these resins function by passing uranium-containing solution down an exchange column containing the material, the separation is based on liquid–liquid extraction. One of these extraction chromatographic resins, TRU Spec resin, consists of octyl(phenyl)-*N*,*N*-diisobutylcarbamoylmethylphosphine oxide in tri(*n*-butyl)phosphate supported by an inert polymeric substrate, Amberlite XAD-7 (Horwitz *et al.*, 1993). The second extraction chromatographic resin, U/TEVA Spec resin consists of diamylphosphonate sorbed on Amberlite XAD-7. This resin possesses tetravalent ion specificity.

Cation exchange is not a commonly used method for the separation of uranium due to the lack of selectivity of the UO_2^{2+} cation over other divalent metal ions. UO_2^{2+} forms strong anionic sulfate and weaker chloride complexes that can be the basis for uranium separation from other metals in solution via anion exchange. Uranium separations can be performed by use of basic anion-exchange resins such as Dowex-1, Dowex-2, Amberlite IRA-400, Amberlite IRA-410, and Bio-Rad AG1X8 from solutions of HCl, HF, HNO_3, H_2SO_4, $(NH_4)_2CO_3$, and H_3PO_4 (Gindler, 1962).

(b) Sample analysis

Total analysis techniques (also known as classical techniques) are the most accurate of all the available methods for uranium determination. Because these techniques provide definitive results, they are typically used as the basis for establishing primary uranium standards and are used extensively in the areas of material control, accountability, and safeguards. Volumetric and gravimetric techniques have both been applied for high accuracy determination of macroscopic quantities of uranium.

Volumetric techniques provide the highest precision and accuracy for uranium determination. Volumetric determination of uranium can be performed via complexation titration with ethylenediaminetetraacetic acid (EDTA). However, the most widely used method is a redox titration where U(VI) is first reduced (e.g. in a Jones reductor) and then back-titrated via oxidation with $KMnO_4$ or Ce(IV) using 1,10-phenanthroline as an indicator (Dean, 1995). The method of Davies and Gray (1964) utilizes excess Fe(II) to reduce U(VI) to U(IV) in a concentrated

H_3PO_4 solution containing H_2NSO_3H. The Fe(II) is selectively oxidized with the addition of HNO_3 in the presence of a Mo(IV) catalyst. After addition of H_2SO_4, U(IV) is titrated with standard Cr(VI) with Ba-diphenylaminesulfonate as an indicator. A modified version of this method has been developed in which the end point is determined potentiometrically (American Society for Testing and Materials, 1994, ASTM C1267–94). This method is exceptionally accurate (relative bias –0.042% and within laboratory variation 0.042%), but requires milligrams of uranium in the sample aliquot.

The necessity for the preparation of redox standard solutions can be circumvented by electrochemical titrations. Coulometric titration of uranium can be performed in both constant-current and controlled-potential titration. Procedures for oxidative coulometric titration of U(IV) and reductive coulometric titration of U(VI) in constant-current mode have been developed. Oxidative coulometric titration of U(IV) is performed via the electrogeneration of Ce(IV) subsequent to preparation of U(IV) by reduction with cadmium amalgam (Furman *et al.*, 1953). Reductive coulometric titration of U(VI) is performed with electrogenerated Ti(III) at a platinum cathode with amperometric endpoint detection (Kennedy and Lingane, 1958). Errors are as low as ±0.3%. An improved version of this method has been developed that is capable of a precision of 0.008% (Marinenko *et al.*, 1983). Methods for oxidative controlled-potential titration of U(IV) and reductive controlled-potential titration of U(VI) have been developed. Oxidative controlled-potential titration of U(IV) can be performed in 1 M $HClO_4$ at a platinum electrode (Boyd and Menis, 1961). The most established controlled-potential coulometric titration of uranium utilizes a mercury pool for reduction of U(VI) (McEwen and DeVries, 1959). Experimental conditions have been established which enable uranium to be determined via controlled-potential coulometric titration at a platinum electrode (Davies *et al.*, 1970). Use of the platinum electrode has several advantages including the possibility of simultaneous consecutive determinations of Fe(III) and U(VI), or Pu(IV) and U(VI) in the same cell.

Gravimetric determination of the uranium content of uranium ores can be performed via the sulfide–carbonate–hydroxide method. In this method, the solid U-containing ore sample is dissolved with HNO_3 and H_2SO_4. Arsenic is first removed via addition of HBr. A treatment of the acidic solution with H_2S precipitates a large number of cations as sulfides; Co and Ni are precipitated with H_2S at low acidity; Al, Cr, and Fe are removed with subsequent addition of NH_4OH and $(NH_4)_2CO_3$;. The solution is then reacidified with HCl and U is precipitated with NH_4OH. The precipitate is filtered, washed, ignited, and determined gravimetrically as U_3O_8. Alternatively, the sample can be decomposed via fluxed fusion followed by dissolution in HCl and precipitation of U(IV) on the addition of 6% cupferron solution. The precipitate is filtered, washed, ignited, and determined gravimetrically as U_3O_8. This separation effectively removes Al, Cr, Mn, Zn, and PO_4^{3-} but the presence of Fe, Ti, V(V), and Zr would interfere with the uranium determination

(Dean, 1995). In general, the use of gravimetric methods is limited due to lack of specificity.

5.12.2 Nuclear techniques

The natural radioactivity inherent to uranium isotopes provides the means for their direct analysis by radiometric analytical techniques. While several radiometric techniques are amenable to the determination of uranium at concentrations higher than 1 μg per gram of sample, the most frequently used are high-resolution alpha and gamma spectrometries. Complete isotopic analysis of the naturally occurring isotopes ^{238}U, ^{235}U, and ^{234}U can be performed via high-resolution alpha spectrometry. Alpha-spectrometric determination requires complete sample dissolution, chemical separation of uranium, followed by preparation of a thin source, typically via electrodeposition or precipitation (Kressin, 1977 and references therein). Either ^{232}U or ^{236}U can be used as isotopic recovery spikes. Backgrounds and efficiencies of typical alpha spectrometers equipped with a 450-mm^2 ion-implanted Si detector would require a total of 0.4 μg of natural uranium to achieve 10% counting statistics for a 24-h sample count. Examples of several applications of alpha spectrometry for the determination of uranium and the measurement of U-series disequilibria are given in Ivanovich and Murray (1992).

High-resolution high-purity germanium (HPGe) detectors are capable of high-specificity measurement of individual radionuclide γ-rays and virtually eliminates the need for chemical treatment of samples. Due to its long half-life, the quantification of ^{238}U is usually based on the measurement of the 92.5 keV or the 63.3 keV γ-ray doublets produced by the short-lived daughter ^{234}Th provided secular equilibrium has been achieved (Harbottle and Evans, 1997). Determination of ^{238}U can also be performed by measurement of the 1001 keV γ-ray from the decay of ^{234m}Pa ($t_{1/2} = 1.175$ minutes). The low branching ratio for this γ-ray precludes its use for samples with uranium concentrations smaller than 10 μg per gram of sample. In the case of ^{235}U, direct quantification can be performed using its 185.7-keV γ-ray. A correction for interference from the 186.1 keV γ-ray, ^{226}Ra ($t_{1/2} = 1600$ years), is required for samples in secular equilibrium.

Radiometric determination of uranium can also be performed utilizing scintillation detection after chemical separation of uranium from interfering radionuclides. A standard test method for the determination of uranium in water by high-resolution alpha liquid-scintillation spectrometry utilizes a selective extractive scintillator solution containing dialkyl phosphoric acid (ASTM D6239–98, 1998).

Activation analysis of uranium is typically performed subsequent to irradiation with thermal neutrons. Uranium is essentially unique among naturally occurring elements in that neutron activation analysis (NAA) can be performed by detection of delayed neutrons (Parry, 1991). This method is highly specific for uranium and has been used for many years in the exploration of uranium ores. NAA with delayed-neutron detection can be automated for online and unattended determination of uranium content in solid and liquid samples.

The coupling of NAA with high-resolution gamma spectrometric detection (instrumental neutron activation analysis, or INAA) yields a highly specific and sensitive method for the determination of uranium. At high concentrations, uranium can be determined by INAA via measurement of the 74 keV γ-ray photo peak from the decay of ^{239}U ($t_{1/2} = 23.5$ minutes). Minor and trace quantities of uranium are typically determined by INAA via the ^{238}U(n,γ)^{239}U(β^-, 23.5 minutes)^{239}Np reaction with measurement of the 105 keV γ-ray photo peak from the decay of ^{239}Np (Parry, 1991). Enhanced sensitivity can be achieved by performing post-irradiation chemical separations (radiochemical neutron activation analysis, or RNAA) (Anders *et al.*, 1988). Both INAA and RNAA are applicable to the determination of trace and ultra trace concentrations of uranium and are further discussed in Chapter 30, section 3.3.

5.12.3 Spectrometric techniques

Uranium is amenable to determination by several fundamentally different spectrometric techniques including spectrophotometry, atomic absorption spectrometry (AAS), atomic emission spectrometry (AES), fluorometry, phosphorimetry, X-ray fluorescence (XRF), and mass spectrometry.

Spectrophotometric determination of uranium can be performed subsequent to sample dissolution, separation of uranium, complexation with an appropriate chromophore, and colorometric determination by comparison with prepared standards. For example, uranium can be determined colorimetrically in the aqueous phase after complexation with 4-(2-pyridylazo)recorcinol (PAR) (Pollard *et al.*, 1959) or as an organic-miscible complex with 4-(2- pyridylazo) napthol (PAN) (Pollock, 1977).

Selectivity of uranium spectrometric determination can be improved using techniques based on atomic absorption and emission. The determination of uranium via AAS techniques can be performed using flame sources (FAAS) or graphite furnace sources (GFAAS). FAAS determination of uranium is performed via the 358.5 nm absorption line using a nitrous oxide/acetylene flame. The detection limit for AAS is 40 μg mL^{-1} for uranium in solution (Dean, 1995). GFAAS can achieve detection limits of 30 ng mL^{-1} in much smaller sample volumes (20 μL). Both AAS and GFAAS are single-element methods that can achieve accuracies greater than $\pm 1\%$ if uranium concentrations are significantly higher than the detection limits.

Sensitivity of atomic spectrometric techniques can be improved via excitation in a high-temperature inductively coupled plasma (ICP) source followed by atomic emission spectrometric (AES) determination. The emission spectrum of U consists of thousands of resolvable lines. ICPAES determination of uranium based on the 385.96 nm emission line can achieve detection limits of 20 ng mL^{-1} with accuracies of ±1% if concentrations are significantly higher than the detection limits (Dean, 1995). While all atomic spectrometric techniques generally determine total uranium concentration without isotopic selectivity, a high-resolution ICPAES has been developed for the determination of uranium isotopic ratios (Edelson, 1992).

Uranium is unique among most elements in that it can be determined directly via fluorometry without the addition of a fluorescent chelating agent. The fluorometric technique can determine uranium concentrations as low as 5 ng mL^{-1} (ASTM D2907–91, 1991a). Superior detection limits can be achieved by utilizing the ability of uranyl ions to phosphoresce when excited to a triplet state. The uranyl ion can be directly determined phosphorometrically in a H_3PO_4 or H_2SO_4 solution. The pulsed-laser phosphorometric technique can determine uranium concentrations as low as 50 pg mL^{-1} (ASTM D5174–91, 1991b). Further discussion of the fluorometric and phosphorometric techniques is given in Chapter 30 (Sections 30.4.1 and 30.4.2, respectively).

X-ray fluorescence (XRF) can provide qualitative identification and quantitative determination of uranium in a variety of matrices. A procedure for the determination of uranium in soils can be found in ASTM C1255-93 (1993). This procedure can be used to determine as little as 20 μg per gram of uranium.

Mass spectrometry is the most sensitive method for the determination of uranium. In contrast to most of the atomic spectrometric techniques outlined previously, mass spectrometry also provides the means for the determination of uranium isotopic composition. As such, mass spectrometry is an essential tool for the determination of uranium in nuclear fuel cycle applications, material control and accountability, environmental chemistry, geochemistry, and cosmo-chemistry. While a variety of mass spectrometric methodologies have been applied to the determination of uranium (Section 30.5; Wolf, 1999 and references therein), the most commonly used mass spectrometric methods for the determination of uranium are electron-impact gas source mass spectrometry, thermal ionization mass spectrometry (TIMS), and inductively coupled plasma mass spectrometry (ICPMS).

Electron-impact gas source mass spectrometry is used specifically for uranium isotopic analysis to monitor U-enrichment processes. Typically, UF_6 is analyzed in ultracentrifuge and thermal diffusion processes and uranium vapor is analyzed in laser enrichment processes (Platzner, 1997). Measurement by gas source mass spectrometry requires approximately 100 mg of sample. Such instruments are used in production line applications and can achieve a precision of ±0.40% for UF_6 with >1% ^{235}U enrichment (Nagatoro *et al.*, 1980). Highly portable quadrupole mass analyzers have been designed for UF_6 isotopic analysis in nuclear safeguard applications (Depaus *et al.*, 1987). A standard method for the isotopic analysis of UF_6 with an electron-impact gas source mass spectrometer utilizing a single standard has been developed for nuclear fuel cycle applications (ASTM C1344-97, 1997).

TIMS is one of the most precise and accurate methods for single element isotope ratio determination and is used when small masses of uranium are analyzed. Instruments configured with multiple Faraday detectors can routinely determine major uranium isotope ratios to a precision better than 0.05% (Walder, 1997) and require less than 1 μg of U. TIMS is a commonly used method in nuclear fuel cycle applications including the isotopic analysis of hydrolyzed UF_6 and uranyl nitrate solutions (ASTM C1413–99, 1999) and for the determination of atom percent fission in irradiated nuclear fuels (ASTM E244-80, 1980). Determination of uranium concentrations is performed via isotope dilution (ID) analysis typically using ^{233}U as an isotopic spike. The high sensitivity of TIMS makes this method suitable for the determination of uranium concentrations and isotopic composition at trace and ultra-trace concentrations such as in geological and cosmo-chemical materials. Procedures and applications of TIMS to uranium measurements in geological samples are summarized in Chen *et al.* (1992) and references therein. The TIMS methodology is capable of determining $^{234}U/^{238}U$ ratios with a precision of 0.5% (2σ) for a sample size of 5×10^9 ^{234}U atoms. The primary disadvantage of TIMS is that extensive sample preparation is required and only one element can be determined in a given prepared sample. Further discussion of the application of TIMS to trace and ultratrace analysis is given in Chapter 30, section 5.1.

A review of the trends of the techniques used for elemental determination indicates that ICPMS is one of the most commonly used methods today (Lipschutz *et al.*, 2001). ICPMS has found applications for the determination of uranium in waters, soils, sludges, wastes, nuclear materials, biological, geological, and cosmo-chemical materials (Chapter 30, section 5.4 and references therein). The strength of ICPMS resides in its high sensitivity, multielement, high sample throughput capabilities. Quantification is typically performed based on external calibration using the most abundant uranium isotope ^{238}U. Solutions can be analyzed with minimal or no sample pre-treatment. Considering the sensitivities of modern state-of-the-art instruments, a minimum detection limit (MDL) of less than 100 fg in a 1 mL sample is readily attainable for uranium determination by ICPMS (Brenner *et al.*, 1998). The combination of an ICP source with a high-precision, double-focusing, mass spectrometer in a single detector configuration (HR-ICPMS) results in an instrument capable of determining less than 1 fg uranium in 1mL solution (Wolf, 1999). This corresponds to a detection limit of approximately 3×10^6 atoms of uranium. Moens and Jakubowski (1998) have published a review of HR-ICPMS instrumentation and applications. Configuration of HR-ICPMS with multiple detectors (MC-ICPMS) yields a method possessing all the attributes of HR-ICPMS with enhanced precision. The routine use of MC-ICPMS in nuclear fuel cycle applications has the potential to dramatically decrease the cost of sample analysis by means of increased sample throughput while maintaining the high precision required for fuel fabrication. A five-fold improvement in sample throughput has been demonstrated for the analysis of hydrolyzed UF_6 with accuracy and precision comparable to TIMS (Walder and Hodgeson, 1994). High sensitivity makes MC-ICPMS particularly attractive for uranium isotope determination in geo-chronological applications. A review of MC-ICPMS instrumentation and applications to uranium isotopic analysis in geological samples has been reported (Halliday *et al.*, 1998). This paper reviews results of replicate analysis of NIST SRM-906 measured by TIMS and MC-ICPMS. Precisions comparable to the best achievable TIMS precisions were achieved. The external reproducibility of MC-ICPMS was superior to TIMS. Further discussion of the application of MC-ICPMS techniques to trace and ultratrace uranium analysis is given in Chapter 30, section 5.4, of this book.

REFERENCES

Aas, W., Moukhamet-Galeev, A., and Grenthe, I. (1998) *Radiochim. Acta*, **82**, 77–82.

Abazli, H., Cousson, A., Tabuteau, A., and Pagès, M. (1980) *Acta Cryst. B*, **36**, 2765–6.

Åberg, M. (1969) *Acta Chem. Scand.*, **23**, 791–810.

Åberg, M. (1971) *Acta Chem. Scand.*, **25**, 368–9.

Åberg, M. (1976) *Acta Chem. Scand. Series A*, **30**, 507–14.

Åberg, M. (1978) *Acta Chem. Scand.*, **A32**, 101–7.

Åberg, M., Ferri, D., Glaser, J., and Grenthe, I. (1983) *Inorg. Chem.*, **32**, 3986–9.

Abraham, B. M. Flotow, H. E. (1955) *J. Am. Chem. Soc.*, **77**, 1446–8.

Abraham, B. M., Osborne, D. W., Flotow, H. E., and Marcus, R. B. (1960) *J. Am. Chem. Soc.*, **82**, 1064–8.

Ackermann, R. J., Gilles, P. W., and Thorn, R. J. (1956) *J. Chem. Phys.*, **25**, 1089–97.

Ackermann, R. J., Thorn, R. J., Alexander, C., and Tetenbaum, M. (1960) *J. Phys. Chem.*, **64**, 350–5.

Ackermann, R. J. and Rauh, E. G. (1969) *J. Phys. Chem.*, **73**, 769–78.

Ackermann, R. J., Rauh, E. G., and Chandrasekharaiah, M. S. (1969) *J. Phys. Chem.*, **73**, 762–9.

Ackermann, R. J. and Rauh, E. G. (1972) *High Temp. Sci.*, **4**, 496–505.

Ackermann, R. J. and Chang, A. T. (1973) *J. Chem. Thermodyn.*, **5**, 873–90.

Ackermann, R. J. and Rauh, E. G. (1973) *J. Inorg. Nucl. Chem.*, **35**, 3787–94.

Ackermann, R. J., Rauh, E. G., and Rand, M. H. (1979) in *Thermodynamics of Nuclear Materials,* Proc. Symp. 1979, International Atomic Energy Agency, Vienna, pp. 11–27.

Addison, C. C. and Hodge, N. (1961) *J. Chem. Soc.*, 2490–6.

Addison, C. C. (1969) *J. Chem. Soc. A*, 2457–9.

Agron, P. A. (1958) in *The Chemistry of Uranium, Collected Papers* (eds. J. J. Katz and E. Rabinowitch), USAEC Technical Information Extension, Oak Ridge, TID-5290 Book 2, pp. 610–26.

Aitken, E. A., Bartram, S. F., and Juenke, E. F. (1964) *Inorg. Chem.*, **3**, 949–54.

Aitken, E. A. and Joseph, R. A. (1966) *J. Phys. Chem.*, **70**, 1090–7.

Akin, G. A., Kackenmaster, H. P., Schrader, R. J., and Strohecker, J. W., Tate, R. E. (1950) *Chemical Processing Plant Equipment: Electromagnetic Separation Process*, Nat. Nucl. En. Ser., Div. I, 12, TID-5232, Oak Ridge, TN.

Alberman, K. B., Blakey, R. C., and Anderson, J. S. (1951) *J. Chem. Soc.*, 1352–6.

Albrecht-Schmitt, T. E., Almond, P. M., Illies, A. J., Raymond, C. C., and Talley, C. E. (2000) *J. Solid State Chem.*, **46**, 87–100.

Alcock, C. B. and Grieveson, P. (1962) *J. Inst. Method.*, **90**, 304–10.

Alcock, C. B. and Grieveson, P. (1963) *Proc. Symp. Thermodyn. Nucl. Mater.*, 1962, International Atomic Energy Agency, Vienna, STI/PUB/58, pp. 563–79.

Alcock, N. W. (1968) *J. Chem. Soc.*, 1588–94.

Alcock, N. W. and Esperas, S. (1997) *J. Chem. Soc. Dalton Trans.*, 893–6.

Alcock, N. W., Kemp, T. J., Sostero, S., and Traverso, O. (1980) *J. Chem. Soc. Dalton Trans.*, 1182–5.

Alcock, N. W., Roberts, M. M., and Chakravorti, M. C. (1980) *Acta Cryst. B*, **36**, 687–90.

Aléonard, K. B., Le Fur, Y., Champarnaud-Mesjard, J. C., Frit, B., and Roux, M. T. (1983) *J. Cryst. Growth*, **217**, 250–4.

Alexander, C. A., and Ogden, J. S., Cunningham, G. C. (1967) Battelle Memorial Institute Report, BMI-1789.

Alibegoff, G. (1886) *Liebig's Ann.*, **233**, 117–43.

Allen, A. L., Anderson, R. W., and McGill, R. M., Powell, F. W. (1950) *Electrochemical Preparation of Uranium Tetrafluoride*, part I, Low Temperature Cell, K-680.

Allen, G. C. and Griffiths, G. C. (1977) *J. Chem. Soc. Dalton Trans.*, 1144–8.

Allen, G. C. Griffiths, A. J., and Suckling, C.W. (1978) *Chem. Phys. Lett.*, **53**, 309–12.

Allen, G. C., Tempest, P. A., and Tyler, J. W. (1982) *Nature*, **295**, 48–9.

Allen, G. C. and Tyler, J. W. (1986) *J. Chem. Soc., Faraday Trans. 1*, **82**, 1367–79.

Allen, G. C. and Holmes, N. R. (1995) *J. Nucl. Mater.*, **223**, 231–7.

Allen, P. G., Bucher, J. J., Clark, D. L., Edelstein, N. M., Ekberg, S. A., Gohdes, J. W., Hudson, E. A., Kaltsyoannis, N., Lukens, W. W., Neu, M. P., Palmer, P. P., Reich, T., Shuh, D. K., Tait, C. D., and Zwick, B. D. (1995) *Inorg. Chem.*, **34**, 4797–807.

Allen, P. G., Shuh, D. K., Bucher, J. J., Edelstein, N. M., Palmer, C. E. A., Silva, R. J., Nguyen, S. N., Marquez, L. N., and Hudson, E. A. (1996a) *Radiochim. Acta*, **75**, 47–53.

Allen, P. G., Shuh, D. K., Bucher, J. J., Edelstein, N. M., Reich, T., Denecke, M. A., and Nitsche, H. (1996b) *Inorg. Chem.*, **35**, 784–7.

Allen, P. G., Bucher, J. J., Shuh, D. K., and Edelstein, N. M. (2000) *Inorg. Chem.*, **39**, 595–601.

Allen, S., Barlow, S., Halasyamani, P. S., Mosselmans, J. F. W., O'Hare, D., Walker, S., and Walton, R. I. (2000) *Inorg. Chem.*, **39**, 3791–8.

Allpress, J. G. (1964) *J. Inorg. Nucl. Chem.*, **26**, 1847–51.

Allpress, J. G. and Wadsley, A. D. (1964) *Acta Cryst.*, **17**, 41–6.

Allpress, J. G. (1965) *J. Inorg. Nucl. Chem.*, **27**, 1521–7.

Allpress, J. G., Anderson, J. S., and Hambly, A. N. (1968) *J. Inorg. Nucl. Chem.*, **30**, 1195–208.

Almond, P. M. and Albrecht-Schmitt, T. E. (2002) *Inorg. Chem.*, **41**, 1177–83.

Almond, P. M., Peper, S. M., Bakker, E., and Albrecht-Schmitt, T. E. (2002) *J. Solid State Chem.*, **168**, 358–66.

Almond, P. M. and Albrecht-Schmitt, T. E. (2004) *Am. Miner.*, **89**, 976–80.

Amberger, H.-D., Grape, W., and Stumpp, E. (1983) *J. Less Common Metals*, **95**, 181–90.

American Society for Testing and Materials (1980) ASTM E244-80, Annual Book of ASTM Standards, vol. 12.01.

American Society for Testing and Materials (1991a) ASTM D2907-91, Annual Book of ASTM Standards, vol. 11.02.

American Society for Testing and Materials (1991b) ASTM D5174-91, Annual Book of ASTM Standards, vol. 11.02.

American Society for Testing and Materials (1993) ASTM C1255-93, Annual Book of ASTM Standards, vol. 12.01.

American Society for Testing and Materials (1994) ASTM D1267-94, Annual Book of ASTM Standards, vol. 12.01.

American Society for Testing and Materials (1997) ASTM C1344-97, Annual Book of ASTM Standards, vol. 12.01.

American Society for Testing and Materials (1998) ASTM D6239-98, Annual Book of ASTM Standards, vol. 11.02.

American Society for Testing and Materials (1999) ASTM C1413-99, Annual Book of ASTM Standards, vol. 12.01.

Amme, M. (2002) *Radiochim. Acta*, **90**, 399–406.

Anders, E., Wolf, R., Morgan, J. W., Ebihara, M., Woodrow, A. B., and Janssens, M.-J., Hertogen, J. (1988) NAS-NS-3117, Office of Scientific and Technical Information, USDOE.

Andersen, R. A. (1979) *Inorg. Chem.*, **18**, 1507–9.

Anderson, A., Chieh, C., Irish, D. E., and Tong, J. P. K. (1980) *Can. J. Chem.*, **58**, 1651–8.

Anderson, R. W., and Allen, A. L., Powell, E. W. (1950) *Electrochemical Preparation of Uranium Tetrafluoride*, Part II, High Temperature Cell, K-681.

Anderson, J. S. and Johnson, K. D. B. (1953) *J. Chem. Soc.*, 1731–7.

Anderson, J. S., Edgington, D. N., Roberts, L. E. J., and Wait, E. (1954) *J. Chem. Soc.*, 3324–31.

Anderson, J. S. and Barraclough, C. G. (1963) *Trans. Faraday Soc.*, **59**, 1572–9.

Anderson, J. S. (1969) *Chimia*, **23**, 438–44.

Anderson, J. S. (1970) in *Modern Aspects of Solid State Chemistry* (ed. C. N. R. Rao), Plenum Press, New York, pp. 29–105.

Andreev, A. V., Bartashevich, M. I., Deryagin, A. V., Havela, L., and Sechovský, V. (1986) *Phys. Status Solidi. A*, **98**, K47–K51.

Andreev, A. V., Zadvorkin, S. M., Bartashevich, M. I., Goto, T., Kamarád, J., Arnold, Z., and Drulis, H. (1998) *J. Alloys Compds*, **267**, 32–6.

Andres, H. P., Krämer, K., and Güdel, H.-U. (1996) *Phys. Rev B*, **54** (6), 3830–40.

Andresen, A. F. (1958) *Acta Crystallogr.*, **11**, 612–14.

Andrieux, L. (1948) *Rev. Met.*, **45**, 49–59.

Andrieux, L. and Blum, P. (1949) *C. R. Acad. Sci.*, **229**, 210–12.

Anonymous (1955) *Purex Technical Manual*, Chemical Development Subsection, Separations Technology Section, Engineering Department, Hanford Atomic Products Operation, declassified with deletion as HW-31000 DEL, ch.II, p. 202, fig. II-1.

Anson, C. E., Al-Jowder, O., Upali, A., Jayasooriya, U. A., and Powell, A. K. (1996) *Acta Cryst. C*, **52**, 279–81.

Anthony, A. M., Kiyoura, R., and Sata, T. (1963) *J. Nucl. Mater.*, **10**, 8–14.

Antill, J. E., Barnes, E., and Gardner, M. (1961) *Prog. Nucl. Energy, Div. V, Metallurgy and Fuels* (eds. H. H. Finniston and J. P. Howe), Pergamon Press, Oxford, vol. 1. pp. 9–18.

Appleman, D. E. and Evans, H. T. (1965) *Am. Miner.*, **50**, 825–42.

Arajs, S. and Colvin, R. V. (1964) *J. Less Common Metals*, 7, 54–66.

Arendt, J., Powell, E. W., and Saylor, H. (1957) A brief guide to UF_6-Handling, K-1323.

Arko, A. J. and Schirber, J. E. (1979) *J. Physique*, Suppl. 40, Coll. C4, 9–14.

Aronson, S. and Belle, J. (1958) *J. Chem. Phys.*, **29**, 151–8.

Aronson, S. and Clayton, J. C. (1960) *J. Chem. Phys.*, **32**, 749–54.

Aronson, S. and Clayton, J. C. (1961) *J. Chem. Phys.*, **35**, 1055–8.

Aronson, S., Rulli, J. E., and Schaner, B. E. (1961) *J. Chem. Phys.*, **35**, 1382–8.

Asami, N., Nishikawa, M., and Taguchi, M. (1975)in *Thermodynamics of Nuclear Materials,* Proc. Symp. 1974, vol. I, International Atomic Energy Agency, Vienna, pp. 287–94.

Atencio, D., Neumann, R., and Silva, A. J. G. C. (1991) *Can. Miner.*, **29**, 95–105.

Atencio, D., Carvalho, F. M. S., and Matioli, P. A. (2004) *Am. Miner.*, **89**, 721–4.

Atoji, M. and McDermott, M. J. (1970) *Acta Crysallogr. B*, **26**, 1540–4.

Aukrust, E., Førland, T., and Hagemark, K. (1962) in *Thermodynamics of Nuclear Materials,* Proc. Symp. 1962, International Atomic Energy Agency, Vienna, pp. 713–22.

Aurov, N. A. and Chirkst, D. E. (1983) *Radiokhimiya*, **25**, 468–73.

Aurov, N. A., Volkov, V. A., and Chirkst, D. E. (1983) *Radiokhimiya*, **25**, 366–72.

Auzel, F. and Malta, O. (1983) *J. Phys.(Paris)*, **44**, 201–6.

Avens, L. R., Bott, S. G., Clark, D. L., Sattelberger, A. P., Watkin, J. G., and Zwick, B. D. (1994) *Inorg. Chem.*, **33**, 2248–56.

Avignant, D. and Cousseins, J.-C. (1971) *Compt. Rend. C*, **272**, 2151–3.

Avignant, D., Vedrine, A., and Cousseins, J.-C. (1977) *Compt. Rend. C*, **284**, 651–4.

Avignant, D., Mansouri, I., Sabatier, R., and Cousseins, J.-C. (1980) *Acta Crystallogr. B*, **36**, 664–6.

Avignant, D., Mansouri, I., Sabatier, R., and Cousseins, J.-C. (1982) *Acta Crystallogr. B*, **24**, 1968–38.

Babelot, J. F., Brumme, G. D., Kinsman, P. R., and Ohse, R. W. (1977) *Atomwirtsch. Atomtech.*, **22**, 387–9.

Bacher, W. and Jacob, E. (1980) Verbindungen mit Fluor, in *Gmelin Handbuch der Anorganischen Chemie,* (1980) System no. 55, Uranium, Suppl. vol. C8, Springer, Berlin.

Bacher, W. and Jacob, E. (1982) *Chemiker-Zeitung*, **106** (3), 117–36.

Bacher, W. and Jacob, E (1986) Uranium hexafluoride, its chemistry related to its major applications, in *Handbook on the Physics and Chemistry of the Actinides* (eds. A. J. Freeman and C. Keller), Elsevier, Amsterdam, vol. 4, ch. 1, 1–38.

Bacmann, M. (1973) *Acta Crystallogr.*, **B29**, 1570–2.

Baes, C. F. Jr, Zingeno, R. A., and Coleman, C. F. (1958) *J. Phys. Chem.*, **62**, 129–35.

Baes, C. F. Jr and Mesmer, R. E. (1976) *The Hydrolysis of Cations,* John Wiley, New York.

Baer, Y. (1984) Electronic spectroscopy studies, in *Handbook on the Physics and Chemistry of the Actinides,* vol. 1, ch. 4, (eds. J. P. Desclaux and A. J. Freeman), Elsevier, Amsterdam, 271–340.

Bagnall, K. W., Brown, D., and Deane, A. M. (1962) *J. Chem. Soc.*, 1655–7.

Bagnall, K. W., Brown, D., and du Preez, J. G. H. (1964) *J. Chem. Soc.*, 2603–8.

Bagnall, K. W., Brown, D., Jones, P. J., and du Preez, J. G. H. (1965) *J. Chem. Soc.*, 350–3.

Bagnall, K. W. (1967) in *Halogen Chemistry of the Actinides,* (ed. V. Gutman), Academic Press, London, vol. 3, ch. 7.

Bagnall, K. W., Brown D., and Easey, J. F. (1968) *J. Chem. Soc. A*, 288–92.

Bagnall, K. W. and Wakerley, M. W. (1974) *J. Less Common Metals*, **35**, 267–74.

Bagnall, K. W., du Preez. J. G. H., Gellatly, B. J., and Holloway, J. H. (1975) *J. Chem. Soc. Dalton Trans.*, 1963–8.

Bagnall, K. W. (1979) Complex compounds of uranium, in *Gmelin Handbook of Inorganic Chemistry*, E 1 Suppl., 1–223.

Bagnall, K. W. (1987) The actinides, in *Comprehensive Coordination Chemistry* vol. 3, ch. 40 (eds. G. Wilkinson, R. D. Gillard, and J. A. McCleverty), Pergamon Press, New York, 1129–228.

Baïchi, M., Chattillon, C., and Guéneau, Le Ny, J. (2002) *J. Nucl. Mater.*, **303**, 196–9.

Baird, C. P. and Kemp, T. J. (1997) *Prog. Reaction Kinetics*, **22**, 87–139.

Bakakin, V. V. (1965) *Zh. Strukt. Khim.*, **6**, 563–6; *J. Struct. Chem.* (*USSR*), **6**, 536–9.

Baker, R. D., Hayward, B. R., Hull, G., Raich, B., and Weiss, A. R. (1946) *Preparation of Uranium Metal by the Bomb Method*, LA-472.

Balzani, V. and Carassiti, V. (1970) *Photochemistry of Coordination Compounds,* Academic Press, London, ch. 15.

Bannister, M. J. (1967) *J. Nucl. Mater.*, **24**, 340–2.

Bannister, M. J. and Taylor, J. C. (1970) *Acta Crystallogr.*, **B26**, 1775–81.

Bannister, M. J. and Buykx, W. J. (1974) *J. Nucl. Mater.*, **55**, 345–51.

Barash, Y. B., Barak, J., and Mintz, M. H. (1984) *Phys. Rev. B*, **29**, 6096–104.

Bard, A. J. and Parsons, R. (1985) *Standard Potentials in Aqueous Solution,* Marcel Dekker, New York.

Bardin, N., Rubini, P., and Madic, C. (1998) *Radiochim. Acta*, **83**, 189–94.

Barnard, R., Bullock, J. I., and Larkworthy, L. F. (1967) *Chem. Comm.*, 1270–2.

Barnard, R., Bullock, J. I., and Larkworthy, L. F. (1972a) *J. Chem. Soc. Dalton Trans.*, 964–70.

Barnard, R., Bullock, J. I., Gellatly, B. J., and Larkworthy, L. F. (1972b) *J. Chem. Soc. Dalton Trans.*, 1932–8.

Barnard, R., Bullock, J. I., Gellatly, B. J., and Larkworthy, L. F. (1973) *J. Chem. Soc. Dalton Trans.*, **6**, 604–7.

Barrett, C. S., Mueller, M. H., Hitterman, R. L. (1963) *Phys. Rev.* **129**, 625–9.

Barton, C. J., Friedman, H. A., Grimes, W. R., Insley, H., Moore, R. E., and Thoma, R. E. (1958) *J. Am. Ceram. Soc.*, **41**, 63–9.

Bartram, S. F., Juenke, E. F., and Aitken, E. A. (1964) *J. Am. Ceram. Soc.*, **47**, 171–5.

Bartram, S. F. (1966) *Inorg. Chem.*, **5**, 749–54.

Bartram, S. F. and Fryxell, R. E. (1970) *J. Inorg. Nucl. Chem.*, **32**, 3701–6.

Bartscher, W. and Sari, C. (1983) *J. Nucl. Mater.*, **118**, 220–3.

Bartscher, W., Boeuf, A., Caciuffo, R., Fournier, J. M., Kuhs, W. F., Rebizant, J., and Rustichelli, F. (1985) *Solid State Commun.*, **53**, 423–6.

Baskin, Y. and Shalek, P. D. (1964) *J. Inorg. Nucl. Chem.*, **26**, 1679–84.

Baskin, Y. (1969) *J. Inorg. Nucl. Chem.*, **29**, 2480–2.

Basnakova, G., Spencer, A. J., Palsgard, E., Grime, G. W., and Macaskie, L. E. (1998) *Environ. Sci. Technol.*, **32**, 760–5.

Bates, J. L. (1964) USAEC Hanford Report, HW-81603.

Bates, J. L. (1966) *J. Am. Ceram. Soc.*, **49**, 395–6.

Bates, J. L., Hinman, C. A., and Kawada, K. (1967) *J. Am. Ceram. Soc.*, **50**, 652–6.

Bates, J. K., Bradley, J. P., Teetsov, A., Bradley, C. R., and Buchholtz ten Brink, M. (1992) *Science*, **256**, 469–71.

Battles, J. E., Shinn, W. A., and Blackburn, P. E. (1972) *J. Chem. Thermodyn.*, **4**, 425–39.

Bayliss, P., Mazzi, F., Munno, R., and White, T. J. (1989) *Miner. Mag.*, **53**, 565–9.

Bayovlu, A. S. and Lorenzelli, R. (1984) *Solid State Ionics*, **12**, 53–66.

Beals, R. J. and Handwerk, J. H. (1965) *J. Am. Ceram. Soc.*, **48**, 271–4.

Bean, A. C., Campana, C. F., Kwon, O., and Albrecht-Schmitt, T. E. (2001a) *J. Am. Chem. Soc.*, **123**, 8806–10.

Bean, A. C., Ruf, M., and Albrecht-Schmitt, T. E. (2001b) *Inorg. Chem.*, **40**, 3959–63.

Beaudry, B. J. and Daane, A. H. (1959) *Trans. Met. Soc. (AIME)*, **215**, 199–203.

Beck, H. P. and Kuehn, F. (1995) *Z. Anorg. Allg. Chem.*, **621**, 1659–62.

Beck, M. T. and Nagypál, I. (1990) *Chemistry of Complex Equilibria,* Harwood Ltd. Publishers, New York.

Becker, E. W. (1979) in *Uranium Enrichment* (ed. S. Villani), Springer, Berlin, p. 245.

Becker, J. S. and Dietze, H.-J. (1998) *Spectrochim. Acta*, **52B**, 177–87.

Becquerel, H. (1896) *C.R. Acad. Sci.*, **122**, 501–3.

Belbeoch, B., Boivineau, J. C., and Pério, P. (1967) *J. Phys. Chem. Solids*, **28**, 1267–75.

Bell, J. T. (1969) *J. Inorg. Nucl. Chem.*, **31**, 703–10.

Bell, J. T. and Buxton, S. R. (1974) *J. Inorg. Nucl. Chem.*, **36**, 1575–9.

Bellamy, R. G. and Hill, N. A. (1963) *The Extraction and Metallurgy of Uranium, Thorium, and Beryllium,* Pergamon Press, Oxford.

Belle, J. (1961) *Uranium Dioxide, Properties and Nuclear Applications,* U.S. Atomic Energy Commission Division of Reactors, U.S. Government Printing Office, Washington, DC.

Belle, J. (1969) *J. Nucl. Mater.*, **30**, 3–15.

Benard-Rocherulle, P., Louer, M., Louer, D., Dacheux, N., Brandel, V., and Genet, M. (1997) *J. Solid State Chem.*, **132**, 315–22.

Bendall, P. J., Fitch, A. N., and Fender, B. E. F. (1983) *J. Appl. Cryst.* **16**, 164–70.

Benedict, U. (1987) *J. Less Common Metals*, **128**, 7–45.

Ben Salem, A., Meerschaut, A., and Rouxel, J. (1984) *Compt. Rend. Hebd. Séances. Acad. Sci. Ser. 2*, **299**, 617–19.

Benson, D. A. (1977) Sandia National Laboratories Report, SAND-77–0429.

Benz, R., Douglas, R. M., Kruse, F. H., and Penneman, R. A. (1963) *Inorg. Chem.*, **2**, 799–803.

Bereznikova, I. A., Ippolitova, E. A., Simanov, Yu. P., and Kovba, L. M. (1961) Argonne National Laboratory Report, ANL-trans-33, p. 176.

Berger, M. and Sienko, M. J. (1967) *Inorg. Chem.*, **6**, 324–6.

Berlincourt, T. G. (1959) *Phys. Rev.*, **114**, 969–77.

Berndt, U. and Erdman, B. (1973) *Radiochim. Acta*, **19**, 45–6.

Berndt, U., Tanamas, R., and Keller, C. (1976) *J. Solid State Chem.*, **17**, 113–20.

Bernstein, E. R., Keiderling, T. A., Lippard, S. J., and Mayerle, J. J. (1972a) *J. Am. Chem. Soc.*, **94**, 2552–3.

Bernstein, E. R., Hamilton, W. C., Keiderling, T. A., LaPlaca, S. J., Lippard, S. J., and Mayerle, J. J. (1972b). *Inorg. Chem.*, **11**, 3009–16.

Bernstein, E. R. and Keiderling, T. A. (1973) *J. Chem. Phys.*, **59**, 2105–22.

Berry, J. A., Poole, R. T., Prescott, A., Sharp, D. W. A., and Winfield, J. M. (1976) *J. Chem. Soc. Dalton Trans.*, 272–4.

Berry, J. A., Prescott, A., Sharp, D. W. A., and Winfield, J. M. (1977) *J. Fluorine Chem.*, **10**, 247–54.

Berthet J.-C., Rivière, C., Miquel, Y., Nierlich, M., Madic, C., and Ephritikhine, M. (2002) *Eur. J. Inorg. Chem.*, 14390–46.

Berthet, J.-C., Nierlich, M., and Ephritikhine, M. (2003) *Chem. Commun.*, 1660–1.

Berthold, H. J., Hien, H. G., and Reuter, H. (1957) *Ber. Dtsch. Keram. Ges.*, **50**, 111–14.

Berthold, H. J. and Knecht, H. (1965a) *Angew. Chem.*, **77**, 428.

Berthold, H. J. and Knecht, H. (1965b) *Angew. Chem.*, **72**, 453.

Berthold, H. J. and Delliehausen, C. (1966) *Angew. Chem.*, **78**, 750–1.

Berthold, H. J. and Knecht, H. (1966) *Z. Anorg. Allg. Chem.*, **348**, 50–7.

Berthold, H. J. and Knecht, H. (1968) *Z. Anorg. Allg. Chem.*, **356**, 151–62.

Bertino, J. P. and Kirchner, J. A. (1945) *U^{233} Purification and Metal Production*, LA-245.

Bertsch, P. M., Hunter, D. B., Sutton, S. R., Bajt, S., and Rivers, M. L. (1994) *Environ. Sci. Technol.*, **28**, 980–4.

Besson, J. and Chevallier, J. (1964) *Compt. Rend. Hebd. Séances Acad. Sci.*, **258**, 5888–91.

Bevan, D. J. M., Grey, I. E., and Willis, B. T. M. (1986) *J. Solid State Chem.*, **61**, 1–7.

Bevz, A. S., Kapshukov, I. I., Vorobei, M. P., and Skiba, O. V. (1970) *Zh. Strukt. Khim.*, **11**, 936; *J. Struct. Chem.* (*USSR*), **11**, 872.

Biennewies, M. and Schäfer, H. (1974) *Z. Anorg. Allg. Chem.*, **407**, 7–44.

Billard, I. and Lützenkirchen, K. (2003) *Radiochim. Acta*, **91**, 285–94.

Birch, W. D., Mumme, W. G., and Segnit, E. R. (1988) *Aust. Miner.*, **3**, 125–31.

Bittel, J. T., Sjodahl, L. H., and White, J. F. (1969) *J. Am. Ceram. Soc.*, **52**, 446–51.

Bjerrum, J., Schwarzenbach, G., and Sillén, L. G. (1956) *Stability Constants. Part I Organic Ligands,* The Chemical Society, London.

Bjerrum, J., Schwarzenbach, G., and Sillén, L. G. (1957) *Stability Constants. Part II Inorganic Ligands,* The Chemical Society, London.

Blackburn, P. E. (1958) *J. Phys. Chem.*, **62**, 897–902.

Blake, C. A., Baes, C. F. Jr, Brown, K. B., Coleman, C. F., and White, J. C. (1958) *Proc. Second Int. Conf. on Peaceful Uses of Atomic Energy*, **vol. 28**, pp. 289–98. Geneva, 1958,

Blank, H. and Ronchi, C. (1968) *Acta Crystallogr.*, **A24**, 657–66.

Blasse, G. (1964) *Z. Anorg. Allg. Chem.*, **331**, 44–50.

Blaton, N., Vochten, R., Peters, O. M., and van Springel, K. (1999) *Neues Jahrb. Miner. Monatsschr.*, pp. 253–64.

Blatov, V. A., Serezhkina, L. B., Serezhkin, V. N., and Trunov, V. K. (1989) *Zh. Neorg. Khim.*, **34**, 162–4; *Russian J. Inorg. Chem.*, **34**, 91–2.

Blum, P. L., Guinet, P., and Vaugoyeau, H. (1963) *C.R. Acad. Sci.(Paris)*, **257**, 3401–3.

Blumenthal, B. and Noland, R. A. (1956) *Progress in Nuclear Energy, Div. V, Metallurgy and Fuels* (eds. H. H. Finniston and J. P. Howe), Pergamon Press, Oxford, vol. 1 pp. 62–80.

Bober, M., Karow, H. U., and Schretzmann, K. (1975) in *Thermodynamics of Nuclear Materials,* Proc. Symp. 1974, vol. I, , International Atomic Energy Agency, Vienna, pp. 295–305.

Boehme, D. R., Nichols, M. C., Snyder, R. L., and Matheis, D. P. (1992) *J. Alloys Compds*, **179**, 37–59.

Boeyens, J. C. A. and Haegele, R. (1976) *Inorg. Chim. Acta*, **20**, L7.

Bogacz, A., Bros, J. P., Gaune-Escard, M., Hewat, A. W., and Taylor, J. C. (1980) *J. Phys. C*, **13**, 5273–8.

Bohrer, R., Conradi, E., and Müller, U. (1988) *Z. Anorg. Allg. Chem.*, **558**, 119–27.

Bohres, E. W., Krasser, W., Schenk, H.-J., and Schwochau, K. (1974) *J. Inorg. Nucl. Chem.*, **36**, 809–13.

Bois, C., Dao, N. Q., and Rodier, N. (1976a) *Acta Crystallogr. B*, **32**, 1541–9.

Bois, C., Dao, N. Q., and Rodier, N. (1976b) *J. Inorg. Nucl. Chem.*, **38**, 755–7.

Bokolo, K., Delpuech, J.-J., Rodehüser, L. R., and Rubini, P. R. (1981) *Inorg. Chem.*, **20**, 992–7.

Bommer, H. (1941) *Z. Anorg. Allg. Chem.*, **247**, 249–58.

Boraopkova, M. N., Kanetsova, G. N., and Novoselova, A. B. (1971) *Izvestia A.N. SSSR, Ser. Neorgan. Mater.*, **7**, 242.

Borène, J. and Cesbron, F. (1971) *Bull. Soc. Fr. Minér. Crystallogr.*, **94**, 8–14.

Borisov, S. K. and Zadneporovskii, G. M. (1971) *At. Energy (USSR),* **31**, 63–5; Sov. At. Energy, **31**, 761–73.

Boroujerdi, A. (1971) Research Center Karlsruhe Report, KFK-1330.

Bougon, R. and Plurien, P. (1965) *Compt. Rend.*, **260**, 4217–18.

Bougon, R., Charpin, P., Desmoulin, J. P., and Malm, J. G. (1976a) *Inorg. Chem.*, **15**, 2532–40.

Bougon, R., Costes, R. M., Desmoulin, J. P., and Michel, J., Person, J. L. (1976b) *J. Inorg. Nucl. Chem.*, Suppl., 99–105.

Bougon, R., Joubert, P., Weulersse, J.-M., and Gaudreau, B. (1978) *Can. J. Chem.*, **56**, 2546–9.

Bougon, R., Fawcett, J., Holloway, J. H., and Russell, D. R. (1979) *J. Chem. Soc. Dalton Trans.*, 1881–5.

Boulet, P., Daoudi, A., Potel, M., Noël, H., Gross, G. M., Andre, G., and Bouree, F. (1997a) *J. Alloys Compds*, **247**, 104–8.

Boulet, P., Daoudi, A., Potel, M., and Noël, H. (1997b) *J. Solid State Chem.*, **129**, 113–16.

Boulet, P., Potel, M., Levet, J. C., and Noël, H. (1997c) *J. Alloys Compds*, **262–3**, 229–34.

Bowen, R. B., Lincoln, S. F., and Williams, E. H. (1976) *Inorg. Chem.*, **15**, 2126–9.

Bowen, R. B., Honan, G. J., Lincoln, S. F., Spotswood, T. M., and Williams, E. H. (1979) *Inorg. Chim. Acta*, **33**, 235–9.

Boyd, C. M. and Menis, O. (1961) *Anal. Chem.*, **33**, 1016–18.

Bradley, M. J. and Ferris, L. M. (1962) *Inorg. Chem.*, **1**, 683–7.

Bradley, M. J. and Ferris, L. M. (1964) *Inorg. Chem.*, **3**, 189–95.

Brandel, V., Dacheux, N., and Genet, M. (1996) *J. Solid State Chem.*, **121**, 467–72.

Branstätter, F. (1981) *Tschermaks Miner. Petrogr. Mitt.*, **29**, 1–8.

Brater, D. C. and Smiley, S. H. (1958) Structural transitions in UCl_4 anticipating melting, in *Progress in Nuclear Chemistry,* Ser. III, *Process Chemistry* vol. 2 (eds. F. R. Bruce, J. M. Fletcher, and H. H. Hyman), Pergamon Press, London, pp. 136–48.

Brauer, G. (1981) *Handbuch der Präparativen Anorganischen Chemie*, 3rd edn, Ferdinand Elke Verlag, Stuttgart.

Braun, R., Kemmler-Sack, S., Roller, H., Seemann, I., and Wall, I. (1975) *Z. Anorg. Allg. Chem.*, **415**, 133–55.

Bredig, M. A. (1972) in *Proc. CNRS Conf. in Odeillo, 1971*, CNRS, Paris, p. 183.

Breeze, E. W., Brett, N. H., and White, J. (1971) *J. Nucl. Mater.*, **39**, 157–65.

Breeze, E. W. and Brett, N. H. (1971) *J. Nucl. Mater.*, **40**, 113–15.

Breeze, E. W. and Brett, N. H. (1972) volume date1972/1973, *J. Nucl. Mater.*, **45**, 131–8.

Breitung, W. (1978) *J. Nucl. Mater.*, **74**, 10–18.

Brendt, U. and Erdman, B. (1973) *Radiochim. Acta*, **19**, 45–6.

Brenner, I. B., Liezers, M., Godfrey, J., Nelms, S., and Cantle, J. (1998) *Spectrochim. Acta*, **53**, 1087–107.

Brisi, C. (1960) *Ric. Sci.*, **30**, 2376–81.

Brisi, C. (1969) *Ann. Chim. (Rome)*, **59**, 400–11.

Brisi, C. (1971) *Rev. Int. Hautes Temp. Réfract.*, **8**, 37–41.

Brisi, C., Montorsi, M., and Burlando, G. A. (1972) *Atti. Acad. Sci. Torino, Cl. Sci. Fis. Mater. Nat.*, **106**, 257.

Brit, D. W. and Anderson, H. J. (1962) USAEC Technical Information Service, TID-7637, p. 408.

Brochu, R. and Lucas, J. (1967) *Bull. Soc. Chim. France*, 4764–7.

Brodsky, M. B., Griffin, N. J., and Odie, M. D. (1969) *J. Appl. Phys.*, **8**, 895–7.

Brookins, D. G. (1990) *Waste Manage.*, **10**, 285–96.

Bros, J. P., Gaune-Escard, M., Szczepaniak, W., Bogacz, A., and Hewat, A. W. (1987) *Acta Crystallogr. B*, **43**, 113–16.

Brown, D. (1966) *J. Chem. Soc.* (*A*), 766–9.

Brown, D. (1968) *The Halides of the Lanthanides and Actinides,* Wiley Interscience, New York.

Brown, D., Fletcher, S., and Holah, D. G. (1968) *J. Chem. Soc. A*, 1889–94.

Brown, D., Hill, J., and Rickard, C. E. F. (1970) *J. Chem. Soc. A*, 476–80.

Brown, D. (1972) The actinide halides and their complexes, in MTP (*Med. Tech. Publ. Co.*) *Intern. Rev. Sci. Inorg. Chem. Ser. One*, 7, 87–137.

Brown, D. and Edwards, J. (1972) *J. Chem. Soc. Dalton Trans.*, 1757–62.

Brown, D. (1973) in *Comprehensive Inorganic Chemistry,* vol. 5, Pergamon Press, Oxford, pp. 151–208.

Brown, D., Whittaker, B., and Lidster, P. E. (1975) Atomic Energy Research Establishment (UK) Report, AERE-R-8035, p. 16.

Brown, D., Lidster, P., Whittaker, B., and Edelstein, N. (1976) *Inorg. Chem.*, **15**, 511–51.

Brown, D. (1979) Compounds of Uranium with Chlorine, Bromine and Iodine, in *Gmelin Handbook of Inorganic Chemistry,* System no. 55, Uranium, Suppl., vol. C9, Springer, Berlin, pp. 1–186.

Brown, D., Berry, J. A., Holloway, J. H., Holland, R. F., and Staunton, G. M. (1983) *J. Less Common Metals*, **92**, 149–53.

Brown, D. R. and Denning, R. G. (1996) *Inorg. Chem.*, **35**, 6158–63.

Brown, G. M. and Walker, L. A. (1966) *Acta Crystallogr.*, **20**, 220–9.

Brown, K. B., Coleman, C. F., Crouse, D. J., Blake, C. A., and Ryan, A. D. (1958) *Proc. Second Int. Conf. on Peaceful Uses of Atomic Energy*, Geneva, 1958, vol. 3, pp. 472–87.

Browning, P., Gillan, M. J., and Potter, P. E. (1978) *Rev. Int. Hautes Tempér. Réfract. Fr.*, **15**, 333–46.

Browning, P. (1981) *J. Nucl. Mater.*, **98**, 345–56.

Browning, P., Hyland, G. J., and Ralph, J. (1983) Oak Ridge National Laboratory Report, *High Temp.-High Press.*, **15**, 169–78.

Brugger, J., Burns, P. C., and Meisser, N. (2003) *Am. Miner.*, **88**, 676–85.

Brugger, J., Krivovichev, S. V., Berlepsch, P., Meisser, N., Ansermet, S., and Armbruster, T. (2004) *Am. Mineral.*, **89**, 339–47.

Brunton, G. D. (1965) Oak Ridge National Laboratory Report, ORNL-3913, p. 10.

Brunton, G. D., Insley, H., and McVay, T. N., Thoma, R. E. (1965) Oak Ridge National Laboratory Report, ORNL-3761, p. 212; (1965) N.S.A. 19, no. 15416.

Brunton, G. D. (1966) *Acta Crystallogr.*, **21**, 814–17.

Brunton, G. D. (1967) *J. Inorg. Nucl. Chem.*, **29**, 1631–6; Oak Ridge National Laboratory Report, ORNL-4076; (1967) N.S.A. 21.

Brunton, G. D. (1969a) *Acta Crystallogr. B*, **25**, 2163–4; **26B**, 2519.

Brunton, G. D. (1969b) *Acta Crystallogr. B*, **25**, 1919–21.

Brunton, G. D. (1971) *Acta Crystallogr. B*, **27**, 245–7.

Brusset, H., Gillier-Pandraut, H., and Dao, N. Q. (1969) *Acta Crystallogr.*, **25B**, 67–73.

Brusset, H. and Dao, N. Q. (1971) *J. Inorg. Nucl. Chem.*, **33**, 1365–72.

Brusset, H., Dao, N. Q., and Rubinstein-Auban, A. (1972) *Acta Cryst. B*, **28**, 2617–19.

Brusset, H., Dao, N. Q., and Chourou, S. (1974) *Acta Cryst.*, **30B**, 768–73.

Buck, E. C., Brown, N. R., and Dietz, N. L. (1996) *Environ. Sci. Technol.*, **30**, 81–8.

Buck, E. C., Wronkiewicz, D. J., Finn, P. A., and Bates, J. K. (1997) *J. Nucl. Mater.*, **249**, 70–6.

Buck, E. C. and Bates, J. K. (1999) *Appl. Geochem.*, **14**, 635–53.

Buck, E. C., Finn, P. A., and Bates, J. K. (2004) *Micron*, **35**, 235–43.

Budnikov, P. P., Tresvyatsky, S. G., and Kushakovsky, V. I. (1958) in *Proc. Second Int. Conf. on Peaceful Uses of Atomic Energy*, Geneva, 1958, vol. 6, United Nations, Geneva, pp. 124–31.

Bugl, J. and Bauer, A. A. (1964) in Waber *et al.* (1964), pp. 215–24.

Buhrer, C. F. (1969) *J. Phys. Chem. Solids*, **30**, 1273–6.

Bullock, J. I. (1969) *J. Chem. Soc. A*, 781– 4.

Bunnell, L. R., Chikalla, T. D., and Woodley, R. E. (1975) *Hydrolysis of Uranium Carbide Fuel Beads*, BNWL-SA-5513.

Burk, W. (1967) *Z. Anorg. Allg. Chem.*, **350**, 92–6.

Burk, W. and Naumann, D. (1969) *Z. Chem. (Leipzig)*, **9**, 189.

Burns, J. H., Osborne, D. W., and Westrum, E. F. Jr (1960) *J. Chem. Phys.*, **33**, 387–94.

Burns, J. H. and Duchamp, D. J. (1962) Oak Ridge National Laboratory Report, ORNL-3262, pp. 14–16; N.S.A. 16, no. 17553.

Burns, J. H., Ellison, R. D., and Levy, H. A. (1968) *Acta Crystallogr. B*, **24**, 230–7.

Burns, P. C., Miller, M. L., and Ewing, R. C. (1996) *Can. Miner.*, **34**, 845–80.

Burns, P. C. (1997) *Am. Miner.*, **82**, 1176–86.

Burns, P. C., Ewing, R. C., and Miller, M. L. (1997a) *J. Nucl. Mater.*, **245**, 1–9.

Burns, P. C., Finch, R. J., Hawthorne, F. C., Miller, M. L., and Ewing, R. C. (1997b) *J. Nucl. Mater.*, **249**, 199–206.

Burns, P. C. (1998a) *Can. Miner.*, **36**, 847–53.

Burns, P. C. (1998b) *Can. Miner.*, **36**, 187–99.

Burns, P. C. (1998c) *Can. Miner.*, **36**, 1061–7.

Burns, P. C. (1998d) *Can. Miner.*, **36**, 1069–75.

Burns, P. C. (1999a) *Rev. Miner.*, **38**, 23–90.

Burns, P. C. (1999b) *Am. Miner.*, **84**, 1661–73.

Burns, P. C. and Finch, R. J. (1999) *Am. Miner.*, **84**, 1456–60.

Burns, P. C. and Hanchar, J. M. (1999) *Can. Miner.*, **37**, 1483–91.

Burns, P. C. (2000) *Am. Miner.*, **85**, 801–5.

Burns, P. C. and Hill, F. C. (2000a) *Can. Miner.*, **38**, 163–73.

Burns, P. C. and Hill, F. C. (2000b) *Can. Miner.*, **38**, 175–82.

Burns, P. C., Olson, R. A., Finch, R. J., Hanchar, J. M., and Thibault, Y. (2000) *J. Nucl. Mater.*, **278**, 290–300.

Burns, P. C. (2001a) *Can. Miner.*, **39**, 1139–46.

Burns, P. C. (2001b) *Can. Miner.*, **39**, 1153–60.

Burns, P. C. and Hayden, L. A. (2002) *Acta Crystallogr. C*, **58**, 121–2.

Burns, P. C. and Li, Y. (2002) *Am. Miner.*, **87**, 550–7.

Burns, P. C. and Hughes, K.-A. (2003) *Am. Mineralogist*, **88**, 1165–8.

Burns, P. C., Deely, K. M., and Hayden, L. A. (2003) *Can. Miner.*, **41**, 687–706.

Burns, P. C., Deely, K. M., and Skanthakumar, S. (2004a) *Radiochim. Acta*, **92**, 151–60.

Burns, C. J., Neu, M. P., Boukhalfa, H., Gutowski, K. E., Bridges, N. J., and Rogers, R. D. (2004) *The Actinides* in *Comprehensive Coordination Chemistry II*, vol. 3, 3.3, 189–345, Elsevier Ltd, Amsterdam.

Burns, P. C., Kubatko, K.-A., Sigmon, G., Fryer, B. J., Gagnon, J. E. Antonio, M. R. and Soderholm, L. (2005) *Angew. Chem. Int. Ed.,* **44**, 2135.

Burrows, H. D. and Kemp, T. J. (1974) *Chem. Soc. Rev.*, **3**, 139–65.

Bursten, B. E. and Strittmatter, R. J. (1987) *J. Am. Chem. Soc.*, **109**, 6606–9.

Busch, G., Hulliger, F., and Vogt, O. (1979a) *J. Physique Colloq.*, **40**, C4 62–3.

Busch, G., Vogt, O., and Bartolin, H. (1979b) *J. Physique Colloq.*, **40**, C4 64–5.

Cahill, C. L. and Burns, P. C. (2000) *Am. Miner.*, **85**, 1294–7.

Caillat, R., Coriou, H., and Perio, P. (1953) *Compt. Rend. Hebd. Séances Acad. Sci.*, **237**, 812–13.

Caillat, R. (1961) in *P. Pascal, Nouveau Traité de Chimie Minérale, Masson et Cie., Paris 1967*, vol. **XV** (2), 59–121; (1967) vol. **XV** (4), 497–517.

Caira, M. R., de Wet, J. F., du Preez, J. G. H., and Gellatly, B. J. (1978) *Acta Crystallogr. B*, **34**, 1116–20.

Caley, E. R. (1948) *Isis*, **38**, 190–3.

Caneiro, A. and Abriata, J. P. (1984) *J. Nucl. Mater.*, **126**, 255–67.

Carbajo, J. J., Yoder, G. L., Popov, S. G., and Ivanov, V. K. (2001) *J. Nucl. Mater.*, **299**, 181–98.

Carlson, E. H. (1969) *Phys. Lett.*, **29A**, 696–7.

Carlson, R. S. (1975) in *Proc. Int. Conf. on Radiation Effects and Tritium Technology for Fusion Reactors*, Gatlinburg, TN, 1975, vol. 4, p. 361.

Carnall, W. T., Neufeldt, S. J., and Walker, A. (1965) *Inorg. Chem.*, **4**, 1808–13.

Carnall, W. T., Walker, A., and Neufeldt, S. J. (1966) *Inorg. Chem.*, **5**, 2135–40.

Carnall, W. T. (1970) Unpublished results.

Carnall, W. T. (1982) in *Gmelin Handbuch der Anorganischen Chemie,* 8th edn, Uranium Suppl., vol. A5, , Springer Verlag, New York, pp. 69–161.

Carnall, W. T. and Crosswhite, H. M. (1985) Argonne National Laboratory Report, ANL 84–90.

Carnall, W. T. (1989) Argonne National Laboratory Report, ANL-89/39.

Carnall, W. T., Liu, G. K., Williams, C. W., and Reid, M. F. (1991) *J. Chem. Phys.*, **95**, 7194–203.

Carter, R. E. and Lay, K. W. (1970) *J. Nucl. Mater.*, **36**, 77–86.

Casto, C. C. (1950) in *Analytical Chemistry of the Manhattan Project* (ed. C. J. Rodden), McGraw-Hill, New York, pp. 511–36.

Catalano, J. G. and Brown, G. E. (2004) *Am. Miner.*, **89**, 1004–21.

Catlow, C. R. A. and Pyper, N. C. (1979) *J. Nucl. Mater.*, **80**, 110–14.

Caville, C. and Poulet, H. (1974) *J. Inorg. Nucl. Chem.*, **36**, 1581–7.

Čejka, J. (1999) *Rev. Miner.*, **38**, 521–622.

Cesbron, F., Ildefonse, P., and Sichere, M.-C. (1993) *Miner. Mag.*, **57**, 301–8.

Chakravorti, M. C., Bharadwaj, P. K., Pandit, S. C., and Mathur, B. K. (1978) *J. Inorg. Nucl. Chem.*, **40**, 1365–7.

Champarnaud-Mesjard, J.-C. and Gaudreau, B. (1976) *Comp. Rend. C*, **282**, 745–7.

Chapman, A. T. and Clark, G. W. (1965) *J. Am. Ceram. Soc.*, **48**, 494–5.

Charpin, P. (1965) *Compt. Rend.*, **260**, 1914–16.

Charpin, P., Montoloy, F., and Nierlich, M. (1968) *Compt. Rend. C*, **266**, 1685–7.

Charpin, P., Montoloy, F., and Nierlich, M. (1969) *Compt. Rend. C*, **268**, 156–8.

Charvillat, J. P., Baud, G., and Besse, J. P. (1970) *Mater. Res. Bull.*, **5**, 933–8.

Chatalet, J. (1967) in *P. Pascal, Nouveau Traité de Chimie Minérale, Masson et Cie.,* Paris (1967) vol. 4, 508–13.

Chen, F., Burns. P. C., and Ewing, R. C. (1999) *J. Nucl. Mater.*, **275**, 81–94.

Chen, F., Burns. P. C., and Ewing, R. C. (2000) *J. Nucl. Mater.*, **278**, 225–32.

Chen, J. H., Edwards, R. L., and Wasserburg, G. J. (1992) in *Uranium Series Disequilibrium Applications to Earth, Marine, and Environmental Sciences* (eds. M. Ivanovich and R. S. Harmon), Clarendon Press, Oxford, pp. 174–206.

Chen, Z., Luo, K., Tan, F., Zhang, Y., and Gu, X. (1986) *Kexue Tongbao*, **31**, 396–401.

Chernyayev, I. I. (1966) *Complex Compounds of Uranium* (translated from Russian by L. Mandel, eds. M. Govre and IPST staff), Israel Program for Scientific Translation, Jerusalem.

Chervet, J. (1960) *Nouveau Traité de Chimie Minérale* (ed. P. Pascal), XV (1), Masson et Cie, Paris., 52–94,

Chevalier, P.-Y., Fischer, E., and Cheynet, B. (2002) *J. Nucl. Mater.*, **303**, 1–28.

Chilton, J. M. (1963) *Proc. First Protactinium Chemistry Symp.*, Gatlinburg, TN, April 25–26, TID-7675, p. 157.

Chiotti, P. (1980) *Bull. Alloy Phase Diagrams*, **1**, 99.

Chiotti, P., Akhachinskij, V. V., Ansara, I., and Rand, M. H. (1981) *The Chemical Thermodynamics of Actinide Elements and Compounds*, part 5, *The Actinide Binary Alloys*, IAEA, Vienna, STI/PUB/424/5.

Chirkst, D. E. (1981) *Koord. Khimiya*, **7**, 3–17.

Chisholm-Brause, C. J., Berg, J. M., Matzner, R. A., and Morris, D. E. (2001) *J. Colloid Interface Sci.*, **233**, 38–49.

Chodos, S. L. (1972) *J. Chem. Phys.*, **57**, 2712–14.

Choppin, G. R., Bokelund, H., and Valkiers, S. (1983) *Radiochim. Acta*, **33**, 229–32.

Christ, C. L., Clark, J. R., and Evans, H. T. Jr (1955) *Science*, **121**, 472–2.

Chukanov, N. V., Pushcharovsky, D. Y., Pasero, M., Merlino, S., Barinova, A. V., Mockel, S., Pekov, I. V., Zadov, A. E., and Dubinchuk, V. T. (2004) *Eur. J. Miner.*, **16**, 367–74.

Cinader, G., Peretz, M., Damir, D., and Hadari, Z. (1973) *Phys. Rev. B*, **8**, 4063–8.

Clark, D. L., Conradson, S. D., Ekberg, S. A., Hess, N. J., Neu, M. P., Palmer, P. D., Runde, W., and Tait, C. D. (1996) *J. Am. Chem. Soc.*, **118**, 2089–90.

Clark, D. L., Conradson, S. D., Donohue, R. J., Keogh, W. D., Morris, D. E., Palmer, P. D., Rogers, R. D., and Tait, C. D. (1999) *Inorg. Chem.*, **38**, 1456–66.

Clausen, K., Hayes, W., Hutchings, M. T., Kjems, J. K., Macdonald, J. E., and Osborn, R. (1985) *High Temp. Sci.*, **19**, 189–96.

Cleaves, H. E., Cron, M. M., and Sterling, J. T. (1945) AEC Report CT2–618.

Clegg, J. W. and Foley, D. D. (1958) *Uranium Ore Processing,* Addison-Wesley, Reading, MA.

Clemente, D. A., Bandoli, G., Benetollo, F., and Marzotto, A. (1974) *J. Cryst. Mol. Struct.*, **4**, 1–14.

Clifton, J. R., Gruen, D. M., and Ron, A. (1969) *J. Chem. Phys.*, **51**, 224–32.

Clusius, K. and Dickel, G. (1938) *Naturwissenschaften*, **26**, 546.

Cody, J. A. and Ibers, J. A. (1995) *Inorg. Chem.*, **34**, 3165–72.

Cody, J. A., Mansuetto, M. F., Pell, M. A., Chien, S., and Ibers, J. A. (1995) *J. Alloys Compds*, **219**, 1239–45.

Cohen, D. and Carnall, W. T. (1960) *J. Phys. Chem.*, **64**, 1933.

Cohen, I. and Schaner, B. E. (1963) *J. Nucl. Mater.*, **9**, 18–52.

Cohen, I. and Berman, R. M. (1966) *J. Nucl. Mater.*, **18**, 77–107.

Colella, M., Lumpkin, G. R., Zhang, Z., Buck, E. C., and Smith, K. L. (2005) *J. Phys. Chem. Miner.*, **32**, 52–64.

Condon, J. B. and Larson, E. A. (1973) *J. Chem. Phys.*, **59**, 855–65.

Contamin, P., Bacmann, J. J., and Marin, J. F. (1972) *J. Nucl. Mater.*, **42**, 54–64.

Conway, J. G. (1959) *J. Chem. Phys.*, **31**, 1002–4.

Cooper, M. A. and Hawthorne, F. C. (1995) *Can. Miner.*, **33**, 1103–9.

Cooper, M. A. and Hawthorne, F. C. (2001) *Can. Miner.*, **39**, 797–807.

Cordfunke, E. H. P. (1961) *J. Inorg. Nucl. Chem.*, **23**, 285–6.

Cordfunke, E. H. P. and Debets, P. C. (1964) *J. Inorg. Nucl. Chem.*, **26**, 1671.

Cordfunke, E. H. P. and Aling, P. (1965) *Trans. Faraday Soc.*, **61**, 50–3.

Cordfunke, E. H. P. and Loopstra, B. O. (1967) *J. Inorg. Nucl. Chem.*, **29**, 51–7.

Cordfunke, E. H. P. (1969) *The Chemistry of Uranium,* Elsevier, Amsterdam.

Cordfunke, E. H. P. and Loopstra, B. O. (1971) *J. Inorg. Nucl. Chem.*, **33**, 2427–36.

Cordfunke, E. H. P. (1975) in *Thermodynamics of Nuclear Materials,* Proc. Symp. 1974, vol. II, International Atomic Energy Agency, Vienna, pp. 185–92.

Cordfunke, E. H. P., van Egmond, A. B., and van Voorst, G. (1975) *J. Inorg. Nucl. Chem.*, **37**, 1433–6.

Cordfunke, E. H. P., Oweltjes, W., and Prins, G. (1976) *J. Chem. Thermodyn.*, **8**, 241–50.

Cordfunke, E. H. P., Prins, G., and van Vlaanderen, P. (1977) *J. Inorg. Nucl. Chem.*, **39**, 2189–90.

Cordfunke, E. H. P. and Westrum, E. F. Jr. (1979) in *Thermodynamics of Nuclear Materials,* Proc. Symp. 1979, vol. II, International Atomic Energy Agency, Vienna, pp. 125–41.

Cordfunke, E. H. P., Oweltjes, W., and van Vlaanderen, P. (1983) *J. Chem. Thermodyn.*, **15**, 237–43.

Cordfunke, E. H. P., van Vlaanderen, P., Goubitz, K., and Loopstra, B. O. (1985) *J. Solid State Chem.*, **56**, 166–70.

Cordier, S., Perrin, C., and Sergent, M. (1997) *Mater. Res. Bull.*, **32**, 25–33.

Cotton, F. A., Marler, D. O., and Schwotzer, W. (1984) *Acta Crystallogr.*, **40C**, 1186–8.

Cousson, A., Pagès, M., Cousseins, J.-C., and Vedrine, A. (1977) *J. Crystal Growth*, **40**, 157–60.

Cousson, A., Tabuteau, A., Pagès, M., and Gasperin, M. (1979) *Acta Crystallogr. B*, **35**, 1198–2000.

Cox, J. D., Wagman, D. D., and Medvedev, V. A. (1989) *CODATA Key Values for Thermodynamics,* Hemisphere, New York.

Crawford, M.-J., Ellern, A., and Mayer, P. (2005) *Angew. Chem. Int. Ed.* 1–5.

Crea, J., Diguisto, R., Lincoln, S. F., and Williams, E. H. (1977) *Inorg. Chem.*, **16**, 2825.

Crosswhite, H. M., Crosswhite, H., Carnall, W. T., and Paszek, A. P. (1980) *J. Chem. Phys.*, **72**, 5103–17.

Cunningham, J. E. and Adams, R. E. (1957) *Fuel Elements Conference*, Paris, November 18–23, TID-7546, Book 1, pp.102–19.

Dao, N. Q. (1972) *Acta Crystallogr. B*, **288**, 2011–15.

Dao, N. Q. and Chourou, S. (1972) *C. R. Acad. Sci. (Paris)*, **275C**, 745–8.

Dao, N. Q. and Chourou, S. (1974) *C. R. Acad. Sci. (Paris)*, **278C**, 879–81.

Dao, N. Q., Chourou, S., Rodier, N., and Bastein, P. (1979) *Compt. Rend. Serie C, Sciences Chimiques*, **289**, 405–8.

Dao, N. Q., Chourou, S., and Heckly, J. (1981) *J. Inorg. Nucl. Chem.*, **43**, 1835–9.

Daoudi, A., Levet, J. C., Potel, M., and Noël, H. (1996) *Mater. Res. Bull.*, **31**, 1213–18.

Davies, W. and Gray, W (1964) *Talanta*, **11**, 1203–11.

Davies, W., Gray, W., and McLeod, K. C. (1970) *Talanta*, **17**, 937–44.

Dawson, J. K. (1951) *J. Chem. Soc.*, 429–31.

Dawson, J. K., D'Eye, R. W. M., and Truswell, A. E. (1954) *J. Chem. Soc.*, 3922–9.

Dawson, J. K., Wait, E., Alcock, K., and Chilton, D. R. (1956) *J. Chem. Soc.*, 3531.

Day, J. P. and Venanzi, L. M. (1966) *J. Chem. Soc. A*, 1365–7.

D'Eye, R. W. M. and Martin, F. S. (1957) N.S.A. 11, no. 3372.

de Alleluia, I. B., Hoshi, M., Jocher, W. G., and Keller, C. (1981) *J. Inorg. Nucl. Chem.*, **43**, 1831–4.

Dean, J. A. (1995) *Analytical Chemistry Handbook,* McGraw-Hill, New York.

Debets, P. C. and Loopstra, B. O. (1963) *J. Inorg. Nucl. Chem.*, **25**, 945–53.

Debets, P. C. (1966) *Acta Crystallogr.*, **21**, 589–93.

Debets, P. C. (1968) *Acta Crystallogr.*, **24B**, 400–2.

de Coninck, R. and Devreese, J. (1969) *Phys. Status Solidi*, **32**, 823–9.

De Jong, W. A., Visscher, L., and Nieupoort, W. C. (1999) *Theochemistry*, **458**, 41–52.

Delamoye, P., Rajnak, K., Genet, M., and Edelstein, N. (1983) *Phys. Rev. B*, **28**, 4923–30.

Deleon, A. and Lazarević, M. (1971) in *The Recovery of Uranium,* Proc. Symp. Sao Paulo, Brazil, August 17–21, 1970, International Atomic Energy Agency, Vienna, STI/PUB/262, pp. 351–61.

Deliens, M. and Piret, P. (1981) *Can. Miner.*, **19**, 553–7.

Deliens, M. and Piret, P. (1982) *Can. Miner.*, **20**, 231–8.

Deliens, M. and Piret, P. (1983a) *Am. Miner.*, **68**, 456–8.

Deliens, M. and Piret, P. (1983b) *Bull. Minér.*, **106**, 305–8.

Deliens, M. and Piret, P. (1984a) *Bull. Minér.*, **107**, 21–4.

Deliens, M. and Piret, P. (1984b) *Bull. Minér.*, **107**, 15–19.

Deliens, M. and Piret, P. (1990a) *Eur. J. Miner.*, **1**, 85–8.

Deliens, M. and Piret, P. (1990b) *Eur. J. Miner.*, **2**, 407–11.

Dell, R. M. and Wheeler, V. I. (1963) *Trans. Faraday Soc.*, **59**, 485.

Della Ventura, G., Bonazzi, P., Oberti, R., and Ottolini, L. (2002) *Am. Miner.*, **87**, 739–44.

Demartin, F., Diella, V., Donzelli, S., Gramaccioli, C. M., and Pilati, T. (1991) *Acta Crystallogr.*, **B47**, 439–46.

Demartin, F., Gramaccioli, C. M., and Pilati, T. (1992) *Acta Crystallogr.*, **C48**, 1–4.

Dempster, A. J. (1935) *Nature*, **136**, 180.

Denes, G., Fonteneau, G., and Lucas, J. (1973) *Compt. Rend. C.*, **276**, 1553–6.

Denning, R. G., Snellgrove, T. R., and Woodwark, D. R. (1976) *Mol. Phys.*, **31**, 419–42.

Dent, A. J., Ramsey, J. D. F., and Swanton, S. W. (1992) *J. Colloid Interface Sci.*, **150**, 45–60.

Depaus, R., Guzzi, G., and Federico, A. (1987) *Proc. Int. Symp. Nuclear Material Safeguards*, Vienna, Austria, IAEA, vol. 2, p. 116.

Dereń, P., Karbowiak, M., Krupa, J. P., and Drożdżyński, J. (1998) *J. Alloys Compds*, **275–7**, 863–6.

Deschaux, M. and Marcantonatos, M. D. (1979) *Chem. Phys. Lett.*, **63**, 283–8.

Destriau, M. and Sériot, J. (1962) *Compt. Rend. Hebd. Séances Acad. Sci.*, **254**, 2982–4.

Deutsch, W. J., Krupka, K. M., Lindberg, M. J., Cantrell, K. J., Brown, C. F., and Schaef, H. F. (2004) *Hanford Tanks 241-C-203 and 241-C-204: Residual Waste Contaminant Release Model and Supporting Data,* PNNL-14903, Pacific Northwest National Laboratory, Richland, Washington.

de Wet, J. F., Caira, M. R., and Gellatly, B. J. (1978) *Acta Crystallogr. B*, **34**, 1121–4.

de Wet, J. F. and du Preez, J. G. H. (1978) *J. Chem. Soc., Dalton Trans.*, 592–7.

Dhar, S. K., Kimura, Y., Kouzaki, M., Sugiyama, K., Settai, R., Onuki, Y., Takeuchi, T., Kindo, K., Manfrinetti, P., and Palenzona, A. (1998) *Physica B* (*Amsterdam, Neth*), **245**, 210–18.

Dharwadkar, S. R., Chandrasekharaiah, M. S., and Karkhanavala, M. D. (1975) *J. Thermal Anal.*, **7**, 219–21.

Dharwadkar, S. R., Chandrasekharaiah, M. S., and Karkhanavala, M. D. (1978) *J. Nucl. Mater.*, **71**, 268–76.

Di Bella, S., Lanza, G., Fragalà, I. L., and Marks, T. J. (1996) *Organometallics*, **15**, 205–7.

Dickens, P. G., Stuttard, G. P., Dueber, R. E., Woodall, M. J., and Patat, S. (1993) *Solid State Ionics*, **63–5**, 417–23.

Diehl, H. G. and Keller, C. (1971) *J. Solid State Chem.*, **3**, 621–36.

Dion, C., Obbade, S., Raekelboom, E., Abraham, F., and Saadi, M. (2000) *J. Solid State Chem.*, **155**, 342–53.

Di Sipio, L., Tondello, E., Pellizzi, G., Ingletto, G., and Montenero, A. (1974a) *Crystal Struct. Commun.*, **3**, 297–300.

Di Sipio, L., Tondello, E., Pellizzi, G., Ingletto, G., and Montenero, A. (1974b) *Crystal Struct. Commun.*, **3**, 731–4.

Di Sipio, L., Tondello, E., Pellizzi, G., Ingletto, G., and Montenero, A. (1974c) *Crystal Struct. Commun.*, **3**, 527–30.

Di Sipio, L., Tondello, E., Pellizzi, G., Ingletto, G., and Montenero, A. (1974d) *Crystal Struct. Commun.*, **3**, 301–3.

Di Sipio, L., Tondello, E., Pellizzi, G., Ingletto, G., and Montenero, A. (1977) *Crystal Struct. Commun.*, **6**, 723–6.

Djogic, R. and Branica, M. (1992) *Electroanalysis*, **4**, 151–9.

Docrat, T. I., Mosselmans, J. F. W., Charnock, J. M., Whitley, M. W., Collison, D., Livens, F. R., Jones, C., and Edmiston, M. J. (1999) *Inorg. Chem.*, **38**, 1879–82.

Dodé, M. and Touzelin, B. (1972) *Rev. Chim. Minér.*, **9**, 139.

Donohue, J. and Einspahr, H. (1971) *Acta Crystallogr. B*, **27**, 1740–3.

Douglas, R. M. and Staritzky, E. (1957) *Anal. Chem.*, **29**, 459.

Douglass, R. M. (1962) *Acta Crystallogr.*, **15**, 505–6.

Downs, A. J. and Gardner, C. J. (1986) *J. Chem. Soc. Dalton Trans.*, 1289–96.

Doyle, G. A., Goodgame, D. M. L., Sinden, A., and Williams, D. L. (1993) *J. Chem. Soc. Chem. Commun.*, 1170–2.

Drożdżyński, J. and Conway, J. G. (1972) *J. Chem. Phys.*, **56**, 883–91.

Drożdżyński, J. (1978) *J. Inorg. Nucl. Chem.*, **40**, 319–23.

Drożdżynski, J. and Kamenskaya, A. N. (1978) *Chem. Phys. Lett.*, **56**, 549–53.

Drożdżyński, J. and Miernik, D. (1978) *Inorg. Chim. Acta*, **30**, 185–8.

Drożdżyński, J. (1979) *Inorg. Chim. Acta.*, **32**, L83–5.

Drożdżyński, J. (1984) *J. Mol. Struct.*, **114**, 449–56.

Drożdżyński, J. (1985) *Inorg. Chim. Acta*, **109**, 79–81.

Drożdżyński, J. (1988a) *Polyhedron*, **7**, 167–8.

Drożdżyński, J. (1988b) *J. Less Common Metals*, **138**, 271–9.

Drożdżyński, J. (1991) Chemistry of tervalent uranium, in *Handbook on the Physics and Chemistry of the Actinides* vol. 6, ch. 5 (eds. A. J. Freeman and C. Keller), North-Holland, Amsterdam, pp. 281–336.

Drożdżyński, J. and du Preez, J. G. H. (1994) *Inorg. Chim. Acta*, **218**, 203–5. no.1–2,

Drożdżyński, J., and Karbowiak, M. (2005) unpublished results.

Drulis, H., Petryński, W., Staliński, B., and Zigmunt, A. (1982) *J. Less Common Metals*, **83**, 87–93.

Ducroux, R. and Baptiste, Ph. J. (1981) *J. Nucl. Mater.*, **97**, 333–6.

Dudney, N. J., Coble, R. L., and Tuller, H. L. (1981) *J. Am. Ceram. Soc.*, **64**, 627–31.

Duff, M. C., Amrhein, C., Bertsch, P. M., and Hunter, D. B. (1997) *Geochim. Cosmochim. Acta*, **61**, 73–81.

Duff, M. C., Coughlin, J. U., and Hunter, D. B. (2002) *Geochim Cosmochim. Acta*, **66**, 3533–47.

du Preez, J. G. H., Gonsalves, J. W., and Steenkamp, P. J. (1977a) *Inorg. Chim. Acta*, **21**, 167–72.

du Preez, J. G. H., Gellatly, B. J., and Gibson, M. L. (1977b) *J. Chem. Soc. Dalton Trans.*, 1062–8.

du Preez, J. G. H. and Zeelie, B. (1987) *Inorg. Chim. Acta*, **134**, 303–8.

du Preez, J. G. H. and Zeelie, B. (1989) *Inorg. Chim. Acta*, **161**, 187–92.

Dusausoy, Y., Ghermain, N.-E., Podor, R., and Chuney, M. (1996) *Eur. J. Miner.*, **8**, 667–73.

Dyall, K. G. (1999) *Mol. Phys.*, **96**, 511–18.

Eastman, E. D., Brewer, L., Bromley, L. A., Gilles, P. W., and Lofgren, N. A. (1950) *J. Am. Chem. Soc.*, **72**, 2248–850; 4019–23.

Eastman, E. D. and Fontana, B. I. (1958) in *Chemistry of Uranium* (*TID –5290*), *Paper 30* (eds. J. Katz and E. Rabinowitch), Oak Ridge, TN, pp. 206–13.

Eastman, M. P., Eller, P. G., and Halstead, G. W. (1981) *J. Inorg. Nucl. Chem.*, **43**, 2839–42.

Ebert, W. L., Bates, J. K., and Bourcier, W. L. (1991) *Waste Manage.*, **11**, 205–21.

Edelson, M. C. (1992) in *Inductively Coupled Plasmas in Analytical Atomic Spectrometry,* 2nd edn (eds. A. Montaser and D. W. Golightly), VCH Publishers, New York, pp. 341–72.

Edelstein, N., Brown, D., and Whittaker, B. (1974) *Inorg. Chem.*, **13**, 563–7.

Edghill, R. (1991) *Radiochim. Acta*, **32**, 381–6.

Eding, H. J. and Carr, E. M. (1961) *High-Purity Uranium Compounds – Final Report*, ANL-6339.

Edwards, R. K. and Martin, A. E. (1966) in *Thermodynamics,* Proc. Symp. 1965, vol. 2, International Atomic Energy Agency, Vienna, pp. 423–9.

Edwards, R. K., Chandrasekharaiah, M. S., and Danielson, P. M. (1969) *High Temp. Sci.*, **1**, 98–113.

Efremova, K. M., Ippolitova, E. A., Simanov, Yu. P., and Spitsyn, V. I. (1959) *Dokl. Akad. Nauk. SSSR*, **124**, 1057–60.

Efremova, K. M., Ippolitova, E. A., and Simanov, Yu. P. (1961a) Argonne National Laboratory Report, ANL-trans-33, p. 44.

Efremova, K. M., Ippolitova, E. A., and Simanov, Yu. P. (1961b) Argonne National Laboratory Report, ANL-trans-33, p. 59.

Efremova, K. M., Ippolitova, E. A., and Simanov, Yu. P. (1961c) Argonne National Laboratory Report, ANL-trans-33, p. 65.

Ehrfeld, W. and Ehrfeld, U. (1980) in *Gmelin Handbuch der Anorganischen Chemie,* Uranium Suppl., vol. A2, Springer, Berlin, p. 57.

Eichberger, K. (1979) *Dissertation,* T.U. Munich, Germany.

Eichberger, K. and Lux, F. (1980) *Ber. Bunsenges. Phys. Chem.*, **84**, 800–7.

Eick, H. A. (1994) Lanthanide and actinide halides, in *Handbook on the Physics and Chemistry of Rare Earths* (eds. K. A. Gschneidner Jr, L. Eyring, G. R. Choppin, and G. H. Lander), Elsevier Science B. V., vol. 18, ch. 124, 365–411.

Ekeroth, E. and Jonsson, M. (2003) *J. Nucl. Mater.*, **322**, 242–8.

Ekstrom, A., Batley, G. E., and Johnson, D. A. (1974) *J. Catalysis*, **34**, 106–16.

Ekstrom, A. and Johnson, D. A. (1974) *J. Inorg. Nucl. Chem.*, **36**, 2549–56.

Eliseev, S. S., Glukhov, I. A., and Vozhdaeva, E. E. (1972) *Zh. Neorg. Khim.*, **17**, 1203–8; *Russ. J. Inorg. Chem.*, **17**, 627–9.

Ellens, A., Krämer, K., and Güdel, H. U. (1998) *J. Lumin.*, **76/77**, 548.

Eller, P. G., Larson, A. C., Peterson, J. R., Ensor, D. D., and Young, J. P. (1979) *Inorg. Chim. Acta*, **37**, 129–33.

Ellert, G. V., Tsapkin, V. V., Mikhailov, Yu. N., and Kuznetsov, V. G. (1965) *Zh. Neorg. Khim.*, **10**, 1572–80; (1965) *Russ. J. Inorg. Chem.*, **10**, 858–62.

Ellert, G. V., Eliseev, A. A., and Slovyanskikh, V. K. (1971) *Zh. Neorg. Khim.*, **16**, 1451; *Russ. J. Inorg. Chem.*, **16**, 768.

Ellert, G. V., Sevast'yanov, V. G., and Slovyanskikh, V. K. (1975) *Zh. Neorg. Khim.*, **20**, 221–7; *Russ. J. Inorg. Chem.*, **20**, 120–3.

Elliot, R. P. (1965) *Constitution of Binary Alloys,* 1st Suppl., McGraw-Hill, New York.

Ellison, A. J. G., Mazer, J. J., and Ebert, W. L. (1994) *Effect of Glass Composition on Waste Form Durability: A Critical Review*, Argonne National Laboratory Report, ANL-94/28, Argonne, IL, USA.

Engmann, R. and de Wolff, P. W. (1963) *Acta Crystallogr.*, **16**, 993–6.

Esch, U. and Schneider, A. (1948) *Z. Anorg. Allg. Chem.*, **257**, 254–66.

Espenson, J. H. (ed.) (1995) *Chemical Kinetics and Reaction Mechanisms,* McGraw-Hill, New York.

Evers, E. C. and Reynolds, M. B. (1954) U.S. Patent 2674518.

Ewing, R. C. (1999) *Proc. Nat. Acad. Sci.*, **96**, 3432–29.

Faber, J. Jr. and Lander, G. H. (1976) *Phys. Rev.*, **B14**, 1151–64.

Faile, S. P. (1978) *J. Crystal Growth*, **43**, 133–4.

Farges, F., Ponader, C. W., Calas, G., and Brown, G. E. (1992) *Geochim. Cosmochim. Acta*, **56**, 4205–20.

Farkas, I., Bányai, I., Szabó, Z., Wahlgren, U., and Grenthe, I. (2000a) *Inorg. Chem.*, **39**, 799–805.

Farkas, I., Grenthe, I., and Bányai, I. (2000b) *J. Phys. Chem. A*, **104**, 1201–6.

Faucher, M. D., Moune, O. K., Garcia, D., and Tanner, P. (1996) *Phys. Rev. B*, **53**, 9501–4.

Fawcett, J., Holloway, J. H., Laycock, D., and Russell, D. R. (1982) *J. Chem. Soc. Dalton Trans.*, 1355–60.

Fazekas, Z., Tomiyasu, H., Park, I.-L., Yamamura, T., and Harada, M. (1998) *Models in Chemistry*, **135** (5), 783–97, Akademiai,Kiadó, Budapest.

Fee, D. C. and Johnson, C. E. (1978) *J. Inorg. Nucl. Chem.*, **40**, 1375–81.

Feng, X., Buck, E. C., Mertz, C., Bates, J. K., Cunnane, J. C., and Chaiko, D. J. (1994) *Radiochim. Acta*, **66/67**, 197–205.

Ferguson, I. F. and Fogg, P. G. T. (1957) *J. Chem. Soc.*, 3679–81.

Ferguson, I. F. and Street, R. S. (1963) AERE Harwell Report, AERE-M 1192.

Fernandes, J. C., Continentino, M. A., and Guimarães, A. P. (1985) *Solid State Commun.*, **55**, 1011–15.

Figgins, P. E. and Bernardinelli, R. J. (1966) *J. Inorg. Nucl. Chem.*, **28**, 2193.

Finch, R. J. and Ewing, R. C. (1992) *J. Nucl. Mater.*, **190**, 133–56.

Finch, R. J., Suksi, J., Rasilainen, K., and Ewing, R. C. (1995) *Mater. Res. Soc. Symp. Proc.*, **353**, 647–52.

Finch, W. I. (1996) *Uranium Provinces of North America – Their Definition, Distribution, and Models*, U.S. Geological Survey Bulletin, 2141.

Finch, R. J., Cooper, M. A., Hawthorne, F. C., and Ewing, R. C. (1996a) *Can. Miner.*, **34**, 1071–88.

Finch, R. J., Suksi, J., Rasilainen, K., and Ewing, R. C. (1996b) *Mater. Res. Soc. Symp. Proc.*, **412**, 823–30.

Finch, R. J. and Ewing, R. C. (1997) *Am. Miner.*, **82**, 607–19.

Finch, R. J., Hawthorne, F. C., and Ewing, R. C. (1998) *Can. Miner.*, **36**, 831–45.

Finch, R. J. and Murakami, T. (1999) *Rev. Miner.*, **38**, 91–180.

Finch, R. J., Buck, E. C., Finn, P. A., and Bates, J. K. (1999a) *Mater. Res. Soc. Symp. Proc.*, **556**, 431–8.

Finch, R. J., Cooper, M. A., Hawthorne, F. C., and Ewing, R. C. (1999b) *Can. Miner.*, **37**, 929–38.

Findley, J. R., Gregory, J. N., and Weldrick, G. (1955) AERE Report, AERE-C/M-265.

Fine, M. A., Mendelson, A., and Schwartz, D. F. (1945) *Purification of Tuballoy by the Thermal Decomposition of Tuballoy Iodide*, CT-2695.

Fink, J. K. (2001) *World Wide Web, INSC Materials Properties Database*, http://www.insc.anl.gov/matprop/

Finnie, K. S., Zhang, Z., Vance, E. R., and Carter. M. L. (2003) *J. Nucl. Mater.*, **317**, 46–53.

Fischer, E. A., Kinsman, P. R., and Ohse, R. W. (1976) *J. Nucl. Mater.*, **59**, 125–36.

Fischer, E. O. and Hristidu, Y. (1962) *Z. Naturforsch.*, **17b**, 275–6.

Fisk, Z., Moreno, N. O., and Thompson, J. D. (2003) *J. Phys. Condensed Matter*, **15**, S1917–21.

Fitzmaurice, J. C. and Parkin, I. P. (1994) *New J. Chem.*, **18**, 825–32.

Flotow, H. E. and Abraham, B. M. (1951) Argonne National Laboratory, IL, Report AEDP-3074.

Flotow, H. E., Lohr, H. R., Abraham, B. M., and Osborne, D. W. (1959) *J. Am. Chem. Soc.*, **81**, 3529–33.

Flotow, H. E. and Osborne, D. W. (1967) *Phys. Rev.*, **164**, 755–8.

Flotow, H. E., Haschke, J. M., and Yamauchi, S. (1984) in *The Chemical Thermodynamics of Actinide Elements and Compounds, part 9, The Actinide Hydrides* (ed. F. L. Oetting), International Atomic Energy Agency, Vienna, pp. 32–44.

Fonteneau, G. and Lucas, J. (1974) *J. Inorg. Nucl. Chem.*, **36**, 1515–19.

Foote, F. (1956) *Proc. Int. Conf. on Peaceful Uses of Atomic Energy*, Geneva, 1955, vol. 9, p. 33.

Formosinho, S. J., Da Graca, M., and Miguel, M. (1984) *J. Chem. Soc., Faraday Trans. I*, **80**, 1745–56.

Formosinho, S. J., Da Graca, M., Miguel, M., and Burrows, H. D. (1984) *J. Chem. Soc., Faraday Trans. I*, **80**, 1717–33.

Fortner, J. A., Kropf, A. J., Finch, R. J., Bakel, A. J., Hash, M. C., and Chamberlain, D. B. (2002) *J. Nucl. Mater.*, **304**, 56–62.

Fournier, J.-M. and Troć, R. (1985) in *Handbook on the Physics and Chemistry of the Actinides* (eds. A. J. Freeman and G. H. Lander), vol. 2, North-Holland, Amsterdam, pp. 29–173.

Fredrickson, D. R. and Chasanov, M. G. (1970) *J. Chem. Thermodyn.*, **2**, 623–9.

Fredrickson, D. R. and Chasanov, M. G. (1972) *J. Chem. Thermodyn.*, **4**, 419–23.

Fredrickson, J. K., Zachara, J. M., Kennedy, D. W., Liu, C., Duff, M. C., Hunter, D. B., and Dohnalkova, A. (2002) *Geochim. Cosmochim. Acta*, **66**, 3247–62.

Freeman, A. J. and Darby, J. B. Jr (1974) *The Actinides: Electronic Structure and Related Properties,* Academic Press, New York.

Freestone, N. P. and Holloway, J. H. (1991) Actinide fluorides, in *Synthesis of Lanthanide and Actinide Compounds* (eds. G. Meyer and L. R. Morss), Kluwer, Dordrecht, pp. 67–133.

Frei, V. and Wendt, H. (1970) *Ber. Bunsenges. Phys. Chem.*, **74**, 593.

Friedman, H. A., Weaver, C. F., and Grimes, W. R. (1970) *J. Inorg. Nucl. Chem.*, **32**, 3131–3.

Friese, J. I., Nash, K. L., Jensen, M. P., and Sullivan, J. C. (1998) *Radiochim. Acta*, **83**, 175–81.

Friese, J. I., Nash, K. L., Jensen, M. P., and Sullivan, J. C. (2001) *Radiochim. Acta*, **89**, 35–41.

Frlec, B., Brčič, B. S., and Slivnik, J. (1966) *Inorg. Chem.*, **5**, 542–6.

Frlec, B. and Hyman, H. H. (1967) *Inorg. Chem.*, **6**, 2233–9.

Frolov, A. A. and Rykov, A. G. (1979) *Radiokhimiya*, **21**, 329–42; *Sov. Radiochem.*, **21**, 281–92.

Frondel, C. (1951a) *Am. Miner.*, **36**, 671–9.

Frondel, C. (1951b) *Am. Miner.*, **36**, 680–6.

Fuchs, L. H. and Gebert, E. (1958) *Am. Miner.*, **43**, 243–8.

Fuger, J. and Brown, D. (1973) *J. Chem. Soc. Dalton Trans.*, 428–34.

Fuger, J., Parker, V. B., Hubbard, W. N., and Oetting, F. L. (1983) *The Chemical Thermodynamics of Actinide Elements and Compounds,* part 8, The Actinide Halides, IAEA, Vienna, STI/PUB/424–8.

Fuji, K., Miyake, C., and Imoto, S. (1979) *J. Nucl. Sci. Technol.*, **16**, 207–13.

Fujino, T. and Naito, K. (1969) *J. Am. Ceram. Soc.*, **52**, 574–7.

Fujino, T. and Naito, K. (1970) *J. Inorg. Nucl. Chem.*, **32**, 627–36.

Fujino, T. (1972) *J. Inorg. Nucl. Chem.*, **34**, 1563–74.

Fujino, T., Masaki, N., and Tagawa, H. (1977) *Z. Kristallogr.*, **145**, 299–309.

Fujino, T., Tateno, J., and Tagawa, H. (1978a) *J. Solid State Chem.*, **24**, 11–19.

Fujino, T., Tagawa, H., Adachi, T., and Hashitani, H. (1978b) *Anal. Chim. Acta*, **98**, 373–83.

Fujino, T., Tagawa, H., and Adachi, T. (1981) *J. Nucl. Mater.*, **97**, 93–103.

Fujino, T., Ouchi, K., Yamashita, T., and Natsume, H. (1983) *J. Nucl. Mater.*, **116**, 157–65.

Fujino, T., Yamashita, T., and Tagawa, H. (1988) *J. Solid State Chem.*, **73**, 544–55.

Fujino, T. and Miyake, C. (1991) in *Handbook on the Physics and Chemistry of the Actinides* vol. 6 (eds. A. J. Freeman and C. Keller), North-Holland, Amsterdam, pp. 155–240.

Fujino, T., Ouchi, K., Mozumi, Y., Ueda, R., and Tagawa, H. (1990) *J. Nucl. Mater.*, **174**, 92–101.

Fujino, T. and Sato, N. (1992) *J. Nucl. Mater.*, **189**, 103–15.

Fujino, T., Sato, N., and Yamada, K. (1995) *J. Nucl. Mater.*, **223**, 6–19.

Fujino, T., Nakama, S., Sato, N., Yamada, K., Fukuda, K., Serizawa, H., and Shiratori, T. (1997a) *J. Nucl. Mater.*, **246**, 150–7.

Fujino, T., Sato, N., and Yamada, K. (1997b) *J. Nucl. Mater.*, **247**, 265–72.

Fujino, T., Sato, N., Yamada, K., Nakama, S., Fukuda, K., Serizawa, H., and Shiratori, T. (1999) *J. Nucl. Mater.*, **265**, 154–60.

Fujino, T., Sato, N., Yamada, K., Okazaki, M., Fukuda, K., Serizawa, H., and Shiratori, T. (2001a) *J. Nucl. Mater.*, **289**, 270–80.

Fujino, T., Park, K., Sato, N., and Yamada, M. (2001b) *J. Nucl. Mater.*, **294**, 104–11.

Fukushima, S., Ohmichi, T., Maeda, A., and Watanabe, H. (1981) *J. Nucl. Mater.*, **102**, 30–9.

Fukushima, S., Ohmichi, T., Maeda, A., and Watanabe, H (1982) *J. Nucl. Mater.*, **105**, 201–10.

Fukushima, S., Ohmichi, T., Maeda, A., and Handa, M. (1983) *J. Nucl. Mater.*, **114**, 312–25.

Fuoss, R. M. (1958) *J. Am. Chem. Soc.*, **80**, 5059–61.

Furman, N. H., Bricker, C. E., and Ditts, R. V. (1953) *Anal. Chem.*, **25**, 482–6.

Furman, S. C. (1957) Knolls Atomic Power Laboratory Report, KAPL-1664.

Gabuda, S. P., Matsutsin, A. A., and Zadneprovskii, G. M. (1969) *Zh. Strukt. Khimii*, **10**, 1115–16; (1969) *J. Struct. Chem.* (*USSR*), **10**, 996–8.

Gagarinskii, Yu. V., Khanaev, E. I., Galkin, N. P., Ananeva, L. A., and Gabuda, S. P. (1965) *At. Energy* (*USSR*)*, 18, 40–5;* (*1965*) *Sov. At. Energy*, **31**, 43–8.

Gagliardi, L., Grenthe, I., and Roos, B. O. (2001) *Inorg. Chem.*, **40**, 2976–8.

Gagliardi, L., Pyykkö, I., and Roos, B. O. (2005) *Phys. Chem. Chem. Phys.* **17**, 2415–17.

Gagliardi, L. and Roos, B. O. (2005a) *Nature*, **433**, 848–51.

Gagliardi, L. and Roos, B. O. (2005b) *Inorg. Chem. Prepublication, ASAP*, Dec. 15.

Gaines, R. V., Skinner, C. W., Foord, E. E., Mason, B., and Rosenzweig, A. (1997) *Dana's New Mineralogy: The System of Mineralogy of James Dwight Dana and Edward Salisbury Dana,* 8th edn, John Wiley, New York.

Gale, W. F. and Totemeier, T. C. (2003) *Smithells Metals Reference Book,* 8th edn, Elsevier, Amsterdam.

Galkin, N. P. and Sudarikov, B. N. (eds.) (1966) *Technology of Uranium*, Israel Program for Scientific Translations, Jerusalem; translated from Tekhnologiya Urana, Atomizdat, Moscow (1964).

Gamp, E., Edelstein, N., Khan Malek, C., Hubert, S., and Genet, M. (1983) *J. Chem. Phys.*, **79**, 2023–6.

Garg, S. P. and Ackermann, R. J. (1977) *Met. Trans.*, **8A**, 239–44.

Garg, S. P. and Ackermann, R. J. (1980) *J. Nucl. Mater.*, **88**, 309–11.

Garrido, F., Ibberson, R. M., Nowicki, L., and Willis, B. T. M. (2003) *J. Nucl. Mater.*, **322**, 87–9.

Gatehouse, B. M., Grey, I. E., and Kelly, P. R. (1979) *Am. Miner.*, **64**, 1010–17.

Gebert, E., Hoekstra, H. R., Reis, A. H. Jr, and Peterson, S. W. (1978) *J. Inorg. Nucl. Chem.*, **40**, 65–8.

Geichman, J. R., Smith, E. A. Trond, S. S., and Ogle, P. R. (1962) *Inorg. Chem.*, **2**, 1012–15.

Geichman, J. R., Smith, E. A., and Ogle, P. R. (1963) *Inorg. Chem.*, **1**, 661–5.

George, A. M. and Karkhanavala, M. D. (1963) *J. Phys. Chem. Solids*, **24**, 1207–12.

Gerdanian, P. (1964) CEA Report, CEA-R 2438.

Gerdanian, P. and Dodé, M. (1965) *J. Chim. Phys. Phys. Chim. Biol.*, **62**, 171–84.

Gerdanian, P. and Dodé, M. (1968) in *Thermodynamics of Nuclear Materials,* Proc. Symp. 1967, International Atomic Energy Agency, Vienna, pp. 41–54.

Gerdanian, P. (1974) *J. Phys. Chem. Solids*, **35**, 163–70.

Gerding, H., Prins, G., and Gabes, W. (1975) *Rev. Chim. Miner.*, **12**, 303–15.

Gesing, T. M. and Jeitschko, W. (1995) *Z. Naturforsch. B: Chem. Sci.*, **50**, 196–200.

Giammar, D. E. and Hering, J. G. (2002) *Geochim. Cosmochim. Acta.*, **66**, 3235–45.

Gibson, G. and Katz, J. J. (1951) *J. Am. Chem. Soc.*, **73**, 5436–8.

Gibson, G., Beintema, C. D., and Katz, J. J. (1960) *J. Inorg. Nucl. Chem.*, **15**, 110–14.

Gieré, R., Williams, C. T., and Lumpkin, G. R. (1998) *Schweiz Miner. Petrogr. Mitt.*, **78**, 433–59.

Gieré, R., Hatcher, C., Reusser, E., and Buck, E. C. (2002) *Mater. Res. Soc. Symp. Proc.*, **713**, 303–10.

Gillan, M. J. (1975) in *Thermodynamics of Nuclear Materials,* Proc. Symp. 1974, vol. I, International Atomic Energy Agency, Vienna, pp. 269.

Gilpatrick, L. O., Stone, H. H., and Secoy, C. H. (1964) Oak Ridge National Laboratory Report, ORNL-3591.

Ginderow, D. and Cesbron, F. (1983a) *Acta Crystallogr.*, **C39**, 1605–7.

Ginderow, D. and Cesbron, F. (1983b) *Acta Crystallogr.*, **C39**, 824–7.

Ginderow, D. and Cesbron, F. (1985) *Acta Crystallogr.*, **C41**, 654–7.

Ginderow, D. (1988) *Acta Crystallogr.*, **C44**, 421–4.

Gindler, G. E. (1962) *Radiochemistry of Uranium*, NAS-NS-3050, Technical Information Center, USAEC.

Gingerich, K. A. (1970) *J. Chem. Phys.*, **53**, 746–8.

Girdhar, H. L. and Westrum, E. F. Jr (1968) *J. Chem. Eng. Data*, **13**, 531–3.

Gittus, J. H. (1963) *Uranium,* Butterworths, Washington.

Gleichman, J. R., Ogle, P. R., and Swaney, L. R. (1961) *Reactions of Molybdenium, Tungsten and Uranium Hexafluoride with Nitrogen Compounds,* III, *Reactions with Nitrogen Dioxide and Nitrogen Oxyhalides*, GAT-T-809.

Gmelin, Handbook of Inorganic, chemistry, System no. 55, *Uran und Isotope mit einem Anhang über Transurane.* (1936) *Main volume,* Verlag Chemie, Berlin.

Gmelin Handbook of Inorganic Chemistry, Suppl. Ser., *Uranium*, Springer-Verlag, Berlin, Heidelberg, and New York.

(1979a) vol. Al, Uranium Deposits.

(1979b) vol. C9, Compounds with Chlorine, Bromine, and Iodine.

(1979c) vol. E1, Coordination Compounds.

(1980a) vol. A2, Isotopes.

(1980b) vol. C8, Compounds with Fluorine.

(1980c) vol. E2, Coordination Compounds (including Organouranium Compounds).

(1981a) vol. A3, Technology Uses.

(1981b) vol. C7, Compounds with Nitrogen.

(1981c) vol. C11, Compounds with Selenium, Tellurium, and Boron.

vol. C12, Carbides.

(1981d) vol. C14, Compounds with P, As, Sb, Bi, Ge.

(1982a) vol. A4, Irradiated Fuel Reprocessing.

(1982b) vol. A5, Spectra.

(1982c) vol. A7, Analytical Chemistry. Determination of the Isotope Composition. Biological Behavior. Health Protection and Safety Control.

vol. B2, Alloys with Alkali metals, Alkaline Earths, and Elements of Main Groups III and IV.

vol. B3, Alloys with Transition Metals of Groups IB to IVB.

(1983a) vol. A6, General Properties – Criticality.

(1983b) vol. C13, Carbonates, Cyanides, Thiocyanates, Alkoxides, Carboxylates, Compounds with Si.

(1983c) vol. D4, Cation Exchange and Chromatography.

(1984a) vol. C4, Uranium Dioxide. Preparation and Crystallographic Properties.

vol. C5, Uranium Dioxide. Physical Properties. Electrochemical Behavior.

(1984b) vol. C10, Compounds with Sulfur.

(1984c) vol. D1, Properties of U ions in Solutions and Melts.

(1982d) vol. D2, Solvent Extraction.

(1982e) vol. D3, Anion Exchange.

(1995a) vol. B4, Alloys with Transition Metals of Groups VB to VIIB.

vol. C1, Compounds with Rare Gases, and Hydrogen.System Uranium-Oxygen.

vol. C2, Oxides U_3O_8 and UO_3. Hydroxides. Oxide Hydrides. Peroxides.

vol. C3, Ternary and Polynary Oxides.

(1995b) vol. D5, Chemistry in Nonaqueous Solutions (Conductivity, Molecular weight, Solubility)

(1996a) vol. C6, Uranium Dioxide. Chemical Behavior.

(1996b) vol. D6, Chemistry in Nonaqueous Solutions (Formation of Complexes and Redox Reactions).

Gnandi, K. and Tobschall, H. J. (2003) *J. African Earth Sci.*, **37**, 1–10.

Gonsalves, J. W., Steenkamp, P. J., and du Preez, J. G. H. (1977) *Inorg. Chim. Acta*, **21**, 167–72.

Gorban, Yu. A., Pavlinov, L. V., and Bykov, V. N. (1967) *Sov. At. Energy*, **22**, 580–4.

Gordon, G. and Taube, H. (1961a) *J. Inorg. Nucl. Chem.*, **16**, 189–91.

Gordon, G. and Taube, H. (1961b) *J. Inorg. Nucl. Chem.*, **16**, 272–8.

Gorokhov, L. N., Emelyanov, A. M., and Khodeev, Y. S. (1974) *Teplofiz. Vyz. Temp.*, **12**, 1307–09.

Gotoo, K. and Naito, K. (1965) *J. Phys. Chem. Solids*, **26**, 1673–7.

Gray, C. W. (1994) *Methods Mol. Biol.*, **22**, 1–12.

Gray, C. W. (2001) *Methods Mol. Biol.*, **148**, 579–87.

Graziani, R., Bombieri, G., Forsellini, E., and Paolucci, G. (1975) *J. Crystal Mol. Struct.*, **5**, 1–14.

Greaves, C. and Fender, B. E. F. (1972) *Acta Crystallogr.*, **B28**, 3609–14.

Greaves, C., Cheetham, A. K., and Fender, B. E. F. (1973) *Inorg. Chem.*, **12**, 3003–7.

Greegor, R. B., Lytle, F. W., Chakoumakos, B. C., Lumpkin, G. R., Warner, J. K., and Ewing, R. C. (1989) *Mater. Res. Soc. Symp. Proc.*, **127**, 261–8.

Greek, B. F., Allen, O. W., and Tynan, D. E. (1957) *Ind. Eng. Chem.*, **49**, 628.

Greenberg, E. and Westrum, E. F. Jr (1956) *J. Am. Chem.Soc.*, **78**, 5144–7.

Gregory, N. W. (1958) in *The Chemistry of Uranium, Collected Papers.* TID-5290 (eds. J. J. Katz and E. Rabinowitch), USA EC Technical Information Extension, Oak Ridge, TN, pp. 465–510.

Grenthe, I., Ferri, D., Salvatore, F., and Diego, F. (1984) *J. Chem. Soc. Dalton Trans.*, 2439–43.

Grenthe, I., Fuger, J., Konings, R. J. M., Lemire, R. J., Muller, A. B., Nguyen-Trung, C., and Wanner, H. (1992) *Chemical Thermodynamics of Uranium,* NEA/OECD, North Holland.

Grenthe, I., Sandino, M. C. A., Puigdomenech, L., and Rand, M. H. (1995) *Corrections to the Uranium NEA-TDB Review. Appendix D in vol. 2. Chemical Thermodynamics of Americium*. By R. J. Silva *et al.* Nuclear Energy Agency, OECD, p. 347–74. Elsevier, Amsterdam.

Grenthe, I., Hummel, W., and Puigdomenech, I. (1997) in *Modelling in Aquatic Chemistry* (eds. I. Grenthe and I. Puigdomenech), Nuclear Energy Agency, OECD, Paris, ch. III.

Griffiths, T. R. and Volkovich, V. A. (1999) *J. Nucl. Mater.*, **274**, 229–51.

Grimes, W. R. (1978) Report CONF-780571-1; *Energy Res. Abstr.*, **3** (22), no. 52726.

Grimes, W. R. and Cuneo, D. R. (1960) in *Reactor Handbook,* vol. 1 (ed. R. Tripton), Interscience Publishers, New York.

Grønvold, F. (1955) *J. Inorg. Nucl. Chem.*, **1**, 357–70.

Grønvold, F., Kveseth, N. J., Sveen, A., and Tichý, J. (1970) *J. Chem. Thermodyn.*, **2**, 665–79.

Gross, E. B., Corey, A. S., Mitchell, R. S., and Walenta, K. (1958) *Am. Miner.*, **43**, 1134–43.

Grossman, L. N. and Priceman, S. (1954) *Nucleonics*, **12 (6)**, 68–9.

Grossman, L. N., Lewis, J. E., and Rooney, D. M. (1967) *J. Nucl. Mater.*, **21**, 302–9.

Gruen, D. M., Koehler, W. C., and Katz, J. J. (1951) *J. Am. Chem. Soc.*, **73**, 1475–9.

Gruen, D. M. (1955) *J. Chem. Phys.*, **23**, 1708–10.

Gruen, D. M. and McBeth, R. L. (1968) *Inorg. Nucl. Chem. Letters*, **4**, 294–8.

Gruen, D. M. and McBeth, R. L. (1969) *Inorg. Chem.*, **8**, 2625–33.

Grunzweig-Genossar, J., Kuznietz, M., and Meerovici, B. (1970) *Phys. Rev. B*, **1**, 1958–77.

Gueguin, M. M. (1964) *Bull. Soc. Chim. France*, 1184–7.

Guéneau, C., Dauvois, V., Pérodeaud, P., Gonella, C., and Dugne, O. (1998) *J. Nucl. Mater.*, **254**, 158–74.

Guéneau, C., Baichi, M., Labroche, D., Chatillon, C., and Sundman, B. (2002) *J. Nucl. Mater.*, **304**, 161–75.

Guest, R. J. and Zimmerman, J. B. (1955) *Anal. Chem.*, **27**, 931–6.

Guilbaud, P. and Wipff, G. (1993) *J. Phys. Chem. A*, **97**, 5685–92.

Guillaumont, R., Fanghänel, T., Fuger, J., Grenthe, I., Palmer, D., Rand, M., and Neck, V. (2003) *Chemical Thermodynamics of Uranium, Neptunium, Plutonium, Americium and Technetium,* NEA/OECD, North Holland.

Guinet, P., Vaugoyeau, H., and Blum, P. L. (1966) *C.R. Acad. Sci.* (*Paris*), **C263**, 17–20.

Gurevich, A. M., Polozhenskaya, L. P., Osicheva, N. P., and Solntseva, L. F. (1971a) *Radiokhimiya*, **13**, 688–692; *Sov. Radiochem.*, **13**, 706–9.

Gurevich, A. M., Polozhenskaya, L. P., and Osicheva, N. P. (1971b) *Radiokhimiya*, **13**, 588–92; *Sov. Radiochem.*, **13**, 604–7.

Gusev, Yu. K., Lychev, A. A., Mashirov, L. G., and Suglobov, D. N. (1985) *Radiokhimiya*, **27**, 412–15.

Güsten, H. (1983) in *Gmelin Handbook of Inorganic Chemistry,* Suppl., vol. A6, Springer-Verlag, Berlin-Heidelberg. ch. 3,

Haas, W. O. Jr and Smith, D. J. (1956) *Thorex Process Development at KAPL,* KAPL-1306 (declassified with deletions).

Habenschuss, A. and Spedding, F. H. (1980) *Crystal Struct. Commun.*, **9**, 71–6.

Haegele, R. and Boeyens, J. C. A. (1977) Nat. Inst. Met. Repub. S. Africa Res. Rep. no 1856.

Hagberg, D., Karlström, G., Roos, B. O., and Gagliardi, L. (2005) *J. Am. Chem. Soc.* **127**, 14250–6.

Hagemark, K. and Broli, M. (1966) *J. Inorg. Nucl. Chem.*, **28**, 2837–50.

Hagemark, K. and Broli, M. (1967) *J. Am. Ceram. Soc.*, **50**, 563–7.

Hagrman, D. T. (1995) SCADAP/RELAP5/MOD 3.1 Code Manual vol. 4, MATPRO, NUREG/CR-6150.

Hahn, O. (1925) *Z. Anorg. Chem.*, **147**, 16–23.

Hahn, O., Meitner, L., and Strassmann, F. (1937) *Ber. Dtsch. Chem. Ges.*, **70**, 1374–92.

Hahn, O. and Strassmann, F. (1939) *Naturwissenschaften*, **27**, 11–12.

Hall, D. A., Rae, A. D., and Waters, T. N. (1966) *Acta Crystallogr.*, **20**, 160–2.

Halliday, A. N., Lee, D.-C., Christensen, J. N., Rehkämper, M., Yi, W., Luo, X., Hall, C. M., Ballentine, C. J., Pettke, T., and Stirling, C. (1998) *Geochim. Cosmochim. Acta*, **62**, 919–40.

Halstead, G. W., Eller, P. G., and Eastman, P. (1979) *Inorg. Chem.*, **18**, 2867–72.

Handler, P. and Hutchison, C. A. (1956) *J. Chem. Phys.*, **25**, 1210–15.

Hansen, M. and Anderko, K. (1958) *Constitution of Binary Alloys,* McGraw-Hill, New York.

Hanson, S. L., Simmons, W. B., Falster, A. U., Foord, E. E., and Lichte, F. E. (1999) *Min. Mag.*, **63**, 27–36.

Hanuza, J., Hermanowicz, K., Macalik, L., Drożdżyński, J., Zych, E., and Meyer, G. (1999) *Vibrational Spectrosc.*, **21**, 111–26.

Harbottle, G. and Evans, C. V. (1997) *Radioact. Radiochem.*, **8**, 38–46.

Harrington, C. D. and Ruehle, A. E. (1959) *Uranium Production Technology,* Van Nostrand, Princeton, p. 461.

Harris, L. A. and Taylor, A. J. (1962) *J. Am. Ceram. Soc.*, **45**, 25.

Hart, F. A. and Tajik, M. (1983) *Inorg. Chim. Acta*, **71**, 169–73.

Haschke, J. M. (1991) in *Synthesis of Lanthanide and Actinide Compounds* (eds. G. Meyer and L. R. Morss), Kluwer Academic Publishers, Dordrecht, pp. 1–53.

Hauck, J. (1969) *Z. Naturforsch.*, **24b**, 1067–8.

Hauck, J. (1973) *Z. Naturforsch.*, **28b**, 215–16.

Hauck, J. (1974) *J. Inorg. Nucl. Chem.*, **36**, 2291–8.

Haug, H. and Weigel, F. (1963) *J. Nucl. Mater.*, **9**, 355–9.

Hay, P. J., Martin, R. L., and Schreckenbach, G. (2000) *J. Phys. Chem. A*, **104**, 6259–70.

Hayden, L. A. and Burns, P. C. (2002) *J. Solid State Chem.*, **163**, 313–18.

Hecht, H. G. and Gruber, J. B. (1974) *J. Chem. Phys.*, **60**, 4872–9.

Hecht, H. G., Malm, J. G., Foropoulos, J., and Carnall, W. T. (1986a) *J. Chem. Phys.*, **84**, 3653–62.

Hecht, H. G., Malm, J. G., and Carnall, W. T. (1986b) *J. Less Common Metals*, **115**, 79–89.

Heckers, U., Jacobs, H., and Kockelmann, W. (2003) *Z. Anorg. Allg. Chem.*, **629**, 2431–2.

Heidt, L. J. and Moon, K. A. (1953) *J. Am. Chem. Soc.*, **75**, 5808–9.

Hein, R. A. and Flagella, P. N. (1968) General Electric Report, GEMP-578.

Hein, R. A., Sjodahl, L. H., and Szwarc, R. (1968) *J. Nucl. Mater.*, **25**, 99–102.

Hellberg, K.-H. and Schneider, H. (1981) in *Gmelin Handbuch der Anorganischen Chemie*, System no. 55, Uranium, Suppl., vol. A3, Springer, Berlin, *Technology*, pp. 121–47.

Helm, L. and Mehrbach, A. E. (1999) *Coord. Chem. Rev.*, **187**, 151–81.

Helm, L. and Mehrbach, A. E. (2002) *J. Chem. Soc. Dalton Trans.*, 633–41.

Henche, G., Fiedler, K., and Gruehn, R. (1993) *Z. Anorg. Allg. Chem.*, **619**, 77–87.

Hendricks, M. E. (1971) DP-MS-71-46, p. 195.

Hendricks, M. E., Jones, E.R. Jr, Stone, J. A., and Karraker, D. G. (1971) *J. Chem. Phys.*, **55**, 2993–7.

Hendricks, M. E., Jones, E. R. Jr, Stone, J. A., and Karraker, D. G. (1974) *J. Chem. Phys.*, **60**, 2095–103.

Henkie, Z., Johanson, W. R., Crabtree, G. W., Dye, D. H., and Arko, A. J., Bazan, C. (1981) *Actinides*, Abstracts of September 1981 Asilomar Conf., Pacific Grove, CA, LBL-12441, pp. 176–8.

Henry, W. E. (1958) *Phys. Rev.*, **109**, 1976–80.

Hermann, J. A. and Suttle, J. F. (1957) *Inorg. Synth.*, **5**, 143–5.

Herrmann, H. (1861) *Uber verschiedene Uranverbindungen,* Dissertation, Göttingen.

Hidaka, H. and Holliger, P. (1998) *Geochim. Cosmochim. Acta*, **62**, 89–108.

Hiernaut, J. P., Hyland, G. J., and Ronchi, C. (1993) *Int. J. Thermophys.*, **14**, 259–83.

Higgins, L. R. and Roberts, J. T. (1956) *Development of the EXCER Process*, Part I, ORNL-1696.

Hildenbrand, D. (1977) *J. Chem. Phys.*, **66**, 4788.

Hill, D. C., Handwerk, J. H., and Beals, R. J. (1963) Argonne National Laboratory Report, ANL-6711.

Hill, F. C. (1999) *Rev. Miner.*, **38**, 635–79.

Hill, F. C. and Burns, P.C. (1999) *Can. Miner.*, **37**, 1283–8.

Hinatsu, Y. and Fujino, T. (1985) *J. Solid State Chem.*, **60**, 244–51.

Hinatsu, Y. and Fujino, T. (1986) *J. Solid State Chem.*, **62**, 342–50.

Hinatsu, Y. and Fujino, T. (1987) *J. Solid State Chem.*, **68**, 255–65.

Hinatsu, Y. and Fujino, T. (1988a) *J. Solid State Chem.*, **73**, 348–55.

Hinatsu, Y. and Fujino, T. (1988b) *J. Solid State Chem.*, **73**, 388–97.

Hinatsu, Y. and Fujino, T. (1988c) *J. Solid State Chem.*, **74**, 163–70.

Hinatsu, Y. and Fujino, T. (1988d) *J. Solid State Chem.*, **74**, 393–400.

Hinatsu, Y., Masaki, N., and Fujino, T. (1988) *J. Solid State Chem.*, **73**, 567–71.

Hinatsu, Y., Fujino, T., and Edelstein, N. (1992a) *J. Solid State Chem.*, **99**, 95–102.

Hinatsu, Y., Fujino, T., and Edelstein, N. (1992b) *J. Solid State Chem.*, **99**, 182–8.

Hines, M. A., Sullivan, J. C., and Nash, K. L. (1993) *Inorg Chem.*, **32**, 1820–3.

Ho, C. I., Powell, R. W., and Liley, P. E. (1972) *J. Phys. Chem. Ref. Data*, **1**, 279–421.

Hoard, J. L. and Stroupe, J. D. (1959) in *The Chemistry of Uranium – Collected Papers*, TID-5290, vol. 1, 325–49.

Hoch, M. and Furman, F. J. (1966) in *Thermodynamics*, Proc. Symp. 1965, International Atomic Energy Agency, Vienna, vol. 2, pp. 517–32.

Hodge, M. (1960) *Advances in Inorganic Chemistry and Radiochemistry,* vol. 2, Academic Press, New York, ch. 7.

Hoekstra, H. R. and Katz, J. J. (1952) *J. Am. Chem. Soc.*, **74**, 1683–90.

Hoekstra, H. R., Siegel, S., Fuchs, L. H., and Katz, J. J. (1955) *J. Phys. Chem.*, **59**, 136–8.

Hoekstra, H. and Siegel, S. (1956) in *Proc. First Int. Conf. on Peaceful Uses of Atomic Energy*, Geneva, vol. 7, P/737, 394–400.

Hoekstra, H. R. and Siegel, S. (1958) in *Proc. Second Int. Conf. on Peaceful Uses of Atomic Energy*, Geneva, paper 15/P/1548.

Hoekstra, H. R., Santoro, A., and Siegel, S. (1961) *J. Inorg. Nucl. Chem.*, **18**, 166–78.

Hoekstra, H. R. and Siegel, S. (1961) *J. Inorg. Nucl. Chem.*, **18**, 154–65.

Hoekstra, H. R. and Siegel, S. (1964) *J. Inorg. Nucl. Chem.*, **26**, 693–700.

Hoekstra, H. R. (1965) *J. Inorg. Nucl. Chem.*, **27**, 801–8.

Hoekstra, H. R. and Marshall, R. H. (1967) in *Lanthanide/Actinide Chemistry* (eds. P. Fields and T. Moeller), (ACS Advan. Chem. Ser. 71), American Chemical Society, Washington, DC, ch. 16, pp. 211–27.

Hoekstra, H. R., Siegel, S., and Charpin, P. (1968) *J. Inorg. Nucl. Chem.*, **30**, 519–23.

Hoekstra, H. R., Siegel, S., and Gallagher, F. X. (1970) *J. Inorg. Nucl. Chem.*, **32**, 3237–48.

Hoekstra, H. R. and Siegel, S. (1973) *J. Inorg. Nucl. Chem.*, **35**, 761–79.

Högfeldt, E. (1982) *Stability Constants of Metal-Ion Complexes. Part A Inorganic Ligands,* IUPAC Chemical Data Series no. 21, Pergamon Press, New York.

Holc, J. and Kolar, D. (1983) *J. Solid State Chem.*, **47**, 98–102.

Holden, A. N. (1958) *Physical Metallurgy of Uranium,* Addison-Wesley, London.

Holden, N. E. (1977) *Isotopic Composition of the Elements and Their Variation in Nature – A Preliminary Report, BNL-NCS-50605; (1979) Pure Appl. Chem.*, **52**, 2371.

Horwitz, E. P., Dietz, M. L., Chiarizia, R., Diamond, H., and Nelson, D. M. (1993) *Anal. Chim. Acta*, **281**, 361–72.

Hoskins, P. W. O. and Burns, P. C. (2003) *Miner. Mag.*, **67**, 689–96.

Howard, C. J., Taylor, J. C., and Waugh, A. B. (1982) *J. Solid State Chem.*, **45**, 396–8.

Howes, K. R., Bakac, A., and Espenson, J. H. (1988) *Inorg. Chem.*, **27**, 791–4.

Howlett, B. (1959/1960) *J. Inst. Met.*, **88**, 91–2.

Hsini, S., Caignol, E., Metin, J., Avignant, D., and Cousseins, J. C. (1986) *Rev. Chim. Minér.*, **23**, 35–47.

Hughes, K.-A. and Burns, P. C. (2003) *Am. Miner.*, **88**, 962–6.

Hughes, K.-A., Burns, P. C., and Kolitsch, U. (2003) *Can. Miner.*, **41**, 677–85.

Hughes-Kubatko, K.-A., Helean, K., Navrotsky, A., and Burns, P. C. (2003) *Science*, **302**, 1191–3.

Hughes-Kubatko, K. A., Helean, K., Navrotsky, A., and Burns, P. C. (2005) *Am. Miner.*, **90**, 1284–90.

Huie, R. E., Clifton, C. L., and Neta, P. (1991) *Radiat. Phys. Chem.*, **38**, 477–81.

Hummel, P., Winkler, J. R., and Gray, H. B. (2006) *J. Chem. Soc. Dalton Trans*. 168–71.

Hund, F., Peetz, U., and Kottenhahn, G. (1965) *Z. Anorg. Allg. Chem.*, **278**, 184–91.

Huntzicker, J. J. and Westrum, E. F. Jr (1971) *J. Chem. Thermodyn.*, **3**, 67–76.

Hutchings, M. T., Clausen, K., Dickens, M. H., Hayes, W., Kjems, J. K., Schnabel, P. G., and Smith, C. (1984) *J. Phys. C*, **17**, 3903–40.

Hutchings, M. T., Clausen, K., Hayes, W., Macdonald, J. E., Osborn, R., and Schnabel, P. (1985) *High Temp. Sci.*, **20**, 97–108.

Hyeon, J.-Y., Gottfriedsen, J., and Edelman, F. T. (2005) *Coord. Chem. Rev.* **249(24)** 2787–844.

Hyman, H. H., Sheft, I., and Katz, J. J. (1955) *Nuclear Engineering and Science Congress,* Cleveland, OH, Preprint 1997.

IAEA (1965) *Thermodynamic and Transport Properties of Uranium Dioxide and Related Phases*, Technical Report Series 39, IAEA, Vienna, STI/DOC/10/39 (1965).

IAEA (1966) *Processing of Low Grade Uranium Ores*, Proc. Panel convened by the International Atomic Energy Agency, Vienna, June 27–July 1, 1966, IAEA, Vienna, STI/PUB/146.

IAEA (1970) *The Recovery of Uranium*, Proc. Symp. Sao Paulo, Brazil, August 17–21, 1970, International Atomic Energy Agency, Vienna, STI/PUB/262.

IAEA (1978) *IWGFR Meeting on Equation of State of Materials of Relevance to the Analysis of Hypothetical Fast Breeder Reactor Accidents*, Harwell, UK, International Atomic Energy Agency,Vienna.

IAEA (1980) *Production of Yellow Cake and Uranium Fluorides*, Proc. Advisory Group Meeting organized by the IAEA, Paris, June 5–8, 1979, International Atomic Energy Agency, Vienna, STI/PUB/553.

Iandelli, A. (1952) *Atti Acad. Lincei, Class. Sci. Fiz. Mat. Nat. Rend.*, **13**, 138–44.

Ifill, R. O., Cooper, W. C., and Clark, A. H. (1996) *CIM Bull.*, **89**, 93–103.

Ikeda, Y., Soya, S., Fukutomi, H., and Tomiyasu, H. (1979a) *J. Inorg. Nucl. Chem.*, **41**, 1333–7.

Ikeda, Y., Tomiyasu, H., and Fukutomi, H. (1979b) *Bull. Res. Lab. Nucl. Reactors*, **4**, 47–59.

Ikeda, Y., Tomiyasu, H., and Fukutomi, H. (1984) *Inorg. Chem.*, **23**, 1356–60.

Imai, H. (1957) *Bull. Chem. Soc. Japan*, **30**, 873.

Inaba, H. and Naito, K. (1973) *J. Nucl. Mater.*, **49**, 181–8.

Inaba, H., Shimizu, H., and Naito, K. (1977) *J. Nucl. Mater.*, **64**, 66–70.

Inada, Y., Wisniewski, P., Murakawa, M., Aoki, D., Miyake, K., Watanabe, N., Haga, Y., Yamamoto, E., and Onuki, Y. (2001) *J. Phys. Soc. Japan*, **70**, 558–68.

Ingamells, C. O. and Pitard, F. (1986) *Applied Geochemical Analysis,* John Wiley, New York.

Ippolitova, E. A., Simanov, Yu. P., Kovba, L. M., Polunina, G. P., and Berznikova, N. A. (1959) *Radiokhimiya*, **1**, 660–4.

Ippolitova, E. A. and Kovba, L. M. (1961) *Dokl. Akad. Nauk. SSSR*, **138**, 377–80.

Ippolitova, E. A., Efremova, K. M., Orlinkova, O. L., and Simanov, Yu. P. (1961a) Argonne National Laboratory Report, ANL-trans-33, p. 52.

Ippolitova, E. A., Bereznikova, I. A., Kosynkin, V. D., Simanov, Yu. P., and Kovba, L. M. (1961b) Argonne National Laboratory Report, ANL-trans-33, p. 180.

Ippolitova, E. A., Bereznikova, I. A., Leonidov, V. Y., and Kovba, L. M. (1961c) Argonne National Laboratory Report, ANL-trans-33, p. 186.

Ippolitova, E. A., Simanov, Yu. P., Kovba, L. M., Murav'eva, I. A., and Krasnoyarskaya, A. A. (1961d) Argonne National Laboratory Report, ANL-trans-33, p. 153.

Ippolitova, E. A., Polunina, G. P., Kovba, L. M., and Simanov, Yu. P. (1961e) Argonne National Laboratory Report, ANL-trans-33, p. 213.

Ishii, T., Naito, K., and Oshima, K. (1970a) *J. Solid State Chem.*, **8**, 677–83.

Ishii, T., Naito, K., and Oshima, K. (1970b) *J. Nucl. Mater.*, **35**, 335–44.

Ishii, T., Naito, K., and Oshima, K. (1970c) *J. Nucl. Mater.*, **36**, 288–96.

Ivanov, V. E., Krugich, A. A., Pavlov, V. C., Kovtun, G. P., and Amonenko, V. M. (1962) in *Thermodynamics of Nuclear Materials,* Proc. Symp. 1962, International Atomic Energy Agency, Vienna, pp. 735–47.

Ivanov, S. B., Mikhailov, Yu. N., Kuznetsov, V. G., and Davidovich, R. L. (1980) *Koord. Khim.* [*Coord. Chem. (USSR)*], **6**, 1746–50.

Ivanov, S. B., Mikhailov, Yu. N., Kusnetsov, V. G., and Davidovich, R. L. (1981) *Zh. Strukt. Khim.*, **22**, 188–91.

Ivanov, S. B., Mikhailov, Yu. N., and Davidovich, R. L. (1982) *Koord. Khim.* (*Coord. Chemistry, USSR*), **8**, 1250–5.

Ivanovich, M. and Murray, A. (1992) in *Uranium Series Disequilibrium Applications to Earth, Marine, and Environmental Sciences* (eds. M. Ivanovich and R. S. Harmon), Clarendon Press, Oxford, pp. 127–73.

Iwasaki, M., Ishikawa, N., Ohwada, K., and Fujino, T. (1981) *Inorg. Chim. Acta*, **54**, L193–4.

Jackson, J. M. and Burns, P. C. (2001) *Can. Miner.*, **39**, 187–95.

Jackson, R. A., Murray, A. D., Harding, J. H., and Catlow, C. R. A. (1986) *Phil. Mag.*, **A53**, 27–50.

Jacob, I., Hadari, Z., and Reilly, J. J. (1984) *J. Less Common Metals*, **103**, 123–7.

Jacobs, H., Heckers, U., Zachwieja, U., and Kockelmann, W. (2003) *Z. Anorg. Allg. Chem.*, **629**, 2240–3.

Jakeš, D., Moravec, J., Křivý, I., and Sedláková, L. (1966) *Z. Anorg. Allg. Chem.*, **347**, 218–22.

Jakeš, D. and Schauer, V. (1967) *Proc. Brit. Ceram. Soc.*, **8**, 123–5.

Jakeš, D. (1973) *Colloq. Czech. Chem. Commun.*, **38**, 1–6.

Jakeš, D. and Křivý, I. (1974) *J. Inorg. Nucl. Chem.*, **36**, pp. 3885.

Jacob, E. and Polligkeit, W. (1973) *Z. Naturforsch.*, **28b**, 120–4.

Jacob, E. (1982) *Angew. Chem. Int. Ed. Engl.*, **21**, 142–3; (1982) *Angew. Chem.*, Suppl., 317.

Janeczek, J. and Ewing, R. C. (1991) *J. Nucl. Mater.*, **185**, 66–77.

Janeczek, J. and Ewing, R. C. (1992) *J. Nucl. Mater.*, **190**, 128–32.

Janeczek, J. (1999) *Rev. Miner.*, **38**, 321–92.

Jayadevan, N. G., Singh Mudher, K. D., and Chackraburtty, D. M. (1974) Bhabha Atomic Research Center Report, BARC-726.

Jensen, K. A., Palenik, C. S., and Ewing, R. C. (2002) *Radiochim. Acta*, **90**, 761–70.

Jerden, J. L. and Sinha, A. K. (2003) *Appl. Geochem.*, **18**, 823–43.

Jiang, J., Sarsfield, M. J., Renshaw, J. C., Livens, F. R., Collison, D., Charnock, J. M., Helliwell, M., and Eccles, H. (2002) *Inorg. Chem.*, **41**, 2799–806.

Jocher, W. G. (1978) Research Center Karlsruhe Report, KFK-2518.

Johansson, G. (1992) Structures of complexes in solution derived from X-ray diffraction measurements, in *Advances in Inorganic Chemistry* (ed. A. G. Sykes), Academic Press, Londonvol. 39.

Johnson, O., Powell, T., and Nottorf, R. (1974) *A Summary, of the Properties, Preparation and Purification of the Anhydrous Chlorides and Bromides of Uranium*, part A, Uranium Chlorides, part B, Uranium Bromides, CC-1974.

Johnson, Q., Biel, T. J., and Leider, H. R. (1976) *J. Nucl. Mater.*, **60**, 231–3.

Johnston, D. R., Satten, R. A., Schreiber, C. L., and Wong. E. (1966) *J. Chem. Phys.*, **44**, 3141–3.

Jones, E. R. Jr, Hendricks, M. E., Stone, J. A., and Karraker, D. G. (1974) *J. Chem. Phys.*, **60**, 2088–94.

Jones, L. H. (1958) *Spectrochim. Acta*, **10**, 395–403.

Jones, L. H. (1959) *Spectrochim. Acta*, **15**, 409–11.

Jones, L. V., Etter, D. E., Hudgens, C. R., Huffman, A. A., Rhinehammer, T. B., Rogers, N. E., and Wittenberg, L. J. (1959) Phase Equilibria in the LiF-BeF_2-UF_4 Ternary Fused Salt System, MLM-1080.

Jones, W. M., Gordon, J., and Long, E. A. (1952) *J. Chem. Phys.*, **20**, 695–9.

Joubert, P. and Bougon, R. (1975) *Compt. Rend.*, **C280**, 193–5.

Joubert, P., Bougon, R., and Gandreau, B. (1978a) *Can. J. Chem.*, **56**, 1874–80.

Joubert, P., Weulersse, J. M., Bougon, R., and Gaudreau, B. (1978b) *Can. J. Chem.*, **56**, 2546–9.

Jove, J. and Cousson, A. (1977) *Radiochim. Acta*, **24**, 73–5.

Jung, W.-S. and Juza, R. (1973) *Z. Anorg. Allg. Chem.*, **399**, 148–62.

Jung, W.-S., Harada, M., Tomiyasu, H., and Fukutomi, H. (1988) *Bull. Chem. Soc. Jpn.*, **61**, 3895–900.

Juza, R. and Sievers, R. (1965) *Naturwissenschaften*, **52**, 538–8.

Juza, R. and Meyer, W. (1966) *Naturwissenschaften*, **53**, 552.

Juza, R. and Meyer, W. (1969) *Z. Anorg. Allg. Chem.*, **366**, 43–50.

Kaltsyoannis, N. (2000) *Inorg. Chem.*, **39**, 6009–17.

Kanellakopulos, B., Henrich, E., Keller, C., Baumgärtner, F., König, E., and Desai, V. P. (1980) *Chem. Phys.*, **53**, 197–213.

Kanellakopulos, B. (1983) Electron paramagnetic resonance, in *Gmelin Handbook of Inorganic Chemistry*, System no. 55, Uranium, Suppl., vol. A6, Springer, Berlin, pp. 241–50.

Karabulut, M., Marasinghe, G. K., Ray, C. S., Day, D. E., Waddill, G. D., Allen, P. G., Booth, C. H., Bucher, J. J., Caulder, D. L., Shuh, D. K., Grimsditch, M., and Saboungi, M.-L. (2000) *J. Mater. Res.*, **15**, 1972–84.

Karbowiak, M. and Drożdżyński, J. (1990) *J.Less Common Metals*, **164**, 159–64.

Karbowiak, M. and Drożdżyński, J. (1993) *J. Alloys Compds*, **190**, 291–4.

Karbowiak, M., Drożdżyński, J., and Hanuza, J. (1996a) *Eur. J. Solid State Inorg. Chem.*, **33**, 1071–8.

Karbowiak, M., Hanuza, J., Drożdżyński, J., and Hermanowicz, K. (1996b) *J. Solid State Chem.*, **121**, 312–18.

Karbowiak, M., Drożdżyński, J., and Janczak, J. (1996c) *Polyhedron*, **15 (2)**, 241–4.

Karbowiak, M., Murdoch, K., Drożdżyński, J., Edelstein, N., and Hubert, S. (1996d) *Acta Phys. Polon.*, **90 (2)**, 371–6.

Karbowiak, M., Simoni, E., Drożdżyński, J., and Hubert, S. (1996e) *Acta Phys. Polon.*, **90 (2)**, 367–70.

Karbowiak, M., Drożdżyński, J., Murdoch, K. M., Edelstein, N. M., and Hubert, S. (1997) *J. Chem. Phys.*, **106**, 3067–77.

Karbowiak, M. and Drożdżyński, J. (1998a) *J. Alloys Compds*, **275–7**, 848–51.

Karbowiak, M. and Drożdżyński, J. (1998b) *J. Alloys Compds*, **271–3**, 863–6.

Karbowiak, M., Edelstein, N., Gajek, Z., and Drożdżyński, J. (1998a) *Spectrochim. Acta A*, **54**, 2035–44.

Karbowiak, M., Drożdżyński, J., Hubert, S., Simoni, E., and Streçk, W. (1998b) *J. Chem. Phys.*, **108**, 10181–8.

Karbowiak, M., Edelstein, N., Gajek, Z., and Drożdżyński, J. (1998c) *Spectrochim. Acta A*, **54**, 2035–44.

Karbowiak, M., Drożdżyński, J., Hubert, S., Simoni, E., and Stręk, W. (1998d) *J. Chem. Phys.*, **108**, 10181–8.

Karbowiak, M., Gajek, Z., and Drożdżyński, J. (2000) *Chem. Phys.*, **261**, 301–15.

Karbowiak, M., Drożdżyński, J., and Gajek, Z. (2001) *J. Alloys.Compds*, **323–4**, 678–82.

Karbowiak, M., Drożdżyński, J., and Sobczyk, M. (2002a) *J. Chem. Phys.*, **117**, 2800–8.

Karbowiak, M. A., Mech, A., Drożdżyński, J., Gajek, Z., and Edelstein, N. M. (2002b) *New. J. Chem.*, **26**, 1651–7.

Karbowiak, M. and Drożdżyński, J. (2003) *Mol. Phys.*, **101**, 971–5.

Karbowiak, M., Zych, E., Dereń, P., and Drożdżyński, J. (2003a) *Chem. Phys.*, **287**, 365–75.

Karbowiak, M., Mech, A., Drożdżyński, J., Edelstein, N. M., and Hubert, S. (2003b) *J. Phys. Chem. B*, **108**, 160–70.

Karbowiak, M., Sobczyk, M., and Drożdżynski, J. (2003c) *J. Solid State Chem.*, **173**, 59–68.

Karbowiak, M., Mech, A., Drożdżyński, J., and Edelstein, N. M. (2003d) *Phys. Rev. B*, **67**, 195108 (1–17).

Karbowiak, M., and Drożdżyński, J. (2004) *J. Phys. Chem. A*. **108**, 6397–406.

Karbowiak, M. (2005a) *J. Phys. chem. A*., **109**, 3569–77.

Karbowiak, M. (2005b) *Chem. Phys.*, **314**, 189–97.

Karbowiak, M., Mech, A., Drozdzynski, J., Ryba-Romanowski, W., and Reid, M. F. (2005a) *J. Phys. Chem. B*, **109**, 155–66.

Karbowiak, M., Mech, A., and Drożdżński, J. (2005b) *Chem. Phys*., **308**, 135–45.

Karchevskĭ, A. I. and Buryak, E. M. (1962) *Sov. Phys. JETP*, **15**, 260–5.

Karmazin, L., Mazzanti, M., Gateau, C., Hill, C., and Pecaut, J. (2002) *Chem. Commun.* (*Cambridge, UK*), **23**, 2892–3.

Karraker, D. G. (1964) *Inorg. Chem.*, **3**, 1618–22.

Katakis, D. and Gordon, G. (1987) *Mechanism of Inorganic Reactions,* Wiley-Interscience, New York.

Kato, Y., Suzuki, K., Fukutomi, H., Tomiyasu, H., and Gordon, G. (1970) *Bull. Tokyo Inst Technol.*, **96**, 133–6.

Katz, J. J. and Rabinowitch, E. (1951) *The Chemistry of Uranium,* Natl. Nucl. En. Ser., Div. VIII, vol. 5, McGraw-Hill, New York.

Katz, J. J. and Rabinowitch, E. (1958) *The Chemistry of Uranium – Collected Papers*, TID-5290, Books I and 2, USAEC Technical Information Service, Oak Ridge, TN.

Katz, J. J. and Sheft, I. (l960) *Advances in Inorganic Chemistry and Radiochemistry,* vol. 2, Academic Press, New York, ch. 5.

Katz, J. J., Seaborg, G. T., and Morss, L. R. (1986) *The Chemistry of the Actinide Elements,* 2nd edn, vol. 1, Chapman and Hall, London, Table 5.68.

Katz, S. (1964) *Inorg. Chem.*, **3**, 1598–600.

Katzin, L. 1. (1952) *Production and Separation of U^{233} – Collected Papers*, Natl Nucl. En. Ser., Div. IV, 17B, Books 1 and 2, USAEC Technical Information Service, Oak Ridge, TN (declassified with deletions as TID-5223, Books 1 and 2).

Katzin, L. I. (1958) *J. Am. Chem. Soc.*, **80**, 5908–10.

Katzin, L. I., Kaplan, L., and Steitz, T. (1962) *Inorg. Chem.*, **1**, 963–4.

Kaufman, A. R., Cullity, B., and Brisianes, G. (1957) *Trans. AIME, J. Met.*, **209**, 23.

Keenan, T. K. (1966) *Inorg. Nucl Chem. Lett.*, **2**, 153–6.

Keenan, T. K. and Asprey, L. B. (1969) *Inorg. Chem.*, **8**, 235–8.

Keller, C. (1962a) *Nukleonik*, **4**, 271–7.

Keller, C. (1962b) *Z. Anorg. Allg. Chem.*, **317**, 241–4.

Keller, C. (1964) KFK Reports, KFK-225.

Keller, C., Koch, L., and Walter, K. H. (1965) *J. Inorg. Nucl. Chem.*, **27**, 1225–32.

Keller, C. and Salzer, M. (1967) *J. Inorg. Nucl. Chem.*, **29**, 2925–34.

Keller, C., Engerer, H., Leitner, L., and Sriyotha, U. (1969) *J. Inorg. Nucl. Chem.*, **31**, 965–80.

Keller, C. (1972) in *MTP International Review of Science, Inorganic Chemistry*, ser. 1, vol. 7 (ed. K. W. Bagnall), Butterworths, London; University Park Press, Baltimore, ch. 2, pp. 47–85.

Keller, C., Berndt, U., Debbabi, M., and Engerer, H. (1972) *J. Nucl. Mater.*, **42**, 23–31.

Keller, C. and Boroujerdi, A. (1972) *J. Inorg. Nucl. Chem.*, **34**, 1187–93.

Keller, C. (1975) in *Gmelin Handbuch der Anorganischen Chemie*, Suppl. Ser., Uranium, part C3, System no. 55, Springer-Verlag, Berlin, Heidelberg, and New York; *Ternäre und Polynäre Oxide des Urans*, pp. 295–359.

Keller, C. (1985) Heptavalent actinides, in *Handbook on the Physics and Chemistry of the Actinides* vol. 3, ch. 3 (eds. A. J. Freeman and G. H. Lander), North-Holland, Amsterdam, 143.

Keller, E. L. (compiler.) (1956) Uranium Hexafluoride Handling Procedures and Container Criteria, ORO-651; Revised Edition, ORO-651.

Keller, E. L., Furrer, A., Fischer, P., Allemspach, P., Krämer, K., Güdel, H. U., Doni, A., and Suzuki, T. (1995) *Phys. Rev. B*, **51** (5), 2881–90.

Kelley, W. E. (1955) *Nucleonics* **13**, 68–71.

Kelly, S. D., Newville, M. G., Cheng, L., Kemner, K. M., Sutton, S. R., Fenter, P., Sturchio, N. C., and Spötl, C. (2003) *Environ. Sci. Technol.*, **37**, 1284–7.

Kemmler-Sack, S. (1965) *Z. Anorg. Allg. Chem.*, **338**, 9–14.

Kemmler-Sack, S. and Rüdorff, W. (1966) *Z. Anorg. Allg. Chem.*, **344**, 23–40.

Kemmler-Sack, S. (1967) *Z. Naturforsch.*, **22B**, 597–79.

Kemmler-Sack, S. and Rüdorff, W. (1967) *Z. Anorg. Allg. Chem.*, **354**, 255–72.

Kemmler-Sack, S., Stumpp, E., Rüdorff, W., and Erfurth, H. (1967) *Z. Anorg. Allg. Chem.*, **354**, 287–300.

Kemmler-Sack, S. (1968a) *Z. Naturforsch. B*, **23**, 1260.

Kemmler-Sack, S. (1968b) *Z. Anorg. Allg. Chem.*, **363**, 295–304.

Kemmler-Sack, S. (1968c) *Z. Anorg. Allg. Chem.*, **363**, 282–94.

Kemmler-Sack, S. (1969) *Z. Anorg. Allg. Chem.*, **364**, 88–99.

Kemmler-Sack, S. and Wall, I. (1971) *Z. Naturforsch.*, **26b**, 1229–31.

Kemmler-Sack, S. (1973) *Z. Anorg. Allg. Chem.*, **402**, 255–78.

Kemmler-Sack, S. and Seemann, I. (1974) *Z. Anorg. Allg. Chem.*, **409**, 23–34.

Kemmler-Sack, S. and Seemann, I. (1975) *Z. Anorg. Allg. Chem.*, **411**, 61–78.

Kennedy, J. H. and Lingane, J. J. (1958) *Anal. Chim. Acta*, **18**, 240–4.

Kepert, D. L. (1982) *Inorganic Stereochemistry,* Springer-Verlag, Berlin.

Kern, D. M. H. and Orleman, E. F. (1949) *J. Am. Chem. Soc.*, **71**, 2102–6.

Kern, S., Hayward, J., Roberts, S., Richardson, J. W. Jr, Rotella, F. J., Soderholm, L., Cort, B., Tinkle, M., West, M., Hoisington, D., and Lander, G. H. (1994) *J. Chem. Phys.*, **101**, 9333–7.

Khanaev, E. I., Teterin, E. G., and Lukyanova, L. A. (1967) *Zh. Prikl. Spektrosk.*, **6**, 789–96; *J. Appl. Spectrosc.* (USSR), **6**, 533–8.

Kharitonov, Yu. Ya., Knyazeva, N. A., Tsapkin, V. V., and Ellert, G. V. (1967) *Radiokhimiya*, **9**, 322–30; (1967) *Sov. Radiochem.*, **9**, 316–23.

Khodadad, P. (1959) *C.R. Acad. Sci.*, **249**, 694–46.

Khodadad, P. (1960) *C.R. Acad. Sci.*, **250**, 3998–4000.

Khodadad, P. (1961) *Bull. Soc. Chim. Fr.*, 133–6.

Khosrawan-Sazedj, F. (1982) *Tschermaks Miner. Petrogr. Mitt.*, **30**, 111–15.

Killeen, J. C. (1980) *J. Nucl. Mater.*, **88**, 185–92.

Kim, K. C. and Olander, D. R. (1981) *J. Nucl. Mater.*, **102**, 192–9.

King, E. G. (1971) Quat. Met. Progr. Rep., no. 51.

Kirslis, S. S., McMillan, T. S., and Bernhardt, H. A. (1950) U.S. Report K-567, 1–36; (1956) N.S.A. Report **10**, no. 7198.

Kiukkola, K. (1962) *Acta Chem. Scand.*, **16**, 327–45.

Kjaerheim, G. and Rolstad, E. (1969) Halden Report, HPR-107.

Klaproth, M. H. (1789) *Chem. Ann.* (*Crell*), **11**, 387–403.

Klein-Haneveld, A. J. and Jellinek, F. (1964) *J. Inorg. Nucl. Chem.*, **26**, 1127–8.

Klein-Haneveld, A. J. and Jellinek, F. (1969) *J. Less Common Metals*, **18**, 123–9.

Klein-Haneveld, A. J. and Jellinek, F. (1970) *J. Less Common Metals*, **21**, 45–9.

Klepfer, H. H. and Chiotti, P. (1957) *Characteristics of the Solid State Transformations in Uranium*, ISC-893.

Kleykamp, H. (1985) *J. Nucl. Mater.*, **131**, 221–46.

Klíma, J., Jakeš, D., and Moravec, J. (1966) *J. Inorg. Nucl. Chem.*, **28**, 1861–9.

Koch, F. and Cohen, J. B. (1969) *Acta Crystallogr.*, **B25**, 275–87.

Kohlmann, H. and Beck, H. P. (1997) *Z. Anorg. Allg. Chem.*, **623**, 785–90.

Kohlmann, H. and Beck, H. P. (2000) *J. Solid State Chem.*, **150**, 336–41.

Kolitsch, U. and Giester, G. (2001) *Min. Mag.*, **65**, 717–24.

Kolitsch, W. and Müller, U. (1974) *Z. Anorg. Allg. Chem.*, **410**, 21–31.

Kolitsch, W. and Müller, U. (1975) *Z. Anorg. Allg. Chem.*, **418**, 235–42.

Kolomiets, A. V., Havela, L., Rafaja, D., Bordallo, H. N., Nakotte, H., Yartys, V. A., Hauback, B. C., Drulis, H., Iwasieczko, W., and De Long, L. E. (2000) *J. Appl. Phys.*, **87**, 6815–17.

Konrad, T. and Jeitschko, W. (1996) *J. Alloys Compds*, **233**, L3–7.

Korba, V. M. (1983) *Zh. Strukt. Khim.*, **24**, 172.

Kotlar, A., Gerdanian, P., and Dodé, M. (1967a) *J. Chim. Phys. Phys. Chim. Biol.*, **64**, 862–8.

Kotlar, A., Gerdanian, P., and Dodé, M. (1967b) *J. Chim. Phys. Phys. Chim. Biol.*, **64**, 1135–44.

Kotlar, A., Gerdanian, P., and Dodé, M. (1968) *J. Chim. Phys. Phys. Chim. Biol.*, **65**, 687–91.

Kovba, L. M., Ippolitova, E. A., Simanov, Yu . P., and Spitsyn, V. I. (1958) *Dokl. Akad. Nauk. SSSR*, **120**, 1042–4.

Kovba, L. M. (1960) *Zh. Strukt. Khim.*, **1**, 390.

Kovba, L. M. (1961) *Zh. Strukt. Khim.*, **2**, 585.

Kovba, L. M., Polunina, G. P., Simanov, Yu. P., and Ippolitova, E. A. (1961a) Argonne National Laboratory Report, ANL-trans-33, p. 17.

Kovba, L. M., Simanov, Yu. P., Ippolitova, E. A., and Spitsyn, V. I. (1961b) Argonne National Laboratory Report, ANL.trans-33, p. 24.

Kovba, L. M. (1962) *Zh. Strukt. Khim.*, **3**, 159.

Kovba, L. M., Vidanskii, L. M., and Lavut, E. G. (1963) *Zh. Strukt. Khim.*, **4**, 627.

Kovba, L. M. (1970) *Sov. Radiochem.*, **12**, 486–7.

Kovba, L. M. (1971a) *Sov. Radiochem.*, **13**, 319–20.

Kovba, L. M. (1971b) *Zh. Neorg. Khim.*, **16**, 3089–91.

Kovba, L. M. and Trunova, V. I. (1971) *Sov. Radiochem.*, **13**, 796–7.

Kovba, L. M. (1972a) *Sov. Radiochem.*, **14**, 746–9.

Kovba, L. M. (1972b) *Zh. Strukt. Khim.*, **13**, 256–9.

Kovba, L. M. (1972c) *Zh. Strukt. Khim.*, **13**, 458–60.

Kovba, L. M., Tsigunov, A. N., Kuz'micheva, E. U., and Kamaratseva, N. I. (1972) *Radiokhimiya*, **14**, 921–3.

Kovba, L. M., Murav'eva, I. A., and Orlova, A. S. (1974) *Sov. Radiochem.*, **16**, 638–9.

Krämer, K. and Meyer, G. (1989) (unpublished results).

Krämer, K., Meyer, G., Karbowiak, M., and Drożdżyński, J. (1991) *J. Less Common Metals*, **175**, 347–52.

Krämer, K., Keller, L., Fischer, P., Jung, B., Edelstein, N. M., Güdel, H. U., and Meyer, G. (1993) *J. Solid State Chem.*, **103**, 152–9.

Krämer, K., Güdel, H. U., Meyer, G., Heuer, T., Edelstein, N., Jung, B., Keller, L., Fischer, P., Zych, E., and Drożdżyński, J. (1994) *Z. Anorg. Allg. Chem.*, **620**, 1339–45.

Kramer, G. M. and Maas, E. T. Jr (1981) *Inorg. Chem.*, **20**, 3514–16.

Krause, W., Effenberger, H., and Brandstätter, F. (1995) *Eur. J. Miner.*, **7**, 1313–24.

Kressin, I. K. (1977) *Anal. Chem.*, **49**, 842–5.

Krol, D. M. (1981) *J. Chem. Soc., Dalton Trans.*, 687–93.

Krivovichev, S. V. and Burns, P. C. (2000a) *Can. Miner.*, **38**, 847–51.

Krivovichev, S. V. and Burns, P. C. (2000b) *Can. Miner.*, **38**, 717–26.

Krivovichev, S. V. and Burns, P. C. (2002a) *J. Solid State Chem.*, **168**, 245–58.

Krivovichev, S. V. and Burns, P. C. (2002b) *Can. Miner.*, **40**, 201–9.

Krivovichev, S. V. and Burns, P. C. (2002c) *Inorg. Chem.*, **41**, 4108–10.

Krivovichev, S. V. and Burns, P. C. (2003) *Can. Miner.*, **41**, 707–19.

Kruger, O. L. and Moser, J. B. (1967) *J. Phys. Chem. Solids*, **28**, 2321–5.

Krupa, J .C. (1987) *Inorg. Chim. Acta*, **139**, 223–41.

Kruse, F. H. (1962) *Inorg. Chem.*, **1**, 137–9.

Kruse, F. H. and Asprey, L. B. (1962a) *J. Inorg. Nucl. Chem.*, **33**, 1625–27.

Kruse, F. H. and Asprey, L. B. (1962b) *Inorg. Chem.*, **1**, 137–9.

Kruse, F. H. (1971) *J. Inorg. Nucl. Chem.*, **33**, 1625–7.

Kubaschewski, O. and Alcock, C. B. (1979) *International Series of Material Science and Technology*, Metallurgical Thermochemistry, vol. 24, 5th edn, Pergamon Press, Oxford.

Kudryashov, V. L., Suglobova, I. G., and Chirkst, D. E. (1978) *Radiokhimiya*, **20**, 366–72.

Kumar, N. and Tuck, D. G. (1984) *Inorg. Chim. Acta*, **95**, 211–15.

Labroche, D., Dugne, O., and Chatillon, C. (2003a) *J. Nucl. Mater.*, **312**, 21–49.

Labroche, D., Dugne, O., and Chatillon, C. (2003b) *J. Nucl. Mater.*, **312**, 50–66.

Lakner, J. F. (1978) University of California, Livermore, Lawrence Livermore National Laboratory, Report UCRL-52518.

Lally, A. E. (1992) in *Uranium Series Disequilibrium Applications to Earth, Marine, and Environmental Sciences* (eds. M. Ivanovich and R. S. Harmon), Clarendon Press, Oxford., pp. 94–126.

Lambertson, W. H. and Mueller, M. H. (1954) Argonne National Laboratory Report, ANL-5312.

Lander, G. H. and Müller, M. H. (1970) *Acta Crystallogr. B*, **26**, 129–36.

Lander, G. H., Fisher, E. S., and Bader, S. D. (1994) *Adv. Phys.*, **43**, 1–111.

Lang, S. M., Knudsen, F. P., Fillmore, C. L., and Roth, R. S. (1956) NBS Circ., no. 568, 32 pp.

Langford, C. H. and Gray, H. B. (1965) *Ligand Substitution Processes*, W. A. Benjamin, New York.

Larson, A. C., Roof, R. B., and Cromer, D. T. (1964) *Acta Crystallogr.*, **17**, 555.

Latta, R. E. and Fryxell, R. E. (1970) *J. Nucl. Mater.*, **35**, 195–210.

Lau, K. H. and Hildenbrand, D. L. (1982) *J. Chem. Phys.*, **76**, 2646.

Lau, K. H. and Hildenbrand, D. L. (1984) *J. Chem. Phys.*, **80**, 1312–17.

Laugier, J., Blum, P. L., and Detourminé, R. J. (1971) *J. Nucl. Mater.*, **41**, 106–8.

Laval, J. P., Mikou, A., Frit, B., Roult, G., and Pannetier, J. (1987) *Rev. Chim. Minér.*, **24**, 165–82.

Laveissière, J. (1967) *Bull. Soc. Franc. Minér. Crist.*, **90**, 308–10.

Lawson, A. C., Severing, A., Ward, J. W., Olsen, C. E., Goldstone, J. A., and Williams, A. (1990) *J. Less Common Metals*, **158**, 267–74.

Lawson, A. C., Goldstone, J. A., Huber, J. G., Giorgi, A. L., Conant, J. W., Severing, A., Cort, B., and Robinson, R. A. (1991) *J. Appl. Phys.*, **69**, 5112–16.

Lay, K. W. (1970) *J. Am. Ceram. Soc.*, **53**, 369–73.

Leask, M. J. M., Roberts, L. E. J., Walker, A. J., and Wolf, W. P. (1963) *J. Chem. Soc.*, 4788–94.

Lebeau, P. and Damien, A. (1913) *C.R. Acad. Sci.*, **156**, 1987–9.

Le Bihan, T., Rogl, P., and Noël, H. (2000) *J. Nucl. Mater.*, **277**, 82–90.

Lederer, C. M. and Shirley, V. S. (1978) *Table of Isotopes*, 7th edn, John Wiley, New York.

Lee, H. M. (1974) *J. Nucl. Mater.*, **50**, 25–30.

Leibowitz, L., Mishler, L. W., and Chasanov, M. G. (1969) *J. Nucl. Mater.*, **29**, 356–8.

Leonidov, V. Y. (1960) *Zh. Fiz. Khim.*, **34**, 1862.

Leroy, J. M. and Tridot, G. (1966) *C.R. Acad. Sci.* (*Paris*), **C262**, 1376–9.

Leslie, B. W., Pearcy, E. C., and Prikryl, J. D. (1993) *Mater. Res. Soc. Symp. Proc.*, **294**, 505–12.

Leung, A. F. and Poon, Y.-M. (1977) *Can. J. Phys.*, **55**, 937–42.

Leuze, R. E., Clinton, S. O., Chilton, J. M. and Vaughen, V. C. A. (1962) in *Transuranium Quarterly Progress Report for period ending Feb. 28, 1962* (compiler D. E. Ferguson), ORNL-3290, p. 79.

Leuze, R. E., Clinton, S. D., Chilton, J. M., and Vaughen, V. C. A. (1963) in *Transuranium Quarterly Progress Report for period ending Aug. 31, 1962* (compiler D. E. Ferguson), ORNL-3375, p. 51.

Levet, J. C. (1965) *Compt. Rend. C*, **260**, 4775–6.

Levet, J. C. (1969) *Compt. Rend. C*, **268**, 703–5.

Levet, J. C., Potel, M., and Le Marouille, J. Y. (1977) *Acta Crystallogr. B*, **33**, 2542–6.

Levet, J. C. and Noël, H. (1979) *J. Solid State Chem.*, **28**, 67–73.

Levet, J. C., Potel, M., and Le Marouille, J. Y. (1980) *J. Solid State Chem.*, **32**, 297–301.

Levet, J. C. and Noël, H. (1981) *J. Inorg. Nucl. Chem.*, **43**, 1841–3.

Levy, J. H., Taylor, J. C., and Wilson, P. W. (1975) *J. Less Common Metals*, **39**, 265–70.

Levy, J. H., Taylor, J. C., and Wilson, P. W. (1976) *J. Chem. Soc. Dalton Trans.*, 219–24.

Levy, J. H., Taylor, J. C., and Wilson, P. W. (1977) *J. Inorg. Nucl. Chem.*, **39**, 1989–91.

Levy, J. H., Taylor, J. C., and Wilson, P. W. (1978) *J Inorg. Nucl. Chem.*, **40**, 1055–7.

Levy, J. H., Taylor, J. C., and Waugh, A. B. (1980) *Inorg. Chem.*, **19**, 672–4.

Levy, J. H., Taylor, J. C., and Waugh, A. B. (1983) *J. Fluorine Chem.*, **23**, 29–36.

Lewis, W. B., Asprey, L. B., Jones, L. H., McDowell, R. S., Rabideau, S. W. Zeltman, A. H., and Levet, J. C. (1965) *Compt. Rend. C*, **260**, 4775–6.

Lewis, W. B., Hecht, H. G., and Eastman, M. P. (1973) *Inorg. Chem.*, **12**, 1634–9.

Lewis, W. B., Asprey, L. B., Jones, L. H., McDowell, R. S., Rabideau, S. W., Zeltman, A. H., and Paine, R. T. (1976) *J. Chem. Phys.*, **65**, 2707–14.

Li, J., Bursten, B. E., Liang, B., and Andrews, L. (2002) *Science*, **295**, 2242–5.

Li, Y.-P. and Burns, P. C. (2000a) *Can. Miner.*, **38**, 737–49.

Li, Y.-P. and Burns, P. C. (2000b) *Can. Miner.*, **38**, 727–35.

Li, Y.-P., Burns, P. C., and Gault, R. A. (2000) *Can. Miner.*, **38**, 153–62.

Li, Y.-P. and Burns, P. C. (2001a) *J. Nucl. Mater.*, **299**, 219–26.

Li, Y.-P. and Burns, P. C. (2001b) *Can. Miner.*, **39**, 1147–51.

Li, Y.-P., Krivovichev, S. V., and Burns, P. C. (2001a) *Miner. Mag.*, **65**, 285–92.

Li, Y.-P., Cahill, C. L., and Burns, P. C. (2001b) *Chem. Mater.*, **13**, 4026–31.

Libowitz, G. G. and Gibb, T. R. P. Jr (1957) *J. Phys. Chem.*, **61**, 793–5.

Libowitz, G. G. (1968) in *Metal Hydrides* (eds. W. Mueller, J. P. Blackledge, and G. G. Libowitz), Academic Press, New York., ch. 11

Lin, S. T. and Kaufmann, A. R. (1956) *Phys. Rev.*, **102**, 640–6.

Lincoln, S. F. (1979) *Pure Appl. Chem.*, **51**, 2059–65.

Lindemann, F. and Aston, F. W. (1919) *Phil. Mag.*, **6(37)**, 523.

Lindemer, T. B. and Besmann, T. M. (1985) *J. Nucl. Mater.*, **130**, 473–88.

Lindemer, T. B. and Brynestad, J. (1986) *J. Am Ceram. Soc.*, **69**, 867–76.

Lindemer, T. B. and Sutton, A. L. Jr (1988) *J. Am. Ceram. Soc.*, **71**, 553–61.

Lipschutz, M. E., Wolf, S. F., Hanchar, J. M., and Culp, F. B. (2001) *Anal. Chem.*, **73**, 2687–700.

Litz, L. M. (1948) *Uranium Carbides – Preparation, Structure and Hydrolysis*, Thesis, Ohio State University, NP-1453.

Litz, L. M., Garrett, A. B., and Croxton, E. C. (1948) *J. Am. Chem. Soc.*, **70**, 1718–22.

Locock, A. J. and Burns, P. C. (2003a) *Am. Miner.*, **88**, 240–4.

Locock, A. J. and Burns, P. C. (2003b) *Min. Mag.*, **67**, 1109–20.

Locock, A. J. and Burns, P. C. (2003c) *Can. Miner.*, **41**, 91–101.

Locock, A. J. and Burns, P. C. (2003d) *Can. Miner.*, **41**, 489–502.

Locock, A. J., Burns, P. C., and Flynn, T. M. (2005a) *Am. Miner.*, **90**, 240–6.

Locock, A. J., Burns, P. C., Flynn, T. M. (2005b) *Can. Miner.*, **43**, 721–33.

Locock, A. J., Kinman, W. S., and Burns, P. C. (2005c) *Can. Miner.* **43**, 989–1003.

Lopez, M. and Birch, D. S. J. (1997) *Chem. Phys. Lett.*, **268**, 125–32.

Loopstra, B. O. (1962) *Acta Crystallogr.*, **17**, 651–4.

Loopstra, B. O. and Cordfunke, E. H. P. (1966) *Rec. Trav. Chim. Pays-Bas*, **58**, 135–42.

Loopstra, B. O. and Rietveld, H. M. (1969) *Acta Crystallogr.*, **B25**, 787–91.

Loopstra, B. O. (1970a) *J. Appl. Crystallogr.*, **3**, 94–6.

Loopstra, B. O. (1970b) *Acta Crystallogr.*, **B26**, 656–7.

Lorenzelli, R. and Touzelin, B. (1980) *J. Nucl. Mater.*, **95**, 290–302.

Lu, W. C., Ree, T., Gerard, V., and Eyring, H. (1968) *J. Chem. Phys.*, **49**, 797.

Lucas, J. (1964) *Rev. Chim. Minér.*, **1**, 479–517.

Lumpkin, G. R., Eyal, Y., and Ewing, R. C. (1988) *J. Mater. Res.*, **3**, 357–68.

Lumpkin, G. R. and Ewing, R. C. (1995) *Am. Miner.*, **80**, 732–43.

Lumpkin, G. R., Hart, K. P., McGlinn, P., Gieré, R., and Williams, C. T. (1995) *Radiochim. Acta*, 469–74.

Lumpkin, G. R., Payne, T. E., Fenton, B. R., and Waite, T. D. (1999) *Mater. Res. Soc. Symp. Proc.*, **556**, 1067–74.

Lundgren, G. (1952) *Arkiv Kemi*, 421–8.

Lupinetti, A. J., Fife, J. L., Garcia, E., Dorhout, P. K., and Abney, K. D. (2002) *Inorg. Chem.*, **41**, 2316–18.

Lychev, A. A., Mashirov, L. G., Smolin, Yu. I., and Shepelev, Yu. F. (1986) *Radiokhimiya*, **28**, 682–5.

Lyon, W. G., Osborne, D. W., Flotow, H. E., and Hoekstra, H. R. (1977) *J. Chem. Thermodyn.*, **9**, 201–10.

Lynch, E. D. (1965) Argonne National Laboratory Report, ANL-6894.

Łyżwa, R. and Erdös, P. (1987) *Phys. Rev. B*, **36**, 8570.

Macaskie, L. E., Bonthrone, K. M., Yong, P., and Goddard, D. T. (2000) *Microbiology*, **146**, 1855–67.

Mac Cordick, J. and Brun, C. (1970) *Compt. Rend. Acad. Sci. Ser. C.*, **270**, 620–3.

Mac Leod, A. C. (1972) *J. Chem. Thermodyn.*, **4**, 699–708.

Mac Wood, G. E. (1958) TID-5290, pp. 543–609.

Maglic, K. and Herak, R. (1970) *Rev. Int. Hautes Tempér. Réfract. Fr.*, **7**, 247.

Mair, M. A. and Savage, D. J. (1986) UK Atomic Energy Agency Report, ND-R-134.

Malek, C. K., Krupa, J.-C., Delamoye, P., and Genet, M. (1986a) *J. Phys.* (*Paris*), **47**, 1763–73.

Malek, C. K., Krupa, J.-C., and Genet, M. (1986b) *Spectrochim. Acta* part A, **42**, 907–12.

Malek, C. K. and Krupa, J.-C. (1994) *J. Chem. Phys.*, **84**, 6584–90.

Maletka, K., Fischer, P., Murasik, A., and Szczepaniak, W. (1992) *J. Appl. Cryst.*, **25**, 1–5.

Maletka, K., Murasik, A., Szczepaniak, W., Rundloef, H., and Tellgren, R. (1995) *Solid State Ionics*, **76**, 115–20.

Maletka, K., Tellgren, R., Rundloef, H., Szczepaniak, W., and Rycerz, L. (1996a) *Solid State Ionics*, **90**, 67–74.

Maletka, K., Ressouche, E., Szczepaniak, W., Rycerz, L., and Murasik, A. (1996b) *Mater. Sci. Forum*, **228**, 711–16.

Maletka, K., Ressouche, E., Rundloef, H., Tellgren, R., Delaplane, R., Szczepaniak, W., and Zablocka-Malicka, M. (1998) *Solid State Ionics*, **106**, 55–69.

Mallett, M. W., Gerds, A. F., and Nelson, H. R. (1952) *J. Electrochem. Soc.*, **99**, 197–204.

Mallett, M. W. and Gerds, A. F. (1955) *J. Electrochem. Soc.*, **102**, 292–6.

Mallett, M. W., Trzeciak, M. J., and Griffith, C. B. (1955) *Nuclear Engineering and Science Congress*, Cleveland, OH, Preprint 334.

Mallett, M. W. and Trzeciak, M. J. (1958) *Trans. Am. Soc. Met.*, **50**, 981–93.

Malm, J. G., Selig, H., and Siegel, S. (1966) *Inorg. Chem.*, **5**, 130–2.

Malm, J. G. (1980) *J. Inorg. Nucl. Chem.*, **42**, 993–4.

Manes, L. (ed.) (1985) *Struct. Bonding*, **59/60**; *Actinide-Chemistry and Physical Properties*, Springer Verlag, New York.

Marakov, E. S. and Bykov, V. N. (1959) *Kristallographica*, **4**, 183–5.

Marchidan, D. I. and Matei-Tanasescu, S. (1972) *Rev. Roum. Chim.*, **17**, 195–202.

Marchidan, D. I. and Matei-Tanasescu, S. (1974) *Rev. Roum. Chim.*, **19**, 1435.

Marchidan, D. I. and Matei-Tanasescu, S. (1975) *Rev. Roum. Chim.*, **20**, 1365.

Marcon, J.-P. (1969) *Contribution à l'Etude des Sulfures d'Actinides*, Thesis, University of Paris, CEA-3919.

Marcon, J. P. (1972) *Rev. Int. Hautes Temp. Réfract.*, **9**, 193.

Marin, J. F. (1968) CEA Report, CEA-N-883.

Marin, J. F. and Contamin, P. (1969) *J. Nucl. Mater.*, **30**, 16–25.

Marinenko, G., Koch, W. F., and Etz, E. S. (1983) *J. Res. Natl. Bur. Stand.*, **88**, 117–24.

Marinsky, J. A. (1956) Development of the EXCER Process, part II, ORNL-1979.

Markin, T. L. and Bones, R. J. (1962a) UKAEA Harwell Report, AERE-R 4178.

Markin, T. L. and Bones, R. J. (1962b) UKAEA Report, AERE-R 4042.

Markin, T. L. and Crough, E. C. (1970) *J. Inorg. Nucl. Chem.*, **32**, 77–82.

Markin, T. L., Street, R. S., and Crough, E. C. (1970) *J. Inorg. Nucl. Chem.*, **32**, 59–75.

Marples, J. A. C. (1976) in *Plutonium 1975 and Other Actinides*, Proc. Fifth Int. Conf. on Plutonium and Other Actinides, Baden-Baden, Germany (eds. H. Blank and R. Lindner), North-Holland, Amsterdam, pp. 353–9.

Martin, A. E. and Edwards, R. K. (1965) *J. Phys. Chem.*, **69**, 1788.

Martin, A. E. and Shinn, W. A. (1971) Argonne National Laboratory Report, ANL-7877.

Martin, P., Ripert, M., Petit, T., Reich, T., Hennig, C., D'Acapito, F., Hazemann, J. L., and Proux, O. (2003) *J. Nucl. Mater.*, **312**, 103–10.

Martinot, L. (1984) Uranium in molten in molten salts and melts, in *Gmelin Handbook of Inorganic Chemistry*, Uranium Suppl., vol. D1, 332–78.

Martinot, L. (1991) Molten-salt chemistry of the actinides, in *Handbook on the Physics and Chemistry of the Actinides* , vol. 6, ch. 4 (eds. A. J. Freeman and C. Keller), North-Holland, Amsterdam, 241–79.

Marzotto, A., Bandoli, G., Clemente, D. A., Benetollo, F., and Galzigna, L. (1973) *J. Inorg. Nucl. Chem.*, **35**, 2769–74.

Marzotto, A., Grazotto, R., Bombieri, G., and Forsellini, E. (1974) *J. Cryst. Mol. Struct.*, **4**, 253–62.

Masaki, N. and Tagawa, H. (1975) *J. Nucl. Mater.*, **58**, 241–3.

Mass, E. T. (1979) *J. Inorg. Nucl. Chem.*, **41**, 991.

Masson, J. P., Desmoulin, R., Charpin, P., and Bougon, R. (1976) *Inorg. Chem.*, **15**, 2529–31.

Masson, J. P., Naulin, C., Charpin, P., and Bougon, R. (1978) *Inorg. Chem.*, **17**, 1858–61.

Masters, B. J. and Schwartz, L. L. (1961) *J. Am. Chem. Soc.*, **83**, 2620–24.

Matonic, J. H., Scott, B. L., and Neu, M. P. (2001) *Inorg. Chem.*, **40**, 2638–9.

Matsika, S., Zhang, Z., Brozell, S. R., Bladeau, J.-P., Wang, Q., and Pitzer, R. M. (2001) *J. Phys. Chem. A*, **105**, 3825–8.

Matson, L. K., Moody, J. W., and Himes, R. C. (1963) *J. Inorg. Nucl. Chem.*, **25**, 795–800.

Matsui, T., Tsuji, T., and Naito, K. (1974) *J. Nucl. Sci. Technol.*, **11**, 216–22.

Matsui, T. and Naito, K. (1975) *J. Nucl. Mater.*, **56**, 327–35.

Matsui, T. and Naito, K. (1985a) *J. Nucl. Mater.*, **132**, 212–21.

Matsui, T. and Naito, K. (1985b) *J. Nucl. Mater.*, **136**, 59–68.

Matsui, T. and Naito, K. (1986) *J. Nucl. Mater.*, **138**, 19–26.

Matzke, Hj. (1981) in *Non-Stoichiometric Oxides* (ed. O. T. Sørensen), Academic Press, New York, ch. 4, pp. 156–232.

Matzke, Hj. (1987) *J. Chem. Soc., Faraday Trans. 2*, **83**, 1121–42.

Maximov, V. (compiler.) (1963) *Uranium Carbides, Nitrides, and Silicides*, vol. I (1961/1963), IAEA Bibliographical Series 14, International Atomic Energy Agency, Vienna, STI/PUB/21/14.

Maximov, V. (compiler.) (1965) *Uranium Carbides, Nitrides, and Silicides*, vol. II (1963/1965), IAEA Bibliographical Series 21, International Atomic Energy Agency, Vienna, STI/PUB/21/21.

Maximov, V. (compiler.) (1967) *Uranium Carbides, Nitrides, and Silicides*, vol. III (1965/1967), IAEA Bibliographical Series 33, International Atomic Energy Agency, Vienna, STI/PUB/21/33.

Mayer, H. and Mereiter, K. (1986) *Tschermaks Miner. Petrogr. Mitt.*, **35**, 133–46.

Mazurak, M., Drożdżyński, J., and Hanuza, J. (1988) *J.Mol. Struct.*, **174**, 443–8.

Mazzi, F. and Munno, R. (1983) *Am. Miner.*, **68**, 262–76.

McDowell, R. S., Asprey, L. B., and Paine, R. T. (1974) *J. Chem. Phys.*, **61**, 3571–80.

McEachern, R. J. and Taylor, P. (1998) *J. Nucl. Mater.*, **254**, 87–121.

McEwen, D. J. and De Vries, T. (1959) *Anal. Chem.*, **31**, 1672–2.

McLaughlin, R. (1962) *J. Chem. Phys.*, **36**, 2699–705.

McNamara, B. K., Buck, E. C., and Hanson, B. D. (2003) *Mater. Res. Soc. Symp. Proc.*, **757**, 401–6.

Mech, A., Karbowiak, M., Lis, T., and Drożdżyński, J. (2005) Polyhedron, in press.

Meinrath, G., Lis, S., Stryla, S., and Noubactep, C. (2000) *J. Alloys Compds.*, **300/301**, 107–12.

Meites, L. (ed.) (1963) *Handbook of Analytical Chemistry*, McGraw-Hill, New York.

Meitner, L., Hahn, O., and Strassmann, F. (1937) *Z. Phys.*, **106**, 249–70.

Mellor, J. W. (1932) *Comprehensive Treatise on Inorganic and Theoretical Chemistry*, vol. XII, , Longmans, Green and Co., London.

Mentink, S. A. M., Mason, T. E., Buyers, W. J. L., and Clausen, K. N. (1998) *Physica B.* (*Amsterdam, Neth.*), **241–243**, 669–71.

Menzies, C. (1966) UKAEA Report, TRG-1119(D).

Mereiter, K. (1982a) *Tschermaks Miner. Petrogr. Mitt.*, **30**, 277–88.

Mereiter, K. (1982b) *Tschermaks Miner. Petrogr. Mitt.*, **30**, 129–39.

Mereiter, K. (1982c) *Tschermaks Miner. Petrogr. Mitt.*, **30**, 47–51.

Mereiter, K. (1984) *Acta Crystallogr.*, **A40**, Suppl. C-247.

Mereiter, K. (1986) *Tschermaks Miner. Petrogr. Mitt.*, **35**, 1–18.

Merritt, R. C. (1971) *The Extractive Metallurgy of Uranium*, Colorado School of Mines Research Institute and USAEC, Golden, CO.

Meunier, G. and Galy, J. (1973) *Acta Crystallogr.*, **B29**, 1251–5.

Meusemann, H. and von Erichsen, L. (1973) *Bundesministerium für Forschung und Technologie*, Report no. BMFT-FBK-73–18.

Meyer, G., Gaebell, H.-Chr., and Hoppe, R. (1983) *J. Less Common. Metals*, **93**, 347–51.

Meyer, H. C., McDonald, P. F., and Settler, J. D. (1967) *Phys. Lett.*, **24A**, 569.

Meyer, R. A. and Wolfe, B. E. (1964) *Trans. Am. Nucl. Soc.*, **7**, 111–12.

Mighell, A. D. and Ondik, H. M. (1977) *J. Phys. Chem. Ref. Data*, **6**, 675–829.

Mignanelli, M. A. and Potter, P. E. (1983) *J. Nucl. Mater.*, **118**, 150–8.

Mignanelli, M. A. and Potter, P. E. (1986) *J. Less Common Metals*, **121**, 605–13.

Miguta, A. K. (1997) *Geol. Ore Deposits*, **39**, 275–93.

Mikhailov, Yu. N. and Kuznetsov, V. G. (1971) *Russ. J. Inorg. Chem.*, **16**, 1340–2.

Mikhailov, Yu. N., Udovenko, A. A., Kuznetsov, V. G., and Davidovich, R. L. (1972a) *Zh. Strukt. Khim.*, **13**, 942–3; (1972) *J. Strukt. Chem.* (*USSR*), **13**, 879–80.

Mikhailov, Yu. N., Udovenko, A. A., Kuznetsov, V. G., and Davidovich, R. L. (1972b) *Zh. Strukt. Khim.*, **13**, 741.

Mikhailov, Yu. N., Ivanov, S. B., Orlova, I. M., Podnebesnova, G. V., Kuznetsov, V. G., and Shchelokov, R. N. (1976a) *Koord. Khim.* [*Coord. Chem.* (*USSR*)], **2**, 1570–3.

Mikhailov, Yu. N., Ivanov, S. B., Kuznetsov, V. G., and Davidovich, R. L. (1976b) *Koord. Khim.* [*Coord. Chem.* (*USSR*)], **2**, 95–8.

Mikhailov, Yu. N., Ivanov, S. B., and Sadikov, G. G. (1979) *Koord. Khim.* [*Coord. Chem.* (*USSR*)], **5**, 1702–5.

Miller, D. (1965) Argonne National Laboratory Report, ANL-7120, p. 641.

Miller, M. L., Finch, R. J., Burns, P. C., and Ewing, R. C. (1996) *J. Mater. Res.*, **11**, 3048–56.

Miller, S. A. and Taylor, J. C. (1986) *Z. Kristallogr.*, **177**, 247–53.

Mills, K. C. (1974) *Thermodynamic Data for Inorganic Sulphides, Selenides, and Tellurides*, Butterworths, London.

Misaelides, P., Godelitsas, A., Filippidis, A., Charistos, D., and Anousis, I. (1995) *Sci. Total Environ.*, **173–174**, 237–46.

Miyake, C., Fuji, K., and Imoto, S. (1977) *Chem. Phys. Lett.*, **46**, 349–51.

Miyake, C., Fuji, K., and Imoto, S. (1979) *Chem. Phys. Lett.*, **61**, 124–6.

Miyake, C., Takeuchi, H., Ohya-Nishiguchi, H., and Imoto, S. (1982) *Phys. Status Solidi*, **A74**, 173–80.

Miyake, C., Kanamaru, M., Imoto, S., and Taniguchi, K. (1986) *J. Nucl. Mater.*, **138**, 36–9.

Miyake, C. (1991) Magnetochemistry of U(V) complexes and compounds, in *Handbook on the Physics and Chemistry of the Actinides* (eds. A. J. Freeman and C. Keller), Elsevier, vol. 6, ch. 5, 337–66.

Miyake, C., Kawasaki, O., Gotoh, K., and Nakatani, A. (1993) *J. Alloys Compds*, **200**, 187–90.

Miyake, C. and Fujino, T. (1998) *J. Alloys Compds*, **271–273**, 479–81.

Moens, L. and Jakubowski, N. (1998) *Anal. Chem.*, **70**, 251A–6A.

Moll, H., Denecke, M. A., Jalilehvand, F., Sandström, M., and Grenthe, I. (1999) *Inorg. Chem.*, **38**, 1795–99.

Moll, H., Reich, T., and Szabó, Z. (2000a) *Radiochim. Acta*, **88**, 411–15.

Moll, H., Reich, T., Hennig, C., Rossberg, A., Szabó, Z., and Grenthe, I. (2000b) *Radiochim. Acta*, **88**, 559–66.

Moll, H., Geipel, G., Reich, T., Bernhard, D., and Grenthe, I. (2003) *Radiochim. Acta*, **91**, 11–20.

Montignie, E. (1947) *Bull. Soc. Chim. Fr.*, 748–49.

Montoloy, F. and Plurien, P. (1968) *C. R. Acad. Sci.*, **267**, 1036.

Moody, D. C. and Odom, J. D. (1979) *J. Inorg. Nucl. Chem.*, **41**, 533–5.

Moody, D. C., Penneman, R. A., and Salazar, K. V. (1979) *Inorg. Chem.*, **18**, 208–9.

Moody, D. C., Zozulin, A. J., and Salazar, K. V. (1982) *Inorg. Chem.*, **21**, 3856–7.

Moore, G. E. and Kelley, K. K. (1947) *J. Am. Chem. Soc.*, **69**, 2105–7.

Morris, D. E., Allen, P. G., Berg, J. M., Chisolm-Brause, C. J., Conradson, S. D., Hess, N. J., Musgrave, J. A., and Tait, C. D. (1996) *Environ. Sci. Technol.*, **30**, 2322–31.

Morss, L. R. (1982) in *Actinides in Perspective* (ed. N. M. Edelstein), Pergamon Press, Oxford, pp. 381–407.

Morss, L. R. (1991) in *Synthesis of Lanthanide and Actinide Compounds* (eds. G. Meyer and L. R. Morss), Kluwer Academic Publishers, Dordrecht., pp. 237–58.

Moriyasu, M., Yokoyama, Y., and Ikeda, S. (1977) *J. Inorg. Nucl. Chem.*, **39**, 2199–203.

Moskvin, A. I. and Zaitseva, V. P. (1962) *Radiokhimiya*, **4**, 73–82; *Sov. Radiochem.*, **4**, 63–9.

Moskvin, A. I. (1968) *Radiokhimiya*, **10**, 13–21; *Sov. Radiochem*, **10**, 10–13.

Mucke, A. and Strunz, H. (1978) *Am. Miner.*, **63**, 941–6.

Mulak, J. and Żołnierek, Z. (1972) *Bull. Acad. Pol. Sci. Ser. Sci. Chim.*, **20**, 1081.

Mulak, J. and Żołnierek, Z. (1977) *Proc. Second Int. Conf. Electron. Struct. Actinides*, Wrocław, Poland., 1976, pp. 125–31.

Mulford, R. N. R., Ellinger, F. H., and Zachariasen, W. H. (1954) *J. Am. Chem. Soc.*, **76**, 297–8.

Müller, U. and Kolitsch, W. (1974) *Z. Anorg. Allgem. Chem.*, **410**, 32–8.

Murakami, T., Ohnuki, T., Isobe, H., and Sato, T. (1997) *Am. Miner.*, **82**, 888–99.

Murasik, A., Suski, W., Troć, R., and Leciewicz, L. (1968) *Phys. Status Solidi*, **30**, 61–6.

Murasik, A., Furrer, A., and Szczepaniak, W. (1980) *Solid State Commun.*, **33**, 1217.

Murasik, A., Fischer, P., and Szczepaniak, W. (1981) *J. Phys. C., Solid State Phys.*, **14**, 1847.

Murasik, A., Fischer, P., Furrer, A., and Szczepaniak, W. (1985) *J. Phys. C, Solid State Phys.*, **18**, 2909–21.

Murasik, A., Fischer, P., Furrer, A., Schmid, B., and Szczepaniak, W. (1986) *J. Less Common Metals*, **121**, 151–5.

Murch, G. E. and Catlow, C. R. A. (1987) *J. Chem. Soc., Faraday Trans. 2*, **83**, 1157–69.

Nagarajan, K., Saha, R., Yadav, R. B., Rajagopalan, S., Kutty, K. V. G., Saibaba, M., Rao, P. R. V., and Matthews, C. K. (1985) *J. Nucl. Mater.*, **130**, 242–9.

Nagatoro, Y., Ochiai, K., and Kaya, A. (1980) *J. Nucl. Sci. Technol.*, **17**, 687–93.

Nagels, P., Devreese, J., and Denayer, M. (1964) *J. Appl. Phys.*, **35**, 1175–80.

Naito, K., Ishii, T., Hamaguchi, Y., and Oshima, K. (1967) *Solid State Commun.*, **5**, 349–52.

Naito, K., Kamagashira, N., and Nomura, Y. (1971) *J. Crystal Growth*, **8**, 219–20.

Naito, K., Tsuji, T., and Matsui, T. (1973) *J. Nucl. Mater.*, **48**, 58–66.

Naito, K. and Kamegashira, N. (1976) in *Advances in Nuclear Science and Technology*, vol. 9, pp. 99–180.

Naito, K., Inaba, H., and Takahashi, S. (1982) *J. Nucl. Mater.*, **110**, 317–23.

Naito, K., Tsuji, T., and Ohya, F. (1983) *J. Nucl. Mater.*, **114**, 136–42.

Naito, K. (1989) *J. Nucl. Mater.*, **167**, 30–5.

Nakagawa, T., Matsuoka, H., Sawa, M., Hirota, M., Miyake, M., and Katsura, M. (1997) *J. Nucl. Mater.*, **247**, 127–30.

Nakajima, K., Ohmichi, T., and Arai, Y. (2002) *J. Nucl. Mater.*, **304**, 176–81.

Nakamura, A. and Fujino, T. (1986) *J. Nucl. Mater.*, **140**, 113–30.

Nakamura, A. and Fujino, T. (1987) *J. Nucl. Mater.*, **149**, 80–100.

Narducci, A. A. and Ibers, J. A. (1998) *Chem. Mater.*, **10**, 2811–23.

Nash, K. L. and Sullivan, J. C. (1998) *J. Alloys Compds*, **271–273**, 712–18.

Nassimbeni, L. R. and Rodgers, A. L. (1976) *Crystal Struct. Commun.*, **5**, 301–8.

Nasu, S. (1964) *Japan. J. Appl. Phys.*, **3**, 664–5.

Navaza, A., Charpin, P., Vigner, D., and Heger, G. (1991) *Acta Crystallogr. C*, **47**, 1842–5.

Neuefeind, J., Skanthakumar, S., and Soderholm, L. (2004a) *Inorg. Chem.*, **43**, 2422–6.

Neuefeind, J., Soderholm, L., and Skanthakumar, S. (2004b) *J. Phys. Chem. A*, **108**, 2733–9.

Neuhaus, A. (1958) *Fortschr. Miner.*, **35**, 151–4.

Neuhaus, A. and Recker, K. (1959) *Z. Elektrochem.*, **63**, 89–97.

Newton, A. S., Warf, J. C., Spedding, F. H., Johnson, O., Johns, I. B., Nottorf, R. W., Ayres, J. A., Fisher, R. W., and Kant, A. (1949) *Nucleonics*, **4** (2), 17–25.

Newton, T. W. and Baker, F. B. (1965) *Inorg. Chem.*, **4**, 1166–70.

Newton, T. W. (1975) *The Kinetics of the Oxidation-Reduction Reactions of Uranium, Neptunium, Plutonium and Americium in Aqueous Solution*, Report TID-26506, Technical Information Center, Office of Public Affairs, US Energy and Development Administration.

Nguyen-Nghi, H., Dianoux, A.-J., and Marquet-Ellis, H. (1964) *Compt. Rend. Acad. Sci.* (*Paris*), **259**, 4683.

Nguyen-Nghi, H., Dianoux, A.-J., Marquet-Ellis, H., and Plurien, P. (1965) *Compt. Rend. Acad. Sci.* (*Paris*), **260**, Group 8, 1963–6.

Niedrach, C. W. and Glamm, A. (1954) *Electrorefining of Uranium – A New Approach*, KAPL-1154.

Nielsen, P. E., Jeppesen, C., and Buchardt, O. (1988) *FEBS Lett.*, **235**, 122–4.

Niinistö, L., Toivonen, J., and Valkonen, J. (1979) *Acta Chem. Scand.*, **33**, 621–4.

Nishioka, T., Motoyama, G., Nakamura, S., Kadoya, H., and Sato, N. K. (2002) *Phys. Rev. Lett.*, **88**, 237203/1–237203/4.

NIST (2004) *NIST Critically Selected Stability Constants of Metal Complexes: version 8.0. NIST Standard Reference Database 46,* National Institute of Standards and Technology, Gaithersburg, MD.

Noël, H. and Prigent, J. (1980) *Physica B+C: Phys. Condensed Matter + Atom Mol. Plasma Phys., Optics*, **102**, 372–9.

Noël, H. and Le Marouille, J. Y. (1984) *J. Solid State Chem.*, **52**, 197–202.

Noël, H. (1985a) *Inorg. Chim. Acta*, **109**, 205–7.

Noël, H. (1985b) *Physica B and C*, **130**, 499–500.

Noël, H. and Levet, J. C. (1989) *J. Solid State Chem.*, **79**, 28–33.

Noël, H., Potel, M., Troć, R., and Shlyk, L. (1996) *J. Solid State Chem.*, **126**, 22–6.

Noland, R. A. and Marzano, C. (1953) *The Electrolytic Refining of Uranium*, ANL-5102.

Norris, D. I. R. and Kay, P. (1983) *J. Nucl. Mater.*, **116**, 184–94.

Northrup, C. J. M. Jr (1975) *J. Phys. Chem.*, **79**, 726–31.

Nowicki, L., Garrido, F., Turos, A., and Thomé, L. (2000) *J. Phys. Chem. Solids*, **61**, 1789–804.

Nriagu, J. O. (1984) Formation and stability of base metal phosphates in soils and sediments, in *Phosphate Minerals* (eds. J. O. Nriagu and P. B. Moore), Springer Verlag, London, pp. 318–29.

Obbade, S., Dion, C., Saadi, M., and Abraham, F. (2004) *J. Solid State Chem.*, **177**, 1567–74.

O'Donnell, T. A., Stewart, D. F., and Wilson, P. W. (1966) *Inorg. Chem.*, **5**, 1438–41.

O'Donnell, T. A. (1983) *J. Fluorine Chem.*, **23**, 97.

OECD-NEA (1982) *Uranium–Resources, Production and Demand*, Paris.

Oetting, F. H., Rand, M. H., and Ackerman, R. J. (1976) *The Chemical Thermodynamics of Actinide Elements and Compounds*, part 1, The Actinide Elements, IAEA, Vienna, STI/PUB/421/1.

Ogard, A. E. and Leary, J. A. (1968) in *Thermodynamics of Nuclear Materials*, Proc. Symp. 1967, International Atomic Energy Agency, Vienna, pp. 651–65.

Ogliaro, F., Cordier, S., Halet, J.-F., Perrin, C., Saillard, J.-Y., and Sergent, M. (1998) *Inorg. Chem.*, **37**, 6199–207.

O'Hare, P. A. G., Shinn, W. A., Mrazek, F. C., and Martin, A. E. (1972) *J. Chem. Thermodyn.*, **4**, 401–9.

O'Hare, P. A. G. and Hoekstra, H. R. (1973) *J. Chem. Thermodyn.*, **5**, 769–75.

O'Hare, P. A. G. and Hoekstra, H. R. (1974a) *J. Chem. Thermodyn.*, **6**, 251–8.

O'Hare, P. A. G. and Hoekstra, H. R. (1974b) *J. Chem. Thermodyn.*, **6**, 1161–9.

O'Hare, P. A. G., Boerio, J., Fredrickson, D. R., and Hoekstra, H. R. (1977) *J. Chem. Thermodyn.*, **9**, 963–72.

Ohmichi, T., Fukushima, S., Maeda, A., and Watanabe, H. (1981) *J. Nucl. Mater.*, **102**, 40–6.

Ohnuki, T., Kozai, N., Samadfam, M., Yasuda, R., Yamamato, S., Narumi, K., Naramoto, H., and Murakami, T. (2004) *Chem. Geol.*, **211**, 1–14.

Ohse, R.W. (1966) *J. Chem. Phys.*, **44**, 1375–8.

Ohse, R. W., Babelot, J. F., Cercignani, C., Kinsman, P. R., Long, K. A., Magill, J., and Scotti, A. (1979) *J. Nucl. Mater.*, **80**, 232–48.

Ohwada, K. (1970a) *J. Inorg. Nucl. Chem.*, **32**, 1209–18.

Ohwada, K. (1970b) *Spectochim. Acta*, **26A**, 1723–30.

Ohwada, K. (1971) *Inorg. Chem.*, **10**, 2281–5.

Ohwada, K. (1972) *J. Chem. Phys.*, **56**, 4951–6.

Ohwada, K., Soga, T., and Iwasaki, M. (1972) *J. Inorg. Nucl. Chem.*, **34**, 363–5.

Ohwada, K. (1976) *J. Inorg. Nucl. Chem.*, **38**, 741–5.

Oikawa, K., Kamiyama, T., Asano, H., Onuki, Y., and Kohgi, M. (1996) *J. Phys. Soc. Japan*, **65**, 3229–32.

Ollier, N., Guittet, M.-J., Gautier-Soyer, M., Panczer, G., Champagnon, B., and Jollivet, P. (2003) *Opt. Mater.*, **24**, 63–8.

Olsen, T., Gerwald, L., and Benedict, U. (1985) *J. Appl. Crystallogr.*, **18**, 37–41.

Olsen, T., Gerwald, L., Benedict, U., Dabos, S., and Vogt, O. (1988) *Phys. Rev. B*, **37**, 8713–8.

Ondruš, P., Veslovský, F., and Rybka, R. (1990) *Neues Jahrb. Miner., Monatsschr.*, **9**, 393–400.

Ondruš, P., Skála, P., Veselovský, F., Sejkora, J., and Vitti, C. (2003) *Am. Miner.*, **88**, 686–93.

Onoe, J., Takeuchi, K., Nakamatsu, H., Mukoyama, T., Sekine, R., Kim, B.-I., and Adachi, H. (1993) *J. Chem. Phys.*, **99**, 6810–17.

Onoe, J., Nakamatsu, H., Mukoyama, T., Sekine, R., Adachi, H., and Takeuchi, K. (1997) *Inorg. Chem.*, **36**, 1934–8.

Onuki, Y., Ukon, I., Komatsubara, T., Takayanagi, S., Wada, N., and Watanabe, T. (1990) *Physica B* (*Amsterdam, Neth.*), **163**, 368–70.

Onuki, Y., Ukon, I., Yun, S. W., Umehara, I., Satoh, K., Fukuhara, T., Sato, H., Takayanagi, S., Shikama, M., and Ochiai, A. (1992) *J. Phys. Soc. Japan*, **61**, 293–9.

Orlandi, P., Pasero, M., Duchi, G., and Olmi, F. (1997) *Am. Miner.*, **82**, 807–11.

Osborne, D. W., Westrum, E. F. Jr, and Lohr, H. R. (1955) *J. Am. Chem. Soc.*, **77**, 2737–9.

Osborne, D. W. and Flotow, H. E. (1972) *J. Chem. Thermodyn.*, **4**, 411–18.

Osborne, D. W., Flotow, H. E., Dallinger, R. P., and Hoekstra, H. R. (1974) *J. Chem. Thermodyn.*, **6**, 751–6.

Otey, M. G. and Le Doux, R. A. (1967) *J. Inorg. Nucl. Chem.*, **29**, 2249–56.

Outebridge, W. F., Staatz, M. H., Meyrowitz, R., and Pommer, A. M. (1960) *Am. Miner.*, **45**, 39–52.

Pabalan, R. T., Prikryl, J. D., Muller, P. M., and Dietrich, T. B. (1993) *Mater. Res. Soc. Symp. Proc.*, **294**, 777–82.

Pabst, A. (1954) *Am. Miner.*, **37**, 137–57.

Pagoaga, M. K., Appleman, D. E., and Stewart, J. M. (1987) *Am. Miner.*, **72**, 1230–8.

Paine, R. T., Ryan, R. R., and Asprey, L. B. (1975) *Inorg. Chem.*, **14**, 1113–17.

Paine, R. T., McDowell, R. S., Asprey, L. B., and Jones, L. H. (1976) *J. Chem. Phys.*, **64**, 3081–3.

Paixão, J. A., Rebizant, J., Blaise, A., Delapalme, A., Sanchez, J. P., Lander, G. H., Nakotte, H., Burlet, P., and Bonnet, M. (1994) *Physica B* (*Amsterdam, Neth.*), **203**, 137–46.

Palenzona, A. and Manfrinetti, P. (1995) *J. Alloys Compds*, **221**, 157–60.

Panlener, R. J., Blumenthal, R. N., and Garnier, J. E. (1975) *J. Phys. Chem. Solids*, **36**, 1213–22.

Papiernik, R., Mercurio, D., and Frit, B. (1980) *Acta Crystallogr. B*, **36**, 1769–74.

Papiernik, R., Mercurio, D., Frit, B., and Baernighausen, H. (1983) *Acta Cryst. C*, **39**, 667–8.

Parks, S. I. and Moulton, W. G. (1968) *Phys. Rev.*, **1973**, 333–7.

Parry, S. J. (1991) in *Activation Spectrometry in Chemical Analysis* (eds. J. D. Winefordner, and I. M. Kolthoff), John Wiley, New York, pp. 206–7.

Partington, J. R. (1949) in *Treatise on Physical Chemistry*, vol. I, Longman, Green, p. 639.

Pascal, P. (ed.) (1962–1970) *Nouveau, Traité de Chimie, Minérale*, vols. VII (1962), IX (1963), XV (2) (1961), XV (3) (1962), XV (4) (1967), and XV (5) (1970), Masson et Cie, Paris.

Pascal, J., Morin, J., and Lacombe, P. (1964) *J. Nucl. Mater.*, **13**, 28–32.

Paszek, A. P. (1978) Ph.D. Dissertation, The John Hopkins University, Baltimore.

Patton, F. S., Googin, J. M., and Griffith, W. L. (1963) *Enriched Uranium Processing*, Int. Ser. Monogr. Nucl. En. Div. IX, vol. 2, Pergamon Press, New York.

Pattoret, A., Drowart, J., and Smoes, S. (1964) *Trans. Faraday Soc.*, **65**, 98.

Pattoret, A., Drowart, J., and Smoes, S. (1968) in *Thermodynamics of Nuclear Materials*, Proc. Symp. 1967, International Atomic Energy Agency, Vienna, pp. 613–36.

Paul, R. (1970) Research Center Karlsruhe Report, KFK-1297.

Paul, R. and Keller, C. (1971) *J. Nucl. Mater.*, **41**, 133–42.

Pearcy, E. C., Prokryl, J. D., Murphy, W. M., and Leslie, B. W. (1994) *Appl. Geochem.*, **9**, 713–32.

Péligot, E. (1841a) *J. Prakt. Chem.*, **1** (24), 442–51.

Péligot, E. (1841b) *C. R. Acad. Sci.*, **12**, 735–7; **13**, 417–26.

Péligot, E. (1842) *Ann. Chim. Phys.*, Series 3, **5**, 5–47.

Péligot, E. (1844) *Ann. Chim. Phys.*, Series 3, **12**, 549–74.

Penneman, R. A., Kruse, F. H., George, R. S., and Coleman, J. S. (1964a) *Inorg. Chem.*, **3**, 309–15.

Penneman, R. A., Sturgeon, G. D., and Asprey, L. B. (1964b) *Inorg. Chem.*, **3**, 126–9.

Penneman, R. A., Keenan, K., and Asprey, L. B. (1967) *Adv. Chem. Ser.*, **71**, 248–55.

Penneman, R. A., Ryan, R. R., and Rosenzweig, A. (1973) *Struct. Bonding*, Berlin, Heidelberg, New York, **13**, 1–52.

Penneman, R. A., Ryan, R. R., and Rosenzweig, A. (1974) *Acta Crystallogr.*, **B30**, 1966–70.

Pepper, R. T. (1964) *Appl. Mater. Res.*, **3**, 203.

Pério, P. (1953a) *Bull. Soc. Chim. Fr*, 256–63.

Pério, P. (1953b) *Bull. Soc. Chim. Fr*, 840–1.

Perrin, A. (1970) *Compt. Rend. C*, **270**, 319–22.

Perrin, A. and Caillet, P. (1976) *Compt. Rend. C*, **282**, 721–4.

Perrin, A. (1977a) *J. Inorg. Nucl. Chem.*, **39**, 1169–72.

Perrin, A. (1977b) *J. Appl. Crystallogr.*, **10**, 359–60.

Perrin, A. and Le Marouille, J. Y. (1977) *Acta Crystallogr. B*, **33**, 2477–81.

Perrin, D. D. (1979) *Stability Constants of Metal-Ion Complexes. Part B Organic Ligands*, IUPAC Chemical Data Series no. 22, , Pergamon Press, New York.

Perron, P. O. (1968) Atomic Energy of Canada Ltd Report, AECL-3072.

Peterson, S. (1961) *J. Inorg. Nucl. Chem.*, **17**, 135–7.

Pfeil, P. C. L. (1956) *Proc. Int. Conf. on Peaceful Uses of Atomic Energy*, Geneva 1955, vol. 9, p. 117.

Picard, C. and Gerdanian, P. (1981) *J. Nucl. Mater.*, **99**, 184–9.

Picon, M. and Flahaut, J. (1968) *Bull. Soc. Chim. Fr.*, 772–80.

Piekarski, C. and Morfeld, P. (1997) *Appl. Occup. Environ. Hyg.*, **12**, 915–18.

Pippin, C. G. and Sullivan, J. C. (1989) *Radiochim. Acta*, **48**, 37–8.

Piret, P., Declerq, J.-P., and Piret-Meunier, J. (1979) *Acta. Crystallogr.*, **B35**, 1880–2.

Piret, P., Declerq, J.-P., and Wauters-Stoop, D. (1980) *Bull. Minér.*, **103**, 176–8.

Piret, P. and Deliens, M. (1982) *Bull. Minér.*, **105**, 125–8.

Piret, P. and Declerq, J.-P. (1983) *Bull. Minér.*, **106**, 383–9.

Piret, P., Deliens, M., Piret-Meunier, J., and Germain, G. (1983) *Bull. Minér.*, **106**, 299–304.

Piret, P. (1985) *Bull. Minér.*, **108**, 659–66.

Piret, P. and Deliens, M. (1987) *Bull. Minér.*, **110**, 65–7.

Piret, P., Deliens, M., Piret-Meunier, J., and Germain, G. (1988) *Bull. Minér.*, **111**, 443–9.

Piret, P., Piret-Meunier, J., and Deliens, M. (1990) *Eur. J. Miner.*, **2**, 399–405.

Plaine, R. T., Ryan, R. R., and Asprey, L. B. (1975) *Inorg. Chem.*, **14**, 1113–17.

Plant, J., Simpson, P. R., Smith, B., and Windley, B. F. (1999) *Rev. Miner.*, **38**, 255–319.

Platzner, I. T. (1997) in *Modern Isotope Ratio Mass Spectrometry* (ed. I. T. Platzner), John Wiley, New York, pp. 363–77.

Plesko, E. P., Scheetz, B. E., and White, W. B. (1992) *Am. Miner.*, **77**, 431–7.

Plumer, M. L. and Caillé, A. (1989) *Phys. Rev. B*, **40**, 396–8.

Pollard, F. H., Hanson, P., and Geary, W. J. (1959) *Anal. Chim. Acta*, **20**, 26–31.

Pollock, E. N. (1977) *Anal. Chim. Acta*, **88**, 399–401.

Polunina, G. P., Kovba, L. M., and Ippolitova, E. A. (1961) Argonne National Laboratory Report, ANL-trans-33, p. 224.

Potol, M., Brochu, R., Padiou, J., and Grandjean, D. (1972) *C.R. Acad. Sci. C*, **275**, 1419–21.

Prescott, C. H., Reynolds, F. L., and Holmes, J. A. (1946) *The Preparation of Uranium Metal by Thermal Dissociation of the Iodide*, MDDC-437.

Prigent, J. (1958) *Compt. Rend. Hebd. Séances Acad. Sci.*, **247**, 1737–9.

Prigent, J. and Lucas, J. (1965) *Bull. Soc. Chim. Fr.*, **4**, 1129–31.

Prins, G. and Cordfunke, E. P. H. (1975) *J. Inorg. Nucl. Chem.*, **37**, 119–27.

Prins, G., Cordfunke, E. P. H., and Ouweltjes, W. (1978) *J. Chem. Thermodyn.*, **10**, 1003–10.

Prins, G. and Cordfunke, E. H. P. (1983) *J. Less Common Metals*, **91**, 177–80.

Privalov, T., Schimmelpfennig, B., Wahlgren, U., and Grenthe, I. (2002) *J. Phys. Chem.*, **106**, 11277–82.

Privalov, T., Macak, P., Schimmelpfennig, B., Fromager, E., Grenthe, I., and Wahlgren, U. (2004) *J. Am. Chem. Soc.*, **124**, 9801–8.

Proceedings (1960a) *Proc. Uranium Carbide Meeting*, Oak Ridge National Laboratory, December 1–2, 1960, TID-7603.

Proceedings (1960b) *Prog. Carbide Fuels, Notes from the Second AEC Uranium Carbide Meeting*, Battelle Memorial Institute, March 22 and 23, 1960, TID-7589.

Proceedings (1961) *Proc. Symp. on Uranium Carbides as Reactor Fuel Materials*, USAEC, April 4, 1961, AEC Headquarters, Germantown, MD, TID-7614.

Proceedings (1963) *Proc. Fourth Uranium Carbide Conf.*, East Hartfield, CT, May 20–21, 1963, TID-7676.

Proceedings (1966) *Proc. Second Int. Thorium Fuel Cycle Symp.*, Gatlinburg, TN, May 3–6, 1966, CONF-660524.

Pushcharovsky, D. Y., Rastsvetaeva, R. K., and Sarp, H. (1996) *J. Alloys Compds.*, **239**, 23–6.

Pyykkö, P., Li, J., and Runeberg, N. J. (1994) *J. Phys. Chem.*, **98**, 4809–13.

Rabinovich, D., Schimek, G. L., Pennington, W. T., Nielsen, J. B., and Abney, K. D. (1998) *Acta Crystallogr. C*, **54**, 1740–2.

Rabinowitch., E. and Belford, R. L. (1964) *Spectroscopy and Photochemistry of Uranyl Compounds*, Pergamon Press, Oxford.

Raetsky, V. M. (1967) *J. Nucl. Mater.*, **21**, 105–8.

Raj, P., Sathyamoorthy, A., Shashikala, K., Kumar, N. H., Rao, C. R. V., and Malik, S. K. (2000) *J. Alloys Compds.*, **296**, 20–6.

Rajnak, K., Gamp, E., Shinomoto, R., and Edelstein, N. M. (1998) *J. Chem. Phys.*, **80**, 5942–50.

Ralph, J. and Hyland, G. J. (1985) *J. Nucl. Mater.*, **132**, 76–9.

Rand, M. H. and Kubaschewski, O. (1963) *The Thermochemical Properties of Uranium Compounds*, Olivier&Boyd, Edinbourgh.

Rand, M. H., Ackermann, R. J., Grønvold, F., Oetting, F. L., and Pattoret, A. (1978) *Rev. Int. Hautes Tempér. Réfract. Fr.*, **15**, 355–65.

Ratho, T. and Patel, T. (1968) *Indian J. Phys.*, **42**, 240–2.

Ratho, T., Patel, T., and Sahoo, B. (1969) *Indian J. Phys.*, **43**, 164–6.

Rebenko, A. N., Brusentsev, F. A., and Opalovskii, A. A. (1968) *Izv. Sib. Otd. Nauk. SSSR, Ser. Khim. Nauk*, **1**, 136–8.

Rebizant, J., Van den Bossche, G., Spirlet, M. R., and Goffart, J. (1987) *Acta Crystallogr.*, **C43**, 1298–300.

Rediess, K. and Sawodny, W. (1982) *Z. Naturforsch.*, **37B**, 524–5.

Reeder, R. J., Nugent, M., Lamble, G. M., Tait, C. D., and Morris, D. E. (2000) *Environ. Sci. Technol.*, **34**, 638–44.

Reeder, R. J., Nugent, M., Drew Tait, C., Morris, D. E., Heald, S. M., Beck, K. M., Hess, W. P., and Lanzirotti. A. (2001) *Geochim. Cosmochim. Acta*, **65**, 3491–503.

Reedy, G. T. and Chasanov, M. G. (1972) *J. Nucl. Mater.*, **42**, 341–4.

Reis, A. H. Jr, Hoekstra, H. R., Gebert, E., and Peterson, S. W. (1976) *J. Inorg. Nucl. Chem.*, **38**, 1481–5.

Reshetov, K. V. and Kovba, L. M. (1966) *Zh. Strukt. Khim.*, **7**, 625–6.

Reynolds, L. T. and Wilkinson, G. (1956) *J. Inorg. Nucl. Chem.*, **2**, 246–53.

Rietveld, H. M. (1966) *Acta Crystallogr.*, **20**, 508–13.

Rigny, P. (1965) CEA Report CEA-R2827, pp. 1–30.

Rigny, P. (1966) N.S.A. 20, no. 1807.

Rigny, P. and Plurien, P. (1967) *J. Phys. Chem. Solids*, **28**, 2589–95.

Rigny, P., Dianoux, A.-J., and Plurien, P. (1971) *J. Chem. Phys. Solids*, **32**, 1175–80.

Rizzo da Rocha, S. M., Rodrigues de Aquino, A., and Abrao, A. (1995) *An. Assoc. Brasil. Quimica*, **44**, 33–40.

Roberts, L. E. J. and Walter, A. J. (1961) *J. Inorg. Nucl. Chem.*, **22**, 213–29.

Roberts, L. E. J. and Walter, A. J. (1966) in *Physico-Chimie du Protactinium* (eds. G. Bouissières and R. Muxart), Colloq. Int. 154, Centre National de la Recherche Scientifique, Paris, pp. 51–9.

Roberts, W. L., Campbell, T. J., and Rapp, G. R. (1990) in *Encyclopedia of Minerals*, Kluwer Academic Publishers, 2nd edn, February 1990.

Robins, R. G. (1961) *J. Nucl. Mater.*, **3**, 294–301.

Rodden, C. J. and Warf, J. C. (1950) in *Analytical Chemistry of the Manhattan Project* (ed. C. J. Rodden), McGraw-Hill, New York, pp. 3–159.

Rodriguez de Sastre, M. S., Philippot, J., and Moreau, C. (1967) CEA Report, CEA-R 3218.

Rogova, V. P., Belova, L. N., Kiziyarov, G. P., Kuznetsova, N. N. (1973) *Zap. Uses. Miner. Obshch.*, **102**, 75–81.

Rona, E. (1950) *J. Am. Chem. Soc.*, **72**, 4339–43.

Ronchi, C. and Hyland, G. J. (1994) *J. Alloys Compds.*, **213/214**, 159–68.

Ronchi, C., Sheindlin, M., Musella, M., and Hyland, G. J. (1999) *J. Appl. Phys.*, **85**, 776–89.

Rosén, A. and Fricke, B. (1979) *Chem. Phys. Lett.*, **61**, 75–8.

Rosenthal, M. W., Briggs, R. B., and Kasten, P. R. (1969) *Molten Salt Reactor Program Semiannual Progress Report for Period Ending August 31, 1968*, ORNL-4344, p. IX.

Rosenthal, M. W., Haubenreich, P. N., and Briggs, R. B. (1972) ORNL-4812, pp. 1–416.

Rosenzweig, A. and Cromer, D. T. (1970) *Acta Crystallogr.*, **B26**, 38–44.

Rosenzweig, A., Ryan, R. R., and Cromer, D. T. (1973) *Acta Crystallogr.*, **B29**, 460–2.

Rosenzweig, A. and Ryan, R. R. (1975) *Am. Miner.*, **60**, 448–53.

Rosenzweig, A. and Ryan, R. R. (1977) *Crystal Struct. Commun.*, **6**, 53–6.

Ross, M. and Evans, H. T. (1964) *Am. Miner.*, **49**, 1578–602.

Ross, J. W. and Lam, D. W. (1968) *Phys. Rev.*, **165**, 617.

Rossetto, G., Zanella, P., Paolucci, G., and de Paoli, G. (1982) *Inorg. Chim. Acta*, **61**, 39–42.

Rossotti, F. J. R. and Rossotti, H. (1961) *The Determination of Stability Constants and Other Equilibrium Constants in Solution*, McGraw-Hill, New York.

Roth, W. L. (1960) *Acta Crystallogr.*, **13**, 140–9.

Rough, F. A. and Bauer, A. A. (1958) *Constitution of Uranium and Thorium Alloys*, BMI-1300.

Roussel, P. and Scott, P. (1998) *J. Am. Chem. Soc.*, **1998**, 1070–1.

Ruch, W. C., Peterson, D. A., Gaskill, E. A., and Tepp, H. G. (1959) *Nuclear Engineering and Science Conf.*, Am. Inst. Chem. Eng., April 6–9, 1959, Cleveland, OH, Preprint V-52.

Rundle, R. E. (1947) *J. Am. Chem. Soc.*, **69**, 1719–23.

Rundle, R. E., Baenziger, N. C., Wilson, A. S., and McDonald, R. A. (1948) *J. Am. Chem. Soc.*, **70**, 99–105.

Rundle, R. E. (1951) *J. Am. Chem. Soc.*, **78**, 4172–4.

Runnals, O. J. C. (1953) *Can. J. Chem.*, **3**, 694.

Rutledge, G. P., Jarry, R. L., and Davis, W. Jr (1953) *J. Phys. Chem.*, **57**, 541–4.

Rüdorff, W. and Pfitzer, F. (1954) *Z. Naturforsch.*, **9b**, 568–9.

Rüdorff, W. and Leutner, H. (1957) *Z. Anorg. Allg. Chem.*, **292**, 193–6.

Rüdorff, W. and Menzer, W. (1957) *Z. Anorg. Allg. Chem.*, **292**, 197–202.

Rüdorff, W., Kemmler, S., and Leutner, H. (1962) *Angew. Chem.*, **74**, p. 429.

Rüdorff, W., Erfurth, H., and Kemmler-Sack, S. (1967) *Z. Anorg. Allg. Chem.*, **354**, 273–85.

Ryan, J. L. (1962) *Proc. Seventh Int. Conf. Coordination Chemistry*, pp. 367–9; and Ryan, J. L. and Keder, W. E., unpublished work.

Ryan, R. R. (1971) *J. Inorg. Nucl.Chem.*, **33**, 153–77.

Ryan, R. R. (1972) *Med. Tech. Pub. Co. Int. Rev. Sci. Inorg. Chem., Ser.1*, **7**, 323–67.

Ryan, R. R. (1974) *Inorg. Synth.*, **15**, 235–43.

Ryan, R. R., Cleveland, J. M., and Bryan, G. H. (1974) *Inorg. Chem.*, **13**, 214–18.

Ryan, R. R., Penneman, R. A., Asprey, L. B., and Paine, R. T. (1976) *Acta Crystallogr. B*, **32**, 3311–13.

Ryan, R. R. and Rosenzweig, A. (1977) *Crystal Struct. Commun.*, **6**, 611–15.

Saito, Y. (1974) *J. Nucl. Mater.*, **51**, 112–25.

Sakurai, T., Kameda, O., and Ishigame, M. (1968) *J. Crystal Growth*, **2**, 236–7.

Saller, H. A. and Rough, F. A. (1954) *Chem. Eng. Prog. Symp. Ser.* 11, **50**, 63–7.

Saller, H. A. and Rough, F. H. (1955) *Compilation of U.S. and U.K. Uranium and Thorium Constitutional Diagrams*, 1st edn, BMI-1000.

Samson, S. and Sillén, L. G. (1947) *Ark. Kemi. Min. Geol.*, **25A** (21), 1–16.

Samsonov, G. V. (1968) *Handbook of the Physicochemical Properties of the Elements*, IFI/Plenum, New York-Washington, p. 437.

Sandell, E. B. (1959) *Colorimetric Determination of Traces of Metals*, 3rd edn, Interscience, New York.

Sandino, A. and Bruno, J. (1992) *Geochim. Cosmochim. Acta.*, **56**, 4135–45.

Santini, P., Lémanski, R., and Erdös, P. (1999) *Adv. Phys.*, **48** (5), 538–653.

Santos, I. G. and Abram, U. (2004) *Inorg. Chem. Commun.*, **7**, 440–2.

Sara, K. H. (1970) *J. Indian Chem. Soc.*, **47**, 88.

Sarp, H., Bertrand, J., and Deferne, J. (1983) *Neues Jahrb. Miner., Monatsschr.*, **6**, 417–23.

Sarsfield, M. J. and Helliwell, M. (2003) *J. Am. Chem. Soc.*, **126**, 1036–7.

Satonnay, G., Ardois, C., Corbel, C., Lucchini, J. F., Barthe, M. F., Garrido, F., and Gosset, D. (2001) *J. Nucl. Mater.*, **288**, 11–19.

Satten, R. A., Schreiber, C. L., and Wong, E. Y. (1983) *J. Chem. Phys.*, **78**, 79–87.

Savage, A. W. (1956) *J. Am. Chem. Soc.*, **78**, 2700–2.

Sawai, H., Kuroda, K., and Hojo, T. (1989) *Bull. Chem. Soc. Japan*, **62**, 2018–23.

Sawai, H., Shibusawa, T., and Kuroda, K. (1990) *Bull. Chem. Soc. Japan*, **63**, 1776–80.

Sawai, H., Higa, K., and Kuroda, K. (1992) *J. Chem. Soc. Dalton Trans.*, 505–8.

Sawai, H., Ito, T., Kokaji, K., Shimazu, M., Shinozuka, K., and Taira, H. (1996) *Biorg Med. Chem. Lett.*, **6**, 1785–90.

Sawodny, W., Rediess, K., and Thewalt, U. (1980) *Z. Anorg. Allg. Chem.*, **469**, 81–6.

Sawodny, W., Rediess, K., and Thewalt, U. (1983) *Z. Anorg. Allg. Chem.*, **499**, 81–8.

Sawyer, J. O. (1963) *J. Inorg. Nucl. Chem.*, **25**, 899–902.

Sawyer, J. O. (1972) *J. Inorg. Nucl. Chem.*, **34**, 3268–71.

Saxena, S. S., Agarwal, P., Ahilan, K., Grosche, F. M., Haselwimmer, R. K. W., Steiner, J. J., Pugh, E., Walker, I. R., Julian, S. R., Monthoux, P., Lonzarich, G. G., Huxley, A., and Shalek, P. D. (1963) *J. Am. Ceram. Soc.*, **46**, 155–61.

Scapolan, S. (1998) *Mise au Point et Evaluation de Techniques de Spéciation pour L'Etudes des Especes Biologiques Circulantes de L'Uranium* (*VI*), Thesis, Université de Paris Sud.

Schaner, B. E. (1960) *J. Nucl. Mater.*, **2**, 110–20.

Schäfer, H. (1975) *Z. Anorg. Allg. Chem.*, **414**, 151–9.

Schindler, M. and Hawthorne, F. C. (2004) *Can. Miner.*, **42**, 1601–27.

Schindler, M., Mutter, A., Hawthorne, F. C., and Putnis, A. (2004) *Can. Miner.*, **42**, 1651–66.

Schirber, J. E., Arko, A. J., and Fischer, E. S. (1975) *Solid State Commun.*, **17**, 553.

Schleid, T., Meyer, G., and Morss, L. R. (1987) *J. Less Common Metals*, **132**, 69–77; Schleid, T. and Meyer, G. (1988) unpublished results.

Schleid, T. and Meyer, G. (1989) *Naturwissenschaften*, **76**, 118.

Schlesinger, H. I. and Brown, H. C. (1953) *J. Am. Chem. Soc.*, **75**, 219–21.

Schlyter, K. (1953) *Ark. Khemi*, **5**, 73.

Schmieder, H., Dornberger, E., and Kanelakopulos, B. (1970) *Appl. Spectrosc.*, **24**, 499.

Schmitz-Dumont, O., Füchtenbusch, F., and Schneiders, H. (1954) *Z. Anorg. Allg. Chem.*, **277**, 315–28.

Schmitz, F., Dean, G., and Halachmy, M. (1971) *J. Nucl. Mater.*, **40**, 325–37.

Schoebrechts, J.-P., Gens, R., Fuger, J., and Morss, L. R. (1989) *Thermochim. Acta*, **139**, 49–66.

Scholder, R. and Brixner, L. (1955) *Z. Naturforsch.*, **10b**, 178–9.

Scholder, R. (1958) *Angew. Chem.*, **70**, 583–94.

Scholder, R. (1960) *Angew. Chem.*, **72**, pp. 120.

Scholder, R. and Gläser, H. (1964) *Z. Anorg. Allg. Chem.*, **327**, 15–27.

Schreckenbach, G., Hay, P. J., and Martin, R. L. (1998) *Inorg. Chem.*, **37**, 4442–51.

Seaborg, G. T. and Katzin, L. 1. (1951) *Production and Separation of U^{233} – Survey*, Natl. Nucl. En. Ser. Div. IV, 17A, USAEC Technical Information Service, Oak Ridge, TN (declassified as TID-5222).

Seijo, L. and Barandiaran, Z. (2001) *J. Chem. Phys.*, **115**, 5554.

Sejkora, J., Čejka, J., Hloušek, J., Novák, M., and Šrein, V. (2004) *Can. Miner.*, **42**, 963–72.

Selbin, J. and Ortego, J. (1969) *Chem. Rev.*, **69**, 657–71.

Selbin, J., Ortego, J. D., and Gritzner, N. (1968) *Inorg. Chem.*, **7**, 976–82.

Selbin, J., Ballhausen, C. J., and Durrett, D. G. (1972a) *Inorg. Chem.*, **11**, 510–15.

Selbin, J., Durret, D. G., Sherrill, H. J., Newkome, G. R., and Wharton, J. H. (1972b) *J. Chem. Soc. Chem. Comm.*, 380–1.

Selbin, J., Durret, D. G., Sherrill, H. J., Newkome, G. R., and Collins, M. (1973) *J. Inorg. Nucl. Chem.*, **35**, 3467–80.

Selbin, J. and Sherrill, H. J. (1974) *Inorg. Chem.*, **13**, 1235–9.

Sémon, L., Boeme, C., Billard, I., Hennig, C., Lützenkirchen, K., Reich, T., Rossberg, A., Rossini, I., and Wipff, G. (2001) *Chem. Phys. Chem.*, **2**, 591–8.

Seppelt, K. and Hwang, I.-C. (2000) *J. Fluorine Chem.*, **102**, 69–72.

Sessler, J. L., Vivian, A. E., Seidel, D., Burrel, A. K., Hoehner, M., Mody, T. D., Gebauer, A., Weghorn, S. J., and Lynch, V. (2001) *Coord. Chem. Rev.*, **216–217**, 411–34.

Seta, K., Matsui, T., Inaba, H., and Naito, K. (1982) *J. Nucl. Mater.*, **110**, 47–54.

Shamir, J. and Silberstein, A. (1975) *J. Inorg. Nucl. Chem.*, **37**, 1173–5.

Shamir, J., Silberstein, A., Ferraro, J. B., and Choca, M. (1975) *J. Inorg. Nucl. Chem.*, **37**, 1429–32.

Shchelokov, R. N. and Belomestnykh, V. I. (1968a) *Zh. Neorg. Khim.*, **13**, 1398–1403; *Russ. J. Inorg. Chem.*, **13**, 733–6.

Shchelokov, R. N. and Belomestnykh, V. I. (1968b) *Zhur. Neorg. Khim.*, **13**, 3386–891; *Russ. J. Inorg. Chem.*, **13**, 1744–7.

Shchelokov, R. N., Tsivadze, A. Yu., Orlova, I. M., and Podnebesnova, G. V. (1977) *Inorg. Nucl. Chem. Lett.*, **13**, 367–74.

Shchukarev, S. A., Vasil'kova, I. V., Drozdova, V. M., and Frantseva, K. E. (1959a) *Zh. Neorg. Khim.*, **4**, 39–41; (1959) *Russ. J. Inorg. Chem.*, **4**, 15–16.

Shchukarev, S. A., Vasilkova, I. V., Drozdova, V. M., and Martynova, N. S. (1959b) *Zh. Neorg. Khim.*, **4**, 33–8; (1959) *Russ. J. Inorg. Chem.*, **4**, 13–15.

Sheikin, I., Braithwaite, D., and Flouquet, J. (2000) *Nature*, **406**, 587–92.

Shen, J. and Peny, Z. (1981) *Acta Crystallogr.*, **A37**, Suppl. C-186.

Shimazu, M., Shinozuka, K., and Sawai, H. (1993) *Angew. Chem. Int. Ed. Engl.*, **32**, 870–2.

Shoesmith, D. W. and Sunder, S. (1994) in *The Electrochemistry of Novel Materials* (eds. J. Lipkowski and P. N. Ross), VCH, New York, p. 297.

Shull, C. G. and Wilkinson, M. K. (1955) *Oak Ridge National Laboratory Report*, *ORNL*-1879, p. 24.

Shunk, F. A. (1969) *Constitution of Binary Alloys*, 2nd Suppl., McGraw-Hill, New York.

Siegel, S. (1956) *Acta Crystallogr.*, **9**, 827.

Siegel, S., Hoekstra, H. R., and Sherry, E. (1966) *Acta Crystallogr.*, **20**, 292–5.

Siegel, S. and Hoekstra, H. R. (1968) *Acta Crystallogr.*, **B24**, 967–70.

Siegel, S. and Hoekstra, H. R. (1971a) *Inorg. Nucl. Chem. Lett.*, **7**, 497–504.

Siegel, S. and Hoekstra, H. R. (1971b) *Inorg. Nucl. Chem. Lett.*, **7**, 455–9.

Siegel, S., Viste, A., Hoekstra, H. R., and Tani, B. (1972) *Acta Crystallogr.*, **B28**, 117.

Silberstein, A. (1972) INIS-mf-36, p. 46.

Sillén, L. G. and Martell, A. E. (1964) *Stability Constants of Metal-Ion Complexes*, The Chemical Society, London.

Sillén, L. G. and Martell, A. E. (1971) *Stability Constants of Metal-Ion Complexes*, Suppl. no. 1, The Chemical Society, London.

Silverman, L. and Sallach, R. A. (1961) *J. Phys. Chem.*, **65**, 370.

Simoni, E., Hubert, S., and Genet, M. (1988) *J. Phys.* (*France*), **49**, 1425–34.

Simoni, E., Louis, M., Gesland, J. Y., and Hubert, S. (1995) *J. Lumin.*, **65**, 153–61.

Simpson, K. A. and Wood, P. (1983) in *Proc. NRC Workshop on Spent Fuel/Cladding Reaction during Dry Storage*, Gaithersburg, MD, NUREG/CP-0049, p. 70.

Singh, R. N. and Coble, R. L. (1974) *J. Crystal Growth*, **21**, 261–6.

Sjkora, J., Čejka, J., Hloušek, J., Šrein, V., Novotná M. (2002) *Neu. Jahr. Miner. Monat.*, **8**, 353–67.

Slain, H. (1950) *Production of Uranium by Electrolysis of Fused Salts*, LA-1056.

Sleight, A. W. and Ward, R. (1962) *Inorg. Chem.*, **1**, 790–3.

Slovyanskikh, V. K., Ellert, G. V., and Yarembash, E. L. (1967) *Izv. Akad. Nauk SSSR, Neorg. Mater.*, **3**, 1088–90; *Inorg. Mater.* (*USSR*), **3**, 969–71.

Slovyanskikh, V. K., Rozanov, I. A., and Gracheva, N. V. (1977) *Zh. Neorg. Khim.*, **22**, 1645–50; *Russ. J. Inorg. Chem.*, **22**, 893–6.

Smiley, S. H. and Brater, D. C. (1956) Current Commission Methods for producing UO_3, UF_4 and UF_6, TID-5295, pp. 245–89.

Smiley, S. H. and Brater, D. C. (1958) K-1379 Del., pp. 1–18.

Smiley, S. H. and Brater, D. C. (1960) N.S.A, **16**, no.1573.

Smith, G. S., Johnson, O., and Elson, R. E. (1967) *Acta Crystallogr.*, **22**, 300–3.

Smith, R. M. and Martell, A. E. (1989) *Critical Stability Constants*, vol. 6, Second Suppl., Plenum Press, New York.

Sobczyk, M., Karbowiak, M., and Drożdżyński, J. (2003) *J. Solid State Chem.*, **170**, 443–9.

Sobczyk, M., Drożdżyński, J., and Karbowiak, M. (2005) *J. Solid. State Chem.*, **178/2**, 536–44.

Soga, T., Ohwada, K., and Iwasaki, M. (1972) *Appl. Spectrosc.*, **26**, 482–3.

Soga, T., Ohwada, K., and Iwasaki, M. (1973) *J. Inorg. Nucl. Chem.*, **35**, 2069–74.

Soulié, E. (1978) *J. Inorg. Nucl. Chem.*, **40**, 351–2.

Souter, P. F., Kushto, G. P., Andrews, L., and Neurock, M. J. (1997) *J. Am. Chem. Soc.*, **119**, 1682–87.

Spedding, F. H., Newton, A. S., Warf, J. C., Johnson, O., Nottorf, R. W., Johns, I. B., and Daane, A. H. (1949) *Nucleonics*, **4** (1), 4–15.

Speer, J. A. (1982) *Rev. Miner.*, **5**, 113–35.

Spencer, S., Gagliardi, L., Handy, N. C., Ioannou, A. G., Skylaris, C.-K., and Willets, A. (1999) *J. Phys. Chem. A*, **103**, 1831–7.

Spirlet, J. C. (1979) *J. Phys. Colloq.*, C4, **40**, 87–94.

Spirlet, J. C., Bednarczyk, E., and Müller, W. (1979) *J. Phys. Colloq.*, **40**, C4, 108–10.

Spirlet, M. R., Rebizant, J., Fuger, J., and Schoebrechts, J. P. (1988) *Acta Crystallogr. C*, **44**, 1300.

Spitsyn, V. I., Ippolitova, E. A., Simanov, Yu. P., and Kovba, L. M. (1961a) Argonne National Laboratory Report, ANL-trans-33, p. 4.

Spitsyn, V. I., Ippolitova, E. A., Efremova, K. M., and Simanov, Yu. P. (1961b) Argonne National Laboratory Report, ANL-trans-33, p. 142.

Spitsyn, V. I., Ippolitova, E. A., Efremova, K. M., and Simanov, Yu. P. (1961c) Argonne National Laboratory Report, ANL-trans-33, p. 148.

Spitsyn, V. I., Tshigunov, A. N., Kovba, L. M., and Kuz'micheva, E. U. (1972) *Dokl. Akad. Nauk SSSR*, **204**, 604–43.

Srirama Murti, P., Yadav, R. B., Nawada, H. P., Vasudeva Rao, P. R., and Mathews, C. K. (1989) *Thermochim. Acta*, **140**, 299–303.

Stadlbauer, E., Wichmann, U., Lott, U., and Keller, C. (1974) *J. Solid State Chem.*, **10**, 341–50.

Staritzky, E. and Singer, J. (1952) *Acta Crystallogr.*, **5**, 536–40.

Staritzky, E., and Douglass, R. M. (1956) *Anal. Chem.*, **28**, 1210–11.

Steinitz, M. O., Burleson, C. E., and Marcus, J. A. (1970) *J. Appl. Phys.*, **41**, 5057.

Stephens, F. M. Jr and McDonald, R. O. (1956) *Proc. First Int. Conf. on Peaceful Uses of Atomic Energy*, Geneva, 1955, vol. 8, pp. 18–25.

Sterns, M. (1967) *Acta Crystallogr.*, **23**, 264–72.

Stoewe, K. (1996a) *Z. Anorg. Allg. Chem.*, **622**, 1419–22.

Stoewe, K. (1996b) *Z. Anorg. Allg. Chem.*, **622**, 1423–7.

Stoewe, K. (1997a) *Z. Anorg. Allg. Chem.*, **623**, 749–54.

Stoewe, K. (1997b) *J. Alloys Compds*, **246**, 111–23.

Stohl, F. V. and Smith, D. K. (1981) *Am. Miner.*, **66**, 610–25.

Stoller, S. M. and Richards, R. B. (1961) *Reactor Handbook*, 2nd edn, vol. II, Fuel Processing, Interscience, New York.

Storms, E. K. (1985) *J. Nucl. Mater.*, **132**, 231–43.

Straka, M., Dyall, K. G., and Pyykkö, P. (2001) *Theor. Chem. Acc.*, **106**, 393–403.

Streitweiser, A. and Müller-Westerhoff, U. (1968) *J. Am. Chem. Soc.*, **90**, 7364.

Strotzer, E. F., Schneider, O., and Biltz, W. (1943) *Z. Anorg. Allg. Chem.*, **243**, 307–21.

Stryer, L. (1988) *Biochemistry*, 3rd edn, W. H. Freeman and Co, New York, p. 705.

Stumpp, E. (1969) *Naturwissenschaften*, **56**, 370.

Stumpp, E. and Piltz, G. (1974) *Z. Anorg Allg. Chem.*, **409**, 53–9.

Sturchio, N. C., Antonio, M. R., Soderholm, L., Sutton, S. R., and Brannon, J. C. (1998) *Science*, **281**, 971–3.

Sugisaki, M., Hirashima, K., Yoshihara, S., and Oishi, Y. (1973) *J. Nucl. Sci. Technol.*, **10**, 387–9.

Sugisaki, M. and Sueyoshi, T. (1978) *J. Inorg. Nucl. Chem.*, **40**, 1543–9.

Sugiyama, K. and Onuki, Y. (2003) *High Magn. Fields*, **2**, 139–70.

Suglobova, I. G. and Chirkst, D. E. (1978a) *Radiokhimiya*, **20**, 361–5; *Sov. Radiochem.*, **20**, 310–14.

Suglobova, I. G. and Chirkst, D. E. (1978b) *Radiokhimiya*, **20**, 352–60; (1978) *Sov. Radiochem.*, **20**, 302–9.

Suglobova, I. G. and Chirkst, D. E. (1981) *Koord. Khimiya*, **7**, 97–102.

Sullivan, J. C., Hindman, J. C., and Zielen, A. J. (1961) *J. Am. Chem. Soc.*, **83**, 3373–8.

Sunder, S., Cramer, J. J., and Miller, N. H. (1996) *Radiochim. Acta*, **74**, 303–7.

Sunder, S., Miller, N. H., and Shoesmith, D. W. (2004) *Corrosion Sci.*, **46**, 1095–111.

Suski, W., Gibifiski, T., Wojakowski, A., and Czaynik, A. (1972) *Phys. Status Solidi*, **9**, 653–8.

Suski, W., Wojakowski, A., Blaise, A., Salmon, P., Fournier, J., and Mydlarz, T. (1976) *J. Magn. Mater.*, **3**, 195–200.

Sutton, S. (1955) *J. Inorg. Nucl. Chem.*, **1**, 68–74.

Swihart, G. H., Sen Gupta, P. K., Schlemper, E. O., Bach, M. E., and Gaines, R. V. (1993) *Am. Miner.*, **78**, 835–9.

Sylwester, E. R., Hudson, E. A., and Allen, P. G. (2000) *Geochim. Cosmochim. Acta*, **64**, 2431–8.

Szabó, Z., Glaser, J., and Grenthe, I. (1996) *Inorg. Chem.*, **35**, 2036–44.

Szabó, Z., Aas, W., and Grenthe, I. (1997) *Inorg. Chem.*, **36**, 5369–75.

Szabó, Z., Moll, H., and Grenthe, I. (2000) *J. Chem. Soc., Dalton Trans.*, 3158–161.

Szabó, Z. and Grenthe, I. (2000) *Inorg. Chem.*, **39**, 5036–43.

Szabó, Z. (2002) *J. Chem. Soc., Dalton Trans.*, 4242–7.

Szabó, Z. Toraishi, T., Vallet, V., and Grenthe, I. (2006) *Coord. Chem. Rev.*, In print.

Szwarc, R. and Latta, R. E. (1968) *J. Am. Ceram. Soc.*, **51**, 264–8.

Tabuteau, A., Jové, J., Pagès, M., and de Novion, C. H. (1984) *Solid State Commun.*, **50**, 357–61.

Tachibana, T., Ohmori, T., Yamanouchi, S., and Itaki, T. (1985) *J. Nucl. Sci. Technol.*, **22**, 155–7.

Tagawa, H. (1975) *J. Inorg. Nucl. Chem.*, **37**, 731–3.

Tagawa, H., Fujino, T., and Tateno, J. (1975) Japan Atomic Research Institute Report, JAERI-M 6180.

Tagawa, H. and Fujino, T. (1977) *Inorg. Nucl. Chem. Lett.*, **13**, 489–93.

Tagawa, H., Fujino, T., and Tateno, J. (1977) *Bull. Chem. Soc. Japan*, **50**, 2940–4.

Tagawa, H. and Fujino, T. (1978) *J. Inorg. Nucl. Chem.*, **40**, 2033–6.

Tagawa, H. and Fujino, T. (1980) *Inorg. Nucl. Chem. Lett.*, **16**, 91–6.

Tagawa, H., Fujino, T., Watanabe, K., Nakagawa, Y., and Saita, K. (1981a) *Bull. Chem. Soc. Japan*, **54**, 138–42.

Tagawa, H., Fujino, T., Ouchi, K., Watanabe, K., and Morimoto, T. (1981b) *J. Nucl Sci. Technol.*, **18**, 811–16.

Tagawa, H., Fujino, T., Ouchi, K., Watanabe, K., Saita, K., and Morimoto, T. (1983) *J. Nucl. Sci. Technol.*, **20**, 467–74.

Takano, Y. (1961) *Am. Miner.*, **46**, 812–22.

Tame, J. R. H. (2000) *Acta Crystallogr.*, **D56**, 1554–9.

Tanaka, H., Kimura, E., Yamaguchi, A., and Moriyama, J. (1972) *J. Jpn. Inst. Metals*, **36**, 633–7.

Tanamas, R. (1974) Research Center Karlsruhe Report, KFK-1910.

Tanner, P. A., Hung, S.-T., Mak, T. C. W., and Wang, R.-J. (1992) *Polyhedron*, **11**, 817–22.

Tanner, P. A., Silvestre, J. P. F., and Dao, N. Q. (1993) *New J. Chem.*, **17**, 263–6.

Tasker, I. R., O'Hare, P. A. G., Lewis, B. M., Johnson, G. K., and Cordfunke, E. H. P. (1988) *Can. J. Chem.*, **66**, 620–5.

Tateno, J., Fujino, T., and Tagawa, H. (1979) *J. Solid State Chem.*, **30**, 265–73.

Tatsumi, K. and Hoffmann, R. (1980) *Inorg. Chem.*, **19**, 2656–8.

Taylor, J. C. (1971) *Acta Crystallogr.*, **B27**, 1088–91.

Taylor, J. C. and Wilson, P. W. (1973a) *Acta Crystallogr. B*, **29**, 1942–4.

Taylor, J. C. and Wilson, P. W. (1973b) *Acta Crystallogr. B*, **29**, 1073–6.

Taylor, J. C. and Wilson, P. W. (1974a) *Acta Crystallogr. B*, **30**, 175–7.

Taylor, J. C. and Wilson, P. W. (1974b) *Acta Crystallogr. B*, **30**, 1481–4.

Taylor, J. C. and Wilson, P. W. (1974c) *Acta Crystallogr. B*, **30**, 169–75.

Taylor, J. C. and Wilson, P. W. (1974d) *J. Chem. Soc. Chem. Commun.*, pp. 598–5.

Taylor, J. C. and Wilson, P. W. (1974e) *Acta Crystallogr. B*, **30**, 2664–7.

Taylor, J. C. and Wilson, P. W. (1974f) *Acta Crystallogr. B*, **30**, 2803–5.

Taylor, J. C. and Wilson, P. W. (1975a) *J. Inorg. Nucl. Chem.*, **39**, 1989–91.

Taylor, J. C., and Wilson, P. W. (1975b) *J. Solid State Chem.*, **14**, 378–82.

Taylor, J. C. (1976a) *Coord. Chem. Rev.*, **20**, 197–273.

Taylor, J. C. (1976b) *Inorg. Nucl. Chem. Lett.*, **12**, 725–8.

Taylor, J. C. and Waugh, A. B. (1980) *J. Solid State Chem.*, **35**, 137–40.

Taylor, J. C., Stuart, W. I., and Mumme, I. A., (1981) *J. Inorg. Nucl. Chem.*, **43**, 2719–23.

Taylor, J. C. and Waugh, A. B. (1983) *Polyhedron*, **2**, 211–16.

Taylor, J. C. (1987) *Z. Kristallogr.*, **181**, 151–60.

Tempest, P. A., Tucker, P. M., and Tyler, J. W. (1988) *J. Nucl. Mater.*, **151**, 251–68.

Templeton, L. K., Templeton, D. H., Bartlett, N., and Seppelt, K. (1976) *Inorg. Chem.*, **15**, 2720–2.

Tetenbaum, M. and Hunt, P. D. (1968) *J. Chem. Phys.*, **49**, 4739–44.

Tetenbaum, M. and Hunt, P. D. (1970) *J. Nucl. Mater.*, **34**, 86–91.

Thibaut, E., Boutique, J.-P., Verbist, J. J., Levet, J.-C., and Noël, H. (1982) *J. Am. Chem. Soc.*, **104**, 5266–73.

Thoma, R. E. and Grimes, W. R. (1957) Phase Equilibria Diagrams for Fused Salt Systems, ORNL-2295.

Thoma, R. E., Insley, H., Landau, B. S., Friedman, H. A., and Grimes, W. R. (1958) *J. Am. Ceram. Soc.*, **41**, 538–44.

Thoma, R.E. (1959) Phase diagrams of Nuclear Reactor Materials, ORNL-2548.

Thoma, R. E. and Penneman, R. A. (1965) ORNL-3789, 33–35; (1965) N.S.A. 19, no. 30066.

Thoma, R. E., Insley, H., Hebert, G. M., Friedman, H. A., and Weaver, C. F. (1963) *J. Am. Ceram. Soc.*, **46**, 37–42.

Thoma, R. E., Friedman, H. A., and Penneman, R. A. (1966) *J. Am. Chem. Soc.*, **88**, 2046–7.

Thoma, R. E. (1971) ORNL-4812, pp. 1–416.

Thoma, R. E. (1972) N.S.A. 26, no. 24796.

Tomiyasu, H. and Fukutomi, H. (1982) *Bull. Res. Lab. Nucl. Reactors*, **7**, 57–80.

Tougait, O., Potel, M., Padiou, J., and Noël, H. (1997) *J. Alloys Compds*, **262**, 320–4.

Tougait, O., Potel, M., and Noël, H. (1998a) *J. Solid State Chem.*, **139**, 356–61.

Tougait, O., Potel, M., Levet, J. C., and Noël, H. (1998b) *Eur. J. Solid State Inorg. Chem.*, **35**, 67–76.

Tougait, O., Potel, M., and Noël, H. (1998c) *Inorg. Chem.*, **37**, 5088–91.

Toussaint, C. J. and Avogadro, A. (1974) *J. Inorg. Nucl. Chem.*, **36**, 781–4.

Toraishi, T., Farkas, I., Szabó, Z., and Grenthe, I. (2002) *J. Chem. Soc. Dalton Trans.*, 3805–12.

Toraishi, T., Aoyagi, N., Nagasaki, S., and Tanaka, S. (2004) *J. Chem. Soc. Dalton Trans.*, 3495–502.

Totemeier, T. C. (1995) *A Review of the Corrosion and Pyrophoricity Behavior of Uranium and Plutonium*, ANL/ED/95–2.

Traverso, O., Portanova, R., and Carassiti, V. (1974) *Inorg. Nucl. Chem. Lett.*, **10**, 771–5.

Troć, R. (1992) *Proc. 22èmes Journées des Actinides*, Méribel, France, p. 97.

Troć, R. and Suski, W. (1995) *J. Alloys Compds*, **219**, 1–5.

Trzebiatowski, W., Śliwa, A., and Staliński, B. (1954) *Rocz. Chem.*, **28**, 12–20.

Trzebiatowski, W. and Jabloński, A. (1960) *Nukleonika*, **5**, 587–96.

Trzebiatowski, W. and Mulak, J. (1970) *Bull. Acad., Polon. Sci. Ser. Sci. Chim.*, **18**, 121–6.

Tsai, H. C., Corington, A., and Olander, D. R. (1975) Lawrence Berkeley Laboratory Report, LBL-6016, p. 188.

Tso, T. C., Brown, D., Judge, A. I., Holloway, J. H., and Fuger, J. (1985) *J. Chem. Soc. Dalton Trans.*, 1853–8.

Tsushima, S., Yang, T., and Suzuki, A. (2001) *Chem. Phys. Lett.*, **334**, 365–73.

Tuller, H. L. (1981) in *Nonstoichiometric Oxides* (ed. O. T. Sørensen), Academic Press, New York, ch. 6. pp. 271–335.

Tutov, A. G., Plakhtii, V. P., Usov, O. A., Bublyaev, R. A., and Chernenkov, Yu. P. (1991) *Kristallografiya*, **36**, 1135–8.

Ugajin, M. (1982) *J. Nucl. Mater.*, **110**, 140–6.

Ugajin, M. (1983) *J. Nucl. Sci. Technol.*, **20**, 228–36.

Ugajin, M., Shiratori, T., and Shiba, K. (1983) *J. Nucl. Mater.*, **116**, 172–7.

Une, K. and Oguma, M. (1982) *J. Nucl. Mater.*, **110**, 215–22.

Une, K. and Oguma, M. (1983a) *J. Am. Ceram. Soc.*, **66**, C179–80.

Une, K. and Oguma, M. (1983b) *J. Nucl. Mater.*, **115**, 84–90.

Une, K. and Oguma, M. (1983c) *J. Nucl. Mater.*, **118**, 189–94.

United Nations, (1955) *Proc. First Int. Conf. on Peaceful Uses of Atomic Energy*, Geneva, 1955, vol. 8, pp. 3–145.

United Nations, (1958) *Proc. Second Int. Conf. on Peaceful Uses of Atomic Energy*, Geneva, 1958, vol. 4, pp. 3–68.

United Nations, (1964) *Proc. Third Int. Conf. on Peaceful Uses of Atomic Energy*, Geneva, 1964, vol. 12, pp. 119–325.

Uvarova, Y. A., Sokolova, E., Hawthorne, F. C., Agakhanov, A. A., and Pautov, L. A. (2004) *Can. Miner.*, **42**, 1005–11.

Vallet, V., Maron, L., Schimmelpfennig, B., Leininger, T., Teichteil, C., Gropen, O., Grenthe, I., and Wahlgren, U. (1999) *J. Phys. Chem. A*, **103**, 9285–9.

Vallet, V., Wahlgren, U., Schimmelpfennig, B., Szabó, Z., and Grenthe, I. (2001) *J. Am. Chem. Soc.*, **123**, 11999–2008.

Vallet, V., Wahlgren, U., Szabó, Z., and Grenthe, I. (2002) *Inorg. Chem.*, **41**, 5626–33.

Vallet, V., Moll, H., Wahlgren, U., Szabó, Z., and Grenthe, I. (2003) *Inorg. Chem.*, **42**, 1982–93.

Vallet, V., Privalov, T., Wahlgren, U., and Grenthe, I. (2004a) *J. Am. Chem. Soc.*, **124**, 7766–7.

Vallet, V., Szabó, Z., and Grenthe, I. (2004b) *J. Chem. Soc. Dalton Trans.*, 3799–807.

Van Axeel Castelli, V., Dalla Cort, A., Mandolini, L., Reinhoudt, D. N., and Schiaffino, L. (2000) *Chem. Eur. J.*, **7**, 1193–8.

Van den Bossche, G., Rebizant, J. G., Spirlet, M. R., and Goffart, J. (1986) *Acta Crystallogr. C*, **42**, 1478–80.

Van den Bossche, G., Spirlet, M. R., Rebizant, J., and Goffart, J. (1987) *Acta Crystallogr. C*, **43**, 383–4.

van Egmond, A. B. (1975) *J. Inorg. Nucl. Chem.*, **37**, 1929–31.

van Egmond, A. B. (1976a) *J. Inorg. Nucl. Chem.*, **38**, 1645–7.

van Egmond, A. B. (1976b) *J. Inorg. Nucl. Chem.*, **38**, 1649–51.

van Egmond, A. B. (1976c) *J. Inorg. Nucl. Chem.*, **38**, 2105–7.

Van Impe, J. (1954) *Chem. Eng. Prog.*, **50**, 230–4.

van Lierde, W., Strumane, R., Smets, E., and Amelinckx, S. (1962) *J. Nucl. Mater.*, **5**, 250–3.

van Lierde, W., Pelsmaekers, J., and Lecocq-Robert, A. (1970) *J. Nucl. Mater.*, **37**, 276–85.

Vance, E. R., Watson, J. N., Carter, M. L., Day, R. A., and Begg, B. D. (2001) *J. Am. Ceram. Soc.*, **84**, 141–4.

Vance, J. E. and Warner, J. C. (1951) *Uranium Technology-General Survey*, Natl. Nucl. En. Ser., Div. VII, 2A, TID-5231, USAEC Technical Information Service, Oak Ridge, TN.

Vaugoyeau, H., Lombard, L., and Morterat, J. P. (1971) *J. Nucl. Mater.*, **39**, 323–9.

Vdovenko, V. M., Mashirov, L. G., Blokhima, V. K., Suglobova, I. G., and Suglobov, D. N. (1963) *Sov. Radiochem.*, **5**, 67–75.

Vdovenko, V. M., Mashirov, L. G., and Suglobov, D. N. (1964) *Radiokhimiya*, **6**, 299–305; *Sov. Radiochem.*, **6**, 289–94.

Vdovenko, V. M., Skoblo, A. I., Suglobov, D. N., Shcherbakova, L. L., and Scherbakov, V. A. (1969) *Zh. Neorg. Khim.*, **12**, 2863–5; *Russ. J. Inorg. Chem.*, **12**, 1513–15.

Vdovenko, V. M., Volkov, V. A., Kozhina, I. I., and Suglobova, I. G. (1972a) *Sov. Radiochem.*, **14**, 492–3.

Vdovenko, V. M., Volkov, V. A., Kozhina, I. I., and Suglobova, I. G. (1972b) *Sov. Radiochem.*, **14**, 489–91.

Vdovenko, V. M., Suglobova, I. G., and Chirkst, D. E. (1973a) *Radiokhimiya*, **15**, 58–61; (1973a) *Sov. Radiochem.*, **15**, 53–5.

Vdovenko, V. M., Kozhina, I. I., Suglobova, I. G., and Chirkst, D. E. (1973b) *Radiokhimiya*, **15**, 172–127; *Soviet Radiochem.*, **15**, 168–72.

Vdovenko, V. M., Kozhina, I. I., Suglobova, I. G., and Chirkst, D. E. (1974a) *Radiokhimiya*, **16**, 369–77; (1974) *Sov. Radiochem.*, **16**, 369–76.

Vdovenko, V. M., Volkov, V. A., and Suglobova, I. G. (1974b) *Radiokhimiya*, **16**, 363–8.

Vdovenko, V. M., Suglobova, I. G., and Chirkst, D. E. (1974c) *Radiokhimiya*, **16**, 203–8.

Védrine, A., Baraduc, L., and Cousseins, J.-C. (1973) *Mater. Res. Bull.*, **8**, 581–8.

Védrine, A., Trottier, D., Cousseins, J.-C., and Chevalier, R. (1979) *Mater. Res. Bull.*, **14**, 583–7.

Vilcu, R. and Misdolea, C. (1967) *J. Chem. Phys.*, **46**, 906.

Viswanathan, K. and Harnett, O. (1986) *Am. Miner.*, **71**, 1489–93.

Vita, O. A., Walker, C. R., and Litteral, E. (1973) *Anal. Chim. Acta*, **64**, 249–57.

Vochten, R. and Deliens, M. (1980) *Phys. Chem. Miner.*, **6**, 129–43.

Vochten, R., Blaton, N., Peeters, O., and Deliens, M. (1996) *Can. Miner.*, **34**, 1317–22.

Vochten, R., Blaton, N., and Peeters. O. (1997) *Can. Miner.*, **35**, 1021–5.

Vochten, R. and Deliens, M. (1998) *Can. Miner.*, **36**, 1077–81.

Vochten, R., Deliens, M., and Medenbach, O. (2001) *Can. Miner.*, **39**, 1685–9.

Vodovatov, V. A., Gorshkov, N. G., Lychev, A. A., Mashirov, L. G., and Leikena, E. V. (1984) *Radiokhimiya*, **26**, 261–4.

Vogt, O. (1982) *Actinides in Perspective* (ed. N. M. Edelstein), Pergamon Press, Oxford, pp. 289–307.

Voliotis, S. and Rimsky, A. (1975) *Acta Crystalogr. B*, **34**, 2612–15.

Volkov, V. A., Suglobova, I. G., and Chirkst, D. E. (1979) *At. Energy.*, **47** (2), 110–12.

Volkov, V. A., Suglobova, I. G., and Chirkst, D. E. (1987) *Radiokhimiya*, **29** (3), 273–6.

Volkovich, V. A., Griffiths, T. R., Fray, D. J., and Fields, M. (1998) *Vibr. Spectrosc.*, **17**, 83–91.

Vorobei, M. P., Siba, O. V., Bevz, A. S., and Kapshukov, I. I. (1971) *Zh. Fiz. Khim.*, **45**, 22–5.

Voronov, N. M., Danilin, A. S., and Kovalev, I. T. (1962) in *Thermodynamics of Nuclear Materials*, Proc. Symp. 1962, International Atomic Energy Agency, Vienna, pp. 789–800.

Voronov, N. M. and Sofronova, R. M. (1972) in *Physical Chemistry of Alloys and Refractory Compounds of Thorium and Uranium* (ed. O. S. Ivanov), Academy of Sciences of the USSR, Israel Program for Scientific Translations, Ltd., Jerusalem, pp. 204–14.

Voronov, N. M., Sofrononova, R. M., and Voitekhova, E. A. (1972) in *Physical Chemistry of Alloys and Refractory Compounds of Thorium and Uranium* (ed. O. S. Ivanov), Academy of Sciences of the USSR, Israel Program for Scientific Translations, Ltd., Jerusalem, pp. 222–8.

Waber, J. T., Chiotti, P., and Miner, W. N. (1964) *Compounds of Interest to Reactor Technology*, IMD Special Report 13, Metallurgical Society of AIME.

Wachter, P. (ed.) (1980) *Proc. Int. Conf. on the Physics of Actinides and Related 4f Materials*, North-Holland, Amsterdam; *Physica*, 102B and 102C.

Wadier, J. F. (1973) CEA Report, CEA-R 4507.

Wadt, W. R. and Hay, P. J. (1979) *J. Am. Chem. Soc.*, **101**, 5198–206.

Wadt, W. R. (1981) *J. Am. Chem. Soc.*, **103**, 6053–7.

Wagner, W., Edelstein, N. M., Whittaker, B., and Brown, D. (1977) *Inorg. Chem.*, **16**, 1021–6.

Wahlgren, U., Moll, H., Grenthe, I., Schimmelpfennig, B., Maron, L., Vallet, V., and Gropen, O. (1999) *J. Phys. Chem. A*, **103**, 8257–64.

Wait, E. (1955) *J. Inorg. Nucl. Chem.*, **1**, 309–12.

Walder, A. J. and Hodgeson, T. (1994) in *DOE-ORNL 1994 Conf. Analytical Chemistry in Energy Technology* (eds. R. W. Morrow and J. S. Crain), ASTM Spec. Tech. Publ. 1291.

Walder, A. J. (1997) in *Modern Isotope Ratio Mass Spectrometry* (ed. I. T. Platzner), John Wiley, New York, pp. 83–108.

Walenta, K. (1965) *Am. Miner.*, **50**, 1143–57.

Walenta, K. (1974) *Am. Miner.*, **59**, 166–71.

Walenta, K. (1976) *Schweiz. Miner. Petrogr. Mitt.*, **56**, 167–85.

Walenta, K. (1983) *Neues Jahrb. Miner. Monatsschr.*, **6**, 259–69.

Walenta, K. (1985) *Tschermaks Miner. Petrogr. Mitt.*, **34**, 25–34.

Walenta, K. (1998) *Aufschluss*, **49**, 253–7.

Wang, W.-D., Bakac, A., and Espenson, J. H. (1995) *Inorg. Chem.*, **34**, 6034–9.

Ward, J. W., Cox, L. E., Smith, J. L., Stewart, G. R., and Wood, J. H. (1979) *J. Phys.* (*Paris*), **40**, C4, 15–17.

Ward, J. W. (1985) in *Handbook on the Physics and Chemistry of the Actinides,* vol. 3 (eds. A. J. Freeman and C. Keller) Elsevier, Amsterdam, pp, 1–74.

Wardman, P. (1989) *J. Phys. Chem. Ref. Data*, **18**, 1637.

Warf, J. C. (1958) in *The Chemistry of Uranium, Collected Papers*, TID-5290 (eds. J. J. Katz and E. Rabinowitch), Oak Ridge, TN, p. 81.

Warner, J. C. (1953) *Metallurgy of Uranium*, Natl Nucl. En. Ser., Div. IV, 12A, , USAEC Technical Information Service, Oak Ridge, TN.

Warner, J. K. and Ewing, R. C. (1993) *Am. Miner.*, **62**, 403–10.

Watkin, D. J., Denning, R. G., and Prout, K. (1991) *Acta Crystallogr. C*, **47**, 2517–19.

Watt, G. W., Baugh, D. W., and Gadd, K. F. (1974) *Inorg Nucl. Chem. Lett.*, **10**, 987–9.

Wedekind, E. and Jochem, O. (1913) *Ber. Dtsch. Chem. Ges.*, **46**, 1204–5.

Wedermeyer, H. (1984) in *Gmelin Handbuch der Anorganischen Chemie*, Suppl. Ser. Uranium, C4, pp. 1–64.

Weeks, J. L. (1955) *AIME, J. Metals*, **203**, 192.

Weigel, F. (1958) in *Handbuch der Präparativen Anorganischen Chemie* (ed. G. Brauer), Enke, Stutttgart, pp. 1197–203.

Weigel, F. and Neufeldt, S. (1961) *Angew. Chem.*, **73**, 468.

Weitzel, H. and Keller, C. (1975) *J. Solid State Chem.*, **13**, 136–41.

Weller, M. T., Light, M. E., and Gelbrich, T. (2000) *Acta Crystallogr.*, **B56**, 577–83.

Wells, A. F. (1990) in *Structural Inorganic Chemistry*, Oxford University Press.

Westrum, E. F. Jr and Grønvold, F. (1959) *J. Am. Chem. Soc.*, **81**, 1777–80.

Westrum, E. F. Jr and Grønvold, F. (1962) in *Thermodynamics of Nuclear Materials*, Proc. Symp. 1962, International Atomic Energy Agency, Vienna, pp. 3–37.

Westrum, E. F. Jr, Takahashi, Y., and Grønvold, F. (1965) *J. Phys. Chem.*, **69**, 3192–3.

White, T. J. (1984) *Am. Miner.*, **69**, 1156–72.

Whitman, C. I., Compton, V., and Holden, R. B. (1955) *Zone Melting of Uranium*, TID-10098.

Wicke, E. and Otto, K. (1962) *Z. Phys. Chem.* (NF), **31**, 222–48.

Wilhelm, H. A., Chiotti, P., Snow, A. I., and Daane, A. H. (1949) *J. Chem. Soc.*, Suppl. 2, 318–21.

Wilhelm, H. A. (1956) *Proc. First Int. Conf. on Peaceful Uses of Atomic Energy*, Geneva, 1955, vol. 8, pp. 162–74.

Wilkins, R. G. (1991) *Kinetics and Mechanism of Reactions of Transition Metal Complexes*, 2nd edn, VCH Publishers, Weinheim, Germany.

Wilkinson, M. K., Shull, C. G., and Rundle, R. E. (1955) *Phys. Rev.*, **99**, 627.

Wilkinson, W. D. and Murphy, W. F. (1958) *Nuclear Reactor Metallurgy*, van Nostrand.

Wilkinson, W. D. (1962) *Uranium Metallurgy*, vol. I, *Uranium Process Metallurgy*, vol. II, *Uranium Corrosion and Alloys*, Interscience, New York.

Williams, C. W., Morss, L. R., and Choi, I.-K. (1984) in *Geochemical Behavior of Disposed Radiochemical Waste* (eds. G. S. Barney, J. D. Navratil, and W. W. Schulz), Am. Chem. Soc. Symp. Ser. 246, American Chemical Society, Washington, DC, pp. 323–34.

Willis, B. T. M. (1964a) *J. Phys.* (*Paris*), **29**, 431–40.

Willis, B. T. M. (1964b) *Proc. Brit. Ceram. Soc.*, **1**, 9–19.

Willis, B. T. M. (1978) *Acta Crystallogr.*, **A34**, 88–90.

Willis, B. T. M. (1987) *J. Chem. Soc., Faraday Trans. 2*, **83**, 1073–81.

Wilmarth, W. R. and Peterson, J. R. (1981) Characterization of selected solid-state actinide (and related) compounds via Raman and absorption spectroscopy, in *Handbook on the Physics and Chemistry of the Actinides*, vol. 6 (eds. A. J. Freeman and C. Keller), North-Holland, Amsterdam, pp. 1–39.

Wilson, W. B., Alexander, C. A., and Gerds, A. F. (1961) *J. Inorg. Nucl. Chem.*, **20**, 242–51.

Wilson, W. W., Naulin, C., and Bougon, R. (1977) *Inorg. Chem.*, **16**, 2252–7.

Winslow, G. H. (1971) *High Temp. Sci.*, **3**, 361–80.

Winslow, G. H. (1973) *High Temp. Sci.*, **5**, 176–91.

Winter, P. W. (1989) *J. Nucl. Mater.*, **161**, 38–43.

Wisnyi, L. G. and Pijunowski, S. W. (1957) USAEC Technical Information Service, TID-7530.

Wolf, A. S., Posey, J. C., and Rapp, K. E. (1965) *Inorg. Chem.*, **4**, 751–4.

Wolf, S. F. (1999) in *Reviews in Mineralogy*, vol. 38 (eds. P. C. Burns and R. Finch), Mineralogical Society of America, Washington, DC, pp. 623–53.

Woodley, R. E. (1981) *J. Nucl. Mater.*, **96**, 5–14.

Woodward, L. A. and Ware, M. J. (1968) *Spectrochim. Acta A*, **24**, 921–5.

Woody, R. J. and George, D. R. (1955) *Nucl. Eng. Sci. Congr.*, Cleveland, OH, Preprint 329.

Wronkiewicz, D. J., Bates, J. K., Gerding, T. J., Veleckis, E., and Tani, B. S. (1992) *J. Nucl. Mater.*, **190**, 107–27.

Wronkiewicz, D. J., Bates, J. K., Wolf. S. F., and Buck, E. C. (1996) *J. Nucl. Mater.*, **238**, 78–95.

Wronkiewicz, D. J. and Buck, E. C. (1999) *Rev. Miner.*, **38**, 475–97.

Yamamoto, T., Kayano, H., Sinaga, S., Ono, S., Tanaka, S., and Yamawaki, M. (1991) *J. Less Common Metals*, **172–174**, 71–8.

Yamamoto, T., Kayano, H., and Yamawaki, M. (1994) *J. Alloys Compds*, **213–214**, 533–5.

Yamamoto, T., Teshigawara, M., Kayano, H., Minakawa, N., and Funahashi, S. (1995) *J. Alloys Compds*, **224**, 36–8.

Yamamoto, T., Ishii, Y., and Kayano, H. (1998) *J. Alloys Compds*, **269**, 162–5.

Yamanaka, S., Iguchi, T., Fujita, Y., Uno, M., Katsura, M., Hoshino, Y., and Saiki, W. (1999) *J. Alloys Compds*, **293–295**, 52–6.

Yamashita, T. and Fujino, T. (1985) *J. Nucl. Mater.*, **136**, 117–23.

Yamashita, T., Fujino, T., and Tagawa, H. (1985) *J. Nucl. Mater.*, **132**, 192–201.

Yang, T., Tsushima, S., and Suzuki, A. (2003) *J. Solid State Chem.*, **171**, 235–41.

Yoshihara, K., Yamagami, S., Kanno, M., and Mukaibo, T. (1971) *J. Inorg. Nucl. Chem.*, **33**, 3323–9.

Young, A. P. and Schwartz, C. M. (1962) Battelle Memorial Institute Report, BMI-1585.

Young, A. P. and Schwartz, C. M. (1963) *J. Inorg. Nucl. Chem.*, **25**, 1133–7.

Young, E. J., Weeks, A. D., and Meyrowitz, R. (1966) *Am. Miner.*, **51**, 651–63.

Young, G. A. (1955) *Feed Materials. A Bibliography of Classified Report Literature*, TID-3081.

Yusov, A. B. and Shilov, V. P. (2000) *Russ. Chem. Bull. Int. Ed.* **49**, 1925–53.

Zachariasen, W. H. (1945) Manhattan Project Report, CP-2611, p. 14.

Zachariasen, W. H. (1946) University of Chicago Metallurgical Laboratory Report, MDDC-1152.

Zachariasen, W. H. (1948a) *Acta Crystallogr.*, **1**, 265–8.

Zachariasen, W. H. (1948b) *Acta Crystallogr.*, **1**, 281–5.

Zachariasen, W. H. (1948c) *J. Chem. Phys.*, **16**, 254.

Zachariasen, W. H. (1948d) *J. Am. Chem. Soc.*, **70**, 2147–51.

Zachariasen, W. H. (1948e) *Acta Crystallogr.*, **1**, 277–81.

Zachariasen, W. H. (1948f) *Acta Crystallogr.*, **1**, 285–7.

Zachariasen, W. H. (1949a) *Acta Crystallogr.*, **2**, 94–9.

Zachariasen, W. H. (1949b) *Acta Crystallogr.*, **2**, 291–6.

Zachariasen, W. H. (1949c) *Acta Crystallogr.*, **2**, 296–8.

Zachariasen, W. H. (1949d) *Acta Crystallogr.*, **2**, 390–3.

Zachariasen, W. H. (1954a) *Acta Crystallogr.*, **7**, 788–91.

Zachariasen, W. H. (1954b) *Acta Crystallogr.*, **7**, 795–9.

Zachariasen, W. H. (1954c) *Acta Crystallogr.*, **7**, 783–7; 792–4.

Zachariasen, W. H. (1954d) *Acta Crystallogr.*, **7**, 783–7.

Zachariasen, W. H. (1975) LA-UR-75–1364, 1977, INIS Atomindex 8, no. 283142.

Zadneporovskii, G. M. and Borisov, S. V. (1971) *Zh. Strukt. Khim.*, **12**, 831–9; *J. Strukt. Chem.*, **12**, 761–9.

Zalkin, A., Templeton, D. H., and Hopkins, T. E. (1967) *Inorg. Chem.*, **5**, 1466–70.

Zalkin, A., Templeton, L. K., and Templeton, D. H. (1989) *Acta Cryst. C*, **45**, 810–11.

Zhang, J., Wan, A., and Gong, W. (1992) *Acta Petrol. Miner.*, **11**, 178–84. (in Chinese).

Zhang, Z. and Pitzer, R. M. (1999) *J. Phys. Chem. A*, **103**, 6880–6.

Zhangru, C., Keding, L., Falan, T., Yi, Z., and Xiaofa, G. (1986) *Kexue Tongbao* (*Chinese Science Bulletin*), **31**, 396–401.

Zhao, D. and Ewing, R. C. (2000) *Radiochim. Acta.*, **88**, 739–49.

Zimmermann, J. I. C. (1882) *Ber. Dtsch. Chem. Ges.*, **15**, 847–51; *Liebig's Ann. Chem.*, **213**, 285–319.

Zogal, O. J., Lam, D. J., Zygmunt, A., Drulis, H., Petryński, W., and Staliński, S. (1984) *Phys. Rev. B*, **29**, 4837–42.

Żołnierek, Z., Gajek, Z., and Khan Malek, Ch. (1984) *Physica B+C* (*Amsterdam, Neth.*), **125**, 199–214.

Zych, E. and Drożdżyński, J. (1986) *Inorg. Chim. Acta, f-Block Elements*, **115**, 219–22.

Zych, E. and Drożdżyński, J. (1990a) *Polyhedron*, **9** (17), 2175–6.

Zych, E. and Drożdżyński, J. (1990b) *J. Less Common Metals*, **164**, 233–8.

Zych, E. and Drożdżyński, J. (1991) *Eur. J. Solid State Inorg. Chem.*, **28**, 575–80.

Zych, E., Starynowicz, P., Lis, T., and Drożdżyński, J. (1993) *Polyhedron*, **12** (13), 1661–6.

CHAPTER SIX

NEPTUNIUM

Zenko Yoshida, Stephen G. Johnson, Takaumi Kimura, and John R. Krsul

6.1 HISTORICAL

The first report on the discovery of neptunium was in 1940 by McMillan and Abelson (1940), although McMillan did the preliminary work in 1939 and published his findings (McMillan, 1939). He did not claim that a new element had been discovered until confirmatory measurements had been undertaken in the following year. The production of neptunium was accomplished by placing a layer of uranium trioxide on paper with several aluminum or paper foils and then exposing this to neutrons from a cyclotron. Examination of the uranium paper sample containing the non-recoiling fraction displayed that two new radioactive components had been created. One component displayed a 23 min half-life, later identified as U-239, while the second exhibited a 2.3 day half-life. Both components decayed via β particle emission. Preliminary chemical analysis was performed to determine the behavior of the 2.3 day component and resulted in the contradictory assignment of this component as that exhibiting an atomic number of 93, but not being transuranic in nature (Segrè, 1939). Segrè noted in his paper that his conclusions were contradictory. However, the following quotation is from his paper, "The necessary conclusion seems to be that the 23 minute uranium decays into a very long-lived 93 and that transuranic elements have not yet been observed." The primary stumbling block to the proper assignment of the material as transuranic in nature was the lack of observation of any alpha decay activity that would emanate from the daughter product of the beta decay of this new material with an atomic number 93. It was this work by Segrè (1939) that led McMillan and Abelson to revisit the chemical analysis and determine its properties in greater depth.

To initiate their work they first had to generate more material. In doing this they were able to confirm the 'linked' nature of the 23 min and 2.3 day half-life materials observed. The ratio of these two materials was observed to remain constant. This also confirmed the earlier suggestion by Hahn *et al.* (Quill, 1938) that the following reaction was possible when uranium underwent neutron bombardment:

$$\mathrm{U} + \text{neutron} \rightarrow \mathrm{U}(23\,\text{minute}) \rightarrow \text{Eka-Re} \tag{6.1a}$$

$$^{238}\mathrm{U}(\mathrm{n},\gamma)^{239}\mathrm{U}(\beta^-, 23\ \text{min}) \rightarrow {}^{239}\mathrm{Np}(\beta^-, 2.3\ \ \text{day}) \rightarrow {}^{239}\mathrm{Pu} \tag{6.1b}$$

Differences between the rare earths and this element were observed immediately by McMillan and Abelson (1940) because it did not form a precipitate when exposed to HF in the presence of bromate, an oxidizing agent, in a strong acid. It did form a precipitate with HF in the presence of SO_2, a reducing agent. This bifurcated behavior in the presence of HF was thought to explain the incorrect assignment of this element as a rare earth by Segrè (1939) since the oxidizing potential of the solution had not been well controlled in earlier experiments (Segrè, 1939). Further evidence strongly suggested that the material was indeed an actinide, such as, precipitation in the reduced state with a thorium carrier by iodate and in the oxidized state with a uranium carrier by acetate. Also the precipitation with thorium carrier in the presence of H_2O_2 and precipitation in a carbonate-free basic solution indicated actinide-like behavior. Careful confirmatory measurements, which involved uranium that had undergone neutron bombardment and subsequent purification via fluoride precipitation in the presence of SO_2, showed the in-growth of the new element with a 2.3 day half-life. The new material was observed to exhibit a beta particle of energy approximately 470 keV. Further speculation by McMillan and Abelson regarding the daughter product, which would have atomic number 94 and a mass number of 239, was also recorded but will be discussed in Chapter 7 of this work. The element discovered by McMillan and Abelson was named after the planet Neptune, which is the first planet beyond Uranus in our solar system. This system was likewise followed for naming plutonium as its orbit was beyond Neptune.

6.2 NUCLEAR PROPERTIES

Twenty-two isotopes of neptunium are now known (Table 6.1). The isotope ^{237}Np has a sufficiently long half-life ($t_{1/2} = 2.144 \times 10^6$ years) that can be handled at weighable quantities. It is the most significant neptunium

Table 6.1 *Nuclear properties of neptunium isotopes.*

Mass number	*Half-life*	*Mode of decay*	*Main radiations* (MeV)	*Method of production*
226	31 ms	EC, α	α 8.044	^{209}Bi(^{22}Ne,5n)
227	0.51 s	EC, α	α 7.677	^{209}Bi(^{22}Ne,4n)
228	61.4 s	EC, α		^{209}Bi(^{22}Ne,3n)
229	4.0 min	$\alpha \geq 50\%$ $\mathrm{EC} \leq 50\%$	α 6.890	^{233}U(p,5n)
230	4.6 min	$\alpha > 99\%$ $\mathrm{EC} \leq 0.97\%$	α 6.66	^{233}U(p,4n)
231	48.8 min	$\mathrm{EC} < 99\%$ $\alpha > 1\%$	α 6.28 γ 0.371	^{233}U(d,4n) ^{235}U(d,6n)
232	14.7 min	EC	γ 0.327	^{233}U(d,3n)
233	36.2 min	$\mathrm{EC} < 99\%$ $\alpha \sim 10^{-3}\%$	α 5.54 γ 0.312	^{233}U(d,2n) ^{235}U(d,4n)
234	4.4 d	EC 99.95% β^+ 0.05%	γ 1.559	^{235}U(d,3n)
235	396.1 d	$\mathrm{EC} > 99\%$ $\alpha\ 1.6 \times 10^{-3}\%$	α 5.022 (53%) 5.004 (24%)	^{235}U(p,2n)
236[a]	22.5 h	β^- 50% EC 50%	β^- 0.54 γ 0.642	^{235}U(d,n)
236[a]	1.54×10^5 yr	EC 87% β^- 13%	γ 0.163	^{235}U(d,n)
237	2.144×10^6 yr $>1 \times 10^{18}$ yr	α SF	α 4.788 (51%) 4.770 (19%) γ 0.086	^{237}U daughter ^{241}Am daughter
238	2.117 d	β^-	β^- 1.29 γ 0.984	^{237}Np(n,γ)
239	2.3565 d	β^-	β^- 0.72 γ 0.106	^{243}Am daughter ^{239}U daughter
240	1.032 h	β^-	β^- 2.09 γ 0.566	^{238}U(α,pn)
240 m	7.22 min	β^-	β^- 2.05 γ 0.555	^{240}U daughter ^{238}U(α,pn)
241	13.9 min	β^-	β^- 1.31 γ 0.175	^{238}U(α,p) ^{244}Pu(n,p3n)
242 g or m	5.5 min	β^-	β^- 2.7 γ 0.786	^{244}Pu(n,p2n) ^{242}Pu(n,p)
242 g or m	2.2 min	β^-	β^- 2.7 γ 0.736	^{242}U daughter
243	1.85 min	β^-	γ 0.288	^{136}Xe + ^{238}U
244	2.29 min	β^-	γ 0.681	^{136}Xe + ^{238}U

[a] Not known whether ground-state nuclide or isomer.

isotope for chemists. ^{237}Np is synthesized by neutron irradiation of uranium according to the reactions (6.2) to (6.4). In conventional nuclear reactors ^{237}Np is generated as a by-product mainly through reactions (6.2) and (6.3). The latter reaction predominates in reactors with fuels of enriched ^{235}U.

$$^{238}\mathrm{U}(n,2n)\,^{237}\mathrm{U}\xrightarrow[6.75\,\mathrm{d}]{\beta^-}\,^{237}\mathrm{Np} \tag{6.2}$$

$$^{235}\mathrm{U}(n,\gamma)\,^{236}\mathrm{U}(n,\gamma)^{237}\mathrm{U}\xrightarrow{\beta^-}\,^{237}\mathrm{Np} \tag{6.3}$$

$$^{238}\mathrm{U}(n,\gamma)\,^{239}\mathrm{U}\xrightarrow{\beta^-}\,^{239}\mathrm{Np}\xrightarrow{\beta^-}\,^{239}\mathrm{Pu}(n,\gamma)^{240}\mathrm{Pu}\xrightarrow{\beta^-}\,^{240}\mathrm{Am}(n,\gamma)^{241}\mathrm{Am}\xrightarrow{\alpha}\,^{237}\mathrm{Np} \tag{6.4}$$

The isotopes ^{238}Np and ^{239}Np have relatively short half-lives and are useful as radioactive tracers for analytical applications or for fundamental chemistry research. They are synthesized by neutron irradiation of ^{237}Np and ^{238}U, respectively, through the following reactions:

$$^{237}\mathrm{Np}(n,\gamma)^{238}\mathrm{Np} \tag{6.5}$$

$$^{238}\mathrm{U}(n,\gamma)^{239}\mathrm{U}\xrightarrow{\beta^-}\,^{239}\mathrm{Np} \tag{6.6}$$

The isotopes ^{235}Np and ^{236}Np are synthesized by cyclotron irradiation of ^{235}U according the following reactions:

$$^{235}\mathrm{U}(d,n)^{236}\mathrm{Np} \tag{6.7}$$

$$^{235}\mathrm{U}(p,n)^{235}\mathrm{Np} \tag{6.8}$$

The isotopes heavier than ^{237}Np are unstable with respect to β^- decay. Isotopes lighter than ^{237}Np decay by electron capture and also are unstable with respect to alpha decay.

6.3 PRODUCTION OF PRINCIPAL NEPTUNIUM ISOTOPES

The principal isotopes of neptunium are generated by irradiation of uranium with neutrons. Of the 22 isotopes listed in Table 6.1, only ^{235}Np, ^{236}Np and ^{237}Np have half-lives long enough to permit accumulation. Neptunium-237 is generated by reactions (6.2), (6.3) and (6.4). However, by irradiating uranium, only ^{237}Np is capable of accumulating. Neptunium-239 is produced from irradiation of ^{238}U and the decay of the resulting ^{239}U, however, the half-life of ^{239}Np, 2.3565 days, is too short for accumulation. Irradiation of uranium by neutrons is unsuitable for the generation of ^{235}Np and ^{236}Np. Therefore only ^{237}Np is produced in any significant quantities. Currently, the production of plutonium is the source of ^{237}Np where the isotope is a by-product of the process. Significant quantities also reside in spent fuel, in high-level waste (HLW), and in solutions containing ^{237}Np stored at various reprocessing facilities. There are no known commercial uses for neptunium. The need for ^{238}Pu as a heat source for radioisotope thermoelectric generators (RTGs) and radioisotope heater units (RHUs) is the main reason to separate and purify ^{237}Np. RTGs are used to supply electricity to space vehicles used in the Galileo, Ulysses, and Cassini NASA missions (see Chapter 7). RHUs are used to provide heat for delicate instruments on space missions. Future needs to separate ^{237}Np and the other actinides from spent fuel and HLW may be required by the proposed transmutation of actinides residing in these materials. Removal of the transuranics, including especially ^{237}Np, has the advantage of eliminating concerns for the long-term storage of radioactive waste. A recent and rather novel use of ^{237}Np is to produce pure ^{236}Pu tracer to assess the amount of plutonium in the environment. Yamana *et al.* (2001) demonstrated that the irradiation of ^{237}Np with bremsstrahlung of an electron beam of 23 and 30 MeV produced ^{236}Pu with low ^{238}Pu impurity. Neptunium-237 could also be used in nuclear weapons; its critical mass is approximately 73 kg.

Plutonium-238 is generated by the reaction shown below:

$$^{237}\mathrm{Np}(\mathrm{n},\gamma)\ ^{238}\mathrm{Np} \xrightarrow{\beta^-} {}^{238}\mathrm{Pu} \qquad (6.9)$$

To obtain ^{238}Pu, ^{237}Np is separated from spent fuel by various modifications of the well-known plutonium and uranium recovery by extraction (Purex) process. After dissolution, neptunium is separated from the spent fuel by solvent extraction and ion exchange by careful adjustments of acid concentrations, oxidations states, and volume percent of tributyl phosphate (TBP). The separated neptunium is precipitated as neptunium oxalate, calcined to neptunium oxide, and fabricated into targets. Targets of the separated isotope are irradiated in a high neutron flux. After irradiation, the targets are cooled for a specific amount of time to allow for fission product decay and then dissolved. ^{238}Pu is then separated from ^{237}Np by taking advantage of the differences in the characteristic oxidation states of the resulting fission products, neptunium, and plutonium.

To date, the reprocessing of irradiated nuclear fuel has focused on the separation of plutonium and uranium from fission products and other actinides. Proposed transmutation and advanced nuclear fuel cycles will require the development of separations that include the actinides and are safe, efficient, and environmentally acceptable. The need for these new technologies will create significant opportunities for research and development activities in the field of actinide chemistry.

6.4 NEPTUNIUM IN NATURE

^{237}Np ($t_{1/2} = 2.144 \times 10^6$ years) has the longest half-life of neptunium isotopes. Because this half-life is considerably shorter than the age of the Earth, which is about 4.5×10^9 years, primordial ^{237}Np no longer exists on Earth.

Neptunium isotopes can be formed by nuclear reactions continuously taking place in the Earth's crust, resulting in a dynamic equilibrium between the rate of formation and the rate of decay. Neutron capture by ^{238}U produces ^{239}Np (see reaction (6.6)), and an (n,2n) reaction on ^{238}U forms ^{237}Np (see reaction (6.2)). The neutrons originate from the spontaneous fission of ^{238}U, the neutron-induced fission of ^{235}U, (α,n) reactions on elements of low atomic number, and/or fission or spallation reactions induced by cosmic rays. Small amounts of ^{239}Np are expected to occur in uranium minerals by continuous formation from ^{238}U, but its half-life of 2.36 days is too short to permit any significant equilibrium concentration to be reached (Garner *et al.*, 1948; Seaborg and Perlman, 1948; Levine and Seaborg, 1951). The isolation of microgram amounts of ^{239}Pu by Peppard *et al.* (1951) from Belgian Congo (now Democratic Republic of the Congo) uranium undoubtedly establishes the existence of ^{239}Np in nature. The isotope ^{237}Np itself has been identified in and isolated from a uranium ore concentrate from Belgian Congo and in other minerals (Peppard *et al.*, 1952). The maximum ratio of ^{237}Np to uranium in such minerals is about 10^{-12}.

The primary sources of neptunium in the biosphere, as with the other transuranium elements, are atmospheric nuclear explosions. On the basis of the analyzed results on global fallout, it was calculated that 2500 kg of ^{237}Np had been generated, which is comparable in mass with the quantity of plutonium (4200 kg of ^{239}Pu and 700 kg of ^{240}Pu) (Efurd *et al.*, 1984). There is little information about the man-made neptunium content of various natural materials, because of the low specific radioactivity of the long-lived ^{237}Np and the systematic difficulties in its determination (Novikov *et al.*, 1989). For global fallout, the ^{237}Np/^{239,240}Pu ratio lies within one order of magnitude $(1\text{–}10) \times 10^{-3}$. When 5×10^{-3} is taken as an average value of the ratio, the concentration of ^{239,240}Pu in seawater is 13×10^{-3} mBq L^{-1}, and the ^{237}Np concentration comprises 6.5×10^{-5} mBq L^{-1} (Holm *et al.*, 1987).

6.5 SEPARATION AND PURIFICATION

Reprocessing of spent nuclear fuels to recover reusable uranium and plutonium and the partitioning of high-level radioactive liquid wastes (HLW) constitute the main processes of the nuclear fuel cycle. ^{237}Np, α emitter with a 2.144×10^{6} years half-life, is one of the major nuclides to be separated from Purex process solutions and HLW. Several separation methods satisfying requirements for process-scale operation have been developed. At the same time, separation methods suitable for relatively small-scale operations are necessary to prepare pure neptunium as a source material in the synthesis of neptunium metal or its compounds, and to isolate or preconcentrate neptunium in analytical samples before determination.

Solvent extraction, ion-exchange chromatography, extraction chromatography, coprecipitation, and electrolytic deposition methods are used for the separation of neptunium ions. Most of the wet-chemical methods involve the control of neptunium ion oxidation states which varies between 3+ and 6+ or even 7+ and utilization of specific chemical behavior of the ion in each oxidation state. Well-established separation methods are reviewed by Burney and Harbour (1974). Choppin and Nash (1995) and Nash and Choppin (1997) recently evaluated separation methods. A report published by OECD/NEA (1997) reviewed separation chemistry of actinides in nuclear waste streams and materials.

6.5.1 Solvent extraction

Many extractants have been employed for the solvent extraction of neptunium ion (cf. reviews by Laskorin *et al.* (1985) and Rozen and Nikolotova (1988)). Multi-dentate β-diketone derivatives, organophosphorus compounds, and amine compounds are commonly used. Mathur *et al.* (2001) reviewed solvent extraction technology from the viewpoints of engineering the management of nuclear spent fuels and radioactive wastes.

Typical β-diketone, 2-thenoyltrifluoroacetone (HTTA, $pK_a = 6.23$), is most widely used for the extraction of neptunium ions. The separation scheme as shown in Fig. 6.1, which is for the analysis of ^{237}Np in sediments and soils by alpha-counting, inductively coupled plasma-mass spectrometry (ICP-MS), or neutron activation analysis, was proposed by Hursthouse *et al.* (1992) and is based on HTTA extraction and anion-exchange chromatography. In this procedure, Np(VI) and Np(V) in the sample solution are reduced to Np(IV), which is extracted from 1 M HNO_3 to 0.5 M HTTA (toluene) phase ($D_{\mathrm{Np(IV)}} \geq 10^3$). Here, D denotes the distribution ratio of a metal ion, which is a ratio of the concentration of the metal in the organic phase to that in the aqueous phase under the extraction equilibrium condition. Coexisting U(VI) and Pu(III) are not extracted ($D_{\mathrm{U(VI)}} \leq 5 \times 10^{-5}$ and $D_{\mathrm{Pu(III)}} \leq 10^{-5}$), which enables the separation of neptunium from plutonium and uranium. Np(IV) in the toluene phase is back-extracted into 8 M HNO_3 solution. Alternatively, Np(IV) in toluene is reduced to Np(V) and back-extracted to 1 M HNO_3 ($D_{\mathrm{Np(V)}} \leq 5 \times 10^{-4}$).

1-Phenyl-3-methyl-4-benzoyl-pyrazol-5-one (HPMBP, cf. Fig. 6.2) and its derivatives are useful extractants for actinide ions. The pK_a of HPMBP (4.11), which is smaller than the pK_a of HTTA, extracts Np(IV) from highly acidic solution, e.g. 1–4 M HNO_3. The ability of HPMBP to extract Np(IV) from such an acidic solution avoids an interference by hydrolysis of Np(IV). Np(VI) and Np(V) are not extracted under this condition.

The synergistic extraction with HPMBP and tri-*n*-octylphosphine oxide (TOPO) was employed to separate Np(V) from Am(III), Cm(III), U(VI), Pu(IV), and lanthanide(III) ions (Pribylova *et al.*, 1987). Zantuti *et al.* (1990) developed a

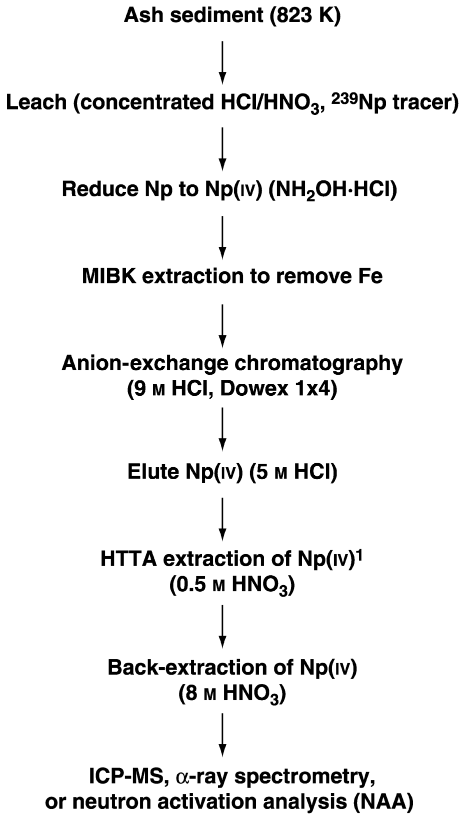

Fig. 6.1 *Procedure for the determination of* ^{237}*Np in sediment samples* (*Hursthouse* et al., 1992). [1]*HTTA extraction is repeated for α-ray spectrometry or NAA.*

method for the separation of a trace amount of neptunium from nitric acid solution containing a large quantity of uranium using the synergistic extraction with HPMBP and di-2-ethylhexylphosphoric acid. Tochiyama *et al.* (1989) showed that Np(V) was extracted efficiently with HPMBP in the presence of methyltrioctylammonium chloride. The 3-phenyl-4-bezoyl-5-isoxazolone was demonstrated to be powerful to extract Np(IV) and the procedure was developed for the separation of ^{237}Np from ^{236}Pu and ^{235}U in the irradiated sample of uranium target (Mohapatra and Manchanda, 1993).

Takeishi *et al.* (2001) studied the extraction behavior of actinide ions using bis (1-phenyl-3-methyl-4-acylpyrazol-5-one) derivatives H_2BPn, where n denotes the number of methylenes in a chain, having a structure as shown in Fig. 6.2. The log D vs $-\log[H^+]$ plots for the extraction of Np(IV) with various derivatives of HBPn ($n = 3, 4, 5, 6, 7, 8, 10, 22$) are shown in Fig. 6.3. The slopes of

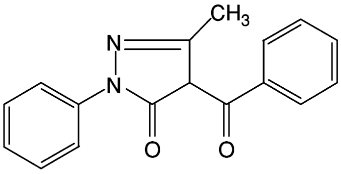

1-Phenyl-3-methyl-4-benzoyl-5-pyrazolone (HPMBP)

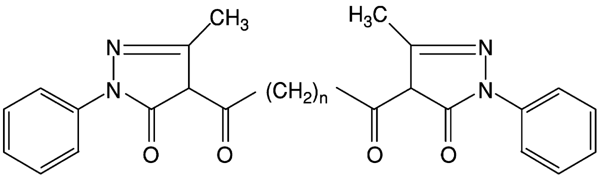

Bis(1-phenyl-3-methyl-4-acylpyrazol-5-one)
(H_2BPn; $n = 3, 4, 5, 6, 7, 8, 10, 22$, etc)

Fig. 6.2 *Structure of pyrazolone derivatives.*

log *D* vs $-\log[H^+]$ plot as well as slopes of log *D* vs $\log[H_2BPn]$ plot suggest $Np(BPn)_2$ as the extracted species. The H_2BPn derivatives are a stronger extractant than HPMBP, which is one of the remarkable characteristics of quadridentate H_2BPn compared with bidentate HPMBP. H_2BP7 and H_2BP8 exhibit higher extractability than the other H_2BPn derivatives examined. Based on their data a procedure for the separation of actinide ions of various oxidation states using H_2BP7 or H_2BP8 was developed.

TBP is the most useful extractant for the separation of actinide ions at the process scale. The early works with TBP are summarized in the reviews by Geary (1955) and Schneider and Harmon (1961), which provide a wide scope of TBP extraction chemistry and engineering. Np(VI) and Np(IV) are extracted as $NpO_2(NO_3)_2(TBP)_2$ and $Np(NO_3)_4(TBP)_2$, respectively, and the extraction efficiency increases with increasing concentrations of TBP and HNO_3 (1–10 M). The distribution ratios of Np(IV) and Np(VI) are 3.0 and 12.0, respectively, between 4 M HNO_3 and 30% TBP(dodecane) at 298 K. The procedure for the separation of neptunium from uranium and plutonium consists in the adjustment of the oxidation state to Np(VI), co-extraction with U(VI) and Pu(IV) and back-extraction of Np(V) by the reduction of Np(VI) to Np(V).

The *n*-octyl(phenyl)-*N*,*N*-diisobutyl-carbamoyl methylphosphine oxide (CMPO) is an effective extractant for the separation of actinide ions from acidic solutions (Kolarik and Horwitz, 1988). The mixed organic solvent of (0.1–0.2) M CMPO + (1.2–1.4) M TBP in dodecane is usually employed. Distribution ratios for Np(IV), Pu(IV), and Pu(III) between nitric acid solution and 0.1 M

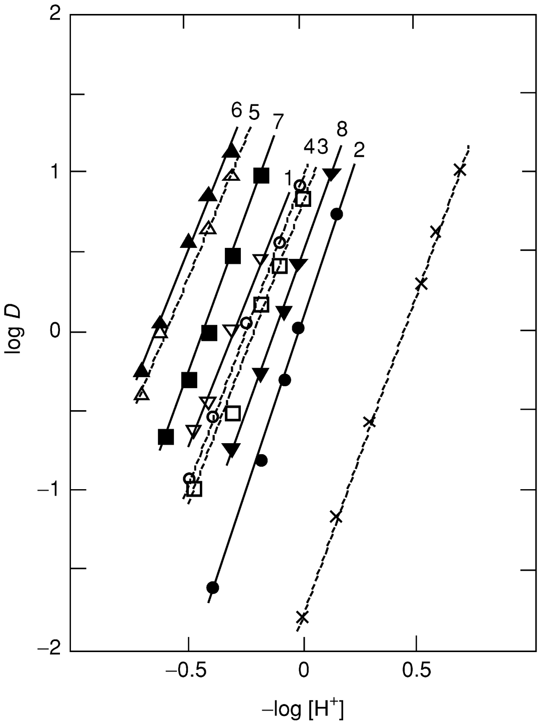

Fig. 6.3 *Log D vs −log* $[H^+]$ *plots for the extraction of* Np^{4+} *in* HNO_3 *solution with* 1×10^{-3} M H_2BPn *and HPMBP in chloroform solution.* (*From Takeishi* et al., 2001, *with permission from Elsevier*). (1) H_2BP_3, (2) H_2BP_4, (3) H_2BP_5, (4) H_2BP_6, (5) H_2BP_7, (6) H_2BP_8, (7) H_2BP_{10}, (8) H_2BP_{22}; *dotted line, HPMBP.*

CMPO + 1.4 M TBP + dodecane are shown in Table 6.2 (Mincher, 1989). For the separation of neptunium and plutonium, the oxidation states are adjusted to Np(IV) and Pu(III) with 0.1 M Fe(II) sulfamate and Np(IV) is then extracted into the CMPO/TBP phase. Pu(III) is removed by stripping with 0.01 M HNO_3 in the presence of 3% hydroxylamine nitrate. Neptunium is removed from the organic phase by an aqueous solution containing complexing agents such as $(COOH)_2$, CO_3^{2-}, or ethylenediaminetetraacetic acid (EDTA). Mathur *et al.* (1996c) compared the extraction behavior of Np(IV), Np(VI), Pu(IV), and U(VI) from nitric acid solutions with CMPO, dibutyldecanamide (DBDA), dihexyldecanamide (DHDA), and bis-2-ethylhexylsulfoxide (BEHSO) in dodecane. The extraction ability is in the order of CMPO > BEHSO > DHDA > DBDA.

Bis(2-ethylhexyl)phosphoric acid (HDEHP), which shows distinguished capability for the extraction of trivalent actinides and lanthanides ions, is also utilized for the separation of neptunium from uranium, plutonium, and

Table 6.2 *Distribution ratios of neptunium and plutonium ions between HNO_3 solution and* 0.1 M *CMPO* + 1.4 M *TBP* (*dodecane*) *at* (278 ± 1) K (*data cited from Mincher,* 1989).

	Concentration of HNO_3 (M)					
Ions	0.5	1.0	2.0	3.0	4.0	5.0
NpO_2^{2+}	43	100	114	133	150	150
NpO_2^{+}	10^{-2}	2×10^{-2}	4×10^{-2}	7×10^{-2}	0.12	0.18
Np^{4+}	0.55	6	113	670	1500	2200
Pu^{4+}	16	40	76	110	144	174
Pu^{3+}	1.6	3.0	5.2	7.1	10	14

americium. After the oxidation state of the actinide ions are adjusted to Np(V), U(VI), Pu(IV), and Am(III) in 1 M HNO_3 by adding $NaNO_2$, all actinide ions except Np(V) are extracted with HDEHP. Np(V) is then oxidized to Np(VI) and extracted with HDEHP. Np(VI) is reduced to Np(V) and back-extracted with 0.1 M HNO_3.

The extraction behavior of Np(IV) and Pu(IV) was investigated using eight kinds of multi-dentate organophosphorus compounds such as dioxides of diphosphine and carbamoyl phosphoryl compounds (Rozen *et al.*, 1988). The extraction behavior of Np(V) was studied systematically with TBP, TOPO, and phosphine oxide derivatives (Rozen *et al.*, 1992). The results of K_{ex} suggested that the stability of the complex between Np(V) and the bidentate extractant was remarkably enhanced in the organic solution.

Solvent extraction with tri-*n*-octylamine (TnOA) has been extensively employed for the separation of ^{237}Np from environmental analytical samples. The separation scheme for ^{237}Np in soils and sediments, which was recommended by Yamamoto *et al.* (1994), is shown in Fig. 6.6 (see Section 6.10). Np(IV) in 10 M HCl is extracted with 10% TnOA (xylene) ($D_{Np(IV)} = 300$). Np(IV) is then back-extracted with a solution of 1 M HCl + 0.1 M HF.

Heptavalent neptunium ion as a form of $NpO_4(OH)_2^{3-}$ produced in 0.1–2 M LiOH (KOH) solution is extracted with various extractants such as TBP, TOPO, crown ether derivatives, HDEHP, etc. (Rozen *et al.*, 1990). The most effective extractant is dicyclohexyl-18-crown-6 ether (in TBP) or HDEHP. Karalova *et al.* (1992a,b) studied the solvent extraction of Np(VII) from alkaline solutions with HPMBP, bis(2-oxy-4-alkyl-benzoyl)amine, bis(2-hydroxy-5-octylbenzyl) amine, and 2-hydroxy-5-*tert*-butylphenyl disulfide. The highest extraction efficiency is obtained when Np(VII) exists as $NpO_4(OH)_2^{3-}$, suggesting that the extraction process involves removal of OH^- from $NpO_4(OH)_2^{3-}$ and H^+ from the OH groups of the extractant molecules. During the extraction process the reduction of Np(VII) to Np(VI) or the oxidation of the extractant is possible, which must be taken into account for the practical use of the Np(VII) extraction procedure.

(a) Neptunium control in advanced Purex process

Currently operated commercial reprocessing plants are based on the Purex process consisting of the solvent extraction of uranium and plutonium with TBP. In principle, all neptunium is rejected into the HLW as a form of inextractable Np(v). The oxidation state of neptunium ion in the process solution, however, varies significantly depending on the chemical environment. Np(v) is oxidized to Np(vi) in the presence of HNO_2 which coexists in nitric acid solution of high concentration; the Np(v) slowly disproportionates generating Np(vi) and Np(iv) in highly acidic solution. Thus, the neptunium behavior is not fully controlled in the Purex process and neptunium distributes in different fractions of the process. Fig. 6.4 shows possible oxidation states of neptunium ions in the main stream of the Purex process. Experimental results at the THORP miniature pilot plant indicated that only 30% of the total neptunium was found in the

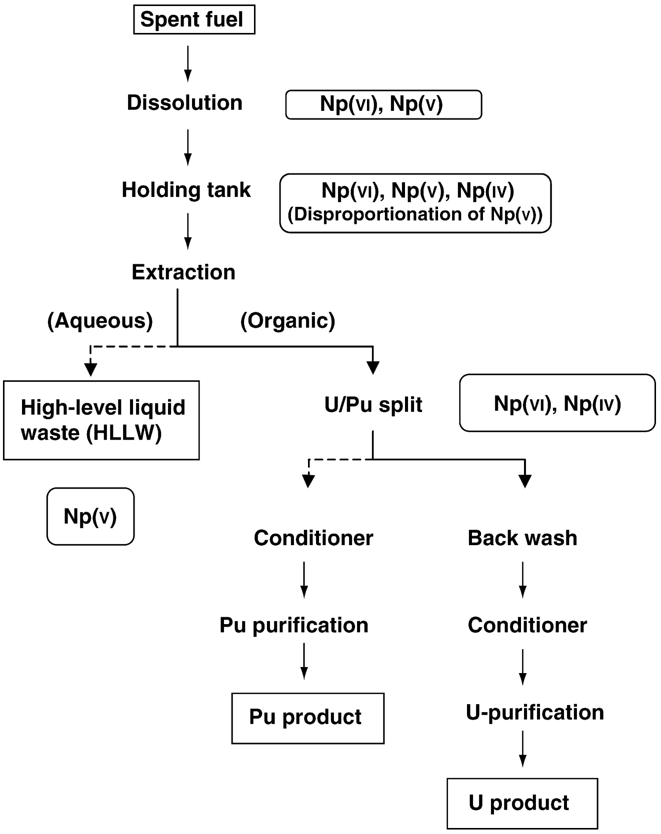

Fig. 6.4 *Flowsheet of the Purex process and the probable oxidation state of neptunium ion in the process solution.*

HLW (Taylor *et al.*, 1997). The remaining neptunium was extracted with uranium and plutonium in the solvent product.

Many attempts have been done to design an advanced Purex process. Taylor *et al.* (1997) summarized the chemical behavior of neptunium in the reprocessing plant. Recent R&D activities at BNFL (UK) attempt to control neptunium in the advanced Purex process. The advanced Purex process is required to satisfy criteria including cost and environmental impact. Reducing the size and complexity of the process and minimizing the secondary waste generation assist in fulfilling these requirements. Efficient control of neptunium within the flowsheet is an important goal assigned to the advanced Purex process. Several scenarios for the control of neptunium in the flowsheet are recommended, i.e. all neptunium is led to: (1) the HLW stream; (2) the Pu fraction; or (3) the U fraction followed by the isolation from uranium, or (4) the recovery in the Np fraction before the U/Pu split process. In all cases, the method to control neptunium behavior is based on precise control of the oxidation state of the ion. Such appropriate redox reagents must be chosen to fulfill all criteria including (1) kinetics of redox reaction, (2) decomposability after the use and (3) stability toward high acidity and radiation.

The back-extraction of Np(V) is an effective way to separate neptunium from Pu(IV) and U(VI) that remain in the organic phase. Many studies have been carried out to select suitable salt-free organic reagents to reduce Np(VI) to Np(V). Taylor *et al.* (1998a) confirmed the selectivity between the reduction of Np(VI) to Np(V) and Pu(IV) to Pu(III) by comparing reduction rates with a wide range of potential reductants such as carboxylic acids, aldehydes, ketones, guanidines, and hydrazine derivatives. The hydrazine derivatives, i.e. *tert*-butyl hydrazine and 1,1-dimethyl hydrazine, are most promising from both viewpoints of the selectivity in the reduction of Np(VI) toward that of Pu(IV) and the reduction kinetics. The results of demonstration solvent extraction tests show that the reduction of Pu(IV) is accelerated by the presence of U(VI).

Uchiyama *et al.* (1998a) studied the reduction kinetics of Np(VI) and Pu(IV) with aldehyde derivatives and concluded that *n*-butyraldehyde was promising as a selective reductant of Np(VI). They proposed an advanced Purex process for the separation of neptunium, technetium, plutonium, and uranium, which consisted of five steps for (1) co-decontamination of these elements, (2) Np oxidation with V(V) and TBP extraction of Np(VI), (3) Np separation by the reduction of Np(VI) to Np(V) with *n*-butyraldehyde, (4) Tc separation using highly acidic scrubbing solution, and (5) U/Pu partitioning by the selective reduction of Pu (IV) to Pu(III) with iso-butyraldehyde.

Taylor *et al.* (1998b) employed hydroxamic acids such as formohydroxamic acid and acetohydroxamic acid, and found that they selectively and rapidly reduced Np(VI) to Np(V). The investigators also reported that the reagent preferentially complexed Np(IV) and Pu(IV) in the aqueous solution. These characteristics may offer advantages in the control of neptunium in the advanced Purex process.

One way to control neptunium separation in the Purex process flowsheet is to extract all neptunium as Np(vi) together with U(vi) and Pu(iv) and then to separate neptunium from U(vi) as the reduced form, Np(v), along with Pu(iii). A suitable reductant to reduce Np(vi) to Np(v) and Pu(iv) to Pu(iii) efficiently and rapidly must be used. Hydroxylamine derivatives such as hydroxylamine and methyl-, dimethyl-, diethyl-, isopropyl-, and dibutyl-hydroxylamines, have been extensively examined for this purpose (Koltunov and Baranov, 1987). Koltunov *et al.* (1999) performed a kinetic study on the reduction of Np(vi) and Pu(iv) with the recently synthesized reductants *N*,*N*-ethyl(hydroxyethyl) hydroxylamine (EHEH). The reduction rates of Np(vi) and Pu(iv) with EHEH are among the highest of the salt-free reductants examined. This rapidity of the reduction makes EHEH particularly suitable for solvent extraction contactors such as centrifugal contactors of very short residence time in the advanced Purex process. A recent study by Koltunov *et al.* (2000) provides data on the rate of the reduction of Np(vi) and Pu(iv) with acetaldoxime in nitric acid solution, and suggests that Np(vi) and Pu(iv) are reductively stripped from 30% TBP (dodecane) phase in the presence of U(vi).

A photochemical procedure for the control of the oxidation state of the neptunium ion in the process solution is attractive due to its potential for minimization of secondary waste generation and simplicity of process design. Enokida and Suzuki (1989) used a KrF excimer laser to induce the reduction of Np(vi) to Np(v) in a 30% TBP (dodecane) phase, which was then stripped into the aqueous solution. Uchiyama *et al.* (1998b) studied the selective reduction of Np(vi) to Np(v) indirectly by nitrous acid produced photochemically with a low-pressure mercury lamp. Using a mixer-settler equipped with a photochemical reactor they demonstrated the applicability of this technique to the selective reduction and stripping of Np(v), leaving Pu(iv) and U(vi) in the 30% TBP (dodecane) phase. Photochemical processes were proposed (Wada *et al.*, 1996) for the selective extraction of Pu(vi) and Pu(iv) from Np(v), the oxidation states of which were controlled by 2 M HNO_3 + 10^{-2} M hydroxylamine nitrate + hydrazine under photoirradiation. A similar photochemical process was used for the coextraction of Pu(vi), Pu(iv), and Np(vi) prepared in 3 M HNO_3 + 10^{-2} M urea solution under irradiation.

(b) Partitioning of neptunium from high-level liquid wastes

The α emitters with a long half-life, such as ^{237}Np and other transplutonium nuclides contained in the HLW from the Purex process, are of great environmental concern. A considerable amount of work has been performed to develop methods for the partitioning of the actinides from the HLW. Several partitioning processes based on the solvent extraction technique using different extractants have been proposed as follows. Mathur *et al.* (1996a) proposed a method based on the TBP extraction for the removal of neptunium and plutonium together with U(VI). Quantitative extraction of Np(VI) and Pu(VI) from various kinds of simulated and real HLW was attained with 30% TBP (dodecane) after oxidizing neptunium and plutonium using 0.01 M $K_2Cr_2O_7$. More than 99% of neptunium and plutonium was stripped from the organic phase by reducing neptunium to Np(V) and plutonium to Pu(III) with 0.01 M ascorbic acid + 0.1 M H_2O_2 + 2 M HNO_3 solution, leaving most of the uranium in the organic phase. Feasibility of this method was confirmed by counter-current experiments using mixer-settlers with simulated HLW (Chitnis *et al.*, 1998). Pentavalent vanadium ion, VO_2^+, is also effective to adjust the oxidation state at Np(VI) and Pu(VI).

CMPO has been evaluated to be one of the best reagents for the partitioning strategy because of its high ability to extract hexavalent, tetravalent, and trivalent actinide ions from an acidic solution of relatively wide range of acid concentrations. The well-known TRUEX process for the recovery of all actinides from various types of nuclear waste solutions is based on CMPO extraction. Kolarik and Horwitz (1988), Wisnubroto *et al.* (1991), and Mathur *et al.* (1996b) accumulated the extraction data of neptunium ion of various oxidation states using TRUEX solvent. Np(V) is inextractable and must be oxidized to Np(VI) with $K_2Cr_2O_7$ or HNO_2 or reduced to Np(IV) with Fe(II) sulfamate or H_2O_2. Wisnubroto *et al.* (1991) showed that Np(V) readily disproportionated to Np(VI) and Np(IV) and the extraction efficiency of neptunium present initially as Np(V) in the sample solution increased, when the acid concentration of the aqueous solution was high enough, e.g. >4 M HNO_3. Np(IV) extracted in the TRUEX solvent was stripped quantitatively into the diluted HNO_3 solution containing complexing agents such as HF, $(COOH)_2$, carbonate, or EDTA. Np(VI) in the organic phase was easily stripped with diluted HNO_3 in the presence of H_2O_2 through the reduction of Np(VI) to Np(V).

The solvent extraction with diisodecylphosphoric acid (DIDPA) was applied to the partitioning of actinides in HLW (Morita *et al.*, 1996). The DIDPA extraction exhibits an advantage in that trivalent actinide ions, Am(III) and Cm(III), can be extracted from an aqueous solution of fairly low acidity, e.g. 0.5 M HNO_3, together with tetravalent and hexavalent ions. Even Np(V) in the sample solution is extracted by DIDPA. The addition of H_2O_2 enhances the rate of the extraction of Np(V) (Morita and Kubota, 1988). Rapid reduction of Np(V) to Np(IV) occurs during the DIDPA extraction in the presence of H_2O_2. The back-extraction of Np(IV) is achieved with 1 M $(COOH)_2$.

Trialkyl(C_6–C_8) phosphine oxides (TRPO) have been studied as an appropriate class of extractants for the recovery of Np, Pu, and Am from HLW (Zhu and Song, 1992). The optimum organic phase is 30 vol% TRPO (kerosene), and >99% of Np(IV) and Np(VI) with U(VI), Pu(VI), and Pu(IV) and >95% of trivalent actinide and lanthanide ions were extracted from 0.2 to 1 M HNO_3. The neptunium ion extracted is stripped with the plutonium ions into 0.5 M $(COOH)_2$ solution. In the recommended flowsheet, the oxidation state of neptunium is adjusted at 4+ by electrolytic reduction.

6.5.2 Chromatography using various resins

(a) Chromatography with ion-exchange resin

Various methods based on ion-exchange chromatography have been used for the separation of neptunium ions (Burney and Harbour, 1974). Cation-exchange chromatography of NpO_2^{2+}, NpO_2^{+}, and Np^{4+} with dilute acid solutions has been developed. The adsorption of ions of different oxidation states differ from each other so that the distribution ratio follows the order $Np^{4+} \gg NpO_2^{2+} \gg NpO_2^{+}$, which enables the mutual separation of neptunium ions of different oxidation states. Utilization of cation-exchange methods is limited because NpO_2^{2+} and NpO_2^{+} are often reduced to Np^{4+} when in contact with the resin; the adsorption behavior of Np^{4+} is not so selective from other coexisting cations.

Np(vi) and Np(iv) form anionic chloride or nitrate complexes in aqueous solutions containing high concentration of chloride or nitrate ions, and the anionic complexes formed are strongly adsorbed on anion-exchange resins. Well-established anion-exchange chromatographic methods are available and have been utilized for the isolation of neptunium from other actinides and fission product elements. From the viewpoint of the selectivity among neptunium ions and the other ions, nitrate media are preferable to chloride media. One such example is the procedure shown in Fig. 6.1 for the separation of ^{237}Np from environmental analytical samples, which consists of anion-exchange chromatography after solvent extraction with HTTA. The common procedure consists of the adjustment of neptunium ion at Np(iv) and the adsorption of Np(iv) nitrate complex, i.e. $Np(NO_3)_6^{2-}$, on the anion-exchange resin from 7 to 8 M HNO_3 solution. The anionic nitrate complexes of Pu(iv) and Th(iv) are also adsorbed on the resin. Pu(iv) is eluted as Pu(iii) with a mixture of 6 M HNO_3 + 0.05 M Fe(ii) sulfamate + 0.05 M hydrazine. Th(iv) is eluted with 8 M HCl. Np(iv) is then recovered by elution with 0.3 M HNO_3. Maiti *et al.* (1992) developed another method for the sequential separation of actinides by anion-exchange chromatography. Np(iv), Pu(iv), and U(vi) in 9 M HCl–0.05 M HNO_3 solution are adsorbed on the anion-exchange resin and Am(iii) is not adsorbed under these conditions. Pu(iv), Np(iv), and U(vi) are eluted successively using 9 M HCl–0.05 M NH_4I, 4 M HCl–0.1 M HF, and 0.5 M HCl–1 M HF, respectively. The Pu(iv) is eluted by the reduction of Pu(iv) to Pu(iii).

(b) Chromatography using chelate resins

Extraction chromatography using porous chelate resin loaded with an extractant is useful for the separation of actinides. A large number of theoretical plates of solvent extraction process is achieved during the column operation, which leads to an improvement of the selectivity in the separation. Maxwell (1997) developed a rapid method for the separation of neptunium using a resin loaded with Aliquat™ 336, which is called TEVA resin. Flowsheet is shown in Fig. 6.5. The oxidation states of neptunium and plutonium are adjusted to Np(IV) and Pu(III) by reducing them in a solution of Fe(II) sulfamate and ascorbic acid. Np(IV) is retained on the resin while >99.9% Pu(III) is eluted and removed. This method can be applied to such samples as nuclear materials process samples, waste solutions, and environmental samples.

TnOA-loaded Teflon resin was used for the rapid and simple separation of ^{237}Np from environmental samples (Ji *et al.*, 2001). Np(IV) in 2 M HNO_3 solution was adsorbed on the resin and eluted with 0.02 M $(COOH)_2$ + 0.16 M HNO_3 at 368 K. The decontamination factor for U(VI) was $>10^5$, allowing direct determination of ^{237}Np by ICP-MS.

Kimura (1990b) and Seranno and Kimura (1993) developed an extraction chromatographic method with TBP-loaded Amberlite XAD-4 resin for the

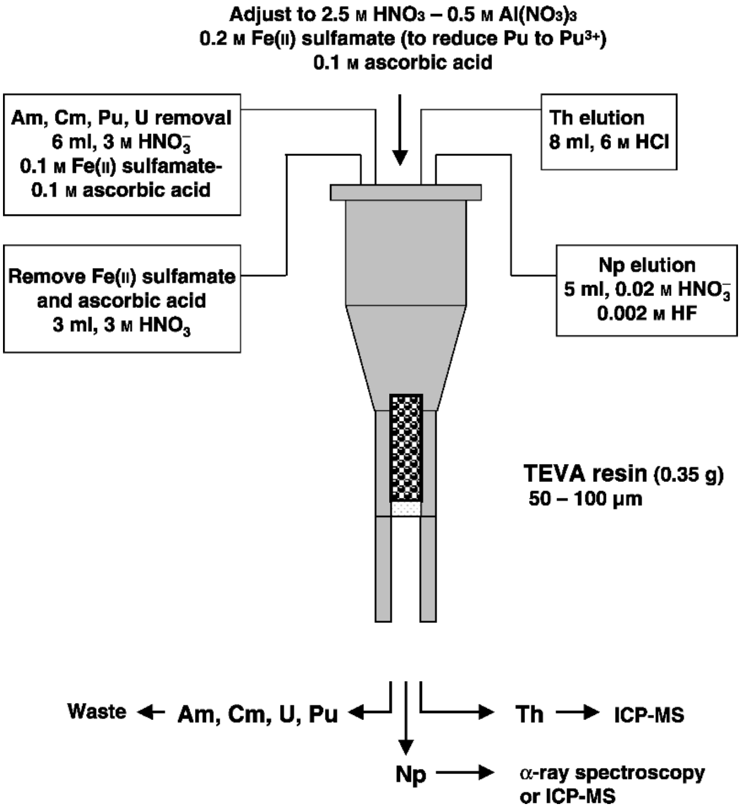

Fig. 6.5 *Procedure for the separation of neptunium ion from other actinide ions using TEVA resin.*

sequential separation of uranium, neptunium, plutonium, and americium. Np(vi) prepared by oxidizing neptunium ion in 3 M HNO_3 with 0.001 M $KBrO_3$ adsorbs on the resin and is eluted as Np(v) with the reductive effluent of 3 M HNO_3 + 0.05 M $NaNO_2$.

Heinrich and Klaus (1999) developed an automatic separation system, that is based on the extraction chromatography with silica gel particles loaded by TOPO, for the pretreatment of samples for nuclear material safeguards analysis. Np(iv), U(vi), and Pu(iv) in 3 M HNO_3 solution adsorb on the resin and are separated from Am(iii), Cm(iii), and fission products. Neptunium is eluted from the column as Np(v) with 0.1 M HNO_3 + 0.3 M H_2O_2 solution, plutonium is then eluted as Pu(iii) with formic acid + ascorbic acid, and finally U(vi) is eluted with $(NH_4)_2CO_3$ solution.

Diphonix resin combines methylenediphosphonate, carboxylate, and sulfonate functional groups in a cross-linked polystyrene resin. This resin has strong affinity toward actinide and lanthanide ions of various oxidation states (Chiarizia *et al.*, 1994). Horwitz *et al.* (1994) obtained data of the adsorption of Np(iv), U(vi), and Am(iii). One of the most distinguished features of this resin is its high adsorption ability of actinide ions from aqueous solutions even of high acidity.

6.5.3 Coprecipitation

Coprecipitation methods are traditional, well-established, and widely used for the separation of trace amounts of radioactive elements and the recovery of actinides such as neptunium. A typical example is the coprecipitation method for the preconcentration of ^{237}Np from a large volume of seawater for analytical purposes. Simplicity, rapidness, and applicability to treat large volumes of sample solution are the main advantages of this method. On the other hand, poor selectivity of coprecipitation often requires additional separation processes by solvent extraction or ion-exchange chromatography for the isolation of neptunium ions.

Several kinds of precipitates such as LaF_3, $BiPO_4$, $BaSO_4$, $Fe(OH)_3$, and MnO_2 have been used as a matrix. Np(iv) coprecipitates quantitatively with LaF_3 together with Pu(iii), Pu(iv), Th(iv), and lanthanide (iii). Because Np(vi) as well as Np(v) do not coprecipitate on LaF_3, neptunium can be separated from these metal ions by adjusting the oxidation state at Np(vi) or Np(v) before the coprecipitation procedure. U(vi) does not coprecipitate on LaF_3 from sulfate medium; therefore, U(vi) can be removed from the coprecipitated ions. Np(iv), Ce(iii), Ba(ii), and lanthanides (iii) coprecipitate on $BiPO_4$ very efficiently. Kimura *et al.* (1986) developed a sequential separation procedure utilizing the coprecipitation of neptunium, plutonium, and americium ions with $BiPO_4$. Hoelgye (1998) employed the $BiPO_4$ coprecipitation method for the separation of neptunium from urine samples.

6.5.4 Electrodeposition methods

The electrodeposition reaction of a metallic actinide at a cathode in a eutectic mixture of LiCl + KCl (ca. 700–900 K) was applied as the separation method for the actinide. This method has been expected to be a novel technology for pyrometallurgical reprocessing of nuclear spent fuels or partitioning of the HLW. Electrolytic reaction reduces an actinide (III) to actinide (0) in LiCl + KCl melt and deposits the metallic actinide at the surface of the solid cathode such as tungsten or dissolves the actinide in the liquid cathode such as bismuth or cadmium melt. There have been fundamental studies on the electrode process between Np(III) and Np(0) to obtain thermodynamic data including the equilibrium redox potential of Np(III)/Np(0), the activity coefficient and the diffusion coefficient of Np(III) in LiCl + KCl (Roy *et al.*, 1996; Sakamura *et al.*, 1998, 2000; Shirai *et al.*, 2001). Martinot (1991) developed a method for the preparation of metallic neptunium of high purity by electrodeposition in LiCl + KCl (723 K). The metal product contained a total of 500 ppm impurities.

6.5.5 Biotechnology

Biotechnological methods exhibit the potential of removal of neptunium from the solution. Lloyd *et al.* (2000) proposed a procedure utilizing a combination of two microbial activities that reduce Np(V) in the sample solution to Np(IV) using the reductive capability of *Shewanella putrefaciens* followed by the formation of Np(IV) precipitate with a phosphate ligand enzymatically liberated by *Citrobacter species*. Immobilized cells of a *Citrobacter species* were prepared and employed for the removal of neptunium and plutonium ions from the sample solution (Macaskie and Basnakova, 1998).

6.6 THE METALLIC STATE

6.6.1 Neptunium metal

Although tracer quantities of neptunium were first produced by McMillan and Abelson (1940), it was not until 1945 that microgram quantities of metallic neptunium were synthesized by Magnusson and LaChapelle (1948). Their method reacted NpF_3 with barium at 1473 K. Several methods are currently used to produce gram-sized quantities of metallic neptunium. The first of these reacts NpF_4 with a stoichiometric excess of calcium and 0.15 mol of iodine 'booster' per mole of neptunium (Haire, 1986). A second method uses NpO_2 as a starting material, although other compounds such as $Cs_2NpO_2Cl_4$ and $Cs_3NpO_2Cl_4$ can be used as starting materials, and applies molten salt electrochemistry (Reavis *et al.*, 1985). A salt of LiCl/KCl is used as the electrolyte maintained at 723 K and the material is subjected to stream of HCl and H_2 gas

(Martinot, 1984). The neptunium produced can be collected either as a solid cathodic deposit on a tungsten mandrel or through use of a vitreous magnesia crucible suspended in the salt and positioned around the tungsten cathode to harvest the drops of neptunium from the cathode. The second method of collection is more challenging due to a higher operating temperature of 1023 K but can yield gram-sized quantities. A third method for producing neptunium is the reduction of NpC using tantalum followed by distillation of the neptunium metal (Spirlet and Vogt, 1984). The purity of the neptunium produced from the methods mentioned above is high, typically 99.95%, although the method involving calcium may require further electrorefining to obtain such an elevated level of purity. Recently, Hasegawa *et al.* (1998) developed a new method for the preparation of metallic neptunium based on the electrodeposition from aqueous solution. Neptunium is amalgamated by electrolysis at a mercury cathode with electrolyte solution of 1 M CH_3COOH + 0.3 M CH_3COONa (pH = 3.5) containing 0.05 M neptunium and then separated from mercury by evaporation at 1523 K.

Metallic neptunium is silvery in appearance and forms a thin oxide layer when exposed to air at ordinary temperatures. The reaction to form oxide is more pronounced at higher temperatures. The metallic form is similar to uranium in physical workability. The accepted values for melting point and density are (912 ± 3) K and 19.38 $cm^3\ g^{-1}$ (Lemire *et al.*, 2001, pp 85–87), respectively. Boiling point has not been determined experimentally; however, a value of 4447 K has been obtained via extrapolation of vapor pressure results (Eick and Mulford, 1964).

The thermodynamic properties of neptunium have been compiled by Oetting *et al.* (1976). Metallic neptunium exists in three crystalline forms (allotropes): α-form (orthorhombic), β-form (tetragonal), and γ-form (body-centered cubic (bcc)). The accepted transition temperatures, obtained by several independent groups (Zachariasen, 1952; Lee *et al.*, 1959; Wittenberg *et al.*, 1970), for the transitions are: $\alpha \rightarrow \beta$ (553 ± 5 K) and $\beta \rightarrow \gamma$ (849 ± 5 K). The enthalpies and entropies of transition for the three allotropes are: (1) for the $\alpha \rightarrow \beta$ transition, 5607 J mol^{-1} (ΔH°) and 10.1 J $K^{-1}mol^{-1}$ (ΔS°) and (2) for $\beta \rightarrow \gamma$ transition, 5272 J mol^{-1} (ΔH°) and 6.23 J $K^{-1}mol^{-1}$ (ΔS°). A later determination of these temperatures and enthalpies of transition using differential thermal analysis has yielded slightly different values: (1) for the $\alpha\rightarrow\beta$ transition (555 K), 4730 J mol^{-1} (ΔH°) and (2) for $\beta \rightarrow \gamma$ transition (856 K), 2990 J mol^{-1} (ΔH°) (Foltyn, 1990). The largest difference between the latter values and earlier set are in the enthalpies of transition. It is reasonable to state that improvement in methods and instrumental techniques could account for this ‘refinement’ of the values of ΔH°. Some mention of a possible fourth allotrope has been advanced in the literature but without conclusive proof at this time (Foltyn, 1990).

The pertinent thermodynamic values at 298 K for metallic neptunium are: entropy, 50.5 J K^{-1} mol^{-1}, heat capacity, 29.6 J $K^{-1}mol^{-1}$, and the enthalpy component, $\{H^\circ(298) - H^\circ(0)\}$ 6.60 kJ mol^{-1}. The enthalpy and entropy of

Table 6.3 *Lattice parameters and space groups for allotropes of neptunium.* (*Lemire* et al., 2001)

Allotrope	*Symmetry*	*Space group*	a_0 (Å)	b_0 (Å)	c_0 (Å)
α-Np	orthorhombic	*Pnma*	6.663	4.723	4.887
β-Np[a]	tetragonal	*P*42	4.897	–	3.388
γ-Np[b]	Body-centered cubic	*Im*3*m*	3.518	–	–

[a] at 586 K.
[b] at 873 K.

fusion for neptunium are 5.19 kJ mol^{-1} and 5.69 J $K^{-1}mol^{-1}$, respectively (Wittenberg, 1970).

The fundamental studies of the crystallography of metallic neptunium were performed by Zachariasen (1952). This work was repeated, to a certain extent and with a different emphasis, by Mardon and Pearce (1959) as a portion of their study of the neptunium–uranium equilibrium diagram. The complete phase diagram for the allotropes of neptunium was first published by Stephens (1966). The lattice parameters for the allotropes are listed in Table 6.3.

The α allotrope of Np is orthorhombic and resembles a highly deformed bcc cell (Zachariasen, 1952). The coordination in this configuration has been reduced from 8 to 4 with a bond length of approximately 2.60 Å. The β allotrope of neptunium is a distorted tetragonal close-packed cell with 4 atoms per unit cell and a bond length of 2.76 Å. The bond length in the γ allotrope of neptunium is 2.97 Å. The phase diagram, fully developed by Stephens (1966), allows for several observations. The region of γ allotrope stability diminishes as the pressure is increased. The melting point of neptunium increases as the pressure is increased. The triple point of β-phase/γ-phase/liquid occurs at 998 K and 3200 MPa.

6.6.2 Neptunium alloys and intermetallic compounds

The past two decades have seen a resurgence of interest in the basic chemistry of neptunium in the area of alloys and intermetallic compounds (Hill, 1971; Aldred *et al.*, 1975; Elliot and Giessen, 1982; Potzel *et al.*, 1983, 1993; Gal *et al.*, 1987; Spitsyn and Ionova, 1987; Schafer *et al.*, 1989; Foltyn, 1990; Kalvius *et al.*, 1992, 1994; Yaar *et al.*, 1992; Gibson and Haire, 1993; Kitazawa *et al.*, 1993; Ogawa, 1993; Sanchez *et al.*, 1993, 1995; Wastin *et al.*, 1993; Zwirner *et al.*, 1993; Gibson *et al.*, 1994, 1996, 1999; Oddou *et al.*, 1994; Rodriguez *et al.*, 1994; Stewart *et al.*, 1994; Seret *et al.*, 1995; Jeandey *et al.*, 1996; Akabori *et al.*, 1997; Keiser *et al.*, 2000; Meresse *et al.*, 2000). The interest in intermetallic compounds in particular has been keen with the focus being the interesting and complex behavior observed due to the presence of f-shell electrons. The actinides and their intermetallic compounds exhibit magnetic behavior ranging from itinerant, band-like character, similar to transition metals, to local moment behavior, similar to the rare earths. The variety of behavior stems from either the overlap of the 5f wave functions or the hybridization of f electrons with the ligand orbitals. For contrasting example, $NpAl_3$ is a ferromagnet, no ordering was found in $NpGe_3$, and $NpSn_3$ was thought to exhibit heavy fermion behavior (Sanchez *et al.*, 1993). The observation of heavy fermion behavior for compounds of several actinides (U, Np, Pu) has been reported by several groups (Potzel *et al.*, 1983, 1993; Gal *et al.*, 1987; Spitsyn and Ionova, 1987; Schafer *et al.*, 1989; Kalvius *et al.*, 1992, 1994; Yaar *et al.*, 1992; Sanchez *et al.*, 1993, 1995; Wastin *et al.*, 1993; Zwirner *et al.*, 1993; Gibson *et al.*, 1994; Oddou *et al.*, 1994; Rodirguez *et al.*, 1994; Seret *et al.*, 1995; Jeandey *et al.*, 1996; Meresse *et al.*, 2000). To restate this unusual behavior in other (more chemical) terms, the 5f electrons of neptunium are relatively unshielded from the crystalline electric field interaction, unlike the rare earths where the 4f electrons are very well shielded thus quenching the angular momentum term leading J to be a good quantum number. In metallic neptunium and other actinides, the spin–orbit coupling is on the same order as the crystalline electric field interaction, leading to possible mixing of the J multiplet and a metallic solid that does not strictly adhere to Hund's rule (Potzel, 1983).

The primary instrumental methods for investigating the various neptunium intermetallics have been: specific heat measurements (Stewart *et al.*, 1994), Mössbauer spectroscopy (Gal *et al.*, 1987; Yaar *et al.*, 1992; Potzel *et al.*, 1993; Sanchez *et al.*, 1993, 1995; Kalvius *et al.*, 1994; Oddou *et al.*, 1994; Jeandey *et al.*, 1996), electrical conductivity (Seret *et al.*, 1995), X-ray diffraction (Wastin *et al.*, 1993; Meresse *et al.*, 2000), magnetization measurements (Yaar *et al.*, 1992; Kitazawa *et al.*, 1993; Sanchez *et al.*, 1993), and neutron diffraction (Oddou *et al.*, 1994).

The investigations of magnetic properties of the intermetallic compounds of neptunium has primarily focused on crystalline compounds, however, some early work was also performed on metallic glasses by Elliott and Giessen (1982). They conducted a study of some 13 metallic glasses containing Np, U, and Pu using X-ray diffraction to determine the interatomic distances. The primary experimental focus has been in the area of crystalline compounds of several types: (1) ternary compounds of composition RMt_2X_2 (R is either Th, Np or Pu, Mt is a 3d, 4d, or 5d transition metal, and X is Si or Ge) (Potzel *et al.*, 1993; Wastin *et al.*, 1993; Jeandey *et al.*, 1996); (2) ternary compounds such as AnT_2Al_3 (where An is either Np or Pu and T is Ni or Pd) or Np_2T_2Sn (where T is Ni, Pd, or Pt) (Zwirner *et al.*, 1993; Sanchez *et al.*, 1995; Seret *et al.*, 1995); (3) binary compounds of composition NpX_3 (where X is Al, Ga, Ge, In, or Sn) (Sanchez *et al.*, 1993; Kalvius *et al.*, 1994; Oddou *et al.*, 1994; Meresse *et al.*, 2000); (4) binary compounds of composition $NpCd_{11}$ (Stewart *et al.*, 1994); (5) binary compounds such as $NpBe_{13}$, $NpRu_2$, $NpOs_2$, and $NpIr_2$ (Gal *et al.*, 1987); (6) ternary compounds of the composition $AnFe_4Al_8$ (where An is Th, U, or Np) (Schafer *et al.*, 1989); and (7) binary compounds of the composition NpM_2 (where M is Al, Cr, Mn, Fe, Co, Ni, Cu, Os, Ir, Ru, or Zn) (Spitsyn and Ionova, 1987).

The effort in the nuclear industry to minimize the amount of the long-lived heavy isotopes of Np, Am, and Pu present in spent fuel so as to make the disposal of the spent fuel more environmentally and economically palatable has led to the efforts in the field of alloying Np with Zr, U, Am, and Pu (Gibson and Haire, 1993; Rodriguez *et al.*, 1994). Modeling efforts have also been employed to better understand the alloying behavior of neptunium with U, Am, Pu, Zr, and Fe (Ogawa, 1993; Gibson *et al.*, 1999). The intent of these efforts is to take long-lived actinides that have been separated from light water reactor spent fuel and recast them into fuel for irradiation in either an accelerator or a breeder reactor and thus transform the long-lived heavy isotopes into shorter-lived isotopes. This work is still underway and the success or failure of these efforts may play a pivotal role in the needed capacity of future geologic repositories for spent fuel in the world.

The formation of binary compounds with stainless steel components such as Fe, Ni, Mn, and Co has been studied from two distinct vantage points. There has been some interest in their magnetic properties (Aldred *et al.*, 1975). More recently intermetallic neptunium compounds (with Fe, Cr, Ni, and Zr) have been formed in a HLW produced from cladding hulls of spent breeder reactor fuel (Keiser *et al.*, 2000). Some neptunium is left in the cladding hulls after electrometallurgical processing for recovery of the uranium. The neptunium that is left forms Laves-type intermetallics with iron, from the stainless steel cladding, and the zirconium, from the metallic alloy fuel, U/10 wt% Zr. More extensive investigations in the general behavior of neptunium with a variety of transition metals have been undertaken by Gibson *et al.* (1994) and Akabori *et al.* (1997).

With the continued interest in making the most economic and environmentally conscious use of the geologic repository for spent fuel and the focus on materials that exhibit possible superconducting properties this area of neptunium chemistry promises to be a lively one for years to come.

6.7 IMPORTANT CLASSES OF COMPOUNDS

Since the discovery of neptunium in 1940 several important activities have directed the synthesis and characterization of neptunium compounds. These activities include the importance of neptunium compounds to fundamental research, as source material for producing Pu-238, and recently neptunium's role as an environmental concern in waste disposal or as a 'burnable' component in future nuclear reactor fuels. As a result of these activities numerous publications are found in the open literature. Synthetic methods, crystal structure, chemical behavior, and thermodynamic properties have been reviewed in a number of books and publications as follows: *The Chemistry of the Transuranium Elements*, Verlag Chemie, Weinheim, Keller (1971); *Gemlin Handbuck der Anorganischen Chemie*, Suppl. Work 8th edn, Transuranium, Verlag Chemie, Weinheim, vol. 4 part C, Compounds (1972); *The Chemical Thermodynamics of Actinide Elements and Compounds*, Part 4, Part 6, Part 8, Part 9 (ed. F. L. Oetting), International Atomic Energy Agency, Vienna, *Comprehensive Inorganic Chemistry* (ed. A. F. Trotman-Dichinson), Pergamon Press, Oxford, vol. 10, pp. 141–429 (1975); *Handbook on the Physics and Chemistry of the Actinides*, vol. 3 (eds. A. J. Freeman and C. Keller), Elsevier Science Publishers B.V., Amsterdam; (1985); *Handbook on the Physics and Chemistry of the Actinides*, vol. 6 (eds. A. J. Freeman and C. Keller), Elsevier Science Publishers B.V., Amsterdam; (1991); *Synthesis of Lanthanide and Actinide Compounds* (eds G. Meyer and L. R. Morss), Kluwer Academic Publishers, Dordrecht, The Netherlands (1991); and *Chemical Thermodynamics of Neptunium and Plutonium* (Lemire, R. J. *et al.*), Elsevier, Amsterdam (2001).

6.7.1 Hydrides

The reaction of neptunium with hydrogen results in the formation of hydrides similar to those produced by the reaction of hydrogen with plutonium (Fried and Davidson, 1948). Two hydrides, NpH_{2+x} and NpH_3, were synthesized and characterized by Mulford and Wiewandt (1965). Mintz *et al.* (1976) and recently Ward *et al.* (1987) confirmed the existence of these phases. A phase diagram proposed by Ward *et al.* (1987) for the neptunium–hydrogen system is shown in Fig. 6.6.

Mulford and Wiewandt (1965) found NpH_{2+x} to be face-centered cubic (fcc) and isostructural with PuH_{2+x} but with increasing lattice constants as hydrogen content increases. This trend is opposite of that expected when compared to the lattice constants for the plutonium–hydrogen system (Mulford and Wiewandt, 1965). Ward *et al.* (1987) confirmed this trend in neptunium–hydrogen lattice constants. A comparison of the lattice constants from the two investigations is given in Table 6.4. Both studies show the NpH_3 phase is hexagonal and isostructural with PuH_3. The lattice parameters found by Ward *et al.* (1987) are $a_0 = 6.5338$ Å and $c_0 = 6.7204$ Å.

Pressure–composition isotherms generated by Mulford and Wiewandt (1965) and later by Mintz *et al.* (1976) show flat plateaus to a [H]/[Np] value of approximately 2.16 in contrast to other actinides and lanthanides that show a phase boundary at 1.90. Another anomalous behavior found by Mulford and Wiewandt (1965) is increasing hydrogen content with increasing temperature as opposed to decreasing hydrogen with increasing temperature in the plutonium–hydrogen system. In addition to the anomalous behaviors described above, a comparison of the two reports show contrasting and conflicting thermodynamic values calculated from the pressure–composition isotherms. Ward *et al.* (1987) gives a detailed review of the two studies.

Thermodynamic data taken from Ward *et al.* (1987) are presented here. These data are selected for reporting because Ward re-examined the neptunium–hydrogen system using ultrapure, double-refined neptunium metal, and a

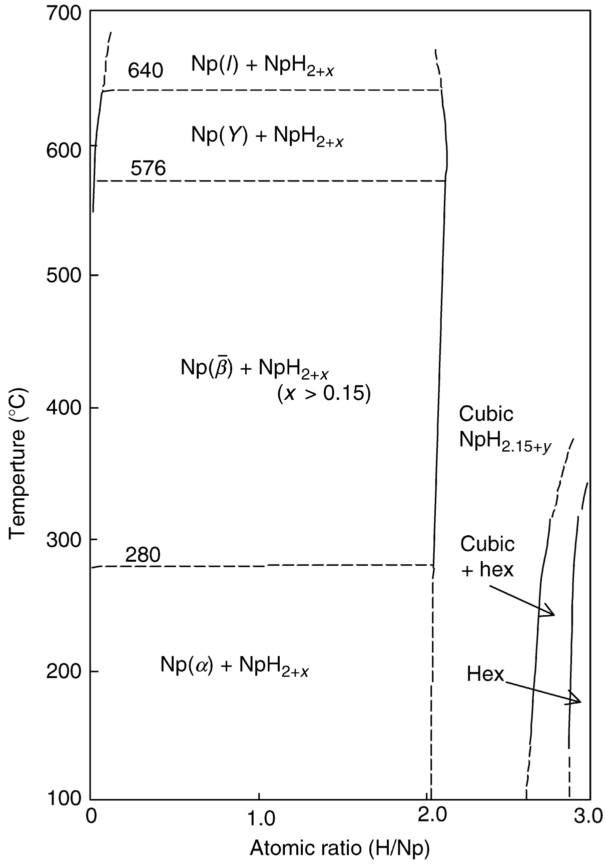

Fig. 6.6 *Partial phase diagram for the neptunium–hydrogen system. Reprinted from Ward* et al. (1987) *with permission from Elsevier Science.*

sophisticated Sievert's type apparatus. The pressure for hydrogen above $NpH_{2.13}$ below 849 K is given by:

$$\ln p \,(\text{pascals}) = 25.043 - 13421T^{-1} \tag{6.10}$$

From this equation enthalpies and entropies of formation for the reaction 0.94 $Np + H_2 = 0.94\ NpH_{2.13}$ are −118.8 kJ mol^{-1} (−28.38 kcal mol^{-1}) and −119.7 J K^{-1} mol^{-1} (−28.6 cal K^{-1} mol^{-1}), respectively. Ward calculated the enthalpy and entropy of formation for NpH_3 to be −153.9 kJ mol^{-1} (−36.78 kcal mol^{-1}) and −174.0 J $K^{-1}mol^{-1}$ (−41.63 cal K^{-1} mol^{-1}), respectively. Ward tabulated calculated partial and integral enthalpies and entropies and compared the data vs the data of Mulford and Wiewandt (1965) and Mintz *et al.* (1976).

There are no known heat capacity data for neptunium hydrides. Flotow *et al.* (1984) estimated the heat capacity of $NpH_2(s)$ from the data of Mulford and

Table 6.4 *Comparison of lattice parameters for cubic neptunium hydride.*

[*H*]/[*Np*]	*Mulford* et al. a_0 (Å)	*Space group*	*Ward* et al.
0.5	5.343	*Fm*3*m*	
1.5		*Fm*3*m*	5.3565
1.78	5.3428	*Fm*3*m*	
2		*Fm*3*m*	5.3475
2.15		*Fm*3*m*	5.3481
2.18	5.3431	*Fm*3*m*	
2.3		*Fm*3*m*	5.349
2.36	5.3463	*Fm*3*m*	
2.42	5.3478	*Fm*3*m*	
2.5	5.36	*Fm*3*m*	5.3516
2.8	5.355	*Fm*3*m*	5.3578

Wiewandt (1965) and Mintz *et al.* (1976). The estimated C_p° at 298 K is 47.279 J K^{-1} mol^{-1}. Flotow *et al.* (1984) lists estimated heat capacities from 298 to 900 K in tabular form.

There are few published data describing chemical behavior of neptunium hydrides. Haschke (1991) reviews the practical aspects of actinide hydrides focusing on safety, compound purity, reaction rates, and preparatory procedures. Recognizing the well-known pyrophoricity of both plutonium and uranium and the fact that neptunium hydride decomposes above 573 K in vacuum, yielding finely divided pyrophoric elemental neptunium, one must take great care in handling neptunium hydrides.

6.7.2 Oxides, hydrated oxides, and hydroxides

Given that neptunium has five oxidation states, it is surprising that there are only two known anhydrous oxides, NpO_2 and Np_2O_5. Attempts to synthesize higher oxides have not been successful (Katz and Gruen, 1949) and the early reported existence of Np_3O_8 has been shown to be the neptunium pentoxide (Sudakov *et al.*, 1972; Fahey *et al.*, 1976a,b). Richter and Sari (1987) on the basis of their work and recent new information on the two-phase boundaries between Np and NpO_{2-x} experimentally determined by Bartscher and Sari (1986) proposed modifications to the partial phase diagram constructed by Belyaev (1983). Their phase diagram, shown in Fig. 6.7, shows the effects of the three metal phases and the substoichiometric range, NpO_{2-x}, first noted by Ackerman *et al.* (1966). However much important work remains to be done to fully understand the neptunium–oxygen system. Recently, Beauvy *et al.* (1998) did not find neptunium metal in their investigation of the preparation of actinide compounds for actinide transmutation, contrary to the data shown in the neptunium–oxygen phase diagram.

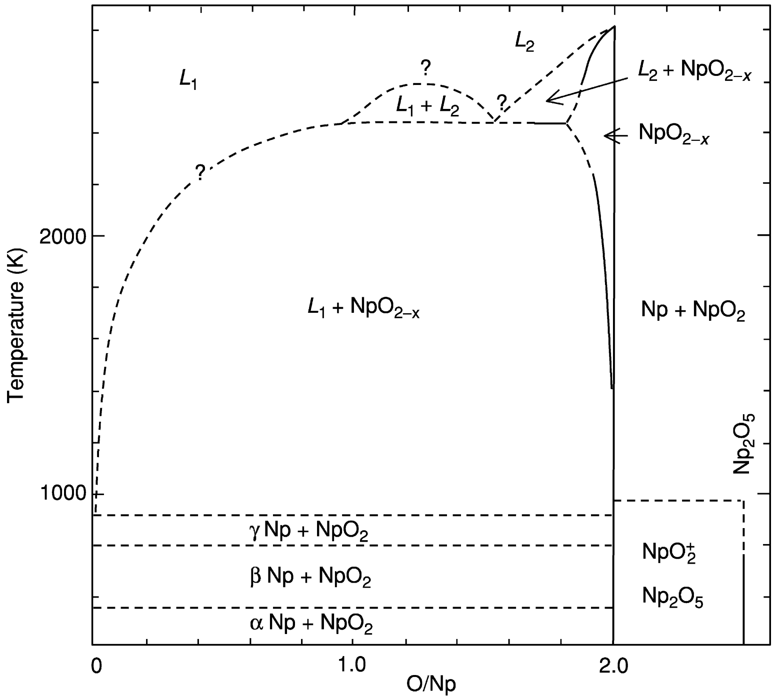

Fig. 6.7 *Phase relation of the neptunium–oxygen system. Reprinted from Richer and Sari* (1987), *with permission from Elsevier Science.*

NpO_2 is synthesized by the thermal decomposition of many neptunium compounds of any oxidation state. The oxide has a fluorite structure with a lattice parameter of (5.4334 ± 0.0003) Å and is isostructural with other actinide oxides (Fahey *et al.*, 1974). Martinot *et al.* (1970) grew single crystals of NpO_2 electrochemically. Spirlet *et al.* (1980) prepared single crystals of NpO_2 by means of a chemical transport reaction using tellurium tetrachloride as a transporting agent in a quartz ampoule at 1233 to 1323 K. X-ray diffraction characterization of the single crystals showed a fluorite lattice parameter of (5.433 ± 0.001) and (5.434 ± 0.001) Å, respectively, in relatively good agreement with literature data of Fahey *et al.* (1974, 1976a,b). Recently, Finch (2002) reported the crystallization of NpO_2 during corrosion experiments in which neptunium-doped U_3O_8 is reacted with humid air at 423 K for several weeks.

NpO_2 is extremely stable over a wide range of temperatures and pressures. The compound does not show a phase transition at low temperatures (Marples, 1975). Benedict *et al.* (1986) studied NpO_2 at pressures up to 50 GPa. Their study shows a phase transition from the fluorite fcc structure to orthorhombic between 33 and 37 GPa. The phase returned to the fcc structure on releasing pressure. The compound is stable at oxygen pressures and temperatures to 2.84 MPa and 673 K (Fahey, 1986). Non-destructive assay standards require materials of known purity for calibration and certification of instruments. Starting with impure NpO_2 and metal, Yarbro *et al.* (1991) synthesized rather pure NpO_2 and metal using two different procedures. Following dissolution, double peroxide precipitations, ion exchange, and an oxalate precipitation of the impurities in the resulting oxides were below 100 ppm each.

The identification of Np_2O_5 and its position in the neptunium–oxygen system result from several investigations of earlier contradictory information (Fahey *et al.*, 1976a,b; Richter and Sari, 1987). Cohen (1963) and Cohen and Walter (1964) obtained Np_2O_5 by precipitation of the compound by bubbling ozone through molten $LiClO_4$ containing NpO_2^+. Bagnall and Laidler (1964) prepared the compound by the thermal decomposition of $NpO_3 \cdot H_2O$ and Sudakov *et al.* (1972) prepared the compound by the decomposition of NpO_2OH(am). Investigations by Fahey *et al.* (1976a,b) and Sudakov *et al.* (1972) provided clarification of early reported contradictory information. Bessonov *et al.* (1989a) reported the synthesis of Np_2O_5 from neptunium(IV) peroxide, double nitrate, and oxalate, apparently contradicting previously published reports. Neptunium peroxide was quantitatively converted to the pentoxide by heating at 573 to 623 K for 2 to 3 h or by heating in an ampoule at 453 to 473 K under a layer of water. The preparation of Np_2O_5 from the double nitrate and oxalate was complex involving several steps for the double nitrate. Attempts to prepare Np_2O_5 by oxidation of NpO_2 at temperatures between 700 and 970 K and oxygen pressures at 0.3 MPa were not successful (Richter and Sari, 1987). Brown Np_2O_5 is monoclinic with the following lattice parameters: $a_0 = (4.183 \pm 0.003)$ Å, $b_0 = (6.584 \pm 0.005)$ Å, and $c_0 = (4.086 \pm 0.003)$ Å, and $\beta = (90.32 \pm 0.03)^\circ$ (Fahey *et al.*, 1976a,b). Np_2O_5 is not very stable decomposing to NpO_2 and O_2 at 693 to 970 K (Bagnall and Laidler, 1964; Richter and Sari, 1987).

Neptunium hydrated oxides and hydroxides are very important in the context of the disposition of nuclear waste. Considerable interest has been devoted to Np(V) since it is the most stable valence of neptunium in the environment. Recent publications reporting the results of studies particularly on chemical thermodynamics have been exhaustively reviewed and summarized by Lemire *et al.* (2001), pp 105–29.

Heptavalent neptunium hydroxide has been precipitated from acidic solutions containing Np(VII) by addition of NaOH or LiOH to a pH at approximately 10 (Krot *et al.*, 1968a; Chaikhorskii and Leikina, 1972). Both studies reported a formula of $NpO_2(OH)_3$. Later, Musikas *et al.* (1974) reported the formula to be $NpO_3(OH)$ based on a titration study showing one hydroxyl ion per Np(VII) ion. Chaikhorskii *et al.* (1972) obtained Np(VII) hydroxide by passing ozone through a suspension of Np(V) hydroxide. The reaction was carried on at 363 K for 5 h or by passing ozone over dried Np(V) hydroxide at 368 to 373 K for 5 h. Nikonov *et al.* (1994) investigated the oxidation of Np(V) hydroxide to form a compound containing Np(VII). The investigators reported the preparation of $(NpO_2OH)(NpO_4) \cdot 4H_2O$.

Several preparations for the synthesis of neptunium(VI) hydrates and hydroxides have been developed. LaChapelle *et al.* (1947) reported the precipitation of neptunium(VI) hydroxide by the addition of ammonia and sodium hydroxide to sulfuric acid solutions containing Np(VI). Cohen (1963) reported the preparation of $NpO_3 \cdot 2H_2O$ by oxidation of Np(V) in a molten $LiNO_3/KNO_3$ eutectic at 423 K with ozone. Bagnall and Laidler (1964), Chaikhorskii *et al.* (1974), and Belyaev *et al.* (1975) precipitated $NpO_3 \cdot H_2O$ and $NpO_3 \cdot 2H_2O$ by adding ozone to aqueous suspensions of neptunium(V) hydroxide. $NpO_2(OH)_2$ was prepared by bubbling ozone into an aqueous solution of NpO_2ClO_4 at $pH = 5$ and 363 K (Belyaev *et al.*, 1979). Kato *et al.* (1996) prepared $NpO_3 \cdot H_2O$ from an acidic solution. The X-ray diffraction pattern and infrared spectrum for their compound was different from that found by Bagnall and Laidler (1964). Recently, Saito *et al.* (1999), to prevent the formation of Np(VII), developed several methods to prepare neptunyl hydroxides. The authors prepared a starting solution containing $NpO_2(NO_3)_2 \cdot xH_2O$. Anhydrous $NpO_2(OH)_2$ and $NpO_2(OH) \cdot H_2O$ (orthorhombic) were precipitated by the addition of pyridine at 373 and 343 K, respectively. $NpO_2(OH) \cdot H_2O$ (hexagonal) and $NpO_2(OH)_2 \cdot xH_2O \cdot yNH_3$ $(x + y = 1)$ were prepared by the addition of LiOH and ammonia water, respectively. The formula reported for the monohydrate has been reported variously as $NpO_3 \cdot H_2O$ and $NpO_2(OH)_2$ (Bagnall and Laidler, 1964; Kato *et al.*, 1996; Saito *et al.*, 1999). The recent review by Lemire *et al.* (2001), p 118 assigns the formula, $NpO_2(OH)_2$, to the dried solid of Bagnall and Laidler (1964) and the formula, $NpO_3 \cdot H_2O$, to the solid of Kato *et al.* (1996). In summary, Lemire *et al.* (2001), p 118 and Saito *et al.* (1999) describe the chemistry of the hydrated oxides and hydroxides of hexavalent neptunium to be a complicated system.

Interest in the solubility and hydrolysis reactions of Np(V) results from the stability and mobility of this oxidation state in the natural environment, the relatively long half-life of ^{237}Np (2.144×10^6 years), and its abundance in nuclear waste (Lierse *et al.*, 1985). Investigators obtained neptunium(V) hydroxide by adding ammonia, NaOH, or LiOH to slightly acidic or basic solutions containing Np(V) (LaChapelle *et al.*, 1947; Chaikhorskii *et al.*, 1974; Neck, 1992; Merli and Fuger, 1994). Neck *et al.* (1992) reported that freshly prepared green NpO_2OH in 1 M $NaClO_4$ turned to a gray-white precipitate with a lower solubility upon aging. The aged precipitate has a lower solubility than that obtained by the addition of ammonia water to a slightly acidic nitrate and $NaClO_4$ solutions containing NpO_2^+. Their preparations did not show any diffraction lines.

Neptunium(IV) hydroxides are formed in the manner of LaChapelle *et al.* (1947). There are apparently very few data on the hydrates/hydroxides of Np(IV) and Np(III) oxides. Keller (1975) reported that hydrous oxides, $MO_2(aq)$ have varying amounts of absorbed water rather than forming distinct compounds such as $M(OH)_4$. In contrast, Rai *et al.* (1987), studying the solubility of $NpO_2 \cdot xH_2O(am)$, reported that hydrous oxides are thermodynamically reproducible material over a period of 2 days to several months when maintained at 298 K. Lemire *et al.* (2001), pp 114–5 however, suggests that the compound is not thermodynamically stable representing a reproducible compound formed under different experimental conditions. Further research is required to fully characterize neptunium oxide hydrates.

Available thermodynamic data for the oxides, hydrates, and hydroxides have been extensively reviewed (Lemire *et al.*, 2001, pp 105–29). Table 6.5 lists the entropies, enthalpies, and Gibbs energies selected from the review Lemire *et al.* (2001).

Ternary oxides are primarily obtained by the reaction of NpO_2 with oxides of many different elements or by precipitation from alkaline solutions. The syntheses and characterization of these oxides have been extensively reviewed (Keller, 1972; Morss, 1982; Tabuteau and Pagès, 1985). Recently Morss *et al.* (1994) reviewed the pioneering work of Keller and co-workers in the synthesis and characterization of alkali neptunates and the importance of these compounds because of their bonding and electronic properties.

The known alkali and alkaline earth Np(VII) ternary oxides include: Li_5NpO_6, $Ba_3(NpO_5)_2$, Ba_2LiNpO_6, Rb_3NpO_5, K_3NpO_5, Cs_3NpO_5, $RbNpO_4$, $KNpO_4$, and $CsNpO_4$ (Keller and Seiffert, 1969; Awasthi *et al.*, 1971; Pages *et al.*, 1971; Mefod'eva *et al.*, 1976). Keller and Seiffert (1969) prepared Li_5NpO_6 by reacting Li_2O with NpO_2 at 673 K for 16 h. Awathi *et al.* (1971) reacted Li_2O_2 with $NpO_3 \cdot H_2O$ at 673 K for 16 h in a quartz tube in flowing oxygen at ambient pressure to obtain the compound. The compound was reported to be Li_5ReO_6 hexagonal structure with lattice parameters: $a_0 = (5.21 \pm 0.03)$ Å and $c_0 = (14.61 \pm 0.05)$ Å, the results of Awasthi *et al.* (1971) differing only slightly from those of Keller and Sieffert (1969). Recently Morss *et al.* (1994) reinvestigated the compound using X-ray and neutron diffractions. The objective of their

Table 6.5 *Thermodynamic properties of neptunium oxides and hydrated oxides at* 298.15 K.

	$\Delta_f H^\circ_m$ (kJ mol^{-1})	S°_m (J K^{-1} mol^{-1})	$\Delta_f G^\circ_m$ (kJ mol^{-1})	C°_{pm} (J K^{-1} mol^{-1})
NpO_2	-1074.0 ± 2.5	80.3 ± 0.4	-1021.731 ± 2.514	66.24 ± 0.5
Np_2O_5	-02162.7 ± 9.5	174 ± 20	-2031.6 ± 11.2	128.6 ± 5
$NpO_3 \cdot H_2O$	-1377 ± 5	129 ± 27	-1239.0 ± 6.1	120 ± 20
$NpO_2 \cdot OH$ (am, fresh)	-1222.9 ± 5.5	60 ± 27	-1114.7 ± 5.7	86 ± 20
$NpO_2 \cdot OH$ (am, aged)		70 ± 28	-1118.1 ± 6.3	
$NpO_2 \cdot$ (hyd,am)			-957.3 ± 8.0	

investigation was the redetermination of the structure based on the earlier finding that Li_5ReO_6 was monoclinic and not in the $R3m$ space group (Betz and Hoppe, 1984). The investigators found the X-ray diffraction patterns to be consistent with past data. However, they did not confirm the originally suggested space group, $R3m$, or any other structure using any plausible model.

$Ba_3(NpO_5)_2$, Ba_2NaNpO_6, and Ba_2LiNpO_6 were obtained by solid state reactions of alkali and alkaline peroxides with $NpO_3 \cdot H_2O$ at temperatures between 673 and 873 K for 15 to 30 h (Awasthi *et al.*, 1971). Interestingly, the reaction between Na_2O_2 and $NpO_3 \cdot H_2O$ was incomplete under the conditions of the experiment. The authors reported the presence of both Np(VI) and Np(VII) absorption spectra in dilute NaOH solution of the dissolved product. Furthermore, X-ray examination of the product showed evidence of unreacted Na_2O_2. Attempts to produce K_5NpO_6 and Ba_2KNpO_6 using the appropriate reactants under similar conditions were not successful. Pagès *et al.* (1971) obtained K_3NpO_5, Rb_3NpO_5, and Cs_3NpO_5 by the general reaction:

$$NpO_2 + 3MO_2 \rightarrow M_3NpO_5(M = K, Cs, Rb) \qquad (6.11)$$

Mefod'eva *et al.* (1976) precipitated $KNpO_4$, $RbNpO_4$, and $CsNpO_4$ from alkaline solutions containing the appropriate alkali metal nitrate, ozone, and Np(VII). Alkali metal to neptunium ratios for these compounds ranged from 1.07 to 1.19. The overestimation of the alkali metal content was explained by an admixture of nitrates.

A large number of hexavalent neptunium ternary oxides are obtained by solid state reactions of NpO_2 and alkali or alkaline earth oxides in a stream of oxygen. These oxides, generally isostructural, with uranates of the same chemical formula include: rhombohedral $Na_2Np_2O_7$, orthorhombic α-Na_2NpO_4 and β-Na_2NpO_4, tetragonal Li_4NpO_5 and α-Na_4NpO_5, orthorhombic β-Na_4NpO_5, Li_6NpO_6, and Na_6NpO_6 (Keller *et al.*, 1965a). Heating a 2:1 mixture of NpO_2 and Na_2O at temperature >673 K results in the formation of $Na_2Np_2O_7$. The heating of $Na_2Np_2O_7$ at >773 K gives α-Na_2NpO_4, which if heated to 1073 K results in the formation of β-Na_2NpO_4. Heating a 1:2 mixture of NpO_2 and Na_2O in an oxygen atmosphere at 673 K produces cubic α-Na_4NpO_5. Heating to >773 K may result in the formation of β-Na_4NpO_5. Further heating to 1073 K β-Na_4NpO_5 decomposes to β-Na_2NpO_4. When a 1:3 mixture of NpO_2 to Na_2O is heated to 773 K Na_6NpO_6 results. Heating a 1:2 mixture of NpO_2 and Li_2O at 673 to 773 K results in Li_4NpO_5 and heating a 1:3 mixture to 673 to 773 K results in Li_6NpO_6. $NaNp_2O_7$ is precipitated from molten salts containing either Np(V) or Np(VI) by reaction with BrO_3^- (Carnall *et al.*, 1965). Keller (1963) synthesized and characterized the following hexavalent Np(VI) alkaline earth oxides: $MNpO_4$ and M_3NpO_6 (where M = Ba, Ca, Sr). Appel *et al.* (1990) using crystallographic and spectroscopic techniques as well as magnetic susceptibility measurement and Mössbauer spectroscopy investigated the structure of $BaNpO_4$. The authors reported that structure to be isostructural with $BaUO_4$ with the lattice contants $a_0 = 5.726$ Å, $b_0 = 8.072$ Å, and $c_0 = 8.165$ Å. Hoekstra and Gebert (1977) synthesized M_2NpO_4 and M_2NpO_7 (where M = K, Rb, and Cs), $Cs_4Np_5O_{17}$, $Cs_2Np_3O_{10}$, and Li_2NpO_4. The researchers obtained the compound by two methods: (1) thermal decomposition of coprecipitated alkali-actinide nitrates and (2) reaction of alkali hydroxides with Np_2O_5.

Compounds of the types $K_2Np_2O_7$, K_2NpO_4, and $BaNpO_4$ have crystal structures made up of linear NpO_2^{2+} groups arranged in layers. By contrast, no NpO_2^{2+} groups are found in the crystal lattice of Li_6NpO_6 (Morss, 1982). Coordination, crystal chemistry, and thermochemistry of these oxides have been reviewed by Morss (1982) and Mössbauer studies have been reported by Jovè *et al.* (1988a,b).

Ternary oxides containing pentavalent neptunium include: Li_3NpO_4, Na_3NpO_4, and Li_7NpO_6 (Keller *et al.*, 1965b). Li_3NpO_4 is obtained by heating Li_6NpO_6 at 1173 to 1273 K apparently in a stream of argon. Na_3NpO_4 results from the heating of a mixture of Na_6NpO_6 and NpO_2 in vacuum at 773 K for 8 h. Li_3NpO_4 is obtained by heating Li_6NpO_6 in vacuum at 1173 to 1273 K for 4 h.

Ternary oxides with Np(IV) compounds with the formula $BaNpO_3$ and $SrNpO_3$ are prepared by reacting NpO_2 with BaO and SrO in an inert and reducing atmosphere between 1373 and 1573 K (Keller, 1963). Mössbauer spectra and magnetic susceptibility of these compounds have been investigated by Kanellakopulos *et al.* (1980a,b), Konig *et al.* (1983), and Bickel and Kanellakopulos (1986).

Neptunium forms a number of ternary oxides with the oxides of group III through group VII elements. Synthesis conditions, structural properties, and phase diagrams have been reviewed by Tabuteau and Pagès (1985). Self-assembled uranyl peroxide nanosphere clusters of 24, 28, and 32 polyhedra (some containing neptunyl) that crystallize from alkaline solution have been characterized (Burns *et al.*, 2005).

6.7.3 Halides, halide complexes, and oxyhalides

The preparation and characterization of neptunium binary halides, oxyhalides, and complex halides have not been as extensively studied with respect to other actinides such as uranium and plutonium and more attention has been given to neptunium–fluorine compounds.

(a) Fluorides, fluoride complexes, and oxyfluorides

There are four known neptunium binary fluorides: NpF_3, NpF_4, NpF_5, and NpF_6. The lower valent neptunium fluorides can be prepared by the following reactions as initially reported by Fried and Davidson (1947):

$$NpO_2 + 1/2H_2 + 3HF \rightarrow NpF_3 + 2H_2O\,(773\,K) \qquad (6.12)$$

$$NpF_3 + 1/4O_2 + HF \rightarrow NpF_4 + 1/2H_2O\,(773\,K) \qquad (6.13)$$

The tetravalent fluoride can also be prepared by the reaction of HF directly with the oxide by the following reaction:

$$NpO_2 + 4HF \rightarrow NpF_4 + 2H_2O \tag{6.14}$$

Trevorrow *et al.* (1968) prepared NpF_4 by treating NpO_2 with a gaseous mixture of HF(75 v/o) and oxygen (25 v/o) at 773 K at approximatetly 101.3 kPa pressure. More recently, Kleinschmidt *et al.* (1992a) prepared NpF_4 by heating NpO_2 between 553 and 603 K in flowing fluorine. Neptunium is apparently transported downstream as NpF_6 and collected as NpF_4. An amorphous NpF_4 can be precipitated from a solution of Np(iv). Fried and Davidson (1947) did report that NpF_4 was not attacked by concentrated HNO_3. The crystal structures for NpF_3 and NpF_4 are shown in Table 6.6.

The preparation of NpF_5 has proved to be difficult. A number of preparations of NpF_5 are reported in the earlier literature (Cohen *et al.*, 1970; Drobyshevskii *et al.*, 1975, 1978; Baluka *et al.*, 1980). These preparations depend on the reaction of I_2 in IF_5 and KrF_2 or PF_3 in anhydrous HF with NpF_6, NpF_4, and NpF_6, respectively. Recently there have been two investigations searching for simpler alternatives to obtain NpF_5 in a pure form. Brown *et al.* (1982) reinvestigated the use of I_2 in IF_5 medium to reduce Np(vi) as shown in the following equation:

$$10NpF_6 + I_2 \rightarrow 10NpF_5 + 2IF_5 \tag{6.15}$$

The authors reported the precipitation of a cream-white precipitate which was determined to be 70.25 wt% Np. NpF_5 is 71.35 wt% Np. There was no evidence of Np(iv) in contrast to the reported contaminant by a similar method employed by Cohen *et al.* (1970). Malm *et al.* (1993) investigated several preparations for NpF_5. NpF_5 is prepared from the reaction of $NONpF_6$ with LiF

Table 6.6 *Crystal structures of neptunium halides.*

			Lattice constants			
Halide	*Symmetry*	*Color*	a_0 (Å)	b_0 (Å)	c_0 (Å)	*Angle (deg)*
NpF_3	trigonal	purple	7.129		7.288	
NpF_4	monoclinic	green	12.68	10.66	8.34	126.3
NpF_5	tetragonal	bluish-white	6.53		4.45	
NpF_6	orthorhombic	orange	9.909	8.997	5.202	
$NpOF_3$	rhombohedral	green	4.185		15.799	
NpO_2F_2	rhombohedral	pink	4.185		15.790	
$NpOF_4$	hexagonal	brown	13.17		5.70	
$NpCl_3$	hexagonal	green	7.413		4.282	
$NpCl_4$	tetragonal	red-orange	8.266		7.475	
$NpOCl_2$	orthorhombic	orange	15.209	17.670	3.948	
$NpBr_3$	hexagonal	green	7.919		4.392	
$NpBr_3$	orthorhombic	green	4.109	12.618	9.153	
$NpBr_4$	monoclinic	dark red	10.89	8.74	7.05	94.19
NpI_3	orthorhombic	brown	4.30	14.03	9.95	
NpOI	tetragonal	?	4.051		9.193	

and BF_3. NpF_6 reacts with CO and light to produce a fine white powder presumed to be a mixture of NpF_5 and unidentified material. NpF_5 did not result from the reaction of NpF_6 with PF_3 in anhydrous HF in contrast to an earlier report (Baluka *et al.*, 1980). Both investigators studied some of the chemical behavior of NpF_5. In summary, NpF_5 does not react with BCl_3 in contrast to UF_5, NpF_5 hydrolyzes in $HClO_4$, NpF_5 reacts with LiF in anhydrous hydrogen fluoride to produce $LiNpF_6$, and NpF_5 thermally decomposes at 591 K to produce NpF_4 and NpF_6. Interestingly, UF_5 decomposes at 423 K into UF_6 and then in a orderly fashion to U_2F_9, U_4F_{17}, and UF_4. The product of both investigations were examined by X-ray diffraction and the patterns were similar to those in the literature (Baluku *et al.*, 1980) and similar to α-UF_5. From the study by Malm *et al.* (1993) the lattice parameters for the tetragonal compound are $a_0 = 6.5358$ Å and $c_0 = 4.4562$ Å (see Table 6.6). Significant differences in the IR data reported by Brown *et al.* (1982) and IR data reported by Drobyshevskii *et al.* (1975, 1978) have apparently not been resolved.

The volatility of NpF_6, presenting possible separation schemes to recover Np from spent nuclear fuel, led to early interest in preparations and characterization of NpF_6 (Malm *et al.*, 1958; Seaborg and Brown, 1961; Trevorrow *et al.*, 1968). The volatility of NpF_6 is similar to that of UF_6 and PuF_6. Florin (1943) first prepared NpF_6 by reacting NpF_3 with fluorine at high temperatures. Malm *et al.* (1958) achieved the preparation of gram quantities of NpF_6 in specially designed fluorination reactors which dripped liquid fluorine onto heated NpF_4. Convection currents moved NpF_6 to a condenser. Trevorrow *et al.* (1968) studied the fluorination of NpF_4 and NpO_2 with fluorine, BrF_3, and BrF_5. The reaction of both BrF_3 and BrF_5 with NpF_4 produced NpF_6 and bromine. The reaction of fluorine with NpF_4 confirmed the production of NpF_6. The researchers identified an intermediate solid, NpF_4, in the preparations of NpF_6 from NpO_2. Similar reactions with UO_2 show an intermediate as UO_2F_2. Later, Henrion and Leurs (1971) reported NpO_2F_2 as an intermediate in the fluorination of NpO_2 with fluorine. The investigators suggest that the NpF_4 identified by Trevorrow *et al.* (1968) was the result of a secondary reaction.

The use of KrF_2 as a fluorinating agent to prepare NpF_6 at low temperatures has been reported by several investigators (Drobyshevskii *et al.*, 1975, 1978; Peacock and Edelstein, 1976; Asprey *et al.*, 1986). Low-temperature fluorinations avoid the safety and material concerns intrinsic to high-temperature fluorinations with F_2. Peacock and Edelstein (1976) reported that NpF_6 resulted when $NpOF_4$ was contacted with KrF_2 at 213 K. Asprey *et al.* (1986) showed that NpF_6 is prepared by the reaction of gaseous KrF_2 and as well KrF_2 dissolved in anhydrous hydrogen fluoride with neptunium substrates.

Eller *et al.* (1998a) investigated the reaction of O_2F_2 with neptunium oxides and fluorides. NpF_6 is prepared by gas–solid reactions as shown below:

$$NpF_4(s) + xO_2F_2(g) \rightarrow NpF_6(g) + xO_2 + (x-1)F_2(g) \qquad (6.16)$$

$$NpO_2(s) + xO_2F_2 \rightarrow NpF_6(g) + (x+1)O_2(g) + (x-3)F_2(g) \qquad (6.17)$$

Both reactions proceed almost quantitatively at ambient temperatures. Reaction (6.16) is >95% complete after 45 min and reaction (6.17) is >95% complete after 30 min. Neptunium hexafluoride is produced by reaction with excess O_2F_2 in anhydrous hydrogen fluoride at 195 K with both NpO_2 and NpF_4, but the reactions are much slower. Reaction with NpF_4 was >95% complete after 2 h and reaction with NpO_2 was >95% complete after 3 h. Under both conditions, NpO_2 is converted to NpF_6 with NpO_2F_2 as one of the intermediates. The investigators attempted to study the reaction of the two substrates by condensing O_2F_2 directly on the solid and allowing the mixture to warm to 195 K. Using this procedure, the reaction became uncontrollable with total decomposition of the O_2F_2 and no detectable NpF_6 was produced.

Neptunium hexafluoride is an orange solid melting at 327.8 K to a liquid. Both solid and liquid evaporate to reddish-brown gas. The crystal structure of NpF_6(s) is orthorhombic and the lattice parameters are given in Table 6.6. The vapor pressure is given by the following:

$$\log p(\text{torr}) = A - B(T(\text{K})) + \text{C} \log(T(\text{K})) \tag{6.18}$$

For the temperature range 273–328.1 K, $A = 18.48130$, $B = 2892.0$, and $C = -2.6990$. For the temperature range 328.1–349.82 K, $A = 0.01023$, $B = 1191.1$, and $C = 2.5825$ (Keller, 1982). Keller (1982) pointed out that NpF_6 has a higher vapor pressure than either UF_6 or PuF_6. As with other volatile radionuclides and radionuclide-containing compounds, $^{237}NpF_6$ is a radiological as well as a chemical hazard and engineered safety precautions are required.

NpF_6 like UF_6 and PuF_6 is a very reactive compound. The chemical behavior has been studied by a number of investigators (Malm *et al.*, 1958; Trevorrow *et al.*, 1968; Peacock and Edelstein, 1976; Eller *et al.*, 1998b). Malm *et al.* (1958) studied the reaction of NpF_6 with both BrF_3 and water. The reaction of NpF_6 with BrF_3 was very slow resulting in a non-volatile product presumed to be NpF_4 in contrast to PuF_6 which reacts very rapidly with BrF_3. Similar to UF_6 and PuF_6, the authors report that NpF_6 reacts vigorously with water to form NpO_2^{2+}. Trevorrow *et al.* (1968) studied the reaction of NpF_6 with sodium fluoride. In this reaction, NpF_6 reacts reversibly with sodium fluoride at 523 to 673 K according to the following reaction:

$$Na_3NpF_8(s) + 1/2F_2(g) \leftrightarrow 3NaF(s) + NpF_6(g) \tag{6.19}$$

This investigaton shows that hexavalent Np is reduced to pentavalent Np; in contrast hexavalent U reacted with NaF under the same conditions results in a hexavalent compound Na_2UF_8. Peacock and Edelstein (1976) investigated the hydrolysis of NpF_6 in anhydrous hydrogen fluoride to form $NpOF_4$. Attempts to oxidize $NpOF_4$ to Np(VII) with KrF_2 were not successful. In the same study, the investigators attempted to produce higher chlorides by an exchange reaction with BCl_3 similar to exchange reactions with uranium and tungsten. In their study, Np(VI) was reduced to Np(IV) by the following reaction:

$$3NpF_6 + 2BCl_3 \rightarrow 3NpF_4 + 3Cl_2 + 2BF_3 \tag{6.20}$$

The investigators reported that NpF_6 reacts with CsF at 298 K to produce $CsNpF_6$. Recently Eller *et al.* (1998b) studied the reactions of neptunium hexafluorides with nitrogen oxides and oxyfluorides. NpF_6 reacts with excess NO. X-ray powder diffraction pattern of a resulting green product indicated NpF_4. NpF_6 reacts with FNO under a UV lamp to produce $(NO)[NpF_6]$ confirming the earlier work of Malm *et al.* (1993). The authors did not observe any reaction between NpF_6 and FNO_2 and F_3NO even when the reaction was carried out under irradiation by UV lamp.

Np(IV), (V), (VI), and (VII) form a number of fluoro complexes. Tetravalent fluoro complexes with Li, Na, K, Rb, NH_3, Ca, Sr, and Ba have all been prepared and are well-characterized. Brown (1972) reviewed and summarized a number of preparatory methods. Examples of these compounds are shown in Table 6.7. Known pentavalent fluoro hexavalent complexes include $CsNpF_6$, Rb_2NpF_7, Na_3NpF_8, and $K_3NpO_2F_5$. Reduction of NpF_6 in contact with alkali metal fluorides or fluorination of tetravalent compounds mixed with the appropriate univalent fluoride leads to the pentavalent compounds. A selection of typical compounds of this class taken in part from a table by Brown (1972) is shown in Table 6.8. Additional information on these complexes is given by Keller (1971) and Penneman *et al.* (1973).

The known or inferred neptunium oxyfluorides are NpO_2F, $NpOF_3$, NpO_2F_2, and $NpOF_4$ (Bagnall *et al.*, 1968a; Henrion and Leurs, 1971; Drobyshevskii *et al.*, 1975, 1978; Peacock and Edelstein, 1976; Holloway and Laycock, 1984; Asprey *et al.*, 1986; Kleinschmidt *et al.*, 1992b; Eller *et al.*, 1998a). These compounds have not been extensively studied and characterized. Fried (1954) first reported the preparation of NpO_2F_2 by reacting $NaNpO_2Ac_3$ with anhydrous hydrogen fluoride at 573 to 625 K. Bagnall *et al.* (1968a) reported the preparation of the compound by reacting $NpO_3 \cdot H_2O$ and Np_2F_5 with anhydrous hydrogen fluoride at 523 to 548 K and fluorine at 603 K, respectively. The authors also reported the preparation of NpO_2F_2 by the reaction of $NpO_3 \cdot H_2O$ with fluorine at 603 K and BrF_3 at 298 K. Henrion and Leurs (1971) reported that NpO_2F_2 was an intermediate compound in the fluorination of NpO_2 with fluorine to produce NpF_6. Kleinschmidt *et al.* (1992b) prepared NpO_2F_2 by reacting NpO_2 with fluorine at 603 K and by the controlled hydrolysis of NpF_6 with trace H_2O in anhydrous hydrogen fluoride. Recently, Eller *et al.* (1998a) inferred that NpO_2F_2 was a dominant intermediate species in the preparation of NpF_6 by the reaction of O_2F_2 with NpO_2 at ambient temperature. NpO_2F_2 is a pink solid that is soluble in water and mineral acid. The crystal structure is rhombohedral and the lattice constants are shown in Table 6.6.

Peacock and Edelstein (1976) investigated the preparation of $NpOF_4$ by hydrolysis of NpF_6 with water in anhydrous hydrogen fluoride. Drobyshevskii *et al.* (1975) prepared $NpOF_4$ by reacting NpO_2 with KrF_2 in anhydrous hydrogen fluoride at ambient temperatures. Malm *et al.* (1993) reported that $NpOF_4$ was an impurity in all reported preparations of Np_2O_5.

Table 6.7 *Crystal structure and lattice constants of selected neptunium halide complexes.*

		Lattice constants			
Compound	*Symmetry*	a_0 (Å)	b_0 (Å)	c_0 (Å)	*References*
Cs_2NpCl_6	trigonal	7.46		6.03	Bagnall and Laidler (1966)
Li_4NpF_8	orthorhombic	9.91 ± 0.01	9.83 ± 0.01	5.98 ± 0.01	Jove and Cousson (1977)
Cs_2NpBr_6	cubic	11.082 ± 0.01			Magette and Fuger (1977)
$(NH_4)Np_3F_{13}$	orthorhombic	7.298 ± 0.005	7.942 ± 0.005	8.392 ± 0.005	Abazli *et al.* (1979)
$CsNpO_2Cl_2(H_2O)$	monoclinic	11.71 ± 0.02	6.99 ± 0.02	8.76 ± 0.02	Tomilin *et al.* (1986)
$Cs_2NaNpCl_6$	cubic	10.9065			Schoebrechts *et al.* (1989)

Table 6.8 *Thermodynamic Properties of Solid Neptunium Halides, Oxyhalides, and Halide Complexes at* 298.15 K.

	$\Delta_f H^\circ_m$ (kJ mol^{-1})	S°_m (J K^{-1} mol^{-1})	$\Delta_f G^\circ_m$ (kJ mol^{-1})	$C^\circ_{p.m}$ (J K^{-1} mol^{-1})
NpF_3	−1529.0 ± 8.3	130.6 ± 3.0	−1460.5 ± 8.3	94.2 ± 3.0
NpF_4	−1874.0 ± 16	148 ± 3	−1783.8 ± 16.0	116.1 ± 4.0
NpF_5	−1941.0 ± 25.0	200.0 ± 15.0	−1834.4 ± 25.4	132.8 ± 8.0
NpF_6	−1970.0 ± 20.0	229.1 ± 0.5	−1841.9 ± 20.0	167.4 ± 0.4
NpO_2F_2				103.2
Na_3NpF_8	−3514.0 ± 21.0	369.0 ± 12.0	−3521.2 ± 21.3	272.3 ± 12.0
$NpCl_3$	−896.8 ± 3.0	165.2 ± 6.0	−829.8 ± 3.0	101.9 ± 4.0
$NpCl_4$	−984.0 ± 1.8	196 ± 5	−895.6 ± 3.0	122.0 ± 6.0
$NpOCl_2$	−1030.0 ± 8.0	143.5 ± 5.0	−960.6 ± 8.1	95.0 ± 4.0
Cs_2NpCl_6	−1976.2 ± 1.9	410.0 ± 15.0	−1833.0 ± 4.9	
$Cs_3NpO_2Cl_4$	−2449.1 ± 4.8			
$Cs_2NpO_2Cl_4$	−2056.1 ± 5.4			
$Cs_2NaNpCl_6$	−2217.2 ± 3.1			
$NpBr_3$	−730.2 ± 2.9	200 ± 6	−705.5 ± 3.8	103.8 ± 6.0
$NpBr_4$	−771.2 ± 1.8	233 ± 5	−737.8 ± 3.5	128.0 ± 4.0
$NpOBr_2$	−950.0 ± 11.0	160.8 ± 4.0	−906.9 ± 11.1	98.2 ± 4.0
Cs_2NpBr_6	−1682.3 ± 2.0	469.0 ± 10.0	−1620.1 ± 3.6	
Npl_3	−512.4 ± 2.2	218 ± 5	−512.5 ± 3.7	110.0 ± 8.0

$NpOF_3$ has been prepared by reacting Np_2O_5 with anhydrous hydrogen fluoride at 313 to 333 K and dehydrating the resulting $NpOF_3$ hydrate at 373 to 423 K or by treating NpO_2 with KrF_2 in anhydrous HF (Bagnall *et al.*, 1968a; Drobyshevskii *et al.*, 1978). Compounds similar to NpO_2F have been obtained by reduction of NpO_2F_2 in hydrogen or the existence of the compound has been inferred as an intermediate in the reaction of NpO_2 with KrF_2 in anhydrous HF, respectively (Bagnall *et al.*, 1968a; Drobyshevskii *et al.*, 1975).

Neptunium tetrachloride has been prepared by at least two methods. One method is to react either neptunium oxalate or neptunium dioxide with CCl_4 at approximately 773 K (Fried and Davidson, 1951). Under these conditions, $NpCl_4$ forms and sublimes and is collected by condensation. Using a modification of this method Choporov and Chudinov (1968) reacted NpO_2 with a stream of CCl_4 vapor at lower temperatures, 553 to 673 K, to obtain $NpCl_4$. Apparently sublimation is minimal at these temperatures. Sublimation under vacuum at 633 to 653 K was used to purify their product. In the second method Bagnall and Laidler (1966) reacted $NpO_2 \cdot OH$ with hexachloropropene to obtain $NpCl_4$. They purified their product by sublimation at 923 K. $NpCl_4(g)$ condenses as a dark red or orange red deposit.

There is still uncertainty in the melting point of $NpCl_4$. Several melting points for $NpCl_4$ have been reported. Fried and Davidson (1951) reported that $NpCl_4$

melts sharply at 811 K. Later, Choporov and Chudinov (1968) using both air and salt baths reported the melting point to be (790.5 ± 2.5) K. More recently, Gruen *et al.* (1976) reinvestigated the melting point of $NpCl_4$. Using data obtained from the spectroscopically measured vapor pressures, the investigators determined that 802.9 K is the best value.

As with most of the early man-made element investigations, $NpCl_4$ was initially identified by X-ray powder diffraction. Fried and Davidson (1951) reported that the crystal structure was tetragonal with lattice parameters $a_0 = (8.25 \pm 0.01)$ Å and $c_0 = (7.46 \pm 0.01)$ Å. Recently, Spirlet *et al.* (1994) performed a complete X-ray examination of single crystals of $NpCl_4$. They confirmed that the crystal structure is tetragonal and the lattice parameters are $a_0 = 8.229$ Å and $c_0 = 7.437$ Å in reasonably close agreement with the earliest work and the crystal structure data shown in Table 6.6.

Neptunium trichloride is prepared by several methods. Fried and Davidson (1951) obtained $NpCl_3$ by reduction of NpO_2 with a mixture of hydrogen and CCl_4 at 623 to 673 K. Brown and Edwards (1972) reported the quantitative synthesis of $NpCl_3$ by reducing $NpCl_4$ with an excess of zinc. In this method, $NpCl_4$ and zinc are sealed under vacuum in a quartz tube. The reactants are heated at 823 to 873 K for 12 to 24 h. After conversion, excess zinc and $ZnCl_2$ are purified by sublimation under high vacuum away from the $NpCl_3$. $NpCl_3$ is sublimed into a clean quartz tube at 1223 to 1273 K. Attempts by Brown and Edwards (1972) to reduce $NpCl_4$ with aluminum were not successful; conversions ranged from 15 to 60%. Recently, Foropoulus *et al.* (1992) prepared anhydrous $NpCl_3$ from aqueous solutions. In their patented method, neptunium is reduced to Np(III) in a chloride solution. The solution is evaporated and the resulting residue, $NpCl_3$ hydrate, is dehydrated by contacting with thionyl chloride. The authors report that an essentially pure $NpCl_3$, ca. 98%, is obtained by their method.

Efforts to prepare higher neptunium chlorides have been unsuccessful. Heating $NpCl_4$ in chlorine at 101.3 kPa does not result in the formation of $NpCl_5$. Efforts were also made to observe the possible formation of $NpCl_5$ spectroscopically in the vapor phase by heating $NpCl_4$ in a chlorine atmosphere. At temperatures up to 1273 K no new features in the absorption spectrum were found (Fried and Davidson, 1951).

Fried and Davidson (1948) reported the preparation of neptunium tetrabromide by reaction of NpO_2 with aluminum bromide at 623 K:

$$3NpO_2 + 4AlBr_3 \rightarrow 3NpBr_4 + 2Al_2O_3 \qquad (6.21)$$

Brown and Edwards (1972) in a method identical to the method described above for the synthesis of $NpCl_3$ reported the quantitative synthesis of $NpBr_3$ by reacting $NpBr_4$ with excess zinc. Brown *et al.* (1970) prepared $NpBr_4$ by direct action of metallic neptunium and bromine. Neptunium metal and bromine were vacuum-sealed in a quartz tube. One end of the tube containing neptunium metal was heated between 673 and 698 K. $NpBr_4$ sublimed and condensed in a cooler section of the tube.

Brown *et al.* (1968) investigated the preparation of $NpBr_3$ by dehydration of $NpBr_3$ hydrates. The authors prepared the hydrates by exposing the anhydrous tribromide to oxygen-free water vapor resulting in $NpBr_3$ hexahydrate. By controlling the temperature and vacuum, the hydrate was easily converted to the anhydrous form. Previously unknown $NpBr_3$ hexahydrate was characterized using X-ray powder diffraction, radioanalytical, and gravimetric methods.

Neptunium triiodide was prepared by Fried and Davidson (1951) with aluminum iodide. Another, perhaps more convenient, method for the preparation of these halides is the direct action of hydrogen bromide/hydrogen iodide on NpO_2 at 773 K. Because the anhydrous gases (HBr and HI) are available in small, easily handled cylinders, this reaction is advantageous for laboratory preparations. The reaction products can be readily purified from unreacted NpO_2 by sublimation at the appropriate temperature. Brown and Edwards (1972) prepared the triiodide by reacting neptunium metal with excess iodine. The reactants were sealed in a tube under vacuum. The reactants were then heated at 773 K. Excess iodine was sublimed from the product, which was identified as NpI_3. Neptunium tetraiodide is predicted to be unstable (Brewer *et al.*, 1949). NpI_3 has been studied by X-ray powder diffraction and the crystal structure and lattice paramters are shown in Table 6.6.

For the synthesis of $NpBr_3$ and NpI_3 described above using aluminum halide, the aluminum halide required for these syntheses is conveniently prepared *in situ* from the elements. This method has the convenience that on the laboratory scale it is unnecessary to handle small amounts of the extremely hygroscopic aluminum halides. In this method, however, if excess aluminum is present, $NpBr_3$ is formed rather than $NpBr_4$. The reaction between NpO_2 and aluminum halide is best carried out in a sealed vessel at 623 to 673 K. Any excess aluminum halide is easily sublimed away at about 523 K. The crystal structures and lattice parameters of neptunium bromides are shown in Table 6.6.

Neptunium oxyhalides have been prepared and characterized. Fried and Davidson (1951) reported $NpOCl_2$ results when $NpCl_4$ was heated in sealed and evacuated capillary. They hypothesized that the compound was the product of the reactions of the tetrachloride with either oxygen or water impurities. The compound was investigated by X-ray powder diffraction and reported to be isostructural with $UOCl_2$. The crystal structure is shown in Table 6.6. Bagnall *et al.* (1968b) reported the synthesis of $NpOCl_2$ by reacting $NpCl_4$ and antimony sesquioxide at 673 K in a vacuum. $NpOCl_2$ can be sublimed at 823 K in vacuum. The synthesis of NpOCl has been observed during efforts to prepare $NpCl_3$ (Brown and Edwards, 1972). Pentavalent neptunium oxychlorides, $NpOCl_2$ and NpO_2Cl, are prepared by the dehydration of a solution containing chloride ions and Np(v) (LaChapelle, 1964). Brown *et al.* (1977) prepared and characterized NpOI. The oxyhalide was prepared by reacting Sb_2O_3 and NpI_3 stoichiometrically in a sealed and evacuated tube at 573 to 773 K. Product SbI_3 was sublimed away from NpOI. The crystal structure is shown in Table 6.6.

Np(III), (IV), (V), and (VI) halide complexes with both alkali metal and alkaline earth elements and ammonia are known and have been characterized (Bagnall and Laidler, 1966; Fuger and Brown, 1971; Jove and Cousson, 1977; Magette and Fuger, 1977; Abazli *et al.*, 1979; Fuger, 1979; Tomilin *et al.*, 1986; Schoebrechts *et al.*, 1989). A selection of compounds collected from the above references is shown in Table 6.7. More recently, Lemire *et al.* (2001, pp 148–53) reviewed the available chemical and thermodynamic data of the following neptunium halide complexes: Na_3NpF_8, Cs_2NpCl_6, $Cs_3NpO_2Cl_4$, $Cs_2NpO_2Cl_4$, $Cs_2NaNpCl_4$, and Cs_2NpBr_6. The information and references therein should be consulted for additional information.

Measured thermodynamic data for the halides is limited. Recently the Nuclear Energy Agency (NEA) published the exhaustive review of the published thermodynamic data (Lemire *et al.* (2001), pp 131–53) and Table 6.8 gives some of the data. In summary much of the thermodynamic data are interpolated from those of the corresponding thorium, uranium, and plutonium compounds. The thermodynamic data are collected from the recommended values in Lemire *et al.* (2001) and those adopted in Chapter 19.

6.7.4 Chalcogenides, pnictides, and carbides

Neptunium pnictides and chalcogenides have been extensively investigated primarily to understand their electronic and magnetic properties. These properties have been studied by magnetic susceptibility, Mössbauer spectroscopy, electrical resistivity, neutron and low-temperature X-ray diffraction experiments (Aldred *et al.*, 1974; Rossat-Mignod *et al.*, 1984, 1989; Burlet *et al.*, 1989; Vogt and Mattenberger, 1994; Lander and Burlet, 1995). The rock salt-type monopnictides and monochalcogenides form ideal models for studying the magnetic properties of the 5f electrons.

(a) Chalcogenides

The known sulfides and oxysulfides are NpS, NpS_3, Np_2S_5, Np_3S_5, Np_2S_3 (α-, β-, and γ-) Np_3S_4, NpOS, Np_4O_4S, and Np_2O_2S (Marcon, 1967, 1969).

NpS has been synthesized by several methods. The compound can be prepared by heating Np_2S_3 and neptunium metal at 1873 K (Marcon, 1967, 1969; Charvillat *et al.*, 1976). Bihan *et al.* (1997) prepared NpS by reacting stoichiometric amounts of the pure elements by vapor reaction in a sealed tube. Details of this method are described by Spirlet and Vogt (1984). A more facile method for preparing the compound was patented by Van Der Sluys *et al.* (1992). In their method NpS was synthesized by heating an admixture of an organometallic precursor, a suitable solvent, and a protic Lewis acid at temperature and for sufficient time to form an intermediate neptunium complex. The complex is then heated at a specific temperature and time to form the monosulfide. NpS is isostructural with PuS and US, exhibiting the NaCl-type structure with lattice parameter $a_0 = (5.532 \pm 0.001)$ Å. Bihan *et al.* (1997)

investigated the compressibility of NpS up to 60 GPa. The authors reported no phase transformation from NaCl to CsCl over the pressure range investigated.

Np_2S_3 was first prepared by treating NpO_2 with a mixture of hydrogen sulfide and carbon disulfide at 1278 K (Fried and Davidson, 1948, 1951). This compound was reported to be isostructural with U_2S_3 with lattice parameters $a_0 = (10.3 \pm 0.1)$ Å, $b_0 = (10.6 \pm 0.1)$ Å, $c_0 = (3.86 \pm 0.5)$ Å (Zachariasen, 1949a, b). Marcon (1967) obtained α-Np_2S_3 by thermal dissociation of Np_3S_5 at 1200 K. The compound is orthorhombic and isotypic with α-Pu_2S_3 and α-Ce_2S_3 with lattice parameters $a_0 = (3.98 \pm 0.01)$ Å, $b_0 = (7.39 \pm 0.02)$ Å, $c_0 = (15.50 \pm 0.03)$ Å. At about 1500 K, α-Np_2S_3 transforms into tetragonal β-Np_2S_3, isotypic with β-Pu_2S_3 and Ce_5S_7, $a_0 = (14.94 \pm 0.02)$ Å, $c_0 = (19.84 \pm 0.02)$ Å. Finally, around 1800 K, change to the cubic Np_2S_3 (γ) with the structure of the Th_3P_4-type occurred ($a_0 = 8.440 \pm 0.001$ Å) (Marcon, 1967). The γ-form can also have the composition of Np_3S_4 (Damien and Berger, 1976). Np_3S_4 was obtained after the heat treatment described above by Charvillat *et al.* (1976). Np_3S_4 is cubic with a lattice parameter of $a_0 = 8.440$ Å.

Np_3S_5 was obtained by thermal decomposition of NpS_3 at 773 K (Marcon, 1967, 1969; Marcon and Pascard, 1968). Blaise *et al.* (1982) reported the preparation of Np_3S_5 by reaction of the appropriate chalcogen and neptunium hydride at 923 K. Np_3S_5 is isostructural with U_3S_5 with lattice parameters $a_0 = (7.42 \pm 0.01)$ Å, $b_0 = (8.07 \pm 0.01)$ Å, $c_0 = (11.71 \pm 0.02)$ Å.

Np_2S_5 is prepared by heating mixtures of Np_3S_5 and sulfur at 773 K (Marcon, 1967, 1969). The crystal structure is tetragonal ($a_0 = (10.48 \pm 0.01)$ Å, $c_0 = (9.84 \pm 0.1)$ Å), and isotypic with Th_2S_5, Th_2Se_5, and U_2S_5.

NpS_3 was prepared from the elements at 773 K by Marcon (1967, 1969). NpS_3 is monoclinic with lattice parameters $a_0 = (5.36 \pm 0.01)$ Å, $b_0 = (3.87 \pm 0.01)$ Å, $c_0 = (18.10 \pm 0.05)$ Å, $\beta = 99.5°$ and isostructural with US_3, USe_3, UTe_3, $NpSe_3$, and $NpTe_3$.

The three oxysulfides NpOS, Np_2O_2S, and $Np_4O_4S_3$ have been reported (Zachariasen, 1949b; Marcon, 1969). Only NpOS has been extensively studied (Thevenin *et al.*, 1985; Collard *et al.*, 1986). Thevenin *et al.* (1985) prepared NpOS by vacuum sealing and heating NpO_2, Np_3S_5, and sulfur in a quartz tube to 1073 K for 1 week. NpOS is tetragonal with lattice parameters $a_0 = b_0 = 3.808$ Å and $c_0 = 6.627$ Å. $Np_4O_4S_3$ and Np_2O_2S were prepared and characterized by Marcon (1969) and Zachariasen (1949b). Hexagonal Np_2O_2S is isostructural with the actinide and lanthanide oxysulfides of the same composition (Zachariasen, 1949b; Haire and Fahey, 1977). Hoffman and Kleykamp (1972) have presented an extensive review of the preparation and properties of these sulfides and oxysulfides.

Known neptunium selenides and oxyselenides are NpSe, Np_3Se_4, γ-Np_2Se_3, Np_2Se_5, Np_3Se_5, $NpSe_3$, NpOSe, and Np_2O_2Se. These compounds have been prepared and characterized by Mitchell and Lam (1971), Damien and Wojakowski (1975), Damien *et al.* (1973), Charvillat *et al.* (1976), and Thevenin and Pagès (1982).

Damien and Wojakowski (1975) and Charvillat *et al.* (1976) obtained NpSe by reacting neptunium hydride with a stoichiometric amount of selenium metal. The reactants, sealed in a quartz tube under vacuum, were heated at 800 K for 24 h. The investigators reported that NpSe crystallizes in the NaCl-type structure with lattice constant $a_0 = (5.804 \pm 0.002)$ Å for samples heated between 1593 and 1783 K. Gensini *et al.* (1993) reported that the selenide transforms from the NaCl to CsCl structure at 23 GPa.

Mitchell and Lam (1971) investigated the alloying behavior of neptunium and selenium and obtained Np_3Se_4. Neptunium and selenium were sealed, in vacuum, in a quartz ampoule. The reactants were heated to the melting point of selenium, 494 K, then heated to and maintained at 1273 K for 5 to 24 h. The final steps in the procedure held the ampoule at 773 K for 15 to 22 days followed by furnace cooling and X-ray diffraction analysis. Damien *et al.* (1973) obtained this phase by decomposition of Np_3Se_5 at 1123 K at high vacuum. After heating at 1323 K and apparently cooling, the lattice parameter decreased from $a_0 = (8.8242 \pm 0.0002)$ to (8.8223 ± 0.0003) Å similar to the cubic structure lattice constant $a_0 = (8.8261 \pm 0.00\,02)$ Å reported by Mitchell and Lam (1971). Damien *et al.* (1973) could not determine if the composition of their product was γ-Np_2Se_3 or Np_3Se_4.

Damien *et al.* (1973) obtained Np_3Se_5 by thermal dissociation of $NpSe_3$ at 693 K in vacuum. Blaise *et al.* (1982) prepared Np_3Se_5 by heating the appropriate amounts of chalcogen with neptunium hydride at 923 K. The crystal structure is orthorhombic and the lattice parameters are $a_0 = (7.75 \pm 0.01)$ Å, $b_0 = (8.43 \pm 0.01)$ Å, and $c_0 = (12.24 \pm 0.02)$ Å. The compound is isostructural with U_3S_5, U_3Se_5, and Np_3S_5.

Np_2Se_5 is prepared either by thermal decomposition of $NpSe_3$ at 823 K for 2 weeks or by reaction of neptunium hydride and selenium metal at 753 K. Both preparations are performed in sealed and evacuated quartz tubes (Thevenin and Pagaès, 1982). The compound has an orthorhombic (pseudotetragonal) crystal structure with lattice parameters $a_0 = b_0 = 7.725$ Å and $c_0 = 10.6225$ Å.

$NpSe_3$ was synthesized by Damien *et al.* (1973) by reaction of neptunium hydride with excess selenium sealed in a quartz tube under vacuum and heating at 620 K for 1 week. Blaise *et al.* (1982) prepared $NpSe_3$ by reacting chalcogen with neptunium hydride at 1273 K. The investigators identified $NpSe_3$ by X-ray powder diffraction pattern to be analogous to that of USe_3. The triselenide crystal structure is monoclinic with lattice constants: $a_0 = (5.64 \pm 0.02)$ Å, $b_0 = (4.01 \pm 0.01)$ Å, $c_0 = (19.06 \pm 0.07)$ Å, $\beta = (79.60 \pm 20)°$.

The known oxyselenides are NpOSe and Np_2O_2Se (Marcon, 1969). Only NpOSe has been investigated (Thevenin *et al.*, 1985). Thevenin *et al.* (1985) prepared NpOSe by vacuum sealing and heating NpO_2 and Np_2Se_5 to 1073 K for 1 week. NpOSe is tetragonal with lattice parameters $a_0 = b_0 = 3.869$ Å and $c_0 = 6.911$ Å. The known neptunium tellurides and oxytellurides are NpTe, Np_3Te_4, $NpTe_3$, $NpTe_{2-x}$, $\eta\gamma$-Np_2Te_3, and Np_2O_2Te.

Damien and Wojakowski (1975) and Charvillat *et al.* (1976) obtained a two-phase NpTe product by reacting neptunium hydride with a stoichiometric amount of tellurium metal sealed in a quartz tube under vacuum at 800 K for 24 h. The product formed was made into a pellet, heated at 1563 K for 4 h in a sealed quartz tube under vacuum, cooled, and examined by X-ray diffraction. Under these circumstances the investigators determined that NpTe crystallizes in the NaCl-type structure with lattice constant $a_0 = (6.197 \pm 0.0001)$ Å. Dabos-Seignon *et al.* (1990) investigated X-ray diffraction patterns of NpTe at pressures up to 51 GPa. The investigators reported that NpTe maintains the NaCl structure to 12 GPa where CsCl-type structure began to appear. Only the CsCl-type structure exists above 20 GPa.

Mitchell and Lam (1971), investigating the alloying behavior of neptunium and tellurium, obtained Np_3Te_4. Neptunium and tellurium were vacuum-sealed in a quartz ampoule. The reactants were heated to the melting point of tellurium, 494 K, then heated to and maintained at 1273 K for 5 to 24 h. The final step in the procedure held the ampoule at 772 K for 15 to 22 days. The lattice constant for the cubic structure was reported to be $a_0 = (8.8261 \pm 0.0002)$ Å (Mitchell and Lam, 1971).

Blaise *et al.* (1976), investigating magnetic properties of some neptunium chalcogenides, prepared $NpTe_3$ by reacting tellurium with neptunium hydride at 628 K. $NpTe_3$ is isostructural with rare earth tritellurides with the lattice parameters $a_0 = b_0 = 4.355$ Å and $c_0 = 25.40$ Å in agreement with literature values (Damien and Berger, 1976).

Thevenin *et al.* (1985) investigated the preparation and crystal structure of Np_2O_2Te. The investigators obtained Np_2O_2Te by reacting Np_2Te_3 and NpO_2 in a vacuum-sealed quartz tube at 1273 K for 1 week. The black compound is tetragonal with lattice constants $a_0 = b_0 = 4.003$ Å, $c_0 = 12.73$ Å and is isostructural with U_2O_2 Te and Pu_2O_2Te.

(b) Pnictides

Neptunium pnictides have been studied because of their solid state properties and relationship to advanced reactor fuels. Neptunium nitride, NpN, was prepared by Sheft and Fried (1953) who reacted ammonia gas and neptunium hydride at 1023 to 1048 K in a quartz X-ray capillary tube. Later preparations by Olson and Mulford (1966), De Novion and Lorenzelli (1968), and Aldred *et al.* (1974) reacted neptunium metal with a mixture of nitrogen and hydrogen at temperatures to 1773 K, NpH_{2+x} with nitrogen at temperatures to 1873 K, and NpH_3 with nitrogen at temperatures between 573 and 623 K, respectively.

In the method of Olson and Mulford (1966) neptunium filings were heated in a tungsten vee with nitrogen 0.5% in hydrogen as a catalyst. The reaction started at 873 K and upon apparent completion the temperature was brought to 1783 K. Gaseous neptunium hydride and neptunium were removed by pumping. De Novion and Lorezelli (1968) directly reacted nitrogen with NpH_{2+x} at 673 K, while Aldred *et al.* (1974) reacted NpH_3 with nitrogen at 573 to 623 K for 5 h. The powder product was formed into pellets and heated at 1273 K for 2.5 h. More recently, Suzuki *et al.* (1994) synthesized NpN by a high temperature, 1823 K, carbothermic reduction of NpO_2 in a stream of N_2 gas. The crystal structure is NaCl-type (fcc) and the lattice parameter is $a = (4.8968 \pm 0.005)$ Å which agrees well with values reported in the literature (Olson and Mulford, 1966; De Novion and Lorenzelli, 1968). NpN is isomorphous with UN and PuN, reacts slowly with dilute hydrochloric and nitric acids, and appears to be relatively inert toward water (Sheft and Fried, 1953). The melting point of NpN has been determined to be 3103 K under a nitrogen pressure of ca. 1 MPa (Olson and Mulford, 1966). There is very little thermodynamic data reported for NpN. Arai *et al.* (1994) derived the following equation for the heat capacity of NpN: $C_p\,(\text{J mol}^{-1}\,\text{K}) = 52.85 + 2.55 \times 10^{-3}T - 8.37 \times 10^{5}T^{-2}$. Suzuki and Arai (1998) reviewed and investigated some thermal and thermodynamic properties of NpN. They reported the free energy of formation to be $\Delta G_f\ (\text{J mol}^{-1}) = 427\,000 - 98.88T(1700\text{–}2100\ \text{K})$.

Lander *et al.* (1973) prepared neptunium monophosphide by a hydriding, dehydriding, and nitriding technique. First the metal is converted to powder by hydriding and dehydriding. Then the powder reacted with phosphine gas at 623 K. NpP is single-phase fcc. The lattice parameter is (5.614 ± 0.001) Å. A compound with the formula, Np_3P_4, is formed by reacting an excess of red phosphorus with neptunium metal at 1013 K in an evacuated and sealed quartz tube (Sheft and Fried, 1953). Excess phosphorus is removed by sublimation in vacuo at 1073 K. The compound does not react with water but does react with 6 M HNO_3 to yield dark-green Np(IV) solution.

$NpAs_2$ and NpAs are prepared by reacting stoichiometrically arsenic and neptunium hydride in a vacuum-sealed tube for 1 week (Charvillat and Damien, 1973; Blaise *et al.*, 1981). In this method NpAs was synthesized at 923 K and $NpAs_2$ synthesized at 723 K. Dabos *et al.* (1986) synthesized NpAs by reacting arsenic vapor and neptunium metal turnings in a vacuum-sealed quartz tube. In this method, the reactants are separated by a quartz membrane and heated to just below the melting point of neptunium metal: arsenic sublimes at 886 K and the melting point of neptunium is 903 K. X-ray studies show that NpAs has the cubic NaCl structure with the lattice parameter $a_0 = (5.8338 \pm 0.0002)$ Å (Charvillat and Damien, 1973). $NpAs_2$ is tetragonal, anti-Fe_2As type with lattice parameter $a_0 = (3.962 \pm 0.001)$ Å, $b_0 = (8.115 \pm 0.002)$ Å (Charvillat and Damien, 1973; Blaise *et al.*, 1981). Wojakowski and Damien (1982) reported the preparation of single crystals of both $NpAs_2$ and Np_3As_4 using iodine as a transporting agent in a transport reaction process in sealed quartz tubes. The investigators reported that $NpAs_2$ single crystals are more stable in air than powder material. $NpAs_2$ crystals are brown to gold and Np_3A_4 are black in color. The reported lattice parameters are in agreement with literature values.

NpSb was prepared by an isothermal annealing technique (Mitchell and Lam, 1971). In this technique, equal atomic percentages of neptunium and 99.999%

pure antimony were sealed in a quartz tube under vacuum, and the mixture was heated at the melting temperature of antimony. The temperature was then raised to 1000°C, held at this temperature for 16 days, and then cooled. In all samples, traces of Np_3Sb_4 were present (Aldred *et al.*, 1974).

There are limited reports for the preparation and characterization of NpBi. Aldred *et al.* (1974) attempted to prepare the compound by reaction of the elements at 1273 K for 16 days and was not successful. Attempts to prepare single crystals of NpBi by Burlet *et al.* (1992) using the mineralization method described by Spirlet and Vogt (1984) were successful.

(c) Carbides

The neptunium compounds NpC, Np_2C_3 and NpC_2 have been reported in the literature with limited characterization. This is unfortunate because of the importance of carbides as advanced reactor fuels. Holley *et al.* (1984) reviewed the earlier literature and determined that two phases had been identified and that the identification of NpC_2 was tentative. Nevitt (1963) reported that the monocarbide exists in the range of $NpC_{0.82}$ to $NpC_{0.96}$. De Novion and Lorenzelli (1968) prepared $NpC_{0.95}$ by heating a mixture of neptunium hydride and graphite to 1673 K. Sandenaw *et al.* (1973) prepared $NpC_{0.91}$ by arc melting the elements using a tungsten electrode. Sheft and Fried (1953) reported the syntheses of NpC_2 by heating NpO_2 at various temperatures between 2933 and 3073 K in a graphite crucible. When an attempt is made to prepare neptunium metal by reaction of lithium vapor on NpF_3 in a graphite crucible at 1373 K, the reaction yields a mixture of NpC and Np_2C_3. When NpC reacts with excess carbon it forms a pure phase with the composition of Np_2C_3 (Lorenzelli, 1968). Sandenaw *et al.* (1973) measured the heat capacity of $NpC_{0.91}$. Holley *et al.* (1984) and Lemire *et al.* (2001), pp 201–2 reviewed the very limited thermodynamic properties of neptunium carbides.

6.7.5 Other inorganic compounds

Many other inorganic neptunium compounds have been synthesized and characterized. Interest has been shown in the preparation and characterization of phosphates, sulfates, and carbonates. The stability of phosphates makes them a candidate for immobilizing radioactive waste (Bamberger *et al.*, 1984; Volkov *et al.*, 1994). Bamberger *et al.* (1984) reported the preparation of green neptunium pyrophosphate, α-NpP_2O_7, by reacting NpO_2 and BPO_4 at 1373 K. The lattice parameter for the cubic compound was (8.593 ± 0.002) Å. Attempts to prepare $Np_3(PO_4)_4$ by a similar reaction were unsuccessful. Volkov *et al.* (1994) studied a series of double phosphate of neptunium with the formula $NpA_2(PO_4)_3$ where A = Li, Na, K, Rb, Cs. The compounds were synthesized by heating the appropriate mixtures of NpO_2, LiOH, $N(K)H_2PO_4$, $Rb(Cs)NO_3$, and H_3PO_4 at 373 to 573 K for 5 h followed by annealing in air from 773 to

1923 K. Monoclinic and trigonal crystalline structures were identified for the double phosphates containing the cations Li^+, Na^+, and K^+. Transitions from the monoclinic to trigonal phases for $NaLi_2(PO_4)_3$, $NaNa_2(PO_4)_3$, and $NaK_2(PO_4)_3$ occurred at 1723, 1623, and 1423 K, respectively. Only the trigonal phase was reported for both $NpRb_2(PO_4)_3$ and $NpCs_2(PO_4)_3$ and the latter compound formed an unidentified high-temperature phase.

A number of neptunium sulfates have been synthesized and characterized. The most recent studies of solid neptunium sulfates are by Weigel and Hellmann (1986) and Budantseva *et al.* (1988). Neptunium hydroxysulfate was synthesized and characterized by Wester *et al.* (1982).

Preparation and characterization of neptunium carbonates is essential to research conducted to understand neptunium behavior in geologic repositories and the environment. Radionuclides placed in repository, particularly the long-lived radiotoxic actinides, may contact carbonate and bicarbonate containing water, forming soluble complexes. Recognizing this concern and the need for research, Clark *et al.* (1995) and Lemire *et al.* (2001, pp 203–83) have exhaustively reviewed the available literature on neptunium carbonates.

6.7.6 Coordination compounds

Interest in the coordination chemistry of neptunium compounds is enhanced by the unique properties of each of the five oxidation states of neptunium and by the changes in coordination chemistry caused by decreasing ionic size across the actinide series. Therefore a number of compounds of neptunium and various ligands have been prepared to characterize neptunium coordination chemistry. A selected listing of these compounds and some reported crystal structures and lattice parameters are given in Table 6.9.

There is little published information of Np(III) coordination compounds. According to Mefod'eva and Gel'man (1971) the reason is in the instability of Np(III) in aqueous solutions to atmospheric oxygen. These investigators, however, reported the reduction of Np(IV) to Np(III) by sodium formaldehyde sulfoxylate, $NaHSO_2 \cdot CH_2O \cdot 2H_2O$. Apparently this compound stabilizes Np(III) and allows the formation of sparingly soluble compounds such as $Np_2(C_2O_4)_3 \cdot nH_2O(n = 11)$, $Np_2(C_6H_5AsO_3)_3 \cdot H_2O$ and $Np_2[C_6H_4(OH)COO]_3$. These compounds were formed by the addition of oxalic acid, phenylarsonic acid, or ammonium salicylate to solutions containing Np(III) reduced by $NaHSO_2 \cdot Ch_2O \cdot 2H_2O$. Atmospheric oxygen was removed from reagent solutions by argon purges and/or covering solutions with benzene. The precipitates were dried with ether and/or acetone and streams of argon.

A number of Np(IV) coordination compounds have been reported. Al-Kazzaz *et al.* (1972) prepared $(Et_4N)Np(NCS)_8$, where Et_4N = tetraethyl ammonium, which is isostructural with the uranium analog. Cousson *et al.* (1985) obtained $CoNp_2F_{10} \cdot 8H_2O$ and $CuNp_2F_{10} \cdot 6H_2O$. The investigators, using the method of Abazli *et al.* (1984), mixed and powdered transition metal cobalt or copper

Table 6.9 *Lattice parameters of selected neptunium coordination compounds.*

Compound	*Symmetry*	*Space group*	*Lattice constants*			Angle (deg)	*References*
			a_0 (Å)	b_0 (Å)	c_0 (Å)		
Np(III)							
$Np_2(C_2O_4)_3{\cdot}nH_2O$							Mefod'eva and Gel'man (1971)
$Np_2(C_6H_5A_5O_3)_3{\cdot}nH_2O$							Mefod'eva and Gel'man (1971)
$Np_2[C_6H_4(OH)COO]_3$							Mefod'eva and Gel'man (1971)
Np(IV)							
$(Net_4)Np(NCS)_8$			11.6		22.89		Al-Kazzaz *et al.* (1972)
$CoNp_2F_{10}\cdot 8H_2O$		$P2_1/a$	8.803	7.04	11.066	94.12	Cousson *et al.* (1985)
$CuNp_2F_{10}{\cdot}6H_2O$		C_2/c	19.043	7.128	8.593	96.63	Cousson *et al.* (1985)
$NpCl_2{\cdot}P(i\text{-}C_4H_9)_3O$							Bagnall *et al.* (1985)
$NpCl_4CH_3CON(i\text{-}C_3H_7)_2$							Bagnall *et al.* (1985)
$NpCl_4{\cdot}2.5HCON(CH_3)$							Bagnall *et al.* (1985)
$NpCl_4{\cdot}3.5P(CH_3)(C_6H_5)_2O$							Bagnall *et al.* (1985)
$Np(NO_3){\cdot}C_{10}H_{10}N_2(NO_3){\cdot}2H_2O$		$P1/2$	8.445	9.013	11.87	102.56	Grigor'ev *et al.* (1986a)
$(C_{10}H_{10}N_2)[NP(NO_3)]{\cdot}2H_2O$		$Pna2_1$	15.61	10.19	14.799		Grigor'ev *et al.* (1987)
Np(V)							
$Na_4(NpO_4)_2C_{12}O_{12}{\cdot}8H_2O$		C_2/c	12.53	11.58	17.81	105.79	Cousson *et al.* (1984)
$(NpO_2)_2CH_2(CO_2)_2{\cdot}1H_2O$							
$(NpO_2)_2CH_2(CO_2)_2{\cdot}3H_2O$		$P2_1$	6.596	8.32	10.308	90.24	Grigor'ev *et al.* (1993b)

$(NpO_2)_2CH_2(CO_2)_2 \cdot 4H_2O$	monoclinic	$P2_1/n$	8.84	15.475	9.07	114.51	Krot *et al.* (1993)
$NH_4NpO_2CH_2(CO_2)_2$		$P2_1/c$	7.703	13.02	7.704	111.08	Krot *et al.* (1993)
$CsNpO_2CH_2(CO_2)_2$		$P2_1/m$	9.184	13.636	7.45	101.97	Krot *et al.* (1993)
$NaNpO_2CH_2(CO_2) \cdot 2H_2O$	monoclinic	$P2_1/n$	12.935	7.645	7.968	97.09	Krot *et al.* (1993)
$NpO_2OOCH \cdot H_2O$							
$NpO_2OOCCH_3 \cdot H_2O$							
$NpO_2SO_3NH_2 \cdot H_2O$			9.067	5.439	12.184		Budantseva *et al.* (1989)
$Cs[NpO_2(SO_4)_2] \cdot 2H_2O$		$P1$	7.522	9.954	10.71	82.24	Grigor'ev *et al.* (1991c)
$[Co(NH_3)_6][NpO_2(SO_4)_2] \cdot 2H_2O$		*Pnma*	17.48	7.143	12.515		Grigor'ev *et al.* (1991b)
$[Co(NH_3)_6]H_8O_3[NpO_2(SO_4)_3]$		*Pbca*	19.437	14.595	12.744		Grigor'ev *et al.* (1991b)
$(NpO_2)_2SO_4 \cdot H_2O$		*Pnma*	15.79	6.932	6.714		Grigor'ev *et al.* (1993c)
$Cs_4(NpO_2)_3Cl_6(NO_3) \cdot H_2O$		$Cmc2_1$	19.6	13.26	8.54		Tomilin *et al.* (1986)
Np(VI)							
$NpO_2C_2O_4$							Mefod'eva *et al.* (1969)
$(NH_4)NpO_2(CO_3)_3$							Marquart *et al.* (1983)
Np(VII)							
$LiCo(NH_3)_6Np_2O_8(OH)_2 \cdot 2H_2O$	monoclinic	C_2/c	10.739	10.45	15.013	116.38	Burns *et al.* (1973)
$NaCo(NH_3)_6Np_2O_8(OH_2) \cdot 2H_2O$			10.865	10.597	14.867	115.13	Burns *et al.* (1973)
$Co(NH_3)_6NpO_4(OH)_2 \cdot 2H_2O$		$P2_1/c$	6.778	8.449	12.448	119.3	Burns *et al.* (1973)
$CsNpO_2Cl_2(H_2O)$	monoclinic	$P2_1(P2_1/n)$	11.71	6.99	8.76	93.1	Tomilin *et al.* (1986)

difluorides and NpF_4. The mixtures were placed into gold tubes with a few drops of 40% HF. The tubes were sealed, placed in an autoclave, the pressure was adjusted to 152 MPa, and temperature increased to the desired reaction temperatures. The cobalt- and copper-containing compounds are reportedly formed at 400 and 600 K, respectively. Bagnall *et al.* (1985) reported the preparation of $NpCl_2 \cdot P(i\text{-}C_4H_9)_3O$, $NpCl_4 \cdot CH_3CON(i\text{-}C_3H_7)_2$, $NpCl_4 \cdot 2.5HCON(CH_3)$, and $NpCl_4 \cdot 3.5P(CH_3)(C_6H_5)_2O$. These compounds were obtained by mixing suspensions of Cs_2NpCl_6 in dichloromethane with the appropriate phosphine oxides and amides by stirring for 7 days and evaporating the solution to dryness. Complex nitrate compounds have been formed. Grigor'ev *et al.* (1986a) prepared $Np(NO_3)_4 \cdot 2C_{10}H_{10}N_2(NO_3)_2 \cdot 2H_2O$ with the intent of investigating the separation of Np(IV) as a more complicated compound. Grigor'ev *et al.* (1987) also prepared the Np(IV) coordination compound $(C_{10}H_{10}N_2)[Np(NO_3)_6] \cdot 2H_2O$. In both nitrate complex studies, the investigators formed single crystals by slow ambient temperature evaporation of solutions of Np(IV) in concentrated HNO_3 and excess 2,2′-pyridine.

The coordination chemistry of Np(V) compounds was stimulated by the discovery of the so-called cation–cation interaction in the solid state by Cousson *et al.* (1984). Interestingly, cation–cation interactions with actinyl ions in solution have been known since 1961 (Sullivan *et al.*, 1961). Cousson *et al.* (1984) obtained the neptunyl dimer, $Na_4(NpO_4)_2C_{12}O_{12} \cdot 8H_2O$, by dissolving neptunyl hydroxide in an aqueous solution of benzenehexacarboxylic acid (mellitic acid). The resulting solution was adjusted with NaOH to a pH of approximately 6.5 and was slowly evaporated, producing green crystals. The investigators reported, based on diffraction studies, the distance between the two neptunium atoms to be 3.4824 Å. Krot *et al.* (1993) and Grigor'ev *et al.* (1993a,b) synthesized and characterized Np(V) malonates and neptunyl malonate hydrates; $(NpO_2)_2CH_2(CO_2)_2 \cdot xH_2O$ where $x = 1, 3, 4$ and $MNpO_2CH_2(CO_2)_2$ where $M = NH_4$ or Cs and $NaNpO_2CH_2(CO_2) \cdot 2H_2O$. Grigor'ev *et al.* (1989) and Logvis' *et al.* (1994) prepared neptunyl formate, $NpO_2OOCH \cdot H_2O$, by reacting NH_4OOCH and HCOOH with a neptunyl(V) nitrate solution. Charushnikova *et al.* (1995) and Grigor'ev *et al.* (1995) prepared neptunyl glycolate by dissolving freshly prepared neptunyl hydroxide into excess glycolic acid and evaporation of the resulting solution until green crystals formed. In the same study Charushnikova *et al.* (1995) precipitated neptunyl trichloroacetate by dissolving the freshly prepared neptunyl hydroxide in equimolar amounts of trichloroacetic acid. The acetate, $NpO_2OOCCH_3 \cdot H_2O$, was obtained either by dissolving freshly prepared neptunyl(V) hydroxide in excess glacial acetic acid and collection of a resulting green precipitate by filtration or by the addition of $NaOOCH_3$ to a solution of Np(V) which had been adjusted to a pH of 4 to 5 with ammonia and collection of the resulting precipitate by filtration (Bessonov *et al.*, 1989b). Charushnikova *et al.* (1992) obtained neptunyl benzoate in a similar manner to the acetate. Ammonium benzoate was added to a solution of Np(V) which had been adjusted to a pH of 4 to 5 with ammonia water. Several oxalate compounds have been prepared and characterized (Jones and Stone, 1972; Tomilin *et al.*, 1984). Grigor'ev *et al.* (1991a) reported the results of their study on two complex neptunium(V) oxalates; $[Co(NH_3)_6][NpO_2(C_2O_4)_2] \cdot nH_2O$ where $n = 3$ and 4. Single crystals of each compound formed were a function of the concentrations of $C_2O_4^{2-}$ and Np(V). Budantseva *et al.* (1989) synthesized and studied some of the properties of neptunyl sulfamate monohydrate. The air-stable compound, $NpO_2SO_3NH_2 \cdot H_2O$, was obtained by eluting Np(V) from a cation-exchange resin in the neptunyl form with sodium sulfamate. The eluent was evaporated in a stream of air at 298 K. Attempts to prepare single crystals were not successful. Simple and complex neptunyl sulfate complexes have been prepared and characterized (Grigor'ev *et al.*, 1991b,c, 1993c). The lattice parameter for these compounds are given in Table 6.9. Saeki *et al.* (1999) studied the correlation between isomer shifts of ^{237}Np Mössbauer spectra and coordination numbers of neptunium atoms in some Np(V) compounds.

Np(VI) coordination compounds include simple compounds such as $NpO_2C_2O_4$ (Mefod'eva *et al.*, 1969) and complex compounds such as $(NH_4)_4NpO_2(CO_3)_3$ (Marquart *et al.*, 1983). The oxalate was obtained by adding oxalic acid to a nitric acid solution of Np(VI) containing $KBrO_3$. The resulting compound is not stable, Np(VI) is reduced to Np(IV) after storage even at cold temperatures. Green $(NH_4)_4NpO_2(CO_3)_3$ was prepared by adding an excess of $(NH_4)_2CO_3$ to a nitric acid solution containing Np(VI). Hexavalent actinide complexes of the formula $M_4AnO_2(CO_3)_3$ (An=U, Np, Pu; M = single valent cation) have been extensively studied (Clark *et al.*, 1995).

Since the discovery of Np(VII) (Krot and Gel'man, 1967) several Np(VII) coordination compounds have been prepared and studied. Krot *et al.* (1968b,c) reported the preparation of a compound with the formulation $Co(NH_3)_6NpO_5 \cdot nH_2O$. Later, Burns *et al.* (1973) suggested the formulation should be $[Co(NH_3)_6][NpO_4(OH)_2] \cdot 2H_2O$ following their efforts to experimentally demonstrate the existence of $[NpO_4(OH)_2]^{3-}$ as the form of Np(VII) in alkaline solution. The investigators, using the method proposed by Krot *et al.* (1968a), precipitated $[Co(NH_3)_6][NpO_4(OH)_2] \cdot 2H_2O$ by the simultaneous dropwise addition of solutions of $Co(NH_3)_6Cl_3$ and Np(VII) in LiOH to a stirred solution of LiOH. In the same study Burns *et al.* (1973) reported the preparation of $LiCo(NH_3)_6Np_2O_8(OH)_2 \cdot 2H_2O$ by slowly diffusing a LiOH solution of Np (VII) into a solution of $Co(NH_3)_6Cl_3$. The investigators also prepared an analog containing sodium from NaOH solution of Np(VII) but attempts to prepare a potassium analog from Np(VII) in KOH was unsuccessful. Apparently, the formation of $[Co(NH_3)_6][NpO_4(OH)_2] \cdot 2H_2O$ or $LiCo(NH_3)_6Np_2O_8(OH)_2 \cdot 2H_2O$ is dependent on rapid precipitation vs slow diffusion, respectively. Grigor'ev *et al.* (1986b) obtained large single crystals of $Co(NH_3)_6NpO_4(OH)_2 \cdot 2H_2O$ by mixing a LiOH solution of Np(VII) with a LiOH solution containing small excess of $Co(NH_3)_6Cl_3$ and placing the mixture into a cooler for several hours. The resulting prismatic crystals were dark green and a maximum length of the edge 0.15–0.4 mm. The crystal structure and lattice parameters are given in Table 6.9. Nakamoto *et al.* (1999) reported the ^{237}Np Mössbauer spectroscopic study of $Co(NH_3)_6NpO_4(OH)_2 \cdot 2H_2O$. The preparation and some properties of $[Pt(NH_3)_5Cl]NpO_5 \cdot nH_2O$ (where $n =$ ca. 1) were reported by Krot *et al.* (1968b). Blackish-green $[Pt(NH_3)_5Cl]NpO_5 \cdot nH_2O$ was obtained by adding a saturated solution of $[Pt(NH_3)_5Cl]Cl_3$ to a basic solution of Np(vii). Mefod'eva *et al.* (1970a,b) synthesized $[CoEn_3]NpO_5 \cdot 3H_2O$ (where En = ethylenediamine) using a method similar to the preparation described above for the preparation of $[Co(NH_3)_6][NpO_4(OH)_2] \cdot 2H_2O$ modified to use more concentration solutions because of the solubility of $[CoEn_3]NpO_5 \cdot 3H_2O$. The precipitates formed are thin green plate-like crystals, which decompose to a brown-colored material after stored for 5 to 6 days in a dry desiccator.

6.7.7 Important organometallic compounds

Neptunium organometallic compounds have been prepared and characterized, but not nearly to the extent of uranium organometallics. A survey of the literature produced a limited number of well-characterized neptunium organometallics. The radioactive hazard associated with neptunium and its scarcity are two reasons for the scarcity of published information. Most investigations reported to date deal with the preparation of neptunium cyclopentadienyl and cyclooctatetraenyl compounds and derivatives of these compounds. These compounds have been extensively reviewed (Gysling and Tsutsui, 1970; Hayes and Thomas, 1971; Legin, 1979; Marks and Ernest, 1982; Mishin *et al.*, 1986). The synthesis, characterization, and catalytic processes of organometallic actinides are discussed in Chapters 25 and 26.

(a) Cyclopentadienyl compounds

A trivalent neptunium cyclopentadienyl complex was synthesized and characterized by Karraker and Stone (1972). The complex is formed by the reduction of $Np(C_5H_5)_3Cl$ with sodium:

$$Np(C_5H_5)_3Cl + Na \rightarrow Np(C_5H_5) \cdot 3THF + NaCl \qquad (6.22)$$

Attempts to obtain $Np(C_5H_5)$ by heating and vacuum to remove tetrahydrofuran (THF) were unsuccessful.

Tetravalent neptunium tetracyclopentadienyl was prepared and characterized by Baumgartner *et al.* (1968). The complex was prepared by reacting $NpCl_4$ with KC_5H_5 in benzene under reflux for 160 h:

$$NpCl_4 + 4KC_5H_5 \rightarrow Np(C_5H_5)_4 + 4KCl \qquad (6.23)$$

The reddish-brown complex dissolved in benzene and THF. The authors reported that the compound is less sensitive to oxygen and water than $Pu(C_5H_5)_3$ and $Am(C_5H_5)_3$.

Other Np(IV) cyclopentadienyl compounds have been prepared and characterized. Two reactions have been reported for the preparation of tricyclopentadienyl chloride, $(C_5H_5)_3NpCl$. Fischer *et al.* (1966) prepared the compound by reacting NpX_4 (X = Cl, F) with potassium cyclopentadienyl, $3K(C_5H_5)$, in THF. Later Karraker and Stone (1972) prepared the compound by reacting $NpCl_4$ with beryllium cyclopentadienyl. Equations describing the two reactions are:

$$NpX_4 + 3K(C_5H_5)_4 \rightarrow Np(C_5H_5)_3X + 3KX \tag{6.24}$$

$$2NpCl_4 + 3BeC_5H_5 \rightarrow 2Np(C_5H_5)_3Cl + 3BeCl_2 \tag{6.25}$$

A number of derivatives can be prepared starting with tetrakiscyclopentadienyl Np(IV), $Np(C_5H_5)_4$, and tris(cyclopentadienyl)Np(IV) chloride, $(C_5H_5)_3NpCl$. These compounds have the general formula $(C_5H_5)_3NpL$ with either inorganic ionic ($L = Br^-$, I^-, $1/2SO_4^{2-}$, NCS^-, $ALCl_4$) or organic ligands ($L = NC_4H_4^-$, $N_2C_3H_3^-$, $C = CH^-$, $1/2C = C_2^-$, $C_2H_5^-$, $C_6H_5^-$) (Bohlander, 1986). An interesting and unusual synthetic method was reported by Baumgartner *et al.* (1965). These authors obtained $Np(C_5H_5)_3Cl$ by (γ,n) reaction with U-238 in $U(C_5H_5)_3Cl$.

(b) Cyclooctatetraene compounds

Karraker *et al.* (1970) prepared bis(cyclooctatetraenyl) Np(IV) by reacting $NpCl_4$ with a THF solution of $K_2(C_8H_8)$:

$$NpCl_4 + 2K_2(C_8H_8) \rightarrow Np(C_8H_8)_2 + 4KCl \tag{6.26}$$

After 16 h of stirring, the compound was precipitated by the addition of deaerated water and recovered by evaporation. The authors report that X-ray diffraction patterns indicate that $Np(C_8H_8)_2$ is isomorphous with $U(C_8H_8)_2$ and $Pu(C_8H_8)_2$. The chemical behavior of the three compounds are identical: the compounds are not sensitive to water or dilute base, they are air-sensitive, reacting quickly to form oxides, and they are very slightly soluble in organic solvents such as benzene and toluene.

Karraker (1973) synthesized both neptunium bis(ethylcyclotetraene) and bis (*n*-butylcyclotetraene) complexes by reacting the alkyl substitued potassium complex in THF with $NpCl_4$ as shown below:

$$2K_2RC_8H_7 + NpCl_4 \rightarrow Np(RC_8H_7)_2 + 4KCl \tag{6.27}$$

where R = ethanol, butanol.

A trivalent neptunium cyclotetraene complex was prepared and characterized by Karraker and Stone (1974) by reacting stoichiometric amounts of NpX_3 (X = Cl, Br, I) and $K_2(C_8H_8)$ in THF:

$$NpXr_3 + 2K_2(C_8H_8) \rightarrow KNp(C_8H_8) \cdot 2THF + 3KX \tag{6.28}$$

The compound is isostructural with $KPu(C_8H_8)_2 \cdot 2THF$ with an orthorhombic unit cell. Both compounds are reported to be air- and water-sensitive, converting to $Np(C_8H_8)_2$ by air oxidation and other trace amounts of oxidizing agents. The compound is soluble in THF but slightly soluble in benzene and toluene.

(c) Other organometallic compounds

Hydrocarbyl compounds of neptunium have been reported. Karraker and Stone (1976) reported the preparation of $Np(C_5H_5)_3R$ where R = *n*-butyl by reacting $Np(C_5H_5)_3Cl$ with RLi.

Recent investigations of suitable precursors for organometallic and inorganometallic compounds suggested the usefulness of solvated triiodide complexes for this purpose (Karraker, 1987; Zwick *et al.*, 1992). Karraker (1987) investigated the reaction of neptunium with diiodoethane. The reaction in THF is:

$$Np + 3/2C_2H_4I_2 \rightarrow NpI_3 \cdot x\mathrm{THF} + 3/2C_2H_4 \qquad (6.29)$$

The reaction was carried out in a dry argon. The mixture of reactants were stirred at ambient temperature at times up to 1 week. A yellow precipitate was mixed with thallous methylcyclopentadienide in THF. The reaction is complete in 5 to 10 min. Two pure products, $NpI_2(MeC_5H_5) \cdot 3THF$ and $NpI(MeC_5H_5)$ 2.3THF can be obtained by evaporation or precipitation with ether. Using $NpI_3(THF)_4$ Zwick *et al.* (1992) reported the preparation of $Np[N(SiMe)_2]_3$, $Np[O\text{-}2,6\text{-}(t\text{-}C_4H_9)_2C_6H_3]_3$, and $Np[CH(SiMe_3)_2]_3$, demonstrating that $NpI_3(THF)_4$ is a precursor to new and existing compounds.

6.8 NEPTUNIUM IN AQUEOUS SOLUTION

6.8.1 Oxidation states of neptunium ions

Neptunium exists in an aqueous solution as ions of oxidation states from 3+ to 7+. These oxidation states are liable to change through reduction and oxidation reactions and disproportionation reaction of Np(v). The stability of the oxidation state is strongly affected by factors such as oxidants or reductants, acidity of the solution, presence of a complex forming ligand, and the concentration of neptunium itself in the solution. The stability of each ion can be simply predicted from the redox potentials as described below.

Trivalent and tetravalent neptunium exist as hydrated Np^{3+} and Np^{4+} in acidic solutions without ligand, Np^{3+} is quickly oxidized to Np^{4+} by air. Even in moderately acidic solutions, Np^{4+} is significantly hydrolyzed. Np(III) and Np(IV) form insoluble hydroxides in aqueous solutions of low acidity and the hydroxide of Np(III) is readily oxidized to the hydroxide of Np(IV) by air. The pentavalent neptunium ion, which is the most stable oxidation state in solution, and hexavalent neptunium ion behave as strong Lewis acids and these ions form dioxo species, NpO_2^+ and NpO_2^{2+}, in acidic solution. NpO_2^{2+} is stable in acidic solution but is relatively easily reduced to NpO_2^+. Np(v) and Np(vi) form hydroxides in neutral and basic solutions. The solubilities of these hydroxides in the aqueous solution are higher than that of Np(iv) hydroxide. Np(vii) was first prepared by Krot and Gelman (1967) in basic solution. The chemical forms of Np(vii) in acidic and basic media are described in Section 6.8.2. NpO_3^+ is quickly reduced to NpO_2^{2+} by water (Spitsyn *et al.*, 1969).

(a) Redox potentials of neptunium ions

(*i*) *Acidic media*

Np(iii), Np(iv), Np(v), and Np(vi) ions exist in solutions of sufficiently high acidity or solutions containing ligands. Standard redox potentials are estimated from experimentally determined formal redox potentials by precise correction for activity coefficients. Alternatively, the standard redox potentials are calculated from standard enthalpies of formation and entropies of the ions. Chapter 19 of this work provides recommended values of the standard potentials of actinide ions as the following potential diagram:

$$\underbrace{\mathrm{NpO_2^{2+}} \xrightarrow{+1.159} \mathrm{NpO_2^{+}} \xrightarrow{+0.604}}_{+0.882} \mathrm{Np^{4+}} \underbrace{\xrightarrow{+0.219} \mathrm{Np^{3+}} \xrightarrow{-1.772} \mathrm{Np}}_{-1.274}$$

Recently, Kihara *et al.* (1999) critically evaluated the redox potentials of uranium, neptunium, and plutonium ions in acidic solutions by extrapolating the formal potentials to the state of zero ionic strength, referring mainly to the works by Riglet *et al.* (1987, 1989) and based on the Bronsted–Guggenheim–Scatchard specific ion-interaction theory (SIT) (Pitzer, 1979).

The $E°$ for such reversible redox couples as NpO_2^{2+}/NpO_2^+ and Np^{4+}/Np^{3+} proposed by Riglet *et al.* (1987, 1989) are reliable and most of the experimental data are in good agreement with these $E°$ if the activity coefficient is properly corrected in the conversion of the formal potential to $E°$. The formal potential for the redox couple between NpO_2^+ and Np^{4+} is difficult to determine by conventional voltammetry or polarography, because the electrode reaction between NpO_2^+ and Np^{4+} is slow or irreversible because Np–O bonds must be made or broken. The $E°$ for NpO_2^+/Np^{4+} couple in the diagram was evaluated from data of Gibbs energy of formation (Martinot and Fuger, 1985). Kihara *et al.* (1999) re-estimated the electromotive force (EMF) data (Cohen and Hindman, 1952) by the activity coefficient correction based on the SIT and obtained $+0.596$ for NpO_2^+/NP^{4+} couple. The $E°$ for NpO_3^+/NpO_2^{2+} estimated by Musikas *et al.* (1974) given in the diagram is recommended at the present time.

(*ii*) *Basic media*

Standard potentials or formal potentials for neptunium ions in basic media are less precise and less reliable than those in acidic media. For some redox reactions even chemical forms of hydrolytic species participating in the processes have not yet been fully understood. The potential diagram for neptunium ions in basic media by Martinot and Fuger (1985) is recommended:

$$\mathrm{NpO_5^{3-}} \xrightarrow{+0.58} \mathrm{NpO_2(OH)_2} \xrightarrow{+0.6} \mathrm{NpO_2OH} \xrightarrow{+0.3} \mathrm{NpO_2} \xrightarrow{-2.1} \mathrm{Np(OH)_3} \xrightarrow{-2.2} \mathrm{Np}$$

Recently a new method for the determination of formal potentials by the use of *in situ* X-ray absorption near-edge structure (XANES) spectroscopy was applied to the redox couples of neptunium ions in 1 M $HClO_4$ (Soderholm *et al.*, 1999). The relative concentrations of Np(VI)/Np(V) or Np(IV)/Np(III) after the controlled potential electrolysis were determined from XANES spectra using the principal component analysis technique. XANES spectra specific for the hydrated neptunium ions of different oxidation states are shown in Fig. 6.8.

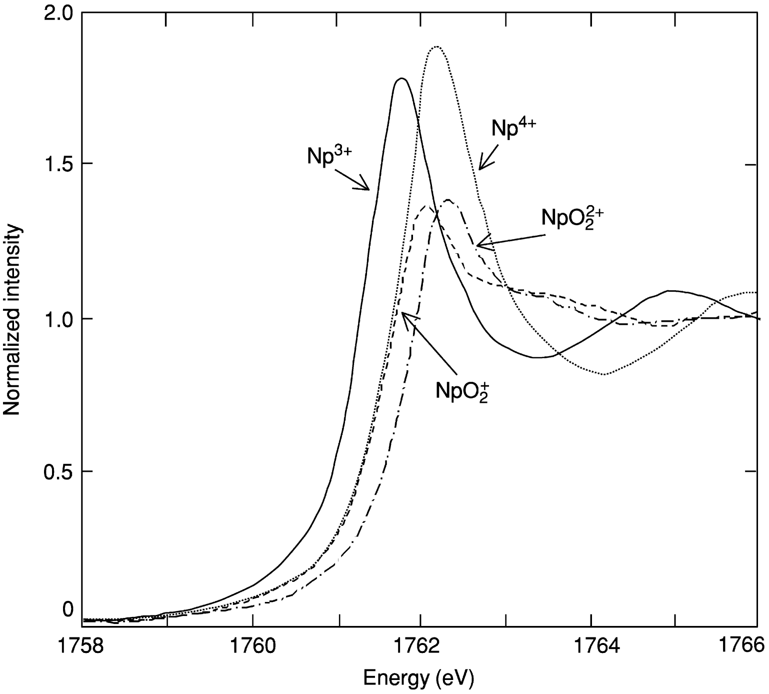

Fig. 6.8 *XANES spectra from the pure Np(III), Np(IV), Np(V), and Np(VI) ions in* $HClO_4$; *reprinted from Soderholm* et al. (1999) *with permission from American Chemical Society.*

The Nernstian plots between log([Np(VI)]/[Np(V)]) or log([Np(IV)]/[Np(III)]) and the applied potential lead to the precise determination of the formal potential, at which [Np(VI)]/[Np(V)] or [Np(IV)]/[Np(III)] equals unity. The formal potentials determined by this method are in good agreement with those determined by traditional voltammetry or polarography. An advantage of this method is that XANES is highly selective to the ion of interest that can interrogate a given redox couple in a complicated mixture such as the test solution containing multiple redox-active species.

(b) Electrolytic behavior of neptunium ions

(*i*) *Voltammetric behavior*

The measurements of current–potential relations by voltammetry, polarography, or related methods are important not only to elucidate the reaction mechanism and estimate the reaction rate but also to determine the formal potential for the evaluation of the standard redox potential. The voltammetric studies of the redox of neptunium ions, however, have not been conducted extensively enough.

Voltammetric data for the redox of neptunium ions in acidic media were provided by Niese and Vecernik (1981). The current–potential curves were recorded by cyclic voltammetry at a glassy carbon electrode with $HClO_4$, HNO_3, H_2SO_4, and acetate buffer solutions containing neptunium ion of a given oxidation state. Clear peaks due to one-electron redox reactions of NpO_2^{2+}/NpO_2^+ and Np^{4+}/Np^{3+} were observed. The peak potentials $E_{p,a}$ and $E_{p,c}$, at which the anodic and cathodic current peaks were observed, for the redox couples of NpO_2^{2+}/NpO_2^+ and Np^{4+}/Np^{3+} are summarized in Table 6.10. A difference between $E_{p,a}$ and $E_{p,c}$, ΔE_p, indicates that the redox processes of NpO_2^{2+}/NpO_2^+ and Np^{4+}/Np^{3+} in the 0.5 M $HClO_4$ or 1 M HNO_3 solutions are practically reversible and those in the H_2SO_4 or acetate buffer solutions are not reversible. The peak potential for NpO_2^{2+}/NpO_2^+ shifts more negatively with acetate buffer solution and the peak potential for Np^{4+}/Np^{3+} in HNO_3, H_2SO_4, and acetate buffer solution are more negative than that in $HClO_4$, which is due to stabilization of NpO_2^{2+} and Np^{4+} by the complex formation of NpO_2^{2+} with acetate ion and Np^{4+} with NO_3^-, SO_4^{2-}, and acetate ion.

The cathodic wave corresponding to further reduction of NpO_2^+ to Np^{4+} or Np^{3+} was not observed in the experiments by Niese and Vecernik (1981). The rate of the redox between Np^{4+} and NpO_2^+ as equation (6.30) is very slow, because the redox process involves formation or rupture of a Np–O bond which requires a large overpotential.

$$NpO_2^+ + 4H^+ + e^- \rightleftarrows Np^{4+} + 2H_2O \tag{6.30}$$

The potential for the reduction of NpO_2^+ to Np^{4+} is, therefore, more negative than that for the reduction of Np^{4+} to Np^{3+}, and the potential for the oxidation

Table 6.10 *Characteristics of voltammograms for redox of neptunium ions in $HClO_4$, HNO_3, H_2SO_4, or acetate buffer solutions.*

		Peak potentials (*V vs SSE*)		
Redox reactions	*Electrolyte*	*Anodic peak,* $E_{p,a}$	*Cathodic peak,* $E_{p,c}$	E_p
$NpO_2^{2+} + e^- = NpO_2^+$	0.5 M $HClO_4$	+1.01	+0.95	0.060
	1 M HNO_3	+1.04	+0.98	0.060
	0.5 M H_2SO_4	+1.02	+0.91	0.110
	0.5 M acetate buffer (pH = 4.2)	+0.84	+0.72	0.120
$Np^{4+} + e^- = Np^{3+}$	0.5 M $HClO_4$	+0.05	–0.02	0.070
	1 M HNO_3	–0.02	–0.08	0.070
	0.5 M H_2SO_4	–0.095	–0.23	0.135
	0.5 M acetate buffer (pH = 4.2)	–0.27	–1.06	0.790

of Np^{4+} to NpO_2^+ is more positive than that for the oxidation of NpO_2^+ to NpO_2^{2+} in $HClO_4$ and HNO_3 media.

Riglet *et al.* (1989) recorded voltammograms for the redox of Np(VI) and Np(V) in perchlorate media of various ionic strengths ($0.5 < I < 3$) for the precise determination of the formal redox potentials and re-evaluation of the standard redox potential at $I = 0$. The current–potential curves shown in Fig. 6.9 were recorded at rotating platinum disk electrode (2 mm in disk diameter) with rotation rate of 1500 rpm by scanning the potential at a rate of 0.002 V s^{-1}. The oxidation state of the neptunium ion in the test solution was controlled by the electrolysis so that NpO_2^+ initially present in the solution was partly oxidized to NpO_2^{2+} step by step (curves 2 to 5). The anodic wave developing at more positive potential and the cathodic wave at more negative potential than ca. +0.77 to +0.78 V correspond to the oxidation of NpO_2^+ and the reduction of NpO_2^{2+}, respectively. The redox reaction between NpO_2^+ and NpO_2^{2+} is not fully reversible at the platinum electrode because the slopes of the logarithmic analysis of the diffusion controlled waves are ca. 0.080 V per log unit, which are larger than the theoretical value.

Voltammetry using a rotating platinum electrode was applied to study the redox behavior of neptunium ions in 0.5– 4 M NaOH solution (Peretrukhin and Alekseeva, 1974). The successive reduction and oxidation among Np(VII), Np (VI), Np(V), and Np(IV) were investigated. The redox behavior of the neptunium ions strongly depends on the concentration of NaOH, which is interpreted as a change of the chemical form of Np(VI) during the electrolytic reduction and oxidation depending on the NaOH concentration.

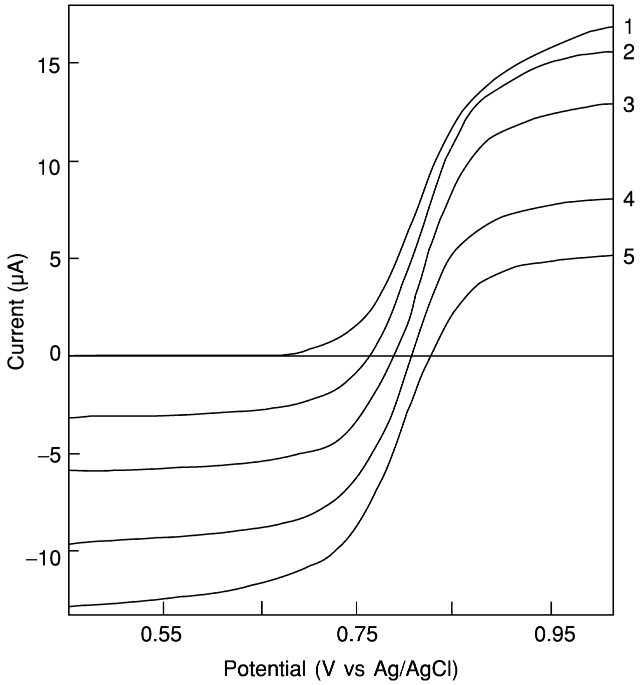

Fig. 6.9 *Current–potential curves for the redox couple of* NpO_2^{2+}/NpO_2^+ *in* 1 M $HClO_4$ + 1 M $NaClO_4$ *at rotating platinum disk electrode* (1500 rpm). *Concentration of Np*; 10^{-3} M, *Potential;* V *vs Ag/AgCl electrode* (E° = 0.3329 V *vs NHE*).

Electrochemical and spectroscopic studies of neptunium ions in concentrated aqueous carbonate and carbonate–hydroxide solutions were carried out by Varlashkin *et al.* (1984). The formal potential of the Np(VI)/Np(V) couple was determined as a function of pH of the solution. The redox reaction between Np(VI) and Np(V) was found to be quasi-reversible at a platinum electrode and the formal potential was estimated to be (+0.23 ± 0.01) V vs saturated calomel electrode (SCE).

(*ii*) *Coulometric behavior*

Flow coulometry using multi-step column electrodes is a powerful technique to investigate a redox reaction even if the reaction is irreversible, because the surface area of the working electrode of the column electrode is very large comparing with a volume of the solution in the column and a quantitative electrolysis can be achieved very rapidly. The electrolysis method using column electrode is also useful for the preparation of ions of a desired oxidation state as well as for the rapid determination or collection of various metals (Fujinaga and Kihara, 1977; Yoshida *et al.*, 1991).

Flow coulometry has been applied to the studies of overall redox behavior of the neptunium ions in acidic aqueous solution. Coulopotentiograms, which are current–potential curves observed by flow coulometry, were measured by using the multi-step column electrodes connected in series. Coulopotentiograms for the redox of neptunium ions of various oxidation states are shown in Fig. 6.10 after correction for the residual current. In the figure, the number of electrons involved in the redox reaction, *n*, converted from the current is plotted on the ordinate instead of the current.

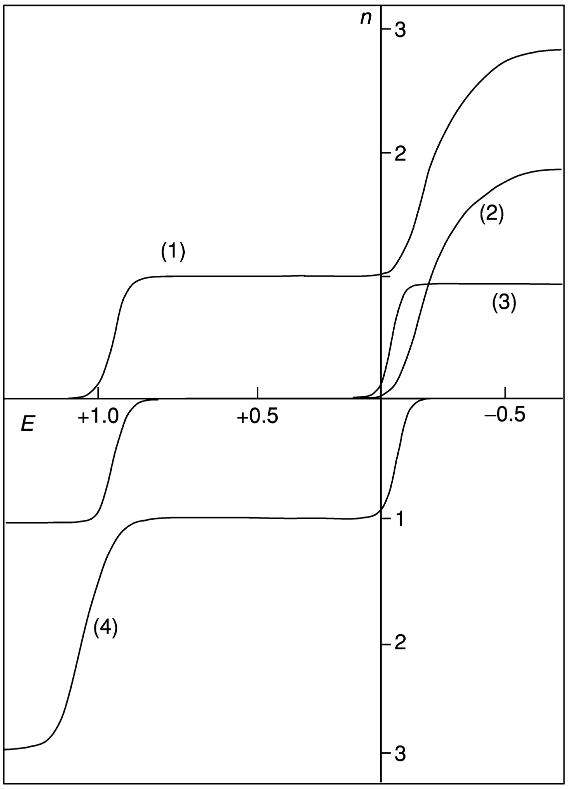

Fig. 6.10 *Coulopotentiograms for the redox of neptunium ions in* 1 M $HClO_4$ *solution.* n, *number of electrons involved in redox reaction;* E, *working electrode potential* (V *vs Ag–AgCl reference electrode*). (1) *Reduction of* NpO_2^{2+}, (2) *reduction and oxidation of* NpO_2^{+}, (3) *reduction of* Np^{4+}, (4) *oxidation of* Np^{3+}. *Sample solution;* 10^{-3} M *Np ion, flow rate,* 1.5 ml min^{-1}; *potential scan rate,* 0.002 V s^{-1}.

Coulopotentiogram 1 in Fig. 6.10 was recorded at a single column electrode with flowing 1 M $HClO_4$ solution containing 10^{-3} M NpO_2^{2+} and scanning the potential. The coulopotentiogram shows the reduction of NpO_2^{2+} to NpO_2^+ at more negative potential than +0.85 V vs Ag–AgCl reference electrode (SSE) and further to Np^{3+} at more negative potential than −0.6 V. Coulopotentiogram 2 was recorded with a two-step column electrode system with the first column electrode kept at +0.5 V and the second column at the scanned potential. Here, NpO_2^{2+} in the test solution is converted to NpO_2^+ quantitatively at the first column, and therefore, the redox behavior of NpO_2^+ can be examined at the second column electrode. Coulopotentiogram 2 shows one-electron oxidation of NpO_2^+ to NpO_2^{2+} at more positive potential than +1.1 V and two-electron reduction to Np^{3+} at more negative potential than −0.6 V. Coulopotentiograms 3 and 4 are recorded identically using two-step or three-step column electrode systems and show the reduction of Np^{4+} to Np^{3+} and the oxidation of Np^{3+} to Np^{4+} and further to NpO_2^{2+}.

(c) Disproportionation of NpO_2^+

NpO_2^+ disproportionates to Np^{4+} and NpO_2^{2+} through the following reaction. The extent of the disproportionation is promoted when the acidity of the solution and the concentration of NpO_2^+ are high:

$$2NpO_2^+ + 4H^+ \rightleftarrows Np^{4+} + NpO_2^{2+} + 2H_2O$$
$$K_{\text{dispro}} = [Np^{4+}][NpO_2^{2+}]/[NpO_2^+]^2[H^+]^4 \tag{6.31}$$

The equilibrium constant is increased by the addition of reagents that form complexes with Np^{4+} and NpO_2^2+ in the solution. For example, it was shown that $K_{\text{dispro}} = 4 \times 10^{-7}$ for Np(V) in 1 M $HClO_4$ and $K_{\text{dispro}} = 2.4 \times 10^{-2}$ for Np(V) 1 M H_2SO_4 solution (Keller, 1971). Hindman *et al.* (1954) suggested that the rate of the disproportionation reaction of equation (6.31) is expressed by equation (6.32).

$$-d[NpO_2^+]/dt = k[NpO_2^+][H^+]^2 \tag{6.32}$$

(d) Methods for the control of oxidation state of neptunium ions

(*i*) *Redox reagents*

The oxidation state of neptunium ions can be adjusted using various redox agents. The agent and chemical procedure feasible for the promotion of the redox between reversible couples such as NpO_2^{2+}/NpO_2^+ or Np^{4+}/Np^{3+} are chosen properly by referring to the redox potentials for neptunium ions and those for the agent as well as a ligand coexisting in the solution. Typical procedures for the control of the oxidation state of neptunium ions are shown

Table 6.11 *Procedures for adjusting the oxidation state of neptunium ion in aqueous solutions using redox agents.*

Oxidation states of neptunium ion		*Procedures*	
Before treatment	*After treatment*	*Agents*	*Conditions*
Oxidative treatment			
Np(iii), Np(iv), Np(v)	Np(vi)	Ce(iv)	HNO_3, H_2SO_4
		MnO_4^-	HNO_3, H_2SO_4
		Ag(ii)	1 M $HClO_4$
		BrO_3^-	
		$HClO_4$	fuming
		Cl_2	1 M HCl (348 K)
Np(iii)	Np(iv)	O_2 (air)	
Reductive treatment			
Np(v), Np(vi)	Np(iv)	Fe^{2+}	H_2SO_4
		I^-	5 M HCl (373 K)
Np(vi)	Np(v)	NH_2NH_2	1 M H^+
		NH_2OH	1 M H^+
		NO_2^-	1 M HNO_3
		H_2O_2	0.5 M HNO_3
		Sn^{2+}	HCl
		SO_2	H_2SO_4
Np(iv), Np(v), Np(vi)	Np(iii)	Zn(Hg)	
		H_2 (Pt black)	

in Table 6.11. The kinetic factors are required to be evaluated to complete slow processes between NpO_2^{2+} and Np^{4+} or between NpO_2^+ and Np^{4+} involved in the procedure for the oxidation state control. The kinetics of the redox reactions for Np(vi)–H_2O_2, Np(v)–V(iii), Np(v)–Cr(ii), and Np(vii)–Hg(i) systems were summarized by Newton (1975). Nakamura *et al.* (1992) proposed a method for the rapid reduction of Np(v) to Np(iv) by hydroxylamine nitrate in the presence of platinum black catalyst.

Recently much attention has been paid to the kinetics of the redox of neptunium ions by various organic agents for the development of an advanced Purex process. These studies aim at screening of the most suitable 'salt-free' redox agent, which enables precise control of the oxidation state of the neptunium ion in the process flowsheet. Taylor *et al.* (1997) reviewed the redox chemistry of neptunium ion in the proposed procedures.

Aldehyde derivatives such as *n*- and isobutyraldehydes are effective reductants for Np(vi) and Pu(iv) as reported by Kolarik and Dressler (1984) and Uchiyama *et al.* (1993). Hydroxylamine- and hydrazine derivatives have been suggested as effective reducing agents for Np(vi) and Pu(iv). Koltunov *et al.* (1993, 1999) investigated the reduction kinetics of Np(vi) by *N*,*N*-ethyl (hydroethyl)hydroxylamine ($HOC_2H_4(C_2H_5)NHOH^+$, EHEH) and *N*,*N*-diethyl hydroxylamine ($(C_2H_5)_2NHOH^+$, DEH) in nitric acid solution. The reduction reactions are expressed as follows.

$$4NpO_2^{2+} + HOC_2H_4(C_2H_5)NHOH^+ + 3H_2O \rightarrow 4NpO_2^+ + 2C_2H_5OH + HNO_3 + 9H^+ \tag{6.33}$$

$$8NpO_2^{2+} + (C_2H_5)_2NHOH^+ + 4H_2O \rightarrow 8NpO_2^+ + CH_3CHO + C_2H_5OH + HNO_3 + 5H^+ \tag{6.34}$$

The different characteristics of reactions by EHEH and DEH are explained by their different structures providing an availability of a hydroxyl group in the EHEH molecule. The kinetics of reactions (6.33) and (6.34) were studied in 0.3 – 2.0 M HNO_3 at ionic strength of 2.0. It was concluded that the reaction is first order relative to Np(VI) with excess reductants. The rate equations of reaction (6.33) and (6.34) are

$$-d[Np(VI)/dt = k[Np(VI)][EHEH][H^+]^{-0.8} \tag{6.35}$$

where k = (334 ± 12) $L^{0.2}\ mol^{-0.2}\ min^{-1}$ (298.6 K), and activation energy (E_A) = (42.3 ± 2.7) kJ mol^{-1}, and

$$-d[Np(VI)/dt = k[Np(VI)][DEH][H^+]^{-0.84} \tag{6.36}$$

where $k = (22.6 \pm 0.8)\ L^{0.16}\ mol^{-0.16}\ min^{-1}$ (298 K), and $E_A = (68.5 \pm 0.9)$ kJ mol^{-1}. Np(VI) and Pu(IV) are reduced faster by EHEH than by DEH, which suggests that the introduction of the hydroxyl group into the reductant molecule enhances the kinetics.

A comprehensive study on the reduction kinetics of Np(VI) and Pu(IV) by Taylor *et al.* (1998a) suggests that 1,1-dimethylhydrazine (DMHz) and *tert*-butylhydrazine (*tert*-BHz) are the most promising agents for the rapid reduction of Np(VI) with high selectivity over Pu(IV) reduction. For example, 99% of Np(VI) (initial concentration (1–2) × 10^{-4} M) in 1 M HNO_3 solution was reduced to Np(V) at 298 K by the addition of 0.1 M DMHz or *tert*-BHz within 1 or 8.7 min, respectively, and only 0.23 or 0.11% of Pu(IV) (initial concentration (2–10) × 10^{-3} M) was reduced to Pu(III) during 99% reduction of Np(VI) under the equivalent condition. It was found that formohydroxamic acid (Taylor *et al.*, 1998b) and acetaldoxime (Koltunov *et al.*, 2000) were also effective reductants for the rapid reduction of Np(VI) to Np(V) in acid solution.

(*ii*) *Electrochemical methods*

Controlled potential electrolysis is available to control the oxidation state of neptunium ions. For example, Np(V) in acidic solutions such as 1 M $HClO_4$ solution is oxidized to Np(VI) completely at +1.20 V vs Ag–AgCl (saturated KCl) reference electrode, Np(v) is quantitatively reduced to Np(iii) at −0.20 V, and Np(iii) is oxidized to Np(iv) at +0.40 V by controlled potential electrolysis using carbon or platinum working electrodes. Controlled potential electrolysis was applied to the preparation of carbonate complexes of neptunium ion of a given oxidation state in neutral or basic solutions (Li *et al.*, 1993).

The electrolytic technique using multi-step column electrodes of glassy carbon fiber working electrode as described in Section 6.8.1b is also useful to adjust the oxidation state of the neptunium ion in the flowing sample solution. The applied potential and the other electrolytic conditions can be chosen consulting with the current–potential relationship as shown in Fig. 6.10.

(*iii*) *Miscellaneous*

A sonochemical technique was applied to oxidize Np(v) efficiently (Nikitenko *et al.*, 1999). Np(v) in HNO_3 solution was found to be oxidized to Np(vi) in the presence of argon under the effect of power ultrasound (20 kHz, 1 W cm^{-2}). The addition of urea which exerts a buffering effect related to nitrous acid concentration helps to stabilize Np(vi) formed under sonification. The oxidation mechanism is related to the formation of HNO_2 by sonolysis of HNO_3, followed by the oxidation of Np(v) with HNO_3 catalyzed by HNO_2.

Photochemical reaction is feasible to oxidize and reduce Np(v) and Np(vi) in nitric acid solution (Fukasawa *et al.*, 1991). Np(vi) is reduced to Np(v) by HNO_2 generated by the photolysis of HNO_3 and is shown in reactions (6.37) to (6.39).

$$HNO_3(\text{photo irradiation}) \rightarrow OH + NO_2 \qquad (6.37)$$

$$2NO_2 + H_2O \rightarrow HNO_2 + HNO_3 \qquad (6.38)$$

$$NpO_2^{2+} + HNO_2 + H_2O \rightarrow 2NpO_2^+ + 3H^+ + NO_3^- \qquad (6.39)$$

Addition of a scavenger for HNO_2, such as urea, allows the oxidation of Np(v) to Np(vi) by the action of OH radical as given by reactions (6.40) and (6.41).

$$2HNO_2 + CO(NH_2)_2 \rightarrow 2N_2 + CO_2 + 3H_2O \qquad (6.40)$$

$$NpO_2^+ + OH + H^+ \rightarrow NpO_2^{2+} + H_2O \qquad (6.41)$$

The kinetics of the photochemical reduction of Np(vi) to Np(v) in HNO_3 solution were investigated (Wada *et al.*, 1995) as a function of irradiation wavelength, the acidity of nitric acid, and the nature of the coexisting agents. It was concluded that the higher the irradiation rate and the HNO_3 concentration, the easier the oxidation reaction of Np(v) progressed.

6.8.2 Optical spectroscopy of neptunium

Optical spectroscopy has been extensively applied to neptunium to better understand the electronic structure of the aquo ions Np(iii) through Np(vii), and of coordination complexes that occur in solution (Gruen, 1952; Waggener, 1958; Dukes and Shuler, 1960; Krot *et al.*, 1968a; Stafsudd *et al.*, 1969; Varga *et al.*, 1970; Chaikhorskii, 1971; Chaikhorskii and Leikina, 1972; Rykov and Frolov, 1972; Tsivadze and Krot, 1972; Kharitonov and Moskvin, 1973; Rykov *et al.*, 1973; Hessler *et al.*, 1980; Kanellakopulos *et al.*, 1980a,b; Lahalle *et al.*, 1986; Carnall *et al.*, 1987; Tait *et al.*, 1995; Matsika and Pitzer, 2000; Neck *et al.*, 2001). An excellent review article has been published by Gruen (1992) describing the development of the knowledge base for the f-electron elements, especially neptunium. Fig. 6.11 shows the visible absorption spectra for the neptunium ions (iii, iv, v, and vi) in 2 M perchloric acid. Optical spectroscopy has been applied in both the visible and infrared portions of the spectrum with a wealth of information being gathered.

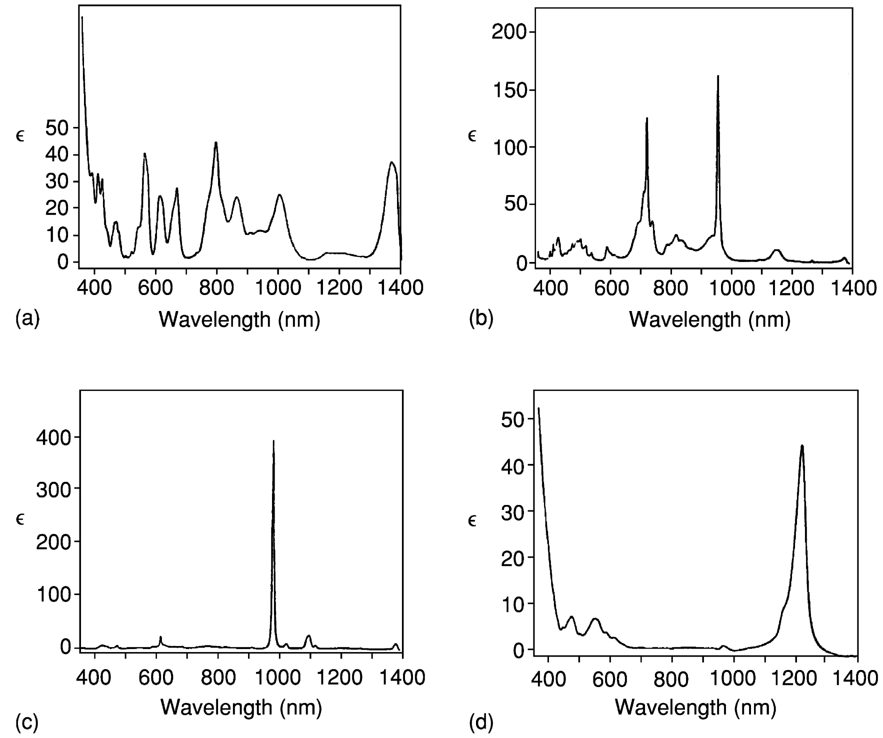

Fig. 6.11 *The absorption spectra of neptunium ions in* 2 M *$HClO_4$ solution:* (*a*)*Np*(*iii*); (*b*) *Np*(*iv*); (*c*) *Np*(*v*); (*d*) *Np*(*vi*).

One of the earliest studies on the subject (Gruen, 1952) used optical means to obtain information on the spin–orbit coupling for NpO_2^{2+} species. A value of 950 cm^{-1} for the spin–orbit coupling energy provided the best agreement between calculated and experimentally observed results for the $5f^2$ configuration. This 'best fit' was obtained by using the intermediate case of mixing the pure spin–orbit coupling and the pure electrostatic case.

The absorption spectrum of neptunium has often been measured in nitric acid solution. This provides straightforward identification of what valence states are present as was shown by Dukes and Shuler (1960). Np(IV) displays a strong absorption band at 715 nm, while Np(V) displays a somewhat weaker band at 617 nm and Np(VI) displays a strong band in the region below 400 nm. The concentration of nitric acid was determined not to be a significant factor in the absorption spectrum from 1 to 6 M.

Absorption spectroscopy of the Np(VII) species is somewhat more difficult in that it can be observed only under basic conditions (Krot *et al.*, 1968a; Williams *et al.*, 2001) in a steady-state manner. The actual form of the Np(VII) in solution is as NpO_6^{5-} in basic solutions and NpO_2^{3+} in acidic solutions. The tetraoxo Np(VII) compound exhibits four 'short' bonded oxygen (~1.85 Å) and two 'long' bonded oxygen (~2.2 Å) in basic solutions. The acidic form can only be observed at room temperature for a matter of minutes before it is reduced to the Np(VI) state. The hydroxide, $NpO_2(OH)_3$ is assumed to have amphoteric properties in solution.

The absorption spectrum for Np(VII) in solution was investigated in more detail by Chaikhorskii (1971). They prepared Np(VII) species in the cationic form and then precipitated it for their study. It was determined that fine structure could be observed in the visible absorption bands (412 and 620 nm). This fine structure was attributed to two causes, electron transfer (oxygen $\pi \rightarrow 5f$) and vibrational states. Several vibrational states were identified with energies between 681 and 2338 cm^{-1}. The vibrational bands identified were consistent with the predicted symmetry of a compound involving the NpO_2^{3+} species.

The infrared spectroscopy study by Chaikhorskii (1971) was extended by Tsivadze and Krot (1972) to include several compounds of Np in the Np(VII) state. Their work validated the earlier work of Chaikhorskii (1971) and furthered the knowledge base in that they determined the neptunium in the solid compounds that contained no isolated NpO_2 groups but that there were chains of 'infinite' length which connected the NpO_6 octahedra.

Stafsudd *et al.* (1969) studied Np(VI) by doping NpO_2^{2+} into a matrix of $Cs_2UO_2Cl_4$ and applying infrared and visible spectroscopies. They identified several pure electronic levels at 6880, 13 277, 15 426, 17 478, and 19 358 cm^{-1}. The ground state and the 6880 cm^{-1} state belong to the $5f^1$ configuration, whereas the other energy levels were thought to likely belong to an excited configuration involving electrons in the non-bonding 5f shell.

A more recent theoretical effort sought to improve the assignments of the electronic states for both Np(VI) and Np(V) species (Matsika and Pitzer, 2000).

This work is more complete than the much earlier effort of Eisenstein and Pryce (1965, 1966). Their work resulted in the calculation of the energy levels of 15 excited states for NpO_2^{2+} and 19 for NpO_2^{+}, as well as their respective wave functions. Their methods used relativistic spin–orbit coupling configuration interactions based on effective core potentials.

Work on the Np(v) species with a focus on its interaction with polyvalent species in different solvents was reported by Rykov and Frolov (1972). Visible spectroscopy of solutions of NpO_2^{+} in several different mixed solvents (water–methanol, water–ethanol, water–acetone) were obtained at room temperature in the presence of Fe^{3+}. The interaction of Fe^{3+} with Np^{5+} ion in mixed solvents was studied and it was reported that the formation of a complex involving both ions mirrored that of the electron exchange for Fe^{2+} and Fe^{3+} for aqueous solutions kinetically. The degree of interaction between the two ions being inversely dependent on the effective dielectric constant of the solvent.

Varga *et al.* (1970) performed an extensive spectroscopic study of the Np(iv) species from 300 to 1800 nm using NpF_4 either dissolved in $CsF \cdot 2HF$ (300–1300 nm) and in a fluorocarbon mull (1300–1800 nm). This study allowed for the assignment of 17 excited-state transitions for Np^{4+}. The experimental values for these transitions were compared to calculated values with good agreement. Infrared spectroscopy was also applied to a Np(iv) species in the form of several oxalate compounds formed with neptunium in the 4+ state (Kharitonov and Moskvin, 1973). This work identified several vibrational bands and their respective force constants and bond lengths (Np–O). The bond length was reported as 1.78 Å, which agreed well with the literature value for this quantity based on the vibrational band of approximately 825 cm^{-1} (Kharitonov and Moskvin, 1973).

Rykov *et al.* (1973) investigated the complexation behavior of Np(iv) in nitrate solutions of varying concentrations. A total of three types (A–B–C) of complexes were observed depending on whether there was very little nitrate present (type 'A' spectra observed) or nitrate solutions with very little free water present (type 'C' spectra observed). Type 'B' spectra were considered as intermediate to 'A' and 'C'. The fundamental distinction between the three types of complexes was assigned to the structure of the first coordination sphere. The type 'A' were thought to be of the M_{aq}^{4+} formula whereas the type 'C' were assigned to be a neptunium ion coordinated with six nitrates. The type 'B' complex had been thought to be an intermediate nitrate complex (less than six coordination) but their results were shown to be consistent with change in the aqueous coordinated complex and did not involve complexation by nitrate at all.

A later study of Np(iv) utilized low temperature spectroscopy (4.2 K) and two different crystalline hosts, $ThSiO_4$ and ThO_2 (Lahalle *et al.*, 1986). The latter of the two crystalline hosts had been used in an earlier study by Gruber and Menzel (1969) and was used for comparison purposes. Their study identified 29 excited-state transitions in the $ThSiO_4$ host and 19 in the ThO_2 host for

Np(IV) using both absorption and fluorescence spectroscopies over the temperature range of 4.2–300 K. Work of a similar nature on alkali and alkaline earth neptunates involving Np(VI) was performed by Kanellakopulos *et al.* (1980a,b).

A spectroscopic investigation of Np(III) was undertaken by Hessler *et al.* (1980) using low-temperature, high-resolution absorption, and fluorescence spectroscopies. A crystalline host of $LaCl_3$ was used. The temperature dependence of the homogeneous linewidth of D_1 to Z_1 (671.51 nm) and the D_1 to Z_2 (677.18 nm) transitions were obtained.

Carnall *et al.* (1987) investigated the interpretation of the spectra of neptunium obtained in silicate glasses with a focus on determining the valence state of the neptunium present. This work was undertaken to assist in the understanding of the local environment of neptunium in waste glasses bound for disposal in a geologic repository. Another spectroscopic investigation that has ramifications in the nuclear waste community is that of Neck *et al.* (2001) which utilized absorption spectroscopy, laser-induced photoacoustic spectroscopy (LIPAS), and laser-induced breakdown spectroscopy to study the colloids formed by neptunium in solution. An aqueous solution of $HClO_4$–$NaClO_4$ with Np(IV) present was used to obtain the solubility product constant of $Np(OH)_4$ at a wide range of pH. Kihara *et al.* (1996) also applied LIPAS to the study of neptunium species in Purex solutions.

A rather extensive study of Np(IV) and Np(V) in hydrolysis and carbonate reactions using optical and NMR spectroscopies was performed by Tait *et al.* (1995). Chaikhorskii and Leikina (1972) had earlier performed a similar study on Np(VII) during hydrolysis using optical spectroscopy.

With the relative importance of neptunium in the field of nuclear waste disposal, due to its long half-life, it is anticipated that the field of optical spectroscopy will continue to be an active one for many years with a particular emphasis on determining its local environment *in situ*.

6.8.3 Hydrolysis behavior

The hydrolysis reaction as a particular case of complex formation is the primary common property of all actinide ions in aqueous solution. The tendency for neptunium ions to undergo hydrolysis is in the order of $Np^{4+} > NpO_2^{2+} > Np^{3+} > NpO_2^+$, following the effective charge of the ions. The pentavalent NpO_2^+ ion is the most stable ion in solution and is not hydrolyzed appreciably at pH below 7. The trivalent Np^{3+} and hexavalent NpO_2^{2+} ions are the predominant species in solution at pH below 4–5 and 3–4, respectively, reflecting that the NpO_2^{2+} ion has an effective charge greater than the Np^{3+} ion. The tetravalent Np^{4+} ion shows a strong tendency towards hydrolysis and considerable hydrolysis is expected at pH 1 or above. Representative equilibrium constants for hydrolysis of neptunium ions, Np^{3+}, Np^{4+}, NpO_2^+, and NpO_2^{2+}, are listed in Table 6.12, together with some solubility products of the oxide or hydroxide.

Table 6.12 *Experimental equilibrium constants for hydrolysis of neptunium ion.*

Ion	*Method*	*Temp.* (°C)	*Medium*	*Equilibrium constants*	*References*
Np^{3+}	pot	25	0.3 M $NaClO_4$	$\log{}^*K_{11} = -7.43 \pm 0.11$	Mefod'eva *et al.* (1974)
Np^{4+}	sp	25	1.0 M	$\log{}^*K_{11} = -1.90$	Paul (1970)
	sol	25	0.0	$\log{}^*K_{14} = -9.8 \pm 0.11$	Rai *et al.* (1987)
				$\log{}^*K_s = 1.5 \pm 1.0$; $NpO_2(s) + 4H^+ \rightleftarrows Np^{4+} + 2H_2O$	Lemire *et al.* (2001)
NpO_2^+	sol	25	0.1 M $NaClO_4$	$\log{}^*K_{11} = -11.36 \pm 0.16$ $\log{}^*K_{12} = -23.50 \pm 0.12$	Neck *et al.* (1992)
			1.0 M $NaClO_4$	$\log{}^*K_{11} = -11.13 \pm 0.20$ $\log{}^*K_{12} = -23.19 \pm 0.14$ $\log{}^*K_s = 4.50 \pm 0.06$; $NpO_2OH(s) + H^+ \rightleftarrows NpO_2^+ + H_2O$	
NpO_2^{2+}	pot	25	1.0 M $NaClO_4$	$\log{}^*K_{11} = -5.17 \pm 0.03$ $\log{}^*K_{22} = -6.68 \pm 0.02$ $\log{}^*K_{35} = -18.25 \pm 0.02$	Cassol *et al.* (1972a)
	sol	25	0.1 M $NaClO_4$	$\log{}^*K_s = 5.87 \pm 0.17$; $NpO_3H_2O(s) + 2H^+ \rightleftarrows NpO_2^{2+} + 2H_2O$	Kato *et al.* (1996)

* K_{mn} is the hydrolysis constant for the equilibrium: $m\mathrm{M}^{a+} + n\mathrm{H_2O} \rightleftarrows \mathrm{M}_m(\mathrm{OH})_n^{am-n} + n\mathrm{H}^+$.

(a) Neptunium(III)

The trivalent Np^{3+} ion is sufficiently stable in acidic solution to allow spectrophotometric studies, but it is rapidly oxidized by air to the tetravalent state. Therefore, Np^{3+} will be stable in the presence of strong reductants and/or in an oxygen-free atmosphere. The tendency of an ion to undergo hydrolysis increases with charge and with decreasing ionic radius. The order of the trivalent actinide ions for ease of hydrolysis should be as follows: $U^{3+} < Np^{3+} < Pu^{3+} < Am^{3+}$, because the stability of hydrolyzed ions increases as z/r_{ion} increases.

As only one experimental study for the equilibrium,

$$Np^{3+} + H_2O \leftrightarrows NpOH^{2+} + H^+ \tag{6.42}$$

Mefod'eva *et al.* (1974) determined $\log {}^*K_{11} = -7.43$ for 298 K and 0.3 M $NaClO_4$ from potentiometric measurements in the pH range 6–8. The Np^{3+} ion was produced by electrolysis of 0.022 M $Cs_2NpCl_6(aq)$ in 0.1 M HCl using a mercury cathode in an inert atmosphere. The titration curves of Np^{3+} were compared with those of Pr^{3+} and Nd^{3+} under the similar conditions to obtain the ratios of the hydrolysis constants.

There has been no systematic study to determine the solubility product for Np(III) and no usable experimental data for $Np(OH)_3(s)$ is available.

(b) Neptunium(IV)

From the same reasons as in the case of the trivalent state, the tendency of the tetravalent actinide ions to undergo hydrolysis follows the order: $Th^{4+} < U^{4+} < Np^{4+} < Pu^{4+}$. There are three reports of the first hydrolysis step of Np^{4+}.

$$Np^{4+} + H_2O \leftrightarrows NpOH^{3+} + H^+ \tag{6.43}$$

Sullivan and Hindman (1959) and Paul (1970) reported $\log {}^*K_{11} = -2.30$ ($I = 2.0$ M) and -1.90 ($I = 1.0$ M), respectively, in aqueous perchlorate solutions by spectrophotometry. From extraction experiments, Duplessis and Guillaumont (1977) reported $\log {}^*K_{11} = -0.50$ in 1.0 M $LiClO_4$. Two values $\log {}^*K_{12}$ for $Np(OH)_2^{2+}$ have been reported with a large discrepancy (three order of magnitude) (Duplessis and Guillaumont, 1977; Schmidt *et al.*, 1980), while there is no experimental evidence for the formation of $Np(OH)_3^+$.

Several groups (Ewart *et al.*, 1985; Rai and Ryan, 1985; Pratopo *et al.*, 1989; Eriksen *et al.*, 1993) measured the solubility of Np(IV) hydrated oxide or hydroxide in neutral to basic solutions at room temperature in the presence of reducing agents, e.g. $Na_2S_2O_4$, Fe, or Zn, and reported a limiting neptunium concentration of $10^{-8.5}$ to $10^{-8.1}$ M. The pH-independence of the solubility indicates that the main species in equilibrium with Np(IV) solids is uncharged $Np(OH)_4^0$ and that $Np(OH)_5^-$ is not an important species for Np(IV) hydrolysis. Rai *et al.* (1987) studied the solubility of $NpO_2 \cdot xH_2O$ in the presence of Cu(I)/Cu(II) buffer and in the pH range from 1.5 to 2.5. Based on the measured redox potentials, pH, and calculated activities of Np^{4+} and NpO_2^+, the thermodynamic equilibrium constants were determined. After recalculation of the results in the NEA/TDB neptunium and plutonium volume (Lemire *et al.*, 2001), $\log{}^*K_s = 1.5$ and $\log{}^*K_{14} = -9.8$ were reported for the following reactions, respectively:

$$NpO_2(s) + 4H^+ \leftrightarrows Np^{4+} + 2H_2O \tag{6.44}$$

$$Np^{4+} + 4H_2O \leftrightarrows Np(OH)_4^0 + 4H^+ \tag{6.45}$$

The experimental $\log{}^*K_s$ values of Th(IV) (Ryan and Rai, 1987), Np(IV) (Rai *et al.*, 1987), and Pu(IV) (Rai, 1984) hydrous oxides show a linear relationship with the inverse square of the M^{4+} ionic radii.

(c) Neptunium(V)

The pentavalent NpO_2^+ ion is stable and disproportionates only at rather high acidities. Many groups have reported the formation constants of the hydroxo species by using various experimental methods (see Lemire *et al.*, 2001). The recent hydrolysis studies by solubility measurements (Lierse *et al.*, 1985; Itagaki *et al.*, 1992; Neck *et al.*, 1992) show smaller constants than found in earlier studies (Kraus and Nelson, 1948; Moskvin, 1971; Sevost'yanova and Khalturin, 1976; Schmidt *et al.*, 1980; Maya, 1983; Bidoglio *et al.*, 1985), which is probably due to the effect of carbonate complexation.

Neck *et al.* (1992) studied the hydrolysis behavior of the NpO_2^+ ion at 298 K by solubility experiments in the pH range 7–14 in 0.1, 1.0, and 3.0 M $NaClO_4$ solutions under CO_2-free argon atmosphere. In 0.1 M $NaClO_4$ Np(V) hydroxide precipitate remained amorphous (green) over several months, while in 1.0 M $NaClO_4$ the precipitate changed from an amorphous to a more stable-aged state (white) within a relatively short time. In 3.0 M $NaClO_4$ the aged modification of $NpO_2OH(s)$ is formed from the beginning. As shown in Table 6.12, the hydrolysis constants and solubility product for aged $NpO_2OH(s)$ were reported for the following reactions:

$$NpO_2^+ + H_2O \leftrightarrows NpO_2OH^0 + H^+ \tag{6.46}$$

$$NpO_2^+ + 2H_2O \leftrightarrows NpO_2(OH)_2^- + 2H^+ \tag{6.47}$$

$$NpO_2OH(s) + H^+ \leftrightarrows NpO_2^+ + H_2O \tag{6.48}$$

The solids (fresh and aged NpO_2OH) were not analyzed for possible incorporation of sodium ions, however the parallel solubility curves obtained for the two solids in 1.0 M $NaClO_4$ strongly suggest that they have similar stoichiometries.

(d) Neptunium(VI)

The hexavalent NpO_2^{2+} ion is not as stable as the UO_2^{2+} and PuO_2^{2+} ions. Cassol *et al.* (1972a) studied the hydrolysis of the NpO_2^{2+} ion in 1 M $NaClO_4$ at 298 K by potentiometric titrations. The NpO_2^{2+} solution was prepared by electrolytic oxidation of a NpO_2^+ solution. The hydrolysis constants shown in Table 6.12 were reported for the following equilibria:

$$NpO_2^{2+} + H_2O \leftrightarrows NpO_2OH^+ + H^+ \tag{6.49}$$

$$2NpO_2^{2+} + 2H_2O \leftrightarrows (NpO_2)_2(OH)_2^{2+} + 2H^+ \tag{6.50}$$

$$3NpO_2^{2+} + 5H_2O \leftrightarrows (NpO_2)_3(OH)_5^+ + 5H^+ \tag{6.51}$$

The value $\log{}^*K_{11} = -5.17$ is consistent with the value ($\log{}^*K_{11} = -5.45$) reported by Schmidt *et al.* (1983), while the hydrolysis scheme proposed by Moskvin (1971) based on solubility measurements is rather different. Comparison of the results (Cassol *et al.*, 1972a) with some available data on the hydrolysis of U(VI) (Rush *et al.*, 1962; Rush and Johnson, 1963) and Pu(VI) (Cassol *et al.*, 1972b) indicates a close analogy in hydrolysis behavior for the three ions. The tendency in acidity with increasing atomic number is in the order of $UO_2^{2+} > NpO_2^{2+} > PuO_2^{2+}$.

Kato *et al.* (1996) have determined the solubility product of neptunium trioxide monohydrate at 298 K in acidic 0.1 M $NaClO_4$ solution prepared with ozone in air.

$$NpO_3H_2O(s) + 2H^+ \leftrightarrows NpO_2^{2+} + 2H_2O \tag{6.52}$$

The solid was characterized to be $NpO_3 \cdot H_2O$, not $NpO_2(OH)_2$, by X-ray diffraction and Fourier transform infrared spectroscopy (FTIR).

(e) Neptunium(VII)

A cationic Np(VII) species in acidic solutions (Shilov *et al.*, 1991) and an anionic species in strongly alkaline solutions (Chaikhorskii *et al.*, 1975) have been reported, but no thermodynamic data are available. Np(VII) hydroxide or hydrated oxide has been prepared by several groups (Chaikhorskii *et al.*, 1974; Nikonov *et al.*, 1994) using different methods. No thermodynamic data for Np(VII) hydroxide and oxide are available.

6.9 COORDINATION COMPLEXES IN SOLUTION

Representative equilibrium constants and the experimental conditions at which they were determined are collected in Tables 6.13 and 6.14 for neptunium complexes with inorganic and organic ligands, respectively. Data on complex formation of neptunium and of other actinides have been compiled in the literature, e.g. Gel'man *et al.* (1962), Degischer and Choppin (1975), Fuger *et al.* (1992), Lemire *et al.* (2001), Smith and Martell (2002), etc., and are reviewed in Chapters 19 and 23.

In Tables 6.13 and 6.14, the following abbreviations are used in experimental methods: cix, cation exchange; dis, distribution between two phases; em, electromigration; emf, electromotive force; ise, ion selective electrode; pot, potentiometry; red, emf with redox electrode; sol, solubility; sp, spectrophotometry. The stepwise stability constants K_i and overall constants β_i are defined for the reaction of a cation M with a ligand L as follows:

$$K_1 = \beta_1 = [\mathrm{ML}]/[\mathrm{M}][\mathrm{L}], K_2 = [\mathrm{ML_2}]/[\mathrm{ML}][\mathrm{L}], K_3 = [\mathrm{ML_3}]/[\mathrm{ML_2}][\mathrm{L}], \mathrm{etc.}$$

$$\beta_2 = [\mathrm{ML_2}]/[\mathrm{M}][\mathrm{L}]^2, \beta_3 = [\mathrm{ML_3}]/[\mathrm{M}][\mathrm{L}]^3, \mathrm{etc.}$$

Therefore

$$\beta_2 = \mathrm{K_1K_2}, \beta_3 = \mathrm{K_1K_2K_3}, \text{ etc.} \qquad (6.53)$$

The other equilibrium constants are indicated in Tables 6.13 and 6.14.

6.9.1 Complexation with inorganic ligands

All of the equilibrium constants listed in Table 6.13 are for complexes of Np (IV), Np(V), and Np(VI). Only a few studies have been carried out on complexes of Np(III) and Np(VII). Shiloh and Marcus (1966) studied the $\mathrm{Np^{3+}}$–halide system quantitatively by measurement of the absorption spectra. The stability constants for $\mathrm{NpX^{2+}}$ and $\mathrm{NpX_2^+}$ ($\mathrm{X = Cl^-, Br^-}$) were obtained in concentrated LiCl and LiBr solutions, respectively. Mefod'eva *et al.* (1970a,b) reported the complex formation of Np(VII)($\mathrm{NpO_2^{3+}}$) with sulfate ion in acid solution. The stability constants obtained for $\mathrm{NpO_2SO_4^+}$ and $\mathrm{NpO_2(SO_4)_2^-}$ were greater than those of $\mathrm{NpO_2^{2+}}$.

The tendency of a neptunium ion for complex formation, as well as the hydrolysis reaction, depends on its ionic potential, i.e. its formal charge divided by its ionic radius. In analogy with neighboring uranium and plutonium, the order of decreasing ability for complex formation is

$$\mathrm{Np^{4+} > NpO_2^{2+} \geq Np^{3+} > NpO_2^+}$$

The relative complex-forming ability of $\mathrm{Np^{3+}}$ and $\mathrm{NpO_2^{2+}}$ may depend on the ligand and/or the solvent with which these ions are associated. It is difficult to

Table 6.13 *Experimental equilibrium constants for neptunium complexes with inorganic ligands.*

Anion	*Ion*	*Method*	*Temp.* (°C)	*Medium*	*Equilibrium constants*	*References*
Fluoride, F^-						
	Np^{4+}	dis	25	1.0 M $HClO_4$	$\log{}^*\beta_1 = 4.60 \pm 0.20$	Choppin and Unrein (1976)
		dis	25	2.0 M $HClO_4$	$\log{}^*\beta_1 = 4.70 \pm 0.15$	Bagawde *et al.* (1976)
		cix, red	20	4.0 M $HClO_4$	$\log{}^*\beta_1 = 4.82 \pm 0.02$	Ahrland and Brandt (1966)
					$\log{}^*\beta_2 = 7.57 \pm 0.15$	
					$\log{}^*\beta_3 = 9.85$	
					$\log{}^*\beta_4 = 11.15$	
					$\log{}^*\beta_n$; $Np^{4+} + nHL \rightleftarrows NpL_n^{4-n} + nH^+$	
	NpO_2^+	dis	23	1.0 M $NaClO_4$	$\log K_1 = 1.26 \pm 0.30$	Choppin and Rao (1984)
		dis	25	2.0 M $NaClO_4$	$\log K_1 = 0.99 \pm 0.10$	Rao *et al.* (1979)
	NpO_2^{2+}	ise	20	0.1 M $NaClO_4$	$\log K_1 = 4.18 \pm 0.15$	Sawant *et al.* (1985)
					$\log \beta_2 = 6.96 \pm 0.15$	
					$\log \beta_3 = 9.64$	
		emf	25	0.5 M $HClO_4$	$\log{}^*\beta_1 = 1.11 \pm 0.20$	Al-Niaimi *et al.* (1970a)
					$\log{}^*\beta_2 = 1.14 \pm 0.40$	
		dis	20	1.0 M $HClO_4$	$\log{}^*\beta_1 = 0.93 \pm 0.11$	Ahland and Brandt (1968a)
					$\log{}^*\beta_2 = 1.11 \pm 0.10$	
					$\log{}^*\beta_n$; $NpO_2^{2+} + nHL \rightleftarrows NpO_2L_n^{2-n} + nH^+$	
Chloride, Cl^-						
	Np^{4+}	dis	20	0.5 M $HClO_4$	$\log K_1 = 0.15 \pm 0.20$	Shilin and Nazarov (1966)
				1.0 M $HClO_4$	$\log K_1 = -0.04 \pm 0.20$	
				2.0 M $HClO_4$	$\log K_1 = 0.04 \pm 0.20$	
		dis	25	2.0 M $HClO_4$	$\log K_1 = -0.05 \pm 0.05$	Patil and Ramakrishna (1975)
	NpO_2^+	dis	25	2.0 M $NaClO_4$	$\log K_1 = -0.42 \pm 0.04$	Rao *et al.* (1979)
	NpO_2^{2+}	emf	25	0.5 M $HClO_4$	$\log K_1 = -0.35 \pm 0.40$	Al-Niaimi *et al.* (1970b)
Bromide, Br^-						
	Np^{4+}	dis	25	2.0 M $HClO_4$	$\log K_1 = -0.21 \pm 0.01$	Raghavan *et al.* (1975)

Iodide, I^-					
Np^{4+}	dis	25	2.0 м $HClO_4$	$\log K_1 = 0.04 \pm 0.30$	Patil *et al.* (1981)
Iodate, IO_3^-					
NpO_2^+	dis	25	2.0 м $HClO_4$	$\log K_1 = 0.32 \pm 0.30$	Rao *et al.* (1979)
NpO_2^{2+}	sp	25	0.3 м $HClO_4$	$\log K_1 = 0.61 \pm 0.02$	Blokhin *et al.* (1972)
Azide, N_3^-					
NpO_2^+	sp	25	5.0 м $NaClO_4$	$\log K_1 = 1.08$ $\log K_2 = 0.77$ $\log K_3 = 0.38$	Musikas and Marteau (1978)
Nitrite, NO_2^-					
NpO_2^+	dis	25	2.0 м $NaClO_4$	$\log K_1 = -0.05 \pm 0.05$	Rao *et al.* (1979)
Nitrate, NO_3^-					
Np^{4+}	dis	20	1.0 м $HClO_4$	$\log K_1 = 0.34 \pm 0.10$ $\log \beta_2 = 0.08$ $\log \beta_3 = -0.26$	Shilin and Nazarov (1966)
	dis	25	4.0 м $NaClO_4$	$\log K_1 = -0.15 \pm 0.12$ $\log \beta_2 = -0.74 \pm 0.15$	Danesi *et al.* (1971)
NpO_2^+	dis	20	2.0 м $NaClO_4$	$\log K_1 = -0.55 \pm 0.09$	Rao *et al.* (1979)
NpO_2^{2+}	pot	25	0.5 м $HClO_4$	$\log K_1 = -0.96 \pm 0.02$	Al-Niaimi *et al.* (1970b)
	dis	25	4.0 м $NaClO_4$	$\log K_1 = -0.68 \pm 0.06$	Danesi *et al.* (1971)
Thiocyanate, SCN^-					
Np^{4+}	dis	25	2.0 м $HClO_4$	$\log K_1 = 1.49 \pm 0.07$ $\log \beta_2 = 2.06 \pm 0.08$ $\log \beta_3 = 2.53 \pm 0.02$	Rao *et al.* (1978)
NpO_2^+	dis	25	2.0 м $NaClO_4$	$\log K_1 = 0.32 \pm 0.02$	Rao *et al.* (1979)
	sp	25	5.0 м $NaClO_4$	$\log K_1 = 0.86$ $\log \beta_2 = 1.05$	Cuillerdier *et al.* (1977)

Table 6.13 (*Contd.*)

Anion	*Ion*	*Method*	*Temp.* (°C)	*Medium*	*Equilibrium constants*	*References*
Sulfate, SO_4^{2-}						
	Np^{4+}	dis	25	2.0 м $HClO_4$	$\log{}^*\beta_1 = 2.49 \pm 0.03$	Patil and Ramakrishna (1973)
					$\log{}^*\beta_2 = 4.06 \pm 0.02$	
		pol	25	3.0 м $NaClO_4$	$\log{}^*\beta_1 = 2.49 \pm 0.03$	Musikas (1963)
					$\log{}^*\beta_2 = 3.57 \pm 0.09$	
		cix	20	4.0 м $HClO_4$	$\log{}^*\beta_1 = 2.70 \pm 0.04$	Ahrland and Brandt (1966)
					$\log{}^*\beta_2 = 4.26 \pm 0.05$	
					$\log{}^*\beta_n$; $Np^{4+} + nHL^- \rightleftarrows NpL_n^{4-2n} + nH^+$	
	NpO_2^+	dis	25	1.0 м $NaClO_4$	$\log K_1 = 0.06 \pm 0.04$	Halperin and Oliver (1983)
		dis	25	2.0 м $NaClO_4$	$\log K_1 = 0.44 \pm 0.09$	Rao *et al.* (1979)
	NpO_2^{2+}	pot	25	0.1 м $HClO_4$	$\log{}^*\beta_1 = 0.88 \pm 0.01$	Al-Niaimi *et al.* (1970a)
				0.5 м $HClO_4$	$\log{}^*\beta_1 = 0.75 \pm 0.01$	
		dis	21	1.0 м $NaClO_4$	$\log{}^*\beta_1 = 0.79 \pm 0.13$	Ahrland and Brandt (1968b)
					$\log{}^*\beta_2 = 0.55 \pm 0.31$	
		dis	25	2.0 м $HClO_4$	$\log{}^*\beta_1 = 1.07 \pm 0.05$	Patil and Ramakrishna (1976)
					$\log{}^*\beta_2 = 0.60 \pm 0.15$	
					$\log{}^*\beta_n$; $NpO_2^{2+} + nHL^- \rightleftarrows NpO_2L_n^{2-2n} + nH^+$	
Carbonate, CO_3^{2-}						
	NpO_2^+	dis	25	0.1 м $NaClO_4$	$\log K_1 = 4.13 \pm 0.03$	Bidoglio *et al.* (1985)
					$\log K_2 = 2.93$	
		sol	25	1.0 м $NaClO_4$	$\log K_1 = 4.49 \pm 0.06$	Maya (1983)
					$\log K_2 = 2.62 \pm 0.09$	
					$\log K_3 = 1.42 \pm 0.11$	

NpO_2^{2+}	sol	25	0.1 M $NaClO_4$	log $K_{sp} = -10.14 \pm 0.04$; $NaNpO_2L(s) \rightleftarrows Na^+ + NpO_2^+ + L^{2-}$ log $K_1 = 9.02 \pm 0.10$ log $\beta_3 = 20.41 \pm 0.09$	Kato *et al.* (1998)
	pot	25	1.0 M $NaClO_4$	log $K_{sp} = -14.04 \pm 0.07$; $NpO_2L(s) \rightleftarrows NpO_2^{2+} + L^{2-}$ log $\beta_2 = 16.51 \pm 0.14$ log $\beta_3 = 21.15 \pm 0.12$ log $\beta_{213} = -1.49 \pm 0.14$; $2NpO_2^{2+} + L^{2-} + 3H_2O \rightleftarrows$ $(NpO_2)_2L\left(OH_3^-\right) + 3H^+$	Maya (1984)
	sp	22	3.0 M $NaClO_4$	log $\beta_{36} = -10.1 \pm 0.1$; $3NpO_2L_3^{4-} \rightleftarrows (NpO_2)_3L_6^{6-} + 3L^{2-}$	Grenthe *et al.* (1986)
Chromate, CrO_4^{2-}					
Np^{4+}	sp	25	0.2 M $LiClO_4$	log $\beta = 1.81 \pm 0.17$; $Np^{4+} + HL^- \rightleftarrows NpL^{2+} + H^+$	Burkhart and Thompson (1972)
Phosphate, PO_4^{3-}					
NpO_2+	cix	20	0.2 M NH_4ClO_4	log $\beta = 2.85 \pm 0.15$; $NpO_2^+ + HL^{2-} \rightleftarrows NpO_2HL^-$	Moskvin and Peretrukhin (1964)
NpO_2^{2+}	dis	25	1.0 M $NaClO_4$	log $\beta = 2.52 \pm 0.50$; $NpO_2^{2+} + H_2L^- \rightleftarrows NpO_2H_2L^+$ log $\beta = 4.54 \pm 0.70$; $NpO_2^{2+} + HL^{2-} \rightleftarrows NpO_2HL$ log $\beta = 7.5 \pm 1.0$; $NpO_2^{2+} + 2HL^{2-} = NpO_2(HL)_2^{2-}$	Mathur and Choppin (1994)

Table 6.14 *Experimental equilibrium constants for neptunium complexes with organic ligands.*

Anion	*Ion*	*Method*	*Temp.* (°C)	*Medium*	*Equilibrium constants*	*References*
Acetate, CH_3COO^-						
	NpO_2^+	em	25	0.3 м $NaClO_4$	$\log K_1 = 0.96$	Rösch *et al.* (1990)
					$\log K_2 = 0.61$	
		spec	25	2.0 м $NaClO_4$	$\log K_1 = 0.87 \pm 0.03$	Rizkalla *et al.* (1990a)
	NpO_2^{2+}	pot	20	1.0 м $NaClO_4$	$\log K_1 = 2.31 \pm 0.02$	Portanova *et al.* (1970)
					$\log \beta_2 = 4.23 \pm 0.05$	
					$\log \beta_3 = 6.00 \pm 0.19$	
Propionate, $C_2H_5COO^-$						
	NpO_2^{2+}	pot	20	1.0 м $NaClO_4$	$\log K_1 = 2.44 \pm 0.03$	Cassol *et al.* (1969)
					$\log \beta_2 = 4.45 \pm 0.03$	
					$\log \beta_3 = 6.49 \pm 0.08$	
Monochloroacetate, CH_2ClCOO^-						
	NpO_2^+	spec	25	2.0 м $NaClO_4$	$\log K_1 = 0.00 \pm 0.05$	Rizkalla *et al.* (1990a)
	NpO_2^{2+}	pot	20	1.0 м $NaClO_4$	$\log K_1 = 1.33 \pm 0.02$	Cassol *et al.* (1969)
					$\log \beta_2 = 2.10 \pm 0.07$	
					$\log \beta_3 = 2.78 \pm 0.34$	
β-Chloropropionate, $CH_2ClCH_2COO^-$						
	NpO_2^{2+}	pot	20	1.0 м $NaClO_4$	$\log K_1 = 1.88 \pm 0.03$	Cassol *et al.* (1969)
					$\log \beta_2 = 3.30 \pm 0.04$	
					$\log \beta_3 = 3.60 \pm 0.32$	
Glycolate, $CH_2(OH)COO^-$						
	NpO_2^+	spec	25	0.1 м $NaClO_4$	$\log K_1 = 1.51 \pm 0.03$	Eberle and Schaefer (1969)
		spec	25	2.0 м $NaClO_4$	$\log K_1 = 1.43 \pm 0.02$	Rizkalla *et al.* (1990a)
					$\log \beta_2 = 1.90 \pm 0.03$	
		dis	25	1.0 м $NaClO_4$	$\log K_1 = 1.31 \pm 0.04$	Tochiyama *et al.* (1992)
					$\log \beta_2 = 2.06 \pm 0.03$	
	NpO_2^{2+}	pot	20	1.0 м $NaClO_4$	$\log K_1 = 2.42 \pm 0.03$	Portanova *et al.* (1972)
					$\log \beta_2 = 3.96 \pm 0.03$	
					$\log \beta_3 = 5.00 \pm 0.10$	

Lactate, $CH_3CH(OH)COO^-$					
NpO_2^+	spec	25	0.1 M $NaClO_4$	$\log K_1 = 1.75 \pm 0.02$	Eberle and Schaefer (1969)
	dis	25	1.0 M $NaClO_4$	$\log K_1 = 1.40 \pm 0.02$	Tochiyama *et al.* (1992)
				$\log \beta_2 = 2.01 \pm 0.02$	
α-Hydroxybutyrate, $C_2H_5CH(OH)COO^-$					
NpO_2^+	spec	25	0.1 M $NaClO_4$	$\log K_1 = 1.62 \pm 0.02$	Eberle and Schaefer (1969)
	dis	25	1.0 M $NaClO_4$	$\log K_1 = 1.64 \pm 0.02$	Tochiyama *et al.* (1992)
				$\log \beta_2 = 2.13 \pm 0.03$	
α-Hydroxyvalerate, $C_3H_7CH(OH)COO^-$					
NpO_2^+	spec	25	0.1 M $NaClO_4$	$\log K_1 = 1.59 \pm 0.03$	Eberle and Schaefer (1969)
α-Hydroxycapronate, $C_4H_9CH(OH)COO^-$					
NpO_2^+	spec	25	0.1 M $NaClO_4$	$\log K_1 = 1.63 \pm 0.02$	Eberle and Schaefer (1969)
α-Hydroxyisobutyrate, $(CH_3)_2C(OH)COO^-$					
NpO_2^+	spec	25	2.0 M $NaClO_4$	$\log K_1 = 1.80 \pm 0.01$	Rizkalla *et al.* (1990a)
	dis	25	1.0 M $NaClO_4$	$\log K_1 = 1.73 \pm 0.02$	Tochiyama *et al.* (1992)
				$\log \beta_2 = 2.46 \pm 0.02$	
NpO_2^{2+}	pot	20	1.0 M $NaClO_4$	$\log K_1 = 3.15 \pm 0.04$	Magon *et al.* (1974)
				$\log K_2 = 2.10 \pm 0.10$	
Glycinate, $NH_2CH_2COO^-$					
NpO_2^+	spec	25	0.1 M $NaClO_4$	$\log K_1 = 3.31 \pm 0.02$	Eberle and Wede (1968)
				$\log \beta_2 = 5.44 \pm 0.07$	
α-Picolinate, $NC_5H_4COO^-$					
Np^{4+}	spec	25	1.0 M $NaClO_4$	$\log K_1 = 6.50 \pm 0.01$	Paul (1970)
NpO_2^+	dis	25	1.0 M $NaClO_4$	$\log K_1 = 3.53 \pm 0.03$	Tochiyama *et al.* (1992)
				$\log \beta_2 = 6.01 \pm 0.03$	
Salicylate, $C_6H_4(OH)COO^-$					
NpO_2^+	spec	25	2.0 M $NaClO_4$	$\log \beta_H = 0.20 \pm 0.01$	Rizkalla *et al.* (1990a)
Oxalate, $(COO^-)_2$ $(=L^{2-})$					
NpO_2^+	pot	20	1.0 M $NaClO_4$	$\log K_1 = 3.74 \pm 0.05$	Magon *et al.* (1972)
				$\log \beta_2 = 6.31 \pm 0.10$	
	dis	25	1.0 M $NaClO_4$	$\log K_1 = 3.71 \pm 0.02$	Tochiyama *et al.* (1992)

Table 6.14 (*Contd.*)

Anion	*Ion*	*Method*	*Temp.* (°C)	*Medium*	*Equilibrium constants*	*References*
					log $\beta_2 = 6.15 \pm 0.02$	
Malonate, $^{-}OOCCH_2COO^{-}$ (=L^{2-})						
	NpO_2^+	pot	20	1.0 M $NaClO_4$	log $K_1 = 2.75 \pm 0.02$	Magon *et al.* (1972)
		dis	25	1.0 M $NaClO_4$	log $K_1 = 2.62 \pm 0.02$	Tochiyama *et al.* (1992)
					log $\beta_2 = 4.22 \pm 0.02$	
Succinate, $^{-}OOC(CH_2)_2COO^{-}$ (=L^{2-})						
	NpO_2^+	pot	20	1.0 M $NaClO_4$	log $K_1 = 1.72 \pm 0.03$	Magon *et al.* (1972)
		dis	25	1.0 M $NaClO_4$	log $K_1 = 1.45 \pm 0.06$	Tochiyama *et al.* (1992)
					log $\beta_2 = 2.43 \pm 0.05$	
Maleate, $^{-}OOC(CH)_2COO^{-}$ (=L^{2-})						
	NpO_2^+	pot	20	1.0 M $NaClO_4$	log $K_1 = 2.20 \pm 0.02$	Magon *et al.* (1972)
Phthalate, $C_6H_4(COO^{-})_2$ (=L^{2-})						
	NpO_2^+	pot	20	1.0 M $NaClO_4$	log $K_1 = 2.22 \pm 0.02$	Magon *et al.* (1972)
		spec	25	1.0 M $NaClO_4$	log $K_1 = 1.62 \pm 0.02$	Choppin *et al.* (1998)
Trimellitate, $C_6H_3(COO^{-})_3$ (=L^{3-})						
	NpO_2^+	spec	25	1.0 M $NaClO_4$	log $K_1 = 1.57 \pm 0.02$	Choppin *et al.* (1998)
Hemimellitate, $C_6H_3(COO^{-})_3$ (=L^{3-})						
	NpO_2^+	spec	25	1.0 M $NaClO_4$	log $K_1 = 2.44 \pm 0.02$	Choppin *et al.* (1998)
Pyromellitate, $C_6H_2(COO^{-})_4$ (=L^{4-})						
	NpO_2^+	spec	25	1.0 M $NaClO_4$	log $K_1 = 1.80 \pm 0.01$	Choppin *et al.* (1998)
Mellitate, $C_6(COO^{-})_6$ (=L^{6-})						
	NpO_2^+	spec	25	1.0 M $NaClO_4$	log $K_1 = 2.34 \pm 0.01$	Choppin *et al.* (1998)
Oxydiacetate, $O(CH_2COO^{-})_2$ (=L^{2-})						
	NpO_2^+	spec	25	0.5 M $NaClO_4$	log $K_1 = 3.72 \pm 0.01$	Rizkalla *et al.* (1990b)
	NpO_2^{2+}	pot	20	1.0 M $NaClO_4$	log $K_1 = 5.16 \pm 0.01$	Cassol *et al.* (1973)
Thiodiacetate, $S(CH_2COO^{-})_2$ (=L^{2-})						
	NpO_2^+	spec	25	0.5 M $NaClO_4$	log $K_1 = 1.18 \pm 0.04$	Rizkalla *et al.* (1990b)

Citrate, $^{-}OOCCH_2C(OH)(COO^{-})CH_2COO^{-}$ (=L^{3-})					
NpO_2^{+}	spec	25	2.0 M $NaClO_4$	log $K_1 = 2.49 \pm 0.01$	Rizkalla *et al.* (1990a)
	spec	25	0.5 M $NaClO_4$	log $K_1 = 2.73 \pm 0.02$	Palade (1997)
			1.0 M $NaClO_4$	log $K_1 = 2.74 \pm 0.02$	
			2.0 M $NaClO_4$	log $K_1 = 2.81 \pm 0.02$	
Iminodiacetate, $^{-}OOCCH_2NHCH_2COO^{-}$ (=L^{2-})					
NpO_2^{+}	spec	25	0.1 M $NaClO_4$	log $K_1 = 6.27 \pm 0.11$ log $\beta_H = 1.35 \pm 0.52$; $NpO_2^{+} + HL^{-} \rightleftarrows NpO_2HL$	Eberle and Wede (1970)
NpO_2^{2+}	pot	20	1.0 M $NaClO_4$	log $K_1 = 8.72 \pm 0.02$	Cassol *et al.* (1973)
N-Methyliminodiacetate, $^{-}OOCCH_2N(CH_3)CH_2COO^{-}$ (=L^{2-})					
NpO_2^{+}	spec	25	0.1 M $NaClO_4$	log $K_1 = 7.37 \pm 0.05$ log $\beta_H = 1.28 \pm 0.48$; $NpO_2^{+} + HL^{-} \rightleftarrows NpO_2HL$	Eberle and Wede (1970)
N-(2-Hydroxyethyl)iminodiacetate, $^{-}OOCCH_2N(C_2H_4OH)CH_2COO^{-}$ (=L^{2-})					
Np^{4+}	spec	25	1.0 M $NaClO_4$	log $K_1 = 12.97 \pm 0.04$ log $K_2 = 10.75 \pm 0.11$	Eberle and Paul (1971)
NpO_2^{+}	spec	25	0.1 M $NaClO_4$	log $K_1 = 6.08 \pm 0.05$ log $\beta_H = 1.45 \pm 0.25$; $NpO_2^{+} + HL^{-} \rightleftarrows NpO_2HL$ $-\log \beta_{OH} = 11.42 \pm 0.03$; $NpO_2L^{-} + H_2O \rightleftarrows NpO_2(OH)L^{2-} + H^{+}$	Eberle and Wede (1970)
Nitrilotriacetate, $NH(CH_2COO^{-})_3$ (=L^{3-})					
Np^{4+}	spec	25	1.0 M $NaClO_4$	log $K_1 = 17.28 \pm 0.02$ log $K_2 = 14.78 \pm 0.07$	Eberle and Paul (1971)
NpO_2^{+}	spec	25	0.1 M $NaClO_4$	log $K_1 = 6.80 \pm 0.10$ log $\beta_H = 1.77 \pm 0.37$; $NpO_2^{+} + HL^{2-} \rightleftarrows NpO_2HL^{-}$ $-\log \beta_{OH} = 11.46 \pm 0.11$; $NpO_2L^{2-} + H_2O \rightleftarrows NpO_2(OH)L^{3-} + H^{+}$	Eberle and Wede (1970)

Table 6.14 (*Contd.*)

Anion	*Ion*	*Method*	*Temp.* (°C)	*Medium*	*Equilibrium constants*	*References*
Nitrilodiacetate mono-*n*-propionate, $–OOC(CH_2)_2N(CH_2COO^-)_2$ ($=L^{3-}$)						
	NpO_2^+	spec	25	0.1 м $NaClO_4$	$\log K_1 = 7.00 \pm 0.09$ $\log \beta_H = 2.35 \pm 0.12$; $NpO_2^+ + HL^{2-} \rightleftarrows NpO_2HL^-$ $-\log \beta_{OH} = 11.57 \pm 0.09$; $NpO_2L^{2-} + H_2O \rightleftarrows NpO_2(OH)L^{3-} + H^+$	Eberle and Wede (1970)
N-(2-Hydroxyethyl)ethylenediamine-*N*,*N′*,*N′*-triacetate, $(HOC_2H_4)(^-OOCCH_2)N(CH_2)_2N(CH_2COO^-)_2$ ($=L^{3-}$)						
	Np^{4+}	spec	25	1.0 м $NaClO_4$	$\log K_1 = 20.82 \pm 0.13$ $\log K_2 = 12.77 \pm 0.16$	Eberle and Paul (1971)
	NpO_2^+	spec	25	0.1 м $NaClO_4$	$\log K_1 = 6.87 \pm 0.11$ $\log \beta_H = 4.06 \pm 0.01$; $NpO_2^+ + HL^{2-} \rightleftarrows NpO_2HL^-$ $-\log \beta_{OH} = 11.37 \pm 0.10$; $NpO_2L^{2-} + H_2O \rightleftarrows NpO_2(OH)L^{3-} + H^+$	Eberle and Wede (1970)
Ethylenediamine-*N*,*N*,*N′*,*N′*,-tetraacetate, $(^-OOCCH_2)_2N(CH_2)_2N(CH_2COO^-)_2$ ($=L^{4-}$)						
	Np^{4+}	spec	25	1.0 м $NaClO_4$	$\log K_1 = 24.55 \pm 0.03$	Eberle and Paul (1971)
	NpO_2^+	spec	25	0.1 м $NaClO_4$	$\log K_1 = 7.33 \pm 0.06$ $\log \beta_H = 5.30 \pm 0.08$; $NpO_2^+ + HL^{3-} \rightleftarrows NpO_2HL^{2-}$ $-\log \beta_{OH} = 11.51 \pm 0.08$; $NpO_2L^{3-} + H_2O \rightleftarrows NpO_2(OH)L^{4-} + H^+$	Eberle and Wede (1970)
Diethylenetriamine-N,N,*N′*,*N″*,*N″*-pentaacetate, $^-OOCCH_2N[(CH_2)_2N(CH_2COO^-)_2]_2$ ($=L^{5-}$)						
	Np^{4+}	spec	20	0.5 м $NaClO_4$	$\log K_1 = 29.29 \pm 0.02$	Piskunov and Rykov (1972)
		spec	25	1.0 м $NaClO_4$	$\log K_1 = 30.33 \pm 0.12$	Eberle and Paul (1971)

compare the data listed in Table 6.13 because of the wide range of experimental conditions used and the lack of data for a given oxidation state of the ions with some ligands. However, the stability sequence for complexes of Np(IV), Np(V), or Np(VI) with monovalent inorganic ligands is seen to be

$$F^- > H_2PO_4^- > SCN^- > NO_3^- > Cl^- > ClO_4^-$$

For divalent inorganic ligands, the sequence is

$$CO_3^{2-} > HPO_4^{2-} > SO_4^{2-}$$

as would be expected from the relative strengths of the corresponding acids. Divalent ligands are more strongly complexing than monovalent ligands.

In addition to the data in Table 6.13, Np(V) (NpO_2^+) is known to form 'cation–cation' complexes with some multiply charged cations. The dioxo cation NpO_2^+ in perchloric acid solution forms complex ions with trivalent cations of Al, Ga, Sc, In, Fe, Cr, and Rh (Sullivan, 1962, 1964). The relative strength of the interaction between NpO_2^+ and M^{3+} was found to follow the following order: Fe > In > Sc > Ga > Al. Some of these polynuclear complexes such as $[NpO_2^+Cr^{3+}]$ and $[NpO_2^+Rh^{3+}]$ have been isolated by using an ion-exchange method, while the others were detected by spectrophotometry. The $[NpO_2^+Cr^{3+}]$ complex is also formed by the reduction of NpO_2^{2+} with Cr^{2+}. The formation of the complex between NpO_2^+ and UO_2^{2+} has extensively been studied by the use of potentiometry, spectrophotometry, Raman spectroscopy, and large-angle X-ray scattering (Sullivan *et al.*, 1961; Guillaume *et al.*, 1982, 1983; Stout *et al.*, 1993).

6.9.2 Complexation with organic ligands

With some exceptions, most of the data in Table 6.14 are for complexes of Np(V) with organic ligands. The following presents the results on several selected systems.

Stability data for complexes of M(VI) ions MO_2^{2+} (M = U, Np, and Pu) with monocarboxylic ligands L (L = acetate, propionate, monochloroacetate, and β-chloropropionate) have been reported and discussed by Cassol *et al.* (1969) and Portanova *et al.* (1970). In the range of ligand concentrations examined, complexes are formed in which the highest average ligand number is three. The stability order of complexes of the various ligands examined is $UO_2^{2+} > NpO_2^{2+} > PuO_2^{2+}$. The stability of complexes of a given MO_2^{2+} ion increases with increasing ligand basicity (pK_a), which suggests a strong 'hard' ionic character of these oxycations.

The stability constants of Np(V) complexes with a series of α-hydroxycarboxylates (e.g. glycolate and lactate) have been obtained by spectrophotometry (Eberle and Schaefer, 1969; Rizkalla *et al.*, 1990a) and solvent extraction (Tochiyama *et al.*, 1992). The stability of the α-hydroxycarboxylate complexes appears to increase a little with pK_a of the ligand, although the stability of these complexes is not much different. The stability of Np(V) complexes with aliphatic dicarboxylates (e.g. oxalate and malonate) has also been studied by potentiometry (Magon *et al.*, 1972), spectrophotometry (Stout *et al.*, 1989), and solvent extraction (Tochiyama *et al.*, 1992). The stability of the complexes is controlled mainly by the size of the chelate ring. In spite of the increase in the basicity of the ligand, the stability of the complexes decreases with increasing the number of carbon atoms between two carboxylate groups in the ligand.

The complexation of Np(v) with aromatic polycarboxylates has been studied by spectrophotometry (Choppin *et al.*, 1998). The stability constants of the 1:1 complexes decreases in the order: hemimellitate > mellitate > pyromellitate > trimellitate≃phthalate. After correction for the number of chelating binding (bidentate) sites, the stability constants with all ligands except hemimellitate are approximately the same. The greater strength of hemimellitate complexation is attributed to an increase in electron density at the binding site through induction from the non-chelating carboxylate group.

With aliphatic aminopolycarboxylate ligands, the complexation of Np(iv) or Np(v) has been studied by spectrophotometry (Eberle and Paul, 1971; Eberle and Wede, 1970). The logarithms of the stability constants of the Np(iv) complexes increase linearly with the number of bound donor atoms of the ligands. On the other hand, the Np(v) ion forms protonated and normal chelates of 1:1 stoichiometry. In addition, at high pH chelate hydroxides with one ligand molecule and one hydroxyl group per NpO_2^+ are formed. The nature of the ligand has only slight or no influence on the stability constants of normal chelates or chelate hydroxides, respectively, suggesting that not more than two carboxylic groups and one amine-nitrogen are bound from one ligand to the central neptunium.

6.10 ANALYTICAL CHEMISTRY AND SPECTROSCOPIC TECHNIQUES

The concentration of ^{237}Np and the radioactivity arising from this nuclide in the environment is extremely low compared to most other α emitters. The background concentration of ^{237}Np in seawater due to global fallout was estimated to be at a level of 10^{-15} to 10^{-14} g L^{-1} (Novikov *et al.*, 1989; Jha and Bhat, 1994). However, with the increase in nuclear power generation, this nuclide has become one of the most important from the viewpoint of long-term disposal of the radioactive waste. In fact, the analytical results showing contamination of ^{237}Np in seawater from nuclear fuel reprocessing plants have been reported, e.g. the concentrations of ^{237}Np were $3 \times 10^{-12} - 5.5 \times 10^{-11}$ g kg^{-1} in some samples from Irish sea (Pentreath and Harvey, 1981), 3×10^{-12} g kg^{-1} from Goury near La Hague, France (Germain *et al.*, 1987), $(2.3 \pm 0.4) \times 10^{-11}$ g kg^{-1} from English disposal area (May *et al.*, 1987), and $2 \times 10^{-12} \sim 2 \times 10^{-11}$ g L^{-1} in a waste discharge point at Trombay, India (Jha and Bhat, 1994). More sensitive methods for measuring such low levels of ^{237}Np must be developed and applied. Novikov *et al.* (1989) reviewed the analytical methods to be applied to

^{237}Np in the environmental samples. Hursthouse *et al.* (1992) performed a comparative study to evaluate the practical advantages and disadvantages of the methods. Lee *et al.* (1995) reported the result of an intercomparison study by eight laboratories of low-level ^{237}Np determination in artificial urine samples in order to evaluate and establish the optimal method for a routine *in vivo* radioassay program. In addition, precise determination of the ^{237}Np in the nuclear spent fuel or HLW from the reprocessing process is still a major concern in the field of nuclear engineering as well as the related research and development works.

6.10.1 Radiometric methods

Radiometric methods that are based on counting of alpha particles from ^{237}Np and neutron activation of ^{237}Np have been widely employed for the quantitative analysis of trace amount of ^{237}Np in environmental samples. The alpha-particle counting method is useful for the rapid and low-cost determination of trace quantity of ^{237}Np (specific radioactivity = 2.6×10^{7} Bq g^{-1}). A recent report by Pavlotskaya (1997) reviewed critically the radiochemical analysis methods for the determination of a trace quantity of neptunium in environmental samples.

(a) Alpha- and gamma-ray spectrometry

Alpha spectroscopy with solid state detectors enables the determination of ^{237}Np in a thin sample of a mixture with other α emitters such as ^{239}Pu and ^{241}Am. A preparation of sufficiently thin counting source is a key in the measurement of a reproducible spectrum without a disturbance from the self-absorption of alpha particles in the source. A simple method adopting an evaporation of the sample solution on the source substrate such as a plate of stainless steel or platinum is typically employed. Methods based on the electrodeposition of neptunium directly on the source substrate are useful to prepare thinner sources. Coprecipitation methods are simple and feasible for the preparation of counting sources but may not yield a sufficiently thin source for energy discrimination. Kimura (1990a) utilized $BiPO_4$ precipitate for the quantitative recovery and the preparation of alpha-counting sources for the simultaneous determination of Np, Pu, Am, and Cm.

Holm *et al.* (1987) applied alpha spectroscopy to the determination of the fallout level of ^{237}Np in large volume samples of seawater. They employed a method for the isolation of ^{237}Np by a hydroxide coprecipitation, ion-exchange chromatography, a LaF_3 coprecipitation, and a solvent extraction with HTTA. Yamamoto *et al.* (1989) developed a method for determination of low levels of ^{237}Np in soil and sediment samples. The separation scheme they developed is shown in Fig. 6.12 and consists of leaching of neptunium by aqua regia, separation and purification by TnOA extraction, LaF_3 coprecipitation, and

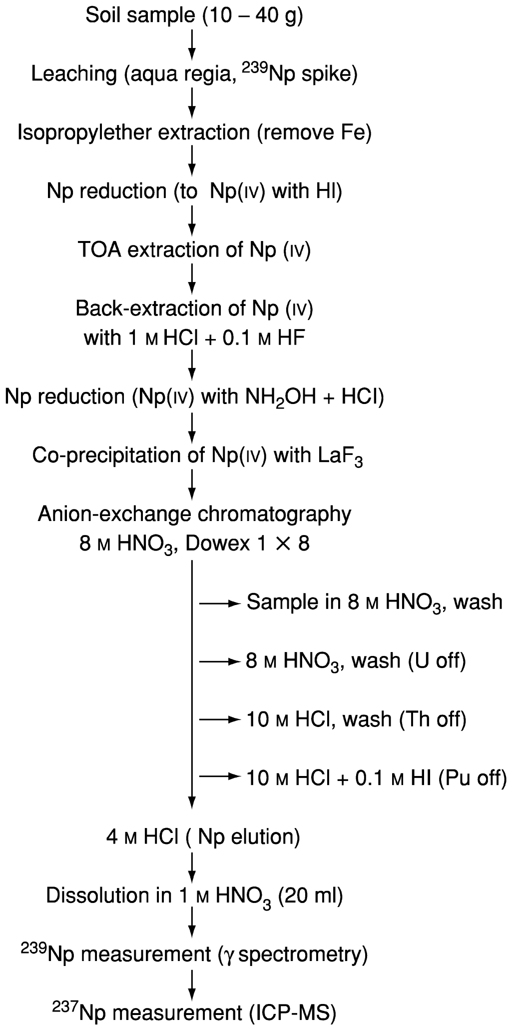

Fig. 6.12 *Chemical separation scheme for the determination of ^{237}Np by high-resolution ICP-MS.* (*Yamamoto* et al., 1994, *with permission from Elsevier Science*).

two steps of anion-exchange chromatography. ^{239}Np was used as a chemical yield monitor. The chemical yield of neptunium ranged from 50 to 84%. The detection limit for ^{237}Np was about 0.1 mBq per sample.

A method for the simultaneous determination of ^{237}Np and ^{239}Np in air, total deposition and sediment samples in ocean was developed (Rosner *et al.*, 1993). Alpha- and gamma-ray spectroscopies were used.

Alpha- and gamma-ray spectroscopies were applied to the determination of ^{237}Np in spent nuclear fuels (Shinohara *et al.*, 1989). After ion-exchange separation of the dissolved fuel solution, the content of ^{237}Np was determined from the activity of ^{237}Np or ^{233}Pa, which is in radioactive equilibrium with ^{237}Np. The chemical yield was determined using inherent ^{239}Np. The proposed method does not require quantitative separation of neptunium and can be applied to routine analyses of burnup for the nuclear spent fuel.

One of the few uses of gamma spectroscopy for Np radioanalysis was that of isotope dilution gamma-ray spectroscopy method using ^{239}Np as a spike for the determination of ^{237}Np in uranium, plutonium, and mixed oxide samples (Sus *et al.*, 1996). Extraction chromatography with trialaurylamine fixed on a SGX-C18 support was used for the isolation of neptunium. A pair of γ-rays of 86.53 keV (^{237}Np) and 106.13 keV (^{239}Np) was employed for the detection. The detection limit was evaluated to be 5×10^{-8} g ^{237}Np.

(b) Liquid scintillation counting method

Liquid scintillation counting method does not require extensive sample preparation and is very sensitive for alpha-decaying radionuclides such as ^{237}Np. The alpha liquid scintillation method with rejection of γ emitters (PERALS spectrometer) is useful because of its high sensitivity, selectivity, and rapid sample preparation. Aupiais *et al.* (1999) developed a method for the determination of ^{237}Np which consists of (1) oxidation of Np(v) to Np(vi) with Ag(ii), (2) extraction of Np(vi) from 0.5 to 0.75 M HNO_3 solution into the extractive scintillation cocktail of TOPO, and (3) gamma liquid scintillation counting with rejection of γ emitters. The method was applied to the biological samples.

The pulse shape discrimination (PSD) technique was introduced to liquid scintillation counting by Yang *et al.* (1994) for the determination of ^{237}Np coexisting with plutonium and americium. Np(iv) was separated from Pu(iii), Am(iii), and fission product elements by two steps of solvent extraction using TTA–xylene and triisooctylamine(TIOA)–xylene. The PDS technique enabled the alpha counting with an efficiency of higher than 99% and a beta discrimination factor of higher than 99.95%. The proposed method was applied to the determination of neptunium, plutonium, and americium in the HLW.

(c) Activation analysis

Neutron activation analysis based on ^{237}Np(n,γ)^{238}Np ($t_{1/2}$ of ^{238}Np = 2.117 days) reaction, for which the activation cross section is large and 170 barns, is one of the most sensitive methods for the determination of ^{237}Np. In general, neutron activation analysis is ca. 500 times more sensitive than the alpha-counting method. The procedure consists of (1) pretreatment of the sample, i.e. the leaching of ^{237}Np from the solid sample and the oxidation state adjustment at Np(iv), (2) the separation and preconcentration of Np(iv), (3) neutron irradiation, (4) separation of Np(iv) from the irradiated sample, and (5) the determination of ^{238}Np by gamma-ray spectroscopy. May *et al.* (1987) applied this method to irradiated nuclear fuels, radioactive waste solutions, and environmental samples such as seawater and submarine fauna and flora of disposal areas. Cation-exchange chromatography with Dowex 1 × 8 was employed to separate Np(IV) both before and after the irradiation. They determined the detection limit to be 5×10^{-13} g ^{237}Np. A similar procedure was applied to the sediment samples around Sellafield, Cumbria (Bryne, 1986) and the samples taken from the marine environment of coastal nuclear sites in India (Jha and Bhat, 1994). Depending on the nature of the sample, the removal of the bulk of the iron is required, and they employed solvent extraction with methylisobutylketone (MIBK) or isopropyl ether. After the irradiation, ^{238}Np purified by solvent extraction of Np(IV) with HTTA (cf. Fig. 6.12). If necessary, neptunium ions in a large volume of the sample solution such as seawater sample was preconcentrated by coprecipitation with iron(III) hydroxide precipitate, and Na^+ (^{24}Na) was removed from the irradiated sample using the flow-through column of the hydrated antimony pentoxide. The chemical yield was monitored, usually with ^{239}Np tracer. Bryne (1986) evaluated the detection limit by this method to be 0.1 to 0.5 mBq ^{237}Np.

Neutron activation analysis using epithermal neutron was applied to the determination of ^{237}Np for the purpose of an environmental monitoring of Yucca Mountain area (Riggle, 1992). The sensitivity obtained by the activation analysis using epithermal neutrons was found to be similar to that by using thermal neutrons. The neutron activation analysis method is also feasible for the determination of ^{235}Np and Zhao *et al.* (1991) applied this method to the determination of ^{235}Np in silicate samples.

Maslov *et al.* (1997) developed a highly sensitive method based on the (γ,f) reaction of ^{237}Np followed by the fission track counting. The proposed method was feasible for the determination of ultra-trace amount of ^{237}Np, e.g. in environmental water, and the detection limit was estimated to be 1×10^{-14} g ^{237}Np.

6.10.2 Spectrophotometric method

Several spectrophotometric methods are available: (1) absorption spectrophotometry of Np ions (direct absorption spectrophotometry); (2) absorption spectrometry of the colored complexes formed by Np ions and a chelating reagent; and (3) fluorescence spectrophotometry. A report by Burney and Harbour (1974) summarized and evaluated traditional spectrophotometric methods.

The direct absorption spectrophotometry is useful for the speciation of the Np ions in a solution by a simple procedure, though the sensitivity is not high. The most appropriate wavelengths for the determination of Np^{3+}, Np^{4+}, NpO_2^+, and NpO_2^{2+} in 2 M $HClO_4$ are 786 nm (molar extinction coefficient ε is approximately 45 $mol^{-1}\ dm^3\ cm^{-1}$), 960 nm ($\varepsilon = 160\ mol^{-1}\ dm^3\ cm^{-1}$), 980 nm

($\varepsilon = 395$ mol^{-1} dm^3 cm^{-1}), and 1223 nm ($\varepsilon = 45$ mol^{-1} dm^3 cm^{-1}), respectively (cf. Fig. 6.11). This method is useful for rapid and non-destructive speciation of the Np ions in acidic solution. The detection limits are approximately 5×10^{-4} M Np^{3+}, 1×10^{-4} M Np^{4+}, 5×10^{-5} M NpO_2^+, and 5×10^{-4} M NpO_2^{2+} simply assuming that the lowest detectable absorption is 0.02.

LIPAS enables the direct detection of the ions of relatively low concentration in the solution (Schrepp *et al.*, 1983; Klenze and Kim, 1988). An utilization of LIPAS leads to an enhancement of the sensitivity by a factor of ten or more compared with traditional absorption spectrophotometry. Pollard *et al.* (1988) realized the sensitivity in the measurement of Np(IV), Np(V), and Np(VI) of ca. 10^{-7} M in acidic solution using a dual beam LIPAS system equipped in Harwell. The LIPAS was applied to the monitoring of Np(V) in the nitric acid solution of the Purex process condition (Kihara *et al.*, 1996).

Colored complexes of neptunium with high absorption ability have been utilized for the sensitive determination of neptunium (Burney and Harbour, 1974). A method using the complex of Np(IV) and 1,8-dihydroxy–3,6-disulfonicnaphthalene–2,7diazo, commonly referred to as arsenazo-III, is one of the most sensitive with a molar extinction coefficient of 10^5 mol^{-1} dm^3 cm^{-1} at 665 nm, when the complex is formed in 4–6 M HNO_3. Uranium, thorium, plutonium, and other ions also form complexes with arsenazo-III, and therefore these ions should be removed from the sample solution before the color formation reaction. Solvent extraction with HDEHP acid or TIOA was used to separate neptunium from these interfering ions. The detection limit obtained by arsenazo-III method is approximately 4×10^{-8} g ml^{-1} of neptunium. Thorin, xylenol orange, and chlorophosphonazo III are other common color-forming reagents for use in the determination of neptunium.

6.10.3 Luminescence methods

Measurement of the luminescence intensity from a phosphor such as CaF_2- or $PbMpO_4$-based crystal that is doped with neptunium makes the sensitive determination of neptunium possible. Aleksandruk *et al.* (1990, 1991a) developed a method that consisted of the leaching of neptunium from solid samples such as soil, the isolation of the neptunium by solvent extraction and extraction chromatography, and counting the luminescence intensity at 651 or 663 nm from a CaF_2(Np) crystal at 77 K using a nitrogen pulsed laser (337 nm) as the excitation source. Neptunium was concentrated on the surface layer of a CaF_2 pellet, which resulted as a remarkable improvement of the sensitivity (Aleksandruk *et al.*, 1990). The detection limit of the absolute amount of neptunium was approximately 10^{-12} to 5×10^{-13} g. The proposed method was applied to the determination of Np in soil samples taken from the 30 km zone of the Chernobyl area.

Several attempts have been made to improve the reliability or the sensitivity of the luminescence method. Stepanov *et al.* (1997) proposed a method using uranium as an internal standard to enhance the reliability of determination of neptunium with CaF_2 phosphor. The procedure was applied to the neptunium analysis of nuclear materials. Ivanova *et al.* (1994) utilized a novel method for the preconcentration of neptunium with high concentrating efficiency by the use of a solid-supported liquid membrane containing trioctylmethylammonium nitrate, which was directly subjected to the preparation of the CaF_2 or $PbMoO_4$ phosphor. The detection limit was 1×10^{-13} g ml^{-1} in pure water and 5×10^{-13} g g^{-1} in soil sample. An alternative membrane technique, which is chemically compatible with the preparation of $PbMoO_4$ phosphor, was utilized by Novikov *et al.* (1997) for the preconcentration of neptunium and plutonium. The elaborate procedure for the determination of neptunium and plutonium consists of the HDEHP solvent extraction of Np(IV) and Pu(IV) from the soil leach and accumulation of these ions on the solid-supported aqueous membrane with $K_{10}P_2W_{17}O_{61}$.

Time-resolved laser-induced fluorescence spectroscopy (TRLFS) was applied for the analysis of Np in plutonium samples (Aleksandruk *et al.*, 1991b) to attain a detection limit of 2×10^{-12} g Np.

6.10.4 X-ray fluorescence spectroscopy (XRF)

The XRF technique, which is essentially a non-destructive method, does not require the removal of uranium, plutonium, and other elements, and can be applied to solid and liquid samples. This technique was utilized to monitor the neptunium content in the products of nuclear spent fuel reprocessing (Akopov *et al.*, 1988). It was found that neptunium of more than 4 mg L^{-1} could be determined by XRF using a high intensity X-ray source and Si:Li detector, when the Np/U and Np/Pu ratios were higher than 1/80 and 1/40, respectively. If the sample contained higher concentration of U or Pu, extraction chromatography was employed to remove these elements from neptunium and the detection limit was lowered to 0.1 mg L^{-1}.

A gamma-ray induced energy-dispersive K-line XRF was applied to the determination of heavy metals such as neptunium, uranium, and plutonium in the Purex process solution using a gamma-ray excitation source of ^{57}Co ($t_{1/2}$ = 27.1 days, 10 mCi), ^{133}Ba ($t_{1/2}$ = 10.7 years, 10 mCi), or ^{192}Ir ($t_{1/2}$ = 74 days, 10 Ci) (Pilz *et al.*, 1989). One of the most distinct advantages of this method is the wide dynamic concentration range from ppm level to 400 g L^{-1}.

6.10.5 Mass spectrometry

(a) Surface ionization mass spectrometry (SIMS)

Isotope dilution mass spectrometry using ^{235}Np or ^{239}Np as a spike is a useful method for the sensitive and precise determination of ^{237}Np. An ion source of surface ionization diffusion (SID)-type, which is prepared by electroplating neptunium and overplating the sample with rhenium or platinum metal film, was applied to the detection of neptunium (Efurd *et al.*, 1986). This technique was applicable to ^{237}Np amounts ranging from 10^{-17} to 10^{-8} g.

(b) ICP-MS

ICP-MS has become one of the most powerful methods for the determination of ultra-trace levels of ^{237}Np in many kinds of samples such as environmental and biological samples, uranium fuels, and Purex process solutions. Distinct advantages of this method are a capability of a simultaneous multi-element analysis providing information on the isotopic composition for a large number of elements with high precision and accuracy, as well as a rapid analysis compared with traditional alpha spectrometry and neutron activation analysis, which require tedious pretreatment and measurement procedures. Interfering elements such as uranium and other heavy elements must be removed from the sample solution using optimum chemical separation methods. The separation of uranium, in particular, is important to avoid the interference from the downmass tailing of ^{238}U.

Kim *et al.* (1989) recommended a separation scheme for the ICP-MS analysis of ^{237}Np in a soil:solvent extraction with isopropyl ether to remove iron, solvent extraction with TOA to recover neptunium, and three-step anion-exchange chromatography. They obtained a detection limit of 0.02 mBq ml^{-1} (ca. 8×10^{-13} g ml^{-1}) of ^{237}Np. Yamamoto *et al.* (1994) conducted ICP-MS analysis of ^{237}Np in paddy field soil samples in Japan using high-resolution ICP-MS equipped with a double-focusing mass spectrometer in order to elucidate the temporal feature of global fallout of ^{237}Np deposition.

Riglet *et al.* (1992) applied ICP-MS to the determination of ^{237}Np in enriched uranium solutions. After extracting neptunium as Np(IV) from 1 M HNO_3 solution into 0.5 M HTTA xylene solution and back-extracting in 10 M HNO_3, the ICP-MS signal of ^{237}Np was recorded. Concentrations of ^{237}Np of more than 5 ng in a 1 g uranium sample could be determined. Fig. 6.13 shows a typical ICP-MS spectrum for ^{237}Np in uranium samples.

Barrero Moreno *et al.* (1997) developed a method for the online separation of neptunium, plutonium, and uranium by ion chromatography using a high-capacity cation-exchange column followed by the direct injection of the effluent to the ICP-MS system to determine neptunium and plutonium in the presence of a high concentration of uranium. The method was applied to various kinds of irradiated UO_2 and MOX fuels.

(c) Other methods based on mass spectrometry

Resonance-ionization mass spectroscopy (RIMS) is expected to be powerful for the ultra-trace analysis of long-lived radioactive elements such as neptunium because of its extremely high sensitivity and selectivity. Riegel *et al.* (1993)

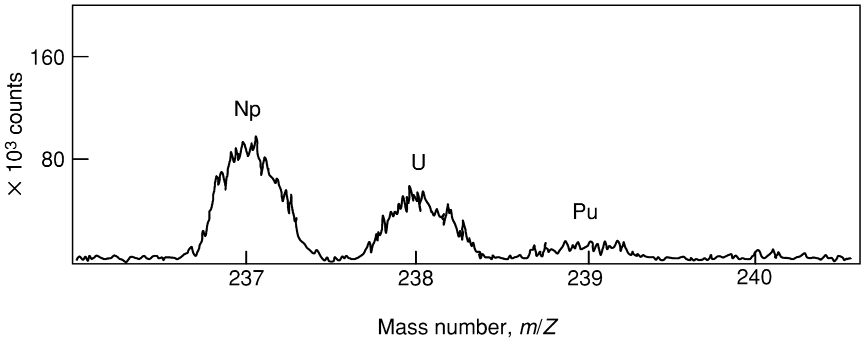

Fig. 6.13 *ICP mass spectrum for* ^{237}*Np in environmental samples. The mean value of the concentration of* ^{237}*Np was obtained to be* 6.2×0.1 Bq kg^{-1} *based on intercomparison analysis using spectrometry by seven laboratories. Reprinted from Kim* et al. (1989), *with permission from Elsevier Sequoia S. A.*

carried out the ^{237}Np detection by RIMS and estimated the detection limit as 4×10^8 atoms (1.6×10^{-13} g) which is almost two orders of magnitude more sensitive than that by alpha spectrometry.

Accelerator mass spectrometry (AMS) was applied to the detection of ^{237}Np in environmental samples such as mud, sediment, and pore water (Fifield *et al.*, 1997). It was estimated that sensitivity by AMS approached 10^5 atoms (4×10^{-17} g) of ^{237}Np. The results obtained by such a highly sensitive method make it possible to elucidate a distribution behavior of neptunium in natural environment and therefore to conclude that neptunium is more mobile than plutonium in the environment.

6.10.6 Electrochemical methods

Electrochemical methods are feasible for the determination of the total concentration and redox speciation of neptunium ions. The reduction–oxidation processes between Np(VI) and Np(V) and between Np(IV) and Np(III) are practically reversible and of simple one-electron transfer characteristics, which enables various electroanalytical performance based on these electrode reactions. The electroanalytical data of neptunium mainly obtained by voltammetry and polarography were reviewed by Kihara *et al.* (1999).

(a) Potentiometric titration and coulometry

Titration methods based on the reduction–oxidation of neptunium ions have been widely used for the accurate and precise determination of 1–10 mg quantities of neptunium. A method proposed by Godbole and Patil (1979) consists of the oxidation of neptunium ions to Np(VI) with Ag(II), destruction of excess

Ag(II) with sulfonic acid, reduction of Np(VI) to Np(IV) by a slight excess of Fe(II) in 2 M H_2SO_4, and potentiometric titration of the excess Fe(II) with standard Ce(IV) solution. The end point was detected potentiometrically using a platinum indicator electrode. Cao *et al.* (1994) proposed an alternative amperometric titration method by the use of Cr(VI) instead of Ce(IV) to titrate Fe(II). They attained less than 0.3% relative standard deviation in the determination of 2 mg of neptunium.

Controlled-potential coulometry is the standard method based on a primary theory, which enables an accurate and precise determination of neptunium. Stromatt (1959) recommended the procedure that consists of the oxidation of neptunium ion to Np(VI) with Ce(IV), the electrolytic reduction of Np(VI) and the excess Ce(IV) to Np(V) and Ce(III), and coulometric determination of Np(V) by the oxidation of Np(V) to Np(VI).

Kasar *et al.* (1991) determined 2–5 mg of neptunium with a relative standard deviation of ±0.25% by controlled-potential coulometry consisting of oxidation to Np(VI) with Ce(IV), decomposition of the excess Ce(IV) with $NaNO_2$, and titration based on the reduction of Np(VI) to Np(IV) with internally and electrolytically generated Fe(II). Karelin *et al.* (1991) developed constant current coulometry adopting amperometric end point detection, which enabled the determination of neptunium in the solution coexisting with uranium, plutonium, cerium, chromium, iron, and manganese. Chemists at the Savannah River Plant, USA, developed an automatically controlled apparatus for coulometry that was applied to the determination of neptunium. Measurement precision within 0.1% was achieved (Holland and Cordaro, 1988). Narrow span controlled-potential coulometry, which can minimize the interference from ions of formal redox potential close to that of the ion to be determined, was developed (Kalsi *et al.*, 1994) and applied to the determination of neptunium with enough high reproducibility, e.g. with relative standard deviation of 0.2%, even in the presence of five times the concentration of plutonium. Kihara *et al.* (1999) proposed a flow-coulometry method using multi-step column electrodes of glassy carbon fibers working electrode for the determination and speciation of neptunium ions in acidic solutions. (The redox behavior of neptunium ions observed by flow-coulometry is described in detail in Section 6.8.1b.)

(b) Voltammetry and polarography

Polarography was applied to the simultaneous determination of Np(V) and U(VI) in samples from the spent nuclear fuel reprocessing process based on the fluoride vaporization (Li *et al.*, 1988). The reduction currents of Np(V) and U(VI) were recorded with the electrolyte solution of a mixture of 2 M acetic acid and 2 M ammonium acetate. Kuperman *et al.* (1988) developed potentiostatic voltammetry for the determination of 2×10^{-8} to 1×10^{-5} M of neptunium and plutonium ions. Yakovlev and Kosyakov (1991) developed anodic stripping voltammetry method for the determination of neptunium using column electrode of carbon fibers as a working electrode whose surface was modified by bis(2-ethylhexyl) phosphate. The recommended procedure consists of the electrolytic preconcentration of Np(VI) at the electrode surface and the measurement of the current peak due to the oxidation of Np(V) to Np(VI). The detection limit was ca. 10^{-7} M.

6.10.7 Mössbauer spectroscopy of ^{237}Np materials

Neptunium–237 is one of the best Mössbauer nuclei in the periodic table. ^{237}Np has the following characteristics which allow the Mössbauer spectroscopic measurement successful: (1) the lifetime of the excited state for Mössbauer transition is long enough, 68 ns, to obtain a sharp resonance line; (2) the spread range of the isomer shift is large enough to differentiate nature of chemical bonds from the shift; and (3) the radiation from a ^{237}Np absorber is low enough to record a spectrum in a standard transmission geometry. The most useful Mössbauer measurement system is the 60 keV radiation from ^{237}Np excited in the alpha decay of ^{241}Am. Nakada *et al.* (1998) developed a source assembly with small sources of ^{241}Am metal and designed the sealed holders to encapsulate the sample without the seepage of liquid helium.

Kalvius (1989) summarized basics and the power of Mössbauer spectroscopy of ^{237}Np in his review article demonstrating examples of study on 5f-electron structure of antiferromagnetic NpAs compounds and various Np(VI) and (VII) compounds. Jovè *et al.* (1991) reviewed applications of Mössbauer spectroscopy to the study of insulating neptunium compounds and discussed correlations between isomer shift, electric field gradient, and bonding or crystallographic structure of neptunium in crystallized or amorphous compounds of Np(III–VII).

Each oxidation state has a characteristic isomer shift range that is correlated with the number of 5f electrons present, and thus the isomer shift is a good indicator of the coordination number as well as the oxidation state of Np in a compound. The isomer shift increases regularly with decreasing oxidation state. Systematic trend of the isomer shift of ^{237}Np in various metal coordination complexes was studied and a linear dependence was found between the isomer shift and the mean neptunium–ligand distance in a series of Np(VI) compounds, which were summarized by Jovè *et al.* (1988a,b, 1991). Ionova and Jovè (1989) proposed a model, which correlated the population of the 5f orbital of ^{237}Np with the isomer shift, for the estimation of covalent effect in neptunium compounds based on the isomer shift. Bickel *et al.* (1987) studied the Mössbauer spectra of such oxoneptunates as $Li_5Np^{(VII)}O_6$, $Li_6Np^{(VI)}O_6$, $BaNp^{(VI)}O_4$, $Np^{(IV)}GeO_4$, $SrNp^{(IV)}O_3$, and $BaNp^{(IV)}O_3$. The isomer shifts were more negative or positive for the bond of ionic or covalent characteristics, respectively.

Sanchez *et al.* (1988) studied the electronic and magnetic properties of a novel intermetallic $NpRh_2Si_2$ by ^{237}Np Mössbauer spectroscopy. The isomer shift ranging from 5.3 (at 4.2 K) to 4.8 mm s^{-1} (at 77 K) with respect to $NpAl_2$ suggested a Np^{4+} electronic configuration in conducting materials.

Nakamoto *et al.* (1998) and Saeki *et al.* (1999) measured Mössbauer spectra of Np(v) compounds such as formate, $NpO_2OOCH \cdot H_2O$, and $NH_4NpO_2(OOCH)_2$, glycolate, $NpO_2OOCCH_2OH \cdot H_2O$, malonate $(NpO_2)_2C_3H_2O_4 \cdot 4H_2O$, and phthalate $(NpO_2)_2(OOC)_2C_6H_4 \cdot 4H_2O$, and found a good correlation between coordination numbers of Np atoms and isomer shifts in the range from –18.6 to –19.1 mm s^{-1} for the compounds with Np atoms surrounded by seven oxygen atoms, i.e. coordination number = 7. The isomer shift for Np of coordination number 8 in the compound is larger than that of coordination number 7. Isomer shifts of Np(iv) to (vii) with different coordination numbers in the compounds are summarized in Fig. 6.14 (Saeki, 2003).

Heptavalent neptunium compounds have been studied by Mössbauer spectroscopy. The characteristic isomer shift of Np(vii) has been reported to be from –64 to –75 mm s^{-1} with respect to $NpAl_2$ (Stone *et al.* 1969; Fröhlich *et al.* 1972; Ilyatov *et al.* 1975; Grigor'ev *et al.* 1979; Ananyev *et al.* 1980). Recently Nakamoto *et al.* (1999) reinvestigated the Mössbauer spectra for Np(vii) in $[Co(NH_3)_6][NpO_4(OH)_2] \cdot 2H_2O$ at 4.2 K. They pointed out that the fitting by using two quadrupole-split peaks did not give a good agreement with the previous data by Stone *et al.* (1969), although the spectrum observed by Nakamoto *et al.* (1999) consisted of two quadrupole-split peaks.

Filin *et al.* (1989, 1990) studied ^{237}Np Mössbauer emission spectra resulting from the alpha decay of ^{241}Am in various solid solutions of actinide dioxides. The oxidation state of ^{237}Np in ^{241}Am(0.6 and 11 at%) + PuO_2 was determined from the isomer shifts of –5.8 and 18.5 mm s^{-1} relative to $NpAl_2$ to be Np^{4+} and Np^{5+}, respectively. They found that the oxidation state strongly depended on the matrix stoichiometry of PuO_2 as well as on the content of the impurity in the sample.

6.10.8 Miscellaneous methods

Speciation of neptunium in samples has been a strong analytical interest and requirement, because the ions of five oxidation states from (iii) to (vii) are stable under certain conditions and the ions form complexes differently with many kinds of ligands. The methods for the speciation were evaluated recently by OECD/NEA (2001).

The redox speciation of neptunium ion of relatively high concentration can be performed by direct absorption spectrophotometry (see Section 6.10.2) or electrochemical methods (see Section 6.10.6). For the redox speciation of neptunium ion at lower concentration, e.g. in environmental samples, a method utilizing chemical separation between ions of different oxidation states followed by the determination of the ions using sensitive methods such as radiometric methods and ICP-MS is employed. Coprecipitation with such precipitates as LaF_3, followed by solvent extraction with, e.g. HTTA, can be used for the separation. It is essential that the separation method does not disturb the

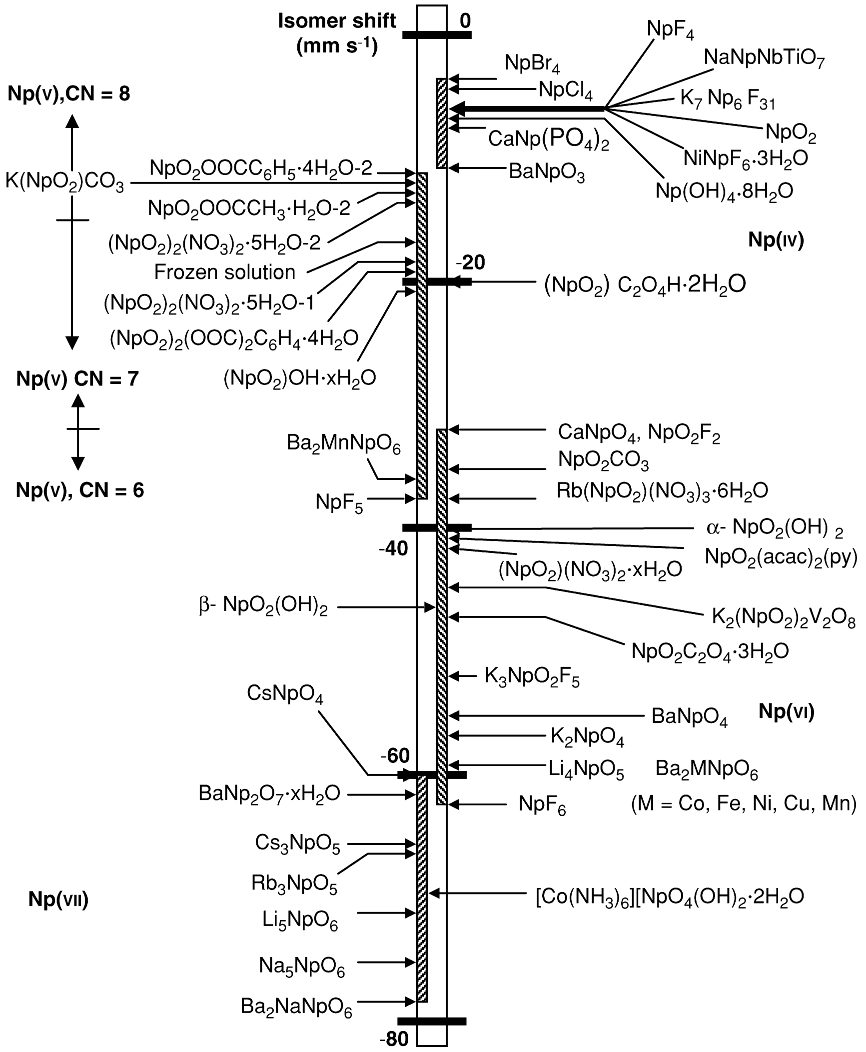

Fig. 6.14 *Isomer shifts of Np(IV), (V), (VI), and (VII) compounds.*

redox equilibrium during the treatment of the sample. Mang *et al.* (1993) investigated a continuous electrophoretic ion focusing method for the separation of Np(vi) from Np(v) at a trace concentration level, e.g. 10^{-14} M level using ^{239}Np tracer. Np(vi) was not stable enough under the recommended conditions. The Np(iv) and Np(v) species were well focused and separated with very reproducible peaks by continuous ion focusing with glycolic acid and tartaric acid.

Chen *et al.* (1992) employed traditional solvent extraction with HTTA and TOPO for the separation of Np(vi), Np(v), and Np(iv). Enokida and Suzuki (1987) employed extraction chromatography with TBP-impregnated resin for the separation of 10^{-5} M levels of neptunium ions of different oxidation states. Nagasaki *et al.* (1988) recommended a paper electrophoresis method for the redox speciation of neptunium ions.

X-ray absorption fine structure (XAFS) was applied to the speciation of Np(v) in an aqueous solution containing high concentration of chloride salt (Allen *et al.*, 1997), and adsorbed at the interface between alpha-Fe hydroxide solid and aqueous solution (Combes *et al.*, 1992).

High-resolution ultraviolet and X-ray photoelectron spectroscopy (UPS and XPS) were applied to characterize the surface of neptunium metal (Naegele *et al.*, 1987). An oxide layer of Np(iii), i.e. Np_2O_3, was found in the near surface of about 10 Å in thickness of the sample.

REFERENCES

Abazli, H., Jovè, J., and Pagès, M. (1979) *C. R. Acad. Sc. Paris C*, **288**, 157–9.

Abazli, H., Cousson, J., Jovè, J., Pagès, M., and Gasperin, M. (1984) *J. Less Common Metals*, **96**, 23–33.

Ackermann, R. J., Faircloth, R. L., Rauh, E. G., and Thorn, R. J. (1966) *J. Inorg. Nucl. Chem.*, **28**, 111–18.

Ahrland, S. and Brandt, L. (1966) *Acta Chem. Scand.*, **20**, 328–46.

Ahrland, S. and Brandt, L. (1968a) *Acta Chem. Scand.*, **22**, 106–14.

Ahrland, S. and Brandt, L. (1968b) *Acta Chem. Scand.*, **22**, 1579–89.

Akabori, M., Haire, R. G., Gibson, J. K., Okamoto, Y., and Ogawa, T. (1997) *J. Nucl. Mater.*, **247**, 240–3.

Akopov, G. A., Krinitsyn, A. P., and Tikhonova, A. E. (1988) *Radiokhimiya*, **30**, 578–83.

Aldred, A. T., Dunlap, B. D., Harvey, A. R., Lam, D. J., Lander, G. H., and Mueller, M. H. (1974) *Phys. Rev. B*, **9**, 3766–78.

Aldred, A. T., Dunlap, B. D., Lam, D. J., Lander, G. H., Mueller, M. H., and Nowik, I. (1975) *Phys. Rev. B*, **11**, 530–44.

Aleksandruk, V. M., Babaev, A. S., Dem'yanova, T. A., and Stepanov, A. V. (1990) *Radiokhimiya*, **32**, 132–8.

Aleksandruk, V. M., Babaev, A. S., Dem'yanova, T. A., and Stepanov, A. V. (1991a) *Radiokhimiya*, **33**, 203–8.

Aleksandruk, V. M., Babaev, A. S., Dem'yanova, T. A., and Stepanov, A. V. (1991b) EUR-13686, pp. 215–18.

Al-Kazzaz, Z. M. S., Bagnall, K. W., Brown, D., and Whittaker, B. (1972) *J. Chem. Soc. Dalton Trans.*, **20**, 2273–7.

Allen, P. G., Bucher, J. J., Shuh, D. K., Edelstein, N. M., and Reich, T. (1997) *Inorg. Chem.*, **36**, 4676–83.

Al-Niaimi, N. S., Wain, A. G., and McKay, H. A. C. (1970a) *J. Inorg. Nucl. Chem.*, **32**, 2331–42.

Al- Niaimi, N. S., Wain, A. G., and McKay, H. A. C. (1970b) *J. Inorg. Nucl. Chem.*, **32**, 977–86.

Ananyev, A. V., Grigoryev, M. S., and Krot, N. N. (1980) *Radiochem. Radioanal. Lett.*, **44**, 217–26.

Appel, H., Bickel, M., Melchior, S., Kanellakopulos, B., and Keller, C. (1990) *J. Less Common Metals*, **162**, 323–34.

Arai, Y., Okamoto, Y., and Suzuki, Y. (1994) *J. Nucl. Mater.*, **211**, 248–50.

Asprey, L. B., Eller, P. G., and Kinkead, S. A. (1986) *Inorg. Chem.*, **25**, 670–2.

Aupiais, J., Dacheux, N., Thomas, A. C., and Matton, S. (1999) *Anal. Chim. Acta*, **398**, 205–18.

Awasthi, S. K., Martinot, L., Fuger, J., and Duyckaerts, G. (1971) *Inorg. Nucl. Chem. Lett.*, **7**, 145–51.

Bagawde, S. V., Ramakrishna, V. V., and Patil, S. K. (1976) *J. Inorg. Nucl. Chem.*, **38**, 2085–9.

Bagnall, K. W. and Laidler, J. B. (1964) *J. Chem. Soc.*, 2693–6.

Bagnall, K. W. and Laidler, J. B. (1966) *J. Chem. Soc. A*, 516–20.

Bagnall, K. W., Brown, D., and Easey, J. F. (1968a) *J. Chem. Soc. A*, 2223–7.

Bagnall, K. W., Brown, D., and Easey, J. F. (1968b) *J. Chem. Soc. A*, 286–91.

Bagnall, K. W., Payne, G. F., and Brown, D. (1985) *J. Less Common Metals*, **109**, 31–6.

Baluka, M., Yeh, S., Banks, R., and Edelstein, N. (1980) *Inorg. Nucl. Chem. Lett.*, **16**, 75–7.

Bamberger, C. E., Haire, R. G., Begun, G. M., and Hellwege, H. E. (1984) *J. Less Common Metals*, **102**, 179–86.

Barrero Moreno, J. M., Betti, M., and Garcia Alonso, J. I. (1997) *J. Anal. Atom. Spectrom.*, **12**, 355–61.

Bartscher, W. and Sari, C. (1986) *J. Nucl. Mater.*, **140**, 91–3.

Baumgartner, F., Fischer, E. O., and Laubereau, P. (1965) *Naturwissenschaften*, **52**, 560

Baumgartner, F., Fischer, E. O., Kanellakopulos, B., and Laubereau, P. (1968) *Angew. Chem. Int. Edn.*, **7**, 634

Beauvy, M., Duverneix, T., Berlanga, C., Mazoyer, R., and Duriez, C. (1998) *J. Alloys Compds.*, **271/273**, 557–62.

Belyaev, Y. I., Il'inskaya, T. A., Kudryavtsev, A. N., Smirnov, N. L., and Tolmachev, Y. M. (1975) *Sov. Radiochem.*, **17**, 847–60.

Belyaev, Y. I., Smirnov, N. L., and Taranov, A. P. (1979) *Radiokhimiya*, **21**, 682–6.

Belyaev, Y. I. (1983) *Radiokhimiya*, **25**, 791–4.

Benedict, U., Dabos, S., Dufour, C., and Spirelet, J. C. (1986) *J. Less Common Metals*, **121**, 461–8.

Bessonov, A. A., Afonas'eva, T. V., and Krot, N. N. (1989a) *Radiokhimiya*, **31**, 9–13.

Bessonov, A. A., Grigor'eva, M. S., Afonas'eva, T. V., and Krot, N. N. (1989b) *Sov. Radiochem.*, **31**, 393–6.

Betz, T. and Hoppe, R. (1984) *Z. Anorg. Allg. Chem.*, **512**, 19.

Bickel, M. and Kanellakopulos, B. (1986) *J. Less Common Metals*, **121**, 291–9.

Bickel, M., Adrian, G., Kanellakopulos, B., Haffner, H., Geggus, G., and Appel, H. (1987) *Inorg. Chim. Acta*, **140**, 101–3.

Bidoglio, G., Tanet, G., and Chatt, A. (1985) *Radiochim. Acta*, **38**, 21–6.

Bihan, T. L., Heathman, S., and Rebizant, J. (1997) *High Press. Res.*, **15**, 387–92.

Blaise, A., Fournier, J. M., Salmon, P., and Wojakowski, A. (1976) *Magnetic Properties of Some Neptunium and Plutonium Compounds. Plutonium and other Actinides.* in (eds. H. Blank and R. Linder), North-Holland, Amsterdam, pp. 635–40.

Blaise, A., Damien, D., and Suski, W. (1981) *Solid State Commun.*, **37**, 659–62.

Blaise, A., Damien, D., and Mulak, J. (1982) *Phys. Stat. Sol.*, **72**, K145–8.

Blokhin, V. I., Bukhtiyarova, T. N., Krot, N. N., and Gel'man, A. D. (1972) *Russ. J. Inorg. Chem.*, **17**, 1742–6.

Bohlander, R. (1986) *Zur Metallorganischen Kompleschemie Des Neptunium*, Dissertation, Kernforshcungszentrum Karlsruhe GmbH, KfK 4152.

Brewer, L., Bromely, L., Gilles, P. W., and Lofgren, N. (1949) in *The Transuranium Elements* (eds. G. T. Seaborg, J. J. Katz, and W. M. Manning), *Natl. Nucl. En. Ser.,* Div. IV, 14B, McGraw-Hill, New York, pp. 1111–18.

Brown, D., Fletcher, S., and Holah, D. G. (1968) *J. Chem. Soc. A*, 1889–94.

Brown, D., Hill, J., and Richard, C. E. F. (1970) *J. Chem. Soc. A*, 476–80.

Brown, D. (1972) in *Gmelin Handbuck der Anorganischen Chemie*, Suppl. Work, 8th edn, *Transuranium*, Verlag Chemie, Weinheim, vol. 4, part C, Compounds.

Brown, D. and Edwards, J. (1972) *J. Chem. Soc. Dalton Trans.*, 1757–62.

Brown, D., Hall, L., Hurtgen, C., and Moseley, P. T. (1977) *J. Inorg. Nucl. Chem.*, **39**, 1464–6.

Brown, W., Whittaker, B., Berry, J. A., and Holloway, J. H. (1982) *J. Less Common Metals*, **86**, 75–84.

Bryne, A. R. (1986) *J. Environ. Radioact.*, **4**, 133–44.

Budantseva, N. A., Fedoseev, M. S., Grigor'ev, M. S., Potemkina, T. I., Afonas'ev, T. V., and Krot, N. N. (1988) *Radiokhimiya*, **30**, 607–10.

Budantseva, N. A., Potemkina, T. I., Grigor'ev, M. S., Fedoseev, A. M., and Krot, N. N. (1989) *Radiokhimiya*, **31**, 5–8.

Burkhart, M. J. and Thompson, R. C. (1972) *J. Am. Chem. Soc.*, **94**, 2999–3002.

Burlet, P., Quezel, J., Rossat- Mignod, J., Spirlet, J. C., Rebizant, J., and Vogt, O. (1989) *Physica B*, **159**, 129–36.

Burlet, P., Bourdarot, F., Rossat- Mignod, J., Sanchez, J. P., Spirlet, J. C., Rebizant, J., and Vogt, O. (1992) *Physica B*, **180&181**, 131–2.

Burney, G. A. and Harbour, R. M. (1974) in *Radiochemistry of Neptunium*, NAS-NS-3060, Technical Information Center, USAEC.

Burns, J. H., Baldwin, W. H., and Stokely, J. R. (1973) *Inorg. Chem.*, **12**, 466–9.

Burns, P. C., Kubatko, K.-A., Sigmon, G., Fryer, B. J., Gagnon, J. E., Antonio, M. R., and Soderholm, L. (2005) *Angew. Chem. Int. Ed.,* **44**, 2135.

Cao, X., Xu, S., Wu, P., and Wen, Z. (1994) *He Huaxue Yu Fangshe Huaxue*, **16**, 43–8.

Carnall, W. T., Neufeldt, S. J., and Walker, A. (1965) *Inorg. Chem.*, **4**, 1808–13.

Carnall, W. T., Goodman, G. L., Veal, B. W., and Lam, D. J. (1987) *J. Less Common Metals*, **133**, 178–9.

Cassol, A., Magon, L., Tomat, G., and Portanova, R. (1969) *Inorg. Chim. Acta*, **3**, 639–43.

Cassol, A., Magon, L., Tomat, G., and Portanova, R. (1972a) *Inorg. Chem.*, **11**, 515–19.

Cassol, A., Magon, L., Portanova, R., and Tondello, E. (1972b) *Radiochim. Acta*, **17**, 28–32.

Cassol, A., Bernardo, P. D., Portanova, R., and Magon, L. (1973) *Inorg. Chim. Acta*, **7**, 353–8.

Chaikhorskii, A. A. (1971) *Radiokimiya* **13**, 320–5.

Chaikhorskii, A. A. and Leikina, E. V. (1972) *Radiokimiya*, **14**, 378–84.

Chaikhorskii, A. A., Zelentov, S. S., and Leikina, E. V. (1972) *Sov. Radiochem.*, **14**, 636.

Chaikhorskii, A. A., Matuzenko, M. Y., and Belyaev, Y. I. (1974) *Radiokhimiya*, **16**, 850–3.

Chaikhorskii, A. A., Matuzenko, M. Y., and Leikina, E. V. (1975) *Sov. Radiochem.*, **17**, 803–11.

Charushnikova, I. A., Afonas'eva, T. V., Perminov, V. P., and Krot, N. N. (1992) *Sov. Radiochem.*, **34**, 648–54.

Charushnikova, I. A., Afonas'eva, T. V., and Krot, N. N. (1995) *Radiochemistry*, **37**, 6–11.

Charvillat, J. P. and Damien, D. (1973) *Inorg. Nucl. Chem. Lett.*, **9**, 337–42.

Charvillat, J. P., Benedict, U., Damien, D., Novion, D., Wojakowski, A., and Muller, W. (1976) in *Tranplutonium Elements* (eds. W. Muller and R. Linder), North-Holland, Amsterdam, p. 79.

Chen, Y., Zhong, J., Zhao, Y., Tan, B., and Lin, Z. (1992) *Yuanzineng Kexue Jishu*, **26**, 63–7.

Chiarizia, R., Horwitz, E. P., and Alexandratos, S. D. (1994) *Solvent Extr. Ion Exch.*, **12**, 211–37.

Chitnis, R. R., Wattal, P. K., Ramanujam, A., Dhami, P. S., Gopalakrishnan, V., Mathur, J. N., and Murali, M. S. (1998) *Sep. Sci. Technol.*, **33**, 1877–87.

Choporov, D. Y. and Chudinov, E. T. (1968) *Radiokhimiya*, **10**, 221–7.

Choppin, G. R. and Unrein, P. J. (1976) in *Transuranium Elements 1975* (eds. W. Müller and R. Lindner), North-Holland, Amsterdam, pp. 97–107.

Choppin, G. R. and Rao, L. F. (1984) *Radiochim. Acta*, **37**, 143–6.

Choppin, G. R. and Nash, K. L. (1995) *Radiochim. Acta*, **70/71**, 225–36.

Choppin, G. R., Stout, B. E., and Pagès, M. (1998) *J. Alloys Compds.*, **271–273**, 774–7.

Clark, D. L., Hobart, D. E., and Neu, M. P. (1995) *Chem. Rev.*, **95**, 25–48.

Cohen, D. and Hindman, J. C. (1952) *J. Am. Chem. Soc.*, **74**, 4682–5.

Cohen, D. (1963) *Inorg. Chem.*, **2**, 866–7.

Cohen, D. and Walter, A. J. (1964) *J. Chem. Soc.*, 2696–9.

Cohen, D., Fried, S., Holloway, J. H., and Selig, H. (1970) Unpublished work at Argonne National Laboratory, Argonne, IL, Quoted by Brown, W., Whittaker, B., Berry, J. A., and Holloway, J. H. (1982). *J. Less Common Metals*, **86**, 75–84.

Collard, J. M., Blaise, A., Boge, M., Bonnisseau, D., Burlet, P., and Fournier, J. M. (1986) *J. Less Common Metals*, **121**, 313–8.

Combes, J-M., Chishoim- Brause, C. J., Brown, G. E., and Parks, G. A. (1992) *Environ. Sci. Technol.*, **26**, 376–82.

Cousson, A., Dabos, S., Abazli, H., Nectoux, F., Pagès, M., and Choppin, G. (1984) *J. Less Common Metals*, **99**, 233–40.

Cousson, A., Abazli, H., and Jovè, J. (1985) *J. Less Common Metals*, **109**, 155–68.

Cuillerdier, C., Musikas, C., and Mateau, M. (1977) Report CEA-CONF-3944.

Dabos, S., Dufour, C., Benedict, U., Spirlet, J. C., and Pagès, M. (1986) *Physica*, **144B**, 79–83.

Dabos-Seignon, S., Benedict, U., Heathman, S., and Spirlet, J. C. (1990) *J. Less Common Metals*, **160**, 35–51.

Damien, D., Damien, N., Jovè, J., and Chavrillat, J. P. (1973) *Inorg. Nucl. Chem. Lett.*, **9**, 649–55.

Damien, D. and Wojakowski, W. (1975) *Radiochem. Radioanal. Lett.*, **23**, 145–54.

Damien, D. and Berger, R. (1976) in Supplement to *J. Inorg. Nucl. Chem*. Proc. Moscow Symp. On the Chemistry of Transuranium Element, 1976 (eds. Spitsyn, V. I. and Katz, J. J.), Pergamon Press, Oxford, pp. 109–16.

Danesi, P. R., Chiarizia, R., Scibona, G., and D'Alessandro, G. (1971) *J. Inorg. Nucl. Chem.*, **33**, 3503–10.

De Novion, C. H. and Lorenzelli, R. (1968) *J. Phys. Chem. Solids*, **29**, 1901–5.

Degischer, G. and Choppin, G. R. (1975) in *Gmelin Handbuch der Anorganischen Chemie, Transurane*, Springer-Verlag, Berlin-Heidelberg, part D1, pp. 129–76.

Drobyshevskii, Y. V., Serik, V. F., and Sokotov, V. B. (1975) *Dokl. Akad. Nauk SSSR*, **225**, 1079–81.

Drobyshevskii, Y. V., Serik, V. F., Sokotov, V. B., and Tul'skii, M. N. (1978) *Radiokhimiya*, **20**, 238–43.

Dukes, E. K. and Shuler, W. E. (1960) Report DP-543, Dupont de Nemours Co.

Duplessis, J. and Guillaumont, R. (1977) *Radiochem. Radioanal. Lett.*, **31**, 293–302.

Eberle, S. H. and Wede, U. (1968) *Inorg. Nucl. Chem. Lett.*, **4**, 661–4.

Eberle, S. H. and Schaefer, J. B. (1969) *J. Inorg. Nucl. Chem.*, **31**, 1523–7.

Eberle, S. H. and Wede, U. (1970) *J. Inorg. Nucl. Chem.*, **32**, 109–17.

Eberle, S. H. and Paul, M. T. (1971) *J. Inorg. Nucl. Chem.*, **33**, 3067–75.

Efurd, D. W., Knobeloch, G. W., Perrin, R. E., and Barr, D. W. (1984) *Health Phys.*, **47**, 786–7.

Efurd, D. W., Drake, J., Roensch, F. R., Cappis, J. H., and Perrin, R. E. (1986) *Int. J. Mass Spectrom. Ion Processes*, **74**, 309–15.

Eick, H. A. and Mulford, R. (1964) *J. Chem. Phys.*, **41**, 1475–8.

Eisenstein, J. C. and Pryce, M. H. L. J. Re. (1965) *Natl. Bur. Stand.*, **A 69**, 217.

Eisenstein, J. C. and Pryce, M. H. L. J. Re. (1966) *Natl. Bur. Stand.*, **A 70**, 165.

Eller, P. G., Asprey, L. B., Kinkead, S. A., Swanson, B. I., and Kissane, R. J. (1998a) *J. Alloys Compds.*, **269**, 63–6.

Eller, P. G., Malm, J. G., Swanson, B. I., and Morss, L. R. (1998b) *J. Alloys Compds.*, **269**, 50–6.

Elliott, R. O. and Giessen, B. C. (1982) *Acta Metall.*, **30**, 785–9.

Enokida, Y. and Suzuki, A. (1987) *J. Nucl. Sci. Technol.*, **24**, 859–61.

Enokida, Y. and Suzuki, A. (1989) *Nucl. Technol.*, **88**, 47–54.

Eriksen, T. E., Ndalamba, P., Cui, D., Bruno, J., Caceci, M., and Spahiu, K. (1993) SKB Report TR-93–18.

Ewart, F. T., Gore, S. J. M., and Williams, S. J. (1985) Report AERE-R11975.

Fahey, J. A., Turcotte, R. P., and Chikalla, T. D. (1974) *Inorg. Nucl. Chem. Lett.*, **10**, 459–65.

Fahey, J. A., Turcotte, R. P., and Chikalla, T. D. (1976a) *Inorg. Nucl. Chem. Lett.*, **10**, 459–65.

Fahey, J. A., Turcotte, R. P., and Chikalla, T. D. (1976b) *J. Inorg. Nucl. Chem.*, **38**, 495–500.

Fahey, J. A. (1986) in *The Chemistry of the Actinide Elements, vol. 1* (eds. J. J. Katz, G. T. Seaborg, L. R. Morss), Chapman & Hall, New York, p. 456.

Fifield, L. K., Clacher, A. P., Morris, K., King, S. J., Cresswell, R. G., Day, J. P., and Livens, F. R. (1997) *Nucl. Instrum. Methods Phys. Res. Sect. B*, **123**, 400–4.

Filin, V. M., Gorbunov, V. F., and Ulanov, S. A. (1989) *Radiokhimiya*, **31**, 13–9.

Filin, V. M., Gorbunov, V. F., and Ulanov, S. A. (1990) *J. Radioanal. Nucl. Chem. Art.*, **143**, 125–34.

Finch, R. J. (2002) in *Scientific Basis for Nuclear Waste Management XXV* (eds. B. P. McGrail and G. A. Cragnolino), Materials Research Society Symp., 2001. The Materials Research Society, Warrendale, Pennsylvania, p. 713, JJ11.60.W.

Fischer, E. O., Laubereau, P., Baumgartner, F., and Kanellakopulos, B. (1966) *J. Organomet. Chem.*, **5**, 583–4.

Florin, A. E. (1943) Report MUC-GTS 2165.

Flotow, H. E., Haschke, J. M., and Yamauchi, S. (1984) in *The Chemical Thermodynamics of Actinide Elements and Compounds* part 9, *The Actinide Hydrides* (ed. F. L. Oetting), International Atomic Energy Agency, Vienna.

Foltyn, E. (1990) *J. Nucl. Mater.*, **172**, 180–3.

Foropoulus, J., Avens, L. R., and Trujillo, E. A. (1992) US Patent No. 5,098,682.

Fried, S. and Davidson, N. R. (1947) MDDC-1332, Argonne National Laboratory, Date Declassified: July 18, 1947.

Fried, S. and Davidson, N. R. (1948) *J. Am. Chem. Soc.*, **70**, 3539–47.

Fried, S. and Davidson, N. R. (1951) US Patent 2,578,416.

Fried, S. (1954) *The Actinide Elements,* Natl. Nucl. En. Ser., Div. IV, 14A (eds. G. T. Seaborg and J. J. Katz), McGraw-Hill, New York, p. 471.

Fröhlich, K., Gütlich, P., and Keller, C. (1972) *Angew. Chem.*, **84**, 26–7.

Fuger, J. and Brown, D. (1971) *J. Chem. Soc. A*, 842–6.

Fuger, J. (1979) *J. de physique, C4 (Suppl. 4)* **40**, 207–13.

Fuger, J., Khodakovsky, I. L., Sergeyeva, E. I., Medvedev, V. A., and Navratil, J. D. (1992) in *The Chemical Thermodynamics of Actinide Elements and Compounds*, part 12, *The Actinide Aqueous Inorganic Complexes*, International Atomic Energy Agency, Vienna.

Fujinaga, T. and Kihara, S. (1977) *CRC Crit. Rev. Anal. Chem.*, **6**, 223–54.

Fukasawa, T., Ikeda, T., and Kawamura, F. (1991) *Eur. J. Solid State Inorg. Chem.*, **28**, 73–6.

Gal, J., Litterst, J., Potzel, W., Moser, J., Potzel, U., Kalvius, G. M., Fredo, S., and Tapuchi, S. (1987) *Phys. Rev. B*, **36**, 2457–60.

Garner, C. S., Bonner, N. A., and Seaborg, G. T. (1948) *J. Am. Chem. Soc.*, **70**, 3453–4.

Geary, N. R. (1955) UKAEA, Risley-5142.

Gel'man, A. D., Moskvin, A. I., Zaitsev, L. M., and Mefod'eva, M. P. (1962) in *Complex Compounds of Transuranium Elements*. Consultants Bureau Enterprises, New York.

Gensini, M., Benedict, U., and Rebizant, J. (1993) *J. Alloys Compds.*, **201**, L19–20.

Germain, P., Guegueniat, P., May, S., and Pinte, G. (1987) *J. Environ. Radioact.*, **5**, 319–31.

Gibson, J. K. and Haire, R. G. (1993) *J. Nucl. Mater.*, **201**, 225–30.

Gibson, J. K., Haire, R. G., Gensini, M. M., and Ogawa, T. (1994) *J. Alloys Compds*, **213/4**, 106–10.

Gibson, J. K., Haire, R. G., Okamoto, Y., and Ogawa, T. (1996) *J. Alloys Compds*, **234**, 34–9.

Gibson, J. K., Haire, R. G., and Ogawa, T. (1999) *J. Nucl. Mater.*, **273**, 139–45.

Godbole, A. G. and Patil, S. K. (1979) *Talanta*, **26**, 330–2.

Grenthe, I., Riglet, C., and Vitorge, P. (1986) *Inorg. Chem.*, **25**, 1679–84.

Grigor'ev, M. S., Glauzunov, M. P., Mefod'eva, M. P., Krot, N. N., Makarov, E. F., Permyakov, Yu. V., and Zemskov, B. G. (1979) *Radiokhimiya*, **21**, 659–64.

Grigor'ev, M. S., Gulev, B. F., and Krot, N. N. (1986a) *Radiokhimiya*, **28**, 685–90.

Grigor'ev, M. S., Gulev, B. F., and Krot, N. N. (1986b) *Radiokhimiya*, **28**, 690–4.

Grigor'ev, M. S., Yanovskii, A. I., Krot, N. N., and Struchkov, Y. T. (1987) *Radiokhimiya*, **29**, 574–9.

Grigor'ev, M. S., Yanovskii, A. I., Struchkov, Y. T., Bessnov, A. A., Afonas'eva, T. V., and Krot, N. N. (1989) *Radiokhimiya*, **31**, 37–44.

Grigor'ev, M. S., Baturin, N. A., Regel', L. L., and Krot, N. N. (1991a) *Radiokhimiya*, **33**, 19–25.

Grigor'ev, M. S., Fedoseev, N. A., Budantseva, N. A., Yanovskii, A. I., Struchkov, Y. T., and Krot, N. N. (1991b) *Radiokhimiya*, **33**, 54–61.

Grigor'ev, M. S., Yanovskii, A. I., Fedoseev, A. M., Budantseva, N. A., Struchkov, Y. T., and Krot, N. N. (1991c) *Radiokhimiya*, **33**, 17–9.

Grigor'ev, M. S., Charushnikova, N. N., Krot, N. N., Yanovskii, A. I., and Struchkov, Y. T. (1993a) *Radiokhimiya*, **35**, 24–30.

Grigor'ev, M. S., Charushnikova, N. N., Krot, N. N., Yanovskii, A. I., and Struchkov, Y. T. (1993b) *Radiokhimiya*, **35**, 31–7.

Grigor'ev, M. S., Baturin, N. A., Budantseva, N. A., and Fedoseev, A. M. (1993c) *Radiokhimiya*, **35**, 29–38.

Grigor'ev, M. S., Charushnikova, I. A., Baturin, N. A., and Krot, N. N. (1995) *Russ. J. Inorg. Chem.*, **40**, 709–12.

Gruber, J. B. and Menzel, E. R. (1969) *J. Chem. Phys.*, **50**, 3772–9.

Gruen, D. M. (1952) *J. Chem. Phys.*, **20**, 1818–9.

Gruen, D. M., McBeth, R. L., and Fried, S. M. (1976) *J. Inorg. Nucl. Chem.*, (Suppl. 2), 27–30.

Gruen, D. M. (1992) in *Transuranium Elements; A Half Century* (eds. L. R. Morss and J. Fuger), American Chemical Society, Washington DC, pp. 63–77.

Guillaume, B., Begun, G. M., and Hahn, R. L. (1982) *Inorg. Chem.*, **21**, 1159–66.

Guillaume, B., Hahn, R. L., and Narten, A. H. (1983) *Inorg. Chem.*, **22**, 109–11.

Gysling, H. and Tsutsui, M. (1970) *Adv. Organomet. Chem.*, **9**, 361–93.

Haire, R. G. and Fahey, J. A. (1977) *J. Inorg. Nucl. Chem.*, **39**, 837–41.

Haire, R. G. (1986) *J. Less Common Metals*, **121**, 379–98.

Halperin, J. and Oliver, J. H. (1983) *Radiochim. Acta*, **33**, 29–33.

Haschke, J. M. (1991) in *Synthesis of Lanthanides and Actinide Compounds* (eds. G. Meyer and L. R. Morss), Kluwer Academic Publishers, The Netherlands, pp. 1–53.

Hasegawa, K., Shiokawa, Y., Akabori, M., Suzuki, Y., and Suzuki, K. (1998) *J. Alloys Compds.*, **271–273**, 680–4.

Hayes, R. G. and Thomas, J. L. (1971) *Organomet. Chem. Rev.*, **7**, 1–50.

Heinrich, Z. and Klaus, M. (1999) *Radiochim. Acta*, **86**, 123–8.

Henrion, P. N. and Leurs, L. (1971) *J. Nucl. Mater.*, **41**, 1–22.

Hessler, J. P., Brundage, R. T., Hegarty, J., and Yen, W. M. (1980) *Optics Lett.*, **5**, 348–50.

Hill, H. (1971) in *Plutonium 1970 and Other Actinide* (ed. W. N. Miner), The Metallurgical Society of AIME, New York, part 2.

Hindman, J. C., Sullivan, J. C., and Cohen, D. (1954) *J. Am. Chem. Soc.*, **76**, 3278–80.

Hoekstra, H. R. and Gebert, E. (1977) *J. Inorg. Nucl. Chem.*, **39**, 2219–21.

Hoelgye, Z. (1998) *J. Radioanal. Nucl. Chem.*, **227**, 127–8.

Hoffman, P. and Kleykamp, H. (1972) in *Gmelin Handbuch der Anorganischen Chemie*, Suppl. Work, 8th edn, *Transuranium*, Verlag Chemie, Weinheim, vol. 4, part C, Compounds.

Holland, M. K. and Cordaro, J. V. (1988) DP-1751.

Holley, C. E. Jr, Rand, M. H., and Storms, E. K. (1984) in *The Chemical Thermodynamics of Actinide Elements and Compounds*, part 6. The Actinide Carbides, International Atomic Energy Agency, Vienna, pp. 49–51.

Holloway, J. H. and Laycock, D. (1984) *Adv. Inorg. Chem. Radiochem.*, **28**, 73–99.

Holm, E., Aarkrog, A., and Ballestra, S. (1987) *J. Radioanal. Nucl. Chem. Art.*, **115**, 5–11.

Horwitz, E. P., Chiarizia, R., and Alexandratos, S. D. (1994) *Solvent Extr. Ion Exch.*, **12**, 831–45.

Hursthouse, A. S. A., Baxter, M. S., McKay, K., and Livens, F. R. (1992) *J. Radioanal. Nucl. Chem. Art.*, **157**, 281–94.

Ilyatov, K. V., Matuzenko, M. Y., Krizhanskii, L. M., and Chaikhorskii, A. A. (1975) *Radiokhimiya*, **17**, 905–9.

Ionova, G. V. and Jovè, J. (1989) *Radiokhimiya*, **31**, 31–6.

Itagaki, H., Nakayama, S., Tanaka, S., and Yamawaki, M. (1992) *Radiochim. Acta*, **58/59**, 61–6.

Ivanova, S. A., Mikheeva, M. N., Novikov, A. P., and Myasoedov, B. F. (1994) *J. Radioanal. Nucl. Chem. Lett.*, **186**, 341–52.

Jeandey, C., Sanchez, J. P., Oddou, J. L., Rebizant, J., Spirlet, J. C., and Wastin, F. (1996) *J. Phys.: Condens. Matter*, **8**, 4259–68.

Jha, S. K. and Bhat, I. S. (1994) *J. Radioanal. Nucl. Chem. Art.*, **182**, 5–10.

Ji, Y. Q., Li, J. Y., Luo, S. G., Wu, Y., and Liu, J. L. (2001) *Fresenius J. Anal. Chem.*, **371**, 49–53.

Jones, E. R. and Stone, J. A. (1972) *J. Chem. Phys.*, **56**, 1343–7.

Jovè, J. and Cousson, A. (1977) *Radiochim. Acta*, **24**, 73–5.

Jovè, J., Cousson, A., and Gasperien, M. (1988a) *J. Less Common Metals*, **139**, 345–50.

Jovè, J., Cousson, H., Abazli, H., Tabuteau, A., Thévenin, T., and Pagès, M. (1988b) *Hyperfine Interact.*, **39**, 1–16.

Jovè, J., He, L., Proust, J., Pagès, M., and Pyykkö, P. (1991) *J. Alloys Compds.*, **177**, 285–310.

Kalsi, P. K., Sawant, L. R., Sharma, R. C., and Vaidyanathan, S. (1994) *J. Radioanal. Nucl. Chem. Lett.*, **187**, 265–75.

Kalvius, G. M. (1989) *J. Nucl. Mater.*, **166**, 5–21.

Kalvius, G. M., Gal, J., Asch, L., and Potzel, W. (1992) *Hyperfine Interact.*, **72**, 77–95.

Kalvius, G. M., Potzel, W., Zwirner, S., Gal, J., and Nowik, I. (1994) *J. Alloys Compds.*, **213/214**, 138–47.

Kanellakopulos, B., Henrich, E., Keller, C., Baumgartner, F., Konig, E., and Desai, V. P. (1980a) *Chem. Phys.*, **53**, 109–213.

Kanellakopulos, B., Keller, C., Klenze, R., and Stollenwerk, A. H. (1980b) *Physica*, **102B**, 221–5.

Karalova, Z. I., Lavrinovich, E. A., and Myasoedov, B. F. (1992a) *J. Radioanal. Nucl. Chem.*, **159**, 259–66.

Karalova, Z. K., Lavrinovich, E. A., Ivanova, S. A., Myasoedov, B. F., Fedorov, L. A., and Sokolovskii, S. A. (1992b) *Radiokhimiya*, **34**, 132–8.

Karelin, A. I., Semenov, E. N., and Mikhailova, N. A. (1991) *J. Radioanal. Nucl. Chem.*, **147**, 33–40.

Karraker, D. G., Stone, J. A., Jones, E. R., Jr, and Edelstein, N. (1970) *J. Amer. Chem. Soc.*, **92**, 4841–5.

Karraker, D. G. and Stone, J. A. (1972) *Inorg. Chem.*, **11**, 1742–6.

Karraker, D. G. (1973) *Inorg. Chem.*, **12**, 1105–8.

Karraker, D. G. and Stone, J. A. (1974) *J. Amer. Chem. Soc.*, **96**, 6885–8.

Karraker, D. G. and Stone, J. A. (1976) *Abstracts*, *172nd National Meeting of the American Chemical Society*, San Francisco, CA, No. INOR 184.

Karraker, D. G. (1987) *Inorg. Chim. Acta*, **139**, 189–91.

Kasar, U. M., Joshi, A. R., and Patil, S. K. (1991) *J. Radioanal. Nucl. Chem. Art.*, **150**, 369–76.

Kato, Y., Kimura, T., Yoshida, Z., and Nitani, N. (1996) *Radiochim. Acta*, **74**, 21–5.

Kato, Y., Kimura, T., Yoshida, Z., and Nitani, N. (1998) *Radiochim. Acta*, **82**, 63–8.

Katz, J. J. and Gruen, D. M. (1949) *J. Amer. Chem. Soc.*, **71**, 2106–12.

Keiser, D. D., Abraham, D. P., Sinkler, W., Richardson, J. W., and McDeavitt, S. M. (2000) *J. Nucl. Mater.*, **279**, 234–44.

Keller, C. (1963) *Nukleonick*, **5**, 89–93.

Keller, C., Kock, L., and Walter, K. H. (1965a) *J. Inorg. Nucl. Chem.*, **27**, 1205–23.

Keller, C., Kock, L., and Walter, K. H. (1965b) *J. Inorg. Nucl. Chem.*, **27**, 1225–32.

Keller, C. and Seiffert, H., (1969) *Inorg. Nucl. Chem. Lett.*, **5**, 51–7.

Keller, C. (1971) *The Chemistry of the Transuranium Elements,* Verlog Chemie, Weinheim.

Keller, C. (1972) in *MTP International Review of Science, Inorganic Chemistry,* ser. 1, 7 (ed. K. W. Bagnall), Butterworths, London.

Keller, C. (1975) in *Comprehensive Inorganic Chemistry,* vol. 10 (ed. A. F. Trotman-Dickinson), Pergamon Press, Oxford, 248 pp.

Keller, C. (1982) *Chemiker-Zeitung*, **106**, 137–42.

Kharitonov, Y. Y. and Moskvin, A.I. (1973) *Radiokimiya*, **15**, 608–12.

Kihara, T., Fujine, S., Fukasawa, T., Matsui, T., Maeda, M., and Ikeda, T. (1996) *J. Nucl. Sci. Technol.*, **33**, 409–13.

Kihara, S., Yoshida, Z., Apyagi, H., Maeda, K., Shirai, O., Kitatsuji, Y., and Yoshida, Y. (1999) *Pure Appl. Chem.*, **71**, 1771–807.

Kim, C., Takaku, Y., Yamamoto, M., Kawamura, H., Shiraishi, K., Igarashi, Y., Igarashi, S., Takayama, H., and Ikeda, N. (1989) *J. Radioanal. Nucl. Chem. Art.*, **132**, 131–7.

Kimura, T., Kobayashi, Y., and Akatsu, J. (1986) *Radiochim. Acta*, **39**, 179–83.

Kimura, T. (1990a) *J. Radioanal. Nucl. Chem. Art.*, **130**, 297–305.

Kimura, T. (1990b) *J. Radioanal. Nucl. Chem. Art.*, **141**, 307–16.

Kitazawa, H., Kwon, Y., Ohe, Y., Amanowicz, M., Ayache, C., Rossat- Mignod, J., Rebizant, J., Sprilet, J. C., Suzuki, T., and Kasuya, T. (1993) *Physica B*, **186/188**, 694–6.

Kleinschmidt, P. D., Lau, K. H., and Hildenbrand, D. L. (1992a) *J. Chem. Phys.*, **97**, 1950–3.

Kleinschmidt, P. D., Lau, K. H., and Hildenbrand, D. L. (1992b) *J. Chem. Phys.*, **97**, 2417–21.

Klenze, R. and Kim, J. I. (1988) *Radiochim. Acta*, **44/45**, 77–85.

Kolarik, Z. and Dressler, P. (1984) *Extraction '84*, *Proc. Symp. On Liquid–Liquid Extraction Science*, Institute of Chemical Engineers Symp. Ser., **88**, 83–90.

Kolarik, Z. J. and Horwitz, E. P. (1988) *Solvent Extr. Ion Exch.*, **6**, 247–63.

Koltunov, V. S. and Baranov, S. M. (1987) *Inorg. Chim. Acta*, **140**, 31–4.

Koltunov, V. S., Baranov, S. M., Zharova, T. P., and Abramina, E. V. (1993) *Radiokhimiya*, **35**, 79–84.

Koltunov, V. S., Taylor, R. J., Baranov, S. M., Mezhov, E. A., and May, I. (1999) *Radiochim. Acta*, **86**, 115–21.

Koltunov, V. S., Taylor, R. J., Baranov, S. M., Mezhov, E. A., Pastuschak, V. G., and May, I. (2000) *Radiochim. Acta*, **88**, 65–70.

Konig, E., Rudowicz, C., and Desai, V. P. (1983) *J. Chem. Phys.*, **78**, 5764–71.

Kraus, K. A. and Nelson, F. (1948) Report AECD-1864.

Krot, N. N. and Gel'man, A. D. (1967) *Dokl. Akad, Nauk SSSR*, **177**, 124–6.

Krot, N. N., Mefodeva, M. P., and Gelman, A. D. (1968a) *Radiokhimiya*, **10**, 634–8.

Krot, N. N., Mefod'eva, M. P., Smirnova, T. V., and Gel'man, A. D. (1968b) *Radiokhimiya*, **10**, 412–8.

Krot, N. N., Mefod'eva, M. P., Zakharova, F. A., Smirnova, T. V., and Gel'man, A. D. (1968c) *Radiokhimiya*, **10**, 630–4.

Krot, N. N., Charushnikova, I. A., Afonas'eva, T. V., and Grigor'eva, M. S. (1993) *Radiokhimiya*, **35**, 14–29.

Kuperman, A. Y., Smirnov, Yu. A., Fedotov, S. N., Nikol'skaya, T. L., and Efimova, N. S. (1988) *Zh. Struk. Khim.*, **30**, 791–7.

LaChapelle, T. J., Magnusson, L. B., and Hindman, J. C. (1947) ANL-4065.

LaChapelle, T. J. (1964) US Patent 3,149,908.

Lahalle, M. P., Krupa, J. C., Guillaumont, R., and Rizzoli, C. (1986) *J. Less -Common Metals*, **122**, 65–73.

Lander, G. H., Dunlap, B. D., Mueller, M. H., Nowik, I., and Reddy, J. F. (1973) *Int. J. Magn.*, **4**, 99–104.

Lander, G. H. and Burlet, P. (1995) *Physica B*, **214**, 7–21.

Laskorin, B. N., Skorovarov, D. I., Filippov, E. A., and Yakshin, V. V. (1985) *Radiokhimiya*, **27**, 156–69.

Lee, A. J., Mardon, P. G., Pearce, J. H., and Hall, R. O. A. (1959) *J. Phys. Chem. Solids*, **11**, 177–81.

Lee, S. C., Hutchinson, J. M. R., Inn, K. G. W., and Thein, M. (1995) *Health Phys.*, **68**, 350–8.

Legin, E. K. (1979) *Radiokhimiya*, **21**, 565–78.

Lemire, R. J., Fuger, J., Nitsche, H., Potter, P., Rand, M. H., Rydberg, J., Spahiu, K., Sullivan, J. C., Ullman, W. J., Vitorge, P., and Wanner, H. (2001) *Chemical Thermodynamics of Neptunium and Plutonium*, Elsevier, Amsterdam.

Levine, C. A. and Seaborg, G. T. (1951) *J. Am. Chem. Soc.*, **73**, 3278–83.

Li, K., Zhang, X., and Dong, W. (1988) *He Huaxue Yu Fangshe Huaxue*, **10**, 107–12.

Li, Y., Kato, Y., and Yoshida, Z. (1993) *Radiochim. Acta*, **60**, 115–9.

Lierse, C., Treiber, W., and Kim, J. I. (1985) *Radiochim. Acta*, **38**, 27–8.

Lloyd, J. R., Yong, P., Macaskie, L. E. (2000) *Environ. Sci. Technol.*, **34**, 1297–301.

Logvis', A. I., Bessonov, A. A., and Krot, N. N. (1994) *Radiokhimiya*, **36**, 6–9.

Lorenzelli, R. (1968) *C. R. Acad. Sci. Paris C*, **226**, 900–2.

Macaskie, L. E. and Basnakova, G. (1998) *Environ. Sci. Technol.*, **32**, 184–7.

Magette, M. and Fuger, J. (1977) *Inorg. Nucl. Chem. Lett.*, **13**, 529–36.

Magnusson, L. B. and La Chapelle, T. J. (1948) *J. Am. Chem. Soc.*, **70**, 3534–8.

Magon, L., Bismondo, A., Tomat, G., and Cassol, A. (1972) *Radiochim. Acta*, **17**, 164–7.

Magon, L., Tomat, G., Bismondo, A., Portanova, R., and Croatto, U. (1974) *Gazz. Chim. Ital.*, **104**, 967.

Maiti, T. C., Kaye, J. H., and Kozelisky, A. E. (1992) *J. Radioanal. Nucl. Chem.*, **161**, 533–40.

Malm, J. G., Weinstock, B., and Weaver, E. E. (1958) *J. Phys. Chem.*, **62**, 1506–8.

Malm, J. G., Williams, C. W., Soderholm, L., and Morss, L. R. (1993) *J. Alloys Compds.*, **194**, 133–7.

Mang, M., Gehmecker, H., Trautmenn, N., and Herrmann, G. (1993) *Radiochim. Acta*, **62**, 49–54.

Marcon, J. P. (1967) *C. R. Acad. Sci. Paris* 265 Series C 235.

Marcon, J. P. and Pascard, R. (1968) *Rev. Int. Hautes Temp. Refract.*, **5**, 51–4.

Marcon, J. P. (1969) Rapport CEA-R 3319.

Mardon, P. G. and Pearce, J. H. (1959) *J. Less Common Metals*, **1**, 467–75.

Marks, T. J. and Ernst, R. D. (1982) in *Comp. Organomet. Chem.* (eds. G. Wilkinson, F. G. A. Stone, and E. W. Abel) Pergamon, Oxford, pp. 211–70.

Marples, J. A. C. (1975) in *Plutonium and Other Actinides* (eds. H. Blank and R. Lindner), North-Holland, Amsterdam, pp. 353–60.

Marquart, R., Hoffman, G., and Weigel, F. (1983) *J. Less Common Metals*, **91**, 119–27.

Martinot, L., Machiels, A., Fuger, J., and Duyckaerts, G. (1970) *Bull. Soc. Chim. Belg.*, **79**, 125–31.

Martinot, L. (1984) Journee d'etude des sels fondus, May 23–25, 1984, Societe Chimie de Belgique, Brussels.

Martinot, L. and Fuger, J. (1985) in *Standard Potentials in Aqueous Solutions* (eds. A. J. Bard, R. Parsons, and J. Jordan), Marcel Dekker, New York.

Martinot, L. (1991) *J. Less Common Metals*, **170**, 121–6.

Maslov, O. D., Dmitriev, S. N., Molokanova, L. G., and Tolmachyov, S. Y. (1997) *J. Radioanal. Nucl. Chem.*, **226**, 181–3.

Mathur, J. N. and Choppin, G. R. (1994) *Radiochim. Acta*, **64**, 175–7.

Mathur, J. N., Murali, M. S., Balarama Krishna, M. V., Iyer, R. H., Chitnis, R. R., Wattal, P. K., Theyyunni, T. K., Ramanujam, A., Dhami, P. S., and Gopalakrishnan, V. (1996a) *Sep. Sci. Technol.*, **31**, 2045–63.

Mathur, J. N., Murali, M. S., Balarama Krishna, M. V., Iyer, R. H., Chitnis, R. R., Wattal, P. K., Bauri, A. K., and Banerji, A. (1996b) *J. Radioanal. Nucl. Chem. Lett.*, **213**, 419–29.

Mathur, J. N., Ruikar, P. B., Balarama Krishna, M. V., Murali, M. S., Nagar, M. S., and Iyer, R. H. (1996c) *Radiochim. Acta*, **73**, 100–206.

Mathur, J. N., Murali, M. S., and Nash, K. L. (2001) *Solv. Extr. Ion Exch.*, **19**, 357–90.

Matsika, S. and Pitzer, R. M. (2000) *J. Phys. Chem.*, **A104**, 4064–8.

Maxwell, S.L., III (1997) *Radioact. Radiochem.*, **8**(4), 36–44.

May, S., Engelmann, Ch., and Pinte, G. (1987) *J. Radioanal. Nucl. Chem. Art.*, **113**, 343–50.

Maya, L. (1983) *Inorg. Chem.*, **22**, 2093–5.

Maya, L. (1984) *Inorg. Chem.*, **23**, 3926–30.

McMillan, E. (1939) *Phys. Rev.*, **55**, 510.

McMillan, E. and Abelson, P. H. (1940) *Phys. Rev.*, **57**, 1185–6.

Mefod'eva, M. P., Krot, N. N., Smirnova, T. V., and Gel'man, A. D. (1969) *Radiokhimiya*, **11**, 193–200.

Mefod'eva, M. P., Krot, N. N., and Gel'man, A. D. (1970a) *Radiokhimiya*, **12**, 232–7.

Mefod'eva, M. P., Krot, N. N., and Gel'man, A. D. (1970b) *Sov. Radiochem.*, **12**, 210–4.

Mefod'eva, M. P. and Gel'man, A. D. (1971) *Radiokhimiya*, **13**, 597–603.

Mefod'eva, M. P., Krot, N. N., Afanas'eva, T. V., and Gel'man, A. D. (1974) *Russ. Chem. Bull.*, **23**, 2285–7.

Mefod'eva, M. P., Krot, N. N., and Gel'man, A. D. (1976) *Radiokhimiya*, **18**, 93–5.

Meresse, Y., Heathman, S., Le Bihan, T., Rebizant, J., Brooks, M. S. S., and Ahuja, R. (2000) *J. Alloys and Compds.*, **296**, 27–32.

Merli, L. and Fuger, J. (1994) *Radiochim. Acta*, **66/67**, 109–13.

Mincher, B. J. (1989) *Solvent Extr. Ion Exch.*, **7**, 45–54.

Mintz, M. H., Hadari, Z., and Bixon, M. (1976) *J. Less Common Metals*, **48**, 183–6.

Mishin, V. Y., Sidorenko, G. V., and Suglobov, D. N. (1986) *Radiokhimiya*, **28**, 292–300.

Mitchell, A. W. and Lam, D. J. (1971) *J. Nucl. Mater.*, **39**, 219–23.

Mohapatra, P. K. and Manchanda, V. K. (1993) *Radiochim. Acta*, **61**, 69–72.

Morita, Y. and Kubota, M. (1988) *Solvent Extr. Ion Exch.*, **6**, 233–46.

Morita, Y., Glatz, J.-P., Kubota, M., Koch, L., Pagliosa, G., Roemer, K., and Nicholl, A. (1996) *Solvent Extr. Ion Exch.*, **14**, 385–400.

Morss, L. R. (1982) in *Actinides – 1981* (ed. N. Edelstein), Pergamon, Oxford, pp. 381–407.

Morss, L. R., Appelman, E. H., Gerz, R. R., and Martin-Rovet, D. (1994) *J. Alloys Compds.*, **203**, 289–95.

Moskvin, A. I. and Peretrukhin, V. F. (1964) *Sov. Radiochem.*, **6**, 198–205.

Moskvin, A. I. (1971) *Sov. Radiochem.*, **13**, 700–5.

Mulford, R. N. R. and Wiewandt, T. A. (1965) *J. Phys. Chem.*, **69**, 1641–4.

Musikas, C. (1963) *Radiochim. Acta*, **1**, 92–8.

Musikas, C., Couffin, F., and Marteau, M. (1974) *J. Chim. Phys.*, **71**, 641–8.

Musikas, G. and Marteau, M. (1978) *Sov. Radiochem.*, **20**, 213–6.

Naegele, J. R., Cox, L. E., and Ward, J. W. (1987) *Inorg. Chim. Acta*, **139**, 327–9.

Nagasaki, S., Tanaka, S., and Takahashi, Y. (1988) *J. Radioanal. Nucl. Chem. Art.*, **124**, 383–95.

Nakada, M., Saeki, M., Masaki, N. M., and Tsutsui, S. (1998) *J. Radioanal. Nucl. Chem.*, **232**, 201–7.

Nakamoto, T., Nakada, M., Masaki, N. M., Saeki, M., and Yamashita, T. (1998) *J. Radioanal. Nucl. Chem.*, **227**, 137–41.

Nakamoto, T., Nakada, M., Masaki, N. M., Saeki, M., Yamashita, T., and Krot, N. N. (1999) *J. Radioanal. Nucl. Chem.*, **239**, 257–61.

Nakamura, T., Takahashi, M., Fukasawa, T., and Utamura, M. (1992) *J. Nucl. Sci. Technol.*, **29**, 393–5.

Nash, K. L. and Choppin, G. R. (1997) *Sep. Sci. Technol.*, **32**, 255–74.

Neck, V., Kim, J. I., and Kanellakopulos, B. (1992) *Radiochim. Acta*, **56**, 25–30.

Neck, V., Kim, J. I., Seidel, B. S., Marquardt, C. M., Dardenne, K., Jensen, M. P., and Hauser, W. (2001) *Radiochim. Acta*, **89**, 439–46.

Nevitt, M. V. (1963) Argonne National Laboratory Report ANL-6868, p. 314.

Newton, T. W. (1975) TID-26506, National Technical Information Service, US Department of Commerce, Springfield, VA.

Niese, U. and Vecernik, J. (1981) *Isotopenpraxis*, **18**, 91–2.

Nikitenko, S. I., Moisy, Ph., and Madic, C. (1999) *Radiochim. Acta*, **86**, 23–31.

Nikonov, M. V., Bessonov, A. A., Krot, N. N., and Perminov, V. P. (1994) *Radiochemistry* (*Moscow*), **36**, 262–3.

Novikov, Y. P., Pavlotskaya, F. I., and Myasoedov, B. F. (1989) *Radiokhimiya*, **31**, 134–42.

Novikov, A. P., Mikheeva, M. N., Gracheva, O. I., and Myasoedov, B. F. (1997) *J. Radioanal. Nucl. Chem.*, **223**, 163–6.

Oddou, J. L., Arons, R. R., Blaise, A., Burlet, P., Colineau, E., Jeandey, C., Ressouche, E., Sanchez, J. P., Larroque, J., Rebizant, J., and Spirlet, J. C. (1994) *J. Magn. and Magn. Mater.*, **135**, 183–90.

OECD/NEA Report (1997) *Actinide Separation Chemistry in Nuclear Waste Streams and Materials*.

OECD/NEA Report (2001) *Evaluation of Speciation Technology*.

Oetting, F. L., Rand, M. H., and Ackermann, R. J. (1976) in *The Chemical Thermodynamics of Actinide Elements and Compounds*, part 1, IAEA, Vienna, pp. 20–3.

Ogawa, T. (1993) *J. Alloys Compds.*, **194**, 1–7.

Olson, W.M. and Mulford, R. N. R. (1966) *J. Phys. Chem. Solids*, **70**, 2932–4.

Pagès, M., Nectoux, F., and Freundlich, W. (1971) *Radiochem. Radioanal. Lett.*, **7**, 155–62.

Palade, D. M. (1997) *Russ. J. Coord. Chem.*, **23**, 636.

Patil, S. K. and Ramakrishna, V. V. (1973) *Radiochim. Acta*, **19**, 27–30.

Patil, S. K. and Ramakrishna, V. V. (1975) *Inorg. Nucl. Chem. Lett.*, **11**, 421–8.

Patil, S. K. and Ramakrishna, V. V. (1976) *J. Inorg. Nucl. Chem.*, **38**, 1075–8.

Patil, S. K., Ramakrishna, V. V., and Gudi, N. M. (1981) in *Proc. Nucl. Chem. Radiochem. Symp. 1980*, Indian Department of Atomic Energy, pp. 388–90.

Paul, M. T. (1970) Report KFK-1210.

Pavlotskaya, F. I. (1997) *J. Anal. Chem.*, **52**, 110–26.

Peacock, R. D. and Edelstein, N. (1976) *J. Inorg. Nucl. Chem.*, **38**, 771–3.

Penneman, R. A., Ryan, R. R., and Rosenzweig, A. (1973) *Struct. Bond*, **13**, 1–52.

Pentreath, R. J. and Harvey, B. R. (1981) *Mar. Ecol. Prog. Ser.* **6**, 243–7.

Peppard, D. F., Studier, M. H., Gergel, M. V., Mason, G. W., Sullivan, J. C., and Mech, J. F. (1951) *J. Am. Chem. Soc.*, **73**, 2529–31.

Peppard, D. F., Mason, G. W., Gray, P. R., and Mech, J. F. (1952) *J. Am. Chem. Soc.*, **74**, 6081–7.

Peretrukhin, V. F. and Alekseeva, D. P. (1974) *Radiokhimiya* **16**, 836–43.

Pilz, N., Hoffmann, P., and Lieser, K. H. (1989) *J. Radioanal. Nucl. Chem. Art.*, **130**, 141–53.

Piskunov, E. M. and Rykov, A. G. (1972) *Sov. Radiochem.*, **14**, 342–4.

Pitzer, K. S. (1979) in *Activity CoeYcients in Electrolyte Solutions,* vol. 1 (ed. R. M. Pytkowicz), CRC Press, Boca Raton, p. 157.

Pollard, P. M., Liezers, M., McMillan, J. M., Phillips, G., Thomason, H. P., and Ewart, F. T. (1988) *Radiochim. Acta*, **44/45**, 95–101.

Portanova, R., Tomat, G., Magon, L., and Cassol, A. (1970) *J. Inorg. Nucl. Chem.*, **32**, 2343–8.

Portanova, R., Tomat, G., Magon, L., and Cassol, A. (1972) *J. Inorg. Nucl. Chem.*, **34**, 1768–70.

Potzel, W., Moser, J., Asch, L., and Kalvius, G. M. (1983) *Hyperfine Interact.*, **13**, 175–98.

Potzel, W., Gleisner, A., Moser, J., Zwirner, S., Potzel, U., Gal, J., and Kalvius, G. M. (1993) *Physica B*, **190**, 98–106.

Pratopo, M. I., Moriyama, H., and Higashi, K. (1989) *Joint Int. Waste Manage. Conf.*, vol. 2, 309–12.

Pribylova, G. A., Chmutova, M. K., and Myasoedov, B. F. (1987) *Radiokhimiya*, **29**, 621–5.

Quill, L. L. (1938) *Chem. Rev.*, **23**, 87–155.

Raghavan, R., Ramakrishna, V. V., and Patil, S. K. (1975) *J. Inorg. Nucl. Chem.*, **37**, 1540–1.

Rai, D. (1984) *Radiochim. Acta*, **35**, 97–106.

Rai, D. and Ryan, J. L. (1985) *Inorg. Chim.*, **24**, 247–51.

Rai, D., Swanson, J. L., and Ryan, J. L. (1987) *Radiochim. Acta*, **42**, 35–41.

Rao, P. R. V., Bagawde, S. V., Ramakrishna, V. V., and Patil, S. K. (1978) *J. Inorg. Nucl. Chem.*, **40**, 339–43.

Rao, P. R. V., Gudi, N. M., Bagawde, S. V., and Patil, S. K. (1979) *J. Inorg. Nucl. Chem.*, **41**, 235–9.

Reavis, J. G., Bowersox, D. F., Christensen, D. C., and Mullins, L. J. (1985) *Radiochim Acta*, **38**, 135–9.

Richter, K. and Sari, C. (1987) *J. Nucl. Mater.*, **148**, 266–71.

Riegel, J., Deissenberger, R., Herrmann, G., Koehler, S., Sattelberger, P., Trautmann, N., Wendeler, H., Ames, F., Kluge, H.-J., Scheerer, F., and Urban, F -J. (1993) *Appl. Phys.*, **B56**, 275–80.

Riggle, K. (1992) DOE/OR/00033-T487.

Riglet, Ch., Vitorge, P., and Grenthe, I. (1987) *Inorg. Chim. Acta*, **133**, 323–9.

Riglet, Ch., Robouch, P., and Vitorge, P. (1989) *Radiochim. Acta*, **46**, 85–94.

Riglet, C., Provitina, O., Dautheribes, J., and Revy, D. (1992) *J. Anal. At. Spectrom.*, **7**, 923–7.

Rizkalla, E. N., Nectoux, F., Dabos-Seignor, S., and Pagès, M. (1990a) *Radiochim. Acta*, **51**, 113–7.

Rizkalla, E. N., Nectoux, F., Dabos-Seignor, S., and Pagès, M. (1990b) *Radiochim. Acta*, **51**, 151–5.

Rodriguez, R. J., Sari, C., and Portal, A. J. C. (1994) *J. Alloys Compds.*, **209**, 263–8.

Rösch, F., Dittrich, S., Buklanov, G. V., Milanov, M., Khalkin, V. A., and Dreyer, R. (1990) *Radiochim. Acta*, **49**, 29–34.

Rosner, G., Winkler, R., and Yamamoto, M. (1993) *J. Radioanal. Nucl. Chem.*, **173**, 273–81.

Rossat-Mignod, J., Lander, G. H., and Burlet, P. (1984) in *Handbook on the Physics and Chemistry of the Actinides,* vol. 1 (eds. A. J. Freeman and G. H. Lander), North-Holland, Amsterdam, pp. 415–500.

Rossat-Mignod, J., Burlet, P., Fournier, J. M., Pleska, E., and Quezel, S. (1989) *J. Nucl. Mater.*, **166**, 56–8.

Roy, J. J., Grantham, L. F., Grimmett, D. L., Fusselman, S. P., Krueger, C. L., Storvick, T. S., Inoue, T., Sakamura, Y., and Takahashi, N. (1996) *J. Electrochem. Soc.*, **143**, 2487–92.

Rozen, A. M. and Nikolotova, Z. I. (1988) *Radiokhimiya*, **30**, 594–606.

Rozen, A. M., Nikolotova, Z. I., and Kartasheva, N. A. (1988) *Radiokhimiya*, **30**, 614–8.

Rozen, A. M., Nikoforov, A. S., Kartasheva, N. A., Nikolotova, Z. I., and Tananaev, I. G. (1990) *Dokl. Akad. Nauk SSSR*, **312**, 897–900.

Rozen, A. M., Nikolotova, Z. I., Kartasheve, N. A., and Tananaev, I. G. (1992) *Radiokhimiya*, **34**, 54–7.

Rush, R. M., Johnson, J. S., and Kraus, K. A. (1962) *Inorg. Chem.*, **1**, 378–86.

Rush, R. M. and Johnson, J. S. (1963) *J. Phys. Chem.*, **67**, 821–5.

Ryan, J. L. and Rai, D. (1987) *Inorg. Chem.*, **26**, 4140–2.

Rykov, A. G. and Frolov, A. A. (1972) *Radiokimiya*, **14**, 717–21.

Rykov, A. G., Blokhin, N. B., and Vasilev, V. Y. (1973) *Radiokimiya*, **15**, 341–7.

Saeki, M., Nakada, M., Nakamoto, T., Yamashita, T., Masaki, N. M., and Krot, N. N. (1999) *J. Radioanal. Nucl. Chem.*, **239**, 221–5.

Saeki, M. (2003) unpublished work, provided for this chapter after revision of the figure in Saeki *et al.* (1999).

Saito, T., Wang, J., Kitazawa, T., Takahashi, M., Takeda, M., Nakada, M., Nakamoto, T., Masaki, N. M., Yamashita, T., and Saeki, M. (1999) *J. Radioanal. Nucl. Chem.*, **239**, 319–23.

Sakamura, Y., Hijikata, T., Kinoshita, K., Inoue, T., Storvick, T. S., Krueger, C. L., Roy, J. J., Grimmett, D. L., Fusselman, S. P., and Gay, R. L. (1998) *J. Alloys Compds.*, **271–273**, 592–6.

Sakamura, Y., Shirai, O., Iwai, T., and Suzuki, Y. (2000) *J. Electrochem. Soc.*, **147**, 642–9.

Sanchez, J. P., Rebizant, J., and Spirlet, J. C. (1988) *Phys. Lett. A*, **128**, 297–301.

Sanchez, J. P., Bouillet, M. N., Colineau, E., Blaise, A., Amanowicz, M., Burlet, P., Fournier, J. M., Charvolin, T., and Larroque, J. (1993) *Physica B*, **186/188**, 675–7.

Sanchez, J. P., Colineau, E., Jeandey, C., Oddou, J. L., Rebizant, J., Seret, A., and Spirlet, J. C. (1995) *Physica B*, **206/7**, 531–3.

Sandenaw, T. A., Gibney, R. B., and Holley, C. E. (1973) *J. Chem. Thermodyn.*, **5**, 41–7.

Sawant, R. M., Chaudhuri, N. K., Rizvi, G. H., and Patil, S. K. (1985) *J. Radioanal. Nucl. Chem.*, **91**, 41–58.

Schafer, W., Will, G., Gal, J., and Suski, W. (1989) *J. Less Common Metals*, **149**, 237–41.

Schmidt, K. H., Gordon, S., Thompson, R. C., and Sullivan, J. C. (1980) *J. Inorg. Nucl. Chem.*, **42**, 611–5.

Schmidt, K. H., Gordon, S., Thompson, M. C., and Sullivan, J. C. (1983) *Radiat. Phys. Chem.*, **21**, 321–8.

Schneider, R. A. and Harmon, K. M. (1961) USAEC Report HW-53368.

Schoebrechts, J. P., Gens, R., Fuger, J., and Morss, L. R. (1989) *Thermochim. Acta*, **139**, 49–66.

Schrepp, W., Stumpe, R., Kim, J. I., and Walther, H. (1983) *Appl. Phys.*, **B32**, 207–9.

Seaborg, G. T. and Perlman, M. L. (1948) *J. Am. Chem. Soc.*, **70**, 1571–3.

Seaborg, G. T. and Brown, H. S. (1961) US Patent No. 2,982,604.

Segrè, E. (1939) *Phys. Rev.*, **55**, 1104–5.

Seranno, J. G. and Kimura, T. (1993) *J. Radioanal. Nucl. Chem. Art.*, **172**, 97–105.

Seret, A., Wastin, F., Waerenborgh, J. C., Zwirner, S., Spirlet, J. C., and Rebizant, J. (1995) *Physica B*, **206/7**, 525–7.

Sevost'yanova, E. P. and Khalturin, G. V. (1976) *Sov. Radiochem.*, **18**, 738–43.

Sheft, I. and Fried, S. (1953) *J. Am. Chem. Soc.*, **75**, 1236–7.

Shilin, I. V. and Nazarov, V. K. (1966) *Sov. Radiochem.*, **8**, 474–8.

Shiloh, M. and Marcus, Y. (1966) *J. Inorg. Nucl. Chem.*, **28**, 2725–32.

Shilov, V. P., Tananaev, I. G., and Krot, N. N. (1991) *Sov. Radiochem.*, **33**, 250–1.

Shinohara, N., Kohno, N., Suzuki, S., and Usuda, S. (1989) *J. Radioanal. Nucl. Chem.*, **130**, 3–12.

Shirai, O., Iizuka, M., Iwai, T., and Arai, Y. (2001) *J. Appl. Electrochem.*, **31**, 1055–60.

Smith, R. M. and Martell, A. E. (2002) in *NIST Critically Selected Stability Constants of Metal Complexes: Version 6.0*, National Institute of Standards and Technology, Geithersburg.

Soderholm, L., Antonio, M. R., Williams, C., and Wasserman, S. R. (1999) *Anal. Chem.*, **71**, 4622–8.

Spirlet, T. E., Bednarcyk, J., Rebizant, J., and Walker, C. T. (1980) *J. Crystal Growth*, **49**, 171–2.

Spirlet, J. C. and Vogt, O. (1984) in *Handbook on the Physics and Chemistry of the Actindes* (eds. A. J. Freeman and G. H. Landers), Elsevier, Amsterdam, pp. 79–151.

Spirlet, M-R., Jemine, X., and Goffart, J. (1994) *J. Alloys Compds.*, **216**, 269–72.

Spitsyn, V. I., Gelman, A. D., Krot, N. N., Mefodiyeva, M. P., Zakharova, F. A., Komkov, Yu. A., Shilov, V. P., and Smirnova, I. V. (1969) *J. Inorg. Nucl. Chem.*, **31**, 2733–45.

Spitsyn, V. I. and Ionova, G. V. (1987) *Dokl. Akad. Nauk SSSR*, **292**, 412–5.

Stafsudd, O. M., Leung, A. F., and Wong, E. Y. (1969) *Phys. Rev.*, **180**, 339–43.

Stepanov, A. V., Nikitina, S. A., Karasev, V. T., Stepanov, D. A., Karmanova, V. Yu., Aleksandruk, V. M., and Dem'yanova, T. A. (1997) *Z. Anal. Khim.*, **52**, 144–9.

Stephens, W. R. (1966) *J. Phys. Chem. Solids*, **27**, 1201–4.

Stewart, G. R., Andraka, B., and Haire, R. G. (1994) *J. Alloys Compds.*, **213/214**, 111–3.

Stone, J. A., Pillinger, W. L., and Karraker, D. G. (1969) *Inorg. Chem.*, **8**, 2519–20.

Stout, B. E., Cacceci, M. S., Nectoux, F., and Pagès, M. (1989) *Radiochim. Acta*, **46**, 181–4.

Stout, B. E., Choppin, G. R., Nectoux, F., and Pagès, M. (1993) *Radiochim. Acta*, **61**, 65–7.

Stromatt, R. W. (1959) USAEC Report HW-59447.

Sudakov, L. V., Solnstsev, V. M., Kapshukov, I. I., Belyaev, Y. I., and Chistyakov, V. M. (1972) V. I. Lenin Scientific Research Institute for Atomic Reactors, Report NIIAR-P-138, Dimitrovgrad, Argonne National Laboratory Trans-935.

Sullivan, J. C. and Hindman, J. C. (1959) *J. Phys. Chem.*, **63**, 1332–3.

Sullivan, J. C., Hindman, J. C., and Zielen, A. J. (1961) *J. Am. Chem. Soc.*, **83**, 3373–8.

Sullivan, J. C. (1962) *J. Am. Chem. Soc.*, **84**, 4256–8.

Sullivan, J. C. (1964) *Inorg. Chem.*, **3**, 315–9.

Sus, F., Parus, J. L., and Raab, W. (1996) *J. Radioanal. Nucl. Chem. Art.*, **211**, 363–74.

Suzuki, Y., Arai, Y., Okamoto, Y., and Ohmichi, T. (1994) *J. Nucl. Sci. Tech.*, **31**, 677–80.

Suzuki, Y. and Arai, Y. (1998) *J. Alloys Compds.*, **271–273**, 577–82.

Tabuteau, A. and Pagès, M. (1985) in *Handbook on the Physics and Chemistry of the Actinides,* vol. 3 (eds. A. J. Freeman and C. Keller), North-Holland, Amsterdam, pp. 184–241.

Tait, C. D., Palmer, P. D., Ekberg, S. A., and Clark, D. L. (1995) Los Alamos National Laboratory Report LA-13012-MS.

Takeishi, H., Kitatsuji, Y., Kimura, T., Meguro, Y., Yoshida, Z., and Kihara, S. (2001) *Anal. Chim. Acta*, **431**, 69–80.

Taylor, R. J., Denniss, I. S., and Wallwork, A. L. (1997) *Nucl. Energy*, **36**, 39–46.

Taylor, R. J., May, I., Koltunov, V. S., Baranov, S. M., Marchenko, V. I., Mezhov, E. A., Pastuschak, V. G., Zhuravleva, G. I., and Savilova, O. A. (1998a) *Radiochim. Acta*, **81**, 149–56.

Taylor, R. J., May, I., Wallwork, A. L., Denniss, I. S., Hill, N. J., Galkin, B. Ya., Zilberman, B. Ya., and Fedorov, Yu. S. (1998b) *J. Alloys Compds.*, **271–273**, 534–7.

Thévenin, T. and Pagès, M. (1982) *J. Less Common Metals*, **84**, 133–7.

Thévenin, T., Jovè, J., and Pagès, M. (1985) *Mat. Res. Bull.*, **20**, 723–30.

Tochiyama, O., Inoue, Y., and Kuroki, Y. (1989) *Solvent Extr. Ion Exch.*, **7**, 289–314.

Tochiyama, O., Inoue, Y., and Narita, S. (1992) *Radiochim. Acta*, **58/59**, 129–36.

Tomilin, S. V., Volkov, Y. F., Visyashcheva, G. I., and Kapshukov, I. I. (1984) *Radiokhimiya*, **26**, 734–9.

Tomilin, S. V., Volkov, Y. F., Melkaya, R. F., Spiryakov, V. I., and Kapshukov, I. I. (1986) *Radiokhimiya*, **28**, 696–700.

Trevorrow, L. E., Gerding, T. J., and Steindler, M. J. (1968) *J. Inorg. Nucl. Chem.*, **30**, 2671–7.

Tsivadze, A. Y. and Krot, N. N. (1972) *Radiokimiya*, **14**, 629–33.

Uchiyama, G., Fujine, S., Hotoku, S., and Maeda, M. (1993) *Nucl. Technol.*, **102**, 341–51.

Uchiyama, G., Asakura, T., Hotoku, S., and Fujine, S. (1998a) *Solvent Extr. Ion Exch.*, **16**, 1191–213.

Uchiyama, G., Kihara, T., Hotoku, S., Fujine, S., and Maeda, M. (1998b) *Radiochim. Acta*, **81**, 29–32.

Van Der Sluys, W. G., Burns, C. J., and Smith, D. C. (1992) Patent No. 67487.

Varga, L. P., Reisfeld, M. J., and Asprey, L. B. (1970) *J. Chem. Phys.*, **53**, 250–5.

Varlashkin, P. G., Hobart, D. E., Begun, G. M., and Peterson, J. R. (1984) *Radiochim. Acta*, **35**, 91–6.

Vogt, O. and Mattenberger, K. (1994) *J. Alloys Compds.*, **213/214**, 248–53.

Volkov, Y. F., Melkaya, R. F., Spiryakov, V. I., and Timofeev, G. A. (1994) *Radiokhimiya*, **36**, 205–8.

Wada, Y., Morimoto, K., Goibuchi, T., and Tomiyasu, H. (1995) *J. Nucl. Sci. Technol.*, **32**, 1018–26.

Wada, Y., Morimoto, K., and Tomiyasu, H. (1996) *Radiochim. Acta*, **72**, 195–204.

Waggener, W. C. (1958) *J. Phys. Chem.*, **62**, 382–3.

Ward, J. W., Bartscher, W., and Rebizant, J. (1987) *J. Less Common Metals*, **130**, 431–89.

Wastin, F., Rebizant, J., Sprilet, J. C., Sari, C., Walker, C. T., and Fuger, J. (1993) *J. Alloys Compds.*, **196**, 87–92.

Weigel, F. and Hellmann, H. (1986) *J. Less Common Metals*, **121**, 415–23.

Wester, D. W., Mulak, J., Banks, R., and Carnall, W. T. (1982) *J. Solid State Chem.*, **45**, 235–40.

Williams, C. W., Blauden, J.-P., Sullivan, J. C., Antonio, M. R., Bursten, B., and Soderholm, L. (2001) *J. Amer. Chem. Soc.*, **123**, 4346–7.

Wisnubroto, D. S., Ikeda, H., and Suzuki, A. (1991) *J. Nucl. Sci. Technol.*, **28**, 1100–06.

Wittenberg, L. J., Vaughn, G. A., and De Witt, R. (1970) *Nucl. Metall. Met. Soc. AIME*, **17**, 659–68.

Wojakowski, A. and Damien, D. (1982) *J. Less Common Metals*, **83**, 263–7.

Yaar, I., Gal, J., Potzel, W., Kalvius, G. M., Will, G., and Schafer, W. (1992) *J. Magn. Magn. Mater.*, **104/7**, 63–4.

Yakovlev, N. G. and Kosyakov, V. N. (1991) *Radiokhimiya*, **33**, 82–7.

Yamamoto, M., Chatani, K., Komura, K., and Ueno, K. (1989) *Radiochim. Acta*, **47**, 63–8.

Yamamoto, M., Kofuji, H., Tsumura, A., Yamasaki, S., Yuita, K., Komamura, M., Komura, K., and Ueno, K. (1994) *Radiochim. Acta*, **64**, 217–24.

Yamana, H., Yamamoto, T., Kobayashi, K., Mitsugashira, T., and Moriyama, H. (2001) *J. Nucl. Sci. Tech.*, **38**, 859–65.

Yang, D., Zhu, Y., and Jiao, R. (1994) *J. Radioanal. Nucl. Chem Art.*, **183**, 245–60.

Yarbo, S. L., Dunn, S. L., and Schreiber, S. B. (1991) LA-11890.

Yoshida, Z., Aoyagi, H., and Kihara, S. (1991) *Fresenius J. Anal. Chem.*, **340**, 403–9.

Zachariasen, W. H. (1949a) *Acta Crystallogr.*, **2**, 291–6.

Zachariasen, W. H. (1949b) *Acta Crystallogr.*, **2**, 60–2.

Zachariasen, W. H. (1952) *Acta Crystallogr.*, **5**, 644–67.

Zantuti, F., Ivanova, S. A., Novikov, Y. P., and Myasoedov, B. F. (1990) *J. Radioanal. Nucl. Chem.*, **143**, 397–401.

Zhao, J., Mao, X., Jin, X., Guo, G., and Fu, Y. (1991) *Microchem. J.*, **44**, 59–62.

Zhu, Y. and Song, C. (1992) in *Transuranium Elements, A Half Century* (eds. L. R. Morss and J. Fuger), American Chemical Society Books, Washington DC, ch. 32.

Zwick, B. D., Sattelberger, A. P., and Avens, L. R. (1992) in *Transuranium Elements* (eds. L. R. Morss and J. Fuger), American Chemical Society, pp. 240–6.

Zwirner, S., Spirlet, J. C., Rebizant, J., Potzel, W., Kalvius, G. M., Geibel, C., and Steglich, F. (1993) *Physica B*, **186/8**, 681–3.

CHAPTER SEVEN

PLUTONIUM

David L. Clark, Siegfried S. Hecker, Gordon D. Jarvinen, and Mary P. Neu

7.1 INTRODUCTION

The element plutonium occupies a unique place in the history of chemistry, physics, technology, and international relations. After the initial discovery based on submicrogram amounts, it is now generated by transmutation of uranium in nuclear reactors on a large scale, and has been separated in ton quantities in large industrial facilities. The intense interest in plutonium resulted from the dual-use scenario of domestic power production and nuclear weapons – drawing energy from an atomic nucleus that can produce a factor of millions in energy output relative to chemical energy sources. Indeed, within 5 years of its original synthesis, the primary use of plutonium was for the release of nuclear energy in weapons of unprecedented power, and it seemed that the new element might lead the human race to the brink of self-annihilation. Instead, it has forced the human race to govern itself without resorting to nuclear war over the past 60 years. Plutonium evokes the entire gamut of human emotions, from good to evil, from hope to despair, from the salvation of humanity to its utter destruction. There is no other element in the periodic table that has had such a profound impact on the consciousness of mankind.

In 2005, approximately 2000 metric tons of plutonium exist throughout the world in the form of used nuclear fuel, nuclear weapons components, various nuclear inventories, legacy materials, and wastes (Albright and Kramer, 2004). This number grows every year by 70 to 75 metric tons through production in irradiated nuclear fuels (Albright and Kramer, 2004). It is clear that the large inventories of plutonium must be prudently managed for many centuries. A complex blend of global political, socioeconomic, and technological challenges must be dealt with to manage these inventories efficiently and safely.

From physical, chemical, and technological perspectives, plutonium is one of the most complex and fascinating elements in the periodic table. The metal exhibits six solid allotropes at ambient pressure and its phases are notoriously unstable with temperature, pressure, chemical additions, and time. With little provocation, the metal can change its density by as much as 25%. It can be as brittle as glass or as malleable as aluminum; it expands when it solidifies, and its freshly machined surface will tarnish in minutes. It is highly reactive in air, has five chemical oxidation states (six if the metal is included), and can form numerous compounds and complexes in the environment and during chemical processing. Plutonium's continuous radioactive decay causes self-irradiation damage of the metal lattice, or modification of solutions containing plutonium ions. Plutonium sits near the middle of the actinide series, which marks the emergence of 5f electrons in the valence shell. Elements to the left of plutonium have delocalized (bonding) electrons, while elements to the right of plutonium exhibit more localized (nonbonding) character. Plutonium is poised in the middle, and in the δ-phase metal, the electrons seem to be in a unique state of being neither fully bonding nor localized, a property that leads to novel electronic interactions and unusual physical and chemical behavior. This position in the periodic table challenges our understanding of relativistic electronic interactions and the nature of chemical bonding in heavy element metals, compounds, and complexes. When the unique nuclear properties are also considered, the study of plutonium is inherently multidisciplinary in nature. The present discussion will be confined to the most recent aspects of the subject. Reviews describing aspects of the chemistry and physics of plutonium can be found by Keller (1971), Cleveland (1979), Wick (1980), Cooper and Schecker (2000), Hecker (2003), Hecker *et al.* (2004), and in the *Gmelin Handbook of Inorganic Chemistry* (Koch, 1972, 1976a,b).

7.2 HISTORICAL

When the first of the transuranium elements, neptunium (Chapter 6) was discovered, it was realized that the radioactive β decay of $^{239}_{93}\mathrm{Np}$ should lead to the formation of element 94. The scale of the experiments at that time, however, precluded its identification. Plutonium was first produced late in 1940 by Seaborg, McMillan, Kennedy, and Wahl (Seaborg *et al.*, 1946, 1949a) by bombarding uranium with deuterons to produce the isotope $^{238}\mathrm{Pu}$:

$$^{238}_{92}\mathrm{U} + ^{2}_{1}\mathrm{H} \rightarrow ^{238}_{93}\mathrm{Np} + 2\,^{1}_{0}\mathrm{n} \qquad (7.1)$$

$$^{238}_{93}\mathrm{Np} \xrightarrow[2.1\mathrm{d}]{\beta^-} {}^{238}_{94}\mathrm{Pu}\ (t_{1/2} = 87.7\,\text{years}) \tag{7.2}$$

The short half-life of ^{238}Pu was conducive to tracer studies, and allowed Seaborg, Wahl, and Kennedy to obtain enough chemical information for subsequent separation and isolation of other plutonium isotopes. The isotope of major importance, ^{239}Pu, was discovered in 1941. Bombardment of $^{238}_{92}$U by neutrons produced $^{239}_{92}$U, which decayed to $^{239}_{93}$Np, and ultimately to $^{239}_{94}$Pu:

$$^{238}_{92}\mathrm{U} + {}^{1}_{0}\mathrm{n} \rightarrow {}^{239}_{92}\mathrm{U} + \gamma \tag{7.3}$$

$$^{239}_{92}\mathrm{U} \xrightarrow[23.5\ \mathrm{min}]{\beta^-} {}^{239}_{93}\mathrm{Np} \xrightarrow[2.36\,\mathrm{days}]{\beta^-} {}^{239}_{94}\mathrm{Pu}\,(t_{1/2} = 24,110\ \text{years}) \tag{7.4}$$

In 1941 Kennedy, Seaborg, Segré, and Wahl established the fissionability of ^{239}Pu with slow neutrons (Kennedy *et al.*, 1941). This crucial experiment revealed the potential of ^{239}Pu as a nuclear energy source. In March 1942, element 94 was christened 'plutonium' with the chemical symbol 'Pu' (Seaborg and Wahl, 1948a). Plutonium was named after the planet Pluto, following the pattern used in naming neptunium.

In August 1942, Cunningham and Werner, working at the wartime Metallurgical Laboratory at the University of Chicago, succeeded in isolating about 1 μg of $^{239}_{94}$Pu, which was prepared by cyclotron irradiation of 90 kg of uranyl nitrate (Cunningham and Werner, 1949a). This experiment made plutonium the first man-made element to be obtained (as Pu(IV) iodate) in a visible quantity. These same investigators carried out the first weighing of this man-made element using a larger sample size of 2.77 μg, on September 10, 1942.

Plutonium is now produced in much larger quantities than any other synthetic element. The large wartime chemical separation plant at Hanford, Washington, was constructed on the basis of investigations performed on the ultramicro chemical scale of investigation. The scale-up between ultramicro chemical experiments and the final Hanford plant corresponds to a factor of about 10^{10} (Seaborg, 1958). Seaborg and Cunningham give detailed first-hand accounts of the early history of plutonium in the *Proceedings of the 1963 Plutonium Chemistry Symposium* (1963). More recent descriptions of this fascinating history have been given by Seaborg (1977, 1978, 1979, 1980, 1983, 1992, 1995), Seaborg and Katz (1990), Seaborg and Loveland (1990), and by Hoffman *et al.* (2000).

7.3 NUCLEAR PROPERTIES

Numerous isotopes of plutonium have been synthesized, all of which are radioactive. These are listed in Table 7.1. The most recent isotope to be discovered is ^{231}Pu, which was reported in 1999 (Laue *et al.*, 1999). For data on nuclear masses the reader is referred to the compilation by Audi and Wapstra (1995),

Table 7.1 *Radioactive decay properties of plutonium isotopes*[a].

Mass number	*Half-life*	*Mode of decay*	*Main radiations* (MeV)	*Method of production*
228	1.1 s	α	α 7.772	^{198}Pt(^{34}S,4n)
229	–	α	α 7.460	^{207}Pb(^{26}Mg,4n)
230	2.6 min	EC, α	α 7.055	^{208}Pb(^{26}Mg,4n)
231	8.6 min	EC 90% α 10%	α 6.72	^{233}U(^{3}He,5n)
232	33.1 min	EC $\geq$80% α $\leq$20%	α 6.600 (62%) 6.542 (38%)	^{233}U(α,5n)
233	20.9 min	EC 99.88% α 0.12%	α 6.30 γ 0.235	^{233}U(α,4n)
234	8.8 h	EC 94% α 6%	α 6.202 (68%) 6.151 (32%)	^{233}U(α,3n)
235	25.3 min	EC >99.99% α 3 × 10^{-3}%	α 5.850 (80%) γ 0.049	^{235}U(α,4n)
236	2.858 yr 1.5 × 10^{9} yr	α SF 1.37 × 10^{-7}%	α 5.768 (69%) 5.721 (31%)	^{235}U(α,3n) ^{236}Np daughter
237	45.2 d	EC >99.99% α 4.24 × 10^{-3}%	5.356 (~17.2%) 5.334 (~43.5%)18 γ 0.059	^{235}U(α,2n) ^{237}Np(d,2n)
238	87.7 yr 4.77 × 10^{10} yr	α SF 1.85 × 10^{-7}%	α 5.499 (70.9%) 5.456 (29.0%)	^{242}Cm daughter ^{238}Np daughter
239	2.411 × 10^{4} yr 8 × 10^{15} yr	α SF 3.0 × 10^{-10}%	α 5.157 (70.77%) 5.144 (17.11%) 5.106 (11.94%) γ 0.129	^{239}Np daughter
240	6.561 × 10^{3} yr 1.15 × 10^{11} yr	α SF 5.75 × 10^{-6}%	α 5.168 (72.8%) 5.124 (27.1%)	multiple n capture
241	14.35 yr	β^- >99.99% α 2.45 × 10^{-3}% SF 2.4 × 10^{-14}%	α 4.896 (83.2%) 4.853 (12.2%) β^- 0.021 γ 0.149	multiple n capture
242	3.75 × 10^{5} yr 6.77 × 10^{10} yr	α SF 5.54 × 10^{-4}%	α 4.902 (76.49%) 4.856 (23.48%)	multiple n capture
243	4.956 h	β^-	β^- 0.582 (59%) γ 0.084 (23%)	multiple n capture
244	8.08 × 10^{7} yr 6.6 × 10^{10} yr	α 99.88% SF 0.1214%	α 4.589 (81%) 4.546 (19%)	multiple n capture
245	10.5 h	β^-	β^- 0.878 (51%) γ 0.327 (25.4%)	^{244}Pu(n,γ)
246	10.84 d	β^-	β^- 0.15 (91%) γ 0.224 (25%)	^{245}Pu(n,γ)
247	2.27 d	β^-		multiple n capture

[a] See Appendix II.

and the update by Audi *et al.* (1997). A more detailed description of the nuclear properties of the individual plutonium isotopes may be found in the book by Hyde *et al.* (1964), in the *Table of Isotopes* (Firestone *et al.*, 1996, 1998), and in *Nuclear Data Sheets* (Tuli, 2004). As mentioned above, ^{238}Pu was the first of the plutonium isotopes discovered. Because of its relatively short half-life, it is a particularly useful tracer for plutonium. ^{238}Pu is readily obtained by neutron bombardment of ^{237}Np in the reaction:

$$^{237}\mathrm{Np}(\mathrm{n},\gamma)^{238}\mathrm{Np} \xrightarrow{\beta^-} {}^{238}\mathrm{Pu} \tag{7.5}$$

The ^{238}Pu is chemically separated from unreacted ^{237}Np by ion-exchange techniques (Burney, 1962; Tetzlaff, 1962; Coogler *et al.*, 1963; Burney and Thompson, 1972, 1974). ^{238}Pu may also be obtained from the α decay of ^{242}Cm and subsequent chemical separation from undecayed curium (Thompson, 1972). Because of its power density of 6.8–7.3 W cm^{-3} (specific power 0.57 W g^{-1}), ^{238}Pu has found important applications in radioisotope power systems – nuclear power systems that derive their energy from the spontaneous decay of radionuclides as distinguished from nuclear fission energy created in a nuclear reactor. Most radioisotope power systems utilize ^{238}Pu as an isotope heat source and an energy conversion system to partially transform the heat produced from ^{238}Pu radioactive decay into electricity (Lange and Mastal, 1994).

In the late 1960s, cardiac pacemakers suffered from early battery exhaustion, and the use of nuclear pacemakers whose battery life could outlive the patient was examined (Boucher and Quere, 1981; Pustovalov *et al.*, 1986). The first implantation of a ^{238}Pu-powered nuclear pacemaker was performed in France on April 27, 1970. Since that time, nuclear pacemakers powered by ^{238}Pu were implanted in patients in a number of countries. The overall results of these studies indicated that nuclear pacemakers required fewer follow-up operations and less maintenance, and were found to be safe and reliable. Subsequent advances in electronics in the intervening years rendered the plutonium-powered devices obsolete, and their use was discontinued. In 2004, there were still a number of living patients with ^{238}Pu pacemakers that had been functioning for over 30 years (Parsonnet *et al.*, 1990; Freedberg *et al.*, 1992; Parsonnet, 2004).

The most prevalent application for ^{238}Pu is as an important fuel for heat and power sources for space exploration (Lange and Mastal, 1994; Rinehart, 2001). For space exploration, heat source fuel is normally enriched to 83.5% in the ^{238}Pu isotope, and the oxygen atoms in ^{238}PuO$_2$ are enriched in ^{16}O to reduce the neutron emission rate to as low as 6000 n s^{-1} g^{-1} ^{238}Pu. In freshly prepared fuel, the specific power is 0.4743 W g^{-1} Pu or 0.4181 W g^{-1} PuO$_2$. The ^{238}Pu isotope provides 99.9% of the thermal power in heat source fuel. Radioisotope thermoelectric generators (RTGs) have been used in the United States to provide electrical power for spacecraft since 1961 (Angelo and Buden, 1985). Early ^{238}Pu-fueled power sources employed Space Nuclear Auxiliary Power (SNAP) units to power satellites and remote instrument packages (DOE, 1987;

Lange and Mastal, 1994). SNAP units served as power sources for instrument packages on the five Apollo missions to the Moon, the Viking unmanned Mars Lander, and the Pioneer and Voyager probes to the outer planets (Jupiter, Saturn, Uranus, Neptune and beyond). The SNAP-3B and SNAP-9A systems were fueled with plutonium metal, the SNAP-19 and Transit systems were fueled with $^{238}PuO_2$–molybdenum cermets, and the SNAP-27 unit was fueled with $^{238}PuO_2$ microspheres (Rinehart, 2001). Voyager missions employed Multihundred Watt Radioisotope Thermoelectric Generators (MHW-RTGs) that consisted of 24 100-W heat sources of $^{238}PuO_2$ (Fig. 7.1) each enclosed in an iridium shell, a graphitic impact material, an ablative heat shield, and a thermoelectric material to convert the decay heat to electrical power at a design voltage of 30 V (Kelly, 1975; De Winter *et al.*, 1999).

The current systems employ General Purpose Heat Source-Radioisotope Thermoelectric Generators (GPHS-RTGs) fueled by $^{238}PuO_2$ pellets. Each GPHS consists of a hot-pressed 150 g pellet of $^{238}PuO_2$ encapsulated in an iridium alloy (iridium-0.3% tungsten) container or clad (Fig. 7.2). Each iridium

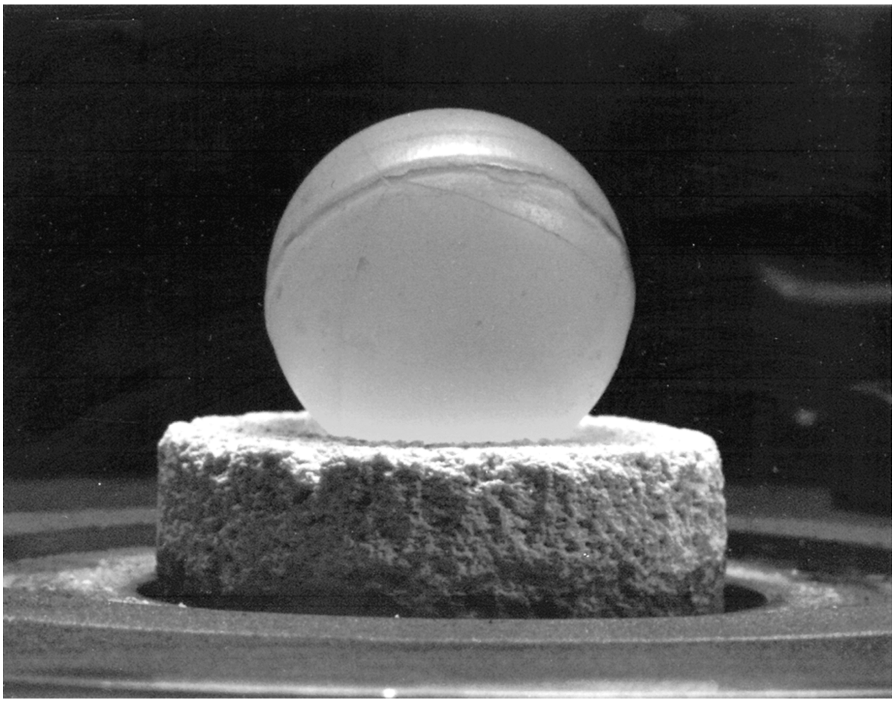

Fig. 7.1 *A* 100 W ^{238}*Pu heat source used in multihundred watt radioisotope thermoelectric generators* (*MHW-RTGs*) *employed in the Voyager space missions. The source contains* 250 g *of* $^{238}PuO_2$ *and was approximately* 3 cm *in diameter. The oxide glowed at red heat after being covered with an insulating ceramic blanket that was removed just before the photograph was taken* (*photograph courtesy of Los Alamos National Laboratory*).

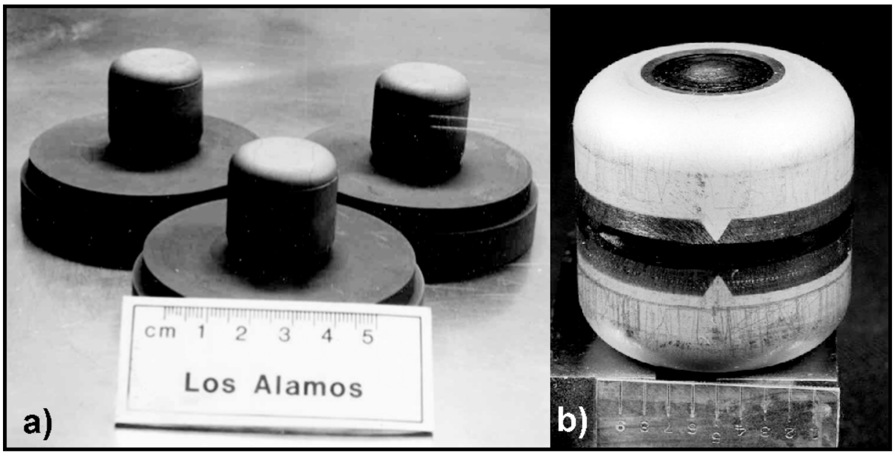

Fig. 7.2 *A modern ^{238}Pu general purpose heat source (GPHS). Hot pressed* 150 g *pellets of ^{238}PuO$_2$ are (a) encapsulated in an iridium*-0.3% *tungsten alloy container, which is then encapsulated in (b) an iridium clad. Each iridium clad contains a sintered iridium powder frit vent designed to release the helium generated by the α-particle decay of the fuel. The iridium is compatible with plutonium dioxide at temperatures greater than* 1773 K, *and melts at* 2698 K. *Each GPHS produces* 62.5 *thermal watts (photographs courtesy of Los Alamos National Laboratory).*

clad contains a sintered iridium powder frit vent designed to release the helium generated by the α-particle decay of the $^{238}PuO_2$. The heat sources are packed in a tightly woven pierced fabric™ graphite aeroshell assembly that protects the fuel from impact, fire, or atmospheric reentry. The RTG consists of 72 GPHS pellets and a thermoelectric converter. The GPHS-RTGs flown on the Galileo, Ulysses, and Cassini spacecraft (3 RTGs per spacecraft) had a mass of 54 kg of PuO_2 and supplied 285 W of electrical power at the beginning of the mission from 4300 W of ^{238}Pu decay heat (Rinehart, 2001). These plutonium power sources have enabled huge advances in our scientific understanding of the solar system. The Cassini–Huygens spacecraft arrived at Saturn on June 30, 2004, and will provide vast amounts of new scientific data on the Saturnian system in the years to come.

Smaller Light Weight Radioisotope Heater Units (LWRHUs) are also used to maintain spacecraft equipment within their normal operating temperature range (Rinehart, 1992). The LWRHUs are cylindrical fueled clads consisting of a hot-pressed, 2.67 g pellet of $^{238}PuO_2$ encapsulated in a Pt-30%Rh container with a sintered platinum powder frit vent to release helium as shown in Fig. 7.3. As in the GPHS, the capsules are contained in a pyrolytic graphite insulator and aeroshell assembly (Rinehart, 2001). These smaller heater units have been employed on the Pioneer 10 and 11, Galileo, Mars Pathfinder, Mars Exploration Rovers (Spirit and Opportunity), and Cassini spacecraft, and are planned for use in many future missions.

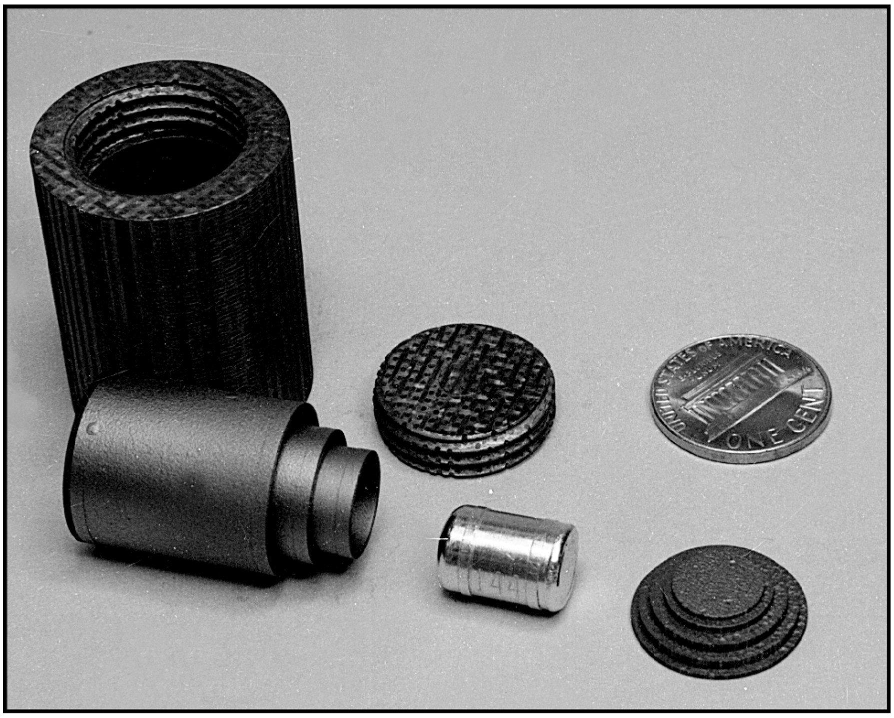

Fig. 7.3 *A* ^{238}*Pu lightweight radioisotope heater unit* (*LWRHU*) *before final assembly. The heat source consists of a fine weave pierced fabric graphite aeroshell, three inner layers of pyrolytic graphite thermal insulators, and a Pt-*30% *Rh-fueled clad containing a hot pressed* 2.67 g *pellet of* $^{238}PuO_2$ *that produces* 1 *thermal watt. The aeroshell serves as the primary heat shield to protect the interior components from aerodynamic forces and thermal heating during accidental atmospheric reentry as well as protecting the fueled clad from mechanical loads during ground impact. The pyrolytic graphite sleeves and plugs serve as thermal shields to keep the fueled clad from melting during an accidental reentry in the atmosphere* (*photograph courtesy of Los Alamos National Laboratory*).

Plutonium-239 is the most important isotope of plutonium. Its half-life (24,110 years) is sufficiently long to permit the preparation of this isotope in large-scale amounts, and to make it feasible to carry out conventional scientific studies. ^{239}Pu has a high cross-section for fission with slow neutrons, and is the isotope that serves as nuclear fuel for both nuclear power and nuclear weapons. By far the greatest portion of the knowledge of the chemical and physical properties of plutonium has been acquired by the use of ^{239}Pu. While its half-life is long enough to permit chemical studies, it is still short enough to present serious problems in handling. These difficulties are discussed in some detail below (Section 7.6). ^{239}Pu has a specific power of 2.2×10^{-3} W g^{-1}. In handling large quantities of ^{239}Pu, the criticality hazard caused by its fissionability becomes an additional problem. Amounts as small as 500 g may become critical

Table 7.2 *Minimum critical parameters of common forms of pure ^{239}Pu (Clark,* 1981).

metal	mass plutonium (kg)	5.0
	cylinder diameter (cm)	4.4
	slab thickness (cm)	0.65
oxide	mass plutonium (kg)	10.2
	mass PuO_2 (kg)	11.5
	cylinder diameter (cm)	7.2
	slab thickness (cm)	1.4
aqueous plutonium nitrate solution		
	plutonium mass (kg)	0.480
	concentration (g Pu L^{-1})	7.3
	H/Pu atomic ratio	3630
	cylinder diameter (cm)	15.4
	volume (L)	7.3

under certain conditions. In Table 7.2 some minimum critical parameters for pure ^{239}Pu obtained in various configurations have been summarized (Clark, 1981). Additional safety and criticality data are available in the compilations by Paxton (1975), Clark (1981), Knief (1985), and Paxton and Pruvost (1987).

The higher plutonium isotopes are formed as a result of successive neutron capture by the various plutonium isotopes:

$$^{239}\mathrm{Pu}(n,\gamma)^{240}\mathrm{Pu}(n,\gamma)^{241}\mathrm{Pu}(n,\gamma)\ \text{etc.} \tag{7.6}$$

The isotopic composition of plutonium produced in a nuclear reactor will therefore vary according to the length of time the plutonium formed is allowed to remain in the neutron flux. From this perspective it is noteworthy that the heavier isotopes ^{244}Pu, ^{245}Pu, and ^{246}Pu were originally discovered in the coral debris of the Mike thermonuclear test conducted in 1952, due to the extremely high neutron fluxes of the event. Hoffman, Ghiorso, and Seaborg described the events that led to the discoveries of these isotopes (Hoffman *et al.*, 2000). When ^{239}Pu targets were irradiated in a high-flux reactor to more than 90% burn-up, the residual plutonium was found to consist mainly of the higher isotopes ^{242}Pu and some ^{244}Pu. Many of the complications arising from the use of the relatively short-lived ^{239}Pu can be greatly ameliorated by the use of these long-lived isotopes of plutonium for fundamental scientific study.

Isotopically pure ^{240}Pu, ^{241}Pu, ^{242}Pu, and ^{244}Pu have become available from various sources. ^{240}Pu may readily be obtained by chemical separation from old ^{244}Cm samples. All the heavier plutonium isotopes have also been isotopically separated by electromagnetic separation in the Y-12 calutron plant in Oak Ridge (Love *et al.*, 1961; Love, 1973), but presently these calutrons have been placed in a standby condition. Gram quantities of these isotopes with isotopic purity above 99% were available from such separations. Russian scientists have also been very successful in producing research quantities of higher plutonium isotopes using electromagnetic mass separation. Ultrapure ^{236}Pu and ^{237}Pu have been produced by Dmitriev and coworkers at the Joint Institute for Nuclear Research in Moscow (Dmitriev *et al.*, 1993, 1995, 1997), and Vesnovskii and Polynov at the Institute of Experimental Physics in Arzamas have been able to produce milligram to gram quantities of ^{240}Pu, ^{241}Pu, ^{242}Pu, and ^{244}Pu at greater than 99% isotopic purity (Vesnovskii and Polynov, 1992a,b). Milligram quantities of ^{244}Pu have been prepared at the IAEA Safeguards Analytical Laboratory in Austria using electromagnetic separation (Deron and Vesnovskii, 1999) and by selective ionization using a pulsed laser beam in Japan (Sasao and Yamaguchi, 1991).

The higher isotopes of plutonium possess interesting nuclear properties, which cannot be discussed in detail here. For further information see Hyde *et al.* (1964).

7.4 PLUTONIUM IN NATURE

Traces of plutonium are found all over the world, predominantly due to 'man-made' plutonium. In addition, two isotopes of plutonium (^{239}Pu and ^{244}Pu) can be found that are 'natural' in origin. Natural ^{239}Pu is produced in nature by nuclear processes occurring in uranium ore bodies, and minute traces of ^{244}Pu exist in nature as remnants of primordial stellar nucleosynthesis.

The presence of small amounts of plutonium in uranium of natural origin was first established in 1942 by Seaborg and Perlman (1948) and by Garner *et al.* (1948). These researchers were able to show that Canadian pitchblende and Colorado carnotite both contain a small amount of alpha activity due to a plutonium isotope, presumed to be ^{239}Pu at the time. Peppard *et al.* (1951) and Levine and Seaborg (1951) conclusively demonstrated the existence of ^{239}Pu in nature. Levine and Seaborg determined the plutonium content of a number of uranium ores, and Peppard and coworkers isolated microgram amounts of ^{239}Pu from uranium process wastes. Recent high-resolution thermal ionization mass spectrometry analyses of plutonium in uranium ore bodies have been described by Curtis *et al.* (1999) and by Dixon *et al.* (1997). The concentrations of plutonium in uranium ore bodies are collected in Table 7.3. No plutonium isotopes other than ^{239}Pu have been conclusively found in any of these experiments. More recently, ^{239}Pu has also been detected in granites from deep boreholes in Germany, and in salt brines from deep boreholes in the United States (Ganz *et al.*, 1991). Alpha pulse analysis and high-resolution mass spectrometry have been the experimental methods of choice for characterization of the isotopic composition of plutonium isolated from natural sources.

With the exception of the very long-lived ^{244}Pu, the half-lives of plutonium isotopes are so short that it is most unlikely that any plutonium except ^{244}Pu

Table 7.3 *Content of plutonium in natural uranium ore deposits.*

Ore	*Uranium content* (wt.%)	*Ratio* ^{239}Pu/U ($\times 10^{12}$)	*References*
Cigar Lake U deposit	31	6.4	Curtis *et al.* (1999)
Beaverlodge U deposit	7.09	14.3	Dixon *et al.* (1997)
Canadian pitchblende	13.5	7.1	Levine and Seaborg (1951)
Belgian Congo pitchblende	38	12	Levine and Seaborg (1951)
Colorado pitchblende	50	7.7	Levine and Seaborg (1951)
Brazilian monazite	0.24	8.3	Levine and Seaborg (1951)
N. Carolina monazite	1.64	3.6	Levine and Seaborg (1951)
Colorado furgusonite	0.25	<4	Levine and Seaborg (1951)
Colorado carnotite	10	<0.4	Levine and Seaborg (1951)

could have survived in nature from primordial times. It is overwhelmingly likely that ^{239}Pu arises in nature by nuclear reactions with ^{238}U and represents a steady-state concentration:

$$^{238}\mathrm{U}(\mathrm{n},\gamma)^{239}\mathrm{U} \xrightarrow{\beta^-} {}^{239}\mathrm{Np} \xrightarrow{\beta^-} {}^{239}\mathrm{Pu} \tag{7.7}$$

Neutrons necessary for the formation of ^{239}Pu from ^{238}U may arise from spontaneous fission of ^{238}U; by neutron multiplication in ^{235}U; from (α,n) reactions caused by the action of α particles (from the radioactive decay of uranium and daughters) on the nuclei of light elements in the ore (Li, B, Be, F, O, Si, Mg); and neutrons produced by cosmic rays. The neutrons from cosmic rays appear to be of negligible importance, since the neutron production from uranium by the capture of μ mesons is considerably less than 0.1% of the neutrons arising from spontaneous fission (Littler, 1952). Spontaneous fission in uranium occurs at the rate of (24.2 ± 0.5) fissions per gram per hour, which produces a neutron flux insufficient to account for the observed plutonium concentration. Neutron multiplication by capture of thermalized neutrons in ^{235}U and the production of fission neutrons will contribute to overcoming the deficiency. The contribution from this source will clearly depend on the uranium concentration, on the composition of the ore, and on the probability that a fission neutron will be slowed down to thermal energies. In all probability, the neutrons produced in (α,n) reactions account for a major portion of the neutrons required for ^{239}Pu formation. Fleming and Thode (1953a,b) found evidence that (α,n) and (α,p) reactions occur to a considerable extent in uranium minerals. This conclusion was reached from a study of the isotopic composition of argon obtained from uranium minerals. In thorium ores containing small amounts of uranium, the neutrons from (α,n) reactions predominate. The amount of plutonium created depends not only on the number of neutrons produced but also on their subsequent fate. Elements with high neutron-capture cross-sections will compete for neutrons and decrease plutonium formation. In carnotite, potassium and vanadium atoms, and in fergusonite, tantalum atoms capture most of the available neutrons, thus accounting for the unusually low plutonium content found in these minerals (Table 7.3).

A fascinating example of the formation of ^{239}Pu by neutron multiplication in ^{235}U was found by French scientists in the uranium deposit at Oklo in the Gabon, Africa. From anomalies in the isotopic composition of rare earths (especially neodymium) and anomalies in the ^{235}U content, it was concluded that, in at least six different locations of this deposit, a self-sustaining nuclear chain reaction must have occurred (Bodu *et al.*, 1972; Neuilly *et al.*, 1972). It was found that, in these locations, a burn-up of part of the original ^{235}U had occurred, but the depletion found was not as great as one would have expected from the observed anomalies in the isotope composition of other elements. It is generally agreed that ^{239}Pu is formed through resonant capture of epithermal neutrons by the ^{238}U present in the matrix, and that subsequent radioactive decay of the ^{239}Pu again regenerates a fraction of the ^{235}U (Holliger and Devillers, 1981; Hidaka and Holliger, 1998; Hidaka, 1999). Since no plutonium has been found in the Oklo deposit, one may conclude that the self-sustaining chain reaction must have taken place around 1.9×10^9 years ago (Cowan, 1976).

A different situation exists with regard to ^{244}Pu, which is sufficiently long-lived to have survived from primordial times. In 1960, Kuroda postulated the existence of ^{244}Pu in the early solar system based on the Xe isotope ratios found in chondritic meteorites (Kuroda, 1960). In 1971, Alexander and coworkers measured the ratios of the Xe isotopes formed by spontaneous fission (SF) of ^{244}Pu and found they agreed with those found in chondritic meteorites, thus strongly supporting this hypothesis and SF decay of ^{244}Pu (Alexander *et al.*, 1971). The discovery of ^{244}Pu fission xenon in extraterrestrial samples such as the Moon (Kuroda and Myers, 1998), Martian (Marty and Marti, 2002), and other meteorites demonstrated that the transuranium elements were synthesized in exploding (supernovae) stars (Kuroda and Myers, 1998).

Conclusive proof for the occurrence of natural ^{244}Pu in a pre-Cambrian bastnasite ore was provided by Hoffman and coworkers (Hoffman *et al.*, 1971). Starting from approximately 85 kg of ore containing 10% bastnasite, these workers isolated 2×10^7 atoms (8×10^{-15} g) of ^{244}Pu corresponding to about 10^{-18} g of ^{244}Pu per gram of pure bastnasite. The presence of ^{244}Pu was conclusively identified using high-resolution mass spectrometry. Thus it seems most probable that this ^{244}Pu sample is a remnant of the stellar debris that coalesced to form the solar system.

That even the richest uranium deposits are not likely to supersede synthetic methods as a source of plutonium can be appreciated from the fact that the microgram amounts of plutonium isolated by Peppard and coworkers (Peppard *et al.*, 1951) required the residues of 100 metric tons of ore concentrate for each microgram of plutonium recovered.

7.5 SEPARATION AND PURIFICATION

7.5.1 Introduction

At the end of 2003, a little more than 60 years after the discovery of the first plutonium isotope in 1940, about 1855 metric tons of plutonium existed, principally within irradiated fuel from nuclear power plants (Albright and Kramer, 2004). About 225 metric tons of plutonium that had been separated and purified for recycling in commercial nuclear fuel cycles was in the unirradiated form. Roughly 260 metric tons of plutonium with a high ^{239}Pu content has been separated for use in nuclear weapons programs worldwide. Some of this weapons plutonium has been declared excess to military needs and will be incorporated into the commercial nuclear power system. Production of plutonium for military use had greatly decreased by early in the 21st century, but the total plutonium inventory will continue to increase as a consequence of nuclear power production for the foreseeable future. The rate of plutonium production in fuel of operating reactors was estimated at 70–75 metric tons per year at the end of 2003. Clearly, the separation of plutonium has been carried out on a large scale. The management of the separated plutonium and the large quantities of highly radioactive by-products of this production will continue to be a challenge in the decades to come.

Plutonium isotopes are produced mainly from neutron absorption by ^{238}U and the subsequent product nuclei as shown in the simplified scheme in Fig. 7.4. The major pathway to plutonium proceeds through absorption of a neutron to give ^{239}U followed by two successive β^- decays to give ^{239}Np and then ^{239}Pu. Neutron absorption by ^{239}Pu produces higher isotopes of plutonium and other transuranic elements, in competition with neutron-induced fission. Beta decay by ^{241}Pu and ^{243}Pu and further neutron absorption leads to the production of higher actinides, americium, curium, etc., but these steps are not shown in the diagram for the sake of clarity. As the scheme for the production of plutonium isotopes suggests, the isotopic composition of plutonium produced in a

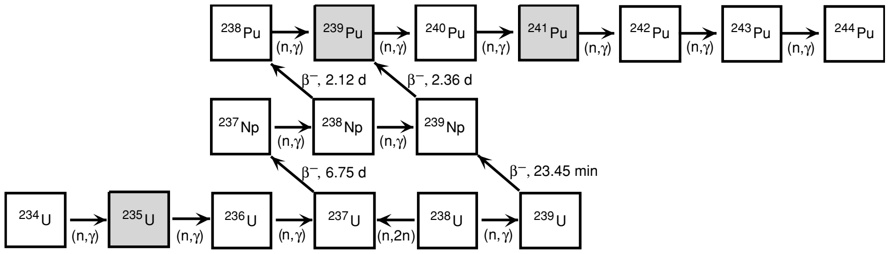

Fig. 7.4 *Major pathways for formation of plutonium isotopes by neutron absorption* (*n, γ*) *and beta decay* (β^-) *in uranium fuels or targets. Shaded boxes indicate most important isotopes undergoing neutron-induced fission in competition with neutron absorption.*

particular portion of the reactor fuel will be a complex function of the total flux and energy distribution of the neutrons that irradiate that fuel segment. The neutron flux and energy distribution will vary with irradiation time and the location of the fuel in the reactor.

The majority of nuclear power reactors around the world use low-enrichment uranium oxide fuels (^{235}U content of 3–5%) and light water (H_2O) to moderate the neutrons and act as the coolant for the system (Neeb, 1997). The uranium oxide fuel is fabricated into cylindrical pellets that are stacked inside a sealed container made of a cladding material such as a zirconium alloy to make a fuel pin. The plutonium content after 'burning' of these fuels amounts to about 1% of the mass of heavy metal content of the used fuel from a 'typical' light water reactor (LWR). Neutron-induced fission of the plutonium generated from neutron absorption by ^{238}U adds substantially to the total power production in commercial nuclear power plants ($\sim$40% of the total). The remaining mass of the used fuel consists of about 95% uranium, 4% fission products, and 0.1% all other transuranic actinides. It is the plutonium content in these 'spent' reactor fuels that provides most of the global plutonium inventory.

The build-up of the plutonium isotopes is accompanied by the production of a great variety of fission product elements. The fission process leads mostly to two product nuclei (only 0.2 to 0.3% of the fission events yield three fragments) that have an asymmetric statistical mass distribution with peaks at mass numbers of 95 and 138 for ^{235}U thermal (low energy) neutron-induced fission. The fission product nuclei commonly have excess neutrons relative to stable nuclei with the same atomic number and thus most are radioactive. The fission products decay primarily by beta/gamma chains to more stable nuclei. A calculation of the principal actinide and fission product isotopes present at the end of irradiation followed by 10 years of storage of a commercial reactor-type fuel is shown in Table 7.4. The burn-up of this fuel is higher than that used in most commercial plants to date, but the nuclear power industry trend is toward such higher burn-ups in the future. The list of fission product masses in Table 7.4 illustrates the two peaks in the fission product yield among the elements Zr through Pd and Xe through Nd. While the fission product masses do not change dramatically for most of the elements in the used fuel after 10 years of storage, the radioactivity has dropped more than two orders of magnitude and the ^{90}Sr and ^{137}Cs decay chains dominate the radioactivity of the used fuel from 10 years out to a few hundred years.

Inspection of Table 7.4 also illustrates that the fission products include elements from all the families of the periodic table. This considerably complicates the chemical problem of separation and purification of plutonium from the irradiated fuel. Additionally, the intense radioactivity requires facilities that use heavy shielding and remotely operated equipment to perform the separation processes. The mixture of plutonium isotopes present in the spent fuel is not so intensely radioactive and can be handled in a gloved box system once the fission products are removed. The term 'decontamination' is often applied to the

Table 7.4 *Actinide and fission product content of neutron-irradiated UO_2 fuel calculated using ORIGEN* 2 *code* (*Croff*, 1980, 1983)[a].

Element	*Weight at discharge* (g)	*Weight after* 10 yr *cooling* (g)	*Activity at discharge* (C_i)	*Activity after* 10 yr *cooling* (C_i)	*Major radioactive isotopes after* 10 yr *cooling and half-lives*
U-234	123	142	0.76	0.88	α, 2.46×10^5 yr
U-235	6 370	6 370	0.01	0.01	α, 7.04×10^8 yr
U-236	5 520	5 520	0.35	0.35	α, 2.34×10^7 yr
U-237	18	<0.1	1.47×10^6	2.76	β^-, 6.75 d
U-238	923 900	923 900	0.31	0.31	α, 4.47×10^9 yr
Np-237	1 020	1 050	0.72	0.74	α, 2.14×10^6 yr
Np-238	2	<0.1	5.23×10^5	0	β^-, 2.34 d
Np-239	100	<0.1	2.32×10^7	1.04×10^2	β^-, 2.34 d
Pu-238	236	242	3.99×10^3	4.09×10^3	α, 87.7 yr
Pu-239	4 900	5 000	3.01×10^2	3.07×10^2	α, 2.41×10^4 yr
Pu-240	2 070	2 130	4.57×10^2	4.70×10^2	α, 6.56×10^3 yr
Pu-241	1 820	1 130	1.85×10^5	1.15×10^5	β^-, 14.4 yr
Pu-242	579	579	2.3	2.3	α, 3.73×10^5 yr
Am-241	48	728	1.64×10^2	2.50×10^3	α, 432 yr
Am-242m	2	2	16.6	15.8	IT, 141 yr
Am-243	538	538	1.04×10^2	1.04×10^2	α, 7.37×10^3 yr
Cm-242	23	<0.1	7.75×10^4	13.0	α, 163 d
Cm-243	2	2	89.3	71.9	α, 29.1 yr
Cm-244	200	136	1.62×10^4	1.10×10^4	α, 18.1 yr
Cm-245	20	20	3.5	3.5	α, 8.5×10^3 yr
Cm-246	4	4	1.2	1.2	α, 4.76×10^3 yr
total An	**947 495**	**947 493**	$\mathbf{2.55 \times 10^7}$	$\mathbf{1.32 \times 10^5}$	
Se	85	85	9.6×10^5	0.58	Se-79 6.5×10^4 yr
Br	33	33	0	0	–
Kr	546	529	3.8×10^6	7.3×10^3	Kr-85 10.7 yr
Rb	520	537	5.4×10^6	<0.01	–
Sr	1 390	1 180	8.6×10^6	8.9×10^4	Sr-90 28.5 yr
Y	722	704	1.2×10^7	8.9×10^4	Y-90 64.1 h
Zr	5 480	5 630	1.0×10^7	2.8	Zr-93 1.5×10^6 yr
Nb	44	<0.01	1.5×10^7	1.1	Nb-93m 13.6 yr
Mo	5 090	5 210	0	0	–
Tc	1 220	1 230	1.2×10^7	21	Tc-99 2.1×10^5 yr
Ru	3 630	3 360	5.6×10^6	757	Ru-106 373 d
Rh	446	504	8.0×10^6	757	Rh-106 2.2 h
Pd	2 140	2 360	7.1×10^5	0.16	Pd-107 6.5×10^6 yr
Ag	73	71	9.4×10^5	0.33	Ag-110m 250 d
Cd	157	159	8.5×10^4	39	Cd-113m 13.7 yr
In	1	1	2.6×10^5	<0.01	–
Sn	76	75	1.5×10^6	1.1	Sn-126 2.5×10^5 yr
Sb	26	14	3.8×10^6	1.2×10^3	Sb-125 2.76 yr
Te	714	717	8.0×10^6	285	Te-125m 58 d
I	363	357	1.2×10^7	0.05	I-129 1.6×10^7 yr
Xe	8 190	8 190	9.0×10^6	<0.01	–
Cs	4 140	3 340	8.6×10^6	1.5×10^5	Cs-137 30.2 yr, Cs-135 2.3×10^6, Cs-134 2.07 yr

Table 7.4 (*Contd.*)

Element	*Weight at discharge* (g)	*Weight after* 10 yr *cooling* (g)	*Activity at discharge* (C_i)	*Activity after* 10 yr *cooling* (C_i)	*Major radioactive isotopes after* 10 yr *cooling and half-lives*
Ba	2 310	3 100	1.0×10^7	1.2×10^5	Ba-137m 2.5 mo
La	1 880	1 870	1.0×10^7	<0.01	–
Ce	4 170	3 690	8.1×10^6	190	Ce-144 284 d
Pr	1 690	1 730	7.0×10^6	193	Pr-144 17.3 mo
Nd	5 770	6 220	1.7×10^6	<0.01	–
Pm	100	7	1.8×10^6	6.9×10^3	Pm-147 2.63 yr
Sm	1 150	1 240	9.6×10^5	1.4×10^3	Sm-151 90 yr
Eu	309	243	6.2×10^5	1.3×10^4	Eu-155 4.73 yr, Eu-154 8.5 yr
Gd	237	309	8.1×10^3	<0.01	–
Tb	3	2	4.8×10^3	<0.01	–
Dy	2	2	1.4×10^3	<0.01	–
total FP	**52 700**	**52 700**	$\mathbf{1.8 \times 10^8}$	$\mathbf{4.8 \times 10^5}$	

[a] Based on an initial uranium loading of 4.25% ^{235}U enrichment (957.5 kg ^{238}U, 42.5 kg ^{235}U, 0.293 kg ^{234}U), burn-up of 50 000 MW-days (metric ton)$^{-1}$ (Hill, 2005).

process of removing the fission products from the plutonium, uranium, or other actinides of interest in the irradiated fuel or target material. The decontamination factor measures the extent to which the concentration of fission products has been removed relative to the original level in the spent fuel at the time processing begins. To allow the product plutonium to be handled by personnel using a gloved box without undue exposure to fission product radioactivity, the decontamination factor required for some fission products is on the order of 10^8. Clearly, the required decontamination factors will vary with the cooling time of the fuel before processing begins.

The fission products and actinides produced from the irradiated uranium fuel are dispersed intimately in the fuel matrix (Neeb, 1997). The fission product nuclei dissipate their kinetic energy after traveling on average 5–10 μm through the uranium oxide matrix, leaving an ionization track and displacement cascade that ultimately generates most of the heat that is used to generate electricity. Atomic mixing occurs from both radiation-induced and thermal mass transport processes. In a typical LWR fuel each atom of the fuel is displaced from its lattice site an average of once a day. Some segregation of the fission product elements occurs under reactor conditions (Neeb, 1997). For example, inert gases such as xenon and krypton can form bubbles in the fuel matrix and even escape into the gas space inside a fuel pin, and some transition elements (Mo, Ru, Rh, Pd, Tc) form small metal inclusions in the uranium oxide. However, the bulk of the fission products and transuranic elements are dispersed fairly homogeneously within the uranium fuel. The uranium matrix must be dissolved into a suitable solution or converted into a volatile compound to allow the fission product and actinide 'impurities' to be separated from the uranium.

The methods used to recover plutonium (and other actinides) from irradiated fuels or targets can be divided into two major groups, aqueous and nonaqueous processes, depending on the primary phase used for the separation process. The major classes of aqueous processes are liquid–liquid extraction (solvent extraction), ion exchange, and precipitation. Examples of nonaqueous processes are electrorefining (ER) in molten salts and fluoride volatility. The separation methods use differences in the chemical properties of the various elements present to segregate some components preferentially between the primary phase and a secondary phase that can be a solid, liquid, or gas. Separation of the two phases partitions the components of the original single phase for further processing steps. These next steps can be additional stages of the same separation method (e.g., a bank of centrifugal contactors for extraction) or a different method (e.g., ion exchange followed by precipitation).

Nearly all of the separation methods take advantage of the multiple oxidation states that plutonium can adopt in its various chemical forms. The chemical properties of plutonium (and other metal ions) change to a large extent depending on the oxidation state. If conditions can be adjusted to obtain various metal ions in a mixture in different oxidation states, the separation of these metals is often straightforward. For example, in aqueous acid solutions it is possible to have uranium in the hexavalent oxidation state (as UO_2^{2+}), neptunium in the pentavalent state (as NpO_2^+), plutonium in the tetravalent state, and americium in the trivalent state. The complexes formed by ions in these different oxidation states in solution are quite different, so that separation by a number of methods is possible. In the case of an irradiated fuel with fission products present, if the chemical behavior of a fission product resembles that of plutonium in one oxidation state, it can be quite different when the plutonium oxidation state or the fission product element oxidation state is changed. The use of oxidation state changes to improve separations will be illustrated in the discussion of specific separation methods below.

The large-scale separation and purification of plutonium has been primarily accomplished using the Plutonium, Uranium, Reduction, EXtraction (PUREX) liquid–liquid extraction process. This process was first developed for separating plutonium from metallic uranium fuels irradiated to produce plutonium for nuclear weapons applications, but has since been adapted to separate uranium and plutonium from many kinds of fuels and targets, including commercial power reactor fuels. While a variety of other processes have been used to separate and purify plutonium from irradiated fuels, many of these are now of only historical interest. More detailed information on the separation technology for plutonium and the other actinides can be found in Chapter 24 of this work, *Actinide Separation Science and Technology*, including extensive documentation of the separation literature. The goal in this chapter is to present the main features of selected separation methods of particular importance to plutonium and to illustrate major factors guiding development of plutonium separation processes. Only brief references to the history of plutonium separations will be made here.

Processes for separation of plutonium from neutron-irradiated uranium metal, uranium oxide, or other irradiated target materials are one important group of plutonium separation and purification methods, but there are additional separation needs. Separated plutonium must be converted into the forms required for various applications, for example, purification of PuO_2 to meet all the specifications for mixed oxide (MOX) fuel fabrication. Recovery and recycle of plutonium from the process and waste streams of these conversion operations constitute another important group of separation processes. A wider variety of separation methods can be employed to accomplish these separations because the high radiation levels of the fission products are not present and the amount of material to be processed is typically much smaller. There is also a need for separation processes to remove plutonium from items that have been contaminated by plutonium-containing materials resulting from normal operations or accidental release to the environment, e.g. equipment, concrete, soils, etc. These types of operations are commonly referred to as decontamination methods; the radioactive contaminant is plutonium in this case rather than a fission product. Finally, a large number of separation methods and reagents have been used to preconcentrate or remove interfering components in analytical procedures for plutonium-containing samples to improve detection limits and accuracy of the results.

As the above discussion indicates, many processes have been developed for separating plutonium from a variety of matrices. There are often variations for a particular method and many combinations of methods possible for accomplishing a specific separation goal. The chosen process can be a result of many factors at a particular facility including available equipment and expertise, safety and operational limits, product specifications, national regulatory requirements, waste management, cost, and schedule. It is possible in some processes to vary operating conditions over a wide range and still obtain a desired result. In the discussion of separation methods that follow, variations in process conditions are common. Defining an 'optimum' process depends on factors like those mentioned above, which can vary even at a single facility over its lifetime. Operational details of this kind are beyond the scope of this chapter.

7.5.2 Introduction to aqueous-based separation methods

Before discussing aqueous separation processes for plutonium in more detail, a brief overview of actinide chemistry in aqueous solution is useful because most actinide separations have been performed using aqueous acid solutions.

The separation of actinides from basic aqueous solutions has been employed less often because the low solubilities of the hydroxides or oxyhydroxides of the high-valent actinide metal ions greatly limit the amount of material that can be processed in a given volume except where strongly complexing ligands, such as carbonate or peroxide, are present. More detailed information on the solution chemistry of plutonium (see Section 7.9) and the other actinide metal ions can be found in the appropriate sections of the chapters for each element and in other chapters of this work.

As noted above, the separation of plutonium and the other early actinides (Th–Am) from fission products and from each other is generally accomplished by adjusting the oxidation state of the actinide ion in aqueous solution to make the coordination chemistry of the actinide ion substantially different from the other species to be separated. The actinides are highly electropositive metals and form cationic species in aqueous solutions. These cations are 'hard' Lewis acids and form strong complexes in solution with hard anions such as hydroxide and fluoride. The oxidation states from III to VI are accessible in aqueous acid solutions of uranium, neptunium, and plutonium. After plutonium the actinides become more lanthanide-like with the coordination chemistry of the trivalent metal ion dominating. The pentavalent and hexavalent actinide ions are found in aqueous solutions as linear dioxo cations, e.g. NpO_2^+ and PuO_2^{2+}. These 'actinyl' species have no close analogs in transition metal oxo complexes and are also hard Lewis acids. Water and other ligands bind to these linear cations in a ring-shaped equatorial region around the metal ion between the two tightly bound oxoanions. The coordination numbers and geometries for the actinide ions are highly variable and reflect the largely ionic bonding in these complexes: generally, 6–12 for An(IV), 6–9 for An(III), and 4–6 in the equatorial ring of AnO_2^+ or AnO_2^{2+}. The trivalent actinides exhibit a slightly stronger bonding to ligands containing soft donor atoms (e.g. sulfur, nitrogen, chloride) than the corresponding lanthanides and this property can be used as a basis for separating these groups of elements.

For plutonium the oxidation states from III to VII are accessible in aqueous solution. The species Pu(III), Pu(IV), and Pu(VI) (PuO_2^{2+}) are most important in acidic aqueous solution. The pentavalent ion PuO_2^+ disproportionates rapidly in acidic solution at moderate plutonium concentrations and is usually a very minor species in acidic aqueous separation systems. Stabilizing Pu(VII) requires strongly complexing ligands such as hydroxide, fluoride, or carbonate in basic solution and, thus, Pu(VII) has not been used in any separation systems.

7.5.3 Precipitation and crystallization methods

As noted above, the oxidation states of the actinide ions in solution produce large differences in coordination chemistry facilitating separation by a variety of methods. An example of this is shown in Table 7.5 which lists the qualitative solubility behavior of the actinides in oxidation states III–VI with some common

Table 7.5 *Precipitation reactions characteristic of various actinide oxidation states (aqueous solution,* 1 M H^+)[a].

Anion	M^{3+}	M^{4+}	MO_2^+	MO_2^{2+}
OH^-	I	I	I	I
F^-	I	I	I[b]	S
IO_3^-	I	I	S	S
O_2^{2-}	–	I	–	–
$C_2O_4^{2-}$	I	I	I	I
CO_3^{2-}	(I)[c]	I[c]	I[d]	S
$CH_3CO_2^-$	S	S	S	I[e]
PO_4^{3-}	I	I	I[f]	I[g]
$Fe(CN)_6^{4-}$	I	I	S	I

I = insoluble, S = soluble.

[a] Unless otherwise stated (the OH^- and CO_3^{2-} precipitations occur in alkaline solution).

[b] At pH = 6, $RbPuO_2F_2$ and $NH_4PuO_2F_2$ may be precipitated by addition of RbF or NH_4F, respectively.

[c] Complex carbonates are formed.

[d] Solid $KPuO_2CO_3$ precipitates on addition of K_2CO_3 to Pu(v) solution.

[e] From solution of Pu(vi) in CH_3CO_2H, $NaPuO_2(CH_3CO_2)_3$ precipitates on addition of Na^+.

[f] Addition of $(NH_4)_2HPO_4$ to Pu(v) solution yields $(NH_4)HPuO_2PO_4$.

[g] On addition of H_3PO_4, $HPuO_2PO_4{\cdot}xH_2O$ precipitates.

anions. These precipitations are very useful for separating mixtures of the actinides and for recovery of solid products from an aqueous stream after using another separation process such as ion exchange or solvent extraction. They are generally not selective enough to be used as the primary process for separation of plutonium or other actinides from all the fission products in irradiated fuel or targets. This is illustrated by a study (Winchester and Maraman, 1958) that used precipitation of Pu(iii) oxalate, Pu(iv) oxalate, Pu(iii) fluoride, and Pu(iv) peroxide to recover plutonium directly from an irradiated plutonium-rich alloy dissolved in nitric acid. The decontamination factors reported in Table 7.6 indicate that none of the precipitation processes achieved high enough fission product or corrosion product (Fe and Co) removal for use as a primary separation process. However, as will be described below, coprecipitations with other metal ion species such as bismuth phosphate were used in the first large-scale separations of plutonium from irradiated uranium. These processes were replaced in time by more efficient solvent extraction processes.

The distinction between crystallization and precipitation is quite often based on the speed of the process and the size of the solid particles produced. The term precipitation commonly refers to a rapid crystallization that gives small crystals that may not appear crystalline to the eye, but still may give very distinct X-ray diffraction (XRD) peaks. Precipitation often involves a relatively irreversible reaction between an added reagent and other species in solution whereas

Table 7.6 *Decontamination factors for plutonium using various precipitation methods.*

Element	*Pu*(*III*) *oxalate*	*Pu*(*IV*) *oxalate*	*Pu*(*IV*) *peroxide*	*Pu*(*III*) *fluoride*
Fe	33	10	50	1.4
Co	47	>95	30	8.6
Zr	3.5	>44	1	1.1
Mo	>13	>15	>140	1.1
Ru	>38	33	>14	36
Ce	1	1	6	1.1

crystallization products can usually be redissolved using relatively simple means such as heating or dilution. The details of the precipitation or crystallization process can be very important to produce a pure product and one that separates well from the liquid phase. Thus, the order and speed of reagent addition, the temperature, and the 'aging' time before filtration or centrifugation can all be important parameters in a precipitation or a crystallization process. The Pu(IV) oxyhydroxide 'polymer' that readily forms in relatively low acid solutions of Pu(IV) is an infamous example of a 'difficult' precipitate that can complicate the processing of plutonium aqueous solutions. The characteristics of this polymer will be described in more detail in Section 7.9.1.d.

(a) Coprecipitation methods

Coprecipitation processes were the first to be used for the recovery of plutonium. The tiny amounts of plutonium present in the first preparations were too small to be precipitated directly, so coprecipitation or 'carrier' precipitations were used to purify and deduce the chemical properties of plutonium and many other radioactive elements. In general, plutonium will coprecipitate if the anion contained in the bulk precipitate forms an insoluble salt with plutonium in the same oxidation state or states present in the solution. Useful carrier precipitation methods for plutonium have been reviewed (Sorantin, 1975). Coprecipitation methods have also been used to purify plutonium in microgram amounts and for recovery on a production scale.

(*i*) *Lanthanum fluoride*

Precipitation of lanthanum fluoride or other lanthanide fluorides from acid solutions carries trivalent and tetravalent actinides, but not the pentavalent and hexavalent ions. The lanthanide and yttrium fission products coprecipitate, but most of the other fission products remain in solution. The behavior of neptunium and plutonium in lanthanum fluoride precipitation was used to establish the existence of two oxidation states of these elements before weighable quantities were available (Seaborg and Wahl, 1948b). The lanthanum fluoride carrier precipitation was also a key step in the first isolation of a weighable plutonium compound to be described below.

Cunningham and Werner isolated a PuO_2 sample that weighed 2.77 μg, the first weighable quantity of any synthetic element, on September 10, 1942 at the Metallurgical Laboratory of the University of Chicago (Cunningham and Werner, 1949b). The plutonium had been separated from about 90 kg of uranyl nitrate hexahydrate that had been irradiated for 1 to 2 months with neutrons produced by bombarding a beryllium target with deuterons at the cyclotron facility at Washington University in St. Louis. The separation of plutonium was accomplished through oxidation state adjustments and a series of LaF_3 precipitations that carried Pu(IV) and Np(IV) but not Pu(VI) or Np(VI). The brief overview that follows provides an example of a coprecipitation separation method and also illustrates the painstaking effort required in these first explorations of plutonium chemistry.

About 90 kg of irradiated $UO_2(NO_3)_2 \cdot 6H_2O$ was mixed with 100 L of diethyl ether to yield about 120 L of ether solution containing uranyl nitrate solvate, $UO_2(NO_3)_2[O(CH_2CH_3)_2]_2$, and a small amount of fission products and 8 L of an aqueous phase that consisted of about 50 wt % uranyl nitrate hydrate with most of the fission products and transuranic elements, principally neptunium and plutonium. This was essentially a solvent extraction step that partitioned most of the U(VI) to the ether phase along with a small amount of the fission products.

The aqueous phase was diluted to 20 L, made 2 M in nitric acid and 0.014 M in La(III) and then HF was added to give a solution 4 M in HF. The resulting 40 g of LaF_3 precipitate contained the transuranium elements and about 25% of the original fission product activity (mostly the lanthanide and yttrium fission products). The separated LaF_3 precipitate was heated in concentrated sulfuric acid to distill HF and then dissolved in and diluted to 5 L with 2 M nitric acid. The Pu(IV) was oxidized to Pu(VI) by using $K_2S_2O_8$ and Ag(I) as a catalyst. The solution was then made 4 M in HF which produced about 40 g of LaF_3 precipitate that was separated by filtration. The LaF_3 precipitate contained most of the remaining fission product activity, while the solution contained the Pu(VI) and Np(VI). The addition of a 6% SO_2 solution to the filtrate and washings reduced the Pu(VI) and Np(VI) and the excess peroxydisulfate. Addition of 2 g of $La(NO_3)_3$ in solution precipitated LaF_3 that carried the tetravalent plutonium and neptunium. Repeated cycles of precipitation with progressively smaller amounts of LaF_3 were used to further decontaminate the plutonium and neptunium. For two of the LaF_3 precipitation cycles, $KBrO_3$ was employed as the oxidizer to selectively oxidize neptunium, but not plutonium. This allowed the separation of the neptunium into the filtrate solutions while plutonium was carried with the LaF_3. These additional cycles of smaller precipitations eventually yielded a 120 μL solution of 1.7 M HNO_3 and 5 M HF that was fumed in a platinum crucible and treated with 10 M ammonium hydroxide to precipitate Pu(VI) hydroxide. The washed precipitate of plutonium hydroxide contained about 40 μg of plutonium. The microliter-scale solution manipulations were performed in a specially designed glass apparatus viewed with a microscope. Additional purification steps yielded a 50 μL solution of plutonium in nitric acid. Ten μL of this solution were placed on a platinum weighing pan, dried, and heated to give the oxide. This sample provided the first weighable quantity of plutonium that is now displayed in the Lawrence Hall of Science at Berkeley, California.

(*ii*) *Bismuth phosphate process*

The bismuth phosphate process was used for the first large-scale purification of plutonium from neutron-irradiated uranium at the Hanford site during the Manhattan Project, and after the war until the 1950s when it was replaced by solvent extraction processes. More detail on the bismuth phosphate process and its replacement by solvent extraction processes can be found in Chapter 24. The precipitation of $BiPO_4$ from acid solutions carries the trivalent and tetravalent actinides, and especially Pu(IV), but not the pentavalent and hexavalent ions. Bismuth phosphate is quite insoluble in moderately concentrated nitric and sulfuric acids. This is an important property because addition of sulfuric acid to a nitric acid solution of neutron-irradiated uranium could be used to keep the relatively large quantity of U(VI) in solution as a sulfate complex while bismuth phosphate was precipitated and carried the plutonium. The $BiPO_4$ precipitate carried only small amounts of the fission products, and could be redissolved in concentrated nitric acid; thus simplifying the process relative to use of a lanthanum fluoride carrier that is difficult to redissolve. A series of oxidation state adjustments and precipitations of $BiPO_4$ from solutions of neutron-irradiated uranium in nitric acid separated the plutonium from the uranium, neptunium and fission products in a scheme that resembles the lanthanum fluoride process described above. In fact, cycles of lanthanum fluoride precipitation from nitric acid were incorporated into the bismuth phosphate process to concentrate and further purify plutonium.

Thompson and Seaborg first developed the bismuth phosphate process (Thompson and Seaborg, 1956). The scale-up of the process from the laboratory to an operating plant by a factor of 10^8 in a short time is a remarkable story (Hill and Cooper, 1958). An overall decontamination factor from the fission products of 10^7 was obtained at Hanford for the plutonium. The disadvantages of the process included discarding the uranium with the fission products, generation of large volumes of high salt wastes, and batch operation. Continuous solvent extraction processes based on extraction of uranium and plutonium from nitric acid solutions of dissolved fuel have replaced the bismuth phosphate process.

(b) Precipitation and crystallization methods for conversion chemistry of plutonium

Solvent extraction processes have displaced the original bismuth phosphate coprecipitation method for production scale plutonium separation from neutron-irradiated uranium fuels and targets. However, precipitation and crystallization from aqueous solutions have always been important processes for preparing and purifying solid compounds for the various applications of plutonium. The major products are plutonium metal for irradiation targets and fuels, weapons components, or storage and PuO_2 for MOX fuels, heat sources (when the ^{238}Pu content is high), and storage.

The bulk of the aqueous processing of plutonium takes place in nitric or hydrochloric acid solutions and most plutonium solids are precipitated from these solutions (Cleveland, 1980; Christensen *et al.*, 1988). The most common precipitations use oxalate, peroxide, hydroxide, and fluoride. The typical reasons for using these precipitations are:

- Good recovery of plutonium can be obtained in the solid in a form suitable for preparing metal or oxide.
- Relatively concentrated plutonium nitrate or chloride solutions can be largely or partially purified from many cationic impurities.
- Precipitation from relatively dilute solutions provides a very quick and convenient method for concentrating plutonium.
- Calcination at 500–800°C readily converts properly precipitated Pu(III) and Pu(IV) oxalates to PuO_2 that is suitable for direct oxide reduction (DOR) with calcium to the metal, or hydrofluorination to PuF_4 that is then reduced to metal (see Section 7.7.2).
- Precipitation of plutonium or americium hydroxides from waste solutions such as oxalate or peroxide filtrates generally provides an effective method to recycle the plutonium and americium in the separated precipitate and to dispose of the alkaline filtrate to low-level waste treatment operations.

This group of common precipitation methods will be briefly reviewed. The detailed procedures used at different facilities vary widely because of the many facility-specific factors that enter into the process design as discussed briefly in Section 7.5.1. Both batch and continuous processes have been developed for these precipitations.

(*i*) *Plutonium*(III) *oxalate precipitation*

Since the time of the Manhattan Project, researchers have found it useful to precipitate the easily filterable turquoise-blue $Pu_2(C_2O_4)_3 \cdot 10H_2O$ by reducing plutonium to the trivalent state in low acid solution and carefully adding an oxalic acid solution. Directly adding solid oxalic acid will produce a crystalline precipitate with a smaller average particle size (Christensen *et al.*, 1988). The solubility of $Pu_2(C_2O_4)_3 \cdot 10H_2O$ can be approximated by the expression

$[\mathrm{Pu}(\mathrm{mg\,L^{-1}})] = 3.24[\mathrm{H^+}]^3[\mathrm{H_2C_2O_4}]^{-3/2}$ (Harmon and Reas, 1957). However, the typical filtrate from a production run will have somewhat higher concentrations of plutonium (0.1–0.5 g L^{-1}) left in solution than that calculated from this equation. The precipitation is useful over a wide range of conditions when the Pu(iii) concentration is more than 1 g L^{-1} and with less than 4 M acid. The Pu(iii) oxalate precipitation gives good decontamination factors from such impurities as Al(iii), Fe(iii), and U(vi). There is less decontamination from sodium, potassium, and calcium and none from Am(iii). Plutonium(iii and iv) can be scavenged from very dilute solutions using Ca(ii) or Pb(ii) oxalates as carriers (Maraman *et al.*, 1954; Akatsu, 1982; Akatsu *et al.*, 1983).

(*ii*) *Plutonium*(*iv*) *oxalate precipitation*

Plutonium(iv) precipitates as the tan solid $\mathrm{Pu(C_2O_4)_2 \cdot 6H_2O}$ from low acid solutions upon addition of oxalic acid, but it is usually a very fine tacky solid at room temperature (Christensen *et al.*, 1988). Precipitation at elevated temperatures can greatly improve the filterability of the solid. Typical losses of plutonium to the filtrate in practical operations are 0.2–0.5 g L^{-1}. The precipitation is used over a wide range of conditions with Pu(iv) concentrations greater than 1 g L^{-1} and acid concentrations between 1 and 5 M. The decontamination factors for impurities such as Al(iii), Fe(iii), and U(vi) are typically higher than for the Pu(iii) oxalate method. There is no decontamination from Am(iii).

(*iii*) *Plutonium*(*iv*) *peroxide precipitation*

Plutonium(iv) peroxide is an olive-green solid formed by the addition of hydrogen peroxide solutions to acid solutions of Pu(iv). The typical range of acid concentration is 2.5–5.5 M. The solutions are often cooled to 10–15°C to reduce the decomposition of hydrogen peroxide. High levels of iron, copper, manganese, or nickel catalyze the decomposition of the H_2O_2 and interfere with precipitation. At higher acid concentrations and with careful H_2O_2 addition, a very filterable hexagonal form of plutonium(iv) peroxide precipitates. At lower acidities a gelatinous cubic form precipitates that is difficult to filter. Plutonium(iv) peroxide is not a stoichiometric compound and its O:Pu ratio may approach 3.5 (Cleveland, 1979, 1980), but does not reach 4.0 as is suggested by the formula $\mathrm{Pu(O_2)_2}$. Anions such as nitrate, chloride, and sulfate, if present in the solution, are incorporated into the solid. Indeed, sulfate is added in some processes at a concentration of 0.1–0.3 M to nitric acid solutions to improve the filterability of the peroxide precipitate.

The Pu(iv) peroxide precipitation is a powerful method for purification of plutonium from many impurity elements except those such as thorium, neptunium, and uranium that form similar peroxides under these conditions. Unlike the oxalate precipitations, Am(iii) is removed to a high degree. The excellent decontamination factors obtained for many elements and the use of one reagent that is easily decomposed to water and oxygen in subsequent operations are the major advantages of using this process. The disadvantages are greater losses of plutonium in the filtrate (typically 0.1–0.5%) and violent decomposition of H_2O_2 that can occur during precipitations in the presence of high concentrations of iron and other metal ion catalysts for the decomposition reaction.

(*iv*) *Plutonium*(*III*) *fluoride precipitation*

Addition of aqueous HF to a solution of Pu(III) in nitric or hydrochloric acid precipitates blue-violet $PuF_3 \cdot xH_2O(x \sim 0.75)$ (Christensen *et al.*, 1988). The Pu(IV) concentration should be kept low because the hydrated PuF_4 precipitate is very gelatinous and much more soluble than the trifluoride. Significant Pu(IV) content will thus increase filtering time and plutonium losses to the filtrate. Reducing agents such as hydroxylamine, sulfamic acid, or ascorbic acid are commonly used. With careful oxidation state control, losses of plutonium to the filtrate are very low (0.05–0.1%). A disadvantage of preparing any fluorine-containing compound of plutonium is increased production of neutrons from α-n reactions relative to the oxygen-, carbon-, and nitrogen-based precipitants. The trifluoride precipitation does not give decontamination factors from cationic impurities that are as high as the oxalate or especially the peroxide precipitations. It gives moderate decontamination from many impurities including iron, but not from aluminum, zirconium, and uranium. Dried PuF_3 can be roasted in oxygen to produce a mixture of PuF_4 and PuO_2 that can be directly reduced with calcium metal to give 95–97% yields of plutonium metal (See Sections 7.7.1 and 7.7.2).

(*v*) *Plutonium hydroxide precipitation*

Hydroxide precipitation is quite useful to produce a filtrate with very low levels of plutonium. Sodium or potassium hydroxide solutions are commonly added to precipitate the gelatinous green Pu(IV) hydroxide (Christensen *et al.*, 1988). If Pu(III) is present, it will slowly oxidize to Pu(IV). Many other metal ions will precipitate as hydroxides as well or be carried by the plutonium hydroxide so that this is not a useful purification procedure. The hydroxide is generally difficult to filter. If large amounts of magnesium or calcium are present, the voluminous hydroxide precipitates of these metal ions make filtration especially difficult, unless they are avoided by carefully controlling the pH. The dried hydroxide cake can be recycled for plutonium recovery by dissolving it in acid. The formation of the Pu(IV) oxyhydroxide polymer should be avoided because this material behaves quite differently from the hydroxide precipitate and can be quite difficult to redissolve in acid. The formation and properties of the polymer are described in more detail in Section 7.9.1.d.

(*vi*) *Miscellaneous precipitations*

Other precipitation methods have been tested for plutonium processing operations, but have not been deployed or as widely used as those reviewed above. These include $CaPuF_6$ and Cs_2PuCl_6 from acid solutions for metal production operations (Christensen *et al.*, 1988; Muscatello and Killion, 1990) and $(NH_4)_4PuO_2(CO_3)_3$ or mixed $(NH_4)_4(Pu, U)O_2(CO_3)_3$ from alkaline solution for the preparation of MOX fuels (Roepenack *et al.*, 1984).

7.5.4 Solvent extraction separation processes

Liquid–liquid (or solvent) extraction partitions solutes between two immiscible liquid phases. The two phases are generally intimately mixed to improve the rate of transfer of solutes between them. The use of a laboratory separatory funnel by a synthetic chemist illustrates the operation of a single stage of liquid–liquid extraction. The two immiscible phases, commonly an organic and an aqueous phase, are shaken vigorously for some time to approach the equilibrium distribution of solutes between the phases and then the phases are allowed to coalesce and reform layers that can be separated. On an industrial scale, the labor-intensive separatory funnel is replaced by a wide variety of equipment that pumps, mixes and separates the phases in a continuous operation so that multiple stages of extraction and back-extraction can be accomplished in an efficient manner. Solvent extraction is a very versatile and useful industrial separation method and has proven to be very important for the recovery and purification of plutonium and other actinides. In fact, as discussed in Chapter 24 of these volumes, the industrial practice of solvent extraction advanced considerably because of the new development work needed to solve the separation challenges of processing neutron-irradiated fuels and targets for military and industrial applications.

In the case of plutonium and other actinide metal ions, the two immiscible phases used in solvent extraction processes are usually an aqueous acid solution and an organic solvent containing components that stabilize certain metal ion complexes in the organic phase. Nitric acid is the most common acidic solution used; hydrochloric acid has seen more limited application. Acids with more strongly complexing anions such as sulfuric, phosphoric, or hydrofluoric acids can have problems with limited solubilities of actinide ions (see Table 7.5) and also some fission product metal ions and are used less commonly. In some cases, these acids with more strongly complexing anions are used in controlled amounts in the acidic aqueous phase as ‘masking agents’ to hold certain metal ions in the aqueous phase and to improve the selectivity of the extraction into the organic phase. They can also be deployed in an aqueous phase to ‘strip’ or back-extract metal ions from an organic phase that has been ‘loaded’ with metal ions in a previous step of the process.

The organic phases used for actinide extractions comprise a wide range of solvents (or diluents) and organic-soluble compounds (extractants) that stabilize metal complexes in an organic phase. Aliphatic and aromatic hydrocarbons, chlorinated hydrocarbons, ethers, and ketones represent some of the major solvent groups. In some cases the solvent and the extractant are the same. For example, chemists used diethyl ether to extract uranyl nitrate from aqueous solutions long before the nuclear age dawned. The influence of the solvent on the extraction system is manifested in various ways such as the solubility of the extractant and metal ion species, the overall thermodynamic activity of the extractant, and the concentration of water in the organic phase (Cox and Flett, 1983).

Metal ions can be stabilized in the organic phase in a variety of structures. While uncharged individual metal ion complexes are solvated in the organic phase in many cases, ion-pairs, reverse micelles, and other aggregated structures are observed, especially as higher concentrations of metal ions are loaded into the organic phase (Borkowski *et al.*, 2003; Chiarizia *et al.*, 2003). For many extraction systems, a third phase can form if the metal ion concentration becomes too high in the organic phase (Rao and Kolarik, 1996). This is a situation to be avoided because the extraction equipment is designed to separate two liquid phases, not three, and any solid phase is particularly troublesome. Phase-modifying reagents are sometimes added to the organic solvent to inhibit third-phase formation and to allow higher levels of metal loading.

When two or more extractant compounds are combined in a single solvent they may act independently or the extraction equilibrium for a metal ion can be enhanced over what each extractant would give independently. This effect is referred to as synergism. It is most typically observed when an acidic extractant is combined with a neutral donor extractant and the major extractant complex contains both extractants bound to the metal ion (Cox and Flett, 1983).

The range and combinations of compounds that have been used in organic solvents to extract plutonium is very extensive and cannot be reviewed here. The extractant compounds can be generally divided into two large groups: compounds with donor atoms that form organic-soluble complexes with the metal ion, and ion-pair reagents that stabilize a charged metal ion complex in the organic phase. Given the hard Lewis acid character of the actinide metal ions, it is not surprising that most of the ligand-type extractants have one or more oxygen donor atom sites that coordinate to the metal ion in the organic phase. The major actinide extractant classes are alkyl and aryl phosphates, $(RO)_3P{=}O$, phosphonates, $(RO)_2RP{=}O$, phosphinates, $(RO)R_2P{=}O$, and phosphine oxides, $R_3P{=}O$; alkyl and aryl phosphoric, $(RO)_2PO_2H$, phosphonic, $(RO)RPO_2H$, and phosphinic acids, R_2PO_2H; ethers, R_2O; ketones, $R_2C{=}O$; 1,3-diketones, $RC(O)CH_2C(O)R$; amides, $RC(O)NR_2$, malonamides, $R_2NC(O)CHRC(O)NR_2$, and carbamoylmethylphosphine oxides, $(RO)_2P(O)CH_2C(O)NR_2$ (the R groups in the formulas can all have different or identical alkyl or aryl functionality). The major ion-pair extractant classes for actinides are tetraalkylammonium salts, $R_4N^+X^-$, and protonated tertiary amines, $R_3NH^+X^-$. More detail on the classes of solvent extraction systems and their use for actinide separations is found in Chapter 24. Tri(*n*-butyl) phosphate (TBP), $(n\text{-BuO})_3P{=}O$, is of particular importance for plutonium separations as the key component of the PUREX process and will be discussed below.

(a) The PUREX process

As mentioned previously, nearly all of the roughly 500 metric tons of plutonium that has been separated to date has been recovered using the PUREX solvent extraction process. The use of TBP to extract nitrate complexes of uranium and other actinides was examined as early as 1944 during the Manhattan Project (Orlemann, 1944; Spedding *et al.*, 1945; Warf, 1945) and a patent application for a solvent extraction process for plutonium based on TBP and other trialkylphosphates was submitted in 1947 – the patent was not issued until 1960 because of security concerns (Anderson and Asprey, 1960). The development work leading to deployment of the process started in the late 1940s principally at Oak Ridge National Laboratory (Coleman and Leuze, 1978). The PUREX process was first used in 1954 at the Savannah River site of the U.S. Atomic Energy Commission and then in 1956 at the Hanford site (Swanson, 1990). With many variations in operational details, the process has since been used around the world as the principal method to separate plutonium and uranium from used reactor fuel and neutron-irradiated actinide materials (McKay *et al.*, 1990). The key to this process is the selective extraction of U(VI) and Pu(IV) from a nitric acid solution of dissolved irradiated fuel into an aliphatic hydrocarbon solvent containing TBP while leaving most of the fission products in the acid solution. The plutonium and then the uranium can be back-extracted separately from the loaded organic solvent into an aqueous strip phase. Additional solvent extraction stages with TBP can be used to further purify the uranium and plutonium or another method such as ion exchange can be used. Most PUREX operations target very pure uranium and plutonium products with high decontamination factors from the fission products of about 10^8 and high recovery (typically about 99.9%).

The following equilibrium equations represent the major separation steps of the PUREX process:

$$\mathrm{Pu}^{4+}_{(\mathrm{aq})} + 4\mathrm{NO}^-_{3\,(\mathrm{aq})} + 2\mathrm{TBP}_{(\mathrm{org})} \rightleftharpoons \mathrm{Pu(NO_3)_4(TBP)}_{2\,(\mathrm{org})} \tag{7.8}$$

$$\mathrm{UO}^{2+}_{2\,(\mathrm{aq})} + 2\mathrm{NO}^-_{3\,(\mathrm{aq})} + 2\mathrm{TBP}_{(\mathrm{org})} \rightleftharpoons \mathrm{UO_2(NO_3)_2(TBP)}_{2\,(\mathrm{org})} \tag{7.9}$$

$$\mathrm{HNO}_{3\,(\mathrm{aq})} + \mathrm{TBP}_{(\mathrm{org})} \rightleftharpoons \mathrm{TBP}\cdot\mathrm{HNO}_{3\,(\mathrm{org})} \tag{7.10}$$

The subscripts (aq) and (org) refer to species present in the aqueous and organic phases, respectively. The distribution coefficient (D) in liquid–liquid extraction is defined as the ratio of the concentration of the solute in the organic phase to that in aqueous phase under a particular set of conditions, e.g. volume ratio of the aqueous to organic phase, temperature, extractant concentration, pH, metal ion concentration. Tetravalent and hexavalent actinide ions are selectively extracted under the PUREX conditions (typically 1–3 M nitric acid and 20–30 vol % TBP in an aliphatic hydrocarbon diluent) but the trivalent and pentavalent oxidation states of the actinides and most of the fission products are poorly extracted. This is illustrated by the data in Table 7.7 that lists the single-stage distribution coefficients for U(VI), Pu(VI), Pu(IV), Pu(III), and a group of fission products for TBP and two other compounds, hexone [$CH_3C(O)CH_2CH(CH_3)_2$] and dibutylcarbitol [$CH_3(CH_2)_3O(CH_2)_2O(CH_2)_2O(CH_2)_3CH_3$] that were the basis for two other competing solvent extraction processes, REDOX and BUTEX (Peterson and Wymer, 1963). The REDOX and BUTEX processes were used for a time at Hanford and in the United Kingdom, respectively, but eventually were replaced by the PUREX process. The data in Table 7.7 illustrate that the modest *D* values like those for uranium of 1.5–8.1 can be exploited for high recovery by using multiple stages of extraction. The data in the table also show that the bulk of the fission product have very low *D* values, but there are exceptions (Zr, Ru, and Tc). These fission product contaminants can be removed in various ways during the additional uranium and plutonium purification operations.

The equations shown above for Pu(IV) and U(VI) extraction indicate that higher nitrate concentrations in the aqueous phase and higher TBP concentrations in the organic phase should increase the *D* values for these metal ions. This is indeed observed as long as the activities of the various species are taken into account and metal ion concentrations are low. However, the extraction of nitric acid by TBP indicated in (7.10) competes with metal ion extraction for the TBP and limits the increase in the *D* value with increasing nitric acid concentration. The *D* values will continue to increase at a low fixed nitric acid concentration if nitrate salts are added to the aqueous phase rather than nitric acid. Pure TBP is

Table 7.7 *Distribution coefficients of uranium, plutonium, and some fission products using TBP, hexone, and Butex extractants.*

Solvent	*U(VI)*	*Pu(VI)*	*Pu(IV)*	*Pu(III)*	*Fission products*[a]
hexone[b]	1.6	2.9	0.84	4.5×10^{-4}	0.03
TBP[c]	8.1	0.62	1.55	0.008	0.001
Butex[d]	1.5	1.8	7	<0.01	~0.02

[a] Combined β emitters (without Zr, Ru, Ca).

[b] From 0.3 M HNO_3/1.0 M $Al(NO_3)_3$/(U,Pu) into hexone at 25°C, or from 0.25 M HNO_3/1.5 M $Al(NO_3)_3/\Sigma FP$ into hexone at 25°C.

[c] From 3.0 M HNO_3 into 30 vol.% TBP in kerosene at 25°C.

[d] From 4 M HNO_3 into dibutylcarbitol (Butex).

a liquid and can be used as the organic phase in an extraction, but it is quite viscous. PUREX plants typically operate with 20–30 vol % TBP in an aliphatic hydrocarbon diluent (Swanson, 1990).

Adjusting the oxidation state of plutonium from Pu(iv) to Pu(iii) is the most commonly used way of selectively stripping plutonium from the loaded organic phase. As shown in Table 7.7, the *D* value of Pu(iii) is quite low and it will preferentially distribute to the aqueous nitric acid phase. Reducing agents that have been used to strip plutonium from the TBP phase are Fe(ii), hydroxylamine, and U(iv). The addition of ferrous sulfamate in the aqueous acid solution used to strip the plutonium has given some of the best results as indicated by the purity of the uranium and plutonium products that result (Miles *et al.*, 1990). The overall equation for the Fe(ii) reduction and stripping reaction is:

$$\mathrm{Pu(NO_3)_4(TBP)_2}_{\,(\mathrm{org})} + \mathrm{Fe}^{2+}_{(\mathrm{aq})} \rightarrow \mathrm{Pu}^{3+}_{(\mathrm{aq})} + 4\mathrm{NO}^{-}_{3\,(\mathrm{aq})} + \mathrm{Fe}^{3+}_{(\mathrm{aq})} + 2\mathrm{TBP}_{(\mathrm{org})} \qquad (7.11)$$

After the removal of plutonium, the uranium can be stripped from the TBP phase with a dilute acid solution. The TBP solution can then be reused to extract more uranium and plutonium. A generalized PUREX flow sheet is shown in Fig. 7.5.

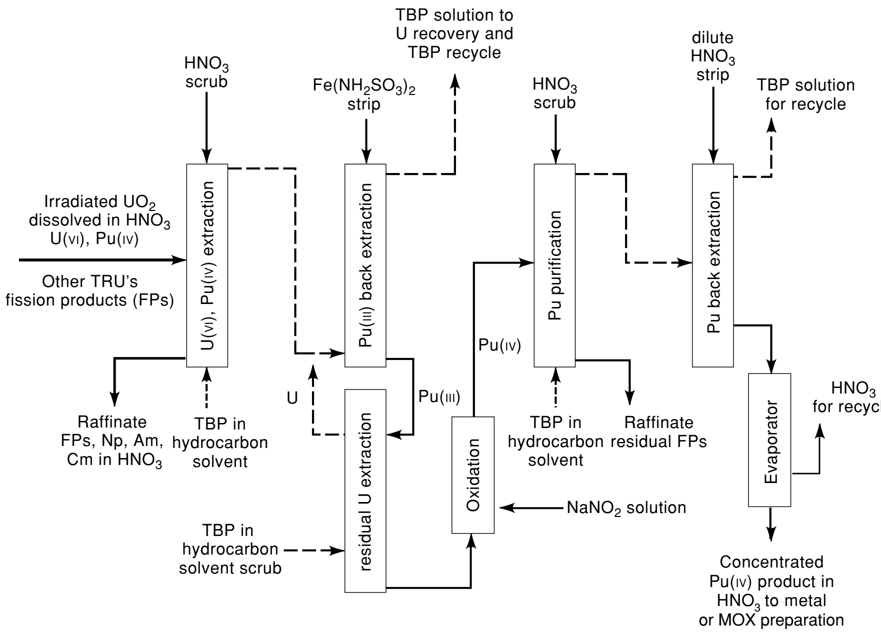

Fig. 7.5 *A generalized PUREX flow sheet where the dashed line indicates the organic stream.*

Of course, there are many other operations needed for running an actual PUREX plant that are not indicated by the simple extraction equations above. A few will be mentioned here and the references can be consulted for more detail. The decladding and dissolution of the fuel in nitric acid in a highly shielded facility are major operations that prepare the feed for the PUREX process. During the extraction process, the organic solvent and TBP undergo degradation reactions because of reactive species produced by the high level of ionizing radiation, particularly in the first extraction cycle where all the fission products are present. Some of the degradation products of TBP, dibutylphosphoric and monobutylphosphoric acids can cause problems by forming solids and modifying the *D* values for certain metal ions. This is dealt with by adding a washing operation to keep the concentration of these compounds below certain levels. The slight solubility of TBP and any entrainment of organic phase droplets in the aqueous phase also cause losses that must be replaced. Maintaining the oxidation states of various actinide and fission product metal ions in the intense radiation field requires careful adjustments at various points in the process. To improve process efficiency and to minimize wastes, evaporators are used to recover nitric acid and concentrate solutions at various points in the process. Finally, the products and wastes from all the operations must be handled properly and transported to their next destination.

During more than 50 years of use around the world, the PUREX process has undergone many improvements. Enhancements continue to be made at operating plants and new plants that will begin operations in the future. As options are considered for advanced nuclear fuel cycles, additional separations operations are under development for potential deployment in PUREX-type plants (see Chapter 24, section 4). Among these operations are solvent extraction processes for recovery of neptunium, americium, and curium to allow their transmutation in advanced reactor systems and for technetium, cesium, and strontium to allow these fission products to be disposed of more efficiently. Solvent extraction systems are certainly the most developed separation processes to accomplish these goals in the near future. The use of other separation approaches to augment or replace solvent extraction in advanced nuclear fuel cycles will require large technology development efforts.

(b) Extraction chromatography and supported liquid membranes

Liquid–liquid extraction can be deployed in forms other than the typical methods of mixing and separating the immiscible liquid phases. In extraction chromatography, the extractant and solvent (in some cases) are prepared in a thin layer on a solid support that usually consists of small spherical particles of a polymer or inorganic material. Inorganic materials such as silica require a surface treatment to generate a relatively hydrophobic surface that will be compatible with the organic extraction components. Aqueous solutions are contacted with the solid and metal ions are extracted into the thin surface layer much as occurs in a liquid–liquid extraction system. However, the composition of the surface layer can be quite different from that of the liquid–liquid system and this must be taken into account when predicting extraction behavior. Extraction chromatography materials are used most commonly for analytical separations of plutonium and other actinides and have been deployed for a limited number of gloved box scale process operations. These materials generally do not have the radiation stability or capacity for use in large-scale processing of irradiated fuels. However, such an approach has been proposed and tested at a small scale with a spent fuel solution using some silica-based extraction materials by Wei and coworkers (Wei *et al.*, 2002).

Supported liquid membranes consist of a liquid phase that separates two fluid phases: two gases, two liquids, or a gas and a liquid. Components in the fluid phases can be separated by differential transport through the liquid membrane phase driven by the chemical potential gradients. For metal ion separations, the fluid phases on each side of the membrane are usually aqueous solutions and the membrane consists of a porous solid support with an organic extractant solution filling the pores. Supported liquid membranes have been demonstrated on the laboratory scale to be an efficient separation method for metal ions, but have seen relatively few industrial applications because of long-term stability problems. With time, the components of the liquid membrane are lost to the aqueous phases and the membrane fails. Many approaches have been considered to overcome this problem, but none have yet seen widespread industrial use (Sastre *et al.*, 1998).

In the extraction chromatography and supported liquid membrane systems the active extractant is not chemically bound to the support. Solids that do contain such chemically bound groups that can selectively bind plutonium and other actinides will be discussed under ion-exchange processes (see Section 7.5.5).

7.5.5 Ion-exchange processes

Ion-exchange materials are insoluble solid materials with groups of one charge fixed in a three-dimensional solid matrix and mobile or exchangeable ions of the opposite charge associated with these fixed sites that balance the charge in the solid. In contact with a liquid phase that contains dissolved ions, the mobile ions will be exchanged for ions of like charge in the solution if the overall free energy of the system is lowered after the exchange. The relative affinity of the ion-exchange material for various cations or anions can be used to separate particular ions from solution. By using a regeneration solution under different conditions, it is usually possible to recover the adsorbed ions from the ion-exchange material (often in more concentrated and pure form) and prepare the ion-exchanger for additional cycles of exchange and regeneration. Both inorganic solids and organic polymers, including natural materials such as clays and zeolites, can function as ion exchangers. Ion exchange has long been an important process for water treatment. One of the first industrial applications of ion exchange described in 1905 was the use of synthetic sodium aluminosilicates (zeolites) to exchange Ca^{2+} from hard water with Na^+ (Simon, 1991).

Ion exchangers are commonly deployed in industrial processes as a packed bed of small particles to obtain a high surface area and accessible exchange sites with minimal diffusion path lengths to the sites. In the loading phase, liquid feed solution is passed through the bed until the mobile ions in the solution have been exchanged for mobile ions in the solid to the extent that the target ion or ions are no longer being removed from solution to the required level. If the ions loaded on the exchanger are to be recovered as a product (e.g. plutonium), one or more wash solutions may be passed through the bed to improve the final purity by removing residual feed solution and exchanging more weakly held ions. In the elution phase a different solution is passed through the column to recover the product ions. The conditions during the elution phase are changed (pH, ion concentration or type, temperature, etc.) so that the target ions bound during the loading phase are exchanged back into the solution. After elution the ion exchanger may be ready for reuse directly or may require an additional regeneration step. Most ion-exchange processes are operated in such a batch mode with separate loading and elution or regeneration steps. Continuous ion-exchange processes have also been developed, but are not as widely used as batch operations (Simon, 1991).

Ion-exchange processes for metal ion separation most commonly use an organic polymer solid phase (often referred to as an ion-exchange 'resin') containing charged functional groups fixed to the polymer structure to selectively bind metal ions or complexes of metal ions with a net opposite charge from an aqueous solution. The organic polymer is usually prepared in the form of small spherical particles or beads with a large internal porosity. The structure of the polymer greatly affects the final ion-exchange properties and the synthetic conditions are adjusted to control properties such as the degree of crosslinking, the number of ion-exchange sites, the size distribution of the pores, and the bead size. The polymer structure in most commercial ion-exchange materials is formed from styrene (vinyl benzene)–divinylbenzene copolymers with the fixed charged groups attached to the phenyl rings. The most common functional groups are sulfonic acid and carboxylic acid groups with protons that exchange for cations (cation exchangers) and alkylamine, alkanolamine, and tetraalkylammonium groups that act as anion exchangers. Other polymer structures have been used to make ion exchangers including polyacrylates and polyvinylpyridines (Simon, 1991; Harland, 1994).

(a) Plutonium ion-exchange separations

Both cation- and anion-exchange processes have been used for concentrating and purifying plutonium from aqueous solutions that result from processing operations ranging from solvent extraction (e.g. PUREX) to recovery of plutonium leached from scrap or debris material. Ion exchange is generally not used as the primary step to separate plutonium and other actinides from fission products in nuclear fuel or neutron-irradiated targets because the intense radiation field degrades the polymer matrix too rapidly. However, organic ion exchangers are very useful for separations in acidic solutions where the radiation dose comes mostly from plutonium and other actinides. Inorganic ion exchangers are generally more radiation-resistant than organic exchangers, but have other problems for large-scale processing such as limited stability over wide pH ranges, difficulty in obtaining reproducible behavior from batch to batch, and the greater difficulty of preparing particles of suitable size and shape for processing (Pekarek and Marhol, 1991).

Plutonium in any of its oxidation states can be taken up onto cation exchangers from dilute acid solutions with weakly binding anions such as nitric, hydrochloric, or perchloric acids. The strength of the binding of the oxidation state decreases in the order $Pu^{4+} > Pu^{3+} > PuO_2^{2+} > PuO_2^+$ as expected with the decreasing net charge on the cation. The ion-exchange process on a strong acid cation exchanger can be represented by the reaction:

$$Pu^{n+}_{(aq)} + nRH_{(org)} \rightarrow Pu(R)_{n\,(org)} + nH^+_{(aq)} \tag{7.12}$$

where RH represents a proton exchange site on the organic resin (usually a sulfonic acid site) and $n+$ is the net charge on the plutonium species. Separations can be made based on the ionic charge alone, but the greater utility of ion exchange results from using the exchange material in combination with complexants in the aqueous solution that bind the various oxidation states of plutonium and other metal ions differently. For example, in dilute hydrofluoric acid, Pu(III) will bind to a cation-exchange resin more strongly than Np(IV), in apparent disagreement with the expected order based on oxidation state alone. This is because Np(IV) forms complexes with fluoride to a greater extent than Pu(III) thereby reducing its overall net charge, e.g. NpF_3^+ and NpF_2^{2+} (Zagrai and Sel'chenkov, 1962). Measuring the change in the ion-exchange equilibrium as a function of metal ion binding in the aqueous phase is one method for determining stability constants and can be particularly useful for radioactive metal ions like plutonium that can be analyzed at low concentrations.

The formation of anionic complexes of plutonium, especially by Pu(IV) and Pu(VI), is the basis for separations using anion-exchange resins. For example, in moderate concentrations of hydrochloric acid (~6 M) both Pu(IV) and Pu(VI) absorb strongly on a Dowex 1 resin (quaternary ammonium exchange sites), but Pu(III) shows no significant uptake even in concentrated HCl. Spectroscopic and ion-exchange capacity data indicate that the anionic species bound in the resin are $PuCl_6^{2-}$ and $PuO_2Cl_4^{2-}$ (Ryan, 1975). If high concentrations of chloride salts (e.g. 10 M LiCl) are used with a relatively low acid concentration, Pu(III) can also be taken up on Dowex 1 as an anionic complex. The absorbed plutonium species can be eluted from the resin by using low concentrations of HCl.

Anion exchange of Pu(iv) from moderate concentrations of nitric acid or nitrate salts is a particularly useful separation method for plutonium and has been applied from the process scale to the analytical scale. Applications range from concentrating and purifying the plutonium product stream from PUREX plants, to recovering and purifying plutonium dissolved from a wide range of scrap, residue, and debris materials, to preparation of analytical samples. The basis for the separation is the strong adsorption of Pu(iv) onto the anion-exchange resin from moderate concentrations of nitric acid or nitrate salts. Few other elements are significantly retained under these conditions by an anion exchanger and large separation factors can be obtained (Faris and Buchanan, 1964). The iii, v, and vi oxidation states of plutonium and other actinides are also not bound strongly. Fig. 7.6 shows the Pu(iv) distribution coefficients (K_d) onto Dowex 1×4 resin plotted as a function of nitrate concentration for HNO_3 and $Ca(NO_3)_2$ solutions at 25 and 60°C (Ryan, 1959). The high distribution coefficients for Pu(iv) near 7 M nitric acid when combined with

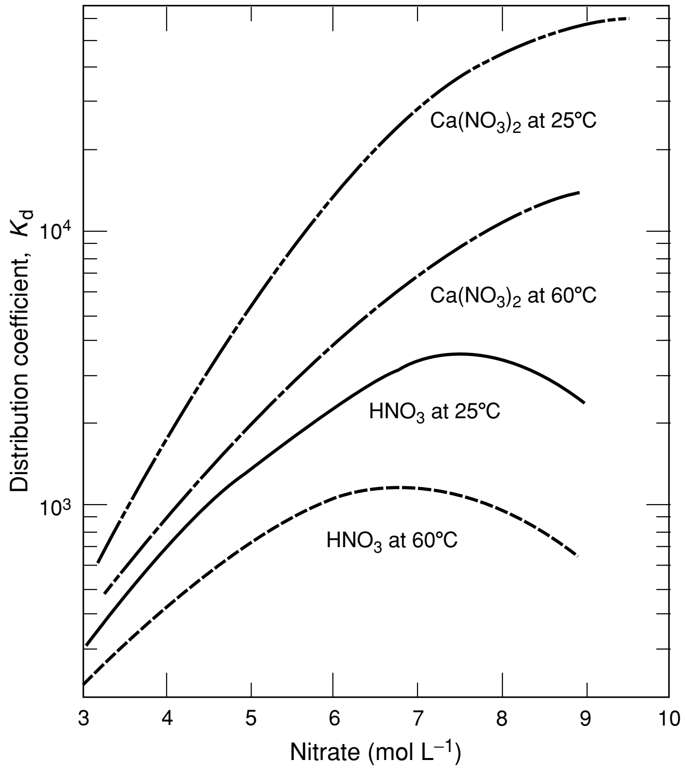

Fig. 7.6 *Plutonium(iv) distribution coefficients from nitric acid and calcium nitrate onto Dowex* 1 × 4 *anion-exchange resin (Ryan,* 1959*).*

an efficient elution method make large concentration factors possible. Elution of the plutonium is usually accomplished using a low nitric acid concentration alone or a low concentration of nitric acid and a reducing agent that generates Pu(III). The data in Fig. 7.6 show that the K_d values are lower at higher temperature, however, the kinetics of loading and elution are faster at higher temperature and this factor can be used as an advantage in process design (Ryan, 1975).

Visible absorption spectroscopy and resin capacity data show that Pu(IV) is absorbed on anion exchangers from nitric acid or nitrate salt solutions as the hexanitrato complex, $Pu(NO_3)_6^{2-}$ (Ryan, 1960, 1975). This has been confirmed by recent extended X-ray absorption fine structure (EXAFS) studies of anion exchange resins loaded with plutonium (Marsh *et al.*, 2000). Visible absorption, nuclear magnetic resonance (NMR), and EXAFS spectra of Pu(IV) and Th(IV) in nitric acid have also refined the information on the complexes formed in nitric acid solution (Veirs *et al.*, 1994; Allen *et al.*, 1996b; Berg *et al.*, 1998, 2000). At low nitric acid concentrations (~0.1 to 3 M) Pu^{4+}, $Pu(NO_3)^{3+}$, and $Pu(NO_3)_2^{2+}$ are the major species present (water molecules fill the rest of the plutonium coordination sphere in these complexes). At high nitric acid concentrations (>10 M), $Pu(NO_3)_6^{2-}$ is the dominant complex. At intermediate nitric acid concentration, in addition to $Pu(NO_3)_2^{2+}$ and $Pu(NO_3)_6^{2-}$, one major additional species is present that has been assigned as $Pu(NO_3)_4$. The trinitrato and pentanitrato complexes do not appear to be present at levels that can be easily observed (See Section 7.9.1.e). The concentration profile of the putative $Pu(NO_3)_4$ complex peaks at about 7 M nitric acid and correlates well with the distribution coefficient profile for Pu(IV) on anion-exchange resins from nitric acid (Marsh *et al.*, 1991). This observation suggests that the uncharged $Pu(NO_3)_4$ species might be important to the mechanism of uptake for Pu(IV) on an anion exchanger, but further work will be needed to verify this.

A general flow sheet for the operation of an anion-exchange process for plutonium recovery is illustrated in Fig. 7.7 (Christensen *et al.*, 1988). The oxidation state of plutonium dissolved in the nitric acid feed solution is carefully adjusted to maximize the amount of Pu(IV) because plutonium in other oxidation states is not retained on the exchanger. A variety of methods can be used for the oxidation state adjustment based on the composition of the feed. If fluoride is present in the feed solution, aluminum may be added to preferentially complex the fluoride and improve plutonium recovery. The nitric acid concentration is adjusted to 7 M and the solution is pumped through the packed bed of anion exchange beads so that $Pu(NO_3)_6^{2-}$ binds to the exchanger. The loaded resin is washed with 7 M nitric acid to remove impurities. Nitric acid at low concentration (0.35–0.6 M) is then pumped through the bed to elute the Pu(IV), or a solution of hydroxylammonium nitrate (or another suitable reducing agent) in dilute nitric acid is used to elute Pu(III). The plutonium in the eluate is commonly precipitated as an oxalate complex of either Pu(III) or Pu(IV) and the washed and dried oxalate solid is calcined to give a PuO_2 product.

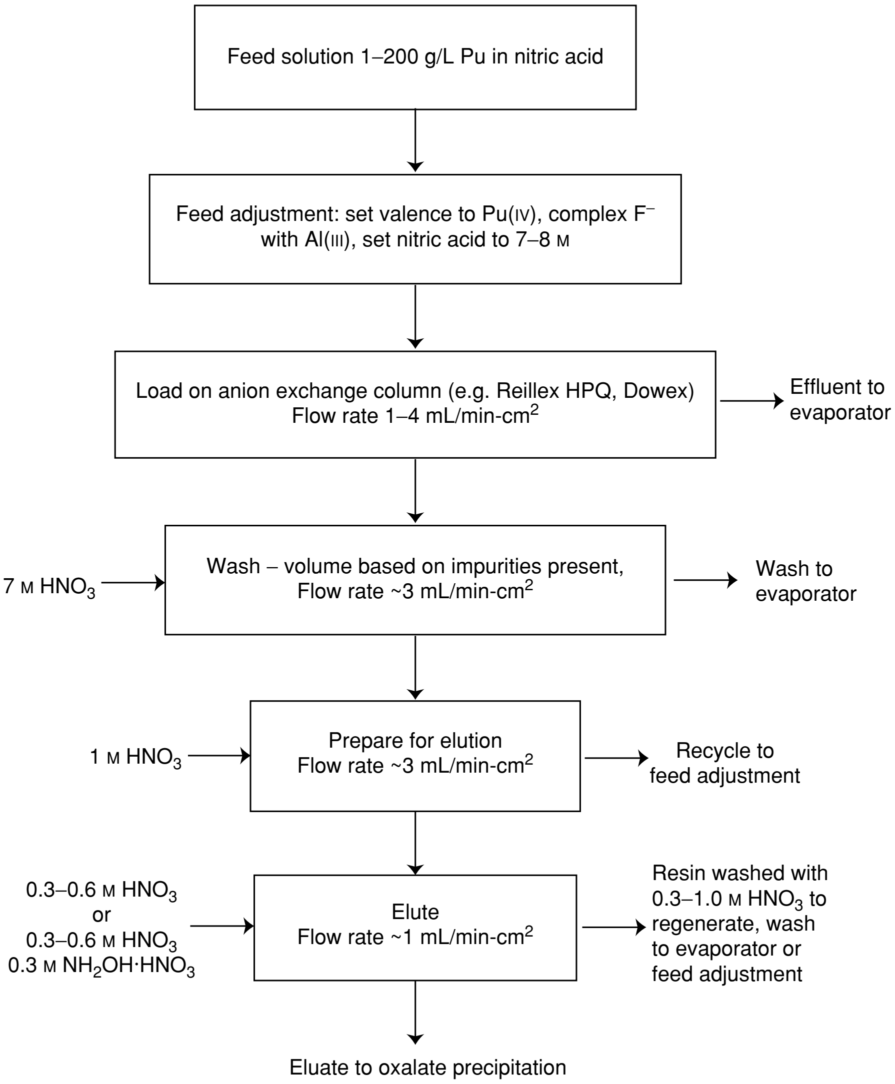

Fig. 7.7 *General flow sheet for operation of Pu*(IV) *anion-exchange purification process in nitric acid.*

There are a number of important features that must be controlled to safely and efficiently operate such an anion-exchange process for plutonium purification. Some of these features will be mentioned here. More detail can be found in the references (Cleveland, 1980; Christensen *et al.*, 1988). The batch size and the geometry of the packed bed are set up so that criticality cannot occur during normal operation. During elution of plutonium from the column, the nitric acid concentration should not drop so low as to allow the formation of the Pu(IV) polymer (see Section 7.9.1.d) as this material can clog the column and can be difficult to redissolve. The nitric acid–organic resin system can undergo a runaway oxidation reaction if temperatures are allowed to reach an initiation point around 160–180°C. A variety of safety devices and operating procedures are used to avoid this situation. For example, in using anion exchange to purify plutonium with a high percentage of the ^{238}Pu isotope for radioisotope heat sources, smaller batch sizes and columns are used to allow removal of the additional heat generated by decay of ^{238}Pu in comparison to 'regular' plutonium with a high ^{239}Pu content (Pansoy-Hjelvik *et al.*, 2001).

Ion exchange has been employed for separating plutonium and studying its chemistry since its discovery of more than 60 years ago. Considerable advances have been made in the processes used to manufacture ion-exchange materials during this time, partly driven by the need to separate plutonium and other actinides more efficiently. Highly uniform ion-exchange beads with reproducible behavior are now standard. The development of methods to synthesize macroporous polymer structures in the beads has reduced swelling and shrinkage of the bed as a function of changing solution conditions while retaining good kinetics of absorption (Simon, 1991). The organic ion-exchange polymers are degraded by radiation-induced reactions as noted above, including the alpha-induced radiolysis reactions of plutonium solutions in nitric acid. Anion exchange polymers made from 4-vinylpyridine crosslinked with divinylbenzene (e.g. Reillex HPQ) were demonstrated to be substantially more resistant to radiation-induced degradation than related polystyrene-based anion exchangers while maintaining excellent properties for plutonium processing (Marsh *et al.*, 1991; Buscher *et al.*, 1999). Reillex HPQ has thus replaced the polystyrene-based materials for plutonium recovery operations at some facilities.

Of course, improvements in ion-exchange technology will continue. Exchange columns that consist of a microporous polymer monolith with uniform flow paths and relatively short diffusion pathways compared to packed beds of beads have been developed. These materials could greatly improve future ion-exchange processes (Buchmeiser, 2001; Viklund *et al.*, 2001). Inorganic ion exchangers are continuing to become more versatile and should see wider applications. Membrane-based ion-exchange processes are also seeing wider application and offer potentially very efficient separation operations, but generally will require membrane materials with better long-term stability, including radiation stability, to replace the more common column method.

(b) Liquid ion exchangers and chelating ion exchangers

The solvent extraction processes discussed in Section 7.5.4 that use organic-soluble tetraalkylammonium salts or trialkylamines to extract anionic metal ion complexes as ion pairs are ion-exchange processes as well. These extractants are sometimes referred to as 'liquid anion exchangers.' Liquid cation exchangers are also used, for example, aliphatic and aromatic sulfonic acid compounds. Also, many types of functional groups have been placed on polystyrene and other polymer supports that can bind directly to the inner coordination sphere of a metal ion and help to stabilize a complex of the metal ion on the solid phases. This includes essentially all of the oxygen donor functionalities that were discussed in Section 7.5.4 (e.g. phosphates, phosphonates, phosphinates, and phosphine oxides). These polymers containing fixed ligand sites resemble solid versions of solvent extraction systems. However, fixing of the ligand to the polymer structure can considerably alter the metal ion-binding properties relative to an analogous ligand in solution. These kinds of materials are often referred to as 'chelating ion-exchange polymers' or resins, but it must be recognized that more than exchange of ion pairs is occurring in such materials and the thermodynamics of complex formation must be included in determining the selectivity and strength of the metal ion binding in these polymers. The use of chelating ion-exchange materials for separations of actinides is reviewed in Chapter 24 and a more general review for metal ion separations was published by Beauvais and Alexandratos (1998).

7.5.6 Separations in aqueous alkaline solutions

As noted in the brief discussion of aqueous actinide chemistry above, alkaline solutions are generally not used for actinide processing because the hydroxide complexes are quite insoluble. Large amounts of high-level caustic waste containing small amounts of actinides have been generated at Hanford and Savannah River as a result of neutralizing nitric acid solutions from PUREX recovery operations. A large body of work has been performed to better define the speciation of the actinides and to examine some potential processes for removing actinides from highly caustic tank wastes, including plutonium removal with various precipitants and absorbents. An overview of this work with references to the extensive literature has been published (Clark and Delegard, 2002).

Alkaline solutions containing strong ligands that can compete with hydroxide such as carbonate, fluoride, and peroxide can give high solubility to actinides in some oxidation states and even stabilize unusual oxidation states such as Pu(vii). The relatively small amount of work that has been done on extraction of actinides from alkaline solutions is reviewed in Chapter 24 (Section 3.7). One method to produce MOX fuels uses crystallization of Pu(vi) and U(vi) from ammonium carbonate solutions as $(NH_4)_4PuO_2(CO_3)_3$ or $(NH_4)_4UO_2(CO_3)_3$, respectively. The ammonium plutonyl and uranyl carbonates can be crystallized separately and blended or coprecipitated as the mixed carbonate (Roepenack *et al.*, 1984). An alkaline processing scheme for separation of the components of spent fuel in sodium carbonate/bicarbonate has been proposed and tested at a small scale on uranium and nonradioactive fission product elements (Asanuma *et al.*, 2001).

7.5.7 Nonaqueous separation processes

As noted above, the recovery of plutonium from irradiated uranium fuels has been dominated by the PUREX process, which requires dissolution of the fuel matrix in nitric acid. Alternative fluid media have been used or are under study to dissolve the uranium matrix and allow separation of the fission products from uranium, plutonium, and the other actinides, but none of these methods have been deployed on a large scale. The types of fluid media used include molten salts, molten metals, volatile halide compounds, ionic liquids, and supercritical fluids. The potential advantages for separation processes using these types of media compared to aqueous-based separations include: (1) greater resistance to radiation damage relative to water and organic solvents, (2) fewer and sometimes less complex steps to obtain products, (3) smaller highly shielded processing area, (4) smaller waste volumes that may also allow ready preparation for disposal, (5) simpler criticality control with reduced amounts of neutron moderating and reflecting materials, and (6) new separation selectivity. The separation selectivity for some of the nonaqueous processes are lower on a per stage basis relative to some of the aqueous technology, but that is not always a disadvantage when considering that more impurities may be acceptable in future reactor fuels and that safeguards benefits may result from keeping some components of the original mixture together. The advantages listed above do not apply to every process, but serve to give an indication of why there is continuing interest around the world in nonaqueous processing for advanced nuclear power systems.

The nonaqueous separation methods have disadvantages as well. The major disadvantage has already been mentioned, in that these processes have not been developed as extensively as the aqueous methods and thus have less well-defined costs, safety envelopes, and operational experience. The chemistry of these nonaqueous separation methods is presented in more detail in Chapter 24, especially as they apply to advanced methods for partitioning of spent nuclear fuel. In this chapter, we will briefly review the nonaqueous separation methods most relevant to plutonium processing.

(a) Pyrochemical separation and conversion processes

After plutonium has been separated from the fission products, pyrometallurgical operations have been used since the days of the Manhattan Project to prepare and purify metallic plutonium from various compounds (Hammel, 1998). Plutonium is a very electropositive and reactive metal, and preparation and purification methods based on molten salts and molten metals under inert atmospheres were adapted from industrial practice with adjustments required for actinide-specific factors such as radioactivity and criticality. The major pyrochemical processes used to prepare and purify plutonium metal (bomb reduction of PuF_4, direct oxide reduction (DOR) of PuO_2, molten salt extraction (MSE) of americium, electrorefining (ER), and pyroredox) are discussed in Sections 7.7.1 and 7.7.2. The pyrochemical operations occur in mixtures of molten Group 1 or 2 chloride or fluoride salts at temperatures of 700–900°C, although temperature spikes near 2000°C may occur during the bomb reduction of PuF_4 with calcium metal. Preparing the feed materials for these pyrochemical operations using aqueous processing operations is reviewed in Section 7.5.3(b).

A wide variety of pyrochemical processes have been considered to separate the components of spent nuclear fuels in advanced nuclear fuel cycles. The processes range from early work on use of molten metals such as silver, cadmium, zinc, and magnesium that are immiscible with molten uranium as extractants for plutonium (Dwyer *et al.*, 1959; Wiswall *et al.*, 1959) to recent work on the pyroelectrochemical deposition of PuO_2 and UO_2 from molten chloride salts for direct fabrication by vibropacking into fast reactor fuel elements (Grachev *et al.*, 2004). An entire reactor system, the Molten Salt Reactor Experiment, based on a molten BeF_2 and ^7LiF core containing fissile UF_4 and fertile ThF_4 was studied at Oak Ridge National Laboratory in the 1960s. Reviews of these processes, both historical and those under development, have been published (Long, 1978; Bychkov and Skiba, 1999).

(b) Room temperature ionic liquids

Room temperature ionic liquids (RTILs) are salts that are liquid at or near room temperature. The RTILs currently under study consist of an organic cation (e.g. quaternary ammonium, $R_1R_2R_3R_4N^+$, or alkylpyridinium) paired with a wide variety of inorganic and organic anions (e.g. $AlCl_4^-$, PF_6^-, $CF_3CO_2^-$). The RTILs are under study for a wide array of applications, such as organic synthesis, battery electrolytes, catalyst systems, and metal ion separations (Rogers and Seddon, 2002). It should be noted that the RTILs and the inorganic molten salts discussed above under pyrochemistry are part of the larger class of ionic liquids. The inorganic salts generally have much higher melting points, but that situation may change to some extent as new classes of ionic liquids are investigated. For example, the sodium/potassium nitrate eutectic has a melting point near 170°C.

Potential applications of RTILs to plutonium and actinide separations are under development in two main areas: use as low temperature ionic liquid solvents for electrochemical deposition of metal or oxide and as liquid–liquid extractants for actinide metal ions from aqueous solutions. A research team led by the Queen's University of Belfast and British Nuclear Fuels, Ltd. has also proposed using RTILs to process spent nuclear fuel (Baston *et al.*, 2002; Pitner *et al.*, 2003). It is not yet known if the present generation of organic-containing RTILS is sufficiently radiation resistant for the processing of spent fuel.

(c) Halide volatility processes

The isotopic separation of volatile UF_6 using processes such as gaseous diffusion or gas centrifugation has been practiced at a large scale since the 1940s. In 1949, Sheft, Andrews, and Katz proposed a separation process for irradiated nuclear fuel based on fluorination using liquid interhalogen compounds. This was the beginning of an extensive research and development program into what is commonly called the fluoride volatility process (Sheft *et al.*, 1949). In this type of process, the irradiated fuel (uranium oxide, uranium alloys, even fuel assemblies with cladding intact) is dissolved in a liquid fluorinating solution, a molten salt sparged with fluorine, or fluorinated directly in a fluidized bed. The volatile UF_6 (along with NpF_6 and PuF_6 depending on the process details) and fission product fluorides such as TcO_3F, RuF_6, NbF_6, and MoF_6 are collected and separated using volatility differences and differences in reactivity of the fluorides with beds of solid reagents. In some proposed fluoride volatility processes, neptunium and plutonium are left with the nonvolatile fission product fluorides and separated by another method such as solvent extraction (Amano *et al.*, 2004).

The major advantages of the fluoride volatility process are relatively simple chemistry, radiation resistance of the reagents, high decontamination factors, and separation of uranium in a form suitable for re-enrichment. The disadvantages are the use of extremely corrosive reagents and the attendant corrosion of materials of construction, the criticality concerns associated with the high reactivity of hexafluorides, especially PuF_6, and controlling their deposition in the process equipment. Investigations of variants of fluoride volatility continue today, but these processes have not yet been deployed on a large scale. A fluoride volatility process for recovery of plutonium from certain scrap materials was demonstrated at the Rocky Flats Plant on a pilot scale, but was never deployed as a regular plant operation (Standifer, 1968).

Chloride volatility processes for separating the components of spent fuels have also been investigated (Bohe *et al.*, 1997). In general, this appears to be a less selective process because of the greater number of volatile fission product chlorides that could accompany the volatile actinide species, but the separation of the various volatile chloride species has not received as much effort as the fluoride system. The removal of zirconium alloy cladding materials by chlorination with HCl or Cl_2 and collection of the volatile $ZrCl_4$ has also been examined (Gens, 1961). This process could potentially provide an attractive alternative to mechanical decladding methods and could allow recycling of the slightly radioactive zirconium.

(d) Supercritical fluid extraction processes

Supercritical fluids, principally carbon dioxide, have been investigated to extract actinides from waste materials, for separating actinides and fission products from spent nuclear fuels, and as an alternative to conventional liquid–liquid extraction. Reagents required for forming metal ion complexes (which include complexing agents, acids, and/or redox reagents) such as 1,3-diketones or $TBP \cdot HNO_3$ are dissolved in supercritical carbon dioxide and this fluid phase is contacted with a solid material (e.g. uranium oxides or a waste solid) or an aqueous phase. The extracted metal ions can be recovered by a number of methods: changing the pressure to modify solubility and filtering a solid product, removing the carbon dioxide as a gas to leave a solid or liquid product, or back-extracting the metal ions into an aqueous phase. The bulk of the studies in this area with actinides have used uranium and thorium, but some work with plutonium and other transuranic elements has appeared. Extraction of U(VI) and Pu(IV) from aqueous nitric acid solutions into supercritical CO_2 solutions of TBP has been studied as a function of temperature and pressure (Iso *et al.*, 2000). Some data on the dissolution of oxides with $TBP \cdot HNO_3$ dissolved in supercritical CO_2 have been reported for PuO_2 and solid solutions of $(Pu,U)O_2$ and $(Pu,Am,U)O_2/Eu_2O_3$ (Trofimov *et al.*, 2004). The use of chelating agents dissolved in supercritical CO_2 or liquid CO_2 with modifiers such as pyridine or water for decontamination of various solid materials including stainless steel, rubber, cotton, plastic, and soil from plutonium and other radionuclides has been studied (Murzin *et al.*, 2002b). The solubility of some 1,3-diketone complexes of U(VI), Np(IV), Pu(IV), and Am(III) in supercritical CO_2 has been measured (Murzin *et al.*, 2002a,b). Removal of plutonium and americium from soil using TBP and thenoyltrifluoroacetone (TTA) or hexafluoroacetone in supercritical CO_2 has been investigated (Mincher *et al.*, 2001; Fox and Mincher, 2002). The studies of supercritical fluid extraction for actinides are reviewed extensively in Chapter 24 (section 3.10).

(e) Combination processes

A great variety of aqueous, nonaqueous, and combined aqueous and nonaqueous processes have been proposed for partitioning of spent fuel. As described above, to prepare and purify plutonium metal, a combination of aqueous (PUREX and precipitation-crystallization methods) and nonaqueous (pyrochemical) processes has been used. A few recent examples proposed in the literature will be briefly described to indicate that combination processes are being considered in future separation facilities for processing used nuclear fuels. Amano and coworkers proposed the use of fluoride volatility on irradiated fuel to separate uranium for re-enrichment. Some volatile fission product fluorides such as technetium would also be collected separate from the uranium. The residual solid would then be dissolved in nitric acid for PUREX-type solvent extraction to separate plutonium and other transuranic actinides from the fission products to recycle the actinides to a fast reactor system, the so-called FLUOREX process (Amano *et al.*, 2004). Another group in Japan has proposed separating uranium, neptunium, and plutonium from spent fuel dissolved in nitric acid by oxidizing the neptunium and plutonium to the hexavalent state and then cooling the nitric acid solution to crystallize out the mixed nitrate complex $(\mathrm{U, Np, Pu})\mathrm{O_2(NO_3)_2} \cdot x\mathrm{H_2O}$ (Kikuchi *et al.*, 2003). A variety of other combined aqueous/nonaqueous processes that have been proposed for processing irradiated fuels are reviewed in Chapter 24.

7.6 ATOMIC PROPERTIES

Plutonium, like all of the heaviest elements, has a very complex electronic structure. The free atom and free ion spectra of plutonium are among the richest and most thoroughly studied of any chemical element. The complexity of the electronic structure is apparent in the spectral properties, such as X-ray absorption and emission spectra, and arc, spark, and discharge emission spectra. Early measurements were made with electrodeless discharge lamps and large grating spectrographs such as the 9.15 m Paschen–Runge spectrograph at Argonne National Laboratory (ANL). Very high-resolution grating spectrographs have been replaced by Fourier transform (FT) spectrometers such as those at the Laboratoire Aimé Cotton (LAC) (built in 1970) and at the Kitt Peak National Solar Observatory. The plutonium free atom, Pu^0, designated Pu I, has 94 electrons of which 86 electrons are in filled shells as found in the radon atom. It is customary in discussing the actinide series to only list the electrons in shells outside the radon core. The outermost electrons of the free actinide atoms and ions outside the radon core are found in the 7s, 7p, 6d, and 5f shells. For example, the ground state (lowest energy) configuration for Pu I is $5f^67s^2$. Identified excited configurations of Pu I within the first 3 eV ($\sim$24,000 cm^{-1}) of the ground state include $5f^56d7s^2$, $5f^66d7s$, $5f^56d^27s$, $5f^67s7p$, $5f^57s^27p$, and $5f^56d7s7p$. In the free atoms and ions, many low-lying configurations interact strongly with each other, giving rise to a large number of electronic states, and tens of thousands of spectral lines. A detailed discussion and review of the spectra of actinide free atoms and ions can be found in Chapter 16, and in reviews by Blaise *et al.* (1983a, 1986), Reader and Corliss (1980), and Blaise and Wyart (1992).

7.6.1 Optical emission spectra of Pu I and Pu II

The emission spectrum of neutral (Pu I) and singly ionized (Pu II) plutonium, which can be excited by arc, spark, hollow cathode, or inductively coupled plasmas, has been extensively studied. The first measurements of plutonium were conducted in 1943 by Rollefson and coworkers (Rollefson and Dodgen, 1943; Dodgen *et al.*, 1944, 1949) who measured the wavelengths and intensities of about 125 spectral lines. In the initial publications of plutonium spectra, only the wavelengths and intensities of unidentified transitions were reported. In 1959, McNally and Griffin reported the first energy level analysis for Pu II, where seven levels of the lowest terms of the $5f^67s$ (^8F and ^6F) electronic configuration were determined (McNally and Griffin, 1959). In 1961, Bovey and Gerstenkorn determined the five lowest levels of $5f^67s^2$ (^7F) for Pu I (Bovey and Gerstenkorn, 1961). In 1961, a collaboration was formed between scientists at ANL, LAC, and Lawrence Livermore National Laboratory (LLNL) to continue studies of the term analyses of Pu I and Pu II spectra. In 1970, the FT spectrometry at LAC was used to record the spectra of ^{240}Pu and of a mixture of ^{240}Pu, ^{242}Pu, and ^{244}Pu isotopes up to 3.59 μm. A portion of one of these spectra is shown in Fig. 7.8. The high resolution and extension into the infrared spectral region greatly enhanced the spectral analysis and allowed the connection between the lowest odd and even levels (Blaise *et al.*, 1983a).

The first comprehensive description of Pu I and Pu II spectra became available in 1983, when Blaise, Fred, and Gutmacher collected wavelengths, wavenumbers, intensities, classifications, and isotope shift data in a 612 page ANL report (Blaise, 1983b). In 1992, Blaise and Wyart published all known energy levels of the actinide elements that had been analyzed up to that time and listed ionization stage, energies, intensities, *J*-values, and level assignments of selected lines (Blaise and Wyart, 1992). The contents of that compilation are available on an updated database at LACs website (www.lac.u-psud.fr).

At the time of this writing (2005), 9500 isotope shifts have been measured, and half of them are in the IR region. More than 31,000 lines of the Pu I and Pu II spectra have been observed, of which 52% have been classified as transitions between pairs of levels (Blaise *et al.*, 1983a, 1986; Blaise and Wyart, 1992). With the aid of Zeeman and isotope-shift data, a total of 606 even and 589 odd levels for Pu I, and 252 even and 746 odd levels for Pu II, have been identified. For all

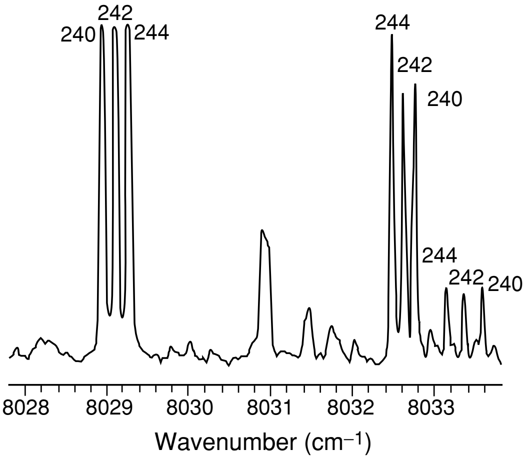

Fig. 7.8 *Fourier transform spectrum of a mixture of ^{240}Pu, ^{242}Pu, and ^{244}Pu isotopes (Blaise* et al., 1983a).

these levels the quantum number J has been assigned, and for many levels Landé g-factors are given. To date, levels belonging to 14 different electronic configurations in Pu I, and 9 electronic configurations in Pu II have been identified. The lowest levels of these configurations are given in Table 7.8 along with the Landé g-factors and experimental isotope shifts (Blaise *et al.*, 1983a; Blaise and Wyart, 1992).

The full-term analysis of plutonium spectra is still not yet complete because, even in 2005, a detailed quantum-mechanical treatment is hindered by the extreme complexity of the spectra. Even though the emission spectra of plutonium are still not completely assigned, they are among the best-understood spectra of the heavy elements.

7.6.2 Ionization potentials

The first ionization potential (IP) is a fundamental physical and chemical property of an element, and it is directly connected to the atomic spectra. Its accurate determination is important for identifying systematic trends within the actinide series of elements. In 1973 and 1974, Sugar derived values for the ionization energies of neutral plutonium and other actinides by using interpolated spectral properties of the atoms (Sugar, 1973, 1974). For neutral plutonium, the first IP was calculated to be 6.06(2) eV or 48,890(200) cm^{-1}. Worden *et al.* (1993) measured the first IP of ^{239}Pu by laser resonance techniques requiring as much as 2 g of ^{239}Pu. The photoionization threshold value for the ^{239}Pu I IP was determined to be 48,582(30) cm^{-1}, and the more accurate value from the Rydberg series measurements was 48,604(1) cm^{-1} or 6.0262(1) eV. In 1998, Erdmann and coworkers reported the first IP of ^{239}Pu using resonance ionization mass spectrometry (RIMS), a technique that requires only a few hundred picograms of material. In this approach, one- or two-step resonant laser excitation in a well-defined electric field promotes the atoms to a highly excited state, and ionization is obtained by scanning the wavelength of an additional tunable laser across the threshold, and extrapolation to zero field strength. From RIMS data, the first IP was found to be 48,601(2) cm^{-1} or 6.0258(2) eV (Erdmann *et al.*, 1998; Waldek *et al.*, 2001).

7.6.3 X-ray spectra

Plutonium X-ray spectra have been studied in detail by several authors (Cauchois *et al.*, 1954; Cauchois and Manescu, 1956; Shacklett and DuMond, 1957; Merrill and DuMond, 1958, 1961; Nelson *et al.*, 1969, 1970), and detailed wavelength and energy tables have been published by Bearden (Bearden, 1967; Bearden and Burr, 1967). The reader is also referred to the *Gmelin Handbook* (Koch, 1973c). The K and L series of the Pu X-ray spectra are known, and a few lines of the M and N series have been measured (Cauchois *et al.*, 1963a,b; Bonnelle, 1976). The L edges of the X-ray absorption spectra have been used

Table 7.8 *The lowest energy level of each electronic configuration of neutral Pu I and monovalent Pu II with their corresponding term symbol, energy, Landé g-values, and isotope shifts* (*Blaise and Wyart*, 1992).

Configuration	*Parity*	*Term*	*Energy* (cm^{-1})	*g*	*IS* (240–239) (10^{-3} cm^{-1})	*References*
Pu I						
$5f^67s^2$	even	$^7F_0$	0.000	–	465	Bovey and Gerstenkorn (1961)
$5f^56d7s^2$	odd	$^7K_4$	6 313.886	0.487	653	Bauche *et al.* (1963b)
$5f^66d7s$	even	$^9H_1$	13 528.246	−0.59	253	Bauche *et al.* (1963b)
$5f^56d^27s$	odd	$^9L_4$	14 912.011	0.496	488	Bauche *et al.* (1963b)
$5f^67s7p$	odd	$^9G_0$	15 449.472	–	336	Brewer (1971a)
$5f^57s^27p$	even	$^7I_3$	17 897.119	0.450	698	Bauche *et al.* (1963b) and Blaise *et al.* (1983a)
$5f^56d7s7p$	even	$^9L_4$	20 828.477	0.352	467	Bauche *et al.* (1963b)
$5f^77s$	odd	$^9S_4$	25 192.231	1.768	273	Blaise *et al.* (1983a,b)
$5f^67s8s$	even	$^9F_1$	31 572.610	2.403	446	Bauche *et al.* (1963b)
$5f^66d^2$	even	$^9I_2$	31 710.912	0.200	115	Blaise *et al.* (1983a)
$5f^67s7p$	odd	$^9I_2$	33 070.58	0.673	293	Blaise *et al.* (1983a, unpublished)
$5f^46d^27s^2$	even	$^7M_6$	36 050.562	0.83	535	Brewer (1971a)
$5f^56d^27p$	even	$^9M_5$	37 415.524	0.980	403	Blaise *et al.* (1983a, unpublished)
$5f^56d7s8s$	odd	$^9K_3$	39 618.16	0.27	503	Blaise *et al.* (1986)
Pu II						
$5f^67s$	even	$^8F_{1/2}$	0.000	3.150	381	McNally and Griffin (1959)
$5f^57s^2$	odd	$^6H_{5/2}$	8 198.665	0.415	896	Fred *et al.* (1966)
$5f^56d7s$	odd	$^8K_{7/2}$	8 709.640	0.310	555	Brewer (1971b) and Blaise *et al.* (1983a)
$5f^66d$	even	$^8H_{3/2}$	12 007.520	−0.019	77	Bauche *et al.* (1963b)
$5f^56d^2$	odd	$^8L_{9/2}$	17 296.88	0.494	242	Brewer (1971b) and Blaise *et al.* (1983a)
$5f^67p$	odd	$^8G_{1/2}$	22 038.95	0.345	287	McNally and Griffin (1959) and Brewer (1971b)
$5f^57s7p$	even	$^8I_{5/2}$	30 956.36	0.650	424	Brewer (1971b) and Blaise *et al.* (1983a)
$5f^57s7p$	even	$^8L_{9/2}$	33 793.30	0.795	208	Blaise *et al.* (1983a)
$5f^46d^27s$	even	$^8M_{11/2}$	37 640.78	0.70	813	Brewer (1971b) and Blaise *et al.* (1983a)

for plutonium oxidation state determination through the X-ray absorption near edge structure (XANES) in a variety of matrices (Conradson *et al.*, 1998, 2004a; Duff *et al.*, 1999; Richmann *et al.*, 1999; Fortner *et al.*, 2002; Antonio *et al.*, 2004; Lechelle *et al.*, 2004).

7.6.4 Core-level spectra

A few core-level spectra on plutonium compounds have been measured and comprehensively reviewed by Teterin and Teterin (2004). Core-level spectra that probe plutonium 4d, 4p, 4f, 5d, 5p, 6s, and 6p levels have been applied to determination of oxidation states and local environment, the magnetic properties of compounds, the nature of the chemical bonding, and secondary electronic processes that accompany photoemission. The use of fine structure spectral parameters, together with the electron binding energies and line intensities, significantly extends the scope of application of the X-ray photoelectron spectroscopy (XPS) method in structural studies. We mention only a few recent applications of core-level spectra.

Kotani and coworkers examined 4f core XPS of PuO_2 and other actinide dioxides and employed the Anderson impurity model to show that PuO_2 is a strongly mixed-valent compound and that a crossover between Mott–Hubbard and charge-transfer insulators occurs near NpO_2 (Kotani and Ogasawara, 1993; Kotani *et al.*, 1993). Allen and coworkers examined Pu 4f XPS of the α, β, γ, and δ phases of plutonium metal. They found that the 4f core-level spectra display features that vary systematically for the α, β, γ, and δ phases. For all phases they observed a sharp feature at binding energy 422 eV and a much broader shoulder that is approximately 2.5 eV higher. Application of an Anderson impurity model indicates that these features represent well-screened ($5f^6$) and poorly screened ($5f^5$) final states, respectively (Allen *et al.*, 1996a; Cox *et al.*, 1999). More recently, Gouder *et al.* (2002) employed 4f core-level spectroscopy to demonstrate dramatic changes in the electronic structure of ultrathin layers of α-Pu, and suggest that the surface of α-Pu should have δ-Pu character.

7.6.5 Mössbauer spectra

It is possible to obtain Mössbauer spectra on plutonium using excited states of ^{238}Pu, ^{239}Pu, and ^{240}Pu. In the case of ^{238}Pu, the β decay of ^{238}Np yields the 44 keV excited state of ^{238}Pu, which decays to the ground state with $T_{1/2} = 183$ ps and E2 dipole radiation. The 44 keV γ-ray may be used in resonance absorption measurements. A disadvantage is the short half-life of the 44 keV level (170 ps), which causes line broadening, and the relatively short half-life (2.1 days) of the source nuclide ^{238}Np, which makes it difficult to prepare sufficient amounts of the latter for a Mössbauer spectroscopy source.

For ^{239}Pu, the β decay of ^{239}Np produces a 57.3 keV state of ^{239}Pu, which decays through E2 γ radiation, which may be used in resonance fluorescence spectroscopy. Gal *et al.* (1972) studied the resonance fluorescence of the 57.3 keV γ ray using a $^{239}NpO_2$–ThO_2 source and ^{239}Pu as the absorber. At 4.2 K, a resonance with a half-width of (5.13 ± 0.10) cm s^{-1} was observed. Assuming a Debye temperature of (250 ± 50) K for PuO_2, they calculated a natural linewidth of (473 ± 0.25) cm s^{-1}. This corresponds to a half-life of (101 ± 5) ps, in agreement with the lifetime of rotational levels, which decay by E2 transitions.

For ^{240}Pu, the α decay of ^{244}Cm yields a 42.9 keV state in ^{240}Pu in 23.3% of all occurring α decays. This state decays to the ground state with $T_{1/2} = 164$ ps. The 42.9 keV transition has an internal conversion coefficient of $\alpha_T = 920$. The use of this transition for Mössbauer spectroscopy was first demonstrated by Kalvius *et al.* (1978), who studied tetravalent $^{240}PuO_2$ and hexavalent $^{240}PuO_2C_2O_4$. In the tetravalent system, at 4.2 and 77 K, a single resonance line was found with a width of about 20% larger than the natural width of about 40 mm s^{-1}. In the hexavalent plutonyl oxalate, $PuO_2C_2O_4$, at 4.2 K a quadrupole interaction $|e^2qQ| = 95$ mm s^{-1} was found, but no isomer shifts were detected.

7.7 PLUTONIUM METAL AND INTERMETALLIC COMPOUNDS

Plutonium metal, alloys, and intermetallic compounds have important technological applications principally because of the nuclear properties of isotope 239. Plutonium metals and alloys are the materials of choice for the nuclear explosive in nuclear weapons and for fuel elements for some advanced reactor designs. The metallic properties of plutonium are important not only for nuclear weapons design, but also for the safe storage and disposition of excess weapons-grade plutonium. Plutonium alloys were used in some early reactor concepts (Anderson *et al.*, 1960; Kiehn, 1961; Burwell *et al.*, 1962) and are under development for advanced designs such as the Integral Fast Reactor (Keiser *et al.*, 2003). Much of the early work on plutonium metal and alloys was done in secrecy in the declared nuclear weapons states (mostly in the United States, Soviet Union, U.K., and France). President Eisenhower's Atoms for Peace initiative, which was launched with his December 8, 1953 speech to the United Nations brought most of the scientific work and many of the engineering properties into the open through a series of international conferences, starting with the first Atoms for Peace Conference in Geneva in 1955. Today, the threats of proliferation and terrorism cause concern about the amount of practical information regarding the construction of nuclear devices available in the open literature. Over the years, the U.S. government has taken the position that the fundamental scientific and engineering properties of plutonium be treated as open information. However, practical manufacturing methods, including those specific to weapons manufacture and the performance of nuclear weapons, remain classified. These guidelines are followed in this chapter.

In addition to its technological importance, plutonium in condensed matter also proves to be fascinating scientifically. The unusual nature of plutonium in the solid state is the result of its peculiar electronic structure. It lies near the middle of the actinide series – precisely at a transition point between the 5f electrons participating in bonding or being localized and chemically inert. Exploring the properties of plutonium and its compounds is an area of great interest in condensed matter physics. From a metallurgical perspective, the peculiarities associated with plutonium's electronic structure cause plutonium to defy most conventional metallurgical wisdom. These peculiarities, along with much of the interesting chemistry of plutonium, have been the subject of several recent reviews (Guerin, 1996; Cooper and Schecker, 2000; Terminello *et al.*, 2001; Hanrahan *et al.*, 2003; Jarvinen, 2003). In this section, we focus on the basic properties of plutonium, but we also explore properties of the neighboring actinides to better understand plutonium within the context of the entire actinide series.

Although our focus is on properties, we state at the outset that to delineate plutonium's metallic behavior it is imperative to understand what is called in the materials science community the processing–structure–properties relationship. Metallurgical practitioners routinely adjust properties by tailoring structure through careful control of chemistry and processing of metals and alloys. By structure we mean crystal structure, grain structure, and defect structure on the nano- and microscale. Plutonium is notoriously unstable with respect to temperature, pressure, and chemical additions, and its surface is reactive, especially in the presence of hydrogen or water. The synthesis and processing of plutonium are quite complex. There is considerable concern over lot-to-lot variations in processing and structure because criticality considerations limit the production of plutonium metal and alloys to small lots (at most on the order of kilograms). Also, microcracks, surface reactions, inclusions from impurities, and retained second phases can affect sample properties. In addition, the self-irradiation of plutonium (especially the prevalent isotopes ^{239}Pu and ^{238}Pu) causes microstructural changes that may affect its properties as it ages. Hence, the age of plutonium samples, or the time elapsed since the material was last molten or heat treated, can affect the properties. Unfortunately, most publications on plutonium properties provide little structural information, and detailed descriptions of processing conditions or sample age are typically limited.

We will draw attention to those cases for which the properties are especially sensitive to structure, processing, and age. The reader is also advised to examine reported density data and X-ray crystal structure information as both provide a good indication of what phases were present in the samples studied.

7.7.1 Preparation of plutonium metal

Plutonium metal may be obtained by a number of reduction reactions of plutonium compounds. Summaries of the various reactions have been given by Harmon *et al.* (1961), Leary and Mullins (1966), McCreary (1955), Christensen and coworkers (Christensen and Mullins, 1983; Christensen *et al.*, 1988), Coops *et al.* (1983), and Baldwin and Navratil (1983). Not all of the reactions that produce plutonium metal are ideally suited for metal preparation in production work. For production processes, the chemical reactions must (a) produce a dense, coherent mass of pure plutonium in high yield; (b) generate sufficient heat to melt both the metal and the resulting slag; (c) result in a slag that stays molten and nonviscous long enough to allow the plutonium to coalesce; and (d) work on the scale desired (a reaction suitable for microgram-scale reductions might be less useful for gram- or multigram-scale reductions and vice versa). In reactions where one of the conditions (a–d) is not initially fulfilled, modified process conditions may still make the technique usable. For example, if the heat of reaction for a Ca reduction is insufficient (condition b), then addition of an iodine booster or use of a laser can provide sufficient heat to make the overall process usable. The resulting CaI_2 in turn helps to improve condition (c).

The pyrochemical preparation of plutonium metal is best carried out by reduction of PuF_4, PuF_3, $PuCl_3$, PuO_2, or a PuO_2–PuF_4 mixture with calcium metal in a high-temperature molten salt. Quite often a booster (such as iodine) initiates the reaction and provides sufficient energy to ensure the complete reaction:

$$PuF_4 + 2Ca^0 \rightarrow Pu^0 + 2CaF_2 \tag{7.13}$$

$$2PuCl_3 + 3Ca^0 \rightarrow 2Pu^0 + 3CaCl_2 \tag{7.14}$$

$$PuO_2 + 2Ca^0 \rightarrow Pu^0 + 2CaO \tag{7.15}$$

These methods of preparation do not produce any purification (Leary and Mullins, 1966); they simply produce metallic plutonium. Of these approaches, the reduction of PuO_2 has become the preferred route for preparation of plutonium metal. $PuCl_3$ is extremely hygroscopic, which poses handling difficulties, particularly for large quantities of material. The plutonium fluorides (PuF_4, PuF_3) are neutron emitters (due to α-n reactions), and working with plutonium fluorides requires considerable protective shielding. A related lithium reduction of PuO_2 has been developed as a pyrochemical process for the recycle of oxide fuels (Usami *et al.*, 2002).

Hydriding and dehydriding or hydriding followed by oxidation can recover plutonium metal scraps adhering to other metal surfaces (Haschke, 1991; Flamm *et al.*, 1998). Even at room temperature, plutonium metal reacts reversibly with hydrogen to form a metallic PuH_x powder (see Section 7.8.1).

$$2Pu^0 + xH_2 \rightleftharpoons 2PuH_x \tag{7.16}$$

The hydride spalls off the inert substrate and subsequent heating of the hydride product in a vacuum recovers the plutonium metal.

7.7.2 Modern pyrochemical preparation and refining

Over time, the general process for obtaining, preparing, and refining plutonium has evolved based on the kinds of feed materials available. Historically, plutonium was first produced in production reactors; extracted, concentrated, and converted to either an oxide or fluoride; and then reduced to metal. The resulting metal was used for fabrication of various parts and components. The fabrication process itself generates major quantities of waste and scrap plutonium that must then be recovered and recycled. In modern times, the feed material for preparation and refining of metallic plutonium has evolved to recovery and recycle of residues and scrap material. This in turn drives the current technology selection for metal preparation and refining. In addition, the technology selection must take nuclear material safeguards, accountability, criticality safety, and radiation exposure into consideration. The major pyrochemical processes that are currently employed in large facilities are bomb reduction of PuF_4, DOR, MSE, anode casting, ER, and pyroredox, and these techniques are integrated into a general processing flow diagram, such as the Los Alamos approach indicated in Fig. 7.9. As the figure shows, each operation produces residues that are treated either by pyrochemical or aqueous means to recover plutonium. We will discuss these pyrochemical processes in some detail.

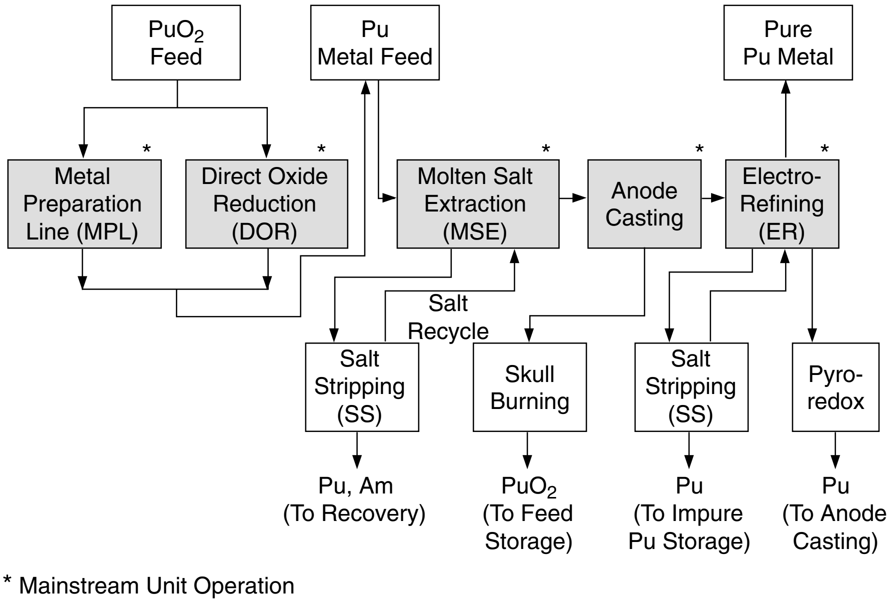

Fig. 7.9 *A general integrated pyrochemical processing system for plutonium metal preparation* (*Christensen* et al., 1988).

(a) Fluorination and reduction

The fluorination and reduction process produces plutonium metal from PuF_4 by the high-pressure reaction between the fluoride and calcium metal (Baker, 1946). Plutonium dioxide is converted to PuF_4 with HF in a hydrofluorination reaction, or by direct fluorination with F_2 (see Section 7.8.6.a). After fluorination of oxide, a chemical booster, such as iodine, initiates the reduction reaction:

$$PuO_2 + 4HF \rightarrow PuF_4 + 2H_2O \tag{7.17}$$

$$PuO_2 + 2F_2 \rightarrow PuF_4 + O_2 \tag{7.18}$$

$$PuF_4 + 3Ca^0 + I_2 \rightarrow Pu^0 + 2CaF_2 + CaI_2 \tag{7.19}$$

An illustration of a typical bomb reduction furnace is shown in Fig. 7.10. The PuF_4, calcium metal, and MgO (magnesia) slag are thoroughly mixed in a molded, open-porosity magnesia crucible. Iodine, added before the equipment is assembled and heated, acts as an initiator and reaction booster. At approximately 325°C, calcium and iodine react exothermically to rapidly raise the temperature. At 600°C, the PuF_4 reduction reaction begins and the system temperature rises rapidly to nearly 2000°C. The slag remains molten while the liquid plutonium sinks to the bottom of the crucible and solidifies. After the equipment has cooled, the crucible is broken to recover the metal button, which is mechanically separated from the slag (Christensen *et al.*, 1988). Little or no purification occurs during the process, and the metal purity is similar to that of the feed material. If the reagents are of high purity, and sufficiently pure plutonium feed is used, then the resulting metal is satisfactory for high-purity applications. Yields usually range from 97 to 99% (Baker and Maraman, 1960). This reaction can be carried out on a relatively large scale, and up to 6 kg batches of plutonium metal are not uncommon.

(b) Direct oxide reduction (DOR)

In the DOR process, plutonium dioxide is reduced with calcium metal to produce plutonium metal and calcium oxide (Mullins *et al.*, 1982; Mullins and Foxx, 1982; Christensen and Mullins, 1983). The reaction takes place in a molten $CaCl_2$ or $CaCl_2$–CaF_2 solvent, which dissolves the resulting CaO and allows the plutonium metal to coalesce in the bottom of the crucible to form a metal button. The PuO_2, calcium metal, and fused $CaCl_2$ are loaded into a vitrified magnesia crucible. The $CaCl_2$ is cast before use and contains no detectable water. The generic DOR apparatus is shown in Fig. 7.11 (Christensen and Mullins, 1983). The crucible is heated in a resistance furnace to 800°C. Once the $CaCl_2$ is molten, a Ta stirrer and a Ta–Ni thermocouple sheath are lowered in the melt. The reaction typically begins at about 820°C with a temperature

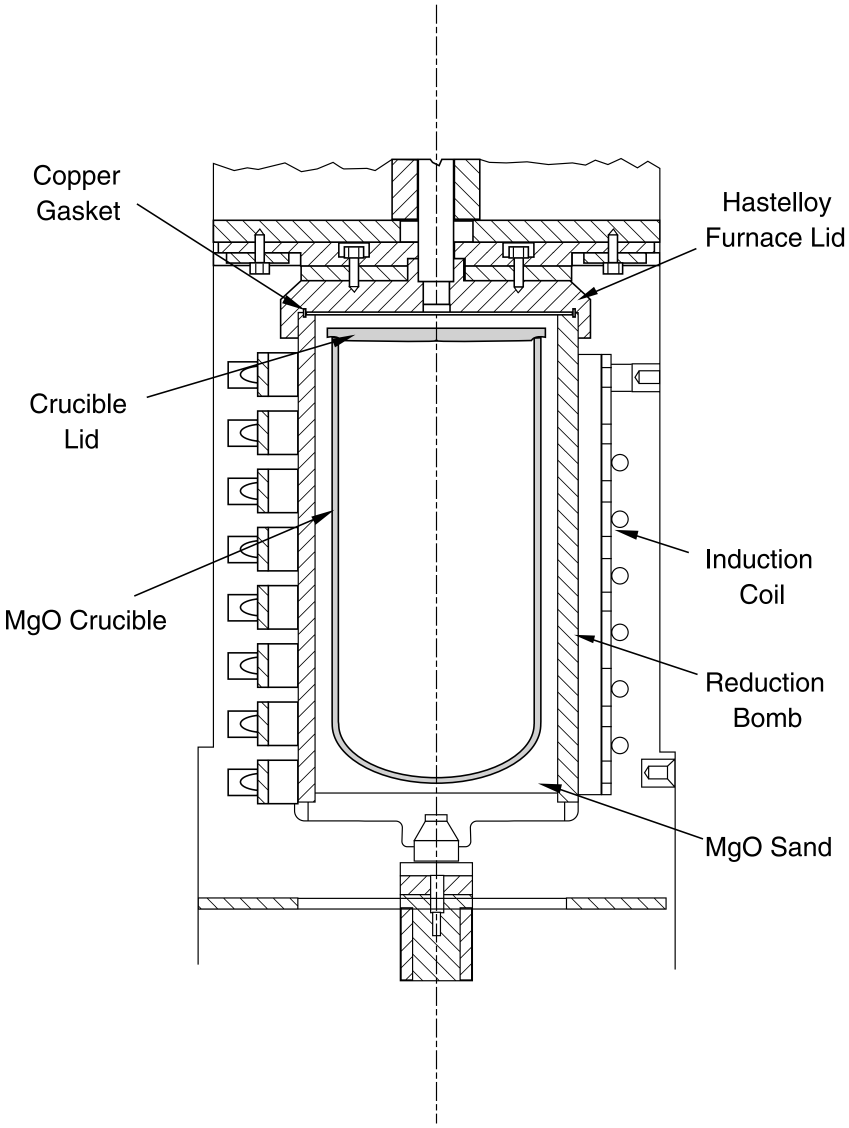

Fig. 7.10 *A furnace assembly for plutonium metal production by reduction of* PuF_4 (*Christensen* et al., 1988).

spike to 875°C. The reaction is complete within 15 min. The reaction proceeds to completion when excess calcium is present, sufficient $CaCl_2$ is available to dissolve the CaO that is produced, and rapid stirring is applied. While stirring, the reaction is monitored with a thermocouple. After completion of the

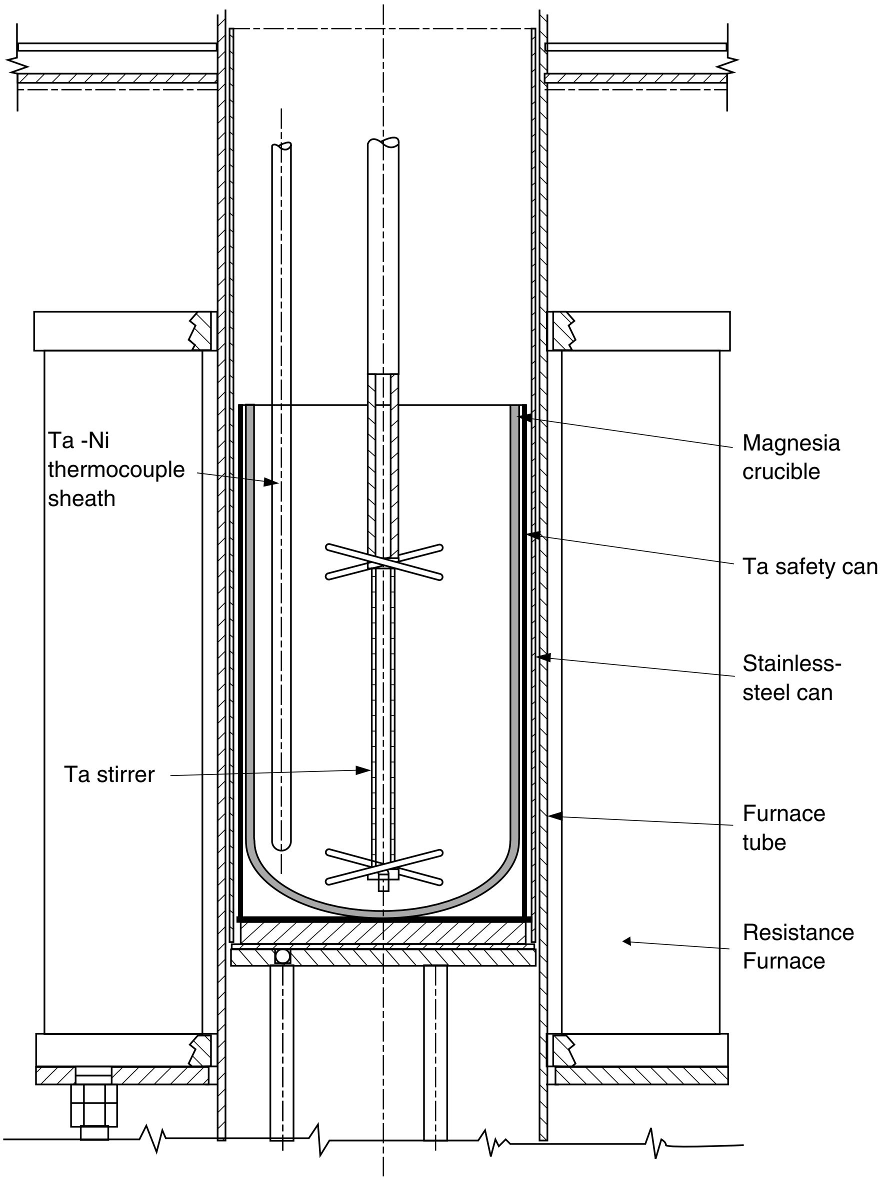

Fig. 7.11 *A general furnace assembly for direct oxide reduction* (*DOR*), *molten salt extraction of americium* (*MSE*) *and pyroredox operations* (*Christensen* et al., 1988).

reaction, the thermocouple well and stirrer are retracted, and the melt is allowed to settle and cool. Almost all the plutonium forms a metal button at the bottom of the crucible, and a typical DOR reaction product is shown in Fig. 7.12. The salt immediately above the button contains a layer of metal shot, and the bulk of

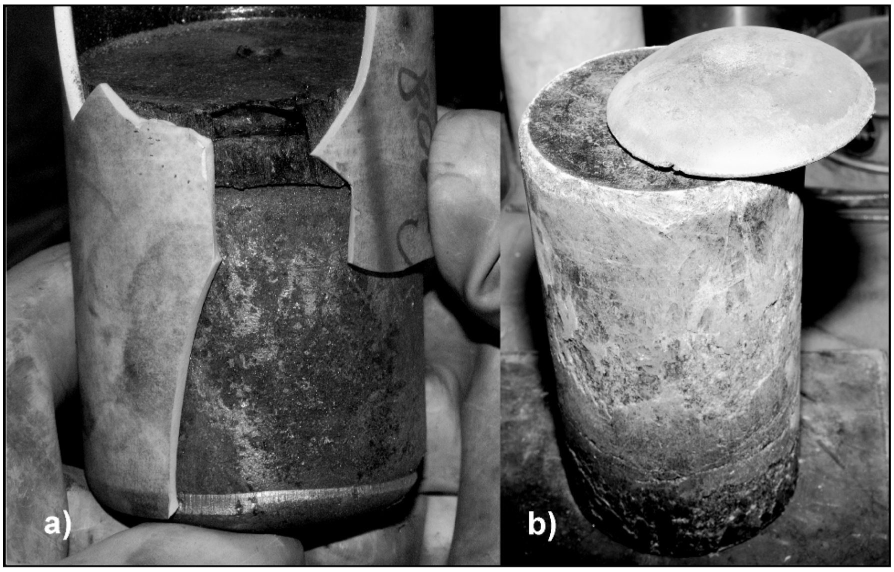

Fig. 7.12 (*a*) *A photograph of a DOR breakout showing the MgO crucible, residues, and metal product at the bottom.* (*b*) *The DOR metal button* (*top*) *and residues* (*photographs courtesy of Los Alamos National Laboratory*).

the salt solidifies above the metal. The plutonium button is mechanically separated, and the shot is recovered by reheating the shot-rich (usually with calcium present) material above the melting point to consolidate the metal. Product yields are greater than 95% (Mullins *et al.*, 1982).

(c) Molten salt extraction (MSE)

The plutonium metal produced in PuF_4 and PuO_2 reduction is impure and needs to be refined. The MSE process is specifically designed to reduce the americium content of plutonium metal (^{241}Am spontaneously grows into plutonium as a result of ^{241}Pu β-decay), but it also separates the more reactive elements, such as rare-earths, alkali-metals, and alkaline-earth metals (Knighton and Steunenberg, 1965; Knighton *et al.*, 1976; Coops *et al.*, 1983). The general principle of MSE is to oxidize the americium to Am(III) to extract it into the salt phase, leaving plutonium in the metallic phase. The extraction procedure is identical to the DOR process and uses essentially the same apparatus shown in Fig. 7.11, with the exception that a reusable tantalum vessel replaces the magnesia crucible, an oxidant is added, and the stirring time is typically 30 min instead of only a few minutes. To run the reaction, workers place impure plutonium metal in contact with a ternary salt, consisting of

$MgCl_2$ as the oxidizing agent in a NaCl/KCl eutectic. The major reactions are (Mullins *et al.*, 1968; Leary and Mullins, 1974):

$$2Am^0 + 3MgCl_2 \rightarrow 2AmCl_3 + 3Mg^0 \tag{7.20}$$

$$2Pu^0 + 3MgCl_2 \rightarrow 2PuCl_3 + 3Mg^0 \tag{7.21}$$

$$Am^0 + PuCl_3 \rightarrow AmCl_3 + Pu^0 \tag{7.22}$$

A typical batch size is 4.5 kg with a 12-h temperature cycle to 750°C. (The actual reaction time is only 30 min.) After the equipment has cooled to room temperature, the fused salt containing the americium and other impurities is separated from the plutonium metal button and crucible. Usually, each feed button goes through two batch extractions. In a typical 4.5-kg run containing 3000 ppm americium, 90% of the americium is oxidized at the expense of ca. 100 g plutonium. A typical product weighs 4.4 kg and contains 98% of the feed plutonium (Christensen and Mullins, 1983; Christensen *et al.*, 1988).

(d) Vacuum melting and casting

After the americium is extracted from the impure metal, the plutonium metal must be cast into a cylindrical geometry that is compatible with the ER cell (Anderson and Maraman, 1962). The ER operation is typically carried out with 6 kg of plutonium, in which case the high-density α phase must be avoided due to nuclear criticality concerns. This requires alloying with sufficient gallium to bring the density from >19 to <16.5 g cm^{-3}. Casting is accomplished by mixing about 6 kg of impure metal with an appropriate amount of gallium in a tantalum pour crucible as shown in Fig. 7.13 (Christensen *et al.*, 1988). The metal and gallium mix upon melting and are bottom-poured from the tantalum crucible into a graphite mold. A casting residue, or "skull", always forms and contains light element impurities, oxide films (thorium, americium, alkali metals, alkaline-earth, and rare-earth metals) or other high melting contaminants. A typical ingot is shown in Fig. 7.14 with yields generally averaging more than 90%.

(e) Electrorefining (ER)

In the ER process, liquid plutonium oxidizes from the anode ingot into a molten-salt electrolyte (Mullins *et al.*, 1960, 1963a,b, 1982; Mullins and Leary, 1965; Mullins and Morgan, 1981). The resulting Pu(III) ion is transported through the salt to the cathode, where it is reduced back to metal. The process is carried out at 740°C in a molten salt consisting of an equimolar mixture of NaCl/KCl containing a small amount of $MgCl_2$ as an oxidizing agent. The $MgCl_2$ reacts with the impure plutonium metal to charge the electrolyte with Pu(III) before a current is passed and ensures the initial reduction of plutonium at the cathode.

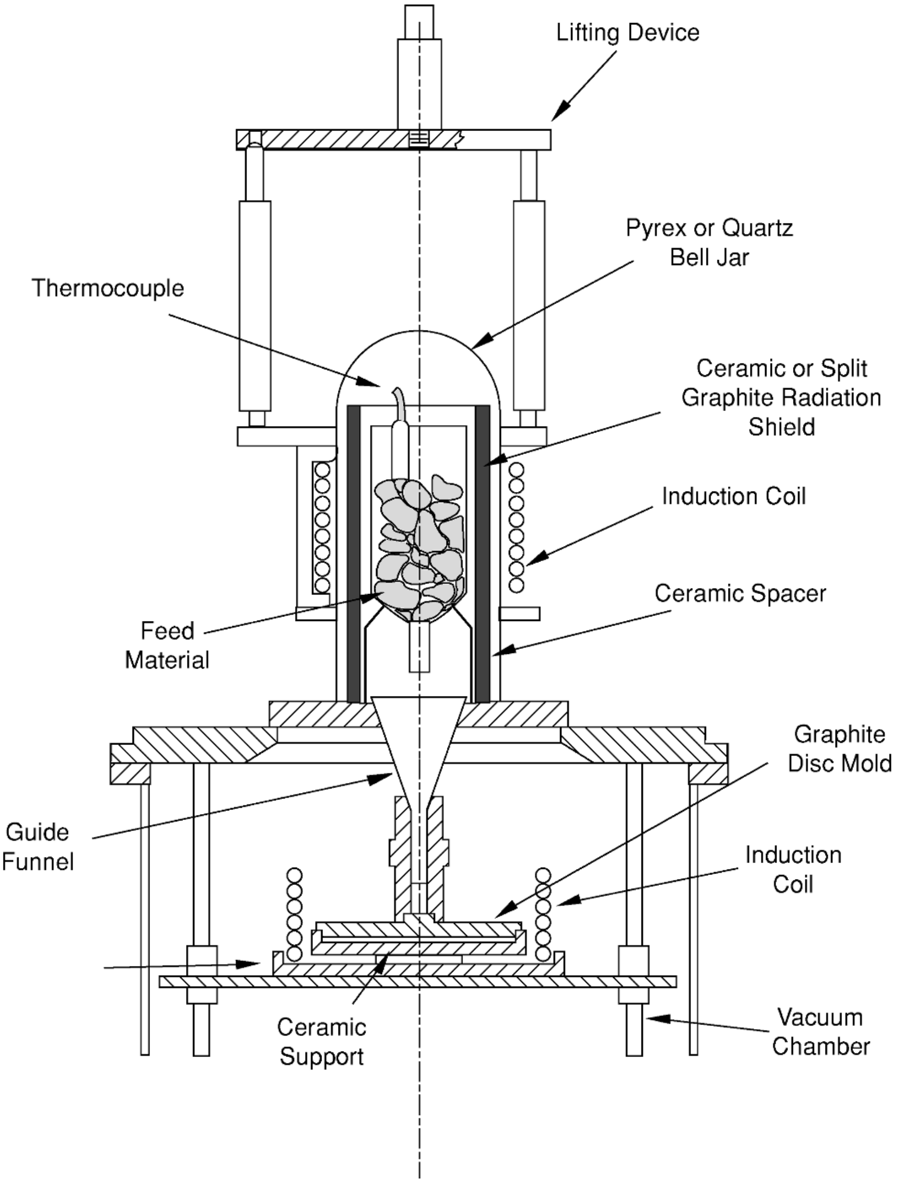

Fig. 7.13 *A general furnace assembly for vacuum casting of plutonium metal* (*Christensen* et al., 1988).

The process is performed in a double-cupped, vitrified magnesia crucible as shown in Fig. 7.15 (Mullins and Morgan, 1981). The inner cup contains the impure metal ingot that serves as the anode material. The electrolyte salt casting is placed on top of the ingot. The crucible is placed inside a tantalum safety can

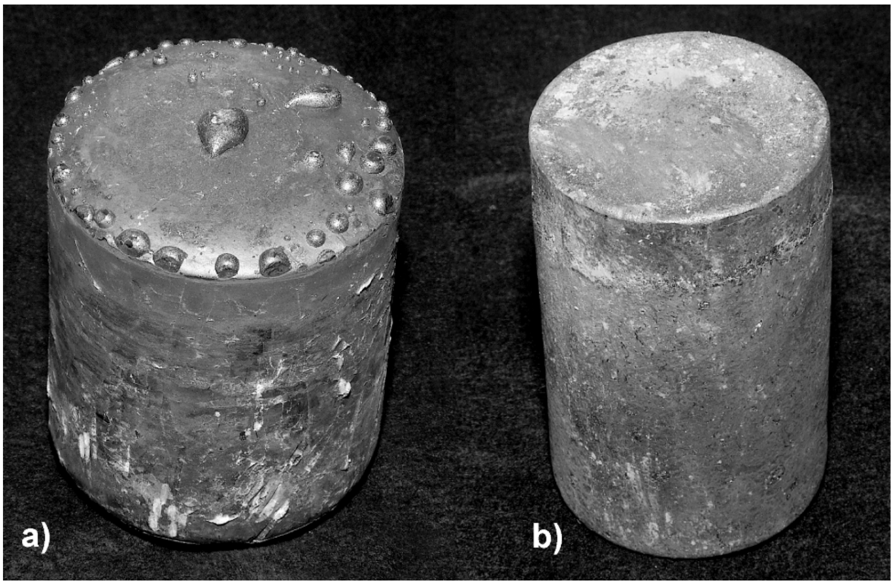

Fig. 7.14 *Photographs of plutonium ingots from vacuum casting.* (*a*) *Metal feed for electrorefining, and* (*b*) *for double electrorefining* (*photographs courtesy of Los Alamos National Laboratory*).

and placed inside the furnace. The assembly is heated using a resistance furnace (the entire assembly is shown in Fig. 7.16). A tantalum or vitrified magnesia stirrer stirs both the impure metal and the molten salt electrolyte. A tungsten rod is suspended in the impure metal pool to serve as the anode rod, and electrically insulated from the salt by a magnesia sleeve. A cylindrically shaped sheet of tungsten is suspended in the annular space between the two cups and serves as the cathode. Stirring and passing a dc current between the anode and cathode accomplish the process. Plutonium oxidizes at the anode and reduces back to metal at the cathode. The liquid metal drips off the cathode and into the annular space. After cooling to room temperature, the cell is broken apart and the plutonium recovered as an annular metal casting, or 'ER ring,' as shown in Fig. 7.17. The product yield from a Pu-1 wt % Ga alloy is greater than 80%. Approximately 10% of the residual plutonium remains in the anode as a very impure anode heel. The rest of the plutonium remains in the salt either as uncoalesced metal shot or as Pu(III), both of which can be recovered and recycled.

(f) Pyroredox or anode recovery

The pyroredox process recovers the plutonium from impure scrap materials and has found application in recovering plutonium from the spent anode heels from

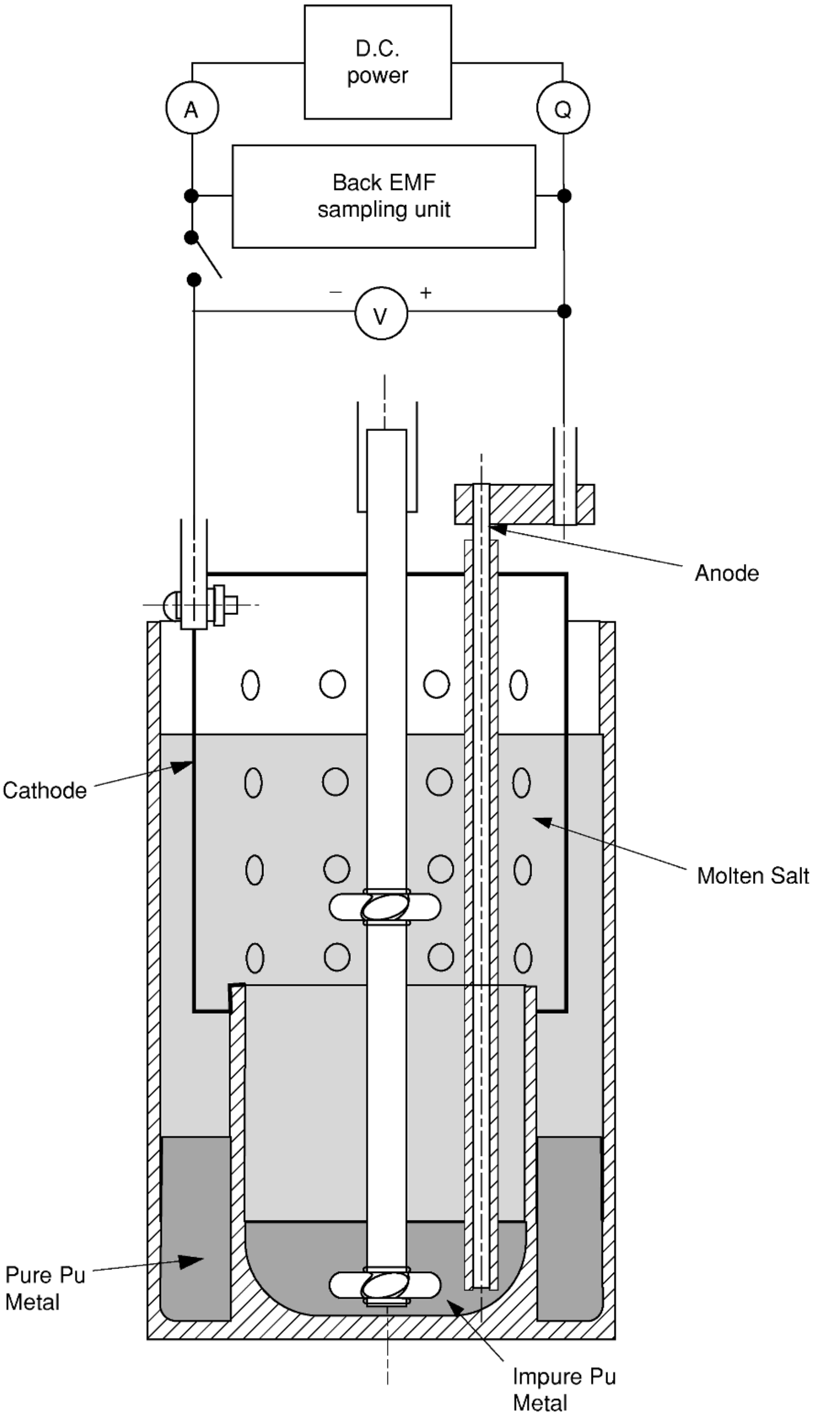

Fig. 7.15 *A general schematic of an electrorefining* (*ER*) *cell showing major features* (*Christensen* et al., 1988).

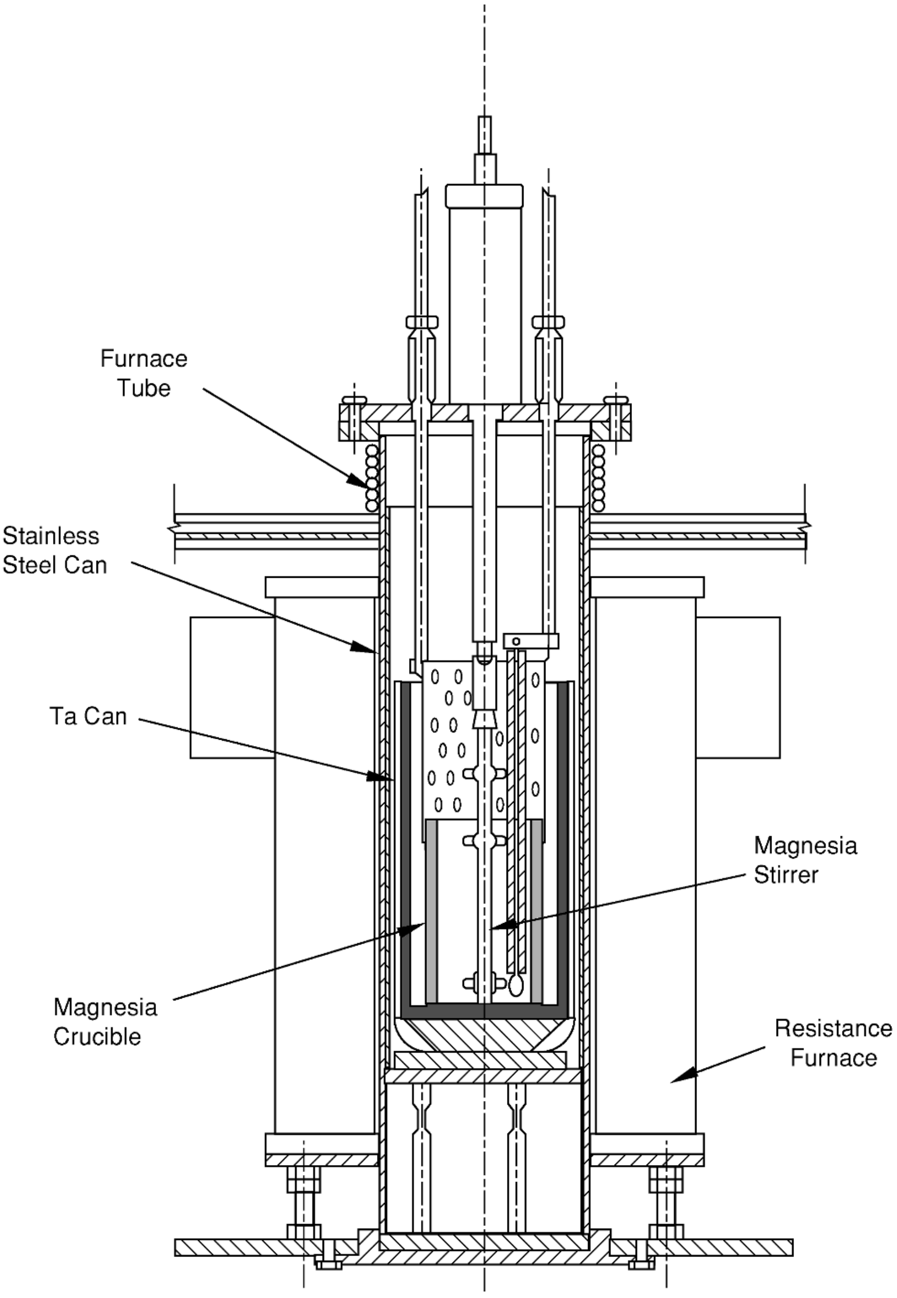

Fig. 7.16 *A general schematic of an electrorefining* (*ER*) *furnace apparatus showing major features* (*Christensen* et al., 1988).

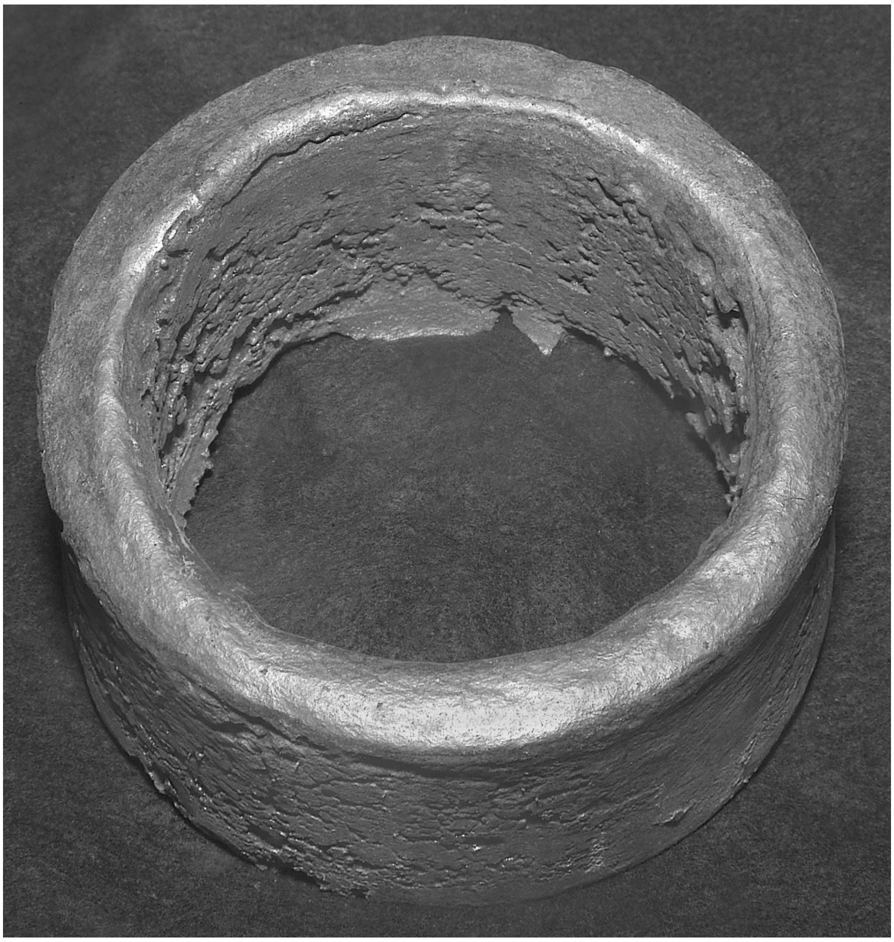

Fig. 7.17 *Photograph of a plutonium product ring from electrorefining* (*ER*) (*photograph courtesy of Los Alamos National Laboratory*).

the ER process (Baldwin and Navratil, 1983; Coops *et al.*, 1983; McNeese *et al.*, 1986; Christensen *et al.*, 1988). The process equipment is identical to that used in DOR (Fig. 7.11). In the pyroredox process, workers initially polish the spent anode with calcium to ensure that all the plutonium is present as metal. The metal is then oxidized to Pu(III) with $ZnCl_2$ dissolved in KCl at 750°C with stirring. After an hour, the mixture is heated to 850°C to promote phase separation. In addition to plutonium, all other elements more active than zinc are oxidized into the salt phase. This process forms a zinc button that may be mechanically separated from the salt and discarded. For the reduction step, the salt containing $PuCl_3$ is crushed and mixed with a $Ca/CaCl_2$ mixture, pressed into an ingot, and placed back into a magnesia crucible and inserted into the furnace assembly. The vessel is heated to 850°C with stirring, and then allowed to cool after removing the stirrer. The chemical reactions are:

$$2Pu^0 + 3ZnCl_2 \rightarrow 2PuCl_3 + 3Zn^0 \qquad (7.23)$$

$$2PuCl_3 + 3Ca^0 \rightarrow 2Pu^0 + 3CaCl_2 \qquad (7.24)$$

The reaction product is a salt phase above a two-phase metal button. The salt phase is mechanically separated and discarded. The bottom, denser metal phase is composed of plutonium and small quantities of calcium and zinc. The upper phase is typically 50% plutonium with the remainder being primarily zinc. Several buttons are allowed to coalesce at 850°C for 6 h to separate the ingots into a plutonium-rich lower phase suitable for ER and a less-pure upper phase that is recycled back to the oxidation step.

(g) Zone-refining of small research samples

Plutonium metal that has been doubly electrorefined is considered of high purity for most applications but still contains small amounts of Fe, U, Mg, Ca, Ni, Al, K, Si, O, C, and H. For small-scale research applications, it can be further purified via levitation zone-refining using a floating molten zone to minimize introduction of impurities from crucible materials. Tate and Anderson (1960) originally observed the phenomenon when they reported that zone melting promoted a reduction of impurity elements within a plutonium rod. Spriet (1965) conducted a more detailed investigation to include quantification of rates and impurity analyses. In more recent work, levitation zone-refining in concert with levitation distillation at reduced pressure has proven to be quite successful at producing ultrahigh purity specimens (Blau, 1998; Lashley *et al.*, 1999). Levitation zone-refining targets metals and metalloids while levitation vacuum-distillation targets daughter products and gases. In the levitation apparatus, radio frequency (rf) power-induced electric current flows into a crucible while the crucible acts as a transformer, inducing a current in the opposite direction to the current in the crucible. Magnetic fields in the crucible and the plutonium are opposed, causing repulsion and levitation of the plutonium a small distance from the crucible walls. Magnetic levitation of plutonium metal rods between 700 and 1000°C enables purification while eliminating plutonium-crucible interactions and minimizing the contact with other elements. The magnetic levitation is the fundamental operating basis for both the zone-refining apparatus and the distillation apparatus.

The zone-refining process involves casting a rod of unalloyed plutonium and then serially passing a molten zone through the rod in one direction at a slow rate. Impurities travel in the same or opposite direction to the direction of motion of the zone, depending on whether it lowers or raises the melting point of the plutonium. Consequently, impurities are swept and become concentrated in the ends of the rod, thereby leaving the remainder purified. The degree of separation approaches an infinitesimal limit as the number of passes increases. Recent work has shown that ten passes through a molten zone can result in the reduction of impurities in double-electrorefined and vacuum-cast unalloyed plutonium from 727 to 184 ppm through levitation zone-refining (Blau, 1998; Lashley *et al.*, 1999).

Since americium exhibits a high vapor pressure relative to plutonium it is possible to remove ^{241}Am daughters from plutonium samples via vaccum distillation. The ^{241}Am is separated when plutonium metal is heated to the liquid state under reduced pressure (10^{-7} Torr). The molten plutonium is levitated while ^{241}Am is distilled off and condensed onto a cold finger. The plutonium is cooled and solidifies. Recent results from levitation distillation show that the concentration of ^{241}Am was reduced from 1100 to 500 ppm (Lashley *et al.*, 1999). These general principles have been combined into a floating zone refining followed by an *in situ* distillation, alloying, and casting technique for high-purity research samples of δ-Pu. In the procedure, a mixture of α-Pu is first levitation zone-refined. The α-Pu and gallium are then added to a levitation crucible. The mixture is heated to the melt while suspended in a magnetic levitation field. As the gallium mixes with the plutonium in the melt, it will stabilize the δ phase upon solidification. While in the melt, ^{241}Am is distilled from the plutonium and collected on a water-cooled condenser. Next, the furnace power is reduced, and plutonium is cast directly from the electromagnetic field into a ceramic mold. The apparatus is illustrated in Fig. 7.18.

7.7.3 Phase stability – allotropes, crystal structures, and transformations

It is important to understand the different allotropic phases of plutonium and the limits of stability with temperature, pressure, chemical additions, and time. We describe the stability of unalloyed plutonium along with the characteristics of its phases as a function of temperature and pressure in this section. We deal with the effects of chemical additions and time subsequently.

C. S. Smith and his Manhattan Project team of metallurgists and chemists were the first to come to grips with the unstable nature of this enigmatic element (Hammel, 1998). During their initial work in 1944, they routinely found the densities of their freshly prepared plutonium samples to vary by more than a factor of two. They quickly determined that unalloyed plutonium has at least five allotropes (a sixth was eventually found) over a very narrow temperature range and that it exhibits large volume changes at the various phase transitions during cooling from the melt, making it difficult to cast. Smith soon found that most of the transformations and the large volume changes could be avoided by alloying pure plutonium with a few atomic percent aluminum or gallium. Such alloying additions retained the high-temperature face-centered cubic (fcc) δ-phase, which is less dense, weak, and ductile, in contrast to the typical room temperature α-phase, which is very dense, strong, and brittle. The profound influence of chemical additions to plutonium on phase stability and the

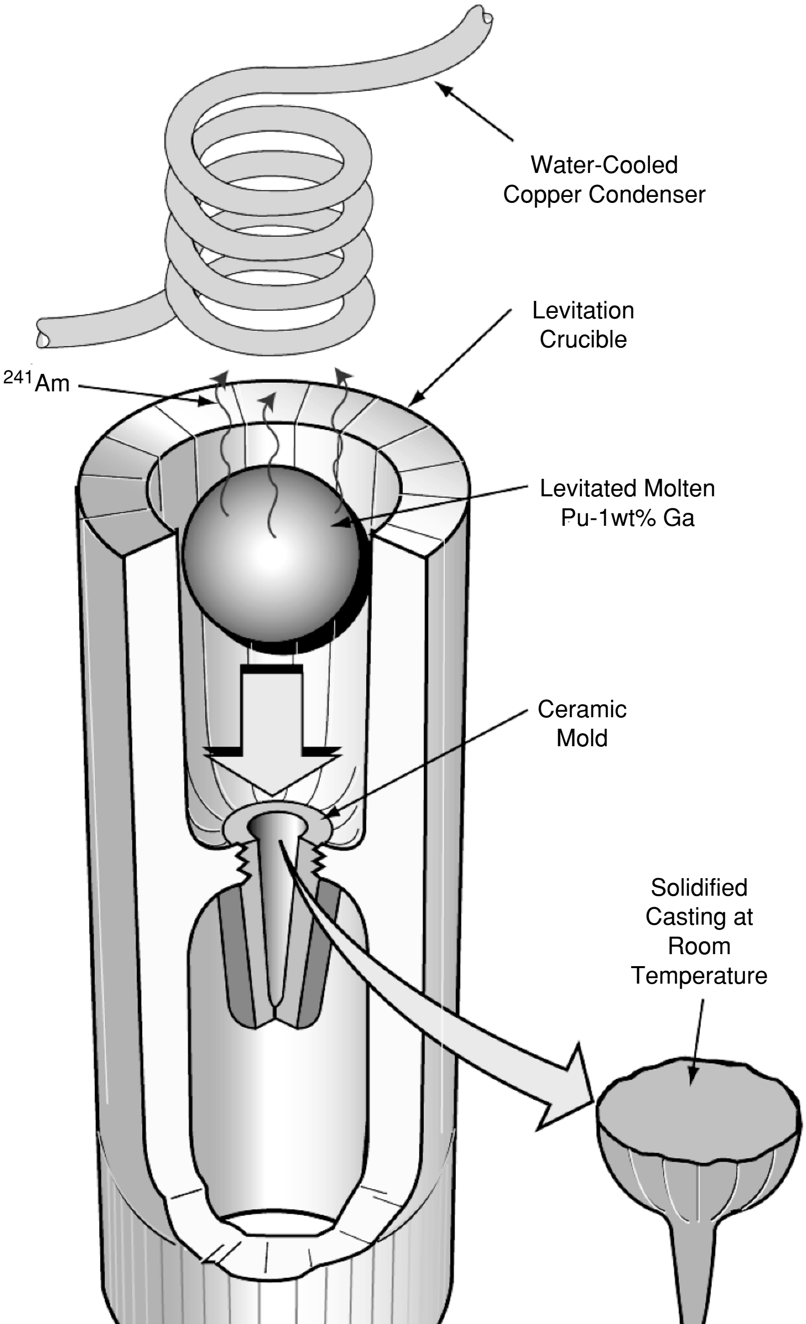

Fig. 7.18 In situ *americium distillation, alloying, and chill casting apparatus* (*Lashley* et al., 1999).

dramatic differences in properties exhibited by the different plutonium allotropes must be kept firmly in mind when considering plutonium and its properties. Moreover, phase transformations between the different allotropes are difficult to avoid during sample preparation, especially if samples are heated, cooled, worked, ground, or polished.

Zachariasen (1944) was the first to suggest that the large density and property variations in the early separated plutonium samples were due to crystallographic modifications of plutonium. Five solid allotropes designated by the Greek symbols α, β, γ, δ, and ϵ were identified during the early studies. A sixth, designated by the symbol δ', was discovered in 1954 by Cramer (Cramer *et al.*, 1961) in high-purity plutonium. An idealized thermal expansion curve is shown for pure plutonium in Fig. 7.19 (Miner and Schonfeld, 1980), along with the crystal structures and densities of the solid phases and the liquid phase. The stability ranges and crystal structure data for the individual allotropes are shown in Table 7.9. The transformation temperatures of the α, β, and γ phases are only approximate because the transformations are kinetically sluggish. The limits represent the approximate transformation temperatures as obtained by dilatometry and thermal analysis at slow heating or cooling rates of 1 to 1.5°C min^{-1}. The actual heating and cooling curves show significant hysteresis.

The data shown in Fig. 7.19 and Table 7.9 demonstrate the idiosyncratic behavior of plutonium. The six solid allotropes at ambient pressure (a seventh was found under pressure by Morgan (1970)) are the most of any element in the periodic table. Plutonium has an unusually low melting point of 640°C, and it contracts upon melting. The maximum density difference between the phases is a very large 20%. Moreover, the classical close-packed fcc phase is the least dense (less dense than the liquid). The two low-temperature phases are low-symmetry monoclinic structures, atypical of metals. The thermal expansion coefficients of these phases are very large and positive, whereas that of the fcc phase is negative.

The low-density, high-temperature phases of plutonium are easily transformed to the higher density phases under hydrostatic pressure as shown in Fig. 7.20 (Liptai and Friddle, 1967). Morgan (1970) clearly demonstrated the existence of a seventh phase at high pressure, designated ζ phase, as shown in Fig. 7.21. Its structure has yet to be determined. Elliott (1980) pointed out the similarity of the new ζ phase to the η phase in the Pu–U and Pu–Np systems. As shown in Fig. 7.20, at 3.0 GPa the ζ phase and all other high-volume phases collapse to the two low-temperature α and β allotropes.

The low-symmetry monoclinic ground-state α phase of plutonium results from the peculiar nature of the 5f electron bonding in plutonium as discussed below. Zachariasen and Ellinger (1957, 1963a) and Zachariasen (1961a) demonstrated that the α phase is a simple monoclinic crystal structure ($P2_1/m$) with 16 atoms per unit cell and eight unique atom positions. All 16 atoms lie in the reflection planes with coordinates $\pm(x,\frac{1}{4},z)$. Several views of the crystal structure of α plutonium are shown in Fig. 7.22. The 16 structural parameter values

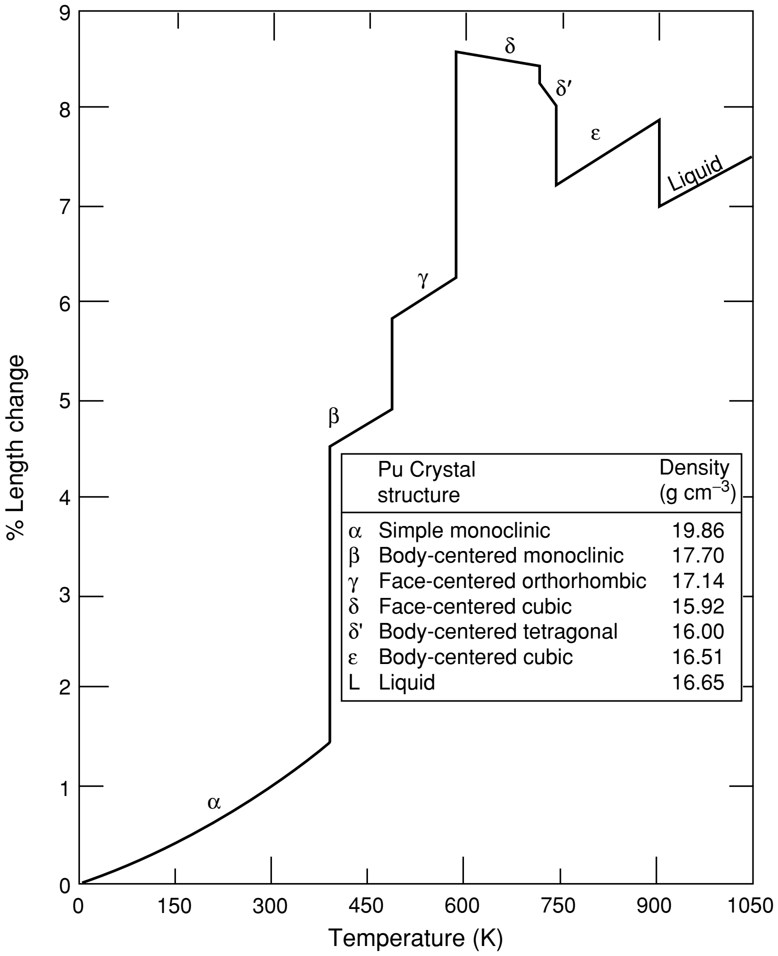

	Pu Crystal structure	Density (g cm^{-3})
α	Simple monoclinic	19.86
β	Body-centered monoclinic	17.70
γ	Face-centered orthorhombic	17.14
δ	Face-centered cubic	15.92
δ'	Body-centered tetragonal	16.00
ε	Body-centered cubic	16.51
L	Liquid	16.65

Fig. 7.19 *Thermal expansion of unalloyed plutonium. This idealized curve was generated by Schonfeld and Tate* (1996) *based on the best available expansion data. Of particular relevance is the correction to the α-Pu thermal expansion, as detailed in Fig.* 7.44.

are listed in Table 7.10 along with the bond lengths. The monoclinic structure of α plutonium is a slight distortion from a hexagonal lattice. This similarity was used by Crocker (1971) in modeling the crystallographic relationships of phase transformations involving the α phase. In addition, the bonding characteristics of the eight atom positions are markedly different. Position 1 has the greatest number of short bonds, whereas position 8 has the fewest short bonds (as shown in Table 7.11). All positions have the same point symmetry. The bonding characteristics are important in determining how the α phase accommodates

Table 7.9 *Crystal structure data for plutonium.*

Phase	*Stability range* (K)	*Crystal lattice and space group*	*Unit cell dimensions* (Å)	*Atoms per unit cell*	*X-ray density* (g cm^{-3})	*Transformation temperature* (K)[b]
α	below 397.6	simple monoclinic P2_1/*m*	at 294 K $a = 6.183(1)$ $b = 4.822(1)$ $c = 10.963(1)$ $\beta = 101.79°(1)$	16	19.85	
β	397.6 – 487.9	body-centered monoclinic I2/*m*[a]	at 463 K $a = 9.284(3)$ $b = 10.463(4)$ $c = 7.859(3)$ $\beta = 93.13°(3)$	34	17.71 (α→β)	397.6
γ	487.9 – 593.1	face-centered orthorhombic F*ddd*	at 508 K $a = 3.159(1)$ $b = 5.768(1)$ $c = 10.162(2)$	8	17.15 (β→γ)	487.9
δ	593.1 – 736.0	face-centered cubic F*m*3*m*	at 593 K $a = 4.6371(4)$	4	15.92 (γ→δ)	593.1
δ′	736.0 – 755.7	body-centered tetragonal I4/*mmm*	at 738 K $a = 3.34(1)$ $c = 4.44(4)$	2	16.03 (δ→δ′)	736.0
ϵ	755.7 – 913.0	body-centered cubic I*m*3*m*	at 763 K $a = 3.6361(4)$	2	16.51 (δ′→ϵ) m.p.	755.7 913.0

[a] Although space group I2/*m* is not one of the 'standard' space groups tabulated in the International Union of Crystallography, *International Tables for X-ray Crystallography*, vol. 1, Kynoch Press, Birmingham, its notation is retained to obtain a β angle of approximately 90° (data from Miner and Schonfeld, 1980).

[b] Data from Lemire *et al.* (2001). The reader is cautioned that the transformation temperatures vary between sources, and are sensitive to heating and cooling rates and metal purity.

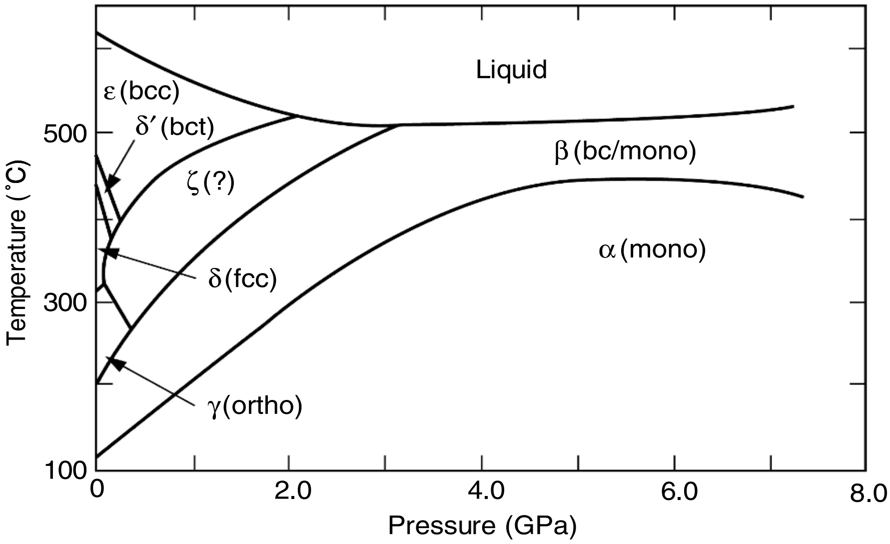

Fig. 7.20 *Pressure–temperature phase diagram of unalloyed plutonium from Liptai and Friddle* (1967).

impurity atoms. Lawson *et al.* (1996) pointed out that with eight unique atom positions, α plutonium looks like a self-intermetallic, much like α manganese. The low-symmetry monoclinic structure of the α phase has a profound influence on its properties; it has no macroscopic ductility, and most properties are highly directional.

The β phase is a body-centered monoclinic (*I2/m*) and equally complex. The atomic coordinates, the structural parameters, and the bond lengths are shown in Table 7.12 (Zachariasen and Ellinger, 1963b). It is considerably less dense than the α phase (17.7 g cm^{-3} compared to 19.85 g cm^{-3}), and it has 34 atoms per unit cell with seven unique atom positions. Properties are also quite anisotropic. The crystal structure of the β phase is compared to the other five allotropes in Fig. 7.23.

The γ phase is a face-centered orthorhombic (*Fddd*) with eight equivalent atoms per unit cell and a density of 17.14 g cm^{-3} (Zachariasen and Ellinger, 1955, 1959; Crocker, 1971). Each atom has four neighbors at 3.026 Å, two at 3.159 Å, and four at 3.228 Å. Roof (cited by Miner and Schonfeld, 1980) pointed out that placing the origin at the center of symmetry places the positions of the eight atoms of the unit cell at ± (1/8,1/8,1/8) + (0,0,0; 0,½, ½; ½,0, ½; ½,½,0). The crystal structure of the γ phase is shown along with the other allotropes in Fig. 7.23.

The δ phase is fcc (*Fm3m*) with four equivalent atoms per unit cell as shown in Fig. 7.23. It is the least dense of the plutonium allotropes at 15.92 g cm^{-3}. Each

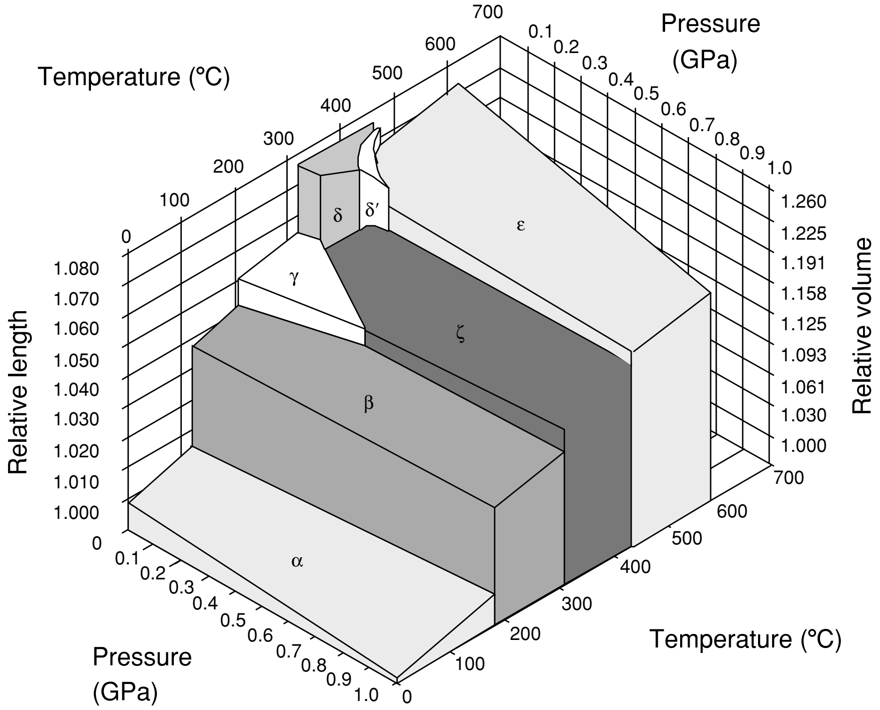

Fig. 7.21 *Pressure–temperature phase diagram from Morgan* (1970) *showing the existence of a seventh phase, ζ.*

atom has 12 neighbors at 3.279 Å in the standard fcc arrangement (0,0,0; 0,½,½; ½,0,½; ½,½,0). The δ′ phase is described by Ellinger (1956) as body-centered tetragonal (*I4/mmm*) with two atoms per unit cell at (0,0,0) and (½,½,½), with a density of 16.00 g cm^{-3}. He pointed out that the structure can be alternatively described as a face-centered tetragonal cell containing four atoms per unit cell, derived from the close-packed arrangement by a slight compression along the [001] direction. The ϵ phase is body-centered cubic (bcc) (*Im3m*) with two equivalent atoms per unit cell at (0,0,0) and (½,½,½). Each atom has eight neighbors at 3.149 Å.

As shown in Figs. 7.20 and 7.21, a seventh solid allotrope, the ζ phase, appears with the application of hydrostatic pressure at elevated temperatures. Very little is known about the precise crystal structure of this phase. However, Elliott (1980) suggested a similarity of this structure with the η phase of the PuU and PuNp systems.

The local coordination and interatomic distances for the four higher-temperature allotropes are shown in Table 7.13. Based on the crystal structure

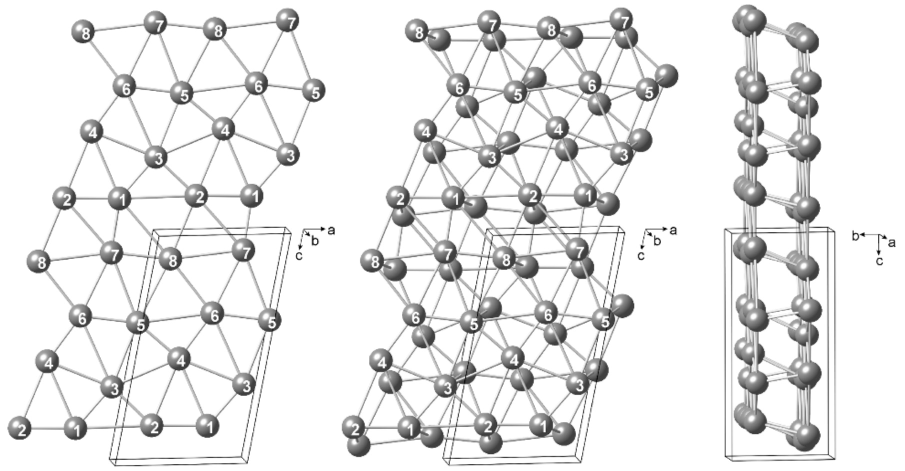

Fig. 7.22 *Several views of the monoclinic α-phase structure of plutonium with* 16 *atoms per unit cell and eight different atom positions.*

Table 7.10 *Structural parameters and bond lengths for α plutonium* (*Miner and Schonfeld*, 1980).

			Short bonds (Å)		*Long bonds* (Å)		*All bonds* (Å)	
Atom	*x*	*z*	*No.*	*Range*	*No.*	*Range*	*No.*	*Mean*
1	0.345(4)	0.162(2)	5	2.57–2.76	7	3.21–3.71	12	3.10
2	0.767(4)	0.168(2)	4	2.60–2.64	10	3.19–3.62	14	3.21
3	0.128(4)	0.340(3)	4	2.58–2.66	10	3.24–3.65	14	3.18
4	0.657(5)	0.457(3)	4	2.58–2.74	10	3.26–3.42	14	3.13
5	0.025(5)	0.618(3)	4	2.58–2.72	10	3.24–3.51	14	3.19
6	0.473(4)	0.653(2)	4	2.64–2.74	10	3.21–3.65	14	3.22
7	0.328(4)	0.926(2)	4	2.57–2.78	10	3.30–3.51	14	3.15
8	0.869(4)	0.894(2)	3	2.76–2.78	13	3.19–3.71	16	3.32

Table 7.11 *Bond characteristics for the eight different atom positions in the α-plutonium structure.*

Atom	*Short bonds*[a]	*Average length* (Å)
1	5	2.67
2–7	4	2.64
8	3	2.77

[a] The short bonds range from 2.57 to 2.78 Å and the long bonds from 3.19 to 3.71 Å. The point symmetry is the same for all eight atom positions.

Table 7.12 *Structural parameters for β plutonium* (*Zachariasen and Ellinger*, 1963*b*).

			Crystallographic parameters			*Bond lengths*			
Type	*No.*	*General atom positions*	*x*	*y*	*z*	*No.*	*Short bonds* (Å)	*No.*	*Long bonds* (Å)
1	2	(0, 0, 0)	0	0	0	4	2.97	8	3.15–3.26
2	4	±(x, 0, z)	0.146(4)	0	0.387(5)	3	3.03–3.10	11	3.26–3.55
3	4	±(x, 0, z)	0.337(4)	0	0.082(5)	4	2.79–3.03	9	3.15–3.43
4	4	±(x, 0, z)	0.434(4)	0	0.672(5)	4	2.79–3.01	8	3.16–3.48
5	4	±(1/2, y, 0)	0.500	0.220(3)	0	4	2.80–2.84	10	3.36–3.63
6	8	±(x, y, z), (x, $\bar{y}$, z)	0.145(3)	0.268(2)	0.108(3)	4	2.91–3.10	10	3.16–3.55
7	8	±(x, y, z), (x, $\bar{y}$, z)	0.167(3)	0.150(2)	0.753(4)	5	2.59–3.05	7	3.14–3.63

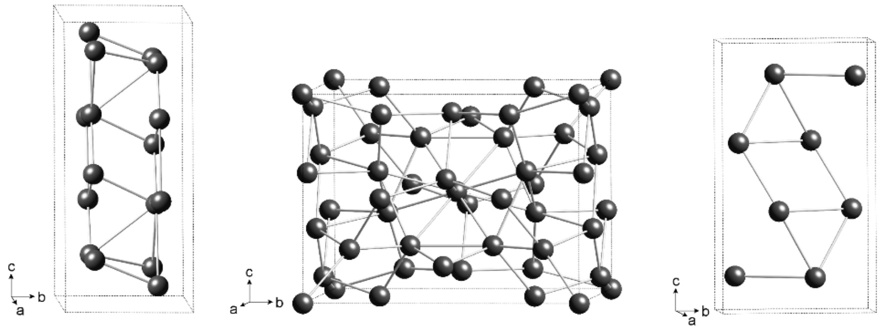

α - simple monoclinic β - body-centered monoclinic γ - face-centered orthorhombic

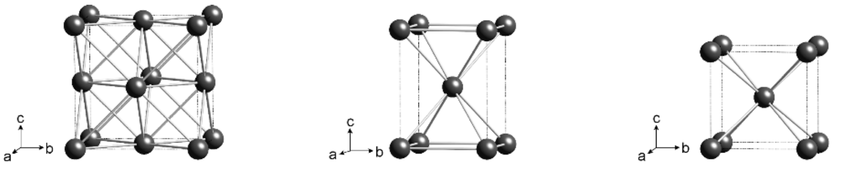

δ - face-centered cubic δ′ - body-centered tetragonal ε - body-centered cubic

Fig. 7.23 *Crystal structures of all six solid phases of plutonium.*

information presented above, Zachariasen (1961b, 1973) derived metallic radii by normalizing the radii to coordination number 12 and extrapolating the high-temperature data to room temperature. His results are shown in Table 7.14. Zachariasen and others also calculated the valences for the plutonium allotropes. We do not present these here because we do not consider these estimates to be useful in considering the complexity of the f-electron bonding. We also list Dormeval's (2001) compilation of atomic volumes for the various allotropes in Table 7.14.

The liquid phase of plutonium is denser than the three highest-temperature solid phases. Density as a function of temperature is listed in Table 7.15, based on the work of Herrick *et al.* (1959) and Serpan and Wittenberg (1961). Extrapolation of the data in Table 7.15 yields a density of 16.65 g cm^{-3} at the melting point of 640°C. Hence, plutonium contracts approximately 2.5% upon melting. Plutonium liquid has a high surface tension and high viscosity.

The transitions (or, in metallurgical terms, phase transformations) between the various allotropes are important. Most studies of such transformations in unalloyed plutonium were conducted before 1970. A typical thermal expansion curve from Goldberg and Massalski (1970) for high-purity, electrorefined plutonium heated and cooled at 4.5°C min^{-1} is shown in Fig. 7.24. The sluggish nature of the transformation among the lower temperature phases results in

Table 7.13 *Coordination and interatomic distances of the higher plutonium allotropes* (*Ellinger* et al., 1956).

Phase	*Symmetry*	*Coordination*	*Distance* (Å)	*Effective coordination number*	*Average distance* (Å)	*Temperature* (°C)
γ	orthorhombic	Pu–4Pu	3.021	10	3.155	210
		Pu–2Pu	3.160			
		Pu–4Pu	3.286			
		Pu–4Pu	3.026	10	3.157	235
		Pu–2Pu	3.159			
		Pu–4Pu	3.288			
		Pu–4Pu	3.041	10	3.165	310
		Pu–2Pu	3.154			
		Pu–4Pu	3.294			
δ	face-centered cubic	Pu–12Pu	3.279	12	3.279	320
		Pu–12Pu	3.275	12	3.275	440
δ′	body-centered tetragonal	Pu–8Pu	3.249	12	3.275	465
		Pu–4Pu	3.327			
		Pu–8Pu	3.239	12	3.275	485
		Pu–4Pu	3.347			
ϵ	body-centered cubic	Pu–8Pu	3.149	8	3.149	490
		Pu–8Pu	3.156	8	3.156	550

Table 7.14 *Metallic radii* (*Zachariasen*, 1961*b; Zachariasen and Ellinger*, 1963*b*) *and volumes* (*Dormeval*, 2001) *of plutonium atoms.*

Phase	*Temperature* (°C)	*Radius* (Å)	*Radius at* 25°C (Å)	*Atomic volume* (Å^3)
α	25	1.580	1.580	20.00
β	93	1.600	1.590	22.43
γ	235	1.601	1.589	23.14
δ	320	1.640	1.644	24.93
δ′	465	1.638	1.644	24.69
ϵ	490	1.622	1.594	24.00

significant hysteresis, compared with the idealized curve shown in Fig. 7.19, and makes it difficult to conclusively determine the transformation temperatures. These temperatures depend on metal purity, microstructural variables (such as grain size and dislocation density), heating or cooling rates, applied stress,

Table 7.15 *Density of liquid plutonium* (g cm^{-3}).

Temperature (°C)	*Serpan and Wittenberg* (1961)[a]	*Olsen* et al. (1955)[b]
664	16.62	16.604
691	16.58	16.554
728	16.52	16.511
746	16.50	16.485
752	16.49	16.476
771	16.46	16.488
788	16.43	16.424

[a] Density equation $\rho = (17.63 - 1.52 \times 10^{-3}\ T) \pm 0.04$; temperature in °C

[b] Density equation $\rho = (17.567 - 0.001451\ T) \pm 0.021$; temperature in °C

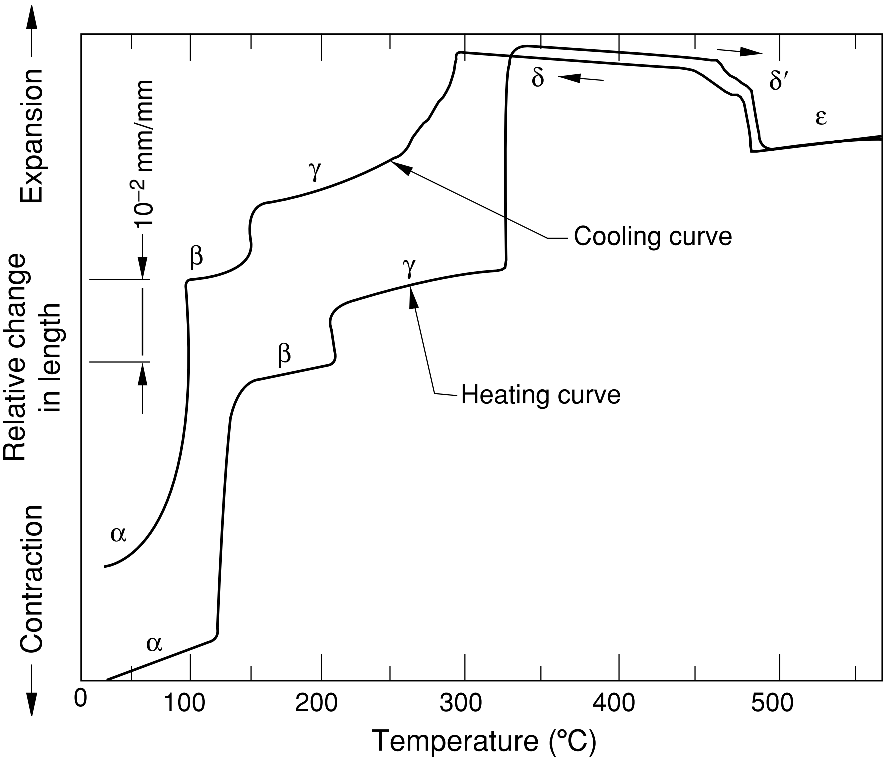

Fig. 7.24 *Experimental thermal expansion curve for heating and cooling of unalloyed plutonium showing typical hysteresis* (*after Goldberg and Massalski,* 1970).

sample size and shapes (resulting in stress effects), and prior transformation history.

Lemire *et al.* (2001) compared various phase transformation studies and compiled the best estimates of transformation temperatures and stability ranges for the various allotropes listed in Table 7.9. Precise transformation temperatures are difficult to measure not only because they depend on the variables mentioned above, but also because all transformations exhibit significant time dependence. The isothermal (as opposed to athermal, where no thermal activation is needed) nature of the α→β and β→α transformations is best illustrated by the so-called time–temperature–transformation (TTT) diagram shown in Fig. 7.25 (after Nelson (1980)). The 'C-curve' shape of the transformation demonstrates how the temperature for the onset of transformation depends on the cooling rate. By determining the curves for both transformations, Nelson was able to establish the equilibrium transformation temperature as 112°C (compared with the average transformation temperature of 122°C during heating at relatively slow rates reported in Table 7.9).

Significant uncertainty still exists about the nature of the transformation mechanisms among the allotropes of plutonium (Hecker, 2000). The transformations among the high-temperature allotropes (δ, δ′, and ϵ) are generally considered to be of a diffusion-controlled (diffusive) nature. However,

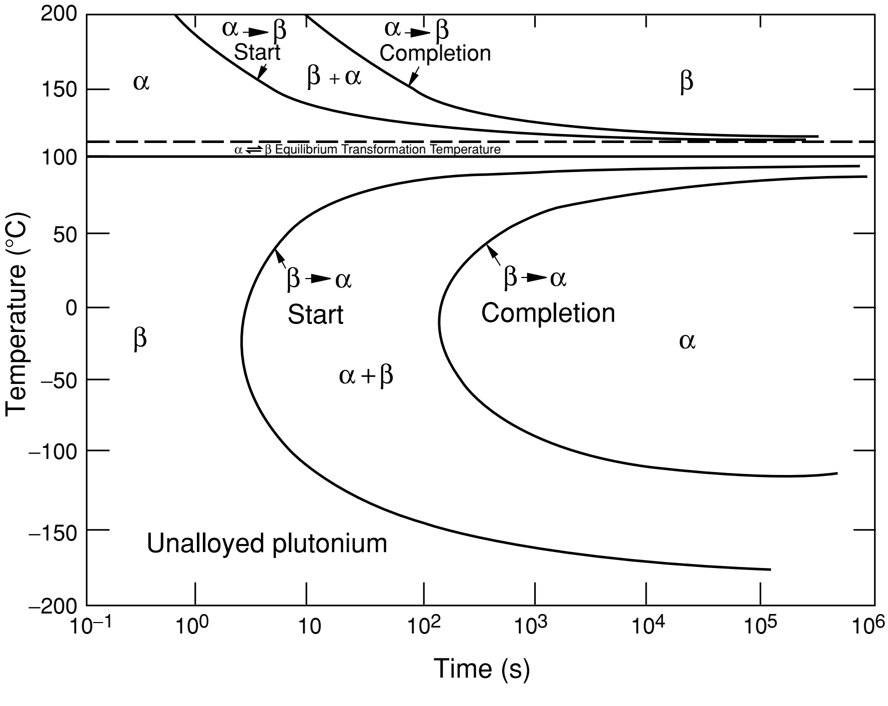

Fig. 7.25 *Representative time–temperature-transformation (TTT) curves of the β→α and α→β transformations in high-purity, electrorefined plutonium. The sample was taken to the β phase for* 45 min *at* 170°C (*from Nelson*, 1980).

transformations at lower temperatures among the δ, γ, β, and α phases show signs of diffusive and diffusionless, shear-type transformations. Shear transformations (of a martensitic nature) involve cooperative shear motion of the atoms and typically result in specific crystallographic relationships between the parent and the transformed phases. The evidence for such relationships was reviewed by Nelson (1980) and by Goldberg and Massalski (1970), who described the highly textured α-phase transformation product that can be formed when the β→α transformation is induced by cooling under applied stress.

Microcracking is difficult to avoid in most unalloyed plutonium as it cools from the melt or from annealing at elevated temperatures. The volume fraction of microcracks can range from 0.1 to 3%. High purity, large sample size, and slow cooling rates result in more extensive microcracking. Thermal cycling between the α and β allotropes greatly exacerbates the microcracking problem and results in sample distortion and surface rumpling (Hecker, 2000). On the other hand, quenching samples from the β phase to –80°C minimizes microcracking. Nelson pointed out that α-phase densities greater than 19.65 g cm^{-3} are generally considered to be good-quality plutonium. Densities around 19.8 g cm^{-3} have been achieved by cooling through the β→α transformation under pressure or by hydrostatic extrusion and concurrent recrystallization (Merz, 1970).

Another important consideration in sample preparation and subsequent property determination is the amount of retained high-temperature phases at ambient temperature. As noted in Figs. 7.24 and 7.25, the transformation from β→α is time-dependent and, hence, not necessarily complete at room temperature, resulting in retained β phase (or sometimes retained γ or δ phases). Impurities generally shift the onset of transformation (the 'C-curve' in Fig. 7.25) to the right. Spriet (1967) demonstrated that the onset of transformation was retarded by a factor of ten as the purity level changed from 200 to 400–1000 ppm. The impurities Ti, Hf, Zr, and U retard the β→α transformation and lead to greater β-phase retention at ambient temperature (Oetting *et al.*, 1976; Hecker, 2000). The impurities Ga, Al, and Si favor retention of the δ phase (Hecker, 2000). The most convenient method to determine the presence of retained high-temperature phases in α plutonium is to measure the density. The best way to identify the retained phases is by XRD; however, by using XRD it is difficult to identify retained phases at the level of less than a few volume percent.

Thermodynamic properties related to phase transformations can be measured directly by calorimetry or estimated from phase diagrams. Such properties are summarized in Table 7.16 along with the best estimates of the equilibrium transformation temperatures and volume changes. The scatter is quite large for reasons mentioned above. Nevertheless, these values are important to help guide the theory and modeling activities. Transformation enthalpies for the pressure-induced ζ phase are shown in Fig. 7.26, as derived from the data of Morgan (1970).

Table 7.16 *Entropies and enthalpies of transformations of the plutonium allotropes.*

Phase transformation	ΔS^a ($J\ K^{-1}\ mol^{-1}$)	ΔS^b ($J\ K^{-1}\ mol^{-1}$)	ΔH^c ($J\ mol^{-1}$)	ΔH^d ($J\ mol^{-1}$)	ΔH^e ($J\ mol^{-1}$)
$\alpha \to \beta$	9.55	8.66	3430	3600	3706 ± 100
$\beta \to \gamma$	1.38	1.34	565	586	478 ± 20
$\gamma \to \delta$	1.05	0.88	586	649	713 ± 40
$\delta \to \delta'$	0.04	0.04	84	41	84 ± 20
$\delta' \to \epsilon$	2.47	2.46	1841	1859	1841 ± 100
$\epsilon \to$ liquid	3.09	3.18	2824	2847	2824 ± 100

[a] Wick (1980); [b] Wittenberg *et al.* (1970); [c] Oetting *et al.* (1976); [d] Deloffre (1997); [e] Lemire *et al.* (2001).

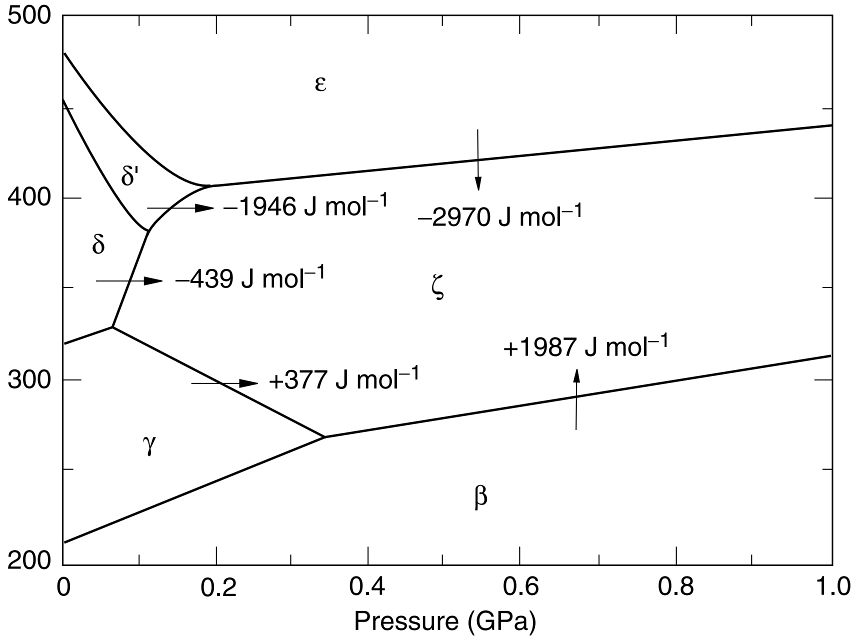

Fig. 7.26 *Transformation enthalpies of ζ plutonium calculated from the Clapeyron equation and slopes from Fig.* 7.21 (*Morgan*, 1970).

7.7.4 Alloys and phase transformations

Equilibrium phase diagrams provide a map of phase stability as a function of chemical concentration and temperature (most of the work of this nature has been done at ambient pressure and for binary alloy systems). All of the early work on phase diagrams of plutonium done during and after the Manhattan Project was classified. It was not until President Eisenhower launched the

'Atoms for Peace' initiative that much of that work was declassified and published. The Russian research group associated with A. A. Bochvar (Konobeevsky, 1955) published the first series of plutonium phase diagrams (with elements Be, Pb, V, Mn, Fe, Ni, and Os, as well as the ternary Pu–U–Fe) at a Moscow conference during the summer of 1955 in the preface to the first Conference on Peaceful Uses of Atomic Energy held in Geneva that fall. The U.S., U.K., and France rapidly followed suit. The Russian group added the Pu–Cu, Pu–Al, Pu–Bi, Pu–Zr, Pu–Mo, Pu–Th, and Pu–U systems at the second Geneva conference held in 1958 (Bochvar *et al.*, 1958). Coffinberry *et al.* (1958), and Schonfeld *et al.* (1959) published plutonium phase diagrams based on their work at Los Alamos Scientific Laboratory. Waldron *et al.* (1958) and Cope *et al.* (1960) published the U.K. results and Hocheid *et al.* (1967) the French results.

By 1968, most of the binary phase diagrams of plutonium were determined and published in the classic report of Ellinger *et al.* (1968b). Additional compilations were published in the *Plutonium Handbook*, edited by Wick (1980) and in the *Plutonium Metallurgy Handbook* (Hasbrouk and Burns, 1965). The most recent compilation is presented by Peterson and Kassner (1988). We review the salient features of binary plutonium phase diagrams below. The reader is referred to the reviews mentioned above for a discussion of available ternary plutonium diagrams. We also note that Blank provides a comprehensive compilation of phase diagram data in Table 2/1 of the *Gmelin Handbook of Inorganic Chemistry* (Blank, 1976). In addition, Blank (1976, 1977) provides a comprehensive treatment of the properties of plutonium alloys.

(a) Elements that expand the δ-phase field

Chemical additions (or alloying) significantly affect plutonium phase stability with temperature and pressure. The dramatic effects of the addition of a few atomic percent gallium to plutonium on its thermal behavior are demonstrated in Fig. 7.27. The addition of gallium retains the attractive feature of expansion during solidification while avoiding all of the large volume perturbations during cooling because the addition of gallium retains the fcc δ phase to room temperature. The thermal expansion is essentially zero, or 'Invar-like,' (Hecker, 2004) making Pu–Ga alloys much easier to cast. Moreover, the soft and ductile nature of the fcc δ phase makes these alloys much easier to shape than unalloyed plutonium. Consequently, most of the detailed work on properties of plutonium alloys has focused on systems that retain the δ phase. However, interest in metallic reactor fuels (Keiser *et al.*, 2003) has also resulted in work on β-phase retainers and on lean plutonium alloys involving uranium.

The complexity of chemical alloying is demonstrated in Fig. 7.28 for the Pu–Ga system. In addition to the six allotropes of plutonium, several new binary phases and 11 intermetallic compounds are formed. The fcc δ phase is retained to room temperature over a substantial range of gallium concentrations.

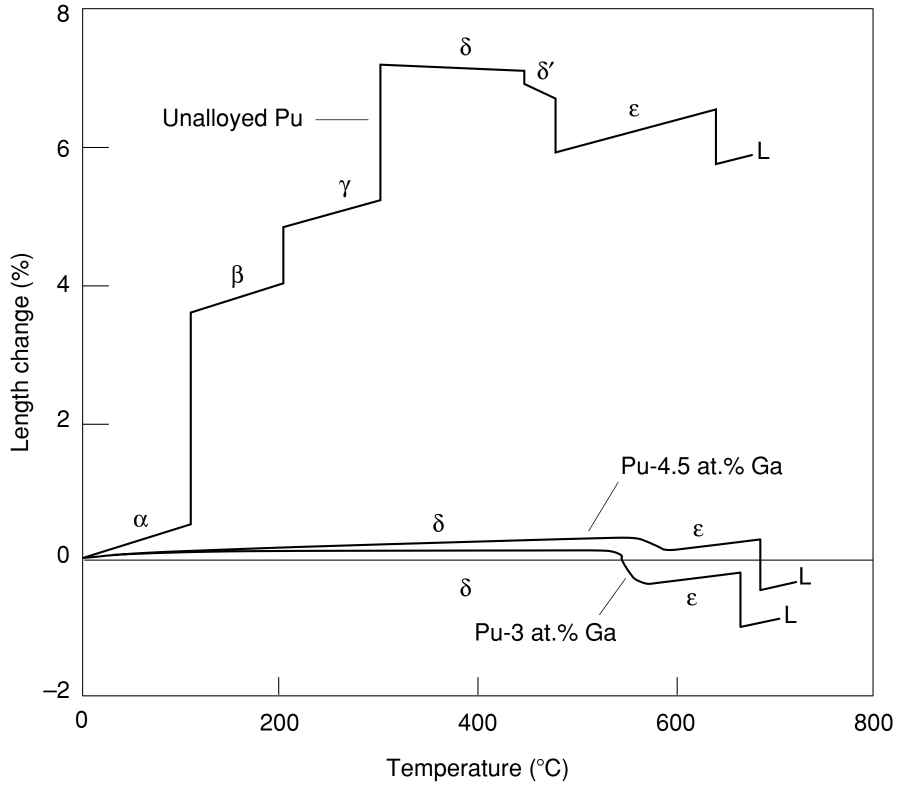

Fig. 7.27 *Length changes for unalloyed plutonium compared to Pu-*3.0 at.% *Ga and Pu-*4.5 at.% *Ga alloys.*

The question of whether the retained δ phase is stable or metastable was resolved only recently when Hecker and Timofeeva (2000) reconciled the U.S. (as well as the U.K. and French) and Russian versions of the Pu–Ga phase diagram. A comparison of the two versions of this fundamental phase diagram is shown in Fig. 7.29. They now believe that the Russian diagram (Fig. 7.29b), which shows an eutectoid point at 97°C and 7.9 at.% Ga, is the true equilibrium phase diagram (or as close a representation as possible, recognizing that radioactive decay in plutonium precludes true equilibrium). This diagram indicates that the δ phase should decompose below 97°C into α-Pu + Pu_3Ga. Such decomposition has never been observed because the kinetics are too slow. Timofeeva (2001) built her case on a clever set of experiments that demonstrated conclusively that the phase boundaries just above the eutectoid temperature clearly point to a decomposition (Hecker and Timofeeva, 2000). In fact, Timofeeva (2001) estimated that such decomposition requires more than 10,000 years at room temperature because the kinetics of the decomposition are exceedingly slow.

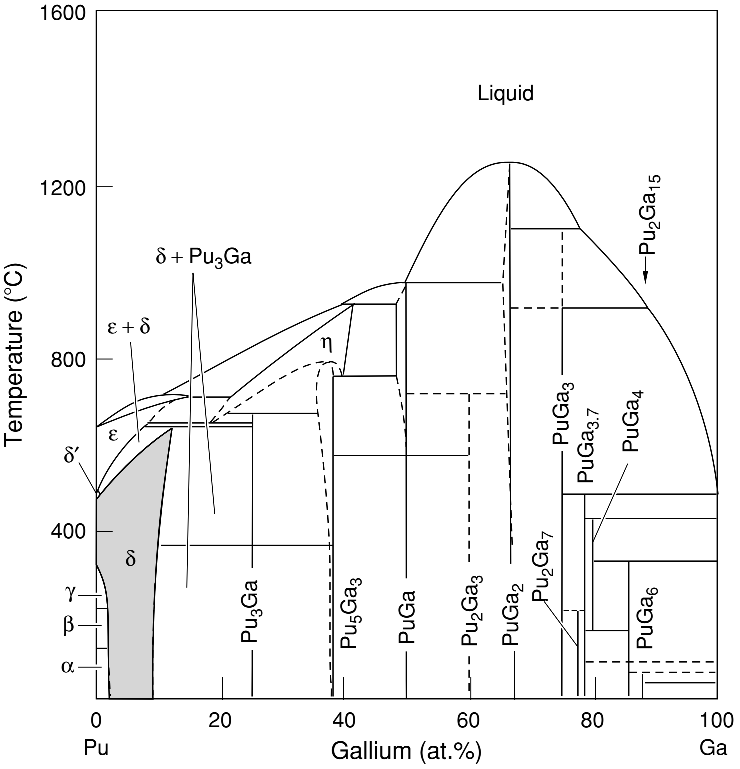

Fig. 7.28 *The Pu–Ga phase diagram at ambient pressure (from Peterson and Kassner*, 1988).

Therefore, the U.S. version (Fig. 7.29a), in which the δ phase is retained at least down to room temperature, represents an adequate 'working' diagram. Blank (1977), in his Table 2/105, presented the most complete table of crystal structures, atom positions, and atomic distances.

Timofeeva (2001) also demonstrated that the Pu–Al system undergoes a similar eutectoid decomposition near 100°C. The plutonium-rich end of the U.S. and Russian diagrams are shown in Fig. 7.30. In addition to the difference in findings related to the stability of the δ phase, Timofeeva also concluded that the intermetallic compound Pu_3Al does not extend to room temperature at thermodynamic equilibrium but rather only to 380°C. The eutectoid decomposition below 93°C is to α-Pu + PuAl (Timofeeva, 2001, 2003a). This finding differs from the conclusions of both the prior U.S. work reported by Ellinger *et al.* (1968b) and the prior Russian work reported by Bochvar *et al.* (1958). Timofeeva (2001) pointed out that the differences result because of slow kinetics. Her experiments allowed for sufficient time to demonstrate that PuAl is the intermetallic compound stable at room temperature.

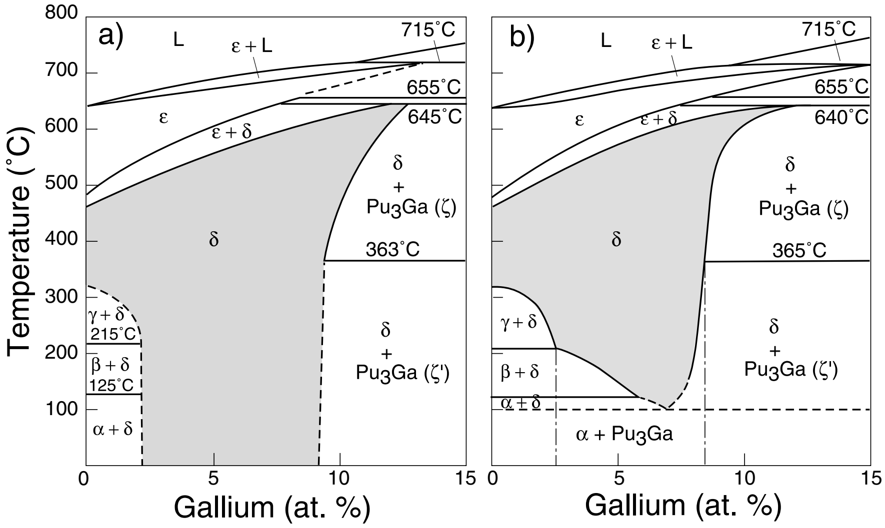

Fig. 7.29 *Comparison of* (*a*) *US and* (*b*) *Russian Pu–Ga phase diagrams from Hecker and Timofeeva* (2000).

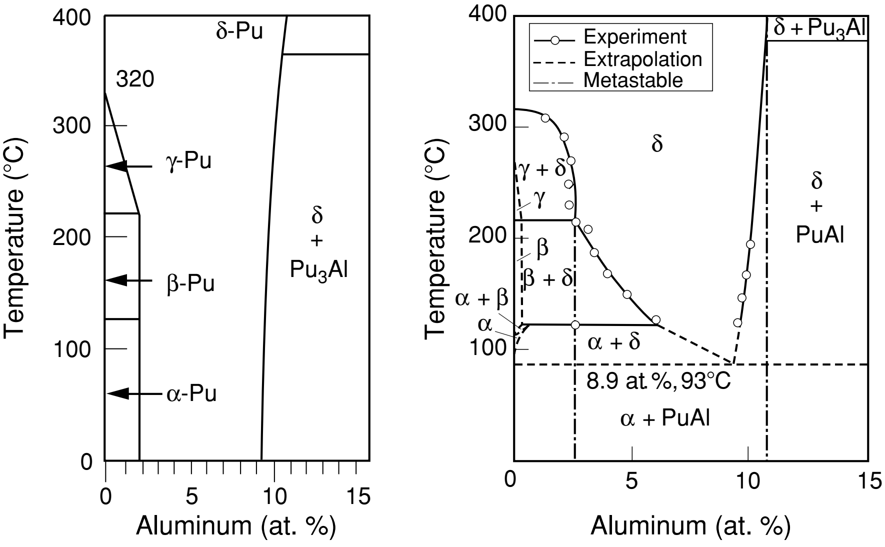

(a)

(b)

Fig. 7.30 *US* (*a*) *and Russian* (*b*) *versions of the Pu-rich side of the Pu–Al phase diagram. The US version is from Ellinger* et al. (1962*b*), *and the Russian version is from Hecker and Timofeeva* (2000).

Timofeeva (2003a) recently published data on 53 eutectoid transformations found in 30 binary plutonium phase diagrams. Eutectoid transformations are observed in binary systems of plutonium with transition metal elements (12), lanthanides (7), actinides, and elements of group IIIB (4 each). Only one eutectoid transformation exists with the elements of groups II, IV, and V. An interesting set of results is shown in Fig. 7.31 for four elements that expand the δ-phase field, Al, Ga, In, and Tl. Timofeeva demonstrated that the compositional range of the δ-phase field decreases and the eutectoid temperature increases monotonically with increasing atomic number of the alloying element. Additions of most trivalent elements expand the δ-phase field (Hecker, 2000), and in addition to Al, Ga, In, and Tl listed above, Ellinger *et al.* (1968b) showed that Sc, Ce, and Am also retain the δ phase. However, as discussed above, the retention appears to be metastable for most of these elements. It is likely that only Am results in a thermodynamically stable δ phase at room temperature. Timofeeva (2003a) reports a eutectoid transformation in Pu–Ce, and Pu–Sc systems that appears not to have received the same scrutiny as the other elements, so its status remains inconclusive.

In addition to the elements that readily retain the δ phase to room temperature (Al, Ga, Ce, Am, Sc, In, and Tl), there is a second class of elements (Si, Zn, Zr, and Hf) that retain the δ phase in a metastable state under conditions of rapid cooling. There are also some indications that the δ phase in Pu–Th alloys can be retained by rapid quenching (Gschneidner *et al.*, 1960).

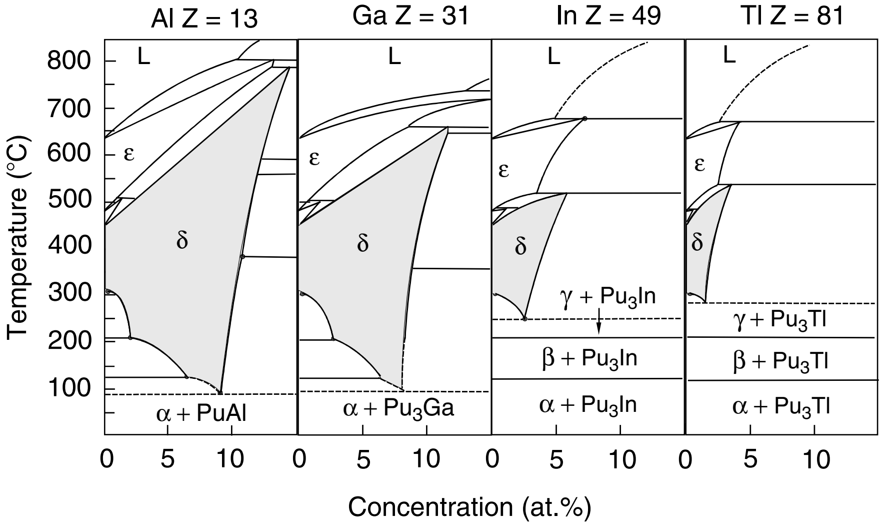

Fig. 7.31 *Phase diagrams of plutonium with several group* III*B elements show the eutectoid parameters and δ-phase region dependence (from Timofeeva,* 2003b).

Gschneidner *et al.* (1960) also found a number of the trivalent lanthanides (Dy, Er, Tm, Lu, and possibly Tb) to favor δ-phase retention, but their phase diagrams exhibit no δ-phase stability. Elliott and coworkers (Elliott and Giessen, 1975; Giessen *et al.*, 1975) demonstrated that retention of the δ phase and the bcc ε-phase can be extended in a metastable manner by splat cooling (rates from 10^6 to 10^8 s^{-1}). For example, both of these phases can be retained in splat-cooled Pu–Ti alloys. In Pu–Ga alloys, the maximum solubility of gallium in plutonium at room temperature is extended from 12.5 to 20 at.%. In Pu–Ce alloys, fcc δ phases can be retained across the entire range of cerium additions by splat cooling.

(b) α-Phase and β-phase stabilizers

Only neptunium has been found to expand the α-phase field. No other element is known to have any equilibrium solubility in the monoclinic α phase. Neptunium is also the only element that significantly expands the β-phase region. However, limited solubility of U, Hf, and Zr has been found in the β phase. Also, additions of Ti, Hf, and Zr will retain the β phase to room temperature and below by rapid quenching. Neptunium and uranium lower the melting point of plutonium slightly. The elements Hf, Zr, and Ti raise it significantly, even with small additions.

(c) Eutectic-forming elements

Additions of Mn, Fe, Co, or Ni lower the melting point of plutonium substantially. These elements form a low-melting eutectic much as does lead alloyed with tin to make solder. For example, the Pu–Fe phase diagram, shown in Fig. 7.32, exhibits the eutectic decomposition at 410°C and close to 10 at.% Fe from the liquid to δ-Pu + Pu_6Fe. This eutectic alloy was used in the first metallic plutonium fuel elements in the Los Alamos Molten Plutonium Reactor (LAMPRE) in the late 1940s (Kiehn, 1961; Burwell *et al.*, 1962). The elements Mn, Co, and Ni exhibit eutectic temperatures at approximately, 525°C, 405°C, and 465°C, respectively. These elements decompose to the intermetallic compounds $PuMn_2$, Pu_6Co, and PuNi, respectively. Other elements form eutectics but at somewhat higher temperatures. These include Si, Mn, Os, Ru, Rh, and Th. Eutectic-forming elements such as Mn, Fe, Ni, or Co are of special significance because they limit the useful temperature range of plutonium and its alloys. For example, plutonium metal heated above 410°C contained in steel will melt through the steel by forming the eutectic. Even when present in small amounts in plutonium, the alloying elements can segregate to grain boundaries, enriching the local alloying concentration and causing local melting or embrittlement at temperatures close to the eutectic temperature. Blank (1977) presented a thorough review of the properties of plutonium alloys and intermetallics with the eutectic-forming elements.

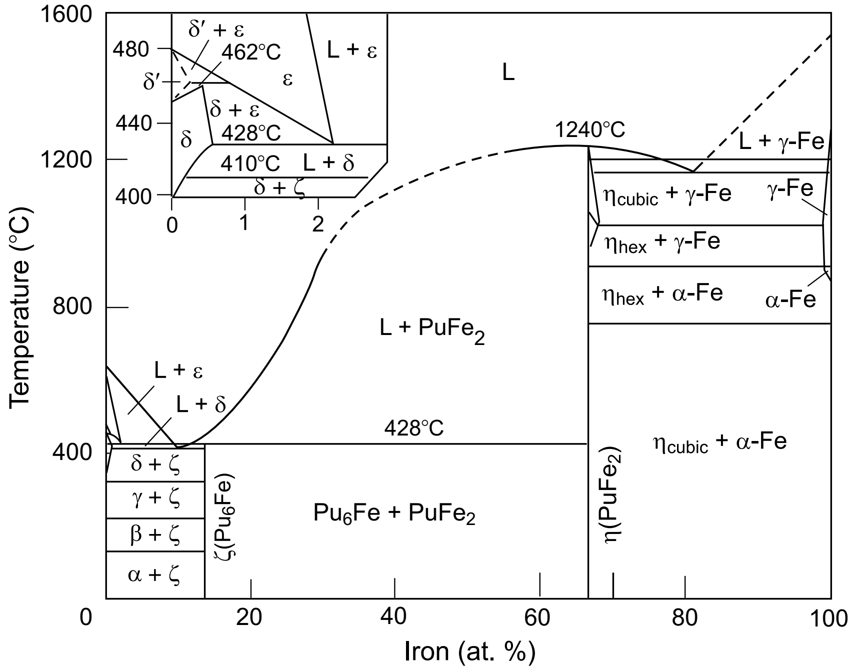

Fig. 7.32 *The Pu–Fe phase diagram at ambient pressure from Ellinger* et al. (1968*b*) *and first reported by Schonfeld* (1961).

(d) Interstitial compounds

When nonmetallic elements with very small radii are alloyed with metals, they tend to form interstitial solid solutions. A general rule of thumb is that if the radius of the nonmetallic element is <0.59 that of the metallic element, then an intermetallic compound with a simple structure (often fcc or hcp) forms. If the ratio is greater, then compounds with complex structures form. The most important nonmetallic elements for plutonium in the solid state are O, C, N, and H. None of these elements shows any solubility in the equilibrium phase diagrams. The Pu–O phase diagram is shown in Fig. 7.90. The elements O, C, and N all form several high-melting, refractory ceramic compounds. The structure and properties of these ceramic compounds will be discussed in greater detail in Section 7.8. Hydrogen also has a tendency to form compounds, but these readily decompose, rather than being refractory.

(e) The rest of the elements

Most other elements show only limited solubility in the δ phase, while some elements such as Ba, Sr, and Ca are immiscible. Most elements increase the melting point. Some have shallow eutectics before the melting point increases. More than half of the elements, namely Th, Np, U, Ti, Ru, Rh, Pt, Os, and most lanthanides, show solubility in the ϵ phase.

Detailed X-ray crystal structure data are presented for many intermetallic compounds of plutonium in Table 7.17.

(f) Microsegregation in δ-phase alloys

Since alloys in which the fcc δ phase is retained to room temperature are of particular interest, we discuss the problem of microsegregation, which can dramatically influence the properties of δ-phase alloys. We use the Pu–Ga system shown in Fig. 7.33 for the purpose of illustration. During solidification and cooling, alloys within the range of gallium content to 13 at.% must cool through the liquid + ϵ and $\epsilon + \delta$ two-phase regions. In a two-phase region, assuming gallium diffusivity is infinite in both phases, the composition of each phase is given by the phase boundaries at that temperature (the lever rule), giving rise to possible microsegregation. We track the gallium content through the $\epsilon + \delta$ two-phase field in Fig. 7.33a. As the temperature reaches point A, the first δ phase to form has the gallium concentration shown at point B. As the temperature is lowered, the gallium concentration in the δ phase moves along the line BD, whereas the gallium concentration in ϵ moves along the line AC – if diffusion is sufficiently rapid to allow migration of gallium consistent with the imposed cooling rate. (Of course, the average gallium concentration in the alloy must be the initial concentration.) The diffusion rate of gallium is approximately 10^4 faster in the ϵ phase (because of its open bcc structure) than the δ phase, thereby not allowing equilibration in the δ phase for typical cooling rates. As a consequence, the gallium concentration of the remaining ϵ phase is pushed to lower values as cooling proceeds, resulting in increased segregation over that expected from equilibrium conditions.

As a result, the microstructure of a typical as-cast δ-phase alloy exhibits a range of gallium concentrations between points B and C. The interior of the δ-phase grains reflects the gallium concentration at point B and the grain boundaries may have very little gallium because they are the last ϵ-phase areas to transform with gallium at or below point C. The resulting microstructure appears heavily 'cored' or segregated as shown in Fig. 7.33b. It consists of gallium-rich δ phase in the center, a gallium-lean δ-phase shell (dark areas) at the core boundaries, and a gallium-lean intercore region that transformed to the α phase during cooling because of insufficient gallium. This type of microsegregation typically occurs during cooling through liquid + solid two-phase regions because diffusion in the liquid is so much faster than in the solid. However, the anomalously high diffusion rate in ϵ-plutonium avoids the problem in the liquid + ϵ region, only to have it reappear in the $\epsilon + \delta$ two-phase region. Equilibrating the gallium concentration requires a sustained return to temperatures high in the δ-phase region, typically hundreds of hours, to achieve

Table 7.17 *X-ray crystal structure data for selected intermetallic compounds of plutonium.*

				Lattice parameters						
Phase	*Structure type*	*Symmetry*	*Space group*	a_0(Å)	b_0(Å)	c_0(Å)	*Angle* (deg)	*Units per cell*	*X-ray density* (g cm^{-3})	*References*
$PuAg_3$(ζ)		hexagonal	P6/*m*	12.730(3)		9.402(5)		16	11.33	Ellinger *et al.* (1968b), Miner (1970), Kutaitsev *et al.* (1967), and Runnalls (1956)
				12.72(5)		9.39(3)				Freeman and Darby (1974) and Blank *et al.* (1962)
$PuAg_{3.6}$	$GdAg_{3.6}$	hexagonal	P6/*m*	12.727(6)		9.392(4)			11.15	Ellinger *et al.* (1968b) and Miner (1970)
$PuAg_2$										Miner (1970)
Pu–Ag phase diagram										Ellinger *et al.* (1968b) and Kutaitsev *et al.* (1967)
Pu_3Al(ζ)	$SrPb_3$	tetragonal	P4/*mmm*	4.499(1)		4.536(1)		1	13.45	Ellinger *et al.* (1968b), Freeman and Darby (1974), Blank *et al.* (1962), and Bochvar *et al.* (1958)
	Ti_3Cu			4.499(2)		4.538(2)			13.45	Coffinberry and Miner (1961)
		cubic		4.500						Ellinger *et al.* (1962b)
				4.530		4.575				
PuAl(η)	related to CsCl	bcc		10.769(1)				29	10.25	Ellinger *et al.* (1968b), Freeman and Darby (1974), Blank *et al.* (1962), and Bochvar *et al.* (1958)
				10.769					10.253	Kay and Waldron (1967)
$PuAl_2$(θ)	Cu_2Mg	cubic	F*d*3*m*	7.831(5)				8	8.09	Ellinger *et al.* (1968b), Freeman and Darby (1974), Blank *et al.* (1962), and Runnalls (1956)
				7.840(1)(Pu-rich)						Bochvar *et al.* (1958)
				7.836(1)(Al-rich)						Bochvar *et al.* (1958)
				7.874						Ellinger *et al.* (1962b)
				7.838(1)(Pu-rich)					8.06	Coffinberry and Miner (1961)
				7.848(1)(Al-rich)						Coffinberry and Miner (1961)

				7.833					8.095	Kay and Waldron (1967)
$\mathrm{PuAl_3}$(ι)	$\mathrm{PuAl_3}$	hexagonal(6H)	$P6_3/mmc$	6.08(1)		14.40(3)				Ellinger *et al.* (1968b), Freeman and Darby (1974), Blank *et al.* (1962), and Runnalls (1956)
				6.084(1)		14.427(2)		6	6.8	Bochvar *et al.* (1958)
				6.10(2)		14.47(4)			6.84	Larson *et al.* (1957)
		hexagonal		6.083		14.410			6.643	Kay and Waldron (1967)
		cubic(3H)	$Pm3m$	4.262					6.604	Kay and Waldron (1967)
		rhomb($9H_\beta$)	$R\bar{3}m$	7.879			$\alpha = 45.94$		6.657	Kay and Waldron (1967)
		rhomb($9H_\alpha$)		7.901			$\alpha = 45.81$		6.634	Kay and Waldron (1967)
$\mathrm{PuAl_4}$(κ)	$\mathrm{UAl_4}$	orthorhombic	*Imma*	4.42(2)	6.26(2)	13.66(3)				Ellinger *et al.* (1968b), Freeman and Darby (1974), and Blank *et al.* (1962)
				4.387(2)	6.262(2)	13.714(4)		4	6.02–6.11	Bochvar *et al.* (1958)
				4.41	6.29	13.79				Ellinger *et al.* (1968b)
α-$\mathrm{PuAl_4}$		orthorhombic	*Imma*	4.396(1)	6.266(1)	13.708(2)		3.6	5.680	Kay and Waldron (1967)
β-$\mathrm{PuAl_4}$		orthorhombic	*Imma*	4.396(1)	6.266(1)	13.708(2)			5.680	Kay and Waldron (1967)
(α- and β-$\mathrm{PuAl_4}$ differ by the distribution of lattice vacancies)										
Pu–Al phase diagram, see Fig. 7.30										Kay and Waldron (1967), Bochvar *et al.* (1958), Waldron *et al.* (1958), Ellinger *et al.* (1962b), and Moeller and Schonfeld (1950)
Pu–Am system, no compounds, phase diagram known										Ellinger *et al.* (1966)
Pu–As system, see Section 7.8, Table 7.33										
$\mathrm{Pu_xAu_y}$(η)										Ellinger *et al.* (1968b) and Kay and Waldron (1967)
PuAu(ζ)										Ellinger *et al.* (1968b) and Kay and Waldron (1967)

Table 7.17 (*Contd.*)

Phase	*Structure type*	*Symmetry*	*Space group*	*Lattice parameters*				*Units per cell*	*X-ray density* (g cm^{-3})	*References*
				a_0(Å)	b_0(Å)	c_0(Å)	*Angle* (deg)			
$PuAu_2$(ι)										Ellinger *et al.* (1968b) and Kay and Waldron (1967)
Pu_xAu_y(κ)										Ellinger *et al.* (1968b) and Kay and Waldron (1967)
$PuAu_3$(λ)		hexagonal	P6/*m*	12.710		9.210		16	17.11	Ellinger *et al.* (1968b), Kay and Waldron (1967), and Kutaitsev *et al.* (1967)
$PuAu_4$(μ)										Ellinger *et al.* (1968b) and Kay and Waldron (1967)
$PuAu_5$(ν)										Ellinger *et al.* (1968b) and Kay and Waldron (1967)
Pu–Au phase diagram										Ellinger *et al.* (1968b), Kay and Waldron (1967), and Kutaitsev *et al.* (1967)
Pu–B system, see Section 7.8, Table 7.28										
Pu–Ba system, no compounds										(Seaborg *et al.* 1946, 1949b), Ellinger *et al.* (1968b), and Bochvar *et al.* (1958)
$PuBe_{13}$	$NaZn_{13}$	cubic	F*m*3*c*	10.284(1)(Be-rich)				8	4.35	Runnalls (1956)
				10.278(1)(Pu-rich)						Runnalls (1956)
				10.274(2)					4.36	Seaborg *et al.* (1946) and Bochvar *et al.* (1958)
				10.282(1)(Be-rich)					4.35	Coffinberry and Miner (1961)
Pu–Be phase diagram										Seaborg *et al.* (1946, 1949b), Konobeevsky (1955), Ellinger *et al.* (1968b), and Bochvar *et al.* (1958)

Pu–Bi system, see Section 7.8, Table 7.33									
Pu–Bi phase diagram									Seaborg *et al.* (1946, 1949b), Ellinger *et al.* (1968b), and Bochvar *et al.* (1958)
Pu–C system, see Section 7.8, Table 7.29									
Pu–Ca system, no compounds									Seaborg *et al.* (1946, 1949b), Ellinger *et al.* (1968b), and Bochvar *et al.* (1958)
PuCd$_2$(ζ)									Etter *et al.* (1965)
PuCd$_4$(η)									Etter *et al.* (1965)
PuCd$_6$(θ)	CeCd$_6$	cubic	I*m*3	15.59(1)				9.61	Etter *et al.* (1965) and Johnson *et al.* (1965)
PuCd$_{11}$(ι)	BaHg$_{11}$	cubic	P*m*3*m*	9.282(2)			3	10.25	Etter *et al.* (1965) and Johnson *et al.* (1965)
Pu–Cd phase diagram									Ellinger *et al.* (1968b), Etter *et al.* (1965), and Johnson *et al.* (1965)
Pu–Ce system, no compounds, phase diagram known									Wilkinson (1960), Ellinger *et al.* (1968b), and Selle and Etter (1964)
Pu$_6$Co(ζ)	U$_6$Mn	tetragonal	I4/*mcm*	10.45(1)		5.32(1)	4	17.6	Bochvar *et al.* (1958)
				10.46(2)		5.33(1)	4	17.00	Coffinberry and Miner (1961)
Pu$_3$Co(η)	Al$_2$CuMg	orthorhombic	C*mcm*	3.501(3)	11.03(3)	9.23(15)(Pu-rich)		14.7	Poole and Nichols (1961)
				3.477(3)	10.99(3)	9.20(15)(Co-rich)			Poole and Nichols (1961)
				3.470	10.939	9.196		14.76	Coffinberry and Miner (1961)
				3.475(4)	10.976(10)	9.220(8)		14.65	Larson *et al.* (1963)
Pu$_2$Co(θ)	Fe$_2$P	hexagonal	P321	7.902(4)(Pu-rich)		3.549(2)	3	14.0	Coffinberry and Miner (1961)
				7.763(2)(Co-rich)		3.648(3)			Coffinberry and Miner (1961)
				7.803(8)(Pu-rich)		3.606(5)			Poole and Nichols (1961)
				7.732(8)(Co-rich)		3.654(5)			Poole and Nichols (1961)
PuCo$_2$(ι)	Cu$_2$Mg	cubic	F*d*3*m*	7.075(5)			8	13.39	Runnalls (1956)
				7.083(10)(Pu-rich)					Bochvar *et al.* (1958)
				7.066(10)(Co-rich)					Bochvar *et al.* (1958)
				7.081(1)(Pu-rich)					Coffinberry and Miner (1961)
				7.095(5)(Pu-rich)					Poole and Nichols (1961)

Table 7.17 (*Contd.*)

				Lattice parameters						
Phase	*Structure type*	*Symmetry*	*Space group*	a_0(Å)	b_0(Å)	c_0(Å)	*Angle* (deg)	*Units per cell*	*X-ray density* (g cm^{-3})	*References*
				7.023(5)(Co-rich)						Poole and Nichols (1961)
PuCo$_3$(κ)	PuNi$_3$	rhombohedral		8.635(10)			$\alpha = 33°40'$	3	11.74	Poole and Nichols (1961)
		(hexagonal setting)		8.327(5)						
Pu$_2$Co$_{17}$(λ)	Th$_2$Ni$_{17}$	hexagonal	P6$_3$/*mmc*	8.325(2)	8.104(3)			2	10.10	Bochvar *et al.* (1958)
				8.327(5)	8.107(5)					Poole and Nichols (1961)
Pu–Co phase diagram										Seaborg *et al.* (1946, 1949b) and Poole and Nichols (1961)
Pu–Cr system, no compounds, phase diagram known										Ellinger *et al.* (1968b), Bochvar *et al.* (1958), and Bowersox and Leary (1968)
Pu–Cs system, no compounds										Seaborg *et al.* (1946, 1949b) and Bochvar *et al.* (1958)
PuCu$_2$(ζ)	CeCu$_2$	orthorhombic	I*mma*	4.332(2)	6.686(1)	7.376(1)		4	11.20	Pons *et al.* (1972)
				4.32(2)	6.69(2)	7.38(2)				Lataillade *et al.* (1971)
PuCu$_4$(η)		orthorhombic		4.320(1)	8.264(3)	9.226(3)		4	10.12	Pons *et al.* (1972)
				4.37(2)	8.37(2)	9.32(2)				Lataillade *et al.* (1971)
Pu$_4$Cu$_{17}$(θ)										Lataillade *et al.* (1971)
PuCu$_6$(ι)	CeCu$_6$	orthorhombic	P*nma*	8.50(3)	5.025(3)	10.059(6)		4	10.12	Kutaitsev *et al.* (1967)
				8.16	5.14	10.06				Wittenberg and Grove (1964)
Pu–Cu phase diagram										Ellinger *et al.* (1968b), Grison *et al.* (1960), and Kutaitsev *et al.* (1967)
Pu–Dy system, miscibility gap, no compounds										Ellinger *et al.* (1968b)
Pu–Er system, miscibility gap, no compounds										Ellinger *et al.* (1968b)
Pu–Eu system, immiscibility, no compounds										Ellinger *et al.* (1968b)
Pu$_6$Fe(ζ)	U$_6$Mn	tetragonal	I4/*mcm*	10.41(1)		5.359(4)		4		Mardon *et al.* (1957)

				10.404(4)	5.355(2)	4	17.07	Coffinberry and Miner (1961)
				10.403	5.347		17.10	Konobeevsky (1955)
				10.405(5)	5.349(3)			Bowersox and Leary (1966)
				10.40(2)	5.345(5)			Coffinberry and Waldron (1956)
PuFe$_2$(η_{cub})	Cu$_2$Mg	cubic	F*d*3*m*	7.150(5)('preparation a')			12.74	Runnalls (1956)
				7.190(5)('preparation b')			12.53	Runnalls (1956)
				7.191(1)(Pu-rich)		4	12.53	Coffinberry and Miner (1961)
				7.178			12.59	Konobeevsky (1955)
				7.189				Mardon *et al.* (1957)
PuFe$_2$(η_{hex})	MgNi$_2$	hexagonal		5.64	18.37			Avivi (1964)
Pu–Fe phase diagram								Ellinger *et al.* (1968b) and Grove (1966)^{f}
Pu–Ga(η)		cubic	I2$_1$3	7.207(18%Ga)			16	Blank and Lindner (1976)
			I2$_1$	7.167(41.6%Ga)				Chebotarev (1976)
		bcc pseudo-cell		3.58				Ellinger *et al.* (1964)
α-Pu$_3$Ga(ζ')	SrPb$_3$	tetragonal	P4/*mmm*	4.470	4.523	1	14.45	Blank and Lindner (1976)
				4.469(1)	4.527(2)	1	14.45	Ellinger *et al.* (1964)
				4.492	4.555			Hocheid *et al.* (1965)
β-Pu$_3$Ga(ζ)	AuCu$_3$	cubic	P*m*3*m*	4.514(Pu-rich)		1	14.27	Blank and Lindner (1976)
				4.497(Ga-rich)				
				4.507(2)		1	14.27	Ellinger *et al.* (1964)
				4.500				Hocheid *et al.* (1965)
Pu$_5$Ga$_3$(θ)	W$_5$Si$_3$	tetragonal	I4/*mcm*	11.736	5.559	4	12.29	Blank and Lindner (1976)
		tetragonal	I4/*mcm*	11.735(3)	5.511(2)	4	12.29	Ellinger *et al.* (1964)
		fcc		5.570				Hocheid *et al.* (1965)
α-PuGa		cubic	I*m*3*m*	3.53		2		Hocheid *et al.* (1965)
β-PuGa(ι)		tetragonal	I4/*mm*	6.641	8.069	8	11.52	Blank and Lindner (1976)
				6.666	7.985(Pu-rich)			Blank and Lindner (1976)
				6.640(1)	8.066(1)	8	11.53	Ellinger *et al.* (1964)
Pu$_2$Ga$_3$ (κ)		hexagonal		4.378	3.792			Blank and Lindner (1976)
PuGa$_2$(λ)	AlB$_2$	hexagonal	P6/*mmm*	4.248(1)	4.120	1	9.76	Ellinger *et al.* (1964)
				4.258	4.120			Hocheid *et al.* (1965)
				4.248	4.107(Pu-rich)	1	9.77	Blank and Lindner (1976)
				4.258	4.139(Ga-rich)			Blank and Lindner (1976)
α-PuGa$_3$(μ)	Ni$_3$Sn	rhombohedral	R$\bar{3}$*m*	6.173	27.99	12	9.66	Blank and Lindner (1976)

Table 7.17 (*Contd.*)

Phase	*Structure type*	*Symmetry*	*Space group*	*Lattice parameters*				*Units per cell*	*X-ray density* (g cm^{-3})	*References*
				a_0(Å)	b_0(Å)	c_0(Å)	*Angle* (deg)			
				6.178(1)		28.031(4)				Larson *et al.* (1965)
				(10.001)			($\alpha =$ 35°59′)	12	9.63	Larson *et al.* (1965)
β-PuGa$_3$(μ')	Mg$_3$Cd	hexagonal	P6$_3$/*mmc*	6.299		4.513		2	9.61	Blank and Lindner (1976)
	Ni$_3$Sn	hexagonal	P6$_3$/*mmc*	6.300(1)		4.514(1)		2	9.59	Ellinger *et al.* (1964)
~Pu$_2$Ga$_7$(?)		tetragonal		4.253		9.695				Blank and Lindner (1976)
Pu$_3$Ga$_{11}$–Pu$_4$Ga$_{15}$										Blank and Lindner (1976)
PuGa$_4$(ν)	UAl$_4$	orthorhombic	*Imma*	4.380(1)	6.290(1)	13.673(4)		4	9.13	Land *et al.* (1965a) and Ellinger and Zachariasen (1965)
			Imma	4.387	6.297	13.663		4	9.11	Blank and Lindner (1976)
α-PuGa$_6$										Blank and Lindner (1976)
β-PuGa$_6$(ζ)	PuGa$_6$	tetragonal	P4/*nbm*	5.942(1)		7.617(1)		2	8.11	Land *et al.* (1965a) and Ellinger and Zachariasen (1965)
			P4/*mbm*	5.941		7.621		2	8.12	Blank and Lindner (1976)
~Pu$_2$Ga$_{15}$		tetragonal		6.206		8.332		1	7.88	Blank and Lindner (1976)
Pu–Ga phase diagram										Ellinger *et al.* (1964), Hocheid *et al.* (1965), and Akhachinskii and Bashlykov (1970)
Pu–Al–Ga phase diagram										Blank and Lindner (1976)
Pu–Gd system, miscibility gap, no compounds										Kutaitsev *et al.* (1967)
Pu$_3$Ge										Coffinberry and Miner (1961)
Pu$_3$Ge$_2$										Coffinberry and Miner (1961)
Pu$_2$Ge$_3$	AlB$_2$	hexagonal	P6/*mmm*	3.975(2)		4.198(2)		0.5	10.16	Coffinberry and Miner (1961)
PuGe$_2$	ThSi$_2$	bc tetragonal	I4/*amd*	4.102(2)		13.81(1)		4	10.98	Coffinberry and Miner (1961)
PuGe$_3$	AuCu$_3$	cubic	P*m*3*m*	4.223(1)				1	10.07	Coffinberry and Miner (1961)
Pu–Ge phase diagram unknown										Ellinger *et al.* (1968b)
Pu–H system, see Section 7.8, Table 7.26										

$Pu_{28}Hf(\zeta)$	$Pu_{28}Zr$	bc tetragonal	$I4_1/a$	18.19		7.851	4	17.57	Zachariasen and Ellinger (1970)
$\sim Pu_{15.7}Hf(\theta)$									Ellinger and Land (1968)
$\sim Pu_{10}Hf(\zeta)$		hexagonal		3.205(1)	5.100(1)			17.07	Kutaitsev *et al.* (1967)
$\sim Pu_9Hf(\theta)$		orthorhombic		10.415(5)	10.428(5)	11.245(5)		17.7	Kutaitsev *et al.* (1967)
Pu–Hf phase diagram									Ellinger *et al.* (1968b), Kutaitsev *et al.* (1967), and Ellinger and Land (1968)
$PuHg_3$(?)	UHg_3(?)								Coffinberry and Miner (1961)
$PuHg_4$		pseudo-cubic		3.61(1)					Coffinberry and Miner (1961)
Pu_5Hg_{21}	γ-brass	distorted bcc	$D8_{1-3}$	21.78(1)			16	13.90	Berndt (1966)
Pu–Hg phase diagram									Seaborg *et al.* (1946, 1949b) and Ellinger *et al.* (1968b)
Pu–Ho system, no compounds									Ellinger *et al.* (1968b)
$Pu_3In(\zeta)$	$AuCu_3$	cubic	P*m*3*m*	4.702(1)(Pu-rich)			1		Bochvar *et al.* (1958)
				4.705(Pu-rich)				13.34	Ellinger *et al.* (1965)
				4.722(In-rich)				12.96	Ellinger *et al.* (1965)
				4.750					Hocheid *et al.* (1965)
				4.703(2)			1	13.3	Coffinberry and Miner (1961)
η phase									Ellinger *et al.* (1965)
$PuIn(\theta)$	AuCu	tetragonal	P4/*mmm*	4.811(1)		4.538(1)	2	11.19	Ellinger *et al.* (1965)
$Pu_3In_5(\iota)$									Ellinger *et al.* (1965)
$PuIn_3(\kappa)$	$AuCu_3$	cubic	P*m*3*m*	4.607(1)					Bochvar *et al.* (1958)
				4.6096(2)				9.22	Ellinger *et al.* (1965)
				4.6185(Pu-rich)					Ellinger *et al.* (1965)
				4.6088(In-rich)					Ellinger *et al.* (1965)
Pu–In phase diagram									Hocheid *et al.* (1965) and Ellinger *et al.* (1965)
Pu_5Ir_3	W_5Si_3	tetragonal	I4/*mcm*	11.0438		5.6115	4	17.18	Beznosikova *et al.* (1974)
				11.043		5.611			Beznosikova *et al.* (1974)
				11.012(3)		5.727(2)	4	16.94	Cromer (1977a)
				11.015		5.621(Ir-rich)			Beznosikova *et al.* (1974)
Pu_5Ir_4	Pu_5Ir_4	orthorhombic	P*nma*	7.245	14.60	7.455	4	16.54	Blank and Lindner (1976)
$PuIr_2$	Cu_2Mg	fcc	F*d*3*m*	7.512(1)–7.528(1)			8		Kutaitsev *et al.* (1967)
				7.518					Erdmann and Keller (1973)

Table 7.17 (*Contd.*)

				Lattice parameters						
Phase	*Structure type*	*Symmetry*	*Space group*	a_0(Å)	b_0(Å)	c_0(Å)	*Angle* (deg)	*Units per cell*	*X-ray density* (g cm^{-3})	*References*
Pu–Ir phase diagram, no information										Erdmann and Keller (1973)
Pu–K system, no compounds										Ellinger *et al.* (1968b)
Pu–La system, miscibility gap, no compounds										Grison *et al.* (1960), Kutaitsev *et al.* (1967), and Ellinger *et al.* (1967)
Pu–Li system, no compounds										Ellinger *et al.* (1968b)
Pu–Lu system, no information										
$PuMg_2(\zeta)$	CaF_2	fcc	F*m*3*m*	7.34(1)				4	4.83	Coffinberry and Miner (1961) and Ellinger *et al.* (1968b)
$PuMg_{2+x}$		hexagonal		13.8(1)		9.7(1)				Coffinberry and Miner (1961) and Ellinger *et al.* (1968b)
Pu–Mg phase diagram										Ellinger *et al.* (1968b) and Knoch *et al.* (1969)
$PuMn_2$	Cu_2Mg	fcc	F*d*3*m*	7.290(5)(Pu-rich)				8	11.96	Runnalls (1956)
				7.292(1)(Pu-rich)					11.95	Coffinberry and Miner (1961)
				7.29(Pu-rich)						Konobeevsky (1955)
				7.26(Mn-rich)						Konobeevsky (1955)
Pu–Mn phase diagram										Konobeevsky (1955), Ellinger *et al.* (1968b), Bochvar *et al.* (1958), and Grove (1966)
Pu–Mo system, no compounds, phase diagram established										Ellinger *et al.* (1968b), Grison *et al.* (1960), and Bochvar *et al.* (1958)
Pu–N system, see Section 7.8, Table 7.33										
Pu–Na system, no compounds										Ellinger *et al.* (1968b)
Pu–Nb system, no compounds, phase diagram established										Ellinger *et al.* (1968b) and Bochvar *et al.* (1958)
Pu–Nd system, miscibility gap, no compounds, phase diagram established										Ellinger *et al.* (1968a,b) and Kutaitsev *et al.* (1967)

$PuNi(\zeta)$	TlI	orthorhombic	C*mcm*	3.59(1)	10.21(2)	4.22(1)		4	12.78	Cromer and Roof (1959)
$PuNi_2(\eta)$	Cu_2Mg	fcc	F*d*3*m*	7.16(1)				8	13.1	Runnalls (1956)
				7.141(1)(Pu-rich)						Coffinberry and Miner (1961)
				7.115(1)(Ni-rich)						
				7.14						
$PuNi_3(\theta)$	$PuNi_3$	rhombohedral	R$\bar{3}$*m*	8.615			$\alpha = 33°44'$	3	11.8	Cromer and Olsen (1959)
$PuNi_4(\iota)$	$PuNi_4$	monoclinic	C2/*m*	4.87(1)	8.46(2)	10.27(2)	$\beta = 100°$	6	11.33	Ellinger *et al.* (1968b) and Cromer and Larson (1960)
$PuNi_5(\kappa)$	$CaZn_5$	hexagonal	P6/*mmm*	4.875(5)		3.970(5)		1	10.8	Runnalls (1956)
				4.872(2)(Pu-rich)		3.980(1)				Coffinberry and Miner (1961)
				4.861(2)(Ni-rich)		3.982(1)				Coffinberry and Miner (1961)
$Pu_2Ni_{17}(\lambda)$	Th_2Ni_{17}	hexagonal	P6$_3$/*mmc*	8.30(1)		8.00(1)				Runnalls (1956)
				8.29(2)		8.01(2)		2	10.3	Coffinberry and Miner (1961)
Pu–Ni phase diagram										Ellinger *et al.* (1968b) and Wensch and Whyte (1951)
Pu–Np										
η phase		orthorhombic		10.86	10.67	10.43		54		Mardon *et al.* (1961) and Cope *et al.* (1960)
Pu–Np phase diagram										Mardon *et al.* (1961) and Cope *et al.* (1960)
Pu–O system, see Section 7.8, Table 7.37										
$Pu_{19}Os(\zeta)$	related to β-Pu	orthorhombic	P*nna*	15.839(5)	7.819(3)	9.151(3)		52	18.02	Cromer (1979b)
$Pu_{19}Os(\eta)$		orthorhombic	C*mca*	5.345(5)	14.884(14)	10.898(15)		2	18.12	Cromer (1978)
Pu_3Os										Konobeevsky (1955)
$Pu_3Os(\eta')$										Ellinger *et al.* (1968b)
$Pu_5Os_3(\theta)$	W_5Si_3	tetragonal	I4/*mcm*	10.8818		5.6645		4	17.48	Beznosikova *et al.* (1974) and Cromer *et al.* (1975)
$PuOs_2(\iota)$	$MbZn_2$	hexagonal	P6$_3$/*mmc*	5.337		8.683		4	19.2	Konobeevsky (1955)
Pu–Os phase diagram										Konobeevsky (1955), Ellinger *et al.* (1968b), and Miner (1970)

Table 7.17 (*Contd.*)

Phase	*Structure type*	*Symmetry*	*Space group*	*Lattice parameters*				*Units per cell*	*X-ray density* (g cm^{-3})	*References*
				a_0(Å)	b_0(Å)	c_0(Å)	*Angle* (deg)			
Pu–P system, see Section 7.8, Table 7.33										
$Pu_3Pb(\zeta)$	Cu_3Au	cubic	$Pm3m$[a]	4.737(1)				1	14.56	Wood *et al.* (1969)
$Pu_5Pb_3(\eta)$	W_5Si_3	tetragonal	$I4/mcm$	12.310(2)		6.084(1)			13.07	Wood *et al.* (1969)
$Pu_5Pb_4(\theta)$	Ti_5Ga_4	hexagonal	$P6_3/mcm$	9.523(4)		6.482(3)			13.31	Wood *et al.* (1969)
$Pu_4Pb_5(\iota)$	Pu_4Pb_5(?)[b]	hexagonal	$P6_322$	16.52(1)		6.440(3)				Wood *et al.* (1969)
$PuPb_2(\kappa)$[c]	$HfGa_2$	tetragonal	$I4_1/amd$	4.621(5)		31.29(3)			12.99	Wood *et al.* (1969)
$PuPb_3(\lambda)$	Cu_3Au	cubic	$Pm3m$	4.8084(Pu-rich)				1		Wood *et al.* (1969)
				4.8077(Pb-rich)					12.86	Wood *et al.* (1969)
				4.808(1)				1	12.86	Bochvar *et al.* (1958) and Wood *et al.* (1969)
				4.81						Coffinberry and Miner (1961), Konobeevsky (1955), and Bochvar *et al.* (1958)
Pu–Pb phase diagram										Bochvar *et al.* (1958) and Wood *et al.* (1969)
Pu_5Pd_4 (probably identical with PuPd)										Kutaitsev *et al.* (1967)
PuPd	FeB	orthorhombic	$Pnma$	7.036(4)	4.550(2)	5.663(2)		4	12.65	Cromer (1975)
				7.028(5)	4.571(1)	5.658(2)		4	12.6	
Pu_3Pd_4	Pu_3Pd_4	rhombohedral (hexagonal setting)	$R\bar{3}$	7.916			$\alpha = 114.2$			Kutaitsev *et al.* (1967)
				13.304		5.783		2	12.8	Kutaitsev *et al.* (1967)
				13.344(2)		5.744(2)			12.85	Cromer *et al.* (1973)
Pu_3Pd_5	Ga_5Zr_3	orthorhombic	$Cmcm$	9.201	7.159	9.771		4	12.89	Cromer (1976)
$PuPd_3$	$AuCu_3$	cubic	$Pm3m$	4.077–4.119				1	13.41[d]	Kutaitsev *et al.* (1967)
				4.095						Erdmann and Keller (1973)
Pu–Pd phase diagram										Ellinger *et al.* (1968b) and Kutaitsev *et al.* (1967)

Pu–Pr system, no compounds, miscibility gap, phase diagram established									Ellinger *et al.* (1968a,b) and Kutaitsev *et al.* (1967)
Pu_5Pt_3(ζ)	Mn_5Si_3	hexagonal	P6_3/*mcm*	8.490		6.094	2		Beznosikova *et al.* (1974)
				8.490(2)		6.084(2)	2	15.57	Cromer and Larson (1975)
$Pu_{31}Pt_{20}$(η)	$Pu_{31}Pt_{20}$	tetragonal	I4/*mcm*	11.302(5)		37.388(23)	4	15.73	Cromer and Larson (1977)
PuPt(θ)	TaB	orthorhombic	C*mcm*	3.816	10.694	4.428		15.95	Kutaitsev *et al.* (1967), Cromer and Roof (1959)
$PuPt_2$(ι)	Cu_2Mg	fcc	F*d*3*m*	7.633			8	18.69	Erdmann and Keller (1973)
				7.631–7.653					Kutaitsev *et al.* (1967)
α-$PuPt_3$(κ)	$AuCu_3$	cubic	P*m*3*m*	4.107			1	19.75	Kutaitsev *et al.* (1967)
				4.105					Erdmann and Keller (1973)
β-$PuPt_3$(κ′)	PNi_3	bc tetragonal	I$\bar{4}$	10.39(1)		4.60(3)			Land *et al.* (1978)
$PuPt_4$(λ)	defect $PuPt_5$	orthorhombic	C*mmm*	5.258(15)	8.759(29)	4.563(13)			Land *et al.* (1978)
$PuPt_5$(μ)	$CaCu_5$	hexagonal	P6/*mmm*	5.262(8)		4.393(8)			Land *et al.* (1978)
	$SmPt_5$	orthorhombic		5.314	9.100	26.51			Erdmann and Keller (1973)
Pu–Pt phase diagram									Kutaitsev *et al.* (1967) and Land *et al.* (1978)[f]
Pu–Rb system, no compounds									Ellinger *et al.* (1968b)
$PuRe_2$	$MgZn_2$	hexagonal	P6_3/*mmc*	5.396(1)		8.729(1)	4	18.45	Coffinberry and Miner (1961)
Pu–Re phase diagram unknown									
Pu_2Rh(ζ)									Kutaitsev *et al.* (1967)
Pu_5Rh_3(η)		tetragonal	P4/*ncc*	10.94		6.020	4		Kutaitsev *et al.* (1967) and Beznosikova *et al.* (1974)
$Pu_{31}Rh_{20}$(θ)	$Pu_{31}Pt_{20}$	tetragonal	I4/*mcm*	11.076(1)		36.933(12)	4	13.87	Cromer and Larson (1977)
Pu_5Rh_4(ι)		orthorhombic	P*nma*	7.276(2)	14.332(4)	7.419(2)	4	13.79	Cromer (1977b)
				7.263	14.48	7.464	4	13.59	Blank and Lindner (1976)
PuRh(κ)									Kutaitsev *et al.* (1967)
Pu_3Rh_4(λ)									Kutaitsev *et al.* (1967)
$PuRh_2$(μ)	Cu_2Mg	fcc	F*d*3*m*	7.488			8	14.07	Kutaitsev *et al.* (1967) and Erdmann and Keller (1973)
$PuRh_3$(ν)	$AuCu_3$	cubic	P*m*3*m*	4.009–4.040			1	13.95	Kutaitsev *et al.* (1967)
				4.042					Erdmann and Keller (1973)
Pu–Rh phase diagram									Kutaitsev *et al.* (1967) and Land *et al.* (1978)

Table 7.17 (*Contd.*)

				Lattice parameters						
Phase	*Structure type*	*Symmetry*	*Space group*	a_0(Å)	b_0(Å)	c_0(Å)	*Angle* (deg)	*Units per cell*	*X-ray density* (g cm^{-3})	*References*
$Pu_{19}Ru(\zeta)$	$Pu_{19}Os$(?)									Ellinger *et al.* (1968b) and Miner (1970)
$Pu_3Ru(\eta)$		(ortho?)		(6.216)	(6.924)	(8.093)		(4)	(15.60)	Berndt (1962)
$Pu_5Ru_3(\theta)$	W_5Si_3	tetragonal	I4/*mcm*	10.7685		5.7473		4	14.93	Beznosikova *et al.* (1974)
				10.745(3)		5.719(2)		4	15.07	Cromer *et al.* (1975)
$PuRu(\iota)$	CsCl	cubic	P*m*3*m*	3.363(1)				1	14.87	Coffinberry and Miner (1961)
				3.3635(6)					14.84	Kutaitsev *et al.* (1967)
$PuRu_2(\kappa)$	Cu_2Mg	fcc	F*d*3*m*	7.476(1)				8	14.06	Coffinberry and Miner (1961)
				7.472(1)–7.476(1)					14.03	Coffinberry and Miner (1961)
				7.4737(1)(Ru-rich)						Kutaitsev *et al.* (1967)
Pu–Ru phase diagram										Seaborg *et al.* (1946, 1949b), Kutaitsev *et al.* (1967), and Cope (1960)
Pu–S system, see Section 7.8, Table 7.39										
'$Pu_{11}Sc_9$'(ζ)		hexagonal	P6_3/*mmc*	3.310(Pu-rich)		10.717		4	10.5	Kutaitsev *et al.* (1967)
				3.308(Sc-rich)		10.709				
'Pu_5Sc_4'										Kutaitsev *et al.* (1967)
Pu–Sc phase diagram										Ellinger *et al.* (1968b), Miner (1970), and Kutaitsev *et al.* (1967)
Pu–Se system, see Section 7.8, Table 7.39										
Pu–Si system, see Section 7.8, Table 7.32										
Pu–Sm phase diagram										Ellinger *et al.* (1968a,b)^f
Pu_3Sn	$AuCu_3$(?)	fcc		4.680						Ellinger *et al.* (1968b)
$PuSn_2$	$HfGa_2$	tetragonal	$I4_1$/*amd*	4.43(2)		31.0(1)				Wallace and Harvey (1974)
$PuSn_3$	$AuCu_3$	fcc	P*m*3*m*	4.630(1)				1	9.96	Coffinberry and Miner (1961)
				4.654(2)						Akhachinskii and Bashlykov (1970)

Pu–Sn phase diagram unknown								
Pu–Sr system, no compounds								Ellinger *et al.* (1968b)
Pu–Ta system, no compounds, phase diagram established								Ellinger *et al.* (1968b)
Pu–Tc system, no information								
Pu–Tb system, no compounds								Ellinger *et al.* (1968b)
Pu–Te system, see Section 7.8								
$Pu_{13}Th_6$		orthorhombic	9.820	8.164	6.681	6		Poole *et al.* (1957)
			7.90	8.43	9.79	8		Bochvar *et al.* (1958)
Pu–Th phase diagram								Seaborg *et al.* (1946, 1949b), Ellinger *et al.* (1968b), Bochvar *et al.* (1958), and Poole *et al.* (1957)
Pu–Ti system, no compounds, phase diagram established								Ellinger *et al.* (1968b) Grison *et al.* (1960) Kutaitsev *et al.* (1967)
Pu_3Tl	$AuCu_3$	cubic	4.723				14.5	Bochvar *et al.* (1958)
$PuTl_3$	disordered Mg	hexagonal	3.458		5.519		12.4	Bochvar *et al.* (1958)
Pu–Tl system, phase diagram not yet established								
Pu–Tm system, no compounds								Bowersox and Leary (1966)
Pu–U(ζ)		primitive cubic						
35 at.%U			10.60(2)					Waldron *et al.* (1958)
35 at.%U			10.692				18.5	Ellinger *et al.* (1959)
50 at.%U			10.61(1)					Waldron *et al.* (1958)
50 at.%U			10.664					Ellinger *et al.* (1959)
65 at.%U			10.65(1)					Waldron *et al.* (1958)
70 at.%U			10.651			58	18.8	Waldron *et al.* (1958)
Pu–U(η)		tetragonal						
25 at.%U			10.57(5)		10.76(5)	52	17.3	Ellinger *et al.* (1959)
20 at.%U			10.44		10.73	56	18.5	Bochvar *et al.* (1958)
Pu–U phase diagram								Coffinberry and Miner (1961) and Ellinger *et al.* (1959)

Table 7.17 (*Contd.*)

				Lattice parameters						
Phase	*Structure type*	*Symmetry*	*Space group*	a_0(Å)	b_0(Å)	c_0(Å)	*Angle* (deg)	*Units per cell*	*X-ray density* (g cm^{-3})	*References*
Pu–V system, no compounds, phase diagram established										Konobeevsky (1955), Ellinger *et al.* (1968b), and Bowersox and Leary (1967)
Pu–W system, no compounds, phase diagram established										Ellinger *et al.* (1968b)
PuY system, no compounds, phase diagram established										Ellinger *et al.* (1968b), Kutaitsev *et al.* (1967), and Wittenberg and Grove (1963)
Pu–Yb system, no compounds										Ellinger *et al.* (1968b)
$\mathrm{PuZn_2}(\zeta)$	$\mathrm{Cu_2Mg}$	bc tetragonal	$\mathrm{F}d3m$	7.760(1)(Pu-rich) 7.747(1)(Zn-rich)				8	10.54 10.5	Cramer *et al.* (1960)
$\mathrm{Pu_2Zn_{\sim 9}}(\eta)$		hexagonal	$\mathrm{P}6_3/mmc$ (?)	28.86(2)		14.14(1)			9.05	Larson and Cromer (1967)
$\mathrm{Pu_{13}Zn_{58}}$	subcell of $\mathrm{Pu_2Zn_{\sim 9}}$	hexagonal	$\mathrm{P}6_3/mmc$ or $\mathrm{P}6_3mc$	(14.43)		(14.14)		2	8.98	Larson and Cromer (1967)
$\mathrm{Pu_3Zn_{22}}(\theta)$		bc tetragonal	$\mathrm{I}4_1/amd$	8.85		21.18		4	8.71	Johnson *et al.* (1967)
$\mathrm{Pu_2Zn_{17}}(\iota)$	$\mathrm{Th_2Zn_{17}}$	rhombohedral (hexagonal setting)	$\mathrm{R}\bar{3}m$	8.95		13.1			8.5	Cramer and Wood (1967)
‘$\mathrm{Pu_2Zn_{17}}$’$(\kappa)^{e}$		hexagonal	$\mathrm{P}6/mmm$	8.9		17.7				Cramer and Wood (1967)

‘Pu_2Zn_{17}’(κ′)[e]		hexagonal	$P6_3/mmc$	8.98		8.85			Cramer and Wood (1967)
‘Pu_2Zn_{17}’(λ)[e]		hexagonal	$P6_322$	8.98		8.85			Cramer and Wood (1967)
Pu–Zn phase diagram									Cramer *et al.* (1960) and Albrecht (1964)
$Pu_{28}Zr$(ζ)	related to β-Pu	bc tetragonal	$I4_1/a$	18.1899(3)		7.8576(2)	4		Cromer (1979a)
				18.19(1)		7.851(3)		17.444	Zachariasen and Ellinger (1970)
~Pu_6Zr		orthorhombic		10.39	10.44	11.18	8	16.7	
Pu_4Zr(ι)		tetragonal	$P4/ncc$	10.893(3)		14.889(7)	16	15.76	Berndt (1967)
$PuZr_{2-3}$(κ)	UZr_2	hexagonal	$P6/mmm$	5.060		3.119	1		Bochvar *et al.* (1958)
				5.055		3.123			Marples (1960)
Pu–Zr phase diagram									Bochvar *et al.* (1958) and Johnson (1954)

---

[a] No superstructure observed (Pu_3Pb).

[b] Preliminary analysis (Pu_4Pb_5).

[c] Low-temperature modification($PuPb_2$).

[d] For 75 at.% Pu ($PuPd_3$).

[e] Assignments to phase regions at the zinc-rich end of the phase diagram (Pu_2Zn_{17}).

[f] Also, F. H. Ellinger, C. C. Land, and K. A. Johnson, unpublished work, Los Alamos Scientific Laboratory.

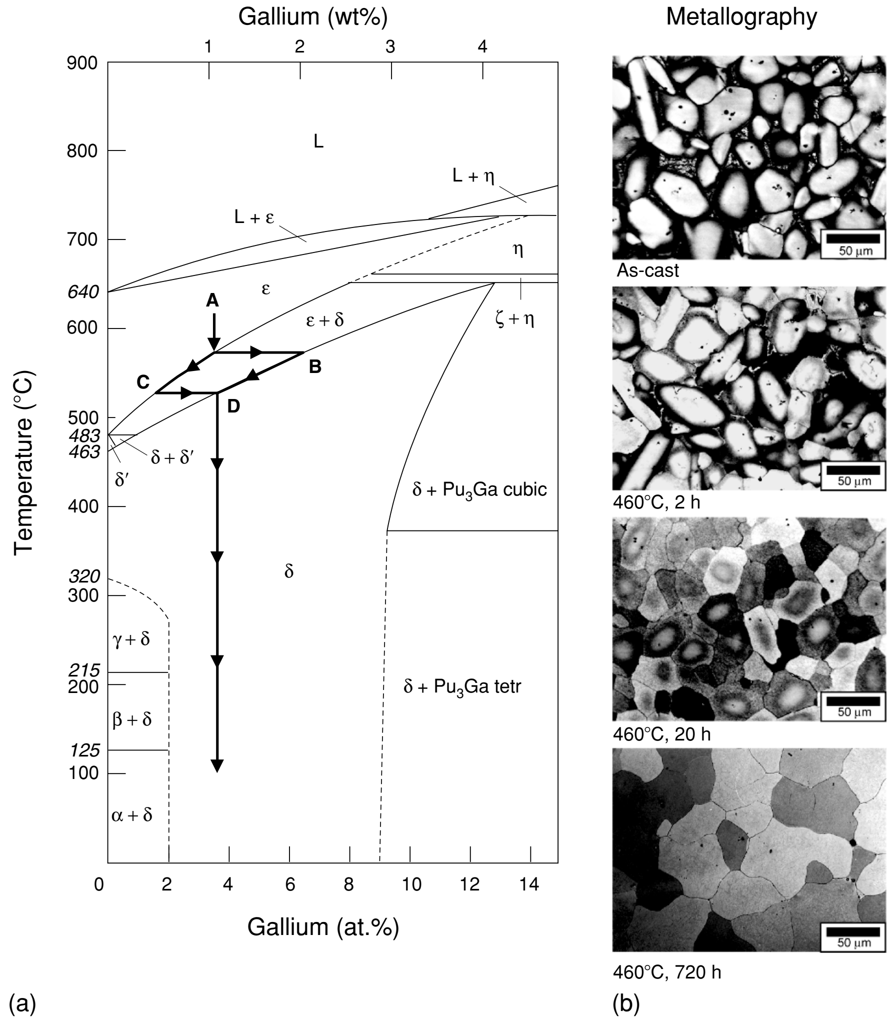

Fig. 7.33 (*a*) *The Pu-rich side of the Pu–Ga phase diagram depicting a typical gallium segregation path.* (*b*) *Typical optical microstructures of a Pu-*3.4 at. *% Ga alloy for various conditions* (*from as-cast to annealed at* 460°C *for* 720 h) (*Mitchell* et al., 2001).

a uniform gallium concentration. The progression of gallium 'homogenization' and consequent change in microstructure are also shown for a homogenization temperature of 460°C in Fig. 7.33(b).

Such microsegregation can occur with any of the alloying elements that retain the δ phase to room temperature. The extent of microsegregation depends on the cooling rate and on the shape of the two-phase field. A typical gallium

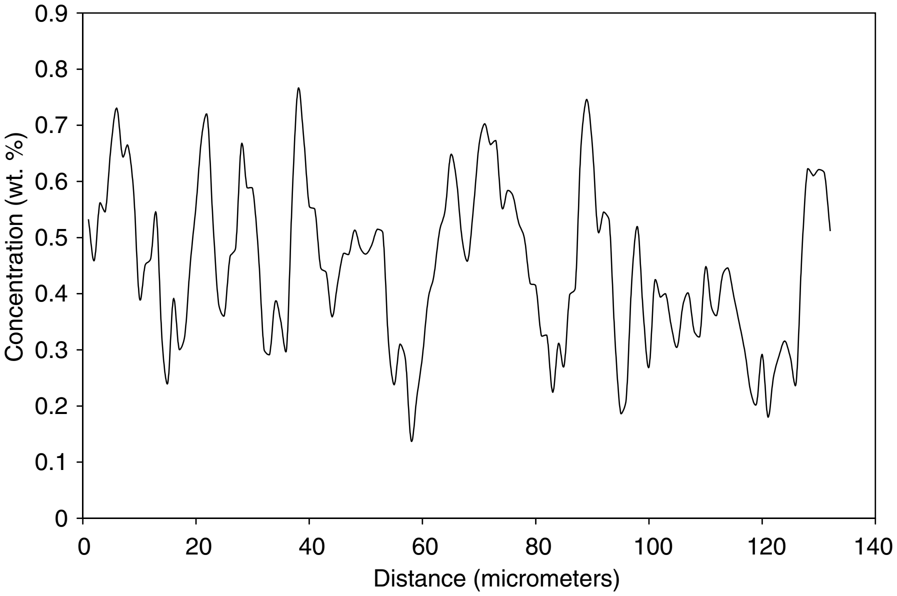

Fig. 7.34 *A typical gallium concentration profile for a nominal Pu-*1.7 at. *% Ga* (0.5 wt. *% Ga*) *alloy by electron microprobe. The grain size was roughly* 30 μm (*from unpublished work of one of the authors, S. S. Hecker*).

profile taken with an electron microprobe is shown in Fig. 7.34 for Pu–1.8 at.% Ga cooled at a rate of ~5°C min^{-1}. At such rates, all areas with <1.4 at.% Ga transform to the α phase upon cooling to room temperature. If initial cooling rates are rapid, and homogenization times of hundreds of hours at 460°C are employed, then the δ phase can be retained to room temperature with as little as 1 at.% Ga. However, the retained δ phase is metastable and will transform at low temperatures and/or hydrostatic compression. Hence, proper homogenization treatments for δ-phase alloys are important in studying plutonium alloys. If not properly homogenized, such alloys exhibit continuously varying gallium gradients (on the scale of the grain size as shown in Fig. 7.34), or they may consist of two-phase mixtures. Either one of these conditions can significantly affect the properties of the alloy.

(g) Phase transformations in δ-phase alloys

Hecker *et al.* (2004) and Deloffre (1997) presented comprehensive overviews of phase transformations in δ-phase plutonium alloys. During cooling the retained fcc δ phase transforms to the monoclinic α phase (sometimes through an intermediate phase such as the β phase or γ phase). The transformation behavior as monitored in a dilatometer is shown for a constant cooling rate for several

Pu–Ga alloys (Hecker *et al.*, 2004) in Fig. 7.35. The transformation is martensitic, that is, diffusionless and displacive (shear). The transformation start temperature depends strongly on the gallium concentration (all three alloys shown were thoroughly homogenized before cooling) as shown in Fig. 7.35. The transformation behavior depends on cooling rate and is, therefore, characterized as an isothermal martensitic transformation. Orme *et al.* (1976) determined the TTT kinetics for Pu–Ga alloys as illustrated by the double C-curves shown in Fig. 7.36. Thermal activation appears to be necessary to nucleate the transformation before the martensite transformation product grows by a shear mechanism at sonic velocities. The C-curve kinetics result from insufficient

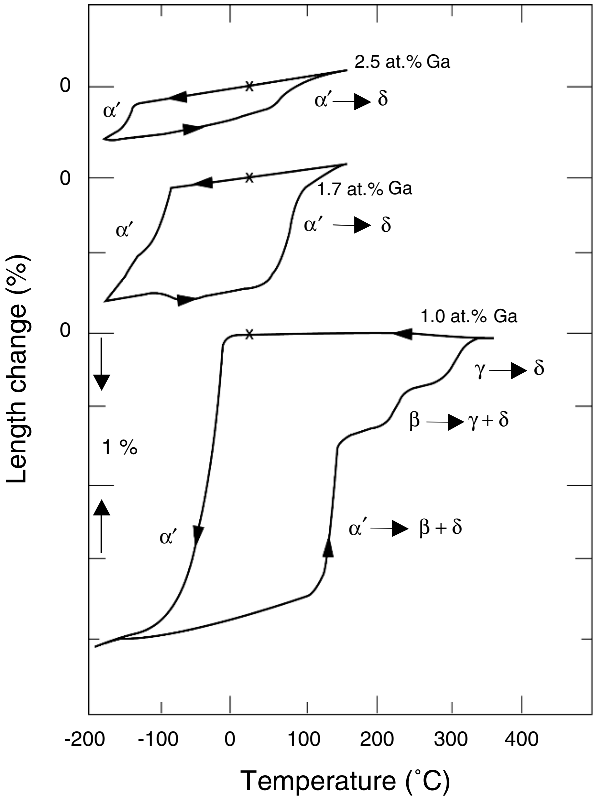

Fig. 7.35 *Thermally induced δ→α′ and reverse transformations for Pu–Ga alloys during cooling and heating. The zero is offset for the three curves as shown. The α′ phase in the* 2.4 *and* 1.7 at. *% Ga alloys revert back to the δ phase. The α′ phase in the Pu-*1 at. *% Ga alloy reverts along a more complex path to mostly β, then γ and finally to the δ phase with a small amount of the α′ phase reverting directly to the δ phase as the rest transforms to the β phase. The x in each of the three figures denotes the onset of the cooling and the end point after heating and cooling* (*Hecker* et al., 2004).

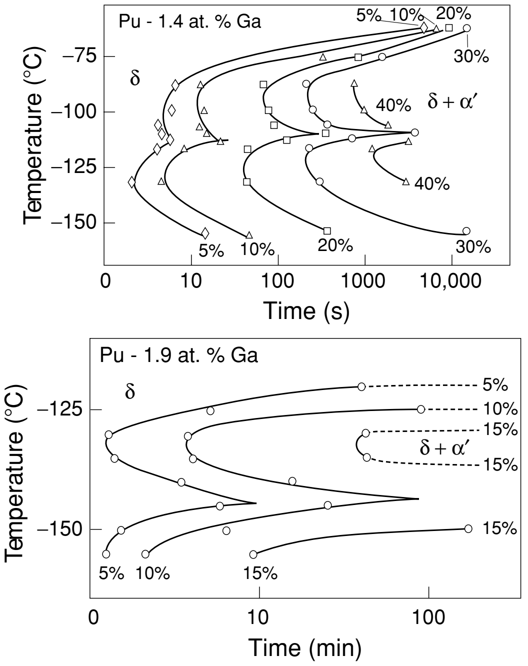

Fig. 7.36 *Time–temperature-transformation curves for* (*top*) *Pu*-1.4 at. *% Ga and* (*bottom*) *Pu*-1.9 at. *% Ga alloys* (*Orme* et al., 1976). *Transformation curves are shown for* 5, 10, 20, *and* 30% *transformation in* (*top*) *and for* 5, 10, *and* 15% *transformation in* (*bottom*) (*from Hecker* et al., 2004).

driving force at the higher temperatures and insufficient thermal activation at the lower temperatures. The overall kinetics is shown to be dependent on gallium concentration.

Similar transformation behavior is observed for δ-phase Pu–Al alloys as demonstrated by Hecker *et al.* (2004) and shown in Fig. 7.37. The well-homogenized Pu–2 at.% Al alloys begin to transform at approximately −130°C during cooling. After cooling to liquid nitrogen temperature and heating back to room temperature, metallographic and X-ray examination showed that the resulting microstructure (shown in Fig. 7.37) consisted of 25% α′ phase (in the form of martensite platelets) and 75% residual δ phase. The α′-phase designation is used here to indicate that the aluminum or gallium atoms, which have no equilibrium solubility in the α phase, are trapped by the martensitic transformation and expand the lattice of the α phase (Hecker *et al.*, 2004). During hydrostatic compression at room temperature, the δ phase collapses just below 0.4 GPa (as shown in Fig. 7.37), transforming martensitically first to the β′ followed by the α′ phase. The microstructure is more complex as shown in Fig. 7.37. If such

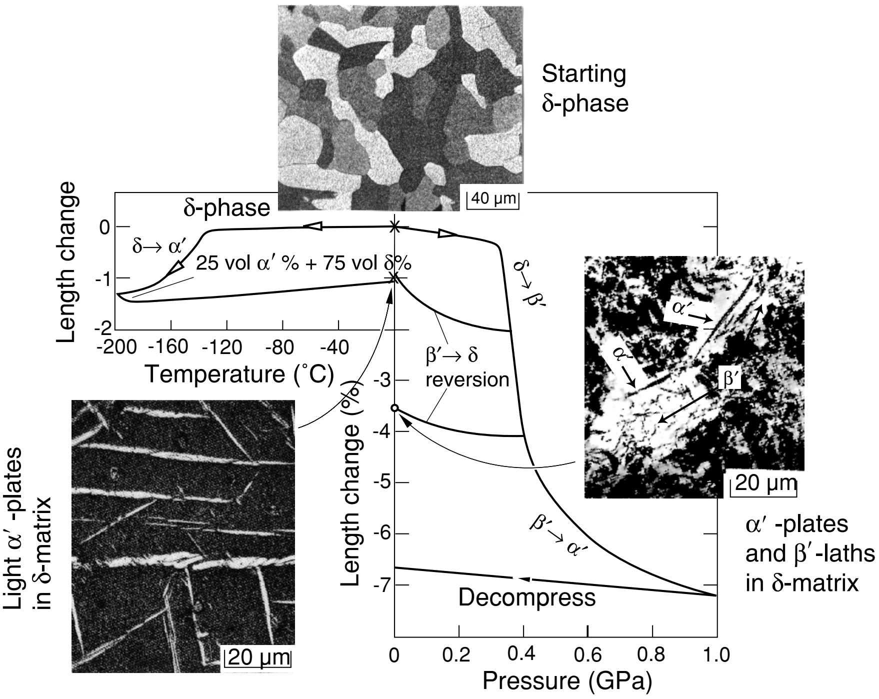

Fig. 7.37 *Temperature and pressure-induced transformations in Pu-*2.0 at. *% Al alloys* (*Zukas* et al., 1981*; Hecker* et al., 1982). *The starting δ-phase microstructure is shown on top and the transformed microstructures on the left and right for temperature and pressure-induced transformations, respectively.*

samples are compressed only partially, then both product phases appear in the residual δ-phase matrix.

Adler and coworkers (Olson and Adler, 1984; Adler *et al.*, 1986) modeled the crystallography of the δ→α′ transformation during cooling. Zocco *et al.* (1990) subsequently confirmed their predictions by transmission electron microscopy (TEM) and determined the lattice correspondence between the parent and product phases and the α′-phase habit plane. The details of the experimental and theoretical results are reviewed by Hecker *et al.* (2004). Heating the transformed α′ phase above room temperature for Pu–Ga alloys results in the transformation behavior shown in Fig. 7.35. The low-gallium alloys transform from α′→β→γ, whereas the higher-gallium alloys transform directly from α′→δ at temperatures significantly lower than the α→β transformation temperature.

Complex stress states such as those found during cold rolling, machining, or mechanical polishing all trigger the δ→α′ transformation. Machining most likely produces a complex mixture of α′ and α-phases (that is, expanded and unexpanded) because of the heat generated. Mechanical polishing is especially effective in promoting the γ'-phase as an intermediary phase (Zukas *et al.*, 1983). These authors also observed that samples that had previously undergone a $\delta\rightarrow\alpha$ transformation were susceptible to the reverse $\alpha'\rightarrow\delta$ transformation at the crack tip of tensile specimens. Hydrostatic tension favors the larger volume δ phase. Hecker and Stevens (2000) reported this behavior for both transformed samples and for unalloyed α plutonium. The reversion results reinforce the importance of the sign and magnitude of the hydrostatic stress component in triggering martensitic transformations in plutonium.

The complex nature of the transformation behavior for plutonium and its alloys must be taken into account during sample synthesis and preparation. In plutonium alloys, the slightest mechanical polishing or machining procedures can leave a layer of transformation product that may influence the properties to be measured. Such transformation products can be avoided or removed, but only if sufficient care is taken. For example, electropolishing is quite effective to remove surface products. Heating is also effective but must be done with care so as to not introduce new artifacts or changes in structure (this is especially true for aged samples in which helium has been generated by self-irradiation damage).

7.7.5 Electronic structure, theory, and modeling

The complex electronic structure of plutonium has been a subject of intense study for theorists and modelers for more than 50 years. Arko *et al.* (2006) present the most recent review of electronic structure in the actinides, including plutonium, in Chapter 21 of this work. As mentioned above, the actinides mark the filling of the 5f atomic subshell much like the rare earths mark the filling of the 4f subshell. Yet, the 5f electrons of the light actinides behave more like the 5d electrons of the transition metals than the 4f electrons of the rare earths. The peculiar properties described in Section 7.7.3, and shown in Fig. 7.19, are telltale signs of novel interactions and correlations among electrons, which result in behavior that cannot be explained by the one-electron band theory of metals. Boring and Smith (2000) point out that such novel interactions typically result from a competition between itinerancy (bonding electrons that form bands in metals) and localization (electrons with local moments that magnetically order at low temperature). In these elements, we find that such novel interactions occur in the d- and f-electron metals near iron, at cerium, and near plutonium. Based on these considerations, Smith and Kmetko (1983) rearranged the periodic table for the transition metals, the rare earths, and the actinides as shown in Fig. 7.38. This representation shows that most transition metals, lanthanides, and actinides have predictable ground states and become either superconducting or magnetic as the temperature is lowered. The elements along the diagonal have two or more partially filled bands that are close in energy. One of the bands is typically relatively narrow with a high density of states (DOS) at the Fermi

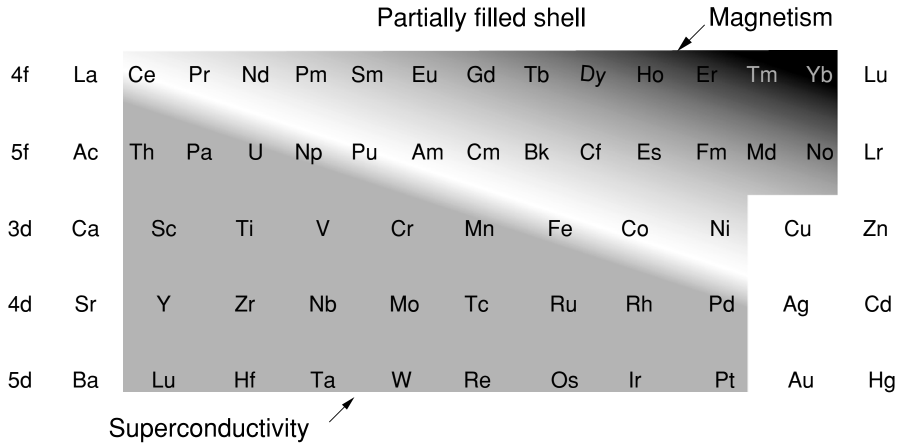

Fig. 7.38 *Smith and Kmetko* (1983) *rearranged periodic table that highlights the transition in electronic behavior from localized electrons* (*resulting in magnetism*) *to itinerant electrons* (*resulting in superconductivity*).

energy (the f-bands are 2 to 4 eV wide and the d-bands span 5 to 10 eV). Narrow bands tend to mix or hybridize with other bands close in energy. The electrons in these narrow bands can be strongly correlated, but still bonding. They spend much more of their time close to their atomic cores than do the 'free' (valence) s-electrons. The electrons in the narrow bands are highly sensitive to small perturbations, which enhances polymorphism and causes instability in the solid state. Smith and Boring point out that in addition to exhibiting multiple crystal structures, the elements along the diagonal also exhibit strong catalytic activity, have a great affinity for hydrogen, and spark easily when struck. Moreover, the behavior of the elements can easily be moved across the diagonal by changes in temperature, pressure, or by alloying.

The electronic configuration of isolated plutonium atoms is $7s^2 5f^6$ (see Section 7.6). In the metallic state the electronic configuration is $7s^2 6d^1 5f^5$. The atomic volumes in the solid state change abruptly across the actinide series at plutonium, as shown in Fig. 7.39. This change indicates a major electronic transition between the light and the heavy actinides. In the light actinides up to plutonium, each additional 5f electron (like each d-electron in the transition metals) goes into the conduction band, where it increases the chemical bonding forces, pulling the atoms closer together and resulting in a decrease in atomic volume. Beginning at americium, the 5f electrons behave like the 4f electrons of the rare earths, localizing at each lattice site and becoming chemically inert. With no 5f contribution to bonding, the atomic volume suddenly increases at americium, and contracts only slightly with increasing atomic number because the 5f electrons remain localized in the remainder of the series. As shown in

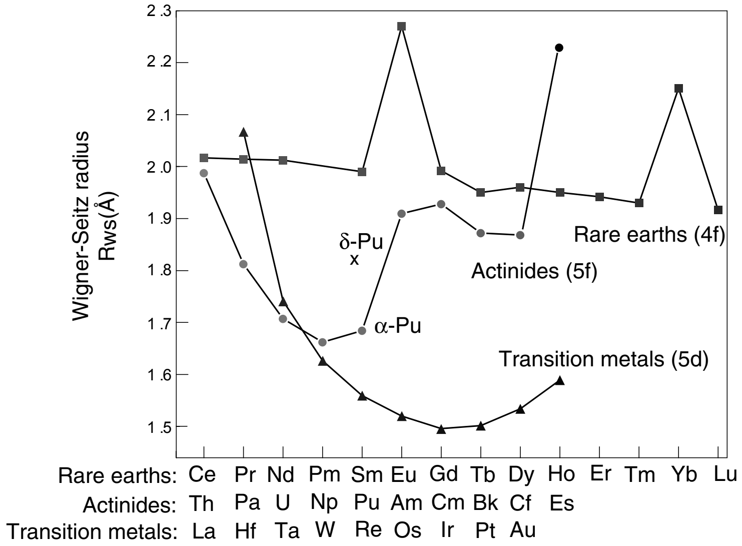

Fig. 7.39 *Wigner–Seitz radii for the actinides compared to the lanthanides and 5d transition metals. The actinides include the data for Es* (*Haire* et al., 2004), *which is divalent with a large volume, much like Eu in the lanthanides.*

Fig. 7.39, this behavior is similar to the lanthanides. The large jump in atomic volume at Es is due to divalent behavior similar to that for Eu and Yb for the lanthanides. The pattern of local moments, another strong indicator of what the electrons are doing, confirms this general picture. The light actinides show no local moments, as expected if all the valence electrons are in the conduction band, whereas the heavy actinides and the lanthanides generally exhibit local moments.

In the α phase, the 5f electrons appear to be bonding (although Savrasov *et al.* (2001) claim that the f-electrons are already strongly correlated in the α phase), whereas in americium the 5f electrons are clearly localized. It is interesting to note here that americium was found to be an ordinary superconductor with no hint of a magnetic moment although it is on the 'magnetic' side of the diagonal in Fig. 7.38 (Smith and Haire, 1978). This is a consequence of the $5f^6$ electronic configuration resulting in a total angular momentum $J = 0$, so that no moment is present even in the free ion limit. As shown by the atomic volumes in Fig. 7.39, the δ phase in pure plutonium falls between the plutonium α phase and the americium dhcp phase. The plutonium δ phase is a state that appears to be unique among the elements. Before addressing the δ phase, we will first consider the α phase ground state.

First-principles total-energy calculations based on density-functional theory (DFT) successfully predict electronic structure and bonding properties of simple metals and the transition metals (Skriver, 1985). With the advent of high-performance computing, it has become possible during the past 10 to 15 years to extend such calculations to the actinides by incorporating low-symmetry crystal structures, relativistic effects, and electron–electron correlations. The complicated electron–electron exchange term arising from the Pauli exclusion principle and electron–electron electrostatic interactions are incorporated through a local density approximation (LDA) or a generalized gradient approximation (GGA), which incorporates the local electron density and the density gradient. Wills and Eriksson (2000), who summarized their efforts and those of their colleagues, successfully predicted the structures and volumes of the low-symmetry ground states of the light actinides, including plutonium. These calculations show that in α plutonium all eight valence electrons are in the conduction band. However, the 5f bands are very narrow – that is, each 5f electron is nearly localized on an atomic site and, hence, spends a long time near this site before it jumps to the next site. Because the bands are narrow, they exhibit a very high DOS. As the number of 5f electrons populating the band increases across the actinide series, the specific properties of the band begin to dominate the bonding properties of the metal.

Wills and Eriksson demonstrated that the α phase is the stable ground state of plutonium because special conditions favor lattice distortions. Specifically, the very narrow band of the 5f electrons with a high DOS at or very near the Fermi energy split the band in certain regions, thereby lowering the total energy through a Jahn–Teller/Peierls-like distortion. We recall that in iron the degeneracy of the d-conduction band is lifted by the electron spins causing the d-band to split spontaneously into spin-up and spin-down bands. In plutonium the degeneracy of the f-band is lifted by a lattice distortion leading to lower energy. Also, because the narrow 5f band overlaps the s, p, and d bands, a number of electronic configurations have nearly equal energy, leading to multiple allotropes in the light actinides and to their great sensitivity to external influences such as temperature, pressure, and chemical additions. Before the insight gained from the calculations of Wills and Eriksson, the low-symmetry ground state in metallic plutonium was attributed to directional or covalent-like bonding, resulting from the angular characteristics of f-electron orbitals (somewhat analogous to molecular bonding, see Section 7.9.3) (Boring and Smith, 2000; Hecker, 2000). Although total-energy electronic structure calculations apply only at zero temperature, they have been remarkably successful in predicting the ground-state properties of the actinides, both at ambient and elevated pressures. In addition, energy differences for various structures can be calculated to give an indication of whether these are thermally accessible. Wills and Eriksson (2000) point out that including temperature effects is not a simple task. One possibility is to integrate existing molecular dynamics or Monte Carlo simulations with electronic structure calculations. It may also be possible that accurate calculations of the phonon spectra of different allotropes may enable reliable calculations of the free energy as a function of temperature.

We now turn to the fcc δ phase, which is the most desirable from an engineering standpoint but the least understood from a physics standpoint. As shown in Fig. 7.39, the volume (the Wigner–Seitz radius is actually plotted) of the δ phase falls between that of α plutonium and americium. The 5f electrons appear to be in some mixed state, neither fully itinerant nor fully localized. Above, we pointed out that the δ phase has other unusual properties, such as a negative thermal expansion coefficient and an unusually large low-temperature electronic specific heat. Unfortunately, even the best calculations based on standard DFT with some LDA do not adequately predict the δ-phase volume or elastic constants in unalloyed plutonium. This failure has spawned numerous attempts to go beyond the LDA. Wills and Eriksson (2000) found that they had to 'constrain' their calculations by localizing four of the five 5f electrons in the δ phase to predict the correct atomic volume using the same formalism as for the ground state of the light actinides. The constrained 5f electrons cannot hop from site to site and do not hybridize with other electrons. In essence, the constrained calculations combine knowledge of DFT and atomic theory. Hecker *et al.* (2004) review other recent attempts to explain the peculiarities of the δ phase. However, none of them currently provide an adequate explanation. The approach of Wills and Eriksson provides the best current guidance for understanding the δ phase and the alloying behavior of plutonium. This is clearly an area where we can expect significant advances in our understanding over the coming decade.

(a) Alloy theory and modeling

Before discussing the alloying behavior, it is instructive to view the behavior of plutonium in context of the other actinides. Fig. 7.40 shows the connected binary alloy phase diagrams of the actinides through curium. At the beginning of the actinides, there is little f-electron influence and, hence, one finds typical metallic crystal structures, few allotropes, and high melting points. As more f-electrons are added (up to plutonium) and participate in bonding (that is, they are itinerant), the crystal structures become less symmetric, the number of allotropes increases, and the melting points decrease. At americium and beyond, crystal structures typical of metals return, the number of allotropes decrease, and the melting points rise – all indications of the f-electrons becoming localized or inert. So we see that the peculiar properties of plutonium are not a single anomaly, but rather the culmination of a systematic trend across the actinides. And, the transition occurs not between plutonium and americium, but right at plutonium – between the ground-state α phase and the elevated-temperature δ phase.

To predict plutonium alloy phase diagrams, we need to know the Gibbs free energy of all the phases and compounds as a function of alloy concentration and temperature. We must calculate the internal energy and the entropy (electronic, vibrational, and configurational). To predict δ-phase stability, we must be able

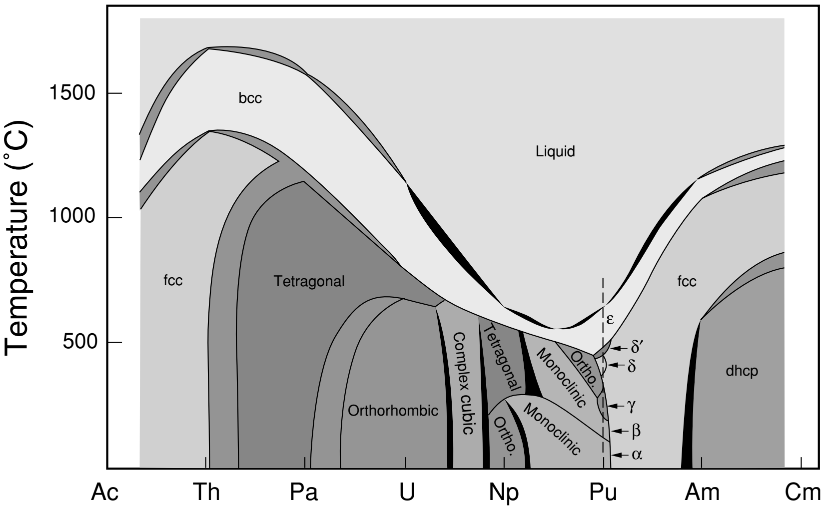

Fig. 7.40 *The experimentally determined, connected binary alloy phase diagram of adjacent actinide elements* (*Smith and Kmetko,* 1983).

to calculate the internal energy of a random substitutional alloy from first principles, which is an immense challenge. So, it is not surprising that semiempirical and phenomenological approaches have guided metallurgical practitioners for many decades. The Hume–Rothery rules, recently reviewed by Massalski (1996) and Gschneidner (1980), relate limits of solid solubility as well as the stability and extent of transition element intermediate phases to three factors:

1. If the atomic size differences of A and B are greater than 15%, solid solubility will be restricted. Significant experimental data support this rule. From a theoretical point of view, large size differences result in large elastic strain energies. The atomic size rule is primarily a ‘negative’ rule stressing that size differences will restrict solid solution formation. Within favorable size ranges, size differences become only of secondary importance.
2. High chemical affinity of A for B (usually denoted by large differences in electronegativity) helps promote intermetallic compounds and, therefore, limits solid solubility.
3. The relative valence rule stresses the importance of electron concentration, which is typically taken as the ratio of all valence electrons to the number of atoms (*e*/*a*).

Darken and Gurry (1953) developed a map that predicts solubility for size differences less than 15% and electronegativity differences of less than 0.4.

Gschneidner (1980) achieved best overall agreement on a large number of known binary alloys by relating solubility to size and similar electronic structures (for which he used the crystal structure as a first approximation) of the constituents. The Darken and Gurry maps for plutonium alloys have been discussed by Blank (1977).

We have not found any of these approaches, or the more sophisticated methods developed by Pettifor (1996) (using tight-binding approximation models) or by Miedema and coworkers (Miedema, 1973, 1976) (using a two-parameter model based on the work function, which is closely related to electronegativity, and on electron density) helpful in predicting solid solubility in δ-phase plutonium. Given the complex electronic structure of plutonium, especially the δ phase, this is not surprising. It is difficult to imagine that these simple approaches would capture the essence of how the electronic structure of plutonium changes with the addition of other elements. However, the Hume–Rothery size rule appears to set a reasonable upper limit on solubility.

Brewer (1965, 2000) developed models based on chemical binding insight to relate phase stability primarily to the total number of valence electrons per atom. Ferro and Cacciamani (2002) recently reviewed the work of Brewer and colleagues on the classification and mapping of alloying patterns. Brewer (1970, 1983) provided some useful insights and general guidance on solubility, melting points, and thermodynamic properties of plutonium and the actinides. For example, he predicted little mutual solubility between plutonium and the alkali metals, the alkaline-earth metals from calcium through radium, and europium and ytterbium. Also, he predicted little solubility of the 4d and 5d transition metals in plutonium, but somewhat greater solubility of the 3d transition metals. He also offered an explanation of the low melting point of plutonium based on the unusually stable liquid phase. He pointed out that plutonium exhibits four or more electronic configurations of comparable energy in the metal. Consequently, atoms of plutonium have different sizes that are readily accommodated in the liquid and pack to very high density. The strain energy resulting from trying to accommodate different-sized atoms into structures such as bcc and fcc with equivalent atom sites destabilizes these structures compared to the liquid. The stability of the liquid, according to Brewer, results from the increased entropy of mixed valence in the liquid state.

A more quantitative, phenomenological approach to predicting phase diagrams was developed by Kaufman and coworkers (Kaufman and Bernstein, 1970; Chang *et al.*, 2002; Kaufman, 2002). The success of CALPHAD (calculation of phase diagrams), a computational thermodynamics approach to predicting phase diagrams of multicomponent alloy systems based on the work of Kaufman and coworkers, was recently reviewed by Turchi *et al.* (2002). Applications of computational thermodynamic modeling to plutonium and its alloys is being developed, but is limited by the lack of good thermodynamic data on plutonium, its alloys, and its compounds. Adler (1991) assessed the Pu–Ga diagram with a calculation using FACT (Facility for the Analysis of Chemical

Thermodynamics, A. Pelton) and retrieved the excess free energy consistent with the Russian phase diagram. Turchi *et al.* (2004) applied the CALPHAD methodology to study the stability and the kinetics of phase transformation and evolution in plutonium-based alloys. They report very good agreement with the thermodynamic properties of pure, unalloyed plutonium. They also predict eutectoid decompositions for both the Pu–Ga and Pu–Al alloy systems.

This brings us back to the first-principles calculations for random alloy systems. In pure materials and perfectly ordered systems, the solution of the many-body Schrödinger equation is simplified by Bloch's theorem that allows us to solve the equation for one cell and use translational symmetry. Random substitutional alloys are disordered by definition and, hence, require some short-range order approximation, typically using an Ising-like cluster expansion. Colinet (2002) recently reviewed the state of the art of deriving phase diagrams by combining quantum mechanics and statistical thermodynamics contributions. Local chemistry affects both the internal energy and the configurational entropy. Statistical treatments of short- or long-range order in solid solutions can use the cluster variation method (CVM) or Monte Carlo simulations. The cluster interactions are either derived experimentally or from first-principles calculations. Local relaxations around the solute atoms are important but also difficult to treat theoretically (Zunger *et al.*, 1990; Abrikosov *et al.*, 1998). Although significant progress has been made in some of the well-studied alloy systems, first-principles calculations of phase stability or phase diagrams are still beyond our grasp. For plutonium, the difficulty is exacerbated by the fact that the parent δ phase is not well understood theoretically and key experimental measurements are sparse.

Baskes (2000) recently extended his semiempirical atomistic embedded-atom method (which is based on DFT) to plutonium. He found reasonable agreement of the calculated energetics and volumes of the phases of plutonium with experimental data. With this method, it is possible to calculate the properties of perfect and defect-containing bulk metal as a function of temperature and pressure. Baskes *et al.* (2003) extended the modified embedded-atom method to model the Pu–Ga phase diagram. They found that a subregular solid solution model is required to describe the properties of the δ phase. They were able to predict the eutectoid decomposition of the δ phase, in qualitative agreement with the Russian phase diagram. However, the accuracy of the calculated temperature and composition of the eutectoid point is limited by inadequate thermodynamic data on Pu_3Ga.

For now, the calculations of Wills and Eriksson (2000) provide good insight into δ-phase stability and alloying. They demonstrated that the low-symmetry ground states in plutonium and the other light actinides require the special conditions of narrow bands and high DOS at or very near the Fermi energy (a natural consequence of the oddity of an f-electron conduction band). It seems reasonable then that anything that destroys these special conditions favors the retention of high-symmetry structures. Their calculations show that energy can be gained (that is, the total energy lowered) either through bonding energy gained from a structural distortion, or through correlation energy gained by localization of the electrons. Plutonium is exactly at that position in the periodic table where either process leads to about the same energy gain. However, alloying or defects disturb the coherence of the 5f bands, thus reducing the bonding energy and leading to at least partial localization of the 5f electrons. Hence, we believe that the fcc δ phase is favored at high temperature in unalloyed plutonium because of 'bond stretching' (in addition to entropy considerations) and in alloys because of 'bond breaking.' Hence, we may expect any alloy addition without bonding 5f electrons to favor the δ phase, assuming it can be dissolved in plutonium. Likewise, defects such as vacancies, vacancy clusters, dislocations, and grain boundaries may favor the retention of the δ phase locally.

Sadigh and Wolfer (2005) recently suggested another mechanism based on their DFT calculations, which showed that the volume decrease that occurs with gallium additions to the δ phase is primarily the result of the reduction in size of the plutonium host atoms. This reduction accounts for roughly two-thirds of the experimentally measured value. The other third is split between the misfit of the gallium in the δ-phase lattice and the elastic strains. The large volume reduction of the plutonium is accompanied by a negative heat of mixing. Their calculations showed that the enthalpy of transformation from the δ→α phase at absolute zero decreases substantially with the addition of gallium solutes. They conclude this reduction accounts for the retention of the δ phase. Clearly one must then invoke a different mechanism for the existence of the δ phase in unalloyed plutonium at high temperature. For example, it could be a combination of entropy effects and possible changes in electronic structure, such as those observed by Manley *et al.* (2001) for uranium. The calculations of Sadigh and Wolfer (as those of Söderlind (2001)) require large local spin moments in the δ phase to get the volume correct.

Considerable debate still exists over these calculational techniques because no local moments have been found experimentally (as recently reviewed by Lashley (2005). The search for magnetic moments has been so elusive, Söderlind explains, because his calculations predict a near zero-ordered moment as the spin and orbital moments are close in magnitude but antiparallel. However, Shick *et al.* (2005), using the *around-the-mean-field* version of the LDA+U method, predict a nonmagnetic ground state for the δ phase. They claim the nonmagnetic character results from $S = 0$ and $L = 0$, rather than the cancellation of spin and orbital parts of the momentum. They claim good agreement with experimental measurements of δ-phase plutonium properties. Shorikov *et al.* (2005) used the LDA+U+SO method to predict nonmagnetic ground states with zero values of spin, orbital, and total moments in both δ-phase and α-phase plutonium. We look forward to future advances in electronic structure theory that provide satisfactory explanations to the enigma surrounding plutonium.

(b) Lattice effects and local structure

We now examine in greater detail some of the interesting electronic structure effects observed in binary plutonium alloys. Binary alloys of plutonium with Am, Ce, Ga, and Al solutes were studied recently by Dormeval *et al.* (2003). Fig. 7.41 shows the approximate range of the δ-phase fields at room temperature for these solutes and the variation in the δ-phase plutonium lattice parameters. The addition of americium or cerium expands the plutonium lattice, whereas gallium and aluminum shrink it. All of them show some deviation from the ideal solution behavior described by Vegard's law, which is not surprising considering the complex electronic interactions expected in plutonium alloys.

In americium, the 5f electrons are completely localized. Substituting large americium atoms into the smaller δ-phase lattice expands the plutonium lattice and causes the 5f electrons in plutonium to become more localized, thereby stabilizing the δ phase over the entire range of americium concentrations. Also,

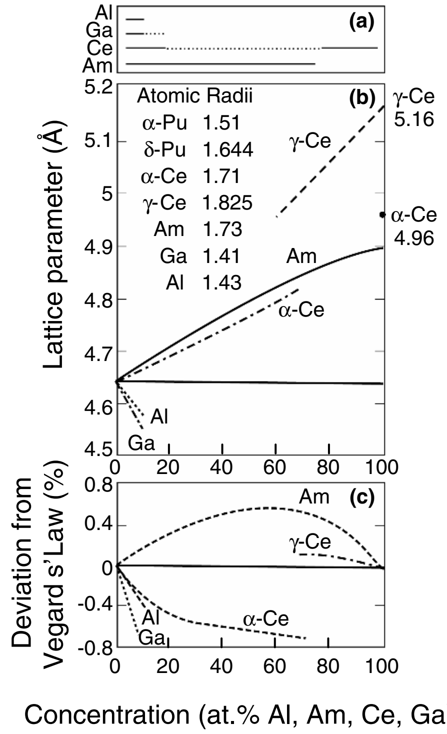

Fig. 7.41 (*a*) *Approximate solubility ranges at room temperature for the δ phase alloyed with Al, Ga, Ce, and Am.* (*b*) *Lattice parameters for these alloys.* (*c*) *Deviation from Vegard's Law* (*Dormeval,* 2001*; Hecker* et al., 2004).

the increased localization of the 5f electrons in plutonium causes the plutonium atoms themselves to increase in size, resulting in a positive deviation from Vegard's law. If a transition from itinerant (bonding) 5f electrons to localized 5f electrons were to suddenly occur in plutonium atoms as the americium concentration is increased, then we would expect a sudden increase in lattice parameter. As seen in Fig. 7.41, no discontinuities in lattice parameters are observed across the entire americium concentration range. This behavior demonstrates that the limited stability of the δ phase in unalloyed plutonium is just the tip of the iceberg for δ-phase stability upon alloying. This is shown most convincingly by looking more closely at the connected binary Np–Pu–Am phase diagrams shown in Fig. 7.42.

In contrast to additions of americium, neptunium stabilizes the α phase of plutonium. In fact, the Pu–Np phase diagram looks strikingly like the plutonium temperature–pressure phase diagram also shown for comparison in Fig. 7.42. Hence, adding neptunium has the same effect as applying pressure to the plutonium lattice, whereas adding americium is equivalent to applying hydrostatic tension.

As shown in Fig. 7.41, the addition of cerium also expands the δ-phase plutonium lattice. The range of stability for the fcc phase was extended across the entire concentration range of cerium by splat cooling (as indicated by the

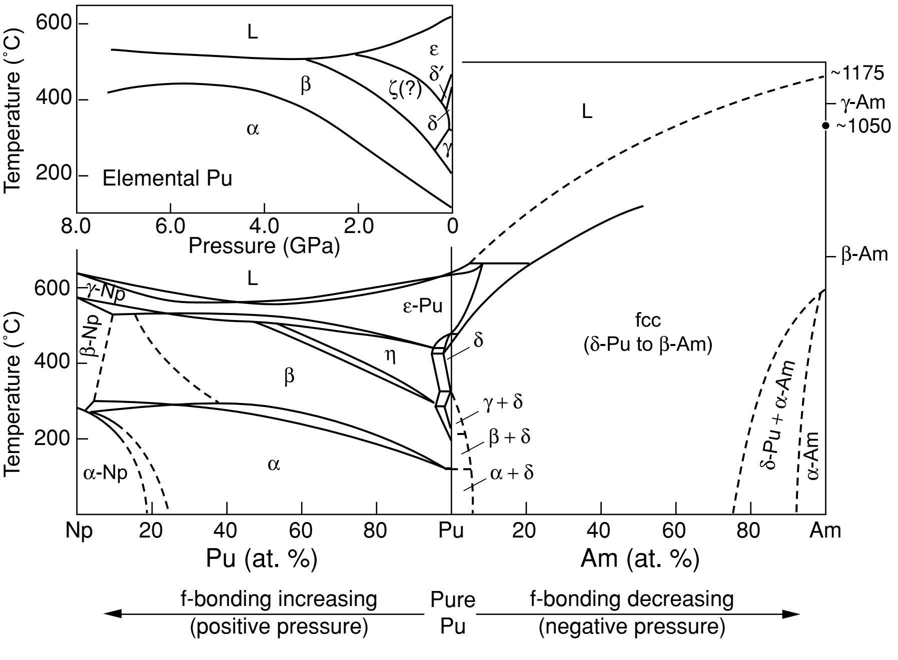

Fig. 7.42 *Plutonium pressure–temperature phase diagram compared to connected Np–Pu–Am binary ambient-pressure phase diagrams* (*Hecker,* 2004).

dotted lines in Fig. 7.41a). In addition to retaining the stable fcc phases of δ plutonium and γ cerium, Giessen *et al.* (1975) were able to retain the metastable fcc α-cerium phase at intermediate concentrations. Unlike americium, which behaves as a rigid sphere because the 5f electrons are well-localized, cerium is a 'soft' sphere, whose diameter adapts to its surroundings. When squeezed into the smaller δ-phase plutonium lattice at the plutonium-rich end, cerium's 4f electrons become delocalized and it takes on the α-phase radius ($r = 1.71$ Å). At 75 at.% Ce, an abrupt transition is observed to γ-cerium (with $r = 1.825$ Å). When viewed from the cerium end, the smaller plutonium atoms substitute in the γ-cerium lattice, until at 25 at.% Pu the pressure is sufficient to collapse the unstable cerium atom to its α-phase radius. Using EXAFS spectroscopy, Conradson (2003) showed that the cerium solute atom was accommodating in the plutonium lattices. It readily adapted its size to fit either into the δ-phase lattice or the even smaller α-plutonium lattice (when trapped in the α lattice under metastable conditions).

Dormeval *et al.* (2003) calculated the deviation of lattice constants from Vegard's law by considering two different limits in the law. As a result of the pressure imposed by the δ-plutonium lattice, cerium is α-like at concentrations below 75 at.% Ce and γ-like above that level. Hence, on the cerium end, there are two different limits corresponding to α-cerium and γ-cerium extrapolated to room temperature and pressure. Following this approach, Dormeval *et al.* found the deviation from Vegard's law to be negative on the plutonium-rich end, while slightly positive at the cerium-rich end as shown in Fig. 7.41c. Based on measurements of lattice constants, electrical resistivity, and magnetic susceptibility, Dormeval *et al.* suggested that the principal cause of the complex alloying behavior of cerium in plutonium is not the plutonium itself but the unstable nature of the cerium atom.

The addition of aluminum or gallium shrinks the δ-phase plutonium lattice (Fig. 7.41). Both show negative deviations from Vegard's law, with the gallium deviation being more than twice that of aluminum. As mentioned above, several investigators have probed the local structure of Pu–Ga alloys using EXAFS (Cox *et al.*, 1995; Faure *et al.*, 1996; Conradson, 2000; Allen *et al.*, 2002). These EXAFS results show that the first-neighbor Pu–Ga bond is 0.13 Å, or 3.7% (the experimental measurements vary from 3.5 to 4%) shorter than the Pu–Pu bond in dilute alloys. Scheuer and Lengeler (1991) and Massalski (1996) pointed out that local distortions in substitutional alloys may bear little or no relation to macroscopic distortions of the unit cell. The local distortions can vary greatly in magnitude and in sign compared to the average change in lattice parameters. The contraction in Pu–Ga is at the upper end of that found in substitutional alloys. Scheuer and Lengeler reported that the change in the next-nearest-neighbor and more distant shells is typically small for substitutional alloys. Conradson (2000) found contractions in the second and third nearest-neighbor shells in Pu–Ga to be almost negligible (0.05 and 0.01 Å, respectively). He also reported a significant change in local order in Pu–Ga alloys as the gallium concentration increases beyond roughly 3.5 at.% Ga. He found the Pu–Ga distance to remain constant with gallium addition, whereas Faure *et al.* (1996) found it to first increase and then decrease. Resolution of the differences in local Pu–Ga arrangements must await additional experiments. However, Ravat *et al.* (2003) recently reported results similar to those of Conradson; that is, the first shell distance for the Pu–Ga bond is 0.1 Å shorter than the Pu–Pu bond, and the second shell bonds are close to the Pu–Pu bond length. We must also heed the caution expressed by Scheuer and Lengeler that alloy additions of roughly 2% or more typically cause complex local ordering effects.

A lattice contraction with the addition of gallium or aluminum to plutonium is expected from purely elastic considerations because the atomic radii of aluminum and gallium are considerably smaller than the radius of δ-phase plutonium. The atoms tend to relax toward their natural bond length rather than retain their average spacing. Harrison (2001) pointed out that each solute atom eliminates 12 f–f bonds in δ-phase plutonium. The f–f bond cutting should counter the elastic contraction of the solutes. However, Harrison's calculations for Pu–Ga alloys showed that the experimentally observed negative deviation from Vegard's law results from a coupling between the core d-states in gallium and the unoccupied d-states in plutonium. Faure *et al.* (1996) suggested that negative deviation to Vegard's law is proof of delocalization. They assume that this negative deviation results from the f–p bonding between Pu 5f and Ga 4p electrons. Thus, in the Pu–Ga alloys the solutes delocalize some of the 5f electrons in alloyed δ plutonium compared to the pure δ plutonium, which, in turn, promotes more bonding and smaller atomic volumes. As pointed out above, using DFT (with spin polarization for the δ phase), Sadigh and Wolfer (2005) predicted that the δ-lattice volume decrease results primarily from the reduction in size of the plutonium host atoms. All of these analyses indicate that electronic effects play a major role in determining the alloying characteristics of plutonium.

Another interesting electronic effect in plutonium is the behavior of alloying elements such as gallium and aluminum in α-phase plutonium. Ellinger *et al.* (1968b) showed that there is no measurable equilibrium solubility of these elements in the α phase. However, as pointed out by Hecker *et al.* (2004), lean δ-phase Pu–Ga and Pu–Al alloys transform to the α phase upon cooling below 0°C or with hydrostatic pressure at ambient temperature and below. Adler *et al.* (1986) and Olson and Adler (1984) concluded that the temperature-induced δ→α transformations are martensitic. Zukas *et al.* (1981) concluded that the pressure-induced δ→α transformations are also martensitic – that is, displacive with no compositional change. Hence, the solute atoms are trapped in the monoclinic α lattice. The crystal structure, as shown in Fig. 7.22, has 16 atoms per unit cell, with eight unique lattice sites and with variable bond lengths.

Hecker *et al.* (2004) reported that XRD measurements and immersion-density measurements of the transformed α phase clearly showed that the gallium is in substitutional lattice positions in the monoclinic lattice, but that it expanded the α lattice (the expanded lattice is called the α′ phase). All three-crystal axes expand, whereas the monoclinic angle remains nearly constant. The volume expansions in the α′ phase with the addition of gallium or aluminum are shown in Fig. 7.43 and contrasted with the volume contractions in the δ phase with alloying additions. With the addition of gallium, the α-phase volume expands ~0.9% per at.% Ga, whereas the δ-phase volume decreases by ~0.6% per at.% Ga.

These results are a most interesting manifestation of the peculiar electronic effects in plutonium. As explained above, the gallium atom, which is 14.2% smaller than the δ-plutonium atom, contracts the lattice significantly more than expected because it is believed to make the plutonium atoms contract in its presence. In other words, the addition of gallium causes more of the 5f electrons in plutonium to bond. This result is conceptually consistent with the calculations of Wills and Eriksson (2000), which indicated that only one of the five 5f electrons appears to be bonding in the unalloyed δ phase. Also, Sadigh and Wolfer (2005) predict the decrease in the size of the plutonium atoms quantitatively.

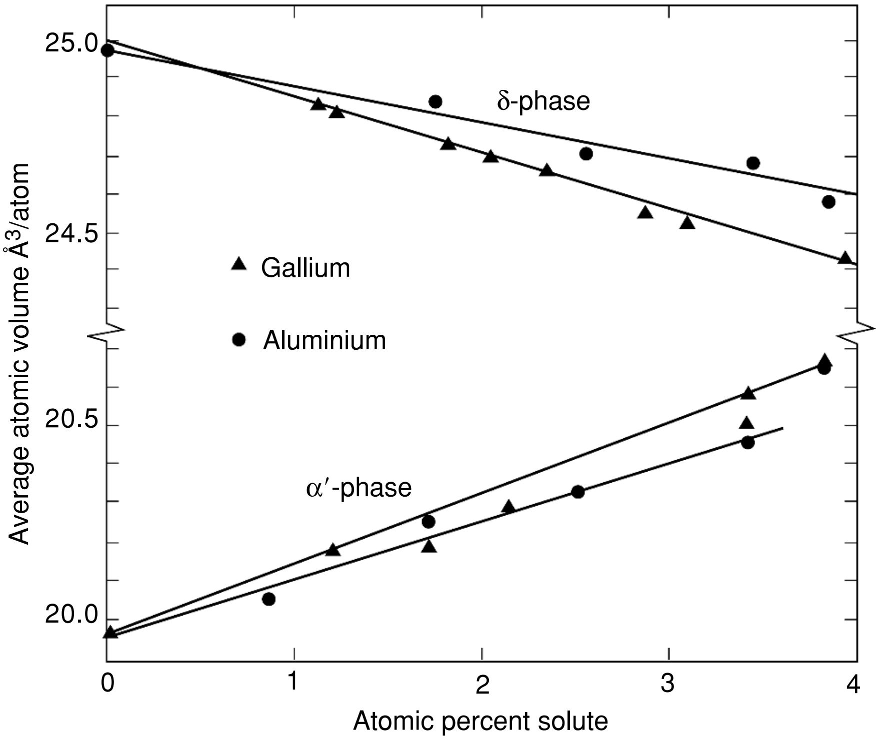

Fig. 7.43 *Atomic volumes of Pu–Ga and Pu–Al alloys in the δ and α′ phases.*

On the other hand, the gallium atom, although 7% smaller than the α-plutonium atom, expands the α lattice, indicating that in the α phase the presence of gallium localizes more of the 5f electrons. The calculations of Wills and Eriksson (2000) showed that all five 5f electrons bond in the α phase, hence it is quite likely that the solute additions disrupt the bonding, causing the volume to expand. Hecker *et al.* (2004) also showed that the lattice expansion in the α′ phase disappears slowly with time at ambient temperature and quite rapidly at slightly elevated temperatures. During the martensitic transformation, the solute atoms are trapped randomly in the α′ lattice, causing it to expand.

However, the eight different lattice sites have different bond lengths as shown in Fig. 7.22. Hecker *et al.* (2004) suggested that there is a strong driving force to rearrange the solute atoms into preferred sites, namely lattice site 8, because it has the fewest number of short bonds (Table 7.10). Based on their recent calculations, Sadigh and Wolfer (2005) showed that site 8 is by far the most favorable substitutional position for gallium. Furthermore, they found that the unit cell of the α phase is not expanded when gallium occupies site 8, while significant expansions are exhibited when gallium is substituted in other sites, with the largest expansion for site 1 occupancy. The energies for gallium substitution correlate with this volume expansion, with a maximum difference of 1.5 eV between site 1 and site 8, confirming the suggestion of Hecker *et al.* (2004) that gallium entrapped in sites other than site 8 will tend to order to this site and in the process contract the unit cell of the α′ phase.

These results demonstrate that plutonium atoms, like cerium atoms, readily change their electronic configurations and adjust their size as their lattice environment changes. It is no surprise then that alloying of plutonium is so complex.

7.7.6 Physical and thermodynamic properties

The physical and thermodynamic properties of plutonium are of great practical interest and present significant engineering challenges; they also represent some of the most puzzling features of solid-state behavior.

(a) Densities and lattice parameters

The densities of the six solid plutonium allotropes and liquid plutonium are summarized in Table 7.18. Of particular note is the fact that the density of liquid plutonium exceeds that of the three high-temperature allotropes and that the δ phase, which is also the closest-packed crystal structure, exhibits a particularly low density compared to the other allotropes. As pointed out above, full density is difficult to achieve in the α phase of unalloyed plutonium because of the propensity for microcracking during cooling and the retention

Table 7.18 *Typical densities for plutonium allotropes, alloys, and compounds.*

Material	*Density* (g cm^{-3}); *References* *calculated*[a]		*Density* (g cm^{-3}); *References* *experimental*	
α-Pu	19.86;	Zachariasen and Ellinger (1963a)	19.82;	Merz (1974)
β-Pu	17.69;	Zachariasen and Ellinger (1963b)		
γ-Pu	17.15;	Zachariasen and Ellinger (1955)		
δ-Pu	15.92;	Ellinger (1956)		
δ′-Pu	16.00;	Ellinger (1956)		
ϵ-Pu	16.51;	Ellinger (1956)		
liquid Pu	16.65;	Miner and Schonfeld (1980)		
Pu-1.24 at.% Ga	15.86		15.83;	Gardner (1965)
Pu-1.7 at.% Ga	15.85		15.82;	Hecker (unpublished)
Pu-2.61 at.% Ga	15.827		15.78;	Gardner (1965)
Pu-3.35 at.% Ga	15.806		15.76;	Hecker (unpublished)
Pu-4.22 at.% Ga	15.787		15.73;	Gardner (1965)
Pu-5.0 at.% Ga	15.77		15.69;	Hecker (unpublished)
Pu-1.2 at.% Al	15.82		15.80;	Elliott *et al.* (1962)
Pu-2 at.% Al	15.76		15.70;	Hecker *et al.* (1982)
Pu-3.4 at.% Al	15.66		15.56;	Elliott *et al.* (1962)
Pu-5 at.% Al	15.55		15.50;	Rosen *et al.* (1969)
Pu-11 at.% Al	15.135		15.19;	Rosen *et al.* (1969)
Pu-5 at.% Ce	15.47		15.45;	Elliott *et al.* (1962)
Pu-10 at.% Ce	15.03		14.93;	Elliott *et al.* (1962)
Pu-18 at.% Ce	14.34		14.24;	Elliott *et al.* (1962)
Pu-5 at.% Am	15.75;	Ellinger *et al.* (1966)		
Pu-10 at.% Am	15.61;	Ellinger *et al.* (1966)		
Pu-15 at.% Am	15.45;	Ellinger *et al.* (1966)		
Pu_6Fe	17.10;	Ellinger *et al.* (1968b)		
Pu_3Ga (cubic)	14.27;	Ellinger *et al.* (1968b)		
Pu_3Ga (tetragonal)	14.45;	Ellinger *et al.* (1968b)		
PuO_2	11.46;	Ellinger *et al.* (1968b)		
Pu_2O_3 (hexagonal)	11.47;	Ellinger *et al.* (1968b)		
PuC_{1-x}	13.6;	Ellinger *et al.* (1968b)		
PuN	14.22;	Ellinger *et al.* (1968b)		

[a] From X-ray data.

of lower-density phases during processing. Merz (1974) achieved exceptionally high density (19.82 g cm^{-3}) in α-phase plutonium by extrusion and concurrent recrystallization, which resulted in very fine grain size (on the order of micrometers). Alpha phase plutonium samples with densities >19.7 g cm^{-3} are typically considered as sound samples.

Alloying plutonium with elements such as aluminum and gallium, which promote δ-phase retention to room temperature, yields densities close to that of the unalloyed high-temperature δ phase. The densities of some δ-phase alloys are also compared to that of the plutonium allotropes and common plutonium compounds in Table 7.18. The densities reported in the middle column were calculated by the authors from the lattice parameters measured by XRD by a number of investigators. Experimental densities are typically measured by liquid immersion techniques. The experimental densities for the δ-phase alloys are usually lower than the calculated densities from X-ray measurements because of impurities and inclusions. Experimental densities higher than X-ray densities are almost always the result of transforming the surfaces of test samples from the δ phase to the α phase during sample preparation (such as punching, machining, filing, or polishing). The compounds Pu_6Fe, PuO_2, PuC, and PuN are common inclusions found in plutonium metal and alloys of typical purity. PuO_2, PuC, and PuN have also been considered for reactor fuels. The compound Pu_3Ga is the most plutonium-rich compound in the Pu–Ga system. Figs. 7.41 and 7.43 show how the lattice parameters of δ-phase plutonium alloys decrease with increasing alloy content.

(b) Thermal expansion

Thermal expansion of the unalloyed α, β, and γ phases of plutonium is large and positive. Thermal expansion of these allotropes is also anisotropic because of their low-symmetry crystal structures. Table 7.19 lists the coefficients of thermal expansion for all allotropes, including coefficients for different lattice directions for the low-symmetry allotropes. The values shown in Table 7.19 were taken primarily from X-ray measurements because of the variability of dilatometric results. Schonfeld and Tate (1996) recently reviewed available thermal expansion results for unalloyed plutonium. We have chosen to present their best fits to the available dilatometric data, as shown in Fig. 7.19. The low-temperature behavior of α-phase plutonium is quite nonlinear, as reported by Cramer *et al.* (1961) and Lallement (1963). On page 37 of the *Plutonium Handbook*, Miner and Schonfeld (1980) show an inflection in thermal expansion near 60 K. However, more recently, Schonfeld and Tate (1996) argued convincingly that the slight lattice expansion in α-phase plutonium reported below 60 K results from self-irradiation damage. Schonfeld and Tate replotted all available thermal expansion data for α-phase plutonium, as shown in Fig. 7.44. They list the average thermal expansion coefficient between 0 and 393 K as 37.8×10^{-6} K^{-1} and that between 294 and 377 K as 53.8×10^{-6} K^{-1} (by dilatometry) and 54×10^{-6} K^{-1}

Table 7.19 *Linear thermal expansion of plutonium.*[a]

Phase	*Principal coefficient*	*Temperature range* (°C)	*Mean coefficient* (10^{-6}°C^{-1})	*Method*	*References*
α	$\bar{\alpha}_p$ (average)	−186 to 101	42.3	dilatometry	Cramer *et al.* (1961)
	$\bar{\alpha}_1 \perp c$-axis	21 to 104	60	X-ray	Zachariasen and Ellinger (1963a)
	$\bar{\alpha}_2 = \bar{\alpha}_b$		75		
	$\bar{\alpha}_3 = \bar{\alpha}_c$		29		
	$\bar{\alpha}_p$ (average)		54		
β	$\bar{\alpha}_1$	93 to 190	94	X-ray	Zachariasen and Ellinger (1963b)
	$\bar{\alpha}_2 = \bar{\alpha}_b$		14		
	$\bar{\alpha}_3 \perp (10\bar{1})$		19		
	$\bar{\alpha}_p$ (average)		42		
γ	$\bar{\alpha}_a$	210 to 310	-19.7 ± 1.0	X-ray	Zachariasen and Ellinger (1955)
	$\bar{\alpha}_b$		39.5 ± 0.6		
	$\bar{\alpha}_c$		84.3 ± 1.6		
	$\bar{\alpha}_p$ (average)		34.6 ± 0.7		
δ	$\bar{\alpha}$	320 to 440	-8.6 ± 0.3	X-ray	Ellinger (1956)
δ'	$\bar{\alpha}_a$	452 to 480	444.8 ± 12.1	X-ray	Elliott and Larson (1961)
	$\bar{\alpha}_c$		-1063.5 ± 18.2		
	$\bar{\alpha}_p$ (average)		-65.6 ± 10.1		
ϵ	$\bar{\alpha}$	490 to 550	36.5 ± 1.1	X-ray	Ellinger (1956)
liquid	$\bar{\alpha}_v$	664 to 788	93[b]	pycnometry	Serpan and Wittenberg (1961)

[a] For low symmetry allotropes, coefficients are given for different lattice directions.

[b] Mean coefficient of volume expansion.

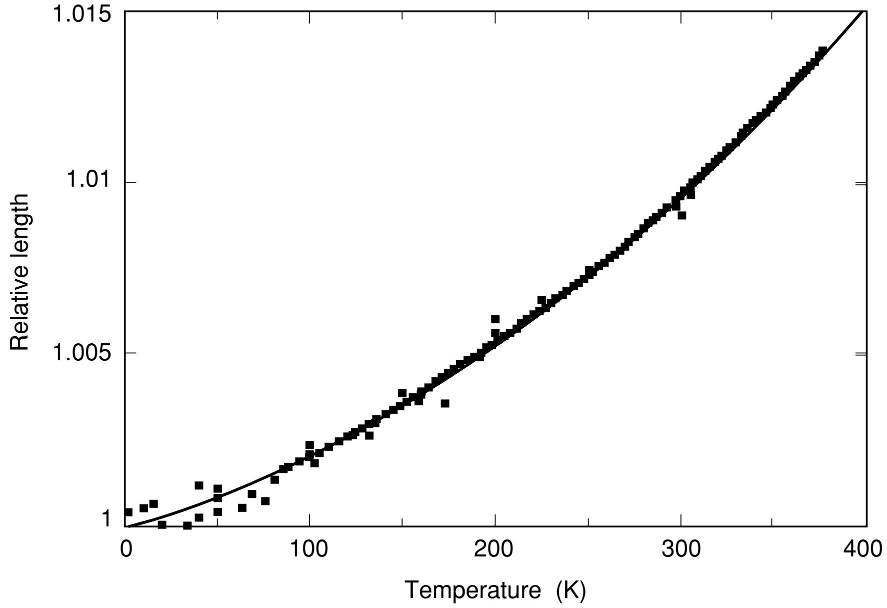

Fig. 7.44 *Thermal expansion of unalloyed α-phase plutonium over most of its temperature region of stability. The curve is a composite generated by Schonfeld and Tate* (1996) *based on data from several references* (*Sandenaw,* 1960*b*; *Cramer* et al., 1961; *Lee* et al., 1965*a*; *Lallement and Solente,* 1967; *Miner and Schonfeld,* 1980; *Lawson* et al., 1994).

(by X-ray measurements). The low-temperature results of Schonfeld and Tate are incorporated into the overall thermal expansion curve shown in Fig. 7.19.

The expansion of the high-temperature δ and ε phases is isotropic. However, the δ and δ′ phases exhibit negative thermal expansion. Thermal expansion of the δ′ phase is also highly anisotropic. The explanation of this unusual behavior has been a contentious issue since the late 1950s. In δ-phase alloys, the thermal expansion coefficient varies from slightly negative to positive, depending on the amount of alloying addition. A graphic example of this behavior is shown for Pu–Ga alloys in Fig. 7.45 (Goldberg *et al.*, 1970). We also show the thermal expansion behavior of various δ-phase plutonium alloys in Fig. 7.46 (taken mostly from the work of Elliott *et al.* (1960) and Lawson *et al.* (2002)). All alloying additions move the coefficient of thermal expansion to more positive values from that of the unalloyed δ phase; that is, alloying results in thermal expansion behavior closer to that observed in normal metals. As shown in Fig. 7.46, significantly less aluminum or gallium is required to increase the coefficient compared to cerium. The properties of Pu–Am alloys were estimated from the measurements of Shumakov *et al.* (1990).

The peculiar thermal expansion behavior of δ-phase plutonium alloys was reviewed by Lawson *et al.* (2002). A negative thermal expansion is associated

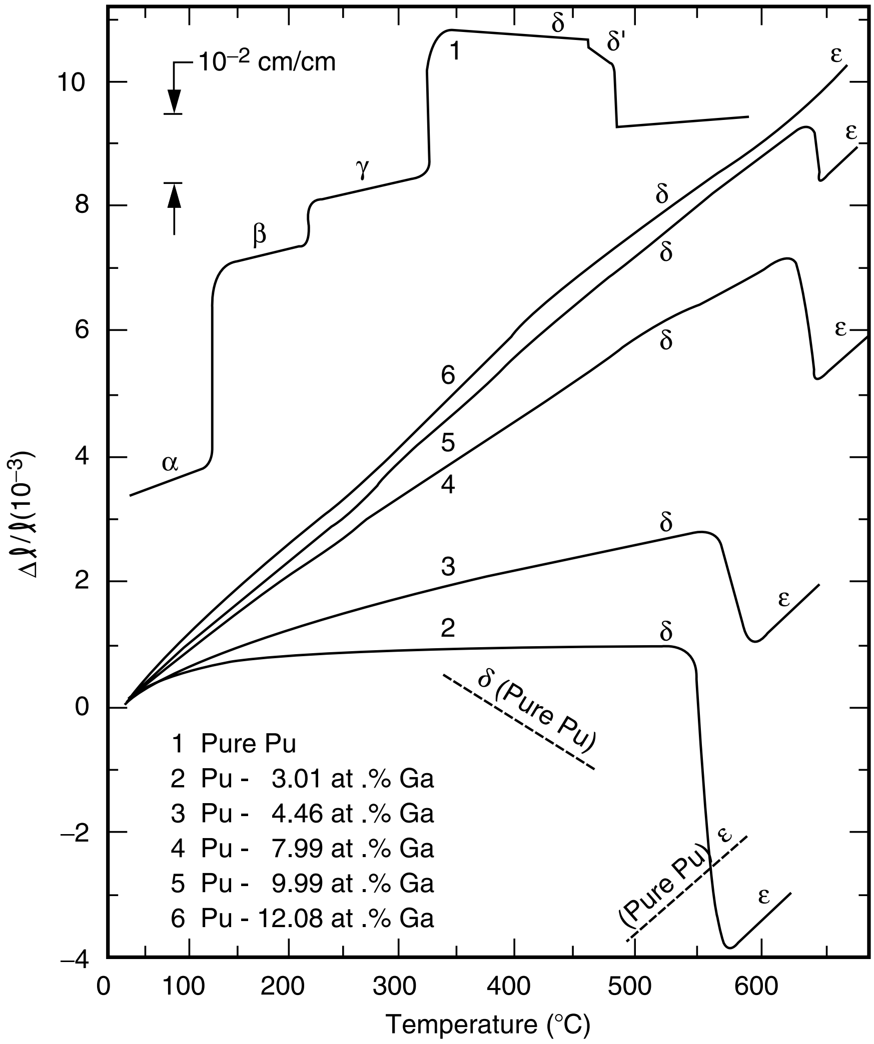

Fig. 7.45 *Corrected dilatometric heating curve* (*at* 4.5°C min^{-1}) *for a series of* δ*-phase Pu–Ga alloys. The curve for unalloyed* (*pure*) *plutonium is based on a scale of one-tenth* (*as shown in insert*) *that used for the alloys. The dashed curves for unalloyed* (*pure*) *plutonium are portions redrawn on the same scale used for the alloys. The scale on the ordinate refers only to the alloys* (*Goldberg* et al., 1970).

with increasing disorder (higher entropy) at higher pressures according to the Maxwell relation $(\partial V/\partial T)_p = -(\partial S/\partial P)_T$, in contrast with the behavior found in ordinary metals. However, for some complex solids with negative thermal expansion, such as the recently discovered ZrW_2O_8, increasing pressure has

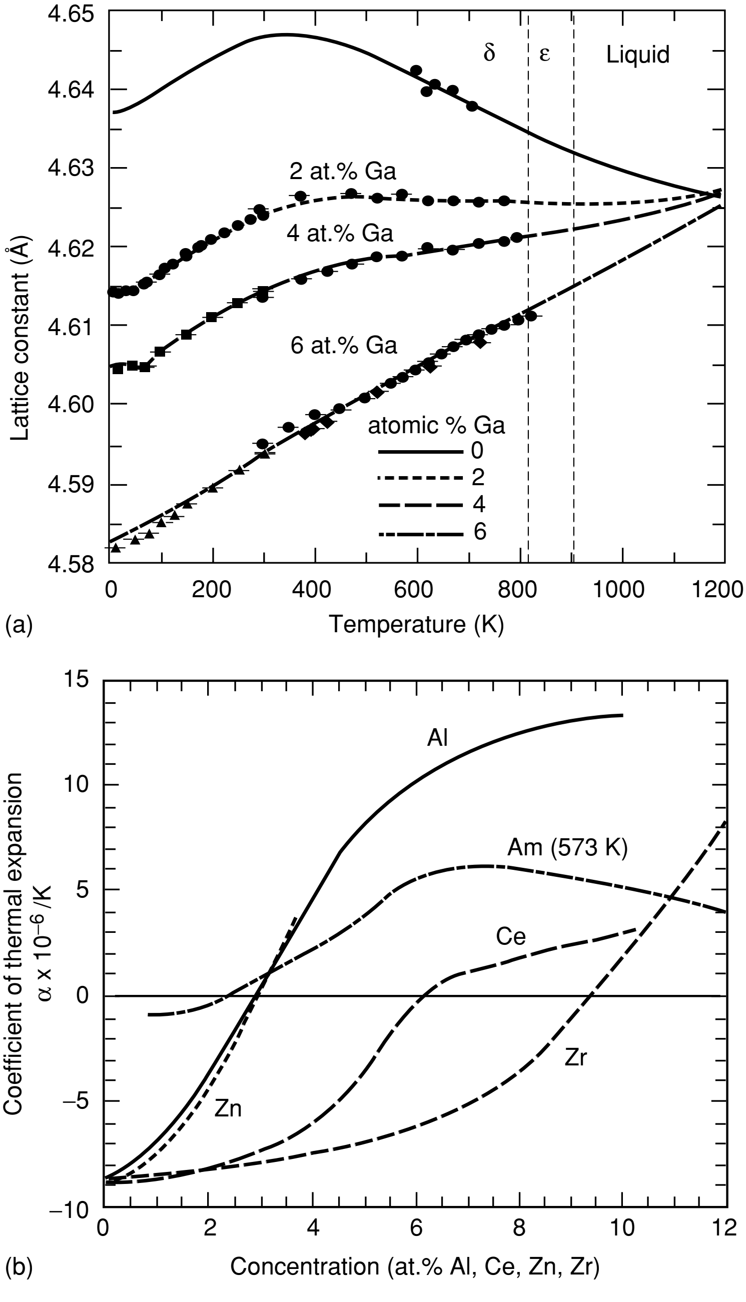

Fig. 7.46 (*a*) *Lattice constants of δ-phase Pu–Ga alloys measured by neutron diffraction by Lawson* et al. (2002). *The line through the data is a fit by the 'Invar' model proposed by Lawson* et al. (*b*) *Coefficient of thermal expansion as a function of solute content for δ-phase plutonium alloys* (*Elliott* et al., 1960). *The results for Pu–Am alloys were estimated from the measurements of Shumakov* et al. (1990) *taken at* 573 K, *where the range of solid solution across the Pu–Am diagram is complete.*

been shown to increase the vibrational entropy of the molecular modes (Evans *et al.*, 1996; Mary *et al.*, 1996; Mittal *et al.*, 2001). For fcc δ plutonium there are no internal vibrational modes, so Lawson *et al.* looked for an electronic degree of freedom whose entropy variation with pressure determines the thermal expansion. They believe zero thermal expansion (Invar-like behavior) of some of the alloys results from a thermal transfer of plutonium atoms from a lower-energy, higher-volume δ_1 state to a higher-energy, lower-volume δ_2 state, comparable to the Weiss two-level model used to explain the Invar behavior in Fe–Ni alloys (Weiss, 1963).

For ordinary metals that follow Grüneisen's law, the thermal expansion behavior can be used to estimate the temperature dependence of the bulk modulus (or the sound speed or Debye temperature); namely, $\mathrm{d}B/\mathrm{d}T = -\gamma\beta B$, where B is the bulk modulus, γ the Grüneisen parameter, and β the volume thermal expansion. The δ-phase plutonium alloys, however, do not follow this relationship since the thermal expansion is small – or even negative – and $\mathrm{d}B/\mathrm{d}T$ is large. For these alloys it is necessary to assume that the elastic stiffness is intrinsically temperature dependent, independent of volume. For unalloyed α-phase plutonium, a recent review by Ledbetter (2004) and by Ledbetter and Migliori (2005) of Grüneisen parameters shows large variations from values of 3.1 to 7.0. They believe the best value is ~3.5. We also note that Hasbrouk and Burns (1965) provide additional listings of thermal expansion in various plutonium allotropes and in several alloys.

(c) Elastic constants and sound velocities

Early elastic constant measurements for unalloyed plutonium and several plutonium alloys by various investigators were compiled by Hasbrouk and Burns (1965). As pointed out by Fisher (1974) in a later compilation, reported elastic constant measurements (particularly the bulk modulus) exhibit significant scatter because of difficulties in fabricating quality samples. Acoustic measurements typically yield the most reliable elastic constants. Calder *et al.* (1981) reported elastic constants of α plutonium and δ-phase Pu–3.4 at.% Ga alloys at elevated temperatures. Migliori *et al.* (2004, 2006) and Ledbetter *et al.* (2004, 2005) recently performed the most accurate acoustic measurements to date on high-quality, high-purity, unalloyed plutonium (with a density >19.7 g cm^{-3}), and Pu–Ga alloys using the resonant ultrasound technique (Migliori *et al.*, 2000). Their room-temperature results are summarized in Table 7.20. Unalloyed α plutonium is soft elastically – its bulk modulus is nearly 50% less than that of α uranium. As shown in Table 7.20, the δ-phase Pu–Ga alloys exhibit substantially reduced elastic constants compared to α plutonium. Typical sound velocities are also listed in Table 7.20.

The temperature dependence of the elastic modulus (Young's modulus), the shear modulus, bulk modulus, and Poisson's ratio is shown for unalloyed plutonium in Fig. 7.47. All but Poisson's ratio are quite sensitive to temperature. The ratio of the bulk modulus at 0 K to the bulk modulus at 300 K for α plutonium is 1.303, compared to 1.104 for lead, 1.03 for iron, and 1.075 for aluminum. There are no single-crystal elastic constant measurements in the literature for α plutonium because of the difficulty of making single crystals of unalloyed plutonium. In addition, making elastic constant measurements of the monoclinic structure of the α phase with 13 independent elastic constants is a daunting task. Moment (2000) and Lashley *et al.* (2000) describe techniques used to prepare single crystals of δ-phase plutonium alloys. Ledbetter and Moment (1976) reported elastic constant measurements on a single crystal δ-phase Pu–3.4 at.% Ga alloy. As shown in Fig. 7.48, the elastic constants are highly anisotropic. The single crystals are stiff in tension and compression and soft in shear in the [111] direction and vice versa in the [100] direction. In fact, the Zener anisotropy ($Z = 2c_{44}/c_{11}-c_{12}$), where c_{ij} are the typical elastic constants is 7.03; whereas lead, the next elastically most anisotropic fcc metal, is roughly 4 and aluminum is nearly isotropic at slightly over 1.0. The elastic constants for a polycrystalline δ-phase Pu–3.35 at.% Ga alloy reported by Calder *et al.* (1981) and shown in Fig. 7.49, exhibit a greater reduction in elastic constants with temperature than that for unalloyed α plutonium. Poisson's ratio for the δ-phase alloy increases monotonically with temperature as is typical for fcc metals.

In addition to providing stiffness data, elastic constants also play an important role in determining the overall mechanical response of materials (Hecker and Stevens, 2000). The Debye temperature at 0 K can be determined by correcting for the temperature dependence of the elastic constants. We will compare these results to the Debye temperatures from specific heat measurements in a subsequent section. Sound velocities provide a convenient way to determine elastic constants. They are also important in dynamic and shock responses of materials. The sound velocities for α plutonium and Pu–Ga alloys are presented in Table 7.20. We also note that Rosen *et al.* (1969) measured elastic properties ultrasonically at low temperatures and found no discontinuities in the elastic constants at low temperature (at the time they were looking for a possible magnetic transition) for α plutonium, and δ-phase Pu–Al and Pu–Ce alloys. However, they observed a sharp peak in the longitudinal wave attenuation accompanied by a normal temperature dependence of the transverse attenuation. Cornet and Bouchet (1968) measured the elastic properties of unalloyed plutonium with temperature, including the bcc ϵ phase (the room-temperature density was 19.1 g cm^{-3}, indicating that the samples contained many microcracks). They reported detailed results for Young's modulus for the δ, δ′, and ϵ phases. They found the ϵ phase to exhibit a large compressibility (0.16 GPa^{-1} at 758 K) and a low Young's modulus (11 GPa at 703 K). As indicated above, however, the sample quality was questionable because of its low density.

Table 7.20 *Elastic constants and sound velocities for plutonium and plutonium alloys at room temperature.*

Material	*Temperature* (°C)	*Density* (g cm^{-3}) *at* 25°C	*Bulk modulus* (GPa)	*Shear modulus* (GPa)	*Young's modulus* (GPa)	*Poisson's ratio*	*Sound speed* (km s^{-1}) (*longitudinal*)	*Sound speed* (km s^{-1}) (*transverse*)	*References*
unalloyed α Pu (high purity)	27	>19.70	54.4	43.7	103.4	0.183	2.39	1.49	Migliori *et al.* (2004) and Ledbetter *et al.* (2005)
unalloyed α Pu (high purity)	~25	19.71	53.43	42.26	100.66	0.186	–	–	Linford quoted in Gardner (1980)
Pu-2.36 at.% Ga	27	15.795	31.2 ± 0.1	16.6 ± 0.01	42.4	0.274	1.86	1.04	Migliori *et al.* (2004)
Pu-2.4 at.% Ga	25	15.75	30.6 ± 0.1	16.3 ± 0.05	41.8 ± 0.1	0.272	–	–	Migliori *et al.* (2006)
Pu-3.3 at.% Ga	27	15.76	29.7 ± 0.4	16.74 ± 0.02	42.3	0.263	1.82	1.03	Migliori *et al.* (2004)
Pu-3.35 at.% Ga	25[a]	15.9	–	15.7	40.5	~0.295	–	–	Calder *et al.* (1981)
Pu-4.64 at.% Ga	27	15.70	30.9	17.1	43.0	0.267	1.86	1.04	Migliori *et al.* (2004)
Pu-5 at.% Al	~25	15.5	–	18.28	45.4	0.24	–	–	Rosen *et al.* (1969)
Pu-6 at.% Al	20	–	–	18.5	46.8	0.264	–	–	Taylor *et al.* (1965)

[a] Extrapolated.

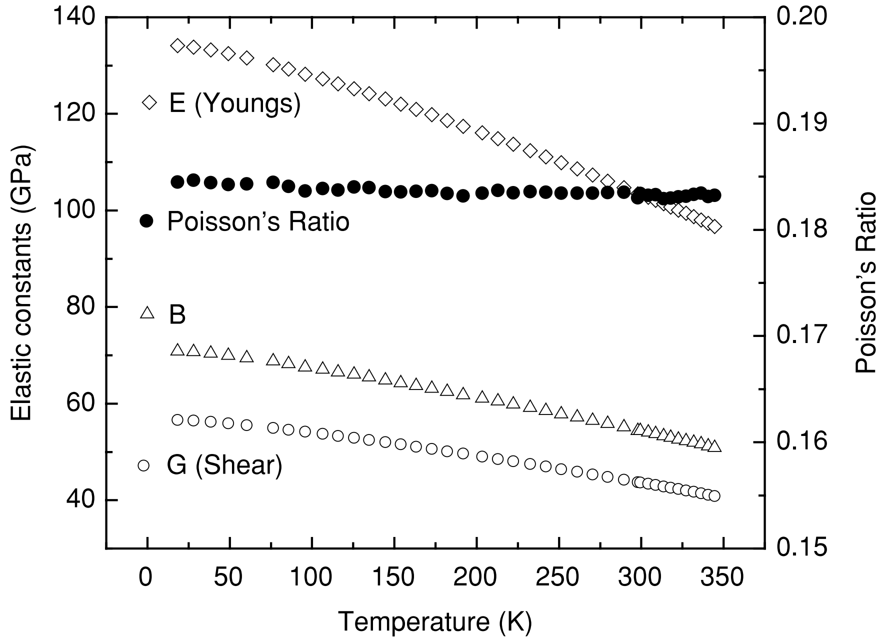

Fig. 7.47 *Elastic moduli of a high-purity, unalloyed α-plutonium polycrystal. Error bars are much smaller than the data points. The primary error is in the determination of density, computed from the dimensions and mass. E denotes Young's modulus, G, the shear modulus, and B, the bulk modulus (data from Ledbetter* et al., 2004; *Migliori* et al., 2004).

(d) Heat capacity

In 1976, Oetting *et al.* (1976) reviewed the early heat capacity measurements on plutonium. Low-temperature measurements of the heat capacity in ^{239}Pu, the most readily available plutonium isotope, have been plagued by self-heating (typically 2.2×10^{-3} W g^{-1} for ^{239}Pu) and by self-irradiation damage, which is especially pronounced at low temperatures where little if any healing of lattice damage occurs (Hecker and Martz, 2001). Although several investigators (Sandenaw and Gibney, 1971; Gordon *et al.*, 1976) minimized the effects of self-irradiation damage by using ^{242}Pu, they still had difficulty in obtaining sufficiently low temperatures to accurately measure the electronic specific heat. Lashley *et al.* (2003b) also reviewed previous low-temperature measurements and extended the measurements to ~2 K on ^{242}Pu using a thermal relaxation method and a specially designed sample mount (Lashley, 2003).

Lashley *et al.* demonstrated conclusively that previously reported anomalies in the heat capacity of plutonium resulted from the effects of self-irradiation damage. They also showed that anomalies in some of the δ-phase plutonium

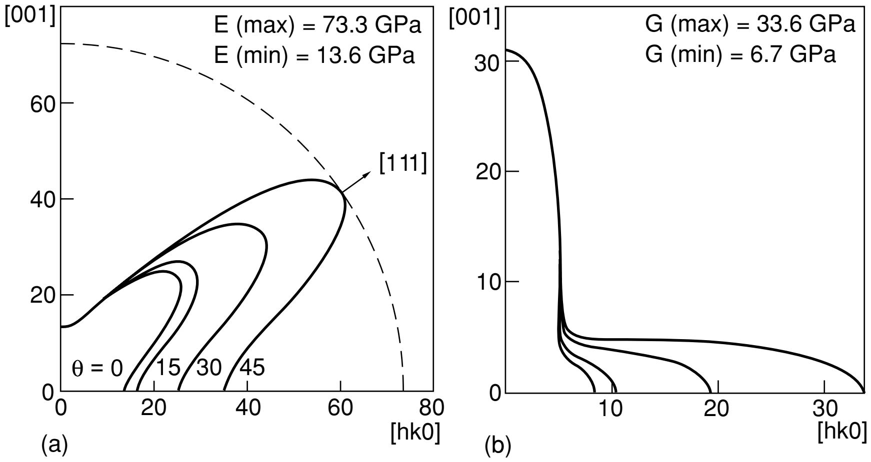

Fig. 7.48 *Elastic constants measured by Ledbetter and Moment* (1976) *on a δ-phase Pu-*3.4 at. *% Ga single crystal.* (*a*) *Young's modulus, E, as a function of crystal direction and* (*b*) *torsion modulus, G, as a function of direction.*

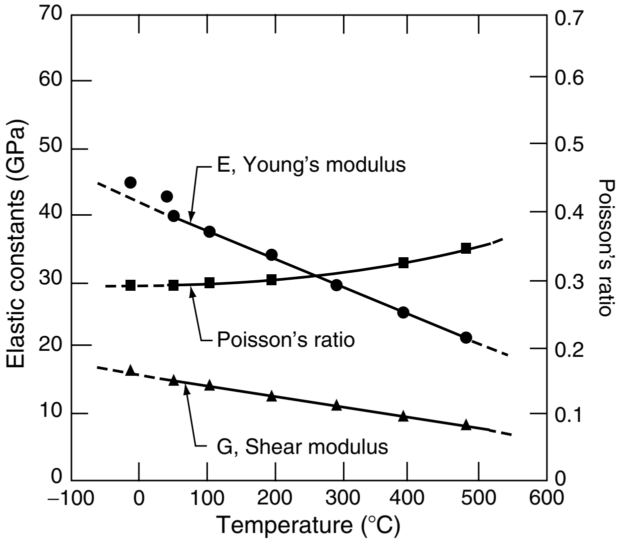

Fig. 7.49 *Elastic moduli of polycrystalline δ-phase Pu-*3.35 at. *% Ga as a function of temperature* (*after Calder* et al., 1981).

alloys at low temperatures resulted from martensitic transformations incurred in such samples when cooled to cryogenic temperatures. The results of Lashley *et al.* for very pure, zone-refined α-phase ^{242}Pu (<200 ppm impurities) are shown in Fig. 7.50 and compared to those reported by Gordon *et al.* (1976).

The electronic contribution to the specific heat can be measured at low temperatures where the phonon contribution is small. It is represented by equation (7.25)

$$(C_p/T) = \gamma + \alpha T^2 + \delta T^4 + \ldots \tag{7.25}$$

where γT and $\alpha T^3 = (12\pi^4 R T^3)/(5\theta_D{}^3)$ are the electronic and phonon contributions to C_p and θ_D is the Debye temperature. The results of Lashley *et al.* (2003b) for low-temperature heat capacity measurements on high-purity ^{242}Pu and a ^{242}Pu–5 at.% Ga alloy are shown in Fig. 7.51. The intercept at $T = 0$, γ, is a measure of the electronic DOS. The low-temperature fit yields $\gamma = (17 \pm 1)$ mJ K^{-2} mol^{-1}, which is within the range of 16 to 23 reported by Gordon *et al.* (1976), but less than the values of 22 to 25 reported by Stewart and Elliott (1981).

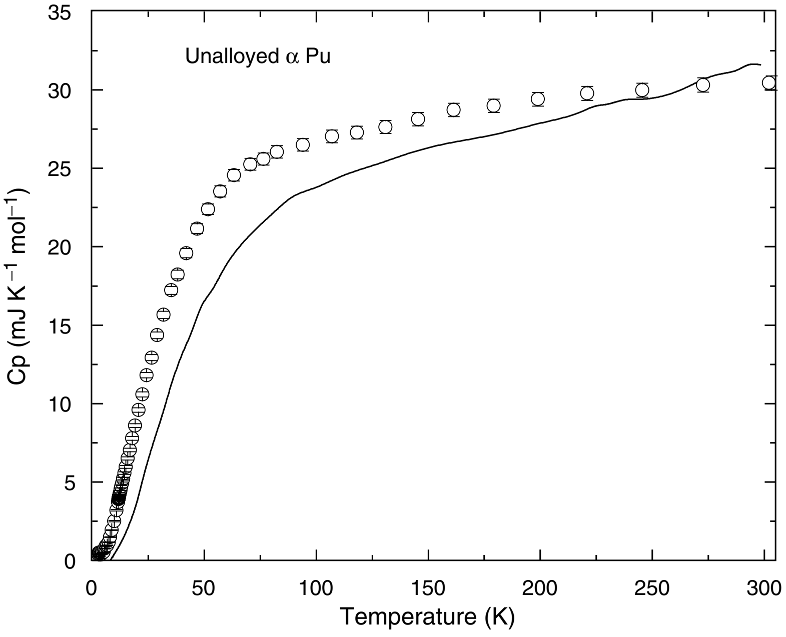

Fig. 7.50 *Heat capacity of unalloyed* ^{242}*Pu* (*solid line from Gordon* et al., 1976) *and high-purity, unalloyed* ^{239}*Pu (symbols) from Lashley* et al. (2003*b*) *who took extraordinary care to avoid self-irradiation damage at low temperatures.*

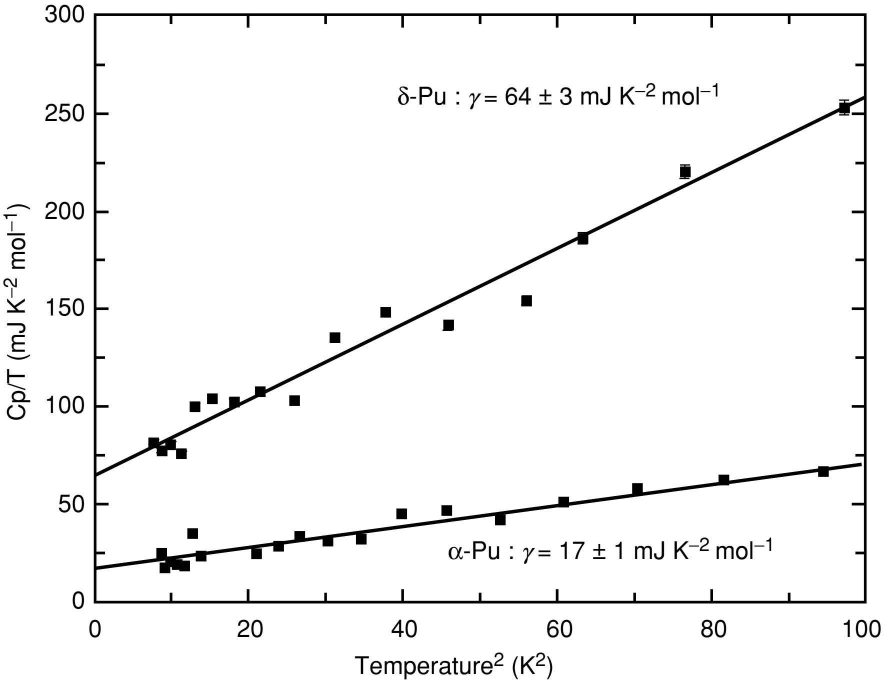

Fig. 7.51 *The low-temperature specific heat of unalloyed* α *plutonium and a* δ*-phase Pu-*5.1 at. *% Al alloy. These data represent the lowest temperature specific heat measurements reported on plutonium* (*after Lashley* et al., 2003*a,b*).

Since Lashley *et al.* reached the lowest temperatures, it is likely that their values are the most accurate. In any case, γ for plutonium is larger than that of any other element (Kittel and Kroemer, 1980). The δ-phase Pu–Al alloy has an even more remarkable γ of (64 ± 3) mJ K^{-2} mol^{-1}. Stewart and Elliott measured γ for Pu–Al alloys of varying aluminum concentration and found γ to vary from 44 to 63 mJ K^{-2} mol^{-1}. Extrapolation of the alloy data to zero alloy content yields $\gamma = 53$ mJ K^{-2} mol^{-1} for pure plutonium in the δ phase. Hence, the δ phase of plutonium, which is known to have less participation by the 5f electrons in bonding than the α phase, nevertheless has three times the electronic DOS at the Fermi energy.

Lashley *et al.* (2003b) calculated a Debye temperature, θ_D, of 153 K for α plutonium. On the other hand, Migliori *et al.* (2004, 2005) report the Debye temperature ($T = 0$ K) as 205 K based on the extrapolation of their elastic constant measurements to absolute zero. This method typically yields more accurate estimates of the Debye temperatures because it is less susceptible to the effects of self-irradiation damage. The literature values for α plutonium as determined from heat capacity, elastic constant, EXAFS, and neutron scattering Debye–Waller measurements (Sandenaw, 1961, 1962; Taylor *et al.*, 1965; Lee *et al.*, 1965b; Gordon *et al.*, 1976; Stewart and Elliott, 1981; Lawson *et al.*, 1994; Lashley *et al.*, 2003b) vary from 118 to 205 K. On the other hand, the Debye temperature for the δ-phase plutonium alloys are reported to vary much less; namely, from 100 to 130 K (Ledbetter and Moment, 1976; Stewart and Elliott, 1981; Lashley *et al.*, 2003b).

Heat capacity measurements below and above room temperature as reported by Oetting and Adams (1983), Taylor *et al.* (1968), and Lashley (2005) for unalloyed plutonium, and by Lashley *et al.* (2003a), Lashley (2005), and Rose *et al.* (1970) are shown in Table 7.21. The heat capacity measurements above room temperature are not affected by self-irradiation damage because defects are sufficiently mobile to heal the damage. As pointed out by Oetting *et al.* (1976) and others, no anomalies in the paramagnetic susceptibility with temperature have been observed, thus the magnetic contribution to heat capacity is negligible, as confirmed by Lashley (2005).

Oetting and coworkers (Oetting *et al.*, 1976) present a comprehensive listing of the thermodynamic functions – enthalpy and entropy – along with the enthalpies of transformation between the various plutonium allotropes. The heat capacity of unalloyed plutonium as a function of temperature taken from Lashley *et al.* (2003b) and Kay and Loasby (1964) is shown in Fig. 7.52. The enthalpies and entropies of transformation are listed for unalloyed plutonium in Table 7.16.

(e) Magnetic behavior

Fig. 7.53 shows the molar magnetic susceptibilities of unalloyed plutonium and a Pu–6 at.% Ga alloy as a function of temperature. The plots are taken from Lashley (2005). The data for unalloyed plutonium above 300 K are those of Comstock, published by Sandenaw (1961) with additional details provided by Olsen *et al.* (1992). These data were obtained by the Gouy method on large samples of ^{239}Pu with a purity of 99.9%. The low-temperature data for the unalloyed α plutonium and all of the data for the alloy is that of Méot-Reymond and Fournier (1996). Their plutonium alloy samples were of high purity, electrorefined, with ferromagnetic impurities constituting <10 ppm. In the plot shown in Fig. 7.53, Lashley *et al.* align Méot-Reymond and Fournier's high- and low-temperature alloy data at 300 K because of the concerns expressed by Méot-Reymond and Fournier about their high-temperature technique.

We note that the susceptibilities of unalloyed plutonium and the alloy are similar – both are quite large, similar to the magnetic susceptibility of manganese. Unlike manganese, which orders antiferromagnetically at 95 K, plutonium shows no anomaly in its susceptibility at low temperatures. Magnetic susceptibilities on the order of those exhibited by plutonium are characteristic of metals with relatively strong paramagnetism caused by electronic band magnetism (such as that for palladium). Lashley *et al.* (2004) recently concluded that a

Table 7.21 *Experimental heat capacities* (C_p) *at various temperatures for* α *plutonium and* δ*-phase Pu–Ga alloys.*

	C_p (*unalloyed* α-*Pu*) (mJ K^{-1} mol^{-1})			C_p (δ-*Pu alloys*) (mJ K^{-1} mol^{-1})	
				Pu-1.7 at.% *Ga*	*Pu*-3.3 at.% *Ga*
T (K)	*Oetting and Adams* (1983)	*Lashley* (2005)	*Taylor* et al. (1968)	*Lashley* et al. (2003b) *and Lashley* (2005)	*Rose* et al. (1970)
2.78		0.227			
3		0.236			
3.5		0.317			
3.7				0.3201	
4		0.414		0.36968	
4.5		0.477		0.46436	
5		0.52		0.58135	
5.5		0.714		0.71759	
6		0.87049		0.87265	
6.5		0.93806		1.05475	
7		1.02		1.24524	
8		1.5		1.70936	
10		2.6		2.81808	
12		4.02757		4.15583	
15		5.92989		6.41797	
20		9.14411	3.65	10.37966	
22		10.36358		11.90103	
25		12.16125		14.26709	
30		14.80288		17.8891	
35		17.10077		21.10807	

40		18.85255		23.92317	
45		20.5505		25.89824	
50		21.95556	16.68	27.62289	
65		24.72443		31.5921	
70		25.19762		32.49775	
75		25.51758		33.19174	
80		25.86718		33.63288	
90		26.33692		34.84199	
100		26.73917	24.09	35.84115	
125		27.46718		34.99518	
150		28.3027		34.62373	
200		29.42604	28.66	33.40867	
250		30.04106		30.59754	
300	31.57	30.43499	32.18	30.80206	31.97
340	33.66				
380	35.16				32.43 (373 K)
400	32.64				
440	33.16				
480	33.69				33.81 (473 K)
500	33.50				
540	34.42				
580	35.34				36.12 (573 K)
600	34.96				
640	35.40				
680	35.83				39.30 (673 K)
700	36.04				
773					43.41
863					33.94
903					33.94

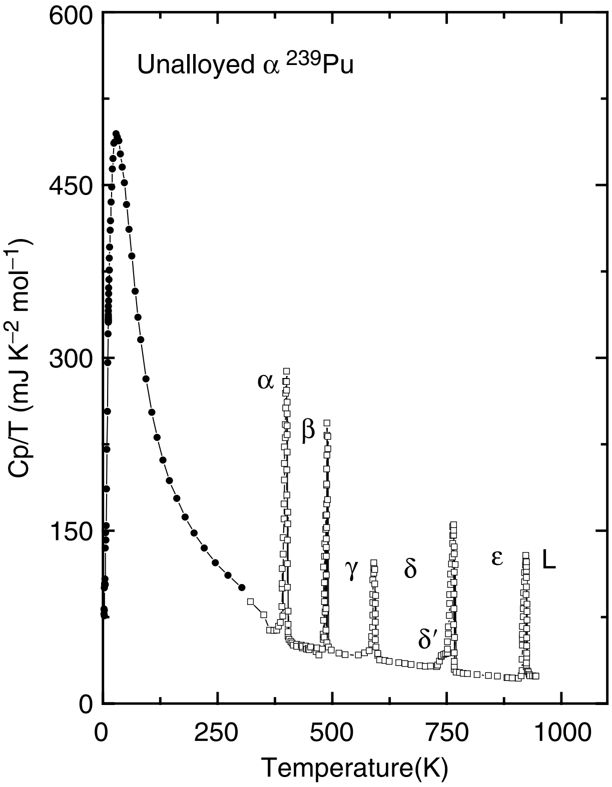

Fig. 7.52 *Heat capacity divided by temperature for high-purity, unalloyed α-phase plutonium. Open symbols are from Kay and Loasby* (1964) *and the solid symbols are unpublished work from Lashley* (2004).

thorough review of experimental data for plutonium (both in the unalloyed α phase and in the alloyed δ phase) provides no evidence for localized magnetic moments. They concluded that neither temperature nor magnetic-field dependencies of measured susceptibilities show evidence for ordered or disordered moments. They reinforce their conclusions with the results of other experimental probes, such as specific heat and NMR.

Magnetic moments and atomic volume are indicators of what the electrons are doing. As shown in Fig. 7.39, the atomic volumes of the actinides exhibit a huge expansion right at plutonium (between the α and δ phases, with an additional expansion at americium). In their review of actinide theory related to magnetic behavior, Lashley *et al.* (2004) show that the consensus among theorists is that a localization of the 5f electrons is required to explain the large volume expansion between the α phase and the δ phase, which leads inexorably

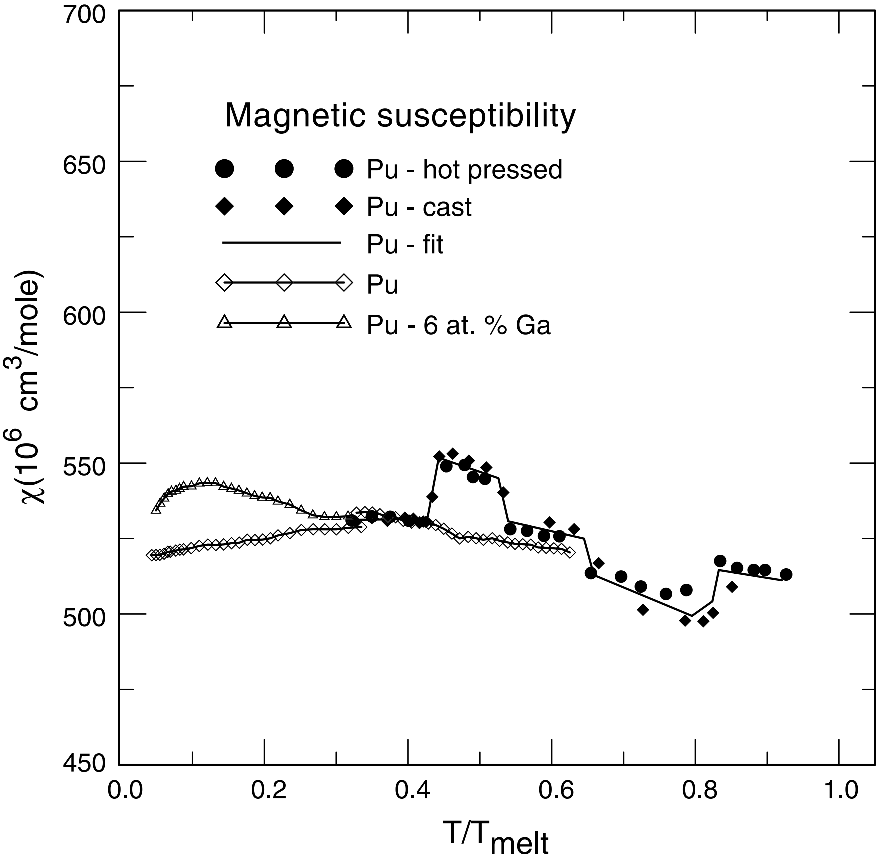

Fig. 7.53 *Molar susceptibility of unalloyed plutonium and δ-phase Pu*-6 at. *% Al alloy plotted as a function of temperature scaled by the melting point* (*from Lashley* et al., 2004). *See text for details of data.*

to magnetic ordering in the δ phase. Some theorists also predict magnetic order in the α phase. The magnetic moments are predicted to be large in both cases. Some of the theoretical treatments have suggested a partial cancellation between the spin and the orbital parts of the moments. However, even with such cancellation, magnetic moments of the order of 1 to $2\mu_B$ are predicted. Yet, the experimental evidence points overwhelmingly to the conclusion reached by Lashley *et al.* namely, neither ordered nor disordered local moments exist. Recent theoretical treatments by Shick *et al.* (2005) and Shorikov *et al.* (2005) predict reasonable volumes without any magnetic moments.

The reader is referred to the *Plutonium Handbook* (Miner and Schonfeld, 1980) and the *Gmelin Handbook of Inorganic Chemistry* (Lesser and Peterson, 1976; Blank, 1977) for additional references to magnetic susceptibility measurements and to the Hall effect in plutonium and its alloys. Recent magnetic susceptibility measurements on plutonium alloys, including Pu–Am and Pu–Ce, are also reported by Dormeval (2001) and Dormeval *et al.* (2000, 2003).

(f) Electrical resistivity, thermal conductivity, thermal diffusivity, and thermoelectric power

The unusual electrical resistivity of unalloyed plutonium is shown in Fig. 7.54 from Sandenaw and Gibney (1958). Unlike most normal metals that exhibit a linear decrease in resistivity at low temperatures, plutonium exhibits an increase and a maximum in resistivity at ~105 K. This low-temperature anomaly was initially believed to result from antiferromagnetic ordering. However, as pointed out above, no magnetic ordering has been found in plutonium or its alloys. Méot-Reymond and Fournier (1996) and Dormeval *et al.* (2000) suggest that the resistivity maximum is an indication of a Kondo effect in plutonium and its alloys. Boring and Smith (2000) make a convincing argument that the resistivity behavior along with other properties (such as the enhanced low-temperature specific heat) is an indication of strong electron–electron correlations involving spin and charge interactions. The resistivity maximum in plutonium is at the level of 150 μΩ cm, which means that an electron is scattered by roughly every atom in the lattice. As pointed out by Boring and Smith (2000), this type of scattering is considered the highest possible simple resistance that a

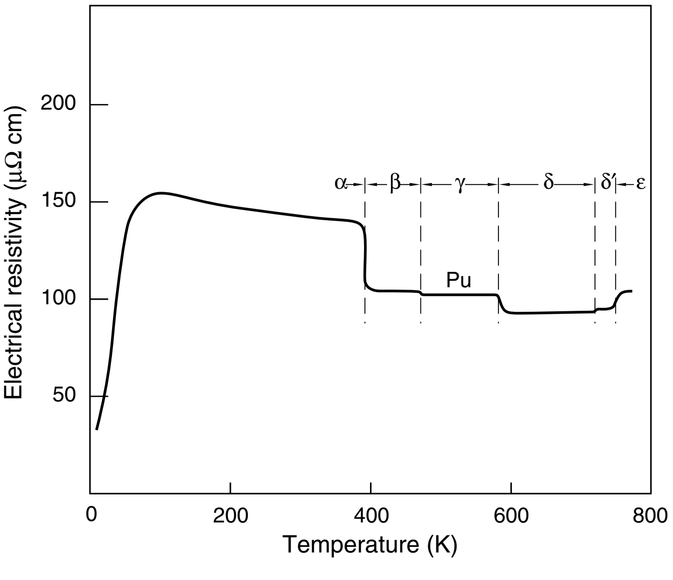

Fig. 7.54 *Electrical resistivity of unalloyed plutonium (from Sandenaw and Gibney,* 1958).

simple metal can exhibit; it is called the unitary limit. We also note that Lee *et al.* (1961) and Smith (1980) showed that plutonium does not become superconducting down to 0.75 K. Boivineau (2001) has extended resistivity measurements into the liquid phase using very high heating rates. He found the resistivity to remain nearly constant over the whole liquid range at a value of approximately 108 μΩ cm.

The resistivity of the δ-phase alloys has been measured by a number of investigators. The room-temperature values typically fall between 105 and 125 μΩ cm, depending on the alloying element and concentration. Extensive measurements have been reported on Pu–Ce alloys (Elliott *et al.*, 1962), Pu–Al alloys (Sandenaw, 1960a; Lee *et al.*, 1961; Elliott *et al.*, 1962), and Pu–Ga alloys (Joel *et al.*, 1971). The low-temperature results of Joel *et al.* (1971) for Pu–Ga alloys with gallium concentrations from 3 to 10 at.% are shown in Fig. 7.55. The results of Elliott *et al.* for Pu–Al alloys are very similar. We do not show the results for Pu–Ga alloys with gallium concentrations <3 at.% because they transform to the α′ phase upon cooling. The resistivities of all alloys are lower than that for unalloyed plutonium shown in Fig. 7.54. They also increase with decreasing temperature and exhibit a broad maximum. Increasing gallium concentration moves the maximum to lower temperatures and leads to higher

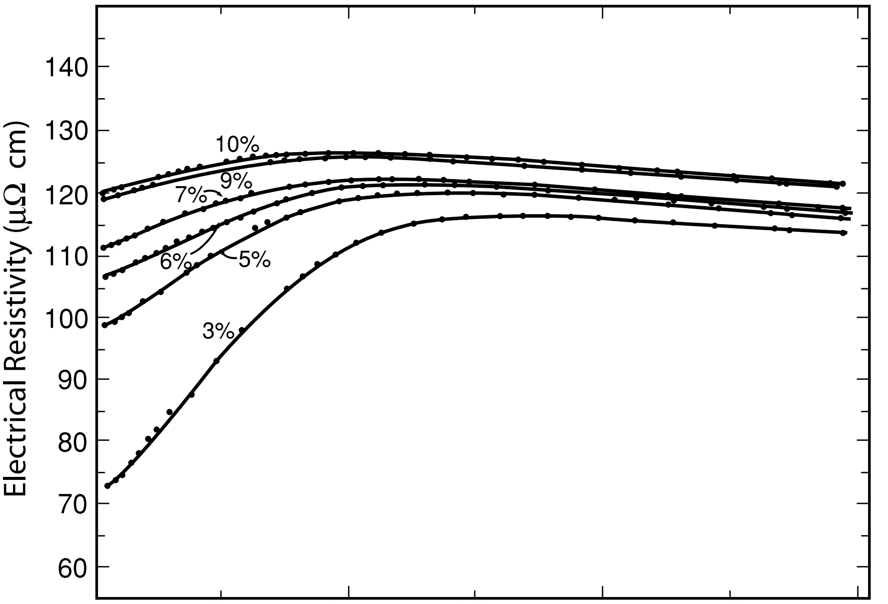

Fig. 7.55 *Electrical resistivity of various δ-phase Pu–Ga alloys (after Joel* et al., 1971).

resistivity. However, the increase with alloy concentration is less than what is typically observed for other metals. The low- and high-temperature regimes are shown together in Fig. 7.56 (taken from Blank (1977) and based on the work of Gibney and Sandenaw (1954)).

Gomez Marin (1997) and Dormeval (2001) recently measured resistivities of Pu–Am alloys across the entire range of δ-phase solubility at low temperatures. The resistivities for the entire range of alloys were considerably higher than any other plutonium alloy system. For example, the values for a Pu–15 at.% Am alloy was reported by Dormeval to be 370 μΩ cm at 293 K and 170 μΩ cm at 4 K. This alloy exhibited a slight maximum at 200 K. Alloys with higher americium contents were shown by Gomez Marin to decrease monotonically although not as rapidly as pure americium. Dormeval also reported resistivities of Pu–Ce alloys and of a number of ternary Pu–Ce–Ga and Pu–Am–Ga alloys. Blank (1977) reported the results of Mortimer and Adamson on Pu_3Al and Pu_6Fe. The resistivities at room temperature were 150 and 140 μΩ cm, respectively, and showed a maximum at lower temperatures. The resistivity for Pu_3Al remained unusually high (142 μΩ cm) at 4 K.

The literature shows large variations in low-temperature electrical resistivities measured in unalloyed plutonium. Much of this problem was a result of impurities. In addition, low-temperature measurements in plutonium are plagued by self-irradiation damage (see Section 7.7.9), which increases the resistivity

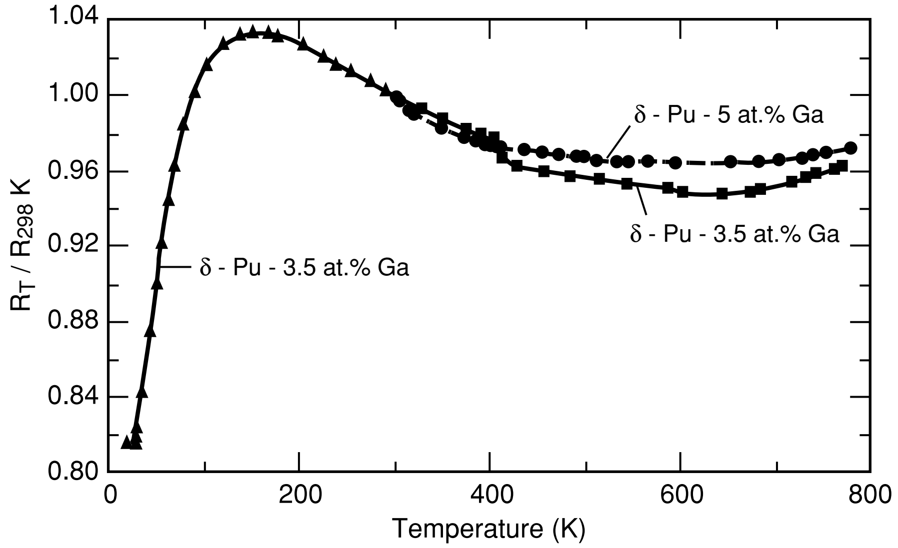

Fig. 7.56 *Electrical resistivity of a δ-phase Pu-*3.5 at. *% Ga alloy between* 25 *and* 750 K *and a δ-phase Pu-*5 at. *% Ga alloy between* 298 *and* 750 K. *The curves were normalized at* 298 K (*taken from Blank,* 1977 *with reference to Gibney and Sandenaw,* 1954).

because there is insufficient mobility of the defects generated to move and heal the lattice (Hecker and Martz, 2001). Olsen and Elliott (1962) reported some of the earliest measurements on the effects of impurities and self-irradiation on the resistivity of α-phase plutonium at low temperatures.

Thermal conductivity measurements on unalloyed plutonium were reported by Sandenaw and Gibney (1958), Lee and Mardon (1961), and Powell (1960). Andrew (1967) measured thermal conductivity of high-purity (99.98%) plutonium, chill-cast to minimize microcracking (density of 19.77 g cm^{-3}), and of preferentially oriented α-phase plutonium (by cooling from the β phase under pressure). The thermal conductivity decreases smoothly from a value of 0.0155 cal s^{-1} cm^{-1} K^{-1} at 300 K to 0.0075 cal s^{-1} cm^{-1} K^{-1} at 80 K for the chill-cast sample. Hence, the mechanisms that cause the increase in electrical resistivity and resistivity maximum at ~100 K do not seem to play a role in the thermal conductivity. Andrew found the thermal conductivity perpendicular to the [020] planes to be about 3 mW cm^{-1} K^{-1} higher than the thermal conductivity parallel to the [020] planes. He also reported a Lorenz number of 3.11×10^{-8} WΩ K^{-2} at 300 K and 5.95×10^{-8} WΩ K^{-2} at 80 K.

Andrew (1969) also reported thermal conductivities for high-purity, well-homogenized δ-phase Pu alloys. The conductivity of the Pu–3.35 at.% Ga alloy varied smoothly from 0.022 cal s^{-1} cm^{-1} K^{-1} at 300 K to 0.0098 cal s^{-1} cm^{-1} K^{-1} at 80 K. The conductivities of a Pu–7 at.% Ga alloy was approximately 10% lower and that of a Pu–10 at.% Ce alloy, approximately 20% higher. As was the case for the unalloyed plutonium, the thermal conductivities do not exhibit the anomalous low-temperature behavior found in resistivity measurements. Lewis *et al.* (1976) reported thermal conductivities calculated from thermal diffusivity measurements on high-purity Pu–3.35 at.% Ga alloys at high temperatures. Their calculated room-temperature value of 0.0205 cal s^{-1} cm^{-1} K^{-1} at 300 K increased to 0.04 cal s^{-1} cm^{-1} K^{-1} at 673 K.

Lewis *et al.* (1976) reported that the thermal diffusivity of high-purity plutonium (<200 ppm impurities) increased approximately linearly from about 0.011 cm^2 s^{-1} at 293 K (α phase) to 0.057 cm^2 s^{-1} at 843 K (ϵ phase). The thermal diffusivities of the δ-phase Pu–3.35 at.% Ga alloy increased smoothly from 0.04 cm^2 s^{-1} at 293 K to 0.065 cm^2 s^{-1} at 673 K.

The thermoelectric power of plutonium at room temperature is large and positive, and it decreases after each allotropic transformation as the temperature is increased, except for the δ′ to ϵ transformation, which shows an increase. The average value and ranges measured are shown in Table 7.22, taken from Wick (1980) and based on the work of Lee and Hall (1959), Costa (1960), Meadon and Lee (1962), and Lallement (1963). The thermoelectric power decreases rapidly at low temperatures with a slight rise at 80 K before falling very rapidly to 4 K. Blank (1977) reviewed thermoelectric power measurements for plutonium alloys. Lee *et al.* (1961) and Brodsky (1961) showed that the thermoelectric power in Pu–Al alloys exhibited an increase with decreasing temperature with a maximum at ~80 K for a δ-phase Pu–6 at.% Al alloy.

Table 7.22 *Thermoelectric power of plutonium* (*Wick*, 1980).

Phase	*Temperature* (K)	*Thermoelectric power, averaged values* (μV K^{-1})	μV K^{-1}, *range*
α	~20	1.75	~1.5–~2
	~80	10.1	8.6–11.6
	~100	9.8	8.2–11.5
	~293	~13	11.2–15.6
	300	11.5	7–15.5
β	400	9.1	7–10.7
γ	500	8.4	7.4–9.4
δ	600	3.0	2.3–3.7
δ'	725	2.32	–
ϵ	800	3.5	3.2–3.8

The value of the thermoelectric power at room temperature was approximately 4 μV K^{-1}, about one third the value of unalloyed plutonium in the α phase.

(g) Diffusion

Diffusion rates in solids depend principally on crystal structure and homologous temperature (T/T_m), that is, how close the temperature is to the melting point (Sherby and Simnad, 1961). Plutonium, of course, has multiple allotropes and a very low melting point. Sherby and Simnad (1961) showed that the Arrhenius-like rate equation for self-diffusion, $D = D_0\exp(-Q/k_BT)$, where D_0 is a constant and Q is the activation energy for self-diffusion (vacancy formation and migration), fits the diffusion data for most solids. The activation energy, Q, was found to depend primarily on the homologous temperature and the crystal structure. Experimental data for plutonium are summarized by Lesser and Peterson (1976), Blank (1977), and Deloffre (1997). The diffusion data presented in Table 7.23 are based on Deloffre's summary (1997) of the work of Tate and coworkers (Tate and Cramer, 1964; Tate and Edwards, 1966), Johnson (1964), Edwards *et al.* (1968), Rafalski and coworkers (Rafalski *et al.*, 1967; Harvey *et al.*, 1971), Dupuy and Calais (1968), Wade (1971), and Wade *et al.* (1978).

The data presented in Table 7.23 contrast self-diffusion rates in the various phases of plutonium. There are no data available for α-phase plutonium because it is stable only below 395 K where diffusion rates are extremely slow. Wade *et al.* (1978) showed that the large variations in diffusion rates in the β and γ phases were a result of short-circuit diffusion along paths such as dislocations or grain boundaries. The diffusion rates in ϵ plutonium are anomalously high even for the open bcc crystal structure. In fact, Cornet (1971) showed that the rate of self-diffusion decreased under pressure, similar to what was previously found for white phosphorus (Nachtrieb and Lawson, 1955). He calculated the

Table 7.23 *Diffusion constants in plutonium and Pu–Ga alloys.*

Pu phase method	*Temperature range* (K)	*Diffusion mechanism*	*Frequency factor* D_0 (cm^2 s^{-1})	*Activation energy* Q (J mol^{-1})	*References*
(a) Self-diffusion in unalloyed plutonium					
ϵ Pu diffusion couple ^{238}Pu tracer	773–893	lattice	2×10^{-2} $3 \times 10^{-3} < D_0 < 9 \times 10^{-2}$	77 400 ± 10 500	Dupuy and Calais (1968)
ϵ Pu thin film ^{238}Pu tracer	765–886	lattice	$(4.5 \pm 1) \times 10^{-3}$	66 940 ± 1 675	Wade (1971)
δ Pu diffusion couple ^{238}Pu tracer	623–713	lattice	4.5×10^{-3}	99 600	Tate and Cramer (1964)
δ Pu thin film ^{238}Pu tracer	594–715	lattice	$(5.17 \pm 0.7) \times 10^{-1}$	126 370 ± 800	Wade *et al.* (1978)
γ Pu diffusion couple ^{238}Pu tracer	488–580	lattice	2.1×10^{-5}	69 870	Tate and Edwards (1966)
γ Pu thin film ^{238}Pu tracer	484–544	lattice	$(3.8 \pm 10) \times 10^{-1}$	118 410 ± 7 500	Wade *et al.* (1978)
	504–564	short circuit	$(1.76 \pm 0.7) \times 10^{-5}$	69 040 ± 1 670	
β Pu thin film ^{238}Pu tracer	409–454	lattice	$(1.69 \pm 0.5) \times 10^{-2}$	108 000 ± 1 200	Wade *et al.* (1978)
		short circuit	$(3.9 \pm 0.05) \times 10^{-7}$	56 070 ± 60	
(b) Self- and interdiffusion in Pu–Ga alloys					
δ phase, thin film ^{238}Pu tracer, self-diffusion	613–781	lattice	76.0	152 000	Wade (1971)
	513–613	grain boundary	1.6×10^{-2}	110 000	
ϵ phase, thin film ^{238}Pu tracer, self-diffusion	847–917	lattice	7×10^{-4}	56 070	Wade (1971)
ϵ phase, diffusion couple, interdiffusion	833–909	lattice	5.3×10^{-4}	55 230	Harvey *et al.* (1971)
δ phase, homogenization interdiffusion	698–798	lattice	65	168 000	Johnson (1964)
δ phase, diffusion couple, interdiffusion	673–807	lattice	9.8×10^{-2}	139 300	Rafalski *et al.* (1967)
δ phase, diffusion couple, interdiffusion	688–790	lattice	1.3×10^{-2}	156 000	Edwards *et al.* (1968)

activation volume to be –4.9 cm^3, which is one-third of the molar volume of plutonium. He suggested an interstitial diffusion mechanism instead of the vacancy mechanism typically associated with lattice diffusion. Hill and Kmetko (1976) agreed with the proposed interstitial mechanism and suggested that the high self-diffusivity in the ϵ phase results from the nature of the 5f electron bonding in plutonium.

As shown in Table 7.23, the frequency factor, D_0, in plutonium is higher for self-diffusion than for interdiffusion. This behavior is shown graphically by the work of Edwards *et al.* (1968) in Fig. 7.57. It also agrees with the general observation that diffusion rates decrease with the addition of elements that raise the melting point of the host metal (Shewmon, 1963). Hilliard *et al.* (1959) showed that diffusion rates decrease significantly with increasing solute concentrations in typical alloy systems. Dupuy and Calais (1968) and Wade (1971) reported decreases in D_0 with additional solute additions. However, as reported by Mitchell *et al.* (2001), Edwards *et al.* (1968), and Rafalski *et al.* (1967) all concluded that the interdiffusion of gallium in plutonium did not vary with concentration over the range studied. Likewise, Tate and Edwards (1966) found no concentration dependence of diffusion rates in a series of δ-phase Pu–Al alloys. They reported values of $D_0 = 2.25 \times 10^{-4}$ and $Q = 106{,}690\ \mathrm{J\ mol^{-1}}$ in the range of 623 to 790 K.

The large differences in interdiffusion rates of gallium between the δ and ϵ phases are particularly important because they lead to microsegregation of gallium in δ-phase plutonium alloys, as discussed in Section 7.7.4. The diffusion data for such alloys were recently summarized by Mitchell *et al.* (2001). Hecker *et al.* (2004) showed that interdiffusion of gallium in the α' phase of plutonium (an expanded α phase resulting from the entrapment of gallium atoms in a martensitically transformed δ-phase plutonium alloy) appears to be quite rapid even at room temperature.

Irradiation enhances both self-diffusion and interdiffusion rates in solids and can lead to phase instability or radiation-enhanced segregation. Such effects are particularly important in plutonium since the radiation is self-induced. Smirnov and Shmakov (1999) provide experimental and theoretical results for the actinides including plutonium and also present a rich Russian literature on this topic.

(h) Liquid plutonium, surface tension, viscosity, and vapor pressure

Liquid plutonium is highly corrosive and easily oxidized. Early measurements of its properties, including compatibility with container materials, were made as part of the LAMPRE program. Comstock (1952) reported some of the first direct measurements on liquid plutonium. There is general agreement today that the melting point of plutonium is (913 ± 2) K. The low melting point (with respect to its position in the periodic table) has many consequences on the practical properties of plutonium. In addition to restricting the temperature

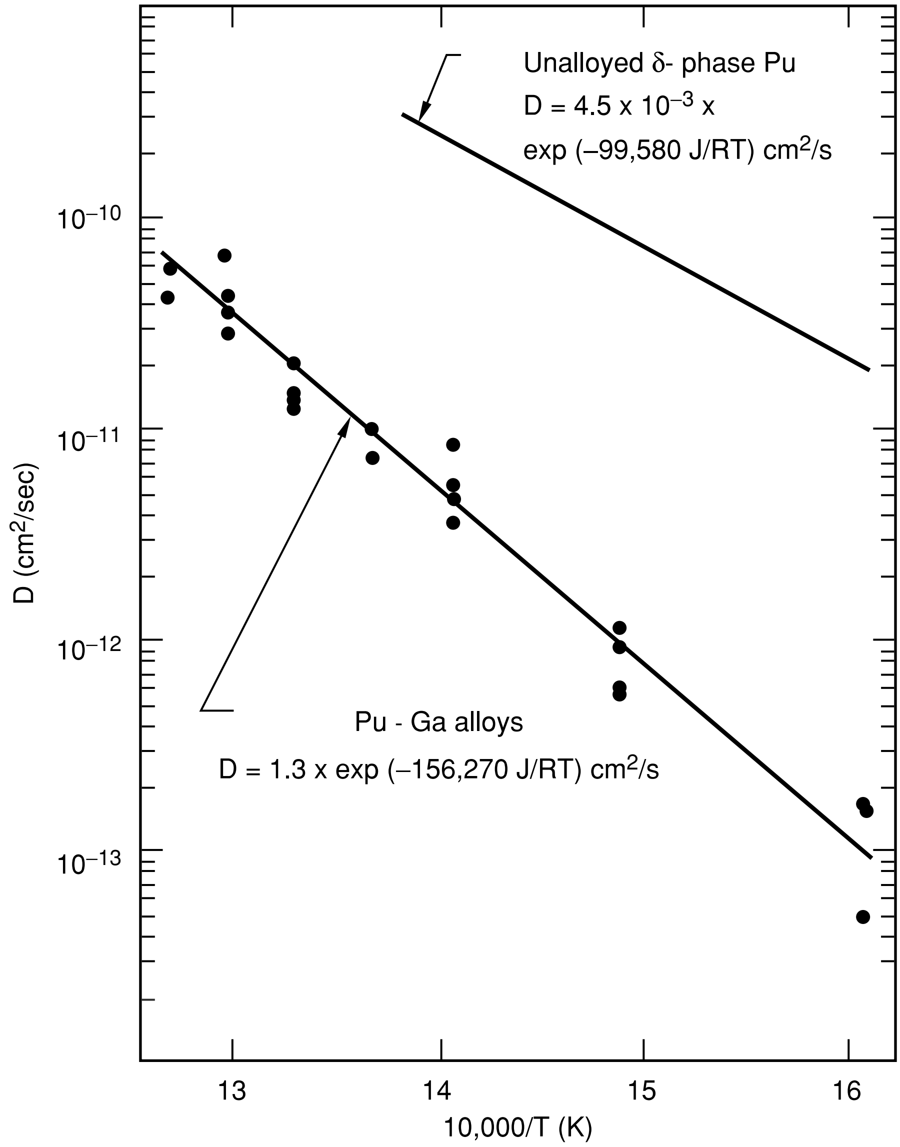

Fig. 7.57 *Diffusion coefficient, D, as a function of temperature for unalloyed plutonium and a δ-phase Pu-*3 at. *% Ga alloy plotted on a customary Arrhenius plot* (*Edwards* et al., 1968).

range of applications, it also affects all thermally activated processes, which scale with the melting point (Hecker, 2000). For example, room temperature represents a homologous temperature of 0.33, a temperature at which many defects become quite mobile. In addition, as pointed out by Nelson *et al.* (1965), the effective melting point of the α phase is significantly lower than that of the ϵ phase, increasing the homologous temperature at room temperature to 0.53 for the α phase (see Hecker *et al.* (2004) for a discussion of the metallurgical consequences).

Liquid plutonium has many peculiarities, including a density greater than the last three solid allotropes, and its heat of fusion ($\sim$2800 J mol^{-1} as shown in Table 7.16) is unusually small. The stability of liquid plutonium has been attributed to the nature of 5f electron bonding in plutonium by Hill and Kmetko (1976) and Brewer (1983). Its melting point decreases with increasing pressure up to 3 GPa (Liptai and Friddle, 1967; Morgan, 1970) consistent with the volume contraction on melting. Other materials such as gallium, bismuth, antimony, germanium, silicon, tellurium, and water show similar behavior. Merz *et al.* (1974) and Boivineau (2001) also reported an increase in sound speed in liquid plutonium with increasing temperature, with a slope of 0.08 to 0.1 m s^{-1} K^{-1}. Using a rapid heating technique, Boivineau showed that the sound speed increases to 2000 K before undergoing a rapid change in slope to a negative value from 2000 to 3600 K. Similar results have been reported for cerium (McAlister and Crozier, 1981), in which 4f electrons also play a role in bonding under pressure. Lawson *et al.* (2000) and Lawson (2001) modified Lindemann's rule for melting to include the temperature dependence of the elastic properties. Lawson *et al.* explain the anomalously low melting point of plutonium and the trend across the light actinides by temperature-induced elastic softening.

The viscosity of liquid plutonium was measured by Wittenberg and coworkers at the Mound Laboratory (Eichelsberger, 1961; Jones *et al.*, 1962; Wittenberg, 1963; Ofte and Rohr, 1965; Ofte *et al.*, 1966). Jones *et al.* (1962) reported the viscosity of liquid plutonium to follow the relation:

$$\log \eta = 672/T + 0.037 \text{ (in centipoise)} \tag{7.26}$$

which yields a viscosity of 6 cP at the melting point. This is one of the highest viscosities measured for metals and is similar to the melting point viscosity of 6.53 cP for uranium (Wittenberg, 1975) and 5.8 cP for iron (Ofte *et al.*, 1966). Ofte *et al.* pointed out that the viscosity of plutonium and its fluid flow properties place it in a class of metals whose melting points are substantially higher than that of plutonium. However, if one accounts for its high mass and low Debye temperature, then plutonium falls only somewhat above the correlation established by Iida *et al.* (1988) for most liquid metals.

Blank (1977) reviewed the measurements of viscosity on liquid Pu–Fe alloys by Ofte and coworkers (Wittenberg *et al.*, 1960; Ofte and Wittenberg, 1964; Wittenberg *et al.*, 1968). The Pu–Fe system is of practical importance because it forms the low-melting eutectic compound, Pu_6Fe. The viscosities of Pu–Fe alloys were uniformly high. That of a Pu–9.5 at.% Fe eutectic alloy (near the compound Pu_6Fe) was a remarkable 25.2 cP at 684 K (and decreased to 6.14 cP at 1081 K). Blank (1977) provides great detail in his summary of the Pu–Fe system. Wittenberg *et al.* (1960) found the activation energy for viscous flow for the eutectic alloy to be 21.9 kJ mol^{-1}. Ofte *et al.* (1966) reported viscosities for Pu–Ce and Pu–Ce–Co alloys in excess of that for plutonium. The viscosity of Pu–28.4 at.% Ce–23.7 at.% Co was reported as 23 cP at its melting point, nearly matching the viscosity of the Pu–Fe eutectic alloy. The Debye temperatures for these alloys are not available, so it is not possible to check if the viscosities fit the correlation established by Iida *et al.* (1988).

The accepted value for the surface tension of unalloyed liquid plutonium is that reported by Spriet (1963), namely 0.55 N m^{-1}. Wittenberg (1975) also reported 0.55 N m^{-1} for plutonium and 1.5 N m^{-1} for uranium. The value for plutonium fits the correlation of surface tension with melting point and molar volume proposed by Iida *et al.* (1988) for most elements in the periodic table. That of uranium appears to be anomalously high.

The optical properties and normal spectral emissivity of liquid Pu–3.4 at.% Ga at 632.8 nm were measured over the temperature range of 2016 to 2189 K using rotating analyzer ellipsometry by Sheldon *et al.* (2001). The temperature dependence of three optical properties ϵ_λ (emissivity), n_λ (index of refraction), and k_λ (extinction coefficient) were reported as:

$$\varepsilon_\lambda = 5.38 \times 10^{-5} + 0.250$$

$$n_\lambda = -1.29 \times 10^{-4}\ \mathrm{T} + 3.82$$

$$k_\lambda = -7.04 \times 10^{-4} + 5.77$$

The value for ϵ_λ is almost a third higher than that measured for uranium by Krishnan *et al.* (1993), demonstrating that the light actinides exhibit significant variations in emissivity.

Phipps *et al.* (1955) reported the vapor pressure of liquid plutonium. Subsequently, Mulford (1965), Kent and Leary (1968), and Kent (1969) added to these measurements, and reported the vapor pressure to be described by the following equation with T in K and P in atmospheres:

$$\log P = (4.924 \pm 0.120) - (17,420 \pm 184)/T \tag{7.27}$$

This relationship extrapolates to a boiling point of (3573 ± 100) K. Hence, the boiling point is quite high, in keeping with the position of plutonium in the periodic table. The combination of a high boiling point and a low melting point results in a wide range of liquid stability. Kent and Leary (1968) also reported the standard enthalpy of vaporization (H°_{298}) as (347.7 ± 2.1) kJ mol^{-1} and the standard entropy of vaporization (S°_{298}) as 123.2 J mol^{-1} K^{-1}. Oetting *et al.* (1976) reviewed the available data and recommended the best average for the enthalpy of vaporization as (345.2 ± 0.4) kJ mol^{-1}. A detailed listing of the thermodynamic properties of plutonium gas is given in Oetting *et al.* The data for the Pu_6Fe intermetallic reported by Sandenaw and Harbur (1973) were summarized by Blank (1977).

(i) New tools, new measurements of physical properties

Arko *et al.* (2006) reviewed the properties of actinides in the metallic state in Chapter 21 of this work. Their emphasis is on those properties that are unique or predominantly found in the metallic solid state. Such properties include magnetism, superconductivity, enhanced mass, spin, and charge density waves as well as quantum critical points. We refer the reader to this chapter for discussion of how plutonium fits into the trends across the actinides. They also provide detailed results of photoemission spectroscopy measurements on plutonium and its alloys.

There has been a revival of experimental work (along with a great increase in theoretical activity) in plutonium over the past 5 years. Some of the modern tools of materials science developed during the past couple of decades are being used to make measurements on plutonium and its alloys. We summarize a few salient ones in this section. One of the key barriers to many of the techniques remains the difficulty in synthesizing single crystals of the various phases of plutonium. No single crystals of α plutonium have been fabricated since the pioneering work in the 1960s by Liptai *et al.* (1967), who grew very large grains by a high-pressure technique. However, Lashley *et al.* (2000, 2001) have refined the strain-anneal technique developed in the 1960s by Moment (1968) to grow large grains of δ-phase plutonium alloys, which are suitable for many of the single-crystal measurements. These large-grained, very high-purity plutonium samples have been used for many recent physics experiments.

Zocco and Schwartz (2003) provide a history of the development of TEM techniques and their application to plutonium and its alloys. This technique is an essential tool for metallurgical studies, first demonstrated for plutonium around 1980 and revived in 2000. Zocco and Schwartz show examples of how TEM has helped answer key questions about phase transformations in plutonium alloys, as well as study the effects of self-irradiation damage. Boehlert *et al.* (2001) demonstrated how electron backscattered diffraction can be used to examine the grain structures in Pu–Ga alloys.

Ledbetter and Moment (1976) raised interest in the phonon spectrum of plutonium with their results nearly 30 years ago on the unusual elastic anisotropy of δ-phase plutonium. In a pioneering paper, Wong *et al.* (2003b) recently reported the first complete phonon dispersion curves of plutonium using inelastic X-ray scattering from a third-generation synchrotron facility (the European Synchrotron Radiation Facility in Grenoble, France). Their results are shown in Fig. 7.58 for a Pu–2 at.% Ga δ-phase alloy large-grained polycrystal grown by the techniques developed by Lashley *et al.* (2001). Wong *et al.* confirmed the large elastic anisotropy found by Ledbetter and Moment. They also found a small shear elastic modulus, C', a Kohn-like anomaly in the T_1 [011] branch, and a pronounced softening of the [111] transverse modes. They relate these findings to a strong coupling between the lattice structure and the 5f valence instabilities in plutonium. Dai *et al.* (2003) predicted the phonon dispersion

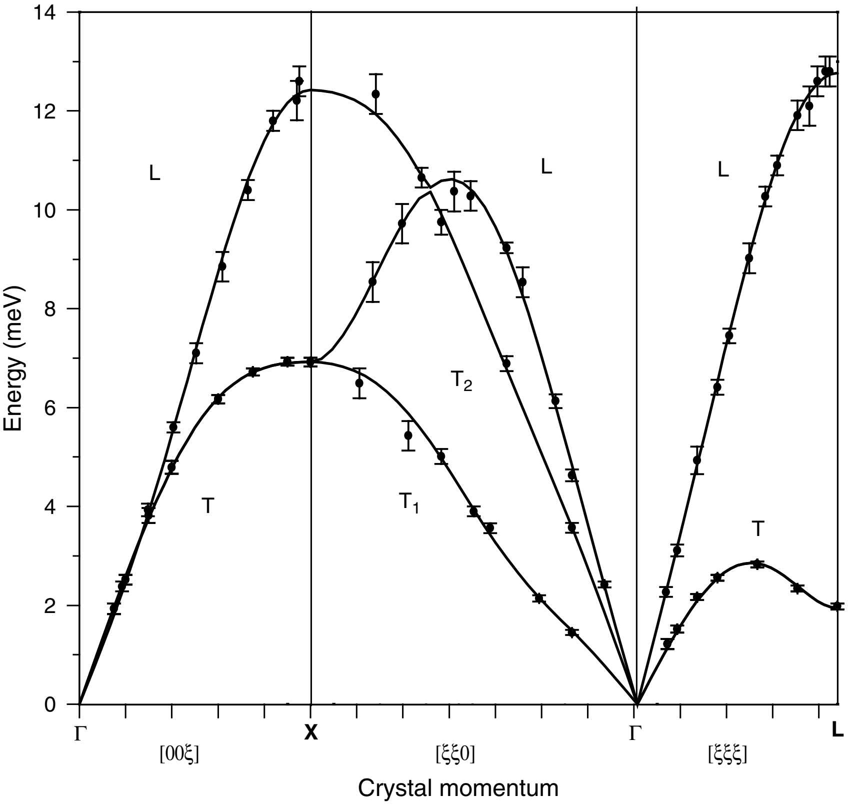

Fig. 7.58 *Phonon dispersion along high-symmetry directions in δ-phase Pu-*2 at. *% Ga alloy. The longitudinal and transverse modes are denoted L and T, respectively. The experimental data are shown with error bars. Along the* [0ξξ] *direction, there are two transverse branches,* [011]<011>(T_1) *and* [011]<100>(T_2)*. The softening of the TA* (*transverse acoustic*) [111] *branch toward the L point is apparent. The curves represent the fourth-nearest neighbor Born–von Kármán model fit* (*Wong* et al., 2003*b*).

curves using dynamical mean-field theory (DMFT), which includes electron correlations that are so important in plutonium. Wong *et al.* point out that although the qualitative agreement between theory and experiment is quite good, there are important quantitative differences. Wong *et al.* (2003a) also developed a thermal diffuse scattering technique to complement their inelastic scattering technique.

McQueeney *et al.* (2004) reported the temperature dependence of the phonon spectrum, as observed from measurements of the phonon DOS and sound velocities as shown in Fig. 7.59. The DOS was measured with inelastic neutron scattering on a polycrystalline ^{242}Pu–5 at.% Al δ-phase alloy. The ^{242}Pu isotope was used because the absorption of thermal neutrons is low compared to the

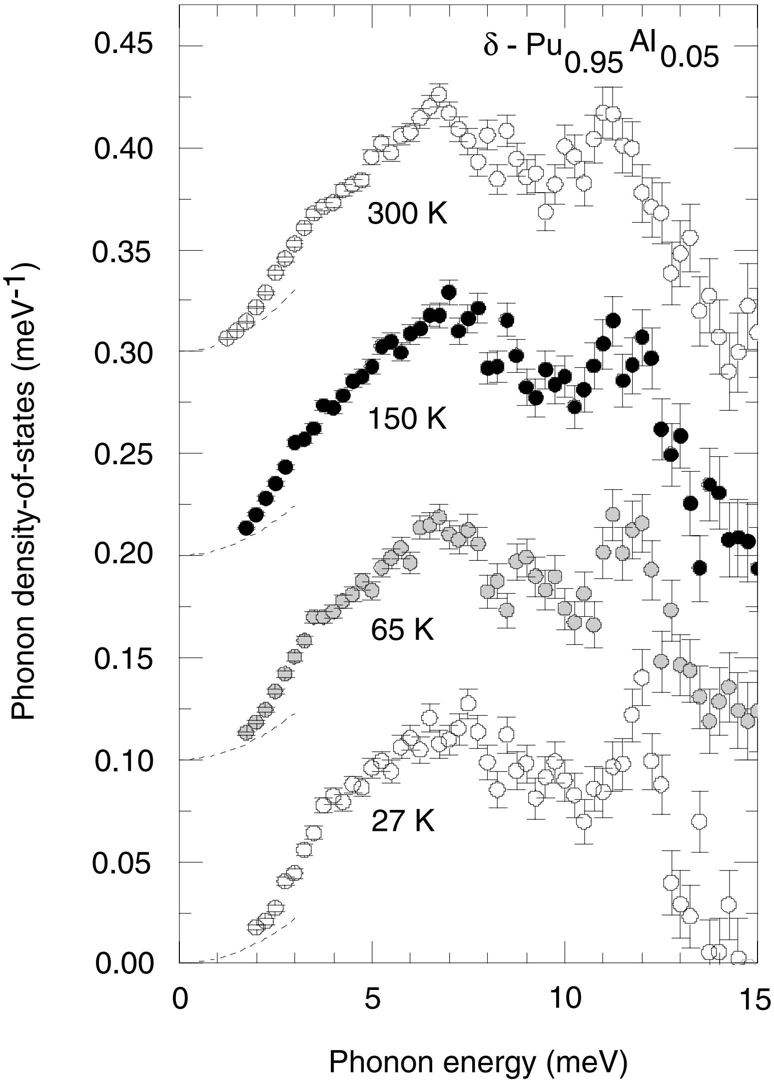

Fig. 7.59 *Phonon density of states of δ-phase Pu-*5 at. *% Al at four temperatures. The dashed line represents the quadratic part of the DOS at each temperature, as estimated by the average sound velocity obtained from resonant ultrasound measurements* (*from McQueeney* et al., 2004).

standard ^{239}Pu isotope. The phonon frequencies and sound velocities soften considerably with increasing temperature in spite of nearly zero thermal expansion over this temperature range. The frequency softening of the transverse branch along the [111] direction is anomalously large (~30%) and sensitive to alloy composition. Based on a comparison to the results of Wong *et al.*, McQueeney *et al.* concluded that the interatomic potential is extremely sensitive to alloy composition, pressure, and temperature, unlike any other metal. They suggest that this behavior may arise from an unusual temperature dependence of the electronic structure.

We referred to local structure measurements at the modern synchrotron sources earlier using EXAFS along with conventional XRD in Section 7.7.5. Allen *et al.* (2002) reported temperature-dependent EXAFS measurements over the temperature range of 20–300 K of the vibrational properties of a Pu–3.3 at. % Ga δ-phase alloy as a means of discerning differences in the vibrational character of the gallium and plutonium sites. They obtained pair-specific, correlated Debye temperatures, θ_{cD}, of (110.7 ± 1.7) K for the Pu–Pu pairs and (202.6 ± 3.7) K for the Pu–Ga pairs. Allen *et al.* concluded that these results indicate that Ga–Pu bonds are significantly stronger than the Pu–Pu bonds. Lynn *et al.* (1998) previously reported a Pu-specific value of $\theta_{\mathrm{D}} = 127$ K and a Ga-specific $\theta_{\mathrm{D}} = 255$ K using neutron-resonance Doppler spectroscopy on a Pu–3.6 at.% Ga alloy. Nelson *et al.* (2003a,b) reported EXAFS measurements on the vibrational properties of both the δ phase and the α′ phase of a Pu–1.9 at. % Ga alloy (in the δ-phase and mixed, α′ + δ, phase conditions). They found a bond-length contraction for the Pu–Ga bond of 0.11 Å in the δ phase, but only 0.03 Å in the α′ phase. They reported correlated Debye temperatures of θ_{cD} (δ) = (120.4 ± 2.6) K and θ_{cD} (α′) = 159.1 ± 12.5 K.

Moore *et al.* (2003) used high-energy electron energy loss spectroscopy (HE-EELS) in a TEM and synchrotron-radiation-based X-ray absorption spectroscopy to determine phase-specific electronic structure information on plutonium. The sample was a dilute Pu–Ga alloy treated to produce a mixture of the α + δ phases. The TEM examination allowed individual grains of each phase to be examined. Moore *et al.* conclude that Russell–Saunders coupling fails for the 5f states of plutonium, and that only the use of JJ or intermediate coupling is appropriate. In addition, they conclude that their results confirm calculations that there is considerable spin–orbit splitting of the occupied and unoccupied 5f states of plutonium, indicating that spin–orbit splitting cannot be neglected in the Hamiltonian for the 5f states of plutonium.

Superconductivity has recently been discovered above 18 K in a plutonium-based nearly magnetic compound, $\mathrm{PuCoGa_5}$ by Sarrao *et al.* (2002, 2003a,b). At the same temperature, this compound exhibits a step-like transition in heat capacity, from which they inferred the electronic specific heat, γ, to be 77 mJ $\mathrm{mol^{-1}\ K^{-2}}$, which points to strong electron–electron correlations. In addition, field-dependent resistivity data gave an upper critical field of 74 T, a surprisingly large value. Other actinide-based superconductors have transition temperatures below a few K. The cerium-based isostructural compounds $\mathrm{CeCoIn_5}$ and $\mathrm{CeIrIn_5}$ are also superconducting but only in the 1-K range, and for $\mathrm{CeRhIn_5}$ only under pressure. The T_{c} of $\mathrm{PuCoGa_5}$ can be further enhanced to about 22 K by applying pressure (Griveau *et al.*, 2004). $\mathrm{PuRhGa_5}$ is superconducting, as well, with $T_c = 8.6$ K (Bauer *et al.*, 2004). The properties of these plutonium-based superconductors are indicative of an unconventional, most likely magnetically mediated, superconductivity (Sarrao *et al.*, 2003b).

7.7.7 Mechanical properties of plutonium metal and alloys

Mechanical properties of metals and alloys depend to first order on their crystal structure and melting point, which indirectly affects all thermally activated processes. The multiple allotropes of plutonium lead to a rich spectrum of mechanical properties as reviewed recently by Hecker and Stevens (2000). The low melting point allows for relatively easy mobility of defects near and above room temperature. Consequently, the mechanical properties of plutonium are especially sensitive to temperature and strain rate. They are also sensitive to chemistry (both intentional alloying and unintentional impurities) and processing, which, in turn, control the microstructure (phases present, their structure and distribution, and the nature and number of defects). Therefore, it is necessary to know the chemistry and the processing history to compare the properties of plutonium.

Gardner (1980) presented the most comprehensive review of the mechanical properties of plutonium and its alloys. His results for the yield and ultimate tensile strengths of unalloyed plutonium (for a range of purities and processing histories) are summarized in Fig. 7.60. These data demonstrate the dramatic temperature and crystal-structure dependence of the strength properties of plutonium. As reported by Gardner, the monoclinic crystal structure of plutonium (the only element in the periodic table with this low-symmetry structure) precludes the necessary conditions for plastic slip (by dislocation glide) in polycrystalline material for extended plastic flow. Consequently, the α phase of plutonium is brittle at and near room temperature. As shown in Fig. 7.60, it is quite strong. However, the tendency for α plutonium to microcrack during typical processing causes significant scatter in the properties. Moreover, certain impurities lead to the retention of second phases (typically the δ or β phases) or the presence of inclusions (such as oxides, nitrides, carbides, or the eutectic intermetallic, Pu_6Fe), which can have a significant effect on the mechanical properties.

Another important variable in determining the mechanical behavior of α plutonium is the grain size. Merz (1970, 1971) demonstrated that in α plutonium with decreasing grain size the mechanism for plastic flow changes. He fabricated very fine-grained α plutonium (1–3 μm) by extrusion and concurrent recrystallization of electrorefined, high-purity plutonium. He demonstrated that the strength decreased substantially with grain size and the ductility increased. At room temperature, he found surprising plastic elongation of 8% at low strain rates. On the high-temperature end of α-phase stability, he found extended plasticity, that is, elongations in excess of 100% (Merz and Allen, 1973;

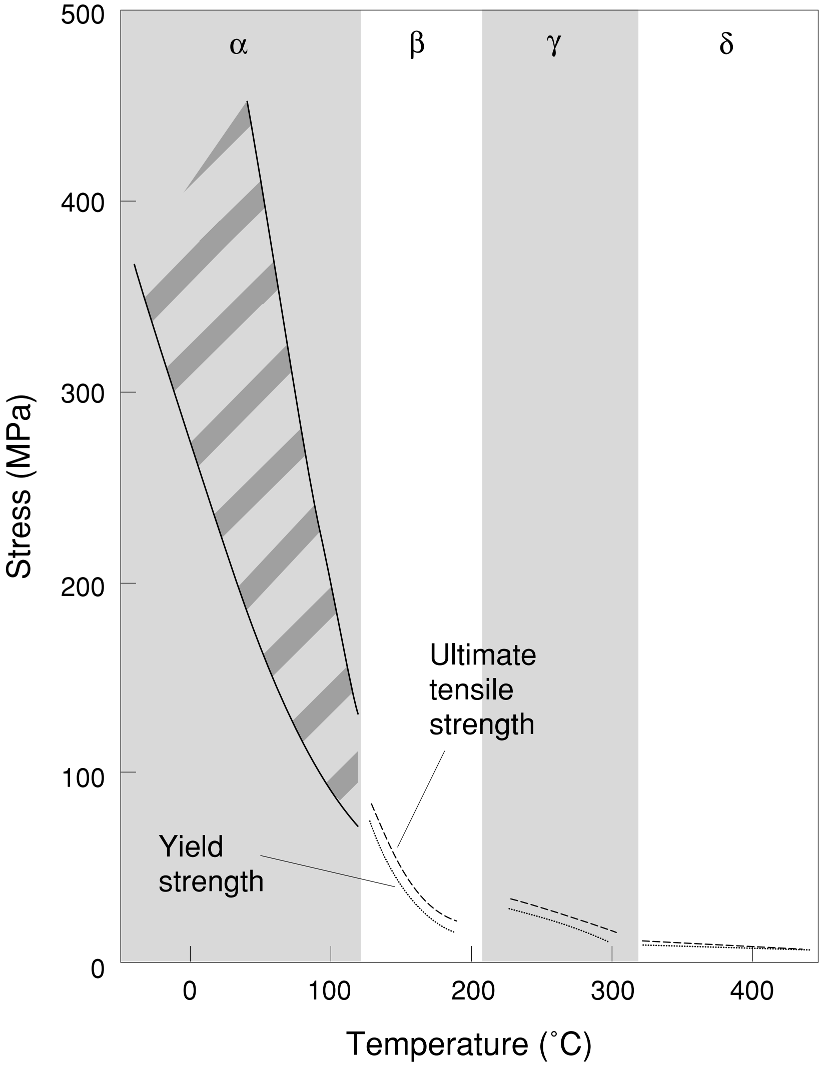

Fig. 7.60 *Strength as a function of temperature for unalloyed plutonium tested in uniaxial tension at nominal strain rates of* 10^{-3} s^{-1} (*after Gardner,* 1980).

Merz, 1974). In the β phase, he found the fine-grained plutonium to exhibit classical superplasticity with several 100% elongation. He explained that the deformation mechanism changed from dislocation glide to grain boundary sliding because of the small grain size and the high homologous temperature of 0.53 at room temperature for the α phase of plutonium. Fig. 7.61 shows the change in Vickers Microhardness with temperature for several grain sizes in α plutonium (Merz and Nelson, 1970). Hecker and Morgan (1976) found that the strength of coarse-grained α plutonium increased moderately at intermediate strain rates. Hecker and Stevens (2000) pointed out several other interesting features about the mechanical behavior of α plutonium in their review.

As shown in Fig. 7.60, the other phases of unalloyed plutonium are relatively weak compared to the α phase. Gardner shows no data for the ε phase. Cornet and Bouchet (1968) showed that the elastic moduli of the ε phase is approximately two-thirds that of the δ phase, and we also expect its strength properties to be lower. The other phases of plutonium are also considerably more ductile than the α phase. As pointed out earlier, a few atom percent of alloying

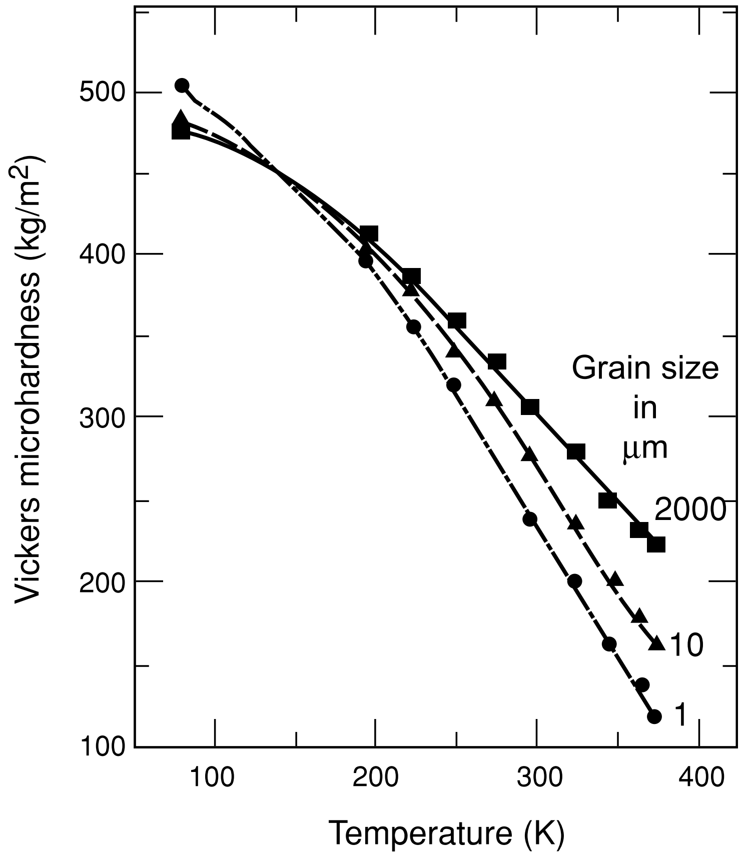

Fig. 7.61 *Vickers microhardness as a function of temperature for unalloyed α plutonium at various grain sizes (after Merz and Nelson,* 1970).

additions of elements such as gallium or aluminum retain the fcc δ phase to room temperature. As expected the δ phase alloys are considerably more ductile than the monoclinic α phase. A comparison of room temperature mechanical behavior is shown in Fig. 7.62 (Hecker and Stevens, 2000). The α phase is shown to be strong and brittle (like cast iron), whereas the δ-phase Pu–Ga alloy is weak and ductile (like commercially pure aluminum). Processing of the δ-phase alloys strongly influences the mechanical properties. Particularly important are gallium segregation, which can be minimized by elevated-temperature annealing treatments and thermo-mechanical treatments (see Fig. 7.33). Robbins (2004) recently reported an extensive compilation of the mechanical properties of Pu–3.4 at.% Ga δ-phase alloys. The compression behavior of a typical, well-homogenized alloy is shown in Fig. 7.63 (from the work of Barmore and Uribe (1970)). We should note that the mechanical properties of δ-phase Pu–Al alloys are similar to Pu–Ga alloys with similar atomic concentrations of the alloying element.

Detailed mechanical properties of plutonium and various alloys, including strength, hardness, ductility, creep, impact strength, and fatigue strength are presented by Gardner (1980), by Lesser and Peterson (1976) for unalloyed

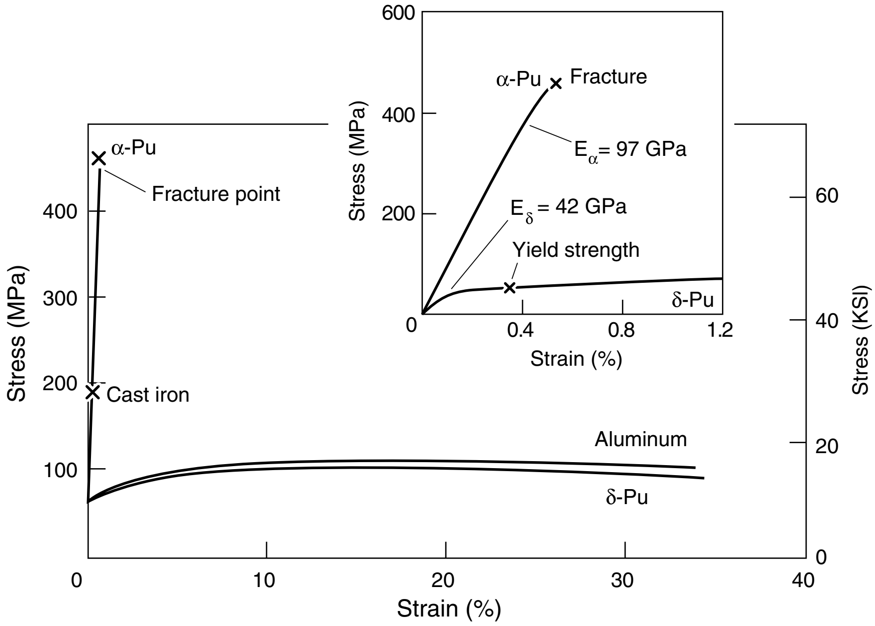

Fig. 7.62 *Typical uniaxial tensile stress–strain curves for unalloyed α plutonium compared to a δ-phase Pu–Ga alloy at a nominal strain rate of* 10^{-3} s^{-1}. *The insert shows the initial stress–strain curve at higher resolution* (*after Hecker and Stevens,* 2000).

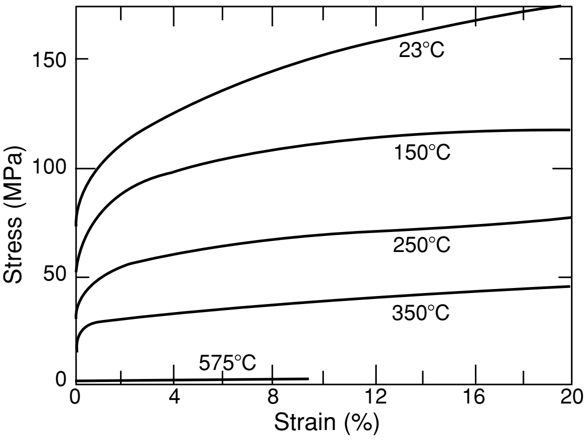

Fig. 7.63 *Uniaxial stress–strain curves in compression for a δ-phase Pu-*3.4 at. % *Ga alloy at different temperatures and a nominal strain rate of* 10^{-2} s^{-1} (*after Barmore and Uribe,* 1970).

plutonium (on pp. 29–33 of their review), and by Blank (1977) for Pu–Al alloys (pp. 180–183) and for Pu–Ga alloys (pp. 221–232). Blank (1976, 1977) also provides mechanical properties for additional alloy systems, with a particularly extensive discussion of the Pu–Fe system (Blank, 1976). Care must be taken during low-temperature experiments on δ-phase alloys to avoid transformation of the retained δ phase to the α′ phase. Since the α′ phase is so much harder than the δ phase, even small amounts of α′ result in significant strengthening.

There are few theoretical treatments of mechanical behavior of plutonium in the literature. The principal problem stems from the fact that the mechanical properties are controlled by microstructure and defects, which are still beyond the reach of *ab initio* calculations for all practical metals. Stout *et al.* (2002) developed a physically based constitutive model to predict the mechanical behavior of fcc δ-phase plutonium alloys. The input to the model was based on previous work with other fcc metals and the published test results on Pu–Ga alloys referenced above. The model is able to predict the temperature and strain-rate effects on the yield and ultimate strengths of Pu–Ga alloys. It also allowed the authors to isolate the effects of microstructural variables such as grain size, alloy content, and impurity content. The effect of gallium solutes has the largest strengthening effect. The yield strength increases by 50% with an increase in gallium from 1 to 6 atomic percent. The grain size effect follows the classical Hall–Petch relationship:

$$\sigma_y = \sigma_0 + \kappa/\sqrt{d} \tag{7.28}$$

where σ_y is the yield strength for a grain diameter d in μm, and σ_0 and κ are measured constants. Hence, decreasing grain size leads to increased strength in the deformation regime controlled by dislocation glide. (We note that in the deformation regime dominated by grain boundary sliding, the relationship is inverted – small grain size leads to lower strength.) The parameters for Pu–Ga alloys are given by Stout *et al.* (2002). The model allowed them to demonstrate that the typical impurities (such as C, O, N, and Fe form hard inclusions of μm to tens of μm in diameter) in these alloys have little effect on strength values at ambient temperature. However, the fracture behavior will be affected negatively by higher impurity contents. In addition, Beitscher (1970) showed that iron impurities at the level >300 ppm lead to dramatic high-temperature embrittlement (at 683 K and low strain rates) because the Pu_6Fe intermetallic inclusions melt and lead to brittle behavior known as 'hot shortness.'

7.7.8 Oxidation and corrosion in plutonium metal and alloys

Degradation of plutonium surfaces under various atmospheric conditions is of concern during handling and for all considerations that require storage of plutonium, its alloys, or its compounds. Although plutonium is a reactive metal as suggested by a standard reduction potential of –2.02 V for the Pu^{3+}/Pu^0 couple (see Fig. 7.116a), its oxidation rate in very dry air (<0.5 ppm H_2O) is a minuscule 20 pm h^{-1} (Haschke *et al.*, 1996). Clean plutonium surfaces have a silvery, metallic sheen, similar to clean iron or nickel. Plutonium loses its metallic sheen quite rapidly in most atmospheres. It takes on a darker appearance and exhibits interference colors before it begins to develop a loose, olive-green powder of PuO_2 'rust' (see Section 7.8.5.a). Although this process occurs quite slowly in most of the protective atmospheres in which plutonium is handled, experience over the years has yielded many surprises, including pyrophoric behavior and anomalous corrosion rates catalyzed under complex atmospheric conditions of hydrogen or moist air that can increase surface corrosion rates by a staggering 13 orders of magnitude. The enhanced oxidation rates in the presence of moisture were already discovered at Los Alamos during the Manhattan Project by Covert and Kolodney (1945). Uncontrolled surface reactions are one of the greatest risks during storage or use of plutonium metal. Not only do these reactions change the geometry of the material, they typically result in finely powdered forms that are more readily dispersed, and hence, increase the health risk of inadvertent release and uptake of plutonium, a safety hazard of paramount importance for long-term plutonium storage (Haschke *et al.*, 1998).

Waber (1980) summarized the available knowledge on corrosion and oxidation of plutonium up to 1964. Subsequent results to 1976 were summarized by Lesser and Peterson (1976). More recently, Haschke *et al.* (2000a) presented a current understanding of corrosion and oxidation, and Hecker and Martz (2001) summarized current understanding and presented practical examples of plutonium corrosion problems. Much of the discussion here is based on the report of Hecker and Martz. We refer the reader to Lesser and Peterson (1976) for a description of the reaction of plutonium with other gases such as nitrogen and ammonia at higher temperatures as well as surface reactions of plutonium with acids and other solvents.

(a) Oxidation in air

Corrosion rates depend greatly on plutonium surface chemistry. Hence, it is crucial to understand the specific surface chemistry for different plutonium substrates and for different atmospheric conditions. In dry air, the reactive plutonium metal surface is passivated by a layer of protective $PuO_{2\pm x}$ that forms rapidly over the entire surface. In the Pu–O system, Pu(IV) is a stable oxidation state and forms a classic fluorite-type crystal structure, with four plutonium cations per unit cell arranged in an fcc lattice, and eight oxygen anions at the tetrahedral interstices in a simple cubic packing (as discussed in Section 7.8.5.a, and shown in Fig. 7.90).

The oxidation rate is controlled by the diffusion of oxygen through the oxide surface to the oxide–metal interface, yielding classic parabolic growth rates. Significant stresses build up at the interface because the density of the oxide is 11.46 g cm^{-3} compared to pure α plutonium at 19.86 g cm^{-3}. The oxide layer reaches a steady-state thickness of 4 to 5 μm because at this thickness the oxide begins to spall, leading to a balance between spalling of the oxide and re-oxidation of the surface (Martz *et al.*, 1994). A constant isothermal oxidation rate is maintained by diffusion of oxygen through an oxide layer of constant average thickness. Fig. 7.64 also shows that corrosion rates depend strongly on temperature and atmospheric conditions. The details of this behavior are presented by Haschke *et al.* (1998) and discussed by Hecker and Martz (2001). Activation energies of oxidation in unalloyed plutonium are reported by Blank (1977), based on the work of Thompson (1965), to be 96.2 kJ mol^{-1} for the α phase, 50.2 kJ mol^{-1} for the β phase, and 58.6 kJ mol^{-1} for the γ phase, each in their temperature range of phase stability. However, Blank points out that significantly different results have been cited by other authors because of the substantial influence of microcracks, impurities, and crystallographic textures. The reader is referred to Haschke *et al.* (1998) for a more detailed discussion of the thermodynamics and kinetics of the oxidation process.

(b) Moisture-enhanced oxidation

Corrosion of plutonium metal in moist air occurs at a rate 200 times greater than in dry air at room temperature and five orders of magnitude greater at 100°C. The mechanisms of water-catalyzed corrosion of plutonium have only recently been elucidated (Haschke *et al.*, 1996). It had been generally accepted that the greatest oxygen concentration possible in plutonium oxide was in the

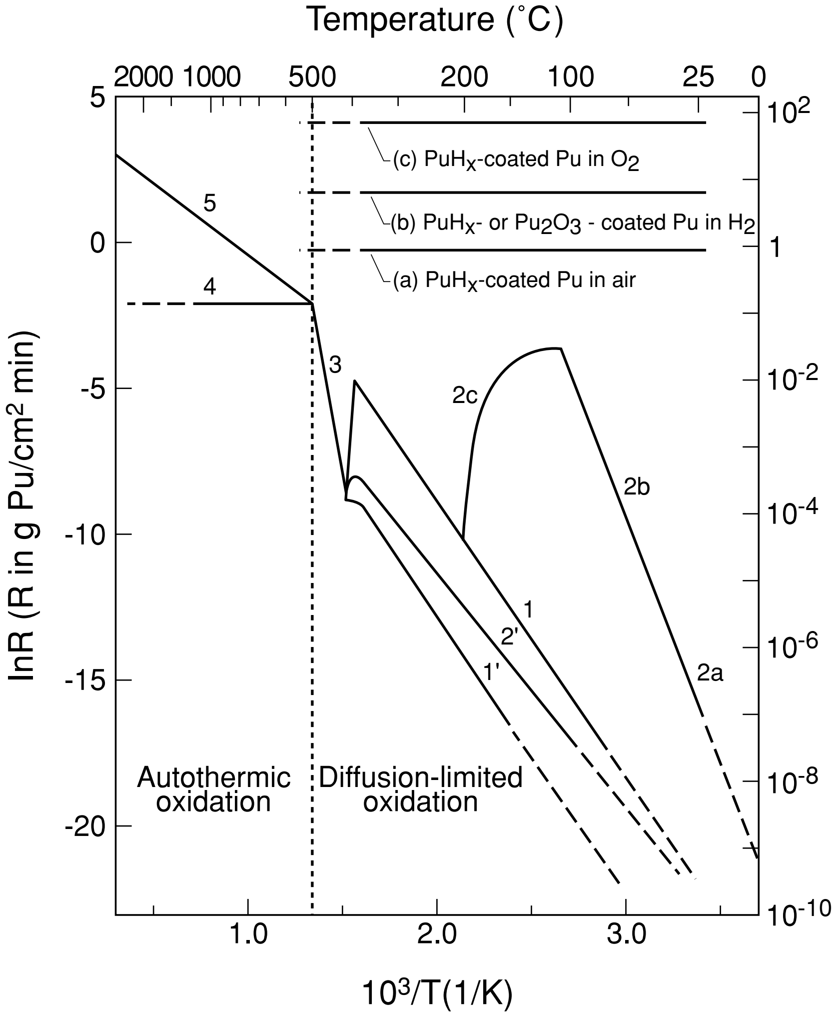

Fig. 7.64 *Oxidation rates of plutonium vs temperature. Curve* 1 *shows the oxidation rate for pure plutonium exposed to dry air or oxygen at an* O_2 *pressure of* 21.3 kPa. *Curve* 2*a presents the oxidation rate when the same, dry Pu samples are exposed to water vapor at the same pressure* (21.3 kPa). *Note the increase of four orders of magnitude in oxidation rate. Curves* 2*b and* 2*c extend the water-exposed oxidation rate to the temperature ranges of* 61–110°C *and* 110–200°C, *respectively. The drop in oxidation rate at higher temperatures is not fully understood, but may be related to the lack of spallation of product oxide at higher temperatures. Curves* 1′ *and* 2′ *present oxidation data for Ga-stabilized* δ *Pu in dry and moist air, respectively. Distinctions in oxidation rates for various alloys and conditions disappear at high temperatures as shown by curve* 3. *Curve* 4 *shows the constant oxidation rate observed under static conditions, while curve* 5 *shows recent data extrapolated from ignited Pu droplets oxidizing during free-fall in air. The reactions of hydride-coated Pu are shown in curves a–c. Curve a shows the constant reaction rate for hydride-coated Pu exposed to dry air. This represents an increase in reaction rate of over* 10^9 *compared to pure Pu. Curve c shows the same material exposed to pure oxygen. This reaction is* 10^{13} *times faster than pure Pu exposed to* O_2. *Finally, curve b shows the constant reaction rate of either hydride- or cubic sesquioxide-coated Pu to hydrogen* (*at* 101 kPa) (*Martz and Haschke,* 1998*; Haschke* et al., 2000*a*).

dioxide, namely $PuO_{2.0}$. However, Stakebake *et al.* (1993) and Haschke *et al.* (2000a, 2001) demonstrated that hyperstoichiometric plutonium oxide, PuO_{2+x}, forms in the presence of either gaseous or liquid water. The largest value they measured for x was 0.26. Rapid oxidation by adsorbed water produces hydrogen at the gas–solid interface and forms a higher oxide as Pu(IV) cations in PuO_2 are replaced by Pu(V) and an equal number of O^{2-} or OH^- ions in interstitial defect sites (see Section 7.8.5). In moist air, product hydrogen combines with disassociatively adsorbed oxygen to reform water on the surface. A water-catalyzed cycle is propagated as Pu and O_2 are transformed into oxide at the rapid rate characteristic of the metal–water reaction. This change in the composition of the oxide is also accompanied by a dull yellow to a khaki-to-green color change.

(c) Oxidation behavior of plutonium alloys

The overall rate of oxidation is less for alloyed plutonium in the fcc δ phase than it is for unalloyed plutonium (shown in Fig. 7.64) because the lowered stresses upon oxide formation (the δ-phase density is 15.8 g cm^{-3} compared to 19.86 g cm^{-3} for the α phase). Haschke (1999) has also speculated that gallium is not incorporated in the PuO_2 lattice and resides in octahedral sites of the fluorite structure. Consequently, since oxygen diffusion occurs via these sites, he suggested transport of oxygen through the oxide layer may be inhibited. Blank (1977) summarized the work of Raynor and Sakman (1965) and Waber (1980) on oxidation of plutonium δ-phase alloys. Pu–Ga alloys were found to oxidize at a lower rate than unalloyed plutonium at all temperatures in moist air. The oxidation rates were found to be greater in moist argon. However, the protection afforded by alloying was less for the case of moist argon than for moist air. Blank (1977) also summarized oxidation results for Pu–Al alloys. A partial summary, presented in Table 7.24, shows that the addition of aluminum lowers the oxidation rate, but that the behavior depends strongly on temperature and relative humidity. As examples of actual weight gain through oxidation, Blank cites the results of Waber *et al.* (1961): 0.1 mg cm^{-2} for Pu–9 to 12 at.% Al alloys after 500 h at 75°C and 50% relative humidity and 0.5 mg cm^{-2} for Pu–8 at.% Al after 8700 h at 35°C and 20% relative humidity. Blank (1977) also provided a summary of the oxidation behavior of Pu–Fe and other alloys.

(d) Pyrophoricity of plutonium metal in air

Fig. 7.64 also shows that at elevated temperatures, plutonium exhibits an autothermic reaction, igniting spontaneously in air when the temperature reaches 500°C. Studies of pyrophoricity of plutonium by Martz *et al.* (1994) helped to elucidate the role of another oxide of plutonium, namely the cubic (bcc) sesquioxide, Pu_2O_3. The revised view of the plutonium–oxygen interface is shown in Fig. 7.65. Although the dioxide is the one observed when plutonium

Table 7.24 *The relative merit given by the merit ratio* (*MR*) *as defined by weight increase of unalloyed α-phase plutonium divided by the weight increase of a δ-phase Pu–Al alloy after the oxidation of the samples by water vapor as compiled by Blank* (1977).

Al content at.%	*T* (°C)	*Relative humidity* (%)	*Time* 12 h	*Time* 50 h	*Time* 1000 h	*Time* 4300 h	*Time* 8700 h	*References*
3.5	30	95			8			Sackman (1960)
3.5	90	95	130					Sackman (1960)
3.5	90	55	50	100	120			Sackman (1960)
3.5	100	0			6			Sackman (1960)
3.0	55	50					~17	Waber (1958)
9	75	50			666			Waber *et al.* (1961)
8	35	20			~19	42.5	51	Waber (1958)

metal is exposed to oxygen or air, there is always a layer of the cubic sesquioxide present at the metal-oxide interface. However, at room temperature, its thickness is small compared to that of the dioxide. The cubic sesquioxide acts as a layer that separates the oxide-rich surface from the plutonium-rich substrate, being simultaneously consumed and formed by competing reactions. The thickness of these various oxides depends upon a variety of factors including temperature and oxygen concentration. At temperatures exceeding 150°C and in oxygen-poor environments, the cubic sesquioxide becomes the predominant phase, appearing as a surface product under oxygen-free environments.

Martz *et al.* (1994) explained the apparent paradox that plutonium metal with low specific surface areas ignites at temperatures above 500°C, whereas metal with large specific surface areas (turnings, chips, and powder) spontaneously ignites in air at temperatures between 150 and 200°C. In such cases, Martz *et al.* concluded that heating metal to 150–200°C in air transforms a large fraction of the surface oxide to cubic sesquioxide. Rapid oxidation of the sesquioxide back to dioxide produces a thermal spike sufficient to heat high-surface-area chips and turnings to the autothermic reaction temperature of 500°C.

(e) Hydrogen- and hydride-catalyzed corrosion

Plutonium reacts readily with hydrogen at rates unprecedented for other metals. It forms an fcc solid solution of PuH_x hydrides with a fluorite structure similar to plutonium oxides (Haschke, 1991; Bartscher, 1996) as discussed in Section 7.8.1 and shown in Fig. 7.72. The hydrogen mole ratio, x, varies from 1.9 to 3.0. As the hydrogen content increases, the hydride exhibits a transition from metallic material near $x = 2$ to a semiconductor near $x = 3$. The electronic structure of the hydride is complex, with electrons apparently being removed from the conduction band and bound as H^- on octahedral sites as the hydrogen concentration is increased in the hydride.

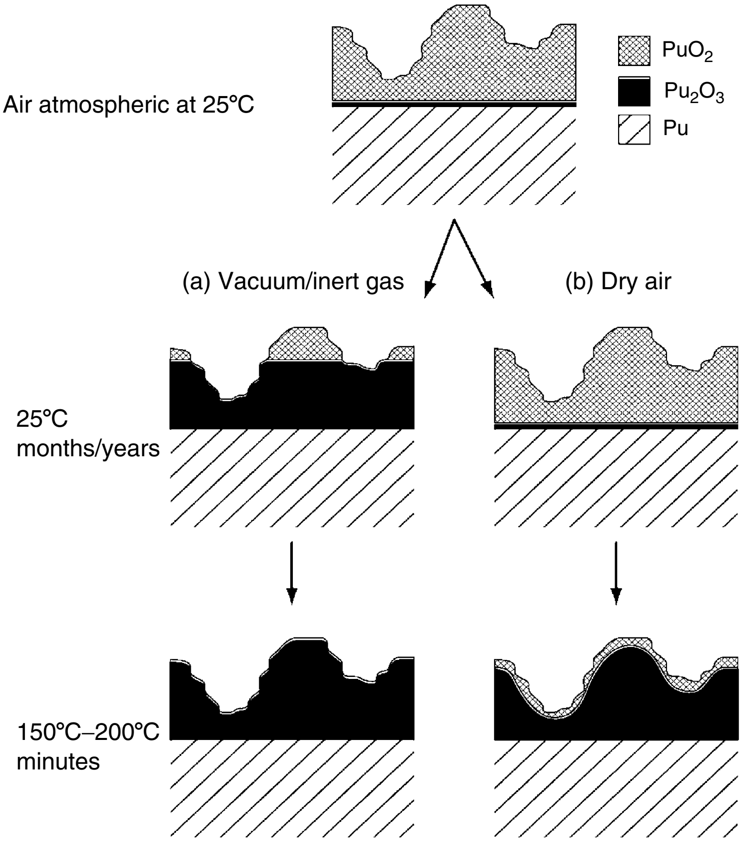

Fig. 7.65 *Evolution of the oxide layer on metallic plutonium. These simplified sketches present the structure of the oxide on Pu. In air, a constant thickness of* PuO_2 *is present on a thin layer of cubic* Pu_2O_3*. If this surface is exposed to inert conditions (vacuum or inert gas), the* PuO_2 *autoreduces to a thicker layer of* Pu_2O_3*. At elevated temperatures, the rate of the autoreduction reaction increases, increasing the thickness of the internal* Pu_2O_3 *layer under all conditions. Oxidation of this layer and its subsequent heat evolution is the attributed cause for the pyrophoric behavior of thin films and small particles (Martz* et al., 1994). *In addition, the growth of* Pu_2O_3 *under inert conditions at elevated temperatures will activate the surface to the hydride reaction, a fact exploited in the hydride–dehydride recovery process for metallic plutonium.*

Reactions of hydrogen on metallic plutonium are complicated by the ever-present layer of plutonium dioxide. Hydrogen gains access to the metal surface only after the dioxide layer is penetrated at cracks or spallation sites, making the nucleation of the hydride reaction heterogeneous. The hydriding rate increases exponentially as nucleation sites grow. Once the entire metal surface is covered with hydride, the reaction occurs very rapidly at rates of 20 cm h^{-1} linear penetration for H_2 at 1 bar compared to the rate of the oxidation reaction of 20 pm h^{-1} in dry air (10^{11} times faster). Haschke (1991) has suggested that this catastrophic enhancement occurs by one of two mechanisms. First, if PuH_x forms, it catalyzes the dissociation of adsorbed H_2 and promotes transport of atomic hydrogen to the hydride–metal interface. Or alternatively, if cubic Pu_2O_3 is exposed to H_2, then the hydride reaction begins instantaneously because Pu_2O_3 also catalyzes the dissociation of H_2 and becomes the medium for hydrogen transport. In either case, rapid dissociation of adsorbed H_2 results in a dramatic enhancement of the reaction rate. Further, the transport of anions in the fluorite structures of PuH_x or cubic Pu_2O_3 is potentially very rapid because in these anion-deficient fluorite structures both tetrahedral and octahedral sites may be vacant and able to participate in the transport of anions such as hydrogen and oxygen (see Sections 7.8.1 and 7.8.5). Another factor is the high self-diffusivity of oxygen in nonstoichiometric PuO_{2-x}, which increases dramatically from PuO_2 to Pu_2O_3.

If a hydride-coated plutonium surface is exposed to oxygen, it has been proposed that PuH_x will promote a dramatic catalytic enhancement of the corrosion rate (Haschke and Martz, 1998a). In this proposed mechanism, oxygen reacts with the pyrophoric plutonium hydride to produce heat and an oxide layer. The temperature is raised sufficiently that the cubic sesquioxide is preferentially formed. The hydrogen produced at the oxide–hydride interface moves through the PuH_x layer increasing the stoichiometry of the hydride. Excess hydrogen is continuously produced at the oxide–hydride interface and consumed at the hydride–metal interface. Thus, hydrogen is involved in a classic catalytic cycle to enhance the oxidation rate. This hydride-catalyzed reaction continues until all the metal is consumed. The rate for reaction of hydride-coated metal with pure oxygen (Fig. 7.64) is 10^{13} times greater than oxidation rates in dry air. Hydride-coated plutonium also reacts rapidly in air. However, the rate is 100 times slower than that in oxygen, apparently due to additional steps involving reaction or transport of nitrogen in air (Haschke, 1991). These fast reactions generate large amounts of heat (approximately 836.8 kJ mol^{-1} of plutonium), which can produce thermal hazards as well. Of additional concern is the possibility of plutonium nitride formation when the temperature exceeds 200–250°C and hydride is exposed to the nitrogen in air. This reaction results in a consumption of all of the major gases in air, preventing the formation of an inert nitrogen 'blanket' and allowing the reaction to proceed to completion within many storage environments. Hecker and Martz (2001) describe some of the practical consequences of enhanced corrosion problems in the storage of plutonium.

7.7.9 Aging and self-irradiation damage in plutonium

The aging of plutonium and its alloys has received increased attention during the past decade because of interest in extending the lifetimes of plutonium components and in the long-term storage of excess weapons-grade plutonium.

Several reviews of the salient aging issues have been reported by Hecker and Martz (2000, 2001), Wolfer (2000), Martz and Schwartz (2003), and Wirth *et al.* (2001). The complexities of plutonium materials are compounded by changes that occur with age. Phase stability is of concern because the various allotropic phases of plutonium are very close in energy and, hence, sensitive to any changes, including kinetic changes, that can occur with time at temperatures close to ambient. The differences in U.S. and Russian phase diagrams for Pu–Ga (Fig. 7.29) demonstrate that we lack definitive information on some basic characteristics of plutonium alloys such as thermodynamic steady-state phase stability. In addition, the very reactive nature of plutonium just described makes it especially susceptible to surface-induced modifications resulting from different atmospheric environments. If that were not sufficient, the most perplexing change is caused by the radioactive decay of the plutonium nucleus in its various isotopic forms. Moreover, in most practical applications the effects of these three types of aging-induced changes occur simultaneously and in synergy causing significant changes in plutonium and its alloys over time. The phase stability and surface behavior were described in some detail above. We will provide additional details of the salient consequences of self-irradiation damage and transmutation resulting from radioactive decay in plutonium and its alloys.

The two primary consequences of plutonium radioactive decay are the displacement damage in the lattice induced by the self-irradiation, and the transmutation of plutonium into its decay products. Displacement damage can cause changes in lattice parameters, the accumulation of defects and, potentially, void swelling. Transmutation may upset the delicate balance of phase stability and lead to phase changes. One of the decay products, helium, is of particular concern because it can form helium bubbles if self-irradiation occurs at temperatures at which helium is mobile. Schwartz *et al.* (2005) provided an excellent overview of the effects of self-irradiation in plutonium. They identified three self-irradiation-related effects that could cause dimensional changes: lattice damage resulting in an initial transient, helium accumulation, and void swelling.

The unstable plutonium nucleus decays principally by α-particle decay. Two primary energetic nuclear particles are produced by α decay – an α particle and a recoil nucleus. These primary particles are created in much less than a femtosecond (10^{-15} s). The range of the 5 MeV α particle is approximately 10 μm within the crystal lattice. The α particle captures two electrons from the plutonium metal and comes to rest in the lattice as a helium atom. The light α particle loses nearly 99.9% of its energy to electrons, heating the plutonium lattice. Some atomic displacements occur near the end of range, producing $\sim$265 Frenkel pairs (vacancies and self-interstitial atoms). Wolfer (2000) calculated the helium generation to be $\sim$41 atomic ppm per year.

The 86 keV ^{235}U recoil nucleus has a range of $\sim$12 nm and creates roughly 2300 Frenkel pairs. Calculations by Wolfer (2000) showed that there are 3×10^{9} α events g^{-1} s^{-1} for a typical ^{239}Pu isotopic mix, resulting in a lattice displacement rate of roughly 0.1 displacements per atom (dpa) per year. Wolfer (2000) and Wirth *et al.* (2001) used molecular-dynamics simulations showing that in the first 200 ns, 90% of the Frenkel pairs return to their original lattice sites, whereas the other 10% remain as free interstitials and vacancies or interstitial/vacancy clusters. In reactor applications, it was shown that these types of microstructural changes ultimately result in property changes that include void swelling, mechanical hardening, and embrittlement. Wirth *et al.* pointed out that although the damage produced by the α particle and the uranium recoil atom are different, it is the eventual interaction and evolution of these spatially uncorrelated primary defects that may, over time, drive materials evolution and the aging process, thus producing microstructural changes over time scales as long as many decades.

(a) Self-irradiation lattice damage

Studies of self-irradiation lattice damage in plutonium at low temperatures (at which little or no annealing of nonequilibrium defect structures is expected) were reported as early as 1962 by American researchers (Olsen and Elliott, 1962) and British researchers (Lee *et al.*, 1962; Wigley, 1964, 1965), and in 1965 by French researchers (Lallement and Solente, 1967). However, more than 40 years later, we still understand little about the mechanisms of defect migration and agglomeration in plutonium. Few measurements and direct observations of the defect structures in plutonium have been made compared to the vast body of literature that exists for irradiation-induced defect structures in other metals and alloys; see Ehrhart *et al.* (1991) for an excellent review. The early work showed that plutonium undergoes substantial lattice damage as determined by increases in electrical resistivity and by length changes. As shown in Fig. 7.66, the α phase in unalloyed plutonium expands during self-irradiation at 4.2 K. Retained β-phase and retained δ-phase plutonium alloys contract. As discussed below, self-irradiation damage of δ-phase plutonium at room temperature results in a volume expansion. All three phases exhibit increases in electrical resistivity with self-irradiation at this temperature; see Hecker and Martz (2001) for more detailed discussions.

Marples and Hall found that if low-temperature irradiation was allowed to proceed sufficiently long, lattice expansion in the α phase saturated at approximately 10.5 vol %. In the δ-phase alloy, lattice contraction saturated at –15 vol %. Their results on all three phases examined are summarized in Table 7.25. Interestingly, all three phases appear to converge to the same density, 18.4 g cm^{-3}. These results may indicate that all three phases are becoming increasingly disordered, approaching an amorphous state. It would not be surprising to create local amorphous regions as a result of the collision cascades following α-decay events. At sufficiently low temperatures, in the absence of significant defect rearrangement, these regions could eventually consume the entire sample. However, the XRD work done at low temperatures showed that

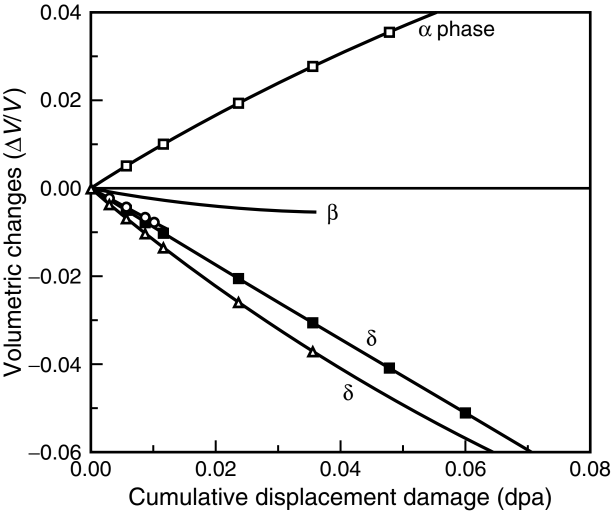

Fig. 7.66 *Volume change vs damage in* dpa (*displacements per atom*) *during self-irradiation of plutonium at* 4.2 K. *The α-Pu data is from Marples* et al. (1970), *as are the data for the δ-phase Pu*-6 at. *% Al alloy* (*solid squares*). *The triangles represent data from Jacquemin and Lallement* (1970) *on a δ-phase Pu*-6 at. *% Al alloy. The β phase was retained by the addition of* 4 at. *% Ti as reported also by Jacquemin and Lallement. Marples* et al. *reported a calculated saturation in volume change of* 10.5% *for the α phase and* –15% *for the δ phase.*

Table 7.25 *Initial and final densities for plutonium self-irradiated at* 4 K (*Marples and Hall,* 1972).

Phase	*Initial density* (g cm^{-3})	*Final density* (g cm^{-3})
α	20.3	18.4
β	18.2	18.4
δ	15.6	17.4 18.3 after correction for presence of 6 at.% Al

the initial crystal structures were retained, although significant line broadening was observed.

At ambient temperature, damage from self-irradiation of plutonium is partially annealed out by thermally activated recovery. Lattice damage created at low temperatures is also annealed out as the temperature is raised. Some of the early experiments of Wigley (1964, 1965) are summarized by Hecker and Martz (2001). Typical damage recovery (based on electrical resistivity measurements)

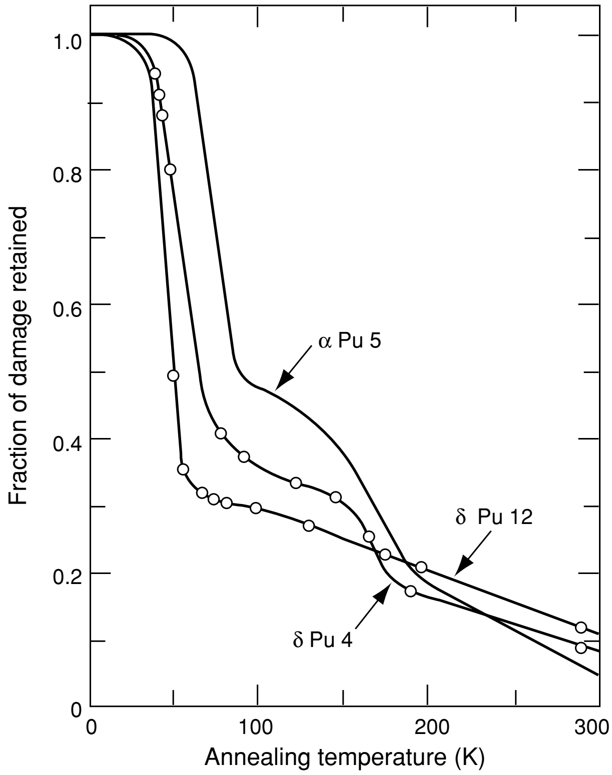

Fig. 7.67 *Damage recovery during isochronal annealing after self-irradiation at* 4.5 K. *δPu*4 *is for an alloy of Pu*-4 at. *% Al with* 920 h *at* 4.5 K. *δPu*12 *is for an alloy of* Pu-12 at. *% Al with* 665 h *at* 4.5 K. *The α-Pu sample, αPu*5, *was self-irradiated for* 640 h *at* 4.5 K (*from Hecker and Martz,* 2001 *based on original data from Wigley,* 1965*; King* et al., 1965).

during isochronal annealing of self-irradiated unalloyed plutonium and δ-phase Pu–Al alloys is shown in Fig. 7.67, based on the work of Wigley (1965) and King *et al.* (1965). Based on comparison to a vast literature of irradiation damage in metals (Ehrhart *et al.*, 1991), Hecker and Martz estimated the following temperatures for the key recovery stages in plutonium alloys: ~18 K for Stage I (recombination and migration of self-interstitials); ~180 K for Stage III (vacancy migration and annihilation); and 410 K for Stage V (thermal dissociation of vacancy and/or interstitial clusters). Unfortunately, the data on plutonium are limited and difficult to interpret quantitatively because of incomplete information about precise isotopic contents, purity levels, prior age, and processing conditions. Wirth *et al.* (2001) reported on recent self-irradiation and isochronal annealing experiments. They found the onset of Stage I to be diffuse and difficult to determine. Their best estimates for the temperatures for the onset of Stage III and Stage V were 190 K and slightly above 320 K. Hence, the defect mobility in plutonium alloys at ambient temperature is substantial. Although much of the damage is healed at room temperature, some of it remains.

For self-irradiation at ambient temperature, we would then expect lattice damage to compete with recovery resulting from the defect mobility. Chebotarev and Utkina (1975) reported a lattice expansion in δ-phase plutonium alloys. Wolfer (2000) showed that the initial transient results in the formation of dislocation loops that lead to expanded lattice parameters, which tend to saturate within approximately 2 years. Unlike at low temperatures, both the unalloyed α-phase plutonium and alloyed δ-phase plutonium exhibit lattice expansion with age. Ellinger *et al.* (1962a) reported that X-ray samples of typical plutonium in the δ phase (alloyed with 12.8 at.% Al) retained their fcc crystal structure with a 0.1% expansion of the lattice constant (0.3% volume change) after 10 years at ambient temperature. Chebotarev and Utkina (1975) also reported slight lattice expansion in δ-phase Pu–Al alloys, with the expansion increasing with increasing aluminum content. For aluminum contents slightly below 10 at.%, they found an expansion of the lattice parameter of 0.25% after 2.5 years at ambient temperature. They also reported that all changes were recovered after a long-term anneal at 423 K.

Morales *et al.* (2003) confirmed that δ-phase alloys expand at ambient temperature and possibly undergo an orthorhombic distortion at long aging times. In recent TEM studies of aged δ-phase plutonium alloys, Schwartz and coworkers observed nanometer-size helium bubbles (see Wirth *et al.*, 2001; Martz and Schwartz, 2003; Schwartz *et al.*, 2005). These will be discussed in greater detail below.

We report one additional important aspect of self-irradiation damage in plutonium described in recent presentations and abstracts by Russian researchers Gorbunov and Seleznev (2001). They studied unalloyed plutonium consisting mostly of ^{238}Pu, which increased the α-decay damage rate by a factor of 240 over the typical ^{239}Pu. They used thin films to keep the temperature close to room temperature. Starting with a sample of α-phase plutonium, their XRD measurements demonstrated that the sample experienced numerous crystallographic transformations over the period of 1 year (equivalent to 240 years of aging for the typical mix of isotopes in plutonium). Specifically, they claim to find evidence that all six phases of plutonium coexisted at 40 to 50 days of age, and that after roughly 1 year, the sample consisted mostly of the α and δ phases. They suggest that the vacancies and vacancy clusters resulting from the intense self-irradiation affect the delicate balance between bonding and localized 5f electrons and, hence, affect phase stability.

(b) Actinide transmutation products and radiogenic helium

In addition to the lattice damage described above, α decay also results in transmutation products. The decay products for plutonium isotopes and

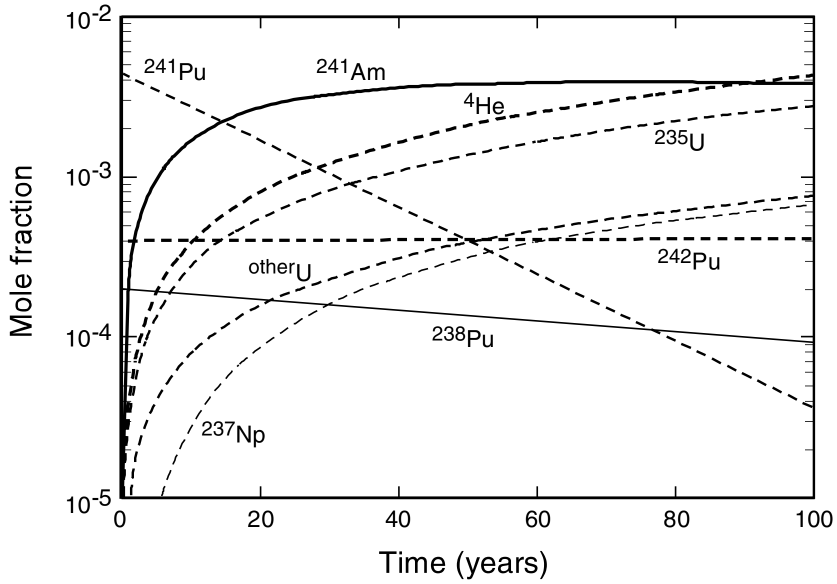

Fig. 7.68 *Transmutation products in typical* ^{239}*Pu metal* (*from Hecker and Martz,* 2001) *as a function of time. For typical* ^{239}*Pu,* 10 years *results in* 1 dpa.

its transmutation products are shown in Fig. 7.68. Helium grows in at the rate of 41.1 atomic ppm per year (based on the assumption made by Wolfer (2000) for typical plutonium). Hence, after 50 years of storage, approximately 2000 ppm helium, 3700 ppm americium, 1700 ppm uranium, and 300 ppm neptunium have grown into plutonium metal. After that length of time, a 1 kg piece of plutonium will contain nearly two-tenths of a liter of helium (measured at standard conditions). Several thousand ppm of americium should help to further stabilize δ-phase alloys. For pure plutonium it is conceivable that the in-growth of americium could stabilize microscopic regions of higher-temperature phases in the monoclinic α phase. However, in both cases, the nonequilibrium conditions that exist immediately following the decay event may further complicate the effects of the transmutation products. Under equilibrium conditions, uranium and neptunium reduce δ-phase stability. As in the case of americium, however, the effect of their presence associated with decay products under the nonequilibrium conditions is not well understood. Our best estimate is that the in-growth of actinides, other than americium, over a time frame of decades should have no major macroscopic effects, but their presence as atomic impurities may influence some microscopic processes. In addition, one must take account of the heat generated during the decay process. For the typical isotopic mixtures discussed above, the heat is a rather modest 2 W kg^{-1}, making kilogram quantities of plutonium warm to the touch. On the other hand, ^{238}Pu used in radioisotope heat sources is roughly 250 times more radioactive.

The accumulation of radiogenic helium, on the other hand, could potentially affect the properties of plutonium significantly. It is well known that less than 100 ppm of helium in fcc stainless steel can cause swelling or dramatic embrittlement. Once helium atoms are generated in the plutonium lattice, they quickly fill nearby vacancies and diffuse through the lattice as helium-filled vacancies (Howell *et al.*, 1999). Wirth *et al.* (2001) calculated that at relatively high helium generation rates, a critical helium bubble nucleus consists of just two helium atoms and one or two vacancies. Russian researchers (Filin *et al.*, 1989) used angle-resolved positron annihilation to study self-irradiation-induced defects in aged δ-phase Pu–3.6 at.% Ga with 800 ppm helium. They concluded that elementary complexes of helium and vacancies are energetically favorable. Their results showed that pores with radii of 0.4–0.8 nm and 17–23 nm formed at temperatures above 200°C. They concluded that the small pores are probably simple helium-vacancy complexes and the larger pores are complex helium-vacancy clusters, possibly also associated with solute atoms. They observed groups of small bubbles with diameters <1 μm by optical metallography after heating the aged plutonium alloy above 425°C. Using TEM, Zocco and Rohr (1988) observed helium bubbles of 3–7 nm and 10–15 nm in diameter in a 10-year-old δ-phase Pu–Ga alloy after annealing at 400°C. Decades-old plutonium will not only swell substantially after heating to such temperatures, but may also suffer major microstructural void damage under these conditions.

Schwartz and coworkers recently observed nanometer-sized helium bubbles using a Fresnel fringe imaging technique in TEM. Schwartz *et al.* (2005) examined Pu–Ga δ-phase alloys ranging in age from 6 months to 42 years. Their observations revealed that the dominant defects attributable to self-irradiation damage at ambient temperature are nanometer-sized, homogeneously distributed helium bubbles as shown in Fig. 7.69. They found no bubbles in the 6-month-old sample above their resolution limit of 0.7 nm. For samples 16–42 years old, they reported a number density of bubbles in the range of $0.6\text{–}2.0 \times 10^{17}$ cm^{-3}, which increases at a steady rate with time. The average diameter of the bubbles in this age range varies from 1.3 to 1.6 nm and is observed to change little with age beyond 16 years. The volume fraction of bubbles increased from roughly 0.01 to 0.03% within the age range of 16–42 years. Based on positron annihilation spectroscopy by Howell and Sterne (personal communications to Schwartz) (Howell and Sterne, 2002), Schwartz *et al.* concluded that helium bubbles containing two to three helium atoms per vacant site must already be present in 6-month old plutonium. Moreover, the characteristic positron lifetime of 180–190 ps remains remarkably constant for

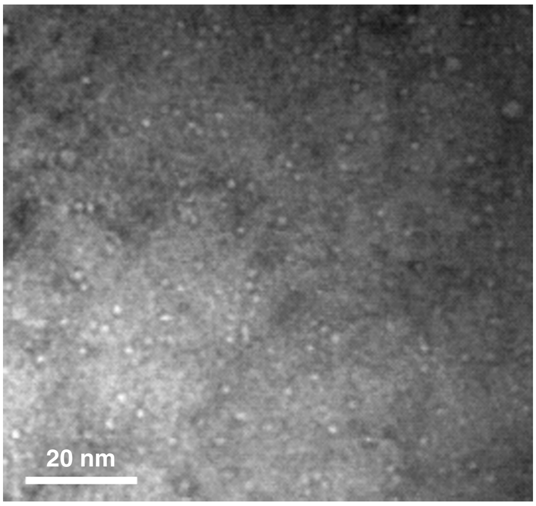

Fig. 7.69 *Transmission electron micrograph of nanometer-scale helium bubbles in a* 30+-year-*old δ-phase Pu*-3.4 at.% *Ga alloy* (*from Martz and Schwartz,* 2003; *Zocco and Schwartz,* 2003; *Schwartz* et al., 2005).

all aged material, implying a constant helium density within the bubbles of 2 to 3 helium atoms per vacant site.

The combination of irradiation-induced lattice damage and the presence of helium can cause void growth and bulk swelling at much lower temperatures without the presence of helium bubbles. Void growth is an obvious potential consequence of vacancy migration and clustering. Sustained void growth requires both the presence of biased defect sinks and the presence of neutral sinks. Wolfer (2000) estimated that for δ-phase plutonium alloys this may vary from 1 to 10 dpa (lifetimes from 10 to 100 years for typical ^{239}Pu). No experimental evidence for void swelling in plutonium has been found to date. In addition, our experience at Los Alamos shows that δ-phase plutonium aged at ambient temperature for 30–40 years retains structural integrity and exhibits no discernable microstructural changes. The influence of aging on the full range of plutonium properties remains to be assessed.

7.8 COMPOUNDS OF PLUTONIUM

From an historical perspective, the early study of plutonium compounds was plagued with difficulties. In addition to the fact that only very small amounts of plutonium were available for early experimentation, there were also special problems associated with the handling and manipulation due to radioactivity.

The problem of handling very small amounts of plutonium was overcome through the introduction of ultramicroscale experimental methods (Cunningham, 1949; Cefola, 1958; Fried *et al.*, 1958), and characterization of small quantities of compounds was masterfully performed by X-ray crystallography by Zachariasen (1954b), who made a major contributions to the structural chemistry of plutonium, almost entirely with Debye–Scherrer X-ray films of polycrystalline samples.

In more modern times, the available quantities of plutonium are large enough that the study of plutonium compounds can be conducted on the milligram and gram scale, and occasionally even on the multigram or kilogram scale. In the latter case, however, special safeguards to prevent criticality have to be taken (cf. Table 7.2) (Clayton, 1965; Thomas, 1969; Hunt and Boss, 1971; Hunt and Rothe, 1974; Paxton and Pruvost, 1987).

The evolution of modern techniques for handling plutonium has taken advantage of specialized high-efficiency particulate air (HEPA) filtered hoods, gloved boxes, and inert atmosphere dry boxes (Maraman *et al.*, 1975; Louwrier and Richter, 1976; Oi, 1995) that make it possible to work with plutonium with confidence, and the health and safety records of laboratories engaged in research with plutonium are very good. It cannot be denied, however, that laboratory work with plutonium and other actinide elements requires more than ordinary foresight and laboratory experience for the investigator. Laboratory safety guides (Peddicord *et al.*, 1998; *Health Physics Manual of Good Practices for Plutonium Facilities*, 1988) have been published that describe handling techniques and operational procedures in plutonium laboratories.

A considerable body of information on the compounds of plutonium has been amassed over the past 65 years, and the sheer volume of data is a testimony to the intense interest in the chemistry of plutonium. Several thorough monographs, conference proceedings, and reviews of the chemistry of plutonium before 1970 are available, and provide fascinating and often personal accounts of the many individual achievements that defined much of our current understanding in this field (Katzin, 1944; Thomas, 1944; Harvey *et al.*, 1947; Seaborg *et al.*, 1949b; Connick, 1954; Cunningham, 1954; Hindman, 1954; Seaborg, 1958; Grison *et al.*, 1960; Taube, 1964; Kay and Waldron, 1967; Miner, 1970; Blank and Lindner, 1976). Since 1970 there have been a number of comprehensive reviews (Keller, 1971; Cleveland, 1979; Wick, 1980; Carnall and Choppin, 1983; Hoffman, 2000) and finally, there are a series of modern reviews concerning a wide range of more specific topics such as chemistry in marine environments (Choppin and Wong, 1998), colloids in groundwater (Kim, 1991, 1994), bioinorganic chemistry in blood (Taylor, 1998), environmental behavior (Guillaumont and Adloff, 1992; Graf, 1994; Silva and Nitsche, 1995), behavior in carbonate media (Clark *et al.*, 1995), behavior in alkaline media (Shilov, 1998; Shilov and Yusov, 2002), actinide–lanthanide separations (Nash, 1993), synthetic methodologies for compounds (Meyer and Morss, 1991; Morss and Fuger, 1992), and a comprehensive compendium of XRD data for plutonium compounds (Roof, 1989).

7.8.1 Plutonium hydrides and deuterides

Plutonium hydrides were first observed in 1944 (Johns, 1944) when Johns found that elemental plutonium would react rapidly with H_2 to form a continuous solid solution of varying stoichiometry, PuH_x, with $1.9 \leq x \leq 3$ according to the equation:

$$Pu(s) + x/2H_2(g) \rightarrow PuH_x(s) \tag{7.29}$$

The reaction proceeds at a range of H_2 pressures. Heating is often required to initiate and sustain the process (Haschke, 1991). The chemical reaction is facile and reversible, making hydride–dehydride cycles a convenient route for preparing powdered plutonium metal samples. It is important to emphasize that stoichiometric compounds such as PuH_2 or PuH_3 do not exist as distinct phases apart from the PuH_x solid solution, though many authors describe reactions in terms of the stoichiometry PuH_2 or PuH_3 to facilitate the balancing of equations (Haschke, 1991).

Recent interest in plutonium hydrides has emerged due to considerations of long-term storage and safe handling of plutonium metal and compounds (Haschke and Allen, 2001) and the application of the plutonium–hydrogen reaction for pyrochemical processing of excess weapons plutonium (Flamm *et al.*, 1998; Mashirev *et al.*, 2001). Several excellent reviews have appeared on the synthesis and kinetics (Haschke, 1991), the thermodynamics (Flotow *et al.*, 1984; Lemire *et al.*, 2001), and the physicochemical characteristics of plutonium and other actinide hydrides (Flotow *et al.*, 1984; Ward, 1985; Ward *et al.*, 1992; Ward and Haschke, 1994; Bartscher, 1996; Haschke and Haire, 2000).

(a) Preparation and reactivity

The only practical method for preparing plutonium hydrides is the direct reaction of plutonium metal with gaseous H_2. In general, there are no good procedures for purification of PuH_x once it is formed, so purity is generally controlled through the use of high-purity metal and gaseous reagents. Plutonium metal must be cleaned to remove surface oxide and other impurities, and this is most conveniently conducted inside a secondary positive pressure chamber within an inert atmosphere gloved box to maintain proper H_2 partial pressures and temperatures. A Sieverts apparatus, and pressure–volume–temperature (PVT) relationships are commonly employed to determine the exact Pu–H stoichiometry, which is crucial because of the stoichiometric variability in the PuH_x product ($1.9 \leq x \leq 3$). Even when the stoichiometry is carefully controlled, differences in preparation or storage can result in differences in homogeneity, morphology, and even crystal structure (see below). Desorption of H_2 is a common problem encountered in working with plutonium hydrides, even under ambient conditions.

Plutonium hydrides are hard, typically black metallic-appearing materials that show different behaviors based on particle size and composition. The color ranges from silver near $x = 2$ to black at higher values of x. Small particles can be extremely reactive towards O_2 and H_2O, and powders near composition PuH_2 can be pyrophoric or ignite spontaneously in air (Flotow *et al.*, 1984; Haschke *et al.*, 1987; Haschke, 1991; Haschke and Allen, 2001). The hydrides can also react with N_2 and CO_2, although these reactions are quite slow. Hence all manipulations and storage should be carried out under inert atmospheres. An excellent and thorough discussion of the practical considerations necessary for preparing plutonium hydrides has appeared (Haschke, 1991).

The kinetics of the Pu–H_2 reaction have been well studied, and the highly complex reaction proceeds through induction, acceleration, parabolic, linear, and terminal stages. Detailed discussions of reaction rates and the role of catalysis are available (Haschke, 1991; Haschke and Allen, 2001). Moreover, hydride stoichiometry and composition changes induced by the addition or removal of H_2 from PuH_x are important in determining plutonium hydride reactivity.

(b) Stoichiometry and phase relationships

The PuH_x phase relationships are remarkably complex. A broad range of nonstoichiometric phases is exhibited that extends from $PuH_{1.9}$ to near stoichiometric PuH_3. Equilibrium data indicate that the hydride composition near the gas–surface interface may also vary from $PuH_{2.3}$ to $PuH_{2.7}$ while the composition at the plutonium metal–plutonium hydride interface remains close to $PuH_{1.95}$ (Ward and Haschke, 1994). The resulting stoichiometry and phase can differ between studies conducted at low temperatures and low pressures, or at high temperatures and high pressures. As a result, two notional phase diagrams, one for slow reaction at low pressure and one for rapid reaction at high pressure, have been proposed and discussed in detail by Haschke and coworkers (Haschke *et al.*, 1987) and by Bartscher (1996). These complex stoichiometry and phase relationships are best understood from consideration of the solid-state structures of the PuH_x system.

The phase relationships in the plutonium–hydrogen system are shown in the phase diagrams of Fig. 7.70 (slow reaction at low pressure) and Fig. 7.71 (rapid reaction at high pressure) (Flotow *et al.*, 1984). Hydrogen dissolves in solid and liquid plutonium (melting point 640°C) to form plutonium metal that is essentially saturated in hydrogen. This is denoted as PuH_s in the figures. Hydrogen-saturated plutonium (PuH_s) coexists with the cubic PuH_x solid solution up to composition $x \approx 1.9$. Between composition $PuH_{1.9}$ and PuH_3, a continuous solid solution forms. The exact value of x is highly dependent upon the

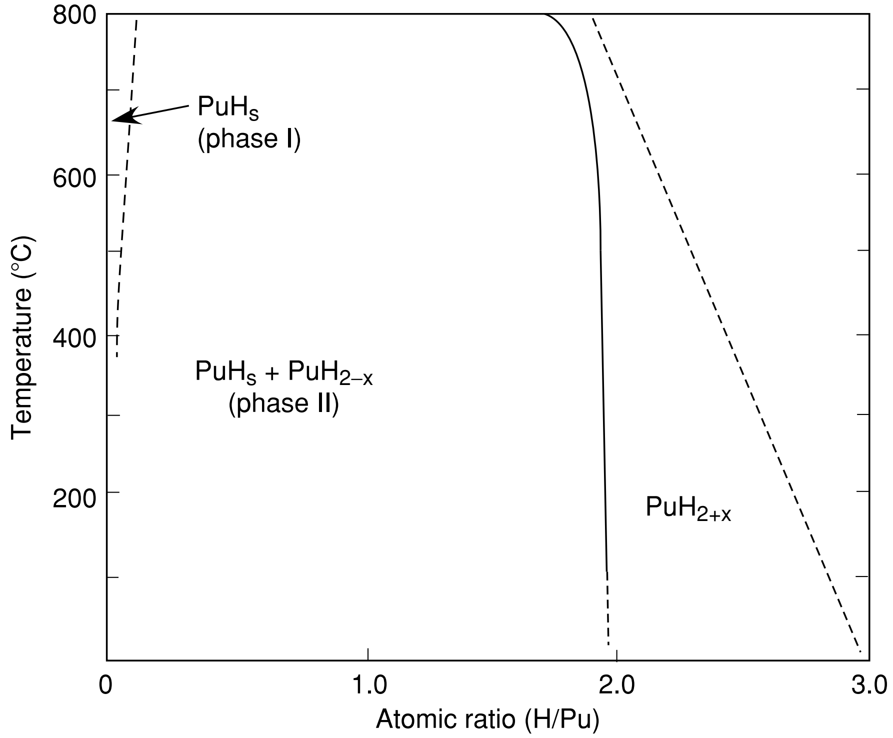

Fig. 7.70 *A plutonium–hydrogen phase diagram depicting equilibrium relationships based on Wick* (1980) *and Flotow* et al. (1984).

conditions of formation (Haschke *et al.*, 1987). The variable composition arises because the hydride reacts reversibly with H_2 between 25 and 500°C and pressures less than 1 bar (Johns, 1944; Haschke *et al.*, 1987). Extrapolation of 25°C data suggests that at 1 bar H_2 pressure, a composition $PuH_{2.93}$ is attained, while at 25 bar H_2, composition PuH_3 is attained. These observations are consistent with the phase diagram for slow reaction at low pressure shown in Fig. 7.70. An alternative phase diagram based on data generated at high pressures and rapid reaction is shown in Fig. 7.71 (Haschke *et al.*, 1987). This diagram is based on measurement of partial molar free energy isotherms that suggest the existence of five hydride phases (indicated as II–VI in Fig. 7.71) in addition to PuH_s (phase I). These data suggest the coexistence of a cubic $PuH_{2.70}$ and a hexagonal $PuH_{2.88}$ in the III + IV two-phase region. Hexagonal phase IV is thought to have a structure similar to that of disordered tysonite (LaF_3), while phase V is thought to be similar to that of orthorhombic YF_3 with a composition near $PuH_{2.95}$. The properties of phase VI are unknown. For a detailed discussion of the plutonium–hydrogen phase equilibria, the reader is

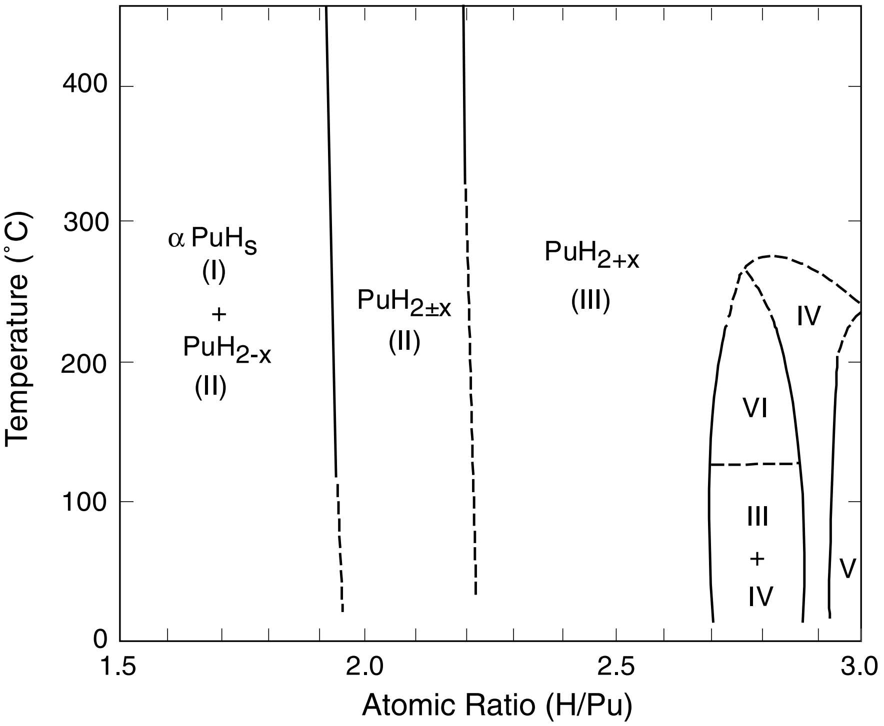

Fig. 7.71 *A plutonium–hydrogen phase diagram for rapid high-pressure reaction conditions, based on Haschke* et al. (1987).

referred to reviews by Flotow *et al.* (1984), Bartscher (1996), and Haschke and Haire (2000).

(c) Solid-state structures

The solid-state crystal structures of plutonium hydrides possess many similarities to those of the lanthanide hydrides, and Haschke and coworkers have suggested a similarity and analogy to the lanthanide trifluoride system (Haschke *et al.*, 1987). A summary of crystallographic data for plutonium hydrides is given in Table 7.26. Plutonium hydride forms a cubic fluorite-type phase over the composition range of PuH_x, where $1.9 < x < 2.7$, and a lanthanum trifluoride-related hexagonal phase beyond $x = 2.9$. The cubic fluorite-type structure based upon CaF_2 is illustrated in Fig. 7.72. As the composition of the fcc PuH_x varies between $1.9 < x < 2.7$, the lattice parameter decreases from 5.360(1) Å at $x = 1.9$ to 5.34(1) Å at $x = 2.7$. Within this fcc arrangement of plutonium metal cations are tetrahedral (*t*) and octahedral (*o*) interstices that may be occupied by the H^- ion. For an idealized PuH_2 structure with lattice

Table 7.26 *Crystal structure data for plutonium hydrides.*

Formula	*Symmetry*	*Space group*	*Lattice parameter* a_0 (Å)	c_0 (Å)	*Formula units per cell*	*Calculated density* (g cm^{-3})	*References*
$PuH_{2.0}$	fcc	F*m*3*m*	5.359(1)		4	10.40	Ellinger (1961)
$PuH_{2.51}$[a]	fcc	F*m*3*m*	5.342(4)		4		Muromura *et al.* (1972)
PuH_3	hexagonal	P6$_3$/*mmc* or P$\bar{3}$*c1*	3.78(1)[b] 6.55(1)	6.76(1)	2	9.608	Ellinger (1961)

---

[a] The values of x between 2.15 and 2.70 are represented by the equation a_0 (Å) = 5.4337 – 0.003575 (H/Pu) (Bartscher, 1996).

[b] Hexagonal LaF_3 (tysonite) has space group P$\bar{3}$*c1*, which is the same as observed in hexagonal lanthanide hydrides, and is the likely space group for PuH_3. To transform from P6$_3$/*mmc* to P$\bar{3}$c*1*, one would use $a_0 = a'\sqrt{3}$, or $a_0 = 6.55$ (Å) for PuH_3.

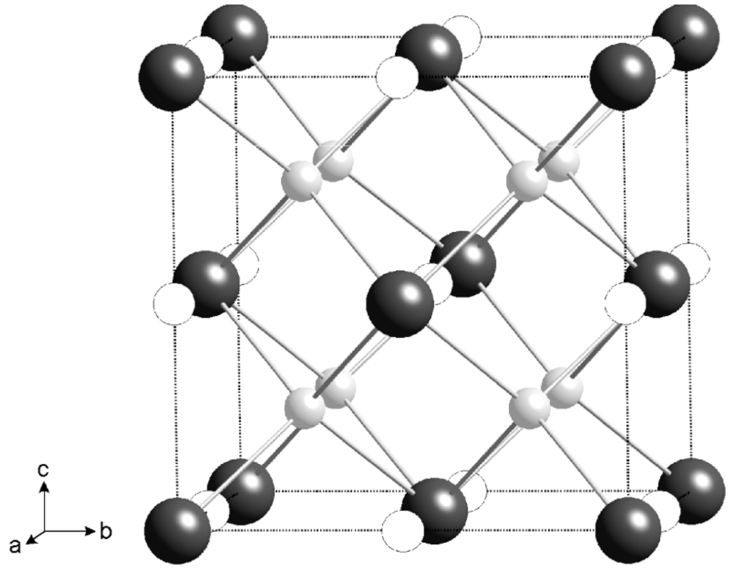

Fig. 7.72 *The cubic* (*Fm*3*m*) *fluorite-like solid-state structure of* PuH_x *showing the fcc arrangement of Pu atoms* (*black*) *with tetrahedral H atoms* (*gray*). *Octahedral vacancies are indicated with white circles, and the unit cell is indicated as a dashed line. For lattice parameter,* $a = 5.336$ Å, *Pu–H* = 2.31 Å, *Pu–Pu* = 3.77 Å, *and Pu-vacancy* = 2.67 Å (*Ellinger,* 1961).

parameter $a = 5.34$ Å, there is eight-fold (cubic) coordination of each plutonium atom by 8 hydrogen atoms, and four-fold tetrahedral (*t*) coordination of hydrogen atoms by 4 plutonium atoms with a Pu–H distance of 2.31 Å. The six-fold octahedral (*o*) sites in this model are vacant. Compositions of PuH_x, where $x < 2$, are likely formed by the creation of hydrogen atom vacancies in the normal *t* sites. At low temperatures, low pressures, and slow reaction times, an extended metastable cubic solid solution can exist all the way up to the PuH_3 phase boundary, and a simplistic model (see discussion below) would have additional hydrogen atoms randomly filling the *o* sites, with a concomitant decrease in lattice parameter.

The simple model of random occupancy of *o* sites in the fluorite lattice by additional hydrogen atoms when H–Pu is greater than two is overly simplistic. Since hydrogen mobility can occur at fairly low temperatures, the hydrogen atom can be disordered between *t* and *o* sites in the lattice (Muromura *et al.*, 1972; Flotow *et al.*, 1984; Haschke *et al.*, 1987; Ward and Haschke, 1994). Bartscher and coworkers employed elastic neutron scattering on deuterated samples of composition $PuD_{2.25}$, $PuD_{2.33}$, and $PuD_{2.65}$ and demonstrated a progressive depletion of *t* sites and occupation of *o* sites relative to PuD_2 (Bartscher *et al.*, 1985). Deuterium atoms in the *o* sites are displaced by 0.4 Å in the [111] direction (body diagonal) toward the *t* sites, in analogy with that observed in lanthanide systems (Ward and Haschke, 1994). In lanthanides, this low-temperature ordering of octahedral hydrogen atoms appears with a concomitant doubling of the *c*-axis of the unit cell. The 'freezing in' of the hydrogen atoms in this structure can be observed by NMR and by heat-capacity measurements (see below) (Cinader *et al.*, 1976; Flotow *et al.*, 1984). Haschke has proposed a conceptual model based on vacancy clusters for interpreting the relative *t*- and *o*-site occupancy factors in this structural model (Haschke *et al.*, 1987).

The structural behavior of the Pu–H system near the PuH_3 phase boundary is complex, and this region remains to be fully characterized. At low temperatures and for compositions above $PuH_{2.7}$, a cubic (fcc) form has been identified (Fig. 7.72). Under the appropriate conditions of rapid (high-temperature and high-pressure) reaction, both hexagonal and orthorhombic phases can also be formed near the PuH_3 boundary. In the range $PuH_{2.9}$–$PuH_{3.0}$, there is a hexagonal, nonstoichiometric phase in which the proposed structure is based on a disordered LaF_3 (tysonite) hexagonal structure ($P\bar{3}c1$), and an orthorhombic phase thought to be based on the YF_3 structure (Haschke *et al.*, 1987). The hexagonal phase was originally reported by Ellinger and assigned space group $P6_3/mmc$ (Ellinger, 1961), but more recent studies of the related lanthanide hydrides and fluorides reveal that trigonal space group $P\bar{3}c1$ is more likely the correct choice (Cheetham *et al.*, 1976). According to Haschke, the two-phase regions separating cubic (fcc) and hexagonal hydrides close in on themselves at 200–400°C, and only the cubic phases exist at higher temperatures (Haschke *et al.*, 1987). For more detailed discussion of these phase relationships, the reader is referred to the recent review by Haschke and Haire (2000).

(d) Physical properties and electronic structure

Trends in electronic properties as a function of x in PuH_x systems are crucial for understanding the nature of chemical bonding in plutonium hydrides. All data are consistent with the general description of cubic plutonium hydrides consisting of a localized 5f shell with a trivalent Pu(III) ion, best formulated as $Pu^{3+}(H^-)_x(e^-)_{3-x}$. Plutonium is trivalent for all compositions and exhibits 'rare-earth like' behavior. For nominal composition PuH_2, XPS shows a 4f intensity at the same 4f binding energy as a Pu(III) standard (Willis *et al.*, 1985). Neutron scattering data display an ordered magnetic moment of $0.71\mu_B$ per plutonium atom, which is the same as the trivalent free ion value (Bartscher *et al.*, 1985). Electrical conductivity decreases with increasing x, indicating that electrons are progressively removed from the conduction band and bound as H^- as the value of x increases (Willis *et al.*, 1985). Moreover, as the conductivity decreases, the hydride color changes from silver to black. Valence band XPS recorded on a (nominal composition) PuH_2 film reveal a large 5f peak consistent with a localized 5f shell, while core-level XPS on the same sample shows $4f^{5/2}$ and $4f^{7/2}$ peaks characteristic of Pu(III) (Ward *et al.*, 1992). Recent XPS data on a thin film of nominal composition PuH_3 shows the disappearance of the 5f peak (Gouder, 2005). Cinader and coworkers studied ^1H NMR spectroscopy on cubic PuH_x (where $x = 1.78$, 2.35, 2.65, and 2.78) between 77 and 300°C (Cinader *et al.*, 1976). Evaluation of line shapes, Knight shifts, and relaxation times are consistent with paramagnetic phases with localized 5f moments. Different line shapes and shifts were observed for *t* and *o* sites, and they were able to observe the 'freeze in' of the hydrogen atoms at low temperature. Enthalpies and entropies of formation for the extended cubic phase composition are given in Table 7.27.

(e) Applications

The hydriding reaction may be used to prepare plutonium metal powder. Compact pieces of plutonium metal can be converted to one of the hydrides and then powdered under an H_2 atmosphere by a magnet hammer. Subsequent

Table 7.27 *Enthalpies and entropies of formation for cubic plutonium hydrides at* 550 K[a].

Product	$\Delta_f H$ (kJ mol^{-1})	$\Delta_f S$ (J K^{-1} mol^{-1})
$PuH_{1.90}$	−155.6 ± 10.9	−138.5 ± 10.9
$PuH_{2.50}$	−190.4 ± 5.0	−175.7 ± 8.4
$PuH_{3.00}$[b]	−205.9 ± 4.6	−211.7 ± 11.7
$PuD_{1.90}$	−141.8 ± 1.7	−125.1 ± 3.8
$PuD_{2.50}$	−174.5 ± 4.2	−160.2 ± 7.5
$PuD_{3.00}$[b]	−189.1 ± 11.7	−188.3 ± 8.4

[a] Data from (Ward and Haschke, 1994).

[b] Based on extrapolated partial molar Gibbs energy data.

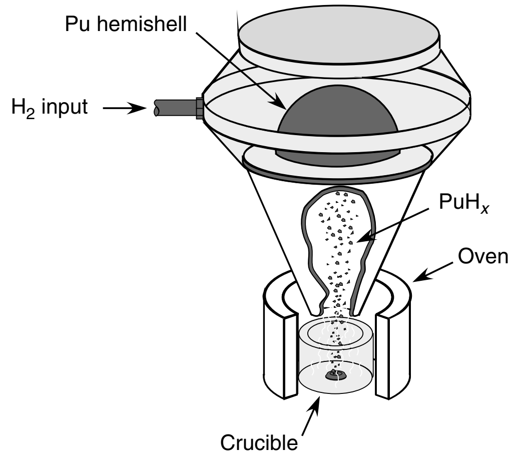

Fig. 7.73 *A schematic representation of the hydride–dehydride or hydride-oxidation chamber for conversion of surplus weapons plutonium. A weapon hemishell sits in the upper chamber, PuH_x spalls off and falls into the lower crucible, where it can be converted to the metal, a nitride or oxide* (*Toevs,* 1997).

decomposition *in vacuo* at more than 400°C leaves finely divided, highly reactive plutonium powder (Stiffler and Curtis, 1960). Both the U.S. and Russian technology for disassembly and conversion of excess plutonium from nuclear weapons employs a hydride–dehydride, or hydride–oxidation process for conversion into an unclassified form that can be examined by inspectors from other nations (Cremers *et al.*, 1995; Toevs, 1997; Nelson, 1998; Mashirev *et al.*, 2001). The U.S. process uses continuous H_2 recycle where the hydride falls into a crucible that is heated, driving off H_2 gas, leaving molten plutonium in the crucible. The H_2 refluxes to the top of the chamber, where it removes additional plutonium from the component. A schematic representation of the reaction chamber employed in this process is shown in Fig. 7.73. For conversion to an oxide, the crucible is not heated, and either O_2 is admitted and the hydride burned to release H_2 and leave an oxide powder, or N_2 is used and burned to a nitride powder. The nitride can then be converted to the oxide by burning with O_2. The three-step process of converting the hydride to the nitride and then the oxide avoids having an H_2–O_2 atmosphere in a glove box (Toevs, 1997). The hydride–dehydride approach to weapons conversion avoids the generation of large volumes of liquid waste from wet chemical methods.

7.8.2 Plutonium borides

Plutonium borides form at stoichiometric compositions PuB_2, PuB_4, PuB_6, PuB_{12}, and PuB_{66}, and at a very restricted solid solution of less than 0.5 at.% Pu in β-rhombohedral boron. These five compounds have high melting points, and with the exception of the preparation and identification of the compounds, very little experimental work is available. Recent detailed reviews describing the plutonium–boron system have appeared (Potter, 1991; Rogl and Potter, 1997).

Plutonium borides were first reported in 1960 (McDonald and Stuart, 1960), when the crystal structures of 'PuB,' PuB_2, PuB_4, and PuB_6 were described. Additional studies of the plutonium boron phase relationships were reported shortly thereafter (Skavdahl, 1963; Skavdahl and Chikalla, 1964; Skavdahl *et al.*, 1964; Weber *et al.*, 1964). Careful structural investigations employing XRD and metallography demonstrated that cubic samples of 'PuB' were contaminated with cubic PuN, and that 'PuB' was not actually a real phase in the Pu–B system (Eick, 1965; Chipaux *et al.*, 1989). Two additional compounds, plutonium dodecaboride, PuB_{12}, and the hectoboride, PuB_{66} were also discovered (Eick, 1965). The hectoboride was originally reported as having composition PuB_{100} (Eick, 1965), but based on analogy with rare-earth elements, which show a YB_{66}-type structure (Kasper, 1976), Rogl and Potter (1997) suggest that PuB_{66} represents a more-likely composition. Using the similarities between rare-earth and actinide boride systems, Rogl and Potter have provided a cautious assessment of the plutonium–boron phase diagram, shown in Fig. 7.74 (Rogl and Potter, 1997).

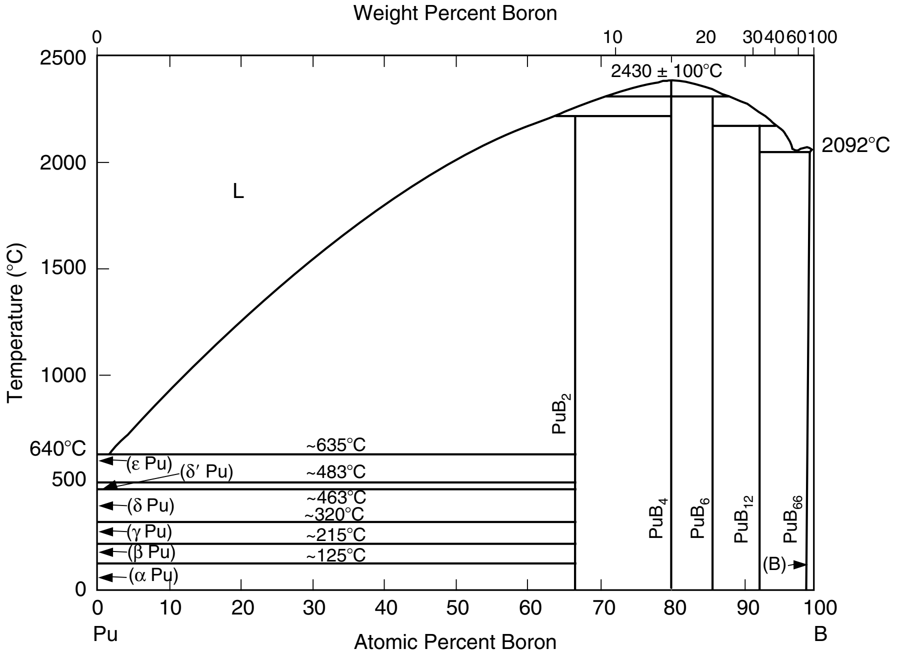

Fig. 7.74 *The plutonium–boron phase diagram* (*redrawn from Rogl and Potter,* 1997).

(a) Preparation

Plutonium borides can be prepared by a variety of methods: heating mixtures of pressed powders of elemental plutonium and boron under vacuum between 900 and 1200°C (McDonald and Stuart, 1960; Weber *et al.*, 1964), arc-melting pure plutonium with crystalline boron under a purified argon atmosphere followed by heat treatment (Eick, 1965), reaction of plutonium hydride with elemental boron at 900°C (Chipaux *et al.*, 1988, 1990), or reduction of PuO_2 by elemental boron and carbon (Skavdahl, 1963; Skavdahl and Chikalla, 1964; Skavdahl *et al.*, 1964; Larroque *et al.*, 1986). All of these reactions are carried out at high temperature (800–1500°C) under Ar or *in vacuo*. A comprehensive listing of preparative methods has been reported (Rogl and Potter, 1997). In view of the recent advances in the low-temperature synthesis of highly refractory materials (Rice, 1983; Wynne and Rice, 1984), and a possible application of actinide borides as an alternative storage form for actinide elements (Lupinetti *et al.*, 2002), it seems likely that this area will grow in interest and importance over the coming decades.

(b) Solid-state structures

The solid-state structures of plutonium borides (as in most metal borides) are dominated by B–B bonding, and the structures are made up of three-dimensional boron atom networks or clusters in which the plutonium atoms occupy otherwise vacant sites (Greenwood and Earnshaw, 1997). The B–B distances in all the plutonium borides are within the same range as those found in elemental boron and other boride complexes, and span 1.73–1.92 Å. The basic structural units in actinide borides, as in all metal borides, are readily described in terms of the B–B bonding configuration, followed by the actinide atom coordination (Potter, 1991; Greenwood and Earnshaw, 1997). Boron bonding units can be conveniently described as belonging to B_2-sp^2, B_6-octahedral, or B_{12}-cubeoctahedral boron atom cluster configurations as shown schematically in **1**, **2**, and **3** below (Potter, 1991; Greenwood and Earnshaw, 1997). To date, the structural characterization of plutonium borides has been performed exclusively by X-ray powder diffraction techniques, and a summary of crystallographic parameters of plutonium borides is given in Table 7.28. No single crystal diffraction studies have been reported.

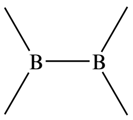

B_2-sp^2

1

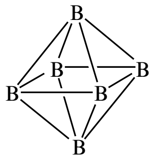

B_6

2

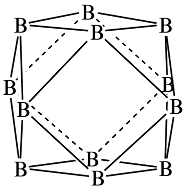

B_{12}

3

Table 7.28 *X-ray crystallographic data for plutonium borides.*

Compound	*Structure type*	*Symmetry*	*Space group*	*Unit cell dimensions* (Å)	*Formula units per cell*	*X-ray density* (g cm^{-3})[a]	*References*
PuB_2	AlB_2	hexagonal	P6/*mmm*	$a = 3.1857(2)$ $c = 3.9485(4)$	1	12.470	Eick (1965)
PuB_4	ThB_4	tetragonal	P4/*mbm*	$a = 7.1018(3)$ $c = 4.0028(1)$	4	9.285	Eick (1965)
PuB_6	CaB_6	cubic	$Pm\overline{3}m$	$a = 4.1134(3)$	1	7.249	Eick (1965)
PuB_{12}	UB_{12}	cubic	$Fm\overline{3}m$	$a = 7.4843(3)$	4	5.842	Eick (1965)
PuB_{66} (‘PuB_{100}’)	YB_{66}	cubic	$Pn\overline{3}n$	$a = 23.43(4)3$	24	2.485	Eick (1965)

[a] Calculated for ^{239}Pu.

Plutonium diboride (PuB_2) exhibits the hexagonal AlB_2 structure in space group *P*6/*mmm* containing one formula unit per unit cell (McDonald and Stuart, 1960; Eick, 1965). The AlB_2 structure is by far the most common phase displayed by metal borides (Spear, 1976). The solid-state structure (Fig. 7.75) consists of graphite-like hexagonal layers of catenated boron atoms with a close B–B contact of 1.84 Å. These hexagonal boron layers are separated by a hexagonal close packed (hcp) layer of plutonium atoms, positioned so that the centroid of a hexagonal ring of boron atoms lies directly above and below each plutonium atom. The closest Pu–B contact in this structure is 2.70 Å, with a closest Pu–Pu separation of 3.19 Å.

Plutonium tetraboride (PuB_4) has a tetragonal lattice (space group *P*4/*mbm*) formed by chains of B_6 octahedra along the *c*-axis and linked in the lateral direction by pairs of B_2 units in the *ab* plane (McDonald and Stuart, 1960;

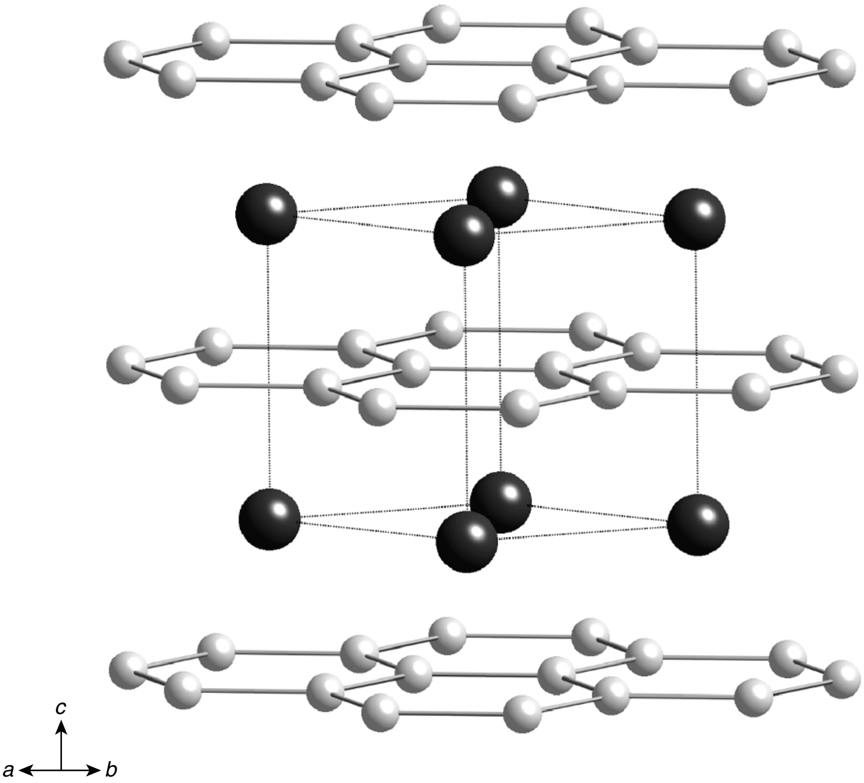

Fig. 7.75 *The solid-state structure of PuB_2 shown perpendicular to the c-axis, and emphasizing the hexagonal graphite-like layers of boron atoms (gray) separated by layers of plutonium atoms (black). The unit cell is indicated as dashed lines.*

Eick, 1965). This forms a three-dimensional network with channels along the *c*-axis that are filled by plutonium atoms. B–B contacts span a narrow range between 1.70 and 1.76 Å, with the shortest Pu–Pu contact of 3.66 Å between chains, and a longer contact of 4.00 Å along the chains. The closest Pu–B contact is 2.72 Å between Pu atoms and B_6 units. This structure type is shown in Fig. 7.76.

Plutonium hexaboride (PuB_6) has a cubic CsCl-type lattice (*Pm3m*) in which the plutonium atom and B_6 octahedra occupy the metal and halogen sites, respectively, as shown in Fig. 7.77(a) (McDonald and Stuart, 1960; Eick, 1965). In this structure, the B_6 octahedra are linked together in all six orthogonal directions. Within this framework, plutonium atoms occupy the corner

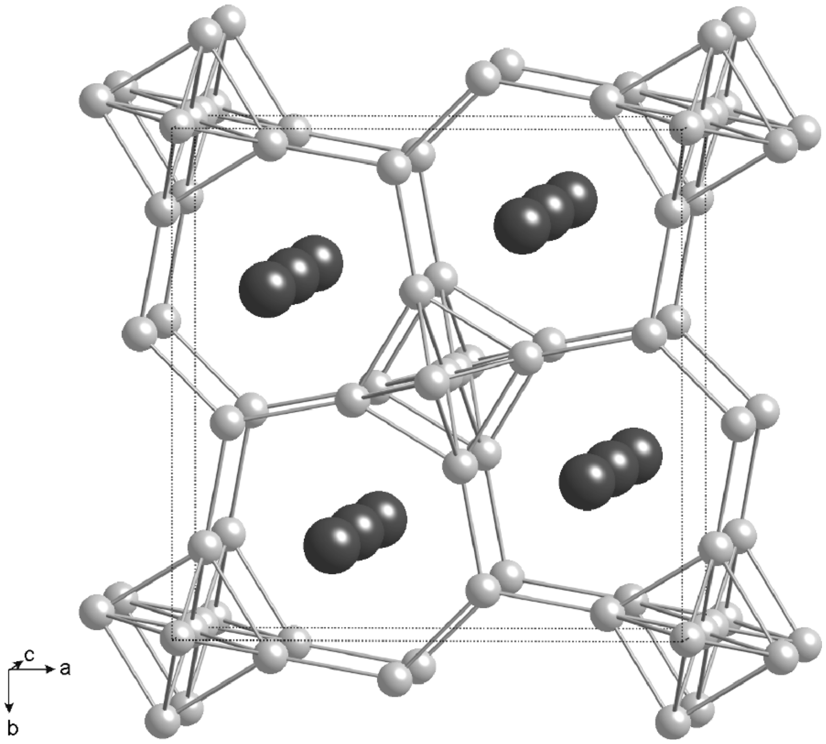

Fig. 7.76 *The solid-state structure of PuB_4 shown looking down the c-axis and emphasizing the open channels filled with plutonium ions (black). Boron atoms (gray) comprise octahedral B_6 units linked by bridging B_2 units within the ab plane. The unit cell is indicated as dashed lines.*

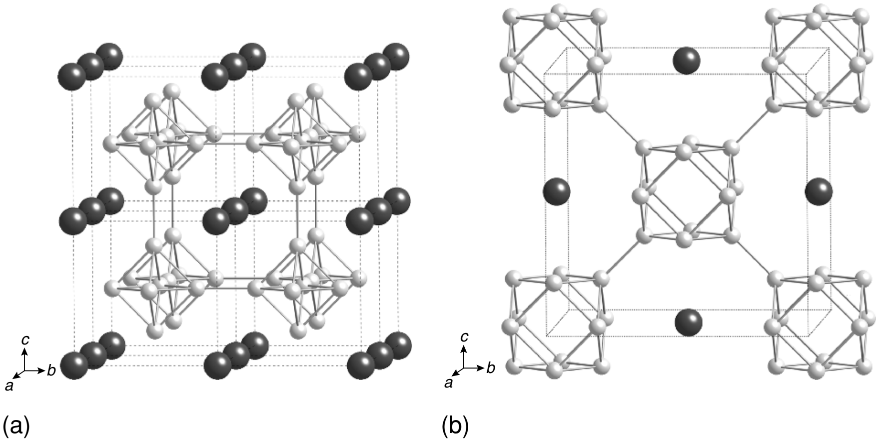

(a) (b)

Fig. 7.77 *The solid-state structure of* PuB_6 (*a*), *and* PuB_{12} (*b*). PuB_6 *has alternating plutonium* (*black*) *and* B_6 *octahedra* (*gray*) *in a 'CsCl-type' lattice.* PuB_{12} *has alternating plutonium* (*black*) *and* B_{12} *cubeoctahedra* (*gray*) *in a 'NaCl-type' lattice.*

positions of an interpenetrating cubic sublattice. B–B contacts within the B_6 unit, and linking adjoining B_6 units, are 1.70 Å, Pu–B contacts are 3.03 Å, and the Pu–Pu nonbonding contact is 4.11Å. Plutonium dodecaboride (PuB_{12}) has a cubic NaCl-type fcc lattice (*Fm3m*) in which the plutonium atoms and B_{12} cubeoctahedral clusters occupy the metal and halogen sites, respectively, as shown in Fig. 7.77(b) (Eick, 1965). B–B distances within the B_{12} unit are 1.76 Å, Pu–B distances between plutonium and B_{12} units are 2.79 Å, and the Pu–Pu nonbonding contact is 5.29 Å.

Plutonium hectoboride was originally formulated as 'PuB_{100}' (Eick, 1965), but this phase is most likely of composition PuB_{66}, belonging to a family of metal hectoborides based on the structure of YB_{66} (Potter, 1991; Rogl and Potter, 1997). This structure is exceedingly complicated, and the reader is referred to Richards and Kasper for a detailed description (Richards and Kasper, 1969). A simplified description is that of a well-known 13-icosahedron unit (156 boron atoms) found in β-rhombohedral boron, comprised of 12 B_{12} icosahedra grouped around a 13th central B_{12} unit. The yttrium atoms in YB_{66} are distributed in channels and coordinate to the cage boron atoms.

(c) Properties

Very little is known about the physicochemical properties of plutonium borides. It seems well established that PuB_4 and PuB_{66} are the only congruently melting plutonium borides (Rogl and Potter, 1997). Magnetic susceptibility measurements of PuB_2 and magnetic susceptibility and Mössbauer measurements on solid solutions of $Np_{1-x}Pu_xB_2$ and NpB_2 suggest a tetravalent oxidation state for neptunium, and presumably plutonium in the diborides. PuB_2 was found to be a weak paramagnet, and the data were fit by a modified Curie–Weiss law with and effective paramagnetic moment of $\mu^*_{\mathrm{eff}} = 0.32\mu_B$ and $\theta_p = -30$ K. Renormalization led to $\mu_{\mathrm{eff}} = 0.75\mu_B$ (Chipaux *et al.*, 1990). Smith and Fisk (1982) reported little temperature dependence in magnetic susceptibility of PuB_6.

7.8.3 Plutonium carbides and silicides

(a) The plutonium–carbon system

Four compounds are known in the plutonium–carbon system: Pu_3C_2, PuC_{1-x}, Pu_2C_3, and PuC_2. All these compounds undergo peritectic decomposition at high temperatures. The Pu–C phase diagram according to Green and Leary (1970), and assessed by Kassner and Peterson (1995), is shown in Fig. 7.78. Pu_3C_2 decomposes between 558 (Rosen *et al.*, 1963) and 575°C (Mulford *et al.*, 1960) to ϵ-Pu + PuC_{1-x} and may be unstable at lower temperatures

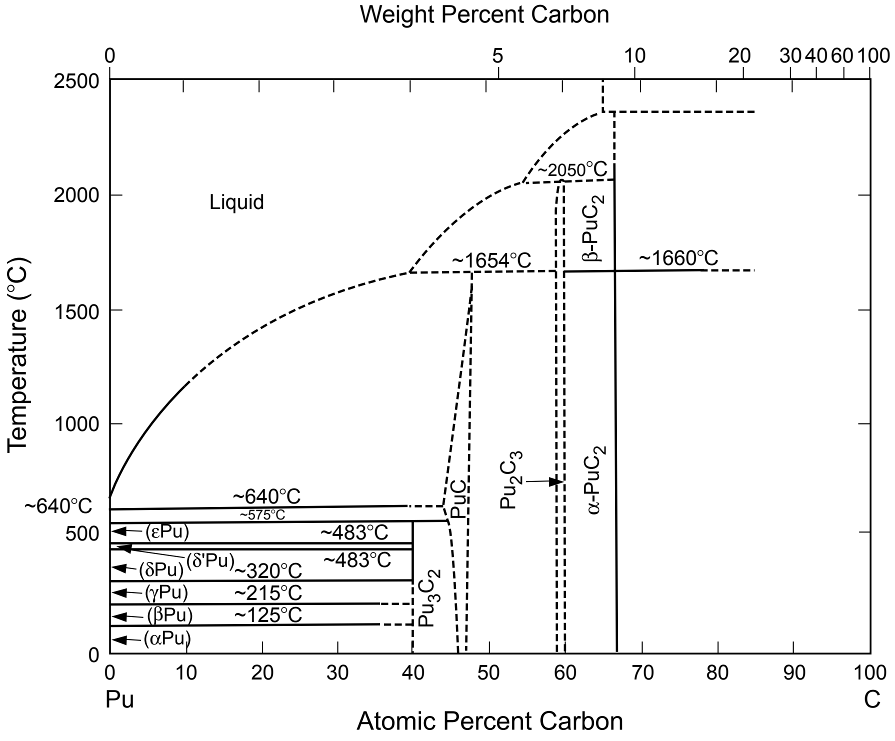

Fig. 7.78 *The plutonium–carbon phase diagram (redrawn from Green and Leary,* 1970*; Kassner and Peterson,* 1995*). See text for discussion of stability of* PuC_2 *below* 1660°C.

(Pascard, 1962). Plutonium monocarbide 'PuC' exists only as substoichiometric PuC_{1-x}, with a stoichiometry ranging from $PuC_{0.6}$ to $PuC_{0.92}$. At 1654°C, PuC_{1-x} decomposes into Pu_2C_3 plus liquid. Plutonium sesquicarbide Pu_2C_3 occurs in a rather narrow phase region around 60 at.% C. It decomposes at 2050°C into the high-temperature cubic phase PuC_2 and liquid (Mulford *et al.*, 1960). Plutonium dicarbide PuC_2 is only stable between 1660 ± 10 and 2230 ± 20°C (Reavis and Leary, 1970). The polymorphic transformation of PuC_2 below 1660°C to give the metastable tetragonal phase was added to the phase diagram in Fig. 7.78 by Kassner and Peterson (1995).

An extensive literature on plutonium carbides exists because actinide carbides have been considered as advanced nuclear fuels. Topical reviews can be found on general behavior (Storms, 1964, 1967; Ogard and Leary, 1970; Potter, 1975), thermodynamics (Holley, 1974; Holley *et al.*, 1984), thermal expansion and density (Andrew and Latimer, 1975), defect and transport properties (Matzke, 1984), and use as nuclear fuel (Russell, 1964; Andrew and Latimer, 1975; Herbst and Matthews, 1982; Handa and Suzuki, 1984).

(*i*) *Preparation*

Quite a few different preparation methods have been used to synthesize plutonium carbides. Carbides of plutonium can be formed by reaction between plutonium metal, plutonium hydrides, or plutonium oxides with elemental carbon at high temperature using furnace or arc-melting techniques (Drummond *et al.*, 1957; Ogard *et al.*, 1962; Pascard, 1962; Kruger, 1963; Chackraburtty and Jayadevan, 1965; Ogard and Leary, 1970). Plutonium oxide reductions using carbon can leave oxygen impurities in the products, and this is particularly true for the cubic monocarbides PuC_{1-x}. The products depend strongly on the temperature of reaction and reaction time. For example, PuC_{1-x} can be prepared by sintering or arc-melting a plutonium carbon mixture at 1000°C for 5 h, by direct reaction of PuO_2 with elemental carbon between 800 and 1350°C, by sintering $PuH_{2.7}$ with carbon in an inert atmosphere between 880 and 1650°C, or by reaction of PuH_2 with Pu_2C_3 at 650–750°C. The sesquicarbide can be obtained by reaction of PuO_2 with carbon under an argon atmosphere between 1250 and 1450°C at 6 h, 1350°C for 2 h or 1300–1400°C under vacuum. Pu_2C_3 can also be obtained by reaction of plutonium hydride with propane at 650–750°C.

(*ii*) *Crystal structures*

The crystal structures of all plutonium carbides, with the exception of Pu_3C_2 have been determined, and crystallographic data are summarized in Table 7.29. The lattice constants depend on the composition and the history of the individual sample. Plutonium monocarbide 'PuC' exists only as substoichiometric PuC_{1-x}, and adopts the cubic NaCl structure with defects in the carbon

Table 7.29 *X-ray crystallographic data for plutonium carbides.*

Compound	*Symmetry*	*Space group*	*Lattice parameters* a_0 (Å)	b_0 (Å)	c_0 (Å)	*Formula units per cell*	*Calculated density* (g cm^{-3})	*References*
PuC_{1-x}	fcc	F*m*3*m*	4.9582(3) (C-poor)			4	13.6	Mulford *et al.* (1960)
			4.9737(3) (C-rich)					Mulford *et al.* (1960)
Pu_2C_3	bcc	I$\bar{4}$3*d*	8.1258(3) (C-poor)			8	12.70	Mulford *et al.* (1960)
			8.1317(3) (C-rich)					Mulford *et al.* (1960)
PuC_2	tetragonal	I4/*mmm*	3.63	3.63	6.094	2	10.88	Chackraburtty and Jayadevan (1965)

sublattice (Zachariasen, 1949c; Mulford *et al.*, 1960). As the carbon content increases, all the carbide carbon atoms are replaced by acetylide C_2 units adopting a stoichiometry $Pu_4(C_2)_3$ (equivalent to Pu_2C_3) and PuC_2. Pu_2C_3 is cubic with 12 C_2 groups in the unit cell, with each plutonium atom bonded to nine carbon atoms, three at 2.48 Å, three at 2.51 Å, and three at 2.84 Å (Zachariasen, 1952). This structure is illustrated in Fig. 7.79, where only the shortest set of three Pu–C bonds are indicated. Due to the difficulty in accurately locating carbon atoms in the presence of the larger plutonium atoms by XRD, the carbon atoms were placed in assumed locations with a C–C single bond distance of 1.54 Å. Neutron diffraction studies on the isostructural U_2C_3 revealed a much shorter C–C distance of 1.295 Å (Austin, 1959), which is considerably lengthened relative to C_2 unit in acetylene at 1.20 Å.

Plutonium dicarbide, PuC_2 is a high-temperature compound that is not stable below ~1750°C (Mulford *et al.*, 1960) and decomposes to Pu_2C_3 and carbon. High temperature XRD revealed an fcc structure at 1710°C with a lattice parameter $a_0 = 5.70(1)$ Å (Harper *et al.*, 1968) which is consistent with

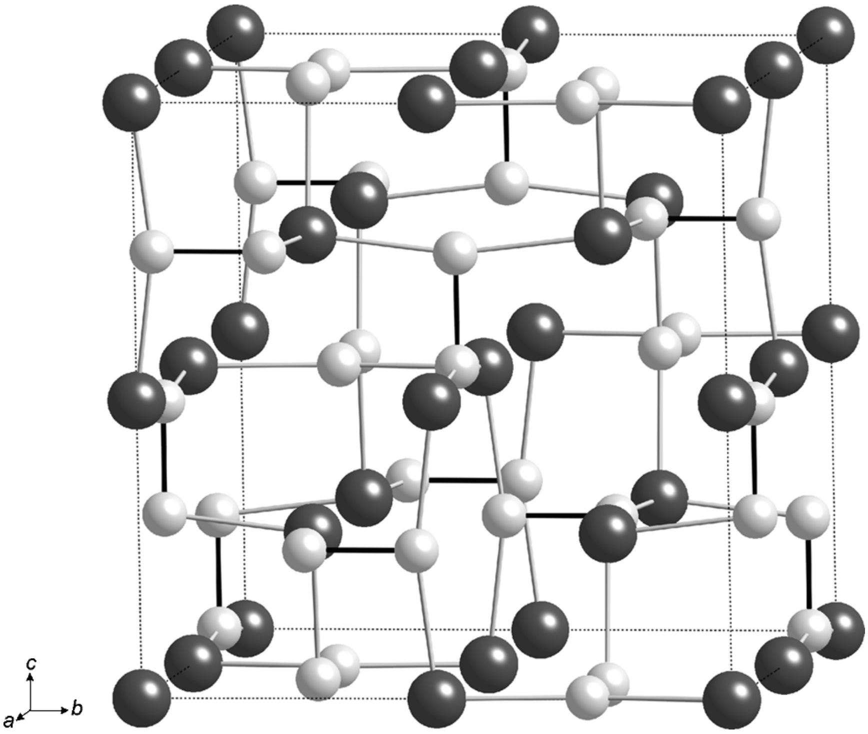

Fig. 7.79 *The solid-state structure of Pu_2C_3 shown looking down the a-axis. Plutonium atoms are black and carbon atoms are gray. The unit cell is indicated as dashed lines. The bold lines between C atoms indicates the* 12 *C_2 groups in the unit cell* (*Zachariasen,* 1952).

the CaC_2 structure that has a NaCl arrangement of Ca atoms and C_2 units (Wells, 1984). A room-temperature structure of what must be considered metastable PuC_2 was found to contain a tetragonal cell, probably due to martensitic transformation on quenching fcc PuC_2 to room temperature (Chackraburtty and Jayadevan, 1965). The tetragonal structure of PuC_2 and its similarity to the NaCl structural unit is shown in Fig. 7.80. For tetragonal PuC_2, the short Pu–C distance is found to be 2.48 Å with Pu–Pu = 3.63 and 3.98 Å (Chackraburtty and Jayadevan, 1965). As in the case of Pu_2C_3, the carbon atom positions are not accurately determined, but a neutron diffraction study on the isostructural tetragonal UC_2 revealed a C–C distance of 1.34 Å (Austin, 1959).

(*iii*) *Chemical properties*

The chemical properties of the plutonium carbides have been studied in some detail (Cleveland, 1979; Wick, 1980). Plutonium monocarbide oxidizes in air at temperatures as low as 200–300°C. It ignites at 400°C in an O_2 atmosphere (Drummond *et al.*, 1957). Compact PuC_{1-x}, kept in air at room temperature, did not show any sign of reaction after 2 months. However, PuC_{1-x} powder was found to be reactive, and sometimes pyrophoric (Ogard *et al.*, 1962). With N_2, PuC_{1-x} reacts more slowly than UC. A PuC_{1-x} sample, kept at 0.5 atm N_2, contains 1 ppm N_2 after 12 h at 200°C and 16 ppm after 12 h at 500°C. If heated

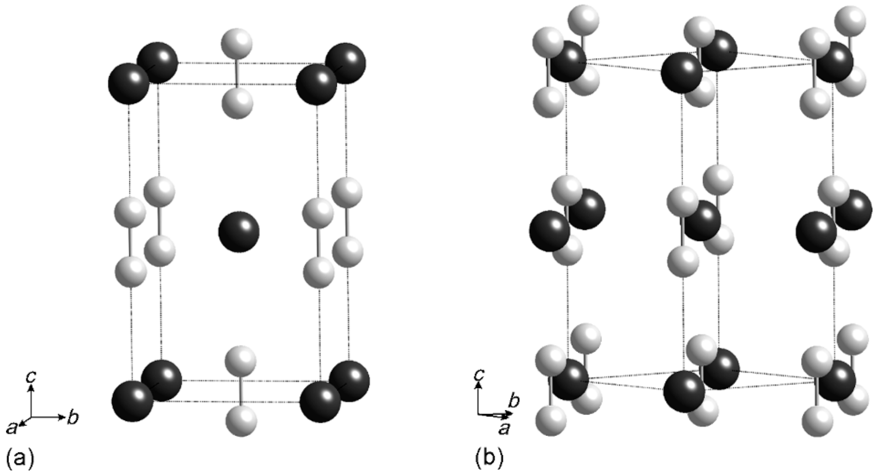

Fig. 7.80 (*a*) *The metastable tetragonal structure of* PuC_2 *shown looking perpendicular to the c-axis, and emphasizing the discrete* C_2 *units within the structure. Plutonium atoms are black and carbon atoms are gray.* (*b*) *The same structure rotated by* 45° *and emphasizing the relationship to the cubic NaCl structure with alternating Pu and* C_2 *units. At high temperature of* 1710°C, $a = b = c = 5.70(1)$ Å.

to 1400°C, the PuC_{1-x} reacts more rapidly to PuN and Pu_2C_3 (Lorenzelli *et al.*, 1966). Plutonium sesquicarbide, Pu_2C_3, shows chemical behavior similar to the monocarbide. It is slightly more stable to oxidation at higher temperatures (Drummond *et al.*, 1957). If heated to 1000°C in H_2, Pu_2C_3 is reduced to $PuC_{0.85}$ (Russell, 1964). PuC_{1-x} reacts with hot water to form $Pu(OH)_3$ and a mixture of H_2 and hydrocarbons. Pu_2C_3 appears to be more stable to hydrolysis in boiling water, but less stable to atmospheric hydrolysis (Drummond *et al.*, 1957).

All the plutonium carbides dissolve in HNO_3–HF mixtures (Storms, 1967). With oxidizing acids, CO_2 is formed. By the dissolution of lower carbides, carbon may be liberated along with hydrocarbons (Storms, 1967) along with organic acids such as mellitic and oxalic acids (Bokelund and Glatz, 1984).

(*iv*) *Thermodynamic properties*

Because of the importance of the plutonium carbides as potential high-temperature reactor fuels, the mechanical, thermal, electrical, magnetic, and thermodynamic properties of these compounds have been determined. For details about these properties and for additional references to the literature, the reader is referred to Holley *et al.* (1984), who reviewed the literature in the 1980s. The 2001 evaluation of plutonium thermodynamic data by the Nuclear Energy Agency (NEA) concludes that little significant thermodynamic information has been published since that time (Lemire *et al.*, 2001) but offers some reassessment of earlier data and provides recommended values for key thermodynamic constants. These are given in Table 7.30.

Monatomic plutonium is the only species that evaporates on heating from Pu–C phases. The equilibria in the solids have been inferred from vapor-pressure measurements (Mulford *et al.*, 1963; Olson and Mulford, 1967; Campbell *et al.*, 1970; Holley *et al.*, 1984). A general survey of the thermal decomposition behavior observed in the plutonium–carbon system has been given by Storms (1967). Specific-heat measurements of plutonium carbides have been reported by numerous authors and reviewed by Holley *et al.* (1984). The NEA review recommends the following temperature dependences (Lemire *et al.*, 2001):

Table 7.30 *Thermodynamic parameters for plutonium carbides.* (*Lemire* et al., 2001).

Compound	$\Delta_f G^\circ_{298}$ (kJ mol^{-1})	$\Delta_f H^\circ_{298}$ (kJ mol^{-1})	S°_{298} (J K^{-1} mol^{-1})	$C^\circ_{p_{298}}$ (J K^{-1} mol^{-1})
$PuC_{0.84}$	−49.8 ± 8.0	−45.2 ± 8.0	74.8 ± 2.1	47.1 ± 1.0
Pu_2C_3	−156.5 ± 16.7	−149.4 ± 16.7	150.0 ± 2.9	114.0 ± 0.4
Pu_3C_2	−123.5 ± 30.0	−113 ± 30	210.0 ± 50	136.8 ± 2.5

$PuC_{0.84}$ ($298.15 \leq T \leq 1875$ K)

$$C_p^o = 71.5910 - 5.95042 \times 10^{-2}T + 4.94346 \times 10^{-5}T^2 - 9.9320 \times 10^5 T^{-2} \mathrm{JK^{-1}mol^{-1}} \quad (7.30)$$

Pu_2C_3 ($298.15 \leq T \leq 2285$ K)

$$C_p^o = 156.000 - 7.9726 \times 10^{-2}T + 7.04170 \times 10^{-5}T^2 - 2.1757 \times 10^6 T^{-2} \mathrm{JK^{-1}mol^{-1}} \quad (7.31)$$

Pu_3C_2 ($298.15 \leq T \leq 850$ K)

$$C_p^o = 120.67 + 4.686 \times 10^{-2}T + 1.9456 \times 10^5 T^{-2} \mathrm{JK^{-1}mol^{-1}} \quad (7.32)$$

(*v*) *Ternary phases*

Several ternary plutonium carbides have been prepared. Of particular importance are the phases formed in the systems Pu–U–C and Pu–Th–C, which may be used in high-temperature reactors and thorium breeders, respectively. The Pu–U–C ternary phase diagram has been reported by Mardon and Potter (1970) and by Rosen *et al.* (1963, 1964). In this system, compounds M_3C_2, MC_{1-x}, M_2C_3, and MC_2 are all observed, where M = (U, Pu), in a wide range of compositions. The Pu–Th–C system has been studied by Reavis and Leary (1970), who reported a partial-phase diagram, and by Dalton *et al.* (1967) and Dalton and Griffin (1964).

A few ternary plutonium carbide phases with transition elements have been prepared by arc melting from the components and have been characterized by their XRD data. These compounds are compiled in Table 7.31. An attempt to estimate ternary phase diagrams for a number of ternary plutonium carbide systems was reported by Holleck (1975). A few mixed carbonitrides, carbide oxides, and carbide hydrides, all of them nonstoichiometric, have been prepared.

(b) The plutonium–silicon system

Five compounds are known in the plutonium–silicon system: Pu_5Si_3, Pu_3Si_2, PuSi, Pu_3Si_5, and $PuSi_2$, melting at 1377, 1441, 1576, 1646, and 1638°C, respectively. The phase diagram determined by Land *et al.* (1965b) and redrawn by Kassner and Peterson (1995) is shown in Fig. 7.81. A recent XRD study by Boulet and coworkers found no new compounds other than the five listed above and confirms the phase diagram (Boulet *et al.*, 2003).

The literature of plutonium silicides is relatively sparse, but there are a few detailed reports on exchange reactions and enthalpies of formation (Krikorian and Hagerty, 1990), physical properties (Taylor, 1966), magnetic properties (Boulet *et al.*, 2003), and the phase diagram (Land *et al.*, 1965b); and an excellent overall review (Potter, 1975).

Table 7.31 *X-ray crystallographic data for selected plutonium ternary carbide phases.*

Compound	*Structure type*	*Space group*	*Lattice parameters* a_0 (Å)	b_0 (Å)	c_0 (Å)	*Formula units per cell*	*Calculated density* (g cm^{-3})	*References*
$PuWC_2$	orthorhombic	P*nma*	5.621(3)	3.245(2)	10.896(7)	4	14.93	Ugajin and Abe (1973)
$PuRh_3C$	cubic	P*m3m*	4.098			1	13.50	Haines and Potter (1975)
$PuRu_3C$	cubic	P*m3m*	4.124			1	13.12	Haines and Potter (1975)

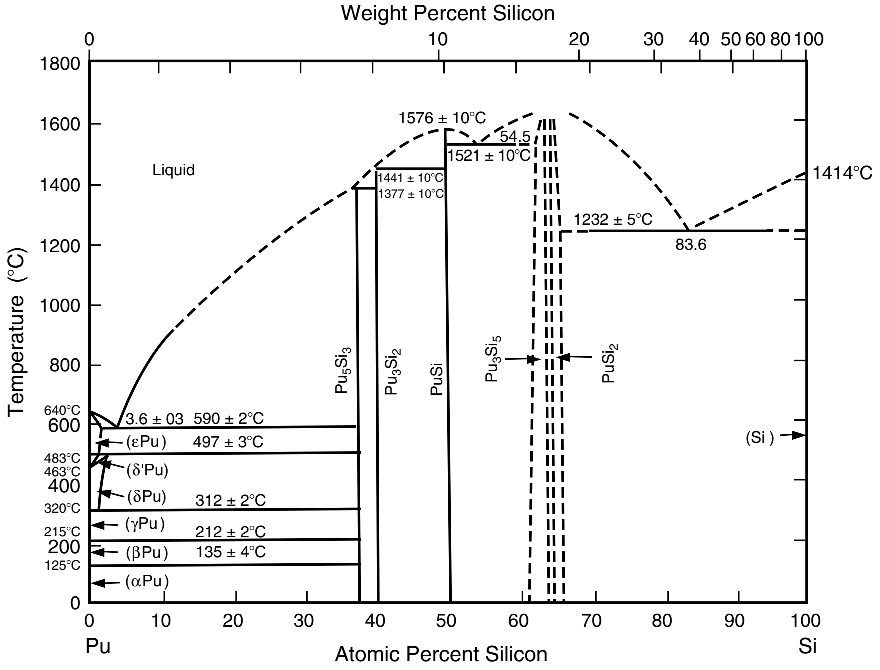

Fig. 7.81 *The plutonium–silicon phase diagram from Land* et al. (1965*b*) *and redrawn from Kassner and Peterson* (1995).

(*i*) *Preparation*

The preparation of plutonium–silicon phases is best carried out by reduction *in vacuo* of plutonium trifluoride with elemental silicon at temperatures above 1200°C in a BeO crucible (Runnalls, 1958):

$$4PuF_3 + (3 + 4x)Si \rightarrow 4PuSi_x + 3SiF_4 \tag{7.33}$$

Volatile SiF_4 is pumped off, and the plutonium silicide remains. The silicides may also be prepared by arc melting of silicon with plutonium metal or plutonium hydride in an argon atmosphere (Pardue *et al.*, 1964b; Land *et al.*, 1965b; Krikorian and Hagerty, 1990), by reduction of PuO_2 with Si or SiC *in vacuo* at 1400°C (Pardue *et al.*, 1964b), and by fluidized-bed reduction of PuO_2 in the presence of SiO_2 with silane (Fletcher *et al.*, 1967).

(*ii*) *Crystal structures*

The crystal structures of all plutonium silicides have been determined. The basic crystallographic data are listed in Table 7.32. Silicon, like boron, is more electropositive than carbon; thus silicides are more closely related structurally to the borides than the carbides. With increasing silicon content, there is an

Table 7.32 *X-ray crystallographic data for plutonium silicides.*

			Lattice parameters					
Compound	*Structure type*	*Space group*	a_0 (Å)	b_0 (Å)	c_0 (Å)	*Formula units per cell*	*Calculated density* (g cm^{-3})	*References*
Pu_5Si_3	W_5Si_3	I4/*mcm*	11.409(3)		5.448(2)	2	11.98	Cromer *et al.* (1964)
			11.407(5)		5.444(3)	2		Land *et al.* (1965b)
			11.4035(8)		5.448(3)	2		Boulet *et al.* (2003)
Pu_3Si_2	U_3Si_2	P4/*mbm*	7.483(2)		4.048(2)	2	11.33	Land *et al.* (1965b)
			7.5061(3)		4.0642(3)	2		Boulet *et al.* (2003)
PuSi	FeB	P*nma*	7.933(3)	3.847(1)	5.727(5)	4	10.15	Land *et al.* (1965b)
			7.9360(1)	3.8510(1)	5.7336(1)	4		Boulet *et al.* (2003)
Pu_3Si_5	AlB_2	P6/*mmm*	3.875(4)		4.102(7)	0.5	8.96	Land *et al.* (1965b)
($PuSi_{2-x}$)			3.884(3)		4.082(3)	0.5		Runnalls and Boucher (1955)
			3.8793(6)		4.0860(8)	0.5		Boulet *et al.* (2003)
$PuSi_2$	$ThSi_2$	I4/*amd*	3.967(1)		13.72(3)	4	9.08	Ellinger (1961)
			3.98(1)		13.58(5)	4		Zachariasen (1949b)
			3.9707(3)		13.6809(5)	4		Boulet *et al.* (2003)

increasing tendency to catenate into isolated Si_2 units, or into chains, layers or three-dimensional networks of silicon atoms. Plutonium silicides adopt examples of all these structure types.

The plutonium-rich compound Pu_5Si_3 adopts the tetragonal W_5Si_3 structure, and this structural unit is shown in Fig. 7.82 (Cromer *et al.*, 1964). In this structure, there is a silicon chain composed of columns of alternating $SiPu_8$ square antiprisms with Pu–Si = 3.025 Å. The linear silicon chain runs parallel to the *c*-axis with a Si–Si distance of 2.72 Å. Interspersed between the square antiprisms is another chain of edge-shared $PuSi_4$ tetrahedra that also runs parallel to the *c*-axis, with Pu–Pu = 2.72 Å. In the linear plutonium chain, each plutonium atom in the $PuSi_4$ tetrahedra shows a Pu–Si distance of 2.89 Å. The silicon atoms in the $PuSi_4$ tetrahedra bridge to the plutonium atoms in the $SiPu_8$ antiprisms with a Si–Pu distance of 3.01 Å. These bridges are omitted

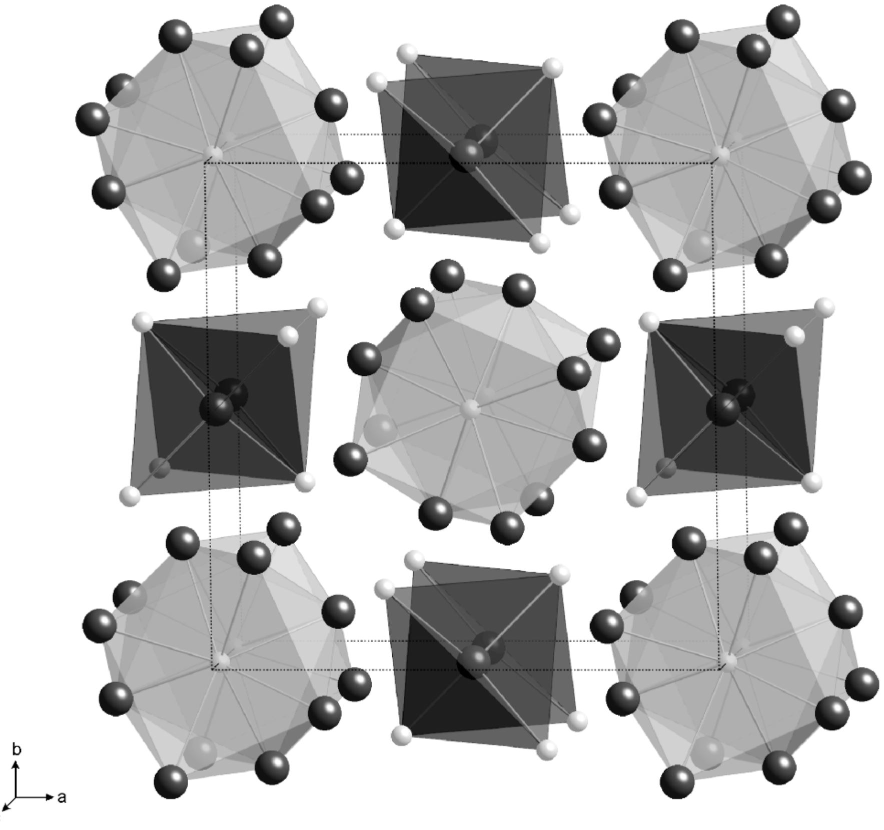

Fig. 7.82 *A polyhedral representation of the solid-state structure of Pu_5Si_3 shown looking down the c-axis, and emphasizing the alternating columns of $SiPu_8$ antiprisms and $PuSi_4$ tetrahedra within the structure. Plutonium atoms are black and silicon atoms are gray.*

from Fig. 7.82 for clarity. Pu_3Si_2 adopts the U_3Si_2 structure, and the basic structural unit is shown in Fig. 7.83. This structure contains a network of Si_2 pairs that are perpendicular to the four-fold axis with Si–Si = 2.35 Å, identical to the Si–Si distance observed in elementary silicon. The plutonium atoms form a puckered cage with Pu–Pu distances of 3.41 Å. The Pu–Si distances range from 2.99 to 3.03 Å.

Plutonium monosilicide is isostructural with ThSi and USi, adopting the FeB structure with infinite one-dimensional zig-zag chains of silicon atoms (Si–Si = 2.35 Å) (Land *et al.*, 1965b). Each silicon atom in the chain is also surrounded by six plutonium atoms at the apices of a trigonal prism with Pu–Si distances spanning the range 2.95–3.03 Å. The PuSi structure is shown in Fig. 7.84. There are four Pu–Pu distances of 3.62 Å, and two Pu–Pu distances of 3.73 Å.

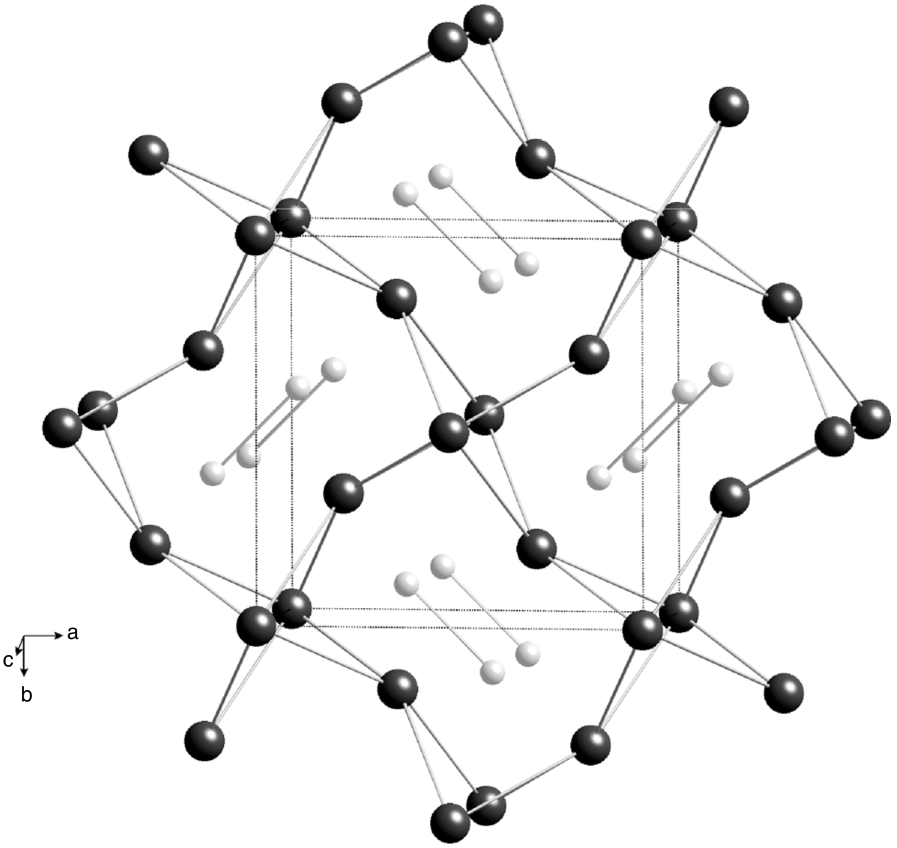

Fig. 7.83 *The solid-state structure of* Pu_3Si_2 *shown looking down the c-axis, and emphasizing the discrete* Si_2 *units within the structure. Plutonium atoms are black and silicon atoms are gray.*

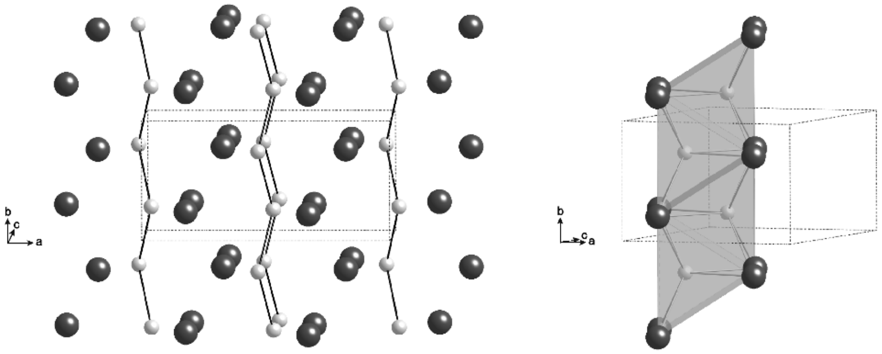

Fig. 7.84 (*left*) *The solid-state structure of PuSi shown looking down the c-axis, and emphasizing the zig-zag chains of Si atoms that run perpendicular to the c-axis. Plutonium atoms are black and silicon atoms are gray.* (*right*) *The same structure rotated by* 45° *and emphasizing the trigonal prismatic* $SiPu_6$ *coordination polyhedra.*

The disilicides form two different structural types that are best considered as defect structures of $PuSi_{2-x}$. There is a hexagonal form of nominal formula Pu_3Si_5 (Runnalls and Boucher, 1955; Ellinger, 1961; Boulet *et al.*, 2003), that adopts the hexagonal AlB_2 structure (discussed for PuB_2, and shown in Fig. 7.75), but the solid is silicon deficient, with vacancies in the silicon sublattice. In this structure there are hexagonal (graphitic) layers of silicon atoms (Si–Si = 2.23 Å) with plutonium atoms interleaved between them (see Fig. 7.75). There is also a tetragonal form that adopts the three-dimensional $ThSi_2$ network structure as shown in Fig. 7.85 (Zachariasen, 1949a,b). In this structure, the silicon atoms form an open, three-coordinated, three-dimensional network. The Si–Si bond lengths are 2.35 and 2.29 Å, which are slightly shorter than that observed in elementary silicon. In the large spaces in this network are the plutonium atoms, each bonded to 12 silicon neighbors with Pu–Si = 3.02 Å. The next nearest neighbors to silicon are six plutonium atoms at this same distance.

(*iii*) *Properties*

The plutonium silicides are hard, brittle, and pyrophoric, with a metallic appearance. They oxidize in air to form PuO_2 (Westrum, 1949b) and are rapidly attacked by water (Pardue and Keller, 1964). Due to their high melting points and high Pu densities, plutonium silicides have been considered as reactor fuels, but the difficulty of preparing them as pure phases has hampered their development for this purpose (Pardue and Keller, 1964; Potter, 1975).

A recent determination of the magnetic properties of PuSi and tetragonal ($ThSi_2$-type) $PuSi_2$ revealed that PuSi orders ferromagnetically around 72 K,

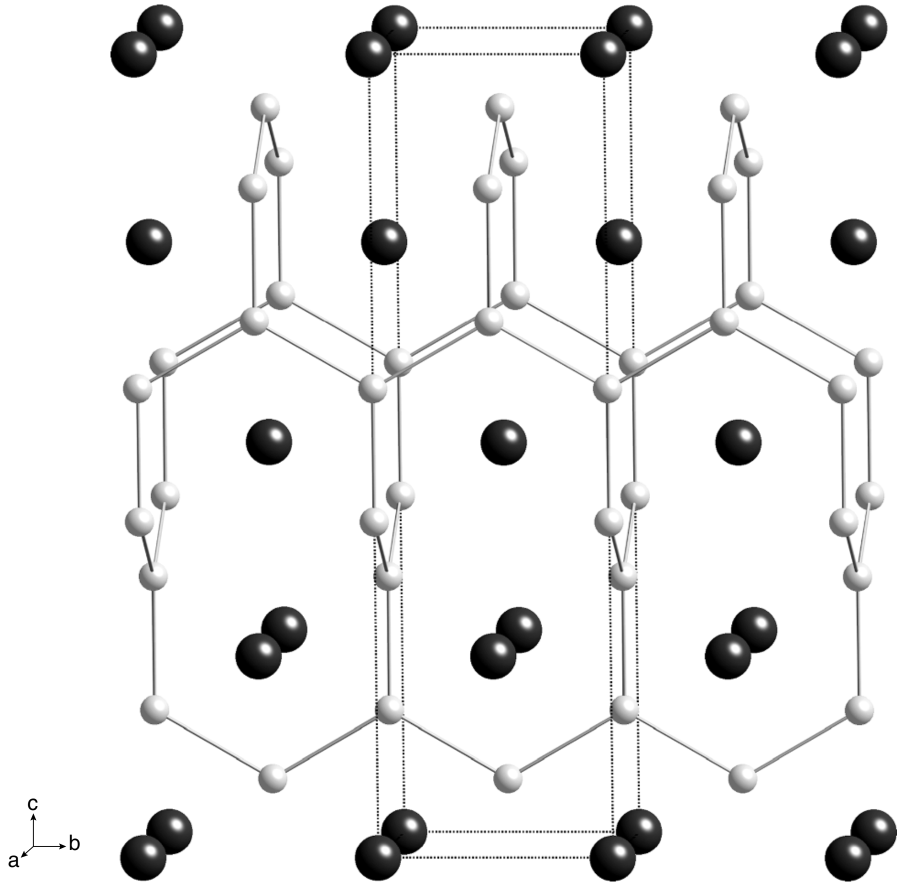

Fig. 7.85 *The solid-state structure of tetragonal $PuSi_2$ shown looking down the a-axis, and emphasizing the three-dimensional network structure of the silicon atoms. Plutonium atoms are black and silicon atoms are gray.*

whereas $PuSi_2$ shows no magnetic ordering (Boulet *et al.*, 2003). The values of the effective moments of PuSi (μ_{eff} ca. $0.72\mu_B$) and $PuSi_2$ (μ_{eff} ca. $0.54\mu_B$) are consistent with a $5f^5$ electronic configuration and a Pu^{3+} oxidation state.

7.8.4 Plutonium pnictides

With pnictogen elements, plutonium forms compounds in three basic families with the highest order composition being PuX_2 that is only found for the heaviest pnictogen elements (X = Sb and Bi). With antimony, thermal dissociation permits the preparation of an intermediate composition Pu_4Sb_3. By far, the most important class of compounds are the monopnictides PuX (N, P, As, Sb, Bi), which form an isostructural series that has played an important role in understanding the degree of localized versus delocalized bonding with 5f electrons.

Plutonium pnictides are generally prepared by reaction of plutonium metal or hydride with the pnictogen in evacuated sealed quartz tubes that are heated to 400–750°C. The monopnictides can be prepared by thermal dissociation of a higher pnictide. Reviews of synthesis (Spirlet, 1991) and structural properties are available (Damien *et al.*, 1986).

(a) The plutonium–nitrogen system

There is only one compound in the plutonium–nitrogen system that is known with certainty: the cubic mononitride PuN. The Pu–N phase diagram has recently been assessed (Wriedt, 1989; Kassner and Peterson, 1995) and is illustrated in Fig. 7.86. The locations of the boundaries on the Pu-rich and N-rich sides of PuN have not been evaluated in detail, but the composition range of PuN is probably quite narrow. PuN decomposes under 1 bar of N_2 pressure at 2570°C into N_2-saturated liquid plutonium and N_2. Liquid plutonium is formed

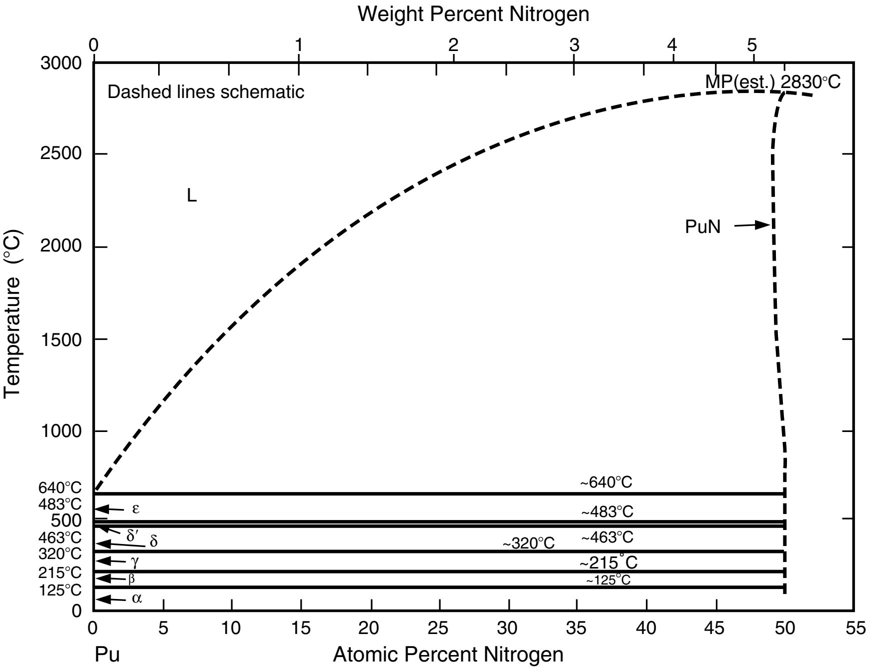

Fig. 7.86 *The plutonium–nitrogen phase diagram* (*Wriedt,* 1989*; Kassner and Peterson,* 1995).

above 1500°C due to incongruent evaporation of PuN. Because of problems associated with sample vaporization, the melting point of PuN has not been observed.

There is a fascinating report by Green and Reedy (1978a) of the observation of matrix isolated PuN_2 containing a molecular N_2 unit and characterized using IR spectroscopy. Theoretical studies discussing the existence, and the nature of chemical bonding in PuN_2 have subsequently appeared (Archibong and Ray, 2000; Tan, 2003).

(*i*) *Preparation*

Cubic PuN can be prepared most conveniently by reaction of metal with H_2 (150–200°C) to produce plutonium hydride, followed by heating the hydride under N_2 at temperatures between 500 and 1000°C (Pardue *et al.*, 1964a, 1967). The preparation can also be accomplished by reaction of plutonium metal with N_2 containing small amounts of H_2 at 250°C (Anselin, 1963a,b; Bridger and Dell, 1967). In view of the facile reactivity of plutonium metal with H_2 (see Section 7.7.1) it is likely that this reaction is catalyzed by surface hydriding of the plutonium metal at 200°C. In the absence of H_2, the direct reaction of pure plutonium metal with N_2, even over a period of 150 h at 1000°C, does not ensure complete conversion to PuN (Brown *et al.*, 1955). The nitride can also be prepared by the carbothermic reduction of PuO_2 under N_2 (Muromura, 1982; Suzuki *et al.*, 1983; Bardelle and Bernard, 1989; Takano *et al.*, 2001), though care must be taken to avoid product contamination with carbon and oxygen impurities. This is a common approach for making nitride fuels as it avoids making large quantities of plutonium hydride in a nuclear facility. The nitride can also be prepared by the reaction of plutonium hydride with ammonia between 600 and 650°C (Abraham *et al.*, 1949c). An interesting low-temperature route to PuN is the reaction of PuI_3 with sodium or potassium metal in liquid ammonia:

$$PuI_3 + NH_{3(l)} + 3M \rightarrow PuN + 3MI + 1.5H_2, \quad M = Na, K \tag{7.34}$$

In this approach, PuI_3 is dissolved in liquid ammonia, followed by reduction with a stoichiometric amount of sodium or potassium metal. The reaction likely proceeds through the *in situ* formation of the active metal amide, MNH_2 (M = Na, K), which undergoes subsequent metathesis with PuI_3. PuN precipitates from liquid ammonia as a black powder, which is washed with liquid ammonia and annealed at 700°C for 24 h (Cleveland *et al.*, 1974, 1975).

Freshly prepared PuN is black, turning brown in moist air due to hydrolysis (Storms, 1964). Formulations of (U, Pu, Zr)N that contain only a few percent of plutonium are golden-yellow. Because of problems with sample vaporization, the melting point of PuN has not been observed, but it has been estimated that congruent melting occurs at 2830 ± 50°C for an N_2 pressure of 50 ± 20 atm (Spear and Leitnaker, 1968).

(*ii*) *Crystal structure*

The crystal structure of PuN was first studied by Zachariasen and shown to exhibit the cubic NaCl structure (Zachariasen, 1949c,d). In cubic PuN, the plutonium and nitrogen atoms alternate in a fcc sphere packing arrangement, with both Pu and N having regular octahedral coordination. Using a lattice parameter of 4.905 Å, the Pu–N and Pu–Pu distances are 2.45 and 3.47 Å, respectively. Many lattice parameter studies of PuN have been reported and recently were summarized (Wriedt, 1989). The rather large variation in lattice parameter is most likely due to the effects of impurities, self-irradiation damage, or nitrogen concentration. A lattice parameter value of 4.918 Å was reported from the results of neutron diffraction on ^{239}PuN at –213°C (Boeuf *et al.*, 1984). Crystallographic properties of PuN and other plutonium pnictides are given in Table 7.33.

(*iii*) *Properties*

Plutonium mononitride is a refractory material with great potential for use as a nuclear reactor fuel (Matzke, 1986; Blank, 1994). It has a high melting point, high density, and high thermal conductivity. Moreover, it is compatible with austenitic steels up to 600°C and with sodium up to its boiling point of 890°C. One drawback is that PuN has a high volatility (due to release of N_2) at the high temperatures possible in a reactor accident. Due to the potential use of PuN in reactor fuels (Sano *et al.*, 1971; Bernard, 1989; Ogawa *et al.*, 1998; Albiol and Arai, 2001), there is an extensive literature on PuN, and topical reviews can be found on the physical and chemical properties (Spear and Leitnaker, 1968; Benedict, 1979), thermodynamic properties (Matsui and Ohse, 1987; Lemire *et al.*, 2001), phase equilibria (Wriedt, 1989), and synthesis (Spirlet, 1991). Selected physical properties of PuN are given in Table 7.34 (Holleck and Kleykamp, 1972; Kleykamp, 1999), and thermodynamic properties of PuN and other plutonium pnictides can be found in Table 7.35.

Powdered PuN reacts with O_2 at 200°C and ignites at 280–300°C to form PuO_2 (Kruger and Moser, 1967a). In moist O_2, the oxidation rate is increased: in the presence of 500 ppm water vapor, the reaction rate at 279°C is three times that without H_2O vapor. In air at room temperature, PuN powder is converted to PuO_2 within 3 days, but compact PuN is oxidized rather slowly (Pardue *et al.*, 1967).

PuN reacts slowly with cold water, but readily with hot water (Bridger *et al.*, 1969). In moist air, PuN decomposes within a few hours at 80–90°C, and within days at room temperature (Storms, 1964). The hydrolysis of PuN was determined in a stream of Ar–H_2O as a function of temperature to give hydrated PuO_2 (Bridger and Dell, 1967). Concentrated mineral acids will decompose PuN with decreasing violence of reaction in the order $HNO_3 > HCl > H_3PO_4 > H_2SO_4 > HF$ (Pardue *et al.*, 1964a).

Table 7.33 *X-ray crystallographic data for plutonium pnictides.*

Compound	*Symmetry*	*Space group*	*Lattice parameter,* a_0 (Å)	*Formula units per cell*	*Calculated density* (g cm^{-3})	*References*
PuN	fcc	F*m*3*m*	4.9055(3)	4	14.22	Ellinger (1961)
			4.9053–4.9056 (N-rich)			Olson and Mulford (1964)
			4.9051 (N-deficient)			Olson and Mulford (1964)
			4.9053 (O-free)			Bridger and Dell (1967)
			4.908 (O-saturated)			Bridger and Dell (1967)
PuP	fcc	F*m*3*m*	5.664(4)	4	9.87	Kruger and Moser (1966a)
			5.6582(1)–5.6613(1)		9.89	Kruger and Moser (1967a)
PuAs	fcc	F*m*3*m*	5.855(4)	4	10.39	Kruger and Moser (1966a)
			5.8586(1)		10.34	Kruger and Moser (1967a)
PuSb	fcc	F*m*3*m*	6.241(1)	4	9.86	Kruger and Moser (1967a)
			6.2396(1)	4		Mitchell and Lam (1971)
Pu_4Sb_3	cubic	$I\bar{4}3d$	9.2406[a]	4		Mitchell and Lam (1974)
			9.2370(5)			Charvillat (1978)
$PuSb_2$	orthorhombic	C*mca*	$a = 6.19(1)$	8	9.735	Charvillat *et al.* (1977)
			$b = 6.05(1)$			
			$c = 17.58(4)$			
PuBi	fcc	F*m*3*m*	6.350(1)	4	11.62	Ellinger (1961)

[a] Labeled as Pu_3Sb_4.

Table 7.34 *Selected properties of PuN of relevance to nuclear fuel.*

Property	*Value*	*References*
Decomposition temperature, 1 bar N_2	2570°C	Oetting (1967)
Nitrogen partial pressure at		
1500°C	2×10^{-7} bar	Alexander *et al.* (1969)
2000°C	1×10^{-4} bar	Alexander *et al.* (1969)
Metal partial pressure at		
1500°C	1×10^{-6} bar	Alexander *et al.* (1969)
2000°C	6×10^{-4} bar	Alexander *et al.* (1969)
Thermal conductivity at		
1000°C	13 W K^{-1} m^{-1}	Alexander *et al.* (1976)
1500°C	14 W K^{-1} m^{-1}	Alexander *et al.* (1976)
2000°C	15 W K^{-1} m^{-1}	Alexander *et al.* (1976)

Table 7.35 *Selected thermodynamic properties of plutonium pnictides, PuX (X = N, P, As, Sb, Bi)* (*Lemire* et al., 2001).

Compound	$\Delta_f G^\circ_{298}$ (kJ mol^{-1})	$\Delta_f H^\circ_{298}$ (kJ mol^{-1})	S°_{298} (J K^{-1} mol^{-1})	$C^\circ_{p_{298}}$ (J K^{-1} mol^{-1})
PuN	−273.7 ± 2.6	−299.2 ± 2.5	64.8 ± 1.5	49.6 ± 1.0
PuP	−313.8 ± 21.1	−318 ± 21	81.3 ± 6.0	50.20 ± 4.00
PuAs	−241.4 ± 20.1	−240 ± 20	94.3 ± 7.0	51.6 ± 4.0
PuSb	−152.1 ± 20.1	−150 ± 20	106.9 ± 7.5	52.8 ± 3.5
PuBi	−119.6 ± 20.2	−117 ± 20	120 ± 10	

(b) The plutonium–phosphorus system

Plutonium monophosphide, PuP, is the only well-defined binary plutonium–phosphorus compound known. Cubic PuP can be prepared by reaction of metal with H_2 (150–200°C) to produce plutonium hydride, followed by heating the hydride with PH_3 (Kruger *et al.*, 1966; Kruger and Moser, 1966b). By employing a stepwise reaction consisting of alternate hydride decomposition and reaction of the decomposition product with PH_3, one can obtain very pure PuP product. At least two cycles of alternate hydride decomposition and reaction with phosphine are required. The conversion cycles are followed by 4 h annealing at 1400°C. The preparation can also be accomplished by reaction of powdered plutonium hydride with excess (100–150%) red phosphorus in tantalum-lined pressure vessels at 600–800°C in an argon atmosphere (Moser and Kruger, 1966). After completion of the reaction, excess phosphorus is removed by distillation at 300°C. Alternatively, the phosphide can be prepared by induction melting of plutonium chips with elemental phosphorus *in vacuo* or under pressure of 1 atm of helium. The exothermal reaction goes to completion at 1400°C (Gorum, 1957). Another method involves the reaction of sol–gel prepared PuO_2 with a stream of PH_3 at temperatures of 1000°C or greater (Cogliati *et al.*, 1969).

PuP has a dark-gray color and melts with decomposition at 2600°C under argon. It exhibits the NaCl structure (see Table 7.33) (Gorum, 1957; Kruger *et al.*, 1966), with lattice constants that depend on sample history. Below 125 K, a tetragonal distortion is observed (Mueller *et al.*, 1979). A number of physical properties (microhardness, thermal expansion, thermoelectric power, temperature conductivity, and heat capacity) have been measured (Hall *et al.*, 1985).

PuP is ferromagnetic below a Curie temperature of $T_c = 126 \pm 1$ K. Above this temperature, the magnetic susceptibility has a temperature dependence given by $\chi_m = 190 \times 10^{-6} + N_L\mu^2/[3k(T–126)]$ cm^3 mol^{-1} where $\mu = 1.06\mu_B$ (Lam *et al.*, 1969). The ferromagnetic moment obtained by extrapolation to 0 K was found to be $0.42/\mu_B$ (Lam *et al.*, 1969). The Landé *g*-factor obtained by a correlation between Knight shift and χ_m is $g = 2/7$ (Fradin, 1970). Thermodynamic and magnetic properties have been discussed (Arai and Ohmichi, 1995).

(c) The plutonium–arsenic system

Plutonium arsenide, PuAs, may be prepared by reaction of plutonium metal with excess arsenic under 1 atm of helium or *in vacuo* at 500–1200 K (Gorum, 1957; Pardue *et al.*, 1964b; Mitchell and Lam, 1974) for a period of 3–7 h. It can also be prepared by reaction of PuH_3 with As *in vacuo* (0.02 Torr, 2.6×10^{-5} atm) at temperatures above 400°C, which are slowly increased to 700°C. The product is homogenized *in vacuo* at a still higher temperature (Kruger and Moser, 1967b; Fradin, 1970; Handwerk and Kruger, 1971; Charvillat and Damien, 1973). Finally, it can be prepared by reaction of plutonium partially converted to the hydride with AsH_3 at 250°C and subsequent recycling at 400, 500, 600, and 700°C in a similar manner as just described for PuP in Section 7.8.4(b) (Anselin, 1963b; Lam *et al.*, 1969). Because of the low decomposition temperature of AsH_3 (300°C), the primary reaction is done at 250°C, and only the annealing cycles are carried out at the higher temperatures mentioned above. Plutonium arsenide is a gray, metallic-looking material, black in finely divided form. Its crystallographic properties are listed in Table 7.33.

(d) The plutonium–antimony system

Arc melting of mixtures of plutonium and antimony yields PuSb (Kruger and Moser, 1966a). In addition to the monopnictide, plutonium also forms a dipnictide $PuSb_2$ (Charvillat *et al.*, 1977), and an intermediate composition, Pu_4Sb_3 (Damien *et al.*, 1986). Cubic PuSb melts at 1980 ± 30°C under 3 atm of argon (Mitchell and Lam, 1974).

The diantimonide exhibits an unusual orthorhombic structure formed by ten layers of atoms, and this structure is shown in Fig. 7.87. Each plutonium atom has four nearest antimony atoms ranging 3.15–3.30 Å away forming a distorted Sb_4 square just below, and another just above but rotated by 45 degrees. The local coordination polyhedron about plutonium is that of a distorted square antiprism. The Sb–Sb distances within the square are 3.095 Å, and the Sb–Sb distances linking the two groups of antiprisms are 2.755 Å. The structure is described in more detail for AB_2 rare-earth compounds by Wang and Steinfink (1967).

(e) Valency and electronic structure in PuX compounds

Plutonium monopnictides show moderately delocalized 5f electrons. The degree of localization increases with atomic number of the pnictogen, with delocalization being largely dominated by plutonium–pnictogen interactions. The lattice parameter is affected by this partial delocalization, making it hard to deduce plutonium valence from the crystal structure or lattice parameter value.

Magnetic susceptibility measurements of plutonium monopnictides show high-temperature Curie–Weiss-like behavior that gives effective moments close to the value of $1.24\mu_B$, consistent with an f^5 ion, and trivalent plutonium (Vogt and Mattenberger, 1993, 1995). The ordered magnetic moments are significantly smaller, and the experimental data suggest partial f-electron localization. For example, X-ray photoemission studies of PuSb clearly indicate localized f-electrons (Gouder *et al.*, 2000), while resistivity measurements show a semimetallic Kondo-like behavior (Blaise *et al.*, 1985). Magnetism experiments show a very strong anisotropy in all PuX compounds, with magnetic moments oriented along the [100] direction (Mattenberger *et al.*, 1986). Neutron scattering experiments (Lander *et al.*, 1984, 1985) support Cooper's interpretation of moderate f-electron delocalization being responsible for the reduction in the ordered moment and strong anisotropy in plutonium monopnictides (Cooper *et al.*, 1983). Recent electronic structure calculations of PuX compounds based upon a self-interaction correlated local spin density (SIC-LSD) approach support the interpretation that the plutonium 5f-electron manifold is best described in a mixed picture of localized and delocalized states (Petit *et al.*, 2002).

7.8.5 Plutonium chalcogenides

(a) The plutonium–oxygen system

Binary plutonium oxides, especially PuO_2, are of tremendous technological importance. They find widespread application as nuclear fuels, as long-term storage forms for both spent nuclear fuels and surplus weapons materials, and

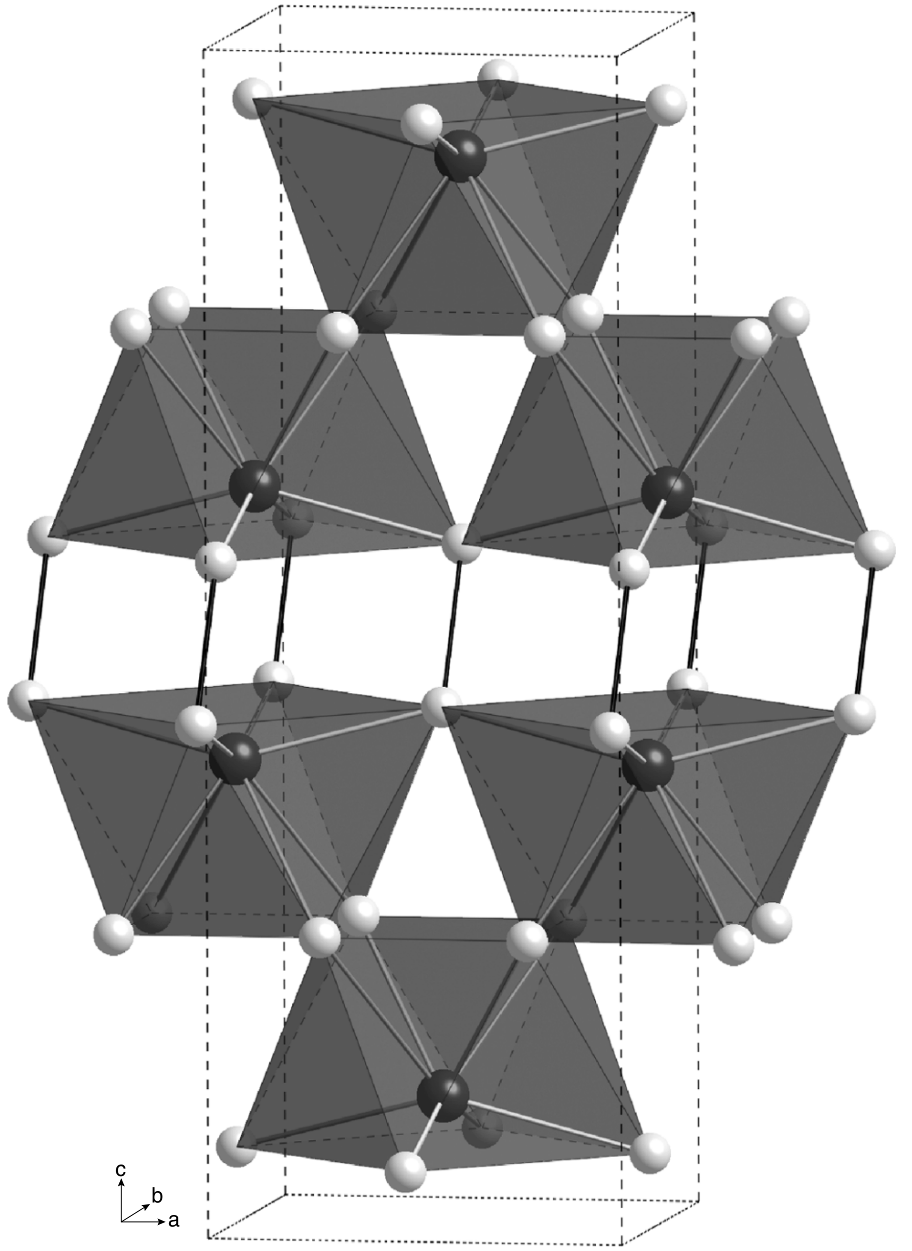

Fig. 7.87 *The solid-state structure of* $PuSb_2$ *shown looking perpendicular to the c-axis, and emphasizing the antiprismatic* $PuSb_8$ *polyhedral layers. Plutonium atoms are black and antimony atoms are gray.*

as heat and power generators (^{238}Pu) for interplanetary exploration. Their properties are also important because oxide particulates contribute to environmental actinide migration, participate in corrosion reactions in nuclear weapons, and exist as chemical intermediates in the purification and preparation of other actinide compounds. This same family of oxides is also of fundamental scientific interest. Even though plutonium oxides were among the first compounds of plutonium to be studied, it is astonishing to consider how much remains unknown about plutonium oxides. A number of reviews on the plutonium–oxygen system have appeared (Chikalla *et al.*, 1962; IAEA, 1967; Wriedt, 1990; Naito *et al.*, 1992).

(*i*) *Phase equilibria*

A good deal of discussion has appeared in the literature regarding the phase diagram for the plutonium–oxygen system, and there are conflicting sets of data for some phases (IAEA, 1967; Wriedt, 1990; Naito *et al.*, 1992; Haschke *et al.*, 2000a). The system is complex, and additional study is still needed to resolve certain issues surrounding the phase diagram. To adequately describe the issues associated with the plutonium–oxygen system, Haschke and Haire (2000) chose to present two diagrams, one based on the most recent assessment with modifications, and another, more pedagogical diagram based upon analogy with the more well-studied and better understood lanthanide oxide systems. There is great utility in this approach, and we have adopted it for our discussion. The proposed phase diagram based on the most recent assessments is shown in Fig. 7.88, and a table of crystallographic data for plutonium oxides is given in Table 7.36.

There are four fundamental equilibrium solid phases in the plutonium–oxygen system. The first of these is the stoichiometric hexagonal sesquioxide of formula Pu_2O_3 with a very small composition range near 60 at.% oxygen and with an ideal stoichiometry of $PuO_{1.5}$. This phase is also commonly known in the literature as hexagonal A-Pu_2O_3, or β-Pu_2O_3, and other designations have also been used (Wriedt, 1990; Haschke and Haire, 2000). We will use the designation A-Pu_2O_3. There is a bcc sesquioxide of composition $PuO_{1.52}$, reported to have only a small composition range near 60.3 at.% oxygen, but this narrow stoichiometry range is not supported by all the available data (Haschke and Haire, 2000). This phase has been commonly referred to as cubic C-Pu_2O_3, α-Pu_2O_3, and α-$Pu_2O_{3+\delta}$, but again, other designations have also appeared in the literature. We will use the designation C-Pu_2O_3.

There is a bcc oxide of intermediate composition $PuO_{1.61}$ with a composition range between 61.7 and 63.0 at.% oxygen that is commonly referred to as C′-Pu_2O_3, α'-Pu_2O_3, $PuO_{1.6+\delta}$, and others. This cubic phase is not stable at room temperature but exists above 335°C. Due to its broad composition range, Haschke and Haire referred to this phase as $PuO_{1.6+\delta}$ to help distinguish this bcc phase from the oxygen-deficient fcc PuO_{2-x}. We will use the designation

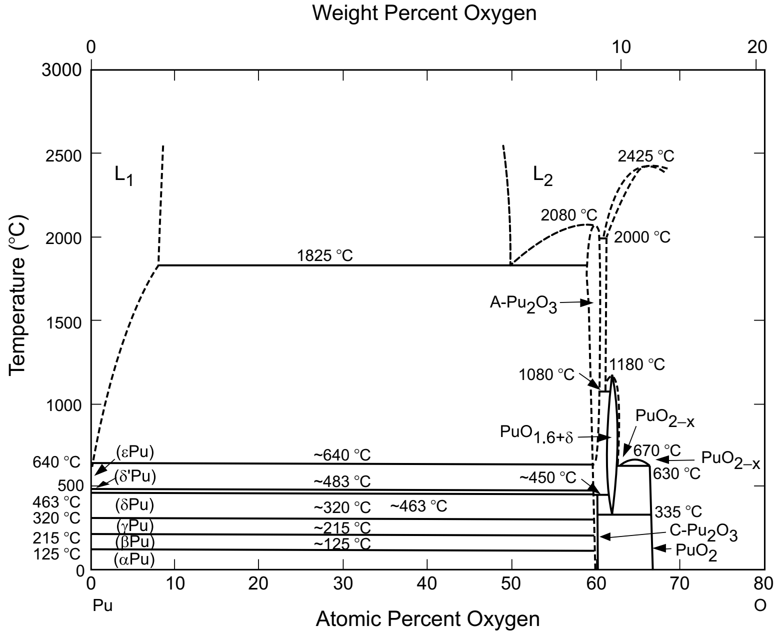

Fig. 7.88 *The plutonium–oxygen phase diagram* (*Wriedt,* 1990; *Naito* et al., 1992; *Haschke* et al., 2000*a*).

$PuO_{1.6+\delta}$. There is a fcc dioxide PuO_2 with a wide composition range that runs from $PuO_{1.6}$ to PuO_2, and sometimes referred to as substoichiometric PuO_2 or PuO_{2-x}. At room temperature, PuO_{2-x} has a fairly narrow composition range between $PuO_{1.98}$ and $PuO_{2.03}$, while at higher temperatures the homogeneity range widens to $PuO_{1.6}$ and PuO_2 as indicated in the phase diagram. Note that the oxygen-deficient fcc $PuO_{1.6}$ (PuO_{2-x}) is not the same as the bcc $PuO_{1.61}$ described above; this is why we prefer the nomenclature $PuO_{1.6+\delta}$ for the bcc phase. On the plutonium-rich side, cubic $PuO_{1.6+\delta}$ coexists with cubic C-Pu_2O_3 until it undergoes a peritectoid decomposition into hexagonal A-Pu_2O_3 and cubic $PuO_{1.6+\delta}$ above 450°C. On the oxygen-rich side of this composition range, C-Pu_2O_3 coexists with PuO_{2-x} below 630°C, and with metal-rich PuO_{2-x} at higher temperatures until it congruently transforms into PuO_{2-x} at 1180°C. Hexagonal A-Pu_2O_3 coexists with oxygen-saturated metal and displays an increasing extent of nonstoichiometry until the congruent melting point of 2080°C is reached. PuO_2 undergoes congruent melting at 2425°C. Only recently has there been enough new data to suggest the addition of a hyperstoichiometric fcc oxide, PuO_{2+x} with composition that runs from stoichiometric PuO_2 to $PuO_{2.27}$ between room temperature and 350°C (Haschke *et al.*, 2000b). This is not shown in Fig. 7.88, but is included in the notional phase diagram shown in Fig. 7.92.

Table 7.36 *X-ray crystallographic data for plutonium oxides.*

Compound or phase	*Structure type*	*Symmetry*	*Space group*	*Unit cell dimensions* (Å)	*Formula units per cell*	*X-ray density* (g cm^{-3})	*References*
PuO	NaCl	fcc	F*m*3*m*	$a = 4.96(1)$	4	13.88	Ellinger (1961)
$PuO_{1.5}$ (A-Pu_2O_3, β-Pu_2O_3)	La_2O_3	hexagonal	$P\bar{3}m1$	$a = 3.841(6)$ $c = 5.958(5)$	1	11.47	Ellinger (1961)
$PuO_{1.51}$ (C-Pu_2O_3, α-Pu_2O_3)	Mn_2O_3	bcc	I*a*3	$a = 11.02(2)$	16	10.44	Ellinger (1961)
$PuO_{1.61}$ ($PuO_{1.6+\delta}$, C′-Pu_2O_3, α′-Pu_2O_3)	Mn_2O_3	bcc	I*a*3	$a = 10.95 - 11.01$			Gardner *et al.* (1965)
PuO_2	CaF_2	fcc	F*m*3*m*	$a = 5.3960(3)$ for stoichiometric composition	4	11.46	Ellinger (1961)
$^{238}PuO_2$	CaF_2	fcc	F*m*3*m*	$a = 5.4141(1)$	4		Roof (1973)
$PuO_{2.26}$	CaF_2	fcc	F*m*3*m*	$a = 5.404$	4		Haschke *et al.* (2000b)

(*ii*) *Preparation*

Plutonium monoxide, PuO

While it has been reported on numerous occasions, the existence of a *stable* condensed oxide of formula PuO is still uncertain and is therefore not indicated in the phase diagram of Fig. 7.88. The material that has been described by many authors is most likely a disordered oxide–carbide $Pu(O_x,C_{1-x})$. Mooney and coworkers (Mooney and Zachariasen, 1949; Zachariasen, 1949d) described powder patterns that could be attributed to cubic PuO, and Holley *et al.* reported a NaCl-type fcc phase with $a_0 = 4.96(1)$ Å as a surface film formed on plutonium metal. Westrum (1949a) describes the material as a semimetallic substance with an almost metallic luster. This surface material has also been observed upon heating oxide-coated plutonium metal *in vacuo* at 250–500°C (Terada *et al.*, 1969). Other reports on the preparation of PuO include the reaction of molten plutonium (microgram quantities) with stoichiometric oxygen generated by thermal decomposition of Ag_2O (Akimoto, 1960), by reduction of PuO_2 with carbon at 1500–1800°C (Skavdahl, 1964), or by reduction of PuOCl or PuO_2 with Ba vapor at 1250°C (Westrum, 1949a). Reshetnikov (2003) has recently claimed to prepare pure PuO by heating PuOCl with calcium at 1200°C, but no characterization data are provided to substantiate the claim. Haschke and Haire (2000) point out that plutonium oxide that results from metal oxidation may be covered with a layer of unbound carbon formed as a result of interaction of the oxide with hydrocarbons or CO_2, and that experiments by Forbes *et al.* (1966) indicate that all products thus obtained contain carbon. The observed lattice parameter is nearly identical to that found for oxide–carbide solid solutions (Mulford *et al.*, 1965; Oetting, 1967). Work on the Pu–O–C phase diagram has shown conclusively that the oxygen-rich limit of the $Pu(O_x,C_{1-x})$ phase lies at a composition of approximately $PuC_{0.3}O_{0.7}$ (Forbes *et al.*, 1966; Taylor *et al.*, 1967; Larson, 1980; Larson and Haschke, 1981). Larson and Haschke (1981) used XPS data to demonstrate that a material believed to be PuO was in fact $PuO_{0.65\pm0.15}C_{0.45\pm0.15}$.

Although the above paragraph argues that most materials that were thought to be PuO were likely contaminated with carbon, and therefore likely to be $Pu(O_xC_{1-x})$ there are several intriguing reports about an unstable, metallic-gray, pyrophoric product that deserve additional study. Reshetnikov (2003) describes an explosion that occurred in 1949 upon grinding a sample thought to be plutonium with a glass rod. Similarly, Haschke described a steel-gray product formed upon the thermal decomposition of PuOH (Haschke *et al.*, 1983; Haschke, 1992). This material underwent a violent exothermic reaction with oxygen, destroying a quartz microbalance container. Such behavior would not be expected for PuO_xC_{1-x}. Thus there may be some instances where a metastable form of solid PuO has indeed been prepared. The full characterization of the material produced by Haschke was not undertaken due its pyrophoric nature (Haschke, 1992), and characterization of the material prepared by Reshetinikov was not provided. We will need to wait for additional characterization data to resolve this issue.

While the existence of solid-phase PuO is unresolved, there is little doubt that gaseous PuO is one of the major species of plutonium oxides in the vaporization process (Green and Reedy, 1978b; Capone *et al.*, 1999; Ronchi *et al.*, 2000). PuO is observed in both the mass spectrum of effusing vapors over PuO_2 (Capone *et al.*, 1999; Ronchi *et al.*, 2000), and in the IR absorption spectra of vapors trapped in argon and krypton matrixes. $Pu^{16}O$ trapped in an argon matrix displays an infrared vibrational frequency of 822.28 cm^{-1} (Green and Reedy, 1978b).

Plutonium sesquioxide phases, Pu_2O_3

There is a good deal of confusion about both the preparative methods and the phase relationships between hexagonal (A-Pu_2O_3) and cubic (C-Pu_2O_3) forms of plutonium sesquioxide. The methods of preparation of hexagonal and cubic forms are very similar, yet these oxides are described as separate and distinct phases at low temperature. As outlined in recent reviews (Wriedt, 1990; Haschke and Haire, 2000), these compounds are thought to be distinct phases because (i) both cubic and hexagonal phases have been observed to coexist; (ii) the transformation between hexagonal and cubic forms has not been observed; and (iii) their regions of composition do not overlap. It has been suggested that kinetic factors may favor the formation of the cubic sesquioxide at low temperature in the presence of plutonium metal (Haschke and Haire, 2000). For example, cubic C-Pu_2O_3 readily forms as a surface layer when PuO_2-coated δ-stabilized plutonium metal is heated to 150–200°C under vacuum (Terada *et al.*, 1969). This observation is highly suggestive that the preexisting fcc lattice of metal atoms in either the underlying metal, the fcc dioxide, or both, imparts some control over the nature of the product in the reaction, and that once the cubic sesquioxide is formed, this phase cannot transform into the hexagonal form unless the temperature exceeds 450°C. The hexagonal form apparently does not transform back into the cubic form at this temperature, suggesting perhaps that more kinetic energy is necessary to rearrange the metal atoms in the lattice. This behavior is not consistent with the known behavior of the isomorphic lanthanide oxides, where hexagonal Nd_2O_3 will transform reversibly to cubic Nd_2O_3 near 600°C (Haire and Eyring, 1994). Thus cubic C-Pu_2O_3 may be only metastable at low temperatures.

Several methods of preparation have been reported for the hexagonal A-Pu_2O_3 sesquioxide. Plutonium dioxide can be reduced with plutonium metal (Holley *et al.*, 1958), dry hydrogen (Flotow and Tetenbaum, 1981), or carbon (Skavdahl, 1964) to form A-Pu_2O_3. Pure hexagonal A-Pu_2O_3 has been prepared by reducing pure PuO_2 with a 20% excess of plutonium turnings or chips in a closed tantalum crucible at 1500°C according to the stoichiometry (Holley *et al.*, 1958):

$$3PuO_2 + Pu \rightarrow 2Pu_2O_3 \qquad (7.35)$$

After a reaction period of 3 h, the excess plutonium metal was removed by sublimation from the open crucible at 1800–1900°C *in vacuo* (Holley *et al.*, 1958; Chikalla *et al.*, 1962, 1964). At higher reaction temperatures, large, flat crystals of hexagonal A-Pu_2O_3 were obtained. In another procedure, Gardner *et al.* (1965) reduced pure PuO_2 powder with a 20% excess of hydride-powdered plutonium metal in a ThO_2 crucible at 1500°C for 3 h in a stream of purified dry hydrogen.

Hydrogen reduction of PuO_2 to produce hexagonal A-Pu_2O_3 can be accomplished at 1550°C in very dry hydrogen purified over titanium turnings (Gardner *et al.*, 1965). Complete reduction of PuO_2 by hydrogen has also been reported to occur in the temperature range 1700–2000°C (Dayton and Tipton, 1961; Flotow and Tetenbaum, 1981). Pure hexagonal A-Pu_2O_3 may be prepared by the stoichiometric reduction of PuO_2 with carbon at (1800 ± 50)°C for 5.5 h in a pure helium atmosphere (Skavdahl, 1964; Forbes *et al.*, 1966) according to the reaction:

$$2PuO_2 + C \rightarrow Pu_2O_3 + CO \tag{7.36}$$

Chikalla and coworkers reported a large-scale preparation (ca. 110 g Pu) of hexagonal A-Pu_2O_3 by sintering pressed compacts of PuO_2 and carbon *in vacuo*, followed by melting under an inert atmosphere (Chikalla *et al.*, 1962, 1964; Skavdahl, 1964). Reaction of PuO_2 with a slight excess of carbon at 1650°C *in vacuo* produced a mixture of hexagonal A-Pu_2O_3 and a small amount of $Pu(O_x,C_{1-x})$. The latter, being more volatile than the Pu_2O_3, could be removed by heating *in vacuo*. Final arc melting resulted in hexagonal A-Pu_2O_3 with an O:Pu ratio of (1.500 ± 0.015), with 175 ppm carbon impurity and 93% theoretical density.

The cubic C-Pu_2O_3 sesquioxide is a silvery, metallic, lustrous solid, which is difficult to prepare by high-temperature methods. Haschke and Haire point out that reports of its preparation by simply heating PuO_2 *in vacuo* to temperatures between 1650 and 1800°C (Westrum, 1949a; Dayton and Tipton, 1961) are suspect because the O:Pu ratio of congruently vaporizing PuO_{2-x} is 1.85–1.90 in this temperature range (Ackermann *et al.*, 1966). The best means of preparation seems to be the heating of PuO_2 coated δ-stabilized plutonium metal to 150–200°C under vacuum (Terada *et al.*, 1969).

Hyperstoichiometric sesquioxide, $PuO_{1.6+\delta}$ (C'-Pu_2O_3, α'-Pu_2O_3, $PuO_{1.61}$)

When PuO_2 is melted, there is an evolution of oxygen resulting in a melt composition of $PuO_{1.62}$, which is the approximate composition of cubic C-Pu_2O_3 (Chikalla *et al.*, 1964). This phase can only be retained with extremely fast quenching. Since it is a high-temperature form of C-Pu_2O_3, it has been given the designation C'-Pu_2O_3 (or α'-Pu_2O_3, $PuO_{1.61}$, $PuO_{1.6+\delta}$). It is likely bcc. Slow cooling of the melt yields a mixture of C-Pu_2O_3 and PuO_{2-x} even in the absence of oxygen. Sari *et al.* (1968) reported that this compound has a composition range from $PuO_{1.62}$ to $PuO_{1.63}$ at 350°C, which extends to a range of $PuO_{1.62}$ to

$PuO_{1.69}$ at 600°C. Because of this broad composition range, we prefer the designation $PuO_{1.6+\delta}$.

Substoichiometric plutonium dioxide, PuO_{2-x}

The oxides between compositions $PuO_{1.61}$ to $PuO_{1.98}$ are mainly single-phase materials at temperatures above about 650°C. They may be prepared by heating PuO_2 at high temperature with carbon, hydrogen, or *in vacuo* (IAEA, 1967). The crystal lattice expands with decreasing oxygen composition (Gardner *et al.*, 1965; IAEA, 1967). Some annealing may be required, but prolonged heating *in vacuo* will cause a change in composition due to incongruent vaporization. This olive-green phase exists in the stoichiometry range $PuO_{1.61}$ to $PuO_{1.98}$ and is closely related to the stoichiometric oxide $PuO_{2.00}$. Its exact composition depends on the temperature and the oxygen partial pressure over the plutonium oxide solid (Drummond and Welch, 1957). Atlas and coworkers performed density measurements at 750°C that are consistent with the formation of oxygen vacancies in the crystal lattice (Atlas *et al.*, 1966). Atlas and Schlehman (1967) conducted a detailed study of the variation in oxygen content, x, with oxygen pressure. The composition–pressure–temperature relationship is shown in Fig. 7.89.

Stoichiometric plutonium dioxide, $PuO_{2.00}$

Plutonium dioxide is formed when metallic plutonium is ignited in air or by calcination of a number of plutonium compounds (except phosphates). Plutonium dioxide often forms when oxygen-containing compounds are heated *in vacuo* or in an inert atmosphere to 1000°C. The most widely used approach to prepare pure, crystalline PuO_2 is by heating Pu(III) or Pu(IV) oxalate to

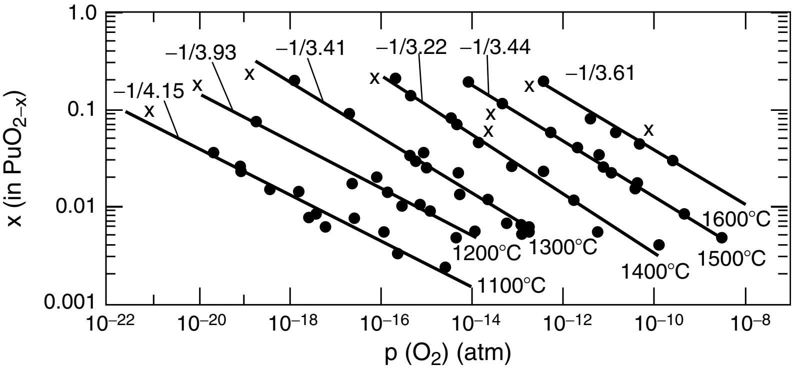

Fig. 7.89 *Variation of x in PuO_{2-x} with temperature and oxygen pressure (Atlas and Schlehman,* 1967*). Slopes (i.e.* –1/4.15, *etc.) of the log–log plots are shown above the lines. Experimental data points marked in x represent values derived from weight change measurements, whereas the circles represent gas-analysis results.*

1000°C in air. The Pu(III) oxalate is often preferred because it forms a powder that is easy to manipulate, while the Pu(IV) oxalate forms a tacky solid (see Section 7.9.1(e)i). The heating rate must be kept slow up to about 700°C to avoid rapid decomposition and gas evolution, followed by heating to 1000°C to remove any residual carbon. Drummond and Welch (1957) studied the stoichiometry of PuO_2 as a function of preparative history, and found that many materials need to be heated to 1250°C to produce reproducible stoichiometric PuO_2.

The method of preparation and process details have a significant influence on the PuO_2 product characteristics, which affect all subsequent uses of the material, such as fabrication and sintering properties of fuel materials containing PuO_2 or its behavior in long-term storage. PuO_2 is normally olive green, but it's observed color is a function of purity, particle size, method of preparation, stoichiometry, and possible reactions with water. The observed colors range from dull yellow, to green, khaki, buff, slate or black. Many of these samples are most likely hyperstoichiometric PuO_{2+x} (see section PuO_{2+x}). All samples turned to a darker, khaki color upon ignition to 1200°C. The qualitative characteristics of various PuO_{2+x} preparations obtained from different starting materials are summarized in Table 7.37 (Drummond and Welch, 1957).

Special preparations of PuO_2

Plutonium dioxide may be pressed and sintered to form pellets or compacts, which may be used in reactor technology or (in the case of $^{238}PuO_2$) in heat- and power-source technology for space exploration. For detailed descriptions, the reader is referred to the *Plutonium Handbook* (Wick, 1980). As an illustrative example of the general pellet-forming process, $^{238}PuO_2$ used to fabricate GPHS and LWRHU fuel pellets (see Section 7.3) for the Cassini mission was subjected to ^{16}O isotope exchange (to reduce neutron emission), ball milling, granulation and seasoning at 1100 and 1600°C to produce $^{238}PuO_2$ granules with <210 μm sized particles. The granules were then blended using those seasoned at

Table 7.37 *Qualitative characteristics of PuO_{2+x} from decomposition of selected materials at* 870°C (*Drummond and Welch,* 1957).

Material	*Color*	*Appearance*
metal	dull yellow	powder
sulfate	yellow-green to green	bulky powder
nitrate	dull yellow	bulky solid
chloride	dull yellow	powder
fluoride	khaki with black traces	granular solid
oxalate	yellow-buff	bulky powder
iodate	buff	very bulky
hydroxide	black with yellow traces	dense, shiny particles

1100°C (60 wt %) with those seasoned at 1600°C (40 wt %) by rolling the granules in a ball-mill jar without balls. After blending, the fuel charges were loaded into a hot press graphite die, placed under vacuum, and heated to 1530°C under a force of 11.8 kN. During hot pressing, the PuO_2 is reduced by the graphite die. After the pellets sat overnight, the PuO_{2-x} stoichiometry was about $PuO_{1.93}$. To oxidize the pellets back to a stoichiometry of PuO_2 and increase their density to meet mission specifications, the pellets were sintered in flowing $Ar–H_2{}^{16}O$ for 6 h at 1000°C, followed by 6 h at 1527°C (Rinehart, 1992, 2001).

Two other forms of PuO_2 also deserve a more detailed description: PuO_2 microspheres and single crystals. Plutonium dioxide microspheres with 10–250 μm diameter may be prepared by the sol-gel process for ^{239}Pu (Wymer and Coobs, 1967; Lloyd and Haire, 1968; Louwrier *et al.*, 1968; Wymer, 1968), ^{238}Pu (Grove *et al.*, 1965; Hass *et al.*, 1966; Hincks and McKinley, 1966), or MOX $(U, Pu)O_2$ (Vaidya *et al.*, 1983; Smolders and Gilissen, 1987; Stratton *et al.*, 1987). In this process, a stable Pu(IV) hydroxide sol is prepared by extraction or evaporation of HNO_3 from $HNO_3–Pu(NO_3)_4$ solution, injection of the resulting sol into a dehydrating organic solvent (for instance, 2-ethylcyclohexanol), and firing the resulting gel to form PuO_2 microspheres (Hass *et al.*, 1966; Lloyd and Haire, 1968; Wymer, 1968).

Very dense microspheres, which have a remarkable freedom from loose α-particle contamination, may be prepared by plasma spheroidization (Jones *et al.*, 1964). In this method, plutonium oxide is first compacted into pellets, which are fired at 1500°C for 1 h in an oxygen-enriched plasma to inhibit loss of oxygen during melting. The resulting compacts are ground to the desired mesh size, and are then fed into an induction-coupled plasma torch, which uses argon, oxygen, or $Ar–O_2$ mixtures as feed gas. In the high temperature of the plasma torch (up to 20,000°C), each plutonium oxide particle immediately melts to a small spherical droplet, which, upon leaving the plasma zone, immediately solidifies into a small sphere with a smooth surface. Depending on the particle size of the feed particles, microspheres from 10 to 250 μm may be obtained (Jones *et al.*, 1964).

Spheres with less than 50 μm diameter are amber-colored and have a clear, vitreous appearance. Those of more than 50 μm diameter do not transmit light and appear opaque black (Jones *et al.*, 1964). If prepared in an O_2 plasma, they have the lattice constants of stoichiometric PuO_2. Each individual sphere usually consists of a single crystal (Jones *et al.*, 1964).

Plutonium dioxide single crystals of considerable size have been prepared by several authors (Phipps and Sullenger, 1964; Schlechter, 1970; Finch and Clark, 1972; Rebizant *et al.*, 2000). Finch and Clark (1972) obtained PuO_2 single crystals from $Li_2O–2MoO_3$ melt in a temperature gradient ranging from 1270 to 1300°C in a tightly closed platinum vessel over a 2 week period. Crystals of 2 × 3 × 3 mm have been obtained in this fashion. Schlechter (1970) grew single crystals of approximately the same size by slow thermal decomposition of

$Pu(SO_4)_2$ either in LiCl–KCl eutectic or in $PbCl_2$–KCl melt at 600–800°C and subsequent cooling at a rate of 2.2°C h^{-1} from 715°C to room temperature. Phipps and Sullenger (1964) obtained PuO_2 single crystals with well-defined faces and edges up to 60 μm long when they prepared plutonium-bearing glass fibers by drawing the molten glass (90% SiO_2–30% Na_2O) from a platinum–rhodium bushing at 1300°C. $(U,Pu)O_2$ single crystals have been grown through a chemical transport reaction (Rebizant *et al.*, 2000).

Higher oxides, PuO_{2+x}, PuO_3, and PuO_4

While plutonium is capable of forming molecular compounds of oxidation state VI and VII, most practitioners have been of the opinion that in the plutonium–oxygen system, the stoichiometric tetravalent oxide $PuO_{2.0}$ represents the highest obtainable binary oxide. The historical basis for this opinion began in 1944, when Moulton (1944) observed that during ignition of plutonyl nitrate, only PuO_2 was formed, but no PuO_3 or any other higher oxide was produced. Moulton took this as evidence for the nonexistence of any oxide of composition higher than PuO_2. In 1953, Brewer (1953) predicted from thermodynamic calculations that any solid anhydrous oxide of plutonium higher than PuO_2 would probably not be stable. This view seemed to be confirmed by the work of Westrum (1949a), who used strongly oxidizing conditions (O_2 at 400°C and 70 atm pressure; ozone at 600–1000°C; atomic oxygen) but failed to oxidize PuO_2. Katz and Gruen (1949) also reported that PuO_2 is not oxidized to a higher oxide with NO_2 or atomic oxygen at 500°C. Moreover, Weigel and coworkers (Marquart *et al.*, 1983) attempted to prepare anhydrous PuO_3 by careful decomposition of PuO_2CO_3, $(NH_4)_2PuO_2(CO_3)_2$, and $PuO_3 \cdot 0.8H_2O$, but did not succeed in preparing any higher oxide. Gouder has attempted to prepare thin films of PuO_3 by reacting PuO_2 with oxygen atoms, and found no evidence for its formation (Gouder, 2005).

A number of recent reports on higher-valent oxides such as $PuO_{2.26}$ in the solid state, and PuO_3 and PuO_4 in the gas phase have challenged these traditional views. While not all of the data are consistent, and there are still disagreements among practitioners, these recent reports strongly suggest that the established views on the oxidation behavior of plutonium are worth reconsideration, and that additional detailed study is appropriate.

PuO_{2+x} As early as 1957, Drummond and Welch (1957) had prepared compositions of PuO_2–$PuO_{2.09}$, and concluded that compounds with O:Pu ratios higher than 2.0 were the result of low temperature ignition of plutonium compounds. Oxygen-rich PuO_2 can also be prepared by heating cubic C-Pu_2O_3 in oxygen at 1000°C, and the material formed in this manner displayed a slightly reduced lattice constant (a_0) of 5.382 Å as compared to 5.396 Å for stoichiometric PuO_2. It was possible that the higher O:Pu ratio in these preparations was attributed to excess oxygen dissolved in the crystal lattice. In other studies, mass changes indicating the formation of $PuO_{2.1}$ during

atmospheric corrosion of plutonium metal had been attributed to adsorption of water (Sackman, 1960).

These views remained widely held until Stakebake and coworkers found evidence for a new fluorite-related phase of composition $PuO_{2.17}$ formed as a surface layer by plutonium metal reaction with water vapor at 200–350°C (Stakebake *et al.*, 1993). XPS data were consistent with the presence of Pu(VI). Confirmatory evidence for the formation of a higher oxide was reported by Haschke *et al.* (2000a,b), who studied the reaction of PuO_2 with water vapor between 25 and 350°C. Mass spectroscopic analysis of the gases produced in this reaction showed that H_2 and H_2O were the only gaseous products and indicated that the reaction proceeds according to the reaction:

$$PuO_2(s) + xH_2O(g) \rightarrow PuO_{2+x}(s) + xH_2(g) \tag{7.37}$$

The final product approached a composition of $PuO_{2.3}$. XRD analyses of the reaction products revealed a single fcc phase with a fluorite-related structure and a slightly expanded lattice. The lattice expansion was accompanied by a linear increase in the O:Pu ratio, consistent with the formation of a solid-solution of PuO_{2+x} in analogy with UO_{2+x} (Allen and Tempest, 1986). Isothermal measurements showed that hydrogen is generated at linear, temperature-dependent rates from which the authors derived an activation energy (E_a) for the reaction of (39 ± 3) kJ mol^{-1}. This was interpreted as being consistent with a chemical reaction, and not with radiolysis, which is expected to be temperature-independent. It should be noted, however, that the rates observed for hydrogen evolution in the reaction of PuO_2 with water vapor at 25°C are in close agreement to the rate of hydrogen evolution observed during exposure of PuO_2 to aqueous salt solutions (Haschke *et al.*, 1983). The report of H_2 being the only gaseous product is not consistent with the observations of Vladimirova and Kulikov (2002), who reported the observation of both H_2 and O_2 in the gas phase during their study of the reaction of PuO_2 with sorbed water using high- and low-burnup plutonium, and therefore different radiolytic dose rates. Their data are consistent with the rates of formation of H_2 and O_2 being in direct proportion to the dose rate. They followed their reactions for 600 days, but did not report on the characterization of the oxide at the end of the experiment.

There is good agreement that water vapor reacts with PuO_2 to generate hydrogen. The generation of hydrogen in storage containers represents a significant safety concern (Haschke and Martz, 1998b), and has led to use of strict standards for stabilization, packaging, and storage of plutonium residue materials that require thermal stabilization using calcinations in air, followed by sealing the materials in nested welded stainless steel containers before storage or transport (Paffett *et al.*, 2003b).

Haschke and coworkers have suggested that the formation of explosive H_2–O_2 mixtures by reaction of water vapor with PuO_2 in air-filled containers is not possible because moisture-enhanced corrosion proceeds via a water-catalyzed cycle (Haschke *et al.*, 2001). In their proposed mechanism, water absorbs strongly on the oxide below 120°C and desorbs as the temperature is increased to 200°C. Dissociative adsorption of water forms surface OH^-, promotes the formation of PuO_{2+x}, and releases H_2. When O_2 is present, they propose a surface catalyzed H_2–O_2 recombination to form surface adsorbed water that then reacts to form PuO_{2+x}, and atomic H on the surface. In the absence of O_2, H atoms associate as H_2 as indicated in equation 7.37 above. Association of H atoms with dissociatively adsorbed oxygen reforms H_2O and prevents the accumulation of H_2 whenever O_2 is present. H_2 appears only after O_2 is depleted.

While this proposed mechanism is plausible, it remains speculative until more data are produced to confirm the proposed mechanisms or to establish an alternative mechanism. What is clear from the above discussion is that our understanding of plutonium oxide chemistry, particularly the associated surface reactions is clearly inadequate.

Gas phase PuO_3 and PuO_4 By analyzing data on transpiration experiments of plutonium oxide, Krikorian and coworkers found that the observed oxygen pressure could only be explained by the presence of a PuO_3 molecule in the gas phase (Krikorian *et al.*, 1997). The presence of gas-phase PuO_3 was confirmed by Ronchi and coworkers a few years later (Ronchi *et al.*, 2000). Knudsen-effusion experiments in combination with mass spectrometry were used to show that PuO_2(s) exposure to oxygen above 1800–1900°C produces gas-phase molecules of PuO_3, along with the expected PuO and PuO_2 gas-phase molecules. These workers concluded that formation of PuO_3(g) was not formed from a gas-phase reaction of PuO_2(g) with oxygen or carbon dioxide gases, but rather the product of a reaction of gaseous oxygen with the surface of the solid PuO_2. In another recent report, Domanov *et al.* (2002) heated PuO_2 in a stream of helium–oxygen and employed a thermogradient tube furnace to separate and condense the volatile components that were subsequently analyzed by α-detection. The data were interpreted as producing volatile or gas-phase PuO_3 and PuO_4. The latter species was expected to have an abnormally high volatility, close to that of OsO_4. As the partial pressure of oxygen was decreased, the yield of the proposed PuO_4 species decreased. These data, while indirect, are quite intriguing. The relationship between the volatile species observed by Domanov *et al.* to those reported by Krikorian *et al.* and Ronchi *et al.* is uncertain. Further study using mass spectrometry as a function of oxygen partial pressure would help to clarify whether gas phase PuO_4 really exists. The clear finding from these studies, however, is that plutonium oxides can exist in oxidation states higher than IV, at least in the gas phase. These findings clearly challenge the traditional view that PuO_2 is the terminal species.

(*iii*) *Solid-state structures*

A summary of crystallographic data for plutonium oxides is given in Table 7.36. The majority of solid-state structures of plutonium oxides are structurally related to the fluorite structure displayed by PuO_2. As a result of these structural similarities, we discuss the fluorite structure first to make the comparison with other oxide structures more understandable.

Cubic PuO_{2-x}

Plutonium dioxide forms a cubic fluorite phase over the composition range of PuO_{2-x}, where $0.4 < x < 0$. The cubic fluorite-type unit cell based upon CaF_2 is illustrated in Fig. 7.72. The lattice consists of an fcc arrangement of plutonium metal cations with O anions occupying most or all the four-fold tetrahedral sites, while the six-fold octahedral sites are vacant. In this structure, when $x = 0$, each plutonium atom is surrounded by eight oxygen atoms at the corners of a cube. Each cubic PuO_8 coordination polyhedron shares an edge with each of 12 neighboring PuO_8 polyhedra as shown in Fig. 7.90a. In this high-symmetry environment, all the Pu–O distances are the same. For a lattice parameter $a_0 = 5.396$ Å, this corresponds to a Pu–O distance of 2.337 Å, and a Pu–Pu distance of 3.816 Å. When $x > 0$, there are disordered oxygen vacancies.

Cubic C-Pu_2O_3

The C-Pu_2O_3 form of the sesquioxide displays the bcc Mn_2O_3 structure that is related to the fluorite structure with a doubled unit cell. The unit cell of the C-type sesquioxide can be considered as consisting of eight fluorite unit cells [a_0(bcc) = $2a_0$(fcc)] from which one-fourth of the oxygen atoms have been removed in an ordered way, and with the metal positions remaining almost unchanged from their fcc positions. The local coordination of the plutonium atom decreases from eight to six, and the PuO_8 cubes become PuO_6 octahedra but now with two types of plutonium atom. For one-fourth of the plutonium atoms, these missing oxygen atoms are at the ends of a body diagonal of the original PuO_8 cube, and for the other three-fourths they are at the ends of a face diagonal. Both PuO_6 coordination groups may be described as distorted octahedral, and each oxygen atom is four-coordinate and approximately tetrahedral. For cubic Pu_2O_3 with $a = 11.02$ Å, one plutonium atom has six equidistant Pu–O distances of 2.367 Å, and another plutonium atom has three pairs of Pu–O distances of 2.342, 2.360, and 2.383 Å. A comparison of the cubic PuO_2 and Pu_2O_3 structures is shown in Fig. 7.90.

Hexagonal A-Pu_2O_3

The A-type hexagonal sesquioxide formed at elevated temperatures displays the A-La_2O_3 crystal structure, typical of light lanthanide sesquioxides (Haire and Eyring, 1994). A striking feature of the hexagonal A-Pu_2O_3 structure is the highly unusual seven-coordination of the plutonium atoms. This gives three different Pu–O distances, three at 2.359, one at 2.353, and three at 2.623 Å. The local PuO_7 geometry is that of a mono-capped octahedron. Actually, there is also an eighth oxygen atom below the opposite face, but a much greater distance of 3.605 Å. This last oxygen atom, together with the seven in the PuO_7

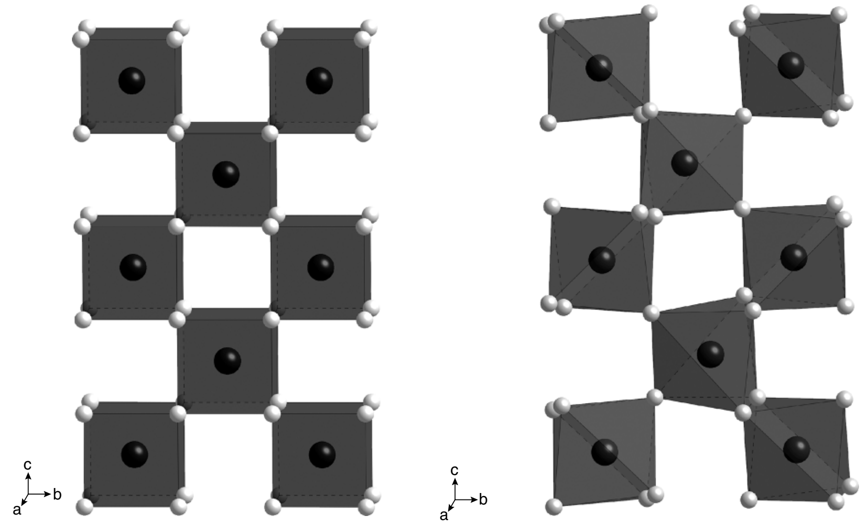

(a) (b)

Fig. 7.90 (*a*) *A polyhedral representation of a layer of the fluorite-type structure of stoichiometric* PuO_2*, emphasizing the alternating cubic* PuO_8 *coordination polyhedra and vacancy sites within the structure, and illustrating the overall face-centered cubic arrangement of Pu metal atoms.* (*b*) *A polyhedral representation of a layer of the cubic C-type* Pu_2O_3 *structure drawn on the same scale and orientation, emphasizing the similarity in the fcc arrangement of Pu metal atoms between the cubic structures of* PuO_2 *and C-*Pu_2O_3*. The local coordination environment around Pu is now reduced to six near neighbors, with alternating* PuO_6 *distorted octahedra. Plutonium atoms are black and oxygen atoms are gray.*

polyhedron forms a distorted cube. These distorted cubes form the basis of the representation given for the A-type lattice given in Fig. 7.91.

Intermediate oxide structures, PuO_{2-x}

Intermediate oxides that display O:Pu stoichiometries between 1.5 and 2.0 (or those with stoichiometry between Pu_2O_3 and PuO_2) are not well characterized for plutonium. In general, intermediate oxides are common to both lanthanides and actinides, although their properties are much better established for the lanthanides. Since both sesquioxides and dioxides are known for plutonium, it is reasonable to assume that plutonium can form a homologous series of intermediate mixed-valent oxide phases Pu_nO_{2n-2} in analogy with the lanthanides. Unfortunately, very few data exist in this stoichiometry region for plutonium, though it is known that heavier actinides, americium, curium, berkelium, and californium form some members of an intermediate An_nO_{2n-2} series

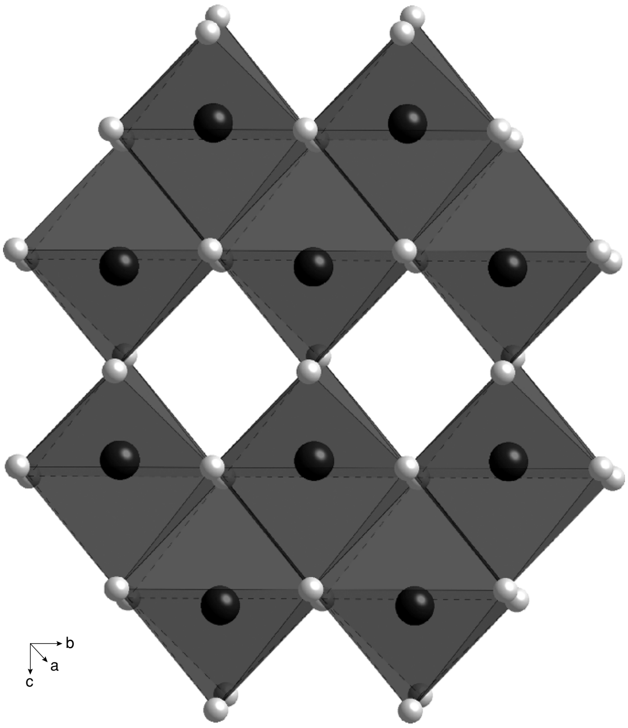

Fig. 7.91 *A polyhedral representation of a layer of the hexagonal A-type* Pu_2O_3 *emphasizing the hexagonal arrangement of Pu atoms. The local coordination environment around Pu has eight near neighbors, giving a highly distorted* PuO_8 *cube. Plutonium atoms are black and oxygen atoms are gray.*

(Haire and Eyring, 1994). Since Pu_2O_3 will take up oxygen to yield a hyperstoichiometric sesquioxide, and PuO_2 will lose oxygen to give a substoichiometric dioxide, the potential for such a series is most intriguing. Upon comparison of the ionic radii and relative free energies of the trivalent and tetravalent oxidation states of plutonium with those of cerium and praseodymium, Haschke concluded that such a mixed-valence series should be stable, and reported data from oxygen titration experiments in which the existence of a series Pu_nO_{2n-2} with $n = 5, 7, 9, 10$, and 12 was inferred (Haschke, 1992). Since the solid phases were not identified, the existence of the Pu_nO_{2n-2} series is not definitive, but clearly this is another area in which more detailed study is warranted.

The possibility of the existence of an intermediate oxide series of formula Pu_nO_{2n-2} is strongly suggested by structural principles established for the more well-studied cerium and praseodymium systems, and forms the basis of the pedagogical phase diagram introduced by Hashke and coworkers (Haschke *et al.*, 2000a), shown in Fig. 7.92. In the structural model upon which this phase diagram is based, there is an fcc array of plutonium atoms in which all (and only) the tetrahedral interstices are occupied with oxygen atoms to form the end-member PuO_2. The intermediate phase compositions and structures are realized by omission of oxygen atoms in a regular way. Except for small shifts away from the vacant oxygen sites, the metal atoms maintain their fcc positions, and this leads to a homologous series Pu_nO_{2n-2} where Pu_2O_3 is the other end-member. Since Pu_2O_3 has a bcc structure, this end-member corresponds to $n = 4$ (Pu_4O_6). With this understanding, it is easy to rationalize the phase diagram of Fig. 7.92. There is a stoichiometric hexagonal sesquioxide (O:Pu = 1.5); a cubic sesquioxide with some vacancies occupied by oxygen (O:Pu = 1.5–1.7), showing variable lattice parameters; an oxide phase corresponding to the Pu_nO_{2n-2} homologous series (rhombohedral, narrow stoichiometry range); a substoichiometric fcc dioxide (O:Pu = 1.8–2.0) with variable and larger lattice parameter than the stoichiometric dioxide; and the stoichiometric and hyperstoichiometric dioxide. Like in the lanthanide systems, the intermediate oxides merge into a continuous PuO_{2-x} solid solution above 700°C. Whether the plutonium oxide system actually contains all of these

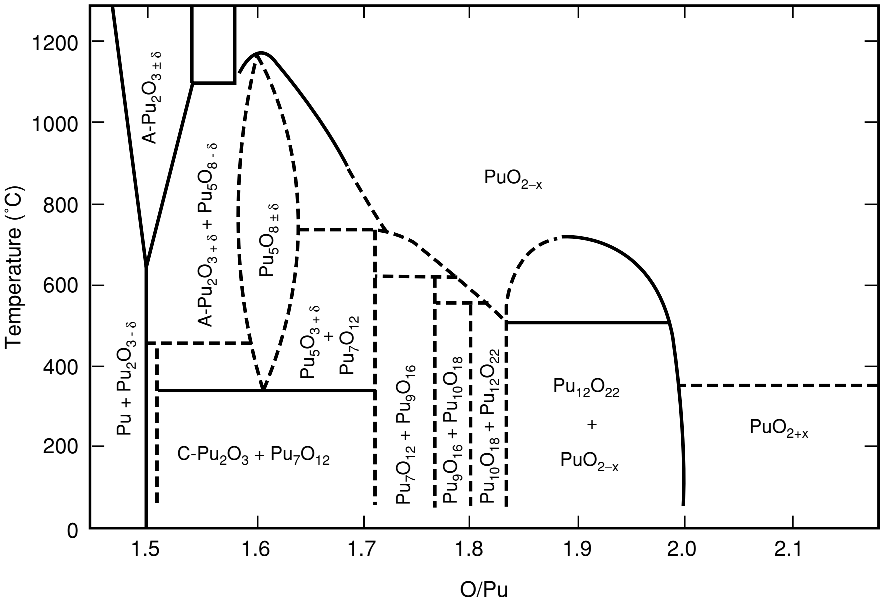

Fig. 7.92 *A pedagogical plutonium–oxygen phase diagram introduced by Hashke and Haire* (2000), *and based upon structural principles established for the more well-studied Ce and Pr oxide systems* (*Haschke* et al., 2000*a*).

features and closely resembles the lanthanide system will require more extensive study.

PuO_{2+x} structural studies

XRD analysis of the products of reaction between PuO_2 and water vapor show a single fcc phase with a fluorite-related structure with an expanded lattice. After reaching a minimum of 5.3975 Å at $PuO_{2.00}$, the lattice parameter increases over a narrow stoichiometry range, consistent with an initial stepwise expansion of the lattice and then a gradual increase with increasing oxygen composition. Results for O:Pu in the 2.016–2.169 range follow Vegard's law, implying that the oxide is a continuous PuO_{2+x} solid solution with a lattice constant given by:

$$a_0 = 5.3643 + 0.01764 \text{ O} : \text{Pu} \tag{7.38}$$

Once the PuO_2 stoichiometry is reached, the lattice parameter is not very sensitive to composition, as shown in Fig. 7.93. Haschke and coworkers proposed that the additional oxygen atoms are accommodated in the vacant octahedral sites in the fluorite lattice, and that charge balance is maintained by replacing Pu(IV) with a higher oxidation state plutonium cation. Initial XPS data were interpreted as being consistent with Pu(VI), but more recent XANES spectroscopy has been interpreted as indicating the presence of Pu(V) (Conradson *et al.*, 2003). Recent EXAFS studies indicate that the original proposal of oxygen atoms in octahedral sites is far too simplistic (Conradson *et al.*, 2004b), and warrants further discussion.

Conradson and coworkers investigated 24 PuO_{2+x} samples prepared by a variety of methods including heterogeneous oxidation of plutonium metal and PuO_2 with gaseous H_2O and/or O_2, and by the hydrolysis and precipitation of the aqueous Pu(IV) ion (Conradson *et al.*, 2003, 2004b). Fourier transforms (FT) of the EXAFS data for selected plutonium oxide compounds are shown in Fig. 7.94. For stoichiometric, ordered $PuO_{2.0}$ the first peak in the Fourier transform is the contribution of the eight nearest neighbor oxygen atoms at 2.33 Å, well separated from the more distant second nearest neighbor peak of 12 plutonium atoms at 3.80 Å (the peaks in Fig. 7.94 are all phase-shifted to lower R). Regular features from the well-ordered extended structure subsequently continue to a very high distance from the central absorbing atom. This spectrum is therefore consistent with the crystal structure of stoichiometric PuO_2 shown in Fig. 7.90a.

However, as x increases from $PuO_{2.00}$ to $PuO_{2.26}$, the amplitudes of all of the peaks in the Fourier transform decrease monotonically, indicative of diminished order via displacements of the plutonium and oxygen atoms from their lattice sites coupled to the incorporation of the nonstoichiometric oxygen atoms into interstitial, essentially defect sites. What contradicts the current models in this process is the splitting of the first oxygen shell in the EXAFS (clearly evident

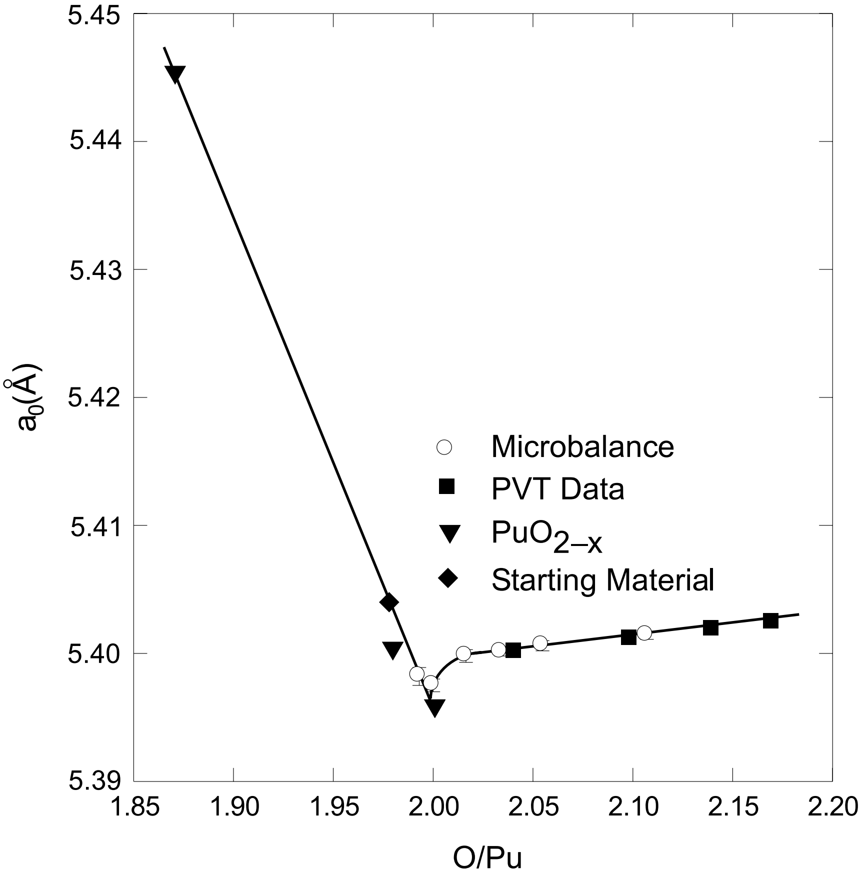

Fig. 7.93 *Variation of the cubic lattice parameter* (a_0) *of* $PuO_{2\pm x}$ *with O:Pu ratio at* 25°C. *Data for* PuO_{2-x} *are shown by gray triangles, microbalance data by open circles, and PVT data by solid squares* (*Haschke* et al., 2000*b*).

in Fig. 7.94) and the appearance of a short Pu–O bond distance of 1.84 Å. Traditional diffraction techniques that probe long-range order have never observed this phenomenon, but the bond distance is similar to the 1.85 Å distance found in axial Pu=O bonds in molecular Pu(v) compounds. Indeed, XANES results were interpreted as being consistent with a mixture of Pu(ɪv) and Pu(v). Combined, these data suggest that as the plutonium center becomes partially oxidized in PuO_{2+x}, there is a strong driving force to form short, strong, covalent Pu=O bonds.

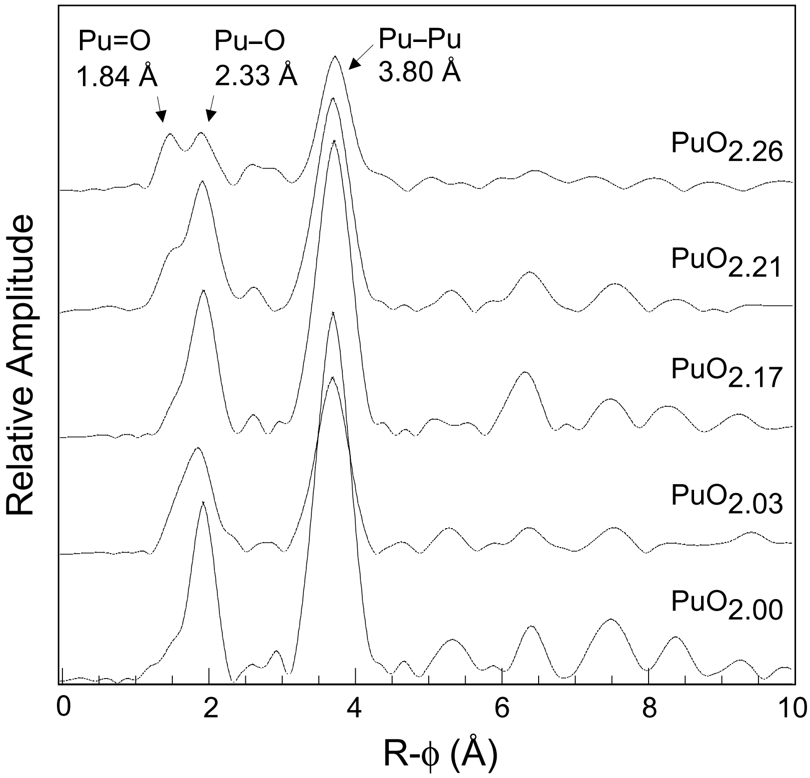

Fig. 7.94 *A comparison of k^3-weighted EXAFS moduli of PuO_{2+x} samples as indicated, and all data are taken from Conradson* et al. (2004*b*). *The peak positions are phase-shifted to lower distance from the actual Pu–O or Pu–Pu distances.*

These data also show that the plutonium atoms retain their essentially fcc positions, and while the plutonium sublattice retains its order through the progression of $PuO_{2.00}$ to $PuO_{2.26}$, the nearest-neighbor oxygen atoms are found in a multisite distribution. In addition to Pu–O distances of 2.33 Å, the additional oxygen atom in PuO_{2+x} generates new bonds both shorter and longer than the 2.33 Å value. These new Pu–O distances were tentatively assigned to bridging O^{2-}/OH^- (2.13, 2.28 Å) and possibly H_2O (2.41 Å) ligands. Based on these observations, Conradson *et al.* suggest that the oxidation produces linear PuO_2^+ moieties that are aperiodically distributed through the lattice, and suggest several structural models that would be consistent with all the observations (Conradson *et al.*, 2004b). Finally, recent XPS results indicate a hydroxylated surface in PuO_{2+x} samples whose thickness depends on exposure conditions (temperature, partial pressure of H_2O) (Paffett *et al.*, 2003a). Much more study in this area is expected in the coming years.

The original report of PuO_{2+x} and its relevance to long-term storage of plutonium through H_2 gas generation has prompted several theoretical studies of this material. To study the electronic structure of PuO_{2+x} with $x = 0.25$, a periodic supercell consisting of four PuO_2 formula units has been used, constituting the conventional fluorite cubic cell of Pu_4O_8 (as shown in Fig. 7.71 for PuH_2). The additional oxygen atom was placed on the octahedral interstitial site, giving rise to a hypothetical Pu_4O_9 compound. Employing a self-interaction correction local spin density method, Petit *et al.* (2003) concluded that stoichiometric PuO_2 displays Pu(IV) with a localized f^4 shell. When oxygen is introduced into the octahedral interstitial site, the nearby plutonium atoms turn into Pu(V) (f^3) by transferring electrons to the oxygen. Oxygen vacancies cause Pu(III) (f^5) to form by taking up electrons released by oxygen (Petit *et al.*, 2003). In another DFT study, Korzhavyi *et al.* (2004) find a similar result, and calculate the thermodynamics for reactions of PuO_2 with either O_2 or H_2O to form PuO_{2+x}. In both cases the reactions are endothermic, i.e. to occur they require a supply of energy. However, the calculations also show that PuO_{2+x} can be formed as an intermediate product by reaction with H_2O radiolysis products such as H_2O_2. While the placement of the interstitial oxygen atom in the octahedral hole of a hypothetical Pu_4O_9 system is not consistent with the experimental findings for PuO_{2+x}, they are consistent with the formation of Pu(V), and offer insights to guide further experimental study.

Penneman and Paffet applied Zachariasen's classic bond strength–bond length relationships (Zachariasen, 1954a,b) to the Pu_4O_9 ($PuO_{2.25}$) entity to suggest that a better description is Pu_4O_8OH containing Pu(V) ions (Penneman and Paffett, 2004, 2005). Bond strength–bond length arguments justify the location of a hydroxide ion, rather than a central oxide ion, in a plutonium dioxide structure, providing an alternative interpretation for the experimental data on plutonium dioxide oxidation by water.

(*iv*) *Properties of plutonium oxides*

Oxygen diffusion

Fluorite-related lanthanide oxides exhibit unusual diffusional properties in that the oxygen substructure (excess interstitial oxygen ions and oxygen vacancies) is mobile below 300°C, which places them in the category of fast-ion conductors (Haire and Eyring, 1994). In actinide oxides of the fluorite structure, interstitial excess oxygen ions and oxygen vacancies are extremely mobile with diffusion rates similar to those of other fluorite-type superionic conductors (Matzke, 1982). Chemical diffusion measurements on PuO_{2-x} reveal relatively high values for diffusion coefficients (Bayoglu and Lorenzelli, 1984), and activation energies in the vicinity of 46 kJ mol^{-1}, which is very close to the migration energy of anion vacancies in UO_{2-x} (49 kJ mol^{-1}) (Chereau and Wadier, 1973; Bayoglu and Lorenzelli, 1979).

For stoichiometric PuO_2, oxygen diffusion has been studied by gas-phase isotope exchange by Bayoglu and coworkers, and by Deaton and Wiedenheft who obtained activation energies of 177 and 187 kJ mol^{-1}, respectively (Deaton and Wiedenheft, 1973; Bayoglu *et al.*, 1983). Murch and Catlow (1987) have suggested that since oxygen interstitials in PuO_2 are almost certainly less mobile than oxygen vacancies, one can assume that the activation energy for oxygen diffusion in stoichiometric PuO_2 can be partitioned into two parts, given by

$$Q = H_F/2 + H_v^m \tag{7.39}$$

where H_v^m is the anion vacancy migration enthalpy and H_F is the enthalpy for anion Frenkel defect formation. With H_v^m given by 46 kJ mol^{-1}, the Frenkel energy is given by 262–282 kJ mol^{-1}.

Melting behavior

The melting behavior of the individual plutonium oxides has been studied by many authors (Holley *et al.*, 1958; Pijanowski and DeLucas, 1960; Chikalla *et al.*, 1962, 1964; Lyon and Baily, 1965, 1967; Chikalla, 1968; Riley, 1970), and has been thoroughly reviewed (IAEA, 1967; Wriedt, 1990; Lemire *et al.*, 2001).

Stoichiometric hexagonal A-Pu_2O_3 ($PuO_{1.50}$) was found to have a melting point of 2085 ± 25°C (Chikalla *et al.*, 1962, 1964), which agrees well with the value of 2075°C reported by Riley (1970). The value of 2080°C was adopted by the IAEA review panel (IAEA, 1967), and by Wriedt (1990) in their reviews.

No melting point can be reported for cubic C-Pu_2O_3 ($PuO_{1.52}$), since this compound undergoes a solid-state peritectoid decomposition to A-Pu_2O_3 ($PuO_{1.5}$) and C′-Pu_2O_3 ($PuO_{1.6+\delta}$) at 450°C (Wriedt, 1990). No melting point for C′-Pu_2O_3 ($PuO_{1.6+\delta}$) can be reported as it transforms congruently to PuO_{2-x} above a temperature of about 1180°C (Wriedt, 1990).

The melting point of PuO_{2-x} depends on the O:Pu ratio. For stoichiometric $PuO_{2.00}$, a number of values have been reported; however, the best values are thought to be those reported by Lyon and Baily (1965, 1967), who found 2390 ± 20°C, or Aitken and Evans (1968) who found a value of 2445°C. These experiments were performed on specimens sealed in tungsten capsules to prevent loss of oxygen. Wriedt (1990) proposed a value of 2445°C, and Adamson *et al.* (1985) recommend the intermediate value of 2428°C.

Vaporization behavior

The plutonium oxide vaporization process is extremely complicated because the solid undergoing vaporization changes its composition during the process. The majority of vapor pressure measurements of plutonium oxides have been carried out by the Knudsen-effusion method (Phipps *et al.*, 1950b; Mulford and Lamar, 1961; Paprocki *et al.*, 1962a; Pardue and Keller, 1964; Ackermann *et al.*, 1966; IAEA, 1967; Capone *et al.*, 1999), with the notable exception of a few mass spectrometry reports (Battles *et al.*, 1968, 1969; Battles and Blackburn, 1969; Kent, 1973). All these data have been reviewed (Wriedt, 1990). The results of these measurements are often conflicting because the condensed oxide phase PuO_{2-x} is at its congruent vaporizing composition, which varies with temperature. When inert containers are used, solid PuO_2 that has a higher O:Pu ratio than the congruent composition will produce vapor with relatively high concentrations of PuO_2(g), O_2(g), and O(g). In contrast, compositions with a lower O:Pu ratio than the congruent composition will produce relatively high concentrations of PuO(g) (Wriedt, 1990). Thus, the early Knudsen measurements yield insufficient information to explain the vaporization behavior of PuO_2 and PuO_{2-x} in detail.

Battles and coworkers (Battles *et al.*, 1968, 1969; Battles and Blackburn, 1969) have determined the species that occur in the vapor of PuO_{2-x} and in the vapor over the binary condensed phase mixture of Pu_2O_3 and $PuO_{1.61}$ over a period of 20 hours. A typical set of data is shown in Fig. 7.95.

In the case of single-phase material, it was found that initially stoichiometric $PuO_{2.00}$ slowly turns into $PuO_{1.831}$ and retains the latter composition. In the vapor, the species PuO_2^+ (g) and PuO^+(g) were observed. At 2219 K the partial pressures of Pu(g) and of O(g) were calculated to be 2.6×10^{-9} and 2.6×10^{-7} atm, respectively. The mass spectrometry results (Battles *et al.*, 1968, 1969; Battles and Blackburn, 1969; Kent, 1973) are in good agreement with those measured by effusion in open containers by Ackermann and coworkers (Ackermann *et al.*, 1966). Partial pressures of O(g), O_2(g), Pu(g), PuO(g) and PuO_2(g) have been tabulated for various PuO_{2-x} compositions and temperatures (Kent and Zocher, 1976; Green *et al.*, 1983).

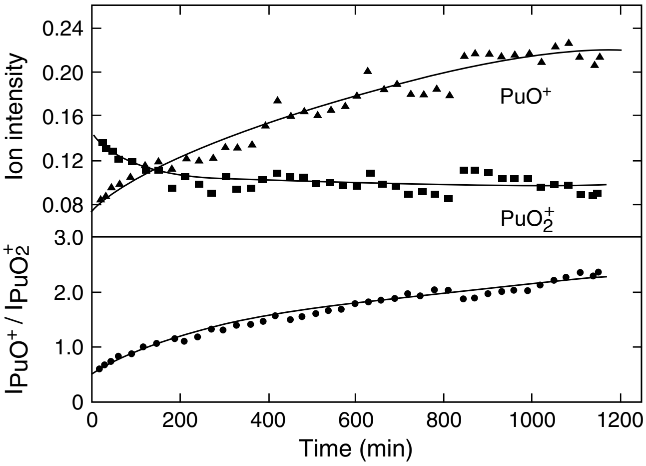

Fig. 7.95 *Mass spectroscopic intensities of gaseous* PuO_2^+ *and* PuO^+, *and the ratio of intensities* $I_{PuO^+}/I_{PuO_2^+}$ *as a function of time at* 2225 K (*Battles* et al., 1968, 1969).

More recently, Krikorian and coworkers suggested that heating PuO_2 in the presence of oxygen produced the PuO_3 molecule in the gas phase (Krikorian *et al.*, 1997), and this was definitively proven by Ronchi and coworkers who used Knudsen-effusion experiments in combination with mass spectrometry to show that PuO_2 exposure to oxygen above 1800–1900°C produces a gas phase molecule PuO_3, along with the expected PuO and PuO_2 gas phase molecules (Ronchi *et al.*, 2000).

Thermodynamic properties of plutonium oxides

The thermodynamic properties of the plutonium oxides have been studied and assessed by numerous authors, and the reader is directed to extensive compilations by Rand (1966), IAEA (1967), Wriedt (1990), and the recent OECD-NEA review of plutonium and neptunium thermodynamics (Lemire et al., 2001). A summary of the most recent OECD-NEA selected thermodynamic data for plutonium oxides is given in Table 7.38.

Stoichiometric Pu_2O_3 ($PuO_{1.5}$) Flotow and Tetenbaum (1981) measured the low-temperature heat capacity from –265 to 77°C on a sample of $^{242}Pu_2O_3$. The heat capacity (C°_p) and entropy (S°) at standard conditions derived from their data were selected by the OECD-NEA reviewers, and are given in Table 7.38 (Lemire *et al.*, 2001). Estimates of the heat capacity of Pu_2O_3 at higher temperatures have been given by IAEA (1967), Glushko (1982), and Besmann and Lindemer (1983). The NEA reviewers recommended the following expressions for heat capacity of Pu_2O_3 over two separate temperature ranges.

(298.15 – 350K)

$$C^\circ_p = 169.466 - 79.98 \times 10^{-3} T - 25.459 \times 10^5 T^{-2} \text{J K}^{-1}\text{mol}^{-1} \quad (7.40)$$

(350 – 2358K)

$$C^\circ_p = 122.953 + 28.548 \times 10^{-3} T - 15.012 \times 10^5 T^{-2} \text{J K}^{-1}\text{mol}^{-1} \quad (7.41)$$

There are no direct measurements of the enthalpy of formation of Pu_2O_3. The value has been derived indirectly from the partial molar Gibbs energies and enthalpies of oxygen in the single-phase oxides Pu_2O_3 and PuO_2, and the two-phase fields between these phases. A thorough discussion of the data and measurement techniques is available in the most recent reviews (IAEA, 1967;

Table 7.38 *Thermodynamic parameters for plutonium oxides* (*Lemire* et al., 2001).

Compound	$\Delta_f G^\circ_{298}$ (kJ mol^{-1})	$\Delta_f H^\circ_{298}$ (kJ mol^{-1})	S°_{298} (J K^{-1} mol^{-1})	C°_{p298} (J K^{-1} mol^{-1})
Pu_2O_3	−1580.4 ± 10.1	−1656.0 ± 10.0	163.0 ± 0.6	117.0 ± 0.5
$PuO_{1.61}$	−834.8 ± 10.1	−875.5 ± 10.0	83.0 ± 5.0	61.2 ± 5.0
PuO_2	−998.1 ± 1.0	−1055.8 ± 1.0	66.13 ± 0.26	66.25 ± 0.26

Wriedt, 1990; Lemire *et al.*, 2001). The recommended values for the enthalpy and Gibbs energy of formation are listed in Table 7.38.

Hyperstoichiometric $PuO_{1.52}$ (*C*-Pu_2O_3) The only thermodynamic data for this phase are the enthalpies of combustion reported by Chereau *et al.* (1977). Their values correspond to an enthalpy of formation of –845 kJ mol^{-1} (Lemire *et al.*, 2001).

Hyperstoichiometric $PuO_{1.6+\delta}$ No experimental data are available. Thermodynamic functions were estimated by NEA reviewers (Lemire *et al.*, 2001).

Stoichiometric $PuO_{2.00}$ The thermodynamic properties of stoichiometric $PuO_{2.00}$ have been the subject of a large number of studies (Sandenaw, 1963; Pardue and Keller, 1964; Ackermann *et al.*, 1966; Rand, 1966; Kruger and Savage, 1968; Engel, 1969; Ogard, 1970; Flotow *et al.*, 1976), and have been extensively reviewed (IAEA, 1967; Cordfunke *et al.*, 1990; Wriedt, 1990; Carbajo *et al.*, 2001; Lemire *et al.*, 2001).

To overcome difficulties performing low-temperature heat capacity measurements on $^{239}PuO_2$, Flotow *et al.* (1976) performed studies with the less radio active isotopes $^{242}PuO_2$ and $^{244}PuO_2$ to avoid problems associated with radiation damage of the solid for low temperatures up to 350 K. These measurements are thought to provide the most reliable values for standard heat capacity (C_p°) and entropy (S°). Their values were selected by the NEA review, and are listed in Table 7.38. High-temperature measurements of enthalpy were measured by Kruger and Savage (1968), Engel (1969), Ogard (1970), and Oetting (1982). Fink (1982) used these data to derive a complex expression for heat capacity, and these were refit to polynomials by Cordfunke *et al.* (1990). The Fink expressions were recently modified by the NEA review to give the following polynomial expression over the temperature range 298.15–2500 K (Lemire *et al.*, 2001):

$$\begin{aligned} C_p^\circ = {} & 84.495 + 10.639 \times 10^{-3} T - 6.1136 \times 10^5 T^2 \\ & - 19.00564 \times 10^5 T^{-2} \text{J K}^{-1}\text{mol}^{-1} \end{aligned} \tag{7.42}$$

The original polynomial functions derived by Fink are far more complex than the NEA modification, and for more information the reader is referred to the original Fink citation (Fink, 1982) or a recent review by Carbajo *et al.* (2001).

There is good agreement between authors on the values for the enthalpy and Gibbs free energy (Holley *et al.*, 1958; Glushko, 1982). The values accepted by the NEA review are given in Table 7.38 (Lemire *et al.*, 2001).

Chemical properties of plutonium oxides

Dissolution of PuO_2 PuO_2 that has been ignited at high temperatures is difficult to dissolve. Christensen and Maraman (1969), Gilman (1965, 1968), Ryan and Bray (1980), and Nikitina *et al.* (1997a,b), have reviewed the methods reported. In general, the rate of dissolution for each reagent often depends on the ignition temperature used to prepare the oxide and on the previous history of the sample. The reagent most frequently used is a boiling mixture of 16 M HNO_3 with 1 M HF as a fluoride complexant. Instead of HF, H_2SiF_6, or Na_2SiF_6 may also be used. High-temperature fired PuO_2 is dissolved only slowly. Irradiated PuO_2 dissolves better, the rate of dissolution being higher, the higher the burnup.

The difficulty in dissolving PuO_2 has led to the search for aggressive approaches to achieve dissolution, such as the use of fused salts (Harvey *et al.*, 1947; Feldman, 1960; Crocker, 1961), dioxygen difluoride, O_2F_2 (Malm *et al.*, 1984), or krypton difluoride, KrF_2 (Asprey *et al.*, 1986). Dioxygen difluoride, and krypton difluoride react readily with PuO_2 to form PuF_6 and/or PuO_2F_2, but this approach has not been pursued on a large scale because of the extreme difficulty in handling KrF_2 and O_2F_2. Two major improvements to the dissolution of PuO_2 have recently appeared. They are based on the electrochemical oxidative dissolution in HNO_3 with Ag(II) as a catalyst (Bourges *et al.*, 1986; Sakurai *et al.*, 1989, 1993; Madic *et al.*, 1992), and oxidative dissolution catalyzed by Ce(IV) in the presence of anions of oxygen-containing acids of group IV–VII elements (Horner *et al.*, 1977; Scheitlin and Bond, 1980). The kinetics and mechanism of these processes and their use for dissolving plutonium from recycled products and wastes have been reviewed (Nikitina *et al.*, 1997a).

Compatibility with Container Materials Because of its importance as a nuclear reactor and heat source fuel, the compatibility of PuO_2 with refractory materials (both metals and ceramics) has been extensively studied. Paprocki *et al.* (1962b) studied the chemical reactions of plutonium dioxide with reactor materials.

An extensive study of the compatibility of $^{238}PuO_2$ with container materials has been reported by Selle *et al.* (1970a,b). They studied the reactions of $^{238}PuO_2$ with container materials such as tantalum, molybdenum, tungsten, rhenium, platinum, rhodium, and their alloys in the temperature range 1000–2500°C and for time periods up to 532 days. For the results, the reader is referred to the comprehensive original reports. Such studies have led to the use of iridium–0.3% tungsten alloys for encapsulation of $^{238}PuO_2$ general-purpose heat sources, and Pt–30%Rh alloys for encapsulation of $^{238}PuO_2$ light weight radioisotope heater units (see Section 7.3).

(b) The plutonium–sulfur, -selenium, and -tellurium systems

With heavier chalcogen elements (X = S, Se, and Te), plutonium forms binary compounds in four basic families (Table 7.39) with the highest-order composition being PuX_3 that is only found for tellurium. All the heavy chalcogen

Table 7.39 *Crystallographic properties of binary plutonium chalcogenides.*

Compound	*Symmetry*	*Space group*	*Lattice parameters*			*Density* (g cm^{-3})	*References*
			a_0 (Å)	b_0 (Å)	c_0 (Å)		
PuX							
$PuS_{0.95}$	fcc	$\mathrm{F}m3m$	5.5280(5)				Marcon (1969)
PuS	fcc	$\mathrm{F}m3m$	5.5400(5)			10.60	Marcon (1969)
PuS	fcc	$\mathrm{F}m3m$	5.5437(3)				Wastin *et al*. (1995)
PuSe	fcc	$\mathrm{F}m3m$	5.79334(1)			10.86	Kruger and Moser (1967a)
PuSe	fcc	$\mathrm{F}m3m$	5.7992(5)				Wastin *et al*. (1995)
PuSe	fcc	$\mathrm{F}m3m$	5.773(3)				Damien (1976)
PuSe	fcc	$\mathrm{F}m3m$	5.776(1)				Marcon (1969)
PuTe	fcc	$\mathrm{F}m3m$	6.183(4)			10.32	Gorum (1957)
PuTe	fcc	$\mathrm{F}m3m$	6.151(3)				Allbutt *et al*. (1970)
PuTe	fcc	$\mathrm{F}m3m$	6.1900(6)				Wastin *et al*. (1995)
Pu_2X_3							
Pu_3S_4	bcc	$\mathrm{I}\bar{4}3d$	8.395			9.41	Damien (1976)
γ-Pu_3S_{4+x}	bcc	$\mathrm{I}\bar{4}3d$	8.4155(5)			8.53	Marcon (1969)
γ-Pu_3S_{3-x}	bcc	$\mathrm{I}\bar{4}3d$	8.4590(5)			8.41	Marcon (1969)
α-Pu_2S_3	orthorhombic	$\mathrm{P}nmm$	3.97(1)	7.37(2)	15.45(3)	8.31	Marcon (1969)
γ-Pu_2S_3	bcc	$\mathrm{I}\bar{4}3d$	8.4585				Damien (1976)
γ-Pu_2Se_3	bcc	$\mathrm{I}\bar{4}3d$	8.7965(5)				Marcon (1969)

γ-Pu_2Se_3	bcc	$I\bar{4}3d$	8.802				Damien (1976)
Pu_3Se_4	bcc	$I\bar{4}3d$	8.768				Damien (1976)
η-Pu_2Se_3	orthorhombic	P*bnm*	4.10(1)	11.10(2)	11.32(2)		Marcon (1969)
γ-Pu_2Te_3	bcc	$I\bar{4}3d$	9.355				Damien (1976)
η-Pu_2Te_3	orthorhombic	P*bnm*	11.94(2)	12.10(2)	4.339(6)		Damien (1976)
PuX_{2-x}							
$PuS_{1.76}$	tetragonal	P4/*nmm*	3.936		7.958		Allbutt and Dell (1967) and Damien (1976)
$PuS_{1.9}$	tetragonal	P4/*nmm*	3.943(3)		7.962(5)		Marcon (1969)
$PuS_{2.0}$	monoclinic	$P2_1/a$	7.962(10)	3.981(5)	7.962(10)		Marcon (1969)
$PuS_{2.0}$	tetragonal	P4/*nmm*	3.974		7.947	8.0	Allbutt and Dell (1967)
$PuSe_{1.8}$	tetragonal	P4/*nmm*	4.100(5)		8.364(5)		Marcon (1969)
$PuSe_{1.814}$	tetragonal	P4/*nmm*	4.088		8.539		Allbutt and Dell (1967) and Damien (1976)
$PuSe_{1.9}$	tetragonal	P4/*nmm*	4.165		8.41(1)		Marcon (1969)
$PuSe_{1.987}$	tetragonal	P4/*nmm*	4.132		8.343		Allbutt and Dell (1967) and Damien (1976)
$PuTe_{1.81}$	tetragonal	P4/*nmm*	4.334		8.984		Damien (1976)
$PuTe_{2.02}$	tetragonal	P4/*nmm*	4.391		8.938		Damien (1976)
PuX_3							
$PuTe_3$	pseudo-tetragonal	B*mmb*	4.338(5) 6.151(3)	4.338(5)	25.60(9)		Damien (1973) Damien (1976)

elements form the series of substoichiometric complexes PuX_{2-x}. For the sesquichalcogenides of formula Pu_2X_3, sulfur forms an α-phase, all the chalcogenides form a γ-phase, while selenium and tellurium form an η-phase. All the heavier chalcogenides form the simple binary PuX.

(*i*) *Preparation*

All of the heavier chalcogenide compounds of plutonium can be prepared by gas–solid reaction between the appropriate stoichiometry of plutonium hydride (PuH_x) and chalcogen element in quartz tubes sealed under secondary vacuum (Damien, 1973, 1976; Damien and De Novion, 1981; Damien *et al.*, 1986). After a typical reaction time of 1 week at 350–750°C, the dichalcogenide, PuX_{2-x} is formed. Compounds with lower X/Pu ratio can be prepared by thermal decomposition of PuX_{2-x} in a sealed tube where one end is kept outside the furnace to allow for the deposition of the chalcogen element. The monochalcogenide, PuX requires much-higher temperature for formation. Typically the quartz tube is heated to 800°C, and the products are pressed into pellets and sintered at 1200–1600°C. This approach works for all the chalcogenide elements except tellurium. Reaction of plutonium hydride with excess tellurium under high vacuum at 350°C for 1 week produces $PuTe_3$ (Damien, 1973). The plutonium tritelluride undergoes decomposition in a stepwise fashion to produce $PuTe_{2-x}$ at 400°C, η-Pu_2Te_3 at 700°C, and γ-Pu_2Te_3 at 900°C (Allbutt *et al.*, 1970; Damien, 1973).

In addition to preparation using plutonium hydride, all the plutonium chalcogenides (sulfur, selenium, tellurium) may be prepared by direct synthesis from the elements (Gorum, 1957; Marcon and Pascard, 1966a,b; Kruger and Moser, 1967a; Marcon, 1969; Wastin *et al.*, 1995). For volatile compounds, the reactions may be carried out in two- or three-zone vacuum-sealed quartz tubes that are placed in a temperature gradient resistance furnace (Spirlet, 1982; Spirlet and Vogt, 1982). The product stoichiometry and phase is controlled by the reaction temperature and stoichiometry of reactants. For compounds that are not highly volatile, excellent results have been obtained when using levitation melting in an induction coil or in a Hukin magnetic levitation cold crucible, by semilevitation melting on a pedestal, or by arc melting (Wastin *et al.*, 1995).

There are other methods for preparation of a few specific plutonium chalcogenide. In the early work of Abraham *et al.* (1949b), PuS was accidentally obtained when PuF_3 was reduced with Ca vapor in a BaS crucible at 1250°C. High-purity PuS may also be obtained when compact plutonium metal is first reacted to give the hydride, the hydride is ground to powder in an inert-gas atmosphere, and, after decomposition to the metal, is reacted with H_2S. A similar reaction of the plutonium hydride with H_2S may also be used to prepare α-Pu_2S_3. Finally, PuSe can be obtained by reacting a higher selenide with plutonium metal (Marcon, 1969).

(*ii*) *Solid-state structures*

Crystallographic properties of binary plutonium chalcogenides are summarized in Table 7.39.

Plutonium tritelluride crystallizes in the orthorhombic $NdTe_3$ structure type (Norling and Steinfink, 1966; Damien, 1973). In this structure, the unit cell contains 12 planar layers each consisting of a single type of atom. Since the separation between the plutonium and tellurium layers is about 0.9 Å, the two layers can be considered as a single puckered layer. In this way, the structure can be described as consisting of four puckered Pu–Te layers and four densely packed tellurium layers. Each plutonium atom is surrounded by nine near-neighbor tellurium atoms, and the $PuTe_9$ coordination polyhedron approximates a capped square antiprism with a distortion of the plutonium atom out of the center of the tellurium prism, as depicted in Fig. 7.96.

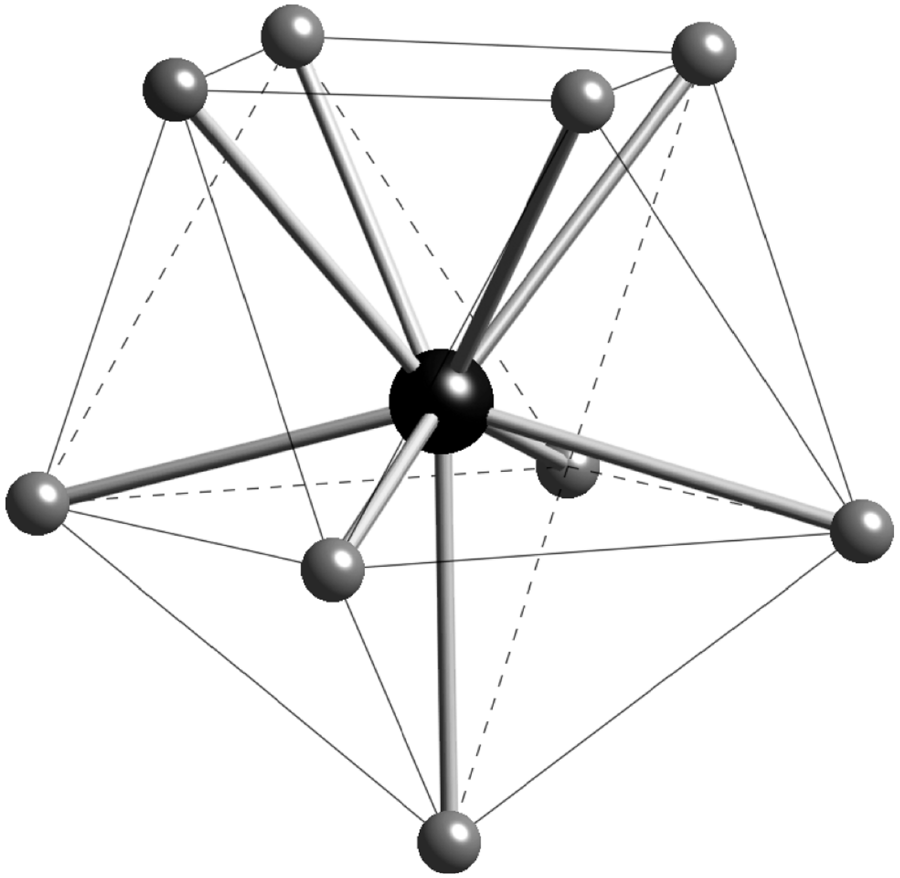

Fig. 7.96 *Local coordination sphere around plutonium in* $PuTe_3$ *and* PuX_2*. The plutonium atom is black and tellurium atoms are gray.*

The ideal structure of plutonium dichalcogenides, PuX_2 is the anti-Fe_2As in space group *P*4/*nmm* ($Z = 2$) (Damien *et al.*, 1986). In this structure, layers of five chalcogen atoms in the basal face-centered square plane are separated by two slabs of alternating Pu^{3+} (nine-fold coordination) and X^{2-} ions. The local PuX_9 coordination polyhedron is identical to that seen in $PuTe_3$, depicted in Fig. 7.96. All the PuX_{2-x} compounds are distorted from this idealized structure due to the formation of X–X bonding pairs within the basal planes. A typical structure is shown in Fig. 7.97. This distortion gives rise to a number of pseudo-cubic, tetragonal, orthorhombic, and monoclinic ($\beta = 90°$) anti-Fe_2As superstructures (Flahaut, 1979; Rolland *et al.*, 1994). From Table 7.39, it can be seen that all PuX_{2-x} ($X =$ S, Se, and Te) compounds display the pseudo-tetragonal cell of the anti-Fe_2As structure, with the exception of PuS_2, which displays the monoclinic ($\beta = 90°$) $CeSe_2$ variant of the structure (Marcon and Pascard, 1968).

The sesquichalcogenides of plutonium are isostructural with the rare-earth analogs (Damien *et al.*, 1986). The low-temperature stoichiometric phase,

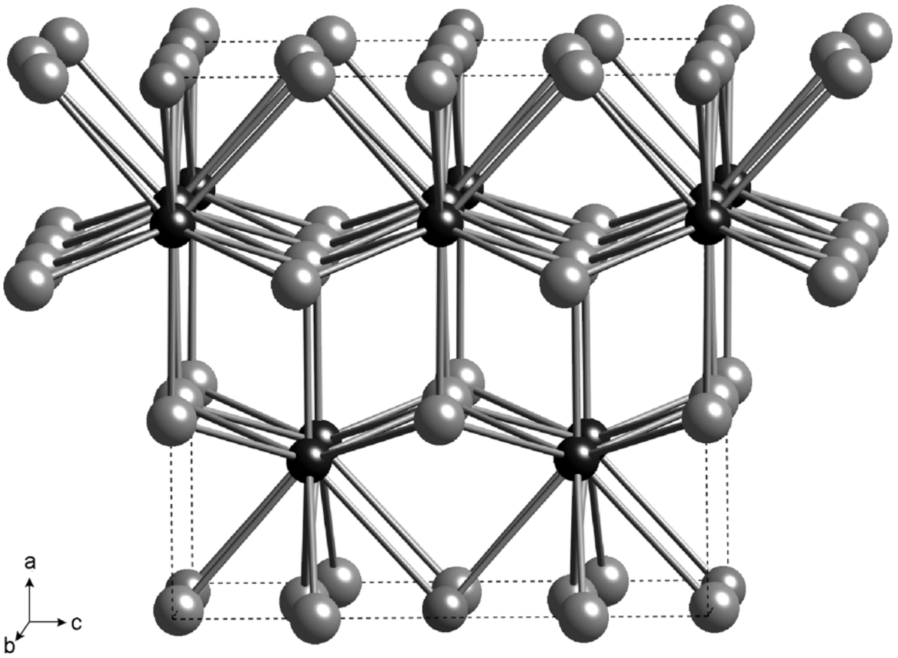

Fig. 7.97 *Solid-state crystal structure of plutonium dichalcogenides,* PuX_2*, emphasizing the local* PuX_9 *coordination. The X–X bonding pairs are not indicated for clarity. The distortions in the chalcogen layers due to X–X bonding are clearly evident in this model, based on monoclinic* $LaTe_2$ (*Stöwe,* 2000). *Plutonium atoms are black and chalcogen atoms are gray.*

referred to as α-Pu_2X_3 only exists for the sulfide, and has the orthorhombic La_2S_3-type structure, with two plutonium sites displaying local PuS_7 and PuS_8 coordination. The high-temperature γ-Pu_2X_3 phase is not a stoichiometric phase, and exists over a range of compositions varying from Pu_2X_3 to Pu_3X_4. This phase displays the cubic Th_3P_4 structure, where the coordination number of the plutonium atom is eight. For selenium and tellurium, there is a η-Pu_2X_3 phase that displays the orthorhombic U_2S_3 structure. The η-Pu_2Se_3 is thermally unstable and transform near 800°C into the cubic γ-Pu_2Se_3 of the Th_3P_4 structure. Early reports of a β-phase for Pu_2S_3 have been shown to be incorrect, as the material is now known to be a ternary oxychalcogenide (Carre *et al.*, 1970). All monochalcogenides of plutonium (PuX) have the cubic NaCl crystal structure.

(*iii*) *Properties*

The monochalcogenides have a metallic luster that can be described as gold, copper, and black for the sulfide, selenide, and telluride, respectively. The monochalcogenides have been the subject of extensive study directed towards understanding valency and the itinerant or localized nature of their 5f electrons. Several excellent overviews are available (Rossat-Mignod *et al.*, 1984; Buyers and Holden, 1985; Dunlap and Kalvius, 1985; Fournier and Troc, 1985; Santini *et al.*, 1999; Wachter, 2003).

Single crystal samples of PuX have been examined by neutron scattering, magnetic susceptibility, and electrical resistivity. All of the PuX compounds ($X = S, Se, Te$) are nonmagnetic with magnetic susceptibilities that are almost temperature independent for temperatures above 50 K (Lander *et al.*, 1987). Electrical resistivity increases continuously from room temperature with two changes of thermal behavior around 200 and 30 K, confirming the hypothesis that the PuX compounds are semiconductors with small energy gaps. Fournier *et al.* (1990) suggest that the ground state of the monochalcogenides is a weak magnetic nonconducting $6d^1$–$5f^5$ Kondo state with a high Kondo temperature of ca. 400 K.

Wachter and coworkers proposed that these properties of PuX compounds can be consistently explained by the assumption that the plutonium chalcogenides are related to the high-pressure intermediate-valent form of the isoelectronic samarium chalcogenides. Pressure in the divalent SmX serves to enhance f–d hybridization to achieve an intermediate valence state, whereas in PuX, f–d hybridization is achieved without pressure because of the larger radial extension of the 5f wave functions relative to the 4f wave functions. Using PuTe as an example, they conclude that SmTe achieves the same state under a pressure of 58 kbars, and achieves an intermediate valence of 2.75 (Wachter *et al.*, 1991). The intermediate valence model is supported by experimental measurement of elastic constants and observation of a negative value for c_{12} (–39 GPa) (Mendik *et al.*, 1993; Wachter *et al.*, 2001). Photoemission measurements on PuSe films

(Gouder *et al.*, 2000) were interpreted as a 5f localization and not an intermediate valent configuration where 5f and 6d states hybridize. Wachter suggested that the existence of a strong Pauli paramagnetism gives a high DOS near the Fermi level, complicating the interpretation. Recent photoemission studies on PuTe single crystals confirm the presence of a strong three-peak structure near the Fermi level in agreement with of an intermediate valence state in PuTe (Durakiewicz *et al.*, 2004).

(c) Ternary and polynary plutonium chalcogenides

A large number of ternary and polynary plutonium/metal chalcogenides have been described in the literature. The majority of these compounds are ternary and quaternary oxide phases, some of which have gained technological importance. The term 'ternary oxide phases' in this context includes two general classes of material. The first are oxoplutonate compounds with PuO_x^{n-} polyhedral anions and mono-, di-, or trivalent metal cations. A typical example would be Ba_3PuO_6. The second general class are oxometallate compounds with MO_x^{n-} polyhedral anions of main group or transition metal elements in which the plutonium serves as the tri- or tetravalent counter cation. A typical example of this class of compound would be $PuCrO_3$.

Ternary and polynary sulfides, selenides, and tellurides are few, generally not well characterized and will not be discussed.

(*i*) *Preparation of alkali metal oxoplutonates*

When plutonium dioxide and alkali metal oxides, hydroxides, peroxides, or carbonates are intimately mixed and heated in a stream of oxygen, inert gas, or vacuum, they react to form ternary oxide phases in which the plutonium is the central atom of an oxoplutonate anion $\left(PuO_x^{n-}\right)$ and may assume any of the oxidation states from IV to VII. Alkali metal oxoplutonates have been prepared with all the alkali metals with the exception of francium.

Pu(IV). The only alkali oxoplutonate(IV) known at the time of writing is greenish brown Li_8PuO_6, which is obtained by heating a Li_2O–PuO_2 mixture (4.2:1) in a sealed evacuated tube at 600°C (Keller *et al.*, 1965b).

Pu(V). For pentavalent plutonium, Li_7PuO_6, Li_3PuO_4, and Na_3PuO_4 have been reported. These compounds may be obtained by reaction of Li_2O or Na_2O with PuO_2 in an oxidizing atmosphere for 8 h at 700–900°C, respectively. Li_3PuO_4 may be prepared by heating a 3:1 mixture of $LiOH \cdot H_2O$ and PuO_2 in an oxygen stream at 900°C for 24 h (Yamashita *et al.*, 1992). M_3PuO_4 compounds are also reportedly obtained by thermal decomposition of hexavalent M_6PuO_6 for 4 h in an argon atmosphere to give the M_3PuO_4 product and PuO_2 (1100°C, M = Li; 1000°C, M = Na) (Keller, 1964). Brownish-green Li_7PuO_6 was prepared by reacting Li_3PuO_4 with two equivalents of Li_2O at 600°C for 6 h in an evacuated quartz tube (Koch, 1964).

Pu(VI). For hexavalent plutonium, M_6PuO_6, M_4PuO_5, (M = Li, Na), and M_2PuO_4 (M = K, Rb, Cs) compounds have been prepared. These compounds may be either dark green (M_6PuO_6) or brown (M_4PuO_5 and M_2PuO_4). The compounds M_4PuO_5 and M_6PuO_6 dissolve in dilute acids to form yellow-brown or yellow-green aqueous solutions (respectively) and show characteristic Pu(VI) absorption spectra (Koch, 1964).

Li_6PuO_6 is obtained by heating a 3:1 mixture of Li_2O and PuO_2 at 400–500°C in an oxygen atmosphere. If a 2:1 mixture is used, Li_4PuO_5 is formed. When Li_4PuO_5 is heated at 900–1000°C, Li_3PuO_4 is formed. Li_4PuO_5 may also be prepared by heating a 4:1 mixture of $LiOH \cdot H_2O$ and PuO_2 under an oxygen stream at 600°C for 24 h (Yamashita *et al.*, 1992).

Heating a 2:1 mixture of Na_2O and PuO_2 in an oxygen atmosphere at 400°C results in the formation of cubic α-Na_4PuO_5, which may be converted to tetragonal β-Na_4PuO_5 by raising the temperature to 500°C. At 900°C, β-Na_4PuO_5 decomposes to Na_3PuO_4. When a 3:1 mixture of Na_2O and PuO_2 is used, α-Na_4PuO_5 is produced at 400°C; and Na_6PuO_6 is produced at 500°C. Upon heating Na_6PuO_6 to 750°C, it is converted to β-Na_4PuO_5 (Koch, 1964; Keller *et al.*, 1965a).

The M_2PuO_4 class of compounds (M = K, Rb, Cs) may be conveniently prepared by reaction of a 2:1 mixture of MOH with PuO_2 in gold crucibles under an oxygen atmosphere, and heated to at least 450°C (Hoekstra and Gebert, 1977). These compounds decompose in air above 650°C. The rubidium and cesium analogs may also be prepared by heating the corresponding oxoplutonates (VII), M_3PuO_5 to temperatures above 320°C (Pagès *et al.*, 1971a,b).

Pu(VII). For heptavalent plutonium, M_5PuO_6 (M = Li, Na) and M_3PuO_5 (M = Rb, Cs) have been reported. Greenish-black Li_5PuO_6 is formed when a 3:1 mixture of Li_2O and PuO_2 is heated in a stream of oxygen at 430°C (Keller and Seiffert, 1969). The corresponding sodium compound, Na_5PuO_6, has not yet been isolated in the pure state. However, the reaction product of Na_2O_2 and PuO_2 in O_2 atmosphere at 400°C, yields a green aqueous solution upon dissolution in dilute aqueous hydroxide, which shows the characteristic absorption spectrum of Pu(VII) (Keller and Seiffert, 1969).

The black compounds M_3PuO_5 (M = Rb, Cs) have been obtained by heating 3:1 mixtures of the corresponding superoxide MO_2 with PuO_2 at 250°C for more than 6 h. These compounds are reportedly less sensitive to air than the corresponding Np compounds, but have a lower thermal stability. At 320°C, they reportedly decompose to M_2PuO_4 and M_2O_2 (Pagès *et al.*, 1971a,b).

(*ii*) *Preparation of ternary and quaternary alkaline-earth oxoplutonates*

The oxoplutonates of the alkaline-earth elements can be prepared in a manner similar to the alkali-metal oxoplutonates. The alkaline-earth oxides, peroxides or carbonates react with PuO_2 to form alkaline-earth oxoplutonates, in which the plutonium may occur in oxidation states III, IV, V, VI, and VII.

Pu(III). The only alkaline-earth oxoplutonate(III) that has been reported is $BaPu_2O_4$, which is formed by reacting a 1:3:2 mixture of BaO, elemental Pu and PuO_2 (Keller, 1962). An intimate mixture of Pu, PuO_2, and BaO is first heated in a stream of hydrogen to convert plutonium metal to hydride (PuH_x). The resulting mixture of PuH_x, PuO_2, and BaO is powdered in an inert-gas atmosphere and then heated in a stream of argon at 600°C for 2 h and at 1200°C for 8 h. At 600°C, the plutonium hydride decomposes, and the resulting finely divided metal reacts with PuO_2 to give Pu_2O_3. The Pu_2O_3 in turn reacts with BaO to form $BaPu_2O_4$, which may be isostructural with the lanthanide compounds $BaPr_2O_4$ and $BaNd_2O_4$ (Keller, 1962). No lattice constants of $BaPu_2O_4$ have been reported.

Pu(IV). Discrete alkaline-earth oxoplutonates(IV) can be prepared with the heavy alkaline-earth elements strontium and barium but not for the lighter alkaline-earth elements beryllium and magnesium. Beryllium and magnesium oxides react with PuO_2 to form solid solutions rather than stoichiometric compounds. The mutual solubilities of $MO–PuO_2$ systems (M = Be, Mg) have been determined by Hough and Marples (1965) and by Carroll (1964). With the heavier alkaline-earth elements, heating stoichiometric mixtures of MO (M = Sr, Ba) with PuO_2 gives $MPuO_3$ (Chackraburtty *et al.*, 1963; Chackraburtty and Jayadevan, 1964). Chackraburtty and coworkers have recommended the use of excess alkaline-earth oxide (3:1 mixtures) to ensure complete conversion of PuO_2 to oxoplutonate. The excess alkaline-earth oxide may be subsequently removed by extraction with methanol (Russell *et al.*, 1960; Keller, 1962, 1964; Chackraburtty and Jayadevan, 1964). $BaPuO_3$ has also been prepared by ball-milling a stoichiometric mixture of $BaCO_3$ and PuO_2, followed by heating under argon at 1197°C for 24 h (Christoph *et al.*, 1988). $SrPuO_3$ and $BaPuO_3$ can also be prepared by reduction of Sr_3PuO_6 or Ba_3PuO_6 in a stream of hydrogen at 1600–1800°C.

Pu(V). Deep black $Ba_3PuO_{5.5}$ is obtained by reacting a mixture of Ba_3PuO_6, PuO_2, and BaO in a stream of argon at 1100–1200°C. It is uncertain whether this compound contains Pu(V) or a mixture of Pu(IV) and Pu(VI) (Keller, 1962, 1964). There are a few quaternary compounds of general formula Ba_2MPuO_6, where M is a trivalent metal ion (M = La, Nd, In). These compounds are prepared by heating a 4:1:1:1 mixture of PuO_2, $PuO_2(NO_3)_2{\cdot}nH_2O$, M_2O_3, and BaO_2 in a platinum crucible at 750–950°C for 8–10 h (Awasthi *et al.*, 1968).

Pu(VI). For hexavalent plutonium, there are ternary alkaline-earth oxoplutonates (VI) of formula $MPuO_4$ and M_3PuO_6 (M = Ca, Sr, Ba) and quaternary compounds of general formula Ba_2MPuO_6, where M is a divalent metal ion (M = Sr, Mn, Pb, Mg, Ca). It is uncertain whether the manganese compound, Ba_2MnPuO_6, contains Mn(II)/Pu(VI) or Mn(III)/Pu(V).

M_3PuO_6 compounds have been prepared by heating 3:1 to 5:1 mixtures of MO (M = Ca, Sr, Ba) with PuO_2 in a stream of oxygen at 950–1050°C

(M = Ca) (Chackraburtty *et al.*, 1963; Awasthi *et al.*, 1968), 900–1200°C (M = Sr), or 800–1300°C (M = Ba) (Keller, 1962, 1964). Sr_3PuO_6 and Ba_3PuO_6 form solid solutions, which range in composition from Ba_3PuO_6 to $Ba_{0.75}Sr_{2.25}PuO_6$.

The reaction of a 1:1 mixture of SrO and PuO_2 in an oxidizing atmosphere at 900–1000°C yields $SrPuO_4$ (Keller, 1962, 1964). $BaPuO_4$ appears to be produced by shaking Ba_3PuO_6 with excess, CO_2-free water for 15–30 min. BaO dissolves and leaves $BaPuO_4$ as the residue (Keller, 1962, 1964).

Pu(VII). Alkaline-earth oxoplutonates(VII) have not yet been prepared by solid-state reactions at elevated temperatures, as has been done with alkali oxoplutonates (VII). However, the compound $Ba_3(PuO_5)_2 \cdot xH_2O$ was obtained by precipitation with $Ba(OH)_2$ from aqueous solutions of Pu(VII) (Komkov *et al.*, 1968).

(*iii*) *Solid-state structures*

Characterization of most alkali and alkaline-earth oxoplutonates are limited to X-ray powder diffraction data. These data have been summarized in Table 7.40. All of the oxoplutonate compounds contain PuO_6^{n-} polyhedra that are octahedral with six equidistant Pu–O bonds, or tetragonally distorted with two short (plutonyl-like) and four long, or four short and two long Pu–O bonds. Representative examples of these structure types will be discussed.

Perovskites – $MPuO_3$

Plutonium (and other light actinides) form an extensive class of complex oxides that are related to the perovskite ($CaTiO_3$) structure in which Pu(IV), Pu(VI), or Pu(VII) ions exist in octahedral PuO_6^{n-} coordination. General structural classifications of perovskites have been discussed (Galasso, 1968; Wells, 1984; Zhou and Goodenough, 2005). The idealized ABO_3 perovskite structure consists of a simple cubic lattice with apex-shared, BO_6 octahedra with large A cations at the center of the unit cell, bonded to 12 oxygen atoms situated at the centers of the cell edges. In this ideal ABO_3 structure, all atomic positions are fixed by symmetry and the packing is very dense. In most perovskites, the actual unit cell symmetry is lower than cubic, which can be accomplished by rotation of the BO_6 octahedra allowing a lengthening of the B–O bonds and lowering the effective A-site coordination number (typically to eight).

Through rotation of a BO_6 unit, the perovskite structure can accommodate a large range of A:B:O radius ratios. Barium plutonate ($BaPuO_3$) is an excellent example of how a 5f element is accommodated into this important structure type. The structure of $BaPuO_3$ had been somewhat controversial, the cell symmetry being reported variously as cubic or orthorhombic (Russell *et al.*, 1960; Keller, 1962; Chackraburtty *et al.*, 1963; Christoph *et al.*, 1988). Christoph and coworkers utilized Zachariasen's bond-length–bond-strength relationships to predict that in the structure of $BaPuO_3$ the PuO_6 octahedra

Table 7.40 *Crystallographic data of alkali and alkaline-earth oxoplutonates.*

Compound	*Symmetry*	*Space group*	*Lattice constants* a_0 (Å)	b_0 (Å)	c_0 (Å)	*Density* (g cm^{-1})	*References*
Pu(IV)							
α-$BaPuO_3$	cubic	F*m*3*m*	4.357(7)			8.34	Keller (1962)
α-$BaPuO_3$	cubic	F*m*3*m*	4.373(3)				Chackraburtty *et al.* (1963)
α-$BaPuO_3$	cubic	P*m*3*m*	4.391 (4.385)				Russell *et al.* (1960)
β-$BaPuO_3$	orthorhombic	P*nma*[a]	5.982(4)	5.976(11)	5.847(4)		Chackraburtty *et al.* (1963)
β-$BaPuO_3$	orthorhombic	P*nma*[b]	6.193(1)	8.744(1)	6.219(1)	8.37	Christoph *et al.* (1988)
$SrPuO_3$	cubic	F*m*3*m*	4.28(3)				Keller (1962)
$SrPuO_3$	orthorhombic	A*mm*2[c]	4.273(4)	5.981(5)	6.124	7.94	Chackraburtty and Jayadevan (1964)
Li_8PuO_6	hexagonal		5.64(2)		15.95(5)		Walter (1965)
Ba_2CePuO_6	cubic	F*m*3*m*	8.72(2)				Awasthi *et al.* (1968)
Ba_2TiPuO_6	cubic	F*m*3*m*	8.06(2)				Awasthi *et al.* (1968)
Pu(V)							
Li_3PuO_4	tetragonal	I4/*mmm*	4.464(2)		8.367(5)	6.45	Keller *et al.* (1965b)
$Ba_3PuO_{5.5}$	cubic	F*m*3*m*	8.813(7)				Keller (1962)
Ba_2LaPuO_6	pseudo-cubic	F*m*3*m*	8.63(2)				Awasthi *et al.* (1968)
Ba_2NdPuO_6	cubic	F*m*3*m*	8.66(2)				Awasthi *et al.* (1968)
Ba_2InPuO_6	cubic	F*m*3*m*	8.50(2)				Awasthi *et al.* (1968)
Pu(VI)							
K_2PuO_4	tetragonal	I4/*mmm*	4.298(3)		13.07(1)	5.22	Hoekstra and Gebert (1977)

Rb_2PuO_4	tetragonal	I4/*mmm*	4.323(3)		13.74(1)		Hoekstra and Gebert (1977)
Cs_2PuO_4	tetragonal	I4/*mmm*	4.368(3)		14.71(1)		Hoekstra and Gebert (1977)
$SrPuO_4$	rhombohedral	$R\overline{3}$	6.51(2)			7.72	Keller (1962)
Li_4PuO_5	tetragonal	I4/*m*	6.677(2)		4.421(3)	5.84	Keller *et al.* (1965a)
α-Na_4PuO_5	cubic	F*m*3*m*	4.718(5)			5.20	Keller *et al.* (1965a)
β-Na_4PuO_5	tetragonal	I4/*m*	7.449(5)		4.590(5)	5.36	Keller *et al.* (1965a)
Li_6PuO_6	hexagonal	$R\overline{3}$	5.184(2)		14.59(5)	5.35	Keller *et al.* (1965a)
Na_6PuO_6	hexagonal	$R\overline{3}$	5.76(2)		15.9(1)	5.16	Keller *et al.* (1965a)
Ba_3PuO_6	cubic	F*m*3*m*	8.844(6)			7.17	Keller (1962)
Ba_2SrPuO_6	cubic	F*m*3*m*	8.780(2)				Keller (1962)
Ba_2SrPuO_6	orthorhombic		6.204(42)	6.188(62)	8.822(32)		Gens *et al.* (1985)
$BaSr_2PuO_6$	cubic	F*m*3*m*	8.717(8)				Keller (1962)
Ba_2MnPuO_6	cubic	F*m*3*m*	8.32(2)				Awasthi *et al.* (1968)
Ba_2ZnPuO_6	pseudo-cubic	F*m*3*m*	8.38(2)				Awasthi *et al.* (1968)
Ba_2PbPuO_6	cubic	F*m*3*m*	8.58(2)				Awasthi *et al.* (1968)
Ba_2MgPuO_6	cubic	F*m*3*m*	8.332(6)				Gens *et al.* (1985)
Ba_2CaPuO_6	cubic	F*m*3*m*	8.611(4)				Gens *et al.* (1985)
***Pu*(*VII*)**							
Li_5PuO_6	hexagonal	$R\overline{3}$	5.19(2)		14.48(2)	3.53	Keller and Seiffert (1969a)
Li_5PuO_6	monoclinic[d]	C2/*m*	5.0679(6)	8.7315(8)	5.0293(6)	5.88	Keller *et al.* (1965a)
Na_5PuO_6	monoclinic[d]	C2/*m*	5.6877(8)	8.7314(13)	5.6074(9)	5.75	Keller *et al.* (1965a)

---

[a] Original space group P*mcm*, recalculated by Roof (1989) in standard setting P*nma*.

[b] Neutron diffraction data; original space group P*bnm*, recalculated by Roof (1989) in standard setting P*nma*.

[c] Original space group B centered, recalculated by Roof (1989) in standard setting A*mm*2.

[d] Keller *et al.* (1965a) reported that Li_5PuO_6 and Na_5PuO_6 are hexagonal and isotypic with rhenium analogs Li_5ReO_6 and Na_5ReO_6. Betz and Hoppe (1984) described the structures of Li_5ReO_6 and Na_5ReO_6 as being monoclinic. Roof (1989) recalculated both Pu structures using the data from Betz and Hoppe, and these are the cell constants reported here with $\beta = 110.24°$ for Li_5PuO_6 and $\beta = 111.01(1)°$ for Na_5PuO_6.

should rotate by about 11 degrees to give the theoretical Pu–O distance predicted by Zachariasen's relationship. This prediction was tested by performing a low-temperature neutron diffraction study on $Ba^{242}PuO_3$ which confirmed the expectations of a distortion away from the cubic perovskite structure (Christoph *et al.*, 1988). The idealized cubic and experimentally confirmed orthorhombic solid-state structures are illustrated in Fig. 7.98. In the low-temperature neutron structure, the PuO_6 octahedra are rotated by about 15 degrees from the idealized position in the cubic perovskite, and this is indicated in Fig. 7.98(b). The PuO_6 rotation gives Pu–O–Pu angles of 157.07 (8) and 160.53(5) degrees. The plutonium atom coordination is only slightly distorted from octahedral with Pu–O distances of 2.2306(5), 2.2295(12), and 2.2230(12) Å. The mean Pu–O distance is 2.228 Å.

Double perovskites M_3PuO_6 and Ba_2MPuO_6

Another important class of plutonium perovskite oxide is the so-called 'double perovskite' typified by M_3PuO_6 (M = Ba, Sr) and Ba_2MPuO_6 (M = Mg, Ca, Sr, Mn, Zn). The double perovskite can be considered as an ideal perovskite with M^{2+} and Pu^{6+} ions occupying alternating octahedral sites in a cubic unit cell with doubled cell edges. The ordered fcc structure (*Fm*3*m*) has the elpasolite (K_2NaAlF_6) structure, and the basic structural unit is shown in Fig. 7.99. This figure maintains the same orientation as Fig. 7.98, and emphasizes the alternating PuO_6 and MO_6 octahedra in the double perovskite structure. As in the ideal

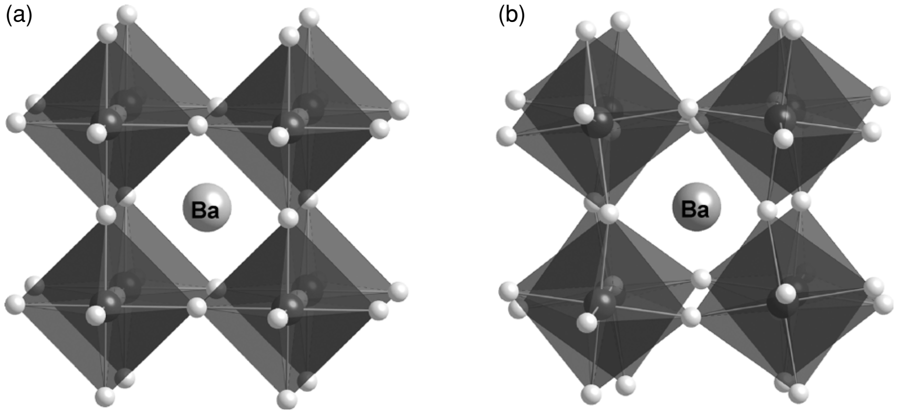

Fig. 7.98 *Idealized cubic (a) and experimental orthorhombic (b) crystal structures of $BaPuO_3$, emphasizing the rotation of the local PuO_6 octahedra between cubic and orthorhombic symmetries. The cubic structure is based on the original report by (Russell* et al., 1960), *and the orthorhombic structure is based on the low-temperature neutron diffraction study (Christoph* et al., 1988). *In this polyhedral representation, the plutonium atoms are dark gray (center of octahedra), oxygen atoms are white, and the central barium atom is light gray.*

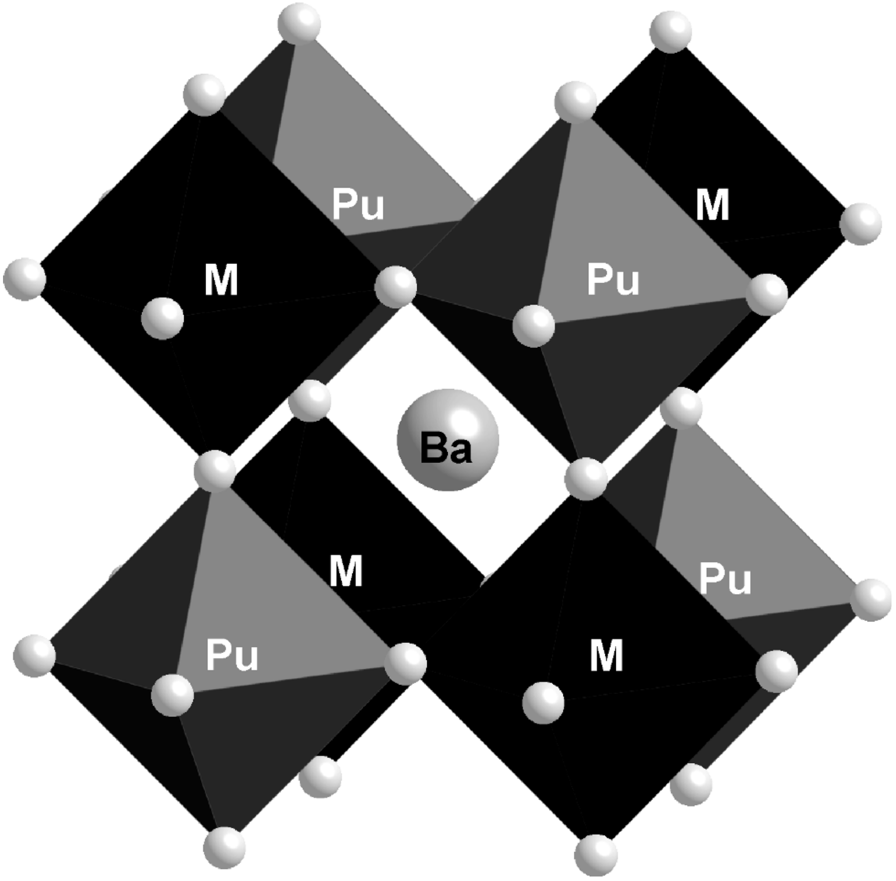

Fig. 7.99 *Polyhedral representation of the idealized double perovskite structure of* Ba_2MPuO_6 *compounds. This polyhedral representation emphasizes the alternating octahedral* PuO_6 *(gray) and* MO_6 *(black) sites in the structure. The central barium ion is light gray.*

perovskite structure, many of these compounds are distorted away from ideal cubic symmetry, and this is often observed as the presence of extra, weak diffraction lines (Gens *et al.*, 1985).

M_4PuO_5

These hexavalent compounds are isostructural with M_4UO_5 (M = Li, Na) and crystallize in tetragonal space group I4/*m*. The solid-state structure of Li_4PuO_5 displays an extended pseudo-octahedral chain of $PuO_4(\mu\text{-}O)_2$ units with a square-planar arrangement of four short equatorial Pu–O bonds of 1.98 Å,

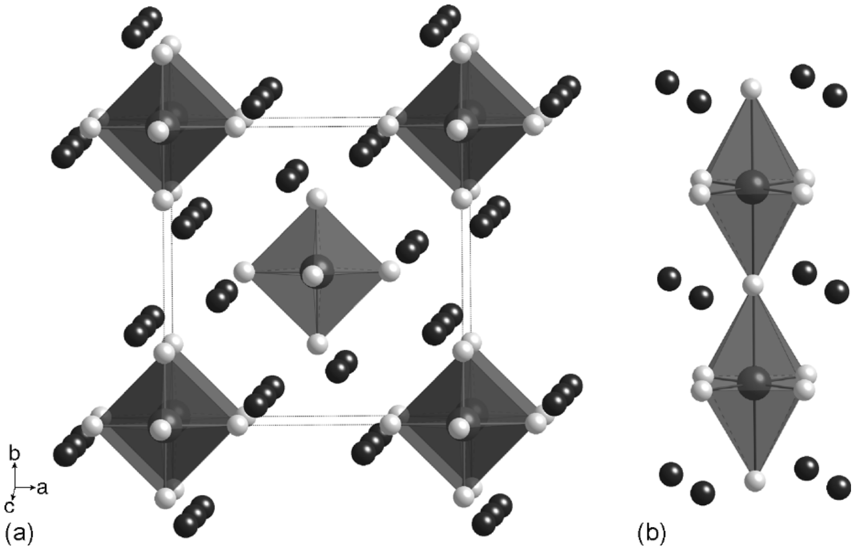

Fig. 7.100 *Polyhedral representation of the solid-state structure of M_4PuO_5 compounds. (a) A view looking down the crystallographic c-axis, and (b) a view perpendicular to the c-axis. The view in (b) emphasizes the distorted PuO_6 polyhedra (gray) surrounded by Li or Na ions (black).*

and two longer axial Pu–O bridging bonds of 2.21 Å that link the planar PuO_4 units together (Keller *et al.*, 1965a). The basic structural unit is shown in Fig. 7.100. This compound is isostructural with β-Na_4PuO_5 that has four short Pu–O bonds of 2.09 Å and two longer Pu–O bonds of 2.29 Å (Keller *et al.*, 1965a). This class of compound is significant in that it demonstrates that hexavalent complex actinide oxides do not necessarily retain actinyl (AnO_2^{2+}) ions with two short metal–oxygen bonds in the solid state.

M_5PuO_6

For heptavalent actinides, Keller reported that M_5PuO_6 (M = Li, Na) compounds were hexagonal and isotypic with rhenium analogs M_5ReO_6 (M = Li, Na) (Keller *et al.*, 1965a). Since Keller's original report, Betz and Hoppe (1984) determined that the structures of M_5ReO_6 were monoclinic and characterized by tetragonally distorted MO_6^{5-} units. In 1994, Morss and coworkers reexamined the structures of both Li_5NpO_6 and Li_5ReO_6 by neutron diffraction and confirmed the monoclinic structure for Li_5ReO_6, but in contrast to the original report, the structure of Li_5NpO_6 was not identifiable (Morss *et al.*, 1994). Thus the actual solid-state structure of M_5PuO_6 compounds remains unresolved.

(*iv*) *Ternary and quaternary oxides of plutonium with main group and transition elements*

A number of ternary oxides of plutonium with the oxides of metallic and semimetallic elements have been prepared. In these compounds plutonium occurs as Pu(III) or Pu(IV), and the tendency for plutonium to assume the role of the cation increases as one proceeds from group III toward group VII elements. A wide variety of compositions are observed, with stoichiometric compounds and nonstoichiometric phases being formed. The crystallographic properties of those compounds having a stoichiometric composition are summarized in Table 7.41. Compounds of the type $PuXO_4$, containing Pu(III) and X = P or As, as well as the phosphates and arsenates of Pu(IV) and Pu(VI) will be discussed in Section 7.8.5.c(i).

Trivalent compounds

Ternary and quaternary oxides containing trivalent plutonium range from simple compounds of the types $PuMO_3$ and $PuMO_4$, to more complex formulae such as $Pu(ReO_4)_3$, or to complicated silicate structures such as $Ba_2Pu_8(SiO_4)_6O_2$ related to apatite.

$PuMO_3$. This class of compound displays the perovskite structure (Fig. 7.98), but with Pu(III) now serving the role of the cation. These compounds have been prepared by Russell *et al.* (1960) for M = Al(III), V(III), Cr(III), and Mn(III), and by Keller *et al.* (1972) for M = Sc(III) by heating mixtures of PuO_2 with the appropriate metal oxide (Al_2O_3, V_2O_5, CrO_3) or carbonate ($MnCO_3$) under argon or hydrogen atmospheres between 1500 and 1600°C for several hours (Russell *et al.*, 1960). Attempts to prepare analogous compounds with M = Fe (III) and Ga(III) were unsuccessful (Chackraburtty and Jayadevan, 1964).

Ba_2PuPaO_6. This is the only known compound in this class, and it shows a double perovskite structure (Fig. 7.99). This compound is prepared as a white powder by heating a 4:1:1 mixture of $BaCO_3$, Pa_2O_5, and Pu_2O_3 at 1350–1400°C *in vacuo* (Keller, 1965b). It is unknown whether this compound contains Pu(III)/Pa(V) or Pu(IV)/Pa(IV).

$PuMO_4$. A few such compounds have been prepared with M = Nb(V) or Ta(V), and contain trivalent plutonium. They are obtained by heating intimate mixtures of Pu_2O_3 and M_2O_3 and M_2O_5 *in vacuo* at 1200°C (Keller and Walter, 1965).

$Pu(ReO_4)_3$. Reaction of plutonium(III) oxalate with Re_2O_7 yields green plutonium(III) perrhenate, $Pu(ReO_4)_3$. This salt-like compound is also obtained by solid-state reaction of PuO_2 with Re_2O_7. $Pu(ReO_4)_3$, is deliquescent in air, and forms hydrates with 1, 2, or $3H_2O$. $Pu(ReO_4)_3$ decomposes at 700°C to PuO_2 and Re_2O_7 (Silvestre *et al.*, 1977). The X-ray powder pattern of anhydrous $Pu(ReO_4)_3$ has not yet been interpreted.

Pu(III) silicates. No simple plutonium(III) silicates are known. However, De Alleluia and coworkers (De Alleluia *et al.*, 1983) have prepared a number of

Table 7.41 *Crystallographic data of ternary oxides of plutonium with main group and transition elements.*

			Lattice constants				
Compound	*Symmetry*	*Space group*	a_0 (Å)	b_0 (Å)	c_0 (Å)	*Density* (g cm^{-1})	*References*
***Pu*(*III*)**							
$PuAlO_3$	orthorhombic	A*mm*2	3.750	5.314	5.350	9.78	Runnalls (1965)
$PuScO_3$	orthorhombic	P*bnm*	5.654	5.839	8.104		Keller *et al.* (1972)
$PuVO_3$	orthorhombic[a]	P*nma*	5.61	7.78	5.48	9.38	Russell *et al.* (1960)
$PuCrO_3$	orthorhombic[a]	P*nma*	5.51	7.76	5.46	9.65	Russell *et al.* (1960)
$PuMnO_3$	orthorhombic[b]	P*nma*	5.497(3)	7.730(4)	5.450(3)	9.72	Russell *et al.* (1960)
$PuAsO_4$	monoclinic[c]	$P2_1/n$	6.92(2)	7.09(2)	6.66(2)		Keller and Walter (1965)
$PuNbO_4$	monoclinic[d]	$I2/a$	5.46	11.27	5.17	8.29	Keller and Walter (1965)
$PuTaO_4$	monoclinic[e]	$C2_1/c$	7.618(1)	5.531(1)	7.767(1)	10.0	Keller and Walter (1965)
$Ba(Pu_{0.5}Pa_{0.5})O_3$	cubic		8.748	5.17			Keller (1965b)
$Pu_{9.33}(SiO_4)_6O_2$	hexagonal	$P6_3m$	9.589(5)		7.019(5)		De Alleluia *et al.* (1983)
$Pu_8(SiO_4)_6$	hexagonal	$P6_3m$	9.595(5)		7.037(5)		De Alleluia *et al.* (1983)
$LiPu_9(SiO_4)_6O_2$	hexagonal	$P6_3m$	9.566(5)		6.999(5)		De Alleluia *et al.* (1983)
$NaPu_9(SiO_4)_6O_2$	hexagonal	$P6_3m$	9.594(5)		7.025(5)		De Alleluia *et al.* (1983)
$Mg_2Pu_8(SiO_4)_6O_2$	hexagonal	$P6_3m$	9.559(5)		6.973(5)		De Alleluia *et al.* (1983)
$Ca_2Pu_8(SiO_4)_6O_2$	hexagonal	$P6_3m$	9.570(5)		7.043(5)		De Alleluia *et al.* (1983)
$Sr_2Pu_8(SiO_4)_6O_2$	hexagonal	$P6_3m$	9.604(5)		7.122(5)		De Alleluia *et al.* (1983)
$Ba_2Pu_8(SiO_4)_6O_2$	hexagonal	$P6_3m$	9.701(5)		7.198(5)		De Alleluia *et al.* (1983)
$Sr_3Pu_6(SiO_4)_6$	hexagonal	$P6_3m$	9.619(5)		7.131(5)		De Alleluia *et al.* (1983)
***Pu*(*IV*)**							
$PuSiO_4$	tetragonal	$I4_1/amd$	6.906(6)		6.221(6)	7.37	Keller (1963)
$PuGeO_4$	tetragonal	$I4_1/a$	5.040(2)		11.11(1)	8.82	Keller (1963)
$Pu(TeO_3)_2$	orthorhombic		5.60	10.46	11.76		Wroblewska *et al.* (1979)
$Pu(NbO_3)_4$	tetragonal[f]	$I4/mmm$	7.67(1)		7.74(1)	5.85	Keller (1965a)

$Pu(TaO_3)_4$	tetragonal[f]	I4/*mmm*	7.654(5)		7.731(5)	Keller (1965a)
$Pu(MoO_4)_2$	orthorhombic[g]	P*mna*	9.422(8)	13.993(10)	10.039(11)	Tabuteau *et al.* (1972)
$Pu(ReO_4)_4 \cdot 4H_2O$	monoclinic[h]		32.4	6.69	16.85	Silvestre *et al.* (1977)
$LiPu_2(VO_4)_3$	tetragonal		7.09		6.35	Pagès and Freundlich (1976)
$NaPu_2(VO_4)_3$	tetragonal		7.14		6.37	Pagès and Freundlich (1976)
$AgPu_2(VO_4)_3$	tetragonal		5.06		11.32	Pagès and Freundlich (1976)
$CdPu(VO_4)_2$	tetragonal		7.04		6.33	Pagès and Freundlich (1976)
$CaPu(VO_4)_2$	tetragonal		7.16		6.33	Pagès and Freundlich (1976)
$SrPu(VO_4)_2$	tetragonal		7.29		6.47	Pagès and Freundlich (1976)
$Na_2Pu(MoO_4)_3$	tetragonal		5.198		11.280	Tabuteau *et al.* (1972)
$Li_4Pu(MoO_4)_4$	tetragonal		11.085		10.600	Tabuteau *et al.* (1972)
$Na_4Pu(MoO_4)_4$	tetragonal		11.20		11.69	Tabuteau *et al.* (1972)
$K_2Pu(MoO_4)_3$	monoclinic[i]	*Cc* or *C*2/*c*	17.538(9)	11.992(6)	5.243(4)	Tabuteau and Pagès, 1980)
$K_8Pu(MoO_4)_6$	monoclinic[j]	*Cc* or *C*2/*c*	10.416(4)	10.416(4)	7.748(4)	Tabuteau and Pagès (1980)
$Rb_2Pu(MoO_4)_3$	monoclinic[k]	*Cc* or *C*2/*c*	17.77(3)	12.068(13)	5.282(7)	Tabuteau and Pagès (1980)
$Rb_8Pu(MoO_4)_6$	monoclinic[l]	*Cc* or *C*2/*c*	10.67(2)	17.71(5)	7.99(12)	Tabuteau and Pagès (1980)
$Cs_2Pu(MoO_4)_3$	orthorhombic		26.516(31)	9.702(25)	5.178(9)	Tabuteau and Pagès (1980)

---

[a] Original space group P*bnm*, atomic positions transformed to standard setting P*nma* by Roof (1989).

[b] Russell *et al.* indicated that $PuMnO_3$ is orthorhombic and perhaps isomorphic with $PuCrO_3$. The structure was refined by Roof using original d-spacings and transformed into standard space group P*nma* (Roof, 1989).

[c] $\beta = 105.45°$.

[d] $\beta = 94.58°$. Keller and coworkers reported lattice constants and suggested that the structure was of the β-fergusonite type (Keller and Walter, 1965). The latter structure was refined in I2/*a* by Santoro *et al.* (1980).

[e] $\beta = 100.94°$. Keller and coworkers reported the structure to be of the $CeTaO_4$ type, whose structure was refined by Santoro *et al.* (1980). Lattice constants, atomic positions and thermal parameters refined by Roof (1989).

[f] Space group assignment described by Roof (1989).

[g] Lattice constants refined by Roof and transformed into standard space group *Pmna* (Roof, 1989).

[h] $\beta = 110.07°$.

[i] $\beta = 104.80(6)°$.

[j] $\beta = 116.59(4)°$.

[k] $\beta = 107.78(10)°$.

[l] $\beta = 116.3(1)°$.

complex silicates of the types $Pu_8(SiO_4)_6$; $Pu_{9.33}(SiO_4)_6O_2$; $M_2Pu_9(SiO_4)_6O_2$ (M = Li, Na), $M_2Pu_8(SiO_4)_6O_2$ (M = Mg, Ca, Sr, Ba), and $Sr_3Pu_6(SiO_4)_6$. All these compounds have hexagonal apatite-type structures, some with lattice defects. All these compounds, which show the blue color of Pu(III), are prepared by reducing mixtures of PuO_2, SiO_2, and the respective alkali or alkaline-earth oxides in ultrapure H_2 at temperatures between 1100 and 1400°C in alumina or iridium vessels for periods up to 3 days. In these systems, the reduction to Pu(III) is accomplished much more readily than the reduction to Pu(III) in other mixed oxide systems.

Tetravalent compounds

$PuMO_4$. Compounds of this type containing M = Si or Ge can be obtained by hydrothermal synthesis from 1:1 mixtures of PuO_2 and MO_2 at 250°C. They may also be prepared by solid-state reactions at 1200°C from the same components (Keller, 1963). $PuSiO_4$ is green; $PuGeO_4$ is pale brown or olive brown.

$Pu(MO_3)_4$. These compounds contain Pu(IV) and M(V) (M = Nb, Ta) and may be obtained by solid-state reaction of a 2:1 mixture of M_2O_5 and PuO_2 (Keller, 1965a).

$Pu(MO_3)_2$. The only representative of this type of compound is white plutonium(IV) tellurite, $Pu(TeO_3)_2$, which is prepared by heating a 1:2 mixture of PuO_2 and TeO_2 for 24 h at 700°C (Wroblewska *et al.*, 1979).

$Pu(MO_4)_2$. The only compound of this type known now is brown-red plutonium(IV) molybdate, $Pu(MoO_4)_2$. This compound may be prepared by heating a stoichiometric mixture of PuO_2 and MoO_3 for 2 h at 500°C, followed by 4 h at 800°C (Tabuteau *et al.*, 1972).

A number of quaternary plutonium(IV) molybdates have been obtained by reaction of $Pu(MoO_4)_2$ with M_2MoO_4 (M = Li, Na, K, Rb, Cs) compounds at high temperature (Tabuteau *et al.*, 1972). Reaction of Li_2MoO_4 with $Pu(MoO_4)_2$ at 500°C gives $Li_4Pu(MoO_4)_4$. $Li_4Pu(MoO_4)_4$ melts congruently at 630°C and has a reversible solid-state transformation at 510°C. Solid-state reaction of Na_2MoO_4 with $Pu(MoO_4)_2$ at 600°C gives $Na_2Pu(MoO_4)_3$ and $Na_4Pu(MoO_4)_4$. Both compounds show peritectic decomposition, $Na_2Pu(MoO_4)_3$ at 714°C and $Na_4Pu(MoO_4)_4$ at 708°C. Similarly, $M_2Pu(MoO_4)_3$ and $M_8Pu(MoO_4)_6$ have been prepared by solid-state reactions between M_2MoO_4 and $Pu(MoO_4)_2$ (M = K, Rb). With Cs_2MoO_4, only $Cs_2Pu(MoO_4)_3$ has been prepared by solid-state reaction with $Pu(MoO_4)_2$ (Tabuteau *et al.*, 1972).

Pu(IV) perrhenates. Plutonium(IV) perrhenate tetrahydrate, $Pu(ReO_4)_4 \cdot 4H_2O$, is obtained as a red powder by dissolving the oxalate $Pu(C_2O_4)_2 \cdot 6H_2O$ in 0.5 M perrhenic acid solution, evaporating the resulting solution to dryness, and heating the residue to a temperature below 100°C. So far, the anhydrous compound has not been prepared. At 250°C, $Pu(ReO_4)_4{\cdot}4H_2O$ decomposes partially to $Pu(ReO_4)_3$ (Silvestre *et al.*, 1977).

Pu(IV) vanadates. No simple plutonium(IV) vanadate has been prepared. However, Pagès and Freundlich (1976) prepared a number of quaternary plutonium(IV) vanadates of the types $MPu_2(VO_4)_3$ (M = Li, Na, Ag) and $M'Pu(VO_4)_2$, (M′ = Ca, Sr, Cd). Heating a 4:3:1 mixture of PuO_2, V_2O_5, and Ag_2O at 500°C produces $AgPu_2(VO_4)_3$. The corresponding alkali compounds (M = Li, Na) are prepared by heating 1:1:3 mixtures of M_2CO_3, PuO_2, and V_2O_5 at 700–750°C. The alkaline-earth compounds are obtained in the same manner from a mixture of $M'CO_3$, PuO_2, and V_2O_5. The compounds $MPu_2(VO_4)_3$ and $M'Pu(VO_4)_2$ have the zircon structure, while $AgPu_2(VO_4)_2$ has the scheelite structure.

(d) Ternary oxides of plutonium with lanthanide oxides

No stoichiometric compounds of plutonium oxides with lanthanide oxides have been observed. The following systems have been studied in some detail: PuO_2–CeO_2 (Farkas, 1966), PuO_{2+x}–$YO_{1.5}$ (Jackson and Rand, 1963), PuO_2–$EuO_{1.5}$ (Haug, 1963; Haug and Weigel, 1963), PuO_2–$HoO_{1.5}$ (Engerer, 1967), PuO_2–$TmO_{1.5}$ (Leitner, 1967), and PuO_2–$LuO_{1.5}$ (Sriyotha, 1968). Preliminary data are available for the systems PuO_{2+x}–$YO_{1.5}$ (Jackson and Rand, 1963) and PuO_{2+x}–$EuO_{1.5}$ (Haug, 1963; Haug and Weigel, 1963), while pseudo-binary phase diagrams have been established for the systems PuO_{2+x}–$HoO_{1.5}$ (Engerer, 1967), PuO_{2+x}–$TmO_{1.5}$ (Leitner, 1967), and PuO_{2+x}–$LuO_{1.5}$ (Sriyotha, 1968) up to temperatures of 1700°C in oxygen-free atmosphere (argon) and in 1 atm O_2. A detailed discussion of all these systems is beyond the scope of this work.

From these phase diagrams, it may be concluded that $PuO_{2\pm x}$ may dissolve considerable amounts of $LnO_{1.5}$ to form a solid solution. For instance, in the system $PuO_{2\pm x}$–$HoO_{1.5}$, 46.0 mol% $HoO_{1.5}$ at 1250°C, and 72.0 mol% at 1700°C. The anion defects formed by inclusion of $LnO_{1.5}$ into the PuO_2 lattice may be partially compensated by oxidation of Pu(IV) to Pu(>IV). For instance, the average oxidation number $\overline{W}$ of plutonium in the system PuO_{2+x}–$HoO_{1.5}$ at $p(O_2) = 1$ atm for a composition of 50 mol% $HoO_{1.5}$ and 1400°C was found to be $\overline{W} = 4.36$ at an O:(Pu + Ho) ratio of 1.84 (Engerer, 1967). At a composition of 70 mol% $HoO_{1.5}$ and 1100°C, it was found to be $\overline{W} = 4.51$ at an O:(Pu + Ho) ratio of 1.68. In general, the average oxidation number of the plutonium in the fluorite phases containing lanthanide elements is lower than the corresponding oxidation number in the uranium or neptunium systems at approximately the same composition in the fluorite phases.

The solubility of $PuO_{2\pm x}$ in $LnO_{1.5}$ (Ln = Ho, Tm, Lu) is considerably larger than the solubility of uranium or neptunium oxides. In the system PuO_{2+x}–$HoO_{1.5}$ and at $p(O_2) = 1$ atm, it is 18.5 mol% PuO_2 at 1100°C, and 25 mol% at 1550°C (Engerer, 1967).

A different situation exists in the system $PuO_{2(+x)}$–CeO_2. At 1000°C, the compositions PuO_2–CeO_2 form a series of solid solutions throughout the whole range of concentrations. Microspheres of PuO_2–CeO_2 have been prepared by the sol-gel process (Farkas, 1966). A detailed X-ray study of the lattice constants of various compositions demonstrates that the solid solutions obey Vegard's law (Mulford and Ellinger, 1958).

(e) Ternary oxides of plutonium with actinides

Ternary oxides of plutonium with actinides have been prepared with thorium, protactinium, uranium, and curium.

(*i*) *The plutonium–thorium system*

At 1000°C the PuO_2–ThO_2 system, forms a series of solid solutions throughout the whole composition range (Mulford and Ellinger, 1958) and these follow Vegard's law. Above 1650°C, under an argon atmosphere, a partial phase separation with formation of C-Pu_2O_3 takes place. The melting points of $(Th,Pu)O_2$ solid solutions are practically constant up to 25 wt % Th and show a linear increase at higher Th contents. $(Pu,Th)O_2$ microspheres have been prepared by the sol–gel process and in the induction-coupled plasma torch.

(*ii*) *The plutonium–uranium–oxygen system*

The plutonium–uranium–oxygen system is one of the best-understood plutonium–actinide oxide systems due to its widespread application in nuclear reactor fuel. For this reason, the mixed plutonium–uranium oxide system has been extensively studied. In spite of this great technological importance, only relatively limited data have been reported in the open literature. There is much more information in the proprietary literature of fuel manufacturing organizations. Plutonium–uranium oxides of general formula $(U,Pu)O_2$ are often referred to as 'mixed oxide' or MOX, and can refer to fuels containing 2–30% PuO_2. These fuels behave very differently depending on the percentage of PuO_2. Fuels for light water reactors (LWR) only contain a small percentage of plutonium (2–6%), and will therefore behave like UO_2 with a small amount of impurity, while fuels for fast breeder reactors (FBR) have a higher percentage of plutonium (15–35%), and behave very differently (Schneider and Roepenack, 1986). Four plants currently produce commercial quantities of MOX fuel. Two are in France, one in Belgium, and one in the United Kingdom. In 2000, about 190 metric tons per year of MOX was produced, incorporating 10–12 metric tons of plutonium. MOX production capacity is presently around 300 metric tons per year, using 18–22 metric tons of plutonium. Since 1963 about 400 metric tons of plutonium have been used in MOX. We only cover the fundamental aspects of the plutonium–uranium–oxygen system; for further details, the reader is referred to part C of the *Gmelin Handbook* (Koch, 1972), to the *Plutonium Handbook* (Wick, 1980), and to a number of original papers (Russell *et al.*, 1962; Markin and Street, 1967; Thuemmler *et al.*, 1967; Benedict and Sari, 1969; Dean *et al.*, 1970; Sari *et al.*, 1970), and reviews (IAEA, 1967; Matzke, 1982; Schneider and Roepenack, 1986; Matthews, 1987; Baily *et al.*, 1989; Bernard, 1989; Bairiot and Deramaix, 1992; Carbajo *et al.*, 2001; Bairiot *et al.*, 2003).

The plutonium–uranium–oxygen phase diagram

The details of the Pu–U–O phase diagram up to 1000°C have been obtained primarily through lattice constant measurements at high temperature and on quenched samples. It is well established that mixed uranium–plutonium oxides with stoichiometric compositions form a continuous solid solution from UO_2 to PuO_2, and the lattice parameters follow Vegard's law (see Fig. 7.101) so long as the stoichiometry is carefully controlled (Markin and Street, 1967; Thuemmler *et al.*, 1967).

The room-temperature phase diagram of the ternary U–Pu–O system is shown in Fig. 7.102 (IAEA, 1967; Markin and Street, 1967; Benedict and Sari, 1969; Koch, 1972). The system is characterized by four single-phase regions: orthorhombic U_3O_8; a cubic fluorite phase, $MO_{2\pm x}$, which occupies the largest area of the single-phase region; a cubic superstructure, M_4O_9; and a fcc C-M_2O_3 phase.

The orthorhombic U_3O_8 phase includes plutonium in its lattice to form $(U, Pu)_3O_{8-x}$ (Benedict, 1970). The maximum amount of plutonium accommodated at 1000°C corresponds to a Pu:(U + Pu) ratio of 0.06, which decreases to 0.02 at 1400°C. It is assumed that the plutonium ions introduced into the lattice occupy the U_{II} positions in U_3O_8.

The fluorite phase $(U,Pu)O_{2\pm x}$ may be hyperstoichiometric, stoichiometric, or substoichiometric with regard to the O:(U + Pu) ratio. The stoichiometric region corresponds to the pseudo-binary system UO_2–PuO_2, in which the lattice constants obey Vegard's law (see Fig. 7.101). Since PuO_2 loses oxygen at high temperature, deviations from Vegard's law can be observed. At room temperature, the range of the single-phase substoichiometric fluorite structure goes up to the ratio $Pu:(U + Pu) = 0.17$. A large region with two cubic phases extends from Pu:(U + Pu) ~0.20 up to the binary Pu–O system. One of these two cubic phases is an fcc phase with $O:(U + Pu) = 1.985$. In the range $0.2 \leq Pu:(U + Pu) \leq 0.5$, this phase is in equilibrium with a second fcc phase; and for higher plutonium contents, in equilibrium with a bcc phase of the C-Pu_2O_3 type. In the region $Pu:(U + Pu) > 0.5$ with low O:(U + Pu) ratios, there exists a bcc single-phase region, which extends up to $Pu:(U + Pu) = 0.95$ and contracts for $Pu:(U + Pu) = 0.97$ to a single line at O:(U + Pu) ~1.51. In the region $Pu:(U + Pu) \geq 0.97$, a hexagonal phase of A-Pu_2O_3 type exists.

Oxidation of $(U,Pu)O_2$ mixtures yields one- or two-phase products, depending on conditions (Brett and Fox, 1966). In the hyperstoichiometric fluorite phase $(U,Pu)O_{2+x}$, only U is oxidized to U (>IV). At room temperature, for a ratio $Pu:(U + Pu) \leq 0.30$ and for $O:(U + Pu) \leq 2.20$, a two-phase region $M_4O_9 + MO_{2+x}$ is observed. The M_4O_9 phase exists in the range $2.20 \leq O:(U + Pu) \leq 2.27$. For $O:(U + Pu) > 2.27$ and $Pu:(U + Pu) < 0.5$, a Pu-rich

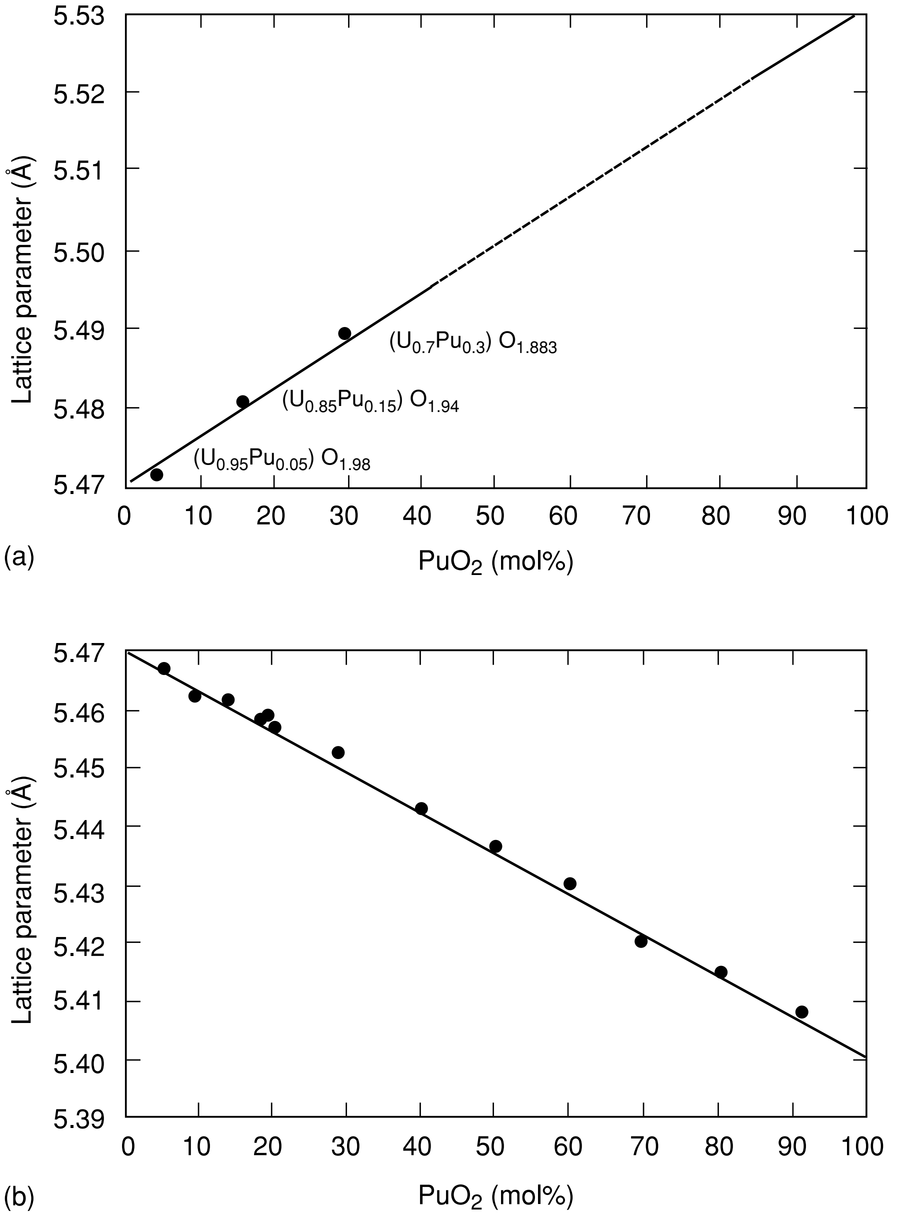

Fig. 7.101 *Lattice parameters of UO_2–PuO_2 mixed oxides that show* (*a*) *the dependence on O*:*M ratio, and* (*b*) *the dependence on PuO_2 concentration* (*Thuemmler* et al., 1967).

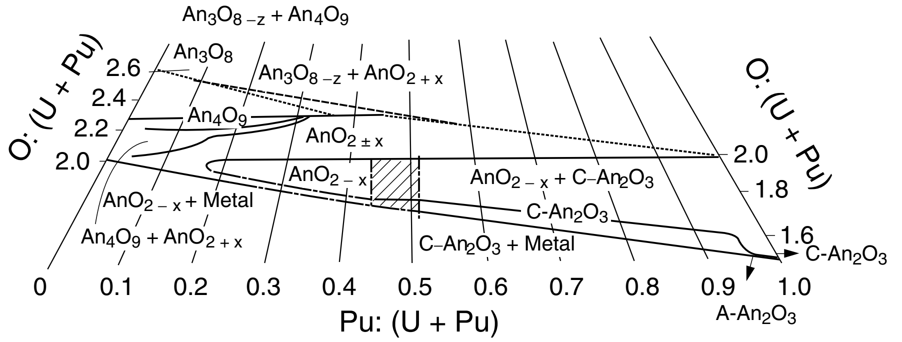

Fig. 7.102 *The phase diagram for the ternary U–Pu–O system in the composition range* (*U,Pu*)O_2–(*U,Pu*)$O_{2.67}$ *at room temperature* (*Benedict and Sari,* 1969).

fluorite phase is in equilibrium with uranium-rich M_3O_8. The oxidation of (U,Pu)O_2 at 600°C yields a metastable U_3O_7 type phase for Pu:(U+Pu) <0.25 and O:(U+Pu) $= 2.28$. Dean and Boivineau (1970) postulate a rhombohedral phase at composition M_7O_{12} for up to 60 at.% plutonium. According to Nakayama (1971), the phase relationships in the U–O system apply to $0.8 > y > 0.7$ in the MOX system $(U_yPu_{1-y})O_{2+x}$. For $y > 0.7$ there exists the tetragonal phase $(U_yPu_{1-y})O_{2+0.36y}$, which is stable up to 600°C.

Preparation

The preparation of well-defined uranium–plutonium mixed oxides is of particular importance because it is applied to the industrial production of nuclear fuel element materials. The majority of all work reported deals with oxides that contain up to 30% PuO_2, the type commonly encountered in fuel element fabrication. Oxides with more than 30% PuO_2 are much less-frequently studied. A large body of literature has been accumulated on the production of (U,Pu)O_2 ceramics for use in nuclear reactors, and a detailed account of all of this work is beyond our scope. The reader is referred to the reviews given in the *Plutonium Handbook* (Wick, 1980), the *Gmelin Handbook* (Koch, 1973c), and the peer-review literature (Schneider and Roepenack, 1986; Baily *et al.*, 1989; Bernard, 1989).

The major technical challenge in preparing (U,Pu)O_2 for fuel applications is to produce a product with the maximum degree of homogeneity. There are two main routes to deliver the required properties: comilling of UO_2 and PuO_2 and coprecipitation of UO_2 and PuO_2. Once the (U,Pu)O_2 material is formed, both processes entail mixing, pressing, sintering, and grinding operations (Schneider and Roepenack, 1986; Baily *et al.*, 1989; Bernard, 1989; Güldner and Schmidt, 1991). Hundreds of tons of mixed oxide (MOX) fuel have been produced using these processes.

Coprecipitation Processes The main process is the ammonium/uranyl/plutonyl/carbonate process (AUPuC) that produces a powder that is soluble in nitric acid. In this approach, gaseous NH_3 and CO_2 are dissolved into a mixed uranyl/plutonyl nitrate aqueous solution (<40% Pu) to generate an AUPuC of formula $[NH_4]_4[(U,Pu)O_2(CO_3)_3]$. The AUPuC precipitates as a coarse green crystalline product. These crystals are calcined into a $(U,Pu)O_2$ powder by firing at 800°C under a reducing atmosphere of N_2/H_2. The resulting $(U,Pu)O_2$ shows good flowability and sinterability (Schneider and Roepenack, 1986).

Comilling Processes Comilling generally involves mechanical grinding of UO_2 and PuO_2 powders followed by a granulation step before pressing into pellets. This process has been employed extensively at the CEA (Commissariat à l'Energie Atomique) plant in Cadarache, France. An alternate comilling approach designed by Belgonucleaire, and practiced at the French MELOX plant is referred to as the micronized master blend (MIMAS) process. In this process, plutonium and uranium oxides are mixed into a master blend that is 30% PuO_2. The master blend is homogenized and micronized in a dry ball mill, and then blended with free-flowing UO_2 powder to achieve the desired plutonium enrichment, and then pellitized (Schneider and Roepenack, 1986; Baily *et al.*, 1989; Bernard, 1989).

Properties

Due to their technological importance, the thermophysical properties of mixed uranium–plutonium oxide phases have been studied in detail. Unfortunately, most of these data are not available in the open literature. The data that are available have been critically reviewed by Fink (1982) and by Carbajo *et al.* (2001). Much of the discussion that follows has been summarized from those critical reviews.

Vaporization Behavior Vapor pressure measurements on the $(U,Pu)O_2$ system were carried out by Dean *et al.* (1970) with a Knudsen-effusion cell using ^{239}Pu and ^{233}U. Mass spectroscopy studies of vaporization of the $(U,Pu)O_2$ system were carried out by Ohse and Olson (1970), Battles *et al.* (1970), and Raj *et al.* (1999) to evaluate the effect of O:M ratio on the nature of gaseous species. These workers found that the total vapor pressure varies with O:M ratio and goes through a minimum value, suggesting there is no congruently vaporizing composition.

Solidus and Liquidus Temperatures There is an extensive literature on melting behavior. UO_2 melts at a higher temperature (2730–2876°C) than PuO_2 (2238–2445°C), and the $(U,Pu)O_2$ solid solution melts at a temperature between that of pure UO_2 and pure PuO_2. The liquidus and solidus curves of the PuO_2–UO_2 system are shown in Fig. 7.103 for the stoichiometric

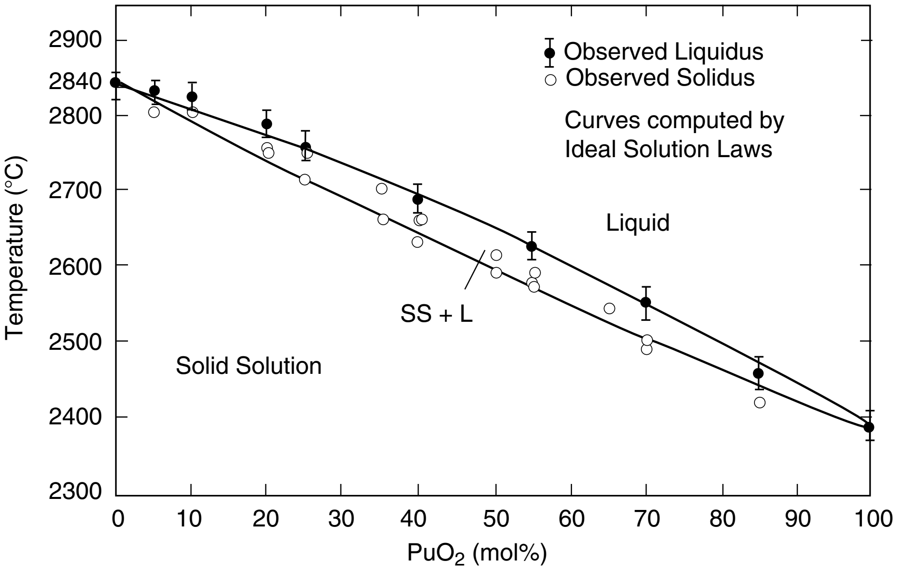

Fig. 7.103 *The solid–liquid phase diagram for the UO_2–PuO_2 system at stoichiometric composition AnO_2 (Lyon and Baily,* 1967*).*

compositions (Lyon and Baily, 1967). In MOX fuel, the actual melting temperature decreases with increasing PuO_2 content of the fuel as shown in Fig. 7.103 and with burnup (Carbajo *et al.*, 2001). Adamson has developed the following equations that predict the liquidus [$T_L(y)$] and solidus [$T_S(y)$] temperatures (in K), where y is the mole fraction of PuO_2 in $(U,Pu)O_2$ (Adamson *et al.*, 1985).

$$T_L(y) = 3120 - 388.1y - 30.4y^2 \tag{7.43}$$

$$T_S(y) = 3120 - 655.3y + 336.4y^2 - 99.9y^3 \tag{7.44}$$

Thermal Expansion and Density MOX fuel density is a function of the fuel composition, temperature, porosity, burnup, and O:M ratio (Carbajo *et al.*, 2001). The $(U,Pu)O_2$ is slightly heavier than UO_2. The density decreases with temperature due to thermal expansion. Fuel burnup changes the porosity and hence the density. At low burnup, the density increases by densification, and at higher burnup the density decreases due to swelling (Carbajo *et al.*, 2001). Martin (1988) developed equations to describe the thermal expansion and density of stoichiometric $(U,Pu)O_2$ compositions. The densities of UO_2 and PuO_2 at 273 K are 10.97 and 11.46 g cm^{-3}, respectively. The density of the solid solution $(U_{1-y}Pu_y)O_2$ changes according to the linear scaling law below, with y being the mole fraction of PuO_2 (Carbajo *et al.*, 2001).

$$\rho_s(273) = 10970 + 490y(\text{kg m}^{-3}) \tag{7.45}$$

Enthalpy and Heat Capacity Enthalpy and heat capacity are functions of the temperature, fuel composition (fractions of UO_2 and PuO_2), gadolinium content (added as a burnable neutron "poison"), O:M ratio, and burnup. The heat capacity is an important thermodynamic property that is necessary for understanding the various chemical interactions likely to occur during the irradiation of the fuel as well for modeling fuel behavior. Temperature and composition are the main influences on both enthalpy and heat capacity. Both enthalpy and heat capacity increase with temperature. The heat capacity reaches a maximum at the melting point, and then decreases. The heat capacity of UO_2 is lower than that of PuO_2. Carbajo *et al.* (2001) recommended the calculation of enthalpy and heat capacity of solid MOX fuel $U_{1-y}Pu_yO_2$ by using the Neumann–Kopp molar additivity rule, since the $(U,Pu)O_2$ system is an almost ideal solid solution. For example, to calculate the specific heat, one would use:

$$\text{Cp}(\text{T}, \text{MOX}) = (1 - y)\text{Cp}(\text{T}, \text{UO}_2) + y\text{Cp}(\text{T}, \text{PuO}_2) \tag{7.46}$$

where the heat capacity values for UO_2 and PuO_2 are calculated using polynomial expressions developed by Fink (2000) for UO_2, and Cordfunke *et al.* (1990) for PuO_2. Enthalpy polynomials were derived by integrating the Cp equations. For a detailed discussion, listings of the polynomial expressions, and tables of the necessary constants used in these equations, the reader is referred to the original publications (Cordfunke *et al.*, 1990; Fink, 2000; Carbajo *et al.*, 2001). A recent study by Kandan and coworkers experimentally verified that the enthalpies of $(U,Pu)O_2$ solid solutions does obey the Neumann–Kopp molar additivity rule (Kandan *et al.*, 2004).

Enthalpy of Fusion There is only one experimental value for the enthalpy of fusion of a MOX fuel of composition $U_{0.8}Pu_{0.2}O_2$, where Leibowitz *et al.* (1974) obtained a value of 67(3) kJ mol^{-1}.

Thermal Conductivity The thermal conductivity of MOX fuels is a function of the temperature, fuel composition, porosity, burnup, and deviation from stoichiometric composition. Thermal conductivity is a property that does not follow the law of mixtures. The existing data have been reviewed by Carbajo *et al.* (2001). The thermal conductivity decreases with temperature up to approximately 2000 K and then increases with temperature. Addition of PuO_2 to the fuel or increasing porosities reduces the thermal conductivity. Burnup, and/or deviations from stoichiometry significantly decrease the thermal conductivity. For fully dense MOX fuel, Carbajo *et al.* recommended an equation that is a combination of that proposed by Dureiz *et al.* (2000) and that of Ronchi *et al.* (1999). For full details and discussion, the reader is referred to the review by Carbajo *et al.* (2001).

7.8.6 Plutonium halides and oxyhalides

The decreasing stability of the higher actinide oxidation states in progressing from uranium through neptunium to plutonium is perhaps most clearly revealed in the halogen compounds of plutonium. With the significant and most important exception of fluorine (and, to a minor degree, chlorine), all the halogens form solid binary trihalides of general formula PuX_3 (X = F, Cl, Br, I). For tetrahalides, the only stable solid is the tetrafluoride, PuF_4, while the binary tetrachloride is only marginally stable in the high temperature gas phase as $PuCl_4(g)$. Gas phase data have been interpreted in terms of PuF_5, but there are no known pentahalides, PuX_5, in the solid state (Jouniaux, 1979; Jouniaux *et al.*, 1979; Kleinschmidt, 1988). Fluorine forms the only binary PuX_6, the technologically important hexafluoride, PuF_6. All the halogens form trivalent oxyhalides PuOX (X = F, Cl, Br, I), while fluorine forms a number of oxyfluorides that include pentavalent $PuOF_3$, and hexavalent $PuOF_4$ and PuO_2F_2.

Complex tetrahalide salts of formula M_2PuX_6 are known for X = F, Cl, Br, where M is a monovalent cation. The fluoride ion forms a range of complex salts of general formula $MPuF_5$, $MPuF_6$, M_2PuF_6, M_3PuF_7, M_4PuF_8, and $M_7Pu_6F_{31}$ for the appropriate choice of monovalent cation, M.

Plutonium hexafluoride is by far the most volatile compound of plutonium and is of extraordinary interest in that it makes possible the study of a gaseous binary compound with a rare-earth-like f^2 electron configuration.

A number of reviews have been published in which the properties of the halides have been discussed in detail (Katz and Sheft, 1960; Hodge, 1961; Bagnall, 1967a,b; Brown, 1968; Peterson, 1995).

(a) Plutonium fluorides

(*i*) *Preparation*

Because of their importance in the preparation of plutonium metal (see Sections 7.7.1 and 7.7.2), the binary plutonium fluorides have received a fair amount of attention. Their preparation has been discussed in detail by Johns and Moulton (1944), Reavis *et al.* (1960), Dawson *et al.* (1951), and Dawson and Truswell (1951). The most common procedures involve hydrofluorination of plutonium dioxide or oxalates to generate PuF_3 and PuF_4, while stronger oxidizing conditions such as F_2 will generate PuF_6.

$$2PuO_2 + H_2 + 6HF \xrightarrow{600^\circ C} 2PuF_3 + 4H_2O \qquad (7.47)$$

$$Pu_2(C_2O_4)_3 + 6HF \xrightarrow{600^\circ C} 2PuF_3 + 3CO + 3CO_2 + 3H_2O \qquad (7.48)$$

$$2Pu(C_2O_4)_2 + 6HF \xrightarrow{600°C} 2PuF_3 + 3CO + 5CO_2 + 3H_2O \tag{7.49}$$

$$PuO_2 + 4HF \xrightarrow[O_2]{550°C} PuF_4 + 2H_2O \tag{7.50}$$

$$PuO_2 + 3F_2 \overset{300°C}{\rightleftharpoons} PuF_6 + O_2 \tag{7.51}$$

$$PuF_4 + F_2 \overset{300°C}{\rightleftharpoons} PuF_6 \tag{7.52}$$

Hydrogen fluoride stored in iron cylinders contains hydrogen, which forms on reaction with the container. Occasionally sulfur dioxide is present. Under reducing conditions like these, PuF_3 results. To secure positive results, either hydrogen may be added, or the absence of reducing agents can be ensured by the addition of oxygen. Between room temperature and 150°C, hydroxyfluorides of the type $Pu(OH)_2F_2$ or $Pu(OH)F_3$ are produced by reaction of PuO_2 with HF. These intermediate compounds are readily converted either to PuF_3 by HF and H_2, or to PuF_4 by HF and O_2 by raising the temperature above 200°C. Instead of plutonium dioxide or one of the oxalates, various other plutonium(III) or plutonium(IV) compounds may also be used as starting materials for fluoride preparations, such as plutonium(IV) nitrate or plutonium peroxide.

Plutonium trifluoride

Plutonium trifluoride is insoluble in water and may therefore be prepared as a hydrate by precipitation from aqueous solution by addition of hydrofluoric acid to an aqueous Pu(III) solution. The preparation of PuF_3 from solution is best accomplished by first reducing Pu(IV) with hydroxylamine (Dawson *et al.*, 1954b) or with SO_2 (Jones, 1953; Weigel, 1965). The purple crystals of the hydrated trifluoride, $PuF_3 \cdot nH_2O$, appear to contain less than one water molecule of hydration. According to Jones (1953), the exact composition of the hydrated compound is $PuF_3 \cdot (0.40 \pm 0.05)H_2O$.

Anhydrous PuF_3 may be obtained by heating $PuF_3 \cdot nH_2O$ in a stream of hydrogen fluoride gas at 200–300°C, or by first heating plutonium(III) oxalate in a stream of hydrogen at 150 to 600°C, followed by hydrogen fluoride at 200 to 300°C (Dawson and Truswell, 1951). The latter method has been used on the 100–350 g scale. PuF_4 may be reduced directly to anhydrous PuF_3 by heating in a stream of hydrogen at 600°C (Garner, 1950).

Plutonium tetrafluoride

Addition of hydrofluoric acid to aqueous plutonium(IV) solutions precipitates pale pink plutonium tetrafluoride hydrate, $PuF_4 \cdot 2.5H_2O$. Attempts to dehydrate this substance by heating *in vacuo* did not yield anhydrous plutonium tetrafluoride, but rather the trifluoride. According to Dawson *et al.* (1954b), this rather surprising result may be accounted for by the following reaction scheme:

$$\mathrm{PuF_4 + H_2O \rightleftharpoons PuO_2 + 4HF} \tag{7.53}$$

$$\mathrm{3PuF_4 + PuO_2 \rightleftharpoons 4PuF_3 + O_2} \tag{7.54}$$

with a net reaction of:

$$\mathrm{4PuF_4 + 2H_2O \rightleftharpoons 4PuF_3 + 4HF + O_2} \tag{7.55}$$

Increasing temperature and high vacuum displaces the equilibrium toward the right and aids in the production of the trivalent fluoride. Both plutonium trifluoride and tetrafluoride hydrates are insoluble in water and will dissolve in acid only sparingly. By contrast, they may be dissolved with comparative ease in aqueous solutions of ions that form stable complexes with fluoride ions, such as Zr(iv), Fe(iii), and Al(iii), or with BO_3^{3-} which forms BF_4^-. Solutions of 0.1 M HNO_3 saturated with boric acid or aluminum nitrate are therefore especially well suited for the dissolution of PuF_3 or PuF_4. Detailed procedures for the dissolution of PuF_4 with nitric acid have been summarized by Navratil (1969a–c).

Plutonium tetrafluoride hydrate, $PuF_4 \cdot 2.5H_2O$, may be dehydrated in a stream of HF gas to anhydrous PuF_4. According to Khanaev *et al.* (1967), the dehydration of $PuF_4 \cdot 2.5H_2O$ proceeds through the successive formation of $PuF_4 \cdot 2.5H_2O$, and ultimately anhydrous PuF_4.

Both plutonium trifluoride and plutonium tetrafluoride react with oxygen at elevated temperatures. Fried and Davidson (1949) concluded that the reaction of plutonium trifluoride with oxygen proceeds according to the equation:

$$\mathrm{4PuF_3 + O_2 \xrightarrow{600^\circ C} 3PuF_4 + PuO_2} \tag{7.56}$$

This conclusion was confirmed by Dawson and Truswell (1951), who measured the oxygen partial pressure for the reverse reaction of PuF_4 with PuO_2. In the presence of water vapor and oxygen, the reaction product is PuO_2 (Dawson and Elliott, 1953). Plutonium tetrafluoride is stable in oxygen at 600°C and *in vacuo* at 900°C. On heating PuF_4 *in vacuo*, some material sublimes and the residue is found to be PuF_3. Fried and Davidson (1949) interpreted this as a disproportionation of PuF_4 into PuF_3 and PuF_5. Dawson *et al.* (1951) confirmed these conclusions but were able to show that the sublimate is probably not PuF_5. It is possible that the compound formed in this process is an oxyfluoride, as observed by Jouniaux *et al.* (1979) for the reaction of PuO_2 with F_2.

Intermediate fluoride and plutonium pentafluoride

During the preparation of plutonium hexafluoride (see below), a brick-red solid residue has been observed. This solid was identified by X-ray powder diffraction and fluorine analysis by pyrohydrolysis to be the mixed-valent compound

Pu_4F_{17} (Mandleberg *et al.*, 1956). Hawkins (1956) and Gendre (1962) have also reported evidence for the existence of this compound, but it has not been isolated in the pure state. Jouniaux and coworkers proposed the formation of gas-phase PuF_5 in their thermochromatographic study (Jouniaux *et al.*, 1979), and Kleinschmidt (1988) also interpreted his mass spectroscopy results on PuF_6 in the presence of alumina in terms of formation of this gas-phase species.

Plutonium hexafluoride

It is well known that fluorine oxidizes transition metals to their highest oxidation states. This general characteristic also holds true for plutonium. The high volatility of PuF_6 has made this compound of great technological importance, and therefore a considerable amount of information about PuF_6 is available.

Plutonium hexafluoride was first prepared at Los Alamos by Florin and coworkers (Florin, 1950a,b, 1953; Florin and Tannenbaum, 1952; Florin *et al.*, 1956). The preparation and determination of some fundamental properties was carried out at Harwell by Mandleberg and colleagues (Hurst *et al.*, 1953; Mandleberg *et al.*, 1953, 1956), while Malm and coworkers (Malm and Weinstock, 1954; Weinstock and Malm, 1956a,b) performed extensive research on the basic properties of PuF_6 at Argonne National Laboratory. Scientists at Argonne (Chemical Engineering Division) performed extensive research on PuF_6 in connection with the development of the fluoride volatility process (Adams *et al.*, 1957; Steindler *et al.*, 1958, 1959; Steindler, 1963). The review by Steindler (1963) gives an excellent summary on the preparation and properties of plutonium hexafluoride.

Plutonium hexafluoride is most easily prepared by using elemental fluorine as an oxidizing–fluorinating agent with PuF_4 or PuO_2, typically at 600°C according to the following reactions:

$$PuO_2 + 3F_2 \rightleftharpoons PuF_6 + O_2 \tag{7.57}$$

$$PuF_4 + F_2 \rightleftharpoons PuF_6 \tag{7.58}$$

The fluorination of plutonium dioxide produces oxygen, which accumulates in any apparatus in which the gases are recirculated over the unreacted solid, and periodic removal of oxygen is required to avoid dilution of fluorine. Since plutonium tetrafluoride is always formed in the fluorination of plutonium dioxide, the preferred method of preparing PuF_6 is the fluorination of PuF_4.

The preparation of PuF_6 from PuF_4 and F_2 proceeds at a reasonable rate only at fairly high temperatures, typically at 300°C. Passage of fluorine over PuF_4, in a conventional tube furnace is possible, but is not very efficient. In order to prevent thermal decomposition of the PuF_6 product, special reaction vessels are employed to permit rapid condensation of the volatile products close to the point of their preparation. Fluorination reactor vessels of this type were first used by Florin and coworkers (Florin, 1950a,b, 1953; Florin and Tannenbaum, 1952; Florin *et al.*, 1956), and by Weinstock and coworkers (Malm and

Weinstock, 1954; Weinstock and Malm, 1956b). Two of these reactor designs are shown in Fig. 7.104. The starting charge of PuF_4 is placed in a nickel dish, which is heated in a fluorine atmosphere by an induction coil. The induction coil consists of copper tubing, through which liquid nitrogen is circulated, such that the coil serves as both the heating element and the product condenser. Once formed, the PuF_6 product collects on the surface of the coil in crystalline form. This type of reactor works very well for gram-quantity preparations. For larger quantities, fluidized-bed fluorination is the preferred method. Quantities up to 500 g of Pu have been volatilized in the fluidized-bed fluorination of PuF_4. For details of the technique, see Levitz *et al.* (1968).

The use of elemental fluorine at elevated temperature is the only known method of economically producing PuF_6. Los Alamos researchers evaluated

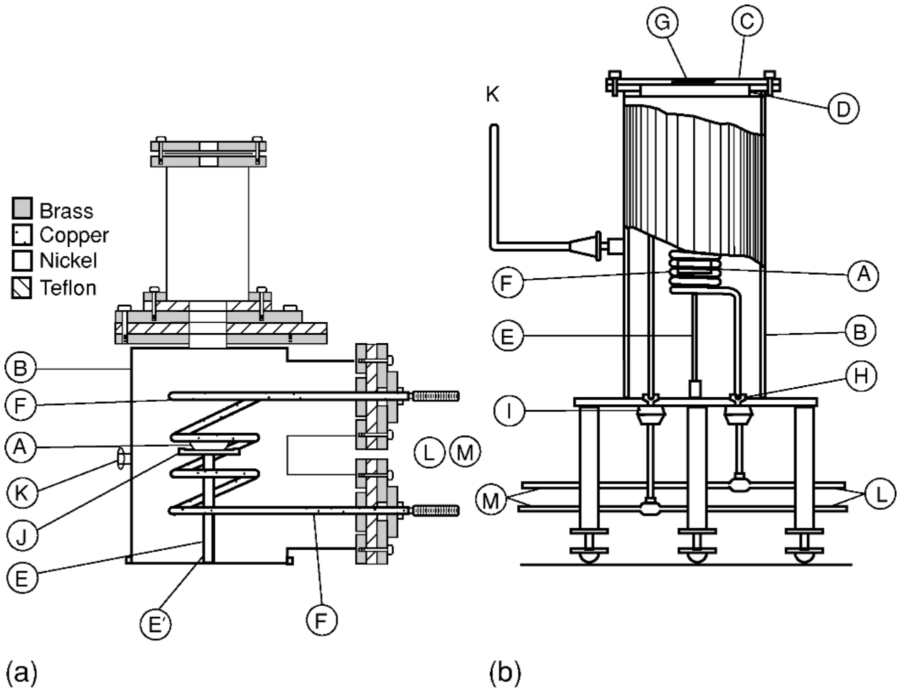

Fig. 7.104 *Two fluorination reactors for the preparation of plutonium hexafluoride. (a) The reactor used by Florin, Tannenbaum and Lemons, and (b) the reactor used by Weinstock and Malm. The legend for both reactors is as follows: A, nickel dish filled with* PuF_4*; B, brass reactor can; C, removable cover for loading the reactor; D, tongue and groove Teflon gasket for closure; E, nickel supporting rod for nickel dish; E′, nickel supporting tube; F, copper tubing induction coil that also serves as cooling coil; G, Fluorothene window; H, Teflon seal and insulator; I, Micalox insulator; J, support for nickel dish; K, connecting line to fluorine source, storage vessels and pumping systems; L, RF connection; M, liquid nitrogen circulation.*

the use of alternative oxidation fluorinating agents that proved capable of producing PuF_6 at or below room temperature (Eller *et al.*, 1992). Plutonium tetrafluoride, oxide, and oxyfluorides are all readily converted to PuF_6 by reaction with gaseous dioxygen difluoride O_2F_2 or O_2F_2/HF solutions at or below room temperature (Malm *et al.*, 1984; Erilov *et al.*, 2002). In a similar fashion, gaseous krypton difluoride, KrF_2 will also produce PuF_6 at ambient or low temperatures (Asprey *et al.*, 1986). The ability of both O_2F_2 and KrF_2 to volatilize plutonium at ambient temperature at moderate rates could have practical applications for recovery of plutonium as volatile PuF_6 from solid wastes.

Plutonium hexafluoride, when rigorously freed from traces of hydrogen fluoride, can be handled in glass equipment. Samples of PuF_6 can be purified by trap-to-trap distillation at cryogenic temperatures to remove HF, F_2, and other impurities. The handling and manipulation of PuF_6 is a very hazardous operation. A broken container means the spreading of hazardous plutonium through the air by the volatile and hydrolytically reactive hexafluoride. An actual multigram release of plutonium from a ruptured container has occurred and has been described by Trevorrow *et al.* (1965). Kessie and Ramaswami (1965) have described methods to prevent the spread of PuF_6 vapor through the ventilation system by operating the vacuum line containing the compound in a moist atmosphere. This hydrolyzes any escaped PuF_6 and converts it to PuO_2F_2, which is a filterable solid.

The rate of formation of plutonium hexafluoride by fluorination of the dioxide and the tetrafluoride was studied by Steindler (1963), who derived activation energies between 43.5 and 52.3 kJ mol^{-1}. These activation energies were found to be greater, the smaller the specific surface area. In the case of a PuF_4 sample having a bulk density of 1.3 g cm^{-3}, the rate of reaction with fluorine was found to follow the relationship

$$\log_{10}(\text{rate/mg PuF}_4\ \text{cm}^{-2}\text{h}^{-1}) = 5.917 - 2719/T \qquad (7.59)$$

The dependence of the reaction rate on the F_2 partial pressure is shown in Fig. 7.105 (Steindler, 1963).

(*ii*) *Solid-state structures*

Crystallographic data for plutonium halide and oxyhalide compounds are given in Table 7.42.

PuF_3. Plutonium trifluoride crystallizes in hexagonal (trigonal) symmetry and adopts the LaF_3 (tysonite) structure. Zachariasen (1949d) indexed the powder pattern based on hexagonal symmetry in space group $P6_3/mmc$. Subsequent work has shown that the tysonite structure has the larger trigonal cell ($P\bar{3}c1$), where $a_0 = a'_0/\sqrt{3}$ (Cheetham *et al.*, 1976). The polymeric structure is complicated, but the simple description is that each plutonium atom is surrounded by nine fluorine atoms, and the plutonium atoms lie on a two-fold axis of symmetry.

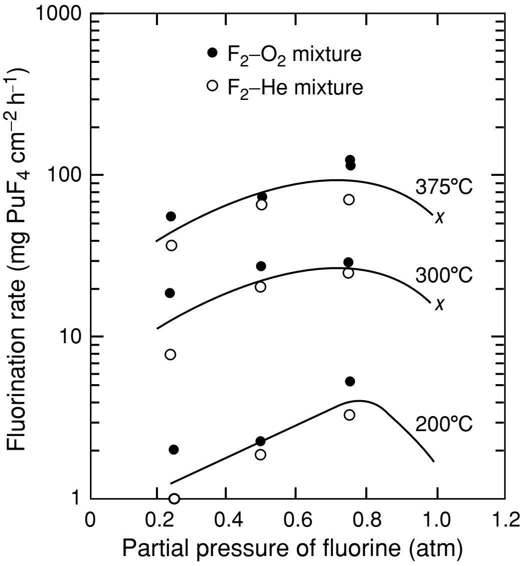

Fig. 7.105 *Fluorination of PuF_4 by fluorine diluted with He/O_2 mixtures to produce PuF_6* (*Steindler,* 1963).

PuF_4. Plutonium tetrafluoride has the ZrF_4 structure and is isostructural with all the lanthanide and actinide tetrafluorides (Wells, 1984). It possesses monoclinic symmetry, space group C2/*c*, with 12 molecules per unit cell (Zachariasen, 1949d). The basic repeating unit contains five plutonium atoms arranged in a distorted pyramid with four plutonium atoms forming a distorted base, and the fifth occupying the apex of the pyramid. Both types of nonequivalent plutonium atom are surrounded by eight fluorine atoms forming a slightly distorted square antiprism that shares vertices with eight other antiprisms. The local PuF_8 pseudo-antiprismatic coordination geometry in PuF_4 is illustrated in Fig. 7.106.

PuF_6. The solid-state structure of PuF_6 was determined by XRD by Florin and coworkers (Florin *et al.*, 1956). Crystalline PuF_6 possesses orthorhombic symmetry with four molecules per unit cell, with Pu–F distances spanning a range from 2.01 to 2.13 Å. The individual PuF_6 molecules in the crystal do not exhibit perfect octahedral symmetry, but spectroscopic studies clearly show that the compound retains octahedral symmetry in the gas phase (see below).

(*iii*) *Properties*

The plutonium trihalides have a small but finite volatility at elevated temperatures. Phipps *et al.* (1949, 1950a) were the first to measure the vapor pressures of the trihalides PuX_3, where X = F, Cl, and Br. In the case of PuF_3, the results are

Table 7.42 *Some physical constants and X-ray crystal structure data for plutonium halides and oxyhalides.*

				Lattice parameters				
Compound	*Color*	*Symmetry*	*Space group*	a_0 (Å)	b_0 (Å)	c_0 (Å)	*Density* (g cm^{-3})	*References*
PuF_3	violet-blue	trigonal	P$\bar{3}$*c1*[a]	7.092		7.254(1)	9.32	Zachariasen (1949d)
PuF_4	pale brown	monoclinic	C2/*c*[b]	12.59(3)	10.69(2)	8.29(4)	7.04	Keenan and Asprey (1969)
$PuF_4 \cdot 2.5H_2O$	pink	orthorhombic	P*nam*	12.66(3)	11.03(5)	6.99(5)	4.89	Dawson *et al.* (1954a)
PuF_6	reddish brown	orthorhombic	P*nma*[c]	9.888(9)	8.961(8)	5.203(5)	5.085	Florin *et al.* (1956)
$PuCl_3$	emerald green	hexagonal	P6_3/*m*	7.394(1)		4.243(1)	5.708	Burns *et al.* (1975)
$PuBr_3$	green	orthorhombic	C*mcm*[d]	4.097(8)	12.617(10)	9.147(10)	6.71	Brown and Edwards (1972)
$PuBr_3 \cdot 6H_2O$	blue	monoclinic	P2/*n*[e]	10.022(5)	6.798(3)	8.181(4)		Brown *et al.* (1968)
PuI_3	bright green	orthorhombic	C*mcm*[d]	4.326(6)	13.962(20)	9.974(20)	6.92	Brown and Edwards (1972)
PuOF	metallic	tetragonal	P4/*nmm*	4.05(1)		5.71(1)	8.20	Zachariasen (1951)
PuOCl	blue-green	tetragonal	P4/*nmm*	4.012(2)		6.792(10)	8.82	Zachariasen (1949d)
PuOBr	dark green	tetragonal	P4/*nmm*	4.022(4)		7.571(11)	9.08	Zachariasen (1949d)
PuOI	green	tetragonal	P4/*nmm*	4.042(2)		9.169(15)	8.47	Zachariasen (1949d)
PuO_2F_2	white	rhombohedral	R$\bar{3}$*m*	4.154		15.84	6.50	Wyckoff (1963)
$PuOF_4$	chocolate brown	trigonal	R3*m*	12.90(2)		5.56(2)		Burns and O'Donnell (1977)

[a] Originally reported by Zachariasen in hexagonal space group P6_3/*mmc*. The hexagonal LaF_3 (tysonite) has trigonal space group P$\bar{3}$*c1*, which is the likely space group for PuF_3. To transform from P6_3/*mmc* to P$\bar{3}$*c1*, one would use $a_0 = a'\sqrt{3}$ to derive $a_0 = 7.092$ (Å), which is the value reported above.

[b] $\beta = 126.0(2)$.

[c] Lattice constants refined from original data by Roof (1989).

[d] Original space group C*cmm*, changed to standard setting C*mcm* by Roof (1989).

[e] $\beta = 92.97(3)$.

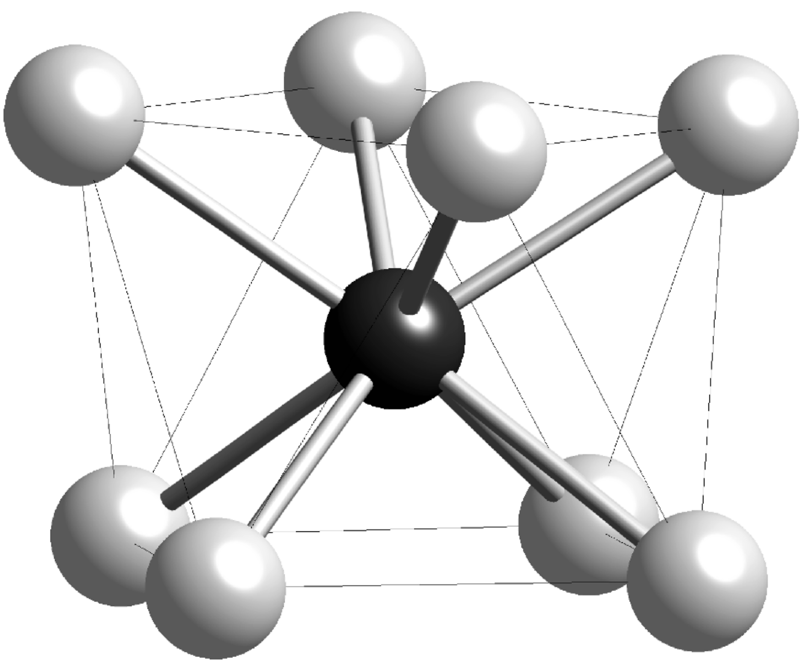

Fig. 7.106 *A view of the local coordination geometry of PuF_4 that emphasizes the local PuF_8 pseudo-antiprismatic coordination environment. The plutonium atoms are black and fluorine atoms gray.*

somewhat conflicting. In the work of Phipps *et al.* (1949, 1950a), an apparent inflection in the vapor–pressure curve implied an improbably low value for the melting point of 1447 K. A direct measurement by Westrum and Wallmann (1951) yielded values of (1698 ± 2) K for the melting point and (1699 ± 2) K for the solidification point, leading these authors to a different interpretation of the data and thus to a vapor–pressure equation that was different from the equation(s) given by Phipps *et al.* (1949, 1950a). Carniglia and coworkers (Carniglia, 1953; Carniglia and Cunningham, 1955) also measured the PuF_3 vapor pressure. Their data, agreed in general with the results of Phipps *et al.* (1949, 1950a), but the calculated enthalpies and entropies are both somewhat smaller. Kent (1968) reinvestigated the PuF_3 vapor pressure in the range 1243–1475 K by evaporating a mixture of PuF_3 and plutonium metal from a tantalum Knudsen cell attached to a mass spectrometer. He observed the species PuF_2^+, PuF^+, and Pu^+, but very little PuF_3^+. Kent used these data to obtain several important thermodynamic quantities, and have been reviewed by Lemire *et al.* (see Table 7.43).

The vapor pressure of PuF_4 has been measured by Mandleberg and Davies (1954, 1961), Chudinov and Choporov (1970), and Berger and Gäumann

(1961). Rand (1966) and Lemire *et al.* (2001) critically assessed these data. They prefer the results of Chudinov and Choporov to the data reported by the two other groups of authors. Chudinov and Choporov used a modified Knudsen method employing a nickel effusion cell, which is not attacked by fluorides. Rand discounts the measurements reported by Mandleberg and Davies because the tantalum effusion cell used by these authors would have reduced PuF_4 to PuF_3. On the basis of the known instability of PuF_5, there is also reason to believe that the disproportionation of PuF_4 into PuF_3 and PuF_5 postulated by Mandleberg and Davies is unlikely to occur, because the calculated pressure of PuF_6 in equilibrium with PuF_4 at 1200 K is 10^{-11} Torr, and because PuF_5 is less stable than PuF_6. The data of Berger and Gäumann (1961) yield too small an entropy change for a sublimation process, suggesting some reduction in their platinum effusion vessel. Another serious objection to these results is the implication that PuF_4 appears to be less volatile than UF_4, something that is not consistent with general trends in vapor pressures of other actinide halides.

In the case of $PuCl_3$ and $PuBr_3$, the only measurements reported are those by Phipps *et al.* (1949, 1950a) and, for $PuCl_3$, those by Weinstock (1944). No other recent measurements are reported. The vapor–pressure equations for PuI_3 were reported by Katz and Sheft (1960).

A detailed assessment and review of the important thermodynamic quantities such as the enthalpy of formation, standard entropy, heat capacity, and fusion data have been given by Lemire *et al.* (2001). Selected thermodynamic constants are given in Table 7.43.

Plutonium hexafluoride is a low-melting, highly volatile solid, whose vapor has the brown color of nitrogen dioxide, and which melts to a deep brown, transparent liquid. The following melting points have been reported: 325 K (52°C), 327 K (54°C), 323.7 K (50.5°C), and 324.74 K (51.59°C), the most-accurate value being the last, measured at $p = 533$ Torr. The boiling point was reported as 335.3 K (62.15°C).

The vapor pressure of PuF_6 has been measured by several authors (Hurst *et al.*, 1953; Mandleberg *et al.*, 1953, 1956; Florin *et al.*, 1956 Adams *et al.*, 1957). The most careful determination and description is that of Weinstock *et al.* (1959), who fit their data to a three-term function of temperature to derive a number of important thermochemical properties. A refit of their data by Lemire *et al.* (2001) gives $\Delta_{\mathrm{subl}}H^{\circ} = (48.65 \pm 1.00)$ kJ mol^{-1} and $\Delta_{\mathrm{f}}H^{\circ} = -(1861.35 \pm 20.17)$ kJ mol^{-1}.

Additional thermodynamic data for PuF_6 have been assessed and compiled by Rand (1966), Fuger *et al.* (1983), and Lemire *et al.* (2001). Thermodynamic data calculated from spectroscopic measurements were reported by Sundaram (1962), Nagarajan (1962), and Hawkins *et al.* (1954).

The PuF_6 molecule has 15 fundamental modes of vibration. These vibrations fall into two groups according to their predominant Pu–F stretching (ν_1, ν_2, ν_3) or bending (ν_4, ν_5, ν_6) modes. The symmetries of these modes indicate that ν_3, ν_4, ν_5, and ν_6 are all triply degenerate, ν_2 doubly degenerate, and ν_1 nondegenerate.

Table 7.43 *Thermodynamic parameters for plutonium halides* (*Lemire* et al., 2001).

Compound	$\Delta_f G^\circ_{298}$ (kJ mol^{-1})	$\Delta_f H^\circ_{298}$ (kJ mol^{-1})	S°_{298} (J K^{-1} mol^{-1})	$C^\circ_{p_{298}}$ (J K^{-1} mol^{-1})[a]
Solids				
PuF_3 (cr)	−1517.4 ± 3.7	−1586.7 ± 3.7	126.1 ± 0.4	92.6 ± 0.3
PuF_4 (cr)	−1756.7 ± 20.0	−1850 ± 20	147.3 ± 0.4	116.2 ± 0.3
PuF_6 (cr)	−1729.9 ± 20.2	−1861.3 ± 20.2	221.8 ± 1.1	168.1 ± 2.0
PuOF (cr)	−1091.6 ± 20.2	−1140 ± 20	96 ± 10	69.4 ± 10
$PuCl_3$ (cr)	−891.8 ± 2.0	−959.6 ± 1.8	161.7 ± 3.0	101.2 ± 4.0
$PuCl_4$ (cr)	−879.4 ± 5.8	−968.7 ± 5.0	201 ± 10	121.4 ± 4.0
$PuBr_3$ (cr)	−767.3 ± 2.7	−792.6 ± 2.0	198 ± 6	101.8 ± 6.0
PuOBr (cr)	−838.4 ± 8.5	−870 ± 8	127 ± 10	73 ± 8
PuI_3 (cr)	−579 ± 4.5	−579.2 ± 2.8	228 ± 12	110 ± 8
PuOI (cr)	−776.6 ± 20.5	−802 ± 20	130 ± 15	75.6 ± 10.0
Cs_2PuCl_6 (cr)	−1838.2 ± 6.7	−1982 ± 5	412 ± 15	
Cs_3PuCl_6 (cr)	−2208.0 ± 9.5	−2364.4 ± 9.0	545.9 ± 11.0	258.6 ± 10.0
$CsPu_2Cl_7$ (cr)	−2235.1 ± 5.3	−2399.4 ± 5.7	424 ± 7.3	254.9 ± 10.0
Cs_2PuBr_6 (cr)	−1636.3 ± 6.1	−1697.4 ± 4.2	470 ± 15	
$Cs_2NaPuCl_6$ (cr)	−2143.5 ± 5.2	−2294.2 ± 2.6	440 ± 15	
Gases				
PuF (g)	−141 ± 10.1	−112.6 ± 10.0	251 ± 5	33.5 ± 3.0
PuF_2 (g)	−626.1 ± 6.7	−614.3 ± 6.0	297 ± 10	51.5 ± 5.0
PuF_3 (g)	−1161.1 ± 4.8	−1167.8 ± 3.7	336.1 ± 10.0	72.2 ± 5.0
PuF_4 (g)	−1517.9 ± 22.2	−1548 ± 22	359 ± 10	92.4 ± 5.0
PuF_6 (g)	−1725.1 ± 20.1	−1812.7 ± 20.1	368.9 ± 1.0	129.3 ± 1.0
$PuCl_3$ (g)	−641.3 ± 3.6	−647.4 ± 2.0	368.6 ± 10.0	78.5 ± 5.0
$PuCl_4$ (g)	−764.7 ± 10.4	−792 ± 10	409 ± 10	103.4 ± 5.0
$PuBr_3$ (g)	−529.8 ± 15.7	−488 ± 15	423 ± 15	81.6 ± 10.0
PuI_3 (g)	−366.5 ± 15.7	−305 ± 15	435 ± 15	82 ± 5

[a] Temperature coefficients of this function are tabulated by Lemire *et al.* (2001) in their Table 4.3.

Only ν_3 (stretching) and ν_4 (bending) are infrared active. The first comprehensive gas-phase absorption spectrum covering 4,000–20,000 cm^{-1} was reported by Steindler and Gunther in 1964 (Steindler and Gunther, 1964a,b). The observed spectrum is shown in Fig. 7.107. These measurements were refined in the wavelength region between 3000 and 9000 cm^{-1} by Walters and Briesmeister (1984) using a very long pathlength cell. In both of these early studies, the spectrometers gave spectral resolutions of several wavenumbers so that vibrational components of the spectra were not resolved. Kugel *et al.* (1976) studied PuF_6 at much higher resolution using an intracavity laser quenching technique. Analysis of the room-temperature absorption spectrum is rendered difficult by the clustering of electronic transitions as well as number of hot bands that result from the low-energy bending vibrations (ν_4, ν_5, ν_6). In a low-temperature matrix, the elimination of rotations and hot bands greatly simplifies the spectral analysis. Dewey *et al.* (1986) studied the absorption and emission of matrix-isolated PuF_6 at 8 K and were able to assign transitions below 17,000 cm^{-1}. From these data, all the vibrational frequencies have been determined from the fundamental or combination bands, and they are compiled in Table 7.44 (Dewey *et al.*, 1986).

Kim and coworkers studied the fine structure in the vibronic band near 800 nm, resolving Coriolis fine structure at the Doppler-limited resolution (Kim *et al.*, 1987). Finally, David and Kim (1988) reported the entire absorption spectrum of PuF_6 in the near IR and visible regions at high sensitivity and high resolution. They measured isotope shifts between $^{239}PuF_6$ and $^{242}PuF_6$ to identify the specific vibrational modes. The Raman spectrum of PuF_6 has not yet been observed, because of the rapid photochemical decomposition at 5641 Å (Hawkins *et al.*, 1954).

The magnetic susceptibility of plutonium hexafluoride was measured at several temperatures by Gruen *et al.* (1956). Molar susceptibilities of 131×10^{-6} cgs units at 81 K and of 173×10^{-6} cgs units at 131 K were observed. Gruen *et al.* indicated that, based on the small susceptibilities observed compared with the susceptibility of isoelectronic compounds of U(IV), Np(V), and PuO_2^{2+}, which show larger, strongly temperature-dependent values, the ground electronic state of plutonium hexafluoride is nondegenerate (see Section 7.9.3). Furthermore, the first excited state of plutonium hexafluoride must be at least 1000 cm^{-1} (0.12 eV) above the ground state, which means that there is a much greater splitting than required for the isoelectronic U(IV) compounds.

Florin *et al.* (1956) studied the equilibrium system

$$PuF_6(g) \rightleftharpoons PuF_4(s) + F_2(g) \tag{7.60}$$

and obtained the equilibrium constant in the range 160–600°C. Their data showed a significant break at 308°C, suggesting a phase change. Weinstock and coworkers (Malm and Weinstock, 1954; Weinstock and Malm, 1956a) reported a measurement of the equilibrium constant at 220°C. Trevorrow and coworkers (Trevorrow and Shinn, 1960; Trevorrow *et al.*, 1961) reexamined this system and made a careful determination of the equilibrium constant in the

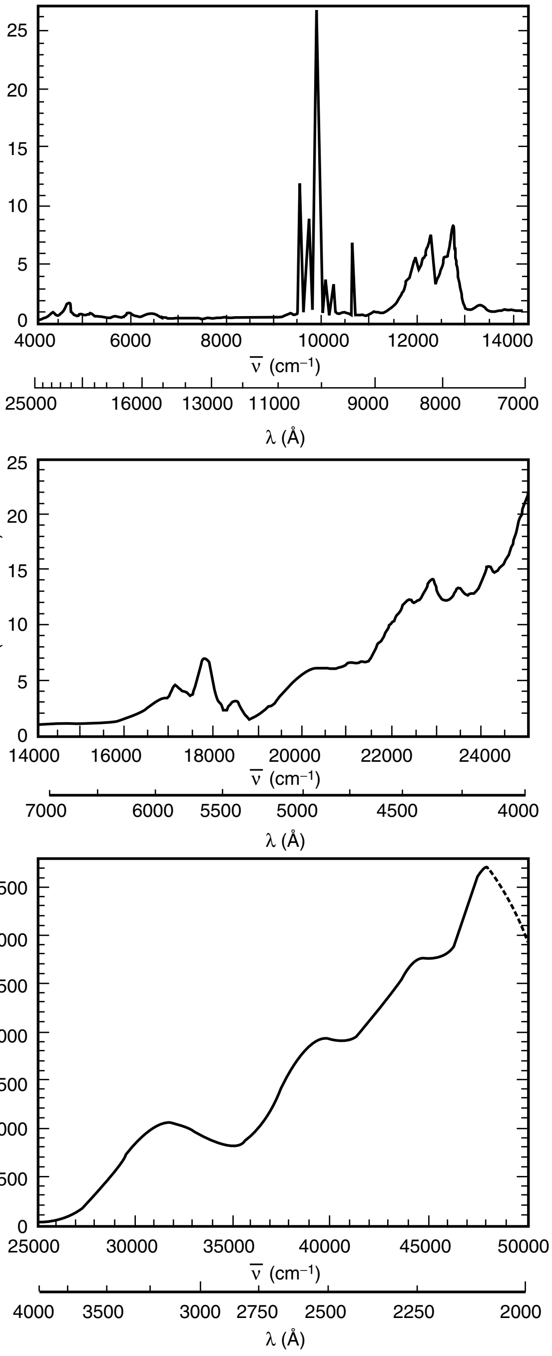

Fig. 7.107 *The absorption spectrum of gaseous PuF_6 from Steindler and Gunther* (1964*a*).

Table 7.44 *Vibrational frequencies of the PuF_6 molecule.*

Mode	*Matrix frequency* (cm^{-1})[a]	*Gas phase frequency* (cm^{-1})[b]
ν_1	(625)	(628)
ν_2	(519)	(523)
ν_3	612	616
ν_4	200[b]	(203)
ν_5	(209)	(211)
ν_6	(177)	(173)
$\nu_1 + \nu_3$	1236	1244
$\nu_2 + \nu_3$	1130	1139
$\nu_3 + \nu_5$	821	827
$\nu_1 + \nu_4$	–	831
$\nu_2 + \nu_4$	–	726
$\nu_4 + \nu_5$	–	414
$\nu_2 + \nu_6$	696	696

[a] From matrix isolation experiments by Dewey *et al.* (1986).

[b] From fluorescence measurements by Weinstock and Goodman (1965).

temperature range 150–400°C. Fig. 7.108 shows a plot of the log of the equilibrium constant K_p versus inverse temperature using the data of various authors (Florin *et al.*, 1956; Trevorrow and Shinn, 1960; Trevorrow *et al.*, 1961). Trevorrow and Shinn (1960) measured the equilibrium constant of the reverse reaction in the temperature range 170–395 K. This equilibrium has been measured at high pressures of fluorine (up to 825 bar) (Steindler *et al.*, 1958) and found to be pressure-independent. The free energy of the reaction

$$PuF_4(s) + F_2(g) \rightarrow PuF_6(g) \tag{7.61}$$

can be calculated from the equation

$$\Delta G^\circ = -RT \ln K = 2.55 \times 10^4 + 5.27T(\mathrm{K})\mathrm{J\ mol^{-1}} \tag{7.62}$$

The calculated value of ΔG° at 275°C is (28.36 ± 0.38) kJ mol^{-1}. The mean value of ΔH° for the reaction is (25.48 ± 0.59) kJ mol^{-1} and the mean value of ΔS° for the reaction is –(5.44 ± 0.84) J K^{-1} mol^{-1}.

Radiation decomposition

The α radioactivity of ^{239}Pu (Table 7.1) causes a continuous decomposition of PuF_6 (Steindler *et al.*, 1963; Wagner *et al.*, 1965). As the emitted α particle travels through the crystal lattice, bonds are ruptured and decomposition of PuF_6 to F_2 and lower plutonium fluorides occurs. The observed rate of decomposition (Gruen *et al.*, 1956) of gaseous PuF_6 is not a linear function of time but decreases with time from 1.78 to 0.064% of the initial PuF_6 (100 Torr) per day in the range from 0.5 to 571 days at 26°C. The initial high decomposition rate of 1.78% per day may be partly attributed to the reaction of the PuF_6 with the

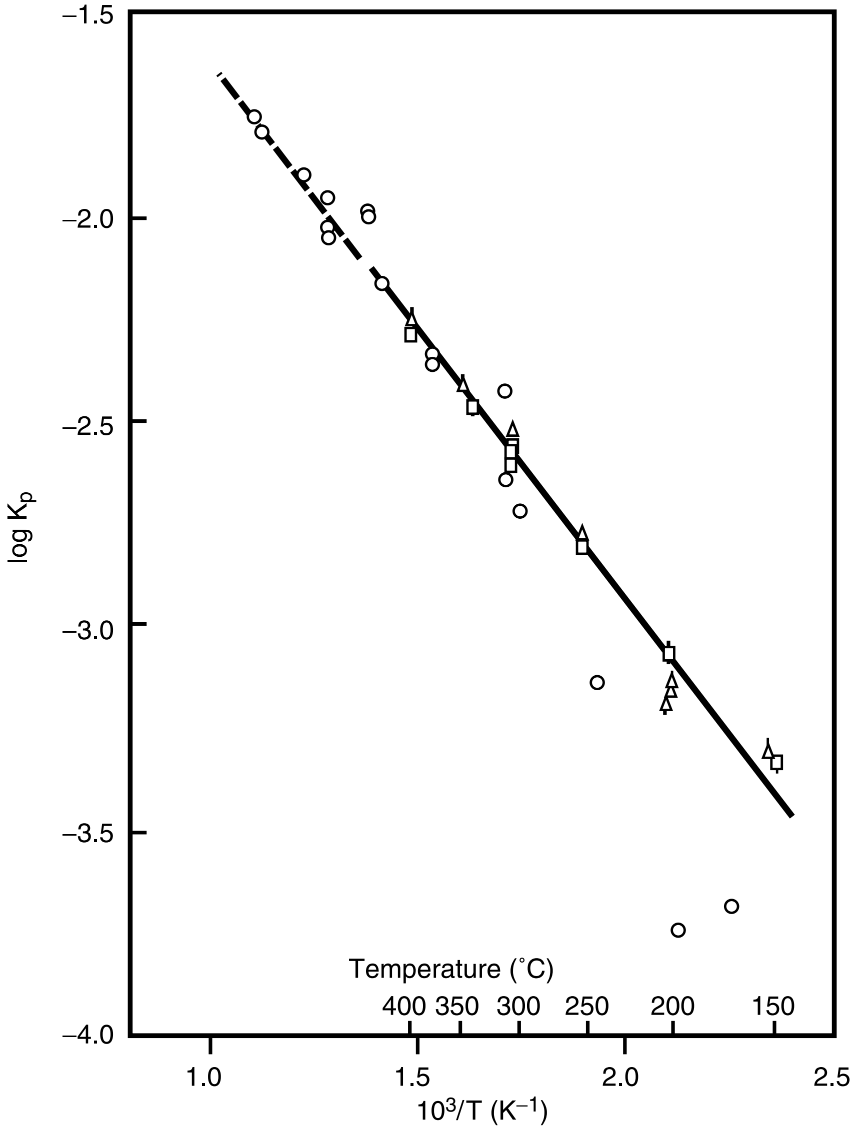

Fig. 7.108 *The relationship between the equilibrium constant and temperature for reaction* 7.60 (*Trevorrow and Shinn,* 1960). *Open circles are data from Florin* et al. (1956), *triangles are from Trevorrow* et al. *with heating to equilibrium, and squares are from Trevorrow* et al. *with cooling to equilibrium* (*Trevorrow* et al., 1961).

container material. If the pressure of the PuF_6 is lowered from 100 to 50 Torr, a lower decomposition rate is observed. Malm measured surprisingly low gas pressure in decades-old, sealed PuF_6 cylinders at ANL, and it was believed to be the result of recombination, probably involving F atoms (Morss, 2005).

Increase of the temperature introduces some thermal decomposition besides radiation decomposition. Observed rates after 77 days were (0.64 ± 0.66)% per day at 82°C, but only (0.18 ± 0.03)% per day at 26°C. Other factors influencing the decomposition of PuF_6 include the initial pressure and presence or absence of PuF_4, and presence or absence and partial pressure of He, Kr, O_2, N_2, or F_2. The exact mechanism of PuF_6 decomposition is still not completely known.

Steindler *et al.* (1963) studied the decomposition of PuF_6 under the influence of γ radiation. This is important because of the possible use of PuF_6 in the fluoride volatility process (see Section 7.5.7(c)). It was observed that PuF_6, if exposed to fission-product radiation, decomposes to form PuF_4 and F_2 with a *G*-value of (7.5 ± 1.7). Addition of 1 atm of He does not significantly change the *G*-value (number of molecules decomposed per 100 eV of radiation absorbed). Krypton, on the other hand, causes a marked enhancement of PuF_6 decomposition by γ radiation. The *G*-value observed in the presence of F_2 or O_2 is less than that observed with pure PuF_6. On the other hand, irradiation of mixtures of $PuF_4 + F_2$ produced larger quantities of PuF_6 than those calculated from the thermodynamic equilibrium constant at the temperature of the irradiation.

Because of the decomposition of PuF_6 by its own α radiation, the compound is best stored in the gaseous state under reduced pressure.

Chemical properties

Because plutonium hexafluoride tends to decompose into PuF_4 and F_2, it is a highly reactive fluorinating agent. The majority of its chemical properties are due to this reactivity.

(b) Plutonium chlorides, bromides, and iodides

In the plutonium–chlorine system, the only stable solid compound is $PuCl_3$, which has been prepared and characterized in large quantities. The only stable higher valent chloride is $PuCl_4$, which is not stable as a solid, and only known as a gaseous species that decomposes upon condensation. For the plutonium–bromine and plutonium–iodine systems, the only stable binary compounds are the trihalides, $PuBr_3$ and PuI_3.

(*i*) *Preparation*

Plutonium trichloride

This was one of the first plutonium compounds to have been prepared and characterized in detail following the initial discovery of the element (Abraham *et al.*, 1949a). Abraham *et al.* (1949a) and Garner (1950) have provided detailed discussions on the fundamental methods for its preparation. Of the various preparative methods, the hydrochlorination of plutonium(III) oxalate hydrate was found to work best on medium-scale reactions (1–10 g) according to the general reaction:

$$Pu_2(C_2O_4)_3 \cdot 10H_2O + 6HCl \rightarrow 2PuCl_3 + 3CO_2 + 3CO + 13H_2O \qquad (7.63)$$

The direct chlorination of plutonium metal at 303–500°C and subsequent sublimation at 600–800°C yields emerald green crystals of $PuCl_3$ on the 500 mg scale (Baumgärtner *et al.*, 1965). If metallic plutonium in 100 g quantities is available, this may be converted to the hydride, which is then reacted with HCl gas at 450°C in a fluid-bed reaction. The resulting $PuCl_3$ is fused at 800°C and sparged with HCl for 45 min to remove oxychlorides. The molten $PuCl_3$ may be purified by filtering through a fritted silica disk (Bjorklund *et al.*, 1959; Reavis *et al.*, 1960).

Chlorination of PuO_2 with either phosgene or carbon tetrachloride at temperatures above 500°C can produce analytically pure samples of $PuCl_3$ (Tolley, 1953; Boreham *et al.*, 1960). This process has been used at Los Alamos to convert large quantities of PuO_2 to anhydrous $PuCl_3$ (West *et al.*, 1988).

Christensen and Mullens (1952) developed a very straightforward procedure that is applicable in most transuranium chemistry laboratories, in which plutonium(III) oxalate is reacted with hexachloropropene at 180–190°C:

$$Pu_2(C_2O_4)_3 \cdot 10H_2O + 3C_3Cl_6 \rightarrow 2PuCl_3 + 3C_3Cl_4O + 3CO_2 + 3CO + 10H_2O \qquad (7.64)$$

The oxalate is refluxed with excess hexachloropropene for 18 h, yielding $PuCl_3$ of 96–98% purity, which is separated by filtration and further purified by sublimation. The method has been applied for preparations on the 100 g scale.

A method for continuous production of 98% $PuCl_3$ at a rate of 250 g h^{-1} was reported by Rasmussen and Hopkins (1961). In this process, $Pu(C_2O_4)_2 \cdot 6H_2O$ is first precipitated from Pu(IV) solution, dried on a filter drum, and calcined to reactive PuO_2. The PuO_2 is chlorinated to $PuCl_3$ with phosgene in a vibrating Hastelloy tube furnace at 500°C.

Plutonium(III) chloride, which is obtained by evaporation of a plutonium(III) solution in HCl, followed by dehydration of the $PuCl_3 \cdot 6H_2O$ residue in a stream of HCl, is a slate-blue solid. $PuCl_3$ prepared by one of the anhydrous methods is a blue-green solid or an emerald green, fine crystalline powder. Emerald green single crystals are obtained by condensation from the vapor phase (Burns *et al.*, 1975). As for other lanthanide and actinide trihalides, sublimation in evacuated, sealed quartz tubes is advisable for purification of $PuCl_3$ (Fuger and Cunningham, 1963).

Plutonium tetrachloride

As early as 1945, Brewer *et al.* (1949) predicted that no solid binary plutonium(IV) chloride should exist. However, from their calculations, the possible existence of gaseous $PuCl_4$ in an atmosphere of Cl_2 over $PuCl_3$ was inferred. Abraham *et al.* (1949a) were the first to observe an enhanced volatility of $PuCl_3$ in a stream of chlorine. This increase in volatility was ascribed to the formation of $PuCl_4$ by the equilibrium

$$\mathrm{PuCl_3 + 0.5\,Cl_2 \rightleftharpoons PuCl_4} \tag{7.65}$$

The $PuCl_4$ gas, on condensation, decomposes again to form solid $PuCl_3$ and Cl_2 gas. Abraham *et al.* (1949a) made the first calculations of the $PuCl_4$ partial pressure over $PuCl_3$ in an atmosphere of Cl_2 and predicted values in the range 10^{-5} mmHg at 500°C to 0.3 mmHg at 800°C. Benz (1962) employed a transpiration technique to determine the equilibrium constant and free energy for the above reaction.

Gruen and deKock (1967) measured the absorption spectrum of the gas phase over solid $PuCl_3$ in 1 atm of Cl_2. The absorption spectrum observed at 928°C is shown in Fig. 7.109, and shows unequivocally the presence of a new species, which is different from Cl_2 and $PuCl_3$. This spectrum is regarded as proof of the existence of gaseous $PuCl_4$.

Even though solid $PuCl_4$ has never been prepared, a number of tetravalent chloro complexes derived from $PuCl_4$, such as Cs_2PuCl_6, have been obtained, and are stable.

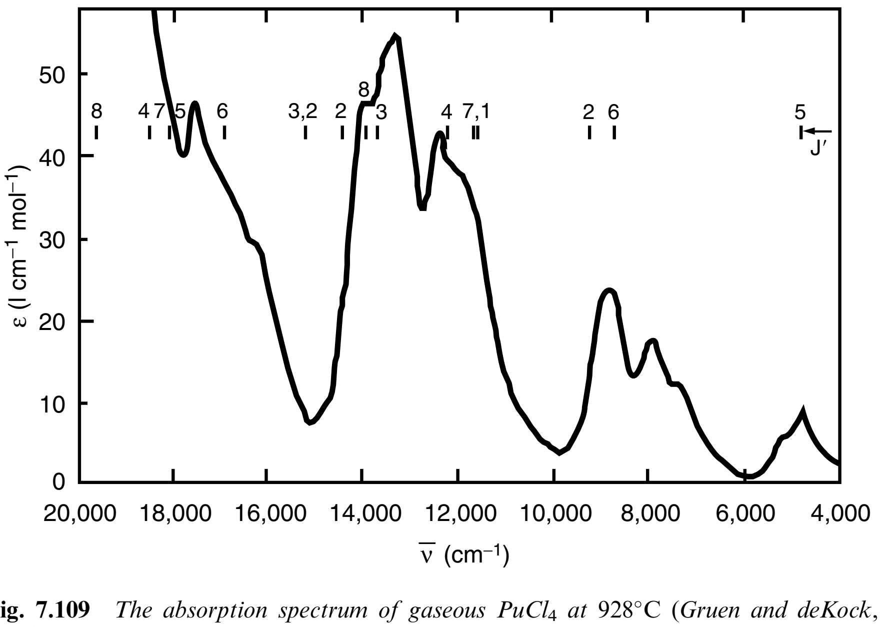

Fig. 7.109 *The absorption spectrum of gaseous* $PuCl_4$ *at* 928°C (*Gruen and deKock*, 1967).

Plutonium tribromide

This compound was first prepared by Hyde *et al.* (1944), and is a light-green solid. The methods for the preparation of $PuBr_3$ have been summarized by Bluestein and Garner (1944) and by Davidson *et al.* (1949). The two best methods for the preparation of $PuBr_3$ are the direct synthesis from the elements (Davidson *et al.*, 1949; Gruen and deKock, 1967), and the hydrobromination of the hydride at 600°C in a stream of HBr (Reavis *et al.*, 1960).

$$2Pu + 3Br_2 \rightarrow 2PuBr_3 \tag{7.66}$$

$$PuH_x + xHBr \xrightarrow{600^\circ C} PuBr_3 + xH_2 \tag{7.67}$$

Other satisfactory methods for the preparation of $PuBr_3$ include the dehydration of $PuBr_3 \cdot 6H_2O$ by controlled vacuum thermal decomposition (Brown *et al.*, 1968) and the hydrobromination of plutonium(III) oxalate at 400–600°C (Bluestein and Garner, 1944; Davidson *et al.*, 1949; Weigel *et al.*, 1982), either with pure HBr (Bluestein and Garner, 1944; Davidson *et al.*, 1949) or an HBr/H_2 mixture (Weigel *et al.*, 1982). These methods have the advantage that they do not require plutonium metal as the starting material, but make use of starting materials such as $Pu_2(C_2O_4)_3 \cdot 10H_2O$, which can be prepared from aqueous solutions (see Section 7.9.1.e.(i)).

Another method involves bromination of $Pu(OH)_4$ (dried at 70°C). This reaction proceeds satisfactorily above 600°C with HBr gas (Davidson *et al.*, 1949; Fomin *et al.*, 1958), and at 800°C with bromine and sulfur dibromide (Davidson *et al.*, 1949; Davidson and Katz, 1958). Plutonium(IV) oxalate or the tribromide hexahydrate react with HBr at 500°C and at 30–300°C, respectively, but the product of the latter reaction is usually contaminated with PuOBr. NH_4Br addition minimizes the PuOBr formation. Finally, one may convert $PuCl_3$ with HBr at 750°C (Davidson *et al.*, 1949; Bonnelle, 1976) and react PuO_2 mixed with carbon, sulfur, or phosphorus with Br_2 at elevated temperatures. Plutonium tribromide is a light green solid.

Plutonium triodide

The first attempts to prepare this compound were made by Hagemann *et al.* (1949). After initial failures, in which the oxyiodide was the reaction product, they finally succeeded in preparing PuI_3 by reacting plutonium metal with HI at 400°C. A more straightforward approach is the redox transmetallation reaction between plutonium metal and mercuric iodide, according to the reaction:

$$2Pu + 3HgI_2 \rightarrow 2PuI_3 + 3Hg \tag{7.68}$$

The plutonium metal and HgI_2 are sealed in a silica tube, and heated for 2 hours at 500°C (Asprey *et al.*, 1964). The mercury byproduct is conveniently separated by distillation away from the product. PuI_3 is extremely sensitive to moisture. Its properties have not been well characterized.

(*ii*) *Solid-state structures*

Crystallographic data on plutonium halides are summarized in Table 7.42.

$PuCl_3$. The crystal structure of $PuCl_3$ was first determined by Zachariasen (1948a) and later refined by Burns *et al.* (1975). Plutonium(III) chloride crystallizes in the hexagonal UCl_3 structure with two formula units per cell. Each plutonium atom has nine-fold coordination with a local tricapped trigonal prismatic coordination environment. Six chlorine atoms form a trigonal prism with Pu–Cl bonds of 2.886(1) Å, and the other three chlorine atoms cap the rectangular faces with Pu–Cl distances of 2.919 (1) Å (Burns *et al.*, 1975). The trigonal prisms share their triangular bases to form infinite chains along the crystallographic *c*-axis. These basic structural features are shown in Fig. 7.110.

$PuBr_3$ and PuI_3. Plutonium tribromide and triiodide are isostructural and display an orthorhombic structure known as the $PuBr_3$ structure. The structures

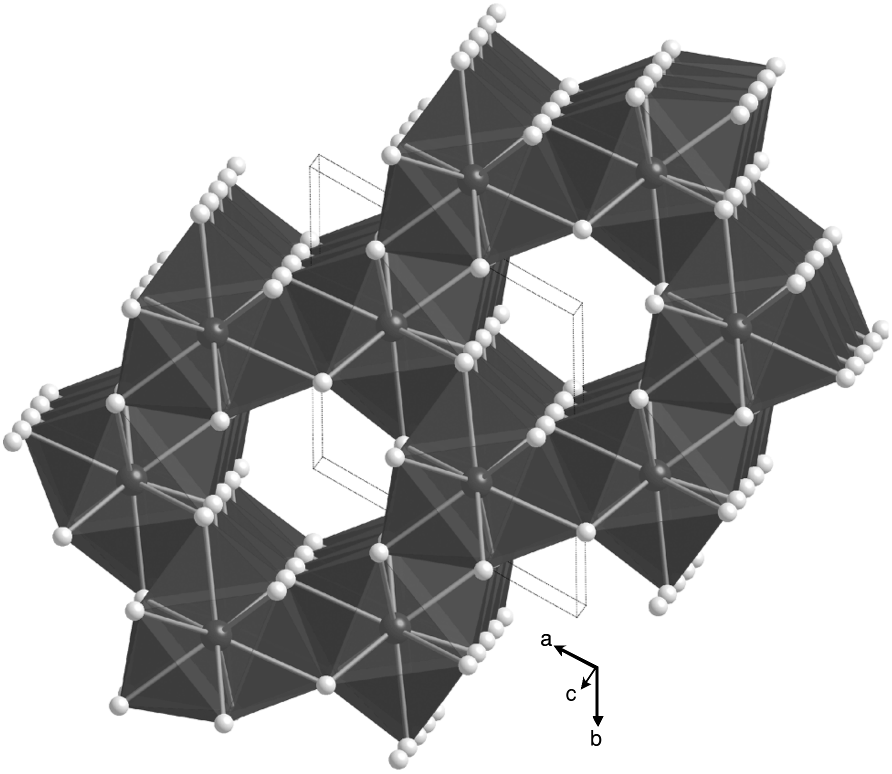

Fig. 7.110 *The solid-state crystal structure of $PuCl_3$ viewed down the c-axis and emphasizing both the hexagonal cell, and the infinite chains of tricapped trigonal prisms. Plutonium atoms are black, and chlorine atoms are light gray.*

of both $PuBr_3$ and PuI_3 were originally determined by Zachariasen (1948a), with subsequent refinements of the iodide reported by Asprey and coworkers (Asprey *et al.*, 1964). For $PuBr_3$, there are six Pu–Br bonds of 3.08 Å that form a trigonal prismatic geometry. There are two additional Pu–Br bonds that cap two of the three rectangular faces with Pu–Br distances of 3.06 Å. As in the $PuCl_3$ structure, these capped trigonal prisms stack in an infinite chain (this time along the *a*-axis) by sharing triangular bases as illustrated in Fig. 7.111. The infinite columns are now separated from each other such that the ninth bromine atom that would complete the tricapped trigonal prism is 4.03 Å away, and outside the bonding radius.

The main difference between the $PuCl_3$ and $PuBr_3$ structures is that in the $PuCl_3$ structure, each plutonium atom is nine-coordinate, while in the $PuBr_3$ structure, each plutonium atom is eight coordinate. This is surprising because the ninth bromine atom in the $PuBr_3$ structure is essentially in the correct position. The change in structure is thought to be due to the larger size of bromine and iodine (Brown, 1968), and the associated electron–electron repulsion between halogen atoms. A comparison of the column stacking between $PuBr_3$ and $PuCl_3$ structures is shown in Fig. 7.112.

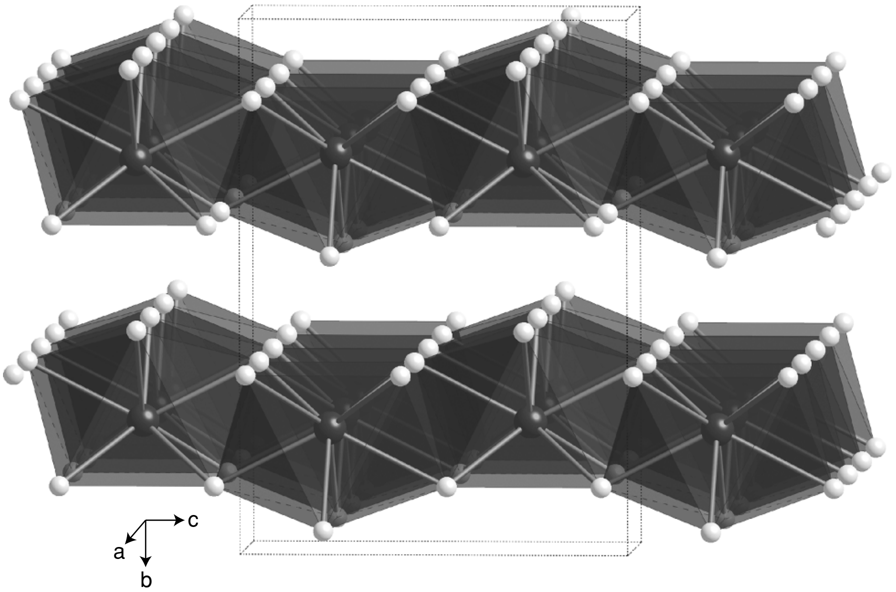

Fig. 7.111 *The solid-state crystal structure of $PuBr_3$ viewed down the a-axis and emphasizing the infinite chains of bicapped trigonal prisms. Plutonium atoms are black, and bromine atoms are light gray.*

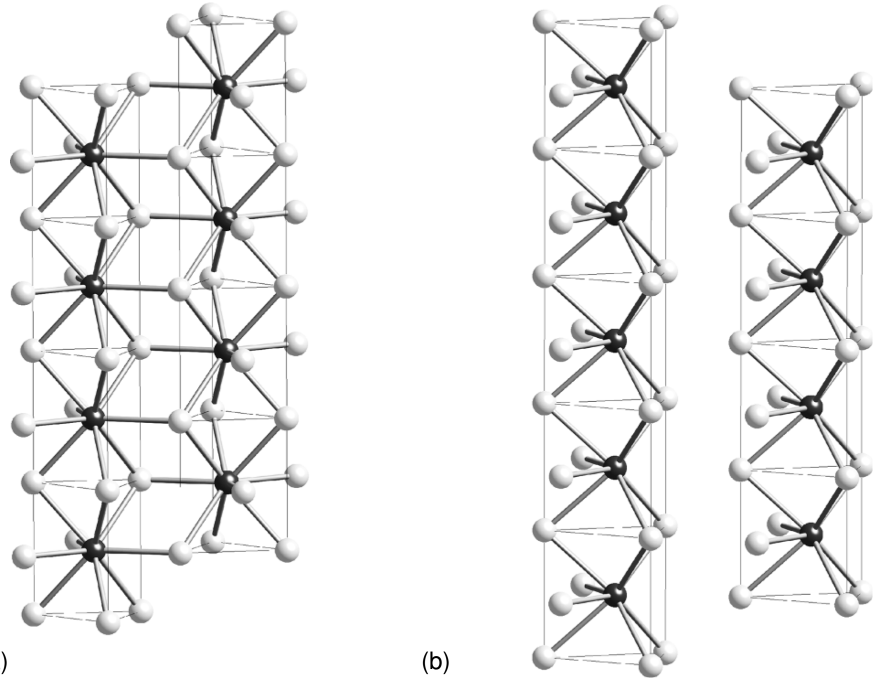

Fig. 7.112 *A comparison of the column stacking of* $PuCl_3$ *and* $PuBr_3$ *units. (a) The column arrangement of* $PuCl_3$ *units showing how tricapped trigonal prisms are formed by linking adjacent trigonal prismatic columns. (b) The column arrangement of trigonal prismatic units in the* $PuBr_3$ *structure, illustrating the vacant coordination site.*

(*iii*) *Properties*

The more important physical properties of plutonium(III) chloride are well known. Thermodynamic data are given in Table 7.43. The enthalpy of formation was first measured by Westrum and Robinson (1949a), then by Fuger and Cunningham (1963) and has been assessed by Fuger *et al.* (1983), and by Lemire *et al.* (2001). The standard free energy of formation as a function of T(K) was determined by Benz (1961), who found the following temperature dependence (958–1014 K):

$$\Delta G = -924.7 + 0.222\,92T(\text{kJ mol}^{-1}) \tag{7.69}$$

By electromotive force (EMF) measurements in fused PuCl–NaCl, Benz and Leary (1961) found the standard free energy and entropy of formation of pure solid $PuCl_3$ at 700°C to be 711 kJ mol^{-1} and 215.9 J K^{-1} mol^{-1}, respectively. From potentiometric measurements based on the Pu/$PuCl_3$ electrode, the free energy of formation of solid $PuCl_3$ in the 755–916 K temperature range was found to fit the expression

$$\Delta G = -909.6 + 0.175T(\text{kJ mol}^{-1}) \tag{7.70}$$

The optical properties of solid and gaseous $PuCl_3$ have been studied. Lipis and Pozharskii (1960) measured the absorption spectrum of $PuCl_3$ in the range 340–1000 nm. This spectrum is altered by water of crystallization, but not by absorbed or occluded water.

Conway and coworkers (Lammermann and Conway, 1963; Conway and Rajnak, 1966) measured the absorption spectrum of Pu^{3+} in an anhydrous $LaCl_3$ matrix and calculated the electrostatic, spin–orbit, and configuration-interaction parameters from these data.

The absorption spectrum of gaseous $PuCl_3$ was measured by Gruen and deKock (1967). Its energies and intensities are summarized in Table 7.45.

The magnetic susceptibility of $PuCl_3$ was measured in the range 90–600 K by Dawson *et al.* (1951). The temperature dependence of χ suggested a $5f^5$ electronic configuration for the Pu^{3+} ion.

The chemical properties of plutonium trichloride have been studied in great detail because of its application in molten-salt chemistry and metal production. $PuCl_3$ may be readily reduced to the metal by Ca, Mg, or La. The phase diagram

Table 7.45 *Energies and intensities of $PuBr_3(g)$ and $PuCl_3(g)$ transitions (Gruen and deKock,* 1967).

	$\bar{\nu}$ (cm^{-1})	ϵ (L cm^{-1} mol^{-1})	$\bar{\nu}$ (cm^{-1})	ϵ (L cm^{-1} mol^{-1})
$PuBr_3$(g)	5 810	2.2	17 390	20
	6 290	3.3	17 600	17 sh
	7 720	2.2 sh	17 860	19
	7 870	7	18 660	25 sh
	8 060	4.8	22 220	170 sh
	8 400	7.5 sh	22 730	210
	8 500	14	23 040	220
	8 930	4.0	23 360	230
	9 520	3.3 sh	23 580	230
	9 710	3.7	23 810	215
	10 870	4.0	24 510	180 sh
	14 490	3.7 sh	24 750	175 sh
	15 380	6 sh	25 000	165 sh
	16 390	9.5 sh	27 500	290 sh
	16 830	16	29 500	420 sh
	17 140	16	31 500	800
$PuCl_3$(g)	22 990	310	24 450	200
	23 360	330	24 940	160
	23 750	290	31 750	1 900

of the system $PuCl_3$–Pu has been studied by Johnson and Leary (1964). The metal solubility at the monotectic (740°C) was found to be 7%, but there was no indication of the formation of divalent plutonium. For the reaction of $PuCl_3$ melts with Am metal, see Mullins *et al.* (1966).

With water, $PuCl_3$ reacts to form several hydrates with 1, 2, or 6 H_2O, depending on the H_2O partial pressure (Abraham *et al.*, 1949a).

Sheft and Davidson (1949b) and Weigel *et al.* (1977) have measured the vapor-phase hydrolysis of $PuCl_3$ by determining the equilibrium constant of the reaction

$$PuCl_3(s) + H_2O(g) \rightleftharpoons PuOCl(s) + 2HCl(g) \qquad (7.71)$$

as a function of temperature. The two groups obtained nearly identical results with regard to the thermodynamic parameters of the above reaction.

With alkaline or alkaline-earth chlorides, a number of ternary chloro complexes are formed. For the individual compounds, see Section 7.8.6(d).

The optical properties of gaseous $PuBr_3$ have been studied by Gruen and deKock (1967). The energies and intensities are summarized in Table 7.45. The absorption spectrum of solid $PuBr_3$ was determined by Lipis and Pozharskii (1960) in the 340–1000 nm range. It was found to be similar to that of aqueous $PuBr_3$, but differed considerably from that of solid $PuCl_3$. This difference, together with the structural difference between $PuCl_3$ and $PuBr_3$, has been interpreted by Fomin *et al.* (1958) to indicate a change in the nature of bonding from predominantly ionic in $PuCl_3$ to predominantly covalent in $PuBr_3$.

The enthalpy of formation of $PuBr_3$ was first determined by Westrum (1949c) from its enthalpy of solution in 6 M HCl. The enthalpy of solution in O_2-free 0.1 and 1.0 M HCl, was also measured by Brown *et al.* (1977).

Sheft and Davidson (1949a) and Weigel *et al.* (1982) have measured the vapor-phase hydrolysis of plutonium(III) bromide by determining the equilibrium constant of the reaction

$$PuBr_3 + H_2O \rightleftharpoons PuOBr + 2HBr \qquad (7.72)$$

as a function of temperature. The results of both groups are in close agreement. The enthalpies of formation derived from these measurements, and reviewed by Lemire *et al.* (2001), are listed in Table 7.43.

$PuBr_3$ reacts with moisture to form the hexahydrate $PuBr_3 \cdot 6H_2O$ (Mullins *et al.*, 1966). The structural data of $PuBr_3 \cdot 6H_2O$ are listed in Table 7.42.

The enthalpy of formation of PuI_3 is reported by Brown *et al.* (1977).

(c) Oxyhalides of plutonium

Plutonium forms a number of oxyhalides in the valence states III and VI. So far, no oxyhalides of Pu(IV) or Pu(V) have been prepared. With Pu(III), the oxyhalides, PuOF, PuOCl, PuOBr, and PuOI are known.

(*i*) *Preparation and properties*

For plutonium(III) oxyfluoride, no direct method of preparation has been reported. Rather, PuOF was accidentally obtained in the attempted reduction of PuF_3 by hydrogen (Cunningham, 1954), and in an attempt to measure the melting point of plutonium metal.

Plutonium(III) oxychloride, PuOCl, was first prepared by Abraham *et al.* (1949a) by heating $PuCl_3 \cdot 6H_2O$ in a sealed tube at 400°C. The resulting preparation contained 60% PuOCl and 40% $PuCl_3$. In another similar preparation, a product containing 60–65% PuOCl and 40–35% $PuCl_3$ was obtained, which could be converted to pure PuOCl by heating in a sealed tube with 95 Torr H_2 and 55 Torr HCl at 675°C.

A preparation method yielding pure PuOCl in a one-step reaction was reported by Westrum and Robinson (1949b). They also made the first determination of the enthalpy of formation using the reaction of $PuCl_3$ with a stream of H_2, HCl and water vapor at 675°C.

The formation of PuOCl in the vapor-phase hydrolysis of $PuCl_3$ (see Section 7.8.6.b.(iii)) has been studied by several authors (Abraham and Davidson, 1949; Sheft and Davidson, 1949b; Weigel *et al.*, 1977), who have also determined the enthalpy of formation. The best values at the time of writing are given in Table 7.43.

Plutonium(III) oxybromide, PuOBr, was first observed by Davidson *et al.* (1949) as a residue from the sublimation of small amounts of $PuBr_3$ in a silica tube. It can be obtained in a pure state by treating gently heated Pu(IV) hydroxide (70°C) with moist hydrogen bromide at 750°C (Davidson *et al.*, 1949; Sheft and Davidson, 1949a), or by vapor-phase hydrolysis (Weigel *et al.*, 1982).

The enthalpy of formation of PuOBr was determined by Weigel *et al.* (1982) by measurement of the equilibrium constant of the vapor-phase hydrolysis of $PuBr_3$. Rand (1966), Fuger *et al.* (1983), and Lemire *et al.* (2001) have assessed previous values of the enthalpy of formation and the recommendations of the latter are listed in Table 7.43.

Plutonium(III) oxyiodide, PuOI, was observed to form in attempts to prepare PuI_3 (Hagemann *et al.*, 1949). In all reactions in which even traces of water are present, or are being formed in the course of the reaction, the bright-green PuOI is formed.

So far, no oxyhalides of tetravalent or pentavalent plutonium have been prepared. However, there is thermochromatographic evidence for the existence of $PuOF_3$ (Jouniaux, 1979; Jouniaux *et al.*, 1979), but this compound has not yet been isolated.

The only oxyhalides of hexavalent plutonium that have been isolated and prepared in substantial quantities are plutonyl fluoride, PuO_2F_2 (Alenchikova *et al.*, 1961a), plutonium(VI) oxytetrafluoride, $PuOF_4$ (Burns and O'Donnell, 1977), and plutonyl chloride, $PuO_2Cl_2 \cdot 6H_2O$ (Alenchikova *et al.*, 1959). $PuOF_4$ is formed when an excess of PuF_6 is condensed on a 0.23% solution of deionized water in HF, and the mixture is warmed to room temperature. After evaporation of unreacted HF and PuF_6, the $PuOF_4$ separates as a chocolate-brown solid. PuO_2F_2 is prepared by slow, low-temperature hydrolysis of PuF_6:

$$PuF_6 + 2H_2O \rightarrow PuO_2F_2 + 4HF \tag{7.73}$$

Alenchikova *et al.* (1961a) studied the system PuO_2F_2–HF–H_2O and observed $PuO_2F_2 \cdot H_2O$, $PuO_2F_2 \cdot HF \cdot 4H_2O$, and anhydrous PuO_2F_2 solids in equilibrium with the solution for 0–1.3% HF, 1.9–0.85% HF, and 87–100% HF, respectively.

Plutonyl chloride hexahydrate, $PuO_2Cl_2 \cdot 6H_2O$, has been prepared by vacuum evaporation at room temperature of Pu(VI) chloride solutions (Alenchikova *et al.*, 1959) formed by oxidation of Pu(IV) chloride solutions with chlorine. The greenish-yellow $PuO_2Cl_2 \cdot 6H_2O$ was identified by chemical and spectrophotometric analysis. $PuO_2Cl_2 \cdot 6H_2O$ is not stable, and gradually decomposes to a Pu(IV) compound.

(*ii*) *Solid-state structures*

All the PuOX compounds with heavier halides (Cl, Br, I) have the well-known PbClF structure type, and were first characterized by Zachariasen (1949d). This basic structure is built up of layers of different atom types. Each complex layer in the PuOX structure consists of a central sheet of coplanar oxygen atoms with a sheet of halogen atoms on each side, and plutonium atoms sandwiched in between. The basic layer structure is shown in Fig. 7.113(a). Within one of these complex layers, the plutonium atoms are coordinated by four oxygen and four chlorine atoms, making a local square antiprismatic coordination geometry. A view of the structure that emphasizes the square antiprismatic geometry is shown in Fig. 7.113(a).

The crystal structure of PuOF was originally reported to be cubic by Zachariasen (1949d), but a subsequent study of powder diffraction data showed that the compound was actually tetragonal (Zachariasen, 1951). In the tetragonal form, the structure fits into a class of MOF structures that display a superstructure that is related to the fluorite structure. In the tetragonal superstructure, the oxygen and fluorine atoms arrange themselves in sheets separated by a layer of plutonium atoms. The local coordination around plutonium is that of cube, with four fluorine atoms on one side, and four oxygen atoms on the opposite side. This cubic PuF_4O_4 coordination environment is compared with the square antiprismatic coordination environment found in PuOX (X = Cl, Br, I) in Fig. 7.113(b).

(d) Ternary halogenoplutonates

With ammonium, alkali, and alkaline-earth halides, and, in a few cases, with transition-metal halides, plutonium(III), (IV), (V), and (VI) halides form a large number of ternary halogenoplutonates.

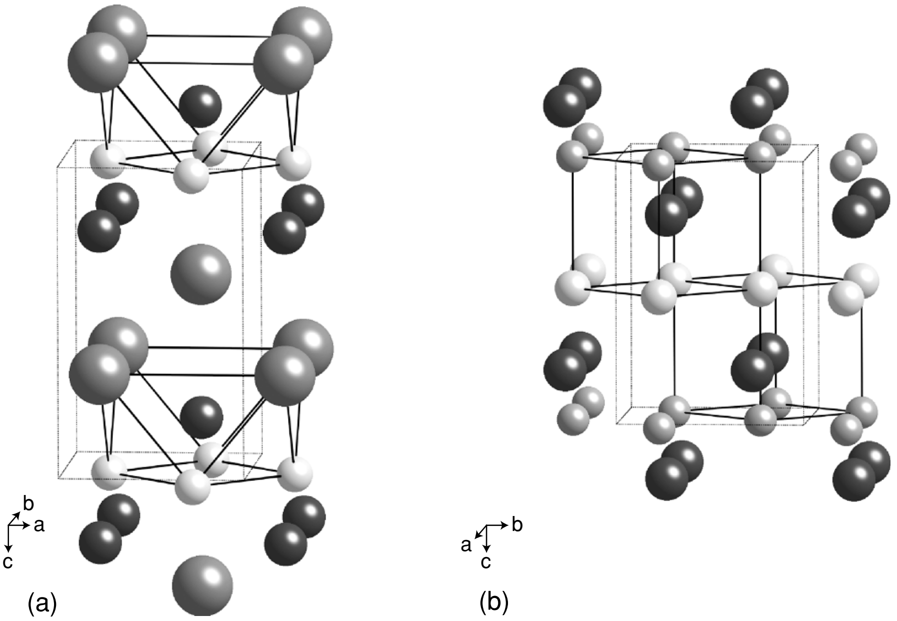

Fig. 7.113 *Comparison of PuOX solid-state structures. (a) The basic structural unit for PuOX (X = Cl, Br, I) illustrating the layered nature of the repeat units, and the local* PuO_4X_4 *square antiprismatic local coordination geometry. (b) The basic structural unit for tetragonal PuOF showing the layered nature of repeat units, and the local cubic* PuO_4F_4 *coordination geometry.*

The fluoroplutonates and pseudo-binary systems containing plutonium fluorides are of major interest as potential materials for molten-salt fuels in high-temperature reactors. Therefore, much work has been devoted to the individual compounds and, in some cases, to pseudo-binary phase diagrams. Leary (1962) has summarized the phase diagram work done up to 1962.

The preparation of individual fluoroplutonates depends on the nature of the compound to be prepared. The following methods are the ones usually employed.

1. A compound is precipitated from aqueous solution, and dried below 100°C.
2. Stoichiometric amounts of alkali halide and plutonium(III) or plutonium(IV) halide in HCl or HF solution(s) are evaporated to dryness. The residue is heated in a platinum boat or a sapphire dish at 300°C in a stream of HF.
3. Stoichiometric amounts of PuF_4 or PuO_2 and alkali or alkaline-earth fluoride are intimately mixed and heated at 300–600°C in a stream of HF, HF + O_2, or HF + H_2 (the latter for preparation of Pu(III) complexes).
4. Stoichiometric amounts of PuF_4 or PuO_2 and NH_4F are heated together in a closed vessel at 70–100°C. The product is pulverized and heated again in

the same manner. This procedure is repeated until a homogeneous product has been obtained.

5. Thermal decomposition of a higher complex, or treatment of another plutonium fluoro complex with elemental fluorine.
6. PuF_6 and alkali or alkaline-earth fluoride are reacted.
7. Alkali carbonate is added to plutonium nitrate solution, the solution evaporated with HF and treated with F_2.
8. PuF_4 is fused with the stoichiometric amount of the corresponding alkali fluoride.
9. PuF_4 is fused with the stoichiometric amount of alkali or metal fluoride.
10. Cooled solution of Pu(v) in dilute acid is added to ice-cold saturated RbF solution.

The known fluoroplutonate complexes have been compiled in Table 7.46. The phase diagrams of the systems LiF–PuF_3 and NaF–PuF_3 have been reported by Barton *et al.* (1961). These two systems are the only ones based on PuF_3 for which phase diagrams have been determined. No other systems, neither based on PuF_3 nor based on PuF_4, have been reported.

With the chloride systems, a different situation exists. Even though only very few compounds have been characterized as individual entities, several phase diagrams have been determined. Most of the compounds occurring in these phase diagrams have never been studied in great detail. Phase diagrams have been reported for solid–liquid equilibria in the binary systems $PuCl_3$–MCl, where M = Li (Bjorklund *et al.*, 1959), Na (Bjorklund *et al.*, 1959), K (Benz *et al.*, 1959), Rb (Benz and Douglass, 1961b), Cs (Benz and Douglass, 1961b), and $PuCl_3$–$M'Cl_2$, where M′ = Mg, Ca, Sr, and Ba (Johnson *et al.*, 1961). An excellent summary of these phase diagrams was reported by Leary (1962). Some of the systems based on $PuCl_3$ have become of practical importance in fused-salt ER of plutonium, and in the DOR and pyroredox processes (see Section 7.7.2). As a representative phase diagram of such a system, the diagram of the system KCl–$PuCl_3$ is shown in Fig. 7.114 (Benz *et al.*, 1959). In these systems based on $PuCl_3$, compounds such as $RbPu_2Cl_7$ (light blue), $CsPu_2Cl_7$ (greenish blue to deep green), $RbPuCl_5$ (brownish to greenish yellow), Cs_3PuCl_6 (green), or M_3PuCl_9 (M = Sr, Ba) (no color given) have been observed, but none of these compounds have been studied in detail.

The hexachloroplutonates M_2PuCl_6, where M = Na, Rb, Cs, $(CH_3)_4N^+$, or $(C_2H_5)_4N^+$, are obtained as pale greenish yellow (alkali compounds) or orange-yellow (alkylammonium compounds) crystals by precipitation from concentrated HCl solution. Except for Cs_2PuCl_6, the properties of these compounds are not known in detail. Cs_2PuCl_6 is sufficiently stable to be useful as a primary plutonium standard (Miner *et al.*, 1963). No bromo or iodo complexes of plutonium(IV) are known, with the sole exception of the red bromo complex, $[(C_2H_5)_4N]_2PuBr_6$, which was prepared by Ryan and Joergensen (1964) by precipitation from ethanolic HBr solution on the addition of acetone.

Table 7.46 *X-ray crystal structure data for plutonium double fluorides.*

Plutonium valence	*Compound*	*Color*	*Symmetry*	*Space group*	*Lattice parameters*			*Angle* (deg)	*Density* (g cm^{-3})	*References*
					a_0 (Å)	b_0 (Å)	c_0 (Å)			
Pu(III)	$NaPuF_4$	blue	hexagonal	P321	6.129(6)		3.753(4)			Zachariasen (1948a)
					6.13(2)		3.76(1)		6.87	Keller and Schmutz (1964)
	$KPuF_4$		orthorhombic	P*nma*	6.23	3.75	15.42		6.53	Jove and Pagès (1977)
	$RbPuF_4$		orthorhombic	P*nma*	6.39	3.80	15.86		6.91	Jove and Pagès (1977)
	KPu_2F_7	blue	cubic	F*m*3*m*	5.880				5.31	Schmutz (1966)
Pu(IV)	$LiPu_4F_{17}$		tetragonal		8.84(1)		11.31(2)		7.25	Jove and Cousson (1977)
	KPu_2F_9	red-brown	orthorhombic[a]	P*nma*	8.58(4)	11.35(6)	6.96(4)		6.74	Zachariasen (1948b)
	$LiPuF_5$	brown	tetragonal	$I4_1/a$	14.67(2)		6.479(5)			Keenan (1966)
			tetragonal	$I4_1/a$	14.65(1)		6.486(5)		6.51	Keller and Schmutz (1966)
	$NaPuF_5$	green	rhombohedral	$R\overline{3}$	8.93(3)			$\alpha = 107.48(16)$	6.03	Zachariasen (1948b)
	$KPuF_5$	green	rhombohedral	$R\overline{3}$	9.27(3)			$\alpha = 107.03(08)$	5.66	Zachariasen (1948b)
	$RbPuF_5$	green	rhombohedral	$R\overline{3}$	9.46(3)			$\alpha = 106.93(16)$	5.88	Zachariasen (1948b)
	α-NH_4PuF_5	light brown	rhombohedral	$R\overline{3}$	9.42					Benz *et al.* (1963)
	β-NH_4PuF_5	yellow-green	orthorhombic		9.83	6.98	6.27			Benz *et al.* (1963)
	$Li_7Pu_6F_{31}$	brown	tetragonal		14.650(1)		6.468(5)		4.96	Schmutz (1966)
	$Na_7Pu_6F_{31}$	brown/green	rhombohedral	$R\overline{3}$	9.006			$\alpha = 107.75$	6.14	Schmutz (1966)
			(hexagonal)		14.52(2)		9.704(3)		6.14	Keller and Schmutz (1966)
	$K_7Pu_6F_{31}$	green/brown	rhombohedral	$R\overline{3}$	9.275(5)			$\alpha = 107.17$	5.77	Schmutz (1966)
			(hexagonal)		14.93(2)		10.28(1)		5.76	Keller and Schmutz (1966)
	$Rb_7Pu_6F_{31}$	green/brown	rhombohedral	$R\overline{3}$	9.466(5)			$\alpha = 106.90(1)$	6.14	Schmutz (1966)
			(hexagonal)		15.21(2)		10.61(1)			Keller and Schmutz (1966)

Table 7.46 (*Contd.*)

Plutonium valence	*Compound*	*Color*	*Symmetry*	*Space group*	*Lattice parameters*			*Angle* (deg)	*Density* (g cm^{-3})	*References*
					a_0 (Å)	b_0 (Å)	c_0 (Å)			
	$(NH_4)_7Pu_6F_{31}$	orange	rhombohedral	R$\overline{3}$	9.42			$\alpha = 107.33$		Benz *et al.* (1963)
	$Tl_7Pu_6F_{31}$		(hexagonal)		15.08		10.40			Jove *et al.* (1976)
	Na_2PuF_6	pink	hexagonal	P321	6.059(5)	7.130(5)			5.84	Keller and Schmutz (1966)
		pink-brown	hexagonal	P321	6.055(3)		3.571(5)			Alenchikova *et al.* (1958)
	Rb_2PuF_6		orthorhombic	C*mcm*	6.971(18)	12.033(16)	7.602(10)			Keenan (1967)
	Cs_2PuF_6		orthorhombic		12.145	7.156	4.056			Riha and Trevorrow (1965)
	$(NH_4)_2PuF_6$	pink								Benz *et al.* (1963)
	Tl_2PuF_6		orthorhombic	P*mma*^{b}	11.35(2)	6.89(1)	4.05(1)			Jove *et al.* (1974)
	$CaPuF_6$	red-brown	hexagonal	P$\overline{3}$*c1*^{c}	3.997		7.097		6.65	Keller and Salzer (1967)
	$SrPuF_6$	red-brown	hexagonal	P$\overline{3}$*c1*^{c}	7.091		7.255		6.95	Keller and Salzer (1967)
	Na_3PuF_7		tetragonal	I4/*mmm*	5.460		10.920		3.98	Riha and Trevorrow (1965)

	Tl_3PuF_7		cubic	F*m*3*m*[d]	9.30				8.13	Jove *et al.* (1974)
	$(NH_4)_4PuF_8$	pink-red								Benz *et al.* (1963)
Pu(v)	Rb_2PuF_7	green	monoclinic	$P2_1/c$	6.270(8)	13.416(8)	8.844(8)	$\beta = 90$		Penneman *et al.* (1965)
	$CsPuF_6$	green	rhombohedral	$R\overline{3}$	8.036(3)		8.388(4)		5.16	Penneman *et al.* (1965)
	$RbPuO_2F_2$	lavender	rhombohedral	$R\overline{3}m$	6.796(8)			$\alpha = 36.28$		Keenan (1965)
	$(NH_4)PuO_2F_2$	lavender	rhombohedral	$R\overline{3}m$	6.817(6)			$\alpha = 36.27$		Keenan (1965)
Pu(vi)	$KPuO_2F_3 \cdot H_2O$		cubic		8.126					Alenchikova *et al.* (1961b)
	$RbPuO_2F_3 \cdot H_2O$		cubic		8.458					Alenchikova *et al.* (1961b)
	$CsPuO_2F_3 \cdot H_2O$		cubic		8.916					Alenchikova *et al.* (1961b)

---

[a] Space group reported as P*nam*, changed to standard setting P*nma* by Roof (1989).

[b] Original lattice constant reported in space group P*mcm*. Changed to standard setting P*mma* by Roof (1989).

[c] Roof (1989) suggests that the original space group $P6_3/mmc$ is likely the trigonal space group $P\overline{3}c1$, hence the *a*-axis lattice constant has been divided by $\sqrt{3}$ to derive the value reported above.

[d] Jove reports the lattice constants, Avignant describes that the structure is isotypic of $(NH_4)_3ZrF_7$ (Avignant and Cousseins, 1971), and this structure is described by Hurst (Hurst and Taylor, 1970).

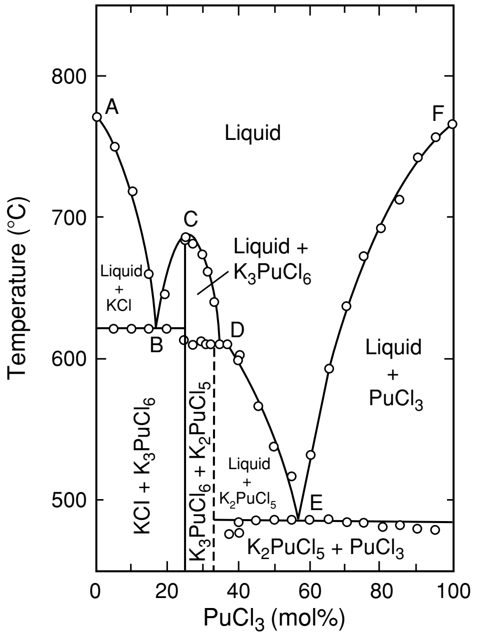

Fig. 7.114 *The phase diagram of the KCl–*$PuCl_3$ *system* (*Benz* et al., 1959). *Key points in the diagram include A, the KCl melting point at* 771°C; *B, eutectic point at* 621°C *corresponding to* 17% $PuCl_3$*; C,* K_3PuCl_6 *melting point at* 685°C; *D, peritectic point at* 611°C *and* 35% $PuCl_3$*; E, eutectic point at* 486°C *and* 57% $PuCl_3$*;and F,* $PuCl_3$ *melting point at* 769°C.

A number of derivatives of plutonyl chloride, PuO_2Cl_2, which is known as the hexahydrate $PuO_2Cl_2 \cdot 6H_2O$ (Alenchikova *et al.*, 1959), have been prepared. These compounds contain the anion $[PuO_2Cl_4]^{2-}$. Probably the best-known compounds of this type are the rubidium salt, $Rb_2PuO_2Cl_4$, and the cesium salt, $Cs_2PuO_2Cl_4$, which form orange-yellow crystals. The lattice constants of both compounds have been determined by Werner (1982) and are listed in Table 7.47. The lattice constants and other crystallographic properties determined for halo complexes of plutonium are listed in Table. 7.47.

7.9 SOLUTION CHEMISTRY

Descriptive solution and coordination chemistry played a key role in the discovery of plutonium and in the formulation of the actinide series concept (Seaborg and Loveland, 1990). The need to separate and purify plutonium from nuclear fuel during the Manhattan Project drove much of the early solution chemistry and included the extraction of plutonium coordinated by organic ligands, pyrochemical processing in molten salts, and the distillation or

Table 7.47 *X-ray crystal structure data for plutonium double chlorides*[a].

Compound	*Color*	*Symmetry*	*Space group*	*Lattice parameters* a_0 (Å)	b_0 (Å)	c_0 (Å)	*Density* (g cm^{-3})	*References*
Pu(III)								
K_2PuCl_5		orthorhombic	P*nma*	12.626(12)	8.674(7)	7.953(5)		Axler *et al.* (1992)
K_2PuCl_5		orthorhombic	P*nma*	12.674(3)	8.727(2)	7.969(2)	3.73	Morss and Fujino (1988b)
Rb_2PuCl_5		orthorhombic	P*nma*	13.093(8)	8.909(5)	8.178(5)	4.09	Morss and Fujino (1988b)
Pu(IV)								
K_2PuCl_6		monoclinic[b]	P2/*m*	7.218(5)	7.611(6)	10.208(7)	3.14	Morss and Fujino (1988a)
Rb_2PuCl_6		hexagonal	$\mathrm{P}6_3mc$	7.377(2)		11.880(7)	3.69	Morss and Fujino (1988a)
Cs_2PuCl_6	pale yellow	trigonal	$\mathrm{P}\bar{3}m$	7.44(1)		6.04(1)	4.10	Zachariasen (1948c)
$[(CH_3)_4N]_2PuCl_6$	orange-yellow	fcc	F*m*3*m*	12.96(5)			1.330	Staritzky and Singer (1952)
$[(C_2H_5)_4N]_2PuCl_6$	yellow	orthorhombic	F*mmm*	14.23(1)	14.53(3)	13.53(5)	1.691	Staritzky and Singer (1952)
Pu(VI)								
$Rb_2PuO_2Cl_4$	orange	monoclinic[c]	I2/*c*	11.60(3)	7.42(5)	5.50(3)		Werner (1982)
$Cs_2PuO_2Cl_4$	orange	monoclinic[d]	I2/*c*	11.879(6)	7.693(6)	11.533(7)		Werner (1982)
$[(CH_3)_4N]_2PuO_2Cl_4$	yellow	tetragonal	I4/*m*	10.00(5)		12.90(5)		Staritzky and Singer (1952)
$[(C_2H_5)_4N]_2PuO_2Cl_4$	yellow	tetragonal	I4/*m*	9.20(5)		11.90(5)		Staritzky and Singer (1952)

[a] All oxidation states Pu(III) through Pu(VI) have been observed in molten salts of the alkali chlorides (Gruen *et al.*, 1960; Benz and Douglass, 1961a; Swanson, 1964).

[b] $\beta = 91.59(4)°$.

[c] $\beta = 100.1(6)°$.

[d] $\beta = 96.99(5)°$.

centrifugation of volatile halide, alkoxide, and borohydride complexes (Koch, 1972, 1973a–c, 1976a,b). Solution and coordination chemistry continues to play a role in modern plutonium processing and separations, and for recycle of plutonium in closed nuclear fuel cycles. More recently, interest has grown in the chemistry of plutonium under biologically and environmentally relevant conditions, as attention has turned to understanding the long-term fate and transport of plutonium stored in geological repositories (Clark *et al.*, 1995; Neu *et al.*, 2002; Silva and Nitsche, 2002). Selected aspects of plutonium coordination chemistry have been reviewed by Cleveland (1979) and Carnall and Choppin (1983), and within broader reviews on actinide elements (Lemire *et al.*, 2001; Burns *et al.*, 2004). In this section we describe the preparation, stability, structure, and spectroscopy, of aqueous and nonaqueous molecular complexes of plutonium.

7.9.1 Aqueous solution chemistry

The chemistry of plutonium in aqueous solution is unique and rich. It is also complicated, primarily due to the small energy separations between the various oxidation states and the extreme oxophilicity of plutonium cations. Five oxidation states, Pu(III), Pu(IV), Pu(V), Pu(VI), and Pu(VII), can be readily prepared and stabilized in aqueous solution under the appropriate conditions. The lower oxidation states, Pu(III) and Pu(IV), are generally more stable in acid solution while the higher oxidation states, Pu(VI) and Pu(VII), are favored under alkaline conditions. Tetravalent plutonium is the most stable and consequently the most studied, followed by plutonium in the trivalent and hexavalent states. In the decades following the discovery of plutonium, its solution chemistry was motivated by the need to separate plutonium from mixtures of actinides and fission products in multiple oxidation states under highly acidic conditions. Processes that used oxidation and/or reduction steps in solution and condensed phases bolstered the study and understanding of aqueous Pu(III) and Pu(VI). In contrast, pentavalent plutonium is most stable in near-neutral pH solutions that are dilute in both plutonium and other ions. Although Pu(V) was identified along with the other common oxidation states, research on the solution complexes of this oxidation state was not widely pursued until the 1990s when the behavior of plutonium in environmental matrices gained importance. Heptavalent plutonium was the last oxidation state to be discovered, and it was first reported in 1967 (Krot and Gel'man, 1967). Plutonium in this oxidation state is stable only in highly alkaline solution and in the presence of strong oxidizing agents, and is therefore the least well studied. There are very recent spectroscopic studies that suggest the possibility of the existence of Pu(VIII) in alkaline solution (Nikonov *et al.*, 2004, 2005). The existence of this oxidation state is equivocal, and we look forward to future research in this area.

Under noncomplexing strongly acidic conditions, such as in perchloric or triflic acid solutions, both Pu(III) and Pu(IV) exist as the simple hydrated (or aquo) ions, $Pu^{3+}_{(aq)}$ or $Pu^{4+}_{(aq)}$, retaining their overall formal charge. In the sections that follow, we refer to the $Pu^{3+}_{(aq)}$ or $Pu^{4+}_{(aq)}$ species as simply Pu^{3+} and Pu^{4+}, or Pu(III) and Pu(IV), respectively. Pentavalent and hexavalent plutonium cations have such large positive charges that in aqueous solution they immediately hydrolyze to form a unique class of trans dioxo cations, $PuO^{+}_{2(aq)}$ and $PuO^{2+}_{2\,(aq)}$, which are commonly referred to as plutonyl ions. Under noncomplexing acid conditions (such as perchloric or triflic acid), both ions exist as the simple hydrated (or aquo) ions, $PuO^{+}_{2(aq)}$ and $PuO^{2+}_{2(aq)}$, and we refer to these as simply PuO_2^+ and PuO_2^{2+}, or Pu(V) and Pu(VI), respectively. These plutonyl cations have estimated effective charges of 2.2 and 3.3, respectively (Choppin, 1983). Heptavalent plutonium is not stable in acid solution, and can only be prepared under highly alkaline solution conditions. Under alkaline conditions, the heptavalent ion forms a tetra-oxo species PuO_4^-, which is always coordinated with hydroxide ions to give $PuO_4(OH)_2^{3-}$. We will refer to this species as Pu (VII). The OECD-NEA has evaluated thermodynamic properties for plutonium ions in aqueous solution, and a selected set of their recommended values is given in Table 7.48 (Lemire *et al.*, 2001).

(a) Stoichiometry and structure of plutonium ions

From an historical perspective, the charge and composition of plutonium ions in acid solution were inferred from solvent extraction studies. For example, plutonium(III) and plutonium(IV) are written as Pu^{3+} and Pu^{4+} in part from an interpretation of charge balances in solvent extraction studies with thenoyltrifluoroacetone (Poskanzer and Foreman, 1961), and also from the lack of hydrogen-ion dependence of the reversible Pu(IV)/Pu(III) redox couple (Rabideau, 1956). The Pu(V)/Pu(IV) redox couple on the other hand, is not rapidly reversible, nor independent of hydrogen-ion concentration, indicating that the two ions differ in degree of oxygenation. The existence of the trans dioxo ions in Pu(V) and Pu(VI) (PuO_2^+ and PuO_2^{2+}, respectively) was originally based on crystallographic data on solid compounds. For Pu(VI), XRD data for $NaPuO_2(O_2CCH_3)_3$ and $Cs_2PuO_2Cl_4$ confirmed that the compounds were isostructural with the corresponding uranium, neptunium, and americium analogs, and contained the linear PuO_2^{2+} unit (Werner, 1982). Similar structural

Table 7.48 *Selected chemical thermodynamic values for plutonium aquo ions* (*Lemire* et al., 2001).

Formula	$\Delta_f G^\circ$ (kJ mol^{-1})	$\Delta_f H^\circ$ (kJ mol^{-1})	S° (J K^{-1} mol^{-1})
Pu^{3+}	−579.0 ± 2.7	−591.8 ± 2.0	−184.5 ± 6.2
Pu^{4+}	−478.0 ± 2.7	−539.9 ± 3.1	−414.5 ± 10.2
PuO_2^+	−852.6 ± 2.9	−910.1 ± 8.9	+1 ± 30
PuO_2^{2+}	−762.4 ± 2.8	−822.0 ± 6.6	−71 ± 22

comparisons were found for other Pu(vi) compounds, and helped to assign the basic formula PuO_2^{2+} to Pu(vi) in solution. Plutonium(v), likewise, was assigned the formula PuO_2^+ because of the existence of the PuO_2^+ unit in the solid-state structure of $KPuO_2CO_3$ (Ellinger and Zachariasen, 1954), and in part because the oxidation–reduction couple Pu(vi)/Pu(v) is reversible and independent of the hydrogen-ion concentration (except for the shift in potential due to hydrolysis). This argued that there was no structural rearrangement during redox, and therefore that the oxygen content was identical in both ions.

Recent X-ray absorption and vibrational spectroscopic studies provide more direct characterization of the solution forms of the ions in all oxidation states. Under noncomplexing acid conditions, Pu(iii), Pu(iv), Pu(v), and Pu(vi) are coordinated by water molecules, resulting in hydrated cations of general formula $Pu(OH_2)_n^{3+}$, $Pu(OH_2)_n^{4+}$, $PuO_2(OH_2)_n^+$, and $PuO_2(OH_2)_n^{2+}$, respectively. Structural analysis in solution using EXAFS spectroscopy has been recently employed to determine the number of coordinated water molecules (n) and the Pu–O distances in the aquo ions (Allen *et al.*, 1997; Conradson *et al.*, 2004a). For the Pu(iii) aquo ion, $Pu(OH_2)_n^{3+}$, EXAFS studies report coordination numbers of 9 (Conradson *et al.*, 2004a) and 10 (Allen *et al.*, 1997), with Pu–O distances of 2.48(1) and 2.51(1) Å, respectively. These coordination number estimates are consistent with previous estimates of 9 that were based upon comparison with Cm(iii) from luminescence lifetime measurements (Kimura and Choppin, 1994), and Am(iii) determined from optical absorption spectroscopy (Carnall, 1989). Relativistic DFT calculations suggest eight or possibly nine water molecules for the Pu(iii) aquo ion, $Pu(OH_2)_9^{3+}$ (Blaudeau and Bursten, 2000). A recent single crystal XRD study of a salt containing the $Pu(OH_2)_9^{3+}$ unit substantiates the coordination number of 9 for the Pu(iii) aquo ion (Matonic *et al.*, 2001) in the solid state. In this compound, the $Pu(OH_2)_9^{3+}$ ion adopts a tricapped trigonal prismatic coordination environment, where all nine coordinated water molecules show a similar Pu–O distance that averages 2.51 Å (Matonic *et al.*, 2001) comparable to the values observed by EXAFS. For Pu(iv), EXAFS analysis indicates the presence of eight water molecules at a shorter Pu–O distance of 2.39(1) Å (Conradson *et al.*, 2004a). For Pu(v) and Pu(vi) aquo ions, EXAFS data reveal two short plutonyl Pu=O bonds at 1.81(1) and 1.75(1) Å (respectively) consistent with expectations for trans dioxo ions. Each plutonyl unit is coordinated by four or five water molecules with Pu–O bond distances of 2.47(1) and 2.41(1) Å, respectively (Conradson *et al.*, 2004a). Similar analyses on the aquo ions of UO_2^{2+}, NpO_2^{2+}, and NpO_2^+ indicate that a coordination number of 5 is the most common, but that this value will be affected by changes in the ionic strength of solution (Antonio *et al.*, 2001). Theoretical analysis of XANES, coupled with experimental measurements, have provided new insights on the electronic structure of these ions, especially the nature of the bonding interactions between plutonium and axial oxygen atoms in the PuO_2^+, and PuO_2^{2+} aquo ions (Ankudinov *et al.*, 1998).

Ions of Pu(vii) also contain Pu=O multiple bonds, and the preponderance of evidence indicates the presence of polyoxo ions with four or more oxo groups depending on solution conditions. The reversibility of the Pu(vii/vi) reduction, similar to the Pu(vi/v) reversible reduction supports the formulation of a polyoxo ion. A series of anionic polyoxo species that form between 0.5 and 18 molar hydroxide has been proposed and includes $PuO_4(OH_2)_2^-$, $PuO_4(OH)(OH_2)^{2-}$, $PuO_4(OH)_2^{3-}$, $PuO_5(OH)^{4-}$, or PuO_6^{5-}, depending on hydroxide concentrations (Spitsyn *et al.*, 1969; Krot, 1975; Tananaev *et al.*, 1992). Of the proposed species, only $PuO_4(OH)_2^{3-}$ has a known analog in neptunium chemistry (Grigor'ev *et al.*, 1986). The neptunium analog, $NpO_4(OH)_2^{3-}$, has a highly unusual geometry with four short Np=O bonds in a square plane, with two axial OH^- ligands (Grigor'ev *et al.*, 1986; Bolvin *et al.*, 2001; Williams *et al.*, 2001). Current research is aimed at defining conditions that favor the various forms, and at identifying their exact structure and reactivity.

Structural representations of the simple aquo ions of plutonium are given in **4**, **5**, **6,** and **7** below.

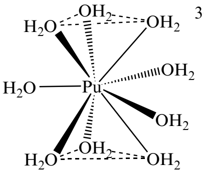

4

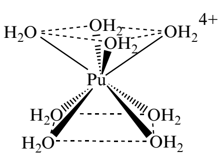

5

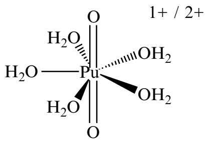

6

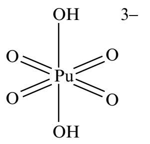

7

(b) Spectroscopic properties of plutonium ions

The electronic absorption spectra of plutonium ions, like those of most other actinide elements, are characterized by the presence of a few very sharp bands with relatively low molar absorptivities compared to those of d-block metal ions. The very sharp bands are strongly reminiscent of spectra of the rare-earth ions, which are attributed to electronic transitions within the shielded 4f–4f manifold of states (Edelstein, 1991). In the actinide elements, similar but relatively less shielded transitions are attributed to the 5f shell (Carnall *et al.*, 1991; Carnall, 1992; Denning, 1992, 1999). The 5f–5f transitions are more intense than the 4f–4f transitions of the lanthanides, due in part to relativistic effects that generate larger spin–orbit coupling. Energy levels for trivalent actinide ions calculated using 5f transitions compare well with experimental spectra, supporting this representation of electronic structure in plutonium (Mikheev *et al.*, 1983; Carnall, 1992). Since these transitions are forbidden by the selection rules, the absorption bands are narrow, but still not very intense.

Internal 5f–5f transitions of the plutonium ions give absorption bands in the visible and near-IR region of the electronic absorption spectrum. These absorption features are characteristic for each oxidation state and therefore frequently used for identification and quantitative analysis of plutonium ions in solution (Cohen, 1961a). Representative electronic absorption spectra of plutonium ions of common oxidation states are given in Fig. 7.115 and molar absorptivities for distinctive bands are given in Table 7.49. Plutonium ions of all oxidation states have strong absorbance in the UV region of the optical spectrum (Stewart, 1956; Cohen, 1961b). In addition to conventional electronic absorption spectroscopy, two-photon optical absorption spectroscopy has also been used to probe the electronic structure of plutonium ions isolated in host matrices and these data have provided useful extrapolations for interpreting the spectra of the solvated ions (Denning, 1991).

Photothermal spectroscopic techniques have been applied to increase the sensitivity and selectivity of the optical absorption method of plutonium analysis. For example, photoacoustic spectroscopy, in which the pressure pulse generated from absorbed light heating the solution is transduced to an electronic signal, generally has 10 to 100 times greater sensitivity (depending on the spectral region) than conventional spectrophotometry (Stumpe *et al.*, 1984; Neu *et al.*, 1994). Thermal-lensing spectroscopy has sensitivities similar to photoacoustic spectroscopy and also uses the heating of the solution due to the absorption of small amounts of energy to detect and quantify analytes. This method optically probes the gradient in the refractive index, which is generated from solution heating, as a 'thermal lens' (Moulin *et al.*, 1988). The use of fiber optics and pulsed laser diode excitation sources with either of these techniques allows for remote or in-process detection and quantification of plutonium ions (Neu *et al.*, 1994; Wruck *et al.*, 1994) in micromolar concentrations or lower. Both methods have been used in solution thermodynamic studies aimed at quantitatively evaluating complexation of plutonyl ions by chelating ligands and even by the oxo ligands of other actinyl ions (Bennett *et al.*, 1992; Stoyer *et al.*, 2000).

Vibrational spectroscopy, both infrared absorption and Raman scattering, are useful for 'fingerprint' comparisons, for structure determination, for analyzing intramolecular bond strength, and for understanding the electronic structure of plutonium ions. Comparison of infrared and Raman spectra of actinyl ions across the actinide series were used to establish that higher valent plutonium (v, vi) species in aqueous solution exist as linear trans dioxo ions with strong covalent Pu=O bonds. The hexavalent actinide ions all show an asymmetric O=An=O stretching frequency (ν_3) in the energy region 930–970 cm^{-1}, with the Pu(vi) aquo ion in noncomplexing perchlorate solution observed at 962 cm^{-1} (Jones and Penneman, 1953). These studies confirmed the symmetric and linear, or nearly linear, structures of both PuO_2^+, and PuO_2^{2+} in a more compelling way than do arguments based on similarities in the fine structure of the visible absorption spectrum. Infrared spectroscopic studies of plutonyl species in condensed phases, using very long pathlengths, powerful excitation sources, and sensitive detectors also contributed to vibrational band assignments for

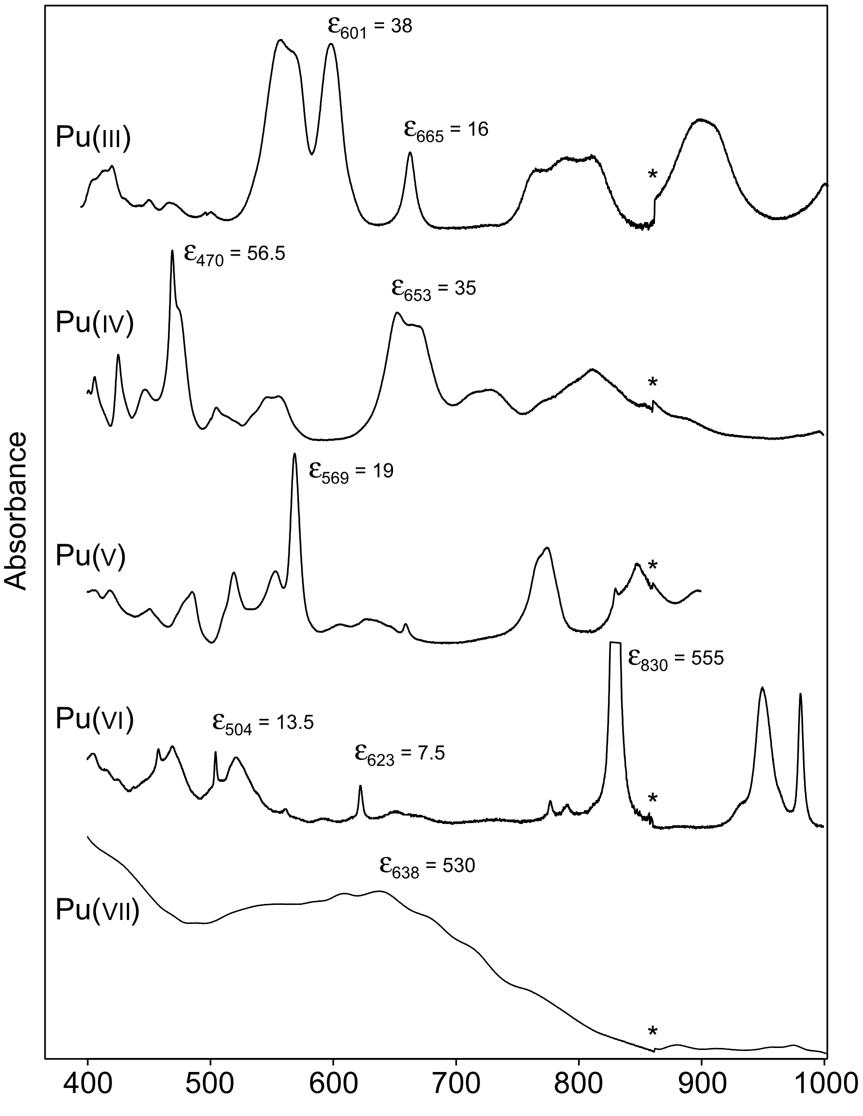

Fig. 7.115 *Electronic absorption spectra of major plutonium aqua ions recorded at* 25°C. *The asterisk marks a spectrophotometer grating change. Plutonium(*III*) recorded on* 1.89 mM *solution in* 1 M $HClO_4$ *using* 1 cm *cell. Plutonium(*IV*) recorded on* 2.91 mM *solution in* 1 M $HClO_4$ *using* 1 cm *cell. Plutonium(*V*) recorded on* 10.2 mM *solution in* 1 M *(Na,H)*ClO_4 *solution at pH* 3.14 *using* 1 cm *cell. Plutonium(*VI*) recorded on* 0.89 mM *solution in* 1 M $HClO_4$ *using* 1 cm *cell. Plutonium(*VII*) recorded on* 20 mM *solution in* 2.5 M *NaOH using* 1 cm *cell (spectra courtesy of Phillip D. Palmer of Los Alamos National Laboratory).*

Table 7.49 *Characteristic optical absorption bands of plutonium aquo ions in* 1 M (*H,Na*) *ClO*$_4$ *at* 25°C *unless noted otherwise* (*Cohen*, 1961*b*).

Species	*Peak max.* (nm)	*Full width at half height* (nm)[a]	*Molar absorption,* ε (L mol^{-1} cm^{-1})
Pu^{3+}	244	broad	1500
	561	broad	38
	601	21.7	38
	665	10.9	16
Pu^{4+}	470	13.6 (shoulder)	56.5
	653	42.7 (shoulder)	35
PuO_2^{+}[b]	569	8.6	19
	1131	32	22
PuO_2^{2+}	504	3.0	13.5
	623	3.8	7.5
	830	2.5	555
$PuO_4(OH)_4^{3-}$[c]	638	broad	530

[a] FWHM estimated from Cohen (1961b).

[b] 10°C, 0.2 M $HClO_4$.

[c] Pu(VII) spectrum from Krot and Gel'man (1967).

ions in solution (Bovey and Steers, 1960; Vdovenko *et al.*, 1973; Kim and Campbell, 1985). Complementary Raman studies assigned the symmetric O=Pu=O stretching frequency (ν_1) for PuO_2^{2+} in 1.0 M (H,Na)ClO_4 at (834 ± 3) cm^{-1}, which compares well with ν_1 for the analogous NpO_2^{2+} and UO_2^{2+} ions at (855 ± 2) cm^{-1} and (865 ± 5) cm^{-1}, respectively. These ν_1 frequencies were assigned to ground state vibrations from both fluorescence spectra intervals and Raman shifts (Madic *et al.*, 1984; Tait *et al.*, 2004). This Raman shift also agrees with the prediction of 830 cm^{-1} based on the visible spectrum of plutonium(VI) in HCl that contains a 708 cm^{-1} frequency interval in the fine structure within the wavelength region 390–430 nm. The Raman shift of PuO_2^{+} in 1.0 M ClO_4^{-} was observed at 748 cm^{-1}. Disproportionation of PuO_2^{+} was evidenced by the decrease of the intensity of the 748 cm^{-1} PuO_2^{+} band and the increase of bands located at 833 and 817 cm^{-1} assigned to PuO_2^{2+} and $(PuO_2)_2(OH)_2{}^{2+}$, respectively (Madic *et al.*, 1984).

Correlations of vibrational frequencies to bond strength and molecular structure of the linear O=An=O moiety have been made. Recent X-ray absorption spectroscopy studies of solution and polycrystalline actinide samples allow for correlation of the energy of the symmetric ν_1 Raman frequency with measured An=O bond lengths. Clear trends can be seen within a particular oxidation state of an actinide and a general trend of heavier actinyl ions having weaker bonds has emerged. The Raman frequency for Pu(VI) is sensitive to complexation environment, showing shifts in ν_1 greater than 40 cm^{-1} between solution species for which the measured changes in the Pu=O bond length are only minimal.

Comparisons of Pu(v) with Np(v), and Pu(vi) with U(vi) and Np(vi) aquo complexes show that as nuclear charge increases across the series uranium to plutonium, the stretching frequencies actually decrease with decreasing An=O bond length. The bond shortening is clearly a result of the actinide contraction, and the weaker bonding is an indication of 5f orbital contraction across the actinide series (Tait *et al.*, 2004). The nature of chemical bonding in the plutonyl ions is discussed in Section 7.9.3 and in Chapter 17.

(c) Oxidation and reduction reactions

(*i*) *Oxidation–reduction equilibria between plutonium ions*

The oxidation–reduction (redox) relationships of the plutonium ions present one of the most complex and fascinating aspects of the aqueous solution chemistry of plutonium. The redox potentials that couple the four common oxidation states (iii, iv, v, vi) of plutonium in acid solution are all of comparable magnitude and very close to 1 V. Moreover, the kinetics of the reactions among oxidation states creates a unique situation where finite amounts of multiple oxidation states can coexist in solution under the appropriate conditions. This situation is unique for plutonium among all the elements in the periodic table. The complications arising from this unusual behavior are responsible for a considerable amount of research devoted to understanding the kinetics and mechanisms of these important reactions. We will discuss these reactions independently, and then discuss several examples to illustrate the complexity of the system. Much of this discussion follows from the excellent reviews by Cleveland (1979) and by Newton (1975, 2002).

The equilibrium concentrations of species involved in these reactions are usually determined from the potentials and the pertinent complex formation constants. Calculating standard potential values for the various couples is challenging since nearly all the data were acquired at high ionic strength, requiring extrapolation to infinite dilution. It is particularly difficult to study tetravalent plutonium independently of its hydrolysis and disproportionation. Redox reactions and corresponding electrochemical potentials that are useful for making predictions of plutonium chemistry in solution are given in Table 7.50. The constants listed for reactions in acid and some of those in base are from direct measurements, while those at pH 8 were estimated from hydrolysis data and standard potentials in acid for Pu(iii), Pu(iv), and Pu(vi) and related ions (Allard *et al.*, 1980). Electrochemical studies and reported potentials have been reviewed in recent publications (Mikheev and Myasoedov, 1985; Capdevila and Vitorge, 1995; Peretrukhin *et al.*, 1995; Lemire *et al.*, 2001) and in Chapter 19 of this work. Formal redox potential schemes for selected plutonium couples at 25°C have been derived for 1 M $HClO_4$ (Lemire *et al.*, 2001), 1 M HCl (Rabideau and Cowan, 1955; Rabideau *et al.*, 1959), and 1 M HNO_3 (Artyukhin *et al.*, 1958), and are shown in Fig. 7.116.

Table 7.50 *Formal electrochemical potentials for redox couples relating the plutonium ions in acidic, neutral, and basic aqueous solution versus the standard hydrogen electrode (SHE).*

Couple	*Acidic*[a]	*Neutral*[b]	*Basic*[c]
Pu(IV)/Pu(III)	+0.982	−0.39	−0.96
Pu(V)/Pu(IV)	+1.170	+0.70	−0.67; +0.52[d]
Pu(VI)/Pu(V)	+0.913	+0.60	+0.12
Pu(VI)/Pu(IV)	+1.043	+0.65	+0.34
Pu(V)/Pu(III)		+1.076	
Pu(VII)/Pu(VI)			+0.85
Pu(V)/Pu(IV)	+1.17		

[a] Formal potential in 1 M $HClO_4$ solution (Lemire *et al.*, 2001).
[b] pH 8 (Allard *et al.*, 1980).
[c] Determined in 1 M NaOH solution (Peretrukhin *et al.*, 1995).
[d] Formal oxidation potential (Allard *et al.*, 1980).

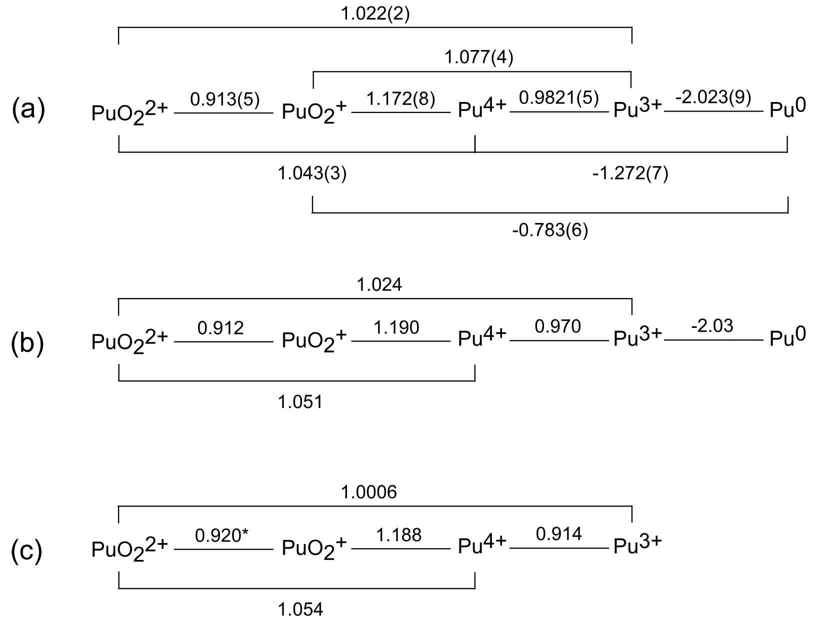

Fig. 7.116 *Formal redox potentials for selected plutonium couples at* 25°C *in V vs SHE* (*a*) *in* 1 M $HClO_4$ (*Lemire* et al., 2001), (*b*) *in* 1 M *HCl* (*Rabideau and Cowan*, 1955*; Rabideau* et al., 1959), *and* (*c*) 1 M HNO_3 (*Artyukhin* et al., 1958).

The formal potential of the Pu(VII)/Pu(VI) couple depends upon the square of the hydroxide ion concentration, and is about 0.85 V in 1 M NaOH, corresponding to the reaction (Spitsyn *et al.*, 1969; Musante and Ganivet, 1974; Krot, 1975):

$$PuO_4(OH)_2^{3-} + 2H_2O \rightleftarrows PuO_2(OH)_4^{2-} + 2OH^- + e^- \tag{7.74}$$

In voltammetric studies performed at lower hydroxide concentration (with a different proposed reaction), the Pu(VII/VI) reduction in 0.01 M hydroxide ion was observed at +1.20 V vs standard hydrogen electrode (Musante and Ganivet, 1974). Due to the instability of Pu(VII) at low hydroxide concentration (and therefore low ionic strength) it is not possible to extrapolate the potential to estimate a standard potential and other standard thermodynamic values.

The redox couples between Pu(V)/Pu(III), Pu(VI)/Pu(III), Pu(V)/Pu(IV), and Pu(VI)/Pu(IV), are quasireversible or irreversible because they involve the breaking or forming of Pu=O multiple bonds. In contrast, the redox couples between species where no Pu=O bond forming or breaking occurs, such as Pu(IV)/Pu(III), Pu(VI)/Pu(V), and Pu(VII)/Pu(VI) couples are reversible. Experimental, standard, and predicted reduction and oxidation potentials have been reported under a wide range of conditions, with the exception of those for Pu(VII). Standard redox potentials in acidic solution are described in greater detail in Chapter 19. Since the redox couples that connect the four main oxidation states (III, IV, V, VI) are relatively similar, it is possible for all four oxidation states to coexist under the appropriate solution conditions. The ability to have multiple oxidation states in solution at the same time will depend upon several key factors. The most important of these are the tendency of Pu(IV) and Pu(V) to disproportionate, and the relatively slow kinetics of reactions that involve the making or breaking of Pu=O bonds in plutonyl ions (PuO_2^+ and PuO_2^{2+}). Other factors are plutonium ion concentration, ionic strength, pH, temperature, and presence or absence of complexing ligands. Thermodynamic and activation data for redox reactions between plutonium ions are summarized in Table 7.51.

(*ii*) *Disproportionation of Pu*(*IV*)

In acid solution in the absence of complexing ligands, the disproportionation of Pu(IV) proceeds according to the following equation:

$$3Pu^{4+} + 2H_2O \rightleftharpoons 2Pu^{3+} + PuO_2^{2+} + 4H^+ \tag{7.75}$$

From this equation one can derive the equilibrium constant expression as:

$$K = \frac{[Pu^{3+}]^2[PuO_2^{2+}][H^+]^4}{[Pu^{4+}]^3} \tag{7.76}$$

Rabideau carefully determined the equilibrium constant for this reaction in $HClO_4/NaClO_4$ solution under a constant ionic strength of 1.0 M (Rabideau, 1953). Rabideau's work on this system is seminal in that it takes into account the plutonium self-reduction by α particle radiolysis, and the hydrolysis of Pu(IV) at low pH. The concentration of Pu(IV) in the equilibrium constant expression above has been corrected for both effects. The equilibrium constant, K, was determined to have a weighted average value of 0.0089 for 1.0 M ionic

Table. 7.51 *Thermodynamics and activation data for plutonium redox reactions* (*Newton,* 2002).

Process	I (M)	ΔG (kJ mol^{-1})	ΔH (kJ mol^{-1})	ΔS (J K^{-1} mol^{-1})	S^* *complex* (J K^{-1} mol^{-1})	*References*
$Pu^{3+} + {}^*Pu^{4+} = Pu^{4+} + {}^*Pu^{3+}$		0.0	0.0	0.0	0.0	
$Pu^{3+} + Pu^{4+} + H_2O = [Pu(Pu)OH^*]^{6+} + H^+$	2	56.1	31.0	−84.2 ± 17	−485	Keenan (1957)
$Pu^{3+} + PuO_2^+ + 4H^+ = 2Pu^{4+} + 2H_2O$		−18.2	−120.9	−344		
$Pu^{3+} + PuO_2^+ + H^+ = [Pu(PuO_2)H^*]^{5+}$	1	82.5	33.5	−164 ± 2	−332	Lavallee and Newton (1972)
	2	78.3	43.1	−117 ± 3	−289	Koltunov *et al.* (1980b)
$Pu^{3+} + PuO_2^{2+} = Pu^{4+} + PuO_2^+$		6.3	−35.6	−140		
$Pu^{3+} + PuO_2^{2+} = [Pu(PuO_2)^*]^{5+}$	1	70.7	20.1	−169 ± 1	−416	Rabideau and Kline (1958)

strength. Rabideau and Cowan (1955) subsequently studied this same disproportion reaction in HCl solution and found the same fourth order dependence on hydrogen ion concentration. It was concluded that the mechanism of Pu(iv) disproportion was identical in both media. The fourth order dependence on hydrogen ion concentration is consistent with experimental observations of essentially no disproportionation of Pu(iv) in strongly acidic solutions. The study in HCl solution is somewhat more straightforward in that α particle reduction was essentially absent. In addition, the value of the equilibrium constant is somewhat smaller ($K = 0.00192$ in 1 M HCl) than observed in perchloric acid ($K = 0.0084$ in 1 M $HClO_4$) and this difference is attributed to stabilization of Pu(iv) ions by complexation with chloride ions in HCl solution. Rabideau and Cowan (1955) also examined the temperature dependence of the equilibria in HCl, and found that raising the temperature from 25 to 45°C increased the value of the equilibrium constant by a factor of 70 ($K = 0.00142$ at 25°C; $K = 0.0967$ at 45.16°C).

Connick studied the kinetics of the disproportionation reaction and found that the overall reaction takes place in two separate steps with a transient Pu(v) intermediate (Connick, 1949). In the first slow step (equation (7.77)), two equivalents of Pu(iv) combine to generate Pu(iii) and Pu(v). This reaction is slow because it involves the formation of a Pu=O bond in forming Pu(v). In the second step (equation (7.78)), the Pu(v) produced in the first step reacts with Pu(iv) in a rapid equilibrium.

$$2Pu^{4+} + 2H_2O \rightleftharpoons Pu^{3+} + PuO_2^+ + 4H^+ \text{ (slow)} \tag{7.77}$$

$$PuO_2^+ + Pu^{4+} \rightleftharpoons Pu^{3+} + PuO_2^{2+} \text{ (fast)} \tag{7.78}$$

Thus, the disproportionation is complete when both reactions (7.77) and (7.78) have reached equilibrium. The addition of equations (7.77) and (7.78) yields the common representation of the Pu(iv) disproportionation reaction that was given in equation (7.75). Equation (7.75) represents a reaction that comes to equilibrium in any plutonium solution, but equation (7.75) does not adequately represent the disproportionation of tetravalent plutonium because it fails to include Pu(v), even as an infinitesimally small intermediate. Silver (1971, 2003) has shown that a linear combination of equations (7.77) and (7.78) produces a new equation for the dissociation of Pu(iv) and is shown in equation (7.79), where the parameter M represents the equilibrium ratio for $[PuO_2^{2+}]/[PuO_2^+]$.

$$\begin{aligned}(2+3M)[Pu^{4+}] + (2M+2)[H_2O] &\rightleftharpoons (1+2M)[Pu^{3+}] \\ &+ [PuO_2^+] + M[PuO_2^{2+}] + (4M+4)[H^+]\end{aligned} \tag{7.79}$$

The value of M was found as the root of the cubic equation (7.80) where $K_{(7.77)}$ and $K_{(7.78)}$ are the equilibrium constants for equations (7.77) and (7.78), respectively.

$$K^2_{(7.78)}[H^+]^4 - K_{(7.77)}(M^2 + 2M^3) = 0 \qquad (7.80)$$

As the value of the ratio M increases, the coefficient of Pu(v) decreases and the stoichiometry of equation (7.79) approaches the stoichiometry of equation (7.75). In 1 M perchloric acid, the value of M is about 50.

(*iii*) *Disproportionation of Pu*(*V*)

In moderately acidic solutions Pu(v) is unstable towards disproportionation reactions. The disproportionation of Pu(v) into Pu(VI) and Pu(IV) or Pu(III) is expected to proceed by either of two possible mechanisms. From a study of the rate of the disproportionation of Pu(v) in 0.5 M HCl, Connick (1949) has shown that the actual mechanism consists of the slow reaction (7.81) coupled with the rapid equilibrium (7.78).

$$PuO_2^+ + Pu^{3+} + 4H^+ \rightleftharpoons 2Pu^{4+} + 2H_2O\,(\text{slow}) \qquad (7.81)$$

$$PuO_2^+ + Pu^{4+} \rightleftharpoons Pu^{3+} + PuO_2^{2+}\,(\text{fast}) \qquad (7.78)$$

with an overall reaction

$$3PuO_2^+ + 4H^+ \rightleftharpoons Pu^{3+} + 2PuO_2^{2+} + 2H_2O \qquad (7.82)$$

Connick (1949) pointed out that the disproportionation of Pu(v) proceeded by the mechanism of equation (7.82) under the conditions of his experiment, but that this mechanism cannot be true under all circumstances. At very low concentrations of Pu(III) the mechanism must necessarily change to that represented by equation (7.83).

$$2PuO_2^+ + 4H^+ \rightleftharpoons Pu^{4+} + PuO_2^{2+} + 2H_2O \qquad (7.83)$$

Thus equations (7.82) and (7.83) are limiting cases for Pu(v) disproportionation, and the actual reaction path depends on the plutonium species present in solution (Connick, 1949). The use of equations (7.82) or (7.83) have been widely cited in the literature, but Connick's original caveats on their intimate connection to solution conditions has not always been kept in mind. Without this understanding, equations (7.82) and (7.83) would appear to be contradictory because they do not predict the same reaction products (Pu^{3+} in (7.82), and Pu^{4+} in (7.83)). Under many solution conditions encountered in the laboratory, Pu(v) disproportionation may follow both mechanisms, in which case neither equation 7.82 or 7.83 by itself adequately describes Pu(v) disproportionation. This apparent discrepancy has been discussed in detail by Silver (1971, 1997, 2002, 2004) who has shown that the disproportionation reaction under any particular solution condition can be expressed as a linear combination of these two limiting cases. In this manner Pu(v) disproportionates in accordance with the stoichiometry of equation (7.84), where the parameter M represents the equilibrium ratio for $[PuO_2^{2+}]/[PuO_2^+]$.

$$\begin{aligned}&(3 + 2M/K_{(7.78)})[PuO_2^+] + (4 + 4M/K_{(7.78)})[H^+] \rightleftharpoons \\ &\quad [Pu^{3+}] + (M/K_{(7.78)})[Pu^{4+}] + (2 + M/K_{(7.78)})[PuO_2^{2+}] \\ &\quad + (2 + 2M/K_{(7.78)})[H_2O]\end{aligned} \tag{7.84}$$

The value of M was found as the positive, real root of equation (7.85) where $K_{(7.78)}$ and $K_{(7.77)}$ are the equilibrium constants for equations (7.78) and (7.77), respectively.

$$2K_{(7.78)}^2[H^+]^4 + (K_{(7.78)}[H^+]^4M - K_{(7.77)}M^3) = 0 \tag{7.85}$$

The mathematical details are beyond the scope of this discussion, and the interested reader should see the works of Silver (1971, 1997, 2002, 2004) for more detail.

It is noteworthy that both reactions 7.82 and 7.83 for the disproportionation of Pu(v) have equilibrium constants with a fourth order dependence on the hydrogen ion concentration. This illustrates why Pu(v) solutions are only stable at near-neutral pH where the hydrogen ion concentration is low. Many workers have used this observation to prepare solutions of Pu(v) in the absence of other oxidation states (Gevantman and Kraus, 1949; Markin and McKay, 1958; Gel'man and Zaitseva, 1965a,b; Newton, Hobart *et al.*, 1986a).

Rabideau studied the kinetics and mechanism of the Pu(v)-Pu(v) reaction in the absence of Pu(III) (Rabideau, 1957).

(*iv*) *Equilibrium between Pu*(*III*), (*IV*), (*V*), *and* (*VI*)

The reaction that describes the equilibrium between all four oxidation states has been used in the discussion of the disproportionation of Pu(IV) and Pu(v). The equilibrium constant for this reaction is given by:

$$K = \frac{[Pu(III)][Pu(VI)]}{[Pu(IV)][Pu(V)]} \tag{7.84}$$

This equilibrium constant has been determined in various media, but not all studies have corrected for the hydrolysis of Pu(IV). Rabideau and Kline (1958) determined this equilibrium constant in unit ionic strength $HClO_4/NaClO_4$ solution for various hydrogen ion concentrations. They obtained a value of $K = (13.1 \pm 0.08)$ at 25°C that is corrected for hydrolysis and is independent of H^+ concentration over the range $0.1 \leq H^+ \leq 1.0$ M. In D_2O solution, the corresponding hydrolysis-corrected value was determined to be (40.6 ± 1.0). Rabideau and Kline studied the kinetics of the reaction in both H_2O and D_2O solution, and determined that a hydrogen atom transfer process is not involved in the reaction. In complexing acids such as HCl and HNO_3, the equilibrium was found to shift to favor higher concentrations of Pu^{4+}.

Because this system is rather complicated, it is instructive to examine a series of figures that describe the system under various conditions. Equilibrium oxidation state distribution diagrams are useful for predicting the behavior of various plutonium stock solutions made up in the laboratory. Equilibrium diagrams showing the predominant oxidation state as a function of pH and average oxidation state for 1.0 M ionic strength are given in Fig. 7.117.

Fig. 7.117(a) shows the distribution for a solution with average oxidation state IV. It is seen that a solution which is initially pure Pu(IV) will contain significant concentrations of Pu(III) and Pu(VI) at equilibrium in 1 M acid. At pH 1 Pu(III) predominates and at pH 2 the solution is primarily a mixture of Pu(III) and Pu(V). The calculations that produced these plots took the first hydrolysis constant for Pu(IV) into account. It should be pointed out that the distribution in the region between pH 1 and 2 is less certain as the second hydrolysis constant was not taken into account. A small amount of irreversible hydrolysis to give colloidal Pu(IV) hydroxide is also expected at very low concentrations. Fig. 7.117(b) shows a distribution for a solution with average oxidation state V, for example an equimolar mixture of Pu(IV) and Pu(VI). Here, Pu(VI) predominates until a pH of about 1.2 is reached. At higher values, Pu(V) becomes predominant.

It is also important to know how rapidly redox equilibria will be reached in plutonium solutions. The rate constants and hydrogen ion dependences for the reactions above are known for solutions at 25°C and unit ionic strength. The kinetics of the system are somewhat complicated in that the forward and reverse

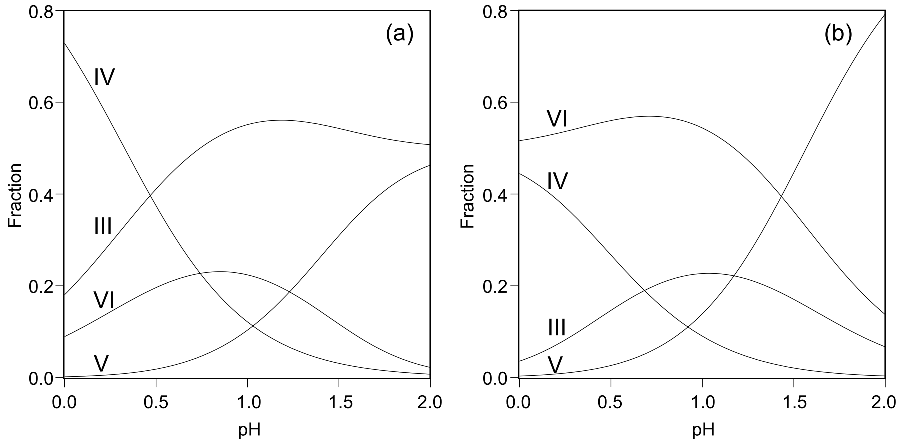

Fig. 7.117 *Oxidation state distribution diagram showing the predominant oxidation state of plutonium in* 1 M *(H,Na)ClO_4 solution as a function of pH and (a) average oxidation state Pu(IV), and (b) average oxidation state Pu(V) (calculations courtesy of T. W. Newton).*

rates of all three of the reactions listed above must be considered. The disproportionation of Pu(IV) in 0.1 M acid has been calculated and the results for 1.0 M ionic strength at pH 1.0 are shown in Fig. 7.118(a). Appreciable concentrations of the other oxidation states appear after relatively short periods of time. The rates depend on the total plutonium concentration, so the time scale is given in units of M s (molar second). The time required to reach any particular distribution is found by dividing the total concentration. For example, Fig. 7.118(a) indicates that if the concentration of Pu(IV) is 0.002 M, then half of the Pu(IV) will be gone in about 3 hours. In a similar fashion, Pu(V) is quite stable at pH 3 and can be formed, for example, by mixing Pu(III) and Pu(VI). The course of this reaction at unit ionic strength is shown in Fig. 7.118(b). For a concentration of 0.001 M, equilibrium is reached in about a day and within about 10% of equilibrium within about 5 hours. Reducing the ionic strength decreases the rate. Selected oxidation and reduction rate data for different plutonium oxidation states are given in Table 7.52.

(*v*) *Preparation and stability of pure oxidation states*

Newton and coworkers have provided excellent experimental procedures for the preparation of oxidation state pure plutonium solutions. The following discussion comes essentially from Newton *et al.* (1986a).

Pu(III). Acidic solutions of Pu(III) are conveniently prepared by dissolving weighed samples of pure α-phase metal in 6 M HCl or $HClO_4$, with cooling, followed by dilution to the desired concentration. Corrosion products on the

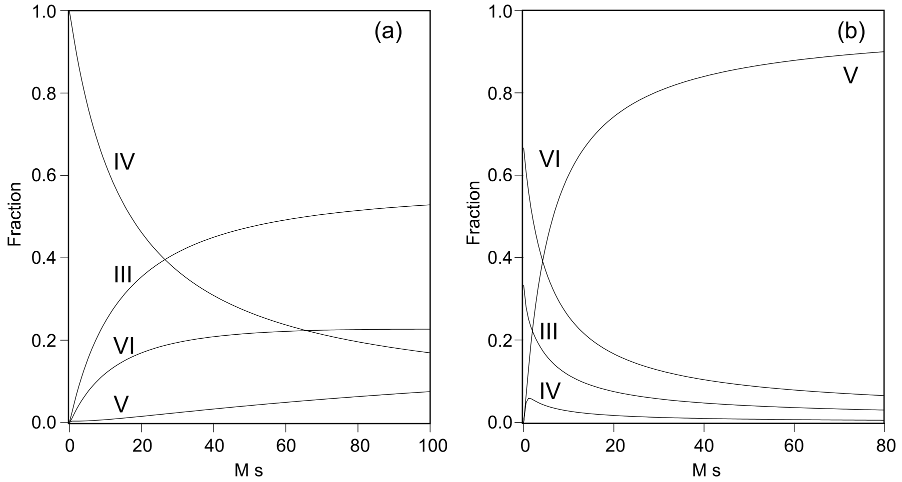

Fig. 7.118 *Kinetics for disproportionation of plutonium in* 1 M *(H,Na)*ClO_4 *solution at (a) pH 1 and average oxidation state Pu(IV), and (b) pH 3 and average oxidation state Pu(V) (calculations courtesy of T. W. Newton of Los Alamos).*

Table 7.52 *Selected plutonium oxidation and reduction rate as compiled by data Newton* (2002).

Agent	*Concentration* (M)	*Solution*	*Temperature* (°C)	*Results*	*References*
Pu(III) oxidation					
NO_3^-	0.2 ($NaNO_3$)	0.5 M HCl	room	$t_{1/2} \approx 600$ h; autocatalytic; rapid in 16 M HNO_3	Connick (1954)
HNO_2	~0.05	2 M HNO_3	16	$k'' = (0.88 \pm 0.03)$ $[HNO_2]^{0.5}[H^+]^{0.5}[NO_3^-]^{0.4}$ M^{-1} min^{-1} E_a (16–32°) = (55.8 ± 3.4) kJ mol^{-1} net reaction is the HNO_2 catalyzed oxidation of Pu(III) by HNO_3	Koltunov and Marchenko (1973) and Newton (2002)
Pu(IV)	3×10^{-6}	2 M (H,Li)ClO_4	25	$k'' = 6.4 \times 10^4 [H^+]^{-1}$ M^{-1} s^{-1} $E_a = (31 \pm 5)$ kJ mol^{-1} also studied in Cl^- and SO_4^{2-} solutions	Keenan (1957) Nikitenko and Ponomareva (1989)
Pu(V)	1.3×10^{-3}	2 M (H,Na)NO_3	38	$k'' = (k + k_1[NO_3^-][H^+])$ M^{-1} s^{-1} $k_o = (0.21 \pm 0.09)$ M^{-2} s^{-1} $k_1 = (0.59 \pm 0.07)$ M^{-3} s^{-1}	Koltunov and Mikhailova (1977) and Newton (2002)
Pu(VI)	10^{-4}	1 M $HClO_4$	25	$k'' = 2.68[H^+]^0$ M^{-1} s^{-1} $\Delta H^* = (20.2 \pm 0.4)$ kJ mol^{-1}	Rabideau and Kline (1958) Alei *et al.* (1967)
Pu(IV) oxidation					
HNO_3	1–5	HNO_3	90	steady-state Pu(IV)–Pu(VI) concentrations reached in about 1 d. Fraction Pu(VI) at the steady state is given by $0.11([Pu(IV)]_0)^{-0.61}([HNO_3])^{-0.74}$	Glazyrin *et al.* (1989)

O_3		1 M (H,Na)NO_3	20	$k = (1.32 \pm 0.13) \times 10^{-2}\,[O_3]^0[H^+]^{-1}\,\text{min}^{-1}$ $[\text{Pu(IV)}] = 10^{-6}–10^{-5}$ M $E_a = (19 \pm 5)\,\text{kJ mol}^{-1}$	Vyatkin *et al.* (1972)
Pu(V) oxidation					
Ce(IV)	6×10^{-5}	2 M $HClO_4$	23	very rapid; $k'' > 7 \times 10^5\,\text{M}^{-1}\,\text{s}^{-1}$	Newton and Burkhart (1971)
O_2	1 atm	4 M NaOH	25 ± 2	$k = 4.5 \times 10^{-4}\,\text{min}^{-1}$	Budantseva *et al.* (1998)
Pu(IV) reduction					
Fe(II)	2×10^{-3}	2 M (H,Li)ClO_4	20	$k'' = 27[H^+]^{-1}\,\text{M}^{-1}\,\text{s}^{-1}$ $E_a = (82 \pm 2.5)\,\text{kJ mol}^{-1}$	Newton and Cowan (1960)
$H_2C_2O_4$ oxalic acid	0.04 excess Pu(IV)	5 M (H,Na)NO_3	98	$k'' = \dfrac{0.215}{[\text{Pu(IV)}] + [H^+]^2/K}\,\text{M}^{-1}\,\text{min}^{-1}$ $K = 86.8\,\text{M} = [PuC_2O_4{}^{2+}][H^+]^2/[Pu^{4+}][H_2C_2O_4]$ (recalculated from the original data)	Newton (2002)
H_2O_2	~0.01	2 M (H,Na)NO_3	25	$k'' = (11.9 \pm 1.0)[H^+]^{-1}[NO_3^-]^{-1}$ E_a (15–45°) = $(95.5 \pm 3.8)\,\text{kJ mol}^{-1}$	Koltunov *et al.* (1981a)
H_2O_2	7.9×10^{-4}	0.5 M HCl	25	$t_{1/2} = 64$ min (excess H_2O_2) complicated by rapid formation of Pu(IV)–H_2O_2	Mazumdar *et al.* (1970)
NH_3OH^+	~0.1	2.5 M (H,Na) (NO_3,ClO_4)	25	$k'' = 13.7/[[H^+]^2\,(1 + [NO_3^-]/0.35)]\,\text{M}^{-1}\,\text{s}^{-1}$ E_a (25–45°) = $(120 \pm 8)\,\text{kJ mol}^{-1}$ for approach to equilibrium in the reaction: $\text{Pu(IV)} + NH_3OH^+ = \text{Pu(III)} + NHOH\bullet + 2H^+$	Barney (1976)

Table 7.52 (*Contd.*)

Agent	*Concentration* (M)	*Solution*	*Temperature* (°C)	*Results*	*References*
			30	$-\mathrm{d[Pu(IV)]}/\mathrm{d}t =$ $(0.27 \pm 0.07)\left(\frac{[\mathrm{Pu(IV)}][\mathrm{NH_3OH^+}]}{[\mathrm{Pu(III)}][\mathrm{H^+}]^2(1+[\mathrm{NO_3^-}]/0.33)}\right)^2$ $\mathrm{M\ min^{-1}}$ E_a (30–45°) = (186 ± 8) kJ mol^{-1} after equilibrium established	
NH_3OH^+ oxidized to N_2	0.2	3 M HNO_3	30	$-\mathrm{d[Pu(IV)]}/\mathrm{d}t =$ $(0.195 \pm 0.013)\left(\frac{[\mathrm{Pu(IV)}][\mathrm{NH_3OH^+}]}{[\mathrm{Pu(III)}][\mathrm{H^+}]^2(1+[\mathrm{NO_3^-}]/0.33)}\right)^2$ $\mathrm{M\ min^{-1}}$ E_a (30–45°) = (205 ± 3) kJ mol^{-1} after equilibrium established	Koltunov and Zhuravleva (1978)
Pu(IV) (disproportionation)	1×10^{-2}	1 M (H,Na)ClO_4	25	$-\mathrm{d[Pu(IV)]}/3\mathrm{d}t = [\mathrm{Pu^{4+}}]^2(2.56 \times 10^{-5}\,[\mathrm{H^+}]^{-3} + 3.9 \times 10^{-6}\,[\mathrm{H^+}]^{-4})\ \mathrm{M\ s^{-1}}$	Rabideau (1953)
				also studied in HNO_3 solutions	Artyukhin *et al.* (1959)
Pu(V) reduction					
ascorbic acid $C_6H_8O_6$	0.02	2 M (H,Na)ClO_4	25	$k' = (4.2 \pm 0.4)10^{-2}[\mathrm{H^+}]^{1.2}\ \mathrm{M^{-1}\ min^{-1}}$ E_a (25.1–44.9°) = (57.3 ± 6.3) kJ mol^{-1}	Koltunov *et al.* (1980a)
		4 M (H,Na)ClO_4	25	$k' = (7.4 \pm 0.5)10^{-2}[\mathrm{H^+}]^{2.2}\ \mathrm{M^{-1}\ min^{-1}}$ *note*: the reaction studied occurs in parallel with the reduction of Pu(V) by Pu(III). Pu(III) is the final product	

Pu(V)	$\sim 10^{-3}$	1 M (H,Na)ClO$_4$	25	$k'' = 3.6 \times 10^{-3}\,[\mathrm{H}^+]\,\mathrm{M}^{-1}\,\mathrm{s}^{-1}$ $\Delta H^* = (79 \pm 4)$ kJ mol^{-1}	Rabideau (1957)
	5.3×10^{-4}	3.3 M NaOH	22	$k'' = 0.024\,\mathrm{M}^{-1}\,\mathrm{s}^{-1}$ E_a (10–30°) = 88 kJ mol^{-1}	Shilov (1997)
Pu(VI) reduction					
EDTA	2×10^{-3}	1 M NaClO$_4$ pH 3–5	room	$k'' = 4.3 \pm 1.6\,\mathrm{M}^{-1}\,\mathrm{s}^{-1}$	Kabanova *et al.* (1960)
Fe(II)	4×10^{-5}	2 M (H,Li)ClO$_4$	25	$k'' = 1000 + (2 \times 10^{-4} + 1.3 \times 10^{-3}\,[\mathrm{H}^+])^{-1}\,\mathrm{M}^{-1}\,\mathrm{s}^{-1}$ evidence for a binuclear intermediate $E_a = (22.6 \pm 0.8)$ kJ mol^{-1} for first rate constant	Newton and Baker (1963) and Beitz *et al.* (1986)
HNO$_2$	0.027	0.55 M (H,Na)NO$_3$	20	$k'' = (2.4 \pm 0.2)/[\mathrm{H}^+]\,\mathrm{M}^{-1}\,\mathrm{min}^{-1}$	Koltunov and Zhuravleva (1968)
	0.02	2 M (H,Na)NO$_3$	22	(a) forward reaction $k'' = (10.55 \pm 0.86)/[\mathrm{H}^+]\,\mathrm{M}^{-1}\,\mathrm{min}^{-1}$ E_a (8–30°) = (111 ± 2) kJ mol^{-1} (b) reverse reaction $k'' = (9.63 \pm 0.42)\,\dfrac{[\mathrm{NO}_3^-]^{0.4}[\mathrm{H}^+]^{0.6}}{[\mathrm{HNO}_2]^{0.5}}\,\mathrm{M}^{-1}\,\mathrm{min}^{-1}$ E_a (8–30°) = (92 ± 3) kJ mol^{-1}	Koltunov and Ryabova (1980)
NH$_3$OH$^+$	0.016	3 M (H,Na)ClO$_4$	60	$k'' = (4.22 \pm 0.12)/[\mathrm{H}^+]\,\mathrm{M}^{-1}\,\mathrm{min}^{-1}$ $E_a = (78 \pm 2)$ kJ mol^{-1}	Koltunov *et al.* (1981b)

Table 7.52 (*Contd.*)

Agent	*Concentration* (M)	*Solution*	*Temperature* (°C)	*Results*	*References*
$N_2H_5^+$	0.02	2 M (H,Na) (NO_3,ClO_4)	40	$k'' = (0.314 \pm 0.042)$ $[H^+]^{-1}[NO_3^-]^0$ M^{-1} min^{-1} $-d[Pu(VI)]/dt = k_a[Pu(VI)]\left(\frac{[N_2H_5^+]}{[H^+]}\right)^{0.85}$ $k_a = (0.243 + 0.024)$ min^{-1} $E_a = (67.4 \pm 0.8)$ kJ mol^{-1} for either rate law	Koltunov and Zhuravleva (1973) and Newton (2002)
EDTA	2×10^{-3}	1 M $NaClO_4$; pH 3–5	room	$k'' = 4.3 \pm 1.6$ M^{-1} s^{-1}	Kabanova *et al.* (1960)

surface of the metal may be removed electrochemically (Bergstresser, 1950) or mechanically. The standard potential for the three-electron oxidation of α-Pu metal is –(2.000 ± 0.009) V (Lemire *et al.*, 2001). Alternatively, plutonium in higher oxidation states in acid solutions may be reduced electrolytically using either a mercury or platinum cathode. The potential should be about 0.75 V (vs NHE) or less (Cohen, 1961a). Chemical reductants such as hydroxylamine or hydrazine may also be used, but these are generally less satisfactory because the oxidized form of the reducing agent is often left in the solution. The Pu(III) aquo ion imparts a blue or blue-violet color to aqueous acidic solutions and exhibits hydrolysis, complexation, and solubility properties similar to the rare-earth ion neodymium(III).

In solutions of noncomplexing acids, Pu(III) is stable with respect to reaction with the oxygen in air. However, in dilute sulfuric acid, for example, the reaction occurs at a conveniently measurable rate (Newton and Baker, 1956). At a pH of 4, Pu(III) is slowly oxidized but at pH values greater than about 4 or 5, or in 0.4 M $NaHCO_3$, Pu(III) is rapidly oxidized by atmospheric oxygen (Newton *et al.*, 1986a). For ^{239}Pu, α-particle induced oxidation occurs in $HClO_4$ solutions at a rate of about 1.5% per day, approaching a steady state containing about 10% Pu(IV) and 90% Pu(III) (Rabideau *et al.*, 1958). In HCl solutions the α-particle induced oxidation proceeds to nearly pure Pu(IV) (Newton *et al.*, 1986a).

Pu(IV). Solutions of Pu(IV) are conveniently prepared by the electrolytic oxidation of Pu(III) at about 1.2 V. At this potential Pu(VI) is thermodynamically stable, but its rate of formation is insignificant due to the slow kinetics of forming the Pu=O bond (Cohen, 1961a). Alternatively, Pu(IV) may be prepared by reacting Pu(III) with Pu(VI) according to the equation:

$$2Pu^{3+} + PuO_2^{2+} + 4H^+ \rightleftharpoons 3Pu^{4+} + 2H_2O \tag{7.86}$$

This reaction is the reverse of the Pu(IV) disproportionation reaction (equation 7.75), and the equilibrium constant is approximately 112 in 1 M $HClO_4$ solution at 25°C (Rabideau, 1953), so at equilibrium under these conditions as much as 28% of the plutonium will be in other oxidation states. Higher acid concentrations or the presence of complexing anions such as chloride will give larger fractions of Pu(IV). This is why it is a common practice to prepare and store Pu(IV) solutions in 3 M HCl (Newton *et al.*, 1986a). Acidic solutions of Pu^{4+} that are free of complexing agents are orange-brown or tan in color.

In acid solutions Pu(IV) is thermodynamically unstable with respect to reaction with oxygen, but the rate of this reaction is negligible. In $HClO_4$, α-particle induced reduction occurs to give the same steady state as described for Pu(III). In HCl solutions, however, Pu(IV) is significantly stabilized (Rabideau *et al.*, 1958). Newton *et al.* (1986a) found that stock solutions of Pu(IV) in about 3 M HCl are stable for many months. Even in 1 M acid, Pu(IV) hydrolyzes appreciably, and, at pH values greater than about 1, significant formation of green colloidal Pu(IV) hydroxide occurs. The rate of colloid formation depends on the plutonium concentration as well as the pH. Rates under specific conditions have been described (Costanzo *et al.*, 1973; Toth *et al.*, 1981; Newton and Rundberg, 1984). Complexation constants for tetravalent plutonium are among the highest for any cation of any element, being most similar to those of Th(IV), U(IV), and Np(IV).

Pu(V). Solutions of Pu(V) are conveniently prepared by the electrolytic reduction of 0.02 M Pu(VI) in $HClO_4$ solution at pH near 3. A potential close to 0.54 V (vs SCE) is suitable (Cohen, 1961a). In most preparations it is necessary to readjust the pH during electrolysis because hydrogen ions are transported from the counter electrode compartment (Newton *et al.*, 1986a). The use of a photochemically produced reducing agent in a two-phase system has also been described (Choppin and Saito, 1984). The PuO_2^+ ion imparts a pink or light purple color to aqueous solutions, has a low effective charge and undergoes hydrolysis only at higher pH (approximately $pH = 9$ for millimolar plutonium).

In acid solution Pu(V) disproportionates with the reaction rate proportional to the fourth power of the hydrogen ion concentration and the square of the Pu(V) concentration (Rabideau, 1957). Thus both the thermodynamics and the kinetics favor Pu(V) at low acidities. However, α-radiolysis effects, even at pH values greater than 3, cause fairly rapid formation of colloidal Pu(IV) and Pu(VI) (Newton *et al.*, 1986b). These effects are more pronounced at higher Pu(V) concentrations, and less pronounced at low concentrations. Pu(V) can persist in near-neutral pH solutions when the total plutonium concentration is very low ($<10^{-6}$ M), as may be the case in slightly-contaminated natural waters and some waste solutions.

Pu(VI). Solutions of Pu(VI) are conveniently prepared by oxidation with hot, concentrated $HClO_4$ (Newton *et al.*, 1986a). Plutonium ions in lower oxidation states, in the absence of coordinating anions are oxidized to Pu(VI) by fuming strongly with $HClO_4$. The remaining free acid may be estimated gravimetrically and traces of chlorine oxides can be removed by boiling the diluted solutions. Acidic solutions of PuO_2^{2+} in the absence of complexing agents are yellow or orange in color. Hexavalent plutonium nitrate can also be generated by heating nitric acid solutions of plutonium almost to dryness at about 170°C. A glassy solid results after cooling the nitrate melt that is a very stable storage form for Pu(VI) and is readily soluble in aqueous solutions (Stoll *et al.*, 1982).

In $HClO_4$ solutions Pu(VI) is unstable with respect to α-particle induced reduction. With millimolar or greater plutonium concentrations, at pH values between about 0 and 2, the rate of reduction is about 1.2 to 2% of the total plutonium per day (Rabideau *et al.*, 1958; Newton *et al.*, 1986b). At very low plutonium concentrations (2.2×10^{-5} M) the rates are much slower. It has also been reported that chloride ions inhibit the α-reduction of Pu(VI) in analogy with Pu(IV) (Rabideau *et al.*, 1958).

Pu(VII). Blue-black heptavalent plutonium is the least stable oxidation state, prepared by vigorous oxidation of highly alkaline solutions of hexavalent plutonium. In alkali solutions, ozonization, anodic oxidation or treatment with peroxydisulfate, or other strong oxidants can produce the heptavalent form (Komkov *et al.*, 1969; Krot *et al.*, 1976; Tananaev *et al.*, 1992). The high formal potential of Pu(VII) puts it outside the region of thermodynamic stability of water for hydroxide concentrations less than about 7 M, and heptavalent plutonium is instantly reduced in acid solutions. This plutonium ion is less stable than the heptavalent neptunium analog (Varlashkin *et al.*, 1984; Tananaev *et al.*, 1992).

(*vi*) *Pu(VI) oxygen exchange with solvent water*

Masters and Rabideau (1963) measured the rate of exchange between PuO_2^{2+} and ^{18}O-enriched water in dilute $HClO_4$ solution. The studies were conducted under chlorine atmosphere to ensure that Pu(VI) was the only oxidation state present. This was done because the rate of exchange was found to be accelerated by the presence of lower oxidation states of plutonium in the solutions (Rabideau and Masters, 1963). Like the exchange for the uranyl ion (Gordon and Taube, 1961), the exchange rate was found to be extremely slow with a half-time of 4.55×10^4 h at 23°C. The exchange rate was found to be the sum of the rates of two separate reaction paths that include the intrinsic $PuO_2^{2+} - H_2^{18}O$ exchange reaction and the exchange induced by the breaking of Pu=O bonds by α-particle reduction. Studies employing ^{238}Pu demonstrated that the exchange rate was much faster than with ^{239}Pu, and extrapolation of the rates to the flux conditions of ^{239}Pu solutions suggested a half-time for radiation-induced exchange of about the same order of magnitude (approximately 10^4 h). This was interpreted as indicating that in 0.15 M Pu(VI) solution, the major contribution to the exchange is from radiation-induced reaction, and that the rate of the intrinsic exchange reaction is even slower.

(*vii*) *Oxidation and reduction by actinide ions*

These reactions have been studied primarily in acidic solutions because hydrolysis and precipitation of these high-valent metal ions limit their solubility at higher pH values. Most of the actinide separations and processing technology has been developed in acid solutions motivating much of the quantitative study of plutonium redox reactions. An important subset of these reactions has been described by Newton (2002) and is given in Table 7.53. The use of catalysts to enhance the rate of reactions has also been studied for plutonium both to accomplish process steps more rapidly on an industrial scale and to determine rate constants that are otherwise difficult to determine because of back reactions, competing reactions, or other complications (Newton, 1975).

The redox reactions between plutonium and other actinides are important because they are applicable to many aqueous solutions used in separation processes and waste operations. These reactions are also useful because the reactions involving ions with similar structures but different reduction potentials can be compared. For example, the rates of reactions (reaction 3 through

Table 7.53 *Thermodynamic constants for plutonium-actinide redox reactions at 25°C (Newton, 2002).*

	ΔG (kJ mol^{-1})	ΔH (kJ mol^{-1})	ΔS (J K^{-1} mol^{-1})	k″ (M^{-1} s^{-1})	I (M)	ΔG* (kJ mol^{-1})	ΔH* (kJ mol^{-1})	ΔS* (J K^{-1} mol^{-1})	*References*
1. $Pu^{3+} + NpO_2^{2+} \rightleftarrows Pu^{4+} + NpO_2^{+}$									
	−15.1	−60.7	−153	$35.5 + 3.1\,[H^+]^{-1}$	1.0	64.2	14.6	−166	Fulton and Newton (1970)
2. $Pu^{3+} + PuO_2^{2+} \rightleftarrows Pu^{4+} + PuO_2^{+}$									
	6.3	−35.6	−140	2.7	1.0	70.5	20.2	−169	Rabideau and Kline (1958)
3. $2Pu^{4+} + 2H_2O \rightleftarrows Pu^{3+} + PuO_2^{+} + 4H^{+}$									
	18.2	121	344	$2.9 \times 10^{-5}\,[H^+]^{-3}$	1.0	101.0	154.5 ± 0.5	180 ± 2	Lavallee and Newton (1972)
				$4.4 \times 10^{-2}\,[H^+]^{a}$	1.0	80.8	33.5 ± 0.5	−158 ± 2	
4. $Np^{4+} + Pu^{4+} + 2H_2O \rightleftarrows NpO_2^{+} + Pu^{3+} + 4H^{+}$									
	−23.4	92	387	$0.253\,[H^+]^{-3}$	2.0	76.6	142 ± 6	218 ± 21	Rykov *et al.* (1969)[b]
				$2.2 \times 10^{-5}[H^+]$	1.0	99.6	50	−167 ± 21	
5. $U^{4+} + Pu^{4+} + 2H_2O \rightleftarrows UO_2^{+} + Pu^{3+} + 4H^{+}$									
	−36.4	68.5	352	$34.4\,[H^+]^{-2}$	2.0	64.3	102 ± 2.5	126 ± 8	Newton (1959)
				$1.9 \times 10^{-5}\,[H^+]^{2}$	1.0	100	33.1	−216 ± 8	

6. $U^{4+} + PuO_2^{2+} + 2H_2O = UO_2^{+} + PuO_2^{+} + 4H^{+}$									
	−30.0	33	213	$[(4.35[H^{+}]^{-1})^{-1} + (11.25[H^{+}]^{-2})^{-1}]^{-1}$	2	69.5	73.6 ± 0.4	15 ± 2	Newton (1958)
						66.9	88.8 ± 1.2	74 ± 5	
6a. $PuO_2^{2+} + U^{4+} + H_2O = [PuO_2(UOH)^{*}]^{5+} + H^{+}$									
	69.5	73.6	14 ± 2		2			−368	Newton (1958)
6b. $PuO_2^{2+} + U^{4+} + H_2O = [PuO_2(UO)^{*}]^{4+} + 2H^{+}$									
	66.9	89.1	75 ± 5		2			−303	Newton (1958)
7. $Np^{4+} + PuO_2^{2+} + 2H_2O \rightleftarrows NpO_2^{+} + PuO_2^{+} + 4H^{+}$									
	−17.1	56.5	247	$3.5 \times 10^{-4}\,[H^{+}]^{-2}$	1.0	92.76	130 ± 4	126 ± 13	Newton and Montag (1976)
				$8.8 \times 10^{-6}\,[H^{+}]^{-3}$	1.0	102	168 ± 8	222 ± 25	
8. $Pu^{4+} + PuO_2^{2+} + 2H_2O \rightleftarrows PuO_2^{+} + 4H^{+}$									
	24.5	85.3	204	$1.2 \times 10^{-7}\,[H^{+}]^{-3}$	2	112.5	164	172	Rabideau (1957)[c]
				$3.6 \times 10^{-3}\,[H^{+}]$[a]		87.0	79 ± 11	25 ± 38	

---

[a] The reaction was measured in the opposite direction, with the result given here.

[b] An estimate for the reverse reaction.

[c] Calculated from the reverse reaction.

8 in Table 7.53) that involve the making of An=O bonds as An^{4+} is oxidized to AnO_2^+ differ by orders of magnitude for the different elements. Four hydrogen ions are produced in the overall reaction, but only two or three are given up in the activation processes. The rate laws for oxidation of U^{4+} and Np^{4+} by PuO_2^{2+} show consecutive rate-determining steps of which only one or two can be redox reactions. This reaction is described below for U^{4+}, as an illustration of the importance of considering multiple intermediates and pathways.

The reaction between U^{4+} and PuO_2^{2+} proceeds through AnO_2^+ intermediates, and in acid solution leads eventually to Pu^{3+} (Newton, 1958, 1975). In dilute solutions (1.8×10^{-4} M Pu(VI) and 0.62×10^{-4} M U(IV) in 1 M $HClO_4$), approximately 96% of the U(IV) reacts according to the following equation:

$$2\mathrm{Pu(VI)} + \mathrm{U(IV)} \rightarrow 2\mathrm{Pu(V)} + \mathrm{U(VI)} \tag{7.87}$$

The remaining U(IV) reacts according to

$$\frac{2}{3}\mathrm{Pu(VI)} + \mathrm{U(IV)} \rightarrow \frac{2}{3}\mathrm{Pu(III)} + \mathrm{U(VI)} \tag{7.88}$$

Equations 7.87 and 7.88 only represent the change in oxidation states of the actinides but do not account for the overall stoichiometry. The reaction rates, as studied by spectrophotometric monitoring of the concentration of Pu(VI), are consistent with the rate law:

$$-\frac{\mathrm{d[Pu(VI)]}}{\mathrm{d}t} = 2k''\mathrm{[Pu(VI)][U(IV)]} \tag{7.89}$$

This requires that the activated complexes be formed from one Pu(VI) and one U(IV), probably according to the reaction

$$\mathrm{Pu(VI)} + \mathrm{U(IV)} \rightarrow \mathrm{Pu(V)} + \mathrm{U(V)} \tag{7.90}$$

followed by the rapid reaction

$$\mathrm{Pu(VI)} + \mathrm{U(V)} \rightarrow \mathrm{Pu(V)} + \mathrm{U(VI)} \tag{7.91}$$

Steady-state calculations show that U(V) disproportionation into U(VI) and U(IV)

$$2\mathrm{U(V)} \rightarrow \mathrm{U(IV)} + \mathrm{U(VI)} \tag{7.92}$$

is too slow to account for the disappearance of U(V) and is unimportant with respect to reaction (7.91). Under these conditions (1 M $HClO_4$) the U(IV) undergoes hydrolysis, while Pu(VI) does not. Thus

$$\mathrm{[U(IV)]} = [\mathrm{U}^{4+}](1 + K/[\mathrm{H}^+]) \tag{7.93}$$

and

$$\mathrm{[Pu(VI)]} = [\mathrm{PuO}_2^{2+}] \tag{7.94}$$

where K is the first hydrolysis constant for U(IV). In terms of the species present, the rate law (7.89) becomes

$$-\frac{\mathrm{d}[\mathrm{Pu(VI)}]}{\mathrm{d}t} = 2k''\left(1+\frac{K}{[\mathrm{H}^+]}\right)[\mathrm{PuO}_2^{2+}][\mathrm{U}^{4+}] \tag{7.95}$$

The hydrogen-ion dependence as a function of temperature suggests that the most important activated complex is that formed by the prior loss of H^+, and that a second activated complex resulting from the loss of two H^+ ions may also be involved. The decrease in the apparent H^+ dependence with decreasing $[H^+]$ is not consistent with parallel rate-determining steps, but suggests consecutive reactions (6a and 6b in Table 7.53) instead.

From the linearity of $\{k''([H^+] + K)\}^{-1}$ vs $[H^+]$ for the data at each temperature (k_1 and k_2 are rate constants distinct from k' or k''). Newton arrived at the following rate law:

$$-\frac{\mathrm{d}[\mathrm{Pu(VI)}]}{\mathrm{d}t} = \frac{2[\mathrm{Pu(VI)}][\mathrm{U(IV)}]}{1+K/[\mathrm{H}^+]}\left(\frac{1}{k_1[\mathrm{H}^+]^{-1}}+\frac{1}{k_2[\mathrm{H}^+]^{-2}}\right)^{-1} \tag{7.96}$$

The rate law (7.96) governs many detailed mechanisms, all of which require a binuclear intermediate that can react to give products or dissociate to give reactants at rates that depend on $[H^+]$. A simple mechanism consistent with the rate law is:

$$\mathrm{U}^{4+} + \mathrm{H_2O} \rightarrow \mathrm{UOH}^{3+} + \mathrm{H}^+ \quad \text{(rapid equilibrium)} \tag{7.97}$$

$$\mathrm{UOH}^{3+} + \mathrm{PuO}_2^{2+} \rightleftarrows \mathrm{PuO_2(UOH)}^{5+} \quad \text{(rate-determining, reversible)} \tag{7.98}$$

$$\mathrm{PuO_2(UOH)}^{5+} \rightarrow \mathrm{PuO_2(UO)}^{4+} + \mathrm{H}^+ \quad \text{(rapid equilibrium)} \tag{7.99}$$

$$\mathrm{PuO_2(UO)}^{4+} + \mathrm{H_2O} \rightarrow \mathrm{UO}_2^+ + \mathrm{PuO}_2^+ + 2\mathrm{H}^+ \quad \text{(rate-determining)} \tag{7.100}$$

The two net activation processes required by the rate law do not depend on the details of the mechanism. The activation parameters ΔG^*, ΔH^*, and ΔS^* for these processes as determined from simultaneous treatment of the hydrogen ion and temperature data are listed in Table 7.53 under reactions 6a and 6b. For a more detailed discussion of redox reactions between plutonium and other actinide ions, the reader is referred to Newton (2002).

(*viii*) *Oxidation and reduction by nonactinide species*

Plutonium ions are well known to undergo redox reactions with ions of almost every element in the periodic table and many inorganic and organic redox reagents. Almost all of the redox reactions of aqueous plutonium ions are first order in the oxidizing or reducing agent, but some are either inhibited or catalyzed by the reaction products. The rates are often strongly influenced by the concentration of H^+ and of complexing ligands. For example, reductions using synthetic and natural organic acids, such as oxalic, ascorbic, hydroxamic, and humic acids are pH dependent with rates that generally increase with increasing $[H^+]$ (Cleveland, 1979; Choppin *et al.*, 1986; Nikitenko, 1988; Czerwinski and Kim, 1997; Ruggiero *et al.*, 2000; Moulin and Moulin, 2001; Taylor *et al.*, 2002). Common strong oxidizing agents that are relatively poor ligands for the actinides, such as dichromate, bromate, and iodate, have comparatively rapid plutonium oxidation rates (Newton, 1975). A large body of empirical observations has been accumulated on the oxidation–reduction behavior of plutonium with various reagents, while quantitative data are available for a relatively small subset. Since among plutonium ions, Pu(IV) forms the strongest complexes, redox reactions of the other ions can be interpreted using similar but simplified reactions and rate laws.

There is a broad qualitative relation between the rates of redox processes and the particular plutonium ions involved. Generally, the reactions of Pu^{4+} with single-electron reductants, such as Fe^{2+}, are rapid. The oxidation of Pu^{3+} or the reduction of Pu^{4+} with two-electron reagents is expected to be slower, although the variation in rate for different reagents varies from slow to a rate too fast to measure. A similar situation exists for one-electron reduction of PuO_2^{2+} to PuO_2^+. In contrast, reactions that make or break Pu=O multiple bonds are inherently slower. Multielectron processes, such as Pu^{4+} oxidation to PuO_2^{2+}, can proceed in one two-electron step or two one-electron steps. Oxidation of Pu^{4+} or reduction of PuO_2^+ can generally proceed by direct reaction with the oxidizing or reducing agent, or by oxidation or reduction through the disproportionation reaction. Reactions of plutonium ions are further complicated in that slight changes in solution conditions can profoundly affect the rate and even the direction of the reaction, particularly for Pu^{4+}, owing to its tendency to form multiple stable molecular complexes. For example, reactions in sulfuric acid or carbonate media may take a different course or proceed at a different rate compared to those in perchlorate solutions. Early observations on the redox behavior of plutonium that were made on tracer level concentrations before all of the oxidation states had been well established cannot be applied directly to higher concentrations without reservations. Many of those experiments were qualitative, designed to determine whether reactions were complete or not, and will not be discussed here. A few important systems that relate to plutonium processing and also illustrate particular details of plutonium chemistry will be described here, including reactions with ferrous ion, nitrate, nitrite, hydroxylamine, and hydrogen peroxide. For additional detailed information or lists of reactions and rates, the reader is directed to reviews by Newton (2002) and Cleveland (1979), and general references that contain oxidation and reduction potentials (Wick, 1980).

The multistep reduction of Pu(VI) by Fe(II) is important in fuel reprocessing and has complicated mechanisms and rate laws that were described by Newton (1958, 2002).

When Fe(II) is added to an excess of Pu(VI), the predominant reaction is

$$\mathrm{PuO_2^{2+} + Fe^{2+} \rightarrow PuO_2^{+} + Fe^{3+}} \tag{7.101}$$

Using a 60% excess of Pu(VI), Newton (1958) found that for each mole of Fe(II) oxidized approximately one mole of Pu(VI) was reduced as the acid concentration was varied from 2.0 to 0.05 M. Although Fe(II) is capable of reducing Pu(VI) all the way to Pu(III), appreciable amounts of Pu(IV) are observed, even if an excess of Fe(II) is used.

In addition to $\mathrm{Pu^{4+}}$ disproportionation, the following reactions were found to be important:

$$\mathrm{PuO_2^{+} + Fe^{2+} + 4H^{+} \rightarrow Pu^{4+} + Fe^{3+} + 2H_2O} \tag{7.102}$$

$$\mathrm{Pu^{4+} + Fe^{2+} \rightarrow Pu^{3+} + Fe^{3+}} \tag{7.103}$$

From sets of individual reactions in which the pH, then ionic strength, then metal ion concentrations were varied, Newton and Baker (1963) found the following rate law:

$$-\frac{\mathrm{d}[\mathrm{PuO_2^{2+}}]}{\mathrm{d}t} = \{A + (B + C[\mathrm{H^+}])^{-1}\}[\mathrm{PuO_2^{2+}}][\mathrm{Fe^{2+}}] \tag{7.104}$$

The necessity of three parameters in the rate law equation indicates three rate-determining steps and three important activated complexes. The above three-parameter equation may be rearranged to give

$$\begin{aligned} -\frac{\mathrm{d}[\mathrm{PuO_2^{2+}}]}{\mathrm{d}t} &= A[\mathrm{PuO_2^{2+}}][\mathrm{Fe^{2+}}] \\ &\quad + \left(\frac{1}{B^{-1}[\mathrm{PuO_2^{2+}}][\mathrm{Fe^{2+}}]} + \frac{1}{C^{-1}[\mathrm{PuO_2^{2+}}][\mathrm{Fe^{2+}}]/[\mathrm{H^+}]}\right)^{-1} \end{aligned} \tag{7.105}$$

In this equation, parameter A is associated with the path that leads directly to products, and the B and C terms involve consecutive reactions that parallel the direct reaction. Newton and Baker found several mechanisms that were consistent with the data. All involve the same three activated complexes formed in both consecutive and parallel paths, as well as $\mathrm{PuO_2^{2+}}$ hydrolysis.

Plutonium reduction and oxidation reactions in nitric acid solutions have been extensively studied. Descriptions of Pu(IV) oxidation and reduction in nitrate solutions benefited from recent spectroscopic studies that measured the formation constants for two Pu(IV) nitrate species, $\mathrm{Pu(NO_3)_n^{4-n}}(n = 1, 2)$ (Berg *et al.*, 2000). Complexation of Pu(IV) by nitrate can decrease the concentration of aquo $\mathrm{Pu^{4+}}$, and thereby slow down the rates of some reactions, or it can provide additional reaction pathways for other reactions. For example, reactions involving Pu(IV) either as a reactant or product with pentavalent metal ions are much faster in nitrate solutions than in perchlorate solutions. Conversely, oxidation of Pu(IV) by Ce(IV) or Np(VI) are both slower in HNO_3. Reductions of Pu(IV) are also generally slower in HNO_3 than in $HClO_4$ (Newton, 2002).

A great deal of information is available for Pu(IV) redox involving nitrous acid, hydroxylamine, and hydrazine in HNO_3, systems that are important for processing applications. Nitrous acid is commonly used to adjust the oxidation state of plutonium, both as a pure reagent and inadvertently as a contaminant in nitric acid. The key to understanding plutonium redox reactions in nitric and nitrous acid is that small equilibrium concentrations of NO_2 are present in HNO_2–HNO_3 mixtures. For example, although Pu(III) is quite stable in dilute nitric acid solutions, in the presence of HNO_2 it is readily oxidized to Pu(IV) by the following reaction:

$$2Pu^{3+} + 3H^+ + NO_3^- \rightleftarrows 2Pu^{4+} + HNO_2 + H_2O \qquad (7.106)$$

An empirical rate law and a plausible mechanism for the reaction were derived by Koltunov and Marchenko (1973). The oxidation may be retarded by the addition of a "holding reductant" to react with the HNO_2 as soon as it is formed. Effective reductants include sulfamic acid, ferrous sulfamate or hydrazine (Cleveland, 1979).

Plutonium(V) is reduced very slowly by nitrous acid (Koltunov *et al.*, 1982b). These studies consistently show that NO_2, formed by reaction of HNO_2 with HNO_3, is the important oxidant in the Pu(III) or Pu(V) oxidation by HNO_3. The rate of the following equilibrium reaction involving Pu(V) and Pu(VI) has been measured in both directions (Koltunov and Ryabova, 1980).

$$2PuO_2^{2+} + HNO_2 + H_2O \rightleftarrows 2PuO_2^+ + NO_3^- + 3H^+ \qquad (7.107)$$

Hydroxylamine and hydrazine are very useful reducing agents for all of plutonium's higher oxidation states, because they are nonmetallic, yield volatile oxidation products, and tend to react rapidly. These reactants are two-electron reducing agents, so one-electron oxidation leads to radical intermediates that can either decompose to stable products or be oxidized by plutonium and therefore influence the overall stoichiometry and the rate law. If the two one-electron oxidations occur at approximately the same rates, the stoichiometry will change during the course of the overall reaction and the rate laws will be very complicated. Additional redox agents and mechanistic complexity are added when the reduction of plutonium by these reagents is conducted in nitric acid solutions.

When hydroxylamine is oxidized by plutonium(IV), the two limiting overall reactions are (Barney, 1976):

$$2Pu^{4+} + 2NH_3OH^+ \rightleftarrows 2Pu^{3+} + N_2 + 4H^+ + 2H_2O \qquad (7.108)$$

and

$$2Pu^{4+} + NH_3OH^+ \rightleftarrows 2Pu^{3+} + 3H^+ + 0.5N_2O + 0.5H_2O \qquad (7.109)$$

The empirical rate law for the plutonium reduction by hydroxylamine in 2.5 M [(H, Na) (NO_3, ClO_4)] was found to be

$$-\mathrm{d}[\mathrm{Pu(IV)}]/\mathrm{d}t = [\mathrm{Pu}^{4+}]^2[\mathrm{NH_3OH^+}]^2/[\mathrm{Pu}^{3+}]^2[\mathrm{H}^+]^4(1+\beta_1[\mathrm{NO_3^-}])^2 \quad (7.110)$$

The factor $(1+\beta_1[\mathrm{NO_3^-}])$ is consistent with the formation of a nitrate complex. An independent investigation using 3 M (H,Na)NO_3 and large excess amounts of NH_3OH^+ gave results at 30°C that agreed reasonably well with the rate law and stoichiometries (Koltunov and Zhuravleva, 1978), yet the rate law does not account for higher nitrate complexes that are known to form when the $[\mathrm{NO_3^-}]$ is greater than ~2–3 M (Berg *et al.*, 1998).

Yarbro *et al.* (1998) recently summarized past studies of Pu(IV) reduction by hydroxylamine and reported results with hydroxylamine nitrate (HAN) in the presence of excess plutonium. Rather than define the kinetic expression in terms of concentrations (although plausible mechanisms and complex stoichiometries were discussed), the following fractional conversion was defined:

$$X = 1 - (N_{\mathrm{A}}/N_{\mathrm{A}^0}) \quad (7.111)$$

where X is the fraction of compound reacted, N_{A^0} is the initial number of moles of the reactant A and N_{A} is the number of moles of reactant A at some time t. If acid and nitrate concentrations are constant, then the fractional conversion of HAN can be described as follows:

$$\begin{aligned}-\mathrm{d}X/\mathrm{d}t = {} & (kk_{\mathrm{H}}^{0.44}/C_{\mathrm{Pu}^0}[\mathrm{H}^+]^{0.56})([\mathrm{H}^+]^{0.65} \\ & + k_{\mathrm{a}}[\mathrm{NO_3^-}])[(1-X)/X]^2([\mathrm{HAN_0}] - C_{\mathrm{Pu}^0}X)^{0.44}\end{aligned} \quad (7.112)$$

where k is the kinetic constant; k_{H} is the dissociation constant for HAN; k_{a} is the dissociation constant for HNO_3; C_{Pu^0} is the initial plutonium molar concentration and [HAN_0] is the initial HAN molar concentration. This expression is useful at low HAN to plutonium molar ratios.

An improved understanding of this system and more broadly applicable rate law requires additional research, including quantitative evaluation of multiple plutonium nitrate complexes (beyond the 1:1 complex), the oxidation of HAN by nitric acid, the reoxidation of Pu(III) by nitrous acid, the disproportionation of Pu(IV), and, for solutions concentrated in Pu, radiolytic oxidation of Pu(III) and reduction of Pu(IV). The Pu(IV) hydroxylamine reaction has also been studied in perchlorate solutions using relatively high $[\mathrm{Pu(IV)}]_o/[\mathrm{NH_3OH^+}]_o$ ratios (Koltunov and Zhuravleva, 1978). These conditions favor the path in which the radical intermediate is oxidized to N_2O. Kinetic studies of Pu(IV) reduction by a derivatized hydroxylamine, where the reducing agent was present in molar excess of plutonium, showed similar dependencies on hydrogen ion and hydroxylamine concentrations (Anyun *et al.*, 2002).

The reduction of Pu(VI) by NH_3OH^+ has been studied in 3 M perchlorate solutions at temperatures near 60°C (Koltunov *et al.*, 1981b). When $[\mathrm{H}^+]$ is

<0.55 M, the disproportionation of Pu(V) is relatively slow and the net reaction is probably as follows:

$$2PuO_2^{2+} + NH_3OH^+ \rightleftarrows 2PuO_2^+ + 3H^+ + 1/2N_2O + 1/2H_2O \qquad (7.113)$$

This reaction requires that a radical intermediate be oxidized by Pu(VI). The rate law was found to be

$$-d[Pu(VI)]/dt = 2k_0[PuO_2^{2+}][NH_3OH^+]/[H^+] \qquad (7.114)$$

This rate law is much simpler than the one for the reduction of Pu(IV), and shows that the rate-determining step is the initial formation of the radical intermediate. At higher $[H^+]$, the disproportionation of Pu(V) becomes important. The Pu(IV) formed is rapidly reduced by NH_3OH^+ to Pu(III), which in turn reacts rapidly with Pu(VI). These steps lead to the catalytic reduction of Pu(VI) by Pu(III). Thus, during the course of the reaction, the concentration of Pu(V) will increase to a maximum, then decrease as the concentration of Pu(III) increases. The complex rate laws for this system have been integrated numerically and give concentrations that are in good agreement with the experimental results (Koltunov *et al.*, 1981b).

The reduction of Pu(IV) by hydrazine has been studied in 2 M $(H,Na)NO_3$ (Koltunov and Zhuravleva, 1974). The limiting overall reactions are probably the following:

$$Pu^{4+} + N_2H_5^+ \rightleftarrows Pu^{3+} + NH_4^+ + H^+ + 1/2N_2 \qquad (7.115)$$

and

$$4Pu^{4+} + N_2H_5^+ \rightleftarrows 4Pu^{3+} + N_2 + 5H^+ \qquad (7.116)$$

The stoichiometric ratio was found to depend on the initial reactant concentrations, just as with hydroxylamine. At 50°C with a $[H^+]$ range between 0.5 and 1.9 M, the rate law for the Pu(IV)–hydrazine reaction was found to be

$$-d[Pu(IV)]/dt = k[Pu^{4+}][N_2H_5^+]/(K_h + [H^+]) \qquad (7.117)$$

This rate law shows that the rate-determining step is the formation of the radical intermediate $(N_2H_4\cdot)$, not its subsequent reaction. The parameter K_h was interpreted as the hydrolysis constant for Pu(IV), but the 1:1 Pu(IV)–nitrate complex should be included in the rate law. An alternative explanation involves the formation of low steady-state concentrations of a plutonium–hydrazine intermediate (Newton, 2002). Additional kinetic studies of the reduction of Pu(IV) have been reported for substituted hydrazines, with similar overall reactions and small changes in reaction rates (Koltunov *et al.*, 1989).

The reduction of Pu(VI) by $N_2H_5^+$ was shown to have features similar to the reduction of Pu(IV) (Koltunov and Zhuravleva, 1973). The initial reaction is most probably

$$PuO_2^{2+} + N_2H_5^+ \rightleftarrows PuO_2^+ + NH_4^+ + 1/2N_2 + H^+ \qquad (7.118)$$

The final reaction product is Pu(III), which arises from the reduction of Pu(IV) described above. The reduction of Pu(V) to Pu(IV) occurs by two parallel pathways: direct reaction of Pu(V) with hydrazine, and comproportionation of Pu(VI) with Pu(III) to give Pu(IV). The kinetics of the reduction of Pu(V) by hydrazine as well as the use of the overall reductions in the nuclear fuel cycle have been described (Koltunov and Baranov, 1993). The rate law in 2 M Na (NO_3,ClO_4) was found to be approximately

$$-\mathrm{d}[\mathrm{Pu(VI)}]/\mathrm{d}t = k[\mathrm{PuO_2^{2+}}][\mathrm{N_2H_5^+}]/[\mathrm{H^+}] \qquad (7.119)$$

The nitrate dependence was found to be zero in the range from 0.15 to 2 M at constant ionic strength. The reduction of Pu(VI) by substituted hydrazines has been shown to proceed with similar overall reactions, some differences in the exponents of the reactants in the rate equation, and small changes in reaction rates (Koltunov *et al.*, 2004).

Both fundamental research and process application of plutonium redox reactions with hydrogen peroxide are complicated by the incomplete characterization of molecular Pu(IV) and Pu(VI) complexes that form with peroxide, and the chemical and radiolytic complexities of plutonium–hydrogen peroxide mixtures. Recent studies indicate the utility of hydrogen peroxide reduction of Pu(VI) and mixtures of Pu(VI) and Pu(IV) on the mM scale by 0.3% H_2O_2 in the presence of extraction resins (Morgenstern *et al.*, 2002). Hydrogen peroxide is more commonly used to reduce Pu(VI) in nitrate solutions. Maillard and Adnet (2001) studied effects of acidity and plutonium and H_2O_2 concentrations on the kinetics of Pu(VI) reduction. The kinetics results generally showed an induction period where the [Pu(VI)] does not change, followed by a linear decrease of [Pu(VI)]. The length of the induction period depends on temperature, $[HNO_3]$, and $[H_2O_2]$, but not on the H_2O_2/Pu(VI) ratio. Total reduction time decreases with increasing [Pu(VI)] and $[HNO_3]$ from 0.5 to 6 M $[HNO_3]$, but increases when $[HNO_3]$ varies from 6 to 8 M. Red-brown peroxo complexes were observed and PuO_2^+ was an intermediate in these reductions.

The kinetics of the reduction of ~1 mM PuO_2^+ by $[H_2O_2]$ has been studied in 1.0 M NaCl solutions at near-neutral pH. The reduction was found to be first order with respect to $[H_2O_2]$ and inverse first order with respect to $[H^+]$ and described by the rate equation (7.119) with $k = 3.59$ to 1.79×10^{-9} min^{-1} (Morgenstern and Choppin, 1999).

$$\mathrm{d}[\mathrm{Pu(V)}]/\mathrm{d}t = k\,[\mathrm{PuO_2^+}][\mathrm{H_2O_2}]/[\mathrm{H^+}] \qquad (7.120)$$

(*ix*) *Autoradiolysis*

When plutonium isotopes undergo radioactive decay in aqueous solution they deposit a great deal of energy (approximately 5 MeV per α particle) in α particle tracks that both heat the solution and produce ions, radicals, and solvated electrons. The predominant products generated by water radiolysis in the bulk solution are H, OH, HO_2, and H_2O_2 (Spinks and Woods, 1990; Vladimirova and Kulikov, 2002). Under plutonium process conditions α radiation generates concentrations of these reactive species that can significantly affect individual stages of reactions as well as the final products. If solute concentrations (most commonly plutonium and nitrate) are less than approximately 1 M, then there will be little direct reaction between the α particles or the transient species and the solute within the tracks.

Reactive species that diffuse out of the alpha-tracks can act as either oxidizing or reducing agents for plutonium and other solutes. For example, in 0.4 M H_2SO_4, 0.53 μmol of Fe(II) is oxidized to Fe(III) per joule of deposited energy (Spinks and Woods, 1990), expressed as $G[\mathrm{Fe(III)}] = 0.53$ μmol J^{-1}; whereas Ce(IV) is reduced with $G[\mathrm{Ce(III)}] = 0.33$ μmol J^{-1} (Spinks and Woods, 1990). The G-values for the reduction of Pu(IV) or Pu(VI) in 1 M $HClO_4$, 0.36 – 0.03 μmol J^{-1}, are similar (for either oxidation state) to those for Fe(II) or Ce(IV) (Kasha, 1949; Newton, 2002). The reduction of Pu(IV) reaches a steady state in which its rate equals the rate of oxidation of Pu(III). At 4°C, the mean oxidation number was found to depend slightly on the total plutonium concentration and/or the dose rate, e.g. 3.05 in 0.022 M Pu, which corresponds to an energy deposition rate of 0.01 Sv L^{-1} (Rabideau *et al.*, 1958).

Plutonium radiolysis in nitrate solution was reviewed by Miner and Seed (1967). Recent research has emphasized the behavior of plutonium in HNO_3 solutions that have much higher dose rates. The results are complicated due to the formation of HNO_2, volatile NO_x, and H_2O_2. Andreichuk *et al.* (1990) studied the oxidation of Pu(III) to Pu(IV) in HNO_3 solutions by using radiation from *in situ* ^{244}Cm. This group first studied the formation of HNO_2 from HNO_3 by ^{244}Cm irradiation in the absence of plutonium (Andreichuk *et al.*, 1984b). These studies, where nitric acid concentrations and dose rates ranged up to 8.6 M and 11.5 W L^{-1}, respectively, showed initial rates of HNO_2 formation to be closely proportional to dose rate, with a yield of 0.21 μmol J^{-1} in 1.89 M HNO_3. A steady-state concentration of 6 mM HNO_2 was reached after 30 h with a dose rate of 3.2 W L^{-1}. In subsequent measurements of Pu(III) oxidation from a dose rate of 3.2 Gy s^{-1}, where $[\mathrm{Pu(III)}]_0 = 10$ mM, and $[HNO_3] < 0.5$ M, steady state was reached within 1 h and approximately 15% of the plutonium had been oxidized. Small concentrations of a Pu(IV) · H_2O_2 complex were observed. At higher acid concentrations, the peroxide complex was not detected and oxidation to Pu(IV) was complete. The reaction was observed to be autocatalytic; that is, initial rates were low but increased to a maximum when approximately one-half the Pu(III) had been oxidized. The corresponding radiation yields of Pu(IV) ranged up to approximately 5 μmol J^{-1} in 2.9 M acid. These yields were relatively high because Pu(III) is readily oxidized in the presence of HNO_2. Plutonium was oxidized further to Pu(VI), but only after no Pu(III) remained. The initial rates for the alpha-radiolytic oxidation of Pu(IV) were similarly found to be proportional to the concentration of the Pu(IV) multiplied by the dose rate

(Andreichuk *et al.*, 1979). For example, for 0.01 M $[\mathrm{Pu(IV)}]_0$, the yield in 6 M HNO_3 is 0.00044 μmol W^{-1}.

The alpha-radiolytic reduction of Pu(VI) is much more complicated. Small steady-state concentrations of Pu(V) are formed initially, followed by the formation of HNO_2. Further reaction is autocatalytic because the Pu(V) disproportionation is catalyzed by both HNO_2 and Pu(IV) (Vladimirova, 1982). The Pu(VI)/Pu(IV) steady-state ratios were found to vary widely, depending on total plutonium concentration, HNO_3 concentration, and dose rate (Andreichuk *et al.*, 1979, 1984a,b). For example, a dose rate of 3.46 W L^{-1} in 1 M HNO_3 for plutonium concentrations of 2.1 and 14.8 mM yielded Pu(VI)/Pu(IV) ratios of 5.1 and 0.047, respectively. For 10 mM Pu in 6 M HNO_3, the dose rates of 1.4 and 13.8 W L^{-1} yielded Pu(VI)/Pu(IV) ratios of 0.76 and 3.15, respectively. Kinetic models for the rates of the radiolytic oxidation of Pu(IV) and the reduction of Pu(VI) have been presented by Vladimirova (1990, 1998) and Frolov *et al.* (1990). In a study designed to mimic conditions of dissolved nuclear fuel in nitric acid, Rance and Zilberman (2002) found that the addition of U and fission products to Pu(VI) solutions eliminates the induction periods for reduction. This study reported *G*-values of 0.6–1.1 for 3 g L^{-1} ^{239}Pu solutions that contained from 0.12 to 9.2% ^{238}Pu.

Haschke and Oversby have proposed an alternate disproportion reaction to explain the instability of Pu(VI) in aqueous solution that does not require water radiolysis (Haschke and Oversby, 2002; Haschke, 2005):

$$\mathrm{PuO_2^{2+}} + 1/2\mathrm{H_2O} \rightleftarrows \mathrm{PuO_2^{+}} + \mathrm{H^+} + 1/4\mathrm{O_2} \tag{7.121}$$

Their proposed mechanism invokes the disproportionation of PuO_2^{2+} to produce PuO_2^{+} and heptavalent PuO_2^{3+}, followed by the water oxidation by PuO_2^{3+} to produce oxygen. The fact that PuO_2^{3+} has never been observed makes this mechanism doubtful. In a subsequent report, Newton and Hobart (2004) reiterate that below pH 6 the instability of Pu(VI) clearly results from reactions with reducing species produced by alpha radiolysis of water.

Chlorine is formed by radiolysis of HCl solutions, counteracting the processes that reduce plutonium, such that neither Pu(IV) nor Pu(VI) appear to be reduced in 1 M HCl (see discussion in Section 7.9.1.c(ii)). However, at lower chloride concentrations, alpha-reduction of ^{239}Pu(IV) does take place. Rabideau and Kline (1958) showed that *G*[Pu(III)] decreases from 0.36 in 1 M $HClO_4$ μmol J^{-1} to approximately 0.077 in 0.5 M HCl–0.5 M $HClO_4$. More recent experiments by Büppelmann *et al.* (1988) using higher chloride concentrations, more nearly neutral acid concentrations, and ^{238}Pu to give higher dose rates, show that Pu(IV) can be oxidized to Pu(V) or Pu(VI). With NaCl concentrations less than 3 M and dose rates of 0.15 W L^{-1}, the product is primarily Pu(V). Higher concentrations of NaCl and/or higher dose rates give Pu(VI). These reactions involve the oxidation of Pu(IV) hydroxide by HClO or ClO^-. The effect of dose rate on the reduction of Pu(VI) in $HClO_4$ is illustrated by the

Table 7.54 *Alpha-induced reduction of Pu*(*VI*) (*Newton,* 2002).

Pu(VI) (mM)	*Dose rate* (W L^{-1})	*Yield* (μeq J^{-1})	*Radiation source*	*References*
<2	<0.002	0.33–0.38	^{239}Pu	Rabideau *et al.* (1958)
1.1	0.15	0.04	^{238}Pu	Büppelmann *et al.* (1988)
1.4	4.16	0.0024	^{244}Cm and ^{239}Pu	Frolov *et al.* (1990)

results of experiments using ^{239}Pu, ^{238}Pu, and ^{239}Pu–^{244}Cm mixtures as summarized in Table 7.54. From the Table it is clear that the yield decreases as the dose rate increases.

(d) Hydrolytic stability of plutonium ions

The hydrolytic behavior of the plutonium ions has been the subject of many studies. This interest has been intensified by the practical importance of hydrolysis in the manipulation of plutonium solutions. This class of solution phenomena is as important in the chemistry of plutonium as it is for the actinide elements generally because of the existence of highly charged positive ions in aqueous solution. Hydrolysis leads to the formation of ionic species or precipitates by the action of water as illustrated in equation (7.122) for trivalent plutonium. While hydrolysis reactions are often written as in equation (7.122), hydrolysis is actually a complexation reaction with the hydroxide ion. Therefore, it is also common to express hydrolysis as a complex formation as indicated in equation (7.123). The hydrolysis constant $^*\beta$ (corresponding to equation (7.122)) is related to the formation constant β (equation (7.123)) by the ion product of water, K_w (Grenthe *et al.*, 1997).

$$Pu^{3+} + H_2O \rightleftharpoons Pu(OH)^{2+} + H^+ \tag{7.122}$$

$$Pu^{3+} + OH^- \rightleftharpoons Pu(OH)^{2+} \tag{7.123}$$

Characterization of the hydrolysis behavior of plutonium is the cornerstone of understanding its aqueous coordination chemistry, particularly the thermodynamic stability of complexes. The tendency to undergo hydrolysis increases with the charge/size ratio of the ion. Therefore hydrolysis is most pronounced for Pu^{4+}, and the least pronounced for PuO_2^+. The tendency for hydrolysis follows the general order

$$Pu^{4+} > PuO_2^{2+} \approx Pu^{3+} > PuO_2^+$$

Plutonium ions hydrolyze readily and thereby limit both the stability fields of individual aquo ions and the overall solubility of plutonium ions in aqueous solution. At the extreme end of the spectrum, Pu(IV) hydrolyzes even in pH 1 solutions and can form complicated polymeric (or colloidal) hydroxides and precipitates (Lemire *et al.*, 2001; Neck and Kim, 2001; Rothe *et al.*, 2004), making even the first hydrolysis product of Pu(IV) difficult to characterize. Each of the other common oxidation states forms more soluble and discrete hydroxide species, although Pu(VI) also forms both monomeric and polymeric hydroxide species. The coordination numbers and structures of all of the pure hydroxides can be inferred from the hydration numbers, the stoichiometry of the hydroxo species, and X-ray structures of corresponding solids. X-ray absorption spectroscopy has been used to determine the bond lengths and coordination numbers more directly. Selected hydrolysis constants for plutonium ions are given in Table 7.55 and follow the usual hydrolysis equilibrium expression and associated hydrolysis constant, $^*\beta_n$ (Lemire *et al.*, 2001).

$$\mathrm{Pu}^{x+} + n\mathrm{H_2O} \rightleftharpoons \mathrm{Pu(OH)}_n^{(x-n)+} + n\mathrm{H}^+ \tag{7.124}$$

$$^*\beta_n = \frac{[\mathrm{Pu(OH)}_n^{(x-n)+}][\mathrm{H}^+]^n}{[\mathrm{Pu}^{x+}]} \tag{7.125}$$

A complete review of hydrolysis products and the solubility of plutonium hydroxides is available in the NEA compilation of the chemical thermodynamics of neptunium and plutonium (Lemire *et al.*, 2001) and its most recent update (Guillaumont *et al.*, 2003). Hydration and hydrolysis of plutonium are compared with that of the other actinide elements in Chapter 23.

Pu(III) The tendency of an ion to displace a proton from water increases with charge and, for a given charge, with decreasing ionic radius. The acidity of the tripositive actinide ions, then, should follow the order

$$\mathrm{Pu}^{3+} > \mathrm{Np}^{3+} > \mathrm{U}^{3+}$$

with Pu^{3+} being the strongest acid and therefore the trivalent actinide ion of this triad that undergoes the most extensive hydrolysis. On the basis of its ionic radius, Pu^{3+} should have an acidity similar to the lanthanide ions, and should have a first hydrolysis constant lying between those of Ce^{3+} and Pr^{3+}.

The hydrolysis of Pu^{3+} can be studied only with careful control of the plutonium solubility and maintenance of an inert or reducing atmosphere to avoid oxidation to Pu^{4+}, which is increasingly favored as the solution pH is raised. The first hydrolysis product, $\mathrm{Pu(OH)}^{2+}$, has been inferred from solvent extraction, potentiometric and spectrophotometric titration studies in acid solutions up to pH ~3 (where it accounts for ca. 70% of plutonium present). Kraus and Dam (1949) have studied the hydrolysis of trivalent plutonium according to equation (7.122). From titration curves of plutonium(III) chloride and perchlorate solutions with alkali, Kraus and Dam (1949) identified the first hydrolysis species $\mathrm{Pu(OH)}^{2+}$ and reported the first hydrolysis constant $^*\beta_1$.

Table 7.55 *Hydrolysis constants for plutonium ions.*

Reaction stoichiometry	*I* (M)	$\log_{10}{}^*\beta_{mn}$	$\log_{10}{}^*\beta^{\circ}_{mn}$	*References*
$Pu^{3+} + H_2O \rightleftarrows Pu(OH)^{2+} + H^+$	0.1	−6.9	−6.9 ± 0.3	Baes and Mesmer (1976) and Lemire *et al.* (2001)
$Pu^{3+} + 2H_2O \rightleftarrows Pu(OH)_2^+ + 2H^+$	–	−15.0	–	Fuger (1992)
$Pu^{4+} + H_2O \rightleftarrows Pu(OH)^{3+} + H^+$	1.0	−0.45	0.6 ± 0.2	Metivier and Guillaumont (1972) and Guillaumont *et al.* (2003)
$Pu^{4+} + 2H_2O \rightleftarrows Pu(OH)_2^{2+} + 2H^+$	1.0	−0.75	0.6 ± 0.3	Metivier and Guillaumont (1972) and Guillaumont *et al.* (2003)
$Pu^{4+} + 3H_2O \rightleftarrows Pu(OH)_3^+ + 3H^+$	1.0	−0.33	−2.3 ± 0.4	Metivier and Guillaumont (1972) and Guillaumont *et al.* (2003)
$Pu^{4+} + 4H_2O \rightleftarrows Pu(OH)_{4(aq)} + 4H^+$	1.0	−0.63	−8.5 ± 0.5	Metivier and Guillaumont (1972) and Guillaumont *et al.* (2003)
$PuO_2^+ + H_2O \rightleftarrows PuO_2(OH)_{(aq)} + H^+$	0.1	−9.73	≤−11.3 ± 1.5	Bennett *et al.* (1992) and Lemire *et al.* (2001)
$PuO_2^{2+} + H_2O \rightleftarrows PuO_2(OH)^+ + H^+$	0		−5.5 ± 0.5[a]	Guillaumont *et al.* (2003)
$PuO_2^{2+} + 2H_2O \rightleftarrows PuO_2(OH)_{2(aq)} + 2H^+$	0		−13.2 ± 0.5[a]	Guillaumont *et al.* (2003)
$2PuO_2^{2+} + 2H_2O \rightleftarrows (PuO_2)_2(OH)_2^{2+} + 2H^+$	0.1	−7.8	−7.5 ± 0.5[a]	Okajima and Reed (1993), Guillaumont *et al.* (2003), Reilly *et al.* (2000), and Madic *et al.* (1984)
$2PuO_2^{2+} + 4H_2O \rightleftarrows (PuO_2)_2(OH)_4 + 4H^+$	0.1	−19.3	–	Okajima and Reed (1993) and Reilly *et al.* (2000)

[a] Asymmetric uncertainties (+0.5, −1.5).

Later studies reported the same species stoichiometry and contributed to the recommended hydrolysis constant of $\log_{10} {}^*\beta_1 = -7.0$ (Baes and Mesmer, 1976; Lemire *et al.*, 2001). The overall formula for $\mathrm{Pu(OH)^{2+}}$ is likely to be $\mathrm{Pu(OH)(OH_2)_8^{2+}}$ based upon the coordination number 9 observed for the $\mathrm{Pu^{3+}}$ aquo ion (see Section 7.9.1(a)) (Matonic *et al.*, 2001). Quantitative evaluation of the formation of higher hydrolysis products is inhibited by oxidation and precipitation of Pu(III/IV) hydroxides. Based on the hydrolysis of other trivalent actinides the second hydrolysis constant for formation of $\mathrm{Pu(OH)_2^+}$ via equation (7.122) is approximately $\log_{10} {}^*\beta_2 = -15.0$ (Baes and Mesmer, 1976; Fuger, 1992).

The solid trivalent plutonium hydroxide that precipitates from aqueous solutions is presumed to be $\mathrm{Pu(OH)_3 \cdot \mathit{n}H_2O}$, by analogy with the known $\mathrm{Am^{3+}}$ hydroxide. Solubility studies that were performed as a function of ionic strength provide a solubility product of $\log_{10} K_{\mathrm{sp}} = -(15.8 \pm 1.5)$ under standard conditions (Felmy *et al.*, 1989).

Pu(IV). On the basis of size and charge, the plutonium(IV) ion should undergo much more extensive hydrolysis than does plutonium(III). For the same reasons as in the case of the III state, the tendency to undergo hydrolysis should be greater in plutonium than for its predecessors in the actinide series:

$$\mathrm{Pu^{4+} > Np^{4+} > U^{4+} > Pa^{4+} > Th^{4+}}$$

In the early stages of hydrolysis, only monomeric species such as $\mathrm{Pu(OH)^{3+}}$ are important. It is likely that $\mathrm{Pu^{4+}}$ hydrolyzes in a stepwise manner to yield monomeric $\mathrm{Pu(OH)}_n^{4-n}$ ($n = 1, 2, 3, 4$); however, the intermediate hydrolysis products ($2 \leq n \leq 4$) undergo irreversible polymerization with the formation of large colloidal aggregates (see below).

The first hydrolysis product for the formation of $\mathrm{Pu(OH)^{3+}}$, has been determined from solution complex formation studies.

$$\mathrm{Pu^{4+} + H_2O \rightleftharpoons Pu(OH)^{3+} + H^+} \tag{7.126}$$

Reported hydrolysis constants for this reaction vary widely, with limited correlation between the experimental technique used and the resulting value of the hydrolysis constant (Baes and Mesmer, 1976; Lemire *et al.*, 2001; Guillaumont *et al.*, 2003). From the many reported values, several are considered the most accurate. Rabideau (1957) carefully measured the pH dependence of the $\mathrm{Pu^{4+}}$/$\mathrm{Pu^{3+}}$ redox couple and calculated a hydrolysis constant of $\log_{10} {}^*\beta_1 = -1.41$ at $I = 0.1$ M using the Nernst equation. Compared with directly measuring the formation of the hydrolysis product, for example, by quantifying the shift in the optical absorption bands for $\mathrm{Pu^{4+}}$ as the hydroxide forms, or calculating a constant to best model the solubility of (oxy)hydroxide solids, this approach explicitly considers the formation and subsequent hydrolysis of $\mathrm{Pu^{3+}}$ at low pH. The 2003 NEA review recommended the value of $\log_{10} {}^*\beta_1 = (0.60 \pm 0.20)$ under standard conditions ($I = 0$) (Guillaumont *et al.*, 2003), which is based on values proposed in recent studies by Knopp *et al.* (1999) and Neck and Kim (2001). The constant for the second hydrolysis product was originally estimated to be $\log_{10} {}^*\beta_2 = -3.7$ at $I = 0.1$ M (Kraus and Nelson, 1950). The 2003 NEA review recommended $\log_{10} {}^*\beta_2 = (0.60 \pm 0.30)$ for $I = 0$ based on the most recent studies (Guillaumont *et al.*, 2003). The overall formulae for $Pu(OH)^{3+}$ and $Pu(OH)_2^{2+}$ are likely to be $Pu(OH)(OH_2)_7^{3+}$ and $Pu(OH)_2(OH_2)_6^{2+}$ based upon the coordination number 8 observed for the Pu^{4+} aquo ion (see Section 7.9.1(a)).

$$Pu^{4+} + 2H_2O \rightleftharpoons Pu(OH)_2^{2+} + 2H^+ \qquad (7.127)$$

Characterization of subsequent third and fourth hydrolysis species [$Pu(OH)_3^+$ and $Pu(OH)_4$] is frustrated by the propensity of these hydroxides to polymerize, as discussed below. The direct observation of the solution species and definitive determination of the constants are prevented by the detection limits of current techniques coupled with the sparing solubility of the (hydr)oxide phases. Attempts to accurately determine these constants from solubility data are focused on the following: identifying discrete solution ion and colloidal species, improving the quantification of the Pu^{4+} ion, refining the operational definitions of the solid/solution phase (commonly delineated by the phase separation method), and better characterizing and controlling the solid phase [crystalline PuO_2, hydrated PuO_2, crystalline or amorphous $Pu(OH)_4$]. Based on the most recent work by Knopp *et al.* (1999), and by Neck and Kim (2001), the 2003 NEA review proposed the value of $\log_{10} {}^*\beta_3 = -(2.3 \pm 0.4)$, and $\log_{10} {}^*\beta_4 = -(8.5 \pm 0.5)$ for the third and fourth hydrolysis constants at $I = 0$, respectively (Guillaumont *et al.*, 2003).

The published solubility product of amorphous Pu(IV) hydroxide, $Pu(OH)_4(s)$, is $\log_{10} K_{sp} = -(58 \pm 1)$ (Capdevila and Vitorge, 1998; Lemire *et al.*, 2001; Neck and Kim, 2001). This value gives a calculated Pu(IV) solution concentration near pH 7 of 10^{-11} M, while observed solubilities span a range of 10^{-8}–10^{-13} M due to interactions with other simple ligands, formation of other hydroxide species, redox instability, and the formation of colloidal species (Neck and Kim, 2001; Rothe *et al.*, 2004).

Pu(IV) polymerization. It has been known for half a century that aqueous solutions of Pu(IV) will form colloidal polymers under the appropriate solution conditions (Kraus and Nelson, 1950; Kraus, 1956). Early emphasis focused on avoiding Pu(IV) polymer because of its intractability and potential for interference in plutonium process chemistry. Newer concerns involve retention of plutonium in nuclear waste repositories where radioactive heating and low acidity of ground waters favor Pu(IV) colloid formation and thus could provide a potential transport pathway for migration of plutonium away from the repository. Radiocolloids are very fine, well-dispersed, intrinsic particles of radioactive compounds, whose formation in the case of the actinides is intimately connected to their hydrolysis chemistry.

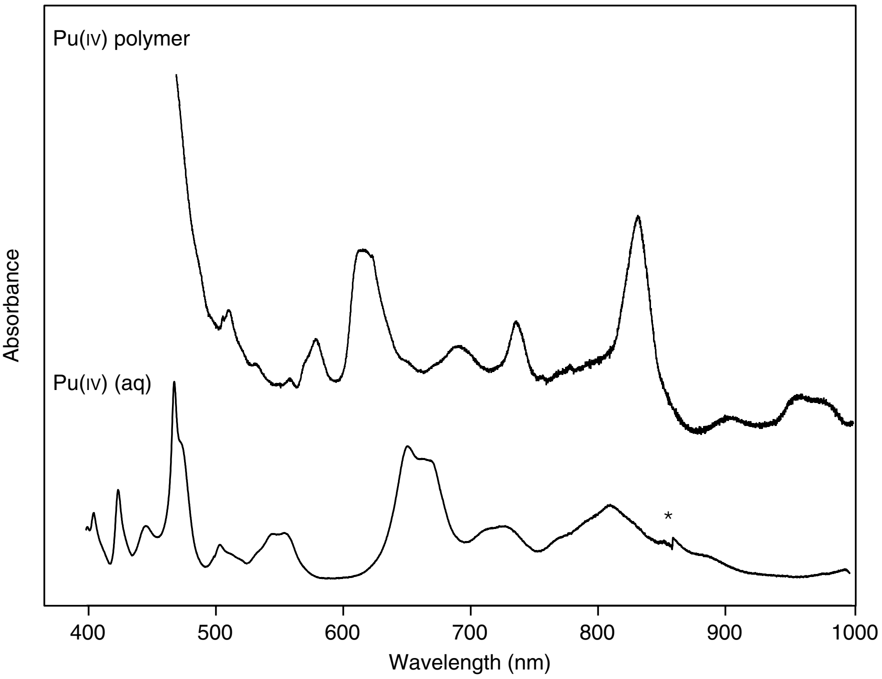

Fig. 7.119 *Electronic absorption spectra of Pu(IV) polymer compared to the Pu(IV) aquo ion. Plutonium(IV) polymer recorded on* 9.0 mM *solution; plutonium(IV) aquo ion recorded on* 2.91 mM *solution in* 1 M *$HClO_4$ using* 1 cm *cell. The asterisk indicated a spectrometer grating change (spectra courtesy of P. D. Palmer of Los Alamos).*

For plutonium (IV) the colloid can form green solution-like sols that are optically clear, display a characteristic absorption spectrum (Fig. 7.119), and do not settle on long-standing (Ockenden and Welch, 1956; Lloyd and Haire, 1978). Under the appropriate conditions, these colloids may decompose or disaggregate into soluble ionic species, or age into relatively insoluble materials (Newton *et al.*, 1986b).

The formation of colloidal Pu(IV) polymer was first reported by Kraus, and much of the early information on it is based on the work of Kraus and his coworkers (Kraus and Nelson, 1950; Kraus, 1956). Pu(IV) polymer can be prepared by a number of methods (Hobart *et al.*, 1989). Precipitation methods include the partial neutralization of Pu(IV) solutions, addition of water to 'dried' acid samples, or precipitation with alkali followed by peptization in dilute acid (90°C). Redox methods include slow oxidation of Pu(III) by oxygen and/or alpha irradiation products, or the reduction of Pu(V). The polymer formation depends on acidity, Pu(IV) concentration, presence of other ions, and temperature (Rainey, 1959). Solutions of Pu(IV) polymer can be very readily obtained when plutonium(IV) hydroxide is treated with less than four equivalents of hydrogen ion per mole of plutonium; when plutonium(IV) hydroxide is dissolved in dilute acid, plutonium polymer forms. Likewise, if a solution of plutonium(IV) in moderately concentrated acid is poured slowly into boiling water, polymeric plutonium is obtained. It is also formed when a plutonium nitrate solution is depleted of nitric acid by extraction with *n*-hexanol. The colloid polymer is ideally formed in nitrate solution in about 0.8 mole per mole of plutonium(IV) (Lloyd and Haire, 1978). This colloidal polymer may be isolated as a solid, which shows the electron diffraction pattern typical of an amorphous substance and has a practical size of up to 20 Å. This colloid can easily be redissolved. On standing or artificial aging, the particle size increases, and the solid becomes finely crystalline and exhibits the XRD pattern of PuO_2. The colloidal character of plutonium(IV) polymer is manifested by the strong absorption of the polymer on glass and on substances such as paper, cotton, and silica, which acquire a negative surface charge when immersed in water.

Until recently, the characterization of plutonium(IV) colloid has met with only limited success. Thiyagarajan *et al.* (1990) measured the structures of Pu(IV) hydrous polymers by small-angle neutron scattering (SANS) in aqueous media and after solvent extraction into an organic phase. The SANS data indicate long, thin, rod-like particles that measured (4.7 ± 0.2) by (190.0 ± 20.0) nm. XRD was consistent with a fcc crystal system similar to that found in crystalline PuO_2 (see Section 7.8.5.a(iii)).

Light scattering methods have also be used to characterize macromolecular Pu(IV) hydroxide solutions. Rundberg *et al.* (1988) and Triay *et al.* (1991) employed autocorrelation photon spectroscopy (APS) to determine the size distribution of Pu(IV) colloidal suspensions that were prepared by dilution, peptization, and autoxidation of Pu(III). The plutonium(IV) colloids measured by APS were assumed to be spherical particles in order to utilize the Stokes–Einstein relationship to calculate a particle diameter. In the initial study by Rundberg *et al.* (1988) the average size of the colloid diameter was measured to be (2.9 ± 0.2) nm. The diameter of a plutonium colloid sample measured over a period of 2 years resulted in reproducible diameters of 180 nm. Subsequently, Triay *et al.* (1991) examined colloid diameters as a function of preparation method, and found that the size of the colloids varied from 1 to 370 nm depending on method of preparation. Small colloid diameters on the order of 1.5 nm were found when the colloid was prepared by the method of Savage and Kyffin (1986) by heating a plutonium nitrate solution with hydrogen peroxide, neutralizing most of the free acid with sodium hydroxide, and diluting to known volume to give 2.5 g L^{-1} solutions. Dilution of a well-characterized Pu(IV) stock solution using distilled water yields colloids in the range of 2–6 nm in diameter (Triay *et al.*, 1991). Peptization gave a mixture of two different sizes (14 and 370 nm). Autoxidation of Pu(III) yielded the largest single-sized colloid.

More recently, Rothe *et al.* (2004) investigated Pu(IV) colloid growth using a combination of laser-induced breakdown detection (LIBD) and X-ray absorption fine structure (XAFS) spectroscopy. LIBD measurements gave colloid sizes ranging from 12 to 25 nm depending on solution conditions.

Rothe *et al.* proposed a model for colloid formation that is consistent with their XAFS, LIBD, and UV-Vis spectroscopic data, based on the stepwise buildup of polynuclear species and loss of water, in analogy to a mechanism proposed by Fujiwara and coworkers (Fujiwara *et al.*, 2001). In this model, they propose hydrolysis of aquo Pu^{4+} to form an eight coordinate monomer $Pu(OH)_2(OH_2)_6^{2+}$ followed by condensation of two monomers to form a dimer of cubic units connected at their edges. The condensation of $Pu(OH)_2^{2+}$ units as reactants satisfies a –2 slope dependency on LIBD data, and the eight coordinate monomer $Pu(OH)_2(OH_2)_6^{2+}$ satisfies the coordination environment from XAFS data. This basic condensation model is described in equation (7.128), and the structural model for the resulting dimer is illustrated in **8**.

$$
\begin{aligned}
2Pu(OH)_2(H_2O)_6^{2+} + xH_2O \rightleftharpoons{}& Pu_2O_p(OH)_{8-2p}(OH_2)_{6+p} \\
&+ 4H^+ + (2+x)H_2O
\end{aligned}
\tag{7.128}
$$

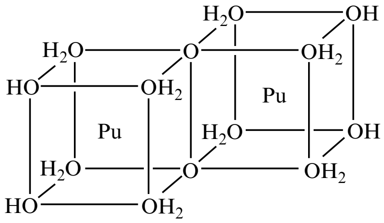

8

In rationalizing the formation of higher order polymers, a trimeric species could be envisioned as forming through the subsequent condensation of monomeric $Pu(OH)_2(OH_2)_6^{2+}$ with the dimer **8**. To be consistent with XAFS data, the new trimer must retain an essentially fcc Pu sublattice with an approximately 3.87 Å distance between Pu centers. This is possible through condensation of the third monomeric $Pu(OH)_2(OH_2)_6^{2+}$ unit along cube edges to form a chain, or by condensing a third monomeric unit along two edges of neighboring cubes of the dimer to form a trimer of cubes sharing one common corner. Examples of these proposed trimeric units are shown in **9** and **10**.

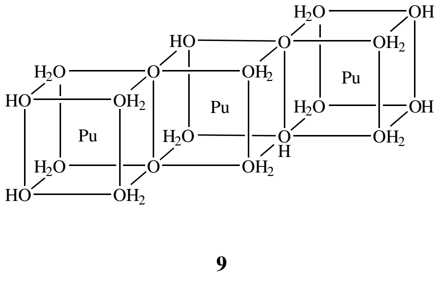

9

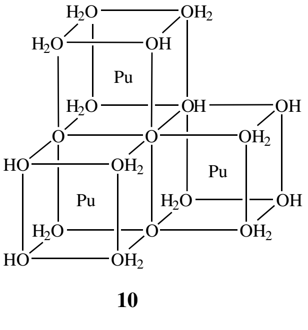

10

The fundamental components of this polymerization mechanism are to grow oligomeric units that maintain a Pu–Pu separation near 3.87 Å, maintain a Pu: OH ratio of 2, and keep the overall cluster size small enough to be consistent with UV-Vis results. Polymerization to larger units can proceed by subsequent condensation of dimers or trimers with each other, or with monomeric units.

The XAFS data from Rothe *et al.* reveal the presence of several different Pu–O distances between 2.20 and 2.42 Å consistent with different coordinating oxygen atoms (–O, –OH, and OH_2). Similarly, the XAFS data show a Pu–Pu distance between 3.86 and 3.89 Å. The fcc cubic environment and the 3.8 Å Pu–Pu separation gives a basic structural unit that is similar to that observed in fcc PuO_2 (see Section 7.8.5(a)). These workers also observed a small feature in their XAFS data near 1.9 Å, and they argued that this feature was too short to be reconcilable with a Pu(IV)–O bond. As this feature had also been observed in ThO_2 XAFS spectra (Rothe *et al.*, 2002), and in XAFS reported by other workers, it was concluded that this feature was most consistent with multiple electron excitation. Essentially identical structural features were observed in XAFS data of Pu(IV) colloid samples reported by Conradson and coworkers (Conradson *et al.*, 2004b). The primary focus of the Conradson study was to examine the structural features of solid PuO_{2+x} materials (see Section 7.8.5(a)). The XAFS data from PuO_{2+x} solids show many remarkable structural similarities to the Pu(IV) colloid samples studied by Rothe *et al.* (2004) and Conradson *et al.* (2004b). Both studies show a range of Pu–O distances consistent with different coordinating oxygen atoms (–O, –OH, and OH_2). In the oxide of stoichiometry of $PuO_{2.26}$, the short interatomic distance near 1.9 Å is no longer a small feature, but has become a dominant spectroscopic feature (see Fig. 7.94). Conradson also reported XAFS data on a number of Pu(IV) colloid samples whose XAFS spectra vary as a function of preparation and aging. Conradson's data show that both Pu(IV) polymers and solid PuO_{2+x} compounds share structural features, and are consistent with an fcc arrangement of plutonium atoms with a 3.8 Å separation. The difference between the two studies is that in solid PuO_{2+x} compounds, the XANES data were consistent with a mixture of Pu(IV) and Pu(V). Conradson *et al.* suggested that the short internuclear distance that averaged 1.86 Å was consistent with the presence of Pu(V), where solution measurements show a distance of 1.85 Å for PuO_2^+. In the freshly prepared samples studied by Rothe *et al.* (2004) this feature was quite small. In the aged samples studied by Conradson *et al.* (2004b) this feature was quite pronounced. These two XAFS studies remind us of the complex nature of the Pu(IV) polymer, and suggest that the elegant polymerization mechanism proposed by Rothe *et al.* may need to be expanded. We look forward to future advances in this area.

Pu(V). Of the common oxidation states of plutonium only Pu(V) is not hydrolyzed until the solution pH becomes basic. Because of the tendency of pentavalent plutonium to disproportionate or be reduced by even weak agents there are very few studies on the hydrolysis of this plutonium ion. Similarly, the presence of inorganic and organic ligands will generally favor the formation of Pu(IV)–ligand complexes in accordance with their relative formation constants. Early conventional spectrophotometric studies showed that Pu(V) hydrolyses above pH 9 to form stepwise products, $PuO_2(OH)$ and $PuO_2(OH)_2^-$ (Baes and Mesmer, 1976; Madic *et al.*, 1984; Fuger, 1992). By analogy with Np(V) hydroxides, which have been studied in detail by optical absorption and Raman spectroscopy (Madic *et al.*, 1984; Sullivan *et al.*, 1991), Pu(V) hydroxide complexes $PuO_2(OH)$ and $PuO_2(OH)_2^+$ likely have two or three inner-sphere water molecules in the equatorial plane and pentagonal bipyramidal coordination geometry. The monohydroxide hydrate solid is amorphous and has not been structurally characterized. Attempts to increase the crystallinity of the $NpO_2(OH)$ analog have produced Np_2O_5 (Runde *et al.*, 2002). Bennett and coworkers used photoacoustic spectroscopy to perform spectrophotometric titrations of millimolar and submillimolar PuO_2^+, which provided a formation constant for the first hydrolysis product of $\log_{10} {}^*\beta_1 = -(9.73 \pm 0.10)$ (Bennett *et al.*, 1992). Mixed hydroxo carbonato complexes, such as $PuO_2(OH)(CO_3)_2^{4-}$ or $PuO_2(OH)_2(CO_3)^{3-}$ may form (by analogy with Np(V) chemistry) but they have not been characterized. In addition, there is some evidence that the superstoichiometric Pu(IV) oxide (PuO_{2+x}) contains Pu(V) (Conradson *et al.*, 2003, 2004b). Thus, Pu(V) hydroxides may be much more important in plutonium chemistry and material science than was previously thought.

Pu(VI). Plutonium(VI) hydrolysis is intermediate between that of Pu(III) and Pu(IV), corresponding to its effective charge of ~3.2. Similar to Pu(IV), low solubility and polymerization challenge the characterization of products above neutral pH. The first hydrolysis products, $PuO_2(OH)^+$ and $PuO_2(OH)_2$ have hydrolysis constants of $\log_{10} {}^*\beta_1 = -(5.5 \pm 0.5)$ and $\log_{10} {}^*\beta_2 = -(13.2 \pm 1.5)$ at $I = 0$, respectively (Lemire *et al.*, 2001), comparable to the analogous U (VI) species (Grenthe *et al.*, 1992). Structurally, these monomeric species likely have three or four water molecules in addition to hydroxide in the equatorial plane and a pentagonal bipyramidal geometry with respect to inner-sphere oxygen atoms as indicated in **11**. There is substantial data from potentiometric, optical absorption, and Raman studies that indicates that at higher plutonium concentrations (estimated to be $\sim 5 \times 10^{-4}$ M) the first hydrolysis product is the dimer, $(PuO_2)_2(OH)_2^{2+}$, with two bridging hydroxides and pseudo-pentagonal bipyramidal coordination as shown in **12** (Madic *et al.*, 1984; Okajima and Reed, 1993; Reilly *et al.*, 2000). The hydrolysis constant for the dimer is estimated to be $\log_{10} {}^*\beta_{22} = -(7.5 \pm 1.5)$ at $I = 0$ (Lemire *et al.*, 2001). Polymerization is less pronounced for Pu(VI) than for U(VI) and there is no evidence for the trimeric hydroxide complexes that have been well characterized for uranyl, e.g. $(UO_2)_3(OH)_5^+$, (Grenthe *et al.*, 1992; Palmer and Nguyen-Trung, 1995). Solids precipitated from these systems have been formulated based on stoichiometry as $PuO_2(OH)_2$ or various hydrated phases, but neither their structures nor solubility products have been determined.

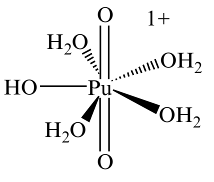

11

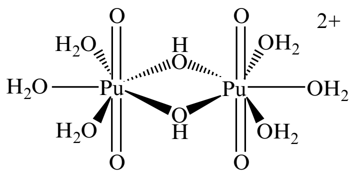

12

Under alkaline solution conditions of 1 M LiOH, Tananaev (1989) presented data to suggest the formation of $PuO_2(OH)_4^{2-}$ that converts to $PuO_2(OH)_3^{-}$ upon lowering the hydroxide concentration. The single crystal XRD structures (Clark *et al.*, 1999a) and solution XAFS data (Wahlgren *et al.*, 1999; Clark *et al.*, 1999a; Moll *et al.*, 2000; Bolvin *et al.*, 2001) have been reported on the $UO_2(OH)_4^{2-}$ and $NpO_2(OH)_4^{2-}$ analogs.

Pu(vii). Heptavalent plutonium has only been studied in strongly alkaline solutions, given its immediate reduction to Pu(vi) under all other conditions. Interest in the coordination environment of Pu(vii) in solution has been renewed because highly alkaline conditions could be technologically useful in nuclear waste processing, and because Pu(vii) hydroxides provide an opportunity to examine structure/bonding relationships in actinide systems with an unusual number of Pu–O multiple bonds. Pu(vii) appears to be analogous to Np(vii) for which many more studies have been reported. A series of anionic polyoxo species that form between 0.5 and 18 M hydroxide has been proposed and includes the following, $PuO_4(OH_2)_2^{-}$, $PuO_4(OH)(OH_2)^{2-}$, $PuO_4(OH)_2^{3-}$, $PuO_5(OH)^{4-}$, or PuO_6^{5-}, depending on hydroxide concentrations (Spitsyn *et al.*, 1969; Krot, 1975; Tananaev *et al.*, 1992). Of the proposed species, only $PuO_4(OH)_2^{3-}$ has a proven analog in neptunium chemistry, and its likely structure is shown in **7** (see Section 7.9.1.a) (Grigor'ev *et al.*, 1986). No hydrolysis constants are known. Crystalline samples of analogous Pu(vii) compounds have been prepared (Zakharova *et al.*, 1972).

(e) Complex ions

In this section we describe the preparation, stability, structure, and in selected cases the spectroscopy and solid-state forms, of molecular complexes of plutonium in aqueous solution. The little information that is available on the nonaqueous coordination and organometallic chemistry of plutonium will be described in Section 7.9.2. The stoichiometry and stability of aqueous plutonium complexes has generally been determined indirectly from proton, ligand, and metal titrations, including the following approaches: measured plutonium extraction efficiencies as a function of extractant ligand concentrations, pH titrations of protic ligands in the absence and presence of plutonium, pH/ligand/plutonium titrations monitored by optical spectroscopy, and less frequently from multinuclear NMR and vibrational spectroscopic analysis. The structures of solution species have also been inferred from the characterization of corresponding solids. More direct methods, including electrospray mass spectroscopy and X-ray absorption spectroscopy, are increasingly being applied to characterize molecular plutonium complexes. Fluorescence spectroscopy has the potential to be used to characterize plutonium species, similar to its application in uranyl chemistry, as emission from plutonium ions has been observed, albeit under very special conditions.

The coordination chemistry of plutonium ions is generally characteristic of exceptionally 'hard' Lewis acids, those that show preference for complexation by hard (i.e. first row donor atom) ligands. Weak Lewis bases, such as HS^- form weak complexes with plutonium and strong Lewis bases, such as CO_3^{2-}, F^-, and PO_4^{3-} form very stable complexes. Plutonium ions have relatively large ionic radii and therefore form complexes with high coordination numbers (8–14). For a given ligand the strength of complexation (the stability of the Pu–ligand complex) and the tendency of ions to hydrolyze decrease following the effective charges:

$$Pu^{4+} > PuO_2^{2+} \approx Pu^{3+} > PuO_2^{+}$$

Overall, the bonding in plutonium complexes can generally be described as ionic, where the geometry of coordination complexes is primarily governed by steric considerations (ligand–ligand repulsions). Plutonium–ligand orbital overlap is considered to be important in some types of complexes, and comparatively more important than in corresponding complexes of lanthanides and lighter actinides with similar ionic radii. Ligand exchange in plutonium complexes is facile, and reaction rates are generally fast.

Complexation in this chapter generally refers to inner-sphere coordination, where the ligand is directly bonded to plutonium and displaces more weakly bound ligands and/or solvent water. Outer sphere complexation and ion pairing are also important interactions, particularly in high ionic strength and otherwise complicated solutions. Equilibrium constants for the reactions of plutonium ions with ligands reflect the competition between protons and plutonium for ligand atom bonding and are experimentally determined. Formation constants are pH independent values calculated from equilibrium constants, ligand pK_as, and plutonium hydrolysis constants and therefore more directly reflect the strength of interaction between the plutonium ion and the deprotonated ligand. For weaker ligands it is important to note that this interaction may be on the order of plutonium–solvent interactions, a factor not easily separated out to provide a quantitative pure plutonium–ligand interaction constant. In the text that follows, we will use K for the consecutive or stepwise formation constants, and β for the cumulative or overall formation constants (Lemire *et al.*, 2001). In cases where complex formation involves a deprotonation of a ligand, the equilibrium constant (K) or formation constant (β) will be denoted by an asterisk as indicated below.

$$\mathrm{PuL}_{n-1} + \mathrm{L} \rightleftharpoons \mathrm{PuL}_n, \quad K_n = \frac{[\mathrm{PuL}_n]}{[\mathrm{PuL}_{n-1}][\mathrm{L}]} \tag{7.129}$$

$$\mathrm{PuL}_{n-1} + \mathrm{HL} \rightleftharpoons \mathrm{PuL}_n + \mathrm{H}^+, \quad {}^*K_n = \frac{[\mathrm{PuL}_n][\mathrm{H}^+]}{[\mathrm{PuL}_{n-1}][\mathrm{HL}]} \tag{7.130}$$

$$\mathrm{Pu} + n\mathrm{L} \rightleftharpoons \mathrm{PuL}_n, \quad \beta_n = \frac{[\mathrm{PuL}_n]}{[\mathrm{Pu}][\mathrm{L}]^n} \tag{7.131}$$

$$\mathrm{Pu} + n\mathrm{HL} \rightleftharpoons \mathrm{PuL}_n + n\mathrm{H}^+, \quad {}^*\beta_n = \frac{[\mathrm{PuL}_n][\mathrm{H}^+]^n}{[\mathrm{Pu}][\mathrm{HL}]^n} \tag{7.132}$$

Selected formation constants and equilibrium constants will be defined and conditions specified in summary tables. The emphasis is on describing the types of molecular plutonium complexes that form and highlighting specific chemical, structural, and physical properties. For a more comprehensive discussion of stability constant determinations and analysis done to compute thermodynamic constants under standard conditions the reader is referred to specialized critical reviews (Grenthe *et al.*, 1997; Lemire *et al.*, 2001; Guillaumont *et al.*, 2003). Comparisons across the actinide series and a fine description of the details of plutonium complexation in solution are given in Chapter 23. Selected formation and equilibrium constants for plutonium complexes are given in Table 7.56.

(*i*) *Oxoanions*

Plutonium ions are oxophilic and therefore readily form complexes with oxo ligands, as exemplified by high hydration numbers and extreme hydrolysis described in Section 7.9.1(d). Anionic inorganic oxo ligands effectively complex plutonium to form complexes whose stability depends on the charge and basicity of the ligand. For a given plutonium ion the order of complexation strength for common oxoanions is: $\mathrm{ClO_4^-}<\mathrm{IO_3^-}<\mathrm{NO_3^-}<\mathrm{SO_4^{2-}}<<\mathrm{CO_3^{2-}}<\mathrm{PO_4^{3-}}$. Perchlorate is often referred to as a noninteracting counter ion, but does coordinate to plutonium at very high concentrations. Nitrate complexes are much more stable than analogous perchlorate species and slightly more stable than chloride complexes of the same stoichiometry. Phosphate is an exceptionally strong ligand for plutonium. These ions usually chelate plutonium ions in a bidentate fashion. The stability of plutonium oxoanionic complexes follow the general trends of Pu(IV) being the strongest and Pu(V) being the weakest.

The coordination numbers of plutonium oxoanion complexes ranges from 7 for $\mathrm{PuO_2^+}$ to up to 12 for $\mathrm{Pu^{4+}}$, where water is successively displaced from the inner coordination sphere by chelating ligands. Water that remains bonded to the Pu center can hydrolyze to form mixed-ligand complexes that contain one or more bidentate oxoanion and one or more hydroxide ligand. These species are favored at near-neutral pH and lower oxoanion concentrations. Solution complex formation constants and solid-state structures are known for relatively few of these species, such as Pu(IV) hydroxo oxalates. It is difficult to distinguish mixed-ligand complexes from the coexistence of individual complexes, which explains the uncertainty in, for example, plutonium(IV) carbonate speciation and thermodynamic stability.

Carbonate

Plutonium carbonates are of interest because of their fundamental chemistry and environmental behavior, including aspects of actinide mineralogy and nuclear waste isolation. Separation schemes based on carbonate that utilize the pH-dependent complexing properties of this ligand have been proposed as alternatives to acid-based or organic extraction processes for used nuclear fuels (Asanuma *et al.*, 2001). Some features are common to the carbonate complexation of plutonium ions. Carbonate binds plutonium in a bidentate fashion and has a small bite angle so that coordination numbers of resulting complexes are generally quite high, 7–10. The actinyl ions, PuO_2^+ and PuO_2^{2+} have pentagonal and hexagonal bipyramidal structures in which the linear triatomic O=An=O unit forms the axis of a pentagonal or hexagonal bipyramidal coordination polyhedron with respect to carbonato and aquo oxygen atoms bound to the metal center. In addition to chelating the plutonium ion, carbonate ligands often hydrogen bond to outer sphere waters or counter ions to produce chains and layers and other less regular hydrogen bond networks in the solid-state structures. For all of the oxidation states the stability constant for the initial monocarbonato complex is known with the greatest accuracy and precision because they can be determined spectrophotometrically from the reduction/shift in the characteristic absorption band for the aquo ion. Thermodynamic constants of the limiting carbonato complexes are better known from the solubility and carbonate titration studies than are those corresponding to intermediate species because the former usually have large stability fields. And the limiting molecular complexes are usually isostructural with the solution species from which they are precipitated. Intermediate carbonate complexes are not well characterized for any of the oxidation states. Several reviews on actinide carbonate and environmental chemistry describe plutonium carbonato complexes in detail (Grenthe *et al.*, 1986b; Newton and Sullivan, 1986; Fuger, 1992; Clark *et al.*, 1995; Choppin and Wong, 1998).

Trivalent plutonium carbonato complexes generally oxidize rapidly to tetravalent species. In aqueous Pu(III) solutions there is evidence for the stepwise formation of the carbonato complexes, $Pu(CO_3)^+$ and $Pu(CO_3)_2^-$. Additional carbonato and hydroxocarbonato complexes may form, but are immediately oxidized to Pu(IV) species. Formation constants of $\log_{10}\beta_1 = 7.5$ and $\log_{10}\beta_2 = 12.4$ have been estimated at low ionic strength (0.1–0.5 M) (Cantrell, 1988). These values have not been verified, but are consistent with well-known constants of Am(III) carbonato complexes (Silva *et al.*, 1995).

Table 7.56 *Formation constants for plutonium oxo anions.*

Reaction stoichiometry	I (M)	$\log_{10}\beta_n$	$\log_{10}\beta_n^\circ$	*References*
carbonate				
$Pu^{3+} + CO_3^{2-} \rightleftarrows PuCO_3^+$	0.1–0.5	7.5		Cantrell (1988)
$Pu^{3+} + 2CO_3^{2-} \rightleftarrows Pu(CO_3)_2^-$	0.1–0.5	12.4		Cantrell (1988)
$Pu^{4+} + CO_3^{2-} \rightleftarrows PuCO_3^{2+}$	0.3	17.0 ± 0.7		Nitsche and Silva (1996) and Rai *et al.* (1999)
$Pu^{4+} + 4CO_3^{2-} \rightleftarrows Pu(CO_3)_4^{4-}$	1.5	44.5	37.0 ± 1.1[a]	Capdevila *et al.* (1996) and Guillaumont *et al.* (2003)
$Pu^{4+} + 5CO_3^{2-} \rightleftarrows Pu(CO_3)_5^{6-}$	0		36.65 ± 1.13[a]	Guillaumont *et al.* (2003)
$Pu(CO_3)_4^{4-} + CO_3^{2-} \rightleftarrows Pu(CO_3)_5^{6-}$	3.0	−1.36 ± 0.09	–	Capdevila *et al.* (1996)
$Pu^{4+} + 2CO_3^{2-} + 4OH^- \rightleftarrows Pu(CO_3)_2(OH)_4^{4-}$	~ 0.1	46.4 ± 0.7[b]		Yamaguchi *et al.* (1994)
$Pu^{4+} + 2CO_3^{2-} + 2OH^- \rightleftarrows Pu(CO_3)_2(OH)_4^{2-}$		44.8[b]		Rai *et al.* (1999)
$PuO_2^+ + CO_3^{2-} \rightleftarrows PuO_2CO_3^-$	0.5	4.60 ± 0.04	5.12 ± 0.14[a]	Bennett *et al.* (1992) and Guillaumont *et al.* (2003)
$PuO_2^+ + 3CO_3^{2-} \rightleftarrows PuO_2(CO_3)_3^{5-}$		7.5	5.025 ± 0.92[a]	Wester and Sullivan (1983), Capdevila *et al.* (1992), and Guillaumont *et al.* (2003)
$PuO_2^{2+} + CO_3^{2-} \rightleftarrows PuO_2CO_3$	3.5	8.6 ± 0.3	9.5 ± 0.5[a]	Robouch and Vitorge (1987) and Guillaumont *et al.* (2003)
	0.1	8.7 ± 0.3		Pashalidis *et al.* (1997)
$PuO_2^{2+} + 2CO_3^{2-} \rightleftarrows PuO_2(CO_3)_2^{2-}$	0.1	13.1 ± 0.1	14.7 ± 0.5[a]	Sullivan *et al.* (1982)
	3.5	13.6 ± 0.7		Robouch and Vitorge (1987) and Guillaumont *et al.* (2003)

$PuO_2^{2+} + 3CO_3^{2-} \rightleftarrows PuO_2(CO_3)_3^{4-}$	0.1	18.2 ± 0.4	18.0 ± 0.5[a]	Ullman and Schreiner (1988), Robouch and Vitorge (1987), and Guillaumont *et al.* (2003)
$3PuO_2(CO_3)_3^{4-} \rightleftarrows (PuO_2)_3(CO_3)_6^{6-} + 3CO_3^{2-}$	3.0	−7.4 ± 0.2		Grenthe *et al.* (1986a)
nitrate				
$Pu^{4+} + NO_3^- \rightleftarrows PuNO_3^{3+}$	2	0.51 ± 0.05	1.95 ± 0.15[a]	Berg *et al.* (2000) and Guillaumont *et al.* (2003)
$Pu^{4+} + 2NO_3^- \rightleftarrows Pu(NO_3)_2^{2+}$	2	1.05 ± 0.08		Berg *et al.* (2000)
phosphate				
$Pu^{4+} + H_3PO_4 \rightleftarrows PuH_3PO_4^{4+}$	2	2.3	2.4 ± 0.3[a]	Denotkina *et al.* (1960) and Guillaumont *et al.* (2003)
$PuO_2^+ + HPO_4^{2-} \rightleftarrows PuO_2HPO_4^-$	1	2.39 ± 0.04		Moskvin and Poznyakov (1979)
sulfate				
$Pu^{3+} + HSO_4^- \rightleftarrows PuSO_4^+ + H^+$			1.93 ± 0.614[a]	Guillaumont *et al.* (2003)
$Pu^{3+} + 2HSO_4^- \rightleftarrows Pu(SO_4)_2^- + 2H^+$			1.74 ± 0.76[a]	Guillaumont *et al.* (2003)
$Pu^{4+} + HSO_4^- \rightleftarrows PuSO_4^{2+} + H^+$			4.91 ± 0.22[a]	Guillaumont *et al.* (2003)
$Pu^{4+} + 2HSO_4^- \rightleftarrows Pu(SO_4)_4 + 2H^+$			7.18 ± 0.32[a]	Guillaumont *et al.* (2003)
$PuO_2^{2+} + SO_4^{2-} \rightleftarrows PuO_2SO_4$			3.38 ± 0.20[a]	Guillaumont *et al.* (2003)
$PuO_2^{2+} + 2SO_4^{2-} \rightleftarrows PuO_2(SO_4)_2^{2-}$			4.4 ± 0.2[a]	Guillaumont *et al.* (2003)

[a] NEA Update Vol 5 (Guillaumont *et al.*, 2003).

[b] Species may not exist, based on later studies of Pu(IV) carbonates (Capdevila *et al.*, 1996).

Tetravalent plutonium probably forms stepwise complexes, $Pu(CO_3)_n^{4-2n}$, $n = 1–5$, with increasing solution pH and carbonate concentration (Newton and Sullivan, 1986; Clark *et al.*, 1995). The end members of this series and the tetracarbonato complex have been characterized, while the bis- and tris-species are inferred from studies of other actinide(IV) carbonates. Monocarbonato Pu(IV) of formula $Pu(CO_3)^{2+}$ is prepared by addition of carbonate to acidic solutions of the ion or from carbonate-mediated dissolution of hydroxide or oxide solids. The formation constant for $Pu(CO_3)^{2+}$ is reported to be $\log_{10} \beta_1 = (17.0 \pm 0.7)$ (Nitsche and Silva, 1996; Rai *et al.*, 1999). Given the generally accepted hydration number of eight for Pu(IV), this complex likely has six additional water molecules in the inner coordination sphere. In concentrated carbonate solutions, $Pu(CO_3)_4^{4-}$ is in equilibrium with $Pu(CO_3)_5^{6-}$. The formation constants for these individual species are highly correlated with each other and with the lower carbonate species.

Capdevila *et al.* (1996) studied the formation of the limiting carbonato complex of formula $Pu(CO_3)_5^{6-}$ by electronic absorption spectroscopy with varying ionic strength. From the study of the equilibrium in equation (7.133), they were able to determine an equilibrium constant for the reaction of $\log_{10} K_5 = -(1.36 \pm 0.09)$, and the formation constant for the limiting complex of $\log_{10} \beta_5 = (35.8 \pm 1.3)$ in 3 M $NaClO_4$ solution. The NEA review recommended a zero ionic strength value of $\log_{10} \beta_5 = (36.65 \pm 1.13)$ (Lemire *et al.*, 2001). By combining the value for β_5 with the equilibrium constant K_5 for equation (7.133), the formation constant for $Pu(CO_3)_4^{4-}$ at zero ionic strength was recommended to be $\log_{10} \beta_4 = (37.0 \pm 1.1)$ (Lemire *et al.*, 2001).

$$Pu(CO_3)_4^{4-} + CO_3^{2-} \rightleftarrows Pu(CO_3)_5^{6-} \qquad (7.133)$$

Recent conventional spectrophotometric and electrochemical studies have focused on refining the thermodynamic constants for the carbonato species and determining the stability field and stoichiometry of mixed hydroxo/carbonato Pu(IV) complexes (Capdevila and Vitorge, 1999). The NEA critical review of thermodynamic data suggests that spectroscopic signatures and solubility characteristics that have been attributed to mixed hydroxo/carbonato complexes are in fact explained by the simultaneous and independent formation of hydrolysis products and carbonato complexes (Lemire *et al.*, 2001). Counter arguments are that colloidal Pu(IV) polymer formation is suppressed by carbonate complexation, and that absorption spectra of Pu(IV) in carbonate solutions over the entire pH range are wholly reproduced by linear combinations of known individual hydroxide and carbonate spectra.

Plutonium(IV) carbonato solids of general formula $M_xAn(CO_3)_y \cdot nH_2O$ have been prepared with a variety of cations ($M = Na^+, K^+, NH_4^+, C(NH_2)_3^+$; $y = 4$, 5, 6, 8) by precipitating or crystallizing the solution species. For example, $[Na_6Pu(CO_3)_5]_2 \cdot Na_2CO_3 \cdot 33H_2O$ was crystallized from 2.5 M Na_2CO_3 solution and characterized by single-crystal XRD (Clark *et al.*, 1998). The structure contains the discrete $Pu(CO_3)_5^{6-}$ ion, which can be viewed as a pseudo-hexagonal bipyramid with three CO_3^{2-} ligands in an equatorial plane and two in axial positions as shown in **13**. Solution XAFS data for Pu(IV) in 2.5 M Na_2CO_3 solution gave bond distances and coordination numbers that corresponded extremely well with the average Pu–O, nonbonding Pu- -C, and distal Pu- -O distances of 2.42(1), 2.87(1), and 4.12(1) Å, respectively, found in the solid-state structure for the $Pu(CO_3)_5^{6-}$ ion. A peak-by-peak correspondence of the optical absorption spectra of the solution and diffuse reflectance spectrum of the ground crystalline solid, together with the solution XAFS data provide conclusive evidence that the $Pu(CO_3)_5^{6-}$ ion is the limiting species in high carbonate solutions. Depending on reaction conditions, green amorphous powders of compositions $K_4Pu(CO_3)_4{\cdot}nH_2O$, $K_6Pu(CO_3)_5{\cdot}nH_2O$, $K_8Pu(CO_3)_6{\cdot}nH_2O$, and $K_{12}Pu(CO_3)_8{\cdot}nH_2O$ have all been reported (Gel'man and Zaitsev, 1958). Since Clark *et al.* identified the $Pu(CO_3)_5^{6-}$ ion as the limiting species, it is reasonable to assume that the latter two solids are more realistically formulated as $[K_6Pu(CO_3)_5][K_2CO_3]{\cdot}nH_2O$ and $[K_6Pu(CO_3)_5][K_2CO_3]_3{\cdot}nH_2O$. Sodium salts of formula $Na_4Pu(CO_3)_4{\cdot}3H_2O$, $Na_6Pu(CO_3)_5{\cdot}2H_2O$, and $Na_6Pu(CO_3)_5{\cdot}4H_2O$ have also been claimed as light green crystalline compounds that appear to dehydrate in air (Gel'man and Zaitsev, 1958). Similarly, the $(NH_4)_4Pu(CO_3)_4{\cdot}4H_2O$ and $[Co(NH_3)_6]_2Pu(CO_3)_5{\cdot}5H_2O$ salts have been reported (Ueno and Hoshi, 1970).

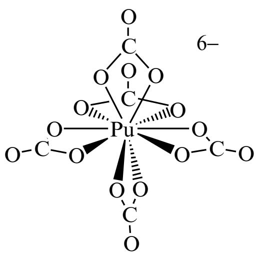

13

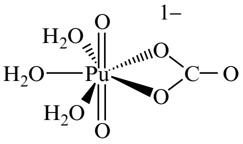

14

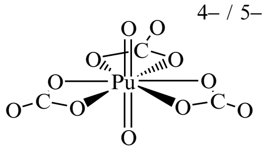

15

Pentavalent plutonium carbonato complexes are prepared by addition of alkali metal carbonate solutions to mildly acidic solutions of PuO_2^+, or by the one-electron reduction of Pu(VI) carbonato complexes. The mono- and triscarbonato complexes, $PuO_2(CO_3)^-$ and $PuO_2(CO_3)_3^{5-}$, have been observed directly by optical absorption spectroscopy, and their formation constants have been determined. In contrast, the biscarbonato complex $PuO_2(CO_3)_2^{3-}$ has not been observed directly, and is only inferred. Sensitive laser photoacoustic spectroscopy was used to determine the formation constant of $\log_{10}\beta_1 = (4.6 \pm 0.04)$ for $PuO_2(CO_3)^-$ (Bennett *et al.*, 1992). Using the Nernst equation, the measured reversible reduction of hexavalent $PuO_2(CO_3)_3^{4-}$ at 339 mV vs SHE in 1 M Na_2CO_3 and comparisons with Np(V) carbonato formation constants, the formation constant for $PuO_2(CO_3)_3^{5-}$ can be estimated to be $\log_{10}\beta_3 = 7.5$

(Wester and Sullivan, 1983; Capdevila *et al.*, 1992). These solution species are likely isostructural with the corresponding $NpO_2(CO_3)(OH_2)_3^-$, and $NpO_2(CO_3)_3^{5-}$ complexes which have been characterized by EXAFS spectroscopy, and illustrated in **14** and **15** (Clark *et al.*, 1996). These complexes have the general actinyl carbonate structure with axial O=An=O units at a bond distance of 1.85 Å and bidentate carbonato and water oxygen atoms arrayed about the equatorial plane to form a pentagonal or hexagonal bipyramidal coordination polyhedron at average bond distances of 2.45 and 2.42 Å, respectively. Optical absorption spectra do not suggest that the biscarbonato complex $PuO_2(CO_3)_2^{3-}$ is ever a predominant solution species, consistent with the small difference between the stability constants for the mono- and tris-species that suggest a very small stability field for this intermediate species. Mixed hydroxo carbonato complexes have been proposed for Np(v) (Sullivan *et al.*, 1991), but the identification and existence of analogous Pu(v) species is questionable.

Solids corresponding to the Pu(v) carbonate solution species have been prepared as microcrystalline powders via precipitation and the orthorhombic solid-state structure of $KPuO_2CO_3$ has been determined (Ellinger and Zachariasen, 1954). Much more data is available for analogous salts of Np(v) carbonates, $MNpO_2CO_3$, and $M_3NpO_2(CO_3)_2$, where M is an alkali metal or ammonium ion (Simakin *et al.*, 1974; Volkov *et al.*, 1974a,b, 1981). These structure types have been reviewed by Clark *et al.* (1995). These compounds show interesting structural changes due to the size similarity of hydrated ions such as K^+ and NpO_2^+, and the extent of hydration. For example, for $MNpO_2CO_3$ where M = Cs^+, Rb^+, NH_4^+, K^+, Na^+, and Li^+, a hexagonal-to-orthorhombic phase change is observed within the NpO_2CO_3 layer at the potassium–sodium boundary. The solids both contain actinyl carbonate layers and the hexagonal and orthorhombic sheets are related by displacement of the chains of actinyl units through half a translation along the crystallographic *a*-axis. These basic layers are illustrated qualitatively in **16** and **17**. The orthorhombic structure **17** is more open than the hexagonal structure **16**, which appears to allow for the closer contacts necessary for the smaller sodium and lithium cations.

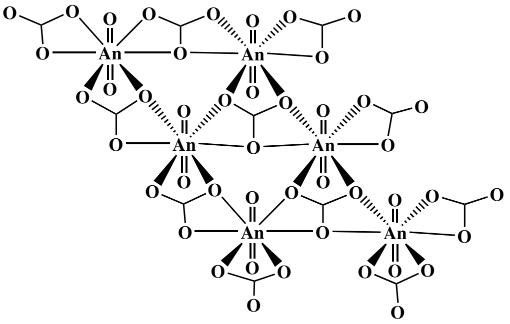

16

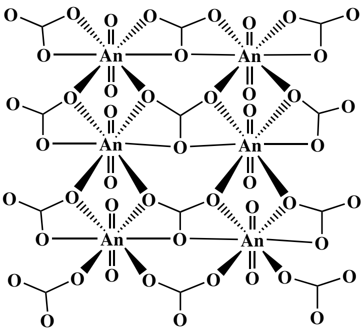

17

The biscarbonato solid $M_3NpO_2(CO_3)_2$ displays an overall orthorhombic structure, but exhibits a pseudo-hexagonal layer similar to **16**, except that one half of the AnO_2^+ ions in the anionic carbonate layer have been replaced by alkali metal cations. One can envision that M^+ and AnO_2^+ cations form alternating chains within the hexagonal sheet and give rise to the approximate composition $[M_{0.5}(AnO_2)_{0.5}(CO_3)]$ within the layer. This arrangement is illustrated qualitatively in **18**. The cation and anion layers are oriented such that an alkali metal cation, M^+, lies directly above and below the linear AnO_2^+ ion of adjacent sheets. The anionic carbonate layer and the cationic potassium layers line up such that they are parallel to the crystallographic *c*-axis, and this allows for an M–O=An interaction between layers and yields a maximally ordered structure (Clark *et al.*, 1995).

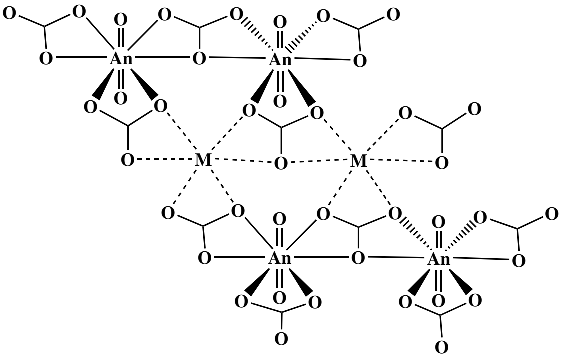

18

Hexavalent plutonium carbonato complexes have been studied primarily as an extension of uranyl carbonate chemistry. Uranyl carbonato complexes are very important in uranium geochemistry actinide contaminant environmental transport, uranium mining, and nuclear fuel production and reprocessing, owing to their high solubility and stability in aqueous solution. Substitution of the plutonyl ion in uranyl phases has the potential to form solid solutions.

Carbonate complexation of Pu(VI) increases with pH and carbonate concentration. Pashalidis *et al.* (1997) studied the solubility of both UO_2CO_3 and PuO_2CO_3 in aqueous carbonate solutions and determined equilibrium constants for the formation of $PuO_2(CO_3)$, $PuO_2(CO_3)_2^{2-}$, and $PuO_2(CO_3)_3^{4-}$. These results are in good agreement with earlier studies on $AnO_2(CO_3)$ solids of uranium, neptunium, and plutonium by Ullman and Schreiner (1988), and $PuO_2(CO_3)$ solids by Robouch and Vitorge (1987). The most recent NEA review recommends $\log_{10}\beta_1 = (9.5 \pm 0.5)$, $\log_{10}\beta_2 = (14.7 \pm 0.5)$, and $\log_{10}\beta_3 = (18.0 \pm 0.5)$ for the corresponding formation constants (Guillaumont *et al.*, 2003).

Both $PuO_2(CO_3)_{(aq)}$ and $PuO_2(CO_3)_3^{4-}$ have been spectroscopically observed. In contrast, while the $AnO_2(CO_3)_2^{2-}$ species has been spectroscopically observed for U(VI) and Np(VI), the stability field of the corresponding $PuO_2(CO_3)_2^{2-}$ analog appears to be so small that it has not been directly observed. Spectrophotometric and calorimetric studies of the formation of the monocarbonato complex from the Pu(VI) hydroxide illustrated that carbonate can outcompete hydroxide to coordinate to plutonium, and provided the first formation constants (Sullivan *et al.*, 1982). Subsequent solubility studies and additional spectrophotometric data provide a formation constant of $\log_{10} \beta_1 = (8.7 \pm 0.3)$ for $PuO_2(CO_3)$ in 0.1 M $NaClO_4$ (Pashalidis *et al.*, 1997). X-ray powder diffraction and XAFS studies of the corresponding $PuO_2(CO_3)$ solid show that it is isostructural with rutherfordine, $UO_2(CO_3)$ (Reilly *et al.*, 2000). This solid has a layered structure where the local coordination environment of the plutonyl ion is a hexagonal bipyramidal arrangement of oxygen atoms with the plutonyl units perpendicular to the orthorhombic plane (Clark *et al.*, 1995). Each plutonium atom forms six equatorial bonds with the oxygen atoms of four carbonate ligands, two in a bidentate manner and two in a monodentate manner. The orthorhombic plane is identical to that shown in **17**. The orthorhombic plane of hexagonal bipyramidal plutonyl units forms infinite, two-dimensional layers.

Solution EXAFS and single crystal XRD studies show the limiting $PuO_2(CO_3)_3^{4-}$ is isostructural with the uranyl analog, which has pseudo-hexagonal pyramidal coordination geometry as illustrated in **15**. The Pu=O distance was found to be 1.74 Å with an average Pu–O distance to carbonate ligands of 2.45 Å (Clark *et al.*, 1999b; Neu *et al.*, 2000; Conradson *et al.*, 2004a). The stability constant for $PuO_2(CO_3)_3^{4-}$ has been determined from solubility, calorimetry, and spectrophotometric studies to be $\log_{10} \beta_3 = (18.2 \pm 0.4)$ in 0.1 M electrolytes (Robouch and Vitorge, 1987; Ullman and Schreiner, 1988). Pashalidis *et al.* determined a value of (17.8 ± 0.2) in 0.1 M $NaClO_4$ solution, and the recent NEA assessment recalculated their value to correct for a systematic error and obtained (18.4 ± 0.2) (Guillaumont *et al.*, 2003). This species can be readily precipitated to form salts with monovalent cations.

In contrast with uranyl carbonate chemistry where the bis carbonato $UO_2(CO_3)_2^{2-}$ and its trimeric oligomer $(UO_2)_3(CO_3)_6^{6-}$ are major species (Allen *et al.*, 1995; Banyai *et al.*, 1995), the bis carbonato plutonyl complex, $PuO_2(CO_3)_2^{2-}$, has a small stability field and neither it nor the trimer $(PuO_2)_3(CO_3)_6^{6-}$ have been characterized. Similar to the hexavalent hydroxides, oligomerization reactions appear to decrease dramatically across the series from uranium to plutonium. Mixed actinyl trimers, $(UO_2)_2(PuO_2)(CO_3)_6^{6-}$ and $(UO_2)(PuO_2)_2(CO_3)_6^{6-}$ have been proposed based on optical absorption and emf studies (Grenthe *et al.*, 1986b). Similarly, additional polymeric species known for uranyl $(UO_2)_2(CO_3)(OH)_3^-$, $(UO_2)_3O(OH)_2(HCO_3)^+$, and $(UO_2)_{11}(CO_3)_6(OH)_{12}^{2-}$ under conditions of high metal ion concentration or high ionic strength (Grenthe *et al.*, 1992) have not been observed for plutonyl.

Nitrate

Nitrates were among the first complexes studied for plutonium and are very important in plutonium processing (Cleveland, 1979). The effectiveness of solvent extraction and ion-exchange processes in nitric acid, for example, depends strongly on the stoichiometry, stability, molecular geometry and molecular charge of nitrate complexes. Nitrate tends to bind plutonium in a bidentate fashion and to retain its planar molecular geometry, similar to carbonate. But it is a much weaker ligand. Because nitric acid solutions of plutonium and nitrate solids of Pu(IV) and Pu(VI) are both prevalent forms in process and synthetic chemistry, a tremendous number of mixed-ligand complexes are known that contain one or more mono- or bidentate nitrates in the inner coordination sphere.

Trivalent nitrate species have been prepared in nitric acid solution, but they are unstable with respect to oxidation.

Aqueous Pu(IV) nitrate complexes are very well studied because of their use in solvent extraction methods and ion-exchange chromatography. The solution species, $Pu(NO_3)_n^{4-n}$ ($n = 1$–6), have been studied in detail. There is evidence from numerous ion exchange and extraction studies and more recent NMR and EXAFS experiments that the mono-, bis-, tetra, and the hexanitrato complexes are significant, but the tris- and pentanitrato complexes are not (Veirs *et al.*, 1994). X-ray absorption data for the system suggest aquo ligation decreases in the inner sphere even before sequential bidentate nitrates bind the metal center. Solution EXAFS data gives coordination numbers of 11–12 for the first coordination sphere, with average Pu–O bond distances of 2.49 and 2.38 Å for nitrate and water ligands, respectively (Allen *et al.*, 1996b). Formation constants measured for the mononitrato complex, $Pu(NO_3)^{3+}$, were critically evaluated by the NEA reviewers, who recommend the constant $\log_{10}\beta_1 = (1.95 \pm 0.15)$ at $I = 0$ (Lemire *et al.*, 2001). A recent spectrophotometric study in 2 molal $HClO_4$ and extensive analysis by Monte Carlo methods sheds new light on the relative importance of the $Pu(NO_3)^{3+}$ and $Pu(NO_3)_2^{2+}$ complexes, and reported the constants $\log_{10}\beta_1 = (0.51 \pm 0.05)$ and $\log_{10}\beta_2 = (1.05 \pm 0.08)$ (Berg *et al.*, 2000).

Cation exchange resins have a strong affinity for the hexanitrato species, $Pu(NO_3)_6^{6-}$. This nitrate-based purification method is used to separate plutonium from most of the elements in the periodic table, and is used on an industrial scale (Section 7.5.5). There has been some discussion over whether the limiting Pu(IV) nitrate in solution is the penta- or hexanitrato species and some experiments suggest that the hexanitrate is only a major species in the presence of resins or in concentrated salt solutions that favor ion pairing (Veirs *et al.*, 1994; Clark and Delegard, 2002).

Plutonium(IV) nitrate solids are readily formed in nitric acid by dissolution of hydroxides or carbonates followed by precipitation or crystallization. Crystalline orthorhombic $Pu(NO_3)_4{\cdot}5H_2O$ can be obtained in this way and also by heating a Pu(VI) nitrate salt (Staritzky, 1956). Hexanitrato complexes, $M_2Pu(NO_3)_6{\cdot}2H_2O$, where M = Rb, Cs, NH_4, and pyridinium, are obtained from moderately concentrated (8 to 14 M) nitric acid. A single crystal XRD study was performed on $(NH_4)_2Pu(NO_3)_6$ by Spirlet *et al.* (1992). In the solid state the icosohedral $Pu(NO_3)_6^{2-}$ unit is characterized by three mutually perpendicular planes formed by the trans NO_3^- ligands giving virtual T_h symmetry as illustrated in **19**. The 12 Pu–O bond distances average 2.487(6) Å.

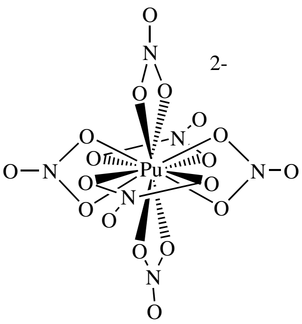

19

Numerous additional solution studies on Pu(IV) mixed ligand-nitrate complexes have been performed in the development and performance testing of extractants. Most notably these include TBP and phosphine oxides. As other examples, a variety of mixed amide-nitrate complexes have been proposed based upon NMR, IR, and extraction behavior (Berthon and Chachaty, 1995; Preston and du Preez, 1995; Romanovski *et al.*, 1999).

No inner-sphere Pu(V) nitrate complexes have been characterized. The existence of the solid nitrates of Np(V) and Pa(V), $NpO_2(NO_3){\cdot}xH_2O$ ($x = 1, 5$), $RbNpO_2(NO_3)_2{\cdot}H_2O$, and $PaO(NO_3)_3{\cdot}xH_2O$ ($x = 1$–4) suggests that it might be possible to isolate solid Pu(V) nitrates if the oxidation state could be stabilized in nitrate solution. Pu(VI) nitrates are weak complexes and only the mononitrate, $PuO_2(NO_3)^+$, species is significant in solution. Mixed TBP-nitrate complexes have been widely studied, including a recent EXAFS study of the structural changes as the actinyl species are reduced to An(IV) (Den Auwer *et al.*, 1999). The hydrated solid, $PuO_2(NO_3)_2{\cdot}xH_2O$, $x = 3{,}6$, has been characterized.

Sulfate

Trivalent plutonium forms at least two stepwise complexes, $PuSO_4^+$ and $Pu(SO_4)_2^-$ in acid solutions according to equations below (Fardy and Buchanan, 1976; Rao *et al.*, 1978; Nash and Cleveland, 1983).

$$\mathrm{Pu^{3+} + HSO_4^- \rightleftharpoons PuSO_4^+ + H^+} \tag{7.134}$$

$$\mathrm{Pu^{3+} + 2HSO_4^- \rightleftharpoons Pu(SO_4)_2^- + 2H^+} \tag{7.135}$$

The NEA reviewers recalculated the formation constants for these species according to the reactions above, extrapolated to zero ionic strength and recommended $\log_{10} {}^*\beta_1 = (1.93 \pm 0.61)$ and $\log_{10} {}^*\beta_2 = (1.74 \pm 0.76)$ (Lemire *et al.*, 2001). The fact that higher order anions such as $Pu(SO_4)_4^{5-}$ are found in solids such as $K_5Pu(SO_4)_4{\cdot}4H_2O$ suggests that higher order ions of formula $Pu(SO_4)_n^{3-2n}$ must form to a small extent in solution (Mudher *et al.*, 1995). There is some evidence for the formation of solid $Pu_2(SO_4)_3{\cdot}xH_2O$. The Pu(III) solid is likely isostructural with $Am_2(SO_4)_3{\cdot}8H_2O$, which is comprised of eight coordinate Am(III) (Bullock *et al.*, 1980). The ternary salts of $MPu(SO_4)_2{\cdot}H_2O$, where M is an alkali metal, are isostructural with the Nd(III) analog (Iyer and Natarajan, 1989, 1990). Similarly, the $(NH_4)Pu(SO_4)_2{\cdot}4H_2O$ is isomorphous with the corresponding Sm(III) compounds; and all of these structures contain nine coordinate metal centers containing water and bidentate sulfate ligands. Salts of other complex anions, such as $K_5Pu(SO_4)_4$, which is isostructural with $K_5La(SO_4)_4$, are also known (Mudher *et al.*, 1995).

Sulfate has high affinity for plutonium(IV). The stability of the complexes has been studied both to understand the properties of the complexes themselves and to evaluate how sulfate competes with extractants (Laxminarayanan *et al.*, 1964; Sokhina *et al.*, 1978; Solovkin and Rubisov, 1983). As for Pu(III), formation constants for Pu(IV) sulfato complexes are accurately expressed as solution reaction constants from bisulfate addition to Pu^{4+} according to reactions (7.136) and (7.137).

$$\mathrm{Pu^{4+} + HSO_4^- \rightleftharpoons PuSO_4^{2+} + H^+} \tag{7.136}$$

$$\mathrm{Pu^{4+} + 2HSO_4^- \rightleftharpoons Pu(SO_4)_{2\,(aq)} + 2H^+} \tag{7.137}$$

The data are most consistent with the formation of two complexes, $PuSO_4^{2+}$ and $Pu(SO_4)_2$, but higher order species $Pu(SO_4)_n^{4-2n}$ are implied by the existence of salts such as $K_4Pu(SO_4)_4{\cdot}2H_2O$. The NEA review recommends the constants $\log_{10} {}^*\beta_1 = (2.75 \pm 0.01)$ and $\log_{10} {}^*\beta_2 = (4.43 \pm 0.01)$ in 2.2 molal $(H, Na)_2SO_4$ solutions (Lemire *et al.*, 2001). Extrapolation to zero ionic strength gives $\log_{10}{}^*\beta_1 = (4.91 \pm 0.22)$ and $\log_{10}{}^*\beta_2 = (7.18 \pm 0.32)$ (Lemire *et al.*, 2001). Based upon the crystal structure of $Pu_2(OH)_2(SO_4)_3(H_2O)_4$, mixed hydroxo sulfato complexes are also thought to form in solution at higher pH (Wester, 1983).

The neutral hydrates can be precipitated as $Pu(SO_4)_2{\cdot}nH_2O$ ($n = 9, 8, 6, 4$), and subsequently dehydrated up to 400°C. The red tetrahydrate Pu(IV) phase is noteworthy because of its high purity (Cleveland, 1979). The common bicapped square antiprismatic geometry of four sulfates and four waters is adopted by the

Pu(IV) centers in the tetra- and octahydrates. Each sulfate group is shared by two Pu(IV) ions, and sulfates not bonded to plutonium are hydrogen bonded to water molecules (Kierkegaard, 1956; Jayadevan *et al.*, 1982). Two orthorhombic polymorphs of the tetrahydrate differ only by hydrogen bonding in the structures (Jayadevan *et al.*, 1982). The octahydrate loses four water molecules at relatively low temperature, and can be fully dehydrated. Ternary salts have also been characterized, such as the green Pu(IV) compounds $M_4Pu(SO_4)_4 \cdot xH_2O$ and $M_6Pu(SO_4)_5 \cdot xH_2O$ ($M = K, NH_4$) (Sood *et al.*, 1992). The structure of the anion in $K_4Pu(SO_4)_4 \cdot 2H_2O$ consists of chains of plutonium atoms linked by pairs of bridging sulfate groups, and the plutonium atom exhibits a tricapped trigonal prismatic coordination geometry. The structure of the Pu(IV) mixed hydroxo-sulfato complex, $Pu_2(OH)_2(SO_4)_3(H_2O)_4$, has been determined and is isomorphous with the hydroxosulfates of Zr, Hf, and Ce (Wester, 1983).

Sulfate complexes of Pu(V) have not been characterized, but they may be important environmental species since sulfate can be a major component of natural waters and minerals. Therefore research on these types of complexes is merited.

Mono- and bis-sulfato complexes of plutonyl(VI), $PuO_2(SO_4)$ and $PuO_2(SO_4)_2^{2-}$, are generally prepared from acidic solutions. Solution equilibrium constants derived in terms of formation constants for the reactions listed below have been measured (Patil and Ramakrishna, 1976; Ullman and Schreiner, 1986).

$$PuO_2^{2+} + SO_4^{2-} \rightleftharpoons PuO_2SO_4(aq) \tag{7.138}$$

$$PuO_2^{2+} + 2SO_4^{2-} \rightleftharpoons PuO_2(SO_4)_2^{2-} \tag{7.139}$$

The NEA reviewers evaluated these results and recommended the zero ionic strength formation constants of $\log_{10} \beta_1 = (3.38 \pm 0.20)$ and $\log_{10} \beta_2 = (4.4 \pm 0.2)$ (Lemire *et al.*, 2001). Changes in the electronic structure of hexavalent plutonium and neptunium as a function of sulfate, selenate, and chromate complexation have been studied by optical and IR spectroscopy and attributed to covalence variation in An=O bonding or distortions in the ligand arrangement (Budantseva *et al.*, 2000).

Plutonyl sulfate solids of formula $M_2PuO_2(SO_4)_2$ have been prepared and are likely isostructural with the neptunyl analogs. The solid state layered structure of $Cs_2NpO_2(SO_4)_2$ is built up by anionic layers $[NpO_2(SO_4)_2]_n^{2n-}$, linked together by Cs^+ ions. Each NpO_2^{2+} ion in the anionic layer is linked via the sulfate ions to three other atoms to form an hexagonal net similar to the actinyl(V) carbonate structures (Fedosseev *et al.*, 1999).

Phosphate

Because of their very low solubility as exemplified by stable minerals and ore bodies, actinide phosphates have been proposed as potential radioactive waste forms (Boatner and Sales, 1988). Phosphate has multiple protonation states, PO_4^{3-}, HPO_4^{2-} and $H_2PO_4^-$, and related condensed phosphate anions such as $P_2O_7^{4-}$ and $(PO_3)_n^{n-}$ with many coordination modes that can lead to intricate three-dimensional structures in the solid state, making the plutonium phosphate compounds particularly challenging to characterize. The limited information that is available for plutonium phosphate solution species comes from solubility studies and X-ray and optical absorption spectroscopic studies. In the solid state, the major classes of actinide phosphate are phosphates, hydrogenphosphates, dihydrogen phosphates, diphosphates (pyrophosphates), and polytrioxophosphates (metaphosphates). In addition there are numerous ternary compounds, mixed valent uranium phosphates, halophosphates, organophosphates, and more recently, open framework and templated phases.

Plutonium(III) phosphate solution species are proposed to have the formula $Pu(H_2PO_4)_n^{3-n}$ ($n = 1$–4), but they have not been spectroscopically or structurally characterized (Moskvin, 1971a). For Pu(III), the blue, hexagonal $PuPO_4 \cdot 0.5H_2O$ has been prepared by precipitation from relatively dilute HNO_3/H_3PO_4 solution, then heated to yield the anhydrous compound (Bamberger, 1985). Anhydrous plutonium pyrophosphate PuP_2O_7 has been prepared by the thermal decomposition of plutonium oxolatophosphates (Bjorklund, 1957; Bamberger, 1985).

By considering the protonation behavior of phosphoric acid (Grenthe *et al.*, 1992) the following plutonium(IV) complexes may form: $Pu(H_3PO_4)_x(H_2PO_4)_y^{(4-y)+}$ ($x = 0, 1$; $y = 0, 1, 2$) under acidic conditions; $Pu(HPO_4)_3(H_2PO_4)_x^{(2+x)-}$ ($x = 1, 2$) at neutral pH; and $Pu(HPO_4)_x^{4-2x}$ ($x = 1$–3) under basic conditions. All of the known Pu(IV) solids have such low solubilities that only experiments with $Pu(HPO_4)_2 \cdot xH_2O$ have yielded solution speciation information. The solution complex in equilibrium with the solids, $Pu(H_3PO_4)^{4+}$, has a formation constant of $\log_{10}\beta_1 = 2.3$ in 2 M $(H,Na)NO_3$ (Denotkina *et al.*, 1960), and the NEA reviewers recommended the value $\log_{10}\beta_1 = (2.4 \pm 0.3)$ at zero ionic strength (Lemire *et al.*, 2001).

The chemistry of tetravalent actinide phosphates has been recently reviewed and a new classification system proposed for these compounds (Brandel and Dacheux, 2004a,b). New characterization data indicates that a number of previously reported actinide phosphate phases appear to be polyphase mixtures, particularly the "$M_3(PO_4)_4$" group of compounds. Solid Pu(IV) phosphates can be considered a subset of known Th(IV) and U(IV) compounds. Plutonium(IV) polytrioxophosphate, $Pu(PO_3)_4$, can be crystallized by dissolving PuO_2 in polyphosphoric acid (Douglass, 1962). The hydrogenphosphate, $Pu(HPO_4)_2 \bullet xH_2O$, is reported to precipitate as a gelatinous solid upon addition of phosphoric acid to nitric acid solutions of Pu(IV) and can be used as precursor for other phosphate phases. Anhydrous plutonium diphosphate PuP_2O_7, has been prepared by the thermal decomposition of plutonium oxolatophosphates or by heating a mixture of PuO_2 and BPO_4 (Bjorklund, 1957; Bamberger, 1985). Additonal Pu(IV) phosphates and diphosphates are likely based on the growing list of thorium and uranium phosphate phases reported. For example, Bénard *et al.* reported two distinct thorium types in $Th_4(PO_4)_4(P_2O_7)$, one eight-coordinate with oxygen from five phosphate and one diphosphate group and around the thorium atom (Bénard, Brandel *et al.*, 1996). Thorium(IV) can be replaced by Pu(IV) up to a maximum value of x = 1.67 for $Th_{4-x}M_x(PO_4)_4(P_2O_7)$ (Dacheux, Brandel *et al.*, 1998). Ternary compounds of the general formula $M(I)Th_2(PO_4)_3$ and $M(II)Th(PO_4)_2$ with M(I) = alkali cation, Tl, Ag, Cu, (Louer, Brochu *et al.*, 1995; Bénard, Brandel *et al.*, 1996) and M(II) = Ca, Sr, Cd, Pb, (Merigou, Genet *et al.*, 1995) are also known for U(IV).

Plutonium(V) phosphate, $NH_4PuO_2HPO_4{\cdot}4H_2O$, was precipitated from solutions of PuO_2^+ in nitric acid with the addition of $(NH_4)_2HPO_4$ (Gel'man and Zaitseva, 1964). There is evidence for $PuO_2HPO_4^-$ from adsorption studies of PuO_2^+ on iron oxides in phosphoric acid, but it has not been fully characterized (Moskvin and Poznyakov, 1979; Morgenstern and Kim, 1996). Its formation constant has been reported to be $\log_{10}\beta_1 = (2.39 \pm 0.04)$ in 1 M NH_4Cl (Moskvin and Poznyakov, 1979). It is likely that additional complexes are formed, but their stoichiometries are not certain.

Denotkina *et al.* reported the first studies of Pu(VI) phosphates (Denotkina, Shevchenko *et al.*, 1965; Denotkina and Shevchenko, 1967). This work was later revised and augmented by Fischer *et al.* who prepared a series of compounds of Pu(VI) with phosphates and arsenates with the general formulas, $MPuO_2XO_4{\bullet}yH_2O$ and $M'(PuO_2XO_4)_2{\bullet}zH_2O$ (X = P, As; M = H^+, K^+, Rb^+, NH_4^+; M′ = Ca^{2+}, Sr^{2+}), and compared the characterization data with analogous uranium and neptunium compounds (Fischer, Werner *et al.*, 1981). The hydrogenphosphate compounds, $PuO_2(HXO_4){\bullet}yH_2O$ (X = P, As), were prepared by reacting Pu(VI) hydroxide with aqueous solutions of H_3PO_4 and H_3AsO_4. The compounds $MPuO_2(PO_4){\bullet}yH_2O$ (M = K^+, NH_4^+) precipitated from aqueous solutions of Pu(VI) in dilute nitric acid upon addition of K_2PO_4 and $(NH_4)_2PO_4$. The acidic proton in the solid arsenate hydrogenarsenate complex was partially exchanged by mixing the solid with a solution of the Group 1 or 2 metal chloride. Weger *et al.* reported preliminary data on the solubility and speciation of Pu(VI) in phosphate solutions and observed evidence for colloid formation from filtration data and for three complexes between pH 2.7 to 12 in the visible–near infrared absorption spectra (Weger, Okajima *et al.*, 1993). Further work is needed to determine if the absorption features are due to soluble or colloidal species.

Iodate

The precipitate of Pu(IV) iodate, $Pu(IO_3)_4$, was one of the first forms of ^{239}Pu isolated and is a common end product in low pH actinide/lanthanide separations (Cleveland, 1979). This useful solid has not been characterized, but likely has the same stoichiometry as the thorium perchlorate analog that forms upon reaction of thorium hydroxide with perchloric acid, $Th(ClO_4)_4{\cdot}4H_2O$. Attempts to prepare Pu(IV) iodates by hydrothermal methods have produced Pu(VI) phases (described below).

Similarly, most conditions that would be used to attempt to prepare Pu(V) iodates have yielded Pu(VI) or Pu(IV) solids. The solid-state structure of $NpO_2(IO_3)$ was recently determined by single crystal XRD (Albrecht-Schmitt *et al.*, 2003). Its structure consists of neptunyl(V) cations linked to one another by $O_2Np{-}O{=}Np{=}O$ bonds and bridging iodate anions, creating a pentagonal bipyramidal NpO_7 unit.

The binary plutonyl(VI) iodate, $PuO_2(IO_3)_2{\cdot}H_2O$, has been prepared under hydrothermal conditions and has a layered structure with PuO_7 pentagonal bipyramids linked by iodate anions. By contrast, $UO_2(IO_3)_2$ is one-dimensional, and contains chains of edge-sharing UO_8 hexagonal pyramids. A second actinyl (VI) compound with water in the inner coordination sphere, $AnO_2(IO_3)_2(H_2O)$, has been characterized for uranyl and neptunyl, but not for the slightly smaller plutonyl ion (Bean *et al.*, 2001; Runde *et al.*, 2003b). The addition of cations to the starting solution for these hydrothermal preparations produces ternary phases where the cations are located between chains and layers in the three-dimensional structure (Shvareva *et al.*, 2005). A dimeric plutonyl hydoxo iodate $(PuO_2)_2(IO_3)(\mu\text{-}OH)_3$ was isolated from a hydrothermal reaction of Pu(IV) in a mixed hydroxide, H_5IO_6 solution. In this structure hydroxide bridges are the primary structural element and seven-coordinate plutonium atoms are bridged by iodate and hydroxide (Bean *et al.*, 2005).

Perchlorate

Because perchlorates and perchloric acid solutions (similar to nitrates) are very common starting materials in actinide chemistry there are numerous examples of perchlorate containing plutonium compounds. However, pure binary plutonium perchlorates have not been characterized in the solution or solid state. Perchlorate is such a weak ligand that it most likely does not form inner-sphere complexes in aqueous solution, but acts as a simple counter ion. For comparison, crystals of uranyl perchlorate, $UO_2(ClO_4)_2{\cdot}nH_2O$ have been obtained with 6 and 7 hydration water molecules. The uranyl is coordinated with 5 water molecules in the equatorial plane with a distance of U–O(aquo) of 2.45 Å. The complex is best formulated as $[UO_2(H_2O)_5][ClO_4]_2{\cdot}nH_2O$ (Alcock and Esperas, 1977).

Oxalate

Oxalates have been widely used in plutonium separations and processing (Cleveland, 1979; Wick, 1980). The rapid formation of microcrystalline phases that are easily filtered from solution is the basis for the large-scale recovery of plutonium from concentrated solutions. In addition, the low solubility of the oxalates makes them useful in 'polishing' or 'finishing' steps where minor amounts of material are recovered. Plutonium oxalates may also be important in environmental chemistry since oxalate is a major byproduct of plant metabolism and can be concentrated in some soils. The stoichiometry for the oxalate complexes has been determined from a combination of thermogravimetric analyses and XRD on solid compounds. The oxalate ligand $\left(C_2O_4^{2-}\right)$ generally binds actinide ions in a mono- or bidentate fashion, and can also bridge metal centers to produce a variety of chains, layers, and intricate three-dimensional structures with high coordination numbers. Solution species are only poorly studied, as expected given their low solubilities.

The solid trivalent plutonium oxalate system is dominated by two hydrates of formula $Pu_2(C_2O_4)_3{\cdot}10H_2O$ and $Pu_2(C_2O_4)_3{\cdot}6H_2O$ that are readily precipitated from solution in the presence of reducing agents, such as hydroxylamine. The blue, monoclinic decahydrate $Pu_2(C_2O_4)_3{\cdot}10H_2O$ forms in concentrated solutions and can be dehydrated or fired to produce highly pure finely divided PuO_2 (Rao *et al.*, 1963). This stoichiometric oxalate is isostructural with lanthanide (III) oxalate decahydrate, which includes nine-coordinate metal centers (Jenkins *et al.*, 1965). A single crystal XRD structure of a nonahydrate $Pu_2(C_2O_4)_3{\cdot}9H_2O$ has been recently reported (Runde *et al.*, 2005a). This two-dimensional solid consists of tricapped trigonal prismatic PuO_9 units that are linked by $C_2O_4^{2-}$ groups and a network of interstitial water molecules. The plutonium atom is coordinated to six oxygen atoms from three bidentate oxalate ligands and three oxygen atoms from coordinated water. The Pu–O distances range from 2.47 to 2.56 Å (Runde *et al.*, 2003a). Complex plutonium(III) oxalates of general formula $MPu(C_2O_4)_2{\cdot}xH_2O$ ($M = Na, K, Cs, NH_4$) have also been prepared (Runde *et al.*, 2005a).

Solution oxalate complexes are mainly of the form, $Pu(C_2O_4)_n^{3-2n}$, $n = 2$–4. The bis-oxalate species is the most important, while the latter complexes have very narrow ranges of stability (Cleveland, 1979; Hasilkar *et al.*, 1994). Numerous mixed-ligand Pu(III) oxalate complexes have been postulated to form but have not been studied in detail.

Tetravalent plutonium oxalates have been prepared with 2, 4, and 5 oxalate ligands bound to plutonium. The binary oxalate hydrates, $Pu(C_2O_4)_2{\cdot}xH_2O$ ($x = 0$, 1, 2, or 6), can be prepared from Pu(III) solutions in the presence of peroxide or other mild oxidizing agents, or precipitated directly from Pu(IV) solutions. Detailed structural analyses of these solids have not been reported. They are likely isostructural with the related binary Th(IV) and U(IV) oxalates, which generally have a coordination number of eight, comprised of bidentate and bridging oxalate and water molecules in the inner sphere arranged in irregular cubic and square antiprismatic coordination geometries. Complex salts of the tetra- and pentaoxalates, including $Na_4[Pu(C_2O_4)_4]{\cdot}5H_2O$, $(NH_4)_6[Pu(C_2O_4)_5]{\cdot}5H_2O$, and $K_6[Pu(C_2O_4)_5]{\cdot}5H_2O$ have been prepared. Uranium and thorium analogs of the tetraoxalate contain a ten-coordinate actinide (IV) atom in an irregular bicapped square antiprism linked to other metal centers by oxalato or aquo bridges (Favas *et al.*, 1983; Harrowfield *et al.*, 1983). Hydrothermal synthesis produced single crystals of $KPu(C_2O_4)_2(OH){\cdot}2H_2O$ (Runde, 2005a). The single-crystal structure of $KPu(C_2O_4)_2(OH){\cdot}2H_2O$ shows a three-dimensional framework built up from oxalate-linked PuO_9 polyhedra. Each PuO_9 polyhedron consists of eight oxygen atoms from four chelating oxalate ligands and one hydroxide ligand. This finding is suggestive that $Pu(C_2O_4)_4(OH)^{5-}$ may be the limiting Pu(IV) solution complex under high oxalate concentrations (Runde, 2005a).

Plutonium(V) in the presence of oxalate disproportionates to a mixture of oxidation states under most conditions (Nikitenko, 1988). Plutonium(V) oxalates (such as $NH_4PuO_2(C_2O_4) \cdot xH_2O$) can be isolated by rapid precipitation from neutral pH solutions and have been identified by optical absorption spectroscopy and chemical analyses (Zaitseva *et al.*, 1973). Plutonium(VI) oxalates that are isostructural with uranyl oxalates have been prepared (Jenkins *et al.*, 1965; Bessonov *et al.*, 1996). The simple binary, $PuO_2(C_2O_4) \cdot 3H_2O$, is the most studied and was recently employed in an EPR study to show the evidence for the participation of 5f electrons in plutonium chemical bonding (Bhide *et al.*, 2000).

Peroxide

Hydrogen peroxide is commonly used to reduce Pu(V) or Pu(VI) to Pu(IV) and to precipitate Pu(IV) from acidic solution, often in the presence of other anions (Balakrishnan and Ghosh Mazumdar, 1964; Hagan and Miner, 1980). Efficient separation and purification processes have been developed from this chemistry (see Section 7.5.3(b)) even though the exact nature of species in solution is not definitively known (Cleveland, 1979; Wick, 1980). Plutonium(IV) can also be reduced by hydrogen peroxide to form Pu(III) or Pu(III)/Pu(IV) mixtures, depending upon the acidity, presence of sulfate, and total plutonium concentration (Balakrishnan and Ghosh Mazumdar, 1964; Koltunov, 1982a).

Connick and McVey (1949) spectroscopically identified two Pu(IV) peroxide complexes in acidic solution. Small amounts of peroxide produced a brown complex with absorption bands at 495 ($\epsilon = 266$ L mol^{-1}cm^{-1}) and 540 nm, with a suggested peroxo-bridged formula of $[Pu(O_2)(OH)Pu]^{5+}$ and corresponding formation constant of 8.8×10^6 in 0.5 M HCl. As more peroxide is added, the brown complex converts to a red complex with an absorption maximum at 513 nm. The equilibrium between these two solution complexes (equilibrium constant of 145 in 0.5 M HCl) suggests intermediates of general composition $[Pu(\mu\text{-}O_2)_2Pu]^{4+}$. While there is no structural information to confirm the proposed solution complex stoichiometries, Runde (2005b) has recently isolated single crystals containing the $Pu_2(\mu\text{-}O_2)_2(CO_3)_6^{8-}$ ion, that confirms the presence of a doubly bridged $Pu_2(\mu\text{-}O_2)_2$ core as illustrated in **20**. When the peroxide concentration is increased, two green precipitates form with different oxygen to plutonium ratios that also incorporate other anions present in the solution, e.g. sulfate, nitrate, and chloride (Leary *et al.*, 1959). The hexagonal form ($a = 4.00$ Å) precipitates preferentially at high acidity and high ionic strength and has an oxygen to plutonium ratio of 3.0–3.4 depending on whether the solid is dry or wet, respectively. At less than 2 M acidity a fcc form ($a = 16.5$ Å) of higher purity and with an oxygen to plutonium ratio of 3.0 is obtained (Hagan and Miner, 1980) regardless of whether the solid is wet or dry.

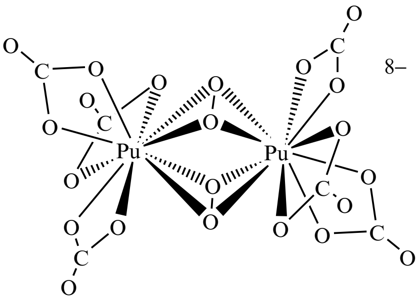

20

Less is known about the complexation of plutonyl ions by peroxide in alkaline media. Nash *et al.* (1980) reported that Pu(VI) in a 3 mM H_2O_2/0.05 M $NaHCO_3$ solution is reduced to Pu(V) via an intermediate reddish-brown colored complex, which was assumed to be a 1:1 Pu(VI) peroxo complex. The rate of formation of this complex was determined to be $(6.9 \pm 0.8) \times 10^3\ M^{-1}\ s^{-1}$ in 0.05 M $NaHCO_3$ (Nash *et al.*, 1980).

(*ii*) *Carboxylate and polyaminocarboxylate complexes*

Plutonium complexes with carboxylates and polyaminocarboxylic acids are important in separations, decontamination, and environmental migration. They have also been studied to achieve a better understanding of fundamental aqueous actinide chemistry. Owing to their multiple anionic chelating oxygen donor atoms, these ligands form highly stable and soluble complexes with plutonium ions. Solution complex formation constants for the plutonium species follow the usual trend where Pu(IV) complexes are the most stable and Pu(V) complexes the least stable. These ligands and other multidentate chelating organic acids stabilize Pu(IV) complexes to such a great extent, that under most conditions plutonium ions of the other oxidation states are rapidly oxidized/reduced to the tetravalent state.

Many studies have been reported for plutonium complexes with citrate, tartrate, malonate, glycine, and other carboxylates and amino acids, most recently by researchers at the Russian Academy of Sciences. Among these the acetate complexes are arguably the most comprehensively studied. The solution chemistry of plutonium complexes of other similar ligands can be inferred by considering the acetate complexes and the comparative basicity of the ligands; hence, only the acetate complexes will be discussed in this section. Among plutonium complexes of the amino polyacetates, iminodiacetate (IDA), nitrilotriacetate (NTA), ethylenediaminetetraacetate (EDTA), diethylenetriamine pentaacetate (DTPA), and derivatives, the EDTA complexes have been studied most extensively and used most broadly in applications. The pentaacetate analog, DTPA, has special application for treatment of internal human plutonium contamination through chelation therapy. The stoichiometry and stability of plutonium polyacetate solution complexes are generally known from spectrophotometric and potentiometric titration experiments. Solution and solid-state structures have been proposed by inference. The chemistry of the lower valent ions, Pu^{3+} and Pu^{4+} is comparative and will be described first, followed by that of the higher oxidation state ions, PuO_2^+ and PuO_2^{2+}. Formation constants for selected carboxylate and aminocarboxylate ligands are given in Table 7.57.

Pu(III) and (IV). Acetate complexes of Pu(III) have been studied primarily for stabilization with respect to oxidation to Pu(IV). Each of the stepwise complexation species from the mono- to pentaacetate has been reported. The formation constants for the first two species are $\log_{10}\beta_1 = 2.02$ and $\log_{10}\beta_2 = 3.34$ in 0.3 M $NaClO_4$ (Moskvin, 1969; Nair and Joshi, 1981). These constants have been reported from independent studies and compare well with values reported for acetate complexes of trivalent lanthanides. The limiting pentaacetate complex has an estimated formation constant of $\log_{10}\beta_5 = 16.7$ (Cleveland, 1979), which is high relative to the formation constants for the mono- and bis complexes and may therefore be considered an upper limit. Similarly, stepwise constants for Pu(IV) have been reported. Values for the first and limiting (penta) species are known with the greatest certainty, $\log_{10}\beta_1 = 5.31$ and $\log_{10}\beta_5 = 22.6$ (Cleveland, 1979). Solid-state structures of the lower valent plutonium acetate complexes are not known.

Plutonium(III) complexes of NTA^{3-} and $EDTA^{4-}$ have been studied directly by optical spectroscopy, voltammetry, and cation exchange, as well as indirectly in the study of Pu(IV) EDTA complexes at very low pH. Multiple species have been identified from pH and ligand titration experiments. In solutions with pH > 5, Pu(III) complexes are rapidly oxidized to Pu(IV). Studies at low pH have yielded the formation constant for the Pu(NTA) complex of $\log_{10}\beta_1 = 10.26$ (Merciny *et al.*, 1978; Anderegg, 1982). The protonated species Pu(EDTA)H forms in strong acid solutions and is deprotonated to $Pu(EDTA)^-$ above pH 3, and then to the mixed EDTA hydroxo complex, $Pu(EDTA)(OH)^{2-}$. Solution formation constants for the first complex and protonated forms have been reported from multiple independent studies (Cauchetier and Guichard, 1973; Merciny *et al.*, 1978). A value for the stability constant of the binary, deprotonated species, $Pu(EDTA)^-$, $\log_{10}\beta_1 = 16.1$ is reported in a critical review of EDTA thermodynamic data (Anderegg, 1977). $DTPA^{5-}$, with an additional bidentate acetate group, forms a more stable 1:1 complex with Pu^{3+}, $\log_{10}\beta_1 = 21.5$ (Merciny *et al.*, 1978).

Tetravalent plutonium–EDTA complexes are important because EDTA stabilizes Pu^{4+} over all other oxidation states sufficient for use in chemical processing, and because the complexes may promote the transport of plutonium contamination in the environment. Studies of Pu–EDTA complexation are challenging because of the extreme hydrolysis of Pu^{4+} and low solubility of

Table 7.57 *Formation constants for selected organic acids and aminopolycarboxylates.*

Ligand	*Complex*	Pu^{+3}	Pu^{+4}	PuO_2^+	PuO_2^{2+}	*References*
acetate, Ac^-	[ML]/[M][L]	2.02	5.31		2.2	Moskvin (1969), Nair and Joshi (1981), Cleveland (1979), Magon *et al.* (1968), and Eberle and Wade (1970)
	$[ML_2]/[M][L]^2$	3.34			3.6	Moskvin (1969) and Nair and Joshi (1981)
	$[ML_5]/[M][L]^5$	16.7	22.6			Cleveland (1979)
IDA^{2-}	[ML]/[M][L]			6.2	8.5	Eberle and Wade (1970) and Cassol *et al.* (1973)
NTA^{3-}	[ML]/[M][L]	10.3	12.9	6.8		Merciny *et al.* (1978), Anderegg (1982), and AlMahamid *et al.* (1996)
$EDTA^{4-}$	[ML]/[M][L]	16.1	26.4	12.3	14.6	Anderegg (1977), Boukhalfa *et al.* (2004), and Cauchetier and Guichard (1975)
	$[ML_2]/[M][L]^2$		35.39			Boukhalfa *et al.* (2004)
$DTPA^{5-}$	[ML]/[M][L]	21.5	29.5			Merciny *et al.* (1978), Anderegg (1982), Moskvin (1969), and Nair and Joshi (1981)
$citrate^{2-}$	[ML]/[M][L]	8.9	15.6			Martell and Smith (2001)
	$[ML_2]/[M][L]^2$		29.8			
$lactate^-$	$[ML_4]/[M][L]^4$		16.2			Martell and Smith (2001)
$oxalate^{2-}$	[ML]/[M][L]		8.30		6.6	Martell and Smith (2001) and Rogozina *et al.* (1973)
	$[ML_2]/[M][L]^2$	9.3	14.9		9.4	
	$[ML_3]/[M][L]^3$	9.4	23.4			
	$[ML_4]/[M][L]^4$	9.9	27.5			
$malonate^{2-}$	[ML]/[M][L]				4.8	Martell and Smith (2001) and Rogozina *et al.* (1973)
$succinate^{2-}$	[ML]/[M][L]				3.4	Martell and Smith (2001)
$glutamate^{2-}$	[ML]/[M][L]	4.7				Martell and Smith (2001) and Rogozina *et al.* (1973)
$aspartate^{2-}$	[ML]/[M][L]	4.8				Martell and Smith (2001) and Rogozina *et al.* (1973)
$glycinate^-$	[ML]/[M][L]	3.2				Martell and Smith (2001) and Rogozina *et al.* (1973)

plutonium hydroxides, inherent limits of analytical and spectrophotometric techniques, large number of potential species, precipitation of EDTA in strong acid solution, and uncertainties in experimental proton concentrations. Despite these limitations, solubility, potentiometric, spectrophotometric, and electrochemical studies provide species formulations that are consistent between techniques (Cauchetier and Guichard, 1973; Rai *et al.*, 2001; Boukhalfa *et al.*, 2004).

In acidic solution ($pH < 4$) and at 1:1 ligand to metal ratio, Pu(EDTA) is the predominant species, with an overall formation constant of $\log_{10} \beta_1 = 26.44$ in 1 M (Na,H)ClO_4. The absorption maximum of the binary complex is at 496 nm. At higher pH the hydrolysis species $Pu(EDTA)(OH)^-$ and $Pu(EDTA)(OH)_2^{2-}$ form with the corresponding overall stability constants of $\log_{10} \beta = 21.95$ and 15.29, respectively. The reduction potential of the complex Pu(EDTA) at $pH = 2.3$ is reported to be $E_{1/2} = 342$ mV (vs SHE). It was recently determined that under conditions of neutral pH and excess EDTA relative to Pu^{4+}, a second ligand coordinates to the ion. The formation of such species, as well as mixed-ligand EDTA complexes, can be anticipated knowing that the Pu^{4+} ions may accommodate up to 12 ligand donor atoms in their inner coordination sphere as in the hexanitrato structure, **19**. The bis chelate complex, $Pu(EDTA)_2^{4-}$, forms with an overall formation constant of $\log_{10} \beta = 35.39$ (Boukhalfa *et al.*, 2004). In the presence of ancillary ligands, mixed-ligand complexes form, as exemplified by the citrate and carbonate complexes $Pu(EDTA)(citrate)^{3-}$ and $Pu(EDTA)(CO_3)^{2-}$ (Boukhalfa *et al.*, 2004).

Dissolution of Pu(IV) hydrous oxides, PuO_2, $PuO_2 \cdot xH_2O$, and '$Pu(OH)_4$' in the presence of EDTA has been studied both to understand how EDTA may promote plutonium solubility in waste and the environment and as a method to determine the thermodynamic stability of the resulting Pu–EDTA solution complexes. Dissolution rates of 0.0074 and 0.42 μmol g^{-1} day^{-1} Pu in the presence of 10 mM EDTA were measured for the oxide and hydroxide, respectively, in a study that measured the solubility over months (Ruggiero *et al.*, 2002). A faster dissolution rate for the oxide has been reported in a study of shorter duration (Rai *et al.*, 2001).

DTPA solution complexes have been studied in pure solutions using the same methods as those employed for the EDTA and NTA complexes. The formation constants are less accurately known because they have been studied by fewer researchers, but mostly because they form in highly acidic solutions where there is uncertainty in the proton concentration and the protonation state of DTPA. The constant, $\log_{10} \beta_1 = 29.5$, can be considered a best estimate (Moskvin, 1971b). Given the high stability constant and positive results from plutonium complexation in aqueous solution, DTPA has been studied as a plutonium decontamination agent (Stradling *et al.*, 1989). It is highly effective in chelating plutonium in complex media that mimic physiological environments, and is the standard against which other potential therapeutic agents are measured. The efficacy of plutonium solubilization and complexation by DTPA has been studied in blood, urine, and cells (Rosenthal *et al.*, 1975). Most mammalian studies are done with Zn and Ca salts ($CaNa_3DTPA$ or $ZnNa_3DTPA$) since early chelation therapy studies indicated that these essential metals were scavenged and depleted in the body. For a more detailed account of *in vivo* actinide chelation, the reader is referred to chapter 31 of this work.

Pu(v) and (vi). Plutonium(vi) acetate complexes have been well studied in solution, and characterized in detail in the solid state. Plutonium(v) acetate complexes are not stable with respect to oxidation or reduction, depending on the solution conditions. Spectrophotometric and potentiometric studies have yielded the following average formation constants for plutonium(vi) acetates $\log_{10}\beta_1 = 2.2$, $\log_{10}\beta_2 = 3.6$, and $\log_{10}\beta_3 = 5.0$, in 1.0 M $(Na,H)ClO_4$ (Magon *et al.*, 1968; Moskvin, 1969; Eberle and Wade, 1970; Cleveland, 1979). In the presence of alkali ions, triacetate complexes of the form $MAnO_2(CH_3COO)_3$ precipitate from solutions containing Pu(vi). The cubic pink sodium plutonyl acetate and the analogous cesium salt are the most studied (Jones, 1955).

Plutonium(v) and plutonium(vi) aminocarboxylate complexes have been identified in electrochemical and pH titration studies (Cauchetier and Guichard, 1975). A stability constant for the complex of Pu(v) with NTA^{3-} was reported to be $\log_{10}\beta_1 = 6.8$ in 0.1 M $(Na,H)ClO_4$ (AlMahamid *et al.*, 1996) consistent with a number of previous studies (Eberle and Wade, 1970). The related iminodiacetate (IDA^{2-}) complex has a reported formation constant $\log_{10}\beta_1 = 6.2$ (Eberle and Wade, 1970), which as expected is somewhat lower than the constant for the Pu(v) complex with NTA^{3-}. A stability constant for a Pu(v) complex with $EDTA^{4-}$ has been estimated to be $\log_{10}\beta_1 = 12.3$ from spectrophotometric titrations (Cauchetier and Guichard, 1975). The reduction to Pu(iv) proceeds at a rate that depends on pH, plutonium concentration, and the ligand to metal ratio. At neutral pH and submicromolar plutonium

Table 7.58 *Formation constants and Gibbs energies for selected aqueous plutonium halides.*[a]

Species	*Reaction*	$\log_{10}\beta^{\circ}_{n}$	$\Delta_r G^{\circ}_m$ (kJ mol^{-1})
PuF^{3+}	$F^- + Pu^{4+} \rightleftarrows PuF^{3+}$	8.84 ± 0.10	−50.46 ± 0.57
PuF_2^{2+}	$2F^- + Pu^{4+} \rightleftarrows PuF_2^{2+}$	15.7 ± 0.2	−89.62 ± 1.14
PuO_2F^+	$F^- + PuO_2^{2+} \rightleftarrows PuO_2F^+$	4.56 ± 0.20	−26.03 ± 1.14
PuO_2F_2 (aq)	$2F^- + PuO_2^{2+} \rightleftarrows PuO_2F_2(aq)$	7.25 ± 0.45	−41.38 ± 2.57
$PuCl^{2+}$	$Cl^- + Pu^{3+} \rightleftarrows PuCl^{2+}$	1.2 ± 0.2	−6.85 ± 1.14
$PuCl^{3+}$	$Cl^- + Pu^{4+} \rightleftarrows PuCl^{3+}$	1.8 ± 0.3	−10.27 ± 1.71
PuO_2Cl^+	$Cl^- + PuO_2^{2+} \rightleftarrows PuO_2Cl^+$	0.23 ± 0.03	−1.31 ± 0.17
PuO_2Cl_2 (aq)	$2Cl^- + PuO_2^{2+} \rightleftarrows PuO_2Cl_2(aq)$	−1.15 ± 0.30	6.56 ± 1.71
$PuBr^{3+}$	$Br^- + Pu^{4+} \rightleftarrows PuBr^{3+}$	1.6 ± 0.3	−9.13 ± 1.71
PuI^{2+}	$I^- + Pu^{3+} \rightleftarrows PuI^{2+}$	1.1 ± 0.4	−6.28 ± 2.28

[a] Data from Lemire *et al.* (2001).

concentrations, the higher oxidation states can persist in the presence of excess NTA and EDTA for weeks (AlMahamid *et al.*, 1996). For Pu(VI), stability constants have been reported for the complexes with IDA^{2-} and $EDTA^{4-}$, $\log_{10}\beta_1 = 8.5$ (Cassol *et al.*, 1973), $\log_{10}\beta_1 = 14.6$ (Cauchetier and Guichard, 1975), respectively. Comparable constants reported for uranyl aminocarboxylates and for other ligand complexes of Pu(VI), suggest that these constants, while not yet confirmed by multiple independent studies, accurately describe the stability of the solution species.

(*iii*) *Halides*

Halide complexes were among the first complexes studied for plutonium and the fluorides and chlorides are of particular importance in plutonium purification and metal production as discussed in Sections 7.5 and 7.7.1. The formation constants for aqueous halide complexes of plutonium(III, IV, and VI) that have been critically evaluated by the NEA reviewers are listed in Table 7.58 (Lemire *et al.*, 2001; Guillaumont *et al.*, 2003). Only the addition of one or two halide ligands to any plutonium aqueous species is considered reliably established by these reviewers.

Many double salts of plutonium(III–VI) fluorides and chlorides have been reported (see Tables 7.46 and 7.47) and these salts have been prepared by aqueous or high temperature methods or combinations of these methods as described in Section 7.8.6(d). Where XRD data are available, the plutonium salts are usually observed to be isostructural with analogous compounds for thorium, uranium, neptunium, or the early lanthanides. For example, K_2PuCl_5 is isostructural with K_2PrCl_5 (Axler *et al.*, 1992) and $[K(18\text{-Crown-}6)]_2PuO_2Cl_4$ is isostructural with $[K(18\text{-Crown-}6)]_2UO_2Cl_4$ (Danis *et al.*, 2001; Clark, in preparation).

(*iv*) *Cation–cation complexes*

Owing to the linear structure and primary ionic bonding in the equatorial plane of actinyl ions AnO_2^{2+} and AnO_2^{+} (see Section 7.9.3), the oxygen atoms within these ions have a negative charge and can form bonds with a second metal center to produce 'cation–cation' complexes. This type of interaction was first characterized for UO_2^{2+} and NpO_2^{+} (Sullivan *et al.*, 1961), and is most well known for NpO_2^{+} (Stout *et al.*, 1993). For example, the structure of $NpO_2(ClO_4)\cdot 4H_2O$ consists of layers of NpO_2^{+} cations where axial O=Np=O units link to the equatorial plane of adjacent NpO_2^{+} units (Grigor'ev *et al.*, 1995). Interactions of this type have also been observed for the plutonyl ions. Newton and Burkhart (1971) oxidized Pu(IV) with Cr(VI) in dilute $HClO_4$ solution to form a $CrOPuO^{4+}$ cation, and recovered the complex by ion exchange. Photoacoustic spectroscopy was used to estimate an equilibrium constant of $K = (2.2 \pm 1.5)$ L mol^{-1} for the interaction between UO_2^{2+} and PuO_2^+ in a 6.0 M perchlorate solution (Stoyer *et al.*, 2000).

7.9.2 Nonaqueous and organometallic chemistry

There is an extensive literature on the nonaqueous and organometallic coordination chemistry of the light actinide elements thorium and uranium. A good deal of this chemistry should, in principle, be accessible to plutonium. Extending this chemistry to plutonium and other transuranium elements would be of great value in elucidating trends in structure and bonding across the actinide series. Unfortunately, the corresponding plutonium chemistry is virtually unexplored, clearly due to the extreme difficulty associated with handling plutonium isotopes, the paucity of synthetic laboratories equipped to conduct this kind of chemical research, and the scarcity of suitable starting materials. The known chemistry has been summarized in several excellent reviews by Ephritikhine (1992), Burns and Sattelberger (2002), Burns *et al.* (2005), and Burns and Eisen in Chapter 25 of this work.

(a) Sigma-bonded ligands

(*i*) *Organic-solvent soluble halides*

As discussed in Section 7.8.6(b), the binary trihalides, PuX_3 (X = F, Cl, Br, I) are polymeric solids that are insoluble in polar organic solvents. Therefore, the PuX_3 compounds have not been particularly useful starting materials for the nonaqueous preparation of other inorganic or organometallic complexes. Over the last two decades, there has been considerable effort to develop organic-solvent soluble forms of plutonium trihalides. Karraker (1987) reported the reaction between alpha plutonium metal and 1,2-diiodoethane in tetrahydrofuran (THF) solvent to give the solvated triiodide complex $PuI_3(THF)_x$, and suggested that such complexes would be useful synthetic starting materials for preparation of nonaqueous inorganic and organometallic compounds. Zwick, Avens and coworkers subsequently reported that stoichiometric amounts of elemental iodine would oxidize plutonium metal in aprotic, coordinating solvents such as THF, pyridine (Py), or dimethylsulfoxide (DMSO) to give hydrocarbon soluble Lewis base adducts of formula PuI_3L_4 in extremely high yields (Zwick *et al.*, 1992; Avens *et al.*, 1994). Unlike the corresponding reaction between uranium metal and iodine, there is no need to rigorously remove any oxide coating from the surface of plutonium metal. The reaction is exothermic, however, and will cause the solvent to boil if the rate of iodine addition is too rapid.

$$2Pu + 3ICH_2CH_2I \xrightarrow[THF]{} 2PuI_3(THF)_x + 3C_2H_4 \qquad (7.140)$$

$$2\text{Pu} + 3\text{I}_2 \underset{\text{L}}{\longrightarrow} 2\text{PuI}_3\text{L}_4, \quad (\text{L} = \text{THF, Py, DMSO}) \qquad (7.141)$$

Infrared spectra of PuI_3L_4 compounds are virtually identical to their UI_3L_4 counterparts, and show vibrational bands characteristic of coordinated ligands. Thermogravimetric analysis demonstrated that upon heating PuI_3L_4, all four coordinated solvent molecules are displaced between 56 and 180°C to give anhydrous PuI_3. Room temperature ^1H NMR spectra of $PuI_3(THF)_4$ in $CDCl_3$ solution shows a single THF ligand environment, consistent with the spectra of the $NpI_3(THF)_4$ and $UI_3(THF)_4$ analogs (Avens *et al.*, 1994). Unlike the uranium and neptunium analog spectra, $PuI_3(THF)_4$ shows reasonably sharp ^1H NMR resonances ($\Delta v_{1/2} = 11.4$ Hz). Subsequent variable temperature ^1H NMR experiments in CD_2Cl_2 solution revealed a dynamic solution process that generates equivalent THF ligand resonances at room temperature, but freezes out a static structure at –90°C with two types of coordinated THF ligand consistent with the solid-state structure of $UI_3(THF)_4$ (**21**). The NMR data were interpreted in terms of the dynamic equilibrium between **21** and **22** shown below. Therefore, while no crystallographic data have been presented for $PuI_3(THF)_4$, the detailed characterization of the series of $AnI_3(THF)_4$ complexes (An = U, Np, Pu) leaves little doubt that in the solid state, the molecule displays the pentagonal bipyramidal coordination geometry, with two trans iodide ligands occupying apical coordination sites, and the third iodide and four THF ligands lying in the equatorial plane as shown in **21** below.

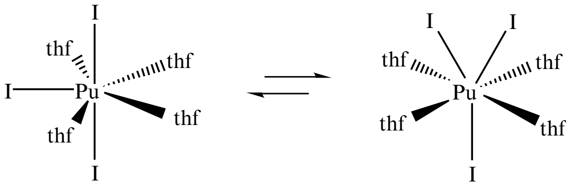

21 **22**

In a variation of the oxidative dissolution of plutonium metal, Enriquez *et al.* (2003) found that plutonium metal will also dissolve in acetonitrile solvent in the presence of three equivalents of thallium or silver hexafluorophosphate as the oxidant to give a blue solution containing $Pu(NCMe)_9^{3+}$. Filtration and cooling gives crystals of $[Pu(NCMe)_9][PF_6]_3 \cdot MeCN$.

$$\text{Pu} \xrightarrow[\text{MeCN}]{3\text{MPF}_6} [\text{Pu(NCMe)}_9][\text{PF}_6]_3 \cdot \text{MeCN}, \quad (\text{M} = \text{Ag, Tl}) \qquad (7.142)$$

The solid-state crystal structure reveals a $Pu(NCMe)_9^{3+}$ cation surrounded by three noncoordinating PF_6^- anions. The $Pu(NCMe)_9^{3+}$ ion displays a nine-coordinate tricapped trigonal prismatic coordination environment as shown in **23**. There is little variation in the Pu–N bond distances between apical and capping ligands, which span the narrow range between 2.554(4) and 2.579(5) Å.

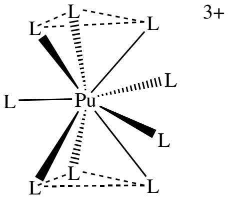

23

While binary $PuCl_4$ is unstable in the solid state (see Section 7.8.6(b)), it can be stabilized by formation of Lewis base adducts. Bagnall and coworkers showed that the reaction of Cs_2PuCl_6 with amide ($RCONR'_2$) or phosphine oxide (R_3PO) ligands in dichloromethane or acetonitrile solvent gives the Lewis base adducts $PuCl_4L_2$ or $PuCl_4L_3$, depending on the steric demands of the Lewis base (Bagnall *et al.*, 1961, 1985a). These adducts were characterized by IR, diffuse reflectance, and X-ray powder diffraction. In many cases, the solids were reported to be isostructural with thorium or uranium counterparts. The $PuCl_4L_2$ complexes were presumed to contain a pseudo-octahedral plutonium center, with trans Lewis base ligands. These Lewis base adducts have the potential to serve as good synthetic starting materials, though their general utility has yet to be explored.

(*ii*) *Amides*

The Lewis base adducts of plutonium triiodide have proven to be useful starting materials for the preparation of a number of trivalent organometallic and nonaqueous coordination compounds. A THF slurry of $PuI_3(THF)_4$ reacts smoothly at room temperature with three equivalents of $NaN(SiMe_3)_2$ to give an air-sensitive yellow-orange $Pu[N(SiMe_3)_2]_3$ in 93–95% yield (Zwick *et al.*, 1992; Avens *et al.*, 1994).

$$PuI_3(THF)_4 + 3NaN(SiMe_3)_2 \xrightarrow{THF} Pu[N(SiMe_3)_2]_3 + 3NaI \qquad (7.143)$$

The tris silylamide complex sublimes at 60°C under reduced pressure, gives an elemental analysis consistent with the formulation of $Pu[N(SiMe_3)_2]_3$, and shows a single ^1H NMR resonance at $\delta = 0.7$ ppm. The infrared spectra display vibrational features nearly identical to the uranium counterpart, and reveal the asymmetric $\nu(PuNSi_2)$ stretch at 986 cm^{-1}. Based on the similarity in spectroscopic properties, it is presumed that this compound will display the well-established pyramidal structure that is shared by the uranium and lanthanide analogs as indicated in **24**.

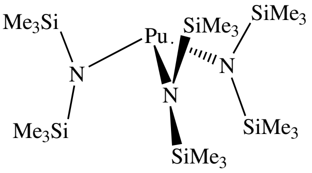

24

(*iii*) *Alkoxides*

Zwick and coworkers reported that the alcoholysis of $Pu[N(SiMe_3)_2]_3$ with the sterically demanding $2,6\text{-}Bu^t_2C_6H_3(OH)$ gives the tan, air-sensitive tris aryloxide derivative $Pu(O\text{-}2,6\text{-}Bu^t_2C_6H_3)_3$ in 70% yield (Zwick *et al.*, 1992). The structural formulation as a monomeric compound is based on the similarity of spectroscopic data (^1H NMR and IR) to the well-characterized uranium analog which shows a monomeric structure in the solid state (Van der Sluys *et al.*, 1988).

$$Pu[N(SiMe_3)_2]_3 + 3HO\text{-}2,6\text{-}Bu^t_2C_6H_3 \xrightarrow{\text{hexane}} Pu(O\text{-}2,6\text{-}Bu^t_2C_6H_3)_3 + 3HN(SiMe_3)_2 \qquad (7.144)$$

The tris aryloxide complex will coordinate Lewis bases to form $LPu(O\text{-}2,6\text{-}Bu^t_2C_6H_3)_3$ complexes (shown in **25**), where L is triphenylphosphine oxide, 4,4′-dimethoxybenzophenone, or *N*,*N*-di-isopropyl-benzamide (Oldham *et al.*, 2000). The relative binding affinities were found to correspond with that observed in process extraction chemistry (see Section 7.5.4), with the phosphine oxide and benzamide showing similar binding affinities, which were much larger than that of the benzophenone. Kinetic investigations of the self-exchange process probed by ^{31}P NMR spectroscopy yielded activation parameters indicative of an associative process, with a five-coordinate $L_2Pu(O\text{-}2,6\text{-}Bu^t_2C_6H_3)_3$ intermediate (**26**).

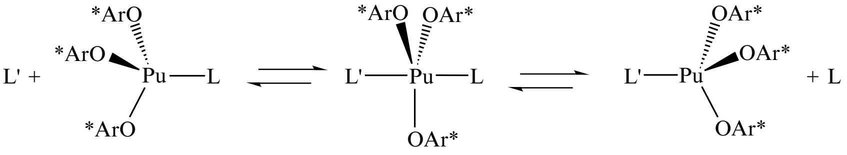

25 **26** **25**

Bradley and coworkers prepared aliphatic alkoxide complexes of general formula $Pu(OR)_4$ using $(Hpy)_2PuCl_6$ and benzene/alcohol solutions containing ammonia (Bradley *et al.*, 1957). With excess isopropanol, the reaction mixture was stirred with NH_3 at room temperature, and then the NH_4Cl and C_5H_6NCl salts removed by filtration. Solvent removal produced a mixture of grass-green $Pu(OPr^i)_4$ and $(Py)Pu(OPr^i)_4$. Recrystallization from isopropanol gives emerald green $Pu(OPr^i)_4(Pr^iOH)$. The base-free, homoleptic $Pu(OPr^i)_4$ compound sublimes at 220°C (0.05 mmHg). A similar reaction employing a large excess of *t*-butanol/benzene gave pale green $Pu(OBu^t)_4$, which sublimes at 112°C (0.05 mmHg). These aliphatic alkoxides were extremely sensitive to moisture, but appeared to be unaffected by dry air. No other characterization data have been reported.

$$(Hpy)_2PuCl_6 + xsPr^iOH \xrightarrow[NH_3/C_6H_6]{} Pu(OPr^i)_4(HOPr^i) + 4(NH_4)Cl + 2HpyCl \tag{7.145}$$

Very little is known about the trivalent isopropoxide, $Pu(OPr^i)_3$, although its use in catalytic reduction of ketones by isopropanol has been reported. Warner and coworkers examined the ability of trivalent and tetravalent lanthanide and actinide isopropoxides to facilitate the Meerwein–Ponndorf–Verley reduction of ketones (Warner *et al.*, 2000). Tetravalent $Pu(OPr^i)_4$ was found to be inactive in ketone reduction, but *in situ* production of $Pu(OPr^i)_3$ by dissolution of $Pu[N(SiMe_3)_2]_3$ in neat isopropanol generated an effective catalyst for the reduction of a range of substituted aryl-alkyl ketones, with yields that were equal or higher than similar reactions employing lanthanides.

(*iv*) *Alkyls*

There is only one example in the literature of an alkyl complex of plutonium, but its characterization data is limited to IR spectroscopy. Zwick and coworkers reported that the reaction of $Pu(O\text{-}2,6\text{-}Bu^t_2C_6H_3)_3$ with three equivalents of $LiCH(SiMe_3)_2$ in hexane solution yields yellow-brown $Pu[CH(SiMe_3)_2]_3$ as an oily solid (Zwick *et al.*, 1992). The IR spectrum was virtually identical to the well-characterized $U[CH(SiMe_3)_2]_3$ analog (Van der Sluys *et al.*, 1989). Other chemical characteristics, such as extreme sensitivity to air, rapid decomposition in solution, and thermal instability are consistent with this formulation. If the formulation is correct, then this complex would be an extremely rare example of a true organometallic complex of plutonium containing metal–carbon sigma bonds.

(*v*) *Borohydrides*

The first attempt to prepare plutonium borohydride was made by Schlesinger and Brown at the University of Chicago Metallurgical Laboratory in 1942 (Schlesinger and Brown, 1943). These authors tried to prepare plutonium borohydride in tracer quantities by reaction of uranium tetrafluoride containing trace amounts of plutonium with aluminum borohydride. Excess aluminum borohydride was removed and the reaction products that were volatile at 60°C were condensed at 20, 0, –23, –80, and –190°C. Only a few percent of the plutonium was recovered from the volatile fractions, the bulk of the plutonium remaining in the nonvolatile residue in the reaction vessel. It was therefore concluded that plutonium borohydride was either not formed or was not volatile at 60°C.

The first unequivocal preparation of plutonium(IV) borohydride was accomplished by Banks, Edelstein and coworkers (Banks *et al.*, 1978; Banks, 1979; Banks and Edelstein, 1980) at the Lawrence Berkeley Laboratory. Treatment of anhydrous PuF_4 with $Al(BH_4)_3$ at 0°C for 4 h in a solvent-free sealed tube reaction gives $Pu(BH_4)_4$ according to the reaction below.

$$PuF_4 + 2Al(BH_4)_3 \rightarrow Pu(BH_4)_4 + 2Al(BH_4)F_2 \qquad (7.146)$$

The unreacted $Al(BH_4)_3$ passes through a dry-ice trap and is collected in a liquid nitrogen trap. The $Pu(BH_4)_4$ is not as volatile and can be collected in the dry-ice trap. By intermolecular exchange in the gas phase with D_2, the deuterated compound $Pu(BD_4)_4$ may also be prepared. $Pu(BH_4)_4$ is a pyrophoric bluish-black liquid that melts at approximately 14°C. Infrared spectroscopy indicates that the compound adopts a monomeric pseudo-tetrahedral coordination geometry similar to $Zr(BH_4)_4$ and $Hf(BH_4)_4$ in the gas phase. Low temperature X-ray powder diffraction was consistent with this assessment, and suggests that the monomeric compound consists of a tetrahedral arrangement of four BH_4^- units coordinated by three B–H bridges per borohydride, giving the 12-coordinate structure shown in **27** below.

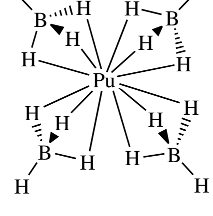

27

(b) Pi-bonded ligands

(*i*) *Cyclooctatetraene complexes*

The synthesis and characterization of the uranium(IV) sandwich complex, U(η-$C_8H_8)_2$, uranocene, was an important milestone in the history of organometallic chemistry, as it represented the logical extension of the bonding concepts that were developing for organotransition metal complexes (Seyferth, 2004). It was only a few years later when the plutonium analog was reported.

Bis(cyclooctatetraenyl)plutonium, or 'plutonocene' has been prepared by metathesis of $[NEt_4]_2[PuCl_6]$ with two equivalents of $K_2(C_8H_8)$ in THF solution to give a bright red product (Karraker *et al.*, 1970). Alternatively, $Pu(C_8H_8)_2$ may be prepared by reaction of degassed cyclooctatetraene, C_8H_8, with finely divided plutonium metal (prepared through hydride–dehydride cycles) in a sealed glass tube. The reaction mixture was heated at 160°C for 15 min, producing a red sublimate of $Pu(C_8H_8)_2$ (Starks and Streitwieser, 1973). Plutonocene reacts rapidly with air, and is only sparingly soluble in aromatic and chlorinated hydrocarbon solvents.

$$(NEt_4)_2PuCl_6 + 2K_2C_8H_8 \rightarrow Pu(\eta\text{-}C_8H_8)_2 + 2(NEt_4)Cl + 4KCl \qquad (7.147)$$

$$Pu + 2C_8H_8 \rightarrow Pu(\eta\text{-}C_8H_8)_2 \qquad (7.148)$$

The hydrocarbon solution solubility of plutonocene is enhanced by adding alkyl groups to the C_8H_8 rings. A number of alkyl substituted derivatives have been prepared, including $Pu(EtC_8H_7)_2$, $Pu(Bu^nC_8H_7)_2$, and $Pu(Bu^tC_8H_7)_2$ using the metathesis route employing $[NEt_4]_2[PuCl_6]$ and the potassium salt of the annulene dianion (Karraker, 1973; Eisenberg *et al.*, 1990). The tetramethyl-substituted complex $Pu(1,3,5,7\text{-}Me_4C_8H_4)_2$ was originally claimed (Solar *et al.*, 1980), but subsequent studies on other alkyl substituted complexes led Streitwieser to conclude that this compound was almost certainly the trivalent complex $[K(THF)_2][Pu(1,3,5,7\text{-}Me_4C_8H_4)_2]$ (Eisenberg *et al.*, 1990).

Single crystal XRD studies on $U(C_8H_8)_2$ shows that this molecule adopts a sandwich-type structure with the uranium center sandwiched between two planar C_8H_8 rings in rigorous D_{8h} symmetry (Zalkin and Raymond, 1969; Avdeef *et al.*, 1972). X-ray powder diffraction, infrared, electronic absorption, solution NMR, and Mössbauer spectroscopy reveal that the neptunium and plutonium analogs maintain the identical D_{8h} structure as shown in **28** (Karraker *et al.*, 1970; Karraker, 1973; Eisenberg *et al.*, 1990). Plutonocene is unique in that it has a $J = 0$ ground state with temperature-independent paramagnetism. Optical spectroscopy shows electronic transitions with intensities approaching 1000 (L mol^{-1} cm^{-1}), which argued against the assignment as 5f–5f transitions, and suggested an unusual 5f–6d orbital mixing with appreciable covalency in the bonding (Karraker *et al.*, 1970; Hayes and Edelstein, 1972).

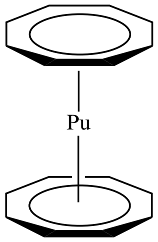

28

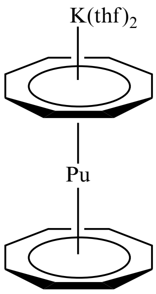

29

A number of trivalent plutonocene complexes of the type $[K(THF)_2][Pu(RC_8H_7)_2]$ have been prepared, where R = an alkyl group or H. These are prepared by reaction of $PuBr_3$ or PuI_3 with $K_2(RC_8H_7)$ in THF solution at –10 to –20°C (Karraker and Stone, 1974). These complexes may also be prepared by the direct reaction of potassium metal with $Pu(RC_8H_7)_2$ in THF solution (Eisenberg *et al.*, 1990).

$$PuX_3 + 2K_2C_8H_8 \underset{\text{THF}}{\longrightarrow} [K(THF)_2][Pu(\eta\text{-}C_8H_8)_2] + 3KX \ (X = Br, I) \quad (7.149)$$

$$Pu(\eta\text{-}C_8H_8)_2 + K \underset{\text{THF}}{\longrightarrow} [K(THF)_2][Pu(\eta\text{-}C_8H_8)_2] \quad (7.150)$$

The trivalent $[K(THF)_2][Pu(C_8H_8)_2]$ complex was described as turquoise-green, and it has been characterized by elemental analysis, X-ray powder diffraction, and magnetic susceptibility measurements (Karraker and Stone, 1974). The lime green $[K(THF)_2][Pu(Bu^tC_8H_7)_2]$ was not isolated, but was produced *in situ* in deuterated THF solvent, and characterized by ^1H NMR (Eisenberg *et al.*, 1990). The change in chemical shifts in the NMR spectrum with temperature was indicative of paramagnetic behavior expected for Pu(III). The solid-state structure of the uranium analog, $[K(diglyme)][U(C_8H_8)_2]$ has been determined by single crystal XRD revealing that the potassium ion is also involved in a multihapto interaction with a C_8H_8 ring. The X-ray powder diffraction data on the plutonium analogs indicate similar structures, as shown in **29** (Karraker and Stone, 1974).

(*ii*) *Cyclopentadienyl complexes*

Cylcopentadienyl ligands (C_5H_5, Cp) have played a central role in the development of the field of organometallic chemistry. The same is true in the field of organoactinide chemistry that was inaugurated with Reynolds and Wilkinson's seminal report on the preparation of $(C_5H_5)_3UCl$ in 1956 (Reynolds and Wilkinson, 1956). The first plutonium compounds containing cyclopentadienyl ligands were reported by Baumgärtner and coworkers in 1965 (Baumgärtner *et al.*, 1965).

The microscale reaction between anhydrous $PuCl_3$ and molten $(C_5H_5)_2Be$ at around 70°C produces tris(cyclopentadienyl)plutonium, $(C_5H_5)_3Pu$, (or Cp_3Pu) (Baumgärtner *et al.*, 1965). Fractional sublimation first removes unreacted $(C_5H_5)_2Be$, and allows the moss green $(C_5H_5)_3Pu$ product to be isolated at a sublimation temperature of approximately 170°C. The transmetallation using $(C_5H_5)_2Be$ has been very useful for preparing transplutonium tris(cyclopentadienyl) complexes, but the nuisance of α-n reactions between the plutonium and beryllium nuclei limit the scale of the reaction. To prepare larger quantities of $(C_5H_5)_3Pu$, Crisler and Eggerman (1974) turned to the reaction between plutonium chloride starting materials with sodium or magnesium metathesis reagents. Both $PuCl_3$ and Cs_2PuCl_6 react with $(C_5H_5)_2Mg$ in THF solution to yield an emerald green product. In THF solution the first product is most likely $(C_5H_5)_3Pu(THF)$, which loses the THF ligand during sublimation to yield $(C_5H_5)_3Pu$ at 140°C under reduced pressure. The reaction is over within minutes when Cs_2PuCl_6 is employed as compared to hours for the reaction with $PuCl_3$. This is most likely because Cs_2PuCl_6 contains discrete $PuCl_6^{2-}$ ions, while $PuCl_3$ displays an extended three-dimensional structure (see Section 7.8.6(b)). Tris(cyclopentadienyl)plutonium can also be prepared from the reaction of $PuCl_3$ with $(C_5H_5)Na$ in THF solution, but the reaction requires 10 days. Zwick and coworkers found that a very convenient way to circumvent this solubility problem is to react $PuI_3(THF)_4$ with three equivalents of $(C_5H_5)Li$ in THF solution (Zwick *et al.*, 1992).

$$2PuCl_3 + 3Be(C_5H_5)_2 \xrightarrow[\text{melt}]{70^\circ} 2(\eta\text{-}C_5H_5)_3Pu + 3BeCl_2 \tag{7.151}$$

$$PuCl_3 + 3Na(C_5H_5) \xrightarrow[\text{THF}]{} (\eta\text{-}C_5H_5)_3Pu(THF) + 3NaCl \tag{7.152}$$

$$2PuCl_3 + 3Mg(C_5H_5)_2 \xrightarrow[\text{THF}]{} 2(\eta\text{-}C_5H_5)_3Pu(THF) + 3MgCl_2 \tag{7.153}$$

$$PuI_3(THF)_4 + 3Li(C_5H_5) \xrightarrow[\text{THF}]{} (\eta\text{-}C_5H_5)_3Pu(THF) + 3LiI \tag{7.154}$$

X-ray powder diffraction data suggest that $(C_5H_5)_3Pu$ is isostructural with $(C_5H_5)_3Ln$ compounds. The lanthanide analogs have been shown to contain polymeric zigzag chains of distinct $(C_5H_5)_2Ln(\mu\text{-}\eta^2\text{-}\eta^5\text{-}C_5H_5)$ units (Hinrichs *et al.*, 1983).

Bagnall and coworkers reported that the reaction between $(C_5H_5)Tl$ and Cs_2PuCl_6 in acetonitrile solution does not give an overall reduction to trivalent plutonium as discussed above, but produces tetravalent $(C_5H_5)_3PuCl$ (Bagnall *et al.*, 1982a). The chloride can be replaced with thiocyanate via a simple metathesis reaction with stirring in a THF solution of K(NCS) for 16 h (Bagnall *et al.*, 1982a). Both the chloride and thiocyanate complexes are dark brown and moisture sensitive, and both are soluble in THF and acetonitrile solution. The anionic analog, $(C_5H_5)_3Pu(NCS)_2^-$, is also reported as a tetraphenylarsonium salt, but little characterization data have been reported (Bagnall *et al.*, 1982b).

$$Cs_2PuCl_6 + 3Tl(C_5H_5) \xrightarrow[CH_3CN]{} (\eta\text{-}C_5H_5)_3PuCl + 2CsCl \tag{7.155}$$

$$(\eta\text{-}C_5H_5)_3PuCl + K(NCS) \xrightarrow[THF]{} (\eta\text{-}C_5H_5)_3Pu(NCS) + KCl \tag{7.156}$$

The chloride compound, $(C_5H_5)_3PuCl$, was found to be isostructural with its uranium counterpart (Bagnall *et al.*, 1982a), which contains a pseudo-tetrahedral unit in which the centroids of the Cp rings occupy three vertices, and the chloride takes up the fourth as illustrated in **30**.

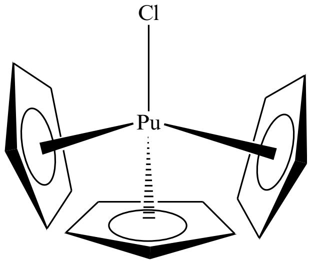

30

Bagnall and coworkers have prepared several examples of mono(cyclopentadienyl) plutonium complexes (Bagnall *et al.*, 1985b). Room temperature reaction of $(C_5H_5)Tl$ with $PuCl_4L_2$ or Cs_2PuCl_6 in dry acetonitrile for 48 h gave $(C_5H_5)PuCl_3L_2$ in 50–85% yield depending on the nature of the Lewis base, L. Neutral Lewis base ligands (L) included a number of phosphine oxide (R_3PO) and amide ($RCONR'_2$) derivatives. Similar reactions employing $(C_5H_5)Tl$ and $Pu(NCS)_4L_2$ produced the analogous $(C_5H_5)Pu(NCS)_3L_2$ complexes (Bagnall *et al.*, 1986). All of these materials have been characterized by infrared and Vis-NIR spectroscopy. It is assumed that these complexes adopt a structure similar to their uranium analogs.

7.9.3 Electronic structure and bonding

(a) Ionic and covalent bonding models

The nature of metal–ligand bonding in light actinide compounds and complexes is quite complicated. In general, the actinides are best viewed as being intermediate between the strongly ionic bonding observed in lanthanide elements, and the more covalent bonding observed in d-block transition elements. There are clearly cases that show ionic behavior, and there are just as clearly cases that show considerable covalency.

Many plutonium–ligand bonds are nondirectional, and determined largely by electrostatic attraction to the metal, electrostatic repulsion between ligands, and steric demands around the metal center. These metal–ligand bonds are relatively weak, and kinetically labile in solution. There are also examples of metal–ligand bonds that are incredibly strong, show a stereochemical orientation, and are kinetically inert. The former situation is often taken as evidence for ionic behavior, while the latter is clearly consistent with covalent interactions. The view that plutonium complexes are generally ionic is supported by the premise that the 5f orbitals are core-like in that they are so contracted they cannot interact in bonding with the ligands. This is generally what is observed, especially for the heavier actinide elements. However, the 5f orbitals of the lighter actinides are much less contracted, and there are certain classes of compounds where the 5f orbitals have been shown to play a significant role in covalent metal–ligand bonding. By consideration of the behavior of the 5f orbitals alone, it is difficult to reconcile these stark differences in chemical behavior.

This is an area where electronic structure calculations have taught us a great deal about how to think about the nature of chemical bonding in molecular plutonium complexes. Electronic structure calculations have demonstrated that for metal–ligand bonding in plutonium (and all light actinides) one cannot consider the 5f orbitals alone, but must consider the relative roles of both the virtual 5f and 6d orbitals as well as the 'semicore' 6s and 6p orbitals. The radial distributions of the plutonium 6s and 6p semicore orbitals lie in the valence region, and they must be considered as active in chemical bonding. In addition, the virtual 6d orbitals are relatively low-lying, and have far larger radial extent than the 5f orbitals. This is illustrated in the radial distribution function for a Pu^{3+} ion shown in Fig. 7.120 (Schreckenbach *et al.*, 1999). Most modern quantum chemical calculations find evidence of mixing of the 6p semicore orbital into metal–ligand bonding combinations. Moreover, there is now a general consensus that the dominant metal–ligand bonding takes place through ligand interactions with the 6d orbitals. The 6d orbitals are strongly split by the presence of a ligand field (as in transition element complexes), but the more contracted 5f orbitals show only weak splitting. The ground state electron configurations are therefore generally governed by the occupation of these closely spaced 5f orbitals, which leads to many open shell states. Spin–orbit coupling and electron correlation effects are extremely important, particularly for understanding spectroscopic properties. In addition to Chapter 17, several excellent reviews exist that describe trends and views on the electronic structure of actinide molecular complexes (Bursten and Strittmatter, 1991; Pepper and Bursten, 1991; Denning, 1992; Schreckenbach *et al.*, 1999; Matsika *et al.*, 2001).

(b) Specific examples

There are a number of specific examples in plutonium chemistry where covalency in metal–ligand bonding plays an important role in the observed chemical

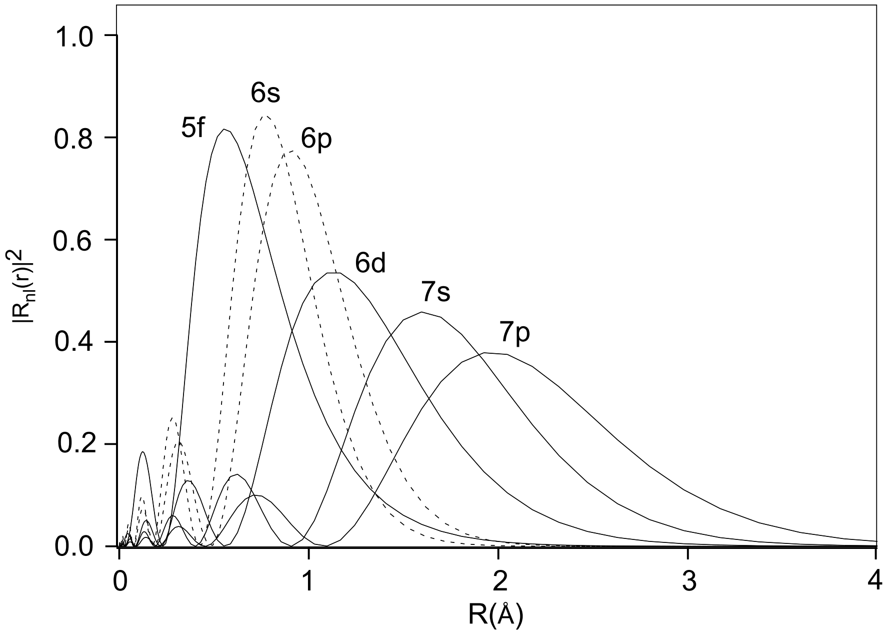

Fig. 7.120 *Radial probability densities of Pu*$^{3+}$ *valence orbitals from relativistic Hartree–Fock orbitals* $\Phi_{nl}(r)$ (*Schreckenbach* et al., 1999). *The authors are grateful to P.J. Hay of Los Alamos for providing the raw data used to prepare this figure.*

behavior. These are plutonium hexafluoride, PuF_6, the linear plutonyl cation, PuO_2^{2+}, and the organoplutonium sandwich compound plutonocene, Pu(η-$C_8H_8)_2$. We provide a qualitative discussion of the bonding in these systems, illustrate the main 6d and 5f orbital interactions, and highlight the 'strong field-weak field' differences in 6d and 5f interactions that make spin–orbit splitting important for understanding spectroscopic properties. Before discussing the examples, we remind the reader that unlike p- or d-orbitals, there is no unique way of representing the angular dependence functions of all seven f-orbitals. In high symmetry cubic point groups, a cubic set of orbitals is used, while in systems containing a high order axis of symmetry, a general set can be used. These two common sets of f-orbital depictions are simply linear combinations of each other, and they are illustrated qualitatively in Fig. 7.121. We will use both the general and cubic orbital sets in describing the bonding in our examples.

(*i*) *PuF*$_6$

As discussed in Section 7.8.6(a), plutonium hexafluoride is a stable molecule in the gas-phase. In view of the electronegativity difference between hexavalent plutonium and the fluoride anion, this observation might seem somewhat surprising in that one might expect Pu–F bonds to show the greatest ionic

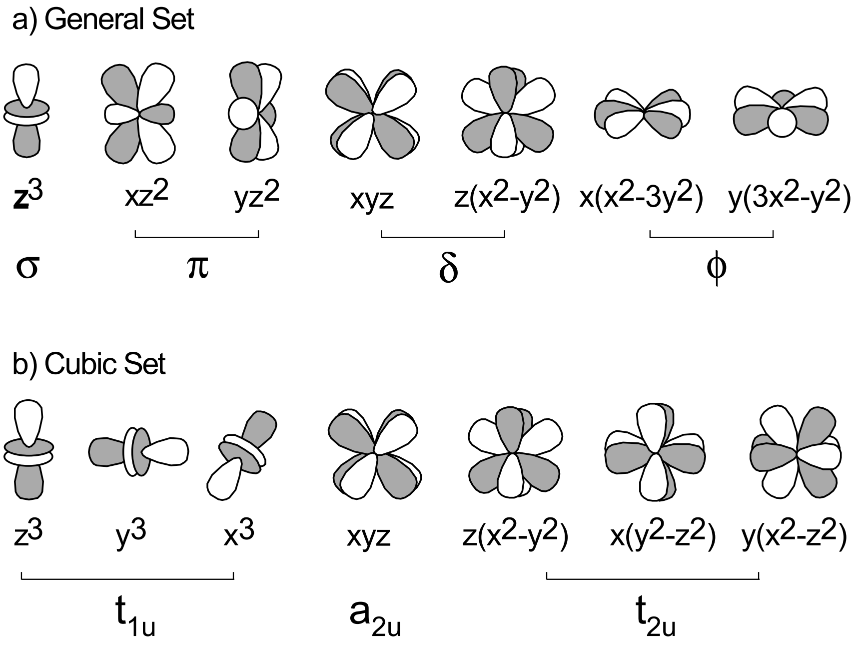

Fig. 7.121 *Qualitative representations of the general* (*a*) *and cubic* (*b*) *sets of valence f orbitals.*

behavior. Spectroscopic properties show that this is clearly not the case. Electronic structure calculations have provided some valuable insights into the nature of Pu–F bonding in this system.

A number of high-level electronic structure calculations have been performed on AnF_6 systems, with the majority of calculations performed on uranium. Calculations on PuF_6 have been reported by Kugel *et al.* (1976), Koelling *et al.* (1976), Boring and Hecht (1978), Wadt (1987), Hay and Martin (1998), Schreckenbach *et al.* (1999), and Onoe (1997). It is clear from all the theoretical calculations that the purely ionic bonding model is an inadequate description of PuF_6. A qualitative molecular orbital diagram for PuF_6 based on an octahedral ligand field that contains the basic features of these calculations is shown in Fig. 7.122. The octahedral point group is relatively straightforward as the 5f and 6d orbitals cannot mix by symmetry. The set of σ lone pairs on the six F atoms transform as $a_{1g} + e_g + t_{1u}$ symmetry under O_h symmetry. The 12 π lone pairs transform as $t_{1u} + t_{1g} + t_{2u} + t_{2g}$ under O_h symmetry. As expected, the set of σ lone pairs interacts most strongly with the Pu atom, resulting in molecular orbitals of a_{1g}, e_g, and t_{1u} symmetry which are lower-lying that the π symmetry orbitals. Of the four triply degenerate sets of F ligand π orbitals, the t_{2g} is of appropriate symmetry to interact with the 6d orbitals of the plutonium atom, the t_{2u} can interact with the 5f orbitals, and the t_{1g} orbital cannot interact with any low-lying metal orbitals, and should remain as an noninteracting set of lone pairs. The t_{1u} orbital can interact with the 5f orbitals of the plutonium atom, but it can also mix with the t_{1u} set of σ orbitals derived from mixing between the semicore 6p and valence 7p orbitals. From simple overlap considerations, one would expect the F lone pair t_{2u} and t_{2g} orbitals to be the most stabilized by donation to the metal, the t_{1g} will be entirely nonbonding, and the t_{1u} will stabilized by π bonding from above, but destabilized by mixing with the σ interaction from below. In all the calculations, appreciable covalency with both 5f and 6d orbitals is present. The covalent interactions are found in Pu–F σ- and π-bonding that takes place through t_{2g} and e_g interactions with Pu 6d orbitals, and σ bonding that takes place through t_{1u} interactions with the 5f and 6p/7p orbitals. These metal–ligand bonding interactions are illustrated qualitatively in the molecular orbital diagram of Fig. 7.122. Wadt employed a Mulliken population analysis to determine the relative amount of plutonium 5f and 6d contribution to bonding (Wadt, 1987). The σ and π components of the t_{1u} interactions are mixed, but the virtual $5t_{1u}$ orbital (the $3t_{1u}$ orbital in Fig. 7.122) was calculated to comprise 71% Pu f, 3% Pu p, and 26% F p character

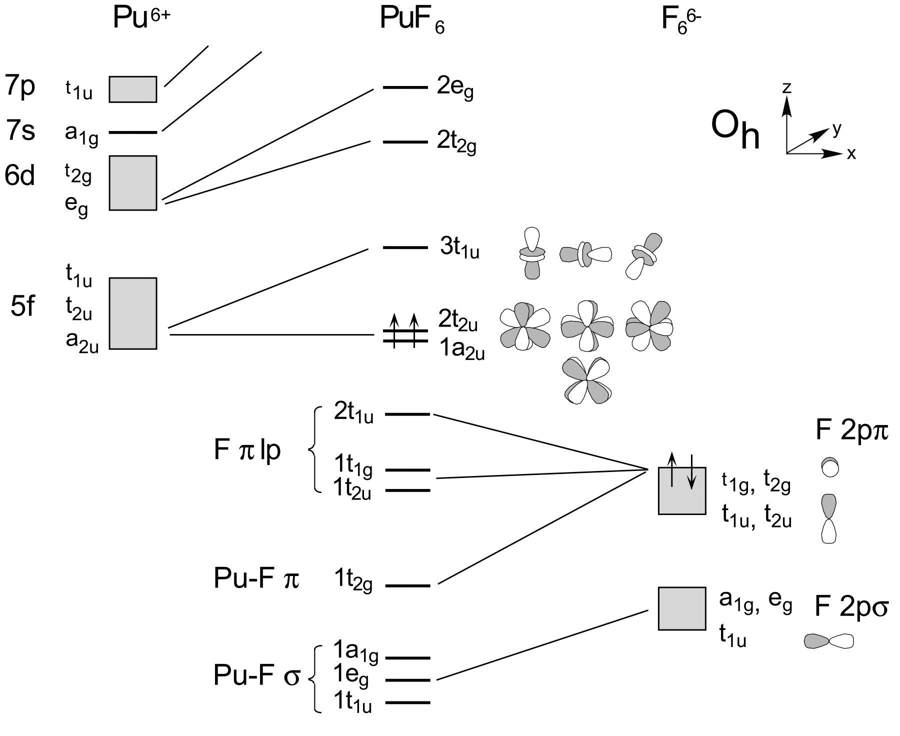

Fig. 7.122 *A qualitative molecular orbital interaction diagram for PuF_6.*

indicating a significant amount of covalency involving Pu 5f orbital interaction with the F ligands. It also shows the importance of mixing 'semicore' 6p character into a f–p σ hybrid orbital that enhances σ bonding. The total population of the Pu 5f orbitals was calculated to be 4.24. Since this system is nominally $5f^2$, the extra 2.24 electrons in 5f orbitals come from σ and π donation from occupied F ligand orbitals into Pu 5f orbitals.

For octahedral PuF_6, a simple filling of this qualitative MO scheme with the 16 valence electrons would give a valence electronic configuration $(1a_{2u})^2$ or $(1a_{2u})^1(2t_{2u})^1$ corresponding to $^1A_{1g}$ or $^3T_{1g}$ ground states, respectively. The 5f ordering in an octahedral ligand field is $a_{2u} < t_{2u} < t_{1u}$, and the calculations indicate that the $1a_{2u}$ and $2t_{2u}$ 5f orbitals are nearly degenerate, suggesting that the $^3T_{1g}$ state would be the likely ground state. This one-electron picture is oversimplistic, because the ligand field splitting of the 5f orbitals is so weak that spin–orbit effects must also be considered. Spin–orbit coupling splits the 5f manifold and gives a $^1\Gamma_{1g}$ (in O_h double group symmetry) ground state. The inclusion of spin–orbit coupling is necessary to understand the stabilization of a singlet ground state, and is in agreement with experiment that shows an absence of temperature-dependent contributions to the magnetic susceptibility, and indicates a nondegenerate ground state. Sophisticated electronic structure calculations are needed to quantify these spin–orbit effects. Wadt employed spin–orbit configuration interaction (CI) calculations that examined all possible arrangements of two electrons in seven 5f levels (Wadt, 1987). Wadt found that the ground $^1\Gamma_{1g}$ state in the octahedral double group representation was comprised of 78% $^3T_{1g}$ and 18% $^1A_{1g}$. More recently, Hay and Martin (1998) performed hybrid DFT calculations on both the $^1A_{1g}$ and $^3T_{1g}$ states and found the $^3T_{1g}$ state to lie lower in energy, consistent with Wadt's study, but did not include the spin–orbit coupling.

(*ii*) PuO_2^{n+}

The linear trans dioxo cations of light actinide elements are among the most well-studied actinide molecular systems. Electronic structure calculations on actinyl ions have revealed a great deal about covalency in metal–oxygen bonds and the relative roles of the valence 5f, 6d, and semicore 6p orbitals. The majority of theoretical studies have been devoted to UO_2^{2+}, but the smaller subset of calculations on PuO_2^{2+} reveals that much of the basic bonding description is essentially the same. The most thorough review on the subject is Denning's 1992 examination of experimental and theoretical work performed up to that time (Denning, 1992). Subsequent reviews build upon that work, and the reader is referred to discussions by Pepper and Bursten (1991), Dyall (1999), Denning *et al.* (2002), and Chapter 17 of this work for additional information.

The trans dioxo cations, AnO_2^{n+}, are invariably linear, regardless of the number of valence 5f electrons. The metal–oxygen bonds are unusually short, strong, and chemically inert. Based on all the experimental and theoretical

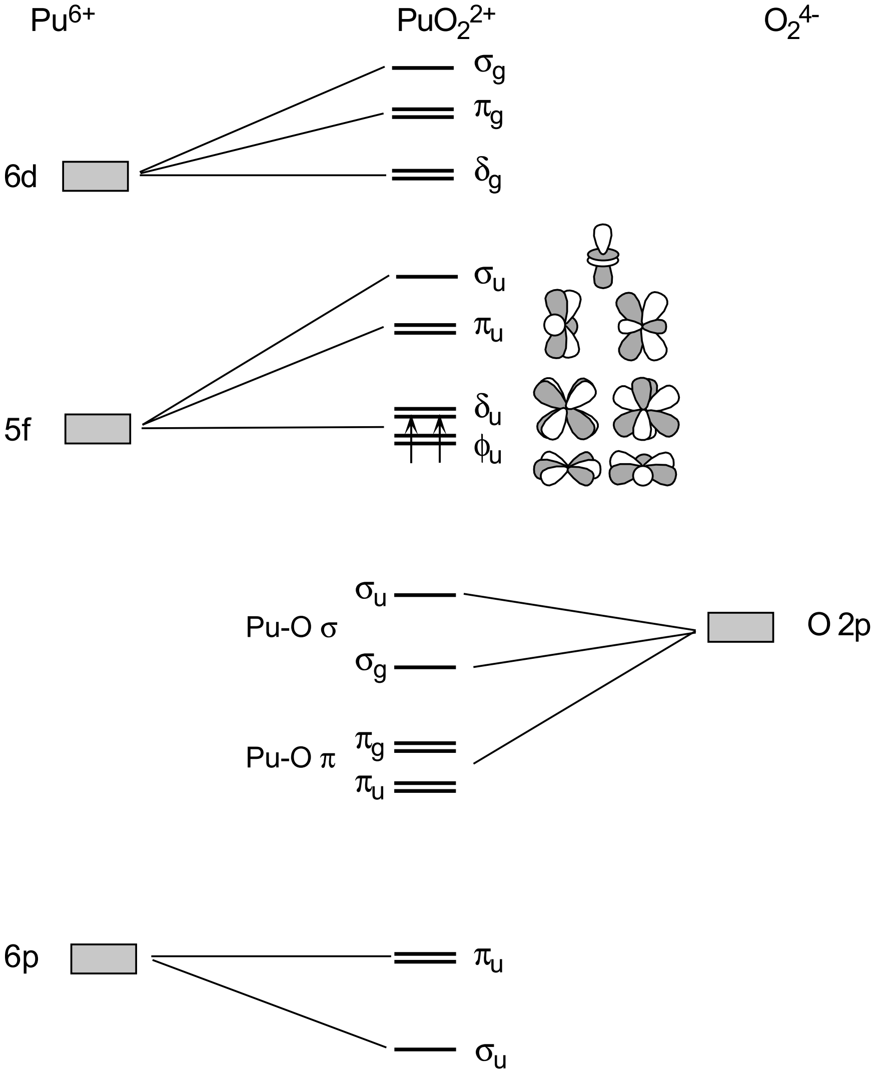

Fig. 7.123 *A qualitative molecular orbital interaction diagram for a linear triatomic PuO_2^{2+} ion.*

studies, there is uniform agreement on the molecular orbital description of bonding in these systems. A qualitative molecular orbital diagram for the linear triatomic PuO_2^{2+} ion that contains the basic features of the calculations is given in Fig. 7.123. In centrosymmetric $D_{\infty h}$ symmetry, the molecular orbitals are conveniently labeled according to their axial symmetry, and the 5f and 6d orbitals cannot mix. The in-phase and out-of-phase combinations of the two O 2p σ orbitals span σ_u and σ_g symmetry, while the corresponding O 2p π orbitals span π_u and π_g symmetry. The metal 6d orbitals span σ_g, π_g, and δ_g symmetry, while the 5f orbitals span σ_u, π_u, δ_u, and φ_u symmetry. Metal–oxygen σ bonds are formed by interaction of the O 2p σ orbitals with metal $6d_{z^2}$ (σ_g) and a hybrid metal orbital formed by mixing $5f_{z^3}$ with the semicore $6p_z$ (σ_u). Metal–oxygen π bonds are formed by interaction of O 2pπ orbitals with metal $6d_\pi$ (π_g) and $5f_\pi$ (π_u) orbitals. The 5f δ_u and φ_u orbitals have no symmetry match with the ligands, and they remain as unperturbed, essentially degenerate, nonbonding 5f orbitals as indicated in Fig. 7.123.

In this qualitative diagram, the 14 valence electrons occupy the molecular orbitals to give a ground state electron configuration of $(\sigma_g^2\pi_g^4\,\sigma_u^2\,\pi_u^4)\,(\delta_u^2)$. Since the δ_u orbital is a nonbonding 5f orbital on the metal, this gives rise to formal Pu–O triple bonds in the linear PuO_2^2+ unit. These four metal–ligand bonding orbitals are shown qualitatively in **31–34** below.

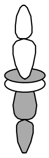

σ_u

31

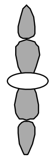

σ_g

32

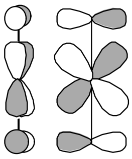

π_g

33

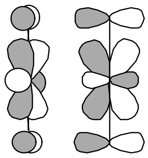

π_u

34

Much discussion and debate has centered around the ordering of the four occupied metal–oxygen bonding orbitals σ_g, π_g, σ_u, and π_u. It is now generally accepted that a filled–filled interaction takes place between the σ_u Pu–O bonding orbital and the lower-lying (semicore) metal $6p_z$ orbital that also has σ_u symmetry. This repulsive interaction keeps the metal–oxygen bonding σ_u at high energy, and this now classical picture has been verified experimentally by Denning and coworkers using polarized oxygen Kα X-ray absorption and emission spectroscopy on a uranyl sample (Denning *et al.*, 2002). The linear trans dioxo cations were the first systems where theoretical calculations revealed that the closed shell (semicore) 6p orbitals were active in chemical bonding. Several studies have focused on the role of semicore 6p involvement, and have shown that $5f_{z^3}$–$6p_z$ hybridization forms an unusually strong metal–oxygen σ bond, and stabilizes the linear geometry (Dyall, 1999; Kaltsoyannis, 2000).

This basic bonding picture holds for all the trans dioxo cations from uranium through plutonium (Hay *et al.*, 2000) and americium. For the 5f orbitals, the overall ordering of levels is $\delta_u \sim \varphi_u < \pi_u << \sigma_u$ because the π_u and σ_u orbitals are destabilized by bonding interactions at lower energy. This basic orbital ordering scheme makes it easy to understand why the AnO_2^{n+} ions remain linear regardless of the number of 5f electrons. As the 5f electron count increases from UO_2^{2+} (f^0) to AmO_2^{2+} (f^3), each successive 5f electron is added to the nonbonding

5f orbitals of δ_u or φ_u symmetry. This is in contrast to transition element complexes where d^0 dioxo complexes are invariably cis, while d^2 dioxo complexes are invariably trans in order to maximize metal–oxygen π bonding. For the actinyl ions, the trans geometry maximizes σ bonding, and the formal metal–oxygen triple bond is retained regardless of the metal 5f electron count.

From this basic molecular orbital description, it is also easy to understand why most equatorial ligands show only a weak interaction with the highly covalent linear AnO_2^{2+} core. Let us consider the D_{4h} symmetry case of four equatorial ligands that only interact via σ bonding to form $PuO_2L_4^{2+}$. The four lone-pair orbitals of the equatorial ligands span a_{1g}, b_{1g}, and e_u symmetry, and these correspond to the $D_{\infty h}$ σ_g, δ_g, and π_u orbitals of the linear PuO_2^{2+} ion. The σ_g orbital has already been significantly destabilized by formation of the axial PuO_2^{2+} σ bonds, and the π_u orbital has very little overlap with incoming ligands in the equatorial plane. This leaves only one component of the degenerate δ_g orbital $\left(d_{x^2-y^2}, d_{xy}\right)$ that is directed towards the incoming ligands. In D_{4h} symmetry, the δ_g orbital $\left(d_{x^2-y^2}, d_{xy}\right)$ transforms as $b_{1g} + b_{2g}$, and only the b_{1g} orbital has the appropriate symmetry to interact. Overall, this gives only one molecular orbital (b_{1g}) that is bonding to all four equatorial bonds with a formal bond order of one quarter. The $PuO_2L_4^{2+}$ molecule therefore has two strong covalent Pu–O triple bonds in the axial direction, and four weak, relatively ionic bonds in the equatorial plane. This qualitative molecular orbital interaction diagram is illustrated in Fig. 7.124.

As in the PuF_6 example, the weak ligand field splitting of the 5f manifold, particularly the δ_u and φ_u orbitals mandates that electron repulsion and spin–orbit interactions be taken into account in order to understand the complexity of molecular electronic spectra. In the actinyl ions, Matsika and coworkers concluded that after consideration of the axial ligand field, electron repulsion was generally larger than spin–orbit coupling, leading them to the use of a Russell–Saunders-like Λ-S coupling scheme to calculate electronic states and optical transitions (Matsika *et al.*, 2001). For the $5f^2$ PuO_2^{2+} system, the $(\delta_u,\varphi_u)^2$ configuration gives two ${}^3\sum_g^-$ states, ${}^3\Pi_g$, ${}^3H_g$ and several higher energy singlets when only considering electron repulsion. When spin–orbit interaction is taken into account, the ${}^3H_g$ is lowered considerably, giving a ground state of ${}^3H_{4g}$ in agreement with spectroscopic data (Bleaney, 1955; Denning, 1992). Hay *et al.* (2000) obtain the same ${}^3H_{4g}$ ground state using spin–orbit configuration interaction (CI) calculations.

(*iii*) *Pu*$(C_8H_8)_2$

Following the discovery of the transition metal sandwich complex ferrocene, $Fe(\eta\text{-}C_5H_5)_2$, R. D. Fischer predicted the existence of the $U(\eta\text{-}C_8H_8)_2$ sandwich complex based on the recognition that the nodal properties of f-orbitals would require an expanded C_8H_8 ring (Fischer, 1963). Five years later uranocene, $U(\eta\text{-}C_8H_8)_2$, was synthesized and only shortly thereafter the plutonium

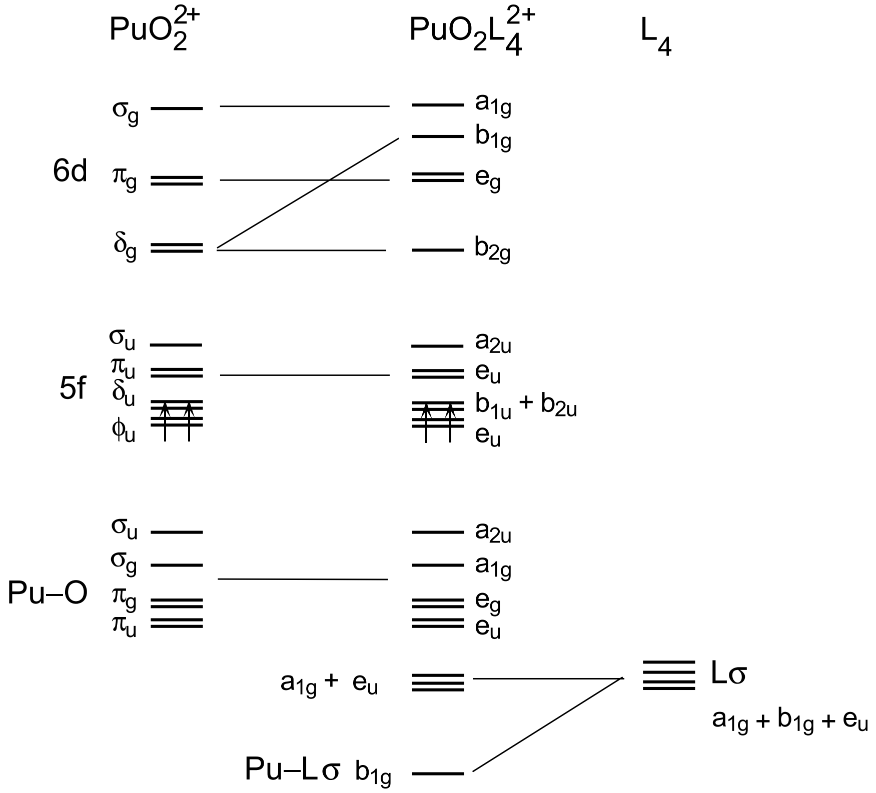

Fig. 7.124 *A qualitative molecular orbital interaction diagram for a linear triatomic* PuO_2^{2+} *ion interacting with four equatorial ligands, L, to form* $PuO_2L_4^{2+}$.

analog was prepared. As one of the first organometallic actinide complexes, the actinocene system has been the topic of much study aimed at understanding the relative roles of 5f and 6d orbitals in bonding (Boerrigter *et al.*, 1988; Brennan *et al.*, 1989; Kaltsoyannis and Bursten, 1997; Li and Bursten, 1998). A qualitative molecular orbital interaction diagram for Pu(η-C_8H_8)$_2$ under D_{8h} symmetry that contains the basic features of the electronic structure calculations is given in Fig. 7.125. The eight carbon $2p_\pi$ orbitals of the planar $C_8H_8^{2-}$ ring transform as a_{2u}, e_{1g}, e_{2u}, e_{3g}, and b_{1u} symmetry in D_{8h}, and these are often referred to as π_0, π_1, π_2, π_3, and π_4. This π_n nomenclature is convenient for visualization because the value of n refers to the number of nodes in the Hückel p_π orbitals of the $C_8H_8^{2-}$ ring. When two $C_8H_8^{2-}$ rings are brought together in D_{8h} symmetry, the in-phase and out-of-phase combinations of these π_n orbitals give rise to 16 orbitals as indicated in Fig. 7.125. These orbitals retain their π_n parentage as π_0 ($a_{1g} + a_{2u}$), π_1 ($e_{1g} + e_{1u}$), π_2 ($e_{2g} + e_{2u}$), π_3 ($e_{3g} + e_{3u}$), and π_4 ($b_{1u} + b_{2g}$). Interaction of these 16 π orbital combinations with Pu 6d atomic

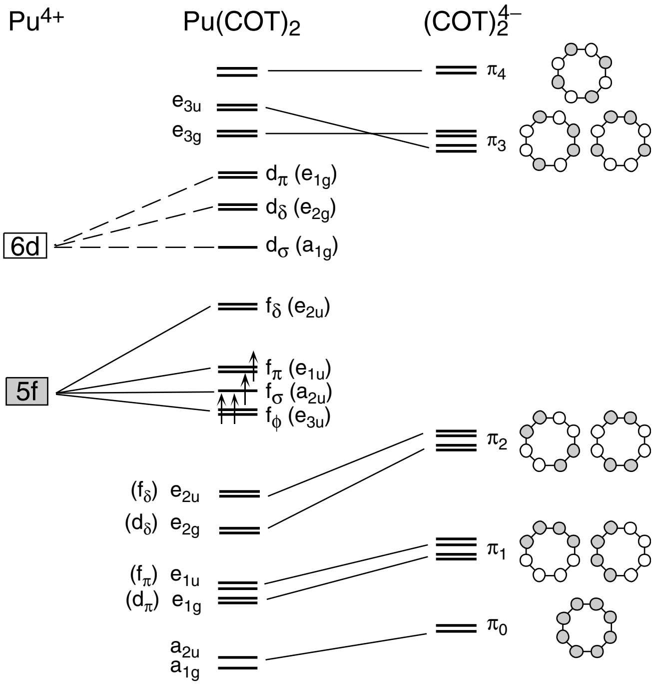

Fig. 7.125 *A qualitative molecular orbital interaction diagram for plutonocene, Pu(η-C_8H_8)$_2$.*

orbitals of d_σ, d_π, and d_δ symmetry gives rise to metal–ligand bonding molecular orbitals of a_{1g}, e_{1g}, and e_{2g} symmetry, respectively. Both the d_π (e_{1g}) and d_δ (e_{2g}) molecular orbitals are significantly destabilized due to strong interactions that occur with ligand orbitals at lower energy. The Pu 5f orbitals are split into the f_σ, f_π, f_δ, and f_φ molecular orbitals of a_{2u}, e_{1u}, e_{2u}, and e_{3u} symmetry, respectively. The lobes of the f_δ orbital are directed towards the $C_8H_8^{2-}$ rings, and interaction with the ligands strongly destabilizes this orbital and moves it significantly higher in energy than the remaining f_σ, f_π, and f_φ orbitals. Ligand interactions with the remaining f_σ, f_π, and f_φ orbitals are significantly weaker, giving rise to an f-orbital splitting pattern where one degenerate set is removed from the 5f manifold, leaving the other five orbitals clustered at lower energy (Boerrigter *et al.*, 1988). These general interactions are illustrated in Fig. 7.125.

As seen in the other examples, the 6d orbital interactions with the ligands are significantly stronger than the 5f interactions. The δ-type interactions have significant metal–ligand overlap and give rise to appreciable covalency through both 6d and 5f orbital interactions. A Mulliken population analysis for nonrelativistic orbitals showed that the $6d_\delta$ orbital is approximately 88% ligand and

11% 6d in character, while the $5f_\delta$ orbital is 48% ligand and 49% 5f in character (Boerrigter *et al.*, 1988). The latter represents significant 5f covalency. In addition, these calculations reveal that the semicore 6p orbitals also have a considerable amplitude at the position of the rings, and that this permits a strong interaction with deeper lying ring orbitals of the appropriate symmetry (Boerrigter *et al.*, 1988). These $6d_\delta$ (e_{2g}) and $5f_\delta$ (e_{2u}) metal–ligand bonding orbitals are illustrated qualitatively in **35** and **36**.

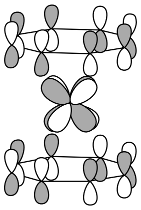

f_δ

35

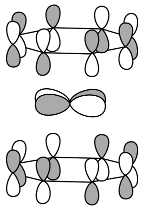

d_δ

36

This general bonding scheme has been experimentally confirmed by Brennan and coworkers who performed variable energy photoelectron spectroscopy on $U(\eta\text{-}C_8H_8)_2$ over a photon energy range of 24–125 eV (Brennan *et al.*, 1989). A mapping of the intensity changes in the ionization from the $5f_\delta$ (e_{2u}) orbital

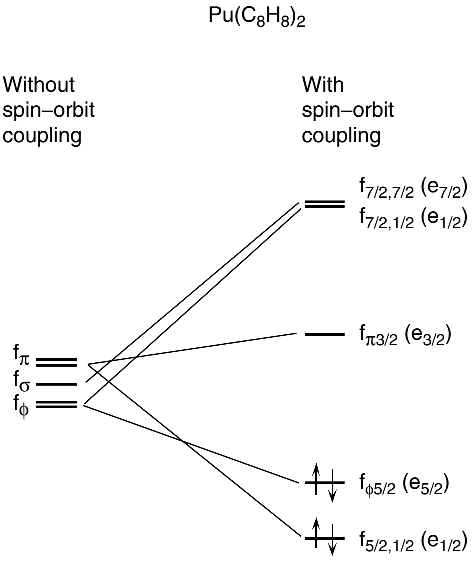

Fig. 7.126 *The effect of spin–orbit coupling on the 5f orbitals of* $Pu(\eta\text{-}C_8H_8)_2$ *adapted from Boerrigter* et al. (1988). *For consistency with Chapter* 17, *the* D_{8h}* *double group notation is given in parentheses.*

provided conclusive spectroscopic evidence for substantial 5f orbital covalency in U(η-C_8H_8)$_2$.

Relativistic calculations employing the HFS LCAO method conclude that the f_σ, f_π, and f_φ orbitals are nearly degenerate, and that they are equally populated with the four valence electrons in Pu(η-C_8H_8)$_2$ (Boerrigter *et al.*, 1988). This is not consistent with the experimental observation of a $M_j = 0$ ground state. As in our other examples, spin–orbit coupling must be taken into account in order to understand spectroscopic data. Boerrigter and coworkers have shown that strong ligand field splitting effectively removes the $5f_\delta$ orbital from the 5f orbital manifold, and this simplifies the discussion of spin–orbit coupling. The spin–orbit interaction on a degenerate set of f_σ, f_π, and f_φ orbitals gives a four-level pattern with two low-lying orbitals, the $f_{5/2,1/2}$ and $f_{\varphi 5/2}$, and three high-lying orbitals, the $f_{\pi 3/2}$, and the degenerate $f_{7/2,7/2}$ and $f_{7/2,1/2}$, as shown in Fig. 7.126. After inclusion of spin–orbit coupling, it is easy to see that Pu(η-C_8H_8)$_2$ is closed shell as both the low-lying $f_{5/2,1/2}$ and $f_{\varphi 5/2}$ are fully occupied leading to a $M_j = 0$ ground state in agreement with the measured magnetic properties.

ACKNOWLEDGMENTS

The authors acknowledge expert assistance from Karen Kippen, Leonard Martinez, Meredith Coonley, Ed Lorusso, and Susan Ramsay in preparing the manuscript. The authors are grateful to Thomas W. Newton and Phillip D. Palmer for electronic absorption spectra and calculations. DLC and MPN acknowledge the Division of Chemical Sciences, Geosciences, and Biosciences, Office of Basic Energy Research, U.S. Department of Energy for their support of actinide chemistry research at Los Alamos National Laboratory.

REFERENCES

(1963) *Plutonium Chemistry Symposium*, Report TID-7683, Argonne National Laboratory, 44 pp.

Abraham, B. M. and Davidson, N. R. (1949) High-temperature Hydrolysis of Plutonium Oxychloride, in *Natl. Nucl. Energy Ser.,* Div IV **14B**(Transuranium Elements, Pt. I) (eds. G. T. Seaborg, J. J. Katz, and W. M. Manning), McGraw-Hill, New York, pp. 779–83.

Abraham, B. M., Brody, B. B., Davidson, N. R., Hagemann, F., Karle, I., Katz, J. J., and Wolf, M. J. (1949a) Preparation and Properties of Plutonium Chlorides and Oxychlorides, in *Natl. Nucl. Energy Ser.,* Div IV **14B**(Transuranium Elements, Pt. I) (eds. G. T. Seaborg, J. J. Katz, and W. M. Manning), McGraw-Hill, New York, pp. 740–58.

Abraham, B. M., Davidson, N. R., and Westrum, E. F., Jr (1949b) Preparation and Properties of Some Plutonium Sulfides and Oxysulfides, in *Natl. Nucl. Energy Ser.,* Div IV **14B**(Transuranium Elements, Pt. I) (eds. G. T. Seaborg, J. J. Katz, and W. M. Manning), McGraw-Hill, New York, pp. 814–17.

Abraham, B. M., Davidson, N. R., and Westrum, E. F., Jr (1949c) Preparation of Plutonium Nitride, in *Natl. Nucl. Energy Ser.,* Div IV **14B**(Transuranium Elements, Pt. I) (eds. G. T. Seaborg, J. J. Katz, and W. M. Manning), McGraw-Hill, New York, pp. 945–8.

Abrikosov, I. A., Ruban, A. V., Johansson, B., and Skriver, H. L. (1998) *Comput. Mater. Sci.,* **10**(1–4), 302–5.

Ackermann, R. J., Faircloth, R. L., and Rand, M. H. (1966) *J. Phys. Chem.,* **70**(11), 3698–706.

Adams, M. D., Steunenberg, R. K., and Vogel, R. C. (1957) *The Transfer of Plutonium Hexafluoride in the Vapor Phase*, Report ANL-5796, Argonne National Laboratory, 14 pp.

Adamson, M. G., Aitken, E. A., and Caputi, R. W. (1985) *J. Nucl. Mater.,* **130**, 349–65.

Adler, P. H. (1991) *Metall. Trans. A,* **22A**(10), 2237–46.

Adler, P. H., Olson, G. B., and Margolies, D. S. (1986) *Acta Metall.,* **34**(10), 2053–64.

Aitken, E. A. and Evans, S. K. (1968) *A Thermodynamic Data Program Involving Plutonium and Urania at High Temperatures*, Report GEAP-5672, General Electric Company, Vallecitos Nucleonics Laboratory, 10 pp.

Akatsu, J. (1982) *Sep. Sci. Technol.,* **17**(12), 1433–42.

Akatsu, J., Moriyama, N., Dojiri, S., Matsuzuru, H., and Kobayashi, Y. (1983) *Sep. Sci. Technol.,* **18**(2), 177–86.

Akhachinskii, V. V. and Bashlykov, S. N. (1970) *Atomnaya Energiya,* **29**(6), 439–47.

Akimoto, Y. (1960) *Chemistry Division Semi-annual Report - June through November 1959*, USAEC Report UCRL-9093, Lawrence Radiation Laboratory.

Albiol, T. and Arai, Y. (2001) *Review of Actinide Nitride Properties with Focus on Safety Aspects*, Report JAERI-Review, Department of Nuclear Energy System, Tokai Research Establishment, Japan Atomic Energy Research Institute, i–vi, pp. 1–50.

Albrecht, E. D. (1964) *J. Nucl. Mater,* **12**(2), 125–130.

Albrecht-Schmitt, T. E., Almond, P. M., and Sykora, R. E. (2003) *Inorg. Chem.,* **42**(12), 3788–95.

Albright, D. and Kramer, K. (2004) *B. Atom. Sci.,* **60**(6), 14–16.

Alcock, N. W. and Esperas, S. (1977) *J. Chem. Soc. Dalton Trans.,* **9**, 893–6.

Alei, M., Johnson, Q. C., Cowan, H. D., and Lemons, J. F. (1967) *J. Inorg. Nucl. Chem.,* **29**, 2327.

Alenchikova, I. F., Zaitseva, L. L., Lipis, L. V., Fomin, V. V., and Chebotarev, N. T. (1958) *Proc. Second UN Int. Conf. Peaceful Uses Atomic Energy*, vol. 28, Geneva, 1958, pp. 309–15.

Alenchikova, I. F., Zaitseva, L. L., Lipis, L. V., and Fomin, V. V. (1959) *Zh. Neorg. Khim.,* **4**, 961–2.

Alenchikova, I. F., Lipis, L. V., and Nikolaev, N. S. (1961a) *Atomnaya Energiya,* **10**, 592–6.

Alenchikova, I. F., Zaitseva, L. L., Lipis, L. V., Nikolaev, N. S., Fomin, V. V., and Chebotarev, N. T. (1961b) *Zh. Neorg. Khim.,* **6**, 1513–19.

Alexander, C. A., Ogden, J. S., and Pardue, W. M. (1969) Report BMI-1862, A7, Batelle Memorial Institute, Columbus, OH.

Alexander, E. C., Jr., Lewis, R. S., Reynolds, J. H., and Michel, M. C. (1971) *Science* **172**(3985), 837–40.

Alexander, C. A., Clark, R. B., Kruger, O. L., and Robbins, J. L. (1976) Fabrication and High-temperature Thermodynamic and Transport Properties of Plutonium Mononitride. *Plutonium 1975 and Other Actinides*, *Proc. Conf. in Baden-Baden,* Sept. 10–13, 1975/*Proc. Fifth Int. Conf. on Plutonium and Other Actinides*, 1975 (eds. H. R. Blank and R. Lindner), pp. 277–86.

Allard, B., Kipatsi, H., and Lilijenzin, J. O. (1980) *J. Inorg. Nucl. Chem.,* **42**(7), 1015–27.

Allbutt, M. and Dell, R. M. (1967) *J. Nucl. Mater.,* **24**(1), 1–20.

Allbutt, M., Dell, R. M., and Junkison, A. R. (1970) Plutonium Chalcogenides, in *Chem. Extended Defects Non-Metal. Solids,* (eds. L. Eyring and M. O'Keefe), Proc. Inst. Advan. Study. Scottsdale, AZ, pp. 124–47.

Allen, G. C. and Tempest, P. A. (1986) *Proc. R. Soc. Lon. Ser. A,* **406**(1831), 325–44.

Allen, P. G., Bucher, J. J., Clark, D. L., Edelstein, N. M., Ekberg, S. A., Gohdes, J. W., Hudson, E. A., Kaltsoyannis, N., Lukens, W. W., Neu, M. P., Palmer, P.D., Reich, T., Shuh, D. K., Tait, C. D., and Zwick, B. D. (1995) *Inorg. Chem.,* **34**(19), 4797–807.

Allen, J. W., Zhang, Y. X., Tjeng, L. H., Cox, L. E., Maple, M. B., and Chen, C. T. (1996a) *J. Electron Spectro. Rel. Phenom.,* **78**, 57–62.

Allen, P. G., Veirs, D. K., Conradson, S. D., Smith, C. A., and Marsh, S. F. (1996b) *Inorg. Chem.,* **35**(10), 2841–5.

Allen, P. G., Bucher, J. J., Shuh, D. K., Edelstein, N. M., and Reich, T. (1997) *Inorg. Chem.,* **36**(21), 4676–83.

Allen, P. G., Henderson, A. L., Sylwester, E. R., Turchi, P. E. A., Shen, T. H., Gallegos, G. F., and Booth, C. H. (2002) *Phys. Rev. B.,* **65**(21), 214107/1–214107/7.

Al Mahamid, I., Becraft, K. A., Hakem, N. L., Gatti, R. C., and Nitsche, H. (1996) *Radiochim. Acta,* **74**, 129–34.

Amano, O., Sasahira, A., Kani, Y., Hoshino, K., Aoi, M., and Kawamura, F. (2004) *J. Nucl. Sci. Technol.,* **41**(1), 55–60.

Anderegg, G. (1977) *Critical Survey of Stability Constants of EDTA Complexes,* Pergamon Press, Oxford.

Anderegg, G. (1982) *Pure Appl. Chem.,* **54**, 2693.

Anderson, H. H. and Asprey, L. B. (1960) *Solvent-extraction Process for Plutonium.* US Patent no. 2924 506. (U.S. Atomic Energy Commission).

Anderson, J. W. and Maraman, W. J. (1962) *Trans. Am. Foundrymen's Soc.,* **70**, 1057–72.

Anderson, J. W., Leary, J. A., and McNeese, W. D. (1960) *Preparation and Fabrication of Plutonium Fuel Alloy for Los Alamos Molten Plutonium Reactor Experiment No. 1*, Report LA-2439, Los Alamos Scientific Laboratory, 30 pp.

Andreichuk, N. N., Vasil'ev, V. Y., Rykova, A. G., Osipov, S. V., Kalashnikov, V. M., and Vysokoostrovskaya, N. B. (1979) *Sov. Radiochem.,* **21**(6), 727–36.

Andreichuk, N. N., Rotmanov, K. V., Frolov, A. A., and Vasil'ev, V. Y. (1984a) *Sov. Radiochem.,* **26**(1), 90–4.

Andreichuk, N. N., Rotmanov, K. V., Frolov, A. A., and Vasil'ev, V. Y. (1984b) *Sov. Radiochem.,* **26**(6), 701–6.

Andreichuk, N. N., Frolov, A. A., Rotmanov, K. V., and Vasil'ev, V. Y. (1990) *J. Radioanal. Nucl. Chem. Lett.,* **143**(2), 427–32.

Andrew, J. F. (1967) *J. Phys. Chem. Solids,* **28**(4), 577–80.

Andrew, J. F. (1969) *J. Nucl. Mater.,* **30**(3), 343–5.

Andrew, J. F. and Latimer, T. W. (1975) *Review of Thermal Expansion and Density of Uranium and Plutonium Carbides*, Report LA-6037-MS, Los Alamos Science Laboratory, Los Alamos, NM, 17 pp.

Angelo, J. A., Jr, and Buden, D. (1985) *Space Nuclear Power,* Orbit Book Company, Malabar, FL, 286 pp.

Ankudinov, A. L., Conradson, S. D., Mustre de Leon, J., and Rehr, J. J. (1998) *Phys. Rev. B,* **57**(13), 7518–25.

Anselin, F. (1963a) *J. Nucl. Mater.,* **10**(4), 301–220.

Anselin, F. (1963b) *Compt. Rend.,* **256**, 2616–19.

Antonio, M. R., Soderholm, L., Williams, C. W., Blaudeau, J.-P., and Bursten, B. E. (2001) *Radiochim. Acta,* **89**(1), 17–25.

Antonio, M. R., Chiang, M.-H., Williams, C. W., and Soderholm, L. (2004) *Mater. Res. Soc. Symp. Proc*., **802**, 157–68.

Anyun, Z., Jingxin, H., Xianye, Z., and Fangding, W. (2002) *J. Radioanal. Nucl. Chem.,* **252**(3), 565–71.

Arai, Y. and Ohmichi, T. (1995) *J. Solid State Chem.,* **115**(1), 66–70.

Archibong, E. F. and Ray, A. K. (2000) *Theochem,* **530**(1,2), 165–70.

Arko, A. J., Joyce, J. J., and Havela, L. (2006) *The Chemistry of the Actinide and Transactinide Elements,* (eds. L. R. Morss, N. M. Edelstein, and J. Fuger), Springer Publishing, New York, ch. 21.

Artyukhin, P. I., Gel'man, A. D., and Medvedovskii, V. I. (1958) *Doklady Akad. Nauk SSSR,* **120**, 98–100.

Artyukhin, P. I., Medvedovskii, V. I., and Gel'man, A. D. (1959) *Zh. Neorg. Khim.,* **4**, 1324–31.

Asanuma, N., Harada, M., Ikeda, Y., and Tomiyasu, H. (2001) *J. Nucl. Sci. Technol.,* **38**(10), 866–71.

Asprey, L. B., Keenan, T. K., and Kruse, F. H. (1964) *Inorg. Chem.,* **3**(8), 1137–240.

Asprey, L. B., Eller, P. G., and Kinkead, S. A. (1986) *Inorg. Chem.,* **25**(5), 670–2.

Atlas, L. M. and Schlehman, G. J. (1967) Defect Equilibria of Nonstoichiometric Plutonium dioxide 1045 to 1505 Deg. *Plutonium 1965, Proc. Third Int. Conf. on Plutonium* (eds. A. E. Kay and M. B. Waldron), Chapman and Hall, London, pp. 838–44.

Atlas, L. M., Schlehman, G. J., and Readey, D. W. (1966) *J. Am. Ceram. Soc.,* **49**(11), 624–5.

Audi, G. and Wapstra, A. H. (1995) *Nucl. Phys. A,* **595**(4), 409–80.

Audi, G., Bersillon, O., Blachot, J., and Wapstra, A. H. (1997) *Nucl. Phys. A,* **624**(1), 1–124.

Austin, A. E. (1959) *Acta Crystallogr.,* **12**, 159–61.

Avdeef, A., Raymond, K. N., Hodgson, K. O., and Zalkin, A. (1972) *Inorg. Chem.,* **11**(5), 1083–8.

Avens, L. R., Bott, S. G., Clark, D. L., Sattelberger, A. P., Watkin, J. G., and Zwick, B. D. (1994) *Inorg. Chem.,* **33**(10), 2248–56.

Avignant, D. and Cousseins, J. C. (1971) *Compt. Rend.,* **272**(26), 2151–3.

Avivi, E. (1964) *Etudes d'Alliages Plutonium - Fer at d'Alliages Uranium - Plutonium-Fer*, Thesis, Universite de Paris, 72 pp.

Awasthi, S. K., Chackraburtty, D. M., and Tondon, V. K. (1968) *J. Inorg. Nucl. Chem.,* **30**(3), 819–21.

Axler, K. M., Roof, R. B., and Foltyn, E. M. (1992) *J. Nucl. Mater.,* **189**(2), 231–2.

Baes, C. F. and Mesmer, R. E. (1976) *The Hydrolysis of Cations,* Wiley, New York, 489 pp.

Baglan, N., Fourest, B., Guillaumont, R., Blain, G., Le Du, J.-F., and Genet, M. (1994) *New J. Chem.,* **18**(7), 809–16.

Bagnall, K. W. (1967a) *Coord. Chem. Rev.,* **2**(2), 145–62.

Bagnall, K. W. (1967b) *Halogen Chem.,* **3**, 303–82.

Bagnall, K. W., Deane, A. M., Markin, T. L., Robinson, P. S., and Stewart, M. A. A. (1961) *J. Chem. Soc.*, *Abstracts*: 1611–17.

Bagnall, K. W., Plews, M. J., and Brown, D. (1982a) *J. Organomet. Chem.,* **224**(3), 263–6.

Bagnall, K. W., Plews, M. J., Brown, D., Fischer, R. D., Klaehne, E., Landgraf, G. W., and Sienel, G. R. (1982b) *J. Chem. Soc., Dalton Trans.*, (10), 1999–2007.

Bagnall, K. W., Payne, G. F., and Brown, D. (1985a) *J. Less-Common Met.,* **109**(1), 31–6.

Bagnall, K. W., Payne, G. F., and Brown, D. (1985b) *J. Less-Common Met.,* **113**(2), 325–9.

Bagnall, K. W., Payne, G. F., and Brown, D. (1986) *J. Less-Common Met.,* **116**(2), 333–9.

Baily, H., Bernard, H., and Mansard, B. (1989) *Mater. Sci. Forum,* **48–49**(Nucl. Fuel Fabr.), 175–83.

Bairiot, H. and Deramaix, P. (1992) *J. Nucl. Mater.,* **188**, 10–18.

Bairiot, H., Blanpain, P., Farrant, D., Ohtani, T., Onoufriev, V., Porsch, D., Stratton, R., Brown, C., Deramaix, P., Golovnin, I., Haas, E., Laraia, M., Nagai, S., Pope, R., Sanchis, H., Shea, T., and Weston, R. (2003) *Status and Advances in MOX Fuel Technology*, Technical Report Series - International Atomic Energy Agency (415), Report 1-179.

Baker, R. D. (1946) *Preparation of Plutonium Metal by the Bomb Method*, Report LA-473, Los Alamos Scientific Laboratory, 65 pp.

Baker, R. D. and Maraman, W. J. (1960) *Extract. Phys. Met. Plutonium and Alloys, Symp.,* San Francisco, California, 43–59.

Balakrishnan, P. V. and Ghosh Mazumdar, A. S. (1964) *J. Inorg. Nucl. Chem.,* **26**(5), 759–63.

Baldwin, C. E. and Navratil, J. D. (1983) *ACS Symp. Ser.* **216** (Plutonium Chem.) (eds. W. T. Carnall and G. R. Choppin), American Chemcial Society, Washington, DC. pp. 369–80.

Bamberger, C. E. (1985) in *Handbook on the Physics and Chemistry of the Actinides* (eds. A. J. Freeman and C. Keller), Elsevier Science, New York, ch. 6, pp. 289–303.

Banks, R. H. (1979) *Preparation and Spectroscopic Properties of Three New Actinide(IV) Borohydrides*, Thesis, Report LBL-10292, Lawrence Berkeley Laboratory, University of California, 209 pp.

Banks, R. H. and Edelstein, N. M. (1980) *ACS Symp. Ser.* **131**(Lanthanide Actinide Chem. Spectrosc.), American Chemcial Society, Washington, DC. 331–48.

Banks, R. H., Edelstein, N. M., Rietz, R. R., Templeton, D. H., and Zalkin, A. (1978) *J. Am. Chem. Soc.,* **100**(6), 1957–8.

Banyai, I., Glaser, J., Micskei, K., Toth, I., and Zekany, L. (1995) *Inorg. Chem.,* **34**(14), 3785–96.

Bardelle, P. and Bernard, H. (1989) *Preparation of Uranium and/or Plutonium Nitride for Use as a Nuclear Reactor Fuel*, (Commissariat a l'Energie Atomique, France). Ep Patent 307311, 5 pp.

Barmore, W. L. and Uribe, F. S. (1970) *Mechanical Behavior of Pu-Ga, Proc. Fourth Int. Conf. on Plutonium and Other Actinides* (ed. W. N. Miner), Santa Fe, NM, The Metallurgical Society of AIME, 1, 414 pp.

Barney, G. S. (1976) *J. Inorg. Nucl. Chem.,* **38**(9), 1677–81.

Barton, C. J., Redman, J. D., and Strehlow, R. A. (1961) *J. Inorg. Nucl. Chem.,* **20**, 45–52.

Bartscher, W. (1996) *Diffusion and Defect Data–Solid State Data, Pt. B. Solid State Phenomena,* **49–50**(Hydrogen Metal Systems I), 159–238.

Bartscher, W., Boeuf, A., Caciuffo, R., Fournier, J. M., Haschke, J. M., Manes, L., Rebizant, J., Rustichelli, F., and Ward, J. W. (1985) *Physica B & C,* **130**(1–3), 530–2.

Baskes, M. I. (2000) *Phys. Rev. B: Condens. Matter,* **62**(23), 15532–7.

Baskes, M. I., Muralidharan, K., Stan, M., Valone, S. M., and Cherne, F. J. (2003) *JOM,* **55**(9), 41–50.

Baston, G. M. N., Bradley, A. E., Gorman, T., Hamblett, I., Hardacre, C., Hatter, J. E., Healy, M. J. F., Hodgson, B., Lewin, R., Lovell, K. V., Newton, G. W. A., Nieuwenhuyzen, M., Pitner, W. R., Rooney, D. W., Sanders, D., Seddon, K. R., Simms, H. E., and Thied, R. C. (2002) Ionic Liquids for the Nuclear Industry: A Radiochemical, Structural and Electrochemical Investigation, in *Ionic Liquids - Industrial Applications to Green Chemistry* (eds. R. D. Rogers and K. R. Seddon), American Chemical Society, Washington, DC, pp. 162–77.

Battles, J. E. and Blackburn, P. E. (1969) *Reactor Development Program Progress Report September 1969*, Report ANL-7618, Argonne National Laboratory, 141 pp.

Battles, J. E., Reishus, J. W., and Shinn, W. A. (1968) *Am. Ceram. Soc. Bull.,* **47**(4), 414.

Battles, J. E., Reishus, J. W., and Shinn, W. A. (1969) *Volatilization Studies of Plutonium Compounds by Mass Spectrometry, in Chemical Engineering Division, Annual Report 1968*, Report ANL-7575, Argonne National Laboratory, pp. 77–82.

Battles, J. E., Shinn, W. A., Blackburn, P. E., and Edwards, R. K. (1970) *Plutonium 1970 and Other Actinides, Proc. Fourth Int. Conf. on Plutonium and Other Actinides,* Santa Fe, NM, Oct. 5–9, 1970 (ed. W. N. Miner), AIME, New York, 733 pp.

Bauche, J., Blaise, J., and Fred, M. (1963) *Compt. Rend.,* **257**(16), 2260–3.

Bauer, E. D., Thompson, J. D., Sarrao, J. L., Morales, L. A., Wastin, F., Rebizant, J., Griveau, J. C., Javorsky, P., Boulet, P., Colineau, E., Lander, G. H., and Stewart, G. R. (2004) *Phys. Rev. Lett.,* **93**(14), 147005/1–4.

Baumgärtner, F., Fischer, E. O., Kanellakopulos, B., and Laubereau, P. (1965) *Angew. Chem.,* **77**(19), 866–7.

Bayoglu, A. S. and Lorenzelli, R. (1979) *J. Nucl. Mater.,* **79**(2), 437–8.

Bayoglu, A. S. and Lorenzelli, R. (1984) *Solid State Ionics,* **12**, 53–66.

Bayoglu, A. S., Giordano, A., and Lorenzelli, R. (1983) *J. Nucl. Mater.,* **113**(1), 71–4.

Bean, A. C., Campana, C. F., Kwon, O., and Albrecht-Schmitt, T. E. (2001) *J. Am. Chem. Soc.,* **123**(36), 8806–10.

Bean, A. C., Abney, K., Scott, B. L., and Runde, W. (2005) *Inorg. Chem.,* **44**(15), 5209–11.

Bearden, J. A. (1967) *Rev. Mod. Phys.,* **39**, 78–124.

Bearden, J. A. and Burr, A. F. (1967) *Rev. Mod. Phys.,* **39**, 125–42.

Beauvais, R. A. and Alexandratos, S. D. (1998) *React. Funct. Polym.,* **36**(2), 113–23.

Beitscher, S. (1970) *Hot Shortness in Plutonium-1 Weight Percent Gallium*, *Proc. Fourth Int. Conf. Plutonium - Other Actinides*, Santa Fe, NM (ed. W. N. Miner), The Metallurgical Society of AIME, 1, pp. 449–56.

Beitz, J., Jonah, C., Sullivan, J. C., and Woods, M. (1986) *Radiochim. Acta,* **40**(1), 7–9.

Benard, P., Brandel, V., Dacheux, N., Jaulmes, S., Launay, S., Lindecker, C., Genet, M., Louer, D., and Quarton, M. (1996) *Chem. Mater.,* **8**(1), 181–8.

Benedict, U. (1970) *J. Nucl. Mater.,* **35**(3), 356–61.

Benedict, U. (1979) *Solid Solubility of Fission Product and Other Transition Elements in Carbides and Nitrides of Uranium and Plutonium*, European Institute for Transuranium Elements, Report 6 pp.

Benedict, U. and Sari, C. (1969) *Ternary System Uranium dioxide-Uranium oxide (U_3O_8)-Plutonium dioxide*, Report EUR-4136, Transuranium Institute, European Atomic Energy Community, Karlsruhe, Germany, 38 pp.

Bennett, D. A., Hoffman, D., Nitsche, H., Russo, R. E., Torres, R. A., Baisden, P. A., Andrews, J. E., Palmer, C. E. A., and Silva, R. J. (1992) *Radiochim. Acta,* **56**(1), 15–19.

Benz, R., Kahn, M., and Leary, J. A. (1959) *J. Phys. Chem.,* **63**, 1983–4.

Benz, R. (1961) *J. Phys. Chem.,* **65**(1), 81–4.

Benz, R. (1962) *J. Inorg. Nucl. Chem.,* **24**(Dec), 1191–5.

Benz, R. and Douglass, R. M. (1961a) *J. Inorg. Nucl. Chem.,* **23**, 134–6.

Benz, R. and Douglass, R. M. (1961b) *J. Phys. Chem.,* **65**, 1461–3.

Benz, R. and Leary, J. A. (1961) *J. Phys. Chem.,* **65**(6), 1056–8.

Benz, R., Douglass, R. M., Kruse, F. H., and Penneman, R. A. (1963) *Inorg. Chem.,* **2**(4), 799–803.

Berg, J. M., Smith, C. A., Cisneros, M. A., Vaughn, R. B., and Veirs, D. K. (1998) *J. Radioanal. Nucl. Chem. Lett.,* **235**(1–2), 25–9.

Berg, J. M., Veirs, D. K., Vaughn, R. B., Cisneros, M. R., and Smith, C. A. (2000) *Appl. Spectrosc.,* **54**(6), 812–23.

Berger, R. and Gäumann, T. (1961) *Helv. Chim. Acta,* **44**(4), 1084–8.

Bergstresser, K. S. (1950) *Plutonium Electropolishing Cell*, Report LA-1106, Los Alamos Scientific Laboratory, 10 pp.

Bernard, H. (1989) *J. Nucl. Mater.,* **166**(1–2), 105–11.

Berndt, A. F. (1962) *On the Use of a Modified Radial Distribution Analysis for Indexing Powder Patterns*, Report ANL-FGF-360, Argonne National Laboratory, 12 pp.

Berndt, A. F. (1966) *J. Less-Common Met.,* **11**(3), 216–19.

Berndt, A. F. (1967) *J. Less-Common Met.,* **12**(1), 82–3.

Berthon, C. and Chachaty, C. (1995) *Solvent Extr. Ion Exc.,* **13**(5), 781–812.

Besmann, T. M. and Lindemer, T. B. (1983) *J. Am. Ceram. Soc.,* **66**(11), 782–5.

Bessonov, A. A., Krot, N. N., Budantseva, N. A., and Afonas'eva, T. V. (1996) *Radiokhimiya,* **38**(3), 223–5.

Betz, T. and Hoppe, R. (1984) *Z. Anorg. Allg. Chem.,* **512**, 19–33.

Beznosikova, A. V., Chebotarev, N. T., Luk'yanov, A. S., Chernyi, A. V., and Smirnova, E. A. (1974) *Sov. At. Energy,* **37**(2), 842–6.

Bhide, M. K., Kadam, R. M., Babu, Y., Natarajan, V., and Sastry, M. D. (2000) *Chem. Phys. Lett.,* **332**(1,2), 98–104.

Bjorklund, C. W. (1957) *J. Am. Chem. Soc.,* **79**, 6347–50.

Bjorklund, C. W., Reavis, J. G., Leary, J. A., and Walsh, K. A. (1959) *J. Phys. Chem.,* **63**(10), 1774–7.

Blaise, A., Collard, J. M., Fournier, J. M., Rebizant, J., Spirlet, J. C., and Vogt, O. (1985) *Physica B & C,* **130**(1–3), 99–101.

Blaise, J., Fred, M. S., Carnall, W. T., Crosswhite, H. M., and Crosswhite, H. (1983a) Measurement and Interpretation of Plutonium Spectra (ACS Symp. Ser. no. 216), (eds. W. T. Carnall and G. R. Choppin), American Chemical Society, Washington, DC, pp. 173–98.

Blaise, J., Fred, M., and Gutmacher, R. G. (1983b) *The Atomic Spectrum of Plutonium*, Report ANL-83-95, Argonne National Laboratory, 612 pp.

Blaise, J., Fred, M., and Gutmacher, R. G. (1986) *J. Opt. Soc. Am.,* **B3**(3), 403–18.

Blaise, J., Fred, M., and Gutmacher, R. G., unpublished results.

Blaise, J. and Wyart, J.-F. (1992) *Energy levels and atomic spectra of actinides,* Tables Internationales de Constantes, Paris, France, ISBN 2-9506414-0-7.

Blank, H. (1976) Transurane: Binare Legierungsysteme 1, in *Gmelin Handbuch der Anorganische Chemie* (ed. K.-C. Buschbeck), Springer-Verlag, Berlin, 38 pp.

Blank, H. (1977) Binary Alloys, in *Gmelin Handbuch der Anorganische Chemie Transurane: The Alloys* (ed. K.-C. Buschbeck), Springer-Verlag, Berlin, pp. 1–275.**39, B3:**

Blank, H. (1994) in *Nuclear Materials* (ed. B. R. T. Frost), VCH publishers, Weinheim, 203 pp.

Blank, H., Brossman, G., Kemmerich, M., and Weitzenmiller, F. (1962) *Zwei- und mehrstoffsysteme mit plutonium. Literaturubersicht, phasendiagramme und daten, teil 1, Pu-Ag bis Pu-Sn.* Karlsruhe, Kernreaktor Bau- und Betriebs-Gesellschaft, 243 pp.

Blank, H. R. and Lindner, R. (eds.) (1976a) *Plutonium 1975 and Other Actinides: Proc. Conf. in Baden-Baden*, Sept. 10–13, 1975/*Proc. Fifth Int. Conf. on Plutonium and Other Actinides*, 1975, American Elsevier Publication, New York; North-Holland, Amsterdam.

Blau, M. S. (1998) *J. Radioanal. Nucl. Chem.,* **235**(1–2), 41–5.

Blaudeau, J.-P. and Bursten, B. E. (2000) *Abstracts of Papers, 220th ACS National Meeting*, Aug. 20–24, 2000, Washington, DC, INOR-419.

Bleaney, B. (1955) *Discuss. Faraday Soc.,* **19**, 112–18.

Bluestein, B. A. and Garner, C. S. (1944) *The Preparation of Plutonium Tribromide*, Report LA-116, Los Alamos Scientific Laboratory, 7 pp.

Boatner, L. A. and Sales, B. C. (1988) in *Monazite,* (eds. W. Lutze and R. C. Ewing), Radioactive Waste Forms for the Future North-Holland, Amsterdam.

Bochvar, A. A., Konobeevsky, S. T., Kutaitsev, V. I., Menshikova, T. S., and Chebotarev, N. T. (1958) *Interaction of Plutonium and Other Metals in Connection with the Arrangement in Mendeleev's Periodic Table, Proc. Second UN Int. Conf. on the Peaceful Uses of Atomic Energy,* Geneva, Switzerland, 6, pp. 184–93.

Bodu, R., Bouzigues, H., Morin, N., and Pfiffelmann, J. P. (1972) *C. R. Acad. Sci., Ser. D,* **275**(16), 1731–2.

Boehlert, C. J., Schulze, R. K., Mitchell, J. N., Zocco, T. G., and Pereyra, R. A. (2001) *Scr. Mater.,* **45**(9), 1107–15.

Boerrigter, P. M., Baerends, E. J., and Snijders, J. G. (1988) *Chem. Phys.,* **122**(3), 357–74.

Boeuf, A., Caciuffo, R., Fournier, J. M., Manes, L., Rebizant, J., Roudaut, E., and Rustichelli, F. (1984) *Solid State Commun.,* **52**(4), 451–3.

Bohe, A. E., Nassini, H. E., Bevilacqua, A. M., and Pasquevich, D. M. (1997) *Chlorination Reactions Applied to Reprocessing of Aluminum–Uranium Spent Nuclear Fuels,* 1997 *Symp. on Scientific Basis for Nuclear Waste Management XXI* (eds. I. G. McKinley and C. McCombie), Materials Research Society, Davos, Switzterland, 506, pp. 535–42.

Boivineau, M. (2001) *J. Nucl. Mater.,* **297**, 97–106.

Bokelund, H. and Glatz, J. P. (1984) *Inorg. Chim. Acta,* **94**(1–3), 131–132.

Bolvin, H., Wahlgren, U., Moll, H., Reich, T., Geipel, G., Fanghaenel, T., and Grenthe, I. (2001) *J. Phys. Chem. A,* **105**(51), 11441–5.

Bonnelle, C. (1976) *Struct. Bond. I,* **31**, 23–48.

Boreham, D., Freeman, J. H., Hooper, E. W., Jenkins, I. L., and Woodhead, J. L. (1960) *J. Inorg. Nucl. Chem.,* **16**, 154–6.

Boring, M. and Hecht, H. G. (1978) *J. Chem. Phys.,* **69**(1), 112–16.

Boring, A. M. and Smith, J. L. (2000) *Los Alamos Science,* **26**(1), 90.

Borkowski, M., Chiarizia, R., Jensen, M. P., Ferraro, J. R., Thiyagarajan, P., and Littrell, K. C. (2003) *Separ. Sci. Technol.,* **38**(12–13), 3333–51.

Boucher, R. and Quere, Y. (1981) *J. Nucl. Mater.,* **100**(1–3), 132–6.

Boukhalfa, H., Reilly, S. D., Smith, W. H., and Neu, M. P. (2004) *Inorg. Chem.,* **43**(19), 5816–23.

Boulet, P., Wastin, F., Colineau, E., Griveau, J. C., and Rebizant, J. (2003) *J. Phys. Condens. Mat.,* **15**(28), S2305–S2308.

Bourges, J., Madic, C., Koehly, G., and Lecomte, M. (1986) *J. Less-Common Met.,* **122**, 303–11.

Bovey, L. and Gerstenkorn, S. (1961) *J. Opt. Soc. Am.,* **51**, 522–5.

Bovey, L. and Steers, E. B. M. (1960) *Spectrochim. Acta,* **16**, 1184–99.

Bowersox, D. F. and Leary, J. A. (1966) *The Solubilities of Selected Elements in Liquid Plutonium. X. Thulium*, Report LA-3623, Los Alamos Scientific Laboratory, 10 pp.

Bowersox, D. F. and Leary, J. A. (1967) *Trans. Amer. Nucl. Soc.,* **10**(1), 106.

Bowersox, D. F. and Leary, J. A. (1968) *The Solubilities of Selected Elements in Liquid Plutonium. XII Chromium*, Report LA-3850, Los Alamos Scientific Laboratory, 5 pp.

Bradley, D. C., Harder, B., and Hudswell, F. (1957) *J. Chem. Soc.*, *Abstracts*: 3318.

Brandel, V. and Dacheux, N. (2004a) *J. Solid State Chem.,* **177**, 4743–54.

Brandel, V. and Dacheux, N. (2004b) *J. Solid State Chem.,* **177**, 4755–67.

Brennan, J. G., Green, J. C., and Redfern, C. M. (1989) *J. Am. Chem. Soc.,* **111**(7), 2373–7.

Brett, N. H. and Fox, A. C. (1966) *J. Inorg. Nucl. Chem.,* **28**(5), 1191–203.

Brewer, L. (1953) *Chem. Rev.,* **52**, 1–75.

Brewer, L. (1965) in *High-strength Materials* (ed. V. F. Zackay), John Wiley, New York, 12.

Brewer, L. (1970) *Proc. Fourth Int. Conf. on Plutonium and Other Actinides,* (ed. W. N. Miner), The Metallurgical Society of AIME, Warrendale, PA, 650 pp.

Brewer, L. (1971a) *J. Opt. Soc. Am.,* **61**(8), 1101–11.

Brewer, L. (1971b) *J. Opt. Soc. Am.,* **61**(12), 1666–82.

Brewer, L. (1983) Systematics of the Properties of the Lanthanides, in *Systematics and the Properties of the Lanthanides* (eds. S. P. Sinha, D. Reidel), Hingham, MA, pp. 17–69.

Brewer, L. (2000) *Metall. Mater. Trans.,* **31B**(4), 603–7.

Brewer, L., Bromley, L., Gilles, P. W., and Lofgren, N. L. (1949) *Natl. Nucl. En. Ser.*, Div IV **14B**(Transuranium Elements, Pt. II) (eds. G. T. Seaborg, J. J. Katz and W. M. Manning), McGraw-Hill, New York, pp. 861–86.

Bridger, N. J. and Dell, R. M. (1967) *Research on Plutonium Nitride*, Report AERE-R-5441, UK Atomic Energy Research Group, Atomic Energy Research Establishment, 14 pp.

Bridger, N. J., Dell, R. M., and Wheeler, V. J. (1969) *Reactivity Solids, Proc. Sixth Int. Symp.*, pp. 389–400.

Brodsky, M. B. (1961) *Comment on J. Friedel Paper, Plutonium 1960,* Grenoble, France (eds. E. Grison, W. B. H. Lord, and R. D. Fowler), Cleaver-Hume Press, London, 1, 210 pp.

Brown, D. (1968) *Halides of the Lanthanides and Actinides.* Wiley-Interscience, New York, 290 pp.

Brown, F., Ockenden, H. M., and Welch, G. A. (1955) *J. Chem. Soc.*, *Abstracts*: 4196–201.

Brown, D., Fletcher, S., and Holah, D. G. (1968) *J. Chem. Soc.*, *(London)* (8), 1889–94.

Brown, D., and Edwards, J. (1972) *J. Chem. Soc., Dalton Trans.: Inorg. Chem.* (1972–1999) (16), 1757–1762.

Brown, D., Hurtgen, C., and Fuger, J. (1977) *Rev. Chim. Miner.,* **14**(2), 189–98.

Buchmeiser, M. R. (2001) *Macromol. Rapid Commun.,* **22**(14), 1081–94.

Budantseva, N. A., Shilov, V. P., and Krot, N. N. (1998) *Radiochemistry,* **40**(6), 565–7.

Budantseva, N. A., Fedosseev, A. M., Bessonov, A. A., Grigoriev, M. S., and Krupa, J. C. (2000) *Radiochim. Acta,* **88**(5), 291–5.

Bullock, J. I., Ladd, M. F. C., Povey, D. C., and Storey, A. E. (1980) *Inorg. Chim. Acta,* **43**(1), 101–8.

Büppelmann, L., Kim, J. I., and Lierse, C. (1988) *Radiochim. Acta,* **44–45**(Pt. 1), 65–70.

Burney, G. A. (1962) *Separation of Neptunium and Plutonium by Anion Exchange*, Report DP-689, E. I. du Pont de Nemours & Co., Aiken, SC, 33 pp.

Burney, G. A. and Thompson, G. H. (1972) *Radiochem. Radioanal. Lett.,* **12**(4–5), 207–14.

Burney, G. A. and Thompson, G. H. (1974) *Separation of Plutonium-238 from Neptunium-237 by Pressurized Anion Exchange*, Report DP-1331, Savannah River Laboratory, E. I. DuPont de Nemours and Co., Aiken, SC, 21 pp.

Burns, C. J. and Sattelberger, A. P. (2002) Organometallic and Nonaqueous Coordination Chemistry, in *Advances in Plutonium Chemistry 1967–2000* (ed. D. C. Hoffman), American Nuclear Society, La Grange Park, IL, pp. 61–76.

Burns, C. J., Neu, M. P., Boukhalfa, H., Gutowski, K. E., Bridges, N. J., and Rogers, R. D. (2004) *Comprehensive Coord. Chem. II,* **3**, 189–345.

Burns, C. J., Clark, D. L., and Sattelberger, A. P. (2005) Actinides: Organometallic Chemistry, in *Encyclopedia of Inorganic Chemistry 2nd Ed.* (ed. R. B. King), Wiley Interscience, New York, 33–59.

Burns, J. H., Peterson, J. R., and Stevenson, J. N. (1975) *J. Inorg. Nucl. Chem.,* **37**(3), 743–9.

Burns, R. C. and O'Donnell, T. A. (1977) *Inorg. Nucl. Chem. Lett.,* **13**(12), 657–60.

Bursten, B. E. and Strittmatter, R. J. (1991) *Angew. Chem., Int. Ed. Engl.,* **30**(9), 1069–85.

Burwell, C. C., Bidwell, R. M., Hammond, R. P., Kemme, J. E., and Thamer, B. J. (1962) *Nucl. Sci. Eng.,* **14**, 123–34.

Buscher, C. T., Donohoe, R. J., Mecklenburg, S. L., Berg, J. M., Tait, C. D., Huchton, K. M., and Morris, D. E. (1999) *Appl. Spectrosc.,* **53**(8), 943–53.

Buyers, W. J. L. and Holden, T. M. (1985) in *Handbook on the Physics and Chemistry of Actinides,* vol. 2, (eds. A. J. Freeman and G. H. Lander), North-Holland, Amsterdam, 239 pp.

Bychkov, A. V. and Skiba, O. V. (1999) Review of Non-aqueous Nuclear Fuel Reprocessing and Separation Methods, in *Chemical Separation Technologies and Related Methods of Nuclear Waste Management* (eds. G. R. Choppin and M. K. Khankhasayev), Kluwer Academic Publishers, Boston, MA, pp. 71–98.

Calder, C. A., Draney, E. C., and Wilcox, W. W. (1981) *J. Nucl. Mater.,* **97**, 126–36.

Campbell, G. M., Kent, R. A., and Leary, J. A. (1970) *Plutonium 1970 and Other Actinides, Proc. Fourth Int. Conf. on Plutonium and Other Actinides,* (ed. W. N. Miner), Santa Fe, NM, Oct. 5–9, 1970 Metallurgical Society of AIME, New York, 781 pp.

Cantrell, K. J. (1988) *Polyhedron,* **7**(7), 573–4.

Capdevila, H. and Vitorge, P. (1995) *Radiochim. Acta,* **68**(1), 51–62.

Capdevila, H. and Vitorge, P. (1998) *Radiochim. Acta,* **82**, 11–16.

Capdevila, H. and Vitorge, P. (1999) *Czech. J. Phys. Sect. B,* **49**(Suppl. 1, Pt. 2, 13th Radiochemical Conference, 1998, 603–9.

Capdevila, H., Vitorge, P., and Giffaut, E. (1992) *Radiochim. Acta,* **58/59**(Pt. 1), 45–52.

Capdevila, H., Vitorge, P., Giffaut, E., and Delmau, L. (1996) *Radiochim. Acta,* **74**, 93–8.

Capone, F., Colle, Y., Hiernaut, J. P., and Ronchi, C. (1999) *J. Phys. Chem. A,* **103**(50), 10899–906.

Carbajo, J. J., Yoder, G. L., Popov, S. G., and Ivanov, V. K. (2001) *J. Nucl. Mater.,* **299** (3), 181–98.

Carnall, W. T. (1989) *J. Less-Common Met.,* **156**, 221–35.

Carnall, W. T. (1992) *J. Chem. Phys.,* **96**(12), 8713–26.

Carnall, W. T., and Choppin, G. R. (eds.) (1983) *ACS Symp. Ser.*, **216**(Plutonium Chem.), American Chemical Society, Washington, DC. 484 pp.

Carnall, W. T., Liu, G. K., Williams, C. W., and Reid, M. F. (1991) *J. Chem. Phys.,* **95** (10), 7194–203.

Carniglia, S. C. (1953) *Vapor-pressures of Americium Trifluoride and Americium Metal.* Thesis, Report UCRL-2389, University of California, Berkeley, 76 pp.

Carniglia, S. C., and Cunningham, B. B. (1955) *J. Am. Chem. Soc.,* **77**(6), 1451–3.

Carre, D., Laruelle, P., and Besancon, P. (1970) *Cr. Acad. Sci. C Chim.,* **270**(6), 537–9.

Carroll, D. F. (1964) *J. Am. Ceram. Soc.,* **47**(12), 650.

Cassol, A., Di Bernardo, P., Portanova, R., and Magon, L. (1973) *Inorg. Chim. Acta,* **7**, 353.

Cauchetier, P. and Guichard, C. (1973) *Radiochim. Acta,* **19**(3), 137–46.

Cauchetier, P. and Guichard, C. (1975) *J. Inorg. Nucl. Chem.,* **37**(7–8), 1771–8.

Cauchois, Y. and Manescu, I. (1956) *Compt. Rend.,* **242**, 1433–6.

Cauchois, Y., Manescu, I., and Le Berquier, F. (1954) *Compt. Rend.,* **239**, 1780–2.

Cauchois, Y., Bonnelle, C., and Bersuder, L. (1963a) *Compt. Rend.,* **257**(20), 2980–3.

Cauchois, Y., Bonnelle, C., and de Bersuder, L. (1963b) *Compt. Rend.,* **256**, 112–14.

Cefola, M. (1958) *Microchem. J.,* **2**, 205–17.

Chackraburtty, D. M. and Jayadevan, N. C. (1964) *Indian J. Phys.,* **38**(11), 585–6.

Chackraburtty, D. M. and Jayadevan, N. C. (1965) *Acta Crystallogr.,* **18**, 811.

Chackraburtty, D. M., Jayadevan, N. C., and Swaramakrishnan, C. K. (1963) *Acta Crystallogr.,* **16**(Pt. 10), 1060–1.

Chang, Y. A., Chen, S. L., Zhang, F., and Oates, W. A. (2002) Improving Multicomponent Phase Diagram Calculations, in *CALPHAD and Alloy Thermodynamics* (eds. P. E. A. Turchi, A. Gonis and R. D. Shull), TMS-Minerals, Metals & Material Society, Warrendale, PA, 53 pp.

Charvillat, J. P. (1978) *Crystal Chemistry of Transuranium Pnictides*, Report CEA-R-4933, CEA, CEN, Fontenay-aux-Roses, France, 364 pp.

Charvillat, J. P. and Damien, D. (1973) *Inorg. Nucl. Chem. Lett.,* **9**(5), 559–63.

Charvillat, J. P., Damien, D., and Wojakowski, A. (1977) *Rev. Chim. Miner.,* **14**(2), 178–88.

Chebotarev, N. T. and Utkina, O. N. (1975) Relation between Structure and Some Properties of δ-plutonium and γ-uranium Alloys. *Plutonium 1975 and Other Actinides, Proc. Fifth Int. Conf.*, Baden-Baden, Germany (eds. H. Blank and R. Lindner), North-Holland Publishing Company, New York, pp. 559–66.

Cheetham, A. K., Fender, B. E. F., Fuess, H., and Wright, A. F. (1976) *Acta Crystallogr. B,* **B32**(1), 94–7.

Chereau, P. and Wadier, J. F. (1973) *J. Nucl. Mater.,* **46**(1), 1–8.

Chereau, P., Dean, G., De Franco, M., and Gerdanian, P. (1977) *J. Chem. Thermodyn.,* **9** (3), 211–19.

Chiarizia, R., Jensen, M. P., Borkowski, M., Ferraro, J. R., Thiyagarajan, P., and Little, K. C. (2003) *Separ. Sci. Technol.,* **38**(12–13), 3313–31.

Chikalla, T. D. (1968) *J. Am. Ceram. Soc.,* **46**(7), 328.

Chikalla, T. D., McNeilly, C. E., and Skavdahl, R. E. (1962) *The Plutonium-Oxygen System*, Report HW-74802, General Electric Company, Hanford Atomic Products Operation, 30 pp.

Chikalla, T. D., McNeilly, C. E., and Skavdahl, R. E. (1964) *J. Nucl. Mater.,* **12**(2), 131–41.

Chipaux, R., Bonnisseau, D., Boge, M., and Larroque, J. (1988) *J. Magn. Magn. Mater.,* **74**(1), 67–73.

Chipaux, R., Larroque, J., and Beauvy, M. (1989) *J. Less-Common Met.,* **153**(1), 1–7.

Chipaux, R., Blaise, A., and Fournier, J. M. (1990) *J. Magn. Magn. Mater.,* **84**(1–2), 132–42.

Choppin, G. R. (1983) *Radiochim. Acta,* **32**(1–3), 43–53.

Choppin, G. R. and Saito, A. (1984) *Radiochim. Acta,* **35**(3), 149–54.

Choppin, G. R. and Wong, P. J. (1998) *Aquat. Geochem.,* **4**(1), 77–101.

Choppin, G. R., Roberts, R. A., and Morse, J. W. (1986) *ACS Symp. Ser.* **305** (Org. Mar. Geochem.), American Chemical Society, Washington, D.C. 382–8.

Christensen, E. L. and Maraman, W. J. (1969) *Plutonium Processing at the Los Alamos Scientific Laboratory*, Report LA-3542, Los Alamos Scientific Laboratory, 85 pp.

Christensen, E. L. and Mullens, L. J. (1952) *Preparation of Anhydrous Plutonium trichloride*, Report LA-1431, Los Alamos Scientific Laboratory, Los Alamos, NM, 8 pp.

Christensen, D. C. and Mullins, L. J. (1983) *ACS Symp. Ser.* **216**(Plutonium Chem.) (eds. W. T. Carnall and G. R. Choppin), American Chemical Society, Washington, DC. pp. 409–31.

Christensen, D. C., Bowersox, D. F., McKerley, B. J., and Nance, R. L. (1988) *Wastes from Plutonium Conversion and Scrap Recovery Operations*, Report LA-11069-MS, Los Alamos National Laboratory, Los Alamos, NM, 96 pp.

Christoph, G. G., Larson, A. C., Eller, P. G., Purson, J. D., Zahrt, J. D., Penneman, R. A., and Rinehart, G. H. (1988) *Acta Crystallogr. B,* **B44**(6), 575–80.

Chudinov, E. G. and Choporov, D., Ya. (1970) *At. Energiya,* **28**(2), 151–3.

Cinader, G., Zamir, D., and Hadari, Z. (1976) *Phys. Rev. B,* **14**(3), 912–20.

Clark, H. K. (1981) *Nucl. Sci. Eng.,* **79**(1), 65–84.

Clark, D. L. (in preparation) Crystal structures of K(18-crown-6)$_2$AnO$_2$Cl$_4$, (An = Np, Pu), Los Alamos National Laboratory, for publication.

Clark, S. B. and Delegard, C. (2002) Plutonium in Concentrated Solutions, in *Advances in Plutonium Chemistry 1967–2000* (ed. D. C. Hoffman), American Nuclear Society, La Grange Park, IL, pp. 118–68.

Clark, D. L., Hobart, D. E., and Neu, M. P. (1995) *Chem. Rev.,* **95**(1), 25–48.

Clark, D. L., Conradson, S. D., Ekberg, S. A., Hess, N. J., Neu, M. P., Palmer, P. D., Runde, W., and Tait, C. D. (1996) *J. Am. Chem. Soc.,* **118**(8), 2089–90.

Clark, D. L., Conradson, S. D., Keogh, D. W., Palmer, P. D., Scott, B. L., and Tait, C. D. (1998) *Inorg. Chem.,* **37**(12), 2893–9.

Clark, D. L., Conradson, S. D., Donohoe, R. J., Keogh, D. W., Morris, D. E., Palmer, P. D., Rogers, R. D., and Tait, C. D. (1999a) *Inorg. Chem.,* **38**(7), 1456–66.

Clark, D. L., Conradson, S. D., Keogh, D. W., Neu, M. P., Palmer, P. D., Runde, W., Scott, B. L., and Tait, C. D. (1999b) *X-ray Absorption and Diffraction Studies of Monomeric Actinide Tetra-, Penta-, and Hexa-Valent Carbonato Complexes*. Speciation, Techniques and Facilities for Radioactive Materials at Synchrotron Light Sources, OECD Nuclear Energy Agency, pp. 121–33.

Clayton, E. D. (1965) *Phys. Today,* **18**(9), 46–8, 50–2.

Cleveland, J. M. (1979) *The Chemistry of Plutonium,* American Nuclear Society, La Grange Park, IL, 680 pp.

Cleveland, J. M. (1980) Section IV: Chemical Processing, in *Plutonium Handbook: A Guide to the Technology,* vol. 2, (ed. O. J. Wick), American Nuclear Society, LaGrange Park, IL, 966 pp.

Cleveland, J. M., Bryan, G. H., Heiple, C. R., and Sironen, R. J. (1974) *J. Am. Chem. Soc.,* **96**(7), 2285–6.

Cleveland, J. M., Bryan, G. H., Heiple, C. R., and Sironen, R. J. (1975) *Nucl. Technol.,* **25**(3), 541–5.

Coffinberry, A. S. and Miner, W. N. (eds.) (1961) *The Metal Plutonium,* University of Chicago Press, Chicago, 446 pp

Coffinberry, A. S. and Waldron, M. B. (1956) Metallurgy and Fuels in *Progress in Nuclear Energy,* (eds. J. P. Howe and H.M. Finniston), ser. V, vol. 1, Pergamon Press, London, pp. 354–410.

Coffinberry, A. S., Schonfeld, F. W., Cramer, E. M., Miner, W. N., Ellinger, F. H., Elliott, R. O., and Struebing, V. O. (1958) *The Physical Metallurgy of Plutonium and its Alloys*. Second United Nations International Conference on the Peaceful Uses of Atomic Energy, Geneva, Switzerland, United Nations, 6, 681 pp.

Cogliati, G., Recrosio, A., and Lanz, R. (1969) *Plutonium Compounds*, (Comitato Nazionale per l'Energia Nucleare) De Patent 1801682, 14 pp.

Cohen, D. (1961a) *J. Inorg. Nucl. Chem.,* **18**, 207–10.

Cohen, D. (1961b) *J. Inorg. Nucl. Chem.,* **18**, 211–18.

Coleman, C. F. and Leuze, R. E. (1978) *J. Tenn. Acad. Sci.,* **53**(3), 102–7.

Colinet, C. (2002) Phase Diagram Calculations: Contribution of *Ab initio* and Cluster Variation Methods, in *CALPHAD and Alloy Thermodynamics.* (eds. P. E. A. Turchi, A. Gonis and R. D. Shull), TMS-Minerals, Metals & Material Society, Warrendale, PA, 21 pp.

Comstock, A. A. (1952) *Measurement of Plutonium Liquid Density*, Report LA-1348, Los Alamos Scientific Laboratory, 23 pp.

Connick, R. E. (1949) *J. Am. Chem. Soc.,* **71**, 1528–33.

Connick, R. E. (1954) Oxidation States, Potentials, Equilibria, and Oxidation–Reduction Reactions of Plutonium, in *The Actinide Elements* (eds. G. T. Seaborg and J. J. Katz), McGraw-Hill, New York, pp. 221–300.

Connick, R. E. and McVey, W. H. (1949) *J. Am. Chem. Soc.,* **71**(5), 1534–42.

Conradson, S. D. (2000) *Los Alamos Science,* **26**(2), 356.

Conradson, S. D. (2003) personal communication, S. S. Hecker, Los Alamos, NM.

Conradson, S. D., Mahamid, I. A., Clark, D. L., Hess, N. J., Hudson, E. A., Neu, M. P., Palmer, P. D., Runde, W. H., and Tait, C. D. (1998) *Polyhedron,* **17**(4), 599–602.

Conradson, S. D., Begg, B. D., Clark, D. L., Den Auwer, C., Espinosa- Faller, F. J., Gordon, P. L., Hess, N. J., Hess, R., Keogh, D. W., Morales, L. A., Neu, M. P., Runde, W., Tait, C. D., Veirs, D. K., and Villella, P. M. (2003) *Inorg. Chem.,* **42**(12), 3715–17.

Conradson, S. D., Abney, K. D., Begg, B. D., Brady, E. D., Clark, D. L., Den Auwer, C., Ding, M., Dorhout, P. K., Espinosa- Faller, F. J., Gordon, P. L., Haire, R. G., Hess, N. J., Hess, R. F., Keogh, D. W., Lander, G. H., Lupinetti, A. J., Morales, L. A., Neu, M. P., Palmer, P. D., Paviet- Hartmann, P., Reilly, S. D., Runde, W. H., Tait, C. D., Veirs, D. K., and Wastin, F. (2004a) *Inorg. Chem.,* **43**(1), 116–31.

Conradson, S. D., Begg, B. D., Clark, D. L., Den Auwer, C., Ding, M., Dorhout, P. K., Espinosa- Faller, F. J., Gordon, P. L., Haire, R. G., Hess, N. J., Hess, R. F., Keogh, D. W., Morales, L. A., Neu, M. P., Paviet- Hartmann, P., Runde, W., Tait, C. D., Veirs, D. K., and Villella, P. M. (2004b) *J. Am. Chem. Soc.,* **126**(41), 13443–58.

Conway, J. G. and Rajnak, K. (1966) *J. Chem. Phys.,* **44**, 348–54.

Coogler, A. L., Craft, R. C., and Tetzlaff, R. N. (1963) *Proc. Conf. on Hot Laboratory Equipment*, vol. 11, pp. 75–87.

Cooper, B. R., Thayamballi, P., Spirlet, J. C., Mueller, W., and Vogt, O. (1983) *Phys. Rev. Lett.,* **51**(26), 2418–21.

Cooper, N. G. and Schecker, J. A. (eds.) (2000) *Los Alamos Science,* Vol. 26, Los Alamos Science, Los Alamos National Laboratory, 493 pp

Coops, M. S., Knighton, J. B., and Mullins, L. J. (1983) *ACS Symp. Ser.* **216**(Plutonium Chem.) (eds. W. T. Carnall and G. R. Choppin), American Chemical Society, Washington, DC. pp. 381–408.

Cope, R. G., Hughes, D. G., Loasby, R. G., and Miller, D. C. (1960) The Plutonium–Ruthenium and Plutonium–Neptunium Binary Phase Diagrams, in *Plutonium 1960,* Grenoble, France (eds. E. Grison, W. B. H. Lord and R. D. Fowler), Cleaver-Hume Publishing, London, 280 pp.

Cordfunke, E. H. P., and Konings, R. J. M., Editors (1990) *Thermochemical Data for Reactor Materials and Fission Products,* North-Holland, Amsterdam, 696 pp.

Cornet, J. A. (1971) *J. Phys. Chem. Solids,* **32**, 1489–506.

Cornet, J. A. and Bouchet, J. M. (1968) *J Nucl. Mater.,* **28**, 303–10.

Costa, P. (1960) *J. Nucl. Mater.,* **2**, 75.

Costanzo, D. A., Biggers, R. E., and Bell, J. T. (1973) *J. Inorg. Nucl. Chem.,* **35**(2), 609–22.

Covert, A. S. and Kolodney, M. (1945) *Protection of Plutonium against Atmospheric Oxidation*, Report LA-314, Los Alamos Scientific Laboratory, 38 pp.

Cowan, G. A. (1976) *Sci. Am.,* **235**(1), 36–47.

Cox, M. and Flett, D. S. (1983) Metal Extractant Chemistry, in *Handbook of Solvent Extraction* (eds. T. C. Lo, M. H. I. Baird, and C. Hanson), Wiley, New York, 980 pp.

Cox, L. E., Martinez, R., Nickel, J. H., Conradson, S. D., and Allen, P. G. (1995) *Phys. Rev. B,* **51**(2), 751–5.

Cox, L. E., Peek, J. M., and Allen, J. W. (1999) *Physica B,* **259–261**, 1147–8.

Cramer, E. M. and Wood, D. H. (1967) *J. Less-Common Met.,* **13**(1), 112–21.

Cramer, E. M., Ellinger, F. H., and Land, C. C. (1960) *Extractive and Physical Metallurgy of Plutonium and its Alloys* (ed. W. D. Wilkinson), Interscience Publishers, New York, 169 pp.

Cramer, E. M., Hawes, L. L., Miner, W. N., and Schonfeld, F. W. (1961) *The Dilatometry and Thermal Analysis of Plutonium Metal,* in *The Metal Plutonium.* (eds. A. S. Coffinberry and W. N. Miner), University of Chicago Press, Chicago, IL, pp. 112–22.

Cremers, T. L., Dworzak, W. R., Brown, W. G., Flamm, B. F., Sampson, T. E., Bronisz, L. E., Nelson, T. O., Bronson, M. C., Colmenares, C. A., and Merrill, R. D. (1995) *Proc. Fifth Int. Conf. on Radioactive Waste Management and Environmental Remediation*, vol. 1, Berlin, Sept. 3–7, 1995, pp. 553–6.

Crisler, L. R. and Eggerman, W. G. (1974) *J. Inorg. Nucl. Chem.,* **36**(6), 1424–6.

Crocker, A. G. (1971) *J. Nucl. Mat.,* **41**(2), 167.

Crocker, H. W. (1961) *Ammonium bifluoride Fusion of Ignited Plutonium dioxide*, Report HW-68655, General Electrical Company, Richland, Washington, 5 pp.

Croff, A. G. (1980) ORIGEN2: *A Revised and Updated Version of the Oak Ridge Isotope Generation and Depletion Code*, Report ORNL-5621, Oak Ridge National Laboratory, 62 pp.

Croff, A. G. (1983) *Nucl. Technol.,* **62**(3), 335–52.

Cromer, D. T. (1975) *Acta Crystallogr.* **B31**, 1760.

Cromer, D. T. (1976) *Acta Crystallogr.* **B32**, 1930.

Cromer, D. T. (1977a) *Acta Crystallogr.* **B33**, 1993.

Cromer, D. T. (1977b) *Acta Crystallogr.* **B33**, 1996.

Cromer, D. T. (1978) *Acta Crystallogr.* **B34**, 913.

Cromer, D. T. (1979a) *Acta Crystallogr.* **B35**, 14.

Cromer, D. T. (1979b) *Acta Crystallogr.* **B35**, 1945.

Cromer, D. T. and Larson, A. C. (1960) *Acta Crystallogr.,* **13**(11), 909–12.

Cromer, D. T. and Larson, A. C. (1975) *Acta Crystallogr.* **B31**, 1758.

Cromer, D. T. and Larson, A. C. (1977) *Acta Crystallogr.* **B33**, 2620.

Cromer, D. T. and Olsen, C. E. (1959) *Acta Crystallogr.,* **12**(9), 689–94.

Cromer, D. T. and Roof, R. B. (1959) *Acta Crystallogr.,* **12**(11), 942–3.

Cromer, D. T., Larson, A. C., and Roof, R. B. Jr., (1964) *Acta Crystallogr.,* **17**(8), 947–50.

Cromer, D. T., Larson, A. C., and Roof, R. B. (1973) *Acta Crystallogr.* **B29**, 564–7.

Cromer, D. T., Larson, A. C., and Roof, R. B. (1975) *Acta Crystallogr.* **B31**, 1756.

Cunningham, B. B. (1949) *Nucleonics,* **5**(No. 5), 62–85.

Cunningham, B. B. (1954) Preparation and Properties of the Compounds of Plutonium, in *The Actinide Elements* (eds. G. T. Seaborg and J. J. Katz), McGraw-Hill, New York, pp. 371–434.

Cunningham, B. B. and Werner, L. B. (1949a) *J. Am. Chem. Soc.,* **71**, 1521–8.

Cunningham, B. B. and Werner, L. B. (1949b) The First Isolation of a Synthetic Element 94Pu239, in *Natl. Nucl. Energy Serv.*, Div IV **14B**(Transuranium Elements, Pt. I) (eds. G. T. Seaborg, J. J. Katz and W. M. Manning), McGraw-Hill, New York, 51–78.

Curtis, D., Fabryka- Martin, J., Dixon, P., and Cramer, J. (1999) *Geochim. Cosmochim. Acta,* **63**(2), 275–85.

Czerwinski, K. and Kim, J.-I. (1997) *Mater. Res. Soc. Symp. Proc.,* **465**(Scientific Basis for Nuclear Waste Management XX), 743–50.

Dacheux, N., Podor, R., Brandel, V. and Genet, C. R. (1998) *J. Nucl. Mater.,* **252,** 179–86.

Dai, X., Savrasov, S. Y., Kotliar, G., Migliori, A., Ledbetter, H., and Abrahams, E. (2003) *Science,* **300**(5621), 953–5.

Dalton, J. T. and Griffin, R. M. (1964) *The Thorium–Plutonium–Carbon System*, Report AERE-R-4742, Atomic Energy Reseach Establishment, Harwell, UK, 20 pp.

Dalton, J. T., Potter, P. E., and Shaw, J. L. (1967) *Plutonium 1965, Proc. Third Int. Conf.*, pp. 775–805.

Damien, D. (1973) *Inorg. Nucl. Chem. Lett.,* **9**(4), 453–6.

Damien, D. (1976) *Synthesis and Crystal Chemistry of Transuranium Element Chalcogenides. Contribution to the Study of the 5f Electron Localization*, Report CEA-R-4783, CEN, CEA, Fontenay-aux-Roses, France, 161 pp.

Damien, D. and De Novion, C. H. (1981) *J. Nucl. Mater.,* **100**(1–3), 167–77.

Damien, D., de Novion, C. H., and Thevenin, T. (1986) Crystal Chemistry of Actinide Chalcogenides and Pnictides, in *Handbook on the Physics and Chemistry of the Actinides* (eds. A. J. Freeman and C. Keller), Elsevier Science, Amsterdam, pp. 39–96.

Danis, J. A., Lin, M. R., Scott, B. L., Eichhorn, B. W., and Runde, W. H. (2001) *Inorg. Chem.,* **40**(14), 3389–94.

Darken, L. S. and Gurry, R. W. (1953) *Physical Chemistry of Metals,* McGraw-Hill, New York, 535 pp.

David, S. J. and Kim, K. C. (1988) *J. Chem. Phys.,* **89**(4), 1780–6.

Davidson, N. R. and Katz, J. J. (1958) *Plutonium halides.* US Patent no. 2859 097. (U.S. Atomic Energy Commission)

Davidson, N. R., Hagemann, F., Hyde, E. K., Katz, J. J., and Sheft, I. (1949) The Preparation and Properties of Plutonium Tribromide and Oxybromide. *Natl. Nucl. Energy Ser.*, Div IV **14B**(Transuranium Element, Pt. I) (eds. G. T. Seaborg, J. J. Katz and W. M. Manning), McGraw Hill, New York, 759–74.

Dawson, J. K. and Elliott, R. M. (1953) *The Thermogravimetry of Some Plutonium Compounds*, Report AERE-C/R-1207, Great Britain Atomic Energy Research Establishment, 20 pp.

Dawson, J. K. and Truswell, A. E. (1951) *The Preparation of Plutonium Trifluoride and Tetrafluoride by the Use of Hydrogen Fluoride*, Report AERE-C/R-662, Great Britain Atomic Energy Research Establishment, 6 pp.

Dawson, J. K., Mandleberg, C. J., and Davies, D. (1951) *J. Chem. Soc.*, 2047–50.

Dawson, J. K., D'Eye, R. W. N., and Truswell, A. E. (1954a) *J. Chem. Soc., Abstracts*: 3922–9.

Dawson, J. K., Elliott, R. M., Hurst, R., and Truswell, A. E. (1954b) *J. Chem. Soc.*, 558–64.

Dayton, R. W. and Tipton, C. R., Jr (1961) *Progress Relating to Civilian Applications during June 1961*, Report BMI-1524(Del.), Battelle Memorial Institute, 104 pp.

De Alleluia, I. B., Berndt, U., and Keller, C. (1983) *Rev. Chim. Miner.,* **20**(4–5), 441–8.

De Winter, F., Stapfer, G., and Medina, E. (1999) *The Design of a Nuclear Power Supply with a 50 Year Life Expectancy: the JPL Voyager's SiGe MHW RTG. Proc. 34th Intersociety Energy Conversion Engineering Conf.*, pp. 433–40.

Dean, G. and Boivineau, J. C. (1970b) *Plutonium 1970 and Other Actinides, Proc. Fourth Int. Conf. on Plutonium and Other Actinides*, Santa Fe, NM, Oct. 5–9, 1970 (ed. W. N. Miner), AIME, New York.

Dean, G., Boivineau, J. C., Chereau, P., and Marcon, J. P. (1970a) *Plutonium 1970 and Other Actinides, Proc. Fourth Int. Conf. on Plutonium and Other Actinides*, Santa Fe, NM, Oct. 5–9, 1970 (ed. W. N. Miner), AIME, New York, 753 pp.

Deaton, R. L. and Wiedenheft, C. J. (1973) *J. Inorg. Nucl. Chem.,* **35**(2), 649–50.

Deloffre, P. (1997) *Etude de la Stabilite de la Phase Delta des Alliages de Plutonium Obtenue par Additions d'elements Deltagenes,* Thesis, Universite de Paris-Sud, Department d'Etudes et Technologies Nucleaires, Paris, 152 pp.

Den Auwer, C., Revel, R., Charbonnel, M. C., Presson, M. T., Conradson, S. D., Simoni, E., Le Du, J. F., and Madic, C. (1999) *J. Synchrotron Radiat.,* **6**(2), 101–04.

Denning, R. G. (1991) *Eur. J. Solid State Inorg.,* **28**(Suppl.), 33–45.

Denning, R. G. (1992) *Structure and Bonding,* **79**(Complexes, Clusters Cryst. Chem.), 215–76.

Denning, R. G. (1999) *Spectrochim. Acta. A,* **55**(9), 1757–65.

Denning, R. G., Green, J. C., Hutchings, T. E., Dallera, C., Tagliaferri, A., Giarda, K., Brookes, N. B., and Braicovich, L. (2002) *J. Chem. Phys.,* **117**(17), 8008–20.

Denotkina, R. G., Moskvin, A. I., and Shevchenko, V. B. (1960) *Russ. J. Inorg. Chem.,* **5**, 387–9.

Denotkina, R. G., Shevchenko, V. B., and Moskvin, A. I. (1965) *Russ. J. Inorg. Chem.,* **10**, 1333–35.

Denotkina, R. G., and Shevchenko, V. B. (1967) *Russ. J. Inorg. Chem.,* **12**, 42–45.

Deron, S. and Vesnovskii, S. (1999) *Nucl. Instrum. Meth. A,* **438**(1), 20–2.

Dewey, H. J., Barefield, II, J. E., and Rice, W. W. (1986) *J. Chem. Phys.,* **84**(2), 684–91.

Dixon, P., Curtis, D. B., Musgrave, J., Roensch, F., Roach, J., and Rokop, D. (1997) *Anal. Chem.,* **69**(9), 1692–9.

Dmitriev, S. N., Oganessian, Y. T., Buklanov, G. V., Kharitinov, Y. P., Novgorodov, A. F., Salamatin, L. I., Starodub, G. Y., Shishkin, S. V., Yushkevich, Y. V., and Newton, D. (1993) *Appl. Radiat. Isot.,* **44**(8), 1097–100.

Dmitriev, S. N., Oganessian, Y. T., Starodub, G. Y., Shishkin, S. V., Bulanov, G. V., Kharitonov, Y. P., Novgorodov, A. F., Yushkevich, Y. V., Newton, D., and Talbot, R. J. (1995) *Appl. Radiat. Isot.,* **46**(5), 307–9.

Dmitriev, S. N., Zaitseva, N. G., Starodub, G. Y., Maslov, O. D., Shishkin, S. V., Shishkina, T. V., Buklanov, G. V., and Sabelnikov, A. V. (1997) *Nucl. Instrum. Methods Phys. Res., Sect. A,* **397**(1), 125–30.

Dodgen, H. W., Chrisney, J., and Rollefson, G. K. (1944) *The Spectrum of Plutonium*, Report ANL-JJK-14B-24, Argonne National Laboratory, 17 pp.

Dodgen, H. W., Chrisney, J., and Rollefson, G. K. (1949) *Natl. Nucl. Energy Ser.*, Div IV **14B**(Transuranium Elements, Pt. II) (eds. G. T. Seaborg, J. J. Katz and W. M. Manning), McGraw Hill, New York, 1327–36.

DOE (1987) *Atomic Power in Space: A History*, Report DOE/NE/32117-H1; DE87010618 (Mar. 1987), 189 pp.

Domanov, V. P., Buklanov, G. V., and Lobanov, Y. V. (2002) *Radiochemistry,* **44**(2), 114–20.

Dormeval, M. (2001) *Structure Electronique d'alliages Pu-Ce(-Ga) et Pu-Am(-Ga) Stabilises en Phase Delta*, Thesis, Chimie - Physique, Dijon, L'Universite de Bourgogne, 194 pp.

Dormeval, M., Baclet, N., and Fournier, J. M. (2000) *AIP Conf. Proc.* **532**(Plutonium Futures–The Science) (eds. K. K. S. Pillay and K. C. Kim), p. 33.

Dormeval, M., Baclet, N., Valot, C., Rofidal, P., and Fournier, J. M. (2003) *J. Alloys Compd.,* **350**(1–2), 86–94.

Douglass, R. M. (1962) *Acta Cryst.,* **15**, 505–6.

Drummond, J. L. and Welch, G. A. (1957) *J. Chem. Soc., Abstracts*: 4781–5.

Drummond, J. L., McDonald, B. J., Ockenden, H. M., and Welch, G. A. (1957) *J. Chem. Soc.,* 4785–9.

Duff, M. C., Newville, M., Hunter, D. B., Bertsch, P. M., Sutton, S. R., Triay, I. R., Vaniman, D. T., Eng, P., and Rivers, M. L. (1999) *J. Synch. Rad.,* **6**(3), 350–2.

Dunlap, B. D. and Kalvius, G. M. (1985) in *Handbook on the Physics and Chemistry of Actinides,* vol. 2, (eds. A. J. Freeman and G. H. Lander), North-Holland, Amsterdam, 329 pp.

Dupuy, M. and Calais, D. (1968) *T. Am. I. Min. Met. Eng.,* **242**, 1679.

Durakiewicz, T., Joyce, J. J., Lander, G. H., Olson, C. G., Butterfield, M. T., Guziewicz, E., Arko, A. J., Morales, L., Rebizant, J., Mattenberger, K., and Vogt, O. (2004) *Phys. Rev. B,* **70**(20), 205103/1–205103/11.

Duriez, C., Alessandri, J. P., Gervais, T., and Philipponneau, Y. (2000) *J. Nucl. Mater.,* **277**(2,3), 143–58.

Dwyer, O. E., Eshaya, A. M., and Hill, F. B. (1959) *Continuous Removal of Fission Products from Uranium-Bismuth Fuels*, *Proc. Second Int. Conf. on the Peaceful Uses of Atomic Energy*, 1958, Geneva, United Nations, New York, 17, pp. 428–37.

Dyall, K. G. (1999) *Mol. Phys.,* **96**(4), 511–18.

Eberle, S. H. and Wade, U. (1970) *J. Inorg. Nucl. Chem.,* **32**, 109.

Edelstein, N. M. (1991) *Eur. J. Solid State Inorg. Chem.,* **28**(Suppl.), 47–55.

Edwards, G. R., Tate, R. E., and Hakkila, E. A. (1968) *J. Nucl. Mater.,* **25**(3), 304–9.

Ehrhart, P., Jung, P., Schultz, H., and Ullmaier, H. (1991) *Atomic Defects in Metals,* vol. 25, (ed. H. Ullmaier), Springer-Verlag, Berlin, 437 pp.

Eichelsberger, J. F. (1961) *Mound Laboratory Progress Report for December 1960*, Report MLM-1108, Mound Laboratory, 16 pp.

Eick, H. A. (1965) *Inorg. Chem.,* **4**(8), 1237–9.

Eisenberg, D. C., Streitwieser, A., and Kot, W. K. (1990) *Inorg. Chem.,* **29**(1), 10–14.

Eller, P. G., Kinkead, S. A., and Nielsen, J. B. (1992) in *Transuranium Elements: A Half Century* (eds. L. R. Morss and J. Fuger), 202–12.

Ellinger, F. H. (1956) *J. Metals,* **8**(AIME Trans. 206), 1256–9.

Ellinger, F. H. (1961) A Review of the Intermetallic Compounds of Plutonium, in *The Metal Plutonium* (eds. A. S. Coffinberry and W. N. Miner), University of Chicago Press, Chicago.

Ellinger, F. H. and Land, C. C. (1968) *J. Nucl. Mater.,* **28**(3), 291–6.

Ellinger, F. H. and Zachariasen, W. H. (1954) *J. Phys. Chem.,* **58**, 405–8.

Ellinger, F. H. and Zachariasen, W. H. (1965) *Acta Crystallogr.,* **19**, 281–3.

Ellinger, F. H., Elliott, R. O., and Cramer, E. M. (1959) *J. Nucl. Mater.,* **1**(3), 233–43.

Ellinger, F. H., Land, C. C., and Miner, W. N. (1962a) *J. Nucl. Mater.,* **1**, 115.

Ellinger, F. H., Land, C. C., and Miner, W. N. (1962b) *J. Nucl. Mater.,* **5**(2), 165–72.

Ellinger, F. H., Land, C. C., and Struebing, V. O. (1964) *J. Nucl. Mater.,* **12**(2), 226–36.

Ellinger, F. H., Land, C. C., and Johnson, K. A. (1965) *Trans. Metall. Soc. AIME,* **233** (7), 1252–8.

Ellinger, F. H., Johnson, K. A., and Struebing, V. O. (1966) *J. Nucl. Mater.,* **20**(1), 83–6.

Ellinger, F. H., Land, C. C., and Johnson, K. A. (1967) *Trans. Metall. Soc. AIME,* **239**(6), 895.

Ellinger, F. H., Land, C. C., and Johnson, K. A., unpublished work, Los Alamos Scientific Laboratory.

Ellinger, F. H., Land, C. C., and Johnson, K. A. (1968a) *J. Nucl. Mater.,* **29**(2), 178–83.

Ellinger, F. H., Miner, W. N., O'Boyle, D. R., and Schonfeld, F. W. (1968b) *Constitution of Plutonium Alloys*, Report LA-3870, Los Alamos Scientific Laboratory, 185 pp.

Elliott, R. O. (1980) personal communication, S. S. Hecker, Los Alamos, NM.

Elliott, R. O. and Giessen, B. C. (1975) Splat Cooling, in *Plutonium and Other Actinides* (eds. H. Blank and R. Lindner), North-Holland, Amsterdam, p. 47.

Elliott, R. O. and Larson, A. C. (1961) Delta-prime Plutonium, in *The Metal Plutonium* (eds. A. S. Coffinberry and W. N. Miner), University of Chicago Press, Chicago, pp. 265–80.

Elliott, R. O., Gschneidner, K. A., and Kempter, C. P. (1960) Thermal Expansion. *Plutonium 1960, Proc. Second Int. Conf. on Plutonium and Other Actinides* (eds. E. Grison, W. B. H. Lord, and R. D. Fowler), Cleaver-Hume Press, London, 142 pp.

Elliott, R. O., Olsen, C. E., and Louie, J. (1962) *J. Phys. Chem. Solids,* **23**(AUG), 1029–44.

Engel, T. K. (1969) *J. Nucl. Mater.,* **31**(2), 211–14.

Engerer, H. (1967) *Phase Equilibrium in the Systems* ThO_2*–*$HoO_{1.5}$*(*$LuO_{1.5}$*,* $ScO_{1.5}$*) and* $HoO_{1.5}$*–*UO_2*,* UO_{2+x}*,* NpO_{2+x}*,* PuO_{2+x}), Thesis, Report KFK-597, Kernforschungszentrum, Karlsruhe, Federal Republic of Germany, 59 pp.

Enriquez, A. E., Matonic, J. H., Scott, B. L., and Neu, M. P. (2003) *Chem. Commun.*, (15), 1892–3.

Ephritikhine, M. (1992) *New J. Chem.,* **16**(4), 451–69.

Erdmann, B. and Keller, C. (1973) *J. Solid State Chem.,* **7**(1), 40–8.

Erdmann, N., Nunnemann, M., Eberhardt, K., Herrmann, G., Huber, G., Kohler, S., Kratz, J. V., Passler, G., Peterson, J. R., Trautmann, N., and Waldek, A. (1998) *J. Alloys Compd.,* **271–273**, 837–40.

Erilov, P. E., Titov, V. V., Serik, V. F., and Sokolov, V. B. (2002) *Atomic Energy (Translation of Atomnaya Energiya),* **92**(1), 57–63.

Etter, D. E., Martin, D. B., Roesch, D. L., Hudgens, C. R., and Tucker, P. A. (1965) *Trans. Metall. Soc. AIME,* **233**(11), 2011–13.

Evans, J. S. O., Mary, T. A., Vogt, T., Subramanian, M. A., and Sleight, A. W. (1996) *Chem. Mater.,* **8**, 2809.

Fardy, J. J. and Buchanan, J. M. (1976) *J. Inorg. Nucl. Chem.,* **38**(3), 579–83.

Faris, J. P. and Buchanan, R. F. (1964) *Anal. Chem.,* **36**(6), 1157.

Farkas, M. S. (1966) *Preparation and Heat Content of Uranium-, Plutonium-, and Neptunium-Containing Microspheres for Use as Intrinsic Thermocouple Flux Probes*, Report BMI-X-10175, Battelle Memorial Institute, Columbus, OH, 19 pp.

Faure, P., Deslandes, B., Bazin, D., Tailland, C., Doukhan, R., Fournier, J. M., and Falanga, A. (1996) *J. Alloys Compd.,* **244**(1–2), 131–9.

Faust, L. G., Brackenbush, L. W., Heid, K. R., Herrington, W. N., Kenoyer, J. L., Munson, L. F., Munson, L. H., Selby, J. M., Soldat, K. L., Stoetzel, G. A., Traub, R. J. and Vallario, E. J. (1988) *Health Physics Manual of Good Practices for Plutonium Facilities*, Report PNL-6534, Pacific Northwest Laboratory, 251 pp.

Favas, M. C., Kepert, D. L., Patrick, J. M., and White, A. H. (1983) *J. Chem. Soc. Dalton Trans.*, (**3**), 571–81.

Fedosseev, A. M., Budantseva, N. A., Grigoriev, M. S., Bessonov, A. A., Astafurova, L. N., Lapitskaya, T. S., and Krupa, J. C. (1999) *Radiochim. Acta,* **86**(1–2), 17–22.

Feldman, C. (1960) *Anal. Chem.,* **32**, 1727–8.

Felmy, A. R., Rai, D., Schramke, J. A., and Ryan, J. L. (1989) *Radiochim. Acta,* **48**(1–2), 29–35.

Ferro, R. and Cacciamani, G. (2002) Chemical Criteria in the Assessment of Alloy Constitutional Properties, in *CALPHAD and Alloy Thermodynamics* (eds. P. E. A. Turchi, A. Gonis and R. D. Shull), TMS, Warrendale, PA, 177 pp.

Filin, V. M., Bulkin, V. I., Timofeeva, L. F., and Polyakova, M. Y. (1989) *Sov. Radiochem.,* **30**, 683–721.

Finch, C. B. and Clark, G. W. (1972) *J. Cryst. Growth,* **12**(2), 181–2.

Fink, J. K. (1982) *Int. J. Thermophys.,* **3**(2), 165–200.

Fink, J. K. (2000) *J. Nucl. Mater.,* **279**(1), 1–18.

Firestone, R. B., Shirley, V. S., Baglin, C. M., Chu, S. Y. F., and Zipkin, J. (eds.) (1996) *Table of Isotopes,* John Wiley & Sons, New York.

Firestone, R. B., Shirley, V. S., Baglin, C. M., Chu, S. Y. F., and Zipkin, J. (eds.) (1998) *Table of Isotopes,* 8th edn, John Wiley & Sons, New York.

Fischer, R. D. (1963) *Theor. Chim. Acta,* **1**(5), 418–31.

Fischer, R., Werner, G.-D., Lehmann, T., Hoffmann, G. and Weigel, F. (1981) *J. Less-Comm. Met.,* **80**, 121–32.

Fisher, E. S. (1974) Ultrasonic Waves in Actinide Metals and Compounds, in *The Actinides: Electronic Structure and Related Properties,* part II, vol. 2 (eds. A. J. Freeman and J. B. Darby), Academic Press, New York, pp. 289–343.

Flahaut, J. (1979) in *Handbook on the Physics and Chemistry of Rare Earths* (eds. K. A. Gschneidner, Jr., and L. Eyring), North-Holland, Amsterdam, p. 2.

Flamm, B. F., Isom, G. M., and Nelson, T. O. (1998) *Proc. Third Topical Meeting on DOE Spent Nuclear Fuel and Fissile Materials Management*, vol. 1, Sept. 8–11, 1998, Charleston, SC, pp. 191–2.

Fleming, W. H. and Thode, H. G. (1953a) *Phys. Rev.,* **90**, 857–8.

Fleming, W. H. and Thode, H. G. (1953b) *Phys. Rev.,* **92**, 378–82.

Fletcher, J. M., Hyde, K. R., and Roberts, F. P. (1967) Germany Patent no. 108 4338.

Florin, A. E. (1950a) *Plutonium Hexafluoride, Plutonium (VI) Oxyfluoride: Preparation, Identification, and Some Properties*, Report LAMS-1118, Los Alamos Scientific Laboratory, Los Alamos, NM, US, 24 pp.

Florin, A. E. (1950b) *Plutonium Hexafluoride: Second Report on the Preparation and Properties*, Report LA-1168, Los Alamos Scientific Laboratory, 18 pp.

Florin, A. E. (1953) *Thermodynamic Properties of Plutonium Hexafluoride: A Preliminary Report*, Report LAMS-1587, Los Alamos Scientific Laboratory, 9 pp.

Florin, A. E. and Tannenbaum, I. R. (1952) *An Improved Apparatus for the Preparation of Plutonium Hexafluoride*, Report LA-1580, Los Alamos Scientific Laboratory, 12 pp.

Florin, A. E., Tannenbaum, I. R., and Lemons, J. F. (1956) *J. Inorg. Nucl. Chem.,* **2**, 368–79.

Flotow, H. E. and Tetenbaum, M. (1981) *J. Chem. Phys.,* **74**(9), 5269–77.

Flotow, H. E., Osborne, D. W., Fried, S. M., and Malm, J. G. (1976) *J. Chem. Phys.,* **65**(3), 1124–9.

Flotow, H. E., Haschke, J. M., and Yamauchi, S. (1984) *The Chemical Thermodynamics of Actinide Elements and Compounds,* part 9, *The Actinide Hydrides,* International Atomic Energy Agency, Vienna, Austria, 115 pp.

Fomin, V. V., Reznikova, V. E., and Zaitseva, L. L. (1958) *Zh. Neorg. Khim.,* **3**, 2231–5.

Forbes, R. L., Fuhrman, N., Andersen, J. C., and Taylor, K. M. (1966) *Uranium-Plutonium Monoxides*, Report UNC-5144, United Nuclear Corporation, Elmsford, New York, 81 pp.

Fortner, J. A., Kropf, A. J., Finch, R. J., Bakel, A. J., Hash, M. C., and Chamberlain, D. B. (2002) *J. Nucl. Mater.,* **304**(1), 56–62.

Fournier, J. M. and Troc, R. (1985) in *Handbook on the Physics and Chemistry of Actinides,* vol. 2 (eds. A. J. Freeman and G. H. Lander), North-Holland, Amsterdam, 29 pp.

Fournier, J. M., Pleska, E., Chiapusio, J., Rossat- Mignod, J., Rebizant, J., Spirlet, J. C., and Vogt, O. (1990) *Physica B,* **163**(1–3), 493–5.

Fox, R. V. and Mincher, B. J. (2002) *ACS Symp. Ser.* **860**(Separ. Processes Using Supercritical Carbon Dioxide) (eds. A. S. Gopalan, C. M. Wai and H. K. Jacobs), American Chemical Society, Washington, DC, pp. 36–49.

Fradin, F. Y. (1970) *Plutonium 1970 and Other Actinides, Proc. Fourth Int. Conf. on Plutonium and Other Actinides*, Santa Fe, NM, Oct. 5–9, 1970 (eds. W. N. Miner), New York, 264 pp.

Fred, M., Blaise, J., and Gutmacher, R. (1966) *J. Opt. Soc. Am.,* **56**, 1416A.

Freedberg, N. A., Antonelli, D., Bloch, L., and Rosenfeld, T. (1992) *Pacing Clin. Electrophysiol.,* **15**(11), 1639–41.

Freeman, A. J. and J. B. Darby, J. (eds.) (1974) *The Actinides, Electronic Structure and Related Properties*, Academic Press, New York.

Fried, S. and Davidson, N. R. (1949) *Nat'l. Nucl. Energy Ser.,* Div IV **14B**(Transuranium Elements, Pt. I) (eds. G. T. Seaborg, J. J. Katz and W. M. Manning), McGraw-Hill, New York, pp. 784–92.

Fried, S., Westrum, Jr, E. F., Baumbach, H. L., and Kirk, P. L. (1958) *J. Inorg. Nucl. Chem.,* **5**, 182–9.

Frolov, A. A., Andreichuk, N. N., Ratmanov, K. V., Frolova, I. M., and Vasiliev, V. Y. (1990) *J. Radioanal. Nucl. Ch. Le.,* **143**(2), 433–44.

Fuger, J. (1992) *Radiochim. Acta,* **58–59**(1), 81–91.

Fuger, J. and Cunningham, B. B. (1963) *J. Inorg. Nucl. Chem.,* **25**(11), 1423–9.

Fuger, J., Oetting, F. L., Hubbard, W. N., and Parker, V. B. (1983) *Chemical Thermodynamics of Actinide Elements and Compounds. Pt. 8. The Actinide Halides.* IAEA, Vienna, Austria, 267 pp.

Fujiwara, K., Yamana, H., Fujii, T., and Moriyama, H. (2001) *Genshiryoku Bakkuendo Kenkyu (J. Nucl. Fuel Cycle Environ. (Japan)),* **7**(1), 17–23.

Fulton, R. B. and Newton, T. W. (1970) *J. Phys. Chem.,* **74**(8), 1661–9.

Gal, J., Hadari, Z., Bauminger, E. R., and Ofer, S. (1972) *Phys. Lett. B,* **41**(1), 53–4.

Galasso, F. S. (1968) *Structure, Properties, and Preparation of Perovskite-type Compounds,* Pergamon Press, Oxford, England.

Ganz, M., Barth, H., Fuest, M., Molzahn, D., and Brandt, R. (1991) *Radiochim. Acta,* **52–53**(Pt. 2), 403–4.

Gardner, H. (1965) Mechanical Properties *Plutonium 1965, Proc. Third Int. Conf.* (eds. A. E. Kay and M. B. Waldron), Chapman and Hall, London, 118 pp.

Gardner, H. R. (1980) Mechanical Properties *The Plutonium Handbook,* vol. 1, (ed. O. J. Wick), American Nuclear Society, La Grange Park, IL, pp. 59–100.

Gardner, E. R., Markin, T. L., and Street, R. S. (1965) *J. Inorg. Nucl. Chem.,* **27**(3), 541–51.

Garner, C. S. (1950) *Los Alamos Technical Series, Chemistry of Uranium and Plutonium*, Report LA-1100, Los Alamos Scientific Laboratory, Los Alamos, NM, pp. 110–16.

Garner, C. S., Bonner, N. A., and Seaborg, G. T. (1948) *J. Am. Chem. Soc.,* **70**, 3453–4.

Gel'man, A. D. and Zaitsev, L. M. (1958) *Zh. Neorg. Khim.,* **3**, 1304–11.

Gel'man, A. D. and Zaitseva, V. P. (1964) *Dokl. Akad. Nauk SSSR,* **157**(6), 1403–5.

Gel'man, A. D. and Zaitseva, V. P. (1965a) *Radiokhimiya,* **7**(1), 49–55.

Gel'man, A. D. and Zaitseva, V. P. (1965b) *Radiokhimiya,* **7**(1), 56–68.

Gendre, R. (1962) *Preparation of Plutonium hexafluoride: Recovery of Plutonium from Waste Dross*, Report CEA-2161, Commissariat a l'Energie Atomique, 109 pp.

Gens, T. A. (1961) *Nucl. Sci. Eng.,* **9**(4), 488–94.

Gens, R., Fuger, J., Morss, L. R., and Williams, C. W. (1985) *J. Chem.Thermodyn.,* **17**(6), 561–73.

Gevantman, L. H. and Kraus, K. A. (1949) *Natl. Nucl. Energy Ser.*, Div IV, **14B** (Transuranium Elements, Pt. I), (eds. G. T. Seaborg, J. J. Katz, and W. M. Manning), pp. 500–18.

Gibney, R. B. and Sandenaw, T. A. (1954) *Electrical Resistivity of Plutonium Metal and of Gallium–Plutonium Alloys over the Temperature Range of 26 K to ~773 K*, Report LA-1883, Los Alamos Scientific Laboratory, 26 pp.

Giessen, B. C., Elliott, R. O., and Struebing, V. O. (1975) *Mat. Sci. Eng.,* **18**(2), 239–43.

Gilman, W. S. (1965) *A Review of the Dissolution of Plutonium Dioxide*, Report MLM-1264, Mound Laboratory, Miamisburg, OH, 12 pp.

Gilman, W. S. (1968) *Review of the Dissolution of Plutonium Dioxide. II*, Report MLM-1513, Mound Laboratory, Miamisburg, OH, 12 pp.

Glazyrin, S. A., Rodchenko, P. Y., and Sokina, L. P. (1989) *Radiokhimiya,* **31**(4), 48–52 (pp 407–410 in English translation).

Glushko, V. P. (ed.) (1982) *Thermodynamic Properties of Individual Substances,* vol. 4, Nauka, Moscow, 623 pp.

Goldberg, A. and Massalski, T. (1970a) *Phase Transformations in the Actinides, Proc. Fourth Int. Conf. on Plutonium and Other Actinides,* Santa Fe, NM (ed. W. N. Miner), The Metallurgical Society of AIME, pp. 875–945.

Goldberg, A., Rose, R. L., and Matlock, D. K. (1970b) *The Delta and Epsilon Thermal Expansion Coefficients and the Delta-to-epsilon Contraction for Some Plutonium-rich Alloys, Proc. Fourth Int. Conf. on Plutonium and Other Actinides 1970, vol. 2,* (ed. W. N. Miner), The Metallurgical Society of AIME, Warrendale, PA, pp. 1056–68.

Gomez Marin, E. (1997) *Etude du Comportement de la Resistivite Electrique des Mono-Chalcogenures de Plutonium et des Alliages de Plutonium et Americium*, Thesis, l'Universite Grenoble, Grenoble.

Gorbunov, S. I. and Seleznev, A. G. (2001) *Radiochemistry,* **43**(2), 111–117.

Gordon, G. and Taube, H. (1961) *J. Inorg. Nucl. Chem.,* **19**, 189–91.

Gordon, J. E., Hall, R. O., Lee, J. A., and Mortimer, M. J. (1976) *Proc. R. Soc. London, Ser. A,* **351**(1665), 179–96.

Gorum, A. E. (1957) *Acta Crystallogr.,* **10**, 144.

Gouder, T., Wastin, F., Rebizant, J., and Havela, L. (2000) *Phys. Rev. Lett.,* **84**(15), 3378–81.

Gouder, T., Havela, L., Wastin, F., and Rebizant, J. (2002) *J. Nucl. Sci. Tech.*, (Suppl. 3), 49–55.

Gouder, T., (2005) *XPS studies of* PuH_3 *thin films, personal communication*, D. L. Clark, Los Alamos, NM.

Grachev, A. F., Maershin, A. A., Skiba, O. V., Tsykanov, V. A., Bychkov, A. V., Kormilitsyn, M. V., and Sokolvskii, Y. S. (2004) *At. Energ.,* **96**(5), 320–6.

Graf, W. L. (1994) *Plutonium and the Rio Grande: Environmental Change and Contamination in the Nuclear Age,* Oxford University Press, New York, 329 pp.

Green, J. L. and Leary, J. A. (1970) *J. Appl. Phys.,* **41**(13), 5121–4.

Green, D. W. and Reedy, G. T. (1978a) *J. Chem. Phys.,* **69**(2), 552–5.

Green, D. W. and Reedy, G. T. (1978b) *J. Chem. Phys.,* **69**(2), 544–51.

Green, D. W., Fink, J. K., and Leibowitz, L. (1983) *ACS Symp. Ser.* **216**(Plutonium Chem.) (eds. W. T. Carnall and G. R. Choppin), American Chemical Society, Washington, DC, pp. 123–43.

Greenwood, N. N. and Earnshaw, A. (1997) *Chemistry of the Elements,* Butterworth-Heinemann, Oxford, England, 1341 pp.

Grenthe, I., Riglet, C., and Vitorge, P. (1986a) *Inorg. Chem.,* **25**(10), 1679–84.

Grenthe, I., Robouch, P., and Vitorge, P. (1986b) *J. Less-Common Met.,* **122**, 225–31.

Grenthe, I., Fuger, J., Konigs, R. J. M., Lemire, R. J., Muller, A. B., Nguyen- Trung, C., and Wanner, H. (1992) *Chemical Thermodynamics of Uranium,* Elsevier Science Publishing Company, New York, 676 pp.

Grenthe, I., Puigdomenech, I., and Allard, B. (1997) *Modelling in Aquatic Chemistry,* Nuclear Energy Agency, OECD, Washington, DC, 724 pp.

Grigor'ev, M. S., Gulyaev, B. F., and Krot, N. N. (1986) *Sov. Radiochem.,* **28**(6), 630–4.

Grigor'ev, M. S., Baturin, N. A., Bessonov, A. A., and Krot, N. N. (1995) *Radiokhimiya,* **37**(1), 15–18.

Grison, E., Lord, W. B. H., and Fowler, R. D. (eds.) (1960) *Plutonium 1960, Proc. Second Int. Conf. on Plutonium Metallurgy,* Grenoble, France, Apr. 19–22, 1960, Cleaver Hume, London.

Griveau, J. C., Pfleiderer, C., Boulet, P., Rebizant, J., and Wastin, F. (2004) *J. Magn. Magn. Mater.,* **272/276**, 154–5.

Grove, G. R. (1966) *Reactor Fuels and Materials Development. Plutonium Research. April–Sept.*, Report MLM-1347, Mound Laboratory, pp. 11–18.

Grove, G. R., Goldenberg, J. A., Kelly, D. P., and Prosser, D. L. (1965) *Plutonium-238 Isotopic Power Sources, a Summary Report*, Report MLM-1270, Mound Laborabory, Miamisburg, OH, 234 pp.

Gruen, D. M. and deKock, C. W. (1967) *J. Inorg. Nucl. Chem.,* **29**(10), 2569–75.

Gruen, D. M., Malm, J. G., and Weinstock, B. (1956) *J. Chem. Phys.,* **24**(4), 905–6.

Gruen, D. M., McBeth, R. L., Kooi, J., and Carnall, W. T. (1960) *Ann. N.Y. Acad. Sci.,* **79**(11), 941–9.

Gschneidner, K. A., Jr (1980) Theory Alloy Phase Form., Proc. Symp, Meeting Date 1979, Metall. Soc. AIME, Warrendale, PA, 1–39.

Gschneidner, Jr, K. A., Elliott, R. O., and Struebing, V. O. (1960) *Pu Phase Diagrams Discussion, Proc. Second Int. Conf. on Plutonium and Other Actinides,* Grenoble, France (eds. E. Grison, W. B. H. Lord, and R. D. Fowler), Cleaver-Hume Press, London, 1, 166 pp.

Guerin, G. (1996) Research on Actinides. CLEFS/CEA. **31**, 1–71.

Guillaumont, R. and Adloff, J. P. (1992) *Radiochim. Acta,* **58–59**(Pt. 1), 53–60.

Guillaumont, R., Fanghaenel, T., Fuger, J., Grenthe, I., Neck, V., Palmer, D. A., and Rand, M. H. (2003) *Update on the Chemical Thermodynamics of Uranium, Neptunium, Plutonium, Americium, and Technetium,* Elsevier, Amsterdam, The Netherlands, 919 pp.

Güldner, R. and Schmidt, H. (1991) *J. Nucl. Mater.,* **178**(2–3), 152–7.

Hagan, P. G. and Miner, F. J. (1980) *ACS Symp. Ser.,* **117**(Actinide Sep.), 51–67.

Hagemann, F., Abraham, B. M., Davidson, N. R., Katz, J. J., and Sheft, I. (1949) The Preparation and Properties of Plutonium Iodide and Plutonium Oxyiodide, in *Natl. Nucl. Energy Ser.,* Div IV **14B**(*Transuranium Elements*, Pt. II), (eds. G. T. Seaborg, J. J. Katz, and W. M. Manning), McGraw-Hill, New York, pp. 957–63.

Haines, H. R. and Potter, P. E. (1975) *Thermodyn. Nucl. Mater*., Proc. Symp., 4th, Meeting Date 1974, **2,** pp. 145–73.

Haire, R. G. and Eyring, L. (1994) Comparison of the Binary Oxides, in *Handbook on the Physics and Chemistry of Rare Earths,* vol. 18, (eds. K. A. J. Gschneidner, L. Eyring, G. R. Choppin, and G. H. Lander), Elsevier Science, New York, pp. 413–505.

Haire, R. G., Heathman, S., Le Bihan, T., Lindbaum, A., and Iridi, M. (2004) *Mater. Res. Soc. Symp. Proc.,* **802**, (Actinides–Basic Science Technol.), 15–20.

Hall, R. O. A., Jeffery, A. J., Lee, J. A., Mortimer, M. J., and Lander, G. H. (1985) *Heat Capacity Measurements on Plutonium Phosphide*, Report AERE-R-11075, Atomic Energy Research Establishment, Harwell, UK, 24 pp.

Hammel, E. F. (1998) *Plutonium Metallurgy at Los Alamos, 1943–1945: Recollections of Edward F. Hammel,* Los Alamos National Laboratory, Los Alamos, NM, 173 pp.

Handa, M. and Suzuki, Y. (1984) *Nihon Genshiryoku Gakkaishi,* **26**(1), 2–7.

Handwerk, J. H. and Kruger, O. L. (1971) *Nucl. Eng. Des.,* **17**(3), 397–408.

Hanrahan, R. J., Boehlert, C., and McDeavitt, S. (2003) *J. Metals*, **55**(9).

Harland, C. E. (1994) *Ion Exchange: Theory and Practice*, 2nd Ed., The Royal Society of Chemistry, Cambridge.

Harmon, K. M. and Reas, W. H. (1957) *Conversion Chemistry of Plutonium Nitrate*, Report HW-49597 A, 15 pp.

Harmon, K. M., Judson, B. F., Lyon, W. L., Pugh, R. A., and Smith, R. C. (1961) in *Reactor Handbook,* 2nd edn, vol. II, (eds. S. M. Stoller and R. B. Richard), Interscience Publishers, New York, 680 pp.

Harper, E. A., Hedger, H. J., and Dalton, J. T. (1968) *Nature,* **219**(5150), 151.

Harrison, W. A. (2001) *Phys. Rev. B,* **64**(23), 235112/1–10.

Harrowfield, J. M. B., Kepert, D. L., Patrick, J. M., White, A. H., and Lincoln, S. F. (1983) *J. Chem. Soc. Dalton Trans.*, (2), 393–6.

Harvey, B. G., Heal, H. G., Maddock, A. G., and Rowley, E. L. (1947) *J. Chem. Soc.*, 1010–21.

Harvey, M. R., Doyle, J. H., Rafalski, A. L., and Riefenberg, D. H. (1971) *J. Less-Common Met.,* **23**, 446.

Hasbrouk, M. E. and Burns, M. P. (1965) *Plutonium Metallurgy Handbook*, Report BNWL-37, Pacific Northwest Laboratory.

Haschke, J. M. (1991) Actinide Hydrides, in *Topics in f-element Chemistry,* vol. 2 (eds. G. Meyer and L. R. Morss), Kluwer Academic Publishers, Boston, MA, pp. 1–53.

Haschke, J. M. (1992) *Hydrolysis of Plutonium. Plutonium–Oxygen Phase Diagram* in *Transuranium Elements: A Half Century* (eds. L. R. Morss and J. Fuger), pp. 416–25.

Haschke, J. M. (1999) Pu Oxidation, personal communication, J. C. Martz, Los Alamos, NM.

Haschke, J. M. (2005) *J. Nucl. Mater.,* **340**(2–3), 299–306.

Haschke, J. M. and Allen, T. H. (2001) *J. Alloys Compd.,* **320**(1), 58–71.

Haschke, J. M. and Haire, R. G. (2000) Crystalline Solids and Corrosion Chemistry, in *Advances in Plutonium Chemistry 1967–2000* (ed. D. C. Hoffman), The American Nuclear Society, La Grange Park, IL, pp. 212–59.

Haschke, J. M. and Martz, J. C. (1998a) *J. Alloys Compd.,* **266**(1–2), 81–9.

Haschke, J. M. and Martz, J. C. (1998b) *Encyclopedia of Environmental Analysis and Remediation, Plutonium Storage,* vol. 6, John Wiley, New York, pp. 3740–55.

Haschke, J. M. and Oversby, V. M. (2002) *J. Nucl. Mater.,* **305**(2–3), 187–201.

Haschke, J. M., Hodges, A. E., III, Bixby, G. E., and Lucas, R. L. (1983) *Reaction of Plutonium with Water. Kinetic and Equilibrium Behavior of Binary and Ternary Phases in the Plutonium + Oxygen + Hydrogen System*, Report RFP-3416, Rockwell International Corporation, Rocky Flats Plant, Golden, CO, 24 pp.

Haschke, J. M., Hodges, III, A. E., and Lucas, R. L. (1987) *J. Less-Common Met.,* **133**(1), 155–66.

Haschke, J. M., Allen, T. H., and Stakebake, J. L. (1996) *J. Alloys Compd.,* **243**(1–2), 23–35.

Haschke, J. M., Allen, T. H., and Martz, J. C. (1998) *J. Alloys Compd.,* **271**, 211–15.

Haschke, J. M., Allen, T. H., and Morales, L. A. (2000a) *Los Alamos Science,* **26**(1), 252–73.

Haschke, J. M., Allen, T. H., and Morales, L. A. (2000b) *Science,* **287**(5451), 285–7.

Haschke, J. M., Allen, T. H., and Morales, L. A. (2001) *J. Alloys Compd.,* **314**(1–2), 78–91.

Hasilkar, S. P., Khedekar, N. B., Chander, K., Jadhav, A. V., and Jain, H. C. (1994) *J. Radioanal. Nucl. Chem.,* **185**(1), 119–25.

Hass, P. A., Lloyd, M. H., Band, W. D., and McBride, J. P. (1966) *Sol-Gel Process Development and Microsphere Preparation*, Report ORNL-P-2159, Oak Ridge National Laboratory, 42 pp.

Haug, H. (1963) *The Systems Uranium Oxide–Europium Oxide and Plutonium Oxide–Europium Oxide*, Thesis, Report NP-13003, University of Munich, Germany, 97 pp.

Haug, H. and Weigel, F. (1963) *J. Nucl. Mater.,* **9**(3), 160–3.

Hawkins, N. J. (1956) *Report of the Chemistry and Engineering Section for February, March, April, 1956*, Report KAPL-1536, Knolls Atomic Power Laboratory, Schenectady, New York, 98 pp.

Hawkins, N. J., Mattraw, H. C., and Sabol, W. W. (1954) *Infrared Spectrum and Thermodynamic Properties of* PuF_6, Report KAPL-1007, Knolls Atomic Power Laboratory, 21 pp.

Hay, P. J. and Martin, R. L. (1998) *J. Chem. Phys.,* **109**(10), 3875–81.

Hay, P. J., Martin, R. L., and Schreckenbach, G. (2000) *J. Phys. Chem. A,* **104**(26), 6259–70.

Hayes, R. G. and Edelstein, N. (1972) *J. Am. Chem. Soc.,* **94**(25), 8688–91.

Hecker, S. S. unpublished work, Los Alamos National Laboratory.

Hecker, S. S. (2000) *Los Alamos Science,* **26**(2), 290.

Hecker, S. S. (2003) *JOM* **55**(9), 13–50.

Hecker, S. S. (2004) *Metall. Mater. Trans. A,* **35 A**(8), 2207–22.

Hecker, S. S. and Martz, J. C. (2000) *Los Alamos Science* **26**(1), 238–43.

Hecker, S. S. and Martz, J. C. (2001) Plutonium Aging: from Mystery to Enigma, in *Aging Studies and Lifetime Extension of Materials* (ed. L. G. Mallinson), Kluwer Academic, New York, pp. 23–52.

Hecker, S. S. and Morgan, J. R. (1976) *Effect of Strain Rate on the Tensile Properties of Alpha - and Delta - Stabilized Plutonium, Proc. Fifth Int. Conf. on Plutonium and Other Actinides 1975, Sept. 10–13, 1975,* Baden-Baden, West Germany, (eds. H. Blank and R. Linder), North-Holland, Amsterdam, The Netherlands, pp. 697–709.

Hecker, S. S. and Stevens, M. F. (2000) *Los Alamos Science* **26**(2), 336–55.

Hecker, S. S. and Timofeeva, L. F. (2000) *Los Alamos Science* **26**(1), 244–51.

Hecker, S. S., Zukas, E. G., Morgan, J. R., and Pereyra, R. A. (1982) *Temperature-Induced Transformation in a Pu-2 at.% Al Alloy. Proc. Int. Conf. on Solid to Solid Phase Transformations;* Pittsburgh, PA, Metallurgical Society of AIME, 1982, Warrendale, PA, pp. 1339–43.

Hecker, S. S., Harbur, D. R., and Zocco, T. G. (2004b) *Prog. Mater. Sci.,* **49**(3–4), 429–85.

Herbst, R. J. and Matthews, R. B. (1982) *Uranium–Plutonium Carbide as an LMFBR Advanced Fuel*, Report LA-9259-MS, Los Alamos National Laboratory, Los Alamos, NM, 24 pp.

Herrick, C. C., Olsen, C. E., and Sandenaw, T. A. (1959) *The Density of Liquid Plutonium Metal*, Report LA-2358, Los Alamos Scientific Laboratory, 17 pp.

Hidaka, H. (1999) *J. Radioanal. Nucl. Chem.,* **239**(1), 53–8.

Hidaka, H. and Holliger, P. (1998) *Geochim. Cosmochim. Acta,* **62**(1), 89–108.

Hill, O. F. and Cooper, V. R. (1958) *Ind. Eng. Chem.,* **50**(4), 599–602.

Hill, H. H. and Kmetko, E. A. (1976) *J. Phys. F: Me. Phys.,* **6**(6), 1025–37.

Hill, R. N. (2005), personal communication, G. Jarvinen.

Hilliard, J. E., Averbach, B. B., and Cohen, M. (1959) *Acta Met.,* **7**, 86.

Hincks, J. A. and McKinley, L. C. (1966) *Heat Source Fabrication*, Report MLM-1365, Mound Laboratory, 35 pp.

Hindman, J. C. (1954) Ionic and Molecular Species of Plutonium in Solution, in *The Actinide Elements* (eds. G. T. Seaborg and J. J. Katz), McGraw-Hill, New York, pp. 301–70.

Hinrichs, W., Melzer, D., Rehwoldt, M., Jahn, W., and Fischer, R. D. (1983) *J. Organomet. Chem.,* **251**(3), 299–305.

Hobart, D. E., Morris, D. E., Palmer, P. D., and Newton, T. W. (1989) *Formation, Characterization, and Stability of Plutonium (IV) Colloid: A Progress Report*, Report LA-UR-89-2541, Los Alamos National Laboratory, 9 pp.

Hocheid, B., Tanon, A., and Despres, J. (1965) *J. Nucl. Mater.,* **15**(3), 241–4.

Hocheid, B., Tanon, A., Bedere, S., Despres, J., Hay, S., and Miard, F. (1967) *Pu-Ga Phase Diagram,* Plutonium 1965, Proc. Third Int. Conf. on Plutonium (eds. A. E. Kay, and M. B. Waldron), Chapman-Hall, London, 321 pp.

Hodge, N. (1961) in *Advances in Fluorine Chemistry,* vol. 2 (eds. M. Stacey, J. C. Tatlow, and A. G. Sharpe), Butterworths, London, England, 138 pp.

Hoekstra, H. R. and Gebert, E. (1977) *J. Inorg. Nucl. Chem.,* **39**(12), 2219–21.

Hoffman, D. C. (ed.) (2000) *Advances in Plutonium Chemistry 1967–2000,* The American Nuclear Society, La Grange Park, IL, 320 pp.

Hoffman, D. C., Lawrence, F. O., Mewherter, J. L., and Rourke, F. M. (1971) *Nature,* **234**(5325), 132–4.

Hoffman, D. C., Ghiorso, A., and Seaborg, G. T. (2000) *The Transuranium People: The Inside Story,* Imperial College Press, London, England, 467 pp.

Holleck, H. (1975) *Proc. Fourth Symp. on Thermodyn. Nucl. Mater.,* vol. 2, pp. 213–64.

Holleck, H. and Kleykamp, H. (1972) *Gmelin Handbook of Inorganic Chemistry, Transuranium Elements, part C,* Verlag Chemie, Weinheim, 83 pp.

Holley, C. E., Jr (1974) *J. Nucl. Mater.,* **51**(1), 36–46.

Holley, C. E., Jr, Mulford, R. N. R., Huber, E. J., Jr, Head, E. L., Ellinger, F. H., and Bjorklund, C. W. (1958) *Proc. Second UN Int. Conf. Peaceful Uses Atomic Energy*, Geneva, 1958, vol. 6, pp. 215–20.

Holley, C. E., Rand, M. H., and Storms, E. K. (1984) The Actinide Carbides, in *Chemical Thermodynamics of Actinide Elements and Compounds: Part. 6,* IAEA, Vienna, Austria, 101 pp.

Holliger, P. and Devillers, C. (1981) *Earth Planet. Sc. Lett.,* **52**(1), 76–84.

Horner, D. E., Crouse, D. J., and Mailen, J. C. (1977) *Cerium-promoted Dissolution of Plutonium dioxide and Plutonium dioxide–Uranium dioxide in Nitric Acid*, Report ORNL/TM-4716, Oak Ridge National Laboratory, TN, 41 pp.

Hough, A. and Marples, J. A. C. (1965) *J. Nucl. Mater.,* **15**(4), 298–309.

Howell, R. H. and Sterne, P. A. (2002) Positron Annihilation Spectroscopy, personal communication, A. J. Schwartz, Livermore, CA.

Howell, R. H., Sterne, P. A., Hartley, J., and Cawan, T. E. (1999) *Appl. Surf. Sci.,* **149**, 103–5.

Hunt, D. C. and Boss, M. R. (1971) *J. Nucl. Energy,* **25**(6), 241–51.

Hunt, D. C. and Rothe, R. E. (1974) *Nucl. Sci. Eng.,* **53**(1), 79–92.

Hurst, H. J. and Taylor, J. C. (1970) *Acta Crystallogr.,* **B26**(Pt. 4), 417–21.

Hurst, R., Mandleberg, C. J., Rae, H. K., Davies, D., Francis, K. E., and Brooks, R. (1953) *Plutonium Hexafluoride*, part II, *Preparation and Some Physical Properties*, Report AERE-C/R-1312, Great Britain Atomic Energy Research Establishment.

Hyde, E. K., Davidson, N. R., Katz, J. J., and Wolf, M. J. (1944) *Chemical Research - Special Chemistry of Plutonium. Report for Month Ending April 1, 1944*, Report CK-1512, Metallurgical Laboratory, pp. 5–7.

Hyde, E. K., Perlman, I., and Seaborg, G. T. (1964) *The Nuclear Properties of the Heavy Elements Vol. I: Systematics of Nuclear Structure and Radioactivity. Vol. II: Detailed Radioactivity Properties*, Prentice-Hall, Englewood Cliffs, NJ, 400 pp.;36 pp.

IAEA (1967) *The Plutonium–Oxygen and the Uranium–Plutonium–Oxygen Systems. A Themochemical Assessment*, Report Tech. Rep Ser. No. 79, STI\DOC-10\79, International Atomic Energy Agency, 86 pp.

Iida, T., Guthrei, R. I. L., and Morita, Z. (1988) *Can. Metall. Quart.,* **27**(1), 1–5.

Iso, S., Uno, S., Yoshihiro, M., Sasaki, T., and Yoshida, Z. (2000) *Prog. Nucl. Energ.,* **37** (1–4), 423–8.

Iyer, P. N. and Natarajan, P. R. (1989) *J. Less-Common Met.,* **146**(1–2), 161–6.

Iyer, P. N. and Natarajan, P. R. (1990) *J. Less-Common Met.,* **159**(1–2), 1–11.

Jackson, E. F. and Rand, M. H. (1963) *Oxidation Behaviour of Plutonium Dioxide and Solid Solutions Containing Plutonium Dioxide*, Report AERE-R-3636, Atomic Energy Research Establishment, Harwell, UK, 13 pp.

Jacquemin, J. and Lallement, R. (1970) *Self-irrad Damage*, *Proc. Int. Conf. on Plutonium and Other Actinides 1970* (ed. W. N. Miner), The Metallurgical Society of AIME, pp. 616–22.

Jarvinen, G. D. (ed.) (2003) *AIP Conf. Proc.*, **673**(Plutonium Futures – The Science). 421 pp.

Jayadevan, N. C., Mudher, K. D. S., and Chackraburtty, D. M. (1982) *Z. Kristallogr.,* **161**(1–2), 7–13.

Jenkins, I. L., Moore, F. H., and Waterman, M. J. (1965) *J. Inorg. Nucl. Chem.,* **27**(1), 77–80.

Joel, J., Roux, C., and Rapin, M. (1971) *J. Nucl. Mater.,* **40**, 297–304.

Johns, I. B. (1944) *Plutonium Hydride And Deuteride*, Report LA-137, Los Alamos Scientific Laboratory, 12 pp.

Johns, I. B. and Moulton, G. H. (1944) *Large-scale Preparation of the Anhydrous Fluorides of Plutonium*, Report LA-193, Los Alamos Scientific Laboratory, Los Alamos, NM, 20 pp.

Johnson, K. W. R. (1954) *Preparation of High-purity Plutonium Metal*, Report LA-1680, Los Alamos Scientific Laboratory.

Johnson, K. A. (1964) *Homogenization of Gallium-stabilized Delta-phase Plutonium*, Report LA-2989, Los Alamos Scientific Laboratory, 43 pp.

Johnson, K. W. R. and Leary, J. A. (1964) *J. Inorg. Nucl. Chem.,* **26**(1), 103–5.

Johnson, K. W. R., Kahn, M., and Leary, J. A. (1961) *J. Phys. Chem.,* **65**, 2226–9.

Johnson, I., Chasanov, M. G., and Yonco, R. M. (1965) *Trans. Metall. Soc. AIME,* **233** (7), 1408–14.

Johnson, Q. C., Wood, D. H., and Smith, G. S. (1967) *The Crystal Structure of* Pu_3Zn_{22}, Report UCRL-70500.

Jones, M. M. (1953) *A Study of Plutonium Trifluoride Precipitated from Aqueous Solution*, Report HW-30384, Hanford Atomic Products Operation, 15 pp.

Jones, L. H. (1955) *J. Chem. Phys.,* **23**, 2105–7.

Jones, L. H. and Penneman, R. A. (1953) *J. Chem. Phys.,* **21**(3), 542–4.

Jones, L. V., Ofte, D., Rohr, L. J., and Wittenberg, L. J. (1962) *Am. Soc. Metals, Trans. Quart.,* **55**, 819–25.

Jones, L. V., Ofte, D., Phipps, K. D., and Tucker, P. A. (1964) *Ind. Eng. Chem. Prod. R. D.,* **3**(2), 78–82.

Jouniaux, B. (1979) *Study by Thermochromatography of Fluorides of Transuranium Elements*, Thesis, Report IPNO-T-79-05, Paris-6 Univ. 75; Paris-11 Univ. 91, Inst. de Physique Nucleaire, Orsay, France, 99 pp.

Jouniaux, B., Legoux, Y., Merinis, J., and Bouissieres, G. (1979) *Radiochem. Radioanal. Lett.,* **39**(2), 129–40.

Jove, J. and Cousson, A. (1977) *Radiochim. Acta,* **24**(2–3), 73–5.

Jove, J. and Pagès, M. (1977) *Inorg. Nucl. Chem. Lett.,* **13**(7), 329–34.

Jove, J., Pagès, M., and Freundlich, W. (1974) *Compt. Rend.,* **278**(12), 873–4.

Jove, J., Pagès, M., and Freundlich, W. (1976) *Inorg. Nucl. Chem. - Herbert H. Hyman Mem. Vol.*, 189–92.

Kabanova, O. L., Danuschenkova, M. A., and Paley, P. N. (1960) *Anal. Chim. Acta,* **22**, 66.

Kaltsoyannis, N. (2000) *Inorg. Chem.,* **39**(26), 6009–17.

Kaltsoyannis, N. and Bursten, B. E. (1997) *J. Organomet. Chem.,* **528**(1–2), 19–33.

Kalvius, G. M., Cohen, D., Dunlap, B. D., and Shenoy, G. K. (1978) *Phys. Rev. B,* **18**(9), 4581–7.

Kandan, R., Babu, R., Nagarajan, K., and Rao, P. R. V. (2004) *J. Nucl. Mater.,* **324**(2–3), 215–19.

Karraker, D. G. (1973) *Inorg. Chem.,* **12**(5), 1105–8.

Karraker, D. G. (1987) *Inorg. Chim. Acta,* **139**(1–2), 189–91.

Karraker, D. G. and Stone, J. A. (1974) *J. Am. Chem. Soc.,* **96**(22), 6885–8.

Karraker, D. G., Stone, J. A., Jones, E. R., Jr, and Edelstein, N. (1970) *J. Am. Chem. Soc.,* **92**(16), 4841–5.

Kasha, M. (1949) Reactions between Plutonium Ions in Perchloric Acid Solutions. Rates, Mechanisms, and Equilibria, in *Natl. Nucl. Energy Ser.*, Div IV **14B**(Transuranium Element, Pt. I) (eds. G. T. Seaborg, J. J. Katz, and W. M. Manning), McGraw-Hill, New York, ch. 3, 295–334.

Kasper, J. S. (1976) *J. Less-Common Met.,* **47**, 17–21.

Kassner, M. E. and Peterson, D. E. (1995) *Phase Diagrams of Binary Actinide Alloys.* ASM International, Materials Park, OH, 489 pp.

Katz, J. J. and Gruen, D. M. (1949) *J. Am. Chem. Soc.,* **71**, 2106–12.

Katz, J. J. and Sheft, I. (1960) Halides of the Actinide Elements, in *Advances in Inorganic Chemistry and Radiochemistry,* vol. 2, (eds. H. J. Emeleus and A. G. Sharpe), Academic Press, San Diego, pp. 195–236.

Katzin, L. I. (1944) *Survey of the Chemistry of Plutonium*, Report CK-2240(Del.), Chicago University Metallurgical Laboratory, 46 pp.

Kaufman, L. (2002) Keynote: Humerothery and Calphad Thermodynamics, in *CALPHAD and Alloy Thermodynamics* (eds. P. E. A. Turchi, A. Gonis and R. D. Shull), TMS, Warrendale, PA, 3 pp.

Kaufman, L. and Bernstein, H. (1970) *Computer Calculation of Phase Diagrams with Special Reference to Refractory Metals.* Academic Press, New York, 334 pp.

Kay, A. E. and Loasby, R. G. (1964) *Philos. Mag.,* **9**(97), 37–49.

Kay, A. E. and Waldron, W. B. (1967) *Plutonium 1965,* Proc. Third Int. Conf. on Plutonium, Institute of Metals, Chapman and Hall, London, 1114 pp.

Keenan, T. K. (1957) *J. Phys. Chem.,* **61**, 1117.

Keenan, T. K. (1965) *Inorg. Chem.,* **4**(10), 1500–1.

Keenan, T. K. (1966) *Inorg. Nucl. Chem. Lett.,* **2**(6), 153–6.

Keenan, T. K. (1967) *Inorg. Nucl. Chem. Lett.,* **3**(10), 463–7.

Keenan, T. K. and Asprey, L. B. (1969) *Inorg. Chem.,* **8**(2), 235–238.

Keiser, D. L. J., Hayes, S. L., Meyer, M. K., and Clark, C. R. (2003) *J. Metals,* **55**(9), 55.

Keller, C. (1962) *Nukleonik,* **4**, 271–7.

Keller, C. (1963) *Nukleonik,* **5**, 41–8.

Keller, C. (1964) *Solid-state Chemistry of the Actinide Oxides*, Thesis, Report KFK-225, Kernforschungszentrum, Karlsruhe, 261 pp.

Keller, C. (1965a) *J. Inorg. Nucl. Chem.,* **27**(6), 1233–46.

Keller, C. (1965b) *J. Inorg. Nucl. Chem.,* **27**(2), 321–7.

Keller, C. (1971) *The Chemistry of the Transuranium Elements* (*Nuclear Chemistry in Monographs,* vol. 3). Verlag Chemie, Weinheim, 675 pp.

Keller, C. and Salzer, M. (1967) *J. Inorg. Nucl. Chem.,* **29**(12), 2925–34.

Keller, C. and Schmutz, H. (1964) *Zeitschr. Naturfors.,* **19b**(11), 1080.

Keller, C. and Schmutz, H. (1966) *Inorg. Nucl. Chem. Lett.,* **2**(11), 355–8.

Keller, C. and Seiffert, H. (1969) *Angew. Chem., Int. Ed. Engl.,* **8**(4), 279–80.

Keller, C. and Walter, K. H. (1965) *J. Inorg. Nucl. Chem.,* **27**(6), 1253–60.

Keller, C., Koch, L., and Walter, K. H. (1965a) *J. Inorg. Nucl. Chem.,* **27**(6), 1205–23.

Keller, C., Koch, L., and Walter, K. H. (1965b) *J. Inorg. Nucl. Chem.,* **27**(6), 1225–32.

Keller, C., Berndt, U., Debbabi, M., and Engerer, H. (1972) *J. Nucl. Mater.,* **42**(1), 23–31.

Kelly, C. E. (1975) MHW [Multihundred Watt] converter (RTG) [radioisotope thermoelectric generator]. *Rec. Intersoc. Energy Convers. Eng. Conf.*, 10, 880–6.

Kennedy, J. W., Seaborg, G. T., Segre, E., and Wahl, A. C. (1941) *Phys. Rev.,* **70**, 555–6.

Kent, R. A. (1968) *J. Am. Chem. Soc.,* **90**(21), 5657–9.

Kent, R. A. (1969) *High Temp. Sci.,* **1**, 169.

Kent, R. A. (1973) *Thermodynamic Analysis of MHW Space Electric Power Generator*, Report LA-5202-MS, Los Alamos Scientific Laboratory, Los Alamos, NM, 108 pp.

Kent, R. A. and Leary, J. A. (1968) *Mass Spectrometric Studies of Plutonium Compounds at High Temperatures, I: the Heats of Vaporization of Gold and Plutonium and the Heat of Decomposition of Plutonium Mononitride*, Report LA-3902, Los Alamos Scientific Laboratory, Los Alamos, NM, 20 pp.

Kent, R. A. and Zocher, R. W. (1976) *Reduction of Plutonia by Carbon Monoxide and Equilibrium Partial Pressures above Plutonia*, Report LA-6534, Los Alamos Scientific Laboratory, Los Alamos, NM, 27 pp.

Kessie, R. W. and Ramaswami, D. (1965) *Removal of Plutonium Hexafluoride from Cell Exhaust Air by Hydrolysis Filtration*, Report ANL-7066, Argonne National Laboratory, Argonne, IL,70 pp.

Khanaev, E. I., Teterin, E. G., and Luk'yanova, L. A. (1967) *Zh. Prikl. Spektrosk.,* **6**(6), 789–96.

Kiehn, R. M. (1961) Pu LAMPRE, in *The Metal Plutonium* (eds. A. S. Coffinberry and W. M. Miner), University of Chicago Press, Chicago, IL, 333 pp.

Kierkegaard, P. (1956) *Acta Chem. Scand.,* **10**(4), 599–616.

Kikuchi, T., Koyama, T., and Homma, S. (2003) *AIP Conf. Proc.,* **673**(Plutonium Futures – The Science), 42–4.

Kim, J. I. (1991) *Radiochim. Acta,* **52–53**(Pt. 1), 71–81.

Kim, J. I. (1994) *MRS Bull.,* **19**(12), 47–53.

Kim, K. C. and Campbell, G. M. (1985) *Appl. Spectrosc.,* **39**(4), 625–8.

Kim, K. C., Krohn, B. J., Briesmeister, R. A., and Rabideau, S. (1987) *J. Chem. Phys.,* **87**, 1538.

Kimura, T. and Choppin, G. R. (1994) *J. Alloys Compd.,* **213–214**, 313–17.

King, E., Lee, J. A., Mendelssohn, K., and Wigley, D. A. (1965) *Proc. R. Soc. Lond. Ser. A,* **284**(1398), 325–43.

Kittel, C. and Kroemer, H. (1980) *Thermal Physics,* Freeman and Company, San Francisco, CA, p. 196.

Kleinschmidt, P. D. (1988) *J. Chem. Phys.,* **89**(11), 6897–904.

Kleykamp, H. (1999) *J. Nucl. Mater.,* **275**, 1–11.

Knief, R. A. (1985) *Nuclear Criticality Safety: Theory and Practice,* American Nuclear Society, La Grange Park, IL, 233 pp.

Knighton, J. B., Auge, R. G., Berry, J. W., and Franchini, R. C. (1976) *Molten Salt Extraction of Americium from Molten Plutonium Metal*, Report RFP-2365, Rocky Flats Plant, Rockwell International, Golden, CO, 24 pp.

Knighton, J. B. and Steunenberg, R. K. (1965) *J. Inorg. Nucl. Chem.,* **27**(7), 1457–62.

Knoch, W., Knighton, J. B., and Steunenberg, R. K. (1969) *Nucl. Metall. Met. Soc. AIME,* **15**, 535–46.

Knopp, R., Neck, V., and Kim, J. I. (1999) *Radiochim. Acta,* **86**(3–4), 101–8.

Koch, L. (1964) *The Ternary oxide of Quinque- and Sexivalent Neptunium and Plutonium with Lithium and Sodium*, Thesis, Report KFK-196, Institute fur Radiochemie, Kernforschungszentrum, Karlsruhe, Germany, 74 pp.

Koch, G. (ed.) (1972) *Gmelin Handbook of Inorganic Chemistry*, vol. 4*: Transuranium Elements, C*, Verlag Chemie, Weinheim, 279 pp.

Koch, G. (ed.) (1973a) *Gmelin Handbook of Inorganic Chemistry*, vol. 7a, *Transuranium Elements, A1, I, The Elements*, Verlag Chemie, Weinheim.

Koch, G. (ed.) (1973b) *Gmelin Handbook of Inorganic Chemistry*, vol. 7b, *Transuranium Elements, A1, II, The Elements*, Verlag Chemie, Weinheim.

Koch, G. (ed.) (1973c) *Gmelin Handbook of Inorganic Chemistry*, vol. 8, *Transuranium Elements, A2, The Elements*, Verlag Chemie, Weinheim.

Koch, G. (ed.) (1976a) *Gmelin Handbook of Inorganic Chemistry, Supplementary Work*, vol. 31, *Transuranium Elements, B1, The Metals*, 8th edn, Springer-Verlag, Berlin.

Koch, G., Ed. (1976b) *Gmelin Handbook of Inorganic Chemistry. Supplementary Work,* vol. 38, *Transuranium Elements, B2: Binary Alloy Systems 1*, 8th edn, Springer-Verlag, Berlin.

Koelling, D. D., Ellis, D. E., and Bartlett, R. J. (1976) *J. Chem. Phys.,* **65**(8), 3331–40.

Koltunov, V. S. (1982a) *Radiokhimiya,* **23**(3), 462.

Koltunov, V. S., Frolov, K. M., Marchenko, V. I., Tikhonov, M. F., Zhuravleva, G. I., Kulikov, I. A., and Ryabova, A. A. (1982b) *Radiokhimiya,* **24**(5), 607–14 (508 pp. in English translation).

Koltunov, V. S. and Baranov, S. M. (1993) *Radiokhimiya,* **35**(6), 11–21.

Koltunov, V. S. and Marchenko, V. I. (1973) *Sov. Radiochem.,* **15**(6), 787–95.

Koltunov, V. S. and Mikhailova, N. A. (1977) *Radiokhimiya,* **19**(3), 342–8 (pp. 282–8 in English translation).

Koltunov, V. S. and Ryabova, A. A. (1980) *Sov. Radiochem.,* **22**(5), 481–7.

Koltunov, V. S. and Zhuravleva, G. I. (1968) *Radiokhimiya,* **10**(6), 662–9 (pp. 648–54 in English translation).

Koltunov, V. S. and Zhuravleva, G. I. (1973) *Sov. Radiochem.,* **15**(1), 73–6.

Koltunov, V. S. and Zhuravleva, G. I. (1974) *Sov. Radiochem.,* **16**(1), 80–3.

Koltunov, V. S. and Zhuravleva, G. I. (1978) *Sov. Radiochem.,* **20**(1), 73–80.

Koltunov, V. S., Frolov, K. M., Tikhonov, M. F., and Shapovalov, M. P. (1980a) *Radiokhimiya,* **22**(4), 491–8 (pp. 386–93 in English translation).

Koltunov, V. S., Tikhonov, M. F., Frolov, K. M., and Shapovalov, M. P. (1980b) *Radiokhimiya,* **22 (1)**, 65–74 (pp. 45–53 in English translation).

Koltunov, V. S., Kulikov, I. A., Kermanova, N. V., and Nikishova, L. K. (1981a) *Radiokhimiya,* **23**(3), 462–5 (pp. 384–6 in English translation).

Koltunov, V. S., Zhuravleva, G. I., and Shapovalov, M. P. (1981b) *Sov. Radiochem.,* **23** (4), 449–553.

Koltunov, V. S., Baranov, S. M., and Zhuravleva, G. I. (1989) *Sov. Radiochem.,* **31**(1), 47–52.

Koltunov, V. S., Pastushchak, V. G., Mezhov, E. A., and Koltunov, G. V. (2004) *Radiochemistry,* **46**(2), 125–30.

Komkov, Y. A., Krot, N. N., and Gel'man, A. D. (1968) *Radiokhimiya,* **10**(6), 625–9.

Komkov, Y. A., Peretrukhin, V. F., Krot, N. N., and Gel'man, A. D. (1969) *Radiokhimiya,* **11**(4), 407–12.

Konobeevsky, S. T. (1955) *Conf. Acad. Sci. USSR, Peaceful Uses of Atomic Energy*, vol. 4, Consultants Bureau, 207.

Korzhavyi, P. A., Vitos, L., Andersson, D. A., and Johansson, B. (2004) *Nat. Mater.,* **3** (4), 225–8.

Kotani, A. and Ogasawara, H. (1993) *Physica B,* **186–188**, 16–20.

Kotani, A., Ogasawara, H., and Yamazaki, T. (1993) *JJAP Series* **8**(Physical Properties of Actinide and Rare Earth Compounds), 117–28.

Kraus, K. A. (1956) *Proc. Int. Conf. Peaceful Uses Atomic Energy,* vol. 7, Geneva, pp. 245–57.

Kraus, K. A. and Dam, J. R. (1949) *in Natl. Nucl. Energy Ser.,* Div IV **14B**(*Transuranium Elements, Pt. I*) (eds. G. T. Seaborg, J. J. Katz, and W. M. Manning), McGraw-Hill, New York, 466.

Kraus, K. A. and Nelson, F. (1950) *J. Am. Chem. Soc.,* **72**(9), 3901–6.

Krikorian, O. H. and Hagerty, D. C. (1990) *J. Nucl. Mater.,* **171**(2–3), 237–44.

Krikorian, O. H., Fontes, A. S., Jr, Ebbinghaus, B. B., and Adamson, M. G. (1997) *J. Nucl. Mater.,* **247**, 161–71.

Krishnan, S., Weber, J. K. R., Anderson, C. D., Nordine, P. C., and Sheldon, R. I. (1993) *J. Nucl. Mater.,* **203**(2), 112–21.

Krot, N. N. (1975) *Radiokhimiya,* **17**(5), 677–83.

Krot, N. N. and Gel'man, A. D. (1967) *Dokl. Akad. Nauk SSSR,* **177**(1), 124–5; see also (1968) Chem. Abstr., **68,** 26372b.

Krott, N. N., Gel'man, A. D., Mefodeva, M. P., Shilov, V. P., Peretrukhin, V. F., and Zakharova, F. A. (1976) *Moscow Symp. on the Chemistry of the Transuranium Elements, V* (eds. I. Spitsyn and J. J. Katz), pp. 249–52.

Kruger, O. L. (1963) *J. Am. Ceram. Soc.,* **46**, 80–5.

Kruger, O. L. and Moser, J. B. (1966a) *J. Am. Ceram. Soc.,* **49**(12), 661–7.

Kruger, O. L. and Moser, J. B. (1966b) *J. Inorg. Nucl. Chem.,* **28**(3), 825–32.

Kruger, O. L. and Moser, J. B. (1967a) *J. Phys. Chem. Solids,* **28**(11), 2321–5.

Kruger, O. L. and Moser, J. B. (1967b) *Chem. Eng. Prog., Symp. Ser.,* **63**(80), 1–10.

Kruger, O. L. and Savage, H. (1968) *J. Chem. Phys.,* **49**(10), 4540–4.

Kruger, O. L., Moser, J. B., and Wrona, B. J. (1966a) *Preparation of Plutonium Monosulfide or Monophosphide*, (United States Atomic Energy Commission). US Patent no. 3282 656, 2 pp.

Kugel, R., Williams, C., Fred, M., Malm, J. G., Carnall, W. T., Hindman, J. C., Childs, W. J., and Goodman, L. S. (1976) *J. Chem. Phys.,* **65**(9), 3486–92.

Kuroda, P. K. (1960) *Nature,* **187**, 36–8.

Kuroda, P. K. and Myers, W. A. (1998) *J. Radioanal. Nucl. Chem.,* **230**(1–2), 175–95.

Kutaitsev, V. I., Chebotarev, N. I., Lebedev, I. G., Adrianov, M. A., Konev, V. N., and Menchikova, T. S. (1967) *Proc. Third Int. Conf. on Plutonium, Plutonium 1965,* (eds. A. E. Kay and M. B. Waldron), Chapman & Hall, London, England, pp. 429–30.

Lallement, R. (1963) *Phys. Chem. Solids* **24**, 1617.

Lallement, R. and Solente, P. (1967) *Low-Temperature Irradiation, Proc. Third Int. Conf. on Plutonium 1965* (eds. A. I. Kay and M. B. Waldron), Chapman and Hall for Institute of Metals, London, pp. 147–61.

Lam, D. J., Fradin, F. Y., and Kruger, O. L. (1969) *Phys. Rev.,* **187**(2), 606–10.

Lammermann, H. and Conway, J. G. (1963) *J. Chem. Phys.,* **38**(1), 259.

Land, C. C., Ellinger, F. H., and Johnson, K. A. (1965a) *J. Nucl. Mater.,* **16**(1), 87.

Land, C. C., Johnson, K. A., and Ellinger, F. H. (1965b) *J. Nucl. Mater.,* **15**(1), 23–32.

Land, C. C., Peterson, D. E., and Roof, R. B. (1978) *J. Nucl. Mater.,* **75**(2), 262–73.

Lander, G. H., Delapalme, A., Brown, P. J., Spirlet, J. C., Rebizant, J., and Vogt, O. (1984) *Phys. Rev. Lett.,* **53**(23), 2262–5.

Lander, G. H., Delapalme, A., Brown, P. J., Spirlet, J. C., Rebizant, J., and Vogt, O. (1985) *J. Appl. Phys.,* **57**(8, Pt. 2B), 3748–50.

Lander, G. H., Rebizant, J., Spirlet, J. C., Delapalme, A., Brown, P. J., Vogt, O., and Mattenberger, K. (1987) *Physica B & C,* **146**(3), 341–50.

Lange, R. G. and Mastal, E. F. (1994) A Tutorial Review of Radioisotope Power Systems, in *A Critical Review of Space Nuclear Power and Propulsion 1984–1993* (ed. M. S. El-Genk), American Institute of Physics, AIP Press, New York, pp. 1–20.

Larroque, J., Chipaux, R., and Beauvy, M. (1986) *J. Less-Common Met.,* **121**, 487–96.

Larson, D. T. (1980) *Effect of Vacuum Heat Treatment on Plutonium Oxide Surfaces as Studied by XPS and AES*, Report RFP-3108, Energy Systems Group, Rockwell International Corporation, Canoga Park, CA, 10 pp.

Larson, A. C. and Cromer, D. T. (1967) *Acta Crystallogr.,* **23**(1), 70–7.

Larson, D. T. and Haschke, J. M. (1981) *Inorg. Chem.,* **20**(7), 1945–50.

Larson, A. C., Cromer, D. T., and Stambaugh, C. K. (1957) *Acta Crystallogr.,* **10**(7), 443–6.

Larson, A. C., Roof, R. B., and Cromer, D. T. (1963) *Acta Crystallogr.,* **16**(8), 835–6.

Larson, A. C., Cromer, D. T., and Roof, R. B. (1965) *Acta Crystallogr.,* **18**(2), 294–5.

Lashley, J. C. (2003) *Cryogenics,* **43**, 369.

Lashley, J. C. (2004) Heat capacity, personal communication, S. S. Hecker, Los Alamos, NM.

Lashley, J. (2005) *Phys. Rev. B: Condens. Matter.*, **71**(17).

Lashley, J. C., Blau, M. S., Staudhammer, K. P., and Pereyra, R. A. (1999) *J. Nucl. Mater.,* **274**(3), 315–19.

Lashley, J. C., Moment, R. L., and Blau, M. S. (2000) *Los Alamos Science,* **26**(1), 226–32.

Lashley, J. C., Stout, M. G., Pereyra, R. A., Blau, M. S., and Embury, J. D. (2001) *Scripta. Mater.,* **44**(12), 2815–20.

Lashley, J. C., Migliori, A., Singleton, J., McQueeney, R. J., Blau, M. S., Pereyra, R. A., and Smith, J. L. (2003a) *J. Metals,* **55**(9), 34.

Lashley, J. C., Singleton, J., Migliori, A., Betts, J. B., Fisher, R. A., Smith, J. L., and McQueeney, R. J. (2003b) *Phys. Rev. Lett.,* **91**(20), 205901/1.

Lashley, J. C., Lawson, A. C., McQueeney, R. J., and Lander, G. H. (2004) *Absence of Magnetic Moments in Plutonium*, Report LA-UR-04-3439 Preprint Archive, Condensed Matter (2004), Los Alamos National Laboratory, pp. 1–30.

Lataillade, F., Pons, F., and Rapin, M. (1971) *J. Nucl. Mater.,* **40**(3), 284–8.

Laue, C. A., Gregorich, K. E., Sudowe, R., Hendricks, M. B., Adams, J. L., Lane, M. R., Lee, D. M., McGrath, C. A., Shaughnessy, D. A., Strellis, D. A., Sylwester, E. R., Wilk, P. A., and Hoffman, D. C. (1999) *Phys. Rev. C,* **59**(6), 3086–92.

Lavallee, C. and Newton, T. W. (1972) *Inorg. Chem.,* **11**, 2616.

Lawson, A. C. (2001) *Philos. Mag. B,* **81**(3), 255–66.

Lawson, A. C., Goldstone, J. A., Cort, B., Sheldon, R. I., and Foltyn, E. M. (1994) *J. Alloys Compd.,* **213/214**, 426–8.

Lawson, A. C., Goldstone, J. A., Cort, B., Martinez, R. J., Vigil, F. A., Zocco, T. G., Richardson, J. W., Jr, and Mueller, M. H. (1996) *Acta Crystallogr.,* **B52**, 32–7.

Lawson, A. C., Martinez, B., Roberts, J. A., and Bennett, B. I. (2000) *Philos. Mag. B,* **80** (1), 53–9.

Lawson, A. C., Roberts, J. A., Martinez, B., and Richardson, J. W. (2002) *Philos. Mag. B,* **82**(18), 1837–45.

Laxminarayanan, T. S., Patil, S. K., and Sharma, H. D. (1964) *J. Inorg. Nucl. Chem.,* **26** (6), 1001–9.

Leary, J. A. (1962) *Temperature-composition Diagrams of Pseudo-binary Systems Containing Plutonium (III) Halides*, Report LA-2661, Los Alamos Scientific Laboratory, Los Alamos, NM, 16 pp.

Leary, J. A. and Mullins, L. J. (1966) *Int. Atomic Energy Agency - Proc. Ser. Thermodynamics*, vol. 1, pp. 459–71.

Leary, J. A. and Mullins, L. J. (1974) *J. Chem.Thermodyn.,* **6**(1), 103–4.

Leary, J. A., Morgan, A. N., and Maraman, W. J. (1959) *Ind. Eng. Chem.,* **51**(1), 27–31.

Lechelle, J., Bleuet, P., Martin, P., Girard, E., Bruguier, F., Martinez, M. A., Somogyi, A., Simionovici, A., Ripert, M., Valdivieso, F., and Goeuriot, P. (2004) *IEEE Trans. Nucl. Sci.,* **51**(4, Pt. 1), 1657–61.

Ledbetter, H. (2004) Grüneisen constants, personal communication, S. S. Hecker, Los Alamos, NM.

Ledbetter, H. M. and Moment, R. L. (1976) *Acta Metall. Mater.,* **24**, 891–9.

Ledbetter, H., Migliori, A., Betts, J., Harrington, S., and El-Khatib, S. (2004) *Elastic Constant Measurements*, Report LA-UR-04-6980, Los Alamos National Laboratory.

Ledbetter, H., Migliori, A., Betts, J., Harrington, S., and El-Khatib, S. (2005) *Phys. Rev. B.*, **71**, 172101/1–4.

Ledbetter, H., and Migliori, A., (2005) Report LA-UR-05-1800, Los Alamos National Laboratory.

Lee, J. A. and Hall, R. O. A. (1959) *J. Less-Common Met.,* **1**, 356.

Lee, J. A. and Mardon, P. G. (1961) Thermal Conductivity, in *The Metal Plutonium* (ed. A. S. Coffinberry), Chicago University Press, Chicago, IL.

Lee, J. A., Hall, R. O. A., King, E., and Meaden, G. T. (1961) Electrical Resistivity, in *Plutonium 1960,* vol. 1, (eds. E. Grison, W. B. H. Lord, and R. D. Fowler), Cleaver-Hume Press Ltd., London, pp. 39–50.

Lee, J. A., Mendelssohn, K., and Wigley, D. A. (1962) *Phys. Lett.,* **1**(8), 325–7.

Lee, J. A., Marples, J. A. C., Mendelssohn, K., and Sutcliffe, P. W. (1965a) Thermal Expansion, in *Plutonium 1965* (eds. K. A. E. and R. G. Loasby), Chapman-Hall Publishers, London, England, pp. 176–88.

Lee, J., Mendelssohn, K., and Sutcliffe, P. (1965b) *Cryogenics,* **5**, 227.

Leibowitz, L., Fischer, D. F., and Chasanov, M. G. (1974) *Enthalpy of Molten Uranium–Plutonium Oxides*, Report ANL-8082, Argonne National Laboratory, Argonne, IL, 19 pp.

Leitner, L. (1967) *Quasibinary Phase Diagrams of the System Thulium Oxide–Actinide Oxide (ThO_2, UO_2, NpO_2, PuO_2) below 1700 deg*, Report KFK-521, Kernforschungszentrum, Karlsruhe, Germany, 86 pp.

Lemire, R. J., Fuger, J., Nitsche, H., Potter, P., Rand, M. H., Rydberg, J., Spahiu, K., Sullivan, J. C., Ullman, W. J., Vitorge, P., and Warner, H. (2001) *Chemical*

Thermodynamics of Neptunium and Plutonium, Elsevier, Amsterdam, The Netherlands, 845 pp.

Lesser, R. and Peterson, J. R. (1976) *Transurane: Die Metalle*, part B1, in *Transurane,* vol. 31, (ed. K.-C. Buschbeck), Springer-Verlag, Berlin, Germany, pp. 40–1.

Levine, C. A. and Seaborg, G. T. (1951) *J. Am. Chem. Soc.,* **73**, 3278–83.

Levitz, N. M., Vogel, G. J., Carls, E. L., Grosvenor, D. E., Murphy, W. F., Kullen, B. J., and Raue, D. J. (1968) *Engineering Development of Fluid-bed Fluoride Volatility Processes*, part 15, *Material Balance Demonstrations, Production Rates, and Fluorine Utilizations in Fluorination of Kilogram Quantities of PuF_4 to PuF_6 with Elemental Fluorine in a Fluid-bed Reactor*, Report ANL-7568, Argonne National Laboratory, Argonne, IL, 28 pp.

Lewis, H. D., Kerrisk, J. F., and Johnson, K. W. (1976) *Effect of a Delta-phase Stabilizer on the Thermal Diffusivity of Plutonium, Proc. 14th Int. Conf. on Therm Conduct,* Jun. 2–4, 1975, University of Connecticut, Storrs, Plenum Press, New York, pp. 201–8.

Li, J. and Bursten, B. E. (1998) *J. Am. Chem. Soc.,* **120**(44), 11456–66.

Lipis, L. V. and Pozharskii, B. G. (1960) *Zh. Neorg. Khim.,* **5**, 2162–6.

Liptai, R. G. and Friddle, R. J. (1967) *J. Nucl. Mater.,* **21**(1), 114.

Liptai, R. G., Lloyd, L. T., and Friddle, R. J. (1967) *J. Phys. Chem. Solids,* **1**, 573.

Littler, D. J. (1952) *Proc. Phys. Soc.,* **65A**, 203–8.

Lloyd, M. H. and Haire, R. G. (1968) *Nucl. Appl. Technol.,* **5**(3), 114–22.

Lloyd, M. H. and Haire, R. G. (1978) *Radiochim. Acta,* **25**(3–4), 139–48.

Long, J. T. (1978) *Engineering for Nuclear Fuel Reprocessing*, American Nuclear Society, La Grange Park, IL, 1025 pp.

Lorenzelli, R., Martin, A., and Schickel, R. (1966) *Reaction of Uranium and Plutonium Carbides with Nitrogen*, Report CEA-R 2997, 21 pp.

Louer, M., Brochu, R., Louer, D., Arsalane, S., and Ziyad, M. (1995) *Acta Crystallogr. B,* **51**(6), 908–13.

Louwrier, K. P. and Richter, K. (1976) *Des. Equip. Hot Lab.*, *Proc. Symp.*, pp. 3–12.

Louwrier, K. P., Ronchi, C., Steemers, T., and Zamorani, E. (1968) *Sol-gel Processes for Ceramic Nuclear Fuels*, *Proc. Panel on Sol-gel Processes for Ceramic Nuclear Fuels*, Report STI/PUB/207, International Atomic Agency, pp. 97–106.

Love, L. O. (1973) *Science,* **182**(4110), 343–52.

Love, L. O., Banic, G. M., Bell, W. A., and Prater, W. K. (1961) *Electromagnetic Separation Radioactive Isotopes, Proc. Int. Symp.,* Vienna, Austria, pp. 141–54.

Lupinetti, A. J., Fife, J. L., Garcia, E., Dorhout, P. K., and Abney, K. D. (2002) *Inorg. Chem.,* **41**(9), 2316–18.

Lynn, J., Kwei, G., Trela, W. J., Yuan, V. W., Cort, B., Martinez, R. J., and Vigil, F. (1998) *Phys. Rev. B,* **65**, 214107–1.

Lyon, W. L. and Baily, W. E. (1965) *Solid-liquid Phase Diagram for the Uranium Oxide–Plutonium Oxide System*, Report GEAP-4878, General Electric Company, 17 pp.

Lyon, W. L. and Baily, W. E. (1967) *J. Nucl. Mater.,* **22**(3), 332–9.

Madic, C., Begun, G. M., Hobart, D. E., and Hahn, R. L. (1984) *Inorg. Chem.,* **23**(13), 1914–21.

Madic, C., Berger, P., and Machuron-Mandard, X. (1992) in *Transuranium Elements: A Half Century*, American Chemical Society, Washington, DC, pp. 457–68.

Magon, L., Portanova, R., and Cassol, A. (1968) *Inorg. Chim. Acta,* **2**, 237.

Maillard, C. and Adnet, J.-M. (2001) *Radiochim. Acta,* **89**(8), 485–90.

Malm, J. G. and Weinstock, B. (1954) *Argonne Plutonium Hexafluoride Program*, Report ANL-5366, Argonne National Laboratory, 14 pp.

Malm, J. G., Eller, P. G., and Asprey, L. B. (1984) *J. Am. Chem. Soc.,* **106**(9), 2726–7.

Mandleberg, C. J. and Davies, D. (1954) *The Vapour Pressure of Plutonium Tetrafluoride*, Report AERE-C/R-1321, Great Britain Atomic Energy Research Establishment, 18 pp.

Mandleberg, C. J. and Davies, D. (1961) *J. Chem. Soc., Abstracts*: 2031–7.

Mandleberg, C. J., Rae, H. K., Hurst, R., Long, G., Davies, D., and Francis, K. E. (1953) *Plutonium Hexafluoride*, part I, *Preparation and Some Physical Properties*, Report AERE-C/R-1172, Great Britain Atomic Energy Research Establishment.

Mandleberg, C. J., Rae, H. K., Hurst, R., Long, G., Davies, D., and Francis, K. E. (1956) *J. Inorg. Nucl. Chem.,* **2**(5–6), 358–67.

Manley, M. E., Fultz, B., McQueeney, R. J., Brown, C. M., Hults, W. L., Smith, J. L., Thoma, D. J., Osborn, R., and Robertson, J. L. (2001) *Phys. Rev. Lett.,* **86**(14), 3076–9.

Maraman, W. J., Beaumont, A. J., Christensen, E. l., Henrickson, A. V., Hermann, J. A., Johnson, K. W. R., Mullins, L. J., and Winchester, R. S. (1954) *Calcium Oxalate Carrier Precipitation of Plutonium*, Report LA-1692, Los Alamos Scientific Laboratory, Los Alamos, NM, 10 pp.

Maraman, W. J., McNeese, W. D., and Stafford, R. G. (1975) *Health Phys.,* **29**(4), 469–80.

Marcon, J. P. (1969) *Actinide Sulfides*, Report CEA-R-3919, Commissariat al'Energie Atomique, France, 99 pp.

Marcon, J. P. and Pascard, R. (1966a) *J. Inorg. Nucl. Chem.,* **28**(11), 2551–60.

Marcon, J. P. and Pascard, R. (1966b) *CR Acad. Sci. C. Chim.,* **262**(24), 1679–81.

Marcon, J. P. and Pascard, R. (1968) *CR Acad. Sci. C. Chim.,* **266**(4), 270–2.

Mardon, P. G. and Potter, P. E. (1970) *Plutonium 1970 and Other Actinides, Proc. Fifth Int. Conf. on Plutonium and Other Actinides,* Baden-Baden, West Germany, (ed. W. N. Miner), North-Holland, New York, 809 pp.

Mardon, P. G., Haines, H. R., Pearce, J. H., and Waldron, M. B. (1957) *J. I. Met.,* **86** (Part 4), 166–71.

Mardon, P. G., Pearce, J. H., and Marples, J. A. C. (1961) *J. Less-Common Met.,* **3**(4), 281–92.

Markin, T. L. and McKay, H. A. C. (1958) *J. Inorg. Nucl. Chem.,* **7**, 298–999.

Markin, T. L. and Street, R. S. (1967) *J. Inorg. Nucl. Chem.,* **29**(9), 2265–80.

Marples, J. A. C. (1960) *J. Less-Common Met.,* **2**(5), 331–51.

Marples, J. A. C. and Hall, R. O. A. (1972) *J. Nucl. Mater.,* **42**(2), 212–16.

Marples, J. A. C., Hough, A., Mortimer, M. J., Smith, A., and Lee, J. A. (1970) *Self-irrad Damage*, in *Proc. Fourth Int. Conf. on Plutonium and Other Actinides 1970* (ed. W. N. Miner), The Metallurgical Society of AIME, pp. 623–34.

Marquart, R., Hoffmann, G., and Weigel, F. (1983) *J. Less-Common Met.,* **91**(1), 119–27.

Marsh, S. F., Day, R. S., and Veirs, D. K. (1991) *Spectrophotometric Investigation of the Pu(IV) Nitrate Complex Sorbed by Ion Exchange Resins*, Report LA-12070, Los Alamos National Laboratory, Los Alamos, NM, 22 pp.

Marsh, S. F., Veirs, D. K., Jarvinen, G. D., Barr, M. E., and Moody, E. W. (2000) *Los Alamos Science,* **26**(2), 454–63.

Martell, A. E. and Smith, R. M. (2001) *Critical Stability Constants,* Standard Reference Database 46, Version 6.0., National Institute of Standards, Gaithersburg, MD.

Martin, D. G. (1988) *J. Nucl. Mater.,* **152**(2–3), 94–101.

Marty, B. and Marti, K. (2002) *Earth Planet. Sc. Lett.,* **196**(3–4), 251–63.

Martz, J. and Haschke, J. (1998) *J. Alloys Compd.,* **266**(1–2), 90–103.

Martz, J. C. and Schwartz, A. J. (2003) *J. Metals,* **55**(9), 19–23.

Martz, J. C., Haschke, J. M., and Stakebake, J. L. (1994) *J. Nucl. Mater.,* **210**(1–2), 130–42.

Mary, T. A., Evans, J. S. O., Vogt, T., and Sleight, A. W. (1996) *Science,* **272**, 90.

Mashirev, V. P., Shatalov, V. V., Grebenkin, K. F., Zuev, Y. N., Panov, A. V., Subbotin, V. G., and Chuvilin, D. Y. (2001) *At. Energ.,* **90**(3), 235–42.

Massalski, T. B. (1996) *Physical Metallurgy* (eds. R. W. Cahn and P. Haasen), Elsevier Science, Amsterdam, The Netherlands, 136 pp.

Masters, B. J. and Rabideau, S. W. (1963) *Inorg. Chem.,* **2**, 1–5.

Matonic, J. H., Scott, B. L., and Neu, M. P. (2001) *Inorg. Chem.,* **40**(12), 2638–9.

Matsika, S., Zhang, Z., Brozell, S. R., Blaudeau, J. P., Wang, Q., and Pitzer, R. M. (2001) *J. Phys. Chem. A,* **105**(15), 3825–8.

Matsui, T. and Ohse, R. W. (1987) *High Temp.-High Press.,* **19**(1), 1–17.

Mattenberger, K., Vogt, O., Spirlet, J. C., and Rebizant, J. (1986) *J. Magn. Magn. Mater.,* **54–57**(1), 539–40.

Matthews, J. R. (1987) *J. Chem. Soc., Faraday Trans., 2,* **83**(7), 1273–85.

Matzke, H. (1982) *Mater. Sci. Monogr.,* **15**(Transp. Non-Stoichiom. Compd.), 203–31.

Matzke, H. (1984) *Solid State Ionics,* **12**, 25–45.

Matzke, H. (1986) *Science of Advanced LMFBR Fuels: Solid State Physics, Chemistry, and Technology of Carbides, Nitrides, and Carbonitrides of Uranium and Plutonium,* North-Holland, New York, 740 pp.

Mazumdar, A. S. G., Natarajan, P. R., and Vaidyanathan, S. (1970) *J. Inorg. Nucl. Chem.,* **32**, 3363.

McAlister, S. P. and Crozier, E. D. (1981) *Solid State Commun.,* **40**, 375.

McCreary, W. J. (1955) *J. Am. Chem. Soc.,* **77**, 2113–14.

McDonald, B. J. and Stuart, W. I. (1960) *Acta Crystallogr.,* **13**, 447.

McKay, H. A. C., Schulz, W. W., Navratil, J. D., Burger, L. L., and Bender, K. P. (1990) The PUREX Process. Part 1: Introduction. Science and Technology of Tributyl Phosphate, vol. 3, *Applications of Tributyl Phosphate in Nuclear Fuel Processing,* CRC Press, Boca Raton, FL, pp. 1–9.

McNally, Jr J. R., and Griffin, P. M. (1959) *J. Opt. Soc. Am.,* **49**, 162–6.

McNeese, J. A., Bowersox, D. F., and Christensen, D. C. (1986) *Proc. Electrochem. Soc.,* **86-1**(Molten Salts), 474–84.

McQueeney, R. J., Lawson, A. C., Migliori, A., Kelley, T. M., Fultz, B., Ramos, M., Martinez, B., Lashley, J. C., and Vogel, S. C. (2004) *Phys. Rev. Lett.,* **92**(14), 146401.

Meadon, G. T. and Lee, J. A. (1962) *Cryogenics,* **2**, 182.

Mendik, M., Wachter, P., Spirlet, J. C., and Rebizant, J. (1993) *Physica B,* **186–188**, 678–80.

Méot-Reymond, S. and Fournier, J. M. (1996) *J. Alloys Compd.,* **232**(1–2), 119–25.

Merciny, E., Gatez, J. M., and Duyckaerts, G. (1978) *Anal. Chim. Acta,* **100**, 329–42.

Merigou, C., Genet, M., Ouillon, N., and Chopin, T. (1995) *New J. Chem.,* **19**(3), 275–85.

Merrill, J. J. and Du Mond, J. W. M. (1958) *Phys. Rev.,* **110**, 79–84.

Merrill, J. J. and Du Mond, J. W. M. (1961) *Ann. Phys. (N.Y.)* **14**, 166–228.

Merz, M. D. (1970) *J. Nucl. Mater.,* **34**, 108–10.

Merz, M. D. (1971) *J. Nucl. Mater.,* **41**, 348–50.

Merz, M. D. (1974) *J. Nucl. Mater.,* **50**, 31–9.

Merz, M. D. and Allen, R. P. (1973) *J. Nucl. Mater.,* **46**, 110.

Merz, M. D. and Nelson, R. D. (1970) Alpha Plutonium, in *Plutonium 1970 and Other Actinides,* vol. 1 (ed. W. N. Miner), The Metallurgical Society of the AIME, Santa Fe, NM, 387 pp.

Merz, M. D., Hammer, J. H., and Kjarmo, H. E. (1974) *J. Nucl. Mater.,* **51**(3), 357–8.

Metivier, H. and Guillaumont, R. (1972) *Radiochem. Radioanal. Lett.,* **10**(1), 27–35.

Meyer, G. and Morss, L. R. (eds.) (1991) Synthesis of Lanthanide and Actinide Compounds, in *Topics in f-element Chemistry*, Kluwer Academic, Boston, MA.

Miedema, A. R. (1973) *J. Less-Common Met.,* **32**(1), 117–36.

Miedema, A. R. (1976) On the Heat of Formation of Plutonium Alloys. *Plutonium 1975 Other Actinides, Proc. Fifth Int. Conf.* (eds. H. Blank and R. Lindner), North-Holland, Amsterdam, The Netherlands, pp. 3–20.

Migliori, A., Baiardo, J. P., and Darling, T. W. (2000) *Los Alamos Science,* **26**(1), 209–25.

Migliori, A., Ledbetter, H., Betts, J., Ramos, M., Harrington, S., and El-Khatib, S. (2004) *Elastic Constants of Plutonium*, Report LA-UR-04-7419, Los Alamos National Laboratory.

Migliori, A., Ledbetter, H., Lawson, A. C., Ramirez, A. P., Miller, D. A., Betts, J. B., Ramos, M., and Lashley, J. C. (2006) *Phys. Rev. B.*, **73**, 052101/1–4.

Mikheev, N. B. and Myasoedov, B. F. (1985) Lower and Higher Oxidation States of Transplutonium Elements in Solutions and Melts, in *Handbook on the Physics and Chemistry of the Actinides* (eds. A. J. Freeman and C. Keller), Elsevier Science, New York, pp. 347–86.

Mikheev, N. B., Rumer, I. A., and Auerman, L. N. (1983) *Radiochem. Radioanal. Lett.,* **59**(5–6), 317–28.

Miles, J. H., Schulz, W. W., Navratil, J. D., Burger, L. L., and Bender, K. P. (1990) The PUREX Process. Part 2: Separation of Plutonium and Uranium. Science and Technology of Tributyl Phosphate, vol. 3. *Applications of Tributyl Phosphate in Nuclear Fuel Processing* (eds. W. W. Schulz and J. D. Navratil), CRC Press, Boca Raton, FL, pp. 11–54.

Mincher, B. J., Fox, R. V., Holmes, R. G. G., Robbins, R. A., and Boardman, C. (2001) *Radiochim. Acta,* **89**(10), 613–17.

Miner, W. N. (1970) *Plutonium 1970 and Other Actinides, Proc. Fourth Int. Conf. on Plutonium and Other Actinides,* Santa Fe, NM (ed. W. N. Miner), Metallurgical Society of AIME, New York, 2 v.

Miner, W. N. and Schonfeld, F. W. (1980) Physical Properties, in *Plutonium Handbook,* vol. 1 (ed. O. J. Wick), American Nuclear Society, La Grange Park, IL, pp. 31–59.

Miner, F. J. and Seed, J. R. (1967) *Chem. Rev.,* **67**, 299–315.

Miner, F. J., De Grazio, R. P., and Byrne, J. T. (1963) *Anal. Chem.,* **35**(9), 1218–23.

Mitchell, A. W. and Lam, D. J. (1971) *J. Nucl. Mater.,* **39**(2), 219–23.

Mitchell, A. W. and Lam, D. J. (1974) *The Actinides: Electronic Structure and Related Properties,* vol. II (eds. A. J. Freeman and J. B. J. Darby), Academic Press, New York, 139 pp.

Mitchell, J. N., Gibbs, F. E., Zocco, T. G., and Pereyra, R. A. (2001) *Metall. Mater. Trans. A,* **32**(3A), 649–59.

Mittal, R., Chaplot, S. L., Schober, H., and Mary, T. A. (2001) *Phys. Rev. Lett.,* **86**, 4692.

Moeller, R. D. and Schonfeld, F. W. (1950) *Alloys of Plutonium with Aluminum*, Report LA-1000, Los Alamos Scientific Laboratory, Los Alamos, NM, 87 pp.

Moll, H., Reich, T., and Szabo, Z. (2000) *Radiochim. Acta,* **88**(7), 411–15.

Moment, R. L. (1968) *J. Cryst. Growth,* **2**(1), 15–25.

Moment, R. (2000) *Los Alamos Science,* **26**(1), 233–7.

Mooney, R. C. L. and Zachariasen, W. H. (1949) *Natl. Nucl. Energy Ser.*, Div IV **14B** (Transuranium Elements, Pt. II) (eds. G. T. Seaborg, J. J. Katz and W. M. Manning), pp. 1442–7.

Moore, K. T., Wall, M. A., Schwartz, A. J., Chung, B. W., Shuh, D. K., Schulze, R. K., and Tobin, J. G. (2003) *Phys. Rev. Lett.,* **90**(19), 196404.

Morales, L. A., Lawson, A. C., Conradson, S., Butler, E. N., Moore, D. P., Ramos, M., Roberts, J. A., and Martinez, B. (2003) *AIP Conf. Proc.,* **673**(Plutonium Futures – The Science), 174–5.

Morgan, J. R. (1970) *Plutonium 1970 and Other Actinides, Proc. Fourth Int. Conf. on Plutonium and Other Actinides,* Santa Fe, NM (ed. W. N. Miner), Metallurgical Society of AIME, 669 pp.

Morgenstern, A. and Choppin, G. R. (1999) *Radiochim. Acta,* **86**(3–4), 109–13.

Morgenstern, A. and Kim, J. I. (1996) *Radiochim. Acta,* **72**(2), 73–7.

Morgenstern, A., Apostolidis, C., Carlos-Marquez, R., Mayer, K., and Molinet, R. (2002) *Radiochim. Acta,* **90**(2), 81–5.

Morss, L. R. (2005) PuF_6 gas pressure in aged cylinders, personal communication, D. L. Clark, Los Alamos, NM.

Morss, L. R. and Fuger, J. (eds.) (1992) *Transuranium Elements: A Half Century,* American Chemical Society, Washington, DC, 562 pp.

Morss, L. R. and Fujino, T. (1988a) *J. Solid State Chem.,* **72**(2), 338–52.

Morss, L. R. and Fujino, T. (1988b) *J. Solid State Chem.,* **72**(2), 353–62.

Morss, L. R., Appelman, E. H., Gerz, R. R., and Martin-Rovet, D. (1994) *J. Alloys Compd.,* **203**(1–2), 289–95.

Moser, J. B. and Kruger, O. L. (1966) *J. Less-Common Met.,* **10**(6), 402–7.

Moskvin, A. I. (1969) *Radiokhimiya,* **11**, 447.

Moskvin, A. I. (1971a) *Sov. Radiochemistry,* **13**, 688–93.

Moskvin, A. I. (1971b) *Radiokhimiya,* **13**, 641.

Moskvin, A. I. and Poznyakov, A. N. (1979) *Russ. J. Inorg. Chem.,* **24**, 1357–62.

Moulin, V. and Moulin, C. (2001) *Radiochim. Acta,* **89**(11–12), 773–8.

Moulin, C., Delorme, N., Berthoud, T., and Mauchien, P. (1988) *Radiochim. Acta,* **44–45**(1), 103–6.

Moulton, G. H. (1944) *Decomposition Products of Plutonyl Nitrate and Plutonium Oxalate*, Report LA-172, Los Alamos Scientific Laboratory, Los Alamos, NM, 10 pp.

Mudher, K. D. S., Krishnan, K., and Iyer, P. N. (1995) *NUCAR 95*, *Proc. Nuclear and Radiochemistry Symp.*, Feb. 21–24, 1995, Kalpakkam, India, pp. 228–9.

Mueller, M. H., Lander, G. H., Hoff, H. A., Knott, H. W., and Reddy, J. F. (1979) *J. Phys. Colloq.*, (4), 68–9.

Mulford, R. N. R. (1965) *Vapor Pressure, Joint Symp. of IUPAC and IAEA on Thermodynamics,* IAEA, Vienna, Austria 231 pp.

Mulford, R. N. R. and Ellinger, F. H. (1958) *J. Phys. Chem.,* **62**, 1466–7.

Mulford, R. N. R., Ellinger, F. H., Hendrix, G. S., and Albrecht, E. D. (1960) The Plutonium–Carbon System. *Plutonium 1960*, *Proc. Int. Conf. on Plutonium Metal*, Grenoble, France (eds. E. Grison, W. B. H. Lord and R. D. Fowler), pp. 301–11.

Mulford, R. N. R., Ellinger, F. H., and Johnson, K. A. (1965) *J. Nucl. Mater.,* **17**(4), 324–9.

Mulford, R. N. R., Ford, J. O., and Hoffman, J. J. (1963) *Thermodynamics of Nuclear Materials, Proc. Symp. on Thermodynamics of Nuclear Materials* 1962, pp.517–25.

Mulford, R. N. R. and Lamar, L. E. (1961) Volatility of Plutonium Oxide. *Plutonium 1960*, *Proc. Int. Conf. on Plutonium Metal*, Grenoble, France (eds. E. Grison, W. B. H. Lord and R. D. Fowler), pp. 411–21.

Mullins, L. J. and Foxx, C. L. (1982) *Direct Reduction of Plutonium-238 Dioxide and Plutonium-239 Dioxide to Metal*, Report LA-9073, Los Alamos National Laboratory, Los Alamos, NM, 19 pp.

Mullins, L. J. and Leary, J. A. (1965) *Ind. Eng. Chem., Process Design Develop.,* **4**(4), 394–400.

Mullins, L. J. and Morgan, A. N. (1981) *Review of Operating Experience at the Los Alamos Plutonium Electrorefining Facility, 1963–1977*, Report LA-8943, Los Alamos National Laboratory, Los Alamos, NM, 24 pp.

Mullins, L. J., Leary, J. A., and Bjorklund, C. W. (1960) *Large-Scale Preparation of High-purity Plutonium Metal by Electrorefining*, Report LAMS-2441, Los Alamos Scientific Laboratory, Los Alamos, NM, 16 pp.

Mullins, L. J., Leary, J. A., and Morgan, A. N. (1963a) *Large Scale Electrorefining of Plutonium from Plutonium–Iron Alloys*, Report LA-3029, Los Alamos Scientific Laboratory, Los Alamos, NM, 35 pp.

Mullins, L. J., Leary, J. A., Morgan, A. N., and Maraman, W. J. (1963b) *Ind. Eng. Chem., Process Design Develop.,* **2**, 20–4.

Mullins, L. J., Beaumont, A. J., and Leary, J. A. (1966) *Distribution of Americium between Liquid Plutonium and a Fused Salt: Evidence for Divalent Americium*, Report LA-3562, Los Alamos Scientific Laboratory, Los Alamos, NM, 26 pp.

Mullins, L. J., Beaumont, A. J., and Leary, J. A. (1968) *J. Inorg. Nucl. Chem.,* **30**(1), 147–56.

Mullins, L. J., Christensen, D. C., and Babcock, B. R. (1982) *Fused Salt Processing of Impure Plutonium dioxide to High-purity Plutonium Metal*, Report LA-9154-MS, Los Alamos National Laboratory, Los Alamos, NM, 26 pp.

Murch, G. E. and Catlow, C. R. A. (1987) *J. Chem. Soc. Faraday Trans. 2,* **83**(7), 1157–69.

Muromura, T. (1982) *J. Nucl. Sci. Technol.,* **19**(8), 638–45.

Muromura, T., Yahata, T., Ouchi, K., and Iseki, M. (1972) *J. Inorg. Nucl. Chem.,* **34**(1), 171–3.

Murzin, A. A., Babain, V. A., Shadrin, A. Y., Kamachev, V. A., Romanovskii, V. N., Starchenko, V. A., Podoinitsyn, S. V., Revenko, Y. A., Logunov, M. V., and Smart, N. G. (2002a) *Radiochemistry,* **44**(4), 410–15.

Murzin, A. A., Babain, V. A., Shadrin, A. Y., Smirnov, I. V., Lumpov, A. A., Gorshkov, N. I., Miroslavov, A. E., and Muradymov, M. A. (2002b) *Radiochemistry,* **44**(5), 467–71.

Musante, Y. and Ganivet, M. (1974) *J. Electroanal. Chem.,* **57**(2), 225–30.

Muscatello, A. C. and Killion, M. E. (1990) *Chloride Anion Exchange Coprocessing for Recovery of Plutonium from Pyrochemical Residues and Cs_2PuCl_6 Filtrate*, Report RFP–4325, EG & G Rocky Flats, Golden, CO, 19 pp.

Nachtrieb, N. H. and Lawson, A. W. (1955) *J. Chem. Phys.,* **23**(7), 1193–5.

Nagarajan, G. (1962) *Bull. Soc. Chim. Belg.,* **71**(1–2), 88–1.

Nair, G. M., and Joshi, J. K. (1981) *J. Indian Chem. Soc.,* **58**, 311.

Naito, K., Tsuji, T., Matsui, T., Fujino, T., Yamashita, T., and Ohuchi, K. (1992) *Defect Chemistry of Plutonium Oxides*, in *Transuranium Elem. Symp.* (eds. L. R. Morss and J. Fuger), American Chemical Society, Washington, DC, pp. 440–50.

Nakayama, Y. (1971) *J. Inorg. Nucl. Chem.,* **33**(12), 4077–84.

Nash, K., Noon, M. E., Fried, S., and Sullivan, J. C. (1980) *Inorg. Nucl. Chem. Lett.,* **16**(1), 33–5.

Nash, K. L. (1993) *Solvent Extr. Ion Exc.,* **11**(4), 729–68.

Nash, K. L. and Cleveland, J. M. (1983) *ACS Symp. Ser.,* **216**(Plutonium Chem.), 251–62.

Navratil, J. D. (1969a) *Dissolution of Impure Plutonium Tetrafluoride in Nitric Acid*, Report RFP-1118, Dow Chemical Company, Rocky Flats Division, Golden, CO, 4 pp.

Navratil, J. D. (1969b) *Dissolution of Plutonium Tetrafluoride in Nitric Acid*, Report RFP-1151, Dow Chemical Company, Rocky Flats Division, Golden, CO, 5 pp.

Navratil, J. D. (1969c) *J. Inorg. Nucl. Chem.,* **31**(11), 3676–80.

Neck, V. and Kim, J. I. (2001) *Radiochim. Acta,* **89**(1), 1–16.

Neeb, K.-H. (1997) *The Radiochemistry of Nuclear Power Plants with Light Water Reactors,* Walter de Gruyter, Berlin, New York, 725 pp.

Nelson, R. D. (1980) Solid State Reactions, in *Plutonium Handbook,* vol. 2, (ed. O. J. Wick), American Nuclear Society, La Grange Park, IL, 101 pp.

Nelson, T. O. (1998) *WM'98 Proc.*, Tucson, AZ, Mar. 1–5, 1998, pp. 1234–9.

Nelson, R. D., Bierlein, T. K., and Bowman, F. E. (1965) *The Steady-State Creep of High-Purity Plutonium*, Report BNWL-32, Battelle Pacific Northwest National Laboratory, 20 pp.

Nelson, G. C., Saunders, B. G., and John, W. (1969) *Phys. Rev.,* **188**(1), 4–6.

Nelson, G. C., Saunders, B. G., and Salem, S. I. (1970) *Z. Phys.,* **235**(4), 308–12.

Nelson, E. J., Blobaum, J. M., Wall, M. A., Allen, P. G., Schwartz, A. J., and Booth, C. H. (2003a) *AIP Conf. Proc.,* **673**(Plutonium Futures – The Science), 187–9.

Nelson, E. J., Blobaum, K. J. M., Wall, M. A., Allen, P. G., Schwartz, A. J., and Booth, C. H. (2003b) *Phys. Rev. B,* **67**(22), 224206.

Neu, M. P., Hoffman, D. C., Roberts, K. E., Nitsche, H., and Silva, R. J. (1994) *Radiochim. Acta,* **66–67**, 251–8.

Neu, M. P., Matonic, J. H., Smith, D. M., and Scott, B. L. (2000) *AIP Conf. Proc.,* **532** (Plutonium Futures – The Science), 381–2.

Neu, M., P., Ruggiero, C. E., and Francis, A. J. (2002) Bioinorganic Chemistry of Plutonium and Interactions of Plutonium with Microorganisms and Plants, in *Advances in Plutonium Chemistry 1967–2000* (ed. D. C. Hoffman), American Nuclear Society and the University Research Alliance, La Grange Park, IL, pp. 169–203.

Neuilly, M., Bussac, J., Frejacques, C., Nief, G., Vendryes, G., and Yvon, J. (1972) *C. R. Acad. Sci., Ser. D,* **275**(17), 1847–9.

Newton, T. W. (1958) *J. Phys. Chem.,* **62**, 943–7.

Newton, T. W. (1959) *J. Phys. Chem.,* **63**, 1493.

Newton, T. W. (1975) *Kinetics of the Oxidation–Reduction Reactions of Uranium, Neptunium, Plutonium, and Americium in Aqueous Solutions*, Los Alamos Scientific Laboratory, Report ERDA Critical Review Series, TID 26506, 131 pp.

Newton, T. W. (2002) Redox Reactions of Plutonium Ions in Aqueous Solutions, in *Advances in Plutonium Chemistry 1967–2000* (ed. D. C. Hoffman), American Nuclear Society and the University Research Alliance, La Grange Park, IL, pp. 24–60.

Newton, T. W. and Baker, F. B. (1956) *J. Phys. Chem.,* **60**, 1417–21.

Newton, T. W. and Baker, F. B. (1963) *J. Phys. Chem.,* **67**, 1425.

Newton, T. W. and Burkhart, M. J. (1971) *Inorg. Chem.,* **10**(10), 2323–6.

Newton, T. W. and Cowan, G. A. (1960) *J. Phys. Chem.,* **64**, 244.

Newton, T. W. and Hobart, D. E. (2004) *J. Nucl. Mater.,* **334**(2–3), 222–4.

Newton, T. W. and Montag, T. (1976) *Inorg. Chem.,* **15(11)**, 2856–61.

Newton, T. W. and Rundberg, V. L. (1984) *Mater. Res. Soc. Symp. Proc.,* **26**(Sci. Basis Nucl. Waste Manage. 7), 867–73.

Newton, T. W. and Sullivan, J. C. (1986) in *Handbook on the Physics and Chemistry of the Actinides* (eds. A. J. Freeman and C. Keller), Elsevier Science Publishers, Amsterdam, p. 387.ch. 10,

Newton, T. W., Hobart, D. E., and Palmer, P. D. (1986a) *The Preparation and Stability of Pure Oxidation States of Neptunium, Plutonium, and Americium*, Report LA-UR-86-967, Los Alamos National Laboratory, Los Alamos, NM, 11 pp.

Newton, T. W., Hobart, D. E., and Palmer, P. D. (1986b) *Radiochim. Acta,* **39**(3), 139–47.

Nikitenko, S. I. (1988) *Radiokhimiya,* **30**(4), 448–52.

Nikitenko, S. I. and Ponomareva, O. G. (1989) *Radiokhimiya,* **31**(2), 58–63 (pp 195–9 in English translation).

Nikitina, G. P., Ivanov, Y. E., Listopadov, A. A., and Shpunt, L. B. (1997a) *Radiochemistry,* **39**(2), 109–22.

Nikitina, G. P., Ivanov, Y. E., Listopadov, A. A., and Shpunt, L. B. (1997b) *Radiochemistry,* **39**(1), 12–25.

Nikonov, M. V., Gogolev, A. V., Tananaev, I. G., and Myasoedov, B. F. (2004) *Radiochemistry,* **46**(4), 340–2.

Nikonov, M. V., Gogolev, A. V., Tananaev, I. G., and Myasoedov, B. F. (2005) *Mendeleev Commun.,* **Mar–Apr 2005**(2), 50–2.

Nitsche, H. and Silva, R. J. (1996) *Radiochim. Acta,* **72**, 65–72.

Norling, B. K. and Steinfink, H. (1966) *Inorg. Chem.,* **5**(9), 1488–91.

Ockenden, D. W. and Welch, G. A. (1956) *J. Chem. Soc., Abstracts*: 3358–63.

Oetting, F. L. (1967) *Chem. Rev.,* **67**(3), 261–97.

Oetting, F. L. (1982) *J. Nucl. Mater.,* **105**(2–3), 257–61.

Oetting, F. L. and Adams, J. B. (1983) *J. Chem. Thermodyn.,* **15**(6), 537–54.

Oetting, F. L., Rand, M. H., and Ackerman, R. J. (1976) *The Chemical Thermodynamics of Actinide Elements and Compounds,* part 1, The Actinide Elements, IAEA, Vienna, Austria, 111 pp.

Ofte, D. and Rohr, W. G. (1965) *J. Nucl. Mater.,* **15**(3), 231.

Ofte, D. and Wittenberg, L. J. (1964) *Am. Soc. Metals, Trans. Quart.,* **57**(4), 916–23.

Ofte, D., Rohr, W. G., and Wittenberg, L. J. (1966) *Trans. Amer. Nucl. Soc.,* **9**, 5–6.

Ogard, A. E. (1970) High-Temperature Heat Content of Plutonium Dioxide. *Plutonium 1970*, *Proc. Fourth Int. Conf. on Plutonium and Other Actinides*, Santa Fe, NM (ed. W. N. Miner), pp. 78–83.

Ogard, A. E. and Leary, J. A. (1970) *Plutonium Carbides*, Report LA-4415, Los Alamos Scientific Laboratory, Los Alamos, NM, 6 pp.

Ogard, A. E., Pritchard, W. C., Douglass, R. M., and Leary, J. A. (1962) *J. Inorg. Nucl. Chem.,* **24**, 29–34.

Ogawa, T., Kobayashi, F., Sato, T., and Haire, R. G. (1998) *J. Alloys Compd.,* **271–273**, 347–54.

Ohse, R. W. and Olson, W. M. (1970) *Plutonium 1970 and Other Actinides, Proc. Fourth Int. Conf. on Plutonium and Other Actinides,* Santa Fe, NM, Oct. 5–9, 1970 (ed. W. N. Miner), AIME, New York, 743.

Oi, N. (1995) *Proc. Fifth Int. Conf. on Radioactive Waste Management and Environmental Remediation,* vol. 1, Berlin, Sept. 3–7, 1995, pp. 469–70.

Okajima, S. and Reed, D. T. (1993) *Radiochim. Acta,* **60**(4), 173–84.

Oldham, S. M., Schake, A. R., Burns, C. J., Morgan, III, A. N., Schnabel, R. C., Warner, B. P., Costa, D. A., and Smith, W. H. (2000) *AIP Conf. Proc.,* **532**(Plutonium Futures – The Science), 230–1.

Olsen, C. E. and Elliott, R. O. (1962) *J. Phys. Chem. Solids,* **23**, 1225.

Olsen, C. E., Sandenaw, T. A., and Herrick, C. C. (1955) *The Density of Liquid Plutonium Metal*, Report LA-2358, Los Alamos Scientific Laboratory, Los Alamos, NM, 17 pp.

Olsen, C. E., Comstock, A. C., and Sandenaw, T. A. (1992) *J. Nucl. Mater.,* **195**, 312.

Olson, G. B. and Adler, P. H. (1984) *Scripta Met.,* **18**(4), 401–6.

Olson, W. M. and Mulford, R. N. R. (1964) *J. Phys. Chem.,* **68**(5), 1048–51.

Olson, W. M. and Mulford, R. N. R. (1967) *Thermodynamics of the Plutonium Carbides*, Report LA-DC-8012, Los Alamos Scientific Laboratory, Los Alamos, NM, 19 pp.

Onoe, J. (1997) *J. Phys. Soc. Jpn.,* **66**(8), 2328–36.

Orlemann, E. F. (1944) *Distribution of 49 [Pu-239] between Aqueous and Non-Aqueous Phases*. Fundamental Chemistry of 49.

Orme, J. T., Faiers, M. E., and Ward, B. J. (1976) The Kinetics of the Delta to Alpha Transformation in Plutonium Rich Pu-Ga Alloys, *5th Int. Conf. on Plutonium and Other Actinides 1975,* Sept. 10–13, 1975, Baden-Baden, West Germany (eds. H. Blank and R. Linder), 1976, North-Holland, Amsterdam, The Netherlands, pp.761–73.

Paffett, M. T., Farr, D., and Kelly, D. (2003a) *AIP Conf. Proc.,* **673**(Plutonium Futures – The Science), 193–5.

Paffett, M. T., Kelly, D., Joyce, S. A., Morris, J., and Veirs, K. (2003b) *J. Nucl. Mater.,* **322**(1), 45–56.

Pagès, M. and Freundlich, W. (1976) Some Actinides Double Orthovanadates and Orthoarsenates: Structural "Evolution" Due to Cationic and Anionic Substitutions. *Plutonium 1975 Other Actinides*, *Proc. Fifth Int. Conf.* (eds. H. Blank and R. Lindner), North-Holland, Amsterdam, pp. 205–7.

Pagès, M., Nectoux, F., and Freundlich, W. (1971a) *Radiochem. Radioanal. Lett.,* **8**(3), 147–50.

Pagès, M., Nectoux, F., and Freundlich, W. (1971b) *CR Acad. Sci. C. Chim.,* **273**(16), 978–80.

Palmer, D. A. and Nguyen- Trung, C. (1995) *J. Solution Chem.,* **24**(12), 1281–91.

Pansoy-Hjelvik, M. E., Brock, J., Nixon, J. Z., Moniz, P., Silver, G., and Ramsey, K. B. (2001) Purification and Neutron Emission Reduction of Plutonium-238 Oxide by Nitrate Anion Exchange Processing. *Space Technology and Applications International Forum (STAIF-2001)*, Albuquerque, NM, American Institute of Physics, *AIP Conf. Proc.*, **52,** 770–3.

Paprocki, S. J., Keller, D. L., Alexander, C. A., and Pardue, W. M. (1962a) *Volatility of Plutonium Dioxide in Nonreducing Atmospheres*, Report BMI-1591, Battelle Memorial Institute, Columbus, OH, 16 pp.

Paprocki, S. J., Keller, D. L., and Purdue, W. M. (1962b) *The Chemical Reactions of Plutonium Dioxide with Reactor Materials*, Report BMI-1580, Battelle Memorial Institute, Columbus, OH, 12 pp.

Pardue, W. M. and Keller, D. L. (1964) *J. Am. Ceram. Soc.,* **47**(12), 610–14.

Pardue, W. M., Storhok, V. W., Smith, R. A., Bonnell, P. H., Gates, J. E., and Keller, D. L. (1964a) *Synthesis, Fabrication, and Chemical Reactivity of Pu Mononitride*, Report BMI-1693, Battelle Memorial Institute, Columbus, OH, 38 pp.

Pardue, W. M., Storhok, V. W., Smith, R. A., and Keller, D. L. (1964b) *An Evaluation of Plutonium Compounds as Nuclear Fuels*, Report BMI-1698, Battelle Memorial Institute, Columbus, OH, 22 pp.

Pardue, W. M., Storhok, V. W., and Smith, R. A. (1967) *Chemical Engineering Progress, Symposium Series,* **63**(80), 142–6.

Parsonnet, V. (2004) personal communication, L. R. Morss.

Parsonnet, V., Berstein, A. D., and Perry, G. Y. (1990) *Am. J. Cardiol.,* **66**(10), 837–42.

Pascard, R. (1962) *Plansee Proc.,* **1961**, 387–419.

Pashalidis, I., Czerwinski, K. R., Fanghanel, T., and Kim, J. I. (1997) *Radiochim. Acta,* **76**(1–2), 55–62.

Patil, S. K. and Ramakrishna, V. V. (1976) *J. Inorg. Nucl. Chem.,* **38**(5), 1075–8.

Paxton, H. C. (1975) *Los Alamos Critical-Mass Data*, Report LA-3067-MS, Los Alamos Scientific Laboratory, Los Alamos, NM, 57 pp.

Paxton, H. C. and Pruvost, N. L. (1987) *Critical Dimensions of Systems Containing Uranium-235, Plutonium-239 and Uranium-233: 1986 Revision*, Report LA-10860-MS, Los Alamos National Laboratory, Los Alamos, NM, 205 pp.

Peddicord, K. L., Lazarev, L. N., and Jardine, L. J. (eds.) (1998) *Nuclear Materials Safety Management, NATO Advanced Research Workshop on Nuclear Materials Safety Management* (*1997: Amarillo, TX*). NATO ASI series. Partnership sub-series 1, Disarmament technologies; vol. 20. Kluwer Academic, Boston, MA, 378 pp.

Pekarek, V. and Marhol, M. (1991) Historical Background of Inorganic Ion Exchangers, their Classification, and Present Status, in *Inorganic Ion Exchangers in Chemical Analysis* (eds. M. Qureshi and K. G. Varshney), CRC Press, Boca Raton, FL, pp. 1–32.

Penneman, R. A. and Paffett, M. T. (2004) personal communication, D. L. Clark.

Penneman, R. A. and Paffett, M. T. (2005) *J. Solid State Chem.,* **178**(2), 563–6.

Penneman, R. A., Sturgeon, G. D., Asprey, L. B., and Kruse, F. H. (1965) *J. Am. Chem. Soc.,* **87**(24), 5803–4.

Peppard, D. F., Studier, N. H., Gergel, N. V., Mason, G. W., Sullivan, J. C., and Mech, J. F. (1951) *J. Am. Chem. Soc.,* **73**, 2529–31.

Pepper, M. and Bursten, B. E. (1991) *Chem. Rev.,* **91**(5), 719–41.

Peretrukhin, V. F., Shilov, V. P., Pikaev, A. K., and Delegard, C. H. (1995) *Alkaline Chemistry of Transuranium Elements and Technetium Elements and Technetium and the Treatment of Alkaline Radioactive Wastes*, Report WHC-EP-0817, Westinghouse Hanford Company, 172 pp.

Peterson, J. R. (1995) *J. Alloys Compd.,* **223**, 180–4.

Peterson, D. E. and Kassner, M. E. (1988) *Bull. Alloy Phase Diagr.,* **9**, 261.

Peterson, S. and Wymer, R. G. (1963) *Chemistry in Nuclear Technology,* Pergamon Press, Oxford, England.

Petit, L., Svane, A., Szotek, Z., and Temmerman, W. M. (2003) *Science,* **301**(5632), 498–501.

Petit, L., Svane, A., Temmerman, W. M., and Szotek, Z. (2002) *Eur. Phys. J. B,* **25**(2), 139–46.

Pettifor, D. G. (1996) in *Physical Metallurgy* (eds. R. W. Cahn and P. Haasen), Elsevier Science, Amsterdam, The Netherlands, 47 pp.

Phipps, K. D. and Sullenger, D. B. (1964) *Science,* **145**(3636), 1048–9.

Phipps, T. E., Sears, G. W., Seifert, R. L., and Simpson, O. C. (1949) *Natl. Nucl. Energy Ser.*, Div. IV, **14B**(Transuranium Elements, Pt. I), (eds. G. T. Seaborg, J. J. Katz, and W. M. Manning), McGraw-Hill, New York, 682–703.

Phipps, T. E., Sears, G. W., Seifert, R. L., and Simpson, O. C. (1950a) *J. Chem. Phys.,* **18**(5), 713–23.

Phipps, T. E., Sears, G. W., and Simpson, O. C. (1950b) *J. Chem. Phys.,* **18**, 724–34.

Phipps, T. E., Sears, G. W., Seifert, R. L., and Simpson, O. C. (1955) *Vapor Pressure of Liquid Plutonium*, *Proc. Int. Conf. on the Peaceful Uses of Atomic Energy*, Geneva, 7, pp. 382–5.

Pijanowski, S. W. and DeLucas, L. S. (1960) *Melting Points in the System* PuO_2-UO_2, Report KAPL-1937, KAPL General Electric Co., Schenectady, N.Y., pp. 1–5.

Pitner, W. R., Bradley, A. E., Rooney, D. W., Sanders, D., Seddon, K. R., Thied, R. C., and Hatter, J. E. (2003) *NATO Sci. Ser. II: Math. Phys. Chem.,* **92**(Green Industrial Applications of Ionic Liquids), 209–26.

Pons, F., Barbe, B., and Roux, C. (1972) *J. Appl. Crystallogr.,* **5**, 47.

Poole, D. M. and Nichols, J. L. (1961) *The Plutonium Cobalt System*, Report AERE-R-3609, UK Atomic Energy Authority Research Group.

Poole, D. M., Williamson, G. K., and Marples, J. A. C. (1957) *J. I. Met.,* **86**(4), 172–6.

Poskanzer, A. M. and Foreman, B. M. (1961) *J. Inorg. Nucl. Chem.,* **16**(3–4), 323–36 and references therein.

Potter, P. E. (1975) *MTP Int. Rev. Sci.: Inorg. Chem., Ser.2,* **7**, 257–315.

Potter, P. E. (1991) The Actinide Borides, in *Handbook on the Physics and Chemistry of the Actinides,* (eds. A. J. Freeman and C. Keller), vol. 6, North-Holland, Amsterdam, The Netherlands, 39 pp.

Powell, R. F. (1960) Thermal Conductivity of Plutonium, in *Plutonium 1960,* (eds. E. Grison, W. B. H. Lord and R. D. Fowler), vol. 1, Cleaver-Hume Press, London, 107 pp.

Preston, J. S. and du Preez, A. C. (1995) *Solvent Extr. Ion Exch.,* **13**(3), 391–413.

Pustovalov, A. A., Shapovalov, V. P., Bovin, A. V., and Fedorets, V. I. (1986) *At. Energ.,* **60**(2), 125–9.

Rabideau, S. W. (1953) *J. Am. Chem. Soc.,* **75**, 798–801.

Rabideau, S. W. (1956) *J. Am. Chem. Soc.,* **78**(12), 2705–7.

Rabideau, S. W. (1957) *J. Am. Chem. Soc.,* **79**(24), 6350–3.

Rabideau, S. W. and Cowan, H. D. (1955) *J. Am. Chem. Soc.,* **77**(23), 6145–8.

Rabideau, S. W. and Kline, R. J. (1958) *J. Phys. Chem. A,* **62**, 617–20.

Rabideau, S. W. and Masters, B. J. (1963) *J. Phys. Chem.,* **67**, 318–23.

Rabideau, S. W., Bradley, M. J., and Cowan, H. D. (1958) *Alpha-particle Oxidation and Reduction in Aqueous Plutonium Solutions*, Report USAEC-LAMS-2236, Los Alamos Scientific Laboratory, 28 pp.

Rabideau, S. W., Asprey, L. B., Keenan, T. K., and Newton, T. W. (1959) *Proc. Second Int. Conf. Peaceful Uses of Atomic Energy,* vol. 28, Geneva, pp. 361–72.

Rafalski, A. L., Harvey, M. R., and Riefenberg, D. H. (1967) *ASM Trans. Q,* **60**(4), 721.

Rai, D., Hess, N. J., Felmy, A. R., Moore, D. A., Yui, M., and Vitorge, P. (1999) *Radiochim. Acta,* **86**(3–4), 89–99.

Rai, D., Bolton, Jr, H., Moore, D. A., Hess, N. J., and Choppin, G. R. (2001) *Radiochim. Acta,* **89**(2), 67–74.

Rainey, R. H. (1959) *Chemistry of Plutonium(IV) Polymer*, Report CF-59-12-95, Oak Ridge National Laboratory, 4.

Raj, D. D. A., Nalini, S., Viswanathan, R., and Balasubramanian, R. (1999) *Proc. Eighth ISMAS Symp. on Mass Spectrometry,* vol. II, Dec. 7–9, 1999 (ed. S. K. Aggarwal), Indian Institute of Chemical Technology, Hyderabad, Indian Society for Mass Spectrometry, Mumbai, p. 847.

Rance, P. and Zilberman, B. (2002) *J. Nucl. Sci. Technol.*, (Suppl. 3), 375–8.

Rand, M. H. (1966) *Atom. Energy Rev.,* **4**(1), 7–51.

Rao, P. R. V. and Kolarik, Z. (1996) *Solvent Extr. Ion. Exch.,* **14**(6), 955–93.

Rao, G. S., Subramanian, M. S., and Welch, G. A. (1963) *J. Inorg. Nucl. Chem.,* **25**(10), 1293–5.

Rao, P. R. V., Bagawde, S. V., Ramakrishna, V. V., and Patil, S. K. (1978) *J. Inorg. Nucl. Chem.,* **40**(1), 123–7.

Rasmussen, M. J. and Hopkins, H. H., Jr (1961) *J. Ind. Eng. Chem.,* **53**, 453–7.

Ravat, B., Jolly, L., Valot, C., and Baclet, N. (2003) *AIP Conf. Proc.,* **673**(Plutonium Futures – The Science), 7–8.

Raynor, J. B. and Sakman, J. F. (1965) Oxidation, in *Proc. Third Int. Conf. on Plutonium 1965* (eds. A. E. Kay and M. B. Waldron), Cleaver - Hume, London, England, 575 pp.

Reader, J. and Corliss, C. H. (1980) *Wavelengths and Transition Probabilities for Atoms and Atomic Ions*, part I, *Wavelengths*, Report NSRDS-NBS 68, Natl. Meas. Lab., Natl. Bur. Stand., Washington, DC, pp. 1–357.

Reavis, J. G. and Leary, J. A. (1970) *Plutonium 1970 and Other Actinides, Proc. Fifth Int. Conf. on Plutonium and Other Actinides,* Baden-Baden, West Germany (ed. W. N. Miner), North-Holland, New York, 809 pp.

Reavis, J. G., Johnson, K. W. R., Leary, J. A., Morgan, A. N., Ogard, A. E., and Walsh, K. A. (1960) *The Preparation of Plutonium Halides for Fused Salt Studies, Extractive and Physical Metallurgy of Plutonium and its Alloys, Symp.,* San Francisco, CA (ed. W. D. Wilkinson), Interscience Publishers, New York, pp. 89–100.

Rebizant, J., Bednarczyk, E., Boulet, P., Fuchs, C., and Wastin, F. (2000) *Single Crystal Growth of* $(U_{1-x}Pu_x)O_2$ *Mixed Oxides. AIP Conf. Proc.,* **532**(Plutonium Futures–The Science), 355–6.

Reilly, S. D., Neu, M. P., and Runde, W. (2000) *AIP Conf. Proc.,* **532**(Plutonium Futures – The Science), 269–71.

Reshetnikov, F. G. (2003) *Mendeleev Commun.*, (4), 155–6.

Reynolds, L. T. and Wilkinson, G. (1956) *J. Inorg. Nucl. Chem.,* **2**, 246.

Rice, R. W. (1983) *Am. Ceram. Soc. Bull.,* **62**(8), 889–92.

Richards, S. M. and Kasper, J. S. (1969) *Acta Crystallogr. B,* **B25**, 237.

Richmann, M. K., Reed, D. T., Kropf, A. J., Aase, S. B., and Lewis, M. A. (1999) *XAFS/XANES Studies of Plutonium-loaded Sodalite/glass Waste Forms*, *Annual Meeting Proc. Institute of Nuclear Materials Management*, 40, pp. 668–75.

Riha, J. and Trevorrow, L. (1965) *Chemical Engineering Division Semiannual Report, January – June 1967*, Report ANL-7375, Argonne National Laboratory, pp. 54–6.

Riley, B. (1970) *Sci. Ceram.,* **5**, 83–109.

Rinehart, G. H. (1992) *Space Nucl. Power Syst.,* **10**, 39–43.

Rinehart, G. H. (2001) *Prog. Nucl. Energ.,* **39**(3–4), 305–19.

Robbins, J. L. (2004) *J. Nucl. Mater.,* **324**(2/3), 125–33.

Robouch, P. and Vitorge, P. (1987) *Inorg. Chim. Acta,* **140**, 239–42.

Roepenack, H., Schneider, V. W., and Druckenbrodt, W. G. (1984) *Am. Ceram. Soc. Bull.,* **63**(8), 1051–3.

Rogers, R. D. and Seddon, K. R., Eds. (2002) *ACS Symp. Ser.* **118**(Ionic Liquids – Industrial Applications for Green Chemistry), American Chemical Society, Washington, DC.

Rogl, P. and Potter, P. E. (1997) *J. Phase Equilib,* **18**(5), 467–73.

Rogozina, E. M., Konkina, L. F., and Popov, D. K. (1973) *Radiokhimiya,* **15**(1), 61–3.

Rolland, B. L., Molinie, P., Colombet, P., and McMillan, P. F. (1994) *J. Solid State Chem.,* **113**(2), 312–19.

Rollefson, G. K. and Dodgen, H. W. (1943) *Report on Spectrographic Analysis Work*, Report CK-812.

Romanovski, V. V., White, D. J., Xu, J., Hoffman, D. C., and Raymond, K. N. (1999) *Solvent Extr. Ion Exch.,* **17**(1), 55–71.

Ronchi, C., Sheindlin, M., Musella, M., and Hyland, G. J. (1999) *J. Appl. Phys.,* **85**(2), 776–89.

Ronchi, C., Capone, F., Colle, J. Y., and Hiernaut, J. P. (2000) *J. Nucl. Mater.,* **280**(1), 111–15.

Roof, R. B., Jr. (1973) *Adv. X. Ray Anal.,* **16**, 396–400.

Roof, R. B. (1989) *X-ray Diffraction Data for Plutonium Compounds: Plutonium and Plutonium Binary Compounds*, Los Alamos National Laboratory, Report LA-11619, 3 volumes.

Rose, R. L., Robbins, J. L., and Massalski, T. B. (1970) *J Nucl. Mater.,* **36**(1), 99–107.

Rosen, S., Nevitt, M. V., and Mitchell, A. W. (1963) *J. Nucl. Mater.,* **10**(2), 90–8.

Rosen, S., Nevitt, M. V., and Mitchell, A. W. (1964) *U-Pu-C Ternary Phase Diagram Below 50 Atomic Percent Carbon*, Report ANL-6435, Argonne National Laboratory, Argonne, IL, 107 pp.

Rosen, M., Erez, G., and Shtrikman, S. (1969) *J. Phys. Chem. Solids,* **30**(5), 1063–70.

Rosenthal, M. W., Rahman, Y. E., Moretti, E. S., and Cerny, E. A. (1975) *Radiat. Res.,* **63**(2), 262–74.

Rossat-Mignod, J., Lander, G. H., and Burlet, P. (1984) in *Handbook on the Physics and Chemistry of Actinides,* vol. 1 (eds. A. J. Freeman and G. H. Lander), North-Holland, Amsterdam, 415 pp.

Rothe, J., Denecke, M. A., Neck, V., Mueller, R., and Kim, J. I. (2002) *Inorg. Chem.,* **41**(2), 249–58.

Rothe, J., Walther, C., Denecke, M. A., and Fanghaenel, T. (2004) *Inorg. Chem.,* **43**(15), 4708–18.

Ruggiero, C. E., Matonic, J. H., Neu, M. P., and Reilly, S. P. (2000) *AIP Conf. Proc.,* **532**(Plutonium Futures – The Science), 284–5.

Ruggiero, C. E., Matonic, J. H., Reilly, S. D., and Neu, M. P. (2002) *Inorg. Chem.,* **41**(14), 3593–5.

Rundberg, R. S., Mitchell, A. J., Triay, I. R., and Torstenfelt, N. B. (1988) *Mater. Res. Soc. Symp. Proc.,* **112**(Sci. Basis Nucl. Waste Manage. 11), 243–8.

Runde, W. (2005a) Preparation and characterization of tetravalent plutonium oxalate compounds, personal communication, D. L. Clark, Los Alamos, NM.

Runde, W. (2005b) Preparation and characterization of peroxocarbonato complexes of tetravalent plutonium, personal communication, D. L. Clark, Los Alamos, NM.

Runde, W., Conradson, S. D., Wes Efurd, D., Lu, N., Van Pelt, C. E., and Tait, C. D. (2002) *Appl. Geochem.,* **17**(6), 837–53.

Runde, W., Bean, A., and Scott, B. L. (2003a) *AIP Conf. Proc.,* **673**(Plutonium Futures – The Science), 23–5.

Runde, W., Bean, A. C., Albrecht-Schmitt, T. E., and Scott, B. L. (2003b) *Chem. Commun.*, 478.

Runnalls, O. J. C. (1956) *Can. J. Chem.,* **34**(2), 133–45.

Runnalls, O. J. C. (1958) *The Preparation of Plutonium–Aluminum and Other Plutonium Alloys*, Report AECL-543, Atomic Energy Canada Ltd., Chalk River, 25 pp.

Runnalls, O. J. C. (1965) *Phase-equilibrium Studies on the Aluminum–Plutonium System*, Report AECL-2275, Atomic Energy Canada Ltd., Chalk River, 20 pp.

Runnalls, O. J. C. and Boucher, R. R. (1955) *Acta Crystallogr.,* **9**, 592.

Russell, L. E., Harrison, J. D. L., and Brett, N. H. (1960) *J. Nucl. Mater.,* **2**, 310–20.

Russell, L. E., Brett, N. H., Harrison, J. D. L., and Williams, J. (1962) *J. Nucl. Mater.,* **5**, 216–27.

Russell, L. E. (1964) *Carbides in Nuclear Energy*, vol. 1, *Physical and Chemical Properties; Phase Diagrams;* vol. 2, *Preparation and Fabrication; Irradiation Behavior*, 966 pp.

Ryan, J. L. (1959) *Concentration and Final Purification of Neptunium by Anion Exchange*, Report HW-59193 Rev, Hanford Works, 22 pp.

Ryan, J. L. (1960) *J. Phys. Chem.,* **64**(10), 1375–85.

Ryan, J. L. (1975) Anion Exchange Reactions, in *Gmelin Handbook of Inorganic Chemistry, Transuranic Elements* (ed. G. Koch), Springer-Verlag, New York. [D2 Chemistry in Solution: 418 and 432.]

Ryan, J. L. and Bray, L. A. (1980) *ACS Symp. Ser.* **117**(Actinide Sep.), American Chemical Society, Washington, DC, 499–514.

Ryan, J. L. and Joergensen, C. K. (1964) *Mol. Phys.,* **7**(1), 17–29.

Rykov, A. G., Timofeev, G. A., and Yakovlev, C. N. (1969) *Radiokhimiya,* **11(4)**, 413–18 (pp 403–407 in English translation).

Sackman, J. F. (1960) The Atmospheric Oxidation of Plutonium Metal. *Plutonium 1960, Proc. Int. Conf. Plutonium Met.*, Grenoble, France (ed. E. Grison, W. B. H. Lord and R. D. Fowler), pp. 222–9.

Sadigh, B. and Wolfer, W. G. (2005) *Phys. Rev. B.* **70**(20), 205122/1–12.

Sakurai, S., Tachimori, S., Akatsu, J., Kimura, T., Yoshida, Z., Mutoh, H., Yamashita, T., and Ohuchi, K. (1989) *Nihon Genshiryoku Gakkaishi,* **31**(11), 1243–50.

Sakurai, S., Usuda, S., Ami, N., Hirata, M., Wakamatsu, S., and Tachimori, S. (1993) *Nihon Genshiryoku Gakkaishi,* **35**(2), 147–54.

Sandenaw, T. A. (1960a) *Phys. Chem. Solids,* **16**, 329.

Sandenaw, T. A. (1960b) *The Thermal Expansion of Plutonium Metal below 300 K, Proc. Second Int. Conf. on Plutonium Metallurgy: Plutonium 1960,* Grenoble, France vol. 1, (eds. E. Grison, W. B. H. Lord, and R. D. Fowler), Cleaver-Hume Press, London, pp. 79–90.

Sandenaw, T. A. (1961) *Results of Measurements of Physical Properties of Plutonium metal*. in *The Metal Plutonium* (eds. A. S. Coffinberry and W. N. Miner), University of Chicago Press Chicago, IL, 154 pp.

Sandenaw, T. A. (1962) *Phys. Chem. Solids,* **23**(Sep), 1241–8.

Sandenaw, T. A. (1963) *J. Nucl. Mater.,* **10**(3), 165–72.

Sandenaw, T. A. and Gibney, R. B. (1958) *Phys. Chem. Solids,* **6**, 81.

Sandenaw, T. A. and Gibney, R. B. (1971) *J. Chem. Thermodyn.,* **3**, 85.

Sandenaw, T. A. and Harbur, D. R. (1973) *J. Phys. Chem. Solids,* **34**(9), 1487–95.

Sano, T., Tanaka, O., Akimoto, I., Imoto, S., Kikuchi, T., Ichikawa, M., Watanabe, H., Nishio, G., and Shimokawa, J. (1971) *Nihon Genshiryoku Gakkaishi,* **13**(11), 642–67.

Santini, P., Lemanski, R., and Erdos, P. (1999) *Adv. Phys.,* **48**(5), 537–653.

Santoro, A., Marezio, M., Roth, R. S., and Minor, D. (1980) *J. Solid State Chem.,* **35**(2), 167–75.

Sari, C., Benedict, U., and Blank, H. (1968) *Metallographic and X-ray Investigations in the Plutonium–Oxygen and Uranium–Plutonium–Oxygen Systems, Proc. Symp. on Thermodynamics of Nuclear Materials*, Vienna, Austria, pp. 587–611.

Sari, C., Benedict, U., and Blank, H. (1970) *J. Nucl. Mater.,* **35**(3), 267–77.

Sarrao, J. L., Morales, L. A., Thompson, J. D., Scott, B. L., Stewart, G. R., Wastin, F., Rebizant, J., Boulet, P., Colineau, E., and Lander, G. H. (2002) *Nature,* **420**(6913), 297–9.

Sarrao, J. L., Morales, L. A., Thompson, J. D., Scott, B. L., Stewart, G. R., Wastin, F., Rebizant, J., Boulet, P., Colineau, E., and Lander, G. H. (2003a) *AIP Conf. Proc.,* **673** (Plutonium Futures – The Science), 12–14.

Sarrao, J. L., Morales, L. A., and Thompson, J. D. (2003b) *J. Metals,* **55**(9), 38–40.

Sasao, N. and Yamaguchi, H. (1991) *Apparatus for Laser Isotope Separation*, (Power Reactor and Nuclear Fuel Development Corp., Japan). Jpn. Patent 03068420, 10 pp.

Sastre, A. M., Kumar, A., Shukla, J. P., and Singh, R. K. (1998) *Sep. Purif. Methods,* **27**(2), 213–98.

Savage, D. J. and Kyffin, T. W. (1986) *Polyhedron,* **5**(3), 743–52.

Savrasov, S. Y., Kotliar, G., and Abrahams, E. (2001) *Nature,* **410**(6830), 793–5.

Scheitlin, F. M. and Bond, W. D. (1980) *Recovery of Plutonium from HEPA Filters by Cerium(IV), Promoted Dissolution of Plutonium Dioxide and Recycle of the Cerium Promoter*, Report ORNL/TM-6802, Oak Ridge National Laboratory, Oak Ridge, TN, 58 pp.

Scheuer, U. and Lengeler, B. (1991) *Phys. Rev. B,* **44**(18), 9883–94.

Schlechter, M. (1970) *J. Nucl. Mater.,* **37**(1), 82–8.

Schlesinger, H. I. and Brown, H. (1943) *Chemical Separation of 94 from Uranium on the Basis of the Volatility of the Borohydrides*, Report CN-441, University of Chicago.

Schmutz, H. (1966) *System Alkali Fluoride–Lanthanide/Actinide Fluoride (Lithium, Sodium, Potassium, Rubidium–Lanthanum, Rare Earths, Yttrium/Neptunium, Americium)*, Report KFK-431, Kernforschungszentrum, Karlsruhe, Germany, 73 pp.

Schneider, V. W. and Roepenack, H. (1986) Fabrication of (U/Pu)O_2-mixed oxide Fuel Elements, in *Handbook on the Physics and Chemistry of the Actinides* (eds. A. J. Freeman and C. Keller), Elsevier Science, New York, 531–55.

Schonfeld, F. W. (1961) Pu Phase Diagrams, in *The Metal Plutonium* (eds. A. S. Coffinberry and W. N. Miner), University of Chicago Press, Chicago, 243.

Schonfeld, F. W. and Tate, R. E. (1996) *The Thermal Expansion Behavior of Unalloyed Plutonium*, Report LA-13034-MS, Los Alamos National Laboratory, pp. 1–34.

Schonfeld, F. W., Cramer, E. M., Miner, W. N., Ellinger, F. H., and Coffinberry, A. S. (1959) *Prog. Nucl. Energy* (eds. H. M. Finniston, and J. P. Howe, Pergamon Press) *Ser. V,* **2**, 579–99.

Schreckenbach, G., Hay, P. J., and Martin, R. L. (1999) *J. Comput. Chem.,* **20**(1), 70–90.

Schwartz, A. J., Wall, M. A., Zocco, T. G., and Wolfer, W. G. (2005) *Philos. Mag.,* **85**, 479–88.

Seaborg, G. T. (1958) *The Transuranium Elements*, Addison-Wesley, Reading, MA, 348 pp.

Seaborg, G. T. (1977) *History of Met Lab section C-I, April 1942 – April 1943*, Report PUB-112(vol.1), Lawrence Berkeley Laboratory, University of California, Berkeley, CA, 708 pp.

Seaborg, G. T. (1978) *History of Met Lab section C-I, May 1943 – April 1944*, Report PUB-112(vol.2), Lawrence Berkeley Laboratory, University of California, Berkeley, CA, 581 pp.

Seaborg, G. T. (1979) *History of Met Lab section C-I, May 1944 – April 1945*, Report PUB-112(Vol.3), Lawrence Berkeley Laboratory, University of California, Berkeley, CA, 625 pp.

Seaborg, G. T. (1980) *History of Met Lab section C-I, May 1945 – May 1946*, Report PUB-112(vol. 4), Lawrence Berkeley Laboratory, University of California, Berkeley, CA, 657 pp.

Seaborg, G. T. (1983) *ACS Symp. Ser.* **216**(Plutonium Chem.) (eds. W. T. Carnall and G. R. Choppin), American Chemical Society, Washington, DC, pp. 1–22.

Seaborg, G. T. (1992) *Transuranium Elements. A Half Century* (eds. L. R. Morss and J. Fuger), American Chemical Society, Washington, DC, pp. 10–49.

Seaborg, G. T. (1995) *Radiochim. Acta,* **70/71**, 69–90.

Seaborg, G. T. and Katz, J. J. (1990) *Proc. Robert A. Welch Found. Conf. Chem. Res.,* **34**, 224–51.

Seaborg, G. T. and Loveland, W. D. (1990) *The Elements beyond Uranium,* John Wiley & Sons, New York, 359 pp.

Seaborg, G. T. and Perlman, M. L. (1948) *J. Am. Chem. Soc.,* **70**, 1571–3.

Seaborg, G. T. and Wahl, A. C. (1948a) *J. Am. Chem. Soc.,* **70**, 1128–34.

Seaborg, G. T. and Wahl, A. C. (1948b) *J. Am. Chem. Soc.,* **70**(3), 1128–34.

Seaborg, G. T., Wahl, A. C., and Kennedy, J. W. (1946) *Phys. Rev.,* **69**, 367.

Seaborg, G. T., Wahl, A. C., and Kennedy, J. W. (1949a) *Natl. Nucl. Energy Ser.,* Div. IV **14B**(Transuranium Elements, Pt. I), (eds. G. T. Seaborg, J. J. Katz and W. M. Manning), McGraw-Hill, New York, 13–20.

Seaborg, G. T., Katz, J. J., and Manning, W. M. (eds.) (1949b) *Natl. Nucl. Energy Ser.,* Div IV **14B** (Transuranium Elements Pt. I), McGraw-Hill, New York.

Selle, J. E. and Etter, D. E. (1964) *Trans. Metall. Soc. AIME,* **230**(5), 1000–5.

Selle, J. E., English, J. J., Teaney, P. E., and McDougal, J. R. (1970a) *Compatibility of Plutonium-238 Dioxide with Various Refractory Metals and Alloys: Interim Report*, Report MLM-1706, Mound Laboratoary, Miamisburg, OH, 214 pp.

Selle, J. E., McDougal, J. R., and Schaeffer, D. R. (1970b) *Compatibility of Plutonium-238 Dioxide with Platinum and Platinum–Rhodium Alloys*, Report MLM-1684, Mound Laboratory, Miamisburg, OH, 124 pp.

Serpan, C. Z. and Wittenberg, L. J. (1961) *Trans. Metall. Soc. AIME,* **221**(5), 1017–20.

Seyferth, D. (2004) *Organometallics,* **23**(15), 3562–83.

Shacklett, R. L. and Du Mond, J. W. M. (1957) *Phys. Rev.,* **106**, 501–12.

Sheft, I. and Davidson, N. R. (1949a) Equilibrium in the Vapor-phase Hydrolysis of Plutonium Tribromide, in *Natl. Nucl. Energy Ser.,* Div **14**B, (Transuranium Elements Pt. I) (eds. G. T. Seaborg, J. J. Katz, and W. M. Manning), McGraw-Hill, New York, pp. 831–40.

Sheft, I. and Davidson, N. R. (1949b) Equilibrium in the Vapor-phase Hydrolysis of Plutonium Trichloride, in *Natl. Nucl. Energy Ser.,* Div **14**B, (Transuranium Elements Pt. I) (eds. G. T. Seaborg, J. J. Katz, and W. M. Manning), McGraw-Hill, New York, pp. 841–7.

Sheft, I., Andrews, H. and Katz, J. J. (1949) *Summary Report for July, August, and September 1949*, Report ANL-4379, Chemistry Division, Section C1, Argonne National Laboratory, Argonne National Laboratory, pp. 43–50.

Sheldon, R. I., Rinehart, G. H., Krishnan, S., and Nordine, P. C. (2001) *Mater. Sci. Eng.,* **B79**, 113–22.

Sherby, O. D. and Simnad, M. T. (1961) *Am. Soc. Metals, Trans. Quart.,* **54**, 227–40.

Shewmon, P. G. (1963) *Diffusion in Solids,* McGraw-Hill, New York, 134 pp.

Shick, A. B., Drchal, V., and Havela, L. (2005) *Europhys. Lett.,* **69**(4), 588–94.

Shilov, V. P. (1997) *Radiokhimiya,* **39**(4), 330–2 (pp. 328–31 in English translation.).

Shilov, V. P. (1998) *Radiochemistry,* **40**(1), 11–16.

Shilov, V. P. and Yusov, A. B. (2002) *Russ. Chem. Rev.,* **71**(6), 465–88.

Shorikov, A. O., Lukoyanov, A. V., Korotin, M. A., and Anisimov, V. I. (2005) *Los Alamos National Laboratory, Preprint Archive, Condensed Matter*: 1–21, arXiv:cond-mat/0412724 v2.

Shumakov, V. D., Kosulin, N. S., and Chebotarev, N. T. (1990) *Phys. Metal Metalloved (Russian),* **37**, 14.

Shvareva, T. Y., Almond, P. M., and Albrecht- Schmitt, T. E. (2005) *J. Solid State Chem.,* **178**(2), 499–504.

Silva, R. J. and Nitsche, H. (1995) *Radiochim. Acta,* **70/71**, 377–96.

Silva, R. J. and Nitsche, H. (2002) *Environmental Chemistry*, in *Advances in Plutonium Chemistry 1967–2000* (ed. D. C. Hoffman), American Nuclear Society and the University Research Alliance, La Grange Park, IL, pp. 89–111.

Silva, R. J., Bidoglio, G., Rand, M. H., Robouch, P. B., Wanner, H., and Puigdomenech, I. (1995) *Chemical Thermodynamics of Americium,* Elsevier Science Publishers, Amsterdam, Netherlands, 392 pp.

Silver, G. L. (1971) *J. Inorg. Nucl. Chem.,* **33,** 577–583.

Silver, G. L. (1997) *Radiochim. Acta,* **77**, 189.

Silver, G. L. (2002) *Appl. Radiat. Isot.* **57,** 1–5.

Silver, G. L. (2003) *Appl. Radiat. Isot.* **59,** 217–20.

Silver, G. L. (2004) *J. Radioanal. Nucl. Chem.* **262**(3), 779–781.

Silvestre, J. P., Freundlich, W., and Pagès, M. (1977) *Rev. Chim. Miner.,* **14**(2), 225–9.

Simakin, G. A., Volkov, Y. F., Visyashcheva, G. I., Kapshukov, I. I., Baklanova, P. F., and Yakovlev, G. N. (1974) *Sov. Radiochem.,* **16**(6), 838–41.

Simon, G. P. (1991) *Ion Exchange Training Manual.* Van Nostrand Reinhold, New York, pp. 1–47.

Skavdahl, R. E. (1963) *Plutonium–Boron System*, Report HW-76302, Article 2.4, US Atomic Energy Commission.

Skavdahl, R. E. (1964) *The Reactions between PuO_2 and Carbon*, Report HW-77906 12 pp.

Skavdahl, R. E. and Chikalla, T. D. (1964) *The Plutonium–Boron System*, Report HW-81602, Article 2.1, US Atomic Energy Commission.

Skavdahl, R. E., Chikalla, T. D., and McNeilly, C. E. (1964) *Trans. Am. Nucl. Soc.,* **7**, 403–4.

Skriver, H. L. (1985) *Phys. Rev. B,* **31**, 1909.

Smirnov, E. A. and Shmakov, A. A. (1999) *Defect Diffus. Forum,* **166**, 63–7.

Smith, J. L. (1980) No superconductivity in plutonium, personal communication, S. S. Hecker, Los Alamos, NM.

Smith, J. L. and Fisk, Z. (1982a) *J. Appl. Phys.,* **53(11)**, 7883–6.

Smith, J. L. and Haire, R. G. (1978) *Science,* **200**(4341), 535–7.

Smith, J. L. and Kmetko, E. A. (1983) *J. Less-Common Met.,* **90**(1), 83–8.

Smolders, A. and Gilissen, R. (1987) *Mater. Sci. Monogr.,* **38C**(High Tech Ceram., Pt. C), 2849–60.

Soderlind, P. (2001) *Europhys. Lett.,* **55**(4), 525–31.

Sokhina, L. P., Solovkin, A. S., Teterin, E. G., Bogdanov, F. A., and Shesterikov, N. N. (1978) *Radiokhimiya,* **20**(1), 28–34.

Solar, J. P., Burghard, H. P. G., Banks, R. H., Streitwieser, A., Jr, and Brown, D. (1980) *Inorg. Chem.,* **19**(7), 2186–8.

Solovkin, A. S. and Rubisov, V. N. (1983) *Radiokhimiya,* **25**(5), 625–8.

Sood, D. D., Jayadevan, N. C., Mudher, K. D. S., Khandekar, R. R., and Krishnan, K. (1992) *Transuranium Elements: A Half Century* (eds. L. R. Morss and J. Fuger), American Chemical Society, Washington, DC, pp. 524–32.

Sorantin, H. (1975) *Determination of Uranium and Plutonium in Nuclear Fuels,* Verlag Chemie, Weinheim, Germany, 285 pp.

Spear, K. E. (1976) *J. Less-Common Met.,* **47**, 195–201.

Spear, K. E. and Leitnaker, J. M. (1968) *Review and Analysis of Phase Behavior and Thermodynamic Properties of the Plutonium–Nitrogen System*, Report ORNL-TM-2106, Oak Ridge National Laboratory, Oak Ridge, TN, 24 pp.

Spedding, F. H., Kant, A., Wright, J. M., Warf, J. C., Powell, J. E., and Newton, A. S. (1945) *Extraction Purification of Thorium Nitrate*, Report CC-2393.

Spinks, J. W. T. and Woods, R. J. (1990) *An Introduction to Radiation Chemistry,* 3rd ed, John Wiley & Sons, New York, Ch. 7, 574 pp.

Spirlet, J. C. (1982) *Nucl. Instrum. Methods,* **200**(1), 45–53.

Spirlet, J. C. (1991) Synthesis of f-element Pnictides, in *Topics in f-element Chemistry,* vol. 2, (eds. G. Meyer and L. R. Morss), Kluwer Academic Publishers, Boston, pp. 353–67.

Spirlet, J. C. and Vogt, O. (1982) *J. Magn. Magn. Mater.,* **29**(1–3), 31–8.

Spirlet, M. R., Rebizant, J., Apostolidis, C., Kanellakopulos, B. K., and Dornberger, E. (1992) *Acta Crystallogr.,* **C48**(7), 1161–4.

Spitsyn, V. I., Gel'man, A. D., Krot, N. N., Mefod'eva, M. P., Zakharova, F. A., Komkov, Y. A., Shilov, V. P., and Smirnova, I. V. (1969) *J. Inorg. Nucl. Chem.,* **31**(9), 2733–45.

Spriet, B. (1963) *Mem. Etud. Sci. Rev. Met.,* **60**, 531.

Spriet, B. (1965) *J. Nucl. Mater.,* **15**(3), 220–30.

Spriet, B. (1967) Study of Allotropic Transformation of Plutonium, in *Plutonium 1965* (eds. A. E. Kay and M. B. Waldron), Chapman and Hall, London, England, pp. 88–117.

Sriyotha, U. (1968) *Phase Equilibrium in the UO_{2+x}-$LuO_{1.5}(ErO_{1.5})$ and $LuO_{1.5}$-$UO_2(NpO_2,NpO_{2+x},PuO_2,PuO_{2+x})$ Systems*, Thesis, Report KFK-737, Kernforschungszentrum, Karlsruhe, Germany, 61 pp.

Stakebake, J. L., Larson, D. T., and Haschke, J. M. (1993) *J. Alloys Compd.,* **202**(1–2), 251–63.

Standifer, R. L. (1968) *Fluoride Volatility 1968, Proc. Rocky Flats Fluoride Volatility Conf.,* Jun. 24–25, 1968, (eds. J. M. Cleveland and M. A. Thompson), Dow Chemical Company, pp. 79–98.

Staritzky, E. (1956) *Anal. Chem.,* **28**(12), 2021–2.

Staritzky, E. and Singer, J. (1952) *Acta Crystallogr.,* **5**, 536–40.

Starks, D. F. and Streitwieser, A., Jr (1973) *J. Am. Chem. Soc.,* **95**(10), 3423–4.

Steindler, M. J. (1963a) *Laboratory Investigations in Support of Fluid-bed Fluoride Volatility Processes*, part II, *The Properties of Plutonium Hexafluoride*, Report ANL-6753, Argonne National Laboratory, 83 pp.

Steindler, M. J. and Gunther, W. H. (1964a) *Laboratory Investigations in Support of Fluid-bed Fluoride Volatility Processes*, part VI, *A. The Absorption Spectrum of Plutonium Hexafluoride. B. Analysis of Mixtures of Plutonium Hexafluoride and Uranium Hexafluoride by Absorption Spectrometry*, Report ANL-6817, Argonne National Laboratory, 16 pp.

Steindler, M. J. and Gunther, W. H. (1964b) *Spectrochim. Acta,* **20**(8), 1319–22.

Steindler, M. J., Steidl, D. V., and Steunenberg, R. K. (1958) *The Fluorination of Plutonium Tetrafluoride*, Report ANL-5875, Argonne National Laboratory, 29 pp.

Steindler, M. J., Steidl, D. V., and Steunenberg, R. K. (1959) *Nucl. Sci. Eng.,* **6**(4), 333–40.

Steindler, M. J., Steidl, D. V., and Fischer, J. (1963) *Laboratory Investigations in Support of Fluid-bed Fluoride Volatility Processes*, part V, *The Radiation Chemistry of Plutonium Hexafluoride*, Report ANL-6812, Argonne National Laboratory, 24 pp.

Stewart, D. C. (1956) *Absorption Spectra of Lanthanide and Actinide Rare Earths. III. Heavier Lanthanide Elements in Aqueous Perchloric Acid Solution*, Report ANL-5624, US Atomic Energy Commission, 16 pp.

Stewart, G. R. and Elliott, R. O. (1981) *Specific Heat Studies of Alpha and Delta Plutonium. Actinides - 1981*, Report LBL-12441, Lawrence Berkeley Laboratory, Berkeley, CA.

Stiffler, G. L. and Curtis, M. H. (1960) *The Preparation of Plutonium Powder by a Hydriding Process: Initial Studies*, Report HW-64, 289, US Atomic Energy Commission, 17 pp.

Stoll, W., Scheider, V., and Ost, C. (1982) German Patent 3, **101**, 505 A.

Storms, E. K. (1964) *A Critical Review of Refractories*, Report LA-2942, US Atomic Energy Commission, 245 pp.

Storms, E. K. (1967) *The Refractory Carbides,* vol. 2 (*Refractory materials series*) Academic Press, New York, 284 pp.

Stout, B. E., Choppin, G. R., Nectoux, F., and Pagès, M. (1993) *Radiochim. Acta,* **61**, 65.

Stout, M. G., Kachner, G. C., and Hecker, S. S. (2002) *Mechanical Behavior of Delta-Phase Plutonium–Gallium Alloys*, Report LA-994458-PR-Revised, Los Alamos National Laboratory, pp. 1–38.

Stöwe, K. (2000) *J. Solid State Chem.,* **149**, 155–66.

Stoyer, N. J., Hoffman, D. C., and Silva, R. J. (2000) *Radiochim. Acta,* **88**(5), 279–82.

Stradling, G. N., Stather, J. W., Gray, S. A., Moody, J. C., Ellender, M., Hodgson, A., Volf, V., Taylor, D. M., Wirth, P., and Gaskin, P. W. (1989) *Int. J. Radiat. Biol.,* **56**(4), 503–14.

Stratton, R. W., Ledergerber, G., Ingold, F., Nicolet, M., and Botta, F. (1987) *Improv. Water React. Fuel Technol. Util., Proc. Int. Symp.*, pp. 353–62.

Stumpe, R., Kim, J. I., Schrepp, W., and Walther, H. (1984) *Appl. Phys. B-Photo,* **34**(4), 203–6.

Sugar, J. (1973) *J. Chem. Phys.,* **59**(2), 788–91.

Sugar, J. (1974) *J. Chem. Phys.,* **60**(10), 4103.

Sullivan, J. C., Hindman, J. C., and Zielen, A. J. (1961) *J. Am. Chem. Soc.,* **83**(16), 3373–8.

Sullivan, J. C., Woods, M., Bertrand, P. A., and Choppin, G. R. (1982) *Radiochim. Acta,* **31**(1–2), 45–50.

Sullivan, J. C., Choppin, G. R., and Rao, L. F. (1991) *Radiochim. Acta,* **54**(1), 17–20.

Sundaram, S. (1962) *Z. Phys. Chem.,* **34**, 225–32.

Suzuki, Y., Arai, Y., and Sasayama, T. (1983) *J. Nucl. Mater.,* **115**(2–3), 331–3.

Swanson, J. L. (1964) *J. Phys. Chem.,* **68**(2), 438–9.

Swanson, J. L. (1990) The PUREX Process. Part 3: PUREX Process Flowsheets. Science and Technology of Tributyl Phosphate, vol. 3, *Applications of Tributyl Phosphate in Nuclear Fuel Processing* (eds. W. W. Schulz, J. D. Navratil, L. L. Burger and K. P. Bender), CRC Press, Boca Raton, FL, pp. 55–79.

Tabuteau, A. and Pagès, M. (1980) *J. Inorg. Nucl. Chem.,* **42**(3), 401–3.

Tabuteau, A., Pagès, M., and Freundlich, W. (1972) *Mater. Res. Bull.,* **7**(7), 691–7.

Tait, C. D., Donohoe, R. J., Clark, D. L., Conradson, S. D., Ekberg, S. A., Keogh, D. W., Neu, M. P., Reilly, S. R., Runde, W. H., and Scott, B. L. (2004) *Actinide Research Quarterly,* Report LA-LP-04-60, Los Alamos National Laboratory, **1,** 20–2.

Takano, M., Itoh, A., Akabori, M., Ogawa, T., Numata, M., and Okamoto, H. (2001) *J. Nucl. Mater.,* **294**(1,2), 24–7.

Tan, J.-h. (2003) *Sichuan Shifan Daxue Xuebao, Ziran Kexueban,* **26**(3), 297–9.

Tananaev, I. G. (1989) *Radiokhimiya,* **31**(3), 46–51.

Tananaev, I. G., Rozov, S. P., and Mironov, V. S. (1992) *Radiokhimiya,* **34**(3), 88–92.

Tate, R. E. and Anderson, R. W. (1960) Some experiments in zone refining plutonium, *Extract. Phys. Met. Plutonium and Alloys, Symposium,* San Francisco, CA, Interscience, New York, pp. 231–42.

Tate, R. E. and Cramer, E. M. (1964) *Trans AIME,* **230**, 639.

Tate, R. E. and Edwards, G. R. (1966) *Diffusion*. Symposium on thermodynamics with emphasis on nuclear materials and atomic transport, Vienna, Austria, 2, 105 pp.

Taube, M. (1964) *Plutonium,* Macmillan Publishing, New York, 258 pp.

Taylor, J. M. (1966) *Physical Properties of Several Pu-base Intermetallic Compounds*, Report BNWLSA-385, Pacific Northwest Laboratory, Battelle Memorial Institute, Richland, WA, 7 pp.

Taylor, D. M. (1998) *J. Alloys Compd.,* **271–273**, 6–10.

Taylor, J. C., Loasby, R. G., Dean, D. J., and Linford, P. F. (1965) Elastic Constants, *Plutonium 1965, Proc. Third Int. Conf.,* London, England (eds. A. E. Kay and M. B. Waldron), Chapman and Hall, New York, 162 pp.

Taylor, J. C., Linford, P. F. T., and Dean, D. J. (1968) *J. Inst. Metals,* **96**(Part 6), 178–82.

Taylor, K. M., Andersen, J. C., Strasser, A., Stahl, D., and Forbes, R. L. (1967) *J. Am. Ceram. Soc.,* **50**(6), 321–5.

Taylor, R. J., Mason, C., Cooke, R., and Boxall, C. (2002) *J. Nucl. Sci. Technol.* (Suppl. 3), 278–81.

Terada, K., Meisel, R. L., and Dringman, M. R. (1969) *J. Nucl. Mater.,* **30**(3), 340–2.

Terminello, L. J., Caturla, M. J., Fluss, M. J., Gouder, T., Haire, R. G., Haschke, J. M., Hecker, S. S., Lander, G. H., Muller, I., Nitsche, H., Rebizant, J., Schwartz, A. J., Silva, R. J., Wall, M. A., Wastin, F., Weber, W. J., Wirth, B. D., and Wolfer, W. G. (2001) *Mater. Res. Soc. Bull.,* **26**(9), 667–71.

Teterin, Y. A. and Teterin, A. Y. (2004) *Russ. Chem. Rev.,* **73**(6), 541–80.

Tetzlaff, R. N. (1962) *Chemical Processing of 238Pu*, E. I. du Pont de Nemours & Co., Aiken, SC, Report DP-729, US Atomic Energy Commission, 30 pp.

Thiyagarajan, P., Diamond, H., Soderholm, L., Horwitz, E. P., Toth, L. M., and Felker, L. K. (1990) *Inorg. Chem.,* **29**(10), 1902–7.

Thomas, C. A. (1944) *The Chemistry, Purification and Metallurgy of Plutonium*, Report MUC-JCW-223 (Books 1 and 2) (Dec. 1944).

Thomas, W. (1969) *Critical and Safe Parameters for Plutonium and Plutonium Compounds*, Report MRR-56, Inst Mess- Regelungstech., Tech. Hochsch. Muenchen, Munich, Germany, 40 pp.

Thompson, M. A. (1965) Plutonium Oxidation, in *Plutonium 1965* (eds. A. E. Kay and R. G. Loasby), London, England, 592 pp.

Thompson, G. H. (1972) *Radiochem. Radioanal. Let.,* **10**(4), 223–30.

Thompson, S. G. and Seaborg, G. T. (1956) First use of bismuth phosphate for separating plutonium from uranium and fission products, *Progress in nuclear energy-Series 3, Process chemistry* (eds. F. R. Bruce, J. M. Fletcher, H. H. Hyman, and J. J. Katz), pp. 163–71.

Thuemmler, F., Theisen, R., and Patrussi, E. (1967) *Phase Relations, Production, and Characteristics of Substoichiometric Uranium and Plutonium oxide Fuels* (UO_{2-x} *and* (*Uranium, Plutonium Uranium*)O_{2-x}), Report KFK-543, Kernforschungszentrum, Karlsruhe, Germany, 44 pp.

Timofeeva, L. F. (2001) Phase Diagrams, in *Ageing Studies and Lifetime Extension of Materials* (ed. L. G. Mallinson), Kluwer Academic Publishers, New York, 191 pp.

Timofeeva, L. F. (2003a) *J. Metals*, (September 2003), 51–4.

Timofeeva, L. F. (2003b) *At.Energ.,* **95**(2), 540–5.

Toevs, J. W. (1997) *Surplus Weapons Plutonium: Technologies for Pit Disassembly/Conversion and MOX Fuel Fabrication*, Report LA-UR-97-4113, Los Alamos National Laboratory, 8 pp.

Tolley, W. B. (1953) *Plutonium Trichloride: Preparation by Reaction with Phosgene or Carbon Tetrachloride, and Bomb Reduction to Metal*, Report HW-30121, General Electric Company, Richland, WA, 28 pp.

Toth, L. M., Friedman, H. A., and Osborne, M. M. (1981) *J. Inorg. Nucl. Chem.,* **43**(11), 2929–34.

Trevorrow, L. E. and Shinn, W. A. (1960) *in Chemical Engineering Division Summary Report for October, November, December 1959* (eds. Lawroski, S, Roedge, W. A., Vogel, R. C., Munnecke, V. H.), Report ANL-6101, Argonne National Laboratory, 80 pp.

Trevorrow, L., Shinn, W. A., and Steunenberg, R. K. (1961) *J. Phys. Chem.,* **65**(3), 398–403.

Trevorrow, L. E., Kessie, R. W., and Steindler, M. J. (1965) *Laboratory Investigations in Support of Fluid-bed Fluoride Volatility Process*, part VIII, *Analysis of an Accidental Multigram Release of Plutonium Hexafluoride in a Glovebox*, Report ANL-7068, Argonne National Laboratory, 20 pp.

Triay, I. R., Hobart, D. E., Mitchell, A. J., Newton, T. W., Ott, M. A., Palmer, P. D., Rundberg, R. S., and Thompson, J. L. (1991) *Radiochim. Acta,* **52–53**(Pt. 1), 127–31.

Trofimov, T. I., Samsonov, M. D., Kulyako, Y. M., and Myasoedov, B. F. (2004) *CR Chim,* **7**(12), 1209–13.

Tuli, J. K. (ed.) (2004) *Nuclear Data Sheets,* Academic Press, San Diego.

Turchi, E. A., Gonis, A., and Shull, R. D. (eds.) (2002) *CALPHAD and Alloy Thermodynamics,* TMS-Minerals, Metals & Materials Society, Warrendale, PA, 281 pp.

Turchi, P. E. A., Kaufman, L., Lui, Z.-K., and Zhou, S. (2004) *Thermodynamics and Kinetics of Phase Transformations in Plutonium Alloys* - part I, Report UCRL-TR-206658, Lawrence Livermore National Laboratory,

Ueno, K. and Hoshi, M. (1970) *J. Inorg. Nucl. Chem.,* **32**, 381.

Ugajin, M. and Abe, J. (1973) *J. Nucl. Mater.,* **47**(1), 117–20.

Ullman, W. J. and Schreiner, F. (1986) *Radiochim. Acta,* **40**(4), 179–83.

Ullman, W. J. and Schreiner, F. (1988) *Radiochim. Acta,* **43**(1), 37–44.

Usami, T., Kurata, M., Inoue, T., Sims, H. E., Beetham, S. A., and Jenkins, J. A. (2002) *J. Nucl. Mater.,* **300**(1), 15–26.

Vaidya, V. N., Kamat, R. V., Joshi, J. K., Iyer, V. S., Suryanarayana, S., Srinivasan, N. L., Pillai, K. T., and Sood, D. D. (1983) *Proc. Nucl. Chem. Radiochem. Symp.*, pp. 549–51.

Van der Sluys, W. G., Burns, C. J., Huffman, J. C., and Sattelberger, A. P. (1988) *J. Am. Chem. Soc.,* **110**(17), 5924–5.

Van der Sluys, W. G., Burns, C. J., and Sattelberger, A. P. (1989) *Organometallics,* **8**(3), 855–7.

Varlashkin, P. G., Begun, G. M., and Peterson, J. R. (1984) *Radiochim. Acta,* **35**(4), 211–18.

Vdovenko, V. M., Vodovatov, V. A., Mashirov, L. G., and Suglobov, D. N. (1973) *Dokl. Akad. Nauk SSSR,* **209**(2), 352–5.

Veirs, D. K., Smith, C. A., Berg, J. M., Zwick, B. D., Marsh, S. F., Allen, P., and Conradson, S. D. (1994) *J. Alloys Compd.,* **213–214**, 328–32.

Vesnovskii, S. P. and Polynov, V. N. (1992a) in *Transuranium Elements: A Half Century* (eds. L. R. Morss and J. Fuger), American Chemical Society, Washington, DC, 131–6.

Vesnovskii, S. P. and Polynov, V. N. (1992b) *Nucl. Instrum. Methods Phys. Res., Sect. B,* **b70**(1–4), 9–11.

Viklund, C., Nordstrom, A., Irgum, K., Svec, F., and Frechet, J. M. J. (2001) *Macromolecules,* **34**(13), 4361–9.

Vladimirova, M. V. (1982) *Sov. Radiochem.,* **24**(4), 393–401.

Vladimirova, M. V. (1990) *J. Radioanal. Nucl. Chem.,* **143**(2), 445–54.

Vladimirova, M. V. (1998) *Sov. Radiochem.,* **40**(5), 395–404.

Vladimirova, M. V. and Kulikov, I. A. (2002) *Radiochemistry (Moscow, Russian Federation)(Translation of Radiokhimiya),* **44**(1), 86–90.

Vogt, O. and Mattenberger, K. (1993) *Handbook on the Physics and Chemistry of Rare Earths,* vol. 17 (eds. K. A. J. Gschneidner, L. Eyring, G. R. Choppin, and G. H. Lander), Elsevier Science, New York, 301 pp.

Vogt, O. and Mattenberger, K. (1995) *J. Alloys Compd.,* **223**(2), 226–36.

Volkov, Y. F., Kapshukov, I. I., Visyashcheva, G. I., and Yakovlev, G. N. (1974a) *Radiokhimiya,* **16**(6), 863–7.

Volkov, Y. F., Kapshukov, I. I., Visyashcheva, G. I., and Yakovlev, G. N. (1974b) *Radiokhimiya,* **16**(6), 868–73.

Volkov, Y. F., Visyashcheva, G. I., Tomilin, S. V., Kapshukov, I. I., and Rykov, A. G. (1981) *Radiokhimiya,* **23**(2), 254–8.

Vyatkin, V. E., Davidov, Y. P., and Shashukov, E. A. (1972) *Radiokhimiya,* **14**(2), 289–93 (pp 299–303 in English translation).

Waber, J. T. (1958) *Plutonium Oxidation*, *Proc. Second UN Int. Conf. Peaceful Uses Atomic Energy*, Geneva, Switzerland, United Nations, 6, 204 pp.

Waber, J. T. (1980) Corrosion and Oxidation, in *Plutonium Handbook,* vol. 1 (ed. O. J. Wick), American Nuclear Society, La Grange, IL, pp. 145–89.

Waber, J. T., Olson, W. M., and Roof, R. B. (1961) *J. Nucl. Mater.,* **3**, 205.

Wachter, P. (2003) *Solid State Commun.,* **127**(9–10), 599–603.

Wachter, P., Marabelli, F., and Bucher, B. (1991) *Phys. Rev. B,* **43**(13-B), 11136–44.

Wachter, P., Filzmoser, M., and Rebizant, J. (2001) *Physica B,* **293**(3&4), 199–223.

Wade, W. Z. (1971) *J. Nucl. Mater.,* **38**, 292.

Wade, W. Z., Short, D. W., Walden, J. C., and Magana, J. W. (1978) *Metall. Trans. A,* **9A**, 965.

Wadt, W. R. (1987) *J. Chem. Phys.,* **86**(1), 339–46.

Wagner, R. P., Shinn, W. A., Fischer, J., and Steindler, M. J. (1965) *Laboratory Investigations in Support of Fluid-bed Fluoride Volatility Processes*, part VII, *The Decomposition of Gaseous Plutonium Hexafluoride by Alpha Radiation*, Report ANL-7013, Argonne National Laboratory, 32 pp.

Wahlgren, U., Moll, H., Grenthe, I., Schimmelpfennig, B., Maron, L., Vallet, V., and Gropen, O. (1999) *J. Phys. Chem. A,* **103**(41), 8257–64.

Waldek, A., Erdmann, N., Gruning, C., Huber, G., Kunz, P., Kratz, J. V., Lassen, J., Passler, G. and Trautmann, N. (2001) *RIMS Measurements for the Determination of the First Ionization Potential of the Actinides Actinium up to Einsteinium.* Melville, NY, American Institute of Physics, *AIP Conf. Proc.,* **584**, 219–24.

Waldron, M. B., Garstone, J., Lee, J. A., Mardon, P. G., Marples, J. A. C., Poole, O. M., and Williamson, G. K. (1958) *Proc. Second Int. Conf. Peaceful Uses of Atomic Energy*, vol. 6, Geneva, United Nations, 162 pp.

Wallace, P. L. and Harvey, M. R. (1974) *J. Nucl. Mater.,* **54**(2), 171–4.

Walter, K. H. (1965) *Ternary oxides of Tri- to Sexivalent Americium. Thesis*, Report KFK-280, Kernforschungszentrum, Karlsruhe, 76 pp.

Walters, R. T. and Briesmeister, R. A. (1984) *Spectrochim. Acta,* **40A**, 587.

Wang, R. and Steinfink, H. (1967) *Inorg. Chem.,* **6**(9), 1685–92.

Ward, J. W. (1985) *Physica B & C,* **130**(1–3), 510–15.

Ward, J. W. and Haschke, J. M. (1994) Comparison of 4f and 5f Element Hydride Properties, in *Handbook on the Physics and Chemistry of Rare Earths,* vol. 18 (eds. K. A. J. Gschneidner, E. L., G. R. Choppin, and G. H. Lander), Elsevier Science, New York, pp. 293–363.

Ward, J. W., Cort, B., Goldstone, J. A., Lawson, A. C., Cox, L. E., and Haire, R. G. (1992) in *Transuranium Elements: A Half Century* (eds. L. R. Morss and J. Fuger), American Chemical Society, Washington, DC, 404–15.

Warf, J. C. (1945) *The Extraction Purification of Cerium*, Report CC-2402.

Warner, B. P., D'Alessio, J. A., Morgan, A. N., III, Burns, C. J., Schake, A. R., and Watkin, J. G. (2000) *Inorg. Chim. Acta,* **309**(1–2), 45–8.

Wastin, F., Spirlet, J. C., and Rebizant, J. (1995) *J. Alloys Compd.,* **219**(1–2), 232–7.

Weber, E. T., Chikalla, T. D., and McNeilly, C. E. (1964) *The Plutonium–Boron System*, Report HW-81603, Article 2.9, US Atomic Energy Commission, 80 pp.

Weger, H. T., Okajima, S., Cunnane, J. C., and Reed, D. T. (1993) *Mater. Res. Soc. Symp. Proc.*, **294**(Scientific Basis Nucl. Waste Manag.), 739–45.

Wei, Y. Z., Arai, T., Hoshi, H., Kumagai, M., Bruggeman, A., Gysemans, M., and Sawa, T. (2002) *JAERI-Conf* **2002–004**(Proc. Int. Symp. NUCEF 2001), 225–36.

Weigel, F. (1965) *Preparation and Roentgenographic Study of Highly Radioactive Material*, Thesis, Report NP-15826, Munich University, 301 pp.

Weigel, F., Wishnevsky, V., and Hauske, H. (1977) *J. Less-Common Met.,* **56**(1), 113–23.

Weigel, F., Güldner, R., and Wishnevsky, V. (1982) *J. Less-Common Met.,* **84**(1), 147–55.

Weinstock, B. (1944) *Vapor Pressure of Plutonium Trichloride*, Report LA-122, Los Alamos Scientific Laboratory, 9 pp.

Weinstock, B. and Goodman, G. L. (1965) *Adv. Chem. Phys.,* **9**, 169–316.

Weinstock, B. and Malm, J. G. (1956a) *J. Inorg. Nucl. Chem.,* **2**(5–6), 380–94.

Weinstock, B. and Malm, J. G. (1956b) *Proc. First Int. Conf. on the Peaceful Uses of Atomic Energy*, vol. 2, New York, pp. 380–94.

Weinstock, B., Weaver, E. E., and Malm, J. G. (1959) *J. Inorg. Nucl. Chem.,* **11**(2), 104–14.

Weiss, R. J. (1963) *Proc. Phys. Soc.,* **62**, 28.

Wells, A. F. (1984) *Structural Inorganic Chemistry,* Oxford University Press, Oxford, England, 1382 pp.

Wensch, G. W. and Whyte, D. D. (1951) *The Nickel Plutonium System*, Report LA-1304, Los Alamos Scientific Laboratory, 29 pp.

Werner, G. D. (1982) *Doctoral Dissertation*, Report, University of Munich.

West, M. H., Ferran, M. D., and Fife, K. W. (1988) *The Chlorination of Plutonium Dioxide*, Report LA-11256, Los Alamos National Laboratory, Los Alamos, NM, 13 pp.

Wester, D. W. (1983) *ACS Symp. Ser.,* **216**(Plutonium Chem.), (eds. W. T. Carnall and G. R. Choppin) American Chemical Society, Washington, DC 49–63.

Wester, D. W. and Sullivan, J. C. (1983) *Radiochem. Radioanal. Lett.,* **57**, 35.

Westrum, E. F., Jr (1949a) Preparation and Properties of Plutonium Oxides, in *Natl. Nucl. Energy Ser.*, Div IV **14**B (Transuranium Elements Pt. II) (eds. G. T. Seaborg, J. J. Katz, and W. M. Manning), McGraw-Hill, New York, pp. 936–44.

Westrum, E. F., Jr (1949b) Preparation and Properties of Plutonium Silicides, in *Natl. Nucl. Energy Ser.*, Div IV **14**B (Transuranium Elements Pt. I) (eds. G. T. Seaborg, J. J. Katz, and W. M. Manning), McGraw-Hill, New York, pp. 729–30.

Westrum, E. F., Jr (1949c) Heat of Formation of Plutonium Tribromide, in *Natl. Nucl. Energy Ser.*, Div IV **14**B (Transuranium Elements Pt. II) (eds. G. T. Seaborg, J. J. Katz and W. M. Manning), McGraw-Hill, New York, pp. 926–9.

Westrum, E. F., Jr and Robinson, H. P. (1949a) Heat of Formation of Plutonium Trichloride, in *Natl. Nucl. Energy Ser.*, Div IV **14**B (Transuranium Elements Pt. II) (eds. G. T. Seaborg, J. J. Katz, and W. M. Manning), McGraw-Hill, New York, pp. 914–21.

Westrum, E. F., Jr and Robinson, H. P. (1949b) Heat of Formation of Plutonium Oxychloride, in *Natl. Nucl. Energy Ser.*, Div IV **14**B (Transuranium Elements Pt. II) (eds. G. T. Seaborg, J. J. Katz, and W. M. Manning), McGraw-Hill, New York, pp. 930–5.

Westrum, E. F., Jr and Wallmann, J. C. (1951) *J. Am. Chem. Soc.,* **73**, 3530–1.

Wick, O. J. (ed.) (1980) *Plutonium Handbook: A Guide to the Technology,* American Nuclear Society, La Grange Park, IL, 992 pp.

Wigley, D. A. (1964) PhD thesis, Oxford University, Oxford, UK.

Wigley, D. A. (1965) *Proc. Roy. Soc. Lond. Ser. A,* **284**(1398), 344–53.

Wilkinson, W. D. (ed.) (1960) *Extractive and Physical Metallurgy of Plutonium and its Alloys,* Interscience Publishers, New York.

Williams, C. W., Blaudeau, J. P., Sullivan, J. C., Antonio, M. R., Bursten, B., and Soderholm, L. (2001) *J. Am. Chem. Soc.,* **123**(18), 4346–7.

Willis, J. O., Ward, J. W., Smith, J. L., Kosiewicz, S. T., Haschke, J. M., and Hodges, A. E., III (1985) *Physica B & C,* **130**(1–3), 527–9.

Wills, J. M. and Eriksson, O. (2000) *Los Alamos Sci.,* **26**(1), 128.

Winchester, R. S. and Maraman, W. J. (1958) *Proc. Second UN Int. Conf. Peaceful Uses Atomic Energy*, vol. 17,Geneva, pp. 168–71.

Wirth, B. D., Schwartz, A. J., Fluss, M. J., Cartula, M. J., Wall, M. A., and Wolfer, W. G. (2001) *Mat. Res. Soc. Bull.,* **26**(9), 679–84.

Wiswall, R. J., Jr, Egan, J. J., Ginell, W. S., Miles, F. T., and Powell, J. R. (1959) *Recent Advances in the Chemistry of Liquid Metal Fuel Reactors*, *Proc. Second Int. Conf. Peaceful Uses of Atomic Energy*, 1958, Geneva, Switzerland, 17, pp. 421–7.

Wittenberg, L. J. (1963) *Symp. on Research at Mound Laboratory,* June 6–7, 1963, Report MLM-1163, Mound Laboratory, 157 pp.

Wittenberg, L. J. (1975) A Model for Liquid Uranium and Plutonium with Implications on the Adjacent Solid Phases, in *Plutonium and Other Actinides,* Baden-Baden, Germany (eds. H. Blank and R. Lindner), North-Holland, New York, pp. 71–83.

Wittenberg, L. J. and Grove, G. R. (1963) *Reactor Fuels and Materials Development. Plutonium Research*, Report MLM-1184, Mound Laboratory, pp. 12–16.

Wittenberg, L. J. and Grove, G. R. (1964) *Reactor Fuels and Materials Development. Plutonium Research*, Report MLM-1244, Mound Laboratory, 56 pp.

Wittenberg, L. J., Jones, L.V., and Ofte, D. (1960) *The Viscosity of a Liquid Pu-Fe Eutectic Alloy, Proc. Second Int. Conf. Plutonium,* Grenoble, France (eds. E. Grison, W. B. H. Lord, and R. D. Fowler), Cleaver-Hume Press, London, 1, pp. 671–83.

Wittenberg, L. J., Ofte, D., and Curtiss, C. F. (1968) *J. Chem. Phys.,* **48**(7), 3253–60.

Wittenberg, L. J., Vaughn, G. A., and DeWitt, R. (1970) *Phase Relationships in Uranium, Neptunium and Plutonium, Proc. Fourth Int. Conf. on Plutonium and Other Actinides,* Santa Fe, NM (ed. W. N. Miner), The Metallurgical Society of the AIME, II, 659–68.

Wolfer, W. G. (2000) *Los Alamos Sci.,* **26**(2), 274–85.

Wong, J., Holt, M., Hong, H., Schwartz, A. J., Zschack, P., Chiang, T. C., and Wall, M. (2003a) *AIP Conf. Proc.,* **673**(Plutonium Futures – The Science), 221–3.

Wong, J., Krisch, M., Farber, D. L., Occelli, F., Schwartz, A. J., Chiang, T. C., Wall, M., Boro, C., and Xu, R. Q. (2003b) *Science,* **301**(5636), 1078–80.

Wood, D. H., Cramer, E. M., Wallace, P. L., and Ramsey, W. J. (1969) *J. Nucl. Mater.,* **32**(2), 193–207.

Worden, E. F., Carlson, L. R., Johnson, S. A., Paisner, J. A., and Solarz, R. W. (1993) *J. Opt. Soc. Am.,* **B10**(11), 1998–2005.

Wriedt, H. A. (1989) *Bull. Alloy Phase Diagr.,* **10**(5), 593–602, 615–16.

Wriedt, H. A. (1990) *Bull. Alloy Phase Diagr.,* **11**(2), 184–202.

Wroblewska, J., Dobrowolski, J., Pages, M., and Freundlich, W. (1979) *Radiochem. Radioanal. Lett.,* **39**(3), 241–6.

Wruck, D. A., Russo, R. E., and Silva, R. J. (1994) *J. Alloys Compd.,* **213–214**, 481–3.

Wyckoff, R. W. G. (1963) *Crystal Structures,* Interscience, New York, 289 pp.

Wymer, R. G. (1968) *Sol-gel Processes for Ceramic Nuclear Fuels*, *Proc. Panel on Sol-gel Processes for Ceramic Nuclear Fuels*, Report STI/PUB–207;CONF-680532, International Atomic Energy Agency, pp. 131–72.

Wymer, R. G. and Coobs, J. H. (1967) *P. Brit. Ceramic Soc.,* **7**, 61–79.

Wynne, K. J. and Rice, R. W. (1984) *Annu. Rev. Mater. Sci.,* **14**, 297–334.

Yamaguchi, T., Sakamoto, Y., and Ohnuki, T. (1994) *Radiochim. Acta,* **66/67**, 9–14.

Yamashita, T., Ohuchi, K., Takahashi, K., and Fujino, T. (1992) Formation of Lithium Plutonates by the Reaction of Lithium Nitrate and Lithium Hydroxide with Plutonium dioxide, in *Transuranium Elements, A Half Century* (eds. L. R. Morss and J. Fuger), American Chemical Society, Washington, DC, pp. 451–6.

Yarbro, S. L., Schreiber, S. B., Ortiz, E. M., and Ames, R. L. (1998) *J. Radioanal. Nucl. Chem.,* **235**(1–2), 21–4.

Zachariasen, W. H. (1944) *X-ray Diffraction Results for Uranium and Plutonium Compounds*, Report CK-1367, Report USAEC Manhattan Project, Metallurgical Laboratory.

Zachariasen, W. H. (1948a) *Acta Crystallogr.,* **1**, 265–8.

Zachariasen, W. H. (1948b) *J. Am. Chem. Soc.,* **70**, 2147–51.

Zachariasen, W. H. (1948c) *Acta Crystallogr.,* **1**, 268–9.

Zachariasen, W. H. (1949a) in *Natl. Nucl. Energy Ser., Div. IV,* **14B**(Transuranium Elements Pt. II), (eds. G. T. Seaborg, J. J. Katz, and W. M. Manning), McGraw-Hill, New York, 1451–3.

Zachariasen, W. H. (1949b) *Acta Crystallogr.,* **2**, 94–9.

Zachariasen, W. H. (1949c) in *Natl. Nucl. Energy Ser., Div. IV,* **14B**(Transuranium Elements Pt. II), (eds. G. T. Seaborg, J. J. Katz, and W. M. Manning), 1448–50.

Zachariasen, W. H. (1949d) *Acta Crystallogr.,* **2**, 388–90.

Zachariasen, W. H. (1951) *Acta Crystallogr.,* **4**, 231–6.

Zachariasen, W. H. (1952) *Acta Crystallogr.,* **5**, 17–19.

Zachariasen, W. H. (1954a) *Acta Crystallogr.,* **7**, 795–9.

Zachariasen, W. H. (1954b) Crystal Chemistry of the 5f Elements, in *The actinide elements* (eds. G. T. Seaborg and J. J. Katz), McGraw-Hill, New York, pp. 769–96.

Zacharaisen, W. H. (1961a) Crystal-structure Studies of Plutonium Metal, in *The Metal Plutonium* (eds. A. S. Coffinberry and W. N. Miner), University of Chicago Press, Chicago, IL, pp. 99–107.

Zachariasen, W. H. (1961b) Crystal-structure Studies of Plutonium Metal, in *The Metal Plutonium* (eds. A. S. Coffinberry and W. N. Miner), University of Chicago Press, Chicago, IL, pp. 104–7.

Zachariasen, W. H. (1973) *J. Inorg. Nucl. Chem.,* **35**(10), 3487–97.

Zachariasen, W. H. and Ellinger, F. H. (1955) *Acta Crystallogr.,* **8**(7), 431–3.

Zachariasen, W. H. and Ellinger, F. H. (1957) *J. Chem. Phys.,* **27**(3), 811–12.

Zachariasen, W. H. and Ellinger, F. H. (1959) *Acta Crystallogr.,* **12**, 175–6.

Zachariasen, W. H. and Ellinger, F. H. (1963a) *Acta Crystallogr.,* **16**(8), 777–84.

Zachariasen, W. H. and Ellinger, F. H. (1963b) *Acta Crystallogr.,* **16**(5), 369–75.

Zachariasen, W. H. and Ellinger, F. H. (1970) *Unit Cell of the Zeta Phase of the Plutonium Zirconium and the Plutonium Hafnium Systems*, Report LA-4367, Los Alamos Scientific Laboratory, 4 pp.

Zagrai, V. D. and Sel'chenkov, L. I. (1962) *Radiokhimiya,* **4**, 181–4.

Zaitseva, V. P., Alekseeva, D. P., and Gel'man, A. D. (1973) *Radiokhimiya,* **15**(3), 385–90.

Zakharova, F. A., Orlova, M. M., and Gel'man, A. D. (1972) *Sov. Radiochem.,* **14**(1), 121–22.

Zalkin, A. and Raymond, K. N. (1969) *J. Am. Chem. Soc.,* **91**(20), 5667–8.

Zhou, J. S. and Goodenough, J. B. (2005) *Phys. Rev. Lett.,* **94**(6), 065501/1–065501/4.

Zocco, T. G. and Schwartz, A. J. (2003) *JOM,* **55**(9), 24–7.

Zocco, T. G., Stevens, M. F., Adler, P. H., Sheldon, R. I., and Olson, G. B. (1990) *Acta Met. Mater.,* **38**(11), 2275–82.

Zocco, T. T. and Rohr, D. L. (1988) *Mater. Res. Soc. Symp. Proc.*, **115** (Specimen Prep. Transm. Electron Mircosc. Mater.), 259–64.

Zubarev, V. G. and Krot, N. N. (1984) *Radiokhimiya,* **26**(2), 176–80.

Zukas, E. G., Hecker, S. S., Morgan, J. R., and Pereyra, R. A. (1981) *Pressure-induced Transformation in a Pu-2.0 at.% Al Alloy*, *Proc. Int. Conf. Solid-Solid Phase Transform.*, Pittsburgh, AIME, 1, 1333–7.

Zukas, E. G., Hecker, S. S., and Pereyra, R. A. (1983) *J. Nucl. Mater.,* **115**(1), 63–8.

Zunger, A., Wei, S. H., Ferreira, L. G., and Bernard, J. E. (1990) *Phys. Rev. Lett.,* **65**(3), 353–6.

Zwick, B. D., Sattelberger, A. P., and Avens, L. R. (1992) in *Transuranium Elements: A Half Century* (eds. L. R. Morss and J. Fuger), American Chemical Society, Washington, DC, 239–46.

CHAPTER EIGHT

AMERICIUM

Wolfgang H. Runde and Wallace W. Schulz

8.1 HISTORICAL

Americium, element 95, was discovered in 1944–45 by Seaborg *et al.* (1950) at the Metallurgical Laboratory of the University of Chicago as a product of the irradiation of plutonium with neutrons:

$$^{239}\mathrm{Pu}(n,\gamma)^{240}\mathrm{Pu}(n,\gamma)^{241}\mathrm{Pu}\xrightarrow{-\beta^-}{}^{241}\mathrm{Am}$$

This reaction is still the best method for the production of pure ^{241}Am. In post-World War II work at the University of Chicago, Cunningham isolated Am(OH)$_3$ and measured the first absorption spectrum of the Am^{3+} aquo ion (Cunningham, 1948). By the 1950s, the major center for americium chemistry research in the world was at Los Alamos. Since the 1970s, the majority of publications on americium have come from researchers in the former USSR and West Germany. Extensive reviews of americium chemistry can be found in Freeman and Keller (1985), Gmelin (1979), Penneman and Asprey (1955), and Schulz (1976).

8.2 NUCLEAR PROPERTIES OF ISOTOPES

To date, 13 americium isotopes with mass numbers 232–247 and half-lives ranging from 55 s to 7370 years are known (Table 8.1). While the isotopes with mass numbers 232, 234, and 237–247 have been known for some time, the neutron-deficient isotopes Am-233, Am-235, and Am-236 have only recently

Table 8.1 *Nuclear properties of americium isotopes.*

Mass number	*Half-life*	*Mode of decay*	*Main radiations* (MeV)	*Method of production*
232	1.4 min	SF isomer		^{230}Th(^{10}B, 8n)
233	3.2 min	α	α 0.00678	^{238}U(^{6}Li, 6n)
234	2.6 min	EC		^{230}Th(^{10}B, 6n)
235	15 min	EC		^{238}Pu(^{1}H, 4n)
236	4.4 min[a]	EC		^{235}U(^{6}Li, 5n)
	3.7 min[b]	EC		^{237}Np(^{6}He, 4n)
237	1.22 h	EC $> 99\%$	α 6.042	^{237}Np(α, 4n)
		α 0.025%	γ 0.280 (47%)	^{237}Np(^{3}He, 3n)
238	1.63 h	EC $> 99\%$	α 5.94	^{237}Np(α, 3n)
		α $1.0 \times 10^{-4}\%$	γ 0.963 (29%)	
239	11.9 h	EC $> 99\%$	α 5.776 (84%)	^{237}Np(α, 2n)
			5.734 (13.8%)	
		α 0.010%	γ 0.278 (15%)	^{239}Pu(d, 2n)
240	50.8 h	EC $> 99\%$	α 5.378 (87%)	^{237}Np(α, n)
		α $1.9 \times 10^{-4}\%$	5.337 (12%)	^{239}Pu(d, n)
			γ 0.988 (73%)	
241	432.7 yr	α	α 5.486 (84%)	^{241}Pu daughter
	1.15×10^{14} yr	SF	5.443 (13.1%)	multiple n capture
			γ 0.059 (35.7%)	
242	16.01 h	β^- 82.7%	β^- 0.667	^{241}Am(n, γ)
		EC 17.3%	γ 0.042 weak	
242 m	141 yr	IT 99.5%	α 5.207 (89%)	^{241}Am(n, γ)
	9.5×10^{11} yr	SF α (0.45%)	5.141 (6.0%)	^{241}Am(n, γ)
			γ 0.0493 (41%)	
243	7.38×10^{3} yr	α	α 5.277 (88%)	multiple n capture
	2.0×10^{14} yr	SF	5.234 (10.6%)	
			γ 0.075 (68%)	
244	10.1 h	β^-	β^- 0.387	^{243}Am(n, γ)
			γ 0.746 (67%)	
244 m	26 min	$\beta^- > 99\%$	β^- 1.50	^{243}Am(n, γ)
		EC 0.041%		
245	2.05 h	β^-	β^- 0.895	^{245}Pu daughter
			γ 0.253 (6.1%)	
246[c]	25.0 min	β^-	β^- 2.38	^{246}Pu daughter
		γ	0.799 (25%)	
246[c]	39 min	β^-	γ 0.679 (52%)	^{244}Pu(α, d)
				^{244}Pu(^{3}He, p)
247	24 min	β^-	γ 0.285 (23%)	^{244}Pu(α, p)

SF, spontaneous fission; EC, electron capture; IT, isomeric transition.

[a] Hall (1989).

[b] Tsukada *et al.* (1998).

[c] Not known whether ground-state nuclide or isomer.

been produced and characterized (Hall, 1989; Tsukada *et al.*, 1998; Weifan *et al.*, 1999; Sakama *et al.*, 2000). The light isotopes up to ^{243}Am mainly decay by electron capture, emission of alpha particles, and spontaneous fission; the isotopes beyond ^{243}Am are short-lived β^--emitters. Data in Table 8.1 are taken primarily from the comprehensive compilation in Gmelin (1973) and others (Hyde *et al.*, 1971; Wapstra and Gove, 1971; Skobelev, 1972; Natowitz, 1973; Schulz, 1976; Lederer and Shirley, 1978; Kuznetsov and Skobelev, 1966). Although not noted in Table 8.1, literature references (e.g. Schulz, 1976) indicate that some of the identified americium isotopes exist in more than one isomeric energy state.

8.3 PRODUCTION OF PRINCIPAL ISOTOPES

The most important isotopes of americium are ^{241}Am and ^{243}Am due to their long half-lives of 433 and 7380 years, respectively. These isotopes have been made in kilogram quantities with high purity. ^{242}Am ($t_{1/2}$ = 141 years) can be produced to the extent of only a few percent in ^{241}Am by neutron capture.

Americium-241 is superior to all competing radionuclides as a low-energy gamma source because of its cost, convenience, spectral purity, and half-life (Crandall, 1971) and its application as a low-energy gamma source may well be the largest of any actinide nuclide (Seaborg, 1970; LeVert and Helminski, 1973). The major use for ^{241}Am is in smoke-detector alarms and in neutron sources to furnish alpha particles for the (α,n) reaction on beryllium. As a source of nearly monoenergetic alpha (5.44 and 5.49 MeV) and gamma (59.6 keV) radiation, ^{241}Am is also widely used in thickness gauging and density and radiographic measurements, and is utilized to produce ^{242}Cm (up to 0.65 g ^{242}Cm per gram of ^{241}Am (Hennelly, 1972)) by thermal neutron capture. The thermal neutron capture sequence involved in producing ^{242}Cm from ^{241}Am is:

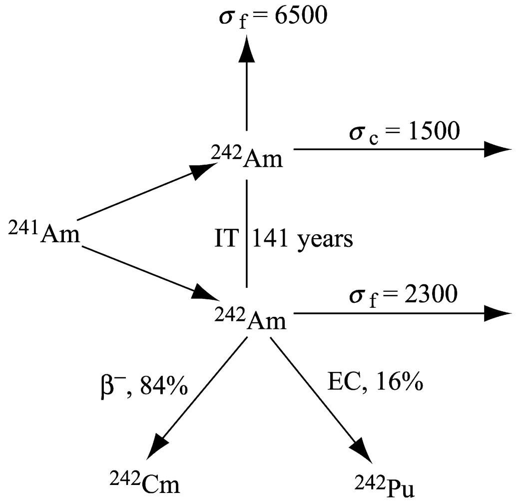

The lower specific activity of ^{243}Am compared to ^{241}Am makes it particularly useful in chemical studies. It is also used in the production of ^{244}Cm, ^{249}Bk/Cf, ^{252}Cf, and other transcurium elements in high neutron-flux reactors.

8.3.1 Production of ^{241}Am by irradiation of ^{239}Pu

Neutron irradiation of ^{239}Pu yields ^{241}Pu, which decays by beta emission with a half-life of 14.4 ± 0.3 years to ^{241}Am. In 1977, more than 1.5 kg of ^{241}Am was isolated from reprocessing aged plutonium at the US Department of Energy (DOE) Rocky Flats site. In 1980, a similar amount was isolated at the DOE Los Alamos site.

8.3.2 Production of ^{243}Am by irradiation of ^{242}Pu

Nearly isotopically pure ^{243}Am results from irradiation of ^{242}Pu with thermal neutrons:

$$^{242}\mathrm{Pu}(\mathrm{n},\gamma)^{243}\mathrm{Pu} \xrightarrow[5\mathrm{h}]{\beta^-} {}^{243}\mathrm{Am}$$

8.3.3 Availability of ^{241}Am and ^{243}Am from power reactor fuel

Commercial nuclear power reactors produce kilogram quantities of both ^{241}Am and ^{243}Am with an isotopic composition dependent on reactor burn-up. The US DOE Savannah River site reactors produced about 9 kg of a ^{243}Am–^{244}Cm mixture over a period of 10 years (Baybarz, 1970). About 1 kg of mixed ^{241}Am and ^{243}Am was recovered at the US DOE Hanford site during reprocessing of the Shippingport reactor blanket fuel (Wheelwright *et al.*, 1968). Approximately 30 kg of americium is reported to remain in the US DOE Hanford site waste tanks (Agnew *et al.*, 1997). But, no industrial reprocessor of commercial nuclear reactor fuel anywhere in the world has opted to pursue systematic recovery of americium. However, a potentially large source of americium is the high-level Purex-process liquid waste from plutonium processing; indeed, future waste storage may require separation of americium.

8.3.4 Critical mass

The calculated minimum critical mass of ^{242}Am in aqueous solution is 23 g at a concentration of 5 g L^{-1} (Bierman and Clayton, 1969). Note that mass separation of ^{242}Am from ^{241}Am is required to obtain pure ^{242}Am.

8.4 SEPARATION AND PURIFICATION OF PRINCIPAL ISOTOPES

Most of the standard methods, aqueous and non-aqueous, for separating and purifying americium from all kinds of sources and materials were developed in the 1950s, 1960s, and 1970s; progress made in this time frame was summarized in the second edition of this work. In contrast to the earlier time period, in the 1980s and 1990s research efforts to develop new or improved technology for recovery and/or purification of americium were largely confined to development and testing of new and improved solvent extraction processes. Worldwide, aside from purely academic investigations mainly in Russia and India, scientists and engineers were motivated by one of two main goals:

(1) In the USA, principally, to find new or modified practicable ways of removing minor amounts of neptunium, plutonium, and americium from various stored defense wastes to convert such wastes from so-called TRU (transuranium) wastes to non-TRU wastes, thus requiring less expensive final disposal procedures and facilities.
(2) To develop and demonstrate practicable technology for removal (partitioning) of long-lived actinides as well as certain long-lived and mobile fission products, e.g. ^{99}Tc, ^{129}I from the high-level aqueous waste (HLW) generated in reprocessing of irradiated commercial nuclear power reactor fuel. Partitioning of these species from the HLW, it is believed, would greatly facilitate and simplify the many current technical and legal obstacles to final geologic disposal of the HLW. Recovered, purified, and concentrated actinides and fission products can, it is further believed, be converted (transmuted) to stable or short-lived radioisotopes by suitable neutron irradiation. Because irradiated commercial nuclear reactor fuel is being reprocessed in Japan, France, and China, investigators in these countries have been active in pursuing partitioning technology options. Several references (ANS, 1993; Prunier *et al.*, 1997; Cohen, 2000; NN, 2002) provide much additional detail concerning the incentives for and status of the development of partitioning and transmutation technology. Particular attention is called to an excellent summary article on actinide partitioning technology (Mathur *et al.*, 2001).

Americium separation technology is presented and discussed here in the same order used in the second edition of this monograph. Significant separation technology developments that have occurred since the second edition was published are incorporated and discussed at appropriate places in the text. (The knowledgeable reader will appreciate that when this text was prepared (early 2002) all the americium separations technologies described in the subsequent parts of Section 8.4 was essentially only of academic and/or historic interest. The present authors are not aware of any current significant effort in any country to actually separate and/or purify americium isotopes from any source.)

8.4.1 Pyrochemical processes

A two-stage, countercurrent molten-salt extraction process was used to extract ^{241}Am from many kilograms of aged plutonium, in which ^{241}Am had grown-in by beta decay of ^{241}Pu. The purification scheme removed about 90% of the americium from plutonium metal, typically containing 200–2000 ppm ^{241}Am (Schulz, 1976).

Mullins and Leary (1969) patented a method of separating americium from plutonium that involves bubbling a mixture of oxygen and argon gas into a molten salt containing both elements. Plutonium precipitates as PuO_2, whereas americium remains in solution.

Ferris *et al.* (1972) determined the equilibrium distribution of americium (and other transuranium elements) between liquid bismuth and molten LiCl, LiBr, and several $LiF–BeF_2–ThF_4$ solutions at temperatures of 600–750°C. Some of the americium appeared to be in the divalent state in the $Am/PuCl_3$ system (Mullins and Leary, 1969). The distribution coefficient, $D =$ (g Am per g metal phase)/(g Am per g salt phase), of americium between molten aluminum metal and molten $AlCl_3–KCl$ is 1.96 (Moore and Lyon, 1959). Mills and Reese (1994) demonstrated that ^{241}Am in aged PuF_4 can be cleanly separated from plutonium by low-temperature reaction with O_2F to generate volatile PuF_6. Americium remains in the fluorination residue from which it can be recovered and concentrated by any of the several aqueous methods.

As part of their comprehensive experimental and theoretical studies of the partitioning of actinides from high-level radioactive fuel reprocessing aqueous waste, Japanese scientists, in collaboration with some US investigators, have been developing a pyrometallurgical partition process (Sakamura *et al.*, 1998). The process consists of four main steps: (1) denitration of the HLW; (2) chlorination to convert oxides to chlorides; (3) reductive extraction to reduce actinides in a molten salt by lithium metal and to extract them into liquid cadmium; and (4) electrorefining in LiCl–KCl eutectic to separate actinides from the liquid cadmium anode. Preliminary experimental tests of the entire process show that uranium, plutonium, and neptunium are relatively easily separated from fission product rare earths but that americium is accompanied by some rare earth elements. In related theoretical studies of actinide partitioning technology, Yamana and Moriyama (1996) concluded that it may be feasible to separate americium and curium from lanthanide elements by electrolytic amalgamation techniques.

8.4.2 Precipitation processes

Initially, only precipitation processes were available for recovery and purification of americium. Later, new ion-exchange and solvent extraction processes largely, but not completely, supplanted the early precipitation recovery/purification processes. Because of their insolubility and other special properties precipitation of certain compounds of americium, e.g. AmF_3, $K_8Am_2(SO_4)_7$, $Am_2(C_2O_4)_3$, $K_3AmO_2(CO_3)_3$, is routinely considered for recovery or purification of a batch of americium. The latter two compounds are useful because oxalate ion prevents certain impurities from accompanying americium in the precipitate and, also, because americium oxalate is a convenient starting point for preparation of AmO_2. The insoluble Am(V) carbonate complex is particularly useful for the large-scale separation of americium from curium (Buijs *et al.*, 1973; King *et al.*, 1973).

Hermann (1956) demonstrated that a substantial separation of americium from lanthanum can be obtained by fractional precipitation of americium and lanthanum oxalates. The precipitation is effected in homogeneous solution; the precipitant is generated by slow hydrolysis of dimethyl oxalate. The oxalate precipitate is greatly enriched in americium; about 50% of the lanthanum can be rejected at each stage with only about 4% of the americium.

Stephanou and Penneman (1952) found that Cm(iii) could be separated from americium by oxidizing the latter to Am(vi) with potassium persulfate and precipitating CmF_3; Am(vi) is soluble under these conditions. Proctor and Connor (1970) at the US DOE Rocky Flats site used precipitation of cerium peroxide to separate gram quantities of americium from cerium. Proctor (1976) also separated Am(vi) from large quantities of rare earths by precipitation of their trifluorides.

Bhanushali *et al.* (1999) have recently proposed a new application of oxalate precipitation technology for separation of americium. Based on some experimental data, these workers suggest that traces of americium and plutonium remaining in the aqueous waste generated during plant-scale precipitation of plutonium oxalate can be effectively removed by simple coprecipitation with thorium oxalate. It is not known if such a coprecipitation step has been incorporated into routine processing of plutonium in India.

8.4.3 Solvent extraction processes

Solvent extraction processes and systems using amine and organophosphorus compounds are extensively used for the initial recovery and separation of gram to kilogram amounts of americium. Excellent reviews of the solvent extraction chemistry of trivalent americium have been published by Weaver (1974) and Shoun and McDowell (1980). Myasoedov *et al.* (1974a) discussed solvent extraction systems useful for the analysis of americium.

(a) Organophosphorus extractants (Gureev *et al.*, 1970)

(*i*) *Tri*-n-*butyl phosphate* (*TBP*)

TBP is the extractant in widest use for nuclear fuel processing. Extraction of Am^{3+} from nitrate media by TBP conforms to the reaction (Weaver, 1974):

$$\mathrm{Am^{3+}(aq) + 3\,NO_3^-(aq) + 3\,TBP(org) \rightarrow Am(NO_3)_3 + 3\,TBP(org)}$$

The equilibrium constant, $K_{\mathrm{ex}} = [\mathrm{Am(NO_3)_3 \cdot 3TBP}]/[\mathrm{Am^{3+}}][\mathrm{NO_3^+}]^3[\mathrm{TBP}]^3$, has the value of 0.4 at zero ionic strength (Zemlyanukhin *et al.*, 1962). While

TBP, even undiluted, extracts americium only weakly from strong nitric acid solutions, americium is extracted by TBP quite strongly from neutral (or low-acid), highly salted nitrate solutions.

As part of their intensive effort to develop feasible partitioning–transmutation technologies, Kamashida and his coworkers investigated TBP extraction of Am(VI) from nuclear reactor fuel reprocessing solutions (Kamashida and Fukasawa, 1996; Kamashida *et al.*, 1998) as a means of removal of americium while separating it from associated trivalent rare earths (good separation of americium from rare earth elements is desirable/necessary to make efficient use of neutrons in the transmutation process). In these studies, Am(VI) was produced by oxidation of Am(III) with silver-catalyzed peroxydisulfate, both in the presence and absence of $(NH_4)_{10}P_2W_{17}O_{61}$ added to stabilize americium in the hexavalent oxidation state. By use of neat TBP to extract Am(VI) from 1 M HNO_3, an americium distribution ratio as high as 4 was realized; the separation factor from Nd(III) was 50.

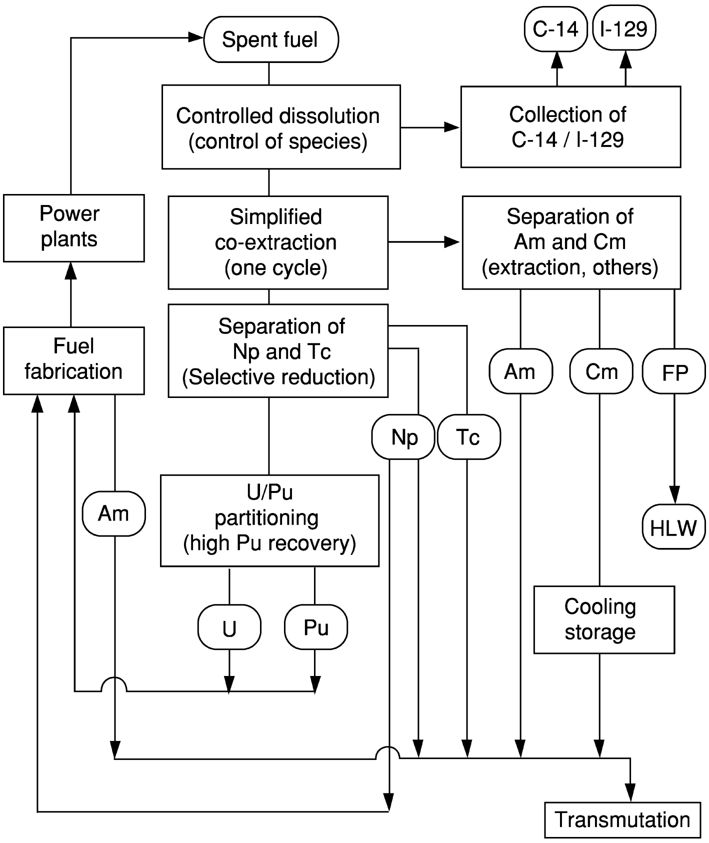

Fig. 8.1 *Schematic of Japanese PARC process* (*Uchiyama* et al., 2000).

In other recent studies, Japanese scientists have developed an advanced Purex process, the PARtitioning Conundrum Key (PARC) process (Uchiyama *et al.*, 2000). Fig. 8.1 shows a schematic diagram of the PARC process concept where americium is not separated in the mainline Purex process, but from HLW generated in the Purex process. The PARC process thus provides for use of certain organic compounds to provide effective Purex process recovery and separation of uranium, neptunium, plutonium, and technetium. Uchiyama *et al.* (2000) conducted tests of parts of the PARC process with aqueous feeds resulting from nitric acid dissolution of highly irradiated (8000 MWD/tU) fuel. Important findings were:

- Np(VI) was reduced to Np(V) by *n*-butyraldehyde selectively in the presence of U(VI), Pu(VI), and Tc(VII);
- high acid scrubbing was effective for separation of technetium;
- isobutyraldehyde reduced Pu(IV) to Pu(III) very effectively;
- *N*-butylamine compounds (carbonate and oxalate) were effective solvent-washing agents.

The French, as stated earlier, are energetically pursuing the partitioning–transmutation alternative for their Purex process HLW. Apparently for proprietary reasons, they have not widely publicized their progress. However, a recent article (NN, 2002) states: "... the Marcoule team have been able to push the current Purex processing technique to enable about 99% of uranium, plutonium, and the minor actinides of most concern, which are neptunium, americium, and curium to be isolated. The separation levels of the main long-lived fission products, which include iodine-129, technetium-99, and cesium-135, are equally impressive. The yields of iodine and technetium extracted are 95 and 90%, respectively. The process for separating cesium is nearing fruition, and technical feasibility is also expected by 2005. These levels of separation provide important benefits as the resulting vitrified waste contains fewer long-lived isotopes. According to the CEA, the radioisotopes of the advanced vitrified product – referred to as 'light glass' – will drop to the level of natural uranium in less than 300 years. This compares to more than 10000 years for the current vitrified HLW and hundreds of thousands for spent fuel." The article in *Nuclear News* does not provide any detail as to the Purex process modifications used to separate americium; it may be, just as in the Japanese PARC process, that the French plan to recover americium from the Purex process HLW by any of several available procedures.

It should be noted that formation constants of complexes formed by Am(III) with aminopolycarboxylic acids are larger than for the comparable complexes of the light lanthanides ($Z = 57$–61). Thus, addition of an aminopolycarboxylic acid to a lithium or aluminum nitrate solution containing Am(III) and rare earth enhances TBP extraction of the lanthanides relative to americium (Koehly and Hoffert, 1967). Americium can be separated from rare earths by TBP extraction from 1 M ammonium thiocyanate solution (Penneman and Keenan, 1960).

The mechanism of Am(III) and Eu(III) extraction from 1 M ammonium thiocyanate media by TBP in both the presence and the absence of a quaternary ammonium thiocyanate compound was investigated by Indian scientists (Khopkar and Narayankutty, 1971).

(*ii*) *Dibutyl butylphosphonate* (*DBBP*)

DBBP, $(C_4H_9O)_2(C_4H_9)PO$, extracts Am(III) from nitrate media more strongly than TBP and was used in a production-scale process at the US DOE Hanford site for several years (Schulz, 1976).

(*iii*) *Trialkylphosphine oxides* (*TRPO*)

It is well known that the basicity of the P–O functionality increases in going from alkyl phosphates (e.g. TBP) to alkyl phosphonates (e.g. DBBP) to alkylphosphine oxides (e.g. TRPO). Corresponding to the increased basicity is increased extractive power for trivalent actinides, e.g. Am(III) and Cm(III) from aqueous 1–2 M HNO_3 solutions. Chinese investigators have made use of the extractive power of TRPOs to develop a process for partitioning actinides, including americium and curium, from acidic Purex process HLW (Zhu and Jiao, 1994). Most of the results of Zhu *et al.* have been published in Chinese language journals, which, apparently, have not been translated into readily available English versions. Zhu and Jiao (1994) presented an admirable English language summary of their work up to 1994. They used a 30 vol% TRPO–kerosene solvent to extract trivalent (Am, Cm, lanthanides), tetravalent (Np, Pu), and hexavalent (U) actinides from both synthetic and actual Purex process HLW adjusted to about 1 M HNO_3. These experimenters used a mixture of C_6–C_8 alkylphosphine oxides available commercially (at least in the early 1990s) from operation of a fertilizer manufacturing plant. Zhu and coworkers found their particular 30% TRPO reagent to be very effective in extracting over 99% of all the actinides and lanthanides from the adjusted HLW. Extracted actinides could be stripped successively with 5.5 M HNO_3, 0.6 M oxalic acid, and 5% Na_2CO_3 solution to yield Am + rare earth, Np + Pu, and U fractions, respectively. Auxiliary experiments showed the TRPO solvent to have excellent actinide extraction kinetics and to be quite resistant to radiolytic degradation. Their highly successful batch and continuous countercurrent extraction–stripping tests led the Chinese to believe (at least in 1994) that their TRPO extractant was eminently suited for use in plant-scale partitioning of actinides from Chinese defense HLW. We, the authors, were not able to establish the present status of development/utilization of the Chinese TRPO extraction process.

Very recently, Murali and Mathur in India revisited use of TRPO for partitioning actinides from Purex process HLW (Murali and Mathur, 2001). They used a 30 vol% solution of a commercially available mixture of alkyl TRPOs (Cyanex-923) in dodecane. Cyanex-923 (Cytec Canada, Inc.) is a mixture of four alkylphosphine oxides, $R_3PO, R'_3PO, R_2R'PO, RR'_2PO$; R = hexyl and R′ = octyl. (Murali and Mathur point out that Cyanex-923 is not the same mixture of alkylphosphine oxides used earlier by the Chinese investigators.) With dodecane as the diluent, the Indian investigators found it necessary to add TBP (5–20 vol%) to the Cyanex-923-dodecane solvent to avoid formation of a third phase even after adjusting the HLW acidity to 1 M HNO_3. Under the latter conditions, Murali and Mathur were able to both successfully extract and strip actinides, including americium, from synthetic Purex process HLW. Despite this successful performance, Murali and Mathur judged, "... the TRUEX solvent (0.2 M CMPO + 1.2 M TBP in dodecane) seems to be a superior extractant for partitioning of minor actinides from HLW solutions as there is no need for any feed adjustment and it tolerates significant amounts of sulfate, fluoride, and oxalate anions." (The TRUEX process is discussed in the later part of Section 8.4.3.)

(*iv*) *Bis*(*2-ethylhexyl*)*phosphoric acid* (*HDEHP*)

HDEHP is an excellent extractant for Am(III) from certain aqueous solutions. This extractant is commercially available in large quantities, can be readily purified, and has been widely used for both analytical purposes and plant-scale recovery and purification of americium (Peppard *et al.*, 1958, 1962; Gureev *et al.*, 1964). A countercurrent HDEHP extraction process was used at the DOE Hanford site in the late 1960s as part of the processing sequence for recovering and purifying 1 kg of americium and 50 g of curium from irradiated Shippingport reactor fuel (Boldt and Ritter, 1969). An HDEHP batch extraction–strip process (Cleanex process) was routinely used in the Transuranium Processing Plant at the DOE Oak Ridge National Laboratory to reclaim americium, curium, and other transuranium elements from rework solution and/or to convert from nitrate to chloride media (Bigelow *et al.*, 1980). The Talspeak HDEHP processes are based upon the results of Weaver and Kappelmann (1964) who were the first to show that HDEHP extracts lanthanides much more strongly than actinides from aqueous carboxylic acid solutions containing an aminopolycarboxylic acid chelating agent. Lactic acid is used to avoid precipitation of solids when the concentration of lanthanides is high. HDEHP solutions have been used to selectively extract Am(VI) from Cm(III) (Musikas *et al.*, 1980a); in such systems rapid reduction of Am(VI) to lower oxidation states is a problem.

Extraction of Am(III) is very sensitive to the nature of compounds used to dilute the HDEHP (Gureev *et al.*, 1964). The kinetics of Am(III) extraction by HDEHP solutions were studied by Choppin and Nash (1977). In 1998, Indian scientists (Mapara *et al.*, 1998) studied solvent extraction of Am(III) from aqueous 0.1–1.0 M HNO_3 solutions using both HDEHP and 2-ethylhexyl phosphonic acid (PC88a in their notation). Before use, 1 M solutions of both extractants in kerosene were partially neutralized (saponified) to varying degrees with NaOH. In agreement with previously well-known chemistry of

HDEHP and PC88a, Am(III) extraction increased as more and more of the acidic extractant was converted to the sodium form.

(*v*) *Diisodecylphosphoric acid* (*DIDPA*)

Morita, Kubota, and other Japanese scientists (Morita and Kubota, 1988; Morita *et al.*, 1993) closely examined properties of solutions of DIDPA for extraction of actinides from acidic Purex process HLW. DIDPA solutions extract hexavalent (U) and tetravalent (Pu,Np) actinides quite efficiently from 1 to 3 M HNO_3 media. (Before extraction of ^{237}Np, however, it must be first reduced to Np(IV) by reduction of Np(V) and Np(VI) with hydrogen peroxide.) But, a disadvantage of the DIDPA extraction technique is that trivalent americium and curium do not extract well at feed acidities much above about 0.5 M HNO_3. Once extracted, Am(III) and Cm(III) can be selectively stripped with a diethylenetriaminepentaacetic acid (DTPA) solution; lanthanides can be easily stripped with 4 M HNO_3; and plutonium and neptunium can be removed from the organic phase by stripping with an aqueous oxalic acid solution. Japanese tests, both batch and countercurrent, of the DIDPA process with simulated Purex process HLW were generally regarded as successful.

(*vi*) *Neutral multifunctional organophosphorus and carbamoylphosphonate reagents*

Monofunctional organophosphorus extractants, e.g. TBP, DBBP, tri-*n*-octylphosphine oxide (TOPO), do not extract Am(III) from strongly acidic (>1 M HNO_3) aqueous solutions. Such behavior is desirable when the goal decades ago was to separate and purify plutonium and uranium from nitric acid solutions of irradiated nuclear fuel, e.g. the Purex process. But, evolving nuclear waste management strategies and policies have driven an urgent need for liquid–liquid extraction agents and processes capable of effective recovery and/or removal of Am(III) and Cm(III) as well as actinides in the +4 and +6 oxidation states from strong nitric acid medium. Thus, in the USA in the 1970s and 1980s there was an economic incentive to convert so-called transuranic acidic waste solutions containing ^{241}Am and various other actinides, chiefly plutonium, to low-level waste, which could be disposed of inexpensively. And, of course, the emergence of the partitioning–transmutation philosophy for advanced nuclear waste management and disposal places a premium on solvent extraction technology for efficient removal of trivalent actinides from acidic HLW solutions.

In the early 1960s, Siddall (1963, 1964) opened the door to the desired practical solvent extraction schemes for extraction of trivalent americium and curium from concentrated nitric acid solutions. Siddall in his papers noted that certain bifunctional organophosphorus reagents, e.g. diphosphonates and carbamoylmethylphosphonates (CMPs), i.e. compounds of the type $(R_1O)_2P(O)$—$(CH_2)_n$—(O)C—N—$(R_2)_2$, were especially effective in extracting trivalent actinides and lanthanides from strong nitric acid solutions.

Siddall's highly significant work lay buried in the literature until resurrected by Schulz and coworkers (Schulz, 1974, 1975; McIsaac and Schulz, 1976; Schulz and Navratil, 1982) in the early and middle 1970s. Both Schulz at the US DOE Hanford site and McIsaac at the US DOE Idaho site were motivated to develop solvent extraction processes for removing Am(III) and Pu(IV) from certain site acid waste solutions to convert the large volumes of these wastes to more easily managed and disposed of low-level wastes.

Based upon Siddall's data, both Schulz and McIsaac elected to use dihexyl-*N*,*N*-diethylcarbamoylmethyl phosphonate (DHDECMP) as the extractant for Am(III) and 4+ and 6+ actinides. Siddall's results indicated that CMPs were better extracting agents for 3+ actinides than diphosphonates. Another candidate, dibutyl-*N*,*N*-diethylcarbamoylmethylphosphonate, was rejected for use because of its high solubility in aqueous phases. Finally, of considerable significance, DHDECMP was available in liter quantities, albeit in a highly impure state (50–70% DHDECMP), from the Wateree Chemical Co. in South Carolina.

Batch tests with the impure DHDECMP solvent at both the Hanford and the Idaho sites quickly confirmed Siddall's results and demonstrated that this particular reagent would indeed permit efficient removal of all actinides from actual candidate acidic wastes. Auxiliary tests soon showed DHDECMP were sufficiently resistant to radiolysis, both alpha and gamma, to have a long useful life in plant-scale continuous countercurrent operations, especially in short residence time contacting equipment. Kinetics of actinide extraction and stripping were sufficiently rapid for satisfactory operation of continuous countercurrent contactors. The propensity of 20–30 vol% DHDECMP–NPH (normal paraffin hydrocarbon) solvents to form a third phase (second organic phase) when contacted with some acidic (HNO_3) waste solutions was overcome by either changing to an aromatic diluent, e.g. tetrachlorobenzene or decalin, or substituting TBP for a large portion of the NPH diluent. All the batch contact experiments culminated in chemical flowsheets (extraction–scrub–strip) that were very successfully demonstrated with both actual Idaho and Hanford sites acid waste solutions.

The only serious discordant note observed in tests with the impure Wateree Chemical Co. DHDECMP arose in attempts to use very dilute, e.g. ~0.01 M HNO_3 solutions to selectively strip 3+ actinides and lanthanides from pregnant organic phases. With as-received DHDECMP extractant D_{Am} instead of decreasing regularly upon successive strip contacts actually increased, resulting in a certain fraction of unstrippable americium. Such behavior is very symptomatic of the presence of an acidic organic compound in an otherwise neutral extractant. To overcome the deleterious effects of the acidic organic impurity, the 20–30 vol% DHDECMP solvent, before use, was subjected to various empirical chemical treatments designed to remove or at least reduce the concentration of the impurity, e.g. washing with ethylene glycol or alternate washing with HCl and NaOH solutions to hydrolyze the organic impurity. These chemical treatments, although cumbersome, removed enough of the offending impurity to allow successful selective stripping of americium in continuous countercurrent flowsheet tests.

Tetravalent actinides and, if not previously removed, trivalent actinides were easily and effectively stripped from the DHDECMP phase with aqueous solutions containing fluoride or oxalate ions. And, as would be expected, dilute NaOH solutions effectively removed all 3+, 4+, and 6+ actinides from the DHDECMP solvent.

Following publication of the Schulz and McIsaac work, many other investigators, both in and outside the USA, conducted comprehensive experimental studies with DHDECMP and various other CMP-type reagents (Martella and Navratil, 1979; Petrzilova *et al.*, 1979; Horwitz *et al.*, 1981; Kalina *et al.*, 1981b; Hugen *et al.*, 1982; McIsaac, 1982; McIsaac and Baker, 1983; Kalina and Horwitz, 1985; Mathur *et al.*, 1991, 1992b). Indeed, as late as 1994, long after the TRUEX process had been proposed (cf. Section 8.4.3a(vi)), Rapko and Lumetta (1994) were still investigating use of a 0.75 M DHDECMP–1.05 M TBP/NPH solvent for extracting U(VI), Pu(IV), and Am(III), as well as competing metal ions, e.g. Fe(III), Zr(IV), from nitric acid solutions. And, in the late 1980s DHDECMP-based flowsheets were still under consideration for removal of all actinides from the DOE Idaho site sodium-bearing waste. Most of the work with CMP-based reagents after the early Schulz and McIsaac studies were done with DHDECMP; some investigators, however, synthesized various other CMP-type compounds to investigate their capability for extracting 3+ as well as 4+ and 6+ actinides from various acid waste solutions.

As discussed in the next section, CMP processes for efficient extraction of Am(III) and other actinides from acidic media have been supplanted and superseded by advanced organophosphorus reagent technology. Even so, the significance of the pioneering work of Schulz and McIsaac cannot be overstated. Through their efforts, scientists and engineers throughout the world became aware of Siddall's papers and the great potential of multifunctional organophosphorus reagents in actinide separation and recovery from many other sources.

Carbamoylphosphine oxide reagents

"CMPO" is a generic acronym for any carbamoylmethylenephosphine oxide. CMPO is also used here and elsewhere in the literature to denote one particular compound, namely, octylphenyl-*N*,*N*-diisobutylmethylenecarbamoylphosphine oxide, $(C_8H_{17})(C_6H_5)P(O){-}CH_2{-}(O)C{-}N{-}N{-}(iC_4H_9)_2$. The actinide separation community is indebted to Dr E. P. Horwitz and his colleagues for their innovative efforts in initially synthesizing this particular CMPO and in evaluating many of its outstanding properties.

Being familiar with the Schulz and McIsaac results with DHDECMP (Section 8.4.3a(vi)), and having worked with this carbamoylphosphonate, Horwitz was motivated to find an improved trivalent actinide extractant with the following highly desirable attributes:

- Greatly increased capability for extracting 3+ actinides.
- Ease of synthesis of high-purity reagent.
- Increased solubility/compatibility with straight-chain hydrocarbon diluents.
- Excellent chemical and radiolytic stability.
- Suitability of extractant-diluent(s) solution for use in centrifugal contactors.
- Satisfactory selectivity for actinide and lanthanide extraction from aqueous media.

Horwitz's aspirations were essentially realized with the synthesis of the octylphenyl CMPO compound and the many successful tests of this reagent.

Gatrone and coworkers (Gatrone and Rickert, 1987; Gatrone *et al.*, 1987, 1989) published complete details of the synthesis of CMPO via a Grignard reaction. The crude CMPO product from the Grignard synthesis contains one or more acidic organophosphorus impurities that seriously interfere with the use of dilute nitric acid solutions to strip trivalent actinides and lanthanides. After testing various purification schemes, Gatrone and coworkers concluded that the most effective way to remove the offending acidic compounds was to first contact a heptane solution of the CMPO with 50 g L^{-1} of a macroporous cation-exchange resin at 50°C and then, without removing the cation resin, contact the heptane–CMPO solution with 50 g L^{-1} of a macroporous anion-exchange resin. This procedure, which Gatrone and his collaborators believe is generic and applicable to removal of acidic compounds from anyneutral organophosphorus extractant, yields solvent extraction-grade CMPO, i.e. $D_{\mathrm{Am}} = <0.02$ in 0.01 M HNO_3/CMPO.

Many different diluents have been used in bench-scale studies of the extraction properties of solvent extraction-grade CMPO. Candidate diluents used at one time or another include aromatic (decalin), chlorinated (tetrachloroethylene), and aliphatic (dodecane) commercially available mixtures of C_{10}–C_{12} NPHs. For plant-scale application of CMPO a mixture of NPHs is the preferred diluent. However, HNO_3 and metal nitrates, e.g. lanthanide nitrates, have only a very limited solubility in CMPO/NPH solutions; once the solubility limit is exceeded, the organic phase splits into two phases (familiar third-phase formation phenomenon). Horwitz *et al.* (1985b) found that a simple and highly effective way to avoid the complications of a third-phase formation is to dilute the CMPO extractant with Purex process solvent to yield, for example, a 0.2 M CMPO/1.2 M TBP/dodecane solution. This solvent composition allows the CMPO fraction to be loaded to near theoretical capacity with trivalent lanthanides without causing a second organic phase to form. And, of course, an added advantage of the latter solvent composition is that its physical properties are little changed from those of familiar Purex process solvent and, therefore, no mechanical difficulties are encountered in operating centrifugal (or other) contactors with the CMPO/TBP/dodecane (or NPH) solvent. Horwitz and coworkers (Kalina *et al.*, 1981a; Horwitz *et al.*, 1982, 1985b, 1986; Horwitz and Kalina, 1984; Kolarik and Horwitz, 1988), as well as many other investigators (Liansheng *et al.*, 1991; Mathur *et al.*, 1992a; Rapko, 1995), conducted comprehensive bench-scale studies to establish the extractive properties of CMPO/TBP/diluent solvents for many different metal ions over a wide range of conditions. Most of these studies were concerned with the extraction of actinides and other metal ions from nitrate-based aqueous media with CMPO/TBP/dodecane (or NPH) solvent, but some work has been done with aqueous HCl solutions (Horwitz *et al.*, 1987). All these bench-scale studies confirmed that the CMPO/TBP/diluent mixture would efficiently extract trivalent actinides and lanthanides as well as 4+ and 6+ actinides from almost any strong, i.e. ca. 1 M, nitric acid solution. Indeed, the more or less constant distribution ratio values for Am(III), Pu(IV), and U(VI) between 1 and 6 M HNO_3 is a very valuable and unique aspect of the CMPO/TBP system.

While the lanthanides and actinides are extracted almost quantitatively by CMPO/TBP/diluent solutions, with only a few exceptions most common metal ions in nuclear waste solutions are not extracted by the CMPO reagent (Horwitz *et al.*, 1985b). Not unexpectedly, Zr(IV) is significantly extracted ($D_{Zr} = \sim 1–3$) by CMPO/TBP/diluent solution from aqueous 1 M HNO_3. Zirconium is one of the major constituents of the DOE Idaho site waste; this particular waste also contains large concentrations of fluoride ion, which, fortunately, greatly inhibits CMPO extraction of inert zirconium (McIsaac and Baker, 1983). Paralleling known Purex process experience, ^{99}Tc, if present, is also well extracted (D_{Tc} = 1–3) from nitric acid feed solutions as the $HTcO_4$ species. (Technetium largely remains in the CMPO phase during actinide scrubbing and stripping stages and is removed when the CMPO phase is washed with alkaline carbonate solutions to remove degradation and other species.) Other metallic contaminants of some interest (D_M = 0.1–0.6) include Mo, Ru, Pd, Ag, and Fe; these constituents are present in nearly all nuclear waste solutions that contain Am and other actinides. Adequate separation of actinides from the latter metal ions in CMPO extraction systems can be controlled by adding oxalic acid to the feed solution and/or by scrubbing the CMPO extract with a dilute oxalic solution before stripping of actinides.

To strip actinides from the CMPO/diluent or, more commonly, CMPO/TBP/NPH phase, conventional practice is to selectively strip, in order, 3+ actinides and lanthanides, 4+, and, if present, 6+ actinides. For this order of actinide stripping, preferred reagents (Mathur *et al.*, 2001) are, respectively, dilute nitric acid, e.g. <0.05 M HNO_3; a dilute oxalic acid, dilute ammonium oxalate, or a mixture of HF and HNO_3, e.g. 0.05 M HNO_3/0.05 M HF; and dilute sodium carbonate, e.g. 0.25 M Na_2CO_3. Sodium carbonate solutions do double duty and also act as a solvent cleanup reagent to remove solvent degradation products. But, in the case where it is desired to strip all the 3+, 4+, and 6+ actinides and lanthanides into a single aqueous phase, Horwitz and Schulz (1990) recommended use of a solution of either vinylidene-1,1-diphosphonic acid (VDPA) or 1-hydroxyethylene-1,1-diphosphonic acid (HEDPA). Also, in a novel approach, Rizvi and Mathur (1997) utilized the ferrocyanide ion to co-strip actinides and lanthanides from CMPO phases. Other stripping agent studies of interest are those of Chitnis *et al.* (1998, 1999) who used a mixture of formic acid, hydrazine hydrate, and citric acid to remove Am(III) and Pu(IV) from CMPO solutions. Finally, Ozawa *et al.* (1998) reported that a mixture of hydrazine oxalate, hydrazine carbonate, and tetramethylammonium hydroxide will selectively strip 3+, 4+, and 6+ actinides from CMPO extractants.

A matter of concern for any liquid–liquid extraction process, especially one dealing with radionuclides, is the resistance of the extractant and its diluents to chemical and radiolytic degradation. Five separate studies (Chiarizia and Horwitz, 1986, 1990; Nash *et al.*, 1988, 1989; Mathur *et al.*, 1998) addressed this concern for CMPO extraction systems. Three of these investigations were concerned only with CMPO/TBP/dodecane solvents while two (Chiarizia and Horwitz, 1986; Nash *et al.*, 1988) also addressed radiolysis of CMPO diluted with decalin or tetrachloroethylene. Test solvents were irradiated both neat and while in contact with aqueous nitric acid solutions. Although results varied to some degree with the reagent used to dilute the CMPO and TBP, the general degradation behavior of CMPO/TBP/diluent solvent was independent of the nature of the diluent. Thus, the general degradation behavior is that chemical hydrolysis produces only acidic degradation products while radiolysis generates both neutral and acidic organophosphorus compounds.

The neutral organophosphorus degradation products of CMPO serve only as diluents for CMPO and TBP. But the acidic radiolytic degradation products are highly troublesome because they seriously interfere with stripping of Am(III) by dilute (<0.05 M HNO_3) solutions. Mathur *et al.* (2001) have published an excellent table, based on data obtained by Mathur *et al.* (1998) that illustrates very markedly the increase in the distribution ratio for Am(III) at 0.04 M nitric acid upon irradiation of a 0.2 M CMPO/1.2 M TBP/dodecane solvent to a total absorbed dose of 26–28 Mrad. According to these data, up to a dose of about 20 Mrad the distribution ratio of Am(III) at 0.04 M nitric acid is less than 1 and, hence, stripping with 0.04 M nitric acid should still be possible. Also, up to a dose of about 20 Mrad washing the spent solvent with a dilute sodium carbonate solution will remove most of the acidic degradation products. But, at higher absorbed radiation doses, in addition to sodium carbonate washing, it is necessary to provide a secondary solvent cleanup step, i.e. treatment with macroporous anion and cation-exchange resins or treatment with basic alumina.

In 1985, Horwitz and his collaborators (Horwitz and Schulz, 1985, 1986, 1990, 1999; Horwitz *et al.*, 1985a,b; Schulz and Horwitz, 1988) proposed a generic actinide solvent extraction process, the TRUEX process (Table 8.2) based on the superior properties of CMPO to remove all 3+, 4+, and 6+ actinides from any nitrate-based aqueous nuclear waste solution. The generic

Table 8.2 *Applications of the TRUEX process.*

Year	*Country*	*References*	*TRUEX process application/demonstration*
1985	USA	[1]	Removal of Am and Pu from Hanford complexant concentrate waste
1985	USA	[1]	Removal of Am and other actinides from Hanford single-shell tank sludges
1985–1991	USA	[2]	Removal of Am and other actinides from Hanford neutralized cladding removal waste
1988	USA	[3]	Removal Am and Pu from Hanford plutonium finishing plant waste
1988–1989	Italy	[4]	Removal of actinides from MOX fuel fabrication waste and waste from analytical laboratories
1992–1998	Japan	[5]	Removal of actinides from actual Purex process high-level waste
1993–1998	India	[6]	Removal of actinides (Am, Cm, Pu, Np, U) from synthetic pressurized water reactor reprocessing Purex process waste
1993–1998	India	[6]	Removal of actinides (Am, Cm, Pu, Np, U) from synthetic Purex process sulfate-bearing high-level waste (SBHLW)
1994–2000	India	[7]	Recovery of Pu and U from oxalate precipitation process waste
1997	USA	[8]	Removal of actinides from actual Argonne National Laboratory analytical wastes
1998	USA	[9]	Removal of actinides from Idaho site actual sodium-bearing waste
1998	USA	[10]	Removal of actinides from actual dissolved Idaho site calcine waste

[1] (Horwitz *et al.*, 1985b); [2] (Swanson, 1991; Lumetta and Swanson, 1993a,b); [3] (Schulz and Horwitz, 1988); [4] (Casarci *et al.*, 1988, 1989); [5] (Ozawa *et al.*, 1992, 1998); [6] (Deshingkar *et al.*, 1993, 1994; Chitnis *et al.*, 1998); [7] (Mathur *et al.*, 1994; Michael *et al.*, 2000); [8] (Chamberlain *et al.*, 1997); [9] (Law *et al.*, 1998a); [10] (Law *et al.*, 1998b).

TRUEX process, which utilizes a nominal 0.2 M CMPO/1.05 M TBP/dodecane (or other NPH-type diluent) solvent, is intended for use in short residence time centrifugal contactors. It typically comprises four separate operations: extraction, scrubbing of the organic phase, one or more stripping steps, and solvent cleanup. The users of the TRUEX process are free to specify whatever the number of extraction stages and organic-to-aqueous phase flow ratios are required to provide the required degree of removal of Am(III) and other actinides. Similarly, the TRUEX process operator is responsible for choosing the number of scrub stages (if any) and the composition of scrub solution(s) needed to adequately remove any co-extracted impurities, e.g. Zr(IV). The generic TRUEX process allows, by choosing particular aqueous phase strip compositions, either selective stripping of 3+, 4+, and 6+ actinides or stripping of combinations of actinides, e.g. 3+ and 4+ or 4+ and 6+. One or two contactor stages for washing the stripped TRUEX process solvent with a dilute sodium carbonate solution are typically included to remove solvent degradation products and any traces of metal ions. Investigators in several countries have conducted continuous countercurrent demonstrations of variations of the TRUEX process with actual radioactive waste solutions of interest to them: references cited in the following list should be consulted for further details:

For various reasons, including the prolonged Cold War syndrome, Russian scientists, largely independent of Western world progress, conducted extensive studies of the actinide extraction properties of multifunctional organophosphorus reagents (Myasoedov *et al.*, 1980, 1986; Chmutova *et al.*, 1983, 1989; Myasoedov and Lebedev, 1991). A recent review paper by Myasoedov (1994) is of special interest. The Russian version of the American TRUEX process utilizes diphenyl-*N*,*N*-dibutylcarbamoylmethylenephosphine oxide dissolved in a commercially available (at least in Russia) fluoroether diluent (Fluoropol 732). According to Russian investigators, use of the fluoroether diluent eliminates any need to dilute the diphenyl CMPO with TBP to avoid third-phase formation; but others (Horwitz and Schulz, 1999) have expressed concern that diluent degradation under plant-scale conditions could lead to undue formation of corrosive HF. The Russian transuranium element extraction process behaves very similarly (Myasoedov, 1994) to the TRUEX process in its efficiency for extracting trivalent americium; in continuous countercurrent tests of the process in centrifugal extractors greater than 99.5% of the actinide elements in the aqueous feed were removed. In addition to the possibility of excessive generation of HF, other possible limitations to the Russian process include difficult americium stripping because of the need to use a very low concentration of nitric acid in the aqueous strip solution and complex solvent cleanup before reuse of the solvent (Horwitz and Schulz, 1999). In addition to the americium extraction results discussed earlier in Section 8.4.3a, certain other, more academically oriented studies of the extraction characteristics of novel phosphate-based reagents are of interest. For example, Paine and his research group (Bond *et al.*, 1997, 1998) investigated the extraction of Am(III) by 1,6-bis(diphenylphosphino)methyl-pyridine-*N*,*P*,*P*′-trioxide solutions from both hydrochloric and nitric acid media. And, Mishra *et al.* (1996) investigated the synergistic extraction of Am(III) by a mixture of Aliquat 336 and TOPO from acidic nitrate medium.

Rais and Tachimori (1994) studied the synergism in extraction and separation of Am(III) and Eu(III) in two systems: (1) dicarbollide anion and dibutyldiethylcarbamoylmethylenephosphonate (DBDECMP) and (2) dicarbollide anion and CMPO. Synergism was observed in both systems at low aqueous phase acidities but the effect was lower with CMPO than with DBDECMP.

Mohapatra and Manchanda (1995, 1999) reported on the unusual extraction behavior of Am(III) and UO_2^{2+} from aqueous picric acid solutions by TBP and TOPO extractants. Surprisingly, under these conditions, the organophosphorus compounds extract Am(III) better than the uranyl ion. Of course, from aqueous nitrate media, TBP and TOPO both extract U(VI) much better than Am(III). Mohapatra and Manchanda attribute the different extraction order from picric acid media to the formation of outer sphere rather than inner-sphere coordination complexes.

(b) Amine extractants

Nitrogen-based extractants, especially tertiary amines and quaternary ammonium compounds, are particularly effective in separating and recovering americium and other actinide elements from aqueous media.

(*i*) *Tertiary amine salts*

Tertiary amine salts extract Am^{3+} poorly from concentrated nitric or hydrochloric acids but extract it very strongly from concentrated nitrate or chloride solutions of low acidity (Myasoedov *et al.*, 1974a). Marcus *et al.* (1963) and Horwitz *et al.* (1966) found that Am^{3+} is extracted from nitrate media as complex $(R_3NH)_2Am(NO_3)_5$. A much more detailed account of the application of tertiary amine salts to extract americium is provided in Schulz (1976); indeed, essentially all the reported results obtained with tertiary amine salts in extraction of americium have been summarized in Schulz (1976).

(*ii*) *Quaternary ammonium salts*

Quaternary alkylammonium nitrate salts were shown by Horwitz *et al.* (1966) to extract Am^{3+} considerably more efficiently from low-acid, highly salted aqueous nitrate solutions than do tertiary alkylamines. The extraction sequence for trivalent actinides into either Aliquat 336 (a mixture of trioctylmethylammonium and tridecylmethylammonium salts made by General Mills, Inc.) nitrate or trilaurylmethylammonium nitrate is Cm<Cf<Am<Es. Horwitz *et al.* (1969) included an extraction step with Aliquat 336 in the preparation of 20–30 Ci of high-purity ^{242}Cm. Koch and Schoen (Koch and Schoen, 1968; Koch, 1969) devised and tested on a laboratory scale a quaternary ammonium extraction process for the isolation of ^{241}Am from aged plutonium scrap. Advantages of a quaternary ammonium nitrate extraction process over other schemes, e.g. Tramex process, for isolating trivalent lanthanides and actinides were discussed by Moore (1966a). Finally, Moore (1964, 1966b) and later Gerontopulos *et al.* (1965) found that the thiocyanate salt of Aliquat 336 preferentially extracts actinides over lanthanides in moderately concentrated NH_4SCN solutions.

(c) Amide extraction reagents

Diamide extractants are generally organic compounds with the generic formula $(R_1,R_2)N–C(O)–CR_3H–C(O)–N(R_1,R_2)$ where R_1, R_2, and R_3 are (typically) alkyl substituents. For various reasons, including doubtlessly their well-recognized nationalistic pride, French investigators have chosen to focus on diamides for possible application in partitioning of americium and other actinides from aqueous Purex process HLW vis-à-vis one of the more well-known and tested carbamoylphosphonates or phosphine oxides. Interestingly, various researchers including the French repeatedly extol the virtues of the carbon, hydrogen, oxygen, nitrogen (CHON) principle, i.e. design and use of liquid–liquid extraction reagents that contain neither sulfur nor phosphorus. Supposedly, degraded CHON-type extractants would be easier to dispose of, e.g. incinerate, than spent extractants that contain phosphorus or sulfur; there are no economic or technical data and/or experience to support the latter claim.

Between 1987 and 2002, numerous diamide compounds have been synthesized and examined for their ability to extract actinides in various oxidation states from aqueous nitric acid solutions. Details and results of these studies were reported (Musikas and Hubert, 1983; Musikas, 1987, 1995; Charbonnel and Musikas, 1988; Cuillerdier *et al.*, 1991a,b, 1993; Musikas *et al.*, 1991; Baudin *et al.*, 1993; Madic *et al.*, 1994; Nigond *et al.*, 1994; Shen *et al.*, 1996; Tan *et al.*, 1999).

Currently, one diamide, namely, *N*,*N*′-dimethyl-*N*,*N*′-dibutyl-2-tetradecylmalonamide (DMDBTDMA) appears particularly suitable for use in plant-scale removal of actinides from Purex process HLW. In France DMDBTDMA has been chosen as the extractant in their DIAMEX process for partitioning of actinides from Purex process HLW. Experiments show that DMDBTDMA is soluble in dodecane and does not produce a third phase when dodecane solutions are contacted with 3–4 M HNO_3. Indian scientists (Mahajan *et al.*, 1998) have also studied DMDBTDMA extraction of Am(III), U(VI), Np(IV), Fe(III), Sr(II), and Cs(I) from various nitric acid solutions and also from a simulated HLW, which would result from reprocessing of commercial pressurized water reactor fuel. These latter experiments confirm that DMDBTDMA is very promising for extraction of Am(III) and other actinides from 3 to 4 M HNO_3, particularly under high solvent loadings of neodymium or neodymium plus uranium.

Even after two decades, diamide extraction of actinides from nitric acid media is a continuing fertile research area. For example, Spjuth *et al.* (2000) have recently prepared seven new malonamide extractants by placing phenyl substituents on the nitrogen atoms in the malonamide or an ether oxygen into the bridging chain. The basicity of such compounds is reported to be less than that of DMDBTDMA, which makes them slightly better extractants for Am(III).

Sasaki and Tachimori (2002) have recently synthesized diamide extractants that they term 'structurally tailored diamides.' The diamides investigated include $(CH_2)_n$–$(CONR_1R_2)_2$ ($n = 0$, 1, 2, and 3); O–$((CH_2)_{n'}$–$CONR_1R_2)_2$; S–$((CH_2)_{n''}$–$CONR_1R_2)_2$; and SS–$((CH_2)_{n'''}$–$CONR_1R_2)_2$, (n', n'', $n''' = 1, 2$). The diglycolamide introducing an ether oxygen into the main structure, O–$(CH_2$–$CONR_1R_2)_2$, exhibits the highest extractability for An(III), An(IV), and An(VI) compared with the other bidentate diamides. The results of Sasaki and Tachimori also demonstrated that the thiaglycolamide, which substitutes an ether sulfur atom or oxygen in the molecule also enhances the extraction of actinides.

(d) Separation of americium from lanthanides

The challenge of separating Am(III) from trivalent lanthanides was first addressed and resolved by Weaver and Kappelmann (1964) as early as 1964. These investigators devised the Talspeak process that is based upon the fact that HDEHP solutions extract trivalent lanthanides much more strongly than trivalent actinides from aqueous carboxylic acid solutions containing an aminopolycarboxylic acid chelating agent.

A reverse Talspeak process involves, naturally, using an aqueous solution of an aminopolycarboxylic acid (e.g. DTPA) to preferentially strip Am(III) (and Cm(III) also if present) from an organic phase containing both trivalent actinides and lanthanides. In the DIDPA extraction process (Section 8.4.3a(v)) an aqueous lactic acid solution containing DTPA is used to strip trivalent americium and curium (Persson *et al.*, 1984); lanthanides remaining in the DIDPA phase are subsequently stripped with 4 M HNO_3.

In yet another application of the Talspeak process technology, the Japanese SETFICS (Solvent Extraction for Trivalent f elements Intragroup separation in CMPO-complexant System), a typical TRUEX process extraction stage, utilizes an aqueous 0.4 M $NaNO_3$ solution containing DTPA (Koma *et al.*, 1998). In a countercurrent test of the SETFICS process with radioactive feed, the reported ^{144}Ce/^{241}Am decontamination factor was 72.

The renewed focus on partitioning–transmutation technology that began in the 1980s (and continues unabated to this day) prompted many new studies of technology for separation of trivalent actinides from trivalent lanthanides. (See the review of the subject of lanthanide/actinide separations (Nash, 1994).) The breakthrough to more efficient lanthanide/actinide separation technology originated with Musikas in France who pointed out that soft-donor extractant molecules containing nitrogen or sulfur functionalities offered great potential to achieve the desired separation (Musikas *et al.*, 1980b; Musikas, 1984). In work published in the late 1970s and mid-1980s, Musikas reported that an extractant consisting of tripyridyltriazene (TPTZ) and dinonylnapthalene sulfonic acid (HDNNS) in carbon tetrachloride preferentially extracted Am(III) from a dilute nitric acid solution containing Am(III) and trivalent lanthanides. In 1985, Musikas in his paper noted that the HDNNS could be replaced by bromocapric acid in an aliphatic hydrocarbon diluent.

Musikas' seminal work in the mid-1980s has triggered a cascade of studies of the ability of other nitrogen (and also sulfur)-containing extractants to provide separation of trivalent actinides from trivalent lanthanides. Noteworthy examples of such research efforts, not in chronological order, include work by Ensor and coworkers (Ensor *et al.*, 1988; Smith *et al.*, 1989), who used the synergistic combination of 4-benzoyl-2,3-dihydro-5-methyl-2-phenyl-3H-pyrazol-3-thione and 4,7-diphenyl-1,10-phenanthroline as an extractant to separate trivalent americium and europium, in the USA; Ensor *et al.* reported Am/Eu separation factors of greater than 10 with this synergistic combination of reagents. In Germany, Kolarik *et al.* (1999) investigated an extraction system based on polyaza ligands, e.g. 2,6-di-(5,6-dipropyl-1,2,4-triazin-3-yl) pyridenes for selective extraction of trivalent actinides from 1.9 M NH_4NO_3/HNO_3 solutions. Kolarik *et al.* reported Am/Eu separation factors in the range 100–120. And, of course Madic and Hudson (1998) as late as 1998 were still investigating TPTZ extraction systems for separating trivalent actinides from associated lanthanides in France. Madic's latest efforts center around attempts to suppress the solubility of TPTZ in aqueous phases by placing alkyl substituents at the 2-pyridyl rings and in replacing bromocapric acid by other anion sources.

An effective nitrogen-based soft-donor extractant for separation of trivalent actinides and lanthanides clearly would adhere to the CHON principle. But, unfortunately, to date at least, research efforts from 1987 to 2002 do not appear to have yielded a nitrogen-based 3+ actinide extractant suitably effective and stable for use on a plant scale with radioactive aqueous nitrate media. Conversely, because of recent breakthrough research results obtained by Zhu and his coworkers, prospects for developing a sulfur-based soft-donor extractant (non-CHON-type) suitable for plant-scale application appear to be reasonably good. In 1996, Zhu and coworkers reported that the compound bis(2,3,4-trimethylpentyl)-dithiophosphinic acid dissolved in a suitable diluent, e.g. heptane, preferentially extracted Am(III) from Eu(III) in aqueous nitrate media (Zhu, 1995; Zhu *et al.*, 1996b, 1998); Zhu and his collaborators found a separation factor as high as 5900 in favor of Am(III). Of particular interest and advantage, bis(2,3,4-trimethylpentyl)-dithiophosphinic acid is marketed commercially by Cyanamide Canada, Inc. under the trade name Cyanex 301; Cyanex 301 contains 77.2% of the dithiophosphinic acid compound. The primary impurities in Cyanex 301 are 14.6% R_3PS, 3.5% R_2POOH, and 0.8% R_2PSOH (Zhu *et al.*, 1996b). Chen *et al.* (1996) developed a scheme for upgrading commercially supplied Cyanex 301 to >99% bis(2,3,4-trimethylpentyl)-dithiophosphinic acid.

The excellent results obtained by Zhu and his coworkers with as-received Cyanex 301 were quickly confirmed in work at Florida State University by Zhu *et al.* (1996a). Data in Fig. 8.2 clearly illustrate the propensity of Cyanex 301 solutions to provide clean separation of Am(III) from trivalent lanthanides in

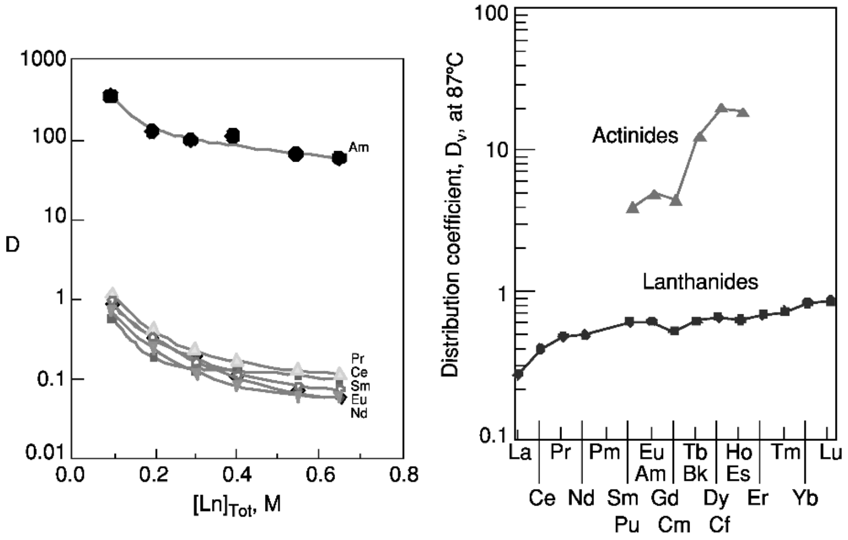

Fig. 8.2 *Distribution ratios of Am*(III) *and Ln*(III) *in* 1.0 M *Cyanex* 301-*heptane* (16 mol% *of Cyanex* 301 *neutralized before extraction contacts*) (*left*) (*Zhu* et al., 1996a). *Distribution coefficients of actinides and lanthanides into Dowex* 1 × 8 *resin from* 10 M *LiCl* (*right*) (*Hulet* et al., 1961).

pH 3 aqueous media. In later work, Modolo and Odoj (1998) also confirmed the initial results of Zhu and his collaborators with Cyanex 301. One very successful continuous countercurrent test of a Cyanex 301-based trivalent actinide/lanthanide separation flowsheet was made; using three extraction and two scrub stages >99.9% of Am(III) was separated from a trace amount of Eu with <0.1% extraction of Eu (Modolo and Odoj, 1998).

An immediate and continuing concern about plant-scale use of Cyanex 301 (or for that matter, any sulfur-based extractant) in a rather hostile environment, e.g. high nitrate concentration–high radiation zone, is its chemical and radiolytic stability. With respect to chemical stability, Sole *et al.* (1993) found that Cyanex 301 exhibits satisfactory resistance to chemical degradation when in contact with aqueous sulfuric acid, hydrochloric acid, and nitric acid solutions provided that the nitric acid concentration is maintained at (or less) than 2 M. With respect to radiolytic stability, one study found that irradiation of Cyanex 301 produces dialkylmonothiophosphonic acid, dialkylphosphinic acid, and other phosphorus compounds (Chen *et al.*, 1996). Purified Cyanex 301 separates tracer amounts of Am(III) from tracer amounts of Eu(III) even after irradiation to a cumulative dose of 10^5 gray; commercially available Cyanex 301 only performs satisfactorily at radiation doses up to 10^4 gray. The practical plant-scale consequences of the relatively poor resistance of Cyanex 301, even purified, to radiolysis would be reflected in the need to conduct countercurrent extraction operations in short residence time equipment, e.g. centrifugal contactors, and, likely, frequent extractant inventory change-outs.

In addition to its relatively poor resistance to radiolytic degradation, Modolo and Odoj (1999) note another serious disadvantage to the use of Cyanex 301 to separate trivalent lanthanides and actinides, namely, the need to conduct extraction operations at an aqueous feed pH of 3 or higher. This latter need derives directly from the mechanism whereby Cyanex 301 humic acid (HA) extracts Am(III) and Eu(III):

$$\mathrm{M}^{3+}_{\mathrm{aq}} + 2(\mathrm{HA})_{2\ \mathrm{org}} \rightarrow \mathrm{MA}_3(\mathrm{HA})_{\mathrm{org}} + 3\mathrm{H}^{+}_{\mathrm{aq}} \text{ where } \mathrm{M} = \mathrm{Am}, \mathrm{Eu}$$

Three protons are released during the extraction operation; thus, Cyanex 301 only becomes an effective extractant at aqueous phase pH of 3 or more.

Modolo and Odoj (1999) recently synthesized and tested a new class of aromatic dithiophosphinic acids as separating agents for trivalent actinides and lanthanides. These compounds are conveniently represented as R_2PSSH with $R = C_6H_5$, ClC_6H_4, FC_6H_4, and $CH_3C_6H_4$. Modolo and Odoj achieved high separation factors (>20) with $D_{\mathrm{Am}} > 1$ in the range 0.1–1.0 M HNO_3 by means of synergistic mixtures of $(C_6H_4Cl)_2PSSH$ with either TBP, TOPO, or tributylphosphine oxide. (Interestingly, none of the R_2PSSH compounds by itself has any capacity to extract trivalent actinides.) Not only do the aromatic dithiophosphinic acids achieve satisfactory separation of trivalent actinides from trivalent lanthanides from low pH (0.1–1.0 M HNO_3) aqueous solutions but they are also reported to be considerably more resistant to radiation degradation than is Cyanex 301. Thus, Modolo and Odoj demonstrated that the selectivity and capacity of all the R_2PSSH–synergist combinations remained intact even at an absorbed dose as high as 10^6 gray. The capability of aromatic compounds to act as radiation 'sinks' is, of course, well known. Finally, it should be noted that none of the R_2PSSH compounds synthesized and studied by Modolo and Odoj are commercially available in large amounts.

Hence, when and if any country commits to plant-scale execution of a partitioning–transmutation approach to nuclear waste management and disposal, it seems quite likely that past and ongoing research and development efforts by many investigators will have culminated in a new solvent extraction process for separation of Am(III) and Cm(III) from lanthanides that operates satisfactorily under plant-scale conditions. The usable fallback technology, even though it may be considered cumbersome, is the Talspeak process.

8.4.4 Ion-exchange processes

The combination of chromatographic elution techniques with cation-exchange resins provides a powerful and sophisticated tool to purify americium from lanthanides and other trivalent actinides. Elution chromatography involves the use of organic chelating agents to produce the largest possible difference in the distribution coefficients of the metal ions to be separated. Both elution-development and displacement-development (also known as barrier-ion or retaining-ion) chromatography have been used in cation-exchange separation and purification of americium. Ryan (1974) points out that displacement-development chromatography is capable of separating macroquantities only, whereas, unless very large columns are used, elution-development chromatography is applicable only to the separation of tracer amounts. Jenkins and Wain (1972) listed publications covering the use of ion exchange to recover and purify ^{241}Am and ^{243}Am.

(a) Cation-exchange resin systems

Cation-exchange resins sorb Am^{3+} very strongly from dilute nitric acid solutions. An important application is to concentrate Am^{3+} and other trivalent and tetravalent ions from dilute acid solutions to separate them, at least partially, from many impurities (Hale and Lowe, 1969; Gmelin, 1979). Before production operations ceased at the US DOE Rocky Flats site, a cation–anion exchange process had replaced the hydroxide precipitation and thiocyanate ion-exchange system formerly used for recovering ^{241}Am from solutions of spent NaCl–KCl–$MgCl_2$ salt residues generated at the site (Proctor, 1975).

(*i*) *Distribution coefficients: separation factors*

Data for the distribution of Am^{3+} between cation-exchange resins and many aqueous solutions were analyzed in a comprehensive review by Ryan (1974). Solutions of α-hydroxycarboxylic acid and aminopolycarboxylic acids are commonly used to elute americium from cation-exchange resins. When these reagents are used in a displacement elution system, they provide excellent separation of americium from trivalent lanthanides and other trivalent actinides. For example, the separation factor for americium from curium ranges from 1.2 to 1.4 for α-hydroxycarboxylic acids and from 1.2 to 2 for aminopolycarboxylic acids (Schulz, 1976).

(*ii*) *Chromatographic elution schemes*

Although citric acid has found use, both lactic and α-hydroxyisobutyric acids provide better separation of americium from curium. Using chromatographic elution from Dowex 50-X12 resin with α-hydroxyisobutyric acid, Campbell (1970) demonstrated the effective use of high-pressure ion-exchange methods for the rapid separation of americium from curium. Highly efficient displacement chromatographic separation schemes that use nitrilotriacetic acid (NTA) and/or DTPA as eluents have been applied at the US DOE Hanford and at Savannah River sites to purify kilogram amounts of americium from curium and lanthanides (Wheelwright *et al.*, 1968; Harbour *et al.*, 1972). Wheelwright *et al.* (1968) successfully used a two-cycle cation-exchange process to separate and purify 1 kg of ^{241}Am and ^{243}Am, about 60 g of ^{244}Cm, and 140 g of ^{147}Pm extracted from 13.5 tons of blanket fuel elements from the Shippingport nuclear reactor. Highly purified americium and curium fractions were obtained by americium–curium displacement elution at 60°C through a series of four Zn^{2+}-form Dowex 50 resins beds with a 0.105 M NTA solution buffered to pH 6.5 with NH_4OH. Harbour *et al.* (1972) adapted the displacement elution scheme to pressurized columns at the Savannah River site.

Nearly 20 years after Wheelwright's work, Chuveleva and some of his colleagues at the Institute of Physical Chemistry in Moscow revisited, as recently as 1999, displacement chromatography for separation of traces of americium and curium (Chuveleva *et al.*, 1999) (interestingly, in these papers Chuveleva *et al.* did not make any reference to Wheelwright's earlier work). The basic system used by the Russian scientists in 1999 utilized their KU-2 cation-exchange resin previously converted to the Ni- (or Zn) form; a NTA solution for elution, and Cd^{2+} as the separating ion. Performance of the Russian system was quite satisfactory; indeed, their results appeared to be in full accord with expectations from Wheelwright's earlier studies.

(b) Anion-exchange resin systems

For routine, large-scale purification of americium, application of anion-exchange resins is limited to sorption from thiocyanate, chloride, and, to a limited extent, nitrate solutions (Hermann, 1956).

(*i*) *Thiocyanate solutions*

Am(III) forms relatively strong complexes, e.g. $AmSCN^{2+}$, $Am(SCN)_2^+$, and Am $(SCN)_3$ in concentrated aqueous thiocyanate solutions, and its thiocyanate species are sorbed on anion-exchange resins considerably more strongly than are the corresponding lanthanide thiocyanate complexes (Coleman *et al.*, 1955, 1957; Surls and Choppin, 1957). Thiocyanate anion-exchange systems have been used to purify americium from rare earths. For example, a plant-scale thiocyanate ion-exchange process has long been used (1960–75) at the US DOE Rocky Flats plant for routine purification of ^{241}Am recovered from aged plutonium metal (Schulz, 1976).

(*ii*) *Chloride solutions*

Am(III) is sorbed much more strongly onto anion-exchange resins from concentrated lithium chloride solutions than are the lanthanides (Hulet *et al.*, 1961). Americium distribution ratios increase with increased lithium chloride concentration whereas increased temperature enhances the separation of americium from rare earths. A lithium chloride-based anion-exchange process for separating milligram amounts of americium and curium from lanthanide fission products and to isolate an Am–Cm fraction free of heavier actinides was routinely operated at the US DOE Oak Ridge facility (Baybarz, 1970).

(c) Inorganic exchangers

Most studies concerned with sorption of Am^{3+} from aqueous solutions have used zirconium phosphate. The order of the distribution coefficients of trivalent actinides and lanthanides on zirconium phosphate is the reverse of the order observed with a typical strong-base cation-exchange resin (Horwitz, 1966). Both American (Moore, 1973) and Russian (Shafiev *et al.*, 1971) scientists utilized the fact that the singly charged AmO_2^+ is not sorbed by zirconium phosphate from dilute acid media to separate americium from curium and other metal ions.

Inorganic exchangers formed by hydrolysis of the alkoxides of titanium, niobium, or zirconium were developed for actinide/lanthanide separation (Lynch *et al.*, 1975) and possible disposal. Schulz *et al.* (1980) investigated the use of sodium titanate [$Na(Ti_2O_5H)$] and bone char (a form of calcium hydroxyapatite) to decontaminate alkaline nuclear waste streams containing minor amounts of americium and other actinides and to separate trivalent curium from trivalent americium.

More recently, as part of the overall Japanese partitioning–transmutation program, Yamagishi *et al.* (1996) reported results of experiments to use the inorganic cation exchanger titanium antimonate 'TiSb' to separate Am(III) from trivalent lanthanides. Before Yamagishi *et al.*'s work the TiSb exchanger had been reported (Kaneko *et al.*, 1992, 1993) to have a high selectivity for Pu^{4+} and trivalent americium and a low selectivity for trivalent lanthanides from concentrated HNO_3 solutions. Yamagishi *et al.* prepared TiSb according to conditions reported by Abe and coworkers (Abe and Tsujii, 1983; Abe *et al.*, 1985) and found that the TiSb exchanger exhibited superior selectivity toward trivalent americium over trivalent europium and other rare earths. The Japanese investigators concluded that TiSb is a promising material particularly for preconcentration of Am^{3+} from HNO_3 solutions containing Am^{3+} and large amounts of La^{3+} without the need for complexing or oxidizing agents.

Ritter (Ebner *et al.*, 1999) and his coworkers synthesized a new magnetic adsorbent material that combines the properties of both organic resin and inorganic material for use in actinide removal from nuclear waste solutions. This new material is called magnetic polyamine–epichlorohydrin (MPE) resin. MPE resin consists of spherical beads of polyamine–epichlorohydrin that have activated iron ferrite (magnetite) particles attached to their outer surfaces. Ferrites have been shown in previous work (Boyd *et al.*, 1986; Kochen, 1987; Kochen and Navratil, 1987; Boyd and Kochen, 1993) to be excellent adsorbents for actinide elements (including Am^{3+}) in wastewaters at relatively low alkaline conditions ($pH > 9$) and independent of a magnetic field. Results obtained by Ritter and his colleagues demonstrated that MPE resin has a significantly enhanced capacity for actinides over conventional-based ferrite surface complexation adsorption processes (where no field is applied) and over traditional high-gradient magnetic separation processes that remove suspended particles.

8.4.5 Extraction chromatographic processes

Extraction chromatography combines the best features of liquid–liquid solvent extraction and chromatographic separation techniques. Extraction chromatographic systems consist of a mobile liquid phase and a stationary liquid phase on an inert support. Separations are achieved by taking advantage of the difference in the distribution of ions between the two liquid phases.

Many systems using either HDEHP or Aliquat 336 as the stationary phase have been studied for extraction chromatographic separation of americium at tracer-level concentrations. An Aliquat 336 (nitrate-form)–kieselguhr system was used both in the USA and in Europe to separate milligram to gram amounts of americium from curium (Horwitz *et al.*, 1967; Müller, 1971).

In the two decades since the publication of the second edition of this monograph extraction chromatographic techniques for separating Am(III) and small amounts of other actinides from various aqueous media have been pursued for routine analytical purposes and for specialized process purposes. Thus far, the analytical applications have met with much greater acceptance and success than the proposed process applications.

Horwitz and his colleagues at the U.S. Argonne National Laboratory have been the prime movers in developing practical extraction chromatographic materials and procedures for analytical-scale separations and determination of Am(III) and other actinides. (Materials developed by Horwitz *et al.* are commercially manufactured and marketed by Eichrom Industries, Darien, Illinois.) Horwitz *et al.* (1990, 1993) initially developed an extraction chromatographic material, which was marketed under the name TRU$^{\mathrm{TM}}$ resin; the TRU$^{\mathrm{TM}}$ resin, which consisted of a solution of CMPO adsorbed on Amberchrom-CG 71 (Rohm & Haas Co.), had a number of attractive features including offering the possibility of sequential elution of individual sorbed actinide elements. However, a major weakness of the TRU$^{\mathrm{TM}}$ resin was that it would not effectively sorb actinides from solutions containing significant concentrations of complexing anions such as fluoride, oxalate, or phosphate. Extraction chromatographic analytical applications of the TRU$^{\mathrm{TM}}$ resin for the separation and determination of Th, U, Pu, Am, and Cm have been described in a series of papers (PilvVo and Bichel, 1998, 2000; PilvVo *et al.*, 1999).

In follow-on development work by Horwitz *et al.* the Diphonix$^{\mathrm{TM}}$ resin, containing geminally substituted diphosphonic acid groups chemically bonded to a styrene-based polymer matrix, was shown to exhibit extraordinarily strong affinity for the actinides particularly the 4+ and 6+ ions. Because of its strong retention of actinides, the Diphonix$^{\mathrm{TM}}$ resin found application in the characterization of mixed and transuranic waste (Chiarizia *et al.*, 1997) and in analytical pre-concentration of actinides from a variety of biological and environmental samples (Smith *et al.*, 1995). Further tests revealed two important weaknesses of the Diphonix^{TM} resin in extraction chromatographic applications, namely (i) insufficient uptake and retention of trivalent actinides and (ii) difficult stripping/recovery of actinides from the loaded resin.

The final important contribution to actinide element extraction chromatography of the Horwitz group at the Argonne National Laboratory was the development and introduction of the DIPEX^{TM} resin (Horwitz *et al.*, 1997). The DIPEX^{TM} resin consists of a new compound, bis(2-ethylhexyl)methanediphosphonic acid (H_2DEH[MDP]) supported on an inert polymeric substrate. Horwitz and his coworkers state that this compound contains the same diphosphonic acid functional group as the Diphonix^{TM} resin but two of the four ionizable hydrogen atoms have been replaced by a C_8 alkyl group to make the molecule more lipophilic. According to the experimental evidence of Horwitz and colleagues, the DIPEX^{TM} resin exhibits stronger affinity for 3+, 4+, and 6+ actinides from acidic chloride media and superior selectivity for Am(III) over Al(III) and Fe(III) than the Diphonix^{TM} resin. Indeed, so strongly does the DIPEX material sorb actinides that the only convenient way to strip sorbed actinides appears to be to wash the resin with isopropanol to completely solubilize the H_2DEH[MDP] for subsequent wet oxidation to liberate the actinides for further treatment and analysis. Despite what appears to be a cumbersome procedure for stripping sorbed actinides, the DIPEX^{TM} resin is considered to be eminently suited for separation and pre-concentration of actinides from complex soil and bioassay matrices.

Nowadays, extraction chromatographic materials and techniques are generally considered to be most suited for analytical aims. But, some process-scale applications of such materials and techniques continue to be proposed from time to time. For example, Akatsu and Kimura (1990) reported on the use of extraction chromatography in the DHDECMP–(XAD-4) HNO_3 system. Also, several investigators (Barney and Cowan, 1992; Lumetta *et al.*, 1993) studied the feasibility of using TRU^{TM} resin and other types of extraction chromatographic supports impregnated with CMPO to separate actinide elements from stored US DOE Hanford site tank wastes including actual neutralized decladding waste and also other acidic waste solutions. Scientists in India (Gopalakrishnan *et al.*, 1995; Mathur *et al.*, 1995) have reported good success in applying an extraction chromatographic material consisting of CMPO adsorbed on Chromosorb-102 to selectively take up U(VI), Pu(IV), and Am(III) from neat nitric acid media, from synthetic sulfate-bearing high-level waste (SBHLW) and actual Purex process oxalate supernatant liquors.

Two other extraction chromatographic process-scale applications for separation of americium and other actinides are noteworthy. Mohapatra *et al.* (2000) found that the diamide DMDBTDMA adsorbed on an inert support was very efficient in taking up tracer concentrations of Am(III) and other actinide ions from 3 to 5 M HNO_3 solutions. Wei and his coworkers (Wei, 2000a,b) prepared and investigated the actinide sorption properties of several novel silica-based extraction chromatographic resins by impregnating organic extractants such as CMPO, HDEHP, and Cyanex 301 into a styrene–divinylbenzene copolymer, which is immobilized in porous silica particles. Recently, these scientists have synthesized 2,6-bis-((5,6-dialkyl)-1,2–4-triazene-3-yl)-pyridine and impregnated such compounds into styrene–divinylbenzene copolymers immobilized in porous silica particles (Wei *et al.*, 2000a,b). The resulting extraction chromatographic material preferentially sorbed Am(iii) over trivalent lanthanides.

A most unusual and intriguing type of extraction chromatographic separation scheme for Am(iii) and other actinides was prepared by Nunez *et al.* (1996). These researchers adsorbed a layer of CMPO/TBP onto polymeric-coated ferromagnetic particles. The CMPO/TBP was very efficient in taking up actinides from 0.01 to 6 m HNO_3 nuclear waste solutions as expected from the results with the TRUEX process (see Section 8.4.3a(vi)). Once loaded with actinides, the ferromagnetic particles could be readily recovered from the waste solutions with a magnet.

8.5 ATOMIC PROPERTIES

8.5.1 Electron configuration

Americium is the sixth member of the actinide series, with electron configurations in its ground and ionized states analogous to those of its lanthanide homolog, europium. Note, however, that the solution chemistries of these two elements show substantial differences, with the major ones being the difficulties in preparing Am(ii) and the absence of Eu(iv), Eu(v), and Eu(vi). Electronic configurations of gaseous americium species as determined from spectroscopic and atomic-beam experiments showed a $5f^77s^2$ ground state for Am(g) and $(5f^7)^{2+}$ state for Am^{2+} (Tomkins and Fred, 1949).

8.5.2 Atomic and ionic radii

Metallic, covalent, and ionic radii of americium in various oxidation states were first calculated by Zachariasen (1948a, 1954). The radius of americium metal with a coordination number (CN) of 12 was reported to be 1.73 Å (McWhan *et al.*, 1960). On the basis of a refined single-crystal structure for $AmCl_3$, Burns and Peterson (1970, 1971) calculated the ionic radius of Am^{3+} (CN 6) in $AmCl_3$ to be 0.984 ± 0.003 Å. Zachariasen (1978) has also deduced some highly useful bond length–bond strength relationships that provide, as a function of americium valence and coordination number, a condensation of many americium–oxygen and americium–halogen distances derived from the best-known structures. For the Am^{3+} and Am^{4+} ions, Zachariasen (1948a) reported crystal radii of 1.00 and 0.85 Å, respectively. Shannon (1976) provided a list of revised effective ionic radii and reported 1.21 Å (CN 6) and 1.26 Å (CN 8) for Am^{2+}, 0.975 Å (CN 6) and 1.09 Å (CN 8) for Am^{3+}, 0.85 Å (CN 6) and 0.95 Å (CN 8) for Am^{4+}. No data are available on Am(V) and Am(VI). David (1986) reported an ionic radius for Am^{3+} of 0.980 Å (CN 6) and 1.106 Å (CN 8).

8.5.3 Ionization potentials

Trautmann and colleagues (Trautmann, 1994; Deissenberger *et al.*, 1995) experimentally determined the first ionization potential of americium to be 5.9738 (2) eV. This determination was made with only 10^{12} atoms of americium using a newly developed method based on resonance ionization mass spectroscopy in the presence of an external electric field. Before the work of Trautmann and colleagues, Carlson *et al.* (1970) calculated the ionization potential values for Am^0 (5.66 eV), Am^+ (12.15 eV), and Am^{2+} (18.8 eV). Penneman and Mann (1976) also estimated the same potentials based on *jj* coupling; these investigators underestimated the first ionization potential but were in good agreement on the potentials for higher ionizations.

8.5.4 Emission spectra

Studies of the arc and spark spectra of americium have been summarized by Carnall (1973a) in *Gmelin's Handbook of Inorganic Chemistry*. Corresponding to the absolute term value (48 767 cm^{-1}) of the ground state, the ionization potential of Am(I) is 6.0 eV (Carlson *et al.*, 1970). As noted above Deissenberger *et al.* (1995) refined the ionization potential to 5.9738(2) eV.

8.5.5 X-ray spectrum

Atomic energy levels (binding energies) of americium have been calculated from experimental measurements of X-ray emission wavelengths; for example, the value for $K–M_{III}$ is 120.319 and 102.041 keV for the $K–L_{II}$ transition (Carnall, 1973b). All K X-ray energies of americium correspond to electric dipole transitions. A critical literature evaluation and a listing of atomic energy levels of americium are given in Bearden (1967).

8.5.6 Photoelectron spectrum

In a highly important experimental measurement, Naegele and coworkers (Naegele *et al.*, 1984) at the European Institute for Transuranium Elements were able in 1984 to directly conduct X-ray and high-resolution ultraviolet photoemission spectroscopy of the conduction band of americium metal. These measurements, parallel to those successfully performed earlier with uranium metal, directly revealed that the 5f electrons in americium metal are localized. Naegele *et al.* state that the final-state multiplet structure arises from a trivalent $5f^6$ Am ground state. In later work, Naegele *et al.* (Martensson *et al.*, 1987) attempted an interpretation of the valence band photoelectron spectrum for americium metal.

8.5.7 Mössbauer spectrum

Beta decay of ^{243}Pu ($t_{1/2} = 4.98$ h) to the 83.9 keV level of ^{243}Am produces an excited nuclear state ($t_{1/2} = 2.34$ ns) of ^{243}Am that is suitable for Mössbauer spectroscopy (Kalvius *et al.*, 1969; Bode *et al.*, 1976). Data obtained with a $^{243}PuO_2$ source at 4.2 K showed the shift of the $^{243}AmF_3$ resonance line relative to $^{243}AmO_2$ to have an unusually large value of 55 mm s^{-1} (Kalvius *et al.*, 1969; Bode *et al.*, 1976).

8.6 METAL AND ALLOYS

8.6.1 Metal preparation

Americium metal has been prepared by the following methods: (1) reduction of AmF_3 with barium (or lithium) metal; (2) reduction of AmO_2 with lanthanum metal; (3) bomb reduction of AmF_4 with calcium metal; and (4) thermal decomposition of Pt_5Am. Lanthanum metal (or thorium metal) reduction of AmO_2 in tantalum equipment and subsequent distillation of the americium metal from the reaction mixture yields americium of very high (>99.9%) purity. Americium is about a factor of 10^4 more volatile than lanthanum. Extensive applications of this technique by the Euratom group led to important new measurements of the physical and thermodynamic properties of americium metal (Oetting *et al.*, 1976). Workers at the U.S. DOE Rocky Flats site also reported similar success with vacuum distillation techniques (Berry *et al.*, 1982).

Preparation of americium metal by thermal decomposition of the intermetallic compound Pt_5Am is a more recent development. Müller *et al.* (1972) produced high-purity americium metal by thermal decomposition of the intermetallic compound at 1550°C and 10^{-6} Torr, followed by further distillation.

8.6.2 Properties

Americium metal is silvery, ductile, non-magnetic, and very malleable. Selected physical properties are listed in Table 8.3. There are two well-established crystalline forms of americium metal, a double hexagonal close-packed (dhcp, *P*6$_3$/*mmc*) phase, stable at room temperature, and a face-centered cubic (fcc, *Fm*3*m*) phase (McWhan *et al.*, 1960; Stephens *et al.*, 1968; Oetting *et al.*, 1976). Differential thermal analysis and dilatometric experiments on americium metal have presented (Rose *et al.*, 1979) evidence for at least three phases existing between room temperature and the melting point (1170°C): an alpha phase

Table 8.3 *Selected properties of americium metal* (*adopted from Schulz* (1976) *and Oetting* et al. (1976); *see also Chapter* 19).

Property	*Values*[a]
Crystallographic data	
symmetry	<658°C, dhcp (α) 793–1004°C, fcc (β) ~1050–1173°C, bcc (?)
space group	$P6_3/mmc$ and $Fm3m$
lattice parameters	dhcp: $a = 3.4681$ Å, $c = 11.241$ Å fcc: $a = 4.894$ Å
density	13.671 g cm^{-3} (calc.); 13.671 g cm^{-3} (obs.)[b]
high-pressure structures[c]	0–5 GPa Am (I): dhcp; 5 to 8–10 GPa Am(II): fcc; 8 to 15–23 GPa Am(III): double body-centered monoclinic, or trigonal distortion of fcc, or monoclinic α-Pu; >15–23 GPa Am(IV): orthorhombic α-U or monoclinic (α-U alloys)
metallic radius (CN 12)	1.73 Å
melting point	(1149 ± 5) K
boiling point	2067°C (calc.)
coefficient of thermal expansion	$\alpha_a = 7.5 \pm 0.2 \times 10^{-6}\ \mathrm{K}^{-1}$ and $\alpha_c = 6.2 \pm 0.2 \times 10^{-6}\ \mathrm{K}^{-1}$
compressibility at 1 atm	0.00277 kbar^{-1} at 23°C
vapor pressure[d]	$\log(p/\mathrm{atm}) = (6.578 \pm 0.046) - (14315 \pm 55)/T$ at 990–1358 K
magnetic susceptibility	$\chi_{20°\mathrm{C}} = (881 \pm 46) \times 10^{-6}\ \mathrm{cm}^3\ \mathrm{mol}^{-1}$
magnetic moment	~0
microhardness (Vickers) at 25°C	800 MN m^{-2}
electrical resistivity	68 μΩ cm (300 K), 71 μΩ cm (298 K)
crystal entropy, $S°298$	55 J K^{-1} mol^{-1}
heat capacity, $(C_P)_{298}$	25.5 J K^{-1} mol^{-1}
heat of vaporization at boiling point	230.2 kJ mol^{-1} (calc.)
entropy of vaporization at boiling point	100.8 J K^{-1} mol^{-1} (calc.)
heat of transformation	5.9 kJ mol^{-1}
heat of fusion	14.4 kJ mol^{-1}
heat of dissolution in aqueous HCl	1 M HCl: −616.3 kJ mol^{-1} 1.5 M HCl: −615.5 kJ mol^{-1} 6 M HCl: −618.0 kJ mol^{-1}

[a] For the dhcp-form unless otherwise indicated.

[b] By immersion in monobromobenzene.

[c] Refer to Section 8.6.2.

[d] Ward *et al.* (1975) give the following equation for americium above its melting point: $\log(p/\mathrm{atm}) = 5.185 - 13191/T$.

existing up to 658°C; a beta phase existing between 793 and 1004°C; and a gamma phase which forms at 1050°C. In studies with high-purity americium metal, Sari *et al.* (1972/73) concluded that there is no phase transition between 600 and 700°C. But, Russian scientists (Seleznev *et al.*, 1979) put forth evidence that the transition from the dhcp structure to the fcc structure occurs at 771 ± 15°C; their observation is in agreement with the conclusions reached from dilatometric and differential thermal analysis measurements.

Smith and Haire (1978) found that americium metal with the dhcp structure became superconducting between 0.55 and 0.75 K; observation of the onset of superconductivity in americium metal confirmed an earlier prediction made from theoretical considerations. In later work, Link *et al.* (1994) found that the superconductivity transition temperature of dhcp americium increases considerably with pressure, reaching a maximum value of 2.3 K at 6.6 GPa. Müller *et al.* (1978), at several laboratories in Europe and in USA, recently measured the electrical resistivity and specific heat of americium metal. These latter investigators observed binding in americium metal to be reduced compared to that in lighter actinide metals and attributed this result to the importance of 5f electrons in electrical conduction. In a later paper, Hall *et al.* (1980) used their data to generate 'best values' for the heat capacity, crystal entropy, and electrical resistivity of americium metal; these 'best values' are shown in Table 8.3.

Owing to its unique position and properties in the actinide series of elements, americium metal has proven to be, over the last quarter of a century, a material of great interest to both theoreticians and experimentalists. In the light actinide metals (Ac–Pu) the 5f electrons are known to be itinerant and not localized. But, there is much evidence, e.g. cohesive properties, magnetic properties, atomic volume, etc. to indicate that the 5f electrons in americium metal at atmospheric pressure are localized and chemically inert. (Indeed, results of recent photoemission spectral studies cited in Section 8.4 essentially prove that 5f electrons in americium metal are localized.) Once the 5f electron localization behavior was noted for americium metal, Johannson (1978) also posited that americium metal under compression will transform to a dense phase where the 5f electrons are itinerant and not localized.

The first experimental study of the behavior and some properties of americium metal above atmospheric pressure was conducted by Stephens *et al.* (1968). These investigators determined the compressibility and electrical resistance of americium metal at room temperature over the range 3.5–12 GPa. They also made an attempt to determine the phase diagram of americium metal over this range of pressures.

Following Johannson's 1978 paper several groups of scientists in the early 1980s determined structural properties from X-ray diffraction data for americium metal at various pressures. The overall goal of these studies was to determine the number and type of different crystalline structures formed as a function of applied pressure and, thereby, obtain experimental evidence for delocalization of the 5f electrons. Thus, Akella and coworkers (Akella *et al.*, 1980;

Roof *et al.*, 1980; Smith *et al.*, 1981; Roof, 1982) established four different crystalline structures in americium metal over the pressure range from 100 kPa (1 atm) to 18 GPa: Am(I)-dhcp; Am(II)-fcc (at 5 ± 1 GPa); Am(III)-not indexed (10 ± 1 GPa); and Am(IV)-not indexed (15 ± 1 GPa). Later Roof (1982) repeated and extended the pressure experiments of Akella and coworkers up to 20 GPa. Roof and his collaborators noted the same four crystalline phases as observed by Akella and coworkers. But, Roof and his collaborators indexed the Am(III) phase (10–15 GPa) as a double-body centered monoclinic structure and the Am(IV) phase (10–20 GPa) as an orthorhombic structure similar to that of alpha uranium metal.

The latest experimental studies of delocalization of 5f electrons in americium metal under pressure were performed by Benedict and colleagues (Benedict *et al.*, 1985, 1986). Benedict *et al.* conducted their experiments over the pressure range 3 to 52 GPa, and, under these conditions, also noted the Am(I)–Am(II)–Am(III)–Am(IV) phase transformation sequence. Benedict *et al.* however, state that the transitions between phases occur at higher pressures than noted by previous workers; in particular, Benedict and his fellow authors state that the Am(III) to Am(IV) transition occurs at 23 GPa, not at 15 GPa. Benedict *et al.* claim that the Am(III) phase is not a monoclinic structure, as previously indexed, but is really a trigonal distortion of the Am(II) fcc structure. Finally Benedict *et al.* state that according to their results, 5f electron delocalization occurs only at a pressure of 23 GPa or above. Lindbaum *et al.* (2001) observed the transition of the normal-pressure double hexagonal close packed ($P6_3/mmc$) structure transforms at 6.1 GPa to the face centered cubic (*Fm3m*) form, which converts at 10.0 GPa to a face centered orthorhombic (*Fddd*) structure. This orthorhombic form converts at 16 GPa to a primitive orthorhombic (*Pnma*) form, which is stable up to at least 100 GPa. Based on the data of americium's pressure behavior the authors concluded that Am f-electrons are involved in the metallic bonding of the AmIII and IV phases.

Coincident with experiments conducted to ascertain the response of americium metal to increasing pressure, theoreticians in several countries have mounted a sustained effort to apply first-principles calculations to deduce the state of 5f electrons both in the presence and absence of applied pressure (Skriver *et al.*, 1980; Johannson, 1984; Nikolaev and Ionova, 1991; Eriksson and Wills, 1992; Eriksson *et al.*, 1993, 1995, 2000; Soderland *et al.*, 2000). The present state of the theoretical calculations is best discussed in a recent paper by Soderland *et al.* (2000). The latter investigators used density functional electronic calculations to study the high-pressure behavior of americium metal. At about 8 GPa, such calculations revealed a phase transition from the fcc structure Am(II) to a dense phase of lower symmetry that Johannson *et al.* were convinced is a monoclinic form similar to the structure of α-plutonium (Fig. 8.3); they state emphatically that it does not have the orthorhombic structure called out by Roof and Benedict *et al.* According to Johannson and collaborators, their calculation results are consistent with a Mott transition;

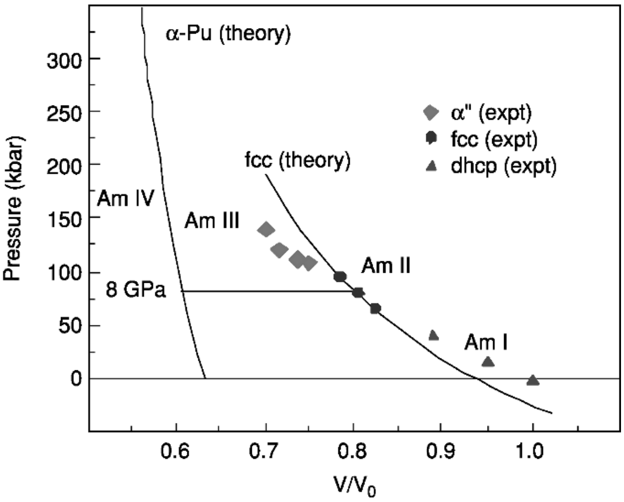

Fig. 8.3 *Calculated equations of state for americium metal from fits to total energies* (*Soderland* et al., 2000)*; equations indicate a volume decrease of* 25% *at* 8 GPa.

the 5f electrons are delocalized and bonding on the high-density side of the transition and chemically inert and non-bonding (localized) on the low-density (fcc phase) side of the transition.

Even at this advanced time in the chemistry of americium, there are still some serious disagreements between experimentally determined and calculated (from theoretical considerations) effects of compression of americium metal. To be sure, both approaches offer strong support for the contention that upon compression the 5f electrons in americium delocalize. Both the experimentalists and the theoreticians concur that at moderate applied pressure, the dhcp structure converts to the fcc phase. And, both groups concur that at some threshold applied pressure the fcc structure transforms to a more dense phase, i.e. Am(III) and, possibly, Am(IV), in which the 5f electrons are delocalized. But, certainly the parties involved do not agree on exactly how many different dense phases (one or two) eventually form on further application of pressure or on the exact pressure of phase transformations and certainly not on the crystal structure of the new dense phase(s). (The data shown in Table 8.3 are listed so as to capture much of the present uncertainty concerning transition pressures and crystalline structures.) Another important point of disagreement and uncertainty, long known and troublesome to theoreticians, is that the experimentally observed volume decreases when the 5f electrons in americium metal are delocalized only to about 6% compared to the 30–35% decrease predicted from theory. The present disagreement between experimental and calculated results point to flaws and deficiencies in both approaches, e.g. difficulties in obtaining and accurately deciphering X-ray diffraction data from a pressurized radioactive system and inadequacies of present calculational tools. It is hoped that future research will resolve the discrepancies between calculation and experiment.

8.6.3 Alloys and intermetallic compounds

Presently, alloy systems involving interaction of americium metal with some 23 different elements have been investigated. One or more intermetallic compounds of definite composition are known to exist in 16 of these systems; Table 8.4 summarizes the significant stoichiometry, structure, and synthesis information for these 16 systems and also provides relevant literature references.

No definite compounds have been observed in the Am–Ce, Am–Hg, Am–La, Am–Np, Am–Pu, Am–Th, or Am–U systems. Phase diagrams for the Am–Np, Am–Pu, and Am–U systems have recently been summarized and published by Okamoto (1998). Okamoto took careful note of the phase diagram for the Am–Pu system constructed earlier by Ellinger *et al.* (1966). Gibson and Haire (1992a) have reported phase relations in the Am–Np system while Adair (1970) prepared alloys of thorium with 0.54–5.0 wt% americium by both levitation and arc melting of prepared mixtures of americium and thorium metal.

Interaction of americium metal with two rare earth metals, lanthanum and cerium, has been investigated, respectively, by Hill and coworkers (Hill and Ellinger, 1971; Hill *et al.*, 1971) and by Connor (1982). Lanthanum–americium alloys containing 0.92–2.37 at% americium dissolved in fcc-beta lanthanum were produced by arc melting the constituent elements. Connor used both co-melting (arc) and co-reduction techniques in his studies of the Am–Ce system. Co-reduction alloy preparation involved calcium metal reduction of an appropriate mixture of AmF_4 and CeF_3 in a sealed vessel.

The Am–Hg system has been studied by Bouissières and Legoux (1965), David and Bouissières (1968), Maly (1969), and Tikhonov *et al.* (1988). A dilute americium amalgam may be prepared either by reduction of Am(III) ions with a sodium amalgam or by electroreduction of Am(III) ions on a mercury electrode. Tikhonov *et al.* also investigated some properties of a concentrated americium amalgam that was prepared electrolytically; their results indicated the formation of an Am–Hg intermetallic compound but no information on the stoichiometry or structure of such a compound was reported. Guminski (1995) recently reviewed and evaluated the equilibrium and thermodynamics of the Am–Hg system.

8.7 IMPORTANT COMPOUNDS

Inorganic compounds containing halides or oxygen-donor ligands are far more numerous than simple oxides, hydroxides, or other binary or ternary compounds. The structures and references to the preparation of about 180 compounds of americium with anionic inorganic ligands are listed in alphabetical order in Table 8.5; compounds of americium with organic ligand coordination are listed in Table 8.6. A group of compounds in which americium could be considered as part of the anionic constituent appears under the heading oxides, ternary.

8.7.1 Inorganic compounds

(a) Oxides and hydroxides

The binary americium oxides are limited to AmO, Am_2O_3, AmO_2, and non-stoichiometric phases between Am_2O_3 and AmO_2. Although the AmO (fcc) phase has been reported twice (Zachariasen, 1949a,c; Akimoto, 1967), the corresponding lattice parameters, 4.95 Å (Zachariasen, 1949a,c) and 5.045 Å (Akimoto, 1967), are not consistent. Accidental exposure of AmH_{2+x} to air at 300°C yielded a fcc phase (Roddy, 1973), which agrees with Akimoto's AmO (Akimoto, 1967) but may in fact be an oxynitride similar to the corresponding 'PuO' (Larson and Haschke, 1981). The difficulty in achieving Am(II) in solution and in solid compounds makes it likely that the monoxide can only be synthesized under high pressure by conproportionation of Am metal and Am_2O_3, analogous to the preparation of the lanthanide monoxide SmO (Leger *et al.*, 1981). Recent evidence that PuO and surface-layer lanthanide monoxides are really oxycarbides or nitrides (Larson and Haschke, 1981) reinforces the uncertainty of whether any claim for AmO is valid.

Phase relationships and thermodynamic data in the $AmO_{1.5}$–AmO_2 systems are well established. The red-brown ('persimmon') sesquioxide, Am_2O_3, is easily prepared in H_2 at temperatures as low as 600°C but it oxidizes very readily in air, even at room temperature. Baybarz (1973a) summarized the transition temperatures of the low-temperature (body-centered cubic (bcc), C-phase) to medium-temperature (monoclinic, B-phase) to high-temperature (hexagonal, A-phase) sesquioxides. The C→B transition temperature appears to be sluggish, occurring between 460 and 650°C and the B→A transition occurs between 800 and 900°C (Chikalla and Eyring, 1968; Hurtgen and Fuger, 1977). The pale tan hexagonal sesquioxide phase undergoes slight swelling with time and self-irradiation causes cubic Am_2O_3 to transform to the hexagonal phase at room temperature within about 3 years (Hurtgen and Fuger, 1977). It is possible that the monoclinic Am_2O_3 is stabilized by small amounts of rare earth impurities (Berndt *et al.*, 1974; Keller and Berndt, 1975) and that pure Am_2O_3 passes directly from the C- to the A-phase; it is also possible that the C→B transition occurs well below 650°C. The hexagonal sesquioxide is stoichiometric but the cubic form may have a lower oxygen limit of $AmO_{1.513}$ (Chikalla and Eyring, 1968). Studies on americium oxides include the measurement of the melting point of Am_2O_3, 2205 ± 15°C (Chikalla *et al.*, 1973), and the enthalpy of formation of AmO_2, -932.2 ± 3.0 kJ mol^{-1} (Morss and Fuger, 1981).

The dioxide AmO_2 was the first reported compound of americium (Zachariasen, 1949a,c). It can be prepared by heating a variety of americium compounds, e.g. hydroxides, carbonates, oxalate, or nitrate, in air or oxygen at

Table 8.4 *Intermetallic compounds in the americium alloy system.*

				Lattice constants			
Class	*Formula*	*Symmetry*	*Structure type*	a_0 (Å)	c_0 (Å)	*Comments*	*References*
aluminide	$AmAl_2$	cubic	$MgCu_2$	7.861		arc melt	[1]
antimonides	AmSb	fcc		6.239		Am/Sb/heat	[2]
	$AmSb_2$		$LaSb_2$				
	Am_4Sb_3	bcc	anti-Th_3	9.239		AmH_3/Sb/heat	[3]
arsenide	AmS	fcc	F*m*3*m*	5.880		Am/As/heat	[4]
				5.875		AmH_3/As/heat	
beryllide	$AmBe_{13}$	fcc	F*m*3*c*	10.283		AmF_3/Be/vac/heat	[6]
						AmO_2/Be/vac/heat	[7]
bismuthide	AmBi	fcc	F*m*3*c*	6.338		Am/Bi/heat	[8]
						AmH_3/Bi/heat	[8]
cobaltide	$AmCo_2$	$MgCu_2$				arc melt	[9]
iridium	Ir_2Am	cubic	F*d*3*m*, Cu_2Mg	7.55		AmO_2/H_2/Ir/1550°C	[10]
iron	Fe_2Am	cubic	Cu_2Mg	7.30		arc melt, ferromagnetic	[9]
lead	Pb_3Am	not reported				PbF_2/AmF_3/Ca/heat	[11]
nickel	Ni_2Am	cubic	F*d*3*m*,Cu_2Mg	6.99		Am/Ni/arc melt	[12]
osmium	Os_2Am	hexagonal	$P6_3/mmc$	5.320	8.849	Am/Os/arc melt	[12]
palladium	Pd_3Am	cubic	P*m*/3*m*	4.158		Am_2O_3/Pd/H_2/heat	[13]
platinum	Pt_2Am	cubic	F*d*3*m*	7.615		AmO_2/Pt/H_2/heat	[13]
	Pt_5Am		$CaCu_5$	5.312	4.411	Am_2O_3/Pt/H_2/heat	[13]
rhodium	Rh_2Am	cubic	F*d*3*m*,Cu_2Mg	7.548		AmO_2/Rh/H_2/heat	[13]
	Rh_3Am	cubic	P*m*3*m*,Cu_3A	4.098		Am_2O_3/Rh/H_2/heat	[14]
ruthenium	Ru_2Am	hexagonal	$MgZn_2$	5.26	8.73	arc melt	[9]
tin	Am_2Ni_2Sn	tetragonal	P4/*mbm*,U_3Si_2				[15]
	Am_2Pd_2Sn	tetragonal					[15]

[1] (Hyde *et al.*, 1971; Aldred *et al.*, 1975); [2] (Mitchell and Lam, 1970a; Roddy, 1974; Charvillat *et al.*, 1975a, 1977); [3] (Charvillat *et al.*, 1975b); [4] (Roddy, 1974); [5] (Charvillat and Damien, 1973); [6] (Runnals and Boucher, 1955, 1956; Benedict *et al.*, 1975); [7] (Brachet and Vasseur, 1969); [8] (Roddy, 1974); [9] (Hyde *et al.*, 1971; Aldred *et al.*, 1975); [10] (Erdmann, 1971; Erdmann and Keller, 1971, 1973; Rebizant and Benedikt, 1978); [11] (Connor, 1982); [12] (Lam and Mitchell, 1972); [13] (Erdmann, 1971; Rebizant and Benedikt, 1978); [14] (Erdmann and Keller, 1971); [15] (Pereira *et al.*, 1997).

Table 8.5 *Inorganic compounds of americium.*

Class	Structural formula	Symmetry	Type	*Lattice constants*			Angle (deg)	Comments	References
				a_0 (Å)	b_0 (Å)	c_0 (Å)			
Aluminates									
	$AmAlO_3$	hexagonal	$R\bar{3}m$, $LaAlO_3$	5.336		12.91		$Am(OH)_3/Al(OH)_3/H_2$/heat	[1,2]
Arsenates									
	$AmAsO_4$	monoclinic	$P2_1/n$	6.89	7.06	6.62	$\beta = 105.5$		[2]
	$NH_4AmO_2AsO_4 \cdot nH_2O$	tetragonal	$P4/nmn$ or $I4/mmm$	7.11		8.93		Am(VI)/0.1 M H_3AsO_4/pH 3.5, lemon yellow	[3]
	$KAmO_2AsO_4 \cdot nH_2O$	tetragonal	$P4/nmn$ or $I4/mmm$	7.10		9.09		Am(VI)/0.1 M H_3AsO_4/pH 3.5, lemon yellow	[3]
	$RbAmO_2AsO_4 \cdot nH_2O$	tetragonal	$P4/nmn$ or $I4/mmm$	7.15		17.73		Am(VI)/0.1 M H_3AsO_4/pH 3.5, lemon yellow	[3]
	$CsAmO_2AsO_4 \cdot vnH_2O$	tetragonal	$P4/nmn$ or $I4/mmm$	7.09		17.72		Am(VI)/0.1 M H_3AsO_4/pH 3.5, lemon yellow	[3]
Borates									
	$AmBO_3$	orthorhombic	$Pnam$	5.053	8.092	5.738		AmO_2/B_2O_3/heat	[1,2]
Borides									
	AmB_4	tetragonal	$P4/mbm$	7.105		4.006		vac. heat Am/B 1:2	[4]
	AmB_6	simple cubic	$Pm3m$	4.115				arc melt Am/B	[4]
Bromides									
	$AmBr_2$	*tetragonal*	$P4/n$, $EuBr_2$	11.59		7.121		$Am/HgBr_2$/vac./heat	[5,6]
	$AmBr_3$	orthorhombic	$Cmcm$, $PuBr_3$	4.064	12.66	9.144			[7,8,9]
	$AmBr_3 \cdot 6H_2O$	monoclinic	$P2/n$	9.955	6.783	8.166	$\beta = 91.75$	$AmBr_3$, H_2O vapor	[9]
	$[(C_6H_5)_3PH]_3AmBr_6$							ethanol pptn.	[10]
	$AmOBr$	tetragonal	$P4/nmm$	3.982		7.644			[11]
Carbides									
	Am_2C_3	bcc	$I\bar{4}3d$	8.276				Am/C arc melt	[12]
Carbonates									
	$AmOHCO_3$	orthorhombic						Am(III)/$NaHCO_3$/0.03% CO_2	[13]
	$Am_2(CO_3)_3 \cdot 2H_2O$							Am(III)/trichloroacetate	[14]
	$Am_2(CO_3)_3 \cdot 4H_2O$							Am(III)/$NaHCO_3/CO_2$	[15]
	$NaAm(CO_3)_2 \cdot nH_2O$	tetragonal	$NaNdO_2CO_3$	13.07		9.93		Am(III)/Na_2CO_3/5 M NaCl	[16]

Table 8.5 (*Contd.*)

Class	*Structural formula*	*Symmetry*	*Type*	*Lattice constants* a_0 (Å)	b_0 (Å)	c_0 (Å)	*Angle* (deg)	*Comments*	*References*
	$NH_4AmO_2CO_3$	hexagonal	*C6/mmc*					Am(III)/$(NH_4)_2CO_3/O_3$	[17]
	$Na_{2x+1}AmO_2(CO_3)_{1+x}$							Am(VI)/Na_2CO_3/heat	[17,18]
	$KAmO_2CO_3 \cdot nH_2O$	hexagonal	*C6/mmc*	5.112		9.740		*n* is variable with H_2O	[18–20]
	$RbAmO_2CO_3$	hexagonal	*C6/mmc*	5.12		10.46		Am(III)/10 M Rb_2CO_3/O_3	[17,21]
	$CsAmO_2CO_3$	hexagonal	*C6/mmc*	5.123		11.538		Am(III)/$CsHCO_3/O_3$	[22]
	$K_3AmO_2(CO_3)_2 \cdot nH_2O$	rhombic (a,b)	*C6/mmc*	5.32	9.21	8.76		(a) 4.7 M, (b) 2.3 M K_2CO_3	[20]
				5.29	9.11	8.83		Am(III)/3.5 M K_2CO_3	[23]
	$K_5AmO_2(CO_3)_3$	orthorhombic						Am(III)/>5 M K_2CO_3/O_3	[17,24]
	$(NH_4)_5AmO_2(CO_3)_3$							Am(VI)/NH_4CO_3	[3]
	$(NH_4)_4AmO_2(CO_3)_3$							Am(VI)/$NaHCO_3/(NH_4)_2CO_3$	[25]
	$Cs_4AmO_2(CO_3)_3$							Am(VI)/$NaHCO_3/Cs_2CO_3$	[25]
Chlorides									
	$AmCl_2$	orthorhombic	*Pbnm*	8.963	7.573	4.532		Am/$HgCl_2$/heat	[5,6]
	$AmCl_3$	hexagonal	P_{63}/m	7.382		4.214		AmO_2/HCl	[7–9,26]
	$AmCl_3 \cdot 6H_2O$	monoclinic	*P2/n*	9.702	6.567	8.009	$\beta = 93.62$		[26,27]
	AmOCl	tetragonal	*P4/nmm*	4.00		6.78			[28]
	$CsAmCl_4$							Am(III)/HCl/CsCl	[29]
	$CsAmCl_4 \cdot 4H_2O$							Am(III)/HCl/CsCl	[29,30]
	Cs_3AmCl_6							Am(III)/HCl/CsCl	[31]
	$Cs_2NaAmCl_6$	fcc	*Fm3m*	10.8548(8)				Am(V)/HCl/CsCl/NaCl	[29,30,32]
	$[(C_6H_5)_3PH]_3$ $AmCl_6$		$Cs_3NpO_2Cl_4$					ethanol pptn.	[10,33]
	$Rb_2AmO_2Cl_4$	monoclinic	*C2/c*	11.53	7.48	5.65	$\beta = 99.19$	Am(V)/HCl/RbCl	[3]
	$Cs_2AmO_2Cl_4$	monoclinic	*C2/c*	11.92	7.61	1167	$\beta = 99.56$	Am(V)/HCl/CsCl	[3]
Chromate									
	$(AmO_2)_2CrO_4 \cdot nH_2O$							20–80°C	[34]
Fluorides									
	AmF_3	hexagonal	$P\bar{3}c1$, LaF_3	7.044		7.225		m.p. 1400°C/v.p.	[35]
	AmF_4	monoclinic	*C2/c*, UF_4	12.538	10.516	8.204	$\beta = 126.8$	AmF_3/F_2/v.p.	[36,37]
	AmO_2F_2	hexagonal	*R3m*	4.136		15.85			[38]
	AmF_6							KrF_2/HF(li); dark brown	[39]

	$NaAmF_4$	hexagonal	*P*6	6.109		3.731		$AmO_2/HF–H_2/NaF$	[40,41]
	$KAmF_4$	orthorhombic	*Pnma*	6.13	3.71	15.2			[42]
	K_3AmF_6	hexagonal	K_3LaF_6	22.75		7.56		$AmO_2/HF–H_2/KF/$ 650°C	[42]
	K_2AmF_5		K_2PrF_5						[42]
	KAm_2F_7	cubic	KEu_2F_7	5.857					[41,42]
	$(NH_4)_4AmF_8$	monoclinic	C2/*c*, $(NH_4)_4UF_8$					$Am(OH)_4/NH_4F$	[43]
	$LiAmF_5$	tetragonal	$I4_1/a$	14.63		6.449			[44]
	$K_7Am_6F_{31}$	hexagonal	*R*3	14.938		10.293		Am(III)/KF	[44,45]
	$Na_7Am_6F_{31}$	hexagonal	*R*3	14.48		9.665			[45]
	$RbAmF_4$	orthorhombic	*Pnma*	6.43	3.76	16.0			[42]
	Rb_2AmF_6	orthorhombic	*Cmcm*	6.962	12.001	7.579			[45,46]
	$KAmO_2F_2$	rhombohedral	*R*3*m*,$CaUO_4$	6.78			$\alpha = 36.25$	AmO_2+/KF	[47]
	$RbAmO_2F_2$	rhombohedral	*R*3*m*	6.789			$\alpha = 36.25$	AmO_2+/RbF	[48]
Germanate									
	$AmGeO_4$	Tetragonal	$I4_1/a$	5.04		11.03			[49]
Hydrides									
	AmH_2	fcc	*Fm*3*m*	5.348				AmH_{2+x}, $x = 0–0.7$	[50,51]
	AmH_3	trigonal	*P*3*c*1	6.68		6.75			[51]
Hydroxide									
	$Am(OH)_3$(am)	hexagonal	$Nd(OH)_3$	6.426		3.745		Am(III)/NaOH, Ksp $\sim 3 \times 10^{-18}$	[52]
	$Am(OH)_3$(cr)							$Am_2O_3(s)/H_2O(g)$	[53]
	$Am(OH)_4$							$Am(OH)_3/NaOCl$	[54]
	$LiAmO_2(OH)_2 \cdot xH_2O$							Am(V)/0.1–2 M LiOH	[55]
	$NaAmO_2(OH)_2 \cdot xH_2O$							Am(V)/0.1–0.5 M NaOH	[55]
	$KAmO_2(OH)_2 \cdot xH_2O$							Am(V)/0.1–0.5 M KOH	[55]
	$RbAmO_2(OH)_2 \cdot xH_2O$							Am(V)/0.1–0.5 M RbOH	[56]
	$CsAmO_2(OH)_2 \cdot xH_2O$							Am(V)/0.1–0.5 M CsOH	[56]
	$Na_2AmO_2(OH)_3 \cdot xH_2O$							Am(V)/2 M NaOH	[55]
	$K_2AmO_2(OH)_3 \cdot xH_2O$							Am(V)/2 M KOH	[55]
	$Rb_2AmO_2(OH)_3 \cdot xH_2O$							Am(V)/>2 M RbOH	[56]
	$Cs_2AmO_2(OH)_3 \cdot xH_2O$							Am(V)/>2 M CsOH	[56]
Iodides									
	AmI_2	monoclinic		7.677	8.311	7.925	$\beta = 98.46$	$Am/H_2/I_2$/vac.	[57]
	α-AmI_3	orthorhombic	*Ccmm*	4.31	14.03	9.92		AmO_2/AlI_3	[8,58]
	β-AmI_3	hexagonal	*R*3	7.42		20.55			[8,58]
	AmOI	tetragonal		4.011		9.204			[8,58]
Iodates									
	$Am(IO_3)_3$	monoclinic	$P2_1/c$	7.243	8.538	13.513	$\beta = 100.123$	$Am/HCl/KIO_4$/180°C	[59]
	$K_3Am_3(IO_3)_{12} \cdot HIO_3$	triclinic		22.096	22.096	13.436	$\gamma = 120$	Am/KIO_4/180°C	[59]

Table 8.5 (*Contd.*)

Class	*Structural formula*	*Symmetry*	*Type*	*Lattice constants*			*Angle* (deg)	*Comments*	*References*
				a_0 (Å)	b_0 (Å)	c_0 (Å)			
Molybdates									
	α-$Am_2(MoO_4)_3$	tetragonal	$I4_1/a$	5.24		11.52		$AmO_2/MoO_3/\sim 825°C$	[60,61]
	β-$Am_2(MoO_4)_3$	orthorhombic		9.095	10.527	10.820		$AmO_2/MoO_3/>850°C$	[60,61]
	$LiAm(MoO_4)_2$	tetragonal	$I4_1/a$, $LiGd(MoO_4)_2$	5.20		11.39		$Am_2(MoO_4)_3/Li_2MoO_4$	[61]
	$Am_2(MoO_4)_3$	tetragonal	scheelite						[60]
	$NaAm(MoO_4)_2$	tetragonal	scheelite	5.25		11.55			[61]
	$Na_5Am(MoO_4)_4$		$Na_5La(WoO_4)_4$	11.515		11.429		solid-state reaction	[61]
	$K_2Am(MoO_4)_4$							solid-state reaction	[61]
	$K_{10}Am(MoO_4)_8$							solid-state reaction	[61]
	$K_3AmO_2(Mo_2O_7)_2 \cdot nH_2O$							$AmO_2NO_3/K_6Mo_7O_{24}$	[62]
	$(NH_4)_3AmO_2(Mo_2O_7)_2 \cdot nH_2O$							$AmO_2NO_3/(NH_4)_6Mo_7O_{24}$	[62]
	$AmO_2Mo_2O_7$							AmO_2SO_4/Na_2MoO_4, <100°C	[62]
Nitride									
	AmN	fcc	$Fm3m$,NaCl	5.000				$Am(AmH_3)/N_2$	[63,64]
Nitrate									
	$CsAmO_2(NO_3)_3$							$Cs_4AmO_2(CO_3)_3$/2M HNO_3/O_3; evap	[25]
Oxides									
	AmO(?)	fcc	$Fm3m$	5.045				Am/Ag_2O	[63,65]
	A-Am_2O_3	hexagonal	$P3m1$	3.817		5.971		$AmO_2/H_2/800°C$	[66,70]
	B-Am_2O_3	monoclinic	$C2/m$	14.38	3.52	8.92	$\beta = 100.4$		[67,68]
	C-Am_2O_3	cubic	$Ia3$	11.03				600°C	[66,69,70]
	AmO_2	fcc	$Fm3m$	5.374				$^{241}AmO_2$, $^{243}AmO_2$	[70,71]
	AmO_{2-x}								[67,74]
	$LiAmO_2$								[1,72,73]
	Li_2AmO_3								[1,72,73]
	Li_8AmO_6	hexagonal	Li_8PbO_6	5.62		15.96			[1,72,73]
	Li_3AmO_4	tetragonal	Li_3UO4	4.459		8.355			[1,72,73]

Li_7AmO_6	hexagonal	*R*3	5.54		15.65			[1,72,73]
Li_4AmO_5	tetragonal	*I4/m*	6.666		4.415			[1,72,73]
Li_6AmO_6	hexagonal	Li_6ReO_6	5.174		14.59			[1,72,73]
K_2AmO_4	tetragonal	*I4/mmm*	4.286		13.05			[73]
Na_2AmO_3	monoclinic	*C2/c*	5.92	10.26	11.23	$\beta = 100.12$		[1,72,73]
Na_3AmO_4	fcc	*Fm3m*	4.757					[1,72,73]
Na_4AmO_5	fcc	*Fm3m*	4.70					[1,72,73]
Na_6AmO_6	hexagonal	Li_6ReO_6	4.76		16.10			[1,72,73]
$BaAm_2O_4$								[1,75]
$BaAmO_3$	cubic	perovskite	4.356					[1,75]
Ba_3AmO_6	cubic	*F43m*	8.81					[1,75]
$SrAm_2O_4$								[1,75]
$SrAmO_3$	cubic	perovskite	4.23					[1,75]
Sr_3AmO_6	cubic	Ba_3WO_6						[1,75]
Cs_2AmO_4	tetragonal	*I4/mmm*	4.364		14.65		$AmO_2/CsOH/O_2/$ 250°C	[76]
Rb_2AmO_4	tetragonal	*I4/mmm*	4.316		13.71		$AmO_2/RbOH/O_2/$ 250°C	[76]
$(Am_{0.30},Cm_{0.70})O_{2.00}$	fcc		5.368				350°C in O_2	[77]
$(Am_{0.30},Cm_{0.70})O_{1.83}$	fcc		5.433				550°C in O_2	[77]
$(Am_{0.30},Cm_{0.70})O_{1.685}$	rhombohedral		6.687			$\alpha = 99.47$	760°C in He	[77]
$(Am_{0.30},Cm_{0.70})O_x$	bcc		10.935				900°C in He	[77]
$(Am_{0.64},Cm_{0.36})O_{1.5}$	monoclinic		14.321	3.665	8.926	$\beta = 100.17$	1100°C in H_2/He	[77]
$(Am_{0.64},Cm_{0.36})O_{1.5}$	hexagonal		3.812		5.980		1500°C in H_2/He	[77]
AmO–ZrO_2	cubic	fluorite					18–100% AmO_2/ZrO_2, SS	[1,78]
AmO–HfO_2							SS, extent unknown	[1,78]
AmO–ThO_2	cubic	fluorite					ThO_2/AmO_2, complete SS	[1]
α-$AmNbO_4$	monoclinic	I2	5.444	11.25	5.141	$\beta = 94.95$	AmO_2/Nb_2O_5	[1,2]
β-$AmNbO_4$	tetragonal	$I4_1/a$	5.30		11.34		α→β ~ 600°C	[1,2]
$Am_{0.33}NbO_3$	pseudo-tetragonal	*P4/mm*, $La_{0.33}TaO_3$	3.819		7.835			[1,2]
Ba_2AmNbO_6	cubic	*F43m*	8.520				$AmNbO_4/BaO$	[1,2]
$AmNbTiO_6$	orthorhombic	*Pnam*	5.34	11.00	7.53		$AmNbO_4/TiO_2$	[1,2]
$AmTaO_4$	monoclinic	*I2*	5.489	11.21	5.115	95.37	AmO_2/Ta_2O_5	[1,2]
$Am_{0.33}TaO_3$	tetragonal	*I41/a*	3.889		7.820		AmO_2/Ta_2O_5	[1,2]
Ba_2AmTaO_6	cubic	*F43m*	8.518					[1,2]
$AmTaTiO_6$	orthorhombic	*Pnam*	5.33	10.95	7.49			[2]
$AmPaO_4$	fcc	*Fm3m*	5.458				AmO_2/Pa_2O_5	[1,2]
Ba_2AmPaO_6	cubic	*F43m*	8.793				$(Am_{0.5}Pa_{0.5})O_2/BaO$	[1,2,79]

Table 8.5 (*Contd.*)

Class	Structural formula	Symmetry	Type	Lattice constants a_0 (Å)	b_0 (Å)	c_0 (Å)	Angle (deg)	Comments	References
Phosphates									
	$AmPO_4$	monoclinic	$P2_1/n$	6.73	6.93	6.41	103.5	stable to 1000°C	[2]
	$AmPO_4 \cdot 0.5H_2O$	Hexagonal		6.99		6.39		pptn. dried at 200°C	[2]
	$NH_4AmO_2PO_4 \cdot 3H_2O$							Am(VI)/$NaHCO_3$/ $NH_4H_2PO_4$	[25]
	$NH_4AmO_2PO_4 \cdot zH_2O$	tetragonal	$P4/nmm$ or $I4/mmm$	6.99		9.06		Am(VI)/0.1 M H_3PO_4/ pH 3.5, lemon yellow	[3]
	$KAmO_2PO_4 \cdot zH_2O$	tetragonal	$P4/nmm$ or $I4/mmm$	6.91		9.00		Am(VI)/0.1 M H_3PO_4/ pH 3.5, lemon yellow	[3]
	$RbAmO_2PO_4 \cdot zH_2O$	tetragonal	$P4/nmm$ or $I4/mmm$	6.94		9.02		Am(VI)/0.1 M H_3PO_4/ pH 3.5, lemon yellow	[3]
	$CsAmO_2PO_4 \cdot zH_2O$	tetragonal	$P4/nmm$ or $I4/mmm$	6.94		8.82		Am(VI)/0.1 M H_3PO_4/ pH 3.5, lemon yellow	[3]
Phosphide									
	AmP	cubic	NaCl	5.711				AmH_3/P/580°C	[63,80]
Rhenate									
	$Am(ReO_4)_3$	hexagonal		10.11		6.26		AmO_2/aq $HReO_4$ AmO_2/Re_2O_7/850°C	[81] [81]
Scandate									
	$AmScO_3$	orthorhombic	$P6mm$, $GdFeO_3$	5.540	5.785	8.005		$AmO_2/H_2/Sc_2O_3$ oxidation yields fluorite	[82] [68]
Selenates									
	AmSe	cubic	NaCl	5.821				AmH_3/Se	[63]
	$AmSe_{2-x}$	tetragonal		4.096		8.347			[83]
	Am_3Se_4	bcc	$I43d$, Th_3P_4	8.799					[63,80,86]
Silicate									
	$AmSiO_4$	tetragonal	zircon	6.87		6.20		hydrothermal	[49]
Silicide									
	Am_5Si_3			11.419		5.538		AmF_3/Si/1050°C	[84]
	AmSi	orthorhombic		8.39	4.09	6.01		AmF_3/Si/1050°C	[85]
	$Am_3Si_5 \ldots Am_2Si_3$	hexagonal	Pu_3Si_5	3.871		4.120		AmF_3/Si/1050°C	[84]
	$AmSi_x$ ($x < 2$)	tetragonal	α-$ThSi_2$	4.02		13.7			[85]

Sulfates							
	$Am_2(SO_4)_3 \cdot 8H_2O$						[37]
	$Am_2O_2SO_4$						[37]
	$Am_2(SO_4)_3 \cdot 5H_2O$						[37]
	$KAm(SO_4)_2$						[37]
	$NaAm(SO_4)_2 \cdot H_2O$						[37]
	$KAm(SO_4)_2 \cdot 2H_2O$						[37]
	$RbAm(SO_4)_2 \cdot 4H_2O$						[37]
	$CsAm(SO_4)_2 \cdot 4H_2O$						[37]
	$TlAm(SO_4)_2 \cdot 4H_2O$						[37]
	$K_3Am(SO_4)_3 \cdot H_2O$						[37]
	$K_8Am_2(SO_4)_7$						[37]
	$Cs_8Am_2(SO_4)_7$						[37]
	$Tl_8Am(SO_4)_7$						[37]
	$\{[Co(NH_3)_6](HSO_4)_2$ $[AmO_2(SO_4)_3]\} \cdot nH_2O$	cubic					[87]
	$(AmO_2)_2SO_4 \cdot nH_2O$					$AmO_2OH/aqH_2SO_4/$ evap	[88]
	$CsAmO_2SO_4 \cdot nH_2O$					aq. $Cs_2SO_4/(AmO_2)_2$ SO_4/evap	[88]
	$Co(NH_3)_6AmO_2(SO_4)_2 \cdot 2H_2O$						[88]
Sulfides							
	AmS	fcc	*Fm3m*	5.592			[89]
	Am_2O_2S	trigonal	*P3m*	3.91		6.772		[52]
	$AmS_{1.9}$	tetragonal		3.938		7.981		[52]
	α-Am_2S_3	orthorhombic	*Pnma*	3.98	6.39	15.36	α→γ ~ 1300°C	[89,90]
	β-Am_2S_3							[91]
	γ-Am_2S_3	bcc	*I43m*	8.434				[91]
	$Am_{10}S_{14}O_3$							[91]
Tellurides							
	$AmTe_2$	tetragonal		4.366		8.969	AmH_3/Te/heat	[63,92]
	$AmTe_3$	orthorhombic	*Bmmb*	4.399	4.339	25.57		[92]
	Am_2Te_3	orthorhombic	*Pbnm*	11.93	12.12	4.33		[93]
	Am_3Te_4	bcc	I43*d*	9.394				[93,96]
Titanates							
	$Am_2Ti_2O_7$	monoclinic		13.07		7.69	$AmO_2/TiO_2/$ 1200–1300°C	[94]
	$SrAm_2Ti_4O_{12}$	tetragonal		3.89		7.75	$SrCO_3/AmO_2/TiO_2/$ 1215°C	[94]
Tungstate							
	$Am_2(WO_4)_3$	tetragonal	*I*4_1/*a*					[60]

Table 8.5 (*Contd.*)

Class	*Structural formula*	*Symmetry*	*Type*	*Lattice constants* a_0 (Å)	b_0 (Å)	c_0 (Å)	*Angle* (deg)	*Comments*	*References*
Vanadates									
	$AmVO_3$	orthorhombic	*Pbnm*, $GdFeO_3$	5.45	5.58	7.76		AmO_2/V_2O_5	[1,2]
	$AmVO_4$	tetragonal	zircon	7.31		6.42			[1,2]
Xenate									
	$Am_4(XeO_6)_3 \cdot 40H_2O$								[95]

[1] (Keller and Walter, 1965); [2] (Keller, 1967); [3] (Lawaldt *et al.*, 1982); [4] (Eick and Mulford, 1969); [5] (Peterson, 1973); [6] (Baybarz, 1973b); [7] (Zachariasen, 1948b; Fried, 1951; Brown *et al.*, 1968; Pappalardo *et al.*, 1969b); [8] (Asprey *et al.*, 1965); [9] (Brown *et al.*, 1968); [10] (Ryan, 1967); [11] (Weigel *et al.*, 1979); [12] (Mitchell and Lam, 1970b); [13] (Runde *et al.*, 1992); [14] (Weigel and ter Meer, 1967); [15] (Fang and Keller, 1969); [16] (Runde and Kim, 1994); [17] (Nigon *et al.*, 1954); [18] (Coleman *et al.*, 1963); [19] (Keenan and Kruse, 1964); [20] (Volkov *et al.*, 1974); [21] (Ellinger and Zachariasen, 1954); [22] (Keenan, 1965); [23] (Burney, 1968); [24] (Yakovlev and Gorbenko-Germanov, 1955); [25] (Fedoseev and Perminov, 1983); [26] (Burns and Peterson, 1970, 1971); [27] (Lohr and Cunningham, 1951; Fuger and Cunningham, 1963); [28] (Weigel *et al.*, 1975); [29] (Bagnall *et al.*, 1968; Morss *et al.*, 1970); [30] (Bagnall *et al.*, 1967); [31] (Marcus and Shiloh, 1969); [32] (Schoebrechts *et al.*, 1989); [33] (Marcus and Bomse, 1970); [34] (Fedoseev *et al.*, 1991); [35] (Jones, 1951; Carniglia and Cunningham, 1955; Burnett, 1965, 1966); [36] (Asprey, 1954; Asprey and Keenan, 1958; Chudinov and Choporov, 1970; Connor, 1971); [37] (Yakovlev and Kosyakov, 1958a,b); [38] (Keenan, 1968); [39] (Drobyshevskii *et al.*, 1980); [40] (Keller and Schmutz, 1964); [41] (Schmutz, 1966); [42] (Jove and Pages, 1977); [43] (Asprey and Penneman, 1962); [44] (Keenan, 1966); [45] (Keenan, 1967); [46] (Kruse and Asprey, 1962); [47] (Asprey *et al.*, 1954a); [48] (Keenan, 1965); [49] (Keller, 1963); [50] (Katz and Seaborg, 1957); [51] (Olson and Mulford, 1966); [52] (Weaver and Shoun, 1971; Haire *et al.*, 1977); [53] (Morss and Williams, 1994); [54] (Cunningham, 1949; Penneman *et al.*, 1961); [55] (Tananaev, 1990b); [56] (Tananaev, 1991); [57] (Baybarz and Asprey, 1972); [58] (Asprey *et al.*, 1964); [59] (Bean *et al.*, 2003b); [60] (Freundlich and Pages, 1969; Tabuteau and Pages, 1978); [61] (Tabuteau *et al.*, 1972); [62] (Fedoseev and Budantseva, 1990); [63] (UCRL, 1959; Akimoto, 1967); [63] (Charvillat *et al.*, 1975a); [64] (Charvillat and Zachariasen, 1977); [65] (Zachariasen, 1949a); [66] (Templeton and Dauben, 1953); [67] (Chikalla and Eyring, 1968; Chikalla *et al.*, 1973); [68] (Berndt *et al.*, 1974; Keller and Berndt, 1975); [69] (Eyring *et al.*, 1949, 1952); [70] (Hurtgen and Fuger, 1977); [71] (Fahey *et al.*, 1974); [72] (Keller *et al.*, 1965b); [73] (Hoekstra and Gebert, 1978); [74] (Chikalla and Eyring, 1967); [75] (Keller, 1964); [76] (Hoekstra and Gebert, 1978); [77] (Mosley, 1970); [78] (Radzewitz, 1966); [79] (Keller, 1965); [80] (Charvillat *et al.*, 1975b); [81] (Silvestre *et al.*, 1977); [82] (Keller *et al.*, 1972); [83] (Damien and Jove, 1971); [84] (Wittmann, 1980); [85] (Burns and Baybarz, 1972; Weigel *et al.*, 1977); [86] (Mitchell and Lam, 1970a; Roddy, 1974); [87] (Ueno and Hoshi, 1971); [88] (Fedoseev and Budentseva, 1989); [89] (Damien, 1971); [90] (Zachariasen, 1949d); [91] (Damien *et al.*, 1972, 1975, 1976); [92] (Burns *et al.*, 1979); [93] (Damien and Charvillat, 1972); [94] (Shoup and Bamberger, 1997); [95] (Marcus and Cohen, 1966).

temperatures of 600–800°C (Eyring *et al.*, 1952; Baybarz, 1960; Chikalla and Eyring, 1967; Hurtgen and Fuger, 1977; Morss and Fuger, 1981). This stoichiometry of the black oxide is believed to be $AmO_{2.00}$ (Chikalla and Eyring, 1967, 1968) and is better than $AmO_{1.99}$ even at 1000°C in oxygen (Chikalla and Eyring, 1967). It undergoes an expansion of its fcc lattice constant due to radiation damage, which reversibly broadens the diffraction lines at low temperatures in both $^{241}AmO_2$ and $^{243}AmO_2$ (Hurtgen and Fuger, 1977; Benedict and Dufour, 1980). Benedict and Dufour (1980) studied the variation of the lattice parameter, of the thermal linear expansion, and of the coefficient of thermal linear expansion for AmO_2 in the range 38–300 K. Upon cooling, AmO_2 contracts more strongly than the dioxides of the lower actinides. The lattice parameters quoted in Table 8.3 represent an extrapolation to zero time for both $^{241}AmO_2$ and $^{243}AmO_2$ (Fahey *et al.*, 1974; Hurtgen and Fuger, 1977).

There is no evidence for any binary oxide of americium higher than AmO_2 (Katz and Gruen, 1949; Templeton and Dauben, 1953). However, ternary oxides are known for Am(III) through Am(VI) (Keller, 1964, 1965; Keller *et al.*, 1965b; Radzewitz, 1966; Mosley, 1970; Keller *et al.*, 1972; Keller and Berndt, 1975; Hoekstra and Gebert, 1978). Stabilization of high oxidation states in complex oxides is frequently observed (Keller, 1964, 1967; Morss, 1982); excellent examples are the thermally stable Am(VI) compounds Cs_2AmO_4 and Ba_3AmO_6. Most complex oxides of americium have been prepared by Keller and Hoekstra and their coworkers (Keller, 1964, 1967; Keller *et al.*, 1965b; Hoekstra and Gebert, 1978).

Initially, americium was prepared in significant quantities as $Am(OH)_3$ and to date hydroxide phases are known for the oxidation states III–VI. Isostructural to its chemical analog $Nd(OH)_3$, the Am(III) hydroxide is by far the most important americium hydroxide for separation and purification purposes and its solubility has been widely studied. The pinkish amorphous hydroxide precipitates by addition of dilute hydroxide to Am(III) solutions under ambient conditions. Rod-like microcrystalline $Am(OH)_3$, similar to $Nd(OH)_3$, is obtained in water after heating at 80°C for about 90 min (Milligan and Beasley, 1968). The transformation rate depends on various experimental parameters, such as solution composition, basicity, temperature, radiolysis, and the (pre)treatment of the precipitate. The crystalline phase can also be obtained by boiling a $^{241}Am(OH)_3$ suspension in 5 M NaOH (Silva, 1982) or hydration of Am_2O_3 with steam at 225°C (Morss and Williams, 1994). The destruction of the crystalline phase by its own alpha-radiation depends strongly on the specific activity of the isotope used: complete degradation is obtained within 1 day using ^{244}Cm(III) (specific activity 3000 MBq mg^{-1}) and 5 months with ^{241}Am(III) (specific activity 120 MBq mg^{-1}) (Haire *et al.*, 1977). The complex aging behavior of $Am(OH)_3$ in aqueous solutions and the changes in particle size result in large differences in its solubility. Nevertheless, two thermodynamic solubility products for the reaction

$$\mathrm{Am(OH)_3 + 3H^+ = Am^{3+} + 3H_2O}$$

have been recommended: $\log K^\circ = 15.2 \pm 0.6$ for crystalline $Am(OH)_3$ and 17.0 ± 0.6 for amorphous $Am(OH)_3$ (Silva *et al.*, 1995).

Few attempts to prepare and characterize $Am(OH)_4$ were reported, probably due to the instability of Am(IV). A black precipitate of $Am(OH)_4$ was obtained by heating $Am(OH)_3$ at 90°C in 0.2 M NaOH with NaOCl or in 7 M KOH with peroxydisulfate (Penneman *et al.*, 1961). The dissolution of this precipitate in sulfuric or nitric acid leads to a mixture of Am(III), Am(V), and Am(VI). Structural and thermodynamic data on $Am(OH)_4$ are not known. $AmO_2(OH)$ has been suggested to precipitate in slightly basic concentrated NaCl solutions under inert atmosphere but the amorphous character of the solid phase inhibited characterization (Magirius *et al.*, 1985; Stadler and Kim, 1988; Giffaut and Vitorge, 1993; Runde and Kim, 1994; Runde *et al.*, 1996). In more concentrated hydroxide solutions ternary Am(V) hydroxides, yellow $MAmO_2(OH)_2 \cdot nH_2O$ at 0.1–0.5 M OH^- and rose-colored $M_2AmO_2(OH)_3 \cdot nH_2O$ (M = Na, K, Rb, Cs) at 0.5–2.0 M OH^- (Tananaev, 1990b, 1991), form, and were characterized by X-ray diffraction. Only the lithium compound appeared to be stable over the entire range of hydroxide concentrations. No information on Am(VI) hydroxides is available.

(b) Hydrides

Olson and Mulford (1966) characterized the ^{241}Am–hydrogen system and found parallels to the lanthanides. The reported AmH_{2+x} (fcc) phase is isostructural with NpH_{2+x}, PuH_{2+x}, and most of the rare earth dihydrides (Roddy, 1973). There is also a phase that approximates hexagonal AmH_3. Although the lattice parameters were reported to be $a_0 = 3.77$ Å and $c_0 = 6.75$ Å (Olson and Mulford, 1966), Keller (1971) has pointed out that recent data on HoD_3 makes the most probable space group $P3c1$ (lattice parameters are given in Table 8.3). A study by Roddy (1973) with ^{243}Am essentially confirms this conclusion.

(c) Halides

A number of americium halides have been synthesized with americium in oxidation states II–VI and the halide systems have been studied extensively. Most remarkable are the halides of americium in extreme oxidation states, i.e. divalent and hexavalent. While solid structures are rare for divalent americium compounds, the black halides, $AmCl_2$ and $AmBr_2$ (Baybarz, 1973b), and AmI_2 (Figure 8.8) (Baybarz and Asprey, 1972) were prepared by reacting metallic americium with the corresponding mercuric halides at 300–400°C. The dihalides cannot be prepared by hydrogen reduction of the Am(III) halides, although hydrogen reduction is successful for the chemical analog lanthanides Sm, Eu, and Yb. Interestingly, all three compounds crystallize in different lattices: orthorhombic $AmCl_2$, tetragonal $AmBr_2$, and monoclinic AmI_2.

(1) Am(III): A number of Am(III) halides have been synthesized and their compositions range from binary AmX_3 adducts such as $AmCl_3 \cdot MCl$ where MCl is LiCl, CsCl, $(C_4H_9)_4NCl$, or $(C_2H_5)_4NCl$, to ternary complexes, i.e. $MAmX_4$, M_2AmX_5, KAm_2F_7, and M_2AmX_6 and M_3AmX_3. In addition, Bagnall *et al.* (1968) and Morss *et al.* (1970) made the cubic derivative $Cs_2NaAmCl_6$, in which the americium atoms are surrounded by six chlorides in an octahedral environment. The iodide AmI_3 is the only actinide triiodide known to be dimorphic; spectrophotometric observations indicate a pressure-induced phase transition from the rhombohedral to the orthorhombic structure (Haire *et al.*, 1985). The compound $(NH_4)_2AmCl_5$ decomposes at 300°C under vacuum to form $AmCl_3$ (Schleid *et al.*, 1987). Crystal structures have been reported for AmF_3 (Templeton and Dauben, 1953), $AmCl_3$ (Burns and Peterson, 1970) and $AmCl_3 \cdot 6H_2O$ (Burns and Peterson, 1971), $AmBr_3$ and AmI_3 (Zachariasen, 1948b; Baybarz and Asprey, 1972), and AmOX (X = Cl Figure 8.8 (Templeton and Dauben, 1953), Br (Weigel *et al.*, 1979) and I (Baybarz and Asprey, 1972)). Octahedral $AmCl_6^{3-}$ and $AmBr_6^{3-}$ can be prepared as triphenyl phosphonium salts in anhydrous ethanol (Ryan, 1967; Marcus and Bomse, 1970).

(2) Am(IV): Orange-pink crystals of orthorhombic Rb_2AmF_6 form in concentrated aqueous fluoride solutions with $RbAmO_2F_2$ or $Am(OH)_4$ (Kruse and Asprey, 1962).

(3) Am(V): The ternary Am(V) fluorides, $KAmO_2F_2$ (Asprey *et al.*, 1954a) and $RbAmO_2F_2$, precipitate from concentrated aqueous fluoride solutions of Am(V) and consist of $AmO_2F_2^-$ connected by K^+ or Rb^+ cations. In contact with acidic RbF solution, $RbAmO_2F_2$ reduces overnight to Rb_2AmF_6 (Kruse and Asprey, 1962). The green chloride $Cs_3AmO_2Cl_4$ precipitates with ethanol from 6 M HCl containing Am(V) hydroxide and CsCl (Bagnall *et al.*, 1968) and is isostructural with the analogous Np(V) compound (Bagnall *et al.*, 1967).

(4) Am(VI): The binary Am(VI) fluoride AmO_2F_2 was prepared by reacting solid sodium Am(VI) acetate with anhydrous HF containing a small amount of F_2 at −196°C (Keenan, 1968). The compound is isostructural with other actinyl(VI) fluorides. Dark-red $Cs_2AmO_2Cl_4$ is obtained by the unusual oxidation of $Cs_3AmO_2Cl_4$ in concentrated HCl (Bagnall *et al.*, 1967). The cubic form of $Cs_2AmO_2Cl_4$ appears to transform to a monoclinic form when washed with small volumes of concentrated HCl (Bagnall *et al.*, 1968). It is suggested that the cubic form is probably a mixed oxidation state compound of formula $Cs_7(AmO_2)(AmO_2)_2Cl_{12}$ (Melkaya *et al.*, 1982).

Conflicting claims have been put forth concerning the existence of AmF_6. Drobyshevskii *et al.* (1980) reported generating a solid by reaction of AmF_3

with KrF_2 in anhydrous HF and inferred its composition to be AmF_6 based upon its volatility, IR spectrum, and hydrolysis to AmO_2^{2+}; the IR absorption band at $604 \pm 3\ cm^{-1}$ is expected for the ν_3 mode of AmF_6. Fargeas *et al.* (1986) also inferred the existence of AmF_6 in their experiments from thermochromatography data. Most recently, Gibson and Haire (1992b) report that they were not able to confirm the existence of AmF_6; in their words, "... but have not been able to identify or provide evidence for the elusive and controversial AmF_6 species, despite having invoked several synthetic approaches and the sensitive analytical tool of mass spectrometry." Given these latest results, we have elected not to list AmF_6 among the identified inorganic compounds of americium in Table 8.5. It is interesting to note, however, that the proposed hexachloro compound of Am(VI) appears to be sufficiently stable to permit X-ray crystallographic studies.

(d) Chalcogenides and pnictides

The chalcogenides of americium comprise a number of compounds with the general formula AmX (X = S, Se, Te), $AmTe_2$, Am_3X_4 (X = S, Se, Te), AmX_3 (X = S, Se, Te), Am_2X_3 (X = S, Se, Te), and substoichiometric compounds AmX_{2-n} (X = S, Se). Some structural and synthetic properties of these chalcogenides, insofar as they have been determined, are briefly listed in Table 8.5; additional details concerning these compounds are provided in this section. The authors of this chapter are not aware that the chalcogenides are of any but academic interest.

The reaction of AmH_3 with stoichiometric amounts of selenium or telluride metal at 800°C in a vacuum yields the monochalcogenides AmSe and AmTe, respectively (Charvillat *et al.*, 1975a, 1977). Further heating of the monochalcogenides at 1100–1200°C produces Am_3X_4 and a second phase that was identified as (probably unreacted) AmX (Charvillat *et al.*, 1975a, 1977). In contrast, α-Am_2S_3 and not AmS is obtained when AmH_3 is heated with elemental sulfur at 500°C; it decomposes to γ-Am_2S_3 and AmS when heated in a vacuum above 650°C (Damien, 1971).

Americium sesquisulfide exhibits a complex structural chemistry and apparently exists in three different crystalline forms. α-Am_2S_3 is obtained by vapor-phase reaction for 4 days of a stoichiometric amount of sulfur with AmH_3 in a quartz and Pyrex tube sealed under high vacuum (Damien, 1971). The quartz end of the tube is heated at 500°C and the Pyrex part is maintained at 300°C to prevent sulfur from condensing. According to Damien *et al.* (1972), α-Am_2S_3 transforms into β-Am_2S_3 when heated at 1100°C. However, the existence of the β-form of americium sesquisulfide is seriously in doubt since the same French scientists believe that β-Am_2S_3 is better considered an oxysulfide, namely $Am_{10}S_{14}O$. When heated in a vacuum at 1300°C, α-Am_2S_3 changes to pure γ-Am_2S_3 (Damien, 1971). The pure γ-Am_2S_3 can also be prepared by passing a mixture of H_2S and CS_2 over heated (1400–1500°C) AmO_2 for 5 min

(Fried, 1951). Zachariasen (1949d) determined the crystal structure of γ-Am_2S_3. Am_2Te_3 is formed by dissociation of $AmTe_2$ at 600°C and is isostructural with the rare earth sesquitellurides (η-form) (Damien and Charvillat, 1972). The Am_2Te_3 phase is stable up to around 850°C and transforms into Am_3Te_4 above 900°C. No sesquiselenide of americium has been reported.

The only americium trichalcogenide yet reported, $AmTe_3$, is prepared by vapor-phase reaction of AmH_3 with excess tellurium for 120 h at 350°C (Damien, 1972; Burns *et al.*, 1979). Orthorhombic $AmTe_3$ is isostructural with the corresponding rare earth tritellurides and is used as a precursor for the synthesis of a number of americium/tellurium compounds. In a high vacuum at 400°C, $AmTe_3$ dissociates to tetragonal $AmTe_2$, which is the only stoichiometric americium dichalcogenide. $AmTe_2$ is isostructural with the rare earth ditellurides and most likely has the Fe_2As-type structure. Roddy (1974) prepared what appeared to be tetragonal $AmSe_2$ by heating ^{243}Am metal or hydride with selenium metal for 24 h at 950°C. However, although two research groups (Charvillat *et al.*, 1977; Burns *et al.*, 1979) reported the preparation and properties of $AmTe_2$, Damien and Jove (1971) state that the $AmTe_2$ prepared as described above is rather a tellurium-deficient compound $AmTe_{2-x}$ with a large homogeneity range between 400 and 600°C. The same homogeneity range seems to exist in the Am–S and Am–Se system and the dichalcogenides actually have a composition near $AmS_{1.9}$ and $AmSe_{1.8}$. The black non-stoichiometric compounds are prepared by heating an excess of sulfur or selenium metal with AmH_3 for 1 week at 400°C under high vacuum (Damien and Jove, 1971).

The americium chalcogenides Am_3Se_4 and Am_3Te_4 are isostructural (bcc) with Th_3P_4 and are without magnetic ordering down to 4.2 K (Dunlap *et al.*, 1972). Both compounds can be prepared by heating ^{243}Am metal with elemental selenium or tellurium for 24 h at 950°C (Roddy, 1974). However, X-ray diffraction measurements show that this synthesis contains at least one other phase (Dunlap *et al.*, 1972). Am_3Se_4 (bcc) is also formed when a mixture of 50 mass% americium metal and 50 mass% elemental selenium is heated for 1 h at 217°C and then for 7 h at 850°C before cooling to room temperature (Mitchell and Lam, 1970a). Am_3Te_4 also forms by decomposition of η-Am_2Te_3 at 900°C (Damien and Charvillat, 1972).

Compounds of americium with all group VB elements N, P, As, Sb, and Bi have been prepared. While AmN is of most interest due to its potential use as nuclear reactor fuel, the americium pnictides are mainly of academic interest. Ogawa *et al.* (1997) note that certain actinide nitrides, e.g. UN, NpN, PuN, can be fabricated by carbothermic reduction of their oxides in a nitrogen atmosphere. Based upon the thermodynamics of the carbothermic synthesis of AmN, calculations indicate that the carbothermic preparation of AmN would be much more difficult than preparation of either UN or PuN.

Americium nitride, AmN, was first prepared by reacting AmH_3 (above 800°C) or americium metal (at 750°C) with nitrogen (Akimoto, 1967; Tagawa, 1971) or in a 99.9% N_2/0.1% H_2 atmosphere (Radchenko *et al.*, 1982). Potter and Tennery (1973) disclosed a cyclic process to prepare finely divided AmN, which consists of incrementally dehydriding AmH_3 and nitriding the metal. Charvillat *et al.* (1975a, 1977) prepared milligram quantities of AmN by heating AmH_3 at 550°C under high-purity nitrogen in a sealed tube. A review of the phase behavior and crystal structure of actinide nitrides has been published (Tagawa, 1971).

The only reported synthesis of AmP was published a quarter of a century ago. Charvillat *et al.* (1975a,b, 1977) synthesized AmP by reacting red phosphorus with AmH_3 in a sealed quartz tube at 580°C.

The product of the vapor-phase reaction of excess elemental arsenic with $^{241}AmH_3$ at 330°C contains both unreacted elemental arsenic and a cubic phase that was assigned as AmAs by analogy with the corresponding NpAs and PuAs (Charvillat and Damien, 1973). Heating ^{243}Am metal and elemental arsenic for 24 h at 675°C and then 7 days at 400°C produces AmAs with slightly higher lattice parameters (Roddy, 1974). However, a slight decrease in the lattice parameters is observed after heating AmAs for 10 h at 1000°C. Weak lines that correspond to AmO are observed in the X-ray diffraction pattern of the resulting product indicating the existence of a solid solution between AmAs and AmO. The slight difference in lattice parameters may have been the result of an isotope effect or may be attributed to other minor americium oxide impurities.

The reaction of ^{243}Am metal with elemental antimony for 23 h at 775–900°C in an evacuated quartz bulb yielded cubic AmSb (Roddy, 1974). Cubic AmSb with almost the same lattice parameters was obtained by heating equimolar amounts of ^{241}Am metal and high-purity elemental antimony under vacuum for 1 h at 630°C (Mitchell and Lam, 1970a). The temperature was gradually raised to 850°C and held at this temperature for 7 h before cooling to room temperature. Finally, the resulting AmSb was heated at 1000°C for 24 h, cooled, and then heated again at 400°C for 10 days. The reaction of a 4:3 stoichiometric ratio of $^{241}AmH_3$: elemental antimony in a Pyrex tube at 550°C produced two phases, AmSb and a second phase with the bcc structure of anti-Th_3P_4-type (Charvillat *et al.*, 1975b).

Like AmP, AmBi has also been investigated. Roddy (1974) produced AmBi by reaction of metallic bismuth vapor with either americium metal or americium hydride in a sealed, evacuated quartz tube for 48 h at 975°C.

The magnetic susceptibilities of actinide chalcogenides and pnictides can be fit by the modified Curie–Weiss law:

$$\chi_{\text{measured}} = \chi_{\text{Curie+Weiss}} + \chi_0 = (C/(T - \theta_{\text{para}})) + \chi_0$$

where C is the Curie constant, θ_{para} is the paramagnetic Curie temperature, and χ_0 is a generally temperature-independent additional term. For the americium compounds, the Curie–Weiss term vanishes and experimentally determined values for χ_0 are reported to be 777 for AmN, 550 for AmAs, 1250 for AmSb, and 500 for AmBi (Kanellakopulos *et al.*, 1975; Vogt *et al.*, 1998).

The effective magnetic moment of AmN is 136 Bohr magnetons (Nellis and Brodsky, 1974; Kanellakopulos *et al.*, 1975) and that of AmAs is 1.14 Bohr magnetons (Kanellakopulos *et al.*, 1975). Kanellakopulos measured the magnetic susceptibility of AmAs between liquid helium and room temperature and observed an antiferromagnetic transition at 13 K. Magnetic susceptibility measurements on AmSb show a temperature-independent value of $\chi_0 = (1250 \pm 100) \times 10^{-6}$ emu mol^{-1} for the range 4.2 K $< T <$ 320 K (Dunlap *et al.*, 1972).

(e) Carbides and carbonates

The binary Am(III) carbide, Am_2C_3, is the only known carbide of americium and is prepared by arc melting americium metal with high-purity graphite in an argon–helium atmosphere (Mitchell and Lam, 1970b). The compound is isostructural with Pu_2C_3.

Carbonate compounds of Am(III) and Am(V) have been synthesized and characterized. They are applied in separation processes and also may form under environmental conditions. No solid carbonates of Am(IV) or Am(VI) are known.

(1) Am(III): The binary Am(III) carbonate, $Am_2(CO_3)_3$, precipitates from a CO_2-saturated solution of $NaHCO_3$ (Meinrath and Kim, 1991b; Runde and Kim, 1994). Thermogravimetric analysis of the precipitated binary compound suggests the formula $Am_2(CO_3)_3 \cdot 2H_2O$ (Weigel and ter Meer, 1967) or $Am_2(CO_3)_3 \cdot 4H_2O$ (Keller and Fang, 1969). The ternary compounds $NaAm(CO_3)_2 \cdot 4H_2O$ and $Na_3Am(CO_3)_3 \cdot 3H_2O$ precipitate from 0.5 M $NaHCO_3$ and 1.5 M Na_2CO_3 solutions, respectively (Keller and Fang, 1969). In analogy to neodymium and europium hydroxycarbonates, orthorhombic $AmOHCO_3$ was characterized by X-ray powder diffraction data (Meinrath and Kim, 1991b; Runde *et al.*, 1992), but the formation of its hexagonal form (Standifer and Nitsche, 1988) could not be confirmed.

(2) Am(V): A number of 'double carbonates' of general formula $MAmO_2CO_3$ where M = K (Nigon *et al.*, 1954; Volkov *et al.*, 1974), Na (Nigon *et al.*, 1954; Runde and Kim, 1994), Rb, Cs, NH_4 (Nigon *et al.*, 1954) have been synthesized by precipitation of Am(V) in dilute bicarbonate solutions of the corresponding cation. The use of large excess of alkali carbonate yields the $K_3AmO_2(CO_3)_2$ and $K_5AmO_2(CO_3)_3$ solids (Yakovlev and Gorbenko-Germanov, 1955; Volkov *et al.*, 1981).

(f) Phosphates and sulfates

Light pink $AmPO_4 \cdot xH_2O$ precipitates by adding dilute solutions of H_3PO_4, Na_2HPO_4, or $(NH_4)_2HPO_4$ to a weakly acidic Am^{3+} solution (Lawaldt *et al.*, 1982; Fedoseev and Perminov, 1983; Rai *et al.*, 1992). Rai and coworkers suggest the precipitation of $AmPO_4 \cdot xH_2O$ from dilute acidic solution but the study lacks characterization of the solid phase. Dehydration of the hydrous precipitate yields hexagonal $AmPO_4 \cdot 0.5H_2O$ at 200°C and $AmPO_4$ at higher temperatures up to 1000°C. The anhydrous compound can also be obtained by reacting AmO_2 with stoichiometric amounts of $(NH_4)_2HPO_4$ at 600–1000°C.

Because of the tendency of Am(VI) towards reduction to Am(V) at near-neutral pH, Am(VI) phosphates can be precipitated only in the narrow pH range of 3.5–4. Four ternary Am(VI) phosphates $MAmPO_4 \cdot xH_2O$ with M = NH_4, K, Rb, Cs have been prepared by Lawaldt *et al.* (1982) by precipitating Am(VI) in 0.1 M H_3PO_4 after adjusting the pH with the corresponding carbonate solution.

Binary sulfate compounds are known for Am(III), Am(V), and Am(VI), especially a large number of double sulfates of Am(III).

(1) Am(III): Evaporation of a neutral solution of ^{243}Am(III) sulfate yields thick, up to 0.5 mm long, tabular, pale yellow-pink crystals of $Am_2(SO_4)_3 \cdot 8H_2O$ (Burns and Baybarz, 1972). Crystals of the octahydrate, after being dried in air, are stable to change in their degree of hydration for several days. On the basis of analyses for americium, sulfate, and water, Yakovlev *et al.* (1958) assign the formula $Am_2(SO_4)_3 \cdot 5H_2O$ to the precipitate obtained by adding ethanol to a solution of Am(III) in 0.5 M H_2SO_4. The white anhydrous Am(III) sulfate, $Am_2(SO_4)_3$, is prepared by heating the hydrate to a temperature of 500–600°C in air (Hall and Markin, 1957). Anhydrous americium sulfate does not take up water when cooled to room temperature in air.

A number of double sulfates of Am(III) with formulas $MAm(SO_4)_2 \cdot xH_2O$ (M = K, Na, Rb, Cs, Tl; x = 0, 1, 2, 4), $K_3Am(SO_4)_3 \cdot xH_2O$, and $M_8Am_2(SO_4)_7$ (M = K, Cs, Tl) have been prepared by adding a metal sulfate solution to a solution of Am^{3+} in 0.5 M H_2SO_4. The concentration ratios M^+/Am^{3+} for the preparation of the various double sulfates as well as the absorption spectra of some Am(III) double sulfates at 80, 200, and 300 K are given by Yakovlev *et al.* (1958). Surprisingly, no X-ray diffraction data were reported for these double sulfates. Coprecipitation of trace amounts of Am(III) with K_2SO_4 and $La_2(SO_4)_3$ has also been published (Grebenshschikova and Babrova, 1958, 1961; Grebenshschikova and Cheinyavskaya, 1962).

(2) Am(V): Fedoseev and Budentseva (1989) claimed the preparation of three solid sulfates of Am(V). $(AmO_2)_2(SO_4) \cdot xH_2O$ crystallizes upon evaporation of an Am(V)-containing sulfuric acid solution. Am(V) sulfate also crystallizes from an ozonated solution of $Am(OH)_3$ after addition of sulfuric acid and subsequent evaporation. Two double salts have been reported: Large light green crystals of $CsAmO_2SO_4 \cdot xH_2O$ were obtained by evaporating a solution containing $(AmO_2)_2(SO_4)$ and Cs_2SO_4 in a 3:1 ratio. According to Fedoseev and Budentseva $Co(NH_3)_6AmO_2(SO_4)_2 \cdot 2H_2O$ can be easily

made by simply including Am(v) among the reagents used to prepare $Co(NH_3)_6(SO_4)_2$.

(3) Am(vi): Addition of hexamine cobalt(iii) ions to an aqueous sulfate solution containing hexavalent americium yields orange cubic crystals of $Co(NH_3)_6(HSO_4)_2(AmO_2(SO_4)_3) \cdot nH_2O$ (Ueno and Hoshi, 1971). The compound is isostructural with the corresponding uranyl and neptunyl compounds. No precipitate forms, however, in an ammonium sulfate solution containing Am(iii) and hexamine cobalt(iii) ions.

(g) Other inorganic compounds

Shirokova *et al.* (2001) reported the complexation of Am(iii) with *N*,*N*-dimethylacetamide and the Keggin-type heteropolyanion $PW_{12}O_{40}^{3+}$. Lawaldt *et al.* (1982) applied the same procedures as used to prepare Am(vi) phosphates for the precipitation of Am(vi) arsenates. The obtained compounds were isostructural to the analogous Am(vi) phosphates.

Only two phases, AmB_4 and AmB_6, have been reported in the boride system in contrast to the richer Np–B system with four phases (Eick and Mulford, 1969).

Weigel *et al.* (1977, 1984) reported the formation of several silicide phases upon reacting AmF_3 with elemental Si at different temperatures. Up to 950°C, the phases Am_5Si_3, AmSi, Am_2Si_3, and $AmSi_2$ have been characterized by X-ray powder diffraction. Orthorhombic AmSi is also prepared at 1050°C and the substoichiometric tetragonal phase $AmSi_x$ ($1.87 < x < 2.0$) forms at 1150–1200°C.

The only silicate known to date, $AmSiO_4$, is obtained as a brown solid by reacting $Am(OH)_4$ with excess SiO_2 in 1 M $NaHCO_3$ solution at 230°C for 1 week (Katz and Seaborg, 1957). $^{241}AmSiO_4$ is patented for the use in manufactured alpha sources.

Large orange needle-like crystals thought to be $AmO_2CrO_4 \cdot H_2O$ were prepared by slowly evaporating a chromic acid (H_2CrO_4) solution containing Am(v) (Fedoseev *et al.*, 1991). Although there is some spectroscopic evidence for the presence of Am(v) in the solid chromate (electronic absorbances at about 518 and 728 nm) the suggested formula of $AmO_2CrO_4 \cdot H_2O$ appears to be erroneous and should rather be $(AmO_2)_2CrO_4 \cdot H_2O$.

Tabuteau and coworkers (Tabuteau *et al.*, 1972; Tabuteau and Pages, 1978) investigated the Am–molybdate and Am–tungstate systems. The solid state reaction of stoichiometric amounts of AmO_2 and MoO_3 or WO_3 at 1080°C resulted in the formation of monoclinic $Am_2(MoO_4)_3$ and $Am_2(WO_4)_3$. Two ternary phases, $KAm(MoO_4)_2$ and $K_5Am(MoO_4)_4$, were found to form at 650°C in the presence of potassium. Fedoseev and Budantseva (1990) report the synthesis of $AmO_2Mo_2O_7 \cdot 3H_2O$ at 100°C, however, no information on the phase characterization was provided.

8.7.2 Compounds of americium with organic ligands

Relatively few solid compounds of americium with organic ligands have been prepared; these are listed in Table 8.6. For detailed reviews of this chemistry see Kanellakopulos (1979) and also Chapters 23 and 25.

(a) Oxalate

Because of its importance for americium separation chemistry $Am_2(C_2O_4)_3 \cdot xH_2O$ (Weigel and ter Meer, 1967) is the most important organic compound of americium. The pink solid precipitates from slightly acidic or neutral solutions of Am^{3+} on addition of oxalic acid or alkali oxalate solution. The hydration number x was previously thought to vary with conditions of preparation and drying and values of 7 (Markin, 1958), 9 (Yakovlev and Kosyakov, 1958a), and 11 (Staritzky and Truitt, 1954) have been reported. Based on their X-ray diffraction studies and in analogy to Nd(III), Pu(III), and Cm(III), Weigel and ter Meer (1967) concluded that the hydration number x is 10. The decahydrate decomposes to the anhydrous form at 340°C through several hydrates and further decomposes to carbonate $Am_2(CO_3)_3$ at about 430°C. The oxalate complexes with general formula $MAm(C_2O_4)_2 \cdot xH_2O$ have been prepared from Am(III) oxalate and $M_2C_2O_4$ ($M = NH_4$, Na, K, Cs) in neutral solution (Zubarev and Krot, 1982, 1983a,b).

(b) Formate

Pink crystals of hexagonal $Am(HCOO) \cdot 0.2H_2O$ form upon evaporation of a concentrated formic acid solution (Weigel and ter Meer, 1967). The formate decomposes at 300–350°C to AmO(HCOO), and at 400–500°C to the oxycarbonate $Am_2O_3CO_3$, which forms at 520°C the sesquioxide Am_2O_3 (Weigel and ter Meer, 1971).

(c) Acetate

Addition of sodium acetate to an acidic Am(VI) solution precipitates lemon-yellow cubic crystals of $NaAmO_2(OOCCH_3)_3$ (Asprey *et al.*, 1950, 1951). The force constant of the Am–O bond in $NaAmO_2(OOCCH_3)_3$ is determined to be 6.12 megadynes/Å (Jones, 1953). The refractive index is 1.528 ± 0.002 (Asprey *et al.*, 1951).

(d) Acetone derivate compounds

Addition of ammonia to aqueous Am^{3+} solution that contains a small amount of acetylacetone precipitates pale-rose $Am(C_5H_7O_2)_3 \cdot H_2O$ at pH 6. The precipitate can be recrystallized in ethanol and dried in air over silica gel or P_2O_5 (Keller and Schreck, 1969). Dropwise addition of aqueous Am^{3+} (pH 4.5) to warm, slightly less than stoichiometric amounts of ammonium benzoylacetone yields pale-rose $Am(C_{10}H_6F_3O_2)_3 \cdot 3H_2O$. Both compounds decompose in air at

Table 8.6 *Organic compounds of americium.*

Organic ligand	*Formula of compound*	*Comments*	*References*
Acetate	$NaAmO_2(OOCCH_3)_3$	lemon yellow	[1]
acetylacetone	$Am(C_5H_7O_2)_3 \cdot H_2O$	pale rose	[2]
benzoyltrifluoroacetone	$Am(C_{10}H_6F_3O_2)_3 \cdot 3H_2O$	pale rose	[2]
cyclooctatetraene	$KAm(C_8H_8)_2 \cdot 2THF^a$	yellow	[3]
cyclopentadiene	$Am(C_5H_5)_3$	flesh	[4]
dipivalomethane	$Am(C_{11}H_{19}O_2)_3$		[5]
formate	$Am(HCOO)_3 \cdot 0.2H_2O$	pink	[6]
hexafluoroacetylacetone	$CsAm(C_5HF_6O_2)_4 \cdot H_2O$	yellow	[7]
hexafluoroacetyl-acetone/TBP	$Am(C_5HF_6O_2)_3 \cdot 2(C_4H_9O)_3PO$	volatile, 175°C	[8]
8-hydroxyquinoline	$Am(C_9H_6NO)_3$	yellow-green	[9]
5-chloro-8-hydroxyquinoline	$Am(C_9H_5ClNO)_3$	dark green	[9]
5,7-dichloro-8-hydroxyquinoline	$Am(C_9H_4Cl_2NO)_3$	green	[9]
oxalate	$Am_2(C_2O_4)_3 \cdot 10H_2O$	pink	[10]
	$KAmO_2C_2O_4 \cdot xH_2O$	color varies from pink to brick red depending on preparation conditions	[11]
	$CsAmO_2C_2O_4 \cdot xH_2O$	green, cubic ($a = 12.5$ Å)	[11]
	$MAmO_2C_2O_4 \cdot xH_2O$	$M = NH_4$, Na	[11]
phthalocyanine	$Am(C_{32}H_{16}N_2)_2$	dark violet	[12]
pyridine-2-carboxylate	$AmO_2(C_5H_4NCOO)_2$	red-brown	[13]
	$HAmO_2(C_5H_4NCOO)_3$	red-brown	[13]
pyridine-*N*-oxo-carboxylate	$AmO_2[C_5H_4N(O)COO]_2$		[14]
salicylate	$Am(C_7H_5O_3)_3 \cdot H_2O$		[15]
thenoyltrifluoroacetate	$Am(C_5H_4F_3O_2S)_3 \cdot 3H_2O$	pale rose	[2]

[a] THF, tetrahydrofuran.

[1] (Asprey *et al.*, 1950, 1951, 1954b); [2] (Keller and Schreck, 1969); [3] (Karraker, 1975, 1977); [4] (Baumgärtner *et al.*, 1966a, 1977; Kanellakopoulos *et al.*, 1970, 1978; Seaborg, 1972); [5] (Danford *et al.*, 1970; Moore, 1970; Sakanoue and Amano, 1975); [6] (Lebedev *et al.*, 1960b, 1962); [7] (Burns and Danford, 1969; Danford *et al.*, 1970; Bagnall, 1972; Sakanoue and Amano, 1975); [8] (Davydov *et al.*, 1975); [9] (Keller *et al.*, 1965a, 1966); [10] (Eyring *et al.*, 1952; Yakovlev and Kosyakov, 1958b; Lebedev *et al.*, 1960a; Weigel *et al.*, 1966; Burney and Porter, 1967; Chikalla and Eyring, 1967; Weigel and ter Meer, 1967, 1971); [11] (Zubarev and Krot, 1982, 1983a); [12] (Kirin *et al.*, 1967; Lux, 1973); [13] (Eberle and Robel, 1970; Robel, 1970); [14] (Robel, 1970); [15] (Burns and Baldwin, 1977).

above 200°C to AmO_2. Yellow $CsAm(C_5HF_6O_2)_4 \cdot H_2O$ crystallizes from $AmCl_3$ solution after addition of excess cesium hexafluoroacetylacetone in 50 vol% ethanol (Burns and Danford, 1969; Danford *et al.*, 1970).

(e) Cyclooctatetraene and cyclopentadiene

Reaction of $^{241}AmI_3$ with $K_2C_8H_8$ in tetrahydrofuran (THF) solution yields the adduct $KAm(C_8H_8)_2 \cdot 2THF$, which is isostructural with its plutonium analog $KPu(C_8H_8)_2 \cdot 2THF$ (Karraker, 1975). The compound decomposes in water and burns in air. Reacting the halides AmF_3 (Moore, 1970) or $AmCl_3$ (Baumgärtner *et al.*, 1966a,b; Kanellakopoulos *et al.*, 1970; Seaborg, 1972) with molten $Be(C_5H_5)_2$ at 65–70°C produces $Am(C_5H_5)_3$ (Moore, 1970). The pure compound can be obtained by fractional sublimation at 10^{-5} Torr and 160–205°C (Baumgärtner *et al.*, 1966a,b). Unlike $Pu(C_5H_5)_3$, $Am(C_5H_5)_3$ is not pyrophoric and decomposes only slowly in air. The IR and absorption spectra of $Am(C_5H_5)_3$ have been reported (Pappalardo *et al.*, 1969a; Kanellakopoulos *et al.*, 1970).

(f) Others

Reaction of AmI_3 at 200°C with phthalodinitride in 1-chloronaphthalene yields the dark violet phthalocyanine compound $Am(C_{32}H_{16}N_8)_2$, which was the first synthesized Am(IV) compound with an organic ligand (Lux, 1973). There is evidence that americium also forms the monophthalocyaninato complex.

Danford *et al.* (1970) precipitated the dipivaloylmethane compound $Am(C_{11}H_{19}O_2)_3$ by adding aqueous Am(III) sulfate to a solution of dipivaloylmethane and NaOH in 70% aqueous ethanol. Sakanoue and Amano (1975) determined the volatility of $Am(C_{11}H_{19}O_2)_3$ and several lanthanide and actinide analog complexes at 180°C and 10^{-3} torr and observed that $Am(C_{11}H_{19}O_2)_3$ is less volatile than its analog compounds of Th, Pu, Cf, or Eu, Gd, or Sc.

The only recorded aliphatic compounds of americium appear to be the citrates $Am(C_6H_5O_7) \cdot xH_2O$ and $[Co(NH_3)_6][Am(C_6H_5O_7)_2] \cdot xH_2O$ (Bouhlassa, 1983), and the salicylate $Am(C_7H_5O_3)_3 \cdot H_2O$ (Burns and Baldwin, 1976); its structure is described in Section 8.9.2.

Hölgye (1982) studied the coprecipitation of Am(III) with various metal cupferrates. With cupferrates of lanthanides and Sc(III), Am(III) coprecipitated quantitatively. But Am(III) coprecipitated only partially with cupferrates of Fe(III), Cu(II), Al(III), In(III), Pb(II), and Bi(III).

8.8 AQUEOUS SOLUTION CHEMISTRY

8.8.1 Oxidation states

In aqueous solutions, americium exhibits the III, IV, V, and VI oxidation states. All four oxidation states can coexist under certain conditions in carbonate media (Bourges *et al.*, 1983). In dilute acid, only the aquo ions Am^{3+} and

AmO_2^{2+} ions are stable, whereas in alkaline solution, americium can exist in all four valence states. In the III and IV oxidation states, americium forms Am^{3+} and Am^{4+} ions in solution, respectively. The highly charged ions in the V and VI states are unstable and hydrolyze instantly to form the linear *trans*-dioxo americyl cations, AmO_2^+ and AmO_2^{2+}, respectively. Analogous to Np(VII) and Pu(VII), americium reportedly can be oxidized to the VII oxidation state in highly alkaline media (Krot *et al.*, 1974a,b; Myasoedov and Kremliakova, 1985).

(a) Preparation

(1) Am(II): In contrast to its chemical analog of the lanthanide series, europium, the divalent state of Am is unstable in aqueous solution. Conditions that stabilize Yb^{2+}, Eu^{2+}, or Sm^{2+} do not reduce Am^{3+} to Am^{2+} (Keenan, 1959). Milyukova *et al.* (1980) claimed electrochemical evidence for unstable Am(II) in acetonitrile; they found that Am(II) was rapidly oxidized to Am(III) by water in the solvent. Sullivan *et al.* (1976, 1978) formed transient Am(II) by pulse radiolysis with an absorption maximum at 313 nm and $t_{1/2} \sim 5 \times 10^{-6}$ s for disappearance. Am(II) can be accessed in the solid state and as dilute solution in CaF_2 (Zachariasen, 1948b; Fried, 1951; Pappalardo *et al.*, 1969b; Baybarz, 1973b; Peterson, 1973). The solid compounds $AmCl_2$ (Baybarz, 1973b), $AmBr_2$ (Baybarz, 1973b), and AmI_2 (Baybarz and Asprey, 1972) have been prepared and characterized.

(2) Am(III): Trivalent americium is the most common and stable oxidation state in aqueous solution. It can be easily prepared by dissolving the metal in acid, dissolving AmO_2 in hot HCl, or by reducing higher valent americium compounds with most common reducing agents, such as NH_2OH, SO_2, or KI (Coleman *et al.*, 1963). Acidic solutions of Am^{3+} are pink in mineral acids but are yellow in concentrated $HClO_4$ or when the Am^{3+} concentration exceeds 0.1 M. Numerous solid compounds of Am(III) have been prepared and characterized.

(3) Am(IV): Tetravalent americium is unstable in non-complexing solutions and is reduced spontaneously to its more stable III oxidation state. Stable Am(IV) can be prepared by dissolving $Am(OH)_4$ in concentrated NH_4F solutions (Asprey and Penneman, 1962). Yanir *et al.* (1969) demonstrated that Am(IV) remains stable in phosphoric and pyrophosphate media. Myasoedov *et al.* (1977) reported that pure Am(IV) is obtained in 8–15 M phosphoric acid by anodic oxidation, while at lower phosphoric acid concentrations impurities of Am(VI) are formed. Similar stability of Am(IV) was reported in an oxidizing mixture of Ag_3PO_4 and $(NH_4)_2S_2O_8$. Electrolytic oxidation of ^{243}Am(III) (<1 V) in 2–5.5 M carbonate solutions resulted in the formation of a golden-yellow Am(IV) carbonate species, which was slowly reduced to Am(III) (Hobart *et al.*, 1982). At potentials exceeding 1.1 V, Am(IV) is oxidized to Am(V) and Am(VI). Am(IV) can be stabilized with heteropolyanions and reduction to Am(III) is caused solely by radiolytic effects

(Saprykin *et al.*, 1976; Kosyakov *et al.*, 1977; Erin *et al.*, 1979). Transient Am(IV) has been observed by pulse radiolysis (Sullivan *et al.*, 1976, 1978).

(4) Am(V): Am(III) can be oxidized to Am(V) in near-neutral and alkaline solution. In acidic media, oxidation of Am(III) yields only Am(VI) because Am(V) is more easily oxidized to Am(VI) than Am(III) is oxidized to Am(V). Solutions of Am(V) can be prepared by oxidation of Am(III) with ozone (Keenan, 1965), hypochlorite (Yakovlev and Gorbenko-Germanov, 1955), and peroxydisulfate (Nigon *et al.*, 1954), or by reduction of Am(VI) with bromide, or by electrolysis (Hobart *et al.*, 1983b). Solid sodium Am(V) carbonate can be precipitated by heating a 2 M Na_2CO_3 Am(VI) solution for 60 min to 60°C (Coleman *et al.*, 1963). Dissolution of the solid in near-neutral solutions yields pure Am(V) solution free of Am(III) and Am(VI). AmO_2^+ solutions free of Am^{3+} can be prepared by first extracting AmO_2^+ from buffered 1 M acetate (pH 3) solutions into 0.1 M thenoyltrifluoroacetone in isobutanol and back-extraction into an aqueous phase (Hara, 1970). More exotic methods include the dissolution of solid Li_3AmO_4 in dilute perchloric acid or the electrolytic oxidation of Am(III) in 2 M $LiIO_3$/0.7 M HIO_3 solutions (pH 1.5) (Keller, 1971).

(5) Am(VI): Powerful oxidants, i.e. peroxydisulfate or Ag(II), oxidize Am(III) and Am(V) in dilute, non-reducing acidic solution to Am(VI) (Myasoedov and Kremliakova, 1985). At acidities above 0.5 M, peroxydisulfate will not oxidize Am(III) completely to Am(VI) because of the interference of acid hydrolysis of $S_2O_8^{2+}$ (Penneman and Asprey, 1955). Ce(IV) oxidizes Am(V) to Am(VI) but only partially oxidizes Am(III) to Am(VI) (Penneman and Asprey, 1955). Electrolytic oxidation of Am(III) in 2 M H_3PO_4 and 6 M $HClO_4$ leads to Am(VI) (Myasoedov *et al.*, 1977) while ozone does not oxidize Am(III) to Am(VI) in acidic medium. In aqueous 2 M carbonate solutions oxidation of Am(III), Am(IV), or Am(V) with ozone or oxidation with $Na_2S_2O_8$ yields an intensely colored red-brown carbonate complex of Am(VI) (Coleman *et al.*, 1963). This complex is also obtained electrolytically at a potential of 1.3 V vs NHE in sodium carbonate solutions (Hobart *et al.*, 1982) or by dissolution of sodium americyl(VI) acetate in sodium carbonate solutions. Ozone oxidation in carbonate solution yields Am(VI) only at 25°C or below while at 90°C oxidation does not proceed past Am(V). Ozone does not oxidize $Am(OH)_3$ or $KAmO_2CO_3$ in 0.1–0.5 M $KHCO_3$ and $K_2S_2O_8$ does not oxidize $Am(OH)_3$ or $NaAmO_2CO_3$ in 0.1 M $NaHCO_3$ (Coleman *et al.*, 1963). This difference to the easy oxidation by $Na_2S_2O_8$ is attributed to the lower solubility of $KAmO_2CO_3$ compared to $NaAmO_2CO_3$. In 0.1–0.5 M $NaHCO_3$, Am(VI) is stable at 90°C to reduction by H_2O, Cl^-, or Br^-, but is easily reduced by I^-, N_2H_4, H_2O_2, NO_2^-, and NH_2OH. Very slow reduction of Am(VI) occurs in 2 M Na_2CO_3. Yellow-colored solutions of Am(VI) in any alkali hydroxide solutions can be prepared by oxidation of solid $Am(OH)_3$ with ozone (Cohen, 1972). Am(VI) in alkali hydroxide solutions undergoes

gradual reduction to form a light-tan solid, which yields Am(v) when dissolved in mineral acid. It is claimed that Am(vi) disproportionates into Am(vii) and Am(v) in >10 M NaOH (Nikolaevskii *et al.*, 1975).

The reaction of KrF_2 with AmF_3 in anhydrous HF yields a dark-brown solid of AmF_6 with a vapor pressure that is similar to that of UF_6 (Drobyshevskii *et al.*, 1980).

(6) Am(vii): While attempts to synthesize Am(vii) from Li_2O–AmO_2 mixtures at 300–400°C failed, oxidation of 3–4 M NaOH solutions containing 0.001–0.002 M Am(vi) with ozone at 0–7°C yields a green-colored solution of Am(vii) (Krot *et al.*, 1974a,b; Myasoedov and Kremliakova, 1985). A similar green-colored solution can be obtained by ^{60}Co gamma irradiation at 0°C of a N_2O-saturated 3 M NaOH solution. (N_2O scavenges hydrated electrons by the reaction $N_2O + e^- (aq) \rightarrow N_2 + O^-$; $S_2O_8^{2-}$ may be substituted for N_2O.) Spectrophotometric studies showed the oxidation of Np(vi) to Np(vii) and Pu(vi) to Pu(vii) under similar conditions, which provides strong evidence that the green solutions indeed contain a powerful oxidant such as Am(vii) (Krot *et al.*, 1974a,b).

(b) Hydration and coordination numbers

Information on the structure of the $Am^{3+}(aq)$ ion has been obtained indirectly from a variety of spectroscopic techniques. From the similar absorption spectra of Am^{3+} in aqueous solution, $AmCl_3$, and Am^{3+} doped into $LaCl_3$, Carnall (1989) concluded that there were nine inner-sphere water molecules associated in $Am^{3+}(aq)$. Horrocks and Sudnick (1979, 1981) and Choppin and coworkers (Barthelemy and Choppin, 1989; Choppin and Peterman, 1998) developed a linear relationship between the decay rate of the lanthanide(iii) and the Am(iii) fluorescence and the number of inner-sphere water molecules: $n_{H_2O} = (x/\tau) - y$. Kimura and Kato (Kimura and Kato, 1998) determined $x = 2.56 \times 10^{-7}$ s and $y = 1.43$ for Am(iii) by measuring the fluorescence lifetime of Am^{3+} in H_2O and D_2O and using Carnall's proposed nine hydration waters. Runde *et al.* (2000) used Kimura's parameters and calculated from the fluorescence lifetime 11 coordinated water molecules for the Am^{3+} ion. Allen *et al.* (2000) determined ten coordinated water molecules around the Am^{3+} aquo ion in dilute aqueous chloride solution using X-ray absorption fine structure (XAFS) spectroscopy. Recently, Matonic *et al.* (2001) crystallized the isostructural Am(iii) and Pu(iii) triflate (trifluoromethanesulfonic acid) salts where the Am^{3+} ion bonds to nine water molecules in a tricapped, trigonal prismatic geometry (Fig. 8.4).

Shilov and Yusov (1999) analyzed reported variations in the Am(v)/Am(vi) potentials and the stability constants of the actinyl(v) oxalate complexes and proposed that the $NpO_2^+(aq)$ and $AmO_2^+(aq)$ ions are coordinated with five water molecules in the equatorial plane, in contrast to the coordination of four waters by $PuO_2^+(aq)$ and $UO_2^+(aq)$.

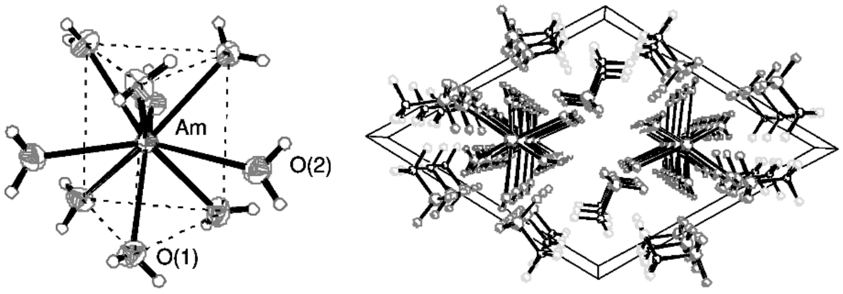

Fig. 8.4 *Coordination environment of* Am^{3+} *and crystal packing in* $[Am(H_2O)_9][CF_3SO_3]$ (*Matonic* et al., 2001).

(c) Electrode potentials and thermodynamic properties

A critical evaluation of available enthalpy and electromotive force (EMF) data were reported (Musikas, 1973b; Fuger and Oetting, 1976; Schulz, 1976; Fuger *et al.*, 1992; Silva *et al.*, 1995). Table 8.7 lists the electrode potentials for americium couples in various aqueous media. The diagram reflects the latest values and data evaluation of Martinot and Fuger (1985), which were accepted with minor changes by the recent Nuclear Energy Agency (NEA) review (Silva *et al.*, 1995). Except for the standard electrode potential ($E°$) of the Am(VI/V) couple, the electrode potentials of all redox couples were measured indirectly.

1. Am(III)/(0): Fuger *et al.* (1972) measured the enthalpy of dissolution of Am metal (dhcp) in hydrogen-saturated HCl solutions and, using the estimated entropy of Am^{3+}(aq), estimated $E°$ to be -2.06 ± 0.01 V in 1 M $HClO_4$; later Martinot and Fuger (1985) recommended -2.07 V.
2. Am(III)/(II): Nugent *et al.* (1973a) estimated the potential to be -2.3 V as a best value by comparing the properties of lanthanide and actinide chloro complexes in relation to their M(II)/M(III) potentials. The estimated value is close to the -2.4 V estimated by Bratsch and Lagowski (1986).
3. Am(IV)/(III): Due to the difficulties in preparing Am(IV) in appreciable amounts, estimating its thermodynamic properties is difficult. The originally estimated 2.44 V in 1 M $HClO_4$ appeared to be too small compared to data on the reduction of $Am(OH)_4$ to $Am(OH)_3$ (Penneman *et al.*, 1961). While the reported electrode potentials in concentrated H_3PO_4 are in agreement, 1.75 ± 0.03 V (Marcus *et al.*, 1972) and 1.78 V in 10 M H_3PO_4 (Nugent *et al.*, 1971a), their extrapolated values, $E° = 2.50 \pm 0.06$ and 2.34 ± 0.22 V, respectively, differ significantly, most likely due to uncertainties in solution speciation. A value of 2.6 ± 0.09 V has been calculated from enthalpy measurements (Morss and Fuger, 1981), and has been confirmed by electrochemical data in carbonate solutions (Hobart *et al.*, 1982). Stabilization by carbonate and phosphotungstate decreases the electrode

Table 8.7 *Electrode potentials of americium redox couples.*

(a) 1 M $HClO_4$ (Schulz, 1976; Silva *et al.*, 1995):

$$\begin{tikzcd}
\text{Am(VI)} \arrow[r, dash, "1.60"] \arrow[rrr, dash, bend left=40, "+1.683"] & \text{Am(V)} \arrow[r, dash, "0.84"] \arrow[rr, dash, bend left=30, "1.727"] & \text{Am(IV)} \arrow[r, dash, "2.62"] \arrow[rrr, dash, bend right=40, "-0.90"'] & \text{Am(III)} \arrow[r, dash, "-2.30"] \arrow[rr, dash, bend right=30, "-2.07"'] & \text{Am(III)} \arrow[r, dash, "-1.95"] & \text{Am(0)}
\end{tikzcd}$$

(b) Phosphoric Acid (Yanir *et al.*, 1959; Nugent *et al.*, 1971a; Myasoedov *et al.*, 1977):

$$\begin{tikzcd}
\text{Am(VI)} \arrow[r, dash, "1.43", "0.54\ \mathrm{M}\ \mathrm{H_3PO_4}"'] & \text{Am(V)}
\end{tikzcd} \text{ and } \begin{tikzcd}
\text{Am(VI)} \arrow[r, dash, "1.32", "4.34\ \mathrm{M}\ \mathrm{H_3PO_4}"'] & \text{Am(V)}
\end{tikzcd}$$

$$\begin{tikzcd}
\text{Am(IV)} \arrow[r, dash, "1.75\text{–}1.78", "10\text{–}14.5\ \mathrm{M}\ \mathrm{H_3PO_4}"'] & \text{Am(III)}
\end{tikzcd}$$

(c) 1 M NaOH (Standard potentials were calculated based on the solubility products of $K_{sp}(Am(OH)_3) = 10^{23.3}$ and $K_{sp}(Am(OH)_4) = 10^{64}$) (Penneman *et al.*, 1961; Musikas, 1973b; Schulz, 1976):

$$\begin{tikzcd}
\text{Am(VI)} \arrow[r, dash, "0.9"] & \text{Am(V)} \arrow[r, dash, "0.7"] & \text{Am(IV)} \arrow[r, dash, "0.5"] & \text{Am(III)} \arrow[r, dash, "-2.5"] & \text{Am(0)}
\end{tikzcd}$$

(d) Carbonate media (Bourges *et al.*, 1983; Hobart *et al.*, 1983b; Berger *et al.*, 1988):

$$\begin{tikzcd}
\text{Am(VI)} \arrow[r, dash, "0.975", "2\ \mathrm{M}\ \mathrm{Na_2CO_3}"'] & \text{Am(V)}
\end{tikzcd} \text{ and } \begin{tikzcd}
\text{Am(IV)} \arrow[r, dash, "0.92", "2\ \mathrm{M}\ \mathrm{Na_2CO_3}"'] & \text{Am(III)}
\end{tikzcd}$$

potential to 0.92 V (Hobart *et al.*, 1982; Bourges *et al.*, 1983) and 1.52 V (Kosyakov *et al.*, 1977), respectively.

(4) Am(VI)/(V): Penneman and Asprey (1950) measured directly the potential of the AmO_2^{2+}/AmO_2^+ couple to be 1.600 ± 0.0005 V in 1 M $HClO_4$ and 1.614 ± 0.001 V in 0.3 M $HClO_4$. From studies of Am(VI) with Pu(VI) in NaOH, Nikolaevskii *et al.* (1974) estimated that the potential for the Am(IV)/Am(V) couple is about 0.65 V rather than 1.1 V.

(5) Am(VII)/(VI): Shilov (1976) reported a value of 1.05 V for the Am(VII)/Am(VI) couple in 1 M NaOH, while Peretrukhin and Spitsyn (1982) reported 0.78 V for this couple in 10 M hydroxide.

The heat of dissolution of americium metal in HCl at 298 ± 0.05 K was redetermined by Fuger *et al.* (1972) with pure americium metal prepared by distillation. Combined with earlier results, Fuger and Oetting (1976) calculated a standard enthalpy of formation of $Am^{3+}(aq)$ at 198 K of -616.7 ± 1.3 kJ mol^{-1}.

The following enthalpies of formation, free Gibbs energies of formation, and standard entropies for the americium aquo ions have been accepted by the NEA review (Silva *et al.*, 1995):

	$\Delta_f H^\circ_m$(298.15 K) (kJ mol^{-1})	$\Delta_f G^\circ_m$(298.15 K) (kJ mol^{-1})	S°_m(298.15 K) (kJ mol^{-1})
$Am^{2+}(aq)$	-355 ± 16	-377 ± 15	-1 ± 15
$Am^{3+}(aq)$	-616.7 ± 1.5	-598.7 ± 4.8	-201 ± 15
$Am^{4+}(aq)$	-406 ± 6	-346 ± 9	-406 ± 21
$AmO_2^+(aq)$	-804.3 ± 5.4	-739.8 ± 6.2	-21 ± 10
$AmO_2^{2+}(aq)$	-650.8 ± 4.8	-585 ± 5.7	-88 ± 10

A correlation function of *P*(M) that connects the trivalent gaseous lanthanide atoms with their aqueous ions changes systematically as a function of atomic number (Nugent *et al.*, 1973b). The same property is moderately well-behaved for trivalent actinides (Nugent *et al.*, 1973b; David *et al.*, 1978; Morss, 1983). The calculated *P*(Am) is about 20 kJ greater than expected from neighboring actinides. This anomaly was attributed to the large positive change in entropy of vaporization of Am (Ward and Hill, 1976).

(d) Autoreduction

Radiolytically produced species in aqueous solution, e.g. H_2O_2 and HO_2 radicals, reduce the higher oxidation states of americium to Am(III). Because of its lower specific activity, the rates of autoreduction of ^{243}Am species are much less than those of ^{241}Am. Zaitsev *et al.* (1960b) account for the autoreduction kinetics of aqueous AmO_2^{2+} and AmO_2^+ ions by assuming that H_2O_2 is consumed only in reducing Am(VI) and Am(V) is reduced only by HO_2 radicals, but that Am(V) may be oxidized to Am(VI) by OH radicals.

All investigators concur that autoreduction is kinetically zero order with respect to the AmO_2^{2+} ion and first order with respect to the total americium concentration:

$$-\mathrm{d}[\mathrm{Am(VI)}]/\mathrm{d}t = \mathrm{d}[\mathrm{Am(V)}]/\mathrm{d}t = k_1[\mathrm{Am_{total}}]$$

In both perchloric and sulfuric acid media, the value of the rate constant k_1 decreases with increasing acid concentration, 0.04 h^{-1} in dilute acid to zero in 12 M $HClO_4$ (Zaitsev *et al.*, 1960b). The autoreduction rate of ^{241}Am(VI) approaches 10% per hour in 9 M HNO_3 (Zaitsev *et al.*, 1960b); a slower rate was found in a later study (Myasoedov *et al.*, 1974b). The rate of autoreduction of ^{243}Am(VI) in 2 M $HClO_4$ solution at 76°C is about six times greater than that at room temperature (Zaitsev *et al.*, 1960b).

The autoreduction of Am(V) to Am(III) is usually stated to depend only on the total americium concentration but to be independent of the Am(V) concentration.

Zaitsev *et al.* (1960b) disagreed and found that under some conditions the rate of autoreduction of Am(v) to Am(iii) does depend on the Am(v) concentration. The autoreduction of $^{241}AmO_2^+$ proceeds more slowly in 0.5 M HCl than in 0.2 M $HClO_4$. The maximum reduction rate of AmO_2^+ is about 1% per hour in 0.5 M HNO_3 and 0.8% per hour in 3 M HNO_3 (Zaitsev *et al.*, 1960b).

In 13 M NH_4F, ^{241}Am(iv) is autoreduced at a rate of about 4% per hour (Asprey and Penneman, 1962), increasing to 10% per hour in 3 M fluoride solution (Yanir *et al.*, 1969). Self-reduction of Am(iv) to Am(iii) in phosphoric acid solution follows first-order reaction kinetics (Yanir *et al.*, 1969; Myasoedov *et al.*, 1973, 1975;). In acidic peroxydisulfate solution, no Am(iii) is observed until all Am(vi) is reduced to Am(v). In the presence of $S_2O_8^{2-}$ ions, the radiolytic reduction of Am(v) proceeds more slowly than that of Am(vi) (Rykov *et al.*, 1970).

(e) Disproportionation

1. Am(iv): Tetravalent americium rapidly disproportionates in nitric and perchloric acid solutions according to the following reaction (Penneman *et al.*, 1961):

$$2\mathrm{Am(IV)} \rightarrow \mathrm{Am(III)} + \mathrm{Am(V)}.$$

Assuming a reaction that is second order in Am(iv) concentration, Penneman *et al.* (1961) estimated k_1 in the equation

$$-\mathrm{d}[\mathrm{Am(IV)}]/\mathrm{d}t = k_1[\mathrm{Am(IV)}]^2$$

to be greater than $3.7 \times 10^{+4}$ L mol^{-1} h^{-1} in 0.05 M HNO_3 at 0°C. The dissolution of $Am(OH)_4$ in 0.05–2 M H_2SO_4 at either 0 or 25°C or of AmO_2 in 1 M H_2SO_4 yields solutions containing Am^{3+} and AmO_2^{2+} (Yakovlev and Kosyakov, 1958b; Penneman *et al.*, 1961). These results are explained by the following mechanism:

$$\text{Disproportionation of Am(IV)}: \ 2\mathrm{Am(IV)} \ \rightarrow \ \mathrm{Am(III)} + \ \mathrm{Am(V)}$$

and

$$\text{Redox Reaction}: \ Am^{4+} \ + \ AmO_2^+ \ \rightarrow \ Am^{3+} \ + \ AmO_2^{2+}$$

The AmO_2^{2+} fraction increases with SO_4^{2-} and HSO_4^- concentrations at constant H^+ concentration, possibly as a result of SO_4^{2-} (or HSO_4^-) stabilization of an Am(iv) complex. Am(iv) is stable only in concentrated H_3PO_4, $K_4P_2O_7$, phosphotungstate, and fluoride (NH_4F, KF) solutions. The average oxidation number of americium remains iv when $Am(OH)_4$ is dissolved in either perchloric, nitric, or sulfuric acids (Penneman *et al.*, 1961), indicating no significant reduction by water, in contrast to the reduction of Cm(iv) (Kosyakov *et al.*, 1977).

2. Am(V): The most thorough study of the disproportionation kinetics of Am(V) was performed by Coleman (1963), who used ^{243}Am to minimize the radiolytically induced redox reactions associated with ^{241}Am. Coleman investigated the disproportionation of Am(V) in 3–8 M $HClO_4$ at 25°C, in 1–2 M $HClO_4$ at 75.7°C, and in about 2 M HCl, H_2SO_4, and HNO_3 solutions at 75.7°C. The disproportionation of Am(V) in 5 M $HClO_4$ and 5 M HCl at 25°C is shown in Fig. 8.5. The disproportionation of Am(V) in all media except HCl follows the reaction

$$3\ \mathrm{AmO_2^+} + 4\mathrm{H^+} \rightarrow \mathrm{Am^{3+}} + 2\mathrm{AmO_2^{2+}} + 2\mathrm{H_2O},$$

reflecting the fourth power dependence on the H^+ concentration. The rate law for this disproportionation reaction is

$$-\mathrm{d[Am(V)]/d}t = k_1\,[\mathrm{AmO_2^+}]^2[\mathrm{H^+}]^4 = k_2\,[\mathrm{AmO_2^+}]^2[\mathrm{H^+}]^2 + k_3\,[\mathrm{AmO_2^+}]^2[\mathrm{H^+}]^3,$$

with $k_2 = (6.94 \pm 1.01) \times 10^{-4}$ $\mathrm{L^3\,mol^{-3}\,s^{-1}}$ and $k_3 = (4.63 \pm 0.71) \times 10^{-4}$ $\mathrm{L^3mol^{-3}s^{-1}}$. The disproportionation rates at 75.7°C in 2 M HNO_3, HCl, and H_2SO_4 are, respectively, 4.0, 4.6, and 24 times greater than in 1 M $HClO_4$, whereas at 25°C the reaction rate increased 450 times in going from 3 to 8 M $HClO_4$. Using the temperature-dependence data from Coleman, Newton (1975) estimated thermodynamic quantities of activation for the disproportionation of Am(V). Note that the formation of Am(VI) in $HClO_4$ reaches a maximum after 5–6 h and then decreases successively with the main end product being Am(III). In 0.5 and 5 M HCl, Am(V) disappears much faster than in the non-complexing perchlorate medium. The formation of Am(VI) has not been observed in HCl media, indicating a fast reduction of Am(VI) by chloride (Hall and Herniman, 1954; Runde and Kim, 1994).

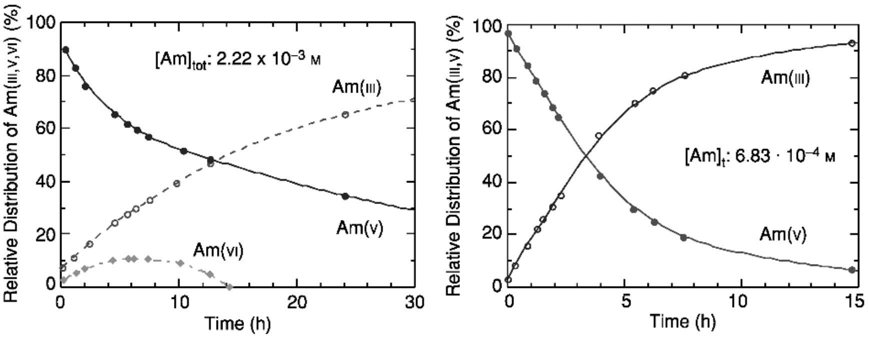

Fig. 8.5 *Disproportionation of Am(V) in 5 M $HClO_4$ (left) and 5 M HCl (right) (Runde and Kim,* 1994).

(f) Kinetics of oxidation–reduction reactions

Data for the few oxidation–reduction reactions that have been studied in detail can now be summarized. This summary supplements information presented by Hindman (1958), Newton and Baker (1967), and Gourisse (1966). An important recent reference on this subject is the critical review by Newton (1975).

(*i*) *Peroxydisulfate oxidation of Am*(III) *in acid media*

Early exploratory work by Asprey *et al.* (1950), the discoverers of the reaction between $S_2O_8^{2-}$ and Am(III) that produces Am(VI), established that the reaction proceeded in the concentration range from 10^{-8} to 10^{-1} M Am(III), implying a low-order dependence of the rate on Am(III) concentration. They further found that acidities greater than a few tenths molar were deleterious, presumably due to the acid-catalyzed decomposition path of $S_2O_8^{2-}$ (Penneman and Asprey, 1955). The general pattern of the oxidation (Fig. 8.6) represents an induction period and a linear region of constant rate followed by a region of gradually decreasing rate at high nitric acid concentrations. Reaction rates are dependent on temperature and on the concentration of HNO_3, $S_2O_8^{2-}$, and, when present, Ag^+. Newton (1975) states that the stoichiometry of the oxidation reaction is

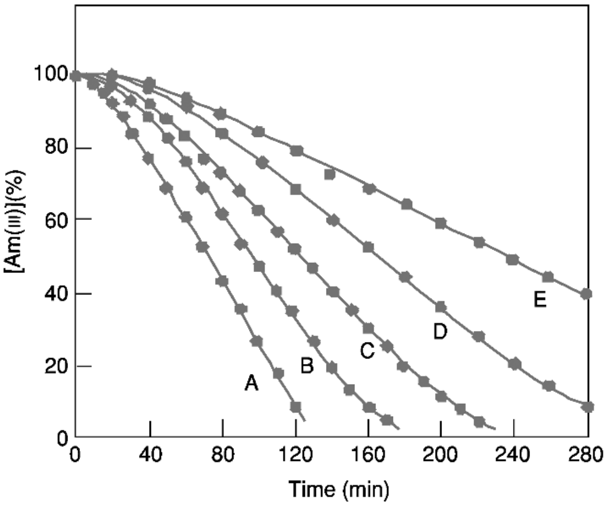

Fig. 8.6 *Kinetics of Am*(III) *oxidation by peroxydisulfate in nitric acid at* 50.6°C ($[S_2O_8^{2+}]_0 = 0.40$ M (*Ermakov* et al., 1971a, 1973, 1974)). *HNO_3 concentrations: A,* 0.09 M; *B,* 0.14 M; *C,* 0.19 M; *D,* 0.24 M; *E,* 0.28 M.

$$3/2\mathrm{S_2O_8^{2-}} + \mathrm{Am^{3+}} + 2\mathrm{H_2O} \rightarrow 3\mathrm{SO_4^{2-}} + \mathrm{AmO_2^{2+}} + 4\mathrm{H^+}$$

All researchers concur that the oxidizing agent is not the $S_2O_8^{2-}$ ion itself but its thermal decomposition products (e.g. $SO_4^{\bullet-}$ or $HS_2O_8^-$).

In contrast to conclusions from studies using micromolar Am(III), Ermakov *et al.* (1971a, 1973, 1974), on the basis of studies with millimolar amounts of ^{243}Am(III), claim that (in the absence of Ag^+) the rate of oxidation of Am(III) in the linear portion of kinetic curves does not depend on the Am(III) concentration and that the rate is given by:

$$\begin{aligned}-\mathrm{d}[\mathrm{Am(III)}]/\mathrm{d}t &= (a + b[\mathrm{H^+}])[\mathrm{S_2O_8^{2-}}][\mathrm{Am(III)}]_0\\ &= 2/3k_1 - (k_4[\mathrm{H^+}]/(1+x))[\mathrm{S_2O_8^{2-}}]_0 = k_{\mathrm{III}}\end{aligned}$$

At 50.6°C, $a = 4.9 \times 10^{-5}$ min^{-1} and $b = 0.9 \times 10^{-4}$ L mol^{-1} min^{-1}. In this equation $[S_2O_8^{2-}]_0$ is the initial concentration of the peroxydisulfate ion, $x = k_5/k_6[H_2O]$, and k_1, k_4–k_6 are rate constants for the following reactions:

$$\mathrm{S_2O_8^{2-}} \xrightarrow{k_1} 2\mathrm{SO_4^{\bullet-}}$$

$$\mathrm{S_2O_8^{2-}} + \mathrm{H^+} \xrightarrow{k_4} \mathrm{HSO_4^-} + \mathrm{SO_4^{\bullet}}$$

$$\mathrm{SO_4^{\bullet}} \xrightarrow{k_5} \mathrm{SO_3} + \mathrm{O}$$

$$\mathrm{SO_4^{\bullet}} + \mathrm{H_2O} \xrightarrow{k_6} \mathrm{H_2O_2} + \mathrm{SO_3}$$

(*ii*) *Peroxydisulfate oxidation of Am*(*V*) *in* HNO_3

Ermakov *et al.* (1971a, 1973, 1974) also investigated the kinetics of the oxidation of Am(V) by $S_2O_8^{2-}$ ion in 0.09–0.6 M HNO_3 media at 45.6–60°C. According to Newton (1975) the stoichiometry of this reaction is

$$1/2\ \mathrm{S_2O_8^{2-}} + \mathrm{AmO_2^{+}} \rightarrow \mathrm{SO_4^{2-}} + \mathrm{AmO_2^{2+}}$$

Ermakov gives the law:

$$-\mathrm{d}[\mathrm{Am(V)}]/\mathrm{d}t = (a' + b'[\mathrm{H^+}])[\mathrm{S_2O_8^{2-}}][\mathrm{Am(V)}]_0$$

At 50.6°C, $a' = 15 \times 10^{-5}$ min^{-1} and $b' = 2.7 \times 10^{-4}$ L mol^{-1} min^{-1}. It follows from this result and the rate data given in the preceding section that

$$-\mathrm{d}[\mathrm{Am(III)}]/\mathrm{d}t = -(1/3)\mathrm{d}[\mathrm{Am(V)}]/\mathrm{d}t$$

The results of Rykov *et al.* (1970) indicate that the mechanism of reduction of Am(VI) in the presence of $S_2O_8^{2-}$ ions is identical with that proposed for the oxidation of Am(V).

(*iii*) *Peroxydisulfate oxidation of Am*(*III*) *in carbonate media*

Peroxydisulfate oxidation of Am(III) in carbonate solutions proceeds through the intermediate formation of Am(V). Ermakov *et al.* (1971a, 1973, 1974) found that the rate of oxidation of Am(III) to Am(V) is independent of the total Am and K_2CO_3 concentrations and is equal to the rate of decomposition of $S_2O_8^{2-}$ ions. However, the rate of oxidation of Am(V) to Am(VI) is directly proportional to both the total americium concentration and the $S_2O_8^{2-}$ concentration, and is inversely proportional to the K_2CO_3 concentration. The effective activation energy of the $S_2O_8^{2-}$ oxidation of Am(III) to Am(V) in K_2CO_3 solutions is close to the activation energy (140 kJ mol^{-1}) of the thermal decomposition of $S_2O_8^{2-}$ ions. Recall that $Na_2S_2O_8$ will oxidize either Am(III) or Am(V) to Am(VI) in Na_2CO_3 or $NaHCO_3$.

(*iv*) *Reduction of Am*(*VI*) *by hydrogen peroxide*

Using ^{243}Am in $LiClO_4$–$HClO_4$ media, Woods *et al.* (1974) studied the kinetics of the reaction of AmO_2^{2+} with H_2O_2 and found the reduction of Am(VI) to be first order in both Am(VI) and H_2O_2 concentrations:

$$2AmO_2^{2+} + H_2O_2 \rightarrow 2AmO_2^{+} + 2H_2$$

(*v*) *Reduction of Am*(*VI*) *by other reductants*

Woods and Sullivan (1974) studied the reaction between AmO_2^{2+} and NpO_2^{+} in 1 M (H,Li)ClO_4. The rate law is:

$$-\mathrm{d}[\mathrm{Am(VI)}]/\mathrm{d}t = k[\mathrm{Am(VI)}][\mathrm{Np(V)}]$$

At 25°C, k is $(2.45 \pm 0.4) \times 10^4$ L mol^{-1} s^{-1}; for this reaction, $\Delta H^* = 27.87 \pm 0.33$ kJ mol^{-1} and $\Delta S^* = -67.8 \pm 1.3$ J K^{-1} mol^{-1}. Oxalic acid reduces Am(VI) rapidly to approximately equal mixtures of Am(III) and Am(V), whereas reagents such as H_2O_2, HCl, HCOOH, HCHO, etc., reduce Am(VI) initially only to Am(V). The reduction of Am(VI) by nitrous acid is first order in each (Woods *et al.*, 1976).

(*vi*) *Reduction of Am*(*V*) *by* H_2O_2

From studies of the reduction of AmO_2^{+} to Am^{3+} by H_2O_2 in 0.1 M $HClO_4$, Zaitsev *et al.* (1960a) deduced the rate law:

$$-\mathrm{d}[AmO_2^{+}]/\mathrm{d}t = k[AmO_2^{+}][H_2O_2]$$

where $k = 14.8 \pm 1.5, 21.6 \pm 2.2$, and 30.3 ± 3.01 mol^{-1} h^{-1} at 25, 30, and 35°C, respectively. The activation energy deduced for the reduction reaction is 55.2 kJ mol^{-1}. The only other reported studies of the Am(III)–Am(V)–H_2O_2–$HClO_4$ system have been made by Damien and Pages (1969, 1970). They reported that the rate at which AmO_2^+ is reduced is inversely proportional to the perchloric acid concentration and is also strongly dependent on the initial $[Am^{3+}]_0/[AmO_2^+]_0$ and $[H_2O_2]_0/[AmO_2^+]_0$ concentration ratios.

(*vii*) *Reduction of Am*(v) *in NaOH solutions*

Shilov *et al.* (1997) investigated the reduction rate of Am(v) in 1.5 and 3 M NaOH at room temperature. Slow reduction of Am(v) is observed in the presence of 0.005–0.4 M of dithionite ($Na_2S_2O_4$), sulfite (Na_2SO_3), or thiourea dioxide ($(NH_2)_2CSO_2$) with a half-reduction time ranging between 0.2 and 9 h. The reduction of Am(v) in 3–14 M NaOH with about 0.01 M hydrazinium nitrate or hydroxylamine is accelerated with reductant concentration and temperature.

(*viii*) *Reduction of Am*(v) *by Np*(iv) *in perchloric acid media*

Blokhin *et al.* (1973) used spectrophotometry to study the kinetics of the Np(iv)–Am(v) reaction in 0.23–1.97 M $HClO_4$ at temperatures in the range 35.0–54.6°C. Depending on the initial concentrations of Np(iv) and Am(v), the reaction products are either Np(v) and Am(iii) or Np(vi) and Am(iii). The reaction rate falls rapidly with increasing acidity. Under the assumption of constant Am(iv) concentration, the kinetic data follow the rate law:

$$d[Am^{3+}]/dt - k'1[Np^{4+}][AmO_2^+] + k'2[NpO_2^+][AmO_2^+]$$

The authors report the following thermodynamic activation parameters: $\Delta H^* = 126 \pm 4$ kJ mol^{-1}, $\Delta G^* = 87 \pm 4$ kJ mol^{-1}, and $\Delta S^* = 130 \pm 13$ J K^{-1} mol^{-1}.

(*ix*) *Reduction of Am*(v) *by Np*(v) *in perchloric acid*

Rykov *et al.* (1973) determined spectrophotometrically the rate of the reaction:

$$2NpO_2^+ + AmO_2^+ + 4H^+ \rightarrow 2NpO_2^{2+} + Am^{3+} + 2H_2O$$

Kinetic data were collected in perchlorate ($\mu = 2.0$ M) at temperatures in the range 24.7–44.1°C. These researchers claim that reduction of Am(v) by Np(v) is an irreversible second-order reaction.

(*x*) *Reduction of Am*(v) *by Np*(v) *in Na_2CO_3*

Kinetics of the reduction of Am(v) by Np(v) in Na_2CO_3 solutions were investigated spectrophotometrically (Chistyakov *et al.*, 1974). The stoichiometry of the reduction is

$$4H^+ + AmO_2^+ + 2NpO_2^+ \rightarrow Am^{3+} + 2NpO_2^{2+} + 2H_2O$$

The kinetics of the Am(v) reactions in aqueous Na_2CO_3 follow the same rate law as in $HClO_4$ media.

(*xi*) *Reduction of Am*(*V*) *by U*(*IV*) *in perchloric acid*

At 11.2 and 3.60°C in 0.51–2.60 M $HClO_4$, the reaction between Am(v) and U(iv) proceeds according to the equation:

$$AmO_2^+ + U^{4+} \rightarrow Am^{3+} + UO_2^{2+}$$

Blokhin *et al.* (1974) derived the following rate law:

$$d[Am^{3+}]/dt = k[AmO_2^{2+}][U^{4+}]$$

In 2.0 M $HClO_4$ at 9.5°C, $k = 725 \pm 30$ L mol^{-1} min^{-1}. Standard thermodynamic activation parameters are $\Delta H^* = 75 \pm 4$ kJ mol^{-1}, $\Delta G^* = 63.6 \pm 0.8$ kJ mol^{-1}, and $\Delta S^* = 37.7 \pm 12.5$ J K^{-1} mol^{-1}.

(*xii*) *Oxidation of Am*(*II*) *by water*

In an elegant experiment carried out at the U.S. Argonne National Laboratory, the absorption spectra of both divalent americium and tetravalent americium were obtained (Sullivan *et al.*, 1976, 1978). This technique involved irradiation of Am(iii) solutions with single electron pulses and recording the spectra with a streak camera at postirradiation times of 50 μs for Am(ii) and 100 μs for Am(iv). Am(ii) disappeared via reaction with water, while the Am(iv) species disproportionated to yield Am(iii) and Am(v).

(g) Radiolysis

The most commonly used americium isotopes, ^{241}Am and ^{243}Am, decay primarily by emitting high-energy alpha particles of about 5.4 and 5.2 MeV, respectively (see Table 8.1). In solution, the energy (1 mg ^{241}Am releases about 7×10^{14} eV s^{-1}) is released in dense tracks producing radicals, ions, and electrons; thus can impact the stability of americium oxidation states in aqueous solutions. There are numerous reports on the effect of the intense alpha radiation of transuranium elements on their chemical behavior in acidic, basic, and highly concentrated chloride solutions. In acidic media, Am(iii) is the most stable oxidation state and Am(v) and Am(vi) are rather rapidly reduced (Vladimirova *et al.*, 1977; Kornilov *et al.*, 1986). The reduction rate is closely related to the dose rate and electrolyte concentration. Vladimirova and coworkers (Vladimirova *et al.*, 1977; Vladimirova, 1986) suggested that Am(v) and Am(vi) reduction in nitric acid solutions cannot be explained by involving only radiolytically produced radicals but also require consideration of chemical reactions with radiolytically produced H_2O_2 and HNO_2:

$$2AmO_2^{2+} + HNO_2 + H_2O \rightarrow 2AmO_2^{+} + 3H^{+} + NO_3^{-}$$

$$2AmO_2^{+} + HNO_2 + 6H^{+} \rightarrow 2Am^{4+} + 3H_2O + HNO_3$$

In perchlorate solutions, alpha-radiolysis produces multiple species, such as Cl_2, ClO_2, or Cl^- that are effective reductants for Am(vi) (Kornilov *et al.*, 1986). A radiolytically enhanced chemical oxidation of Am(iii) to Am(v) and Am(vi) (at large gamma doses) is observed in perchlorate solutions at pH 3–6 in the presence of excess of N_2O, $S_2O_8^{2-}$, or XeO_3 (Pikaev *et al.*, 1977). As expected the stability of higher oxidation states increases with pH and Am(iii) is radiolytically oxidized to Am(v) in carbonate solutions under the exposure of intense alpha-radiation from ^{244}Cm (3–8 KCi L^{-1}) (Osipov *et al.*, 1977). The formation of oxidizing species in concentrated chloride solutions, i.e. Cl_2 and ClO^-, leads to the autoradiolytical oxidation of Am(iii) to Am(v) (Magirius *et al.*, 1985; Runde and Kim, 1994). The radiolytical formation of hypochlorite in basic 5 M NaCl is directly correlated with the alpha-specific activity of ^{241}Am.

8.8.2 Complexation reactions

A critical review of the chemical thermodynamics of experimental data and chemical thermodynamics for americium inorganic compounds was recently published by the NEA (Silva *et al.*, 1995). Nearly all formation constants listed in Table 8.8 are for complexes formed by Am(iii), as little work has been done on complexes with Am in higher oxidations states. Color changes of Am(iii)-containing solutions indicate existence of Am(vi) nitrate, sulfate, and fluoride complexes. Some spectroscopic evidence exists for a Am(v) peroxide complex in 1 M NaOH (Musikas, 1973a). In agreement with the behavior of other actinide (iii) and (iv) ions, the stability of Am(iii) complexes with monovalent inorganic ligands follows the sequence:

$$F^- > H_2PO_4^- > SCN^- > NO_3^- > Cl^- > ClO_4^-.$$

As a Chatt–Ahrland ‘A’ type or Pearson ‘hard’ cation, Am^{3+} association with inorganic ligands proceeds initially through electrostatic interactions to form outer-sphere complexes, such as chlorides or perchlorates. Spectrophotometric results suggested the inner-sphere formation of chloride and nitrate ions in concentrated Na/LiCl and $LiNO_3$ solutions (Marcus and Shiloh, 1969; Allen *et al.*, 2000). Inner-sphere complexes are also found to form with harder ligands, such as fluoride or sulfate. In most cases, the stability of Am(iii) complexes is similar to those that contain lanthanide ions with similar ionic radii, e.g. Nd(iii) and Eu(iii). In some cases, the stability of the Am(iii) complex is slightly greater than that of the corresponding lanthanide complex presumably because of the participation of f-electrons in the bonding (Moskvin, 1967, 1971, 1973). As discussed earlier, this difference in stability can be used to separate Am(iii) effectively from lanthanide elements.

Table 8.8 *Selected formation constants and solubility products of inorganic americium complexes* (*Silva* et al., 1995).

Complex	*log* β° *or* *log* K°_{sp}	$\Delta_f G^o_m$(298.15K) (kJ mol^{-1})	$\Delta_f H^o_m$(298.15K) (kJ mol^{-1})
Solution species			
$AmOH^{2+}$	–6.4 ± 0.7	–799.31 ± 6.21	
$Am(OH)_2^+$	–14.1 ± 0.6	–992.49 ± 5.86	
$Am(OH)_3(aq)$	–25.7 ± 0.5	–1163.42 ± 5.55	
$Am(CO_3)^+$	7.8 ± 0.3	–1171.12 ± 5.07	
$Am(CO_3)_2^-$	12.3 ± 0.4	–1724.71 ± 5.33	
$Am(CO_3)_3^{3-}$	15.2 ± 0.6	–2269.16 ± 5.98	
$AmSCN^{2+}$	1.3 ± 0.3	–513.42 ± 6.45	
AmF^{2+}	3.4 ± 0.4	–899.63 ± 5.32	
AmF_2^+	5.8 ± 0.2	–1194.85 ± 5.08	
$AmCl^{2+}$	1.05 ± 0.1	–735.91 ± 4.77	
$AmSO_4^+$	3.85 ± 0.03	–1364.68 ± 4.78	
$Am(SO_4)_2^-$	5.4 ± 0.8	–2117.53 ± 6.27	
$AmNO_3^{2+}$	1.33 ± 0.2	–717.08 ± 4.91	
$AmH_2PO_4^{2+}$		–1752.97 ± 5.76	
Solid phases			
$Am(OH)_3(am)$	–17.0 ± 0.6		
$Am(OH)_3(cr)$	–15.2 ± 0.6		
$AmO_2(cr)$		–874.49 ± 4.27	–932.20 ± 3.00
Am_2O_3 (cr)		–1613.32 ± 9.24	–1690.40 ± 8.00
AmF_3 (cr)		–1518.83 ± 13.10	–1588.00 ± 13.00
AmF_4 (cr)		–1616.83 ± 20.06	–1710 ± 20.00
$Am_2(CO_3)_3$ (cr)	16.7 ± 1.1	–2971.74 ± 15.79	
$Am(OH)CO_3$ (cr)	21.2 ± 1.4	–1404.83 ± 9.31	
$AmPO_4$ (am)	24.8 ± 0.6	–1752.97 ± 5.76	

(a) Hydrolysis

(1) Am(III): The hydrolysis of Am(III) has been studied extensively, partly because the hydrolysis reactions are strongly favored in aqueous systems. It is established that Am(III) is complexed by hydroxide above pH 5 to form complexes of general formula $Am(OH)_n^{3-n}$ where $n = 1$–3. Thermodynamic stabilities of these complexes were calculated from data obtained by a variety of methods, such as solubility studies, solvent extraction, and potentiometric and electromigration measurements. Spectroscopic characterization or structural information of these complexes is absent because of their low solubilities. The existence of the anionic species $Am(OH)_4^-$ has been postulated, which would increase the Am(III) solubility at high pH. However, an increase in solubility is not observed at pH > 13 and contamination of the solution by carbonate may have produced anionic carbonate complexes that increase

the overall Am(III) solubility. There is substantial uncertainty about the formation of polynuclear complexes, as common in the U(VI) hydrolysis system.

(2) Am(V): Kim and coworkers (Magirius *et al.*, 1985; Stadler and Kim, 1988) measured the solubility of autoradiolytically formed $^{241}AmO_2(OH)$ (s) in 3 and 5 M NaCl. Runde and coworkers (Runde and Kim, 1994; Runde *et al.*, 1996) reported an increased solubility of $^{241}AmO_2(OH)(s)$ over $^{237}NpO_2(OH)(s)$ in 5 M NaCl. Slope analysis of the solubility data indicated formation of only two americyl(V) hydrolysis products in solution, $AmO_2(OH)(aq)$ and $AmO_2(OH)_2^-$. Tananaev (1990a) suggested the formation of $AmO_2(OH)_3^{2-}$ (with an absorption peak at 750 nm) and $AmO_2(OH)_4^{3-}$ in highly alkaline media based on spectroscopic measurements of Am(V) in 0.001–1 M LiOH solutions. Because of the radiolytic formation of oxidizing species (such as OCl^-) and the subsequently increased stability of Am(V), the few solubility studies of Am(V) were performed in concentrated chloride solutions. The reported apparent stability constants for $AmO_2(OH)(aq)$ and $AmO_2(OH)_2^-$ are close to those for the analogous Np(V) species (Runde *et al.*, 1996). However, the solubility of $^{241}AmO_2OH$ appears to be higher than that of $^{237}NpO_2OH$, probably due to higher alpha-radiation damage of the Am(V) solid.

(3) Am(IV) and Am(VI): The hydrolysis of Am(IV) and Am(VI) remains rather unexplored because of the instabilities of these oxidation states in aqueous solutions under ambient conditions. There is spectroscopic evidence for the formation of Am(VI) hydrolysis species of general formula $AmO_2(OH)_n^{2-n}$ where $n = 1$–4.

(b) Carbonate complexation

(1) Am(III): The carbonate complexation of Am(III) has been widely investigated using a variety of methods, such as solvent extraction, spectrophotometry, electromigration, and solubility. Meinrath and Kim (1991a) monitored the solubility and complexation reactions of Am(III) in carbonate-containing solutions spectroscopically. Three solution species, $Am(CO_3)_n^{3-2n}$ with $n = 1$–3, were characterized by their distinct absorbances at 505.4 nm ($\varepsilon = 385$ L mol^{-1} cm^{-1}), 506.5 nm ($\varepsilon = 350$ L mol^{-1} cm^{-1}), and 507.8 nm ($\varepsilon = 330$ L mol^{-1} cm^{-1}), respectively. Wruck *et al.* (1999) determined the formation constant of the monocarbonato complex, $Am(CO_3)^+$, at 25, 50, and 75°C at 0.1 m ionic strength using laser-induced photoacoustic spectroscopy. There is no experimental or spectroscopic proof for the proposed formation of bicarbonato complexes, $Am(HCO_3)_n^{3-2n}$, and mixed hydroxocarbonato species, $Am(OH)_m(CO_3)_n^{3-m-2n}$ (Bernkopf and Kim, 1984). These complexes were used to explain extraction and solubility data although the experimental data can be explained by pure carbonato

and hydroxo species. The solid phases $AmOHCO_3$ and $Am_2(CO_3)_3$ were found as solubility-controlling phases in aqueous carbonate solutions (Meinrath and Kim, 1991b; Runde *et al.*, 1992). The double carbonate $NaAm(CO_3)_2 \cdot nH_2O$ was identified by X-ray diffraction to form at increased NaCl concentrations (Runde and Kim, 1994; Rao *et al.*, 1996).

(2) Am(IV): There is only one carbonato complex of Am(IV) discussed in the literature. From combined spectroscopy and cyclic voltammetry data in bicarbonate/carbonate solutions (Bourges *et al.*, 1983), it was concluded that $Am(CO_3)_5^{6-}$ is the limiting carbonate complex of Am(IV). Its logarithmic stability constant, $\log \beta_5^{\circ} = 39.3 \pm 2.1$ (Silva *et al.*, 1995), is comparable to those of the analogous U(IV) (34.0 ± 0.9 (Grenthe *et al.*, 1992)) and Np(IV) complexes (33.9 ± 2.6 (Kaszuba and Runde, 1999)).

(3) Am(V): Giffaut and Vitorge (1993) studied the solubility of $NaAmO_2CO_3$ in carbonate-containing 4 M NaCl solution and claimed the formation of two Am(V) carbonate complexes, $AmO_2(CO_3)^-$ and $AmO_2(CO_3)_2^{3-}$. Runde and coworkers (Runde and Kim, 1994; Runde *et al.*, 1996) reported identical solubility and speciation behavior of Am(V) and Np(V) in carbonated 3 and 5 M NaCl solutions. In analogy to the well-characterized Np(V) system in 5 M NaCl, the solubility data were interpreted with the formation of $AmO_2(CO_3)_n^{1-2n}$ ($n = 1$–3) in solution and $NaAmO_2CO_3 \cdot nH_2O$ as the solid equilibrium phases.

Spectroscopic evidence suggests that an Am(V) carbonate complex in $NaHCO_3$, presumably the triscarbonato complex $AmO_2(CO_3)_3^{5-}$, has an absorbance at 727 nm (Tananaev, 1990a).

(4) Am(VI): The appearance of a burgundy-red color upon introducing Am(VI) into carbonate-containing solutions indicates the coordination of AmO_2^{2+} with carbonate ions. However, spectroscopic studies of the carbonate complexation of Am(VI) are few. Based on electrochemical measurements, it is assumed that the limiting complex is the $AmO_2(CO_3)_3^{4-}$ anion (Bourges *et al.*, 1983; Silva *et al.*, 1995).

(c) Organic ligands

With few exceptions, the data in Table 8.9 are for complexes of Am(III). Generally, the higher oxidation states of americium are reduced by organic complexing agents. Aminopolycarboxylic acids complex Am(III) more strongly than either hydroxycarboxylic or aminoalkylpolyphosphoric acids (e.g. ethylenediamine bis(methylene)phosphonic acid). Keller (1971) observed that in the series of α-hydroxycarboxylic acids (e.g. glycolic and lactic), the stability of the Am(III) complex decreases with increasing number of carbon atoms. The logarithm of the stability constant of the Am(III) complexes with aminopolycarboxylic acids increases linearly (Fig. 8.7) with the number of bound donor atoms of the ligand.

Table 8.9 *Complexes of Am(*III*) with organic ligands (unless otherwise noted, see the compilation by Schulz (1976) and references therein).*

				Log of formation constants			
Ligand	*Method*	*Temp.* (°C)	*Ionic strength, medium* μ (mol L^{-1})	β_1	β_2	*Other constants*	*References*
acetic acid (HAc)	IX	20	9.0 M HAc	2.28 ($AmAc^{2+}$)	3.84($AmAc_2^+$)	$\beta_3 = 4.78$ ($AmAc_3$)	[1]
						$\beta_4 = 5.7$ ($AmAc_4^+$)	[1]
						$\beta_5 = 6.66$ ($AmAc_5^{2+}$)	[1]
						$\beta_6 = 7.62$ ($AmAc_3^{6+}$)	[1]
	PT	20	1.0 M NH_4ClO_4	1.81	3.20	$\beta_3 = 4.57$; $\beta_4 = 5.7$	[1]
						$\beta_5 = 6.73$; $\beta_6 = 7.73$	[1]
	SX	25 ± 0.1	2.0 M NH_4ClO_4	1.95 ± 0.11			[2]
	IX	20	0.5 M NaClO4	1.99 ± 0.01	3.27 ± 0.07	$\beta_3 = 3.9$	[3]
	IX	25	$\mu = 0.2$	2.15	3.83		[4]
		25	$\mu = 0.5$	2.30	3.81		[4]
		25	$\mu = 1.0$	2.08	3.62		[4]
	SX	~25	0.1–1.0 M Ac	1.40 (AmO_2Ac)	2.51($AmO_2Ac_2^-$)		[5]
	SX	25 ± 0.5	0.5 M NH_4ClO_4	2.39 ± 0.05			[6]
α-alanine	SX	25	2.0 M $NaClO_4$	0.79 ($AmAla^{2+}$)			[7]
(Ala)	Spec	18 ± 2	1.0 M KCl	3.9 ± 0.2			[8]
anthranil-*N*,*N*-diacetic acid (H_3ADA)							
	IX	25	0.1 M NH_4ClO_4	8.92 (AmADA)	14.5($Am(ADA)_2^{3-}$		[26,52]
arginine				3.8 ± 0.3			[8]
aspartic acid	Spec	18 ± 2	1.0 M KCl	5.1 ± 0.02			[8]
Benzoyltrifluoroacetone (HBTA)							
	SX	25	0.1 M NH_4ClO_4			$\beta_3 = 14.84$ ($Am(BTA)_3$)	[9]
citric acid (H_3Cit)	Spec	25	1.0 M $NaClO_4$	6.96 (AmCit)	10.3($Am(Cit)_2^{3-}$)	$\beta'_1 = 4.53$ ($AmHCit^+$)	[10,11]
	SX	25	0.1 M(H,Li)ClO_4		12.15	$\Delta G^\circ = 44.98$ kJ mol^{-1} ($AmHCit^{2-}$)	[12]
	IX	25	0.1 M $NaClO_4$	9.16 ± 0.03		$\beta'_1 = 7.00$	[11]
			0.5 M $NaClO_4$	8.73 ± 0.066		$\beta'_1 = 6.29$	[11]
			1.0 M $NaClO_4$	6.72 ± 0.05		$\beta'_1 = 4.24$	[11]
	IX	25	0.1 M NaH_2 Cit	6.74	11.55	$\beta'_1 = 5.31$	[13]
						$\beta'_2 = 8.23$ ($Am(HCit)_2^-$)	[13]
	IX		1.0 M NH_4Cl	7.11	14.0	$\beta''_3 3 = 8.29$ ($Am(H_2Cit)_3$)	[14]
	PEP		0.04 M		9.66		[15]
	SX		0.1 M $LiClO_4$	10.1 ($Am(HCit)^+$)			[16]

				8.0 (Am(Cit))			[16]
				20 (Am(HcCit)_2^-)			[16]
				16.3 $(\text{Am(HCit)(Cit)}^{2-})$			[16]
				12.1 (Am(Cit)_2^{3-})			[16]
	PT		0.1 м LiClO_4	11.36 (Am(HCit)^+)			[16]
				8.69 (Am(Cit))			[16]
				18.97 $(\text{Am(HCit)(Cit)}^{2-})$			[16]
				14.29(Am(Cit)_2^{3-})			[16]
				10.53 (Am(OH)(Cit)^-)			[16]
				22.80 $(\text{Am(OH)(Cit)}_2^{2-})$			[16]
	SX	25	0.3 м NaCl	5.9 ± 0.1			[17]
			1.0 м NaCl	5.2 ± 0.1			[17]
			2.0 м NaCl	5.0 ± 0.1			[17]
			3.0 м NaCl	4.84 ± 0.04			[17]
			4.0 м NaCl	5.38 ± 0.06			[17]
			5.0 м NaCl	5.10 ± 0.15			[17]
15-crown-5	SX	25	0.1 м	0.21 ± 0.02			[18]
18-crown-6	SX	25	0.1 м	0.55 ± 0.06			[18]
cysteine	Spec	18 ± 2	1.0 м KCl		4.3 ± 0.3		[8]
1,2-diaminocyclohexanetetraacetic acid (H_4DCTA)							
	EM	20 ± 0.5	0.1 м KCl/HCl	18.34 (AmDCTA^-)		$\beta_1' = 2.87$ (AmHDCTA^-)	[19]
	IX	25 ± 1	0.1 м NH_4ClO_4	18.79			[20]
	IX	80	0.001 м H_4DCTA +0.02 м ammonium-α-hydroxyisobutyrate	18.79[e]			[21]
	SX	20	0.1 м NH_4Cl	18.21		$\beta_1''' = 2.85 \pm 0.04$ $(\text{AmO}_{22}\text{DTPA})^{2-}$	[22]
1,2-diaminopropanetetraacetic acid $(\text{H}_4\text{DTPrA}^-)$							
	IX	25	0.1 м NaClO_4	17.69 (AmDTPrA^-)		$\beta_1' = 9.79$ (AmHDTPrA)	[11]
1,10-diaza-4,7,13,16-tetraoxacyclooctadecane (diaza-crown ether; kryptofix 22; K22)							
	SX	25	1.0 м NaCl	6.05 ± 0.3			[23]
dibutyl-P,P′-ethane-1,2-diphosphonic acid $(\text{H}_2\text{B}_2\text{EDP})$							
	SX	25	1.0 м NaClO_4			$\beta_1' = 14.52$ $(\text{Am(HB}_2\text{EDP)}_3)$	[24]
5,7-dichloro-8-hydroxyquinoline (HDCO)							
	SX	25 ± 0.5	0.1 м $(\text{NH}_4\text{, H)ClO}_4$			$\beta_3 = 21.93$ (Am(DCO)3)	[25]

Table 8.9 (*Contd.*)

Ligand	*Method*	*Temp.* (°C)	*Ionic strength, medium* μ (mol L^{-1})	*Log of formation constants*		*Other constants*	*References*
				β_1	β_2		
diethylenetriaminepentaacetic acid (H_5DTPA)							
	IX	25	0.1 M NH_4ClO_4	23.07 ($AmDTPA^{2-}$)		$\beta_1' = 14.06$ ($AmHDTPA^+$)	[26]
	IX	25	0.1 M NH_4ClO_4	22.92			[27]
	EM	25 ± 0.2	0.1 M KNO_3	22.74		$\beta_1' = 14.3$	[28]
	SX		$\mu = 0.1$	23.2			[29]
	Spec	25	$\mu = 0.1$	23.2			[30]
	Spec	25	0.1 M NH_4ClO_4	24.03			[31]
	Spec	20 ± 0.1	0.5 M $HClO_4/HNO_3$	22.09			[32]
	IX	25	0.1 M NH_4ClO_4	23.32			[33]
	IX	25	1.0 M NH_4ClO_4	21.3		$\beta_1' = 15.46$	[1]
diethylphosphinylpropionic acid (HDEPP)							
	IX	25	0.5 M NH_4ClO_4; $HClO_4$	1.76 ($AmDEPP^{2+}$)	3.16 ($Am(DEPP)_2^+$)		[34]
diglycolic acid (H_2DGA)							
	Spec	25.2	0.1 M NH_4ClO_4	6.47 ($AmDGA^+$)	10.96 ($Am(DGA)_2^-$)	$\beta_3 = 13.83$ ($Am(DGA)_3^{3-}$)	[35]
dioctyl-P,P′-ethane-1,2-diphosphonic acid (H_2O_2 EDP)							
	SX	25	1.0 M NaClO4			$\beta_1' = 19.53$ ($Am(HO_2EDP)_3$)	[24]
diphosphine dioxides (1,1-DiPO=$(C_6H_{13})_2P(O)CH_2(O)P(C_6H_{13})_2$; 1,4-DiPO=$(C_6H_{11})_2P(O)(CH_2)_4(O)P(C_6H_{11})_2$; 1,5-DiPO=$(C_6H_{11})_2P(O)(CH_2)_5(O)P(C_6H_{11})_2$)							
	SX	2.0	2.0 M $NaNO_3$	1.43 ($Am(NO_3)_3 \cdot$ (1,1-DiPO))			[36]
				6.56 ($Am(NO_3)_3 \cdot$ 2(1,4-DiPO))			[36]
				5.92 ($Am(NO_3)_3 \cdot$ 2(1,5-DiPO))			[36]
ethylenediaminebis(isopropyl)phosphonic acid (H_4EDIP)							
	EM	25	0.1 M KNO_3	18.00 ($AmEDIP^-$)		$\beta_1' = 6.26$ (AmH_3EDIP^{2+})	[28]
						$\beta_1' = 8.94$ (AmH_2EDIP^+)	[28]
						$\beta_1' = 13.95$ (AmHEDIP)	[28]

ethylenediaminebis(methyl)phosphonic acid (H_4EDMP)							
	EM	25	0.1 м KNO_3	16.52 ($AmEDMP^-$)		$\beta_1' = 6.3$ (AmH_3EDMP^{2+})	[37]
						$\beta_1' = 8.48$ (AmH_2EDMP^+)	[37]
						$\beta_1' = 12.3$ ($AmHEDMP$)	[37]
	IX	25	0.5 м NH_4ClO_4			$\beta_1' = 6.12$ (AmH_2EDMP^+)	[38]
ethylenediaminetetraacetic acid (H_4EDTA)							
	IX	25	0.1 м $NaClO_4$	18.15 ($AmEDTA^-$)			[11]
			0.5 м $NaClO_4$	16.36		$\beta_1' = 9.68$ ($AmHEDTA$)	[11]
			1.0 м $NaClO_4$	15.72			[11]
	Spec	25 ± 0.2	1.0 м $NaClO_4/HClO_4$	15.33	22.10 ($Am(EDTA)_2^{5+}$	$\beta_1' = 8.94$ ($AmHEDTA$)	[11]
	SX	20	0.1 м NH_4Cl	16.91 ± 0.04			[39]
	Spec	25	0.1 м NH_4ClO_4	18.06			[31]
	IX	25 ± 0.02	0.1 м NH_4ClO_4	18.16 ± 0.10			[40]
	IX		1.0 м NH_4ClO_4	18.03 ± 0.13		$\beta_1' = 10.29$ ($AmHEDTA$)	[41]
	EM	25 ± 0.5	0.1 м HCl/KCl	17.0		$\beta_1' = 9.21$ ($AmHEDTA$)	[42]
	IX	80	0.001 м H_4EDTA + 0.2 м α-hydroxyisobutyrate	17.14			[43]
	EM	25 ± 0.1	0.1 м KNO_3	17.00 ± 0.09		$\beta_1' = 9.21$ ($AmHEDTA$)	[22,44]
	Spec	25	$\mu = 0.1$			$\beta = 19.98$ (AmO_2HEDTA^{2+})	[22,44]
						$\beta_1''' = 4.88 \pm 0.05$ (AmO_2HEDTA^{2+})	[22,44]
ethylenediaminetetramethylphosphonic acid (H_8EDTMP)							
	EM	25 ± 0.1	0.1 м KNO_3	22.47 ± 0.08 ($AmEDTMP^{5-}$)		$\beta_1' = 4.8 \pm 0.6$ (AmH_5EDTMP)	[44]
						$\beta_1'' = 7.33 \pm 0.09$ (AmH_4EDTMP)	[44]
						$\beta_1''' = 11.17 \pm 0.07$ (AmH_3EDTMP)	[44]
						$\beta_1'''' = 14.90 \pm 0.06$ (AmH_2EDTMP)	[44]
						$\beta_1''''' = 18.45 \pm 0.08$ ($AmHEDTMP$)	[44]

Table 8.9 (*Contd.*)

Ligand	*Method*	*Temp.* (°C)	*Ionic strength, medium* μ (mol L^{-1})	*Log of formation constants*		*Other constants*	*References*
				β_1	β_2		
ethylenediaminetetrapropionic acid (H_4EDTP)							
	Spec	25 ± 0.2	1.0 M $NaClO_4/HClO_4$	18.84 ± 0.02 ($AmEDTP^-$)	$\beta'_1 = 12.31$ (AmHEDTP)		[11]
ethyleneglycol*bis*(2-aminoethyl)tetraacetic acid (H_4EGTA)							
	IX	25	0.1 M NH_4ClO_4	18.22 (AmEGTA)			[26]
formate	Sol	25	2.0 M $NaClO_4$	2.54 (lg β_1)	4.02 (lg β_2)	$\log \beta_3 = 4.64$ $\log \beta_4 = 4.5$	[45]
formate (Am(v))	Spec	25	2.0 M $NaClO_4$	1.22 ± 0.3			[46]
fulvic acid	Spec	25	0.1 M $NaClO_4$	5.78 ± 0.07			[22]
	SX	25	3 M NaCl	4.7 ± 0.1			[13]
			6 M NaCl	6.0 ± 0.7			
glutamic acid	Spec	18 ± 2	1.0 M KCl	5.6 ± 0.1			[8]
glycine (HGlyn)	SX	25	2.0 M $NaClO_4$	0.69 ± 0.02 ($AmGlyn^{2+}$)			[47]
	Spec	18 ± 2	1.0 M KCl	4.1 ± 0.02			[8]
glycolic acid (HGlyc)							
	IX	0.5	0.5 M $NaClO_4$	2.82 ($AmGlyc^{2+}$)	4.85($Am(Glyc)_2^+$)	$\beta_3 = 6.30$ ($Am(Glyc)_3$)	[3]
	SX	25	2.0 M $NaClO_4$	2.59			[48]
	Spec	25 ± 0.2	1.0 M $NaClO_4/HClO_4$	2.44 ± 0.02	4.29 ± 0.2	$\beta_3 = 5.20$	[11]
	IX	25	0.5 M $NaClO_4$	2.57 ± 0.02	4.01 ± 0.1		[11]
histadine	Spec	18 ± 2	1.0 M KCl	4.8 ± 0.2			[8]
hydrazine-*N,N*-diacetic acid (H_2HyDA)							
	IX	25	0.1 M $NaClO_4$	10.74 ($AmHyDA^+$)	20.20 ($Am(HyDA)_2^+$)		[11]
	EM	25	$\mu = 0.1$	11.01	19.78		[37]
hydrazineiminodiacetic acid (H_2HyIDA)							
	EM	25	0.1 M KNO_3	10.98 ($AmHyIDA^+$)	19.97 ($AmHyIDA)_2^-$)	$\beta'_1 = 4.13$ ($AmHHyIDA^{2+}$)	[49]
2-hydroxycyclohexylethlenediaminetriacetic acid ($H_3HCEDTA$)							
	IX	25	0.1 M $NaClO_4$	16.09 (AmHCEDTA)		$\beta'_1 = 7.44$ ($AmHHCEDTA^+$)	[11]

N (2-hydroxyethyl)ethylene-*N,N,N'*-triacetic acid ($H_3NHEDTA$)						
	IX	25	0.1 M $HClO_4/NH_4ClO_4$	15.72 (AmNHEDTA)	22.47 $(Am(NHEDTA)_2^{3-})$		[26,50]
	Spec	25 ± 0.2	1.0 M $HClO_4/NH_4ClO_4$	14.84	22.18		[13]
	Spec	25	0.1 M NH_4ClO_4	16.18			[31]
	IX	22	0.15 M HCl/KCl	15.34			[51]
N′ (2-hydroxyethyl)iminodiacetic acid (H_2NHIDA)						
	IX	25	0.1 M NH_4ClO_4	9.14 (\rm Am(NHIDA^{+})	17.04 $(Am(NHIDA)_2^{-})$		[26,52]
	Spec	25	0.1 M NH_4ClO_4	9.80	17.01		[31]
	SX			9.3 ± 0.1			[53]
	EM	25	0.1 M KNO_3	9.3 ± 0.13	16.5 ± 0.2		[54]
α-hydroxyisobutyric acid (HIBA)						
	Spec	25 ± 0.2	1.0 M $HClO_4/NaClO_4$	2.68 ($AmIBA^{2+}$)	4.38 $(Am(IBA)_2^{+})$		[11]
	IX	25 ± 0.2	0.5 M NH_4ClO_4	2.88 ± 0.01	4.03 ± 0.02		[11]
	IX		0.5 M NH_4ClO_4/NH_4IBA	2.38	4.67	$\beta_3 = 5.12$ (Am(IBA)3)	[55]
	IX			2.72	4.69	$\beta_3 = 5.64$	[56]
	SX					$\beta_3 = 6.1$	[57]
bis(hydroxymethyl)phosphonic acid (HMP′A)						
	IX	25		1.76 ± 0.06 ($AmMPA^{2+}$)	2.48 ± 0.02 $(Am(MPA)_2^{+})$		[58]
hydroxymethylphosphonic acid (HMP′A)						
	IX	25	0.2 M NH_4ClO_4	1.55 $AmMP'A^{2+}$)	3.18 $(Am(MP'A)_2^{+})$		[59]
o-hydroxyphenyliminodiacetic acid (H_2HPIDA)						
	SX	25 ± 0.1	0.1 M NH_4ClO_4	6.80 $(Am(HPIDA)^{2+})$	11.9 (Am($HPIDA_2^{+}$)		[60]
8-hydroxyquinoline-5-sulfonic acid (H_2OXSA)						
	IX	25 ± 0.2	0.1 M NH_4ClO_4	8.64 ± 0.09 ($AmOXSA^{+}$)			[61]
iminodiacetic acid (H_2IDA)						
	IX	25	0.1 M NH_4ClO_4	7.37 ($AmIDA^{+}$)	12.39 $(Am(IDA)_2)$		[26]
	Spec	25 ± 0.2	1.0 M $HClO_4/NaClO_4$	6.14		$\beta_5 = 3.34$ $(Am(IDA)_5^{7-})$	[11]
	Spec	25	0.1 M NH_4ClO_4	6.94			[31]
7-iodo-8-hydroxyquinoline-5-sulfonic acid (H_2IOXSA)						
	IX	25 ± 0.2	0.1 M NH_4ClO_4	6.92 ($AmIOXSA^{+}$)			[61]
β-isopropyltropolone (HIPT)						
	IX		0.1 M NH_4ClO_4			$\beta_3 = 22.22 \pm 0.15$ (Am(IPT)3)	[9]
	SX	25	0.1 M NH_4ClO_4			$\beta_3 = 21.37$	[9,62]

Table 8.9 (*Contd.*)

Ligand	*Method*	*Temp.* (°C)	*Ionic strength, medium* μ (mol L^{-1})	*Log of formation constants*		*Other constants*	*References*
				β_1	β_2		
lactic acid (HLact)	SX	25	2.0 M NH_4ClO_4	2.52 ($AmLact^{2+}$)	4.77 ($Am(Lact)_2^+$)	$\beta_3 = 5.98$ (Am(Lact)3)	[63]
	IX		0.5 M NH_4ClO_4	2.77	4.64		[64]
	SX	20	0.5 M NH_4ClO_4			$\beta_3 = 5.71 \pm 0.03$	[65]
	IX	20	0.5 M NH_4ClO_4			$\beta_3 = 5.73$	[65]
	PEP	10	1.5 M KCl/HLact	2.57	4.21		[66]
methionine	Spec	18 ± 2	1.0 M KCl	4.8 ± 0.2			[8]
N-methyliminodiacetic acid (H_2MIDA)							
	IX	25	0.1 M NH_4ClO_4	7.01 ($AmMIDA^+$)	12.51 ($Am(MIDA)_2^-$)		[26]
6-methyl-2-picoline acid (HMAPS)							
	IX	25 ± 0.2	0.1 M NH_4ClO_4	4.26 ($AmMAPS^{2+}$)			[61]
6-methyl-2-picolyliminodiacetic acid (H_2MPIDA)							
	IX	25	0.1 M NH_4ClO_4	8.38 ($AmMPIDA^+$)			[26]
methylolethylphosporic acid (HMEPA)							
	IX	25	0.2 M NH_4ClO_4	1.79 ± 0.12 ($AmMEPA^{2+}$)			[59]
(methylphenylphosphinyl)methylphenylposphinic acid (HMPPA)							
	SX	25	0.2 M NH_4ClO_4	3.35 ($AmMPPA^{2+}$)			[59]
methylphosphinic acid (HMPA)							
	IX	25 ± 0.2	0.5 M NH_4ClO_4	2.79 ($AmMPA^{2+}$, at $\mu = 0$)			[67]
naphthoyltrifluoroacetone (HNTA)							
	SX	25	0.1 M NH_4ClO_4			$\beta_3 = 18.31$ ($Am(NTA)_3$)	[9]
nitrilodiacetomonobutyric acid (H_3NDMBA)							
	IX	25	0.1 M NH_4ClO_4			$\beta_1' = 3.53$ (AmHNDMBA)	[68,69]
nitrilodiacetomonopropionic acid (H_3NDAPA)							
	IX	25	0.1 M NH_4ClO_4	10.54 (AmNDAPA)	17.83 ($Am(NDAPA)_2^{3-}$)	$\beta_1' = 4.02$ (AmHNDAPA)	[68,69]
nitrilodiacetomonovaleric acid (H_3NDAVA)							
	IX	25	0.1 M NH_4ClO_4			$\beta_1' = 3.47$ (AmHNDAVA)	[68,69]

nitrilotriacetic acid (H_3NTA)							
	IX	25 ± 0.2	0.1 M $NaClO_4$	11.72 ± 0.02 (AmNTA)			[11]
			0.5 M $NaClO_4$	10.84 ± 0.06			[11]
	SX	20	0.1 M NH_4ClO_4	10.70	19.71$(Am(NTA)_2^{3-})$		[39]
	IX	20	1.0 M NH_4ClO_4	10.87			[1]
	IX	25.6	0.1 M NH_4ClO_4	11.91	20.18		[35]
	IX	25	0.1 M NH_4ClO_4–$HClO_4$	11.52	20.24		[68]
	IX	25	0.1 M (NH_4, $HClO_4$)	11.68	20.47		[69]
	Spec	24.6	0.1 M NH_4ClO_4	11.99	21.1		[70]
		20		11.65	19.52	$\beta_3 = 13.56$ $(AmNTA(HNTA)^{2-})$	[71]
oxalic acid (H_2Ox)	SX	20	0.1 M NH_4Cl		8.3 $(Am(Ox)_2^-)$	$\beta_3 = 11.8$ $(Am(Ox)_3^{3-})$	[39]
	IX		1.0 M NH_4Cl		9.95	$\beta'_4 = 11.0$ $(Am(HOx)_4^-)$	[41]
	Sol	25	$HClO_4/H_2Ox$	7.10 $(AmOx^+)$	11.2	$\beta_3 = 12.3$	[72]
	IX	20–25	0.2 M NH_4ClO_4	5.99	10.1		[73]
	EM	25	0.1 M NH_4Cl/HCl	6.45	10.5		[73]
	SX	25	1.0 M $NaClO_4$	4.63	8.35	$\beta_3 = 11.2$	[74,75]
	IX	25	0.5 M $NaClO_4$	3.8 ± 0.02	8.61 ± 0.01		[28]
	Spec	25 ± 0.1	$\mu = 0.25$; oxalate,pH1–5	3.27 (AmO_2Ox^+)	2.09 $(AmO_2(Ox)_2^{3-})$		[75]
	SX	21	0.7 M Na NaCl	4.58 ± 0.05 (pH 6.0) 3.95 ± 0.15 (pH 8.05)	7.91 ± 0.10 (pH 6.0) 7.54 ± 0.20 (pH 8.05)		[76]
	Sol	25 ± 0.2	I = 0	6.68	9.94	11.62	[77]
	EM	25	0 M $NaClO_4$		9.6		[78]
			0.01 M $NaClO_4$		9.0		[78]
			0.05 M $NaClO_4$		8.3		[78]
			0.1 M $NaClO_4$		8.2		[78]
	SX	25.0	1.0 M $NaClO_4$	4.61 ± 0.06	8.39 ± 0.12		[79]
			3.0 M $NaClO_4$	4.65 ± 0.04	8.67 ± 0.13		[79]
			5.0 M $NaClO_4$	4.83 ± 0.06	9.24 ± 0.09		[79]
			7.0 M $NaClO_4$	4.93 ± 0.11	9.42 ± 0.06		[79]
			9.0 M $NaClO_4$	4.54 ± 0.06	8.77 ± 0.05		[79]
phenylalanine	Spec	18 ± 2	1.0 M KCl	5.1 ± 0.3			[8]
1-phenyl-3-methyl-4-acetylpyrazolone-5 (HPMAP)							
	SX	25	0.1 M NH_4ClO_4			$\beta_3 = 12.23$ $(Am(PMAP)_3)$	[80]
1-phenyl-3-methyl-4-benzoylpyrazolone-5 (HPMBP)							
	SX	25	0.1 M NH_4ClO_4			$\beta_3 = 16.49$ $(Am(PMBP)_3)$	[80]
1-phenyl-3-methyl-4-trichloroacetylpyrazolone-5 (HPMTCP)							
	SX	25	0.1 M NH_4ClO_4			$\beta_3 = 7.47$ $(Am(PMTCP)_3)$	[80]

Table 8.9 (*Contd.*)

Ligand	*Method*	*Temp.* (°C)	*Ionic strength, medium* μ (mol L^{-1})	*Log of formation constants* β₁	β₂	*Other constants*	*References*
1-phenyl-3-methyl-4-trifluoroacetylpyrazolone-5 (HPMTFP)							
	SX	25	0.1 M NH_4ClO_4			$\beta_3 = 9.70$ $(Am(PMTFP)_3)$	[80]
phosphonoacetic acid (H_3PAA)							
	IX	0.2 M NH_4ClO_4				$\beta_1'' = 2.75$ $(Am(H_2PAA)^2)$	[81]
						$\beta_1''' = 5.15$ $(AmHPAA^+)$	[81]
						$\beta_2''' = 8.5$ $(Am(HPAA)_2^-)$	[81]
pyridine-2-carbonic acid (HAPS)							
	IX	25 ± 0.2	0.1 M NH_4ClO_4	4.28 ± 0.05 $(AmAPS^{2+})$	7.99 ± 0.03 $(Am(APS)_2^+)$	$\beta_3 = 10.51 \pm 0.05$ (Am(APS)3)	[61]
α-picolinic acid-*N*-oxide (HAPSNO)							
	IX	25 ± 0.2	0.1 M NH_4ClO_4	3.09 ± 0.07 $(AmAPSNO^{2+})$	5.49 ± 0.07 $(Am(APSNO)_2^+)$		[61]
2-picolyliminodiacetic acid (H_2PIDA)							
	IX	25	0.1 M NH_4ClO_4	8.96 $(Am(PIDA^+))$	17.71 $(Am(PIDA)_2^+)$		[26,52]
	Spec	25	0.1 M	0.94 ± 0.01 $(Am(PIDA)^+)$			[82]
				1.24 ± 0.001 $(Am(PIDA)_2^-)$			[82]
propanetricarboxylic acid (H_3PTA)							
	Spec	25	1.0 M $NaClO_4$	5.61 ± 0.07 (AmPTA)		$\beta_1' = 4.96 \pm 0.02$ $(AmHPTA^+)$	[10,11]
α-pyridiylacetic acid (HAPAA)							
	IX	25 ± 0.2	0.1 M NH_4ClO_4	3.63 ± 0.07 $(AmAPPA^{2+})$			[61]
pyridine-3-carboxylic acid (Nicotinic acid) (HNIC)							
	IX	25 ± 0.2	0.1 M NH_4ClO_4	3.18 ± 0.07 $(AmNIC^{2+})$			[61]
pyridine-2,6-dicarboxylic acid (H_2PDA)							
	IX	25 ± 0.2	0.1 M NH_4ClO_4	9.33 ± 0.09 $(AmPDA^+)$	16.51 ± 0.09 $(Am(PDA)_2^-)$		[61]
pyruvic acid (HPruv)							
	SX	25	2.0 M $NaClO_4$	2.03 $(AmPruv^{2+})$	3.34 $(Am(Pruv)_2^+)$	$\beta_3 = 3.87$ $(Am(Pruv)_3)$	[63]

bis(3-methoxysalicylidenaldehyde)ethylenediimine (B3MOXSEDI)							
	SX	25	0.3 M KNO_3			$\beta'_2 = 0.59$ (AmH (B3MoxSEDI)$_2$)	[83]
bis(salicylidenaldehyde)ethylenediimine (BSEDI)							
	SX	25	0.3 M KNO_3			$\beta'_2 = 4.94$(AmH (BSEDI)$_2$)	[83]
serine		Spec	18 ± 2	1.0 M KCl	4.3 ± 0.1		[8]
squaric acid (H_2Sq, Diketocyclobutenediol)							
	IX	25	1.0 M (H,NH_4)ClO_4	2.17(AmSq$^+$)	3.10 (Am(Sq)$_2$)		[84]
5-sulphosalicylic acid							
	PT	25	1.0 M $NaClO_4$	8.06 ± 0.02	15.34 ± 0.02		[85]
tartaric acid (H_2Tart)							
	IX		1.0 M NH_4Cl		10.7 (Am(Tart)$_2^+$)		[14,86]
	SX	20	0.1 M NH_4Cl	3.9 (AmTart$^+$)	6.8		[39]
	PEP	(?)	(?)		7.88		[87]
	SX	25 ± 0.5	0.5 M NH_4ClO_4	4.20 ± 0.06	6.84 ± 0.07		[6]
taurine-*N,N*-diacetic acid (H_3TDA)							
	IX	25	0.1 M NH_4ClO_4	8.08 (AmTDA)		$\beta'_1 = 2.29$ (AmHTDA$^+$)	[26]
	Spec	25	0.1 M	0.89 ± 0.001 (Am(H_3TDA))			[82]
				1.14 ± 0.005 (Am(H_3TDA)$_2^{3-}$)			[82]
N,*N*,*N*′,*N*′-tetrakis(2-pyridylmethyl)ethylenediamine (TPEN)							
	PT	25	0.1 M $NaClO_4$	6.69 ± 0.03 (Am(TPEN)$^{+3}$)			[88]
	Spec	25	0.1 M $NaClO_4$	6.77 ± 0.01 (Am(TPEN)$^{+3}$)			[88]
thenoyltrifluoroacetone (HTTA)							
	SX	25	0.1 M NH_4ClO_4	3.4 (AmTTA^{2+})	8.5(Am(TTA)$_2^+$)	$\beta_3 = 13.3$ (Am(TTA)$_3$)	[9]
	SX	10.40	0.1 M $HClO_4$/ClO_4			$\Delta G^\circ = 43.9$ kJ mol^{-1} (Am(TTA)3)	[12]
thiodiglycolic acid (H_2TDGA)							
	Spec	25.6	0.1 M NH_4ClO_4	3.52 ± 0.08 (AmTDGA$^+$)	5.66 ± 0.07 (Am(TDGA)$_2^+$)	$\beta'_1 = 2.06 \pm 0.08$ (AmHTDGA^{2+})	[35]
thioglycolic acid (HTGlyc)							
	IX	20	0.5 M NH_4ClO_4	1.55 (AmGlyc^{2+})	2.60(Am(TGlyc)$_2^+$)		[3]
p-toluenesulfonic acid (pTSAH)							
	SX	25	2.0 M $HClO_4$/pTSAH	–0.028 ± 0.028 (AmpTSA2$^+$)			[89]
	SX	25	2.0 M HBF_4/pTSAH	0.075 ± 0.018			[89]

Table 8.9 (*Contd.*)

Ligand	*Method*	*Temp.* (°C)	*Ionic strength, medium* μ (mol L^{-1})	*Log of formation constants* β₁	β₂	*Other constants*	*References*
triethylenetetraaminehexaacetic acid (H_6TTHA)							
	IX	25	0.1 M NH_4ClO_4			$\beta_1' = 18.13$ ($AmHTTHA^{2+}$)	[26]
						$\beta_1'' = 11.85$ (AmH_2TTHA^-)	[26]
	Spec	25	0.1 M NH_4ClO_4	27.61 ($AmTTHA^{3-}$)		$\beta = 30.97$ (Am2TTHA)	[1,31]
						$\beta = 9.15 (Am_2H_2(TTHA)_3^{10-})$	[1,31]
Tropolene	SX	25	0.1 M $HClO_4$			$\beta_3 = 16.17 \pm 0.08$	[62]
Tryptophan	Spec	18 ± 2	1.0 M KCl	4.7 ± 0.2			[8]

[1] (Moskvin, 1967, 1971, 1973); [2] (Choppin, 1965, 1970, 1975); [3] (Grenthe, 1962); [4] (Gureev *et al.*, 1970); [5] (Hara, 1970); [6] (Rao *et al.*, 1987); [7] (Aziz and Lyle, 1971); [8] (Rogozina *et al.*, 1974); [9] (Keller and Schreck, 1969); [10] (Eberle and Moattar, 1972); [11] (Moattar, 1971); [12] (Hubert *et al.*, 1974, 1975); [13] (Ohyoshi and Ohyoshi, 1971); [14] (Moskvin *et al.*, 1962); [15] (Marcu and Samochocka, 1966); [16] (Bouhlassa and Guillaumont, 1984); [17] (Wall *et al.*, 2002); [18] (Mohapatra and Manchanda, 1991); [19] (Stepanov *et al.*, 1967); [20] (Baybarz, 1966); [21] (Elesin and Zaitsev, 1971a); [22] (Shilov *et al.*, 1976); [23] (Mohapatra and Manchanda, 1995); [24] (Zur Nedden, 1969); [25] (Keller *et al.*, 1965a, 1966); [26] (Bayat, 1970); [27] (Baybarz, 1965); [28] (Lebedev and Shalinets, 1968; Lebedev *et al.*, 1968); [29] (Burch, 1964); [30] (Hafez, 1968); [31] (Delle Site and Baybarz, 1969); [32] (Piskunov and Rykov, 1972); [33] (Brandau, 1971); [34] (Elesin and Zaitsev, 1972); [35] (Grigorescu-Sabau, 1972); [36] (Goffart and Kuyckaerts, 1969; Vorob'eva *et al.*, 1973a); [37] (Shalinets and Stepanov, 1971, 1972); [38] (Elesin *et al.*, 1973); [39] (Stary, 1966); [40] (Fuger, 1958); [41] (Moskvin *et al.*, 1959); [42] (Lebedev *et al.*, 1967); [43] (Elesin and Zaitsev, 1971b); [44] (Shalinets, 1972a,c); [45] (Anan'ev and Krot, 1985; Anan'ev and Shilov, 1985); [46] (Buckau *et al.*, 1992); [47] (Tanner and Choppin, 1968); [48] (Choppin and Degischer, 1972); [49] (Levakov and Shalinets, 1971); [50] (Eberle and Bayat, 1967); [51] (Mercing and Duyckaerts, 1967); [52] (Eberle and Bayat, 1969); [53] (Ermakov *et al.*, 1971c); [54] (Shalinets, 1972b); [55] (Dedov *et al.*, 1961); [56] (Graus Odenheimer and Choppin, 1956); [57] (Stary, 1965); [58] (Vorob'eva *et al.*, 1973b); [59] (Elesin *et al.*, 1972a,b); [60] (Ermakov *et al.*, 1971b); [61] (Al Rifai, 1970); [62] (Cilindro and Keller, 1974); [63] (Aziz and Lyle, 1971); [64] (Lebedev and Yakovlev, 1961); [65] (Ermakov and Starπ, 1967); [66] (Sakanque and Nakatani, 1972); [67] (Borisov *et al.*, 1967); [68] (Eberle and Ali, 1968); [69] (Ali, 1968); [70] (Eberle and Sabau, 1972); [71] (Gedeonov *et al.*, 1967); [72] (Lebedev *et al.*, 1960a); [73] (Stepanov and Makarova, 1965; Stepanov, 1971); [74] (Sekine, 1965); [75] (Shilov *et al.*, 1974); [76] (Caceci and Choppin, 1983); [77] (Pazukhin *et al.*, 1987); [78] (Rosch *et al.*, 1989); [79] (Choppin and Chen, 1996); [80] (Backer and Keller, 1973); [81] (Elesin *et al.*, 1972c); [82] (Bayat and Moattar, 1982); [83] (Stronski and Rekas, 1973); [84] (Cilindro *et al.*, 1972); [85] (Nair and Chander, 1983); [86] (Gel'man *et al.*, 1967); [87] (Marcu and Samochocka, 1965); [88] (Jensen *et al.*, 2000); [89] (Baisden *et al.*, 1972).

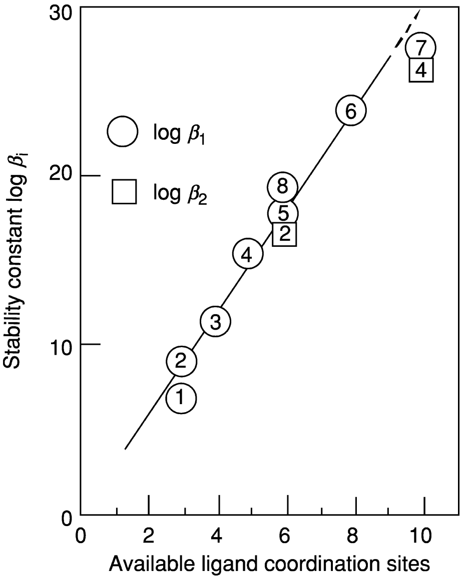

Fig. 8.7 *Correlation of stability constants with number of available coordination sites.* 1, *iminidiacetic acid;* 2, *N-hydroxy-ethyliminodiacetic acid;* 3, *nitrilotriacetic acid;* 4, *N-hydroxyethylenediaminetriacetic acid;* 5, *ethylenediaminetetraacetic acid;* 6, *diethylenetriaminepentaacetic acid;* 7, *triethylenetetraaminehexaacetic acid;* 8, *diaminocyclohexanetetraacetic acid* (*Keller*, 1971).

Methods are being sought to estimate and correlate the strengths of Am(III) complexes and other trivalent actinides and lanthanides with various organic ligands. Shalinets and Stepanov (1971, 1972) suggests a 'rule of additivity of the strength of rings' according to which, under similar conditions, the logarithm of the thermodynamic formation constant of the complex is proportional to the sum of the strengths of the individual rings. In a few cases, formation constants of americium chelates calculated by Shalinets are in good agreement with experimental data. For a more detailed discussion of the nature and stability of organic complexes of americium, refer to Chapters 23 and 25.

It is not surprising that a number of studies focus on the complexation of Am(III) with natural organic substances because of its importance for the assessment of nuclear waste disposal in geologic formations. The majority of naturally occurring organic materials derive from the decomposition of organic matter to soluble polymeric HA and fulvic acid (FA). The surfaces of these substances have a number of hydrophilic functional groups, such as amine, hydroxyl, carboxyl, and phenolic. As a hard cation, Am^{3+} interacts predominantly with the oxygen-donating phenolic and carboxylic groups. A large number of experimental data exist that are usually interpreted by the charge neutralization model or a polyelectrolyte model (Choppin and Labonne-Wall, 1997). The charge neutralization model is based on the cation complexation by a number of carboxylate groups expressed as an experimentally determined loading capacity of the organic substance. The polyelectrolyte model can better accommodate the chemical behavior of the humic/fulvic acids and takes into account the nature of the binding functional group (carboxylate). The concentration of binding sites and the ionization degree is determined experimentally via pH titration. For a more detailed discussion of these two models and of the impact of humate and fulvate complexation on the environmental behavior of americium, refer to Chapters 27 and 29.

Choppin and coworkers (Bertha and Choppin, 1978) performed ion-exchange studies at pH 4.5 to determine log $\beta_1 = 6.83$ and log $\beta_2 = 10.58$ for a Lake Bradford, Florida (USA), humic substance. These results agree well with log $\beta_1 = 6.4$ and log $\beta_2 = 10.58$ determined for HA from Mount Kanmuri, Japan (Yamamoto and Sakanoue, 1982). Applying a degree of ionization of the HA, Choppin and coworkers (Torres and Choppin, 1984) reported log $\beta_1 =$ 6.8–11.6 and log $\beta_2 =$ 11.9–14.3 for the Am(III)—HA (Lake Bradford) complex determined at pH 3.75–5.7. Using UV–VIS and laser-induced photoacoustic spectroscopy Kim *et al.* (1993) determined log $\beta_1 = 6.4 \pm 0.1$ at pH = 6 ($I = 0.1$) for HAs obtained from natural water at the German Gorleben (Gohy-573) site and from a commercial HA (Aldrich Chemical Co.). For the calculation of the Am(III)–HA stability constant, Kim *et al.* determined a loading capacity of 62.2% for Gohy-573 HA and of 81.5% for Aldrich HA. The Am(III) absorption band at 506 nm was assigned to an Am(III)–HA complex and was used for data analysis. Moulin *et al.* (1987) spectroscopically monitored the complexation of Am(III) with Aldrich HA at pH 4.65 ($I = 0.1$) and calculated log $\beta_1 =$ 7–7.5.

The stability constants found for Am(III) fulvate are slightly smaller than those found for humate. Buckau *et al.* (1992) determined log $\beta_1 = 5.9$ for FA extracted from the Gohy-573 groundwater using UV–VIS absorption spectroscopy. This FA is characterized by a proton exchange capacity of 5.7 meq g^{-1} and a loading capacity of 64.9% at pH 6.0. Interestingly, the stability constant of the Am(III)–FA complex is constant in the Am(III) concentration range of 4×10^{-5} to 5×10^{-8} mol L^{-1} at [HA] = 10^{-6} mol L^{-1}.

Complexation of Am(III) with the hexadentate ligand *N*,*N*,*N*′,*N*′-tetrakis (2-pyridylmethyl)ethylenediamine (TPEN) in 0.1 M $NaClO_4$ at 25°C to form $Am(TPEN)^{3+}$ is about two orders of magnitude higher than that of Sm(III), reflecting the stronger bonding of the trivalent actinide cations with softer ligands as compared to lanthanides (Jensen *et al.*, 2000).

(d) Others

The stability constants of Am(III) fluoride complexes are much larger than for the other halides (Silva *et al.*, 1995). Positive enthalpies for the reaction of Am^{3+} with F^- anions indicate that the AmF_n^{3-n} are inner-sphere complexes.

Two Am(III) fluoride solution species have been identified, AmF^{2+} and AmF_2^+, with recommended formation constants of log $\beta_1^o = 3.4 \pm 0.4$ and log $\beta_2^o = 5.8 \pm 0.2$, respectively. In contrast, the recommended formation constant for $AmCl^{2+}$, log $\beta_1^o = 1.05 \pm 0.06$, suggests a very weak bonding of chloride ions.

Few reliable data have been reported for the sulfate complexation of Am(III). Stability constants for two complexes, $AmSO_4^+$(log $\beta_1^o = 3.85 \pm 0.03$) and $Am(SO_4)_2^-$(log $\beta_2^o = 5.4 \pm 0.7$), were recommended (Silva *et al.*, 1995). There is no evidence for the formation of $Am(III) - HSO_4^-$ complexes.

The formation of Am(III) thiocyanate complexes was studied intensively because of the use of such complexes in separation of lanthanide and actinide elements. Three complexes of general formula $Am(SCN)_n^{3-n}$ (n = 1–3) have been identified from spectroscopic and solvent extraction data. The complexation of Am(III) by thiocyanate is quite weak and the accepted thermodynamic constant for the 1:1 complex is log $\beta_1^o = 1.3 \pm 0.3$ (Silva *et al.*, 1995).

Nitrate complexes of Am(III) are weak complexes and two complexes, $AmNO_3^{2+}$ and $Am(NO_3)_2^+$, have been used to interpret solvent extraction data in nitric acid media. The recommended formation constant of the 1:1 complex is log $\beta_1^o = 1.33 \pm 0.20$ (Silva *et al.*, 1995).

A number of studies of Am(III) complexation in phosphate media have been reported with only a few reliable data interpretations and complex characterizations. The system is complicated by the presence of multiple (hydrogen) phosphate species in solution. The solution complexes $AmHPO_4^+$ and $Am(H_2PO_4)_n^{3-n}$ (n = 1–4) have been used to interpret cation exchange, solvent extraction, and spectroscopic data. Lebedev *et al.* (1979) attributed the changes of the characteristic absorption band of Am^{3+} at 503 nm to the formation of $Am(III) - H_2PO_4^-$ complexes. With increasing phosphoric acid concentration (up to 13 M), the absorbance maximum is shifted to about 502 nm and the characteristic shoulder in the Am^{3+} band at 506 nm almost disappears. It remains unclear if these changes are due to inner-sphere complexation with phosphate or to changes in the number of coordinated water molecules in these extreme experimental conditions. The NEA recommends a stability constant only for the complex $AmH_2PO_4^{2+}$, log $\beta_1^o = 3.0 \pm 0.5$ (Silva *et al.*, 1995).

Am(IV) can be stabilized in acidic media by complexation with heteropolyanions. Chartier *et al.* (1999) reported spectroscopic evidence for the formation of $AmP_2W_{17}O_6^{16-}$ and $Am(P_2W_{17}O_{61})_2^{16-}$ via their absorbance bands at 789 and 560 nm, respectively. Chartier *et al.* reported log $\beta_1 = 19.2 \pm 0.2$ and log $\beta_2 = 22.8 \pm 0.2$ in 1 M HNO_3. The rate of autoradiolytic reduction of Am(IV) in these complexes is independent of the complex composition. Th(IV) causes the destruction of the complexes and subsequent disproportionation of free Am(IV) into Am(III) and Am(VI). Complex formation of Am(III) with $W_{10}O_{36}^{12-}$, $PW_{11}O_{39}^{7-}$, and $SiW_{11}O_{39}^{8-}$ was discussed qualitatively by Yusov (1989). Chartier *et al.* (1999) determined the apparent formation constants for $AmSiW_{11}O_{39}^{4-}$ and for $Am(SiW_{11}O_{39})_2^{12-}$ in 1 M HNO_3, log $\beta_1 = 21.3 \pm 0.3$ and log $\beta_2 = 26.2 \pm 0.2$, respectively. In contrast, Williams *et al.* (2000) used extended X-ray absorption fine structure (EXAFS) to determine that the Am center cation is trivalent when integrated in the Preyssler anion, $AmP_5W_{30}O_{110}^{12-}$.

Sullivan *et al.* (1961) discovered cation–cation interaction between pentavalent and hexavalent actinides. Subsequently, Guillaume *et al.* (1981) found spectroscopic evidence for the Am(V)–U(VI) interaction in perchlorate medium where the interaction between AmO_2^+ and UO_2^{2+} shifts the main absorbance peak of AmO_2^+ at 716–733 nm and a new band appears at 765 nm. Both bands are close to the absorbances reported for the solid $KAmO_2CO_3$ (733 and 770 nm (Varga *et al.*, 1971)). Upon interaction of Am(V) with U(VI), the symmetrical stretching (Raman) frequency of AmO_2^+ at 732 cm^{-1} is shifted to 719 cm^{-1} (Guillaume *et al.*, 1982). The Am(V)–U(VI) ($K = 0.35 \pm 0.07$ at $I = 10$) and Am(V)–Np(VI) ($K = 0.095 \pm 0.03$ at $I = 6$) (Guillaume *et al.*, 1981, 1982) complexes appeared to be much weaker than the corresponding Np(V) complexes: Np(V)–U(VI) ($K = 3.7 \pm 0.1$ at $I = 7$) and Np(V)–Np(VI) ($K = 3.0 \pm 0.1$ at $I = 7$ (Madic *et al.*, 1979)).

8.9 COORDINATION CHEMISTRY AND COORDINATION COMPLEXES

Although over 250 compounds of americium have been synthesized and characterized, the coordination chemistry of americium is relatively unknown. As of 2001, the crystal structures of 39 americium compounds with inorganic ligands and only seven americium compounds with organic ligands have been structurally characterized. However, the majority of phase identification and characterization relied on X-ray powder diffraction and comparison to isostructural lanthanide, neptunium, or plutonium compounds. Certainly, the application of EXAFS provides useful insight into coordination and bonding of solution complexes and amorphous solid phases. As hard metal ions Am(III to VI) have a high affinity for hard donor atoms, such as O or N, and the light halides, and their coordination will be discussed in this section. Because of its high redox stability, trivalent americium coordination complexes are the most common. Generally, higher dimensional structures are found containing Am^{2+}, Am^{3+}, or Am^{4+} while the introduction of the linear americyl unit forces Am(V) and Am(VI) to form layered structures.

8.9.1 Compounds with inorganic ligands

(a) Halides

Americium exhibits different coordination environments in halide complexes with coordination numbers of 7, 8, 9, and 11. In the orthorhombic M_2AmCl_5 ($M = K, NH_4$, or Rb) trivalent americium is seven-coordinate in $AmCl_5^{2-}$ chains with two of the five chlorides bridging to adjacent Am atoms. In the monoclinic hexahydrate, $AmCl_3 \cdot 6H_2O$, americium is coordinated to two chlorides and six water molecules forming $AmCl_2(H_2O)_6^+$ cations that are linked through chloride anions in the lattice and an extensive hydrogen bond network (Burns and Peterson, 1971). Considering the inner-sphere bonding of the water molecules, the formula of this compound is better represented by $AmCl_2(H_2O)_6 \cdot Cl$. Eight-coordinate americium is also found in the tetrafluoride AmF_4. $AmO_2F_2^-$ layers held together by K^+ ions form the rhombohedral $KAmO_2F_2$, in which americium is eight-coordinate with two axial oxygen atoms (Am–O = 1.936 Å) and six fluorides (Am–F = 2.473 Å) in the equatorial plane (Asprey *et al.*, 1954a). The isostructural oxyhalides AmOCl (Weigel *et al.*, 1975) and AmOI (Asprey *et al.*, 1964, 1965) also contain nine-coordinate americium that is surrounded by four oxygen (2.343 Å) and five iodine atoms (4 Am–I of 2.994 Å and 1 Am–I of 3.0035 Å). Interestingly, AmOBr (Weigel *et al.*, 1979) is reported to be built up from linear Br–Am–O units stacked along the *c*-axis with reported interatomic distances of 2.415 Å for Am–O and 3.21 and 3.36 Å for Am–Br. Using the atomic coordinates reported for AmOBr, we calculate 2.339 and 2.979 Å for Am–O and 3.145 and 3.801 Å for Am–Br bond distances. Considering the discrepancies in the bond distances and the structural anomaly within the AmOX series, there are serious doubts about the reported structure of AmOBr. The trifluoride AmF_3 crystallizes in the 11-coordinate LaF_3 structure (Templeton and Dauben, 1953). In the anhydrous $AmCl_3$, the americium atom is bonded to six chlorine atoms at 2.874 Å and three chlorine atoms at 2.915 Å (Burns and Peterson, 1970) (Fig. 8.8).

(b) Oxides

Several americium oxides of varying stoichiometry have been prepared and structural data rely principally on X-ray powder diffraction powder data. The binary oxide AmO (CN 6) crystallizes in a cubic structure with octahedral O and Am atoms (Zachariasen, 1949b). Interatomic distances are calculated to be 2.480 Å for Am–O and 3.507 Å for Am–Am. However, AmO may be an oxynitride, as discussed in Section 8.7.1. As discussed in Section 8.7.1, three Am_2O_3 phases are known. Templeton and Dauben (1953) report the lattice parameters $a = 11.03 \pm 0.01$ Å for the low-temperature cubic form and $a = 3.817 \pm 0.005$ Å, $c = 5.971 \pm 0.010$ Å for the high-temperature hexagonal form. In the cubic phase two crystallographically different americium atoms exist: distorted $[Am(1)O_6]$ octahedra with Am(1)–O bond lengths of 2.369 Å are bridged through their oxygens to six Am(2) atoms. The Am(2) atoms are centered within a distorted octahedral environment of six oxygen atoms with Am–O distances of 1.984, 2.678, and 2.774 Å. The Am(2)–O distances of 1.984 Å are unusually short for trivalent actinide–oxygen bonds and only slightly longer than the reported bond lengths of about 1.935 Å for the linear Am=O bonds in Am(v) compounds (Asprey *et al.*, 1954a; Ellinger and Zachariasen, 1954). The intermediate-temperature monoclinic AmO_2 is isostructural with

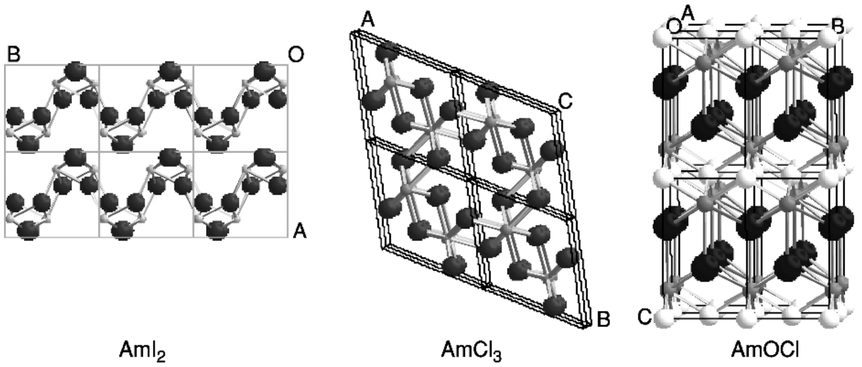

Fig. 8.8 *Structures of americium halide compounds: AmI_2 (Baybarz and Asprey,* 1972), *$AmCl_3$ (Burns and Peterson,* 1970), *and AmOCl (Templeton and Dauben,* 1953).

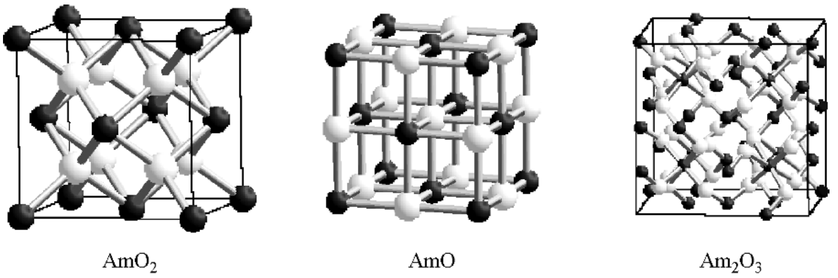

Fig. 8.9 *Unit cells of americium oxides: AmO_2 (Templeton and Dauben,* 1953; *Chikalla and Eyring* 1967, 1968), *AmO (Zachariasen,* 1949a,b), *and Am_2O_3, (Templeton and Dauben,* 1953).

PuO_2 with eight Am–Am distances of 3.803 Å and a tetrahedral arrangement of four Am atoms around each oxygen atom (Am–O is 2.480 Å) (Templeton and Dauben, 1953). The three-dimensional ternary oxide $BaAmO_3$ (cubic perovskite structure, $a = 4.35$ Å, although possibly distorted as are $BaPuO_3$ and $BaLnO_3$) is built from edge-sharing $[AmO_6]$ octahedra with large Ba^{2+} cations in 12-coordinated sites (Keller, 1964). Each AmO_6 octahedron shares all oxygen atoms with six adjacent octahedra. The Am–O distances are calculated to be 2.175 Å (Fig. 8.9).

(c) Chalcogenides and pnictides

The americium monochalcogenides AmX (X = S, Se, Te) crystallize in the cubic NaCl-type structure (CN 6) with the lattice parameters increasing with chalcogen atomic number. Early work of Zachariasen (1949d) concluded from powder

X-ray diffraction data that the sesquisulfide Am_2S_3 is isostructural with cubic Ce_2S_3 and contains 16 sulfur atoms and $10^{2/3}$ americium atoms per unit cell. The calculated interatomic Am–S distances of 2.94 Å are indicative of an ionic bonding between Am^{3+} and S^{2-} and compare well with the value of 2.93 Å reported by Damien and Jove (1971) in the substoichiometric compound $AmS_{1.9}$. The substoichiometric ditelluride, $AmTe_{1.73}$ (CN 9), crystallizes in a tetragonal anti-Fe_2As-type structure (Burns *et al.*, 1979). Layers of Te atoms are interleaved with puckered double layers of AmTe. The bond length between Te atoms in the pure Te layer is much shorter than the Te^{2-} interionic distances, suggesting some covalency within the pure Te layer. Random vacancy at sites within the pure Te layers causes the variable stoichiometry in Am–Te_2. The Am–Te bond lengths within the AmTe layers are only slightly shorter (3.258 and 3.208 Å) than the 3.269 Å from the Am atoms to the nearest Te atoms in the pure Te layer.

The structural information on the known pnictides of general formula AmX (X = N, P, Sb, As) was obtained from X-ray powder diffraction data. All binary pnictides crystallize in the cubic NaCl-type structure; both lattice parameters and Am–X bond length increase along the series: in AmN (a = 5.005 Å) Am–N is 2.503 Å, in AmP (a = 5.711 Å) Am–P is 2.856 Å, in AmAs (a = 5.875 Å) Am–As is 2.938 Å, and in AmSb (a = 5.6.24 Å) Am–Sb is 3.120 Å.

(d) Silicides

Weigel *et al.* (1977, 1984) reported structural information of several silicide phases. The layered structure of the binary AmSi is built up from corner-sharing [$AmSi_3$] pyramids with μ_3-Si atoms and Am–Si distances of 2.56 and 2.66 Å. The tetragonal $AmSi_2$ is isostructural with α-$ThSi_2$ and Am–Si distances range between 2.01 and 2.70 Å. In the sesquisilicide Am_2Si_3 americium atoms are coordinated to Si atoms at Am–Si distances of 3.04 Å.

(e) Oxoanionic ligands

Six oxygen atoms from three bidentately bonded carbonate ligands in the equatorial plane and two axial americyl oxygens form the inner coordination sphere of Am(V) in $RbAmO_2CO_3$ (Ellinger and Zachariasen, 1954) (Fig. 8.10). The Am=O and Am–O_{eq} bond distances are calculated from X-ray powder diffraction data to be 1.935 and 2.568 Å, respectively. Both distances are significantly longer than those in the Np(V) compounds, i.e. 1.75 Å for Np=O and 2.46 Å for Np–O_{eq} in aqueous $NpO_2(CO_3)_n^{1-2n}$ complexes (Clark *et al.*, 1996).

In the pseudotetragonal molybdate $Am_2(MoO_4)_3$ one-third of the Am sites are replaced by ordered vacancies (Tabuteau and Pages, 1978). The molybdate is isostructural to several lanthanide molybdates that crystallize in the pseudo-scheelite structure. The Am(III) tungstate, $Am_2(WO_4)_3$, is structurally analogous to $Eu_2(WO_4)_3$ and is built up from [AmO_8] dodecahedra and [WO_4] tetrahedra.

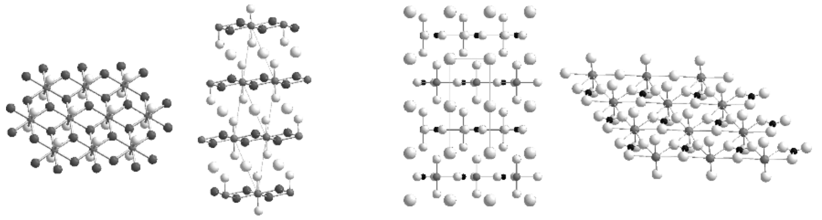

$KAmO_2F_2$ $RbAmO_2CO_3$

Fig. 8.10 *Sheet structures and crystal packing of the Am*(V) *compounds* $KAmO_2F_2$ (*Asprey* et al., 1954a) *and* $RbAmO_2CO_3$ (*Ellinger and Zachariasen*, 1954).

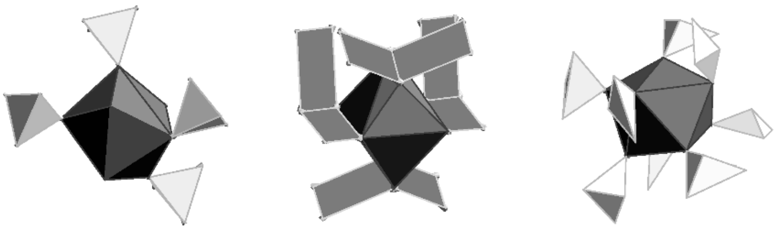

$Am_2(SO_4)_3 \cdot 8H_2O$ $Am_2(MoO_4)_3$ α-$Am(IO_3)_3$

Fig. 8.11 *Coordination of oxyanions in the Am*(III) *compounds* $Am_2(SO_4)_3 \cdot 8H_2O$ (*Burns and Baybarz*, 1972), $Am_2(MoO_4)_3$ (*Tabuteau and Pages*, 1978), and α-$Am(IO_3)_3$ (*Bean* et al., 2003).

Burns and Baybarz (1972) reported the synthesis and single-crystal structure analysis of $Am_2(SO_4)_3 \cdot 8H_2O$. Eight-coordinate americium bonded to eight O atoms from four sulfate ligands (Am–O distances range from 2.381 to 2.951 Å) and four water molecules (Am–O range from 2.406 to 2.553 Å). The sulfate tetrahedra share edges and bridge americium atoms within the layers; extensive hydrogen bonding involving the lattice waters occurs between the layers.

Very recently, Bean *et al.* (2003) synthesized the anhydrous Am(III) iodate, α-$Am(IO_3)_3$, which is isostructural to the Gd(III) compound (Liminga *et al.*, 1977), and a new f-element iodate of composition $K_3Am_3(IO_3)_{12} \cdot HIO_3$ (Runde *et al.*, 2003) (Fig. 8.11). In both compounds, oxygens from eight iodate pyramids and Am^{3+} ions are located within a distorted $[AmO_8]$ dodecahedron that form a three-dimensional network with Am–O bond distances ranging from 2.34 to 2.60 Å and averaged I–O distances of 1.80 Å. Runde and coworkers also reported the synthesis of β-$Am(IO_3)_3$, that exhibits a novel two-dimensional architecture type within the f-element iodates. The nine-coordinate Am atoms are coordinated with only 7 iodate ligands via a combination of edge-sharing and corner-sharing $[IO_3]$ groups (Bean *et al.*, 2003).

(f) Others

The hydride AmH_3 crystallizes in a cubic structure with eight hydrogen atoms surrounding each Am atom and a tetrahedral arrangement of four Am atoms around each H atom. The bond lengths for Am–H and Am–Am are calculated to be 2.316 and 3.782 Å (Olson and Mulford, 1966).

8.9.2 Compounds with organic ligands

Only seven compounds of americium are listed in the Cambridge Structural Database (version 5.22, October 2001) that compiles complexes of metal cations with organic molecules. However, it is noteworthy that structures obtained from single crystal X-ray diffraction are reported only for two compounds. For the other five compounds, only cell constants and space groups were obtained from X-ray powder patterns and information on bond distances remains unavailable. Information on the overall structure was obtained by analogy to the corresponding compounds of rare earth elements. For a more detailed discussion of the preparation and reactivity of organic americium compounds, refer to Chapters 23 and 29.

(a) Oxygen-donor ligands

A wide variety of oxygen-donor ligands have been used to complex and separate americium. The most synthesized compounds of Am(III) are those with carboxylic acids, because of their applications in separation (Weigel and ter Meer, 1967). However, only the single-crystal structure of the hydrated Am(III) salicylate, $Am(C_7H_5O_3)_3(H_2O)$, has been reported. In this compound, americium is nine-coordinate to one water molecule and six salicylato ligands (Burns and Baldwin, 1976). The six salicylato ligands display three different coordination modes: (i) monodentate binding through the carboxylic oxygens of four ligands; (ii) bidentate binding through its carboxyl group; and (iii) and bidentate binding through a combination of carboxylic and phenolic oxygens. Salicylato complexes have been reported for rare earths and plutonium and are important because the ligands contain carboxylic and hydroxo functional groups, which are typical for the more complex natural humic materials.

The sodium acetate, $NaAmO_2(CH_3CO_2)_3$, is the only characterized complex of americyl(VI) (Jones, 1955). Lychev *et al.* (1980) synthesized the cesium salt of Am(V), $CsAmO_2(CH_3CO_2)_3$, but solved the crystal structure only of the isostructural analogous Np(V) compound. In both americyl acetate compounds, three carboxylates are coordinated bidentately in the equatorial planes of AmO_2^+ and AmO_2^{2+}. Burns and Danford (1969) obtained single crystals of orthorhombic $CsAm(hfa)_4$ (hfa = hexafluoro-acetylacetone) when recrystallizing monoclinic $CsAm(hfa)_4 \cdot H_2O$ (Danford *et al.*, 1970) in 1-butanol. The compound is composed of Am(hfa)-chains that interact with Cs^+ ions. The Am^{3+} ion is chelated by the eight acetone–oxygen atoms of the four hfa ligands with Am–O bond distances between 2.36 and 2.45 Å. $CsAm(hfa)_4$ and CsAm $(hfa)_4 \cdot H_2O$ sublimes at about 135°C. Both hydrated and the anhydrous compounds are metastable and degrade after about 1 week with AmF_3 identified as one of the degradation products (Fig. 8.12).

EXAFS studies of the structure of the solvent-containing $Am(NO_3)_3$ $(TEMA)_2$ complexes (TEMA = *N*,*N*,*N*,*N*′-tetraethylmalonamide) resulted in Am–O distances of 2.52 ± 0.01 Å and a coordination polyhedron similar to that of the corresponding Nd compound, where Nd is ten-coordinate (DenAuwer *et al.*, 2000).

In recent years, the reactions of americium ions with a number of organic molecules were studied in the gas phase. As an example, the gas-phase reaction of laser-ablated americium ions with alcohols yields a mixture of hydroxides and alkoxides, i.e. $Am(OR)^+$ and $Am(OR)^{2+}$ (Gibson, 1999b). The reaction with dimethylether yields the methoxy ion $Am(OCH_3)^+$ as the primary product. Although these reactions do not reveal any structural details, they provide some understanding of potential interaction mechanisms in americium organometallic chemistry. Other products of laser-ablated Am^+ or AmO^+ ions reacting with polyimide, nitriles, or butylamines are AmC_2H^+, $AmC_2H_4^+$, $AmC_2H_2^+$, several cations of general formula $AmC_xH_yN_z^+$, and metal oxide clusters such as Am_2O^+ an $Am_2O_2^+$ (Gibson, 1998a, 1999a). An interesting anomaly was the observation of dimeric Am_2^+ clusters that were not formed by any other actinides studied (Gibson, 1999a).

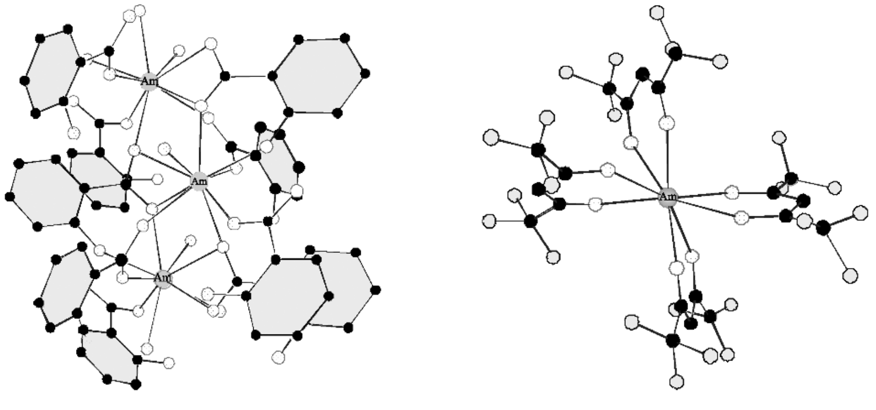

$Am(C_7H_5O_3)_3(H_2O)$ $CsAm(hfa)_4$

Fig. 8.12 *Nine-fold coordination of Am(III) in* $Am(C_7H_5O_3)_3(H_2O)$ *(Burns and Baldwin,* 1976) *and eight-coordinate Am(III) in* $CsAm(hfa)_4$ *(Burns and Danford,* 1969).

(b) Nitrogen donors

Only a few complexes of americium with N-donating ligands have been studied yet; structural details are limited. The bis-phthalocyanine complex has been synthesized and displays a sandwich-type complex with eight-coordinate americium (Moskalev *et al.*, 1979). Yaita *et al.* (2001) studied the Am(III) benzimidazole complex using XAFS spectroscopy and found a bidentate coordination of Am through two nitrogen atoms with the bond distance Am–N of 2.63 Å. The overall coordination number of Am(III) is reported to be close to 10.

(c) Sulfur donors

Only few structural studies are reported involving compounds with Am–S bonds. Gibson (1999b) observed SH abstraction from thiols and formation of the hydrosulfide $Am(SH)^+$ in the gas phase. The gas-phase reaction with propanethiol yielded the thiolate $Am(PrS)^+$. Tian *et al.* (2002) used EXAFS to study the structure of extraction complexes of Am(III) with di-*n*-octyldithiophosphinic acid and di(2,4,4-trimethylpentyl)dithiophosphinic acid in kerosene. The two extraction complexes appear to be similar in coordination with eight sulfur atoms in the inner sphere and four phosphorus atoms in the second shell with average Am–S and Am–P bond distances of 2.9 and 3.5 Å, respectively.

(d) Cyclopentadienyl and cyclooctatetraenyl compounds

The organometallic chemistry of americium remains essentially unstudied. The most studied compound is the cyclopentadiene complex, $Am(C_5H_5)_3$, which crystallizes in the orthorhombic *Pbcm* space group and is isostructural with, but not pyrophoric like $Pu(C_5H_5)_3$ (Baumgärtner *et al.*, 1966a). Pappalardo *et al.* (1969a) reported the absorbance spectrum of $Am(C_5H_5)_3$ films from which Nugent *et al.* (1971b) calculated a bond covalency of only 2.8 ± 0.2% (relative to the corresponding bands of $Am(aq)^{3+}$) indicating that the organometallic bonding in $Am(C_5H_5)_3$ is highly ionic. Consequently, Nugent *et al.* suggested that the compound should be designated as a tris-cyclopentadienide rather than a tricyclopentadienyl compound. Bursten and coworkers (Bursten *et al.*, 1989; Li and Bursten, 1997) calculated the electronic structure of $AnCl_3$, $An(C_7H_7)_2$, and $An(C_5H_5)_3$, and discussed the relative role of the 5f and 6d atom orbitals. Karraker (1975, 1977) reported the synthesis of the potassium salt of a bis-cyclooctatetraenyl Am(III) complex, $KAm(C_8H_8)_2$, and obtained the absorbance spectrum in THF. The compound $KAm(C_8H_8)_2 \cdot 2THF$ decomposes in water and burns when exposed to air. The X-ray powder diffraction data show that $Am(C_8H_8)_2$ is isostructural with the analogous Np and Pu compounds and the sandwich complex uranocene. The gas-phase reaction of Am^+ ions with 1.5-cyclooctadiene and cyclooctatetraene produced the dehydrogenation complexes $Am-C_8H_8^+$ and $Am-C_8H_6^+$ that were detected by mass spectrometry

(Gibson, 1998b). The gas-phase reaction of laser-ablated Am^+ with pentamethylcyclopentadiene (HCp*) yielded the fragments $AmC_8H_{14}^+$, $AmC_9H_{12}^+$, and $AmC_{10}H_{14}^+$ (Gibson, 2000). In contrast to the multiple dehydrogenation reactions observed with Np^+ and Pu^+, the Am^+ ion appeared unreactive and induced exclusively single hydrogen loss. Gibson concludes from this finding that the valence 5f electrons of Am^+ are too inert to form σ-bonds with carbon or hydrogen atoms and therefore do not participate in the Am–HCp interaction.

8.10 ANALYTICAL CHEMISTRY AND SPECTROSCOPY

8.10.1 Radioanalytical chemistry

(a) Alpha spectroscopy

Common analytical procedures include alpha spectrometry for the detection of ^{241}Am and ^{243}Am. The typical alpha-spectrum of ^{241}Am exhibits a peak at 5.49 MeV. The energy of the main alpha particles of ^{243}Am (5.28 MeV) differs by only about 0.2 MeV, which can result in peak broadening and overlap with α-peaks of other radionuclides (Lin *et al.*, 2002). Quantitative analysis by alpha spectrometry requires extensive radiochemical purification, preparation of a high-quality americium source by a skilled radiochemist, and correction for absorption and backscattering from the planchet. Scintillation counting has largely replaced alpha spectrometry in many radioanalytical procedures.

(b) Gamma spectroscopy

Nuclide identification and analysis of biological and environmental samples mainly use high-sensitivity gamma counting in a germanium multichannel detector. ^{241}Am emits two main γ-rays at 59.5 (36%) and 26.3 keV (2.4%). Scintillation counting is also commonly used when only one γ-emitting isotope is in the sample.

8.10.2 Spectroscopy

(a) Solution absorption

(1) Am(III): UV–VIS–NIR absorption spectroscopy has been widely used to characterize americium solution species. The major absorbance that has been measured to speciate Am(III) corresponds to the transition $^7F_0 \rightarrow {}^5L_6$ with its maximum at 503.2 nm ($\varepsilon \sim 410$ L mol cm^{-1}) for Am^{3+}(aq). The molar absorptivity may change with spectral slit widths, temperature, and ionic strength of the solution. Shifts in the position of the absorbance bands

and changes in molar absorbance are evidence of changes in the number of inner-sphere coordinated water molecules and/or coordination of ligands, i.e. carbonate or sulfate. Theoretical calculations of the electronic energy bands in the Am^{3+} ion have been performed by a number of investigators (Conway, 1963, 1964; Carnall and Wybourne, 1964; Carnall *et al.*, 1964; Carnall and Fields, 1967). An unexpected predicted $^7F_0 \rightarrow {}^5D_1$ transition was found in more concentrated Am(III) solution. Carnall (1989) analyzed the energy levels of the Am^{3+} ion by comparing the absorption spectra of $AmCl_3$ and $LaCl_3$ that was doped with Am(III).

Barbanel *et al.* (1997, 2001) studied the transitions in the octahedral complexes AmX_6^{3+} in the Cs_2NaLuX_6 (X = Cl, Br) crystal. The absorption spectra showed excitation to the ground level states $^7F_2$, $^7F_4$, $^7F_6$ and to the exited states $^5L_6$, $^5G_2$, and $^5D_2$. Absorbance spectra have been recorded in H_2SO_4, H_3PO_4, HNO_3, HCl, $HClO_4$, and in carbonate media (Keenan, 1959; Marcus and Shiloh, 1969; Shiloh *et al.*, 1969; Stadler and Kim, 1988; Meinrath and Kim, 1991a; Runde and Kim, 1994) (Fig. 8.13).

(2) Am(IV): The spectrum of Am(IV) in acid media is characterized by broad absorption features and has been measured in 13 M HF (Asprey and Penneman, 1961, 1962), 12 M KF (Varga *et al.*, 1973), 12 M H_3PO_4 (Myasoedov *et al.*, 1977), and in 2 M Na_2CO_3 (Bourges *et al.*, 1983; Hobart *et al.*, 1983b). The spectrum of Am(IV) in concentrated fluoride solution resembles very closely that of solid AmF_4 (Fig. 8.14).

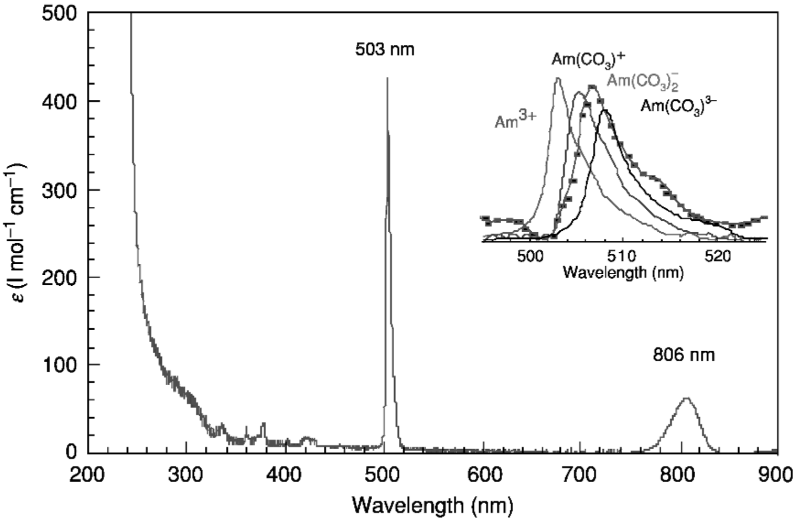

Fig. 8.13 *Electronic absorption spectra of* Am^{3+} *in* 1 M $HClO_4$ *and of the predominant Am*(III) *species in carbonate-containing solutions* (*inset*) (*Meinrath and Kim*, 1991a).

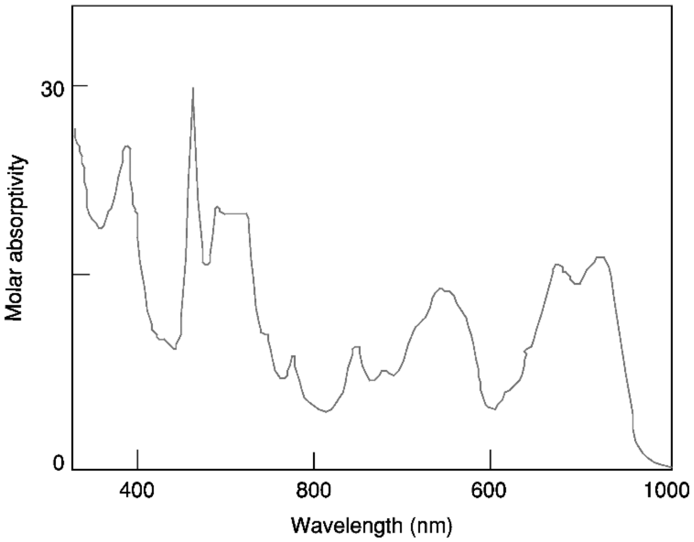

Fig. 8.14 *Absorption spectrum of Am(IV) in* 13 M NH_4F (*Asprey and Penneman*, 1962).

(3) Am(v): The Am(v) transitions $^5I_4 \rightarrow ^3G_5$ and $^5I_4 \rightarrow ^3I_7$ with their absorbance peaks at 513.7 nm ($\varepsilon \sim 45$ L mol cm^{-1}) and 716.7 nm ($\varepsilon \sim 60$ L mol cm^{-1}), respectively, are the main absorbance bands of the AmO_2^+ ion in aqueous solutions. Absorbance spectra of Am(v) have been recorded in H_2SO_4 (Werner and Perlman, 1950), HCl (Hall and Herniman, 1954; Stadler and Kim, 1988; Runde and Kim, 1994), $HClO_4$ (Asprey *et al.*, 1951; Stephanou *et al.*, 1953), NaCl (Stadler and Kim, 1988; Runde and Kim, 1994), and in 2 M Na_2CO_3 (Bourges *et al.*, 1983; Hobart *et al.*, 1983b) (Fig. 8.15).

(4) Am(vi): The spectrum of Am(vi) in acid media is characterized by the sharp absorption band at about 996 nm with $\varepsilon \sim 100$ L mol cm^{-1} in $HClO_4$ and ~100 L mol cm^{-1} in H_3PO_4. A less intense absorbance appears at 666 nm. Bell (1969) has compared band positions of transuranium actinyl spectra, including those of AmO_2^+ and AmO_2^{2+}, with the spacings between positions of the UO_2^{2+} bands. His results indicate that a single molecular orbital model can represent any of the actinyl ions when the uranyl ion is assumed to have the bonding orbitals exactly filled; the transuranium actinyl ions are represented with the uranyl core and a progressive increase of electrons in the first two lowest unoccupied molecular orbitals (LUMOs). Although the Am(vi) absorbance appears when Am(v) disproportionates in $HClO_4$, the absorbance is absent in HCl media potentially because of the formation of chloride complexes of lower molar absorptivity or due to the instability of Am(vi) in acidic chloride media (Fig. 8.16).

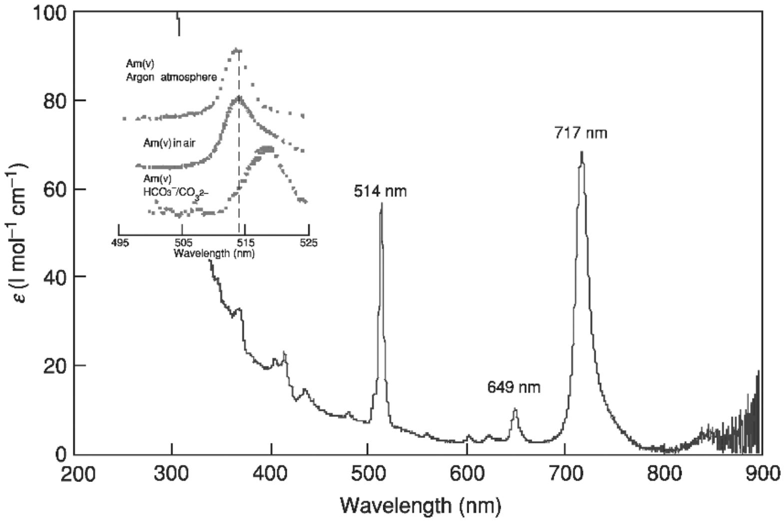

Fig. 8.15 *Electronic absorption spectra of AmO_2^+ in* 1 M *$HClO_4$ and in carbonate-containing solutions* (*inset*) (*Stadler and Kim*, 1988).

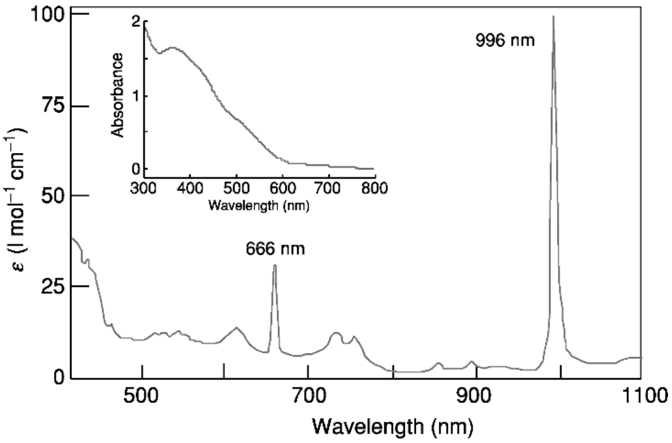

Fig. 8.16 *Absorption spectrum of Am*(*VI*) *in* 1 M *$HClO_4$ and in carbonate solution* (*inset*) (*Penneman and Asprey*, 1955).

(5) Am(VII): Green-colored solutions, believed to be Am(VII), are prepared by oxidation of Am(VI) in 3–5 M NaOH at 0–7°C with either ozone or the O^- radical. The spectrum of Am(VI) and Am(VII) was measured in 3.5 M NaOH solution by Krot *et al.* (1974a,b) and exhibited a broad absorbance

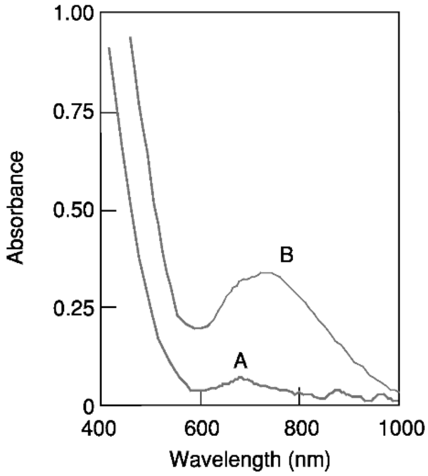

Fig. 8.17 *Absorption spectra of Am*(*VI*) *and Am*(*VII*) *in* 3.5 M *NaOH* (*Krot* et al., 1974a). *A*, 0.0194 M *Am*(*VI*); *B*, 0.0194 M Am_{tot} *with* 50% *Am*(*VI*) *and* 50% *Am*(*VII*).

at 740 nm (Fig. 8.17). Heptavalent americium is unstable and reduces to Am (VI) within minutes. It can be easily reduced by hydrogen peroxide, hydrazine, hydroxylamine, sulfite, and ferrocyanide ions, and Np(VI) and Pu(VI) (Shilov, 1976). A review on the chemistry of heptavalent transplutonium elements can be found in Mikheev and Myasoedov (1985).

(b) Luminescence

Luminescence has been observed only for Am(III). Reviews of Am(III) luminescence studies can be found in Beitz (1994) and Yusov (1993). The first study on the luminescence properties of Am(III) was reported by Beitz *et al.* (1989). Excitation of Am(III) from the $^7F_0$ ground state to the $^5L_6$ state at 503 nm results in the emission from the lowest luminescent level to the ^7F_J ground-state manifold. From seven expected transitions only two are experimentally accessible. The two most populated transitions are the $^5D_1 \rightarrow {}^7F_1$ band at 685 nm and the $^5D_1 \rightarrow {}^7F_2$ band at 836 nm. These transitions can be used for the determination of trace concentrations of Am(III) in solution or solid-state matrices (Thouvenot *et al.*, 1993). Beitz and coworkers (Liu *et al.*, 1997) investigated the crystal field splitting and hyperfine energy level structure in the $^5D_1$ level of $^{243}Am^{3+}$ in $LaCl_3$ and $CaWO_4$.

The fluorescence lifetime of the Am^{3+} ion(aq) is reported to be 20.4 ± 2.1 ns (Runde *et al.*, 2000), 24.6 ± 0.6 ns (Kimura and Kato, 1998), and 22 ± 3 ns (Beitz, 1994) in aqueous systems. The lifetime increases dramatically to 155 ± 4 ns (Beitz, 1994) in D_2O. Complexation of the Am^{3+} ion changes the position of the emission bands and the duration of the fluorescence lifetime; e.g. the fluorescence of the triscarbonato complex, $Am(CO_3)_3^{3+}$, is observed at 693 nm with a lifetime of 34.5 ± 2.4 ns (Runde *et al.*, 2000). The luminescence spectra of Am^{3+} have been also measured in Am-doped powdered ThO_2 (Hubert and Thouvenot, 1992), $Cs_2NaLuCl_6$ (Barbanel *et al.*, 1998), $LiYF_4$ (Cavellec *et al.*, 1997), heavy metal fluoride glass containing AmF_3 (Beitz, 1994), and in fluorozirconate glass (Valenzuela and Brundage, 1990; Brundage, 1994) (Fig. 8.18) .

(c) Vibrational (IR and Raman)

There are few data on the IR spectra of americium compounds. Tananaev (1991) reported the antisymmetric vibration frequency of the AmO_2^+ group in $CsAmO_2(OH)_2 \cdot nH_2O$ at 802 cm^{-1}. Hobart *et al.* (1983a) reported the Raman spectra of $AmPO_4$ and $Am(PO_3)_3$ with the most intense Raman frequencies for the symmetric stretching mode of PO_4^{3-} at 973 cm^{-1} and of PO_3^- groups at 1195 cm^{-1}. Jones and Penneman (1953) studied the infrared absorption assigned to the infrared O–An–O asymmetric stretch of actinyl(v) and (vi) ions, concluding that these ions were linear or very nearly so. For the solid $NaAmO_2(CH_3COO)_2$ the vibrational frequencies $\nu_1 = 749$ and $\nu_2 = 914$ cm^{-1} were reported (Jones, 1955). Data on Raman scattering of americyl(v) and (vi) ions have been reported in non-complexing perchloric acid and complexing carbonate solutions (Basile *et al.*, 1974). The values for the polarized symmetric stretching frequencies (ν_1) of AmO_2^+ and AmO_2^{2+} were found to be 730 and 796 cm^{-1}, respectively (Basile *et al.*, 1974). The Raman scattering in carbonate solutions showed a shift of ν_1 to 747 cm^{-1} for Am(v) (Madic *et al.*, 1983) and to 760 cm^{-1} for Am(vi) (Basile *et al.*, 1978). A study of the correlation of the Raman spectra of actinyl(v) and (vi) ions in perchlorate and carbonate

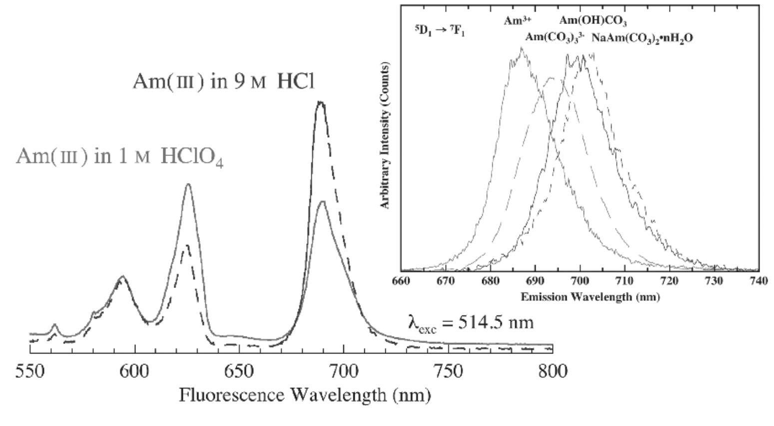

Fig. 8.18 *Luminescence spectrum of Am^{3+} in acidic media and of Am(III) carbonate complexes*. (*Runde* et al., 2000, 2002).

solutions, as well as the spectra of solid actinide(v) double carbonate compounds, $Na_3AnO_2(CO_3)_2 \cdot H_2O$, was published by Madic *et al.* (1983).

(d) X-ray absorption

Although X-ray absorption spectroscopy (XAS, see Chapter 28) has been increasingly used since 1990 to obtain structural information of actinide compounds, only a small number of XAS studies on americium compounds have been reported. Bearden and Burr (1967) reported the edge energy of americium metal at 18 504 eV. Soderholm *et al.* (1996) observed the Am edge energy at 18515 eV in the Am(IV) compound $Pb_2Sr_2AmCu_3O_8$, which is about 4 eV higher in energy compared to the solid Am(III) reference compounds AmF_3 and $Cs_2NaAmCl_6$. EXAFS has been used to study the coordination of americium in organic complexes (DenAuwer *et al.*, 2000; Yaita *et al.*, 2001) and inorganic complexes with $P_5W_{30}O_{110}^{15-}$ (Williams *et al.*, 2000), chloride (Allen *et al.*, 2000), and carbonate (Runde *et al.*, 2002).

REFERENCES

Abe, M. and Tsujii, M. (1983) *Chem. Lett.*, 1561.

Abe, M., Chitrakar, R., Tsujii, M., and Fukumoto, K. (1985) *Solvent Extr. Ion Exch.*, **3**, 149.

Adair, H. L. (1970) *J. Inorg. Nucl. Chem.*, **32**, 1170.

Agnew, S. F., Boyer, J., Corbin, R. A., Duran, T. B., Fitzpatrick, J. R., Jurgensen, K. A., Ortiz, T. P., and Young, B. L. (1997) *Hanford Tank Chemical and Radionuclide Inventories: HDW Model Rev. 4*, Los Alamos National Laboratory.

Akatsu, J. and Kimura, T. (1990) *J. Radioanal. Nucl. Chem.*, **140**, 195.

Akella, J., Johnson, Q., and Schock, R. N. (1980) *J. Geophys. Res.*, **85**, 7056–8.

Akimoto, Y. (1967) *J. Inorg. Nucl. Chem.*, **29**, 2650–2.

Al Rifai, S. (1970) *Complex Formation between Trivalent Transuranium Elements and Ligand which Contain the Pyridinie or Quinoline Ring*. German Report IRCH-10/70-2.

Aldred, A. T., Dunlap, B. D., Lam, D. J., and Shenoy, G. K. *Transplutonium 1975, Proc. 4th Int. Symp.,* Baden-Baden, Germany 1975; Ed. by W. Müller and R. Lindner, North-Holland, Amsterdam; p. 191–5.

Ali, S. (1968) *Chelatbildung der Dreiwertigen Transplutoniumelemente mit Nitrilotriessigsaeure und Ihren Derivaten.*

Allen, P. G., Bucher, J. J., Shuh, D. K., Edelstein, N. M., and Craig, I. (2000) *Inorg. Chem.*, **39**, 505–601.

Anan'ev, A. V. and Krot, N. N. (1985) *Sov. Radiochem.* (*Engl. Transl.*), **26**(6), 716–9.

Anan'ev, A. V. and Shilov, V. P. (1985) *Sov. Radiochem.* (*Engl. Transl.*), **26**(6), 768–70.

ANS (1993) *Int. Conf. and Tech. Exposition on Future Nuclear Systems: Emerging Fuel Cycles and Waste Disposal Options*, *Global '93*. Seattle, WA. 1993; Amer. Nucl. Soc., La Grange Park, IL. ISBN 0894481827.

Asprey, L. B., Stephanou, S. E., and Penneman, R. A. (1950) *J. Am. Chem. Soc.*, **72**, 1425–6.

Asprey, L. B., Stephanou, S. E., and Penneman, R. A. (1951) *J. Am. Chem. Soc.*, **73**, 5715–7.

Asprey, L. B. (1954) *J. Am. Chem. Soc.*, **76**, 2019–20.

Asprey, L. B., Ellinger, F. H., and Zachariasen, W. H. (1954a) *J. Am. Chem. Soc.*, **76**, 5235–7.

Asprey, L. B., Stephanou, S. E., and Penneman, R. A.: patent number 2681 923. US, (1954).

Asprey, L. B. and Keenan, T. K. (1958) *J. Inorg. Nucl. Chem.*, **7**, 27–31.

Asprey, L. B. and Penneman, R. A. (1961) *J. Am. Chem. Soc.*, **83**, 2200.

Asprey, L. B. and Penneman, R. A. (1962) *Inorg. Chem.*, **1**, 134–6.

Asprey, L. B., Keenan, T. K., and Kruse, F. H. (1964) *Inorg. Chem.*, **3**, 1137–40.

Asprey, L. B., Keenan, T. K., and Kruse, F. H. (1965) *Inorg. Chem.*, **4**, 985–6.

Aziz, A. and Lyle, S. J. (1971) *J. Inorg. Nucl. Chem.*, **33**, 3407.

Backer, W. and Keller, C. (1973) *J. Inorg. Nucl. Chem.*, **35**, 2945.

Bagnall, K. W., Laidler, J. B., and Stewart, M. A. A. (1967) *Chem. Commun.*, **1**, 24–5.

Bagnall, K. W., Laidler, J. B., and Stewart, M. A. A. (1968) *J. Chem. Soc.* **A**, 133–6.

Bagnall, K. W. (1972) *The Actinide Elements,* Elsevier, New York.

Baisden, P. A., Choppin, G. R., and Kinard, W. K. (1972) *J. Inorg. Nucl. Chem.*, **34**, 2029.

Barbanel, Y. A., Chudnovskaya, G. P., Dushin, R. B., Kolin, V. V., Kotlin, V. P., Nekhoroshkov, S. N., and Pen'kin, M. V. (1997) *Radiochim. Acta*, **78**, 69–72.

Barbanel, Y. A., Chudnovskaya, G. P., Dushin, R. B., Kolin, V. V., Kotlin, V. P., Nekhoroshkov, S. N., and Penkin, M. V. (1998) *J. Alloys Compd.*, **277**, 295–300.

Barbanel, Y. A., Dushin, R. B., Kolin, V. V., Kotlin, V. P., and Nekhoroshkov, S. N. (2001) *Radiochemistry*, **43**, 118–23.

Barney, G. S. and Cowan, R. G. (1992) Separation of actinide ions from radioactive waste solutions using extraction chromatography, *American Chemical Society National Meeting*, San Francisco, CA, USA, April 5–10, p. 77.

Barthelemy, P. and Choppin, G. R. (1989) *Inorg. Chem.*, **28**, 3354–7.

Basile, L. J., Sullivan, J. C., Ferrarro, J. R., and La Bonville, P. (1974) *Appl. Spectrosc.*, **28**, 142–5.

Basile, L. J., Ferrarro, J. R., Mitchell, M. L., and Sullivan, J. C. (1978) *Appl. Spectrosc.*, **32**, 535–7.

Baudin, G., Lefevre, J., Prunier, C., and Salvatore, M. (1993) IAEA Report TECDOC-783, p. 37.

Baumgärtner, F., Fischer, E. O., and Kanellakopulos, B. (1966a) *Angew. Chem. Int. Edn.*, **5**(1), 134–5.

Baumgärtner, F., Fisher, E. O., Kanellakopulos, B., and Laubereau, P. G. (1966b) *Angew. Chem. Int. Edn.*, **78**, 112–3.

Baumgärtner, F., Fisher, E. O., Kanellakopulos, B., and Laubereau, P. G. (1977) *J. Inorg. Nucl. Chem.*, **39**, 87–9.

Bayat, I. (1970) *Über Komplexe dreiwertiger Transurane mit Aminopolykarbonsäuren*, German Report, KFK-1291.

Bayat, I. and Moattar, F. (1982) *Radiochem. Radioanal. Lett.*, **51**(3), 171–9.

Baybarz, R. D. (1960) *Preparation of Americium Dioxide by Thermal Decomposition of Americium Oxalate in Air*, Oak Ridge National Laboratory.

Baybarz, R. D. (1965) *J. Inorg. Nucl. Chem.*, **27**, 1831.

Baybarz, R. D. (1966) *J. Inorg. Nucl. Chem.*, **28**, 1055.

Baybarz, R. D. (1970) *At. Energy Rev.*, **8**, 327–60.

Baybarz, R. D. and Asprey, L. B. (1972) *J. Inorg. Nucl. Chem.*, **34**, 3427–31.

Baybarz, R. D. (1973a) *J. Inorg. Nucl. Chem.*, **35**, 4149–58.

Baybarz, R. D. (1973b) *J. Inorg. Nucl. Chem.*, **35**, 483–7.

Bean, A. C., Scott, B. L., Albrecht- Schmitt, T., and Runde, W. (2003) *Plutonium Futures – the Science, Third Topical Conference on Plutonium and Actinides*, pp. 233–5.

Bearden, J. A. (1967) *Rev. Mod. Phys.*, **39**, 78.

Bearden, J. A. and Burr, A. F. (1967) *Rev. Mod. Phys.*, **39**, 125–42.

Beitz, J. V., Jursich, G., and Sullivan, J. C. (1989) Fluorescence studies of Am3+ in aqueous solution, in *Rare Earth 1988* (eds. L. R. M. H. B. Silber and L. E. Delony), Elsevier Sequoia, Amsterdam.

Beitz, J. V. (1994) *J. Alloys Compd.*, **207/208**, 41–50.

Bell, J. T. (1969) *J. Inorg. Nucl. Chem.*, **31**, 703–10.

Benedict, U., Bujis, K., Dufour, S., and Toussaint, J. C. (1975) *J. Less Common Metals*, **42**, 345–54.

Benedict, U. and Dufour, C. (1980) *Physica*, **102B**, 303–7.

Benedict, U., Itíe, J. P., Dufour, C., Dubos, S., and Spirlet, J. C. (1985) in *Americium and Curium Chemistry and Technology* (eds. N. Edelstein, J. Navratil, and W. Schulz), D. Reidel, The Netherlands.

Benedict, U., Itíe, J. P., Dufour, C., Dubos, S., and Spirlet, J. C. (1986) *Physica*, B&C, **139**, 284.

Berger, P., Blanc, P., and Bourges, J. (1988) *Radiochim. Acta*, **43**, 217–22.

Berndt, U., Tanamas, R., Maier, D., and Keller, C. (1974) *Inorg. Nucl. Chem. Lett.*, **10**, 315–21.

Bernkopf, M. F. and Kim, J. I. (1984) *Hydrolydsereaktionen und Karbonatkomplexierung von dreiwertigem Americium in natürlichen aquatischen Systemen*, Technische Universität München.

Berry, J. W., Knoghton, J. B., and Nannie, C. A. (1982) *Vacuum Distillation of Americium Metal*, US Department of Energy.

Bertha, E. I. and Choppin, G. R. (1978) *J. Inorg. Nucl. Chem.*, **40**, 655–8.

Bhanushali, R. D., Pius, I. C., Muherjee, S. K., and Vaidya, V. N. (1999) *J. Radioanal. Nucl. Chem.*, **240**, 977–9.

Bierman, S. R. and Clayton, E. D. (1969) *Trans. Am. Nucl. Soc.*, **12**, 887–8.

Bigelow, J. E., Collins, E. d., and King, L. J. (1980) *The Cleanex Process: A Versatile Solvent-Extraction Process for Recovery and Purification of Lanthanides*, *Americium*, *and Curium, Amer. Chem. Soc.* pp. 147–55.

Blokhin, N. B., Ermakov, V. A., and Rykov, A. G. (1973) *Radiokhimiya*, **16**, 189–92.

Blokhin, N. B., Ermakov, V. A., and Rykov, A. G. (1974) *Radiokhimiya*, **16**, 551–3.

Bode, D. D., Wild, J. F., and Hulet, E. K. (1976) *J. Inorg. Nucl. Chem.*, **38**, 1291–7.

Boldt, A. L. and Ritter, G. L. (1969) *Recovery of Am, Cm, and Pm from Shipping Port Reactor Fuel Reprocessing Wastes by Successive TBP and D2EHPA Extractions*, Atlantic Richfield Hanford Company.

Bond, E. M., Engelhardt, U., Deere, T. P., Rapko, B. M., Paine, R. T., and FitzPatrick, J. R. (1997) *Solvent Extr. Ion Exch.*, **15**, 381.

Bond, E. M., Engelhardt, U., Deere, T. P., Rapko, B. M., Paine, R. T., and Fitz Patrick, J. R. (1998) *Solvent Extr. Ion Exch.*, **16**, 967.

Borisov, M. S., Elesin, A. A., Lebedev, I. A., Piskunov, E. M., Filimonof, V. T., and Yakovlev, G. N. (1967) *Radiokhimiya*, **9**, 166.

Bouhlassa, S. (1983) *Chem. Abstr.*, **98**, 82730.

Bouhlassa, S. and Guillaumont, R. (1984) *J. Less Common Metals*, **99**(1), 157–71.

Bouissières, G. and Legoux, Y. (1965) *Bull. Soc. Chim. Fr.*, **2**, 386.

Bourges, J. Y., Guillaume, B., Koehly, G., Hobart, D. E., and Peterson, J. R. (1983) *Inorg. Chem.*, **22**, 1179–84.

Boyd, T. E., Cusick, M. J., and Navratil, J. D. (1986) *Recent Developments in Separation Science,* CRC Press, Boca Raton, FL.

Boyd, T. E. and Kochen, R. L. (1993) *Ferrite Treatment of Actinide Waste Solutions: Continuous Processing of Rocky Flats Process Waste,* Rockwell International, Golden, CO.

Brachet, G. and Vasseur, C. (1969) *Reduction of Americium Oxide by Beryllium for Neutron-Source Production,* CEA, France.

Brandau, E. (1971) *Inorg. Nucl. Chem. Lett.*, **7**, 1177.

Bratsch, S. G. and Lagowski, J. J. (1986) *J. Phys. Chem.*, **90**, 307–12.

Brown, D., Fletcher, S., and Holah, D. G. (1968) *J. Chem. Soc.* **A**, 1889–94.

Brundage, R. T. (1994) *J. Alloys Compd.*, **213**, 199–206.

Buckau, G., Kim, J. I., klenze, R., Rhee, D. S., and Wimmer, H. (1992) *Radiochim. Acta*, **57**(2–3), 105–11.

Buijs, K., Müller, W., Reul, J., and Toussaint, J. C. (1973) *Separation and Purification of Americium on the Multigram Scale*, Euratom.

Burch, W. D. (1964) *Transuranium Quarterly Progress Report for Period Ending February* 29, 1963, Oak Ridge National Laboratory.

Burnett, J. L. (1965) *Trans. Am. Nucl. Soc.*, **8**, 335.

Burnett, J. L. (1966) *J. Inorg. Nucl. Chem.*, **28**, 2454–6.

Burney, G. A. and Porter, J. A. (1967) *Inorg. Nucl. Chem. Lett.*, **3**, 79–85.

Burney, G. A. (1968) *Nucl. Appl.*, **4**, 217–21.

Burns, J. H. and Danford, M. D. (1969) *Inorg. Chem.*, **8**, 1780–4.

Burns, J. H. and Peterson, J. R. (1970) *Acta Crystallogr. B*, **26**, 1885–7.

Burns, J. H. and Peterson, J. R. (1971) *Inorg. Chem.*, **10**, 147–51.

Burns, J. H. and Baybarz, R. D. (1972) *Inorg. Chem.*, **11**, 2233–7.

Burns, J. H. and Baldwin, W. H. (1976) *Inorg. Chem.*, **16**(2), 289–94.

Burns, J. H. and Baldwin, W. H. (1977) *Inorg. Chem.*, **16**, 289–94.

Burns, J. H., Damien, D., and Haire, R. G. (1979) *Acta Crystallogr. B*, **35**, 143–4.

Bursten, B. E., Rhodes, L. F., and Strittmatter, R. J. (1989) *J. Less Common Metals*, **149**, 207–11.

Caceci, M. and Choppin, G. (1983) *Radiochim. Acta*, **33**(2/3), 101–4.

Campbell, D. O. (1970) *Ind. Eng. Chem. Process Des. Dev.*, **9**, 95–9.

Carlson, T. A., Nestor, C. W. J., Wasserman, N., and McDowell, J. D. (1970) *Comprehensive Calculations of Ionization Potentials and Binding Energies for Multiply-Charged Ions*, Oak Ridge National Laboratory.

Carnall, W. T. and Wybourne, B. G. (1964) *J. Chem. Phys.*, **40**, 3428–33.

Carnall, W. T., Fields, P. R., and Wybourne, B. G. (1964) *J. Chem. Phys.*, **41**, 2195–6.

Carnall, W. T. and Fields, P. R. (1967) in *Lanthanide/Actinide Chemistry* (ed. R. F. Gould), American Chemical Society, Washington, DC, pp. 86–101.

Carnall, W. T. (1979a) Emission Spectra, in *Gmelins Handbuch der Anorganischen Chemie*, Transurane, Teil A2, vol. 8, (ed. G. Koch), Verlag Chemie, Weinheim, Germany, p. 42.

Carnall, W. T. (1979b) X-ray spectra, in *Gmelins Handbuch der Anorganischen Chemie,* Transurane, Teil A2, vol. 8, (ed. G. Koch), Verlag Chemie, Weinheim, p. 80.

Carnall, W. T. (1989) *J. Less Common Metals*, **156**, 221–35.

Carniglia, S. C. and Cunningham, B. B. (1955) *J. Am. Chem. Soc.*, **77**, 1451–3.

Casarci, M., Chiarizia, R., Gasparini, G. M., Puzzuoli, G., and Valeriani, G. (1988) in *Proc. of ISEC '88,* Moscow, USSR.

Casarci, M., Gasparini, G. M., and Grossi, G. (1989) in *Proc. of Actinides – 89*, Tashkent, Russia.

Cavellec, R., Hubert, S., and Simoni, E. (1997) *J. Solid State Chem.*, **129**, 189–95.

Chamberlain, D. B., Conner, C., Hutter, J. C., Leonard, R. A., Wygmans, D. G., and Vandegrift, G. F. (1997) *Sep. Sci. Technol.*, **32**, 303.

Charbonnel, M. C. and Musikas, C. (1988) *Solvent Extr. Ion Exch.*, **6**, 461.

Chartier, D., Donnet, L., and Adnet, J. M. (1999) *Radiochim. Acta*, **85**, 25–31.

Charvillat, J. P., Benedict, U., Damien, D., de Novion, C., Wojakowski, A., and Müller, W. (1975a) in *Transplutonium 1975*, *Proc. 4th Int. Symp.*, pp. 79–93.

Charvillat, J. P., Benedict, U., Damien, D., and Müller, W. (1975b) *Radiochem. Radioanal. Lett.* **20**, 371–381.

Charvillat, J. P. and Damien, D. (1973) *Inorg. Nucl. Chem. Lett.*, **9**, 559–63.

Charvillat, J. P. and Zachariasen, W. H. (1977) *Inorg. Nucl. Chem. Lett.*, **13**, 161–3.

Charvillat, J. P., Benedict, U., Damien, D., de Novion, C., Wojakowski, A., and Müller, W. (1977) *Rev. Chim. Minér.*, **14**, 178–88.

Chen, J., Jiao, R., and Zhu, Y. (1996) *Solvent Extr. Ion Exch.*, **14**, 555.

Chiarizia, R. and Horwitz, E. P. (1986) *Solvent Extr. Ion Exch.*, **4**, 677.

Chiarizia, R. and Horwitz, E. P. (1990) *Solvent Extr. Ion Exch.*, **8**, 907.

Chiarizia, R., Horwitz, E. P., Alexandratos, S. D., and Gula, M. J. (1997) *Separation Science and Technology*, **32**(1–4), 1–35.

Chikalla, T. D. and Eyring, L. (1967) *J. Inorg. Nucl. Chem.*, **29**, 2281–93.

Chikalla, T. D. and Eyring, L. (1968) *J. Inorg. Nucl. Chem.*, **30**, 133–45.

Chikalla, T. D., McNeilly, C. E., Bates, J. L., and Rasmussen, J. J. (1973) in *Proc. Int. Colloq. on High Temp. Phase Transform.*, CNRS Publ. No. 205, pp. 351–60.

Chistyakov, V. M., Ermakov, V. A., and Rykov, A. G. (1974) *Radiokhimiya*, **16**, 553–5.

Chitnis, R. R., Wattal, P. K., Ramanujam, A., Dhami, P. S., Gopalakrishnan, V., Mathur, J. N., and Murali, M. S. (1998) *Sep. Sci. Technol.*, **33**, 1877.

Chitnis, R. R., Wattal, P. K., Ramanujam, A., Dhami, P. S., Gopalalkrishnan, V., Bauri, A. K., and Bannerji, A. (1999) *J. Radioanal. Nucl. Chem.*, **240**, 721.

Chmutova, M. K., Kochetkova, N. E., Koiro, O. E., Myasoedov, B. F., Medved, T. Y., Nesterova, N. P., and Kabachnik, M. I. (1983) *J. Radioanal. Chem.*, **80**, 63.

Chmutova, M. K., Kochetkova, N. E., and Myasoedov, B. G. (1989) *J. Inorg. Nucl. Chem.*, **42**, 897.

Choppin, G. R. (1965) *Inorg. Chem.*, **4**, 1250–4.

Choppin, G. R. (1970) *J. Inorg. Nucl. Chem.*, **32**, 3283–8.

Choppin, G. R. and Degischer, G. (1972) *J. Inorg. Nucl. Chem.*, **34**, 3473–7.

Choppin, G. R. and Unrein, P. J. (1975) in *Transplutonium 1975, Proc. 4th Int. Symp.*, Baden-Baden, Germany, Ed. by W. Müller and R. Lindner, North-Holland, Amsterdam, Netherlands, p. 97–107.

Choppin, G. R. and Nash, K. L. (1977) *Rev. Chim. Minér.*, **14**, 230–6.

Choppin, G. R. and Chen, J. F. (1996) *Radiochim. Acta*, **74**, 105–10.

Choppin, G. R. and Labonne-Wall, N. (1997) *J. Radioanal. Nucl. Chem.*, **221**(1–2), 67–71.

Choppin, G. R. and Peterman, D. R. (1998) *Coord. Chem. Rev.*, **174**, 283–99.

Chudinov, E. G. and Choporov, D. Y. (1970) *At. Energy (USSR)*, **28**, 62–4.

Chuveleva, E. A., Peshkov, A. S., Kharitonov, O. V., and Firosova, L. A. (1999) *Radiochemistry* (*Eng. Transl.*), **41**, 442–4, 445–7, and 465–7.

Cilindro, L. G., Stadlbauer, E., and Keller, C. (1972) *J. Inorg. Nucl. Chem.*, **34**, 2577.

Cilindro, L. G. and Keller, C. (1974) *Radiochim. Acta*, **21**, 29–32.

Clark, D. L., Conradson, S. D., Ekberg, S. A., Hess, N. J., Neu, M. P., Palmer, P. D., Runde, W., and Tait, C. D. (1996) *J. Am. Chem. Soc.*, **118**, 2089–90.

Cohen, D. (1972) *Inorg. Nucl. Chem.*, **8**, 533–5.

Cohen, K. P. (2000) *Nucl. News*, **43** (Nov), 45–6.

Coleman, J. S., Armstrong, D. E., Asprey, L. B., Keenan, T. K., La Mar, L. E., and Penneman, R. A. (1955) *Purification of Gram Amounts of Americium*, Los Alamos Scientific Laboratory.

Coleman, J. S., Armstrong, D. E., Asprey, L. B., Keenan, T. K., La Mar, L. E., and Penneman, R. A. (1957) *J. Inorg. Nucl. Chem.*, **3**, 327–8.

Coleman, J. S. (1963) *Inorg. Chem.*, **2**, 53–7.

Coleman, J. S., Keenan, T. K., Jones, L. H., Carnall, W. T., and Penneman, R. A. (1963) *Inorg. Chem.*, **2**, 58–61.

Conner, W. V. (1971) *J. Less Common Metals*, **25**, 379–84.

Connor, W. V. (1982) *Nucl. Instrum. Methods*, **200**, 55–66.

Conway, J. G. (1963) University of California, Lawrence Laboratory.

Conway, J. G. (1964) *J. Chem. Phys.*, **40**, 2504–7.

Crandall, J. L. (1971) *Applications of Transplutonium Elements*, Savannah River Laboratory.

Cuillerdier, C., Musikas, C., and Hoel, P. (1991a) in *New Separations Technology for Radioactive Waste and Other Specific Applications* (eds. L. Cecille, M. Cesarci, and L. Pietrelli), Elsevier Applied Science, p. 41.

Cuillerdier, C., Musikas, C., Hoel, P., Nigond, L., and Vitart, X. (1991b) *Sep. Sci. Technol.*, **26**, 1229.

Cuillerdier, C., Musikas, C., and Nigond, L. (1993) *Sep. Sci. Technol.*, **28**, 155.

Cunningham, B. B. (1948) *Isolation and Chemistry of Americium*, Argonne National Laboratory.

Cunningham, B. B. (1949) in *The Transuranium Elements* (eds. G. T. Seaborg and J. J. Katz), Natl. Nucl. En. Ser., Div. IV, 14B, McGraw-Hill, New York, pp. 1363–70.

Damien, D. and Pages, M. (1969) in *Rapport Semestriel du Department de Chimie No.* 6, *Juin* 1968–*Novembre*1968, CEA, p. 407.

Damien, D. and Pages, M. (1970) in *Rapport Semestriel du Department de Chimie No.* 8, *Juin* 1969–*Novembre*1969, CEA, p. 472.

Damien, D. (1971) *Inorg. Nucl Chem. Lett.*, **7**, 291–7.

Damien, D. and Jove, J. (1971) *Inorg. Nucl. Chem. Lett.*, **7**, 685–8.

Damien, D. (1972) *Inorg. Nucl Chem. Lett.*, **8**, 501.

Damien, D. and Charvillat, J. P. (1972) *Inorg. Nucl. Chem. Lett.*, **8**, 705–8.

Damien, D., Jove, J., and Marcon, J. P. (1972) *Inorg. Nucl. Chem. Lett.*, **8**, 317–20.

Damien, D., Marcon, J. P., and Jove, J. (1975) *Radiochem. Radioanal. Lett.*, **23**, 145–54.

Damien, D., Marcon, J. P., and Jove, J. (1976) *Bull. D'Inform. Sci. Tech. (fr.)*, **217**, 67–76.

Danford, M. D., Burns, J. H., Higgins, C. E., Stokeley, J. R. J., and Baldwin, W. H. (1970) *Inorg. Chem.*, **9**, 1953–5.

David, F. and Bouisissiéres, G. (1968) *Inorg. Nucl. Chem. Lett.*, **4**, 153–9.

David, F., Samhoun, K., Guillaumont, R., and Edelstein, N. (1978) *J. Inorg. Nucl. Chem.*, **40**, 69–74.

David, F. (1986) *J. Less Common Metals*, **121**, 27.

Davydov, A. V., Myasoedov, B. F., and Travnikov, S. S. (1975) *Dokl. Akad. Nauk SSSR*, **225**, 1075–8.

Dedov, V. B., Lebedev, I. A., Ryzhov, M. N., Trakhlyaev, P. S., and Yakovlev, G. N. (1961) *Radiokhimiya*, **3**, 701.

Deissenberger, R., Kohler, S., Ames, F., Eberhardt, K., Erdmann, N., Funk, H., Herrmann, G., Kluge, H., Nunnemann, M., Passler, G., Riegel, J., Scheerer, F., Trautmann, N., and Urban, F. J. (1995) *Angew. Chem. Int. Edn.*, **34**, 814–5.

Delle Site, A. and Baybarz, R. D. (1969) *J. Inorg. Nucl. Chem.*, **31**, 2201.

Den Auwer, C., Charbonnel, M. C., Drew, M. G. B., Grigoriev, M., Hudson, M. J., Iveson, P. B., Madic, C., Nierlich, M., Presson, M. T., Revel, R., Russell, M. L., and Thuery, P. (2000) *Inorg. Chem.*, **39**, 1487–95.

Deshingkar, D. S., Chitnis, R. R., Theyyunni, T. K., Wattal, P. K., Ramanujam, A., Dhami, P. S., Gopalakrishnan, V., Rao, M. K., Mathur, J. N., Murali, M. S., Iyer, R. H., Badheka, L. P., and Bannerji, A. (1993) Report BARC.

Deshingkar, D. S., Chitnis, R. R., Wattal, P. K., Theyyunni, T. K., Nair, M. K. T., Ramanujam, A., Dhami, P. S., Gopalakrishnan, V., Rao, M. K., Mathur, J. N., Murali, M. S., Iyer, R. H., Badheka, L. P., and Bannerji, A. (1994) Report BARC.

Drobyshevskii, I. V., Prusakov, V. N., Serik, V. F., and Sokolov, V. B. (1980) *Radiokhimiya*, **22**(44), 591–4.

Dunlap, B. D., Lam, D. J., Kalvius, G. M., and Shenoy, G. K. (1972) *J. Appl. Phys.*, **42**, 1419.

Eberle, S. H. and Bayat, I. (1967) *Radiochim. Acta*, **7**, 214.

Eberle, S. H. and Ali, S. (1968) *Z. Anorg. Allg. Chem.*, **361**, 1.

Eberle, S. H. and Bayat, I. (1969) *Inorg. Nucl. Chem. Lett.*, **5**, 229.

Eberle, S. H. and Robel, W. (1970) *Inorg. Nucl. Chem. Lett.*, **6**, 359–65.

Eberle, S. H. and Moattar, F. (1972) *Inorg. Nucl. Chem. Lett.*, **8**, 265.

Eberle, S. H. and Sabau, C. S. (1972) *Radiochem. Radioanal. Lett.*, **11**, 77.

Ebner, A. D., Ritter, J. A., Ploehn, H. J., Kochen, R. L., and Navratil, J. D. (1999) *Sep. Sci. Technol.*, **34**, 1277–300.

Eick, H. A. and Mulford, R. N. R. (1969) *J. Inorg. Nucl. Chem.*, **31**, 371–5.

Elesin, A. A. and Zaitsev, A. A. (1971a) *Radiokhimiya*, **13**, 902.

Elesin, A. A. and Zaitsev, A. A. (1971b) *Radiokhimiya*, **13**, 775.

Elesin, A. A. and Zaitsev, A. A. (1972) *Radiokhimiya*, **14**, 370.

Elesin, A. A., Zaitsev, A. A., Ivanovich, N. A., Karaseva, V. A., and Yakovlev, G. N. (1972a) *Radiokhimiya*, **14**, 546.

Elesin, A. A., Zaitsev, A. A., Karaseva, V. A., Nazarova, I. I., and Petukhova, I. V. (1972b) *Radiokhimiya*, **14**, 374.

Elesin, A. A., Zaitsev, A. A., Kazakova, S. S., and Yakovlev, G. N. (1972c) *Radiokhimiya*, **14**, 541.

Elesin, A. A., Zaitsev, A. A., Sergeev, G. M., and Nazarova, I. I. (1973) *Radiokhimiya*, **15**, 64.

Ellinger, F. H. and Zachariasen, W. H. (1954) *J. Phys. Chem.*, **58**, 405–8.

Ellinger, F. H., Johnson, K. A., and Struebing, V. O. (1966) *J. Nucl. Mater.*, **20**, 83–6.

Ensor, D. D., Jarvinen, G. D., and Smith, B. F. (1988) *Solvent Extr. Ion Exch.*, **6**, 439.

Erdmann, B. (1971) *Darstellung von Actiniden/Lanthaniden-Edelmetall (Pt, Pd, Ir, Rh)-Legierungsphasen durch gekoppelte Reduktion*, Kernforschungszentrum karlsruhe.

Erdmann, B. and Keller, C. (1971) *Inorg. Nucl. Chem. Lett.*, **7**, 675–83.

Erdmann, B. and Keller, C. (1973) *J. Solid State Chem.*, **7**, 40–8.

Eriksson, O. and Wills, J. M. (1992) *Phys. Rev. B*, **45**, 3198–203.

Eriksson, O., Soderland, J. M., Wills, J. M., and Boring, A. M. (1993) *Physica B*, **190**, 5–11.

Erin, E. A., Kopytov, V. V., Rykov, A. G., and Kosyakov, V. N. (1979) *Radiokhimiya*, **21**, 63–7.

Ermakov, V. A. and Star, I. (1967) *Radiokhim.*, **9**, 197.

Ermakov, V. A., Rykov, A. G., Timofeev, G. A., and Yakovlev, G. N. (1971a) *Radiokhimiya*, **13**, 826–32.

Ermakov, V. A., Vorob'eva, V. V., Zaitsev, A. A., and Yakovlev, G. N. (1971b) *Radiokhimiya*, **13**, 692.

Ermakov, V. A., Vorob'eva, V. V., Zaitsev, A. A., and Yakovlev, G. N. (1971c) *Radiokhimiya*, **13**, 840.

Ermakov, V. A., Rykov, A. G., Timofeev, G. A., and Yakovlev, G. N. (1973) *Radiokhimiya*, **15**, 380–5.

Ermakov, V. A., Rykov, A. G., Timofeev, G. A., and Yakovlev, G. N. (1974) *Radiokhimiya*, **16**, 810–17.

Eyring, L., Lohr, H. R., and Cunningham, B. B. (1949) University of California Radiation Laboratory.

Eyring, L., Lohr, H. R., and Cunningham, B. B. (1952) *J. Am. Chem. Soc.*, **74**, 1186–90.

Fahey, J. A., Turcotte, R. P., and Chikalla, T. D. (1974) *Inorg. Nucl. Chem. Lett.*, **10**, 459–65.

Fang, D. and Keller, C. (1969) *Radiochim. Acta*, **11**, 123–7.

Fargeas, M., Fremont- Lamouranne, R., Legoux, Y., and Morini, O. J. (1986) *J. Less Common Metals*, **121**, 439.

Fedoseev, A. M. and Perminov, V. F. (1983) *Sov. Radiochem.* (*Engl. Transl.*), **25**, 522–3.

Fedoseev, A. M. and Budentseva, N. A. (1989) *Sov. Radiochem.* (*Engl. Transl.*), **31**, 525–37.

Fedoseev, A. M. and Budantseva, N. A. (1990) *Radiokhimiya*, **32**, 14–18 and 19–24.

Fedoseev, A. M., Budantseva, N. A., Grigor'ev, M. S., and Perminov, V. P. (1991) *Radiokhimiya*, **33**, 7–19.

Ferris, L. M., Smith, F. J., Mailen, J. C., and Bell, M. J. (1972) *J. Inorg. Nucl. Chem.*, **34**, 2921–33.

Freeman, A. J. and Keller, C. (1985) in *Handbook on the Physics and Chemistry of Actinides*, Elsevier Science Publishers.

Freundlich, W. and Pages, M. (1969) *C. R. Acad. Sci. Ser. C*, **269**, 392–4.

Fried, S. (1951) *J. Am. Chem. Soc.*, **73**, 416–18.

Fuger, J. (1958) *J. Inorg. Nucl. Chem.*, **5**, 332.

Fuger, J. and Cunningham, B. B. (1963) *J. Inorg. Nucl. Chem.*, **25**, 1423–9.

Fuger, J., Spirlet, J. C., and Müller, W. (1972) *Inorg. Nucl. Chem. Lett.*, **8**, 709–23.

Fuger, J. and Oetting, F. L. (1976) *The Chemical Thermodynamics of Actinide Elements and Compounds,* part 2, *The Actinide Aqueous Ions*, IAEA, Vienna.

Fuger, J., Khodakovsky, I. L., Serfeyeva, E. I., Medvedev, V. A., and Navratil, J. D. (1992) *Part 12, The Actinide Aqueous Inorganic Complexes*, IAEA, Vienna.

Gatrone, R. C., Kaplan, L., and Horwitz, E. P. (1987) *Solvent Extr. Ion Exch.*, **5**, 1075.

Gatrone, R. C. and Rickert, P. G. (1987) *Solvent Extr. Ion Exch.*, **5**, 1117.

Gatrone, R. C., Horwitz, E. P., Rickert, P. G., and Diamond, H. (1989) *Solvent Extr. Ion. Exch.*, **7**, 793.

Gedeonov, L. I., Lebedev, I. A., Stepanov, A. V., Shalinets, A. B., and Yakovlev, G. N. (1967) *Chemistry of the Transuranium and Fission Elements*, Izd. Nauka, p. 140.

Gel'man, A. D., Moskvin, A. I., Zaitsev, L. M., and Medfod'eva, M. P. (1967) *Complex Compounds of Transuranides* (*Engl. transl.*), Israel Program for Scientific Translations, Jerusalem.

Gerontopulos, P. T., Rigali, L., and Barbano, P. G. (1965) *Radiochim Acta*, **4**, 75.

Gibson, J. K. and Haire, R. G. (1992a) *J. Nucl. Mater.*, **195**, 156–65.

Gibson, J. K. and Haire, R. G. (1992b) *J. Alloys Compd.*, **181**, 23–32.

Gibson, J. K. (1998a) *J. Phys. Chem. A*, **102**, 4501–8.

Gibson, J. K. (1998b) *Organometallics*, **17**, 2583–9.

Gibson, J. K. (1999a) *Inorg. Chem.*, **38**, 165–73.

Gibson, J. K. (1999b) *J. Mass Spectrom.,* **34**(11), 1166–77.

Gibson, J. K. (2000) *Int. J. Mass Spectrom.*, **202**, 19–29.

Giffaut, E. and Vitorge, P. (1993) *Mat. Res. Soc. Symp. Proc.*, **294**, 747–51.

Gmelin (1973) in *Gmelins Handbuch der Anorganischen Chemie*, Suppl. Work, 8th edition, Verlag Chemie, Weinheim, Germany: Vol. 4, Transurane, Teil C Verbindungen (Compounds); Vol. 7a, Die Elemente (The Elements), Teil A1 (1973); Vol. 8, Teil A2, Die Elemente (The Elements) (1973).

Gmelin (1979) in *Gmelin Handbook of Inorganic Chemistry*, vol. *Transuranium*, Parts A1, A2, B1–3, C, D1, D2, Verlag Chemie, Weinheim.

Goffart, J. and Kuyckaerts, G. (1969) *Anal. Chim. Acta.*, **43**, 99.

Gopalakrishnan, V., Dhami, P. S., Ramanujam, A., Balaramarkishna, M. V., Murali, M. S., Mathur, J. N., Iyer, R. H., Bauri, A. K., and Bannerji, A. (1995) *J. Radioanal. Nucl. Chem. Art.*, **191**, 279.

Gourisse, D. (1966) *Cinetique des Reactions D'Oxydo-Reduction des Elements Transuraniens en Solution*, CEA.

Graus Odenheimer, B. and Choppin, G. R. (1956) *Stability Constants of Alpha hydroxyisobutyric Acid Complexes with Actinide Elements*, University of California Radiation Laboratory, Berkeley.

Grebenshchikova, V. I. and Babrova, V. N. (1958) *Zhur. Neorg. Khim.*, **3**, 400.

Grebenshschikova, V. I. and Babrova, V. N. (1961) *Radiochemistry USSR* **3**, 32.

Grebenshschikova, V. I. and Cheinyavskaya, N. B. (1962) *Sov. Radiochem.* (*Engl. Transl*), **4**, 207.

Grenthe, I. (1962) *Acta. Chem. Scand.*, **16**, 1695.

Grenthe, I., Fuger, J., Konings, R. J. M., Lemire, R. J., Muller, A. B., Nguyen-Trung, C., and Wanner, H. (1992) *Chemical Thermodynamics of Uranium*, Elsevier Science Publishers, North-Holland.

Grigorescu-Sabau, C. S. (1972) *Über die Temperaturabhangigkeit von Komplexgleichgewichten der Transplutone*, Kernforschungszentrum Karlsruhe.

Guillaume, B., Hobart, D. E., and Bourges, J. Y. (1981) *J. Inorg. Nucl. Chem.*, **43**(12), 3295–9.

Guillaume, B., Begun, G. M., and Hahn, R. L. (1982) *Inorg. Chem.*, **21**, 1159–66.

Guminski, C. (1995) *J. Phase Equilib.*, **16**, 333.

Gureev, E. S., Kosyakov, V. N., and Yakovlev, G. N. (1964) *Sov. Radiochem.*, **6**, 639–47.

Gureev, E. S., Dedov, V. B., Karpacheva, S. M., Shvetsov, I. K., Ryzhov, M. N., Trukchlayev, P. S., Yakovlev, G. N., and Lebedev, I. A. (1970) in *Progress in Nuclear Energy, Process Chemistry*, ser. III, vol. 4, (eds. C. E. Stevenson, E. A. Mason, and A.T. Gresky), Pergamon Press, New York, p. 631.

Hafez, M. B. (1968) *Spectrophotometric Study of the Complexes of Cerium and Uranides with Diethylenetriaminepentaacetic Acid* (DTPA).

Haire, R. G., Lloyd, M. H., Milligan, W. O., and Beasley, M. L. (1977) *J. Inorg. Nucl. Chem.*, **39**(5), 837–41 and 843–7.

Haire, R. G., Benedict, U., Young, J. P., Peterson, J. R., and Begun, G. M. (1985) *J. Phys. C: Solid State Phys.*, **18**(24), 4595–601.

Hale, W. H. and Lowe, J. T. (1969) *Inorg. Nucl. Chem. Lett.*, **5**, 363–9.

Hall, G. R. Herniman, and P. D. (1954) *J. Chem. Soc.*, 2214–21.

Hall, G. R. and Markin, T. L. (1957) *J. Inorg. Nucl. Chem.*, **4**, 137–42.

Hall, R. O. A., Lee, J. A., Mortimer, M. J., McElroy, D. L., Müller, W., and Spirlet, J. C. (1980) *J. Low Temp. Phys.*, **41**, 397–403.

Hall, H. L. (1989) Report USDOE LBL-27878, University of California, Berkeley, USA.

Hara, M. (1970) *Bull. Chem. Soc. Jpn.*, **43**, 89–94.

Harbour, R. M., Hale, W. H., Burney, G. A., and Lowe, J. T. (1972) *At. Energy Rev.*, **10**, 379–99.

Hennelly, E. J. (1972) in *Radioisotope Engineering* (ed. G. G. Eichholz), Marcel Dekker, New York, pp. 44–134.

Hermann, J. A. (1956) *Coprecipitation of Am*(*III*) *with Lanthanum Oxalate*, Los Alamos Scientific Laboratory.

Hill, H. H. and Ellinger, F. H. (1971) *J. Less Common Metals*, **23**, 92.

Hill, H. H., Lindsey, J. D. G., White, R. W., Asprey, L. B., Streubing, V. O., and Matthias, B. T. (1971) *Physica*, **55**, 615.

Hindman, J. C. (1958) Proc. of the *Second Int. Conf. on the Peaceful Uses of Atomic Energy*, Geneva, United Nations, p. 349–60.

Hobart, D., Samhoun, K., and Peterson, J. R. (1982) *Radiochim. Acta*, **31**, 139–45.

Hobart, D. E., Begun, G. M., Haire, R. G., and Hellwege, H. E. (1983a) *J. Raman Spectrosc.*, **14**(1), 59–62.

Hobart, D. E., Samhoun, K., and Peterson, J. R. (1983b) *Radiochim. Acta*, **31**, 139–45.

Hoekstra, H. and Gebert, E. (1978) *Inorg. Nucl. Chem. Lett.*, **14**, 189–91.

Hölgye, Z. (1982) *Radiochem. Radioanal. Lett.*, **53**, 285–90.

Horrocks, W. D. Jr and Sudnick, D. R. (1979) *Science,* **206**(7), 1194–6.

Horrocks, W. D. Jr and Sudnick, D. R. (1981) *Acc. Chem. Res.*, **14**, 384–92.

Horwitz, E. P. (1966) *J. Inorg. Nucl. Chem.*, **28**, 1469–78.

Horwitz, E. P., Bloomquist, C. A. A., Sauro, L. J., and Henderson, D. J. (1966) *J. Inorg. Nucl. Chem.*, **28**, 2313–24.

Horwitz, E. P., Bloomquist, C. A. A., Orlandini, K. A., and Henderson, D. J. (1967) *Radiochim. Acta*, **8**, 127–32.

Horwitz, E. P., Bloomquist, C. A. A., and Griffin, H. E. (1969) Argonne National Laboratory.

Horwitz, E. P., Kalina, D. G., and Muscatello, A. C. (1981) *Sep. Sci. Technol.*, **16**, 403.

Horwitz, E. P., Kalina, D. G., Kaplan, L., Mason, G. W., and Diamond, H. (1982) *Sep. Sci. Technol.*, **17**, 1261.

Horwitz, E. P. and Kalina, D. G. (1984) *Solvent Extr. Ion Exch.*, **2**, 179.

Horwitz, E. P. and Schulz, W. W. (1985) in *Solvent Extraction and Ion Exchange in the Nuclear Fuel Cycle* (eds. D. H. Logsdail and A. L. Mills), Ellis Horwood, Chichester, p. 137.

Horwitz, E. P., Kalina, D. G., Diamond, H., Kaplan, L., Vandegrift, G. F., Leonard, R. A., Steindler, M. J., and Schulz, W. W. (1985a) in *Actinide/Lanthanide Separations* (eds. G. R. Choppin, J. D. Navratil, and W. W. Schulz), World Scientific, Singapore, p. 43.

Horwitz, E. P., Kalina, D. G., Diamond, H., Vandegrift, G. F., and Schulz, W. W. (1985b) *Solvent Extr. Ion Exch.*, **3**, 75.

Horwitz, E. P. and Schulz, W. W. (1986) in *Proc. ISEC '86.*

Horwitz, E. P., Martin, K. A., Diamond, H., and Kaplan, L. (1986) *Solvent Extr. Ion Exch.*, **4**, 449.

Horwitz, E. P., Diamond, H., Martin, K. A., and Chiarizia, R. (1987) *Solvent Extr. Ion Exch.*, **3**, 419 and 447.

Horwitz, E. P. and Schulz, W. W. (1990) *Symposium on New Separation Chemistry for Radioactive Waste and Other Specific Applications.*

Horwitz, E. P., Dietz, M. L., Nelson, D. M., La Rosa, J. J., and Fairman, W. B. (1990) *Anal. Chim. Acta.*, **238**, 263.

Horwitz, E. P., Chiarizia, R., Dietz, M. L., and Diamond, H. (1993) *Anal. Chem.*, **281**, 361.

Horwitz, E. P., Chiarizia, R., and Dietz, M. L. (1997) *React. Funct. Polym.*, **33**, 25.

Horwitz, E. P. and Schulz, W. W. (1999) in *Metal Ion Separation and Preconcentration: Progress and Opportunities* (eds. A. H. Bond, M. L. Dietz, and R. D. Rogers), American Chemical Society, Washington, DC, p. 20.

Hubert, S., Hussonnois, M., Brillard, L., Goby, G., and Guillaumont, R. (1974) *J. Inorg. Chem.*, **36**, 2361.

Hubert, S., Hussonois, M., Brillard, L., and Guillaumont, R. (1975) in *Transplutonium Elements, Proc. 4th Int. Symp.*, Baden-Baden, Sept. 13–17, Ed. by Müller, W. Lindner, R., North-Holland/Amer. Elsevier, p. 109–118.

Hubert, S. and Thouvenot, P. (1992) *J. Lumin.*, **54**, 103–11.

Hugen, Z., Yuxing, Y., and Xuexian, Y. (1982) *Actinide Recovery from Waste and Low-Grade Source*, Harwood Academic Publishers, New York, USA.

Hulet, E. K., Gutmacher, R. G., and Coops, M. S. (1961) *J. Inorg. Nucl. Chem.*, **17**, 350–60.

Hurtgen, C. and Fuger, J. (1977) *Inorg. Nucl. Chem. Lett.*, **13**, 1186–90.

Hyde, E. K., Perlman, I., and Seaborg, G. T. (1971) *The Nuclear Properties of the Heavy Elements*, Prentice-Hall, New York.

Jenkins, I. L. and Wain, A. G. (1972) *Rep. Prog. Appl. Chem.*, **57**, 308–19.

Jensen, M. P., Morss, L. R., Beitz, J. V., and Ensor, D. D. (2000) *J. Alloys Compd.*, **303**, 137–41.

Johannson, B. (1978) *J. Phys. Chem. Solids*, **39**, 467.

Johannson, B. (1984) *Phys. Rev B*, **30**, 3533–55.

Johannson, B. (1995) *J. Phys. Compds.*, **223**, 211–15.

Johannson, B. (2000) *Physics World*, 26–7.

Jones, M. E. (1951) *The Vapor Pressure of Americium Trifluoride* (Thesis), University of California Radiation Laboratory.

Jones, L. L. (1953) *J. Chem. Phys.*, **23**, 2105.

Jones, L. H. and Penneman, R. A. (1953) *J. Chem. Phys.*, **21**, 542–4.

Jones, L. H. (1955) *J. Chem. Phys.*, **23**, 2105–7.

Jove, J. and Pages, M. (1977) *Inorg. Nucl. Chem.*, **13**, 329–34.

Kalina, D. G., Horwitz, E. P., Kaplan, L., and Muscatello, A. C. (1981a) *Sep. Sci. Technol.*, **16**, 1127.

Kalina, D. G., Mason, G. W., and Horwitz, E. P. (1981b) *J. Inorg. Nucl. Chem.*, **43**, 159.

Kalina, D. G. and Horwitz, E. P. (1985) *Solvent Extr. Ion Exch.*, **3**, 235.

Kalvius, G. M., Ruby, S. L., Dunlap, B. D., Shenoy, G. K., Cohen, D., and Brodsky, M. B. (1969) *Phys. Lett. B*, **29**, 489–90.

Kamashida, M. and Fukasawa, T. (1996) *J. Nucl. Sci. Technol.*, **33**, 403–8.

Kamashida, M., Fukasawa, T., and Kawamura, F. (1998) *J. Nucl. Sci. Technol.*, **35**, 185–9.

Kaneko, H., Tsujii, M., Abe, M., Morita, Y., and Kubota, M. (1992) *J. Nucl. Sci. Technol.*, **29**, 988.

Kaneko, H., Tsujii, M., and Tamaura, Y. (1993) *Solvent Extr. Ion Exch.*, **11**, 693.

Kanellakopoulos, B., Fisher, E. O., Dornberger, E., and Baumgärtner, F. (1970) *J. Organomet. Chem.*, **24**, 507–14.

Kanellakopulos, B., Charvillat, J. P., Maino, F., and Müller, W. (1975) in *Transplutonium Elements*, *Proc. 4th Int. Symp.*, Baden-Baden, Sept. 13–17, Ed. by Müller, W. Linder, R., North-Holland/Amer. Elsevier.

Kanellakopulos, B., Aderhold, C., Dornberger, E., Müller, W., and Baybarz, R. D. (1978) *Radiochim. Acta* **25** (2), 89–92.

Kanellakopulos, B. (1979) in *Organometallics of the f-Elements* (eds. T. J. Marks and R. D. Fischer), Reidel, Dordrecht, pp. 1–35.

Karraker, D. G. Potassium Bis(Cyclooctatetraenyl) Americium(III). in *Transplutonium Elements, proc. 4th Int. Symp.,* Baden-Baden, Sept. 13–17, Ed. by Müller, W. Lindner, R., North-Holland/Amer. Elsevier, p. 131–5.

Karraker, D. G. (1977) *J. Inorg. Nucl. Chem.,* **39**(1), 87–9.

Kaszuba, J. P. and Runde, W. (1999) *Environ. Sci. Technol.*, **33**, 4427–33.

Katz, J. J. and Gruen, D. M. (1949) *J. Am. Chem. Soc.*, **71**, 2106–12.

Katz, J. J: Seaborg, G. T. (1957) *The Chemistry of the Actinide Elements*, Methuen, London, UK.

Keenan, T. K. (1959) *J. Chem. Educ.*, **36**, 27–31.

Keenan, T. K. and Kruse, F. H. (1964) *Inorg. Chem.*, **3**, 1231–2.

Keenan, T. K. (1965) *Inorg. Chem.*, **4**, 1500–1.

Keenan, T. K. (1966) *Inorg. Nucl. Chem. Lett.*, **2**, 153–6 and 211–14.

Keenan, T. K. (1967) *Inorg. Nucl Chem. Lett.*, **3**, 391–6 and 463–7.

Keenan, T. K. (1968) *Inorg. Nucl. Chem. Lett.*, **4**, 381–4.

Keller, C. (1963) *Nukleonik*, **5**, 41–8.

Keller, C. (1964) *Über die Festkörperchemie der Actiniden-Oxide*, Kernforschungszentrum Karlsruhe.

Keller, C. and Schmutz, H. (1964) *Z. Naturf. B*, **19**, 1080.

Keller, C. (1965) *J. Inorg. Nucl. Chem.*, **27**, 321–7.

Keller, C. and Walter, K. H. (1965) *J. Inorg. Nucl. Chem.*, **27**, 1247–51 and 1253–60.

Keller, C., Eberle, S. H., and Mosdzelewski, K. (1965a) *Radiochim. Acta*, **4**, 141–5.

Keller, C., Koch, L., and Walter, K. H. (1965b) *J. Inorg. Nucl. Chem.*, **27**, 1205–23 and 1225–32.

Keller, C., Eberle, S. H., and Mosdzelewski, K. (1966) *Radiochim. Acta*, **5**, 185–8.

Keller, C. (1967) in *Lanthanide/Actinide Chemistry* (ed. R. F. Gould), American Chemical Society, Washington, DC, , pp. 228–47.

Keller, C. and Fang, D. (1969) *Radiochim. Acta*, **11**, 123.

Keller, C. and Schreck, H. (1969) *J. Inorg. Nucl. Chem.*, **31**, 1121–32.

Keller, C. (1971) *Chemistry of the Transuranium Elements*, Verlag Chemie, Weinheim.

Keller, C., Berndt, U., Debbabi, M., and Engerer, H. (1972) *J. Nucl. Mater.*, **42**, 23–31.

Keller, C. and Berndt, U. (1975) in *Transplutonium, Proc. 4th Int. Symp.,* Baden-Baden, Sept. 13–17, Ed. by Müller, W. Lindner, R., North-Holland/Amer. Elsevier, p. 85–93.

Khopkar, P. K. and Narayankutty, P. (1971) *J. Inorg. Nucl. Chem.*, **33**, 495–502.

Kim, J. I., Rhee, D. S., Wimmer, H., Buckau, G., and Klenze, R. (1993) *Radiochim. Acta*, **62**, 35.

Kimura, T. and Kato, Y. (1998) *J. Alloys Compd*, **271**, 867–71.

King, L. J., Bigelow, J. E., and Collins, E. D. (1973) *Transuranium Processing Plant Semiannual Report of Production*, *Status*, *and Plans for Period Ending June* 30, 1972, Oak Ridge National Laboratory.

Kirin, I. S., Moskalev, P. N., and Mishin, V. Y. (1967) *Zh. Obshch. Khim.*, **37**, 1065–8.

Koch, G. and Schoen, J. (1968) German Report KFK-783, Kernforschungszentrum Karlsruhe, Germany.

Koch, G. (1969) Conf. Report CONF-690426, Liege, Belgium.

Kochen, R. L. (1987) *Actinide Removal from Aqueous Solution with Activated Magnetite*, Rockwell International, Golden, CO.

Kochen, R. L. and Navratil, J. D. (1987) *Lanthanide/Actinide Res.*, **2**, 9.

Koehly, G. and Hoffert, F. (1967) *Semiannual Report of the Chemistry Department*, *Center for Nuclear Studies at Fontenay-aux-Roses*, *December* 1966–*May* 1967, Argonne National Laboratory.

Kolarik, Z. J. and Horwitz, E. P. (1988) *Solvent Extr. Ion Exch.*, **6**, 247.

Kolarik, Z., Müllich, U., and Gassner, F. (1999) *Solvent Extr. Ion Exch.*, **17**, 23 and 1155.

Koma, Y., Watanabe, M., Nemoto, S., and Tanaka, Y. (1998) *Solvent Extr. Ion Exch.*, **16**, 1357.

Kornilov, A. S., Frolov, A. A., and Vasil'ev, V. Y. (1986) *Radiokhimiya*, **28**(5), 656–60.

Kosyakov, V. N., Timofeev, G. A., Erin, E. A., Andreev, V. I., Kopytov, V. V., and Simakin, G. A. (1977) *Radiokhimiya*, **19**, 511–7.

Krot, N. N., Shillov, V. P., Nikolaevskii, V. B., Nikaev, A. K., Gel'man, A. D.,and Spitsyn, V. I. (1974a) *Dokl. Acad. Sci. USSR*, **217**(3), 525–7.

Krot, N. N., Shillov, V. P., Nikolaevskii, V. B., Nikaev, A. K., Gel'man, A. D., and Spitsyn, V. I. (1974b). Oak Ridge National Laboratory.

Kruse, F. H. and Asprey, L. B. (1962) *Inorg. Chem.*, **1**(1), 137–9.

Kuznetsov, V. I. and Skobelev, N. K. (1966) ORO-tr-3346-15, Joint Inst. for Nuclear Research, Dubna (USSR), translation of Russian report JINR-p7-2984.

Lam, D. J. and Mitchell, A. W. (1972) *J. Nucl. Mater.*, **44**, 279–84.

Larson, D. T. and Haschke, J. M. (1981) *Inorg. Chem.*, **20**, 1945–50.

Law, J. D., Brewer, K. N., Herbst, R. S., Todd, T. A., and Olsen, L. G. (1998) Report INEL/EXT-98-00004, Idaho National Engineering and Environmental Laboratory, Idaho Falls, Idaho, USA.

Law, J. D., Brewer, K. N., Herbst, R. S., and Todd, T. A. (1998) Report INEL/EXT-97-00837, Idaho National Engineering and Environmental Laboratory, Idaho Falls, Idaho, USA.

Lawaldt, D., Marquart, R., Werner, G.-D., and Wigel, F. (1982) *J. Less Common Metals*, **85**, 37–41.

Lebedev, I. A., Pirozhkov, S. V., Razbitnoi, V. M., and Yakovlev, G. N. (1960a) *Radiokhimiya*, **2**, 351–6.

Lebedev, I. A., Pirozhkov, S. V., and Yakovlev, G. N. (1960b) *Radiokhimiya*, **2**, 549–58.

Lebedev, I. A. and Yakovlev, G. N. (1961) *Radiokhimiya*, **3**, 455.

Lebedev, I. A., Pirozhkov, S. V., and Yakovlev, G. N. (1962) *Radiokhimiya*, **4**, 304–8.

Lebedev, I. A., Maksimova, A. M., Stepanov, A. V., and Shalinets, A. B. (1967) *Radiokhimiya*, **9**, 707.

Lebedev, I. A. and Shalinets, A. B. (1968) *Radiokhimiya*, **10**, 233.

Lebedev, I. A., Filimonov, V. T., Shalinets, A. B., and Yakovlev, G. N. (1968) *Radiokhimiya*, **10**, 93.

Lebedev, I. A., Frenkel, V. Y., Kulyako, Y. M., and Myasoedov, B. F. (1979) *Radiokhimiya*, **21**(6), 809–16.

Lederer, C. M. and Shirley, V. S. (1978) in *Table of Radioactive Isotopes*, John Wiley, New York.

Leger, J. M., Yacoubi, N., and Loriers, J. (1981) *J. Solid State Chem.*, **36**, 261–70.

Levakov, B. I. and Shalinets, A. B. (1971) *Radiokhimiya*, **13**, 295.

Le Vert, F. E. and Helminski, E. L. (1973) *Literature Review and Commercial Source Evaluation of Americium-241*, Tuskegee Institute.

Li, J. and Bursten, B. E. (1997) *J. Am. Chem. Soc.,* **119**(38), 9021–32.

Liansheng, W., Casarci, M., and Gasparini, G. M. (1991) *Solvent Extr. Ion Exch.*, **8**, 49.

Liminga, R., Abrahams, S. C., and Bernstein, J. L. (1977) *J. Chem. Phys.*, **67**(3), 1015–23.

Lin, Z., Berne, A., Cummings, B., Filliben, J. J., and Inn, K. G. W. (2002) *Appl. Radiat. Isot.*, **56**, 57–63.

Lindbaum, A., Heathman, S., Litfin, K., Meresse, Y., Haire, R. G., Le Bihan, T., and Libotte, H. (2001) *Phys. Rev. B*, **63**, 214101 (1–10).

Link, P., Braithwaite, D., Wittig, J., Benedict, U., and Haire, R. G. (1994) *J. Alloys Compd.*, **213/214**, 148–52.

Liu, G. K., Beitz, J. V., Huang, J., Abraham, M. M., and Boatner, L. A. (1997) *J. Alloys Compd.*, **250**, 347–51.

Lohr, H. R. and Cunningham, B. B. (1951) *J. Am. Chem. Soc.*, **73**, 2025–8.

Lumetta, G. J. and Swanson, J. L. (1993a) *Sep. Sci. Technol.*, **28**, 43.

Lumetta, G. J. and Swanson, J. L. (1993b) Pacific Northwestern Laboratory.

Lumetta, G. J., Wester, D. W., Morrey, J. R., and Wagner, M. J. (1993) *Solvent Extr. Ion Exch.*, **11**, 663.

Lux, F. (1973) *Proc. Tenth Rare Earth Reasearch Conf.,* Carefree, Arizona, April 30-May 3, Ed. by Kevane, C. J. and Moeller, T., pp. 871–80.

Lychev, A. A., Mashirov, L. G., Smolin, Y. I., Suglobov, D. N., and Shepelev, Y. F. (1980) *Radiokhimiya*, **22**, 43–8.

Lynch, R. W., Dosch, R. G., Kenna, B. T., Johnstone, J. K., and Nowak, E. J. (1975) *The Sandia Solidification Process: A Broad Range Aqueous Waste Solidification Method.*

Madic, C., Guillaumont, B., Morisseau, J. C., and Moulin, J. P. (1979) *J. Inorg. Nucl. Chem.*, **83**, 3373.

Madic, C., Hobart, D. E., and Begun, G. M. (1983) *Inorg. Chem.*, **22**, 1494–503.

Madic, C., Blanc, P., Condamines, N., Baron, P., Berthon, L., Nicol, C., Pozo, C., Lecomte, M., Phillipe, M., Masson, M., Hequet, C., and Hudson, M. J. (1994) French Report CEA-CONF-12297.

Madic, C. and Hudson, M. J. (1998) Report EUR 18038 EN.

Magirius, S., Carnall, W. T., and Kim, J. I. (1985) *Radiochim. Acta*, **38**, 29–32.

Mahajan, G. R., Prabhu, D. R., Manchanda, V. K., and Badheka, L. P. (1998) *Waste Manage.*, **18**, 125.

Maly, J. (1969) *J. Inorg. Nucl. Chem.*, **31**, 1007–17.

Manchanda, V. K. and Mohapatra, P. K. (1995) *Radiochim. Acta*, **69**, 81.

Mapara, P. M., Godbole, A. G., Rajendra, S., and Thakur, N. V. (1998) *Hydrometallurgy*, **49**, 197–201.

Marcu, G. and Samochocka, K. (1965) *Stud. Univ. Babes-Bolyai, Ser. Chem.*, **10**, 71.

Marcu, G. and Samochocka, K. (1966) *Stud. Univ. Babes-Bolyai, Ser. Chem.*, **11**, 15.

Marcus, Y., Givon, M., and Choppin, G. R. (1963) *J. Inorg. Nucl. Chem.*, **25**, 1457–63.

Marcus, Y. and Cohen, D. (1966) *Inorg. Chem.*, **5**, 1740–3.

Marcus, Y. and Shiloh, M. (1969) *Israel J. Chem.*, **7**, 31–43.

Marcus, Y. and Bomse, M. (1970) *Israel J. Chem.*, **8**, 901–11.

Marcus, Y., Yanir, E., and Givon, M. (1972) The standard potential of the americium III/IV couple. An estimate from the formal potential and complex stabilities in phosphoric acid, in *Coordination Chemistry in Solution*, Vol. kungl. Tek. Högsk. Handl. Nr. 265 (ed. E. Högfeldt), Swedish Nat. Sci. Res. Council, pp. 227–38.

Markin, T. L. (1958) *J. Inorg. Nucl. Chem.* **7**, 290–2.

Martella, L. L. and Navratil, J. D. (1979) US Report.

Martensson, N., Johansson, B., and Naegele, J. R. (1987) *Phys. Rev. B*, **35**, 1437–9.

Martinot, L. and Fuger, J. (1985) *The Actinides* in *Standard Potentials in Aqueous Solution*, ed. by Bard, A. J., Parsons, R., Jordan, J., Dekker, New York, USA, p. 631–74.

Mathur, J. N., Murali, M. S., and Natarajan, R. R. (1991) *J. Radioanal. Nucl. Chem.*, **152**, 127.

Mathur, J. N., Murali, M. S., Natarajan, P. R., Bodheka, L. P., and Benerji, R. (1992a) *Talanta*, **39**, 493.

Mathur, J. N., Murali, M. S., and Natarajan, R. R. (1992b) *J. Radioanal. Nucl. Chem.*, **155**, 195.

Mathur, J. N., Murali, M. S., Rizvi, G. H., Iyer, R. H., Michael, K. M., Kapoor, S. C., Dhumwad, R. K., Badheka, L. P., and Bannerji, A., (1994) *Solvent Extr. Ion Exch.*, **12**, 745.

Mathur, J. N., Murali, M. S., Iyer, R. H., Ramanujam, A., Dhami, P. S., Gopalakrishnan, V., Badheka, L. P., and Bannerji, A. (1995) *Nucl. Technol.*, **109**, 216.

Mathur, J. N., Murali, M. S., Ruikar, P. B., Nagar, M. S., Sipahimalani, A. R., Bauri, A. K., and Bannerji, A. (1998) *Sep. Sci. Technol.*, **33**, 2179.

Mathur, J. N., Murali, M. S., and Nash, K. L. (2001) *Solvent Extr. Ion Exch.*, **19**, 357–90.

Matonic, J. H., Scott, B. L., and Neu, M. P. (2001). *Inorg. Chem.*, **40**, 2638.

McIsaac, L. D. and Schulz, W. W. (1976) *Transplutonium 1975*, North-Holland, Amsterdam.

McIsaac, L. D. (1982) *Sep. Sci. Technol.*, **17**, 387.

McIsaac, L. D. and Baker, J. D. (1983) *Solvent Extr. Ion Exch.*, **1**, 72.

McWhan, D. B., Wallmann, J. C., Cunningham, B. B., Asprey, L. B., Ellinger, F. H., and Zachariasen, W. H. (1960) *J. Inorg. Nucl. Chem.*, **15**, 185–7.

Meinrath, G. and Kim, J. I. (1991a) *Radiochim. Acta*, **52/53**, 29.

Meinrath, G. and Kim, J. I. (1991b) *Eur. J. Inorg. Solid State Chem.*, **28**, 383–8.

Melkaya, R. F., Volkov, Y. F., Sokolov, E. I., Kapshukov, I. I., and Rykov, A. G. (1982) *Dokl. Chem.* (*Engl. Transl.*), **262/7**, 42.

Mercing, E. and Duyckaerts, E. (1967) *Anal. Lett.*, **1**, 23.

Michael, K. M., Rizvi, G. H., Mathur, J. N., and Ramanujam, A. (2000) *J. Radioanal. Nucl. Chem.*, **246**, 355.

Mikheev, N. B. and Myasoedov, B. F. (1985) Lower and higher oxidation states of transplutonium elements in solutions and Metals, in *Handbook on the Physics and Chemistry of the Actinides*, ch. 9 (eds. J. A. Freeman and C. Keller), Elsevier Science Publishers, pp. 347–86.

Milligan, W. O. and Beasley, M. L. (1968) *Acta Crystallogr. B*, **24**, 979–81.

Mills, T. R. and Reese, L. W. (1994) *J. Alloys Compd.*, **213/214**, 360–2.

Milyukova, M. S., Litvina, M. N., and Myasoedov, B. F. (1980) *Radiochem. Radioanal. Lett.,* **44**(4), 259–68.

Mishra, S., Chakravortty, V., and Vasudeva Rao, P. R. (1996) *Radiochim. Acta*, **73**, 89.

Mitchell, A. W. and Lam, D. J. (1970a) *J. Nucl. Mater.*, **37**, 349–52.

Mitchell, A. W. and Lam, D. J. (1970b) *J. Nucl. Mater.*, **36**, 110–12.

Moattar, F. (1971) *Compounds of Trivalent Transuranium Compounds Appearing in Mixtures of Complexing Agents.* Report KFK-1416, Kernforschungszentrum Karlsruhe, Germany.

Modolo, G. and Odoj, R. (1998) *J. Radioanl. Nucl. Chem.*, **228**, 83.

Modolo, G. and Odoj, R. (1999) *Solvent Extr. Ion Exch.*, **17**, 33.

Mohapatra, P. K. and Manchanda, V. K. (1991) *Radiochim. Acta*, **55**(4), 193–7.

Mohapatra, P. K. and Manchanda, V. K. (1995) *Polyhedron,* **14**(13–14), 1993–7.

Mohapatra, P. K. and Manchanda, V. K. (1999) *J. Radioanal. Nucl. Chem.*, **240**, 259.

Mohapatra, P. K., Sriram, S., Manchanda, V. K., and Badheka, L. P. (2000) *Sep. Sci. Technol.*, **35**, 39.

Moore, R. H. and Lyon, W. L. (1959) *Distribution of Actinide Elements in Molten System KCl-AlCl*$_3$*-Al*, General Electric Company, Hanford Atomic Products Operation.

Moore, F. L. (1964) *Anal. Chem.*, **36**, 2158.

Moore, F. L. (1966a) *Anal. Chem.*, **38**, 510.

Moore, F. L. (1966b) US Patent 3 194 494.

Moore, G. E. (1970) *Chemistry Division Annual Progress Report for Period Ending May* 20, 1970, Oak Ridge National Laboratory.

Moore, F. L. (1973) US Patent 3 687 641.

Morita, Y. and Kubota, M. (1988) *Solvent Extr. Ion Exch.*, **6**, 233.

Morita, Y., Yamaguchi, L., Kondo, Y., Shirahashi, K., Yamagishi, I., Fugiwara, T., and Kubota, M. (1993) in Proc. of Technical Committee on *Safety and Environmental Aspects of Partitioning and Transmutation of Actinides and Fission Products*. Report IAEA-TECDOC-783, Vienna, Austria.

Morss, L. R., Siegal, M., Stenger, L., and Edelstein, N. (1970) *Inorg. Chem.*, **9**(7), 1771–5 .

Morss, L. R. and Fuger, J. (1981) *J. Inorg. Nucl. Chem.*, **43**(9), 2059–64.

Morss, L. R. (1982) in *Actinides in Perspective* (ed. N. Edelstein), Pergamon Press, New York, pp. 381–407.

Morss, L. R. (1983) *J. Less Common Metals*, **93**, 301–21.

Morss, L. R. and Williams, C. W. (1994) *Radiochim. Acta*, **66/67**, 99–103.

Moskalev, P. N., Shapkin, G. N., and Darovskikh, A. N. (1979) *Zh. Neorg. khim.*, **24**, 340–6.

Moskvin, A. I., Khalturin, G. V., and Gel'man, A. D. (1959) *Radiokhimiya*, **1**, 141.

Moskvin, A. I., Khalturin, G. V., and Gel'man, A. D. (1962) *Radiokhimiya*, **4**, 162.

Moskvin, A. I. (1967) *Radiokhimiya*, **9**, 718–20.

Moskvin, A. I. (1971) *Radiokhimiya*, **13**, 221–3, 224–30, 575–81, and 668–74.

Moskvin, A. I. (1973) *Radiokhimiya*, **15**, 504–13.

Mosley, W. C. (1970) in *Proc. 4th Internat. Conf. on Plutonium and other Actinides*, Santa Fe, NM, USA, USAEC CONF-701001, Parts II, pp 762–771.

Moulin, V., Robouch, P. B., Vitorge, P., and Allard, B. (1987) *Inorg. Chim. Acta*, **140**, 303.

Müller, W. (1971) *Angew. Chem.*, **83**, 625.

Müller, W., Reul, J., and Spirlet, J. C. (1972) *Atomwirtschaft*, **17**, 415.

Müller, W., Schenkel, R., Schmick, H. E., Spirlet, J. C., McElroy, D. L., Hall, R. O. A., and Mortimer, M. J. (1978) *J. Low Temp. Phys.*, **40**, 361–78.

Mullins, L. J. and Leary, J. A. (1969) US Patent 3420639.

Murali, M. S. and Mathur, J. N. (2001) *Solvent Extr. Ion Exch.*, **19**, 61–77.

Musikas, C. (1973a) *Radiochem. Radioanal. Lett.*, **13**, 255–8.

Musikas, C. C. (1973b) Electrochimie en solution aqueuse, in *Gmelin Handbook of Inorganic Chemistry*, vol. part D1, Verlag Chemie, Weinheim, pp. 5–23.

Musikas, C., Germain, M., and Bathelier, A. (1980a) in *Actinide Separations* (eds. J. D. Navratil and W. W. Schulz) (*ACS Symp. Ser. 117*), American Chemical Society, Washington, DC, pp. 157–73.

Musikas, C., Le Marois, G., Fitoussi, R., and Cuillerdier, C. (1980b). in *Actinide Separations* (eds. J. D. Navratil and W. W. Schulz), (*ACS Symp. Ser. 117*), American Chemical Society, Washington, DC, pp. 131–45.

Musikas, C. and Hubert, H. (1983) *Proc. ISEC '83*, p. 449.

Musikas, C. (1984) *Actinide/Lanthanide Separations, Proc., Int. Symp.*, 19–30.

Musikas, C. (1987) *Inorg. Chim. Acta*, **140**, 197.

Musikas, C., Condamines, C., Cuillerdier, C., and Nigond, L. (1991) *International Symposium on Radiochemistry and Radiation Chemistry*.

Musikas, C. (1995) *Nuclear and Radiochemistry Symposium*.

Myasoedov, B. F., Mikhailov, V. M., Lebedev, I. A., Litvina, M. N., and Frenkel, V. Y. (1973) *Radiochem. Radioanal. Lett.*, **14**, 17–24.

Myasoedov, B. F., Guseva, L. I., Lebedev, I. A., Milyukova, M. S., and Chmutova, M. S. (1974a) *Analytical Chemistry of the Transplutonium Elements,* John Wiley, New York.

Myasoedov, B. F., Lebedev, I. A., Frenkel, V. Y., and Vyatkina, I. I. (1974b) *Sov. Radiochem.*, **16**, 803–7.

Myasoedov, B. F., Milyukova, M. S., Lebedev, I. A., Livina, M. N., and Frenkel, V. Y. (1975) *J. Inorg. Nucl. Chem.*, **37**, 1475–8.

Myasoedov, B. F., Lebedev, I. A., and Milyukova, M. S. (1977) *Rev. Chem. Minér.*, **14**, 160–71.

Myasoedov, B. F., Chmutova, M. K., and Karalova, Z. K. (1980) in *Actinide Separations* (eds. J. D. Navratil and W. W. Schulz), American Chemical Society, Washington, DC, p. 101.

Myasoedov, B. F. and Kremliakova, N. Y. (1985) Studies of americium and curium solution chemistry in the USSR, in *Americium and Curium Chemistry and Technology* (ed. N. M. Edelstein), D. Reidel, Germany, pp. 53–79.

Myasoedov, B. F., Chmutova, M. K., Kochetkova, N. E., Koiro, O. E., Priibylova, G. A., Nesterova, N. P., Medved, T. Y., and Kabachnik, M. I. (1986) *Solvent Extr. Ion Exch.*, **4**, 61.

Myasoedov, B. F. and Lebedev, I. A. (1991) in *Handbook on the Physics and Chemistry of the Actinides* (eds. A. J. Freeman and C. Keller), Elsevier, New York, p. 551.

Myasoedov, B. F. (1994) *J. Alloys Compd.*, **290**, 213–14.

Naegele, J. R., Manes, L., Spirlet, J. C., and Müller, W. (1984) *Phys. Rev. Lett.*, **52**, 1834–7.

Nair, G. M. and Chander, K. (1983) *J. Less Common Metals*, **92**(1), 29–34.

Nash, K. L., Gatrone, R. C., Clark, G. A., Rickert, P. G., and Horwitz, E. P. (1988) *Sep. Sci. Technol.*, **23**, 1355.

Nash, K. L., Gatrone, R. C., Clark, G. A., Rickert, P. G., and Horwitz, E., (1989) *Solvent Extr. Ion Exch.*, **7**, 644.

Nash, K. L. (1994) in *Handbook on the Physics and Chemistry of Rare Earths, Gschneidner* (eds. K. A. Gschneidner, Jr, L. Eyring, G. R. Choppin, and G. H. Lander), New York, Elsevier North-Holland, pp. 197–235.

Natowitz, J. B. (1973) USAEC Report ORO-3924–14.

Nellis, W. and Brodsky, M. B. (1974) in *The Actinides: Electronic Structure and Related Properties*, Academic Press, New York.

Newton, T. W. and Baker, F. (1967) in *Lanthanide/Actinide Chemistry* (ed. R. F. Gould), ACS Adv. Chem. Ser., American Chemical Society, Washing DC, pp. 268–95.

Newton, T. W. (1975) *The Kinetics of the Oxidation–Reduction Reactions of Uranium, Neptunium, Plutonium, and Americium Ions in Aqueous Solutions.*

Nigon, J. P., Penneman, R. A., Staritzki, E., Keenan, T. K., and Asprey, L. B. (1954) *J. Phys. Chem.*, **58**, 403–4.

Nigond, L., Musikas, C., and Cuillerdier, C. (1994) *Solvent Extr. Ion Exch.*, **12**, 261 and 297.

Nikolaev, A. V. and Ionova, G. V. (1991) *Phys. Stat. Sol. (6)* **167**, 613–23.

Nikolaevskii, V. B., Shilov, V. P., and Krot, N. N. (1974) *Radiokhimiya*, **16**, 122–3.

Nikolaevskii, V. B., Shilov, V. P., Krot, N. N., and Peretrukhin, V. F. (1975) *Radiokhimiya*, **17**, 420–2 and 431–3.

NN (2002) *Nucl. News*, **45**(Jan), 58–60.

Nugent, L. J., Baybarz, R. D., Burnett, J. L., and Ryan, J. L. (1971a) *J. Inorg. Nucl. Chem.*, **33**, 2503–30.

Nugent, L. J., Laubereau, P. G., Werner, G. K., and Vander Sluis, K. L. (1971b) *J. Organomet. Chem.*, **27**(3), 365–72.

Nugent, L. J., Baybarz, R. D., Burnett, J. L., and Ryan, J. L. (1973a) *J. Phys. Chem.*, **77**, 1528–39.

Nugent, L. J., Burnett, J. L., and Morss, L. R. (1973b) *J. Chem. Thermodyn.*, **5**, 665–78.

Nunez, L., Buchholz, B. A., Kaminski, M., Aase, S. B., Brown, N. R., and Vandegrift, G. F. (1996) *Sep. Sci. Technol.*, **31**, 1393.

Oetting, F. L., Rand, M. H., and Ackermann, R. J. (1976) in *The Chemical Thermodynamics of Actinide Elements and Compounds, part 1, The Actinide Elements*. IAEA.

Ogawa, T., Shirasu, Y., Minato, K., and Serizawa, H. (1997) *J. Nucl. Mater.*, **247**, 151–7.

Ohyoshi, E. and Ohyoshi, A. (1971) *J. Inorg. Nucl. Chem.*, **33**, 4265.

Okamoto, H. (1998) *J. Phase Euilib.*, **20**, 450–2.

Olson, W. M. and Mulford, R. N. R. (1966) *J. Phys. Chem.*, **70**, 2934–7.

Osipov, S. V., Andreichuk, N. N., Vasil'ev, V. Y., and Rykov, A. G. (1977) *Radiokhimiya*, **19**(4), 522–4.

Ozawa, M., Nemoto, S., Togashi, A., Kawata, T., and Onishi, K. (1992) *Solvent Extr. Ion Exch.*, **10**, 829.

Ozawa, M., Koma, Y., Nomura, K., and Tanaka, Y. (1998) *J. Alloys Compd.*, **538**, 272–3.

Pappalardo, R., Carnall, W. T., and Fields, P. R. (1969a) *J. Chem. Phys.*, **51**(2), 842–3.

Pappalardo, R. G., Carnall, W. T., and Fields, P. R. (1969b) *J. Chem. Phys.*, **51**, 1182–2000.

Pazukhin, E. M., Krivokhatskii, A. S., and Kochergin, S. M. (1987) *Sov. Radiochem.*, **29**(1), 9–13.

Penneman, R. A. and Asprey, L. B. (1950) *The formal potential of the Am(V)-Am(VI) couple*, Los Alamos National Laboratory.

Penneman, R. A. and Asprey, L. B. (1955) *A Review of Americium and Curium Chemistry, Proc. First Int. Conf. on the Peaceful Uses of Atomic Energy*, pp. 355–62.

Penneman, R. A. and Keenan, T. K. (1960) *The Radiochemistry of Americium and Curium*, National Academy of Sciences.

Penneman, R. A., Coleman, J. S., and Keenan, T. K. (1961) *J. Inorg. Nucl. Chem.*, **17**, 138–45.

Penneman, R. A. and Mann, J. B. (1976) *J. Inorg. Nucl. Chem.*, Suppl., 257–63.

Peppard, D. F., Mason, G. W., Driscoll, W. J., and Sironen, R. J. (1958) *J. Inorg. Nucl. Chem.*, **7**, 276–85.

Peppard, D. F., Mason, G. W., Driscoll, W. J., and Sironen, R. J. (1962) *J. Inorg. Nucl. Chem.*, **24**, 881–8.

Pereira, L. C. J., Wastin, F., Winand, J. M., Kanellakopoulos, B., Rebizant, J., Spirlet, J. C., and Almeida, M. (1997) *J. Solid State Chem.*, **134**, 138–47.

Peretrukhin, V. F. and Spitsyn, V. I. (1982) *Izv. Akad. Nauk SSSR, Ser. Khim.*, **31**, 826–31.

Persson, G. E., Svantesson, S., Wingefors, S., and Liljenzin, J. O. (1984) *Solvent Extr. Ion Exch.*, **2**, 89.

Peterson, J. R. (1973) in *Proc. 10th Rare Earth Research Conf.* (eds. C. J. Kevane and T. Moeller), April 30-May 3, Carefree, Arizona.

Petrzilova, H., Binka, J., and Kuca, L. (1979) *J. Radioanal. Nucl. Chem.*, **51**, 107.

Pikaev, A. K., Shilov, V. N., Nikolaevskii, V. B., Krot, N. N., and Spitsyn, V. I. (1977) *Radiokhimiya*, **19**(5), 720–4.

Pilv Vo, R. and Bickel, M. (1998) *J. Alloys Compd.*, **49**, 271.

Pilv Vo, R., La Rosa, J. J., Mouchel, D., Nardel, R., Bichel, M., and Altzizaglau, T. (1999) *J. Environ. Radioact.*, **43**, 343.

Pilv Vo, R. and Bichel, M. (2000) *Appl. Radiat. Isot.*, **53**, 273.

Piskunov, E. M. and Rykov, A. G. (1972) *Radiokhimiya*, **14**, 638.

Potter, R. A. and Tennery, V. J. (1973) US Patent, 3,758, 669.

Proctor, S. G. and Connor, W. V. (1970) *J. Inorg. Nucl. Chem.*, **32**, 3699–701.

Proctor, S. G. (1975) *Cation Exchange Process for Molten Salt Extraction Residues*, Rocky Flats Plant, Dow Chemical Company.

Proctor, S. G. (1976) *J. Less Common Metals*, **44**, 195–9.

Prunier, C., Guérin, L., Faugére, J.-L., Cocuaud, N., and Pidnet, J.-M. (1997) *Nucl. Technol.*, **120**, 110–20.

Radchenko, V. M., Ryabinin, M. A., Selezenev, A. G., Shimbarev, E. V., Sudakov, L. V., Kapashukov, I. I., and Vasil'ev, V. Y. (1982) *Sov. Radiochem.* (*Engl. Trans.*), **24**, 144–6.

Radzewitz, H. (1966) *Festkörperchemische Untersuchungen über die Systeme* $SeO_{1.5}$–ZrO_2 (HfO_2, $AmO_{1.5}$–ZrO_2 (HfO_2, ThO_2)–O_2, und TiO_2–NpO_2 (PuO_2), Kernforschungszentrum Karlsruhe.

Rai, D., Felmy, A. R., and Fulton, R. W. (1992) *Radiochim. Acta*, **56**(1), 7–14.

Rais, J. and Tachimori, S. (1994) *J. Radioanal. Nucl. Chem. Lett.,***188**, 157.

Rao, V. K., Mahajan, G. R., and Natarajan, P. R. (1987) *Inorg. Chim. Acta*, **128**(1), 131–4.

Rao, L. F., Rai, D., Felmy, A. R., Fulton, R. W., and Novak, C. F. (1996) *Radiochim. Acta*, **75**(3), 141–7.

Rapko, B. M. and Lumetta, G. J. (1994) *Solvent Extr. Ion Exch.*, **12**, 967.

Rapko, B. M. (1995) in *Separations of Elements* (eds. K. L. Nash and G. R. Choppin), Plenum Press, New York, p. 99.

Rebizant, J. and Benedikt, U. (1978) *J. Less Common Metals*, **58**, 31–3.

Rizvi, G. H. and Mathur, J. N. (1997), Report BARC/P004, p. 56.

Robel, W. (1970) *Complex Compounds of Hexavalent Actinides with Pyridine Carboxylic Acids*. KFK.

Roddy, J. W. (1973) *J. Inorg. Nucl. Chem.*, **35**, 4141–8.

Roddy, J. W. (1974) *J. Inorg. Nucl. Chem.*, **36**, 2531–3.

Rogozina, E. M., Konkina, L. F., and Popov, D. K. (1974) *Radiokhimiya*, **16**, 383–6.

Roof, R. B., Haire, R. G., Schiferl, D., Schwalbe, L., Kmetko, E. A., and Smith, J. L. (1980) *Science*, **207**, 1353–5.

Roof, R. B. (1982) *Z. Kristallogr.*, **158**, 307–12.

Rosch, F., Reimann, T., Ludwig, R., Dreyer, R., Buklanov, G. V., Khalkhin, V. A., Milanov, M., and Tran Kim, H. (1989) in *Actinides-89 Abstracts*, Tashkent, USSR.

Rose, R. L., Kelly, R. E., and Lesuer, D. R. (1979) *J. Nucl. Mater.*, **79**, 414–16.

Runde, W., Meinrath, G., and Kim, J. I. (1992) *Radiochim. Acta*, **58/59**, 93–100.

Runde, W. and Kim, J. I. (1994) *Chemisches Verhalten von Drei- und Fünfwertigem Americium in Salinen NaCl-Lösungen*, Institut für Radiochemie, Technische Universität München.

Runde, W., Neu, M. P., and Clark, D. L. (1996) *Geochim. Cosmochim. Acta*, **60**(12), 2065–73.

Runde, W., Van Pelt, C., and Allen, P. G. (2000) *J. Alloys Compd.*, **303/304**, 182–90.

Runde, W., Neu, M. P., Conradson, S., and Tait, C. D. (2002) American Chemical Society Meeting ACS 2002, Orlando, Florida, USA.

Runde, W., Bean, A., and Scott, B. (2003) *Chem. Commun.*, 1848–9.

Runnals, O. J. C. and Boucher, R. R. (1955) *Nature*, **176**, 1019–20.

Runnals, O. J. C. and Boucher, R. R. (1956) *Can. J. Phys.*, **34**, 949–58; Great Britain Patent 741441 (1956); and US Patent 2809887 (1975).

Ryan, J. L. (1967) Octahedral complexes of trivalent actinides, in *Lanthanide/Actinide Chemistry* (ed. R. F. Gould), American Chemical Society, Washing DC, pp. 331–4.

Ryan, J. L. (1974) Ion exchange, in *Gmelins Handbuch der Anorganischen Chemie*, vol. 21, *Transurane*, part D2, Verlag Chemie, Weinheim.

Rykov, A. G., Ermakov, V. A., Timofeev, G. A., Chistyakov, V. M., and Yakovlev, G. N. (1970) *Sov. Radiochem.*, **13**, 858–61.

Rykov, A. G., Timofeev, G. A., and Chistyakov, V. M. (1973) *Radiokhimiya*, **15**, 872–4.

Sakama, M., Tsukada, K., Asai, M., Tchikawa, S., Haka, H., Gata, S., Oura, Y., Nishanaka, I., Nagama, Y., Shibata, M., Kojima, Y., Kawada, K., Ebihara, M., and Nikahara, H. (2000) *Eur. Phys. J. A*, **9**, 303–5.

Sakamura, Y., Hijkata, T., Kinoshita, K., Inoue, T., Storvik, T. S., Kreuger, C. L., Grantham, L. F., Fusselman, S. F., Grimmett, D. L., and Roy, J. J. (1998) *J. Nucl. Sci. Technol.*, **35**, 49–59.

Sakanoue, M. and Amano, R. (1975) in *Transplutonium 1975*, *Proc. 4th Int. Symp.*, pp. 123–9.

Sakanque, M. and Nakatani, M. (1972) *Bull. Chem. Soc. Jpn.*, **45**, 3429.

Saprykin, A. S., Spitsyn, V. I., and Krot, N. N. (1976) *Dokl. Akad. Nauk SSSR*, **228**, 649–51.

Sari, C., Müller, W., and Benedict, U. (1972/73) *J. Nucl. Mater.*, **45**, 73–5.

Sasaki, Y. and Tachimori, S. (2002) *Solvent Extr. Ion Exch.*, **20**, 21.

Schleid, T., Morss, L. R., and Meyer, G. (1987) *J. Less Common Metals*, **127**, 183–7.

Schmutz, H. (1966) *Untersuchungen in den Systemem Alkalifluorid-Lanthaniden/Actinidenfluorid* (*Li*, *Na*, *K*, *Rb-La*, *S. E.*, *Y/Np*, *Pu*, *Am*), KFK.

Schoebrechts, J. P., Gens, R., Fuger, J., and Morss, L. R. (1989) *Thermochim. Acta*, **139**, 49–66.

Schulz, W. W. (1974) *Bidentate Organophosphorus Extraction of Americium and Plutonium from Hanford Plutonium Reclamation Facility Waste*, Atlantic Richfield Hanford Company.

Schulz, W. W. (1975) *Trans. Am. Nucl. Soc.*, **21**, 262–3.

Schulz, W. W. (1976) *The Chemistry of Americium*, DOE Technical Information Center.

Schulz, W. W., Koenst, J. W., and Tallant, D. R. (1980) *Actinide Separations,* American Chemical Society, Washington, DC.

Schulz, W. W. and Navratil, J. D. (1982) in *Recent Developments in Separation Science*, vol. 7 (ed. Li, N.), CRC Press, Boca Raton, FL.

Schulz, W. W. and Horwitz, P. (1988) *Sep. Sci. Technol.*, **23**, 1191.

Seaborg, G. T., James, R. A., Ghiorso, A., and Morgan, L. O. (1950) *Phys. Rev.*, **78**, 472.

Seaborg, G. T. (1970) *Nucl. Appl. Technol.*, **9**, 830–50.

Seaborg, G. T. (1972) *Pure Appl. Chem.*, **30**, 539–49.

Sekine, T. (1965) *Acta Chem. Scand.*, **19**, 1476.

Seleznev, A. G., Shushakov, V. D., and Kosulin, N. S. (1979) *Phys. Met. Metall.* (*Engl. Transl.*), **46**, 193–4.

Shafiev, A. I., Efremov, Y. V., Nikolaev, V. M., and Yakovlev, G. N. (1971) *Sov. Radiochem.*, **13**, 123–5.

Shalinets, A. B. and Stepanov, A. V. (1971) *Radiokhimiya*, **13**, 566–70.

Shalinets, A. B. and Stepanov, A. V. (1972) *Radiokhimiya*, **14**, 280–3.

Shalinets, A. B. (1972a) *Radiokhimiya*, **14**, 275.

Shalinets, A. B. (1972b) *Radiokhimiya*, **14**, 33.

Shalinets, A. B. (1972c) *Radiokhimiya*, **14**, 269.

Shannon, R. D. (1976) *Acta Crystallogr. B*, **A32**, 751–67.

Shen, C., Bao, B., Zhu, J., Wang, Y., and Cao, Z. (1996) *J. Radioanal. Nucl. Chem. Art.*, **212**, 187.

Shiloh, M., Givon, M., and Marcus, Y. (1969) *J. Inorg. Nucl. Chem.*, **31**, 1807–14.

Shilov, V. P., Nikolaevskii, V. B., and Krot, N. N. (1974) *Zh. Neorg. Khim.*, **19**, 469.

Shilov, V. P. (1976) *Radiokhimiya*, **18**, 659–60.

Shilov, V. P., Nikalagevsky, V. B., and Krot, N. N. (1976) in *Chemistry of Transuranium Elements* (eds. V. I. Spitsyn and J. J. Katz), Pergamon Press, New York, pp. 225–8.

Shilov, V. P., Garnov, A. Y., Krot, N. N., and Yusov, A. B. (1997) *Radiochemistry* (*Eng. Transl.*), **39**(6), 504–7.

Shilov, V. P. and Yusov, A. B. (1999) *Radiochemiya* (*Moscow*), **41**(5), 445–7.

Shirokova, I. B., Grigor'ev, M. S., Makarenkov, V. I., Den Auwer, C., Fedoseev, A. M., Budantseva, N. A., and Bessonov, A. A. (2001) *Russ. J. Coord. Chem.*, **27**, 729–30.

Shoun, R. R. and McDowell, W. J. (1980) *Actinide Separation*, ch 6.

Shoup, S. and Bamberger, C. (1997) *Radiochim. Acta*, **76**, 63–9.

Siddall, T. H. I. (1963) *J. Inorg. Nucl. Chem.*, **25**, 883–92.

Siddall, T. H. J. (1964) *J. Inorg. Nucl. Chem.*, **26**, 1991.

Silva, R. J. (1982) *Thermodynamic Properties of Chemical Species in Nuclear Waste. Topical Report*: *The Solubilities of Crystalline Neodymium and Americium Trihydroxides*, Lawrence Berkeley National Laboratory, p. 57.

Silva, R. J., Bidoglio, G., Rand, M. H., Robouch, P. B., Wanner, H., and Puigdomenech, I. (1995) *Chemical Thermodynamics of Americium,* Elsevier, New York.

Silvestre, J. P., Freundlich, A., and Pages, M. (1977) *Rev. Chim. Minér.*, **14**, 225–9.

Skobelev, N. K. (1972) *Sov. J. Nucl. Phys.* (*Engl. Transl*), **15**, 249.

Skriver, H. L., Anderson, O. K., and Johannson, B. (1980) *Phys. Rev. Lett.*, **44**, 1230–3.

Smith, J. L. and Haire, R. G. (1978) *Science*, **200**, 535–7.

Smith, G. S., Akella, J., Reichlin, R., Johnson, Q., Schock, R. N., and Schwab, M. (1981) *Actinides – 1981*, Lawrence Berkeley Laboratory.

Smith, B. F., Jarvinen, G. D., Jones, M. M., and Hay, P. J. (1989) *Solvent Extr. Ion Exch.*, **7**, 749.

Smith, L. L., Crain, J. P., Yeager, J. P., Horwitz, E. P., Diamond, H., and Chiarizia, R. (1995) *J. Radioanal. Chem.*, **15**, 194.

Soderholm, L., Skanthakamur, S., Antonio, M. R., and Conradson, S. (1996) *Z. Phys. B*, **101**, 539–45.

Soderland, P., Ahuja, R., Eriksson, O., Johannson, B., and Wills, J. M. (2000) *Phys. Rev. B*, **61**, 8119–24.

Sole, K. C., Hiskey, J. B., and Ferguson, T. L. (1993) *Solvent Extr. Ion Exch.*, **11**, 1993.

Spjuth, L., Liljenzin, J. O., Hudson, M. I., Drew, M. G. B., Iveson, P. B., and Madic, C. (2000) *Solvent Extr. Ion Exch.*, **18**, 1.

Stadler, S. and Kim, J. I. (1988) *Radiochim. Acta*, **44/45**, 39–44.

Standifer, E. M. and Nitsche, H. (1988) *Lanthanide and Actinide Res.*, **2**, 383.

Staritzky, E. and Truitt, A. L. (1954) Optical properties of some compounds of Uranium, Plutonium, and related elements, in *The Actinide Elements* (eds. G. T. Seaborg and J. J. Katz), Natl. Nucl. En. Ser., Div. IV, Vol. 14A, McGraw-Hill, New York, chapter 9.

Stary, J. (1965) *Talanta*, **13**, 421.

Stary, I. (1966) *Radiokhimiya*, **8**, 504.

Stepanov, A. V. and Makarova, T. P. (1965) *Radiokhimiya*, **7**, 670.

Stepanov, A. V., Makarova, T. P., Maksimova, A. M., and Shalinets, A. B. (1967) *Radiokhimiya*, **9**, 710.

Stepanov, A. V. (1971) *Zh. Neorg. Khim.*, **16**, 2981.

Stephanou, S. E. and Penneman, R. A. (1952) *J. Am. Chem. Soc.*, **74**, 3701–2.

Stephanou, S. E., Nigon, J. P., and Penneman, R. A. (1953) *J. Chem. Phys.*, **21**, 42–5.

Stephens, D. R., Stromberg, H. D., and Lilley, E. M. (1968) *J. Phys. Chem. Solids*, **29**, 815–21.

Stronski, I. and Rekas, M. (1973) *Radiochem. Radioanal. Lett.*, **14**, 297.

Sullivan, J. C., Hindman, J. C., and Zielen, A. J. (1961) *J. Am. Chem. Soc.*, **83**, 3373.

Sullivan, J. C., Gordon, S., Mulac, W. A., Schmidt, K. M., Cohen, D., and Sjoblom, R. (1976) *Inorg. Nucl. Chem. Lett.*, **12**, 599–601.

Sullivan, J. C., Gordon, S., Mulac, W. A., Schmidt, K. M., Cohen, D., and Sjoblom, R. (1978) *Inorg. Chem.*, **17**, 294–6.

Surls, J. P. J. and Choppin, G. R. (1957) *J. Inorg. Nucl. Chem.*, **4**, 62–73.

Swanson, J. L. (1991) Reports PNL-7716, 7734, and 7780, Pacific Northwestern Laboratory, Richland, Washington, USA.

Tabuteau, A., Pages, M., and Freundlich, W. (1972) *Radiochem. Radioanal. Lett.*, **12**, 139–44.

Tabuteau, A. and Pages, M. (1978) *J. Solid State Chem.*, **26**(2), 153–8.

Tagawa, H. (1971) *Nippon Genshiryoku Gakkaishi*, **5**, 267.

Tan, X.-F., Wang, U.-S., Tan, T.-Z., Zhou, G.-F., and Bao, B.-R. (1999) *J. Radioanal. Nucl. Chem. Art.*, **242**, 123.

Tananaev, I. G. (1990a) *Radiokhimiya*, **32**(5), 53–7.

Tananaev, I. G. (1990b) *Radiokhimiya*, **32**(4), 4–6.

Tananev, I. G. (1991) *Sov. Radiochem.*, **33**, 224–30.

Tanner, S. P. and Choppin, G. R. (1968) *Inorg. Chem.*, **7**, 2046.

Templeton, D. H. and Dauben, C. H. (1953) *J. Am. Chem. Soc.*, **75**, 4560–2.

Thouvenot, P., Hubert, S., Moulin, C., Decambox, P., and Mauchien, P. (1993) *Radiochim. Acta*, **61**, 15–21.

Tian, G. X., Zhu, Y. J., Xu, J. M., Hu, T. D., and Xie, Y. N. (2002) *J. Alloys Compd.*, **334**, 86–91.

Tikhonov, M. F., Nepomnyaskeru, V. Z., Kalinina, S. V., Khokhlov, A. D., Bulkin, V. I., and Filin, B. M. (1988) *Radiokhimiya*, **28**, 804–9.

Tomkins, F. S. and Fred, M. (1949) *J. Opt. Soc. Am.*, **39**, 357–63.

Torres, R. A. and Choppin, G. R. (1984) *Radiochim. Acta*, **35**, 143.

Trautmann, N. (1994) *J. Alloys Compd.*, **213/214**, 28–32.

Tsukada, K., Ichikawa, Y., Hatsukawa, Y., Nishinaka, I., Hata, K., Nagame, Y., Oura, Y., Ohyama, T., Sueki, K., Nakahara, H., Asai, M., Kojima, Y., Hirose, T., Yamamoto, H., and Kawade, K. (1998) *Phys. Rev. C*, **57**, 2057–60.

Uchiyama, G., Mineo, H., Hataku, S., Asakura, T., Kansi, K., Watanabe, M., Nakano, Y., Kimura, S., and Fujine, S. (2000) *Prog. Nucl. Energy*, **35**, 151–6.

UCRL (1959) Chemistry Division Semiannual Report for December 1958 Through May 1959 and Chemistry Division Semiannual Report for June Through December 1959.

Ueno, K. and Hoshi, M. (1971) *J. Inorg. Nucl. Chem.*, **33**, 1765 and 2631–3.

Valenzuela, R. W. and Brundage, R. T. (1990) *J. Chem. Phys.*, **93**, 8469–73.

Varga, L. P., Mann, J. B., Asprey, L. B., and Reisfeld, M. J. (1971) *J. Chem. Phys.*, **55**(9), 4230..

Varga, L. P., Baybarz, R. D., Reisfeld, M. J., and Asprey, L. B. (1973) *J. Inorg. Nucl. Chem.*, **35**, 2775–85.

Vladimirova, M. V., Ryabova, A. A., ulikov, I. A., and Milovanova, A. S. (1977) *Radiokhimiya*, **19**(5), 725–31.

Vladimirova, M. V. (1986) *Radiokhimiya*, **28**(5), 649–56.

Vogt, O., Mattenberger, K., Löhle, J., and Rebizant, J. (1998) *J. Alloys Compd.*, **271–273**, 508–12.

Volkov, Y. F., Kapshukov, I. I., Visyasheva, G. I., and Yokovlev, G. N. (1974) *Radiokhimiya*, **16**, 859–63, 863–7, and 868–73.

Volkov, Y. F., Visyasheva, G. I., Tomilin, S. V., Kapshukov, I. I., and Rykov, A. G. (1981) *Sov. Radiochem.*, **23**, 195.

Vorob'eva, V. V., Elesin, A. A., and Zaitsev, A. A. (1973a) *Complexing of Trivalent Americium, Curium, Californium, Promethium, and Yttrium Ions with Dioxymethylphosphinic Acid.*

Vorob'eva, V. V., Elesin, A. A., and Zaitsev, A. A. (1973b) *Complexing Trivalent Americium, Curium, Californium, and Yttrium Ions with Bis(hydroxymethyl)phosphinic Acid.*

Wall, N., Borkowski, M., Chen, J., and Choppin, G. (2002) *Radiochim. Acta*, **90**(9–11), 563–8.

Wapstra, A. H. and Gove, N. B. (1971) *Nucl. Data Tables*, **9**, 265–468.

Ward, J. W., Müller, W., and Kramer, G. F. (1975), in *Transplutonium Elements, Proc. 4th Int. Symp.*, Baden-Baden, Sept. 13–17, (eds. W. Müller and R. Lindner), Elsevier, North-Holland/Amer. Elsevier, p. 161–71.

Ward, J. W. and Hill, H. H. (1976) *Heavy Elements Properties,* North-Holland, Amsterdam.

Weaver, B. and Kappelmann, F. A. (1964) *Talspeak: A New Method of Separating Americium and Curium from the Lanthanides by Extraction from and Aqueous Solution of an Aminopolyacetic Acid Complex with a Monoacidic Organophosphate or Phosphonate*, Oak Ridge National Laboratory.

Weaver, B. and Shoun, R. R. (1971) in *Proc. 9th Rare Earth Research Conf.*, p. 322.

Weaver, B. (1974) in *Ion Exchange and Solvent Extraction,* (eds. J. A. Marinsky and Y. Marcus), A Series of Advances, vol. 6 , Marcel Dekker, New York.

Wei, Y. Z., Kumagai, M., Takashima, Y., Modolo, G., and Odoj, R. (2000a) *Nucl. Tech.*, **132**, 413–23.

Wei, Y. Z., Sabharwal, K. N., Kumagi, M., Asakara, T., Uchiyama, G., and Fujine, S. (2000b) *J. Nucl. Sci. Technol.*, **37**, 1108–10.

Weifan, Y., Junsheng, G., Wantong, M., Keming, F., Zaiguo, G., Hongye, L., Lijun, S., Shuifa, S., Shuanggui, Y., Shuhong, W., Denming, K., and Jimin, Q. (1999) *J. Radioanal. Nucl. Chem.*, **240**, 379–81.

Weigel, F., Ollendorff, W., Scherer, V., and Hagenbruch, R. (1966) *Z. Anorg. Allg. Chem.*, **345**, 119–28.

Weigel, F. and Meer, ter N. (1967) *Inorg. Nucl. Chem. Lett.*, **3**, 403–8.

Weigel, F. and Meer, ter N. (1971) *Z. Naturf. B*, **26**, 504–12.

Weigel, F., Wishnevsky, V., and Hauske, H. (1975), in *Transplutonium Elements, Proc. 4th Int. Symp.*, Baden-Baden, Sept. 13–17, (eds. W. Müller and R. Lindner), Elsevier, North-Holland/Amer., p. 217–26.

Weigel, F., Wittmann, F. D., and Marquart, R. (1977) *J. Less Common Metals*, **56**, 47–53.

Weigel, F., Wishnevsky, V., and Wolf, M. (1979) *J. Less Common Metals*, **63**, 81–6.

Weigel, F., Wittmann, F. D., Schuster, W., and Marquart, R. (1984) *J. Less Common Metals*, **102**(2), 227–38.

Werner, L. B. and Perlman, I. (1950) *J. Am. Chem. Soc.*, **73**, 495–6.

Wheelwright, E. J., Roberts, F. P., and Bray, L. A. (1968) *Simultaneous Recovery and Purification of Pm, Am, and Cm by the Use of Alternating DTPA and NTA Cation-Exchange Flowsheets*, Pacific Northwest Laboratories.

Williams, C. W., Antonio, M. R., and Soderholm, L. (2000) *J. Alloys Compd.*, **303/304**, 509–13.

Wittmann, F. D. (1980) University of Munich.

Woods, M., Cain, A., and Sullivan, J. C. (1974) *J. Inorg. Nucl. Chem.*, **36**, 2605–7.

Woods, M. and Sullivan, J. C. (1974) *Inorg. Chem.*, **13**, 2774–5.

Woods, M., Montag, T. A., and Sullivan, J. C. (1976) *J. Inorg. Nucl. Chem.*, **38**, 2059–61.

Wruck, D. A., Palmer, C. E. A., and Silva, R. J. (1999) *Radiochim. Acta*, **85**, 21–4.

Yaita, T., Tachimori, S., Edelstein, N. M., Bucher, J. J., Rao, L., Shuh, D. K., and Allen, P. G. (2001) *J. Synchrotron Radiation*, **8**, 663–5.

Yakovlev, G. N. and Gorbenko- Germanov, D. S. (1955) in *Proc. Int. Conf. on the Peaceful Uses of Atomic Energy*, pp. 306–8.

Yakovlev, G. N., Gorbenko- Germanov, D. S., Zenkova, R. A., Razbitnoi, V. L., and Kazanski, K. S. (1958) *J. Gen. Chem. USSR*, **28**(2653).

Yakovlev, G. N. and Kosyakov, V. N. (1958a) *An Investigation of the Chemistry of Americium*, *Proc. 2nd Int. Conf. on the Peaceful Uses of Atomic Energy*, pp. 373–84.

Yakovlev, G. N. and Kosyakov, V. N. (1958b) *Spectrophotometric Studies of the Behaviour of Americium Ions in Solutions*, *Proc. 2nd Int. Conf. on the Peaceful Uses of Atomic Energy*, pp. 363–8.

Yamagishi, I., Morita, Y., and Kubota, M. (1996) *Radiochim. Acta*, **75**, 27–32.

Yamamoto, M. and Sakanoue, M. (1982) *J. Radiat. Res.*, **23**, 261.

Yamana, H. and Moriyama, H. (1996) *J. Nucl. Sci. Technol.*, **33**, 288–97.

Yanir, E., Givon, M., and Marcus, Y. (1959) *Inorg. Nucl. Chem. Lett.*, **6**, 415–9.

Yanir, E., Givon, M., and Marcus, Y. (1969) *Inorg. Nucl. Chem. Lett.*, **5**, 369–72.

Yusov, A. B. (1989) Photoluminescence of americium(III) in aqueous and organic solutions, in *Actinides '89*, p. 240 and pp. 241–2.

Yusov, A. B. (1993) *Radiochem. Radioanal. Lett.*, **35**, 1–14.

Zachariasen, W. H. (1948a) *Phys. Rev. B*, **73**, 1104–5.

Zachariasen, W. H. (1948b) *Acta Crystallogr.*, **1**, 265–9.

Zachariasen, W. H. (1949a) *Acta Crystallogr.*, **2**, 288–91.

Zachariasen, W. H. (1949b) *Acta Crystallogr.*, **2**, 388–90.

Zachariasen, W. H. (1949c) *Phys. Rev.*, **73**, 1104.

Zachariasen, W. H. (1949d) *Acta Crystallogr.*, **2**, 57–60.

Zachariasen, W. H. (1954) in *The Actinide Elements* (eds. G. T. Seaborg, L. R. Morss and J. J. Katz), McGraw-Hill, New York, pp. 769–95.

Zachariasen, W. H. (1978) *J. Less Common Metals*, **62**, 1–7.

Zaitsev, A. A., Kosyakov, V. N., Rykov, A. G., Sobolev, Y. B., and Yakovlev, G. N. (1960a) *Radiokhimiya*, **2**(3), 348–50.

Zaitsev, A. A., kosyakov, V. N., Rykov, A. G., Sobolov, Y. P., and Yakovlev, G. N. (1960b) *Sov. At. Energy*, **7**, 562–9.

Zemlyanukhin, V. I., Savoskina, G. P., and Pushlenkov, M. F. (1962) *Sov. Radiochem.*, **4**, 501–5.

Zhu, Y. (1995) *Radiochim. Acta*, **68**, 1995.

Zhu, Y., Chen, J., and Choppin, G. R. (1996a) *Solvent Extr. Ion Exch.*, **14**, 543.

Zhu, Y., Chen, J., and Jiao, R. (1996b) *Solvent Extr. Ion Exch.*, **14**, 61.

Zhu, Y. and Jiao, R. (1994) *Nucl. Technol.*, **108**, 361–9.

Zhu, Y., Xu, J., Chen, J., and Chen, Y. (1998) *J. Alloys Compd.*, **742**, 271–3.

Zubarev, V. G. and Krot, N. N. (1982) *Sov. Radiochem.* (*Engl. Transl.*), **24**, 264–7.

Zubarev, V. G. and Krot, N. N. (1983a) *Sov. Radiochem.*, **25**, 601.

Zubarev, V. G. and Krot, N. N. (1983b) *Sov. Radiochem.*, **25**, 594.

Zur Nedden, P. (1969) *Z. Anal. Chem.*, **247**, 236.

CHAPTER NINE

CURIUM

Gregg J. Lumetta, Major C. Thompson, Robert A. Penneman,
and P. Gary Eller

9.1 HISTORICAL

Curium, element 96, is named after Pierre and Marie Curie, by analogy with its lanthanide congener, gadolinium (named after the Finnish chemist, J. Gadolin). Curium is not a naturally occurring terrestrial element.

The first curium isotope, ^{242}Cm, was prepared by Seaborg, James, and Ghiorso in mid-1944 by cyclotron helium ion (He^{2+}) bombardment of ^{239}Pu, and was identified by its characteristic alpha radiation (Seaborg *et al.*, 1949). The discovery of curium preceded that of americium (element 95). G. T. Seaborg described this discovery in a fascinating historical account (Seaborg, 1985). Werner and Perlman (1951) separated the first weighable quantity of curium (40 μg of impure ^{242}Cm oxide), which was prepared by prolonged neutron irradiation of ^{241}Am.

Curium is the element of highest atomic number that is available on the gram scale. However, chemical studies are typically done on the milligram scale using glove boxes, although microchemical techniques were originally used (Seaborg, 1972; Stevenson and Peterson, 1975). Larger scale work usually requires remote handling. Because of the limited availability of long-lived isotopes (especially ^{248}Cm), the high radioactivity of its most common isotopes (^{242}Cm and ^{244}Cm), and its general occurrence in aqueous systems as a 3+ ion, considerably less physical and chemical information about curium is available than for americium. Excellent reviews have been published on various aspects of curium chemistry (Katz and Seaborg, 1957; Brown, 1968; Keller, 1971; Bagnall, 1972; Gmelin, 1972–74; Penneman *et al.*, 1973; Edelstein *et al.*, 1985; Navratil and Schulz, 1993).

This chapter provides an overview of curium chemistry, with emphasis on advances since the publication of the 1986 version of this chapter (Eller and Penneman, 1986). The technical literature indicates that chemical investigations during this period have focused on the following general areas:

- Separations chemistry related to high-level waste management: This topic is addressed in Section 9.5.
- High-temperature superconductivity studies of curium compounds: Soderholm (1992) has provided an excellent review in this area. Additional discussion can be found in Section 9.7 and in Chapter 20.
- Behavior of curium in the environment: This topic is addressed in Chapter 27.
- Use of curium isotopes as targets to prepare superheavy elements: Hoffman (1985) and Lobanov *et al.* (1997) provide examples. This subject is discussed in Chapter 14.
- Use of curium isotopes in analytical space applications: Radchenko *et al.* (1999, 2000), Abramychev *et al.* (1992), and Vesnovskii *et al.* (1996) provide illustrative examples of this type of work applied to alpha spectrometry analysis of extraterrestrial rocks and soils.
- Transmutation in reactors and accelerators: Artisyuk *et al.* (1999), Gerasimov *et al.* (2000), and Raison and Haire (2001) describe this topic.

9.2 NUCLEAR PROPERTIES

Properties of the known curium isotopes, which range in mass from 238 to 251, are summarized in Table 9.1. Additional information is available in the appendix. Electron binding energies, radiation energies, X-ray spectra, and L-shell fluorescence data are available, as well as both alpha and spontaneous fission data (see Chu, 1972; Kerrigan and Banick, 1975; Lederer and Shirley, 1978; Lougheed *et al.*, 1978; Holden, 1989). Three isotopes (^{242}Cm, ^{244}Cm, and ^{248}Cm) are available in quantities sufficient for chemical study. Macroscopic studies with ^{242}Cm and ^{244}Cm are complicated by the high specific alpha activities of these isotopes (half-lives of 163 days and 18.1 years, respectively). The practical limit for chemical operations with ^{248}Cm in glove boxes is 10–20 mg because of the significant neutron exposure hazard from the 8% spontaneous fission yield of this isotope.

Both ^{242}Cm and ^{244}Cm have been used in power sources (thermal and electrical) for space and medical applications (Groh *et al.*, 1965; Abramychev *et al.*, 1992; Vesnovskii *et al.*, 1996). The isotope ^{242}Cm has a specific heat output (122 W g^{-1}) about 43 times higher than that of ^{244}Cm (2.8 W g^{-1}),

Table 9.1 *Nuclear properties of curium isotopes.*

Mass number	*Half-life*	*Mode of decay*	*Main radiations* (MeV)	*Method of production*
237	–	EC, α	α 6.660	^{237}Np(^{6}Li,6n)
238	2.3 h	EC < 90% α > 10%	α 6.52	^{239}Pu(α,5n)
239	2.9 h	EC	γ 0.188	^{239}Pu(α,4n)
240	27 d 1.9×10^{6} yr	α SF	α 6.291 (71%) 6.248 (29%)	^{239}Pu(α,3n)
241	32.8 d	EC 99.0% α 1.0%	α 5.939 (69%) 5.929 (18%) γ 0.472 (71%)	^{239}Pu(α,2n)
242	162.8 d 7.0×10^{6} yr	α SF	α 6.113 (74.0%) 6.070 (26.0%)	^{239}Pu(α,n) ^{242}Am daughter
243	29.1 yr	α 99.76% EC 0.24%	α 5.785 (73.5%) 5.741 (10.6%) γ 0.278 (14.0%)	^{242}Cm(n,γ)
244	18.10 yr 1.35×10^{7} yr	α SF	α 5.805 (76.7%) 5.764 (23.3%)	multiple n capture ^{244}Am daughter
245	8.5×10^{3} yr	α	α 5.362 (93.2%) 5.304 (5.0%) γ 0.175	multiple n capture
246	4.76×10^{3} yr 1.80×10^{7} yr	α SF β stable	α 5.386 (79%) 5.343 (21%)	multiple n capture
247	1.56×10^{7} yr	α	α 5.266 (14%) 4.869 (71%) γ 0.402 (72%)	multiple n capture
248	3.48×10^{5} yr	α 91.61% SF 8.39%	α 5.078 (82%) 5.034 (18%)	multiple n capture
249	64.15 min	β^{-}	β^{-} 0.9 γ 0.634 (1.5%)	^{248}Cm(n,γ)
250	$\sim 8.3 \times 10^{3}$ yr	SF		multiple n capture
251	16.8 min	β^{-}	β^{-} 1.42 γ 0.543 (12%)	^{250}Cm(n,γ)

This table is reproduced directly from the compilations in Appendix II of this volume by I. Ahmad.

and a cake of $^{242}Cm_2O_3$ weighing a few grams can be photographed using its own incandescence for illumination. These isotopes provide convenient energy sources for short-period/high-output and long-period/moderate-output applications. However, because of its greater availability and high-energy density, ^{238}Pu has supplanted both ^{242}Cm and ^{244}Cm for many such uses. The isotope ^{248}Cm has been a favored nuclide for accelerator studies attempting to form superheavy elements (Hoffman, 1985; Lobanov *et al.*, 1997).

9.3 PRODUCTION

Intense neutron exposure of ^{242}Pu and ^{243}Am in nuclear reactors forms significant quantities of the isotopes ^{244}Cm, ^{246}Cm, and ^{248}Cm, with lesser amounts of the odd-mass isotopes, ^{245}Cm and ^{247}Cm. Most curium isotopes heavier than ^{244}Cm have longer half-lives, but cannot be prepared isotopically pure by neutron capture. Except for ^{248}Cm, which is available as an essentially pure isotope from the decay of ^{252}Cf, curium isotope enrichment is accomplished in mass separators. The isotope ^{248}Cm is particularly desirable for chemical studies because of its long half-life (3.48×10^5 years). Approximately 100 mg of ^{248}Cm was produced in the 1970s and 1980s in the United States by purification from parent ^{252}Cf.

By far, the greatest quantity of curium exists as the isotope ^{244}Cm, which has been produced on the several kilogram scale at the Savannah River Site (Groh *et al.*, 1965; Baybarz, 1970; Gmelin, 1972–74). This isotope is produced by successive neutron capture starting with ^{239}Pu, ^{242}Pu, or ^{243}Am:

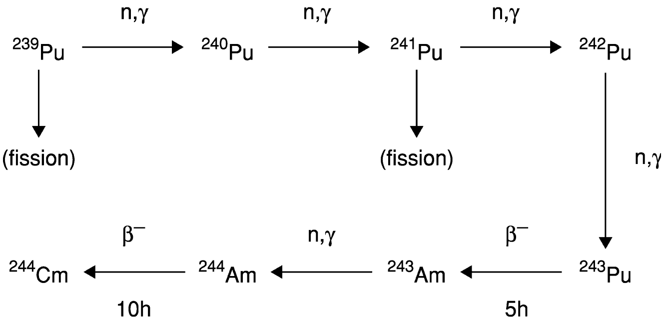

For 20 years following the discovery of curium, only milligram amounts of curium were available from the irradiation of ^{241}Am. It was not until Glenn T. Seaborg became Chairman of the US Atomic Energy Commission that a large-scale national program was instituted. Kilograms of ^{239}Pu were transferred from the weapons program for irradiation at Savannah River Site. This 'expenditure' of plutonium required a Presidential Directive. The authors note that, especially in 1960, this transfer from programmatic use was extraordinary and stands in striking contrast to current views regarding the disposition of many tons of excess weapons-grade plutonium. The aim of the irradiation campaign was to produce major amounts of the higher-mass isotopes of plutonium and elements of higher atomic number for research. The demand for large quantities of higher isotopes has diminished, resulting in the disposal of 2–3 kg of Cm from the Savannah River Site in 2002 (Peters *et al.*, 2002).

Initially, 8.5, then 12.0 kg for a total of 20.5 kg of ^{239}Pu, was staged in a Savannah River reactor. This approach was necessary to remove the immense heat produced (3×10^6 Btu h^{-1} ft^{-2}) from ^{239}Pu and ^{241}Pu fission. The yield from 20.5 kg of initial ^{239}Pu was 930 g of ^{242}Pu and 630g of ^{243}Am and ^{244}Cm combined (Penneman and Ferguson, 1971). The mixture was sent for separation to the Oak Ridge National Laboratory (ORNL), where the high-mass plutonium was fabricated into cermet targets for the High Flux Isotope Reactor (HFIR). A neutron flux of 5×10^{15} neutrons cm^{-2} s^{-1} was used for the specific purpose of creating higher-mass/higher-atomic-number isotopes. The plutonium feed composition was initially ^{238}Pu (0.43%), ^{239}Pu (1.12%), ^{240}Pu (1.8%), ^{241}Pu (0.91%), and ^{242}Pu (95.7%) (Bigelow, 2002).

At the height of production, about 1 g of ^{252}Cf was produced per year. Its short alpha decay half-life (2.6 years) yields ^{248}Cm. Production of ^{252}Cf has diminished, but continues because it is desirable for neutron irradiation in health applications. Its decay currently yields 35–50 mg of ^{248}Cm annually (Knauer, 2002).

The relatively stable isotope ^{248}Cm can be obtained in multi-milligram quantities by milking aged, prepurified ^{252}Cf materials that have undergone alpha decay. This method routinely yields milligram amounts of ^{248}Cm with an isotopic purity of 97%. Even so, 99.9% of the alpha activity arises from ^{244}Cm and ^{246}Cm impurities.

$$^{252}\mathrm{Cf} \xrightarrow[2.6\ \mathrm{y}]{\alpha} {}^{248}\mathrm{Cm}$$

Small (microgram) amounts of ^{245}Cm have been separated from alpha decay products of ^{249}Cf, itself a daughter of ^{249}Bk.

To isolate ^{244}Cm, irradiated material is dissolved in nitric acid and tetravalent plutonium is removed by solvent extraction (Groh *et al.*, 1965; Baybarz, 1970). The trivalent species (americium, curium, and the lanthanides) remaining in the aqueous phase are then extracted with 50% tributyl phosphate (TBP) in kerosene, and then back-extracted into dilute acid. For purification from lanthanides, Am/Cm chlorides are extracted with tertiary amines from slightly acidic 11 M LiCl (Tramex process), and then back-extracted into aqueous 7 M HCl. Subsequent precipitation of Am(V) as the potassium double carbonate effectively separates americium, leaving soluble Cm(III) in the K_2CO_3 medium.

The isotope ^{242}Cm is best obtained by neutron irradiation of ^{241}Am at an intermediate flux level. High neutron fluxes diminish the yield of ^{242}Cm because of the increased fission of ^{242}Am:

$$^{241}\mathrm{Am} \xrightarrow{\mathrm{n},\gamma} {}^{242}\mathrm{Am} \xrightarrow[16\,\mathrm{h}]{\beta^-} {}^{242}\mathrm{Cm}$$

Following irradiation of $\mathrm{AmO_2/Al}$ cermet targets, hot NaOH is used to dissolve the aluminum. Dissolution in HCl also can be used, in which case $\mathrm{Al^{3+}}$ must be removed before further processing. For small-scale separations, the Am/Cm/lanthanide fraction is dissolved in HCl; the solution is then made 11 M in LiCl, and passed through an anion-exchange column. Under these conditions, trivalent actinides (but not rare earth elements) are retained on the column. Alternatively, a tertiary amine extractant can be substituted for the anion-exchange resin to provide a group separation between actinides (extracted) and lanthanides (Baybarz, 1970). A subsequent americium/curium separation step is then required. A combination of anion and cation exchange was used successfully to separate about 1 g of $^{242}\mathrm{Cm}$ from neutron-irradiated $^{241}\mathrm{Am}$ (Thompson, 1972).

Numerous other techniques, including high-pressure ion exchange, extraction chromatography, and di(2-ethylhexyl)phosphoric acid (HDEHP) extraction also have been used for Cm separation and purification (Dedov *et al.*, 1965; Baybarz, 1970; Gmelin, 1972–74; Thompson, 1972; Buijs *et al.*, 1973; Haug, 1974; Lebedev *et al.*, 1974; Bigelow *et al.*, 1980; Bond and Leuze, 1980). Pressurized displacement ion-exchange chromatography has been applied to large-scale $^{244}\mathrm{Cm}/^{243}\mathrm{Am}$ separation and purification using Dowex® 50 resin in the $\mathrm{Zn^{2+}}$ form and diethylenetriaminepentaacetic acid (DTPA) as eluant (Stephanou and Penneman, 1952). Where sufficient quantities of Cm are present to give a substantial band, a pure curium cut can be obtained, since it leads the americium band.

9.4 ATOMIC PROPERTIES

Selected properties of curium-free atoms and ions are summarized in Table 9.2. A set of recommended thermodynamic parameters is available in the recent publication of Konings (2001b). Thermodynamic properties of actinides are addressed in Chapter 19.

The great stability of the $5f^7$ configuration of Cm(III) and its lanthanide congener Gd(III) is shown by the large M(III)–(IV) oxidation potentials (see Section 9.7.1). In contrast, it is noteworthy that the tendency of americium to attain the $5f^7$ configuration by assuming a divalent state is much weaker than that displayed by europium. Isolated Cm(II) compounds are unknown and a value of –2.78 V has been estimated for the Cm(III)/Cm(II) redox potential (Mikheev *et al.*, 1992).

The spectra of the Cm(III) aquo ion and of a metastable Cm(IV) aqueous fluoride solution complex ion are shown in Figs. 9.1 and 9.2, respectively. In contrast to solutions of Gd(III) (Moeller and Moss, 1951), aqueous solutions of

Table 9.2 *Selected properties and references of curium ions and metal.*

Property	*Value*	*Reference*	*Comment*
Cm(0) electronic configuration	$5f^7ds^2$ ($^9D_2$)	Keller (1971, p. 79)	
Cm(III) electronic configuration	$5f^7$	Katz and Seaborg (1957, Chapter 5)	
Metallic radius	1.743 Å	Reichlin *et al.* (1981); Zachariasen (1973)	dhcp form
Cm(III) ionic radius	0.97 Å	Shannon (1976)	six coordination
Cm(IV) ionic radius	0.85 Å	Shannon (1976)	six coordination
first ionization potential	5.99 eV	Deissenberger *et al.* (1995)	
Cm(0)–Cm(III) potential	−2.06 V	Fuger *et al.* (1975)	
Cm(II)–Cm(III) potential	−2.8 V	Mikheev (1983)	
Cm(III)–(IV) potential	−3.1 V	Keller (1971, p. 212)	1 M $HClO_4$
metal cell constants	dhcp, $a = 3.496(3)$ Å, $c = 11.331(5)$ Å; fcc, $a = 5.039$ (2) Å	Reichlin *et al.* (1981); Stevenson and Peterson (1979); Baybarz *et al.* (1976)	
melting point	1345 ± 50°C	Oetting *et al.* (1976); Fuger and Oetting (1976)	
boiling point	3110°C (calcd.)	Ward *et al.* (1975)	
ΔH_{fus}	13.85 kJ mol^{-1}	Ward *et al.* (1975)	
gaseous entropy	47.2 J K^{-1} mol	Edelstein *et al.* (1985, p. 139)	
density	13.5 g cm^{-3}	Reichlin *et al.* (1981)	dhcp form
magnetic moment	8.07 μ_B	Reichlin *et al.* (1981); Kanellakopulos *et al.* (1976)	100–550°K

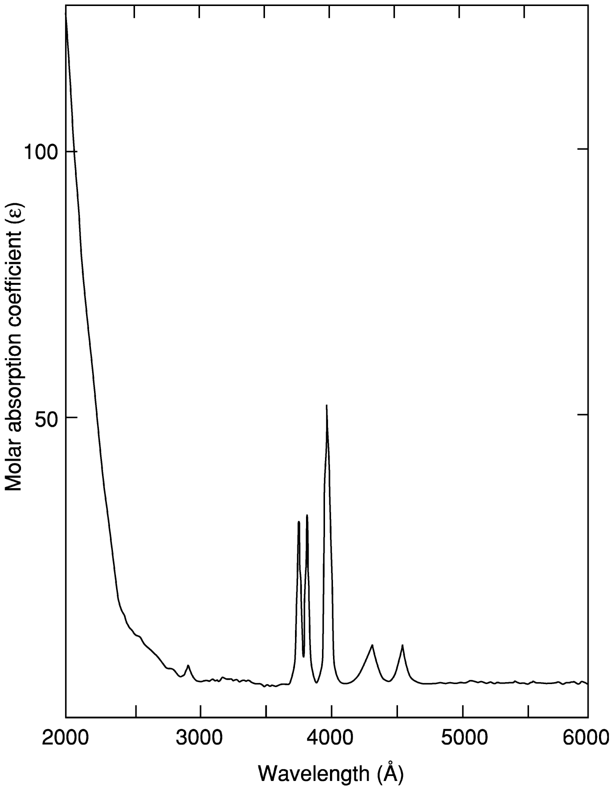

Fig. 9.1 *The absorption spectrum of Cm(*III*) in* 0.04 N *HclO*$_4$ *(aq). (Adapted from Carnall* et al., 1958.)

Cm(III) have weak absorption bands in the near-violet region, although intense absorptions are present in the ultraviolet region (Asprey and Keenan, 1958; Keenan, 1961; Barbanel *et al.*, 1977). The absorption spectra of metastable Cm(IV) was measured at Los Alamos by dissolving CmF_4 prepared by fluorination of dry CmF_3, and that of Cm(III) was measured at both Los Alamos and Argonne using curium solutions carefully purified from rare earths and americium. The principal peaks of Cm(IV) strongly resemble those of Am(III), with which it is isoelectronic (Carnall *et al.*, 1958).

Electronic transitions for Cm(III) solutions are shifted 20–30 Å to longer wavelengths compared to the solid state. The addition of complexing ions normally produces a diminution of intensities, and small changes in band positions. The transition energies for CmF_3 are considerably lower than those of GdF_3, due to smaller electrostatic repulsion terms and larger spin–orbit coupling in Cm(III). The spectra in both cases may be interpreted in terms of a $5f^7$ ground-state configuration. The spectrum of $Cs_2NaCmCl_6$, which

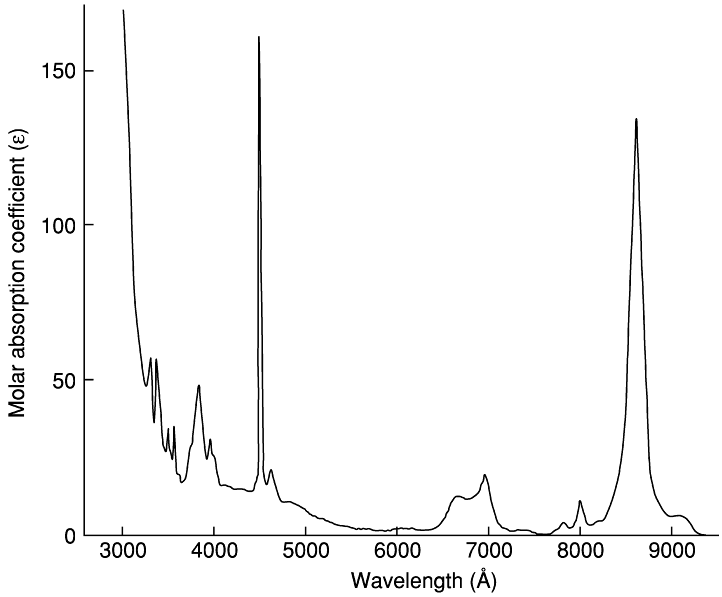

Fig. 9.2 *The absorption spectrum of Cm*(IV) *in* 15 M *CsF* (*aq*). (*Adapted from Keenan,* 1961.)

contains octahedrally coordinated Cm(III), was reported for both the solid and molten phases (Barbanel *et al.*, 1977). The most notable spectral effect is a sharp diminution in intensity compared to that of aqueous Cm(III) because of the highly symmetric curium coordination, which precludes observation of symmetry-forbidden f–f electronic transitions.

Time-resolved laser-induced fluorescence spectroscopy has been shown to be an especially valuable tool for determining curium concentration and speciation (Elesin *et al.*, 1973; Dem'yanova *et al.*, 1986; Yusov *et al.*, 1986b; Decambox *et al.*, 1989; Kim *et al.*, 1991; Myasoedov and Lebedev, 1991; Myasoedov, 1994; Moulin *et al.*, 1997; Dacheux and Aupais, 1998). Curium solutions have the unique property of strongly fluorescing in the range of 595–613 nm when irradiated with a laser or a mercury-discharge lamp (Myasoedov and Lebedev, 1991; Myasoedov, 1994). The broad unresolved fluorescence emission band is attributed to relaxation from the $^6D_{7/2}$ (*A*) state to the $^8S_{7/2}$ (*Z*) ground state (Kim *et al.*, 1991).

The energy of the emission band is dependent on the ligands attached to the curium ion. Taking advantage of this feature, time-resolved laser-induced fluorescence spectroscopy has been used extensively since the mid-1980s to investigate the fundamental solution chemistry of Cm (see Section 9.8). The method has been used to determine the hydration number for curium in solution (Kimura *et al.*, 1996) and complexation constants for a number of ligands. Furthermore,

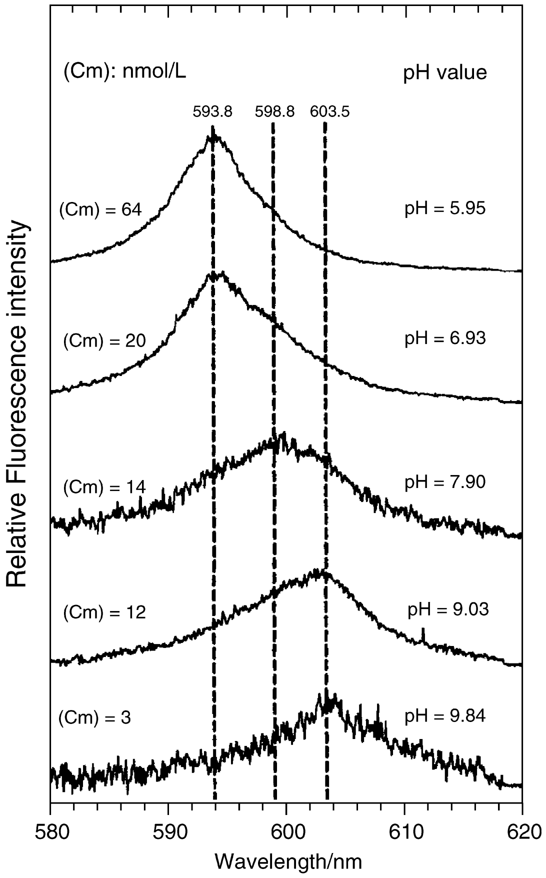

Fig. 9.3 *Curium(III) fluorescence emission spectra taken in the course of hydrolysis reaction in the pH range of* 5.05–9.84. *Used with permission from Wimmer* et al. (1992).

time-resolved laser-induced fluorescence spectroscopy has been used to characterize the Cm species present in groundwater taken from sites being considered for disposition of nuclear wastes (Wimmer *et al.*, 1992). Fig. 9.3 displays examples of fluorescence spectra for aqueous Cm species (Wimmer *et al.*, 1992). The examples presented are for Cm(III) as a function of pH and indicate the successive conversion of Cm(III) ion to $[Cm(OH)]^{2+}$ and $[Cm(OH)_2]^+$ (see Section 9.8 for a more detailed discussion of this topic).

For more thorough discussions of actinide ion absorption and luminescence spectra, see the sections on this subject by Carnall and Crosswhite (Gmelin, 1972–74). Chapter 18 of this work covers additional recent spectroscopic studies, including high-resolution spectra.

9.5 SEPARATION AND PURIFICATION OF PRINCIPAL ISOTOPES

The chemistry of curium in separation and purification is similar to that of other trivalent actinides and lanthanides and involves a series of steps, the number depending on the source of the curium. For example, separation of curium from irradiated uranium or plutonium materials requires more steps than separation of ^{248}Cm from decay of ^{252}Cf. Section 9.3 covers separation of curium from irradiated fuels and targets. This section covers separation and purification from high-level waste and other solutions, which has received more emphasis in recent years. In addition, Section 9.9 contains references to separations done for analysis of curium. Some of the analytical separations are also applicable to separation and purification.

9.5.1 Solvent extraction

Myasoedov and Kremliakova (1985) reviewed Russian literature up to the mid–1980s on americium and curium chemistry, including separations. A subsequent review has updated the work up to 1994 (Myasoedov, 1994). A recent book on separations for nuclear waste management contains reviews of work in the United States, France, and Russia (Choppin, 1999; Jarvinen, 1999; Musikas, 1999).

Extractions with organic phosphates (e.g. TBP, phosphine oxides, dialkylphosphoric acids, high-molecular-weight amines, β-diketones, and combinations of these) have been studied. Extraction by alkylphosphates depends on the structure and nature of the alkyl groups (Myasoedov, 1994; Zhu and Jiao, 1994). For example, mixed alkylphosphates with alkyl chains of six to eight carbons in length are reported to have properties superior to TBP (Zhu and Jiao, 1994). Extraction also depends on the salting agent present in solution. HDEHP has been widely studied for americium and curium extractions from both HNO_3 and LiCl solutions (Myasoedov and Kremliakova, 1985; Choppin, 1999). The latter solution has been used to separate the actinides from the lanthanides. Trioctylamine has been used to separate americium and curium from the lanthanides, with the salting agent and the diluent being important factors for extraction of curium, but not the lanthanides (Myasoedov and Kremliakova, 1985; Choppin, 1999). Russian researchers have studied the β-diketone, 1-phenyl-3-methyl-4-benzoyl-pyrazol-5-one, extensively (Myasoedov and Kremliakova, 1985). More recently, studies have been done with 1-phenyl-3-methyl-4-acylpyrazol-5-one in which the length of the carbon chain for the acyl group was varied from 2 to 22 (Takeishi *et al.*, 2001). A flowsheet was demonstrated with an acyl chain length of 8, which resulted in separate uranium, plutonium, and transplutonium fractions. All actinides were extracted from a 1 M HNO_3 solution and sequentially stripped by adjusting the pH with NaOH (Takeishi *et al.*, 2001).

Extensive studies have been done using bifunctional extractants, especially compounds such as octyl(phenyl)-*N*,*N*-diisobutyl carbamoylmethylphosphine oxide (CMPO) to recover transuranium elements, including curium, from high-level waste solutions (Horwitz and Schulz, 1991; Ozawa *et al.*, 1992; Myasoedov, 1994; Felker and Benker, 1995; Choppin, 1999; Musikas, 1999). This class of extractants can extract all the actinides from acid solutions, with separation of uranium, plutonium, and trivalent cations, by using selective stripping solutions. The separation results in a product with both the trivalent lanthanides and the actinides in the same solution, which requires further processing to isolate a pure curium stream.

French researchers have done extensive work on diamides for the extraction of trivalent actinides and lanthanides from plutonium and uranium recovery by extraction (Purex) waste solutions (Musikas, 1999). These bifunctional ligands are stronger extractants than monofunctional ligands and can be destroyed thermally without leaving a solid residue (phosphorus-containing ligands leave a solid residue when incinerated). They have also investigated nitrogen donor ligands for separation of actinides from lanthanides. The neutral tridentate ligand 2,4,6-tris-(2-pyridyl)-1,3,5-triazine has promise, but requires an additive to increase nitrate ion solubility in the organic phase (Musikas, 1999).

The largest separation factors for actinides and lanthanides have been shown with ligands containing sulfur, a ‘soft’ donor that forms stronger covalent bonds with the actinides than with lanthanides (Jarvinen, 1999; Musikas, 1999). Thio derivatives of acylpyrazolones containing both nitrogen and sulfur donor atoms are good extractants, but give best separation when combined with TBP or a phosphine oxide (Jarvinen, 1999). Dithiophosphoric or phosphinic acids have shown the highest separation factors for actinides and lanthanides (Jarvinen, 1999; Musikas, 1999).

Separation of actinides has also been done with salt mixtures and polyethylene glycol (Myasoedov and Kremliakova, 1985; Myasoedov, 1994). Cm(III) has been extracted from sulfate, carbonate, phosphate, and nitrate solutions. Extraction requires addition of complexants to the salt solutions, with arsenazo-III and xylenol orange being the most effective solution (Molochnikova *et al.*, 1992). Potassium phosphotungstate in salt solution aids in the separation of neptunium from trivalent actinides (Myasoedov, 1994).

Recovery of curium from carbonate and hydroxide solutions has been demonstrated with quaternary ammonium bases, primary amines, alkylpyrocatechols, β-diketones, and *N*-alkyl derivatives of amino-alcohols or phenols (Myasoedov and Kremliakova, 1985; Bukina *et al.*, 1988; Karalova *et al.*, 1988; Novikov *et al.*, 1988; Myasoedov, 1994). This method requires the addition of a complexant to the aqueous phase to maintain the solubility of the actinides in the solutions. The strength of the complexant must differ depending on the mechanism for extraction. Some extractants form ion pairs in the organic phase, while others extract the complexes. In the case of alkylpyrocatechols, the kinetics of extraction of lanthanides and actinides are significantly different, allowing group separation (Novikov *et al.*, 1988).

Am(iii) and Cm(iii) have also been separated using supported liquid membranes with 1 m HDEHP in hexane (Novikov and Myasoedov, 1987). The separation factor between Am and Cm was increased from 1.1 for simple extraction to 5.0 with the membrane in which potassium phosphotungstate is added to one solution to increase the chemical potential of the membrane and speed the kinetics of the process (Novikov and Myasoedov, 1987).

9.5.2 Ion exchange

Ion exchange in almost all forms has been used for curium separation from americium and the lanthanides. Organic cation and anion resins, chelating resins, chromatographic columns, and inorganic sorbents have been used (Ryan, 1975; Myasoedov and Kremliakova, 1985; Bokelund *et al.*, 1989; Choppin, 1999).

A review in 1975 summarizes the work on ion exchange, with sections on cation, anion, and chelating resins as well as inorganic sorbents (Ryan, 1975). The trivalent actinides and lanthanides are strongly adsorbed from low concentrations of common monovalent acid solutions. Separation of lanthanides from actinides is accomplished by elution with a variety of organic complexants, such as α-hydroxyisobutyric acid, ethylenediaminetetracetic acid (EDTA), or DTPA. Such complexants can also be used to separate trivalent actinides from each other (Lebedev *et al.*, 1974; Ryan, 1975; Myasoedov and Kremliakova, 1985; Bokelund *et al.*, 1989). Extraction chromatography with Zn^{2+} and DTPA was used for separation of kilograms of curium from americium (Haug, 1974). Thiocyanate solutions are also useful in accomplishing similar separations.

Anion-exchange resins have been used with HCl, LiCl, and HNO_3 in both aqueous and aqueous–alcohol mixtures (Ryan, 1975; Myasoedov and Kremliakova, 1985; Bokelund *et al.*, 1989; Choppin, 1999). Solutions of LiCl have been used extensively (Ryan, 1975; Choppin, 1999). A time-resolved laser-induced fluorescence spectroscopic study of a $LiCl/H_2O/CH_3OH$ anion-exchange system suggested the primary Cm species in the solution phase (at 14 m LiCl) is $CmCl_4^-$, but the number of coordinated chloride ions is greater than 4 for the species sorbed to the anion-exchange resin (Arisaka *et al.*, 2002). Thiocyanate solutions have also been used for separation (Myasoedov and Kremliakova, 1985). Solvents that are a mixture of alcohols and acids have been widely used for curium separations (Ryan, 1975).

A variety of zirconium-based inorganic sorbents have been used for separation of Am(iii) and Cm(iii), either using solutions similar to those employed with organic cation-exchange resins, or by oxidizing Am(iii) to Am(v), which does not adsorb (Moore, 1971; Ryan, 1975).

Extraction chromatography with CMPO on an organic support allows ready separation of an americium and curium fraction (Cunningham and Wallmann, 1964; Fuger and Oetting, 1976; Oetting *et al.*, 1976). A commercially available resin based on CMPO has been used in studies (Kaye *et al.*, 1995; Maxwell, 1996).

Different chelate groups have been tried to increase selectivity of resins for curium (Ryan, 1975; Myasoedov and Kremliakova, 1985). A column containing the tertiary amine base, Aliquat-336, was used in combination with a column of HDEHP to obtain 6 g of pure ^{244}Cm (Bokelund *et al.*, 1989). Curium was first loaded onto the Aliquat column from $LiNO_3$, eluted, loaded onto the HDEHP column, and finally eluted with 1 M lactic acid containing DTPA. Other ion-exchange methods are described in Section 9.9.2.

9.5.3 Precipitation

Precipitation has been used for the separation of Cm(III) from americium in its higher valence states of V and VI. Separation at Savannah River was achieved by adjusting the solution to an Am(Cm) concentration of 10 g L^{-1} and 3.5 M K_2CO_3, oxidizing the Am(III) to Am(V) with hypochlorite, peroxydisulfate, or ozone, and precipitating the double carbonate $K_5AmO_2(CO_3)_3$ at 85°C (Groh *et al.*, 1965). Am(III) has also been oxidized to Am(V) electrochemically (Myasoedov and Kremliakova, 1985). A second precipitation is sometimes used to remove residual Am from the Cm solution. This process is based on the original work of Stephanou and Penneman (1952). After precipitation of Am(V) as the complex carbonate, Cm(III) can be precipitated with oxalate, hydroxide, or fluoride. It is noteworthy that the choice of cation is critical; if sodium is used in place of potassium, oxidation of americium proceeds past Am(V) to form the magenta-colored Am(VI) carbonate complex, which is soluble. Based on this observation, and utilizing the insolubility of $Cm(OH)_3$ in $NaHCO_3$, the americium content in the $Cm(OH)_3$ precipitate can be reduced to low levels (Coleman *et al.*, 1963).

9.6 THE METALLIC STATE

9.6.1 Physical properties

Curium is a lustrous, malleable, silvery metal with many properties comparable to those of the lighter actinide elements. The melting point of Cm (dhcp form) is 1345 ± 50°C (Fuger and Oetting, 1976; Oetting *et al.*, 1976), much higher than for the immediately preceding actinide elements, Np–Am (639–1173°C), but very similar to that of gadolinium (1312°C), its lanthanide analog (Cunningham and Wallmann, 1964; Reichlin *et al.*, 1981).

Curium metal exists in two modifications, a double hexagonal close-packed (dhcp) structure (α-lanthanum type) and a high-temperature cubic close-packed (fcc) structure. Using ^{244}Cm, the dhcp form was found to have lattice constants $a = 3.496(3)$ and $c = 11.331(5)$ Å, giving a calculated density of 13.5 g cm^{-3} and a metallic radius of 1.74 Å (Stevenson and Peterson, 1979; Reichlin *et al.*, 1981). Baybarz and Adair (1972) and Baybarz *et al.* (1976) reported the high-temperature fcc phase with $a = 5.039(2)$ Å, prepared by metal volatilization at 1650°C.

Using ^{248}Cm, Stevenson and Peterson (1979) also obtained this phase with $a = 5.065$ Å. Other preparations of Cm metal using ^{248}Cm have been reported. They exhibit the dhcp structure with $a = 3.500 \pm 0.003$ Å and $c = 11.34 \pm 0.01$ Å, and with $a = 3.490 \pm 0.006$ Å and $c = 11.308 \pm 0.018$ Å (Reichlin *et al.*, 1981). Other X-ray diffraction studies of ^{248}Cm metal have yielded evidence for an orthorhombic form as well as delocalization and compressibility data (Benedict *et al.*, 1985; Haire *et al.*, 1985).

The entropy of vaporization for Cm metal is similar to that of gadolinium; its vapor pressure is about double that of gadolinium over the measured range. The vapor pressure of triply distilled ^{244}Cm metal has been measured between 1300 and 2000 K and obeys the following relations (Ward *et al.*, 1975):

$$\log_{10}(p/(\text{atm})) = (6.082 \pm 0.129) - (19\,618 \pm 193)/T(\text{K}) \quad (\text{solid}, 1327\text{–}1639\ \text{K})$$

$$\log_{10}(p/(\text{atm})) = (5.586 \pm 0.157) - (18\,894 \pm 275)/T(\text{K}) \quad (\text{liquid}, 1640-1972\ \text{K})$$

From the latter equation the calculated boiling point of Cm is 3110°C. The derived heat of fusion, entropy of fusion, and average second-law entropy are 13.85 kJ mol^{-1}, 9.16 J K^{-1} mol^{-1}, and 106.7 ± 3.0 J K^{-1} mol^{-1}, respectively. Determination of low-temperature condensed-phase thermodynamic parameters awaits the availability of long-lived isotopes. For excellent discussions of thermodynamic, electronic, and magnetic effects in curium and other actinide and lanthanide metals, the reader is referred to articles by Ward and Hill (1975) and Ward *et al.* (1980). Konings (2001b) has reevaluated the thermodynamic data for curium metal in the solid, liquid, and gaseous states and has reported a set of recommended values that are similar to values by Ward *et al.* (1980).

Metallic curium obeys a Curie–Weiss magnetic susceptibility relationship between 100 and 550 K with a magnetic moment of 8.07 μ_B (Kanellakopulos *et al.*, 1976; Nave *et al.*, 1981; Reichlin *et al.*, 1981), comparable to earlier values of 7.85–8.15 μ_B (Marei and Cunningham, 1972), although a lower value of 6.0 μ_B was reported recently (Fujita *et al.*, 1976). However, the form of the metal was not identified by X-ray diffraction in the latter case. Schenkel (1977) performed electrical resistance measurements on ^{244}Cm metal, and showed that curium is the first reported magnetically ordered actinide metal, with a Néel temperature of 52.5 K. A neutron diffraction study of the dhcp (α-La) form indicated no structural change down to 5 K and also showed antiferromagnetic ordering below 52 K (Fournier *et al.*, 1977). A careful susceptibility study with ^{248}Cm metal confirmed an antiferromagnetic transition at about 65 K, but the fcc phase reveals a ferrimagnetic transition near 200 K (Eubanks and Thompson, 1969).

9.6.2 Preparation of curium metal

Curium metal can be prepared from CmF_3 by reduction with barium or lithium metal. Dry, oxygen-free CmF_3 is required and the temperatures used (>1600 K) are well above the melting point of the metal. One to ten micrograms of

Cm metal was made using tungsten coils and tantalum crucibles (tantalum is reported to dissolve slightly in Cm) (Cunningham and Wallmann, 1964; Stevenson and Peterson, 1979; Reichlin *et al.*, 1981). Gram quantities of the metal have been prepared in 75–90% yield by reduction with a magnesium–zinc alloy of CmO_2 suspended in a $MgF_2/MgCl_2$ melt (Eubanks and Thompson, 1969). When CmO_2 or Cm_2O_3 and pure hydrogen are heated to temperatures between 1200 and 1500°C in the presence of Pt, Ir, or Rh, alloy phases result with compositions of Pt_5Cm, Pt_2Cm, Ir_2Cm, Pd_3Cm, and Rh_3Cm (Erdmann and Keller, 1971, 1973). Similar alloys with Ni (Radchenko *et al.*, 1995), Al (Radchenko *et al.*, 1996), and Si (Radchenko *et al.*, 1998) have also been reported. Reports on CmPd alloys showed formation of a solid solution of Cm in Pd, with the fcc lattice parameter increasing linearly with at.% Cm (Radchenko *et al.*, 1985, 1989). The Cm–Pu phase diagram has been reported, which indicates that α-Cm (dhcp) predominates at lower wt% Pu and temperature, with β-Cm (fcc) forming as the Pu concentration and temperature increase, ultimately leading to γ-Cm (space group $Im3m$) (Okamoto, 2000). Pure curium metal has been prepared by decomposition of these intermetallic compounds (Müller *et al.*, 1972, 1977). The dhcp form of curium has also been prepared by reducing the dioxide or sesquioxide with thorium metal, followed by volatilization and condensation of the curium metal vapor on a tantalum condenser (Baybarz and Adair, 1972; Damian *et al.*, 1975; Baybarz *et al.*, 1976).

9.6.3 Chemical properties of the metallic state

Metallic curium appears to be even more susceptible to corrosion than the earlier actinide elements, a property due at least in part to radioactive self-heating. The metal dissolves rapidly in dilute acid solutions. The metal surface rapidly oxidizes in air to form a film that may begin as CmO (Cunningham and Wallmann, 1964; Burney, 1980; Reichlin *et al.*, 1981), progresses to Cm_2O_3 at room temperature, and further to CmO_2 at elevated temperatures. The metal is pyrophoric when finely divided.

The direct reactions of curium metal with non-metals such as Bi, P, As, Sb, S, and Se have been reported, and binary compounds with N, P, As, and Sb have been prepared by reactions using curium hydride (see Sections 9.7.5 and 9.7.6) (Charvillat *et al.*, 1975, 1976; Gibson and Haire, 1987; Zhu and Jiao, 1994).

9.7 CLASSES OF COMPOUNDS

9.7.1 General

Because curium is available in macro quantities, a number of Cm compounds have been synthesized and structurally characterized. Table 9.3 lists crystallographic data for Cm metal, alloys, and compounds.

Table 9.3 *Crystallographic data for curium metal, alloys, and compounds.*

				Lattice constants		
	References	*Lattice type*	*Crystal system-space group*	a_0 (Å)	b_0 (Å)	c_0 (Å)
Metal						
α-Cm	Cunningham and Wallmann (1964 Müller *et al.* (1972, 1977)	α-La	hexagonal-$P6_3/mmc$	3.496		11.331
β-Cm	Baybarz and Adair (1972); Baybarz *et al.* (1976)		fcc	5.039		
Alloys						
Pd_3Cm	Erdmann and Keller (1973); Radchenko *et al.* (1985)	Cu_3Au	cubic-$Pm3m$	4.147		
Rh_3Cm	Erdmann and Keller (1973); Radchenko *et al.* (1985)	Cu_3Au	cubic-$Pm3m$	4.106		
Ir_2Cm	Erdmann and Keller (1973); Radchenko *et al.* (1985)	Cu_2Mg	cubic-$Fd3m$	7.561		
Pt_5Cm	Erdmann and Keller (1973); Radchenko *et al.* (1985)	Pt_5Sm	orthorhombic	5.329	9.108	26.38
Pt_2Cm	Erdmann and Keller (1973); Radchenko *et al.* (1985)	Cu_2Mg	cubic-$Fd3m$	7.625		
Ni_5Cm	Radchenko *et al.* (1995)	Cu_5Ca	hexagonal	4.871		4.018
$Ni_{15}Cm_2$	Radchenko *et al.* (1995)	$Ni_{17}Th_2$	hexagonal	8.348		8.071
Al_2Cm	Radchenko *et al.* (1996)	Cu_2Mg	cubic	7.878		
CmSi	Radchenko *et al.* (1998)		orthorhombic	8.288	3.912	5.966
Cm_2Si_3	Radchenko *et al.* (1998)		hexagonal	3.879		4.147
$CmSi_2$	Radchenko *et al.* (1998)		tetragonal	3.977		13.719
$CmSi_{1.88}$	Radchenko *et al.* (1998)		tetragonal	4.029		13.715
Oxides and chalcogenides						
α-Cm_2O_3	Noé *et al.* (1970)	α-La_2O_3	hexagonal- $P\bar{3}m1$	3.7952		5.985
β-Cm_2O_3	Noé *et al.* (1970); Morss *et al.* (1983)	β-La_2O_3	monoclinic	14.282	3.641 $\beta = 100.29$	8.883

Table 9.3 (*Contd.*)

	References	*Lattice type*	*Crystal system-space group*	*Lattice constants*		
				a_0 (Å)	b_0 (Å)	c_0 (Å)
γ-Cm_2O_3	Noé *et al.* (1970)	γ-Mn_2O_3	cubic-*Ia*3	11.002		
CmO_2	Wallmann (1964); Noé and Fuger (1971); Peterson and Fuger (1971); Mosley (1972)	fluorite	cubic-*Pm*3*m*	5.3584		
CmO	Cunningham and Wallmann (1964)		cubic-*Fm*3*m*	5.09		
CmS	Damien *et al.* (1979a,b)		fcc	5.5754		
CmSe	Damien *et al.* (1979a,b)		fcc	5.791		
CmTe	Damien *et al.* (1979a,b)		fcc	6.150		
Cm_2S_3	Damien *et al.* (1975)	Th_3P_4	bcc	8.452		
$CmS_{1.98}$	Damien *et al.* (1975)	Fe_2As	tetragonal	3.926		8.01
Cm_2Se_3	Damien *et al.* (1975)	Th_3P_4	bcc	8.788		
$CmSe_{1.98}$	Damien *et al.* (1975)	Fe_2As	tetragonal	4.096		8.396
$CmTe_3$	Damien *et al.* (1976)	$NdTe_3$	orthorhombic (pseudotetragonal)	4.34		25.7
$CmTe_2$	Damien *et al.* (1976)	Fe_2As	tetragonal	4.328		8.93
Cm_2Te_3	Damien *et al.* (1976)	η-U_2S_3	orthorhombic	11.94	12.13	4.330
Cm_2O_2S	Haire and Fahey (1977)	Pu_2O_2S	hexagonal	3.889		6.736
Cm_2O_2Te	Damien *et al.* (1976)	La_2O_2Te	tetragonal	3.98		12.58
$Cm_2O_2SO_4$	Haire and Fahey (1977)	$Nd_2O_2SO_4$	orthorhombic	4.209	4.087	13.270
$BaCmO_3$	Haire and Fahey (1977)	perovskite				
$CmAlO_3$	Haire and Fahey (1977)	perovskite				

Pnictides						
CmN	Charvillat *et al.* (1976)	NaCl	fcc	5.041		
CmP	Damien *et al.* (1979a,b)	NaCl	fcc	5.743		
CmAs	Damien *et al.* (1979a,b)	NaCl	fcc	5.887		
CmSb	Damien *et al.* (1979a,b)	NaCl	fcc	6.242		
Cm_2O_2Sb	Charvillat and Zachariasen (1977)	La_2O_2Te	tetragonal–14/*mmm*	3.920		13.41
Cm_2O_2Bi	Charvillat and Zachariasen (1977)	La_2O_2Te	tetragonal–14/*mmm*	3.957		13.359
Halides						
CmF_3	Stevenson (1973); Asprey *et al.* (1965)	LaF_3	trigonal- $P\overline{3}\,Cl$	7.019		7.198
$CmCl_3$	Asprey *et al.* (1965); Peterson and Burns (1973)	UCl_3	hexagonal-$P6_3/m$	7.3743		4.1850
$CmBr_3$	Asprey *et al.* (1965); Burns *et al.* (1975)	$PuBr_3$	orthorhombic-*Cmcm*	4.041	12.709	9.135
CmI_3	Asprey *et al.* (1965)	BiI_3	hexagonal-$R\overline{3}$	7.44		20.4
CmF_4	Asprey and Haire (1973); Haug and Baybarz, (1975)	UF_4	monoclinic-$C2/c$	12.500 $\beta = 126.10$	10.488	8.183
$LiCmF_5$	Keenan (1966a)	$LiUF_5$	tetragonal-$I14_1/a$	14.579		6.437
$K_7Cm_6F_{31}$	Keenan (1966b)	$Na_7Zr_6F_{31}$	hexagonal-$R\overline{3}$	14.41		9.661
$Na_7Cm_6F_{31}$	Keenan (1967a)	$Na_7Zr_6F_{31}$	hexagonal-$R\overline{3}$	14.89		10.254
Rb_2CmF_6	Keenan (1967b)	Rb_2UF_6	orthorhombic-*Cmcm*	6.931		7.56
CmOCl	Peterson (1972)	PbClF	hexagonal	3.98		6.75
Hydrides						
CmH_{2+x}	Gibson and Haire (1985)	fluorite	fcc	5.322		
$CmH_{3-\delta}$	Gibson and Haire (1985)	PuH_3	trigonal-$P\overline{3}\,ClCl$	3.769		6.732

The most important chemical characteristic that distinguishes curium from the lighter actinides is the great stability of the 3+ state with respect to oxidation or reduction. The stability of Cm(III) has been attributed to the relative stability of a half-filled ($5f^7$) configuration, and causes a chemical resemblance to lanthanides. All known Cm(IV) compounds are either fluorides or oxides.

In contrast to americium, the oxidation of Cm(III) to Cm(IV) is achieved only with the strongest oxidizing agents, and only two reports claim evidence for an oxidation state greater than IV (Peretrukhin *et al.*, 1978; Fargeas *et al.*, 1986). Transient divalent and tetravalent states have been observed in aqueous perchlorate media using pulse radiolysis techniques (Sullivan *et al.*, 1976). Attempts have been made to induce Cm(III)–Cm(IV) oxidation chemically (using ozone (Pages and Demichelis, 1966) and perxenate (Holcomb, 1967)) or electrochemically (Myasoedov *et al.*, 1973). These attempts have failed, an effect clearly not attributable solely to radiolytic reduction.

However, formation of a red Cm(IV) complex in phosphotungstate solution was achieved by the use of peroxydisulfate as the oxidant (Saprykin *et al.*, 1976). Kosyakov *et al.* (1977) demonstrated that, in such solutions, the Cm(IV) is reduced much more rapidly than can be accounted for by radiolytic effects, while Am(IV) in such solutions is much more stable, being reduced at a rate attributable to radiolytic effects alone. This behavior stands in contrast to the reduction of Cm(IV) in 15 M CsF, which does proceed at the slower radiolytic rate (Keenan, 1961). No value for the $E°$(Cm(IV)/Cm(III)) is known, but, from existing data, it is substantially more positive than $E°(Am^{4+}/Am^{3+})$ and probably about as positive as $E°(Pr^{4+}/Pr^{3+})$.

With the more common isotopes ^{242}Cm and ^{244}Cm, intense alpha self-irradiation and heating effects cause aqueous-solution instability (peroxide is always present) and solid-state instability (lattice changes and compound alteration). In some cases, these effects are sufficiently large that certain compounds may be identified in bulk only with the more stable isotopes, e.g. $^{244}CmF_4$ and $^{248}Cm(n\text{-}C_5H_5)_3$ (Asprey and Keenan, 1958; Laubereau and Burns, 1970b).

9.7.2 Hydrides

The hydrides of Cm are relatively little explored. The first Cm hydride was prepared by Bansal and Damien (1970) by reacting ^{244}Cm metal with hydrogen at 200–250°C. Based on its X-ray diffraction pattern, this hydride was characterized as the face-centered cubic (fcc) CmH_{2+x}, by analogy to NpH_{2+x}, PuH_{2+x}, and AmH_{2+x}. The existence of the dihydride was confirmed by Gibson and Haire (1985), who prepared the dihydride from ^{248}Cm metal. In the latter work, the hexagonal $CmH_{3-\delta}$ was also prepared. The trihydride was characterized from its x-ray diffraction pattern by analogy to those of known lanthanide and actinide trihydrides.

The dissociation enthalpy for CmH_2 has been reported to be 187 ± 14 kJ mol^{-1}, consistent with the trend in stability of the actinide dihydrides becoming more like that of the lanthanide dihydrides with increasing atomic number (Gibson and Haire, 1990). The order of stability of f-element dihydrides can be summarized as follows:

$$\text{Ln(most stable)} > \text{Cm} > \text{Am} > \text{Pu}$$

9.7.3 Halides

The halides represent by far the most extensively characterized class of curium compounds (see Table 9.3). The complete CmX_3 series (X = F, Cl, Br, I), as well as CmF_4 and several complex Cm(IV) fluorides, have been prepared and studied. Several reviews deal specifically with actinide halides; for further information (especially for cross-comparisons of Cm with other actinide halides) the reader is referred to these articles (Katz and Sheft, 1960; Bagnall, 1967; Brown, 1968; Penneman *et al.*, 1973).

Curium trifluoride is a white, sparingly soluble (~10 mg L^{-1}) compound (Cunningham, 1966) with the LaF_3 structure, which precipitates when fluoride ion is added to weakly acidic Cm(III) solutions, or HF to $Cm(OH)_3$. The anhydrous trifluoride is obtained by desiccation over P_2O_5 or by treatment with hot HF(g). The trifluoride melts at 1406 ± 20°C; its standard enthalpy and entropy of formation have been estimated to be 1660 kJ mol^{-1} (Ionova *et al.*, 1997) and 121 J K^{-1} mol^{-1} (Burnett, 1966; Cunningham, 1966) at 298 K, respectively. Curium has an irregular tricapped trigonal prismatic coordination in CmF_3 (Penneman *et al.*, 1973).

Curium trichloride is a white compound that can be obtained by treating curium oxides or CmOCl with anhydrous hydrogen chloride at 400–600°C (Wallmann *et al.*, 1967). The hydrate has been reported to be light green. A single-crystal study showed that $CmCl_3$ has the hexagonal UCl_3-type structure common among the actinide trichlorides. Based on the lattice constants for $CmCl_3$ (Table 9.3), a radius of 0.971 Å has been calculated for Cm(III) (Peterson and Burns, 1973). Curium has nine chloride neighbors in the form of a tricapped trigonal prism, with Cm–Cl lengths of 2.859 and 2.914 Å. A melting point of 695°C (Peterson and Burns, 1973) and an enthalpy of formation (298 K) of −974 ± 4 kJ mol^{-1} (Fuger *et al.*, 1975; Oetting *et al.*, 1976) have been reported. The entropy of formation of $CmCl_3$ at 298 K has been estimated to be 163 ± 6 J K^{-1} mol^{-1} (Konings, 2001a).

Curium tribromide has been prepared by heating the trichloride with NH_4Br at 400–450°C in a hydrogen atmosphere (Asprey *et al.*, 1965) and also by hydrogen bromide treatment of the calcined oxide at 600°C (Burns *et al.*, 1975). The compound melts at 625°C and has the $PuBr_3$ (orthorhombic) structure (Burns *et al.*, 1975). The metal ion is surrounded by eight bromide ions, two at 2.865 Å, four at 2.983 Å, and two at 3.137 Å. An analogous procedure ($CmCl_3+NH_4I$) has been used to prepare CmI_3, a colorless material having the BiI_3 structure (Asprey *et al.*, 1965). Preparation from elemental curium and iodine has also been reported (Seaborg *et al.*, 1949). The standard enthalpies of formation of $CmBr_3$ and CmI_3 are estimated to be 794 and 564kJ mol^{-1}, respectively, at 298 K (Ionova *et al.*, 1997).

The halides of tetravalent curium include the simple fluoride CmF_4 (Keenan and Asprey, 1969; Asprey and Haire, 1973; Haug and Baybarz, 1975), and a series of complex fluorides of the type $M_7Cm_6F_{31}$ (Keenan, 1966b, 1967a), M_2CmF_6 (Keenan, 1967b), and $MCmF_5$ (Keenan, 1966a), where M is an alkali metal. As with terbium, the only reported method for preparing the tetrafluoride is by fluorine oxidation of the trifluoride. CmF_4 is a brownish-tan solid with a monoclinic ZrF_4-type structure, in which curium has an antiprismatic eight coordination (Asprey and Haire, 1973; Penneman *et al.*, 1973; Haug and Baybarz, 1975). Magnetic susceptibility measurements suggest a fluoride-deficient structure, CmF_{4-x} (Haire *et al.*, 1982; Nave *et al.*, 1983).

Evidence for the existence of CmF_6 and $CmOF_3$ (as well as $NpOF_3$, NpF_7, PuO_3F, AmF_5, AmF_6, and EsF_4) has been reported using thermochromatographic techniques (Fargeas *et al.*, 1986). These fluorides were claimed to form in low yield when a deposit of Cm (chemical form not reported) on Ni metal was treated with a mixture of BF_3 and F_2 at 800°C. However, there has been no independent confirmation of these species.

A prominent series of isostructural complex actinide(IV) fluorides, $M_7An_6F_{31}$, with the $Na_7Zr_6F_{31}$ structure have been prepared (Keenan, 1966b, 1967a). With curium, the Na and K salts are known. The compounds were prepared by direct fluorination of evaporated salt mixtures of MX and CmX_3 at about 300°C. This 7:6 type of compound predominates with the larger alkali cations. The basic coordination polyhedron is a square antiprism (Penneman *et al.*, 1973). In tetragonal $LiCmF_5$, the curium coordination is tricapped trigonal prismatic (Penneman *et al.*, 1973). The compound Rb_2CmF_6 is orthorhombic with the Rb_2UF_6 structure, which consists of chains of fluoride dodecahedra (Penneman *et al.*, 1973). The oxychloride CmOCl has been synthesized by treatment of $CmCl_3$ (or Cm_2O_3) at 500–600°C, with the vapor in equilibrium with a 10 M HCl solution (Peterson, 1972):

$$CmCl_3 + H_2O \leftrightarrow CmOCl + 2HCl$$

From the equilibrium and known heats of formation, ΔH°_{f298} for CmOCl was calculated (Weigel *et al.*, 1977, Table 17.4). Marei and Cunningham (1972) found that the magnetic susceptibility of CmOCl follows the Curie–Weiss law over the temperature range 77–298 K, with $\mu_{eff} \sim 7.58\ \mu_B$ and a Curie temperature of approximately 22 K. The structure of CmOCl is of the PbClF-type (hexagonal), with each metal surrounded by four oxides and five chlorides (Peterson, 1972).

9.7.4 Oxides

Konings (2001a,b) has recently reviewed the thermochemical and thermophysical properties of Cm oxides. Crystallographic data for the various oxides are compiled in Table 9.3.

The white to faint tan sesquioxide Cm_2O_3 (m.p. 2270 ± 25°C) (Konings, 2001b) was prepared by thermal decomposition of $^{244}CmO_2$ at 600°C and 10^{-4} torr pressure (Asprey *et al.*, 1955). This material has the Mn_2O_3-type cubic-C lattice, which gradually changes at room temperature to a hexagonal A-form because of self-irradiation effects (Wallmann, 1964; Noé *et al.*, 1970). Haug (1967) prepared monoclinic B-type Cm_2O_3 by reduction of $^{244}CmO_2$ with hydrogen. This study showed that the cubic form described by Asprey *et al.* (1955) predominates at reaction temperatures below 800°C, changing to the monoclinic B-form at higher temperatures (Haug, 1967). These three crystal modifications correspond to the three types observed for lanthanide sesquioxides. Structural data, enthalpy of formation, and magnetic susceptibility were obtained by Morss *et al.* (1983) with B-form $^{248}Cm_2O_3$. The enthalpy of formation at 25°C has been estimated as –1684 ± 14 kJ mol^{-1} for the monoclinic Cm_2O_3 (Konings, 2001b), with the corresponding entropy of formation estimated to be 167 ± 5 J K^{-1} mol^{-1} (Konings, 2001a).

Preparation of the black curium dioxide by ignition in air was first claimed by Asprey *et al.* (1955). The product had a cubic (fcc) structure. The compound is also formed by thermal decomposition of ^{244}Cm(III)-loaded resin (Hale and Mosley, 1973) and by heating $^{244}Cm_2O_3$ to 650°C in 1 atm of oxygen, followed by cooling in oxygen (Noé and Fuger, 1971; Peterson and Fuger, 1971). Others have shown that the dioxide is the stable oxide form in an oxygen atmosphere at temperatures below 400°C (Chikalla and Eyring, 1969). At temperatures between 380 and 420°C, CmO_2 is reduced to $CmO_{1.95}$; above 430°C, rapid decomposition occurs via various intermediate oxides to Cm_2O_3 (Mosley, 1972). The enthalpy of formation at 25°C has been estimated as −912 ± 7 kJ mol^{-1} for CmO_2 (Konings, 2001b).

Curium oxalate, $Cm_2(C_2O_4)_3$, is routinely used for calcination to CmO_2. For example, oxalate precipitation has been used to process kilograms of ^{244}Cm, with subsequent metathesis with 0.5 M hydroxide to $Cm(OH)_3$ (Scherer and Fochler, 1968; Bibler, 1972).

Morss *et al.* (1989) reported a neutron diffraction and magnetic susceptibility study of CmO_2 prepared by calcination of Cm(III) oxalate at 775°C in flowing O_2, followed by annealing for 4 days at 350°C in flowing O_2. Based on the lattice parameter (a_0 = 5.359 ± 0.002 Å), the stoichiometry of this material was reported to be $CmO_{1.99 \pm 0.01}$, indicating that the material essentially contained only Cm(IV). Nevertheless, the effective paramagnetic moment was found to be $(3.36 \pm 0.06)\mu_B$, a value which had previously been attributed to the presence of Cm(III). Based on these data, it has been suggested that the electronic ground states in actinide dioxides may need to be reexamined.

The curium–oxygen phase diagram studies show a great similarity to analogous Pu, Pr, and Tb systems, and indicate the possible existence of two additional Cm_2O_3 phases which have not yet been isolated (Eyring, 1967; Stevenson and Peterson, 1975). Two intermediate oxides, $CmO_{1.72}$ and $CmO_{1.82}$, and two other non-stoichiometric phases close to the composition of CmO_2 and $CmO_{1.5}$, have also been detected (Chikalla and Eyring, 1969). A cubic (fcc) phase, CmO, was reported in an early preparation of the metal (Cunningham and Wallmann, 1964).

The ternary oxides $BaCmO_3$ (Fuger *et al.*, 1993) and Cm_2CuO_4 (Soderholm *et al.*, 1999) have recently been reported. The latter is of interest by its analogy to M_2CuO_4 (M= La, Pr–Eu), which are parent compounds for high-temperature superconductors. When doped with Th^{4+}, the M_2CuO_4 (M = Pr–Eu) materials become superconducting, with T_c of ~32 K. Although Cm_2CuO_4 is isostructural with the M_2CuO_4 (M = Pr–Gd) series, its Th-doped analog is not superconducting. This effect may be due to its high magnetic ordering temperature relative to other M_2CuO_4.

Hale and Mosley (1973) have reported the preparation of curium oxysulfate, $^{244}Cm_2O_2SO_4$, by heating Cm(III)-loaded resin (sulfonate form) in a stream of oxygen at 900°C. The thermogravimetric analysis indicated that heating to 1175°C under otherwise similar conditions yielded Cm_2O_3, which on cooling formed CmO_2. Haire and Fahey (1977) have prepared $Cm_2O_2SO_4$ by calcination of the hydrated sulfate in air at about 750°C. The brown $Cm_2O_2SO_4$ has a body-centered orthorhombic structure, similar to $Nd_2O_2SO_4$ and $Cf_2O_2SO_4$. The computed Cm(III) radius in $Cm_2O_2SO_4$, 0.980 Å, agrees with the value of 0.979 Å derived from Cm_2O_3. The oxysulfide Cm_2O_2S is formed when the sulfate is heated to about 800°C in H_2/Ar (Haire and Fahey, 1977). Cell constants for Cm_2O_2Sb and Cm_2O_2Bi have been reported (Charvillat and Zachariasen, 1977).

9.7.5 Chalcogenides

Damien *et al.* (1975) prepared $^{244}CmS_2$ and $^{244}CmSe_2$ by slow reaction of excess sulfur or selenium vapor with curium hydride in vacuum. The resulting solids gave powder patterns indicating the tetragonal Fe_2As-type cell (isostructural with AmS_2 and $AmSe_2$) with lattice parameters (Table 9.3) showing the materials to be non-stoichiometric.

The sesquisulfide Cm_2S_3 forms a defect body-centered cubic (bcc) phase of the Th_3P_4-type (Damien *et al.*, 1975). The sesquiselenide was obtained by thermal dissociation of $CmSe_2$ at 620°C, again yielding a Th_3P_4-type phase (Damien *et al.*, 1975). Unlike gadolinium or plutonium, no other sesquiselenide forms were observed, even after thermal treatment at various temperatures.

The monochalcogenides were prepared by heating stoichiometric mixtures of chalcogen and curium metal at 700–750°C for 15 h, followed by heating at 1250–1500°C under high vacuum (Damien *et al.*, 1979a). The monochalcogenides have fcc structures. In these preparations, accessory phases, possibly γ-Cm_2S_3, Cm_2O_2S, γ-Cm_2Se_3, and Cm_2O_2Te, were detected.

The oxysulfide Cm_2O_2S was prepared by partial oxidation of CmS_2 at 700°C (Damien *et al.*, 1975; Haire and Fahey, 1977). This compound has a hexagonal structure and is isostructural with the Np, Pu, and Cf analogs (Haire and Fahey, 1977).

Damien *et al.* (1976) have reported the preparation of $CmTe_3$ by the reaction of the hydride with tellurium at 400°C. At temperatures above 400°C, the tritelluride decomposes to form the successive lower tellurides $CmTe_2$ and Cm_2Te_3. At 1100°C in a quartz tube, the oxytelluride Cm_2O_2Te is formed.

9.7.6 Pnictides

The syntheses of the pnictide compounds CmX, where X = N, P, As, and Sb, have been reported (Charvillat *et al.*, 1975, 1976; Kanellakopulos *et al.*, 1976; Damien *et al.*, 1979a,b; Stevenson and Peterson, 1979; Nave *et al.*, 1981). The compounds were obtained by heating curium hydride or metal with the respective pnictide element in a sealed tube to temperatures of 350–950°C. The N, P, As, and Sb compounds all have the NaCl structure (Charvillat *et al.*, 1975, 1976; Kanellakopulos *et al.*, 1976; Damien *et al.*, 1979a,b; Nave *et al.*, 1981). Damien *et al.* (1979a,b) prepared the monopnictides (N, P, As, Sb) by directly heating stoichiometric mixtures of the elements. CmN and CmAs are ferromagnetic, with T_c of 109 and 88 K, respectively (Kanellakopulos *et al.*, 1976; Nave *et al.*, 1981). The calculated effective magnetic moments are 7.02 and 6.58 μ_B, lower than expected for a pure $5f^7$ configuration, probably because of strong spin–orbit coupling and crystal field effects (Kanellakopulos *et al.*, 1976; Nave *et al.*, 1981).

The possibility of using mixed nitride fuels for transmutation of minor actinides has gained recent attention because it is anticipated that the actinide nitrides are mutually miscible. The miscibility of CmN and PuN has been confirmed by the carbothermic synthesis of (Cm,Pu)N (Takano *et al.*, 2001). This was achieved by heating graphite and $(Cm_{0.4}Pu_{0.6})O_{2-x}$ at 1773 K in N_2. The lattice parameter of the resulting mixed nitride was close to that expected from the known lattice parameters for CmN and PuN.

9.7.7 Miscellaneous compounds

The trihydroxide, $Cm(OH)_3$, has been prepared from aqueous solution and crystallized by aging in water (Haire *et al.*, 1977). The compound has the lanthanide trihydroxide (hexagonal) structure. Although there have been no reports of Cm carbide, the silicides CmSi, $CmSi_2$, Cm_2Si_3, and Cm_5Si_3 have been reported (Weigel and Marquardt, 1983; Radchenko *et al.*, 2000).

The oxalate $Cm_2(C_2O_4)_3 \cdot 10H_2O$ forms when aqueous Cm(III) and oxalic acid are mixed. The compound dehydrates in a stepwise fashion when heated *in vacuo*, yielding the anhydrous oxalate at 280°C, which then converts to a carbonate above 360°C (Scherer and Fochler, 1968). A differential thermal analysis (DTA) investigation of the hydrated Cm oxalate under helium revealed endothermic events centered at 145 and 400°C, corresponding to the release of water and the formation of $Cm_2O_2CO_3$, respectively. Above 500°C, the $Cm_2O_2CO_3$ converts to Cm_2O_3 (Vasil'ev *et al.*, 1989). The hydrated oxalate dissolves readily in aqueous alkali-metal carbonate solutions (Bibler, 1972; Burney and Porter, 1967). The compound has a solubility (~0.8 mg Cm per liter at 23°C) lower than that of the americium analog in 0.1 M $H_2C_2O_4$/0.2 M HNO_3. The solubility increases rapidly with temperature.

Curium nitrate can be isolated by evaporation of solutions formed by dissolving curium oxide in nitric acid. DTA analysis of the freshly prepared $^{244}Cm(NO_3)_3$ indicated the decomposition pathway is the same under an oxygen atmosphere as it is under helium (Vasil'ev *et al.*, 1990). The thermal decomposition is characterized by endothermic events centered at 90, 180, 400, and 450°C. By analogy to the thermal decomposition of lanthanide nitrates, the first two endotherms have been assigned to melting of the crystalline hydrated nitrate and its dehydration, respectively. The last two endotherms (which overlap) are associated with the decomposition of the anhydrous Cm nitrate. The final product of the thermal decomposition is CmO_2, indicating the Cm is oxidized to Cm(IV) during the decomposition process. The enthalpy of formation of the anhydrous crystalline $Cm(NO_3)_3$ was estimated to be -700 kJ mol^{-1} from the DTA data.

Complex sulfates of the type $MAn(SO_4)_2 \cdot xH_2O$, where M = alkali metal, have been precipitated from solutions of M_2SO_4 and the appropriate trivalent actinide ion in dilute HCl or H_2SO_4 (Dedov *et al.*, 1965). Structural characterization is lacking for these compounds.

A series of actinide phosphates having the formulation $AnPO_4 \cdot 0.5H_2O$ has been prepared (An = Pu, Am, Cm) (Weigel and Haug, 1965; Kazantsev *et al.*, 1982). These compounds form when aqueous Cm(III) solutions are mixed with Na_2HPO_4 or $(NH_4)_2HPO_4$. The structures of the $AnPO_4 \cdot 0.5H_2O$ compound are unknown. The hydrated phosphate of Cm(III) dehydrates at 300°C to $CmPO_4$, which has the monazite structure (Weigel and Haug, 1965; Kazantsev *et al.*, 1982).

The compound $Cm[Fe(CN)_6]$ forms as a dark red precipitate when $K_3[Fe(CN)_6]$ is added to a solution of Cm nitrate in 0.2 M HNO_3 (Kulyako *et al.*, 1993). This contrasts to the lanthanides (Eu, Ce, Pr) that do not form precipitates under identical conditions, but is similar to the behavior of Am.

The compounds $CmNbO_4$ and $CmTaO_4$ are isotypic with the corresponding lanthanide compounds and are obtained by heating the precipitated, mixed hydroxide/hydrous oxides at 1200°C (Keller and Walter, 1965).

Heating mixtures of curium oxide and alumina affords $CmAlO_3$, which gives either a rhombohedral or a cubic product depending upon the quenching conditions (Mosley, 1971). The rhombohedral phase transforms to the cubic phase at room temperature. $BaCmO_3$ has also been reported (Haire, 1980; Nave *et al.*, 1983). The addition of K_2CO_3 to Cm(III) solution precipitates $Cm_2(CO_3)_3$ (Dedov *et al.*, 1965). The compound is soluble in 40% K_2CO_3.

The salt $CsCm(HFAA)_4 \cdot H_2O$, where HFAA = hexafluoroacetylacetone, has been studied in detail (Nugent *et al.*, 1969). This compound, as well as the Eu, Gd, Tb, Nd, Am, Bk, Cf, and Es analogs, forms readily when HFAA is added to ethanol solutions of Cm(III) in the presence of cesium ion. Of the actinides studied for possible laser properties, only Cm displayed UV-excited, sharp-line sensitized luminescence (Nugent *et al.*, 1969). Cm(III) was found to be a highly efficient emitter (resembling Eu(III)) in the crystalline state, in ethanol solution, and doped into a $CsGd(HFAA)_4$ crystal matrix; hence laser emission should be demonstrable. Strong luminescence has been observed from ^{244}Cm (III) on an anion-exchange resin and in solution (Gutmacher *et al.*, 1964; Beitz and Hessler, 1980).

A number of adducts of the type $CmL_3 \cdot n$Q have been prepared, where L is a fluorinated β-diketonate and Q is TBP or trioctylphosphine oxide (Davydov, 1978). The volatility, thermal, and radiation stabilities were studied with consideration of such compounds for gas chromatographic separation of Am and Cm.

9.7.8 Organometallics

Despite substantial recent advances in the organometallic chemistry of other actinide elements, progress with curium has been slow. This lack of progress apparently results from the radiolytic properties of the element rather than an inherent chemical instability of the organometallic compounds. For more detailed discussion of actinide organometallic compounds, the reader is directed to Chapters 25 and 26.

The synthesis and spectroscopic characterization of milligram quantities of white, crystalline tris(η^5-cyclopentadienyl)curium, $Cm(C_5H_5)_3$, has been reported from the reaction of $^{248}CmCl_3$ with $Be(C_5H_5)_2$ (Baumgärtner *et al.*, 1970; Laubereau and Burns, 1970b). The compound can be sublimed in vacuum at 180°C and is isostructural with the Pr, Pm, Sm, Gd, Tb, Bk, and Cf analogs (Laubereau and Burns, 1970a,b). Mass spectrometric evidence for volatile $Cm(C_5H_5)_3$ using microgram amounts of ^{244}Cm was obtained (Baumgärtner *et al.*, 1970).

In terms of structural properties, volatility, thermal stability, and solubility, $Cm(C_5H_5)_3$ closely resembles other actinide and lanthanide tris(cyclopentadienide) compounds and hence the bonding must be similar. Nugent *et al.* (1971) studied the optical spectrum of $^{248}Cm(C_5H_5)_3$ and found weak bands, typical for Cm(III). These workers derived a value for the nephelauxetic parameter $d\beta$ of 0.050 ± 0.004, corresponding to very weak covalency in the organometallic bond. Thus, like the lanthanide analogs, the bonding in $Cm(C_5H_5)_3$ appears to have rather little covalent character. The ^{248}Cm compound fluoresces bright red under 360 nm irradiation (Nugent *et al.*, 1971).

Gas-phase reactions of Cm^+ and CmO^+ ions with small organic compounds have been investigated (Gibson and Haire, 1998, 1999). The gas-phase Cm ions used in these studies were generated by laser ablation of Cm_7O_{12} and the reaction products were characterized by mass spectroscopy. Using this methodology, a number of Cm organometallic fragments have been identified, including Cm_2^+, CmC_2H^+, $CmCN^+$, and a series of $CmC_xH_y^+$ species. The relative ability of Cm^+ to activate C–H bonds is less than that for U^+ or Tb^+ ions.

9.8 AQUEOUS CHEMISTRY

9.8.1 Inorganic

The aqueous solution chemistry of curium is almost exclusively that of Cm(III). Relatively little non-aqueous solution chemistry has been reported with curium other than that related to separations and environmental applications. Dilute Cm(III) solutions are normally colorless, but Cm(III) in concentrated HCl appears greenish. Curium-242 solutions with concentrations of about 1 g l^{-1} will boil unless cooled. The hydration number for the Cm(III) ion is estimated to be 9, based on fluorescence lifetimes (Kimura and Choppin, 1994; Kimura *et al.*, 1996). In HCl solution, the hydration number for the Cm(III) ion remains 9 up until 5 M HCl, then decreases with increasing HCl concentration (Kimura *et al.*, 1998). At 11 M HCl, the hydration number is 7. In contrast, the hydration number for Cm(III) drops steadily with increasing HNO_3 concentration from 0 to 13 M, with the hydration number being 5 at 13 M HNO_3. The differences between the HCl and HNO_3 systems are presumably simply due to the stronger binding affinity of the nitrate ion compared to chloride.

For dissolution of dhcp Cm metal in 1 M HCl, the value of ΔH is -615 ± 4 kJ mol^{-1} at 298.2 K, which, with an estimated $S° = -194$ J mol^{-1} h^{-1} for the Cm^{3+} (aquo) ion, yields an estimated -2.06 ± 0.03 V for the Cm(III)/Cm(0) couple (Fuger *et al.*, 1975) (see Chapter 17). Raschella *et al.* (1981) found $\Delta H = -606.5 \pm 11.7$ kJ mol^{-1} for dissolution using ^{248}Cm metal. From electron-transfer spectra, the Cm(III)/Cm(II) couple was estimated at -4.4 V (Nugent *et al.*, 1973), but the results of the pulse radiolysis study and the potential of the hydrated electron place a lower value on this couple (Sullivan *et al.*, 1976). From studies in a melt, Mikheev (1983) obtained –2.8 V for $E°$(Cm(III)/Cm(II)). Fuger and Martinot (1985) report $E°$(Cm(III)/Cm(IV)) to be -3.1 V.

Solution reactions of Cm(III) resemble those of the trivalent lanthanides and other trivalent actinides. The fluoride, oxalate, phosphate, iodate, and hydroxide are essentially water-insoluble, and the chloride, iodide, perchlorate, nitrate, and sulfate are water-soluble. The first hydrolysis constant for Cm(III), i.e. for the reaction

$$\mathrm{Cm(III)} + H_2O \rightarrow CmOH^{2+} + H^+$$

is 1.2×10^{-6} ($\mu = 0.1$; 23°C), which is within experimental error of the value for Am^{3+} but ten times greater than that for Pu^{3+} (Désiré *et al.*, 1969; Korotkin, 1974). The formation constants for $[Cm(OH)]^{2+}$ and $[Cm(OH)_2]^+$ have been determined by time-resolved laser-induced fluorescence spectroscopy (Fanghänel *et al.*, 1994). The measurements were made under high ionic strength (up to 6 M NaCl). Extrapolation to zero ionic strength yielded values of $\log \beta_{11} = 6.44$ and $\log \beta_{12} = 12.3$. Ionic strength significantly affects the distribution of hydrolyzed species with the Cm(III) ion becoming more easily hydrolyzed as the ionic strength increases (Fig. 9.4).

Stability constants for Cm(III) complexes have been determined for a number of inorganic and organic liquids in aqueous solution (Table 9.4). Most recent stability constant measurements for Cm(III) have been performed using time-resolved laser-induced fluorescence spectroscopy; these studies provide the most self-consistent set of stability constant data for Cm(III). Cm(III) is a 'class A' or 'hard' metal ion, and thus complexes far more strongly to oxygen and fluoride donors than to more polarizable donors such as chloride or sulfur. This is reflected in the fact that β_1 for F^- is three orders-of-magnitude greater than that for Cl^-. The stability constants for oxygen donors (e.g. OH^- and CO_3^{2-}) are even higher than that for F^-.

Cm(III) forms complexes with a number of polytungstate and heteropolytungstate anions and the luminescence properties of these complexes have been extensively studied. Included in this class of compounds are $CmW_{10}O_{36}^{9-}$, $Cm(SiW_{11}O_{39})_2^{13-}$, $CmSiW_{11}O_{39}^{5-}$, $Cm(PW_{11}O_{39})_2^{11-}$, $CmPW_{11}O_{39}^{4-}$, $Cm(P_2W_{17}O_{61})_2^{17-}$, and $CmP_2W_{17}O_{61}^{7-}$ (Yusov and Fedoseev, 1989b, 1990). The polytungstate ligands quench the luminescence of Cm(III), evidently due to charge transfer between the excited Cm*(III) and W(VI). This effect is magnified when the solutions of these complexes are frozen, resulting in a sharp decrease in

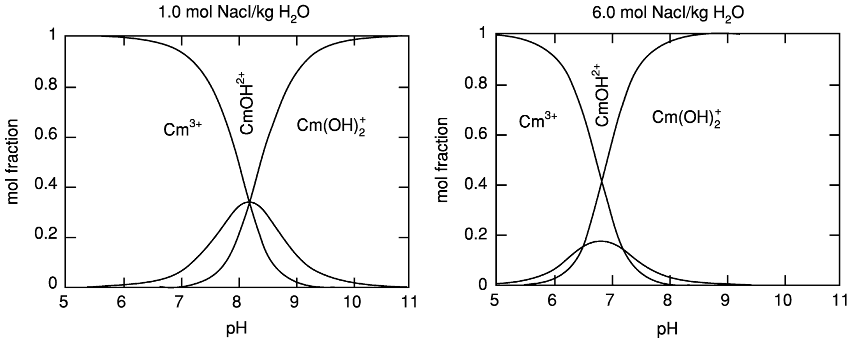

Fig. 9.4 *Comparison of Cm*(III) *species distribution as function of pH at two NaCl molalities. The speciation determination is based on Cm*(III) *fluorescence spectra. Used with permission from Fanghänel* et al. (1994).

Table 9.4 *Stability constants for selected Cm(III) complexes.*

Ligand	*Conditions*	*Stability constants*	*References*
OH^-	time-resolved laser fluorescence spectroscopy extrapolated to $\mu = 0$	$\beta_1 = 2.75 \times 10^6$; $\beta_2 = 2.00 \times 10^{12}$	Fanghänel *et al.* (1994)
F^-	time-resolved laser fluorescence spectroscopy, $\mu = 0$	$\beta_1 = 1.45 \times 10^3$	Aas *et al.* (1999)
F^-	extraction with di(2-ethylhexyl) phosphoric acid, pH = 3.6, $\mu = 0.50$	$\beta_1 = 2.21 \times 10^3$: $\beta_2 = 1.50 \times 10^6$: $\beta_3 = 1.2 \times 10^9$	Aziz and Lyle (1969)
F^-	extraction, $\mu = 1.0$	$\beta_1 = 4 \times 10^2$	Choppin and Unrein (1976)
Cl^-	extraction with dinonylnaphthalene sulfonic acid, $\mu = 1.0$	$\beta_1 = 1.6$; $\beta_2 = 0.9$	Khopkar and Mathur (1980a)
Cl^-	time-resolved laser fluorescence spectroscopy, $\mu = 6.8$ m, $T = 25°C$	$\beta_1 = 0.02$; $\beta_2 = 0.0007$	Fänghanel *et al.* (1995)
Cl^-	time-resolved laser fluorescence spectroscopy and Pitzer parameterization, $\mu = 0$ m, $T = 25°C$	$\beta_1 = 1.7$; $\beta_2 = 0.2$	Könnecke *et al.* (1997)
N_3^-	extraction with dinonylnaphthalene sulfonic acid pH = 5.9, $\mu = 0.5$, $T = 25°C$	$\beta_1 = 4.36$	Choppin and Barber (1989)
SCN^-	extraction with dinonylnaphthalene sulfonic acid pH = 2.8, $\mu = 1.0$	$\beta_1 = 1.53$; $\beta_2 = 4.08$	Khopkar and Mathur (1974, 1980b)

NO_2^-	extraction with dinonylnaphthalene sulfonic acid	$\beta_1 = 6.6$	Vasudeva Rao *et al.* (1978)
NO_3^-	extraction with dinonylnaphthalene sulfonic acid, $\mu = 1$, $T = 30°C$	$\beta_1 = 2.2$; $\beta_2 = 1.3$	Khopkar and Mathur (1980a)
CO_3^{2-}	time-resolved laser fluorescence spectroscopy and Pitzer parameterization, $\mu = 0$ m, $T = 25°C$	$\beta_1 = 1.3 \times 10^7$; $\beta_2 = 1.0 \times 10^{13}$; $\beta_3 = 1.6 \times 10^{15}$; $\beta_4 = 1.0 \times 10^{13}$	Fänghanel *et al.* (1999)
SO_4^{2-}	extraction, pH = 3.0, $\mu = 2.0$, $T = 25°C$	$\beta_1 = 22$; $\beta_2 = 73$	de Carvalho and Choppin (1967)
SO_4^{2-}	ion exchange	$\beta_1 = 32$; $\beta_2 = 241$	Khopkar and Mathur (1980a)
SO_4^{2-}	time-resolved laser fluorescence spectroscopy, $\mu = 3$ m	$\beta_1 = 8.5$; $\beta_2 = 4.1$	Paviet *et al.* (1996)
$P_3O_9^{3-}$	ion exchange	$\beta_1 = 4.4 \times 10^3$	Elesin *et al.* (1967)
$PW_{11}O_{39}^{7-}$	luminescence spectroscopy 0.1 м HNO_3	$\beta_1 = 5.0 \times 10^6$	Ioussov and Krupa (1997)
$SiW_{11}O_{39}^{8-}$	luminescence spectroscopy 0.1 м HNO_3	$\beta_1 = 3.2 \times 10^6$	Ioussov and Krupa (1997)
acetate	ion exchange, $\mu = 0.5$, $T = 20°C$	$\beta_1 = 114$; $\beta_2 = 1240$	Grenthe (1963)
glycolate	ion exchange, $\mu = 0.5$, $T = 20°C$	$\beta_1 = 700$; $\beta_2 = 5.6 \times 10^4$	Grenthe (1963)
glycinate	extraction, $\mu = 2.0$, $T = 25°C$	$\beta_1 = 6.4$	Tanner and Choppin (1968)
lactate	extraction, $\mu = 0.5$	$\beta_1 = 5.5 \times 10^2$; $\beta_2 = 3.0 \times 10^2$; $\beta_3 = 1.3 \times 10^6$	Nikolaev and Lebedev (1975)
2-hydroxyisobutyrate	cation exchange, $\mu = 0.5$	$\beta_1 = 2.7 \times 10^3$; $\beta_2 = 5.1 \times 10^4$; $\beta_3 = 1.7 \times 10^5$	Dedov *et al.* (1961)

Table 9.4 (*Contd.*)

Ligand	*Conditions*	*Stability constants*	*References*
5-sulfosalicylate	time-resolved laser fluorescence spectroscopy, $\mu = 0.05$	$\beta_1 = 2.8 \times 10^6$; $\beta_2 = 9.8 \times 10^8$	Klenze *et al.* (1998)
$C_4O_4^{2-}$	solubility ion exchange, $\mu = 0.2$	$\beta_1 = 9.1 \times 10^5$; $\beta_2 = 1.40 \times 10^{10}$	Lebedev *et al.* (1960, 1962)
citrate	extraction, $\mu = 0.1$	$\beta_1 = 4.9 \times 10^{10}$; $\beta_2 = 8.5 \times 10^{11}$	Hubert *et al.* (1974)
ethylenediaminetetraacetate	cation exchange, $\mu = 0.1$	$\beta_1 = 2.5 \times 10^{17}$	Elesin and Zaitsev (1971)
nitrilotriacetate	ion exchange, $\mu = 0.1$, $T = 25°C$	$\beta_1 = 6.3 \times 10^{11}$; $\beta_2 = 4.0 \times 10^{20}$	Eberle and Ali (1968)
ethylenediamine-bis(methyl) phosphonic acid	ion exchange, $\mu = 0.5$, $T = 25°C$	$\beta_1 = 2.5 \times 10^6$	Elesin *et al.* (1973)
thenoyltrifluoroacetone	extraction ($CHCl_3$), $\mu = 0.1$, $T = 25°C$	$\beta_3 = 2.5 \times 10^{13}$	Keller and Schreck (1969)

the luminescence lifetimes. However, upon further cooling, the luminescence quenching decreases and sharp luminescence bands are observed for these complexes at 77 K. The luminescence quenching is severe in Cm(III) complexes with $P_2W_{17}O_{61}^{10-}$ as these complexes do not luminesce in solution at 293 K. In contrast, $CmW_{10}O_{36}^{9-}$, $CmPW_{11}O_{39}^{4-}$, $CmSiW_{11}O_{39}^{5-}$, $Cm(SiW_{11}O_{39})_2^{13-}$, and $Cm(PW_{11}O_{39})_2^{11-}$ all display luminescence in D_2O at 293 K. At 77 K, the luminescence spectra of the $P_2W_{17}O_{61}^{10-}$ complexes are very similar to the other Cm(III) polytungstate complexes. Addition of molybdate to solutions of the Cm(III) polytungstate or heteropolytungstate complexes results in rapid quenching of the Cm(III) luminescence (Yusov and Fedoseev, 1992a,b). This behavior is the opposite of what is observed for the analogous Eu, Nd, and Yb systems.

The trends for the complexation of carboxylate ligands to Cm(III) are somewhat difficult to interpret. The β_1 values at $\mu = 0.5$ can be compared for acetate, glycolate, lactate, and 2-hydroxyisobutyrate (Table 9.4). The β_1 value increases from 114 to 700 in going from acetate to glycolate, which could be due to interaction of the hydroxyl group in glycolate with the Cm(III) center. One would expect that the inductive effect of an added methyl group would lead to a further increase in β_1 for complexation of lactate ion, but the β_1 value drops to 550 for lactate. On the other hand, addition of yet another methyl group does result in a significant increase in β_1 for 2-hydroxyisobutyrate ($\beta_1 = 2700$). The anomaly for lactate may simply reflect the differing experimental conditions under which the measurements were made. As would be expected, the chelating carboxylate ligands display substantially stronger binding to Cm(III) than the monocarboxylate ligands.

There are a limited number of reports concerning Cm(IV) in aqueous media. A fluoride complex of Cm(IV) was obtained when CmF_4 was dissolved in concentrated (15 M) MF solution (M = alkali–metal ion) (Asprey and Keenan, 1958; Keenan, 1961) (see Fig. 9.2). Even under these conditions, and using ^{244}Cm, the self-reduction rate because of alpha decay is about 1% per minute. When CmF_4 is added to aqueous NH_4F, an immediate oxidation–reduction reaction occurs, with deposition of CmF_3. This is in sharp contrast to the stability of Am(IV) in NH_4F solution (Asprey and Penneman, 1962).

Other than the CmF_4/MF system, the only claims for chemically generated Cm(IV) in solution are the reports that red solutions result when aqueous Cm(III) solutions are mixed with potassium peroxydisulfate and heteropolyanions such as $[P_2W_{17}O_{61}]^{10-}$ (Saprykin *et al.*, 1976; Kosyakov *et al.*, 1977). Cm(IV), produced by persulfate oxidation of Cm(III) in phosphotungstate solution, converts back to Cm(III) at a rate that suggests that the reduction involves both radiolytic mechanisms and direct reduction by water (Kosyakov *et al.*, 1977). In contrast, reduction of Am(IV) to Am(III) under similar conditions is dominated by radiolytic processes. Electrochemical generation of Cm(IV) in phosphate solutions was unsuccessful, owing to the large Cm(IV)/Cm(III) potential, estimated to be greater than 2 V in these systems (Myasoedov *et al.*, 1973, 1974). Other attempts to prepare Cm(IV) by oxidation of Cm(III) in solution have failed. These attempts include electrochemical methods (Myasoedov *et al.*, 1973, 1974; Ionova and Spitsyn, 1978) and the use of sodium perxenate (Holcomb, 1967) and ozone (Pages and Demichelis, 1966), agents which readily oxidize Am(III) to Am(V) or Am(VI). $Cm(OH)_3$ in $NaHCO_3$ is not oxidized by ozone or $Na_2S_2O_8$, conditions which produce Am(VI) as a carbonate complex (Coleman *et al.*, 1963).

The polytungstate Cm(IV) complexes – $CmW_{10}O_{36}^{8-}$, $Cm(SiW_{11}O_{39})^{12-}$, and $Cm(PW_{11}O_{39})_2^{10-}$ – display chemiluminescence upon reduction to Cm(III) (Yusov *et al.*, 1986a,b). The brightest chemiluminescence was observed when the initial complexes were treated with 1–3 M alkali, in which case water in the system most probably served as reductant. Chemiluminescence has also been observed during dissolution of the Cm(IV) double oxide Li_xCmO_y in mineral acids (Yusov and Fedoseev, 1989a, 1991).

Despite the numerous unsuccessful attempts to oxidize Cm(III) and Cm(IV) compounds to higher oxidation states, some theoretical work suggests the possibility that Cm(VI) may be even more stable than Am(VI), and the lack of success in preparing Cm(VI) may result from the low stability of Cm(V) and the high Cm(IV)/Cm(III) potential (Ionova and Spitsyn, 1978; Spitsyn and Ionova, 1978). One report claims the synthesis of Cm(VI) by beta decay of $^{242}AmO_2^+$ (Peretrukhin *et al.*, 1978).

$$^{242}AmO_2^+ \xrightarrow[16h]{\beta^-} CmO_2^{2+}$$

The $K_3AmO_2(CO_3)_2$ starting material was aged 18–40 h and then dissolved in 0.1 M $NaHCO_3$ in the presence of ozone, followed by addition of $Na_4UO_2(CO_3)_3/K_2CO_3$ solution to precipitate MO_2^{2+} species as $K_4MO_2(CO_3)_3$. From the enhancement of Cm in the precipitate over that expected for Cm(III), it was concluded that a 30–60% conversion to Cm(VI) had occurred.

Cm(II) is unknown other than as a transient aqueous species and a species coprecipitated from melts, and possibly in CmO. Pulse radiolysis, producing OH radicals as oxidant and the aquo electron as reductant, produced changes in aqueous americium and curium perchlorate solutions. The new absorbances were attributed to transient formation of Cm(II), A_{max} 240 nm, and Cm(IV), A_{max} 260 nm (Sullivan *et al.*, 1976).

9.8.2 Organic

Studies of Cm chemistry in pure organic solvents are rare. The solvation of Cm(III) in non-aqueous and binary mixed solvents has been investigated by luminescence spectroscopy (Kimura *et al.*, 2001). This study revealed that the relative preference for solvation of Cm(III) ion is dimethylsulfoxide > dimethylformamide > H_2O > methanol.

Very few curium compounds containing organic ligands have actually been isolated (see Section 9.7.8), although it seems likely that efforts to isolate such compounds would prove fruitful. Because of the interest in extraction schemes for treating radioactive wastes, a substantial number of studies have determined stability constants and distribution coefficients for solutions containing curium and various organic ligating agents. However, these experiments have often involved tracer amounts of curium and have employed a variety of experimental conditions (ionic strength, temperature, concentrations, etc.); therefore, quantitative comparisons of the determined values are difficult. As with the inorganic anions, values, and in some cases even trends, can vary markedly under seemingly similar conditions. Most studies do not involve isolation or definitive formulation of the actual species in solution, and it is possible that complicated structures occur, e.g. $CmF_3 \cdot (HDEHP)_x$ (Aziz and Lyle, 1969).

Furthermore, crystal structure determinations for a number of pertinent lanthanide and actinide extractant complexes illustrate that surprises may be expected when more definitive structural information becomes available (Burns, 1982; Bowen *et al.*, 1984). Because of these complications, we have not tried to analyze the voluminous Cm extraction data that are available, but included in Table 9.4 the data for only a few of the more important extractants. The reader is referred to a more extensive compilation for additional data of this type (Jones and Choppin, 1969).

Keller and Schreck (1969) have shown that Cm(III), as well as Ac(III), Am(III), and Cf(III), are extracted with β-diketone ligands as 1:3 chelates only, with stability constants ($\log\beta_3$) decreasing in the series Cf > Cm ~ Am > Ac. Keller *et al.* (1966) have also shown that Am(III) and Cm(III) are extracted from aqueous solutions into chloroform solutions of 8-hydroxyquinoline ligands as AnL_2Y, where L is the 8-hydroxyquinolate anion and Y is probably OH^-, in contrast to the lanthanides, which are extracted as LnL_3 chelates.

Distribution ratios (chloroform–water) have been reported for curium complexes with 8-hydroxyquinoline, cupferron, and *N*-benzoylphenylhydroxylamine (Akatsu *et al.*, 1968). Only 1:3 complexes with Cm(III) and Am(III) were reported, and extraction into the organic phase appears to be very high at pH values above 5. Solution interaction of Cm(III) with bis(salicylidene)ethylenediimine and derivatives has also been studied (Stroński and Rekas, 1973). With the reagent arsenazo-III, both Cm(III) and Am(III) form 1:1 and 1:2 complexes (Myasoedov *et al.*, 1970).

During the last 20 years, the use of neutral bifunctional compounds as extractants for trivalent actinides has been extensively investigated. These compounds include carbamoylmethylphosphonates, CMPOs, and diamides. The mechanism by which these extractants operate is still open to debate. Slope analysis studies often give varied results. For example, Mincher (1992) has reported the extraction of trivalent actinides (including Cm) by CMPO to be due to formation of $M(NO_3)_3(CMPO)_4$ complexes, whereas most other studies indicate a stoichiometry of the type $M(NO_3)_3L_3$ (Horwitz *et al.*, 1981). Similar confusion can be cited for the diamide extractants, although mechanistic studies have not been performed specifically with Cm for this class of ligands.

9.9 ANALYTICAL CHEMISTRY

The analysis for curium has been done by the typical methods for metal ions and alpha-emitting actinides, such as alpha, gamma, and neutron spectroscopy, nuclear track detection, photon/electron-rejecting alpha liquid scintillation, mass spectrometry, spectrophotometry of highly colored complexes such as arsenazo, and time-resolved laser-induced fluorescence or luminescence spectroscopy (Buijs, 1973). In most cases, at least some separations are required before analysis of curium.

9.9.1 Analysis of curium

The curium isotopes, 242, 243, and 244, emit high-energy alpha particles (see Table 9.1) that are easily quantified in the presence of lower-energy α emitters without extensive separations. Curium isotopes 245–248 emit lower-energy alpha particles and generally require more extensive separations before alpha analysis. Alpha spectrometry is typically used for curium determination, although photon/electron-rejecting alpha liquid scintillation has been shown to have lower detection limits when combined with extractive scintillators (Metzger *et al.*, 1995; Dacheux and Aupais, 1998). One extractive scintillator was a combination of HDEHP and CMPO, allowing the separation and analysis to occur in one step (Metzger *et al.*, 1995). The key to alpha spectrometry is the preparation of counting plates with minimal solids to degrade the energy of the alpha particles. Various deposition techniques have been used, including electrodeposition, evaporation, and precipitation of insoluble compounds (Trautmann and Folger, 1989; Kaye *et al.*, 1995; Gascon *et al.*, 1996; Rameback and Skalberg, 1998; Diakov *et al.*, 2001). Precipitation can involve addition of a lanthanide ion to act as a carrier for curium (Kaye *et al.*, 1995). Nuclear track analysis has been shown to be useful for very low concentrations of curium, such as environmental samples and waste streams at nuclear power plants (Lancsarics *et al.*, 1988; Espinosa *et al.*, 1995). The alpha energies were determined by the size of the track after calibration with sources of known energy.

Spontaneous fission occurs for the even isotopes of curium, allowing neutron counting to be used for their determination, especially for ^{244}Cm and ^{248}Cm, but this method requires pure isotopes for quantification (Trautmann and Folger, 1989). Curium analyses have been done by inductively coupled mass spectrometry and isotope dilution thermal ionization mass spectrometry after separation to obtain a pure curium solution (Kinard *et al.*, 1995; Niese and Gleisberg, 1995; Chartier and Aubert, 1999).

As has been mentioned previously, time-resolved laser-induced fluorescence spectroscopy has been shown to be an especially valuable tool for investigating Cm solution chemistry, but it has also proved useful for quantitative determination of Cm (Elesin *et al.*, 1973; Dem'yanova *et al.*, 1986; Yusov *et al.*, 1986a,b; Decambox *et al.*, 1989; Kim *et al.*, 1991; Myasoedov and Lebedev, 1991; Myasoedov, 1994; Moulin *et al.*, 1997; Dacheux and Aupais, 1998). The Cm fluorescence emission signal is strong enough that no separations from other transuranium or lanthanide elements are required to use this technique to quantify Cm ion in solution. Sensitivity for curium detection is about 5×10^{-11} M in carbonate solution without separation from matrix elements (Radchenko *et al.*, 1999). An even lower detection limit of 5×10^{-13}M has been observed at 612 nm (Moulin *et al.*, 1997).

9.9.2 Separations for analysis

Separations are a primary component of most analytical procedures. Initial separation is from non-radioactive elements and the large quantity of uranium that may be present in the sample. Plutonium is often separated to allow determination without interference from the higher actinides. Separation of curium from americium and the lanthanides is possible, but may not be necessary, depending on the method of final analysis. A variety of separation methods have been reported, including ion exchange, extraction chromatography, and solvent extraction, or combinations of several of these methods. Early work was summarized in Gmelin (Buijs, 1973). A more recent review summarizes many of the methods for analytical separations (Myasoedov, 1994).

Anion-exchange resins have been used with HCl and HNO_3 in both aqueous and aqueous–alcohol mixtures (Trautmann and Folger, 1989; Gascon *et al.*, 1996; Diakov *et al.*, 2001). Anion exchange alone usually results in a product containing all trivalent actinides and lanthanides. Cation exchange from HCl solutions has been used to separate lanthanides from actinides, or with α-hydroxyisobutyric acid to separate both lanthanides and actinides (Myasoedov, 1994). Anion exchange from HCl has also been used to remove uranium and plutonium, followed by a rapid separation of curium from americium by high-pressure liquid chromatography (HPLC) using 2-hydroxy-2-methylbutyric acid as the eluent (Trautmann and Folger, 1989). Americium–curium separation was rapid, with no overlap between curium and americium peaks. Anion exchange has been combined with HDEHP to separate an americium–curium product (Gascon *et al.*, 1996).

Another method involves a combination of extraction of plutonium with trioctylphosphine oxide in cyclohexane from HNO_3, then absorbing the metal ions onto Dowex® 50 resin from an HCl solution containing oxalic acid.

Washing the column with 2 M HCl removed impurities, followed by americium–curium elution in 6 M HNO_3 (Niese and Gleisberg, 1995).

Extraction chromatography with CMPO on an organic support allows ready separation of an americium and a curium fraction. A commercially available resin based on CMPO has been used (Kaye *et al.*, 1995; Maxwell, 1996).

Separations by solvent extraction include extraction of all the actinides into HDEHP, with selective back-extraction of americium and curium into 5 M HNO_3 (Rameback and Skalberg, 1998). Another method used extraction of plutonium from HCl solution with triisooctylamine in xylene. Americium and curium were then extracted with dibutyl-*N*,*N*-diethylcarbamoyl phosphonate and stripped into dilute acid (Kimura *et al.*, 1996). CMPO has been used extensively for solvent extraction separations of americium and curium (Myasoedov and Lebedev, 1991). Other separation methods are given in the review by Myasoedov (1994).

ACKNOWLEDGMENT

This work was performed under the auspices of the U.S. Department of Energy. The authors gratefully acknowledge the excellent editorial support of Paula Ložar and helpful suggestions by Calvin Delegard (Pacific Northwest National Laboratory) and anonymous peer reviewers.

REFERENCES

Aas, W., Steinle, E., Fanghänel, Th., and Kim, J. I. (1999) *Radiochim. Acta*, **84**, 85–8.

Abramychev, S. M., Balashov, N. V., Vesnovskii, S. P., Vjachin, V. N., Lapin, V. G., Nikitin, E. A., and Polynov, V. N. (1992) *Nucl. Instrum. Methods*, **B70**, 5–8.

Akatsu, E., Hoshi, M., Ono, R., and Ueno, K. (1968) *J. Nucl. Sci. Tech.*, **5**, 252–5.

Arisaka, M., Kimura, T., Suganuma, H., and Yoshida, Z. (2002) *Radiochim. Acta*, **90**, 193–7.

Artisyuk, V., Chmelev, A., Saito, M., Suzuki, M., and Fujii, E.Y. (1999) *J. Nucl. Sci. Tech.*, **36**, 1135–40.

Asprey, L. B., Ellinger, F. H., Fried, S., and Zachariasen, W. H. (1955) *J. Am. Chem. Soc.*, **77**, 1707–8.

Asprey, L. B. and Keenan, T. K. (1958) *J. Inorg. Nucl. Chem.*, **7**, 27–31.

Asprey, L. B. and Penneman, R. A. (1962) *Inorg. Chem.*, **1**, 134–6.

Asprey, L. B., Keenan, T. K., and Kruse, F. H. (1965) *Inorg. Chem.*, **4**, 985–6.

Asprey, L. B. and Haire, R. G. (1973) *Inorg. Nucl. Chem. Lett.*, **9**, 1121–8.

Aziz, A. and Lyle, S. J. (1969) *J. Inorg. Nucl. Chem.*, **31**, 3471–80.

Bagnall, K. W. (1967) *Coord. Chem. Rev.*, **2**, 145–62.

Bagnall, K. W. (1972) *The Actinide Elements,* Elsevier, New York.

Bansal, B. M. and Damien, D. (1970) *Inorg. Nucl. Chem. Lett.*, **6**, 603–6.

Barbanel, Yu. A., Kotlin, V. P., and Kolin, V. V. (1977) *Radiokhimiya*, **19**, 497–501; *Sov. Radiochem.*, **19**, 406–9.

Baumgärtner, F., Fischer, E. O., Billich, H., Dornberger, E., Kanellakopulos, B., Roth, W., and Stieglitz, L. (1970) *J. Organomet. Chem.*, **22**, C17–18.

Baybarz, R. D. (1970) *At. Energy Rev.*, **8**, 327–60.

Baybarz, R. D. and Adair, M. L. (1972) *J. lnorg. Nucl. Chem.*, **34**, 3127–30.

Baybarz, R. D., Bohet, J., Buijs, K., Colsen, L., Müller, W., Reul, J., Spirlet, J. C., and Toussaint, J. C. (1976) in *Transplutonium 1975* (eds. W. Müller and R. Lindner), North-Holland, Amsterdam, pp. 61–8.

Beitz, J. V. and Hessler, J. P. (1980) *Nucl. Tech.*, **51**, 169–77.

Benedict, U., Haire, R. G., Peterson, J. R., and Itié, J. P. (1985) *J. Phys. F*, **15**, L29–35.

Bibler, N. E. (1972) *Inorg. Nucl. Chem. Lett.*, **8**, 153–6.

Bigelow, J. E., Collins, E. D., and King, L. J. (1980) in *Actinide Separations* (ACS Symp. Ser. 117), American Chemical Society, Washington DC, pp. 147–55.

Bigelow, J. (2002) Oak Ridge National Laboratory, personal communication.

Bokelund, H., Apostolidis, C., and Glatz, J. P. (1989) *J. Nucl. Mater.*, **166**, 181–8.

Bond, W. D. and Leuze, R. E. (1980) in *Actinide Separations* (ACS Symp. Ser. 117), American Chemical Society, Washington DC, pp. 441–53.

Bowen, S. M., Dresler, E. N., and Paine, R. T. (1984) *Inorg. Chim. Acta*, **84**, 221; also see earlier articles by these authors.

Brown, D. (1968) *Halides of the Lanthanides and Actinides,* Wiley-Interscience, New York.

Buijs, K. (1973) in *Handbook of Inorganic Chemistry, Transuranics*, part A2 (ed. G. Koch), Verlag Chemie, Weinheim, pp. 164–73.

Buijs, K., Müller, W., Reul, J., and Toussaint, J. C. (1973) Euratom Report 5040. *Nucl. Sci. Abstr.*, **29**, 02573.

Bukina, T. I., Khizhnyak, P. L., Karalova, Z. K., and Myasoedov, B. F. (1988) *Radiokhimiya.*, **31**, 94–98; *Sov. Radiochem.*, **31**, 452–56.

Burnett, J. (1966) *J. Inorg. Nucl. Chem.*, **28**, 2454–6.

Burney, G. A. and Porter, J. A. (1967) *Inorg. Nucl. Chem. Lett.*, **3**, 79–85.

Burney, G. A. (1980) *Sep. Sci. Technol.*, **15**, 163–82.

Burns, J. H., Peterson, J. R., and Stevenson, J. N. (1975) *J. Inorg. Nucl. Chem.*, **37**, 743–9.

Burns, J. H. (1982) Oak Ridge National Laboratory Report, ORNL/TM–8221.

Carnall, W. T., Fields, P. R., Stewart, D. C., and Keenan, T. K. (1958) *J. Inorg. Nucl. Chem.*, **6**, 213–16.

Chartier, F. and Aubert, P. (1999) *Fresenius J. Anal. Chem.*, **364**, 320.

Charvillat, J. P., Benedict, U., Damien, D., and Müller, W. (1975) *Radiochem. Radioanal. Lett.*, **20**, 371–81.

Charvillat, J. P., Benedict, U., Damien, D., de Novion, C. H., Wojakowski, A., and Müller, W. (1976) in *Transplutonium 1975* (eds. W. Müller and R. Lindner), North-Holland, Amsterdam, , pp. 79–84.

Charvillat, J. P. and Zachariasen, W. H. (1977) *Inorg. Nucl. Chem. Lett.*, **13**, 161–3.

Chikalla, T. D. and Eyring, L. (1969) *J. Inorg. Nucl. Chem.*, **31**, 85–93.

Choppin, G. R. and Unrein, P. J. (1976) in *Transplutonium 1975* (eds. W. Müller and R. Lindner), North-Holland, Amsterdam, pp. 97–105.

Choppin, G. R. and Barber, D. W. (1989) *J. Less Common Metals*, **149**, 231–5.

Choppin, G. R. (1999) in *Chemical Separation Technologies and Related Methods of Nuclear Waste Management* (eds. G. R. Choppin and M. Kh. Khankhasayev), Kluwer Academic Publications, Dordrecht, pp. 1–16.

Chu, Y. Y. (1972) *Phys. Rev. A*, **5** (1), 67–72.

Coleman, J. S., Keenan, T. K., Jones, L. H., Carnall, W. T., and Penneman, R. A. (1963) *Inorg. Chem.*, **2**, 58–61.

Cunningham, B. B. and Wallmann, J. C. (1964) *J. Inorg. Nucl. Chem.*, **26**, 271–5.

Cunningham, B. B. (1966) *Prep. Inorg. Reactions*, **3**, 79–121.

Dacheux, N. and Aupais, J. (1998) *Anal. Chim. Acta* **363**, 279–94.

Damien, D., Charvillat, J. P., and Müller, W. (1975) *Inorg. Nucl. Chem. Lett.*, **11**, 451–7.

Damien, D., Wojakowski, W., and Müller, W. (1976) *Inorg. Nucl. Chem. Lett.*, **12**, 441–9.

Damien, D. A., Haire, R. G., and Peterson, J. R. (1979a) *J. Less Common Metals*, **68**, 159–65.

Damien, D. A., Haire, R. G., and Peterson, J. R. (1979b) *J. Phys. Colloq.*, 95–100.

Davydov, A. V., Myasoedov, B. F., Travnikov, S. S., and Fedoseev, E. V. (1978) *Radiokhimiya*, **20**, 257–64; *Sov. Radiochem.*, **20**, 217–24.

de Carvalho, R. G. and Choppin, G. R. (1967) *J. Inorg. Nucl. Chem.*, **29**, 725–35.

Decambox, P., Mauchien, P., and Moulin, C. (1989) *Radiochim. Acta*, **42**, 23–8.

Dedov, V. D., Lebedev, I. A., Ryzhov, M. N., Trukhlyaev, P. S., and Yakovlev, G. N. (1961) *Radiokhimiya*, **3**, 701–5; *Sov. Radiochem.*, **3**, 197–201.

Dedov, V. D., Volkov, V. V., Gvozdev, B. A., Ermakov, V. A., Lebedev, I. A., Razbitnoi, V. M., Trukhlyaev, P. S., Chuburkov, Yu. T., and Yakovlev, G. N. (1965) *Radiokhimiya*, **7**, 453–61; *Sov. Radiochem.*, 7, 452–8.

Deissenberger, R., Köhler, S., Ames, F., Eberhardt, K., Erdman, N., Funk, H., Herrmann, G., Kluge, H.-J., Munnemann, M., Passler, G., Riegel, J., Scheere, F., Trautmann, N., and Urban, F.-J. (1995) *Angew. Chem. Int. Ed. Engl.*, **34**, 814–15.

Dem'yanova, T. A., Stepanov, A. V., Babaev, A. S., and Aleksandruk, V. M. (1986) *Radiokhimiya*, **28**, 494–8; *Sov. Radiochem.*, **28**, 450–3.

Désiré, B., Hussonnois, M., and Guillaumont, R. (1969) *C. R. Acad. Sci. Paris C*, **269**, 448–51.

Diakov, A. A., Perekhozheva, T. N., and Zlokazova, E. I. (2001) *Rad. Meas.*, **34**, 463–6.

Eberle, S. H. and Ali, S. A. (1968) *Z. Anorg. Allg. Chem.*, **361**, 1–14.

Edelstein, N. M., Navratil, J. D., and Schulz, W. W. (eds.) (1985) *Americium and Curium Chemistry and Technology,* Reidel Publishing Co, Boston.

Elesin, A. A., Lebedev, I. A., Piskunov, E. M., and Yakovlev, G. N. (1967) *Radiokhimiya*, **9**, 161–6; *Sov. Radiochem.*, **9**, 159–63.

Elesin, A. A. and Zaitsev, A. A. (1971) *Radiokhimiya*, **13**, 775–8; *Sov. Radiochem.*, **13**, 798–801.

Elesin, A. A., Zaitsev, A. A., Sergeev, G. M., and Nazarova, I. I. (1973) *Radiokhimiya*, **15**, 64–8; *Sov. Radiochem.*, **15**, 62–6.

Eller, P. G. and Penneman, R. A. (1986) in *The Chemistry of the Actinide Elements*, Chapman and Hall, New York, ch. 9.

Erdmann, B. and Keller, C. (1971) *Inorg. Nucl. Chem. Lett.*, **7**, 675–83.

Erdmann, B. and Keller, C. (1973) *J. Solid State Chem.*, **7**, 40–8.

Espinosa, G., Gammage, R. B., Meyer, K., Wheeler, R. B., and Salasky, M. (1995) *Rad. Prot. Dos.*, **59**, 227–9.

Eubanks, I. D. and Thompson, M. C. (1969) *Inorg. Nucl. Chem. Lett.*, **5**, 187–91.

Eyring, L. (1967) in *Adv. Chem. Ser.*, **71**, pp. 67–85. American Chemical Society, Washington DC.

Fanghänel, Th., Kim, J. I., Paviet, P., Klenze, R., and Hauser, W. (1994) *Radiochim. Acta*, **66/67**, 81–7.

Fanghänel, Th., Kim, J. I., Klenze, R., and Kato, Y. (1995) *J. Alloys Compds*, **225**, 308–11.

Fanghänel, Th., Könnecke, Th., Weger, H., Paviet-Hartmann, P., Neck, V., and Kim, J. I. (1999) *J. Soln. Chem.*, **28**, 447–62.

Fargeas, M., Fremont- Lamouranne, R., Legoux, Y., and Merini, J. (1986) *J. Less Common Metals*, **121**, 439–44.

Felker, L. K. and Benker, D. E. (1995) *Application of the TRUEX Process to Highly Irradiated Targets*, USDOE Report ORNL/TM–12784.

Fournier, J. M., Blaise, A., Müller, W., and Spirlet, J. C. (1977) *Physica*, **87–88B**, 30–1.

Fuger, J., Reul, J., and Müller, W. (1975) *Inorg. Nucl. Chem. Lett.*, **11**, 265–75.

Fuger, J. and Oetting, F. L. (1976) in *The Chemical Thermodynamics of Actinide Elements and Compounds*, part 2, *The Actinide Aqueous Ions*, IAEA, Vienna, p. 48.

Fuger, J. and Martinot, L. (1985) The Actinides, Standard Potentials in Aqueous Solutions in (eds. A. J. Bard, R. Parsons, and J. Jordan), Marcel Dekker, New York, ch. 21, pp. 631–73.

Fuger, J., Haire, R. G., and Peterson, J. R. (1993) *J. Alloys Compds*, **200**, 181–5.

Fujita, D. K., Parsons, T. C., Edelstein, N., Noe, M., and Peterson, J. R. (1976) in *Transplutonium 1975* (eds. W. Müller and R. Lindner), North-Holland, Amsterdam, pp. 173–8.

Gascon, J. L., Rodriguez, M., and Suarez Del Rey, J. A. (1996) *J. Radioanal. Nucl. Chem.*, **207**, 63–9.

Gerasimov, A. S., Zaritskaya, T. S., Kiselev, G. V., and Myrtsymova, L. A. (2000) *At. Energy*, **89**, 663–7.

Gibson, J. K. and Haire, R. G. (1985) *J. Solid State Chem.*, **59**, 317–23.

Gibson, J. K. and Haire, R. G. (1987) *J. Less Common Metals*, **132**, 149–54.

Gibson, J. K. and Haire, R. G. (1990) *J. Phys. Chem.*, **94**, 935–9.

Gibson, J. K. and Haire, R. G. (1998) *J. Phys. Chem. A*, **102**, 10746–53.

Gibson, J. K. and Haire, R. G. (1999) *Organometallics*, **18**, 4471–7.

Gmelin Handbook of Chemistry Inorganic (1972–74) Suppl. Work, 8th edn, *Transuranium*, part A1, II (1973); part A1, II (1974); part A2 (1973); part C (1972),Verlag Chemie, Weinheim.

Grenthe, I. (1963) *Acta. Chem. Scand.*, **17**, 1814–15.

Groh, H. J., Huntoon, R. T., Schlea, C. S., Smith, J. A., and Springer, F. H. (1965) *Nucl. Appl.*, **1**, 327–36.

Gutmacher, R. G., Hulet, E. K., and Conway, J. G. (1964) *J. Opt. Soc. Am.*, **54**, 1403–4.

Haire, R. G. and Fahey, J. A. (1977) *J. Inorg. Nucl. Chem.*, **39**, 837–41.

Haire, R. G., Lloyd, M. H., Milligan, W. O., and Beasley, M. L. (1977) *J. Inorg. Nucl. Chem.* **39**, 843–7.

Haire, R. G. (1980) *Proc. 10th Journée des Actinides*, Stockholm, p. 19.

Haire, R. G., Nave, S. E., and Huray, P. G. (1982) *12th Journée des Actinides*, Orsay.

Haire, R. G., Benedict, U., Peterson, J. R., Dufour, C., and Itié, J. P. (1985) *J. Less Common Metals*, **109**, 71–8.

Hale, W. H. Jr and Mosley, W. C. (1973) *J. Inorg. Nucl. Chem.*, **35**, 165–71.

Haug, H. O. (1967) *J. Inorg. Nucl. Chem.*, **29**, 2753–8.

Haug, H. O. (1974) *J. Radioanal. Chem.*, **21**, 187–98.

Haug, H. O. and Baybarz, R. D. (1975) *Inorg. Nucl. Chem. Lett.*, **11**, 847–55.

Hoffman, D. C. (1985) in *Americium and Curium Chemistry and Technology* (eds. N. M. Edelstein, J. D. Navratil, and W. W. Schulz), Reidel Publishing, Boston, pp. 241–260.

Holcomb, H. P. (1967) *J. Inorg. Nucl. Chem.*, **29**, 2885–8.

Holden, N. E. (1989) *Pure Appl. Chem.*, **61**, 1483–504.

Horwitz, E. P., Muscatello, A. C., Kalina, D. G., and Kaplan, L. (1981) *Sep. Sci. Technol.*, **16**, 417–37.

Horwitz, E. P. and Schulz, W. W. (1991) The Truex process: A vital tool for disposal of U.S. defense nuclear waste, in *New Separation Chemistry Techniques for Radioactive Waste and Other Specific Applications*, Elsevier Applied Science, Amsterdam.

Hubert, S., Hussonnois, M., Brillard, L., Goby, G., and Guillaumont, R. (1974) *J. Inorg. Nucl. Chem.*, **36**, 2361–6.

Ionova, G. V. and Spitsyn, V. I. (1978) *Dokl. Akad. Nauk SSSR*, **241**, 590–1; *Dokl. Acad. Sci. USSR*, **241**, 348–9.

Ionova, G., Madic, C., and Guillaumont, R. (1997) *Radiochim. Acta*, **78**, 83–90.

Ioussov, A. and Krupa, J. C. (1997) *Radiochim. Acta*, **78**, 97–104.

Jarvinen, G. D. (1999) in *Chemical Separation Technologies and Related Methods of Nuclear Waste Management* (eds. G. R. Choppin and M. Kh. Khankhasayev), Kluwer Academic Publications, Dordrecht, pp. 53–70.

Jones, A. D. and Choppin, G. R. (1969) *Actinide Rev.*, **1**, 311–36.

Kanellakopulos, B., Charvillat, J. P., Maino, F., and Müller, W. (1976) in *Transplutonium 1975* (eds. W. Müller and R. Lindner), North-Holland, Amsterdam, pp. 181–90.

Karalova, Z. K., Myasoedov, B. F., Bukina, T. I., and Lavrinovich, E. A. (1988) *Solvent Extr. Ion Exch.*, **6**, 1109–35.

Katz, J. J. and Seaborg, G. T. (1957) *The Chemistry of the Actinide Elements,* Methuen, London.

Katz, J. J. and Sheft, I. (1960) *Adv. Inorg. Chem. Radiochem.*, **2**, 195–236.

Kaye, J. H., Strebin, R. S., and Orr, R. D. (1995) *J. Radioanal. and Nucl. Chem.*, **194**, 191–6.

Kazantsev, G. N., Skiba, O. V., Burnaevà, A. A., Kolesnikov, V. P., Volkov, Yu. F., Kryukova, A. I., and Korshunov, I. A. (1982) *Radiokhimiya*, **24**, 88–91.

Keenan, T. K. (1961) *J. Am. Chem. Soc.*, **83**, 3719–20.

Keenan, T. K. (1966a) *Inorg. Nucl. Chem. Lett.*, **2**, 153–6.

Keenan, T. K. (1966b) *Inorg. Nucl. Chem. Lett.*, **2**, 211–4.

Keenan, T. K. (1967a) *Inorg. Nucl. Chem. Lett.*, **3**, 391–6.

Keenan, T. K. (1967b) *Inorg. Nucl. Chem. Lett.*, **3**, 463–7.

Keenan, T. K. and Asprey, L. B. (1969) *Inorg. Chem.*, **8**, 235–8.

Keller, C. and Walter, K. H. (1965) *J. Inorg. Nucl. Chem.*, **27**, 1253–60.

Keller, C., Eberle, S. H., and Mosdzelewski, K. (1966) *Radiochim. Acta*, **5**, 185–8.

Keller, C. and Schreck, H. (1969) *J. Inorg. Nucl. Chem.*, **31**, 1121–32.

Keller, C. (1971) *The Chemistry of the Transuranium Elements,* Verlag Chemie, Weinheim.

Kerrigan, W. J. and Banick, C. J. (1975) *J. Inorg. Nucl. Chem.*, **37**, 641.

Khopkar, P. K. and Mathur, J. N. (1974) *J. Inorg. Nucl. Chem.*, **36**, 3819–25.

Khopkar, P. K. and Mathur, J. N. (1980a) *J. Inorg. Nucl. Chem.*, **42**, 109–13.

Khopkar, P. K. and Mathur, J. N. (1980b) *Thermochim. Acta*, **37**, 71–8.

Kim, J. I., Klenze, R., and Wimmer, H. (1991) *Eur. J. Solid State Inorg. Chem.*, **28**, 347–56.

Kimura, T. and Choppin, G. R. (1994) *J. Alloys Compds*, **213/214**, 313–17.

Kimura, T., Choppin, G. R., Kato, Y., and Yoshida, Z. (1996) *Radiochim. Acta*, **72**, 61–4.

Kimura, T., Kato, Y., Takeishi, H., and Choppin, G. R. (1998) *J. Alloys Compds*, **271/274**, 719–22.

Kimura, T., Nagaishi, R., Kato, Y., and Yosida, Z. (2001) *Radiochim. Acta*, **89**, 125–30.

Kinard, W. F., Bibler, N. E., Coleman, C. J., Dewberry, R. A., Boyce, W. T., and Wyrick, S. B. (1995) *ASTM Spec. Tech. Publ.*, STP **1291**, 48–58.

Klenze, R., Panak, P., and Kim, J. I. (1998) *J. Alloys Compds*, **271–273**, 746–50.

Knauer, J. B. (2002) Oak Ridge National Laboratory, personal communication.

Konings, R. J. M. (2001a) *J. Nucl. Mater.*, **295**, 57–63.

Konings, R. J. M. (2001b) *J. Nucl. Mater.*, **298**, 255–68.

Könnecke, Th., Fänghanel, Th., and Kim, J. I. (1997) *Radiochim. Acta*, **76**, 131–5.

Korotkin, Yu. S. (1974) *Radiokhimiya*, **16**, 221–5; *Sov. Radiochem.*, **16**, 223–6.

Kosyakov, V. N., Timofeev, G. A., Erin, E. A., Andreev, V. I., Kopytov, V. V., and Simakin, G. A. (1977) *Radiokhimiya*, **19**, 511–17; *Sov. Radiochem.*, **19**, 418–23.

Kulyako, Yu. M., Trofimov, T. I., Malikov, D. A., Lebedev, I. A., and Myasoedov, B. F. (1993) *Radiokhimiya*, **35**, 38–41; *Radiochemistry*, **35**, 399–401.

Lancsarics, G., Feher, I., Sagi, L., and Palfalvi, J. (1988) *Rad. Prot. Dos.*, **22**, 111–3.

Laubereau, P. G. and Burns, J. H. (1970a) *Inorg. Chem.*, **9**, 1091–5.

Laubereau, P. G. and Burns, J. H. (1970b) *Inorg. Nucl. Chem. Lett.*, **6**, 59–63.

Lebedev, I. A., Pirozhkov, S. V., and Yakovlev, G. N. (1960) *Radiokhimiya*, **2**, 549–58; *Sov. Radiochem.*, **2** (5), 39–47.

Lebedev, I. A., Pirozhkov, S. V., and Yakovlev, G. N. (1962) *Radiokhimiya*, **4**, 304–8; *Sov. Radiochem.*, **4**, 273–6.

Lebedev, I. A., Myasoedov, B. F., and Guseva, L. I. (1974) *J. Radioanal. Chem.*, **21**, 259–66.

Lederer, C. M. and Shirley, V. S. (eds.) (1978). *Table of Isotopes,* 7th edn, Wiley-Interscience, New York.

Lobanov, Yu. V., Buklanov, G. V., Abdullin, F. Sh., Polyakov, A. N., Shirokovsky, I. V., Tsyganov, Yu. S. and Utyonkov, V. K. (1997) *Nucl. Instrum. Methods*, **A397**, 26–29.

Lougheed, R. W., Wild, J. F., Hulet, E. K., Hoff, R. W., and Landrum, J. H. (1978) *J. Inorg. Nucl. Chem.*, **40**, 1865–9.

Marei, S. A. and Cunningham, B. B. (1972) *J. Inorg. Nucl. Chem.*, **34**, 1203–6.

Maxwell, S. L. (1996) *Nucl. Mater. Manage.*, **25**, 686–90.

Metzger, R. L., Jessop, B. H., and McDowell, B. L. (1995) *Radioact. Radiochem.*, **6**, 46–50.

Mikheev, N. B. (1983) *Radiochim. Acta*, **32**, 69.

Mikheev, N. B., Kazakevich, M. Z., and Rumer, I. A. (1992) *Radiokhimiya*, **34**, 31–4; *Radiochemistry*, **34**, 293–5.

Miles, J. H. (1965) *J. Inorg. Nucl. Chem.*, **27**, 1595–600.

Mincher, B. J. (1992) *Solvent Extr. Ion Exch.*, **10**, 615–22.

Moeller, T. and Moss, F. A. (1951) *J. Am. Chem. Soc.*, **73**, 3149–51.

Molochnikova, N. P., Shkinev, V. M., and Myasoedov, B. F. (1992) *Solvent Extr. Ion Exch.*, **10**, 679–712.

Moore, F. L. (1971) *Anal. Chem.*, **43**, 487–9.

Morss, L. R., Fuger, J., Goffart, J., and Haire, R. G. (1983) *Inorg. Chem.*, **22**, 1993.

Morss, L. R., Richardson, J. W., Williams, C. W., Lander, G. H., Lawson, A. C., Edelstein, N. M., and Shalimoff, G. V. (1989) *J. Less Common Metals*, **156**, 273–89.

Mosley, W. C. (1971) *J. Am. Ceram. Soc.*, **54**, 475–9.

Mosley, W. C. (1972) *J. Inorg. Nucl. Chem.*, **34**, 539–55.

Moulin, C., Decambox, P., and Mauchien, P. (1997) *J. Radioanal. Nucl. Chem.*, **226**, 135–8.

Müller, W., Reul, J., and Spirlet, J. C. (1972) *Atomwirt. Atomtech.*, **17**, 415–16.

Müller, W., Reul, J., and Spirlet, J. C. (1977) *Rev. Chim. Miner.*, **14**, 212–24.

Musikas, C. (1999) in *Chemical Separation Technologies and Related Methods of Nuclear Waste Management* (eds. G. R. Choppin and M. Kh. Khankhasayev), Kluwer Academic Publications, Dordrecht, pp. 99–122.

Myasoedov, B. F., Milyukova, M. S., and Ryzhova, L. V. (1970) *Radiochem. Radioanal. Lett.*, **5**, 19–23.

Myasoedov, B. F., Lebedev, I. A., Mikhailov, V. M., and Frenkel, V. Ya. (1973) *Radiochem. Radioanal. Lett.*, **14**, 131–4; (1974) *Radiochem. Radioanal. Lett.*, **17**, 359–65.

Myasoedov, B. F. and Kremliakova, N. Yu. (1985) in *Americium and Curium Chemistry and Technology* (eds. N. M. Edelstein, J. D. Navratil, and W. W. Schulz), Reidel Publishing Co, New York, pp. 53–79.

Myasoedov, B. F. and Lebedev, I. A. (1991) *Anal. Chem.*, **147**, 5–26.

Myasoedov, B. F. (1994) *J. Alloys Compds*, **213/214**, 290–9.

Nave, S. E., Huray, P. G., Peterson, J. R., Damien, D. A., and Haire, R. G. (1981) *Physica*, **107B**, 253–4.

Nave, S. F., Haire, R. G., and Huray, P. G. (1983) *Phys. Rev. B*, **28**, 2317–27.

Navratil, J. D. and Schulz, W. W. (1993) *J. Miner. Metals Mater.*, **45**, 32–4.

Niese, S. and Gleisberg, B. (1995) *J. Radioanal. Nucl. Chem. Lett.*, **200**, 31–41.

Nikolaev, V. M. and Lebedev, V. M. (1975) *Zh. Neorg. Khim.*, **20**, 1359–61; *Sov. J. Inorg. Chem.*, **20**, 765–7.

Noé, M., Fuger, J., and Duyckaerts, G. (1970) *Inorg. Nucl. Chem. Lett.*, **6**, 111–19.

Noé, M. and Fuger, J. (1971) *Inorg. Nucl. Chem. Lett.*, **7**, 421–30.

Novikov, A. P. and Myasoedov, B. F. (1987) *Solvent Extr. Ion Exch.*, **5**, 117–27.

Novikov, A. P., Bukina, T. I., Karalova, Z. K., and Myasoedov, B. F. (1988) *Radiokhimiya*, **29**, 184–9.

Nugent, L. J., Burnett, J. L., Baybarz, R. D., Werner, G. K., Tanner, J. P., Tarrant, J. R., and Keller, O. L. (1969) *J. Phys. Chem.*, **73**, 1540–9.

Nugent, L. J., Laubereau, P. G., Werner, G. K., and Vander Sluis, K. L. (1971) *J. Organomet. Chem.*, **27**, 365–72.

Nugent, L. J., Baybarz, R. D., Burnett, J. L., and Ryan, J. L. (1973) *J. Phys. Chem.*, **77**, 1528–39.

Oetting, F. L., Rand, M. H., and Ackermann, R. J. (1976) *The Chemical Thermodynamics of Actinide Elements and Compounds,* part 1, *The Actinide Elements*, IAEA, Vienna, p. 34.

Okamoto, H. (2000) *J. Phase Equil.*, **21**, 108.

Ozawa, M., Nemeto, S., Togashi, A., Kawata, T., and Onishi, K. (1992) *Solvent Extr. Ion Exch.*, **10**, 829–46.

Pages, M. and Demichelis, R. (1966) *C. R. Acad. Sci. Paris C*, **263**, 938–40.

Paviet, P., Fanghänel, Th., Klenze, R., and Kim, J. I. (1996) *Radiochim. Acta*, **74**, 99–103.

Penneman, R. A. and Ferguson, D. E. (1971) *Proc. Sem. Radiat. Prot. Problems Relating to Transuranium Elements,* Karlsruhe, West Germany, September 21–25, 1970, CID, Luxembourg, pp. 85–98.

Penneman, R. A., Ryan, R. R., and Rosenzweig, A. (1973) *Struct. Bonding*, **13**, 1–52.

Peretrukhin, V. F., Enin, E. A., Dzyubenko, V. I., Kopytov, V. V., Polyukhov, V. G., Vasil'ev, V. Ya., Timofeev, G. A., Rykov, A. G., Krot, N. N., and Spitsyn, V. I. (1978) *Dokl. Akad. Nauk SSSR*, **242**, 1359–62; *Dokl. Acad. Sci. USSR*, **242**, 503–6.

Peters, T. B., Hobbs, D. T., Diprete, D. P., Diprete, C. C., and Fink, S. D. (2002) *Final Report on the Demonstration of Disposal of Americium and Curium Legacy Material Through the High Level Waste System*, US Report WSRC-TR–2001–00503.

Peterson, J. R. and Fuger, J. (1971) *J. Inorg. Nucl. Chem.*, **33**, 4111–7.

Peterson, J. R. (1972) *J. Inorg. Nucl. Chem.*, **34**, 1603–7.

Peterson, J. R. and Burns, J. H. (1973) *J. Inorg. Nucl. Chem.*, **35**, 1525–30.

Radchenko, V. M., Seleznev, A. G., Shushakov, V. D., Ryabinin, M. A., Lebedeva, L. S., Karelin, E. A., and Vasil'ev, V. Ya. (1985) *Radiokhimiya*, **27**, 33–7; *Sov. Radiochem.*, **27**, 33–6.

Radchenko, V. M., Seleznev, A. G., Lebedeva, L. S., Droznik, R. R., Ryabinin, M. A., and Shushakov, V. D. (1989) *Radiokhimiya*, **31**, 1–7; *Sov. Radiochem.*, **31**, 145–50.

Radchenko, V. M., Seleznev, A. G., Ryabinin, M. A., Droznik, R. R., and Vasil'ev, V. Ya. (1995) *Radiokhimiya*, **37**, 317–321; *Radiochemistry*, **37**, 292–6.

Radchenko, V. M., Seleznev, A. G., Ryabinin, M. A., Droznik, R. R., and Vasil'ev, V. Ya. (1996) *Radiokhimiya*, **38**, 391–4; *Radiochemistry*, **38**, 369–72.

Radchenko, V. M., Seleznev, A. G., Droznik, R. R., and Ryabinin, M. A. (1998) *Radiokhimiya*, **40**, 6–8; *Radiochemistry*, **40**, 4–6.

Radchenko, V. M., Andreichikov, B. M., Wänke, H., Gavrilov, V. D., Korchuganov, B. N., Rieder, R., Ryabinin, M. A., and Economou, T. (1999) *Radiokhimiya*, **41**, 150–2; *Sov. Radiochem.*, **41**, 155–8.

Radchenko, V., Andreichikov, B., Wänke, H., Gavrilov, V., Korchuganov, B., Rieder, R., Ryabinin, M., and Economou, T. (2000) *Appl. Rad. Isot.*, **53**, 821–4.

Raison, P. E. and Haire, R. G. (2001) *Prog. Nucl. Energy*, **38**, 251–4.

Rameback, H. and Skalberg, M. (1998) *J. Radioanal. Nucl. Chem.*, **235**, 229–33.

Raschella, D. L., Fellows, R. L., and Peterson, J. R. (1981) *J. Chem. Thermodyn.*, **13**, 303–12.

Reichlin, R. L., Akella, J., Smith, G. S., and Schwab, M. (1981) in *Actinides – 1981*, Lawrence Berkeley Laboratory Report LBL-12441.

Ryan, J. L. (1975) *Gmelin Handbook of Inorganic Chemistry, Transuranics,* part D2 (ed. G. Koch), Springer-Verlag, Berlin, pp. 373–436.

Saprykin, A. S., Shilov, V. P., Spitsyn, V. I., and Krot, N. N. (1976) *Dokl. Akad. Nauk SSSR*, **226**, 853–6; *Dokl. Acad. Sci. USSR*, **226**, 114–16.

Schenkel, R. (1977) *Solid State Commun.*, **23**, 389–92.

Scherer, V. and Fochler, M. (1968) *J. Inorg. Nucl. Chem.*, **30**, 1433–7.

Seaborg, G. T., James, R. A., and Ghiorso, A. (1949) in *The Transuranium Elements* (eds. G. T. Seaborg, J. J. Katz, and W. W. Manning), Natl. Nucl. En. Ser., Div. IV, 14B, McGraw-Hill, New York, pp. 1554–71.

Seaborg, G. T. (1972) *Pure Appl. Chem.*, **30**, 539–49.

Seaborg, G. T. (1985) The 40th Anniversary of the Discovery of Americium and Curium, in *Americium and Curium Chemistry and Technology* (eds. N. M. Edelstein, J. D. Navratil, and W. W.Schulz), Reidel Publishing, Boston, MA, pp. 3–17.

Shannon, R. D. (1976) *Acta Crystallogr.*, **A32**, 751–67.

Soderholm, L. (1992) *J. Alloys Compds*, **181**, 13–22.

Soderholm, L., Skanthakumar, S., and Williams, C. W. (1999) *Phys. Rev. B*, **60**, 4302–8.

Spitsyn, V. I. and Ionova, G. V. (1978) *Radiokhimiya*, **20**, 328–32; *Sov. Radiochem.*, **20**, 279–83.

Stephanou, S. E. and Penneman, R. A. (1952) *J. Am. Chem. Soc.*, **74**, 3701.

Stevenson, J. N. (1973) Oak Ridge National Laboratory Report TID–26453, 28, 30534.

Stevenson, J. N. and Peterson, J. R. (1975) *Microchem. J.*, **20**, 213–20.

Stevenson, J. N. and Peterson, J. R. (1979) *J. Less Common Metals*, **66**, 201–10.

Stroński, I. and Rekas, M. (1973) *Radiochem. Radioanal. Lett.*, **14**, 297–304.

Sullivan, J. C., Gordon, S., Mulac, W. A., Schmidt, K. M., Cohen, D., and Sjoblom, R. (1976) *Inorg. Nucl. Chem. Lett.*, **12**, 599–601.

Takano, M., Itoh, A., Akabori, M., Ogawa, T., Numata, M., and Okamoto, H. (2001) *J. Nucl. Mater.*, **294**, 24–7.

Takeishi, H., Kitatsuji, Y., Kimura, T., Meguro, Y., Yoshida, Z., and Kihara, S. (2001) *Anal. Chim. Acta*, **431**, 69–80.

Tanner, S. P. and Choppin, G. R. (1968) *Inorg. Chem.*, **7**, 2046–8.

Thompson, G. H. (1972) *Ion Exch. Membranes*, **1**, 87–9.

Trautmann, N. and Folger, H. (1989) *Nucl. Instrum. Methods*, **A282**, 102–6.

Tuli, J. K. (ed.) (2002) *Nucl. Data Sheets* 95.

Vasil'ev, V. I., Kalevich, E. S., Radchenko, V. M., Egunov, V. P., Izmalkov, A. N., Shimbarev, E. V., and Vasil'ev, V. Ya. (1989) *Radiokhimiya*, **31**, 35–7; *Sov. Radiochemistry*, **31**, 651–3.

Vasil'ev, V. I., Kalevich, E. S., Radchenko, V. M., Egunov, V. P., Izmalkov, A. N., Shimbarev, E. V., and Vasil'ev, V. Ya. (1990) *Radiokhimiya*, **32**, 6–8; *Sov. Radiochem.*, **32**, 141–3.

Vasudeva Rao, P. R., Kusumakumari, M., and Patil, S. K. (1978) *Radiochem. Radioanal. Lett.*, **33**, 305–14.

Vesnovskii, S. P., Vjachin, V. N., and Kavitov, P. N. (1996) *J. Radioanal. Nucl. Chem.*, 105–12.

Wallmann, J. C. (1964) *J. Inorg. Nucl. Chem.*, **26**, 2053–7.

Wallmann, J. C., Fuger, J., Peterson, J. R., and Green, J. L. (1967) *J. Inorg. Nucl. Chem.*, **29**, 2745–51.

Ward, J. W. and Hill, H. H. (1975) in *Heavy Element Properties* (eds. W. Müller and M. Blank), vol. I, North-Holland, Amsterdam, pp. 65–79.

Ward, J., Ohse, R. W., and Reul, R. (1975) *J. Chem. Phys.*, **62**, 2366–72.

Ward, J. W., Kleinschmidt, P. D., Haire, R. G., and Brown, D. (1980) in *Lanthanide and Actinide Chemistry and Spectroscopy* (ACS Symp. Ser. 131), American Chemical Society, Washington DC, pp. 199–220.

Weigel, F. and Haug, H. (1965) *Radiochim. Acta*, **4**, 227–8.

Weigel, F., Wishnevsky, V., and Hauske, H. (1977) *J. Less Common Metals*, **56**, 113–23.

Weigel, F. and Marquardt, R. (1983) *J. Less Common Metals*, **90**, 283–90.

Werner, L. B. and Perlman, I. (1951) *J. Am. Chem. Soc.*, **73**, 5215–17.

Wimmer, H., Klenze, R., and Kim, J. I. (1992) *Radiochim. Acta*, **56**, 79–83.

Wimmer, H., Kim, J. I., and Klenze, R. (1992) *Radiochim. Acta*, **58/59**, 165–71.

Yusov, A. B., Fedoseev, A. M., Spitsyn, V. I., and Krot, N. N. (1986a) *Dokl. Akad. Nauk SSSR*, **289**, 1441–4.

Yusov, A. B., Perminov, V. P., and Krot, N. N. (1986b) *Radiokhimiya*, **28**, 72–8; *Sov. Radiochem.*, **28**, 63–8.

Yusov, A. B. and Fedoseev, A. M. (1989a) *Radiokhimiya*, **31**, 16–19; *Sov. Radiochem.*, **31**, 538–41.

Yusov, A. B. and Fedoseev, A. M. (1989b) *Radiokhimiya*, **31**, 19–23; *Sov. Radiochem.*, **31**, 541–4.

Yusov, A. B. and Fedoseev, A. M. (1990) *Radiokhimiya*, **32**, 73–6; *Sov. Radiochem.*, **31**, 69–71.

Yusov, A. B. and Fedoseev, A. M. (1991) *J. Radioanal. Nucl. Chem. Articles*, **147**, 201–6.

Yusov, A. B. and Fedoseev, A. M. (1992a) *Radiokhimiya*, **34**, 61–70; *Sov. Radiochem.*, **34**, 314–20.

Yusov, A. B. and Fedoseev, A. M. (1992b) *Radiokhimiya*, **34**, 70–77; *Sov. Radiochem.*, **34**, 320–5.

Zachariasen, W. H. (1973) *J. Inorg. Nucl. Chem.*, **35**, 3487–97.

Zhu, Y. and Jiao, R. (1994) *Nucl. Tech.*, **1083**, 361–9.

CHAPTER TEN

BERKELIUM

David E. Hobart and Joseph R. Peterson

10.1 HISTORICAL

As was the case for the previously discovered transuranium elements, element 97 was first produced via a nuclear bombardment reaction. In December 1949 ion-exchange separation of the products formed by the bombardment of ^{241}Am with accelerated alpha particles provided a new electron-capture activity eluting just ahead of curium (Thompson *et al.*, 1950a,b). This activity was assigned to an isotope (mass number 243) of element 97. The new element was named berkelium after Berkeley, California, USA, the city of its discovery, in a manner parallel to the naming of its lanthanide analog, terbium, after Ytterby, Sweden. The initial investigations of the chemical properties of berkelium were limited to tracer experiments (ion exchange and coprecipitation), and these were sufficient to establish the stability of Bk(III) and the accessibility of Bk(IV) in aqueous solution and to estimate the electrochemical potential of the Bk(IV)/Bk(III) couple (Thompson *et al.*, 1950b,c). Because a complete study of the chemistry of an element is not possible by tracer methods alone, a program for long-term neutron irradiation of about 8 g of ^{239}Pu was initiated in 1952 in the Materials Testing Reactor (Arco, Idaho, USA) to provide macroquantities of berkelium (Cunningham, 1959). In 1958 about 0.6 μg of ^{249}Bk was separated, purified, and used in experiments to determine the absorption spectrum of Bk(III) in aqueous solution and to measure the magnetic susceptibility of Bk(III) (Cunningham, 1959). No Bk(III) absorption was observed over the wavelength range 450–750 nm, but an upper limit of about 20 was set for the molar absorptivity of any

Bk(III) absorption in this wavelength region. The magnetic susceptibility, measured from 77 to 298 K with the Bk(III) ions sorbed in a single bead of cation-exchange resin, was found to conform to the Curie–Weiss law with an effective moment of 8.7 μ_B, suggesting a $5f^8$ electronic configuration for the Bk(III) ion. The first structure determination of a compound of berkelium, the dioxide, was carried out in 1962 (Cunningham, 1963). Four X-ray diffraction lines were obtained from 4 ng of BkO_2 and indexed on the basis of a face-centered cubic (fcc) structure with $a_0 = (0.533 \pm 0.001)$ nm. In the intervening years since this initial work to characterize element 97, considerable information about the physicochemical properties of berkelium has been obtained in spite of the rather limited availability and the short half-life (330 days) of ^{249}Bk, the only isotope available in bulk quantities.

The authors have focused this review of the chemistry of berkelium on open literature references in English or English translation, except where it was deemed necessary to cite a research institution report or technical memorandum or personal communication. References to theses, dissertations, and patents are minimal. The biologic and metabolic effects of exposure to and/or ingestion of berkelium on humans and animals have not been reviewed here (see Chapter 31). Also excluded are references dealing with the determination and/or use of the nuclear properties of the various isotopes of berkelium, with the notable exception of a few modern references dealing with the use of ^{249}Bk as a target material for the production of transactinide elements. The references cited herein are not necessarily inclusive or always the original ones, yet they should be adequate to permit the interested reader to access easily the broader literature beyond.

Earlier reviews of the physicochemical properties of berkelium are available in Keller (1971), in several new supplement series volumes of the *Gmelin Handbuch der Anorganischen Chemie* (e.g. Peterson, 1976), Peterson and Hobart (1984), and in Hobart and Peterson (1986).

10.2 NUCLEAR PROPERTIES, AVAILABILITY, AND APPLICATIONS

Selected nuclear properties of the 14 known isotopes of berkelium, ranging from mass numbers 238 to 251, are listed in Table 10.1 (Appendix II). Included in this list are two neutron-deficient isotopes that have been identified since the publication of the second edition of this text in 1986. These are ^{238}Bk with an electron-capture decay half-life of 2.4 min (Kreek *et al.*, 1994) and ^{241}Bk with an electron-capture decay half-life of 4.6 min (Asai *et al.*, 2003). Only ^{249}Bk is available in bulk quantities for chemical studies, as a result of prolonged neutron irradiation of Pu, Am, or Cm (Bigelow *et al.*, 1981). About 1 g of this isotope has been isolated from target rods irradiated in the High Flux Isotope Reactor (HFIR) at Oak Ridge National Laboratory (ORNL) in east Tennessee, USA, over the period 1967–2001 (Knauer, 2002). The relative atomic mass of

Table 10.1 *Nuclear properties of berkelium isotopes.*[a]

Mass number	*Half-life*	*Mode of decay*	*Main radiations* (MeV)	*Method of production*
238	2.4 min	EC		^{241}Am(α,7n)
240	4.8 min	EC		^{232}Th(^{14}Ne,6n)
241	4.6 min	EC	γ 0.2623	^{239}Pu(^{6}Li,4n)
242	7.0 min	EC		^{232}Th(^{14}N,4n) ^{232}Th(^{15}N,5n)
243	4.5 h	EC 99.85% α 0.15%	α 6.758 (15%) 6.574 (26%) γ 0.755	^{243}Am(α,4n)
244	4.35 h	EC > 99% α 6×10^{-3}%	α 6.667 (~50%) 6.625 (~50%) γ 0.218	^{243}Am(α,3n)
245	4.94 d	EC > 99.88% α 0.12%	α 6.349 (15.5%) 6.145 (18.3%) γ 0.253 (31%)	^{243}Am(α,2n)
246	1.80 d	EC	γ 0.799 (61%)	^{243}Am(α,n)
247	1.38×10^{3} yr	α	α 5.712 (17%) 5.532 (45%) γ 0.084 (40%)	^{247}Cf daughter ^{244}Cm(α,p)
248[b]	23.7 h	β^- 70% EC 30%	β^- 0.86 γ 0.551	^{248}Cm(d,2n)
248[b]	>9 yr	decay not observed		^{246}Cm(α,pn)
249	330 d	β^- > 99% α 1.45×10^{-3}%	α 5.417 (74.8%) 5.390 (16%) β^- 0.125 γ 0.327 weak	multiple n capture
250	3.217 h	β^-	β^- 1.781 γ 0.989 (45%)	^{254}Es daughter ^{249}Bk(n,γ)
251	55.6 min	β^-	β^- ~ 1.1 γ 0.178	^{255}Es daughter

[a] Appendix II.

[b] Not known whether ground state nuclide or isomer.

^{249}Bk was given as 249.075 (Audi and Wapstra, 1995), and the most recent determination of its half-life yielded a value of (330 ± 4) days (Popov and Timofeev, 1999).

Besides the research use of ^{249}Bk for the characterization of the chemical and physical properties of element 97, its relatively rapid decay to ^{249}Cf (ca. 0.22% per day) makes it a valuable source of this important isotope of californium for chemical study. This genetic relationship has been exploited in studies of the chemical consequences of beta (β^-) decay in the bulk-phase solid state (Young *et al.*, 1980; Ensor *et al.*, 1981; Young *et al.*, 1984; Peterson *et al.*, 1986).

As a consequence of recent interest in nuclear power reactors to increase fuel burn-up and in the areas of nuclear waste transmutation, nuclear deterrence, and astrophysics, more accurate data on the nuclear characteristics of heavier actinides, including berkelium, are in demand. A recent compilation of the decay characteristics of actinides, including ^{249}Bk and ^{250}Bk, has been published (Popov and Timofeev, 1999). Fission fragment angular distributions for the compound nucleus ^{246}Bk have been measured (Behera *et al.*, 2001). ^{246}Bk was produced via two nuclear reaction pathways, lying on either side of the Businaro–Gallone critical asymmetry parameter.

By combining measured fission probabilities for reactions such as ^{248}Cm(^{3}He, d)^{249}Bk → fission (Gavron *et al.*, 1977) with calculated total neutron inelastic cross sections, empirical predictions for the neutron-induced fission cross sections for several actinides have been obtained (Britt and Wilhelmy, 1979). These predictions ignore differences in angular momentum distributions between the direct reaction products and the incident neutrons when populating the same energy levels in the compound nucleus. As demonstrated by Britt and Wilhelmy (1979), this assumption is reasonably good for equivalent neutron energies (energy of an incident neutron that would leave the identical residual nucleus at the same energy as is reached by the direct nuclear reaction) of greater than about 0.5 MeV. For Bk the equivalent (n,f) cross sections were extracted for the berkelium isotopes with mass numbers 244 to 248. Odd-mass-number Bk nuclei exhibit a strong reduction in the fission probability for excitation energies above the neutron-binding energy that is presumably caused by the opening of a large number of competing decay channels (Britt and Wilhelmy, 1979). Although no experimentally measured fission cross section for $^{248\mathrm{m}}$Bk has been determined, estimates of up to 1000 barns have been predicted based on correlations with other actinides having similar characteristics (Ronen, 1998).

The intrinsic single-particle states of ^{249}Bk have been studied by measuring the gamma radiations emitted after the alpha decay of ^{253}Es. The low spin states were studied by measuring gamma rays in the beta decay of ^{249}Cm. Levels in ^{249}Bk were also studied by the reaction ^{248}Cm(α,t)^{249}Bk. A diagram of the intrinsic states for ^{249}Bk, deduced from these decay studies, has been constructed. This well-established nuclear structure information, available only for the heaviest elements for which macro amounts are obtainable, can be used either to determine the parameters of a single-particle potential or to test the nuclear models of super-heavy elements (Ahmad, 2002).

Although currently there are no practical or commercial applications for any known berkelium isotopes, ^{249}Bk has been used extensively as a target material for the production of still heavier actinides such as lawrencium (Brüchle *et al.*, 1988; Scherer *et al.*, 1988) and transactinide elements such as element 104, rutherfordium, and element 107, bohrium (Gregorich *et al.*, 1988; Kratz *et al.*, 1992; Gobrecht *et al.*, 1999; Paulus *et al.*, 1999; Eichler *et al.*, 2000; Wilk *et al.*, 2000).

10.3 PRODUCTION

Methods of production for each of the isotopes of berkelium are listed in Table 10.1 (Appendix II). Only ^{249}Bk is available in bulk quantities for chemical studies, as a result of prolonged neutron irradiation of Pu, Am, or Cm (Bigelow *et al.*, 1981). About 0.73 g of this isotope was isolated from target rods irradiated with neutrons in the ORNL HFIR over the period 1967–1985 (Ferguson and Bigelow, 1969; King *et al.*, 1981; Bigelow, 1985). Toward the end of 1986, HFIR was shut down for an extended period of time for major maintenance and safety considerations. This action resulted from the nuclear reactor accident at Chernobyl (former USSR) earlier that year. After a 4+ year hiatus, HFIR was restarted with a power limit of 85 MW, down from the previous 100 MW level. Through the HFIR product campaign that started in late 2000, an additional 0.28 g of ^{249}Bk was recovered during the period 1986–2001. It is not known to the present authors how much ^{249}Bk has been produced elsewhere in the world, for instance, in the former USSR.

10.4 SEPARATION AND PURIFICATION

Berkelium may be purified by many methods that are also applicable to other actinide elements. Therefore, only those methods that apply specifically to berkelium separation and purification are treated here.

Because berkelium can be readily oxidized to Bk(IV), it can be separated from other, non-oxidizable transplutonium elements by combining oxidation–reduction (redox) methods with other separation techniques. The first application of this approach was performed by oxidizing Bk(III) with BrO_3^- in nitric acid solution (Peppard *et al.*, 1957). The resultant Bk(IV) was then extracted with bis(2-ethylhexyl)phosphoric acid (HDEHP) in heptane followed by back-extraction with nitric acid containing H_2O_2 as a reducing agent. In addition to other reports of the use of BrO_3^- as an oxidizing agent in berkelium purification procedures (Knauer and Weaver, 1968; Weaver, 1968; Fardy and Weaver, 1969; Overman, 1971; Erin *et al.*, 1979b), the use of CrO_4^{2-} (Knauer and Weaver, 1968; Milyukova *et al.*, 1980), $Cr_2O_7^{2-}$ (Moore, 1966; Shafiev *et al.*, 1974; Milyukova *et al.*, 1980), $Ag(I)/S_2O_8^{2-}$ (Milyukova *et al.*, 1978, 1980), PbO_2 (Myasoedov *et al.*, 1971; Myasoedov, 1974; Shafiev *et al.*, 1974), BiO_3^- (Shafiev *et al.*, 1974), O_3 (Myasoedov, 1974), and photochemical oxidation (Myasoedov, 1974) has also been reported.

Separation of the oxidized berkelium has been accomplished by the use of: (1) liquid–liquid extraction with HDEHP (Peppard *et al.*, 1957; Knauer and Weaver, 1968; Kosyakov *et al.*, 1977; Erin *et al.*, 1979b; Yakovlev and Kosyakov, 1983), trioctylphosphine oxide (Kosyakov and Yakovlev, 1983), alkylpyrocatechol (Karalova *et al.*, 1983), 2-thenoyltrifluoroacetone (TTA) (Moore 1966, 1969), primary, tertiary, or quaternary amines (Moore, 1969;

Milyukova and Myasoedov, 1978; Milyukova *et al.*, 1978, 1980; Malikov *et al.*, 1983), or tri(*n*-butyl)phosphate (TBP) (Milyukova *et al.*, 1981; Yakovlev *et al.*, 1982); (2) extraction chromatography with HDEHP (Kooi and Boden, 1964; Kooi *et al.*, 1964; Overman, 1971; Erin *et al.*, 1979a) or zirconium phosphate adsorbant (Myasoedov *et al.*, 1971; Shafiev and Efremov, 1972; Myasoedov, 1974; Shafiev *et al.*, 1974); (3) precipitation of the iodate (Weaver, 1968; Fardy and Weaver, 1969); or (4) ion-exchange methods (Moore, 1967; Overman, 1971; Shafiev and Efremov, 1972; Guseva and Stepushkina, 1987; Guseva *et al.*, 1987, 1991; Firsova *et al.*, 1996, 1998a,b). These techniques can be applied separately or in combination with one another.

The purification procedures outlined above provide separation of berkelium from all trivalent lanthanides and actinides with the notable exception of cerium. Because berkelium and cerium exhibit nearly identical redox behavior, most redox separation procedures include a Bk–Ce separation step (Moore, 1967; Horwitz *et al.*, 1969; Guseva *et al.*, 1971; Chudinov and Pirozhkov, 1972; Shafiev and Efremov, 1972; Shafiev *et al.*, 1974). Separation of Bk(III) from Ce(III) and other trivalent lanthanide and actinide elements can also be accomplished without the use of redox procedures (Moore and Jurriaanse, 1967; Farrar *et al.*, 1968; Horwitz *et al.*, 1969; Aly and Latimer, 1970; Guseva *et al.*, 1971; Chudinov and Pirozhkov, 1972; Harbour, 1972; Shafiev and Efremov, 1972; Horwitz and Bloomquist, 1973; Korpusov *et al.*, 1975; Khopkar and Mathur, 1980; Mathur and Khopkar, 1982; Ensor and Shah, 1984).

During the period 1967–2001, personnel at ORNL isolated and purified a total of about 1 g of ^{249}Bk (King *et al.*, 1981; Bigelow, 1985; Knauer, 2002) using the procedure outlined in Fig. 10.1.

The transcurium elements, partitioned by LiCl-based anion exchange, are precipitated as hydroxides, filtered, and dissolved in nitric acid. Initial isolation is accomplished by high-pressure elution from cation-exchange resins with α-hydroxyisobutyrate solution. The berkelium fraction is oxidized and extracted into HDEHP/dodecane from HNO_3–$NaBrO_3$ solution. The organic fraction containing Bk(IV) is treated with 2,5-di(*t*-butyl)hydroquinone (DBHQ) to reduce the Bk(IV) to Bk(III) before back-extracting (stripping) it into HNO_3–H_2O_2 solution. Then another oxidation/extraction, reduction/back-extraction cycle is carried out. The solution at this point is radiochemically pure except for the fission product cerium. After solvent cleanup and evaporation to dryness, the berkelium is dissolved in 0.1 M HCl for final ion-exchange purification steps including alcoholic HCl elution from cation-exchange resin and cation cleanup columns (Baybarz *et al.*, 1973).

Procedures for the rapid separation of berkelium from other actinides, lanthanides, and fission products have been developed in order to measure the decay properties of short-lived isotopes. Berkelium and cerium were separated from other elements using solvent extraction with HDEHP followed by cation-exchange high-pressure liquid chromatography (HPLC) using α-hydroxyisobutyrate as the eluant (Liu *et al.*, 1981). The elution curve, showing

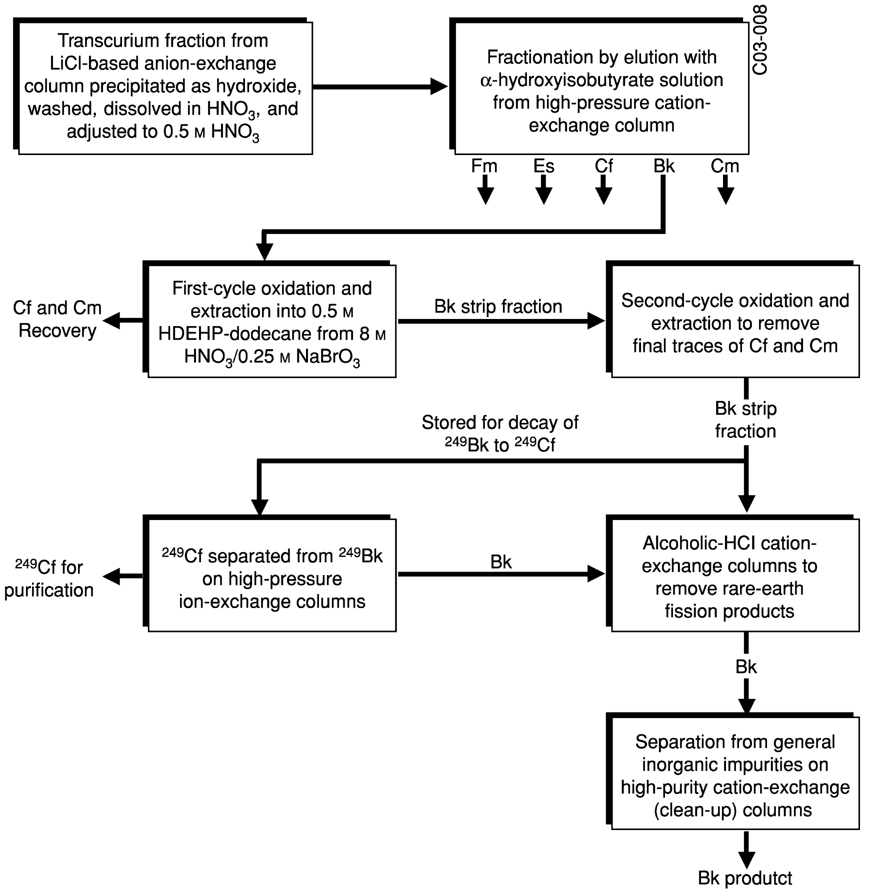

Fig. 10.1 *Schematic diagram of procedures used in the final isolation and purification of berkelium in the transuranium processing plant at the Oak Ridge National Laboratory.* (*Adapted from Baybarz* et al., 1973.)

a clean separation of Bk from Ce, is shown in Fig. 10.2. The total separation time was reported to be 8 min. (*Note*: A discrepancy exists in the drop number in the abscissa of Fig. 10.2; however, this figure is presented as it appeared in Liu *et al.* (1981).)

The fast separation of berkelium from beryllium foil targets and gold catcher foils has been published (Liu *et al.*, 1983). New, fast separation techniques, involving volatile mineral acid–alcohol solvent systems used to isolate very short-lived isotopes, have been reported (Maruyama *et al.*, 2002).

For additional discussion of berkelium separation procedures, the reader is referred to several reviews and comprehensive texts on the subject (Korkisch, 1966; Ulstrup, 1966; Müller, 1967; Bigelow, 1974; Myasoedov *et al.*, 1974;

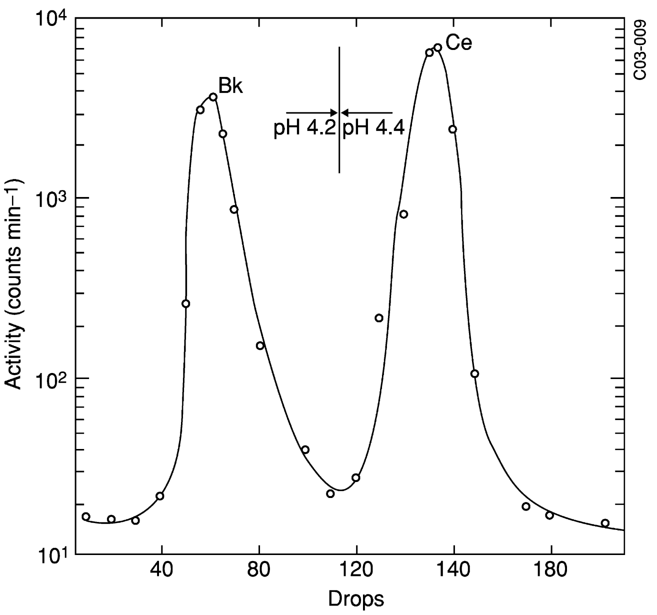

Fig. 10.2 *HPLC elution curve of Bk and Ce using* 0.5 M *ammonium α-hydroxyisobutyrate on a cation-exchange column* (*Liu* et al., 1981).

Campbell, 1981; Collins *et al.*, 1981; Myasoedov, 1987; Myasoedov and Lebedev, 1991).

10.5 PROPERTIES OF FREE ATOMS AND IONS

10.5.1 Thermochromatographic behavior of neutral atoms

The adsorption of ^{250}Bk atoms on niobium foils in a sapphire support tube has been studied (Hübener *et al.*, 2000). A deposition temperature of 1535 K was found in two separate experiments, and the enthalpy of adsorption was calculated to be –332 kJ mol^{-1}. A regular trend in the adsorption enthalpies of Bk–Fm and No is consistent with Bk adsorption on niobium in its trivalent $5f^86d^17s^2$ state (Taut *et al.*, 1998; Hübener *et al.*, 2000). In another approach by the same research group, the adsorption of elemental ^{248}Bk onto niobium was measured thermochromatographically (Taut *et al.*, 2000). The enthalpy of adsorption was determined to be –(349 ± 15) kJ mol^{-1}, in agreement with the above value, taking into account the experimental uncertainties.

10.5.2 Electronic energies

The ionization potential of neutral berkelium ($5f^97s^2$) was initially derived from spectroscopic data to be (6.229 ± 0.025) eV (Sugar, 1974). The changes in entropy associated with the stepwise ionization of gaseous berkelium atoms have also been calculated (Krestov, 1966). The energy interval between the ground level ($^7H_8$) and the first excited level ($^5H_7$) of singly ionized berkelium was determined from measurements done on plates using a high-resolution emission spectrograph and was found to be 1.48752×10^5 m^{-1} (Worden *et al.*, 1969). Several authors have calculated the energies of, and energy intervals between, the lowest-lying levels of the various electronic configurations of neutral berkelium (Nugent and Vander Sluis, 1971; Brewer, 1971a; Vander Sluis and Nugent, 1972, 1974) and of singly, doubly, and triply ionized berkelium (Brewer, 1971b; Vander Sluis and Nugent, 1974).

More recently, experimental determination of the first ionization potential of neutral berkelium was accomplished by resonance ionization mass spectroscopy (Erdmann *et al.*, 1998; Passler *et al.*, 1998; Waldek *et al.*, 2001). In this elegant approach (Kohler *et al.*, 1997) an atomic beam of Bk atoms was produced from heating a tantalum foil onto which Bk had been electrodeposited and then covered with a thin layer of titanium to reduce the Bk species to the metallic state. The Bk atoms were ionized in the presence of an electric field by multiple resonant laser excitation, and the Bk^+ ions were mass-selectively detected in a time-of-flight spectrometer. The first ionization potential was obtained by scanning the wavelength of the laser used for the last excitation step across the ionization threshold (indicated by a sudden increase in the Bk^+ count rate) at various electric field strengths. A linear plot of the ionization threshold against the square root of the electric field strength, extrapolated to zero field strength, yielded the first ionization potential of Bk to be (6.1979 ± 0.0002) eV. This value is just below the one derived from an extrapolation of spectral properties (Sugar, 1974). In addition the resonant excitation scheme used provided the energies of three of the excited energy levels of neutral Bk: 17666.0, 31541.3, and 32710.3 cm^{-1} (Kohler *et al.*, 1997; Erdmann *et al.*, 1998; Passler *et al.*, 1998).

From measurements of the energies of a number of internal conversion lines in ^{249}Bk (produced by the alpha decay of ^{253}Es), the atomic electron-binding energies in berkelium were calculated for the K through O shells (Hollander *et al.*, 1965). The K-series X-ray energies and intensities of berkelium were later measured, and the K-shell electron-binding energy was calculated (Dittner and Bemis, 1972). The measured energies and relative transition probabilities agreed well with theoretical predictions (Carlson *et al.*, 1969; Lu *et al.*, 1971). Also available are the results of relativistic relaxed-orbital *ab initio* calculations of L-shell Coster–Kronig transition energies for all possible transitions in berkelium atoms (Chen *et al.*, 1977), relativistic relaxed-orbital Hartree–Fock–Slater calculations of the neutral-atom electron binding energies in berkelium (Huang *et al.*, 1976), and calculations of the K- through O-shell binding energies and K and L X-ray energies for berkelium (Carlson and Nestor, 1977). Relativistic Hartree–Slater values of the X-ray emission rates for the filling of K- and L-shell vacancies in berkelium have been tabulated (Scofield, 1974). X-ray emission rates for the filling of all possible single inner-shell vacancies in berkelium by electric dipole transitions have been calculated using nonrelativistic Hartree–Slater wave functions (Manson and Kennedy, 1974).

10.5.3 Emission spectra

Twenty emission lines, produced from 0.2 μg of berkelium in a high-voltage spark, were reported by Gutmacher *et al.* (1965). In 1967 between 3000 and 5000 lines were recorded in the wavelength region 250–900 nm from 38 μg of ^{249}Bk in an electrodeless discharge lamp (Worden *et al.*, 1967). Many of the emission lines exhibited a well-resolved eight-component hyperfine structure, which established the nuclear spin of ^{249}Bk to be 7/2 (Worden *et al.*, 1967). This value is in agreement with that derived from nuclear decay systematics.

The ground state electronic configurations (levels) of neutral and singly ionized berkelium were identified as $5f^97s^2$ ($^6H_{15/2}$) and $5f^97s^1$ ($^7H_8$), respectively (Worden *et al.*, 1970). A nuclear magnetic dipole moment of 1.5 μ_N (Worden *et al.*, 1969) and a quadrupole moment of 4.7 barns (Conway, 1976) were determined for ^{249}Bk, based on analysis of the hyperfine structure in the berkelium emission spectrum.

The wavenumbers, wavelengths, and relative intensities of 1930 of the stronger emission lines from ^{249}Bk in the 254–980 nm wavelength region are available (Worden and Conway, 1978). The infrared emission spectrum of ^{249}Bk from 830 to 2700 nm has been recorded (Conway *et al.*, 1977). The emission profile of ^{249}Bk(III) in a silicate matrix has been studied as a function of excitation power and temperature (Assefa *et al.*, 1998). With both experimental parameters it was found that the two primary emission bands (believed to originate from f→f transitions) decreased in intensity at different rates with increasing excitation power or temperature, such that the higher-energy band became dominant over the lower-energy one. Thermal quenching and/or energy transfer between neighboring ions are possible factors responsible for this behavior (Assefa *et al.*, 1998).

A preliminary report on the self-luminescence of ^{249}Bk(III) in a $LaCl_3$ host lattice was published by Gutmacher *et al.* (1963), and the self-luminescence spectra of ^{249}Bk-doped BaF_2 and $SrCl_2$ were reported by Finch *et al.* (1978). The fluorescence and excitation spectra of Bk^{3+} ions (<0.001 mol fraction) in single-crystal $LaCl_3$ were determined using dye laser techniques (Hessler *et al.*, 1978). Selective laser excitation was used to excite specific Bk^{3+} levels, and then the subsequent fluorescence spectrum was recorded. Determining fluorescence lifetimes of all fluorescing levels and grouping the lines by lifetimes precluded confusion caused by transference of the excitation energy to a fluorescing level of another ion. The fluorescing manifolds of Bk^{3+} were found to be $J = 6$ at 1.540 μm^{-1} and $J = 4$ at 1.953 μm^{-1} (Hessler *et al.*, 1978). The absence of UV-excited sharp-line sensitized luminescence of ^{249}Bk-doped gadolinium hexafluoroacetyl acetonate has been observed (Nugent *et al.*, 1969, 1970). Such luminescence was absent also in cesium berkelium hexafluoroacetyl acetonate chelate in anhydrous ethanol (Nugent *et al.*, 1969). A study of Bk^{3+} fluorescence in H_2O and D_2O solutions has been reported, and a basis for assessing the use of fluorescence detection for transuranic ions established (Beitz *et al.*, 1981).

The first report of fluorescence from the Bk^{4+} ion included establishment of the total ground state splitting of this ion and probing the higher-lying electronic states of its $5f^7$ configuration (Jursich *et al.*, 1987). The Bk^{4+} ions were stabilized in CeF_4, where it is known that there are two distinct low-symmetry sites to accommodate them. Two Bk^{4+} bands were detected and assigned to transitions to the ground state. From laser excitation spectra taken at 4 K, a $5f^7$ energy-level diagram was proposed, which is consistent with the authors' assumption of a single average D_{4d} site symmetry. Mixing of higher lying states into the ground state caused the total ground state crystal-field splitting of Bk^{4+} in CeF_4 to be 58 cm^{-1} (Jursich *et al.*, 1987). The results of a detailed, systematic spectral analysis of these data, along with those obtained in additional site-selective laser excitation studies of another sample of Bk^{4+} in CeF_4, have been reported (Liu *et al.*, 1994a). A complete set of crystal-field parametric values was given and compared with those derived from the previous five tetravalent actinides. In addition an observed and calculated line list out to about 27 000 cm^{-1} was published (Liu *et al.*, 1994a). Another paper from the same research group focused on the use of fluorescence line narrowing spectra of 0.1 at% Bk^{4+} in CeF_4 to study emissions from the lowest energy component of $^6D_{7/2}$ at 16375 cm^{-1} to the four components of the $^8S_{7/2}$ ground multiplet (Liu *et al.*, 1994b). A linear relationship was observed between the excitation-laser photon energy and the energies of the Bk^{4+} emission lines. A subsequent study of the influence of the crystal field on the $^8S_{7/2}$ ground state splitting of Bk^{4+} ion in CeF_4, based on the 24 energy levels observed in their earlier work (Liu *et al.*, 1994a), was carried out (Brito and Liu, 2000). The parametric model used a set of nine nonzero parameters (corresponding to C_{2v} point symmetry) and yielded a good correlation between the experimental and calculated energy levels in Bk^{4+} ion. Compared with the isoelectronic Cm^{3+} ion, the large ground state splitting of Bk^{4+} ion in CeF_4 is attributed to the smaller energy gap between the ground state and the low-lying excited states (Brito and Liu, 2000). Subsequently, a model that included relativistic effects in an effective way was used to improve the theoretical reproduction of the splitting of the energy levels for such S-state f-electron ions (Smentek *et al.*, 2001). It was concluded in this work that the fitting procedure applied for the determination of the crystal-field parameters had to be done within the parametrization scheme that included the relativistic weights of the various parameters.

10.5.4 Solid-state absorption spectra

The absorption spectrum of Bk(iii) in a lanthanum chloride host matrix at 77 K was first obtained by Gutmacher (1964). A prediction of the energy-level structure of Bk(iii) was made by others the same year (Fields *et al.*, 1964). Extensive, low-temperature spectroscopic studies of $BkCl_3$ showed the absence of transitions to excited $J = 0$ and $J = 1$ states (Carnall *et al.*, 1972, 1973). This provided good evidence for a $\mu = 0$ ground level for Bk(iii), consistent with that of Tb(iii):$LaCl_3$ (Carnall and Fried, 1976). Experimental and theoretical studies of the crystal-field parameters of Bk(iii) in a $LaCl_3$ host lattice have also been reported (Carnall *et al.*, 1977).

Microscale spectrophotometric techniques, using 0.5–10 μg berkelium samples, have been applied for identification and characterization of berkelium halides and oxyhalides (Young *et al.*, 1978). The spectra of orthorhombic and hexagonal $BkCl_3$ have been recorded (Peterson *et al.*, 1986) and are shown in Fig. 10.3. Spectra of orthorhombic and monoclinic $BkBr_3$ (Peterson *et al.*, 1977a,b), trigonal and orthorhombic BkF_3 (Ensor *et al.*, 1981), and monoclinic BkF_4 (Ensor *et al.*, 1981) have been reported. This technique has also been applied to the study of the chemical consequences of radioactive decay in bulk-phase solid-state samples (Young *et al.*, 1980, 1981). It was found that the ^{249}Cf daughter growing into crystalline $^{249}BkBr_3$ exhibited the same oxidation state and crystal structure as its berkelium parent (Young *et al.*, 1980).

The absorption spectra of Bk(iii) and Bk(iv) hydroxides as suspensions in 1 m NaOH have been reported (Cohen, 1976). The solid-state absorption spectrum (Haire *et al.*, 1983) and Raman spectrum (Hobart *et al.*, 1983) of berkelium(iii) orthophosphate have been obtained, as well as those for berkelium(iii) oxalate decahydrate, $Bk_2(C_2O_4)_3 \cdot 10H_2O$ (Morris *et al.*, 2005). Line lists of the absorption bands of two organoberkelium compounds, $Bk(C_5H_5)_3$ (Laubereau and Burns, 1970) and $[Bk(C_5H_5)_2Cl]_2$ (Laubereau, 1970), have been published.

For additional information (Carnall, 1973) and discussion of the development of the theoretical treatment of berkelium spectra, the reader is referred to other sources (Carnall and Fried, 1976; Conway, 1976; Carnall *et al.*, 1984; Liu *et al.*, 1994a) and to Chapters 16 and 18.

10.5.5 Ion–molecule reactions in the gas phase

Organoberkelium ions have been produced by laser ablation of Bk_2O_3 dispersed in polyimide (Gibson and Haire, 2001a). Characterization of the resulting products via time-of-flight spectrometry identified the primary species as $BkCH_3^+$, BkC_2^+, BkC_2H^+, $BkCN^+$, BkC_4H^+, $Bk(OH)(CN)^+$, $BkOCN^+$, $BkOH^+$, $Bk(OH)_2^+$, and BkO^+, as shown in Fig. 10.4. The product ion compositions and abundance distributions were reasonably explained in the context of the electronic structure and energetics of the Bk^+ ion. Several of these organoberkelium species incorporate direct metal ion–carbon bonding via a single

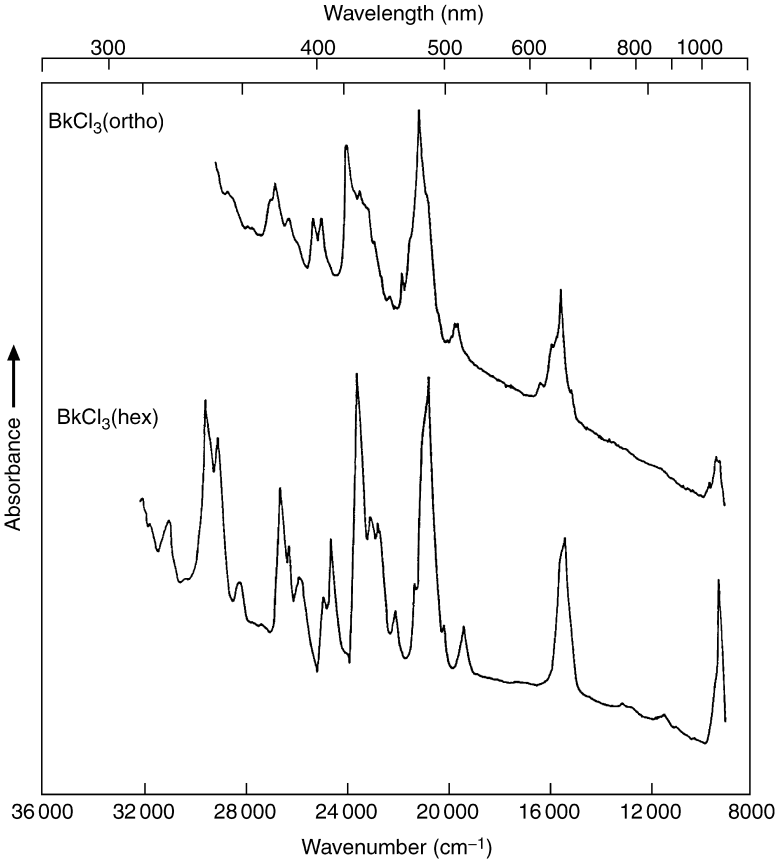

Fig. 10.3 *The solid-state absorption spectra of orthorhombic and hexagonal* $BkCl_3$ (*Peterson* et al., 1986).

σ-type covalent bond. Comparisons of the product ion compositions and abundance distributions of similarly produced organoactinide and lanthanide species provided correlations with the electronic promotion energies required to create a divalent or a monovalent state, capable of forming two or one covalent bonds, respectively (Gibson and Haire, 2001a). In an extension of the above work, gas-phase reactions of Bk^+ ion with several alkenes, butylamine, butyronitrile, and other reagents were studied in concert with similar reactions with Pu^+ ion or homologous Tb^+ ion to aid in the interpretation of the results in the context of the electronic structure and energetics of berkelium (Gibson and Haire, 2001b). A key result of this work was the finding that the efficiency of hydrocarbon, nitrile, and amine activation by Bk^+ ion directly reflected the energy required to excite the ion from its ground electronic state, $5f^97s^1$, to the lowest lying state with two spin-unpaired non-5f valence electrons, $5f^86d^17s^1$. Thus it appears that

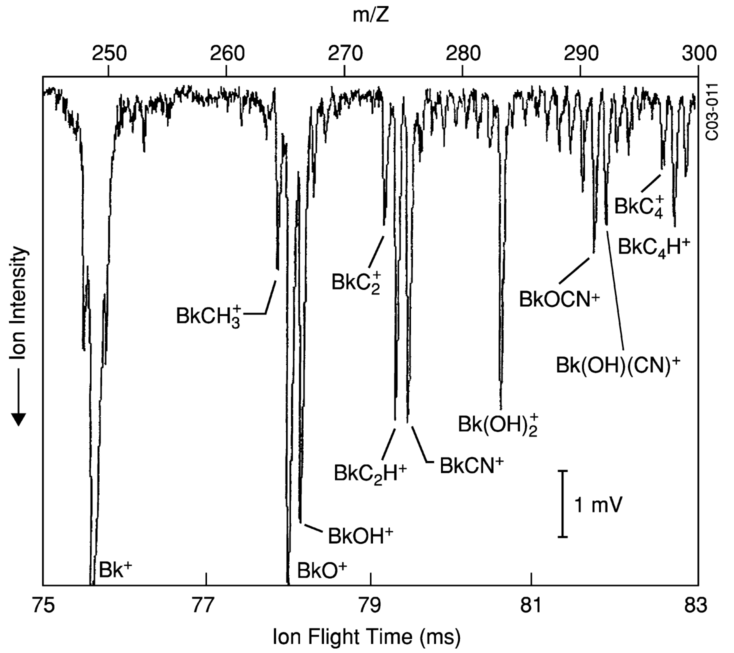

Fig. 10.4 *The mass spectrum of positive ions ablated from a Bk–polyimide target.* (*Reprinted figure with permission from Gibson and Haire* (2001*a*). *Copyright* 2001 *by Oldenbourg Verlag.*)

the 5f electrons in Bk^+ ions do not participate in organometallic bond activation. A variety of organoberkelium species were identified, as well as a few inorganic ones, e.g. BkF^+. A covalent bonding model was used to estimate the Bk^+–O bonding energy as (610 ± 40) kJ mol^{-1} (Gibson and Haire, 2001b).

10.6 THE METALLIC STATE

10.6.1 Pure metal

(a) Preparation

The first bulk (>1 μg) samples of berkelium metal were prepared in early 1969 by the reduction of BkF_3 with lithium metal vapor at about 1300 K (Peterson *et al.*, 1971). The BkF_3 samples were suspended in a tungsten wire spiral above a charge of Li metal in a tantalum crucible. Berkelium metal samples up to 0.5 mg each have been prepared via the same chemical procedure (Fuger *et al.*, 1975). Elemental berkelium can also be prepared by reduction of BkF_4 with lithium metal and by reduction of BkO_2 with either thorium or lanthanum metal

(Spirlet *et al.*, 1987). The latter reduction process is better suited to the preparation of thin metal foils unless multi-milligram quantities of berkelium are available.

(b) Physical properties

Berkelium metal exhibits two crystallographic modifications: double hexagonal close-packed (dhcp) and fcc. Thus, it is isostructural with the two preceding actinide elements, both of which also exhibit the fcc structure at high temperature. The room-temperature lattice constants of the dhcp (α) form are $a_0 = (0.3416 \pm 0.0003)$ nm and $c_0 = (1.1069 \pm 0.0007)$ nm, yielding a calculated density of 14.78 g cm^{-3} and a metallic radius (coordination number, CN 12) of 0.170 nm (Peterson *et al.*, 1971). The room-temperature metastable fcc (β) lattice parameter is $a_0 = (0.4997 \pm 0.0004)$ nm, from which the X-ray density and metallic radius (CN 12) are calculated to be 13.25 g cm^{-3} and 0.177 nm, respectively (Peterson *et al.*, 1971). The metallic radius of berkelium, assuming a metallic valence of 3- and 12-fold coordination, has been calculated to be 0.1739 nm (Sarkisov, 1966). On the other hand, the radii (CN 12) of berkelium were predicted to be 0.184 nm for a trivalent metal and 0.1704 nm for a tetravalent metal; so it was proposed that the observed dhcp form corresponds to tetravalent metal, while the fcc form represents a metallic valence of ~3.5 (Zachariasen, 1973).

Although berkelium metal is dimorphic, the transformation temperature is not known with certainty. A change in the appearance of Bk metal samples at (1203 ± 30) K during the course of two melting point determinations might correspond to the dhcp→fcc phase transformation, which should be accompanied by a 12% change in the volume of the sample (Fahey *et al.*, 1972). By analogy with the behavior of neodymium, a phase-transition temperature of (1250 ± 50) K was assigned by Ward *et al.* (1982), in agreement with the Fahey *et al.* (1972) observation. The melting point of berkelium metal was first determined to be (1259 ± 25) K from measurements on two samples (Fahey *et al.*, 1972). The melting and boiling points of elemental berkelium have been reported to be (1323 ± 50) K and (2900 ± 50) K, respectively (Ward *et al.*, 1982). These two melting-point determinations are in agreement, considering their experimental uncertainties.

The first studies of berkelium metal under pressure were performed with a diamond anvil pressure cell using energy-dispersive X-ray powder diffraction analysis (Haire *et al.*, 1984). Three different metallic phases were observed as the pressure was increased to 57 GPa. The normal-pressure dhcp form changed to an fcc form at about 8 GPa. Above 22 GPa (reported to be at about 32 GPa in later reports; Itié *et al.*, 1985; Peterson *et al.*, 1987), the fcc form was transformed to the alpha-uranium-type orthorhombic structure (Haire *et al.*, 1984). A 12% shrinkage in volume accompanied the latter transition. This collapse was associated with delocalization of the 5f electrons (Benedict *et al.*, 1984).

Below 22 GPa, a bulk modulus (compressibility) of (30 ± 10) GPa was estimated for berkelium metal (Haire *et al.*, 1984). This bulk modulus only for the normal-pressure dhcp phase of Bk metal was reported later to be 52 GPa (Itié *et al.*, 1985). Berkelium metal under pressure behaves similarly to americium, curium, and some light lanthanide metals and does not appear to undergo an isostructural phase transition corresponding to a change in metallic valence before delocalization of the 5f electrons (Johansson *et al.*, 1981).

Retention of the fcc phase in Bk metal after release of pressure (pressure quenched) allows comparison of the atomic volume of this cubic phase at room temperature and pressure (RTP) with the atomic volume of the same phase produced via thermal treatment and quenching to RTP (temperature quenched) (Haire *et al.*, 1986). The values obtained were 2.80×10^{-2} nm^3 for the pressure-quenched fcc phase and 3.12×10^{-2} nm^3 (Peterson *et al.*, 1971) for the temperature-quenched fcc phase. Similar results were found in the cases of Cm and Cf metals. In fact, for the three metals, the atomic volumes of their temperature-quenched fcc phases are all larger than those of their RTP dhcp phases. In contrast, the atomic volumes of their pressure-quenched fcc phases at RTP are in good agreement with those of their RTP dhcp phases (Haire *et al.*, 1986). The argument is made that the lattice parameter of the pressure-quenched fcc phase of these metals is preferred to that of the temperature-quenched fcc phase, in that it provides consistency with the atomic volumes of their RTP dhcp phases and the known trend in lattice parameters of their corresponding mononitrides (Haire *et al.*, 1986).

In the first experiments to measure the vapor pressure of metallic berkelium using Knudsen effusion target-collection techniques, the preliminary data were fitted with a least-squares line to give a provisional vaporization equation for the temperature range 1326–1582 K and $\Delta_{\mathrm{v}}H^0_{298} = (382 \pm 18)$ kJ mol^{-1} (Ward *et al.*, 1980). Later measurements of the vapor pressure of Bk metal over the temperature range 1100–1500 K, using combined Knudsen effusion mass-spectrometric and target-collection techniques (Ward *et al.*, 1982), led to the vaporization equations:

$$\log p(\mathrm{atm}) = (5.78 \pm 0.21) - (15718 \pm 253)/T(\mathrm{K})$$

for solid Bk between 1107 and 1319 K, and

$$\log p(\mathrm{atm}) = (5.14 \pm 0.17) - (14902 \pm 244)/T(\mathrm{K})$$

for liquid Bk between 1345 and 1528 K. The enthalpy of fusion was calculated to be 7.92 kJ mol^{-1}, and the enthalpy associated with the dhcp→fcc transition was calculated to be 3.66 kJ mol^{-1} (Ward *et al.*, 1982). The crystal entropy, S^0_{298}, of berkelium was estimated to be (76.2 ± 1.3) J K^{-1} mol^{-1} (Ward and Hill, 1976) and then later to be (78.2 ± 1.3) J K^{-1} mol^{-1}, and the average of data according to the second and third law data analysis yielded (310 ± 6) kJ mol^{-1} for its enthalpy of vaporization, $\Delta_{\mathrm{v}}H^0_{298}$ (Ward *et al.*, 1982). Earlier correlation systematics had suggested that the standard enthalpy of sublimation of berkelium metal, $\Delta_f H^0$(Bk(g)), is 280 kJ mol^{-1}, and that the standard enthalpy of formation of aqueous Bk(III), $\Delta_f H^0$ (Bk^{3+}(aq)), is −615 kJ mol^{-1} (Nugent *et al.*, 1973a; Johansson and Rosengren, 1975). A later modification of the systematics (Nugent *et al.*, 1973a) led to values of (320 ± 8) kJ mol^{-1} and −(590 ± 21) kJ mol^{-1} for $\Delta_f H^0$ (Bk(g)) and $\Delta_f H^0$ (Bk^{3+}(aq)), respectively (David *et al.*, 1976). There is very good agreement between the value of (320 ± 8) kJ mol^{-1} for $\Delta_f H^0$ (Bk(g)) derived from systematics and the value of (310 ± 6) kJ mol^{-1} for $\Delta_v H^0_{298}$, which is the same thermodynamic quantity, derived from experiment.

The enthalpy of solution of Bk metal (dhcp) to Bk^{3+}(aq) in 1 M HCl at 298 K was determined from five measurements to be −(576 ± 25) kJ mol^{-1} (Fuger *et al.*, 1975). The error limits reported did not reflect the precision of the calorimetric measurements but rather the uncertainties in the purity of the berkelium metal. A new determination of the enthalpy of solution of Bk metal (dhcp) in 1 M HCl at (298.15 ± 0.05) K has yielded a value of −(600.2 ± 5.1) kJ mol^{-1} (Fuger *et al.*, 1981). From this value $\Delta_f H^0$ (Bk^{3+}(aq)) was derived to be −(601± 5) kJ mol^{-1}, in good agreement with the value from systematics (David *et al.*, 1976), and, using reasonable entropy estimates, the standard potential of the Bk(III)/Bk(0) couple was calculated to be −(2.01 ± 0.03) V (Fuger *et al.*, 1981).

Studies of the magnetic susceptibility of berkelium metal have been hampered by the difficulty in obtaining well-characterized, single-phase bulk samples containing minimal amounts of daughter californium. Recent results obtained from a 21 μg sample of dhcp Bk metal (~12 at% Cf) indicated a transition to antiferromagnetic behavior at about 34 K and paramagnetic behavior between 70 and 250 K (Nave *et al.*, 1980). Applying the Curie–Weiss susceptibility relationship to the berkelium data obtained at fields greater than 0.08 T (where the field dependency was saturated) yielded $\mu_{\text{eff}} = 9.69\ \mu_B$ and $\theta = 101.6$ K. The agreement of this value with the theoretical free-ion effective moment (9.72 μ_B) calculated for trivalent berkelium with LS coupling suggests that dhcp Bk metal exhibits high-temperature magnetic behavior like its lanthanide homolog, terbium. The results of earlier magnetic measurements on smaller samples of berkelium metal exhibiting mixed phases were reported by others (Fujita, 1969; Peterson *et al.*, 1970).

(c) Chemical properties

During the handling of microgram-sized samples of berkelium metal, it was observed that the rate of oxidation in air at room temperature is not extremely rapid, possibly due to the formation of a ‘protective’ oxide film on the metal surface (Peterson *et al.*, 1970). Berkelium is a chemically reactive metal, and berkelium hydride (Fahey *et al.*, 1972), some chalcogenides (Fahey *et al.*, 1972; Damien *et al.*, 1979, 1981), and pnictides (Stevenson and Peterson, 1979; Damien *et al.*, 1980) have been prepared directly from the reaction of Bk metal with the appropriate nonmetallic element. Berkelium metal dissolves rapidly in aqueous mineral acids, liberating hydrogen gas and forming Bk(III) in solution.

(d) Theoretical treatment

A hybridized nondegenerate 6d and 5f virtual-bound-states model has been used to describe the properties of the actinide metals, including berkelium (Jullien *et al.*, 1972). It accounted for the occurrence of localized magnetism in Bk metal. A review of the understanding of the electronic properties of berkelium metal as derived from electronic band theory was published shortly thereafter (Freeman and Koelling, 1974). Included was the relativistic energy band structure of fcc Bk metal ($5f^86d^17s^2$), and the conclusion was that berkelium is a rare earth-like metal with localized (ionic) 5f electrons resulting from less hybridization with the 6d and 7s itinerant bands than occurs in the lighter actinides.

A phenomenological model based on crystal structure, metallic radius, melting point, and enthalpy of sublimation has been used to arrive at the electronic configuration of berkelium metal (Fournier, 1976). An energy difference of 0.92 eV was calculated between the $5f^97s^2$ ground state and the $5f^86d^17s^2$ first excited state. The enthalpy of vaporization of trivalent Bk metal was calculated to be 2.99 eV (288 kJ mol^{-1}), reflecting the fact that berkelium metal is more volatile than curium metal. It was also concluded that the metallic valence of the fcc form of berkelium metal is less than that of its dhcp modification (Fournier, 1976).

A relativistic Hartree–Fock–Wigner–Seitz band calculation has been performed for Bk metal in order to estimate the Coulomb term U (the energy required for a 5f electron to hop from one atomic site to an adjacent one) and the 5f electron excitation energies (Herbst *et al.*, 1976). The results for berkelium, in comparison to those for the lighter actinides, show increasing localization of the 5f states, i.e. the magnitude of the Coulomb term U increases through the first half of the actinide series with a concomitant decrease in the width of the 5f level.

10.6.2 Intermetallics

There have been no reports of berkelium intermetallics. Bk–Cf alloys formed from the natural decay of ^{249}Bk metal samples have been studied and are discussed in Section 10.6.3.

10.6.3 Alloys

^{249}Bk ($t_{1/2}$ = 330 days) decays by β^- emission to ^{249}Cf, and because this transition occurs on an atomic scale at randomly distributed lattice sites, truly homogeneous solid solutions (alloys) result. Two such alloys, one Bk-rich (65%)

and the other Cf-rich (60%), have been studied under pressure via energy-dispersive X-ray powder diffraction (Itié *et al.*, 1985; Peterson *et al.*, 1987). The Bk-rich alloy exhibited the same phases with increasing pressure as did pure Bk metal, and the Cf-rich alloy exhibited the same phases with increasing pressure as did pure Cf metal (Peterson *et al.*, 1987). Continuity was observed between the values for pure Bk and Cf metals in the phase-transition pressures, the relative volume and volume decrease upon delocalization (point at which the α-uranium structure is first exhibited), and the bulk modulus. Thus one can consider these alloys as actinide metals with nonintegral atomic numbers (Itié *et al.*, 1985).

Two ^{248}Cm–Bk alloys have been prepared by reduction of their mixed anhydrous trifluorides (precipitated from aqueous solution and treated with fluorine) with lithium metal (Heathman and Haire, 1998). One alloy contained 30% Bk and the other contained 54% Bk. The stated goal of this work was to understand the phase and relative volume behavior of both alloys in terms of chemical bonding, each element's electronic configuration, and the alloys' pressure behavior relative to that reported for the pure Am–Cf metals (Heathman and Haire, 1998). The structural behavior of these two alloys was monitored by energy-dispersive X-ray powder diffraction. Both exhibited the expected RTP dhcp phase that transformed to the fcc phase at 12 GPa (30% Bk) or 8 GPa (54% Bk). The fcc phase changed to a third, unidentified phase at 35 GPa (30% Bk) or at 24 GPa (54% Bk), which was retained up to the maximum pressure studied (53 GPa) (Heathman and Haire, 1998). These results are consistent with the phase-transition pressures in pure Cm and Bk metals, i.e. the greater the concentration of Bk in the alloy, the lower the corresponding phase transition pressure.

10.7 COMPOUNDS

10.7.1 General summary

The trivalent oxidation state of berkelium prevails in the known berkelium compounds, although the tetravalent state is exhibited in BkO_2, BkF_4, Cs_2BkCl_6, and $[N(CH_3)_4]_2BkCl_6$. Selected crystallographic data for a number of berkelium compounds are collected in Table 10.2. In cases where there have been multiple reports of lattice parameters for a particular compound, the ones considered more reliable by the present authors are given in Table 10.2. The interested reader is encouraged to refer to the citations given in the table and text for complete details. An inherent difficulty, not addressed here, in the determination of lattice constants of 'pure' ^{249}Bk compounds concerns the ingrowth of daughter ^{249}Cf at the rate of about 0.22% per day. Two experimental methods to address this problem are: (1) the determination of the lattice parameters of berkelium compounds as a function of californium content and then extrapolation to zero californium content; and (2) the utilization of Vegard's law to correct measured berkelium lattice parameters for the presence of a known amount of californium (assuming, of course, that the lattice parameters of the isostructural 'pure' californium compound are known).

A summary and discussion of the structural aspects of solid-state actinide chemistry are presented in Chapter 22, so no attempt is made to do so here for the compounds of berkelium. Estimated thermochemical values for many compounds of berkelium can be found in Chapter 19. Only those values determined by direct experiment are discussed here.

An empirical set of 'effective' ionic radii in oxides and fluorides, taking into account the electronic spin state and coordination of both the cation and the anion, have been calculated (Shannon and Prewitt, 1969). For six-coordinate Bk(III), the radii values are 0.096 nm, based on a six-coordinate oxide ion radius of 0.140 nm, and 0.110 nm, based on a six-coordinate fluoride ion radius of 0.119 nm. For eight-coordinate Bk(IV), the corresponding values are 0.093 and 0.107 nm, respectively, based on the same anion radii (Shannon and Prewitt, 1969). Other self-consistent sets of trivalent and tetravalent lanthanide and actinide ionic radii, based on isomorphous series of oxides (Peterson and Cunningham, 1967a; Shannon, 1976) and fluorides (Peterson and Cunningham, 1968b; Shannon, 1976), have been published. Based on a crystal radius for Cf(III), the ionic radius of isoelectronic Bk(II) was calculated to be 0.114 nm (Ionova *et al.*, 1977). It is important to note, however, that meaningful comparisons of ionic radii can only be made if the values compared are calculated in like fashion from the same type of compound, with respect to both composition and crystal structure (Shannon, 1976).

The thermal decomposition of $Bk(NO_3)_3 \cdot 4H_2O$, $BkCl_3 \cdot 6H_2O$, $Bk_2(SO_4)_3 \cdot 12H_2O$, and $Bk_2(C_2O_4)_3 \cdot 4H_2O$ has been studied in air, argon, and H_2–Ar atmospheres and compared to that of the corresponding hydrates of cerium, gadolinium, and terbium (Haire, 1973). In air or Ar the final berkelium product was BkO_2; in H_2–Ar it was Bk_2O_3.

10.7.2 Hydrides

The preparation of berkelium hydride has been accomplished by treatment of berkelium metal at 500 K with H_2 gas derived from thermal decomposition of UH_3 (Fahey *et al.*, 1972). The product exhibited an fcc structure with lattice parameter $a_0 = (0.523 \pm 0.001)$ nm determined from nine observed X-ray diffraction lines. By analogy with the behavior of the lanthanide hydrides (Holley *et al.*, 1955), the stoichiometry BkH_{2+x} $(0 < x < 1)$ was assigned. Later studies of the berkelium–hydrogen system resulted in products with either fcc symmetry, identified as the dihydride, or hexagonal symmetry, which was taken to be berkelium trihydride, BkH_{3-x} $(0 < x < 1)$ (Gibson and Haire, 1985). Additional work is required to characterize fully the berkelium–hydrogen system.

Table 10.2 *Selected crystallographic data for berkelium compounds.*

Substance	*Structure type*	*Crystal system*	*Lattice parameters*[a] a_0 (nm)	b_0 (nm)	c_0 (nm)	β (degree)	*Other*[b]	*References*
Hydrides								
BkH_{2+x}	CaF_2	cubic (fcc)	0.523					Fahey *et al.* (1972)
BkH_{2+x}	CaF_2	cubic (fcc)	0.5248					Gibson and Haire (1985)
BkH_{3-x}	LaF_3	trigonal	0.6454		0.6663			Gibson and Haire (1985)
Oxides								
BkO_2	CaF_2	cubic (fcc)	0.53315					Fahey *et al.* (1974)
Bk_2O_3	$(Fe,Mn)_2O_3$	cubic (bcc)	1.0887					Peterson and Cunningham (1967a)
Bk_2O_3	Sm_2O_3	monoclinic	1.4197	0.3606	0.8846	100.23		Baybarz (1973)
Bk_2O_3	La_2O_3	hexagonal	0.3754		0.5958		V72.7	Baybarz (1973)
Halides								
BkF_4	UF_4	monoclinic	1.2396	1.0466	0.8118	126.33	V70.7	Haug and Baybarz (1975)
BkF_3	LaF_3	trigonal	0.697		0.714		ρ10.15	Peterson and Cunningham (1968b)
BkF_3	YF_3	orthorhombic	0.670	0.709	0.441		ρ9.70	Peterson and Cunningham (1968b)
$BkCl_3$	UCl_3	hexagonal	0.7382		0.4127			Peterson and Cunningham (1968a)
Cs_2BkCl_6	Rb_2MnF_6	hexagonal	0.7451		1.2097		ρ4.155	Morss and Fuger (1969)
$Cs_2NaBkCl_6$	$(NH_4)_3AlF_6$	cubic (fcc)	1.0805				ρ3.952	Morss and Fuger (1969)
$BkCl_3 \cdot 6H_2O$	$GdCl_3 \cdot 6H_2O$	monoclinic	0.966	0.654	0.797	93.77	ρ3.06	Burns and Peterson (1971)
$BkBr_3$	$PuBr_3$	orthorhombic	0.403	1.271	0.912		V116.8	Burns *et al.* (1975)

$BkBr_3$	$AlCl_3$	monoclinic	0.723	1.253	0.683	110.6	V144.8	Burns *et al.* (1975)
BkI_3	BiI_3	hexagonal	0.7584		2.087			Fellows *et al.* (1977)
Chalcogenides								
BkS_{2-x}	anti-Fe_2As	tetragonal	0.3902		0.792			Damien *et al.* (1981)
Bk_2S_3	deficit Th_3P_4	cubic (bcc)	0.8358					Damien *et al.* (1981)
$BkSe_{2-x}$	anti-Fe_2As	tetragonal	0.404		0.828			Damien *et al.* (1981)
Bk_2Se_3	deficit Th_3P_4	cubic (bcc)	0.8712					Damien *et al.* (1981)
$BkTe_3$	$NdTe_3$	orthorhombic	0.4318	0.4319	2.5467			Damien *et al.* (1979, 1981)
$BkTe_{2-x}$	anti-Fe_2As	tetragonal	0.4314		0.8945			Damien *et al.* (1979)
Bk_2Te_3	Sc_2S_3	orthorhombic	1.226	0.8685	2.605			Damien *et al.* (1979)
Pnictides								
BkN	NaCl	cubic (fcc)	0.4951					Damien *et al.* (1980)
BkP	NaCl	cubic (fcc)	0.5669					Damien *et al.* (1980)
BkAs	NaCl	cubic (fcc)	0.5829					Damien *et al.* (1980)
BkSb	NaCl	cubic (fcc)	0.6191					Damien *et al.* (1980)
Other inorganic compounds								
BkOCl	PbFCl	tetragonal	0.3966		0.6710		ρ9.45	Peterson and Cunningham (1967b)
BkOBr	PbFCl	tetragonal	0.395		0.81			Cohen *et al.* (1968)
BkOI	PbFCl	tetragonal	0.3986		0.9149			Fellows *et al.* (1977)
$Bk_2O_2SO_4$	$La_2O_2SO_4$	orthorhombic	0.4195	0.4083	1.3110			Haire and Fahey (1977)
Bk_2O_2S	Pu_2O_2S	trigonal	0.3861		0.6686			Haire and Fahey (1977)
$Bk_2(C_2O_4)_3{\cdot}10H_2O$	$La_2(C_2O_4)_3{\cdot}10H_2O$	monoclinic	1.112	0.9746	0.987	114.1		Morris *et al.* (2005)
Coordination compounds								
$[Bk(C_5H_5)_2Cl]_2$	$[Sm(C_5H_5)_2Cl]_2$							Laubereau (1970)
$[N(CH_3)_4]_2BkCl_6$	K_2PtCl_6	cubic (fcc)	1.308					Morss *et al.* (1991)
Organometallic compounds								
$Bk(C_5H_5)_3$	$Pr(C_5H_5)_3$	orthorhombic	1.411	1.755	0.963		ρ2.47	Laubereau and Burns (1970)

---

[a] See original source for precision claimed on these room-temperature values and for information regarding sample purity.

[b] ρ = density in 10^3 kg m^{-3}(g cm^{-3}); V = formula volume in 10^6 pm^3($Å^3$).

10.7.3 Oxides

The first compound of berkelium identified on the basis of its characteristic X-ray powder diffraction pattern was BkO_2 (Cunningham, 1963). Other researchers have since confirmed its CaF_2-type fcc structure with $a_0 = 0.533$ nm (Peterson and Cunningham, 1967a; Baybarz, 1968, 1973; Fahey *et al.*, 1974; Sudakov *et al.*, 1977). The thermal expansion of BkO_2 in 1 atm of oxygen was determined and shown to be reversible with temperature (Fahey *et al.*, 1974). The data were fitted by the expression

$$a_0(t) = 5.3304 + (4.32 \times 10^{-5})t + (15.00 \times 10^{-9})t^2,$$

where $a_0(t)$ is the unit cell edge (in Å) at temperature t (in °C). In addition, the instantaneous expansion coefficients at 25 and 900°C were calculated to be $8.25 \times 10^{-6}\ °C^{-1}$ and $13.2 \times 10^{-6}\ °C^{-1}$, respectively (Fahey *et al.*, 1974).

The results of a preliminary study of a sample of berkelium oxide (BkO_2, Bk_2O_3, or a mixture of the two) via X-ray photoelectron spectroscopy (XPS) included measured core- and valence-electron-binding energies (Veal *et al.*, 1977). The valence-band XPS spectrum, which was limited in resolution by phonon broadening, was dominated by 5f electron emission. The photoelectron spectrum of the 4f lines of Bk in BkO_2 was recorded, and the binding energies of the $4f_{5/2}$ electrons determined to be 515.6(4) eV, and those of the $4f_{7/2}$ electrons, 499.6(4) eV (Krause *et al.*, 1988). These values were reported to be slightly lower than theoretical estimates, but the spin–orbit splitting of the 4f levels, 16.0 (3) eV, was in good agreement with the results of relativistic Hartree–Slater calculations (Krause *et al.*, 1988).

A capacitance manometer system was used to measure the equilibrium oxygen decomposition pressures over non-stoichiometric BkO_x $(1.5\ x < 2.0)$ (Turcotte *et al.*, 1971). Three broad non-stoichiometric phases were defined: $BkO_{1.5–1.77}$; $BkO_{1.81–1.91}$; and BkO_{2-x} $(x \leq 0.07)$. Later, an X-ray diffraction investigation of this BkO_x system under equilibrium conditions was undertaken to correlate the above data with structural behavior (Turcotte *et al.*, 1980). A phase diagram was suggested, showing above 673 K two widely non-stoichiometric phases: body-centered cubic (bcc) for $1.5 < O/Bk \leq 1.70$ and fcc for $1.78 \leq O/Bk < 2.00$. Interestingly, no evidence was found for the formation of Bk_7O_{12}, expected to exhibit a rhombohedral structure based on its common presence in other MO_x $(1.5 < x < 2.0)$ systems. Using the data from the work of others (Peterson and Cunningham, 1967a; Baybarz, 1968, 1973; Turcotte *et al.*, 1980), a berkelium–oxygen phase diagram was constructed over the range from 59 to 67 at% oxygen and from 200 to 900°C (Okamoto, 1999). Also provided is a summary of Bk–O crystal structure data.

The stable room-temperature form of berkelium sesquioxide exhibits the bixbyite-type bcc structure with $a_0 = 1.0887$ nm (Peterson and Cunningham, 1967a). This has been corroborated by an independent study (Baybarz, 1968, 1973). The cubic sesquioxide has also been analyzed by electron diffraction

(Haire and Baybarz, 1973). The high-temperature behavior of Bk_2O_3 has been studied, with the finding that the cubic-to-monoclinic transition at (1473 ± 50) K is irreversible, while the monoclinic-to-hexagonal transition at about 2025 K is reversible (Baybarz, 1973). In addition, the melting point of Bk_2O_3 was determined to be (2193 ± 25) K. Thus berkelium continues the trend of actinide sesquioxides exhibiting trimorphism; with increasing temperature, the structure of Bk_2O_3 changes from bcc (C-form) to monoclinic (B-form) to hexagonal (A-form).

The possibility of the existence of BkO has been considered (Fahey *et al.*, 1972). The true identity of the brittle, gray material exhibiting an fcc structure with $a_0 = 0.4964$ nm is still in doubt. This phase might represent a nitride or an oxide nitride.

A preliminary report of the synthesis and structural characterization of polycrystalline $Bk_2M_2O_7$ and solid solutions of $(Bk,M)O_2$, where M = Zr or Hf, has been given, but no specifics were provided (Haire and Raison, 2000). In a later report the lattice parameter for $Bk_2Zr_2O_7$ was presented to be 1.058 nm in a graph (Haire *et al.*, 2002).

As part of an investigation of the fundamental chemistry and materials science of the 4f and several 5f elements in glass matrices, berkelium was put into two high-temperature (850 and 1450°C), silicate-based glasses and into one sol–gel glass (formed by the hydrolysis of a silicate ester) (Haire *et al.*, 1998). Berkelium (along with cerium and americium) provided an exception to the general observation that the oxidation state of the f element in the high-temperature glasses correlated with that in the element's usual binary oxide produced in air. The same correlation also applied to the f elements in the sol–gel glasses after they had been heated to 200–400°C. The authors only observed Bk(III) in the three glasses and reasoned that without the added stability afforded by the fluorite lattice in BkO_2, Bk(III) was the more stable oxidation state in these glasses (Haire *et al.*, 1998). The anomalous dependence on excitation power of the emission profile of Bk(III) in the 850°C silicate-based glass (Assefa *et al.*, 1998) has been discussed in Section 10.5.3.

10.7.4 Halides

The only reported binary Bk(IV) halide is BkF_4 (Asprey and Keenan, 1968; Keenan and Asprey, 1969; Asprey and Haire, 1973; Haug and Baybarz, 1975), prepared by fluorination of BkO_2 or BkF_3. Although these researchers agree that it exhibits the UF_4-type monoclinic structure, there is some variance in the reported lattice parameters. This could result from the complexity of the X-ray powder diffraction pattern of BkF_4. A molecular volume of 7.07×10^7 pm^3 is calculated from the lattice constants given in Table 10.2, in contrast to those of 7.148×10^7 pm^3 (Asprey and Haire, 1973) and 7.28×10^7 pm^3 (Asprey and Keenan, 1968; Keenan and Asprey, 1969) derived from the other reported lattice parameters. The solid-state absorption spectrum of BkF_4 was obtained by Ensor *et al.* (1981). Mixed alkali metal (M)–Bk(IV) fluoride compounds of the types $MBkF_5$, M_2BkF_6, M_3BkF_7, and $M_7Bk_6F_{31}$, although at present unreported, should be readily prepared. The structural systematics of such actinide fluoride complexes have been discussed elsewhere (Thoma, 1962; Penneman *et al.*, 1973).

In addition to $[N(CH_3)_4]_2BkCl_6$ (discussed in Section 10.7.7), one other Bk(IV) halide compound, Cs_2BkCl_6, has been characterized by its crystallographic properties (Morss and Fuger, 1969). This orange compound precipitated upon dissolution of Bk(IV) hydroxide in chilled, concentrated HCl solution containing CsCl, and was found to crystallize in the Rb_2MnF_6-type hexagonal structure with $a_0 = 0.7451$ nm and $c_0 = 1.2097$ nm. Using a separated halogen atom model, the lattice energy of this compound has been calculated to be 1295 kJ mol^{-1} and the average radius of the $BkCl_6^{2-}$ ion to be 0.270 nm (Jenkins and Pratt, 1979).

The trihalides of berkelium can be prepared by hydrohalogenation of BkO_2, Bk_2O_3, or a lighter berkelium halide. BkF_3 (Peterson and Cunningham, 1968b; Ensor *et al.*, 1981), $BkCl_3$ (Peterson and Cunningham, 1968a; Young *et al.*, 1978; Peterson *et al.*, 1981, 1986), and $BkBr_3$ (Burns *et al.*, 1975; Peterson *et al.*, 1977b) have been shown by X-ray powder diffraction and absorption spectrophotometric studies to be dimorphic. Berkelium is the lightest actinide whose trifluoride exhibits the YF_3-type orthorhombic structure as the room-temperature alpha phase and the LaF_3-type trigonal structure as the high-temperature phase (Peterson and Cunningham, 1968b).

In the case of dimorphic $BkCl_3$, the UCl_3-type hexagonal structure (Peterson and Cunningham, 1968a) represents the low-temperature form, while the $PuBr_3$-type orthorhombic structure is exhibited by the high-temperature modification (Peterson *et al.*, 1981, 1986). The phase-transition temperature appears to be close (Peterson *et al.*, 1981, 1986) to the $BkCl_3$ melting point (876 K) (Peterson and Burns, 1973). The volatilization behavior of many of the binary actinide chlorides including $BkCl_3$ has been studied and correlated with the oxidation state and atomic number ($Z < 92$ or $Z \geq 92$) of the actinide (Merinis *et al.*, 1970). More recent thermochromatographic studies of berkelium chloride using ^{250}Bk confirmed these early results, in that under non-oxidizing conditions, only one deposition peak was observed, corresponding to $BkCl_3$ (Yakushev *et al.*, 2003). With oxidizing conditions (Cl_2 or $Cl_2/SOCl_2$), however, a lower temperature deposition peak grows slowly over time and was assigned to more volatile $BkCl_4$. The adsorption enthalpies were calculated via a Monte Carlo simulation method (Zvara, 1985) and found to be $-(201 \pm 6)$ and $-(154 \pm 6)$ kJ mol^{-1} for $BkCl_3$ and $BkCl_4$, respectively (Yakushev *et al.*, 2003). White $Cs_2NaBkCl_6$ was crystallized from aqueous CsCl–HCl solution by increasing the HCl concentration and cooling to −23°C, and it was found to exhibit an fcc structure in which the Bk(III) ions (O_h site symmetry) are octahedrally coordinated by chloride ions (Morss and Fuger, 1969). The unique properties of such compounds stimulated the synthesis and study of an isostructural set of Cs_2NaMCl_6 compounds containing trivalent cations (including M = U, Np, Pu, Am, and Cf) whose ionic radii ranged from 0.065 to 0.106 nm (Morss *et al.*, 1970; Schoebrechts *et al.*, 1989).

X-ray diffraction from a powder sample of $BkCl_3 \cdot 6H_2O$ showed that it is isostructural with $AmCl_3 \cdot 6H_2O$, whose structure was refined by single-crystal diffraction methods (Burns and Peterson, 1971). By analogy, the basic units of the berkelium structure are $BkCl_2(OH_2)_6^+$ cations and Cl^- anions, the latter being octahedrally coordinated by water molecules.

From X-ray powder diffraction patterns of $BkBr_3$ obtained as a function of the sample's thermal treatment, it was concluded that the $PuBr_3$-type orthorhombic structure is the low-temperature form of $BkBr_3$, and the $AlCl_3$-type monoclinic structure is the high-temperature form (Burns *et al.*, 1975). Because these two crystallographic modifications differ by 2 in the Bk(III) CN, absorption spectrophotometric analysis easily distinguishes between them (Peterson *et al.*, 1977b). The possibility of a third polymorph of $BkBr_3$ has been suggested on the basis of eight lines of low intensity in one powder pattern (Burns *et al.*, 1975). If it does exist, it would be the form intermediate between the $PuBr_3$- and $AlCl_3$-type structures and would exhibit the $FeCl_3$-type rhombohedral structure with $a_0 = 0.766$ nm and $\alpha = 56.6°$ (Burns *et al.*, 1975). There is one additional report (Cohen *et al.*, 1968) with lattice parameters for the orthorhombic form of $BkBr_3$ and for BiI_3-type hexagonal BkI_3.

Samples of berkelium trifluoride, trichloride, tribromide, and triiodide have been studied over time to ascertain the physicochemical effects of beta decay in the bulk-phase solid state (Young *et al.*, 1984). In each case Bk^{3+} was found to transform to Cf^{3+}, and the crystal structure of the solid remained unchanged. Maintenance of oxidation state would seem to be a chemical effect of this transformation, whereas maintenance of crystal structure is more of a physical effect, the structure of the progeny being controlled by its environment. Details of the characterization and study of dimorphic $BkCl_3$, via X-ray powder diffraction and absorption spectrophotometry, have been published (Peterson *et al.*, 1986). The results of monitoring each of the crystal forms of $BkCl_3$ over a period of almost 3 years are included. Justification (and some limitations) for the use of electronic f→f absorption peaks in the spectra of berkelium (and other actinide) compounds for the elucidation of the crystal structures of these compounds (crystal-field effects) has been published (Peterson *et al.*, 1990). In addition to absorption spectrophotometry, phonon Raman spectroscopy has been shown to be an effective way to elucidate the structure of a solid-state compound. Each crystal type possesses a unique set of fundamental crystal vibrations resulting from the positions, coordinations, bonding, and masses of its atoms. A catalog of phonon Raman spectral data for selected actinide compounds, including both crystallographic and spectroscopic parameters for each individual crystal structure exhibited, is available (Wilmarth and Peterson, 1991). A discussion of the comparative science of the lanthanide and actinide halides, mainly focusing on the trivalent chlorides and bromides, provides the systematics into which berkelium fits as expected (Peterson, 1995).

10.7.5 Chalcogenides and pnictides

The only other crystallographic result reported for a berkelium chalcogenide besides those summarized in Table 10.2 is a cubic lattice parameter of 0.844 nm for Bk_2S_3 (Cohen *et al.*, 1968). The microscale synthesis of the brownish-black sesquisulfide was carried out by treatment of berkelium oxide at 1400 K with a mixture of H_2S and CS_2 vapors. In a later work (Damien *et al.*, 1979, 1981), the higher chalcogenides were prepared on the 20–30 μg scale in quartz capillaries by direct combination of the elements. These were then thermally decomposed *in situ* to yield the lower chalcogenides. The stoichiometries of these compounds have not been determined directly.

The berkelium monopnictides have been prepared on the multi-microgram scale by direct combination of the elements (Damien *et al.*, 1980). In all cases the lattice constants of the NaCl-type cubic structures were smaller than those of the corresponding curium monopnictides but comparable to those of the corresponding terbium compounds. This supports the semimetallic classification for these compounds. One additional report of BkN has appeared (Stevenson and Peterson, 1979). The lattice parameter derived from the sample exhibiting a single phase was (0.5010 ± 0.0004) nm, whereas that extracted from the mixed-phase sample of BkN resulting from incomplete conversion of a hydride was (0.4948 ± 0.0003) nm. Additional samples of BkN should be prepared to establish more firmly its lattice constant.

10.7.6 Other inorganic compounds

BkOCl (Peterson and Cunningham, 1967b), BkOBr (Cohen *et al.*, 1968), and BkOI (Cohen *et al.*, 1968; Fellows *et al.*, 1977) have been synthesized and are found to exhibit the PbFCl-type tetragonal structure. Although presently unreported, BkOF certainly can be prepared and probably exhibits polymorphism.

Both the oxysulfate (body-centered orthorhombic) and the oxysulfide (trigonal) of Bk(III) have been studied by X-ray powder diffraction (Haire and Fahey, 1977). $Bk_2O_2SO_4$ resulted from the decomposition of $Bk_2(SO_4)_3 \cdot nH_2O$ in an argon atmosphere (to prevent oxidation to BkO_2) at about 875 K, whereas Bk_2O_2S was formed upon thermal decomposition of the sulfate hydrate in a 4% H_2/96% Ar atmosphere. No decomposition of the oxysulfide was observed up to 1300 K in the H_2/Ar gas mixture (Haire and Fahey, 1977). Both $Bk_2O_2SO_4$ and Bk_2O_2S are isostructural with the corresponding lanthanide and actinide compounds.

Berkelium(III) orthophosphate has been prepared and characterized by X-ray powder diffraction and solid-state absorption and Raman spectroscopies (Haire *et al.*, 1983; Hobart *et al.*, 1983). Analysis of the X-ray data has shown this compound to be isostructural with samarium and europium orthophosphates and to exhibit similar lattice parameters (Haire *et al.*, 1983). The structure type was confirmed by the direct correlation of the Raman spectrum of $BkPO_4$ with those of the isostructural lanthanide orthophosphates (Hobart *et al.*, 1983).

The preparation of berkelium(III) sesquioxalate decahydrate has been reported, along with its monoclinic unit cell parameters and its absorption and Raman spectra. It was observed that the Bk(III) compound underwent oxidation in about 24 h to a non-stoichiometric Bk(IV) oxalate complex, presumably the result of its self-irradiation (Morris *et al.*, 2005).

10.7.7 Coordination compounds

A β-diketonate compound of Bk(III) has been prepared and reported to be stable when volatilized. The possibility of using this volatile compound in transport and subsequent separation of berkelium from other actinides has been proposed (Fedoseev *et al.*, 1983).

More recently $[N(CH_3)_4]_2BkCl_6$ samples were prepared from cold, concentrated HCl(aq) on the milligram scale and studied via X-ray powder diffraction and optical spectroscopy in KBr and KCl pellets (Morss *et al.*, 1991). The powder patterns were indexed on fcc symmetry, with $a_0 = 1.308(2)$ nm, although from systematics a smaller lattice parameter was expected. No fluorescence attributable to Bk^{4+} was found under several modes of excitation. Strong f-center absorptions, due to radiation damage, and several very weak absorptions, presumably due to transitions to the first excited state of Bk^{4+}, were noted (Morss *et al.*, 1991).

10.7.8 Organometallic compounds

Two cyclopentadienylberkelium(III) compounds have been reported, but only one of them, $Bk(C_5H_5)_3$, has been characterized crystallographically (Laubereau and Burns, 1970). In addition to the data given in Table 10.2, the formula volume of this compound is 2.98×10^8 pm^3. The amber-colored tris(cyclopentadienyl)berkelium(III) was isolated from a reaction mixture of $BkCl_3$ and molten $Be(C_5H_5)_2$ by sublimation in vacuum at 475–495 K. It decomposes to an orange melt at 610 K (Laubereau and Burns, 1970).

During vacuum sublimation from a mixture of $BkCl_3$ and molten $Be(C_5H_5)_2$ at temperatures above 500 K (up to 600 K), a second berkelium fraction was obtained (Laubereau, 1970). Its identity was established to be bis(cyclopentadienyl)berkelium(III) chloride dimer, $[Bk(C_5H_5)_2Cl]_2$, based on the similarities of its X-ray powder diffraction pattern and sublimation behavior to those of known $[Sm(C_5H_5)_2Cl]_2$. The solid-state absorption spectrum of $[Bk(C_5H_5)_2Cl]_2$ was obtained and noted to be very similar to that of $Bk(C_5H_5)_3$ (Laubereau, 1970).

10.7.9 Magnetic behavior of berkelium ions

In order to improve upon the precision (±10%) of the initial measurements of the magnetic susceptibility of Bk(III) ions (Cunningham, 1959) and to extend the range of measurements to lower temperatures, single beads of cation-exchange resin were saturated with Bk(III) and subjected to susceptibility measurements over the temperature range 9–298 K (Fujita, 1969). The magnetic behavior of Bk(III) over the entire temperature range was described well by the Curie–Weiss relationship with $\mu_{\mathrm{eff}} = (9.40 \pm 0.06)\ \mu_{\mathrm{B}}$ and $\Theta = (11.0 \pm 1.9)$ K. The magnetic susceptibility of Bk(III) in an octahedral environment of host matrix $Cs_2NaLuCl_6$ was measured; temperature-independent paramagnetism was observed over the temperature range 10–40 K, with the lowest level of Bk(III) determined to be Γ_1 and with a Γ_1–Γ_4 separation of $8.5 \times 10^3\ \mathrm{m}^{-1}$ (Hendricks *et al.*, 1974).

Results of electron paramagnetic resonance (Boatner *et al.*, 1972) and magnetic susceptibility (Karraker, 1975) studies of Bk(IV) in ThO_2 have been reported. The eight-line hyperfine pattern confirmed that the nuclear spin of ^{249}Bk is 7/2; the estimated nuclear moment was $(2.2 \pm 0.4)\ \mu_{\mathrm{N}}$ (Boatner *et al.*, 1972). Two regions of temperature-dependent paramagnetism of BkO_2 in ThO_2 were observed over the temperature range 10–220 K; the possibility of an antiferromagnetic transition at 3 K was noted (Karraker, 1975).

The first measurements of the magnetic susceptibilities of bulk-phase samples of some berkelium compounds (BkO_2, BkF_3, BkF_4, and BkN) were made in 1981. The effective moments were found to agree with the calculated free-ion values, assuming Bk(IV) or Bk(III) cores and LS coupling (Nave *et al.*, 1981). The paramagnetic effective moments for BkF_4 and BkO_2 were determined from a Curie–Weiss fit to the data displayed in Fig. 10.5. The experimentally determined μ_{eff} values for BkF_4 and BkO_2 of $(7.93 \pm 0.03)\ \mu_{\mathrm{B}}$ and $(7.92 \pm 0.1)\ \mu_{\mathrm{B}}$, respectively, are in good agreement with a localized $5f^7$ ionic model where μ_{eff} (theory) $= 7.94\ \mu_{\mathrm{B}}$ (Nave *et al.*, 1983).

10.8 IONS IN SOLUTION

10.8.1 Oxidation states

Berkelium exhibits both III and IV oxidation states in solution, as would be expected from the oxidation states displayed by its lanthanide counterpart, terbium. Evidence has been offered for the existence of Bk(II), but there is only speculation on the possible existence of Bk(V). Bk(III) is the most stable oxidation state in non-complexing aqueous solutions. Bk(IV) is reasonably stable in solution in the absence of reducing agents because of the stabilizing influence of the half-filled $5f^7$ subshell. Bk(III) and Bk(IV) exist in aqueous solution as simple hydrated ions, Bk^{3+}(aq) and Bk^{4+}(aq), respectively, unless complexed by ligands. Bk(III) is green in most mineral acid solutions. Bk(IV) is yellow in HCl solution and orange-yellow in H_2SO_4 solution.

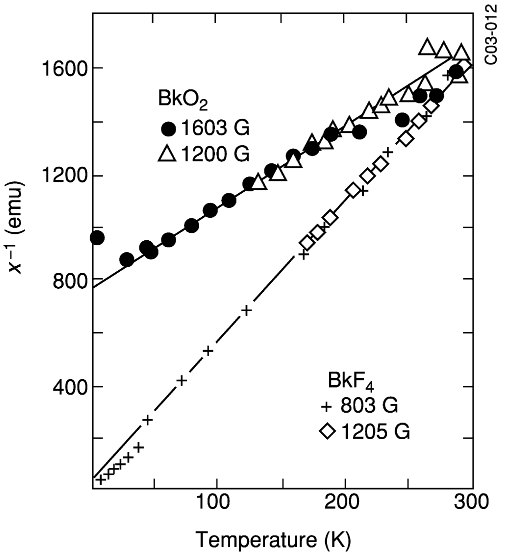

Fig. 10.5 *Inverse magnetic susceptibility of* BkF_4 *at* 803 *and* 1205 G *and* BkO_2 *at* 1200 *and* 1603 G *as a function of temperature.* (*The solid lines are least-squares fits of the data to the Curie–Weiss law.*) (*Reprinted figure with permission from Nave* et al. (1983). *Copyright* 1983 *by the American Physical Society.*)

The possible existence of divalent berkelium was studied by polarography in acetonitrile solution. Because of high background currents, caused by radiolysis products obscuring the polarographic wave, evidence for Bk(ii) was not obtained (Friedman and Stokely, 1976). Divalent berkelium has been reported to exist in mixed lanthanide chloride–strontium chloride melts. The claim is based on the results of the distribution of trace amounts of berkelium between the melt and a solid crystalline phase (co-crystallization technique) (Mikheev *et al.*, 1979; D'yachkova *et al.*, 1980). As discussed in Section 10.8.2, additional evidence for the transient existence of Bk(ii), generated via pulse radiolysis of an aqueous bicarbonate–ethanol solution, has been reported (Sullivan *et al.*, 1988).

10.8.2 Spectra in solution

The first attempts to measure the absorption spectrum of Bk(iii) involved the use of a single ion-exchange resin bead (Cunningham, 1959). Later the spectrum of a 3.6×10^{-3} M Bk(iii) solution was recorded in a microcell (Gutmacher *et al.*, 1967). Sixteen absorption bands of Bk(iii) were identified in the solution spectrum recorded in a 'suspended-drop' microcell over the wavelength range 320–680 nm (Peterson, 1967, 1980). The results of additional observations identified a total of 23 absorption bands in the 280–1500 nm wavelength region (Fujita, 1969).

The first attempts to record the Bk(IV) solution absorption spectrum were hindered by the presence of cerium impurities (Gutmacher *et al.*, 1967). The positions of the Bk(IV) absorption bands, superimposed on the strong Ce(IV) bands, suggested the assignment of $5f^7$ for the electronic configuration of Bk(IV), which is in agreement with the actinide hypothesis.

The absorption spectra of Bk(III) and Bk(IV) have been recorded in a variety of solutions (Baybarz *et al.*, 1972). New absorption bands were reported as the result of using larger quantities of ^{249}Bk of higher purity. Observations of the spectrum of Bk(III) were extended further into the UV wavelength region (to 200 nm), and nine new absorption bands were reported (Gutmacher *et al.*, 1973). An interpretation of the low-energy bands in the solution absorption spectra of Bk(III) and Bk(IV) was published (Carnall *et al.*, 1971). Later experimental work using larger quantities of berkelium than had been available previously, coupled with a new technique for rapidly separating small quantities of daughter ^{249}Cf, has resulted in a Bk(III) solution absorption spectrum with minimal interference from radiolysis products and significantly higher resolution than those of previously published spectra (Carnall *et al.*, 1984). A parametric fit of the data was performed in order to obtain the energy-level structure of the Bk^{3+} aquo ion. The band intensities were analyzed using the Judd–Ofelt theory, and fluorescent branching ratios were computed from theoretical parameters (Carnall *et al.*, 1984).

The spectra of Bk(III) and Bk(IV) in complexing, concentrated aqueous carbonate solutions have been reported (Hobart *et al.*, 1990). Bk(III) rapidly oxidizes in strongly basic carbonate solutions, and thus the Bk(III) spectrum could only be obtained by electrochemically reducing Bk(IV) in such solutions in a semi-micro cell. The stable Bk(IV) carbonate solution spectrum exhibited a strong charge transfer band peaking at 282 nm in 2 M carbonate solution and at 274 nm in 5 M carbonate solution. The Bk(III) carbonate spectrum showed characteristic f–f transitions superimposed on remnants of the Bk(IV) spectrum. The spectra of Bk(III) in 0.1 M citrate solution at pH values of 1 and 4 have also been reported (Hobart *et al.*, 1990).

The solution absorption spectra of 1×10^{-4} M solutions of yellow Bk(IV) nitrate- and brown Bk(IV) perchlorate–triphenylarsine oxide adducts in acetonitrile were recorded as a result of ozonolysis of initial Bk(III) adduct solutions. Both Bk(IV) spectra exhibited a charge transfer UV cutoff around 300 nm (Payne and Peterson, 1987).

Fluorescence X-ray absorption near-edge spectra (XANES) and the L_3-edge fluorescence X-ray absorption fine structure (XAFS), and their Fourier transforms, of Bk(III) and Bk(IV) aquo ions have been published (Antonio *et al.*, 2002).

Although there have been a number of elegant solid-state studies that provided indirect evidence for the existence of the divalent state of berkelium (e.g. Young *et al.*, 1981), an attempt was made to generate Bk(II) in an aqueous bicarbonate–ethanol solution via pulse radiolysis (Sullivan *et al.*, 1988). The absorption

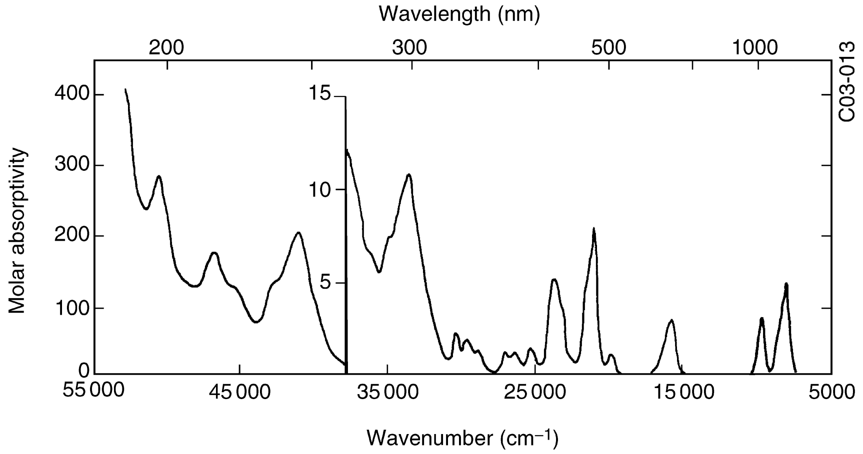

Fig. 10.6 *Solution absorption spectrum of Bk(*III*) in* 0.2 M *$HClO_4$ (DCl solutions were used for portions of the infrared spectrum) (Carnall* et al., 1984).

spectrum of Bk(II), obtained by subtracting out the contributions of the ethanol radical, yielded a peak with a maximum at 310 nm and a molar absorptivity of $(2.3 \pm 0.2) \times 10^3$ cm^{-1} M^{-1}. Bk(II) is unstable in this medium, and the rate of its disappearance was reported to be $(1.53 \pm 0.25) \times 10^5$ s^{-1} (Sullivan *et al.*, 1988).

The solution absorption spectrum of non-complexed Bk(III) is shown in Fig. 10.6. This spectrum is characterized by sharp absorption bands of low molar absorptivity attributed to 'Laporte-forbidden' f–f transitions and by intense absorption bands in the UV region attributed to f–d transitions (Gutmacher *et al.*, 1973). The spectra of Bk(IV) shown in Fig. 10.7 are dominated by a strong absorption band at 250–290 nm, the peak position of which is strongly dependent on the degree of complexation of Bk(IV) by the solvent medium. This dominant band is attributed to a charge transfer mechanism (Gutmacher *et al.*, 1973).

Electronic spectra of Bk(III) (Varga *et al.*, 1973b; Carnall *et al.*, 1984) and Bk(IV) (Varga *et al.*, 1973c) and a prediction of the electronic spectrum of Bk(II) (Varga *et al.*, 1973a) have been published. Spin–orbit coupling diagrams for these berkelium ions, based on a free-ion interpretation of the f–f spectra, were proposed. Further discussion of the absorption spectra of berkelium ions in solution can be found in Chapter 18.

10.8.3 Hydrolysis and complexation behavior

Although Bk(IV) is well known in solution, only stability constants of complexes with Bk(III) have been reported, most of which were determined during investigations of separation procedures. A compilation of the stability constants of Bk(III) complexes with various anions is given in Table 10.3. In most cases the

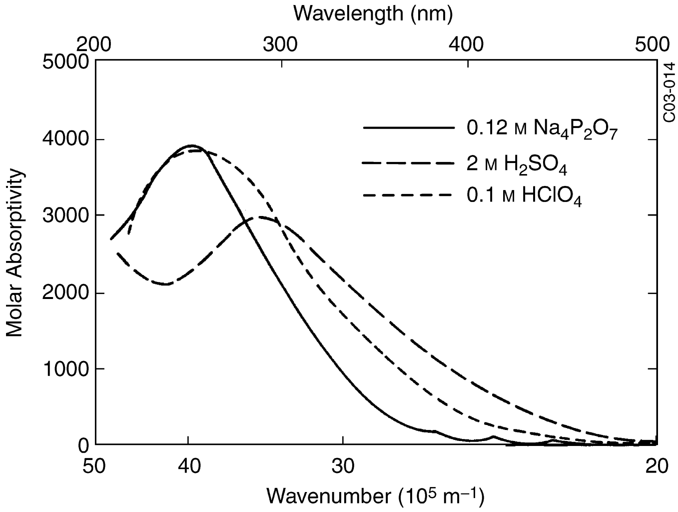

Fig. 10.7 *Solution absorption spectra of Bk*(IV) *in various media* (*Gutmacher* et al., 1973).

lack of replicate results precludes an assessment of the accuracy of the reported values. The reader should consult the original sources for any information regarding the precision of the stability constant values. Although the number of directly measured stability constants for complexes of Bk(III) is rather small, a number of additional, reasonably accurate values for other complexes of Bk(III) can be obtained by interpolation of the stability constant data for the corresponding complexes of Am(III), Cm(III), and Cf(III).

Attempts to obtain thermodynamic data for solvent extraction of Bk(III) by thenoyltrifluoroacetone (TTA) in benzene and for complexation of Bk(III) by hydroxide and citrate ions were unsuccessful (Hubert *et al.*, 1976). The high extractibility and complexibility of the easily accessible tetravalent state of berkelium probably accounts for the difficulty encountered in this study. However, TTA was used successfully to determine the first hydrolysis constant (Désiré *et al.*, 1969; Hussonnois *et al.*, 1973) and citrate complexation constants (Aly and Latimer, 1970; Stepanov, 1971) of Bk(III).

Although no complexation constant values have been reported for Bk(IV), one study is worth noting (Makarova *et al.*, 1979). The electromigration behavior of Bk(IV), Ce(IV), and other actinide(IV) ions was studied in perchloric and nitric acid solutions and mixtures of these acids. In pure 6 M $HClO_4$ both Bk(IV) and Ce(IV) have equal mobilities of $(13.0 \pm 1.0) \times 10^{-5}$ cm^2 V^{-1} s^{-1} and behave as free hydrated ions. As HNO_3 is added to $HClO_4$ solution, keeping the total acid concentration constant at 6 M, the mobility of both ions decreases, with the Bk(IV) mobility decreasing more sharply and then remaining constant (4×10^{-5} cm^2 V^{-1} s^{-1}) between 3 and 6 M HNO_3 (Makarova *et al.*, 1979). The decreased mobility is attributed to changes in the charge of the berkelium species, possibly

Table 10.3 *Stability constants of Bk(III) complexes with various anions.*

Ligand	*Conditions*[a]	*Stability constants*[b]	*References*
fluoride ion, F^-	solv. extrn., 298 K, $\mu = 1.0$, pH = 2.72	$\beta_1 = 7.8 \times 10^2$	Choppin and Unrein (1976)
chloride ion, Cl^-	solv. extrn., 298 K, $\mu = 1.0$ pH = 2	$\beta_1 = 0.96$	Harmon *et al.* (1972a)
	solv. extrn., ca. 293 K, $\mu = 3.0$, pH = 0.82	$\beta_1 = 0.59$ $\beta_2 = 0.25$	Fukasawa *et al.* (1982)
bromide ion, Br^-	solv. extrn., ca. 293 K, $\mu = 3.0$, pH = 0.82	$\beta_1 = 0.15$ $\beta_2 = 0.29$	Fukasawa *et al.* (1982)
hydroxide ion, OH^-	solv. extrn., 293 K, $\mu = 0.1$	$\beta_1 = 2.2 \times 10^8$	Désiré *et al.* (1969), Hussonnois *et al.* (1973)
sulfate ion, SO_4^{2-}	solv. extrn., 298 K, calc. values for $\mu = 0$ (meas. $\mu \leq 0.5$)	$\beta_1 = 5.1 \times 10^3$ $\beta_2 = 3.9 \times 10^5$ $\beta_3 = 1.1 \times 10^5$	McDowell and Coleman (1972)
thiocyanate ion, SCN^-	solv. extrn., 298 K, $\mu = 5.0$	$\beta_1 = 7.21$	Kinard and Choppin (1974)
	$\mu = 1.0$, pH = 2	$\beta_1 = 3.11$, $\beta_2 = 0.31$ $\beta_3 = 2.34$	Harmon *et al.* (1972b)
oxalate ion, $C_2O_4^{2-}$	electromigrn. rates, 298 K, $\mu = 0.1$, pH ~ 1.8	$\beta_1 = 2.8 \times 10^5$ $\beta_2 = 1.4 \times 10^9$	Stepanov (1971)
acetate ion, CH_3COO^-	solv. extrn., 298 K, 2.0 M $NaClO_4$	$\beta_1 = 1.11 \times 10^2$	Choppin and Schneider (1970)
glycolate ion, $CH_2(OH)COO^-$	solv. extrn., 298 K, 2.0 M $NaClO_4$	$\beta_1 = 4.4 \times 10^2$ $\beta_2 = 5.0 \times 10^4$	Choppin and Degischer (1972)
lactate ion, $CH_3CH(OH)COO^-$	ion exch., $\mu = 0.5$	$\beta_3 = 7.9 \times 10^5$ (est.)	Stary (1966)
2-methyllactate ion, $(CH_3)_2C(OH)COO^-$	solv. extrn., 10^{-2} to 1 M	$\beta_1 = 6.39 \times 10^3$	Aly and Latimer (1970)
α-hydroxyisobutyrate ion, $CH_3CH_2CHOHCOO^-$	ion exch. $\mu = 0.5$	$\beta_3 = 4.0 \times 10^6$ (est.)	Stary (1966)

Table 10.3 (*Contd.*)

Ligand	*Conditions*[a]	*Stability constants*[b]	*References*
malate ion, $CH(OH)(COO)CH_2COO^{2-}$	solv. extrn., 10^{-2}–1 M	$\beta_1 = 1.07 \times 10^7$	Aly and Latimer (1970)
tartrate ion, $[CH(OH)COO]_2^{2-}$	solv. extrn., 10^{-2} to 1 M	$\beta_1 = 6.80 \times 10^5$	Aly and Latimer (1970)
citrate ion, $C(OH)(COO)(CH_2COO)_2^{3-}$	electromigrn. rates, 298K, $\mu = 0.1$	$\beta_1 = 7.8 \times 10^7$ $\beta_2 = 1.5 \times 10^{11}$	Stepanov (1971)
	solv. extrn., 10^{-2}–1 M	$\beta_1 = 3.00 \times 10^{11}$	Aly and Latimer (1970)
ethylenediamine-tetraacetate ion (EDTA) $C_2H_4N_2(CH_2COO)_4^{4-}$	ion exch., 298K, $\mu = 0.1$	$\beta_1 = 7.59 \times 10^{18}$	Fuger (1961)
trans-1,2-diaminecyclohexane-tetraacetate ion (DCTA) $C_6H_{10}N_2(CH_2COO)_4^{4-}$	ion exch., 298K, $\mu = 0.1$	$\beta_1 = 1.44 \times 10^{19}$	Baybarz (1966)
diethylenetriamine-pentaacetate ion (DTPA) $C_4H_8N_3(CH_2COO)_5^{5-}$	ion exch., 298K, $\mu = 0.1$	$\beta_1 = 6.2 \times 10^{22}$	Baybarz (1965)

---

[a] Solv. extrn. = solvent extraction; calc. = calculated; meas. = measured; electromigrn.= electromigration; exch.= exchange.

[b] Overall stability constants, e.g.

$$\beta_1 = \frac{\left[BkL^{(3-n)+}\right]}{\left[Bk^{3+}\right]\left[L^{n-}\right]},\ \beta_2 = \frac{\left[BkL_2^{(3-2n)+}\right]}{\left[Bk^{3+}\right]\left[L^{n-}\right]^2},\ \text{and}\ \beta_3 = \frac{\left[BkL_3^{(3-3n)+}\right]}{\left[Bk^{3+}\right]\left[L^{n-}\right]^3}.$$

forming $[Bk(H_2O)_x(NO_3)_3]^+$ between 3 and 6 M HNO_3. It was also reported that Bk(IV) does not form negatively charged species up to 10 M HNO_3. This study provides an explanation for the differences observed in the ion-exchange and solvent extraction behavior of Bk(IV) as compared to that of Ce(IV), Th(IV), Np(IV), and Pu(IV) (Makarova *et al.*, 1979).

The extraction of Bk(III) by organophosphorus acids has been studied, and activity coefficients for Bk(III) in nitric acid solution were estimated (Chudinov *et al.*, 1976). In addition a mechanism for the extraction of Bk(IV) by HDEHP from nitric acid solution was proposed. The self-diffusion coefficients (D) of Bk(III) ion in perchloric acid media were measured using the open-end capillary method (Latrous and Oliver, 1999). The limiting value, D_0, at zero ionic strength was reported to be 5.95×10^{-6} cm^2 s^{-1}. This value is in good agreement with $D_0 = 5.81 \times 10^{-6}$ cm^2 s^{-1}, calculated by using a microscopic version of the Stokes–Einstein law (Mauerhofer *et al.*, 2003). Both reported values correlate well with experimentally determined values for neighboring trivalent actinide and analog lanthanide ions.

The kinetics of exchange of Bk(III) with $EuEDTA^-$ (EDTA = ethylenediaminetetraacetic acid) in aqueous acetate solutions of 0.1 M ionic strength has been studied (Williams and Choppin, 1974). The exchange was found to be first order with both acid-dependent and acid-independent rate terms. Rate values were calculated and compared to other actinide reaction rates.

The aqueous solubilities of Bk(III) oxalate and Bk(IV) iodate have been reported to be 1.5 and 10 mg L^{-1}, respectively (Erin *et al.*, 1977).

10.8.4 Redox behavior and potentials

Berkelium(III) in solution can be oxidized by strong oxidizing agents such as BrO_3^- (Knauer and Weaver, 1968; Weaver, 1968; Fardy and Weaver, 1969; Overman, 1971; Erin *et al.*, 1979b; Malikov *et al.*, 1980), AgO (Erin *et al.*, 1976), $Ag(I)S_2O_8^{2-}$ (Milyukova *et al.*, 1977, 1978, 1980), perxenate (Lebedev *et al.*, 1975), and ozone (Myasoedov *et al.*, 1973, 1974, 1975; Myasoedov, 1974).

Oxidation of green Bk(III) hydroxide as a suspension in 1 M NaOH to yellow Bk(IV) hydroxide was performed by bubbling ozone through the slurry (Cohen, 1976). In hydroxide solution, Bk(III) is unstable toward oxidation by radiolytically produced peroxide (Cohen, 1976). This 'self-oxidation' has also been observed in carbonate solutions (Baybarz *et al.*, 1972; Timofeev *et al.*, 1987; Hobart *et al.*, 1990; Morris *et al.*, 1990). Bk(III) can be stabilized in these solutions, however, by the presence of a reducing agent such as hydrazine hydrate (Cohen, 1976).

$BkCl_3$ is reported to be soluble in acetonitrile saturated with tetraethylammonium chloride (Nugent *et al.*, 1971). A colorless 7.6×10^{-4} M $BkCl_6^{3-}$ solution was formed that could be completely oxidized to red-orange $BkCl_6^{2-}$ by treatment with chlorine gas. The color of this Bk(IV) solution was quite similar to that observed for crystalline Cs_2BkCl_6 (Morss and Fuger, 1969).

Investigation of the amalgamation behavior of actinides in aqueous acetate and citrate solutions by treatment with sodium amalgam showed that berkelium and the lighter actinides do not readily form the amalgam. Those lanthanides that are known to exist only in the trivalent or the tetravalent state in solution also do not readily amalgamate. This behavior is in contrast to that of the heavier actinides californium, einsteinium, fermium, and mendelevium, and those lanthanides that exhibit stable divalent states, all of which readily amalgamate (Malý, 1967, 1969). This has been extensively studied as a basis for lanthanide/actinide and actinide/actinide separations and for determining redox reactions, kinetics, potentials, and other thermodynamic parameters (David *et al.*, 1990).

Bk(IV) is a strong oxidizing agent, comparable to Ce(IV) (Weaver and Stevenson, 1971). It can be coprecipitated with cerium iodate (Weaver, 1968) or zirconium phosphate (Cunningham, 1959). The stability of Bk(IV) solutions is a function of the degree of complexation of Bk(IV) by the solvent medium (Baybarz *et al.*, 1972). Bk(IV) is reduced by radiolytically generated peroxide in acidic and neutral solutions. The rate of reduction of Bk(IV) can be accelerated by the introduction of a reducing agent such as hydrogen peroxide (Peppard *et al.*, 1957; Kazakova *et al.*, 1975), hydroxylamine hydrochloride (Kazakova *et al.*, 1975), or ascorbic acid (Kazakova *et al.*, 1975).

Potentials of berkelium redox couples are summarized in Table 10.4. Replicate values for the Bk(IV)/Bk(III) couple under various conditions are in reasonable agreement with one another. The first estimate of the Bk(IV)/Bk(III) potential was made in 1950, only a short time after the discovery of the element. A value of 1.6 V was reported, based on tracer experiments (Thompson *et al.*, 1950a). Later, a refined value of (1.62 ± 0.01) V was reported for the couple, based on the results of experiments with microgram quantities of berkelium (Cunningham, 1959). The potential of the Bk(IV)/Bk(III) couple has subsequently been determined by several workers using direct potentiometry (Stokely *et al.*, 1969; Propst and Hyder, 1970; Nugent *et al.*, 1973b; Simakin *et al.*, 1977a; Kulyako *et al.*, 1981) or indirect methods (Musikas and Berger, 1967; Weaver and Fardy, 1969; Weaver and Stevenson, 1971). A recent, novel determination of the Bk(IV)/Bk(III) potential in $HClO_4$ solution, using *in situ* X-ray absorption spectroelectrochemistry, was reported to be (1.595 ± 0.005) V (Antonio *et al.*, 2002), in close agreement with some of the other values in perchloric acid solution listed in Table 10.4.

All of the above-mentioned determinations were performed in media of relatively low complexing capability. The potential of the Bk(IV)/Bk(III) couple is significantly shifted to less positive values in media containing anions that strongly complex Bk(IV). Values of 1.36 V (Stokely *et al.*, 1969; Kulyako *et al.*, 1981) and 1.12 V (Stokely *et al.*, 1972) have been reported for the couple in sulfuric and phosphoric acid solutions, respectively. Carbonate ions, apparently forming the strongest complex with Bk(IV) of the anions listed in Table 10.4, provide conditions for the least positive potential, 0.26 V (Stokely *et al.*, 1972), as compared to the potential of 1.6 V for the couple in non-complexing

Table 10.4 *Potentials of berkelium redox couples.*

Redox couple	*Potential* (V versus *NHE*)	*Conditions*[a]	*References*
Bk(IV)–Bk(III)	1.6 ± 0.2	calc.	Nugent *et al.* (1973b, 1976)
	1.664	calc.	Simakin *et al.* (1977b)
	1.54 ± 0.1	1 M $HClO_4$, dir. pot.	Stokely *et al.* (1972)
	1.597 ± 0.005	1 M $HClO_4$, dir. pot.	Simakin *et al.* (1977a)
	1.595 ± 0.005	1 M $HClO_4$, spectroelectro.	Antonio *et al.* (2002)
	1.735 ± 0.005	9 M $HClO_4$, dir. pot.	Simakin *et al.* (1977a)
	1.54 ± 0.1	1 M HNO_3, dir. pot.	Stokely *et al.* (1972)
	1.562 ± 0.005	1 M HNO_3, dir. pot.	Simakin *et al.* (1977a)
	1.56	6 M HNO_3, solv. extrn.	Musikas and Berger (1967)
	1.6	3–8 M HNO_3, coprecip.	Thompson *et al.* (1950a)
	1.543 ± 0.005	8 M HNO_3, dir. pot.	Simakin *et al.* (1977a)
	1.43	0.1 M H_2SO_4, dir. pot.	Propst and Hyder (1970)
	1.44	0.25 M H_2SO_4, solv. extrn.	Musikas and Berger (1967)
	1.38	0.5 M H_2SO_4, dir. pot.	Stokely *et al.* (1969)
	1.42	0.5 M H_2SO_4, solv. extrn.	Musikas and Berger (1967)
	1.37	1 M H_2SO_4, dir. pot.	Stokely *et al.* (1969), Kulyako *et al.* (1981)
	1.36	2 M H_2SO_4, dir. pot.	Stokely *et al.* (1969), Kulyako *et al.* (1981)
	1.12 ± 0.1	7.5 M H_3PO_4, dir. pot.	Stokely *et al.* (1972)
	0.85	0.006 M $K_{10}P_2W_{17}O_{61}$, $pH = 0$, dir. pot.	Baranov *et al.* (1981)
	0.65	0.006 M $K_{10}P_2W_{17}O_{61}$, $pH > 4$, dir. pot.	Baranov *et al.* (1981)
	0.24	1 M Na_2CO_3, dir. pot.	Timofeev *et al.* (1987)
	0.26 ± 0.1	2 M K_2CO_3, dir. pot.	Stokely *et al.* (1972)
Bk(III)–Bk(II)	–2.8 ± 0.2	calc.	Nugent *et al.* (1976)
	–2.75	calc.	Lebedev (1978)
Bk(III)–Bk(0)	–2.03 ± 0.05	calc.	Nugent (1975)
	–2.4	calc.	Krestov (1965)
	–1.99 ± 0.09	calc.	David *et al.* (1976)
	–2.18 ± 0.09	0.1 M LiCl, radiopol.	Samhoun and David (1976, 1979)
	–2.01 ± 0.03	calc.	Fuger *et al.* (1981)

[a] Calc. = calculated value; dir. pot. = direct potentiometry; spectroelectro. = spectroelectrochemistry; solv. extrn. = solvent extraction; coprecip. = coprecipitation; radiopol. = radiopolarography.

perchlorate solutions (Stokely *et al.*, 1972; Simakin *et al.*, 1977a). Other studies of the Bk(IV)/Bk(III) couple in complexing concentrated carbonate solutions also yielded potential values significantly shifted from those in non-complexing perchloric acid media (Timofeev *et al.*, 1987; Hobart *et al.*, 1990; Morris *et al.*, 1990). This behavior closely parallels that of the Ce(IV)/Ce(III) couple. In fact the

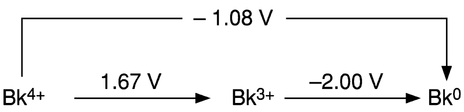

Fig. 10.8 *Standard reduction potential diagram for berkelium ions in acid solution* (*Chapter* 19).

Bk(iv)/Bk(iii) couple markedly resembles the Ce(iv)/Ce(iii) couple in its redox chemistry.

The overall thermodynamic and electrochemical data support a value of (1.67 ± 0.07) V for the standard potential (E°) of the Bk(iv)/Bk(iii) couple (Fuger and Oetting, 1976; Martinot and Fuger, 1985), which is 0.05 V less positive than the accepted value of (1.72 ± 0.02) V for the corresponding cerium couple (Morss, 1985), though within the stated uncertainties.

The potential of the Bk(iii)/Bk(0) couple has been investigated using radiopolarography (Samhoun and David, 1976, 1979) and theoretical calculations (Krestov, 1965), as well as by correlation with data concerning enthalpy of formation (David *et al.*, 1976; Fuger *et al.*, 1981). Estimates of the potentials of berkelium redox couples have also been made from correlation plots of electron-transfer and f–d absorption band energies versus redox potential and by theoretical calculations (Nugent *et al.*, 1971, 1973b, 1976; Nugent, 1975). The overall data support a value of –(2.00 ± 0.02) V for the standard potential of the Bk(iii)/Bk(0) couple.

Theoretical estimates of the potentials of the Bk(v)/Bk(0) and Bk(v)/Bk(iv) couples have been reported as 0.2 and 3.5 V, respectively (David *et al.*, 1976). These estimates suggest that Bk(v) would be very unstable in aqueous solution.

The scatter in the potential values of the Bk(iii)/Bk(ii) and Bk(iii)/Bk(0) couples in Table 10.4 reflects the necessary requirement of making estimates of thermodynamic quantities that have not been directly determined. A standard reduction potential diagram for berkelium ions is shown in Fig. 10.8. Additional information on the redox behavior of berkelium can be found in reviews by Martinot (1978) and Martinot and Fuger (1985).

10.8.5 Thermodynamic properties

Values of thermodynamic properties for the formation of berkelium ions in solution, according to the reactions:

$$\mathrm{Bk(cr,dhcp)} + 3\mathrm{H}^+(\mathrm{aq}) \rightarrow \mathrm{Bk}^{3+}(\mathrm{aq}) + 3/2\,\mathrm{H}_2(\mathrm{g})$$

and

$$\mathrm{Bk(cr,dhcp)} + 4\mathrm{H}^+(\mathrm{aq}) \rightarrow \mathrm{Bk}^{4+}(\mathrm{aq}) + 2\mathrm{H}_2(\mathrm{g}),$$

are summarized in Table 10.5. These values result from the evaluation of experimental measurements on the enthalpy of formation of Bk^{3+}(aq)

Table 10.5 *Thermodynamic quantities for simple aqueous berkelium ions at* 298 K.[a]

Bk ion	$\Delta_f H^o$ (kJ mol^{-1})	$\Delta_f G^o$ (kJ mol^{-1})	S° (J K^{-1} mol^{-1})
Bk^{3+}(aq)	–(601 ± 5)	–(578 ± 7)	–(194 ± 17)
Bk^{4+}(aq)	–(483 ± 5)	–(417 ± 7)	–(402 ± 17)

[a] Chapter 19.

(Fuger *et al.*, 1981), on the temperature dependence of the Bk(IV)/Bk(III) couple (Simakin *et al.*, 1977b), and on estimated entropies. These values are discussed in more detail in Chapter 19.

An electrostatic hydration model has been applied to the trivalent lanthanide and actinide ions in order to predict the standard Gibbs energy ($\Delta_{\text{hydr}}G_t^0$) and enthalpy ($\Delta_{\text{hydr}}H_t^0$) of hydration for these series. Assuming crystallographic and gas-phase radii for Bk(III) to be 0.096 and 0.1534 nm, respectively, and using 6.1 as the primary hydration number, $\Delta_{\text{hydr}}G_{298}^0$ was calculated to be –3357 kJ mol^{-1} and $\Delta_{\text{hydr}}H_{298}^0$ to be –3503 kJ mol^{-1} (Goldman and Morss, 1975). Later efforts to calculate semi-empirically entropy and enthalpy effects associated with hydration (David, 1986a,b), as well as an effort to intercorrelate non-complexed di-, tri-, and tetravalent actinide aquo ions based on crystallographic radii, have been published (David, 1986c). More recently the hydration enthalpy of Bk(III) has been derived by interpolation from data for the neighboring actinides attained by combining previously published thermodynamic and structural data with new data on high-symmetry elpasolites ($Cs_2NaAnCl_6$) using Born–Haber cycles (Schoebrechts *et al.*, 1989). The value obtained for Bk(III), $\Delta_{\text{hydr}}H_{298}^0 = -3501$ kJ mol^{-1}, is in excellent agreement with that calculated by Goldman and Morss (1975). A more comprehensive treatment of the thermodynamic properties of berkelium, including correlations of berkelium hydration enthalpies and Gibbs hydration energies with those of other actinides, can be found in Chapter 19.

Activity coefficients for Bk(III) in aqueous $NaNO_3$ solutions have been calculated from distribution data for the ion between the aqueous phase and a tertiary alkylamine organic phase (Chudinov and Pirozhkov, 1973). The activity coefficient values were reported as a function of the $NaNO_3$ concentration. Additional discussion of, and derived thermochemical properties for, a number of compounds of berkelium can be found in Chapter 19.

10.9 ANALYTICAL CHEMISTRY

The analytical determination of berkelium is dominated by radioanalytical methods, usually after separation from other radionuclides by procedures outlined in Section 10.4. ^{249}Bk, the most common isotope available, emits primarily (>99%) beta (β^-) particles up to a maximum energy of 125 keV. A proportional flow or liquid scintillation counter is used to measure this radiation. The use of scintillators for this determination is complicated by the fact that most substances quench the weak scintillations induced by the beta particles; however, a detection limit of ~0.1 Bq can be attained with an error of about 0.1% (Myasoedov, 1987). The beta decay of ^{249}Bk results in the ingrowth of daughter ^{249}Cf ($t_{1/2} = 351$ years) at about 0.22% per day. This has been utilized for an analytical determination of the parent berkelium. After an initial Bk/Cf separation, the ingrowth decay product is measured over time (Propst and Hyder, 1970) to determine the original berkelium amount.

Methods other than radioanalytical techniques have been developed for berkelium determination. Coulometric determinations of berkelium utilizing the Bk(IV)/Bk(III) couple have been reported (Propst and Hyder, 1970; Timofeev *et al.*, 1986). A spectrophotometric titration method for determination of microgram amounts of berkelium has been proposed (Frolova *et al.*, 1986). Berkelium is electrolytically oxidized to Bk(IV) in nitric acid solution and titrated with H_2O_2 or $NaNO_2$ solution with the equivalence point determined by the disappearance of the high molar absorptivity peak of Bk(IV) at 350 nm. The error in the determination of >70 mg of Bk is reported to be 3–5% (Frolova *et al.*, 1986).

Mass spectrometric techniques that provide increased sensitivity for detection of lanthanides and other actinides in berkelium samples have been developed. In 0.1 μg of berkelium, californium can be determined at the 0.03% level with an error of 10–20% (Tikhomirov *et al.*, 1981). The ionization efficiency of ^{250}Bk has been investigated utilizing an on-line isotope separator, which may have valuable applications in analytical determinations (Asai *et al.*, 2002).

A sensitive neutron-activation method for Bk determination in mixtures of curium and californium has been developed (Ivanov *et al.*, 1979). Thermal neutron irradiation of ^{249}Bk produces ^{250}Bk ($t_{1/2} = 3.217$ h) which emits intense gamma radiation at 989 keV that can be measured using a semiconductor detector. The absolute measurement error for Bk in a 2 μg sample was 1.8×10^{-4} %, and a detection limit for Bk of 4 pg was observed (Ivanov *et al.*, 1979).

The emission spectrum of berkelium over the range from 250 to 336 nm excited by an alternating current arc has been investigated in an effort to develop a semi-quantitative analysis method for berkelium in solutions containing large amounts of curium, cerium, and other elements. The reported detection limit for berkelium is 30 ng over the concentration range 1–100 μg of total metal per milliliter (Myasoedov, 1987).

10.10 CONCLUDING REMARKS

Berkelium is the first member of the second half of the actinide series of elements. Extended knowledge of the stability and accessibility of the various oxidation states of berkelium is important to the understanding and predictability of its physicochemical behavior. In addition such information would enable more accurate extrapolations to the physicochemical behavior of the transberkelium elements for which experimental studies are severely limited by lack of material and/or by intense radioactivity.

Although berkelium oxidation states 0, III, and IV are known in bulk phase, further work is required to characterize more completely the solid-state and solution chemistries of this element. The synthesis of divalent berkelium in bulk should be possible via the metallothermic reduction of its trihalides, e.g.

$$\mathrm{Bk} + 2\mathrm{BkBr}_3 \rightarrow 3\mathrm{BkBr}_2,$$

in an inert reaction vessel. It is quite possible that nature accomplishes this synthesis through alpha decay of the dihalides of ^{253}Es. A direct synthesis, however, would allow both absorption spectrophotometric and X-ray powder diffraction analyses, the results of which would aid in the identification of Bk(II) species in aged einsteinium dihalide samples that also contain Cf(II) (Peterson *et al.*, 1979; Young *et al.*, 1981).

Intermetallic compounds, various alloys, and additional semimetallic compounds of berkelium should be prepared and characterized to extend the knowledge of the physicochemical behavior of berkelium in these kinds of solids. Studies of such materials under pressure would be of interest in determining the effects of the non-berkelium component on physical properties such as bulk modulus (compressibility), pressure for the onset of 5f electron delocalization, and possible volume collapse associated with a change in the metallic valence of berkelium from three to four.

The range of oxidation states accessible to berkelium in solution should be further examined by using strong complexing agents in an effort to stabilize Bk(II), Bk(IV), and possibly Bk(V), produced chemically or electrochemically in nonaqueous or molten salt media. The complexation of Bk(III) with additional organic ligands should be studied to improve solvent extraction separation procedures. Also lacking to date, but experimentally obtainable, are stability constants of any complexes of Bk(IV). With an estimated potential of 3.5 V for the Bk(V)/Bk(IV) couple, it may be possible to prepare Bk(V) in a noncomplexing molten salt solution.

In the intervening years since the 1986 publication of the second edition of this work, a surprisingly large number of berkelium research reports have been published. This is significant because berkelium is quite rare and its longest-lived isotope has a half-life of a little less than 1 year. This continued interest must be attributed, in part, to the extensive use of ^{249}Bk as a nuclear target for creating still heavier elements. New research on this fascinating element will continue to contribute to the knowledge of the physicochemical properties of berkelium and will aid in elucidating the intricacies of the structure of the atom and in extending the limits of the periodic table.

ACKNOWLEDGMENTS

The authors gratefully acknowledge the assistance of Ms Kathy Garduno at the Los Alamos National Laboratory for gathering some of the references included herein and of Ms Annie Loweere and Mr Josh Smith for graphics support. The cooperation of numerous colleagues in supplying and/or verifying information, identifying oversights, and in commenting on the manuscript is greatly appreciated. J.R.P. acknowledges with gratitude Professor B. B. Cunningham (University of California, Berkeley; deceased), whose guidance, inspiration, and personal interest during the first systematic study of the physicochemical properties of berkelium are still fondly remembered. D.E.H. acknowledges with sincere appreciation his coauthor, Professor Emeritus J.R.P., for his dedication in the early education and mentoring of his young protégé and in his continued rewarding collaborations in the exciting area of actinide chemistry.

The preparation of this chapter was sponsored by the Division of Chemical Sciences, Geosciences, and Biosciences, Office of Basic Energy Sciences, U.S. Department of Energy, under contracts W-7405-ENG-36 with Los Alamos National Laboratory, operated by the University of California, and DE-ACO5-00OR22725 with Oak Ridge National Laboratory, managed and operated by UT-Battelle, LLC.

REFERENCES

[NOTE: In citations to *Sov. Radiochem.* and *Radiochem.*, both of which are English translations of *Radiokhimiya*, the year given herein is that of the original publication in Russian. This date is the same or one year later in the English translation.]

Ahmad, I. (2002) *J. Nucl. Radiochem. Sci.*, **3**, 179–82.

Aly, H. F. and Latimer, R. M. (1970) *Radiochim. Acta*, **14**, 27–31.

Antonio, M. R., Williams, C. W., and Soderholm, L. (2002) *Radiochim. Acta*, **90**, 851–6.

Asai, M., Sakama, M., Tsukada, K., Ichikawa, S., Haba, H., Nishinaka, I., Nagame, Y., Goto, S., Akiyama, K., Toyoshima, A., Kojima, Y., Oura, Y., Nakahara, H., Shibata, M., and Kawade, K. (2002) *J. Nucl. Radiochem. Sci.*, **3**, 187–90.

Asai, M., Tsukada, K., Ichikawa, S., Sakama, M., Haba, H., Nagame, Y., Nishinaka, K., Akiyama, K., Toyoshima, A., Kaneko, T., Oura, Y., Kojima, Y., Shibata, M. (2003) *Eur. Phys. J. A*, **16**, 17–19.

Asprey, L. B. and Keenan, T. K. (1968) *Inorg. Nucl. Chem. Lett.*, **4**, 537–41.

Asprey, L. B. and Haire, R. G. (1973) *Inorg. Nucl. Chem. Lett.*, **9**, 1121–8.

Assefa, Z., Haire, R. G., and Stump, N. A. (1998) *J. Alloys Compds*, **271–273**, 854–8.

Audi, G. and Wapstra, A. H. (1995) *Nucl. Phys. A*, **595**, 409–80.

Baranov, A. A., Simakin, G. A., Kosyakov, V. N., Erin, E. A., Kopytov, V. V., Timofeev, G. A., and Rykov, A. G. (1981) *Sov. Radiochem.*, **23**, 104–6.

Baybarz, R. D. (1965) *J. Inorg. Nucl. Chem.*, **27**, 1831–9.

Baybarz, R. D. (1966) *J. Inorg. Nucl. Chem.*, **28**, 1055–61.

Baybarz, R. D. (1968) *J. Inorg. Nucl. Chem.*, **30**, 1769–73.

Baybarz, R. D., Stokely, J. R., and Peterson, J. R. (1972) *J. Inorg. Nucl. Chem.*, **34**, 739–46.

Baybarz, R. D. (1973) *J. Inorg. Nucl. Chem.*, **35**, 4149–58.

Baybarz, R. D., Knauer, J. B., and Orr, P. B. (1973) *Final Isolation and Purification of the Transplutonium Elements from the Twelve Campaigns Conducted at TRU During the Period August 1967–December 1971*, U.S. Atomic Energy Commission Document ORNL-4672, Oak Ridge National Laboratory.

Behera, B. R., Jena, S., Satpathy, M., Kailas, S., Mahata, K., Shrivastava, A., Chatterjee, A., Roy, S., Basu, P., Sharan, M. K., and Datta, S. K. (2001) *Phys. Rev. C*, **64**, 041602 (R)1–3.

Beitz, J. V., Carnall, W. T., Wester, D. W., and Williams, C. W. (1981) in *Actinides – 1981*, Pacific Grove, California, September 1981, Abstracts Volume (ed. N. M. Edelstein), U.S. Department of Energy Document LBL-12441, University of California, Lawrence Berkeley Laboratory, pp. 108–9.

Benedict, U., Peterson, J. R., Haire, R. G., and Dufour, C. (1984) *J. Phys. F: Met. Phys.*, **14**, L43–7.

Bigelow, J. E. (1974) in *Gmelin Handbuch der Anorganischen Chemie*, System No. 71, *Transurane*, New Suppl. Ser., vol. 7b, part A1, II, *The Elements*, Springer-Verlag, New York, pp. 326–36.

Bigelow, J. E., Corbett, B. L., King, L. J., McGuire, S. C., and Sims, T. M. (1981) in *Transplutonium Elements – Production and Recovery* (eds. J. D. Navratil and W. W. Schulz) (ACS Symp. Ser. 161), American Chemical Society, Washington, DC, pp. 3–18.

Bigelow, J. E. (1985) Oak Ridge National Laboratory, personal communication.

Boatner, L. A., Reynolds, R. W., Finch, C. B., and Abraham, M. M. (1972) *Phys. Lett. A*, **42**, 93–4.

Brewer, L. (1971a) *J. Opt. Soc. Am.*, **61**, 1101–11.

Brewer, L. (1971b) *J. Opt. Soc. Am.*, **61**, 1666–82.

Brito, H. F. and Liu, G. K. (2000) *J. Chem. Phys.*, **112**, 4334–41.

Britt, H. C. and Wilhelmy, J. B. (1979) *Nucl. Sci. Eng.*, **72**, 222–9.

Brüchle, W., Schädel, M., Scherer, U. W., Kratz, J. V., Gregorich, K. E., Lee, D., Nurmia, M., Chasteler, R. M., Hall, H. L., Henderson, R. A., and Hoffman, D. C. (1988) *Inorg. Chim. Acta*, **146**, 267–76.

Burns, J. H. and Peterson, J. R. (1971) *Inorg. Chem.*, **10**, 147–51.

Burns, J. H., Peterson, J. R., and Stevenson, J. N. (1975) *J. Inorg. Nucl. Chem.*, **37**, 743–9.

Campbell, D. O. (1981) in *Transplutonium Elements – Production and Recovery* (eds. J. D. Navratil and W. W. Schulz) (ACS Symp. Ser. 161), American Chemical Society, Washington, DC, pp. 189–201.

Carlson, T. A., Nestor, C. W. Jr, Malik, F. B., and Tucker, T. C. (1969) *Nucl. Phys. A*, **135**, 57–64.

Carlson, T. A. and Nestor, C. W. Jr (1977) *At. Data Nucl. Data Tables*, **19**, 153–73.

Carnall, W. T., Sjoblom, R. K., Barnes, R. F., and Fields, P. R. (1971) *Inorg. Nucl. Chem. Lett.*, **7**, 651–7.

Carnall, W. T., Fried, S., Wagner, F. Jr, Barnes, R. F., Sjoblom, R. K., and Fields, P. R. (1972) *Inorg. Nucl. Chem. Lett.*, **8**, 773–4.

Carnall, W. T. (1973) in *Gmelin Handbuch der Anorganischen Chemie*, System No. 71, *Transurane*, New Suppl. Ser., vol. 8, part A2, *The Elements*, Springer-Verlag, New York, pp. 35–80.

Carnall, W. T., Fried, S., and Wagner, F. Jr (1973) *J. Chem. Phys.*, **58**, 3614–24.

Carnall, W. T. and Fried, S. (1976) in *Proc. Symp. Commemorating the 25th Anniversary of Elements 97 and 98*, January 20, 1975, U.S. Energy Research and Development Administration Document LBL–4366, University of California, Lawrence Berkeley Laboratory, pp. 61–9.

Carnall, W. T., Crosswhite, H. M., Crosswhite, H., Hessler, J. P., Aderhold, C., Caird, J. A., Paszek, A., and Wagner, F. W. (1977) in *Proc. 2nd Int. Conf. on the Electronic Structure of the Actinides,* Wrocław, Poland, September 1976 (eds. J. Mulak, W. Suski, and R. Troć), Ossolineum, Wrocław, pp. 105–10.

Carnall, W. T., Beitz, J. V., and Crosswhite, H. (1984) *J. Chem. Phys.*, **80**, 2301–8.

Chen, M. H., Crasemann, B., Huang, K., Aoyagi, M., and Mark, H. (1977) *At. Data Nucl. Data Tables*, **19**, 97–151.

Choppin, G. R. and Schneider, J. K. (1970) *J. Inorg. Nucl. Chem.*, **32**, 3283–8.

Choppin, G. R. and Degischer, G. (1972) *J. Inorg. Nucl. Chem.*, **34**, 3473–7.

Choppin, G. R. and Unrein, P. J. (1976) in *Transplutonium Elements 1975* (eds. W. Müller and R. Lindner), *Proc. 4th Int. Transplutonium Element Symp.*, Baden-Baden, September 1975, North-Holland, Amsterdam, pp. 97–107.

Chudinov, E. G. and Pirozhkov, S. V. (1972) *J. Radioanal. Chem.*, **10**, 41–6.

Chudinov, E. G. and Pirozhkov, S. V. (1973) *Sov. Radiochem.*, **15**, 195–9.

Chudinov, E. G., Kosyakov, V. N., Shvetsov, I. K., and Vereshchaguin, Yu. I. (1976) in *Transplutonium 1975* (eds. W. Müller and R. Lindner), *Proc. 4th Int. Transplutonium Element Symp.*, Baden-Baden, September 1975, North-Holland, Amsterdam, pp. 49–56.

Cohen, D., Fried, S., Siegel, S., and Tani, B. (1968) *Inorg. Nucl. Chem. Lett.*, **4**, 257–60.

Cohen, D. (1976) *J. Inorg. Nucl. Chem.*, Suppl., 41–9.

Collins, E. D., Benker, D. E., Chattin, F. R., Orr, P. B., and Ross, R. G. (1981) in *Transplutonium Elements – Production and Recovery* (eds. J. D. Navratil and W. W. Schulz) (ACS Symp. Ser. 161), American Chemical Society, Washington, DC, pp. 147–60.

Conway, J. G. (1976) in *Proc. Symp. Commemorating the 25th Anniversary of Elements 97 and 98*, January 20, 1975, U.S. Energy Research and Development Administration Document LBL-4366, University of California, Lawrence Berkeley Laboratory, pp. 70–5.

Conway, J. G., Worden, E. F., Blaise, J., Camus, P., and Vergès, J. (1977) *Spectrochim. Acta*, **32B**, 101–6.

Cunningham, B. B. (1959) *J. Chem. Edn.*, **36**, 32–7.

Cunningham, B. B. (1963) in *Proc. Robert A. Welch Foundation Conf. on Chemical Research*, vol. VI, *Topics in Modern Inorganic Chemistry*, Houston, Texas, November 1962, (ed. W. O. Milligan), The Robert A. Welch Foundation, Houston, pp. 237–59.

Damien, D. A., Haire, R. G., and Peterson, J. R. (1979) *J. Physique***, 40** (C4), 95–100.

Damien, D., Haire, R. G., and Peterson, J. R. (1980) *J. Inorg. Nucl. Chem.*, **42**, 995–8.

Damien, D., Haire, R. G., and Peterson, J. R. (1981) Oak Ridge National Laboratory, unpublished results.

David, F., Samhoun, K., Guillaumont, R., and Nugent, L. J. (1976) in *Heavy Element Properties* (eds. W. Müller and H. Blank), *Proc. Joint Session, 4th Int. Transplutonium Element Symp. & 5th Int. Conf. on Plutonium and Other Actinides*, Baden-Baden, September 1975, North-Holland, Amsterdam, pp. 97–104.

David, F. (1986a) *J. Less Common Metals*, **121**, 27–42.

David, F. (1986b) *J. Chim. Phys.*, **83**, 393–401.

David, F. (1986c) in *Handbook on the Physics and Chemistry of the Actinides*, vol. 4 (eds. A. J. Freeman and C. Keller), North-Holland, Amsterdam, pp. 97–128.

David, F., Maslennikov, A. G., and Peretrukhin, V. P. (1990) *J. Radioanal. Nucl. Chem.*, **143**, 415–26.

Désiré, B., Hussonnois, M., and Guillaumont, R. (1969) *C. R. Acad. Sci. Paris C*, **269**, 448–51.

Dittner, P. F. and Bemis, C. E. Jr (1972) *Phys. Rev. A*, **5**, 481–4.

D'yachkova, R. A., Auérman, L. N., Mikheev, N. B., and Spitsyn, V. I. (1980) *Sov. Radiochem.*, **22**, 234–8.

Eichler, R., Brüchle, W., Dressler, R., Düllmann, Ch. E., Eichler, B., Gäggler, H. W., Gregorich, K. E., Hoffman, D. C., Hübener, S., Jost, D. T., Kirbach, U. W., Laue, C. A., Lavanchy, V. M., Nitsche, H., Patin, J. B., Piguet, D., Schädel, M., Shaughnessy, D. A., Strellis, D. A., Taut, S., Tobler, L., Tsyganov, Y. S., Türler, A. Vahle, A., Wilk, P. A., and Yakushev, A. B. (2000) *Nature*, **407**, 63–5.

Ensor, D. D., Peterson, J. R., Haire, R. G., and Young, J. P. (1981) *J. Inorg. Nucl. Chem.*, **43**, 1001–3.

Ensor, D. D. and Shah, A. H. (1984) *Solvent Extr. Ion Exch.*, **2**, 591–605.

Erdmann, N., Nunnemann, M., Eberhardt, K., Herrmann, G., Huber, G., Köhler, S., Kratz, J. V., Passler, G., Peterson, J. R., Trautmann, N., and Waldek, A. (1998) *J. Alloys Compds*, **271–273**, 837–40.

Erin, E. A., Kopytov, V. V., and Vityutnev, V. M. (1976) *Sov. Radiochem.*, **18**, 446–8.

Erin, E. A., Kopytov, V. V., Vasil'ev, V. Ya., and Vityutnev, V. M. (1977) *Sov. Radiochem.*, **19**, 380–2.

Erin, E. A., Vityutnev, V. M., Kopytov, V. V., and Vasil'ev, V. Ya. (1979a) *Sov. Radiochem.*, **21**, 85–8.

Erin, E. A., Vityutnev, V. M., Kopytov, V. V., and Vasil'ev, V. Ya. (1979b) *Sov. Radiochem.*, **21**, 487–9.

Fahey, J. A., Peterson, J. R., and Baybarz, R. D. (1972) *Inorg. Nucl. Chem. Lett.*, **8**, 101–7.

Fahey, J. A., Turcotte, R. P., and Chikalla, T. D. (1974) *Inorg. Nucl. Chem. Lett.*, **10**, 459–65.

Fardy, J. J. and Weaver, B. (1969) *Anal. Chem.*, **41**, 1299–302.

Farrar, L. G., Cooper, J. H., and Moore, F. L. (1968) *Anal. Chem.*, **40**, 1602–4.

Fedoseev, E. V., Ivanova, L. A., Travnikov, S. S., Davidov, A. V., and Myasoedov, B. F. (1983) *Sov. Radiochem.*, **25**, 343–7.

Fellows, R. L., Young, J. P., and Haire, R. G. (1977) in *Physical–Chemical Studies of Transuranium Elements* (Progress Report April 1976–March 1977) (ed. J. R. Peterson), U.S. Energy Research and Development Administration Document ORO-4447-048, University of Tennessee, Knoxville, pp. 5–15.

Ferguson, D. E. and Bigelow, J. E. (1969) *Actinides Rev.*, **1**, 213–21.

Fields, P. R., Wybourne, B. G., and Carnall,W. T. (1964) *The Electronic Energy Levels of the Heavy Actinides* $Bk^{3+}(5f^8)$, $Cf^{3+}(5f^9)$, $Es^{3+}(5f^{10})$, and $Fm^{3+}(5f^{11})$, U.S. Atomic Energy Commission Document ANL-6911, Argonne National Laboratory.

Finch, C. B., Fellows, R. L., and Young, J. P. (1978) *J. Lumin.*, **16**, 109–15.

Firsova, L. A., Chuveleva, E. A., and Kharitonov, O. V. (1996) *Radiochemistry*, **38**, 407–9.

Firsova, L. A., Chuveleva, E. A., and Kharitonov, O. V. (1998a) *Radiochemistry*, **40**, 254–6.

Firsova, L. A., Chuveleva, E. A., and Kharitonov, O. V. (1998b) *Radiochemistry*, **40**, 257–61.

Fournier, J. M. (1976) *J. Phys. Chem. Solids*, **37**, 235–44.

Freeman, A. J. and Koelling, D. D. (1974) in *The Actinides: Electronic Structure and Related Properties,* vol. 1 (eds. A. J. Freeman and J. B. Darby Jr), Academic Press, New York, pp. 51–108.

Friedman, H. A. and Stokely, J. R. (1976) *Inorg. Nucl. Chem. Lett.*, **12**, 505–13.

Frolova, L. M., Vityutnev, V. M., Vasil'ev, V. Ya. (1986) *Sov. Radiochem.*, **28**, 349–53.

Fuger, J. (1961) *J. Inorg. Nucl. Chem.*, **18**, 263–9.

Fuger, J., Peterson, J. R., Stevenson, J. N., Noé, M., and Haire, R. G. (1975) *J. Inorg. Nucl. Chem.*, **37**, 1725–8.

Fuger, J. and Oetting, F. L. (1976) in *The Chemical Thermodynamics of Actinide Elements and Compounds,* part 2, *The Actinide Aqueous Ions.* (eds. V. Medvedev, M. H. Rand, E. F. Westrum Jr and F. L. Oetting), IAEA, Vienna, pp. 50–3.

Fuger, J., Haire, R. G., and Peterson, J. R. (1981) *J. Inorg. Nucl. Chem.*, **43**, 3209–12.

Fuger, J. (1982) in *Actinides in Perspective, Proc. Actinides – 1981*, Pacific Grove, California, September 1981 (ed. N. M. Edelstein), Pergamon Press, New York, pp. 409–31.

Fujita, D. K. (1969) *Some Magnetic, Spectroscopic, and Crystallographic Properties of Berkelium, Californium, and Einsteinium*, PhD Thesis, U.S. Atomic Energy Commission Document UCRL-19507, University of California, Lawrence Berkeley Radiation Laboratory.

Fukasawa, T., Kawasuji, I., Mitsugashira, T., Satô, A., and Suzuki, S. (1982) *Bull. Chem. Soc. Jpn.*, **55**, 726–9.

Gavron, A., Britt, H. C., Goldstone, P. D., Schoenmackers, R., Weber, J., and Wilhelmy, J. B. (1977) *Phys. Rev. C*, **15**, 2238–40.

Gibson, J. K. and Haire, R. G. (1985) *J. Less Common Metals*, **109**, 251–9.

Gibson, J. K. and Haire, R. G. (2001a) *Radiochim. Acta*, **89**, 363–9.

Gibson, J. K. and Haire, R. G. (2001b) *Radiochim. Acta*, **89**, 709–19.

Gobrecht, J., Zehnder, A., Kubik, P., Kettle, P.-R., Junker, K., Herlach, D., and Gaeggler, H. (1999) *Particles and Matter*, vol. 1, Paul Sherrer Institute Scientific Report INIS-CH-019.

Goldman, S. and Morss, L. R. (1975) *Can. J. Chem.*, **53**, 2695–700.

Gregorich, K. E., Henderson, R. A., Lee, D. M., Nurmia, M. J., Chasteler, R. M., Hall, H. L., Bennett, D. A., Gannet, C. M., Chadwick, R. B., Leyba, J. D., Hoffman, D. C., and Hermann, G. (1988) *Radiochim. Acta*, **43**, 223–31.

Guseva, L. I., Gregor'eva, S. I., and Tikhomirova, G. S. (1971) *Sov. Radiochem.*, **13**, 802–4.

Guseva, L. I. and Stepushkina, V. V. (1987) *Sov. Radiochem.*, **29**, 611–14.

Guseva, L. I., Tikhomirova, G. S., and Stepushkina, V. V. (1987) *Sov. Radiochem.*, **29**, 733–9.

Guseva, L. I., Tikhomirova, G. S., and Stepushkina, V. V. (1991) *Sov. Radiochem.*, **33**, 193–8.

Gutmacher, R. G., Hulet, E. K., Worden, E. F., and Conway, J. G. (1963) *J. Opt. Soc. Am.*, **53**, 506.

Gutmacher, R. G. (1964) *Atomic Spectroscopy of Berkelium* (Abstract), U.S. Atomic Energy Commission Document UCRL-12275-T, University of California, Lawrence Livermore Radiation Laboratory.

Gutmacher, R. G., Hulet, E. K., and Lougheed, R. (1965) *J. Opt. Soc. Am.*, **55**, 1029–30.

Gutmacher, R. G., Hulet, E. K., Lougheed, R., Conway, J. G., Carnall, W. T., Cohen, D., Keenan, T. K., and Baybarz, R. D. (1967) *J. Inorg. Nucl. Chem.*, **29**, 2341–5.

Gutmacher, R. G., Bodé, D. D., Lougheed, R. W., and Hulet, E. K. (1973) *J. Inorg. Nucl. Chem.*, **35**, 979–94.

Haire, R. G. (1973) in *Proc. 10th Rare Earth Research Conf.,* Carefree, AZ, April–May 1973, vol. II (eds. C. J. Kevane and T. Moeller), National Technical Information Service, U.S. Department of Commerce, Springfield, VA, pp. 882–91.

Haire, R. G. and Baybarz, R. D. (1973) *J. Inorg. Nucl. Chem.*, **35**, 489–96.

Haire, R. G. and Fahey, J. A. (1977) *J. Inorg. Nucl. Chem.*, **39**, 837–41.

Haire, R. G., Hellwege, H. E., Hobart, D. E., and Young, J. P. (1983) *J. Less Common Metals*, **93**, 358–9.

Haire, R. G., Peterson, J. R., Benedict, U., and Dufour, C. (1984) *J. Less Common Metals*, **102**, 119–26.

Haire, R. G., Benedict, U., Peterson, J. R., Dufour, C., and Dabos, S. (1986) *Physica*, **144B**, 19–22.

Haire, R. G., Assefa, Z., and Stump, N. (1998) *Mat. Res. Soc. Symp. Proc.*, **506**, 153–60.

Haire, R. G. and Raison, P. E. (2000) *AIP Conf. Proc.*, **532**, 173–4. (Plutonium Futures – The Science, Santa Fe, NM, July 10–13, 2000.)

Haire, R. G., Raison, P. E., and Assefa, Z. (2002) *J. Nucl. Sci. Technol.*, Suppl. 3, 616–19.

Harbour, R. M. (1972) *J. Inorg. Nucl. Chem.*, **34**, 2680–1.

Harmon, H. D., Peterson, J. R., and McDowell, W. J., (1972a) *Inorg. Nucl. Chem. Lett.*, **8**, 57–63.

Harmon, H. D., Peterson, J. R., McDowell, W. J., and Coleman, C. F. (1972b) *J. Inorg. Nucl. Chem.*, **34**, 1381–97.

Haug, H. O. and Baybarz, R. D. (1975) *Inorg. Nucl. Chem. Lett.*, **11**, 847–55.

Heathman, S. and Haire, R. G. (1998) *J. Alloys Compds*, **271–273**, 342–6.

Hendricks, M. E., Jones, E. R. Jr, Stone, J. A., and Karraker, D. G. (1974) *J. Chem. Phys.*, **60**, 2095–103.

Herbst, J. F., Watson, R. E., and Lindgren, I. (1976) *Phys. Rev. B*, **14**, 3265–72.

Hessler, J. P., Caird, J. A., Carnall, W. T., Crosswhite, H. M., Sjoblom, R. K., and Wagner, F. Jr (1978) in *The Rare Earths in Modern Science and Technology* (eds. G. J. McCarthy and J. J. Rhyne), Plenum, New York, pp. 507–12.

Hobart, D. E., Begun, G. M., Haire, R. G., and Hellwege, H. E. (1983) *J. Raman Spectrosc.*, **14**, 59–62.

Hobart, D. E. and Peterson, J. R. (1986) in *The Chemistry of the Actinide Elements,* 2nd edn (eds. J. J. Katz, G. T. Seaborg, and L. R. Morss), Chapman & Hall, London, pp. 989–1024.

Hobart, D. E., Morris, D. E., Palmer, P. D., Haire, R. G., and Peterson, J. R. (1990) *Radiochim. Acta*, **49**, 119–24.

Hollander, J. M., Holtz, M. D., Novakov, T., and Graham, R. L. (1965) *Ark. Fys.*, **28**, 375–9.

Holley, C. E. Jr, Mulford, R. N. R., Ellinger, F. H., Koehler, W. C., and Zachariasen, W. H. (1955) *J. Phys. Chem.*, **59**, 1226–8.

Horwitz, E. P., Bloomquist, C. A. A., Henderson, D. J., and Nelson, D. E. (1969) *J. Inorg. Nucl. Chem.*, **31**, 3255–71.

Horwitz, E. P. and Bloomquist, C. A. A. (1973) *J. Inorg. Nucl. Chem.*, **35**, 271–84.

Huang, K., Aoyagi, M., Chen, M. H., Crasemann, B., and Mark, H. (1976) *At. Data Nucl. Data Tables*, **18**, 243–91.

Hübener, S., Taut, S., Vahle, A., Eichler, B., Trautmann, N., and Peterson, J. R. (2000) in *Annual Report 1999*, Laboratory for Radio- and Environmental Chemistry, University of Bern and Paul Scherrer Institute, Switzerland, p. 16.

Hubert, S., Hussonnois, M., Brillard, L., and Guillaumont, R. (1976) in *Transplutonium 1975* (eds. W. Müller and R. Lindner), *Proc. 4th Int. Transplutonium Element Symp.*, Baden-Baden, September 1975, North-Holland, Amsterdam, pp. 109–18.

Hussonnois, M., Hubert, S., Brillard, L., and Guillaumont, R. (1973) *Radiochem. Radioanal. Lett.*, **15**, 47–56.

Ionova, G. V., Spitsyn, V. I., and Mikheev, N. B. (1977) in *Proc. 2nd Int. Conf. on the Electronic Structure of the Actinides,* Wrocław, Poland, September 1976 (eds. J. Mulak, W. Suski, and R. Troć), Ossolineum, Wrocław, pp. 39–47.

Itié, J. P., Peterson, J. R., Haire, R. G., Dufour, C., and Benedict, U. (1985) *J. Phys. F: Met. Phys.,* **15**, L213–19.

Ivanov, O. I., Krainov, E. V., and Sviridov, A. F. (1979) *Sov. At. Energ.*, **45**, 924–6.

Jenkins, H. D. B. and Pratt, K. F. (1979) *Prog. Solid State Chem.*, **12**, 125–76.

Johansson, B. and Rosengren, A. (1975) *Phys. Rev. B*, **11**, 1367–73.

Johansson, B., Skriver, H. L., and Andersen, O. K. (1981) in *Physics of Solids Under High Pressure* (eds. J. S. Schilling and R. N. Shelton), North-Holland, Amsterdam, pp. 245–62.

Jullien, R., Galleani d'Agliano, E., and Coqblin, B. (1972) *Phys. Rev. B*, **6**, 2139–55.

Jursich, G. M., Beitz, J. V., Carnall, W. T., Goodman, G. L., Williams, C. W., and Morss, L. R. (1987) *Inorg. Chim. Acta*, **139**, 273–4.

Karalova, Z. K., Myasoedov, B. F., Rodionova, L. M., and Kuznetsov, V. S. (1983) *Sov. Radiochem*, **25**, 175–9.

Karraker, D. G. (1975) *J. Chem. Phys.*, **62**, 1444–6.

Kazakova, G. M., Kosyakov, V. N., and Erin, E. A. (1975) *Sov. Radiochem.*, **17**, 315–18.

Keenan, T. K. and Asprey, L. B. (1969) *Inorg. Chem.*, **8**, 235–8.

Keller, C. (1971) *The Chemistry of the Transuranium Elements,* Verlag Chemie, Weinheim, pp. 553–66.

Khopkar, P. K. and Mathur, J. N. (1980) *J. Radioanal. Chem.*, **60**, 131–40.

Kinard, W. F. and Choppin, G. R. (1974) *J. Inorg. Nucl. Chem.*, **36**, 1131–4.

King, L. J., Bigelow, J. E., and Collins, E. D. (1981) in *Transplutonium Elements – Production and Recovery* (eds. J. D. Navratil and W. W. Schulz) (ACS Symp. Ser. 161), American Chemical Society, Washington, DC, pp. 133–45.

Knauer, J. B. and Weaver, B. (1968) *Separation of Berkelium from Trivalent Actinides by Chromate Oxidation and HDEHP Extraction*, U.S. Atomic Energy Commission Document ORNL-TM-2428, Oak Ridge National Laboratory.

Knauer, J. B. Jr (2002) Oak Ridge National Laboratory, personal communication.

Kohler, S., Deissenberger, R., Eberhardt, K., Erdmann, N., Herrmann, G., Huber, G., Kratz, J. V., Nunnemann, M., Passler, G., Rao, P. M., Riegel, J., Trautmann, N., and Wendt, K. (1997) *Spectrochim. Acta Part B*, **52**, 717–26.

Kooi, J. and Boden, R. (1964) *Radiochim. Acta*, **3**, 226.

Kooi, J., Boden, R., and Wijkstra, J. (1964) *J. Inorg. Nucl. Chem.*, **26**, 2300–2.

Korkisch, J. (1966) *Oesterr. Chem. Ztg.*, **67**, 273–9.

Korpusov, G. V., Patrusheva, E. N., and Dolidze, M. S. (1975) *Sov. Radiochem.*, **17**, 230–6.

Kosyakov, V. N., Yakovlev, N. G., Kazakova, G. M., Erin, E. A., and Kopytov, V. V. (1977) *Sov. Radiochem.*, **19**, 397–400.

Kosyakov, V. N. and Yakovlev, N. G. (1983) *Sov. Radiochem.*, **25**, 172–5.

Kratz, J. V., Gober, M. K., Zimmerman, H. P., Schädel, M., Brüchle, W., Schimpf, E., Gregorich, K. E., Türler, A., Hannink, N. J., Czerwinski, K. R., Kadkhodayan, B., Lee, D. M., Nurmia, M. J., Hoffman, D. C., Gäggeler, H., Jost, D., Kovacs, J., Scherer, U. W., and Weber, A. (1992) *Phys. Rev. C*, **45**, 1064–9.

Krause, M. O., Haire, R. G., Keski-Rahkonen, O., and Peterson, J. R. (1988) *J. Electron. Spectrosc. Relat. Phenom.*, **47**, 215–26.

Kreek, S. A., Hall, H. L., Gregorich, K. E., Henderson, R. A., Leyba, J. D., Czerwinski, K. R., Kadkhodayan, B., Neu, M. P., Kacher, C. D., Hamilton, T. M., Lane, M. R., Sylwester, E. R., Türler, A., Lee, D. M., Nurmia, M. J., and Hoffman, D. C. (1994) *Phys. Rev. C,* **49**, 1859–66.

Krestov, G. A. (1965) *Sov. Radiochem.*, **7**, 69–77.

Krestov, G. A. (1966) *Sov. Radiochem.*, **8**, 200–3.

Kulyako, Yu. M., Frenkel, V. Ya., Lebedev, I. A., Trofimov, T. I., Myasoedov, B. F., and Mogilevskii, A. N. (1981) *Radiochim. Acta*, **28**, 119–22.

Latrous, H. and Oliver, J. (1999) *J. Mol. Liq.*, **81**, 115–21.

Laubereau, P. G. (1970) *Inorg. Nucl. Chem. Lett.*, **6**, 611–16.

Laubereau, P. G. and Burns, J. H. (1970) *Inorg. Chem.*, **9**, 1091–5.

Lebedev, I. A., Chepovoy, V. I., and Myasoedov, B. F. (1975) *Radiochem. Radioanal. Lett.*, **22**, 239–42.

Lebedev, I. A. (1978) *Sov. Radiochem.*, **20**, 556–62.

Liu, Y.-F., Luo, C., von Gunten, H. R., and Seaborg, G. T. (1981) *Inorg. Nucl. Chem. Lett.*, **17**, 257–9.

Liu, Y.-F., Luo, C., Moody, K. J., Lee, D., Seaborg, G. T., and von Gunten, H. R. (1983) *J. Radioanal. Chem.*, **76**, 119–24.

Liu, G. K., Carnall, W. T., Jursich, G., and Williams, C. W. (1994a) *J. Chem. Phys.*, **101**, 8277–89.

Liu, G. K., Jursich, G., Huang, J., Beitz, J. V., and Williams, C. W. (1994b) *J. Alloys Compds*, **213–214**, 207–11.

Lu, C. C., Malik, F. B., and Carlson, T. A. (1971) *Nucl. Phys. A*, **175**, 289–99.

Makarova, T. P., Fridkin, A. M., Kosyakov, V. N., and Erin, E. A. (1979) *J. Radioanal. Chem.*, **53**, 17–24.

Malikov, D. A., Almasova, E. V., Milyukova, M. S., and Myasoedov, B. F. (1980) *Radiochem. Radioanal. Lett.*, **44**, 297–305.

Malikov, D. A., Milyukova, M. S., Kuzovkina, E. V., and Myasoedov, B. F. (1983) *Sov. Radiochem.*, **25**, 293–6.

Malý, J. (1967) *Inorg. Nucl. Chem. Lett.*, **3**, 373–81.

Malý, J. (1969) *J. Inorg. Nucl. Chem.*, **31**, 1007–17.

Manson, S. T. and Kennedy, D. J. (1974) *At. Data Nucl. Data Tables*, **14**, 111–20.

Martinot, L. (1978) in *Encyclopedia of Electrochemistry of the Elements* (ed. A. J. Bard), Marcel Dekker, New York, ch. VIII-2, pp. 196–8.

Martinot, L. and Fuger, J. (1985) in *Standard Potentials in Aqueous Solution* (eds. A. J. Bard, R. Parsons, and J. Jordan), Marcel Dekker, New York, ch. 21, pp. 631–73.

Maruyama, T., Kaji, D., Kaneko, T., Goto, S., Tsukada, K., Haba, H., Asai, M., Ichikawa, S., Nagame, Y., and Kudo, H. (2002) *J. Nucl. Radiochem. Sci.*, **3**, 155–8.

Mathur, J. N. and Khopkar, P. K. (1982) *Sep. Sci. Technol.*, **17**, 985–1002.

Mauerhofer, E., Zhernosekov, K., and Rösch, F. (2003) *Radiochim. Acta*, **91**, 473–7.

McDowell, W. J. and Coleman, C. F. (1972) *J. Inorg. Nucl. Chem.*, **34**, 2837–50.

Merinis, J., Legoux, Y., and Bouissières, G. (1970) *Radiochem. Radioanal. Lett.*, **3**, 255–61.

Mikheev, N. B., D'yachkova, R. A., and Spitsyn, V. I. (1979) *Dokl. Chem.*, **244**, 18–20.

Milyukova, M. S., Malikov, D. A., and Myasoedov, B. F. (1977) *Radiochem. Radioanal. Lett.*, **29**, 93–101.

Milyukova, M. S. and Myasoedov, B. F. (1978) *Sov. Radiochem.*, **20**, 324–30.

Milyukova, M. S., Malikov, D. A., and Myasoedov, B. F. (1978) *Sov. Radiochem.*, **20**, 762–8.

Milyukova, M. S., Malikov, D. A., and Myasoedov, B. F. (1980) *Sov. Radiochem.*, **22**, 267–72.

Milyukova, M. S., Malikov, D. A., Kuzovkina, E. V., and Myasoedov, B. F. (1981) *Radiochem. Radioanal. Lett.*, **48**, 355–61.

Moore, F. L. (1966) *Anal. Chem.*, **38**, 1872–6.

Moore, F. L. (1967) *Anal. Chem.*, **39**, 1874–6.

Moore, F. L. and Jurriaanse, A. (1967) *Anal. Chem.*, **39**, 733–6.

Moore, F. L. (1969) *Anal. Chem.*, **41**, 1658–61.

Morris, D. E., Hobart, D. E., Palmer, P. D., Haire, R. G., and Peterson, J. R. (1990) *Radiochim. Acta*, **49**, 125–34.

Morris, D. E., Hobart, D. E., Palmer, P. D., Begun, G. M., Young, J. P., and Haire, R. G. (2005) *Structural characterization of berkelium and californium oxalates*, U.S. Department of Energy Document LA-UR-05-4597, University of California, Los Alamos National Laboratory.

Morss, L. R. and Fuger, J. (1969) *Inorg. Chem.*, **8**, 1433–9.

Morss, L. R., Siegal, M., Stenger, L., and Edelstein, N. (1970) *Inorg. Chem.*, **9**, 1771–5.

Morss, L. R. (1985) in *Standard Potentials in Aqueous Solution* (eds. A. J. Bard, R. Parsons, and J. Jordan), Marcel Dekker, New York, ch. 20, pp. 587–629.

Morss, L. R., Carnall, W. T., Williams, C. W., Fahey, J. A., Fuger, J., Meyer, G., and Irmler, M. (1991) *J. Less Common Metals*, **169**, 1–8.

Müller, W. (1967) *Actinides Rev.*, **1**, 71–119.

Musikas, C. and Berger, R. (1967) in *Lanthanide/Actinide Chemistry* (eds. P. R. Fields and T. Moeller) (ACS Adv. Chem. Ser. 71), American Chemical Society, Washington, DC, pp. 296–307.

Myasoedov, B. F., Barsukova, K. V., and Radionova, G. N. (1971) *Radiochem. Radioanal. Lett.*, **7**, 269–74.

Myasoedov, B. F., Chepovoy, V. I., and Lebedev, I. A. (1973) *Radiochem. Radioanal. Lett.*, **15**, 39–45.

Myasoedov, B. F. (1974) *Sov. Radiochem.*, **16**, 716–21.

Myasoedov, B. F., Guseva, L. I., Lebedev, I. A., Milyukova, M. S., and Chmutova, M. K. (1974) in *Analytical Chemistry of Transplutonium Elements* (ed. D. Slutzkin), John Wiley, New York, pp. 122–32.

Myasoedov, B. F., Chepovoy, V. I., and Lebedev, I. A. (1975) *Radiochem. Radioanal. Lett.*, **22**, 233–8.

Myasoedov, B. F. (1987) *Talanta*, **34**, 31–40.

Myasoedov, B. F. and Lebedev, I. A. (1991) *J. Radioanal. Nucl. Chem.*, **147**, 5–26.

Nave, S. E., Huray, P. G., and Haire, R. G. (1980) in *Crystalline Electric Field and Structural Effects in f-Electron Systems* (eds. J. E. Crow, R. P. Guertin, and T. W. Mihalisin), Plenum, New York, pp. 269–74.

Nave, S. E., Haire, R. G., and Huray, P. G. (1981) in *Actinides – 1981,* Pacific Grove, California, September 1981, Abstracts Volume (ed. N. M. Edelstein), U.S. Department of Energy Document LBL-12441, University of California, Lawrence Berkeley Laboratory, pp. 144–6.

Nave, S. E., Haire, R. G., and Huray, P. G. (1983) *Phys. Rev. B*, **28**, 2317–27.

Nugent, L. J., Burnett, J. L., Baybarz, R. D., Werner, G. K., Tanner, S. P., Tarrant, J. R., and Keller, O. L. Jr (1969) *J. Phys. Chem.*, **73**, 1540–9.

Nugent, L. J., Baybarz, R. D., Werner, G. K., and Friedman, H. A. (1970) *Chem. Phys. Lett.*, **7**, 179–82.

Nugent, L. J. and Vander Sluis, K. L. (1971) *J. Opt. Soc. Am.*, **61**, 1112–5.

Nugent, L. J., Baybarz, R. D., Burnett, J. L., and Ryan, J. L. (1971) *J. Inorg. Nucl. Chem.*, **33**, 2503–30.

Nugent, L. J., Burnett, J. L., and Morss, L. R. (1973a) *J. Chem. Thermodyn.*, **5**, 665–78.

Nugent, L. J., Baybarz, R. D., Burnett, J. L., and Ryan, J. L. (1973b) *J. Phys. Chem.*, **77**, 1528–39.

Nugent, L. J. (1975) *J. Inorg. Nucl. Chem.*, **37**, 1767–70.

Nugent, L. J., Baybarz, R. D., Burnett, J. L., and Ryan, J. L. (1976) *J. Inorg. Nucl. Chem.*, Suppl., 37–9.

Okamoto, H. (1999) *J. Phase Equilib.*, **20**, 351.

Overman, R. F. (1971) *Anal. Chem.*, **43**, 600–1.

Passler, G., Nunnemann, M., Huber, G., Deissenberger, R., Erdmann, N., Köhler, S., Kratz, J. V., Trautmann, N., Waldek, A., and Peterson, J. R. (1998) *AIP Conf. Proc.*, **454**, 183–8. (Resonance Ionization Spectroscopy, Manchester, UK, June 21–25, 1998)

Paulus, W., Kratz, J. V., Strub, E., Zauner, S., Brüchle, W., Pershina, V., Schädel, M., Schausten, B., Adams, J. L., Gregorich, K. E., Hoffman, D. C., Lane, M. R., Laue, C., Lee, D. M., McGrath, C. A., Shaughnessy, D. A., Strellis, D. A., and Sylwester, E. R. (1999) *Radiochim. Acta*, **84**, 69–77.

Payne, G. F. and Peterson, J. R. (1987) *Inorg. Chim. Acta*, **139**, 111–12.

Penneman, R. A., Ryan, R. R., and Rosenzweig, A. (1973) *Struct. Bond.*, **13**, 1–52.

Peppard, D. F., Moline, S. W., and Mason, G. W. (1957) *J. Inorg. Nucl. Chem.*, **4**, 344–8.

Peterson, J. R. (1967) *The Solution Absorption Spectrum of* Bk^{3+} *and the Crystallography of Berkelium Dioxide*, *Sesquioxide*, *Trichloride*, *Oxychloride*, *and Trifluoride*, PhD Thesis, U.S. Atomic Energy Commission Document UCRL-17875, University of California, Lawrence Berkeley Radiation Laboratory.

Peterson, J. R. and Cunningham, B. B. (1967a) *Inorg. Nucl. Chem. Lett.*, **3**, 327–36.

Peterson, J. R. and Cunningham, B. B. (1967b) *Inorg. Nucl. Chem. Lett.*, **3**, 579–83.

Peterson, J. R. and Cunningham, B. B. (1968a) *J. Inorg. Nucl. Chem.*, **30**, 823–8.

Peterson, J. R. and Cunningham, B. B. (1968b) *J. Inorg. Nucl. Chem.*, **30**, 1775–84.

Peterson, J. R., Fahey, J. A., and Baybarz, R. D. (1970) *Nucl. Metall.*, **17**, 20–34.

Peterson, J. R., Fahey, J. A., and Baybarz, R. D. (1971) *J. Inorg. Nucl. Chem.*, **33**, 3345–51.

Peterson, J. R. and Burns, J. H. (1973) *J. Inorg. Nucl. Chem.*, **35**, 1525–30.

Peterson, J. R. (1976) in *Gmelin Handbuch der Anorganischen Chemie,* New Suppl. Ser., vol. 31 (ed. G. Koch), Springer-Verlag, New York, pp. 72–6.

Peterson, J. R., Fellows, R. L., Young, J. P., and Haire, R. G. (1977a) in *Proc. 2nd Int. Conf. on the Electronic Structure of the Actinides,* Wrocław, Poland, September 1976 (eds. J. Mulak, W. Suski, and R. Troć), Ossolineum, Wrocław, pp. 111–16.

Peterson, J. R., Fellows, R. L., Young, J. P., and Haire, R. G. (1977b) *Rev. Chim. Minér.*, **14**, 172–7.

Peterson, J. R., Ensor, D. D., Fellows, R. L., Haire, R. G., and Young, J. P. (1979) *J. Physique*, **40**(C4), 111–13.

Peterson, J. R. (1980) in *Lanthanide and Actinide Chemistry and Spectroscopy* (ed. N. M. Edelstein) (ACS Symp. Ser. 131), American Chemical Society, Washington, DC, pp. 221–38.

Peterson, J. R., Young, J. P., Ensor, D. D., and Haire, R. G. (1981) in *Actinides – 1981,* Pacific Grove, California, September 1981, Abstracts Volume (ed. N. M. Edelstein), U.S. Department of Energy Document LBL-12441, University of California, Lawrence Berkeley Laboratory, pp. 118–20.

Peterson, J. R. and Hobart, D. E. (1984) in *Adv. Inorg. Chem. Radiochem.,* vol. 28 (eds. H. J. Emeléus and A. G. Sharpe), Academic Press, New York, pp. 29–72.

Peterson, J. R., Young, J. P., Ensor, D. D., and Haire, R. G. (1986) *Inorg. Chem.*, **25**, 3779–82.

Peterson, J. R., Haire, R. G., Benedict, U., and Young, J. P. (1987) *J. Less Common Metals*, **33**, 143–53.

Peterson, J. R., Young, J. P., Wilmarth, W. R., and Haire, R. G. (1990) *Appl. Spectrosc.*, **44**, 461–5.

Peterson, J. R. (1995) *J. Alloys Compds*, **223**, 180–4.

Popov, Yu. S. and Timofeev, G. A. (1999) *Radiochem.*, **41**, 26–30, and references therein.

Propst, R. C. and Hyder, M. L. (1970) *J. Inorg. Nucl. Chem.*, **32**, 2205–16.

Ronen, Y. (1998) *Ann. Nucl. Energy*, **25**, 983–5.

Samhoun, K. and David, F. (1976) in *Transplutonium Elements 1975* (eds. W. Müller and R. Lindner), *Proc. 4th Int. Transplutonium Element Symp.*, Baden-Baden, September 1975, North-Holland, Amsterdam, pp. 297–304.

Samhoun, K. and David, F. (1979) *J. Inorg. Nucl. Chem.*, **41**, 357–63.

Sarkisov, E. S. (1966) *Dokl. Akad. Nauk SSSR*, **166**, 627–30.

Scherer, U. W., Kratz, J. V., Schädel, M., Brüchle, W., Gregorich, K. E., Henderson, R. A., Lee, D., Nurmia, M., and Hoffman, D. C. (1988) *Inorg. Chim. Acta*, **146**, 249–54.

Schoebrechts, J.-P., Gens, R., Fuger, J., and Morss, L. R. (1989) *Thermochim. Acta*, **139**, 49–66.

Scofield, J. H. (1974) *At. Data Nucl. Data Tables*, **14**, 121–37.

Shafiev, A. I. and Efremov, Yu. V. (1972) *Sov. Radiochem.*, **14**, 754–6.

Shafiev, A. I., Efremov, Yu. V., and Yakovlev, G. N. (1974) *Sov. Radiochem.*, **16**, 31–4.

Shannon, R. D. and Prewitt, C. T. (1969) *Acta Crystallogr. B*, **25**, 925–46.

Shannon, R. D. (1976) *Acta Crystallogr. A*, **32**, 751–67.

Simakin, G. A., Kosyakov, V. N., Baranov, A. A., Erin, E. A., Kopytov, V. V., and Timofeev, G. A. (1977a) *Sov. Radiochem.*, **19**, 302–7.

Simakin, G. A., Baranov, A. A., Kosyakov, V. N., Timofeev, G. A., Erin, E. A., and Lebedev, I. A. (1977b) *Sov. Radiochem.*, **19**, 307–9.

Smentek, L., Wybourne, B. G., and Kobus, J. (2001) *J. Phys. B*, **34**, 1513–22.

Spirlet, J. C., Peterson, J. R., and Asprey, L. B. (1987) in *Advances in Inorganic Chemistry,* vol. 31 (eds. H. J. Emeléus and A. G. Sharpe), Academic Press, Orlando, FL, pp. 1–41.

Stary, J. (1966) *Talanta*, **13**, 421–37.

Stepanov, A. V. (1971) *Russ. J. Inorg. Chem.*, **16**, 1583–6.

Stevenson, J. N. and Peterson, J. R. (1979) *J. Less Common Metals*, **66**, 201–10.

Stokely, J. R., Baybarz, R. D., and Shults, W. D. (1969) *Inorg. Nucl. Chem. Lett.*, **5**, 877–84.

Stokely, J. R., Baybarz, R. D., and Peterson, J. R. (1972) *J. Inorg. Nucl. Chem.*, **34**, 392–3.

Sudakov, L. V., Erin, E. A., Kopytov, V. V., Baranov, A. Yu., Shimbarev, E. V., Vasil'ev, V. Ya., and Kapshukov, I. I. (1977) *Sov. Radiochem.*, **19**, 394–6.

Sugar, J. (1974) *J. Chem. Phys.*, **60**, 4103.

Sullivan, J. C., Schmidt, K. H., Morss, L. R., Pippin, C. G., and Williams, C. (1988) *Inorg. Chem.*, **27**, 598–9.

Taut, S., Hübener, S., Eichler, B., Türler, A., Gäggeler, H. W., Timokhin, S. N., and Zvara, I. (1998) *J. Alloys Compds*, **271–273**, 316–21.

Taut, S., Vahle, A., Hübener, S., Eichler, B., Jost, D., and Türler, A. (2000) in *Annual Report 1999,* Laboratory for Radio- and Environmental Chemistry, University of Bern and Paul Scherrer Institute, Switzerland, p. 17.

Thoma, R. E. (1962) *Inorg. Chem.*, **1**, 220–6.

Thompson, S. G., Cunningham, B. B., and Seaborg, G. T. (1950a) *J. Am. Chem. Soc.*, **72**, 2798–801.

Thompson, S. G., Ghiorso, A., and Seaborg, G. T. (1950b) *Phys. Rev.*, **77**, 838–9.

Thompson, S. G., Ghiorso, A., and Seaborg, G. T. (1950c) *Phys. Rev.*, **80**, 781–9.

Tikhomirov, V. V., Chetverikov, A. P., and Gabeskiriya, V. Ya. (1981) *Sov. Radiochem.*, **23**, 722–5.

Timofeev, G. A., Chistyakov, V. M., and Erin, E. A. (1986) *Sov. Radiochem.*, **28**, 454–8.

Timofeev, G. A., Chistyakov, V. M., Erin, E. A., and Baranov, A. A. (1987) *Sov. Radiochem.*, **29**, 147–51.

Turcotte, R. P., Chikalla, T. D., and Eyring, L. (1971) *J. Inorg. Nucl. Chem.*, **33**, 3749–63.

Turcotte, R. P., Chikalla, T. D., Haire, R. G., and Fahey, J. A. (1980) *J. Inorg. Nucl. Chem.*, **42**, 1729–33.

Ulstrup, J. (1966) *At. Energy Rev.*, **4**, 3–82.

Vander Sluis, K. L. and Nugent, L. J. (1972) *Phys. Rev. A*, **6**, 86–94.

Vander Sluis, K. L. and Nugent, L. J. (1974) *J. Opt. Soc. Am.*, **64**, 687–95.

Varga, L. P., Baybarz, R. D., Reisfeld, M. J., and Asprey, L. B. (1973a) *J. Inorg. Nucl. Chem.*, **35**, 2775–85.

Varga, L. P., Baybarz, R. D., Reisfeld, M. J., and Volz, W. B. (1973b) *J. Inorg. Nucl. Chem.*, **35**, 2787–94.

Varga, L. P., Baybarz, R. D., and Reisfeld, M. J. (1973c) *J. Inorg. Nucl. Chem.*, **35**, 4313–7.

Veal, B. W., Lam, D. J., Diamond, H., and Hoekstra, H. R. (1977) *Phys. Rev. B*, **15**, 2929–42.

Waldek, A., Erdmann, N., Grüning, C., Huber, G., Kunz, P., Kratz, J. V., Lassen, J., Passler, G., and Trautmann, N. (2001) *AIP Conf. Proc.*, **584**, 219–24. (Resonance Ionization Spectroscopy, Knoxville, TN, October 8–12, 2000.)

Ward, J. W. and Hill, H. H. (1976) in *Heavy Element Properties* (eds. W. Müller and H. Blank), *Proc. Joint Session, 4th Int. Transplutonium Element Symp. & 5th Int. Conf. on Plutonium and Other Actinides,* Baden-Baden, September 1975, North-Holland, Amsterdam, pp. 65–79.

Ward, J. W., Kleinschmidt, P. D., Haire, R. G., and Brown, D. (1980) in *Lanthanide and Actinide Chemistry and Spectroscopy* (ed. N. M. Edelstein) (ACS Symp. Ser. 131), American Chemical Society, Washington, DC, pp. 199–220.

Ward, J. W., Kleinschmidt, P. D., and Haire, R. G. (1982) *J. Chem. Phys.*, **77**, 1464–8.

Weaver, B. (1968) *Anal. Chem.*, **40**, 1894–6.

Weaver, B. and Fardy, J. J. (1969) *Inorg. Nucl. Chem. Lett.*, **5**, 145–6.

Weaver, B. and Stevenson, J. N. (1971) *J. Inorg. Nucl. Chem.*, **33**, 1877–81.

Wilk, P. A., Gregorich, K. E., Türler, A., Laue, C. A., Eichler, R., Ninov, V., Adams, J. L., Kirbach, U. W., Lane, M. R., Lee, D. M., Patin, J. B., Shaughnessy, D. A., Strellis, D. A., Nitsche, H., and Hoffman, D. C. (2000) *Phys. Rev. Lett.*, **85**, 2697–700.

Williams, K. R. and Choppin, G. R. (1974) *J. Inorg. Nucl. Chem.*, **36**, 1849–53.

Wilmarth, W. R. and Peterson, J. R. (1991) in *Handbook on the Physics and Chemistry of the Actinides,* vol. 6 (eds. A. J. Freeman and C. Keller), North-Holland, New York, pp. 1–38.

Worden, E. F., Hulet, E. K., Lougheed, R., and Conway, J. G. (1967) *J. Opt. Soc. Am.*, **57**, 550.

Worden, E. F., Gutmacher, R. G., Conway, J. G., and Mehlhorn, R. J. (1969) *J. Opt. Soc. Am.*, **59**, 1526.

Worden, E. F., Gutmacher, R. G., Lougheed, R. W., and Conway, J. G. (1970) *J. Opt. Soc. Am.*, **60**, 1555.

Worden, E. F. and Conway, J. G. (1978) *At. Data Nucl. Data Tables*, **22**, 329–66.

Yakovlev, N. G., Kosyakov, V. N., and Kazakova, G. M. (1982) *J. Radioanal. Chem.*, **75**, 113–20.

Yakovlev, N. G. and Kosyakov, V. N. (1983) *Sov. Radiochem.*, **25**, 687–92.

Yakushev, A., Eichler, B., Türler, A., Gäggeler, H. W., and Peterson, J. (2003) *Radiochim. Acta*, **91**, 123–6.

Young, J. P., Haire, R. G., Fellows, R. L., and Peterson, J. R. (1978) *J. Radioanal. Chem.*, **43**, 479–88.

Young, J. P., Haire, R. G., Peterson, J. R., Ensor, D. D., and Fellows, R. L. (1980) *Inorg. Chem.*, **19**, 2209–12.

Young, J. P., Haire, R. G., Peterson, J. R., Ensor, D. D., and Fellows, R. L. (1981) *Inorg. Chem.*, **20**, 3979–83.

Young, J. P., Haire, R. G., Peterson, J. R., and Ensor, D. D. (1984) in *Geochemical Behavior of Disposed Radioactive Waste* (eds. G. S. Barney, J. D. Navratil, and W. W. Schulz) (ACS Symp. Ser. 246), American Chemical Society, Washington, DC, pp. 335–46.

Zachariasen, W. H. (1973) *J. Inorg. Nucl. Chem.*, **35**, 3487–97.

Zvara, I. (1985) *Radiochim. Acta*, **38**, 95–101.

CHAPTER ELEVEN

CALIFORNIUM

Richard G. Haire

11.1 INTRODUCTION

The discovery of californium came in the era of the syntheses and identifications of other transplutonium elements, following the end of World War II. The discovery of the element californium, like many of the other actinide elements, hinged on the development of new experimental techniques in conjunction with predictions based on nuclear systematics. Californium was named after the University and State of California where many of the transuranium elements were first identified. This element was discovered by Thompson, Street, Ghiorso, and Seaborg (Hyde *et al.*, 1971; Seaborg and Loveland, 1990) in February, 1950. The discovery of californium came only 2 months after the preparation and identification of the first isotope of berkelium, element 97 (see Chapter 10). An account of the discovery and reminiscences about the early work on californium has been given by Ghiorso (1983).

The first preparative method for californium was to bombard microgram targets of ^{242}Cm with 35 MeV helium ions in a 60 in. cyclotron. This produced ^{244}Cf by a (α,2n), reaction which decayed primarily by alpha emission ($t_{1/2}$ = 19.4 min, with two different alpha energies having a 75% and 25% branching ratios; see Table 11.1). This isotope also has a small decay branch that proceeds via electron capture. Since element 98 ('eka-dysprosium') was expected to have a stable tripositive oxidation state in aqueous solution, its elution behavior in chromatographic separation schemes was predicted and this was used as a guide to estimate which collection fractions should be examined for the new element. In addition to acquire a high degree of decontamination

Table 11.1 *Nuclear properties of californium isotopes*.*

Mass number	*Half-life*	*Mode of decay*	*Main radiations* (MeV)	*Method of production*
237**	2.1 s	EC, SF		^{206}Pb(^{34}S,3n)
238**	21 ms	EC, SF		^{207}Pb(^{34}S,3n)
239	39 s	α	α 7.63	^{243}Fm daughter
240	1.06 min	α	α 7.59	^{233}U(^{12}C,5n)
241	3.8 min	α	α 7.335	^{233}U(^{12}C,4n)
242	3.7 min	α	α 7.385 (∼ 80%)	^{233}U(^{12}C,3n)
			7.351 (∼ 20%)	^{235}U(^{12}C,5n)
243	10.7 min	EC ∼ 86%	α 7.06	^{235}U(^{12}C,4n)
		α ∼ 14%		
244	19.4 min	α	α 7.210 (75%)	^{244}Cm(α,4n)
			7.168 (25%)	^{236}U(^{12}C,4n)
245	45.0 min	EC ∼ 70%	α 7.137	^{244}Cm(α,3n)
		α ∼ 30%		^{238}U(^{12}C,5n)
246	35.7 h	α	α 6.758 (78%)	^{244}Cm(α,2n)
	2.0×10^{3} yr	SF	6.719 (22%)	^{246}Cm(α,4n)
		β stable		
247	3.11 h	EC 99.96%	α 6.296 (95%)	^{246}Cm(α,3n)
		α 0.035%	γ 0.294 (1.0%)	^{244}Cm(α,n)
248	334 d	α	α 6.258 (80.0%)	^{246}Cm(α,2n)
	3.2×10^{4} yr	SF	6.217 (19.6%)	
		β stable		
249	351 yr	α	α 6.194 (2.2%)	^{249}Bk daughter
	6.9×10^{10} yr	SF	5.812 (84.4%)	
			γ 0.388 (66%)	
250	13.08 yr	α	α 6.031 (83%)	multiple n capture
	1.7×10^{4} yr	SF	5.989 (17%)	
251	898 yr	α	α 5.851 (27%)	multiple n capture
			5.677 (35%)	
			γ 0.177 (17%)	
252	2.645 yr	α 96.91%	α 6.118 (84%)	multiple n capture
		SF 3.09%	6.076 (15.8%)	
253	17.81 d	β^- 99.69%	α 5.979 (95%)	multiple n capture
		α 0.31%	5.921 (5%)	
254	60.5 d	SF 99.69%	α 5.834 (83%)	multiple n capture
		α 0.31%	5.792 (17%)	
255	1.4 h	β^-		^{254}Cf(n,γ)
256	12.3 min	SF		^{254}Cf(t,p)

SF = spontaneous fission: EC = electron capture

* See Appendix II.

** The existence of these isotopes has been questioned but included for completeness.

from other radionuclides, it was also necessary that the chemical separations be completed rapidly (within about 1 h) due to the short half-life projected for this isotope of californium.

Californium, element 98, is in the second half of the actinide series, where its 5f electrons are further removed from the valence electrons than in the lighter actinide elements. It is this effect that makes californium more 'lanthanide-like' in many compounds and in solutions. However, in progressing across this half of the actinide series, there is also an increasing tendency for a divalent metallic state and the formation of a divalent state in compounds, and several compounds containing Cf(II) are known. Thus, its comparison to the lanthanide elements has limitations, as seen from topics discussed throughout this chapter. Unlike members of the second half of the lanthanide series, which may exhibit either a divalent or tetravalent oxidation state in addition to their more common trivalent state, californium is known to exhibit a divalent, trivalent, and tetravalent state in compounds. In solution, the trivalent state is dominant, although the II, IV states, and a potential V state have been reported. In its elemental state, californium properties differ from those exhibited by its lanthanide homolog, dysprosium.

When the existence of californium was established, scientific interests and efforts progressed to prepare other isotopes of this element, to determine their nuclear properties, and to investigate the chemistry of the element. These initial studies were performed using only small numbers of atoms, but it is to the credit of the early investigators that considerable amounts of chemical and nuclear data were accumulated in their work. Tracer experiments were sufficient to establish the stability of Cf(III) in solution, as well as some of the element's basic chemistry. Additional information on the chemistry of californium was generated as microgram quantities became available, which also permitted the preparation and study of solid compounds. The first compound of californium of a definitive structure (the oxychloride by Cunningham and Wallmann) was determined a decade after the discovery of the element (Seaborg and Loveland, 1990).

Larger quantities of the transplutonium elements, including californium, subsequently became available by the development of a reactor irradiation program that was initiated in the mid-1960s by the former U.S. Atomic Energy Commission. The U.S. Department of Energy retains the ability to produce these transplutonium elements, including sub-gram amounts of the different californium isotopes yearly in the High-Flux Isotope Reactor (HFIR) at Oak Ridge National Laboratory, Oak Ridge, Tennessee. The continued production at HFIR may be limited in the future. Transplutonium elements are also produced in high-flux reactors at Dimitrovgrad in the Russian Federation, and potentially in other reactors. Smaller amounts of californium can be generated by irradiation of special targets in accelerators, but in the best case these smaller quantities only serve for chemical tracer studies or for determining their nuclear properties.

Reactor-produced californium consists of californium isotopes from ^{249}Cf through ^{254}Cf, with the major isotope produced being ^{252}Cf. Californium isotopes produced in accelerators normally have lower atomic masses and obtained in much smaller quantities. Considering these production schemes and the californium daughters formed as daughter products of other decaying isotopes, californium isotopes with masses as small as 237 and as large as 256 have been reported. An example of accelerator-produced californium is the generation of ^{242}Cf reported by Sikkeland and Ghiorso (1967), in the time frame when HFIR was producing californium isotopes through successive neutron capture processes.

This chapter focuses on the chemistry and physical properties of californium that are available in the open literature, and supplementing/evaluating this information when appropriate. An effort was made to minimize the number of references to technical reports, unpublished information, etc., except for cases when such a citation was warranted. The number of publications dealing with technological and medical applications of neutrons from ^{252}Cf is very large. There are numerous references to work done with californium covering biological studies, radiotherapy, neutron radiography, neutron activation analyses, dosimetry, etc. Some 70% of the work published during the last decade concerns efforts in these arenas using the ^{252}Cf isotope. The remaining reports deal with chemical studies and separation work, which normally employ the longer-lived ^{249}Cf isotope.

A significant amount of the basic chemical work on californium has been reported in different publications, but this should not be construed to interpret that additional chemical or physical studies are not needed! Indeed, given some of the recent advances in scientific techniques (i.e. those involving synchrotron sources, such as extended X-ray absorption fine structure (EXAFS), X-ray absorption near edge structure (XANES), photoelectron scattering, etc.), new studies should be pursued with californium and its compounds, and such investigations would be expected to yield even further insights into this element's science. Some of the more recent thrusts in the chemistry and physics of californium have involved its gas-phase chemistry, high-pressure studies of the metal and compounds, and new separation science. These topics are covered in the different sections of this chapter.

11.2 PREPARATION AND NUCLEAR PROPERTIES

It is unlikely that, nor have there been reports or evidence of, primordial californium in nature. Thus, isotopes of californium with mass numbers between 237 and 256 have been prepared as man-made isotopes. A summary of methods for the preparation of and nuclear data for these isotopes is given in Table 11.1, and in Appendix II. The lighter masses (neutron deficient) are produced by accelerator methods, (e.g. the helium bombardment of curium isotopes) which was the initial technique used to generate and discover californium. But californium isotopes can also be prepared by heavy-ion bombardment of elements other than curium. Examples of the latter are bombarding thorium with oxygen ions, and uranium with carbon or nitrogen ions. These preparations involve high-energy accelerators and produce only limited numbers of atoms of the product nucleus, and therefore are not useful for producing weighable quantities (i.e. even micrograms quantities) of californium needed for the preparation of pure solid compounds. An excellent discussion on the history, preparation, and nuclear properties of californium isotopes is given by Hyde *et al.* (1971) and Seaborg and Loveland (1990).

Californium isotopes with larger neutron contents (higher mass numbers) are usually prepared by irradiation of targets (plutonium through curium) in nuclear reactors that have a high neutron flux ($>10^{15}$ neutrons cm^{-2} s^{-1}). These and even heavier californium isotopes are also generated in nuclear explosions, where for short periods of time the neutron flux is even higher (fluence $> 10^{29}$ neutrons cm^{-2}). In the latter case, the formation of higher-Z elements and heavier isotopes is favored due to the high density of neutrons and in time spans that are short relative to the various decay half-lives of the materials formed. In principle, the objective would be to favor the significant neutron capture by the uranium to plutonium atoms present in such devices over the decay process of the products formed. This builds very rapidly by capture beyond the particularly short-lived isotopes before they can decay appreciably. Although transplutonium elements have been intentionally produced in underground nuclear explosions, processing of large amounts of 'ore material' (rock debris) in reasonable time periods makes this preparation procedure for these elements impracticable. Thus, weighable quantities of californium are best obtained as direct or indirect products from irradiation of materials in nuclear reactors.

Since the mid-1960s californium has been produced in special nuclear reactors (i.e. the HFIR at Oak Ridge National Laboratory). Most recently the intial targets consist mainly of curium isotopes (^{244}Cm through ^{248}Cm isotopes), which are irradiated in the reactor by neutrons to produce californium isotopes from ^{249}Cf through ^{255}Cf with the major isotope being ^{252}Cf. The HFIR located at Oak Ridge National Laboratory can produce currently up to 0.5 g of ^{252}Cf (together with other californium isotopes) per year. By using larger reactors, this quantity could be conceivably be increased to produce several grams of ^{252}Cf per year, and at one time this was planned in the U.S. but the greater need for this isotope never materialized.

The ^{252}Cf isotope has a 2.6 year alpha decay half-life, and a 85 year spontaneous fission branching half-life, which is the source of the neutrons it emits. Neutrons from its fission offer the main use for this isotope (i.e. neutron activation analysis, medical treatments, neutron radiography, etc.), but it is also useful for chemical tracer work, given its high specific alpha activity and greater availability. However, the neutron field (3×10^{6} neutrons s^{-1} $\mu\text{g}^{-1}$and the gamma radiation accompanying fission and/or the alpha decay of ^{252}Cf (up to 7 MeV gammas)) normally precludes its use for basic chemical/physical studies, as considerable shielding is required to protect personnel and equipment from even microgram amounts of it (gloved box limits are normally only a few micrograms). As a result, the mixture of californium isotopes obtained directly from reactors (which contains ^{252}Cf as the primary isotope) is not generally considered when multiple micrograms or more of californium are needed for studies without extensive shielding. Instead, the ^{249}Cf isotope is used.

Although in principle, ^{251}Cf has the most desirable radiation characteristics with regard to performing research studies, and it could be isolated from mixed californium isotopes using a mass separator, the cost and low yields (10%) makes this process unattractive. This isotope is only formed at low concentrations, as a result of its high-neutron capture and fission cross sections.

Another isotope, ^{253}Cf, is important as a parent for obtaining isotopically pure ^{253}Es (see Chapter 12). If a chemically pure (i.e. free of einsteinium) fraction of mixed californium isotopes from a reactor is obtained, and the ^{253}Cf present is allowed to decay, then a subsequent chemical separation of this californium fraction allows recovery of its pure ^{253}Es daughter.

For the majority of basic studies, especially those requiring weighable quantities of californium, the ^{249}Cf isotope is desired. Its alpha half-life of 351 years makes it suitable for chemical/physical experiments in gloved boxes, although there is still significant gamma radiation associated with its decay, which may require some shielding for protection. Typically, gloved box studies are rather limited to less than 10 mg because of radiation levels.

Isotopically pure ^{249}Cf is best obtained form the decay of ^{249}Bk (beta emitter, half-life of 330 days; see Appendix II). This latter isotope is the major berkelium isotope obtained from reactor irradiations (^{250}Bk is also formed in reactors but it has a 3.217 h half-life and rapidly decays; see appendix II). Thus, to obtain ^{249}Cf free of other californium isotopes for research studies, it is necessary to generate berkelium in a reactor and then separate it chemically from the other transplutonium elements present. After sufficient decay of the ^{249}Bk to ^{249}Cf, the latter can be subsequently separated chemically from the berkelium fraction. It is possible to obtain multi-milligrams (up to 60 mg at the HFIR at Oak Ridge National Laboratory) per year in this manner. And, as the half-life of ^{249}Cf is 351 years, it is possible to accumulate larger amounts of it over time by recovery operations. The only other known production source of ^{249}Bk in significant quantities, and hence a source of isotopically pure ^{249}Cf by its decay, is in Russia but the quantity available there is often smaller. It is then possible to provide in relatively short time frames multi-milligram amounts of ^{249}Cf.

The half-life of ^{250}Cf (13.08 years), which is produced along with other californium isotopes in reactors, has been determined recently (Popov *et al.*, 1996). The ^{238}Cf nuclide had been reported from bombardment of lead isotopes (^{207}Pb and ^{208}Pb) with ^{34}S and ^{36}S ions (Lazarev *et al.*, 1995). Its mode of decay is suggested to occur by spontaneous fission.

The K series of X-rays generated form californium has been discussed by Dittner and Bemis (1972), and can be used for the identification of californium during its decay processes. The vibration states in californium nuclei have been discussed by Ahmad (1980).

11.3 APPLICATIONS

As mentioned in Section 11.2, californium produced in nuclear reactors is mainly comprised of ^{252}Cf, and only a small quantity of this isotope mixture can be employed for chemical/physical studies outside of heavy shielding or hot cells. Thus, the applications for this ^{252}Cf isotope are for: (1) neutron emissions; (2) a target material for producing transcalifornium elements; (3) a californium tracer, using its higher specific alpha activity; and/or (4) a parent for obtaining ^{248}Cm (^{248}Cm is the alpha-decay product of ^{252}Cf; see Chapter 9). This long-lived isotope of curium is very useful for basic studies of curium. In practice, a mixture of ^{246}Cm, ^{248}Cm, and small amounts of other curium isotopes are obtained from the decayed californium reactor products (~97% ^{248}Cm and 3% ^{246}Cm from the alpha decays of ^{252}Cf and ^{250}Cf isotopes present).

Although it is beyond the scope of this work to review such applications of ^{252}Cf fully, or mixtures where this is the main californium isotope, its potential usefulness warrants some coverage here. The reader is also referred to: the ^{252}Cf Information Center at the Savannah River Laboratory (USAEC Rept, 1969) , Georgia, U.S.A. or the ^{252}Cf User Facility located at Oak Ridge National Laboratory. More extensive information is also given by Martin *et al.* (1997, 2000) and by Osborne-Lee and Alexander (1995). When ^{252}Cf is used as a neutron source, the data listed in Table 11.2 may be useful. Martin *et al.* (1998; 2004) have discussed applications of ^{252}Cf.

Considering the spontaneous fission half-lives, ^{252}Cf has the shortest one (85 years), a 3.09% fission fraction and yields 3.767 neutrons per fission. One observes a range from 2 to 3.8 neutrons per event for other fissioning actinide isotopes. The calculated neutron emission rate for ^{252}Cf is 2.3×10^{12} neutrons s^{-1} g^{-1}, although one would rarely expect to have a gram. In contrast, high-flux reactors have fluxes of three orders of magnitude higher. But, this rate for ^{252}Cf is lower than that for ^{254}Cf (1.2×10^{15} neutrons s^{-1} g^{-1}) due to its 99.7% fission fraction and 3.83 neutrons per fission event. But, this later isotope is not readily available in any significant quantities. For comparison, the neutron emission for ^{248}Cm, which also undergoes spontaneous fission, is only 4.2×10^{7} neutrons s^{-1} g^{-1}. It has a long alpha decay having a half-life of 3×10^{5} years, 8.39% fission fraction, and 3.2 neutrons per fission event. Data are summarized in Table 11.2.

Applications of ^{252}Cf can be broadly classified as medical, analyses, and biological studies, where the majority of the work involves in one way or the other the spontaneous-fission neutrons emitted from ^{252}Cf (Karelin *et al.*, 1997). These sources have been useful in such areas as neutron activation analysis, neutron radiography (a technique that complements X-ray radiography), and medical therapy for treatment of cancer. They are most useful where access to nuclear reactors is not possible, or convenient, and/or where a lower neutron flux is adequate for the need at hand. An important application for ^{252}Cf is to

Table 11.2 *Data for ^{252}Cf and other selected neutron sources*.*

Isotope	*Half Life* (yrs)	*Specific Activity* (Ci g^{-1})	*Spontaneous Fission Half-Life* (yrs)	*Fission Fraction* (%)	*Neutrons per Fission*	*Neutron Rate* (n $s^{-1}g^{-1}$)
^{252}Cf	2.645	5.38×10^2	85	3.09	3.767	2.3×10^{12}
^{252}Cf alpha energies:			6.118 (84%) 6.076 (16%)			
Specific heat from decay of ^{252}Cf			38 W g^{-1}			
Neutrons from (α, n) reaction on Al metal: 1.3×10^7 n s^{-1} g^{-1}						
^{254}Cf	0.17	8.45×10^3	–	99.7	3.83	1.2×10^{15}
^{248}Cm	3.4×10^5	4.25×10^{-3}	41	8.39	3.16	4.2×10^7

**Sources*: The Health Physics and Radiological Health Handbook (1998); Osborne-Lee and Alexander (1995).

provide neutrons for the initial start-up of nuclear reactors (Osborne-Lee and Alexander, 1995).

Portable neutron activation analysis systems using ^{252}Cf have been designed for use in deep-sea exploration for minerals, or for space probes (Senftle *et al.*, 1969; Wiggins *et al.*, 1969; Filippov, 1979; Bakiev *et al.*, 1991).

Various sizes and forms of ^{252}Cf sources have been designed for medical applications, both for external irradiation and for internal implantation. How extensive the practical applications of ^{252}Cf can be determined by the success of experiments using this nuclide. The more extensive shielding hinders medical applications needed for the neutrons (greater thickness of paraffin for neutrons versus that of lead for shielding X-rays). Remote operation/delivery of the californium sources to the application site aids in this respect. A large number of such applications have been reported (Castro *et al.*, 1973; Poda and Hall, 1975; Zech *et al.*, 1976a,b; Maruyama *et al.*, 1978, 1980, 1991; Belenkll *et al.*, 1991; Yanch *et al.*, 1993; Patchell *et al.*, 1997; Knapp *et al.*, 1999; Rivard, 1999a,b, 2000a–c; Rivard *et al.*, 1999, 2002, 2004; Wanwilairat *et al.*, 2000; Tacev *et al.*, 2003a,b, 2004a,b).

Studies involving the injection of ^{252}Cf into beagles (Lloyd *et al.*, 1972a,b, 1976; Taylor *et al.*, 1972) and into swine (Mahony *et al.*, 1973; Beamer *et al.*, 1974) have also been reported. Investigations involving mouse mammary-carcinoma and bone were also reported (Fu and Phillips, 1973).

Several biological studies have used ^{252}Cf to examine the effects of neutron radiation. Work on DNA (Tacev *et al.*, 1998; Florjan *et al.*, 1999) has been done, as well as work on its bioefficiency (Cebulska-Wasilewska *et al.*, 1999). The biokinetics of it in marine isopods (Carvalho and Fowler, 1985) and the survival of human cells under irradiation (Todd *et al.*, 1984) have also been published. A solvent extraction/liquid scintillation counting method for determining ^{252}Cf in biological samples has been discussed (Miglio, 1978).

There is an extensive list of reports and publications dealing with the applications. The reader is referred to these for more extensive information. One useful source in this regard is an ORNL Report (Osborne-Lee and Alexander, 1995). Other sources of information involve the use of ^{252}Cf: for cervical carcinoma treatment (a 12 year review by Tacev *et al.*, 2004a,b); a review of other clinical applications (Mignano and Rivard, 2004); and advances in neutron radiographic techniques (Berger, 2004). Dullmann *et al.* (2003) also discuss fission fragment sources using ^{252}Cf.

11.4 SEPARATION AND PURIFICATION

The choice of a separation and purification scheme for californium depends on the nature of its source, the particular isotopes of californium involved, the amount of material, the impurities present, as well as several other factors. In short, the best procedure needs to be customized to the particular situation at hand. Usually, ion exchange is involved either as the main separation technique, or at least in some secondary capacity. Since californium in aqueous solutions is normally stable only in its tripositive state, oxidation–reduction cycles are not useful for separation. Due to the very similar chemical behavior of the tripositive transplutonium elements, as well as lanthanide ions of comparable ionic radii (i.e. Sm–Tb), the separation chemistry for californium employed must often rely on small differences in chemical behaviors for the different materials to be separated.

The separation procedure most suitable for californium isotopes generated in accelerators may not be the same as that used for californium produced in reactor targets. In some accelerator experiments, the desired californium isotopes generated may be physically separated via recoil mechanisms from the targets, which simplifies the separations and shortens the time required for the shorter-lived isotopes. The need for nuclear or radioactive purity, as opposed to chemical purity, will also affect the particular separation processes to be used. A considerable amount of information on californium chemistry was determined using tracer levels of californium, usually using ^{252}Cf isotope. The major purification schemes for californium at tracer levels have frequently involved ion-exchange techniques to separate californium from other transcurium elements.

For purposes of separation, the transplutonium elements can be placed into two groups: (1) americium and curium and (2) the group of the next several transcurium elements, which includes californium. The separation of californium from its neighbors, especially einsteinium, is therefore more difficult than separating it from americium/curium or from the lighter actinides. Separation of californium from berkelium is simplified by the ability to oxidize berkelium in an aqueous medium, which then permits the solvent extraction of Bk(IV) away from Cf(III).

A number of procedures have been used for the separation/purification of californium. One of the early ion-exchange methods involved the use of cation-exchange resin (Dowex 50) and ammonium citrate or ammonium lactate as eluants. A superior eluant, ammonium α-hydroxyisobutyrate (α-HIBA), was first used over 30 years ago (Choppin *et al.*, 1956), and this reagent is still in use today for the separation of californium from other actinides. Thompson *et al.*, (1954). A very useful group separation between the lanthanides and actinides can be accomplished using concentrated hydrochloric acid as an eluant for the transcurium elements sorbed on cation resin; the separation is improved by using an ethanol–hydrochloric acid mixture as an eluant (Street and Seaborg, 1950). Another method for separation elements from the two groups, especially with smaller quantities has been the use of TEVA™ columns (Horwitz *et al.*, 1992, 1993, 1995; Porter *et al.*, 1997). These resin columns are available commercially (Eichrom Industries) and employ thiocyanate and formic acid solutions. The greater complexing ability of the transplutonium elements is evident as they desorb ahead of the lanthanide elements when using these separation approaches. The separation of californium from its actinide neighbors, using cation- or anion-exchange resins, or elution with either hydrochloric or ethanol–hydrochloric acid mixture, alone is not feasible.

Anion-exchange separation procedures using slightly acidic $LiNO_3$ or $Al(NO_3)_3$ solutions (Surls and Choppin, 1957; Adar *et al.*, 1963; Marcus *et al.*, 1963) or ethylenediaminetetraacetic acid (EDTA; Baybarz, 1966a,b) as eluants have also been reported. Several extraction procedures have been used, such as the extraction of trivalent actinides from concentrated LiCl or $LiNO_3$ (slightly acidic) solutions and the use of trilaurylamine or other trialkylamines (Baybarz *et al.*, 1963) or quaternary ammonium salts (Moore, 1964, 1966; Horwitz *et al.*, 1966). Extraction chromatography using quaternary ammonium salts or bis(2-ethylhexyl)phosphoric acid (HDEHP) as a stationary phase has also been employed (Gavrilov *et al.*, 1966; Horwitz *et al.*, 1967, 1969a,b). Inorganic ion exchangers such as zirconium phosphate materials have limited applications for californium separations due to their lower selectivity as compared to organic-type extractant materials.

Several summaries of separation procedures have been discussed and can be found in: Miller (1967), Keller (1971), Myasoedov *et al.* (1974), Bigelow (1974), Ishimori (1980), King *et al.* (1981), Collins *et al.* (1981), Benker *et al.* (1981), and Campbell (1981).

Most extraction procedures are useful for separating californium from americium/curium or from lighter actinides, but are limited for separating it from other transcurium elements. For example, HDEHP dissolved in an aromatic diluent has been used to separate Cf and Cm providing a separation factor of about 50, but it is not useful for californium–einsteinium separations. Efforts continue to find new and better extractants with the aim of improving separation factors and selectivity. It is unlikely that a specific extractant for californium alone will be developed but new materials may provide improved separation factors over methods presently used or known. Reviews that discuss californium extraction chemistry are available (Bigelow *et al.*, 1980, 1981; Myasoedov *et al.*, 1980; Shoun and McDowell, 1980).

One application of HDEHP on an inert support material, such as porous glass (i.e. Bioglass), is worth noting. An excellent separation between curium and californium can be achieved using this approach, which is important process for recovering $^{248}Cm/^{246}Cm$ from their $^{252}Cf/^{250}Cf$ parents. In this procedure, the actinides are loaded onto a column with the agent, and then eluted with 0.1 M HNO_3. As the californium is retained more strongly due to complexation, the curium is eluted first.

It is also useful to note that berkelium and californium can be readily separated by solvent extraction of Bk(IV) away from Cf(III). This separation is important since isotopically pure ^{249}Cf is obtained from the beta decay of ^{249}Bk. The berkelium can be readily oxidized to Bk(IV) in aqueous solution with a strong oxidant (i.e. bromate ion) in nitric acid solution.

Since the majority of californium is produced in nuclear reactors, or obtained as a by-product from reactor-produced ^{249}Bk, it is appropriate to discuss briefly a flowsheet for the separation techniques employed in recovering californium for reactor targets. If uranium or plutonium is present as the main target material, then these elements must also be separated from the transplutonium element group (containing the californium) in addition to fission products (lanthanide elements, transition metals, etc.) and other products (aluminum from target assemblies, etc.). If americium and curium, or pure curium, is the main starting material, then only small amounts (if any) of the lighter actinides may be present, which simplifies the situation.

The general separation scheme, Scheme A in Fig. 11.1, is for separating and purifying californium from the HFIR products containing uranium and plutonium at the Oak Ridge National Laboratory. Reports on different aspects of these purification processes are available (Baybarz *et al.*, 1973; King *et al.*, 1981; Bigelow *et al.*, 1981). The procedure begins with alkali dissolution of the aluminum target holders used for the reactor. This leaves the insoluble actinide oxides, which are subsequently dissolved in hydrochloric or nitric acid to generate a solution of the elements to be separated.

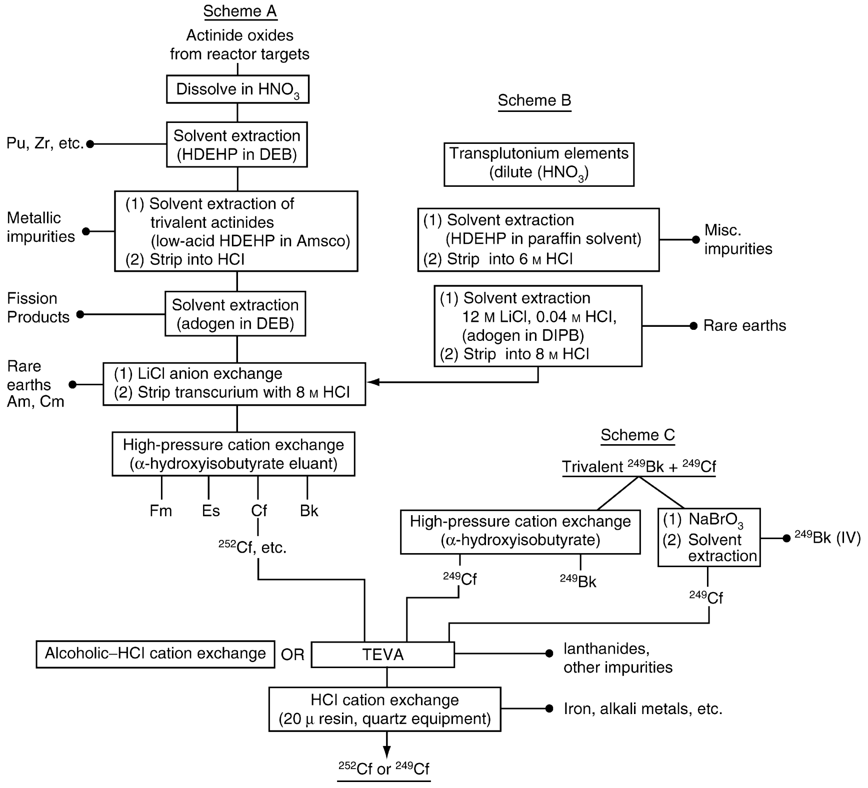

Fig. 11.1 *Separation and purification scheme for californium.*

Solvent extraction (HDEHP in an aromatic diluent as diethylbenzene) (DEB) removes plutonium and zirconium from the system. Scheme B is given for the situation where only the transplutonium elements are present (i.e. starting with americium and curium targets rather than plutonium).

In both cases, the transplutonium elements are then extracted with HDEHP in an aliphatic solvent, and a subsequent amine extraction (adogen) of these actinides removes them from most of the fission products. At this point, the product contains the transplutonium elements and any lanthanides present (fission products). A LiCl anion-exchange process partitions the transcurium elements from americium, curium, and the lanthanides, leaving the transcurium elements as a separate fraction. Scheme B in the figure considers only mixtures of the transplutonium elements.

The transcurium elements (Bk, Cf, Es, and some Fm) are then separated on high-pressure cation-exchange columns. Using a buffered α-hydroxyisobutyric acid solution as an eluant, californium is obtained as a separate fraction using a high-pressure ion-exchange process (very small resin particles, elevated temperature, at 80°C). The subsequent treatment of the different fractions obtained from this process depends on several factors, which include the final use of the material. The purification requirements for the californium isotopes produced directly in the reactor are based on whether Es or Cm daughters will be recovered, or the medical/industrial uses of the californium isotopes.

The californium fraction is further treated to remove residual lanthanide elements; this is especially important for nuclear studies where traces of radioactive lanthanide isotopes are detrimental, or for target materials, where unwanted reaction products may be generated from any impurities present. An ethanol–hydrochloric column is shown in Fig. 11.1, but it could also be replaced by a TEVA™ column. Horwitz *et al.*, (1992, 1993, 1995); Porter *et al.*, (1997).

Since most basic research studies involving milligram quantities of californium make use of ^{249}Cf obtained from the decay of ^{249}Bk, the purification requirements and processes for the californium produced in this manner is different, and shown in Scheme C in Fig. 11.1. Here, the material normally consists of only ^{249}Bk and ^{249}Cf isotopes plus any non-actinide impurities (i.e. accumulated from berkelium used in research studies). The objective is then to separate californium from its berkelium parent and any other impurities that may be present. To achieve the very high chemical purity desired for basic research work on californium, different things must be considered and the necessary separation processes must be addressed on an individual basis. The easiest situation is when the ^{249}Bk precursor for ^{249}Cf is already available in a highly pure state, and the separation of the californium involves only its separation from a relatively pure parent material. It this case, Scheme C in the figure could apply. For separating berkelium and californium, either a cation-exchange column (with α-hydroxyisobutyrate as the complexing agent) or the solvent extraction of berkelium as Bk(IV) away from trivalent californium (several different extracts schemes can be used). In the latter process, the berkelium is first oxidized to Bk(IV) in solution with bromate ions, and the californium remains trivalent. An advantage with the ion-exchange process is that it avoids generating higher acid solutions and does not add bromide or bromate ions to the californium fraction.

In general, the purification of ^{249}Cf normally involves multiple pressurized cation-exchange columns with 0.25 M α-hydroxyisobutyric acid as an eluant (using solutions of variable pH from 3.8 to 4.2 at 80°C) to separate californium from other transplutonium elements, which also provides a general purification from other impurities than actinides. Then, a cation-exchange column with an ethanol–hydrochloric acid as an eluant, or a TEVA column, can remove lanthanide elements, alkaline earths, alkali metals, iron, nickel, etc. The columns, especially the final column and product receiver, are often constructed of acid-leached quartz. Special alpha detectors are used to determine the fractions that contain the californium. Using this process, a very pure californium chloride product is obtained, which can then be used for preparing compounds or the metal of californium for research.

Additional separation approaches have been reported in more recent publications. Firsova *et al.* (1998) have used bis(1-phenyl-3-methyl-4-acylpyrazolol-5-one) and its derivatives for solvent extraction, and other chromatographic separation methods (Firsova *et al.*, 1996) for separating berkelium and californium. Extractions using 4-benzoyl-2, 4-dichloro-5-methyl-2-phenyl-3H-pyrozol-3-thione, and tri-*n*-octylphosphine oxide (TOPO) have also been tested (Hannink *et al.*, 1992). Separation exclusion chromatography techniques have also been applied for separating californium from americium, curium, and lanthanides (Firsova *et al.*, 1990). The transplutonium elements have also been extracted from carbonate solutions using oligomers and alkylphenol derivatives (Karalova *et al.*, 1990), and extraction chromatography results with *DHDECMP* in nitric acid and characterization of DHDECMP/XAD-4 resins have been tested in the purification process (Kimura and Akatsu, 1991).

Extractions approaches for Cf(III) have also been done with aqueous pyrophosphates and lithium polyphosphate solutions with HDEHP (Chakravortty *et al.*, 1989). Extractions have also used HDEHP in nitric acid solutions (Kasimov and Skobelev, 1987). A modified ion-exchange procedure using α-hydroxyl-2-methyl butyrate was reported by Vobecky (1989). The separation of einsteinium from californium irradiation targets by ion exchange has been discussed by Elesin *et al.* (1986). The separation of californium using different salts of HDEHP was published by Dedov *et al.* (1986a,b). The extraction of magnesium and its influence on californium extraction via HDEHP for citric acid–magnesium nitrate systems has also been discussed (Kovantseva *et al.*, 1986). The effect of cations on exchange chromatography of curium and californium has been reported (Erin *et al.*, 1981) and the complexation of Cf(III) in perchlorates was also reported (Lebedev and Mazur, 1981). A simple separation approach for special applications has been suggested by Guseva *et al.* (1973), and a curium–californium extraction chromatography approach was published by Aly and Abdelras (1972). The use of 8-hydroxyquinoline and 5,7-dichloro-8-hydroxyquinoline for extraction of californium was suggested by Feinauser and Keller (1969).

Three extraction studies involving californium were reported by Horwitz and coworkers. One study involved bis(2-ethyl)orthophosphoric acid (Horwitz *et al.*, 1969a); a second report was made on the same system (Horwitz *et al.*, 1969b); and the third effort was an extraction using high molecular weight quaternary amines in ammonium nitrate solutions (Horwitz *et al.*, 1967). The chelating and extraction of Cf(III) by acetylacetone and derivatives of it were also reported by Keller and Schreck (1969). Fused salt, molten metal processes have also been examined for separating californium (Knighton and Steunenberg, 1966; Mailen and Ferris, 1971). The analytical chemistry of the actinides has been reviewed by Myasoedov and Lebedev (1991), and several aspects of separation chemistry are also discussed in this work.

In principle, an alternative procedure for the separation of californium in special circumstances may be to reduce a mixture of actinide oxides with thorium metal under vacuum, and distill away the more volatile californium metal and then condense it on a suitable receiver (Haire, 1982). The separation of californium oxide from curium oxide using a vacuum sublimation procedure was also suggested (Aleksandrov *et al.*, 1972).

11.5 ELECTRONIC PROPERTIES AND STRUCTURE

A considerable amount of spectroscopic data has been obtained for californium and a number of theoretical calculations have been made concerning its energy levels. The californium neutral atom's ground state is assigned as $5f^{10}7s^2$ ($^5I_8$) and the Cf^+ ground state as $5f^{10}7s$ ($^6I_{17/2}$) (Worden and Conway, 1970; Martin *et al.*, 1974; Blaise and Wyart, 1992; for further details see Chapter 16). The ionization energy for the neutral californium atom has been calculated from spectroscopic data and were found to be 6.298 eV or 50800 (200) cm^{-1} (Sugar, 1973), respectively, but it now has been determined experimentally and found to be 6.2817(2) eV or 50665(200) cm^{-1}, respectively (Erdmann *et al.*, 1996, 1998) using resonance ionization mass spectrometry. Some of the lowest energy levels and the representative configurations are given in Tables 11.3 and 11.4, and experimental F^k(ff) and Hartree–Fock values are listed in Table 11.5. These values were determined using the ^{249}Cf isotope. Ionova *et al.* (1977) have also discussed the electronic levels of californium.

From limited absorption and self-luminescence spectra for californium, an early partial energy-level scheme was published for the $5f^9$ configuration (Conway *et al.*, 1962a,b). Predictions of the energy-level structure for Cf(III) appeared in 1964 (Fields *et al.*, 1964), and work on the triply ionized form of californium has also been published (Carnall *et al.*, 1973; Varga *et al.*, 1973a,b).

Table 11.3 *Lowest californium electronic levels for configurations listed.*

Species	*Configuration*	*Parity term*	*Level* (cm^{-1})	G_{obs}	*Hfs* (10^{-3} cm^{-1})
^{249}Cf(II)	5f^{10}6s	E ^{6}I$_{17/2}$	0.00	1.28	
^{249}Cf(II)	5f^{10}6d	E $J = 15/2$	19 359.06		
^{249}Cf(II)	5f^{9}6d7s	O $J = 19/2$	24 213.34	1.27	
^{249}Cf(II)	5f^{107}p	O $J = 15/2$	26 858.90	1.26	
^{249}Cf(I)	5f^{10}7s^2	E ^{5}I$_8$	0.000	1.213	0
^{249}Cf(I)	5f^{9}6d7s^2	O $J = 8$	16 909.355	1.301	–40
^{249}Cf(I)	5f^{10}7s7p	O $J = 8$	17 459.210	1.277	–140
^{249}Cf(I)	5f^{10}6d7s	E $J = 8$	20 043.930		–210
^{249}Cf(I)	5f^{9}7s^{2}7p	E $J = 7$	24 727.600		60
^{249}Cf(I)	5f^{10}7s8s	E ^{7}I$_9$	32 983.180	1.300	–490
^{249}Cf(I)	5f^{9}6d7s7p	E $J = 8$	33 952.135		–200
^{249}Cf(I)	5f^{10}7s8p	O $J = 8$	38 225.945		–410
^{249}Cf(I)	5f107s7d	E $J = 8$	39 091.175	1.245	
^{249}Cf(I)	5f^{9}7s^{2}8s	O $J = 8$	45 183.155		–150

Source: Chapter 16 and references therein.

Table 11.4 *Lowest electronic levels for neutral californium configurations.*

Configuration	*Level* (cm^{-1})
5f^{9}6d7s^2	16 909
5f^{9}6d^{2}7s	31 500
5f^{9}6s^{2}7p	24 728
5f^{9}6d7s7p	33 952
5f^{10}7s^2	0
5f^{10}6d7s	20 044
5f^{10}6d^2	50 000
5f^{10}7s7p	17 459

Source: Chapter 16 and references therein.

Table 11.5 *Selected experimental values of* F^k(ff), *Hartree–Fock values and* F^k/F^2 *ratios for californium.*

Configuration	*Element*	*Parameter* (r)	*Exp.*	*Hartree–Fock*	F^k/F^2 (exp.)	F^k/F^2 (calc.)	*Exp./H.F.*	*H.F.-exp.*
5f^{10}7s^2	Cf(I)	F^2	57 870	84 799	1.000	1.000	0.682	26 929
5f^{10}7s^2	Cf(I)	F^4	45 052	55 085	0.779	0.650	0.818	10 033
5f^{10}7s^2	Cf(I)	F^6	31 873	40 345	0.551	0.476	0.790	8472

Source: Chapter 16 and references therein.

Blaise and Wyart (1992) and Wyart *et al.* (2005) have more recently reported a comprehensive list of electron energy levels for californium, which are recommended values. Additional information is given in Chapter 15.

Absorption spectra of Cf(III) are mainly characteristic of f–f transitions (Laporte forbidden) within the $5f^{10}$ configuration. Spectra of Cf(III) in $DClO_4$–D_2O have been used to make term assignments and energy levels for californium (Varga *et al.*, 1973a). The electronic spectrum and estimated energies of the electronic configurations of Cf(IV) has also been predicted from spin–orbit coupling (Varga *et al.*, 1973b). Estimated energies of the electronic configurations for californium had appeared earlier (Brewer, 1971a,b), where values were given for singly, doubly, and triply charged californium ions.

A detailed theoretical interpretation of solid-state absorption spectra of $CfCl_3$ has also been published (Carnall *et al.*, 1973), and energy level assignments made for several californium absorption bands. The observed and calculated free-ion energy levels for Cf(III) have also been compared to the lower energy levels in californium's analog, Dy(III) (Carnall *et al.*, 1973). An attempt to correlate the electronic excitation energies for 4f and 5f elements suggested that the $f^ns^2 \rightarrow f^{n-1}ds^2$ excitation values for californium compare best with the lighter lanthanide elements (Mikheev *et al.*, 1979). A valence-band approach for high-coordination bonding in the californium compounds has also been suggested by Carter (1979); this approach implies d- and f-orbital splitting into bonding hybrids. From quantum chemistry considerations, the monopositive ion of californium should be more stable than monopositive lanthanide or lighter actinide ion, based on its lower calculated excitation energy. Calculations have also shown that, from berkelium to nobelium, the excitation (promotion) energies for the $f^ns^2 \rightarrow f^{n-1}ds^2$ configuration, which is taken as a measure of the stability of the divalent state, increases with the atomic number up to element 103 (Spitsyn, 1977). Thus, Cf(II) should be more stable than Bk(II) but less stable than Es(II). These promotion energies are discussed throughout this chapter and play an important role in the californium chemistry.

Predictions for excitation energies for $7s^2 \rightarrow 7s7p$ and $7s^26d$ levels have also been given (Carnall *et al.*, 1977). Experimental data were obtained and crystal field calculations have been made for Cf(III) in different crystal hosts (Carnall *et al.*, 1977). Relativistic Hartree–Fock–Slater calculations have yielded neutral-atom electron binding energies for californium (Haung *et al.*, 1976), and relativistic relaxed-orbital calculations of L-shell Coster–Kronig transition energies have been reported for californium (Chen *et al.*, 1977). An interpolation scheme for cohesive energies provides binding energies for electrons, which can correlate and compare the divalent nature of transplutonium elements; this approach has predicted a divalent metallic state for einsteinium rather than for californium (Johansson and Rosengren, 1975a,b). The divalent metallic state for einsteinium has been verified (see Chapter 12) but this state is less likely for bulk forms of californium (see Section 11.6).

Photoelectron spectrometry of californium has been performed on Cf_2O_3 and Cf_7O_{12}, using an MgKα excitation source (Krause *et al.*, 1988). Values for the

4f doublet ($4f_{5/2}$ and $4f_{7/2}$) of californium were determined in that work. The spin–orbit splitting for californium was estimated to be 17.5 eV.

The energy spectrum of electrons in ^{252}Cf has been given (Rykov and Yudin, 1998) and the energy levels of ^{249}Cf, both neutral Cf(I) and singly ionized Cf(Ii), are also available (Blaise and Wyart, 1992; Conway *et al.*, 1995; and Chapter 16). Ionova *et al.* (1989a,b) has reported computational results for the electronic structure of californium. Also see subsequent sections of this chapter regarding discussions of the absorption spectra of Cf(II) in solids and Cf(III) in solution, and californium's electronic behavior in the gas-phase studies (see Section 11.9). The nuclear magnetic moment of ^{249}Cf has been determined and found to be –0.28 nuclear magnetons, and its nuclear spin is accepted as being 9/2 (see Ahmad, Appendix I).

11.5.1 Emission spectra

The first emission spectrum for californium was reported by Conway *et al.* (1962a,b) and obtained via the copper-spark method. The majority of subsequent work on californium has been carried out using electrodeless lamps, where multi-microgram amounts of material are sealed in quartz envelopes and the californium is excited by external radiation. Emission spectra of californium have been observed from 2400 to 2.5 μm, with approximately 25000 lines having been recorded and accurately measured (Conway, 1976; Conway *et al.*, 1977). Fourier transform analyses of data obtained from californium lamps have been carried out with the goal of resolving the hyperfine structure (Blaise and Wyart, 1992; Wyart *et al.*, 2005). The $5f^{10}7s^2$ ground state, the $5f^{10}7s8s$, and $5f^96d7s^2$ configurations have been established from californium spectra (Warden *et al.*, 1970; Conway, 1976; Conway *et al.*, 1977; for further details see Chapter 16).

11.5.2 X-ray emission spectroscopy

The characteristic X-rays resulting from atomic readjustment to inner shell vacancies provide a very useful means for identification of an element (see Dittner and Bemis, 1972). Several X-ray emissions for heavy elements and their bonding energies are known, and such data have been tabulated for californium (Carlson and Nestor, 1977).

Similar calculations using nonrelativistic Hartree–Slater wave functions (Manson and Kennedy, 1974) and relativistic Hartree–Slater theory (Scofield, 1974) have also provided data for californium. The atomic form factors, the incoherent scattering functions (Hubbell *et al.*, 1975), and a total Compton profile have been tabulated for californium (Biggs *et al.*, 1975).

Systematic X-ray photoelectron spectroscopy (XPS) studies have also been carried out on transplutonium oxides through californium, providing experimental binding energies for their electrons, which can be compared to the calculated energies (Veal *et al.*, 1977). An interpolation scheme has also been reported for determining the binding energies of some lanthanides and actinides, including californium (Johansson and Rosengren, 1975a). The nature of the 5f electrons in the actinide series including californium has also been discussed (Johansson and Rosengren, 1975b).

11.6 THE METALLIC STATE

11.6.1 Preparation

The first attempt to prepare californium metal was made in the late 1960s (Fujita and Cunningham, 1969). Subsequently, several additional attempts have been made to prepare and study this metal. The relatively high volatility of californium metal has made its preparation and study on the microscale more difficult than the first three transplutonium metals. The possibility that the metal may exist in two different metallic valence states has also made it an interesting candidate for study, but it has also complicated the full understanding of californium's metallic state. The potential for californium to exist in two metallic valence states arises due to its f → d electron promotion or excitation energy (see subsequent discussion).

Two preparative approaches have been utilized for californium metal. The first approach utilizes the reduction of the trifluoride with lithium metal at elevated temperatures; the excess reductant and lithium fluoride are removed by vacuum distillation. The second preparative method employs thorium or lanthanum metal to reduce one of the californium oxides, permitting the distillation and subsequent condensation of the metal (Haire, 1982) and leaving the thorium or lanthanide metal and their oxides as residues. With thorium metal, the reaction is a solid–solid reaction and thorium has a lower vapor pressure, which should reduce the presence of the reductant in the vaporized product. With lanthanum, one encounters a liquid–solid reaction, as the lanthanum melts at 920°C; it also has a higher vapor pressure than thorium at high temperatures. The latter property must be considered to avoid incorporating lanthanum into the distilled californium product.

With the halide reduction process, where californium is to be retained as a solid residue, the volatility of californium is greater than that of lithium fluoride. This makes it difficult to volatilize the lithium fluoride completely from the californium product without simultaneously volatilizing away significant amounts of californium. In the oxide reduction procedure, the distillation of microgram quantities of metal yields thin films that are difficult to remove from the collection substrate. Also, a very good vacuum (free of residual materials such as hydrogen, oxygen, water or oil vapor, etc.) is required to avoid the formation of undesired compounds during the distillation of the reactive metal. With multi-milligram quantities, the distillation procedure is the best preparative route. The limited availability of the ^{249}Cf isotope and the radiation fields encountered with this isotope do limit the amount of metal that can be prepared in an unshielded gloved box to 10–20 mg. There is little information about the preparation of ^{252}Cf metal using these procedures, and it is likely little if any has been made by this route.

Some work has been done on preparing californium–palladium alloys via hydrogen reduction of oxide–palladium metal mixtures in conjunction with medical applications of this isotope (Haire and Sato, 1998; Rivard *et al.*, 1999). The latter products are not pure alloys but sufficient for pressing or making extruded sources if the californium content is kept below 20 at%. The malleability of the products is found to decrease with higher californium contents. The reduction in this procedure is driven by the stability of actinide–noble metal alloys. Radchenko *et al.* (1986b) have discussed the formation of $CfPt_5$ on platinum surfaces.

The preparation of pure ^{249}Cf metal to date has been in the 2–10 mg range, with the largest known amount prepared at one time being about 10 mg (Haire, 1978, 1980, 1982). A picture of a 10 mg ^{249}Cf product is shown in Fig. 11.2, where it is compared to the head of a common safety pin. A more detailed account of the preparation of californium metal is available (Haire, 1982).

The limited quantities of californium metal have placed restrictions on the amount of analytical data that can be obtained for products; normally it is not possible to analyze for hydrogen, nitrogen, and oxygen contents. The quality of the metal has then been ascertained mainly by diffraction analysis, total metal impurities by mass spectrometry, its physical properties and appearance and its behavior (such as the rate and extent of dissolution for enthalpy-of-solution

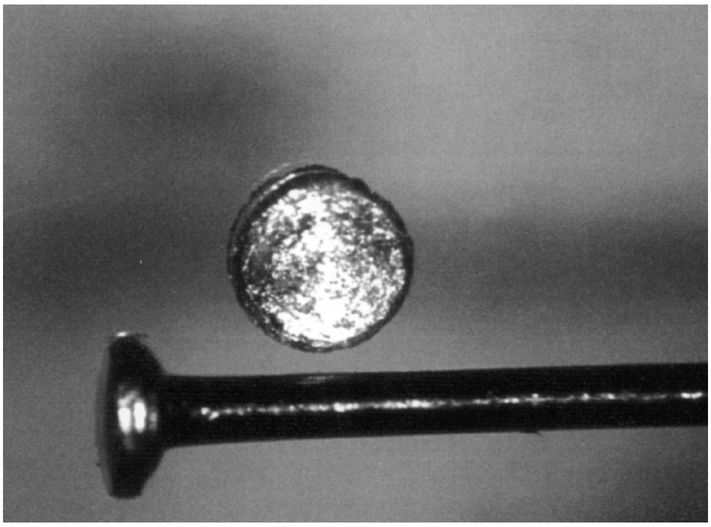

Fig. 11.2 *Ten milligram disc of californium compared to a straight pin.*

measurements) in experiments performed with the metal. Ideally, a larger quantity of metal would be prepared, characterized, and then used for a number of scientific measurements or experiments. But with californium (and some of the other transcurium metals), the preparation of the metal often becomes an integral part of a subsequent study, and either the major portion or the entire preparation is needed and often consumed in the study at hand (i.e. dissolved in acid in determining the enthalpy-of-solution of the metal) in an experiment.

11.6.2 Physical properties

There have been several different reports regarding the crystal data for californium over the years, and these are summarized in Table 11.6. Based on extrapolations from trivalent americium, curium, and berkelium metals, a double hexagonal close-packed structure with parameters on the order of $a_0 = 3.4$ Å and $c_0 = 11.0$ Å, and a face-centered cubic (fcc) high-temperature phase with $a_0 \sim 4.8$ Å would be expected for trivalent californium metal.

In earlier work, a face-centered structure with a parameter of 5.40 Å was reported, which was from a product obtained by the lithium reduction of its fluoride (Cunningham and Parsons, 1970). This is a difficult technique for preparing californium metal (see Section 11.6.1) and this work also involved very small quantities of californium. A potential explanation for this reported parameter is that it represents a poorly crystallized sesquioxide (body-centered cubic (bcc)), lattice parameter of 10.831 Å (see Section 11.7.4), which with the absence of weak diffraction lines in a diffraction pattern of marginal quality may be interpreted as arising from a face-centered material of 5.42 Å (10.831/2).

Subsequently, cubic and hexagonal structures were observed by Haire and Baybarz (1973a,b) in very thin films (<2.5 Å) of californium distilled onto electron microscopy grids and then analyzed by electron diffraction. These data suggested a metallic radius of slightly greater than 2.0 Å, suggesting californium may be a divalent metal. An extrapolation by Zachariasen (1975) also suggested that californium metal would be a cubic lattice and a larger radius than the trivalent metal. Subsequently, very small quantities of apparent metal were also analyzed by X-ray diffraction (Noé and Peterson, 1976) that duplicated the 5.747 Å cubic structure reported by Haire and Baybarz (1973a,b, 1974). Thus, these early data thus suggested californium may be a divalent metal.

With larger quantities of californium, its crystallographic data (Haire and Asprey, 1976; Noé and Peterson, 1976) independently showed that the metal was trivalent with a room temperature double hexagonal close-packed parameters of $a_0 = 3.384$ Å and $c_0 = 11.040$ Å, which suggests an atomic radius of 1.69 Å, which is in line with radii reported for americium, curium, and berkelium metals. The crystal forms of californium metal were also determined by Radchenko *et al.* (1986a) and Seleznev *et al.* (1989) for 1.5 mg of californium.

Table 11.6 *Crystallographic data reported for californium metal.*

Crystal System	*Lattice Parameters*		*Atomic Volume* (Å)^3	*Crystal Density* (g cm^{-3})	*Metallic Radius* (Å)	*References*
	a_0 (Å)	c_0 (Å)				
fcc	5.40	–	39.4	10.5	1.91	Cunningham and Parsons (1970)
fcc	5.743	–	47.4	8.72	2.03	Haire and Baybarz (1970)
hcp	3.988	6.887	47.4	8.72	2.07	Haire and Baybarz (1970)
dhcp	4.002	12.804	44.4	9.31	1.99	Haire and Asprey (1976)
dhcp	3.384	11.040	27.4	15.1	1.69	Haire and Asprey (1976)
fcc	4.94	–	30.1	13.7	1.75	Noé and Peterson (1976)
fcc	5.75	–	47.4	8.72	2.03	Noé and Peterson (1976)
dhcp	3.39	11.01	27.4	15.1	1.69	Noé and Peterson (1976)
fcc	4.78	–	27.4	15.1	1.69	Haire *et al.* (1986)
dhcp	3.380	11.025	27.3	15.0	1.69	Radchenko *et al.* (1986); Seleznyov *et al.* (1989)
fcc	4.994	–	30.1	13.7	1.75	Stevenson (1973)
CfN, fcc	4.94	–	30.1	13.7	–	Haire *et al.* (1986)

Recommended values for californium are: (a) dhcp 3.384(3) Å and 11.040(10) Å and (b) fcc = 4.78(1) Å. Both yield a metallic radius of 1.69 Å, a volume of 27.4 Å and a density of 15.1 g cm^{-3}.

From these efforts double hexagonal lattice parameters of: $a = 3.380(2)$ Å and $c = 11.025(2)$ Å were reported.

A fcc-form (high-temperature form and also a high-pressure form at modest pressures) have been observed for californium. This form of californium was reported to have a fcc structure with a parameter of 4.94 Å (Noé and Peterson, 1976), but this parameter gives an atomic radius for californium that is too large. It agrees better with the parameter for californium nitride ($a_0 = 4.94$ Å; Haire *et al.*, 1986), with an oxynitride (oxygen and nitrogen exchanged in the crystal sites), or could have represented an expanded lattice that was 'quenched in' at elevated temperatures. The proper lattice parameter (4.78 Å) for this cubic form of californium at room temperature and at a pressure 1 atm was observed both with pressure-quenched samples (Haire *et al.*, 1986) and also from larger quantities of californium obtained as foils prepared by distillation (Haire, 1978). The atomic radius derived from this smaller cubic parameter agrees well with that obtained from the ambient temperature, double hexagonal parameters. Pressure-quenched cubic parameters for curium, berkelium, and californium metals have also been found to give identical atomic radii and atomic volumes as obtained from their room temperature, double hexagonal forms, while earlier work with samples quenched from elevated temperatures also resulted in larger (expanded) parameters for curium and berkelium metals (Haire *et al.*, 1986). The preparation and lattice parameters for the californium metal have also been reported by Radchenko *et al.* (1986a) and by Seleznev *et al.* (1989). An alloy of californium and platinum ($CfPt_5$) was obtained when thin films of californium were vapor deposited on platinum surfaces. The products were analyzed as formed on the surfaces (Radchenko *et al.*, 1986b).

The transition temperature for the hexagonal to cubic phase of californium is not well-established, and only limited efforts have been made to determine it (Noé and Peterson, 1976). It is likely to be in the region of 600–800°C. The dhcp to fcc structural transition occurs under pressure at about 16 GPa (Peterson *et al.*, 1983; Benedict *et al.*, 1984). This cubic phase formed under pressure can be retained at atmospheric pressure and 25°C (Haire *et al.*, 1986), and provides a lattice parameter of 4.78 Å. This transition from a hexagonal to cubic state is a low-energy transition in the transplutonium metals. The different crystal data for californium that have been reported are summarized in Table 11.6.

Californium lies very close to the 'border' between a divalent and trivalent metal due to its f- to d-electron promotion energy (see Fig. 12.4 and discussion in Chapter 12). It is possible that in very thin films californium metal may retain a divalent state (i.e. a metastable state) under the conditions of preparation. A similar situation has been observed previously with very thin films of samarium metal (Allen *et al.*, 1978), where the surface atoms of samarium metal in these films remain divalent, although atoms in bulk metal are normally trivalent. Samarium also exhibits a unique rhombohedral crystal form in bulk form. The next element after samarium in the lanthanide series is europium, and it is a divalent metal. Thus, the situation with the californium structures may be similar to the samarium case, as the next element after californium, einsteinium, is also a divalent metal (see Chapter 12). However, californium metal is correctly identified as being a trivalent metal in bulk forms, but does display aspects of this 'closeness' to being divalent (see discussion of its enthalpy of sublimation of the metal in section 11.6). The best lattice parameters for both the dhcp and fcc crystal forms of californium metal are those that give an atomic radius of about 1.69 Å.

There has been only one reported value for the melting point of californium metal, which is (900 ± 30)°C (Haire and Baybarz, 1973a,b). This value was obtained by observing the 'puddling' of metal particles in an electron microscope with thin films of californium metal. This melting point is lower than those reported for americium, curium, and berkelium metals, but is close to the melting point of einsteinium metal (Haire and Baybarz, 1979). Californium's lower melting point is also in accord with some of its physical properties, and the trend toward divalency (which would yield lower melting points) in going across the actinide series. The properties for californium and the other transplutonium metals are compared in an ASM report by Haire (1990).

Californium metal has been examined under high pressure using X-ray diffraction techniques. Early high-pressure studies showed that its dhcp form transformed to a fcc form at 16 GPa (Peterson *et al.*, 1983). A bulk modulus of (50 ± 5) GPa was derived from those data, which is similar to moduli for many of the trivalent lanthanide metals but much lower than those of the earlier actinides with itinerant 5f electrons (i.e. Pa–Pu). Subsequent work with californium metal under higher pressures up to 48 GPa showed a transition of the fcc structure to a new lower symmetry structure (reported to be orthorhombic, alpha-uranium structure; Benedict *et al.*, 1984). Formation of this structure was interpreted as reflecting the delocalization of californium's 5f electrons and their participation in the metal's bonding. Very recently californium metal has been reexamined under much higher pressures and with the use of synchrotron radiation (Haire *et al.*, 2004). These studies have provided much higher quality data, which have shown the occurrence of three structural transitions, and confirmed that the 5f electrons of californium do indeed delocalized and become involved in bonding at these higher pressures. But the new californium structures observed at higher pressures (after the fcc phase), are very similar to those noted in the behavior of americium metal under pressure (Heathman *et al.*, 2000). Work on the structures of californium observed at pressures above 40 GPa are being finalized and details will be published later. However, in this work on californium, it was very clear that when progressing across the actinide series, it takes higher and higher pressures to force the delocalization of the 5f electrons, as they become further withdrawn from the Fermi surface due to the greater nuclear charges (Haire *et al.*, 2004). Thus, californium requires much higher pressures to force the delocalization of its 5f electrons than do the first three transplutonium metals.

The vapor pressure and enthalpy of sublimation of californium metal have been measured using the Knudsen effusion technique (Ward *et al.*, 1979). The vaporization of californium metal, starting at 298 K with the dhcp crystal form, and over the temperature range of 733–973 K, is described by the following equation:

$$\log p(\text{atm}) = (5.675 \pm 0.0319) - (9895 \pm 34)\ \mathrm{T}^{-1}$$

The $\Delta_{\text{sub}}H^{\circ}_{298.15\ \text{K}}$ was calculated to be (196.23 ± 1.26) kJ mol^{-1}, and $\Delta_{\text{sub}}S^{\circ}_{298.15\ \text{K}}$ was derived to be 120.6 J K^{-1} mol^{-1}. The estimated boiling point for the metal is 1745 K. Nugent *et al.* (1973b) had estimated the enthalpy of sublimation of californium to be 163 kJ mol^{-1} and David *et al.* (1976a,b) had predicted a value of 197 kJ mol^{-1}. By comparison, the vapor pressure behavior of californium is intermediate between that of samarium metal (a trivalent metal) and europium metal (a divalent metal), which is discussed by Ward *et al.* (1979).

The enthalpy of sublimation is an important bulk property of an element, and can be a measure of the metal's cohesive energy. From the magnitude of the enthalpy, the number of bonding electrons can be inferred from it, and this allows systematic comparisons to be made between the two f-electron elements series.

The experimental sublimation data for californium (Ward *et al.*, 1979) are in accord with it being a trivalent metal up to 1026 K, although it is one of the most volatile (has one of the lowest sublimation enthalpies) of the trivalent actinide metals; its high volatility precludes vaporization studies of it above 1073 K. Evidence for CfO was not obtained in this mass spectrometry study, and this finding is in accord with subsequent studies on californium oxides (Haire, 1994; see Section 11.7.3).

Thermochromatographic studies (involving sublimation and adsorption) of californium, einsteinium, and fermium using different metal columns (titanium, tantalum, etc.) were performed to yield enthalpies of adsorption for these actinides. Attempts have been made to relate these adsorption enthalpies to enthalpies of sublimation, but there is a significant difference in the actual numerical values, as they measure different properties. A comparison between the enthalpies of sublimation for the americium through californium trivalent actinide metals and their enthalpies of absorption is striking, and efforts have been made to compare them (Haire, 1997). Fig. 11.3 shows plots of these values for selected actinides. The enthalpies of sublimation range irregularly for the first four transplutonium elements with the values reflecting in part differences in 5f to 6d promotion energies – smaller promotion energies link with larger, more positive enthalpies of sublimation.

The enthalpy of sublimation for californium is 196 kJ mol^{-1} (Ward *et al.*, 1979, 1986). In contrast, the enthalpy of adsorption for californium ranges from –302 to –310 kJ mol^{-1} (Hübener, 1980; Hübener *et al.*, 1994). The exact value depends on the particular metal substrate used for its adsorption. A comparison between these enthalpies of vaporization and adsorption is shown

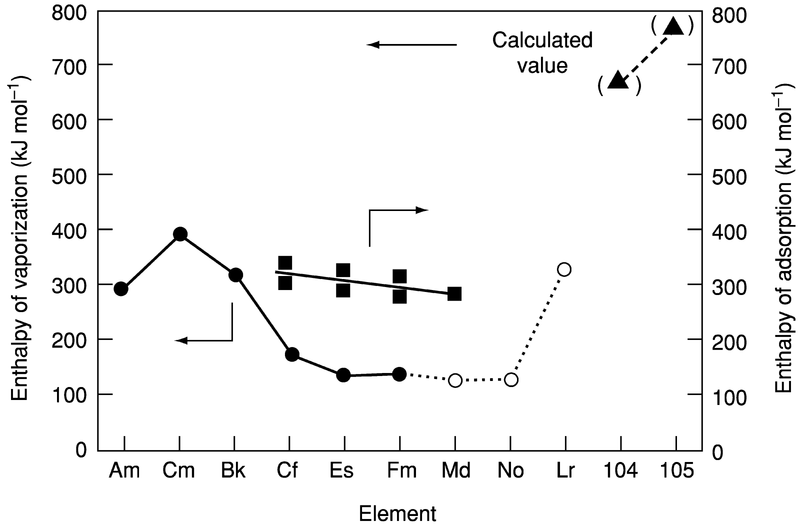

Fig. 11.3 *Vaporization and adsorption enthalpies for selected actinides.*

in Fig. 11.3 (Haire, 1997) for californium through mendelevium elements, and using some extrapolated values for sublimation of the two transfermium elements. The sublimation values for element 104 (Johnson and Fricke, 1991) and 105 (Pershina *et al.*, 1994) are calculated values, and are included here for comparison purposes. Their larger more positive enthalpies of sublimation reflect that greater bonding (i.e. greater than three electrons) is present in these latter two elements. One advantage of the adsorption technique versus the sublimation method is the former can be used for smaller quantities of materials (tracer levels).

It can be seen from Fig. 11.3 that the sublimation enthalpy for californium and the adsorption enthalpy are close to the comparable enthalpies for divalent einsteinium and fermium; the sublimation enthalpy for californium is considerably smaller (less positive, lower energy required) than values for americium, curium, and berkelium, which are trivalent metals.

Initially, the adsorption behavior (i.e. temperature of adsorption) of californium with different metal columns was taken as an indication of a metallic divalency (Hübener and Zvara, 1982) but more recent interpretations of adsorption enthalpies and the relative behavior of californium through nobelium elements suggests that californium is trivalent but close to the divalent–trivalent border Eichler *et al.* (1997). Using adsorption enthalpies, fermium is considered unquestionably as being divalent (Taut *et al.*, 1997), while californium is trivalent an atomic from source for actinide elements has been discussed (Eichler *et al.* 1997.)

The initial enthalpy of solution of californium metal (dhcp crystal form, trivalent metal) in 1.0 M HCl at 298 K is $-(617 \pm 11)$ kJ mol^{-1} (Raschella *et al.*, 1982).

This value was corrected in a subsequent determination of this important thermodynamic quantity using larger samples of well-characterized metal to yield an enthalpy of solution value of $-(576.1 \pm 3.1)$ kJ mol^{-1} for 1 M HCl (Fuger *et al.*, 1984; for further details see Chapter 19). This less-negative enthalpy value shows a trend among the transplutonium metals from americium through californium of less-negative enthalpies with increasing atomic numbers, and is in accord with an increasing trend toward metallic divalency in progressing across the series. This enthalpy of solution of the metal is important for providing the enthalpy of formation of the Cf(III) ion in solution and discussed in a subsequent section (see Section 11.8.3) on thermodynamic properties.

Several efforts have been made to obtain the magnetic susceptibility of californium metal. Magnetic information is valuable in ascertaining the metallic valence of metals and the bonding present. However, in the case of californium, such information is not useful and cannot differentiate between a divalent form (presumable a $5f^{10}$ state) that would have an effective moment of 10.22 μ_B, while the trivalent form (for an $5f^9$ state) would have an effective moment of 10.18 μ_B.

The first magnetic measurements were made by Fujita *et al.* (1976) using two samples believed to represent a fcc form of divalent californium metal from 22 to 298 K. Both samples followed a Curie–Weiss relationship, and the data produced an average moment of 9.75 μ_B. Subsequent magnetic measurements were made on well-characterized samples of the dhcp, trivalent form of californium from 4.2 to 350 K and in applied fields of up to 50 kG (Nave *et al.*, 1983, 1984). These data showed that californium exhibits at least two differing magnetic behaviors as a function of temperature. Below 51 K, the metal was either ferro- or ferrimagnetic; a distinction between the transition type could not be made owing to the inability to obtain a saturated moment of greater than 6.1 μ_B in the highest field of 50 kG. There was also evidence for antiferromagnetic behavior in the temperature range of 48–66 K. Additional magnetic studies of californium compounds (i.e. oxides and nitrides in particular) need to be done to rule out the possibility that their presence as impurities may be responsible for this latter behavior. Above 160 K, californium exhibits paramagnetic behavior. An average effective moment of (10.6 ± 0.2) μ_B was obtained for three different samples, whereas a fourth sample produced a moment of (9.7 ± 0.2) μ_B. Results from Nave *et al.* (1983) indicate that the magnetic behavior of californium is similar in some respects to that of its electronic homolog, dysprosium. Additional comments on magnetic behavior of californium and its compounds are given in Section 11.7.5 and in Table 11.11.

11.6.3 Chemical and mechanical properties

Californium is a fairly reactive metal, comparable to those of the lighter lanthanide metals but is less reactive than europium, which is considered as the most reactive lanthanide metal. This reactivity of europium is related to several factors but in part arises from it being a divalent metal. On standing to air or when exposed to moisture at room temperature, small bulk pieces or foils of californium quickly form an oxide, but it is not a violent reaction. Moisture and temperature increase the rate of the reaction. One of the difficulties of preparing small quantities of californium metal is that it only takes small amounts of impurities to form reaction products with it. When the temperature is elevated, the reactivity of californium metal increases, and reactions occur readily with hydrogen, nitrogen, the chalcogen elements, etc. The silver colored, relatively soft californium metal quickly adopts a golden or bluish color on its surface when reacting with small amounts of other materials. Pure californium metal is easily cut with a 'razor' blade and is also malleable in its pure state.

When californium is sealed in evacuated quartz containers and when heated to 300°C, especially when it is a film on the quartz surface, the metal quickly deteriorates. Solid pieces of californium metal stored in quartz under vacuum and heated to moderate temperatures (i.e. 300°C) can vaporize sufficiently to form 'mirrors' on the quartz surface. Vaporization and reaction with the quartz worsens at higher temperatures. Products are usually oxides or silicates.

The metal reacts very rapidly with dry gaseous hydrogen halides and aqueous mineral acids to evolve hydrogen. In aqueous media, a Cf(III) solution is obtained, except with the case of hydrogen fluoride, where an insoluble californium trifluoride precipitate is formed.

Californium forms alloys when heated with the lanthanide metals but these products have not been well-characterized. When heated, it 'wets' tantalum, which usually limits the use of tantalum containers for high-temperature work with it. Tungsten containers are preferred, especially those made from single crystals, which prevents the metal from entering the grain boundaries of the containers.

11.6.4 Theoretical treatments

The chemistry of the actinide series can be complex and changes considerably when progressing across the actinide series. The development of a self-consistent model for these elements has had limited success in the past but more recent computational approaches have been more successful. However, even plutonium is still not completely understood, and total agreement on details of its fundamental science is not realized fully even after some 60 years of extensive studies. In comparison, far less effort has been done on californium, although its behavior is more lanthanide-like and has fewer complexities than plutonium, which has delocalized 5f electrons. However, the increased promotion energy for the 5f electrons of californium makes it close to being a divalent metal, and therefore its properties and behavior deviate somewhat from those of the americium through berkelium metals, as well as some of the trivalent lanthanide metals.

Efforts have been made to describe the overall fundamental aspects of these actinide metals, and be able to correlate them with other members of the periodic table (Brewer, 1971a,b; Nugent *et al.*, 1973a,b; Johansson and Rosengren, 1975a,b; Nugent, 1975; David *et al.*, 1976a,b, 1978; Samhoun and David, 1979;

Brooks *et al.*, 1984). These authors provide useful considerations for understanding the series in general and the changes that are observed when moving across it.

With respect to californium, the important questions often have to do with the role of its 5f electrons, their position with respect to the Fermi level, the narrowing of its 5f levels relative to earlier members of the series and the position of the 5f electrons with respect to the other outer electrons. The concept of promotion energy for the 5f electrons (f → d) is an important factor here. At 1 atm and room temperature, the 5f electrons in californium and its compounds are fully localized, much like the 4f electrons in the lanthanide series.

Several predictions for the properties of californium have been made with regard to its 5f electrons. One of the predictions was addressed by Brooks *et al.* (1984). It was accepted that californium was close to the divalent–trivalent metallic boundary. This pseudo-boundary considered that the crystal energy gained from acquiring three bonding electrons versus two in isolated atoms, had to be greater than the promotion energy needed for promoting a 5f electron to a d-state (to provide three bonding electrons). As with many of the other actinide metals, atomic californium in the vapor state has only two bonding electrons, but upon condensation, a third bonding electron can be acquired by promoting a 5f electron to a '6d' state. True divalency in the metallic state is believed to occur first in the higher members of the series, starting with einsteinium and fermium metals (see Chapters 12 and 13, and Johansson and Rosengren, 1975a,b; Brooks *et al.*, 1984). Additional discussions in this regard on the nature of californium can be found in the literature and in Section 11.9.

Correlation between crystal entropy and metallic radius, atomic weight, magnetic properties, and electronic structure have permitted an accurate calculation of unknown entropies for the actinide elements, including californium (Ward and Hill, 1976). This required a defined electronic structure to predict the entropy values. In addition, thermodynamics for the transplutonium metals have been summarized (Ward *et al.*, 1980; Ward, 1983). A pattern of superconductivity in f-band metals has also received attention over the years. It is unlikely that californium would show superconductivity, due to its large magnetic moment (see Section 11.6.2 on metal properties) and localized 5f electrons. Prospects for superconducting behavior in other actinides have been discussed (Smith, 1979, 1980; Baring and Smith, 2000). Of the first four transplutonium metals, ending with californium, only americium metal (Smith and Haire, 1978) is known to become superconducting at low temperature.

11.7 SOLID COMPOUNDS

11.7.1 General comments

A wide variety of californium compounds have been reported, even though only small amounts of this element (especially the ^{249}Cf isotope) have been available an overview of Cf solid state chemistry is available (Haire & Gibson, 1989). Most of the expected halides and oxides for californium are established. It is accepted that californium exhibits three oxidation states, II, III, IV, in solids. There are reports that suggest the possibility of a Cf(V) state in solution (see Section 11.8); this state for californium is questionable. The II, III, and IV states are observed in different halides, and the III and IV states are found in oxides. The existence of stable, solid CfO is less probable and a minor product (see Section 11.9 on gas-phase behavior of californium). The trivalent state is the most prevalent state in both compounds and solutions, and the tetravalent state is only observed in the compounds, CfO_2, $BaCfO_3$, and CfF_4 and special solutions. The divalent state is found in the pure solids $CfCl_2$, $CfBr_2$, and CfI_2.

There are other compounds of californium where the oxidation state is less well-defined, such as in compounds with pnictogens, chalcogens, hydrides, etc. For example, in CfN, a formal state of Cf(III) can be assigned but it is not fully clear if this state is correct for a potentially more covalent material, as expected in its nitride. With hydrides, stoichiometries can range between a value of two (dihydride) and three (trihydride), in addition to intermediate hydrogen stoichiometries (i.e. CfH_{2+x} cubic materials and CfH_{3-y} hexagonal products.). This suggests that the bonding in hydrides is other than purely ionic.

Ionic radii for each oxidation state of californium can be established from crystallographic data for these compounds, and some radii are provided in Table 11.7 for comparison. Many similarities in behavior between californium

Table 11.7 *Comparison of selected radii of californium and some lanthanides.*

Ion	*Compound*	*Radius* (Å)	*References*
Cf^{2+}	$CfBr_2$	1.08	Peterson and Baybarz (1972)
Eu^{2+}	$EuBr_2$	1.09	Peterson and Baybarz (1972)
Cf^{3+}	$CfCl_3$	0.932[a]	Burns *et al.* (1973)
Gd^{3+}	$GdCl_3$	0.938[a]	Burns *et al.* (1973)
Cf^{3+}	Cf_2O_3	0.942[b]	Baybarz *et al.* (1972)
Cf^{3+}	Cf_2O_3	0.95	Shannon (1976)
Gd^{3+}	Gd_2O_3	0.938[b]	Haire and Baybarz (1973a,b)
Eu^{3+}	Eu_2O_3	0.950[b]	Haire and Baybarz (1973a,b)
Cf^{4+}	CfO_2	0.859[c]	Baybarz *et al.* (1972)
Cf^{4+}	–	0.821[d]	Shannon (1976)
Ce^{4+}	CeO_2	0.898[c]	Haire and Eyring (1994)
Pr^{4+}	PrO_2	0.890[c]	Haire and Eyring (1994)
Tb^{4+}	TbO_2	0.817[c]	Haire and Eyring (1994)

[a] Derived from apical distances of hexagonal trichloride cells; six-coordinated metal atom.

[b] Derived from sesquioxide lattice parameters, using an oxygen radius of 1.46 Å and adding 0.08 Å for covalent M–O bond character; six-coordinate metal ion. (Lattice parameters for are taken from Haire and Eyring, 1994).

[c] Derived from dioxide lattice parameters, using an oxygen radius of 1.46 Å, correcting for covalent character of M–O bond (+0.10 Å) and for coordination number of 8 to 6 (−0.08 Å).

[d] Radius from plot of r^3 vs volume.

and other actinides and the lanthanides can be made based on ionic radii. It is important when making such comparisons that the radii were calculated in the same manner and perhaps even from the same compounds. In many cases, the transplutonium elements (i.e. californium specifically) with similar radii will likely form the same compounds, have the same structures, display similar phase behaviors, and may even have similar lattice parameters. This affords some predictability for properties of different californium compounds.

It must be recognized that a shift in radii is found between the lanthanide and actinide series, such that Cf(III) has a similar radius to Gd(III) rather than Dy(III), its apparent electronic homolog. Crystallographic data for a number of californium compounds are given in Table 11.8. This ionic radius relationship contrasts with the behaviors of the f-electron metals; metallic radii for the trivalent actinide metals are smaller than their lanthanide counterparts, and the metallic radius for californium is smaller than that of the smallest lanthanide metal, lutetium.

11.7.2 Halides and oxyhalides

Based on the estimated IV and III reduction potentials (Nugent *et al.*, 1971; David *et al.*, 1978) for californium, it would be expected that the only stable, bulk binary Cf(IV) halide would be its tetrafluoride. This compound can be prepared by fluorinating materials such as the oxides or CfF_3 with F_2 or ClF_3 (Asprey, 1970; Asprey and Haire, 1973; Haug and Baybarz, 1975). General preparative routes for the halides are summarized in Table 11.9 and their preparations have been summarized by Haire (1982).

The tetrafluoride has limited thermal stability and decomposes to CfF_3 (Haire and Asprey, 1973a,b) at 300–400°C. This temperature has limited the degree of crystallinity that can be obtained for it. There has been some variation in the lattice parameters reported for CfF_4, which arises mainly from indexing the monoclinic structure using powder diffraction data from samples of moderate crystallinity. A solid-state absorption spectrum has been obtained for the compound, its thermal stability examined and new X-ray data for the compound evaluated using small differences between the reported values (Haire *et al.*, 1980).

Ternary alkali-metal fluoride complexes of the types $MCfF_5$, M_2CfF_6, M_3CfF_7, and $M_7Cf_6F_{31}$ ($M = $ Li through Cs) are expected to exist, and these complexes should provide added stability for the Cf(IV) state. These complex salts are well-established for the tetravalent state of lanthanides (Brown, 1968). The existence of CfF_4 in the vapor state has been claimed based on high-temperature (>500°C) chromatographic studies using tracer quantities of californium (Jouniaux, 1979; Bouissières *et al.*, 1980), which appears to conflict with the thermal decomposition of bulk CfF_4 at low temperatures (i.e. 300–400°C).

All of the trihalides and oxyhalides of Cf(III) are known (see Table 11.8), and many of these compounds were among the first prepared and reported for

Table 11.8 *Crystallographic data for californium compounds.*

Substance	*Structure Type*	*Crystal System*	*Lattice Parameters*				*References*
			a_0 (Å)	b_0 (Å)	c_0 (Å)	*Angle* (deg)	
Oxides							
Cf_2O_{Green}	Mn_2O_3	bcc	10.839			$\beta = 100.3$	Copeland and Cunningham (1969);
	Sm_2O_3	monoclinic	14.12	3.591	8.809		Green and Cunningham (1967)
	La_2O_3	hexagonal	3.72		5.96		Baybarz and Haire (1976)
Cf_7O_{12}	Tb_7O_{12}	rhombohedral	6.596			$\alpha = 99.40$	Turcotte and Haire (1976)
CfO_2	CaF_2	fcc	5.310				Baybarz *et al.* (1972); Haire (1976) [see also Haire and Eyring (1994) for oxides]
Halides							
CfF_3	LaF_3	trigonal	6.945		7.101		Stevenson and Peterson (1973)
CfC_3	YF_3	orthorhombic	6.653	7.039	4.393		Stevenson and Peterson (1973)
CfC_4	UF_4	monoclinic	12.42	10.47	8.126	$\beta = 126.0$	Haire and Asprey (1973)
	UF_4	monoclinic	12.33	10.40	8.113	$\beta = 126.44$	Haug and Baybarz (1975)
$CfCl_3$	UCl_3	hexagonal	7.379		4.090		Green and Cunningham (1967)
$CfCl_3$	$PuBr_3$	orthorhombic	3.859	11.748	8.561		Burns *et al.* (1973)
$CfBr_2$	$SrBr_2$	tetragonal	11.50		7.109		Peterson and Baybarz (1972)
$CfBr_3$	$AlCl_3$	monoclinic	7.215	12.423	6.825	$\beta = 110.7$	Fried *et al.* (1968)
$CfBr_3$	$FeCl_3$	rhombohedral	7.58			$\alpha = 56.2$	Burns *et al.* (1975)
CfI_2	$CdCl_2$	rhombohedral	7434			$\alpha = 35.83$	Wild *et al.* (1978)
	CdI_2	hexagonal	4.557		6.992		Wild *et al.* (1978)
CfI_3	BiI_3	hexagonal	7.587		20.814		Wild *et al.* (1978)
		rhombohedral	8.205			$\alpha = 55.08$	Wild *et al.* (1978)

Oxyhalides						
CfOF	CaF_2	cubic	5.561				Peterson and Burns (1968)
CfOCl	PbFCl	tetragonal	3.956		6.662		Copeland and Cunningham (1969)
CfOBr	PbFCl	tetragonal	3.90		8.		Fried *et al.* (1968)
CfOI	PbFCl	tetragonal	3.97		9.14		
$Cf(IO_3)_3$	$Bi(IO_3)_3$	monoclinic	8.7994(2)	5.9388(7)	15.157(2)	96.833(2)	Sykora *et al.* (2006)
pnictides							
CfN	NaCl	fcc	4.98				Haire (1974)
CfAs	NaCl	fcc	5.809				Damien *et al.* (1980)
CfSb	NaCl	fcc	6.165				Damien *et al.* (1980)
hydride							
CfH_{2+x}	NaCl	cubic	5.285				Gibson and Haire (1985)
oxysulfide and oxysulfate							
CfO_2S	La_2O_2S	trigonal	3.844		6.656		Barbarz *et al.* (1974)
$Cf_2I_2SO_4$	$La_2O_2SO_4$	orthorhombic	4.187	4.072	13.008		
cyclopentadienyl							Laubereau and Burns (1970)
$Cf(C_5H_5)_3$		orthorhombic	1.410	1.750	0.969		
pyrochlore							
$Cf_2Zr_2O_7$		cubic	10.55				Haire *et al.* (2002)

Table 11.9 *Preparation of californium halides.*

tetrafluoride
CfF_3 or Cf oxide $+ F_2 \rightarrow CfF_4$
trihalides
Cf oxide $+ HX \rightarrow CfX_3 (X = F, Cl, Br)$
$Cf^0 + HX \rightarrow CfX_3$
$Cf^0 + X_2 \rightarrow CfX_3$
$CfX_3 + 3HI \rightarrow CfI_3 + 3HX$
oxyhalides
Cf oxide or $CfX_3 + HX/H_2O \rightarrow CfOX$
dihalides (X = Cl, Br, I)
$CfX_3 + Cf^0 \rightarrow CfX_2$
$CfX_3 + H_2 \rightarrow CfX_2$

californium. Their crystal structures vary between the different compounds, but are often isostructural with the lanthanide trihalides for lanthanides having comparable ionic radii (i.e. Gd(III)).

The oxyhalides can be prepared by incomplete halide formation starting from oxides, careful hydrolysis of the anhydrous halides or thermal decomposition of hydrated halides. They are also prepared by hydrohalogenation of Cf_2O_3 or via treatment of a californium oxide with moist interhalogens at an elevated temperature. The anhydrous trihalides can be prepared by treating californium oxides with dry hydrogen halides or the metals with hydrogen halides or elemental halogens. However, the reaction of the oxide with hydrogen iodide does not give satisfactory results; the triiodide can be prepared by treating $CfBr_3$ or $CfCl_3$ with hydrogen iodide, or the metal with iodine. The trihalides have relatively low-melting temperatures and can be melted in inert atmospheres and/or in vacuum. Careful melting and cooling of such anhydrous halide melts have been used to create single crystals.

The trifluoride is dimorphic (orthorhombic, YF_3-type; high-temperature form, trigonal, LaF_3-type) with the transition temperature above 600°C (Cunningham and Ehrlich, 1970; Stevenson and Peterson, 1973). Treatment of CfF_3 with water vapor above 700°C or non-purified/moist HF produces CfOF (Peterson and Burns, 1968). The enthalpy of formation of CfF_3 at 298.15 K is accepted as being –1553(35) kJ mol^{-1} (see Chapter 19).

Californium trichloride is also dimorphic, exhibiting the UCl_3-type hexagonal structure (low-temperature form) and the $PuBr_3$-type orthorhombic structure (Green and Cunningham, 1967; Burns *et al.*, 1973). The melting point of $CfCl_3$ is 545°C (Burns *et al.*, 1973).

Treatment of Cf_2O_3 with moist hydrogen chloride, or $CfCl_3$ with water vapor, at elevated temperatures produces tetragonal CfOCl (Copeland and Cunningham, 1969). The preparation and measurement of the enthalpy of solution for CfOCl was also reported (Burns *et al.*, 1998). From the solution data, the enthalpy of formation ($\Delta_f H°(CfOCl_{cr})$) at 298 K was calculated to be –970(7) kJ mol^{-1}. This value is also discussed in Chapter 19.

Californium tribromide is trimorphic, but only two of these forms have been prepared by a direct synthetic route. The high-temperature form (>500°C) is an $AlCl_3$-type, monoclinic structure (Fried *et al.*, 1968; Burns *et al.*, 1975; Young *et al.*, 1976). A less well-characterized form, a $FeCl_3$-type rhombohedral structure, has also been reported (Burns *et al.*, 1975). A third form, a $PuBr_3$-type orthorhombic structure was acquired indirectly, aged (after a few half-lives of decay) from an orthorhombic form of its $BkBr_3$ parent (Young *et al.*, 1980). Interestingly, when mixed tribromides of californium–berkelium were synthesized, the orthorhombic structure did not form if the californium content exceeded 45 at%. And, when heating the orthorhombic $CfBr_3$ above 330°C, it immediately transforms into the monoclinic structure, which illustrates that the orthorhombic form is limited to the region of the ionic radius of californium (Young *et al.*, 1980). In contrast, applying pressure on monoclinic $CfBr_3$ (>3 GPa) transforms it to the orthorhombic structure (Peterson *et al.*, 1985). The oxybromide of californium, CfOBr (Fried *et al.*, 1968), is isostructural with CfOCl (Copeland and Cunningham, 1969), and both are prepared by the same methods (see Table 11.9). The molar enthalpy of formation of $CfBr_3$ has been reported to be –752.5 (3.2) kJ mol^{-1} at 298.15 K (Fuger *et al.*, 1990; see Chapter 19).

Californium triiodide is monophasic, and exhibits the BiI_3-type hexagonal structure (Fried *et al.*, 1968; Wild *et al.*, 1978). It is prepared by treating 'californium hydroxide' with hydrogen iodide at 800°C (Fried *et al.*, 1968), but a preferred synthetic route is to heat $CfBr_3$ or $CfCl_3$ with hydrogen iodide (Wild *et al.*, 1978). The CfOI is isostructural with CfOCl and CfOBr, and is prepared by the same procedure used for the latter two compounds (see Table 11.9).

The dichloride, dibromide, and diiodide of californium have all been prepared but the difluoride has not been reported. It would be expected that the Gibbs energy change between the di- and trivalent compounds would be the least for the iodides and hence the diiodide would be the most stable. The first compound of Cf(II) was $CfBr_2$ prepared by hydrogen reduction of $CfBr_3$ at elevated temperature (Peterson and Baybarz, 1972; Fried *et al.*, 1973). Subsequently, it was observed, and shown by absorption spectra, that lime-green $CfBr_3$ could also be reduced by thermal treatment alone (760°C) to produce an amber-colored $CfBr_2$ (Young *et al.*, 1975). The structure of $CfBr_2$ is tetragonal ($SrBr_2$-type; Peterson and Baybarz, 1972). Table 11.8 gives some crystallographic data for these compounds.

The first preparation of CfI_2 produced the high-temperature CdI_2-type hexagonal form (Young *et al.*, 1975); subsequently, a second structural form ($CdCl_2$-type rhombohedral structure) was reported (Wild *et al.*, 1978). The diiodide can be obtained via hydrogen or thermal reduction of the triiodide.

Of the three californium dihalides, $CfCl_2$ proved to be the most difficult to prepare, and many early attempts to prepare it were unsuccessful (Fujita and Cunningham, 1969; Young *et al.*, 1980). It was eventually prepared by hydrogen reduction of the trichloride at 700°C (Peterson *et al.*, 1977). The X-ray structure of $CfCl_2$ still has not been resolved; the existence of this compound is based on its solid-state spectra. It is expected that $CfCl_2$ would exhibit either the $PbCl_2$-type orthorhombic or the $SrBr_2$-type tetragonal structure (Young *et al.*, 1975; Peterson *et al.*, 1977).

There is some evidence that californium halides may form so-called mixed-valence compounds (M_5X_{11}, $M_{11}X_{24}$ or M_6X_{13}, where M = metal ion and X = halide ion) like those reported for some of the lanthanide elements (Bärnighausen, 1976; Haschke, 1976; Luke and Eick, 1976). To avoid the necessity of carefully controlling reduction of californium to the proper stoichiometry, mixtures of gadolinium and californium (both have comparable III radii; see subsequent section) were used such that total reduction of the californium to Cf(II) would produce the desired cation II/III stoichiometry for formation of the structures, Cf_4GdCl_{11} and Cf_4GdBr_{11} (Haire *et al.*, 1978).

It has been reported that Cf(II) can be obtained in crystalline strontium tetraborate matrices (Peterson and Xu, 1996). It appears that this tetraborate matrix provides stability for the divalent state of the lanthanides and actinides. It was concluded from spectral data that Cf(II) existed in the material.

Except for the trifluoride, anhydrous californium trihalides are hygroscopic and must be protected from moisture. The dihalides are very sensitive to both moisture and oxygen. Normally, their syntheses are carried out in glass (except for the fluorides) so that products can be flame-sealed *in situ*, avoiding subsequent transfers of the products. Some preparative and experimental techniques for studying californium halides have been reviewed (Young *et al.*, 1978; Haire, 1982). In general, californium forms the same halide compounds and structures as lanthanide elements having a similar ionic radius.

11.7.3 Oxides

Oxides of californium have received a great deal of study, in part because they are primary compounds of interest and use, and were among the first compounds of this element that were investigated given their ease of formation. Oxides often serve as starting materials for preparing other compounds and can be obtained by calcining in air different materials (e.g. nitrates, oxalates, etc.) obtained from solutions. The stoichiometries (O/M ratios), crystal structures, and oxidation states of the californium oxide obtained, all depend on the experimental conditions employed. Haire *et al.* (1972) have discussed the californium-oxygen system.

Oxides of both Cf(III) and Cf(IV) (the sesquioxide and dioxide) are well known, as well as oxides with intermediate oxide compositions (i.e. between O/M of 1.5 and 2.00). The compound, Cf_7O_{12}, which is isostructural with Tb_7O_{12}, has also been established and its crystal structure and stability are known. It exists as a rhombohedral structure over a very narrow stoichiometry range (Turcotte and Haire, 1976). Although the monoxide has been observed in the vapor state, a true CfO solid has not been identified. This is in accord with the difficulty of preparing a true monoxide of ytterbium, although EuO is known. It is likely that a oxynitride (i.e. Cf(O,N)) or oxycarbonitride (i.e. Cf(O, N,C)) may exist as a solid phase; if so, a variation of lattice parameter (likely fcc-type structure) would be expected for these compounds depending on the actual O/N/C ratios. The formation of californium monoxide may be possible by reacting stoichiometric quantities of the metal and sesquioxide under high pressure and at elevated temperatures. If formed, it would be expected to exhibit a fcc structure with a parameter of 4.8–5.0 Å. This high-pressure preparation of monoxides has been used with selected lanthanides to prepare their monoxides (Leger *et al.*, 1980), but often small residues of metal or oxides remain in the products.

Crystallographic data for the sesquioxides are listed in Table 11.8. Three structures are known for californium sesquioxide: a bcc, a monoclinic, and a hexagonal form. A phase diagram for the transneptunium sesquioxides is shown in Fig. 11.4, where it can be seen that the hexagonal form of californium sesquioxide exists only over a very narrow temperature range up to its melting point of about 1750°C (Haire and Eyring, 1994). There is a trend of decreasing melting point of the actinide sesquioxides with atomic number, which contrasts with the trend observed with the lanthanide compounds. The cubic sesquioxide exists below 1400°C but the monoclinic to cubic transition is very difficult to achieve and appears irreversible, whereas the reverse transition occurs readily. Fig. 11.5 shows the relationship in the molecular volumes for the sesquioxides of the f-elements, where it can be seen that the density for the three californium

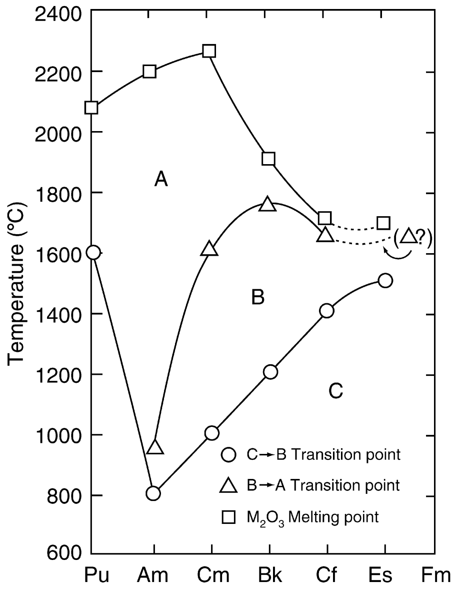

Fig. 11.4 *Phase diagram for the Pu through Es sesquioxides.*

forms increases in going from the cubic to the monoclinic to the hexagonal structures (Baybarz and Haire, 1976; Haire and Eyring, 1994). This trend for the californium compounds is in accord with those seen for the other f-element sesquioxides.

The monoclinic form of Cf_2O_3 (Sm_2O_3-structure type) was established early (Green and Cunningham, 1967) and the bcc (α-Mn_2O_3-type) was observed subsequently (Copeland and Cunningham, 1969). It was noted that slight oxidation of the bcc form may occur when it was heated in air. The hexagonal form of Cf_2O_3 was established later and was difficult to retain on cooling – it could be retained in samples quenched rapidly with helium from the melt (Baybarz, 1973; Baybarz and Haire, 1976; Haire and Eyring, 1994). One aspect of this monoclinic sesquioxide is its oxygen to metal ratio is 'fixed' at 1.5, whereas the cubic sesquioxide readily adds oxygen to its lattice up to a oxygen to metal ratio of 1.67.

As stated above, the hexagonal form of the californium sesquioxide exists over a narrow temperature region (Fig. 11.4). This structural form of berkelium sesquioxide is known and the hexagonal form of californium sesquioxide has also been observed in old samples of hexagonal Bk_2O_3 after berkelium has decayed to californium.

The transition temperature for the bcc to monoclinic form of californium sesquioxide was reported to be both 1100°C (Green and Cunningham, 1967) and 1400°C (Baybarz, 1973; Baybarz and Haire, 1976). The transition from the monoclinic to the hexagonal form was set at 1700°C, just 50°C below the oxide's melting point. While the monoclinic to cubic transition appears irreversible, the hexagonal to monoclinic form is readily reversible.

The fcc dioxide has been prepared by heating lower oxides of californium with atomic oxygen or under high-pressure molecular oxygen (Baybarz *et al.*, 1972; Haire, 1976). It usually appears as a black or dark-brown material, whereas the sesquioxide is very light green to light-tan color. With time, the dioxide's lattice parameter increases slightly, due to swelling and/or small losses of oxygen, both processes probably being due to self-irradiation. When heated in air above 200°C, the dioxide begins to lose oxygen and eventually forms Cf_7O_{12} or lower oxides at temperatures above 400°C (Haire, 1976).

A capacitance manometer system, capable of analyzing oxygen overpressures for samples as small as 1.4 mg of californium, together with X-ray diffraction analyses have established the californium–oxygen system between $1.50 < O/Cf < 1.72$ (Turcotte and Haire, 1976). In that work it was shown that Cf_7O_{12} (a rhombohedral structure) was the stable oxide in air or oxygen up to 750°C. At higher temperatures this compound loses oxygen to eventually form the sesquioxide. A stoichiometric bcc sesquioxide is obtained when these higher oxides of californium are heated in vacuum to 800–1000°C, or when an air-calcined oxide is subsequently treated in hydrogen or carbon monoxide at 850–1000°C.

Thus, the californium sesquioxide system is trimorphic, and there are also the established Cf_7O_{12} and CfO_2 compounds. The bcc sesquioxide lattice can also accept additional oxygen, and this structure exists for an O/M ratio of 1.5 to 1.67. It is expected that californium oxides with O/M compositions between 1.8 and 2.0 would have fcc structures but this has not been well established. Both the bcc lattice parameters for the sesquioxides up to an O/M of 1.67, and the fcc lattice parameters for the oxides having an O/M of 1.8–2.0, decrease in magnitude with the addition of oxygen to the lattices. In many respects (e.g., stability, formation of specific oxides, structures with specific O/M ratios, etc.), the californium–oxygen system is similar to that of the terbium–oxygen system (Haire and Eyring, 1994).

One other aspect regarding californium oxides is the behavior of (Bk,Cf) oxides as a function of the californium content (Turcotte, 1980). It appears that with californium contents up to 25 at%, the actinides can be oxidized up to an O/M of 2.0 (behaving like pure berkelium oxide). When the californium content is 64 at% or greater, the californium now controls the behavior of berkelium and limits the stoichiometry of the products to M_7O_{12}.

Although the preparation of CfO_2 normally requires strong oxidizing conditions and moderate temperatures, under certain conditions lower oxides of californium stored in air or oxygen can 'self-oxidize,' presumably due to an active oxygen species (atomic oxygen?) generated by the alpha radiation field (Haire, 1976); in contrast, small (few micrograms) samples of CfO_2 may lose oxygen under these conditions. The exact composition of aged californium oxides is difficult to ascertain by X-ray analyses alone, as the lattice parameters measured reflect both radiation damage to the lattice (swelling, larger parameter) and/or oxidation that affects the O/M ratios (decrease in parameter with greater oxygen content). Both effects may be operational in these systems. There are reviews on the effects of radiation damage on actinide oxides (Fuger, 1975; Fuger and Matzke, 1991).

The high-temperature vaporization of californium oxides has been explored by Knudsen effusion studies (Haire, 1994). With californium, oxides with O/M ratios > 1.5 lose oxygen, especially in vacuum, when heated (see above discussion) so that vaporization studies at higher temperatures basically deal with the sesquioxide. From the phase behavior in Fig. 11.4, vaporization from solid Cf_2O_3 should involve its monoclinic or hexagonal phases. Vaporization products observed for Cf_2O_3 were atomic Cf and CfO, in a ratio of $\sim$1:10 at 1800 K. This low concentration of CfO (i.e. CfO is not a dominant species, even though CfO may be expected) is due to the relatively low dissociation energy of CfO (about 498 kJ mol^{-1}) as compared to CmO (about 728 kJ mol^{-1}; Cm/CmO < 0.1) (Haire, 1994). A value for the enthalpy of formation of the Cf_2O_3 from the vaporization studies was reported as between –1650 and –1700 kJ mol^{-1} (Haire, 1994), which compares to –1653(10) kJ mol^{-1} obtained from solution calorimetry experiments (see Chapter 19).

A systematic treatment of data for the lanthanide and actinide oxides has generated estimated thermochemical values for the oxides of californium (Morss, 1983). A comparison of the lanthanide and actinide oxygen systems in detail, which includes discussions of the californium oxides, is also available (Haire and Eyring, 1994). In Section 11.9, discussions on the gas-phase behavior of californium are presented and include other chemical aspects of californium oxides. Both experimental and computational thermochemical data for californium oxides are given in Chapter 19.

There are a number of more complex oxide materials (i.e. ternary systems for one) that are outside the scope of the present chapter. However, one system, the zirconium–californium oxide pyrochlores, is discussed given its potential applications and systematic comparisons with other comparable actinide pyrochlores. The zirconium–californium–oxygen compound has the stoichiometry of $Cf_2Zr_2O_7$. These f-element materials are called pyrochlores given their similarity of their structures to that of the mineral, 'pyrochlore.' A related system to these pyrochlores involves solid solutions of zirconium and californium dioxides, which can be prepared from the pyrochlores by adding oxygen to their lattice.

Applications for the americium and curium pyrochlore counterparts include transmutation and nuclear waste matrices, although these uses are not considered for the californium products. The californium–zirconium oxide pyrochlore is cubic with a lattice parameter of 10.57 Å, and it is isostructural with comparable compounds formed with the trivalent actinides plutonium through presumable einsteinium and zirconium or hafnium (Haire *et al.*, 2002). The fit of the lattice parameter of the californium compound with the plutonium through californium and lanthanide zirconium pyrochlores is shown in Fig. 11.6, which can be used to generate a linear equation for the parameters of mixed f-elements or ascertain the oxygen content of a particular pure pyrochlore. This relationship is useful to analyze mixed actinide or lanthanide–actinide pyrochlores when encountered.

11.7.4 Other compounds of californium

In addition to the oxides and halides, several other compounds of californium have been prepared and their crystallographic data reported (see Table 11.8). Some of these data represent preliminary values or even results from a single experiment. In some cases (pnictides, chalcogenides, etc.), the limited supply of californium metal has precluded the preparation of specific compounds via the reaction of the metal, especially where close control of the stoichiometries is required (for example, the preparation of the potential compound, CfS). The general preparative techniques for the different pnictides and chalcogenides of the transuranium elements have been reviewed (Damien *et al.*, 1979).

Stoichiometries other than 1:1 ratio are not expected for the californium pnictides. These materials can be prepared by direct reaction of the elements, and exhibit a NaCl-type, cubic structure. From preparations of CfN, a fcc lattice constant of 4.94 Å has been derived (Haire, 1988). This parameter is only slightly different or the same as reported for samples of fcc californium metal (4.994 Å, Stevenson, 1973; or 4.94 Å, Noé and Peterson, 1976; see Section 11.6)

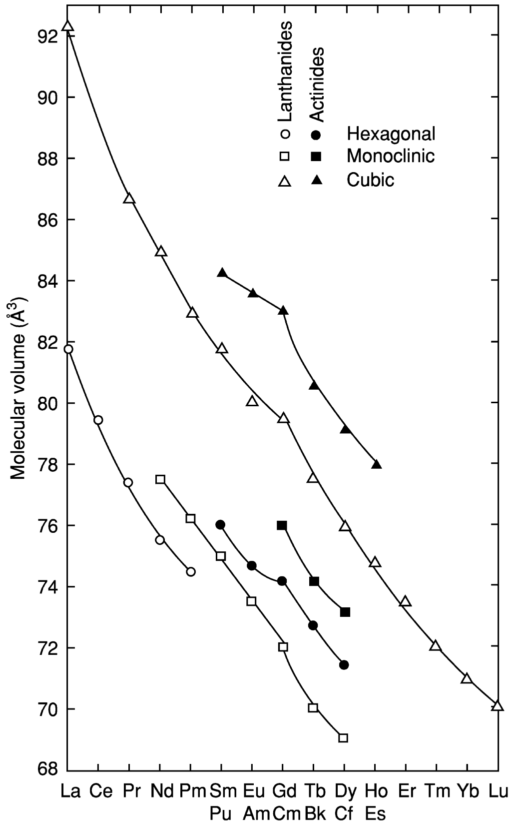

Fig. 11.5 *Molecular volumes of f-element sesquioxides.*

but much larger than the 4.78 Å parameter reported for the metal by Haire (1978) and Haire *et al.* (1986). It should be noted that carbon, nitrogen, and oxygen can replace one another in f-element, cubic NaCl-type compounds as the mononitride. The substitution going from carbon to nitrogen to oxygen increases the compound's parameter. For the remaining pnictogens, the monophosphide of californium has not been reported, but the monoarsenide and monoantimonide have been prepared (Damien *et al.*, 1980; see Table 11.8).

In contrast to the pnictides, californium chalcogenides of different stoichiometries can be prepared (Damien *et al.*, 1980). Preparation of the monochalcogenides requires close control of the reactant stoichiometries to avoid the formation of higher chalcogenides, and attempts to prepare californium monochalcogenides as single-phase products have not been successful to date. Another difficulty is that the monosulfide can convert to higher sulfides by volatilizing californium metal and driving the stoichiometry to a higher sulfide. The tritelluride, ditelluride, diselenide, disulfide, sesquiselenide, and sesquisulfide of

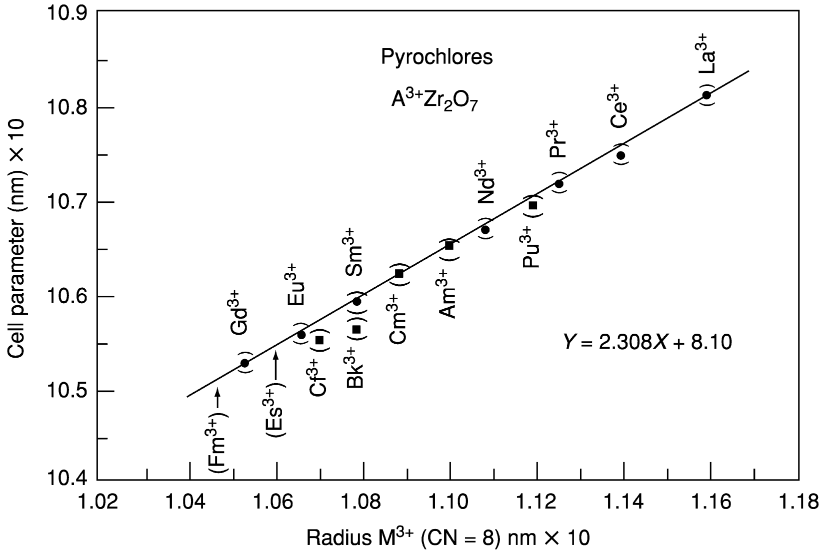

Fig. 11.6 *Relationship of lattice parameters and radii for f-element pyrochlore oxides. (units shown are equivalent to Ångströms)*

californium have all been prepared (Damien *et al.*, 1980). These higher chalcogenides are normally prepared by direct combination of the elements, and lower stoichiometries can be obtained by thermal decomposition of compounds having higher compositions. Lattice parameters for many of these californium compounds have not been reported. It is believed the tritelluride of californium has an orthorhombic structure isomorphous with the NdFe structure. All the dichalcogenide compounds crystallize in the anti-FeAs-type of tetragonal structure (as do the corresponding plutonium, americium, curium, and berkelium compounds). Four transuranium sesquichalcogenide structure types are known; but the sesquisulfide and sesquiselenide of californium have been obtained as the alpha form (bcc; anti-Th_3P_4 type of structure; Damien *et al.*, 1980).

There have been different reports on the preparation of californium hydrides (Gibson and Haire, 1985). The hydrides are generally prepared by reaction of californium metal with hydrogen at elevated temperatures. It was believed that the stoichiometries of the products were close to that for the dihydride (CfH_{2+x}). The products exhibited fcc structures with an average lattice parameter of $a = 5.285$ Å, which is slightly larger than expected for the compound based on extrapolations of parameters for preceding actinide dihydrides. This larger parameter and the inability to prepare a trihydride of californium in the initial efforts were believed to reflect a tendency for californium to be divalent. In the lanthanide–hydrogen system, the hydrides of divalent europium and ytterbium metals also deviate from the behavior of the other lanthanide hydrides (Topp, 1965). Reports of californium hydrides up to trihydride were subsequently published, which also included stoichiometries intermediate to the dihydride and trihydride (Gibson and Haire, 1987).

The oxysulfate (orthorhombic) and the oxysulfide (trigonal) of californium have also been reported (see Table 11.8); Baybarz *et al.*, 1974). These compounds can be prepared by thermally decomposing either Dowex ion-exchange resin beads containing Cf(III) or hydrated $Cf_2(SO_4)_3$ salt. The oxysulfide is obtained by heating these materials in a vacuum or a reducing (hydrogen-containing) atmosphere. The oxysulfate does not decompose to the sesquioxide when heated in air until the temperature exceeds 860°C.

A solid organocalifornium compound, $Cf(C_5H_5)_3$, has been prepared and characterized crystallographically (Laubereau and Burns, 1970a,b; see Table 11.8). Both powder and single-crystal X-ray data were obtained for this orthorhombic, cyclopentadienyl compound, which was prepared by reacting anhydrous $CfCl_3$ and molten $Be(C_2H_5)_2$, and the crystalline product was isolated by vacuum sublimation (135–200°C). A solid-state absorption spectrum of Cf $(C_5H_5)_3$ was obtained from these crystals, which showed a broad absorption from 600 nm to lower wavelengths. This was accredited to the presence of an electron-transfer process in the system.

Some work has also been reported on a californium dipivaloylmethanato complex, where the volatility of the complex was compared to complexes of other lanthanides and actinides (Sakanoue and Amano, 1976). These tracer studies suggested that the californium complex deposited at lower temperatures than the americium or plutonium complexes. Other studies have been done on formation of californium β-diketonates, and their thermochromatography behavior has been described (Aizenberg *et al.*, 1988).

11.7.5 Magnetic properties of compounds

A limited amount of magnetic work has been reported for californium and its compounds. Magnetic data for the metallic state of californium have been described in Section 11.6. The transplutonium metals with localized 5f electrons behave as though they consist of ions embedded in a sea of conduction electrons. It is these 5f electrons that are then mainly responsible for the susceptibility. With this simple model, the effective moment for californium metal should be the same as that for a californium ion, where the same number of nonbonding 5f electrons is present.

In Table 11.10 magnetic data for some f-element metal ions are listed, including californium, and their calculated magnetic moments based on LS coupling and Hund's rule. On this basis, the moments of Cf(IV), Tb(III), or Bk(III) would be the same, the moments of Cf(III), Dy(III), or Es (IV) would be identical, and the moments of Cf(II), Es(III), or Ho(III) would be equal. It is unfortunate that the measured moments cannot differentiate between Cf(II) and Cf(III),

Table 11.10 *Electronic states* (3+) *and effective magnetic moments given by LS coupling and Hund's rule: expected moments of californium.*[a]

Lanthanide	*Actinide*	3+ *Ion configuration*	*Basic level*	*L*	*S*	*J*	g_J	g_J $[J(J+1)]^{1/2}$	μ^*_{eff}
Gd	Cm	f^7	$^8S_{7/2}$	0	7/2	7/2	2	7.94	7.66
Tb	Bk	f^8	$^9F_6$	3	3	6	3/2	9.7	9.40
Dy	Cf	f^9	$^6H_{15/2}$	5	5/2	15/.2	4/3	10.63	10.22
Ho	Es	f^{10}	$^5I_8$	6	2	8	5/4	10.60	10.18

Based on these assumptions: Cf(II) = 10.60 μ_B; Cf(III) = 10.63 μ_B; and Cf(IV) = 9.72 μ_B.

[a] Edelstein and Karraker (1976) and Huray and Nave (1987). Based on intermediate coupling as opposed to pure *LS* coupling.

and that the calculated difference between Cf(III) and Cf(IV) is only 0.9 Bohr magnetons (see Table 11.10). However, the magnetic behavior of these materials as a function of temperature and/or magnetic field can still provide very useful information, and by itself may be sufficient to differentiate between these states.

The first magnetic data reported for californium compounds were obtained from 56 ng of californium; this small quantity required a microscope to measure the deflections of a Faraday apparatus (Cunningham, 1959). The objective of this experiment was to confirm that californium, deposited on an ion-exchange resin bead, had a radon core plus $5f^9$ electrons. The results showed that the sample followed the Curie–Weiss law and produced a moment of 9.2 μ_B. A subsequent experiment with larger samples (0.3–1.2 μg) of californium on resin beads gave effective moments of 9.1–9.2 μ_B. Magnetic studies on oxides, Cf_2O_3, Cf_7O_{12}, CfO_2, and $BaCfO_3$, have been reported (Moore *et al.*, 1986). The magnetic moments obtained in these studies were in agreement with the charge states assigned to californium based on the stoichiometries in the materials. Magnetic studies have also been carried out on three monopnictides, CfN, CfAs, and CfSb (Nave *et al.*, 1985) and on the two structure types of $CfCl_3$ (Nave *et al.*, 1986).

In other studies, the moment of californium in a Cs_2NaYCl_6 host has been measured (Karraker and Dunlap, 1976). An electron paramagnetic resonance study on Cf(III) in a cubic $NaLuCl_4$ host (<1% Cf by weight) produced a 10-line spectrum to confirm the nuclear spin to be 9/2 (Edelstein and Karraker, 1976). The crystal field ground state was also identified in this work and the nuclear dipole moment of ^{249}Cf was determined to be –0.28 μ_n. The magnetic properties of californium compounds and metal are summarized and compared in Table 11.11.

11.7.6 Solid-state absorption spectra

The anhydrous transplutonium halides have been extensively studied by absorption spectrophotometry. The f–f and f–d transitions in californium spectra

Table 11.11 *Effective magnetic moments of californium metal and compounds.*

Material	*T range* (K)	θ (K)	μ_{eff} (μ_{B})	T_{N} (K)	*References*
CfO_2	80–320	–70	9.1(2)	7(2)	Nave *et al.* (1981)
Cf_7O_{12}	80–320	95	9.5(2)	8(2)	Moore *et al.* (1986)
CfF_4	150–340	–51	9.4(1)		Chang *et al.* (1990)
CfF_4 (aged)	150–340	–33	9.1(1)	9–12	Chang *et al.* (1990)
Cf^{3+} (on a resin bead)	77–298	–5.6	9.14(6)		Fujita and Cunningham (1969)
$BaCfO_3$	80–320	–210	9.2(2)	7(2)	Moore *et al.* (1986)
Cf_2O_3 (monoclinic)	80–320	–80	10.1(2)	8(2)	Moore *et al.* (1986)
Cf_2O_3 (bcc)	80–320	–115	9.8(2)	19(2)	Moore *et al.* (1986)
Cf_2O_3 (bcc)	90–300	–80	9.7	–	Morss *et al.* (1987)
CfF_3	150–340	–20	10.2(1)	6–7	Chang *et al.* (1990)
$CfCl_3$	60–340	13	10.1(2)	7	Moore *et al.* (1988)
$Cs_2NaCfCl_6$	2–14	–2.8	7.36(20)	–	Karraker and Dunlap (1976)
$Cs_2NaCfCl_6$	20–100	–13.5	10.0(1)	–	Karraker and Dunlap (1976)
Cf metal	28–298	3.24	9.84		Fujita *et al.* (1976)
	22–298	–3.00	9.67		
Cf metal	100–340	40	9.7(2)		Nave *et al.* (1985)
CfN	4–340	41	10.3(2)	25	Nave *et al.* (1986)
CfAs	4–340	29	10.3(2)	25	Nave *et al.* (1986)
CfSb	4–340	18	10.3(2)	25	Nave *et al.* (1986)

can be utilized to ascertain the oxidation state and coordination number of californium in the compounds. A valuable technique in these spectroscopy studies was the use of a 'fingerprint' approach, where spectra of materials with known structures were used to compare with other compounds. Some of these experimental techniques employed for studying microgram quantities of californium halides have been reported (Green, 1965; Green and Cunningham, 1966; Fujita and Cunningham, 1969; Young *et al.*, 1978). One of the first absorption spectra for californium was obtained from a single crystal of anhydrous $CfCl_3$. Subsequently, other spectra have also been obtained for this compound (Carnall *et al.*, 1972; Peterson *et al.*, 1977) and for $CfCl_2$ (Peterson *et al.*, 1977). Absorption spectra have also been obtained for anhydrous $CfBr_3$ (Young *et al.*, 1975, 1980); $CfBr_2$ (Young *et al.*, 1980), CfI_3 and CfI_2 (Wild *et al.*, 1978), plus CfF_4 and CfF_3 (Haire *et al.*, 1980).

In Fig. 11.7 solid-state absorption spectrum for $CfCl_2$ is shown, which is compared with a spectrum for $CfCl_3$. There is a distinct difference between the absorption spectrum for Cf(III) and Cf(II) states. For a given oxidation state, differences in absorption spectra as well as emission spectra can be noted when the crystal structures are different. This arises from symmetry conditions and how they affect the splitting of electronic levels in the californium compounds. These spectra, once assigned to specific structures, may be used to identify the

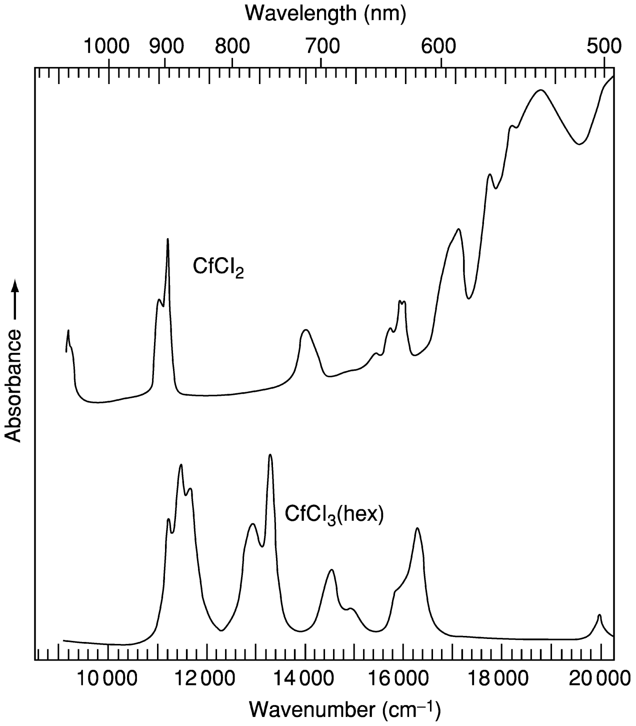

Fig. 11.7 *Solid-state spectra for $CfCl_2$ and $CfCl_3$.*

structure type by a 'fingerprint' technique. Thus, one finds the spectral envelops of the absorption spectrum for the hexagonal form of $CfCl_3$ differs from that of the orthorhombic form of this compound. A review of solid-state spectral studies on californium halides is available (Wilmarth and Peterson, 1991a,b). In this review the authors also give a discussion of Raman spectra obtained for californium.

Laser-induced fluorescence of Cf^{3+} in a $LaCl_3$ host has also been reported (Caird *et al.*, 1976; Hessler *et al.*, 1978). A limited amount of spectral information has been reported for the dicyclopentadienyl californium compound, where Cf exists as Cf(III) (Laubereau and Burns, 1970a,b). The spectra of Cf(IV) in CeF_4 matrices has also been discussed (Liu *et al.*, 1993) and information obtained was interpreted in terms of line broadening.

Infrared spectra for californium materials have also been obtained (Conway *et al.*, 1977). Crystal field calculations and parameters for the trivalent actinides in crystal hosts have been made and published (Carnall and Fried, 1976; Conway *et al.*, 1977; Crosswhite, 1977). The spectroscopic properties of californium compounds pertinent to potential laser applications have also been discussed, and the transition from the $J = 11/2$ state at 6500 cm to the $^6H_{15/2}$ ground state appears to be a likely candidate in this regard (Weber, 1980). Free-ion energy levels and the optical properties for californium have also been published (Hessler and Carnall, 1980).

In addition, absorption spectra of californium halides have been obtained and examined as a function of time, looking at the daughter or granddaughter products in studies that examined the chemical and structural consequences of the radioactive decay processes (Young *et al.*, 1980, 1981, 1984). Following the chemistry and structural forms through radioactive decay processes by examining the californium granddaughter products produced from the decay of Es-253 halides (i.e.Es-253 → Bk-249 → Cf-249 → ⋯) is an example. It is worthwhile to note that in the latter decay sequence, Cf(III) halide product was produced from an initial Es(III) halide product and a Cf(II) halide product when starting with a Es(II) halide. Essentially, the oxidation state was retained through two decay events, first an alpha and then a beta decay). This implies that a Bk(II) product was formed in the transition although Bk(II) has not been synthesized directly.

11.8 SOLUTION CHEMISTRY

11.8.1 General comments

Although californium exhibits oxidation states of II, III, and IV in the solid state, its solution chemistry is basically that of a trivalent ion. There has been only a couple of unsubstantiated reports of an oxidation state above Cf(IV) in solution even though formation of Cf(V) presumably would acquire some stabilizing influence by attaining a half-filled, 5f-orbital state ($5f^7$).

To retain the tetravalent state in solution is also more difficult than generating it in the solid state, and for solutions it requires a high degree of complexation to afford sufficient stabilization to maintain this state. It has been reported (Kosyakov *et al.*, 1977) that Cf(IV) was stabilized in phosphotungstate solutions, where M(IV)/M(III) couples can be shifted by as much as 1.0 V (Barnanov *et al.*, 1981). Another report for stabilizing Cf(IV) in solution involved the use of triphenylarsine oxide in acetonitrile (Payne and Peterson, 1987).

It is expected to be easier to stabilize Cf(II) than Cf(IV) in solutions. Nonaqueous solvents also offer some promise for obtaining both the II and IV oxidations states of californium. But in all cases, the effects of self-irradiation and the potential for generating oxidizing and/or reducing conditions must be considered and factored into the picture.

Although californium is the electronic homolog of dysprosium, its divalent–trivalent behavior in solution should be considered to be more similar to that of samarium, and its trivalent–tetravalent behavior may be comparable to that of terbium. Thus, samarium and terbium can be used as template elements for testing the oxidation behavior of californium.

Trivalent californium's behavior in solution is very similar to the behaviors of the trivalent lanthanide ions in solution, except californium has a greater tendency to form complexes (is more covalent). This arises from the somewhat extended 5f orbitals of actinides compared to the 4f orbitals, which provides a slightly greater degree of complexing ability to afford californium's greater covalent nature. The higher degree of complexation found with the transplutonium (III) ions in ethanol–HCl solution, as compared to the lanthanide (III) ions (see Section 11.4), has used this condition as one method for a group separation.

As with the lanthanides, both fluoride and oxalate ions will precipitate trivalent californium from dilute acid solutions. Addition of hydroxide to a Cf(III) solution produces a gelatinous, light green-tinted precipitate, which is presumably its trihydroxide. In non-complexing solutions (i.e. dilute acid solutions, 0.1 M perchloric or hydrochloric acids), Cf(III) exists as a hydrated cation; at higher acid concentrations (i.e. 6 M HCl), complexation is sufficient so that californium will not be held on cation-exchange resins but will elute as an anion complex. This difference in complexation forms the basis for a number of group separations between trivalent lanthanides and actinide ions. The greater complexing nature of the actinides allows them to be removed from cation-exchange resins with different reagents while the lanthanides are retained on the columns.

11.8.2 Oxidation–reduction reactions

Several reduction potentials for californium have been derived from both experimental data and from systematic calculations, and some of these values are given in Table 11.12. The calculated Cf(IV)/(III) couple of 3.2 V (Nugent *et al.*, 1971) is in accord with the inability to obtain Cf(IV) in most aqueous media. This value for californium can be compared to the Tb(IV)/Tb(III) couple of 3.1–3.3 V, the Am(IV)/Am(III) couple of 2.2–2.5 V, and the Cm(IV)/Cm(III) couple of 3.1–3.5 V (Nugent *et al.*, 1973a,b). It is difficult to maintain Am(IV) and essentially not feasible to produce Cm(IV) in most aqueous solutions. Preparation of these higher oxidation states for the actinides in general should be more favorable in alkaline than acidic media, but complexation can also offer stabilization. Thus, in principle, the ease of forming Cf(IV) should be comparable to forming Tb(IV) or Cm(IV) in solution, which are more difficult than forming Am(IV) in solution. This relative behavior of californium in solution may be likened to that in the solid state: the formation of californium dioxide is comparable to preparing terbium dioxide, with both being more difficult to prepare than americium or curium dioxide (see Section 11.7.3).

The ability to oxidize Cf(III) to Cf(IV) in a phosphotungstate solution has been summarized in a paper on the solution behavior of the transplutonium elements (Myasoedov, 1982). Both Tb(IV) and Am(IV) can be stabilized in strong carbonate; thus, it would appear possible to prepare Cf(IV) in a strong carbonate medium, utilizing the expected shift of 1.7 V in the Cf(IV)/Cf(III) couple arising from carbonate complexation of the Cf(IV). Two conflicting reports exist on the

Table 11.12 *Reduction potentials for californium.*

Couple	*Potential* (V vs NHE)	*Method*	*References*
Cf(IV)/Cf(III)	3.3; 3.2	calculated	Nugent *et al.* (1971, 1973a,b)
Cf(IV)/Cf(III)	3.2		Chapter 19
Cf(III)/Cf(II)	–2.0; –1.9	calculated; spectra	Nugent *et al.* (1969)
	–1.6		Chapter 19
	–1.4	calculated	David (1970a,b,c)
	–1.6	calculated; spectra	Friedman *et al.* (1972)
	–1.47	polarographic/voltammetric	Musikas *et al.* (1981)
	–1.6	polarographic (acetonitrile)	Friedman *et al.* (1972)
Cf(III)/Cf(0)	–2.32	calculated	David (1980)
	–2.01	radiopolarography	David *et al.* (1978) and Samhoun and David (1976)
	–2.06	calculated	Raschella *et al.* (1982)
	–1.93		Chapter 19
Cf(III)/Cf(Hg)	–1.61	Calculated	Musikas *et al.* (1981)
Cf(III)/Cf(Hg)	–1.503	radiopolarography	Samhoun and David (1976)
Cf(II)/Cf(Hg)	–1.68	polarographic/voltammetric	Samhoun and David (1976)
Cf(II)/Cf(0)	–2.1		Chapter 19

oxidation of Cf(III) in carbonate. One group (Hobart *et al.*, 1981, 1983) was unable to find evidence for Cf(IV) after chemical or electrical treatments, while a second team (Myasoedov *et al.*, 1986) reported that 20% of the Cf(III) present in a K_2CO_3 solution could be oxidized electrochemically.

The behavior of californium and the next two actinide elements in molten salts where strong reducing agents were present has been reported (Kulyukhin *et al.*, 1997). The ease of preparing the divalent state increases in going across the series to einsteinium.

A number of studies have supported the potential for the existence of Cf(II) in solution. In one study, the tendency for californium to form amalgams rapidly is compared to the behavior of the lanthanides known to acquire a divalent state (Maly, 1967; Maly and Cunningham, 1967; Nugent, 1975). In early work, the inability to reduce Cf(III) in 0.1 M NH_4Cl suggested a potential limit of −1.4 V for the Cf(III)/Cf(II) couple (Cunningham *et al.*, 1970). David (1970a–c) also proposed a value of –1.4 V from radiopolarographic and amalgamation behaviors using tracers.

Studies on the coprecipitation behavior of californium (Cohen *et al.*, 1968; Fried and Cohen, 1968; Mikheev *et al.*, 1972a,b) have also supported the existence for Cf(II) in solution. The difference in formal potentials between the Sm(III)/Sm(II) and Cf(III)/Cf(II) couples has been estimated to be 0.045 V (californium being more negative) by studies on coprecipitation of chloride salts in aqueous ethanol solutions (Mikheev *et al.*, 1972a,b). Another comparison between the reduction behavior of californium and samarium was made in anhydrous acetonitrile (Friedman *et al.*, 1972), where the Cf(III)/Cf(II) and Sm(III)/Sm(II) couples were found to be nearly identical; a value of –1.58 V was proposed for the Cf(III)/Cf(II) couple. Essentially the same value (–1.60 V) for this couple was reported from co-crystallization studies (Mikheev *et al.*, 1972a,b). Nugent *et al.* (1969, 1973a) have suggested the potential for the Cf(III)/Cf(II) couple is –1.6 V, based on systematic analyses of electron-transfer bands. Radiopolarographic experiments on californium have resulted in two reports regarding its behavior. The first report (David, 1970a) suggested two couples: –2.32 V for Cf(III)/Cf(0) and –1.4 V for Cf(III)/Cf(II). Subsequent work (Samhoun and David, 1976) concluded that the first radiopolarographic results were incorrect, and that Cf(III) is reduced directly to Cf(Hg) in one step ($E_{1/2} =$ 1.503 V): correcting for the amalgamation process yields a Cf(III)/Cf(0) couple of –2.01 V. Guminski (1996) has discussed the Hg-Cf system.

Subsequently, a polarographic and voltammetric study (Musikas *et al.*, 1981) on larger amounts of californium concluded that californium is reduced via a two-step process as is found with samarium: (1) Cf(III) → Cf(II) and (2) Cf(II) → Cf(Hg). Potentials for these processes were given as –1.47 and –1.68 V, respectively. These data yield a calculated value of –1.61 V for Cf(III)/Cf(0). An evaluation of earlier amalgamation experiments has also led to a proposed value of –2.2 V for the Cf(II)/Cf(0) couple (Nugent, 1975).

These reported differences for californium have not been resolved and additional work needs to be done to resolve the system. Since Cf(II) can be prepared and maintained in the solid state, there still remains a good possibility that Cf(II) can be stabilized in aqueous and/or nonaqueous solvents. David *et al.* (1990a,b) and David and Bouissières (1968) discuss the electrochemical reduction in aqueous solution for separations, and for the formation of intermetallic compounds and amalgams. Other work on the radiopolarography of californium has also been published (Skiokawa and Suzuki, 1984).

Evidence for Cf(II) in molten-salt systems has also been reported (Ferris and Mailen, 1971). The distribution coefficient of californium between molten lithium chloride and lithium–bismuth metals at 640°C indicated that divalent californium was present in the salt phase. However, evidence for the existence of Cf(II) was not found in lithium fluoride–beryllium fluoride melts (Ferris and Mailen, 1970).

It is generally accepted that the stability of the divalent state increases for the second half of the actinide series of elements, and it has been accepted that californium metal is close to being a metal having only two bonding electrons (see earlier section). Starting with californium, the M(III)/M(II) couples increase regularly in the order: No > Md > Fm > Es > Cf, with values ranging from –1.45 V for nobelium to –1.60 V for californium (Myasoedov, 1982).

In discussing the oxidation states of californium in solution, the possibility of attaining Cf(V) could be enhanced by the attainment of a $5f^7$ electronic state.

Some early coulometric data obtained with a few micrograms of californium suggested that Cf(v) may have been attained in a 1 M H_2SO_4 solution (Propst and Hyder, 1969), but these results have not been confirmed and are likely to be incorrect. More recently, a claim for the generation of Cf(v) in a carbonate media was made based on results of coprecipitation experiments (Kosyakov *et al.*, 1982a,b). In this work, small amounts (<10%) of californium, generated from the decay of Bk(IV) in the solution, were found in $Na_4UO_2(CO_3)_3$ 'wet' solids precipitated from the solutions. The presence of 'co-precipitated' californium in these precipitates was interpreted as reflecting the presence of an oxidized form of californium (Cf(IV) or Cf(v) i.e. as the CfO^{2+} or CfO_2^+ ion) within the uranium precipitate. These results must be accepted with some caution, as other explanations for the behavior can be given. It is likely that Cf(IV) would accompany Bk(IV) in such situations. Thermodynamic (David *et al.*, 1978) and quantum-chemical calculations (Ionova *et al.*, 1980) have been made that indicate it may be possible to obtain Cf(v) state in the solid state, which could be considered for the solid phases mentioned above. However, it would seem most plausible that Cf(IV) or Cf(v) would be stabilized in alkaline conditions/materials, oxygenated complexes, complex polyanion materials (i.e. polytungstates), etc.

11.8.3 Complexation chemistry

A considerable portion of the published data dealing with californium concerns the complexation and solvent extraction chemistry of Cf(III). This is in part a consequence of the fact that a large amount of this information could be obtained using tracer quantities of the more abundant ^{252}Cf isotope, which also has a higher specific activity. In addition, there was an impetus to perform this type of study using the small quantities available during the investigation/development of californium's separation chemistry for processing. A compilation of stability constants for californium complexes and chelates is given in Table 11.13.

Some of the first data on californium complexes involved materials such as halides, citrates, lactates, α-hydroxyisobutyrate complex, etc., as these materials played a role in early separation/purification schemes (Katz and Seaborg, 1957; Keller, 1971) for californium (see Section 11.4). In general, it is expected that only small differences in stability would exist between Cf(III) and its two trivalent near neighbors, Bk(III) and Es(III), with potentially larger differences existing between Cf(III) and Am(III). A general discussion of actinide complexes (including californium) in aqueous solution is available (Jones and Choppin, 1969). Horwitz *et al.* (1997) discuss complexer in solution.

From the initial studies on Cf(III) and sulfate ions (De Carvalho and Choppin, 1967) it was concluded that 1:1 and 1:2 complexes $Cf(SO_4)^+$ and $Cf(SO_4)_2^-$ were formed, but subsequent work in the sulfate system suggested that mono-, di-, and trisulfate species were formed (McDowell and Coleman, 1972).

Table 11.13 *Stability constants of Cf(III) complexes and chelates.*

Ligand	*Experimental method*	*Log of stability constants*[a] *at* 25°C	*References*
fluoride ion	solv. extract.	$\beta_1 = 3.03$ $\mu = 1.0$	Choppin and Unrein (1976)
hydroxide ion	solv. extract	$\beta_1 = 5.62$ $\beta_1 = 5.05$ $\mu = 2.00$	Desiré *et al.* (1969)
sulfate ion	solv. extract.	$\beta_1 = 1.36$ $\beta_2 = 2.07$ $\mu = 2.0$ $K_{01} = -3.73$ $K_{02} = -5.58$ $K_{03} = -5.09$ $\mu = 0$	De Carvalho and Choppin (1967)
thiocyanate ion	solv. extract.	$\beta_1 = 3.06$	Choppin and Ketels (1965)
	solv. extract.	$\beta_1 = 3.71$ $\beta_2 = 0.28$ $\beta_3 = 2.65$	Coleman (1972)
acetate ion	solv. extract.	$\beta_1 = 2.11$ $\mu = 1.0$	Choppin and Schneider (1970)
oxalate ion	–	$\beta_3 = 12.5$ $\mu = 0.1$	Stary (1966)
	electromigr.	$\beta_1 = 5.50$ $\beta_2 = 3.87$ $\mu = 0.1$	Stepanov (1971)
lactic acid	–	$\beta_3 = 6.08$ $\mu = 0.15$	Stary (1966)
	solv. extract.	$\beta_3 = 6.09$ $\mu = 0.5$	Ermakov and Stary (1967)
	ion exchange	$\beta_3 = 6.08$ $\mu = 0.5$	Ermakov and Stary (1967)

α-hydroxyisobutyric acid	ion exchange	$\beta_3 = 6.9$ $\mu = 0.5$	Desiré *et al.* (1969)
tartaric acid	–	$\beta_2 = 6.8$ $\mu = 0.1$	Desiré *et al.* (1969)
	solv. extract.	$\beta_2 = 5.86$	Aly and Latimer (1970)
ethylenediaminetetraacetic acid	ion exchange	$\beta_1 = 19.09$	Fuger (1958)
1,2-diaminocyclohexane-tetraacetic acid	ion exchange	$\beta_1 = 19.42$	Baybarz (1966a,b)
diethylenetriaminepentaacetic acid	–	$\beta_1 = 22.6$	Stary (1966)
	ion exchange	$\beta_1 = 22.57$	Baybarz (1965)
	ion exchange	$\beta_1 = 25.19$	Brandau (1971)
glycolate ion	solv. extract.	$\beta_1 = 2.63$ $\beta_2 = 1.97$ $\mu = 2.0$ (53°C)	Choppin and Degischer (1972)
2-methyllactic acid	solv. extract.	$\beta_1 = 4.10$ $\mu = 0.1$	Aly and Latimer (1970)
malic acid	solv. extract.	$\beta_1 = 7.02$ $\mu = 0.1$	Aly and Latimer (1970)
citric acid	solv. extract.	$\beta_1 = 11.61$ $\mu = 0.1$	Aly and Latimer (1970)
	electromigr.	$\beta_1 = 7.93$ $\beta_2 = 3.3$ $\mu = 0.1$	Stepanov (1971)
	solv. extract.	$\beta\left(C\frac{2-}{2}\right) = 10.90$ $\mu = 0.1$ $\beta\left(C\frac{3-}{2}\right) = 12.26$ $\mu = 0.1$	Hubert *et al.* (1974)
	solv. extract.	$\beta(\mathrm{M(HCit^-)_2} = 5.8;$ $\mu = 0.1$ $\beta(\mathrm{M(HCit)(Cit^{2-})} = 9.9;$ $\mu = 0.1$	Guillaumont and Bourderie (1971)

Table 11.13 (*Contd.*)

Ligand	*Experimental method*	*Log of stability constants*[a] *at* 25°C	*References*
thenoyltrifluoroacetone	solv. extract.	$\beta_3 = 14.94$ $\mu = 0.1$	Keller and Schreck (1969)
benzoyltrifluoroacetone	solv. extract.	$\beta = 16.06$ $\mu = 0.1$	Keller and Schreck (1969)
naphthoyltrifluoroacetone	solv. extract.	$\beta = 18.83$ $\mu = 0.1$	Keller and Schreck (1969)
nitrilodiaceto-monopropionic acid	ion exchange	$\beta_1 = 10.94$ $\beta_2 = 18.45$	Eberle and Ali (1968) Eberle and Ali (1968)
nitrilotriacetic acid	ion exchange	$\beta_1 = 11.92$ $\beta_1 = 11.3$ $\beta_2 = 21.0$ $\mu = 0.1$	Stary (1966)
N-2-hydroxyethyl-ethylenediaminetriacetic acid	ion exchange	$\beta_1 = 16.27$ $\beta_2 = 28.5$ $\mu = 0.1$	Eberle and Ali (1968) Eberle and Bayat (1967)
2-hydroxy-1,3diamino-propane tetraacetic acid		$\beta_1 = 13.18$ $\mu = 0.1$	Baybarz (1967)
5,7-dichloro-8-hydroxyquinoline	solv. extract.	$\beta_3 = 22.59$	Feinauser and Keller (1969)
4-benzolyl-3-methyl-1-phenyl-2-pyrozolin-5-one	solv. extract	$\beta_3 = 17.78$ $\mu = 0.1$	Keller (1971)

4-acetyl-3-methyl-1-phenyl-2-pyrozolin-5-one	solv. extract	$\beta_3 = 13.48$ $\mu = 0.1$	Keller (1971)
2-hydroxyethyl-iminodiacetic acid	solv. extract.	$\beta_1 = 9.61$ $\mu = 0.1$	Ermakov *et al.* (1971b)
o-hydroxyphenyl-iminodiacetic acid		$\beta_1 = 7.38$ $\beta_2 = 12.28$ $\mu = 0.1$	Ermakov *et al.* (1971)
2-ethylhexylphenyl-phosphoric acid		$\beta_1 = 6.03$ $\beta_2 = 2.00$ $\mu = 0.1$	Barketov *et al.* (1975)
thenoyltrifluoroacetone		$\beta_1 = 6.90$ $\mu = 0.1$	Khopkar and Mathur (1977)

[a] Overall formation constants:

$$\beta_1 = \frac{[\mathrm{CfA}^{(3-n)+}]}{[\mathrm{Cf}^{3+}][\mathrm{A}^{n-}]}, \quad \beta_2 = \frac{[\mathrm{CfA}_2^{(3-2n)+}]}{[\mathrm{Cf}^{3+}][\mathrm{A}^{n-}]^2} \quad \text{etc.}$$

stepwise constants:

$$K_2 = \frac{[\mathrm{CfA}^{(3-2n)+}]}{[\mathrm{CfA}^{(3-n)+}][\mathrm{A}^{n-}]} \quad \text{etc.}$$

A similar situation exists for the thiocyanate complexes reported for Cf(III). Initially a 1:1 complex, $Cf(SCN)^{2+}$, was reported (Choppin and Ketels, 1965), but subsequent work indicated that three different complexes could form: $Cf(SCN)^{2+}$, $Cf(SCN)_2^+$, and $Cf(SCN)_3$, where the 1:3 complex was of the inner-sphere type (Coleman, 1972).

The hydrolysis behavior of Cf(III) is expected to be similar to that of trivalent lanthanides, and more specifically to that of Eu(III) or Gd(III), which have nearly the same ionic radii. The first hydrolysis reaction (i.e. $Cf^{3+} + H_2O \rightarrow CfOH^2 + H^+$; i.e. the K_1 value) has also been determined for Cf(III); log K_1 values for it were given as –5.62 (Desiré *et al.*, 1969) and –5.05 (Hussonnois *et al.*, 1973).

Several quite stable complexes can be formed with Cf(III) (see Table 11.13). Complexes of diketones and aminopolycarboxylic acids have been found to be considerably more stable than those of tartrate, lactate, oxalate, etc. In some cases, adduct chelates can also form with Cf(III), such as with the californium thenoyltrifluoroacetone (TTA) chelate and methyl isobutyl ketone (MIBK) (i.e. $Cf(TTA)^{3+}$ and $Cf(TTA) \rightarrow$ MIBK or Cf(TTA)3–2 MIBK; Desiré *et al.*, 1969).

With the monodentate ligands, such as tributyl phosphate (TBP), the extractable californium adduct from nitric acid solutions has been assigned as being a 1:3 species $Cf(NO_3)_3 \cdot 3\,TBP$ (Healy and McKay, 1956). Quaternary ammonium bases and alkylpyrocatechols (i.e. 4-dioctylethyl pyrocatechol) can form californium complexes in alkaline solutions (Derevyanko *et al.*, 1976), which affords a different medium for complexation. One recent extraction study has examined the influence of the extractant's structure on the extraction behavior of californium (Derevyanko *et al.*, 1976). A large number of materials have been investigated for forming extractable complexes of californium, and the reader is referred to reviews on the subject (Ishimori, 1980; Myasoedov *et al.*, 1980; Shoun and McDowell, 1980). Takeiski *et al.* (2001) have discussed the solvent extraction of californium by deratives of bis(1-phenyl-3-methyl-4-acylpyrazol-5-one) .

Exchange kinetics of Cf(III) with europium ethylenediaminetetraacetate (Eu EDTA) in aqueous solution ($\mu = 0.1$) has also been reported (Williams and Choppin, 1974). The exchange was found to be a first-order reaction having both acid-dependent and acid-independent terms.

From a study of the relationship between distribution coefficients for californium with sodium nitrate in extractions using organic ammonium nitrates, the apparent mean molar activity coefficient of Cf(III) was calculated in terms of a polynomial (log $k = a + bm + cm^2 + dm^3$, where $a = 0.00397$, $b = –0.154$, $c = 0.0252$, and $d = 0.00119$) (Chudinov and Pirozhkov, 1973).

Some initial studies of californium complexes involving 6-methyl 2-(2-pyridyl)-benzimidazole and derivatives of it have been carried out. The initial studies involved photoluminescence and Raman spectroscopy investigations, where it was concluded that 1:1, 1:2, 1:3, and 1:4 complexes were formed (Assefa *et al.*, 2005).

A general discussion of the hydrolysis of actinide ions is given in a review by Ahrland (1991). Although little is mentioned about californium, several general concept discussed there are useful for the trivalent actinides. In another review, Bhattacharyya and Natarajan (1991) discuss the radiation chemistry of actinide solutions. A rate constant for the oxidation of Cf^{2+} by water ($K = 7 \times 10^4\ \text{M}^{-1}\ s^{-1}$) and a rate constant for the reduction of Cf^{3+} ($K = 3 \times 10^9\ \text{M}^{-1}\ s^{-1}$) at a pH of 5.3 are quoted.

11.8.4 Thermodynamic data

The thermodynamic behavior of californium has been addressed in Chapter 19. Given there are the recommended values for californium that have been arrived at after considering various reports.

Selected thermodynamic data for the formation of Cf(III) in solution (according to the following reaction):

$$\mathrm{Cf}_{(s,a)} + 3\mathrm{H}^+_{(aq)} = \mathrm{Cf(III)}_{(aq)} + 3/2\mathrm{H}_{2(g)}$$

are given in Table 11.14 (also see Section 11.6.2 on californium metal for comments on its enthalpy of solution), which has been used for calculating the enthalpy of formation of aqueous ions. The enthalpy of formation, $\Delta H^{\circ}_{298,f}(Cf^{3+},aq))$ was derived from the enthalpy of solution (Fuger *et al.*, 1984) as being –577(5) kJ mol^{-1}. The entropy, S° (Cf^{3+}, aq)), has been accepted as –197(17) J $K^{-1} \cdot mol^{-1}$ (see Chapter 19). Using these values and S°(Cf, cr, α phase, 298.15 K) = 81(5) (Ward, 1983; see Chapter 19) one obtains $\Delta_f G(Cf^{3+},aq)$ = –533(7) kJ mol^{-1}. A standard potential for the Cf(III)/Cf(0) couple was calculated to be –(1.92 ± 0.03) V in that work. Earlier estimates for this potential ranged from –1.95 to –2.03 V (Nugent, 1975; David *et al.*, 1976a,b; David *et al.*, 1978; Samhoun and David, 1979).

Other estimates for ΔH_f (Cf^{3+},aq) have appeared in the literature. Nugent *et al.* (1973a,b) proposed a value of –623 kJ mol^{-1}; David *et al.* (1986) suggested −(586 ± 21) kJ mol^{-1}; and Nugent (1975) subsequently arrived at a value of –(602 ± 21) kJ mol^{-1}. A value of –603 kJ mol^{-1} was estimated for californium in a comparison given for thermochemical properties for the lanthanide and actinide elements (Morss, 1983). This latter work also presents other thermochemical values for californium.

Predictions of the standard free energy (ΔG_f) and the enthalpy of hydration (ΔH_{hyd}) for the trivalent californium ion have been made based on an electrostatic hydration model (Goldman and Morss, 1975). Assuming a crystallographic radius of 0.94 Å and a gas-phase radius of 1.516 Å for Cf(III), and using a primary hydration number of 6.1, ΔG°_{298} and ΔH°_{298} were calculated to be –3385 and –3582 kJ mol^{-1}, respectively.

Thermodynamic data for the 1:1 complex, $Cf(SO_4)^+$, have been calculated from the temperature dependence of the stability constant (De Carvalho and

Table 11.14 *Thermodynamic data for californium.*

A. Metal, crystal at 298.15 K and 10^5 Pa

S° (J K^{-1} mol^{-1})	$\Delta_{sub}H^\circ$ (kJ mol^{-1})
81(5)	196 (10)

B. Metal, gas at 298.15 K and 10^5 Pa

S° (J $K^{-1}mol^{-1}$)	Cp (J $K^{-1}mol^{-1}$)
201.3(30)	20.786(20)

C. High temperature heat capacity of the metal [$Cp/J\ K^{-1}\ mol^{-1} = a(T/K)^{-2} + b + c(TK) + d(T/K)^2 + e(T/K)^3$]

form	$A\times10^{-6}$	b	$C\times10^3$	$D\times10^6$	e	T/K	$\Delta_{trs}H$ (kJ mol^{-1})
dhcp		23.651	9.7865	9.0983		863	2.64
fcc	0.0580	37.6				1173	7.51

D. Aqueous ions at 298.15 K

Cf^{3+}	Cf^{3+}	Cf^{4+}	Cf^{4+}
S° (J K^{-1} mol^{-1})	Δ_fH° (kJ mol^{-1})	S° (J K^{-1} mol^{-1})	Δ_fH° (kJ mol^{-1})
–197(17)	–577(5)	–405(17)	–483(5)

E. Solid CfO_2 at 298.15 K

S_{exs} (J K^{-1} mol^{-1})	S° (J K^{-1} mol^{-1})	Δ_fH° (kJ mol^{-1})
21.3	87(5)	–858

F. Standard entropy and enthalpy of formation of Cf_2O_3 at 298.15 K

S° (J K^{-1} mol^{-1})	Δ_fH° (kJ mol^{-1})
176.0(50)	–1653(10)

G. Properties of californium halides at 298.15 K.

Halide	S° (J K^{-1} mol^{-1})	Δ_fH° (kJ mol^{-1})
CfF_4		–1623
CfF_3		–1553(35)
$CfCl_3$	167.2(6)	–965(20)
$CfBr_3$	202(5)	–752.5
CfI_2	154	–669

Source: Chapter 19.

Choppin, 1967). Values for this complex are: $\Delta G_{298} = -7.9$ kJ mol^{-1}, $\Delta H_{298} =$ 19 kJ mol^{-1}, and $\Delta S_{298} = 88$ kJ mol^{-1}. Similarly, data for the 1:1 CfF^{2+}complex have been calculated (Nugent *et al.*, 1973a,b), and have been given as: $\Delta G_{298} =$ 17.3 kJ mol^{-1}, $\Delta H_{298} = 27.2$ kJ mol^{-1}, and $\Delta S_{298} = 14$ kJ mol^{-1}.

Other thermodynamic data have also been reported for californium (David *et al.*, 1978). The reader is also referred to Chapter 19 for a more complete summary of thermodynamic data for californium.

11.8.5 Solution absorption spectra

The first absorption spectrum for Cf(III) was obtained from the solid state (Green, 1965; see Section 11.7.6). The first solution absorption spectrum was obtained shortly thereafter, using 592 μg of mainly ^{252}Cf isotope, which introduced experimental problems regarding both shielding and radiolytic gassing. Nineteen absorption bands were recorded between 280 and 1600 nm from a 1 M $DClO_4$ solution (see Table 11.15; Fig. 11.6). The absorption spectrum from this work was confirmed using milligram quantities of ^{249}Cf (Carnall and Fried, 1976).

Table 11.15 *Absorption data for Cf(III) in 1 M $DClO_4$.*[a]

Wavelength (nm)	*Wavelength* (cm^{-1})	*Absorption coefficient*, μ (L mol^{-1} cm^{-1})
1560.0	6410	5.3
1211.0	8260	1.6
840.3	11 900	2.5
769.8	12 990	6.3
745.2	13 420	6.4
673.8	14 840	2.5
640.2	15 620	1.7
602.0	16 610	4.9
490.0	20 410	1.9
469.9	21 280	8.9
442.1	22 620	10.3
434.8	23 000	9.8
401.9	24 880	0.9
353.4	28 300	1.0
334.0	29 940	1.5
325.0	30 770	3.8
304.9	32 800	1.1
295.0	33 900	2.4
284.0	35 210	1.9

[a] Conway *et al.* (1966).

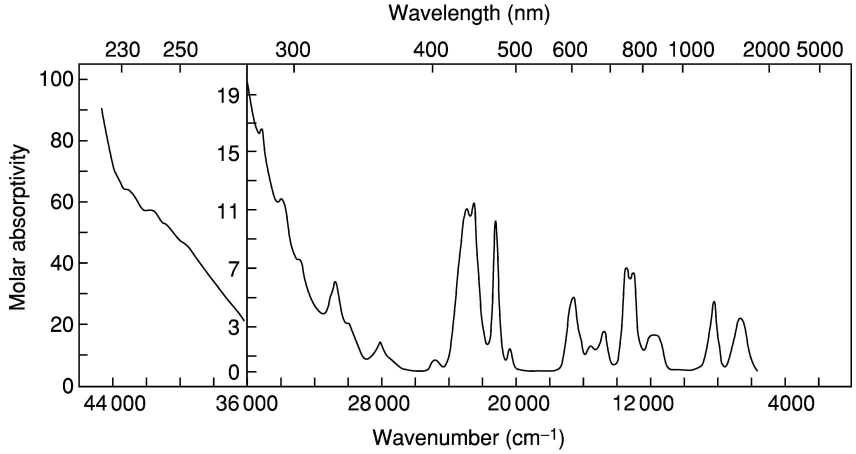

Fig. 11.8 *Solution absorption spectrum of Cf(*III*) in* 0.1 M *$HClO_4$–$DClO_4$.*

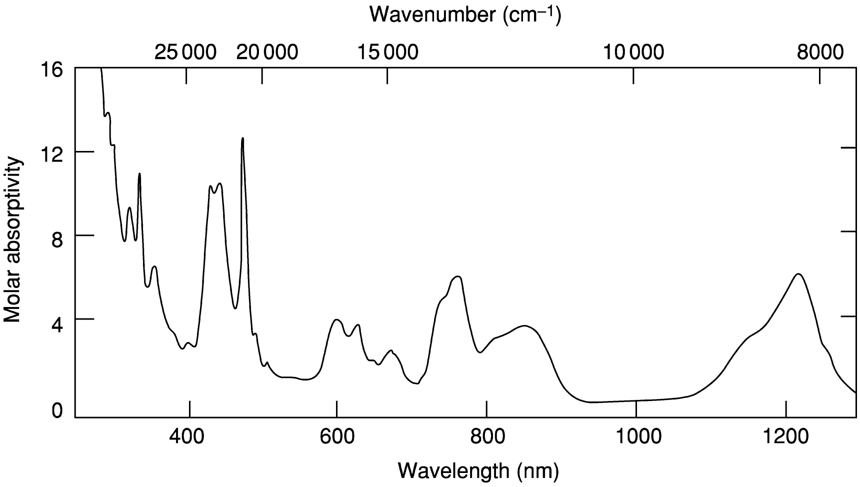

Fig. 11.9 *Solution absorption spectra of Cf(*III*) in* 0.12 M *Na_2CO_3 at pH* 12.

Fig. 11.8 shows the Cf(III) absorption spectrum obtained from a 0.1 M $HClO_4$–$DClO_4$ solution. The absorption spectrum of Cf(III) in 2 M Na_2CO_3 (Hobart *et al.*, 1982) is shown in Fig. 11.9, and the intensities of the absorptions in the carbonate solution is given in Table 11.16. The spectrum of Cf(III) in the Na_2CO_3 solution is similar to that observed in 1 M $DClO_4$, but shifts in wavelength and enhancement of intensity occur for some peaks. See Chapter 16 for a comprehensive overview of actinide spectroscopy.

Table 11.16 *Absorption data for Cf(III) in* 2 m *Na_2CO_3*.[a]

Wavelength (nm)	*Wavelength* (cm^{-1})	*Absorption coefficient,* μ (L mol^{-1} cm^{-1})
293	34 100	14
303	33 000	12
322	31 000	9.3
336	29 800	11
355	28 200	6.5
402	24 900	2.9
430	23 200	10
443	22 600	11
474	21 100	13
491	20 400	3.3
506	19 800	2.0
600	16 700	4.0
625	16 000	3.8
674	14 800	2.4
740	13 500	4.9
757	13 200	6.0
850	11 800	3.7
1140	770	2.8
1214	8 240	6.1

[a] Hobart *et al.* (1983).

The absorption spectrum of Cf(IV) and Cf(III) in a potassium phosphotungstate medium has been reported (Kosyakov *et al.*, 1977; Myasoedov, 1982). The phosphotungstate ion stabilizes the Cf(IV) oxidation state sufficiently to permit spectra to be obtained (half-life approximately 70 min at room temperature). This Cf(IV) oxidation state was achieved by using potassium persulfate at elevated temperatures; attempts to oxidize (Cf(III) electrochemically in this medium were not successful. The absorption spectrum of Cf(IV) in this medium is characterized by a broad absorption band beginning at 1030 nm and increasing in intensity down to 390 nm. The maximum absorption appears at about 450 nm, which is similar to the absorption maximum obtained for Cm(IV) and Tb(IV) in this medium (Myasoedov, 1982). The absorption of a comparable Cf(III) phosphotungstate solution did not show a significant absorbance over this spectral region.

11.9 GAS-PHASE STUDIES

In addition to studies in the solid phase and in solution, investigations of reactions in the gas phase provide important insights into the chemistry and electronic make-up of californium. These studies in the gaseous state examine the reactions of Cf ions with other molecules, as opposed to addressing the vaporization of the metal (see Section 11.6), or other solids such as oxides (see Section 11.7.3), which can provide important thermodynamic parameters for these materials (i.e. their enthalpies of vaporization and formation).

The gas-phase chemistry of californium has been studied by mass spectrometry time-of-flight, and Fourier transform ion resonance mass spectrometry (FTIRMS), and the latter offers an especially powerful technique in this regard. In this technique, metal ions can be isolated and then reacted with other specific materials, which can lead to bond dissociation energies, reaction kinetics, and ionization potentials for the metal ions being studied. Important information about californium's electronic configuration, which can be used for systematic comparisons with other actinides, is also be obtained from these gas-phase reactions.

One area of this californium gas-phase chemistry has involved the dehydrogenation of alkenes, thiols, ethers, and perfluorohydrocarbons by Cf^+ (Gibson and Haire, 2000). The emphasis in that work was on the efficiency of dehydrogenation of alkenes by Cf^+ ions, and direct comparisons with the comparable reactivities of Cm^+, Pr^+, and Tm^+ for similar reactions. It was determined that Cf^+ is inefficient at C–H bond activation, due to its particular electronic structure and energy levels, and evidence was not found for the direct participation of its 5f electrons in the reactions studied.

In related studies, organometallic ions of californium were produced in the gas phase by laser ablation of Cf_2O_3 dispersed in polyimide matrices. This process was followed by mass spectrometric analyses (Gibson and Haire, 2001). Primary products formed were: CfC_2H^+, $CfCN^+$, CfC_4H^+, $Cf(OH)(CN)^+$, $CfOCN^+$, $CfOH^+$, $Cf(OH)_2^+$, and CfO^+. Some of these products represent the first organometallic materials for californium where it is directly bonded to carbon. It was concluded that the composition and abundance of the products are dependent on the ability of californium to have two non–5f valence electrons at the Cf^+ center for participation in the bonding, which involves a single sigma-type bond with the organic material. Thus californium exhibits 'monovalent character' (one direct actinide–carbon bond; as do americium and berkelium) versus 'divalent character' of thorium, uranium, neptunium, plutonium, and curium (two direct actinide-carbon bonds)

This behavior is electronically orientated and associated with the $f \rightarrow d$ promotion energies of the actinides to give a chemically active 6d orbital. As the promotion energy for californium is higher (i.e. ~ 200 kJ mol^{-1}, see Fig. 11.10) than earlier actinides, this diminishes the generation of reaction products for it. More recent work with Cf^+ and Es^+ (see Chapter 12) has shown that a greater reactivity is observed with pentamethylcyclopentadiene than with most other alkenes. It was found that Cf^+ reacts with this reagent to produce $[MCp^*]^+$ and other products. This behavior of Cf^+ allows estimates for low-lying electronic levels (Gibson and Haire, 2005).

In studies of californium with several alkenes (Gibson and Haire, 2004), it was determined that the relative C–H activation of Cf^+ was $<1\%$ of that for Cm^+. Thus, instead of C–H activation from insertion of the metal center into a

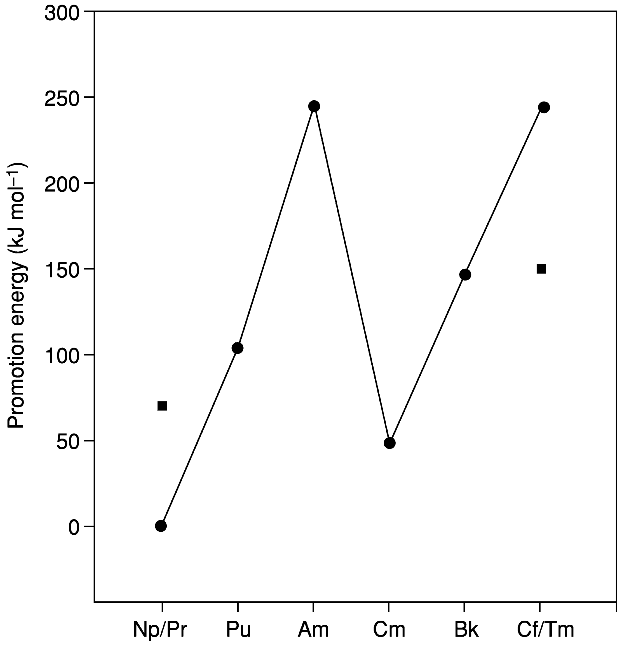

Fig. 11.10 *The f–d promotion energies for selected actinides. Values for Pr and Tm (solid blocks) are given for comparison. (Gibson,* 2003).

C–H bond (i.e. C–Cf^+–H), reactions of Cf^+ with butryonitrile produces an adduct, M^+-butrynitrile. Californium also resisted the formation of CfO^+ ions, consistent with its preference to be 'divalent' rather than 'trivalent' – attempts to oxidize Cf^+ with N_2O to yield CfO^+ in the gas phase were not successful.

In reactions of Cf^+ with perfluorophenanthrene (Gibson and Haire, 2005) only minor yields of CfF_2^+ were observed, again in accord with its propensity to remain divalent. This is also in accord with results noted in the vaporization of Cf_2O_3 at high-temperatures (Haire, 1994). Very little CfO is found in the vapor state as compared to atomic Cf vapor (see Section 11.7.3). This latter behavior is similar to that observed with Eu_2O_3 and Yb_2O_3 and results from the lower dissociation energy of CfO compared to CmO (Haire, 1994). The dissociation energies of the monoxides are also linked to the f–d promotion energies for f-electrons and the formation and availability of active 6d orbital–7s electron orbitals (Haire, 1994; Gibson, 2003).

11.10 CONCLUDING REMARKS

A considerable quantity of chemical and physical data have been acquired for californium over the years. In many instances this information was obtained using tracer levels or microgram quantities of the element, often using the ^{252}Cf isotope. With the availability of multi-milligram amounts of ^{249}Cf isotope, it became possible to expand studies of californium and prepare pure samples of the metal. This allowed important information to be obtained for californium; acquiring the enthalpy of solution (Fuger *et al.*, 1984) and the sublimation of californium metals (Ward *et al.*, 1980) are two such examples. These data then allowed thermodynamic cycles to be established for the element and many of its compounds.

Given the limited supplies of ^{249}Cf (i.e. perhaps a total of some 50–100 mg exist) as well as other experimental limitations (given its radioactive decay process, the accompanying heat, personnel radiation exposures, etc.) it may not be possible to perform all the desired experiments or to be able to carry them out to the degree of perfection that may be desired. However, californium is the element with the highest atomic number in the periodic table expected to be available in weighable amounts (milligrams) and that has a reasonably long half-life. This allows many studies with it that cannot be done with higher members of the actinide series or periodic table. The next element, einsteinium (see Chapter 12) is available in only multi-microgram amounts, but its very high specific radioactivity and the short half-lives of its isotopes severely limit the experiments can be performed with it. Therefore, data on californium can provide insights/extrapolations into the chemical/physical properties of the higher members of the actinide series, in addition to the importance of its own data in providing a better understanding of the architecture of the periodic table.

Oxidation states of 0, II, III, and IV have been established for Cf, with the III state being the most prevalent and the only state presently known to have a reasonable stability in aqueous solutions. The existence of Cf(V) has been suggested but needs confirmation. In may be more probable to generate this oxidation state in solids or nonaqueous solutions and/or molten salts than in aqueous solutions. Future investigations of californium may place emphasis on stabilizing oxidation states other than Cf(III).

Studies of californium in the gaseous state offer important new thrusts in californium chemistry. Using ion cyclotron resonance mass spectrometry, californium ions can be selected, held, and then reacted with a variety of materials to establish important parameters, thermodynamic properties, bond dissociation energies, reaction kinetics, etc.

Although a considerable amount of information has been acquired for californium metal, there are still unanswered questions about it, for example, concerning a potential divalent form of the metal under certain conditions. Recent high-pressure diffraction studies on the metals have provided important new aspects about the behavior of their 5f electrons under pressure and reduced interatomic distances. Indeed, under these very high pressures (i.e. 100 GPa or higher), the electronic nature of californium metal changes, and it adopts lower-symmetry structures normally displayed by the lighter actinide metals (Pa–Pu), which have itinerant 5f electrons at atmospheric pressure. These high pressures on californium metal forces the involvement of its 5f electrons into its bonding and changes its physical properties. Thus, pressure can bring about a form of modern alchemy in californium metal with regard to its structure and properties.

There is also a considerable amount of work that can be done on californium compounds, such as the monopnictides and chalcogenides – the mononitride and monosulfide both offer interesting compounds to study in detail. Investigations of its compounds under high pressure should also provide new findings about californium's chemistry. Applying modern tools (synchrotron-based, EXAFS, XANES, photon scattering, etc.) offers the potential to learn new facets about californium materials.

In short, there is a considerable amount of scientific work that needs to be done on californium, perhaps the highest atomic numbered element available for performing the usual actinide studies. The scope of such studies will be limited only by the imagination and skill of the investigators.

ACKNOWLEDGMENTS

The author gratefully acknowledges the assistance of several personnel at the Oak Ridge National Laboratory, as well as other institutions, for helpful discussions, references, comments, and in some cases collaborative studies on californium. The research reported herein was sponsored by the Division of Chemical Sciences, U.S. Department of Energy, under contract DE-AC05-00OR22725 with UT-Battelle, LLC.

REFERENCES

Adar, S., Sjoblom, R. K., Barnes, R. F., Fields, P. R., Hulet, E. K., and Wilson, H. D. (1963) *J. Inorg. Nucl. Chem.*, **25**, 447–52.

Ahmad, I. (1980) *Abstr. Pap. Am. Chem. Soc.*, **179** (Mar) 122-NUCL.

Ahrland, S. (1991) in *Handbook on the Chemistry and Physics of the Actinides,* vol. 6 (eds. A. J. Freeman and C. Keller), North-Holland, New York, pp. 471–510.

Aizenberg, M. I., Fedoseev, E. V., and Travnikov, S. S. (1988) *Sov. Radiochem.*, **30**(3), 299–302.

Aleksandrov, B. M., Malysheva, L. P., Savoskina, G. P., Smirnova, E. A., and Krivokhat-skii, A. S. (1972) *Radiokhimiya*, **19**, 472–7.

Allen, J. W., Johanson, L. I., Bauer, R. S., and Lindau, I. (1978) *Phys. Rev. Lett.*, **41**, 1499–502.

Aly, H. F. and Latimer, R. M. (1970) *Radiochim. Acta*, **14**, 27–31; and (1979) in *Actinide Chemistry and Spectroscopy* (ed. N. M. Edelstein) (ACS Symp. Ser. 131), American Chemical Society, Washington, DC, pp. 199–220.

Aly, H. F. and Abdelras, A. A. (1972) *Z. Anorg. Allg. Chem.*, **387**(2), 252–7.

Asprey, L. B. (1970) unpublished results; cited in Baybarz, Haire and Fahey (1972) *J. Inorg. Nucl. Chem.*, **35**, 1171–7.

Asprey, L. B. and Haire, R. G. (1973) *Inorg. Nucl. Chem. Lett.*, **9**, 1121–8.

Assefa, Z., Yaita, T., Haire, R. G., and Tachimori, S. (2005) *J. Solid State Chem.*, **178**, 505–11.

Bakiev, S. A., Kist, A. A., Rakhmanov, Z., and Flitsiyan, E.S. (1991) *J. Radioanal. Nucl. Chem.*, **147**(1), 59–68.

Baring, A.M. and Smith, J. L. (2000) USDOE Report LA-UR-00-4100, pp. 90–128.

Barketov, E. S., Zaitsev, A. A., and Felermonov, V. T. (1975) *Sov. Radiochem.*, **17**, 383–7.

Barnanov, A. A., Simakin, G. A., Kosyakov, V. N., Rin, E. A., Kopytov, V. V., Timofeev, G. A., and Rykov, A. G. (1981) *Radiokhimiya*, **23**(1), 127–9; (1981) *Sov. Radiochem.*, **23**, 104–6.

Bärnighausen, H. (1976) in *Proc. 12th Rare Earth Research Conf.* (ed. C. E. Lundin), Vail, Colo., July 1976, pp. 404–13.

Baybarz, R. D., Weaver, B. S., and Kinser, H. B. (1963) *Nucl. Sci. Eng.*, **17**, 457–62.

Baybarz, R. D. (1965) *J. Inorg. Nucl. Chem.*, **2**, 1831–9.

Baybarz, R. D. (1966a) *J. Inorg. Nucl. Chem.*, **28**, 23–31.

Baybarz, R. D. (1966b) *J. Inorg. Nucl. Chem.*, **28**, 1055–61.

Baybarz, R. D. (1967) USAEC Report ORNL-4145, p. 225.

Baybarz, R. D., Haire, R. G., and Fahey, J. A. (1972) *J. Inorg. Nucl. Chem.*, **34**, 5576–85.

Baybarz, R. D., Knauer, J. B., and Orr, P. B. (1973) USAEC Report ORNL-4672, Oak Ridge National Laboratory.

Baybarz, R. D. (1973) *J. Inorg. Nucl. Chem.*, **35**, 4149–58.

Baybarz, R. D., Fahey, J. A., and Haire, R. G. (1974) *J. Inorg. Nucl. Chem.*, **36**, 2023–7.

Baybarz, R. D. and Haire, R. G. (1976) *J. Inorg. Nucl. Chem.*, Suppl., 7–12.

Beamer, J. L., Mahony, T. D., and Sullivan, M. F. (1974) *Radiat. Res.*, **36**(6), 1295–302.

Belenkll, B. G., Bondarenko, P. V., Gankina, E. S., *et al.* (1991) *Vysokomol Soedin*, A**33**(9), 2020–6.

Benedict, U., Peterson, J. R., Haire, R. G., and Dufour, C. (1984) *J. Phys. F.: Metal Phys.*, **14**, L43–7.

Benker, D. E., Chattin, F. R., Collins, E. D., Knauer, J. B., Orr, P. B., Ross, R. G., and Wiggins, J. T. (1981) in *Transplutonium Elements – Production and Recovery* (eds. J. D. Navratil and W. W. Schulz) (ACS Symp. Ser. 161), American Chemical Society, Washington, DC, pp. 161–72.

Berger, H. (2004) *Appl. Radiat. Isot.*, **61**(4), 437–42.

Bhattacharyya, P. K. Natarajan, R. and (1991) in *Handbook on the Chemistry and Physics of the Actinides,* vol. 6 (eds. A. J. Freeman and C. Keller), North-Holland, New York, pp. 597–640.

Bigelow, J. E. (1974) in *Gmelin Handbuch der Anorganischen Chemie*, Suppl. Ser., *Transuranium*, Springer-Verlag, New York, vol. 7b, part Al, II, The Elements, pp. 326–36.

Bigelow, J. E., Collins, E. D., and King, L. J. (1980) in *Actinide Separations* (eds. J. D. Navratil, and W. W. Schulz) (ACS Symp. Ser. 117), American Chemical Society, Washington, DC, pp. 147–55.

Bigelow, J. E., Corbett, B. L., King, L. J., McGuire, S. C., and Sims, T. M. (1981) in *Transplutonium Elements – Production and Recovery* (eds. J. D. Navratil and W. W. Schulz) (ACS Symp. Ser. 161), American Chemical Society, Washington, DC, pp. 3–18.

Biggs, F., Mendelsohn, L. B., and Mann, J. B. (1975) *At. Data Nucl. Data Tables*, **16**, 201–309.

Blaise, J. and Wyart, J. F. (1992) Energy levels and atomic spectra of actinides, in *International Tables of Selected Constants*, Curie University, Paris, pp. 401–7; and the WEB, www.lac.u-psud.fr/Database/Tab-energy-californium.

Bouissières, G., Jouniaux, B., Legoux, Y., Merinis, J., David, F., and Samhoun, K. (1980) *Radiochem. Radioanal. Lett.*, **45**(2), 121–8.

Brandau, E. (1971) *Inorg. Nucl. Chem. Lett.*, **7**, 1177–81.

Brewer, L. (1971a) *J. Opt. Soc. Am.*, **61**, 1101–11.

Brewer, L. (1971b) *J. Opt. Soc. Am.*, **61**, 1666–82.

Brooks, M. S. S., Johansson, B., and Skriver, H. L. (1984) in *Handbook on the Physics and Chemistry of the Actinides* (eds. A. J. Freeman and G. H. Lander), North-Holland, New York, pp. 153–271.

Brown, D. (1968) in *Halides of the Lanthanides and Actinides*, John Wiley, London, pp. 48–78.

Burns, J. H., Peterson, J. R., and Baybarz, R. D. (1973) *J. Inorg. Nucl. Chem.*, **35**(4), 1171–7.

Burns, J. H., Peterson, J. R., and Stevenson, S. N. (1975) *J. Inorg. Nucl. Chem.*, **37**, 743–9.

Burns, J. B., Haire, R. G., and Peterson, J. R. (1998) *J. Alloys. Compd.*, **271**, 676–9.

Caird, J. A., Hessler, J. P., Paszek, A. P., Carnall, W. T., Crosswhite, H. M., Crosswhite, H., Diamond, H., and Williams, C. W. (1976) *Bull. Am. Phys. Soc.*, **21**, 1284–7.

Californium (^{252}Cf) Progress Reports and Bibliography are available from: (a) Californium Information Center, Savannah River Laboratory, Aiken, SC 29801, USAEC Report 1969; (b) Oak Ridge User Facility, Oak Ridge, TN 37831.

Campbell, D. O. (1981) in *Transplutonium Elements – Production and Recovery* (eds. J. D. Navratil and W. W. Schulz) (ACS Symp. Ser. 161), American Chemical Society, Washington, DC, pp. 189–202.

Carlson, T. A. and Nestor, C. W. Jr (1977) *At. Data Nucl. Data Tables*, **19**(2), 15373.

Carnall, W. T., Fried, S. M., Wagner, F. Jr, Barnes, R. F., Sjoblom, R. K., and Fields, P. R. (1972) *Inorg. Nucl. Chem. Lett.*, **8**, 773–4.

Carnall, W. T., Fried, S., and Wagner, F. Jr (1973) *J. Chem. Phys.*, **58**, 1938–49.

Carnall, W. T. and Fried, S. (1976) in *Proc. Symp. Commemorating the 25th Anniversary of the Elements 97 and 98*, Lawrence Berkeley Laboratory LBL-Report 4366, pp. 61–9.

Carnall, W. T., Crosswhite, H. M., Crosswhite, H., Hessler, J. P., Aderhold, C., Caird, J. A., Paszek, A., and Wagner, F. W. (1977) in *Proc. 2nd Int. Conf. on Electronic Structure of the Actinides* (eds. J. Mulak, W. Suski, and R. Troc), Wroclaw, Poland, pp. 105–10.

Carter, F. L. (1979) *J. Physique*, Suppl. **C–4**, 228–9.

Carvalho, F. P. and Fowler, S. W. (1985) *Mar. Biol.*, **89**(2), 173–81.

Castro, J. R., Oliver, G. D., and Withers, H. R. (1973) *Am J. Roentgenol.*, **117**(1), 182–94.

Cebulska- Wasilewska, A., Rekas, K., and Kim, J. K. (1999) *Nukleonika* **44**(1), 15–30.

Chakravortty, V., Perevalov, S. A., and Kulyako, Y. M. (1989) *J. Radioanal. Nucl. Chem. Lett.*, **136**(2), 85–94.

Chang, C. T. P, Haire, R. G., and Nave, S. E. (1990) *Phys. Rev.*, **B41**(13-A), 9045–8.

Chen, M. H., Crasemann, B., Huang, K.-N., Aoyagi, M., and Mark, H. (1977) *At. Data Nucl. Data Tables*, **19**(2), 97–151.

Choppin, G. R., Harvey, B. G., and Thompson, S. G. (1956) *J. Inorg. Nucl. Chem.*, **2**, 66–8.

Choppin, G. R. and Ketels, J. (1965) *J. Inorg. Nucl. Chem.*, **27**, 1335–9.

Choppin, G. R. and Schneider, J. K. (1970) *J. Inorg. Nucl. Chem.*, **32**, 3283–8.

Choppin, G. R. and Degischer, G. (1972) *J. Inorg. Nucl. Chem.*, **34**, 3473–7.

Choppin, G. R. and Unrein, P. J. (1976) in *Transplutonium 1975* (eds. W. Müller and R. Lindner), North-Holland, New York, 97–107.

Chudinov, E. G. and Pirozhkov, S. V. (1973) *Sov. Radiochem.*, **15**, 195–9.

Cohen, L. H., Aten, A. H. W. Jr, and Kooi, J. (1968) *Inorg. Nucl. Chem. Lett.*, **4**, 249–52.

Coleman, C. F. (1972) *J. Inorg. Nucl. Chem.*, **34**, 1381–97.

Collins, E. D., Benker, D. E., Chattin, F. R., Orr, P. B., and Ross, R. G. (1981) in *Transplutonium Elements – Production and Recovery* (eds. J. D. Navratil and W. W. Schulz) (ACS Symp. Ser. 161), American Chemical Society, Washington, DC, pp. 147–60.

Conway, J. G., Bruger, J. B., Hulet, E. K., Morrow, R. J., and Gutmacher, R. G. (1962a) *J. Chem. Phys.*, **36**, 189–90.

Conway, J. G., Hulet, E. K., and Morrow, R. J. (1962b) *J. Opt. Soc. Am.*, **52**, 222.

Conway, J. (1976) in *Proc. Symp. Commemorating the 25th Anniversary of the Elements 97 and 98*, Lawrence Berkeley Report LBL 4366, pp. 70–5.

Conway, J. G., Worden, E. F., Blaise, J., and Verges, J. (1977) *Spectrochim. Acta B*, **32**, 97–9.

Conway, J. G., Worden, E. F., and Blaise, J. (1995) *J. Opt. Soc. Am.*, **B12**(7), 1186–202.

Copeland, J. C. and Cunningham, B. B. (1969) *J. Inorg. Nucl. Chem.*, **31**, 733–40.

Crosswhite, H. M. (1977) *Coll. Int. CNRS*, Spectroscopie des Eléments de Transition et des Elements Lourds dans les Solides, Editions du CNRS, Paris, pp. 65–9.

Cunningham, B. B. (1959) *J. Chem. Educ.*, **36**, 32–7.

Cunningham, B. B. and Ehrlich, P. (1970) USAEC Report UCRL-205426, p. 239.

Cunningham, B. B. and Parsons, T. C. (1970) USAEC Report UCRL-205426, pp. 239–40.

Cunningham, B. B., Morss, L. R., and Parsons, T. C. (1970) USAEC Report UCRL-19530, p. 276.

Damien, D. A., Haire, R. G., and Peterson, J. R. (1979) *J. Physique*, Suppl. **C–4**, 95–100.

Damien, D., Haire, R. G., and Peterson, J. R. (1980) *Inorg. Nucl. Chem. Lett.*, **16**, 537–41.

Damien, D., Haire, R. G., and Peterson, J. R., unpublished data.

David, F. and Bouissières, G. (1968) *Inorg. Nucl. Chem. Lett.*, **4**, 153–9.

David, F. (1970a) *C. R. Acad. Sci. Paris C*, **270**, 2112–15.

David, F. (1970b) *Radiochem. Radioanal. Lett.*, **5**, 279–85.

David, F. (1970c) *Rev. Chim. Minér.*, **7**, 1–10.

David, F. (1986) *J. Less-Common Metals*, **121**, 27–42.

David, F., Samhoun, K., and Guillaumont, R. (1976a) in *Transplutonium 1975* (eds. W. Müller and R. Lindner), North-Holland, Amsterdam, pp. 297–304.

David, F., Samhoun, K., Guillaumont, R., and Nugent, L. J. (1976b) in *Heavy Element Properties* (eds. W. Müller and H. Blank), North-Holland, New York, pp. 97–104.

David, F., Samhoun, K., Guillaumont, R., and Edelstein, N. (1978) *J. Inorg. Nucl. Chem.*, **40**, 69–74.

David, F., Maslennikov, A. G., and Peretrukhin, V. P. (1990a) *J. Radioanal. Nucl. Chem.*, **143**(2), 415–26.

David, F., Peretrukin, V. F., and Maslennikov, A. G. (1990b) *Radiochim. Acta.*, **50**(3), 151–4.

De Carvalho, R. H. and Choppin, G. R. (1967) *J. Inorg. Nucl. Chem.*, **29**, 725–36.

Dedov, V. B., Trukhlyaev, P. S., and Kalinichenko, B. S. (1986a) *Sov. Radiochem.*, **28**(5), 579–82.

Dedov, V. B., Trukhlyaev, P. S., and Kalinichenko, B. S. (1986b) *Sov. Radiochem.*, **28**(5), 583–6.

Derevyanko, E. P., Pirozkhov, S. V., and Chudinov, E. G. (1976) *Sov. Radiochem.*, **17**(2), 295–9.

Desiré, B., Hussonnois, M., and Guillaumont, R. (1969) *C. R. Acad. Sci. Paris C*, **269**, 448–51.

Dittner, P. E. and Bemis, C. E. (1972) *Phys. Rev. A*, **5**(2), 481–8.

Dullmann, C. E., Eichler, B., Eichler, R. *et al.* (2003) *Nucl. Instrum. Method A*, **512**(3), 595–605.

Eberle, S. H. and Bayat, I. (1967) *Radiochim. Acta*, **7**, 214–17.

Eberle, S. H. and Ali, S. A. (1968) *Z. Anorg. Allg. Chem.*, **361**, 1–14.

Edelstein, N. and Karraker, D. (1976) in *Proc. Symp. Commemorating the 25th Anniversary of Elements 97 and 98*, Lawrence Berkeley Laboratory Report LBL4366, pp. 75–84; and (1975) *J. Chem. Phys.*, **62**, 3–8.

Eichler, B., Hubener, S., and Erdmann, N. (1997) *Radiochim. Acta*, **79**(4), 221–33.

Elesin, A. A., Nikolaev, V. M., and Shalimov, V. V. (1986) *Sov. Radiochem.*, **28**, 723–6.

Erdmann, N., Nunnemann, M., Eberhardt, K., Herrmann, G., Huber, G., Kohlër, S., Kratz, J. V., Passler, G., Peterson, J. R., Trautmann, N., and Waldek, A. (1998) *J. Alloys Compd.*, **271–273**, 837–40.

Erin, E. A., Vityutnev, V. M., and Kopytov, V. V. (1981) *Sov. Radiochem.*, **23**(3), 277–80.

Ermakov, V. A. and Stary, J. (1967) *Sov. Radiochem.*, **9**, 195–8.

Ermakov, V. A., Vorob'eva, V. V., Zaitsev, A. A., and Yakovlev, G. N. (1971) *Sov. Radiochem.*, **13**, 710–13.

Feinauser, D. and Keller, C. (1969) *Inorg. Nucl. Chem. Lett.*, **5**, 625–30.

Ferris, L. M. and Mailen, J. C. (1970) *J. Inorg. Nucl. Chem.*, **32**, 2019–35.

Ferris, L. M. and Mailen, J. C. (1971) *J. Inorg. Nucl. Chem.*, **33**, 1325–35.

Fields, P. R., Wybourne, B. G., and Carnall, W. T. (1964) Argonne National Laboratory Report ANL-6911.

Filippov, E. M. (1979) *Sov. At. Energy*, **47**(4), 841–3.

Firsova, L. A., Chuveleva, E. A., and Kharitonov, O. V. (1990) *Sov. Radiochem.*, **32**(2), 372–5.

Firsova, L. A., Chuveleva, E. A., and Kharitonov, O. V. (1996) *Radiochemistry*, **38**(5), 407–9.

Firsova, L. A., Chuveleva, E. A., and Kharitonov, O. V. (1998) *Radiochemistry*, **40**(3), 254–6.

Florjan, D., Niedzwiedz, W., and Schneider (1999) *Neoplasma*, **46** (Suppl. S), 88–9.

Frenkel, V. Y., Kulyako, Y. M., and Chistyakov, V. M. (1986) *J. Radioanal. Nucl. Chem.*, **104**(4), 191–200.

Fried, S. and Cohen, A. (1968) *Inorg. Nucl. Chem. Lett.*, **4**, 611–15.

Fried, S., Cohen, D., Siegal, S., and Taire, B. (1968) *Inorg. Nucl. Chem. Lett.*, **4**, 4948.

Fried, S. M., Wagner, F. Jr, and Carnall, W. T. (1973) Argonne National Laboratory Report ANL-7996, p. 5.

Friedman, H. A., Stokely, J. R., and Baybarz, R. D. (1972) *Inorg. Nucl. Chem. Lett.*, **8**, 433–41.

Fu, K. and Phillips, T. L. (1973) *Radiat. Res.*, **55**(3), 605.

Fuger, J. (1958) *J. Inorg. Nucl. Chem.*, **5**, 332–8.

Fuger, J. (1975) in *MTP International Review of Science,* (eds. H. J. Emeleus and K. W. Bagnall), Inorganic Chemistry, ser. II, vol. 7 , Butterworths, London, pp. 151–94.

Fuger, J., Haire, R. G., and Peterson, J. R. (1984) *J. Less Common Metals*, **98**, 315–21.

Fuger, J., Haire, R. G., and Wilmarth, W. R. (1990) *J. Less Common Metals*, **158**(1), 99–104.

Fuger, J. and Matzke, H. J. (1991) in *Handbook on the Chemistry and Physics of the Actinides* vol. 6 (eds. A. J. Freeman and C. Keller), North-Holland, New York, pp. 641–84.

Fujita, D. K. and Cunningham, B. B. (1969) USAEC Report UCRL-19507, p. 136.

Fujita, D. K., Parsons, T. C., Edelstein, N., Noé, M., and Peterson, J. R. (1976) in *Transplutonium Elements 1975* (eds. W. Müller and R. Lindner), North-Holland, Amsterdam, pp. 173–9.

Gavrilov, K. A., Gwozdz, E., Stary, J., and Seng, W. T. (1966) *Talanta*, **13**, 471–6.

Ghiorso, A. (1983) *Int. J. Mass Spectrom.*, **53**, 21–6.

Gibson, J. K. and Haire, R. G. (1985) *Radiochim. Acta*, **38**(4), 193–6.

Gibson, J. K. and Haire, R. G. (1987) *J. Less Common Metals*, **127**, 257–67.

Gibson, J. K. and Haire, R. G. (2000) *Int. J. Mass Spectrom.*, **203**(1–3), 127–42.

Gibson, J. K. and Haire, R. G. (2001) *Radiochim. Acta*, **89**(6), 363–9.

Gibson, J. K. (2003) *J. Phys. Chem.* A **107**, 7891–9.

Gibson, J. K. and Haire, R. G. (2004) *J. Alloys and Compounds*, **363**, 112–16.

Gibson, J. K. and Haire, R. G. (2005) *Organometallics*, **24**, 119–26.

Goldman, S. and Morss, L. R. (1975) *Can. J. Chem.*, **53**, 2685–700.

Green, J. L. (1965) PhD Thesis, UCRL Report 16516, pp. 41–9.

Green, J. L. and Cunningham, B. B. (1966) *Inorg. Nucl. Chem. Lett.*, **2**, 365–71. 157.

Green, J. L. and Cunningham, B. B. (1967) *Inorg. Nucl. Chem. Lett.*, **3**, 43–9.

Gruen, D. M., Koehler, W. C., and Katz, J. J. (1951) *J. Am. Chem. Soc.*, **73**, 1475–9.

Guillaumont, R. and Bourderie, L. (1971) *Bull. Soc. Chim. Fr.*, **8**, 2806–9.

Guminski, C. (1996) *J. Phase Equilib.*, **17**(5), 443–4.

Guseva, L. I., Myasoedov, B. F., and Tikhomir, G. S. (1973) *J. Radioanal. Chem.*, **13**(2), 292–300.

Haire, R. G., Baybarz, R. D., and Fahey, J. A. (1972) *Inorg. Nucl. Chem.*, **34**, 557–62.

Haire, R. G. and Asprey, L. B. (1973) *Inorg. Nucl. Chem. Lett.*, **9**, 869–74.

Haire, R. G. and Baybarz, R. D. (1973a) *J. Inorg. Nucl. Chem.*, **35**, 489–96.

Haire, R. G. and Baybarz, R. D. (1973b) *Inorg. Nucl. Chem. Lett.*, **9**, 1121–4.

Haire, R. G. and Baybarz, R. D. (1974) *J. Inorg. Nucl. Chem.* **36**, 1295–302.

Haire, R. G. and Baybarz, R. D. (1979) Proc. 3rd International Conference on Electronic Structure of the Actinides, *J. de Physique Suppl.* C4 195.

Haire, R. G. (1974) USAEC Report 4966, p. 19.

Haire, R. G. and Asprey, L. B. (1975) *Proc. Berkelium and Californium Symposium*, Berkeley, CA, Jan. 20, 1975.

Haire, R. G. and Asprey, L. B. (1976) *Inorg. Nucl. Chem. Lett.*, **12**, 73–84.

Haire, R. G. (1976) in *Proc. 12th Rare Earth Research Conf.*, vol. II (ed. C. E. Lundin), Vail, Colo., July 1976, Denver Research Institute, pp. 584–93.

Haire, R. G., Young, J. P., Peterson, J. R., and Fellows, R. L. (1978) in *The Rare Earths in Modern Science and Technology* (eds. G. J. McCarthy and J. J. Rhyne), Plenum, New York, pp. 501–6.

Haire, R. G. (1978) USDOE Report ORNL–5485, p. 52; (1980) USDOE Report ORNL-5665, p. 71; and (1981) USDOE Report–5817, p. 65.

Haire, R. G., Young, J. P., Peterson, J. R., Ensor, D. D., and Asprey, L. B. (1980) unpublished data, presented at SE/SW Regional ACS Meeting, December 1980, New Orleans.

Haire, R. G. (1982) in *Actinides in Perspective* (ed. N. Edelstein), Pergamon Press, New York, pp. 309–42.

Haire, R. G., Benedict, U., Peterson, J. R., Dufour, C., and Dabos, S. (1986) *Physica*, **144B**, 19–22.

Haire, R. G. (1988) USDOE Report ORNL-5485, 52.

Haire, R. G. and Gibson, J. K. (1989) *J. Radioanal. Nucl. Chem.*, **143**(1), 35–51.

Haire, R. G. (1990) in *Metals Handbook*, ASM International, Materials Park, OH, pp. 1198–201.

Haire, R. G. (1994) *J. Alloys Compd.*, **213**, 185–90.

Haire, R. G. and Eyring, L. (1994) in *Handbook on the Physics and Chemistry of the Rare Earths* (eds. K. A. Gschneidner, L. Ewing, G. R. Choppin, and G. H. Lander), North-Holland, Amsterdam, pp. 449–505.

Haire, R. G. (1997) *J. Nucl. Mat.*, **247**, 1–6.

Haire, R. G. and Sato, T. (1998) unpublished work.

Haire, R. G., Raison, E. P., and Assefa, Z. (2002) *J. Nucl. Sci. and Technol.*, **3** (Suppl.), 616–19.

Haire, R. G., Heathman, S., Le Bihan, T., Lindbaum, A., and Iridi, M. (2004) *Mat. Res. Symp. Proc.*, **802**, 15–21.

Hannink, N. J., Hoffman, D. C., and Smith, B. F. (1992) *Solvent Extr. Ion Exch.*, **10**(3), 431–8.

Haschke, J. M. (1976) *Inorg. Chem.*, **15**, 298–303.

Haug, H. W. and Baybarz, R. D. (1975) *Inorg. Nucl. Chem. Lett.*, **11**, 847–55.

Haung, K., Aoyagi, M., Chen, M. H., Crasemann, B., and Mark, H. (1976) *At. Data Nucl. Data Tables*, **18**, 243–91.

Healy, T. V. and McKay, H. A. C. (1956) *Rec. Trav. Che. Pay-Bas*, **75**, 730–6.

Heathman, S., Haire, R. G., Le Bihan, T., Lindbaum, A., Litfin, K., Mèresse, Y., and Libotte, H. (2000) *Phys. Rev. B*, **63**, 214101.

Hessler, J. P., Caird, J. A., Carnall, W. T., Crosswhite, H. M., Sjoblom, R. K., and Wagner, F. Jr (1978) in *The Rare Earths in Modern Science and Technology* (eds. G. J. McCarthy and J. J. Rhyne), Plenum, New York, pp. 507–12.

Hessler, J. P. and Carnall, W. T. (1980) in *Lanthanide and Actinide Chemistry and Spectroscopy* (ed. N. M. Edelstein) (ACS Symp. Ser. 131), American Chemical Society, Washington, DC, pp. 349–68.

Hobart, D. E., Samhoun, K., Young, J. P., Norvell, V. E., Mamantov, G., and Peterson, J. R. (1981) *Inorg. Nucl. Chem. Lett.*, **16**, 321–8.

Hobart, D. E., Samhoun, K., and Peterson, J. R. (1982) *Radiochim. Acta*, **31**, 139–45.

Hobart, D. E., Varlashkin, P. G., Samhoun, K., Haire, R. G., and Peterson, J. R. (1983) *Rev. Chim. Minér.*, **20**, 817–27.

Horwitz, E. P., Bloomquist, C. A., Sauro, L. J., and Henderson, D. J. (1966) *Inorg. Nucl. Chem.*, **28**(10), 2313–24.

Horwitz, E. P., Sauro, L. J., Bloomquist, C. A. (1967) *Inorg. Nucl. Chem.*, **29**(8), 2033–46.

Horwitz, E. P., Bloomquist, C. A., Henderson, D. J. (1969a) *Inorg. Nucl. Chem.*, **31**(4), 1149–59.

Horwitz, E. P., Bloomquist, C. A., Henderson, D. J., *et al.* (1969b) *Inorg. Nucl. Chem.*, **31**(10), 3255–64.

Horwitz, E. P., Chiarizia, R., and Dietz, M. L. (1992) *Solvent Extr. Ion Exch.*, **10**, 313–16.

Horwitz, E. P., Chiarizia, R., and Dietz, M. L. (1993) *Anal. Chim. Acta*, **281**, 361–7.

Horwitz, E. P., Dietz, M. L., Chiarizia, R., Diamond, H., Maxwell, S. L. III, and Nelson, M. R. (1995) *Anal. Chim. Acta*, **310**, 63–8.

Hübener, S. and Zvara, I. (1982) *Radiochim. Acta*, **31**, 89–93.

Hübener, S., Eichler, B., and Schadel, M. (1994) *J. Alloys Compd.*, **213**, 429–32.

Hubert, S., Hussonnois, M., Brillard, L., Goby, G., and Guillaumont, R. (1974) *J. Inorg. Nucl. Chem.*, **36**(10), 2361–6.

Huray, P. G. and Nave, S. A. (1987) in *Handbook of the Physics and Chemistry of the Actinides,* vol. 2 (eds. A. J. Freeman and G. L. Lander), North-Holland, Amsterdam, pp. 311–72.

Hussonnois, M., Hubert, S., Brillard, L., and Guillaumont, R. (1973) *Radiochem. Radioanal. Lett.*, **15**, 47–56.

Hyde, E. K., Perlman, I., and Seaborg, G. T. (1971) *The Nuclear Properties of the Heavy Elements,* vol. II, Dover, New York, pp. 923–43.

Ionova, G. V., Spitsyn, V. I., and Pershina, V. G. (1980) in *Proc. 10ème Journées des Actinides* (eds. B. Johansson and A. Rosengren), Stockholm, Sweden, May 27–28, 1980, pp. 126–59.

Ionova, G. V., Pershina, V. G., and Suraeva, N. I. (1989a) *Sov. Radiochem.*, **31**(1), 9–14.

Ionova, G. V., Pershina, V. G., and Suraeva, N. I. (1989b) *Sov. Radiochem.*, **31**(4), 379–86.

Ishimori, T. (1980) in *Actinide Separations* (eds. J. D. Navratil and W. W. Schulz) (ACS Symp. Ser. 117), American Chemical Society, Washington, DC, pp. 333–50.

Johansson, B. and Rosengren, A. (1975a) *Phys. Rev. B*, **11**(4), 1367–73.

Johansson, B. and Rosengren, A. (1975b) *Phys. Rev. B*, **11**(4), 2740–3.

Johnson, E. and Fricke, B. (1991) *J. Phys. Chem.*, **95**, 7082.

Jones, A. D. and Choppin, G. R. (1969) *Actinides Rev.*, **1**, 311–36.

Jouniaux, B. (1979) Thesis, University of Paris, pp. 34–86.

Karalova, Z. K., Lavrinovich, E. A., and Myasoedov, B. F. (1990) *Sov. Radiochem.*, **32**(2), 93–6.

Karraker, D. G., and Dunlap, B. D. (1976) *J. Chem. Phys.* **65**, 2032–3.

Karelin, Y. A., Gordeev, Y. N., and Karasev, V. I. (1997) *Appl. Radiat. Isot.*, **48**(10–12), 1563–6.

Kasimov, F. D. and Skobelev, N. F. (1987) *Sov. Radiochem.*, **29**(5), 591–4.

Katz, J. J. and Seaborg, G. T. (1957) *The Chemistry of the Actinide Elements,* John Wiley, New York, pp. 386–99.

Keller, C. and Schreck, H. (1969) *J. Inorg. Nucl. Chem.*, **31**, 1121–32.

Keller, C. (1971) *The Chemistry of the Transuranium Elements,* Verlag Chemie, Weinheim, pp. 217–49 and 565–80.

Khopkar, P. K. and Mathur, J. N. (1977) *J. Inorg. Nucl. Chem.*, **39**, 2063–7.

Kimura, T. and Akatsu, J. (1991) *J. Radioanal. Nucl. Chem.*, **149**(1), 25–31.

King, L. J., Bigelow, J. E., and Collins, E. D. (1981) in *Transplutonium Elements – Production and Recovery* (eds. J. D. Navratil and W. W. Schulz) (ACS Symp. Ser. 161), American Chemical Society, Washington, DC, pp. 133–46.

Knapp, F. F., Beets, A. L., and Mirzadeh, S. (1999) *Czech. J. Phys.*, **49**, 799–809.

Knighton, J. B. and Steunenberg, R. K. (1966) US Patent 3276 861.

Kosyakov, V. N., Timofeev, G. A., Erin, E. A., Kopytov, V. V., and Andreev, V. J. (1977) *Radiokhimiya*, **19**(1), 82–4; (1977) *Sov. Radiochem.*, **19**, 66–7.

Kosyakov, V. N., Erin, E. A., and Vityutnev, V. M. (1982a) *Sov. Radiochem.*, **24**(5), 455–7.

Kosyakov, V. N., Erin, E. A., Vityutnev, V. M., Kopytov, V. V., and Rykov, A. G. (1982b) *Radiokhimiya*, **24**(5), 551–3.

Kovantseva, S. N., Kasimova, V. A., and Filimonov, V. T. (1986) *Sov. Radiochem.*, **28**(2), 174–7.

Krause, M. O., Haire, R. G., Keski-Rahkonen, O., and Peterson, J. R. (1988). *J. Electron Spectrosc. Relat. Phenom.*, **47**, 215–26.

Kulyukhin, S. A., Mikheev, N. B., and Rumer, I. A. (1997) *Radiochemistry*, **39**(2), 130–2.

Laubereau, P. G. and Burns, J. H. (1970a) in *Proc. 8th Rare Earth Research Conf.*, vol. I (T. Henrie and R. Lindstrom), Reno, Nev., pp. 258–65.

Laubereau, P. G. and Burns, J. H. (1970b) *Inorg. Chem.*, **9**, 1091–5.

Lazarev, Y. A., Shirokovsky, I. V., Utyonkov, V. K., *et al.* (1995) *Nucl. Phys.*, **A588**(2), 501–9.

Lebedev, I. A. and Mazur, Y. F. (1981) *Sov. Radiochem.*, **23**(3), 291–9.

Leger, J. M., Yacoubi, N., and Loriers, J. (1980) in *The Rare Earths in Modern Science and Technology,* vol. II (eds. G. J. McCarthy, J. J. Rhyne, and H. B. Silber), Plenum Press, New York, pp. 203–8.

Liu, G. K., Huang, J., and Beitz, J. V. (1993) *Phys. Rev. B*, **48**(18), 13351–60.

Lloyd, R. D., Atherton, D. R., and Taylor, G. N. (1972a) *Radiat. Res.*, **51**(2), 542–7.

Lloyd, R. D., Mays, C. W., and Taylor, G. N. (1972b) *Health Phys.*, **22**(6), 667–71.

Lloyd, R. D., May, C. W., and McFarland, S. S. (1976) *Radiat. Res.*, **65**(3), 462–73.

Luke, H. and Eick, H. A. (1976) in *Proc. 12th Rare Earth Research Conf.* (ed. C. E. Lundin), Vail, Colo., July 1976, Denver Research Institute, pp. 424–32.

Mahony, T. D., Beamer, J. L., and Sullivan, M. F. (1973) *Radiat. Res.*, **55**(3), 606.

Mailen, J. C. and Ferris, L. M. (1971) *Inorg. Nucl. Chem. Lett.*, **7**(5), 431–8.

Maly, J. and Cunningham, B. B. (1967) *Inorg. Nucl. Chem. Lett.*, **3**, 445–51.

Maly, J. (1969) *J. Inorg. Nucl. Chem.*, **31**, 1007–18.

Manson, S. T. and Kennedy, D. J. (1974) *At. Data Nucl. Data Tables*, **14**(2), 111–20.

Marcus, Y., Givon, H., and Choppin, G. R. (1963) *J. Inorg. Nucl. Chem.*, **25**, 1457–63.

Martin, W. C., Hagan, L., Reader, J., and Sugar, J. (1974) *J. Phys. Chem. Ref. Data*, **3**(3), 771–5.

Martin, R. C., Laxson, R. R., and Knauer, J. B. (1997) *Appl. Radiat. Isot.*, **48**(10–12), 1691–5.

Martin, R. C., Byrne, T. E., and Miller, L. F. (1998) *J. Radioanal. Nucl. Chem.*, **236**(1–2), 5–10.

Martin, R. C., Knauer, J. B., and Balo, P. A. (2000) *Appl. Radiat. Isot.*, **53**(4–5), 785–92.

Martin, R. C., Glasgow, D. C., and Martin, M. Z. (2004) in *ACS Symp. Ser. 868*, American Chemical Society, Washington, DC, pp. 88–104.

Maruyama, Y., Feola, J. M., Tai, D., Wison, L. C., Van Nagel, J. R., and Yoneda, J. (1978) *Oncology*, **35**(4), 172–8.

Maruyama, Y., Yoneda, J., and Krolikiewicz, H. (1980) *Int. J. Radiat. Oncol.*, **6**(12), 1629–37.

Maruyama, Y., Vannagell, J. R., and Yoneda, J. (1991) *Cancer*, **68**(6), 1189–97.

McDowell, W. J. and Coleman, C. F. (1972) *J. Inorg. Nucl. Chem.*, **3**, 2837–50.

Miglio, J. J. (1978) *Int. J. Appl. Radiat. Isot.*, **29**(9–10), 581–4.

Mignano, J. and Rivard, M. (2004) *Radiothermodyn. Oncol.*, **71** (Suppl. 2), S77–8.

Mikheev, N. B., Spitsyn, V. I., Kamenskaya, A. N., Rozenkevich, N. A., Rumer, I. A., and Auerman, L. N. (1971) *Radiokhimiya*, **14**, 486–7; (1972) *Sov. Radiochem.*, **14**, 494–5.

Mikheev, N. B., Auerman, L. N., Spitsyn, V. I. (1972a) *Inorg. Nucl. Chem. Lett.*, **8**(10), 869–73.

Mikheev, N. B., Kamenskaia, A. N., Rumer, I. A., Spitsyn, V. I., Diatokova, R. A., and Rosenkevitch, N. A. (1972b) *Radiochem. Radioanal. Lett.*, **9**, 247–54.

Mikheev, N. B., Spitsyn, V. I., Dyachkova, R. A., and Auerman, L. N. (1979) *J. Physique*, **C-4**(Suppl.), 230–2.

Miller, W. (1967) *Actinides Rev.*, **1**, 71–119.

Moore, F. L. (1964) *Anal. Chem.*, **36**, 2158–62.

Moore, F. L. (1966) *Anal. Chem.*, **38**, 510–14.

Moore, J. R., Nave, S. E., Haire, R. G., and Huray, P. G. (1986) *J. Less Common Metals*, **121**, 187–92.

Moore, J. R., Nave, S. E., Haire, R. G. and Hurray, P. G. (1998) Unpublished work presented at the Rare Earths Conference (1988), Lake Geneva, WI, Sept. 12-16.

Morss, L. R. (1983) *J. Less Common Metals*, **93**, 301–21.

Morss, L. R., Fuger, J., Goffart, J., and Haire, R. G. (1983) *J. Less Common Metals*, **127**, 79–85.

Morss, L. R., Fuger, J., Goffart, J., Edelstein, N. M., and Shalimoff, G. V. (1987) *J. Less Common Metals*, **127**, 251–7.

Musikas, C., Haire, R. G., and Peterson, J. R. (1981) *J. Inorg. Nucl. Chem.*, **43**, 2935–41.

Myasoedov, B. F., Guseva, L. I., Lebedev, I. A., Milyukova, M. S., and Chmutova, M. K. (1974) in *Analytical Chemistry of Transplutonium Elements* (ed. D. Slutzk), John Wiley, New York, pp. 122–32.

Myasoedov, B. F., Chmutova, M. K., and Karalova, Z. K. (1980) in *Actinide Separations* (eds. J. D. Navratil and W. W. Schulz) (ACS Symp. Ser. 117), American Chemical Society, Washington, DC, pp. 101–15.

Myasoedov, B. F. (1982) in *Actinides in Perspective* (ed. N. M. Edelstein), Pergamon Press, New York, pp. 509–40.

Myasoedov, B. F., Leedev, I. A., Khizhnyak, P. L. Timofeev, G. A., and Frenkel, V. Y. A. (1986) *J. Less Common Metals*, **122**, 189–93.

Myasoedov, B. F. and Lebedev, I. A. (1991) in *Handbook on the Chemistry and Physics of the Actinides,* vol. 6 (eds. A. J. Freeman and C. Keller), North-Holland, Amsterdam, pp. 551–96.

Nave, S. E., Haire, R. G. and Hurray, P. G. (1981) Actinides-81 Conference abstracts, Asilomar, CA., Sept. 10-15, p. 144.

Nave, S. E., Haire, R. G., and Huray, P. G. (1983) in USDOE Report ORNL-5954, pp. 63–5.

Nave, S. E., Haire, R. G., and Huray, P. G (1984) in *Proc. Conf. on Electronic Structure and Properties of Rare Earth and Actinide Intermetallics*, St. Polten, Austria, Sept. 3–6, pp. 220–7.

Nave, S. E., Moore, J. R., Spaar, M. T., Haire, R. G., and Huray, P. G. (1985) *Physica B*, **130B**, 225–7.

Nave, S. E., Moore, J. R., Haire, R. G., Peterson, J. R., Damien, D. A., and Huray, P. G. (1986) *J. Less Common Metals*, **121**, 319–24.

Noé, M. and Peterson, J. R. (1976) in *Transplutonium 1975* (eds. W. Mller and R. Lindner), North-Holland, Amsterdam, pp. 69–77.

Nugent, L. J., Baybarz, R. D., and Burnett, J. L. (1969) *J. Phys. Chem.*, **73**, 1177–8.

Nugent, L. J., Baybarz, R. D., Burnett, J. L., and Ryan, J. L. (1971) *J. Inorg. Nucl. Chem.*, **33**, 2503–30.

Nugent, L. J., Baybarz, R. D., Burnett, J. L., and Ryan, J. L. (1973a) *J. Phys. Chem.*, **77** (12), 1528–39.

Nugent, L. J., Burnett, J. L., and Morss, L. R. (1973b) *J. Chem. Thermodyn.*, **5**, 665–78.

Nugent, L. J. (1975) *J. Inorg. Nucl. Chem.*, **37**, 1767–75.

Osborne-Lee, I. W. and Alexander, C. W. (1995) ORNL/TM–12760, pp. 1–43, and references therein.

Patchell, R. A., Yaes, R. J., Beach, L., Kryscio, R. J., Davis, D. G., Tibbs, P. A., and Young, B. (1997) *Br. J. Radiol.*, **70**(839), 1162–8.

Payne, G. L. and Peterson, J. R. (1987) *Inorg. Chim. Acta*, **139**, 111–12.

Pershina, V., Fricke, B., Inova, G. V., and Johnson, E. (1994) *J. Phys. Chem.*, **98**, 1482.

Peterson, J. R. and Burns, J. H. (1968) *J. Inorg. Nucl. Chem.*, **30**, 2955–8.

Peterson, J. R. and Baybarz, R. D. (1972) *Inorg. Nucl. Chem. Lett.*, **8**, 423–31.

Peterson, J. R., Fellows, R. L., Young, J. P., and Haire, R. G. (1977) *Radiochem. Radional. Lett.*, **31**(4–5), 277–82.

Peterson, J. R., Benedict, U., Dufour, C., Birkel, I., and Haire, R. G. (1983) *J. Less Common Metals*, **93**, 353–6.

Peterson, J. R., Young, J. P., and Haire, R. G. (1985) *Abstr. Am. Chem. Soc. Natl. Meeting* I985 S190:334-INR.

Peterson, J. R. and Xu, W. (1996) *J. Radioanal. Nucl. Chem.*, **203**(2), 301–7.

Poda, G. A. and Hall, R. M. (1975) *Health Phys.*, **29**(3), 407–9.

Popov, Y. S., Efremov, Y. V., and Borisenkov, V. I. *et al.* (1966) *Radiochemistry* **38**(2), 124–6.

Porter, C. E., Riley, F. D., and Vandergriff, R. D. (1997) *Sep. Sci. Technol.*, **32**(1–4), 83–92 and 227–34.

Propst, R. L. and Hyder, M. L. (1969) *Nature*, **221**, 1141–2.

Radchenko, V. M., Seleznev, A. G., and Droznik, R. R. (1986a) *Sov. Radiochem.*, **28**(4), 401–4.

Radchenko, V. M., Shushakov, V. D., and Seleznev, A. G. (1986b) *Sov. Radiochem.*, **28**(4), 405–8.

Raschella, D. L., Haire, R. G., and Peterson, J. R. (1982) *Radiochim. Acta*, **30**, 41–3.

Rivard, M. J. (1999a) *Med. Phys.*, **26**(1), 87–96.

Rivard, M. J. (1999b) *Med. Phys.*, **26**(8), 1503–14.

Rivard, M. J., Wierzbicki, J. G., den Heuvel, Van Chuba, P. J., Fontanesi, J., Martin, R., Mahon, C., and Haire, R. G. (1999) *Med. Phys.*, **26**(1), 87–96.

Rivard, M. J. (2000a) *Med. Phys.*, **27**(8), 1761–9.

Rivard, M. J. (2000b) *Med. Phys.*, **27**(12), 2803–15.

Rivard, M. J. (2000c) *Med. Phys.*, **27**(12), 2816–20.

Rivard, M. J., Sganga, J. K., d'Errico, F., Tsai, J.-S., Ulin, K., and Engler, M. J. (2002) *Nucl. Instrum. Methods A*, **476**(1–2), 119–22.

Rivard, M. J., Evans, K. E., Leal, L. C., and Kirk, B. L. (2004) *Nucl. Instrum. Methods B*, **213**, 621–5.

Rykov, V. A. and Yudin, G. L. (1998) *Dokl. Akad. Nauk.*, **360**(2), 186–9.

Sakanoue, M. and Amano, R. (1976) in *Transplutonium 1975* (eds. W. Müller and R. Lindner), North-Holland, Amsterdam, pp. 123–9.

Samhoun, K. and David, F. (1976) in *Transplutonium 1975* (eds. W. Müller and R. Lindner), North-Holland, Amsterdam, pp. 297–304.

Samhoun, K. and David, F. (1979) *J. Inorg. Nucl. Chem.*, **41**, 357–63.

Scofield, J. H. (1974) *At. Data Nucl. Data Tables*, **14**(2), 121–37.

Seaborg, G. T. and Loveland, W. D. (1990) *The Elements Beyond Uranium,* John Wiley, New York, p. 28.

Seleznev, A. G., Radchenko, V. M., and Shushakov, V. D. (1989) *Sov. Radiochem.*, **(6)**, 637–41.

Seleznev, A. G., Radchenko, V. M., and Shushakov, V. D. (1990) *J. Radioanal. Nucl. Chem.*, **143**(1), 253–9.

Senftle, F. E., Duffey, D., and Wiggins, P. E. (1969) *Mar. Technol. Soc. J.*, **3**(5), 9–11.

Shannon, R. D. (1976) *Acta Crystallogr.*, **A32**, 751–64.

Shleien, B., Slaback, L. A. Jr, and Birky, B. K. (eds) (1998) in *Handbook of the Health Physics and Radiological Health*, 3rd edn, Williams and Wilkins, Baltimore, p. 14.

Shoun, R. R. and McDowell, W. J. (1980) in *Actinide Separations* (eds. J. D. Navratil and W. W. Schulz) (ACS Symp. Ser. 117), American Chemical Society, Washington, DC, pp. 71–87.

Sikkeland, T. and Ghiorso, A. (1967) *Phys. Lett. B*, **24**(7), 333–4.

Skiokawa, Y. and Suzuki, S. (1984) *Bull. Chem. Soc. Jpn.*, **57**(10), 2910–13.

Smith, J. L. and Haire, R. G. (1978) *Science*, **200**, 535–9.

Smith, J. L. (1979) USDOE Report LA-UR-79–1666, pp. 1–13.

Smith, J. L. (1980) USDOE Report LA-UR-80–762, pp. 1–5.

Spitsyn, V. I. (1977) in *Proc. 2nd Int. Conf. on Electronic Structure of the Actinides* (eds. J. Mulak, W. Suski, and R. Troc), Wroclaw, Poland, pp. 25–38.

Stary, J. (1966) *Talanta*, **13**, 421–37.

Stepanov, A. V. (1971) *Russ. J. Inorg. Chem.*, **16**, 1583–6.

Stevenson, J. N. (1973) PhD Thesis University of Tennessee, (Knoxville), U. S. Energy Research and Development Admin. Doc. ORO-4447-004 (TID-26453) p. 49.

Stevenson, J. N. and Peterson, J. R. (1973) *J. Inorg. Nucl. Chem.*, **35**, 3481–6.

Street, K. Jr and Seaborg, G. T. (1950) *J. Am. Chem. Soc.*, **72**, 2790–2.

Sugar, J. (1973) *J. Chem. Phys.*, **59**, 788.

Surls, Jr and J. P. Choppin, G. R. (1957) *J. Inorg. Nucl. Chem.*, **4**, 62–73.

Sykora, R. E., Raison, P. E. and Haire, R. G. (2005) *J. Solid State Chemistry*, **178**(2), 578–83.

Sykora, R. E., Assefa, Z., Haire, R. G., and Albrecht-Schmitt, T. E. (2006) *Inorg. Chem.*, **45**, 475–77.

Tacev, T., Zaloudik, J., Janakova, L., and Vagunda, V. (1998) *Neoplasma*, **45**(2), 96–101.

Tacev, T., Grigorov, G., Papirek, T., and Kolarik, V. (2003a) *Strahlenther. Onkol.*, **179** (6), 113–17.

Tacev, T., Ptackova, B. N., and Strnad, V. (2003b) *Strahlenther. Onkol.*, **179**(6), 377–84.

Tacev, T., Grigorov, G., Papirek, T., and Kolarik, V. (2004a) *Nucl. Instrum. Methods B*, **213**, 626–8.

Tacev, T., Ptackova, B. N., and Strnad, V. (2004b) *Radiothermodyn. Oncol.*, **71**, S8–18.

Taut, S., Hübener, S., and Eichler, B. (1997) *Radiochim. Acta*, **78**, 33–8.

Taylor, G. N., Jee, W. S., Mays, C. W., Dell, R. B., Williams, J. L., and Shabestari, L. (1972) *Health Phys.*, **22**(2), 691–3.

Todd, P., Feola, J. M., and Maruyama, Y. (1984) *Am. J. Clin. Oncol. – Cancer*, **7**(5), 495–8.

Topp, N. E. (1965) in *Chemistry of the Rare Earth Elements*, Elsevier, New York, pp. 71–3.

Turcotte, R. P. and Haire, R. G. (1976) in *Transplutonium Elements 1975* (eds. W. Müller and R. Lindner), North-Holland, Amsterdam, pp. 267–77.

Turcotte, R. P. (1980) *J. Inorg. Nucl. Chem.*, **42**, 1735–7.

Varga, L. P., Baybarz, R. D., Reisfeld, M. J., and Asprey, L. B. (1973a) *J. Inorg. Nucl. Chem.*, **35**, 2775–86.

Varga, L. P., Baybarz, R. D., Reisfeld, M. J., and Volz, W. B. (1973b) *J. Inorg. Nucl. Chem.*, **35**, 2787–94.

Veal, B. W., Lam, D. J., Diamond, H., and Hoekstra, H. R. (1977) *Phys. Rev. B*, **15**(6), 2929–42.

Vobecky, M. (1989) *J. Radioanal. Nucl. Chem.*, **135**(3), 165–9.

Wanwilairat, S., Schmidt, R., and Vilaithong, T. (2000) *Med. Phys.*, **27**(10), 2357–62.

Ward, J. W. and Hill, H. H. (1976) in *Heavy Element Properties* (eds. W. Müller and H. Blank), North-Holland, Amsterdam, pp. 65–79.

Ward, J. W., Kleinschmidt, P. D., and Haire, R. G. (1979) *J. Physique*, **C–4**(Suppl.), 233–5.

Ward, J. W., Kleinschmidt, P. D., Haire, R. G., and Brown, D. (1980) in *Lanthanide and Actinide Chemistry and Spectroscopy* (ed. N. M. Edelstein) (ACS Symp. Ser. 131), American Chemical Society, Washington, DC., pp. 199–221.

Ward, J. W. (1983) *J. Less Common Metals*, **93**, 279–92.

Ward, J. W., Kleinschmidt, P. D. and Peterson, D. E. (1986) in *Handbook of the Physics and Chemistry of the Actinides,* vol. 4 (eds. A. J. Freeman and C. Keller), North-Holland, Amsterdam ch. 7.

Warden, J., Gutmacher, R. G., and Lougheed, R. W. (1970) *J. Opt. Soc. Am.*, **60**, 1555.

Weber, M. J. (1980) in *Lanthanide and Actinide Chemistry and Spectroscopy* (ed. N. Edelstein) (ACS Symp. Ser. 131), American Chemical Society, Washington, DC., pp. 275–311.

Wiggins, P. F., Senftle, F. E., and Duffey, D. (1969) *Trans. Am. Nucl. Soc.*, **12**(2), 492–7

Wild, J. F., Hulet, E. K., Lougheed, R. W., Hayes, W. N., Peterson, J. R., Fellows, R. L., and Young, J. P. (1978) *J. Inorg. Nucl. Chem.*, **40**, 811–17.

Williams, K. R. and Choppin, G. R. (1974) *J. Inorg. Nucl. Chem.*, **36**, 1849–53.

Wilmarth, W. R., Young, J. P., Haire, R. G., and Peterson, J. R. (1988) *J. Less Common Metals*, **143**(1–2), 183–93.

Wilmarth, W. R. and Peterson, J. R. (1991a) in *Handbook on the Chemistry and Physics of the Actinides,* vol. 6 (eds. A. J. Freeman and C. Keller), North-Holland, New York, pp. 61–38.

Wilmarth, W. R. and Peterson, J. R. (1991b) in *Handbook on the Chemistry and Physics of the Actinides,* vol. 6 (eds. A. J. Freeman and C. Keller), North-Holland, New York, pp. 1–38.

Worden, E. F. and Conway, J. G. (1970) *J. Opt. Soc. Am.*, **60**, 1144–5.

Yanch, J. C., Kim, J. K., and Wilson, M. J. (1993) *Phys. Med. Biol.*, **38**(8), 1145–55.

Young, J. P., Vander Sluis, K. L., Werner, G. K., Peterson, J. R., and Noé, M. (1975) *J. Inorg. Nucl. Chem.*, **37**(12), 2497–501.

Young, J. P., Haire, R. G., Fellows, R. L., Noé, M., and Peterson, J. R. (1976) in *Transplutonium 1975* (eds. W. Müller and R. Lindner), North-Holland, Amsterdam, pp. 227–33.

Young, J. P., Haire, R. G., Fellows, R. L., and Peterson, J. R. (1978) *J. Radioanal. Chem.*, **43**, 479–88.

Young, J. P., Haire, R. G., Peterson, J. R., Ensor, D. D., and Fellows, R. L. (1980) *Inorg. Chem.*, **19**, 209–12.

Young, J. P., Haire, R. G., Peterson, J. R., Ensor, D. D., and Fellows, R. L. (1981) *Inorg. Chem.*, **20**, 3979–83.

Young, J. P., Haire, R. G., Peterson, J. R., and Ensor, D. D. (1984) in *Geochemical Behavior of Disposed Radioactive Waste* (eds. G. S. Barney, J. D. Navratil, and W. W. Schulz) (ACS Symp. Ser. 246), American Chemical Society, Washington, DC, pp. 335–46.

Zachariasen, W. H. (1975) *J. Inorg. Nucl. Chem.*, **37**(6), 1441–2.

Zech, P., Guey, A., Leitienne, P., Meary, M. F., Pozet, N., Moskovtchenko, J. F., and Traeger, J. (1976a) *J. Urol. Nephrol.*, **82**(4–5), 315–19.

Zech, P., Guey, A., and Leitienne, P. (1976b) *Kidney Int.*, **9**(6), 524.

CHAPTER TWELVE

EINSTEINIUM

Richard G. Haire

12.1 INTRODUCTION

The discovery of einsteinium, element 99, came about during the analyses of nuclear products produced in and then recovered from test debris following a thermonuclear explosion (weapon test device, 'Mike', November 1952) at Eniwetok Atoll in the Pacific Ocean. The uranium present in this device was subjected to a very intense neutron flux (integrated fluence of about 10^{24} neutrons) in an extremely short time frame (few nanoseconds), which allowed a large number of multiple neutron captures with a minimal degree of decay of the products formed. Nuclei were formed with usually high neutron/proton ratios (very 'heavy' uranium isotopes), which then rapidly beta-decayed into new, transuranium isotopes through element 100. Scientists from several U.S. Government laboratories separated and analyzed extensively the debris samplings in the following weeks. From these investigations came the discovery and identification of einsteinium and fermium. The first element was named in honor of Albert Einstein, and assigned the symbol, E (later changed to the current symbol, Es). Additional details and discussions about the discovery of this element and the scientists involved are given in several references (Thompson *et al.*, 1954; Ghiorso *et al.*, 1955; Fields *et al.*, 1956; Hyde *et al.*, 1964; Seaborg and Loveland, 1990).

Subsequently, einsteinium has been produced in accelerator targets, and in reactors via successive neutron captures, starting with targets of plutonium or higher actinides. The first macroscopic and weighable quantities of einsteinium (few hundredths of a microgram of ^{253}Es) were obtained in 1961. Today, up to $\sim$2 mg can be present in special high-flux isotope reactor targets at the time of release from a reactor.

The transplutonium elements, where einsteinium is the fifth, have chemistries similar to those of the lanthanide elements, especially in their ionic states and in compounds. In essence, elements in the series sequentially add one f-electron in progressing to higher atomic numbers. Einsteinium is therefore an f-electron element, and its 5f electrons are considered fully localized, as opposed to those in the protactinium through plutonium grouping.

Oxidation states of II, III, and IV have been reported for einsteinium, where the best-established state is III (state normally observed in solution) followed by divalent einsteinium, which can be obtained in solid compounds. The tetravalent state has been postulated from vapor transport studies using tracer levels of einsteinium, but this state has not been established fully. More remote is the potential for a hexavalent state, based on the conception that this state may acquire stability from attaining a half-filled, 5f shell (5f^{11} down to 5f^{7}), by losing a total of six electrons (Liebman, 1978).

An exception of this similarity of einsteinium to the regular lanthanide elements occurs with the elemental state of einsteinium, where its properties and bonding compare more closely to those for europium and ytterbium metals, rather than to the other lanthanide elements, or more specifically to its apparent lanthanide homolog, holmium. This difference in behavior for einsteinium is readily seen by examining the atomic volumes of the two f-series that are shown in Fig. 12.1. Einsteinium is therefore unique in that it is the first divalent

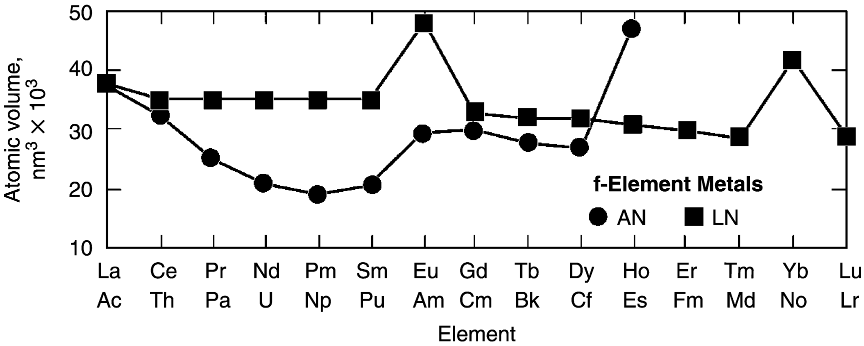

Fig. 12.1 *Atomic volumes of the two f-electron series of elements are shown. The behavior of einsteinium shows it is the first divalent actinide metal, with bonding similar to that for europium and ytterbium metals. This behavior for einsteinium metal is very different than that observed with Es(II) and Es(III) in compounds, which is similar to that for the lanthanides in these states.* (*Haire* et al., 2004).

actinide metal. In the lanthanide elements, europium and ytterbium are also divalent metals (two bonding electrons rather than three). The rationale for their metallic divalency is due to stabilization from a half-filled (Eu) or full (Yb) 4f-orbital arrangement. But this is not an appropriate explanation for the divalency of einsteinium metal. As discussed in Section 12.4, this situation for einsteinium is explained by its high 5f-electron promotion energy (energy to change an $f \rightarrow d$).

There are 16 established isotopes of einsteinium (with three isomers), with many having very short half-lives. The longest-lived isotope is ^{252}Es ($t_{1/2} = 471.7$ days), but the ^{253}Es ($t_{1/2} = 20.47$ days) isotope is available in the largest quantity and obtained primarily from nuclear reactors. The quantities of the latter isotope are normally limited to hundreds of micrograms, but frequently only a few micrograms are employed in studies at one time. Up to 2 mg can be discharged from special reactors (i.e. High Flux Isotope Reactor (HFIR) at Oak Ridge National Laboratory, ORNL) once every 6 months to 2 years, depending on the production schedule used. Even so, studies with it are also severely hindered by its half-life ($\sim$3% daughter 'impurity' ingrowth per day) and intense self-radiation (6.6 MeV alpha, self-heating of 1000 W g^{-1}), which are often detrimental to the studies being performed. A feeling for the magnitude of the energy released by the decaying einsteinium is obtained by looking at Fig. 12.2. The illumination is associated with the radioactive decay from 300 μg of ^{253}Es solid that is in the bottom of a 9 mm diameter quartz cone.

In essence, there are not many practical applications for einsteinium isotopes. Applications are found as target materials for producing elements with even higher atomic numbers, use of the self-irradiation fields of einsteinium for damage studies, and the use of its radiation for medical treatments. The latter application has been limited, but in principle would employ einsteinium chemically bound to biological agents that could deliver the radiation of einsteinium to biological sites for treatment of different disorders. In this regard, studies have been performed where beagles have been injected einsteinium citrate (Lloyd *et al.*, 1975). Other experiments along this line have been tried with the shorter-lived ($\sim$20 h) ^{255}Fm isotope, a daughter product of ^{255}Es; the latter is present in einsteinium products from reactors.

Einsteinium can also be useful in certain chemical studies, where its intense self-irradiation can be used for evaluating radiation damage and radiolysis effects both in solution and in the solid phase. One example of the latter would be to prepare a compound of einsteinium and then follow the chemistry of the daughter and granddaughter (i.e. from ^{253}Es one obtains ^{249}Bk, and ^{249}Cf, respectively) products as they grow into the einsteinium material (Young *et al.*, 1981). The main point is that knowing and understanding the science of einsteinium is important for actinide systematics and understanding the changing role of 5f electrons across the series.

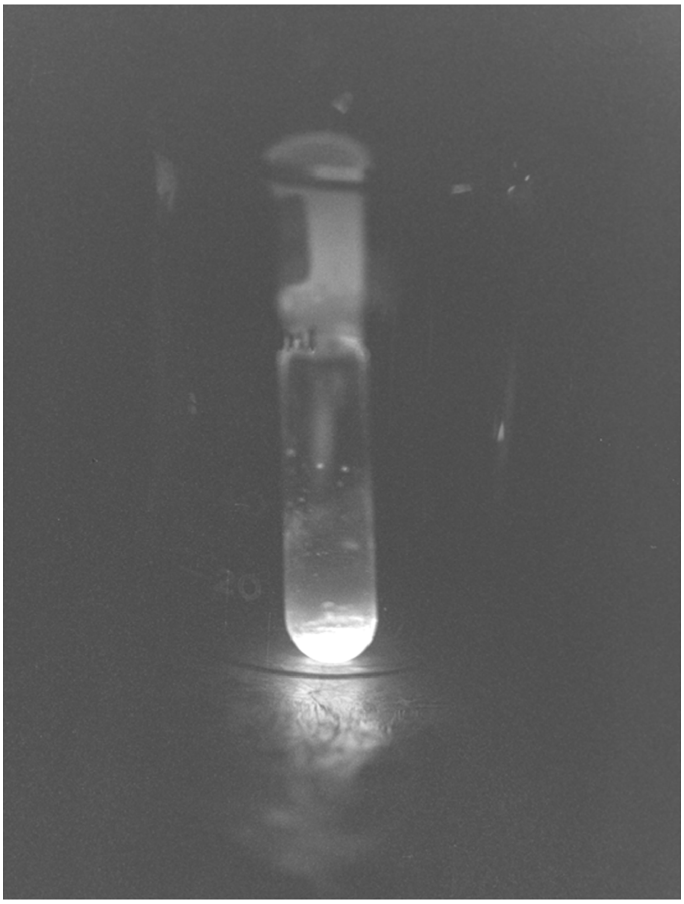

Fig. 12.2 *Self-luminescence arising from the intense radiation from* ~300 μg *of* ^{253}*Es in a quartz cone. The heat and radiation accompanying decay often generate detrimental effects in studies of Es.*

12.2 PRODUCTION AND NUCLEAR PROPERTIES

The primary nuclear properties and production schemes for einsteinium are outlined in Table 12.1 and in Appendix II. The reader is also directed in this regard to references discussing these isotopes (Hyde *et al*., 1964; Seaborg and Loveland, 1990). The nuclear levels of their daughters and the exact atomic mass of each isotope can be established by relating the total decay energies with the masses of the daughter products through studies of the decay processes.

The discovery of einsteinium in nuclear debris involved primarily the ^{253}Es and ^{255}Es isotopes, which have half-lives of 20.47 days and 39.8 h, respectively.

Table 12.1 *Nuclear properties of einsteinium isotopes.*[a]

Mass number	*Half-life*	*Mode of decay*	*Main radiations* (MeV)	*Method of production*
241	8 s	α	α 8.11	^{245}Md daughter
242	13.5 s	α	α 7.92	^{233}U(^{14}N,5n)
243	21 s	α	α 7.89	^{233}U(^{15}N,5n)
244	37 s	EC 96% α ~ 4%	α 7.57	^{233}U(^{15}N,4n) ^{237}Np(^{12}C,5n)
245	1.1 min	EC 60% α ~ 40%	α 7.73	^{237}Np(^{12}C,4n)
246	7.7 min	EC 90% α 10%	α 7.35	^{241}Am(^{12}C,α3n)
247	4.55 min	EC ~ 93% α ~ 7%	α 7.32	^{241}Am(^{12}C,α2n) ^{238}U(^{14}N,5n)
248	27 min	EC 99.7% α ~ 0.3%	α 6.87 γ 0.551	^{249}Cf(d,3n)
249	1.70 h	EC 99.4% α 0.57%	α 6.770 γ 0.380	^{249}Cf(d,2n)
250[b]	8.6 h	EC	γ 0.829	^{249}Cf(d,n)
250[b]	2.22 h	EC	γ 0.989	^{249}Cf(d,n)
251	33 h	EC 99.5% α 0.49%	α 6.492 (81%) 6.463 (9%) γ 0.177	^{249}Bk(α,2n)
252	472 d	α 78% EC 22%	α 6.632 (80%) 6.562 (13.6%) γ 0.785	^{249}Bk(α,n)
253	20.47 d 6.3×10^5 yr	α SF β stable	α 6.633 (89.8%) 6.592 (7.3%)	multiple neutron capture
254g	275.7 d $>2.5 \times 10^7$ yr	α SF	α 6.429 (93.2%) 6.359 (2.4%) γ 0.062	multiple neutron capture
254m	39.3 h $>1 \times 10^5$ yr	β^- 99.6 SF α 0.33% EC 0.08%	α 6.382 (75%) 6.357 (8%)	^{253}Es(n,γ)
255	39.8 d	β^- 92.0% α 8.0% SF 4×10^{-3}%	α 6.300 (88%) 6.260 (10%)	multiple neutron capture
256[b]	25.4 min	β^-		^{255}Es(n,γ)
256[b]	~7.6 h	β^-		^{254}Es(t,p)

[a] Appendix II.

[b] Not known whether ground state nuclide or isomer (Appendix II).

EC = Electron capture

SF = Spontaneous fission

Both elution behavior during ion-exchange purification and the nuclear properties of these isotopes were used to establish the existence of this new element. These two isotopes together with ^{254g}Es ($t_{1/2}$ = 275.7 d) are produced by neutron-capture processes. All three isotopes are obtained in high-flux reactors designed to produce synthetic elements, but ^{253}Es and ^{254g}Es are the isotopes normally used for physicochemical studies other than for tracer work given their greater quantities.

The lighter isotopes of einsteinium are prepared in smaller quantities using accelerators and often other actinides as target materials (see Table 12.1). The synthesis of einsteinium isotopes using bombardment of targets with nitrogen isotopes has been discussed (Mikheev *et al.*, 1967), as has been the alpha decay properties of some lighter einsteinium isotopes (Ahmad and Wagner, 1977). The half-life of ^{252}Es is also addressed specifically in Ahmad *et al.* (1970). McHarris *et al.* (1966) have addressed the decay scheme of ^{254g}Es. Einsteinium isotopes have also been produced by bombardment of ^{209}Bi with ^{40}Ar ions (Ninov *et al.*, 1996). The electron-capture decay fission processes in neutron-deficient einsteinium isotopes have also been discussed (Shaugnessy *et al.*, 2000).

At the present time, einsteinium can be produced in the HFIR at the ORNL, Oak Ridge, Tennessee, and at the Research Institute of Atomic Reactors in Dimitrovgrad, Russia. At the HFIR, the targets for neutron irradiation consist mainly of curium isotopes (^{244}Cm through ^{248}Cm), which are irradiated in the reactor to produce the transcurium elements through fermium. The process involves successive neutron captures and beta decays to reach ^{253}Cf, which then β^- decays to ^{253}Es. The latter einsteinium isotope captures neutrons to reach ^{256}Es (possibility even ^{257}Es) but the einsteinium isotopes removed from the reactor targets consist of essentially ^{253}Es, ^{254g}Es, and ^{255}Es. The HFIR can produce einsteinium once every 12–24 months. The SM-2 loop reactor in Russia has similar power and flux levels, also giving it the potential for producing quantities of these transcurium isotopes.

The direct production in the HFIR in the U.S. is less than 2 mg of ^{253}Es, with the ^{254g}Es and ^{255}Es contents being ~0.3 and 0.06%, respectively, at discharge. However, ^{253}Cf is present in the californium isotope fraction that is chemically separated and it β^- decays to ^{253}Es. By subsequent chemical separation of the californium fraction of isotopes, it is possible to obtain chemically the ^{253}Es daughter from the californium fraction at a later time (weeks) and recover isotopically pure ^{253}Es at levels up to 200 μg.

From the mixed einsteinium isotope fraction received from the reactor there are two considerations to be addressed for using this einsteinium fraction. The first concerns the decay of the ^{255}Es present, which is a source of ^{255}Fm at the nanogram level (the longer-lived ^{257}Fm is produced directly in the reactor at only a 1 pg level). Chemical separations of the einsteinium fraction for multiple weeks (i.e. for about a total of four ^{255}Es half-lives) produces a repeated source of a few nanograms of ^{255}Fm. Another aspect is that after decay of —six to ten half-lives of ^{253}Es, the original einsteinium fraction is almost pure ^{254g}Es, and some 4 μg of it can be obtained essentially free of ^{253}Es. The latter isotope is highly desirable for nuclear syntheses but is of more limited value for physiochemical work, despite its longer half-life. This is due not only to the smaller amounts of it but also to the highly penetrating radiation field generated from its short-lived ^{250}Bk daughter ($t_{1/2} = 3.217$ h with β^- decay having a 45% branching ratio for a ~1 MeV gamma emission) in equilibrium with it. Thus, decisions must be made regarding the needs and the different choices available for the einsteinium products generated.

More detailed discussions on the nuclear properties, preparation of einsteinium isotopes, and their decay schemes are provided in the references. The K-series X-ray energies of einsteinium isotopes are discussed in Dittner and Bemis (1972). The electron-capture delayed fission processes of neutron-deficient isotopes, ^{242}Es and ^{244}Es, have also been reported, and highly asymmetric mass distributions have been noted (Kosyakov *et al.*, 1974). Average pre-neutron total kinetic energies of (183 ± 18) and (186 ± 9) MeV, respectively, were found. The probability of delayed fission was determined to be $(6 \pm 2) \times 10^{-3}$ and $(1.2 \pm 0.4) \times 10^{-4}$, respectively; smaller probabilities were given for the ^{246}Es and ^{248}Es isotopes.

12.3 PURIFICATION AND ISOLATION

The techniques used for the isolation, recovery, and purification of einsteinium isotopes are very dependent on the method of production. Accelerator production often involves thin foils or targets, where the einsteinium products are either recovered simply (washed off) from the target or from 'catcher' foils located behind a thin target. Recovery from 'catcher' foils can be straightforward, and recovery of products may only involve dissolution or washing of the foil followed by a minor purification of the einsteinium product.

In contrast, recovery of einsteinium following a neutron irradiation process can be rather complex. Larger quantities of very radioactive materials are involved in this process and it requires hot cell operations. The actinide targets are placed in some form of 'container' for the reactor irradiation (normally in aluminum rods), which must then be removed mechanically or chemically to reach the irradiated starting and product materials. At that point, one is faced with the starting material (i.e. curium oxide) and various fission products, in addition to the desired transcurium products (i.e. berkelium, californium, einsteinium, and some fermium). The purification and recovery of einsteinium then involves: (1) separation from lanthanide fission products; and (2) separation from curium, berkelium, and the adjacent actinides, californium and fermium. The major obstacle is the great similarity in the chemical properties of their trivalent actinide ions in solution, given their similar ionic radii.

There is only a small contraction in radii with increasing atomic number in the case of transplutonium elements, which provides a small increase in covalency and complexing ability, but these are sufficient to allow chromatographic methods to be used for separations. An advantage is acquired in the case of berkelium (which is also a daughter product of einsteinium), as this element can be oxidized to a tetravalent state and separated from the curium through fermium trivalent elements. Separation of einsteinium from its berkelium daughter product can be accomplished by solvent extraction. If solvent extraction is used to remove tetravalent berkelium, the extraction can then leave trivalent californium, einsteinium, and fermium ions together. These elements would have to be separated by subsequent ion exchange or chromatography techniques. A schematic for the separation of einsteinium is given in Fig. 12.3, parts A and B.

The details of various chemical separation processes have been published and presented as reviews. Two earlier reviews cover the approaches in the U.S. (Hulet and Bodé, 1972) and in Russia (Myasoedov *et al.*, 1974). A more general overview for separation of the transuranium elements is also available (Hyde *et al.*, 1964), and individual accounts of procedures used worldwide have been published (Müller, 1967; Bigelow, 1974; Ishimori, 1980; King *et al.*, 1981; Collins *et al.*, 1981). The early scheme used for products from the HFIR at ORNL has also been published in separate reports (Baybarz *et al.*, 1973; Benker *et al.*, 1981). Many of these procedures have not changed significantly over the years.

The removal of lanthanides from the actinides can be accomplished in different ways. An early method, suited for laboratory separations of smaller quantities, was through the use of alcoholic hydrochloric acid as an elutant for the

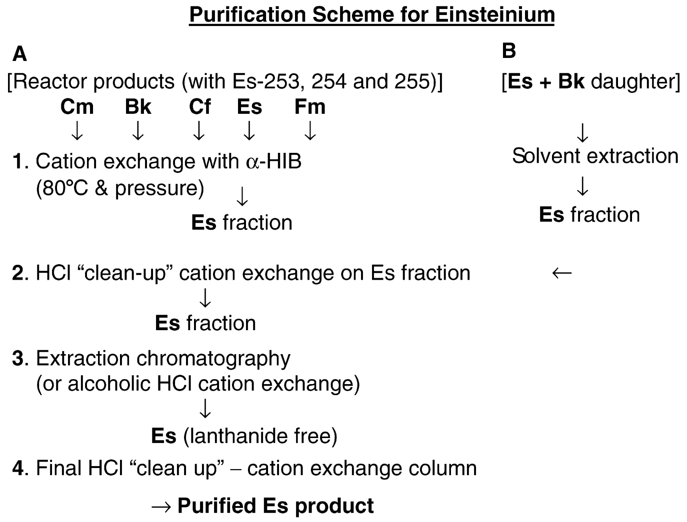

Fig. 12.3 *Einsteinium purification scheme.*

transcurium elements sorbed on cation resin (Street and Seaborg, 1950), where the greater complexing ability of the actinides allowed their desorption as chloride complexes ahead of the lanthanides. A preferred method for larger-scale operations is a lithium chloride anion-exchange process (Shoun and McDowell, 1980), which partitions the actinides from the lanthanides. For small amounts of lanthanides from einsteinium (i.e. the final removal of trace amounts of lanthanides of similar ionic radii) an extraction chromatography column employing ammonium thiocyanate and formic acid can be used (TEVA™ columns; see Horwitz *et al.*, 1994; Porter *et al.*, 1997). These special columns are also available commercially and give excellent separations between the lanthanide and actinide groups.

When the three elements californium, einsteinium, and fermium are considered, the individual elements can be separated by cation-exchange processes. One method that has been used for several decades is to sorb the three ions on a cation resin from dilute acids (i.e. 0.1 M hydrochloric acid) and selectively elute them with ammonium alpha-hydroxyisobutyrate (α-HIB) solutions at a pH in the range 3.8–4.2 (Choppin and Silva, 1956; Baybarz *et al.*, 1973; Bigelow *et al.*, 1980; Myasoedov *et al.*, 1980; Shoun and McDowell, 1980; Campbell, 1981). The elution order is fermium, einsteinium, and then californium; a high-pressure, ion-exchange column operated at 80°C gives the best results. Separation factors are not great but sufficient, ranging from 1 to 2 for different conditions. Details of using high-pressure columns for separation of f-elements have been given by Campbell (1981). However, even when working with only 10–20 μg of ^{253}Es, care must be exercised, as its radiation level is sufficient to char the resin upon standing and makes it difficult to recovery fully the einsteinium from the resin.

Another approach employs extraction chromatography, where either bis(2-ethylhexyl)phosphoric acid (HDEHP) or 2-ethylhexylphenylphosphonic acid (HEMΦP) are placed on an inert (i.e. fine glass particles) support. The actinides are loaded on this column and eluted with a dilute 0.3 M nitric acid solution (Hulet and Bodé, 1972). Separation factors for these actinide elements are again between 1 and 2. Ion-exchange separations of einsteinium from irradiated californium have also been discussed by Elesin *et al.* (1986).

The extraction chromatography behavior of einsteinium with a quaternary ammonium nitrate has been discussed (Horwitz *et al.*, 1966), and extraction of einsteinium with bis(2-ethylhexyl)phosphoric acid was also reported (Horwitz *et al.*, 1969). The extraction of einsteinium by bis(2-ethylhexyl)phosphoric acid and the stability constants for hydroxycarboxylic acids is reported by Aly and Latimer (1970a). The extraction of Es by dibutyl *N*,*N*,-diethyl carbamyl phosphate is also discussed (Aly and Latimer, 1970b). The current separation procedure for einsteinium from neutron-irradiated targets at ORNL dates back many years and has been summarized by Campbell (1970). Other separation methods for einsteinium have been provided by Horwitz *et al.* (1994).

12.4 ELECTRONIC PROPERTIES AND STRUCTURE

Chapter 16 is concerned with spectra and electronic structure of free actinide atoms and ions, and these topics are only touched upon here. As einsteinium belongs to the actinide series of elements it can be considered a 5f electron element, which has localized (non-bonding) 5f electrons, and potentially a 'dsp' or an 's^2' type of bonding. In addition, both non-relativistic and relativistic approaches (appropriate because of its high atomic number einsteinium) should be considered with regard to its behavior.

From non-relativistic considerations, the radial probability distributions of the 5f electrons are well within the principal confines of the 6d, 7s, and 7p orbitals, although there is some 'tailing' to the outer regions. This tailing or extension relative to the 7s and 7p orbitals lends itself to a slightly greater degree of covalency than found for the lanthanide's 4f electrons. With the transplutonium elements, the degree of covalency increases slightly when moving to elements with increased atomic number for a given ionic state.

For the relativistic situation, the binding of the electrons becomes greater with higher atomic numbers, which can affect the energies for the different electronic states. Also, potential effects may be found with regard to radii and energies of certain orbitals, spin–orbit splitting, and the expansion of the d- and f-orbitals, all of which can affect chemical behavior. An overview of this electronic picture has been given (Seaborg and Loveland, 1990).

The electronic configurations of einsteinium in neutral and singly ionized gaseous atoms have been analyzed via emission spectra (Gutmacher *et al.*, 1967; Conway, 1979), although full characterization of the ~20000 lines collected is still incomplete. Worden *et al.* (1974) have provided term assignments to a small number of these lines, and Brewer (1971a,b) had estimated energies for the lower spectroscopic terms. Brewer estimated that for a singly ionized atom the $f^{10}s^2$, f^{12}, and $f^{11}d$ levels should be lower in energy than the $f^{11}p$ level reported by Worden *et al.* (1974).

For the gaseous atom of einsteinium, a $5f^{11}7s^2$ ground state is assumed, and the successively ionized neutral gaseous atom loses first one, then two 7s electrons, while the third and even fourth electron lost are 5f electrons, to give a $5f^9$ configuration for the potential ion. It must be remembered that the gaseous atom configurations are different from those encountered in the metals, which are influenced by other factors including crystal energies.

Brewer (1971a,b) has calculated that for einsteinium metal the bonding configuration could be $5f^{10}dsp$, where the 6d and 7p orbitals play important roles. In this case, einsteinium would have three bonding electrons in its conduction band. Alternative configurations would be $5f^{11}sp$ or $5f^{11}s^2$, where only two bonding electrons are present, and in this case, einsteinium would be the first divalent actinide metal. The latter configuration appears to be the correct configuration for einsteinium metal. The reason for the divalency of einsteinium metal can be found in the promotion energy for changing an f-electron to a d-electron, which would then provide three electrons rather than two electrons for the metallic bonding.

A plot of promotion energies for the actinide is shown in Fig. 12.4 (Haire, 1994), which shows einsteinium's promotion energy as being just above the border between divalent and trivalent metal bonding. This 'borderline' energy relates to the crystal energy recovered when the metal atoms crystallize. Thus, when gaseous atomic einsteinium ($5f^{11}7s^2$) condenses to form a crystal, promotion of a 5f electron must occur to provide three rather than two bonding electrons in the solid if a trivalent metal (i.e. with a ds^2 configuration) is to form. For the earlier transplutonium metals, this promotion energy is provided from the greater crystal energy acquired, but with einsteinium, the promotion

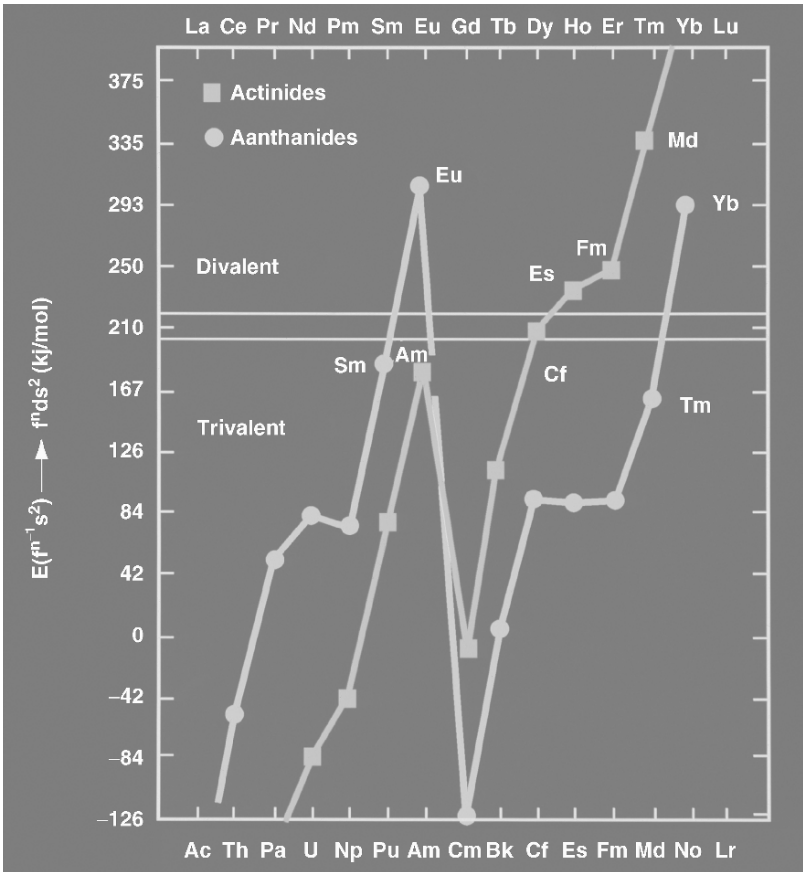

Fig. 12.4 *The f→d promotion energies for the f-elements (bar across figure is estimate of crystal energy needed to compensate for promotion of an electron from an f to a d level).*

energy needed exceeds the crystal energy recovered. Thus, einsteinium remains a divalent metal, as do the next three metals in the series.

Recent gas-phase studies of einsteinium have also provided important new insights into its chemistry. The behavior of einsteinium ions in the gas phase is discussed in Section 12.6.6 and the concept of f→d promotion energy again is seen as being important for the different gas species and their reactions.

Blaise and Wyart (1992) have provided tabulated values for einsteinium's energy levels and atomic spectra. Tabulated values for the newer values are given in Table 12.2 for Es(I). The reader is referred to Blaise and Wyart (1992) or Wyart *et al.* (2005) for more extensive data and values for Es(II). Some other atomic values for einsteinium and its ionization potentials are also given in Table 12.3. Estimations of the first ionization potential for einsteinium were earlier given to be 6.42(3) eV (Rajnak and Shore, 1978) but the ionization potential has now been determined accurately by resonance ionization mass spectroscopy using some 10^{12} atoms of ^{254g}Es in an atomic beam (Erdmann *et al.*, 1998; Peterson *et al.*, 1998). The method used is based on measuring photoionization thresholds as a function of an applied electric field, followed by an extrapolation to a zero electric field. The first ionization potential determined experimentally was found to be to be 6.367(5) eV (see Table 12.3). Goodman *et al.* (1975) also examined the nuclear and quadrupole moments of einsteinium. Table 12.3 provides some basic values for Es, but the reader may find more details in the references.

12.5 THE METALLIC STATE

The scarcity and the high specific radioactivity of einsteinium isotopes have in general impeded the investigation of its chemistry, but particularity so for its metallic state. The self-radiation and accompanying heat are imposing factors, and the former rapidly destroys the metal's crystal lattice. The transplutonium elements are all electropositive metals, and react with water and the oxygen in air, but einsteinium metal is even more reactive. Strong reducing agents are needed to convert einsteinium oxide or its halides to the metal. Einsteinium is the most volatile of all the actinides preceding it, which dictates the preparative methods that can be used. It has been concluded that einsteinium is the first divalent actinide metal, in the sense that there are two bonding electrons in its conduction band compared to three or higher for the preceding actinide metals (see Section 12.4). It is followed by divalent fermium metal, and presumably divalent mendelevium and nobelium metals. The last member of the series, lawrencium, is presumably again a trivalent metal. It is likely to have a filled 5f level and a single d-electron; therefore, the promotion of an f-electron is not necessary for it to become trivalent. Thus, einsteinium is divalent like europium and ytterbium metals, but not trivalent like its homolog holmium, the other lanthanide metals, or the americium through californium metals.

Table 12.2 *Atomic properties of einsteinium*(I).[a]

Configuration	*Term*	J	*Energy* (cm^{-1})	w (10^{-3} cm^{-1})	A (10^{-3} cm^{-1})	B (10^{-3} cm^{-1})
$5f^{11}7s^2$	$^4I^0$	15/2	0.00	1543	2 725 729	−1 438 749
$5f^{11}7s^2$	$^4F^0$	9/2	7894.54	>792	25 905	159.1
$5f^{11}7s^2$	$^2H^0$	11/2	8759.27	1216	29 109	36
$5f^{11}7s^2$		137/2	10 244.29	>1391	3113	−1922
$5f^{11}(^4I_{15/2})7s8s$	$(15/2,1)^0$	17/2	33 829.35	6252		
$5f^{11}(^4I_{15/2})7s8s$	$(15/2,1)^0$	15/2	34 068.94	4153		
$5f^{11}7s7p$	^6I	15/2	17 803.09	3838	68 293	−793
$5f^{11}7s7p$	^6I	17/2	19 209.15	5938	93 954	−2173
$5f^{10}6d7s^2$	^6I	17/2	19 367.85	−245	−3777	14
$5f^{11}7s7p$		13/2, 15/2	19 788.32	−2103		
$5f^{10}6d7s^2$		13/2	28 118.65	2170	43 477	−289
$5f^{10}6d7s^2$		13/2, 15/2, 17/2	28 372.78	52		
$5f^{11}7s7p$		13/2	28 447.02	4576	92 872	−1714
$5f^{10}6d7s^2$		15/2, 17/2	28 578.60	−266		
$5f^{10}6d7s^2$		15/2, 17/2	28 689.74	837		
		15/2, 17/2	29 159.28	952		
$5f^{11}7s7p$		13/2	29 204.89	3138	63 762	−763
		11/2	31 829.03	4037	96 233	203
$5f^{10}6d7s^2$		13/2	31 886.3	1590		
		13/2	32 770.06	4437	91 272	573
		9/2	34 192.6			
		13/2	35 507.74			
		11/2	38 634.04			

[a] See Blaise and Wyart (1992) or Wyart *et al.* (2005) for complete set of data including Es(I) and Es(II) and references.

Table 12.3 *Properties of* ^{253}*Es.*

Property	*Value*	*References*
first ionization potential	6.42(3) eV (calc.)	Sugar (1974); Rajnak and Shore (1978)
first ionization potential	6.3676(5) eV (exp.)	Peterson *et al.* (1998); Erdmann *et al.* (1998)
nuclear spin	$I = 7/2$	Appendix I
electronic ground state	$J = 15/2$	
nuclear dipole moment, μ	$4.10(7)\mu_N$	Appendix I
nuclear quadrupole moment, Q_s	6.7(8)	Appendix I
K X-ray energies	$K\alpha_2$ 112.501(10)	Dittner and Bemis (1972)
	$K\alpha_1$ 118.018(10)	Dittner and Bemis (1972)
	$K\beta_3$ 131.848(20)	Dittner and Bemis (1972)
	$K\beta_1$ 133.188(20)	Dittner and Bemis (1972)

Small quantities of transplutonium metals have traditionally been prepared by different methods, two of which are mentioned here (Haire, 1982). The first is reduction of an actinide halide by an active metal (alkali or alkaline earth), and the desired actinide metal is left as a product. This is a suitable technique if the actinide has a lower volatility than the reductant or its halide product (i.e. lithium and lithium fluoride, which are both sufficiently volatile). The second approach is to reduce the actinide oxide with thorium or lanthanum metal and distill away the actinide product. The choice frequently depends on the volatility of the actinide metal. In the case of einsteinium, the latter technique is the most appropriate given its higher volatility. If einsteinium fluoride was reduced with lithium metal, it would be difficult to obtain the metal free of lithium fluoride in the distilled/condensed product.

The first reported attempt to prepare einsteinium metal (Cunningham and Parsons, 1971) used less than 1 μg of einsteinium, and involved distilling lithium metal onto EsF_3. The temperature was raised to 800°C and the sample than quench-cooled to give a material contaminated with lithium fluoride. Thin films of pure einsteinium were prepared subsequently by reducing Es_2O_3 with lanthanum metal followed by collecting the einsteinium metal distillate on electron microscopy grids (Haire and Baybarz, 1979). This reduction approach has become the normal preparative route for einsteinium metal, and has provided the first diffraction data from pure einsteinium metal.

Electron diffraction data for the metal prepared by oxide reduction consisted of over 14 diffraction lines and were obtained from 10–200 ng deposits. The very thin films reduced effects from both self-irradiation damage and self-heating in the metal from the ^{253}Es isotope, and they also allowed diffraction powder patterns to be obtained in a few seconds versus the 30–120 min often needed for X-ray powder analysis. The diffraction data obtained showed a face-centered cubic (fcc) (*Fm*3*m*) symmetry and generated a lattice parameter of 5.75(1) Å, which corresponds to a metallic radius of 2.03 Å. This radius compares with radii of 2.042 and 1.940 Å (Topp, 1965) for divalent europium and ytterbium metals, respectively, compared to much smaller radii (i.e. 1.734–1.877 Å) for the trivalent lanthanide metals and 1.691–1.725 Å for the trivalent americium through californium metals (Haire, 1990). The radii of Ba, Eu, Es, and Yb form a smooth curve, if radii are plotted versus atomic number (see Fig. 12.1 for the volume behavior of the latter three elements). These findings led to the conclusion that einsteinium is indeed the first divalent actinide metal, and this was subsequently supported by studies of the enthalpy of sublimation of einsteinium (see subsequent discussion) and thermochromatography studies with tracer levels of einsteinium. Selected data for einsteinium and selected f-element metals are given in Tables 12.4 and 12.5.

The elements americium through californium are trivalent metals and exhibit a double hexagonal close-packed (dhcp) room-temperature and an

Table 12.4 *Structural and physical properties of Es versus other f-electron metals.*

		Lattice parameters					
Metal	*Structure type*	a_0 (Å)	b_0 (Å)	c_0 (Å)	*Atomic radius* (Å)	*Atomic volume* (Å)	*References*
Es	fcc (*Fm*3*m*)	5.75(1)			2.03	47.5	Haire and Baybarz (1979)
Eu	bcc	4.578(1)			2.04	48.0	Topp (1965)
Yb	fcc	5.481(1)			1.940	41.2	Topp (1965)
Cf	fcc	4.78(1)			1.69	27.3	Haire (1990)
Cf	dhcp ($P6_3/mmc$)	3.384		11.040	1.691	27.37	Haire (1990)

Table 12.5 *Physical properties of Es versus Cf metals.*[a]

Metal	*Structure type*	*Density* (g cm^{-3})	*Melting point* (K): *boiling point* (K)	*Enthalpy of sublimation at* 298 K (kJ mol^{-1})	*Entropy* (J K^{-1} mol^{-1})	*Bulk modulus* (GPa)	*References*
Es	fcc (*Fm*3*m*)	8.84	1133:1269	134	89.4	15	Haire (1990)
Cf	dhcp ($P6_3/mmc$)	15.10	1173:2018	196	80.3	50	Haire (1990)

[a] Note: Am, Cm, and Bk metal values are similar to those for Cf; all four are 'trivalent' metals, while Es is a 'divalent' metal.

elevated-temperature fcc structure. The densities of the four trivalent transplutonium metals range from 13.6 to 15.1 g cm^{-3}, while einsteinium has a density of 8.84 g cm^{-3} (Haire, 1990). The cubic structure of einsteinium should be considered as reflecting its electronic bonding configuration rather than being a high-temperature form, as are the room temperature structures of europium (body-centered cubic, bcc) and ytterbium (fcc) in the lanthanide series. Europium remains bcc down to 5 K, even with 'cold working' of the material. In contrast, ytterbium transforms from its fcc structure to a hcp form below 270 K, which can be retained at room temperature. Einsteinium metal has been examined at liquid nitrogen temperature (Haire, 1980), where evidence for a hexagonal structure was obtained. However, it was not resolved in that work whether this was a temperature-induced change (comparable to ytterbium metal) or reflected a change from the effects of radiation damage to the einsteinium lattice.

Alloys of einsteinium with europium and with ytterbium ($\sim$1 mol%) have also been prepared by co-distilling the metals (Haire, 1982) from mixed oxides (einsteinium–europium and einsteinium–ytterbium) after reacting the oxide mixtures with lanthanum metal. With 100 μg of ^{253}Es, the self-heating/radiation in an Es–Yb alloy was sufficient to give rise to partial sublimation of the einsteinium product when it was isolated in vacuum.

A value for the melting point of einsteinium was obtained by observing the heating of deposits in an electron microscope (Haire and Baybarz, 1979). The melting point was taken as the point where "micro-puddles" were formed, in conjunction with calibration studies with other known metals done in a similar fashion. A value of (1133 ± 50) K was reported for the melting point of einsteinium metal. This value can be compared to the melting points of 1099 and 1097 K for europium and ytterbium metals, respectively, while the values for the trivalent lanthanide and americium through californium metals are higher, being (1173–1620) K (Haire, 1990).

At the tracer level, einsteinium–calcium metal mixtures were prepared and studied via thermochromatographic metal columns, where their sorption/condensation behaviors were monitored (Hübener, 1980). Data from this work supported the divalency of einsteinium metal. It was determined that ytterbium, einsteinium, fermium, and mendelevium all condensed at the same column length ($\sim$700 K), but deviations were found for europium, samarium, and calcium, where their behaviors were intermediate to the divalent and trivalent metals. One aspect of this thermochromatographic technique has been variation in results when different metals are used for the sorbers or columns.

Volatilities of these metals are correlated with f-electron promotional energies and the number of bonding electrons – the fewer the bonding electrons the higher the volatility. Estimates have been given by Nugent *et al.* (1969a) for the enthalpy of sublimation of these metals via extrapolations. Kleinschmidt *et al.* (1984, 1985) and Haire and Gibson (1989) have also reported experimental data for the enthalpies of sublimation and entropies of einsteinium metal.

The enthalpy for einsteinium also supports that it is a divalent metal. The enthalpy of sublimation of einsteinium is given as 133 kJ $mol^{-1}$and was found to agree closely with that for fermium (143 kJ mol^{-1}) (Haire and Gibson, 1989), the second divalent actinide metal. In the latter work on fermium, the enthalpy for einsteinium was reevaluated, and a value of 134 kJ mol^{-1} was determined for einsteinium, this value being slightly lower than that for fermium. However, this difference is not significant, given that error bars were estimated at ± 12 kJ mol^{-1}. In essence, the two values for einsteinium and that for fermium can be considered the same.

Subsequent studies of heavy elements (including einsteinium) via thermochromatography have been performed (Hübener *et al.*, 1994; Taut *et al.*, 1997, 1998) and results varied significantly with the metal of the columns used – five different metals were used in the work. With iron columns, californium, einsteinium, and fermium behaved the same; with niobium columns, einsteinium was intermediate to positions for californium and fermium, and in titanium columns, einsteinium and fermium behaved similarly (Hübener *et al.*, 1994). It was concluded that einsteinium and fermium were acting as divalent actinide metals while californium was 'borderline' between divalent and trivalent. Subsequently, similar studies with californium, einsteinium, and fermium tracers estimated einsteinium's enthalpy of sublimation to be 167 kJ mol^{-1} (Taut *et al.*, 1997), a significantly higher value than reported earlier by more direct methods (134 kJ mol^{-1}) but still lower than the enthalpy for californium determined by this technique (close to 200 kJ mol^{-1}). It was stated in Taut *et al.*'s work (1997) that the value for einsteinium is still typical for a divalent metal, although it was higher than that for fermium. Additional discussions on einsteinium thermochromatography are given together with the work on nobelium, where the two models are discussed in conjunction with *ab initio* calculations for actinide adsorption enthalpies (Eichler *et al.*, 2002), and in diffusion studies into tantalum (Legoux and Merinis, 1986).

The crystal entropy of einsteinium has been calculated using a correlation (Ward and Hill, 1976; Ward *et al.*, 1980; Ward, 1986) based on ytterbium metal, and a value of (89.4 ± 0.8) J K^{-1} mol^{-1} at 298 K was determined. For the 1133 K melting point of einsteinium (Haire and Baybarz, 1979), the enthalpy of melting was calculated to be 9.40 kJ mol^{-1} and the entropy as 8.30 J K^{-1} mol^{-1} by Ward and Hill (1976). The magnetic entropy for a $5f^{11}$ configuration gives a total angular momentum of $J = 15/2$ for the divalent einsteinium. A boiling point of 1269 K was also calculated (Kleinschmidt *et al.*, 1984) for the metal. One additional piece of information has been reported for the metal; its thermal conductivity has been estimated to be 10 W m^{-1} K^{-1} at 300 K (Ho *et al.*, 1972). The bulk modulus of einsteinium was estimated to be similar to those for europium and ytterbium metals. See Tables 12.4 and 12.5 for selected properties and values of einsteinium.

More recent work on the preparation of einsteinium metal provided the first isolated piece of pure einsteinium metal (~100 μg) and a 60 μg deposit (~200 μm in diameter) on platinum. These efforts were in conjunction with attempts to study the high-pressure behavior of the metal (Haire and Heathman, 2000) by energy-dispersive X-ray diffraction using high-intensity tungsten radiation. The pressure behavior of einsteinium metal is very interesting, as it could become a trivalent metal under pressure, where pressure provides the energy necessary to promote an f-electron to a bonding state. In essence, the volume of einsteinium may be reduced under pressure to force additional bonding, similar to that found in the trivalent Am through Cf metals. It was anticipated that applying additional pressure on a potential trivalent einsteinium product could even lead to a further reduction in volume and result in the formation of an einsteinium metal product with itinerant 5f electrons (Haire *et al.*, 2004). This can be understood by examining the volume curves shown in Fig. 12.1, where the volume reduction induces greater bonding. However, the intended study of einsteinium under pressure was not successful, as the intense self-irradiation of einsteinium destroyed both its crystal lattice and the platinum pressure marker present within a few minutes. But the recent preparative effort with einsteinium allowed a new level to be reached in obtaining elemental einsteinium – namely, an einsteinium metal product free of a supporting substrate (i.e. a 100 μg 'bulk form' of pure einsteinium metal).

12.6 COMPOUNDS OF EINSTEINIUM

12.6.1 Crystal data

Once the existence of a new element has been established, scientists strive to determine its chemical and physical properties. The extent to which this is possible depends on the availability and nature of the material, and the techniques that are or can be established to study it. With the availability of multiple micrograms of einsteinium it became feasible to prepare and examine 'bulk forms' of its compounds, although not without perturbations and limitations caused by its short half-life, high self-radiation field, and the heat associated with the decay (^{253}Es alpha decay corresponds to 15312 kJ mol^{-1} min^{-1}). For the preparation of compounds, one normally uses the ^{253}Es isotope (see earlier discussion on isotopes), given its greater availability. Some of the techniques used for microgram-sized samples of einsteinium have been discussed (Haire, 1981, 1982).

Only a few compounds of einsteinium have been prepared and have had their crystal structures identified. In this realm, there are induced changes or destruction of crystal lattices by the isotope's self-irradiation (alpha emission plus nucleus recoil) and the rapid ingrowth of the berkelium daughter (~3% per day, berkelium 'impurity'). For diffraction studies, the accompanying penetrating radiation (L, M and N X-rays, the gamma emissions from ^{254g}Es and its short-lived daughter, ^{250}Bk, also have serious effects on both X-ray detectors and/or X-ray film in a short time frame (the film is often used for small 1–2 μg sized samples).

Even with rotating anode-type generators with higher X-ray intensities, these difficulties with einsteinium are not overcome. Electron diffraction techniques do afford major advantages, as only small, very thin samples (which can be smaller than the alpha particle's range, where a minimum amount of its energy is transferred) are needed. This technique requires very short exposure times (seconds) and that the detection mode is located approximately 1 m from the sample, which avoids film or detector problems from the einsteinium radiations.

Although synchrotron radiation can supply more intense radiation for diffraction studies with einsteinium samples, two difficulties are encountered: (1) the destruction of the crystal lattice during the time of 'transportation' to the synchrotron beamline; (2) the difficulty of obtaining approvals to use the activity levels from the einsteinium at the synchrotron, or for setting up an apparatus for *in situ* preparation of the compounds on the beamline. Yet, the latter remains an option for dealing with some of the experimental problems with einsteinium's rapid radioactive decay.

As with many of the transuranium compounds, halides and oxides were among the first compounds of einsteinium to be prepared and studied, which is in accord with the fact that these have frequently been among the first to be prepared for new elements. These are also used often as a starting platform for synthesizing other materials. To overcome the experimental difficulties encountered with diffraction analysis of ^{253}Es or ^{254g}Es compounds, three approaches have been successful. One has been constant resynthesis of the compound during X-ray analysis, while another has been the use of very thin films, especially in conjunction with electron diffraction. The third has been to use very short exposures as can be accomplished by electron diffraction. Crystal data have been collected for the following materials: $EsCl_3$, EsOCl, Es_2O_3, $EsBr_3$, and EsI_3 (See Table 12.6). A discussion of X-ray diffraction techniques for einsteinium compounds is also available (Haire and Peterson, 1979).

The first crystal data for einsteinium compounds were obtained for the trichloride and the oxychoride via the constant synthesis technique (Fujita *et al.*, 1969a,b). The approach was to resynthesize these materials *in situ* at ~430°C. The trichloride was found to be hexagonal, isostructural with the actinium through californium trichlorides and the lanthanum through gadolinium trichlorides (UCl_3-type, space group $C^2_{6h}-C6_3/m$). The oxychloride was found to crystallize in the tetragonal PbFCl structure (space group $D^7_{4h}-P4/nmm$) and is isostructural with the trivalent lanthanum through erbium oxychlorides and the known actinium through californium oxychlorides. The lattice parameters, corrected to 298 K, are given in Table 12.6.

Einsteinium sesquioxide was the next compound for which diffraction data were acquired, and this involved the use of the electron diffraction technique. The samples were prepared by calcining an einsteinium nitrate salt *in situ* on

Table 12.6 *Compounds of di- and trivalent einsteinium characterized by structural and/or spectroscopic analysis.*

		Lattice parameters					
Compound	*Structure type*	a_0 (Å)	b_0 (Å)	c_0 (Å)	β(degree)	*Major absorption bands* (cm^{-1})	*References*
Es_2O_3	Mn_2O_3-bcc	10.766(6)				–	Haire and Baybarz (1973)
Es_2O_3	monoclinic	14.1	3.59	8.80	100	–	Haire and Eyring (1994)
Es_2O_3	La_2O_3-hexagonal	3.7		6.0		–	Haire and Eyring (1994)
$EsCl_3$	UCl_3-hexagonal	7.40(2)		4.07(2)		12 800,20 000, 23 000	Fujita *et al.* (1969a,b)
$EsCl_2$	–					11 100, 18 500, 24 500	Peterson *et al.* (1979); Fellows *et al.* (1977)
EsOCl	PbFCl-tetragonal	3.948(4)		6.702(19)		12 800,16 300	Young *et al.* (1981)
$EsBr_3$	$AlCl_3$-monoclinic	7.27(2)	12.59(3)	6.81(2)	110.8(2)	12 600, 19 800	Fellows *et al.* (1975)
$EsBr_2$	–					11 100,18 300	Young *et al.* (1976)
EsOBr	–					12 700	Peterson *et al.* (1979)
EsI_3	BiI_3-hexagonal	7.53(4)		20.84(5)		12 300	Haire (1978); Peterson (1979)
EsI_2	–					11 100	Young *et al.* (1981)
EsOI	–					12 700,16 100	Young *et al.* (1981)
EsF_3	–					13 200, 20 300, 27 000	Ensor *et al.* (1981)

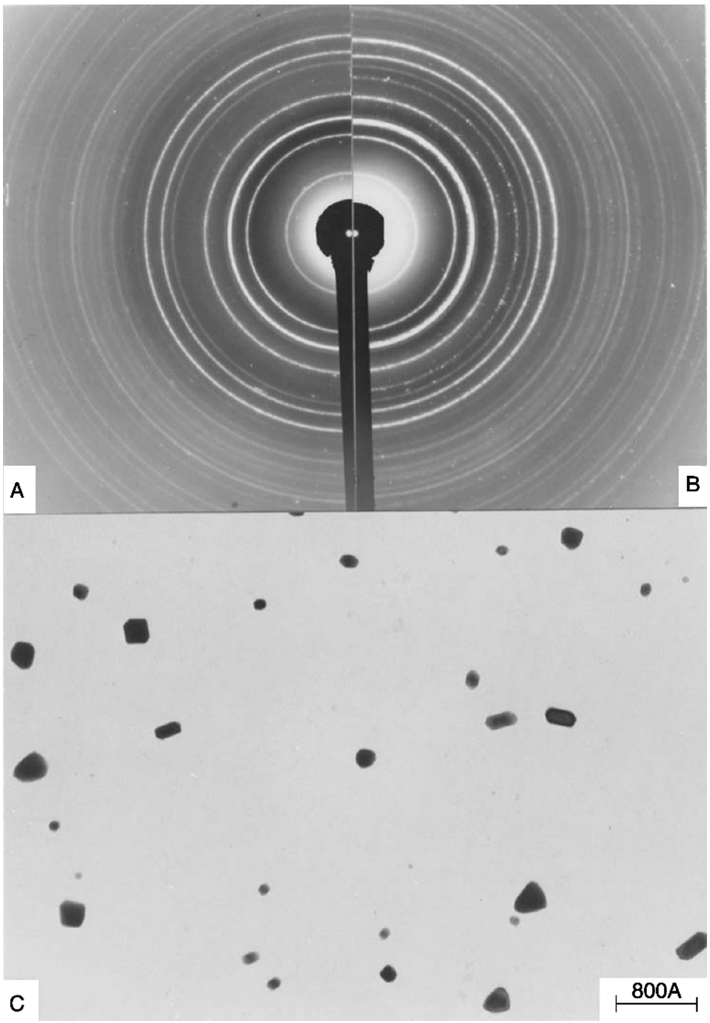

Fig. 12.5 *Electron diffraction patterns of* (*a*) Es_2O_3 *and* (*b*) Gd_2O_3; *particles of* (*c*) Es_2O_3 (*Haire and Baybarz*, 1973).

electron microscope grids in different atmospheres up to 1000°C, and then analyzing the products by electron diffraction (Haire and Baybarz, 1973).

Fig. 12.5 shows an electron diffraction pattern of cubic Es_2O_3 together with isostructural Gd_2O_3 and the small particles from which the einsteinium pattern was obtained. A bcc (α-Mn_2O_3-type, space group *Ia*3) Es_2O_3 was formed, which had a lattice parameter of 10.766(6) Å. Evidence for a higher oxide of einsteinium was not obtained. The parameter and ionic metal radius (calculated to be

Table 12.7 *Ionic radii of einsteinium and selected f-elements.*[a]

Ion	M^{2+} (CN 6)	M^{3+} (CN 6)	M^{3+} (CN 8)	M^{4+} (CN 6)	M^{4+} (CN 8)	*References*
Selected values from calculations						
Cf	1.125	0.945	1.066	0.827	0.925	David (1986)
Es	1.102	0.934	1.053	[0.818]	[0.914]	David (1986)
Fm	1.083	0.922	1.040	[0.811]	[0.906]	David (1986)
Eu	1.166	0.946	1.065	[0.807]	[0.903]	David (1986)
Gd	[1.140]	0.937	1.055	[0.799]	[0.894]	David (1986)
Tb	[1.119]	0.923	1.040	0.792	0.886	David (1986)
Calculated from consistent set of experimental oxide data						
Cf	–	0.949	–	0.859	–	Haire and Eyring (1994)
Es	–	0.928	–	–	–	Haire and Eyring (1994)
Eu	–	0.950	–	–	–	Haire and Eyring (1994)
Gd	–	0.938	–	–	–	Haire and Eyring (1994)
Tb	–	0.920	–	0.817	–	Haire and Eyring (1994)

[a] Radii are given in Å; [–] indicates interpolations.

0.928 Å) for this oxide were intermediate to those for Gd_2O_3 and Tb_2O_3, and just smaller than those for Cf_2O_3 (see Table 12.7).

Lattice parameters and ionic radii for the cubic sesquioxides of the f-elements are shown in Fig. 12.6, where a smooth relationship can be seen. These behaviors differ from the volume behaviors of the metals (see Fig. 12.1). The properties of einsteinium oxide and a comparison of its properties are also discussed in reviews (Baybarz and Haire, 1976; Haire and Eyring, 1994). As opposed to the metal, compounds of einsteinium (i.e. the oxide here) display lattice parameters and ionic radii similar to the comparable transplutonium and lanthanide compounds. All of the first five transplutonium sesquioxides form this cubic crystal form, but some may also exist in a monoclinic structure (Sm_2O_3-type, space group *C*2/*m*) or a hexagonal form (La_2O_3-type, space group *P*3*m*1), depending on the thermal history and the particular element in question (see Haire and Eyring, 1994).

Self-irradiation may also convert one structural form of the sesquioxide to another; this radiation effect has been discussed in an earlier review (Fuger, 1975). For einsteinium sesquioxide, both a monoclinic and a hexagonal form have been recorded (Haire *et al.*, 1985; Haire and Eyring, 1994). The monoclinic form was observed during oxidation of metal films below 1273 K, and this effect has also been observed with gadolinium metal films. The hexagonal oxide was observed in 'aged' cubic einsteinium sesquioxide. It could not be ascertained whether the monoclinic and/or hexagonal forms of Es_2O_3 resulted from being heated, from self-heating, or from self-irradiation damage. It is probable that the hexagonal form resulted from one of both of the latter two consequences; the hexagonal form of Es_2O_3 would be expected from systematics to be formed

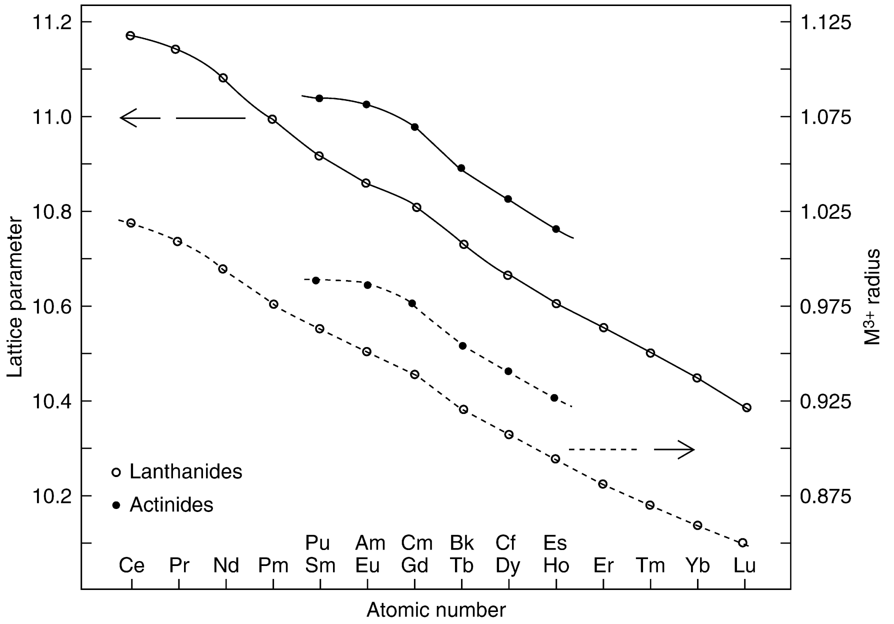

Fig. 12.6 *Lattice parameters and calculated radii for the cubic sesquioxides. A regular trend is observed with Es(*III*), as opposed to the different behavior observed with Es metal* (*Haire and Eyring*, 1994). *Parameters and radii are given in Å.*

only near its melting point (Baybarz and Haire, 1976; Haire and Eyring, 1994). Lattice parameters for the monoclinic and/or hexagonal structural forms of einsteinium sesquioxide must also be considered in this context. The monoclinic form of einsteinium sesquioxide was obtained after heating at temperatures lower than would be expected to bring about the thermal transformation from its cubic form. The values for the lattice parameters of the monoclinic and hexagonal forms of Es_2O_3 are however reasonable, based on ionic systematics for the lanthanide and first four transplutonium sesquioxides (Haire and Eyring, 1994), and allowing for some lattice expansion due to self-irradiation.

X-ray data were also obtained for $EsBr_3$ (Fellows *et al.*, 1975, 1977) and EsI_3 (Peterson, 1979; Haire, 1980). The $EsBr_3$ data were acquired from very small (~1 μg) pieces immediately after annealing at 400°C. Fifteen diffraction lines were obtained and indexed as a monoclinic $AlCl_3$-type structure, which is isostructural with $BkBr_3$ and $CfBr_3$ (Burns *et al.*, 1975). The information for EsI_3 was obtained from freshly sublimed films formed in a quartz capillary. The diffraction lines were indexed as belonging to a hexagonal BiI_3-type structure, which is also formed by the transneodymium triiodides and the five transplutonium triiodides. The first four lanthanide triiodides form a $PuBr_3$-type structure (Brown, 1968). Important factors in obtaining these diffraction data were the very small samples or thin films and some luck.

12.6.2 Spectrometry – solids

Another important technique for characterizing einsteinium compounds was the use of absorption spectrometry of solids (as well as for actinides in solution, see Section 12.6.3). Divalent compounds of einsteinium were characterized entirely by this technique, given the difficulties in obtaining diffraction data. A great aid in this technique was incorporation of a 'fingerprint' approach, where correlations between spectra and short-range local environment ('crystal environment'; X-ray diffraction requires 'longer-range order') allowed important conclusions to be drawn for the einsteinium compounds. This technique depends partly on the changes in metal ion coordination in the structures. One advantage of this technique is it allows samples to be prepared, annealed, and/or chemically converted in quartz capillaries, while permitting spectral analyses of intermediate products to follow the completeness of the changes being sought (i.e. reduction of a trihalide with hydrogen) in the same system. This approach was particularly suited to halides, as they had modest melting points, and with care, the melts can be solidified to transparent solids or even single crystals. The technique employed a microscope–spectrometer system, which has been described (Young *et al.*, 1976, 1978, 1981). The einsteinium solid-state absorption spectra are characterized normally by sharp electronic f–f transitions. In addition, luminescence spectra have been obtained but the self-radiation of einsteinium also excites trace amounts of impurities and the quartz envelopes containing it, producing an additional source of luminescence that must be considered. Some of the solid-state absorption spectra for einsteinium compounds are shown in Fig. 12.7.

As discussed in Section 12.6.5, potentials ranging from –1.6 to –1.2 V are reported for the Es^{3+}–Es^{2+} couple in aqueous solutions; a value of –1.3V is adopted in Chapter 19. This potential offers an explanation for the ability to reduce einsteinium trihalides with hydrogen at elevated temperatures. This potential for einsteinium contrasts with the more negative $Am^{3+}-Am^{2+}$ through $Bk^{3+}-Bk^{2+}$ potentials, whose trihalides cannot be reduced by hydrogen. This smaller potential is in accord with the greater tendency for obtaining divalency with einsteinium (also see Section 12.6.5).

Several halide materials have been prepared and their solid-state absorption spectra obtained: $EsCl_2$ (Fellows *et al.*, 1975, 1977; Peterson *et al.*, 1977, 1979; Peterson, 1979; Young *et al.*, 1981); $EsBr_2$ and EsI_2 (Young *et al.*, 1976, 1978; Peterson *et al.*, 1979); for EsF_3 (Ensor *et al.*, 1981); and $EsBr_3$ and $EsCl_3$ (Fellows *et al.*, 1975, 1977; Peterson *et al.*, 1979; Young *et al.*, 1981). Efforts to prepare EsF_2 have not been successful and attempts to prepare EsI_3 have encountered difficulties involving the thermal reduction to EsI_2. The spectra obtained for the three divalent halides of einsteinium and that for $EsBr_3$ are shown in Fig. 12.7 (Peterson *et al.*, 1979). The distinct differences between the spectra of $EsBr_2$ and $EsBr_3$ are obvious, while the similarities in the spectra for the three dihalides are also evident. The cutoff in the near UV for the diiodide reflects charge transfer occurring in this sample. The absorption spectrum of

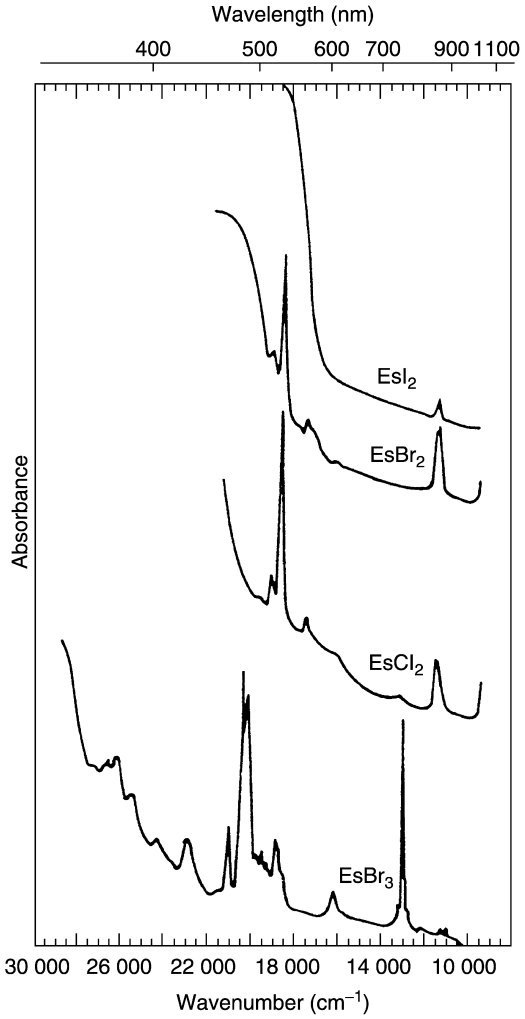

Fig. 12.7 *Solid-state absorption spectra for Es halides* (*Peterson* et al., 1979).

EsOBr is similar to that of $EsBr_3$, but it is sufficiently different to differentiate between the spectra of the two compounds and identify them.

Absorption spectrometry has also been used to study EsF_3 (Ensor *et al.*, 1981) and to then follow the decay products (^{249}Bk and ^{249}Cf, daughter and granddaughter) as they formed in the solid-state sample. From the spectrometric data, it was concluded that EsF_3 initially formed as a LaF_3-type trigonal phase.

Silicate matrices containing ^{253}Es have also been prepared. Results of recent spectroscopic investigations of their properties have been reported (Assefa *et al.*, 1999; Assefa and Haire, 2000, 2001). These studies concentrated on

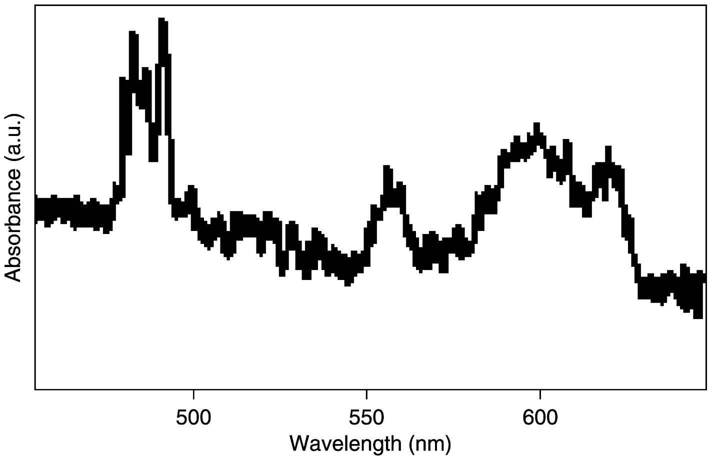

Fig. 12.8 *Absorption spectrum of Es in a borosilicate glass: absorption bands correspond to Es(*III*) (Assefa and Haire,* 2001).

self-luminescence from the materials, and examined the effects of the excitation source used, power of excitation, sample age, and nature of the sample matrix. Also obtained in that work were the absorption spectra of the einsteinium in this host matrix. The self-luminescence arising from einsteinium in these matrices was attributed to defect centers within the Si–O–Si network, nonbonding oxygen holes and Si cluster sites. It was determined that Es(III) was present; evidence for Es(II) was not found. The different spectra obtained for einsteinium in silicate matrices are shown in Figs. 12.8 and 12.9.

12.6.3 Other results – solids

Electron paramagnetic resonance spectra have been obtained for einsteinium placed in single-crystal hosts of CaF_2 (Edelstein *et al.*, 1970; Edelstein, 1971), in BaF_2 and SrF_2 (Bouissières *et al.*, 1980), and in BaF_2 and $SrCl_2$ (Boatner *et al.*, 1976). The spectra of Es^{2+} were similar in CaF_2 and BaF_2. The immediate reduction of Es(III) to Es(II) in the matrix from electron displacement via the alpha radiation field was suggested as the cause of the einsteinium reduction observed in these efforts. A $5f^{11}$ configuration with a ground state close to the $^4I_{15/2}$ (with a small admixture of a $^2K_{15/2}$ state) state was assigned to einsteinium. This indicated that only a minor perturbation of the inner 5f orbitals occurred from the crystal fields in the solids. A value of $\mu_n = 3.62(50)$ nm was reported for einsteinium.

Some information has also been acquired for the magnetism of einsteinium compounds. Preliminary magnetic measurements on einsteinium metal did not show a low temperature transition (Huray *et al.*, 1983). Studies on Es_2O_3 and EsF_3 indicated moments of 10.2(1) and 10.5(1) Bohr magetons, respectively. When corrected for the berkelium ingrowth present in the oxide sample, a value

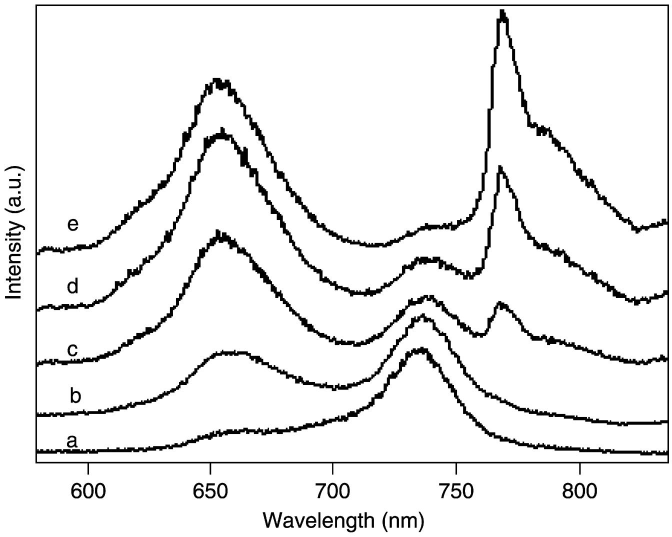

Fig. 12.9 *Photoluminescence spectra from a borosilicate glass doped with Es: excitation was with* 488 nm. *Spectra were recorded at laser powers of* (*a*) 100; (*b*) 310; (*c*) 600; (*d*) 800; *and* (*e*) 1000 mW (*Assefa and Haire*, 2001).

of 10.6(1) is obtained, which is in excellent agreement with a calculated $5f^{10}$ free-ion value (Huray *et al.*, 1983; Huray and Nave, 1987).

Preliminary information for the vaporization behavior of Es_2O_3 has been reported (Haire, 1994). The primary mode of vaporization for this oxide is the generation of atomic metal vapor, rather than via a monoxide (Es/EsO in the vapor was greater than 10:1). This situation arises as a result of the lower dissociation energy of EsO, which was estimated to be 460 kJ mol^{-1}. More recent calculations and work (Gibson, 2003; Gibson and Haire, 2003) discuss the electronic states, dissociation energies, and gaseous behavior of einsteinium. A brief discussion on these topics is given in Section 12.6.6.

The thermal behavior of einsteinium sesquioxide and the reduced formation of EsO(g) compares closely to the behaviors of europium and ytterbium oxides. The sesquioxides of europium and ytterbium also decompose mainly to atomic europium and ytterbium rather than form monoxides. A calculated estimate for the standard Gibbs energy of formation of Es_2O_3 at 298 K has been given as –1605 kJ mol^{-1}, and that for EsO_2 as –701 kJ mol^{-1} (Chapter 19). A tentative value for the Gibbs energy of formation for Es_2O_3 based on experimental behavior was given to be between –1650 and –1700 kJ mol^{-1} (Haire, 1994). Attempts to form EsO_2 or other compounds containing Es(IV) (i.e. $BaEsO_3$ or other materials that might help stabilize Es(IV)) have produced negative results (Haire and Bourges, 1980). Several estimated values for thermodynamics of formation of Es_2O_3, EsO_2, EsF_3, EsF_4, $EsCl_2$, and $EsCl_3$ are also given in Chapter 19.

12.6.4 Spectrometry – solutions

Spectrometry of einsteinium in solution has also been pursued, but only its trivalent state has been observed. The solution properties of the trivalent state are similar to those of the previous four transplutonium elements, and coordination number is an important variable. Given that the trivalent ion is present, bonding with ligands is often due to electrostatic effects. But as covalence for a given oxidation state increases across the series, second-order contributions from covalent interactions are possible. The ionic radius of einsteinium in solution should be only slightly smaller than that of californium(III). The free-ion energy levels for trivalent actinides have been given by Blaise and Wyart (1992) and Wyart *et al.* (2005). The ground state of einsteinium (Es(I)) is given as $^5I_8$, with the first excited state appearing at $\sim 10 \times 10^3$ cm^{-1} higher in energy (see Table 12.2).

The first observation of a solution spectrum was for $EsCl_3$ in hydrochloric acid by Cunningham *et al.* (1967), which was obtained by a special technique, where the micro-sized volume of the solution was kept constant by 'pumping' in liquid to overcome evaporation/radiolysis effects. Superior results were obtained subsequently with larger amounts of einsteinium, and 18 peaks between 370 and 1060 nm were obtained in a later work (Fujita *et al.*, 1969b). Electronic energy level and intensity correlations have also been made for Es(III) aquo ion, using data from dilute perchloric acid solutions (Carnall *et al.*, 1973). The absorption spectrum of Es(III) in solution, as demonstrated by Carnall *et al.*, is shown in Fig. 12.10. The band structure and intensities of einsteinium have also been discussed (Nugent *et al.*, 1969b, 1970; Varga *et al.*, 1973a,b).

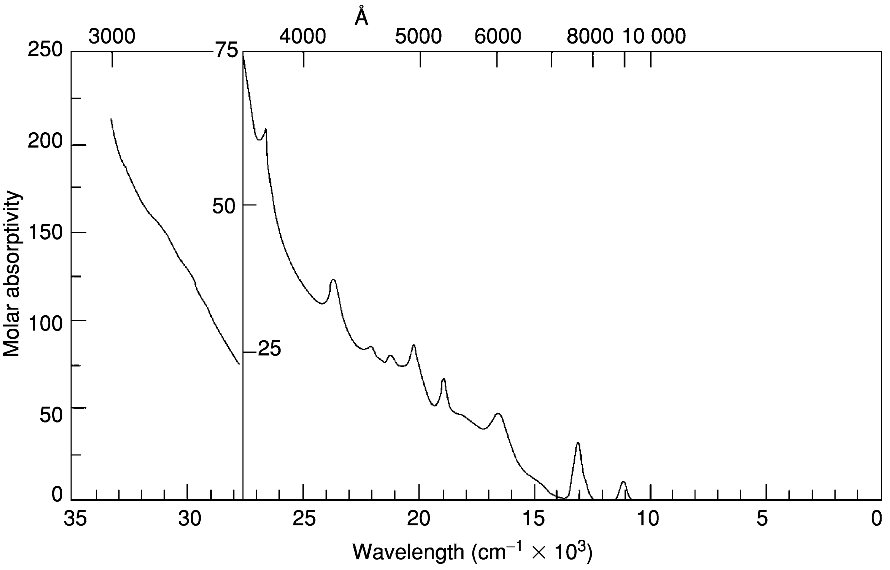

Fig. 12.10 *Solution spectrum of Es(III) in dilute perchloric acid (Carnall* et al., 1973).

The spectra fit the behavior expected for an Es(III) free ion, where the f–f transitions were believed to arise from mixed eigenstates, due to coupling that was intermediate between LS and jj.

Photoelectron spectrometry of einsteinium oxide provided spectra of the 4f lines obtained with MgKα excitation (Krause *et al.*, 1988). Binding energies for $4f_{5/2}$ (569.3(4) eV) and $4f_{7/2}$ (550.8(3) eV) of einsteinium were reported and compared to values for other actinides. These values compared well (within –1.0 and –0.1 eV, respectively) with theoretical binding energies The spin–orbit splitting for the 4f level was also measured and compared to the values obtained from theory. Beitz *et al.* (1992, 1998) have reported on the spectrometry and dynamics of the 5f electron states in Es(III) placed in a LaF_3 matrix.

The consequences of self-irradiation from einsteinium on selected clay minerals for waste isolation have also been probed employing ^{253}Es in solution. The einsteinium was sorbed from aqueous solution using two different clay minerals (kaolin and attapugite) and the morphology of the clay was followed with time using electron microscopy (Haire and Beall, 1979). The conclusion reached was that although the clay structure became damaged, einsteinium was still retained by the clay debris and not released to the solution.

12.6.5 Related studies in solution

The complex-ion chemistry of einsteinium has often been studied in conjunction with an examination of the stabilities of other trivalent actinide ions in solution, and often at the tracer level. Although einsteinium exhibits oxidation states of II, III with a potential for IV in the solid state, its solution chemistry is essentially that of a trivalent ion, and is often comparable to the actinide and lanthanide ions having similar radii. A list of the reported stability constants for einsteinium is given in Table 12.8. It has been concluded that chloride and possibly some thiocyanate complexes are the only outer-sphere complexes (water of hydration found between the ligand and the metal ion). The majority of the complexes are instead the inner-sphere type, which has been inferred from an increased stability constant as a function of increased atomic number, and from the enthalpy and entropy values for the formation of the complexes. Several different complexes have been studied, and these are shown in Table 12.8.

The radii and hydration numbers for actinide(III) ions have been derived from the Stokes' law approach using migration rates in electric fields or diffusion coefficients of tracers in electrolytes (Lundqvist *et al.*, 1981; Latrous *et al.*, 1982; Fourest *et al.*, 1983). David (1986) have also discussed the radii of actinides. In line with an expected greater covalent nature when progressing across the series, the Es(III) and Fm(III) hydrated ions are larger than those for earlier members of the series. A value of 0.492 nm (with up to ~16 molecules of water in the hydration sphere) has been estimated for the radius of einsteinium(III).

Several thermodynamic values have also been reported for einsteinium: (1) the molar activity coefficient in sodium nitrate solutions (Chudinov and Pirozhkov,

Table 12.8 *Cumulative stability constants of einsteinium complexes.*

	Log stability constants			
*Complex**	β_1	β_2	β_3	*References*
$EsCl^{2+}$	–0.18			Harmon and Peterson (1972a)
$EsOH^{2+}$	8.86			Hussonnois *et al.* (1973)
$Es(SO_4)_n^{3-2n}$	−2.19	−4.3	−4.93	McDowell and Coleman (1972)
$Es(SCN)_n^{3-n}$	0.559	−1.4	0.468	Harmon and Peterson (1972b)
$EsHCit^{2-}$	10.6			Hubert *et al.* (1974)
$Es(Cit)_2^{3-}$	12.1			Hubert *et al.* (1974)
$Es(\alpha HIB)^{2+}$	4.29			Aly and Latimer (1970a)
$Es(tartrate)^{+}$	5.86			Aly and Latimer (1970a)
$Es(malate)^{+}$	7.06			Aly and Latimer (1970a)
$EsDTPA^{2-}$	22.62			Myasoedov *et al.* (1974)
$EsDCTA^{-}$	19.43			Myasoedov *et al.* (1974)
$EsEDTA^{-}$	19.11			Myasoedov *et al.* (1974)
Es(II) PB (water)	6.2	106.4		Mikheev *et al.* (1988a)
Es(II) PB (acetonitrile)	6.6			Mikheev *et al.* (1988a)
Es(II) 18-6	log $K = 2.64$ water log $K = 4.70$ ethanol–water			Mikheev *et al.* (1986, 1988a,b, 1993a,b); Veleshko *et al.* (1993)

* Cit = citrate ion; αHIB = alphahydroxyisobutyrate; DTPA = diethylenetriaminepentaacetate; DCTA = trans-1,2 diamino cyclohexanetetraacetate ion; EDTA = ethylenediaminetetraacetate ion; PB = tetraphenyl borate; 18-6 = 18-crown-6.

1973); and (2) the Gibbs energy, enthalpy, and entropy of formation (Nugent, 1975; David *et al.*, 1978, 1986; Lebedev, 1978). The following values given were: enthalpy of formation, $\Delta_f H^0 = -603\,\text{kJ mol}^{-1}$; the entropy of formation, $\Delta_f S^0 = -100\,\text{J K}^{-1}\,\text{mol}^{-1}$; and the Gibbs energy, $\Delta_f G^0 = -573\,\text{kJ mol}^{-1}$.

Morss (1986) has provided estimates for several thermodynamic properties of einsteinium, ranging from the formation of aqueous ions, the activity products for the trihydroxide and dioxide, hydration enthalpies and ionization energies, and the enthalpies of formation and solution for the sesquioxide and dioxide. Also given are the calculated enthalpies of formation and solution for the dichlorides and trihalides (fluoride, chloride, bromide, and iodide) and the enthalpy of formation of the four tetrahalides.

Electrode potentials and diffusion coefficients for einsteinium were measured by radiopolarography using solutions and a dropping mercury cathode (Samhoun and David, 1979). A single half-wave for the III to 0 standard potential for reduction/amalgamation was reported as –1.460(5) V and a diffusion coefficient of $6 \times 10^{-6}\,\text{cm}^2\,\text{s}^{-1}$. Nugent (1975) suggested a corrected, more negative value (−1.98(7) V; after correcting for the amalgamation energy) as given in

Chapter 19. David (1986) discussed other values and gave selected ionic radii for several actinides, including einsteinium.

The amalgamation behavior of einsteinium and other actinide elements had been investigated earlier, where it was noted that amalgams of californium, einsteinium, and fermium displayed an anomalous behavior (Maly, 1969). This work suggested that these three elements may display a divalent state, given their preference to form amalgams in comparison to other actinides. Radiopolarography frequently employs mercury as one phase but phase diagrams for mercury alloys or dilute amalgams are not available for many of the transplutonium elements. One report (Guminski, 1996) has tabulated information from pre-1970 publications that contained incorrect data, which makes this publication of limited value.

Although einsteinium is the first element in the series to be divalent, the divalent ionic states of americium and californium have also been reported (see Chapters 8 and 11). The III → II reduction potential for einsteinium was initially estimated to be –1.6V, based on the lowest state for electron transfer (Nugent *et al.*, 1969b; Nugent, 1975), but was later suggested to be –1.21 V (from work with chloroaluminate salts (Duyckaerts and Gilbert, 1977)) and –1.18 V from radiopolarographic experiments (David *et al.*, 1978). Using a method of cocrystallization of einsteinium tracer with $SmCl_2$, Mikheev *et al.* (1972a,b) and Mikheev and Rumer (1972) had suggested einsteinium's reduction potential should be close to that for samarium ($-1.55(6)$ V). A value of -1.3 V is adopted in Chapter 19 for the standard potential of the Es^{3+}–Es^{2+} couple.

A series of papers over several years have dealt with Es^{2+} in selected solutions. These have been tracer-level studies involving different facets of the co-crystallization technique and of complexation studies. One of these papers (Mikheev *et al.*, 1986) investigated the cocrystallization of divalent ions of californium, einsteinium, fermium, samarium, europium, and ytterbium with SrI_2 (18-crown-6) using tetrahydrofuran as a solvent. The Tm^{2+} ion controlled the oxidation potential of the solution. Cocrystallization coefficients relative to strontium were given as close to 1, where the coefficients of the three actinides fell between values of 1.10 for samarium and 0.83 for ytterbium.

The behavior of einsteinium (together with other Am, Cf, and Fm) in $LiCl$–$NdCl_2$–$NdCl_3$ and in LiI–PrI_2 systems was examined (Kulyukhin *et al.*, 1997a,b). In the first molten salt, Nd(II) reduced Cf and Fm to a divalent state. In the second salt system, it was not clear if these actinides were reduced to their divalent or monovalent states. Ratios of the actinide distribution coefficients to those of samarium were reported for both salt systems. Mikheev *et al.* (2004) have reviewed the lower oxidation states of actinides with regard to cocrystallization coefficients in melts, and provided a distribution coefficient for einsteinium versus strontium ($D_{Es/Sm} = 0.94$).

Complexation and cocrystallization of einsteinium with 18-crown-6 in water and water–ethanol mixtures were reported by Mikheev *et al.* (1993a,b). Log K values measured for water and the water–ethanol mixtures were 2.64

and 4.70, respectively. The solvent effects on cocrystallization of Es^{2+} with $SrCl_2$ were reported by Mikheev *et al.* in the 1993b reference. Mikheev *et al.* (1986) had also looked at cocrystallization of Es^{2+} with SrI_2–18-crown-6 complexes, and the effects of water on the cocrystallization and solubility of einsteinium in $Sr(Sm)SO_4$ systems (Mikheev *et al.*, 1987). In the latter work, hydration values could be estimated for Es^{2+} from radii considerations of the different ions. Solubility products for einsteinium complexes with 18-crown-6, boron tetrafluoride, and boron tetraphenyl in tetrahydrofuran were discussed by Kulyukin and Mikheev (1997a,b). The distribution of einsteinium in molten salts containing reductants was described by Kulyukin *et al.* (1997). Veleshko *et al.* (1993) discussed the complexation of Es^{2+} with tetraphenylborate in acetonitrile, and Mikheev *et al.* (1988b) reported the data for the latter with water–ethanol mixtures.

Another study examined the effects of water on the cocrystallization of divalent europium, ytterbium, and einsteinium ions in the $Sr(Sm)SO_4$–ethanol system (Mikheev *et al.*, 1988a,b). Water affected the Es^{2+} coefficients up to 10 M water. The Gibbs energies of hydration were given for Eu^{2+}, Yb^{2+}, and Sr^{2+} ions and were assumed to extend to Es^{2+}. Values ranged from 1361 to 1461 kJ mol^{-1}. The coordination of these three ions was also examined with sodium tetraphenylborate in water–ethanol solutions (Mikheev *et al.*, 1988b). The coordination constants, β_1 and β_2, were determined and the observed trend suggested that the hydrated Es^{2+} ion was smaller than the two divalent lanthanide ions. The β_1 and β_2 values were given as log values: 6.2 and 106.4 for Es^{2+}; 1.7 and 52.7 for Eu^{2+}; and 6.5 and 25.7 for Yb^{2+}.

The effect of the solvent on the cocrystallization of Es^{2+} complexed with tetraphenylborate in acetonitrile and tetrahydrofuran was reported (Mikheev *et al.*, 1993a,b), where the einsteinium was complexed in the acetonitrile but not in the other solvent. The stability constants of the Es^{2+} complexes in acetonitrile were given as $\log \beta_1 = 6.6$ and $\log \beta_2 = 16.0$. Additional work on the complexation of Eu^{2+}, Yb^{2+}, and Es^{2+} with this reagent in different solvents suggested that outer sphere complexes are formed due to electron tunneling from the cation into the unsaturated π-bonds of the anion to form a single-electron bond (Mikheev *et al.*, 1993). The β_1 and β_2 values were given for the three divalent ions in water–ethanol mixtures, acetonitrile, and tetrahydrofuran. From the complexation of Es^{2+} in ethanol–water, acetonitrile, and tetrahydrofuran with the tetraphenylborate ion, it was concluded that complexes are not formed in tetrahydrofuran, as the solvent molecule is too large (Veleshko *et al.*, 1993). In the other two solvents, the smaller solvent molecule is inner sphere and complexes are formed.

The complexation of Es^{2+} with 18-crown-6 in aqueous ethanol and in water was studied, and the stability constants of the complex were determined (Mikheev *et al.*, 1993a,b). The log *K* values for einsteinium were given as 2.70 in water and 4.70 in ethanol–water (10 M). In both solvents, the log *k* varied in the order: $Eu^{2+} > Es^{2+} > Yb^{2+}$. The effect of perchlorate, tetrafluoroborate, and tetraphenylborate ions on the crystallization behavior of Es^{2+} with Sr–10-crown-6)I in tetrahydrofuran was reported (Kulyukhin and Mikheev, 1997a,b). The first two ions affected the cocrystallization constants but the tetraphenylborate ion did not, as it did not form complexes with the metal ion in this solvent. The stability constants were found to increase in going from the tetrafluoroborate to the perchlorate ions.

12.6.6 Compounds in the vapor state

The chemistry of elemental einsteinium in the vapor state was covered in Section 12.5. Elemental einsteinium vapor was generated by direct vaporization of it while ions as Es^+ or EsO^+ were produced by laser ablation of solid matrices or by heating oxides.

Recent gas-phase studies of einsteinium have provided important new insights into its chemistry. The concept of f→d promotion energy is also very important for different gas species and their reactions. The promotion energies for einsteinium's 5f electrons in the elemental state and in different ions are given in Figs. 12.11–12.13, which are taken from Gibson and Haire (2003). One plot is for the promotion energies for An^+ and Ln^+ ions from their ground state electronic configuration to the lowest-lying configurations that have two unpaired non-f valence electrons (i.e. $5f^{n-2}6d7s$), where the value for einsteinium requires some 150 kJ mol^{-1} more energy than its homolog, holmium. The second plot in Fig. 12.12 compares promotion energies for an An^+ ion from the ground state to a configuration having two non-5f valence electrons, a $5f^{n-2}6d7s$ versus a $5f^{n-2}7s^2$ state. The promotion energy for an einsteinium ion having two unpaired 7s electrons is lower. The third comparison in

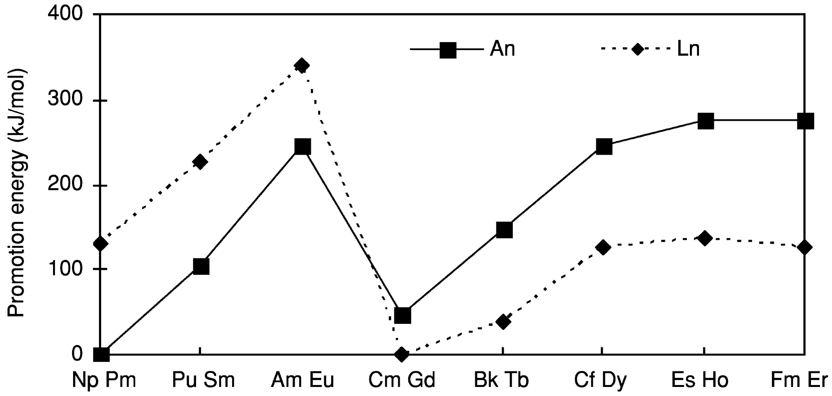

Fig. 12.11 *Promotion energies for An^+ and Ln^+ from ground states to the reactive lowest lying onfiguration having two unpaired, non-f electrons.* (*Gibson and Haire*, 2003). *Note the different trend with the higher members of each series.*

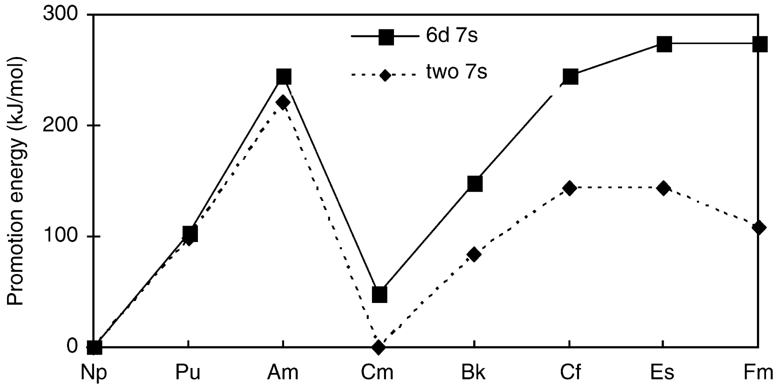

Fig. 12.12 *Promotion energies for An$^+$ ground state to produce a reactive state with two unpaired f electrons and a* 6d7s state (*solid line*) *versus a paired* 7s^2 *state* (*dashed line*). *Additional energy is needed to acquire the* 6d7s *reactive state.* (*Gibson and Haire*, 2003).

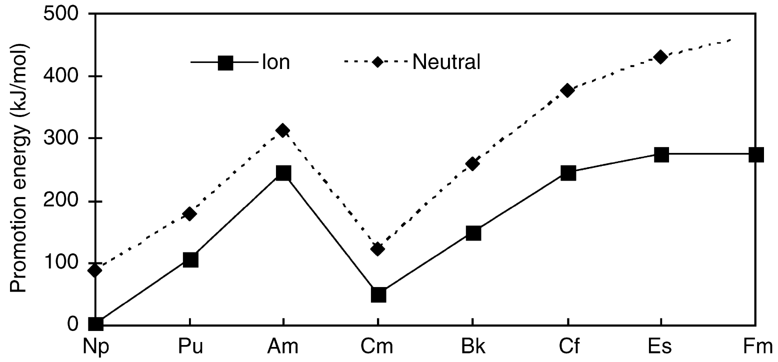

Fig. 12.13 *Promotion energies for An$^+$ for atomic ions and for An neutral atoms. The energies are for excitation from the ground states to* 6d7s *"divalent" configurations for An$^+$ and for* 6d7s *"trivalent" configurations for the atoms.* (*Gibson and Haire*, 2003).

Fig. 12.13 is made for the promotion energies from the ground state to the neutral atom ('trivalent' configuration, 5f^{n-3} 6d^{2}7s) and the Es$^+$ ion ('divalent' configuration, 5f^{n-2}6d7s), where the neutral atom has a promotion energy twice that for forming the An$^+$ ion.

Important information has been acquired from gas-phase studies of einsteinium, where laser ablations were used in conjunction with mass spectrometry (Gibson and Haire, 2003). The small yields of EsO$^+$ obtained relative to Es$^+$ ions indicated that the Es$^+$–O bond is significantly weaker than that for the earlier actinides.

Fluorination of Es^+ by extraction of fluorine atoms from hexafluoropropene demonstrated the stability of the divalent state of einsteinium. Using this technique, the first organometallic complex of einsteinium was observed ($EsC_4H_8^+$) in the gas phase. From this work the bond dissociation energy for EsO^+ was established and it was found to be smaller than those for EuO^+ and YbO^+, being more similar to that for TmO^+.

Systematic trends of einsteinium's chemistry terms of electronic structure and the energetics of the actinides and lanthanides were developed in this work (Gibson and Haire, 2003). The bond dissociation energy for Es^+–O was estimated to be (470 ± 60) kJ mol^{-1}, higher than the values for Eu^+–O (389 kJ mol^{-1}) and Yb^+–O (372 kJ mol^{-1}), but similar to that for Tm^+–O (478 kJ mol^{-1}) (Gibson and Haire, 2003). The dissociation energy for EsO was earlier reported to be 443 kJ mol^{-1} (Haire, 1994), smaller than dissociation energies for the americium through californium monoxides but similar to those for europium and ytterbium. Thus, einsteinium sesquioxide at high temperatures produces mainly elemental einsteinium rather than a monoxide, where the latter is found when heating curium sesquioxide to very high temperatures.

An important finding was that for einsteinium to become a reactive species, it was necessary to promote the Es^+ ion's ground state electronic configuration to the lowest-lying configuration having two unpaired non-5f valence electrons (i.e. 6d7s rather than $7s^2$). The Es^+ ion was found to be the least efficient of the Th^+ through Cf^+ ions at the dehydrogenation of organic materials, although it was only slightly less efficient than Am^+ and Cf^+ ions (Gibson and Haire, 2003).

In conjunction with the proposal that a hexavalent state of einsteinium could exist based on the added stability acquired from formation of a half-filled 5f orbital (i.e. $[Rn]5f^{11}7s^2 \rightarrow [Rn]5f^7$ for Es(VI)); Liebman, 1978), a potential compound could be the hypothetical EsF_6. As a molecular material, it would be expected to be volatile like UF_6 and PuF_6. From limited attempts to make this material, there is no experimental evidence to support its existence. Attempts to prepare AmF_6 have also proven it to be an elusive material, and far less stable than UF_6 or PuF_6. Therefore, it is unlikely that EsF_6 would be stable.

Studies have also been performed on the formation of volatile molecules using the concepts of thermochromatography (see Section 12.5), and the idea that a molecule in an unusual oxidation state may have a greater potential to form or to exist in the vapor state. From tracer experiments with ^{254}Es, evidence was claimed to support the existence of EsF_4 (Bouissières *et al.*, 1980). The technique consisted of treating EsF_3 with flowing fluorine and determining the temperature where the einsteinium's activity was deposited. This temperature was correlated with deposition temperatures for five other (Pu–Cf) actinide materials, also assumed to be transported as tetrafluorides. The volatility of fluorides should increase with higher oxidation states, so that the order of volatility would be expected to be hexafluoride > tetrafluoride > trifluoride. A point of concern with einsteinium may be the ability to form a tetrafluoride from its trifluoride at temperatures above the expected decomposition temperature of the tetrafluoride, as estimated from the behaviors of other actinide tetrafluorides.

Thermochromatography of ^{254g}Es in chlorinating carrier gas was used to estimate the adsorption of $EsCl_3$, and was found to be in agreement with a Monte Carlo model for its behavior (Eichler *et al.*, 2002). Volatile einsteinium hexafluoroacetylacetonate (HHFA) complexes have also been reported (Fedoseev *et al.*, 1987a,b). At the tracer level, these materials can form by passing vapors of the HHFA over einsteinium chloride solids at 200°C. A thermochromatographic study was then used to follow the reaction products. Mixed ligand complexes and lanthanide complexes were also studied. Solvated complexes of HHFA (as well as other organic materials) and the oxychlorides were found to be less volatile in the system. It was concluded that the complexes contained Es(III) rather than Es(II), the latter having a lower volatility.

The gas-phase chemistry of Es^+ and EsO^+ ions has been studied by a laser ablation technique (Gibson and Haire, 2003). The behavior of the Es^+ ion was found to be comparable to that of other actinide ions. The yield of EsO^+ ions suggests that the Es^+–O bond energy is significantly lesser that that of other such actinide ions (i.e. Bk^+–O). By performing chemical reactions in the gas phase between these einsteinium ions and other materials (halogenated organics, alkenes, etc.), it was possible to ascertain important aspects of the chemical behavior of einsteinium in the gas phase, and the ability to form organometallic compounds of einsteinium.

12.7 ATOMIC AND IONIC RADII, AND PROMOTION ENERGIES – THEIR IMPORTANCE IN EINSTEINIUM'S OVERALL SCIENCE

The radii of ions, molecules, and atoms are important in the chemistry and physics of materials as well as for estimation/interpolation of their behaviors. For einsteinium there is a considerable difference in its atomic radius compared to the four previous transplutonium elements, and this is reflected in its properties and science. For divalent and trivalent einsteinium ions, much of their solid and solution behaviors reflect their radii, and in these states einsteinium often behaves similarly to the comparable oxidation states of the other transplutonium and lanthanide ions. In the gas state, bonding energies and potentials (oxidation and promotion) are also of major chemical importance.

The atomic and ionic radii for a given number of bonding electrons or for an oxidation state of the f-elements, in principle, should decrease in a uniform manner across each series (well-established f-element contraction phenomena). This contraction with atomic number has been found to be is in good agreement with multidimensional Dirac–Fock calculations (Desclaux and Freeman, 1984). Ionova *et al.* (1978) have also calculated einsteinium's radius via Hartree–Fock approximations. Thus, these radii are often useful for extrapolations of behavior and properties.

In the case of atomic radii, one observes that einsteinium's radius compares well with radii of europium and ytterbium; as a result of it being a divalent rather than a trivalent metal (see Section 12.5 and Fig. 12.1). The divalent atomic radii of these elements are considerably larger than the trivalent atomic radii of these f-elements, as expected from one less bonding electron. This comes about in part due to the larger promotion energy for changing an f-electron in einsteinium to a 'd' state to enable additional bonding. As a result, einsteinium is the first divalent actinide metal.

With ionic compounds, many are found to form similar, isostructural phases, which is well established in oxide systems (Haire and Eyring, 1994). The ion-exchange behavior of the trivalent ions in solution also shows this correlation (Seaborg and Loveland, 1990). The ionic radius of Es(III), which varies with the coordination number, has been determined from different compounds. From sesquioxide lattice parameters for the actinides and lanthanides (Haire and Eyring, 1994), the ionic radius of Es^{3+} (0.928 Å) is slightly smaller than that of Cf^{3+}, and midway between the radii for Tb^{3+} (0.920 Å) and Gd^{3+} (0.938 Å). Another set of ionic radii has been given by David (1986), which shows a similar relationship. Thus, similar oxide-phase behavior is expected for these ions. The relative behaviors of the sesquioxide lattice parameters and the ionic radii are shown in Fig. 12.6 and Table 12.7, including calculated radii for Es(II) ions. Values are also given for potential Es(IV) ions; these ions would have different coordination numbers and show somewhat different behaviors than the Es(II) and Es(III) ions.

Einsteinium's sesquioxide and trivalent halide-phase behaviors in several solid compounds are found to be comparable to the lanthanides discussed above. In the case of cation-exchange behavior, the elution behavior from ion-exchange columns for a given oxidation state is generally in the order of the radii of the hydrated ions, with the largest or more readily complexed ions eluting first (einsteinium before californium). With elution from a cation column using α-HIB, einsteinium is found at a position between dysprosium and holmium (einsteinium's lanthanide homolog; Seaborg and Loveland, 1990).

Thus, einsteinium's atomic and ionic radii are important factors in the science of einsteinium. They often serve as useful information to understand, predict, and/or extrapolate the behavior of einsteinium. And the $f \rightarrow d$ electron promotion energy is also very important to understanding elemental einsteinium, as well as several facets of einsteinium's gas-phase chemistry.

ACKNOWLEDGMENTS

Research was sponsored by the Division of Chemical Sciences, Geosciences and Biosciences, Office of Basic Energy Sciences, U.S. Department of Energy, under contract DE-ACO5-00OR22725 with Oak Ridge National Laboratory, managed and operated by UT-Battelle, LLC.

REFERENCES

Ahmad, I., Sjoblom, R. K., and Barnes, R. F. (1970) *Nucl. Phys. A*, **141**, 141–7.

Ahmad, I. and Wagner, F. (1977) *J. Inorg. Nucl. Chem.*, **39**, 1509–11.

Aly, H. F. and Latimer, R. M. (1970a) *Radiochim. Acta*, **14**, 27–31.

Aly, H. F. and Latimer, R. M. (1970b) *J. Inorg. Nucl. Chem.*, **32**, 3081–7.

Aly, H. F., Sjoblom, R. K., and Barnes, R. F. (1970) *Radiochim Acta*, **14**, 27–31.

Assefa, Z., Haire, R. G., and Stump, N. A (1999) Abstract NUCL-164 American Chemical Society, 218th National Meeting, New Orleans, LA.

Assefa, Z. and Haire, R. G. (2000) Abstract NUCL-146, American Chemical Society, 219th National Meeting, San Francisco, CA.

Assefa, Z. and Haire, R. G. (2001) ACS Symp. Ser. 778 (eds. P. G. Elter and W. R. Heineman), American Chemical Society, Washington, DC, ch. 20, pp. 329–66.

Baybarz, R. D., Knauer, J. B., and Orr, P. B. (1973) USAEC Report, ORNL-4672, Oak Ridge National Laboratory.

Baybarz, R. D. and Haire, R. G. (1976) *J. Inorg. Nucl. Chem.*, Suppl., pp. 7–11.

Beitz, J. V., Liu, G. K., Morss, L. R, and Williams, C. W. (1992) Abstract NUCL-105 American Chemical Society, 203th National Meeting, San Francisco, CA.

Beitz, J. V., Williams, C. W., and Liu, G. K. (1998) *J. Alloys Compds*, **271**, 850–3.

Benker, D. E., Chattin, F. R., Collins, E. D., Knauer, J. B., Orr, P. B., Ross, R. G., and Wiggens, J. T. (1981) in *Transplutonium Elements, Production and Recovery,* ACS Symp. Ser. 161 (eds. J. D. Navratil and W. W. Schultz), American Chemical Society, Washington, DC, pp. 161–72.

Bigelow, J. E. (1974) in *Gmelin Handbuch der Anorganischen Chemie, Suppl. Ser., Transuranium*, vol.7b, part A1, II, *The Elements*, Springer-Verlag, Berlin, pp. 326-36.

Bigelow, J. E., Collins, E. D., and King, L. J. (1980) in *Actinide Separations* ACS Symp. Ser. 117 (eds. J. D. Navratil and W. W. Schulz), American Chemical Society, Washington, DC, pp.147–55.

Blaise, J. and Wyart, J.-F. (1992) Energy Levels and Atomic Spectra of Actinides. in *International Tables of Selected Constants*, Curie University, Paris, pp. 401–7; and the WEB, www.lac.u-psud.fr/Database/Tab-energy (einsteinium).

Boatner, L. A., Reynolds, R. W., Finch, C. B., and Abraham, M. M. (1976) *Phys. Rev. B*, **13**, 953–8.

Bouissières, G. Jouniaux, B., Legoux, Y., Mérinis, J., David, F., and Samhoun, K. (1980) *Radiochem. Radioanal. Lett.*, **45**, 121–8.

Brewer, L. (1971a) *J. Opt. Soc. Am.*, **61**, 1101–11.

Brewer, L. (1971b) *J. Opt. Soc. Am.*, **61**, 1666–82.

Brooks, M. S. S., Johansson, B., and Skriver, H. K. (1984) Electronic Structure and Bulk Ground State Properties of the Actinides. in *Handbook on the Physics and Chemistry of the Actinides* vol.1 (eds. A. J. Freeman and G. H. Lander), North-Holland, Amsterdam, pp. 165–76.

Brown, D. (1968) *Halides of the Lanthanides and Actinides,* John Wiley, London, pp. 117–71.

Burns, J. H., Peterson, J. R., and Baybarz, R. D. (1975) *J. Inorg. Nucl. Chem.*, **35**, 1171–7.

Campbell, D. O. (1970) *Ind. Eng. Chem. Process. Des. Dev.*, **9**, 95–9.

Campbell, D. O. (1981) in *Transuranium Elements – Production and Recovery,* ACS Symp. Ser. 161 (eds. J. D. Navratil and W. W. Schulz), American Chemical Society, Washington, DC, pp. 133–46.

Carnall, W. T., Cohen, D., Fields, P. R., Sjoblom, R. K., and Barnes, R. F. (1973) *J. Chem. Phys.*, **59**, 1785–9; and references therein.

Choppin, G. R. and Silva, R. J. (1956) *J. Inorg. Nucl. Chem.*, **3**, 153–4.

Chudinov, E. G. and Pirozhkov, S. V. (1973) *Sov. Radiochem.*, **15**, 195–9.

Collins, E. D., Benker, D. E., Chattin, F. R. Orr, P. B., and Ross, R. G. (1981) in *Transuranium Elements – Production and Recovery,* ACS Symp. Ser. 161 (eds. J. D. Navratil and W. W. Schulz), American Chemical Society, Washington, DC, pp. 147–60.

Conway, J. G. (1979) in *Proc. Symp. Commemorating the 25th Anniversary of Elements 99 and 100*, Report LBL-7701 (ed. G. T. Seaborg), Nat. Tech. Serv., Springfield, VA, p. 9.

Conway, J. G. (1986) in *The Chemistry of the Actinide Elements,* 2nd edn, vol. 2 (eds. J. J. Katz, G. T. Seaborg, and L. R. Morss), Nuclear Spins and Moments of the Actinides, Appendix I, Chapman & Hall, New York, pp. 1647–48; and references therein.

Cunningham, B. B., Peterson, J. R., Baybarz, R. D., and Parsons, T. C. (1967) *Inorg. Nucl. Chem. Lett.*, **3**, 519–21.

Cunningham, B. B. and T. C. Parsons, (1971) USAEC Doc. URCL-20426, p. 239.

David, F., Samhoun, K., Guillaumont, R., and Edelstein, N. (1978) *J. Inorg. Nucl. Chem.*, **40**, 69–74.

David, F. (1986) *J. Less Common Metals*, **121**, 27–42.

Desclaux, J. P. and Freeman, A. J. (1984) Atomic Properties of the Actinides, in The Handbook on the Physcis and Chemistry of the Actinides (eds. A.J. Freeman and G. H. Lander), Elsevier, North-Holland, Amsterdam, pp. 1–78.

Dittner, and P. E. Bemis, C. E. (1972) *Phys. Rev A*, **5**, 481–7.

Duyckaerts, and G. Gilbert, B. (1977) *Inorg. Nucl. Chem. Lett.*, **13**, 537–42.

Edelstein, N., Conway, J. G., and Fujita, D. (1970) *J. Chem. Phys.* **52** (12), 6425–30.

Edelstein, N. (1971) *J. Chem. Phys.*, **54**, 2488–91.

Eichler, B., Adams, J., Eichler, R., Gäggeler, H. W., and Peterson, J. R. (2002) *Radiochim. Acta*, **90**, 895–7.

Elesin, A. A., Nikolaev, V. M., and Shalimov, V. V. (1986) *Sov. Radiochem.*, **28**, 723–6.

Ensor, D. D., Peterson, J. R., Haire, R. G., and Young, J. P. (1981) *J. Inorg. Nucl. Chem.*, **43**, 2425–7.

Erdmann, N., Nunnemann, M., Eberhardt, K., Huber, G., Köhler, S., Kratz, J. V., Passler, G., Peterson, J. R., Trautmann, N., and Waldek, A. (1998) *J. Alloys Compds*, **271/273**, 837–40.

Fedoseev, E. V., Aizenberg, M. I., and Travnikov, S. S. (1987a) *Sov. Radiochem.*, **29**(6), 677–81.

Fedoseev, E. V., Aizenberg, M. I., and Travnikov, S. S. (1987b) *Sov. Radiochem.*, **116**(1), 183–92.

Fellows, R. L., Peterson, J. R., Noé, M., Young, J. P., and Haire, R. G. (1975) *Inorg. Nucl. Chem. Lett.*, **11**, 737–42.

Fellows, R. L., Young, J. P., Haire, R. G., and Peterson, J. R. (1977) in *The Rare Earths in Modern Science and Technology* (eds. G. J. McCarthy and J. J. Rhyne), Plenum Press, New York, pp. 493–9; also cited in Report LBL-7701, p. 55.

Fields, P. R., Studier, M. H., Diamond, H., Mech, J. F., Inghram, M. G., Pyle, G. L., Stevens, C. M., Fried, S., Manning, W. M., Ghiorso, A., Thompson, S. G., Higgins, G. H., and Seaborg, G. T. (1956) *Phys. Rev.*, **102**, 180–2.

Fourest, B., Duplessis, J., and David, F. (1983) *J. Less Common Metals*, **92**, 17–27.

Fuger, J. J. (1975) in*International Review of Science, Inorganic Chemistry,* ser. II, vol.7 *Lanthanides and Actinides* (ed. K. W. Bagnall), Butterworths, London, pp. 151–94.

Fujita, D. K., Cunningham, B. B., Parsons, T. C., and Peterson, J. R. (1969a) *Inorg. Nucl. Chem. Lett.*, **5**, 245–50.

Fujita, D. K., Cunningham, B. B., and Parsons, T. C. (1969b) *Inorg. Nucl. Chem. Lett.*, **5**, 307–13.

Ghiorso, A., Thompson, S. G., Higgins, G. H., Seaborg, G. T., Studier, M. H., Fields, P. R., Fried, S. M., Diamond, H., Mech, J. F., Pyle, G. L., Huizenga, J. R., Hirsch, A., Manning, W. M., Browne, C. I., Smith, H. L., and Spence, R. W. (1955) *Phys. Rev.*, **99**, 1048–9.

Gibson, J. K. (2003) *J. Phys. Chem. A*, **107**, 7891–9.

Gibson, J. K. and Haire, R. G. (2003) *Radiochim. Acta*, **91**, 441–8.

Goodman, L. S., Diamond, H., and Shanton, H. E. (1975) *Phys. Rev. A*, **11**, 499–504.

Guminski, C. (1996) *J. Phase Equilib.*, **17**(5), 443–4.

Gutmacher, R. G., Evans, J. E., and Hulet, E. K. (1967) *J. Opt. Soc. Am.*, **57**, 1389–90.

Haire, R. G. and Baybarz, R. D. (1973) *J. Inorg. Nucl. Chem.*, **35**, 489–96.

Haire, R. G. (1978) unpublished data, ORNL Report 5485.

Haire, R. G. and Baybarz, R. D. (1979) *J. Phys. Colloq.*, **40**(C4), 101–2.

Haire, R. G. and Beall, G. W. (1979) in *Consequences of Radiation from Sorbed Transplutonium Elements on Clays Selected for Waste Isolation,* ACS Symp. Ser. 100 (ed. S. Fried), American Chemical Society, Washington, DC, pp. 291–5.

Haire, and R. G. Peterson, J. R. (1979) *Advances in X-ray Analysis,* vol. 22 (eds. G. J. McCarthy, C. S. Barrett, and C. O. Rund), Plenum Press, New York, pp. 101–9.

Haire, R. G. (1980) in USDOE Report, ORNL-5665, 71.

Haire, R. G. and Bourges, J. (1980) Presented at Journées de Actinides, Stockholm, Sweden, unpublished work.

Haire, R. G. (1981) in USDOE Report, ORNL-5817, p. 60.

Haire, R. G. (1982) Preparation of Transplutonium Metals and Compounds in *Actinides in Perspective* (ed. N. M. Edelstein), Pergamon, Oxford, pp. 309–42.

Haire, R. G., Young, J. P., and Peterson, J. R. (1985) Abstract NUCL-24, American Chemical Society, 189th National Meeting, Miami Beach, FL.

Haire, R. G. and Gibson, J. K. (1989) *J. Chem. Phys.*, **91**, 7085–96.

Haire, R. G. (1990) in *Properties of the Transplutonium Metals*, ASM International, Materials Park, Ohio, pp. 1198–201.

Haire, R. G. (1994) *J. Alloys Compds*, **213/214**, 185–93.

Haire, R. G. and Eyring, L. (1994) in *Handbook on the Physics and Chemistry of Rare Earths,* vol. 18 *Lanthanides and Actinides Chemistry* (eds. K. A. Gschneidner, Jr, L. Eyring, G. R. Choppin, and G. H. Lander), North-Holland, New York, pp. 414–505.

Haire, R. G. and Heathman, S. (2000) unpublished data.

Haire, R. G., Heathman, S., Le Bihan, T., Lindbaum, A., and Iridi, M. (2004) Investigations of Actinide Metals and Compounds Under Pressure Provide Important Insights Into Bonding and Chemistry. in *Materials Research Society Proceedings, Actinides –Basic Science, Applications and Technology,* vol. 802 (eds. L. Soderholm, J. J. Joyce, M. F. Nichols, D. K. Shuh, and J. G. Tobin), MRS, Warrendale, PA, pp. 15–21.

Harbour, R. M. (1972) *J. Inorg. Nucl. Chem.*, **34**, 2680–1.

Harmon, H. D. and Peterson, J. R. (1972a) *Inorg. Nucl. Chem. Lett.*, **8**, 57–63.

Harmon, H. D. and Peterson, J. R. (1972b) *J. Inorg. Nucl. Chem.*, **34**, 1381–97.

Hatsukaway, Y., Ohtsuki, T., and Sueki, K. (1989) *Nucl. Phys. A*, **500**(1), 90–110.

Ho, C. Y., Powell, R. W., and Lilly, P. E. (1972) *J. Phys. Chem. Ref. Data*, **1**, 418

Horwitz, E. P., Sauro, L. J., and Bloomquist, C. A. (1966) *J. Inorg. Nucl. Chem.*, **29**, 2033–7.

Horwitz, E. P., Bloomquist, C. A. A., and Henderson, D. J. (1969) *J. Inorg. Nucl. Chem.*, **31**, 1149–70.

Horwitz, E. P., Chiarizia, R., Dietz, M. L., Diamond, H., and Nelson, D. M. (1993) *Anal. Chim. Acta*, **281**, 361–72.

Horwitz, E. P., Chiarixia, R., and Alexandratos, S. (1994) *Solv. Extr. Ion Exch.*, **12**(4), 831–45.

Hübener, S. (1980) *Radiochem. Radioanal. Lett.*, **44**, 79–86.

Hübener, S., Eichler, S. B., and Schädel, M. (1994) *J. Alloys Compds*, **213**, 429–32.

Hubert, S., Hussonnois, M., Billard, L., Goby, G., and Guillaumont, R. (1974) *J. Inorg. Nucl. Chem.*, **36**, 2361–6.

Hulet, E. K., Gutmacher, R. G., and Coops, M. S. (1961) *J. Inorg. Nucl. Chem.*, **17**, 350–60.

Hulet, E. K. and Bodé, D. D. (1972) in *MTP International Review of Science, Inorganic Chemistry,* Ser. I, vol. 7 *Lanthanide and Actinides* (ed. K. W. Bagnall), Butterworths, London, pp. 1–46.

Huray, P. G., Nave, S. E., and Haire, R. G. (1983) *Magnetism of the Heavy 5f Elements,* in *The Rare Earths in Modern Science and Technology* (eds. J. J. Rhyne, H. B. Silber, and G. J. McCarthy), Elsevier, New York, pp. 293–300.

Huray, P. G. and Nave, S. E. (1987) Magnetic studies of the Transplutonium Actinides, in *Handbook on the Physics and Chemistry of the Actinides* (eds. A. J. Freeman and G. H. Lander), vol. 5, 311–72.

Hussonnois, M., Hubert, S., Billard, L., and Guillaumont, R. (1973) *Radiochem. Radioanal. Lett.*, **15**, 4756

Hyde, E. K., Perlman, I., and Seaborg, G. T. (1964) The Transuranium Elements. in *The Nuclear Properties of the Heavy Elements II,* Prentice-Hall, Englewood Cliffs, NJ, pp. 946–64.

Ionova, G. V., Mikheev, N. B., and Spitsyn, V. I. (1978) *Sov. Radiochem.*, **20**, 89–92.

Ishimori, T. (1980) in *Actinide Separations,* ACS Symp. Ser. 117 (eds. J. D. Navratil and W. W. Schulz), American Chemical Society, Washington, DC, pp. 333–50.

King, L. J., Bigelow, J. E., and Collins, E. D. (1981) in *Transuranium Elements – Production Recovery,* ACS Symp. Ser. 161 (eds. J. D. Navratil and W. W. Schulz), American Chemical Society, Washington, DC, pp. 133–46.

Kleinschmidt, P. D., Ward, J. W., Matlack, G. M., and Haire, R. G. (1984) *J. Chem. Phys.*, **81**, 473–7.

Kleinschmidt, P. D., Ward, J. W., Matlack, G. M., and Haire, R. G. (1985) *High Temp. Sci.*, **19**(3), 267–74.

Kosyakov, V. N., Chudinov, N., and Shvetsov, I. K. (1974) *Sov. Radiochem.*, **16**, 722–8.

Krause, M. N., Haire, R. G., Keski-Rahkonen, O., and Peterson, J.R. (1988) *J. Electron Spectrosc. Related Phenom.*, **47**, 215–26.

Kulyukhin, S. A. and Mikheev, N. B. (1990) *J. Radioanal. Nucl. Chem.*, **143**(2), 415–26.

Kulyukhin, S. A. and Mikheev, N. B. (1997a) *Radiochemistry*, **39**(2), 123–5.

Kulyukhin, S. A. and Mikhee, N. B. (1997b) *Radiochemistry*, **39**(2), 126–7.

Kulyukhin, S. A., Mikheev, N. B., and Rumer, I. A. (1997) *Radiochemistry*, **39**(2), 130–32; and references therein.

Latrous, H., Oliver, J., and Chemla, M. (1982) *Radiochem. Radioanal. Lett.*, **53**, 81–8.

Lebedev, I. A. (1978) *Sov. Radiochem.*, **20**, 556–62.

Legoux, Y. and Merinis, J. (1986) *J. Less Common Metals*, **121**, 49–54.

Liebman, J. F. (1978) *Inorg. Nucl. Chem. Lett.*, **14**, 245–7.

Lloyd, R. D., Dockum, J. G., and Atherton, D. R. (1975) *Health Phys.*, **28**(5), 585–9.

Lundqvist, R. D., Hulet, E. K., and Baisden, P. A. (1981) *Acta Chem. Scand. A*, **35**, 653–61.

Maly, J. (1969) *J. Inorg. Nucl. Chem.*, **31**, 1007–17.

McDowell, W. J. and Coleman, C. F. (1972) *J. Inorg. Nucl. Chem.*, **34**, 2837–50.

McHarris, W., Stephens, F. S., and Asaro, F. (1966) *Phys. Rev.*, **144**, 1031–7.

Mikheev, N. B. and Rumer, I. A. (1972) *Sov. Radiochem.*, **14**, 502–3.

Mikheev, N. B., Spitsyn, V. I., Kamenskaya, A. N., Rozenkevich, N. A., Rumer, I. A., and Auerman, L. N. (1972a) *Sov. Radiochem.*, **14**, 494–5.

Mikheev, N. B., Auerman. and L. N., Spitsyn, V. I. (1972b) *Inorg. Chem. Lett.*, **8**(10), 869–73; *Sov. Radiochem.*, **14,** 494–5.

Mikheev, N. B. (1986) *J. Less Common Metals*, **121**, 652–3.

Mikheev, N. B., Kamenskaya, A. N., and Kulyukhin, S. A. (1986) *Sov. Radiochem.*, **28**(5), 532–34.

Mikheev, N. B., Kamenskaya, A. N., and Kulyukhin, S. A. (1988a) *Sov. Radiochem.*, **30**(2), 196–200.

Mikheev, N. B., Kulyukhin, S., and Rumer, I. A. (1988b) *Sov. Radiochem.*, **30**(2), 200–4.

Mikheev, N. B. and Kamenskaya, A. N. (1992) in *Transuranium Elements: a Half Century*, ACS Symp. (eds. L. Morss and J. Fuger), Americian Chemical Society, Washington, DC, pp. 469–80; and references therein.

Mikheev, N. B., Kulyukhin, S. A., and Veleshko, I. E. (1993a) *Radiochemistry*, **35**(5), 527–30.

Mikheev, N. B., Veleshko, I. E., And Kulyukhin, S. A. (1993b) *Radiochemistry*, **35**(5), 518–20; and references therein.

Mikheev, and N. B. Rumer, I. A. (1999) *Radiochim. Acta*, **85**(1–2), 49–55.

Mikheev, N. B., Kulyukhin, S. A., Kamenskaya, A. N., Rumer, I. A., and Konovalova, N. A. (2004) *Radiochemistry*, **46**(4), 324–39; and references therein.

Mikheev, V. L., Ilyushch, V. I., and Miller, M. B. (1967) *Sov. J. Nucl. Phys.*, **5**, 35–7.

Morss, L. R., (1986) in *The Chemistry of the Actinide Elements*, (eds. Katz, Seaborg and Morss) Chapter 17, Thermodynamics, Chapman and Hall, New York, pp. 1278–360.

Müller, W. (1967) *Actinides Rev.*, **1**, 71–119.

Myasoedov, B. F., Guseva, L. I., Lebedev, I. A., Milyukova, M. S., and Weinheim, M. K. (1974) in *Analytical Chemistry of the Transplutonium Elements* (ed. D. Slutzkin), John Wiley, New York, pp. 122–32.

Myasoedov, B. F., Chmutova, M. K., and Karalova, Z. K. (1980) in *Actinide Separations,* ACS Symp. Ser. 117 (eds. J. D. Navratil and W. W. Schulz), American Chemical Society, Washington, DC, pp. 101–15.

Ninov, V., Hessberger, F. P., and Hofmann, S. (1996) *Z. Phys. A-Hadron Nucl.*, **356**(1), 11–12.

Nugent, L. J., Burnett, J. L., Baybarz, R. D., Werner, G. K., Tanner, S. R., Tarrant, J. R., and Keller, O. L. Jr (1969a) *J. Phys. Chem.*, **73**, 1540–9.

Nugent, L. J., Baybarz, R. D., and Burnett, J. L. (1969b) *J. Phys. Chem.*, **73**, 1177–8.

Nugent, L. J., Baybarz, R. D., Werner, G. K., and Friedman, H. A. (1970) *Chem. Phys. Lett.*, **7**, 179–82.

Nugent, L. J., Baybarz, R. D., Burnett, J. L., and Ryan, J. L. (1971) *J. Inorg. Nucl. Chem.*, **33**, 2503–30.

Nugent, L. J., Burnett, J. L., and Morss, L. R. (1973) *J. Phys. Chem.*, **77**, 1528–39.

Nugent, L. J. (1975) *J. Inorg. Nucl. Chem.*, **37**, 1767–70.

Peterson, J. R., Ensor, D. D., Fellows, R. L., Haire, R. G., and Young, J. P. (1977) *Rev. Chim. Minér.*, **14**, 172–7.

Peterson, J. R. (1979) in *Proc. Symp. Commemorating the 25th Anniversary of Elements 99 and 100* (ed. G. T. Seaborg), Report LBL-7701, p. 55; and references therein.

Peterson, J. R., Ensor, D. D., Fellows, R. L., Haire, R. G., and Young, J. P. (1979) *J. Phys. Colloq.*, **40**(C4), 111–13; and references therein.

Peterson, J. R. (1994) American Chemical Society, Abstract NUCL-14, 207th National Meeting, San Diego, CA.

Peterson, J. R., Erdmann, N., Nunnemann, M., Eberhardt, K., Huber, G., Kratz, J. V., Passler, G., Stetzer, O., Thorle, P., Trautmann, N., and Waldek, A. (1998) *J. Alloys Compds*, **271/273**, 876–78.

Porter, C. E., Riley, F. D., Vandergrift, R. D., and Felker, L. K. (1997) *Sep. Sci. Technol.*, **32**(1–4), 83–92.

Rajnak, and K. Shore, B. W. (1978) *J. Opt. Soc. Am.*, **68**, 360–7.

Samhoun, and K. David, F. (1979) *J. Inorg. Nucl. Chem.*, **41**, 357–63; and references therein.

Seaborg, G. T. and Loveland, W. D. (1990) *The Elements Beyond Uranium,* John Wiley, New York, pp. 28–38.

Shaugnessy, D. A., Gregorich, K. E., Adams, J., Laue, C. A., Lane, M., Lee, D., McGrath, C. A., Patin, J. B., Strellis, D. A., Sylwester, E. R., Wilk, P. A., and Hoffman, D. C. (2000) American Chemical Society, Abstract NUCL-78, 220th National Meeting, Washington, DC.

Shoun, and R. R. McDowell, W. J. (1980) in *Actinide Separations,* ACS Symp. Ser. 117 (eds. J. D. Navratil and W. W. Schulz), American Chemical Society, Washington, DC, pp. 71–87.

Sugar, J. (1974) *J. Chem. Phys.*, **60**, 4103–10.

Street, K. J., and Seaborg, G. T. (1950) *J. Am. Chem. Soc.*, **72**, 2790–2.

Taut, S. S., Hübener, S., Eichler, B., Gäggeler, H. W., Schädel, M., and Zvara, I. (1997) *Radiochim. Acta*, **78**, 33–8.

Taut, S. S., Hübener, S., Eichler, B., Turler, A., Gäggeler, H. W., Timokhin, S. N., and Zvara, I. (1998) *J. Alloys Compds*, **271**, 316–21.

Thompson, S. G., Harvey, B. G., Choppin, G. R., and Seaborg, G. T. (1954) *J. Am. Chem. Soc.*, **76**, 6229–303.

Topp, N. E. (1965) *The Chemistry of the Rare-Earth Elements,* Elsevier, New York, pp. 125–55.

Varga, L. P., Baybarz, R. D., Reisfeld, M. J., and Asprey, L. B. (1973a) *J. Inorg. Nucl. Chem.*, **35**, 2775–85.

Varga, L. P., Baybarz, R. D., Reisfeld, M. J., and Mann, J. B. (1973b) *J. Inorg. Nucl. Chem.*, **35**, 2303–10.

Veleshko, I. E., Mikheev, N. B., and Kulyukhin, S. A. (1993) *Radiochemistry*, **35**(5), 523–26.

Ward, J. W. and Hill, H. H. (1976) in *Heavy Element Properties* (eds. W. Müller and H. Blank), Elsevier, New York, p. 65.

Ward, J. W., Kleinschmidt, P. D., Haire, R. G., and Brown, D. (1980) in *Lanthanides and Actinides Chemistry and Spectroscopy* (ed. N. Edelstein), ACS Symp. Ser. 131, American Chemical Society, Washington, DC, p. 199.

Ward, J. W. (1986) *J. Less Common Metals*, **121**, 1–15.

Worden, E. F., Lougheed, R. W., Gutmacher, R. G., and Conway, J. G. (1974) *J. Opt. Soc. Am.*, **64**, 77–85.

Wyart, J. F., Blaise, J., and Worden, E. F. (2005) *J. Solid State Chem.*, **178**(2), 589–602.

Young, J. P., Haire, R. G., Fellows, R. L., Noé, M., and Peterson, J. R. (1976) Spectroscopic and X-ray Diffraction Studies of the Bromides of Cf-249 and Es-253, in *Transplutonium 1975* (eds. W. Müller and R. Lindner), North-Holland, Amsterdam, pp. 227–34.

Young, J. P., Haire, R. G., Fellows, R. L., and Peterson, J. R. (1978) *J. Radioanal. Chem.*, **43**, 479–88.

Young, J. P., Haire, R. G., Peterson, J. R., Ensor, D. D., and Fellows, R. L. (1981) *Inorg. Chem.*, **20**, 3979–83.

CHAPTER THIRTEEN

FERMIUM, MENDELEVIUM, NOBELIUM, AND LAWRENCIUM

Robert J. Silva

13.1 GENERAL

Because of conflicting claims, the International Union of Pure and Applied Chemistry (IUPAC) recently reviewed the names of all the trans-fermium elements; Münzenberg (1999) has published a detailed discussion of the problems and the resolution. First, a Transfermium Working Group decided the priority of discoveries. Next, the discoverers proposed names to the IUPAC and names were officially accepted by that body. The names for the elements mendelevium, nobelium, and lawrencium were retained as originally proposed at the time of their discoveries.

As of this writing, the number of known isotopes of Fm, Md, No, and Lr is 58, ranging in half-life from as short as 0.25 ms for ^{250}No to as long as 100.5 days for ^{257}Fm. Relativistic effects have been predicted to affect ground state electronic configurations, ionic radii, and oxidation state for the heavier actinides. While the 3+ oxidation state remains a dominant feature of the heavier actinides, a tendency toward the formation of lower oxidation states has emerged. Divalency had been observed in solution for fermium through nobelium, in fact, the elements Fm, Md, and No are divalent in the metallic state. Due to increased 5f electron binding of the filled 5f^{14} shell, the 2+ oxidation state is the most stable in aqueous solution for nobelium. However, lawrencium, the last member of the actinide series, returns to the 3+ oxidation state as the most stable in aqueous solution, as predicted (Seaborg, 1949).

Due to the short half-lives and low production yields of Fm–Lr, all available chemical information has been obtained from experiments with tracer quantities. In fact, in many cases, chemical experiments were performed with only a few atoms or even one atom at a time. These experiments have necessarily been rather simple in principle, aimed primarily at making comparative studies with elements of known chemical properties. Nevertheless, all available experimental and theoretical evidence supports the original prediction of an actinide series (Seaborg, 1945) involving filling of the 5f electron shell, analogous to the lanthanide series resulting from the filling of the 4f electron shell, and that element 103 is the last member of this series of elements (Seaborg, 1949). The next element, atomic number 104, would be expected to fall into the next chemical group, i.e. Group IVB, of the periodic table.

13.2 FERMIUM

13.2.1 Introduction

The first isotope of element 100 was discovered in heavy-element samples obtained after the ‘Mike’ thermonuclear explosion of 1952, during the same set of experiments that resulted in the discovery of element 99. A joint effort by the researchers from the Lawrence Berkeley National Laboratory, the Argonne National Laboratory, and the Los Alamos National Laboratory resulted in the chemical isolation and identification of the 20 h half-life isotope ^{255}Fm (Ghiorso *et al.*, 1955a). The production involved rapid, multiple neutron capture by uranium nuclei in the nuclear device to form neutron-rich uranium isotopes of heavy mass followed by beta decay to elements of higher atomic number. The ^{255}Fm in the samples, produced from the beta decay of the longer-lived ^{255}Es, was purified and chemically identified by cation-exchange chromatography and detected through the use of alpha particle energy analysis. The name, fermium, was proposed in 1955 in honor of the leader in nuclear science, Enrico Fermi, and the name was subsequently accepted by the IUPAC.

13.2.2 Isotopes of fermium

As can be seen in Table 13.1, there are 19 known isotopes of element 100, ranging from atomic masses 242 through 260. Isotopes with masses 254 through 257 have been identified in samples of plutonium or elements of higher atomic number following neutron irradiation in nuclear reactors. All the other isotopes can only be produced by charged-particle bombardments of targets of elements of lower atomic number at charged-particle accelerators, e.g. cyclotrons, linear accelerators, etc.

The isotope that can be produced in largest quantities on an atomic basis is ^{257}Fm. This isotope is also the nuclide of highest atomic and mass number ever

Table 13.1 *Nuclear properties of fermium isotopes.*

Mass number	*Half-life*	*Mode of decay*	*Main radiations* (MeV)	*Method of production*
242	0.8 ms	SF		^{204}Pb(^{40}Ar,2n)
243	0.18 s	α	α 8.546	^{206}Pb(^{40}Ar,3n)
244	3.3 ms	SF		^{206}Pb(^{40}Ar,2n) ^{233}U(^{16}O,5n)
245	4.2 s	α	α 8.15	^{233}U(^{16}O,4n)
246	1.1 s	α 92% SF 8%	α 8.24	^{235}U(^{16}O,5n) ^{239}Pu(^{12}C,5n)
247[a]	35 s	$\alpha \geq 50\%$ EC $\leq 50\%$	α 7.93 ($\sim$ 30%) 7.87 ($\sim$70%)	^{239}Pu(^{12}C,4n)
247[a]	9.2 s	α	α 8.18	^{239}Pu(^{12}C,4n)
248	36 s	α 99.9% SF 0.1%	α 7.87 (80%) 7.83 (20%)	^{240}Pu(^{12}C,4n)
249	2.6 min	α	α 7.53	^{238}U(^{16}O,5n) ^{249}Cf(α,4n)
250	30 min	α SF 5.7×10^{-4}%	α 7.43	^{249}Cf(α,3n) ^{238}U(^{16}O,4n)
250 m	1.8 s	IT		^{249}Cf(α,3n)
251	5.30 h	EC 98.2% α 1.8%	α 6.834 (87%) 6.783 (4.8%)	^{249}Cf(α,2n)
252	25.39 h	α SF 2.3×10^{-3}%	α 7.039 (84.0%) 6.998 (15.0%)	^{249}Cf(α,n)
253	3.0 d	EC 88% α 12%	α 6.943 (43%) 6.674 (23%) γ 0.272	^{252}Cf(α,3n)
254	3.240 h	$\alpha > 99\%$ SF 0.0592%	α 7.192 (85.0) 7.150 (14.2%)	^{254m}Es daughter
255	20.07 h	α SF 2.4×10^{-5}%	α 7.022 (93.4%) 6.963 (5.0%)	^{255}Es daughter
256	2.63 h	SF 91.9% α 8.1%	α 6.915	^{256}Md daughter ^{256}Es daughter
257	100.5 d	α 99.79% SF 0.21%	α 6.695 (3.5%) 6.520 (93.6%) γ 0.241	multiple n capture
258	0.37 ms	SF		^{257}Fm(d,p)
259	1.5 s	SF		^{257}Fm(t,p)
260	4 ms	SF		^{260}Md daughter

[a] Not known whether ground-state nuclide or isomer.

isolated from either reactor or thermonuclear-produced materials. The neutron capture production chain essentially terminates at mass 257 owing to the very short spontaneous fission half-lives of the heavier isotopes. The current annual reactor production rate is in the picogram range (Porter *et al.*, 1997). However, in the thermonuclear explosion of 1969 called ‘Hutch,’ about 10^8 higher production was achieved (Hoff and Hulet, 1970), but only one part in 10 million of the total number of atoms of ^{257}Fm imbedded in tons of geologic debris was recovered, i.e. a 10 kg sample of debris yielded about 10^{10} atoms.

Though ^{257}Fm is produced in larger amounts, ^{255}Fm has been more available on a regular basis from the beta decay of reactor-produced ^{255}Es ($t_{1/2} = 38.3$ days) and is more frequently used for chemical studies at the tracer level. Radioactivity levels in excess of 10^8 alpha disintegrations per minute of ^{255}Fm can be obtained from periodic chemical separations of Fm, 'milkings,' from purified Es samples.

13.2.3 Preparation and purification

Because of their strong chemical similarity, the only satisfactory methods of separation of the trivalent actinides are by cation exchange or solvent extraction chromatography. The procedure most often selected is separation by elution from a cation-exchange resin column, e.g. Dowex 50 × 8 or × 12 resin, using an aqueous solution of the chelating agent ammonium α-hydroxyisobutyrate (α-HIB) as eluant. This combination, developed in 1956 (Choppin *et al.*, 1956) primarily for the isolation and identification of new actinide elements, remains the main process method for the separation of trivalent actinides (Porter *et al.*, 1997). The actinides exhibit increasing complexation strength with the organic ligand with increasing atomic number, attributed to the decreasing ionic radii due to the actinide contraction (Katz *et al.*, 1986) and are eluted from the column in a regular sequence with the higher atomic number elements eluting first. Fig. 13.1 shows a typical separation of trace amounts of trivalent actinides using this method.

Vobecký *et al.* (1991) have obtained similar sequential elution and separation of 3+ actinides from a column of the spheroidal cation exchanger OSTION using a solution of ammonium α-hydroxy-α-methylbutyrate as the eluant.

Porter *et al.* (1997) have described a process method for the isolation and purification of fermium from other actinides and from rare earth fission produce from reactor target material. In addition to the standard series of transcurium actinide separations through the use of ammonium α-HIB eluant and cation-exchange resin, final purification of the fermium from small amounts of rare earth impurities that could contribute to the mass of the sample was accomplished using a solvent extraction chromatographic resin (the quaternary amine, Aliquat-336, impregnated into Amberchrom CG-71 ms support resin) that is marketed under the trade name TEVA.

Mikheev *et al.* (1983) have developed a rapid method for the separation of fermium from californium, einsteinium, and lanthanide elements based on the cocrystallization of reduced ^{254}Fm(II) with sodium chloride in aqueous ethanol solutions containing Yb(II). The coefficient of separation of Fm

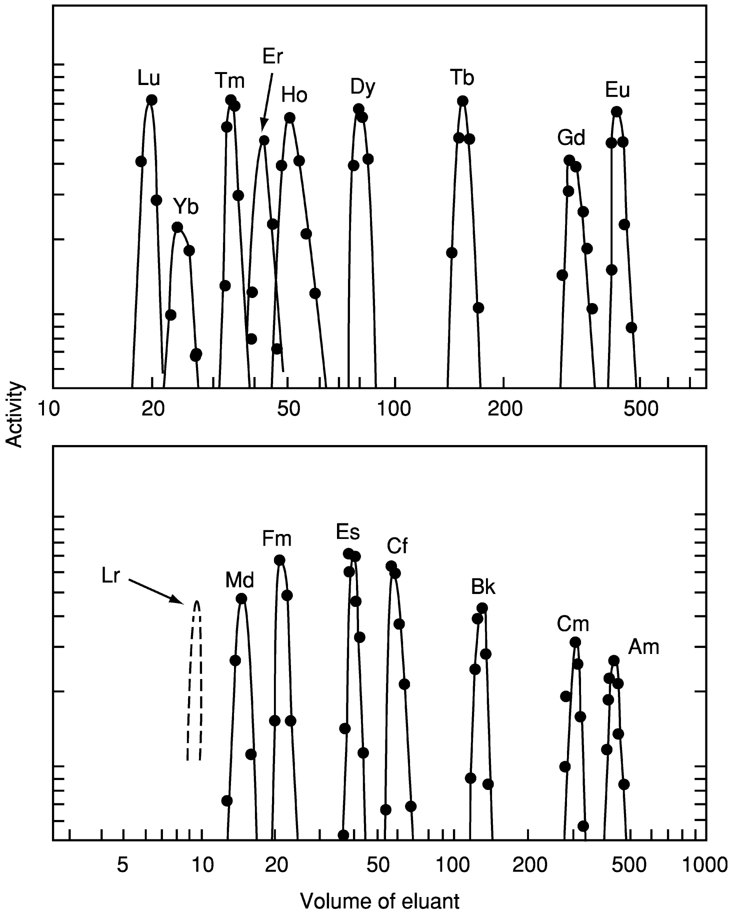

Fig. 13.1 *Elution of homologous trivalent actinides and lanthanides from a Dowex* 50 *cation-exchange resin column at* 87°C *with ammonium α-hydroxyisobutyrate as eluant. The broken curve for element* 103 (*Lr*) *is an estimate based on its predicted radius.*

from its elemental analogs in one cocrystallization step is 10^3 to 10^4 and the separation takes about 10 min.

Fermium has also been separated rapidly from the other transplutonium elements via chromatography using strongly basic anion-exchange resin and mixtures of nitric acid and methyl alcohol at elevated temperatures for the elutions (Usuda *et al.*, 1987).

Volatile hexafluoroacetylacetonates of Md and Fm have been prepared and could be the bases for chemical isolation by thermochromatography (Fedoseev *et al.*, 1990).

13.2.4 Atomic properties

Goodman *et al.* (1971) have used the atomic-beam magnetic resonance technique, adapted to the measurement of radioactive samples, to determine the magnetic moment, g_j, of the atomic ground state of neutral atoms of ^{254}Fm to be 1.16052 ± 0.00014. A comparison of the experimentally measured value with values obtained from intermediate coupling calculations for several likely electron configurations was made. The measured value of g_j was found to be in close agreement only with that calculated for the $^3H_6$ level of the $5f^{12}7s^2$ electronic configuration. This agreement was taken as a conclusive evidence for the assignment of this configuration to the ground state of fermium.

The inner-shell binding energies and X-ray energies for the heavy elements have been estimated from total energies obtained from a Dirac–Fock computer code of Desclaux by Carlson and Nestor (1977). In these calculations, small empirical corrections were added as a result of comparing calculations with experimentally determined binding energies for elements of $Z > 95$. Where comparisons have been made for higher Z elements, the results of the calculations have agreed well with the experimentally measured values. Fricke *et al.* (1972) have also published electron binding energies in fermium obtained from Dirac–Fock calculations and compared them to the values of Porter and Freedman (1971) measured experimentally via spectroscopic measurements of internal conversion electrons emitted following the beta decay of ^{254m}Es to ^{254}Fm. Das (1981) calculated the binding energies in fermium by using a relativistic local density functional theory. Porter and Freedman (1978) have recommended atomic binding energies of the K, L, M, N, O, and P shells for heavy elements from $Z = 84$ to 103. A table of electron binding energies based on the latter is given by Firestone *et al.* (1996). The values for Fm differ slightly from their earlier experimental values (Porter and Freedman, 1971). The results of the three theoretical calculations are compared with the recommended values of Porter and Freedman in Table 13.2. The agreement is quite good and demonstrates that these types of theoretical calculations are consistent and quite useful for predictive purposes.

Dittner *et al.* (1971) have measured the K-series X-rays of ^{251}Fm emitted following the alpha decay of ^{255}No. The K-series X-ray energies derived experimentally from these studies are compared with the values calculated using the binding energies of Porter and Freedman (1978) in Table 13.2.

13.2.5 The metallic state

Fermium metal has not been prepared, however, measurements have been performed on alloys with rare earth metals and a number of predictions about it have been made.

Johansson and Rosengren (1975) have correlated the measured and predicted cohesive energies of the lanthanide and actinide elements in both the divalent and trivalent metallic states. They concluded that the gain in energy of binding

Table 13.2 *Comparison of calculated and measured electron binding and X-ray energies for fermium.*

	Binding energy (−eV)					*X-ray energy* (keV)	
Shell	*Calc.*[a]	*Calc.*[b]	*Calc.*[c]	*Meas.*[d]	*Transition*	*Calc.*[e]	*Meas.*[f]
1s	1 41 943	1 41 953	1 42 573	1 41 962			
2s	27 584	27 581	27 503	27 573			
$2p_{1/2}$	26 643	26 646	26 608	26 644	$K_{\alpha 2}$ ($2p_{1/2} \rightarrow 1s_{1/2}$)	115.285	115.280
$2p_{3/2}$	20 872	20 869	20 783	20 868	$K_{\alpha 1}$ ($2p_{3/2} \rightarrow 1s_{1/2}$)	122.058	121.070
3s	7 206	7 213	7 127	7 200			
$3p_{1/2}$	6 783	6 783	6 710	6 779	$K_{\beta 3}$ ($3p_{1/2} \rightarrow 1s_{1/2}$)	135.150	135.2
$3p_{3/2}$	5 414		5 341	5 408	$K_{\beta 1}$ ($3p_{3/2} \rightarrow 1s_{1/2}$)	136.521	136.6
$3d_{3/2}$	4 757		4 726	4 746			
$3d_{5/2}$	4 497		4 460	4 484			
4s	1 954		1 904	1 940			
$4p_{1/2}$	1 753		1 712	1 743	$K_{\beta 2}$ ($4p_{1/2} \rightarrow 1s_{1/2}$)	140.177	140.1
$4p_{3/2}$	1 383		1 340	1 371			
$4d_{3/2}$	1 071		1 046	1 059			
$4d_{5/2}$	1 005		979	989			
$4f_{5/2}$			591				
$4f_{7/2}$			572				
5s			440				
$5p_{1/2}$			361				
$5p_{3/2}$			264				
$5d_{3/2}$			150				
$5d_{5/2}$			144				

[a] Carlson and Nester (1977).
[b] Fricke *et al.* (1972).
[c] Das (1981).
[d] Porter and Freedman (1971).
[e] Porter and Freedman (1978).
[f] Dittner *et al.* (1971).

of the $5f^n6d^17s^2$ (trivalent) configuration over the $5f^{n+1}7s^2$ (divalent configuration) is less than the energy necessary to promote one 5f electron to the 6d state in the final members of the actinide series. Therefore, Es, Fm, Md, and No prefer a divalent metallic state similar to Eu and Yb rather than a trivalent one. However the energy difference is small for Es and Fm and, at modest compression, the divalent metallic state may convert to the trivalent one.

The sublimation enthalpy, a fundamental metallic property, is connected directly with the valence electronic structure of the metal. The enthalpy of sublimation of fermium has been determined directly by measuring the partial pressure of Fm over Fm–Sm and Fm, Es–Yb alloys for the temperature range 642–905 K (Haire and Gibson, 1989). Based on their combined second law and third law measured values for the enthalpy of sublimation of Fm, they reported a value of (142 ± 13) kJ mol^{-1} for ΔH_{298}. Because the enthalpy of sublimation of Fm was similar to those of divalent Es, Eu, and Yb, it was concluded that Fm is divalent in the metallic state. Comparisons with radii and melting points of Eu, Yb, and Es metals have yielded estimated values of 0.198 nm and 1125 K for Fm by these authors. David *et al.* (1978) have estimated a divalent metallic radius of 0.194 nm for Fm, in close agreement.

Because the heaviest actinides are available only in trace amounts, innovative experimental approaches must be used in order to characterize their elemental state properties. Zvara and coworkers (Zvara *et al.*, 1976) compared the evaporation rates of trace amounts of Es, Fm, and Md from molten La with those of Ce, Eu, Yb, Am, and Cf to obtain information on their metallic states. Hübener (1980) compared the thermochromatographic behavior of Es, Fm, and Md evaporated from molten La in titanium columns with those of Na, Sc, Sm, Eu, Yb, Bk, and Cf. The conclusion reported in both of these papers supported the idea that Es, Fm, and Md prefer the divalent metallic state. The adsorption behavior of Cf, Es, Fm, and Md on titanium and molybdenum thermochromatographic columns was compared to a number of monovalent, divalent, and trivalent elements and enthalpies of adsorption determined (Hübener and Zvara, 1982). From the data, the authors also concluded that Es, Fm, and Md are divalent in the metallic state and that the position of the f-energy levels relative to the Fermi-energy is lower than in the cases of Cf and Yb. A nearly linear correlation was found between the experimental enthalpies of adsorption of the heavy actinides and their predicted enthalpies of sublimation.

Thermochromatographic studies of the adsorption of Cf, Es, and Fm on several metals were conducted by Taut *et al.* (1997) and enthalpies of sublimation inferred from the measured enthalpies of adsorption. The results support the value of the enthalpy of sublimation of Fm published by Haire and Gibson (1989).

13.2.6 Solution chemistry

The chemical properties of fermium have been studied only with trace quantities. The chemical properties of Fm have been discussed by Thompson *et al.* (1954). Under conditions not strongly reducing, fermium behaves in aqueous solution as expected for a trivalent actinide ion. Fermium coprecipitates with rare earth fluorides and hydroxides. The elution of fermium just before einsteinium from cation-exchange resin columns with hydrogen ion and the complexing ligands citric acid, lactic acid, and α-HIB is consistent with the existence of a trivalent ion (Katz and Seaborg, 1957). In concentrated hydrochloric acid, nitric acid, and ammonium thiocyanate solutions, fermium forms anion complexes with these ligands that can be adsorbed onto and subsequently eluted from anion-exchange columns (Thompson *et al.*, 1954). In this case, fermium follows einsteinium in the elution sequence. Both types of column results indicate that Fm forms a slightly stronger complex with the ligands than Es, which is due to the slightly smaller ionic radius of Fm as a result of the actinide contraction

(Katz *et al.*, 1986). Fermium also exhibits a more acidic behavior than the preceding actinides in aqueous solution, having a first hydrolysis constant of 1.6×10^{-4} (Hussonnois *et al.*, 1972).

David *et al.* (1978) have estimated some thermodynamic properties of the 5f elements obtained from theoretical considerations and empirical correlations drawn from observed trends in the 4f series. They proposed an ionic radius of 0.0922 nm for Fm^{3+}. From the linear correlation of log distribution coefficients with ionic radius obtained from elution positions from α-HIB/cation-exchange column separations, a value of 0.0911 nm was calculated for the ionic radius of Fm^{3+} (Brüchle *et al.*, 1988). Lundqvist *et al.* (1981) have studied the migration rates of Fm^{3+} in an electrical potential gradient using paper electrophoresis and reported a hydrated radius of 0.495 nm and a hydration number of 16.9 in aqueous perchlorate solutions.

Fermium readily forms complexes with a variety of organic ligands, e.g., β-diketones (Hussonnois *et al.*, 1972), hydroxycarboxylic acids (Thompson *et al.*, 1954; Choppin *et al.*, 1956; Baybarz, 1965, 1966; Ermakovl and Stary, 1967; Hubert *et al.*, 1974), organophosphorus esters (Baybarz, 1963; Stary, 1966; Horwitz *et al.*, 1969), and alkylamines (Müller, 1967). α-HIB has long been used as the eluant for inner series separation of trivalent actinides by cation-exchange chromatography as stated above. However, bis(2-ethylhexyl)phosphoric acid (HDEHP) (Horwitz and Bloomquist, 1973) and Alamine 336 (a mixed *n*-octyl and *n*-decyl tertiary amine) (Leuze *et al.*, 1963) have also been used for similar separations of Fm by solvent extraction column chromatography. Gorski *et al.* (1990) have investigated the complex formation of several transplutonium elements, including Fm, with 1,2-diaminocyclohexane tetraacetic acid (DCTA) and shown the correlation of ionic radii with the values of the log of the complex stability constants. A linear dependence is observed for lanthanides while it deviates from linearity for the heavy actinides. The author's postulate that, since the stability of chelate complexes are determined by the positive change of entropy of the reaction, the change in stability constants of the heavy actinides is due to an entropy effect rather than to the change in the ionic radii.

The behavior of Sr, Y, Sm, Eu, Am, Cf, Es, and Fm in the molten salt mixtures $LiCl–NdCl_2–NdCl_3$ and $LiI–PrI_2$ have been studied (Kulyukhin, 1997). In the presence of Nd^{2+}, Cf, Es, and Fm are reduced to the 2+ oxidation state. The results obtained in the $LiI–PrI_2$ system were ambiguous as to whether the actinides Cf–Fm were reduced to the 1+ or 2+ oxidation states.

The tendency of Fm to form a divalent ion under strong reducing conditions was first suggested by the work of Maly (1967). Mikheev *et al.* (1972) reported the reduction of Fm^{3+} to Fm^{2+} in 1972 from the results of reduction/cocrystallization experiments with $SmCl_2$. The reduction of Fm^{3+} to Fm^{2+} with $SmCl_2$ has also been observed by Hulet *et al.* (1979). Mikheev *et al.* (1977) were able to estimate the reduction potential to be very nearly the same as the $Yb^{3+} \rightarrow Yb^{2+}$ couple or −1.15 V. This value is in reasonably good agreement with the value of –(1.1 ± 0.2) V calculated by Nugent (1975) using refined electron-spin-pairing theory.

Using a refined radiopolarographic technique, Samhoun and David (1976) measured the half-wave potential for the $Fm^{2+} \rightarrow Fm(Hg)$ reduction at a dropping mercury electrode as –(1.47 ± 0.01) V. By applying an estimated amalgamation potential correction of 0.90 V obtained from correlations of other divalent ions, a value for E° ($Fm^{2+} \rightarrow Fm^0$) of –(2.37 ± 0.1) V was reported. Using this latter value of Samhoun and David, combined with Mikheev's value of –1.15 V for the $Fm^{3+} \rightarrow Fm^{2+}$ couple, a value of –(1.96 ± 0.13) V can be calculated for E° ($Fm^{3+} \rightarrow Fm^0$). Nugent (1975) has estimated $E^\circ(Fm^{4+} \rightarrow Fm^{3+})$ to be +4.9 V. These values (Table 13.8) are consistent within uncertainties with those in Chapter 19 (Fig. 19.9).

Unless otherwise indicated, all electrode potentials in this chapter are with reference to the normal hydrogen electrode (NHE) and the 1969 IUPAC convention, i.e. the more positive the potential the more stable the reduced form (McGlashan, 1970).

13.3 MENDELEVIUM

13.3.1 Introduction

The first isotope of element 101 was produced in 1955 by Ghiorso *et al.* (1955b). It was synthesized in the bombardment of approximately one billion atoms of ^{253}Es with 41 MeV alpha particles and produced at a rate of only about two atoms per 3 h bombardment. A chemical identification was made on the basis of its elution position just before Fm from a cation-exchange resin column using ammonium α-HIB as eluant in a series of repetitive experiments. It was not detected directly but by the observation of spontaneous fission events arising from its electron-capture daughter ^{256}Fm. Additional analysis of the data, coupled with further experimentation, showed the isotope to have mass 256 and to decay by electron capture with a half-life of 1.5 h. The name mendelevium was proposed for the element in honor of Dimitri Mendeleev, in recognition of his contributions to the development of the chemical periodic system, and it was accepted by IUPAC.

13.3.2 Isotopes of mendelevium

Sixteen isotopes of mendelevium from mass 245 to 260 are known (see Table 13.3) . All of its isotopes can only be produced through charged-particle irradiations at accelerators. Although ^{258}Md, with a half-life of 51 days, is the longest-lived isotope, ^{256}Md remains the isotope most often used in chemical experiments because it can be produced in relatively larger quantities. Using microgram amounts of ^{253}Es presently available, more than a million

Table 13.3 *Nuclear properties of mendelevium isotopes.*

Mass number	*Half-life*	*Mode of decay*	*Main radiations* (MeV)	*Method of production*
245	0.4 s	α	α 8.680	^{209}Bi(^{40}Ar,4n)
	0.9 ms	SF		
246	1.0 s	α	α	^{209}Bi(^{40}Ar,3n)
247	1.12 s	α 80%	α 8.424	^{209}Bi(^{40}Ar,2n)
	0.27 s			
248	7 s	EC $\sim$ 80%	α 8.36 ($\sim$25%)	^{241}Am(^{12}C,5n)
		α $\sim$ 20%	8.32 ($\sim$75%)	^{239}Pu(^{14}N,5n)
249	24 s	EC $\leq$ 80%	α 8.03	^{241}Am(^{12}C,4n)
		$\alpha \geq$ 20%		
250	52 s	EC 94%	α 7.830 ($\sim$25%)	^{243}Am(^{12}C,5n)
		α 6%	7.750 ($\sim$75%)	^{240}Pu(^{15}N,5n)
251	4.0 min	EC $\geq$ 94%	α 7.55	^{243}Am(^{12}C,4n)
		$\alpha \leq$ 6%		^{240}Pu(^{15}N,4n)
252	2.3 min	EC > 50%	α 7.73	^{243}Am(^{13}C,4n)
		α < 50%		
253	6 min		^{238}U(^{19}F,5n)	
254[a]	10 min	EC		^{253}Es(α,3n)
254[a]	28 min	EC		^{253}Es(α,3n)
255	27 min	EC 92%	α 7.333	^{253}Es(α,2n)
		α 8%	γ 0.453	^{254}Es(α,3n)
256	1.27 h	EC 90.7%	α 7.205 (63%)	^{253}Es(α,n)
		α 9.9%	7.139 (16%)	
257	5.52 h	EC 90%	α 7.069	^{254}Es(α,n)
		α 10%		
258[a]	51.5 d	α	α 6.790 (28%)	^{255}Es(α,n)
			6.716 (72%)	
258[a]	57 min	EC ?		^{255}Es(α,n)
259	1.60 h	SF		^{259}No daughter
260	31.8 d	SF > 73%		^{254}Es(^{18}O,^{12}C)
		EC < 15%		

[a] Not known whether ground-state nuclide or isomer.

atoms per hour of ^{256}Md can be produced by alpha-particle bombardments (Hulet *et al.*, 1967).

13.3.3 Preparation and purification

The isotope ^{256}Md can best be produced for chemical study by the ^{253}Es(α,n) or ^{254}Es(α,2n) reactions at cyclotrons or linear accelerators. The isotope ^{254}Es would be the target material of choice if available. It has a half-life of 276 days compared to only 20.5 days for ^{253}Es and thus it would have a longer usable target lifetime.

The discovery experiments on mendelevium were the first in which the recoil momentum imparted by the bombarding ion to a product atom during its formation was used to carry out an instantaneous physical separation of the product atom from the target material (Seaborg, 1963). The recoil atoms were collected on a thin metal foil placed behind the target in an evacuated reaction chamber. This eliminated the time needed to separate the product atoms from the target atoms, previously accomplished by chemical means, and made it possible to use the same valuable target in repeated bombardments. A few years later, it was found that the recoil atoms could be slowed down and stopped in a gaseous atmosphere, frequently helium. The gas could be pumped out of the reaction chamber through a small orifice to form a 'gas-jet.' If this jet was impinged onto the surface of a foil, some fraction (frequently 75% or more) of the nonvolatile product atoms carried along with the gas were deposited permanently on the foil surface (Ghiorso, 1959; Macfarlane and Griffioen, 1963). The foil could be removed periodically for processing and a new foil installed. A good description of this system has been giving by Hoffman (1994).

After removal of the Md atoms from the collector foil by acid etching or following total dissolution of the thin metal foil, they can be purified and isolated from other product activities by several other techniques.

Md can be separated from the dissolved 'catcher' foil material, e.g. Be, Al, Pt, or Au, and most fission-product activities by coprecipitation with lanthanum fluoride. Subsequent separation of trivalent actinides from lanthanide fission products and La carrier can be accomplished with a cation-exchange resin column using a 90% water/10% ethanol solution saturated with HCl as eluant (Thompson *et al.*, 1954). When a very thin gold foil is used as the 'catcher' foil, after dissolution with aqua regia, a rapid separation of the Md from the Au can be made by anion-exchange chromatography using 6 M HCl as eluant. The gold remains on the column while the Md and other actinides pass through.

Final isolation of Md^{3+} from other trivalent actinides can be accomplished by selective elution from a cation-exchange resin column using ammonium α-HIB (Choppin *et al.*, 1956). When using the gas-jet system, the first two steps can frequently be eliminated.

In more recent years, it was found that, using the 'gas-jet' method, the recoil product atoms could be transported many meters with the stopping gas through a long capillary tube to the chemistry/counting area (Macfarlane and McHarris, 1974). In this case, effective transport over long distances requires the presence of large clusters, frequently KCl aerosols, in the 'carrier' gas. By this method, it is possible to transport and collect individual product atoms in a fraction of a second some tens of meters away from the target area. This method is quite generally used nowadays in the production and isolation of transeinsteinium elements.

A good separation of Md and Fm has been performed on a spheroidal cation-exchanger OSTIN using ammonium α-hydroxy-α-methylbutyrate (Vobecký *et al.*, 1991). The isotope ^{256}Md is most easily detected through the measurement of the spontaneous fission activity of its daughter ^{256}Fm; however, in the presence of other fissioning nuclides, the detection of alpha particles of the characteristic energy of ^{256}Md associated with the 10% alpha decay branch can be used for identification.

Intragroup separation of the 3+ actinides has also been achieved by solvent extraction chromatography using HDEHP as the stationary organic phase and HNO_3 as the mobile aqueous phase (Horwitz and Bloomquist, 1969). Here, the actinide elution sequence is reversed from that of the cation-exchange resin column. This method gives a somewhat better final separation of Md from Fm than the cation-exchange resin column. It has the advantage that the final solution containing the Md is free of organic complexing agents compared to the resin column but has the disadvantage that Md elutes after Fm late in the sequence.

Following the discovery that Md can form a divalent state, extraction chromatography using HDEHP was used to show that the elution behavior of Md^{2+} is dissimilar to that of Es^{3+} and Fm^{3+} (Hulet *et al.*, 1967). This became the basis for a rapid separation method for the isolation of Md (Hulet *et al.*, 1979; Lundqvist *et al.*, 1981). After the initial steps of dissolution from the 'catcher' foil and coprecipitation with terbium fluoride, the mendelevium and 50 mg of Cr (added as a holding reductant) in 0.1 M HCl are co-reduced with Zn(Hg). The solution is passed through a solvent extraction column containing HDEHP on an inert support as the stationary organic phase. The actinides in the trivalent and tetravalent states as well as the trivalent lanthanides are extracted by the HDEHP and are retained on the column while the divalent Md is not appreciably extracted and appears in the 0.1 M HCl washes of the column. After reoxidation of the Md and Cr to the trivalent states with H_2O_2, the residual impurities, including the Cr, are separated from the Md by selective elution with 2 M (to remove the impurities) and 6 M HCl (to remove the Md) from a small column of Dowex 50 × 12 colloidal resin. Guseva *et al.* (1988) have reported a similar method for isolating Md where, using one column with cationite and zinc amalgam and a solution of 1 M HCl as the eluant, Md is reduced and washes through the column with the alkaline earth elements.

Volatile hexafluoroacetylacetonates of Md and Fm have been prepared and could be the bases for chemical isolation by thermochromatography (Fedoseev *et al.*, 1990).

13.3.4 Atomic properties

The electronic structure of the ground state of gaseous mendelevium atoms has been predicted to be the $^2F_{7/2}$ level of the $5f^{13}7s^2$ configuration (Martin *et al.*, 1974). An experimental confirmation has not yet been made. No experimental measurements of inner-shell binding energies or X-ray energies have been reported but estimated values have been reported by Firestone *et al.* (1996)

Table 13.4 *Estimated electron binding and X-ray energies for mendelevium, nobelium, and lawrencium.*

	Binding energy (–eV)				*X-ray energy* (keV)		
Shell	*Md*	*No*	*Lr*	*Transition*	*Md*	*No*	*Lr*
1s	1 46 526	1 49 208	1 52 970	$K_{\alpha1}$ $(2p_{3/2} \rightarrow 1s)$	125.17	127.36	130.61
				$K_{\alpha2}$ $(2p_{1/2} \rightarrow 1s)$	119.09	120.95	123.87
2s	28 387	29 221	30 083	$K_{\alpha3}$ $(2s \rightarrow 1s)$	118.14	119.99	122.89
$2p_{1/2}$	27 438	28 255	29 103				
$2p_{3/2}$	21 356	21 851	22 359	$K_{\beta1}$ $(3p_{3/2} \rightarrow 1s)$	140.97	143.51	147.11
				$K_{\beta2}$ $(4p_{3/2,1/2} \rightarrow 1s)$	144.91	147.53	151.23
3s	7 440	7 678	7 930	$K_{\beta3}$ $(3p_{1/2} \rightarrow 1s)$	139.53	141.98	145.50
$3p_{1/2}$	7 001	7 231	7 474	$K_{\beta4}$ $(4d_{5/2,3/2} \rightarrow 1s)$	145.46	148.10	151.82
$3p_{3/2}$	5 552	5 702	5 860	$K_{\beta5}$ $(3d_{3/2,1/2} \rightarrow 1s)$	141.77	144.32	147.94
$3d_{3/2}$	4 889	5 028	5 176				
$3d_{5/2}$	4 615	4 741	4 876	$L_{\alpha1}$ $(3d_{5/2} \rightarrow 2p_{3/2})$	16.74	17.10	17.48
				$L_{\alpha2}$ $(3d_{3/2} \rightarrow 2p_{3/2})$	16.47	16.82	17.18
4s	2 024	2 097	2 180				
$4p_{1/2}$	1 816	1 885	1 963	$L_{\beta1}$ $(3d_{3/2} \rightarrow 2p_{1/2})$	22.55	23.23	23.93
$4p_{3/2}$	1 424	1 469	1 523	$L_{\beta2}$ $(4d_{5/2,3/2} \rightarrow 2p_{3/2})$	20.29	20.74	21.21
$4d_{3/2}$	1 105	1 145	1 192	$L_{\beta3}$ $(3p_{3/2} \rightarrow 2s)$	22.84	23.52	24.22
$4d_{5/2}$	1 034	1 070	1 112	$L_{\beta4}$ $(3p_{1/2} \rightarrow 2s)$	21.39	21.99	22.61
$4f_{5/2}$	618	645	680	$L_{\beta5}$ $(5d_{5/2,1/2} \rightarrow 2p_{3/2})$	21.21	21.70	22.20
$4f_{7/2}$	597	624	658	$L_{\beta6}$ $(4s \rightarrow 2p_{3/2})$	19.33	19.75	20.18
5s	471	490	516	$L_{\gamma1}$ $(4d_{3/2} \rightarrow 2p_{1/2})$	26.33	27.11	27.91
$5p_{1/2}$	389	406	429	$L_{\gamma2}$ $(4p_{1/2} \rightarrow 2s)$	26.57	27.34	28.12
$5p_{3/2}$	272	280	296	$L_{\gamma3}$ $(4p_{3/2} \rightarrow 2s)$	26.96	27.75	28.56
$5d_{3/2}$	154	161	174	L_{l} $(3s \rightarrow 2p_{3/2})$	13.92	14.17	14.43
$5d_{5/2}$	137	142	154	L_{v} $(3s \rightarrow 2p_{1/2})$	20.00	20.58	21.17
$5f_{5/2}$	12.9	13.6	19.9				
$5f_{7/2}$	10.5	11.1	17.0				

based on the values recommended by Porter and Freedman (1978). The results are given in Table 13.4.

13.3.5 The metallic state

While mendelevium metal has not been prepared, Johansson and Rosengren (1975) predicted that, for the same reasons as discussed above for Fm, Md would prefer a divalent metallic state similar to Eu and Yb rather than a trivalent one.

As was the case with Fm, thermochromatographic studies conducted with trace amounts of Md by Zvara *et al.* (1976), Hübener (1980), and Hübener and Zvara (1982) led to the conclusion that Md forms a divalent metal. If the enthalpies of sublimation determined for Es and Fm from alloys are accepted, then, using the measured enthalpies of adsorption and the established correlation between the sublimation and adsorption enthalpies, Haire and Gibson (1990) estimated that Md has an enthalpy of sublimation in the range of

134–142 kJ mol^{-1}. Using empirical correlation methods, David *et al.* (1978) have estimated a divalent metallic radius of (0.194 ± 0.010) nm.

13.3.6 Solution chemistry

Before mendelevium was discovered, the trivalent state was predicted to be the most stable in aqueous solution and, therefore, it was expected to exhibit a chemical behavior similar to the other 3+ actinides and lanthanides (Seaborg and Katz, 1954). The elution of Md just before Fm in the elution sequence of trivalent actinides from a cation-exchange resin column observed in the discovery experiments appeared to confirm this prediction. Later, Md was indeed found to form insoluble hydroxides and fluorides that are quantitatively coprecipitated with trivalent lanthanides (Hulet *et al.*, 1967). Both the cation-exchange resin column (Choppin *et al.*, 1956) and HDEHP solvent extraction column (Horwitz and Bloomquist, 1969) elution data are consistent with a trivalent state for Md and an ionic radius slightly smaller than Fm.

Using empirical correlations, David *et al.* (1978) have estimated an ionic radius of 0.0912 nm (coordination number (CN) 6) for Md^{3+}. In addition to the ionic radius, a number of enthalpies and entropies of formation and sublimation were also estimated for Md. Hoffman *et al.* (1988) and Brüchle *et al.* (1988) compared the distribution coefficients for Lr, Md, and Fm with those of Tm, Er, and Ho obtained from ammonium α-HIB elutions from cation-exchange resin columns. Using the known ionic radii for the trivalent rare earths and the linear correlation of log distribution coefficient with ionic radius (for the same coordination number), an average ionic radius of 0.0896 nm was estimated for Md^{3+} and a heat of hydration of −(3654 ± 12) kJ mol^{-1} calculated using empirical models and the Born–Haber cycle.

Gorski *et al.* (1990) have studied the extraction behavior of Md with trioctylphosphine oxide in the presence of complexing agents and compared it to other transplutonium elements. They have also investigated the complex formation of several transplutonium elements, including Md, with DCTA and shown the correlation of ionic radii with the values of the log of the complex stability constants. The observed deviation from linearity by the heavy actinides is discussed in Section 13.2.5.

Hulet *et al.* (1967) first observed an anomalous chemical behavior for Md in certain chemical systems involving reducing conditions. With 10^5 to 10^6 atoms per experiment, coprecipitation with $\mathrm{BaSO_4}$ and solvent extraction chromatography experiments using HDEHP were carried out in the presence of a number of different reducing agents. These experiments showed that Md^{3+} could be easily reduced to a stable Md^{2+} in aqueous solution. An estimate was made for the standard potential of the half-reaction $E^\circ(\mathrm{Md}^{3+} \rightarrow \mathrm{Md}^{2+})$ of approximately −0.2 V. Maly and Cunningham (1967) also produced the divalent state of Md and, from experiments similar to Hulet *et al.*, estimated $E^\circ(\mathrm{Md}^{3+} \rightarrow \mathrm{Md}^{2+})$ at −0.1 V. David (1986a) estimated $E^\circ(\mathrm{Md}^{3+} \rightarrow \mathrm{Md}^{0})$ to be −1.74 V. David *et al.* (1981, 1990a) measured $-(1.51 \pm 0.01)$ V for the polarographic $E_{1/2}$ of the couple $Md^{2+} \rightarrow Md^0$ which (with correction for amalgamation potential of 1.0 V) yields an estimated $E°(Md^{2+} \rightarrow Md^0) = -2.5$ V (SHE). These values (Table 13.8) are consistent with those in Chapter 19 (Fig. 19.9).

Guseva *et al.* (1988) compared the elution behavior of Md^{2+} with Sr^{2+} and Eu^{2+} from a cationite and zinc amalgam ion-exchange column using 1 M HCl. On the basis of the elution peak position of Md relative to the Sr and Eu and the known ionic radii of the latter two elements, a value for the ionic radius of Md^{2+} was estimated to be 0.115 nm. Using this value for the radius, the enthalpy of hydration of Md^{2+} was calculated to be -1413 kJ mol^{-1}.

In 1973, Mikheev *et al.* reported that a stable monovalent Md ion could be produced in neutral water–ethanol solutions and that it cocrystallized with CsCl (Mikheev *et al.*, 1973). However, studies of the overall reduction of Md^{3+} to Md^0 (Hg) using controlled potential radiocoulometry (Samhoun *et al.*, 1979) and radiopolarography (David *et al.*, 1981) led to the conclusion that Md could not be considered as a cesium-like element and no evidence was obtained consistent with the formation of a monovalent state. Electrode reduction proceeded in two steps, $3+ \rightarrow 2+$ and $2+ \rightarrow 0$. Hulet *et al.* (1979) repeated some of the cocrystallization experiments of Mikheev and performed a series of new experiments in an attempt to prepare Md^+ by reduction with Sm^{2+} in ethanol solutions and also in fused KCl. In these experiments, the coprecipitation behavior of Md was compared to tracer quantities of Es, Fm, Eu, Sr, Y, and Cs. Md consistently followed the behavior of Fm^{2+}, Eu^{2+}, and Sr^{2+} rather than Cs^+. They concluded that Md could not be reduced to a monovalent state with Sm^{2+} as claimed by Mikheev. However, on the basis of the results of further thermodynamic studies of the cocrystallization process of mendelevium with chlorides of alkali metals, the Russian investigators maintain that Md can be reduced to the monovalent state in water–ethanol solutions and that the cocrystallization of Md^+ with salts of divalent ions can be explained as being due to the formation of mixed crystals (Mikheev *et al.*, 1980, 1981a; Spitsyn *et al.*, 1982). An ionic radius of 0.117 nm was calculated for Md^+ from the results of the cocrystallization studies (Mikheev *et al.*, 1981b, 1982).

Unsuccessful attempts have been made to oxidize Md^{3+} to Md^{4+} using the strong oxidant sodium bismuthate (Hulet *et al.*, 1967). Thus, Md^{3+} is not readily oxidized as would be expected from the value of +5.4 V predicted by Nugent (1975) for the $E°(Md^{4+} \rightarrow Md^{3+})$ couple.

13.4 NOBELIUM

13.4.1 Introduction

The discovery of element 102 was first reported in 1957 by an international research team working at the Nobel Institute in Stockholm, Sweden (Fields *et al.*, 1957). During the bombardment of a ^{244}Cm target with ^{13}C ions from the

Nobel Institute cyclotron, an 8.5 MeV alpha particle activity was produced which decayed with a half-life of approximately 10 min. The alpha activity eluted just before Es and Fm from a cation-exchange resin column using ammonium α-HIB as eluant and also appeared in the trivalent actinide fraction along with Cf and Fm, also produced in the irradiations, from a cation-exchange resin column using 6 M HCl as eluant. This behavior was taken as chemical evidence for the production of an isotope of element 102. From half-life systematics and reaction energetics, an isotope with a mass number of 253 or 255 was thought to have been produced. The name, nobelium, was proposed in honor of Alfred Nobel, in recognition of his support of the natural sciences, and in honor of the Nobel Institute where the experiments were conducted.

During the following 10 years, researchers at both the Lawrence Berkeley National Laboratory and the Dubna Research Center, Russia, attempted to repeat the Nobel Institute experiments, but were unsuccessful. However, the Berkeley group did succeed in identifying an alpha-emitting isotope of element 102 in 1958 using a newly developed method called the ‘double recoil technique’ (Ghiorso *et al.*, 1958) and assigned a mass of 254. Where the same isotopes have been studied, the Dubna and Berkeley groups are in substantial agreement (Ghiorso and Sikkeland, 1967). The results of the efforts of both groups exclude the likelihood of any isotope of element 102 having a half-life of 10 min with the emission of 8.5 MeV alpha particles. Further, chemical studies by Maly *et al.* (1968) showed that, because of its divalency in aqueous solutions, element 102 could not have exhibited the trivalent cation-exchange column elution behavior attributed to the 10 min activity. On the basis of their 1958 and later work, the Berkeley group claimed discovery of element 102 and, because of the wide use of the name over many years, suggested that nobelium be retained as the name of element 102 (Ghiorso and Sikkeland, 1967).

Because No is normally a divalent ion in aqueous solution and is difficult to oxidize and hold in the trivalent state, it has not been possible to make a chemical identification of the atomic number in the same manner as the preceding 3+ actinides, i.e. identification by their unique positions in the elution sequence from a cation-exchange resin column. However, in 1971, the atomic number of ^{255}No was unequivocally determined through the observance of characteristic K-series X-rays from the daughter isotope ^{251}Fm in coincidence with the alpha particles from the decay of the parent, ^{255}No (Dittner *et al.*, 1971).

13.4.2 Isotopes of nobelium

The known isotopes of nobelium range from mass 250 through 262, with the exception of 261 (Table 13.5) . The isotope ^{259}No is the longest-lived with a half-life of 58 min. However, the isotope ^{255}No has a considerably higher production rate and is most often used for chemical studies.

Table 13.5 *Nuclear properties of nobelium isotopes.*

Mass number	*Half-life*	*Mode of decay*	*Main radiations* (MeV)	*Method of production*
250	0.25 ms	SF		^{233}U(^{22}Ne,5n)
251	0.8 s	α	α 8.68 (20%) 8.60 (80%)	^{244}Cm(^{12}C,5n)
252	2.27 s	α 73% SF 27%	α 8.415 (~ 75%) 8.372 (~ 25%)	^{244}Cm(^{12}C,4n) ^{239}Pu(^{18}O,5n)
253	1.62 min	α	α 8.01	^{246}Cm(^{12}C,5n) ^{242}Pu(^{16}O,5n)
254	51 s	α	α 8.086	^{246}Cm(^{12}C,4n) ^{242}Pu(^{16}O,4n)
254 m	0.28 s	IT		^{246}Cm(^{12}C,4n) ^{249}Cf(^{12}C,α3n)
255	3.1 min	α 61.4% EC 38.6%	α 8.121 (46%) 8.077 (12%)	^{248}Cm(^{12}C,5n) ^{249}Cf(^{12}C,α2n)
256	2.91 s	α ~ 99.7% SF ~ 0.3%	α 8.43	^{248}Cm(^{12}C,4n)
257	25 s	α	α 8.27 (26%) 8.22 (55%)	^{248}Cm(^{12}C,3n)
258	1.2 ms	SF		^{248}Cm(^{13}C,3n)
259	58 min	α ~ 75% EC ~ 25%	α 7.551 (22%) 7.520 (25%)	^{248}Cm(^{18}O,α3n)
260	106 ms	SF, α		^{254}Es(^{18}O,x)
262	5 ms	SF		^{262}Lr daughter

13.4.3 Preparation and purification

The isotope ^{255}No can be produced for chemical study via the ^{249}Cf (^{12}C,α2n) reaction; about 1200 atoms were produced in a 10 min irradiation of a 350 μg cm^{-2} target of ^{249}Cf with 3 × 10^{12} particles per second of 73 MeV ^{12}C ions (Dittner *et al.*, 1971).

As with Md, the physical separation of the nobelium atoms from the target material can be made using the recoil-atom catcher foil technique. It is preferable to combine this with the 'gas-jet' technique since the product atoms can be deposited on the 'catcher' foil in a chemistry area separate from the bombardment area. The nearly monolayer of collected atoms can then be easily rinsed off the surface of the foil with dilute acid without dissolution of the foil. Isolation of the No from other actinides produced in the bombardment and from any target material transferred to the foil can be readily made using schemes based on the separation of divalent ions from trivalent ones, e.g. selective elution by solvent extraction chromatography using HDEHP as the stationary organic phase and 0.05 M HCl as the mobile aqueous phase (Silva *et al.*, 1969). Under these conditions, No passes through the column in the first few column volumes while the trivalent actinides are strongly adsorbed on the column. Selective elution from a cation-exchange resin column, e.g. Dowex 50 × 4, can also be made using 3 M HCl as eluant. Here, No again elutes in a few column volumes and the trivalent actinides remain on the column (Silva *et al.*, 1973). When using a direct 'catcher' foil, e.g. gold, a more elaborate scheme involving separation of the gold by anion-exchange chromatography is necessary (David *et al.*, 1990b). This can be followed by selective isolation of the No from contaminants by elution from a chromatographic extraction column using HDEHP.

13.4.4 Atomic properties

The electronic ground state of gaseous nobelium atoms has been predicted to be the $^1S_0$ level of the $5f^{14}7s^2$ configuration (Martin *et al.*, 1974). No experimental information is available. No experimental measurements of inner-shell binding energies have been reported but estimated values have been published by Firestone *et al.* (1996), along with X-ray energies, based on the values recommended by Porter and Freedman (1978). The results are given in Table 13.4.

The characteristic K-series X-rays of ^{253}No emitted following the alpha decay of ^{257}Rf have been measured in alpha/X-ray coincidence experiments by Bemis *et al.* (1973). Values for $K_{\alpha 2}$ and $K_{\alpha 1}$ were reported as (120.9 ± 0.3) and (127.2 ± 0.3) keV, respectively.

13.4.5 The metallic state

Nobelium metal has not been prepared; however Johansson and Rosengren (1975) predicted that, for the same reasons as discussed above for Fm, No would prefer a divalent metallic state similar to Eu and Yb rather than a trivalent one. An estimate of 126 kJ mol^{-1} for the enthalpy of sublimation of No has been reported (David, 1986a). This value is similar to that of Es, Fm, and Md and supports the suggestion that No would form a divalent metal (Haire and Gibson, 1990). David (1986a) estimated a divalent metallic radius of 0.197 nm.

13.4.6 Solution chemistry

Before discovery, nobelium was expected to be a trivalent ion in aqueous solution and to exhibit a chemical behavior similar to the elements preceding it in the actinides series. However, in 1949, Seaborg (1949) predicted that a relatively stable 2+ state might exist for element 102 due to the special stability of the filled $5f^{14}$ shell in the $5f^{14}7s^2$ electronic configuration. Twenty years later, this prediction was confirmed.

In over 600 experiments, Maly *et al.* (1968) subjected about 50000 atoms of ^{255}No to cation-exchange chromatography and coprecipitation experiments. These tracer experiments showed that nobelium exhibits a chemical behavior substantially different from the trivalent actinides but similar to the divalent alkaline earth elements, Sr, Ba, and Ra. Thus, the divalent ion of nobelium was shown to be the most stable species in aqueous solution in the absence of strong oxidizing agents.

Chuburkov *et al.* (1967) have compared the behavior of nobelium to those of Tb, Cf, and Fm during experiments where the atoms were first chlorinated and subsequently were carried by gas along a tube with a thermal gradient. From the position of deposition of atoms along the tube, they concluded that the chloride of No undergoes strong adsorption on solid surfaces and therefore is not very volatile; its volatility is close to the chlorides of Tb, Cf, and Fm. The chloride of either divalent or trivalent nobelium would be expected to exhibit a low volatility.

Silva *et al.* (1974) have conducted solvent extraction and cation-exchange chromatography studies of nobelium. Its complexing ability with chloride ions were compared with that of divalent mercury, cadmium, copper, cobalt, and barium in a tri-*n*-octylamine chloride/HCl liquid extraction system, and it was found to be most similar to the relatively weakly complexed alkaline earth element. The elution behavior of nobelium was also compared with that of Be, Mg, Ca, Sr, Ba, and Ra in a cation-exchange resin column/4 M HCl system and found to elute with Ca^{2+}. Further, comparison with these alkaline earth elements in an HDEHP/HCl liquid chromatography system showed nobelium to elute between Ca^{2+} and Sr^{2+}. The ionic radius of No^{2+} was estimated as 0.11 nm from a linear correlation of ionic radius with log distribution coefficient for several divalent ions obtained using an HDEHP/HNO_3 liquid–liquid extraction system. Using a similar correlation, a value of 0.10 nm was obtained from the cation-exchange chromatography data. From the results of relativistic Hartree–Foch–Slater calculations (Lu *et al.*, 1971), a value of 0.11 nm was suggested for the ionic radius of No^{2+}. The single-ion heat of hydration, calculated using an empirical form of the Born equation (Phillips and Williams, 1966) was 1486 kJ mol^{-1}. From correlations of ionic radii of actinides and lanthanides with atomic number, an ionic radius for No^{3+} of 0.90 and 1.02 Å for CNs 6 and 8, respectively, have been estimated. (David *et al.*, 1978; David, 1986b).

The formation of divalent nobelium complexes with citrate, oxalate, and acetate ions in aqueous solution of 0.5 M NH_4NO_3 have been studied by McDowell *et al.* (1976) using solvent extraction techniques. In general, the complexing tendency of nobelium with these ligands is between that of Ca and Sr, being somewhat more like Sr.

Silva *et al.* (1969) have studied the reduction potential of the No(III)–No(II) couple in aqueous solution with 50–100 atoms per experiment using HDEHP extraction column chromatography to distinguish between No^{2+} and No^{3+}. By comparing the extraction of nobelium from dilute acid solutions containing oxidants of differing potentials with the extraction behavior of tracer quantities of Cf, Cm, Ra, Tl, and Ce, the standard potential $E^\circ(No^{3+} \rightarrow No^{2+})$ was estimated to be between +1.4 and +1.5 V.

Meyer *et al.* (1976) used a modified radiopolarographic technique and ^{255}No to measure the half-wave potential for the reduction of nobelium at a mercury electrode and reported a value for $E^\circ(No^{2+} \rightarrow No^0(Hg))$ of −1.6 V. After applying an estimated amalgamation potential correction, a value of -2.6 V was calculated for the standard potential of the $\mathrm{No}^{2+} \rightarrow \mathrm{No}^0$ couple. More recently David *et al.* (1990b) have measured amalgamation potentials of nobelium using radiocoulometry with the isotope ^{259}No. From the data, they estimated the $\mathrm{No}^{2+} \rightarrow \mathrm{No}^0$ couple standard potential as $-(2.49 \pm 0.06)$ V. This couple, combined with the measured $3+ \rightarrow 2+$ potential of 1.45 V (Silva *et al.*, 1969) resulted in an estimated value for E° ($\mathrm{No}^{3+} \rightarrow \mathrm{No}^0$) of -1.18 V by David *et al.* (1990b). David (1986a, 1986b) estimated E° ($\mathrm{No}^{3+} \rightarrow \mathrm{No}^0$) to be -1.26 V, which leads to a calculated E° ($\mathrm{No}^{2+} \rightarrow \mathrm{No}^0$) $= -2.61$ V; these values were selected for Table 13.8 and Fig. 19.9 because of the consistent systematics (David, 1986a, 1986b) among many actinide species. David *et al.* (1990b) also estimated Gibbs energies of formation of -480 and -342 kJ mol^{-1} for No^{2+} (aq) and No^{3+} (aq), respectively. From a semiempirical technique for the linearization of actinide and lanthanide electrode potentials, Nugent (1975) has calculated a value of $+6.5$ V for $E^\circ(\mathrm{No}^{4+} \rightarrow \mathrm{No}^{3+})$.

13.5 LAWRENCIUM

13.5.1 Introduction

In 1961, Ghiorso, Sikkeland, Larsh, and Latimer of the Lawrence Berkeley National Laboratory reported the discovery of element 103 (Ghiorso *et al.*, 1961). An alpha particle activity of 8.5 MeV energy with a half-life of 8 s was produced in bombardments of a Cf target with both ^{10}B and ^{11}B ions. Owing to the short half-life, a chemical identification was not possible but the alpha activity was attributed to an isotope of element 103 on the basis of convincing nuclear evidence, i.e. the results of cross-bombardments with other targets and projectiles. However, because the target consisted of a mixture of californium isotopes, masses 249 through 252, an unambiguous mass assignment was not possible. Though isotopes of masses 255–259 could have been produced, based on cross-section considerations, the highest yield was expected for mass 257. The discoverers suggested the name lawrencium, symbol Lw, for the new element in honor of E. O. Lawrence, inventor of the cyclotron and founder of the Lawrence Berkeley National Laboratory. The name was accepted by IUPAC, but the symbol was changed to Lr.

The results of subsequent studies on the production and identification of ^{255}Lr, ^{256}Lr, and ^{257}Lr by researchers at the Joint Institute for Nuclear Research (JINR) at Dubna, Russia, appeared to conflict with the Berkeley mass assignment because none of the above isotopes had the decay properties of the original Berkeley alpha activity (Druin, 1971). However, in 1971, six alpha particle emitting isotopes of lawrencium, masses 255–260, were identified at Berkeley in bombardments of nearly isotopically pure targets of ^{248}Cm with ^{14}N and ^{15}N and ^{249}Cf with ^{10}B and ^{11}B ions, respectively, and an explanation for the discrepancy was suggested (Eskola *et al.*, 1971). From the Berkeley experiments, ^{257}Lr was found to emit alpha particles of 8.8 MeV with a half-life of only 0.6, but ^{258}Lr was found to have a half-life of 4.2 s with the emission of 8.62 MeV alpha particles. Thus, Ghiorso and associates considered that the mass assignment made in 1961 should have been 258. The difference in the new half-life value compared to the 1961 value was attributed to relatively poor counting statistics resulting from the small number of alpha particle events observed in the earlier work.

13.5.2 Isotopes of lawrencium

Twelve isotopes of lawrencium are known with masses ranging from 252 through 262 (Table 13.6). The longest-lived isotope is ^{262}Lr, with a half-life of 3.6 h. The isotope ^{256}Lr, half-life of 26 s, was used in the early chemical studies; however, the longer-lived isotope ^{260}Lr ($t_{1/2} = 3$ min) has been used in more recent experiments.

13.5.3 Preparation and purification

The production of ^{256}Lr is best accomplished through the ^{249}Cf(^{11}B,4n) reaction using 70 MeV boron ions while ^{260}Lr is produced via the ^{249}Bk(^{18}O, α3n) reaction using 117 MeV oxygen ions.

As with Md and No, the physical separation of the Lr atoms from the target material and subsequent rapid collection is best accomplished using a recoil-atom gas-jet system coupled to a capillary transport system of some type (Hoffman *et al.*, 1988).

Because of their short half-lives, there is insufficient time to obtain a rigorous chemical purification of ^{256}Lr or ^{260}Lr. The isotope, ^{256}Lr was first isolated from

Table 13.6 *Nuclear properties of lawrencium isotopes.*

Mass number	*Half-life*	*Mode of decay*	*Main radiations* (MeV)	*Method of production*
252	0.36 s	α	α 9.018 (75%)	^{256}Db daughter
253 m	1.5 s	α	α 8.722	^{257}Db daughter
253	0.57 s	α	α 8.794	^{257}Db daughter
254	13 s	α	α 8.460 (64%)	^{258}Db daughter
255	21.5 s	α	α 8.43 (40%) 8.37 (60%)	^{243}Am(^{16}O,4n) ^{249}Cf(^{11}B,5n)
256	25.9 s	α	α 8.52 (19%) 8.43 (37%)	^{243}Am(^{18}O,5n) ^{249}Cf(^{11}B,4n)
257	0.65 s	α	α 8.86 (85%) 8.80 (15%)	^{249}Cf(^{11}B,3n) ^{249}Cf(^{14}N,α2n)
258	3.9 s	α	α 8.621 (25%) 8.595 (46%)	^{248}Cm(^{15}N,5n) ^{249}Cf(^{15}N,α2n)
259	6.2 s	α	α 8.45	^{248}Cm(^{15}N,4n)
260	3.0 min	α	α 8.03	^{248}Cm(^{15}N,3n)
261	39 min	SF		^{254}Es(^{22}Ne,x)
262	3.6 h	SF, EC		^{254}Es(^{22}Ne,x)

reaction products by a rapid solvent extraction technique using the chelating agent thenoyltrifluoroacetone (TTA) dissolved in methyl isobutyl ketone (MIBK) as the organic phase and buffered acetate solutions as the aqueous phase (Silva *et al.*, 1970). This method did not separate individual trivalent actinides so identification of Lr was made on the basis of its unique alpha particle energy of 8.24 MeV.

When the capillary transport system is used, the longer-lived isotope, ^{260}Lr, can be washed from the 'catcher' foil along with the small amount of aerosol carrier particles with 0.05 M HCl. Kept to a few drops of volume, this solution can be placed on the top of a cation-exchange resin column and isolation of Lr^{3+} from other trivalent actinides can be accomplished by selective elution with ammonium α-HIB (Hoffman *et al.*, 1988). An automated system called Automated Rapid Chemistry Apparatus (ARCA) has been developed and used to carry out this separation (Brüchle *et al.*, 1988).

13.5.4 Atomic properties

The electronic structure of the ground state of neutral atoms of Lr was predicted in 1970 as the $^2D_{3/2}$ level of the $5f^{14}6d^{1}7s^{2}$ configuration (Moeller, 1970) similar to the rare earth homolog Lu, $4f^{14}5d^{1}6s^{2}$, as one would expect from a simple extrapolation from the chemical periodic table. This prediction was brought into question in 1971 by Brewer who calculated, by a semiempirical method, a configuration of $5f^{14}7s7p^{1}$ (Brewer, 1971). Later the results of relativistic Dirac–Hartree–Fock calculations by Nugent *et al.* (1974) concluded that the energy difference between these two configurations was quite small and either configuration could be the ground state. On the basis of the results of multiconfiguration Dirac–Fock calculations, Desclaux and Fricke (1980) predicted the $5f^{14}7s^{2}7p^{1}$ configuration as the ground state. Later, multiconfiguration Dirac–Hartree–Fock calculations by Wijesundera *et al.* (1995) and relativistic Fock-space coupled-cluster method by Eliav *et al.* (1995) led to a similar conclusion, i.e. the s^2p $J = 1/2$ is energetically favored over the s^2d $J = 3/2$ state. This result is due to the relativistic mass increase of the electrons that are strongly accelerated near the highly charged nucleus. This effect is strongest for the spherical s and $p_{1/2}$ orbitals that have high densities near the nucleus.

In 1988, Eichler and coworkers proposed gas adsorption chromatography experiments to distinguish between the two ground state configurations s^2d and s^2p. They calculated that there should be a measurable difference in the enthalpies of adsorption on metal surfaces for the two different configurations (Eichler *et al.*, 1988). The s^2p was predicted to be less volatile, perhaps similar to the p-element Pb, than the s^2d configuration with estimated sublimation energies of about 134 and 400 kJ mol^{-1}, respectively. Online gas chromatography was applied to study the volatility of Lr by Jost *et al.* (1988) and to determine the enthalpy of adsorption. No evidence for Lr as a volatile element was found under reducing conditions at a temperature of about 1000°C. Their

Table 13.7 *Comparison of calculated and measured L-series X-rays for Lr.*

	X-ray energy (keV)	
Transition	*Calculated*[a]	*Measured*[b]
$L_{\gamma 1}$ ($4d_{3/2} \rightarrow 2p_{1/2}$)	27.91	27.97 (15)[c]
$L_{\beta 1}$ ($3d_{3/2} \rightarrow 2p_{1/2}$)	23.93	24.03 (14)
$L_{\beta 4}$ ($3p_{1/2} \rightarrow 2s$)	22.61	22.61 (18)
$L_{\beta 2}$ ($4d_{5/2} \rightarrow 2p_{3/2}$)	21.21	21.35 (20)
$L_{\alpha 1}$ ($3d_{5/2} \rightarrow 2p_{3/2}$)	17.48	17.57 (12)
L_{l} ($3s \rightarrow 2p_{3/2}$)	14.43	14.43 (20)

[a] Firestone *et al.* (1996).
[b] Bemis *et al.* (1977).
[c] Error in last two digits.

results gave a lower limit for the adsorption enthalpy for Lr on quartz and Pt surfaces at 290 kJ mol^{-1}, significantly higher than the estimated values for Lr (s^2p). The configuration of the ground state of lawrencium is still in doubt.

No experimental measurements of inner-shell binding energies have been reported but estimated values have been published by Firestone *et al.* (1996), along with X-ray energies, based on the values recommended by Porter and Freedman (1978). The results are given in Table 13.4.

The characteristic L-series X-rays of ^{256}Lr have been observed in coincidence with alpha particles of the parent ^{260}Db by Bemis *et al.* (1977). The results are presented in Table 13.7. They agree very well with those given by Firestone *et al.* (1996).

13.5.5 Metallic state

Lawrencium metal has not been prepared. An estimate of 352 kJ mol^{-1} for the enthalpy of sublimation of Lr has been reported (David *et al.*, 1978). This value is similar to that of Lu and supports the suggestion that Lr would prefer the formation of a trivalent metal as expected for the last member of the actinide series. Systematic properties of heats of vaporization, bulk modulus, and atomic volumes suggest that Lr would be a trivalent metal with a volume similar to that of Lu (Haire and Gibson, 1990). David *et al.* (1978) estimated a trivalent metallic radius of 0.171 nm.

13.5.6 Solution chemistry

In 1949, element 103 was predicted by Seaborg (1949) to be the last member of the proposed actinide or 5f series of elements and to be similar to lutetium with respect to the stability of the 3+ oxidation state in aqueous solution. It required nearly 20 years to finally synthesize this element and to conduct chemical experiments to confirm this prediction.

Silva *et al.* (1970) employed a fast solvent extraction procedure using MIBK containing the chelating agent TTA as the organic phase and buffered acetate solutions of differing pH as the aqueous phase to distinguish between the 2+, 3+, and 4+ oxidation states. In over 200 separate experiments, approximately 1500 atoms of ^{256}Lr were produced for study and the extraction behavior of Lr was compared with a number of tetravalent (Th, Pu), trivalent (Fm, Cf, Cm, Am, Ac), and divalent ions (No, Ba, Ra). In these experiments, lawrencium was found to extract into the organic phase over the pH range of 3+ ions along with Fm and Cf. Thus, it was concluded that the 3+ oxidation state is the most stable oxidation state for Lr in aqueous solution. Unfortunately, because of the short half-life, there was insufficient time to perform a cation-exchange resin column separation to confirm its predicted elution position just ahead of Md^{3+}.

From studies comparing the retention times of chlorinated atoms of several different actinides and transactinides as they passed through a heated glass column, Chuburkov *et al.* (1969) concluded that the chloride of element 103 has an adsorbability on solid surfaces, and hence volatility, similar to the chlorides of Cm, Fm, and No and to be much less volatile than the chlorides of element 104, Rf.

Because Lr is a trivalent ion in aqueous solution, it should exhibit a chemical behavior similar to the other 3+ actinides and lanthanides, e.g. insoluble fluoride and hydroxide. One would expect Lr^{3+} to have a slightly smaller ionic radius than Md^{3+}, due to the actinide contraction, and to elute just before Md from a cation-exchange resin column using ammonium α-HIB as eluant (see Fig. 13.1). From correlations of ionic radius with atomic number for actinide and lanthanide elements, David *et al.* (1978) estimated an ionic radius of 0.0893 nm for Lr^{3+}.

By 1987, a longer-lived isotope of lawrencium, ^{260}Lr, with a half-life of 3 months and alpha particle energy of 8.03 MeV, was available for chemical studies. Hoffman *et al.* (1988) repeated the solvent extraction experiments of Silva *et al.* (1970) and confirmed the trivalent nature of Lr in aqueous solution. Further, elutions of Lr from a cation-exchange resin columns using ammonium α-HIB as eluant were conducted and compared with the elution behavior of Md and the rare earths Tm, Er, and Ho (Hoffman *et al.*, 1988). Lr was found to elute between Ho and Tm, and approximately with the Er tracer. Seven alpha events attributable to Lr^{260} were detected. The distribution coefficients were determined from the elution positions and, using the linear correlation of ionic radius with log distribution coefficient, an ionic radius was calculated for each Lr event. The average Lr^{3+} radius was found to be 0.0886 ± 0.0003 nm assuming an ionic radius of 0.0881 nm for Er for CN 6 (Templeton and Dauben, 1954). This result was surprising to the authors because it gave a difference of only 0.0015 nm for the step of 2 in atomic number between Md, with an ionic radius of 0.0896 nm, and Lr. This is substantially smaller than the 2Z difference of 0.0021 for the analogous trivalent rare earth ions Tm and Lu and indicates an ionic radius for Lr larger than expected. Therefore, Lr elutes later than predicted in Fig. 13.1.

In later experiments, a German–American collaboration (Brüchle *et al.*, 1988) used the ARCA (Automated Rapid Chemistry Apparatus) system to check the earlier results of Hoffman *et al.* (1988) and to increase the number of Lr atoms studies and thus the statistical significance. The earlier work was confirmed and a value of 0.0881 ± 0.0001 nm was obtained from the elution data for Lr. A heat of hydration of $-(3685 \pm 13)$ kJ mol^{-1} was calculated from the radius using empirical models and the Born–Haber cycle. Brüchle *et al.* (1988) pointed out that the difference between the radii of $\mathrm{Md^{3+}}$, $\mathrm{Fm^{3+}}$, and $\mathrm{Es^{3+}}$ is 0.0016 nm while this difference is 0.0012 nm for the analogous lanthanide ions. This suggests that the contraction at the end of the actinides series is larger than the analogous lanthanide contraction, perhaps due to relativistic effects (Seth *et al.*, 1994), with the exception of the last member of the actinide series, Lr.

It is possible that relativistic effects could stabilize the $7s^2$ closed shell so that only the $7p_{1/2}$ or 6d electron would be ionized under reducing conditions to give a monovalent Lr. Several attempts have been made to reduce $\mathrm{Lr^{3+}}$ to a divalent or monovalent ion in aqueous solution. Hoffman *et al.* (1988) used a solvent extraction column with HDEHP as the stationary organic phase and dilute HCl as the mobile aqueous phase to separate 1+ and 2+ ions from 3+ and 4+ ions, the former passing through the column while the latter remain fixed. Solutions containing $^{260}\mathrm{Lr^{3+}}$ were passed through the column where the Lr remained fixed. The reducing agent hydroxylamine hydrochloride was added to the HCl and the resulting solution passed through the column for 20 s at 80°C in an attempt to reduce and elute any Lr. The attempt was unsuccessful, however, as the authors noted, the kinetics of the reduction are slow. In companion experiments, Scherer *et al.* (1988) used the HDEHP solvent extraction column

Table 13.8 *Summary of chemical properties of elements* 100–103.

Element	100	101	102	103
electronic configuration[a]	$5f^{12}7s^2$	$5f^{13}7s^2$	$5f^{14}7s^2$	$5f^{14}6d^1(7p^1)7s^2$
stable oxidation states[b]	$\underline{3}$, 2	$\underline{3}$, 2	3, $\underline{2}$	$\underline{3}$
ionic radius of indicated ion (nm)	0.0911(3+)	0.0896(3+)	0.105(2+)	0.0886(3+)
standard electrode potentials (V)[c]				
3+ → 2+	−1.15	−0.15	+1.45	<−0.44
3+ → 0	−1.96	*−1.74*	*−1.26*	*−2.06*
2+ → 0	−2.37	*−2.5*	*−2.61*	
first ionization potential (V)[d]	6.50	6.58	6.65	

[a] Free neutral atom + Rn core.

[b] Most stable state in aqueous solution underlined.

[c] Values in italics are estimates.

[d] From Martin *et al.* (1974).

method, with the ARCA system, to attempt reductions of Lr to di- or monovalent ions (Scherer *et al.*, 1988). In a series of experiments using the reducing agents V^{2+} and Cr^{2+} in the dilute HCl-eluting solutions, there was no evidence for the reduction of Lr^{3+} to either the 2+ or 1+ oxidation state. From the results, a limit of <-0.44 V was estimated for the $Lr^{3+} \rightarrow Lr^{2+,\,1+}$ reduction potential. Using the newly discovered Lr^{262} ($t_{1/2} = 3.6$ h), Lougheed *et al.* (1988) attempted to reduce Lr with Sm^{2+}, $E°(Sm^{3+} \rightarrow Sm^{2+}) = -1.55$ V, and coprecipitate Lr^{1+} with Rb using sodium tetraphenylborate or chloroplatinic acid but were unsuccessful. The 2+ and 3+ actinide ions do not coprecipitate under these conditions. On the basis of 20 Lr events, they calculated an upper limit of -1.56 V for $E°(Lr^{3+} \rightarrow Lr^{1+})$ and concluded that it is unlikely that Lr^{1+} can exist in aqueous solutions. Nugent (1975) has calculated values of -2.06 V for $E°(Lr^{3+} \rightarrow Lr^{0})$ and $+7.9$ V for $E°(Lr^{4+} \rightarrow Lr^{3+})$.

A summary of some of the chemical properties of fermium, mendelevium, nobelium, and lawrencium is given in Table 13.8.

REFERENCES

Baybarz, R. D. (1963) *Nucl. Sci. Eng.*, **17**, 463–7.

Baybarz, R. D. (1965) *J. Inorg. Nucl. Chem.*, **27**, 1831–9.

Baybarz, R. D. (1966) *J. Inorg. Nucl. Chem.*, **28**, 1055–61.

Bemis, C. E. Jr, Silva, R. J., Hensley, D. C., Keller, O. L. Jr, Tarrant, J. R., Hunt, L. D., Dittner, P. F., Hahn, R. L., and Goodman, C. D. (1973) *Phys. Rev. Lett.*, **31**, 647–50.

Bemis, C. E. Jr, Dittner, P. F., Silva, R. J., Haoh, R. L., Tarrant, J. R., Hunt, L. D., and Hensley, D. C. (1977) *Phys. Rev. C*, **16**, 1146–58.

Brewer, L. (1971) *J. Opt. Soc. Am.*, **61**, 1101–11.

Brüchle, W., Schädel, M., Scherer, U. W., Kratz, J. V., Gregorich, K. E., Lee, D., Nurmia, M., Chasteler, R. M., Hall, H. L., Henderson, R. A., and Hoffman, D. C. (1988) *Inorg. Chim. Acta*, **146**, 267–76.

Carlson, T. A. and Nestor, C. W. Jr (1977) *At. Data Nucl. Data Tables*, **19**, 153–73.

Choppin, G. R., Harvey, B. G., and Thompson, S. G. (1956) *J. Inorg. Nucl. Chem.*, **2**, 66–8.

Chuburkov, Y. T., Caletka, R., Shalaevskii, M. R., and Zvara, I. (1967) *Radiokhimiya*, **9**, 637–42.

Chuburkov, Y. T., Belov, V. Z., Caletka, R., Shalaevsky, M. R., and Zvara, I. (1969) *J. Inorg. Nucl. Chem.*, **31**, 3113–18.

David, F., Samhoun, K., Guillaumont, R., and Edelstein, N. (1978) *J. Inorg. Nucl. Chem.*, **40**, 69–74.

David, F., Samhoun, K., Hulet, E. K., Baisden, P. A., Dougan, R., Landrum, J. H., Lougheed, R. W., Wild, J. F., and O'Kelley, G. D. (1981) *J. Inorg. Nucl. Chem.*, **43** (11), 2941–5.

David, F. (1986a) Oxidation Reduction and Thermodynamic Properties of Curium and Heavier Actinide Elements, in *Handbook on the Physics and Chemistry of the Actinides,* vol. 4 (eds. A. J. Freeman and C. Keller), North-Holland, Amsterdam, pp. 97–128.

David, F. (1986b) *J. Less Common Metals*, **121**, 27–35.

David, F., Maslennikov, A. G., and Peretrukhin, V. P. (1990a) *J. Radioanal. Nucl. Chem. Articles*, **143**(2), 415–26.

David, F., Samhoun, K., Lougheed, R. W., Dougan, R. J., Wild, J. F., Landrum, J. H., Dougan, A. D., and Hulet, E. K. (1990b) *Radiochim. Acta*, **51**, 65–70.

Das, M. P. (1981) *Phys. Rev. A*, **23**(2), 391–4.

Desclaux, J. P. and Fricke, B. (1980) *J. Phys.*, **41**, 943–6.

Dittner, P. F., Bemis, C. E. Jr, Hensley, D. C., Silva, R. J., and Goodman, C. C. (1971) *Phys. Rev. Lett.*, **26**, 1037–40.

Druin, V. A. (1971) *Sov. J. Nucl. Phys.*, **12**, 146–7.

Eichler, B., Hübener, S., Gäggeler, H. W., and Jost, D. T. (1988) *Inorg. Chim. Acta*, **146**, 261–5.

Eliav, E., Kaldor, U., and Ishikawa, Y. (1995) *Phys. Rev. A*, **52**, 291–6.

Ermakovl, V. A. and Stary, I. (1967) *Radiokhimiya*, **9**, 197–201.

Eskola, K., Eskola, P., Nurmia, M., and Ghiorso, A. (1971) *Phys. Rev. C*, **4**, 632–42.

Fedoseev, E. V., Aizenberg, I., Timokhin, S. N., Travnikov, S. S., Zvara, I., Davydov, A. V., and Myasedov, B. F. (1990) *J. Radioanal. Nucl. Chem. Articles*, **142**(2), 459–65.

Fields, P. R., Friedman, Am. M., Milstead, J., Atterling, H., Forsling, W., Holm, L. W., and Aström, B. (1957) *Phys. Rev.*, **107**, 1460–2.

Firestone, R. B., Shirley, V. S., Baglin, C. M., Chu, S. Y., and Zipkin, J. (1996) *Table of Isotopes,* 8th edn, vol. 2, Appendix F, John Wiley, New York, pp. F37–9; F47.

Fricke, B., Desclaux, J. P., and Waber, J. T. (1972) *Phys. Rev. Lett.*, **28**(12), 714–16.

Ghiorso, A., Thompson, S. G., Higgens, G. H., Seaborg, G. T., Studier, M. H., Fields, P. R., Fried, S. M., Diamond, H., Mech, J. F., Pyle, G. L., Huizengo, J. R., Hirsch, A., Manning, W. M., Browne, C. I., Smith, H. L., and Spencer, R. W. (1955a) *Phys. Rev.*, **99**, 1048–9.

Ghiorso, A., Harvey, B. G., Choppin, G. R., Thompson, S. G., and Seaborg, G. T. (1955b) *Phys. Rev.*, **5**, 1518–19.

Ghiorso, A., Sikkeland, T., Walton, J. R., and Seaborg, G. T. (1958) *Phys. Rev. Lett.*, **1**, 18–20.

Ghiorso, A. (1959) LBNL Report UCRL-8714, Berkeley, CA, USA.

Ghiorso, A., Sikkeland, T., Larsh, A. E., and Latimer, R. M. (1961) *Phys. Rev. Lett.*, **6**, 473–5.

Ghiorso, A. and Sikkeland, T. (1967) *Phys. Today*, **20**(9), 25–32.

Goodman, L. S., Diamond, H., Stanton, H. E., and Fred, M. S. (1971) *Phys. Rev. A*, **4**, 473–5.

Gorski, B., Buklanov, G. V., Dok, L. D., Gleisberg, B., Timokhin, S. N., Milek, A., and Salamatin, L. I. (1990) *Radiochim. Acta*, **51**, 59–63.

Guseva, L. I., Tikhomirova, G. S., Buklanov, G. V., Pkhar, Z. Z., Lebedev, I. A., Katargin, N. V., and Myasoedov, B. F. (1988) *Radiokhimiya*, **30**(1), 21–5.

Haire, R. G. and Gibson, J. K. (1989) *J. Chem. Phys.*, **91**(11), 7085–96.

Haire, R. G. and Gibson, J. K. (1990) *J. Radioanal. Nucl. Chem. Articles*, **143**, 35–51.

Hoff, R. W. and Hulet, E. K. (1970) *Proc. Am. Nucl. Soc. Symp.*, in *Engineering with Nuclear Explosives*, vol. 2, pp. 1283–94.

Hoffman, D. C., Henderson, R. A., Gregorich, K. E., Bennett, D. A., Chasteler, R. M., Gannett, C. M., Hall, H. L., Lee, D. M., Nurmia, M. J., Cai, S., Agarwal, R., Charlop, A. W., Chu, Y. Y., Seaborg, G. T., and Silva, R. J. (1988) *J. Radioanal. Nucl. Chem. Articles*, **124**, 135–44.

Hoffman, D. C. (1994) The Heaviest Elements, in *Chem. Eng. News*, **72**(18), 24–34.

Horwitz, E. P. and Bloomquist, C. A. A. (1969) *Chem. Lett.*, **5**, 753–9.

Horwitz, E. P., Bloomquist, C. A. A., and Henderson, D. J. (1969) *J. Inorg. Nucl. Chem.*, **31**, 1149–66.

Horwitz, E. P. and Bloomquist, C. A. A. (1973) *J. Inorg. Nucl. Chem.*, **35**, 271–84.

Hübener, S. (1980) *Radiochem. Radioanal. Lett.*, **44**(2), 79–86.

Hübener, S. and Zvara, I. (1982) *Radiochim. Acta*, **31**, 89–94.

Hubert, S., Hussonnois, M., Brillard, L., Goby, G., and Guillaumont, R. (1974) *J. Inorg. Nucl. Chem.*, **36**, 2361–6.

Hulet, E. K., Lougheed, R. W., Brady, J. D., Stone, R. E., and Coops, M. S. (1967) *Science*, **158**, 486–8.

Hulet, E. K., Lougheed, R. W., Baisden, P. A., Landrum, J. H., Wild, J. F., and Lundqvist, R. F. (1979) *J. Inorg. Nucl. Chem.*, **41**, 1743–7.

Hussonnois, H., Hubert, S., Aubin, L., Guillaumont, R., and Boussieres, G. (1972) *Radiochem. Radioanal. Lett.*, **10**, 231–8.

Johansson, B. and Rosengren, A. (1975) *Phys. Rev. B*, **11**, 1367–73.

Jost, D. T., Gäggeler, H. W., Vogel, Ch., Schädel, M., Jäger, E., Eichler, B., Gregorich, K. E., and Hoffman, D. C. (1988) *Inorg. Chim. Acta*, **146**, 255–9.

Katz, J. J. and Seaborg, G. T. (1957) *Chemistry of the Actinide Elements,* Methuen, London, p. 404.

Katz, J. J., Seaborg, G. T., and Morss, L. R. (1986) *The Chemistry of the Actinide Elements*, Chapman & Hall, London, p. 1165.

Kulyukhin, S. A., Mikheev, N. B., and Rumer, I. A. (1997) *Radiochemistry*, **39**(2), 130–2.

Leuze, R. E., Baybarz, R. D., and Weaver, B. (1963) *Nucl. Sci. Eng.*, **17**, 252–8.

Lougheed, R. W., Moody, K. J., Dougan, R. J., Wild, J. F., and Hulet, E. K. (1988) LLNL report, Nuclear Chemistry Division FY 1988 Annual Report, Livermore.

Lu, C. C., Carlson, T. A., Malik, F. B., Tucker, T. C., and Nester, C. W. Jr (1971) *At. Data*, **3**, 1–131.

Lundqvist, R., Hulet, E. K., and Baisden, T. A. (1981) *Acta. Chem. Scand.*, **A35**, 653–61.

Macfarlane, R. D. and Griffioen, R. D. (1963) *Nucl. Inst. Methods*, **24**, 461–4.

Macfarlane, R. D. and McHarris, W. (1974) in *Nuclear Spectroscopy and Reactions,* vol. A (ed. J. Cerny), Academic Press, New York, p. 24.

Maly, J. (1967) *Inorg. Nucl. Chem. Lett.*, **3**, 373–81.

Maly, J. and Cunningham, B. B. (1967) *Inorg. Nucl. Chem. Lett.*, **2**, 445–51.

Maly, J., Sikkeland, T., Silva, R. J., and Ghiorso, A. (1968) *Science*, **160**, 1114–15.

Martin, W.C., Hagan, L., Reader, J., and Sugar, J. (1974) *J. Phys. Chem. Ref. Data*, **3**, 771–9.

McDowell, W. J., Keller, O. L. Jr, Dittner, P. F., Tarrant, J. R., and Case, G. N. (1976) *J. Inorg. Nucl. Chem.*, **38**, 1207–10.

McGlashan, M. L. (1970) *J. Pure Appl. Chem.*, **21**, 1–44.

Meyer, R. I., McDowell, W. J., Dittner, P. F., Silva, R. J., and Tarrant, J. R. (1976) *J. Inorg. Nucl. Chem.*, **38**, 1171–3.

Mikheev, N. B., Spitsyn, V. I., Kamenskaya, A. N., Gvozdec, B. A., Druin, V. A., Rumer, I. A., Dyachkova, R. A., Rozenkevitch, N. A., and Auerman, L. N. (1972) *Inorg. Nucl. Chem. Lett.*, **8**, 929–36.

Mikheev, N. B., Spitsyn, V. I., Kamenskaya, A. M., Rumer, I. A., Gvozdev, B. A., Rozenkevich, N. A., and Auerman, L. N. (1973) *Dokl. Akad. Nauk SSSR*, **208**, 1146–9.

Mikheev, N. B., Spitsyn, V. I., Kamenskaya, A. N., Konovalova, N. A., Rumer, I. A., Auerman, L. N., and Podorozhnyi, A. M. (1977) *Inorg. Nucl. Chem. Lett.*, **13**, 651–6.

Mikheev, N. B., Spitsyn, V. I., Kamenskaya, A. N., Mikulski, J., and Petryna, T. (1980) *Radiochem. Radioanal. Lett.*, **43**, 85–92.

Mikheev, N. B., Kamenskaya, A. N., Spitsyn, V. I., Mikul'skil, Ya., Petryna, T., and Konovalova, N. A. (1981a) *Radiokhimiya*, **23**(5), 736–42.

Mikheev, N. B., Kamenskaya, A. N., Berdonosov, S. S., and Klimov, S. I. (1981b) *Radiochimiya*, **23**(6), 793–5.

Mikheev, N. B., Spitsyn, V. I., Kamenskaya, A. N., and Berdonosov, S. S. (1982) *Radiochem. Radioanal. Lett.*, **51**(4), 257–64.

Mikheev, N. B., Kamenskaya, A. N., Konovalova, N. A., Rumer, I. A., and Kulyukhin, S. A. (1983) *Radiokhimiya*, **25**(2), 158–61.

Moeller, T. (1970) *J. Chem. Educ.*, **47**, 417–23.

Müller, W. (1967) *Actinides Rev.*, **1**, 71–119.

Münzenberg, G. (1999) *J. Phys G: Nucl. Part. Phys.*, **25**, 717–25.

Nugent, L. J., Vander Sluis, K. L., Fricke, B., and Mann, J. B. (1974) *Phys. Rev. A*, **9**(6), 2270–2.

Nugent, L. J. (1975) in *MTP Review of Inorganic Chemistry*, vol. 7 (ed. K. W. Bagnall), Butterworths, London, pp. 195–219.

Phillips, C. S. G. and Williams, R J. P. (1966) in *Inorganic Chemistry*, vol. 2, Oxford University Press, London, p. 56.

Porter, C. E., Riley, F. D. Jr, Vandergriff, R. D., and Felker, L. K. (1997) *Sep. Sci. Technol.*, **32**, 83–92.

Porter, F. T. and Freedman, M. S. (1971) *Phys. Rev. Lett.*, **27**, 293–7.

Porter, F. T. and Freedman, M. S. (1978) *J. Phys. Chem. Ref. Data*, **7**(4), 1267–84.

Samhoun, K. and David, F. (1976) in *Transplutonium Elements, Proc. 4th Int. Transplutonium Elements Symp.*, 1975 (eds. W. Müller and R. Lindner), North-Holland, Amsterdam, pp. 1297–304.

Samhoun, K., David, F., Hahn, R. L., O'Kelley, G. D., Tarrant, J. R., and Hobart, D. E. (1979) *J. Inorg. Nucl. Chem.*, **41**, 1749–54.

Scherer, U. W., Kratz, J. V., Schädel, M., Brüchle, W., Gregorich, K. E., Henderson, R. A., Lee, D., Nurmia, M., and Hoffman, D. C. (1988) *Inorg. Chim. Acta*, **146**, 249–54.

Seaborg, G. T. (1945) *Chem. Eng. News*, **23**, 2190–3.

Seaborg, G. T. (1949) in *The Transuranium Elements* (eds. G. T. Seaborg, J. J. Katz, and W. M. Manning), Natl. Nucl. Energy Ser., Div. IV, 14B, McGraw-Hill, New York, pp. 1492–524.

Seaborg, G. T. and Katz, J. J. (1954) in *The Transuranium Elements,* Natl. Nucl. Energy Ser., Div. IV, 14A, McGraw-Hill, New York, pp. 733–68.

Seaborg, G. T. (1963) *Man-Made Transuranium Elements,* Prentice-Hall, Englewood Cliffs, NJ, pp. 26–30.

Seth, M., Dolg, M., Fulde, P., and Schwerdtfeger, P. (1994) *J. Am. Chem. Soc.*, **117**, 6597–8.

Silva, R. J., Sikkeland, T., Nurmia, M., and Ghiorso, A. (1969) *J. Inorg. Nucl. Chem.*, **31**, 3405–9.

Silva, R. J., Sikkeland, T., Nurmia, M., and Ghiorso, A. (1970) *Inorg. Nucl. Chem. Lett.*, **6**, 733–9.

Silva, R. J., Dittner, P. F., Keller, O. L. Jr, Eskola, K., Eskola, P., Nurmia, M., and Ghiorso, A. (1973) *Nucl. Phys. A*, **216**, 97–108.

Silva, R. J., McDowell, W. J., Keller, O. L. Jr, and Tarrant, J. R. (1974) *J. Inorg. Nucl. Chem.*, **13**, 2233–7.

Spitsyn, V. I., Mikheev, N. B., Kamenskaya, A. N., Berdonosov, S. S., and Mikul'skii, Ya. (1982) *Radiokhimiya*, **24**(5), 615–17.

Stary, I. (1966) *Talanta*, **13**, 421–37.

Taut, S., Hübener, S., Eichler, B., Gäggeler, M., Schädel, M., and Zvara, I. (1997) *Radiochim. Acta*, **78**, 33–8.

Templeton, D. H. and Dauben, C. H. (1954) *J. Am. Chem. Soc.*, **76**, 5237–9.

Thompson, S. G., Harvey, B. G., Choppin, G. R., and Seaborg, G. T. (1954) *J. Am. Chem. Soc.*, **76**, 6229–36.

Usuda, S.,Shinohara, N., Yoshikawa, S., and Suzuki, T. (1987) *J. Radioanal. Nucl. Chem. Articles*, **116**(1), 125–32.

Vobecký, M., Buklanov, G. V., Maslov, O. D., Salamatin, L. I., Schumann, D., Sen, W. G., and Yakushev, A. B. (1991) *J. Radioanal. Nucl. Chem. Lett.*, **154**(1), 73–8.

Wijesundera, W. P., Vosko, S. H., and Parpia, F. A. (1995) *Phys. Rev. A*, **51**, 278–82.

Zvara, I., Belov, V. Z., Domanov, V. P., Zhuikov, B. L., Huebener, S., and Shalaevskii, M. R. (1976) Joint Inst. Nucl. Res. Report JINR P6-10334, Dubna, Russia.

CHAPTER FOURTEEN

TRANSACTINIDE ELEMENTS AND FUTURE ELEMENTS

Darleane C. Hoffman, Diana M. Lee, and Valeria Pershina

14.1 INTRODUCTION

This chapter gives a brief summary of the reported discoveries, confirmation, and nuclear properties of the claimed and confirmed transactinide elements through the year 2004. However, the primary emphasis is on the chemical properties – experimental, theoretical, and predicted – of the transactinides and a comparison of measured properties with theoretical predictions. The experimental studies of chemical properties are especially challenging because of the low production rates and the short half-lives and the need for very special facilities and the use of atom-at-a-time chemistry. The discovery of a new element must furnish evidence that its atomic number is different from those of all the currently known elements and first claims to discovery often lacked such positive identification. As a result, there were uncertainties and controversies over priority of discovery, nuclear and chemical properties, and assignment of names. The first *positive identification* of the atomic number of all these elements was accomplished using 'physical' rather than chemical techniques.

The authors of this chapter have made a conscientious effort to present a balanced view of research on the properties of the transactinides. The chapter also includes predictions of the nuclear and chemical properties of the

SuperHeavy Elements (SHEs). The term originally referred to an 'island of nuclear stability' around the predicted closed spherical shells at 112 to 114 protons and 184 neutrons. Revisions due to recent experiments and theoretical calculations are discussed.

As of 1997, discoveries of the transactinide elements 104 through 109 had been recognized by the International Union of Pure and Applied Chemistry (IUPAC) and the International Union of Pure and Applied Physics (IUPAP). The names and symbols for these elements as finally approved by IUPAC in 1997 (CNIC, 1997) and the year of discovery are given in Table 14.1.

Claims to the discovery of element 110 were made by researchers at the Lawrence Berkeley National Laboratory (LBNL) (Ghiorso *et al.*, 1995a,b), by researchers at the Gesellschaft für Schwerionenforschung (GSI) in Darmstadt, Germany (Hofmann *et al.*, 1995a), and by a Dubna/Livermore group working at the Joint Institute for Nuclear Research (JINR) in Dubna, Russia (Lazarev *et al.*, 1996).

The published analysis of these claims by a Joint Working Party (JWP) of IUPAC/IUPAP (Karol *et al.*, 2001) gave credit for the synthesis of element 110 to the GSI group and invited them to propose a name. They proposed the name 'Darmstadtium' with the symbol Ds after the place in Germany where the element 110 discovery experiments were conducted. The IUPAC Commission on Nomenclature of Inorganic Chemistry (CNIC) considered the proposal and in March 2003 (Corish and Rosenblatt, 2003) recommended to the IUPAC Bureau that it be accepted. It was officially approved by the IUPAC Council at the 42nd General Assembly in Ottawa, Canada, on August 16, 2003.

The discovery of elements 111 and 112 was reported by the GSI group in 1995 (Hofmann *et al.*, 1995b, 1996) and confirmatory experiments were reported in 2002 (Hofmann *et al.*, 2002). In mid-2003 the JWP assigned credit for discovery of element 111 to the GSI group and asked them to propose a name (Corish and Rosenblatt, 2003; Karol *et al.*, 2003), but judged that the evidence for assigning

Table 14.1 *CNIC/IUPAC compromise recommendation for names of transactinide elements. Approved by IUPAC, August* 30, 1997, *Geneva, Switzerland.*

Element	*Name*	*Symbol*	*Discovery year*
104	Rutherfordium	Rf	1969
105	Dubnium (Hahnium)[a]	Db (Ha)[a]	1970
106	Seaborgium	Sg	1974
107	Bohrium	Bh	1981
108	Hassium	Hs	1984
109	Meitnerium	Mt	1982

[a] Many publications of chemical studies before 1997 use hahnium (Ha) for element 105.

credit for the discovery of element 112 was insufficient. The element 111 discovery team proposed the name 'Roentgenium' with symbol Rg after Wilhelm Conrad Roentgen, the discoverer of X-rays. A provisional recommendation for approval of the proposal was sent (Corish and Rosenblatt, 2004) to the IUPAC Bureau and Council and was approved in late 2004. A modern periodic table showing elements through $Z = 154$ is given in Fig. 14.1.

Evidence for elements 112 through 116 has been reported from 1999 to early 2004 by groups working at Dubna (Oganessian, 1999a–c, 2001, 2002; Lougheed *et al.*, 2000; Oganessian *et al.*, 2000a,b, 2002, 2004a–c). However, it should be emphasized that as yet there is no confirmation by other groups of the isotopes of these elements and their decay products. Nuclear properties of the transactinide elements including half-life, mode of decay, main radiations, and method of production based on reports published through early 2004 are given in Table 14.2 and in Appendix II. Nuclides for which only one decay chain has been reported are not listed. Charts of the isotopes of Lr (the last of the actinides) through 109 and for 110 through 116 are shown in Fig. 14.2(a) and (b).

The transactinide elements begin with element 104 (rutherfordium) and include all the elements beyond lawrencium, the element that ends the actinide series with the filling of the 5f electron shell. According to results of atomic relativistic calculations (Fricke, 1975), the filling of the 6d shell takes place in the

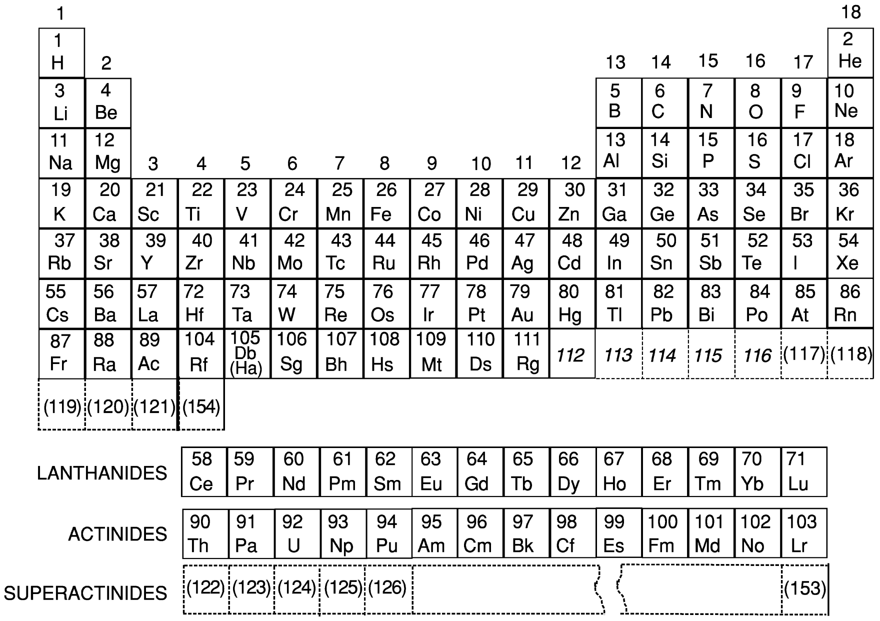

1	2	3	4	5	6	7	8	9	10	11	12	13	14	15	16	17	18
1 H																	2 He
3 Li	4 Be											5 B	6 C	7 N	8 O	9 F	10 Ne
11 Na	12 Mg											13 Al	14 Si	15 P	16 S	17 Cl	18 Ar
19 K	20 Ca	21 Sc	22 Ti	23 V	24 Cr	25 Mn	26 Fe	27 Co	28 Ni	29 Cu	30 Zn	31 Ga	32 Ge	33 As	34 Se	35 Br	36 Kr
37 Rb	38 Sr	39 Y	40 Zr	41 Nb	42 Mo	43 Tc	44 Ru	45 Rh	46 Pd	47 Ag	48 Cd	49 In	50 Sn	51 Sb	52 Te	53 I	54 Xe
55 Cs	56 Ba	57 La	72 Hf	73 Ta	74 W	75 Re	76 Os	77 Ir	78 Pt	79 Au	80 Hg	81 Tl	82 Pb	83 Bi	84 Po	85 At	86 Rn
87 Fr	88 Ra	89 Ac	104 Rf	105 Db (Ha)	106 Sg	107 Bh	108 Hs	109 Mt	110 Ds	111 Rg	*112*	*113*	*114*	*115*	*116*	(117)	(118)
(119)	(120)	(121)	(154)														

LANTHANIDES	58 Ce	59 Pr	60 Nd	61 Pm	62 Sm	63 Eu	64 Gd	65 Tb	66 Dy	67 Ho	68 Er	69 Tm	70 Yb	71 Lu
ACTINIDES	90 Th	91 Pa	92 U	93 Np	94 Pu	95 Am	96 Cm	97 Bk	98 Cf	99 Es	100 Fm	101 Md	102 No	103 Lr
SUPERACTINIDES	(122)	(123)	(124)	(125)	(126)									(153)

Fig. 14.1 *Periodic table showing placement of transactinides through element* 154. (*Italics indicate elements reported but not yet confirmed. Undiscovered elements are shown in parentheses.*)

Table 14.2 *Nuclear properties of transactinide elements.*

Mass number	*Half-life*	*Mode of decay*	*Main radiations* (MeV)	*Method of production*
rutherfordium (Rf)				
253	∼48 μs	SF		^{206}Pb(^{50}Ti,3n)
254	22.3 μs	SF		^{206}Pb(^{50}Ti,2n)
255	1.64 s	α 48%	α 8.722 (94%)	^{207}Pb(^{50}Ti,2n)
		SF 52%		
256	6 ms	SF, α	α 8.79	^{208}Pb(^{50}Ti,2n)
257	4.7 s	α ∼ 80%	α 9.012 (18%)	^{208}Pb(^{50}Ti,n)
		SF ∼ 2%	8.977 (29%)	^{249}Cf(^{12}C,4n)
		EC ∼ 18%		
258	12 ms	SF		^{246}Cm(^{16}O,4n)
259	3.1 s	α 93%	α 8.87 (∼40%)	^{249}Cf(^{13}C,3n)
		SF 7%	8.77 (∼60%)	^{248}Cm(^{16}O,5n)
260	20 ms	SF		^{248}Cm(^{16}O,4n)
261	75.5 s	α	α 8.28	^{248}Cm(^{18}O,5n)
	4.2 s	α, SF	8.52	
262	2.1 s	SF		^{248}Cm(^{18}O,4n)
	47 ms	SF		
dubnium (Db)				
256	1.6 s	EC, α	α 9.014 (∼67%)	^{209}Bi(^{50}Ti,3n)
257	1.5 s	α, SF	α 8.967, 9.074	^{209}Bi(^{50}Ti,2n)
257 m	0.76 s	α, SF	9.163	^{209}Bi(^{50}Ti,2n)
258	4.4 s	α	α 9.19	^{262}Bh daughter
			9.07	
259	0.51 s	α	α 9.47	^{241}Am(^{22}Ne,4n)
260	1.5 s	α $\geq$ 90%	α 9.082 (25%)	^{249}Cf(^{15}N,4n)
		SF $\leq$ 9.6%	9.047 (48%)	^{243}Am(^{22}Ne,5n)
		EC $\leq$ 2.5%		
261	1.8 s	α ∼ 75%	α 8.93	^{243}Am(^{22}Ne,4n)
		SF ∼ 25%		^{249}Bk(^{16}O,4n)
262	34 s	α $>$ 67%	α 8.66 (∼20%)	^{249}Bk(^{18}O,5n)
		SF + EC $<$ 33%	8.45 (∼80%)	
263	27 s	α, SF	α 8.36	^{249}Bk(^{18}O,4n)
268	16 h	SF		115 decay product
seaborgium (Sg)				
258	2.9 ms	SF		^{209}Bi(^{51}V,2n)
259	0.48 s	α	α 9.62 (78%)	^{208}Pb(^{54}Cr,3n)
260	3.6 ms	α	α 9.77 (83%), SF	^{208}Pb(^{54}Cr,2n)
261	0.23 s	α, SF	α 9.56 (60%)	^{208}Pb(^{54}Cr,n)
262	6.9 ms	α $\leq$ 22%		^{270}110 decay product
		SF $\geq$ 78%		
263	0.9 s	α	α 9.06 (90%)	^{249}Cf(^{18}O,4n)
	0.3 s	α	α 9.25	
265	7.4 s	α	α 8.84 (46%)	^{248}Cm(^{22}Ne,5n)
266	21 s	α	α 8.77, 8.52	^{248}Cm(^{22}Ne,4n)

Table 14.2 (*Contd.*)

Mass number	*Half-life*	*Mode of decay*	*Main radiations* (MeV)	*Method of production*
bohrium (Bh)				
261	12 ms	α	α 10.10 (40%)	^{209}Bi(^{54}Cr,2n)
262	0.1 s	α	α 10.06, 9.91, 9.74	^{209}Bi(^{54}Cr,n)
	8.0 ms	α	α 10.37, 10.24	^{209}Bi(^{54}Cr,n)
264	1.0 s	α	α 9.48, 9.62	111 decay product
266	~1 s	α	α 9.3	^{249}Bk(^{22}Ne,5n)
267	17 s	α	α 8.85	^{249}Bk(^{22}Ne,4n)
272	9.8 s	α	α 9.02	115 decay product
hassium (Hs)				
264	0.26 ms	α, SF	α 10.43	^{207}Pb(^{58}Fe,n)
265	1.7 ms	α	α 10.30 (90%)	^{208}Pb(^{58}Fe,n)
	0.8 ms	α	α 10.57 (63%)	^{208}Pb(^{58}Fe,n)
266	2.3 ms	α	α 10.18	^{270}110 daughter
267	59 ms	α	α 9.88, 9.83, 9.75	^{271}110 daughter
269	14 s	α	α 9.23, 9.17	112 decay product
270	~4 s	α		^{248}cm(^{26}Mg,4n)
meitnerium (Mt)				
266	1.7 ms	α	α 10.46, 11.74	^{209}Bi(^{58}Fe,n)
268	42 ms	α	α 10.10, 10.24	111 daughter
276	0.72 s	α	α 9.71	115 decay product
darmstadtium (Ds)				
267	3.1 μs	α	α 11.6	^{209}Bi(^{59}Co,n)
269	0.17 ms	α	α 11.11	^{208}Pb(^{62}Ni,n)
270	0.10 ms	α	α 11.03	^{207}Pb(^{64}Ni,n)
	6.0 ms	α	α 12.15	^{207}Pb(^{64}Ni,n)
271	56 ms	α	α 10.71	^{208}Pb(^{64}Ni,n)
	1.1 ms	α	α 10.74, 10.68	
273	0.15 ms	α	α 11.08	112 daughter
280	7.6 s	SF		114 decay product
roentgenium (Rg)				
272	1.6 ms	α	α 11.0	^{209}Bi(^{64}Ni,n)
280	3.6 s	α	α 9.75	115 decay product
element 112				
277	0.6 ms	α	α 11.65, 11.45	^{208}Pb(^{70}Zn,n)
283	3 min	α, SF		^{238}U(^{48}Ca,3n); 114 daughter
284	0.75 min	α	α 9.15	114 daughter
element 113				
284	0.48 s	α	α 10.00	115 daughter
element 114				
287	5 s	α	α 10.29	^{242}Pu(^{48}Ca,3n)
288	2.6 s	α	α 9.82	^{244}Pu(^{48}Ca,4n)
element 115				
288	87 ms	α	α 10.46	^{243}Am(^{48}Ca,3n)
element 116				
292	53 ms	α	α 10.53	^{248}Cm(^{48}Ca,4n)

Mt 109									266 1.7 ms α		268 42 ms α								276 0.72 s α
Hs 108								264 0.3 ms α, SF	265 0.8 ms | 1.7 ms α	266 2.3 ms α	267 59 ms α		269 14 s α	270 ~4 s α					
Bh 107							261 12 ms α, SF	262 8 ms | 0.1 s α		264 1.0 s α		266 ~1 s α	267 17 s α					272 9.8 s α	
Sg 106					258 2.9 ms SF	259 0.5 s EC,α	260 3.6 ms α, SF	261 0.2 s α, SF	262 7 ms SF, α	263 0.9 s | 0.3 s α, SF		265 7.4 s α	266 21 s α						
Db(Ha) 105				256 1.6 s α, EC	257 0.8 s | 1.5 s α, SF	258 4.4 s EC,α	259 0.5 s α	260 1.5 s α, SF	261 1.8 s α, SF	262 34 s EC,α	263 27 s SF, α					268 16 h SF			
Rf 104	253 0.05ms SF	254 0.02ms SF	255 1.6 s α, SF	256 6 ms SF, α	257 4.7 s α, SF	258 13 ms SF, α	259 3.0 s α, SF	260 20 ms SF	261 1.3 m | 4.2 s α, SF	262 47 ms | 2 s SF									
Lr 103	252 0.36 s α	253 1.5 s | 0.6 s α	254 13 s α	255 22 s α ,EC	256 26 s α ,EC	257 0.65 s α ,EC	258 3.9 s α	259 6.2 s α ,SF	260 3 m α ,EC	261 39 m SF	262 3.6 h SF,EC								
		150		**152**		**154**		**156**		**158**		**160**		**162**		**164**		**166**	

N

Fig. 14.2 (*a*) *Chart of all isotopes reported for elements* 103 *through* 109.

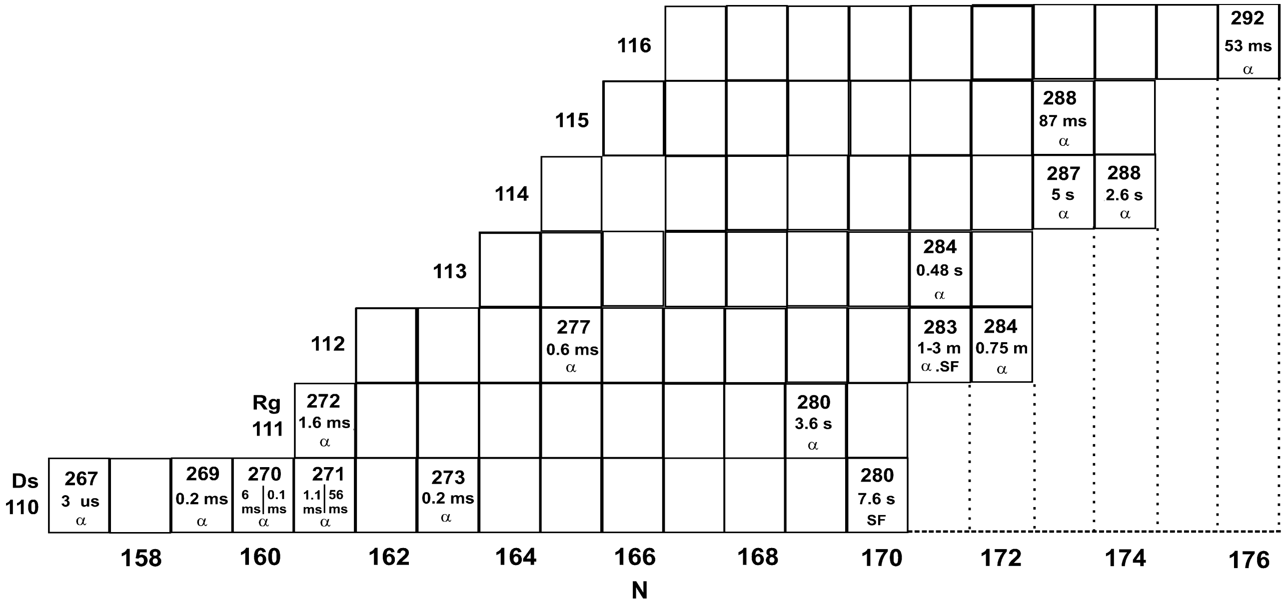

Fig. 14.2 (*b*) *Chart of all isotopes reported for elements* 110 *through* 116.

first nine of the transactinide elements (Z = 104 through 112). In elements 113 through 118 the 7p shell is being filled and element 118 is the heaviest member of the noble gas group. Filling of the 8s shell is expected to occur with elements 119 and 120, making them homologs of elements in groups 1 and 2. Accurate relativistic calculations (Eliav *et al.*, 1998a) show that element 121 will have an 8p electron in its ground state configuration in contrast to the 7d electron expected from simple extrapolation of the members of group 3 in the periodic table. A 7d electron will be added in element 122 to give it the [118] $8s^27d8p$ configuration (Eliav *et al.*, 2002), in contrast to thorium, which has the configuration $[Rn]7s^26d^2$.

No accurate calculations exist beyond element 122 (Eliav *et al.*, 1992), where the situation becomes more complicated because the energy spacings for the 7d, 6f, and 5g levels and later on for the 9s, $9p_{1/2}$, and $8p_{3/2}$ become so close that in the region of $Z = 160$ the usual classification on the basis of a simple electronic configuration may become invalid. Clear structures on the basis of pure p-, d-, f-, and g-blocks are no longer distinguishable. Chemical properties of the elements influenced by these mixed electronic shells will then be so different from anything currently known that classification on the basis of the known periodic table will be impossible.

In order to positively identify a new element and place it in its proper position in the periodic table, its atomic number (proton number) must be determined or deduced in some way. For transactinide elements it became necessary to develop new methods for positive identification of atomic number. One widely used technique is that of correlation of the unknown element's decay to a known daughter and/or granddaughter, which can be identified either chemically or by its decay characteristics. The method of $\alpha-\alpha$ correlations has been widely used for elements that decay by alpha emission to subsequent known α emitters. Another definitive method is measurement of the characteristic X-rays of the new element. This technique was used by Bemis *et al.* (1973, 1977) to confirm the discovery and reported properties of elements 104 and 105, but it requires considerably larger samples than the α–α correlation method. Although detection of spontaneous fission (SF) is a very sensitive technique, determination of the Z of the parent fissioning nuclide is extremely difficult and depends on some other indirect method such as excitation functions, half-life systematics, production in other reactions, or determination of the atomic number of *both primary fragments* from the same SF event in order to add them together to get the Z of the fissioning new element. Detection of only SF decay has led to many controversies concerning discoveries of the transactinide elements.

In 1974, IUPAC and IUPAP appointed an *ad hoc* committee of neutral experts, consisting of three members from the USA, three from the USSR, and three from other countries (including the chairman), to consider the claims of priority to discovery of elements 104 and 105 and attempt to get agreement between the research groups at Berkeley (USA) and Dubna (USSR). The committee was finally disbanded without finishing the report, but the American members eventually published their own in-depth report (Hyde *et al.*, 1987) that summarized the claims and counterclaims together with a critical assessment of both the physical and the chemical evidence relating to discovery of these elements during the period 1960–77. Reference tables with all the known information for each element, a comprehensive bibliography including internal laboratory reports from Dubna and Berkeley, and all articles published in refereed journals related to the first synthesis and identification of the isotopes of elements 104 and 105, and a summary and conclusions were presented. They concluded that the information published for element 104 (Ghiorso *et al.*, 1969) and element 105 (Ghiorso *et al.*, 1970, 1971) was correct and fully met the criteria for discovery of new elements stated by Harvey *et al.* (1976) and Flerov and Zvara (1971) and that priority for discovery of elements 104 and 105 clearly belonged to the Berkeley group and endorsed their proposal that they be named rutherfordium (Rf) and hahnium (Ha).

However, the combined IUPAC and IUPAP Transfermium Working Group (TWG) came to different conclusions in their reports (Barber *et al.*, 1991, 1992, 1993) on the final assignment of credit for discovery of elements 101 through 109. An immediate rebuttal to the initial assignments of credit for discovery (Barber *et al.*, 1991) of element 102 to Dubna, and assignment of shared credit to Berkeley/Dubna for elements 104 and 105, and to GSI/Dubna for element 107 was sent in 1991 in a message from Ghiorso and Seaborg to the chairman of the joint IUPAC/IUPAP TWG. A longer response is found in Ghiorso and Seaborg (1993a), as part of the responses invited from Berkeley, Dubna (Oganessian and Zvara, 1993), and GSI (Armbruster *et al.*, 1993). These were published immediately following the TWG report (Barber *et al.*, 1993). The response from Ghiorso and Seaborg (1993b) was also published in *Progress in Particle and Nuclear Physics* because IUPAP had given them no opportunity to respond to the companion 'discovery' article published there (Barber *et al.*, 1992). A long period of dissent ensued after the CNIC resolved that 'an element could not be named after a living person' and, therefore, the name seaborgium for element 106 already approved by the American Chemical Society could not be accepted. The names for elements 101 through 103 were accepted as mendelevium, nobelium, and lawrencium, but dubnium (Db), joliotium (Jl), rutherfordium (Rf), bohrium (Bh), hahnium (Ha), and meitnerium (Mt) were recommended for elements 104 through 109 by IUPAC/CNIC and approved by the IUPAC Bureau in September 1994. This resulted in protest and criticism from around the world as names that had been in common use were scrambled and the historical right of discoverers of a new element to name it was ignored. A long period of negotiation ensued and resulted in 1995 in the suggestion of still another 'compromise' set of names. This time nobelium (102) was replaced with the name flerovium (Fl), and dubnium, joliotium, seaborgium, nielsbohrium, hahnium, and meitnerium were suggested for elements 104 through 109. This slate did not meet with any more approval than the previous one and in an unprecedented step the IUPAC Bureau rescinded the previously approved names and solicited comments over a 5-month period. Finally, the CNIC/IUPAC compromise recommendation shown in Table 14.1 was approved by the IUPAC Bureau on August 30, 1997. The long negotiations and final compromise that resulted in the naming of elements 104 through 106 as rutherfordium, dubnium, and seaborgium, and elements 107 through 109 as bohrium, hassium, and meitnerium have been described in detail in the book *The Transuranium People* (Hoffman *et al.*, 2000a).

14.2 NUCLEAR PROPERTIES OF THE TRANSACTINIDE ELEMENTS

All known isotopes of the transactinides are radioactive. The longest known confirmed half-life for these elements ranges from 75 s for ^{261}Rf to only 42.7 ms for ^{268}Mt, the daughter of ^{272}111 (see Fig. 14.2). No transactinide elements have been found in nature although early predictions (Myers and Swiatecki, 1966; Meldner, 1967) that an ‘island of SHEs’ well beyond uranium might exist around elements with atomic numbers 114 or 126 raised the tantalizing possibility that very long-lived SHEs might still exist on Earth after having been formed during the last nucleosynthesis in our solar system some 5 billion years ago. Later theoretical studies based on new theories of nuclear structure (Strutinsky, 1966; Nilsson *et al.*, 1969a,b; Fiset and Nix, 1972; Randrup *et al.*, 1974) confirmed that an island of nuclear stability stabilized by spherical nuclear shells should be centered around 110 to 114 protons and 184 neutrons. Some calculations even indicated that element 110 with 184 neutrons (^{294}110) should be the longest-lived, with a half-life in the range of hundreds of thousands to a billion years. These predictions sparked a host of experimental investigations to try to detect SHEs in a wide variety of natural sources, but by 1987 no credible evidence for SHEs in nature remained (Hoffman *et al.*, 2000b).

14.3 ONE-ATOM-AT-A-TIME CHEMISTRY

14.3.1 Challenges

Special challenges are involved in studying the chemical properties of the transactinide elements because of their short half-lives, low production rates, the presence of many other unwanted activities, the necessity for producing them in accelerators with high-intensity beams, and the need to build special radiochemistry laboratory and detection facilities nearby. In addition, it is often necessary to prepare and use highly radioactive and rare targets, e.g. ^{248}Cm, ^{249}Bk, ^{249}Cf. Techniques have been developed for detection of a single atom at a time, usually by measuring its radioactive decay. Often the longest-lived known isotope of the element that is used for chemical studies is not the isotope first discovered. Knowledge of the nuclear decay properties and a measurement technique that positively shows that the detected decay arises from the element in question are required. The technique of α–α correlation to known daughter or granddaughter activities can provide such positive identification and has been widely used because many of the transactinide isotopes decay by alpha emission to known alpha-decaying daughter isotopes. Measurement of characteristic X-rays associated with the decay can also provide positive identification of atomic number, but the technique is difficult to apply when only a few atoms can be detected.

14.3.2 Production methods and facilities required

Chemical studies require use of an isotope with a half-life long enough to permit chemical separation and a reasonable production and detection rate, which for the transactinide elements may range from a few atoms per minute for Rf to only an atom per week in the case of Hs. In addition, the isotope must have unique decay characteristics so that it can be positively identified even on an atom-at-a-time basis in order to prove that it belongs to the element whose chemistry is being studied. The isotopes of elements Rf through Hs that were used in the first definitive chemical studies for each element, their production modes, approximate cross sections, and approximate detection rates for the initial experiments that had different overall efficiencies and transport times are listed in Table 14.3, together with those for Lr, the last of the actinides.

14.3.3 Chemical procedures

The chemical procedures used in atom-at-a-time studies must be fast enough to be accomplished in times comparable to the half-lives of the isotopes used in those studies and must give the same results for a few atoms as for macro

Table 14.3 *Isotopes used in first definitive chemical studies of Lr through Hs.*

Nuclide (*half-life*)	*Reaction*	*Cross section*	*Estimated rate*	*Year*
^{256}Lr (26 s)	^{249}Cf (^{11}B,4n)	∼5 nb	3 min^{-1}	1970[a]
^{261}Rf (75 s)	^{248}Cm(^{18}O,5n)	∼5 nb	3 min^{-1}	1970[b]
^{262}Ha (34 s)	^{249}Bk(^{18}O,5n)	∼6 nb	1 min^{-1}	1988[c]
^{266,265}Sg (21 s, 7 s)	^{48}Cm(^{22}Ne,4n,5n)	0.03 nb	1-2 d^{-1}	1997[d]
^{267}Bh (17 s)	^{249}Bk(^{22}Ne,4n)	∼60 pb	2 week^{-1}	2000[e]
^{270,269}Hs (∼4 s, 14 s)	^{248}Cm(^{26}Mg,4,5n)	∼5 pb	1 week^{-1}	2001[f]

[a] Silva *et al.* (1970a).
[b] Silva *et al.* (1970b).
[c] Gregorich *et al.* (1988).
[d] Schädel *et al.* (1997b).
[e] Eichler *et al.* (2000).
[f] Düllmann *et al.* (2002a,b); Kirbach *et al.* (2002).

amounts. Chemical methods in which a single atom rapidly participates in many identical chemical interactions in two-phase systems with fast kinetics that reach equilibrium quickly have proven to be valid. Adloff and Guillaumont (1993) have given a thorough discussion of the validity of conclusions about chemical behavior obtained from very small numbers of atoms. An equilibrium constant was defined for such reactions in terms of the probabilities of finding the species in one phase or the other. Adloff and Guillaumont concluded that it is valid to combine the results of many separate one-atom-at-a-time experiments in order to get statistically significant results. Thus the results obtained from many identical experiments, each performed with only a single atom, can be added together to obtain statistically significant information about chemical behavior (Guillaumont *et al.*, 1989, 1991).

In early studies, activities recoiling from the target were deposited on a thin 'catcher' foil placed directly behind the target in the production chamber of the accelerator. The foil was then removed manually or remotely shuttled to a detection system without disturbing the accelerator vacuum, and its alpha and SF activity measured with appropriate radiation detectors. Alternatively, the collector foil was removed and chemically processed. In either case, the valuable target is not destroyed, and considerable decontamination from all of the activity remaining in the target itself is achieved. Later, gas transport systems using a variety of gases and aerosols were developed to rapidly and efficiently transport reaction products to collection sites outside the radiation field where chemistry can be carried out within a few seconds, either manually or with computer-controlled automated systems that have been developed for both aqueous- and gas-phase chemistry. Although the automated systems are not necessarily faster, they usually give more reproducible results and are more appropriate for carrying out the many repetitive, around the clock experiments lasting weeks at a time that are required to get statistically significant information. Several detailed reviews (Gäggeler, 1990; Hoffman, 1994; Wierczinski and Hoffman, 1996; Hoffman and Lee, 1999; Kratz, 1999a) of these methods have been given.

(a) Gas-phase chemistry

Both thermochromatographic and isothermal methods have been used to study gas-phase properties of the heaviest elements. These methods are particularly useful for short-lived isotopes because the lengthy process of evaporating liquid samples that is required in most aqueous chemistry experiments is avoided. Gas-phase chromatographic methods permit determination of the adsorption enthalpy, ΔH_{ads}, by using correlations between measured properties such as temperature of adsorption and ΔH_{ads}. The latter were shown to be linearly related to the sublimation enthalpy, ΔH_{sub} (Zvara *et al.*, 1970), which is used to compare the volatilities with lighter homologs.

Pioneering studies of the volatilities of the halides of elements 104 and 105 were carried out in the late 1960s and 1970s by Zvara *et al.* (1974, 1976) using thermochromatographic separations. In this method, a longitudinal, negative temperature gradient is established along a chromatographic column through which a gas stream is conducted. It contains the volatile species of interest that deposit on the surface of the column according to their volatilities. Later, the deposition zones are determined from fission tracks registered in detectors positioned along the column. These fissions are associated with specific deposition temperatures, which are then correlated with ΔH_{ads}. The advantage of this method is that production and separation of the detected species takes place very rapidly and species with half-lives as short as a few seconds can be measured. It also has some disadvantages. Positions of the deposition zones are determined only after the experiments are finished. This makes the interpretation of the results very difficult because it is necessary to correct for the half-lives of the various species involved before their volatilities can be compared. Furthermore, real-time observation of the nuclear decay and the determination of the half-lives of the detected species are not possible. Another difficulty is that if only SF activity is measured in the experiments, it is difficult to prove what the atomic number of the detected species actually was because only the fission fragments are detected (see discussion in Section 14.1).

Improved gas thermochromatographic systems have now been developed in which volatile species are transported through a thermochromatographic column (TC) where they are deposited directly on the surface of the pairs of opposing (Si) photodiode detectors that form the column. Both the radiations from the radioactive species and their deposition positions as a function of temperature along the column can be determined simultaneously and recorded. In this way, the isotope (and element) being studied can be positively identified and its deposition temperature at various positions along the TC (Si) (subjected to an appropriate negative temperature gradient) can be determined. Such a cryogenic on-line TC system was used (Düllmann *et al.*, 2002b) to perform the first successful chemical studies of element 108 (Hs) using the alpha-emitting isotopes ^{269,270}Hs and compare the behavior of Hs with Os, its lighter group 8 homolog. These investigations are described in detail in Section 14.6.4b.

Recent studies of gas-phase chemistry have utilized isothermal chromatographic systems such as the On-Line Gas Analyzer (OLGA) developed by Gäggeler (1994) and the Heavy Element Volatility Instrument (HEVI) developed by Kadkhodayan *et al.* (1996) and the alpha-emitting isotopes shown in Table 14.3 to compare the behavior of the halides and oxyhalides of elements 104 through 107 with those of their lighter homologs in groups 4 through 7 of the periodic table. In such systems the entire chromatographic column (usually quartz) is kept at a constant temperature. Volatile species pass through the column and undergo numerous sorption/desorption steps. Chromatographic experiments are carried out at a series of temperatures and the chemical yield of the volatile, short-lived species is studied as a function of temperature. Retention time is indicative of the volatility at each isothermal temperature and can be deduced from the observed changes in the yield from low to high values. The half-life of the nuclide under investigation serves as an 'internal' clock for the process. Just half of the atoms introduced into the isothermal gas chromatographic column will exit from the other end when the time it takes for an atom to pass through the column (the retention time) corresponds to its half-life. That is, the retention time in the chromatographic column at the temperature where the yield is 50% ($T_{50\%}$) of this maximum value is equal to the half-life of the short-lived nuclide (Gäggeler, 1997) and can be used as a relative measure of volatility. If the retention time is very short compared to the known half-life, the yield through the column will approach 100%. A Monte Carlo program taking account of all the experimental conditions is used to deduce the ΔH_{ads} for the measured species. Examples of these studies are discussed in Section 14.6.

(b) Solution chemistry

The Automated Rapid Chemistry Apparatus (ARCA) and the microcentrifuge system SISAK (Special Isotopes Studied by the AKUFE, Swedish acronym for the centrifuge liquid–liquid extraction technique) are examples of automated, computer-controlled systems that have been used in studies of solution chemistry of the heaviest elements.

(*i*) *ARCA*

ARCA can be used to perform rapid, repeated, high-pressure liquid chromatography column experiments on a timescale of seconds. The separations usually are carried out using microscale ion-exchange resin columns. After sorption on the column, the absorbed species are eluted and distribution coefficients are determined from the retention times of the species on the column. The collected liquid samples must then be dried before measurement of alpha emission and/or SF decay with high-resolution solid-state detectors, thus limiting detection to nuclides with half-lives longer than ~30 s. However, longer-lived daughter products can be detected in subsequent steps and used to infer properties of the parent element. The ARCA system has been used successfully for separations of elements 104 through 106, as described in detail in several reviews (Hoffman, 1994; Schädel, 1995; Hoffman and Lee, 1999; Kratz, 1999a,b).

(*ii*) *SISAK*

SISAK is a well-established on-line technique that has been used for studies of gamma-emitting nuclides with half-lives as short as 0.8 s, e.g., ^{109,110}Tc (Alzitzoglou *et al.*, 1990) and was later adapted for use with alpha emitters (Alstad *et al.*, 1995). The SISAK system can be used to perform liquid–liquid extractions on the timescale of a few seconds and has been coupled to a flowing liquid scintillation system to provide continuous separation and measurement of α–α correlations and SFs for nuclides as short as a few seconds (Omtvedt *et al.*, 1998). This permits chemical studies of shorter-lived nuclides, but the detection energy resolution is not as good. However, a recent experiment by Omtvedt *et al.* (2002) showed that rapid pre-separation by the Berkeley Gas-filled Separator (BGS) furnished sufficient decontamination from the extremely high background of unwanted activities so that the SISAK system could be used to obtain more detailed information about the chemical properties of Rf using 4.7-s ^{257}Rf produced in the ^{208}Pb(^{50}Ti,n) reaction. The same technique can be extended to studies of 4.4-s ^{258}Db produced via ^{208}Pb(^{51}V,n) or ^{209}Bi(^{50}Ti,n) reactions as well as to still heavier elements although the production rates are steadily decreasing as Z increases. Additional developments to increase production rates will be required. Another limitation will be the requirement to choose extraction systems with fast enough kinetics to achieve equilibrium.

14.4 RELATIVISTIC EFFECTS ON CHEMICAL PROPERTIES

14.4.1 Relativistic effects on atomic electronic shells

The relativistic mass increase can be expressed as $m = m_0\sqrt{1-(v/c)^2}$ where m_0 is the rest mass and v is the velocity of an electron. As the Z of the heavy elements increases, the stronger attraction to the core causes the electrons to move faster, and the resultant mass increase leads to a decrease in the Bohr radius of the hydrogen-like s and $p_{1/2}$ electrons: $a_{\mathrm{B}} = \hbar^2/mc^2 = a_{\mathrm{B}}^0\sqrt{1-(v/c)^2}$. The contraction and stabilization of these orbitals is the direct relativistic effect; it was shown to originate from the region of the inner K- and L-shells (Schwarz *et al.*, 1989; Baerends *et al.*, 1990). This effect was originally thought to be large only for the 'fast' electrons in inner core shells of heavy atoms. Later, it was also found to be large for the outer s and $p_{1/2}$ valence electrons. For example, the relativistic contraction for the 7s orbital in Db is $\Delta_{\mathrm{R}}\langle r\rangle_{ns} = (\langle r\rangle^{nr} - \langle r\rangle^{\mathrm{rel}}/\langle r\rangle^{nr}) = 25\%$, as shown in Fig. 14.3. As a consequence, the relativistic stabilization of this 7s orbital is 2.6 eV, as shown in Fig. 14.4.

The effect of the *n*s orbital contraction reaches its maximum in the 6th period with Au (17.3%) and in the 7th period with element 112 (31%); the phenomenon has been called the relativistic effect gold maximum and group 12 maximum, respectively (Pyykkö, 1988; Schwerdtfeger and Seth, 1998). The same maximum is, consequently, observed with the relativistic stabilization of the 6s and 7s orbitals (Fig. 14.5). The shift of the maximum to element 112 in the 7th period in contrast to gold in the 6th period is due to the fact that in both elements 111 and 112 the ground state electronic configuration is d^qs^2, while the electronic configuration changes from Au ($d^{10}s^1$) to Hg ($d^{10}s^2$). (See the discussion of relativistic effects in relation to electronic configurations by Autschbach *et al.* (2002).)

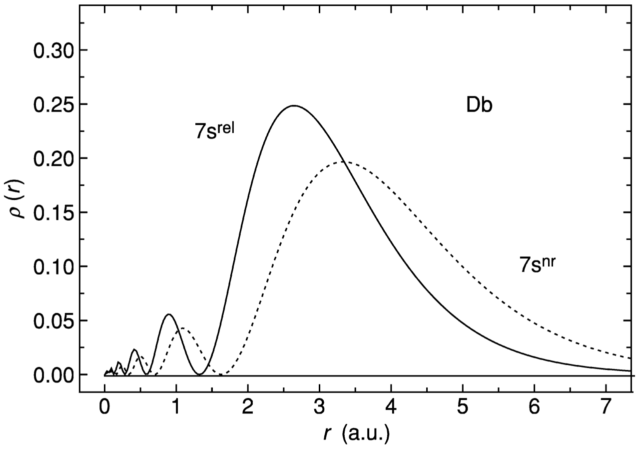

Fig. 14.3 *Relativistic (solid line) and nonrelativistic (dashed line) radial distribution of the 7s valence electrons in Element* 105, *Db.*

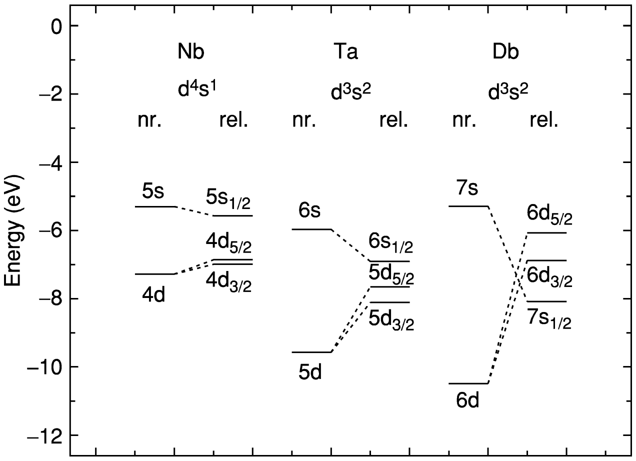

Fig. 14.4 *Relativistic stabilization of the* n*s orbitals, the destabilization of the* (n − 1)*d orbitals and their SO splitting for the group* 5 *elements. Dirac–Fock values are from Desclaux* (1973).

The contraction of the outer s and $p_{1/2}$ orbitals was recently explained as due to the admixture of higher bound and (partially) continuum orbitals due to relativistic perturbations (Schwarz *et al.*, 1989; Baerends *et al.*, 1990).

The relativistic contraction of the s and $p_{1/2}$ shells results in a more efficient screening of the nuclear charge so that orbitals of the outer d- and f-electrons, which never come close to the core, become more expanded and energetically destabilized. This is called the second or indirect relativistic effect. It was

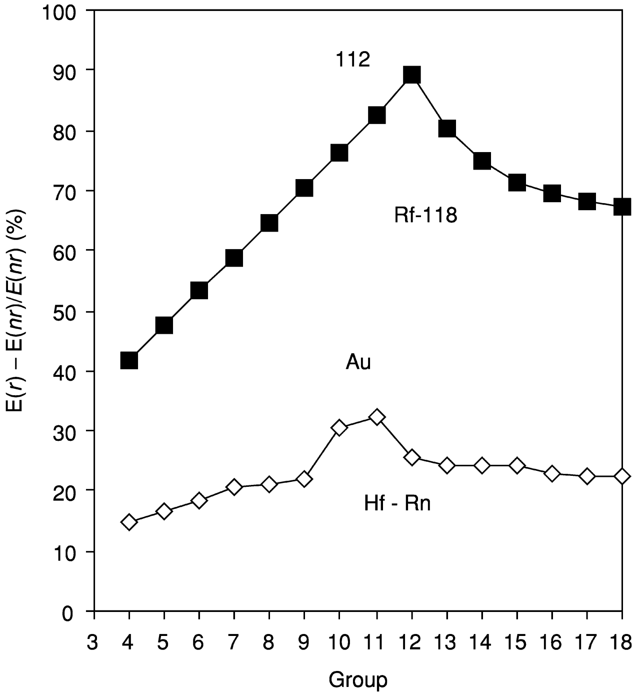

Fig. 14.5 *Relativistic stabilization of the* 6*s and* 7*s orbitals in the* 6*th and* 7*th periods of the periodic table. Redrawn from the data of Schwerdtfeger and Seth* (1998). *Relativistic Dirac–Fock data are from Desclaux* (1973). E(r) *is the relativistic orbital energy and* E(nr) *is the nonrelativistic orbital energy.* (*Figure from Pershina,* 2003).

realized that though contracted s and $p_{1/2}$ core (innermost) orbitals cause indirect destabilization of the outer orbitals, relativistically expanded d- and f-orbitals cause the indirect stabilization of the outer valence s- and p-orbitals. That partially explains the very large relativistic stabilization of the 6s and 7s orbitals in Au and in element 112, respectively (Fig. 14.5). Since both d-shells and f-shells become fully populated at the end of the d- and f-series, respectively, a maximum of indirect stabilization of the valence s- and p-orbitals will occur (Schwarz *et al.*, 1989) there. An example of the relativistic destabilization of the $(n - 1)$d orbitals is shown in Fig. 14.4 for the group 5 elements. This figure shows that trends in the relativistic and nonrelativistic energies of the valence electrons are opposite in going from the 5d to the 6d elements. Their spatial distributions show a similar effect (Fig. 14.3). Thus, only the relativistic description of the wave function can give the appropriate predictions of trends in properties within the chemical groups.

The third relativistic effect is the well-known spin–orbit (SO) splitting of levels with $l > 0$ (p-, d-, f-electrons, etc.) into $j = l \pm 1/2$. It also originates in the vicinity of the nucleus. The SO splitting decreases with increasing *l* quantum number: SO(np$_{1/2}$ – np$_{3/2}$) > SO(nd$_{3/2}$ – nd$_{5/2}$) > SO(nf$_{5/2}$ – nf$_{7/2}$). All three of these effects are of the same order of magnitude and increase roughly as Z^2. The effects can be seen from the energies of one-electron levels of the 7th series of the elements shown in Fig. 14.6.

Breit effects (accounting for magnetostatic interactions) on energies of the valence orbitals and on ionization potentials (IPs) are usually small, e.g. 0.02 eV for element 121 (Eliav *et al.*, 1998a). They can, however, reach a few percent for the fine structure level splitting, e.g. 3.6% of the total amount of the Tl ^{2}P splitting. Quantum electrodynamic (QED) effects are known to be very important for the inner shells, e.g. in accurate calculations of x-ray spectra. The effects were shown to be small, but not negligible for the valence electron shells, and are of the order of 1–2% of the kinetic relativistic effects. That means that existing studies of relativistic effects have uncertainties of no more than 2% (Pyykkö *et al.*, 1998). Recent monographs are recommended for a discussion of relativistic effects on chemical properties (Schwarz, 1990; Wilson *et al.*, 1991).

14.4.2 Current relativistic quantum-chemical methods

Early predictions of chemical properties of the heaviest elements were made in the 1970s on the basis of relativistic atomic electronic structure calculations and extrapolations of properties from the lighter elements (Keller *et al.*, 1970, 1973; Fricke and Waber, 1971; Fricke, 1975; Penneman and Mann, 1976). Influenced by the success of chemical experiments on the heaviest elements and due to the further development of the quantum-mechanical theory, a new wave of predictions of chemical properties based on relativistic molecular calculations

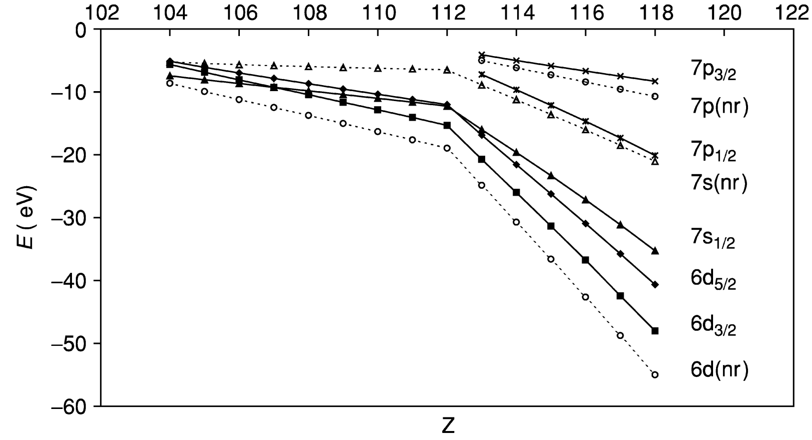

Fig. 14.6 *Relativistic* (*Dirac–Fock, solid lines*) *and nonrelativistic* (*Hartree–Fock, dashed lines*) *orbital energies for elements* 104 *through* 118. *The Dirac–Fock data are from Desclaux* (1973); *Hartree–Fock data are from Schwerdtfeger and Seth* (1998).

appeared, beginning in the 1990s. These calculations were performed using the most advanced quantum-chemical methods at the time. Overviews of their application to transition elements are given by Pyykkö (1988), to actinides by Pepper and Bursten (1991), and to transactinides by Pershina (1996, 2003), Pershina and Hoffman (2003), and Schwerdtfeger and Seth (1998). All-electron *ab initio* methods based on the Dirac–Coulomb–Breit (DCB) Hamiltonian with some possible corrections such as the radiative correction, the extension of the finite nuclei, and coupling with nuclear spin offer fully relativistic treatment of any atomic system. Since the Dirac equation is written for one electron, the real problem of *ab initio* methods is the treatment of the instantaneous electron–electron interaction, called electron correlation. Correlation effects are taken into account by the configuration interaction (CI) technique, the many-body perturbation theory (MBPT) and currently, most accurately by the Fock-space coupled cluster (CC) procedure, called single double CC excitations (CCSDs) (Ishikawa and Kaldor, 1996; Kaldor and Eliav, 1998, 2000). However, the CCSD method is presently limited to treating electronic configurations with no more than two electrons or holes beyond the closed shell. The DCB CCSD calculations have been performed for elements as heavy as 103, 104, 111–115, 118–122 (Kaldor and Eliav, 2000; Eliav *et al.*, 2002).

Atomic calculations using approximations of the DCB equations and some numerical techniques were very successful in the past. Calculations of the electronic structures of the heaviest elements up to very high Z were performed by Desclaux (1973), Mann and Waber (1970), Fricke and Waber (1971), and Fricke *et al.* (1971) using the one-configuration Dirac–Fock (DF) or the Dirac–Slater (DS) methods. (The DS method contains the Slater potential for the exchange-correlation term.) Later, a correlated method, the multi-configuration Dirac–Fock (MCDF) in some slightly different modifications (Desclaux, 1975; Grant, 1986; Parpia *et al.*, 1996), was applied in calculations of the electronic structures of many of the heaviest elements up to $Z = 118$ (Desclaux and Fricke, 1980; Pyper and Grant, 1981; Glebov *et al.*, 1989; Johnson *et al.*, 1990, 1999, 2002; Fricke *et al.*, 1993).

Molecular fully relativistic DF linear combination of atomic orbitals (DF-LCAO) codes including correlation effects are still under development (Grant, 1994; Grant and Quiney, 2000). Calculations are restricted to molecules with very few atoms, such as $(113)_2$ (Wood and Pyper, 1981), 111H, 117H, (113), (117), and $114H_4$ (Saue *et al.*, 1996; Seth *et al.*, 1996; Faegri and Saue, 2001). Algebraic solution of the molecular Dirac equation encounters difficulties due to the fact that the Dirac operator is unbound. Some special techniques like the projection operator technique are used to avoid the variational collapse connected with it. In contrast to nonrelativistic calculations, large basis sets are needed to describe accurately the inner-shell region where relativistic perturbation operators are dominant. The condition of kinetic balance relating the large and small components of the four-component wave function (Grant, 1986) must be observed. Kinetically balanced Gaussian type wave functions with a Gaussian distribution for the nuclear potential are presently the best suited for these purposes. These methods place heavy demands on computer memory and computational time.

Some pseudopotentials (PPs) (Schwerdtfeger *et al.*, 1989; Schwerdtfeger and Seth, 1998) or relativistic effective core potentials (RECPs) (Ermler *et al.*, 1988; Nash *et al.*, 1997; Han and Lee, 1999) are used to solve the many-electron problem in an efficient way. According to these approximations, frozen inner shells are omitted and replaced in the Hamiltonian by an additional PP term. As a result, the number of basis functions is drastically reduced, and, hence the number of two-electron integrals is reduced. Then, the one-electron integrals are solved for the valence basis functions and this additional term by applying *ab initio* schemes at the self-consistent-field (SCF) level or with electron correlation (CI, MBPT, or CCSD) included. The RECP and the PP have been generated for the transactinides (Nash *et al.*, 1997; Schwerdtfeger and Seth, 1998) and quite a number of calculations have been performed for gas-phase compounds of the heaviest elements.

The next group of methods that can successfully be applied to the calculations of the ground state properties of large, chemically interesting systems are methods based on the density functional theory (DFT). This is a theory of the electronic ground state structure couched in terms of the electronic density distribution $\rho(r)$ (Kohn *et al.*, 1996; Rosen, 1997). It has become increasingly useful in calculations of the ground state density and energy of molecules, clusters, and solids, as well as of solvation and adsorption processes. It is an alternative and complementary approach to the traditional methods of quantum chemistry expressed in terms of the many-electron wave function $\psi(r_1, \ldots, r_N)$. The modern DFT is exact and the methods are accurate upon the introduction of the non-local effects via accurate exchange-correlation potentials, like the relativistic general gradient approximation (RGGA). The electronic structures of a number of the heaviest element compounds have been calculated (Bastug *et al.*, 1993; Varga *et al.*, 1999; Pershina and Bastug, 2000; Pershina *et al.*, 2001, 2002a,b) using the fully relativistic four-component RGGA DFT method. A slightly different Beijing DFT code (Liu *et al.*, 1997; Liu and van Wüllen, 1999) was used for some calculations on the simple heaviest systems. The DS discrete-variational (DS-DV) method, a predecessor of the RGGA DFT method which is intrinsically approximate, was extensively used previously by Pershina *et al.* Reviews of the systems for the heaviest elements are given in Pershina (1996), Pershina and Fricke (1999), Pershina and Hoffman (2003), and Pershina (2003).

There are many other theoretical methods appropriate for calculations of the electronic structures of the heaviest element systems, with some limitations. Their descriptions can be found elsewhere (Pepper and Bursten, 1991; Pershina, 1996; Schwerdtfeger and Seth, 1998). Presently, the combination of the PP (RECP) and DFT methods is the best way to study the electronic structures of the heaviest systems.

14.5 PREDICTIONS OF CHEMICAL PROPERTIES FOR ELEMENTS 104 THROUGH 112

14.5.1 Atomic properties

(a) Electronic configurations

Table 14.4 shows the current best calculations of the electronic configurations of the 6d element atoms and ions in comparison with their 5d homologs. The filling of the 6d shell takes place in the first nine of the transactinide elements, $Z = 104$ through 112. Relativistic changes in the energies of the 7s and 6d electrons (Fig. 14.6) result in the stabilization of the $7s^2$ electronic pair in the ground and first ionized states over the entire 7th period of the periodic table, which is different from the ground states of Pt($5d^96s$) and Au($5d^{10}6s$) or from some of the 1+ and 2+ ionized states, as shown in Table 14.4. For example, the nonrelativistic configuration of element 111 is $6d^{10}7s$ according to Eliav *et al.* (1994). It was thought earlier that the relativistic stabilization of the $7p_{1/2}$ electrons of Rf (the $7s^27p6d$ ground state) indicated by MCDF calculations (Glebov *et al.*, 1989; Johnson *et al.*, 1990) would influence the properties of its compounds, but the $7s^27p6d$ electronic configuration was not confirmed by the more accurate CCSD calculations of Eliav *et al.* (1995a). Inclusion of dynamic correlation was required to obtain the correct $6d^27s^2$ ground state for Rf. However, the CCSD calculations of Eliav *et al.* (1995b) did confirm the $7s^27p_{1/2}$ ground state of Lr obtained earlier from the MCDF calculations of

Table 14.4 *Electronic configurations of* 5d *and* 6d *elements.*

5d elements[a]				*6d elements*			
Element	Atom	M^+	M^{2+}	Element	Atom	M^+	M^{2+}
Hf	$5d^26s^2$	$5d6s^2$	$5d^2$	Rf[b]	$6d^27s^2$	$6d7s^2$	$7s^2$
Ta	$5d^36s^2$	$5d^36s$	$5d^3$	Db[c]	$6d^37s^2$	$6d^27s^2$	$6d^3$
W	$5d^46s^2$	$5d^46s$	$5d^4$	Sg[d]	$6d^47s^2$	$6d^37s^2$	$6d^37s$
Re	$5d^56s^2$	$5d^46s^2$	$5d^5$	Bh[e]	$6d^57s^2$	$6d^47s^2$	$6d^37s^2$
Os	$5d^66s^2$	$5d^66s$	$5d^56s$[e]	Hs[e]	$6d^67s^2$	$6d^57s^2$	$6d^57s$
Ir	$5d^76s^2$	$5d^66s^2$?	$5d^7$?	109[f]	$6d^77s^2$	$6d^67s^2$	?
Pt	$5d^96s$	$5d^9$	$5d^8$	110[f]	$6d^87s^2$	$6d^77s^2$	?
Au	$5d^{10}6s$	$5d^{10}$	$5d^9$	111[g]	$6d^97s^2$	$6d^87s^2$	?
Hg	$5d^{10}6s^2$	$5d^{10}6s$	$5d^{10}$	112[h]	$6d^{10}7s^2$	$6d^97s^2$	$6d^87s^2$

[a] Experimental values (Moore, 1958).
[b] CCSD calculations (Eliav *et al.*, 1995a).
[c] MCDF calculations (Fricke *et al.*, 1993).
[d] MCDF calculations (Johnson *et al.*, 1999).
[e] MCDF calculations (Johnson *et al.*, 2002).
[f] DF calculations (Fricke, 1975).
[g] CCSD calculations (Eliav *et al.*, 1994).
[h] CCSD calculations (Eliav *et al.*, 1995b).

Desclaux and Fricke (1980). The relativistic stabilization of the $7p_{1/2}$ electrons manifests itself in some excited states of the transactinides that are different from those of their lighter homologs. For example, the first excited state of Rf is $6d7s^27p(^3D_2)$, only 0.3 eV above its $6d^27s^2(^3F_2)$ ground state (Eliav *et al.*, 1995a), in contrast to Hf, whose first excited state is $5d^26s^2(^3F_3)$, although its ground state is $5d^26s^2(^3F_2)$. Ionized states of elements 104 through 112 show no 7p character, so properties of their compounds in the most typical oxidation states also should not be influenced by this orbital.

(b) Stabilities of oxidation states and ionization potentials

The most accurate IPs calculated for the 6d elements are given in Table 14.5. IPs for elements of the 7th period are shown in Fig. 14.8 in comparison with those of elements of the 6th period. Earlier predictions of stable oxidation states were made on the basis of atomic DF calculations as given in the review of Fricke (1975). They indicated the 4+, 5+, and 6+ states as the most stable for gaseous compounds of Rf, Db, and Sg, respectively, although in solutions the 4+ state was suggested as the most stable for Sg, though not confirmed by later calculations (Pershina *et al.*, 1999). The close proximity of the energy levels of the 7s and 6d electrons (Fig. 14.6) is the reason for the increased stability of the maximum oxidation states of the 6d elements. Indeed, recent MCDF calculations for elements 104 through 108 (Johnson *et al.*, 1990, 1999, 2002; Fricke *et al.*, 1993) have shown a decrease in the multiple IP ($0 \rightarrow Z^+_{\mathrm{max}}$) within the transition element groups 4 through 8, as illustrated in Fig. 14.7. This is also the reason that lower oxidation states are not stable at the beginning of the 6d series: the 7s and 6d levels are spatially so close to each other that the stepwise ionization process, for example, for Db or Sg, results in the $6d^2$ and not in the $7s^2$ configuration of Db^{3+} or Sg^{4+} (Pershina *et al.*, 1999). Since the 6d orbitals of the 6d elements are more destabilized than the 4d and 5d orbitals of the 4d and

Table 14.5 *Calculated ionization potentials for the* 6d *elements.*

IP	*Rf*[a]	*Db*[b]	*Sg*[b]	*Bh*[b]	*Hs*[b]	109[c]	110[c]	111	112
IP_1	6.01	6.89	7.85	7.7	7.6	8.3	9.9	10.6[a]	11.97[a]
IP_2	14.4	16.03	17.96	17.5	18.2	(18.9)	(19.6)	(21.5)	22.49[a]
IP_3	23.8	24.65	25.74	26.6	29.3	(30.1)	(31.4)	(31.9)	(32.8)
IP_4	31.9	34.19	35.40	37.3	37.7	(40)	(41)	(42)	(44)
IP_5		44.62	47.28	49.0	51.2	(51)	(53)	(55)	(57)
IP_6			59.24	62.1	64.0				
IP_7				74.9	78.1				
IP_8					91.8				

[a] CCSD calculations: 104 (Eliav *et al.*, 1995a), 111 (Eliav *et al.*, 1994), and 112 (Eliav *et al.*, 1995b).
[b] MCDF calculations; 104 (Johnson *et al.*, 1990), 105 (Fricke *et al.*, 1993), 106 (Johnson *et al.*, 1999), 107, and 108 (Johnson *et al.*, 2002).
[c] DF calculations, best expectation value (Fricke, 1975). Values in parentheses are estimates.

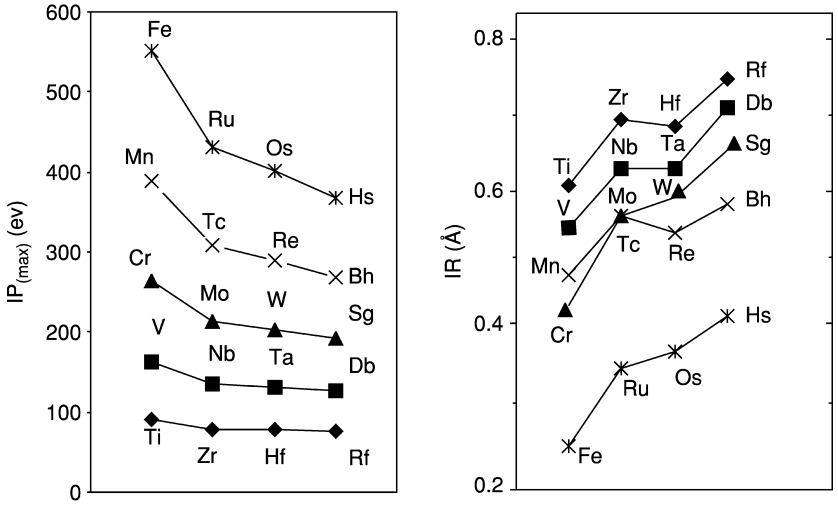

Fig. 14.7 *Ionization potentials (IP$_{max}$) and ionic radii (IR) for elements* 104 *through* 108 *in their maximum oxidation states obtained as a result of the MCDF calculations (Johnson* et al., 1990, 1999, 2002; *Fricke* et al., 1993).

5d elements, respectively, Db^{3+} and Sg^{4+} will be even less stable than Ta^{3+} and W^{4+}. Redox potentials estimated on the basis of these MCDF calculations, as discussed in Section 14.5.3a, indicate that the 6+ state of Sg will also be the most stable in solutions (Pershina *et al.*, 1999).

Predicted stable oxidation states of elements 107 through 110 vary widely. They were discussed in an early paper of Penneman and Mann (1976) that used relativistic Hartree–Fock calculations of the gaseous ion and the hydration parameters of Jorgensen to predict that the most stable oxidation states of elements 107 through 110 in aqueous solutions would be 3+, 2+, 1+, and 0. Earlier, Cunningham (1969) predicted 7+, 8+, 6+, 6+, respectively, for oxidation states of these elements, based on extrapolation by group in the periodic table. Since the Jorgensen hydration parameters did not consider the stabilizing effects of oxyanion formation as observed experimentally for W(vi) and for Re and Os, the higher oxidation states suggested by Cunningham are probably more realistic for solutions where oxyanions can be formed. No predictions based on modern relativistic calculations have been reported for elements 107 through 110.

A most stable oxidation state of 3+ was suggested for element 111, predicted to be a noble metal. It was considered to be as reactive as Au^{3+}, but with more extensive complex formation. Oxidation state 1− was also thought to be possible by analogy to Au^{-}, while 1+ was predicted to be less stable than for Au. The destabilization of the 6d orbitals at the end of the transactinide series is a reason for the 6d electrons to be chemically active. As a consequence, an enhanced stability of higher oxidation states can be expected, for example, of the 5+ states of element 111, and of the 4+ state of element 112 (Fricke, 1975; Schwerdtfeger and Seth, 1998).

It was suggested that the 2+ oxidation state of element 112 would be less stable than that of Hg as its IP_2 of 22.49 eV is larger than that for Hg of 18.75 eV (see Table 14.5). The 1+ state of element 112 also will be less stable than that of Hg (see Fig. 14.8) and probably will not be realized in element 112 at all, since compounds of Hg(I) exhibit the diatomic species $(Hg–Hg)^{2+}$. Higher oxidation states such as 4+ will surely be important in aqueous solutions and in compounds. The neutral state of element 112 is also likely to be very stable due to the inertness of the $7s^2$ electrons.

(c) Ionic radii and polarizability

The ionic radii (IR) of elements are defined by the maximum of the radial charge density, $r_{\max}$, or the expectation values $\langle r_{nj} \rangle$ of an outer valence orbital of an ion. The DF $\langle r_{nj} \rangle$ values for elements up to $Z = 120$ were tabulated by Desclaux (1973). The MCDF $r_{\max}$ for elements 104 through 108 in various oxidation states were calculated by Johnson *et al.* (1990, 1999, 2002) and by Fricke *et al.* (1993). Using these $r_{\max}$, IR of elements 104 through 108 were estimated by these workers using a linear correlation between $r_{\max}$ and the experimentally known IR for the lighter group 4 to 8 elements (Shannon, 1976). The predictions

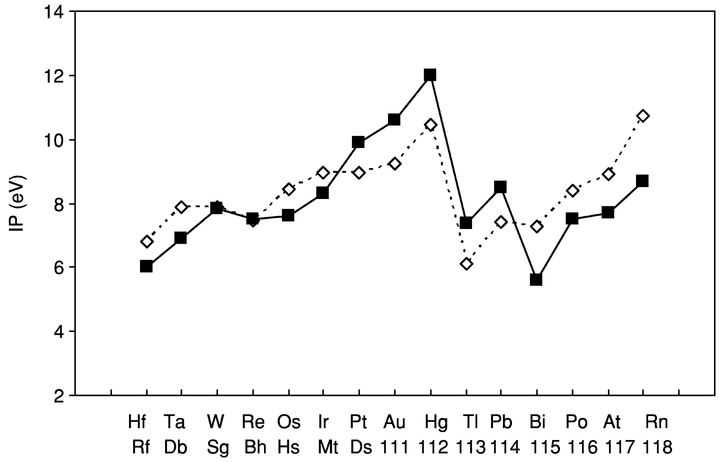

Fig. 14.8 *First ionization potentials for the* 7*th period* (*calculated, solid line*) *and the* 6*th period elements* (*experimental, dashed line*). *CCSD calculations for Rf and elements* 111 *through* 115 (*Eliav* et al., 1994, 1995*b*, 1996*a*, 1998*a*,*b*; *Landau* et al., 2001); *MCDF for elements* 105 *through* 108 (*Fricke* et al., 1993; *Johnson* et al., 1999, 2002; *Pyper and Grant*, 1981).

for the IR of Rf through Hs in their highest oxidation states are summarized in Table 14.6 and Fig. 14.7 together with experimental values for the lighter elements.

The indicated IR of the 4d and 5d elements are almost equal due to the lanthanide contraction, which is 86% a nonrelativistic effect, while the IR of the transactinides are about 0.05 Å larger than the IR of the 5d elements due to an orbital expansion of the $6p_{3/2}$ orbitals, the outer orbitals for the maximum oxidation state. Nevertheless, they are still smaller than the IR of the actinides due to actinide contraction (of 0.030 Å), which is mostly a relativistic effect. Relativistic effects on polarizability (α) change roughly as Z^2 and α should be the smallest in group 12 and in the 7th period for element 112. Its α is relativistically decreased from 74.66 to 25.82 a.u., as shown by PP CCSD(T) calculations (Seth *et al.*, 1997). As a consequence, element 112 is expected to have the weakest van der Waals bond and be extremely volatile.

14.5.2 Gas-phase compounds

(a) Electronic structures of Rf through element 112 and role of relativity

(*i*) *Rf through Hs*

A large series of calculations were performed for halides, oxides, and oxyhalides of Rf through Hs using the DFT and RECP methods: MCl_4 (M = Zr, Hf, and Rf), MCl_5 and MBr_5, $MOCl_3$, and $MOBr_3$ (M = V, Nb, Ta, and Db), MF_6 and MCl_6, $MOCl_4$, MO_2Cl_2, and MO_4^{2-} (M = Mo, W, and Sg) (Pershina, 1996, Pershina and Fricke, 1999), MO (M = Nb, Ta, and Db) (Dolg *et al.*, 1993), $M(CO)_6$ (M = Mo, W, and Sg) (Nash and Bursten, 1995; Nash and Bursten, 1999b), MO_3Cl (M = Tc, Re, and Bh) (Pershina and Bastug, 2000), and MO_4 (M = Ru, Os, and Hs) (Pershina *et al.*, 2001). Various electronic structure

Table 14.6 *MCDF values of IR* (*in* Å) *for the coordination number CN* = 6 *of elements* 104 *through* 108 *in the maximum oxidation states estimated by Johnson* et al. (1990, 1999) *and Fricke* et al. (1993). *Experimental data* (*Shannon,* 1976) *where available are given for the lighter elements.*

Group 4		*Group* 5		*Group* 6		*Group* 7		*Group* 8^a	
Ti^{4+}	0.61	V^{5+}	0.54	Cr^{6+}	0.44	Mn^{7+}	0.46	Fe^{8+}	0.23
Zr^{4+}	0.72	Nb^{5+}	0.64	Mo^{6+}	0.59	Tc^{7+}	0.57	Ru^{8+}	0.36
Hf^{4+}	0.71	Ta^{5+}	0.64	W^{6+}	0.60	Re^{7+}	0.53	Os^{8+}	0.39
Rf^{4+}	0.79^b	Db^{5+}	0.74^b	Sg^{6+}	0.65	Bh^{7+}	0.58	Hs^{8+}	0.45

[a] For CN = 4.

[b] More realistic values obtained from the geometry optimization of molecular compounds are IR = 0.76 Å for Rf^{4+} (Varga *et al.*, 2000) and 0.69 Å for Db^{5+} (Han *et al.*, 1999a).

properties such as IP, electron affinity (EA), electron transition energies, charge density distribution and bonding, as well as their trends in the groups, have been predicted.

Bonding in the compounds of Rf through Hs was shown to be typical of d-element compounds. The bonding is dominated by the large participation of both $6d_{3/2}$ and $6d_{5/2}$ orbitals. The 7s orbital, as well as both $6p_{1/2}$ and $6p_{3/2}$ orbitals, each contribute about 15% to the bonding, and this contribution is increased relative to that of the lighter homologs. The contribution of the $7p_{1/2}$ orbital of 9.4% in $DbCl_5$ is, for example, 50% larger than the contribution of the $5p_{1/2}$ orbital of Nb in $NbCl_5$ (Pershina *et al.*, 1992a). The contribution of the 6d orbitals with respect to that of the 7s and $7p_{1/2}$ orbitals is thus decreased, although it does not change the d-character of the chemical properties.

Molecular orbital (MO) levels for the highest chlorides of Rf, Db, and Sg are shown in Fig. 14.9. They are similar to those of d-element compounds. The group of binding (occupied) levels (with the upper MOs of predominantly 3p character of Cl) is separated from the group of the unoccupied levels of d-character by the energy gap ΔE. A decrease in ΔE from $RfCl_4$ to $SgCl_6$ is indicative of a decrease in the metal–ligand overlap of the atomic wave functions.

The most common feature found in the calculations for all these compounds is an increase in covalence, i.e. a decrease in the effective charge, Q_M, and an increase in the overlap population (OP), as shown in Figs. 14.10 and 14.11. The OP is the amount of the electronic density localized on the bond between atoms in a molecule and is a direct counterpart of the covalent contribution to the

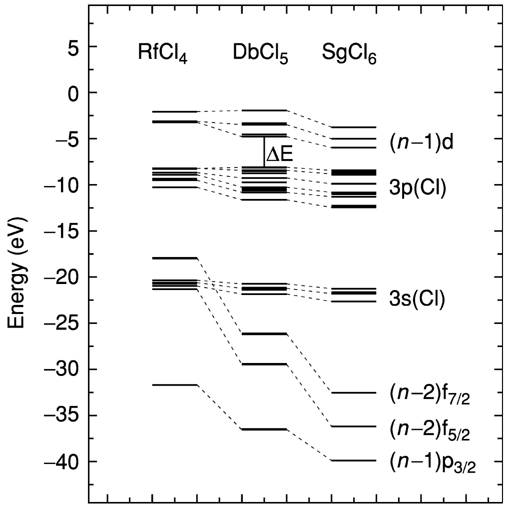

Fig. 14.9 *MO levels for $RfCl_4$, $DbCl_5$, and $SgCl_6$ (Pershina and Fricke,* 1994).

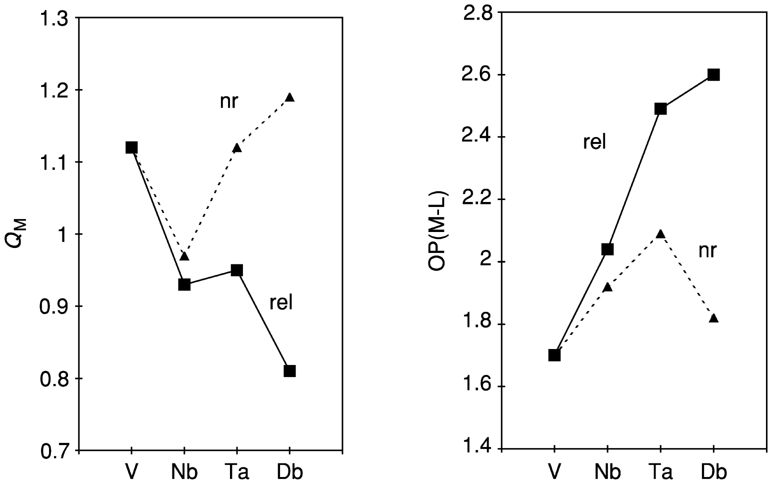

Fig. 14.10 *Relativistic (rel) and nonrelativistic (nr) values of the effective charge* (Q_M) *and overlap population (OP) in* MCl_5*, where* $M = V, Nb, Ta,$ *and Db (Pershina and Fricke,* 1993).

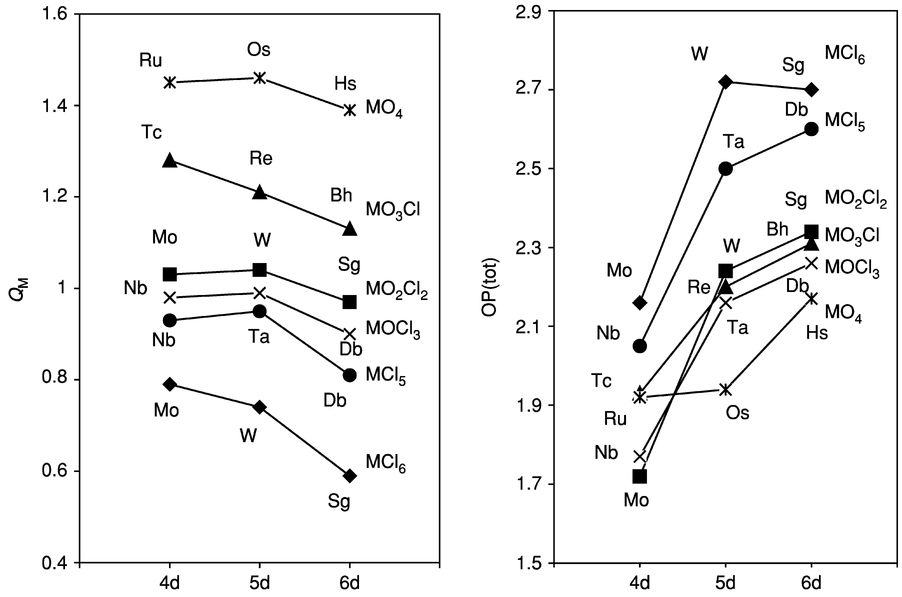

Fig. 14.11 *Effective charges* (Q_M) *and total overlap populations (OPs) for group* 4 *through* 8 *halides and oxyhalides obtained in various calculations (Pershina,* 2003).

binding energy (Mulliken, 1955). Comparison of the relativistic with nonrelativistic calculations (Fig. 14.10) shows this increase to be a purely relativistic effect due to the increasing contribution of the relativistically stabilized and contracted 7s and $7p_{1/2}$ atomic orbitals (AOs), as well as of the expanded 6d AOs in bonding (Pershina and Fricke, 1993).

Calculated molecular properties of gas-phase chlorides, oxychlorides, and oxides of groups 4 through 8 elements and of their homologs studied experimentally are summarized in Table 14.7. Results of molecular calculations (Pershina and Fricke, 1993; Pershina, 1996) have shown that relativistic effects increase IP, decrease EA, and increase the stability of the maximum oxidation state in each compound of the *n*d transition elements, with these effects increasing with increasing Z within the chemical groups. As a consequence, IP, ΔE, and the stabilities of the maximum oxidation states increase from the 4d to the 6d compounds, while the EAs decrease. Nonrelativistically, trends in all these properties would just be reversed from the 5d to the 6d compounds, similarly to the Q_M and OP shown in Fig. 14.10.

Trends in binding energies, D_e, and equilibrium bond distances, R_e, for various types of compounds are depicted in Fig. 14.12. There is a decrease in D_e for almost all of the 6d relative to the 5d element compounds except for MO_4 (M = Ru, Os, and Hs) and MCl_6 (M = Mo, W, and Sg). Within all the groups, relativistic effects enhance bonding of the compounds with increasing Z, though increasing SO splitting of the d-orbitals partially diminishes the binding energy, reaching a decrease of about 1.5 eV for 6d element compounds like SgO_2Cl_2, as shown by RECP calculations (Han *et al.*, 1999a). This is one of the reasons that most of the transactinide compounds have atomization energies lower than those of the homologous 5d elements. The other reason is a decrease in the ionic contribution to bonding, which is also a relativistic effect. The calculated R_e (Fig. 14.12) reflect the experimentally known similarities of bond lengths for the 4d and 5d compounds (due to the lanthanide contraction) and they show an increase in R_e of about 0.05 Å in the transactinide compounds compared to the 5d compounds.

Another important trend is the decrease in the metal–ligand single bond strength in going from the group 4 to the group 6 halides, as well as a decrease in the relative stability of the maximum oxidation state. As a consequence, volatile species such as $SgCl_6$ and $SgOCl_4$ are expected to decompose (a weak Sg–Cl bond) into compounds of Sg(v) at high temperatures by analogy with $MoCl_6$ and $MoOCl_4$. SgO_2Cl_2 was found to be the most stable of all the halides or oxyhalides and was, therefore, recommended (Pershina, 1996) for gas-phase chromatography experiments (Schädel *et al.*, 1997a). An increase in dipole moment, μ, of the low-symmetry molecules within the transition element groups was predicted for all the group 4 to 7 compounds (Table 14.7). The μ and α, as well as the molecular sizes, are decreased by relativistic effects. The PP calculations performed for the gas-phase MO (M = Nb, Ta, and Db) (Dolg *et al.*, 1993) have shown that relativistic effects stabilize the $^2\Delta$ ground state by 2.74 eV

Table 14.7 *Calculated molecular properties of transactinide compounds and of some lighter homologs experimentally studied: ionization potentials (IPs), electron affinities (EAs), energies of the lowest charge-transfer transitions* ($E_{\pi\rightarrow d}$)*, equilibrium bond lengths* (R_e)*, bond strengths* (D_e)*, or dissociation energies* (ΔH_{diss})*, and dipole moments* (μ).

Compound	*IP* (eV)	*EA* (eV)	$E_{\pi\rightarrow d}$ (eV)	R_e (Å)	D_e (eV) (ΔH_{diss})	μ (D)	*Reference*
$ZrCl_4$				2.32[a]	20.32[b]		Girichev *et al.* (1981) (exp.)
$HfCl_4$				2.318[a]	20.53[b]		Girichev *et al.* (1981) (exp.)
$RfCl_4$				2.36	18.97		Han *et al.* (1999a)
				2.38	18.8		Varga *et al.* (2000)
$NbCl_5$	10.77	2.04	2.98	2.34/2.24[c]	19.25[b]		Pershina *et al.* (1992a)
$TaCl_5$	10.73	1.53	3.41	2.37/2.23[c]	19.47[b]		Pershina *et al.* (1992a)
$DbCl_5$	10.83	1.49	3.70	2.42/2.26[c]	17.76		Pershina *et al.* (1992a)
$NbOCl_3$	11.60	0.77	4.57	1.66/2.24[c]		0.91	Pershina *et al.* (1992b)
$TaOCl_3$	11.57	0.29	4.98	1.67/2.25[c]		0.99	Pershina *et al.* (1992b)
$DbOCl_3$	11.64	0.45	4.94	1.72/2.30[c]		1.27	Pershina *et al.* (1992b)
$MoCl_6$	11.06		1.92	2.25	19.29[b]		Pershina and Fricke (1994)
WCl_6	11.13		2.37	2.36[d]	21.65[b]		Pershina and Fricke (1994)
			2.32		19.9		Han *et al.* (1999a)
$SgCl_6$	11.17		2.65	2.38	20.05		Pershina and Fricke (1994)
				2.36	19.9		Han *et al.* (1999a)
$MoOCl_4$				1.658/2.279[e]	20.5[b]	0.14	Pershina and Fricke (1995)
$WOCl_4$				1.685/2.280[e]	22.1[b]	0.49	Pershina and Fricke (1995)
				1.670/2.317	21.5	0.24	Han *et al.* (1999a)

$SgOCl_4$				21.2	1.03	Pershina *et al.* (1995)
			1.720/2.364	21.0	0.77	Han *et al.* (1999a)
MoO_2Cl_2		4.06	1.698/2.259[f]	21.08[b]	1.04	Pershina and Fricke (1996)
WO_2Cl_2		4.48	1.710/2.27[g]	23.5[b]	1.35	Pershina and Fricke (1996)
			1.70/2.28	22.2	1.51	Han *et al.* (1999a)
SgO_2Cl_2		4.33		21.8	1.83	Pershina *et al.* (1996b)
			1.75/2.34	21.0	2.39	Han *et al.* (1999a)
TcO_3Cl	12.25		1.69/2.30[c]	23.12	0.93	Pershina and Bastug (2000)
ReO_3Cl			1.761/2.23			Amble *et al.* (1952) (exp.)
	12.71		1.71/2.28	24.30	1.29	Pershina *et al.* (2000)
BhO_3Cl	13.05		1.77/2.37	22.30	1.95	Pershina *et al.* (2000)
RuO_4	12.19[i]		1.706[h]	27.48		Pershina *et al.* (2001)
OsO_4	12.35[i]		1.711[h]	27.71		Pershina *et al.* (2001)
HsO_4	12.28		1.775	28.44		Pershina *et al.* (2001)

---

[a] Exp. (Girichev *et al.*, 1981).
[b] From a Born–Haber cycle.
[c] Estimated from IR.
[d] Exp. (Brown, 1973).
[e] Exp. (Lijima and Shibata, 1974, 1975)
[f] Exp. (Zharskii *et al.*, 1975).
[g] Exp. (Jampolskii, 1973).
[h] Exp. (Krebs and Hasse, 1976).
[i] Exp. (Burroughs *et al.*, 1974).

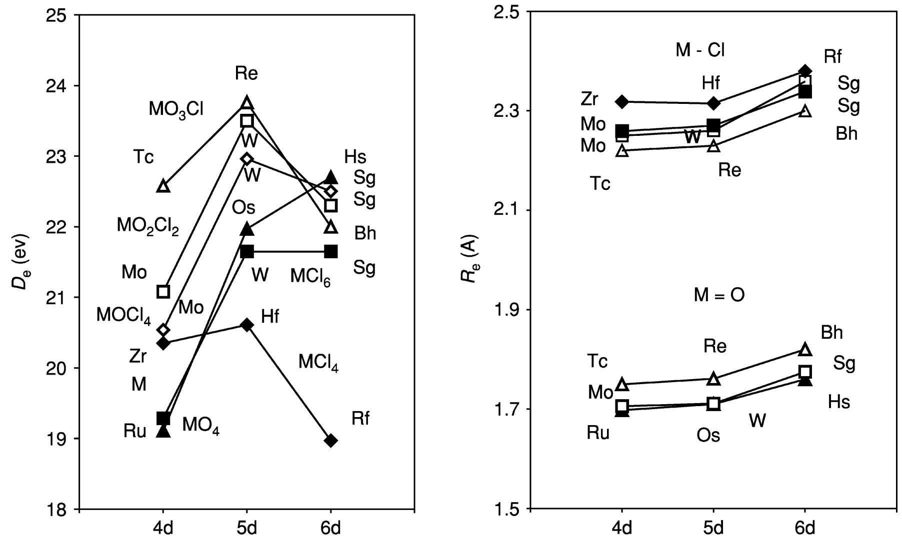

Fig. 14.12 *Binding energies* (D_e, *the dissociation energy of the molecule into its atoms*) *and optimized bond lengths* (R_e) *for various halides, oxides, and oxyhalides of group* 4 *through* 8 *elements* (*Pershina,* 1996; *Han* et al., 1999*a*; *Pershina and Bastug,* 2000; *Pershina* et al., 2001). *Symbols for both* D_e *and* R_e *are open triangles* = MO_3Cl, *open squares* = MO_2Cl_2, *open rhomboids* = $MOCl_4$, *solid rhomboids* = MCl_4, *solid triangles* = MO_4, *solid squares* = MCl_6.

(the nonrelativistic configuration is $^4\Sigma^-$) in contrast to the $^4\Sigma^-$ state observed for NbO. The relativistic effects also stabilize the binding energy of DbO by 1.93 eV. (Σ and Δ denote molecular spectroscopic states.)

(*ii*) *Mt through element* 112

Elements 109 (Mt) and 110 (Ds) have received little attention in recent years. The position of these elements in the periodic table indicates that they should be noble metals. Volatile hexafluorides and octafluorides might be produced and used for chemical separations. The relativistic DS-DV molecular calculations of Rosen *et al.* (1979) and of Waber and Averill (1974) performed for DsF_6 have shown that its electronic structure is very similar to that of PtF_6, with similar values of IP.

Earlier detailed predictions of chemical properties of element 111 based on atomic calculations were made by Keller *et al.* (1973). Due to the fact that the maximum of relativistic effects in the *n*s shell in group 11 occurs at element 111, there has been widespread interest in the electronic structure of its compounds. The effect of the 7s orbital contraction was investigated for the simplest molecule, 111H, whose electronic structure was calculated by a variety of methods including the fully relativistic DCB *ab initio* method (Seth *et al.*, 1996; Liu and van Wüllen, 1999). The bonding was shown to be considerably increased by relativistic effects, which doubled the dissociation energy, though the SO splitting diminished it by 0.7 eV. Calculations (Liu and van Wüllen, 1999) were also performed for other dimers, AuX and 111X where X = F, Cl, Br, O, Au, and 111.

The stability of higher oxidation states of element 111 was examined in calculations of energies of the decomposition reactions $MF_6^- \rightarrow MF_4^- + F_2$ and $MF_4^- \rightarrow MF_2^- + F_2$ using the relativistic PP method (Seth *et al.*, 1998a,b). The results support the earlier predictions that the 3+ and 5+ oxidation states will be more stable for this element than they are for Au (due to a larger participation of the 6d orbitals in bonding) and that the 1+ oxidation state of element 111 may be difficult to prepare. The SO coupling was shown to stabilize the molecules in the following order: $MF_6^- > MF_4^- > MF_2$. This order is consistent with the relative involvement of the $(n-1)$d electrons in bonding for each type of molecule.

The most interesting among the heaviest elements from the chemical point of view is element 112, where the maximum of relativistic effects on the 7s shell in the entire 7th period and within group 12 occurs (see Fig. 14.5). Due to the strong relativistic contraction and stabilization of the 7s orbitals (and accordingly its highest IP in group 12) and its closed-shell configuration, it is expected to be rather inert and may be a distinctly noble metal. It was suggested that the interatomic interaction in the metallic state will be small, possibly even leading to high volatility as in the noble gases. Pitzer (1975a) estimated that the very high excitation energy of about 8.6 eV for the $6d^{10}7s^2 \rightarrow 6d^{10}7s7p$ transition into the configuration of the metallic state will not be compensated by the energy gain of the metal–metal bond formation. An extrapolation of the sublimation enthalpy from its homologs, Zn, Cd, and Hg, also suggests that element 112 should be quite volatile (Eichler, 1974). Recently, a similar conclusion was obtained by using a more sophisticated empirical model (Ionova *et al.*, 1996).

Estimates of adsorption enthalpies of element 112 on various metal surfaces using some adsorption models suggest, nevertheless, that element 112 can be deposited on some metals, like Ag, Au, Pd, or Pt (Eichler and Rossbach, 1983). The ability of element 112 to form a metal–metal bond was also predicted by recent relativistic MO calculations for 112M, where M = Cu, Pd, Pt, Ag, and Au (Pershina *et al.*, 2002a). Element 112 was calculated to form a rather strong bond with the above-mentioned transition elements, only about 15–20 kJ mol^{-1} weaker than that of HgM, with the D_e of 112Pd being the largest.

Molecular relativistic PP calculations (Seth *et al.*, 1997) have predicted that the 2+ oxidation state of element 112 will be less stable than that of Hg. They have calculated that $112F_2$ is, indeed, less stable than HgF_2 and that it will decompose readily into 112 and F_2. Seth *et al.* (1997) also came to the conclusion that element 112 should exhibit a typical transition element character in higher oxidation states, because its 6d orbitals are relativistically destabilized and, therefore, should participate more in coordination bonding. Thus, for example, the 4+ oxidation state of element 112 as in $112F_4$ may be accessible while the 2+ state may not. In combination with an appropriate polar solvent, the species $112F_5^-$ and/or $112F_3^-$ should be formed rather than $112F_4$ or $112F_2$, although these compounds will probably undergo strong hydrolysis in aqueous solutions, and perhaps bromides or even iodides will be more stable and would be better for experimental investigations.

(b) Predictions of volatilities

A more extensive series of the DFT calculations (Pershina, 1996; Pershina and Bastug, 2000; Pershina *et al.*, 2001) permitted establishment of some relationships between molecular properties such as covalence or dipole moment and volatility. Because covalent compounds are typically more volatile than ionic compounds, the higher covalence of high-symmetry halides or oxides of the transactinides is expected to result in their higher volatilities compared with those of their 4d and 5d homologs. For example, $RfCl_4$ is expected to be more volatile than $HfCl_4$ since it is more covalent and is expected to have the T_d symmetry shown by $HfCl_4$ in the vapor phase. Low-symmetry compounds, e.g. oxyhalides of C_n symmetry, have dipole moments and, therefore, are attracted more strongly to the surface of a chromatographic column due to an additional electrostatic (dipole moment–surface charge) interaction than are high-symmetry compounds of the same element such as pure halides. Therefore, one expects that $DbCl_5$ (D_{3h} symmetry) will be more volatile than $DbOCl_3$ (C_{3v} symmetry). For low-symmetry compounds, a trend in volatility in a chemical group will be opposite to the trend in μ, since larger dipole moments cause stronger electrostatic interactions with the surface of a chromatography column. Accordingly, the following decreasing trends in volatility were predicted: $MoO_2Cl_2 > WO_2Cl_2 > SgO_2Cl_2$ and $TcO_3Cl > ReO_3Cl > BhO_3Cl$. These trends are opposite to the increasing dipole moments. Indeed, these trends were confirmed experimentally by the observations (Kadkhodayan, 1993; Kadkhodayan *et al.*,1996; Türler *et al.*, 1998b; Sylwester *et al.*, 2000) that $RfCl_4$ is more volatile than $HfCl_4$, while $DbOCl_3$ (Türler *et al.*, 1996), SgO_2Cl_2 (Schädel *et al.*, 1997a; Türler *et al.*, 1999), and BhO_3Cl (Eichler *et al.*, 2000) are less volatile than the corresponding compounds of their lighter homologs in the respective chemical groups.

In addition, enthalpies of adsorption, $\Delta H_{ads}(BhO_3Cl) = -78.5$ kJ mol^{-1} compared to $\Delta H_{ads}(TcO_3Cl) = -48.2$ kJ mol^{-1} and ΔH_{ads} $(ReO_3Cl) = -61$ kJ mol^{-1}, on the quartz surface of the chromatography column were predicted by Pershina and Bastug (2000) using a model of physisorption and by performing calculations of the electronic structures of those molecules. The obtained adsorption enthalpies indicate that volatility decreases as $TcO_3Cl > ReO_3Cl > BhO_3Cl$, in excellent agreement with the experimental value $\Delta H_{ads}(BhO_3Cl) = -77.8$ kJ mol^{-1} (Eichler *et al.*, 2000). In a similar way, $\Delta H_{ads} = -(36.7 \pm 1.5)$ kJ mol^{-1} on a quartz surface was predicted by Pershina *et al.* (2001) for HsO_4

as compared to $\Delta H_{\mathrm{ads}}(\mathrm{RuO_4}) = -(40.4 \pm 1.5)$ kJ mol^{-1} and ΔH_{ads} $(\mathrm{OsO_4}) = -(38.0 \pm 1.5)$ kJ mol^{-1}. Thus, the volatility of group 8 tetroxides in the specific experiments is expected to change as $\mathrm{RuO_4} < \mathrm{OsO_4} \leq \mathrm{HsO_4}$. Such a sequence is also expected from an extrapolation of this property within the group (Düllmann *et al.*, 2002b). This trend is in accord with the idea of increasing volatility with increasing covalence of compounds.

14.5.3 Solution chemistry

(a) Redox potentials

Some earlier estimates of oxidation states of the transactinides made on the basis of empirical modifications of the Born–Haber cycle were reviewed by Fricke (1975). They were mostly related to simple M^{z+} ions, and the results were rather inconsistent. Recently, redox potentials ($E°$) for complex species of Rf, Db, and Sg in aqueous solutions were estimated (Ionova *et al.*, 1992; Pershina and Fricke, 1994; Pershina *et al.*, 1999) using correlations between the MCDF-calculated IPs (Johnson *et al.*, 1990; 1999; Fricke *et al.*, 1993) and the tabulated redox potentials for group 4, 5, and 6 elements (Bratsch, 1989). Two correlation plots for groups 5 and 6 are shown in Fig. 14.13.

These estimates indicate that the stability of the maximum oxidation state increases with Z within groups 5 and 6, while that of lower oxidation states decreases. Thus, the 5+ and 6+ states of Db and Sg will be more stable than their 3+ and 4+ states, respectively. The 3+ state of Db will be less stable than the 3+ states of Nb or Ta, and the 4+ state of Sg will be less stable than the 4+ states of Mo and W.

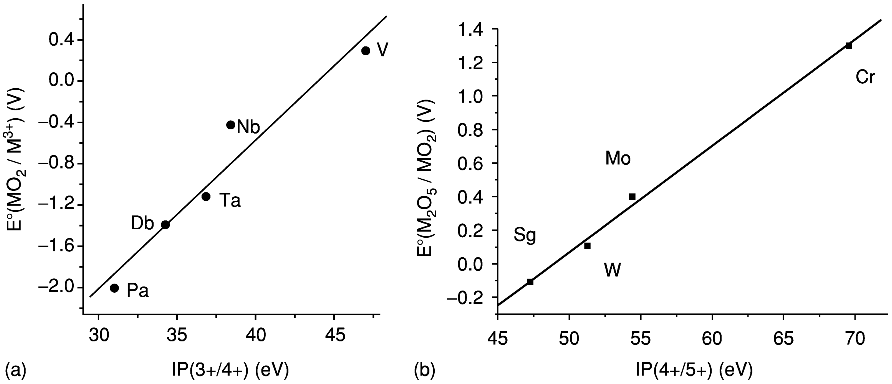

Fig. 14.13 (*a*) *Correlation between IP*(3+/4+) *and the standard potentials* $\mathrm{E}^o(MO_2/M^{3+})$ *where* $M = V$*, Nb, Ta, Db, Pa. The standard potential for Db is from Ionova* et al. (1992). *The standard potentials for Nb, Ta, and Pa are from Bratsch* (1989). (*b*) *Correlation between IP*(4+/5+) *and the standard potentials* $\mathrm{E}^o(M_2O_5/MO_2)$ *where M=Cr, Mo, W, and Sg* (*Pershina* et al., 1999).

The increasing stability of the maximum oxidation state and the decreasing stability of lower oxidation states at the beginning of the 6d series is a relativistic effect caused by destabilization of the 6d orbitals, as discussed earlier. Along the 6d series, the stability of the maximum oxidation state decreases in the order: $\mathrm{Lr}^{3+} > \mathrm{Rf}^{4+} > \mathrm{Db}^{5+} > \mathrm{Sg}^{6+}$. For comparison, the results are summarized in Table 14.8, together with those for Lr, the last of the actinides.

(b) Hydrolysis

Aqueous ions of transition elements undergo strong hydrolysis, as do their heaviest homologs. In acidic solutions, hydrolysis involves either the cation $\mathrm{M(H_2O)}_n^{Z+} \Leftrightarrow \mathrm{MOH(H_2O)}_{n-1}^{(Z-1)+} + \mathrm{H}^+$ or the anion, or both. The hydrolysis of cations of a given oxidation state is known to decrease within groups 4, 5, and 6 as one proceeds down the periodic table and it increases from group 4 to group 6 (Baes and Mesmer, 1976). Hydrolysis/protonation of group 4, 5, and 6 cations and of their compounds was considered theoretically on the basis of relativistic DFT calculations (Pershina, 1998a,b; Pershina and Kratz, 2001; Pershina *et al.*, 2002b).

For group 4 elements, about 50% of each type of the species indicated in the following equilibrium exists in aqueous solutions at pH = 0: $\mathrm{M(H_2O)}_8^{4+} \Leftrightarrow \mathrm{MOH(H_2O)}_7^{3+}$. For this reaction, the following trend in hydrolysis of the group 4 elements was predicted from the calculated Gibbs energy changes: Zr > Hf > Rf (Pershina *et al.*, 2002b). The first hydrolysis constant

Table 14.8 *Calculated redox potentials of Lr, Rf, Db, and Sg in aqueous acidic solutions.*

Potential	*Lr*[a]	*Rf*	*Db*[b]	*Sg*[c]
$E°(\mathrm{M}^{6+}/\mathrm{M}^{5+})$	–	–	–	–0.046 $(\mathrm{MO_3/M_2O_5})$ –0.05 $(\mathrm{M}^{6+}, \mathrm{H}^+/\mathrm{M})$
$E°(\mathrm{M}^{5+}/\mathrm{M}^{4+})$	–	–	–1.0 $(\mathrm{M_2O_5/MO_2})$ –1.13 $(\mathrm{MO_2^+/MO^{2+}})$	0.11 $(\mathrm{M_2O_5/MO_2})$ –0.35 $(\mathrm{M}^{5+}, \mathrm{H}^+/\mathrm{M}^{4+}, \mathrm{H}^+)$
$E°(\mathrm{M}^{4+}/\mathrm{M}^{3+})$	8.1	–1.5 $(\mathrm{M}^{4+}/\mathrm{M}^{3+})$[d]	–1.38 $(\mathrm{MO_2/M^{3+}})$	–1.34 $(\mathrm{MO_2/M^{3+}})$ –0.98 $(\mathrm{M(OH)_2^{2+}/M^{3+}})$
$E°(\mathrm{M}^{3+}/\mathrm{M}^{2+})$	–2.6	–1.7 $(\mathrm{M}^{3+}/\mathrm{M}^{2+})$[d]	–1.20	–0.11
$E°(\mathrm{M}^{3+}/\mathrm{M})$	–1.96[e]	–1.97 $(\mathrm{M}^{3+}/\mathrm{M})$[f]	–0.56	0.27
$E°(\mathrm{M}^{4+}/\mathrm{M})$	–	–1.85 $(\mathrm{M}^{4+}/\mathrm{M})$[g] –1.95 $(\mathrm{MO_2/M})$[g]	–0.87 $(\mathrm{MO_2/M})$[f]	–0.134 $(\mathrm{MO_2/M})$ –0.035 $(\mathrm{M(OH)_2^{2+}/M})$
$E°(\mathrm{M}^{5+}/\mathrm{M})$	–	–	–0.81 $(\mathrm{M_2O_5/M})$	–0.13 $(\mathrm{M_2O_5/M})$[f]
$E°(\mathrm{M}^{6+}/\mathrm{M})$	–	–	–	–0.12 $(\mathrm{MO_3/M})$ –0.09 $(\mathrm{M}^{6+}, \mathrm{H}^+/\mathrm{M})$

[a] Bratsch and Lagowski (1986).
[b] Ionova *et al.* (1992).
[c] Pershina *et al.* (1999).
[d] Johnson and Fricke (1991).
[e] Bratsch (1989).
[f] Roughly estimated from the other $E°$.
[g] Pershina *et al.* (1994).

log K_{11}(Rf) ≈ –4 was then calculated and compared to log K_{11}(Zr) = 0.3 and log K_{11}(Hf) = –0.25. This hydrolysis sequence is in agreement with the order of extraction of group 4 elements into thenoyltrifluoroacetone (TTA) obtained in the experiments described in Section 14.6.1c(iv).

For group 5 elements and Pa, hydrolysis proceeds very rapidly, with the ultimate formation of products such as M(OH)$_5$(aq). Hydrolysis of group 5 cations was studied theoretically for the following reaction: $M(H_2O)_6^{5+} \Leftrightarrow M(OH)_6^- + 6H^+$ where M = Nb, Ta, Db, and Pa. Calculations (Pershina, 1998a) of the Gibbs energy changes of this reaction showed that the trend toward decreasing hydrolysis is continued with Db, giving the sequence Nb > Ta > Db >> Pa.

Hydrolysis of group 6 elements proceeds even further than that of the group 5 elements, with the formation of MO_4^{2-} at higher pH according to the following scheme: $M(H_2O)_6^{6+}$ (this species is not observed) ⇔ … ⇔ $[M(OH)_4(H_2O)]^{2+}$ ⇔ $[MO(OH)_3(H_2O)_2]^+ \Leftrightarrow MO_2(OH)_2(H_2O)_2 \Leftrightarrow [MO_3(OH)]^- \Leftrightarrow MO_4^{2-}$. The protonation process, the reverse of the reaction shown above, was considered theoretically (Pershina and Kratz, 2001). The resulting relative values of Gibbs energy changes suggest that for the first two protonation steps (see Table 14.12) the trend in group 6 should be W > Sg ≥ Mo rather than Sg > W > Mo. For the third and subsequent protonation processes, the trend should be Sg > W > Mo. The values of log *K* were defined for Sg, as shown in Table 14.9. The predicted trends in log *K* are in agreement with experiments on Mo and W at various pH values (Baes and Mesmer, 1976) and with Sg for the protonation/hydrolysis of the positively charged complexes (Schädel *et al.*, 1998).

(c) Complexation

If one molecular complex ML_i, among many others, is extracted into an organic phase, the distribution coefficient, K_d (expressed in terms of the complex formation constant β_i), is a good measure of its stability and the sequence in the K_d values for a given series should reflect the sequence in the stability of the complexes (Ahrland *et al.*, 1973). Thus, by predicting $\log\beta_i = \Delta G^r/2.3RT$ one

Table 14.9 *Values of log* K *for the stepwise protonation of* MO_4^{2-} (*M = Mo, W, and Sg*) (*Pershina and Kratz*, 2001).

	log K$_n$		
Reaction	*Mo*	*W*	*Sg*
$MO_4^{2-} + H^+ \Leftrightarrow MO_3(OH)^-$	3.7	3.8	3.74
$MO_3(OH)^- + H^+ + 2H_2O \Leftrightarrow MO_2(OH)_2(H_2O)_2$	3.8	4.3	4.1 ± 0.2
$MO_4^{2-} + 2H^+ + 2H_2O \Leftrightarrow MO_2(OH)_2(H_2O)_2$	7.50	8.1	8.9 ± 0.1
$MO_2(OH)_2(H_2O)_2 + H^+ \Leftrightarrow MO(OH)_3(H_2O)_2^+$	0.93	0.98	1.02

can predict sequences in the extraction of complexes into an organic phase or their sorption by cation- or anion-exchange resins.

Complex formation is known to increase within the transition element groups with increasing Z. However, in aqueous solutions it competes with hydrolysis as described by the following equilibrium: $x\mathrm{M(H_2O)}_{w^{\circ}}^{z+} + y\mathrm{OH}^- + i\mathrm{L}^- \Leftrightarrow \mathrm{M}_x\mathrm{O}_u\mathrm{(OH)}_{z-2u}\mathrm{(H_2O)}_w\mathrm{L}_a^{(xz-y-i)} + (xw^{\mathrm{o}} + u - w)\mathrm{H_2O}$. This may change trends in the stabilities of the complexes and, consequently, their extraction into an organic phase.

(*i*) *Rf through Sg*

Complexation of group 4 elements in HF solutions is described by the following equilibria:

$$\mathrm{M(H_2O)}_8^{4+} \Leftrightarrow \mathrm{MF(H_2O)}_7^{3+} \Leftrightarrow \mathrm{MF_3(H_2O)}_5^{-} \Leftrightarrow \tag{14.1}$$

$$\mathrm{MF_4(H_2O)_4} \Leftrightarrow \mathrm{MF_5(H_2O)}^{-} \Leftrightarrow \mathrm{MF}_6^{2-}. \tag{14.2}$$

Results of DFT calculations of the relative Gibbs energy changes of these equilibria (Pershina *et al.*, 2002b) suggest that the trend in the formation of the positively charged complexes according to equation (14.1) should be Zr $\geq$ Hf $>$ Rf. This means that the K_d values for sorption by a cation resin of the positively charged complexes formed at HF concentrations below <0.01 M will have the following trend in group 4: Rf $>$ Hf $\geq$ Zr. (In the case of the formation of positively charged complexes of a lower charge from complexes with a higher charge (equation (14.1)), the sequence in the K_d values is opposite to the sequence in the complex formation, since complexes with a lower positive charge are more poorly sorbed on cation exchange resin than those with a higher charge.) For the formation of anionic complexes (equation (14.2)) sorbed by an anion-exchange resin, the trend becomes more complicated depending on the pH, i.e. depending on whether the fluorination process starts from the hydrated or the hydrolyzed species. Thus, for experiments conducted at HF concentrations above 0.001 M where some hydrolyzed or partially fluorinated species are present, the trend for the formation of MF_6^{2-} (equation (14.2)) and hence of K_d should be reversed in group 4: Rf $\geq$ Zr $>$ Hf.

The predicted sequences are in agreement with experiments on cation- and anion-exchange resin separations of Zr, Hf, and Rf from mixed HF/HCl solutions, where fluorinated complexes were sorbed on the resin and Cl^- ions served as counter-ions competing for its active centers (Trubert *et al.*, 1999). At high HCl concentrations, where no hydrolysis takes place, the complexation reaction is $\mathrm{M(H_2O)}_8^{4+} + 6\mathrm{HCl} \Leftrightarrow \mathrm{MCl}_6^{2-}$. Results of the DFT calculations of Gibbs energy changes for this reaction (Pershina *et al.*, 2002b) suggest that the trend in complex formation and in the K_d values should definitely be continued with Rf to give the sequence Zr $>$ Hf $>$ Rf.

Group 5 elements form a large variety of complexes, such as $M(OH)_2Cl_4^-$, $MOCl_4^-$, $MOCl_5^{2-}$, and MCl_6^- (M = Nb, Ta, Db, and Pa), in HCl solutions with different degrees of hydrolysis. Their formation is described in a general form by the following equilibrium reactions: $M(OH)_6^- + iL^- \Leftrightarrow MO_u(OH)_{z-2u}L_i^{(6-i)-}$. The DFT calculations of Gibbs energy changes for these reactions (Pershina, 1998b) showed the following trend in the complex formation and extraction of group 5 elements: Pa >> Nb ≥ Db > Ta. Thus, a reversal of the trend from Ta to Db was predicted for group 5 elements. The following sequence in the formation of various types of complexes as a function of increasing acid concentration was predicted (Pershina and Bastug, 1999): $M(OH)_2Cl_4^- > MOCl_4^- > MCl_6^-$. For the acids of interest, the sequence was predicted as: $MF_6^- > MCl_6^- > MBr_6^-$.

Complex formation of the group 6 elements, Mo, W, and Sg, in HF solutions is described as: MO_4^{2-} (or $MO_3(OH)^-$) + HF $\Leftrightarrow MO_3F^- \Leftrightarrow MO_2F_2(H_2O)_2 \Leftrightarrow MO_2F_3(H_2O)^- \Leftrightarrow MOF_5^-$. The calculated Gibbs energy changes of these reactions show a very complicated dependence of trends in the complex formation on HF concentration and pH. Thus, at low [HF] < ~0.1 M, a reversal of the trend from W to Sg should occur, while at high [HF] > 0.1 M, the trend is continued with Sg: Sg > W > Mo. It should be noted that such complicated trends could not be obtained by any extrapolation of properties within the group, but are the result of considering complex formation in equilibrium with hydrolysis and by calculating relativistically the electronic structure of the complexes.

(*ii*) *Bh through element* 112

The aqueous chemistry of these elements promises to be very interesting and should provide extensive information about complexing ability as well as information about the potential reduction reactions. Some general considerations on the basis of atomic calculations are presented by Fricke and Waber (1971); Fricke (1975). Some aspects of the complex formation of elements 107 through 112 in aqueous solution were discussed by Keller and Seaborg (1977) and Seaborg and Keller (1986). It is expected that element 112 will have extensive complex-ion chemistry, as do other elements of the second half of the 6d transition series. From early relativistic atomic calculations, Pitzer (1975a) postulated some very interesting properties for element 112 caused by relativistic effects on the $7s^2$ shell. He suggested that element 112, eka-Hg, would be more noble than Hg, and even though the oxide, the chloride, and the bromide would be unstable, $112Cl_4^{2-}$ and $112Br_4^{2-}$ would exist in solution, and $112F_2$ would be stable.

Recently, Seth *et al.* (1997) have considered the possibility of formation of $112F_5^-$ and $112F_3^-$, by analogy with Hg where the addition of F^- to HgF_2 or HgF_4 was found to be energetically favorable. However, in aqueous solutions these complexes probably undergo strong hydrolysis. Thus, experiments might only be possible with $112Br_5^-$ or $112I_5^-$.

14.6 MEASURED CHEMICAL PROPERTIES FOR ELEMENTS 104 THROUGH 112

The experimental results for Rf, Db, and Sg, the results of the first experimental investigations for Bh and Hs, and a preliminary report of experiments designed to study element 112 are briefly reviewed. Several more detailed reviews of the experimental techniques, measured chemical properties of Rf, Db (Ha), and Sg, and prospects for studies of still heavier elements are available and should be consulted for additional information (Schädel, 1995, 2002; Gregorich, 1997a; Hoffman and Lee, 1999; Kratz, 1999b).

A summary of some predicted chemical properties of elements 104 through 112 is given in Table 14.10. First experimental investigations of the chemical properties of the transactinides focused on the most fundamental and simplest properties. For example, the determination that the most stable oxidation states of elements 104 and 105 in aqueous solutions were 4+ and 5+, respectively, allowed their placement at the bottom of groups 4 and 5 in the periodic table as members of the 6d transition series. In later experiments, attempts were made to perform more complex studies of transactinide properties for comparison with their lighter homologs in the periodic table. Such studies present even greater challenges because of the need to investigate the transactinides and their lighter homologs under exactly the same chemical conditions – the ideal situation being to measure them all in the same on-line experiments conducted at the accelerators where they are produced.

14.6.1 Chemistry of rutherfordium (104)

(a) Historical

In early gas-phase studies at Dubna, Zvara *et al.* (1969, 1970) reported that the chloride of a 0.3-s SF activity produced in the ^{242}Pu(^{22}Ne,4n) reaction and initially assigned to ^{260}Rf formed a chloride, presumably $RfCl_4$, that was less volatile than $HfCl_4$. However, the existence of such an isotope has never been confirmed (see Fig. 14.2) and these claims were apparently incorrect as discussed in detail by Kratz (1999b). Zvara *et al.* (1972) later proposed that they were actually measuring the SF branch of the known alpha-emitting 3-s ^{259}104, which was produced in the same experiments via the ^{242}Pu(^{22}Ne,5n) reaction. They then reported that the volatility of the Rf tetrachloride was similar to that of $HfCl_4$ and much more volatile than the chlorides of the actinides and Sc. They concluded from their results that Rf properly belonged to group 4 of the periodic table. However, only SF events were measured and there is still some doubt about the magnitude of the SF branch of ^{259}104, which decays predominantly by alpha emission. The results could not be considered definitive because positive identification of the element being studied was not possible since only SF decay was detected.

Table 14.10 *Predicted chemical properties of elements* 104 *through* 112.

	Rf	Db	Sg	Bh	Hs	Mt	110	111	112
chemical group	4	5	6	7	8	9	10	11	12
stable oxidation states[a,b]	$\underline{\mathbf{4}}$,3	$\underline{\mathbf{5}}$,4,(3)	$\underline{\mathbf{6}}$,5,4,(3)	$\underline{7}$,5,4,$\underline{3}$	$\underline{\mathbf{8}}$,6,$\underline{4}$,$\underline{3}$	6,$\underline{3}$,1	6,4,2,$\underline{0}$	5,$\underline{\mathbf{3}}$,–1	$\underline{\mathbf{4}}$,2,$\underline{\mathbf{0}}$
first ionization potential (eV)[c]	6.01	6.89	7.85	7.7	7.6	8.7	9.6	10.6	11.97
standard electrode potential in aqueous solution (V)[d]	(4+→0)	(5+→0)	(6+→0)	(5+→0)	(4+→0)	(3+→0)	(2+→0)	(3+→0)	(2+→0)
	–1.85	–0.81	–0.12	+0.1	+0.4	+0.8	+1.7	+1.9	+2.1
ionic radius of indicated ion (Å)[e]	0.76(4+)	0.69(5+)	0.65(6+)	0.83(5+) 0.58(7+)	0.80(4+) 0.45(8+)	0.83(3+)	0.80(2+)	0.76(3+)	0.75(2+)
atomic radius (Å)[f]	1.50	1.39	1.32	1.28	1.26	1.22	1.18	1.14	1.10
density (g cm^{-3})[f]	23	29	35	37	41	37.4	34.8	28.7	23.7
ΔH_{sub} (kJ mol^{-1})[g]	694	795	858	753	628	594	481	335	29
boiling point (K)[g]	5800								
melting point (K)[g]	2400								

[a] Bold type: most stable in gas phase; underlined = most stable in aqueous solutions; non-bold: less stable; ( ) = least stable.

[b] Fricke (1975), Pershina *et al*. (1999), Schwerdtfeger and Seth (1998).

[c] See Table 14.5.

[d] See Table 14.8 for Rf through Sg; see Seaborg and Keller (1986) for elements Bh through 112.

[e] See Table 14.6 for maximum oxidation states of Rf through Hs; see Seaborg and Keller (1986) for Mt through 112.

[f] See Seaborg and Keller (1986) for Rf through Hs and Fricke (1975) for Mt through 112.

[g] Seaborg and Keller (1986).

Studies of the solution chemistry of element 104 were conducted in 1970 by Silva *et al.* (1970b) using 75-s ^{261}Rf (see Table 14.3). Positive identification of ^{261}Rf was made by measuring its known half-life and characteristic alpha-decay sequence. Elutions with α-hydroxyisobutyrate solutions from cation-exchange resin columns were used to compare the behavior of ^{261}Rf with No^{2+}, trivalent actinides, Hf^{4+}, and Zr^{4+}. In several hundred repetitive experiments in which 100 atoms were produced for study, the behavior of element 104 was shown to be similar to that of the group 4 elements Zr and Hf, which did not sorb on the column. Its behavior was entirely different from that of No^{2+} and the trivalent actinides that did sorb on the column at pH 4.0.

Some time later, Hulet *et al.* (1980) used ^{261}Rf to perform further experiments to compare the anionic chloride complexes of Rf with those of Hf, Cm, and Fm. Extraction chromatography with a column containing trioctylmethylammonium chloride on an inert fluorocarbon powder was used rather than an ion-exchange resin column because of the faster kinetics. The products recoiling from the nuclear reaction were transported to a fast computer-controlled apparatus that performed the many repetitive experiments necessary to get statistically significant information. The results showed that in 12 M HCl solutions the anionic chloride complexes of Rf and the Hf tracer were strongly extracted by the quaternary amine while the trivalent actinides were not and ran through the column. The chloride complexation of Rf was clearly similar to Hf and much stronger than that of the trivalent actinides, again confirming its position in group 4 of the periodic table. This experiment is especially noteworthy in that it was the first sophisticated, computer-controlled automated system to be used to perform very rapid solution chemistry experiments on an atom-at-a-time basis.

Following these pioneering studies of Rf, a rather long period of time elapsed before additional experiments were conducted in the late 1980s. MCDF calculations (Desclaux and Fricke, 1980; Glebov *et al.*, 1989) indicated that relativistic effects might cause replacement of the expected 6d orbital in Lr by $7p_{1/2}$ orbitals. Spurred by Keller's (1984) extrapolation that Rf might have the configuration $7s^27p^2$ rather than $6d^27s^2$ as expected by analogy to the $5d^26s^2$ configuration of Hf, experimental investigations of relativistic effects in Rf were undertaken. In 1989, Zhuikov *et al.* (1989) examined the volatility of 3-s ^{259}Rf relative to Au, Tl, and Pb tracers in on-line measurements in a quartz column at 1170°C. Under reducing conditions using Ar/H_2 carrier gas, they found that Hf and Rf did not pass through the column while the other elements did. They deduced a lower limit of 370 kJ mol^{-1} for the sublimation enthalpy of metallic 104, much higher than for Pb and other heavy 'p-elements'. Later MCDF relativistic calculations (Glebov *et al.*, 1989; Johnson *et al.*, 1990) indicated that the ground state of Rf is 80% [$6d7s^27p$] while the $7s^27p^2$ state is 2.9 eV above the ground state. Zhuikov *et al.* (1990) and Ryzhkov *et al.* (1992) further concluded that there was no basis for expecting any distinct 'p-character' in the chemical properties of Rf and evaluated various experimental approaches for investigating relativistic effects, including volatilities in the elemental state, thermochromatography of tetrahalides, and the stability of lower oxidation states. Zhuikov *et al.* warned that gas chromatography experiments that depend on Rf or Hf in the atomic state are not useful for investigating relativistic effects because of the difficulty in stabilizing the atomic states at the temperatures above 1500°C that are needed for chromatography columns. However, they suggested that thermochromatography of the tetrahalides appeared promising.

(b) Gas-phase chemistry

In the late 1980s an international team of scientists from Switzerland, Germany, and the USA studied the gas-phase properties of the tetrahalides of Rf using the automated isothermal systems OLGA (Türler *et al.*, 1996) and HEVI (Kadkhodayan *et al.*, 1992). The alpha-emitting isotope 75-s ^{261}Rf (see Table 14.3), produced at the LBNL 88-Inch Cyclotron, was used in the experiments and was positively identified by using surface barrier detectors to measure α–α correlations from its known decay scheme. The Zr and Hf activities were identified via gamma spectroscopy. A schematic diagram of HEVI and the arrangement used in some of the gas-phase studies of element 104 tetrachlorides and tetrabromides at LBNL is shown in Fig. 14.14.

The adsorption enthalpies on the SiO_2 surface of the column were calculated from Monte Carlo fits to the measurements of the relative yields as a function of the isothermal temperature between about 100 and 600°C. The Monte Carlo model was introduced by Zvara (1985) and adapted for use with isothermal gas chromatography by Türler (1996). The calculation takes account of the flow rate, half-life of the isotope, temperature, and other variables to generate yield curves as a function of temperature. A rather complete description of this model has been given by Gäggeler (1997). The adsorption enthalpies resulting from the most recent experiments on the tetrabromides (Sylwester *et al.*, 2000) are shown, together with those for the tetrachlorides (Kadkhodayan *et al.*, 1996), in Fig. 14.15.

Under these conditions, Rf produced volatile $RfCl_4$ at about the same temperature as $ZrCl_4$, indicating their similar volatilities. $HfCl_4$ was unexpectedly less volatile. The analysis of the data using the Monte Carlo model gave the following ΔH_{ads} for group 4 chlorides on SiO_2: $-(74 \pm 5)$ kJ mol^{-1} for Zr, $-(96 \pm 5)$ kJ mol^{-1} for Hf, and $-(77 \pm 6)$ kJ mol^{-1} for Rf (Fig. 14.14). $RfCl_4$ showed about the same volatility as $ZrCl_4$ within the error bars as expected from relativistic calculations (Pershina and Fricke, 1994). 'Nonrelativistic' extrapolations gave lower volatility for $RfCl_4$ (Türler *et al.*, 1996). The observation of the relatively high volatily of $RfCl_4$ was a confirmation of the influence of relativistic effects. Experiments with the bromides showed that they are generally less volatile than the chlorides and that $RfBr_4$ is more volatile than $HfBr_4$ (Fig. 14.14), in agreement with theoretical predictions (Pershina and Fricke, 1999). No attempts to measure the volatilities of the fluorides have yet been reported.

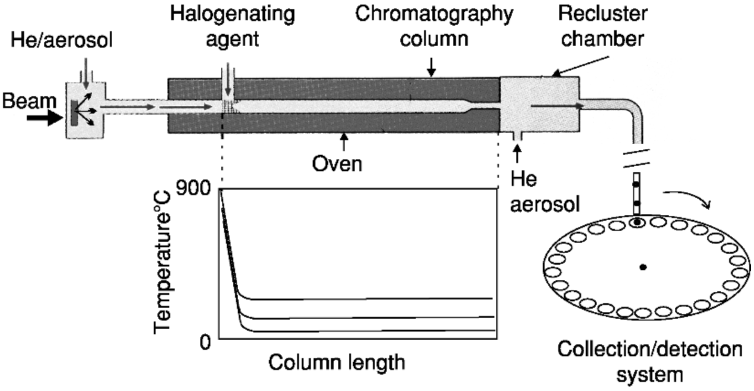

Fig. 14.14 *Schematic diagram of a system used for gas-phase studies is shown. The recoiling products from the reaction are attached to either KCl, KBr, or MoO_3 aerosols and transported in He gas to the entrance to HEVI where they were deposited on a quartz wool plug and halogenated at* 900°C. *Volatile products are transported through the quartz column in flowing He gas and are again attached to aerosols and transported in a gas-jet system and deposited on thin polypropylene films placed on the periphery of a horizontal wheel that is rotated so as to position the foils successively between pairs of surface barrier detectors for* alpha *and SF spectroscopy.*

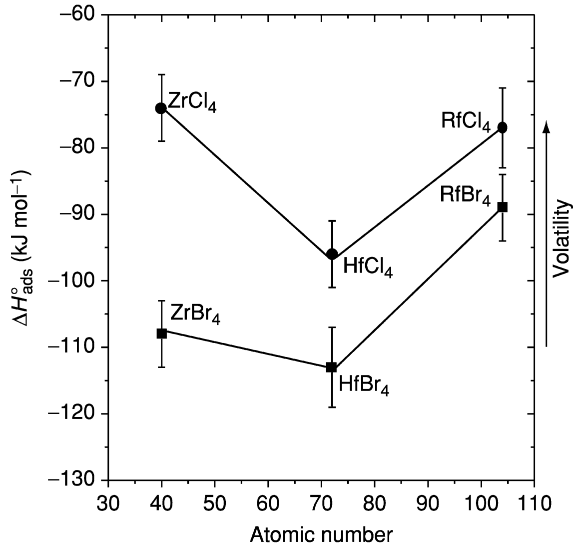

Fig. 14.15 *Adsorption enthalpy values on SiO_2 for Zr, Hf, and Rf chlorides and bromides* (*Kadkhodayan,* 1993*; Kadkhodayan* et al., 1996*; Sylwester* et al., 2000).

(c) Solution chemistry

Additional experimental investigations of the solution chemistry of Rf were initiated in the late 1980s. Manual studies to compare the extraction from aqueous solutions into triisooctylamine (TIOA), tri-*n*-butylphosphate (TBP), and TTA of 75-s ^{261}Rf, its lighter homologs Zr and Hf, and the pseudohomologs Th(IV) and Pu(IV) were reported by the Berkeley group (Czerwinski, 1992b; Czerwinski *et al.*, 1994a,b; Bilewicz *et al.*, 1996; Kacher *et al.*, 1996a,b; Hoffman and Lee, 1999). A comprehensive review and summary, as of 1997, of the results from experiments on the extraction behavior of Rf was given by Gregorich (1997a). Later studies used ARCA for repeated chromatographic studies and SISAK for very rapid automated liquid–liquid extractions (Alstad *et al.*, 1995; Omtvedt *et al.*, 2002).

(*i*) *Extraction of anionic species*

Batch extractions

In repeated manual extractions taking about a min each and using only microliters of each phase, the effect of chloride concentration and pH on extractions into TIOA were investigated. In general, these extractions (Czerwinski *et al.*, 1994a,b; Kacher *et al.*, 1996a,b) confirmed the earlier results (Hulet *et al.*, 1980), showing that Rf generally behaves as a group 4 element, and unlike the trivalent actinides, forms negatively charged complexes in concentrated HCl that are extracted efficiently. Rf is nearly 100% extracted into TIOA from 12 M HCl, as are Zr and Nb, while Th and trivalent actinides and lanthanides are poorly extracted.

Extractions into TIOA/xylene from HF solutions were also performed (Kacher *et al.*, 1996b). Although there were some experimental difficulties with the experiments, they clearly showed that Rf was extracted from 0.5 M HF but not from 4 M HF. This was attributed to the extraction of F^- at the higher fluoride concentrations, which complexes all of the TIOA, thus limiting the extraction of the anionic metal fluoride complexes. The extractability of the group 4 elements was found to decrease in the order: Ti $>$ Zr $\sim$ Hf $>$ Rf. This behavior was cited as evidence that the equilibria for the group 4 elements are the same and that Rf is extracted in the chemical form RfF_6^{2-} similarly to Ti, Zr, and Hf, which are extracted as MF_6^{2-} complexes.

Column separations

Pfrepper *et al.* (1998) produced ^{261}Rf and $^{165-169}$Hf isotopes (few-minute half-lives) simultaneously at the Dubna U-400 cyclotron and devised a multi-column technique for continuous on-line processing and detection of ^{253}Es, the long-lived descendant of ^{261}Rf. Using an anion-exchange column with 0.27 M HF/ 0.1–0.2 M HNO_3 as the eluant, Es was eluted and measured to obtain the K_d values for Rf, which were nearly the same as those for Hf. The ionic charge of the Rf complex was obtained from measurements of K_d vs. [HNO_3]. The ionic charge was calculated to be –(1.9 ± 0.2), similar to that of Hf, indicating formation of RfF_6^{2-}. This again indicates that Rf is similar to Hf and to other members of group 4. The technique, though extremely complex, ensures that equilibrium has been attained and has the virtue of measuring both Rf and Hf in the same experiment. However, it does not give any additional information about specific differences in the chemical behavior of Rf and of its lighter homologs and pseudohomologs.

Other researchers (Haba *et al.*, 2002) used batch extractions with an anion-exchange resin (CA08Y) to determine K_d values for the Rf homologs Zr and Hf, and the pseudohomologs Th(IV) and Pu(IV) as a function of HCl and HNO_3 concentrations in order to determine appropriate conditions for on-line studies with ^{261}Rf and ^{169}Hf at the same time. They then performed on-line measurements of ^{261}Rf and ^{169}Hf produced in ^{18}O-induced reactions with a ^{248}Cm target containing natural Gd, to study their sorption behavior on this anion-exchange resin in solutions of 1.0–11.5 M HCl and in 8 M HNO_3 using an automated ion-exchange separation apparatus coupled to an alpha-spectroscopy detection system. They found that the adsorption of Rf increased steeply with increasing HCl concentration between 7.0 and 11.5 M, as did the adsorption of Zr and Hf, indicating that like Zr and Hf, anionic complexes such as $Rf(OH)Cl_5^{2-}$ or $RfCl_6^{2-}$ are formed. Their results are consistent with previous experiments with Aliquat 336 (Hulet *et al.*, 1980) and TIOA (Czerwinski *et al.*, 1994a). The adsorption order in the region of 9 M HCl was Rf > Zr > Hf. This behavior is quite different from that of Th(IV), whose distribution coefficients are less than 1 and further decrease in this region. In 8 M HNO_3, more than 80% of Rf, Hf, and Zr were eluted while 99% of the pseudohomolog Th(IV) was retained, indicating that Rf, like Hf and Zr, formed cationic or neutral species, unlike Th(IV) or Pu(IV).

(*ii*) *Extraction of neutral complexes with TBP*

It is well known that TBP extracts neutral complexes by forming adducts with neutral metal salts that are extractable into the TBP organic phase. The adduct is presumed to have the form $ML_4 \cdot x\mathrm{TBP}_{(org)}$ where x can be determined by measuring the slope of log K_d as a function of log [TBP]. If the TBP concentration is too high, aggregation of the TBP molecules may give erroneous results. Furthermore, there are very large statistical uncertainties in determination of K_d values when the small number of atoms produced is measured only in the organic phase. The calculation of K_d = (extraction yield)/(1−extraction yield) is probably only accurate for relatively small K_d values because if the K_d values are high the denominator becomes a very small difference between two very similar numbers with large errors. Extractions from HCl into TBP are also unusually dependent on both [H^+] and [A^-], indicating that hydrolysis plays an important role.

Batch extractions

Extractions of ^{261}Rf, Hf, Zr, Th, and Pu into TBP were first studied by Czerwinski *et al.* (1994b) using manual extractions from aqueous solutions of 8, 10, and 12 M HCl, with $[H^+]$ held constant at 8, 10, and 12 M and $[Cl^-]$ adjusted with LiCl to 8, 10, and 12 M. The Zr, Th, and Pu(IV) results were obtained from off-line tracer experiments. In pure HCl solutions, the extraction of Pu, Th, and Zr was nearly 100% at all three molarities, consistent with previously reported (Peppard *et al.*, 1956) data for Zr and Th, while extraction of Rf and Hf was low at 8 M and increased to higher values at 10 and 12 M HCl. Extraction of Hf remained lower than that of Rf at all molarities. With $[H^+]$ held at 8 M, an increase in $[Cl^-]$ to 10 and 12 M resulted in significant decreases of both Rf and Pu extraction into TBP/benzene while extraction of Zr, Hf, and Th remained high. This was interpreted as indicating that chloride complexation is stronger for Rf than for Zr, Hf, and Th, and that Rf, similarly to Pu(IV), forms anionic species of the type MCl_6^{2-}, which does not extract into TBP. The trends in extraction yields vs. $[H^+] = 8$, 10, and 12 M for $[Cl^-]$, which are constant at 12 M, show that the Hf yields are independent of $[H^+]$ and remain nearly constant between 75 and 80% while the extraction yields for Rf sharply increase, indicating different extraction mechanisms for Rf and Hf. At the highest $[Cl^-]$ concentrations, the extraction yield for Hf follows that of Th, which does not form anionic chloride complexes, while the trend for Rf follows Pu(IV), which does. Problems with losses of Rf and Hf on Teflon collector foils used in some of the on-line studies resulted in absolute values that were probably too low for the higher K_d values. Nevertheless, much useful information can be obtained from an examination of relative extraction yields.

The extractability decreases in the order Zr > Pu > Rf > Hf > Th for 8 M HCl, in the order Zr > Pu > Rf ~ Th > Hf for 10 M HCl, and in the order Zr ~ Rf ~ Pu > Th > Hf for 12 M HCl. A striking observation that needs to be investigated further is that with $[H^+]$ held constant at 8 M the extraction of Rf increases to ~80% when $[Cl^-]$ is increased to 10 M and then decreases sharply to ~25% when $[Cl^-]$ is increased to 12 M, similar to the extraction of Pu(IV), which decreases to less than 20% while that of Zr remains at ~100% and Hf and Th increase to 80–90%. This would indicate formation of an anionic species of Rf similar to $PuCl_6^{2-}$ and unlike all the other group 4 elements and Th. Extraction as a function of $[H^+]$ between 8 and 12 M with $[Cl^-]$ constant at 12 M indicated little effect on the extraction of Zr and Hf, but the extraction of Rf increased from 25 to ~100%. The extracted complex might be of the type $RfCl_4 \cdot x HCl \cdot y TBP$, where x is 1 or 2, values that have been observed in extraction of other elements into TBP.

Kacher *et al.* (1996a) conducted studies to compare extractions of these elements from HBr solutions into TBP with the results of the previous HCl/TBP experiments. They expected the stability of the bromide complexes to differ from that of the HCl complexes because bromide is a larger and more polarizable anion than chloride. They found that the most likely extracted form of Zr was $ZrBr_4 \cdot {\sim}1TBP$ for the HBr/TBP system and ~2TBP for the HCl/TBP system. In general, the extraction of these elements from HBr is much lower than from HCl, and 0.35 M TBP was used to obtain increased extraction. At 9 M HBr, essentially no Rf was extracted but increasing $[Br^-]$ with LiBr to 10, 12, and 13 M resulted in more than 88% extraction of Zr and Rf and ~80% extraction of Th throughout this range while extraction of Pu(IV) increased from about 25 to 70%. In these experiments, Pt collection foils were used to avoid losses of the on-line cyclotron-measured isotopes Rf and Hf. (The Pu tracer was fumed with $NaNO_2$ to make sure it was in the tetravalent state.) Extraction as a function of [HBr] from 7.75 to 9 M HBr solutions was investigated, but without addition of LiBr neither Th nor Rf was extracted. Zr begins to extract at a somewhat lower concentration than Hf, indicating a somewhat stronger tendency to form neutral complexes; Ti extracted only above 9 M HBr. Thus the order of extractability is $Zr > Hf >> Ti \sim Rf$, a reversal in the trend $Zr > Rf > Hf$ seen in the HCl/TBP extractions. Experiments to examine the extraction at concentrations up to 12 M HBr are necessary to confirm this trend.

Column experiments

In order to check and resolve some of the differences in the previously reported results for the TBP/HCl system, Brüchle *et al.* (1998) and Günther *et al.* (1998) measured K_d values for the TBP/HCl system for the carrier-free radionuclides ^{98}Zr (from fission), and ^{169}Hf and ^{261}Rf produced on-line at the Paul Scherrer Institute (PSI) cyclotron. The recoiling products were transferred via He(KCl) jet to ARCA II whose 40 microchromatographic columns (1.6-mm diameter × 8-mm long) were filled with the inert support Voltalef™ (Lehmann & Voss, Hamburg, Germany) coated with undiluted TBP. The use of undiluted TBP is expected to shift the complete extraction of both Zr and Hf to higher HCl concentrations, as shown earlier (Czerwinski *et al.*, 1994b), and prior batch experiments from >10 M HCl confirmed this. From 8 M HCl, 80% Zr and only 20% Hf extraction was found. Chromatographic separations of Zr and Hf were then conducted with ARCA. The radioactive ions were sorbed from 12 M HCl. Most (75%) of the Hf and no Zr were eluted with 8 M HCl and then the remaining Hf and Zr were stripped with 2 M HCl. The K_d for Hf was calculated to be 53 from the relationship, $K_d = [(100)(\%aq)^{-1}{-}1][vol_{aq}/vol_{org}]$, consistent with batch measurements. Subsequent experiments to determine the K_d for Rf in 8 M HCl were conducted at the PSI cyclotron in the same way. After 90 s collection times, the reaction products were sorbed on the columns in 12 M HCl. Hf and Zr fractions were eluted with 8 and 2 M HCl, respectively, and analyzed for alpha decays from ^{261}Rf and its daughter ^{257}No. Two α–α mother–daughter correlations were observed in the Hf fraction and three in the Zr fraction, indicating that Rf extraction is somewhere between that of Hf and Zr in 8 M HCl. After lengthy and complex considerations of contributions from random and background effects, they (Günther *et al.*, 1998) concluded that the K_d for Rf is 150 compared to the K_d of 1180 for Zr and of 60 for Hf obtained from the batch experiments with 8 M HCl, giving the order of decreasing extraction Zr > Rf > Hf. The percentage extraction in their work, 52% for Rf and 25% for Hf from 8 M HCl, appears to be consistent with that of ~60% for Rf and ~25% for Hf obtained by Czerwinski *et al.* (1994b). In a detailed discussion of corrections for the differences in volumes used in the two studies and the dependence of the equilibrium constant on the differences in the TBP concentrations in the organic phase, they finally concluded that Czerwinski's K_d values for Hf and probably for Rf are significantly too low (probably due to sorption on the Teflon collection foils), but that their K_d values were also lower than expected for undiluted TBP because of aggregation effects.

Thus it appears that measurements of relative extractability can be obtained for experiments carried out under exactly the same conditions, but that determination of absolute K_d values is subject to numerous difficulties. The inconsistencies in the K_d results reported by various researchers are probably due in large part to differences in the exact details of the experimental conditions and can greatly affect the measurements, as pointed out above. In addition, results of on-line experiments for the transactinides often are compared with results of off-line tracer studies of their homologs. Furthermore, in the very rapid separations with ion-exchange resin columns required in the study of short-lived isotopes it is necessary to make sure that equilibrium is attained in order to obtain valid results. Some evidence of non-equilibrium effects was reported by Paulus *et al.* (1999) for most amines other than Aliquat 336 and will require further study. Care must be taken in batch experiments to remove any fluoride ion that may have been present in stored tracer solutions. Kacher *et al.* (1996b) found that fluoride ion concentrations as low as 0.02 M reduced the K_d values for extraction into TBP from HBr by about 2 for Hf and 10 for Zr.

(*iii*) *Extraction of fluoride complexes*

Cationic complexes

The fluoride complexation of Zr, Hf, ^{261}Rf, and Th in mixed HNO_3/HF solutions was investigated (Strub *et al.*, 2000) by studying K_d values for both anion- and cation-exchange resins using ARCA. A detailed study of the complexation as a function of fluoride- and nitrate-ion concentrations was performed. They found all four elements to be strongly sorbed on the cation-exchange resin Aminex A6 at HF concentrations below 0.001 M. The K_d values for Zr and Hf decreased between 0.001 and 0.01 M HF, presumably due to the formation of fluoride complexes. Those for Rf and Th decreased at an order of magnitude higher HF concentrations, and the K_d for Rf remained very high even in 0.01 M HF. The K_d for Rf was found to be >148 in 0.1 M HNO_3/ 5×10^{-4} M HF while under these conditions ^{265}Sg had been found to elute (Türler *et al.*, 1998a). As discussed in Section 14.5.3c (Eqs. 14.1 and 14.2) at [HF] < 0.01 M, positively charged complexes of higher charge will be formed, which will sorb on the cation resin. The observed order of sorption Rf > Hf $\geq$ Zr corresponds to the opposite trend in the complex formation, as discussed in Section 14.5.3c, in agreement with theoretical predictions.

Anionic complexes

Trubert *et al.* (1999) determined distribution coefficients for Zr, Hf, and Rf on the macroporous anion exchanger Bio-Rad (Bio-Rad Laboratory, Hercules, CA, USA) AG® MP-1 from HF/HCl media with concentrations between 0.02 M and concentrated HF and [HCl] $\leq$ 0.8 M. They used batch experiments with Zr and Hf tracers and examined the K_d values as a function of free H^+, Cl^-, and F^- species in solution. They performed on-line column experiments using their automated system at the tandem accelerator at Orsay where ^{261}Rf and ^{167}Hf were produced.

A rather complicated two-column technique (Pfrepper *et al.*, 1998) was used in which the Rf or Hf parents were partially sorbed on a first anion-exchange resin column and the remainder plus the trivalent decay products Fm and Lu are sorbed on a subsequent cation-exchange resin column. One-hour irradiation times were used and the longer-lived ^{253}Fm–^{253}Es granddaughters of ^{261}Rf were finally measured to deduce the K_d for Rf. The one K_d value for Rf obtained for 0.02 M HF/0.4 M HCl was slightly higher than those for Zr and Hf, respectively, in agreement with the theoretically predicted trend Rf $>$ Hf $\geq$ Zr (Section 14.5.3c), but more data are needed before any conclusions can be drawn.

An increase in K_d values for Zr and Hf was observed by Strub *et al.* (2000) with the anion-exchange resin (similar to Bio-Rad AG®1-X8) and solutions between 0.001 and 0.01 M HF, consistent with the observation of decreasing values in the HF range for the cation-exchange resin. Surprisingly, the results of the experiments showed that again Rf and Th behaved differently from Zr and Hf and did not show the high K_d values expected for anionic fluoride complexes even at HF concentrations as high as 1 M. Rf seemed to resemble Th rather than Zr and Hf, which was different from the theoretical predictions (Pershina *et al.*, 2002b). There were indications that the action of the counter-ion was responsible for the unexpected behavior, and by varying the NO_3^- concentration Strub *et al.* (2000) were able to show that Rf did form anionic species, but apparently NO_3^- competed more effectively than F^- for the binding sites on the anion resin. Additional experiments are needed to investigate the effect of varying [NO_3^-] at constant [F^-] and varying [F^-] at much lower [NO_3^-].

(*iv*) *Extraction of cationic complexes*

TTA batch extractions

The chelating agent TTA extracts cationic species from aqueous solutions. Its electron donor groups are oxygen atoms and the tendency for different metals to be extracted is a measure of their affinity for oxygen atoms. This affinity should have a strong correlation with the log of the first hydrolysis constants of the metal ions. Thus TTA can be used to obtain information about hydrolysis of the group 4 ions.

The Berkeley group (Czerwinski, 1992b) performed some preliminary measurements of the extraction of the group 4 elements, Th, and Pu from 0.1 and 0.4 M HCl into 0.5 M TTA/benzene. The initial measurements gave K_d values, decreasing in the order Zr > Hf ~ Pu > Rf > Th, similar to the decreasing values of the logs of the first hydrolysis constants that have been measured for Zr, Hf, Th, and Pu (Baes and Mesmer, 1976). These extraction results are discussed by Gregorich (1997b), who states that on this basis the tendency for Rf to hydrolyze should be between that for Th and Pu and less than that for Zr and Hf. This prediction is in agreement with the theoretical calculation for the hydrolysis of group 4 elements (Pershina *et al.*, 2002b). However, more tracer measurements of the effect on extraction as a function of [HCl] and [TTA] are needed to determine if the equilibria involved in the extraction of Pu and Th are the same as for the group 4 elements. The kinetics of TTA extractions are relatively slow so they may not be the best choice for rapid separations of short-lived species.

HDBP extractions with SISAK

The SISAK microcentrifuge liquid–liquid extraction system described in Section 14.3.3b was used to study extraction of 4.7-s ^{257}Rf [1] from 6 M HNO_3 and 0.25 M dibutylphosphoric acid (HDBP) in toluene. ^{257}Rf was produced at the LBNL 88-Inch Cyclotron in the ^{208}Pb(^{50}Ti,n) reaction, with a cross section of ~10 nb.[1] In preliminary test experiments, ^{257}Rf was pre-separated in the BGS, which reduced unwanted background activities by more than three orders of magnitude, and then transferred to the specially designed Recoil Transfer Chamber (RTC) attached at the BGS focal plane (Kirbach *et al.*, 2002). The Rf ions passed from the BGS detector chamber (held at a pressure of only 1.3 mbar) through a thin Mylar window into the RTC containing He gas whose pressure could be varied from 480 to 2000 mbar, as appropriate, to stop the separated ions. The positive identification of Rf atoms entering the RTC was accomplished by measuring their α decay with an array of Si-strip detectors and six to seven ^{257}Rf–^{253}No α–α correlations per hour were found in these experiments. They were then sorbed on aerosols in a He/KCl gas-jet system and transported without chemical separation directly to the SISAK liquid scintillation detection cells. The transport time was measured with $^{170-x}$Hf isotopes (half-lives > 1 min) produced at the same time in ^{120}Sn(^{50}Ti,xn) reactions. An alpha event in the appropriate preset energy range caused the cell to close and to switch to daughter mode. The cell remained closed for more than five ^{253}No ($t_{1/2}$ = 1.6 min) daughter half-lives. In this way an α–α correlation matrix was successfully obtained and clearly showed that the SISAK liquid scintillation system could detect nuclides at a rate of less than one atom per hour. A number

---

[1] ^{257}Rf has been reported (Hessberger *et al.*, 1997) to have a metastable state with a half-life of ~4.0 s from which ~60% of the α-decay is estimated to originate and a ground state that α-decays with a half-life of ~3.5 s, but this has not yet been confirmed. Both decay primarily by α-emission so for the purposes of this experiment it makes very little difference.

of other important improvements including pulse-shape discrimination to reduce the beta-background, real-time scintillation yield monitoring by continuous measurement of the Compton edge of ^{137}Cs γ-rays, and improvements in the detection cell efficiencies were also made. Experimental details of the system have been published (Omtvedt *et al.*, 2002). The pre-separation thus permits designing studies of the chemical properties of Rf without the necessity for adding time-consuming and yield-loss steps to remove radioactive isotopes that would interfere with its detection and measurement.

After this successful demonstration, liquid–liquid extraction experiments were performed to compare the extraction behavior of Rf from 6 M HNO_3 into 0.25 M HDBP/toluene with that of its lighter homologs Zr and Hf. A schematic diagram of the setup is shown in Fig. 14.16. The activity-containing aerosols in the He jet are dissolved in the 'de-gasser' centrifuge containing 6 M HNO_3 and the He gas is removed. The main extraction is performed in the next centrifuge. An important step is to wash any dissolved HNO_3 from the organic phase before adding the scintillator ingredients because the acid will cause degradation of the energy resolution, as will any O_2. It is removed by sparging with He, which is removed in the last centrifuge. Flow rates of the order of 0.4–0.8 ml s^{-1} were used and the centrifuges typically operate at 25000–40000 rpm. This was the first time a transactinide, Rf, was extracted and unequivocally identified by the SISAK liquid scintillation system and demonstrates that this method can be used to investigate the chemical properties of the transactinides. The results indicate that Rf behaves similarly to Zr and Hf, as expected. In this demonstration, the conditions were chosen to maximize extraction of Rf and the other group 4 elements rather than to investigate possible differences among them. The next step will be to use the pre-separation technique to conduct experiments with chemical systems designed to distinguish differences in the behavior of individual elements within a periodic table group.

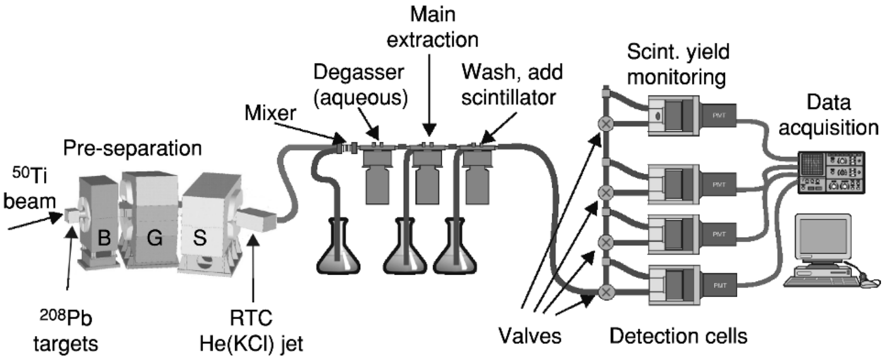

Fig. 14.16 *Schematic diagram of a typical SISAK liquid–liquid extraction configuration with BGS as a pre-separator.*

14.6.2 Chemistry of dubnium/(hahnium) (105)

As discussed in Section 14.5 and shown in Tables 14.4–14.6, the ground state configuration for element 105 is predicted to be $6d^37s^2$ although the relativistic destabilization of the 6d electrons and the close proximity of the 7s and 6d levels should stabilize the higher oxidation states of the 6d elements relative to their 5d homologs. Thus, the most stable oxidation state of Db is expected to be 5+ and the 3+ and 4+ states are even less stable than in its lighter homolog Ta.

(a) Historical

In the only published studies of the early chemistry of element 105, Zvara *et al.* (1974, 1976) reported investigations of the volatilities of the chlorides and bromides of element 105 with 1.8-s ^{261}Db compared to those of Nb and Hf. They used a thermochromatographic system similar to that used in the studies of Rf. Again, they detected SF events from the SF branch in mica track detectors placed along the chromatography column. After corrections for the much shorter half-life of ^{261}Db, the distribution of the fission tracks was compared with the adsorption zones of the tracers (3.3-min ^{169}Hf and 14.6-h ^{90}Nb). From these experiments, Zvara *et al.* concluded that the volatility of Db bromide was less than that of Nb bromide and about the same as that of Hf bromide. Again, only SF events were detected and because the SF branch ($\leq$18%?) is still not well known, it is not certain that the detected fissions belonged to element 105. A complete discussion of these early results was given by Hyde *et al.* (1987), who interpreted these results as indicating that Db behaved more like the group 4 element Hf than like Nb and Ta.

(b) Solution chemistry

No further studies of element 105 chemistry were reported until 1988 when Gregorich *et al.* (1988) reported the very first study of its behavior in aqueous solutions. These experiments were undertaken simply to show whether its most stable oxidation state in aqueous solution was 5+. At that time it had been postulated (Keller, 1984) that Ha might have a $7s^26d7p^2$ rather than a $6d^37s^2$ valence configuration expected by analogy with Ta, whose most stable state in aqueous solution is 5+. The α-emitting, 35-s ^{262}Db (then called Ha), produced in the reaction of ^{18}O with the radioactive target, 320-d ^{249}Bk (see Table 14.3) at the LBL 88-Inch Cyclotron, was used. The recoiling reaction products attached to KCl aerosols were transferred from the target system and outside the cyclotron shielding via a He gas-jet system to a 4-position collection site in a fume hood located outside the radiation area. Here very simple 'manual' chemistry was performed using only a few microliters of solution. The sorption of Ha on glass cover slips after fuming twice with concentrated nitric acid and washing with 1.5 M HNO_3 was compared with that of tracers of the group 5 elements Nb and Ta and with the group 4 elements Zr and Hf produced on-line under similar conditions. These group 5 elements are known to sorb on glass surfaces while the group 4 elements do not. Measurements of the energy and time distribution of the alpha decay and of time-correlated pairs of alphas from ^{262}Db and its 4-s daughter ^{258}Lr were recorded and analyzed to provide positive identification that element 105 was detected. Some 800 manual extractions taking about 50-s each were performed and a total of 26 alpha and 26 SF events were recorded. Element 105, like its group 5 homologs Nb(v) and Ta(v), was found to sorb on the glass surfaces while Zr and Hf and the trivalent actinides did not. This confirmed the group 5 character of Ha and demonstrated that it properly belonged in the periodic table as the heaviest member of group 5. Its extraction behavior into methylisobuytlketone from mixed HNO_3/HF solutions under conditions in which Ta was extracted but Nb was not was also investigated (Gregorich *et al.*, 1988). Surprisingly, it was found that element 105 did not extract and that its behavior was more like Nb than Ta, indicating that details of complexing behavior cannot be predicted based only on simple extrapolations of trends within a group in the periodic table. This behavior was explained much later (Pershina, 1998b), as discussed in detail in Sections 14.5.3b and 14.5.3c.

This surprising result provided the impetus for further exploration of the complex behavior of element 105. Chromatographic experiments using ARCA II to carry out the thousands of required repetitive experiments were performed jointly by the GSI/Mainz, PSI/Bern, and LBL/Berkeley groups in 1988, 1990, and 1993 at LBL, and in 1992 at GSI. In the first extraction chromatography column separations with the anion exchanger TIOA on inert supports, all the group 5 elements and Pa(v) were extracted from concentrations of HCl > 10 M. At lower concentrations of HCl, small amounts of added HF gave selective back extraction, showing different chemical behavior for these elements (Kratz *et al.*, 1989; Zimmermann *et al.*, 1993). Element 105 showed a marked non-Ta-like behavior at concentrations below 12 M HCl and follows the behavior of Nb and the pseudohomolog Pa(v). Because of this similarity to Nb and Pa, it was concluded that the complex was $DbOX_4^-$ or $[Db(OH)_2X_4]^-$. ARCA was also used to investigate the extraction of Db from HBr into diisobutyl carbinol (DIBC), a specific extractant for Pa, with subsequent elutions with mixed HCl/HF and HCl. The extraction sequence Pa $>$ Nb $>$ Db was obtained and attributed to the increasing tendency to form non-extractable polynegative complexes (Gober *et al.*, 1992). Due to the difficulties encountered in the theoretical interpretation of the results of these experiments because of the small amounts of HF added to the various halide solutions (long recommended for reducing hydrolysis of group 5 elements to prevent them from unwanted sorption on containers, etc.), it was recommended that future experiments be carried out in pure rather than mixed halide solutions (Pershina, 1998b).

Experiments conducted with ARCA also showed that Ha was eluted promptly from cation-exchange columns with α-hydroxyisobutyrate (Kratz *et al.*, 1992;

Schädel *et al.*, 1992) together with Nb, Ta, and Pa, whereas trivalent and tetravalent ions were retained, again confirming that Ha is most stable in aqueous solution as a pentavalent species. The new isotope 27-s ^{263}105 was also identified in these experiments.

Subsequently, Pershina (1998b) and Pershina and Bastug (1999) predicted the sequence Pa >> Nb $\geq$ Db > Ta for extraction into the anion exchanger TIOA from halide solutions. Paulus *et al.* (1999) remeasured K_d values for Nb, Ta, and Pa in new batch extraction experiments with the quaternary ammonium salt Aliquat-336 and pure HCl, HBr, and HF solutions. New chromatographic column separations with ARCA II were then conducted to study chloride and fluoride complexation separately. The Aliquat-336/HCl experiments confirmed the extraction sequence Pa >> Nb $\geq$ Db > Ta, as theoretically predicted. In the Aliquat 336/HF system the K_d value for element 105 in 4 M HF was >570, close to those for Nb and Ta of >1000 and different from that of ~10 for Pa.

In his review of transactinide chemistry, Kratz (1999b) discussed all the results for the ARCA experiments on element 105 in detail and concluded that the amine extraction behavior of dubnium halide complexes is always close to Nb, consistent with the predicted inversion of the trend in properties between the 5d and the 6d elements. In pure HF solution, Db differs most from Pa, and in pure HCl solution, it differs from both Pa and Ta. In mixed HCl/HF solutions, it differs markedly from Ta. The experimental results are in agreement with the calculated Gibbs energy changes (see Section 14.5.3c) of 12, 20, and 22 eV for the reactions for complex formation (Pershina *et al.*, 2002b) of the fluorides, chlorides, and bromides, respectively. For example, the equilibrium between hydrolysis and halogenation always favors formation of an extractable fluoride complex rather than the hydrolyzed species even at very low HF concentrations, whereas [HCl] > 3 M is required for formation of extractable chloride complexes, and [HBr] > 6 M is required for the formation of extractable bromide complexes.

(c) Gas-phase chemistry

The first on-line isothermal gas chromatography experiments were performed by an international group (Gäggeler *et al.*, 1992; Türler *et al.*, 1992) using OLGA II with 35-s ^{262}Db. The volatile species were deposited on a moving tape that was subsequently stepped in front of six large-area-passivated implanted planar Si detectors to measure alpha particles and SF events to identify element 105. From the yields as a function of isothermal temperature measured for the bromides of Nb, Ta, and Db, adsorption enthalpies of –88, –94, and –155 kJ mol^{-1}, respectively, were obtained from least-squares fits of Monte Carlo simulations to the isothermal yield curves. Within the error limits, the adsorption enthalpies (volatilities) are nearly the same for Nb and Ta, but Db appears to be significantly less volatile. It was postulated that traces of oxygen in the system might have led to formation of the oxytribromide of Db, which was predicted to be less volatile than the pentabromide (Pershina *et al.*, 1992b), and Db was also predicted to have a much stronger tendency to form oxyhalides than Nb or Ta, as discussed in Section 14.5.2b.

Investigations (Kadkhodayan *et al.*, 1996; Türler, 1996) of the volatility of the chlorides of the group 5 elements showed that they were more volatile than their respective bromides, with element 105 being similar to Nb, but for Ta, only a species with much lower volatility, presumably $TaOCl_3$, was observed. In more recent experiments conducted by Türler *et al.* (1996) the volatilities of Db and Nb chlorides were studied as a function of controlled partial pressures of O_2. It was shown that the concentrations of O_2 and oxygen-containing compounds were extremely important in determining whether or not the oxychlorides were formed and in determining the resultant volatilities of the Nb and Db compounds. The results showed that for pO_2 between 1 ppm (vol.) and 80 ppm (vol.) both a volatile species and a less volatile species, presumably MCl_5 and $MOCl_3$, were formed in about equal amounts. The more volatile species, $NbCl_5$, was shown to be the major component at $pO_2 \leq 1$ ppm (vol.). Subsequent experiments with Db were conducted under similar conditions and a two-step yield curve was obtained indicating that both $DbCl_5$ and $DbOCl_3$ were present. Adsorption enthalpies of –80 and –99 kJ mol^{-1} for the Nb species and –98 and –117 kJ mol^{-1} for the Db species were deduced, indicating that the Db species are less volatile than those of Nb. As predicted, the oxychlorides are less volatile than the chlorides, but the experiments need to be extended to lower temperatures for Db with pO_2 kept as low as possible to see if $DbCl_5$ can be measured as a single component, and the measurements need to be extended to Ta.

14.6.3 Chemistry of seaborgium (106)

(a) Historical

Early attempts were made to study the chemistry of Sg using 0.9-s ^{263}Sg produced in the ^{249}Cf(^{18}O,4n) reaction at the U-400 cyclotron at Dubna (Timokhin *et al.*, 1996; Yakushev *et al.*, 1996). Recoiling reaction products were thermalized and carried in Ar gas from the target chamber into a fast on-line TC consisting of a 3.5 mm i.d. by 120 cm long tube of fused SiO_2 where air saturated with $SOCl_2$ was used as a chlorinating agent. The inner surface of the silica column served as a solid-state detector for SF events. In two experiments, Timokhin *et al.* (1996) found a total of 29 fission tracks in zones in the temperature region of 150–250°C, close to the deposition temperature of 16-s ^{166}W. No tracks were found in the start zone or outside the indicated region while alpha activities from actinide products were seen mostly in the start zone. They claimed that this was the first chemical identification of element 106 as SgO_2Cl_2 and that it formed an oxychloride similar to that of W. However, the assignment of the fissions to element 106 based on detection of a small fission branch of ^{263}Sg is uncertain because it was not shown that the observed fissions did not belong to elements 104 or 105. Kratz (1999b) gave a detailed critique of the Timokhin reports and concluded that their conclusions were not justified.

The discovery by a Dubna–Lawrence Livermore National Laboratory (LLNL) collaboration (Lazarev *et al.*, 1994; Lougheed *et al.*, 1994) of the longer-lived isotopes ^{266}Sg and ^{265}Sg in ^{248}Cm(^{22}Ne,4n,5n) reactions with cross sections of ~80 and 260 pb for 116 and 121 MeV ^{22}Ne projectiles, respectively, made chemical studies of element 106 much more feasible. These new isotopes were separated and identified using the gas-filled recoil separator at the Dubna U-400 cyclotron. The partial alpha half-lives of 2–30 s for ^{265}Sg and 10–30 s for ^{266}Sg had to be estimated from the measured alpha-decay energies because the time intervals between the Sg isotopes and their Rf daughters were not measured as the signals from the implanted Sg isotopes were below the threshold of their detector system. On-line procedures for studying the chemistry of element 106 with both OLGA and ARCA were developed using W and Mo, the presumed lighter group 6 homologs of element 106.

(b) Gas-phase chemistry

Theoretical predictions (Pershina and Fricke, 1996) based on relativistic MO calculations indicated that SgO_2Cl_2 was the most stable of the Sg oxychlorides. Based on this prediction, the gas-phase chromatography experiments discussed in Section 14.5.2b were conducted under conditions designed to study and identify SgO_2Cl_2. The trend in volatilities of these oxychlorides within group 6, which was predicted using relationships between molecular properties such as covalence or dipole moment and volatility, was $MoO_2Cl_2 > WO_2Cl_2 > SgO_2Cl_2$. Eichler *et al.* (1999) estimated the thermochemical quantities for chlorides, oxychlorides, and oxides of Sg by extrapolation. By the use of empirical correlations, they also found SgO_2Cl_2 to be the most suitable compound for the gas-phase chemistry experiments and expected its standard sublimation enthalpy to be between 125 and 144 kJ mol^{-1}, resulting in an adsorption enthalpy between –97 and –108 kJ mol^{-1} and less volatile than its W homolog.

OLGA III was used in experiments to study the behavior of fission-product Mo isotopes and short-lived W isotopes produced at the PSI Philips cyclotron in preparation for studies of element 106 (Gärtner *et al.*, 1997). The reactive gas mixture O_2, Cl_2, and $SOCl_2$ at 900°C was used; adsorption enthalpies of −90 and −100 kJ mol^{-1} were measured for MoO_2Cl_2 and WO_2Cl_2, respectively, in agreement with predictions. The isothermal yield curve was measured for 58-min ^{229}U produced in the ^{232}Th(α,7n) reaction and the resulting adsorption enthalpy of −91 kJ mol^{-1} was interpreted as indicating formation of UCl_6.

The first chemical experiments on Sg were conducted in 1995 and in 1996 at the Universal Linear Accelerator (UNILAC) at GSI using the ^{248}Cm

(^{22}Ne,4n,5n) reactions to produce ^{266,265}Sg. The reaction products recoiling out of the target were thermalized in helium gas containing carbon aerosols (~0.1 – 1 μm diameter, generated using a spark discharge generator). In about 3 s, the flowing helium gas continuously transported the reaction products attached to the carbon aerosols through a capillary to a quartz wool plug in the reaction chamber (900–1000°C) at the inlet of OLGA III. There the reactive chlorinating gas consisting of O_2, Cl_2, and $SOCl_2$ was added to form volatile compounds, which were transported through the 1.5-mm i.d. × 1.8 m long isothermal quartz chromatography column to a recluster chamber where the chemically separated volatile Sg compounds were again attached to aerosol particles. They were transported within about 6 s to a rotating wheel system and collected on thin polypropylene foils placed in the 64-collection positions located around the periphery of a wheel that was stepped every 10 s to move the collected activity consecutively between pairs of Passivated Ion-implanted Planar Silicon (PIPS) detectors for measurement of alpha and SF activities. The times, energies, and positions of all events were recorded in list mode by a computer. A mother–daughter stepping mode was used to avoid interference from 45-s ^{212}Po^{m} contamination in the alpha energy region of interest (8.8 MeV). In this mode every other position on the 64-position wheel was left empty. When an alpha particle with the decay energy of ^{265,266}Sg was detected in a bottom detector, the daughter Rf nucleus was assumed to have recoiled out of this aerosol deposit onto the top detector. This initiated the daughter mode, causing a single step that positioned the empty collection sites between the detector pairs. The system waited for 2 min to permit the Rf daughter on the detector to decay in an environment clean of contamination. In the first experiment, two decays of ^{265}Sg were identified in daughter mode, one triple correlation was observed in parent mode, and one α–α correlation from ^{266}Sg–^{262}Rf was recorded (Schädel *et al.*, 1997a).

The isothermal temperature was varied in the second experiment conducted in 1996 (Türler *et al.*, 1999) to obtain the adsorption enthalpy for Sg. The experimental conditions were similar except that a 200 s wait in the daughter mode was used. The yield of short-lived W isotopes produced from ^{22}Ne reactions with ^{152}Gd incorporated in the ^{248}Cm target was measured with a high-purity Ge detector and used to monitor the yield of the chemical separation. An adsorption enthalpy of –(96 ± 1) kJ mol^{-1} was obtained for $^{168}WO_2Cl_2$, in agreement with the previous measurement. The isothermal yield curves obtained for SgO_2Cl_2 along with those for the Mo and W compounds are shown in Fig. 14.17. Based on detection of 11 events attributable to Sg, an adsorption enthalpy of –(100 ± 4) kJ mol^{-1} was derived. Adsorption enthalpies of –(90 ± 3) kJ mol^{-1} and –(96 ± 1) kJ mol^{-1} were obtained for Mo and W oxychlorides, respectively. Thus the volatility sequence is $MoO_2Cl_2 > WO_2Cl_2 > SgO_2Cl_2$, as theoretically predicted. Türler *et al.* (1998a) analyzed the decay properties of the 13 correlated chains of ^{265}Sg and ^{266}Sg observed in these experiments and recommended the following half-lives and cross sections for

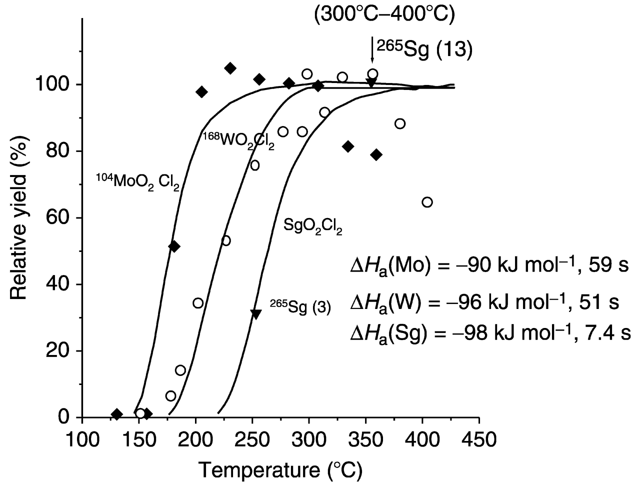

Fig. 14.17 *Relative yields vs. isothermal temperatures for* MoO_2Cl_2 *(solid diamonds),* WO_2Cl_2 *(open circles), and* SgO_2Cl_2 *(solid triangles). (Data from Türler* et al., 1999).

^{22}Ne energies between 120 and 124 MeV: ^{265}Sg, $t_{1/2} = 7.4^{+3.3}_{-2.7}$ s, cross section ~240 pb; ^{266}Sg, $t_{1/2} = 21^{+20}_{-12}$ s, cross section ~25 pb.

Hübener *et al.* (2001) reported that Sg forms volatile oxide-hydroxides similar to those of U and the group 6 elements Mo and W. They used high-temperature on-line isothermal gas chromatography with quartz columns to study Sg and W in the O_2–$H_2O(g)/SiO_2$ system. ^{266}Sg, produced as above, was transported in a He/MoO_3 gas-jet system into the chromatography system. Group 6 elements formed oxide-hydroxides that were volatile at a temperature of 1325 K upon addition of O_2. ^{266}Sg was unambiguously identified by measuring its decay chain. They postulated a dissociative adsorption and associative desorption process to explain their results.

(c) Solution chemistry

The first successful studies of the chemical properties of Sg in aqueous solution were reported by Schädel *et al.* (1997a,b) using ^{265,266}Sg produced in the reaction of 121 MeV ^{22}Ne projectiles with ^{248}Cm targets of 0.15 mg cm^{-2} in the first experiment and 0.95 mg cm^{-2} in the second experiment at the UNILAC at GSI. The emphasis in these experiments was on rapid preparation of samples for alpha spectroscopy with decontamination from the high-energy Bi and Po alpha activities and of trivalent actinides, and efficient separation of the Rf and No daughter activities from Sg. If these conditions are met, Rf and No isotopes observed later in the chemically separated Sg fraction can be presumed to be daughters of Sg precursor nuclei. A system with anionic or possibly neutral oxy- and oxyfluoride compounds was chosen because the formation of neutral and anionic complexes with F^- ions is a characteristic property of group 4, 5, and 6 elements, with distinct differences between the behaviors of the three groups. Based on previous on-line tracer experiments, a solution of 0.1 M HNO_3/5 × 10^{-4} M HF was used to elute the activity from the columns of the cation-exchange resin Bio-Rad AG Aminex A6. The recoiling activities attached to KCl aerosols were swept from the recoil chamber with He gas into a capillary and transported in flowing He some 18 m to ARCA II where they were collected, dissolved, and fed into the 1.8-mm i.d. × 8-mm chromatographic columns filled with the cation-exchange resin Aminex A6. The transport and collection efficiency of about 45% was monitored frequently by checking the production rate of $^{252-255}$Fm isotopes of known cross section. Although the mean separation time of Sg from Rf and No took only 5 s, the evaporation of the eluted samples took about 20 s and on the average, α-particle and SF measurements using a system of eight PIPS detectors were not begun until 38 s after the end of the collection. The energies, times, and detector positions were recorded in list mode on a magnetic disk and tape for later data analysis and identification of the Sg isotopes. Collections times of 45 s were used for most of the 3900 collection and elution cycles. Observation of three correlated α–α events identified as the ^{261}Rf(78 s)$\rightarrow$^{257}No(26 s)$\rightarrow$decay sequence indicated the decay of ^{265}Sg in the chemically separated Sg fractions. From this observation, it was concluded that Sg behaved as a typical hexavalent group-6 element as did W studied previously in similar on-line experiments. This indicated the formation of SgO_2F_2 by analogy to its Mo and W homologs and showed behavior different from the pseudohomolog U(VI), which remained on the column, presumably as UO_2^{2+}.

An investigation of the fluoride complexation of Zr, Hf, Rf, and Th in mixed HNO_3/HF solutions was undertaken (Strub *et al.*, 2000) to verify experimentally that under the conditions of the first experiments on the solution chemistry of Sg using ARCA, ^{261}Rf would not be eluted from the cation-exchange resin. These detailed studies of sorption on both cation- and anion-exchange resins using ARCA confirmed the validity of the assumption in the Sg experiments that Rf would remain on the Aminex A6 cation-exchange resin column. Therefore, it was concluded that Rf could only have been in the Sg fraction as a result of the alpha decay of 7-s ^{265}Sg.

A new series of 4575 experiments was conducted (Schädel *et al.*, 1998) with ARCA using the same Aminex A6 cation-exchange resin to determine if Sg would form SgO_4^{2-} under the same conditions as before if fluoride ions were not present. The activity was dissolved in 0.1 M HNO_3 without any HF; subsequent analysis of the effluent showed that Sg still remained on the column while W was eluted with 0.1 M HNO_3. This non-tungsten-like behavior of Sg was tentatively attributed to its weaker tendency to hydrolyze in dilute HNO_3 so that its hydrolysis stopped at $M(OH)_4(H_2O)_2^{2+}$ or $MO(OH)_3(H_2O)_2^{+}$ while hydrolysis of Mo and W proceeded to the neutral species $MO_2(OH)_2$. Thus, in the previous experiments in the presence of fluoride ions, Sg might have been eluted from the cation-exchange column as neutral or anionic fluoride complexes of the type SgO_2F_2 or $SgO_2F_3^-$ rather than as SgO_4^{2-}.

This hypothesis has been examined theoretically by considering hydrolysis of group 6 elements, as described in Sections 14.5.3b and 14.5.3c. The calculations (Pershina and Kratz, 2001) show that between a pH of 0 and 1, Sg forms complexes with charges of 1+ or 2+ while W forms neutral complexes. Hydrolysis of group-6 elements proceeds even faster at higher pH and a reversal of the trend in group-6 should be observed at pH > 4 (see Section 14.5.3b). Theoretical considerations of complex formation in HF solutions (Pershina *et al.*, 2002b) indicate that it competes with hydrolysis in aqueous solutions, that the dependence on pH and HF concentrations is very complicated, and that reversals of the trends occur. Further experiments can be planned based on the theoretical predictions that cover a wide range of pH values. These reversals of trends among the group 6 elements and U(IV) should be investigated experimentally.

14.6.4 Chemistry of bohrium (107) and hassium (108)

(a) Bohrium

The isotope, 17-s ^{267}Bh (Wilk *et al.*, 2000), produced in the ^{249}Bk(^{22}Ne,4n) reaction, was used in studies to compare the volatility of the oxychloride of Bh with those of its group 7 homologs Re and Tc in on-line isothermal gas chromatographic experiments using the OLGA system (Eichler *et al.*, 2000) conducted at the PSI cyclotron. The recoiling reaction products were sorbed on carbon particles suspended in He gas and continuously transported over a distance of a few meters to the OLGA where they were treated with HCl and oxygen to produce the volatile oxychlorides. These were conducted into the quartz chromatographic column, where their retention time is primarily dependent on the sorption interaction with the chlorinated column surface at a given isothermal temperature and the carrier gas velocity. The molecules passing through the column were attached to aerosols and then deposited stepwise on foils placed in positions on the circumference of a rotating wheel where their decay by alpha emission and SF was measured to identify them positively as ^{267}Bh based on their decay sequences to known daughter activities as reported in Wilk *et al.* (2000). Six such decay chains were observed over nearly 1 month of irradiation time. The relative yields for the trioxychlorides of ^{267}Bh as well as for those for Re and Tc obtained in similar experiments as a function of the isothermal temperatures are shown in Fig. 14.18.

A Monte Carlo program based on a microscopic model of the adsorption process was used to deduce ΔH_{ads} of –75 kJ mol^{-1} with a 68% confidence interval of –66 to –81 kJ mol^{-1} for BhO_3Cl, the most probable oxychloride under these conditions. The ΔH_{ads} values for the Tc and Re oxychlorides studied under the same conditions are –51 and –61 kJ mol^{-1}, respectively. Thus Bh oxychloride shows a stronger adsorption interaction with the chlorinated quartz

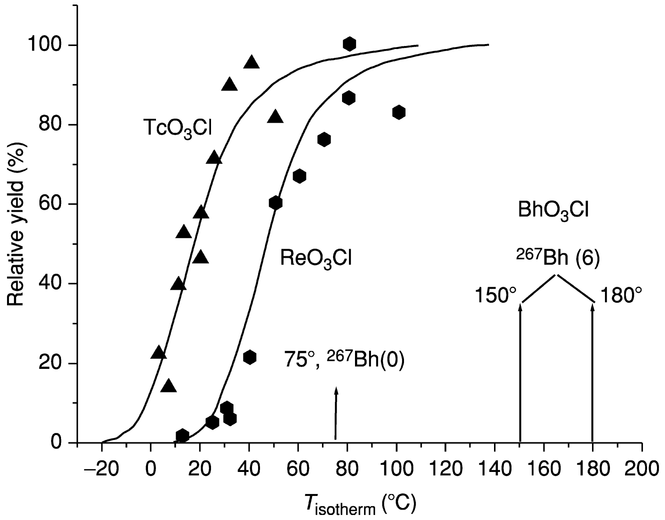

Fig. 14.18 *Relative yields vs. isothermal temperatures for* TcO_3Cl *(solid triangles) and* ReO_3Cl *(solid hexagons). A total of six events attributed to* ^{267}Bh *were detected at the isothermal temperatures of* 150 *and* 180°*C* (*Eichler* et al., 2000). *No events were detected at* 75°*C.*

surface than either Tc or Re compounds and it is less volatile than Re and Tc. This is in very good agreement with the calculations (Pershina and Bastug, 2000) where ΔH_{ads} of –48.2 kJ mol^{-1} for Tc and –78.5 kJ mol^{-1} for Bh were predicted, giving a volatility sequence of $TcO_3Cl > ReO_3Cl > BhO_3Cl$ (see discussion in Section 14.5.2).

(b) Hassium

Systems were developed for separating and detecting Hs as a volatile oxide based on the expectation that it would form a highly volatile tetroxide, as do its group 8-homologs osmium and ruthenium. Fully relativistic density functional calculations have been performed for MO_4 (M = Ru, Os, and Hs), as discussed in Section 14.5.2b. The volatility sequence for the tetroxides was predicted to be $HsO_4 \geq OsO_4 > RuO_4$ based on the calculated adsorption enthalpies of –(36.7 ± 1.5), –(38.0 ± 1.5), and –(40.4 ± 1.5) kJ mol^{-1}, respectively (Pershina *et al.*, 2001).

In preparation for experiments with Hs, Kirbach *et al.* (2002) developed the Cryo-Thermochromatographic Separator (CTS) to perform on-line investigations of the oxides of the α-emitters ^{171,172}Os (8 s,19 s) produced in ^{118,120}Sn (^{56}Fe,3–5*n*) reactions at the LBNL 88-Inch Cyclotron. The CTS consists of a channel formed by two facing rows of 32 PIN (Positive Implanted N-type silicon) diode α-particle detectors upon which a negative temperature gradient from 247 K at the entrance to 176 K at the exit was maintained. The volatile species deposit on the detector surfaces at a characteristic temperature and are identified from their measured α-decay energies.

After pre-separation with the BGS to remove unwanted transfer reaction products and scattered beam particles, the separated Os ions were stopped in the RTC (described earlier) in a mixture of He gas containing 10 vol% O_2 at 100 kPa. The Os activities were transferred in a continuously flowing He/O_2 mixture through a Teflon capillary to a quartz tube heated to 1200 K where OsO_4 was formed and then transported through another capillary to the CTS. The detector pair in which the activity was deposited and the alpha spectra at each position were recorded to identify these activities. The temperature was determined from thermocouple measurements and also from the measured resistances of the PIN diodes. Monte Carlo fits to the adsorption distributions were obtained by adjusting the model to more closely approximate the slit-like CTS cross section and resulted in an adsorption enthalpy of –(40.2 ± 1.5) kJ mol^{-1} for quartz surfaces.

Düllmann *et al.* (2002a) devised the *In-situ* Volatilization and On-line detection apparatus (IVO) in which products recoiling from a nuclear reaction are thermalized and stopped in a recoil chamber containing He gas while the high-energy beam particles travel directly through the chamber to a beam stop, thus removing them from the system. The thermalized recoil products are then converted *in situ* to the volatile species to be studied and are swept by the carrier gas to a chromatography column. Volatile species pass through the column to a recluster chamber where they are sorbed on aerosols and transported via gas jet either to an additional quartz column to measure the retention times of the volatile species or directly to an on-line detection system. Short-lived Os isotopes were used to test IVO for future chemical studies with Hs. From the Monte Carlo simulations an adsorption enthalpy of –(38.0 ± 1.5) kJ mol^{-1} was obtained for $^{173}OsO_4$ on quartz surfaces, in agreement within the uncertainty limits with the value of –(40.2 ± 1.5) kJ mol^{-1} obtained by Kirbach *et al.* (2002). Subsequent to these prototype experiments, an international team of scientists (Düllmann *et al.*, 2002b) conducted the first studies of the chemistry of hassium, the heaviest element to date whose chemistry has been successfully investigated. The ^{248}Cm(^{26}Mg,5n,4n) reactions with estimated production cross sections of only a few picobarns were used to produce ~10 s ^{269}Hs reported previously (Hofmann *et al.*, 1996, 2002) and possibly ^{270}Hs (~4 s) (Türler *et al.*, 2003) at the UNILAC at GSI. Three ^{248}Cm targets were positioned on a rotating wheel to increase the production rate. The IVO device was used to transport recoiling products to a quartz wool plug where Os and Hs were oxidized to the tetroxides by treatment with oxygen at 600°C. They were transported in helium through a Teflon capillary to the entrance to the Cryo On-Line Detector (COLD) TC formed by 12 pairs of opposing Si PIN-photodiode detectors with an outermost layer of Si_3N_4 positioned so that the gas flow was confined to the active detector surfaces. A schematic diagram of the system is shown in Fig. 14.19.

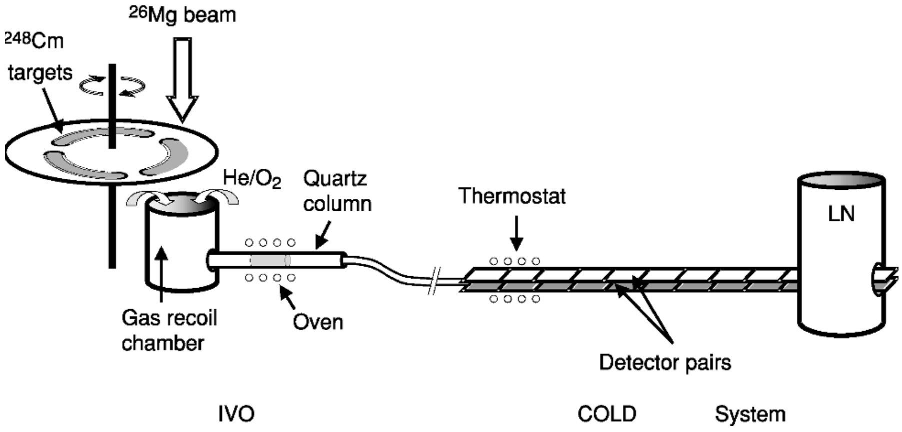

Fig. 14.19 *Schematic of IVO-COLD system for study of gas-phase properties of* HsO_4 *and lighter homologs* (*adapted from Düllmann* et al., 2002*b*).

Spectra of the alpha particles and SFs of the species deposited within each of the detectors of the array were measured and recorded to provide identification of the ^{269,270}Hs isotopes. The detection efficiency was about 77% for detection of a single alpha particle. A negative temperature gradient from –20 to –170°C was established along the TC formed by the detector array and measured at five positions. The system was checked at the beginning and at the end of the experiment by on-line measurements of the short-lived Os isotopes. In the 64 h experiment performed to produce Hs, three α–α-correlated decay chains were detected and assigned to the decay of ^{269}Hs. Two others, possibly due to the new nuclide ^{270}Hs or an isomer of ^{269}Hs, were detected, but a definite assignment could not be made. Based on detection of the three decay chains attributable to ^{269}Hs and two to a new nuclide ^{270}Hs (Türler *et al.*, 2003), HsO_4 was found to condense at a higher temperature than OsO_4 under similar conditions, indicating that the Hs oxide is less volatile than that of Os. The data for Hs and Os are shown in Fig. 14.20.

The Monte Carlo simulations that best fit these data give an adsorption enthalpy of –(39 ± 1) kJ mol^{-1} for OsO_4 on the silicon nitride surface, in good agreement with the previously measured values for SiO_2. An adsorption enthalpy of –(46 ± 2) kJ mol^{-1} was deduced for HsO_4 using only the three events assigned to ^{269}Hs and a $t_{1/2}$ value of 11 s in the analysis. This value is considerably more negative than the predicted value of –(36.7 ± 1.5) kJ mol^{-1} and suggests that HsO_4 is less volatile than OsO_4, in disagreement with calculations (Pershina, 1998a) that indicated that they should be nearly the same. More data and a better half-life measurement for ^{269}Hs are needed to investigate this discrepancy further. The possibility of different behaviors of HsO_4 on the Si_3N_4 detector surface compared to the SiO_2-coated detector surfaces should

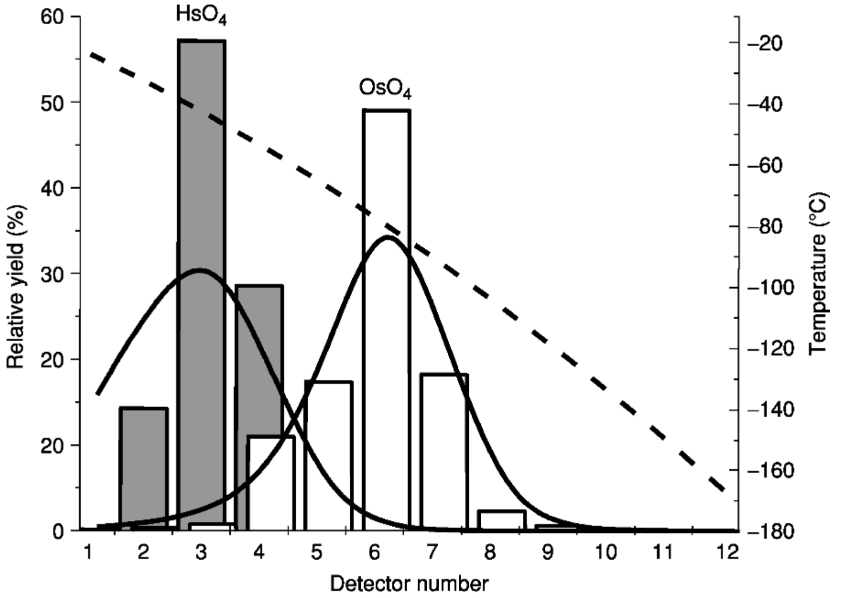

Fig. 14.20 *Combined thermochromatograms for Hs and Os oxides based on deposition positions (temperatures) for each of the* 12 *detector pairs. Dashed line indicates the temperature profile. The bars represent measured values and the curves result from Monte Carlo simulations of the migration process along the column.*

be considered and experiments with the tetroxide of Ru, predicted to be more volatile than those of either Os or Hs, should be conducted on both surfaces to investigate possible differences and the possibility that other oxides may be formed.

14.6.5 Summary of measured compared to predicted chemical properties

(a) Gas-phase studies

Observed trends in the volatility of the compounds of groups 4 through 8 compared to the theoretical predictions are summarized in Table 14.11. It can be seen that the measured and predicted trends in volatilities of the halide and oxyhalide compounds are in excellent agreement. However, in the case of the presumed tetroxides of Os and Hs there appears to be a discrepancy. This discrepancy emphasizes the need for additional investigations because few Hs disintegrations events were measured and their nuclear characteristics have not been unequivocally established.

Table 14.11 *Comparison of measured and predicted trends in volatilities of the compounds of Rf, Db, Sg, Bh, and Hs and their lighter homologs in periodic table groups* 4 *through* 8.

Group	*Compounds*	*Predicted volatility*	*Reference*	*Measured volatility*	*Reference*
4	MCl_4, MBr_4	Rf>Hf	Pershina and Fricke (1999)	Rf >Hf	Kadkhodayan *et al*. (1996); Sylwester *et al*. (2000)
5	ML_5 (L = Cl, Br)	Db >Ta > Nb	Pershina *et al*. (1992b)	(DbO_3Br)	Türler *et al*. (1996)
		$DbCl_5 > DbOCl_3$	Pershina *et al*. (1992b)	$DbCl_5 > DbOCl_3$	Türler *et al*. (1996)
6	MO_2Cl_2	Mo > W > Sg	Pershina and Fricke (1996)	Mo > W > Sg	Schädel *et al*. (1997a); Türler *et al*. (1999)
7	MO_3Cl	Tc > Re > Bh	Pershina and Bastug (2000)	Tc > Re > Bh	Eichler *et al*. (2000)
8	MO_4	Hs = Os >Ru	Pershina *et al*. (2001)	Os > Hs	Düllmann *et al*. (2002b)

(b) Aqueous-phase studies

The measured trends in hydrolysis, complex formation, and extraction of complexes of Rf, Db, and Sg and their lighter homologs in groups 4 through 6 of the periodic table under a variety of experimental conditions compared to theoretical predictions for the same systems are summarized in Table 14.12. Care must be taken to ensure that the conditions for the experimental studies are the same as for the theoretical predictions since small differences in pH, purity of halide solutions, etc. can affect the equilibria that determine whether hydrolysis or complex formation dominates and whether the resultant complexes are neutral or charged. The order of extraction into organic solvents and sorption in cation- and anion-exchange chromatography differs greatly, depending on the charge on the complex. In general, agreement of the experimental results with the predictions is excellent when these factors are carefully controlled, as discussed in Section 14.5.3c.

There are some prospects for studies of the aqueous chemistry of elements heavier than 106 as well as for more detailed studies of elements 104, 105, and 106 using shorter-lived isotopes that may have higher production rates. The RTC (Kirbach *et al.*, 2002) coupled with the BGS could be used so that the separated isotopes can be transported to different rapid chemical separation systems such as SISAK-III described earlier (Omtvedt *et al.*, 2002) for few-second liquid–liquid extractions or other automated systems such as ARCA. This might permit detailed studies of complex formation of elements Bh and Hs that would be of special interest in acid solutions.

14.6.6 Prospects for experimental studies of chemistry of Mt through element 112

(a) Predictions of half-lives and production modes

Prospects for chemical studies of Mt depend on the confirmation of longer-lived isotopes than ^{268}Mt, currently the longest-lived known isotope of Mt. This isotope decays primarily by alpha emission, with a half-life reported to be about 40 ms; it was detected as the alpha-decay product of ^{272}111 produced with a cross section of 2.5 pb in the ^{209}Bi(^{64}Ni,n) reaction (Hofmann *et al.*, 2002). The half-lives of the ^{264}Bh daughter and the ^{260}Db granddaughter of ^{268}Mt are only about 1 s, so even techniques involving chemical separation of the daughters to infer the parent chemical properties do not appear feasible. Longer-lived isotopes of Mt are expected around the deformed nuclear shell at 162 neutrons and might be produced using the ^{238}U(^{37}Cl,4n) or the ^{249}Bk (^{26}Mg,4n) reaction to make ^{271}Mt. The half-life of this odd-proton, odd-neutron isotope was estimated from interpolation of Smolańczuk's (1997) calculations

Table 14.12 *Comparison of measured with predicted trends in hydrolysis and complex formation of some compounds of Rf, Db, and Sg and their lighter homologs in periodic table groups* 4 *through* 6.

Group	*Complexes*	*Experimental conditions*	*Predictions*	*Reference*	*Measured*	*Reference*
4	hydrolysis of M^{4+}	$pH \leq 2$	Zr > Hf > Rf	Pershina *et al.* (2002b)	Zr > Hf > Rf	Czerwinski (1992a)
	$MF_x(H_2O)_{8-x}^{z-x}(x \leq 4)$	$[HF] < 10^{-1}$ M	Zr > Hf > Rf	Pershina *et al.* (2002b)	Zr > Hf > Rf	Strub *et al.* (2000)
	MF_6^-	$[HF] > 10^{-3}$ M	Rf ≥ Zr > Hf	Pershina *et al.* (2002b)	Rf ≥ Zr > Hf	Trubert *et al.* (1999)
	MCl_6^-	4–8 M [HCl]	Zr > Hf > Rf	Pershina *et al.* (2002b)	Rf > Zr > Hf	Haba *et al.* (2002)
5	hydrolysis of M^{5+}	all pH	Nb > Ta > Db	Pershina (1998a)	Nb > Ta	Baes and Mesmer (1976)
	$M(OH)_2Cl_4^-$ $MOCl_4^-$, MCl_6^-	all [HCl]	Pa >> Nb ≥ Db > Ta	Pershina (1998b)	Pa >> Nb ≥ Db >Ta	Paulus *et al.* (1999)
6	hydrolysis of M^{6+}	$0 < pH < 1$	Mo > W > Sg	Pershina and Kratz (2001)	Mo > W > Sg	Schädel *et al.* (1998)
	hydrolysis of $MO_2(OH)_2$	$pH > 1$	Mo > Sg > W	Pershina and Kratz (2001)	Mo > W	Baes and Mesmer (1976)

for even proton–even neutron nuclides to be a few seconds and decay primarily by alpha emission. The cross section for the first reaction is expected to be similar to that of 2.5 pb, measured for the ^{238}U(^{34}S, 5n)→^{267}Hs reaction (Lazarev *et al.*, 1995) as the enhancement of the cross section due to the extra two neutrons in ^{37}Cl compared to ^{34}S is expected to balance the decrease due to the higher Z of Mt. Based on this cross section, detection of two or three chains a week might be expected using multiple ^{238}U targets in the BGS. The BGS is capable of positively separating and identifying such a new nuclide based on measurement of the known alpha-decay chain of its daughters even if the ^{271}Mt half-life is as short as a few tenths of a second. The overall yield for the reaction with the highly radioactive target ^{249}Bk will be much lower because the cross section is expected to be only a few tenths of 1 pb and it is much more difficult to use multiple targets.

The production of longer-lived isotopes of elements 110, 111, and 112 with half-lives in the range of seconds to minutes have now been reported using 'warm/hot' fusion reactions or as decay products of elements 114 and 115. (See Table 14.2 and Fig. 14.2(b) and discussion in Section 14.1.) It may be possible to produce ^{277}110 directly in the 'warm' fusion reaction ^{232}Th(^{48}Ca,3n), but the cross section may be low and the systematics of these reactions need to be investigated further. The isotope ^{280}110 with a half-life of 7.6 s has been reported as the granddaughter of ^{288}114 produced in a four neutron out reaction in the bombardment of ^{244}Pu targets with ^{48}Ca (Oganessian *et al.*, 2000a; Oganessian, 2001), but this indirect production method is not favorable for chemical studies. Currently, there appear to be no suitable reactions for direct production of the very neutron-rich isotopes of Ds.

Some isotopes of the odd-proton element 111 should have half-lives of seconds or more and hindrances toward fission and alpha decay should exist. An isotope with mass number 280 and with a half-life of 3.6 s has been reported in the alpha-decay chain of ^{288}115 produced in the bombardment of ^{243}Am with ^{48}Ca projectiles (Oganessian *et al.*, 2004a).

SF activity attributed to ^{283}112 produced in the ^{238}U(^{48}Ca,3n) reaction and from the alpha decay of ^{287}112 produced via the ^{242}Pu(^{48}Ca,3n) reaction has been reported by Oganessian *et al.* (1999a,c, 2004b) who obtained a half-life of $\sim$5 min by averaging these results. However, as discussed in Section 14.1, it is difficult to positively identify a new nuclide that decays only by SF and even if this assignment is verified, its positive identification in chemical studies would be equally difficult and likely to be inconclusive. The production of 112 isotopes in ^{238}U(^{48}Ca,xn) reactions should be investigated further to determine the cross sections and if there is an alpha branch in ^{283}112 or ^{284}112. Then more definitive chemical studies could be undertaken. Such experiments would also help to assess the usefulness of 'warm' fusion reactions for production of a broad range of heavy element reactions for chemical studies.

(b) Chemical methods

Even though it appears that isotopes of the elements from Mt through element 112 can exist with half-lives long enough for chemical studies, the most difficult problem will be to increase the production rates and to perform on-line experiments with continuous separation and detection capabilities that can be operated for times long enough to obtain statistically significant results. These times will be of the order of weeks or months and will certainly require computer-controlled automated systems to carry out both gas-phase and solution chemistry. As the production cross sections for the elements of interest become ever smaller, the use of some pre-separation technique – either physical such as BGS or chemical such as IVO – will become mandatory in order to separate out the multitude of unwanted products before use of the more selective systems mentioned below.

The stable oxidation states of these elements both in the gas phase and in solution are predicted to vary widely, as shown in Table 14.10. From element 107 on, the maximum oxidation state is expected to be relatively unstable in aqueous solutions. Experimental studies designed simply to try to determine the most stable oxidation states in aqueous solution should be devised. Thus, for example, the stability of Bh(IV) relative to Bh(VII), or Hs(IV) relative to Hs(VIII) could be investigated by performing anion-exchange separations from HCl solutions in which the 4+ states might form negatively charged complexes that would be retained on the anion column. The relative positions of the peaks of the elution curves associated with reduction would give information about relative stabilities of lower oxidation states. Complex formation can also be studied for elements 109 and heavier. The imaginative gas-separation techniques developed for study of Bh and Hs can be applied to Mt and Ds, which are predicted to form volatile hexafluorides and octafluorides, as discussed in Section 14.5.2b.

Some preliminary chemical experiments on element 112 have been reported by Yakushev *et al.* (2001) and by Yakushev (2002) using the spontaneously fissioning nuclide $^{283}112$ (~5 min) reported by Oganessian *et al.* (1999a, 2004b) to be formed in the $^{238}U(^{48}Ca,3n)$ reaction with a cross section of 5 pb. The experiment was designed to determine whether element 112 behaved similarly to its periodic table homolog Hg, which had been shown to deposit on Au- or Pd-coated silicon surface barrier detectors (Yakushev *et al.*, 2001), or whether it behaved as a noble gas like Rn and remained in the gas phase. An unambiguous answer about the physical or chemical properties of element 112 was not obtained. The system was improved by introducing a special ionization chamber after the silicon detectors to measure alpha decays and SF events of nuclei remaining in the gas. More than 95% of the simultaneously produced Hg isotopes were deposited on the first Au-coated detector. Again, no events attributable to element 112 were detected on either the Au- or the Pd-coated silicon detectors, but eight SF events were registered in the ionization chamber (Yakushev, 2002). These SF events were attributed to element 112, which indicates that it is more chemically inert than Hg and remained in the gas phase. The ΔH_{ads} of element 112 was deduced to be more positive than -55 kJ mol^{-1}. Further experiments with a temperature gradient in the chromatography column are now planned to better define ΔH_{ads}. It is also important to confirm that the observed SF events actually belong to element 112. If an alpha-decaying isotope of element 112 with a suitable half-life and production rate can be identified it would be much more suitable for chemical studies because it could be positively identified from its half-life and characteristic alpha-decay chain.

Experiments on element 112, similar to those conducted in Dubna, are planned by researchers at PSI (Soverna *et al.*, 2001) using a chromatographic column with a negative temperature gradient from 35 to –190°C. Silicon detectors coated with Au and Pd will be placed along the chromatographic column to detect element 112 and its deposition temperature will be determined relative to those of Hg at 115°C and Rn at –115°C in order to deduce ΔH_{ads}.

Eichler and Schädel (2002) investigated the adsorption of Rn on polycrystalline surfaces of transition metals and found the strength of adsorption to decrease in the order: $\mathrm{Ni} > \mathrm{Pd} \approx \mathrm{Cu} > \mathrm{Au} > \mathrm{Ag}$. They suggest that low-temperature vacuum thermochromatographic techniques could be used to rapidly separate element 112 from 114 and Rn and to determine whether its behavior is more like its lighter homolog Hg or an inert noble gas.

Isotopes of Hg have been studied by carrying them on Pd aerosols to serve as a model system for possible studies of elements 112 or 114 (Düllmann *et al.*, 2002a). Recoiling Hg isotopes produced in $^{168}\mathrm{Yb}(^{22}\mathrm{Ne},xn)^{190-x}\mathrm{Hg}$ reactions in the IVO setup at the PSI Philips cyclotron were thermalized in He, swept through an isothermal quartz column at 800°C to the re-cluster chamber, and transported on Pd aerosols to a suitable detection device for measurement of alpha spectra. The short-lived nuclides $^{183-185}\mathrm{Hg}$ were identified, indicating that volatile metals such as Hg can be transported in gas-flow systems without the presence of aerosol particles and then quickly adsorbed on metal aerosols if the enthalpy of adsorption is sufficiently large. The aerosols can then be transported to a detection system for measurements at low pressure and room temperature. Such a technique may also be applicable to measurements of transactinides with $Z = 112$ to 117.

Plans to separate elements with $Z > 108$ as noble metals by electrochemical deposition from aqueous solutions have been described (Kratz, 1999a). The choice of an appropriate electrode material is very important and estimates of suitable electrodes have been made for lighter homologs of the heaviest elements (Eichler and Kratz, 2000). Pd and Pt were found to be suitable electrode metals for the deposition of Hg, Tl, Pb, Bi, and Po, the homologs of elements 112 through 116.

14.7 FUTURE: ELEMENTS BEYOND 112 (INCLUDING SHEs)

14.7.1 Predictions of electronic structures and chemical properties

(a) Introduction

The ground state configurations of the free neutral atoms of elements 113 through 184 obtained from relativistic DF calculations are summarized in Table 14.13.

Table 14.13 *Dirac–Fock ground state configurations of free neutral atoms of elements* 113 *through* 184.[a]

Rn 'core' + $5f^{14}$ + $6d^{10}$ + $7s^2$ +								*Element* 120 *'core'* + $5g^{18}$ + $8p^2_{1/2}$ +					
	$5g$	$6f$	$7p_{1/2}$	$7p_{3/2}$	$7d$	$8s$	$8p_{1/2}$		$6f$	$7d$	$9s$	$9p_{1/2}$	$8p_{3/2}$
113			1					145	3	2			
114			2					146	4	2			
115			2	1				147	5	2			
116			2	2				148	6	2			
117			2	3				149	6	3			
118			2	4				150	6	4			
119			2	4		1		151	8	3			
120			2	4		2		152	9	3			
121			2	4		2	1	153	11	2			
122			2	4	1	2	1	154	12	2			
123		1	2	4	1	2	1	155	13	2			
124		3	2	4		2	1	156	14	2			
125	1	3	2	4		2	1	157	14	3			
126	2	2	2	4	1	2	1	158	14	4			
127	3	2	2	4		2	2	159	14	4	1		
128	4	2	2	4		2	2	160	14	5	1		
129	5	2	2	4		2	2	161	14	6	1		
130	6	2	2	4		2	2	162	14	8			
131	7	2	2	4		2	2	163	14	9			
132	8	2	2	4		2	2	164	14	10			
133	8	3	2	4		2	2	165	14	10	1		
134	8	4	2	4		2	2	166	14	10	2		
135	9	4	2	4		2	2	167	14	10	2	1	
136	10	4	2	4		2	2	168	14	10	2	2	
137	11	3	2	4	1	2	2	169	14	10	2	2	1
138	12	3	2	4	1	2	2	170	14	10	2	2	2
139	13	2	2	4	2	2	2	171	14	10	2	2	3
140	14	3	2	4	1	2	2	172	14	10	2	2	4
141	15	2	2	4	2	2	2	. . .					
142	16	2	2	4	2	2	2	. . .					
143	17	2	2	4	2	2	2	184	172 'core' + $6g^5 7f^4 9d^3$				
144	18	1	2	4	3	2	2						

[a] Fricke (1975).

Chemical properties for elements 113 through 121, as predicted by various researchers, are summarized in Table 14.14. A rather complete discussion and summary of the chemical properties predicted for these elements as of 1986 was given by Seaborg and Keller (1986).

(b) Elements 113 through 115

In elements 113 through 118, the filling of the 7p shell is expected to takes place. Chemistry of these elements will be strongly influenced by relativistic effects: the large relativistic stabilization of the $7s^2$ electron pair (a large 7s–7p gap hindering the hybridization) and a very large SO splitting of the 7p levels into $7p_{1/2}$ and $7p_{3/2}$, reaching 11.8 eV for element 118 (Fig. 14.21). Since the electrons occupying the $7p_{1/2}$ orbital will then form a closed subshell, an enhanced stability of lower oxidation states of these elements is expected. However, destabilization of the 6d levels would contribute to a more transition element character for the earlier 7p elements (Han *et al.*, 1999b; Seth *et al.*, 1999).

(*i*) *Element* 113

Element 113 has one electron in the $7p_{1/2}$ valence shell. Due to relativistic stabilization of the $7p_{1/2}$ electrons, its first IP of 7.306 eV, as shown in Table 14.15, is the largest in group 13 (Eliav *et al.*, 1996a). The 1+ state is thus predicted to be the most stable.

The CCSD calculations (Eliav *et al.*, 1996a) revealed a dramatic reduction in the excitation energy of an electron from the d^{10} shell: the $d^{10}s \rightarrow d^9s^2$ energy of 113^{2+} is 0.1 eV as compared to 8 eV for Tl^{2+}. It is, therefore, predicted that divalent or trivalent compounds of element 113 with an open $6d^9$ shell could exist. The calculated EA of Tl and element 113 are 0.4 and 0.68 eV, respectively.

The very large SO splitting of the 7p orbital will influence the chemistry of element 113 compounds by destabilizing the binding energy by almost 1 eV in the monohydride 113H. In this molecule, the 6d and 7s orbitals were shown to participate little in bonding (Han *et al.*, 1999a,b, 2000; Seth *et al.*, 1999) and all the effects are defined by the large participation of the $7p_{1/2}$ shell. Element 113 was calculated to be more electronegative than Ga, In, Tl, and even Al among all the monohydrides. Involvement of the 6d electrons in bonding in element 113 was confirmed by PP calculations (Han *et al.*, 1999b; Seth *et al.*, 1999) for $113H_3$, $113F_3$, and $113Cl_3$. As a consequence, a T-shape geometric configuration rather than a trigonal planar was predicted for these molecules. The stability of a high-coordination compound MF_6^- with the metal in the 5+ oxidation state is foreseen. $113F_5$ will probably be unstable since the energy of the reaction $113F_5 \rightarrow 113F_3 + F_2$ is only –53.4 kJ mol^{-1} (Seth *et al.*, 1999). The calculated energies of the decomposition reaction $MX_3 \rightarrow MX + X_2$ (M = B, Al, Ga, In, Tl and element 113) confirmed a decrease in the stability of the 3+ oxidation state in group 13.

Table 14.14 *Predicted chemical properties of elements* 113 *through* 121.

	113	114	115	116	117	118	119	120	121
Chemical group	13	14	15	16	17	18	1	2	3
stable oxidation states[a,b,c]	$\underline{\mathbf{1}}$,3	**2**,0,(4)	$\underline{\mathbf{1}}$,$\underline{3}$	**2**,4	$\underline{\mathbf{1}}$,**3**,5,(–1)	**4**,2,–1,(6)	**1**,3	2,4	**3**
first ionization potential (eV)[d]	7.306[d]	8.539[d]	5.58[d]	7.5[c]	7.7[c]	8.7[c]	4.53[e]	6.0[c]	4.45[f]
standard electrode potential in aqueous solution (V)	+0.6	+0.9	–1.5	+0.1	–0.25, 0.5		–2.7	–3.0	+2.1
	+0.6	+0.9	–1.5	+0.1	–0.25, 0.5		–2.7	–3.0	+2.1
ionic radius of indicated ion (Å)	1.4(1+)	1.2(2+)	1.5(1+) 1.0(3+)	0.83(4+) 0.58(7+)	0.80(4+) 0.58(7+)		1.8(1+)	1.6(2+)	
atomic radius (Å)[b]	1.7	1.6	2.0				2.4[c]	2.0[c]	
density (g cm^{-3})[b]	18 (16[c])	22 (14[c])	11 (13.5[c])	12.9[c]			3[c]	7[c]	
ΔH_{sub} (kJ mol^{-1})[b]	142(129[c])	42	142	197[c]			42	138	
boiling point (K)[b]	1400	420	~1400		883	263			
melting point (K)[b]	700	340	~700		623–823[c]	258[c]	273–303[c]	953[c]	

[a] Bold type: most stable in gas phase; underlined = most stable in aqueous solutions; non-bold: less stable; ( ) = least stable.
[b] Keller and Seaborg (1977) and Seaborg and Keller (1986).
[c] Fricke (1975).
[d] See Table 14.15.
[e] Lim *et al.* (1999).
[f] Eliav *et al.* (1998a).

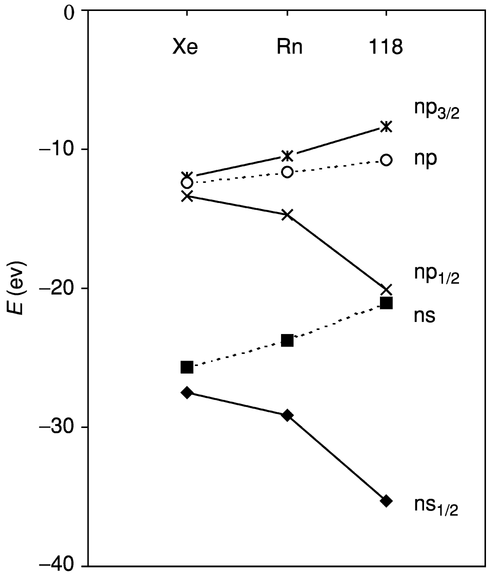

Fig. 14.21 *Relativistic stabilization of the ns and np*$_{1/2}$ *orbitals and the spin–orbit splitting of the np orbitals for the noble gases Xe, Rn, and element* 118. *DF atomic energies* (—) *are from Desclaux* (1973) *and HF values* (---) *are from Schwerdtfeger and Seth* (1998).

The standard electrode potential $E°(113^+/113)$ was predicted to be +0.6 eV and 113^+ is expected to be more easily complexed than Tl^+ and to be similar to Ag^+ (Keller *et al.*, 1970). For example, the solubility of TlCl in water is not increased much by adding excess HCl (Alekseeva *et al.*, 1972) or NH_3, whereas AgCl dissolves when NH_3 is added. Element 113 is expected to be more like silver in this respect. The smallest sublimation enthalpy in the group was predicted for element 113 by extrapolation (Keller *et al.*, 1970) and can be explained by the relativistic stabilization of the $7p_{1/2}$ orbital.

(*ii*) *Element* 114

The most interesting among the 7p elements is element 114 where a very large SO splitting of the 7p orbital and the relativistically stabilized 7s and $7p_{1/2}$ electrons result in a closed-shell ground state $7s^27p_{1/2}{}^2$, suggesting that the element should be rather inert. This is also reflected by the largest IP in group 14 (Table 14.15). One of the most striking features seen in Table 14.14 is the great decrease in boiling point in going from element 113 to element 114. This decrease was predicted by Keller *et al.* (1970) on the basis of extrapolations of the heats of sublimation of the group 13 and 14 elements versus periods of the periodic system. The boiling points were then calculated using Trouton's rule. This effect is a result of adding a second $7p_{1/2}$ electron in element 114 to form a

Table 14.15 *Ionization potentials (in* eV) *for the 7p elements.*

Calculated	113	114	115	116	117	118	*Reference*
DF	7.4[a]	8.5[a]	5.5[a]	7.5[a]	7.7	8.7	Fricke (1975)
MCDF	7.11	8.04 (8.51[b])	4.65	5.96	6.51	7.74 (7.6[b])	Pyper and Grant (1981)
CCSD	7.306[c]	8.539[d]	5.58[e]	–	–		Eliav *et al.* (1996a),[c] Eliav *et al.* (1998b),[d] Landau *et al.* (2001)[e]

[a] DF values corrected for the difference between theoretical and experimental values for the elements of the 6th period.

[b] Relativistic CI version of RECP (Nash and Bursten, 1999a).

[c] Eliav *et al.* (1996a).

[d] Eliav *et al.* (1998b).

[e] Landau *et al.* (2001).

closed-shell $7p_{1/2}{}^2$ configuration, similar to the s^2 one, making this configuration responsible for much weaker bonding in a metallic state.

The group 14 elements show increasing stability of the 2+ oxidation state relative to the 4+ state as one goes to higher atomic numbers. Lead is known to be most stable of the group 14 elements in the 2+ oxidation state. Due to the very large 7s orbital stabilization, the sp^3 hybridization energy needed for the 4+ valence is very large in element 114, so that the 4+ oxidation state of element 114 is expected to be unstable, while the 2+ state should be the most stable in the group. Recent calculations (Liu *et al.*, 2001) have, indeed, shown $114O_2$ to be thermodynamically unstable in contrast to PbO_2. Energies of the decomposition reactions $MX_4 \rightarrow MX_2 + X_2$ and $MX_2 \rightarrow M + X_2$ (M=Ge, Sn, and Pb; X = H, F, and Cl) were calculated at the PP level (Seth *et al.*, 1998b; Nash and Bursten, 1999a). The results confirm a trend of decreasing stability of the 4+ oxidation state in the group. The neutral (monatomic) state was calculated to be more stable for element 114 than for Pb. Element 114 should also have a greater tendency to form complexes in solutions than Pb. Because the stability of the 2+ state increases within group 14, element 114 would probably form MX^+, MX_2, MX_3^-, or MX_4^{2-} (X = Cl, Br, and I) by analogy with Pb. $114F_6^{2-}$, suggested by Seth *et al.* (1998b), will probably be unstable in the aqueous phase due to strong hydrolysis of the fluorides in aqueous solutions. Thus, aqueous complexes of element 114 such as $114Br_3^-$ or $114I_3^-$ should be preferentially formed. Pitzer (1975a) predicted stable $(114)X_2$ (X = F, Cl, and Br). The standard electrode potential $E°(114^{2+}/114)$ was estimated as +0.9 V by Keller *et al.* (1970). We thus see that relativistic effects on the $7p_{1/2}$ electrons cause a diagonal relationship to be introduced into the periodic table near element 114, causing 114^{2+} to be somewhere between Hg^{2+} or Cd^{2+} and Pb^{2+} in its chemistry and causing 113^+ to act more like Ag^+ than Tl^+.

(*iii*) *Element* 115

In element 115, one electron is located in the relativistically destabilized $7p_{3/2}$ orbital and, therefore, is loosely bound,while $7p_{1/2}{}^2$ serves as an inert pair. Thus, the 1+ oxidation state of element 115, like that of Tl^+, should be preferred. This is also supported by a drastic decrease in the first IP between 114 and 115 (Fig. 14.8). Furthermore, calculations show that element 115 has the smallest IP in group 15 and in the 7th period, as shown in Table 14.15 and Fig. 14.8. Keller *et al.* (1974) made some detailed predictions of the chemical properties of element 115 based on extrapolations of the properties of group 15 elements and relativistic atomic DS and DF calculations. Their results indicate that the chemical properties of element 115 should be analogous through a diagonal relationship to those of Tl (group 13) as well as to those of Bi. They predicted a standard electrode potential $E°(115^+/115) = –1.5$ V, indicating that element 115 metal should be quite reactive. They also suggested that 115(III) should be relatively stable and have some chemical properties somewhat similar to Tl(III), but that its chemical properties will be closer to those of Bi(III). The 5+ state seems unlikely. Melting and boiling points of the metal should be close to those of element 113.

(c) Elements 116 through 118

The chemistry of elements 116 through 118 will be defined mostly by the participation of the $7p_{3/2}$ orbital in bonding. Certain predicted volatility characteristics of elements 116, 117, and 118 or their compounds may offer advantages for chemical identification. This will be especially true for element 118. The chemical properties of element 116 can be deduced by extrapolations from Po, though the 2+ state should be more stable than the 4+ state because the $7p_{1/2}^2$ electrons are expected to be rather inert. Estimates of formation enthalpies of MX_2 and MX_4 ($X = F$, Cl, Br, I, SO_4^{2-}, CO_3^{2-}, NO_3^-, and PO_4^{3-}) for Po and element 116 (Grant and Pyper, 1977) on the basis of the MCDF atomic calculations are consistent with the expected instability of 116^{4+}. The chemistry of element 116 is expected to be mainly cationic, i.e. the relative ease of formation of the divalent compounds should approach that of Be or Mg, and tetravalent compounds such as $116F_4$ should be formed only with the most electronegative atoms.

In element 117, the 1– oxidation state becomes less important than that of the lighter group 17 halide ions due to the destabilization of the $7p_{3/2}$ orbital. The EA of element 117 is the smallest in the group (2.6 eV as predicted by Cunningham, 1969 and 1.8 eV as given by Waber *et al.*, 1969). Therefore, the 3+ state should be at least as important as the 1– state, so that element 117 might resemble Au^{3+} in its ion-exchange behavior in halide media. The trend to decreasing participation of the $np_{1/2}$ orbital bonding in group 17 was found to be continued further with element 117 (Hoffman, 1996; Saue *et al.*, 1996; Nash and Bursten, 1999c; Han *et al.*, 2000). In the group HI, HAt, and H117, an increasing trend in R_e and a decreasing trend in D_e are continued with H117. Analogous to its lighter homologs, Element 117 should form dimers X_2. The DCB CCSD(T) calculations for X_2 ($X = F$ through At) (Visscher *et al.*, 1996) found a considerable antibonding σ-character in the HOMO of At_2 due to the SO coupling while without the SO coupling it is an antibonding π-orbital. The bonding in $(117)_2$ is predicted to continue this trend and have a strong π-character.

The elements in the noble gas group become less inert with increasing Z. Earlier predictions of properties of element 118 were made by extrapolation from lighter homologs within the group (Grosse, 1965; Pitzer, 1975a,b). Early calculations of Penneman and Mann (1976) indicated that ionization energies of element 118 should be less than the experimental values for xenon, and that chemical compounds should be expected for 118. The first IP of element 118 is 8.7 eV (see Table 14.15), about the same as the $IP(114) = 8.54$ eV and smaller than $IP(Rn) = 10.74$ eV and $IP(112) = 11.97$ eV. The outer 8s orbital of element 118 is relativistically stabilized to give the atom a positive EA of 0.056 eV, as shown by recent CCSD calculations (Eliav *et al.*, 1996b). The polarizability of 118 is expected to be the largest in group 18. Its largest polarizability, together with its smallest IP, implies that it will have the highest reactivity in the group. It should be stable in the 4+ oxidation state, and should form stable tetrafluorides and tetrachlorides as well. Recent RECP calculations (Han and Lee, 1999) of free energies of the reactions $M + F_2 \rightarrow MF_2$ and $MF_2 + F_2 \rightarrow MF_4$, where M = Xe, Rn, and element 118, confirmed an increase in the stabilities of the 2+ and 4+ oxidation states in group 18. The SO effects were shown to stabilize $118F_4$ by a significant amount, about 2 eV, though they elongate R_e by 0.05 Å. The influence of the SO interaction on the geometry of MF_4 was investigated by RECP calculations (Han and Lee, 1999; Nash and Bursten, 1999a,b). It was found that the D_{4h} geometrical configuration for XeF_4 and RnF_4 becomes slightly unstable for $118F_4$. A T_d configuration was shown to be more stable than D_{4h} by about 0.20 eV. The reason was the availability of only stereochemically active $7p_{3/2}$ electrons for bonding. An important observation was made that the fluorides of element 118 will most probably be ionic rather than covalent as is the case of Xe. Therefore, they are predicted to be non-volatile.

(d) Elements 119 through 121

In elements 119 and 120, the filling of the 8s shell will take place, so that these elements should be homologs of the alkali and alkaline earth elements in groups 1 and 2 and will be stable in the 1+ and 2+ oxidation states, respectively. Their first IPs (Fricke, 1975) should be about 0.5 eV higher than those of Fr and Ra, respectively, due to the relativistic stabilization of the 8s electrons, and closer to the values of Rb and Sr. Thus, an upturn in the IPs from Cs to element 119 and from Ba to element 120 (see Fig. 14.22) was predicted (Penneman and Mann, 1976). Recent DK CCSD calculations (Lim *et al.*, 1999) showed the first IP of element 119 to be relativistically increased from 3.31 to 4.53 eV, while polarizability is decreased from 693.94 to 184.83 a.u. Due to the relativistic stabilization of the 8s orbital, the EA for element 119, of 662 meV, is 20 meV higher (being the highest in the group) than that for Fr, according to recent DCB CCSD calculations (Landau *et al.*, 2001).

The atomic radii of elements 119 and 120 are expected to be 2.4 and 2.0 Å, respectively, very similar to the values of Rb and Sr, as shown in Fig. 14.23. They show the same reversal of the trend (a downturn from Cs/Ba to 119/120) as do the IPs in groups 1 and 2 (Fricke, 1975). Thus, the chemical properties of elements 119 and 120 should be close to those of Rb and Sr, respectively, rather than to Fr and Ra in the 1+ and 2+ oxidation states. On the other hand, the ions will have larger radii than Rb^+ and Sr^{2+} because of the larger extension of the filled 7p shell compared to the lower p-shells. Another important point is that due to the relatively small ionization energy of the outer $7p_{3/2}$ electrons and their spatial extension, higher oxidation states like 3+ or 4+, respectively, could be reached in elements 119 and 120.

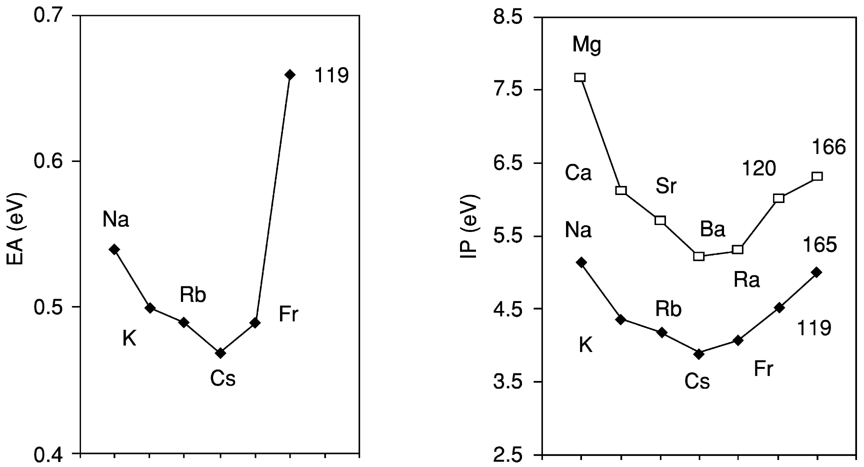

Fig. 14.22 *Electron affinities (EAs) and ionization potentials (IPs) for alkali and alkaline-earth elements. The data for Na through Fr and Mg through Ra are experimental. The value for Element* 119 *is from DF CCSD calculations (Landau* et al., 2001). *The values for elements* 120, 165 *and* 166 *are from DF calculations (Fricke,* 1975).

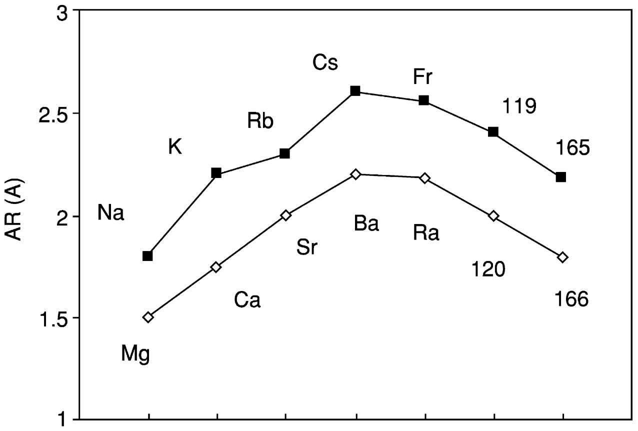

Fig. 14.23 *Atomic radii (AR) of alkali and alkaline earth elements. The data for Na through Cs and Mg through Ra are experimental. The other data are from DS calculations. (Redrawn from Fricke,* 1975).

The next element, 121, will have a relativistically stabilized 8p electron in its ground state electronic configuration $8s^28p_{1/2}$ (see Table 14.13) in contrast to that of $8s^27d$ predicted by a simple extrapolation within the group. As early as 1969, Griffin *et al.* (1969) showed that the large SO splitting brings an 8p electron into the stable atomic ground state. Recent CCSD calculations for element 121 (Eliav *et al.*, 1998a) gave $IP_1 = 4.45$ eV and EA = 0.75 eV, the highest EA in group 3. Griffin *et al.* also showed that large changes occur in the spatial distribution of the valence orbitals in going from element 120 to 121. For example, the effective radius of the 5g electrons changes from 25 Bohr units for element 120 in the excited configuration $8s^15g^1$ to 0.8 Bohr units for element 121 in the configuration $8s^17d^15g^1$. This phenomenon, called 'radial collapse', occurs as late as element 125 as a consequence of indirect relativistic effects. Due to the proximity of the valence levels, higher oxidation states are possible.

(e) Superactinide elements and beyond

Element 122 belongs to a very long, unprecedented transition series that is characterized by the filling of not only 6f but also 5g orbitals with partially filled $8p_{1/2}$ orbitals, which is a direct relativistic effect. These elements were dubbed 'superactinides' by Seaborg (1968) as early as 1968. Quite a number of theoretical calculations of the ground state electronic configurations (Griffin *et al.*, 1969; Mann, 1969; Mann and Waber, 1970; Fricke *et al.*, 1971) were performed for this region and the results have been summarized by Fricke (1975). The calculated ground state configurations of the free neutral atoms of elements 113 through 184 are listed in Table 14.13. Here, at the beginning of the superactinides, not only two but four electron shells, namely $8p_{1/2}$, $7d_{3/2}$, $6f_{5/2}$, and $5g_{7/2}$, are expected to compete simultaneously. These open shells, together with the 8s electrons, determine the chemistry.

As shown in Table 14.13, a 7d electron is added to the ground state in element 122 and the 8p electron is relativistically stabilized so that the configuration is $8s^27d8p$, in contrast to the $7s^26d^2$ state of Th. This is the last element where accurate CCSD calculations (Eliav *et al.*, 2002) exist. The first four calculated IPs of element are 5.6, 11.3, 20.4, and 27.14 eV as compared to the first and the fourth IPs, 6.54 and 28.75 eV, of Th. A decrease in the first IP from Th to element 122 is due to the ionized $8p_{1/2}$ electron.

Elements 122 through 152 might have chemical properties somewhat similar to those of the actinides but there will be some differences. The very small binding energies of all the valence electrons will cause the higher oxidation states to be reached in these elements. This will be a continuation of the trend from the lanthanides (where 3+ states are highest) to the superactinides.

For ionic compounds it is important to establish which external orbitals are left after all outer s-, p-, and d-electrons are removed. Will there be some g- and f-electrons left or will they be easily excited to an outer electron shell, so that they can be removed as well? Some investigations showed that for element 126 in the divalent state, one g-electron will move to an f-electronic state, and the 8s electrons will not be the first to be removed. Thus, the divalent ions are expected to act as soft Lewis acids and possibly form covalent complex ions readily. From some calculations of excited states, it is assumed that very high oxidation states may be possible around element 128 in complex compounds, but that normally these elements will have 4+ as their main oxidation state in ionic compounds. The maximum valence will be reduced to 6+ at element 132 and in the region of 140, it will be 3+ to 4+. At the end of the superactinide series, the normal oxidation states are expected to be only 2+ because the 6f shell will be buried deep inside the electron core and the 8s and $8p_{1/2}$ orbitals will be strongly bound. At element 156, only two 7d relativistically destabilized electrons will be available for bonding. This behavior should be similar to that of the low oxidation states of elements at the end of the actinides. Thus, at the end of the superactinide series, the elements will be more noble.

A contraction of bond lengths, analogous to the actinide contraction, is expected for the superactinide series. The total effect will be very large because of the 32 electrons, with the expected contraction of 0.02 Å per element. The predictions of chemical properties by extrapolation will be very difficult und unreliable in this area, since most of the elements have no homologs. From atomic calculations, one can already say that the behavior will be very different due to the stronger relativistic effects.

The fifth series of transition elements is expected to begin beyond the superactinides. Several early DF calculations in this region were performed. In elements 155 to 164, the filling of the 7d shell will take place so that they will be the d transition elements of the 8th period. The 8s and $8p_{1/2}$ electrons will be bound so strongly in these elements that they will not participate in the chemical bonding in contrast to the 7s electrons of the 7th period. Nevertheless, the 9s and $9p_{1/2}$ states will be easily available in 164 for hybridization so that the chemical behavior is expected to be similar to that of other d-elements. From DF calculations of excited states of element 164, Penneman and Mann (1976) suggested that the 7d orbitals will be chemically very active. Thus, in aqueous solutions, strong ligands can form tetra- and hexavalent bonds in addition to the predominant bivalent bonds. Consequently, tetrahedral $164(CO)_4$, $164(PF_3)_4$, and linear $164(CN)_2^{2-}$ might be prepared, which would be a striking contrast to lead (Fricke, 1975). The softness of element 164 should be similar to that of Hg, so that its location in the same group in the periodic table is justified. The metallic state of element 164 should have a larger cohesive energy than almost any other element because of covalent bonding, so that the melting point should be high (Fricke and Waber, 1971). The same authors indicated that the properties of elements 118 and 164 might also be analogous.

In elements 165 and 166, the 9s shell will be filled, suggesting that they should be homologs of group 1 and 2 elements and that their IPs and IR (Fricke, 1975) will be similar to those of the group 1 and 2 elements, respectively. Nevertheless, because of the underlying 7d shell, elements 165 and 166 might exhibit properties similar to those of the group 13 and 14 elements. Therefore, higher oxidation states than 1+ and 2+, respectively, might occur.

In elements 167 through 172 the $9p_{1/2}$ shell will fill before the $8p_{3/2}$ shell. The energies of these orbitals are so close to each other that this situation is analogous to the nonrelativistic p-shell in the 3d period. Thus, the common oxidation states of elements 167 to 179 will be 3+ to 6+. Element 171 is expected to have many states from 1– to 7+, as do halogens. H(171) would form due to its high electron affinity of 3.0 eV (Fricke *et al.*, 1971). Compounds with F and O are also expected. Element 172 might be a noble gas similar to Xe due to the similar values of their IPs. The major difference is that element 172 is predicted to be a liquid or a solid at normal temperatures because of its large atomic weight.

Mann reported that his program was unable to go beyond $Z = 176$. Model calculations of Fricke and Waber (1972) took into account a phenomenological formulation of quantum electrodynamic effects and made it possible to extend the DF calculations to even higher elements. They calculated the DF ground state for element 184, as shown in Table 14.13. The 10s and $10p_{1/2}$ electrons do not appear in the ground state configuration and only $8d^3$ and $7f^4$ electrons might be available for chemical bonding. The chemical behavior will be then even simpler than that of the early superactinides. With increasing ionization of the 184 ion, a redistribution of electrons occurs between the 6g and 7f shells so that the number of electrons in the 6g shell increases. Since the 6g electrons are very deep inside the ion, only 7f electrons will be available for bonding. By analogy to U, the 5+ and 6+ states may be easily reached, but in aqueous solution the 4+ oxidation state will be the most stable. Higher oxidation states are not likely because the binding energy of the electrons in the deeply buried 6g shell will increase rapidly with higher ionization. Thus, in the very long SHE transition series, where many outer electron shells are being filled simultaneously in the neutral atom, a large increase in ionization energies will occur so that extremely high or unusual oxidation states are not expected.

In summary, in the area of the SHEs, the relativistic effects are so strong that any classification based on the knowledge of their electronic configurations or extrapolations of properties from the known elements is inappropriate. It is interesting to note that even without relativistic effects, the chemistry of the heaviest SHEs would be different from that of their lighter homologs due to very large shell-structure effects. The nonrelativistic expansion and destabilization of the *n*s valence orbitals and contraction and stabilization of the *n*d, *n*f, and orbitals of higher angular quantum number *l* with very large *n* also would have drastically changed the properties of the SHEs. However, due to the opposite actions of relativistic and shell-structure effects, the relativistic and nonrelativistic changes are predicted to go in opposite directions. A more detailed periodic table up to element 172 was given by Fricke (1975). Some discussions of the chemistry of SHEs can be found in Penneman *et al.* (1971), Fricke (1975), and Jorgensen (1968), and more recently in a review of the evolution of the periodic table by Seaborg (1996).

14.7.2 Prospects for experimental studies of chemistry of elements beyond element 112, including SHEs

The prerequisites for successful studies of the chemistry of elements beyond 112 will be similar to those discussed previously for Mt through 112. These include the existence of isotopes with long enough half-lives for chemical studies, knowledge of their nuclear decay properties so that they can be positively identified as belonging to the element being studied, synthesis reactions with the highest possible cross sections, techniques for increasing the production rates such as cooled, multiple targets, the highest possible beam currents at accelerators with facilities for conducting these studies, and, ideally, dedicated beamlines for optimal utilization of facilities by international groups of scientists. After the chemistry of a given element is known, the atomic number of new isotopes can be positively assigned based on their established chemical properties and detailed studies of nuclear properties such as SF can be conducted on chemically separated samples.

(a) Chemical methods

A useful technique that should prove invaluable in the study of very low-yield, short-lived elements is pre-separation of the nuclides of interest from the host of unwanted activities using a dedicated on-line separator such as the BGS at the appropriate accelerator. At the focal plane the separated isotopes can be stopped in an RTC containing an appropriate gas and can even be treated chemically to adjust oxidation states and volatility. The resultant volatile species can then be rapidly and continuously transported to a cryo-thermochromatographic separator or any other desired chemical separation/detection system.

The ingenious isothermal gas-phase techniques that have already been applied in the studies of volatile Hs oxides can be used to study other volatile species that can be similarly swept in carrier gas directly to an on-line detection system or to a cryogenic TC composed of the particle detectors. In this way, simultaneous on-line measurements can be performed of the decay properties of the radioactive nuclides in the volatile species and their deposition temperature on the surface of the detectors that form the chromatography column. Vacuum cryo-thermochromatographic techniques in which the relative reactivity of elements 114 through 118 are determined based on their sorption on a variety of transition metal surfaces might be used to assess whether their behavior is more like their lighter homologs or the inert noble gases.

The continuous, computer-controlled automated procedures discussed in the previous sections can be used and other procedures designed specifically to exploit the chemistry predicted for each of these elements. Continuously operating, rapid systems for liquid–liquid extractions followed by detection in flowing liquid-scintillation detectors such as the SISAK-III/liquid scintillation system (Omtvedt *et al.*, 1998, 2002) can be used for on-line studies of isotopes with half-lives as short as a few seconds provided chemical systems that rapidly come to equilibrium can be devised. Alternatively, they could be used to continuously purify longer-lived SHEs. A variety of computer-controlled, continuous multi-ion-exchange column techniques that include automated transport of samples to the detection equipment have been developed (Haba *et al.*, 2002; Nagame *et al.*, 2002) for performing rapid separations of isotopes with half-lives as short as a few seconds and then inferring their presence based on detection of their longer-lived daughters in subsequent chemical separations. Such continuous systems might also be adapted for processing longer-lived SHEs for subsequent off-line detection.

New methods for studying gas-phase ion chemistry in a Penning trap have been reported by Rieth *et al.* (2002) and it has been shown by the ISOLTRAP group at the Centre Européen pour la Recherche Nucléaire (CERN) (Kugler *et al.*, 1992; Bollen *et al.*, 1996) that nuclides as short as a few tenths of a second can be used with Penning trap mass spectrometers. These techniques have potential application to gas-phase studies of elements beyond 112. Kinetic data on ion–molecule interactions can be obtained with single-ion detection, and mass spectrometry can be used to unambiguously determine the stoichiometry of the reaction products. However, the reaction rates must be increased in order to make the technique viable for the low production rates of less than one atom per week expected for the heaviest elements.

(b) Predicted and reported half-lives and nuclear properties of SHEs

One of the most significant nuclear properties of elements 107 through 112 is that they decay predominantly by alpha emission rather than SF, contrary to earlier predictions. This experimental discovery sparked a renewal of interest in searching for elements beyond 112 and revived hope that the long-predicted island of SHEs might finally be reached. Armbruster and Münzenberg (1989) proposed that even though the neutron-deficient isotopes of elements 107 through 112 are probably not spherical, they should qualify as SHEs because without the stabilization of nuclear shells they would not exist. These elements have not been generally recognized as SHEs.

The discovery of longer-lived isotopes in this region, ^{265,266}Sg, ^{267}Bh, and ^{269,270}Hs, substantiated the theoretical model and calculations (Sobiczewski *et al.*, 1994; Smolańczuk *et al.*, 1995) predicting a doubly magic deformed region of extra stability in the vicinity of proton number 108 and neutron number 162 in addition to the island of spherical stability originally predicted to be around $Z = 114$ and $N = 184$, as shown in Fig. 14.24.

Evidence for three isotopes of element 114, ^{287,288,289}114, has been reported (Oganessian *et al.*, 1999a) although only one event of 21-s ^{289}114 was detected

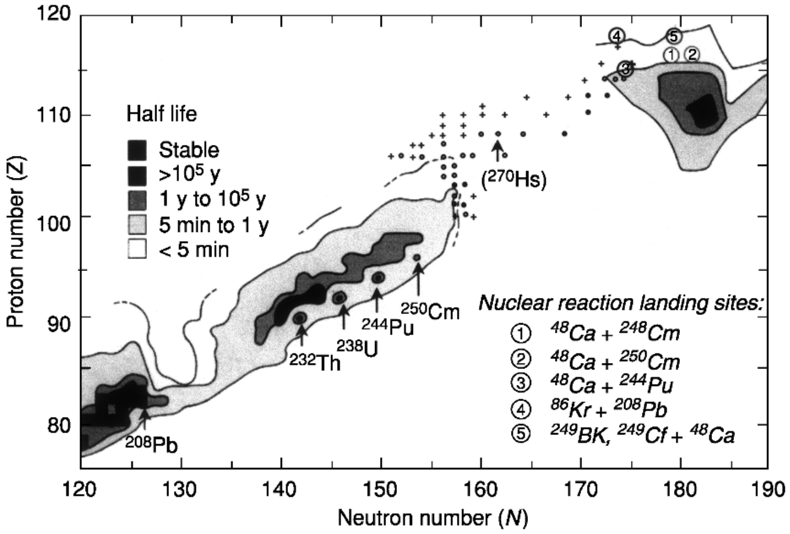

Fig. 14.24 *Updated plot of heavy element topology from* 1978 *showing some landing points for proposed reactions. Heavy element isotopes reported since* 1978 *up to mid-*2002 *are indicated with symbols denoting the following half-life ranges:* 0.1 ms to 0.1 s (+); 0.1 s to 5 min (○); > 5 min (●).

and it was not confirmed in subsequent experiments (Lougheed *et al.*, 2000). The discovery of isotopes of element 116, $^{292}116$, has been discussed by Oganessian (2002) and Oganessian *et al.* (2002, 2004c). Calculations (Smolańczuk, 1997) indicate that these isotopes are nearly spherical with deformation energies ranging from only about 0.1 MeV for $^{292}116$ to 0.3–0.2 MeV for the 114 isotopes, compared to zero deformation energy for the spherical doubly magic $^{298}114$ and 7.8 MeV for the doubly deformed magic nucleus, $^{270}108$. Thus, element 114 and 116 isotopes qualify as spherical SHEs even though they do not have the full complement of 184 neutrons. However, their existence still awaits confirmation by other groups.

Recent theoretical predictions (Chasman and Ahmad, 1997; Smolańczuk, 2001a,b) indicate that isotopes with half-lives of microseconds or longer will exist all along the way to the predicted islands of stability. However, the half-lives predicted for nuclei in the region of the spherical island of stability have decreased dramatically since the 1970s when half-lives of billions of years were predicted. For example, Smolańczuk (2001a,b) predicted that the spherical doubly magic superheavy nucleus $^{298}114$ will decay predominantly by alpha emission with a half-life of only 12 min, but that ^{292}Ds may alpha decay with a half-life of about 50 years.

Some other recent calculations (Kruppa *et al.*, 2000) predict that the strongest spherical shell effects might be at $Z = 124$ or 126 and $N = 184$ while still others propose the maximum effect might be at $Z = 120$ and $N = 172$. Doughnut-like, toroidal nuclear shapes with lower densities or a hole in the middle to alleviate the effects of Coulomb repulsion have even been postulated. How many more elements can exist is still unclear and it is even more unclear how many of these we can actually produce.

(c) Production reactions

So-called 'cold' fusion reactions in which the compound nucleus is produced with small excitation energy and emits only a single neutron were used to discover the elements from Bh through 112 (Hofmann, 1998). After the discovery of element 112 in 1996 (Hofmann *et al.*, 1996), researchers at GSI unsuccessfully attempted to produce element 113 using the cold fusion reaction ^{209}Bi (^{70}Zn,n) ^{278}113 (Hofmann and Münzenberg, 2000). From two experiments lasting about 3 weeks each, they set a limit of 0.6 pb on the cross section at a mean excitation energy of 10.5 MeV. They concluded that the cross section for production of element 116 would be only 1 femtobarn and that their experimental setup would have to be greatly improved in order to investigate this region further. Contrary to these expectations that the production cross sections for the 1n evaporation channel in cold fusion reactions to produce elements above 112 would continue to decrease exponentially with the proton number of the projectile, Smolańczuk (1999a) suggested that the cold fusion reaction ^{208}Pb(^{86}Kr,n) reaction to produce the hypothetical spherical SHE nuclide ^{293}118 with an excitation energy of only 13 MeV would have an unusually large cross section of a few hundred picobarns. The predicted increase in formation cross section was attributed to the fact that ^{86}Kr contains the magic number of 50 neutrons, which leads to a larger Q value with a subsequent increase in the transmission probability through the Coulomb barrier. He also predicted that ^{293}118 would decay by a unique decay sequence of six high-energy alpha particles. However, the results of Gregorich *et al.* (2002) setting upper limits of less than 1 pb for the formation cross section for this reaction based on detection of the predicted high-energy alpha-decay chain make the use of cold fusion reactions appear less attractive for production of SHEs. Estimates of the predicted cross section were later lowered to about 6 pb (Smolańczuk, 2001b), and it was pointed out that the excitation functions are quite narrow and have a rather sharp threshold (Smolańczuk, 1999c) so use of too low a bombarding energy might result in a negative result and the idea should not be totally abandoned.

Similar cold fusion reactions with ^{208}Pb or ^{209}Bi targets with ^{87}Rb or ^{86}Kr projectiles could be used to produce ^{294}119 (Smolańczuk, 1999a,b), whose half-life is estimated to be only microseconds. However, ^{294}119 is predicted to decay to isotopes of the new longer-lived, odd-Z elements 117, 115, and 113 via a succession of alpha emissions, ending with the known isotope 3.6-h ^{262}Lr. Production of ^{295}120 ($\sim$2 μs) via the ^{208}Pb(^{88}Sr,1n) reaction and detection of its high-energy alpha-decay chain have also been proposed (Smolańczuk, 2001a).

The reported elements 114 and 116 were synthesized using reactions of ^{244}Pu and ^{248}Cm with ^{48}Ca projectiles to form the compound nuclei ^{292}114 and ^{296}116, which then emitted four neutrons to produce 2.6-s ^{288}114 and 53-ms ^{292}116 (Oganessian *et al.*, 2000a,b; Oganessian, 2001, 2002). They were calculated to have excitation energies of only 33 and 31 MeV, respectively, due to the stability of the doubly magic projectile, compared to >45 MeV for 'hot' fusion reactions. The detection limit of these experiments was about 0.5 pb, several orders of magnitude more sensitive than in the unsuccessful attempt reported in 1984 by an international group of nuclear scientists, both chemists and physicists (Armbruster *et al.*, 1985), who conducted an exhaustive 'final' investigation of the reaction of ^{248}Cm with ^{48}Ca projectiles to produce SHEs. Oganessian also proposed that the reaction of ^{48}Ca with ^{249}Cf targets be used to produce element ^{294}118 via the '3n out' reaction. However, the viability of the '3n out' reactions in this region has yet to be confirmed. Loveland *et al.* (2002) set a limit of <2 pb for SF and alpha events for the ^{238}U(^{48}Ca,3n)^{283}Ds reaction. Hot fusion reactions between ^{48}Ca projectiles and ^{249}Bk and ^{249}Cf targets to produce elements ^{293,294}117 and ^{293,294}118, respectively, are under investigation by the Dubna/LLNL group.

The ^{237}Np and ^{249}Bk targets with ^{48}Ca projectiles can probably be used to make the odd-proton element 113 and more neutron-rich isotopes of element 117, respectively. Other highly radioactive targets such as ^{249}Cf or even ^{254}Es with appropriate projectiles might be used to make more neutron-rich isotopes of elements as heavy as 118, but considerable development work will be required.

Reactions that can produce a higher ratio of neutrons to protons will certainly be most advantageous and need to be investigated. Myers and Swiatecki (2000) have suggested that so-called 'unshielded' reactions in which the Coulomb barrier has sunk below the bombarding energy may result in enhanced production yields for some of the higher Z elements. Their hypothesis that the cross section for ^{277}112 produced in the symmetric reaction ^{142}Ce(^{136}Xe,n) might be much larger than that for the 112 discovery reaction ^{208}Pb(^{70}Zn, n)^{277}112 should be tested experimentally. If so, the unshielded reaction ^{170}Er (^{136}Xe,n) reaction to make ^{305}122, which has 183 neutrons, might be a method for getting closer to these regions. It should decay by successive alpha emission to the isotope ^{289}114, reported by the Dubna/LLNL group. Whether additional SHEs can be produced depends very much upon whether the cross sections for the 'cold' fusion reactions in which only a single neutron is emitted and the 'warm'/'hot' fusion reactions with three or four neutrons emitted are large enough to permit detection.

It now appears likely that many more relatively long-lived nuclides can exist than are presently known, but a major research effort to explore new types of production reactions, imaginative techniques for optimizing overall yields by using multiple targets and higher beam currents, innovative chemical separations, and a dedicated on-line installation for chemical studies at an appropriate accelerator with access to a pre-separator will be required in order to fully explore their chemical properties. If, on the other hand, relatively long-lived new elements are discovered, then methods for 'stockpiling' them for off-line studies or producing them as by-products of other experiments must be devised to facilitate studies of their chemistry. The prospect lies ahead of a whole new landscape for the exploration of the chemical properties of the heaviest elements and their compounds, determining the influence of relativistic effects, assigning their positions in the periodic table, and extending and further defining the architecture of the periodic table.

REFERENCES

Adloff, J. -P. and Guillaumont, R. (1993) *Fundamentals of Radiochemistry*, CRC Press, Boca Raton, pp. 327–52.

Ahrland, S., Liljenzin, J. O., and Rydberg, J. (1973) in *Comprehensive Inorganic Chemistry*, vol. 5 (ed. J. Bailar), Pergamon Press, Oxford, pp. 519–42.

Alekseeva, T. E., Arkhipova, N. F., and Rabinovitch, V. A. (1972) *Russ. J. Inorg. Chem.* **17**, 140–1.

Alstad, J., Skarnemark, G., Haberberger, F., Herrmann, G., Nähler, A., Pense-Maskow, M., and Trautmann, N. (1995) *J. Radioanal. Nucl. Chem. Articles*, **189**, 133.

Alzitzoglou, T., Rogowski, J., Skålberg, M., Alstad, J., Herrmann, G., Kaffrell, N., Skarnemark, G., Talbert, W., and Trautmann, N. (1990) *Radiochim. Acta*, **51**, 145–50.

Amble, E., Miller, S. L., Schawlaw, A. L., and Townes, C. H. (1952) *J. Chem. Phys.,* **20**, 192.

Armbruster, P., Agarwal, Y. K., Brüchle, W., Brügger, M., Dufour, J. P., Gäggeler, H., Hessberger, F. P., Hofmann, S., Lemmertz, P., Münzenberg, G., Poppensieker, K., Reisdorf, W., Schädel, M., Schmidt, K. H., Schneider, J. H. R., Schneider, W. F. W., Sümmerer, K., Vermeulen, D., Wirth, G., Ghiorso, A., Gregorich, K. E., M., D. L., Leino, M., Moody, K. J., Seaborg, G. T., Welch, R. B., Wilmarth, P., Yashita, S., Frink, C., Greulich, N., Herrmann, G., Hickmann, U., Hildebrand, N., Kratz, J. V., Trautmann, N., Fowler, M. M., Hoffman, D. C., Daniels, W. R., Gunten, H. R. V., and Dornhöfer, H. (1985) *Phys. Rev. Lett.,* **54**, 406–9.

Armbruster, P. and Münzenberg, G. (1989) *Sci. Am,* **66**, 66–72.

Armbruster, P., Hessberger, F. P., Hofmann, S., Leino, M., Münzenberg, G., Reisdorf, W., and Schmidt, K.-H. (1993) *Pure Appl. Chem.*, **65**, 1822–4.

Autschbach, J., Siekierski, S., Seth, M., Schwerdtfeger, P., and Schwarz, W. H. E. (2002) *J. Comput. Chem.*, **23**, 804–13.

Baerends, E. J., Schwarz, W. H. E., Schwerdtfeger, P., and Snijders, J. G. (1990) *J. Phys. B,* **23**, 3225–40.

Baes, C. F. and Mesmer, R. E. (1976) *The Hydroysis of Cations*, Wiley Interscience, New York, pp. 152–91.

Barber, R. C., Greenwood, N. N., Hrynkiewicz, A. Z., Jeannin, Y. P., Lefort, M., Sakai, M., Ulehla, I., Wapstra, A. H., and Wilkinson, D. H. (1991) *Pure Appl. Chem.*, **63**, 879–86.

Barber, R. C., Greenwood, N. N., Hrynkiewicz, A. Z., Jeannin, Y. P., Lefort, M., Sakai, M., Ulehla, I., Wapstra, A. H., and Wilkinso, D. H. (1992) *Prog. Part. Nucl. Phys.*, **29**, 453–530.

Barber, R. C., Greenwood, N. N., Hrynkiewicz, A. Z., Jeannin, Y. P., Lefort, M., Sakai, M., Ulehla, I., Wapstra, A. H., and Wilkinso, D. H. (1993) *Pure Appl. Chem.,* **65**, 1757–813.

Bastug, T., Heinemann, D., Sepp, W.-D., Kolb, D., and Fricke, B. (1993) *Chem. Phys. Lett.*, **211–224**, 119–24.

Bemis, C. E. Jr, Silva, R. J., Hensley, D. C., Keller, O. L. Jr, Tarrant, J. R., Hunt, L. D., Dittner, P. F., Hahn, R. L., and Goodman, C. D. (1973) *Phys. Rev. Lett.,* **31**, 647–50.

Bemis, C. E. Jr, Dittner, P. F., Silva, R. J., Hahn, R. L., Tarrant, J. R., Hunt, L. D., and Hensley, D. C. (1977) *Phys. Rev. C,* **16**, 1146–57.

Bilewicz, A., Kacher, C. D., Gregorich, K. E., Lee, D. M., Stoyer, N. J., Kadkhodayan, B., Kreek, S. A., Lane, M. R., Sylwester, E. R., Neu, M. P., Mohar, M. F., and Hoffman, D. C. (1996) *Radiochim. Acta*, **75**, 121–6.

Bollen, G., Becker, S., Kluge, H.-J., Konig, M., Moore, R. B., Otto, T., Raimbault-Hartmann, H., Savard, G., Schweikhard, L., and Stolzenberg, H. (1996) *Nucl. Instrum. Methods A,* **368**, 675–97.

Bratsch, S. G. and Lagowski, J. J. (1986) *J. Phys. Chem.,* **90**, 307–12.

Bratsch, S. G. (1989) *Phys. Chem. Ref. Data,* **18**, 1–21.

Brown, D. (1973) *Comprehensive Inorganic Chemistry*, vol. 3, Pergamon Press, Oxford, pp. 553–622.

Brüchle, W., Jäger, E., Pershina, V., Schädel, M., Schausten, B., Günther, R., Kratz, J. V., Paulus, W., Seibert, A., Thörle, P., Zauner, S., Schümann, D., Eichler, B., Gäggeler, H., Jost, D., and Türler, A. (1998) *J. Alloy Compds*, **271–273**, 300–2.

Burraghs, P., Evans, S., Hamnett, A., Orchard, A. F., and Richardson, N. V. (1974) *J. Chem. Soc. Faraday Trans.* 2, **70**, 1895.

Chasman, R. R. and Ahmad, I. (1997) *Phys. Lett. B,* **392**, 255–61.

CNIC, Commission on Nomenclature of Inorganic Chemistry of IUPAC (1997) *Pure Appl. Chem.*, **69**, 2471–3.

Corish, J. and Rosenblatt, G. M. (2003) *Pure Appl. Chem.*, **75**, 1613–15.

Corish, J. and Rosenblatt, G. M. (2004) *Pure Appl. Chem.* **76**, 2101–3.

Cunningham, B. B. (1969) in *Proc. Robert A. Welch Foundation, XIII, The Transuranium elements – The Mendeleev Centennial*, pp. 307–22, Houston, Texas.

Czerwinski, K. R. (1992a) *Studies of Fundamental Properties of Rutherfordium (element 104) Using Organic Complexing Agents*, Doctoral Thesis, LBL-32233, Berkeley.

Czerwinski, K. R. (1992b) *Studies of Fundamental properties of Rutherfordium (element 104) Using Organic Complexing Agents*, Ph.D. Thesis, Berkeley, LBL-32233, pp. 83–102.

Czerwinski, K. R., Gregorich, K. E., Hannink, N. J., Kacher, C. D., Kadkhodayan, B. A., Kreek, S. A., Lee, D. M., Nurmia, M. J., Türler, A., Seaborg, G. T., and Hoffman, D. C. (1994a) *Radiochim. Acta,* **64**, 23–8.

Czerwinski, K. R., Kacher, C. D., Gregorich, K. E., Hamilton, T. M., Hannink, N. J., Kadkhodayan, B. A., Kreek, S. A., Lee, D. M., Nurmia, M. J., Türler, A., Seaborg, G. T., and Hoffman, D. C. (1994b) *Radiochim. Acta,* **64**, 29–35.

Desclaux, J. P. (1973) *Data Nucl. Data Tables*, **12**, 311–406.

Desclaux, J. P. (1975) *Comp. Phys. Commun.*, **9**, 31–45.

Desclaux, J. P. and Fricke, B. (1980) *J. Phys.*, **41**, 943–6.

Dolg, M., Stoll, H., Preuss, H., and Pitzer, R. M. (1993) *J. Phys. Chem.*, **97**, 5852–9.

Düllmann, C. E., Eichler, B., Eichler, R., Gäggeler, H. W., Jost, D. T., Piguet, D., and Türler, A. (2002a) *Nucl. Instrum. Methods A*, **479**, 631–9.

Düllmann, C. E., Brüchle, W., Dressler, R., Eberhardt, K., Eichler, B., Eichler, R., Gäggeler, H. W., Ginter, T. N., Glaus, F., Gregorich, K. E., Hoffman, D. C., Jäger, E., Jost, D. T., Kirbach, U. W., Lee, D. M., Nitsche, H., Patin, J. B., Pershina, V., Piguet, D., Qin, Z., Schädel, M., Schausten, B., Schimpf, E., Schött, H.-J., Soverna, S., Sudowe, R., Thörle, P., Timokhin, S. N., Trautmann, N., Türler, A., Vahle, A., Wirth, G., Yakushev, A. B., and Zielinski, P. M. (2002b) *Nature,* **418**, 859–62.

Eichler, B. (1974) Dubna Report JINR P12–7767.

Eichler, B. and Rossbach, H. (1983) *Radiochim. Acta,* **33**, 121–5.

Eichler, B., Türler, A., and Gäggeler, H. W. (1999) *J. Phys. Chem. A,* **103**, 9296–306.

Eichler, B. and Kratz, J. V. (2000) *Radiochim. Acta,* **88**, 475–82.

Eichler, R., Brüchle, W., Dressler, C. E., Düllman, C. E., Eichler, B., Gäggeler, H. W., Gregorich, K. E., Hoffman, D. C., Hübener, S., Jost, D. T., Kirbach, U. W., Laue, C. A., Lavanchy, V. M., Nitsche, H., Patin, J. B., Piguet, D., Schädel, M., Shaughnessy, D. A., Strellis, D. A., Taut, S., Tobler, L., Tsyganov, Y. S., Türler, A., Vahle, A., Wilk, P. A., and Yakushev, A. B. (2000) *Nature (Lett.),* **407**, 63–5.

Eichler, R. and Schädel, M. (2002) *J. Phys. Chem. B,* **106**, 5413–20.

Eliav, E., Landau, A., Ishikawa, Y., and Kaldor, U. (1992) *J. Phys. B,* **35**, 1693.

Eliav, E., Kaldor, U., Schwerdtfeger, P., Hess, B. A., and Ishikawa, Y. (1994) *Phys. Rev. Lett.,* **73**, 3203–6.

Eliav, E., Kaldor, U., and Ishikawa, Y. (1995a) *Phys. Rev. Lett.,* **74**, 1079–82.

Eliav, E., Kaldor, U., and Ishikawa, Y. (1995b) *Phys. Rev. A,* **52**, 2765–9.

Eliav, E., Kaldor, U., Ishikawa, Y., Seth, M., and Pyykkö, P. (1996a) *Phys. Rev. A,* **53**, 3926–33.

Eliav, E., Kaldor, U., Ishikawa, Y. M., and Pyykkö, P. (1996b) *Phys. Rev. Lett.*, **77**, 5350–2.

Eliav, E., Shmulyian, S., Kaldor, U., and Ishikawa, Y. (1998a) *J. Chem. Phys.*, **109**, 3954–8.

Eliav, E., Kaldor, U., and Ishikawa, Y. (1998b) *Mol. Phys.*, **94**, 181–7.

Eliav, E., Landau, A., Ishikawa, Y., and Kaldor, U. (2002) *J. Phys. B,* **35**, 1693–700.

Ermler, W. C., Ross, R. B., and Christiansen, P. A. (1988) *Adv. Quant. Chem.,* **19**, 139–82.

Faegri, K. and Saue, T. (2001) *J. Chem. Phys.*, **115**, 2456–64.

Fiset, E. O. and Nix, J. R. (1972) *Nucl. Phys.*, **A193**, 647.

Flerov, G. N. and Zvara, I. (1971) Joint Institute of Nuclear Research, Dubna, USSR, Report D7-6031, August 1971.

Fricke, B., Greiner, W., and Waber, J. T. (1971) *Theor. Chim. Acta,* **21**, 235–60.

Fricke, B. and Waber, J. T. (1971) *Actinides Rev.*, **1**, 433–85.

Fricke, B. and Waber, J. T. (1972) *J. Chem. Phys.*, **56**, 3246.

Fricke, B. (1975) in *Structure and Bonding*, vol. 21 (ed. J. D. Dunitz), Springer-Verlag, Berlin, pp. 89–144.

Fricke, B., Johnson, E., and Rivera, G. M. (1993) *Radiochim. Acta,* **62**, 17–25.

Gäggeler, H. W. (1990) Chemistry of the transactinide elements, in *The Robert A. Welch Foundation Conference on Chemical Research XXXIV. Fifty Years with Transuranium Elements*, pp. 255–76, Houston, Texas.

Gäggeler, H. W., Jost, D. T., Kovacs, J., Scherer, U. W., Weber, A., Vermeulen, D., Türler, A., Gregorich, K. E., Henderson, R. A., Czerwinski, K. R., Kadkhodayan, B., Lee, D. M., Nurmia, M., Hoffman, D. C., Kratz, J. V., Gober, M. K., Zimmermann, H. P., Schädel, M., Bruchle, W., Schimpf, E., and Zvara, I. (1992) *Radiochim. Acta,* **57**, 93–100.

Gäggeler, H. W. (1994) *J. Radioanal. Nucl. Chem. Articles,* **183**, 261.

Gäggeler, H. W. (1997) Fast chemical separation procedures for transactinides, in *The Robert A. Welch Foundation 41st Conference on Chemical Research the Transuranium Elements*, pp. 47–51, Houston, Texas.

Gärtner, M., Boettger, M., Eichler, B., Gäggeler, H. W., Grantz, M., Hubener, S., Jost, D. T., Piguet, D., Dressler, R., Türler, A., and Yakushev, A. B. (1997) *Radiochim. Acta,* **78**, 59–68.

Ghiorso, A., Nurmia, M., Harris, J., Eskola, K., and Eskola, P. (1969) *Phys. Rev. Lett.,* **22**, 1317.

Ghiorso, A., Nurmia, M., Eskola, K., Harris, J., and Eskola, P. (1970) *Phys. Rev. Lett.,* **24**, 1498–503.

Ghiorso, A., Nurmia, M., Eskola, K., and Eskola, P. (1971) *Phys. Rev C,* **4**, 1850–5.

Ghiorso, A. and Seaborg, G. T. (1993a) *Pure Appl. Chem.*, **65**, 1815–20.

Ghiorso, A. and Seaborg, G. T. (1993b) *Prog. Part. Nucl. Phys.*, **31**, 233–7.

Ghiorso, A., Lee, D., Somerville, L. P., Loveland, W., Nitschke, J. M., Ghiorso, W., Seaborg, G. T., Wilmarth, P., Leres, R., Wydler, A., Nurmia, M., Gregorich, K., Czerwinski, K., Gaylord, R., Hamilton, T., Hannink, N. J., Hoffman, D. C., Jarzynski, C., Kacher, C., Kadkhodayan, B., Kreek, S., Lane, M., Lyon, A., McMahan, M. A., Neu, M., Sikkeland, T., Swiatecki, W. J., Türler, A., Walton, J. T., and Yashita, S. (1995a) *Nucl. Phys.*, **583**, 861–6.

Ghiorso, A., Lee, D., Somerville, L. P., Loveland, W., Nitschke, J. M., Ghiorso, W., Seaborg, G. T., Wilmarth, P., Leres, R., Wydler, A., Nurmia, M., Gregorich, K., Czerwinski, K., Gaylord, R., Hamilton, T., Hannink, N. J., Hoffman, D. C., Jarzynski, C., Kacher, C., Kadkhodayan, B., Kreek, S., Lane, M., Lyon, A., McMahan, M. A., Neu, M., Sikkeland, T., Swiatecki, W. J., Türler, A., Walton, J. T., and Yashita, S. (1995b) *Phys. Rev. C,* **51**, R2293–7.

Girichev, G. V., Petrov, V. M., Giricheva, N. I., Utkin, A. N., and Petrova, V. N. (1981) *Zh. Strukt. Khim.,* **22**, 6.

Glebov, V. A., Kasztura, L., Nefedov, V. S., and Zhuikov, B. L. (1989) *Radiochim. Acta*, **46**, 117–21.

Gober, M. G., Kratz, J. V., Zimmermann, H. P., Schädel, M., Brüchle, W., Schimpf, E., Gregorich, K. E., Türler, A., Hannink, N. J., Czerwinski, R. K., Kadkhodayan, B., Lee, D. M., Nurmia, M. J., Hoffman, D. C., Gäggeler, H., Jost, D., Kovacs, J., Scherer, U. W., and Weber, A. (1992) *Radiochim. Acta*, **57**, 77–84.

Grant, I. P. and Pyper, N. C. (1977) *Nature (Lett.)*, **265**, 715–17.

Grant, I. P. (1986) *J. Phys. B,* **19**, 3187–205.

Grant, I. P. (1994) *Adv. Mol. Phys.,* **32**, 169–86.

Grant, I. P. and Quiney, H. (2000) *Int. J. Quant. Chem.*, **80**, 283–97.

Gregorich, K. E., Henderson, R. A., Lee, D. M., Nurmia, M. J., Chasteler, R. M., Hall, H. L., Bennett, D. A., Gannett, C. M., Chadwick, R. B., Leyba, J. D., Hoffman, D. C., and Herrmann, G. (1988) *Radiochim. Acta*, **43**, 223–31.

Gregorich, K. E. (1997a) Radiochemistry of rutherfordium and hahnium, in *The Robert A. Welch Foundation 41st Conference on Chemical Research the Transuranium Elements*, pp. 95–124, Houston, Texas.

Gregorich, K. E. (1997b) Radiochemistry of rutherfordium and hahnium, in *The Robert A. Welch Foundation 41st Conference on Chemical Research the Transuranium Elements*, pp. 103–8, Houston, Texas.

Gregorich, K. E., Ginter, T., Loveland, W., Peterson, D., Patin, J. B., Folden, C. M. III, Hoffman, D. C., Lee, D. M., Nitsche, H., Omtvedt, J. P., Omtvedt, L. A., Stavsetra, L., Sudowe, R., Wilk, P. A., Zielinski, P., and Aleklett, K. (2002) *Eur. Phys. J. A,* **18**, 633–8.

Griffin, D. C., Andrew, K. L., and Cowan, R. D. (1969) *Phys. Rev.,* **177**, 62–71.

Grosse, A. V. (1965) *J. Inorg. Nucl. Chem.,* **27**, 509–20.

Guillaumont, R., Adloff, J.-P., and Peneloux, A. (1989) *Radiochim. Acta,* **46**, 169–76.

Guillaumont, R., Adloff, J.-P., Peneloux, A., and Delamoye, P. (1991) *Radiochim. Acta,* **54**, 1–15.

Günther, R., Paulus, W., Kratz, J. V., Seibert, A., Thorle, P., Zauner, S., Bruchle, W., Jager, E., Pershina, V., Schädel, M., Schausten, B., Schumann, D., Eichler, B., Gäggeler, H. W., Jost, D. T., and Türler, A. (1998) *Radiochem. Acta,* **80**, 121–8.

Haba, H., Tsukada, K., Asai, M., Goto, S., Toyoshima, A., Nishinaka, I., Akiyama, K., Hirata, M., Ichikawa, S., Nagame, Y., Shoji, Y., Shigekawa, M., Koike, T., Iwasaki, M., Shinohara, A., Kaneko, T., Maruyama, T., Ono, S., Kudo, H., Oura, Y., Sueki, K., Nakahara, H., Sakama, M., Yokoyama, A., Kratz, J. V., Schädel, M., and Brüchle, W. (2002) *J. Nucl. Radiochem. Sci.,* **3**, 143–6.

Han, Y.-K. and Lee, Y. S. (1999) *J. Phys. Chem. A,* **103**, 1104–8.

Han, Y.-K., Son, S.-K., Choi, Y. J., and Lee, Y. S. (1999a) *J. Phys. Chem.,* **103**, 9109–15.

Han, Y.-K., Bae, C., and Lee, Y. S. (1999b) *J. Chem. Phys.,* **110**, 8986–75.

Han, Y.-K., Bae, C., Son, S.-K., and Lee, Y. S. (2000) *J. Chem. Phys.,* **112**, 2684–91.

Harvey, B. G., Gunther, H., Hoff, R., Hoffman, D. C., Hyde, E. K., Katz, J. J., and Seaborg, G. T. (1976) *Science,* **193**, 271–3.

Hessberger, F. P., Hofmann, S., Ninov, V., Armbruster, P., Folger, H., Munzenberg, G., Schott, H. J., Popeko, A. G., Yeremin, A. V., Andreyev, A. N., and Saro, S. (1997) *Z. Phys. A,* **359**, 415–25.

Hoffman, D. C. (1994) *Chem. Eng. News*, 24–34.

Hoffman, D. C. (1996) *Radiochim. Acta,* **72**, 1–6.

Hoffman, D. C. and Lee, D. M. (1999) *J. Chem. Educ.,* **76**, 331–47.

Hoffman, D. C., Ghiorso, A., and Seaborg, G. T. (2000a) *The Transuranium People: The Inside Story*, Imperial College Press, London, pp. 258–98; 379–96.

Hoffman, D. C., Ghiorso, A., and Seaborg, G. T. (2000b) *The Transuranium People: The Inside Story*, Imperial College Press, London, pp. 400–17.

Hofmann, S., Ninov, V., Hessberger, F. P., Armbruster, P., Folger, H., Münzenberg, G., Schott, H. J., Popeko, A. G., Yeremin, A. V., Andreyev, A. N., Saro, S., Janik, R., and Leino, M. (1995a) *Z. Phys.,* **A350**, 277–80.

Hofmann, S., Ninov, V., Hessberger, F. P., Armbruster, P., Folger, H., Münzenberg, G., and Leino, M. (1995b) *Z. Phys.,* **A350**, 281–2.

Hofmann, S., Ninov, V., Hessberger, F. P., Armbruster, P., Folger, H., Münzenberg, G., Schott, H. J., Popeko, A. G., Yeremin, A. V., Saro, S., Janik, R., and Leino, M. (1996) *Z. Phys.,* **A354**, 229–30.

Hofmann, S. (1998) *Rep. Prog. Phys.,* **61**, 639–89.

Hofmann, S. and Munzenberg, G. (2000) *Rev. Modern Phys.,* **72**, 733–67.

Hofmann, S., Hessberger, F. P., Ackermann, D., Münzenberg, G., Antalic, S., Cagarda, P., Kindler, B., Kojouharova, J., Leino, M., Lommel, B., Mann, R., Popeko, A. G., Reshitko, S., Saro, S., Uusitalo, J., and Yeremin, A. V. (2002) *Eur. Phys. J. A,* **14**, 147–57.

Hübener, S., Taut, S., Vahle, A., Dressler, R., Eichler, B., Gäggeler, H. W., Jost, D. T., Piguet, D. T., Türler, A., Brüchle, W., Jäger, E., Schädel, M., Schimpf, E., Kirbach, U., Trautmann, N., and Yakushev, A. B. (2001) *Radiochim. Acta,* **89**, 737–41.

Hulet, E. K., Lougheed, R. W., Wild, J. F., and Landrum, J. H. (1980) *J. Inorg. Nucl. Chem.,* **42**, 79–82.

Hyde, E. K., Hoffman, D. C., and Keller, O. L. Jr (1987) *Radiochim. Acta,* **42**, 57–102.

Ionova, G. V., Pershina, V., Johnson, E., Fricke, B., and Schädel, M. (1992) *J. Phys. Chem.,* **96**, 11096–101.

Ionova, G. V., Pershina, V., Zuraeva, I. T., and Suraeva, N. I. (1996) *Sov. Radiochem.,* **37**, 282–91.

Ishikawa, Y. and Kaldor, U. in *Computational Chemistry, Reviews of Current Trends* (1996) (ed. J. Leszczynski), Worlds Scientific, Singapore, Vol. 1, pp. 1–52.

Jampolskii, V. I. (1973) Doctoral Thesis, Moscow State University.

Johnson, E., Fricke, B., Keller, O. L. Jr, Nestor, C. W. Jr, and Ticker, T. C. (1990) *J. Chem. Phys.,* **93**, 8041–50.

Johnson, E. and Fricke, B. (1991) *J. Phys. Chem.,* **95**, 7082–4.

Johnson, E., Pershina, V., and Fricke, B. (1999) *J. Phys. Chem.,* **103**, 8458–62.

Johnson, E., Fricke, B., Jacob, T., Dong, C. Z., Fritzsche, S., and Pershina, V. (2002) *J. Chem. Phys.,* **116**, 1862–8.

Jorgensen, C. K. (1968) *Chem. Phys. Lett.,* **2**, 549–50.

Kacher, C. D., Gregorich, K. E., Lee, D. M., Watanabe, Y., Kadkhodayan, B., Yang, B. J., Hsu, M., Hoffman, D. C., and Bilewicz, A. (1996a) *Radiochim. Acta,* **75**, 127–33.

Kacher, C. D., Gregorich, K. E., Lee, D. M., Watanabe, Y., Kadkhodayan, B., Wierczinski, B., Lane, M. R., Sylwester, E. R., Keeney, D. A., Hendricks, M., Hoffman, D. C., and Bilewicz, A. (1996b) *Radiochim. Acta,* **75**, 135–9.

Kadkhodayan, B., Türler, A., Gregorich, K. E., Nurmia, M. J., Lee, D. M., and Hoffman, D. C. (1992) *Nucl. Instrum. Methods,* **A317**, 254–61.

Kadkhodayan, B. (1993) *On-Line Gas Chromatographic Studies of Rutherfordium (element 104), Hahnium (element 105), and Homologs*, Doctoral Thesis, LBL-33961, Berkeley.

Kadkhodayan, B., Türler, A., Gregorich, K. E., Baisden, P. A., Czerwinski, K. R., Eichler, E., Gäggeler, H. W., Hamilton, T. M., Stoyer, N. J., Jost, D. T., Kacher, C. D., Kovacs, A., Kreek, S. A., Lane, M. R., Mohar, M. F., Neu, M. P., Sylwester, E. R., Lee, D. M., Nurmia, M. J., Seaborg, G. T., and Hoffman, D. C. (1996) *Radiochim. Acta,* **72**, 169–78.

Kaldor, U. and Eliav, E. (1998) *Adv. Quantum. Chem.,* **31**, 313–36.

Kaldor, U. and Eliav, E. (2000) Energies and other properties of heavy atoms and molecules, in *Quantum Systems in Chemistry and Physics,* vol. II (eds. A. Hernandes-Laguna, J. Maruani, R. McWeeny, S. Wilson), Kluwer, Dordrecht, vol. 1, pp. 161–176.

Karol, P. J., Nakahara, H., Petley, B. W., and Vogt, E. (2001) *Pure Appl. Chem.,* **73**, 959–67.

Karol, P. J., Nakahara, H., Petley, B. W., and Vogt, E. (2003) *Pure Appl. Chem.,* **75**, 1601–11.

Keller, O. L. Jr, Burnett, J. L., Carlson, T. A., and Nestor, C. W. J. (1970) *J. Phys. Chem.,* **74**, 1127–34.

Keller, O. L. Jr, Nestor, C. W., Carlson, T. A., and Fricke, B. (1973) *J. Phys. Chem.,* **77**, 1806–9.

Keller, O. L. Jr, Nestor, C. W., and Fricke, B. (1974) *J. Phys. Chem.,* **78**, 1845–9.

Keller, O. L. Jr and Seaborg, G. T. (1977) *Annu. Rev. Nucl. Sci.,* **27**, 139–66.

Keller, O. L. Jr (1984) *Radiochim. Acta,* **37**, 169–80.

Kirbach, U. W., Folden, C. M. III, Ginter, T. N., Gregorich, K. E., Lee, D. M., Ninov, V., Omtvedt, J. P., Patin, J. B., Seward, N. K., Strellis, D. A., Sudowe, R., Türler, A., Wilk, P. A., Zielinski, P. M., Hoffman, D. C., and Nitsche, H. (2002) *Nucl. Instrum. Methods A,* **484**, 587–94.

Kohn, W., Becke, A. D., and Parr, R. G. (1996) *J. Phys. Chem.,* **100**, 12974–80.

Kratz, J. V., Zimmermann, H. P., Scherer, U. W., Schädel, M., Brüchle, W., Gregorich, K. E., Gannett, C. M., Hall, H. L., Henderson, R. A., Lee, D. M., Leyba, J. D., Nurmia, M. J., Hoffman, D. C., Gäggeler, H. W., Jost, D., Baltensperger, U., Ya, N. Q., Türler, A., and Lienert, C. (1989) *Radiochim. Acta,* **48**, 121–33.

Kratz, J. V., Gober, M. K., Zimmermann, H. P., Schädel, M., Brüchle, W., Schimpf, E., Gregorich, K. E., Türler, A., Hannink, N. J., Czerwinski, K. R., Kadkhodayan, B., Lee, D. M., Nurmia, M. J., Hoffman, D. C., Gäggeler, H. W., Jost, D., Kovacs, J., Scherer, U. W., and Weber, A. (1992) *Phys. Rev. C,* **45**, 1064–9.

Kratz, J. V. (1999a) Fast chemical separation procedures for transactinides, in *Heavy Elements and Related New Phenomena* (eds. W. Greiner and R. K. Gupta), World Scientific, Singapore, pp. 43–63.

Kratz, J. V. (1999b) Chemical properties of the transactinide elements, in *Heavy Elements and Related New Phenomena* (eds. W. Greiner and R. K. Gupta), World Scientific, Singapore, pp. 129–93.

Krebs, B., and Hasse, K. D. (1976) *Acta Crystallogr., B* **32**, 1334

Kruppa, A. T., Bender, M., Nazarewicz, W., Reinhard, P. G., Vertse, T., and Cwiok, S. (2000) *Phys. Rev. C,* **61** 034313-1–13.

Kugler, E., Fiander, D., Jonson, B., Haas, H., Przewloka, A., Ravn, H. L., Simon, D. J., and Zimmer, K. (1992) *Nucl. Instrum. Methods. B,* **70**, 41–9.

Landau, A., Eliav, E., Ishikawa, Y., and Kaldor, U. (2001) *J. Chem. Phys.,* **114**, 2977–80.

Lazarev, Y. A., Lobanov, Y. V., Oganessian, Y. T., Utyonkov, V. K., Abdullin, F. S., Buklanov, G. V., Gikal, B. N., Iliev, S., Mezentsev, A. N., Polyakov, A. N., Sedykh, I. M., Shirokovsky, I. V., Subbotin, V. G., Sukhov, A. M., Tsyganov, Y. S., Zhuchko, V. E., Lougheed, R. W., Moody, K. J., Wild, J. F., Hulet, E. K., and McQuaid, J. H. (1994) *Phys. Rev. Lett.,* **73**, 624–7.

Lazarev, Y. A., Lobanov, Y. V., Oganessian, Y. T., Tsyganov, Y. S., Utyonkov, V. K., Abdullin, F. S., Iliev, S., Polyakov, A. N., Rigol, J., Shirokovsky, I. V., Subbotin, V. G., Sukhov, A. M., Buklanov, G. V., Gikal, B. N., Kutner, V. B., Mezentsev, A. N., Sedykh, I. M., Vakatov, D. V., Lougheed, R. W., Wild, J. F., Moody, K. J., and Hulet, E. K. (1995) *Phys. Rev. Lett.,* **75**, 1903–6.

Lazarev, Y. A., Lobanov, Y. V., Oganessian, Y. T., Utyonkov, V. K., Abdullin, F. S., Polyakov, A. N., Rigol, J., Shirokovsky, I. V., Tsyganov, Y. S., Iliev, S., Subbotin, V. G., Sukhov, A. M., Buklanov, G. V., Gikal, B. N., Kutner, V. B., Mezentsev, A. N., Subotic, K., Wild, J. F., Longheed, R. W., and Moody, K. J. (1996) *Phys. Rev. C,* **54**, 620–5.

Lijima, K. and Shibata, S. (1974) *Bull. Chem. Soc. Jpn.,* **47**, 1393.

Lijima, K. and Shibata, S. (1975) *Bull. Chem. Soc. Jpn.,* **48**, 666.

Lim, I., Pernpointner, M., Seth, M., and Schwerdtfeger, P. (1999) *Phys. Rev. A,* **60**, 2822–8.

Liu, W., Hong, G., Dai, D., Li, L., and Dolg, M. (1997) *Theor. Chem. Acc.,* **96**, 75–83.

Liu, W. and van Wüllen, C. (1999) *J. Chem. Phys.,* **110**, 3730–5.

Liu, W., van Wüllen, C., Han, Y. K., Choi, Y. J., and Lee, Y. S. (2001) *Adv. Quant. Chem.,* **39**, 325–55.

Lougheed, R. W., Moody, K. J., Wild, J. F., Hulet, E. K., McQuaid, J. H., Lazarev, Y. A., Lobanov, Y. V., Oganessian, Y. T., Utyonkov, V. K., Abdullin, F. S., Buklanov, G. V., Gikal, B. N., Iliev, S., Mezentsev, A. N., Polyakov, A. N., Sedykh, I. M., Shirokovsky, I. V., Subbotin, V. G., Sukhov, A. M., Tsyganov, Y. S., and Zhuchko, V. E. (1994) *J. Alloys Compds,* **213**, 61–6.

Lougheed, R. W., Moody, J., Wild, J. F., Stoyer, N. J., Stoyer, M. A., Oganessian, Y. T., Utyonkov, V. K., Lobanov, Y. V., Abdullin, F. S., Polyakov, A. N., Shirokovsky, I. V., Tsyganov, Y. S., Gulbekian, G. G., Gobomolov, S. L., Gikal, B. N., Mezentsev, A. N., Iliev, S., Subbotin, V. G., Sukhov, A. M., Buklanov, G. V., Subotic, K., and Itkis, M. G. K. (2000) NUCL Abstract 19, San Francisco, CA, March 27.

Loveland, W., Gregorich, K. E., Patin, J. B., Peterson, D., Rouski, C., Zielinski, P., and Aleklett, K. (2002) *Phys. Rev. C,* **66** 044617-1–5.

Mann, J. B. (1969) *J. Chem. Phys.,* **51**, 841.

Mann, J. B. and Waber, J. T. (1970) *J Chem. Phys.,* **53**, 2397.

Meldner, H. (1967) *Ark. Fys.,* **36**, 593–8.

Moore, C. E. (1958) Atomic Energy Levels, Natl. Bur. Stand. (U. S.) Circ. No. 467 (U. S. GPO, Washington, DC, 1952), Vol. II; III.

Mulliken, R. S. (1955) *J. Chem. Phys.,* **23**, 1833–46.

Myers, W. D. and Swiatecki, W. J. (1966) *Nucl. Phys.,* **81**, 1.

Myers, W. D. and Swiatecki, W. J. (2000) *Phys. Rev. C,* **6204**, 312–17.

Nagame, Y., Asai, M., Haba, H., Tsukada, K., Goto, S., Sakama, M., Nishinaka, I., Toyoshima, A., Akiyama, K., and Ichikawa, S. (2002) *J. Nucl. Radiochem. Sci.,* **3**, 129–32.

Nash, C. S. and Bursten, B. E. (1995) *New J. Chem.,* **19**, 669–75.

Nash, C. S., Bursten, B. E., and Ermler, W. C. (1997) *J. Chem. Phys.,* **106**, 5133–42.

Nash, C. S. and Bursten, B. E. (1999a) *J. Phys. Chem. A,* **103**, 402–10.

Nash, C. S. and Bursten, B. E. (1999b) *Angew. Chem. Int. Ed. Engl.,* **38**, 151–3.

Nash, C. S. and Bursten, B. E. (1999c) *J. Phys. Chem. A,* **103**, 632–6.

Nilsson, S. G., Tsang, C. F., Sobiczewski, A., Szymanski, Z., Wycech, S., Gustafsson, G., Lam, I. L., Möller, P., and Nilsson, B. (1969a) *Nucl. Phys.,* **A131**, 1.

Nilsson, S. G., Thompson, S. G., and Tsang, C. F. (1969b) *Phys. Lett.,* **28B**, 458.

Oganessian, Y. T. and Zvara, I. (1993) *Pure Appl. Chem.,* **65**, 1820–1.

Oganessian, Y. T., Yeremin, A. V., Popeko, A. G., Bogomolov, S. L., Buklanov, G. V., Chelnokov, M. L., Chepigin, V. I., Gikal, B. N., Gorshkov, V. A., Gulbekian, G. G., Itkis, M. G., Kabachenko, A. P., Lavrentev, A. Y., Malyshev, O. N., Rohac, J., Sagaidak, R. N., Hofmann, S., Saro, S., Giardinas, G., and Morita, K. (1999a) *Nature,* **400**, 242–5.

Oganessian, Y. T., Utyonkov, V. K., Lobanov, Y. V., Abdullin, F. S., Polyakov, A. N., Shirokovsky, I. V., Tsyganov, Y. S., Gulbekian, G. G., Gobomolov, S. L., Gikal, B. N., Mezentsev, A. N., Iliev, S., Subbotin, V. G., Sukhov, A. M., Buklanov, G. V., Subotic, K., Itkis, M. G., Moody, K. J., Wild, J. F., Stoyer, N. J., Stoyer, M. A., and Lougheed, R. W. (1999b) *Phys. Rev. Lett.,* **83**, 3154–7.

Oganessian, Y. T., Yeremin, A. Y., Gulbekian, G. G., Bogomolov, S. L., Chepigin, V. I., Gikal, B. N., Gorshkov, V. A., Itkis, M. G., Kabachenko, A. P., Kutner, V. B., Lavrentev, A. Y., Malyshev, O. N., Popeko, A. G., Rohac, J., Sagaidak, R. N., Hofmann, S., Münzenberg, G., Veselsky, M., Saro, S., Iwasa, N., and Morita, K. (1999c) *Eur. Phys. J. A,* **5**, 63–8.

Oganessian, Y. T., Utyonkov, V. K., Lobanov, Y. V., Abdullin, F. S., Polyakov, A. N., Shirokovsky, I. V., Tsyganov, Y. S., Gulbekian, G. G., Bogomolov, S. L., Gikal, B. N., Mezentsev, A. N., Iliev, S., Subbotin, V. G., Sukhov, A. M., Ivanov, O. V., Buklanov, G. V., Subotic, K., Itkis, M. G., Moody, K. J., Wild, J. F., Stoyer, N. J., Stoyer, M. A., and Lougheed, R. W. (2000a) *Phys. Rev. C,* **62** 041604 (R) 1–4.

Oganessian, Y. T., Utyonkov, V. K., Lobanov, Y. V., Abdulin, F. S., Polyakov, A. N., Shirokovsky, I. V., Tsyganov, Y. S., Gulbekian, G. G., Bogomolov, S. L., Gikal, B. N., Mezentsev, A. N., Iliev, S., Subbotin, V. G., Sukhov, A. M., Ivanov, O. V., Buklanov, G. V., Subotic, K., Itkis, M. G., Moody, K. J., Wild, J. F., Stoyer, N. J., Stoyer, M. A., Lougheed, R. W., Laue, C. A., Karelin, Y. A., and Tatarinov, A. N. (2000b) *Phys. Rev. C,* **63** 011301 (R) 1–2.

Oganessian, Y. T. (2001) *Nucl. Phys. A,* **685**, 17c.

Oganessian, Y. T. (2002) *J. Nucl. Radiochem. Sci.,* **3**, 5–8.

Oganessian, Y. T., Utyonkov, V. K., Lobanov, Y. V., Abdullin, F. S., Polyakov, A. N., Shirokovsky, I. V., Tsyganov, Y. S., Gulbekian, G. G., Bogomolov, S. L., Gikal, B. N., Mezentsev, A. N., Iliev, S., Subbotin, V. G., Sukhov, A. M., Ivanov, O. V., Buklanov, G. V., Subotic, K., Voinov, A. A., Itkis, M. G., Moody, K. J., Wild, J. F., Stoyer, N. J., Stoyer, M. A., Lougheed, R. W., and Laue, C. A. (2002) *Eur. Phys. J. A,* **15**, 201–4.

Oganessian, Y. T., Utyonkoy, V. K., Lobanov, Y. V., Abdullin, F. S., Polyakov, A. N., Shirokovsky, I. V., Tsyganov, Y. S., Gulbekian, G. G., Bogomolov, S. L., Mezentsev, A. N., Iliev, S., Subbotin, V. G., Sukhov, A. M., Voinov, A. A., Buklanov, G. V., Subotic, K., Zagrebaev, V. I., Itkis, M. G., Patin, J. B., Moody, K. J., Wild, J. F., Stoyer, M. A., Stoyer, N. J., Shaughnessy, D. A., Kenneally, J. M., and Lougheed, R. W. (2004a) *Phys. Rev. C,* **69**, 021601(R).

Oganessian, Y. T., Yeremin, A. V., Popeko, A. G., Malyshev, O. N., Belozerov, A. V., Buklanov, G. V., Chelnokov, M. L., Chepigin, V. I., Gorshkov, V. A., Hofmann, S., Itkis, M. G., Kabachenko, A. P., Kindler, B., Munzenberg, G., Sagaidak, R. N., Saro, S., Schott, H.-J., Streicher, B., Shutov, A. V., Svirikhin, A. I., and Vostokin, G. K. (2004b) *Eur. Phys. J. A,* **19**, 3–6.

Oganessian, Y. T., Utyonkov, V. K., Lobanov, Y. V., Abdullin, F. S., Polyakov, A. N., Shirokovsky, I. V., Tsyganov, Y. S., Gulbekian, G. G., Bogomolov, S. L., Gikal, B. N., Mezentsev, A. N., Iliev, S., Subbotin, V. G., Sukhov, A. M., Voinov, A. A., Buklanov, G. V., Subotic, K., Zagrebaev, V. I., Itkis, M. G., Patin, J. B., Moody, K. J., Wild, J. F., Stoyer, M. A., Stoyer, N. J., Shaughnessy, D. A., Kenneally, J. M., and Lougheed, R. W. (2004c) *Phys. Rev. C,* **69**, 054607.

Omtvedt, J.-P., Alstad, J., Eberhardt, K., Fure, K., Malmbeck, R., Mendel, M., Nähler, A., Skarnemark, G., Trautmann, N., Wiehl, N., and Wierczinski, B. J. (1998) *J. Alloys Compds,* **271**, 303.

Omtvedt, J. P., Alstad, J., Breivik, H., Dyve, J. E., Eberhardt, K., Folden, C. M. III, Ginter, T., Gregorich, K. E., Hult, E. A., Johansson, M., Kirbach, U. W., Lee, D. M., Mendel, M., Nahler, A., Ninov, V., Omtvedt, L. A., Patin, J. B., Skarnemark, G., Stavsetra, L., Sudowe, R., Wiehl, N., Wierczinski, B., Wilk, P. A., Zielinski, P. M., Kratz, J. V., Trautmann, N., Nitsche, H., and Hoffman, D. C. (2002) *J. Nucl. Radiochem. Sci.,* **3**, 121–4.

Parpia, F. A., Froese-Fisher, S., and Grant, I. P. (1996) *CPC,* **94**, 249–71.

Paulus, W., Kratz, J. V., Strub, E., Zauner, S., Brüchle, W., Schädel, M., Schausten, B., Adams, J. L., Gregorich, K. E., Hoffman, D. C., Laue, C., Lee, D. M., McGrath, C. A., Shaughnessy, D. K., Strellis, D. A., and Sylwester, E. R. (1999) *Radiochim. Acta,* **84**, 69–77.

Penneman, R. A., Mann, J. B., and Jorgensen, C. K. (1971) *Chem. Phys. Lett.,* **8**, 321–6.

Penneman, R. A. and Mann, J. B. (1976) Calculational Chemistry of the Superheavy Elements; Comparison with elements of the 7th Period, in *J. Inorg. Chem. Suppl., Proc. Moscow Symp. on Chemistry of the Transuranium Elements,* pp. 257–63.

Peppard, D. F., Mason, G. W., and Maier, J. L. (1956) *J. Inorg. Nucl. Chem.,* **3**, 215.

Pepper, M. and Bursten, B. E. (1991) *Chem. Rev.,* **91**, 719–40.

Pershina, V., Sepp, W.-D., Fricke, B., and Rosen, A. (1992a) *J. Chem. Phys.,* **96**, 8367–78.

Pershina, V., Sepp. W.-D., Bastug, T., Fricke, B., and Ionova, G. V. (1992b) *J. Chem. Phys.,* **97**, 1123–31.

Pershina, V. and Fricke, B. (1993) *J. Chem. Phys.,* **99**, 9720–9.

Pershina, V. and Fricke, B. (1994) *J. Phys. Chem.,* **98**, 6468–73.

Pershina, V. and Fricke, B. (1995) *J. Phys. Chem.,* **99**, 144–7.

Pershina, V. (1996) *Chem. Rev.,* **96**, 1977–2010.

Pershina, V. and Fricke, B. (1996) *J. Phys. Chem.,* **100**, 8748–51.

Pershina, V. (1998a) *Radiochim. Acta,* **80**, 65–73.

Pershina, V. (1998b) *Radiochim. Acta,* **80**, 75–84.

Pershina, V. and Bastug, T. (1999) *Radiochim. Acta,* **84**, 79–84.

Pershina, V. and Fricke, B. (1999) Electronic Structure and Chemistry of the Heaviest Elements, in *Heavy Elements and Related New Phenomena,* vol. 1, (eds. W. Greiner and R. K. Gupta), World Scientific, Singapore, pp. 184–262.

Pershina, V., Johnson, E., and Fricke, B. (1999) *J. Phys. Chem. A,* **103**, 8463–70.

Pershina, V. and Bastug, T. (2000) *J. Chem. Phys.,* **113**, 1441–6.

Pershina, V., Bastug, T., Fricke, B., and Varga, S. (2001) *J. Phys. Chem.,* **115**, 792–9.

Pershina, V. and Kratz, J. V. (2001) *Inorg. Chem.,* **40**, 776–80.

Pershina, V., Bastug, T., Jacob, T., Fricke, B., and Varga, S. (2002a) *Chem. Phys. Lett.,* **365**, 176–83.

Pershina, V., Trubert, D., Le Naour, C., and Kratz, J. V. (2002b) *Radiochim. Acta,* **90**, 869–77.

Pershina, V. (2003) Theoretical chemistry of the heaviest elements, in *The Chemistry of Superheavy Elements* (ed. M. Schädel), Kluwer Academic Publishers, Dordrecht, The Netherland, pp. 31–94.

Pershina, V. and Hoffman, D. C. (2003) The chemistry of the heaviest elements, in *Theoretical Chemistry and Physics of Heavy and Superheavy Elements* in the series Comput. Phys. Commun. *Progress in Theoretical Chemistry and Physics* (eds. U. Kaldor and S. Wilson), Kluwer Academic Publishers, Dordrecht, The Netherlands, ch. 3, pp. 55–114.

Pfrepper, G., Pfrepper, R., Krauss, D., Yakushev, A. B., Timokhin, S. N., and Zvara, I. (1998) *Radiochim. Acta,* **80**, 7–12.

Pitzer, K. S. (1975a) *J. Chem. Phys.,* **63**, 1032–3.

Pitzer, K. S. (1975b) *J. Chem. Soc., Chem. Commun.*, 760–1.

Pyper, N. C. and Grant, I. P. (1981) *Proc. R. Soc. Lond. A,* **376**, 483–92.

Pyykkö, P. (1988) *Chem. Rev.,* **88**, 563–94.

Pyykkö, P., Tokman, M., and Labzowsky, L. N. (1998) *Phys. Rev. A,* **57**, R689–92.

Randrup, J., Larsson, S. E., Moller, P., Sobiczewski, A., and Kukasiak, A. (1974) *Phys. Scr.,* **10A**, 60–4.

Rieth, U., Herlert, A., Kratz, J. V., Schweikhard, L., Vogel, M., and Walther, C. (2002) *Radiochim. Acta,* **90**, 337–43.

Rosen, A., Fricke, B., Morovic, T., and Ellis, D. E. (1979) *J. Phys. C4, Suppl. 4,* **40**, C4/218–19.

Rosen, A. (1997) *Adv. Quant. Chem.,* **29**, 1–30.

Ryzhkov, M. V., Gubanov, V. A., and Zvara, I. (1992) *Radiochim. Acta,* **57**, 11–14.

Saue, T., Faegri, K., and Gropen, O. (1996) *Chem. Phys. Lett.,* **263**, 360–6.

Schädel, M., Brüchle, W., Schimpf, E., Zimmermann, H. P., Gober, M. K., Kratz, J. V., Trautmann, N., Gäggeler, H., Jost, D., Kovacs, J., Scherer, U. W., Weber, A., Gregorich, K. E., Türler, A., Czerwinski, K. R., Hannink, N. J., Kadkhodayan, B., Lee, D. M., Nurmia, M. J., and Hoffman, D. C. (1992) *Radiochim. Acta,* **57**, 85–92.

Schädel, M. (1995) *Radiochimica Acta,* **70/71**, 207–23.

Schädel, M., Brüchle, W., Dressler, R., Eichler, B., Gäggeler, H. W., Günther, R., Gregorich, K. E., Hoffman, D. C., Hübener, S., Jost, D. T., Kratz, J. V., Paulus, W., Schumann, D., Timokhin, S., Trautmann, N., Türler, A., Wirth, G., and Yakuschev, A. (1997a) *Nature* (*Lett.*), **388**, 55–7.

Schädel, M., Brüchle, W., Schausten, B., Schimpf, E., Jäger, E., Wirth, G., Günther, R., Kratz, J. V., Paulus, W., Seibert, A., Thorle, P., Trautmann, N., Zauner, S., Schumann, D., Andrassy, M., Misiak, R., Gregorich, K. E., Hoffman, D. C., Lee, D. M., Sylwester, E. R., Nagame, Y., and Oura, Y. (1997b) *Radiochim. Acta,* **77**, 149–59.

Schädel, M., Brüchle, W., Jäger, E., Schausten, B., Wirth, G., Paulus, W., Günther, R., Eberhardt, K., Kratz, J. V., Seibert, A., Strub, E., Thörle, P., Trautmann, N., Waldek, W., Zauner, S., Schumann, D., Kirbach, U., Kubica, B., Misiak, R., Nagame, Y., and Gregorich, K. E. (1998) *Radiochim. Acta,* **83**, 163–5.

Schädel, M. (2002) *J. Nucl. Radiochem. Sci.,* **3**, 113–20.

Schwarz, W. H. E., Van Wezenbeek, E. M., Baerends, E. J., and Snijders, J. G. (1989) *J. Phys. B,* **22**, 1515–30.

Schwarz, W. H. E. (1990) *Theoretical Models of Chemical Bonding,* Springer, Berlin, pp. 593–643.

Schwerdtfeger, P., Dolg, M., Schwarz, W. H. E., Bowmaker, G. A., and Boyd, P. W. D. (1989) *J. Chem. Phys.,* **91**, 1762–74.

Schwerdtfeger, P. and Seth, M. (1998) Relativistic effects on the superheavy elements, in *Encyclopedia on Computational Chemistry*, vol. 4, John Wiley, New York, pp. 2480–99.

Seaborg, G. T. (1968) *Annu. Rev. Nucl. Sci.,* **18**, 53.

Seaborg, G. T. and Keller, O. L. Jr (1986) Future elements, in *The Chemistry of the Actinide Elements,* 2nd edn, vol. II (eds. J. J. Katz, G. T. Seaborg, and L. R. Morss), Chapman & Hall, London, pp. 1635–43.

Seaborg, G. T. (1996) *J. Chem. Soc., Dalton Trans.*, 3899–907.

Seth, M., Schwerdtfeger, P., Dolg, M., Faegri, K., Hess, B. A., and Kaldor, U. (1996) *Chem. Phys. Lett.,* **250**, 461–5.

Seth, M., Schwerdtfeger, P., and Dolg, M. (1997) *J. Chem. Phys.,* **106**, 3623–32.

Seth, M., Cooke, F., Schwerdtfeger, P., Heully, J.-L., and Pelissier, M. (1998a) *J. Chem. Phys.,* **109**, 3935–43.

Seth, M., Faegri, K., and Schwerdtfeger, P. (1998b) *Angew. Chem. Int. Ed. Engl.,* **37**, 2493–6.

Seth, M., Schwerdtfeger, P., and Faegri, K. (1999) *J. Chem. Phys.,* **111**, 6422–33.

Shannon, R. D. (1976) *Acta Crystallogr. A,* **32**, 751–67.

Silva, R. J., Sikkeland, T., Nurmia, M., and Ghiorso, A. (1970a) *Inorg. Nucl. Chem. Lett.,* **6**, 733–9.

Silva, R., Harris, J., Nurmia, M., Eskola, K., and Ghiorso, A. (1970b) *Inorg. Nucl. Chem. Lett.,* **6**, 871–7.

Smolańczuk, R., Skalski, J., and Sobiczewski, A. (1995) *Phys. Rev. C,* **52**, 1871–80.

Smolańczuk, R. (1997) *Phys. Rev. C,* **56**, 812–24.

Smolańczuk, R. (1999a) *Phys. Rev. C,* **59**, 2634–9.

Smolańczuk, R. (1999b) *Phys. Rev. Lett.,* **83**, 4705–8.

Smolańczuk, R. (1999c) *Phy. Rev. C,* **61** 011601-1–4.

Smolańczuk, R. (2001a) *Phys. Lett. B,* **509**, 227–30.

Smolańczuk, R. (2001b) *Phys. Rev. C,* **63** 044607-1–8.

Sobiczewski, A., Smolańczuk, R., and Skalski, J. (1994) *J. Alloys Compds,* **213**, 38–42.

Soverna, S., Aebersold, H. U., Düllman, C. E., Eichler, B., Gäeggeler, H. W., Tobler, L., Türler, A., and Thi, Q. (2001) The GDCh Conference, Würzburg, Germany, September 2001.

Strub, E., Kratz, J. V., Kronenberg, A., Nähler, A., Thörle, P., Zauner, S., Brüchle, W., Jäger, E., Schädel, M., Schausten, B., Schimpf, E., Zongwei, L., Kirbach, U., Schumann, D., Jost, D., Türler, A., Asai, M., Nagame, Y., Sakara, M., Tsukada, K., Gäggeler, H. W., and Glanz, J. P. (2000) *Radiochim. Acta,* **88**, 265–71.

Strutinsky, V. M. (1966) *Sov. J. Nucl. Phys.,* **3**, 449–57.

Sylwester, E. R., Gregorich, K. E., Lee, D. M., Kadkhodayan, B., Türler, A., Adams, J. L., Kacher, C. D., Lane, M. R., Laue, C. A., McGrath, C. A., Shaughnessy, D. A., Strellis, D. A., Wilk, P. A., and Hoffman, D. C. (2000) *Radiochim Acta,* **88**, 837–43.

Timokhin, S. N., Yakushev, A. B., Xu, H. G., Perelygin, V. P., and Zvara, I. (1996) *J. Radioanal. Nucl. Chem. Lett.,* **212**, 31–4.

Trubert, D., Le Naour, C., Hussonois, M., Brillard, L., Montroy Gutman, F., Le Du, J. F., Constantinescu, O., Barci, V., Weiss, B., Gasparro, J., and Ardisson, G. (1999) in *Abstracts of the 1st Int. Conf. on Chemistry and Physics of the Transactinides*, Seeheim, September 26–30.

Türler, A., Gäggeler, H. W., Gregorich, K. E., Barth, H., Bruchle, W., Czerwinski, K. R., Gober, M. K., Hannink, N. J., Henderson, R. A., Hoffman, D. C., Jost, D. T., Kacher, C. D., Kadkhodayan, B., Kovacs, J., Kratz, J. V., Kreek, S. A., Lee, D. M., Leyba, J. D., Nurmia, M. J., Schädel, M., Scherer, U. W., Schimpf, E., Vermeulen, D., Weber, A., Zimmermann, H. P., and Zvara, I. (1992) *J. Radioanal. Nucl. Chem. Articles,* **160**, 327–39.

Türler, A. (1996) *Radiochim. Acta,* **72**, 7–17.

Türler, A., Eichler, B., Jost, D. T., Piguet, D., Gäggeler, H. W., Gregorich, K. E., Kadkhodayan, B., Kreek, S. A., Lee, D. M., Mohar, M., Sylwester, E., Hoffman, D. C., and Hübener, S. (1996) *Radiochim. Acta,* **73**, 55–66.

Türler, A., Dressler, R., Eichler, B., Gäggeler, H. W., Jost, D. T., Schädel, M., Bruchle, W., Gregorich, K. E., Trautmann, N., and Taut, S. (1998a) *Phys. Rev. C,* **57**, 1648–55.

Türler, A., Buklanov, G. V., Eichler, B., Gäggeler, H. W., Grantz, M., Hübener, S., Jost, D. T., Lubedev, V. Y., Piguet, D., Timokhin, S. N., Yakushev, A. B., and Zvara, I. (1998b) *J. Alloys Compds,* **271**, 287–91.

Türler, A., Brüchle, W., Dressler, R., Eichler, B., Eichler, R., Gäggeler, H. W., Gartner, M., Glatz, J. P., Gregorich, K. E., Hübener, S., Jost, D. T., Lebedev, V. Y., Pershina, V. G., Schädel, M., Taut, S., Timokhin, S. N., Trautmann, N., Vahle, A., and Yakushev, A. B. (1999) *Angew. Chem Int. Ed. Engl.,* **38**, 2212–13.

Türler, A., Düllman, C. E., Gäggeler, H. W., Kirbach, U. W., Yakushev, A. B., Schädel, M., Brüchle, W., Dressler, R., Eberhardt, K., Eichler, B., Eichler, R., Ginter, T. N., Glaus, F., Gregorich, K. E., Hoffman, D. C., Jäger, E., Jost, D. T., Lee, D. M., Nitsche, H., Patin, J. B., Pershina, V., Piguet, D., Qin, Z., Schausten, B., Schimpf, E., Schött, H.-J., Soverna, S., Sudowe, R., Thörle, P., Timokhin, S. N., Trautmann, N., Vahle, A., Wirth, G., and Zielinski, P. (2003) *Eur. Phys. J. A,* **17**, 505–8.

Varga, S., Engel, E., Sepp, W.-D., and Fricke, B. (1999) *Phys. Rev. A,* **59**, 4288–94.

Varga, S., Fricke, B., Hirata, M., Bastug, T., Pershina, V., and Fritzsche, S. (2000) *J. Phys. Chem. A,* **104**, 6495–8.

Visscher, L., Lee, T. J., and Dyall, K. G. (1996) *J. Chem. Phys.,* **105**, 8769–76.

Waber, J. T., Cromer, D. T., and Liberman, D., (1969) *J. Chem. Phys.* **51**, 664.

Waber, J. T. and Averill, F. W. (1974) *J. Chem. Phys.,* **60**, 4460–70.

Wierczinski, B. and Hoffman, D. C. (1996) Instrumentation for atom-at-a-time chemistry of the heavy elements, in *IANCAS Frontiers in Nuclear Chemistry* (eds. D. D. Sood, P. K. Reddy, and A. V. R. Pujari), Perfect Prints, Thane, India, pp. 171–91.

Wilk, P. A., Gregorich, K. E., Türler, A., Laue, C. A., Eichler, R., Ninov, V., Adams, J. L., Kirbach, U. W., Lane, M. R., Lee, D. M., Patin, J. B., Shaughnessy, D. A., Strellis, D. A., Nitsche, H., and Hoffman, D. C. (2000) *Phys. Rev. Lett.,* **85**, 2697–700.

Wilson, S., Grant, I. P., and Gyoffry, B. L. (1991) *The Effects of Relativity in Atoms, Molecules and the Solid State,* Plenum, New York.

Wood, C. P. and Pyper, N. C. (1981) *Chem. Phys. Lett.,* **84**, 614–21.

Yakushev, A. B., Timokhin, S. N., Vedeneev, M. V., Xu, H. G., and Zvara, I. (1996) *J. Radioanal. Nucl. Chem. Articles,* **205**, 63–7.

Yakushev, A. B., Buklanov, G. V., Chelnokov, M. L., Chepigin, V. I., Dmitriev, S. N., Gorshkov, V. A., Hübener, S., Lebedev, V. Y., Malyshev, O. N., Oganessian, Y. T., Popeko, A. G., Sokol, E. A., Timokhin, S. N., Türler, A., Vasko, V. M., Yeremin, A. V., and Zvara, I. (2001) *Radiochim. Acta,* **89**, 743–5.

Yakushev, A. B. (2002) Workshop on Recoil Separator for Superheavy Element Chemistry, March 20–21, 2002, Darmstadt.

Zharskii, I. M., Zasorin, E. Z., Spiridonov, V. P., Novikov, G. I., and Kupreev, V. N. (1975) *Koord. Khim.,* **1**, 574.

Zhuikov, B. L., Chuburkov, Y. T., Timokhin, S. N., Jin, K. U., and Zvara, I. (1989) *Radiochim. Acta,* **46**, 113–17.

Zhuikov, B. L., Glebov, V. A., Nefedov, V. S., and Zvara, I. (1990) *Radioanal. Nucl. Chem. Articles,* **143**, 103–11.

Zimmermann, H. P., Gober, M. K., Kratz, J. V., Schädel, M., Brüchle, W., Schimpf, E., Gregorich, K. E., Türler, A., Czerwinski, K. R., Hannink, N. J., Kadkhodayan, B., Lee, D. M., Nurmia, M. J., Hoffman, D. C., Gäggeler, G., Jost, D., Kovacs, J., Scherer, U. W., and Weber, A. (1993) *Radiochimica Acta,* **60**, 11–16.

Zvara, I., Chuburkov, Y. T., Tsaletka, R., and Shalaevskii, M. R. (1969) *Sov. Radiochem.,* **11**, 161–70.

Zvara, I., Chuburkov, Y. T., Belov, V. Z., Buklanov, G. V., Zakhvataev, B. B., Zvarova, T. S., Maslov, O. D., Caletka, R., and Shalaevsky, M. R. (1970) *J. Inorg. Nucl. Chem.,* **32**, 1885–94.

Zvara, I., Belov, V. Z., Domanov, V. P., Korotkin, Y. S., Chelnokov, L. P., Shalaevsky, M. R., Shchegolev, V. A., and Hussonois, M. (1972) *Sov. Radiochem.,* **14**, 115–18.

Zvara, I., Aikhler, V., Belov, V. Z., Zvarova, T. S., Korotkin, Y. S., Shalaevskii, M. R., Shchegolev, V. A., and Yussonnua, M. (1974) *Sov. Radiochem.,* **16**, 709–15.

Zvara, I., Belov, V. Z., Domanov, V. P., and Shalaevskii, M. R. (1976) *Sov. Radiochem.,* **18**, 328–34.

Zvara, I. (1985) *Radiochim. Acta,* **38**, 95–101.

SUBJECT INDEX

Vol. 1: 1–698, Vol. 2: 699–1395, Vol. 3: 1397–2111, Vol. 4: 2113–2798, Vol. 5: 2799–3440.

Page numbers suffixed by t and f refer to Tables and Figures respectively.

AUTHOR INDEX

Vol. 1: 1–698, Vol. 2: 699–1395, Vol. 3: 1397–2111, Vol. 4: 2113–2798, Vol. 5: 2799–3440.

Page numbers suffixed by t and f refer to Tables and Figures respectively.

Vol. 1: 1–698, Vol. 2: 699–1395, Vol. 3: 1397–2111, Vol. 4: 2113–2798, Vol. 5: 2799–3440

Vol. 1: 1–698, Vol. 2: 699–1395, Vol. 3: 1397–2111, Vol. 4: 2113–2798, Vol. 5: 2799–3440

Vol. 1: 1–698, Vol. 2: 699–1395, Vol. 3: 1397–2111, Vol. 4: 2113–2798, Vol. 5: 2799–3440

Vol. 1: 1–698, Vol. 2: 699–1395, Vol. 3: 1397–2111, Vol. 4: 2113–2798, Vol. 5: 2799–3440

Vol. 1: 1–698, Vol. 2: 699–1395, Vol. 3: 1397–2111, Vol. 4: 2113–2798, Vol. 5: 2799–3440

Vol. 1: 1–698, Vol. 2: 699–1395, Vol. 3: 1397–2111, Vol. 4: 2113–2798, Vol. 5: 2799–3440

Vol. 1: 1–698, Vol. 2: 699–1395, Vol. 3: 1397–2111, Vol. 4: 2113–2798, Vol. 5: 2799–3440

Vol. 1: 1–698, Vol. 2: 699–1395, Vol. 3: 1397–2111, Vol. 4: 2113–2798, Vol. 5: 2799–3440

Vol. 1: 1–698, Vol. 2: 699–1395, Vol. 3: 1397–2111, Vol. 4: 2113–2798, Vol. 5: 2799–3440

Vol. 1: 1–698, Vol. 2: 699–1395, Vol. 3: 1397–2111, Vol. 4: 2113–2798, Vol. 5: 2799–3440

Vol. 1: 1–698, Vol. 2: 699–1395, Vol. 3: 1397–2111, Vol. 4: 2113–2798, Vol. 5: 2799–3440

Vol. 1: 1–698, Vol. 2: 699–1395, Vol. 3: 1397–2111, Vol. 4: 2113–2798, Vol. 5: 2799–3440